Laboratory Directed Research and Development

Los Alamos National Laboratory

FY10 Annual Progress Report

LA-UR 11-01736

innovation for our nation

Los Alamos NATIONAL LABORATORY EST. 1943

About the Cover

There are enough wind resources in the US to provide 10 times the electric power we currently use, however wind power only accounts for 2% of our total electricity production. One of the main limitations to wind use is cost. Wind power currently costs 5-to-8 cents per kilowatt-hour, which is more than twice the cost of electricity generated by burning coal. In an LDRD project titled “Intelligent Wind Turbines,” Curtt Ammerman is applying Los Alamos National Laboratory’s leading-edge engineering expertise in modeling and simulation, experimental validation, and advanced sensing technologies to challenges faced in the design and operation of modern wind turbines.

Disclaimer

Issued March 2011

LA-UR 11-01736

Structure of this Report

In accordance with U.S. Department of Energy Order (DOE) 413.2B, the Laboratory Directed Research and Development (LDRD) annual report for fiscal year 2009 (FY09) provides summaries of each LDRD-funded project for the fiscal year, as well as full final reports on completed projects. The report is organized as follows:

Overview: An introduction to the LDRD Program at Los Alamos National Laboratory (LANL), the program's structure and strategic value, the LDRD portfolio management process, and highlights of outstanding accomplishments by LDRD researchers.

Project Summaries: The project summaries are organized first by science and technology categories: Physics, Chemistry and Material Sciences, Environmental and Biological Sciences, Information Science and Technology, and Technology. Within each category, summaries are organized by LDRD component: Directed Research (DR) projects first, Exploratory Research (ER) second, and Postdoctoral Research and Development (PRD) projects last. Full final reports are included at the end of each section.

Projects are listed in numerical order according to their project identification number, which consists of three parts. The first is the fiscal year in which the project began; the second is a unique numerical identifier; and the third identifies the project component.

Acknowledgements

Technical Review
William Priedhorsky
Robert Kraus Jr.

Publication Editor and Designer
Andrea Maestas

Team Contributors
Benjamin Brown
Lennett Rendon
Stephen Schultz
Debbie Martinez
Adrienne Sena
Susan Whittington
Douglas Wokoun

Table of Contents

Environmental and Biological Sciences

Information Science and Technology

Physics

Technology

by William Priedhorsky, LDRD Program Manager

R&D is one of the best investments a country can make. As quoted in *Rising Above the Gather Storm, Revisited*, "Robert Solow received a Nobel Prize in economics in part for his work that indicated that well over half of the growth in United States output per hour during the first half of the twentieth century could be attributed to advancements in knowledge, particularly technology." The impact of research and development (R&D) has only continued to grow in the half century since.

America competes with the world not only economically, but also in the hard currency of national security. A small but critical fraction of the nation's investment in national security – less than 10% – is R&D. Indeed, science and technology are arguably the nation's best option for advantage against our adversaries.

Los Alamos National Laboratory has contributed to national security since 1943. Our mission is to develop and apply science and technology to

- ensure the safety and reliability of U.S. nuclear deterrent,
- reduce the threat of weapons of mass destruction, proliferation, and terrorism, and
- solve national problems in defense, energy, environment, and infrastructure.

These missions demand that we *anticipate, innovate, and deliver* to solve the unsolved and know the unknown. We seek innovation that can drive breakthroughs in mission performance, whether that mission demands prediction of weapons aging, the remediation of legacy contamination, or the mitigation of transnational terrorism.

At Los Alamos, LDRD is an open market for ideas, inspired by mission. We succeed because of the diversity of our investments, which mix applied and fundamental research. Although no single project can guarantee results, the aggregate results of LDRD investment drive the Laboratory forward. Margaret Thatcher spoke in 1988 about the powerful but unpredictable benefits of R&D: "…although basic science can have colossal economic rewards, they are totally unpredictable. And therefore the rewards cannot be judged by immediate results. Nevertheless, the value of Faraday's work today must be higher than the capitalization of all shares on the stock exchange… . The greatest economic benefits of scientific research have always resulted from advances in fundamental knowledge rather than the search for specific applications … transistors were not discovered by the entertainment industry … but by people working on wave mechanics and solid state physics. [Nuclear energy] was not discovered by oil companies with large budgets seeking alternative forms of energy, but by scientists like Einstein and Rutherford…"

Our missions require breadth and depth in science and technology. Their complexity demands a span of excellence that crosses nearly every discipline in science. For example, the core nuclear weapons program demands prediction and control of materials in extreme conditions, computing at the petascale and soon the exascale, the understanding of turbulent fluid flow, miniaturized smart sensors, and advances in nuclear and high-energy density physics.

By investing in LDRD, Los Alamos builds its vision: to be the National Security Science Laboratory of choice, ready to take on whatever complex issue that the nation asks of us.

Maintaining our leadership in research and technology is crucial to America's success.

- President Obama

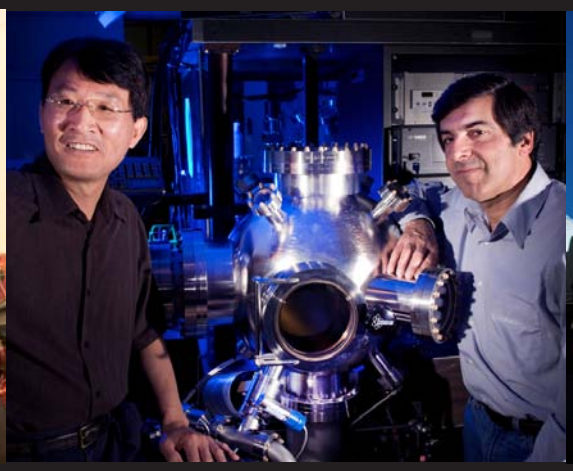

LDRD is the most prestigious source of research and development funding at the Laboratory. It follows a strategic guidance derived from the missions of DOE, the National Nuclear Security Administration, and the Laboratory. To execute that strategy, the Los Alamos LDRD program creates a free market for ideas that draws upon the bottom-up creativity of the Laboratory's best and brightest researchers. The combination of strategic guidance and free-market competition provides a continual stream of capabilities that position the Laboratory to accomplish its missions.

The LDRD program provides the Laboratory Director with the opportunity to strategically invest in forward-thinking, potentially high-payoff research that strengthens the Laboratory's capabilities for national problems. Funded in FY10 with approximately 5.8% of the Laboratory's overall budget, the LDRD program makes it possible for the best and brightest researchers to pursue cutting-edge research and development. This in turn enables the Laboratory to anticipate, innovate, and deliver world-class science, technology, and engineering.

PROGRAM STRUCTURE

The LDRD program is organized into three program components with distinct institutional objectives: Directed Research (DR), flagship investments in mission solutions; Exploratory Research (ER), smaller projects that invest in people and skills; and Postdoctoral Research and Development (PRD), recruiting bright, qualified, early-career scientists and engineers. In FY10, the LDRD program funded 269 projects with total costs of $126.4 million. These projects were selected through a rigorous and highly competitive peer-review process and are reviewed formally and informally throughout the fiscal year.

Directed Research

The DR component makes long-range investments in multidisciplinary scientific projects in key competency or technology-development areas vital to LDRD's long-term ability to execute Laboratory missions. In FY10, LDRD funded 51 DR projects, which represents approximately 58% of the program's research funds. Directed Research projects are typically funded up to a maximum of $1.7M per year for three years.

The DR component is guided by the LDRD Strategic Investment Plan, which is in turn guided by eight Grand Challenges that define the advances in science and technology that are needed to address Los Alamos missions. These challenges were originally set out in the Los Alamos National Security LLC contract and refined in a Laboratory-wide

workshop. The Grand Challenges have evolved in their four years in response to an ever-changing world. Figure 1 shows how the Grand Challenges align with the Laboratory's three "Science that Matters" thrusts.

Exploratory Research

The ER component is focused on developing and maintaining technical staff competencies in key strategic disciplines that form the foundation of the Laboratory's readiness for future national missions. Largely focused on a single discipline, ER projects explore highly innovative ideas that underpin Laboratory programs. In FY10, LDRD funded 135 ER projects, which represents approximately 35% of the program's research funds. Exploratory Research projects are typically funded up to a maximum of $375K per year for three years.

Unlike DR proposals, division endorsements are not required for ER proposals; instead, this component of the LDRD program is operated as an open and competitive path for every staff member to pursue funding for his/her great idea. The ER component is a critical channel for purely bottom-up creativity at the Laboratory. Nonetheless, it is strongly driven by mission research and development needs via the definition of the 12 research categories, and the assignment of investment between them.

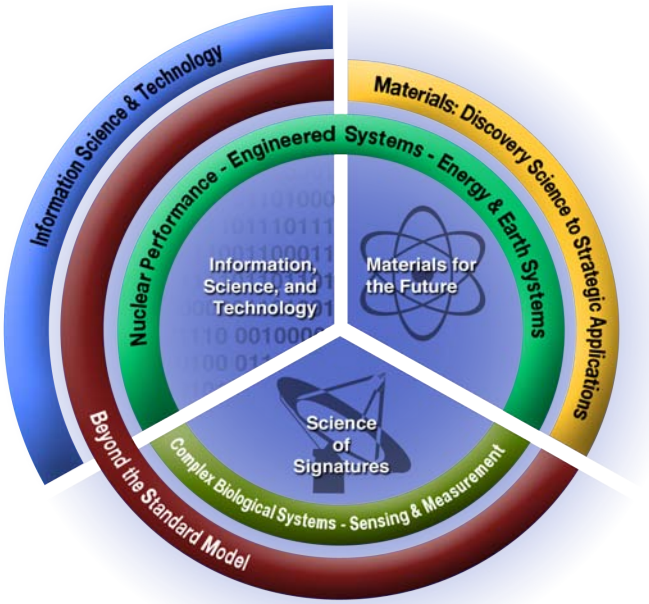

Figure 1: The science and technology Grand Challenges that guide the LDRD program's investment in Directed Research are aligned with the Laboratory's three "Science that Matters" thrusts.

Directed Research Grand Challenges	Mission Impact
Beyond the Standard Model	Sensitive instrumentation and tools to manipulate massive data volumes, in support of national security missions
Materials: Discovery Science to Strategic Applications	Energy sources, efficiency and storage; sensing for threat reduction; materials underpinnings of stockpile security
Complex Biological Systems	Energy, national security, health and the environment
Information Science and Technology	Overarching capability supporting all Laboratory missions
Earth and Energy Systems	Energy and climate security
Nuclear Performance	Stockpile safety, surety and reliability
Sensing and Measurement Science for Global Security	Nuclear weapons of mass destruction, space situational awareness, global environmental treaty monitoring and emerging threats
Engineered Systems	Systems-level solutions for all missions

Exploratory Research Technical Categories	Laboratory Capability
Nuclear Physics, Particle Physics, Astrophysics and Cosmology	Nuclear physics, astrophysics and cosmology
Materials Science	Materials
Earth and Environmental Sciences and Space Physics	Earth and space sciences
Chemistry and Chemical Sciences	Chemical sciences
Engineering and Engineering Sciences	Weapons science and engineering, advanced manufacturing, sensors, remote sensing and sensor systems
Computational, Information and Knowledge Sciences	Information and knowledge sciences, computer and computational sciences
High-Energy Density, Plasma and Fluid Physics	High-energy density plasmas and fluids
Biological Science, Biosecurity and Cognitive Sciences	Biosciences
Atomic, Optical and Quantum Physics	Chemical sciences
Energy Sciences, Technology and Engineering	Energy sciences, technology and engineering

Postdoc Research and Development

The PRD component of the program ensures the vitality of the Laboratory by recruiting early-career researchers. Through this investment, the LDRD program funds postdoctoral fellows to work for two years under the mentorship of PIs on highly innovative projects. The primary criterion for selection of LDRD-supported postdocs is the raw scientific and technical talent and performance of the candidate, with the exact specialty of the candidate a secondary factor. In FY10, LDRD funded 83 PRD projects, which represents 7% of the program's research funds. Postdoctoral Research and Development researchers are supported full-time for two years.

In addition to approximately 50 "Director's Postdocs," the LDRD program supported 10 distinguished postdoctoral fellows at a higher salary and for a three-year term. Distinguished postdoctoral fellow candidates typically show evidence of solving a major problem or providing a new approach or insight to a major problem; in other words, they show evidence of having a major impact in their research field. To recognize their role as future science and technology leaders, these appointments are named after some of the greatest leaders of the Laboratory's past.

Even more LDRD-funded postdocs are hired through DR and ER projects than directly through PRD appointments. Counting both avenues, the LDRD program supported almost 60% of the Laboratory's 547 postdocs in FY10. Among the DOE labs, the LANL postdoc population is exceeded only by Lawrence Berkeley National Laboratory, which has a special relationship with the neighboring University of California campus.

As the principal pipeline for new technical staff, the health of the postdoctoral program is of vital interest to the Laboratory. There is strong evidence that the postdoctoral program is excelling:

- Acceptance rate for Laboratory offers of postdoc appointments remains high, at 89%.
- 68% of US citizen distinguished postdocs selected since 1999 are still at the Laboratory as staff.
- The quality of postdocs hired at Los Alamos reveals a clear upward trend, evidenced by the high numbers of publications and citations at the time of their hire.

Post-doctoral appointments offer the single largest source of new scientific and engineering talent for the DOE laboratories and are therefore essential to maintaining their institutional vitality. - 2010 LDRD Report to Congress

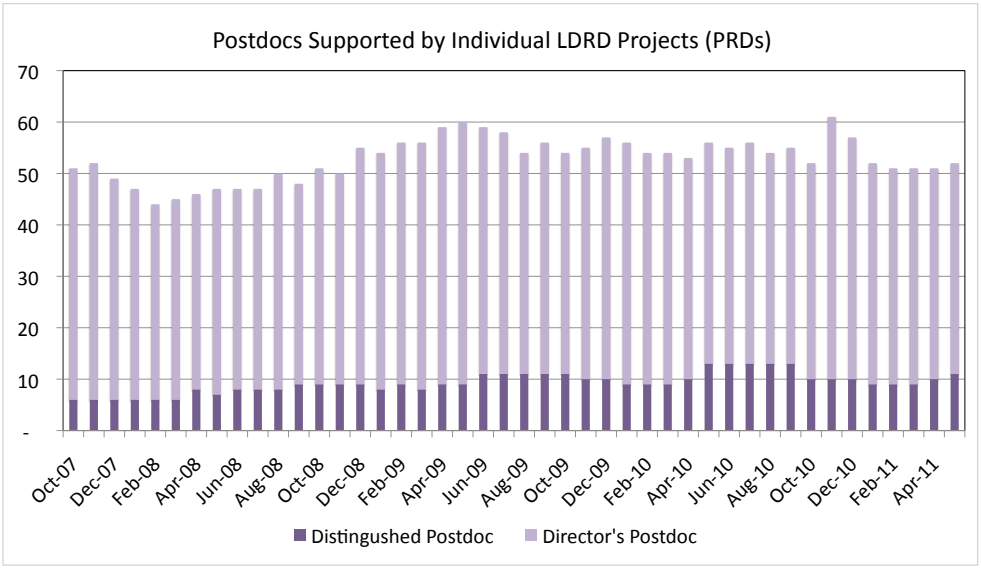

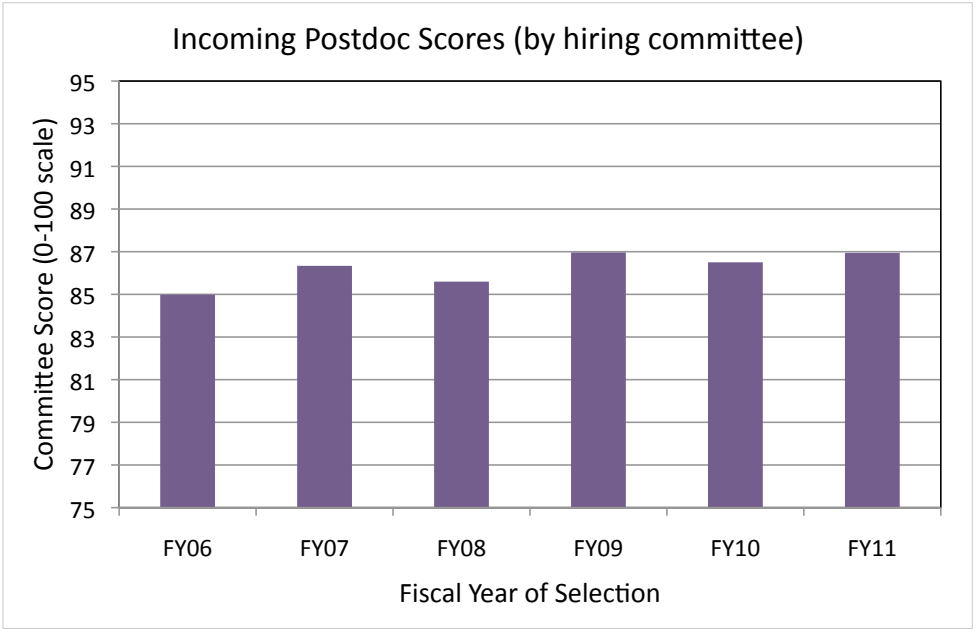

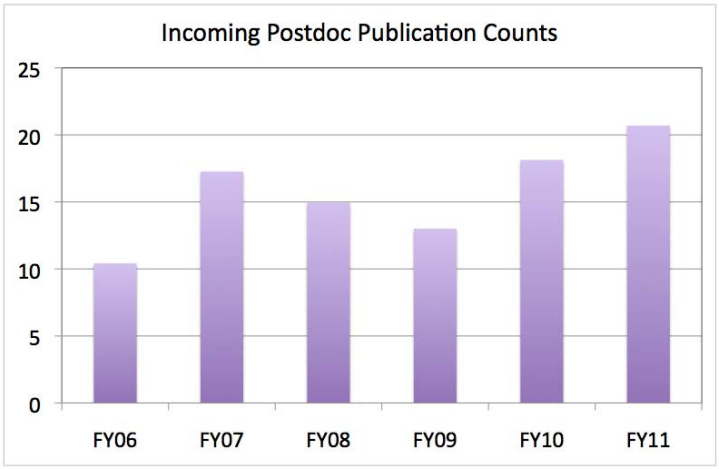

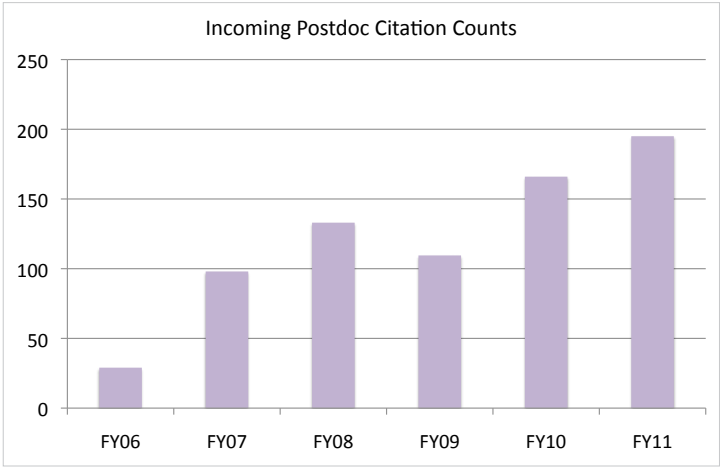

Program Reserve

Most LDRD investments are selected in a rigorous, multi-step peer-review process during the nine months preceding the new fiscal year. However, in a fast-changing world, there are needs that cannot wait until the next cycle of competition. The LDRD Program Office holds a reserve each year for these needs. This reserve is small on a program basis, but allowed the opportunity to make modest investments that address new opportunities. In FY10, the reserve budget was approximately $3M.

The top priority for the reserve is feasibility studies: short projects aimed at a key proof-of-principle, which open the door to either external or more substantial LDRD funding in the out years. Reserve is held foremost to exploit opportunity, rather than fix problems, and the expectation is that reserve projects will be the first step in a chain that leads to bigger things.

Reserve decisions are guided by strategic priorities articulated by Division Leaders, Associate Directors, and more senior management. They are also informed by the just-concluded competitive cycle, in which selection panels sometimes identify ideas that are exciting but just not mature enough for a full-scale investment.

Reserve calls often attract first-time LDRD proposers. In FY10 LDRD supported 27 reserve projects, ten of which were led by first-time LDRD PIs. Half of those projects resulted in internal or external follow-on funding. In collaboration with the Laboratory's Energy Security Center, Information Science and Technology Center, and Center for Bio-Security Science (also known as mission incubator centers), a portion of FY10 LDRD reserve funds were invested in ten mission incubator projects. One project in particular exemplifies how early LDRD investment enables spectacular results: Jane Nordholt's Quantum Communications work has resulted in two patent disclosures and interest from nine major companies. The work has also been submitted for an R&D 100 Award.

Quantum Cryptographic QKarD Proof-Of-Concept

In today's highly networked world, point-to-point communications that cannot take advantage of the network have limited to no commercial interest and very little use even in high-security, government systems. Quantum communications provide unconditional security using the laws of physics and information theory but have not been able to take advantage of networked communications or portable systems. The objective of this project is to make quantum communications commercially viable by demonstrating the key components of a quantum smartcard or

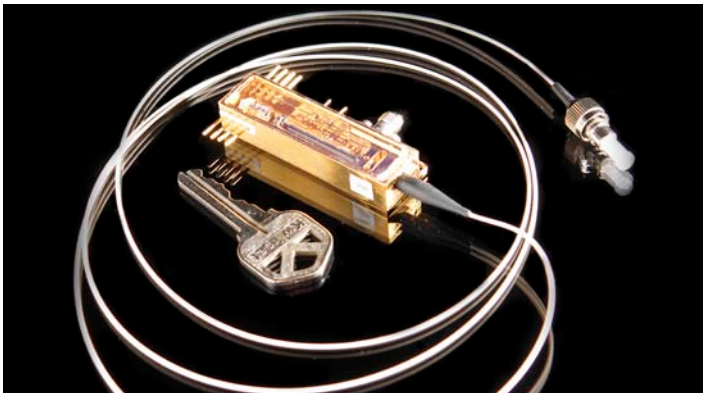

The prototype QKarD electro-optics module with its fiber optic pigtail.

QKarD. A QKarD would be a portable QC system that would communicate with a Trusted Authority (TA). The TA would authenticate users; produce unconditionally secure key with each user; and provide the information to users that would allow them to communicate with other users using quantum security. Such a QKarD could be part of a smart phone or used as a fillgun load key into user computers, smart phones, or encryptors at remote locations. Not only would the QKarD store quantum keys in secure memory, but it would also store a nonsecret database, which when used with the quantum keys would provide secure keys in common with any desired user. Should a user wish to communicate with a user not in the database, the QKarD would contact the TA using whatever communication methods it has available such as cellular telephone or Internet and without reducing the security of the quantum keys, receive information that would allow secure communication with the other user. This flexibility provides the portability and security needed to make QC commercially viable.

Although the Los Alamos QC team has already shown its ability to perform QC over active fiber optics and miniaturize things such as the conventional protocol processing needed for QKD into an FPGA, a miniaturized electro-optics module capable of QC is needed as well as theoretical development of the security protocols a QKarD would implement.

Many parts of the US government have a need for increased cybersecurity and, with the coming advent of the quantum computer, better cryptography. The QKarD opens up new ways to use quantum cryptography and offers flexibility and portability that will allow QKD to enable solutions in these areas. This work will make the QKarD feasible for secure communications and personnel authentication. The QKarD will also make it possible to miniaturize QKD transmitters for space and treaty verification. QKarD can also be used as part of a system for securing infrastructure such as the smartgrid or supervisory, control, and data acquisition (SCADA) systems.

From early career to senior scientist... LDRD supports a diverse pool of the Laboratory's best and brightest

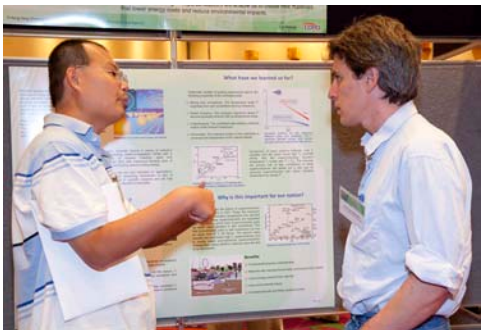

An evaluation of who leads and contributes to LDRD projects revealed that the program is supporting a diverse cross section of the Laboratory population.

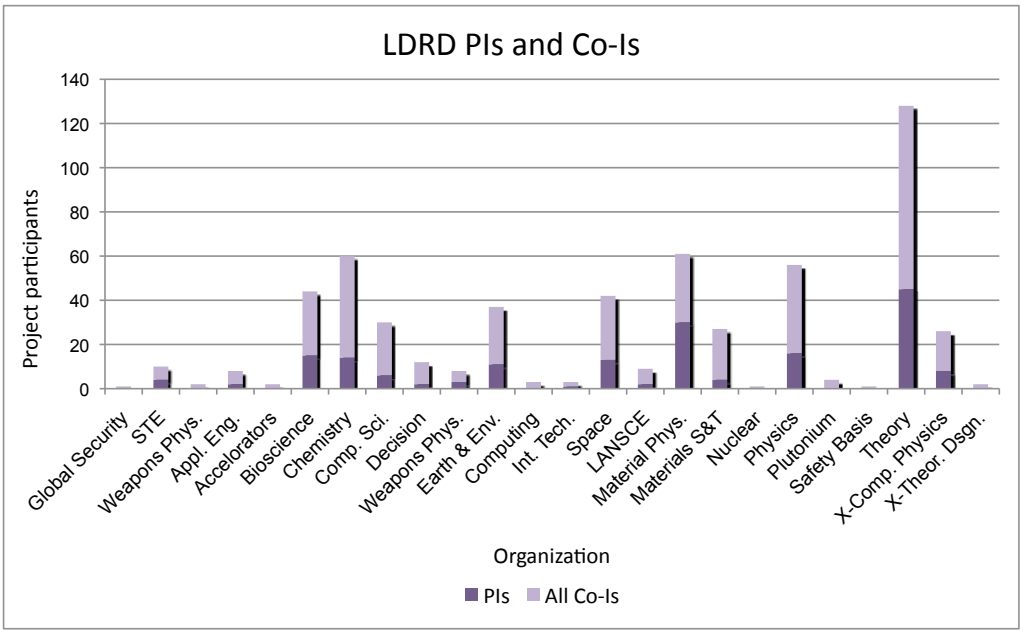

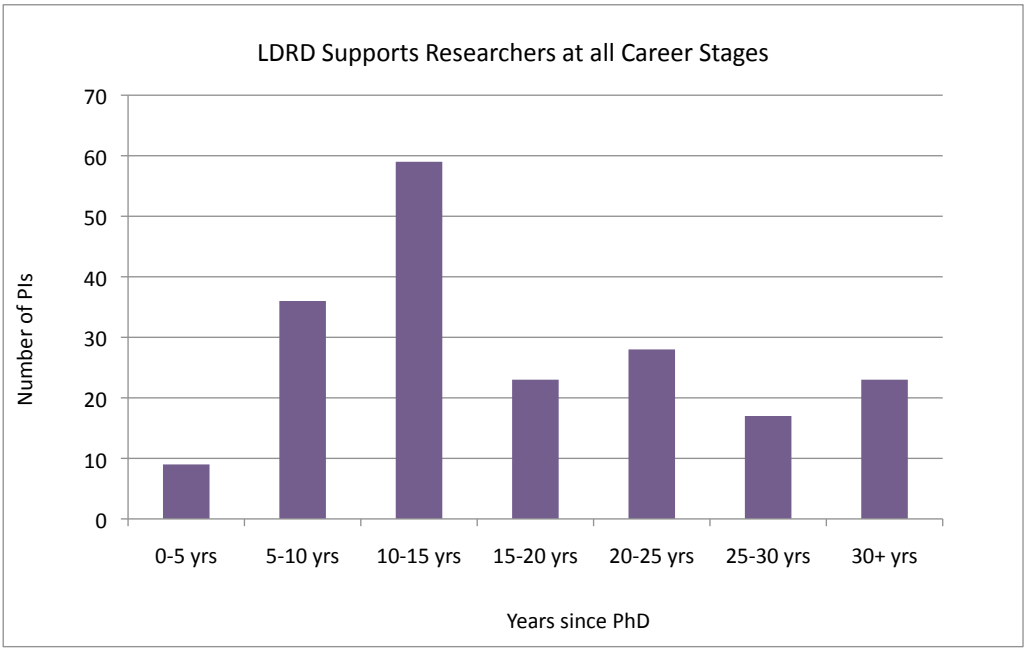

PROJECT SELECTIONS

The Los Alamos LDRD program operates as a free market for ideas driven by Laboratory strategy: Senior Laboratory leadership set science and technology priorities, then open an LDRD competition for ideas across the breadth of the Laboratory. Proposals are rigorously reviewed by panels drawn from Laboratory's intellectual leaders. Conflict of interest is carefully regulated. Evaluation criteria include innovation and creativity, potential scientific impact, viability of the research approach, qualifications of the team and leadership, and potential impact on Laboratory missions. The selection processes are modeled on best practices established by the National Science Foundation (NSF) and National Institutes of Health (NIH).

To guarantee fairness and transparency, and to ensure that the strongest proposals are funded, the selection panels include managers and technical staff drawn from the full range of technical divisions. Serving on an LDRD selection panel, such as the DR Strategy Team, is often a starting point on the path to leadership roles in the scientific community. Past LDRD panelists have gone on to be Laboratory fellows, division leaders, program directors, association fellows, and chief scientists, while others have transitioned from the Laboratory to become leaders in academia.

LDRD Encourages team building

A priority for the Laboratory is to build the capabilities and teams for continued excellence in the future. The value of LDRD is that it provides the opportunity to develop innovative new capabilities *and* build integrated, multi-disciplinary teams across capabilities, resulting in projects that can easily transition to programs and provide scientific vibrancy for the future of the Laboratory. There is strong evidence that proposals that partner increase their chances of funding by about 40%. In FY07-FY10, 448 pre-proposals were submitted. Of the 70 selected for funding, more than 50% partnered across principal directorates, while only 34% of the unfunded proposals were partnered. LDRD thus encourages integrated, multi-disciplinary teams that cut across capabilities to provide new, improved, and more efficient approaches mission solutions.

Independent project appraisals validate mission relevance

In FY10, the LDRD Program Office conducted an appraisal of every ongoing project it intended to fund in the next fiscal year. The primary objective is to assess progress and provide peer input to help PIs maintain the highest quality of work. The appraisals also help the LDRD Program

Where are they now? FY02-04 Strategy Team Members

Dana Berkeland, Program Manager at federal agency

Tanmoy Bhattacharya

Greg Boebinger, Director, National High Magnetic Field Lab

David Clark, Director, Seaborg Institute

Harry Crissman, Lab Fellow, retired

Maya Gokhale, Computer Scientist, LLNL

Wu-Chun Feng, Director, Synergy Laboratory, Virginia Tech

Michael Fisk, Cybersecurity Technical Lead, LANL

Hans Frauenfelder, Senior Lab Fellow

Herb Funsten, Cheif Scientist, ISR, LANL

David Funk, WX Division Leader, LANL

Salman Habib, in transition to ANL

David Janecky, Deputy Group Leader, Environment Stewardship, LANL

Mikkel Johnson, Lab Fellow, retired

Paul Johnson, Lab Fellow, Acoustical Society of America Fellow

Sallie Keller-McNulty, Dean of Engineering, Rice University

Hui Li, American Physical Society Fellow

Tracy Light, Space and Remote Sensing Team Leader, ISR, LANL

Ferenc Mezei, Hungarian Academy of Sciences and Academia Europaea

Albert Migliori, Director, Seaborg Institute

Jeremy Mitchell

James Morel

Chris Morris, Lab Fellow

William Parkinson

Alan Perelson, Lab Fellow

William Priedhorsky, Director, LDRD, LANL

Art Ramirez

Gary Resnick, Bioscience Division Leader, LANL

John Sarrao, Program Director, Office of Sciences

Nan Sauer, Acting Associate Director, CLES, LANL

Andrew Shreve, former acting Director, CINT, LANL

Karl Staudhammer

Tom Terwilliger, Lab Fellow, Biosecurity Center Leader

Les Thode, Lab Fellow, retired

Frans Trouw

David Vieira

Office monitor and manage the program portfolio. In addition to formal project appraisals, which are conducted annually, the LDRD Program Director and Deputy Program Director meet informally with PIs in their labs at least once a year to discuss their projects. The purpose of these one-on-one meetings is to give PIs individualized assistance and to determine what the LDRD Program Office can do to positively impact the success of the project. Each DR project has also been assigned a Program Development Mentor to assist the transition of LDRD successes to mission.

Continuing DR projects are appraised every year of the life of the project, with at least one of the reviews including external reviewers. The internal-external review is open to all Laboratory staff and leaders. Four project appraisers – two internal and two external – are nominated by the PI and approved by the LDRD Program Director. When possible, the appraisal is held as part of a broader workshop hosted by the Laboratory.

DR Project Appraisals Average "Excellent" to "Outstanding"

Analysis of FY10 project appraisals shows a mean rating of 4.25, which is between outstanding and excellent. The appraisals involved internal and external reviewers.

Written appraisals, held in the LDRD archives, address: (1) Brief summary of accomplishments; (2) Assessment of quality of science and technology, relevance to Laboratory and national missions, progress toward goals and milestones, project leadership, and the degree to which the project may establish or sustain a position of scientific leadership for the Laboratory; and (3) Recommendations by the committee for changes in the scope or approach of the project. The criteria for the most important point – number (2) above – are derived from criteria developed by the National Academy of Science to assess all federally sponsored research.

Continuing ER projects are appraised in their first and second years. The LDRD Deputy Program Director collaborates with the technical divisions to conduct project appraisals. PIs are now required to submit self-assessment to the LDRD Program Office addressing the following points: introduction to the problem and goals of the project; background and significance of the work in terms of impact of the work; methods developed during the course of the project; results and accomplishments; and future work for the upcoming year and/or efforts to develop new funding.

Once the PI appraisal inputs are complete, the LDRD Program Office forwards the presentations to the respective division leadership for a formal appraisal. The projects are appraised according to the Federal criteria of quality, performance, leadership, and relevance.

MISSION RELEVANCE

The LDRD Program Office treats mission relevance as one of the most important criteria in the evaluation of a potential LDRD project. Mission impact is considered carefully in project selection. Later, the mission impact of funded projects is tracked annually through the data sheet process. Because of the basic science and engineering nature of most LDRD projects, the work often proves to be relevant to numerous missions and agencies. In the chart below, the sum of the total LDRD investment in DOE missions is significantly greater than the annual LDRD budget because LDRD investment in a single project is often relevant to more than one mission area.

Our space science studies provide compelling examples of research that has broad-reaching relevance across many mission areas and sponsor interests.

Space is no longer just a place to explore; it has become an indispensable part of the nation's infrastructure for civil and national security missions. The high ground of space supports communications, remote sensing, and navigation, every one of which is needed for the nation to defend itself. For example, nuclear nonproliferation depends on satellites to detect weapons programs and nuclear testing. LDRD invests in a range of science and technology to enable the space mission. Our projects build capabilities to collect and interpret remote sensing data. They let us track and understand activities in space, making possible Space Situational Awareness. Space missions are almost all solar powered and might benefit from new solar cells explored by LDRD. They are vulnerable to cosmic rays and trapped radiation in the Van Allen belts; LDRD projects aim at better predicting the fluctuations of this "space weather," and its impact on satellites. The capabilities needed for space national security are diverse. More than 25% of the Los Alamos LDRD portfolio supports the space mission, either addressing known mission challenges, or building the underlying capability for challenges both current and yet unrealized.

Modeling the Earth's Magnetosphere with the DREAM system

The Dynamic Radiation Environment Assimilation Model (DREAM) was developed at Los Alamos to understand and predict hazards from the natural space environment and artificial radiation belts produced by high altitude nuclear explosions (HANE) such as Starfish. DREAM was initially developed in 2005 as part of an LDRD Directed Research project. It uses Kalman filter techniques to assimilate data from space environment instruments with a physics-based model of the radiation belts.

DREAM can assimilate data from a variety of types of instruments and data with various levels of resolution and fidelity by assigning appropriate uncertainties to the observations. Data from any spacecraft orbit can be assimilated, but DREAM was originally designed to work with input from the Los Alamos space environment instruments on Geosynchronous and GPS platforms. With those inputs, DREAM can be used to specify the energetic electron environment at any satellite in the outer electron belt whether space environment data are available in those orbits or not. Even with very limited data input and relatively simple

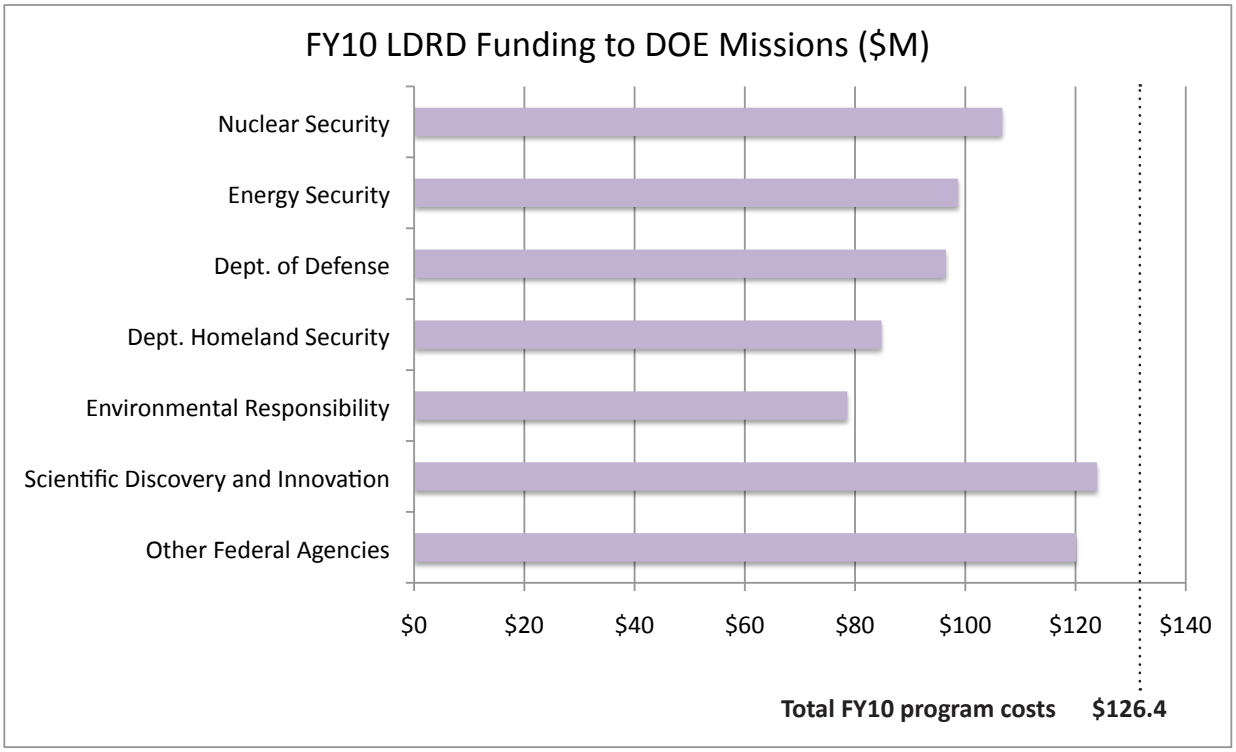

physics models, DREAM specifies the space environment in the radiation belts to a high level of accuracy.

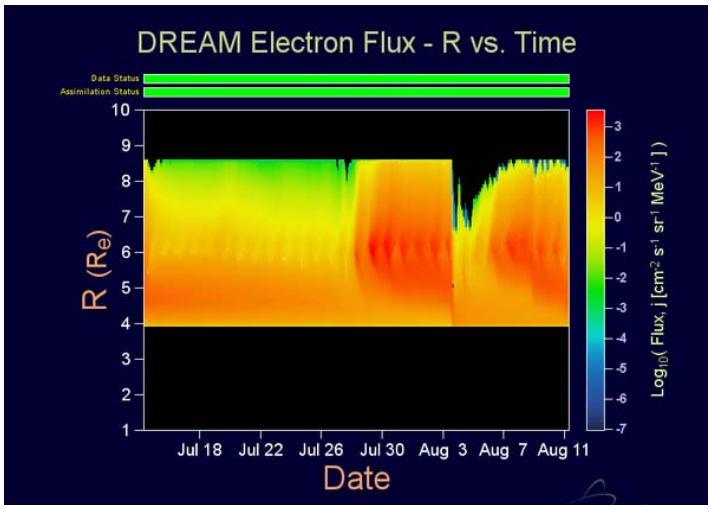

The DREAM system tracks space weather throughout near-earth space using real-time data from NOAA GOES satellites.

DREAM was selected for funding in 2009 by DOE NA-22 for work on the natural space environment, and by WFO for work on the HANE environment. The DOE funds are an open-ended Mission Sustainment Program, and the WFO funding is a four-year project that started May 2010.

Exploiting the Last Spectral Frontier

According to the National Science Foundation, the portion of the electromagnetic spectrum referred to as Terahertz is considered a science frontier because it lies between, and combines the benefits of, the familiar microwave and optical regions. THz can propagate like radio waves, image structures like optical light, and even reveal material composition.

The THz band yields unprecedented opportunities to interrogate, image, and uniquely identify substances and structures. However, well established techniques for generating and controlling microwave and optical radiation have proven ineffective for the THz band, despite decades of intense effort. Among the greatest impediments to exploiting this regime of the electromagnetic spectrum are the difficulties in building sources with sufficient power and sensors with the needed sensitivity.

Nathan Moody leads an ER project that aims to go beyond what nature provides for materials. Imposing new periodic structures enables us to create an artificial media sensitive to THz radiation. Artificial media composed of metamaterials (MMs) and/or photonic band gap (PBG) structures can respond to THz radiation in a variety of ways.

This work has and will continue to extend our knowledge of and provide raw materials for a new, portable mechanism for creating non-ionizing THz radiation, which is ideal for determining certain properties of materials that are not apparent when using other types of radiation (such as microwave, light, or x-rays). THz radiation can be used to actively interrogate a variety of environments, including human subjects, in search of dangerous materials to protect both soldiers and civilians. Our work could also lead to tissue-safe low cost THz imaging, which could be used to supplement and/or replace carefully regulated x-ray doses typical in medical imaging.

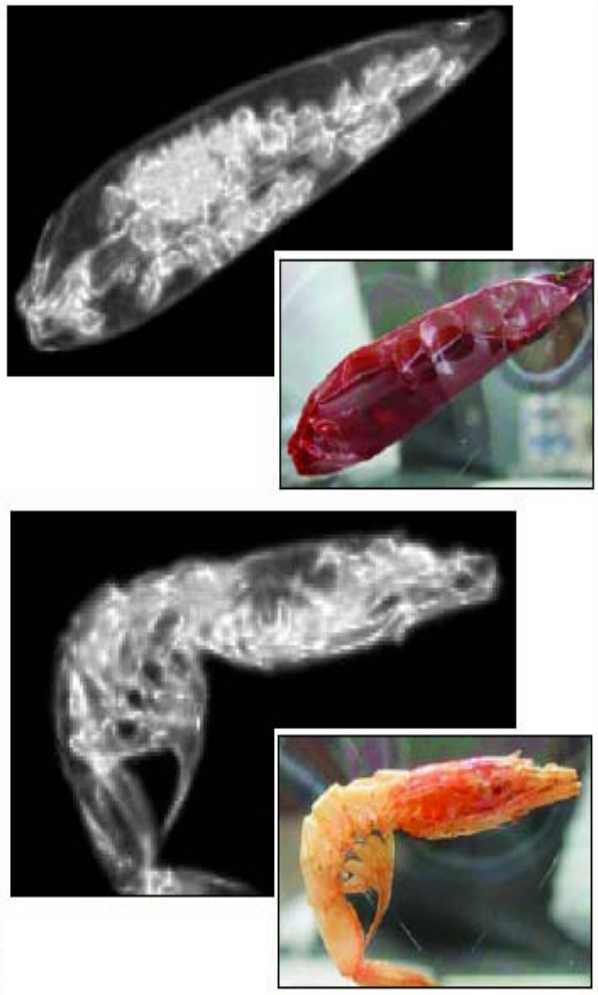

THz imaging can reveal the internal composition of some materials, as well as their structure.

MISSION IMPACT

LDRD delivers capabilities and explores solutions for all Los Alamos missions: Nuclear Security, Global Security, Energy Security, and Scientific Discovery. In some cases these lead to clearly identified follow-on projects. In part, this can be attributed to the program development mentors who help transition these projects from LDRD to external funding.

Putting a quantitative metric on mission impact is difficult. The obvious metric –follow-on funding – omits other benefits like new ideas and approaches that feed into ongoing work. Counting dollars is also imperfect because, although LDRD is part of what enables new mission solutions, the Laboratory brings other assets to bear, including facilities, ideas, and personnel from a range of programs.

Nonetheless, if we look at admittedly rough numbers, we find that projects active in FY10 played an important part on the path to $98M of externally funded R&D. Even this is not the end of the story, because follow-on projects often do not begin immediately upon the conclusion of the LDRD. A study carried out in FY08 showed that follow-on projects over a five-year period totaled approximately twice the original LDRD investment.

The path from LDRD to mission is clearly demonstrated by follow-on projects from sponsors that range, inside DOE, from the nuclear weapons program to nonproliferation programs, applied energy programs, and the Office of Science, and more broadly, across a range of sponsors that include DoD (DARPA, ONR, and DTRA), DHS and DNDO, NIH and CDC, classified agencies, and a range of industrial partners. The capabilities sustained by these external sponsors feed back once again to enable the Laboratory's execution of NNSA missions.

Here we highlight just a few successful projects that have transitioned from LDRD to external funding:

The project "Genomes to Behavior: Predicting Bacterial Response by Constrained Network Interpolation" set out to create a fundamental capability that could transform comparative genomics and reduce the need for experimentation 10 to 100-fold, profoundly cutting costs and accelerating solutions to central problems in biosecurity, bioenergy, carbon management, and bioremediation. The research team solved several fundamental problems and acquired experimental data that exceeded the original goals for the project, establishing a solid foundation to pursue the project with more than $11M in external funding from the National Institutes of Health and Department of Defense.

Investment in "Foundations for Practical Pattern Recognition Systems" led to advancements in state-of-the-art pattern recognition, taking us several steps closer toward an ability to digest and analyze orders of magnitude more data than we currently can, and vastly reducing data storage and exploitation costs. The research team developed a theoretical base for a new class of pattern recognition system that allows users to inspect and understand how the system makes predictions. They also developed a number of pattern recognition solutions to specific problems encountered in real-world data analysis environments. The Department of Homeland Security has invested $3M to further the research in a project titled, "Knowledge Capture Tool Kit for Forensic Signatures using Nuclear Material Images."

A recent project focused on "Enhancing Radiation Damage Resistance via Manipulation of the Properties of Nanoscale Materials" resulted in a spin-off project funded by the DOE Energy Frontier Research Center at Los Alamos. The project, funded at $19M, seeks to understand, at the atomic scale, the behavior of materials subject to extreme radiation doses and mechanical stress in order to synthesize new materials that maintain their desired properties under such conditions.

The project "Hot Spot Physics and Chemistry in Energetic Materials Initiation" resulted in state-of-the-art experimental and computational studies that significantly advanced us toward a robust, rapid-response predictive capability for multi-agency needs relating to energetic materials, including developing quantitative understanding of the safety and initiation of stockpile explosive materials. Follow-on projects have been established through the Office of Naval Research, Department of Homeland Security and the Department of Energy, resulting in more than $2.5M in external funding. This LDRD work supported a major milestone for the Advanced Simulation and Computing Program, and was one of the first simulations on Roadrunner, the Laboratory's supercomputer.

METRICS OF EXCELLENCE

The LDRD program is a key resource for addressing the long-term science and technology goals of the Laboratory, as well as for enhancing the scientific capabilities of Laboratory staff. Through careful investment of LDRD funds, the Laboratory builds its reputation, recruits and retains excellent scientists and engineers, and prepares to meet evolving national needs. The impacts of the LDRD program are particularly evident in the number of publications and citations resulting from LDRD-funded research; the number of postdoctoral candidates supported by the program; and the number of awards LDRD researchers received.

Publications

LDRD produces a large volume of high-quality scientific contributions relative to its portion of the Laboratory's budget. The numerous publications made possible with LDRD funding help the Laboratory maintain a strong presence and scientific reputation in the broader scientific community. In calendar year 2009, LDRD researchers generated 376 publications, accounting for 22% of the Laboratory's peer-reviewed publications. The quality of these publications is evidenced by the number of times they were cited. LDRD publications published in 2009 were cited 2,652 times, accounting for 37% of the Laboratory's citations, as well as a significant number of the Laboratory's top 50 most highly cited publications. LDRD supported the #1 most highly cited papers published in 2009 and 2007, with 299 and 359 citations, respectively, as of the date of this report.

Peer-Reviewed Publications			
	CY07	CY08	CY09
LANL Pubs	1928	1780	1743
LDRD Supported	401	452	376
% due to LDRD	21%	25%	22%

Citations			
	CY07	CY08	CY09
LANL Citations	20550	13830	7075
LDRD Supported	7796	4756	2652
% due to LDRD	38%	34%	37%
Top 50 Most Highly Cited Publications			
LDRD Supported	25	21	22

Patents and Disclosures

Another indication of the cutting-edge nature of the research funded by LDRD is the contribution the program makes to the intellectual property of the Laboratory. In FY10, LDRD-supported research resulted in 12 patents, 21% of the Laboratory's total, and 16 disclosures, 28% of the Laboratory's total.

Patents				
	FY07	FY08	FY09	FY10
LANL Patents	49	28	52	56
LDRD Supported	22	8	12	12
% due to LDRD	45%	29%	23%	21%

Disclosures				
	FY07	FY08	FY09	FY10
LANL Disclosures	166	116	110	116
LDRD Supported	49	36	38	16
% due to LDRD	29%	31%	38%	21%

Postdoctoral Support

In an increasingly competitive job market, LDRD remains an important vehicle for recruiting the brightest researchers to the Laboratory, where they become innovators and scientific leaders. In FY10, LDRD supported 325 postdocs, accounting for 59% of the Laboratory's total.

Postdoc Support				
	FY07	FY08	FY09	FY10
LANL Postdocs	473	477	470	547
LDRD Supported	284	274	291	325
% due to LDRD	60%	61%	62%	59%

Postdoc Conversions				
	FY07	FY08	FY09	FY10
LANL Conversions	35	39	37	53
LDRD Supported	22	21	14	33
% due to LDRD	63%	54%	38%	62%

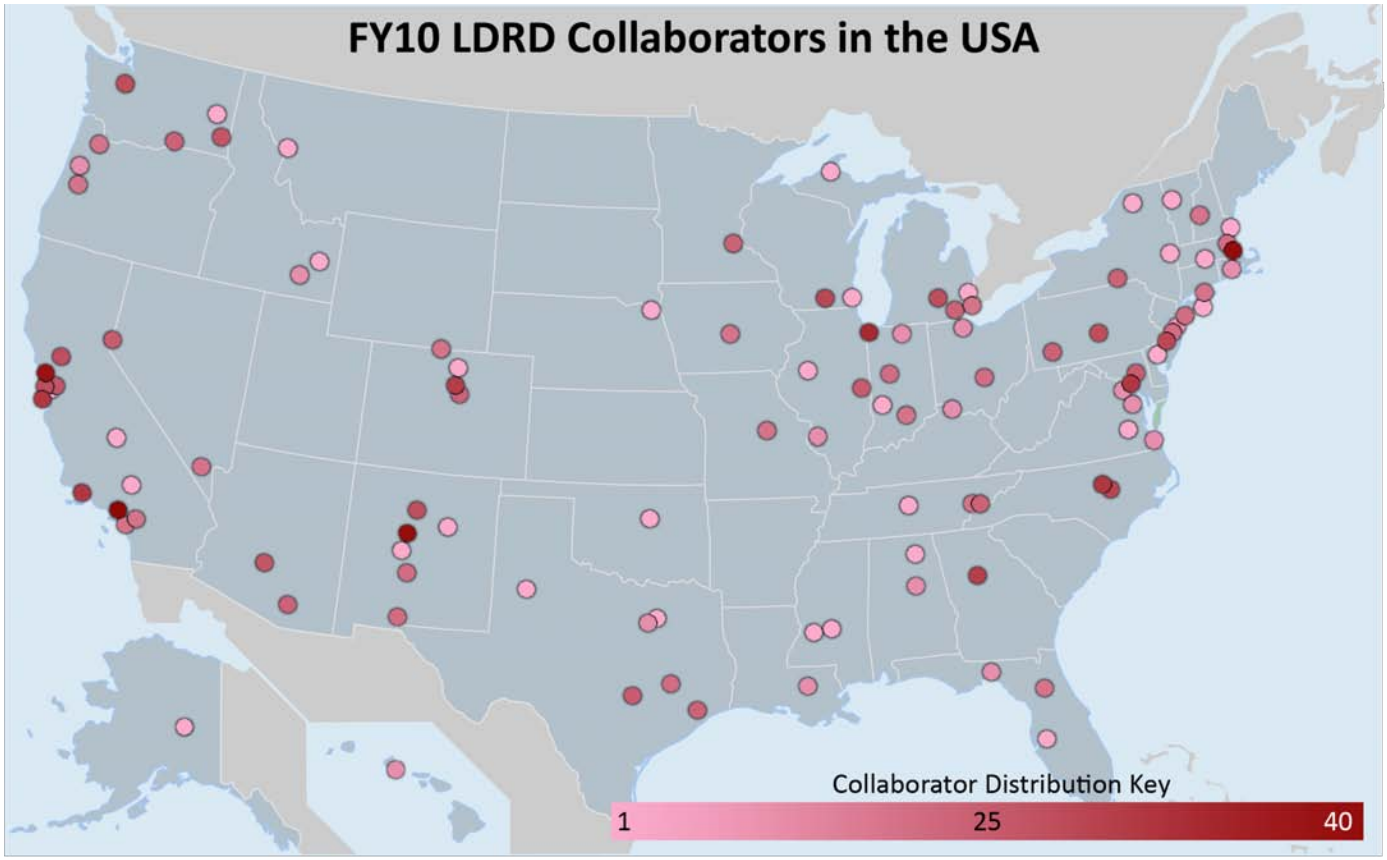

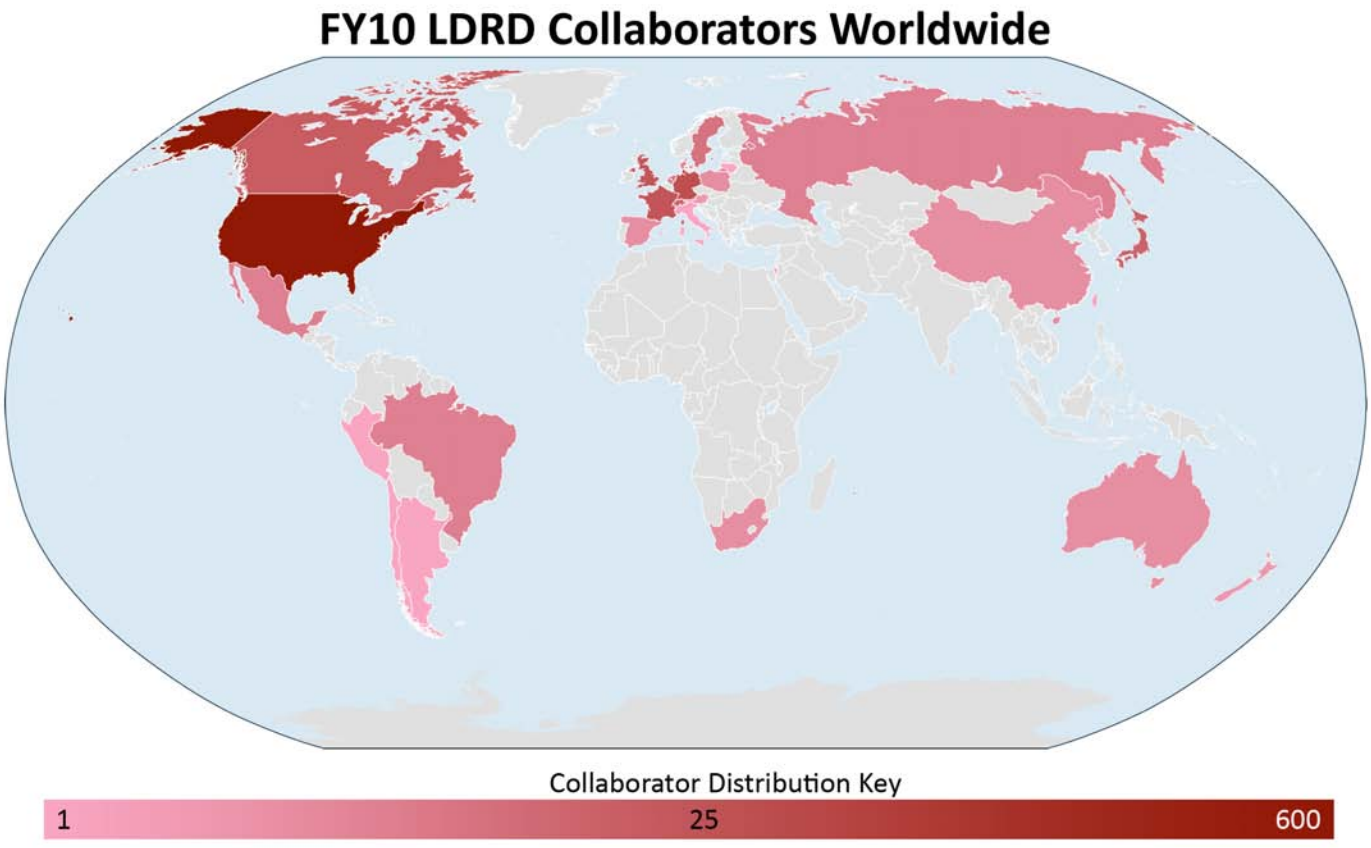

External collaborations are often critical to a successful LDRD project. Formal collaborations between LDRD PIs and researchers at other national laboratories, academia, and industry enable access to world-leading facilities and knowledge. Such collaborations enable LDRD researchers to be active and prominent members of the broad scientific community. The figures above illustrate the far-reaching collaborations established by LDRD researchers in FY10.

FY10 LDRD METRICS SUMMARY

Metric	Evidence
LDRD work is of high technical quality and impact	● Peer-reviewed publications remain a large fraction of Laboratory output (25%) **- LDRD supports approximately 23% (3-year average)** ● Patents and disclosures remain a large fraction of Laboratory output (25%) **- LDRD supports approximately 30% (3-year average)** ● Top-cited papers are dominated by LDRD work **- LDRD supports more than 45% (3-year average)** ● Quantitative appraisal scores for ongoing projects show a pattern of excellence **- Independent project appraisal scores average outstanding to excellent** ● Citation counts show that LDRD makes a major contribution to Laboratory technical output **- LDRD supports 37% of the Laboratory's total (3-year total)**
LDRD is essential to the Laboratory's ability to deliver mission solutions	● Success stories show clear path from LDRD investment to major mission impacts ● Funded follow-on projects show LDRD prepares the Laboratory to meet national needs **- Active projects resulted in approximately $89M in external funding** ○ Proposals and briefings tracked by the program development mentor program show sponsor engagement - Considering returning direct program engagement to line management
LDRD builds the Laboratory's human capital	● Number of postdocs supported by LDRD provides a strong pool for future Laboratory needs **- LDRD supports approximately 60% of Laboratory postdocs (4-year average)** ● LDRD supports researchers at all career stages, from postdocs to senior staff **- Analysis of PI career stages revealed LDRD is supporting a diverse cross section of the Laboratory population** ● LDRD supports numerous and substantive national and international collaborations that reinforce internal capabilities **- LDRD researchers established 735 collaborations worldwide**
LDRD is a major factor behind the Laboratory's technical reputation	● LDRD work contributes significantly to awards such as R&D 100, Lab and Society Fellows, and others ● Journal covers based on LDRD work show a prominent national impact (FY11+)

● **Excellent** ● **Satisfactory** ● **Improvement sought**

The strategy and outcomes of the LDRD program are tracked by these metrics. The results show that LDRD is on track to meet the challenging goals we have set for ourselves.

INVESTING IN THE BEST AND BRIGHTEST

America is currently facing energy, security and environmental challenges that, in their scope and complexity, are perhaps unparalleled in the nation's history. The LDRD program plays a vital role in the Laboratory's ability to develop a world-class scientific, technical, and engineering workforce capable of responding to those challenges. LDRD supports some of the Laboratory's most accomplished researchers, as well as many of the Laboratory's most promising young scientists and engineers. In FY10, LDRD researchers received well over 100 awards and recognitions, including R&D 100 Awards; fellowships from the American Physical Society, American Ceramic Society, Materials Research Society, and American Association for the Advancement of Science; the Presidential Early Career Award for Science and Engineering, and many others. Here we highlight only a few:

Awards and Recognitions

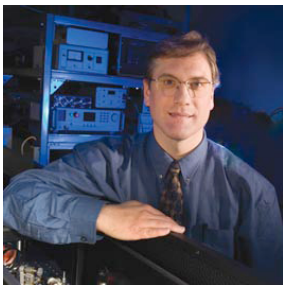

Maxwell wins three prestigious R&D 100 Awards

James Maxwell of the Laboratory's Nuclear Counterterrorism Response has enjoyed the prestige of an R&D 10 Award for his work for the past three years in a row. Maxwell has been involved in laser and microchemical processing for more than 14 years. His work has pushed the frontiers of nanotechnology with groundbreaking technologies that have won an R&D 100 Award each year since 2008.

In 2008, Maxwell won an R&D 100 Award for Laser-Weave, a process involving hyperbaric laser chemical vapor deposition that grows high-strength inorganic fibers into useful shapes and complex patterns, or braid or weave strong, cost-effective cables, cloth, or composites for micro-electrical mechanical systems used in industry.

Maxwell's success continues with his most recent win of a 2010 R&D 100 Award for Ultraconductus, a technology that has the potential to increase the conductivity of metallic wiring by at least 100 times, useful for high-voltage cables used in power transmission, as well as electrical wires used in cell phones and specialized devices.

The LDRD program supported Maxwell's early laser processing work through a 2000 Exploratory Research project on boron carbon nitride growth.

American Physical Society Fellows

The APS Fellows Program recognizes members who have made advances in knowledge through original research and publication, or who have made significant and innovation contributions in the application of physics to science and technology. The following four LDRD researchers were named APS fellows in 2010.

Mark B. Chadwick was cited for significant and innovative contributions to applied nuclear physics, including medical radiation therapy, nonproliferation, homeland security, the physics of nuclear weapons, and especially to development of the modern ENDF/B-VII data base. Chadwick, now Deputy Division Leader of the Theoretical Division, came to the Lab in 1995 as a Director's Fellow in the Theoretical Division. He received the 2007 ASC research prize in 2007, the Criticality Safety Program Manager's Award in 2005, two LANL Distinguished Performance Team Awards and five NNSA Awards of Excellence. He has 250 publications of which over 100 are in refereed research journal papers. Chadwick's research work is in applied nuclear physics. His work on modeling neutron cross sections on plutonium, americium, uranium and radiochemistry materials — with measurements by collaborators at LANSCE — has established robust metrics for validating nuclear weapons simulations. LDRD invested in Chadwick's work through a 2005 Directed Research project titled "New Americium Delta-A Metric for Primary Certification."

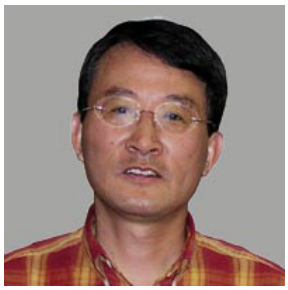

Quanxi Jia was cited for pioneering contributions in epitaxial functional metal-oxide films for coated conductors and electronic devices. Jia came to Los Alamos in 1993 as a staff member. He has more that 300 refereed journal articles, 32 issued patents, and two R&D 100 Awards. Named the Asian- American Engineer of the Year by the Chinese Institute of Engineers USA in 2005, he was also the 2008 recipient of the Federal Laboratory Consortium for Technology Transfer Awards for excellence in technology transfer and a 2008 recipient of an Outstanding Women's Career Development Mentoring Award at LANL. He is known for his innovations in the field of electronic materials and high-temperature superconductivity. Jia is currently working on a 2011 reserve project to build capabilities that will enable us to achieve novel functionalities and to explore new physics of a wide range of materials. He is

also leading a Directed Research project aiming to develop a conceptually new approach to understand the emergent physics that evolves over multiple length and time scales in order to design new materials with entirely new or significantly improved functionalities.

Michael Murillo was cited for theoretical and computational research in several areas of non-ideal plasmas, including non-equilibrium properties of ultra-cold plasmas, collective properties of dusty plasmas, transport in strongly coupled plasmas, and atomic physics in dense plasmas. Murillo is a former Director's Postdoctoral Fellow, funded by LDRD. In 2006 he was a UC, Berkeley Visiting Scholar and in 1997 a Long-Term Visitor at Harvard University. He is a member of the editorial advisory board of High Energy Density Physics and an American Physical Society Outstanding Referee. He is now primarily working on influenza epidemiology. Murillo is Co-PI of a 2010 Exploratory Research project aiming to develop a mathematical model of the annual global movement and evolution of influenza virus as a function of weather phenomena over several geographical regions.

Wojciech H. Zurek was cited for his seminal contributions to the theory of quantum decoherence, and his contributions to quantum foundations more generally. Zurek came to LANL as J. Robert Oppenheimer Fellow, funded by LDRD. He was the leader of the Theoretical Astrophysics Group at Los Alamos from 1991 until he was elected a Laboratory Fellow in the Theory Division in 1996. Developing the theory of decoherence and elucidating its significance for the quantum-to-classical transition is Zurek's major contribution to physics. He also demonstrated (with Wootters) that an unknown quantum cannot be cloned. This is a fundamental result, and an essential distinction between classical and quantum information. Zurek has vastly extended Kibble's cosmological scenario to develop a successful general theory of phase transition dynamics ("Kibble-Zurek mechanism"), which been verified experimentally in superconductors and superfluids (including Bose Einstein condensation). Zurek's extensive work in quantum phase transitions has been supported through several Directed Research projects since 2004.

SAGE Magazine Recognizes Bette Korber's HIV Research

SAGE magazine, the *Albuquerque Journal's* monthly magazine for women, has announced the winners of its SAGE 20 Women Making a Difference award. The list of women throughout New Mexico was selected from a flood of nominations from readers and others. The list is being created in honor of SAGE's 20th anniversary, and the women were featured in the November 1 edition. In addition, winners were honored at a special luncheon hosted by the Greater Albuquerque Chamber of Commerce. Two women were selected from each of 10 categories. LDRD researcher Bette Korber, an immunologist who is working on a global HIV database and an AIDS vaccine, was one of two women selected in the science category. Korber is a Laboratory Fellow at LANL and an external professor at the Santa Fe Institute. She has led an HIV sequence and immunology database project at LANL for the past decade. In part using the collected data in the HIV database as a foundation for her work, and in part working with experimentalist collaborators from around globe, she has co-authored over 190 scientific papers. Most of these studies focus on HIV, but occasionally involve work on other pathogens, the immune response, and human genetics. Her primary areas of research include: HIV vaccine design; HIV evolution; and the impact of the human immune response on HIV, and conversely the potential for a pathogen to impact human populations. She received the E.O. Lawrence Award, the highest scientific honor from the DOE, for her achievements in the Life Sciences, and was an Elizabeth Glaser Scientist.

Early Career Award

Jasper Vrugt, a Distinguished Postdoctoral Fellow funded by LDRD, was selected for the 2010 Outstanding Young Scientist Award. Vrugt, who was jointly sponsored by Computational Earth Science and Applied Mathematics and Plasma Physics, made seminal contributions to geosciences by developing general purpose algorithms and numerical approaches to extract information from the mismatch between model predictions and observations, quantifying individual error sources, and improving theory, understanding, and predictability of environmental systems. Elsevier, a scientific journal publisher, also selected Vrugt as one of the Top 50 most talented young people from the Netherlands.

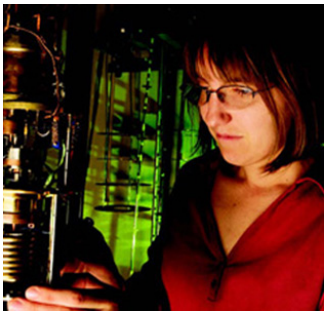

Vivien Zapf is the recipient of the 2010 Lee Osheroff Richardson U.S. Prize for research in physical science. The annual award, sponsored by Oxford Instruments NanoScience, which designs and manufactures tools and systems for industry and research in science and technology, is given to promote and support the career development of early career scientists in North America who conduct research employing low temperatures and/or high magnetic fields. A committee of senior academics throughout North America selects the recipient.

LDRD supported Zapf's work on Bose-Einstein condensation in quantum magnets through a 2005 Postdoctoral Research and Development project. She studies the fundamental properties of materials, including quantum magnets, superconductors and other correlated-electron systems, at high magnetic fields and low temperatures. Zapf is currently researching magneto-electric and multiferroic effects in quantum magnets that are composite organic-metallic hybrids. She also investigates the physics of quantum magnets at low temperatures, including the Bose-Glass to Bose-Einstein condensation phase transition, which is analogous to the metal-to-insulator transition for fermions, and the effect of quantum fluctuations on boson masses. Zapf has published nearly 60 journal articles.

Journal Covers

Research may aid characterization and development of nanoparticles and sensing applications

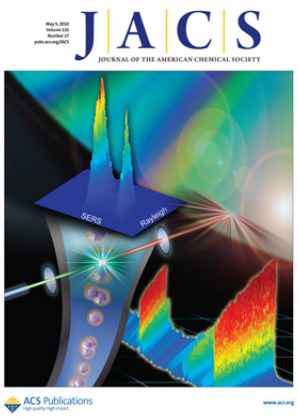

The development of a full spectral, in-flow Raman instrument created by LDRD researchers is a powerful new tool for nanomaterials development. The instrument has uses beyond traditional biological applications of flow cytometry. The capability could have an expanded role in the characterization and development of nanoparticles and sensing applications. In research that appears on the May 5 cover of the *Journal of the American Chemical Society*, a team that led by PI Steve Doorn of the Center for Integrated Nanotechnologies reported on this new capability.

Plasmonic nanoparticles functionalized with molecular dyes can be designed to provide stable and intense surface enhanced Raman (SERS) spectral fingerprint signatures. Changing the adsorbed dye molecule can vary the spectral signature of these "SERS tags," thus providing a route to advanced multiplexing in sensing applications. Such spectral tags have potential for applications in bioassays and imaging. However, development of the spectral tags has been limited by the lack of rapid, high-throughput characterization tools to correlate the observed spectral responses with particle structure for feedback into synthesis optimization.

The research team demonstrated flow-based instrumentation that directly addresses this problem. The new approach uses a modified flow cytometry platform to acquire full, high-resolution Raman spectra of single SERS-tag particles in applications-relevant detection times of 20 microseconds. This new capability will aid the Laboratory's development of SERS tags for next generation bioassays by providing rapid feedback on synthesis strategies for spectral tag optimization. It also will allow a first-time direct particle-by-particle comparison of SERS response for different nanoparticle architectures. In addition, the unique sorting capability of flow cytometry will enable isolation of selected particle populations to permit analysis of SERS enhancements.

Controlled synthesis of self-assembled nanotubes with rectangular cross-sections

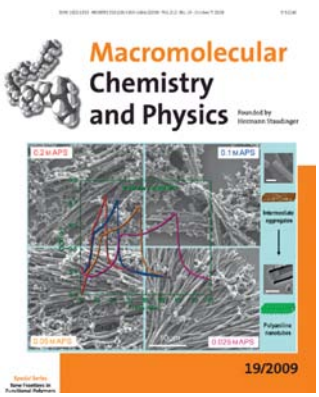

Nanomaterials made from the conducting polymer polyaniline (PANI) have unique applications due to their high surface area and ease of processing. The applications include antistatic coatings, anticorrosion coatings, sensors, supercapacitors, and batteries. Because of their high surface area and ease of processing, PANI nanomaterials are also useful in chemical sensing, microelectronics, and gas storage. During the PANI synthesis, different condition leads to different morphologies - nanotube, nanofiber, and nanoparticles. These morphologies possess different surface properties and thus different physical and chemical properties. Nanotubes provide high surface area and a more ordered form. Therefore, control over the synthesis and morphology of PANI nanofibers and nanotubes is important. PANI nanotubes with different diameters, wall thickness, cross-sections, and yields have been synthesized. Typically, PANI nanotubes are prepared using a variety of acid dopants (usually weak acids), or in pure water, using a self-assembly method without hard a template

such as porous alumina, porous silica, etc. While most PANI nanotubes have circular cross sections, nanotubes with rectangular hollow interiors have been rarely observed and are expected to have unique properties.

LDRD PI Yusheng Zhao and colleagues developed a simple, high yield self-assembly method to make PANI nanotubes with rectangular holes and outer contours. The scientists controlled the reaction rate through adjusting acid and oxidant concentrations to slow the aggregation rate of the intermediates. This enhanced the yield of nanotubes with rectangular cross sections. The aggregation of detectable and separable reaction intermediates is directly correlated with PANI nanotube formation. The scientists systematically examined the control over intermediate aggregates morphology. Their work establishes the relationship between reactant ratio, aggregation of intermediates, and product morphology. This information contributes to the conducting polymer field to understand how reaction kinetics impact the polymerization process and thus to the morphology of the final products. This work appeared as the cover article of the October 2009 edition of *Macromolecular Chemistry & Physics*.

SHOWCASING LDRD RESULTS TO STAKEHOLDERS

LDRD Tri-lab Symposium

On June 9, 2010, at the University of California Washington Center in Washington, D. C., the LDRD program convened an open symposium to review program highlights and discuss program initiatives and directions. The symposium focused on the research and development investments the LDRD program is making at the NNSA national laboratories to reduce the global danger of weapons of mass destruction. The keynote presentations and poster session addressed research and development in the critical areas of nuclear counterterrorism, arms control and treaty monitoring, and biological chemical threats.

More than 200 participants attended the symposium, including staff from the national laboratories, the Nevada Test Site, the weapons manufacturing plants (Y-12, Kansas City, and Savannah River), as well as from other federal agencies and organizations, including general and science news media.

Los Alamos took the lead in organizing the symposium, and with strong support from the other laboratories, it was a great success.

LDRD Day 2010

Serving the nation through cutting-edge science and technology

The Los Alamos LDRD Program Office hosted its Second Annual LDRD Day in September 2010, in Santa Fe, NM. Keynote speaker Heather Wilson spoke about the importance of science and technology for the future, and especially emphasized the important role the Laboratory plays in recruiting and retaining bright, young researchers. Other presentations by Laboratory leaders focused on the capabilities of the Laboratory in nuclear security and global security, specifically space situational awareness. The highlight of the day was the 45 posters that showcased LDRD work benefiting all Laboratory mission areas, including energy security and scientific discovery.

LDRD Day 2011 will be held September 13, 2011 in Santa Fe, NM. More information can be found online at http://www.lanl.gov/science/ldrd/ldrdday/.

EXTERNAL REVIEWS AT THE PROGRAM LEVEL

As noted elsewhere in this report, independent assessments of individual LDRD projects range from excellent to outstanding. At the broader program level, our self-assessment is that the Los Alamos LDRD program is in good shape, producing excellent science with high mission impact, and carefully stewarding taxpayer monies. However, it is useful from time to time to validate our assessment via an independent external analysis. Based on interactions with NNSA (Site Office and Headquarters), we have collaborated with the LANL managing partnership, Los Alamos National Security (LANS) LLC, to commission two independent reviews during FY11.

The first was a "Functional Management Review of LANL LDRD Business Practices", held March 15-17, 2011. The objective of this review was to "determine whether LANL has developed a management approach to the stewardship of LDRD monies that achieves the objectives of legislation, DOE order, and sound charging practices." The independent panel was chaired by John Birely, consultant to the University of California Office of the President, and included Todd Hansen, LBNL LDRD Program Director; Paul Rosenkoetter, director, Prime Contract Management Office and manager, LANS LLC office; and Ross Thomas, chief technical officer for Babcock & Wilcox. Every member of the panel was a senior manager experienced in the stewardship of taxpayer funds.

While their final report is still in preparation, their preliminary conclusions were quite positive regarding the management of the Los Alamos LDRD program. The panel noted that LDRD is uniformly viewed as vital to the health and future of Lab, that the Laboratory has been responsive to issues raised in recent audits and reviews and has since then significantly improved systems for management of LDRD program. The panel concluded that Laboratory business process provided reasonable assurance of systems-based good management, and that LANL has developed a management approach to the stewardship of LDRD monies that achieves the objectives of applicable legislation and DOE Order 413.2B.

A second functional management assessment will concentrate on the effectiveness of the Los Alamos LDRD program, with the objective of (1) validating that LDRD investments effectively and efficiently meet the goals of the program; and (2) assessing the impact of these investments on national missions, current and anticipated. This assessment will consider the quality, relevance, and impact of LDRD-supported science and technology at the program level. Scheduled for August 17-19, the assessment will be chaired by Professor Raymond Jeanloz of UC Berkeley, a member of LANS S&T advisory committee. Jeanloz is an AAAS Fellow, Macelwane medal winner for the AGU, MacArthur "genius" grantee, Szilard prize winner, and a member of the National Academy.

Chemistry & Material Sciences

LABORATORY DIRECTED RESEARCH AND DEVELOPMENT

Predictive Design of Noble Metal Nanoclusters

Jennifer Martinez
20090017DR

Introduction

The next revolution in materials science will be the first principles design and "atom-by-atom" assembly of nanoarchitectures having specific properties. Recent advances in the synthesis of fluorescent noble metal nanoclusters (NCs), for example, suggest that they will likely permit the manipulation of light at the molecular scale, if only their size and structure can be controlled at the atomic level. NCs are collections of silver or gold atoms (2-31 atoms). They are small and fluorescent.

Biological systems make materials with: 1. Precise structure. 2. Controlled function. In Nature, the design of materials is encoded by DNA. From this genetic blueprint, protein and peptide templates are produced. These templates control the assembly of inorganic atoms. These blueprints lead to materials with controlled structure and properties that span many length scales. However, Nature's materials fabrication is not perfect. Most materials Nature makes are: 1. Structural (i.e. the foundation of the house). 2. Neither electronic nor optical. A major opportunity in materials science is to develop methods to create inorganic optical nanomaterials using atom-by-atom assembly approaches inspired by and derived from Nature.

We are mimicking biology to develop NCs with exquisite synthetic precision. We are using state-of-the-art experimental and theoretical tools to develop an understanding of the electronic structure and remarkable photophysical properties of these materials.

Benefit to National Security Missions

This project supports the DOE mission in Threat Reduction by enhancing our understanding of the design and synthesis of materials with defined properties for application in chem/biothreat reduction, imaging, and the biosciences missions of the DOE Office of Science.

Progress

While fluorescent clusters have tremendous potential for use as fluorescent probes, there are a number of fundamental challenges that prevent their widespread use:

1. Nanoclusters are difficult to make.
2. Nanoclusters are difficult to characterize.
3. There is little detailed chemical, physical, or theoretical understanding.
4. Nanoclusters are difficult to use for bioimaging and sensing.

From our theoretical studies we have determined the effect of cluster geometry and ligand environment. We find that while the jellium model can describe the clusters in the gas phase, it poorly describes clusters with attached ligands. Further, while dogma posits that the nanocluster fluorescence scales as a function of cluster size, our computational results suggest that the cluster geometry, ligand functionality, and ligand number are the critical factors for determination of fluorescence properties. Further, we show that strong binding ligands (i.e. phosphine or thiol) will not produce fluorescent species, while poor binding ligands (i.e. amine or carboxylate) do. We have experimentally validated the predictions in two recently accepted papers and in a mechanistic study. Traditionally, nanoclusters have been synthesized using soft ligands, such as phosphines or thiols that form strong bonds with gold, and, with the exception of a mixed-ligand protected cluster, tend to exhibit low fluorescence quantum yields. We have instead produced fluorescent metallic gold nanoclusters stabilized by small molecule amine ligands (hard ligands). The morpholine and piperazine backbones of Good's buffers were used to template fluorescent clusters, through a process of etching of nanoparticles first formed in the reaction. The clusters are found to be subnanometer sized, with nanosecond fluorescence lifetimes and as bright, or brighter, than the commercial dye norharmane. Additionally, from our mechanistic studies we better understand the nature of the fluorescent clusters (both stoichiometry and charge) and the ligand environment, which directly correlates with our theoretical predictions (currently being submitted to *Angew. Chemie*.)

Toward production of clusters in stable templates that allow ease in biolabeling, we have reported the synthesis and photophysical properties of silver-nanoclusters

templated on DNA. We have produced a suite of clusters with distinct excitation and emission wavelengths, tuned to common laser lines. Utilizing these clusters for multiplex protein detection, we have developed an intrinsically fluorescent recognition ligand that combines the strong fluorescence of oligonucleotide templated AgNCs with the specificity and strong binding affinity of DNA aptamers for their target proteins, to develop a new strategy for detection of specific proteins (Figure 1).

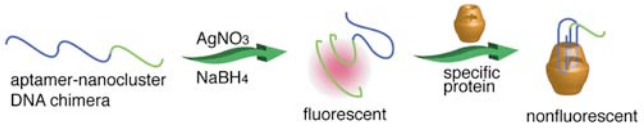

Figure 1. Characterization of protein binding induced fluorescence change.

This new recognition ligand and detection scheme is simple, inexpensive, and a sensitive method for protein detection. Further, we find that the red fluorescence of oligonucleotide-templated silver nanoclusters (DNA/Ag NCs) can be enhanced 500 fold when placed in proximity to guanine-rich DNA sequences. Based upon this newly observed phenomenon, we have designed a **DNA detection probe (NanoCluster Beacon, NCB) that "lights up"** upon target binding (Figure 2).

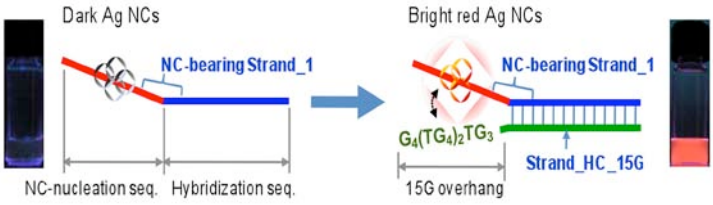

Figure 2. Guanine enhancement upon hybridization.

In a separation-free assay, a signal-to-background ratio of 76 was demonstrated for the detection of a human oncogene target (Braf) and 175 for H1N1 detection. In addition to eliminating the need to purify DNA nanocluster probes that do not bind targets, there is no need to remove the silver nanocluster precursors used during nanocluster formation. Since the observed fluorescence enhancement is caused by intrinsic nucleobases, our detection technique is simple, inexpensive, and compatible with commercial DNA synthesizers. *This exciting new discovery is currently being submitted for the R&D 100 award competition.* More recently we have developed "chameleon" NanoCluster Beacons. Like the reptile, these chameleons change their colour, in addition to lighting up, based on subtle differences in their environment. We have used these chameleons to detect single nucleotide polymorphisms (SNPS). SNPS are important in human disease (patent and paper in preparation). Further, for the first time in fluorescent NC science we have proven by EXAFS analysis: 1. NCS are clusters and have Ag-Ag bonds. 2. NCs have Ag-DNA bonds. 3. NC size is between 4-10 atoms (EXAFS: extended x-ray absorption fine structure).

Future Work

The overall goal is to produce of a full color palette of stable, biologically compatible, luminescent nanoclusters. The production of stable, bright, and small fluorescent nanoclusters will impact diverse scientific and applied areas such as electronics, light harvesting, and biological imaging, with corresponding implications in laboratory mission areas of energy science and biological sensor or assay development.

To achieve this goal, we will: a) explore bio-inspired and traditional methods of cluster synthesis [tasks: 1. Design DNA for nanocluster synthesis. 2. Conduct phage display panning to find peptides that template nanoclusters. 3. Clone peptides into proteins. 4. Develop and understand small molecule templates for cluster synthesis.], b) characterize cluster morphology and photophysical properties [tasks: Characterize morphology of clusters by: 1. Raman. 2. EXAFS. 3. FCS. 4. Mass spectrometry 5. Fluorescence as ensemble and single molecules.] Critical to the success and advancement of this field is better characterization. We strive, particularly in this next year, to set the foundation for cutting edge characterization of clusters. In addition to the spectroscopies above, we have formed collaboration with UCSD to characterized NCs by neutron scattering and have recently finished our first beam time. c) correlate these experimental measurements with electronic structure and dynamics calculations to improve fundamental understanding of cluster properties [tasks: 1. Use first-principles-based-calculations to model electronic structure and photoexcited state dynamics of clusters. 2. Better understand the mechanisms for fluorescence. 3. Better understand the transition to nanoparticles.], and d) demonstrate the utility of the clusters for applications in biological imaging and sensing.

Conclusion

We have made tremendous progress in producing NCs that can be used in medical imaging and sensing. These NCs are in user-friendly formats. We have made substantial progress in modeling the clusters and have corroborated these predictions experimentally (Figure 3), beginning to reach the ultimate goal in materials science: predictive design. Out team has published many papers this year and has gained international recognition (invited talks to international symposium and constant requests to review papers on fluorescent NCs). We expect, and are actively pursuing projects, to impact Lab missions in biothreat reduction for, fieldable, organism specific detection.

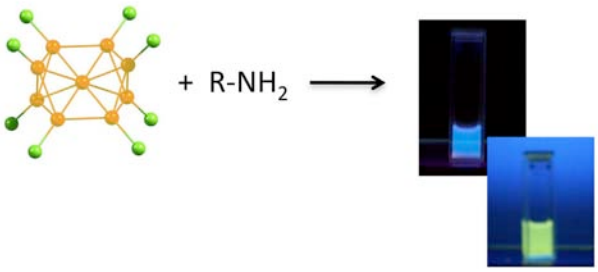

Figure 3. Amine exchange produces fluorescent species.

References

1. Yeh, H., J. Sharma, H. Yoo, J. Martinez, and J. Werner. Photophysical characterization of fluorescent metal nanoclusters synthesized using oligonucleotides, proteins and small molecule ligands. 2010. In *Reporters, Markers, Dyes, Nanoparticles, and Molecular Probes for Biomedical Applications II ; 20100125 - 20100127 ; San Francisco, CA, United States.* Vol. 7576, p. var.pagings.

2. Sharma, J., H. Yeh, H. Yoo, J. Werner, and J. Martinez. A complementary palette of fluorescent silver nanoclusters. 2010. *CHEMICAL COMMUNICATIONS.* **46** (19): 3280.

3. Yeh, H., J. Sharma, J. Han, J. Martinez, and J. Werner. A DNA-silver nanocluster probe that fluoresces upon hybridization. 2010. *Nano Letters.* **10** (8): 3106.

4. Bao, Y., H. Yeh, C. Zhong, S. Ivanov, J. Sharma, M. Neidig, D. Vu, A. Shreve, R. Brian. Dyer, J. Werner, and J. Martinez. Formation and stabilization of fluorescent gold nanoclusters using small molecules. 2010. *Journal of Physical Chemistry C.* **114** (38): 15879.

5. Sharma, J. K., H. C. Yeh, H. Yoo, J. H. Werner, and J. S. Martinez. In-situ generation of aptamer templated silver nanoclusters for label-free protein detection. To appear in *Chemical Communications.*

6. Arachchige, I., and S. Ivanov. Synthesis of luminescent gold species from cationic clusters . *Angewante Chemie Int. Ed.*

7. Goel, S., K. Velizhanin, A. Piryatinski, S. Tretiak, and S. Ivanov. DFT Study of Ligand Binding to Small Gold Clusters. 2010. *JOURNAL OF PHYSICAL CHEMISTRY LETTERS.* **1** (6): 927.

8. Goel, S., K. Velizhanin, A. Piryatinski, S. Ivanov, and S. Tretiak. Ligand Effects on Optical Absorption of Small Gold Clusters: A TDDFTStudy . *Journal of Physical Chemistry C.*

Publications

Bao, Y., H. Yeh, C. Zhong, S. Ivanov, J. Sharma, M. Neidig, D. Vu, A. Shreve, R. Brian. Dyer, J. Werner, and J. Martinez. Formation and stabilization of fluorescent gold nanoclusters using small molecules. 2010. *Journal of Physical Chemistry C.* **114** (38): 15879.

Goel, S., K. A.Velizhanin, A. Piryatinski, S. Tretiak, and S. Ivanov. DFT study of ligand binding to small gold clusters satyende. 2010. *Journal of Physical Chemistry Letters.* **1** (6): 927.

Sharma, J. K., H. C. Yeh, H. Yoo, J. H. Werner, and J. S. Martinez. In-situ generation of aptamer templated silver nanoclusters for label-free protein detection. To appear in *Chemical Communication.*

Sharma, J., H. Yeh, H. Yoo, J. Werner, and J. Martinez. A complementary palette of fluorescent silver nanoclusters. 2010. *CHEMICAL COMMUNICATIONS.* **46** (19): 3280.

Yeh, H., J. Sharma, H. Yoo, J. Martinez, and J. Werner. Photophysical characterization of fluorescent metal nanoclusters synthesized using oligonucleotides, proteins and small molecule ligands. 2010. In *Reporters, Markers, Dyes, Nanoparticles, and Molecular Probes for Biomedical Applications II ; 20100125 - 20100127 ; San Francisco, CA, United States.* Vol. 7576, p. var.pagings.

Yeh, H., J. Sharma, J. Han, J. Martinez, and J. Werner. A DNA-silver nanocluster probe that fluoresces upon hybridization. 2010. *Nano Letters.* **10** (8): 3106.

Yeh, H., J. Sharma, Y. Bao, J. Martinez, and J. Werner. Photophysical characterization of fluorescent metal nanoclusters synthesized using oligonucleotides, proteins, and small reagent molecules. Presented at *2010 BiOS SPIE Photonics West.* (San Francisco, January 23-28, 2010).

Understanding Anisotropy to Develop Superconductors by Design

Filip Ronning
20090022DR

Introduction

Condensed matter physics is entering an exciting age where our emerging ability to control materials properties holds tremendous promise for addressing the world's most basic needs. Superconductivity, the perfect flow of electricity resulting from quantum mechanics on a macroscopic scale, will be critical for meeting the energy demands of the future. Unconventional superconductors, with their inherent strong electronic correlations that allow the flow of current without loss at temperatures nearly half that of room temperature, provide the best opportunity for meeting these energy needs. To date, the inability to design superconducting materials from basic principles has plagued the international scientific community and represents one of its greatest challenges. Recent experimental discoveries reveal materials-specific anisotropic characteristics of these complex electronic oxides and metals that enhance their superconducting properties, but their microscopic origins are completely unknown. Our scientific objective utilizes a novel approach to discover the fundamental atomic-scale, structure-property materials' characteristics that generate this unconventional superconductivity, by employing a comprehensive suite of experimental probes and state-of-the-art theoretical tools. Success will take condensed matter to a whole new level of understanding in superconductivity and materials research.

Benefit to National Security Missions

This project will support the DOE mission in nuclear weapons by enhancing our understanding of actinide materials in general. In addition, we will directly support the DOE mission in energy security by enhancing our understanding of superconductors.

Progress

In the past year we have spent a great deal of time and effort studying the spin degrees of freedom in the so called "115" family of superconductors. The reason is that the fluctuations in the spin degrees of freedom are believed to be the glue which creates superconductivity. Muon spin resonance measurements have revealed the emergence of magnetism within the superconducting state in the compound CeCoIn5 (one of the "115" materials) in agreement with the above speculation. Nuclear magnetic resonance measurements have also shown that the magnetism which arises in the "115"s is of the "local" variety. This has implications on the details of the spin fluctuation spectrum which acts as the glue holding superconductivity together. By further exploring these ideas with nuclear magnetic resonance we have discovered an even more exciting relationship between the anisotropy of those spin fluctuations and the superconducting transition temperature. The more anisotropic the fluctuations, the higher the transition temperature, Tc, becomes. This is precisely the type of microscopic information we had hoped to uncover in the work proposed. The effort will now be to try and understand how the structure and bonding in these materials causes the spin fluctuations to become anisotropic, and whether we can suggest new compounds which would further enhance this anisotropy.

In addition to studying the spin degrees of freedom we have also devoted a great deal of effort to studying the single crystals we have discovered in the first year. Namely, CePt2In7 is a compound which is more structurally layered than other superconductors in this family. Work on single crystals has revealed that the phase diagram under pressure is identical to that found in polycrystalline samples. Additionally, by measuring the electronic structure with quantum oscillations in high magnetic field we have demonstrated a striking similarity between this compound, and the parent compound CeIn3, which is a 3 dimensional analog of CePt2In7. These results support our notion that reduced dimensionality is good for superconductivity. However, the transition temperature was not as high as we expected, and trying to understand this will be a focus of work in the next year. For instance determining the degree of anisotropy of the spin fluctuations is a high priority for the following year.

With the discovery of CePt2In7 single crystals, came the knowledge of how additional materials with a similar structure could be synthesized. We have been able to exploit this knowledge to discover several related plu-

tonium compounds. PuCoIn5 is a new compound we have succeeded to grow with this new found information, and it is the third known plutonium based material to exhibit superconductivity. In addition, it has the remarkable property that another transition (likely magnetic) precedes the superconducting transition at higher temperature. If confirmed, this will be the first example of a plutonium compound in which magnetism coexists with superconductivity. More importantly, it will be the long sought after proof that the plutonium compounds are directly related to the cerium compounds. Consequently, this will justify the argument that to increase the superconducting transition temperature further we will need to increase the coupling between the magnetic moments and the conducting electrons further. Most likely this can be accomplished by replacing plutonium with transition metal elements such as iron, nickel or copper.

To help identify whether such compounds could be structurally stable we are investigating the structural stability of hypothetical compounds using brute force theoretical calculations coupled with chemical intuition provided by our chemists. This approach has already predicted several new compounds. Although we did not expect that they had the correct microscopic elements for superconductivity, we confirmed the validity of this approach by synthesizing one of these predicted compounds (CeIr4In). Additional theoretical work has demonstrated how we can interpret point contact tunneling experiments. This experiment will be performed on the new plutonium superconductor, and this theoretical work is crucial for us to correctly interpret the significance of these results.

Our theoretical work continues to investigate the effects of the strength of the coulomb repulsion on the physics of these interesting materials. Work on theoretical models has developed new techniques as well as revealed the emergence of competing energy scales (and corresponding competing phenomena). We have also investigated the result of weakening the hybridization in the new class iron-based superconductors. The result predicted by theory is that the system goes from a superconductor to an insulating state, and this has been confirmed experimentally. Based on these experimental and theoretical insights we continue to attempt to grow new structures which will optimize these features.

Future Work

Understanding the strong electronic correlations that give rise to the anisotropies beneficial to unconventional superconductivity is the most direct path to move beyond serendipity into designing improved superconductors. The entwined spin, charge, and lattice degrees of freedom in strongly correlated systems require closely coupled experimental and theoretical efforts combined within a non-trivial (but direct) approach. To be successful in this endeavor, we must:

1. experimentally identify and subsequently decouple the momentum-dependent spin and charge anisotropies and energy scales relevant for unconventional superconductivity. We will focus on the compounds CePt2In7 and PuCoIn5 to see how they are similar and how they are different to the 10 other structurally related superconductors in this family.

2. theoretically determine the microscopic aspects of the underlying crystal structure/chemistry that lead to these correlation-driven anisotropies. Specifically we will look at the proximity to a magnetic instability in this family of compounds

3. integrate these experimental and theoretical thrusts to produce a microscopic understanding of the interactions that enable prediction and synthesis of new enhanced unconventional superconductors.

Conclusion

We expect to develop a playbook to design new superconducting materials. We will achieve this by learning how tuning a material's structure drives specific material properties which we can correlate with superconducting properties. Los Alamos is uniquely poised to capitalize on this new understanding for designing the next generation of improved correlated electron superconductors, through an integrated experimental and theoretical approach performed by its assembled team of world-class experts in superconductivity that will test and expand the limits of research at high magnetic fields and pressure, materials synthesis, and of theory and simulation. We now possess the capability of synthesizing the cleanest samples possible, which will allow us to detect what are the key factors for generating superconductivity, and we will be able to address the observation of why layered superconductors with increased spin fluctuations appear to be favorable for superconductivity.

Publications

Baek, S. -H., H. Sakai, E. D. Bauer, J. N. Mitchell, J. A. Kennison, F. Ronning, and J. D. Thompson. Anisotropic spin fluctuations and superconductivity in "115" heavy fermion compounds: Co59 NMR study in PuCoGa₅. 2010. *Physical Review Letters.* **105** (21): 217002.

Baek, S.-H., H. Lee, S. E. Brown, N. J. Curro, E. D. Bauer, F. Ronning, T. Park, and J. D. Thompson. NMR Investigation of Superconductivity and Antiferromagnetism in CaFe[sub 2]As[sub 2] under Pressure. 2009. *Physical Review Letters.* **102** (22): 227601.

Bauer, E. D., H. O. Lee, V. A. Sidorov, N. Kurita, K. Gofryk, J. -X. Zhu, F. Ronning, R. Movshovich, J. D. Thompson, and T. Park. Pressure-induced superconducting state and effective mass enhancement near the antiferromagnetic quantum critical point of CePt2In7. 2010.

PHYSICAL REVIEW B. **81** (18): 180507.

Bauer, E. D., T. Park, R. D. McDonald, M. J. Graf, L. N. Boulaevskii, J. N. Mitchell, J. D. Thompson, and J. L. Sarrao. Possible two-band superconductivity in PuRhGa₅ and CeRhIn₅. 2009. *Journal of Alloys and Compounds.* **488** (2): 554.

Bauer, E. D., V. A. Sidorov, H. Lee, N. Kurita, F. Ronning, R. Movshovich, and J. D. Thompson. Coexistence of Antiferromagnetism and Superconductivity in CeP-t2In7. 2010. *Journal of Physics: Conference Series.* **200**: 20110.

Bobev, S., S. Q. Xia, E. D. Bauer, F. Ronning, J. D. Thompson, and J. L. Sarrao. Nickel deficiency in RENi2-xP2 (RE = La, Ce, Pr). Combined crystallographic and physical property studies. 2009. *Journal of Solid State Chemistry.* **182** (6): 1473.

Curro, N., B. Young, R. Urbano, and M. Graf. Hyperfine Fields and Magnetic Structure in the B Phase of Ce-CoIn5. 2009. *JOURNAL OF LOW TEMPERATURE PHYSICS.* **158** (3-4): 635.

Dai, J. H., J. X. Zhu, and Q. M. Si. f-spin physics of rare-earth iron pnictides: Influence of d-electron antiferromagnetic order on the heavy-fermion phase diagram. 2009. *Physical Review B.* **80** (2): 020505.

Dai, J. H., Q. M. Si, J. X. Zhu, and E. Abrahams. Iron pnictides as a new setting for quantum criticality. 2009. *Proceedings of the National Academy of Sciences of the United States of America.* **106** (11): 4118.

Fogelstrom, M., W. K. Park, L. H. Greene, G. Goll, and M. Graf. Point-contact spectroscopy in heavy-fermion superconductors. 2010. *PHYSICAL REVIEW B.* **82** (1): 014527.

Harrison, N., R. D. McDonald, C. H. Mielke, E. D. Bauer, F. Ronning, and J. D. Thompson. Quantum oscillations in antiferromagnetic CaFe/sub 2/As/sub 2/ on the brink of superconductivity. 2009. *Journal of Physics: Condensed Matter.* **21** (32): 322202 (4 pp.).

Hu, X., C. S. Ting, and J. X. Zhu. Vortex core states in a minimal two-band model for iron-based superconductors. 2009. *Physical Review B.* **80** (1): 014523.

Klimczuk, T., T. M. McQueen, A. J. Williams, Q. Huang, F. Ronning, E. D. Bauer, J. D. Thompson, M. A. Green, and R. J. Cava. Superconductivity at 2.2 K in the layered oxypnictide La[sub 3]Ni[sub 4]P[sub 4]O[sub 2]. 2009. *Physical Review B (Condensed Matter and Materials Physics).* **79** (1): 012505.

Kurita, N., F. Ronning, C. F. Miclea, E. D. Bauer, J. D. Thompson, A. S. Sefat, M. A. McGuire, B. C. Sales, D. Mandrus, and R. Movshovich. Low-temperature thermal conductivity of BaFe[sub 2]As[sub 2]: A parent compound of iron arsenide superconductors. 2009. *Physical Review B (Condensed Matter and Materials Physics).* **79** (21): 214439.

Kurita, N., F. Ronning, Y. Tokiwa, E. D. Bauer, A. Subedi, D. J. Singh, J. D. Thompson, and R. Movshovich. Low-Temperature Magnetothermal Transport Investigation of a Ni-Based Superconductor BaNi[sub 2]As[sub 2]: Evidence for Fully Gapped Superconductivity. 2009. *Physical Review Letters.* **102** (14): 147004.

Qi, Y. N., J. X. Zhu, and C. S. Ting. Validity of the equation-of-motion approach to the Kondo problem in the large-N limit. 2009. *Physical Review B.* **79** (20): 205110.

Ronning, F., E. D. Bauer, T. Park, N. Kurita, T. Klimczuk, R. Movshovich, A. S. Sefat, D. Mandrus, and J. D. Thompson. Ni2X2 (X = pnictide, chalcogenide, or B) based superconductors. 2009. *Physica C-Superconductivity and Its Applications.* **469** (9-12): 396.

Ronning, F., E. D. Bauer, T. Park, S.-H. Baek, H. Sakai, and J. D. Thompson. Superconductivity and the effects of pressure and structure in single-crystalline SrNi[sub 2]P[sub 2]. 2009. *Physical Review B (Condensed Matter and Materials Physics).* **79** (13): 134507.

Sakai, H., S. -H. Baek, E. D. Bauer, F. Ronning, and J. D. Thompson. 29Si-NMR study of magnetic anisotropy and hyperfine interactions in the uranium-based ferromagnet UNiSi2. 2010. *IOP Conference Series: Materials Science and Engineering.* **9**: 012097 (7 pp.).

Sefat, A. S., D. J. Singh, R. Y. Jin, M. A. McGuire, B. C. Sales, F. Ronning, and D. Mandrus. BaT2As2 single crystals (T = Fe, Co, Ni) and superconductivity upon Co-doping. 2009. *Physica C-Superconductivity and Its Applications.* **469** (9-12): 350.

Sefat, Athena S., Michael A. McGuire, Brian C. Sales, and E. D. Bauer. Structure and anisotropic properties of BaFe[sub 2 - x]Ni[sub x]As[sub 2] (x = 0, 1, and 2) single crystals. 2009. *Physical Review B (Condensed Matter and Materials Physics).* **79** (9): 094508.

Si, Q. M., E. Abrahams, J. H. Dai, and J. X. Zhu. Correlation effects in the iron pnictides. 2009. *New Journal of Physics.* **11**: 045001.

Spehling, J., R. H. Heffner, J. E. Sonier, N. Curro, C. H. Wang, B. Hitti, G. Morris, E. D. Bauer, J. L. Sarrao, F. J. Litterst, and H. -H. Klauss. Field-Induced Coupled Superconductivity and Spin Density Wave Order in the Heavy Fermion Compound CeCoIn5. 2009. *PHYSICAL REVIEW LETTERS.* **103** (23): 237003.

Talbayev, D., K. S. Burch, E. M. Chia, S. A. Trugman, J. -X. Zhu, E. D. Bauer, J. A. Kennison, J. N. Mitchell, J. D.

Thompson, J. L. Sarrao, and A. J. Taylor. Hybridization and superconducting gaps in the heavy-fermion superconductor PuCoGa5 probed via the dynamics of photo-induced quasiparticles. 2010. *Physical Review Letters.* **104** (22): 227002.

Tobash, P., F. Ronning, J. D. Thompson, S. Bobev, and E. Bauer. Magnetic order and heavy fermion behavior in CePd_{1+x}Al_{6-x}: Synthesis, structure, and physical properties. 2010. *Journal of Solid State Chemistry.* **183** (3): 707.

Zhu, J., R. Yu, H. Wang, L. Zhao, M. D. Jones, J. Dai, E. Abrahams, E. Morosan, M. Fang, and Q. Si. Band narrowing and mott localization in iron oxychalcogenides La2O2Fe2O(Se,S)2. 2010. *Physical Review Letters.* **104** (21): 216405.

Spatial-temporal Frontiers of Atomistic Simulations in the Petaflop Computational World

Timothy C. Germann
20090035DR

Introduction

In recent years there have been two exciting developments in the field of computational materials science at the direct atom-by-atom level. First, continuing advances in high-performance computing, in particular massively parallel supercomputers consisting of tens to hundreds of thousands of processors working in concert, have enabled the study of complex phenomena in fluids and solids by "molecular dynamics" (MD) modeling of systems containing millions to billions of atoms. Secondly, "accelerated MD" algorithms, developed at Los Alamos over the past decade, are enabling the modeling of timescales of seconds or longer, far beyond the nanoseconds (billionths of a second) that traditional MD simulations have been able to reach. The basic idea underlying such methods is that a wide class of material behavior consists of a sequence of thermally activated, "rare event" processes; it is only such processes that are important, and not the atoms vibrating about their equilibrium positions. However, such accelerated MD simulations have thus far been limited to systems of only several hundred to a few thousand atoms at most. The goal of this project is to develop and validate techniques for combining the accelerated and large-scale MD techniques, enabling for the first time atomistic simulations with both large size and long time scales. In certain cases, such simulations may directly overlap those of ultrafast, high-resolution experimental measurements. We pursue two distinct approaches for achieving this integration, and focus on two specific scientific materials science problems for study: (1) the nucleation, growth, and coalescence of voids leading to failure in metals; and (2) the interaction of a dislocation pileup forced against a grain boundary, a fundamental issue underlying material strength. These two phenomena are representative of a large class of problems that have until now been tantalizingly just out-of-reach of current simulation techniques: requiring timescales of microseconds to milliseconds that have eluded direct MD, and sample dimensions as large as a micrometer that accelerated MD techniques have not been able to reach.

Benefit to National Security Missions

This project will support DOE missions in the Office of Science and Nuclear Weapons (NNSA Advanced Simulation and Computing) programs, by proving new computational tools and enhancing our understanding of the fundamental dynamics of materials, in particular under extreme loading conditions that are difficult to probe experimentally. The methods demonstrated here should have applications beyond these materials science issues that we will focus on; similarly, the materials science questions addressed here have impacts in nuclear energy, DOD programs (e.g. armor/anti-armor), and beyond.

Progress

During the past year, we have made significant progress in both the method and algorithm development aspects as well as the materials science problems we are studying.

On the algorithm side, two techniques have been demonstrated for the first time. The local bond-boost hyperdynamics technique has the capability for accelerating billion-atom (or even larger) systems for the first time, far beyond the thousand-atom size of most previous accelerated molecular dynamics (AMD) techniques. We have implemented this technique in the SPaSM (Scalable Parallel Short-range Molecular dynamics) code, and demonstrated that it gives accurate results for a test problem in which several copper adatoms run around the top of a copper surface at various temperatures. We have also performed initial prototype runs for a 10 million atom copper crystal with a distribution of bulk vacancies, for instance resulting from radiation damage, and shown that the subsequent evolution of such a system can be modeled for tens of microseconds in a single day of computational time. The second technique for integrating accelerated and large-scale MD techniques is an embedding technique, in which active regions are carved out of a larger material, and AMD used to speed up the search for transition pathways to new atomic configurations, or states. When such a transition is detected, it may result in the rapid (athermal) propagation of a dislocation loop, requiring the larger-scale

simulation model. We have demonstrated this for the void growth aspect of spall failure, in which a crystal containing a preexisting void is stretched using AMD at experimentally relevant strain rates which are not directly accessible to MD (e.g. 10^5/second), and then upon dislocation emission embedded into a suitably relaxed larger crystal so that dislocation propagation and reactions on the picosecond time scale (10^{-12} sec) can be followed (Figure 1).

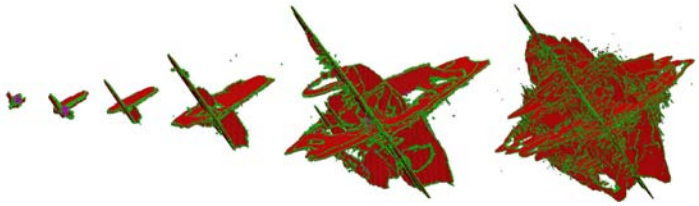

Figure 1. Void growth via dislocation emission studied by a combined accelerated and large-scale MD simulation. An initial 13-atom void in a copper crystal containing 13 thousand atoms is stretched at experimental strain rates using accelerated MD until the first dislocation emission event is detected. At that point, the sample is embedded into a larger (108 million atom) crystal that allows the subsequent processes of dislocation loop emission, growth, and intersection to evolve.

On the materials science side, the void growth process just mentioned is being further studied to inform our ductile spall model, and its component elements of void nucleation, growth, and coalescence. During the Roadrunner open science period, we were also able to carry out direct large-scale MD studies of spall failure in ~100 million-atom copper bicrystals, observing a transition between high strain rate (short timescale) nucleation-dominated failure within grains, to a low strain rate (long timescale) growth-dominated failure between grains. The extrapolation of this transition (vs. strain rate and lengthscale) is in quantitative agreement with recent experiments; the accelerated large-scale techniques being developed here may be able to bridge the remaining gap between experiment and simulation.

The second problem we are studying, dislocation pileup transmission through a grain boundary, has also yielded scientific insight. Small-scale (quasi-two-dimensional) simulations have revealed the sequence of events involved in slip transmission across an asymmetric aluminum grain boundary, and the energy landscape involved (Figure 2), which is important for the subsequent application of AMD techniques. Large-scale (multimillion-atom) simulations, on the Cerrillos Turquoise network partition of Roadrunner, have been used to determine the critical bow-out length scale for fully three-dimensional slip transmission. The more complicated energy landscape for this problem is challenging to the techniques we are developing, but is representative of a broad class of phenomena so its solution is being actively pursued.

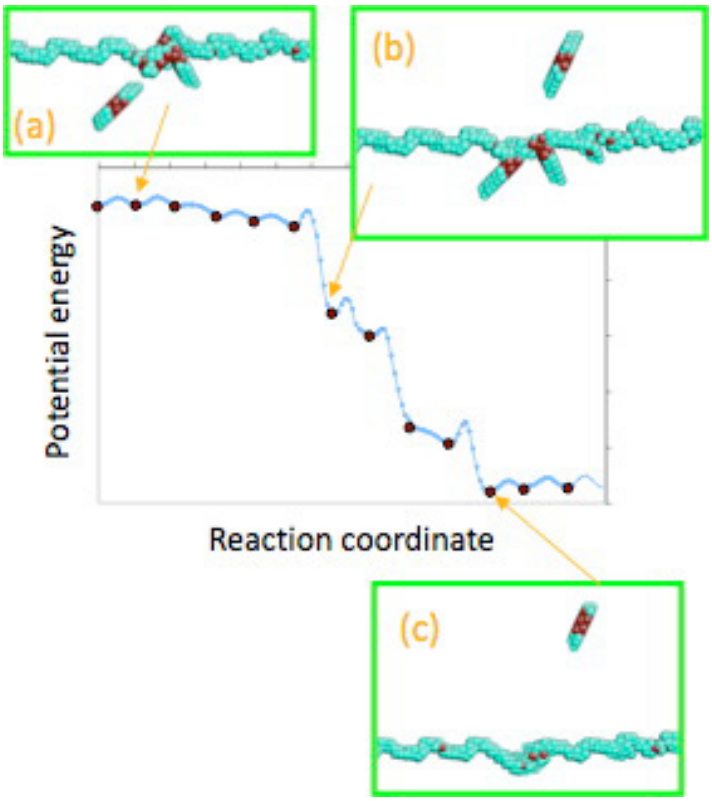

Figure 2. Energy landscape for dislocation transmission across a grain boundary. (a) Initial configuration, in which the leading two dislocations have been absorbed into the grain boundary and modified its local structure, but the third dislocation is still in the lower grain. (b) The transmission event involves a coupled emission of one dislocation from the grain boundary into the upper grain, and absorption of the third dislocation from the lower grain. (c) Final state, in which one dislocation is in the upper grain and two are in the grain boundary.

Future Work

Atomistic-scale simulations are playing an increasing role in fundamental and applied materials science. Los Alamos has two distinct internationally recognized capabilities in this area: large-scale molecular dynamics (MD) simulations, specifically the SPaSM code supported primarily by the weapons program (ASC), and accelerated molecular dynamics algorithm development and implementation under the auspices of LDRD and Basic Energy Sciences (BES). The goal of this project is to develop and demonstrate the coupling of these two capabilities to address heretofore inaccessible problems in materials science, building a transformational capability with potential future applications in the BES, nuclear energy, and weapons programs.

Two different routes are being pursued to couple large-scale and accelerated MD: (1) for situations where likely sites of interest can be identified (e.g. void locations), SPaSM will provide the long-range stress boundary conditions for accelerated zones, partitioning the available pro-

cessors (e.g. on Roadrunner) between the two concurrent models. Alternatively, (2) a newly developed "local-bias hyperdynamics" offers a way to simultaneously accelerate the dynamics across a large system. At the end of this project we expect to have developed and applied both of these algorithms, as demonstrated by computer codes that effectively utilize Roadrunner, as well as a firm understanding of the strengths and weaknesses of each approach for model problems, that will be published in peer-reviewed scientific journals.

The two specific materials science problems that we have chosen to study with these new capabilities are: (1) the nucleation, growth, and coalescence of voids leading to ductile failure of metals ("spall") following shock release; and (2) the interaction of a dislocation pileup forced against a grain boundary, a fundamental issue underlying material strength. We expect that each of these studies will lead to unprecedented insight, resulting in one or more high-profile scientific publications (e.g. suitable for the journals Science or Nature).

The work that we have performed under this project has led to a proposed Exascale Co-Design Center for Materials in Extremes. The basic idea is that materials simulation codes at individual scales, including the atomic scale and grain level, as well as coupled scales such as the large-scale/accelerated MD work developed here, will be used to evaluate potential "exascale" supercomputer designs capable of reaching 1 exaflop (1,000,000,000,000,000,000 floating point operations per second) by the end of the decade, and conversely the potential hardware design space will be used to guide the development of simulation codes, algorithms, and libraries such that they can effectively utilize such a machine. Since the commercial market is dominated by either highly specialized graphics processors (e.g. for video streaming or games) or simplified low-power processors (e.g. for cell phones and PDAs), exploiting them for scientific computation is becoming increasingly difficult, as demonstrated by LANL's Roadrunner hybrid platform, which uses the IBM/Sony/Toshiba Cell processor developed for the Sony Playstation; therefore such a "co-design" process is critical for the future of high-end, or "bleeding edge," scientific computing.

Conclusion

This project is expected to lead to one or more algorithms and practical computer codes that will effectively utilize DOE supercomputer platforms - in particular LANL's Roadrunner - to study microscopic phenomena at an atom-by-atom level, for size and time scales that are both larger and longer than currently possible. We will then utilize this unique capability to investigate fundamental materials science questions that have eluded direct study for a half-century or longer. Through this effort, we will help maintain America's leadership role in advanced high-performance computing and nanotechnology.

Publications

Arman, B., S. Luo, T. Germann, and T. Cagin. Dynamic response of Cu46Zr54 metallic glass to high-strain-rate shock loading: Plasticity, spall, and atomic-level structures. 2010. *PHYSICAL REVIEW B.* **81** (14): 144201.

Germann, T.. LARGE-SCALE CLASSICAL MOLECULAR DYNAMICS SIMULATIONS OF SHOCK-INDUCED PLASTICITY IN BCC NIOBIUM. 2009. In *16th Conference of the American-Physical-Society-Topical-Group on Shock Compression of Condensed Matter ; 20090628 - 20090703 ; Nashville, TN.* Vol. 1195, p. 761.

Germann, T., and K. Kadau. LARGE-SCALE MOLECULAR DYNAMICS SIMULATIONS OF THE FCC-FCC VOLUME COLLAPSE TRANSITION IN SHOCKED CESIUM. 2009. In *16th Conference of the American-Physical-Society-Topical-Group on Shock Compression of Condensed Matter ; 20090628 - 20090703 ; Nashville, TN.* Vol. 1195, p. 1209.

Han, L., Q. An, S. Luo, and T. Germann. THE EFFECTS OF DEFECTS ON MELTING OF COPPER. 2009. In *16th Conference of the American-Physical-Society-Topical-Group on Shock Compression of Condensed Matter ; 20090628 - 20090703 ; Nashville, TN.* Vol. 1195, p. 1187.

Luo, S. N., Q. An, T. C. Germann, and L. B. Han. Shock-induced spall in solid and liquid Cu at extreme strain rates. 2009. *Journal of Applied Physics.* **106** (1): 013502.

Luo, S., Q. An, T. Germann, and L. Han. Shock-induced spall in solid and liquid Cu at extreme strain rates. 2009. *JOURNAL OF APPLIED PHYSICS.* **106** (1): 013502.

Luo, S., T. Germann, Q. An, and L. Han. SHOCK-INDUCED SPALL IN COPPER: THE EFFECTS OF ANISOTROPY, TEMPERATURE, DEFECTS AND LOADING PULSE. 2009. In *16th Conference of the American-Physical-Society-Topical-Group on Shock Compression of Condensed Matter ; 20090628 - 20090703 ; Nashville, TN.* Vol. 1195, p. 1015.

Luo, S., T. Germann, T. Desai, D. Tonks, and Q. An. Anisotropic shock response of columnar nanocrystalline Cu. 2010. *JOURNAL OF APPLIED PHYSICS.* **107** (12): 123507.

Luo, S., T. Germann, and D. Tonks. The effect of vacancies on dynamic response of single crystal Cu to shock waves. 2010. *JOURNAL OF APPLIED PHYSICS.* **107** (5): 056102.

Luo, S., T. Germann, and D. Tonks. The effect of vacancies on dynamic response of single crystal Cu to shock waves. 2010. *JOURNAL OF APPLIED PHYSICS.* **107** (5): 056102.

Luo, S., T. Germann, and D. Tonks. Spall damage of copper under supported and decaying shock loading. 2009. *JOURNAL OF APPLIED PHYSICS.* **106** (12): 123518.

Pozzi, C., T. C. Germann, and R. G. Hoagland. MOLECULAR DYNAMICS SIMULATION OF DISLOCATION EMISSION FROM SHOCKED ALUMINUM GRAIN BOUNDARIES. 2009. In *16th Conference of the American-Physical-Society-Topical-Group on Shock Compression of Condensed Matter ; 20090628 - 20090703 ; Nashville, TN.* Vol. 1195, p. 765.

Ravelo, R., B. L. Holian, and T. Germann. HIGH STRAIN RATES EFFECTS IN QUASI-ISENTROPIC COMPRESSION OF SOLIDS. 2009. In *16th Conference of the American-Physical-Society-Topical-Group on Shock Compression of Condensed Matter ; 20090628 - 20090703 ; Nashville, TN.* Vol. 1195, p. 825.

Enhance Radiation Damage Resistance via Manipulation of the Properties of Nanoscale Materials

Michael A. Nastasi
20090061DR

Introduction

We propose to enhance the radiation resistance of materials by manipulating their properties at the nanoscale to directly affect the evolution of damage cascades. The design of future nuclear power reactors, including advanced fuel cycles, Gen IV and fusion reactors places high demands on reactor cladding and structural materials. These extreme operating conditions include extremely high irradiation doses, corrosive liquid metal environments, and higher operating temperatures with minimal change in mechanical properties. At present, the best engineered materials for high dose nuclear applications reach their structural limit at relatively low irradiation dose. Their elevated temperature mechanical integrity at even lower irradiation doses. Thus, the transformative research in materials development is required to meet the needs of future nuclear reactors.

The reason why materials fail under irradiation can be traced at the most fundamental level to the accumulation of the defects produced during the irradiation process. Left unbridled such processes lead to swelling, and chemical changes that compromise the material's mechanical and corrosion resistant properties. Therefore, the principal challenge in the development of materials with radically extended performance limits in extreme radiation environments is to increase the recovery efficiency of radiation-induced defects.

Our approach in addressing this problem is to develop materials that will contain special internal features, i.e., interfaces, that can be designed at the atomic-scale to attract, absorb and annihilate radiation-induced defects, thereby allowing design of nanostructured materials for radiation damage tolerance. This will build on recent scientific breakthroughs at LANL that presents a new paradigm in designing materials with the specific property of radiation damage tolerance. The central idea of this proposal is atomic-scale design of stable internal interfaces that impart radiation tolerance to materials by attracting, absorbing, and annihilating point defects.

Benefit to National Security Missions

This work will support the mission of the DOE Office of Science, explicitly the BES-stated Basic Research Needs for Advanced Nuclear Energy Systems, included a priority research direction on Nanoscale Design of Materials and Interfaces that Radically Extend Performance Limits in Extreme Radiation Environments.

Progress

The critical He concentration at which bubbles are resolved in through-focus transmission electron microscopy images was measured to be orders of magnitude higher in fcc-bcc nanolayered composites than in pure metals. The general trend was observed in several composites: Cu-Nb, V-Ag, Cu-Mo and Cu-V. This implies increased helium trapping at fcc-bcc interfaces that may originate from the atomic structure of the interface. By comparison, coherent twin boundaries appear to have low solubility for helium.

The magnitude of hardening, as measured by micropillar compression tests, in helium ion implanted Cu-Nb nanolayered composites decreases significantly with decreasing layer thickness. At layer thicknesses less than approximately 5 nm, no irradiation hardening is measured. This is consistent with the experimentally observed decrease in the density of radiation-induced bubbles and interstitial loops with reducing layer thickness.

We have finished a density functional theory study of Cu-He and Nb-He interactions and defect properties. On the basis of this finding, we constructed a predictive Cu-Nb-He embedded atom model (EAM) potential, which predicts the correct formation energies and volumes of He defects in fcc Cu and bcc Nb, despite not being fitted to them. The reason for the predictive capability of the potential was explained in terms of the ground state electron density in condensed phases of Cu and Nb containing He. A manuscript describing this work is currently under review in Modeling and Simulation in Materials Science and Engineering.

We have applied this potential to study the binding energy of He interstitials and substitutionals as a function of location in several atomic configurations of Cu-Nb interfaces. We find that constitutional vacancies formed at misfit dislocation intersections are preferential He trapping sites. Whether or not trapped He clusters remain in solution depends on the availability of (regular, i.e. not constitutional) vacancies in the neighboring Cu and Nb, with high availability favoring clustering. Current work is focusing on determining the effect of He trapped at Cu-Nb interfaces on the mechanical properties of these interfaces, namely shear resistance and cohesive stress.

Another area of our study is the thermodynamics of heterogeneous He precipitation, which focuses on the determination of preferential location for He bubbles, and the form He bubbles adopt. Simulations are done with a parallel Metropolis Monte Carlo code under the assumption of He/vacancy ratio equal to 1, a sensible assumption for He implantation occurring simultaneously with some irradiation damage. For fcc metals, it has been shown experimentally that pure twist Au grain boundaries, formed by a square array of screw dislocations show dislocation intersection as preferential sites for He precipitation (Figure 1). Our simulations are done for an equivalent fcc material, Cu, using the He-Cu potential develop by our MIT collaborators, which fully confirm this result. Moreover, simulations show the decomposition of initial perfect screw dislocation into partials that leave the (100) plane of the interface, in agreement with energetic considerations about dislocation configurations.

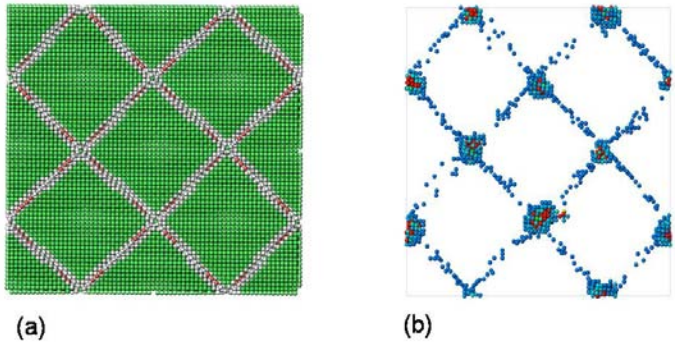

Figure 1. (a) atomic scale view of a slice of the grain boundary plane containing the network of dislocations prior to the introduction of He. (b) After the introduction of He (red atoms), precipitation of He at the nodes of the network takes place.

We have also examined the role that grain boundaries play in the radiation tolerance of nanostructured materials, using grain boundaries in Cu as model systems. We have examined three types of grain boundaries – $\Sigma 11$ symmetric tilt, $\Sigma 11$ asymmetric tilt, and $\Sigma 5$ twist – and are investigating a more general combined twist/tilt boundary. We focused on two time-scale regimes: the ps time scale over which damage (primarily interstitials and vacancies) is created by collision cascades (using molecular dynamics) and the longer time scales over which those defects annihilate and aggregate (using accelerated molecular dynamics). We found that during the damage production stage, the grain boundaries absorb very large numbers of interstitials, so many that less vacancy-interstitial recombination occurs than if the grain boundary is not present. This implies that under conditions in which thermally active annealing processes are not possible, nanocrystalline materials may behave worse than polycrystalline materials. However, when long-time behavior is accounted for, we find that grain boundaries exhibit an enhanced self-healing capability and that interstitials absorbed at the boundary during the cascade can be reemitted to annihilate with vacancies in the bulk. This "interstitial emission" mechanism occurs with relatively small barriers of about 0.2 eV (compared to 0.7 eV for bulk vacancy migration) and can annihilate vacancies that are up to 1 nm from the boundary. This mechanism leads to superior radiation tolerance at temperatures where vacancies are essentially immobile. These results explain experimental observations of radiation damage effects in nanocrystalline gold, which show worse tolerance than large-grained counterparts at low temperature but enhanced recovery at intermediate temperatures.

Future Work

Following our discovery of "super sink" interfaces we have a truly unique opportunity to develop highly radiation tolerant nanocomposite materials. We have shown that such interfaces stabilize material microstructure and efficiently heal radiation damage by attracting, absorbing, and catalyzing the annihilation of radiation-induced point defects. Our objectives in this work are to: 1) develop a generalized description, applicable to any interface in any material, of the properties that make an interface a "super sink" for radiation-induced defects; 2) explore the irradiation stability of nano-composites over a broad spectrum of extreme environments (high irradiation dose, long time, high temperature, and corrosion to simulate real reactor environments conditions); and 3) explore the effect of irradiation (particularly at high doses) on mechanical properties such as strength and ductility. Our approach integrates theory, modeling, and experiments to formulate, validate, and test the limits of strategies for enhancing radiation damage resistance of materials by maximizing their content of super sink interfaces. Our findings will lay the scientific foundations for intelligently designing radiation tolerant materials for future nuclear reactors.

With the startup of our Energy Frontiers Research Center, we have refocused this project to retain clear boundaries between the EFRC and LDRD work. The focus of the LDRD-DR is be on studying the behavior of interfaces at high ratio of helium gas to DPA (displacements per atom). This is of direct relevance to fusion reactors where the production of helium via transmutation reactions per DPA is high. Our research objectives remain essentially remain the same, but the focus is on fusion relevant environment. We therefore focus on identifying interfaces that are 'super sinks' for he-

lium; stability of nanocomposites at high ratios of helium to DPA, and influence of helium gas bubbles on mechanical behavior of nanocomposites.

Conclusion

We have 3 objectives in this research that we believe will lead to the development of materials with high radiation tolerance. First, to develop a generalized description, applicable to any interface in any material, of the properties that make an interface a "super sink" for radiation-induced defects. Second, explore the irradiation stability of nanocomposites over a broad spectrum of extreme conditions (high irradiation dose, long time, high temperature, and corrosion). Third, explore the effect of irradiation (particularly at high doses) on mechanical properties such as strength and ductility.

Publications

Bai, X. M., A. F. Voter, R. G. Hoagland, M. Nastasi, and B. P. Uberuaga. Efficient annealing of radiation damage near grain boundaries via interstitial emission. 2010. *Science.* **327**: 1631.

Demkowicz, M. J., D. Bhattacharyya, I. Usov, A. Misra, Y. Q. Wang, and M. Nastasi. The Role of the atomic structure of the Cu-Nb interface on helium bubble formation at interfaces. 210. *Applied Physics Letters.* **97**: 161903.

Fu, E. G., A. Misra, H. Wang, and X. Zhang. Interface enabled defects reduction in helium ion irradiated Cu/V nanolayers. To appear in *Journal of Nuclear Materials.*

Kashinath, A., and M. J. Demkowicz. A predictive interatomic potential for He in Cu and Nb. *Modeling and Simulation in Materials Science and Engineering .*

Li, N., J. J. Carter, A. Misra, L. Shao, and X. Zhang. The influence of interfaces on the formation of bubbles in He ion irradiated Cu/Mo multilayers. To appear in *Philosophical Magazine Letters.*

Wei, Q. M., Y. Q. Wang, M. Nastasi, and A. Misra. Nucleation and growth of bubbles in He ion implanted V/Ag multilayers. To appear in *Philosophical Magazine.*

Zhang, X., E. G. Fu, A. Misra , and M. J. Demkowicz. Interface-enabled defect reduction in He ion irradiated metallic multilayers. To appear in *Journal of Metals.*

Seaborg Institute Fellows

Albert Migliori
20090475DR

Introduction

This project is directed toward development of new actinide science capabilities to respond to the future national security mission environment, nuclear energy, weapons complex transformation, and the evolution of actinide science and technology that will be applicable to national security. We will address fundamental science that will enhance stockpile stewardship, reduce global nuclear threats, and lead to sustainable nuclear energy. Los Alamos strengths in actinide chemistry, material synthesis, condensed matter physics, complex systems, emergent phenomena, and theory and modeling provides a world-class foundation from which to develop these capabilities, and help transform the Laboratory mission over the next five years.

Benefit to National Security Missions

Knowledge and expertise in actinide science is central to the mission of DOE and the NNSA, including national defense, threat reduction, nuclear forensics, fundamental science, energy security, environmental restoration, and radioactive waste management.

Progress

We describe here highlights of progress made in FY 2010 by the (at present) 14 Seaborg postdocs. This year, several noteworthy accomplishments occurred, supported by this program. One was the conversion to permanent staff of two Seaborg postdocs. The other was the very high profile work by Rob Thompson, mentored by Jacqueline Kiplinger. This work resulted in a Nature Chemistry cover by Thompson et al. , and a "Best Mentor" award for Kiplinger.

Uranium Nitride Complexes

Molecular uranium nitride complexes $[UN]_x$ are important for alternate nuclear fuel. Synthetic work directed towards the goal of preparing terminal uranium nitride complexes that has been supported by the LDRD office is summarized by three publications from 2010[1],[2,3] This work has been the subject of a great deal of media attention, including press release highlights through *Nature*, *LANL*, *DOE Pulse*, the *LDRD offices of LANL*, *Sandia National Laboratory*, *and LLNL.* Articles highlighting this work have also appeared in *Discovery News*, *ARS Technica*, *Chemical & Engineering News (C&EN)*, *New Scientist*, *Chemistry World*, and an upcoming issue of *Vision Magazine*, published by Futurelab in the U.K. Additional exposure was also bestowed on this work through a news and views article[4] in *Nature Chemistry* and selection for the cover of the issue in *Nature Chemistry*.

Spectroscopic Analysis of Actinyl Systems

Actinyl cations are ubiquitous for higher oxidation state actinides and are pertinent to environmental remediation and nuclear fuel separation technologies. The goal of this research was to increase our understanding of the electronic structure and bonding properties of the actinyls through polyoxometalate coordination. This work has been presented at an Office of Basic Energy Science, Heavy Element Chemistry Contractors Meeting and the 239th ACS National Meeting & Exposition and the Plutonium Futures - The Science 2010.

Systematic trends in the covalency of dithiophosphinates using X-ray absorption spectroscopy (XAS)

A significant challenge for creating proliferation-resistant separation technologies to reprocess spent nuclear fuel is developing methods to efficiently partition trivalent actinides from lanthanide ions, a separation hampered by the similar chemical properties of the 5*f*- and 4*f*-elements. Work has resulted in the synthesis and characterization of 15 previously unreported compounds. These results will be the subject of several papers, and should provide crucial guidance for the development and optimization of new f-metal extractants.

Elastic moduli of beta plutonium

Using high precision elastic moduli measurements via resonant ultrasound spectroscopy (RUS) technique, the elastic moduli measured for beta plutonium have been

extended and analyzed, Figure 1. These have been submitted for publication and are the first high accuracy measurements of this phase. The results, shown in the figure, lead to the conjecture that these three studied phases of plutonium behave as if they are three entirely different metals.

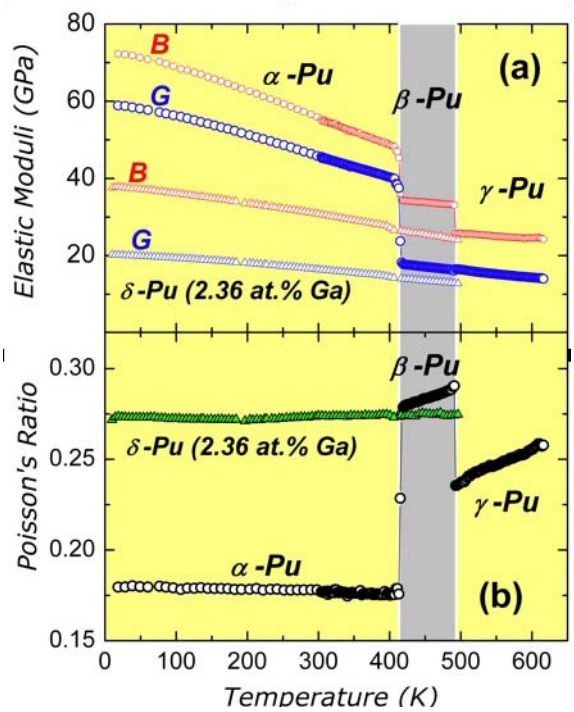

Figure 1. (a) Temperature dependence of the bulk (red symbols) and shear (blue symbols) moduli for pure plutonium phases (circles) and 2.36% gallium alloyed delta plutonium (triangles). (b) Temperature dependence of the Poisson's ratio for pure plutonium phases (circles) and gallium alloyed delta plutonium (green triangles).

Synthesis and Characterization of Novel Uranium Imido Complexes

Imido complexes of the actinide elements continue to generate great interest amongst scientists as a means to study multiple bonding throughout the actinide series. We studied reactions of UCl_4.

X-ray Absorption Spectroscopy

To improve our understanding of the interplay between the electronic structure and physical properties of transition metal and actinide materials, investigation have begun with two series of structurally-related molecules which formed a basis for early descriptions of metal-ligand covalent bonding. Preliminary findings will likely lead to changes in how scientists view electronic structure for all *d*- and *f*-block materials.

Grain Boundaries and heat transport in nuclear fuels

Thermal transport is an important performance metric for nuclear fuels because a high thermal conductivity is needed for efficient transfer of thermal energy. Thermal transport is limited by the presence of grain boundaries and Xe gas. This work has concentrated on how mass and thermal transport are affected by grain boundaries and Xe gas. Some modeling of such boundaries is shown in Figure 2.

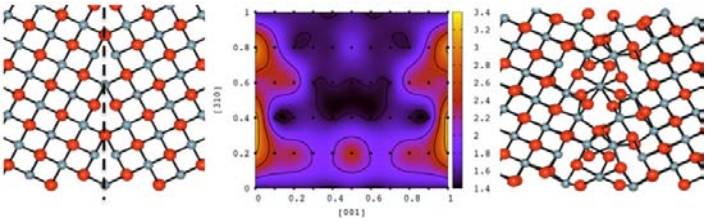

Figure 2. Structure of the S5 tilt boundary in UO_2:__ (a) __idealized__, (b) __g-surface plot, and (c) translated and relaxed. The relaxed structure exhibits an electric field strong enough to influence thermal and mass transport properties. (Part of this figure was used on the cover of the Consortium for Advanced Simulation of Light Water Reactors – the first Energy Innovation Hub).

Developing Actinide Catalysts for Cleaning Dirty Fossil Feedstocks

Using Density Functional Theory (DFT) calculations to study homogeneous Actinide catalysts for removing contaminants from low-quality feedstocks, two catalysts, were studied in terms of reactivity towards thiophene, furan, and pyridine, three common contaminants of crude oil containing S, O, and N atoms, respectively.

"Crystal chemistry" of well known heavy fermion superconductors

This task uses specific structural units to construct new intermetallic compounds. We still do not yet have a firm grasp on the origins of unconventional superconductivity in intermetallic and oxide compounds. Our approach therefore is to bridge the structure/property relationships to move towards a rational design of superconductivity through crystal chemistry. We have had some success with several new superconductors.

Ligand Development for Lanthanide/Actinide Separation

Several terdentate and tetradentate ligands were prepared from the Schiff-base condensation of chelating amines to sterically hindered ketones. The addition of these ligands to various lanthanide precursors was then explored to determine the reaction conditions under which ligation occurs and assay their viability for use as sequestering agents in the selective removal of minor actinides from PUREX waste streams.

UCu_5 and $UAuPt_4$

Geometric magnetic frustration occurs when localized magnetic moments (spins) can not satisfy all of their nearest neighbor magnetic interactions because of their relative positions on a regular crystal lattice. The consequences of geometric frustration have been extensively studied in

insulating materials but geometric frustration in metallic systems is virtually unexplored. One material we are currently studying is the 5f-electron metal UCu_5. The large ratio of the Weiss temperature to T_N and a measured magnetic entropy that is only about 1/3 of that expected are good evidences that this material is frustrated.

Ionic Scintillators
The primary synthetic targets of the current research are intrinsic scintillators that are promising candidates for actinide detection. Investigations into the size-dependent behavior of ionic scintillators have received little attention in part because they are hygroscopic. We developed a strategy for a general, mild synthesis of monomeric cerium halide fragments that would permit the incorporation of a broad spectrum of solvating ligands.

Actinide based f-electron systems
f-electron systems (compounds) composed of elements like plutonium (Pu), uranium (U) and cerium (Ce) have f-electrons in their valance band that play an important role in determining the physical properties in these systems. Different types of critical phenomena occur with temperature, pressure and magnetic field. These critical phenomena include phase transitions (e.g., magnetic transitions), quantum criticality and unconventional superconductivity

where the electrical resistivity becomes zero. This task focuses on such effects in two important systems: URu2Si2 (Ru: Ruthenium and Si: Silicon) and PuCoGa5 (Pu based superconductivity, Co: Cobalt and Ga: Gallium).

Publications

Altarawneh, M. M., N. Harrison, R. D. McDonald, F. F. Balakirev, C. H. Mielke, P. H. Tobash, J. X. Zhu, J. D. Thompson, F. Ronning, and E. D. Bauer. The fermi surface of CePt2In7: a two-dimensional analog of CeIn3. *Physical Review B.*

Bauer, E. D., P. H. Tobash, J. N. Mitchell, J. A. Kennison, F. Ronning, B. L. Scott, and J. D. Thompson. Magnetic order in Pu2Ni3Si5. To appear in *Condensed Mater Physics Conference Proceedings.* (New Mexico, June 27 - July 2, 2010).

Bauer, E. D., P. H. Tobash, J. N. Mitchell, J. A. Kennison, J. J. Joyce, T. Durakiewicz, B. L. Scott, J. L. Sarrao, L. A. Morales, and J. D. Thompson. Complex magnetic order in PuSb2 single crystals. 10. In *Plutonium Futures - The Science 2010.* (Keystone, 19-23 Sept 2010). , p. 315. Illinois: American Nuclear Society.

Chantis, A. N., R. C. Albers, A. Svane, and N. E. Christensen. GW correlation effects on plutonium quasiparticle energies: changes in crystal-field splitting. 2009. *Philosophical Magazine.* **89**: 1801.

Chantis, A. N., R. C. Albers, M. D. Jones, M. van Schilfgaarde, and T. Kotani. Many-body electronic structure for metallic uranium. 2008. *Physical Review B (Rapid Communications.* **78**: 811101.

Jilek, R. E., L. P. Spencer, D. L. Kuiper, B. L. Scott, U. J. Williams, J. M. Kikkawa, E. J. Shelter, and J. M. Boncella. A general and modular synthesis of monoimido uranium(IV) dihalides. *Journal of the American Chemical Society.*

Nerikar, P. V., C. R. Stanek, S. R. Phillpot, S. B. Sinnott, and B. P. Uberuaga. Intrinsic electrostatic effects in nanostructured ceramics. 2010. *Physical Review B.* **80**: 064111.

Nerikar, P. V., K. Rudman, T. G. Desai, D. Byler, C. Unal, K. J. McClellan, S. R. Phillpot, S. B. Sinnott, P. Peralta, B. P. Uberuaga, and C. R. Stanek. Grain boundaries in uranium dioxide: scanning electron microscopy experiments and atomistic simulations. To appear in *Journal of the American Ceramic Society.*

Placzek, C. J., J. Quade, P. J. Patchett, and R. Seager. Magnitudes and causes of Pleistocene large-lake episodes in the central Andes. To appear in *Quaternary Science Reviews.*

Soderlind, P., A. Landa, J. A. Klepeis, Y. Suzuki, and A. Migliori. Elastic properties of Pu metal and Pu-Ga alloys. 2010. *Physical Review B.* **81**: 224110.

Spencer, L. P., S. A. Kozimor, P. Yang, R. E. Jilek, T. W. Hayton, R. L. Gdula, B. L. Scott, E. R. Batista, and J. M. Boncella. Tetrahalide complexes of the [U(NR)2]2+ ion: systhesis, theoretical, and Cl K-edge x-ray absorption spectroscopic analysis. *Journal of the American Chemical Society.*

Stroe, I., J. Betts, A. Trugman, C. H. Mielke, J. N. Mitchell, M. Ramos, A. Migliori, and H. Ledbetter. Polycrystalline gamma-plutonium's elastic moduli versus temperature. 2010. *Journal of the Acoustical Society of America.* **127**: 741.

Thomson, R. K., T. Cantat, B. L. Scott, D. E. Morris, E. R. Batista, and J. L. Kiplinger. Uranium azide photolysis results in C-H bond activation and provides evidence for a terminal uranium nitride. 2010. *Nature Chemistry.* **2** (9): 723.

Thomson, R., B. Scott, D. Morris, and J. Kiplinger. Synthesis, structure, spectroscopy and redox energetics of a series of uranium(IV) mixed-ligand metallocene complexes. 2010. *COMPTES RENDUS CHIMIE.* **13** (6-7, SI): 790.

Thomson, R., C. Graves, B. Scott, and J. Kiplinger. Organometallic uranium(IV) fluoride complexes: Preparation using protonolysis chemistry and reactivity with trimethylsilyl reagents. 2010. *Dalton Transactions.* **39** (29):

6826.

Tobash, P. H., B. L. Scott, V. A. Sidorov, F. Ronning, K. Gofryk, J. D. Thompson, R. C. Albers, J. X. Zhu, M. D. Jones, and E. D. Bauer. Heavy fermion behavior in the new anitferomagnetic compound UIr4Al15. To appear in *Journal Condensed Mater Physics Conference Proceedings.* (New Mexico, June 27-July 2, 2010).

Tobash, P. H., F. Ronning, J. D. Thompson, and S. Bobev. Magnetic order and heavy fermion behavior in CePd1+xAl6-x: Synthesis, structure, and physical properties . 2010. *Journal of Solid State Chemistry.* **183**: 707.

Tobash, P. H., Y. Jiang, F. Ronning, C. H. Booth, J. D. Thompson, B. L. Scott, and E. D. Bauer. Synthesis, structure, and physical properties of YbNi3Al9.23. *New Journal of Physics.*

Isolating the Influence of Kinetic and Spatial Effects on Dynamic Damage Evolution

Darcie Dennis-Koller
20100026DR

Introduction

While Los Alamos has been a leader in the field of shock physics and dynamic damage prediction, our current ability to simulate evolving deformation and damage during dynamic loading remains limited. Reasons for this are related not only to previous limitations in our abilities to characterize damage both during and after deformation, but also our abilities to experimentally mimic well-modeled shock deformation conditions. Specifically, while we believe that both time and length scale of a dynamic loading event are critically important to the development of damage leading to component failure [1], we have not been able to perform the experiments that allow us to isolate these effects, interrogate their unique contribution to material behavior, and then incorporate this physical understanding into predictive models. Recent advances in bulk characterization techniques and newly developed dynamic loading techniques have made isolation of these effects possible for the first time [1]. This project proposes a combined experimental and theoretical approach for examining the influence of time and length scales on dynamic damage. Experimental are communicated with a modeling team that incorporates this understanding into materials models to advance the state of the art in damage modeling and shed light on materials performance parameters critical to the design of next-generation materials.

Benefit to National Security Missions

The incorporation of the physics of small length-scale damage evolution during dynamic loading into predictive models has important implications for a number of programs. Currently, accurately predicting damage and ultimately failure in structural metals is critical to the nuclear weapons, nuclear energy, insensitive munitions, transportation, and infrastructure maintenance programs supported by DOE, DoD, DHS, and NASA. Understanding critical materials, design, parameters for damage evolution is necessary as we consider the design of next generation metals to meet future energy demands.

Progress

The first year of this project was dedicated to interrogating the influence of spatial effects on dynamic damage evolution and then utilizing this understanding to change the way in which damage models predict failure of structural metals. It is generally accepted that damage in structural metals initiates at defects in materials caused by the processing or manufacturing of the material. However, combined influence of dynamic loading condition and distribution of these defects on damage evolution leading to failure is not understood and therefore is not predicted by current damage simulations.

To examine the spatial effect (distribution of processing defects) on damage evolution, a very early stage of damage evolution was examined. To ensure that experiments captured this early stage of damage a number of scoping calculations were completed using current Los Alamos damage simulation tools. These calculations were utilized to determine initial experimental design requirements. Six dynamic scoping experiments were completed (including two dimensional (2D) and three dimensional (3D) metallography) to validate the calculation and determine experimental design. Figure 1 shows the comparison between simulation and experiment for a dynamic loading condition that imparts an early stage of damage and one that imparts almost complete failure.

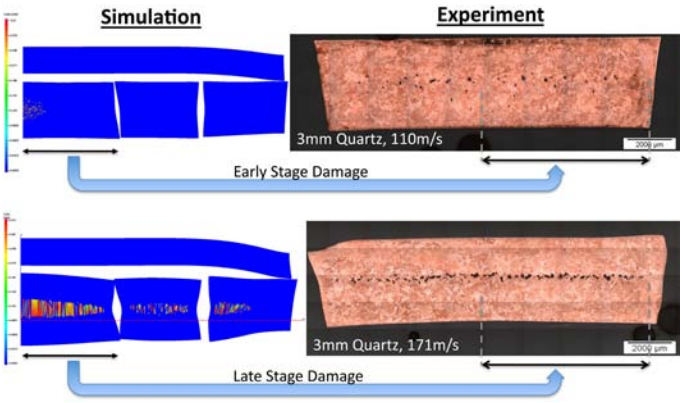

Figure 1. Simulations and corresponding experimental characterizations of dynamically induced damage are shown. The simulations were performed to identify a dynamic loading condition that would impart an early

stage of damage to a test specimen. Experiments were strategically performed to validate the simulations. From this figure, the loading configuration that imparted the early stage damage in the top of the figure, was selected for the spatial study.

Then using the experimental design parameters for the early stage of damage, a series of twelve experiments probing length scale effects in high purity copper were performed. Analysis of these experiments has utilized cutting edge capabilities in 3D x-ray micro tomography and has shown never before observed evidence of a transition in damage evolution mode as a function of the grain size distribution. Figure 2 is an example of the type of 3D measurement of damage that is possible using x-ray tomography. Experimental work has also resulted in demonstrating the nucleation-dominated nature of dynamic damage and exposed the need for a nucleation model in our damage models, which are currently limited to a simple accounting of damage growth.

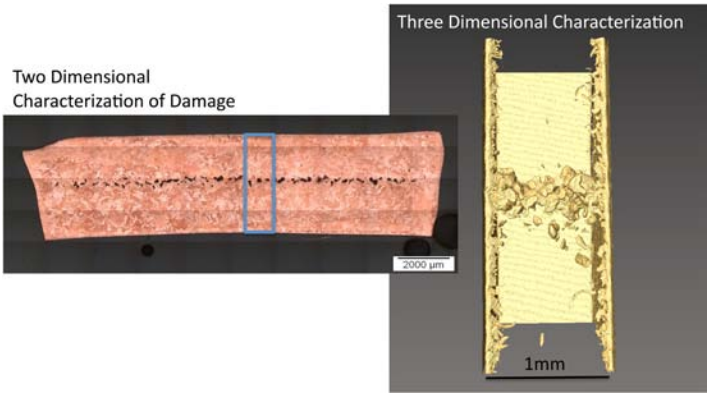

Figure 2. Experimental two dimensional and three dimensional characterization of dynamic damage is shown. The blue box in the two dimensional characterization is the area analyzed in the three dimensional case. While the two dimensional characterization gives insight into damage evolution coupling this with three dimensional characterization techniques lends more insight into statistics of damage initiation in metals.

Theoretical advances have been made in finite element model (FEM) formulations representing strain localization in dynamically deforming materials. By tracking evolving damage in a sub-grid fashion (behind the scenes of the finite element simulation) we can account for small length-scale damage in a computationally efficient way. This sub-grid formulation is being implemented into the FEM code ABAQUS/Explicit. This allows us, for the first time, to predict when and where localization/shear bands (types of damage that typically lead to catastrophic failure) are formed [2]. In addition to this, at a still smaller length-scales, a new single crystal plasticity model has been created to track defects on the atomistic scale that form during deformation. Our model examines the contribution of defects to damage not just in traditional low-rate loading conditions, but also in high-rate regimes. Finally, a new capability has been developed to generate 3D microstructure models of our materials, allowing us to track and capture the 3D effects of microstructure on the overall material response to dynamic loading conditions [3].

Our work so far has resulted in an understanding of the role of microstructures, and therefore material processing, on dynamic damage and also in the development of necessary building blocks to support new predictive capabilities that capture the microstructural evolution of materials under extreme condition of high strain rate deformation. So far this has lead to thirty-five related publications in peer review journals and thirty-eight invited talks, lectures and posters by team members at both domestic and international venues.

Future Work

Model driven shock experiments will be used to answer a second question that is fundamental to dynamic failure: What is the role of kinetics on dynamic damage evolution? The answer to this question can be utilized to unify data collected across multiple dynamic testing platforms (gas gun, laser, high explosive) as well as advance the state of the art in damage modeling. Tailored wave shape experiments along with post mortem materials characterization (metallography and tomography) and our new understanding of the influence of spatial effects on damage will be utilized to probe kinetic effects on dynamic damage and test hypotheses of the relative influences of spatial and kinetic parameters on plastic processes leading to failure. In-situ diagnostics along with three-dimensional characterization will be performed to allow real time and statistical measurements of deformation processes that lend important physics to damage models. New tools developed and data acquired in the proposed work will make possible, for the first time, direct measurement and prediction of the influence of kinetics and spatial effects on dynamic failure.

Conclusion

This research has three broad impact results: (1) advanced, physically-based, damage models, (2) an unclassified data base of modeled dynamic damage data, and (3) a parameter basis for diagnostic needs for future user facilities. Each result has implications for the weapons and energy programs as current structural materials are pushed to new design requirement expectations. These results will also be critical for transportation and energy industries as future applications will call for design of next generation metals requiring a fundamental understanding of the behavior of materials in extreme environments such as dynamic loading.

References

1. Koller, D. D., R. S. Hixson, G. T. Gray, P. A. Rigg, L. B. Addessio, E. K. Cerreta, J. D. Maestas, and C. A. Yablinsky. Influence of shock-wave profile shape on dynamically

induced damage. 2005. *Journal of Applied Physics.* **98** (10): 103518.

2. Bronkhorst, C. A., E. K. Cerreta, Q. Xue, P. J. Maudlin, T. A. Mason, and G. T. Gray III. An Experimental and Numerical Study of the Localization Behavior of Tantalum and Stainless Steel. 2006. *International Journal of Plasticity.* **22**: 1304.

3. Prakash, A., and R. A. Lebensohn. Simulation of Micromechanical Behavior of Polycrystals: Finite Elements Versus Fast Fourier Transforms. 2009. *Modelling and Simulation in Materials Science and Engineering.* **17**: 64010(p16).

Publications

Abeele, K. Van Den, T. J. Ulrich, P. Le Bas, M. Griffa, B. Anderson, and R. Guyer. Vector Component Focusing in Elastic Solids using a Scalar Source in Three Component Time Reversal. 2010. In *International Congress on Ultrasonics ; 20090111 - 20090117 ; Univ Santiago Chile, Santiago, CHILE.* Vol. 3, 1 Edition, p. 685.

Bronkhorst, C. A., A. R. Ross, B. L. Hansen, E. K. Cerreta, and J. F. Bingert. Modeling and Characterization of Grain Scale Strain Distribution in Polycrystalline Tantalum . To appear in *Computers, Materials, and Continua.*

Bronkhorst, C. A., P. J. Maudlin, G. T. Gray III, E. K. Cerreta, E. N. Harstad, and F. L. Addessio. Accounting for Microstructure in large Deformation Models of Polycrystalline Metallic Materials. 2010. In *Computational Methods for Microstructure-Property Relationships.* Edited by Ghosh, S., and D. Dimiduk. Vol. 1, First Edition, p. -. Norwell: Springer.

Bronkhorst, C. A., S. R. Kalidindi, and S. R. Zavaliangos. Editorial - Special Issue in Honor of Lallit Anand. 2010. *International Journal of Plasticity.* **26**: 1071.

Cao, F., I. J. Beyerlein, F. L. Addessio, B. H. Sencer, C. P. Trujillo, E. K. Cerreta, and G. T. Gray III. Orientation Dependence of Shock Induced Twinning and Substructures in a Copper Bi-Crystal. 2010. *Acta Materialia.* **59**: 549.

Hansen, B. L., C. A. Bronkhorst, and M. Ortiz. Dislocation Subgrain Structures and Modelingthe Plastic Hardening of Metallic Single Crystals. 2010. *Modelling and Simulation Materials Science and Engineering.* **18**: 055001.

Lebensohn, R. A., M. I. Idiart, P. Ponte Castaneda, and P. G. Vincent. Dilatational Visco-plasticity of Polycrystalline Solids with Intergranular Cavities. *Philospohical Magazine.*

Lebensohn, R. A., M. I. Idiart, P. Ponte Castaneda, and P. G. Vincent. Dilatational Viscoplasticity of Polycrystalline Voided Solids. *Philosophical Magazine.*

Lebensohn, R., C. Hartley, C. Tome, and O. Castelnau. Modeling the mechanical response of polycrystals deforming by climb and glide. 2010. *PHILOSOPHICAL MAGAZINE.* **90** (5): 567.

Luscher, D. J., D. L. McDowell, and C. A. Bronkhorst. Essential Features of Fine Scale Boundary Conditions for Second Gradient Multi-scale Homogenization of Statistical Volume Elements. *International Journal of Multi-scale Computer Engineering.*

Luscher, D. J., D. L. McDowell, and C. A. Bronkhorst. A Second Gradient Theoretical Framework for Hierarchical Multi-scale Modeling of Materials. 2010. *International Journal of Plasticity.* **26**: 1248.

Patterson, B. M., J. Campbell, and G. J. Havrilla. Integrating 3D Images Using Laboratory-based micro x-ray computed tomography and confocal x-ray fluorescence techniques. 2010. *X-ray Spectrometry.* **39** (3): 184.

Patterson, B. M., and C. E. Hamilton. Dimensional Standard for Micro-CT for the Quantification of 3D Voids Structures. 2010. *Analytical Chemistry.* **82** (20): 8537.

Preston, D. L., V. I. Levitas, and D. W. Lee. Interface Propagation and Microstructure Evolution in Phase Field Models of Stress-Induced Martensitic Phase Transformations. 2010. *International Journal of Plasticity.* **26**: 395.

Rollett, A. D., R. A. Lebensohn, M. Groeber, Y. Choi, J. Li, and G. S. Rohrer. Stress hot spots in viscoplastic deformation of polycrystals. 2010. *Modelling and Simulation in Materials Science and Engineering.* **18** (7): 074005 (16 pp.).

Tonks, D. L., and J. Bingert. Mesoscale Polycrystal Calculations of Damage Histories in Shock Loaded Metals. To appear in *TMS 2010.* (Seattle, WA, 2010).

Tonks, D. L., and J. Bingert. Mesoscale Polycrystal Calculations of Damage in Shock Loaded Copper. To appear in *European Physics Journal, Web of Conference.*

Understanding and Controlling Complex States Emerging from Frustration

Ivar Martin
20100043DR

Introduction

Our national security relies on technologies made possible by magnetism, because magnetism underpins our ability to compute and store huge bodies of information as well as to move things and sense the world. Most of these technologies have relied on ferromagnetism, i.e. the large-scale parallel alignment of magnetic spins, like in a refrigerator magnet. Antiferromagnetism is a related phenomena in which spins alternate in a regular pattern from one molecule to the next. Only recently have discoveries been made that take advantage of antiferromagnetism to enable, for example, spintronics devices. In certain crystal structures, however, the desire for the spins to align antiparallel to each other can be frustrated, so that it cannot be satisfied locally or globally within the material. A triangular pattern of three spins is the canonical example of frustrated magnetism. While there is no perfect solution to a frustrated system, there can be many approximate solutions with similar energies. As a result, frustration leads to the proximity of multiple thermodynamically stable complex magnetic states of matter, none of which is a perfect antiferromagnet. Transitions between these states can be controlled by even a small perturbation in parameters such as composition, pressure, or temperature. This tunability is one reason why frustrated systems are fundamentally interesting and highly desirable for applications. Another is the complex, non-coplanar patterns often adopted by frustrated systems. These low-symmetry states can enable coupling between magnetism and electric effects in both insulators and conductors. In particular, quantum magnetoelectric amplification can result from coupling of itinerant electrons to frustrated magnetic textures and that can enable entirely new technologies. The coherent effect of frustrated magnetic states on itinerant electrons can generate magnetic fields that are orders of magnitude larger than possible in a laboratory, and that can be controlled by small changes in a tuning variable. Our objective is to pioneer a new direction for condensed matter science at the Laboratory as well as for international community by discovering, understanding and controlling effects that emerge from frustrated spin textures.

Benefit to National Security Missions

The frustration-induced mechanisms for magnetoelectric coupling that we will study operate both in insulators and metals. Among the possibilities that they enable are:

- Controlled electronic transport in metals, both magnetoresistance and Hall conductance;
- Strong coupling of magnetization and electrical polarization in insulators with the ability to switch magnetization by an electric field or electrical polarization by a magnetic field;
- Electrical control of optical properties of materials;
- New concepts for binary magnetic storage. These rich possibilities can be used to create entirely new classes of devices as well as improve the energy efficiency of existing ones.

Progress

We have synthesized and studied both conducting and insulating materials that hold promise for frustration and magneto-electric effects. In conductors we have synthesized single and polycrystalline metallic samples that contain U and Ce, which carry magnetic electrons and sit on special sites that frustrate their interactions. We have studied these materials using a variety of techniques, for example, magnetic susceptibility and magnetization, specific heat, electrical resistivity and Hall effect, over broad temperature ranges above 0.350K and in magnetic fields up to 13 tesla. One system in particular, UCu_5, has shown indications of an unusual quantum state that we have hoped to discover, and this is being pursued aggressively by measurements to lower temperatures, higher magnetic fields and by neutron scattering techniques. In addition, we have begun investigating the effects of chemical disorder on this unusual state in UCu_5 and evidence for related states in similarly frustrated Ce-based materials, $CeCu_4Ga$, $CeIr_4In$ and $CePt_4In$. Measurements at temperatures down to 50 mK are in progress to explore the competition between frustrated magnetic interactions in these metals and to determine the extent

to which they manifest a special universality of signatures in their thermodynamic properties.

In addition to these frustrated metals, we are studying electrically insulating materials to determine how magnetic frustration leads to complex magnetic patterns that couple to the underlying crystal lattice and thereby create polarization of electrical charge. The goal is to understand and ultimately design compounds with electric and magnetic polarizations that are closely coupled such that a change in magnetic field produces a change in electric polarization. We have focused on insulators including those where a soft organic lattice incorporates magnetic transition metal ions. The magnetic forces of the transition metal ions can distort the organic lattice and modify the electric polarization. We have grown single crystals of Ni, Mn, and Co compounds with the highly polarizable ligand thiourea. We have found significant field-electric polarization coupling in the Ni and Co members and are in the process of investigating the remaining materials for magnetic and electric properties. We also are working on a magnetically frustrated Cr-based organic system and an inorganic material, Lu_2MnCoO_6, in which we observe electric polarization coupled to its magnetism. Three manuscripts on the experimental results in $NiCl_2$-4SC$(NH_2)_2$ (Figure 1) and $CuCl_2$-2SO$(CH_3)_2$ are submitted or accepted.

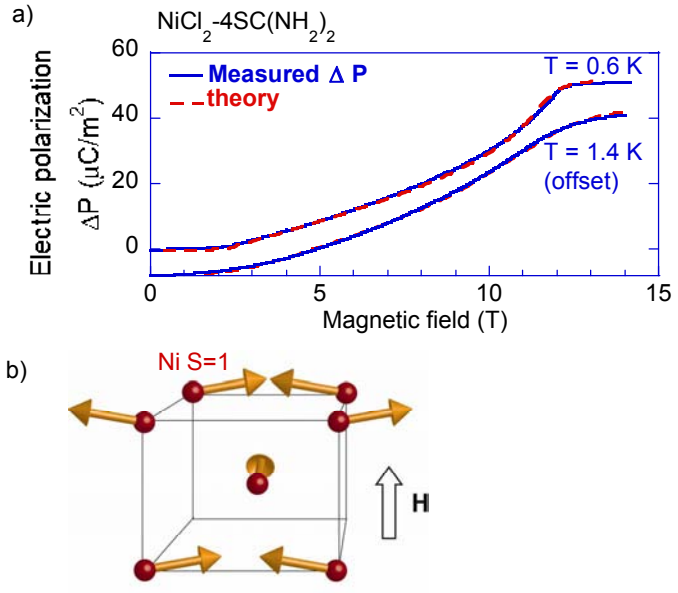

Figure 1. Magneto-electric coupling for the organo-metallic material $NiCl_2$-4SC(NH_2)2 containing S= 1 Nickel magnetic moments and electrically polar thiourea molecules, indicating that strong magneto-electric coupling can occur in this family of compounds. A) Experimental data and theoretical predictions are shown for the magnetic field-induced electric polarization at two different temperatures. B) The magnetic structure of the Nickel magnetic moments is shown for magnetic fields between 2 and 12 T arising from the antiferromagnetic frustrated interactions.

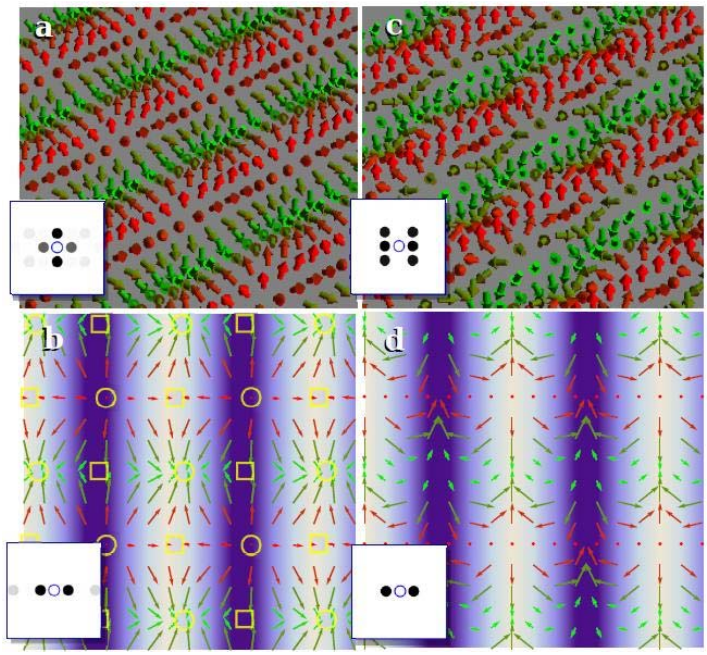

Figure 2. Calculated chiral magnetic structures in quasi-2D isotropic systems containing local and itinerant magnetic moments interacting via the Kondo effect. Arrows represent local magnetic moments (e,g, those attached to individual atoms rather than conduction electrons) with the color encoding the direction of the arrows. Circles and squares indicate the centers of spontaneously formed vortices and antivortices, respectively. The insets indicate the strength of magnetic (a and c) and chiral Bragg peaks in momentum space. These calculations demonstrate that complex non-coplanar magnetic order can arise spontaneously due to interactions mediated by scattering between local and itinerant magnetic moments, without requiring spin-orbit interactions.

Theory

Theory provides guidance for what materials should be measured as well as a framework for interpreting experimental results. We have exactly solved a theoretical problem in which magnetic electrons with spin-1/2 sit in a one-dimensional zigzag ladder arrangement. We have extended this result to a two-dimensional model in which magnetic electrons sit at vertices of an anisotropic triangular lattice, which is prone to produce frustration.

Using both numerical and analytical techniques, we have computed the specific heat and magnetic excitation spectrum of $NiCl_2$-4SC$(NH_2)_2$ as a function of the magnetic field and temperature. Agreement with our experimental observations is excellent.

We have also determined the nature of a transition that takes place in magnetic materials that are comprised of two interpenetrating magnetic subsystems, which are cou-

pled by a frustrated interaction. This transition is weakly first order for three-dimensional systems. This result has important consequences for understanding magnetic frustration in classes of materials.

For two-dimensional systems that contain both localized magnetic electrons and mobile electrons, we have demonstrated that the magnetic moments carried by magnetic electrons will order in a non-coplanar pattern in which the chirality (or "handedness") of moments varies spatially, Figure 2. Chirality has an effect on itinerant electrons equivalent to an applied magnetic field of a very large strength. Our finding is in stark contrast to the "common sense" expectation that the pattern of magnetic moments is a simple (non-chiral) magnetic spiral. These results have implications for interpreting behaviors of several itinerant magnetic systems that currently are receiving much attention.

Future Work

Frustrated compounds represent a sweet spot of the many-dimensional space of materials. The reason is simple: frustration, by definition, leads to the proximity of multiple thermodynamically stable states of matter. Even a small perturbation in parameters, such as composition, pressure, or temperature, can lead to a phase transformation with dramatic consequences for thermal and transport properties. This tunability makes frustrated systems highly desirable for applications.

The range of emergent phenomena resulting from the coupling of electrons to frustrated magnetic states has been barely tapped. Most of the magnetic compounds that have been studied so far have collinear orderings that do not generate quantum magnetoelectric amplification. Moreover, the desirable non-coplanar magnetic states are difficult to identify experimentally and can be often confused with their simpler cousins – coplanar (e.g., spiral or helical) or even collinear (e.g., simple antiferromagnetic) states. A suite of experimental techniques combined with theory and modeling is needed to unambiguously identify, understand, and exploit these unusual and promising states of matter. To develop the fundamental understanding of the interplay between frustrated magnetism and charge degrees of freedom, we will focus on the following four objectives:

- Identification of the unconventional broken symmetry (low-temperature) states and phase transitions
- Understanding of the "normal" (high-temperature disordered) state
- Determination of the necessary conditions for large magneto-transport responses in magnetically-frustrated metals
- Enhancement of magneto-electric effects in weakly-insulating frustrated magnets

We will achieve these objectives by a coordinated approach combining theory, including both analytical and numerical approaches, and a wide range of experimental techniques, including neutron scattering, nuclear magnetic resonance (NMR), magnetization, transport, thermodynamic, de Haas-van Alphen, electron spin resonance (ESR), and electric polarization measurements.

Conclusion

Materials with complex magnetic properties resulting from frustration could produce revolutionary new functionalities due to the interplay between electric and magnetic properties at the quantum level. This work provides the basic understanding that will open a new field of applications ranging from energy storage to computing to novel magnetic sensors.

Publications

Al-Hassanieh, K. A., C. D. Batista, G. Ortiz, and L. N. Bulaevskii. Field-Induced Orbital Antiferromagnetism in Mott Insulators. 2009. *PHYSICAL REVIEW LETTERS.* **103** (21): 216402.

Al-Hassanieh, K. A., C. D. Batista, P. Sengupta, and A. E. Feiguin. Robust pairing mechanism from repulsive interactions. 2009. *PHYSICAL REVIEW B.* **80** (11): 115116.

Al-Hassanieh, K. A., Y. Yang, I. Martin, and C. D. Batista. Effective Low-Energy Model for f-Electron Delocalization. 2010. *PHYSICAL REVIEW LETTERS.* **105** (8): 086402.

Batista, C. D.. Canted spiral: An exact ground state of XXZ zigzag spin ladders. 2009. *PHYSICAL REVIEW B.* **80** (18): 180406.

Batista, C. D.. Canted spiral: An exact ground state of XXZ zigzag spin ladders. 2009. *PHYSICAL REVIEW B.* **80** (18): 180406.

Kamiya, Y., N. Kawashima, and C. Batista. Finite-Temperature Transition in the Spin-Dimer Antiferromagnet BaCuSi2O6. 2009. *JOURNAL OF THE PHYSICAL SOCIETY OF JAPAN.* **78** (9): 094008.

Kamiya, Y., N. Kawashima, and C. D. Batista. Crossover behavior from decoupled criticality. 2010. *PHYSICAL REVIEW B.* **82** (5): 054426.

Samulon, E. C., K. A. Al-Hassanieh, Y. -J. Jo, M. C. Shapiro, L. Balicas, C. D. Batista, and I. R. Fisher. Anisotropic phase diagram of the frustrated spin dimer compound Ba3Mn2O8. 2010. *PHYSICAL REVIEW B.* **81** (10): 104421.

Samulon, E. C., K. A. Al-Hassanieh, Y. -J. Jo, M. C. Shapiro, L. Balicas, C. D. Batista, and I. R. Fisher. Anisotropic phase diagram of the frustrated spin dimer compound Ba3Mn2O8. 2010. *PHYSICAL REVIEW B.* **81** (10): 104421.

Seo, J. W., W. Prellier, P. Padhan, P. Boullay, J. -. Kim, H. Lee,

C. D. Batista, I. Martin, E. M. Chia, T. Wu, B. Cho, and C. Panagopoulos. Tunable Magnetic Interaction at the Atomic Scale in Oxide Heterostructures. 2010. *PHYSICAL REVIEW LETTERS.* **105** (16): 167206.

Stone, M. B., M. D. Lumsden, S. Chang, E. C. Samulon, C. D. Batista, and I. R. Fisher. Singlet-Triplet Dispersion Reveals Additional Frustration in the Triangular-Lattice Dimer Compound Ba3Mn2O8 (vol 100, 237201, 2008). 2010. *PHYSICAL REVIEW LETTERS.* **105** (16): 169901.

Zapf, V. S., M. Kenzelmann, F. Wolff-Fabris, F. Balakirev, and Y. Chen. Magnetically induced electric polarization in an organometallic magnet. 2010. *PHYSICAL REVIEW B.* **82** (6): 060402.

Zenker, B., H. Fehske, and C. D. Batista. Competing chiral and multipolar electric phases in the extended Falicov-Kimball model. 2010. *PHYSICAL REVIEW B.* **82** (16): 165110.

First Principles Predictive Capabilities for Transuranic Materials: Mott Insulators to Correlated Metals

Richard L. Martin
20100044DR

Introduction

We combine experiment and theory in an effort to develop a computational tool which is predictive for 'strongly correlated' materials. These materials lie at the heart of many technologically important applications, and a predictive theory is critically needed to be able to predict, control and manipulate their properties. Unfortunately, no such tool currently exists, nor is it precisely clear exactly what it should contain. This is therefore a basic research effort, and carries with it the associated risk. Breakthroughs in theory over the past year, however, suggest a path forward. We approach the problem by examining materials where these effects are paramount: the carbides, nitrides and oxides of uranium, neptunium, and plutonium. These materials are important in nuclear weapons (Pu), as advanced nuclear energy fuels (UC), and in nuclear reactor waste forms (PuO2). Advances in synthesis and spectroscopy over the past year now allow us to make extremely high quality samples which can be probed with state-of-the-art experimental measurements. These measurements will confront the theory, critically test its predictions, and stimulate refinements. In this manner, we hope to produce a predictive tool for 'strongly correlated' materials.

Benefit to National Security Missions

The development and experimental validation of a first principles predictive capability for transuranic materials principally addresses the area of scientific discovery and innovation. These materials currently defy quantitative theoretical treatments, but have direct implications to DOE/NNSA and DOE/BES in the areas of nuclear security (Pu metal), nuclear energy (advanced actinide carbide fuels), and environmental remediation (PuO2). A successful theory will also have ramifications for more general (non-actinide) materials which share the feature of "strong correlations" with the transuranics studied here. The most important applications in this regard involve renewable energy.

Progress

The synthesis team has made a thin film of PuO_2. This was the first technical goal of our project. The x-ray results show a well-defined diffraction pattern. This is a real accomplishment, as it represents the first single crystal quality thin film of PuO_2, a grail of synthetic actinide chemistry for over 50 years. In addition, the synthesis team has prepared thin films of NpO_2 and U_3O_8. The optical gap of U_3O_8 has been measured, demonstrating the capability to provide data on this important oxide (another first in terms of single crystal quality samples). Work on the nitrides has commenced. UN_2 has been made and will be used as the basic material in our attempts to synthesize UN.

The PuO_2 film has been transferred to our angle-resolved photoemission spectroscopy (ARPES) facilities and an initial spectrum taken. ARPES finds significant orbital hybridization and band dispersion, verifying the predictions of previous hybrid DFT calculations. This is an exciting step for this team, and confirms a hypothesis concerning unexpected covalency in the later members of the actinide series. At the risk of exaggerating the importance of this work, we believe it represents a fundamental sea change in the way that the community will view bonding and covalency in actinide compounds.

X-ray absorption (XAS) spectroscopy have also been performed. The metal edge in NpO_2 and PuO_2 compare favorably with powder samples. The principal goal of this subtask is to measure the O K-edge, and our first experiments in December showed that the oxygen content of the substrate upon which the film was grown interfered with getting a clean spectrum of the AnO_2 samples. This will be remedied in runs in June at Stanford using grazing incidence techniques in order to emphasize the film over the substrate.

Theory has made progress. The diffusion Quantum Monte Carlo (DQMC) code at North Carolina State University has been extended to allow studies on actinides. Work is now in progress to generate a relativistic effective core potential to use for the actinides. Progress at Rice has been rapid, on both the post-Kohn-Sham (RPA) front and on a many-body method called constrained pair mean-field theory (CPMFT). These methods are being developed for molecules and will be extended

to solids over the next two years. At LANL, we have benchmarked the hybrid DFT results for the series AnN (An=U,Np,Pu). We have also developed a new approach to treating multiplets and simple pair functions which we believe are robust and may be extended to the periodic case.

Future Work

This work will combine synthesis, spectroscopy and theory in an effort to develop a first principles predictive tool for strongly correlated transuranic materials. We will focus on the series AnC, AnN, and AnO_2, An=(U, Np, Pu). Their behaviors span the range from strongly correlated metals (AnC, AnN) to Mott insulators (AnO_2), and thereby provide a systematic evolution of the transition from strongly correlated metals to Mott insulators as a function of ligand. Our approach combines several facilities unique to LANL which now allow the properties of these materials to be studied with single_crystal quality samples, a requirement for the angle-resolved photoemission measurements we propose. Specifically we will:

1. Synthesize, via the polymer assisted deposition (PAD) technique developed at LANL, quality thin films of AnC, AnN, and AnO_2.

2. As they become available, the samples will be characterized with X-ray crystallography, IR and optical spectroscopy.

3. Energy and angle-resolved photoemission experiments will be undertaken on the thin films to determine their electronic structure.

4. Ligand K-edge X-ray absorption spectroscopy experiments will determine the character and metal-ligand interactions in the unoccupied levels.

5. Screened hybrid density functional theory (DFT) calculations will be performed for all members of the series in order to see where, and in what manner, the current state-of-the-art fails.

6. New mergers of DFT and wavefunction theory (the random-phase approximation) will be developed in order to address the spin correlations important in the correlated metals.

7. A capability to perform Quantum Monte Carlo calculations for actinide containing species will be developed and applied to selected materials.

8. These steps will be thoroughly integrated and support one another. The structure, band gaps, photoemission spectra and x-ray absorption spectra computed will be compared with experiments (2,3,4).

Conclusion

Many materials that lie at the heart of many technologically important applications currently cannot be described by predictive theories. In this effort, we combine experiment and theory in order to develop a computational tool applicable to these 'strongly correlated' materials. This is a basic research effort; no such tool currently exists. It is critically needed, however, in order to be able to predict, control and manipulate the properties of materials of importance in nuclear weapons (Pu), advanced nuclear energy fuels (UC), and in nuclear reactor waste forms (PuO_2).

Molecular Forensic Science of Nuclear Materials

Marianne P. Wilkerson
20100048DR

Introduction

Our project aims to exploit chemical speciation resulting from aging, process chemistry, or chemical reactivity to revolutionize nuclear forensics. This necessitates advances in the fundamental science required to collect and interpret chemical signatures. Traditional techniques for forensic analysis rely upon physical, isotopic, and elemental measurements, but these techniques do not exploit the full range of chemical information available from intercepted nuclear materials [1]. Processes employed to convert actinide precursors to nuclear-grade quality material are chemical in nature, often leaving clues as to how the material was prepared, when the material was chemically manipulated, or where the material has been. Weathering of material with air and water also induces changes in chemical speciation. Although analyses of bulk materials for chemical speciation have been available for some time, new capabilities developed for analyzing small samples could provide an unprecedented ability to assess sample origin, intended use, and history of particles [2]. In order to determine the usefulness of chemical speciation for forensics, we have carried out measurements and analyses on a variety of samples of known history. Key techniques used for understanding actinide oxide speciation include synchrotron-based X-ray Absorption Spectroscopy [3-6], as well as the more traditional tools of Scanning Electron Microscopy, X-ray fluorescence, and optical spectroscopy [1,7].

Benefit to National Security Missions

A revolutionary approach to nuclear particle analysis has direct benefit to three national security challenges: 1) forensics associated with illicit material handling and trafficking; 2) locating clandestine facilities producing, processing, and weaponizing nuclear material; and 3) detecting undeclared operations within nuclear facilities under IAEA safeguards.

Progress

We are developing an understanding of forensics-critical molecular signatures carried by actinide materials ranging from bulk to the micron scale. Specifically, we have carried out measurements and analyses on particles collected from a variety of scenarios, including the BOMARC incident, Chernobyl, the Hanford Z-Plant complex, and a hydrotest involving uranium.

In 1960, a BOMARC air defense missile in ready storage condition was destroyed by explosion and fire after a high-pressure helium tank exploded and ruptured the missile's fuel tanks. The warhead was also destroyed by the fire although the high explosives did not detonate. The primary radiological contaminant released throughout the site was weapons grade plutonium, with lesser activities of highly-enriched and depleted uranium. Environmental samples from this site are excellent analogs for soils where debris from a low-yield/no-yield undeclared nuclear test has been obscured in some manner. Scanning electron microscopy of post-remediation soil reveals particle sizes from 100 micron to 1 mm in diameter. Synchrotron-based X-ray fluorescence analyses reveal particles of plutonium that contain varying distributions of uranium and gallium (Figure 1). Initial analyses by X-ray diffraction and X-ray Absorption Fine Structure suggest the presence of PuO_{2+x} and UO_2.

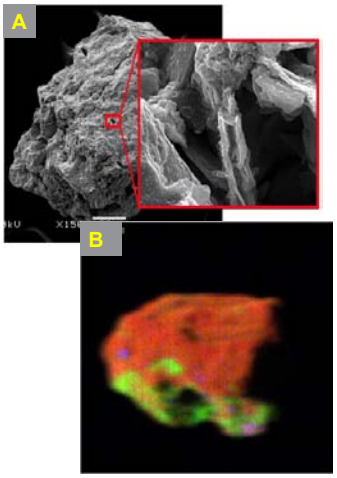

Figure 1. Scanning Electron Microscope image (A) and X-ray fluorescence image (B) of a BOMARC particle showing morphology and elemental composition.

We have examined environmental samples collected 1.5 km northwest from the accident at the Chernobyl Nuclear Power Plant in April 1986. This accident resulted in dispersal of large quantities of radioactive fuel and core materials into the atmosphere. Reports in the literature suggest that fuel particles released during the initial explosion are characterized by UO_2 cores with a surrounding shell of reduced uranium, but fuel particles released following the subsequent fires are characterized by a similar UO_2 core surrounded by a shell of oxidized uranium [8,9]. However, chemical speciation was not identified, and this model continues to be debated. Synchrotron-based imaging of five particles reveals a larger range of chemical species. Two of these particles are composed of UO_2, and two more particles are composed of U_4O_9 (Figure 2). Analysis of the speciation of the fifth particle is ongoing, but the uranium in this particle is clearly correlated with zirconium.

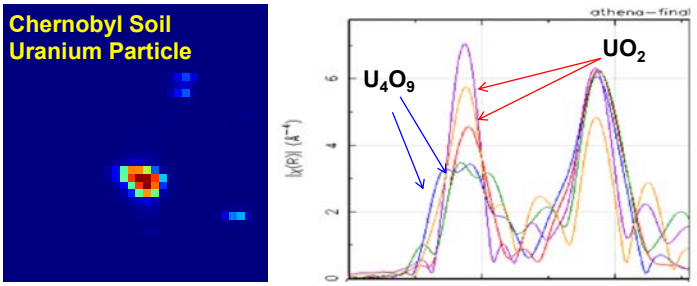

Figure 2. The image of a soil particle collected from Chernobyl identifies the presence of uranium (left). Analyses of X-ray Absorption Spectra identify the chemical speciation as UO_2 and U_4O_9 (right).

Three soil samples were obtained from waste streams at the Hanford Site Z-Plant Complex where purified plutonium nitrate was processed to weapons grade Pu with the Plutonium Finishing Plant. These samples represent Pu material that was isolated from aqueous colloids. Bulk analyses of soils from within the cribs is definitive for PuO_{2+x}. Analysis of spectra images measured from two plutonium-containing particles reveals that the Pu are not associated with any minerals in the environment, but rather are present as isolated particles, some of which may be associated with low molecular weight chemical species (Figure 3). Preliminary results suggest that the chemical composition of these particles is disordered PuO_{2+x}, which is consistent with the previously reported bulk measurements on materials collected from this site.

We obtained a filter used to collect air particulate samples from a hydrotest involving uranium. Analyses of X-ray fluorescence measurements indicate the presence of uranium, iron, copper, and zirconium. Preliminary analyses suggest that the chemical speciation of the uranium-containing particles is U_3O_8.

In order to understand the interactions of actinide materials with aging conditions, we are studying the oxidation of uranium oxides and plutonium oxides on both bulk and particulate scales. Corrosion of plutonium-gallium alloys has been carried out to understand the interaction of plutonium with water, hydrogen and other gases. Current views of this corrosion are that water and oxygen react with the metal alloy to form a uniform plutonium-oxide film on the surface, but our results from this past year suggest that this process is much more complicated. Measurements on corroded plutonium metal reveal segregated regions of ordered plutonium metal mixed with regions of highly disordered plutonium oxides ($PuO_{1.5+x}$). In particular, it appears that the gallium is associated with the ordered metallic plutonium regions, resulting in the creation of channels of corroded plutonium oxides within the uncorroded plutonium gallium alloy.

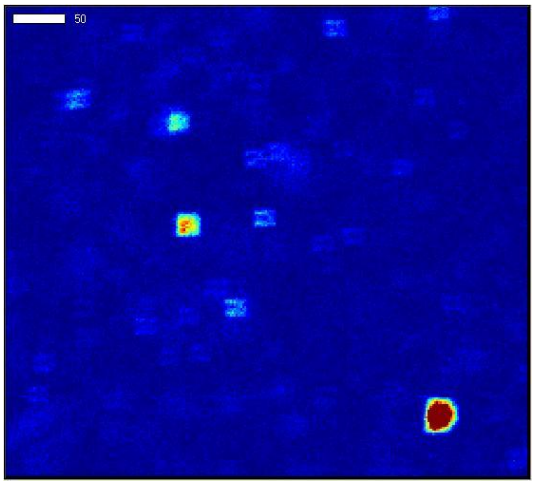

Figure 3. Plutonium-bearing particles collected from Hanford may be associated with low molecular weight chemical species possibly produced from processes use to make the waste.

We have initiated investigations to reveal how oxygen atoms add to UO_2 surfaces using density functional theory calculations, which apply quantum mechanics to describe the interaction among atoms and electrons. In bulk UO_{2+x} the extra oxygen ions tend to form clusters due to favorable interactions at the electronic level, and individual oxygen ions would only exist in certain concentration regimes and at very high temperature. In contrast, surface oxidation attributed to individual extra oxygen atoms (no cluster formation) is thermodynamically just as stable as the most favorable clusters found in bulk UO_{2+x}. We have also investigated bulk oxidation of stoichiometries between UO_2 and U_3O_8. Our results illustrate that the new split quad-interstitial cluster identified in UO_{2+x} for $x<0.25$ [10] also constitutes the fundamental structural building block up to (approximately) the U_3O_7 composition, after which re-arrangement of both the uranium and oxygen atoms occurs. This transformation corresponds to formation of U_3O_8, and the reverse reaction is observed when oxygen atoms were removed from U_3O_8. These findings are all in good agreement with available ex-

perimental observations and provide new mechanistic insights to the UO_{2+x} oxidation/reduction process [10,11], and these results should eventually allow us to predict oxidation rates to be compared with experiments.

Recent reports in the literature suggest that hydrolysis of UF_6 produces a variety of uranium oxyfluoride particles [12-15], based upon Secondary Ionization Mass Spectrometry, Scanning Electron Microscopy and micro-Raman spectroscopy. We are carrying out studies to prepare these materials and investigate the chemical speciation of these products using synchrotron-based measurements. There are significant dangers associated with UF_6, and we have identified expertise and capabilities appropriate for preparing these materials. For the initial spectroscopic characterization, we have initiated synchrotron-based measurements on a number of uranium oxide samples that were contaminated with fluorine. Comparison of the spectra with chemical standards indicate significant amounts of $UO_2F_{2+x}^{x-}$ (x = 0, 1, 2, 3) are present in the uranium material.

Important to all of these studies is a capability for handling and measuring single particles. In order to first identify and visualize particles that are mounted on a substrate, we purchased (capital) and received an Olympus LEXT4000, a laser scanning confocal visible microscope. This system will also be tested for visible identification of various uranium oxide systems, many of which change color with oxidation state. We purchased (capital) and received a Zyvex DCG S200 nanomanipulator that has been interfaced to our Thermo-Electron Field Emission Environmental Scanning Electron Microscope that will allow development of protocols for routine manipulation of particles under an electron beam that range in size from several hundred nanometers to several hundred microns.

Future Work

Our research plan is designed to answer the fundamental scientific questions required to exploit both new and "traditional" forensic signatures at the particle level. Future work in the coming year will include training of two post-docs and two graduate students that have joined our research team on this project. We will complete analyses on particle measurements described above and carry out additional particle measurements, *in-situ* oxidation of UO_2 as a function of particle size and measurements using powder X-ray diffraction analyses in a sealed stage under controlled temperature and humidity conditions. In order to submit these particles to various analytical platforms for measurements, we are developing a sample setup upon which we can register the location of a particle. Because the samples that we are working with are radioactive, containment is required in this setup, based on encapsulation that does not inhibit measurements by electron microscopy, X-ray absorption, or optical spectroscopy. We have carried out a variety of sample preparation methods, and are testing this setup on various analytical platforms.

Conclusion

We will use information from chemical speciation to develop process models allowing better quantification of potential forensic tools such as speciation and radiometric clocks. Measurements on environmental samples of known history will provide useful analytes for our synchrotron studies of chemical speciation. Controlled exposure experiments using bulk coupons and particle of various sizes, along with quantitative modeling will allow us to study processes and rate dependencies. This new approach will be further aimed at identifying useful "fingerprints" in order to reduce ambiguities in the interpretation of forensic analytical results.

References

1. Nuclear Forensics Role, State of the Art, and Program Needs. 2008. *Joint Working Groups of the American Physical Society and the American Association for the Advancement of Science.* : 1.

2. Schofield, E. J., H. Veeramani, J. O. Sharp, E. Suvorova, R. Bernier-Latmani, A. Mehta, J. Stahlman, S. M. Webb, D. L. Clark, S. D. Conradson, and E. S. Ilton. Structure of biogenic uraninite produced by Shewanella oneidensis strain MR-1. 2008. *Environ. Sci. Technol..* **42**: 7898.

3. Conradson, S. D., B. D. Begg, D. L. Clark, C. den Auwer, M. Ding, P. K. Dorhout, F. J. Espinosa-Faller, P. L. Gordon, R. G. Haire, N. J. Hess, R. F. Hess, D. W. Keogh, G. H. Lander, D. Manara, L. A. Morales, M. P. Neu, P. Paviet-Harmann, J. Rebizant, V. V. Rondinella, W. Runde, C. D. Tait, D. K. Veirs, P. M. Villella, and F. Wastin. Charge distribution and local structure and speciation in the UO2+x and PuO2+x binary oxides for x,0.25. 2005. *J. Solid State Chem..* **178**: 521.

4. Conradson, S. D., B. D. Begg, D. L. Clark, C. den Auwer, F. J. Espinosa-Faller, P. L. Gordon, N. J. Hess, R. Hess, D. W. Keogh, L. A. Morales, M. P. Neu, W. Runde, C. D. Tait, D. K. Veirs, and P. M. Villella. Speciation and unusual reactivity in PuO2+x. 2003. *Inorg. Chem..* **42**: 3715.

5. Rousseau, G., L. Desgranges, J. C. Niepce, G. Baldinozzi, and J. F. Berar. Contribution of the synchrotron diffraction study of the oxidation of uranium dioxide at 250 C. 2004. *J. Phys. IV France.* **118**: 127.

6. Clark, D. L., D. R. Janecky, and L. J. Lane. Science-based cleanup of Rocky Flats. 2006. *Phys. Today.* : 34.

7. Reeder, R. J., E. J. Elzinga, C. D. Tait, K. D. Rector, R. J. Donohoe, and D. E. Morris. Site-specific incorporation of uranyl carbonate species at the calcite surface. 2004. *Geochim. Cosmochim. Acta.* **68**: 4799.

8. Salbu, B., T. Krekling, O. X. Lind, D. H. Oughton, M. Drakopoulos, A. Simionovici, I. Snigireva, A. Snigirev, T. Weitkamp, F. Adams, K. Janssens, and V. A. Kashparov.

High energy X-ray microscopy for characterisation of fuel particles. 2001. *Nucl. Instrum. Methods Phys. Res., Sect. A.* **467-468**: 1249.

9. Salbu, B., T. Krekling, and D. H. Oughton. Characterisation of radioactive particles in the environment. 1998. *Analyst.* **123**: 843.

10. Andersson, D. A., J. Lezama, B. P. Uberuaga, C. Deo, and S. D. Conradson. Cooperativity among defect sites in AO2+x and A4O9 (A=U,Np,Pu): density functional calculations. 2009. *Phys. Rev. B: Condens. Matter.* : 24110.

11. Andersson, D. A., T. Watanabe, C. Deo, and B. P. Uberuaga. Role of di-interstitial cluster in oxygen transport in UO2+x from first principles. 2009. *Phys. Rev. B: Condens. Matter.* **80**: 60101.

12. Kips, R.. Development of uranium reference particles for nuclear safeguards and nonproliferation control. 2007. *Ph.D. Dissertation, Universiteit Antwerpen, Belgium.*

13. Kips, R., A. J. Pidduck, M. R. Houlton, A. Leenaers, J. D. Mace, O. Marie, F. Pointurier, E. A. Stefaniak, P. D. Taylor, S. Van den Berghe, P. Van Espen, R. Van Grieken, and R. Wellum. Determination of fluorine in uranium oxyfluoride particles as an indicator of particle age. 2009. *Spectrochim. Acta, Part B.* **64**: 199.

14. Kips, R. S., and M. J. Kristo. Investigation of chemical changes in uranium oxyfluoride particles using secondary ion mass spectrometry. 2009. *J. Radioanal. Nucl. Chem..* **282**: 1031.

15. Hu, S. -W., X. -Y. Wang, T. -W. Wang, and X. -Q. Liu. Theoretical mechanism study of UF6 hydrolysis in the gas phase. 2008. *J. Phys. Chem. A.* **112**: 8877.

Publications

Andersson, D. A., F. J. Espinosa-Faller, B. P. Uberuaga, and S. D. Conradson. Configurational stability and migration of large oxygen clusters in UO2+x: Density functional theory calculations. 2010. *Manuscript in preparation.*

Batuk, O. N., I. E. Vlasova, A. L. Costello, S. N. Kalmykov, S. D. Conradson, M. P. Wilkerson, and D. L. Clark. Characterization of U and Pu oxide particles formed during the accident at the Chernobyl NPP by various spectroscopic and microscopic techniques. 2010. In *Plutonium Futures - The Science 2010.* (Keystone, Colorado, 19-23 September 2010). , p. 89. LaGrange Park, Illinois: American Nuclear Society.

Bowen, J. M., W. Kinman, H. D. Selby, S. Glover, and H. Spitz. Characterization of residual plutonium particles extracted from soil contaminated by the 1960 BOMARC incident. 2010. *Manuscript in preparation.*

Bowen, J. M., W. Kinman, M. Smith, S. Glover, and H. Spitz. Method for identifying and isolating residual particles of plutonium in soil. 2010. *Manuscript in preparation.*

Conradson, S. D., A. L. Costello, D. E. Hobart, P. T. Martinez, J. Mitchell, and F. Espinosa-Faller. Atomic scale mechanism of corrosion of metallic Pu from X-ray absorption fine structure (XAFS) and synchrotron X-ray diffraction (XRD) measurements. 2010. *Manuscript in preparation.*

Conradson, S. D., A. L. Costello, F. J. Espinosa-Faller, D. E. Hobart, J. N. Mitchell, and P. T. Martinez. Atomic scale mechanism of plutonium corrosion. 210. In *Plutonium Futures - The Science 2010.* (Keystone, Colorado, 19-23 September 2010). , p. 232. LaGrange Park, Illinois: American Nuclear Society.

Daly, S. R., K. S. Boland, S. A. Kozimor, S. G. Minassian, D. K. Shuh, T. Tyliszczak, G. L. Wagner, and M. P. Wilkerson. F K-edge X-ray absorption spectroscopy in nuclear forensics. 2010. *Manuscript in preparation.*

Felmy, A. R., K. J. Cantrell, and S. D. Conradson. Plutonium contamination issues in Hanford soils and sediments: discharges from the Z-plant (PFP) complex. 2010. *Physics and Chemistry of the Earth.* **35** (6-8): 292.

Hobart, D. E., D. S. Peterson, S. A. Kozimor, K. S. Boland, M. P. Wilkerson, and J. N. Mitchell. Diffuse reflectance spectroscopy of plutonium metal, alloys, and compounds. 2010. In *Plutonium Futures - The Science 2010.* (Keystone, Colorado, 19-23 September 2010). , p. 61. LaGrangePark, Illinois: American Nuclear Society.

Reilly, D. D., K. S. Boland, S. A. Kozimor, G. L. Wagner, and M. P. Wilkerson. Na22 generation from actinide fluorides. 2010. *Manuscript in preparation.*

Reilly, D., O. N. Batuk, A. L. Costello, R. Gostic, M. P. Wilkerson, S. D. Conradson, and K. Czerwinski. Analysis of BOMARC plutonium hot particles with synchrotron techniques. 2010. *Manuscript in preparation.*

Wilkerson, M. P., A. D. Andersson, J. M. Berg, K. S. Boland, C. J. Burns, D. L. Clark, S. D. Conradson, A. L. Costello, D. E. Hobart, P. K. Kennedy, S. A. Kozimor, P. T. Martinez, J. Mitchell, K. D. Rector, D. Reilly, L. R. Riciputi, L. Tandon, and G. L. Wagner. Application of chemical structure and bonding of actinide oxide materials for forensic science. To appear in *Institute of Nuclear Materials Management 51st Annual Meeting.* (Baltimore, Maryland, 11-15 July 2010).

Understanding, Exploiting, and Controlling Competing Interactions in Complex Oxides

Quanxi Jia
20100073DR

Introduction

Epitaxial nanocomposites, in which emergent behaviors can be achieved through interfacing different strongly correlated materials at the nanoscale, provide a new design paradigm to produce enhanced and/or novel properties that cannot be obtained in the individual constituents. Several recent experimental results have shown that new functionalities and emergent behaviors in complex metal-oxides can be obtained through constituent interactions on micro-, meso-, and macro-scopic scales. However, empirical rules are currently used to guide research on such materials, and the state of the art remains at the "observation/validation" stage. We cannot yet control or predict their properties. We propose an innovative approach to controlling emergent behavior in hybrid complex oxide nanostructures. More specifically, we target intrinsic control and manipulation of competing interactions by designing and synthesizing complex oxide nanocomposites using ferroelectric, ferromagnetic, and high-temperature superconducting materials as the functional components. We pursue a conceptually new approach to design new materials with entirely new or significantly improved functionalities, by understanding the emergent physics that evolves over multiple length and time scales in these systems. Our ultimate objective is to develop a framework for understanding and controlling the states that emerge from strong electronic correlations. The impact of this project is expected to reach well beyond these particular phenomena as this study will enable the transition from "observation and validation" to "prediction and control."

Benefit to National Security Missions

This research strongly supports the LDRD Materials Grand Challenge, specifically, "Strategies exploring and developing the ability to control emergent phenomena," and it underpins three of the five Scientific Grand Challenges identified in the DOE-BES Report, "Directing Matter and Energy: Five Challenges for Science and the Imagination." This research will result in materials with tunable, enhanced or novel functionality, such as enhanced magnetoelectric materials, which will enable next-generation devices for sensing, information storage, advanced detection, or spintronics of interest to DOE-BES, DOD, IC, and industry. Finally, this work exploits the capabilities at CINT, a DOE National User Facility.

Progress

Our capability to synthesize different complex metal-oxide materials with controlled architectures paves the way for new physics through the manipulation of structural, thermodynamic, and transport properties. We have used laser molecular beam epitaxy (or laser MBE), one of the most powerful techniques for the growth of high performance metal-oxide films, to grow multilayered structures needed for this project. We prepared both single layer and multilayer films for scanning tunneling microscopy (STM) and ultrafast optical spectroscopy (UOS) studies. We optimized the processing parameters to prepare high quality ferroelectric, ferromagnetic, and superconducting films on crystal $LaAlO_3$, $SrTiO_3$, and MgO substrates. For instance, we deposited single layer $BiFeO_3$, $TbMnO_3$, $La_{0.7}Sr_{0.3}MnO_3$ (LSMO), and $YBa_2Cu_3O_{7-x}$ (YBCO) films. These films are of high quality as confirmed by both x-ray diffraction and transmission electron microscopy. We further deposited multilayered YBCO/LSMO, YBCO/$TbMnO_3$, and $BiFeO_3$/LSMO films with different layer thicknesses. These films were characterized by the structural and transport property.

Investigation of the inhomogeneity in surface morphology and local electronic/magnetic properties as a function of composition of heterostructured complex oxides is crucial for understanding the mechanisms of the competition between multiple orders in these materials. We have applied STM to characterization of the electronic properties of superconducting YBCO films deposited onto $SrTiO_3$ substrate. Our experimental results showed that the film surface contains ridge-like structures with characteristic height of 0.5-2 nm and width in the range of 5-10 nm. Such structure has been observed before on YBCO films grown by MBE method at low temperatures and high deposition rates.

We carried out optical pump-probe measurements on (LSMO/YBCO/LSMO/MgO) samples (as described above) with varying thicknesses of the top LSMO layer (0, 25,

50, 75, 100 nm) along with LSMO/MgO and YBCO/SrTiO3 samples for comparison. We observed some discrepancies in the physics between the earlier (0, 100 nm, YBCO/STO) and new (LSMO/MgO, 25, 50, 75 nm) samples: we qualitatively reproduced the data on the earlier samples from previous measurements, but had some issues in understanding the data between the new and earlier samples. Regardless, these were the first ultrafast optical measurements on high-temperature superconductor (HTSC) and ferromagnetic (FM) oxides multilayers or HTS/FM multilayers. We should be able to submit a publication once we figure out the dynamics in conjunction with the theorists on the project.

We have performed pump-probe spectroscopy (OPOP) on different complex oxide heterostructures described above in order to understand the interactions between superconductors, ferromagnets, antiferromagnets, and ferroelectrics when combined in a controlled manner. For example, we have depicted the photoinduced change in reflectivity ($\Delta R/R$) at 800 nm on a sample consisting of a $TbMnO_3$ film deposited on a YBCO film on a STO substrate. The initial rapid decay and recovery is due to pair breaking and recovery dynamics in YBCO, nearly identical to that measured on YBCO alone. The dynamics at longer times can be attributed primarily to quasiparticle excitations in TMO; however, the measured decay times significantly differ from those measured on TMO alone, indicating the influence of the superconducting state on quasiparticle dynamics in TMO. We are currently analyzing this data to understand the mechanism by which this occurs.

We have also performed the first OPOP experiments on multiferroic $BiFeO_3$ (BFO) as well as superlattices of $BiFeO_3$ and LSMO, to the best of our knowledge. BFO is both ferroelectric and antiferromagnetic at room temperature, while LSMO is a CMR manganite that is a ferromagnetic metal below T_c=360 K. Our temperature-dependent OPOP measurements at 400 nm on a BFO film deposited on an STO substrate reveal a two-component relaxation, with the fast component increasing in amplitude with temperature. This is likely due to the decrease of the BFO band gap with increasing temperature, causing the optical excitation to create carriers higher above the band edge that then relax through electron-phonon coupling. We also observed damped oscillations in the signal below ~250 K that may be due to the excitation of electromagnons in this system. Finally, our experiments on $BiFeO_3$/LSMO superlattices (with 15 periods, each consisting of a few monolayers of BFO and LSMO) reveal extremely large oscillations in the $\Delta R/R$ signal at 200 K, possibly due to photoinduced strain wave propagation at this temperature.

We have further used OPOP to explore the interplay between superconductivity and ferromagnetism in layered YBCO/LSMO heterostructures. Our initial experiments on a heterostructure consisting of a single layer of YBCO deposited on a single layer of LSMO on an MgO substrate reveal that the quasiparticle dynamics are qualitatively similar to the sum of the responses from individual YBCO and LSMO layers. Our results show that the dynamics at early times are dominated by YBCO, while the longer time dynamics are governed by the LSMO response. This is somewhat unexpected, as we would expect the magnetization of the LSMO film to affect the dynamics of quasiparticles and Cooper pairs in YBCO.

Theoretically, we applied a time-domain terahertz spectroscopic study of magnetic excitations in ferroelectric antiferromagnet $BiFeO_3$. We further studied the electronic structure and transport properties in a multilayer system formed by d-wave superconducting (DSC) and antiferromagnetic (AFM) layers, that is DSC/AFM/DSC. The interplay between the superconductivity and antiferromagnetism is considered within an effective model with the corresponding competing interaction by injecting the supercurrent. In the weak AFM regime, the system functions as a weak link. In the strong AFM regime, the system operates like a Josephson junction. Interestingly, we discovered that, for a given weak AFM interaction, the AFM magnetism can be generated in a special condition of phase difference between two superconducting contacts. A calculation of local electronic structure showed that this phenomenon is related to the existence of midgap states at the Fermi energy. We are now developing theoretical formulation to calculate the optical properties of the system.

Future Work

Interfaces and surfaces have played a critical role in determining the physical properties of a broad range of electronic materials. We use the broken symmetry at controlled interfaces in complex oxide heterostructures to perturb the subtle balance between competing physical phenomena. Specifically, we synthesize and investigate epitaxial ferroelectric/ferromagnetic and ferromagnetic/superconductor nanocomposites of different geometries and controlled dimensions using laser molecular beam epitaxy. We explore two architectures: the layered laminar-like and the vertically aligned pillar-like nanocomposites. A fundamental understanding of these material systems necessitates the use of advanced characterization techniques to study their physics. We use ultrafast temperature-dependent optical spectroscopy from THz through UV frequencies to probe electronic, lattice, and spin dynamics in these materials. We also employ scanning tunneling microscopy to characterize electronic phase inhomogeneities as well as magnetic force microscopy and magnetic resonance force microscopy to characterize the magnetic properties on a nanometer scale. The emergent behaviors (such as the magnetoelectric effect, proximity-induced metal-insulator transition, and giant superconductivity-induced modulation of the ferromagnetic magnetization) and enhanced functionalities (such as magnetic-domain-induced flux pinning in superconductors) of the materials enable us to understand the coupling between these components. In a coupled synthesis, characterization and theory effort, we

further use ultrafast optical spectroscopy and nanoscale scanning probes to investigate, and ultimately control, the character of competing electronic, magnetic, and lattice interactions as a function of structure and material composition.

Conclusion

We are using a conceptually new approach to understand the emergent physics that evolves over multiple length and time scales in order to design new materials with entirely new or significantly improved functionalities. The integration of nanoscale synthesis and coherent control, guided by forefront condensed matter theory, is poised to forge a new paradigm in the design of novel functionality through both intrinsic and extrinsic control of competing interactions. Our experimental results are emerging and expected to result in materials with tunable, enhanced or novel functionality, which will enable next-generation devices for sensing, information storage, and advanced detection.

Publications

Balatsky, A. V., D. N. Basov, and J. X. Zhu. Induction of charge density waves by spin density waves in iron-based superconductors. 2010. *Phys. Rev. B.* **82**: 144522.

Bi, Z., O. Anderoglu, X. Zhang, J. L. MacManus-Driscoll, H. Yng, Q. X. Jia, and H. Wang. Nanoporous thin films with controlable nanopores processed from vertically aligned nanocomposites. 2010. *Nanotechnology.* **21**: 285606.

Bi, Z., O. Anderoglu, X. Zhang, J. MacManus-Driscoll, Q. X. Jia, and H. Wang. Nanoporous thin films with controllable nanopores processed from BiFeO3:Sm2O3 vertically aligned nanocomposites. Presented at *2010 MRS Spring Meeting.* (San Francisco, CA, April 5 – 9, 2010).

Jia, Q. X.. Synthesis and characterization of nanocomposite films. Invited presentation at *2010 MRS Spring Meeting, San Francisco.* (San Francisco, CA, April 5-9, 2010).

Jia, Q. X.. Control of lattice strain and electrical properties of epitaxial nanocomposite films. Invited presentation at *Control of lattice strain and electrical properties of epitaxial nanocomposite films.* (Lake Buena Vista, FL, Jan. 20 - 22, 2010).

MacManus-Driscoll, J. L., S. Harrington, L. Jew, E. Weal, H. Wang, H. Yang, Z. Bi, and Q. X. Jia. Vertical nanocomposites for multiferroics and enhanced single phase functionality. Invited presentation at *Electronic Materials and Applications 2010.* (Lake Buena Vista, FL, Jan. 20 - 22, 2010).

She, J. H., J. Zaanen, and A. R. Bishop. Stability of quantum critical points in the presence of competing orders. 2010. *Phys. Rev. B.* **82**: 165128.

Sheng, G., Y. L. Li, J. X. Zhang, S. Choudhury, Q. X. Jia, V. Gopalan, D. G. Schlom, Z. K. Liu, and L. Q. Chen. A modified Landau-Devonshire thermodynamic potential for strontium titanate. 2010. *Appl. Phys. Lett..* **96**: 232902.

Sheng, G., Y. L. Li, J. X. Zheng, S. Choudhury, Q. X. Jia, V. Gopalan, D. G. Schlom, Z. K. Liu, and L. Q. Chen. Phase transitions and domain stabilities in biaxially strained (001) SrTiO3 epitaxial thin films. 2010. *J. Appl. Phys..* **108**: 083903.

Talbayev, D., A. D. LaForge, N. Hur, T. Kimura, S. A. Trugman, A. V. Balatsky, D. N. Basov, A. J. Taylor, and R. D. Averitt. Dynamic investigations of multiferroics: terahertz and beyond. 2009. *J. Phys: Conf. Series.* **148**: 01203.

Talbayev, D., K. S. Burch, E. E. M. Chia, S. A. Trugman, J. X. Zhu, E. D. Bauer, J. A. Kennison, J. N. Mitchell, J. D. Thompson, and J. L. Sarrao. Hybridization and superconducting gaps in heavy-fermion superconductor PuCoGa5 probed via the dynamics of photoinduced quasiparticles. 2010. *Phys. Rev. Lett.* **104**: 227002.

Talbayev, D., S. A. Truman, S. Lee, S. W. Cheong, and A. J. Tayloe. Long wavelength magnetic excitations in the ferroelectric antiferromagnet BiFeO3. *preprint.*

Wimbush, S. C., J. H. Durrell, C. F. Tsai, H. Wang, Q. X. Jia, and M. G. Blamire. Enhanced critical current in YBa2Cu3O7 thin films through pinning by ferromagnetic YFeO3 nanoparticles. 2010. *Supercond. Sci. Technol..* **23**: 045019.

Upgrading Renewable and Sustainable Carbohydrates for Production of High Energy Density Fuels.

John C. Gordon
20100089DR

Introduction

We are executing a transformational strategy to obtain high-density hydrocarbon fuels from non-food derived carbohydrates. In order to transform sugars into diesel and gasoline, we need to remove oxygen atoms and do so efficiently and environmentally soundly. The development of effective biomass conversion technologies that integrate with existing fuel production and distribution infrastructure would permit a shift away from our dependence on foreign petroleum imports. In fact, efficient conversion of renewable biomass can account for 100% of current U.S. petroleum imports. Even a 5% contribution from biofuels eliminates approximately 375 million tons of CO2 per year. This area of transformational research directly addresses important national security transportation issues (tanks, jets and helicopters) and can meet the mission needs of a wide range of sponsors.

Initially, we will extend the carbon skeletons of biomass-derived carbohydrates through a class of environmentally friendly, carbon-chain extension reactions with other naturally occurring polyalcohols. Inexpensive, water soluble metal catalysts will then be developed for efficient deoxygenation and hydrogenation of the resulting extended chain polyalcohols, allowing facile separation of the resulting chain-extended hydrocarbons. An essential element of our strategy is the development of highly functional catalysts that operate at low temperatures, thus enabling dramatically higher conversion efficiencies and selectivities than current methods. Successful execution of the proposed work will provide the transformational science (especially in aqueous phase homogeneous catalysis) required to obtain useful fuels from cellulose-derived feedstocks without wasting energy or carbon.

Benefit to National Security Missions

This area of transformational research directly addresses important National security transportation issues and represents significant opportunities to address nationally significant WFO missions. For example, the DOD, the largest consumer of petroleum in the world, has significant interest in the future development of domestically sourced biologically derived fuels. DOE's OBP has seen a dramatic increase in mission priority. With the successful demonstration of the novel energy efficient conversion of carbohydrates to high energy density fuels proposed herein, LANL will demonstrate its capabilities for the OBP mission and be successful in fostering a biomass-related research and development program dedicated to energy security.

Progress

We have made excellent progress in several of the subtask areas of the project. In the first area of organocatalyzed aldol carbon-carbon chain extension, we have been able to demonstrate the generality of this chemistry to generate fragments of various chain lengths that vary from C9 to C15. Various conditions have been worked out to provide these molecules in high yield under ambient conditions. Several different sugar derived synthons have been investigated in this regard as have different classes of organocatalysts in an attempt to understand the optimal catalyst/substrate combinations.

We have continued to investigate oxygen removal chemistries from chain extended products (necessary for the synthesis of hydrocarbon based chains), and we have also focused on a number of methodologies with which to ring open the furan based systems that result from the C-C coupling step (again a necessary goal in order to provide linear hydrocarbon chains). We have demonstrated the viability of ring opening chemistries pertinent to the overall goal of providing hydrocarbon-based fuels and we have also examined various approaches for oxygen removal (hydrogenation, reduction) with a number of substrates and a number of catalysts/reagents. Again we have made significant progress in this project task, and in the case of a nine-carbon system mentioned above, we have been able to demonstrate the feasibility of converting this into the desired hydrocarbon (in this case, nonane) using simple reactions and reagents under relatively mild conditions.

In combination with our synthesis/catalysis work and in collaboration with our colleagues in T-Division we have begun to try to understand the nature of various cata-

lyst/substrate interactions pertinent to the chain extension chemistries as well as the transition state pathways and energies involved in these conversions. This will allow us to gain a better understanding of why a particular catalyst appears to work better than another in the aldol chemistry, as well as in the ring opening and oxygen removal chemistries that are required downstream of the carbon-carbon chain extension steps.

We are currently extending the scope of organocatalysis to other biorenewable substrates and we are examining a variety of Lewis and Bronsted acids capable of catalyzing the ring opening of a variety of hydrogenated furan systems derived from the C-C chain extension task. Two new T-Division postdocs have arrived, so we are accelerating our work with their help to understand the mechanism of Lewis-Acid catalyzed ring openings. We are at the stage now where we can begin to think about the possibility of hydrogenating/reducing aldol condensation products and ring opening of the resultant furan systems in one pot and we are in the process of investigating a variety of catalysts to address this.

This project was chosen by Chemistry Division management for review during the recent LANL Chemical Sciences Capability Review in May 2010 (i.e. only seven months into the duration of the project). The committee were very supportive of the effort, gave very positive reviews of the goals of the project and the progress made-to-date. Several manuscripts are currently in preparation that describe the progress made in various subtasks of this project.

Future Work

Lignocellulose-derived polyalcohols constitute the most abundant renewable organic carbon source on the planet. In contrast to hydrocarbons, these polyalcohols are characterized by an abundance of oxygen and typically possess C3-6 chain lengths. Therefore, we seek to perfect the chemical and engineering methods required to selectively extend the carbon chain length and remove the oxygen content of the starting material, while minimizing energy input and loss of carbon (in the form of CO2). Maintaining a focus toward large-scale industrial viability, it is critical to develop thermally efficient (e.g. < 100 deg C) and “atom economical” processes for these transformations. With appropriately designed catalysts, the slight driving force required for these reactions could be harnessed from industrial waste heat that is presently discarded. The use of waste heat as a energy source for fuel upgrading removes the need to drive a high temperature process using a (sizable) portion of the feed stock as the fuel. In addition, direct use of waste heat in biomass conversion obviates the need for cooling towers (where huge amounts of useful potable water are consumed by evaporation). However, before this can be realized, the required fundamental molecular science must be perfected. The objective of this proposal is to develop the transformational science needed to enable the high yield, energy-efficient production of hydrocarbon fuels from biomass-derived polyalcohols.

Conclusion

Within the next 30 years, world energy consumption is projected to double. With decreasing global production of crude oil, it is essential to our National security that renewable alternatives to petrochemical feedstocks for hydrocarbon fuels are developed. A constant, reliable supply of these fuels would ensure that the transportation of food, medicine, and consumer goods about the country remains uninterrupted, regardless of sociopolitical conflict. This project will integrate expertise in catalysis, stable isotope chemistry, reaction engineering and theory/modeling to forge a unique technical approach for energy-efficient, carbon-neutral conversion of biomass-derived polyalcohols to high energy density fuels.

Hot Spot Physics and Chemistry in Energetic Materials Initiation

Dana M. Dattelbaum
20080015DR

Abstract
In this project, we performed state-of-the-art experimental and computational studies to isolate and interrogate energy localization phenomena in initiating explosives (commonly known as "hot spots") on scales ranging from nanometers to millimeters, and picoseconds to milliseconds. We developed new tools for interrogating hot spot physics, and we have defined key features pertaining to effective hot spot activity in initiating explosives. The results from this project have advanced us toward new predictive capabilities for National security needs pertaining to both the safety and performance of our stockpile materials, and understanding characteristics of improvised explosives.

Background and Research Objectives
Explosives are often "initiated," or induced to chemically react to a run-away, self-sustained reaction called detonation, by shock waves. As a shock wave passes over the heterogeneous (non-uniform) microstructure of most commonly encountered explosives, such as the plastic-bonded explosives used in weapons, localization of energy occurs in regions known as "hot spots" [1-12]. It is within "hot spots" that chemistry occurs at high temperatures and pressures. The potential origins of hot spots are numerous and include shock-induced collapse of voids or porosity, plastic deformation, friction from motion along cracks, or shock wave reflections from in-situ interfaces such as explosive grain boundaries. Despite many decades of research into the physics of high explosives, we have just a very basic understanding of the broad mechanisms underlying hot spot ignition, interactions, and reaction spread leading to detonation. A detailed understanding of these processes is absent. Consequently, all current high explosive burn models treat hot spot physics empirically, have poor predictive capabilities, and require substantial calibration to experimental results. A new generation of predictive models for all types of explosives can only come from a fundamental understanding of hot spot physics.

The principal goal of this effort was to fill in critical gaps in our knowledge of how hot spots dictate details of the shock initiation of explosives. Until recently, the field has lacked the ability to produce and interpret well-defined, scientific studies that probe hot spot physics at the time and length scales characteristic of their growth and evolution (nanoseconds-to-microseconds, and nanometers-to-micrometers). Substantial advances in the spatial and temporal capabilities of experimental techniques, coupled with improvements in modeling & simulation mean a deeper understanding of hot spot physics can now be made. By capitalizing on these advancements, we will substantially improve our understanding regarding several fundamental yet longstanding questions regarding hot spot physics and chemistry, including:

How do hot spots form, evolve and interact?

- What combinations of parameters define critical conditions of hot spot effectiveness vs. criticality?
- What is the influence of specific hot spot parameters on the initiation mechanisms, overall sensitivities, and signatures of chemical reactions behind the detonation front?

Scientific Approach and Accomplishments
The scientific approach taken in this project was to focus on the careful study of well-defined, prototypical explosives seeded with defect sources that will form hot spots under shock conditions. By studying well-defined materials, hot spots and their influence on how the explosive reacts or "builds up" to detonation can be isolated. Because explosive initiation occurs over decades in length and time scale, the project established parallel theoretical and experimental efforts matched by scale to facilitate an overall improved knowledge of the details of the physics. The major research accomplishments of this project are:

- Establishment of a new technique, femtosecond laser drilling, to create arrays of holes in explosive crystals to act as hot spot seeds when shocked;
- Development of ultrafast temperature diagnostics to

probe hot spot temperatures during shock compression;

- Definition of several key parameters dictating hot spot effectiveness vs. criticality in shock-initiating explosives;
- Elucidation of hot spot formation mechanisms, and their associated temperatures and pressures for a well-defined model system.

Details of these research accomplishments are summarized below.

Femtosecond laser drilling of hot spot "seeds" in explosive crystals

The relevant size scale for features associated with dynamic hot spot formation in real explosive microstructures is believed to be 1-100 micrometers [1]. Fabrication and characterization of controlled heterogeneities in explosive samples at this length scale are essential to interpreting hot spot effects on initiation. Spatially placed hot spot seeds offer an opportunity to examine the details of hot spot formation at well-defined locations under shock compression.

A major accomplishment of this project was the development of a new capability to introduce holes into pristine HE crystals *without causing them to initiate or degrade during fabrication*. The highest quality single crystals of HMX, RDX, and PETN explosives were micromachined using a 100 femtosecond pulse-length laser, in which the spatial extent of the pulses is ~30 micrometers.[14]. While this method had been previously applied to inorganic crystals such as quartz and sapphire,[15] it had never been attempted on fragile explosive crystals. Single laser pulses were focused by a high power microscope *inside* the explosive crystals, vaporizing material to form spherical voids less than one micrometer in diameter. Coupling microscopy with spectroscopy, it was verified that the spheres were really voids, not pockets of high-pressure gas products. 2- and 3- dimensional arrays of thousands of voids can be produced by scanning the crystal position with sub-micrometer accuracy, as required for hot spot interaction studies. Some examples are shown in Figure 1.

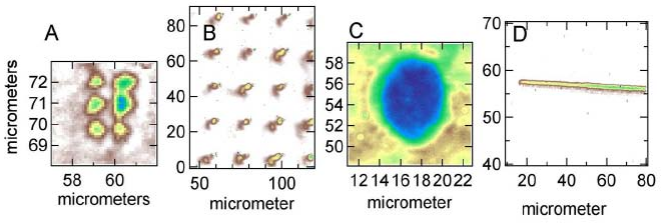

Figure 1. Voids produced by femtosecond micromachining of explosive single crystals. Examples of a 2-dimensional array (A), a 3-dimensional array where deeper voids are out of focus and appear to be a column (B), a consolidated spherical void machined from thousands of smaller voids (C), and a linear array of voids (D) are shown.

We also examined the ability to make larger voids that could be resolved by optical diagnostics on gas gun studies (exceeding 10 micrometers). We found that the explosive crystals could not maintain the stresses induced by large-scale (>10 micrometer) internal voids, leading to reproducible microcracking. However, millimeter-scale machining of the crystal surface was performed successfully, since the stress was released at the surface by expansion of the product gases into the air.

Development of ultrafast temperature diagnostics to quantify hot spot temperatures

The ability to place hot spot seeds in explosive samples offers an opportunity to probe the physics of individual hot spots under shock compression. Before attempting to measure temperature of an individual shocked hot spot, we needed to prove that we could actually measure temperature in a solid with coherent Raman, and that it could be sensitive enough to be performed in a single laser shot. For experimental simplicity, we chose to cool a single crystal of quartz in a liquid helium cryostat to measure the effect of temperature on coherent Raman. At 30 degrees Kelvin (-243 degrees C), the vibrational motion is almost frozen out. As the temperature rises to room temperature of 298 degrees Kelvin, the vibrational motion increases. This has a characteristic signature in the coherent Raman spectrum, which has been predicted theoretically, but never observed. We have verified the theoretical prediction, as shown in Figure 2, and now can proceed to utilize this spectroscopy for measurements of unknown temperatures. While we have performed this spectroscopic measurement in a single shot, we have yet to perform a spatially resolved temperature measurement, or the measurement of temperature in a shock wave. While we have not yet achieved the measurement of spatially resolved temperature across a micrometer size shocked void, we have built the experimental tools that will make that difficult measurement possible.

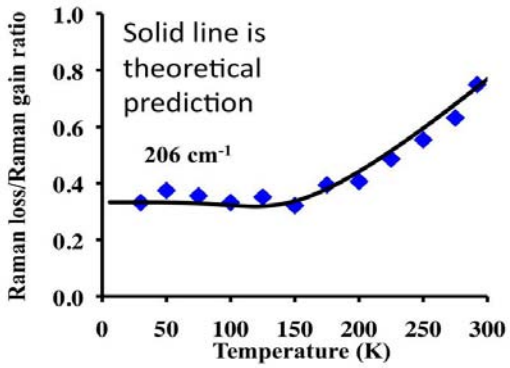

Figure 2. Femtosecond stimulated Raman spectroscopy was shown to be an effective picosecond temperature measure-

ment, matching previously untested theoretical predictions. The figure shows the ratio of Raman band intensities for the 206 cm-1 vibrational mode compared with theoretical prediction as a function of temperature, showing excellent agreement between the two.

Definition of key hot spot parameters and their influence on explosives initiation

To narrow in on the critical parameters pertaining to hot spot activity, we chose gelled nitromethane (NM) with added particles as a flexible model system that offers an ability to vary features of the microstructure in the mixture while maintaining the basic explosive. This proved to be extremely useful for interrogating the importance of hot spot type, size, shape, and number density. Both solid and hollow glass spheres, of relevant sizes in the micron-range, have been intentionally introduced into gelled NM [16-19]. The solid and hollow spheres mimic two types of purported hot spots– density (shock impedance) mismatches, and porosity [1-3]. The sizes of the particles, as well as their inter-particle separations were varied to determine their influence on initiation. Detailed insights into the initiation process or mechanism were obtained from the response of *in-situ* electromagnetic gauges placed at ten depths into the sample [20]. Homogeneous explosives, such as neat liquid nitromethane, exhibit fundamentally different shock initiation behaviors compared with solid, multi-phase explosives. The initiation "mechanism" for liquid or homogeneous explosives is marked by shock heating of the material, giving rise to a thermal explosion that occurs behind the incident shock front.[26-28] Following thermal explosion, growth of a reactive wave behind the front is observed, building up over measureable time and distance until it reaches a steady condition or overtakes the initial shock [17-19]. The initiation and build up of chemical reactions are observed as changes in the shock wave profiles, e.g. as increasing particle velocity. By contrast, when hot spots are responsible for initiating chemistry, the particle velocity growth occurs very close to the shock front because the energy release from the reactions occurs locally near the shock due to the energy focusing in hot spots formed due to the microstructure. Figure 3 shows the evolution of shock wave profiles for NM/glass bead solutions where the mechanism is thermal explosion-dominated (left) and hot spot-dominated (right). As the shock wave initiates chemical reactions, the shock profiles evolve, Figure 3, but there are clear differences in the build-up to detonation, depending on which underlying mechanism dominates.

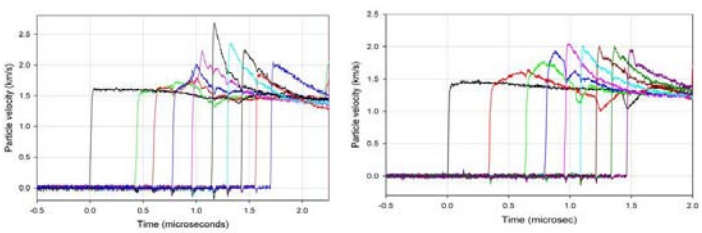

Figure 3. (right) Example in-situ shock wave profiles of nitromethane containing 6 wt% 40 micron solid glass beads shocked to 9.5 GPa. Despite containing particles, the initiation behavior is like that of a neat liquid explosive (thermal explosion-based), as noted by the growth of a sharp wave behind the shock front. (left) Smaller solid particles (1-4 micron diameter) spaced closer together spatially show a hot spot-derived mechanism with reactions observed near the shock front and a steady growth to detonation.

A large number of gas gun-driven shock experiments were performed on NM/particle mixtures. The experiments focused on 1-4 micron and 40 micron diameter solid beads at 6 wt% (inter-bead spacing's of 6 and 106 microns respectively), and 40 micron hollow spheres at 1.2 and 0.36 wt% (inter-particle spacing of 106 and 164 microns). The data reveal that in general, the addition of silica has a sensitizing effect (e.g. lowering initiation thresholds) due to hot spot production; however, different behaviors are observed for small (1-4 mm) vs. large (40 mm) beads at 6 wt% loading. A transition from homogeneous initiation behavior to a hot spot-driven initiation behavior was observed in *the same 40 micron bead samples* depending on shock input pressure [17]. This is one of the few, if any, observations of homogeneous initiation behavior in a heterogeneous mixture – e.g. the hot spots are not effective on the time scale of the shock initiation at this size and spacing (~2.5 diameters apart). Smaller beads, at a greater number density and closer spacing (~ 6 micrometers), were found to result in more effective hot spots, Figure 3 right [18,19]. Furthermore, exchanging hollow microballoons (porosity) for solid particles at the same size (40 micrometers) and number density was found to be more effective at producing hot spot-driven flow due to collapse of the porosity.[19] The initiation thresholds were reduced by almost 3.0 GPa or 30 kilobars compared with solid beads. Lastly, an additional limit of hot spot effectiveness was found by decreasing the number density of the hollow particles so that they were spaced ~ 4 diameters apart, where again, the initiation was dominated by thermal explosion in the nitromethane.

Overall, we have found that the initiation mechanism and shock pressure threshold for initiation can be substantially "tuned" or tailored by varying the type and number density of hot spots [19]. We have found that if the hot spots derived from *large* density inclusions (40 micrometer solid beads) are spaced ~2 diameters apart, they are not effective at high input pressures. Smaller particles spaced closer together form effective hot spots, regardless of shock strength. Finally, microballoons (porosity) are more sensitizing than solid beads.

Meso-scale Multi-material Hot Spot Simulations.

Very high resolution simulations of NM/particle mixtures were performed to lend insight into how hot spots are formed, and what peak temperatures and pressures they

reach for a given shock wave strength. First, improvements to the NM equation of state and chemical reaction rate model were performed [21-22]. The LANL NOBEL/xRAGE hydrodynamic code was used to perform non-reactive simulations of NM/particle mixtures [23]. Figure 4 (left) shows the computational cell used in the simulation, which consists of three 20 micron diameter glass beads in NM. A 10 GPa shock was introduced into the simulation. Figure 5 (right) shows the temperature field following shock passage. Hot spots are formed, not from shock reflections at the beads, but rather from transverse shock interactions between the beads. The bulk temperature of the shocked nitromethane was ~ 1000K, with the hot spot temperature higher by 50-100%, $T_{hotspot}$ = 1800 K. Likewise, the pressure field showed increased pressure focusing between the beads, and a spatial distribution of pressure set up along the leading shock front.

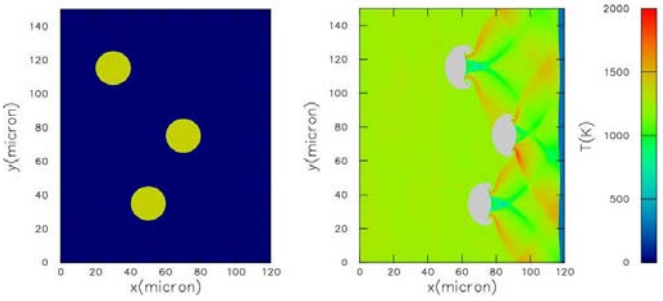

Figure 4. Simulations of shock interactions with glass beads in nitromethane have been performed to understand how hot spots are formed. (Left) Computational cell at the start of the simulation showing three 20 micrometer diameter glass beads in nitromethane. A 10 GPa is introduced into the simulation, traveling from left to right. (Right) Temperature field following shock passage over the computational cell (t = 25 ns). Regions of high temperature are found to form between the beads as a result of transverse shock collisions. The temperature of the shocked nitromethane (bulk) is ~ 1000 K, and the hot spot temperatures are 50-100 % higher.

Reactive chemistry modeling is a promising tool for understanding how shock compression energy is deposited into collective molecules leading to chemical reaction. It can also inform continuum chemical reaction rate models. The decomposition mechanisms of NM were studied using ReaxFF, a reactive force field developed with W. Goddard's group at Caltech. Simulations of NM decomposition were performed on collections of 240 molecules, compressed to relevant (detonation) volumes, and then heated to high temperatures (2500-4500 K). The decomposition processes were then tracked. Analysis of the change in potential energy of the system showed an initial increase in potential energy, followed by an exponential decrease. This type of behavior was previously observed for related explosives, and is consistent with an initial endothermic process, followed by at least one exothermic process. The activation energy for the exothermic process is ~35 kcal/mol, which is in good agreement with the effective activation barrier need to simulate the detonation wave profiles for NM [21-22].

Impact on National Missions

The research described supports LANL's principal mission in stockpile stewardship, and the Laboratory's emerging roles in threat reduction and homeland security, as well as DOE-DoD collaborative programs. Understanding hot spots could have future implications for designing in the performance of our plastic-bonded explosives, and lead to new concepts, such as "on-off" explosives [25-26]. Furthermore, this work has stimulated hot spot simulations and the development of "homogenization" models that are intermediate between explicit microstructure simulations and currently calibrated models. These models aim to capture salient features of hot spot ignition and reaction spread [27-28].

Follow-on projects have been established through the Office of Naval Research, DHS, and DOE/NNSA. The work supported a major milestone for the Advanced Simulation and Computing Program, and was one of the first simulations on Roadrunner, LANL's new supercomputer. The project also helped develop individual scientists both at LANL and at national universities. Four post-doctoral fellows (including a Director's funded Fellow) were converted to staff members at LANL. Additional students (4) and post-docs (4) were supported at LANL and at US universities.

References

1. Bowden, F. P., and A. D. Yoffe. Initiation and growth of explosion in liquids and solids. 1952.

2. Field, J. E.. . 1992. *Accounts of Chemical Research.* : 489.

3. Bourne, N. K., and J. E. Field. . 1999. *Proceedings: Mathematical, Physical, Engineering Science.* : 2411.

4. Simpson, R. L., and F. H. Helm. . 1989. In *9th Symposium (International) on Detonation.* (,). , p. 25. Washington, D. C.: Office of Naval Research.

5. Setchell, R. E.. . 1985. In *Eight Symposium (International) on Detonation.* (,). , p. 15. Washington, D.C.: Office of Naval Research.

6. Moulard, H.. . 1989. In *Ninth Symposium (International) on Detonation.* (,). , p. 18. Washington, D.C.: Office of Naval Research.

7. Moulard, H., J. W. Kury, and A. Delclos. . 1985. In *Ninth Symposium (International) on Detonation.* (,). , p. 902. Washington, D. C.: Office of Naval Research.

8. Lee, E. L., and C. M. Tarver. . 1980. *Physics of Fluids.* : 2362.

9. Engelke, R.. . 1979. *Physics of Fluids.* : 1623.

10. Engelke, R.. . 1983. *Physics of Fluids.* : 2420.

11. Presles, H. N.. . 1995. *Shock Waves.* : 325.

12. Khasainov, B. A., B. S. Ermolaev, and H. N. Presles. . 1997. *Shock Waves.* : 89.

13. Bouton, E.. . 1999. *Shock Waves.* : 141.

14. McGrane, S. D., A. Grieco, K. J. Ramos, D. E. Hooks, and D. S. Moore. . 2009. *Journal of Applied Physics.* : 073505.

15. Juodkazis, S., K. Nishimura, H. MIsawa, T. Ebisui, R. Waki, S. Matsuo, and T. Okada. . 2006. *Advanced Materials.* : 1361.

16. Patterson, B. M., and C. E. Hamilton. . To appear in *Analytical Chemistry.*

17. Dattelbaum, D. M., S. A. Sheffield, D. B. Stahl, and A. M. Dattelbaum. . 2009. In *APS Shock Compression of Condensed Matter Topical Group.* (Nas,). , p. 261. Melville, NY: AIP.

18. Dattelbaum, D. M., S. A. Sheffield, D. B. Stahl, and A. M. Dattelbaum. Hot spot-derived shock initiation phenomena in heterogeneous nitromethane. To appear in *25th JANNAF Propulsion Hazards Subcommittee Meeting.* (La Jolla CA,).

19. Dattelbaum, D. M., S. A. Sheffield, D. B. Stahl, A. M. Dattelbaum, and W. Trott. Influence of hot spot features on the initiation characteristics of heterogeneous nitromethane. To appear in *14th International Detonation Symposium.* (Coeur D'Alene, Idaho ,).

20. Gustavsen, R. L., S. A. Sheffield, R. R. Alcon, and L. G. Hill. Shock initiation of new and aged PBX 9501 measured with embedded electromagnetic particle velocity gauges. . *Los Alamos National Laboratory Report, LA-13634-MS.*

21. Hardesty, D. R., and P. C. Lysne. Shock initiation and detonation properties of homogeneous explosives. 1974. *Sandia Report No. SLA-74-165.*

22. Menikoff, R.. Hot spot formation from shock reflections. *Shock Waves.*

23. Menikoff, R., and M. S. Shaw. Modeling detonation waves in nitromethane. 2010. *intended for Journal of Combustion and Flame.*

24. Perry, W. L., T. D. Sewell, B. B. Glover, and D. M. Dattelbaum. Electromagnetically-induced localized ignition in secondary high explosives. 2008. *Journal of Applied Physics.* **104**: 094906.

25. Perry, W. L., B. B. Glover, J. G. Gunderson, and D. M. Dattelbaum. A numerical and experimental study of electromagnetically induced ignition of explosives. *Journal of Applied Physics.*

26. Hill, L. G.. Reactive thermal waves in energetic materials. To appear in *25th JANNAF Propulsion Hazards Subcommittee Meeting.* (La Jolla, CA,).

27. Hill, L. G., B. Zimmermann, and A. Nichols III. On the burn topology of hot-spot initiated reactions. 2009. In *APS Shock Compression of Condensed Matter Topical Group Meeting.* (Nashville, TN, 28 June-03 July, 2009). , p. 432. Melville, N: AIP.

Publications

Bedrov, D., O. Borodin, G. Smith, T. Sewell, D. Dattelbaum, and L. Stevens. A molecular dynamics simulation study of crystalline 1,3,5-triamino-2,4,6-trinitrobenzene as a function of pressure and temperature. 2009. *JOURNAL OF CHEMICAL PHYSICS.* **131** (22): 224703.

Bouyer, V., S. A. Sheffield, D. M. Dattelbaum, R. L. Gustavsen, and D. B. Stahl. Experimental measurements of the chemical reaction zone of detonating liquid explosives. 2009. In *16th Conference of the American Physical Society Topical Group on Shock Compression of Condensed Matter.* (Nashville, TN, 28 June - 03 July, 2009). , p. 177. Melville, NY: AIP.

Cawkwell, M. J., K. J. Ramos, D. E. Hooks, and T. Sewell. Homogeneous dislocation nucleation in cyclotrimethylene trinitramine under shock loading. 2010. *JOURNAL OF APPLIED PHYSICS.* **107** (6): 063512.

Cawkwell, M. J., T. D. Sewell, L. Zheng, and D. L. Thompson. Shock-induced shear bands in an energetic molecular crystal: Application of shock-front absorbing boundary conditions to molecular dynamics simulations. 2008. *Physical Review B.* **78** (1): 014107.

Chen, J., M. Kim, C. Yoo, D. Dattelbaum, and S. Sheffield. Phase transition and chemical decomposition of hydrogen peroxide and its water mixtures under high pressures. 2010. *JOURNAL OF CHEMICAL PHYSICS.* **132** (21): 214501.

Crouzet, B., S. A. Sheffield, N. Carion, D. M. Dattelbaum, R. Engelke, P. Manczur, R. R. Alcon, D. B. Stahl, and R. L. Gustavsen. Homogeneous Shock Initiation Process in Neat and Chemically-Sensitized Nitromethane. 2008. *EUROPYRO 2007-37th IPS.* : xxxx.

Dattelbaum, D. M., S. A. Sheffield, D. B. Stahl, A. M. Dattelbaum, W. Trott, and R. Engelke. Influence of hot spot features on the initiation characteristics of heterogeneous nitromethane. To appear in *25th JANNAF Propulsion Hazards Subcommittee Meeting.* (La Jolla, CA,).

Dattelbaum, D. M., S. A. Sheffield, D. B. Stahl, and A. M. Dattelbaum. Influence of Hot spot features on the shock initiation of heterogeneous nitromethane. 2009. In *16th Conference of the American Physical Society Topical Group on Shock Compression of Condensed Matter.* (Nashville, TN, 28 June to 3 July, 2009). , p. 263. Melville, NY: AIP.

Dattelbaum, D. M., S. A. Sheffield, D. B. Stahl, and A. M. Dattelbaum. Hot spot-derived shock initiation phenomena in heterogeneous nitromethane. To appear in *25th JANNAF Propulsion Hazards Subcommittee Meeting.* (La Jolla, CA,).

Dawes, R., A. Siavosh-Haghighi, T. Sewell, and D. Thompson. Shock-induced melting of (100)-oriented nitromethane: Energy partitioning and vibrational mode heating. 2009. *JOURNAL OF CHEMICAL PHYSICS.* **131** (22): 224513.

Engelke, R., N. Blais, and S. Sheffield. Mass-Spectroscopic Observations of Glycine Subjected to Strong Shock Loading. 2010. *JOURNAL OF PHYSICAL CHEMISTRY A.* **114** (32): 8234.

Heim, A., N. Gronbech-Jensen, E. Kober, J. Erpenbeck, and T. Germann. Interaction potential for atomic simulations of conventional high explosives. 2008. *PHYSICAL REVIEW E.* **78** (4, 2): 046709.

Hill, L. G.. Reactive thermal waves in energetic materials. To appear in *25th JANNAF Propulsion Hazards Subcommittee Meeting.* (La Jolla, CA,).

Hill, L. G., B. Zimmermann, and A. Nichols III. On the burn topology of hot-spot initiated reactions. 2009. In *APS Shock Compression of Condensed Matter Topical Group Meeting.* (Nashville, TN, 28 June - 03 July, 2009). , p. 432. Melville, NY: AIP.

McGrane, S. D., A. Grieco, K. J. Ramos, D. E. Hooks, and D. S. Moore. Femtosecond micromachining of internal voids in high explosive crystals for studies of hot spot initiation. 2009. *Journal of Applied Physics.* : 073505.

Menikoff, R., and M. S. Shaw. Hot spot formation from shock reflections. *Shock Waves.*

Menikoff, R., and M. Shaw. Review of the Forest Fire Model for High Explosives," Combustion Theory and Modelling. 2008. *Combustion Theory and Modelling.* **12** (3): 569.

Perry, W. L., B. B. Glover, J. G. Gunderson, and D. M. Dattelbaum. A numerical and experimental study of electromagnetically induced ignition of explosives. *Journal of Applied Physics.*

Perry, W. L., T. D. Sewell, B. B. Glover, and D. M. Dattelbaum. Electromagnetically-induced localized ignition in secondary high explosives. 2008. *Journal of Applied Physics.* **104**: 094906.

Ramos, K. J., D. F. Bahr, and D. E. Hooks. Nanoindentation of cyclotrimethylene trinitramine: new slip systems from anisotropic deformation and a reliable method to characterize dislocation content. To appear in *Philosophical Magazine.*

Ramos, K. J., and D. E. Hooks. Measurement of the Hugoniot Elastic Limit in Cyclotrimethylene Trinitramine at 1.0 GPa Peak Stress. *Journal of Applied Physics.*

Ramos, K., D. Hooks, and D. Bahr. Direct observation of plasticity and quantitative hardness measurements in single crystal cyclotrimethylene trinitramine by nanoindentation. 2009. *PHILOSOPHICAL MAGAZINE.* **89** (27): 2381.

Robbins, D. L., S. A. Sheffield, D. M. Dattelbaum, N. Velisavljevic, D. B. Stahl, and L. L. Gibson. Equation of state of ammonium nitrate. 2009. In *16th Conference of the American Physical Society Topical Group on Shock Compression of Condensed Matter.* (Nashville, TN, 28 June-03 July, 2009). , p. 552. Melville, NY: AIP.

Siavosh-Haghighi, A., R. Dawes, T. Sewell, and D. Thompson. Shock-induced melting of (100)-oriented nitromethane: Structural relaxation. 2009. *JOURNAL OF CHEMICAL PHYSICS.* **131** (6): 064503.

Stevens, L. L., A. Migliori, and D. E. Hooks. A Brillouin scattering and resonant ultrasound study of the mechanical properties of pentaerytritol tetranitrate. To appear in *Journal of Applied Physics.*

Stevens, L. L., N. Velisavljevic, D. E. Hooks, and D. M. Dattelbaum. Hydrostatic compression curve for triaminotrinitrobenzene (TATB) determined to 13.0 GPa with powder X-ray diffraction. 2008. *Pyrotechics, Explosives, and Propellants.* **33** (4): 286.

Stevens, L. L., N. Velisavljevic, D. E. Hooks, and D. M. Dattelbaum. The high pressure phase behavior and compressibility of 2,4,6-trinitrotoluene (TNT). 2008. *Applied Physics Letters.* **93**: 081912.

Stevens, L. L., and D. M. Dattelbaum. Equations-of-state of Non-crystalline Materials: High Explosive Binders and Related Polymers. 2008. In *Energetic Materials at Static High Pressures.* Edited by Peiris, S., and G. Peirmarini. , p. 127. Berlin: Springer-Verlag.

Sun, B., J. M. Winey, Y. M. Gupta, and D. E. Hooks. Determination of second-order elastic constants of cyclotetramethylene tetranitramine (β-HMX) using impulsive stimulated thermal scattering. To appear in *Journal of Applied Physics.*

Zhang, L., S. Zybin, A. T. van Duin, S. Dasgupta, W. Goddard, and E. Kober. Carbon Cluster Formation during Thermal Decomposition of Octahydro-1,3,5,7-tetranitro-1,3,5,7-tetrazocine and 1,3,5-Triamino-2,4,6-trinitrobenzene High Explosives from ReaxFF Reactive Molecular Dynamics Simulations. 2009. *JOURNAL OF PHYSICAL CHEMISTRY A.* **113** (40): 10619.

Design, Synthesis, and Theory of Molecular Scintillators

Rico E. Del Sesto
20080037DR

Abstract

Our project involved the development of new scintillator materials for large-scale, high resolution, real time radiation detection. We targeted hybrid organic-inorganic materials in order to achieve the performance of the individual components used in scintillators today. Studies on existing materials over the last several decades have provided some understanding of the process of scintillation, but there are still missing pieces that are much less well understood. Using what we know now about the interaction with incident radiation with a material, we proposed to design materials using synthetic chemistry to incorporate functional units that optimize the known processes of scintillation. Designing these functional units, along with characterizing the resulting materials and theoretical predictions of the response of a material to radiation, promised an in-depth understanding of the entire process including the missing pieces. From the knowledge gained in this project, we hoped to optimize the materials for their response to radiation. Additionally, with the materials being organic in nature, they can be processed and scaled up as typical plastic scintillators are now, but with added inorganic components that provide the energy resolution necessary for efficient isotope identification.

Background and Research Objectives

Utilizing chemical synthesis, this project aimed to develop new materials specifically designed to interact with incident ionizing radiation, and convert that energy to visible light output. This process of scintillation can be broken down into several steps – (1) interaction of the incident radiation, which generates charged particles within those materials; (2) interaction of those charged particles with components of the material, creating excitations; (3) transport of those excitations through the materials to sites where (4) luminescence can occur. This process is generalized in Figure 1. We therefore designed materials to address each of these steps – high-Z (atomic number) for gamma and charged particle interactions, or boron-10 for neutron interactions; ionic or polymeric materials for transport and transparency to the luminescent sites; and a luminescent site to emit visible light, which in general can be an organic dye or lanthanide. Many materials were synthesized, characterized to ionizing radiation (generally X-ray), and theoretical models were used to help understand the processes in specific materials, but also to understand the process of high-energy electrons (charged particles) and their fate as they progress through many common scintillator materials.

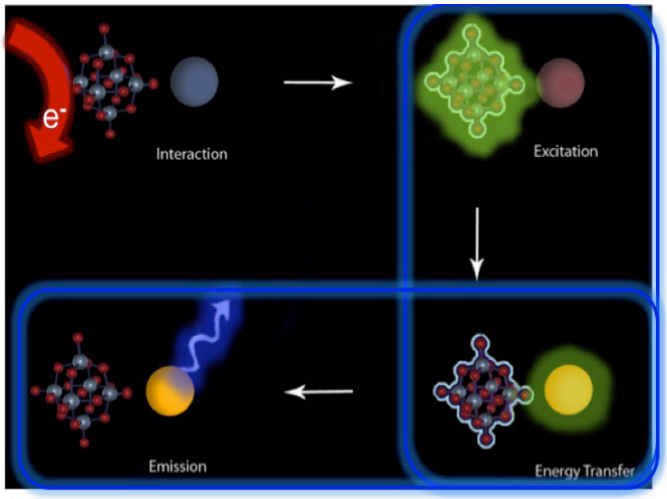

Figure 1. Generalized view of the steps that contribute to the scintillation process.

Scientific Approach and Accomplishments

Design and Synthesis

High-Z organic liquids and polymers – Materials containing high-Z tungsten polyoxometalates (POMs) were synthesized. This includes both ionic liquids, which are liquid at room temperature, and polymer composites that contain pendant POMs. The POMs incorporated lanthanide cations that provide the materials with a luminescent center for use as phosphors in radiation detection. The ILs were obtained from the coupling of an organic phosphonium cation with an anionic cluster, $[Ln(W_5O_{18})_2]^{8/9-}$ (Ln= La^{3+}, Ce^{4+}, Tb^{3+}, Eu^{3+}, Dy^{3+}) to form liquids with an average melting point of -77 ºC. The polymer composites were obtained from the encapsulation

of these anionic clusters with cations that have polymerizable groups, including acroyl and styryl cations. Materials with improved transparency could be synthesized by incorporation of various co-monomers. As lanthanide based materials, they all emit in the visible region when exposed to UV-light. The ionic liquids and polymer composites with Ln= Tb^{3+}, Eu^{3+}, and Dy^{3+} all showed emission corresponding to its respective Ln^{3+} cation that result from O → W LMCT to the lanthanide cation. The materials also respond to ionizing radiation. The radioluminescence (RL), which is X-ray stimulated luminescence, of a Tb(III) transparent polymer is shown in Figure 2. We attempted to obtain spectra of these materials when exposed to gamma-radiation as well. However, the lifetimes of most lanthanides are excessively long – on the order of milliseconds to seconds – which is far too long to record their response due to the electronics used for gamma characterization, and because successive pulses would be confused as they pile up, one upon the other.

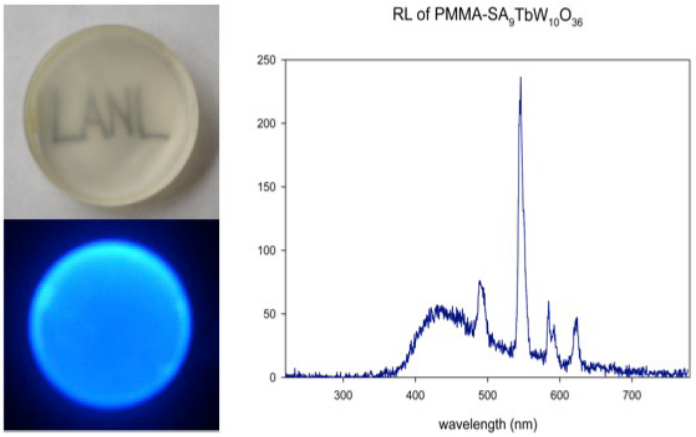

Figure 2. Tb-POM polymer under visible and UV-light, and (right) response of the polymers to ionizing (X-ray) radiation.

Hybrid Framework Materials - Organic-inorganic hybrid framework materials, sometimes known as Metal-Organic Frameworks (MOFs), are another class of compounds being investigated as gamma ray scintillators. Their composition allows the easy combination of a high-Z metal (gamma ray absorber), with a chromophoric ligand (visible light emitter), into a crystalline solid having a known structure. Ideal structures for efficient energy transfer will feature dense, highly connected arrays of metal centers along with multiply bridging coordination of polyfunctional ligands, typically large aromatic polycarboxylates. Some of the materials synthesized include metal (Cs, Ba, La) stilbenedicarboxylates. Solid products have been obtained in good yield, and powder x-ray diffraction (XRD) shows that they are crystalline, with large unit cell dimensions consistent with framework materials. Radioluminescence spectra of these powders show emission of visible light upon irradiation with Mo-K_a x-rays (17.4 keV). In addition, the significant Stokes shift in this particular ligand system, which limits potential self-absorption, can be seen in the photoluminescence spectra.

Molecular analogs of existing scintillators – In addition to newly designed materials for gamma detection, we also synthesized molecular analogs to known single-crystalline scintillators. In particular, the Ce:$LaBr_3$ scintillator is one of the brightest known single crystal materials. We therefore developed the molecular analog, which is a solvent adduct, in $CeBr_3(THF)_4$. This material represents the smallest of building blocks for the known scintillator. The molecular analog responds to X-ray irradiation, exhibiting strong fluorescence. Due to limited solubility, however, we could not put enough into solution to measure its response to gamma radiation. The molecular species is also unique in that modeling the behavior in response to ionizing radiation is more approachable than a bulk material. Thus, the $CeBr_3(THF)_4$ was used as a common material to develop several components of the theoretical modeling tasks of this project.

Carborane materials for neutron detection - Ionic liquid molecular scintillators for neutron detection were synthesized, formulated at 2% boron in toluene, and tested for radioluminescence, photoluminescence, and emission in the presence of a neutron source and a gamma source. The carborane anion $B_9C_2H_{12}^-$ was synthesized from o-carborane and the ionic liquids $[PC_6C_6C_6C_{14}][B_9C_2H_{12}]$ and $[NC_6C_6C_6C_6][B_9C_2H_{12}]$ were synthesized by salt. The phosphonium ionic liquid was a room temperature ionic liquid and the ammonium ionic liquid melted just above room temperature (between 40 and 60°C). The emission of these ionic liquids was examined in PPO/POPOP liquid scintillator. Neither of these ionic liquids showed a detectable signal in the presence of the neutron source and the gamma signal was quenched at least 5-fold relative to the signal obtained with only the liquid scintillator. Also using the synthesized carborane anion $B_9C_2H_{12}^-$, a cerium-containing molecular scintillator, cerium dicarbollide (CeCB), was synthesized. This molecule was of particular synthetic interest because the synthesis had not previously been published. The ionic liquid of this molecule was synthesized by salt metathesis with CYPHOS 101 and tested for emission in toluene. The gamma signal was similar to that of toluene and no signal was detected in the neutron experiment.

Monte Carlo Code for Electron-Hole Pair Statistics in Gamma-ray Detector Materials

The purpose of this component of the project has been to develop a Monte Carlo code capable of calculating the statistics of electron-hole pair production in gamma ray detector materials in the context of determining energy resolution. For a given semiconductor or scintillation detector material, a realistic model for inelastic electron scattering is constructed from electron energy loss spectra (EELS), optical data for the complex index of refraction, and calculated valence band densities of states. Results from this

code can be used for evaluating potential detector materials and for studying the effects of material properties on energy resolution.

The nature of the model allows one to study the effects of material properties by varying a number of parameters that include the bandgap, valence bandwidth, and the plasmon energy. The variation of the Fano factor (defined as S^2_n/n, where n electron-hole pairs are produced for a given shower) with plasmon resonance energy has been calculated. A smaller Fano factor implies better energy resolution, as desired. In Figure 3, the Fano factor is plotted against the energy of the initial fast electron in silicon. The four different curves in the plot represent scattering models based on different assumptions. That the Fano factor saturates at higher energies is consistent with previous work on the subject.

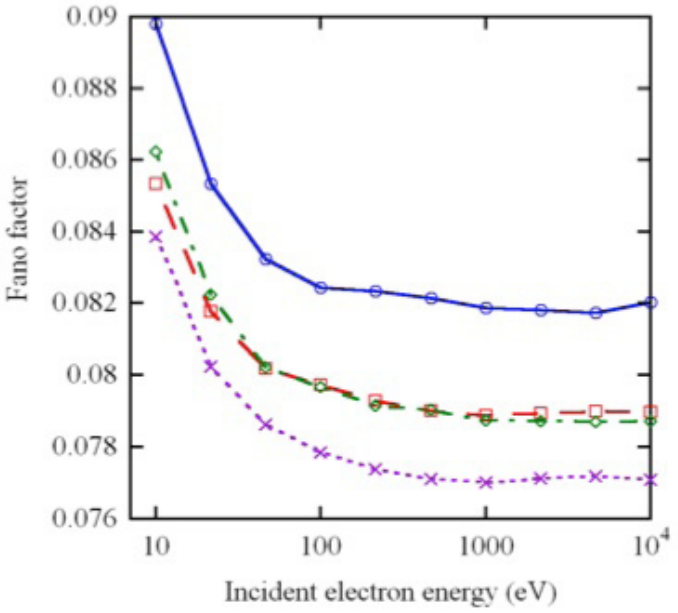

Figure 3. Fano factor vs. incident electron energy for silicon using a measured EELS spectrum and a calculated valence band density-of-states (DOS) (solid curve). Also shown are results using a uniform energy-loss DCS (dashed curve), a uniform valence band DOS of width ~11 eV (dot-dashed curve), and both a uniform energy-loss DCS and a uniform valence band DOS (dotted curve).

This model is incorporated into the Penelope radiation transport code, where it takes the place of Penelope's treatment of inelastic electron scattering. This allows one to calculate the statistics of electron-hole pair production for showers that begin with a single gamma-ray. On output one obtains a histogram of the number of counts (electron-hole pairs) per shower. Since Penelope tracks all particles through the material, any effects due to the escape of photons and electrons will be included. In future work, when the EELS spectrometer on our microscope has been repaired, we shall record spectra from CeF_3 and LSO . We shall then use our new version of the Penelope Monte Carlo code to calculate the energy resolution of gamma rays incident on these scintillator materials, as well as semiconductors such as Si, Ge and GaAs. A paper on this work will be submitted for publication either towards the end of 2010 or early 2011.

Theory and Modeling of Molecular Scintillators

The theory and modeling component of this project includes first principles calculations of the electronic structure of the constituent components of the molecular scintillators, and modeling of the dynamics of the excitation generation, excitation transfer between the constituents, and luminescence of the scintillators. The first principles electronic structure calculations provide essential input parameters to the dynamics models. When radiation (gamma ray or neutron) interacts with the scintillator material, high-energy charged particles, such as electrons, are generated. These high-energy charged particles generate secondary electrons and electronic excitations as they traverse the scintillator material. The electronic excitations are transferred to luminescent centers in the scintillator and light emitted from the luminescent centers is detected by a photo-detector indicating the presence of the radiation.

The molecular scintillators under investigation in the project consist of composites of high-Z particles, in which the high-energy charged particles generate electronic excitations, and luminescent centers. We performed Time Dependent Density Functional Theory (TDDFT) calculations of the electronic structure of both the dyes and the particles or clusters. Calculated optical absorption and emission properties are in good agreement with our experimental observations for the dye Coumarin-120 and the scintillator material $CeBr_3(THF)_4$. Calculated transition energies and dipole strengths play an essential role in the energy transfer modeling. As a specific example, a large Stokes shift of 0.3-0.5 eV was observed in the calculated optical spectra of Coumarin-120 and of the particles and clusters of interest, which was consistent with experiment. We have extended our calculations of the optical properties of the scintillator materials to bis-polyoxometallates of Ce. We found that, when the influence of the solvent is included in the calculations, a very reasonable energy level diagram is obtained, and consistent with experimental results. We have examined other members in this series, including the cases where the Ln ion is Yb(III), and Eu(III). Finally, our calculations determine details of the emission spectra and lifetimes of these states.

We have also developed: (a) an effective dielectric model of the wide band gap scintillator material for the calculation of the excitation transition rates and energy loss functions, and (b) rate equations for the calculation of TSL (thermally stimulated luminescence), OSL (optically stimulated luminescence) and PL (photoluminescence) characteristics of the scintillators. The energy loss function

is a central property of the material describing the loss of energy and stopping length of secondary electrons created after the initial excitation with a gamma ray. In Figure 4 we show results for the calculated effective dielectric function and energy loss function with the relevant characteristic plasmon of the electronic excitations. We used the Penn model to describe scintillator materials with an energy gap typical for wide band gap materials. In order to couple the energy loss function with the first-principles TDDFT efforts of this project. The Monte Carlo simulations described earlier can be integrated with either the TDDFT or effective dielectric medium model calculations for a more materials specific modeling of radiation interacting with scintillators.

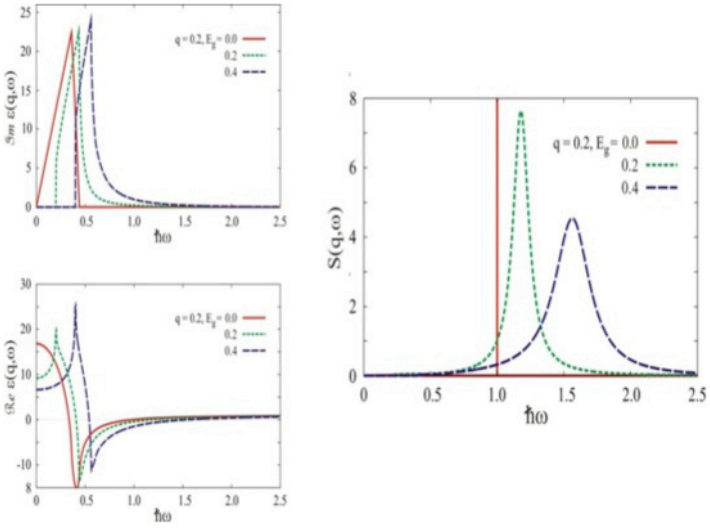

Figure 4. The energy loss is dominated by plasmons. Left panels: Dielectric functions (real and imaginary part) for the Penn model with different energy gaps E(g). Right panel: scattering cross section S(q,ω) derived from the dielectric function e(q,ω). The energy loss is dominated by plasmons and the plasmon peak shifts to higher energies with increasing energy gap

We also developed model rate equations for calculating photoluminescence using phenomenological transition rates fitted to experiments of known scintillators like $CeBr_3(THF)_4$ to benchmark our models (see Figure 5). The experimental luminescence data are generally underconstrained. In order to benchmark our model it was sufficient to describe the measured photoluminescence by assuming a three-site model for the energy transfer between luminescence sites and final relaxation of the electronic excitations. The three sites include transfers between two sites with radiative transitions and the third site is a trap that allows after a long escape time to transfer back to one of the luminescence sites. To close the modeling loop, we started implementing materials specific dipole moments and oscillator strengths of excited states from TDDFT calculations for $CeBr_3(THF)_4$ to calculate the intrinsic radiative transition rates needed as input parameters for the rate equation models. Additionally, we established an approach for calculating the energy loss function from the electronic structure input parameters. A major challenge that remains at the end of this project is the full integration of the first-principles calculations of the excited electronic states of a real scintillator material with the effective dielectric model energy loss functions, the Monte Carlo simulation of the excitation distributions, and the model rate equations for luminescence.

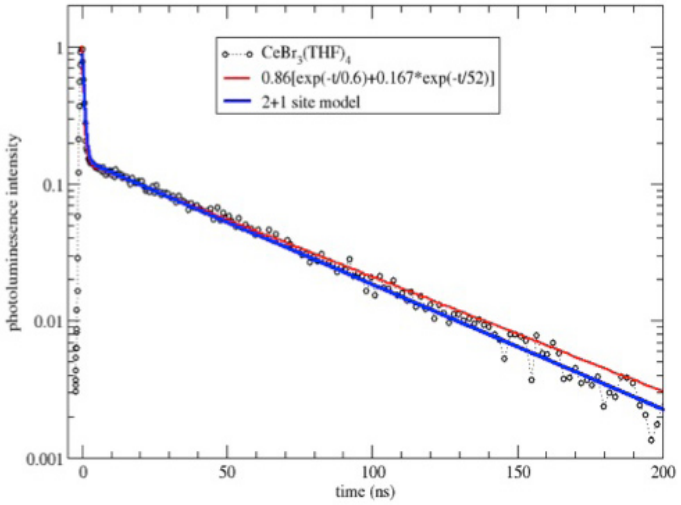

Figure 5. Modeling and fitting of the photoluminescence intensity of $CeBr_3(THF)_4$ assuming a three-site (2+1) energy transfer model with back transfer.

Impact on National Missions

This project supports the DOE mission of Threat of Weapons of Mass Destruction through enhancement of current capabilities for detecting nuclear threats. Existing scintillators lack characteristics to fully address radiation detector needs. Specifically, it is necessary to have large-volume, low-cost, high-performance materials to satisfy radiation detector requirements. Through this project, we have been able to begin understanding the effects in the scintillation mechanism at the molecular and nanomaterial size regimes, and how that relates to bulk behavior. While the materials presented are not ideal for a large-scale detector, they provided tools by which to study scintillation processes in more detail.

Publications

Ortiz-Acosta, D., G. M. Purdy, B. Scott, B. L. Bennett, R. E. Muenchausen, E. A. McKigney, R. D. Gilbertson, and R. E. Del Sesto. Ionic liquid polyoxometalates as light emitting materials. 2008. In *Molten Salts and Ionic Liquids 16 - 214th ECS Meeting ; 20081012 - 20081017 ; Honolulu, HI, United States.* Vol. 16, 49 Edition, p. 171.

Roy, L., D. Ortiz-Acosta, E. Batista, B. Scott, M. Blair, I. May, R. Del Sesto, and R. Martin. Luminescence in Ce-IV polyoxometalate [Ce(W5O18)(2)](8-): a combined experimental and theoretical study. 2010. *CHEMICAL COMMUNICATIONS.* **46** (11): 1848.

Ultrafast Nanoscale XUV Photoelectron Spectroscopy

George Rodriguez
20080097DR

Abstract

The overall goal of this project was to study materials' properties from a novel perspective by developing a new scientific instrument that allows us to merge two experimental techniques, angle-resolved photoemission spectroscopy and ultrafast spectroscopy, leading us to a deeper understanding of dynamical physical processes occurring in complex materials. The technique, coined "ultrafast time-resolved angle-resolved photoemission spectroscopy (trARPES)" because it measures the *dynamical* response of the material, and provides complementary information to the more traditional method, static ARPES. Time-resolved ARPES is still in its early demonstration stages of scientific discovery for materials science studies because of lack of suitable ultrafast laser-based coherent light sources in the extreme ultraviolet (XUV) portion of the electromagnetic spectrum. Only recently have sufficiently energetic laser pulses with pulse durations in the femtosecond (1 fsec = 10^{-15} sec) time regime come available that have enough flux to generate XUV light for ARPES based spectroscopic detection. Over the course of this project, we demonstrated a table-top ultrafast laser-based XUV light source and then used the source to perform trARPES on materials. The project is a first demonstration of the scientific capabilities of ultrafast trARPES. Below is a description describing the background and research objectives of the project, the scientific approach and accomplishments, and its Laboratory relevant impact on national mission priorities.

Background and Research Objectives

Angle-resolved photoemission spectroscopy (ARPES) is an experimental technique aimed at determining the electronic structure of solids [1-4]. It is based on the photoelectric effect, explained by Einstein more than 100 years ago: a beam of high-energy photons, impinging on the surface of a solid-state material liberates electrons, whose kinetic energy and direction angle carry direct information about the state (energy and momentum) of the electrons within the sample (see Figure 1.). With the advance of powerful sources of high-energy XUV photons (typically from synchrotron accelerator facilities), and the significant improvement in the development of highly-sensitive photoelectron detectors, the ARPES technique has been established as an accurate scientific spectroscopic method for studying the occupied states in condensed-matter physics [1-4]. By "occupied states", we refer to the quantum mechanical ordering of electrons in an atom that comprise a crystalline solid to form ordered discrete energy levels called the electronic band structure. It is the detailed ordering of the occupied states that are often responsible for the material's properties such as thermal and electric conduction, magnetism, superconductivity, and optical light response [5-9]. Thus by using the ARPES spectroscopic technique, one may understand the complex electronic ordering in the material and then use that information to engineer new materials with different properties for desired function.

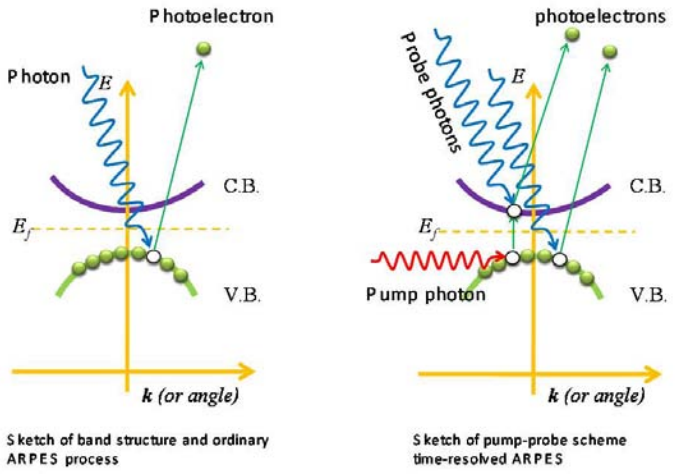

Figure 1. Band structure sketch diagramming the comparison of traditional static ARPES and trARPES. The plots represent an energy (E) versus momentum (k) diagram about the Fermi midpoint energy (Ef) that distinguishes between occupied electronic states in the valence band (V.B.) and conduction band (C.B.). In the trARPES case, time-dependent relaxation processes are measured stroboscopically by varying the temporal delay between the pump and probe beam photons. In both cases, the photoelectrons are ejected from the surface and the energy and momentum of the electron are mea-

sured with a hemispherical electron momentum-energy analyzer.

New to the field of ARPES is our extension to investigate normally unoccupied states. Unoccupied states are those that are normally not populated with electrons in the material's electronic band structure and ground state configuration, but are quantum mechanically allowed to be populated if stimulated or excited by promoting ground state electrons to excited state energy levels. For many materials such as metals, semiconductors, superconductors, insulators, etc., these energies for promotion of electrons to previously unoccupied states are easily accessible with existing external stimuli such as optical lasers, electric current, heat, etc. In our project we use ultrashort laser pulses to excite material electrons into unoccupied states. The unoccupied sates are populated with this "pump" photon from laser pulse, and then the new excited state configuration of the material is subsequently "probed" with a second ultrashort XUV laser pulse for producing a trARPES recordable signal [10-13]. In the so-called pump/probe configuration (see Figure 1): the first, pump pulse, excites electrons from filled to empty states, while the second, probe pulse, which is the high-energy photon beam used for conventional ARPES, ejects these excited electrons and subjects them to measurement. In this fashion besides the usual information obtained from ARPES, trARPES can trace the dynamics of the excited electrons by varying the delay between the pump and probe pulses. The dynamics of the excited electrons is very fast: typically a few picoseconds after excitation, the sample has recovered to its normal state. Multiple relaxation processes are responsible for electron recovery to its normal state. The excited electrons can relax by scattering with adjacent electrons, or by coupling to quantum crystalline lattice vibrations called phonons. Other fundamental quantum particles such as holes, quasiparticles, excitons, polarons, etc., all are of scientific interest to the materials physics community. It is the dynamical energy interaction and exchange of these fundamental particles that intrigues materials scientists and thus forms the basis of trARPES instrumentation development. A better understanding of these dynamical interactions help scientists refine complex materials physics models and design new materials with engineered properties for applications such as nano-electronics, superconductivity, magnetism, and for other energy efficient technologies.

Research objectives for this project were several-fold. The first half of the project was dedicated to design, construction, and demonstration of the trARPES instrument. This required a novel and unique ultrafast XUV light source coupled to a high resolution angle resolved photoemission (ARPES) analyzer. The second half of the project consisted of a set of scientific materials experiments and measurement tasks. The experiments and measurements work can be divided into several sub tasks: (i) trARPES, (ii) static ARPES at synchrotron facilities, and (iii) ultrafast optical spectroscopic measurements. These subtasks are complementary efforts aimed at providing alternative pieces experimental information that cannot be obtained with one instrument/technique alone. We focused our material studies to several systems of interest: gallium arsenide (GaAs) semiconductor, correlated *f*-electron actinide materials (URu_2Si_2 and UO_2), and a *d*-wave high-temperature superconductor $Bi_2Sr_2CaCu_2O_8$ (known as BSCCO-2212). In addition to materials measurement, a theoretical modeling component was supported.

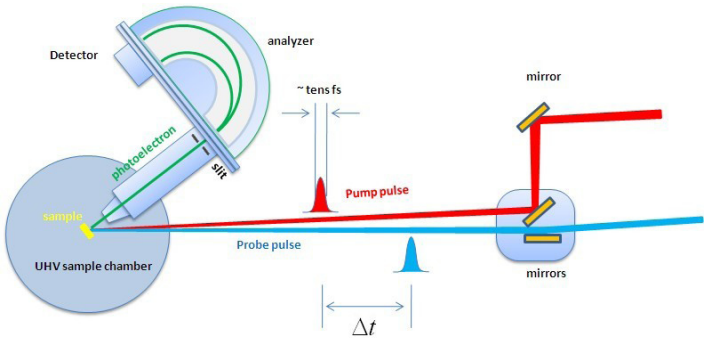

Figure 2. Experimental setup illustrating how in trARPES pump and probe laser beams are launched into the the ultra-high vacuum (UHV) chamber containing the material sample under study. Both, pump and probe, beams have temporal pulse widths of few tens of femtoseconds each while an adjustable time delay allows for measuring time dependent process on the femtosecond to picosecond time scale. The pump beam photon energy is in the visible portion of the electromagnetic spectrum of light, typically 1.5 eV or 3 eV, and the probe beam photon energy is an XUV pulse tunable between 15 eV and 50 eV. After impinging the surface with photons, the material surface releases photoelectrons that are subsequently analyzed for their energy and momentum states. These photoelectron states are directly correlated with the material's electronic band structure.

Scientific Approach and Accomplishments

Time-Resolved ARPES

A significant fraction of the project effort focused on construction of the trARPES instrument and initial testing on metal samples for determining the spectrometer resolution, XUV flux and spectral range [13]. An outline of the experimental trARPES setup is shown in more detail in Figure 3. At the heart of the apparatus lies the amplified laser system, capable of delivering strong (1.5 mJ), ultrashort (30 fs), visible (1.5 eV) pulses at repetition rate of 10 kHz suitable for fast data acquisition. The beam is split in two arms, in accordance with the pump/probe configuration, with one of the beams designated as pump (at the fundamental wavelength) traversing a delay stage which controls the timing between the pump and probe pulses. The photon energy of the beam in the other arm is insufficient for ARPES: at least 4-5 eV photons are needed to

overcome the work function (almost a constant regardless of the material) and produce photoelectrons for ARPES study. This increase in photon energy is achieved through the highly-nonlinear process of High-Harmonic Generation (HHG), which occurs when a very intense laser beam interacts with typically a noble gas: the electromagnetic pulse frees an electron and accelerates it to a high energy, which can be emitted in the form of a far-more energetic photon upon the electron's recombination. Physically this occurs in the first round chamber where the fundamental beam is focused on a small target containing argon; all subsequent chambers are evacuated to progressively lower pressure to ensure that the high-energy photons produced via HHG are not absorbed in ambient air, and to reach the necessary base pressure at the ARPES chamber. An image of the HHG beam is shown (camera image inset to Figure 3), indicating that the beneficial properties of the fundamental laser beam are "transferred" to the high-energy XUV photon beam as confirmed by the Young-type double-pinhole interference pattern shown.

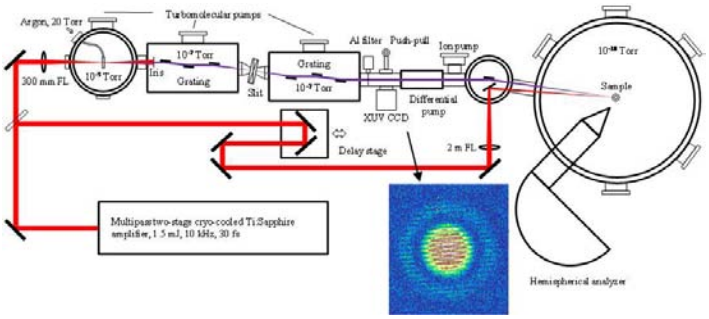

Figure 3. A detailed view of the experimental optical-pump/XUV-probe setup for trARPES. The inset figure shows a Young-type double-pinhole diffraction CCD image of the XUV beam profile to illustrate excellent spatial coherence in the XUV beam.

In general, a multitude of high harmonic lines, separated by twice the fundamental photon energy, is generated, while for the purpose of ARPES just one of these harmonics, chosen for the particular experiment, needs to be extracted with maximum efficiency. We pick the harmonic by passing the beam through a home-built double-grating monochromator (the two rectangular boxes in Figure 3). The first grating spatially disperses the beam containing all harmonics, then the necessary photon energy is selected with a slit; at this point the HHG pulse is also stretched in time which is inherent in the diffraction process. To re-sharpen the pulse, the beam reflects off of a second grating (in opposite diffraction order), which compresses the pulse back to its original duration. This gives us a single high-harmonic, with energy suitable for ARPES and sufficiently short duration for time-resolved studies, heading towards the sample chamber, where it is made to hit the sample almost collinearly with the visible pump beam. To demonstrate this basic capability of the apparatus we have acquired an angle-integrated photoemission spectrum from uranium dioxide (UO_2), shown in Figure 4(a), and compared it to similar data obtained from a synchrotron source (inset to Figure 4(a)). The two spectra are seen to be in excellent qualitative agreement. This is rather a coup, because we are comparing our table-top experiment to a facility costing hundreds of millions of dollars. The spectra obtained in UO_2 were the first -ever examples of 5*f* electronic structure measured with a laser-based harmonic generator source. We plan further studies on this material because it is important for nuclear fuels.

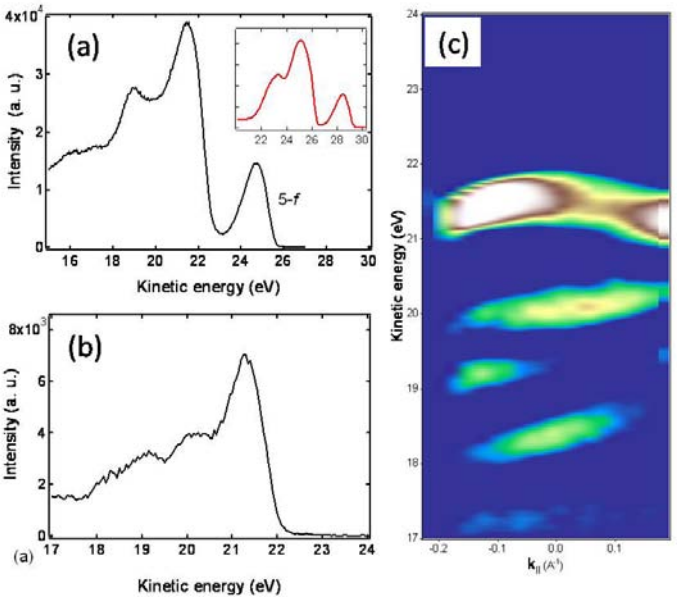

Figure 4. Examples of ARPES measurements in two material systems: (a) angle integrated ARPES spectrum from the Mott insulator UO_2 using the trARPES system compared to synchrotron data (inset) obtained at SRC (Stoughton, WI); (b) angle integrated ARPES spectrum from the semiconductor GaAs; (c) angle- and energy-resolved full ARPES spectrum from GaAs in an energy versus momentum map plot.

The ability of the instrument to record simultaneously energy and angle of the emitted photoelectrons results in the possibility to reconstruct the electronic band structure of different materials. In Figures 4(b) and 4(c) we show the angle integrated (non-momentum resolved) and angle resolved (momentum resolved) photoemission spectrum of the semiconductor gallium arsenide (GaAs). The intensity map in Figure 4(c) is a portion of the band structure of GaAs at a temperature of 12 Kelvin. Acquisition of such precise and direct ARPES data allows for detailed comparison between experiment and various theoretical models. Finally, we also showed the full capability of the trARPES instrument (time-, angle-, and energy-resolved) by successfully measuring the first time-resolved ARPES in an *f*-electron system: the heavy-fermion system URu_2Si_2. This material is of interest to the condensed matter physics community because of its unusual magnetic and superconducting properties at low temperature. The plot in Figure 5

shows an energy and momentum (angle) map for ground state dynamics near the Fermi edge at T=12 Kelvin at two separate optical-pump XUV-probe time delays (Δt=0 and -150 fs). Notice the spectral weight transfer from below the Fermi edge (E_f) to unoccupied states above E_f (indicated by arrows) at different photoemission angle. These results are the first ever recorded time-resolved ARPES spectra from an *f*-electron heavy fermion material. The data show that at a time scale of 100 femtoseconds, the excited electrons/quasiparticles (induced by the pump pulse) rearrange themselves and alter the material band structure. Time-resolved ARPES is able to capture this process and its subsequent relaxation history. Key data such as this is only obtainable with trARPES, and the first trARPES measurements show how detailed information about ultrafast energy exchange processes amongst the various particles can be tracked in time yielding their energy and momentum histories.

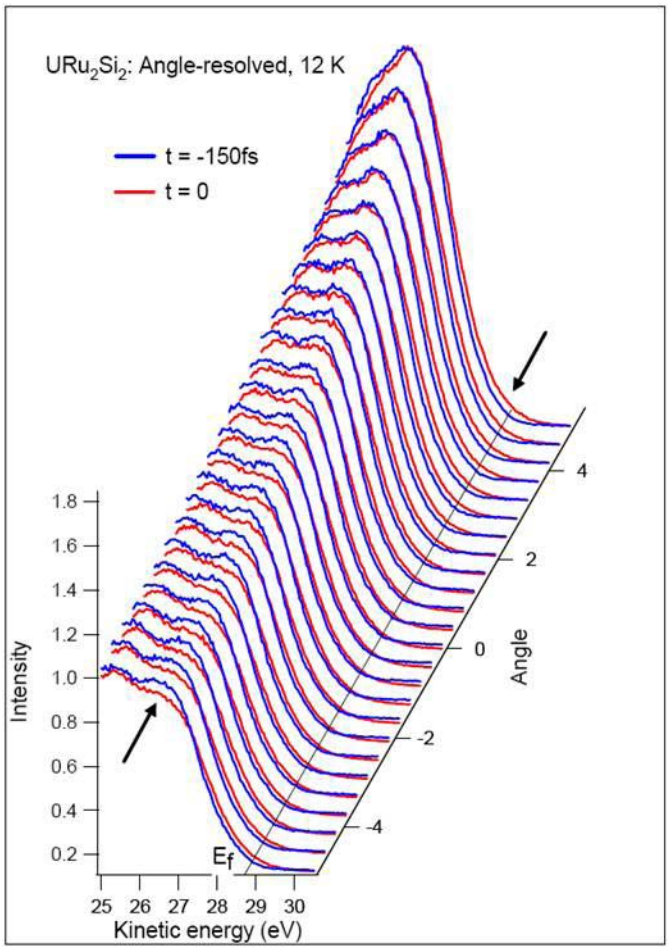

Figure 5. Full (time-, angle-, and energy-resolved) trARPES spectrum of URu_2Si_2 near the Fermi edge at T=12K (in the hidden order phase) for two pump-probe time delays. Arrows indicate electron kinetic energy regions of significant changes in the spectrum.

Static ARPES

High resolution photoemission spectra of URu_2Si_2 were obtained at the Wisconsin Synchrotron Radiation Center (SRC at Stoughton, WI) to complement spectra measured by the Los Alamos ultrafast trARPES instrument. The motivation was to investigate the changes in Fermi surface of this compound at the complex hidden order transition which occurs at T=18 Kelvin in this material. SRC-based ARPES data contain information about the band structure evolution with emergence of coherence and hidden order. However, static ARPES does not provide the information about electronic structure above the Fermi edge energy (E_f), and the information about the quasiparticle lifetime and dynamics is convoluted. Nonetheless, a static ARPES measurement from SRC is valuable because it is able to discern detailed state information that the Los Alamos trARPES instrument cannot because of the superior energy and momentum resolution from a synchrotron based measurement. Synchrotron static ARPES measurement runs were performed and detected formation of several complex quasiparticle states near the Fermi energy edge beginning at a temperature of T=70 Kelvin where coherence sets in and then continuing down to T=18 Kelvin where additional states form at the hidden order phase transition. The results of this measurement have been submitted for publication [14,15].

Ultrafast Optical Spectroscopy

In addition to ARPES based measurements, the project also supported complementary ultrafast optical spectroscopy measurements [16-18] on UO_2. Motivated by understanding the nature of conduction electron transport in this material, we studied the ultrafast dynamics of photoexcited carriers in this system. It was discovered that upon photoinjection of carriers across the Mott energy gap (>2 eV) with 3 eV photons, a hopping conduction between excited carriers is observed; 5f electrons instantly hop to neighboring uranium (U) sites and subsequently cause lattice deformation on picosecond (ps) time scales that then induce acoustic phonon emission. The relaxation is found to be on microsecond (μs) time scale at low temperatures and is assigned to the decay from bound $U^{3+}(5f^3)$-$U^{5+}(5f^1)$ exciton pairs. Additional magnetic ordering mediation is also observed as the temperature is dropped below the magnetic phase transition temperature T_N = 31 Kelvin, thus indicating an effect on the binding of the U^{3+}-U^{5+} exciton [16-18].

Theory

The combination of ultrafast laser sources with angle-resolved photoemission spectroscopy is a powerful technique because the time-resolved ARPES monitors the temporal evolution of electronic states. During the tenure of this project, we have been able to develop a theory for the time-resolved spectral function in high-temperature superconductors [19]. This theory is based on an assumption

that the characteristic time for the individual electronic and lattice baths to reach the local equilibrium is much shorter than the energy relaxation time between the electronic and lattice baths. This approximation is especially valid for the strongly correlated electron systems, which represent most of the complex functional materials ranging from high-temperature cuprate superconductors to heavy fermions. It then allows us to construct an effective temperature model to describe the time dynamics of electronic and lattice degrees of freedom. We have applied this line of strategy to the high-temperature cuprates [19] and established the time-resolved quasiparticle spectral function with the electron-lattice coupling. The signature as a consequence of the coupling is identified to evolve with time. The same line of strategy can be used to study other strongly correlated materials.

Impact on National Missions

The research in this project was aimed at developing a novel instrument capable of time-, momentum- and energy-resolved ARPES measurements for application to strategic materials science. It supports fundamental experimental facility capability not currently available elsewhere in the Department of Energy (DOE) complex. We used the experimental capability for fundamental understanding of electronic structure and behavior of complex correlated electronic materials. Our fundamental experiments served as a foundation for future energy technologies,by improving our understanding of emergent phenomena for the discovery of new material properties. Hence, this project embraces the Laboratory's Materials Strategy, as well as the LDRD Grand Challenge in Materials. Broadening our knowledge about phenomena such as superconductivity, magnetism, electrical transport, and physics of low dimensional electron systems is relevant to DOE energy security mission, and ultimately National Security, by providing the scientific base for next generation energy efficient technologies.

References

1. Damascelli, A.. Probing the electronic structure of complex systems by ARPES. 2004. *Physica Scripta.* **T109**: 61.

2. Cardona, M., and L. Ley. Introduction [to `Photoemission in solids']. 1978. In *Introduction [to `Photoemission in solids'].* , p. 1.

3. Feuerbacher, B., B. Fitton, and R. F. Willis. Introduction [to photoemission and the electronic properties of. 1978. In *Introduction [to photoemission and the electronic properties of.* , p. 1.

4. Grioni, M.. Special issue: Strongly correlated systems - Foreword. 2001. *Journal of Electron Spectroscopy and Related Phenomena.* **117**: IX.

5. Dagotto, E.. Complexity in strongly correlated electronic systems. 2005. *Science.* **309** (5732): 257.

6. Mathur, N. D., F. M. Grosche, S. R. Julian, I. R. Walker, D. M. Freye, R. K. Haselwimmer, and G. G. Lonzarich. Magnetically mediated superconductivity in heavy fermion compounds. 1998. *Nature.* **394** (6688): 39.

7. Coleman, P.. The Lowdown on Heavy Fermions. 2010. *Science.* **327** (5968): 969.

8. Bostwick, A., T. Ohta, T. Seyller, K. Horn, and E. Rotenberg. Quasiparticle dynamics in graphene. 2007. *Nature Physics.* **3** (1): 36.

9. Bostwick, A., T. Ohta, J. L. McChesney, T. Seyller, K. Horn, and E. Rotenberg. Band structure and many body effects in graphene. 2007. *European Physical Journal - Special Topics.* **148**: 5.

10. Haight, R.. Photoemission with laser-generated harmonics tunable to 80 eV. 1996. *Applied Optics.* **35** (33): 6445.

11. Mathias, S., M. Wiesenmayer, F. Deicke, A. Ruffing, L. Miaja-Avila, M. M. Murnane, H. C. Kapteyn, M. Bauer, and M. Aeschlimann. Time and angle resolved photoemission spectroscopy using femtosecond visible and high-harmonic light. 2009. In *63rd Yamada Conference on Photo-Induced Phase Transition and Cooperative Phenomena (PIPT3) ; 20081111 - 20081115 ; Osaka, JAPAN.* Vol. 148, p. 012042.

12. Mathias, S., L. Miaja-Avila, M. M. Murnane, H. Kapteyn, M. Aeschlimann, and M. Bauer. Angle-resolved photoemission spectroscopy with a femtosecond high harmonic light source using a two-dimensional imaging electron analyzer. 2007. *Review of Scientific Instruments.* **78** (8): 083105.

13. Dakovski, G. L., Y. Li, T. Durakiewicz, and G. Rodriguez. Tunable ultrafast XUV source for time- and angle-resolved photoemission spectroscopy. 2010. *Review of Scientific Instruments.* **81** (7): 073108.

14. Oppeneer, P. M., J. Rusz, S. Elgazzar, M. T. Suzuki, T. Durakiewicz, and J. Mydosh. Electronic structure theory of the hidden order material URu2Si2. To appear in *Physical Review B.*

15. Li, Y., T. Durakiewicz, J. J. Joyce, and K. Graham. Electronic structure of URu2Si2 from ARPES. *Journal of Physics: Conference Series, Strongly Correlated Electron Systems (SCES) Conference 2010.*

16. An, Y. Q., A. J. Taylor, S. D. Conradson, T. Durakiewicz,

S. A. Trugman, and G. Rodriguez. Ultrafast hopping dynamics of 5f electrons in the Mott insulator UO2 studied by femtosecond pump-probe spectroscopy. *Physical Review Letters..*

17. An, Y. Q., A. J. Taylor, and G. Rodriguez. Pump-probe reflectivity study of ultrafast dynamics of strongly correlated 5f electrons in UO2. *Journal of Physics: Conference Series, Strongly Correlated Electron Systems (SCES) 2010 .*

18. An, Y. Q., A. J. Taylor, T. Durakiewicz, and G. Rodriguez. Probing ultrafast dynamics of 5f electrons in crystalline UO2. To appear in *Ultrafast Phenomena XVII, Proceedings of the 16th International Conference on Ultrafast Phenomena.* (Snowmass, CO USA, 18-23 Jul. 2010).

19. Tao, J., and J. X. Zhu. Theory of the time-resolved spectral function of high-temperature superconductors with bosonic modes. 2010. *Physical Review B.* **81** (22): 224506.

Publications

An, Y. Q., A. J. Taylor, S. D. Conradson, S. A. Trugman, T. Durakiewicz, and G. Rodriguez. Ultrafast hopping dynamics of 5f electrons in the Mott insulator UO2 studied by femtosecond pump-probe spectroscopy. *Physical Review Letters.*

An, Y. Q., A. J. Taylor, T. Durakeiwicz, and G. Rodriguez. Ultrafast dynamics of photoexcited 5f electrons in the Mott insulator UO2. Presented at *American Physical Society March Meeting 2010.* (Potland, OR, USA, 15-19 Mar. 2010).

An, Y. Q., A. J. Taylor, T. Durakeiwicz, and G. Rodriguez. Pump-probe reflectivity study of ultrafast dynamics of strongly correlated 5f electrons in UO2. Presented at *International Conference on Strongly Correlated Electron Systems 2010.* (Santa Fe, NM, USA, 27 Jun. - 2 Jul. 2010).

An, Y. Q., A. J. Taylor, T. Durakiewicz, and G. Rodriguez. Probing ultrafast dynamics of 5f electrons in crystalline UO2. To appear in *Ultrafast Phenomena XVII, Proceedings of the 17th International Conference on Ultrafast Phenomena.* (Snowmass, CO, USA, 18-23 Jul. 2010).

An, Y. Q., A. J. Taylor, and G. Rodriguez. Pump-probe reflectivity study of ultrafast dynamics of strongly correlated 5f electrons in UO2. *Journal of Physics: Conference Series, International Conference on Strongly Correlated Electron Systems 2010.*

Dakovski, G. L., Y. Li, T. Durakiewicz, and G. Rodriguez. High-harmonic XUV source for time- and angle-resolved photoemission spectroscopy. Presented at *Ultrafast Optics (UFO VII) and High Field Short Wavelength (HFSW XIII) Conference 2009.* (Arcachon, France, 31 Aug. - 4 Sep. 2009).

Dakovski, G. L., Y. Li, T. Durakiewicz, and G. Rodriguez. Tunable high-harmonic source for time- and angle-resolved photoemission spectroscopy. Presented at *37th International Conference on Vacuum Ultraviolet and X-ray Physics.* (Vancouver, Canada, 11 - 16 Jul. 2010).

Dakovski, G. L., Y. Li, T. Durakiewicz, and G. Rodriguez. Tunable ultrafast XUV source for time- and angle-resolved photoemission spectroscopy. 2010. *Review of Scientific Instruments.* **81** (7): 073108.

Durakiewicz, T.. Quest for band renormalization and self-energy in correlated f-electron systems. Presented at *Meeting of the Polish Synchrotron Society.* (Podlesice, Poland, 24-26 Sept, 2009).

Durakiewicz, T.. Band renormalization and kink structures in correlated f-electron systems. Presented at *International Workshop on the Dual Nature of f-Electrons.* (Dresen, Germany, 24-7 May 2010).

Durakiewicz, T.. Band renormalization in f electron systems - novel findings from ARPES. Presented at *9th Prague Colloquium on f-Electron Systems.* (Prague, Czech Republic, 31 May - 3 Jun. 2010).

Durakiewicz, T.. Band renormalization and kink structure in correlated f-electron materials. Presented at *2009 North American Calorimetry Conference.* (Santa Fe, NM, USA, 28 Jun. - 2 Jul. 2010).

Durakiewicz, T.. Band renormalization and kink structures in correlated f-electron systems. Presented at *The 23rd General Conference of the Condensed Matter Division of the European Physical Society 2010.* (Warsaw, Poland, 30 Aug. - 3 Sep. 2010).

Durakiewicz, T., P. S. Riseborough, C. D. Batista, Y. F. Yang, P. M. Oppeneer, J. J. Joyce, E. D. Bauer, and K. S. Graham. Quest for band renormalization and self-energy in correlated f-electron systems. 2010. *Acta Physica Polonica A.* **117** (2): 264.

Durakiewicz, T., P. S. Riseborough, C. G. Olson, J. J. Joyce, E. Bauer, J. L. Sarrao, S. Elgazzar, P. M. Oppeneer, E. Guziewicz, D. P. Moore, M. T. Butterfield, and K. S. Graham. Observation of a kink in the dispersion of f-electrons. 2008. *Europhysics Letters.* **84** (3): 3003.

Durakiewicz, T., P. S. Riseborough, C. G. Olson, J. J. Joyce, P. M. Oppeneer, S. Elgazzar, E. D. Bauer, J. L. Sarrao, E. Guziewicz, D. P. Moore, M. T. Butterfield, and K. S. Graham. Kink in the dispersion of f-electrons. Presented at *American Physical Society March Meeting 2009.* (Pitts-

burgh, PA, USA, 16-20 Mar. 2009).

Durakiewicz, T., P. S. Risebourough, C. G. Olson, J J. Joyce, Y. Li, P. M. Oppeneer, S. Elgazzar, E. D. Bauer, J. L. Sarrao, E. Guziewicz, D. P. Mpore, M. T. Butterfield, and K. S. Graham. Kinks in the dispersion of f-electrons: first results from ARPES. To appear in *Actinides 2009 Conference Proceedings.* (San Francisco, CA, USA, 12-17 Jul. 2009).

Durakiewicz, T., Y. Li, P. S. Riseborough, P. M. Oppeneer, J. J. Joyce, E. D. Bauer, and K. S. Graham. Near-Fermi level band renormalization effects in f electron systems. Presented at *American Physical Society March Meeting 2010..* (Portland, OR, USA, 15-19 Mar. 2010).

Durakiewicz, T., Y. Li, P. S. Riseborough, P. M. Oppeneer, J. J. Joyce, E. D. Bauer, and K. S. Graham. Band renormalization and self energy in correlated f-electron systems. Presented at *International Conference on Strongly Correlated Electron Systems 2010.* (Santa Fe, NM, USA, 28 Jun. - 2 Jul. 2010).

Kim, K. Y., A. J. Taylor, J. H. Glownia, and G. Rodriguez. Coherent control of THz supercontinuum generation in ultrafast laser-gas interactions. 2008. *Nature Photonics.* **2** (10): 605.

Li, Y., G. Dakovski, T. Durakiewicz, G. Rodriguez, and K. S. Graham. Table-top femtosecond ultrafast time resolvable ARPES facility at LANL. Presented at *American Physical Society March Meeting 2010.* (Portland, OR, USA, 1-19 Mar. 2010).

Li, Y., T. Durakiewicz, J. J. Joyce, P. Tobash, E. D. Bauer, and K. S. Graham. Electronic structure of URu2Si2 from ARPES. Presented at *International Conference on Strongly Correlated Electron Systems 2010.* (Sana Fe, NM, USA, 28 Jun. - 2 Jul. 2010).

Prasankumar, R. P., S. G. Choi, G. T. Wang, S. T. Picraux, and A. J. Taylor. Ultrafast carrier dynamics in semiconductor nanowires. 2009. In *Proceedings of the 16th International Conference on Ultrafast Phenomena.* (Stresa, Italy, 9-13 Jun. 2008). , p. 271. New York: Springer.

Prasankumar, R. P., S. G. Choi, G. T. Wang, S. T. Picraux, and A. J. Taylor. Ultrafast carrier dynamics in semiconductor nanowires. Invited presentation at *Conference on Lasers and Electro-Optics.* (San Jose, CA, USA, 4-9 May 2008).

Prasankumar, R. P., S. G. Choi, S. A. Trugman, S. T. Picraux, and A. J. Taylor. Ultrafast electron and hole dynamics in Germanium nanowires. 2008. *Nano Letters.* **8** (6): 1619.

Rodriguez, G., and K. Y. Kim. THz supercontinuum generation in gas filaments: ‘current ‘ perspective and applications. Invited presentation at *Second International Symposium on Filamentation.* (Paris, France, 22-25 Sep. 2008).

Tao, J., and J. X. Zhu. Theory of the time-resolved spectral function of high-temperature superconductors with bosonic modes. 2010. *Physical Review B.* **81** (22): 224506.

Trugman, S. A.. Quasiparticles, dynamics, and coupled nanowires. Presented at *XXXIII International Workshop on Condensed Matter Theories.* (Quito, Ecuador, 16-22 Aug. 2009).

Yang, X., P. S. Riseborough, T. Durakiewicz, P. M. Oppeneer, and S. Elgazzar. Effect of Electronic Correlations on the Quasiparticle Dispersion of USb2. 2010. *Journal of Physics: Conference Series, International Conference on Magnetism 2009.* **200**: 012164.

Yang, X., P. S. Risebourough, T. Durakiewicz, C. G. Olson, J. J. Joyce, E. D. Bauer, J. L. Sarrao, D. P. Moore, K. S. Graham, S. Elgazaar, P. Oppeneer, E. Guziewicz, and M. T. Butterfield. Unusual quasiparticle renormalizations from angle resolved photoemission on USb2. 2009. *Philosophical Magazine.* **89** (22-24): 1893.

Advanced Fuel Forms with Microstructures Tailored to Naturally Induce Fission Product Separation During Service

Kurt E. Sickafus
20080114DR

Abstract

The objective of our project was to investigate key scientific and technological issues underpinning the design of a revolutionary nuclear fuel form possessing desirable attributes of conventional nuclear fuel (i.e., uranium oxide fuel), but with a tailored microstructure that radically eases separation of fission products, drastically reduces separation costs, and substantially mitigates proliferation risks of the separated material. Our advanced nuclear fuel design is based on a *dispersion fuel* concept (i.e., two separate solid phases co-existing in one solid body). The goal of this project was NOT to develop a dispersion fuel form that could be readily licensed by the Nuclear Regulatory Commission (NRC). Rather, our goal was to develop the underpinning science to facilitate more rapid evaluation and acceptance of new, advanced fuel forms such as dispersion fuels, which are not currently used in commercial (light-water) nuclear reactors. This supports the overarching mission of the Department of Energy (DOE): "to advance the national, economic, and energy security of the United States and to promote scientific and technological innovation in support of this mission." Our project promotes a designed merger of two portions of the nuclear fuel cycle: (*i*) fuel burning and (*ii*) fuel reprocessing (these ordinarily are managed independently).

Background and Research Objectives

When nuclear reactor fuel such as uranium dioxide (UO_2) burns in a nuclear reactor, it produces heat that is converted to electricity. The heat is derived from nuclear *fission* reactions, wherein a fissionable isotope of uranium, usually ^{235}U, captures a neutron and then transmutes to form a variety of energetic particles and radiation. Two of the particles formed by fission of ^{235}U are atomic nuclei with masses of about 95 and 139 atomic mass units (amu). These atomic particles are known as *fission products*. Very often these fission products are radioactive and herein lies the problem with nuclear energy: these radioactive fission products (which cannot undergo further fissioning to produce additional energy) are classified as radioactive waste and destined for disposal in a geological repository.

Unfortunately, fission is an inefficient process and a large concentration (several atom percent) of "burnable" actinides remain in *spent nuclear fuel* (SNF) at fuel "end-of-life".[1] An engineering challenge is to chemically remove these burnable actinides from SNF. The process typically used to do this is known as aqueous "reprocessing." Aqueous reprocessing is expensive and leads to significant waste (both wet and dry) compared to unprocessed. SNF. But what if it were possible to produce a fuel form that burned in such a way that the actinides (An) and fission products (FPs) segregated within the fuel so that they could be readily separated from one another? If this were possible, this natural, in-service separations strategy would greatly reduce both technological challenges and costs compared to conventional reprocessing. This is the concept that we set out to investigate over the course of our project.

The objective of our project was to design a nuclear fuel form possessing the desirable attributes of conventional nuclear fuel (UO_2), but with a tailored microstructure that makes it easier to separate FPs from residual An species. Our strategy to achieve this was to develop a *composite* nuclear fuel, i.e., a fuel with two phases, one an An-bearing phase (such as UO_2), the other a non-fertile, inert matrix phase. Composite materials are designed to combine the good properties of each of the constituent phases. For instance, it was recently proposed to produce a composite inert matrix fuel by combining the oxide zirconia (ZrO_2) that is compatible with An species and has excellent radiation stability but poor thermal conductivity, with the oxide magnesia (MgO), which is not compatible with An species but has superior thermal conductivity [1]. In our case, we proposed to disperse small particles of an An-bearing "kernel" phase in a matrix phase that is compatible with FPs. The idea is that if the An kernel particles are small enough, the FP species born upon neutron-induced transmutation of ^{235}U will have sufficient energy to escape the kernel particles and come to rest in the matrix phase. Thus, the FPs and the residual An are spatially separated during the burning process. With appropriate selection of kernel

and matrix phases in this "dispersion" fuel, it should then be possible to separate these two phases once the fuel completes its reactor service.

Scientific Approach and Accomplishments

In the course of our project, we performed three types of experiments: (1) composite sample synthesis; (2) irradiation tests on composite samples; and (3) characterization of composite samples structure and properties, before and after irradiation. The purpose of the irradiation tests was to assess the relative durability of composite materials in extreme environments. Relatively little is known about the behavior of composites in energetic particle environments (neutrons, ions, electrons, gamma rays), such as the environment in a nuclear reactor core. Also, conventional nuclear fuel burns at a high temperature (1000°C or more). At such high temperatures, atomic constituents of fuel, such as FPs and An species, can migrate and redistribute. This has implications for our dispersion fuel separations strategy. Thus, much of our project was devoted to developing a high-temperature irradiation capability in order to examine chemical and microstructural evolution in model composite materials exposed to extreme conditions (high temperature and high radiation environments). Before describing our irradiation experiments, we first describe the model composite materials that we fabricated during this project.

Our composite synthesis experiments involved fabricating three types of samples: (1) bulk ceramic composite samples, produced by conventional powder ceramic processing; (2) thin film multilayer ceramic composite samples; and (3) spherical particle synthesis as kernels for a dispersion fuel.

For bulk ceramic composites, we fabricated the following the following ceramic-ceramic (CERCER) composites: (1) MgO-UO_2; (2) MgO-CeO_2; and (3) MgO-HfO_2. We used "depleted" uranium, i.e., uranium highly enriched in ^{238}U, in the MgO-UO_2. The MgO was intended to represent an inert matrix with relatively high thermal conductivity. The ceria (CeO_2) and hafnia (HfO_2) were isostructural surrogates for an An-bearing fuel kernel such as UO_2. We varied the volume fraction of the constituent oxides in these composites over a wide range, though the samples most closely approximating a dispersion fuel contained MgO as the majority phase and UO_2, CeO_2, or HfO_2 as the minority phase. Select microstructures obtained in these bulk composite synthesis experiments are shown in Figure 1. We also prepared two ceramic-metal (CERMET) composites on this project: NiAl-UO_2 and NiAl-CeO_2. The nickel-aluminide (NiAl) was used as a matrix phase with very high thermal conductivity and high temperature stability. These bulk ceramic composite samples allowed us to test composite stability under high temperature/high radiation conditions. However, these samples did not meet the dispersion fuel criterion of small kernel size described in the previous section. The kernel particles in our bulk ceramic composites tended to be quite large, ranging from 10 – 100 μm in diameter. The particles also tended to aggregate.

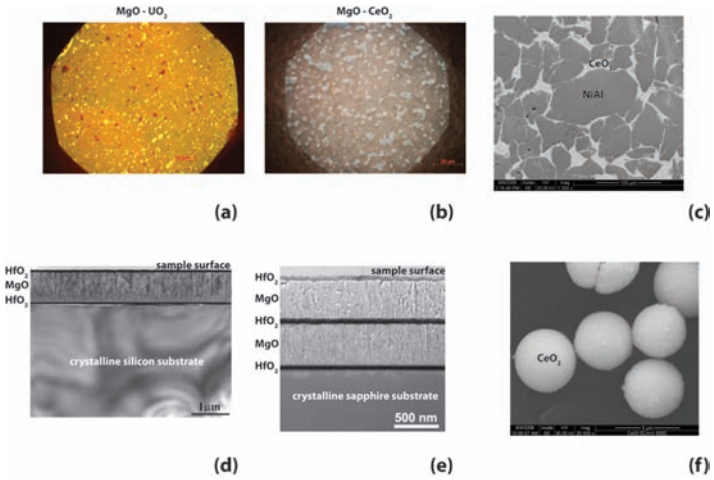

Figure 1. Various pristine samples produced during the course of this project. (a) optical micrograph, MgO/UO_2 (UO_2 light phase); (b) optical micrograph, MgO/CeO_2 (CeO_2 light phase); (b) scanning electron micrograph, NiAl/CeO_2 (CeO_2 light phase); (c) cross-sectional transmission electron micrograph, HfO_2/MgO/HfO_2/Si tri-layer (HfO_2, thin dark layers); (d) cross-sectional transmission electron micrograph, HfO_2/MgO/HfO_2/MgO/HfO_2/Al_2O_3 penta-layer (HfO_2, thin dark layers); (e) scanning electron micrograph, CeO_2 particles.

For thin film ceramic composites, we fabricated both 3-layer and 5-layer thin films on substrates such as silicon (Si) and sapphire (Al_2O_3). Most of our thin film work was devoted to the following two architectures: (1) HfO_2 / MgO / HfO_2 / Si (substrate) tri-layer thin films; and (2) HfO_2 / MgO / HfO_2 / MgO / HfO_2 / Al_2O_3 (substrate) penta-layer thin films (Figure 1). As with the bulk composite samples, the HfO_2 in these thin film multilayer samples was intended to serve as a surrogate for UO_2. The HfO_2 layers were made very thin (~50-70 nm), while the MgO layers were made thick (~500-900 nm). We used this design so that if FPs were born inside the HfO_2 "kernel" layers (assuming fission events were possible), they would have a high probability of escaping the HfO_2 and being deposited within the MgO layers. This was an attempt to simulate small kernel particles in a dispersion fuel, though here we were using a planar, "plate-like" composite geometry.

For the spherical particle synthesis, of the methods and recipes we explored, the best for achieving micron size particles was a spray method. This method allowed us to achieve small (≤ 5 μm diameter) spheres of CeO_2 (Figure 1). Once again, the CeO_2 was intended to serve as a surrogate for UO_2. In the spray method, we begin with an aqueous solution of $Ce(NO_3)_3$. This solution is atomized with a 120 kHz ultra sonic nozzle and directed into a solution of 2-ethyl-hexanol and ethyl acetate (4:1) with a few percent NH_3. Under these condition $Ce(OH)_3$ is precipitated within the droplets. Heating in air results in decomposition with

all the weight loss occurring below 300°C. The particles shown in Figure 1 were calcined at 600 °C for 1 hour. To use these particles in a dispersion fuel application, they must be combined with a non-fissile matrix material. This will likely be achieved using a conventional ceramic powder processing procedure, but this was not attempted during the course of this project.

To test composite sample stability under extreme conditions (high temperature, high radiation field), we performed ion beam irradiations at high temperature in the Ion Beam Materials Laboratory (IBML) at Los Alamos National Laboratory (LANL). For these experiments, we designed and built a new, high-temperature ion beam irradiation chamber and installed it on a dedicated beamline in the IBML (Figure 2). The source of ions for these experiments was a 3.2 MV NEC Tandem accelerator. Using this accelerator, we produced beams of highly-energetic, 10 MeV gold (Au) ions and implanted them into our composite samples (either bulk or thin film). During ion implantation, these composite substrates were held at temperatures ranging from 90 K to 800 °C.

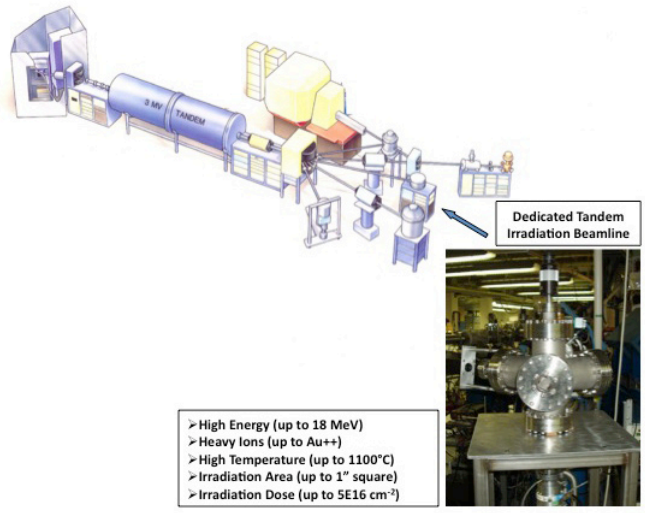

Figure 2. Schematic diagram showing the 3 MV Tandem Ion Accelerator in the IBML at LANL, as well as the dedicated beamline for high-energy / high-temperature ion irradiations. Also shown is a photograph of the high-temperature end-station completed during the course of this project.

Figure 3 shows a typical composite microstructure following a 10 MeV Au ion irradiation to an ion fluence of $5x10^{15}$ Au/cm^2. This is considered a rather large ion dose. Thus, this experiment should be considered as a test of the composite's ability to resist radiation damage. The sample in Figure 3 is an HfO_2 / MgO / HfO_2 / Si tri-layer thin film sample. This image was obtained using transmission electron microscopy (TEM). The image shows the oxide layers in "cross-section," i.e., viewed with the electron beam oriented parallel to the thin layers. Our TEM image analyses, along with additional characterization results obtained from the same sample using grazing incidence X-ray diffraction (GIXRD), indicate that the HfO_2 and MgO layers are not significantly degraded by the ion irradiation. The layers are crystalline following irradiation, and the grains in the microstructure are similar in appearance to how they looked before irradiation. By contrast, the silicon substrate is significantly affected by the irradiation, in the sense that the image in Figure 3 shows that the part of the Si substrate exposed to Au ions has completely *amorphized* at this dose. These results suggest that a composite made from oxides MgO and HfO_2 will be relatively stable against detrimental microstructural changes induced by radiation damage.

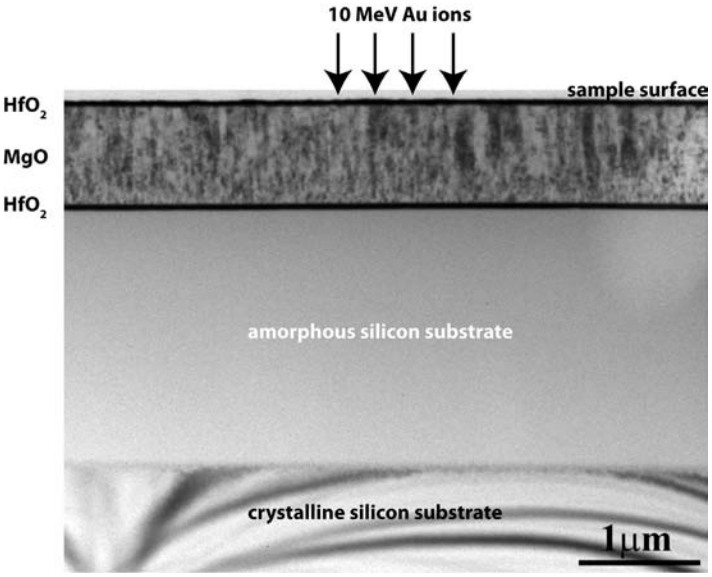

Figure 3. Cross-sectional transmission electron micrograph showing the microstructure of an HfO_2/MgO/HfO_2/Si tri-layer following ion irradiation with 10 MeV Au+ ions to a fluence of 5x1015 Au/cm2 (irradiation performed at room temperature).

During the course of this project, we also performed experiments and computer modeling studies regarding the thermodynamic stability and mobility of FPs in the constituent phases of various two-phase composite materials. The experiments that we performed involved implanting various FP species, such as strontium (Sr), xenon (Xe) and krypton (Kr) into thin film bi-layer samples, such as MgO/HfO_2. We then post-annealed these samples to allow redistribution of the FPs within the bi-layer microstructures of these samples. Unfortunately, the migration of FPs during these experiments was far too complicated to be analyzed in any meaningful way. One recommendation from our project is that future studies of FP behavior in composite nuclear fuel forms must involve systematic studies using very carefully-designed experiments.

We also performed density functional theory (DFT) calculations of FP stability in oxide phases such as MgO, CaO, SrO, BaO, UO_2, HfO_2, CeO_2, and ZrO_2. We found that the solution energies for placing various FPs such as Xe, Cs, and

Sr, in an oxide matrix varies significantly depending on the oxide. This further substantiates our thesis that we may be able to design a dispersion fuel in which FPs preferentially segregate to an inert matrix phase (a phase where the FPs are thermodynamically more stable than in the An kernel phase. This is illustrated in Figure 4 where we show FP solution energies for Xe, Cs, and Sr in four different alkaline earth oxides (MgO, CaO, SrO, and BaO) compared to hafnia (HfO_2). It is apparent in Figure 4 that the energy cost to place either Xe or Cs in an alkaline earth oxide decreases with increasing alkaline earth cation ionic size ($Mg^{2+} \rightarrow Ca^{2+} \rightarrow Sr^{2+} \rightarrow Ba^{2+}$. In fact, for Xe, the solution energies in SrO and BaO are significantly lower than in HfO_2. So, we expect that SrO and BaO should be effective "getters" for Xe, were these oxides to be used as inert matrices in a dispersion fuel.

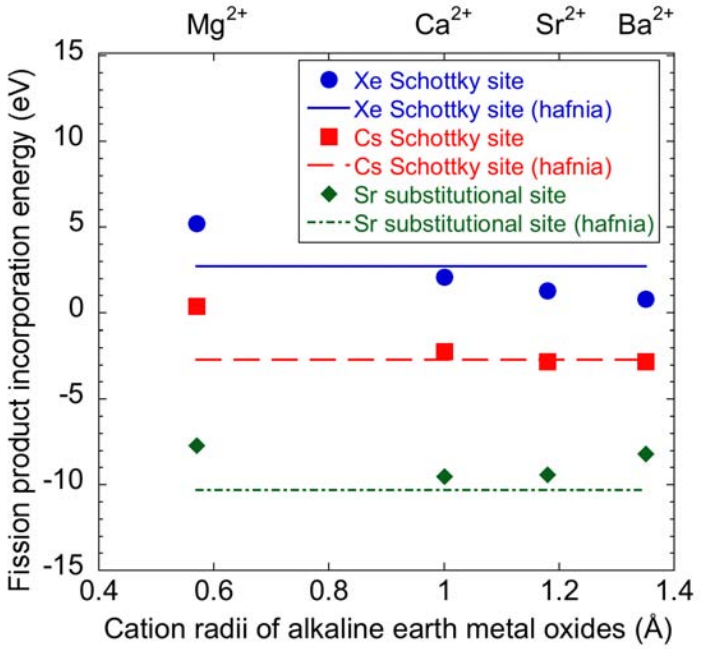

Figure 4. Xe, Cs, and Sr incorporation energies in alkaline earth oxides, in comparison with HfO_2.

This project produced 16 publications (11 published, 5 submitted or in press). Eight of our publications are devoted to theory, the other 8 to experiments. We had one patent awarded (Patent Pending (DOE docket # S-116, 249), New Generation Nuclear Fuel Structures: Dense Particles In Selectively Soluble Matrix) and one additional patent disclosure (Los Alamos Disclosure # LAD-10-181, Coatings Resistant to Irradiation Induced Swelling).

Impact on National Missions

This project supports the DOE mission for Energy Security, especially the DOE overarching mission: "to advance the national, economic, and energy security of the Unites States and to promote scientific and technological innovation in support of this mission." This project has led to two new projects that will be funded in fiscal year 2011 (FY-11). One project, "High burn-up ceramic composite fuel" is a direct outgrowth of our LDRD-DR project and will be funded by the Office of Nuclear Energy (NE), Fuel Cycle Research & Development (FCR&D) Program. The initial funding expected on this project is $600 K for FY-11. The second project, "A novel method for incorporating fission gas elements into solids," is the subject of a patent disclosure that we submitted near the end of our LDRD-DR project. Figure 5 shows the concept of this patent disclosure and this new project. We propose to use Ion Beam Assisted Deposition (IBAD) to implant FPs (Xe in the example shown in Figure 5) into thin oxide films, while the oxide films are being deposited (deposited by electron beam evaporation in the example shown in Figure 5). Following thin film synthesis, we will then anneal the samples at high temperature and study FP redistribution and segregation. We believe that this will be a revolutionary way to investigate FP behavior in advanced fuel forms. This new project will also be sponsored by NE-FCR&D. We anticipate funding in FY-11 of about $200 K. These new projects will be led by new, young technical staff members at LANL, particularly Drs. Igor Usov and Jonghan Won.

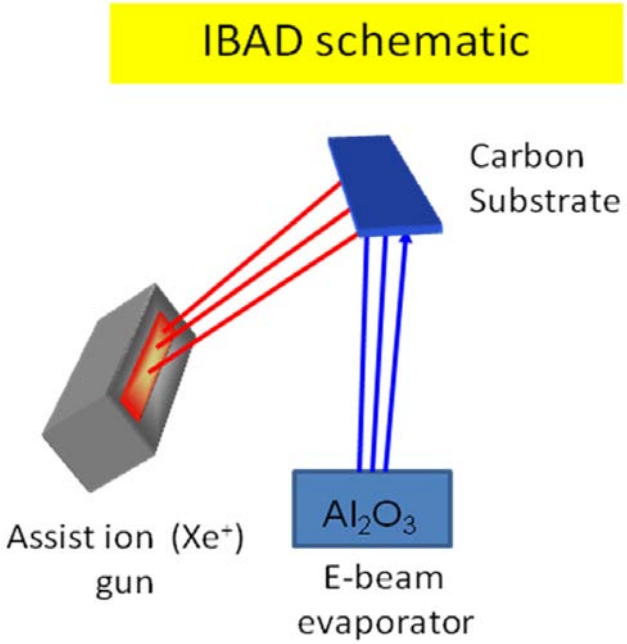

Figure 5. Schematic diagram showing electron beam thin film deposition of alumina (Al_2O_3) onto a carbon (C) substrate, while simultaneously implanting xenon (Xe) ions into the growing thin Al_2O_3 film. This process is known as Ion Beam Assisted Deposition or IBAD.

References

1. Medvedev, P. G., S. M. Frank, T. P. O,ÄôHolleran, and M. K. Meyer. Dual phase MgO-ZrO2 ceramics for use in LWR inert matrix fuel. 2005. *JOURNAL OF NUCLEAR MATERIALS.* **342** (1-3): 48.

Publications

Devlin, D. J., G. D. Jarvinen, B. Patterson, S. Pattillo, J. A. Valdez, X. Y. Liu, and J. Phillips. New generation nuclear fuel structures: dense particles in selectively soluble matrix. 2009. *Journal of Nuclear Materials.* **394**: 190.

Hawley, M. E., D. J. Devlin, C. J. Rechhardt, K. E. Sickafus, I. O. Usov, J. A. Valdez, and Y. Q. Wang. AFM characterization of model nuclear fuel oxide multilayer structures modified by heavy ion beam irradiation. 2010. *Nuclear Instruments and Methods in Physics Research B.* **268**: 3269.

Jeon, B., M. Asta, S. M. Valone, and N. Gronbech-Jensen. Simulation of ion-track ranges in uranium dioxide. 2010. *Nuclear Instruments and Methods in Physics Research Section B.* **268**: 2688.

Jeon, B., and N. Gronbech-Jensen. Efficient parallel algorithm for statistical ion track simulations in solids. 2009. *Computer Physics Communications.* **180**: 231.

Jiang, C., X. -Y. Liu, and K. E. Sickafus. First principles prediction of thermodynamic stability of xenon in monoclinic, tetragonal, and yttrium stabilized cubic zirconia. *Physical Review B.*

Liu, X. -Y., B. P. Uberaga, A. D. Andersson, C. R. Stanek, and K. E. Sickafus. New mechanism for transient migration of xenon in UO2. *Applied Physics Letters .*

Liu, X. -Y., B. P. Uberuaga, and K. E. Sickafus. First-principles study of fission product (Xe, Cs, Sr) incorporation and segregation in alkaline earth metal oxides, HfO2, and the MgO-HfO2 interface. 2009. *Journal Of Physics: Condensed Matter.* **21**: 45403.

Liu, X. Y., B. P. Uberuaga, P. V. Nerikar, and C. R. Stanek. Thermodynamics of fission products in dispersion fuel designs - first-principles modeling of defect behavior in bulk and at interfaces. 2010. *Nuclear Instruments and Methods in Physics Research B.* **268**: 3014.

Liu, X. Y., and K. E. Sickafus. Lanthanum energetics in cubic ZrO2 and UO2 from DFT and DFT+U studies. *Journal of Nuclear Materials.*

Nerikar, P. V., X. Y. Liu, B. P. Uberauga, C. R. Stanek, S. R. Phillpot, and S. B. Sinnott. Thermodynamics of fission products in UO2±x. 2009. *Journal of Physics: Condensed Matter.* **21**: 435602.

Usov, I. O., J. A. Valdez, J. Won, D. J. Devlin, and K. E. Sickafus. Medium energy ion irradiation capability for studies of radiation damage effects over a wide temperature range. *Journal of Nuclear Materials.*

Usov, I. O., J. A. Valdez, J. Won, M. E. Hawley, D. J. Devlin, R. M. Dickerson, B. P. Uberuaga, C. J. Olson Reichhardt, G. D. Jarvinen, and K. E. Sickafus. Irradiation effects in an HfO2/MgO/HfO2 tri-layer structure induced by 10 MeV Au ions. 2009. *Nuclear Instruments and Methods in Physics Research B.* **267**: 1918.

Usov, I. O., J. Won, D. J. Devlin, Y. -B. Jiang, J. A. Valdez, and K. E. Sickafus. A novel method for incorporating fission gas elements into solids. *Journal of Nuclear Materials.*

Usov, I. O., J. Won, J. A. Valdez, M. E. Hawley, D. J. Devlin, G. D. Jarvinen, and K. E. Sickafus. Radiation damage effects in layered thin film MgO/HfO2 structures. 2010. *Nuclear Instruments and Methods in Physics Research B.* **268**: 3044.

Valdez, J. A., I. O. Usov, J. Won, M. Tang, R. M. Dickerson, G. D. Jarvinen, and K. E. Sickafus. 10 MeV Au ion irradiation effects in an MgO-HfO2 ceramic-ceramic (CERCER) composite. 2009. *Journal of Nuclear Materials.* **393**: 126.

Valone, S. M., B. P. Uberuaga, X. Y. Liu, B. Jeon, A. Chaudhry, and N. Gronbech-Jensen. Cascade-driven mixing at metal oxide interfaces. 2010. *Nuclear Instruments and Methods in Physics Research B.* **268**: 3114.

Molecular Scale Shock Response of Explosive1

Shawn D. Mcgrane
20090186ER

Introduction

The initial events that occur upon shock loading explosives are crucial in determining the sensitivity of the material. Various theories have been proposed regarding the reaction mechanisms, but there are few experiments to test them. This project develops experiments sensitive to the time and length scales needed to observe chemical kinetics in shocked explosives.

Our measurements look into a shocked explosive at time scales of a millionth of a millionth of a second (a picosecond, or ps) and length scales 100 times smaller than a human hair. By making direct measurements of the energy flow at the molecular level, mechanistic insights can be obtained that will impact modeling and optimization of explosive safety and performance.

The state of the art experimental developments in optical measurement of ultrafast phenomena in materials have many scientific applications. These techniques are expected to impact fields such as energy sciences (photovoltaics) and matter under extreme conditions (such as material testing of power plant alloys). These small-scale custom experiments have been developed into a world-class ultrafast shock physics laboratory, illustrated in Figure 1.

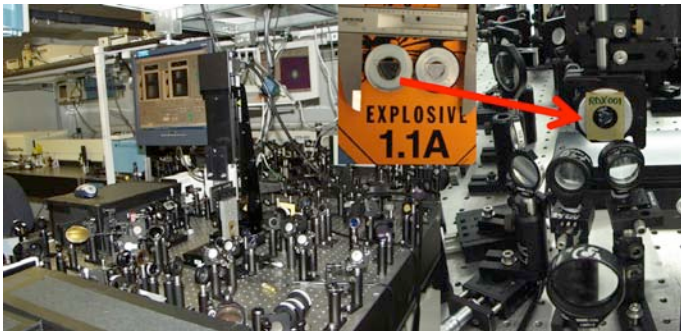

Figure 1. The ultrafast shock experiment allows testing and introduction of numerous diagnostics that allow observation of shock dynamics in explosives, such as the ~ 1 cm RDX crystal shown, on molecular time scales.

Benefit to National Security Missions

This project supports the Department of Energy (DOE) mission in Nuclear Weapons by enhancing our knowledge of explosive issues important to the aging stockpile. This project supports Department of Defense (DoD) missions that require better predictions and optimization of explosive behavior. DOE Office of Science missions are supported through development of new ultrafast laser methods.

Progress

We have observed strong broadband (<400 to >850 nm) shock induced absorptions in single crystals of the explosives PETN and RDX shocked to 23 gigapascal, or GPa (230,000x atmospheric pressure) and the explosive polymer polyvinylnitrate shocked to 17 GPa. Sample data are shown in Figure 2. These data are the first experimental indications of chemical reactions occurring on these time scales in explosive crystals. Further work is needed to definitively identify the origin of the absorptions; these studies were planned in the original work proposal and will be completed in the final year of the project.

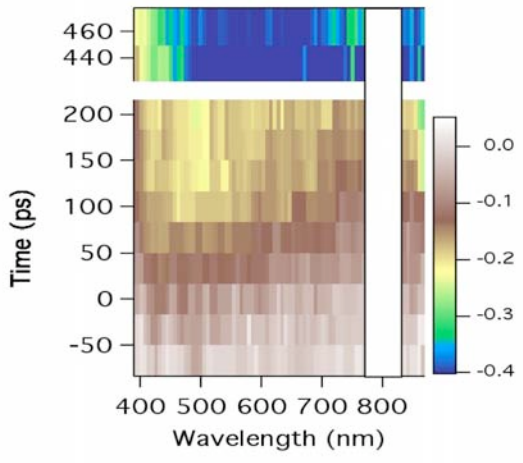

Figure 2. An explosive crystal of RDX is transparent in the visible wavelength region, but becomes absorbing in less than half a nanosecond when shocked to 230,000 times atmospheric pressure.

A second experimental thrust to develop a picosecond temperature measurement in condensed phase materials has come to fruition. The first data establishing the validity of this new technique have been acquired and a publication is in preparation. We have produced data verifying that the measurement of temperature jumps can performed with picosecond temporal resolution. This is the first time this method has been used for temperature measurement, and the technique should have broad ranging applications.

The progress of this project has led to the acceptance or publication or four peer reviewed conference publications and a peer reviewed journal publication is in press. The results to date have been presented at five international conferences and three domestic meetings. Two international and three domestic collaborations have grown from the work funded under this project.

Future Work

The goals of this project are to experimentally address fundamental underpinnings of explosive initiation and detonation physics. Achieving these goals involves advancement of experimental measurement and analysis beyond the current state of the art. These advances are expected to have broad scientific applicability- the development of which is a corollary goal of the project.

The project has a clear path forward for continuing experiments through the remainder of the timeline. Diagnostics of shock-induced chemistry will be added to confirm the interpretation of the transient absorption data. PETN (explosive) thin films obtained from Sandia National Laboratory will be used for this effort. Studies as a function of shock drive stress will be performed to look for mechanistic changes.

Conclusion

Explosives are composed of molecular crystals that undergo extremely fast reaction once stimulated by shock or heat. Understanding how explosives react to stimuli that may set off their destructive power is crucial for modeling explosive safety and performance.

The data provided in this project seeks to experimentally measure molecular scale mechanisms of reactivity in shocked explosives. These data are necessary to answer even qualitative questions regarding explosive initiation. These questions must be answered to identify the correct theoretical framework to understand, predict, and simulate explosive initiation.

Publications

McGrane, S. D., C. A. Bolme, V. H. Whitley, and D. S. Moore. Ultrafast Dynamic Ellipsometry And Spectroscopy Of Laser Shocked Materials. 2010. In *International Symposium on High Power Laser Ablation 2010 ; 18-22 April 2010 ; Santa Fe, NM, USA.* Vol. 1278, p. 392.

McGrane, S. D., D. S. Moore, V. H. Whitley, C. A. Bolme, and D. E. Eakins. MOLECULAR SHOCK RESPONSE OF EXPLOSIVES: ELECTRONIC ABSORPTION SPECTROSCOPY. 2009. In *16th Conference of the American-Physical-Society-Topical-Group on Shock Compression of Condensed Matter ; 20090628 - 20090703 ; Nashville, TN.* Vol. 1195, p. 1301.

Multifunctional Materials

James E. Gubernatis
20090187ER

Introduction

An outstanding challenge in materials science is "bridging the gaps." Materials science typically is studied at three different length scales: the macroscopic (what we see unaided), the mesocopic (what we see with conventional microscopy); and the microscopic (what we can see with sophisticated microscopy). Our understanding of materials must be consistent among the scales. Establishing this consistency however has been difficult. For a particular class of materials, the multifunctionals, we are proposing to achieve consistency in a novel way by placing the Landau phenomenological theory for the free energy, typically used at the mesoscale, at the center of our analysis and fixing as many of its unspecified parameters as possible by deriving them from microscopic theory and by measuring them experimentally. The question to be answered is: With the theory parameterized better than ever, can we predict the many phase transitions exhibited by multifunctional materials and also predict the evolution of their mesoscale structure which is so important for the design of such devices as new switches, sensors, and actuators.

Multifunctional materials are those that have cross-field responses between two (or more) applied fields. For example, in a piezoelectric material, electric polarization and strain both respond to a stress or to an electric field. Normally, stress and strain pair their responses as does electric field and polarization. It is the cross-field responses that makes the materials interesting scientifically and important technologically. Typically, a Landau phenomenology lacks such responses. Our objective in co-generating a Landau theory on the mesoscopic and microscopic scales is the assurance of "uploading" maximal information from the microscopics to mesoscopics. Such information will include these responses. Experiment plays a special role in our research. We recently developed new unique capabilities that enable the measurement of two important classes of cross-field responses, the magneto-electric and magneto-strictive responses. These measurements will enable benchmarking the theory in a way never before possible.

Benefit to National Security Missions

This project will support the DOE mission in the Office of Science by enhancing our understanding of multifunctional materials and establishing a theoretical paradigm for addressing their properties. In particular it supports the DOE Basic Energy Science program office mission for fundamental materials science research for energy independence.

Progress

We have been studying tin-tellurium as a simple manifestation of a multifunctional material. For about fifty years, it has been widely regarded as a ferroelectric and ferroelastic material whose structural phase transition involved changes between relatively simple crystal structures. Further, when small amounts of a magnetic material, such as chromium, are added, the resulting alloy becomes a ferromagnet. The prefix "ferro" in these different states of matter refers to the ability, in principle, to reverse the direction, let us say, of the magnetism, with the application of an external field, which in the case of magnetism would be a magnetic field. The ability to reverse the directions of multiple ferro-states and the coupling between these states makes the material multifunctional.

In the past, the widely accepted ferroelectricity in tin-tellurium had been inferred from indirect evidence. In the first year of the project, we kept finding that tin-tellurium behaved more like a metal (a good conductor of electricity) than a semiconductor or insulator (poor or bad conductors of electricity). Ferroelectricity cannot exist in a metal. In this project year, we executed a suite of experimental measurements, backed by theoretical calculations, to resolve this matter. We established that tin-tellurium is neither ferroelectric nor ferroelastic.

We performed the first angular-resolved photoemission spectroscopy of the electronic structure of tin-tellurium. These photoemission measurements found a Fermi surface, which is a signature of a metal, and both simple and state-of-the-art electronic structure calculations agreed with the principal features of the measured

Fermi surface topology. Figure 1 shows both a result of the experiment and of our calculations. We also performed the first piezoelectric measurements of the material. For a piezoelectric material, applying an electric field across its body changes the volume of the material and vice versa. Ferroelectricity is the spontaneous development of an electric polar state. All ferroelectrics are piezoelectric. We found no piezoelectricity.

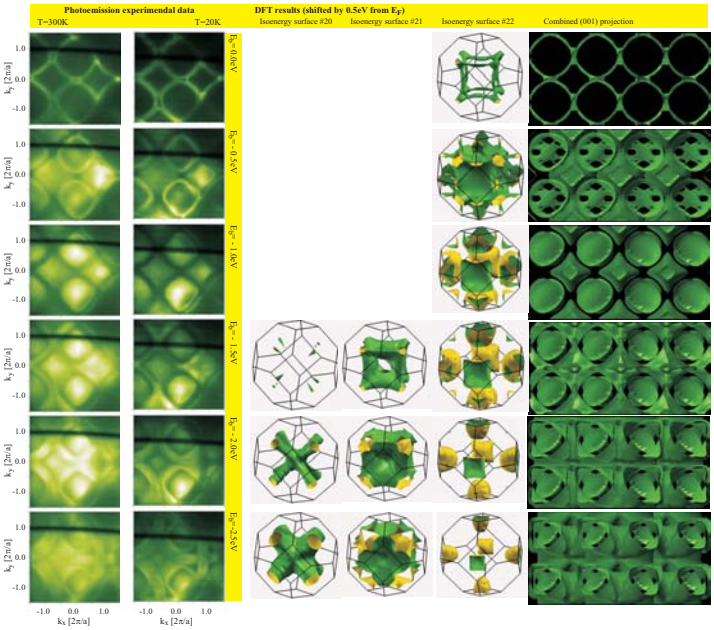

Figure 1. The experimental (left columns) and the theoretical (right column) angle-resolved photoemission spectroscopy energy cross-sections of tin tellurium corresponding to various values of the energy of the photoemission beam. The middle columns are three-dimensional reconstructions of these energy states. The two energy cross-sections on the left are at temperatures above and below the temperature of the structural phase transition. The small change indicates the transition is weak. The existence of energy states at the top of the column indicates the material is a metal at temperatures both above and below the transition. The energy reference point of the left two columns and right column differ. Shifting the right column down one panel brings theory and experiment into closer agreement.

We also performed the first resonant ultrasound spectroscopy of the elastic properties of the material. This technique measures the material's elastic constants. While we saw the structural phase transition, we were unable to confirm the previously reported and widely accepted low-temperature rhombohedral crystal structure. We found that on transforming key elastic constants of the material, instead of jumping in value, as they should for a ferroelastic, barely changed. Barely measureable changes were also found for the expected jumps in specific heat and thermal expansion. A Landau theory for the material was constructed, several of its parameters were fitted to the experiments, and from them we inferred that material is not ferroelastic but rather co-elastic. For a co-elastic material, the directions of the elastic deformations are not reversible. The measured changes in the properties of tin-tellurium on structurally transforming are among the smallest ever reported for a co-elastic material. With the formulation of the Landau theory for this material and its successful application to the elastically driven phase transition, we accomplished one objective of our proposal.

Adding small amounts of chromium to tin-tellurium did result in the alloy becoming ferromagnetic. In fact, with only a few percent of chromium, a room temperature ferromagnetic material resulted. A temperature this high for such small alloying is a rather surprising result. Further, measurements of the resonant ultrasound spectroscopy indicated the alloy was distinctly ferroelastic. The changing of the elastic material classes upon such dilute alloying is an even more surprising result. Figure 2 presents the results of one of our resonant ultrasound measurement for both the pure tin tellurium and the tin tellurium with a small amount of chromium. On the vertical axes is an elastic constant. On the horizontal axis is the temperature. In the vicinity of the structural phase transition, which is around one hundred degrees, clearly the two materials behave very differently.

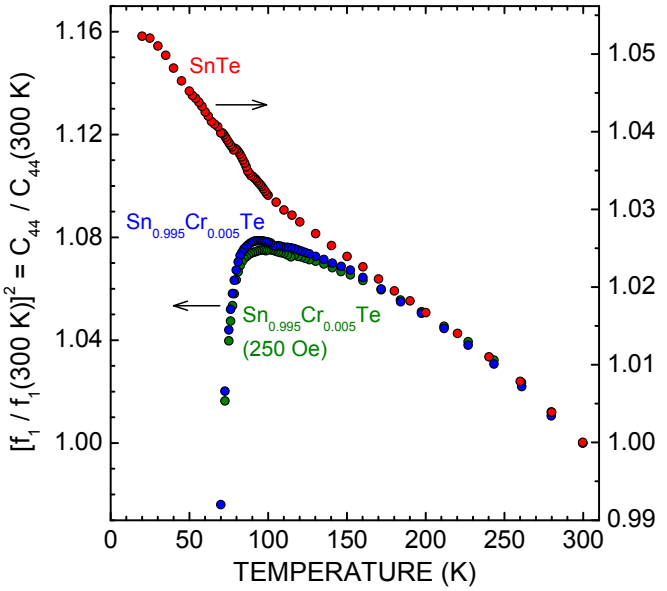

Figure 2. The temperature dependent resonant ultrasound spectroscopy measurement of an elastic constant, called the shear modulus, of both tin tellurium and tin tellurium with a small amount of chromium impurities. The structural phase transition, which occurs around one hundred degrees in temperature, is very evident in the tin tellurium with the chromium but is barely detectable in the unalloyed tin tellurium.

Our paper describing our angular-resolved photoemission spectroscopy measurements and calculations was

accepted for publication, and we drafted and submitted for publication a second paper reporting the results of the other measurements and calculations. The latter paper contains what is likely the most extensive study of the thermodynamic and structural properties of tin tellurium ever published.

Future Work

Unfortunately, our surprising finding that the properties of tin tellurium differ so essentially from what had been believed for 50 years has the consequence of it being an unsuitable multifunctional material. We will not continue studying it. Fortunately, many other options exist. Presently, we are beginning to study iron mono-oxide: It has the same simple crystal structure as tin tellurium, but its structural phase transition occurs only under the application of an external pressure. In the absence of an external pressure, it does undergo a metal-to-insulator transition as a function of temperature, that is, a phase transition from a state that conducts electrical current well to one that conducts it poorly. Accompanying this transition is a second transition from an anti-ferromagnetic to non-magnetic phase. An anti-ferromagnetic state is an ordered magnetic state, like a ferromagnetic state, but one in which that material does not attract or repel itself from a magnet.

For iron mono-oxide we have already assessed and assembled the theoretical capabilities needed to make comparisons with the suite of experiments necessary to quantify its properties. We will co-ordinate band structure and many-electron mean-field approximations to describe the metal-to-insulation and the anti-ferromagnetic to non-magnetic transitions. Critical will be properly modeling the coupling of the magnetism to the structural transition. From this microscopic approach we will derive a Landau phenomenology that has comparable terms as the one already derived on the mesoscopic scale. Then we will study the mesoscopic development and growth of the grains. The key task here will be predicting the development and growth of twin boundaries between the grains. Twin boundaries occur when two crystals of the same type grow with only a slight mis-orientation between them. The interface is highly symmetrical, with the atoms being shared by the two crystals at regular intervals. This specific type of interface has a lower energy than the grain boundaries that form from arbitrary crystalline orientations. Experimentally, we plan to execute many of the same measurements we used to unravel the properties of tin tellurium, the core ones being angle-resolved photoemission spectroscopy, neutron scattering, and resonant ultrasound spectroscopy. The key measurement will be of the strength of the magnetostriction that will give us the cross-field coupling of the anti-ferromagnetic state with the transforming lattice structure. The strength of this coupling is hard to predict theoretically. Presently, we are preparing to grow the crystals needed for these measurements. To date, we have prepared reasonably pure iron mono-oxide in powder form. The next step is fusing this powder into large crystals.

Conclusion

We remain committed to the challenge of "bridging the gap" and believe we can successfully produce a Landau free energy theory for the newly targeted material. Available experimental data is likely insufficient for fitting the theory over large ranges of parameters. We will thus be less interested in quantitative agreement with experiment but will be more interested in answering such questions as: Are we capturing the right phase transitions? Are they located in the right places? Are our predictions of microstructure reasonable? Do they suggest additional experiments? What does their interplay suggest about multifunctionality? In short, have we bridged the gaps?

Publications

Lashley, J. C., S. M. Shapiro, B. L. Winn, C. P. Opeil, M. E. Manley, A. Alatas, W. Ratcliff, T. Park, R. A. Fisher, B. Mihaila, P. Riseborough, E. K. H. Salje, and J. L. Smith. Observation of a continuous phase transition in a shape-memory alloy. 2008. *Physical Review Letters.* **101**: 135703.

Littlewood, P. B., B. Mihaila, R. K. Schulze, D. J. Safarik, J. E. Gubernatis, A. Bostwick, E. Rotenberg, C. P. Opeil, T. Durakiewicz, J. L. Smith, and J. C. Lashley. Band structure of SnTe studied by photoemission spectroscpy. 2010. *Physical Review Letters.* **105**: 86404.

Lookman, T., and P. B. Litlewood. Nanoscale heterogeneity in functional materials. 2009. *Materials Research Society Bulletin.* **34**: 822.

Porta, M., T. Lookman, and A. Saxena. Piezoelectric properties of ferroelectrics: effect of criticality and disorder. 2010. *Journal of Physics: Condensed Matter.* **22**: 345902.

Salje, E. K. H., D. J. Safarik, J. C. Lashley, J. E. Gubernatis, K. A. Modic, J. C. Cooley, R. D. Taylor, B. Mihalia, A. Saxena, T. Lookman, J. L. Smith, R. A. Fischer, M. Pasternik, C. P. Opeil, and P. B. Littlewood. Tin telluride: a weakly co-elastic material. *Physical Review B.*

Saxena, A., and G. Aeppli. Phase transitions at the nanoscale in functional materials. 2009. *Material Research Society Bulletin.* **34**: 804.

Yang, X. D., P. S. Riseborough, K. A. Modic, R. A. Fisher, C. P. Opeil, T. R. Finlayson, J. C. Cooley, J. L. Smith, P. A. Goddard, A. V. Silhanek, and J. C. Lashley. Influence of magnetic fields on structural martensitic transitions . 2009. *Philosophical Magazine.* **89**: 2083–2091.

Photodynamics and Photochemistry of Carbon Nanotube Materials

Sergei Tretiak
20090253ER

Introduction

Carbon nanotubes (CNT) constitute a class of the most promising technological materials for high-strength materials with desirable - and tunable - electrical properties. Our progress in understanding and manipulating nanotube's fundamental electronic properties, and subsequent practical applications has been slow due to difficulties in synthesizing sample materials. A lack of the experimental knowledge of electronic processes in carbon nanotubes has impeded advances in theory and simulations.

We have still not achieved a quantitative understanding and prediction of nanotube materials properties, however, several challenges in nanotube science are expected to be overcome in the near future. Carbon nanotube and graphene based electronics are rapidly becoming today's reality given the huge R&D effort in the industry. This creates a need for modeling and simulation effort to predict physical phenomena and deliver comprehensive theoretical framework of electronic structure and dynamics in carbon nanotubes. Such theory should provide guidance and a platform for future experimental studies, and impact technology. We will conduct systematic theoretical investigation of electronic structure and excited state dynamics in carbon nanotube materials. Our modeling will use LANL-developed quantum chemical tools, which outperform similar techniques world-wide. Time dependent semiempirical and density functional theory will be used as the basic quantitative framework for computing electronic structure and photoexcited trajectories and dynamics. Our research program involving the necessary expertise in quantum chemistry, condensed matter, spectroscopy, synthesis, and optical physics, will provide detailed understanding of fundamental physical processes which, in particular, govern the operation of nanotube-based electronic devices.

We expect to answer many outstanding questions in nanotube science. Namely, an interplay between excitonic and vibrational effects in photochemistry, the role of dark excitons and chemical defects in luminescence, formation of polarons and triplet states, transport, intertube and solvent interactions, nonlinear dynamics and localization effects will be investigated in detail.

Benefit to National Security Missions

This project will make a significant contribution to our basic understanding of materials, a LANL Grand Challenge. Carbon nanotube technology is widely expected to impact many areas including energy security, threat reduction, ubiquitous sensing, among others. These are major mission areas within DOE, DHS, DOD, and other government agencies.

Progress

During the second year of the project our effort focused on several areas.

We continue to study structural relaxation of DNA molecules in a presence of the CNTs. Simulated structures well agree with experimentally resolved STM images showing a stable wrapping period of DNA at ~60 degrees which coincide with natural tube coordinates of the tube (6,5) [1,2]. We have extended our investigations by simulating CNT/DNA structures with different wrapping angles, different DNA sequences, and different CNT chiralities. All structures we studied show DNA wrapping angles of about 50-60 degrees, independent on the tube chirality, while being very stable (with ~0.8 eV binding energy per base). Such a structure and stability suggest that DNA is unlikely be detached from the CNT because of external fluctuations, such as thermal vibrations and solvent effects, that is a very reliable property for drug delivery systems. This work has been recently submitted for publication [8]. On the experimental side, to improve the Scanning Tunneling Microscopy (STM) image quality we recently started to collaborate with Ming Zheng from NIST, who can fabricate the CNT/DNA hybrids with the specific DNA sequence and nanotube chirality. These samples allegedly contain nanotubes with certain chirality, and will allow us to verify our previous results for (6,5) nanotube. Moreover, we will be able to independently vary the type of nanotubes and DNA sequence in order to study the dependence of the electronic properties and structure of the hybrids on both paramethers.

Preliminary atomic force microscopy measurements show good dispersibility of the CNT-DNA hybrids and overall good quality and low residual contamination of the sample after deposition onto flat gold substrate.

We also carry out structure-property studies on CNTs functionalized by small organic molecules and conjugated polymers. Unlike CNT/DNA hybrids, the interaction between conjugated polymers and the nanotube is relatively weak (with ~0.1-0.3 eV binding energy per base). Our simulations predict the most stable polymer wrapping angles of about 15-20 degrees, which is well compared with available experimental data for these systems. Despite a weak interaction, the wrapping affects the first and second optical excitations (E11 and E22 bands) of the nanotube slightly shifting them to the red, compared to pristine tubes. Moreover, the conformational changes in the wrapped polymer strongly affect its optical spectra resulted in the significant blue shift of the excited energy and broader linewidth. The obtained results have been finalized in a paper "Effects of Wrapping on Optical Spectra of Carbon Nanotube/Conjugated Polymer Hybrids", to be submitted to the Journal of Physical Chemistry soon, and have been presented on several seminars and conferences.

Our most recent experimental efforts have focused on understanding surfactant structure at the CNT interface [3], with an aim of determining the limits of tunability of that structure for optimizing photoluminescence (PL) response. Density gradient ultracentrifugation (DGU) and fluorescence spectroscopy were used to probe the dynamic response of surfactant structure at the CNT surface to reorganizing forces, including changes in surfactant concentration and electrolyte screening. A diameter-dependent enhancement is observed in photoluminescence intensities from semiconducting CNTs upon initial titration with NaCl. This response to electrostatic screening diminishes as surfactant concentration is increased. The results are understood as a saturation of the surfactant (sodium dodecyl sulfate, SDS) structural response, defined as both a loss in ability to increase SDS loading at the SWNT surface, and as a loss in ability to reorient surface structure in response to a reorganizing force. These results confirm several aspects of recent molecular dynamics simulations of SDS behavior on CNTs and have important implications both for tunability of density based separations approaches using cosurfactant systems that include SDS and as routes for optimizing PL response for sensing, photonics, and imaging applications. This work has recently appeared in the Journal of the American Chemical Society [6]. We have also been extending the work to understand how changing of surfactant structure and composition impacts the ability to incorporate the nanotubes into various gel matrices for sensing applications and for fundamental photophysical measurement. To date we have demonstrated generation of high quality sol-gel hybrid structures, with the ability to tune the interfacial behavior of the nanotubes in these matrices to modulate surface access by various chemical species. The work has recently been submitted to Nature Nanotechnology [7].

In general, our research establishes a systematic and insightful understanding of photoinduced electronic dynamics [4,5] in nanotube based materials, which will guide the design of new experimental probes, and potentially lead to new nanotechnological applications.

Future Work

Our team has pioneered applications of methodologies we previously developed for molecular materials to carbon nanotubes. We applied our experience and theoretical methodologies well characterizing molecular systems such as conjugated polymers, to nanotubes. This resulted in a number of studies addressing virtually every aspect of photophysics of an isolated tube from the very different perspective with respect to what has been published before. In this proposal we consider real nanotube materials. We apply 'molecular-type' approach, which assumes analysis of finite-size systems. This method is ideally suited to study inhomogeneous structures (from amorphous materials to perfect periodic systems), various disorders, local defects, chemical functionalizations, intertube interactions, etc. Molecular modeling software we are using and developing, can routinely compute excited state structure and follow the ultrafast dynamics on femto- to picosecond timescales in large molecular systems of thousands of atoms in size (tens of nm length-scale).

Using our theoretical modeling, we intend to reach detailed understanding of electro- and photo-dynamics in carbon nanotubes and related hybrid materials, which govern the operation of molecular electronic devices. This includes charge transport and energy transfer in the presence of defects, functional groups, and intertube interactions. For example, the interplay between ballistic, polaronic, and incoherent hopping charge transfer regimes is critical for transistor electronics based on nanotubes. We further pose a question: how could we engineer nanotube materials to gain specific functionalities (i.e. materials by design)? For example, nanotubes are weakly luminescent materials, by knowing all the 'bells and whistles' of their electronic structure, can we suggest specific chemical functionalizations to enhance dramatically their luminescent efficiency? Our theoretical results will be immediately tested and verified by experiment (synthesis, spectroscopy and STM) at LANL. The experimental component of the project is greatly enhanced by our well established experimental collaborations world-wide.

Conclusion

Our proposal will achieve a quantitative description and a fundamental understanding of electronic processes in nanotube materials, provide novel material design strategies, and suggest practical nanotube applications.

We expect to develop synthetically viable strategies in

order to improve dramatically photoluminescence and electroluminescence of carbon nanotubes. Development of novel hybrid materials such as nanotubes wrapped with polymers/DNA and tubes with intercalated dyes opens new and exciting functionalities.

The results will be immediately implemented synthetically and experimentally tested using spectroscopic and STM facilities at LANL. This will provide guidance to world-wide efforts in development of new functional nanotube-based electronic materials and devices.

References

1. Yarotski, D., A. Balatsky, S. Kilina, A. Talin, J. X. Zhu, S. Tretiak, and A. Taylor. Scanning Tunneling Microscopy of DNA-Carbon Nanotube Hybrids. 2009. *Nano Letters* . **9**: 12.

2. Structure of DNA-wrapped carbon nanotubes revealed. 2009. *PADSTE HIGHLIGHTS* .

3. Niyogi, S., C. G. Densmore, and S. K. Doorn. Electrolyte Tuning of Surfactant Interfacial Behavior for Enhanced Density-Based Separations of Single-Walled Carbon Nanotubes. 2009. *Journal of the American Chemical Society.* **131**: 1144.

4. Kilina, S., E. Badaeva, A. Piryatinski, S. Tretiak, A. Saxena, and A. Bishop. Bright and Dark Excitons in Semiconductor Carbon Nanotubes. 2009. *Physical Chemistry Chemical Physics.* **11**: 4113.

5. Wong, C. Y., C. Curutchet, S. Tretiak, and G. D. Scholes. Ideal dipole approximation fails to predict electronic coupling between semiconducting single wall carbon nanotubes. 2009. *Journal of Chemical Physics.* **130**: 081104.

6. Duque, J., C. Densmore, and S. Doorn. Saturation of Surfactant Structure at the Single-Walled Carbon Nanotube Surface. To appear in *the Journal of the American Chemical Society* .

7. Duque, J., G. Gupta, S. Doorn, and A. Dattelbaum. Maximizing Fluorescence Intensity and Environmental Sensitivity of Single Walled Carbon Nanotubes. *Nature Nanotechnology.*

8. Kilina, S., D. A. Yarotski, A. A. Talin, S. Tretiak, A. J. Taylor, and A. V. Balatsky. Unveiling Stability Criteria of DNA-Carbon Nanotubes Constructs by Scanning Tunneling Microscopy and Computational Modeling. *Journal of Drug Delivery.*

9. Duque, J., H. Chen, A. K. Swan, A. P. Shreve, S. Kilina, S. Tretiak, X. Tu, M. Zheng, and S. K. Doorn. Violation of the Condon Approximation in Semiconducting Carbon Nanotubes. *Nature.*

Publications

Structure of DNA-wrapped carbon nanotubes revealed. 2009. *PADSTE HIGHLIGHTS* .

Duque, J., C. Densmore, and S. Doorn. Saturation of Surfactant Structure at the Single-Walled Carbon Nanotube Surface. To appear in *the Journal of the American Chemical Society* .

Duque, J., G. Gupta, S. Doorn, and A. Dattelbaum. Maximizing Fluorescence Intensity and Environmental Sensitivity of Single Walled Carbon Nanotubes. *Nature Nanotechnology.*

Duque, J., H. Chen, A. K. Swan, A. P. Shreve, S. Kilina, S. Tretiak, X. Tu, M. Zheng, and S. K. Doorn. Violation of the Condon Approximation in Semiconducting Carbon Nanotubes. *Nature.*

Kilina, S., D. A. Yarotski, A. A. Talin, S. Tretiak, A. J. Taylor, and A. V. Balatsky. Unveiling Stability Criteria of DNA-Carbon Nanotubes Constructs by Scanning Tunneling Microscopy and Computational Modeling. *Journal of Drug Delivery.*

Kilina, S., E. Badaeva, A. Piryatinski, S. Tretiak, A. Saxena, and A. Bishop. Bright and Dark Excitons in Semiconductor Carbon Nanotubes. 2009. *Physical Chemistry Chemical Physics.* **11**: 4113.

Niyogi, S., C. G. Densmore, and S. K. Doorn. Electrolyte Tuning of Surfactant Interfacial Behavior for Enhanced Density-Based Separations of Single-Walled Carbon Nanotubes. 2009. *Journal of the American Chemical Society.* **131**: 1144.

Wong, C. Y., C. Curutchet, S. Tretiak, and G. D. Scholes. Ideal dipole approximation fails to predict electronic coupling between semiconducting single wall carbon nanotubes. 2009. *Journal of Chemical Physics.* **130**: 081104.

Yarotski, D., A. Balatsky, S. Kilina, A. Talin, J. X. Zhu, S. Tretiak, and A. Taylor. Scanning Tunneling Microscopy of DNA-Carbon Nanotube Hybrids. 2009. *Nano Letters* . **9**: 12.

Compositionally Graded InGaN-based High Efficiency Photovoltaic Devices

Mark A. Hoffbauer
20090260ER

Introduction

Photovoltaic (PV) technology will significantly impact our nation's energy portfolio only when the costs are significantly reduced. Three materials systems are being aggressively explored for use in single p-n junction PV devices: Si, CdTe, and CIGS (Cu-In-Ga-Se). PV devices are made from either expensive single crystalline Si (efficiency ~24.7%) or from relatively inexpensive polycrystalline Si, CdTe, or CIGS based devices (all presently limited to about 10% efficiency). Clearly, breakthroughs in the cost and efficiency of PVs are needed for widespread deployment.

This project seeks to use an alternative materials system for creating high-efficiency PV devices, namely compositionally graded InGaN, offering inexpensive, single-junction PV device efficiencies approaching 30%. These devices will combine the advantages of the high efficiency of single-crystalline Si PV devices with the low cost and simplicity of CdTe and CIGS based devices. Our device architectures are based on p-i-n semiconductor structures functioning like a single junction PV device but made from compositionally-graded, device-quality InGaN films using a unique LANL technology called ENABLE.

Success of this project will have important consequences for our nation's energy security. The newly emerging InGaN materials system will be grown using a new technology for creating compositionally graded materials for PV devices combining the advantages of high-efficiency single crystalline Si-based PV devices with the low cost and simplicity of thin film-based PV devices. Because the bandgap of InGaN system can be tuned from the infrared to the ultraviolet by varying the In and Ga concentrations (0.7eV for InN to 3.4eV for GaN), the PV materials and device architectures can be optimized for maximum light-harvesting efficiency.

In nearly all conventional PV devices, the material's bandgap is fixed at a single value (e.g. Si = 1.1eV), limiting device efficiency because of two basic issues. Photon energies below a material's band gap are not absorbed, and the extra photon energy above of the band gap is converted into heat without producing charge carriers (electricity). The ideal PV device would encompass two demonstrated methods for improving efficiency. Fabrication from a single material system having tunable (multiple) band gaps tailored to match the full solar spectrum, and the use of PV films with high mobility charge carriers. For widespread use, PVs must be manufactured inexpensively from stable and non-toxic materials. Graded InGaN-based PV devices offer several advantages: absorption of photons over a wide spectral range creates more charge carriers; the polar material generates an electric field enhancing carrier transport; and the high bandgap active layer increases output power. The potential of the InGaN materials system offers a real opportunity for realizing low-cost, high-efficiency PV devices.

Benefit to National Security Missions

This research will directly support LANL and DOE core missions in national energy security and threat reduction by developing a new electronic and photonic material system for photovoltaic applications with unprecedented efficiency and lower costs that are key elements in several DOE programs including the Solar America Initiative. The results of this project will position us to compete for follow-on funding from DOE (e.g. DOE/BES, ARPA-E, and EERE initiatives) to expand this effort into a much larger program. Our results will have important consequences for our nation's energy security, national security, and environment.

Progress

Significant progress towards our project goals have been achieved for this project. The developments are summarized as follows:

Isothermal growth of GaN, InN and high-In-content InGaN is now routinely achieved and shows excellent crystallinity and optical properties. The temperature variation observed in x-ray diffraction (XRD) and photoluminescence (PL) measurements for ~500nm thick, ~37% In-content films of InGaN grown on sapphire substrates at relatively low temperatures are shown in Figure 1. In all cases the films show excellent crystallinity and bright PL. These results are critical for this project since creating

graded composition structures over wide ranges requires isothermal growth. We have also demonstrated growth of graded composition films and are investigating methods for forming the uniform gradients in InGaN composition needed for prototype PV devices, and are exploring the rate at which changes in the graded composition can be made to define the graded layer thickness.

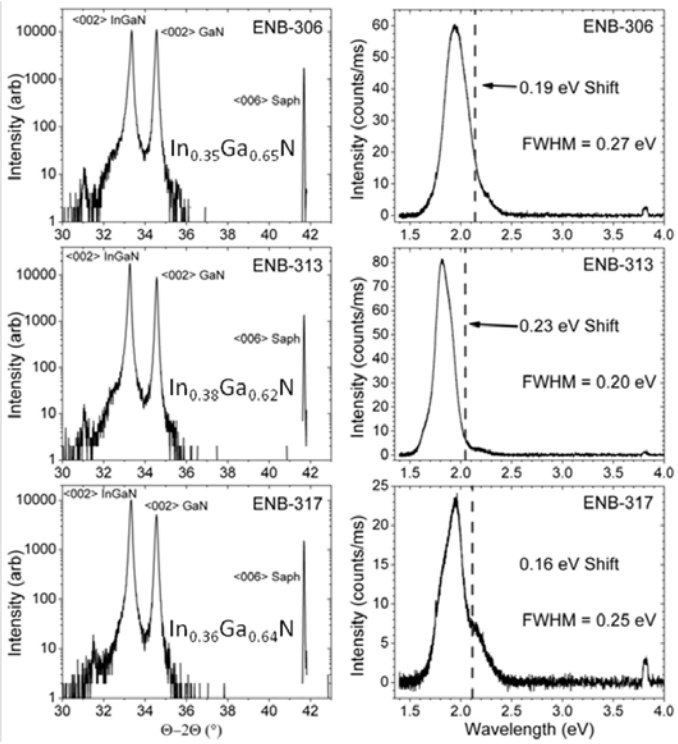

Figure 1. X-ray diffraction theta-2theta scans (left column) and photoluminescence spectra (Right column) of a series of ~500nm thick InxGa1-xN films grown by ENABLE showing the <0002> diffraction peak (left) and bandgap luminescence (right). These films had In compositions of 35% to 38%. ENB-306 (top) was grown at 570°C, ENB-313 (middle) was grown at 530°C, and ENB-317 (bottom) was grown at 490°C. The dashed lines indicate energy shifts in the PL spectra (right column) from the expected position of the bandgap luminescence based on the composition determined from the XRD scans.

By carefully controlling impurities and other sources of contamination in our source gas streams and in the Ga and In evaporators, we now routinely achieve background carrier concentration in semiconducting GaN-related films in the low $10^{17}cm^{-3}$ range, allowing p-type doping of the films. Intrinsic InGaN-related films show carrier mobilities in the 200 to >500 cm^2/Vsec range, fully acceptable for prototype PV devices.

P-type doping of GaN with a high concentration of active Mg is now well established. We have solid preliminary evidence indicating successful p-type doping of high-In-content InGaN films. Spectrally resolved electroluminescence measurements (EL) indicate that Mg can be doped into InGaN at In contents up to ~50% yielding bright, tunable band edge EL. These results are being improved upon and verified by electrical transport measurements. We have grown our first p-n junctions in InGaN films that are being optically and electrically tested by our colleagues. These steps are all critical for creating actual PV devices and measuring their efficiencies, particularly since the bottom n- and p-type films needed for our proposed device structure will be doped In-rich InGaN.

In addition, we are designing and will be moving our ENABLE technology to a new platform that will allow us to routinely grow GaN-related thin films over larger substrate areas. We have successfully transitioned our substrates from one square cm areas to 5 cm diameter substrate wafers, the standard size for research grade devices. Even larger substrate sizes will facilitate the low-cost fabrication of prototype PV devices.

The growth of high-quality high-In-content InGaN on crystalline and polycrystalline silicon substrates has been demonstrated. These experiments yield highly-crystalline InGaN films of similar quality to that observed for growth on sapphire (see Figure 1 above). Once optimized, the ability to grow InGaN-related thin film materials on inexpensive Si substrates will significantly reduce the costs of PV devices by providing a path forward for adding value to existing Si-based PV device architectures.

Future Work

Preliminary results show a clear path to making device-quality compositionally-graded InGaN materials. One of our first tasks is to further improve (reduce) the background (intrinsic) carrier concentration for ENABLE grown InGaN films to levels suitable for demonstrating active p-n junctions and for fabricating prototype PV devices. High-quality compositionally graded InGaN will be grown over well-defined, relatively narrow composition ranges optimized for performance in single junction PV devices and these devices will be fully characterized. These graded InGaN films will also be grown on Si substrates and fabricated into working PV devices to measure their overall efficiency. Our ultimate goal is to achieve ~30% PV efficiency for these graded composition devices and explore fabricating these devices on inexpensive substrates.

Conclusion

Significant progress has been achieved towards our goal of creating a new type of PV device based on compositionally graded InGaN thin film materials. A unique LANL technology is the only one shown to be capable of growing high-quality compositionally graded InGaN over the full composition range, allowing the development of this important PV technology. Substantial work has set the basis for creating these materials and understanding their use in PV devices. These single-junction PV devices will be alternatives to current thin film single-junction PV devices that are be-

ing aggressively researched. Compositionally graded InGaN devices have the potential to achieve record efficiencies of ~30%, allowing them to produce electricity at $0.05/kWh (cost competitive with fossil fuel generated electricity).

Publications

Williamson, Todd L., Alicia L. Salazar, Joshua J. WIlliams, and Mark A. Hoffbauer. Improvements in the Compositional Uniformity of In-rich InxGa1-xN Films Grown at Low Temperatures by ENABLE. *Physica Status Solidi (c).*

Williamson, Todd L., Joshua J. WIlliams, Jonathan C. Hubbard, and Mark A. Hoffbauer. High-In-Content InxGa1-xN Grown by Energetic Neutral Atom Beam Lithography & Epitaxy under Slightly N-rich Conditions. *Journal of Vacuum Science and Technology B.*

Plasmonic Bandgap Materials: Fusion of Interparticle and Particle-Photon Interactions at the Nanoscale

Stephen K. Doorn
20090325ER

Introduction

Optical excitation of surface electrons (plasmons) within multiple interacting metal nanoparticles can result in huge amplification of associated surface enhanced Raman Spectroscopy (SERS) responses from adsorbed molecules, providing single-molecule sensitivity. Gaining a fundamental understanding of these interparticle plasmonic interactions is essential for future exploitation of this phenomenon for next-generation sensing needs. Engineering such plasmonic nanoparticles into ordered arrays that also exhibit tunable photonic bandgap properties (with well-defined optical resonances) will present a novel system for exploring optical behaviors that will provide new modes for sensing opportunity. Our broad goal is to probe, understand, and manipulate the interparticle and particle-photon interactions required to realize a functional plasmonic/photonic-bandgap material hybrid.

To do so, we will pursue a fundamental understanding of how particle architecture impacts SERS response through single-particle in-flow measurements. Additionally, the interparticle plasmonic interactions responsible for SERS signal amplification will be probed via controlled 2-Dimensional and 3-Dimensional assemblies of SERS-active particle aggregates. We will also generate a new class of nanoparticles that combine magnetic and plasmonic properties. These hybrids will allow self-assembly of interacting nanoparticles with long-range 3-Dimensional order to generate and characterize a manipulable dynamic photonic bandgap material that displays SERS activity. Finally, we will incorporate functional elements into this dynamic plasmonic/photonic lattice to impart a chemoresponsive route to manipulation of its optical properties.

Our efforts represent the development of novel fabrication and self-assembly routes for producing 2- and 3-D plasmonic and plasmonic/photonic-bandgap hybrid nanoparticle assemblies. These new materials will be a powerful testbed for understanding the fundamental properties of coupled photonic/plasmonic metamaterials and will lead to novel sensing approaches not previously explored. We anticipate this novel approach will generate more sensitive and more tunable sensing platforms than are currently available.

Benefit to National Security Missions

We address DOE's goal of developing advanced functional nanomaterials. DOE is also interested in materials that function at the nano-bio interface. Our plasmonic bandgap materials will ultimately be functionalized to interact with bioanalytes at the nanoscale. These materials also have applications relevant to mission areas in other government agencies.

Progress

In this FY, our efforts have been devoted to developing multiple nanoparticle architectures through both collaborative in-house synthesis efforts. The primary goal is to produce multifunctional particles that match spectroscopic signatures with suitable physical traits for efficiently manipulating inter-particle interactions. In parallel with this synthetic work, we have been developing our particle manipulation capabilities to include inflow single particle analysis as well as approaches to 2-d and 3-d particle assemblies for subsequent spectroscopic study.

We are currently investigating the spectroscopic properties of superparamagnetic nano-aggregates (of interest for magnetic manipulation of particle interactions, provided by Yin, UC Riverside) that are encapsulated in a silica shell then functionalized with a plasmonic metal film. Additionally, we are studying bulk spectral properties of silver nano-cubes (of interest as unique geometries for interaction studies, provided by Xia, Washington U.). Finally, we are studying a variety of high aspect ratio gold nano-rods (Khanal, LANL), to probe any potential 'tip' enhancement effects present at the rod ends.

In addition to synthetic collaborations, we have been developing and characterizing the synthesis of metallic nanoshell particles. These architectures typically have an oxide central core (silica) that is encapsulated by a thin metallic shell (gold). This work has revealed detailed light mediated reaction pathways that have

not been previously reported and is the subject of a manuscript in preparation.

In addition to colloidal synthetic approaches, we have extensively studied surface directed growth of metallic nanoparticles in an attempt to reveal inter-pariticle interactions in-situ as the particles are nucleated and formed. This parallel approach has the significant advantage over colloidal solutions in that we are not required to manipulate the particle once they are formed; the surface dictates how the particles interact. These studies typically involve conducting polymer thin films that are used to reduce metal ions to zero valent metallic particles. The subsequent particle morphologies formed on the polymer surface are found to be highly dependent on the polymer processing conditions and solution properties of the metal ions. This work has resulted in publications in Langmuir and Nanoscale.

We have also been developing techniques for particle manipulation. In a slight change in scope we are using recent advances in full-spectral flow-based analysis of nanoparticles to observe spectroscopic signatures of plasmonic nanoparticles at the single particle level. This newly-developed high-throughput instrumentation enables multi-parametric spectral analysis of 100s of particles per second. This enables us to assemble particle structure-property relationships using statistically relevant particle population sizes. In many ways, this flow-based work is merely a 1-d extension of the 2-d and 3-d manipulation approaches proposed in this project. This work not only drives cutting edge instrument development, but also has resulted in a publication (as the May 5th cover article) in the Journal of the American Chemical Society, "High Resolution Analysis of Individual Surface-Enhanced Raman-Active Nanoparticle Spectral Tags in Flow". In addition to allowing probing of fundamental particle properties, the new instrumentation also promises to be a powerful new tool for advancing development of a variety of nanoparticle types.

Additionally, we have made significant strides towards 2-d surface manipulation of our particles. In an effort to create well-defined nanoparticle aggregates and to attempt to control the inter-particle interactions, we have been using electron beam lithography to generate patterned arrays of holes into polymer thin films. By carefully controlling solvent evaporation, we are now able to deposit colloidal particles into the patterned arrays. This has been successfully demonstrated for 2 micron wide lines using 200 nm spherical particles to produce a small particle crystal only several particles wide. Current efforts are working to lower this feature size to <1 micron and extend the deposition process to the wide variety of particles we now have available. We will also be moving ahead with Raman characterization of the interacting geometries within the next month.

Future work on this project will seek to apply the various particle manipulation techniques towards the range of particle architectures all developed in this FY. This will position us ideally, in the next FY, for full spectroscopic analysis of novel engineered nanomaterials with an emphasis on resolving differences, for the first time, in overall SERS activity as a function of nano-morphology.

Future Work

We will pursue self-assembly of 3-D photonic lattices whose optical properties are coupled to plasmonic behavior of its constituent SERS-active particles. Noble metal nanoparticles, when induced to interact can be used as highly effective SERS substrates, serving as easily accessible starting points for SERS-active metamaterials. However, control of these particle aggregates is difficult, with few fundamental studies having investigated the ideal aggregate size and geometry for maximum SERS excitation. Using new concepts in surface-based particle patterning techniques, we will introduce a combinatorial approach to assembling simple metallic particle aggregates in an effort to deduce ideal aggregate structures for efficient intra-particle SERS hot spot generation.

These particle architectures will then be extended to 3-D through the assembly of particle aggregates via optical trapping as well as magnetic assembly. By manipulating the aggregates into 3-D architectures, we hope to generate readily observed intense SERS hot spots within the core of the particle aggregate, the results of which will have broad reaching impacts on the understanding of the underlying mechanisms responsible for SERS. By assembling the plasmonic aggregates into arrays with long range order, we will leverage the high sensitivity aspect of SERS based substrates with the unique optical properties of a fully 3-D photonic crystal.

Our assemblies will represent the first tunable photonic/plasmonic hybrid metamaterials, providing a route to probing unexplored behaviors of these emerging novel materials. Optimized geometries for the hybrid material with the most efficient coupling between these two optical phenomena will be isolated by immobilizing the aggregate array in a hydrogel matrix that is preloaded with analyte receptor sites. This novel nanocomposite will yield a multimodal approach to sensing via analyte modulation of the photonic lattice properties and inter-particle plasmon field overlap which will result in greatly improved SERS-based analyte detection.

Conclusion

Ultimately, this project will produce a better understanding of the critical parameters associated with surface enhanced Raman (SERS) responses that yield single-molecule sensitivity. This is critical to the realization of new sensing materials capable of the stringent sensitivity and confidence requirements of the threat reduction community. Our efforts will also produce a totally new class of materials that combine SERS-active "plasmonic" properties with ordered "bandgap materials" that provide highly tunable

optical properties. This fusion of properties opens up novel sensing approaches that will be explored.

Publications

Brady, C. I., N. H. Mack, L. O. Brown, and S. K. Doorn. Self-assembly approach to multiplexed SERS encoder beads. 2009. *Analytical Chemistry.* **81**: 7181.

Goddard, G., L. Brown, R. Habbersett, C. Brady, J. Martin, S. Graves, J. Freyer, and S. Doorn. High-resolution spectral analysis of individual sers-active nanoparticles in flow. 2010. *Journal of the American Chemical Society.* **132** (17): 6081.

Xu, P., B. Zhang, N. MacK, S. Doorn, X. Han, and H. Wang. Synthesis of homogeneous silver nanosheet assemblies for surface enhanced Raman scattering applications. 2010. *Journal of Materials Chemistry.* **20** (34): 7222.

Xu, P., N. Mack, S. Jeon, S. Doorn, X. Han, and H. Wang. Facile Fabrication of Homogeneous 3D Silver Nanostructures on Gold-Supported Polyaniline Membranes as Promising SERS Substrates. 2010. *LANGMUIR.* **26** (11): 8882.

Xu, P., S. Jeon, N. MacK, S. Doorn, D. Williams, X. Han, and H. Wang. Field-assisted synthesis of SERS-active silver nanoparticles using conducting polymers. 2010. *Nanoscale.* **2** (8): 1436.

Probing the Origin and Consequences of Quantum Critical Fluctuations

Tuson Park
20090335ER

Introduction

Electronic technology has advanced in step with our increased understanding of how electrons behave in materials. In recent years, however, we have witnessed a crisis in our fundamental knowledge of the way electrons behave in certain materials in which the electrons interact strongly with each other. Our historical understanding of the electron cannot be applied to these correlated electron metals and requires a new paradigm. Initial studies have revealed that quantum effects, usually only significant at very low temperatures, dominate the character of electrons even at finite temperature and may be responsible for producing new forms of unconventional superconductivity at unexpectedly high temperatures. The goal of this project is to create a proper understanding of the new quantum phenomena and with this knowledge to transform the modern crisis into an opportunity that will advance our scientific understanding as well as create new technology.

In our research, we propose to identify the spectrum of electronic fluctuations that results from the quantum effects and that can be tuned by applied magnetic field and pressure. Anisotropic electrical resistivity and momentum-dependent superconducting properties depend on the nature of the quantum fluctuations, and these are precisely the properties that we will measure to explore the origin and consequences of quantum fluctuations. A triple axis vector magnet, which has three sets of independent magnets, will enable us to probe these anisotropic properties at any arbitrary magnetic field direction while a single crystal is subjected to high pressure, a unique capability that is needed to guide a theoretical description of these phenomena.

Benefit to National Security Missions

This project directly supports the DOE mission in Energy Security by enhancing our fundamental understanding of materials with high superconducting temperatures, which hold promise for efficient transmission and storage of electricity.

Progress

We describe our recent progress for understanding of the origin and consequences of the magnetic fluctuations from a quantum critical point in complex electronic materials. Our efforts have been centered on two classes of strongly correlated electron systems, namely f-electron and d-electron based correlated materials. In the study of the f-electron based metallic compounds, we confirmed that the magnetic quantum critical point hidden under the dome of superconductivity of CeRhIn5 (cerium-rhodium-indium) is responsible for the strange metallic behavior in the normal state. In addition, disorder effects on the quantum criticality have been systematically investigated with cadmium (Cd) doping at the percent level in CeCoIn5 (cerium-cobalt-indium). Electric transport meaurements have played a significant role in probing quantum criticality, in which their temperature dependence strongly depends on the nature of quantum fluctuations. In order to study the unconventional normal state of CeRhIn5, we applied magnetic fields that are strong enough to suppress completely superconductivity. At the optimal pressure where the superconducting transition temperature of CeRhIn5 is highest, the electrical resistivity shows a sub-linear temperature dependence above the superconducting transition temperature (Tc) and extends to the lowest temperature when the superconductivity is suppressed by applied magnetic field. The temperature-squared-coefficient of the resistivity becomes singular as the magnetic field approaches the upper critical field, indicating that the unconventional normal state of CeRhIn5 is a direct consequence of the magnetic quantum critical point. When disorder is coupled to quantum fluctuations, physical properties may differ depending on the nature of the quantum critical point. Cd-doping into the quantum critical superconductor CeCoIn5 at the percent level induces an antiferromagnetic ground state, which could be reversed back to its original superconducting state by applied pressure. Measurements of specific heat and electrical resistivity of Cd-doped CeCoIn5 showed that disorder associated with the Cd-doping moves the system away from a quantum critical state. These studies leave open the questions of the nature of the distinct quantum fluc-

tuations associated with either an incommensurate spiral (CeRhIn5) or a commensurate (CeCo(In1-xCdx)5) structure and their relation to the occurrence of quantum criticality. Furthermore, this avoided quantum criticality in a slightly disordered heavy fermion material is expected to guide theoretical efforts to properly understand disorder as a new degree of freedom in controlling physical properties in correlated electronic compounds.

In the study of d-electron based superconductors, we measured low-temperature specific heat of the electron doped BaFe1.8Co0.2As2 (barium-iron-cobalt-arsenic) to explore the nature of the superconductivity—one of the most important unanswered questions in this new family of high-temperature superconductors. Earlier studies of the specific heat of similar compounds found an anomalous upturn at low temperatures, making an interpretation of the symmetry of the superconducting order parameter rather ambiguous. Our results on the slightly overdoped compound grown by a closed Bridgman method, however, did not show any hint of this Schottky-like feature at low temperatures or in magnetic fields up to 9 tesla. This enabled us to unambiguously identify the enhanced low-temperature excitations and also study the anisotropy of the linear term of the specific heat. These results cannot be explained by an isotropic s-wave superconducting gap symmetry, but is consistent with multi-gap superconductivity with nodes on the Fermi surface. We also studied quasiparticle relaxation dynamics in hole doped (Ba,K)Fe2As2 (barium-potassium-iron-arsenic) and found a new type of ordered state that suppresses magnetic order. We speculate that this is a precursor to superconductivity, very reminiscent of the other class of d-electron high-temperature cuprate superconductors. Further investigations using anisotropic electrical transport meaurements of the relationship between quantum criticality and non-Fermi-liquid behavior in these two classes of high-temperature superconductors is under way.

Future Work

A quantum critical point (QCP) is an instability between ordered and disordered electronic states at T=0K, with the transition between them driven by Heisenberg's uncertainty principle. Strongly correlated f-electron materials have been a prime testing ground to explore the consequences of such an instability. Among many anomalous properties associated with the QCP, two consequences stand out: a strange metallic state that persists from very low to high temperatures and the emergence of unconventional superconductivity nearby the QCP. A microscopic understanding of these phenomena poses a fundamental challenge in the condensed matter community.

Identification of the relevant fluctuation spectrum is needed to guide a theoretical description of these phenomena. Compared to chemical substitution that induces chemical disorder and modifies the fluctuations, applying pressure is an ideal knob to tune compounds to a QCP without additional complication. Though microscopic measurements, such as neutron scattering, are well-suited to characterize the fluctuation spectrum, they are impossible to perform with sufficient resolution under high pressure conditions. Instead, relatively simple anisotropic transport and thermodynamic measurements under pressure place strong constraints on the fluctuation spectrum and their origin. Field-angle-dependent transport and thermodynamic measurements complimented with point contact spectroscopy will be exploited to determine the order parameter symmetry of pressure-induced or pressure-tuned superconducting states, which will allow us to critically determine the relationship between quantum fluctuations and unconventional superconductivity.

We will study representative correlated f-electron systems, including antiferromagnetic CeRhIn5 and ferromagnetic UGe2, which can be tuned by pressure to quantum critical and superconducting states. The high purity of these stoichiometric compounds with energy scales amenable to detailed study makes them ideal test systems. The generality of understanding gleaned from the f-electron compounds will be tested by complementary experiments on electron doped cuprates and charge-density-wave/superconducting systems.

Conclusion

The unique combination of the vector magnet and high pressures will allow us to probe the nature of electrons in correlated materials in ways never before possible. Specifically, we expect to: (i) determine the origin of quantum fluctuations that are responsible for a strange metallic state in correlated f-electron compounds, and (ii) to make the first determination of the superconducting order parameter for any pressure-induced superconductor. Knowledge obtained through this study will be applied to d-electron high-temperature superconductors, providing fundamental information to superconducting technology that will help to ensure the Nation's energy security.

Publications

Baek, S. H., H. Lee, S. E. Brown, N. J. Curro, E. D. Bauer, F. Ronning, T. Park, and J. D. Thompson. NMR investigation of superconductivity and antiferromagnetism in CaFe2As2 under pressure. 2009. *Physical Review Letters.* **104**: 227601.

Bauer, E. D., H. O. Lee, V. A. Sidorov, N. Kurita, K. Gofryk, J. X. Zhu, F. Ronning, R. Movshovich, J. D. Thompson, and T. Park. Pressure-induced superconducting state and effective mass enhancement near the antiferromagnetic quantum critical point of CePt2In7. 2010. *Physical Review B.* **81**: 1805071.

Bauer, E. D., T. Park, R. D. McDonald, M. J. Graf, L. N. Boulaevskii, J. N. Mitchell, J. D. Thompson, and J. L. Sarrao. Possible two-band superconductivity in PuRhGa5 and CeRhIn5. 2009. *Journal of Alloys and Compunds.* **488**: 554.

Chia, E. E., D. Talbayev, J. X. Zhu, H. Q. Yuan, T. Park, J. D. Thompson, C. Panagopoulos, G. F. Chen, J. L. Luo, N. L. Wang, and A. J. Taylor. Ultrafast pump-probe study of phase separation and competing orders in the underdoped (Ba, K)Fe2As2 superconductor. 2010. *Physical Review Letters.* **104**: 027003.

Lee, H. O., E. Park, T. Park, V. A. Sidorov, F. Ronning, E. D. Bauer, and J. D. Thompson. Pressure-Induced Superconducting State of Antiferromagnetic CaFe2As2. 2009. *Physical Review B.* **80**: 024519.

Park, T., V. A. Sidorov, H. Lee, F. Ronning, E. D. Bauer, J. L. Sarrao, and J. D. Thompson. Unconventional quantum criticality in the pressure-induced heavy-fermion superconductor CeRhIn5. To appear in *Journal of Physics: Condensed Matter.*

Park, T., Y. Tokiwa, F. Ronning, H. Lee, E. D. Bauer, R. Movshovich, and J. D. Thompson. Field-induced quantum critical point in the pressure-induced superconductor CeRhIn5. 2010. *Physica Status Solidi.* **247**: 553.

Park, T., and J. D. Thompson. Magnetism and Superconductivity in Strongly Correlated CeRhIn5. 2009. *New Journal of Physics.* **11**: 055062.

Ronning, F., E. D. Bauer, T. Park, S. H. Baek, H. Sakai, and J. D. Thompson. Superconductivity and the effects of pressure and structure in single-crystalline SrNi2P2. 2009. *Physical Review B.* **79**: 134507.

Linear Scaling Quantum-Based Interatomic Potentials for Energetic Materials

Marc J. Cawkwell
20090369ER

Introduction

The fundamental mechanical and chemical events that lead to the detonation of explosives occur over time scales so short that they are extremely difficult to study experimentally. Furthermore, the postmortem analysis of samples is usually impossible. For these reasons, the computational modeling of atomic level events in energetic and reactive materials using molecular dynamics (MD) simulations is one of the few tools available to study the phenomena leading to detonation. However, the reliability of the predictions provided by such calculations is almost entirely dependent on the mathematical description of interatomic bonding employed. Unfortunately, highly accurate descriptions of bonding tend to be very expensive computationally, leading to simulations of limited scale and duration. This project has developed methods and an open source supporting code that enable long duration molecular dynamics simulation with quantum mechanical accuracy to reveal shock-induced phenomena and reactions in real materials.

Benefit to National Security Missions

This project supports the DOE/NNSA mission in Nuclear Weapons by enhancing our understanding of the initial mechanical and chemical events that lead to the detonation of conventional explosives. Furthermore, the predictive capabilities the project will provide will enhance DOD and DHS programs on energetic materials. The deliverables of this project will see applications to basic research on the physical properties of several classes of complex materials. Hence, mission relevance extends to all areas where a fundamental understanding of materials is required.

Progress

The project has pursued self-consistent charge transfer tight-binding (SCC-TB) as a fast, yet explicitly quantum mechanical alternative to fully quantum or fully empirical descriptions of interatomic bonding in organic materials [1 – 2]. The SCC-TB formalism is the simplest quantum-based method that captures the making and breaking of covalent bonds, the self-consistent transfer of charge between species of differing electronegativity, long-range electrostatic interactions, and weak van der Waals-type bonding. Around this formalism we have developed the MD code 'LATTE' (Los Alamos Transferable Tight-binding for Energetics) [3] which is actively being used in research on four continents. The source code for LATTE has received an open source Gnu Public License (GPL) and is available for download from.

The LATTE code offers a number of methods for computing the energy of, and forces acting on, atoms in organic molecules within the SCC-TB framework. We find that the optimal method depends on the system under study, its size, whether chemical bonds are expected to break, and the computational platform available to the user. Of particular note in this regard, especially with respect to the tailoring of algorithms to computational architecture, is our pursuit of multi-core central processing unit (CPU), many-core graphics processing unit (GPU) hybrid computing. It is clear that the generations of supercomputer that follow LANL's Roadrunner will utilize hybrid architectures in order to maximize the number of calculations that can be performed per watt of power consumed and per $ expended on hardware. We have demonstrated that Niklasson's density matrix purification algorithm [4] is well suited to execution on a many-core GPU, especially when the algorithm is constructed such that communication between the CPU and GPU is minimized. In Figure 1 we show the wall time required for the calculation of the total energy of a 512 atom system (1088 orbitals) using density matrix purification on a multi-core CPU cluster and on modern, general purpose, NVIDIA Tesla and Fermi GPUs. Figure 1 illustrates clearly that when used efficiently, the performance of a single GPU exceeds the shared memory performance of all 16 CPU cores on a node of a supercomputer while using far less power and with a much lower cost. Furthermore, as CPU performance scales less than ideally with increasing numbers of cores, it unlikely that increasing the number of CPU cores further will eclipse the performance of the GPU. Uniquely for an electronic structure code, LATTE can be executed robustly in single precision arithmetic, nevertheless, we see that the performance in double

precision of the latest generation of Fermi-based GPUs exceeds that of 16 CPU cores.

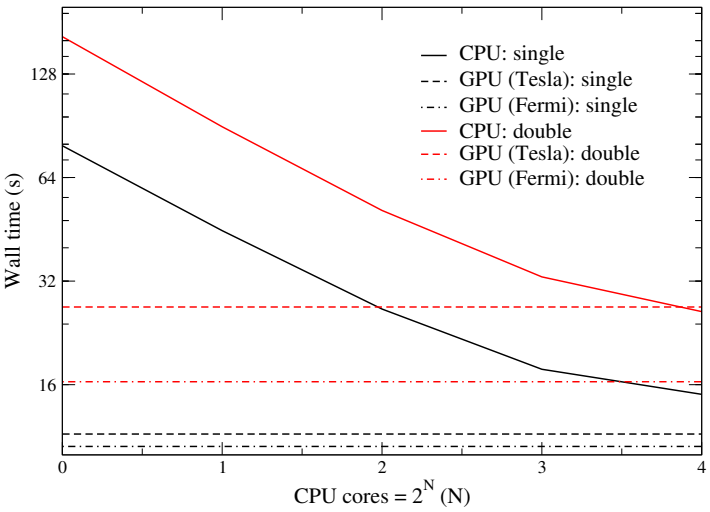

Figure 1. Wall time for the calculation of the total energy of a 512 atom system using density matrix purification as function of the number of CPU cores for CPU and hybrid CPU/GPU code in single and double precision.

The overall aim of this project is the simulation of mechanical events and chemical reactions stimulated by shock compression. As a result, it is essential that our MD simulations allow adiabatic shock heating and exothermic chemistry to be captured accurately. Temperature changes can be captured with high fidelity within MD if the total energy (potential energy plus kinetic energy) is conserved precisely over the duration of the simulation. For many years quantum-based MD codes suffered from a poor conservation of the total energy that could be overcome only at very high computational expense. A remedy for these fundamental issues was put forward recently by Niklasson and implemented into LATTE. Niklasson's extended Lagrangian Born-Oppenheimer MD framework [5] has enabled us to perform the first quantum-based MD simulation of exothermic chemistry under explicit shock compression with an accurate underlying dynamics and with no requirement for either thermostats or full numerical convergence. These new capabilities were demonstrated by a study of shock-induced chemistry in tert-butylacetylene (TBA), using our SCC-TB parameterization for hydrocarbons, in collaboration with experimental work by Dattelbaum, Sheffield, and co-workers.

Flyer plate-driven shock compression experiments on TBA provided evidence for a two stage chemical reaction leading to an increase in the density at pressures greater than 3.6 GPa [6]. To identify the reactions that occurred during the experiments we performed simulations of shock compression in 160 and 256 atom systems. The uniaxial compression of the shock was captured in our simulations using a simple 'hugoniostat' whereby the length, l, of an axis of the periodic simulation cell was compressed according to $l(t) = l_0 - U_p t$, where $0 \le t < l_0/U_s$, and U_s and U_p are the experimentally measured shock and particle velocities, respectively, and t is time. This hugoniostat ensures the system reaches the appropriate density by uniaxial compression in the period of time required for the shock wave to cross the simulation cell. In Figures 2(a) and 2(b) we plot the temperature and total energy of the system, respectively, as a function of time during the first 30 ps of the simulation. During the first 1.0 ps the system is thermalized to a temperature of 300 K, followed by energy conserving MD using Niklasson's formalism. The shock compression manifests itself as a rapid increase in the total energy owing to the work done on the system, but once the compression ends the system returns seamlessly to a precise conservation of the total energy. The shock compression gives a rapid initial rise in the temperature because of the adiabatic compression followed by a longer, more gradual rise caused by exothermic chemical reactions that are driven by the shock wave. We also resolve another exothermic chemical reaction at a time of about 25 ps.

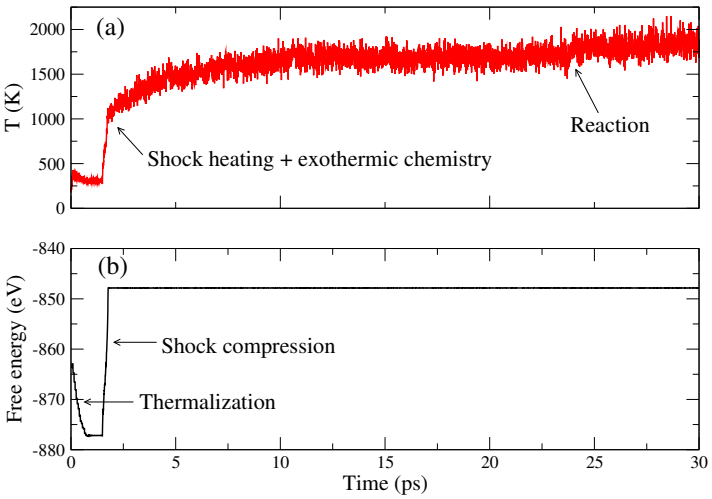

Figure 2. (a) Temperature, and (b) total energy as a function of time during a molecular dynamics simulation of the shock compression and subsequent radical chain polymerization of tert-butylacetylene.

Our molecular dynamics simulations showed that TBA undergoes a radical chain polymerization under shock compression whereby many TBA molecules form join at their carbon triple bonds to form polymer chains (see Figure 3) [2]. These reactions can be expected to increase density and are in full qualitative agreement with the experimental work on this system.

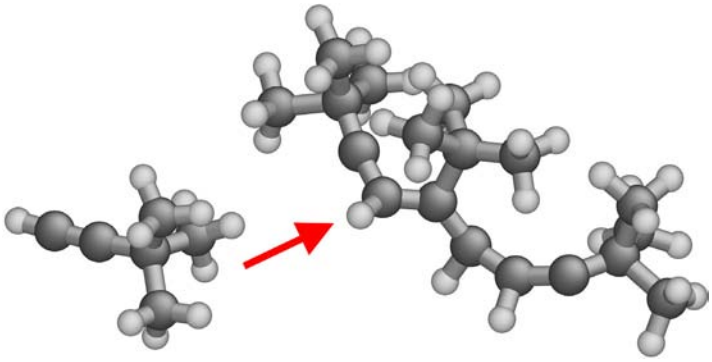

Figure 3. Intermediate step during the radical chain polymerization of tert-butylacetylene molecules from a LATTE simulation. The small and large spheres are hydrogen and carbon atoms, respectively.

Future Work

The current version of LATTE employs only dense matrix algebra and as a result computational time scales with the cube of the number of atoms, or $O(N^3)$. This aspect of LATTE limits severely the maximum number of atoms that can be modeled. However, we have pursued algorithms that are suited to implementation in sparse matrix schemes such that the computational cost will scale linear with system size, or O(N). LATTE will be extended over the coming year to employ sparse matrix algebra and we expect to be able to perform simulations with orders of magnitude more atoms than is possible today.

Our SCC-TB parameterization for hydrocarbons is both accurate and transferable. Unfortunately, the development a transferable model for oxygen has been more difficult. In order to improve the quality of our materials models will we extend our SCC-TB formalism to better describe the environmental dependencies of interatomic bonding via the addition of non-orthogonal basis sets.

We will continue to port algorithms from CPUs to GPUs and develop, support, and release high performance, user-friendly code to research groups worldwide.

The work started during this LDRD-ER project became the main theoretical thrust of the 2011 new-start LDRD-DR project "First Reactions: Simple Molecule Chemistry Behind the Shock Front", PI: D. M. Dattelbaum. Hence, we have demonstrated both the relevance of our simulations to the wider LANL community and our ability to secure follow-on funding.

Conclusion

Computer modeling and molecular dynamics simulations are one of the few tools available for the study of the initial mechanical and chemical events at the atomic scale that lead to detonation in energetic materials. To push LANL's capabilities in this area we have developed from scratch a quantum-based molecular dynamics code that displays exceptional levels of performance and which is aligned with emerging trends in the architectures of high performance computing. Furthermore, we have released our code under a GPL to stimulate and facilitate research at institutions worldwide. Our materials models and simulation methodologies have enabled simulations of shock-induced chemical reactions that capture without approximation their endo- or exothermicity and adiabatic shock heating. We will also pursue theoretical and computational advances over the coming year to improve further the accuracy of our predictions and the increase significantly the size and duration of our simulations.

References

1. Elstner, M., D. Porezag, G. Jungnickel, J. Elsner, M. Haugk, T. Frauenheim, S. Suhai, and G. Seifert. Self-consistent-charge density-functional tight-binding method for simulations of complex materials properties. 1998. *PHYSICAL REVIEW B.* **58** (11): 7260.

2. Sanville, E. J., N. Bock, A. M. N. Niklasson, M. J. Cawkwell, T. D. Sewell, D. M. Dattelbaum, and S. A. Sheffield. Extended Lagrangian quantum molecular dynamics simulations of shock-induced chemistry in hydrocarbons. To appear in *14 International Detonation Symposium.* (Coeur D'Alene, 1-16 April 2010).

3. Sanville, E. J., N. Bock, A. M. N. Niklasson, and M. J. Cawkwell. LATTE (LA-CC 10-004). 2010. .

4. Niklasson, A. M.. Expansion algorithm for the density matrix. 2002. *Physical Review B (Condensed Matter and Materials Physics).* **66** (15): 155115.

5. Niklasson, A. M.. Extended Born-Oppenheimer molecular dynamics. 2008. *Physical Review Letters.* **100** (12): 123004.

6. Sheffield, S. A., D. M. Dattelbaum, R. R. Alcon, D. L. Robbins, D. B. Stahl, and R. L. Gustavsen. Shock-induced chemical reactions in organic and silicon based liquids. 2006. In *Shock Compression of Condensed Matter - 2005.* (Baltimore, 31 July - 5 Aug. 2005). , p. 921. : American Institute of Physics.

Publications

Sanville, E. J., N. Bock, A. M. N. Niklasson, M. J. Cawkwell, T. D. Sewell, D. M. Dattelbaum, and S. A. Sheffield. Extended Lagrangian quantum molecular dynamics simulations of shock-induced chemistry in hydrocarbons. To appear in *14th International Detonation Symposium.* (Coeur d'Alene, 11-16 April 2010).

Transparent Organic Solar Cells

Ian H. Campbell
20090393ER

Introduction

The ideal solar cell would convert every bit of energy in photons originating from the sun into usable energy. We propose a completely novel approach which would "milk" a small amount of energy from solar photons in a most unobtrusive fashion. We propose to develop a new class of truly transparent solar cells using organic semiconductors. A transparent solar cell is designed to have > ~85% transmission in the visible region of the solar spectrum. Although, transparency necessarily decreases the maximum possible efficiency of the cell, it enables two specialty applications: windows and stealth. A transparent solar cell for windows is designed to use window glass as the substrate for the solar cell and thus reduce costs associated with fabrication and installation. Many of the materials required for transparent solar cells are already used in high performance windows and transparent solar cells can be designed to also function as low-e window coatings. Transparent solar cells for stealth applications are designed to provide power in applications where the solar cell should be difficult to detect, for example, it can be added to an existing surface to provide power for surreptitious electronic devices.

Benefit to National Security Missions

This work will contribute to enhancing the national energy security, a key DOE mission area. The ability to incorporate solar cells into conventional windows, using many of the materials and coatings already used in high performance windows, could provide an economic method to deploy solar cells.

Progress

We are using a closely coupled fabrication/measurement/theory approach to demonstrate and optimize transparent organic solar cells. We are fabricating specialized material test structures and prototype solar cells to understand the semiconductor and device parameters that control the cell performance. Simultaneously, the electronic structure and optical properties of semiconductors are being calculated and the results used to interpret the test structure and device performance and, most importantly, to guide materials design modifications needed to maximize device performance. We are using our established relationships with organic chemical companies to obtain new, specialized organic semiconductors. The project naturally divides into work focusing on two tasks: 1) understanding the relevant properties of the organic semiconductors and 2) designing and fabricating solar cells made from these materials.

The organic semiconductors we are working with are naphthalocyanine compounds that are transparent in the visible spectrum and absorb strongly in the near infrared. We are exploring two major types of naphtalocyanine compouds: those that can be solution processed and those that can be thermally evaporated in vacuum. Solution processing is a very low cost method of producing thin films and electronic devices but the chemical purity of the materials can be difficult to control. Thermal evaporation in vacuum is also a low cost technique for device fabrication and it has the advantage that the materials used may be purified by a variety of sublimation techniques. The solution processed materials are part of the family of octabutoxy naphthalocyanines (OctNc). We are making chemical substitutions to the base OctNc molecule by adding a central metal atom or varying the ligands attached to the naphthalocyanine core to control the molecule's absorption in the infrared. The vacuum processed materials are part of the family of naphthalocyanines (Nc) where we are again making chemical substitutions to control the molecular optical properties. These two classes of molecules are very similar as they share the naphthalocyanine core. In addition to their processing and purity differences, the two molecular families have very different intermolecular interactions in the solid state. In the solid state, the absorption of the smaller, vacuum evaporated molecules can red shift by ~ 100 nm, significantly improving their infrared response. In contrast, the absorption properties of the solution processed molecules are essentially unchanged in the solid state. We are performing theoretical calculations of the electronic structure of these molecules to understand them and design new molecules with improved properties.

We are fabricating and testing transparent, organic so-

lar cells using these naphthalocyanine compounds as the critical, infrared absorbing layer. Indium tin oxide (ITO) is used as a transparent electrode. When combined with special surface layers, ITO can function as either an electron or hole injecting material. This is critical to retain the high transparency required in these devices. We are using very thin layers of C60 to dissociate excitons produced in the Nc layer and we have also explored large energy gap organic semiconductors such as bathocuproine to serve as an exciton blocking layer. The prototype device results are very encouraging. We have made structures that are > 80% transparent throughout the visible spectrum and have strong absorption in the infrared (IR). These devices have near ideal IR quantum efficiency, i.e. every photon absorbed produces one electron of photocurrent. We are now designing improved molecules and alternate solar cell device architectures that increase the IR absorption while maintaining visible transparency. This work has now been published in two Applied Physics Letters articles and widely disseminated in the trade journal Laser Focus World.

Future Work

The goals of this work are to demonstrate, for the first time, a truly transparent solar cell by exploiting the unique electronic structure of organic semiconductors, and to understand and optimize the electronic structure of these materials for this application. Technologically, organic semiconductors are of increasing importance for large area low cost applications such as displays, solid state lighting, large area electronics, and solar cells. From a scientific perspective, organic semiconductors offer a model system for studying multiscale physics involving, for example, the properties of individual molecules and their solid state intermolecular interactions.

Solar cell performance is controlled by exciton processes (transport and dissociation), charge carrier transport, and device open circuit voltage. Electronic processes in organic semiconductors are poorly understood: exciton processes are difficult to calculate and they have been reliably measured in few materials; charge carrier transport can be measured reliably but predicting the carrier mobility of solid films from molecular properties is problematic; and the open circuit voltage is determined by organic material/electrode interactions which only follow general relationships such as approximate scaling with electrode work function. Because organic semiconductors are condensed phases of organic molecules or polymers there is an essentially unlimited variety of organic semiconductors that can be created. Fundamental understanding is required in order to provide insight to develop new materials with properties tailored for this application.

We will use a closely coupled fabrication/measurement/theory approach to demonstrate and optimize transparent organic solar cells. We will fabricate specialized material test structures and prototype solar cells to understand the semiconductor and device parameters that control the cell performance. Simultaneously, the electronic structure and optical properties of semiconductors will be calculated and the results used to interpret the test structure and device performance and, most importantly, to guide materials design modifications needed to maximize device performance.

Conclusion

We propose to create a new class of truly transparent solar cells. A transparent solar cell is designed to use window glass as the substrate for the solar cell and thus reduce costs associated with fabrication and installation. Simply replacing the glass on office buildings could generate a large fraction of the building's electric power requirements. This would help the U.S. become energy independent in a cost effective manner.

Publications

Campbell, I.. Low-cost organic photodiodes reach into the infrared. 2010. *LASER FOCUS WORLD.* **46** (3): 45.

Campbell, I. H.. Transparent organic photodiodes with high quantum efficiency in the near infrared. 2010. *APPLIED PHYSICS LETTERS.* **97** (3): 033303.

Campbell, I. H., and B. K. Crone. A near infrared organic photodiode with gain at low bias voltage. 2009. *APPLIED PHYSICS LETTERS.* **95** (26): 263302.

Uranium Imido Complexes as Catalysts for the Reduction of Carbon Dioxide

James M. Boncella
20090397ER

Introduction

This project will attempt to use the chemical properties of uranium compounds in a method for the conversion of carbon dioxide into fuel. It will also attempt to utilize this unusual chemistry for the conversion of acid to hydrogen, a fuel that generates only water as a byproduct when used to produce energy. By generating gaseous products from uranium, the project attempts to quell concerns related to the use of radioactive materials to make useful products. The separation of gaseous products from the uranium will occur with absolutely no uranium contamination of the products or environment. This work is cutting edge science because it will develop new chemistry of uranium and apply it to develop a practical solution to an important problem in the field of energy production. Even if the project does not result in the development of a practical system for carbon dioxide conversion, the lessons learned will undoubtedly be useful to anyone working in this general area of chemical research. Thus, this project, if successful, will enable progress toward a carbon neutral fuel cycle and will reduce the production of greenhouse gases.

Benefit to National Security Missions

This project directly supports the U.S. drive for energy security and to maintain a safe nuclear stockpile by enhancing our understanding of actinide coordination chemistry. The work is basic science that supports DOE energy security and nuclear weapons missions.

Progress

Thus far in this project, we have been able to demonstrate that the novel uranium(VI) bis(imido) (imido compounds have a double bond between nitrogen and uranium) complexes that we discovered several years ago are capable of being reduced to lower oxidation states. We have succeeded in the synthesis of three new classes of uranium complexes that have these ligands. The compounds have uranium in the +5 and +4 oxidation states with either one or two imido ligands. The ability to access lower valent U complexes is the first step in investigating whether or not such compounds have the ability to reduce carbon dioxide. The initial U(V) complexes that were formed have structures in which the f1 metal centers interact with one another. This is only the second example of such electronic communication in a molecular actinide complex. Further chemistry of these U (V) complexes have led to the synthesis of U(IV) mono imido complexes through reaction with U(III) complexes. This revealed the fact that simple U(IV) mono imido complexes are stable and has led us to develop simple, high yielding syntheses of a family of U(IV) mono imido complexes that originate from readily available starting materials. The reaction chemistry of these new molecules demonstrates that the compounds are potent reducing agents forming U(VI) compounds, which provides a significant driving force for the chemistry. They do react with carbon dioxide or alkyl isocyanates (a carbon dioxide surrogate), though the products of these reactions are still being determined at the present time.

We have also been able to generate a U(IV) bis-imido complex that is extremely reactive. This compound is a molecular analogue of uranium dioxide, which is an ionic solid. The complex readily forms mono nuclear U(V) and U(VI) bis(imido) complexes and it will reduce the protons in an N-H bond of an amine to hydrogen. This demonstrates, in a general way, one of the fundamental premises of the project. The new molecules promise to provide us with information on the bonding in uranium and actinide complexes in general. Qualitatively, the observed extreme reactivity of some of these compounds shows that simple theories of actinide bonding and reactivity are clearly incorrect. The observed reactivity is clearly not predicted by the standard theories. The ability of these molecules to undergo oxidation reactions will allow us to begin to understand this type of reactivity of uranium. Surprisingly, this reaction chemistry is not well-developed despite the fact that uranium has 4 stable oxidation states. It is likely that the typical compounds that have been used throughout the development of uranium chemistry do not allow oxidation chemistry to occur. It is the combination of the imido ligand with the other ancillary ligands that we are using that will allow us to investigate and exploit uranium oxidation chemistry.

Future Work

The goal of this research is to develop the chemistry of this series of unique uranium complexes and apply it to the formation of useful products. The uranium compounds that are the focus of this proposal have the potential to function as catalysts for the reduction of carbon dioxide generating products that can be used as fuels. They also have the potential to generate hydrogen from protons. This is a fundamental process that is central to the function of light driven water splitting reactions, and is carried out in biology by enzymes. Understanding these kinds of chemical reactions will be central to solving some of the most vexing and important energy problems that our society currently faces. This research will be the first example of using 5f electron species (actinides) to perform these types of reactions. It is enabled by our ability to access a new class of bis(imido) uranium complexes. The successful reduction of carbon dioxide or the conversion of protons to hydrogen will demonstrate that it is possible for actinide complexes to be used in this manner. It could make the practical application of actinide catalysis a real possibility. It is unlikely that the complexes that are now in hand will be the best catalysts that we will develop. The search for better catalysts through modification of the uranium compounds is the approach that we will take. Ultimately, this work will answer the question of whether it is possible dictate the reaction chemistry of uranium. Such tuning would represent a giant advance in actinide chemistry of the type that would be fitting for an institution with LANL's tradition in actinide chemistry.

Conclusion

This project will attempt to produce a method for the conversion of the green house gas, carbon dioxide, into a usable fuel or fuels. If successful, this project will contribute to the realization of the goal of a carbon neutral fuel cycle while providing a use for the significant stocks of depleted uranium that exist in the United States. If successful, this project will convert an environmental liability into a useful resource that has the potential to make a positive impact on carbon dioxide emissions and therefore global warming.

Publications

Spencer, L., E. Schelter, P. Yang, R. Gdula, B. Scott, J. Thompson, J. Kiplinger, E. Batista, and J. Boncella. Cation-Cation Interactions, Magnetic Communication, and Reactivity of the Pentavalent Uranium Ion [U(NtBu)(2)] (+). 2009. *ANGEWANDTE CHEMIE-INTERNATIONAL EDITION.* **48** (21): 3795.

Spencer, L., P. Yang, B. Scott, E. Batista, and J. Boncella. Uranium(VI) Bis(imido) Chalcogenate Complexes: Synthesis and Density Functional Theory Analysis. 2009. *INORGANIC CHEMISTRY.* **48** (6): 2693.

Spencer, L., P. Yang, B. Scott, E. Batista, and J. Boncella. Uranium(VI) bis(imido) disulfonamide and dihalide complexes: Synthesis density functional theory analysis. 2010. *COMPTES RENDUS CHIMIE.* **13** (6-7, SI): 758.

Spencer, L., P. Yang, B. Scott, E. Batista, and J. Boncella. Oxidative Addition to U(V)-U(V) Dimers: Facile Routes to Uranium(VI) Bis(imido) Complexes. 2009. *INORGANIC CHEMISTRY.* **48** (24): 11615.

Spencer, L., R. Gdula, T. Hayton, B. Scott, and J. Boncella. Synthesis and reactivity of bis(imido) uranium(VI) cyclopentadienyl complexes. 2008. *CHEMICAL COMMUNICATIONS.* (40): 4986.

Swartz, D., L. Spencer, B. Scott, A. Odom, and J. Boncella. Exploring the coordination modes of pyrrolyl ligands in bis(imido) uranium(VI) complexes. 2010. *DALTON TRANSACTIONS.* **39** (29): 6841.

Earth Tremor, Time Reversal and Earthquake Forecasting

Paul A. Johnson
20100141ER

Introduction

Along tectonic plate boundaries, two plates move relative to each other. Under circumstances not well understood, portions of the plates become locked due to friction. As a result, the locked portions accumulate stress while the surrounding rock continues to deform. When the locked region reaches a critical state and releases catastrophically, an earthquake occurs. It is this scenario that has produced the largest and most devastating earthquakes in history, and the details of which we must ultimately understand if earthquake forecasting is to become a reality. A recent phenomena has been discovered that could have a profound impact on forecasting large earthquakes: an Earth rumbling called non-volcanic tremor comprised of long seismic signals with no discrete beginning or end. Tremor has been observed in an increasing number of active tectonic environments, including subduction zones and transform faults such as the San Andreas. Tremor, if it is located on the plate interface, may be the manifestation of slip on a series of faults, that may organize and accelerate before reaching a critical size where the system destabilizes catastrophically and an earthquake occurs. However, we cannot be certain tremor originates at the plate interface because tremor cannot be located applying classical seismic means. A number of tremor location schemes are in development that are based on unproven assumptions; the tremor locations resulting from these procedures are literally all over the map. Until tremor is definitely located, we have no hope of taking the next step and testing it as an earthquake precursor. We know how to locate tremor using our unique expertise in seismology and time reversal. That is the goal of our work.

Benefit to National Security Missions

In addition to impacting the national security by enabling earthquake prediction, there are numerous other problems of interest to DOE where location of long-duration sources would have direct application, such as locating underground structures that broadcast long duration signals from machinery located within. Other pertinent problems include locating moving vehicles (aircraft, ships, submarines), as well as swimmers.

Progress

We have made significant progress in three areas of our tremor work:

- Continuing tremor location using time reversal;
- Continuing laboratory studies where we are trying to understand how tremor originates, how it may be triggered by seismic waves, and its association with other kinds of slip events, especially slow slip. Tremor and slow slip are frequently associated, and triggered slow slip and tremor are exciting new observations in Earth that are poorly understood;
- Developing new models that help us understand the physics of how tremor originates. The models are coupled to both experiment and Earth observations.

In the following, we present details of each of these areas.

For the first progress item, we published an overview paper in the August issue of Physics Today [1] regarding applying time reversal to earthquake source location. That paper contained a portion describing location of tremor. Our test bed data set is that of tremor that was triggered southeast of the Park field, CA, by seismic waves emanating from the August, 2009, magnitude 5.8 Mexicali Earthquake. We find that, by using a seismic recording array located on Earth's surface very near to the triggered tremor source, we can locate the tremor source at about 23 km depth along a fault associated with the San Andreas Fault. We also published a paper describing our approach to the time reversal imaging problem [2]. We are currently outlining a manuscript before we submit it for publication. This work is being led by post doc Caréne Larmat.

For the second progress item, we have made much progress in regards to characterizing slow-slip and tremor in the laboratory and relating it to field observations. The experimental studies are being conducted at the Pennsylvania state university. We observe both phenomena and the experiments are helping us understand

the physical regimes in which they occur. We are comparing the experimental results to field observations of tremor and slow slip that occurred along the Parkfield segment of the San Andreas Fault in 2004. For the observational component, we are collaborating with David Shelly at the USGS in Menlo Park, CA. A manuscript describing the observations is currently 80% complete and will be submitted very soon.

For the third progress item, our modeling work is comprised of two approaches. At Los Alamos we are developing a physical based frictional model that encompasses all types of slip including slow slip and tremor. This work is being led by post doc Eric Daub at Los Alamos. A manuscrpt describing the initial results is in review currently [2]. In collaboration with ETH Zurich, we are developing a Molecular Dynamical model of slip in granular media. This model provides the means to understand the physics of slow slip and tremor at the grain scale, which is not the case with the other modeling procedure. The work is being led by ex-LANL post doc and now researcher at the Swiss National Laboratory (EMPA), Michele Griffa. We have a manuscript describing these results that is currently in review [3].

Future Work

Our approach is comprised of: (a) laboratory experiments, (b) modeling (c) location of actual tremor. Our goal is to locate tremor understand the physics of tremor and associated slow slip and how the relate to earthquakes.

Laboratory studies. We will continue laboratory studies of tremor and slow slip in sheared granular media as described above. These experiments will guide the numerical and Earth tremor studies.

Model studies. We will continue to develop the two modeling approaches in order to understand how tremor and slow slip may take place, and to characterize the physics of the process.

Tremor location in Earth. We will continue to hone our skills for locating tremor in Earth. We have developed a number of novel procedures for locating tremor and we expect these will become important as we proceed and will eventually be used by others for earthquake location.

Conclusion

At the end of three years we will have definitively answered the question of where tremor originates for a given region—and will have made tremendous progress on understand the physics of tremor and slow slip. By doing so, we will resolve whether or not tremor can be tested in the framework of a new earthquake forecasting tool. We will create a new goal at LANL in locating noisy underground structures, swimmers/divers with nefarious intent, location of moving vehicles, and aircraft, all difficult problems at present for the same reason as tremor: no discrete wave arrivals.

References

1. Larmat, C., R. Guyer, and P. Johnson. Time-reversal methods in geophysics. 2010. *PHYSICS TODAY.* **63** (8): 31.

2. Larmat, C., R. Guyer, and P. Johnson. Tremor source location using Time Reversal: selecting the appropriate imaging field. 2009. *Geophysical Research Leters.* **36** (L22304): 4.

3. Daub, E., D. Shelly, R. Guyer, and P. Johnson. Brittle and ductile friction and the physics of tectonic tremor. *Nature Geoscience.*

4. Griffa, M., E. Daub, R. Guyer, P. A. Johnson, and C. Marone. Vibration-induced unjamming of sheared granular layers and the micromechanics of dynamic earthquake triggering. *Physical Review Letters.*

Publications

Larmat, C., R. Guyer, and P. A. Johnson. Tremor source location using Time Reversal: selecting the appropriate imaging field. 2009. *GEOPHYSICAL RESEARCH LETTERS.* **36**: L22304.

Larmat, C., R. Guyer, and P. Johnson. Time-reversal methods in geophysics. 2010. *PHYSICS TODAY.* **63** (8): 31.

New Generation "Giant" Nanocrystal Quantum Dots for Transformational Breakthrough in Solid State Lighting

Han Htoon
20100144ER

Introduction

The incandescent lamps, which are currently utilized for 42% of the general lighting applications, are capable of converting only 5% of electrical energy into light, wasting remaining 95% to useless heat. For this reason, tremendous research efforts have been invested into the development of new solid-state lighting technologies (SSL) which ultimately aim to generate light without heat. Group III-nitride-based light emitting diodes (LEDs) and thin-film organic LEDs (OLEDs) have been at the forefront of these research efforts. Although these two technologies have delivered LEDs that are 5 to 10 times more efficient than that of incandescent lamps, they are not yet cost efficient for an average consumer and far from reaching the ultimate goal of SSL.

Since their initial discovery, nanocrystal quantum dots (NQDs) have been considered as a key material for SSL because they not only exhibit robust optical characteristics but also can be synthesized and processed into LED devices in very cost efficient ways. However, NQD-based LEDs (NQD LEDs) reported to date suffer from low efficiency (external quantum efficiency, EQE < 2%) and short device lifetimes (<300 h).

The overarching goal of this proposal is to develop the first, all-solid-state NQD-LED for a paradigm shift in efficiency and stability by integrating two of LANL's unique inventions: (1) a new class of colloidal NQD – the so-called 'giant' (core)shell NQD (g-NQD), that exhibits transformational optical, mechanical and chemical characteristics, and (2) the polymer-assisted deposition (PAD) technology that enables cost-effective growth of semiconductor-nanoparticle composite films.

Benefit to National Security Missions

The proposed g-NQD based, low-cost, all-solid-state LED architecture has the potential to become the key enabling technology for energy-efficient SSL applications. Furthermore, it could also pave the way for electrically pumped NQD lasers and single-photon sources that have applications in defense and intelligence programs. Our project, therefore, directly addresses the main mission of DOE "Discovering the solution to power and secure America's future" through strategic themes of "energy security" and "scientific discovery and innovation".

Progress

Integration of g-NQDs with PADs

Achieve chemical compatibility between g-NQD and PAD processes: While as-prepared, g-NQDs are soluble in nonpolar solvents, e.g., hexane and toluene, the PAD process requires g-NQDs to be soluble in water. Although ligand exchange procedures that would render g-NQD water soluble already exist, they provided limited absolute concentrations—insufficient to afford the growth of densely packed g-NQD/PAD composite films. To this end, Jennifer Hollingsworth's team had explored ligand-exchange parameters that influence transfer efficiency and nanoparticle solubility in water: stirring conditions, concentration of exchange-ligand, concentration of base, temperature, and time. The relatively large size of g-NQDs make this optimization more difficult than in the case of conventional smaller NQDs, nevertheless, we have managed to achieve adequately high concentrations.

Identify a key road block in the growth of g-NQD/PAD composite films: We propose to fabricate our g-NQD composite active layer by spin coating the premixed solution of stable metal-polymer precursors and polymer-coated g-NQDs, followed by heat treatment in an appropriate gas environment (e.g. NH_4 for GaN). The success of this approach depends upon whether g-NQDs will withstand the heat treatment that is necessary for removal of the organic component of the metal-polymer precursor mixture and crystallization. Based on g-NQDs' capability of emitting efficient PL after the removal of ligand layer together with previous melting studies of NQDs, we preliminarily assessed that PAD processing is not anticipated to impact g-NQD PL. However, we observed that the PL of the g-NQD is strongly quenched when g-NQD/PAD composite films were grown via conventional PAD approach. Further systematic studies by Guifu Zou and Quanxi Jia reveal that the quenching is

mainly caused by the presence of oxygen in the annealing environment. Specifically, annealing of g-NQDs-PAD precursor films to 350 °C under high vacuum condition does not cause any degradation in PL emission property of the film, however, annealing in a furnace with flowing argon gas at the same temperature causes complete quenching of the PL. Based on this observation, we are developing a vacuum thermal process for the growth of functional g-NQD/PAD composite films.

Fabrication and characterization of LEDs

Established thin film deposition and LED characterization capabilities: Don Werder and Bhola N. Pal have established capabilities to deposit various types of thin films required for fabrication of all in-organic LED (i.e NiO, ZnO, Zn:SnO, etc). Sergio Brovellei has designed and built the facility for quantitative characterization of LED device performance.

Achieve >0.1% EQE in very simple proto-type LED: In parallel with g-NQD-PAD integration, Bhola N. Pal is determining which of the g-NQD structures is most appropriate for LED device by incorporating g-NQDs into a very simple device structure: ITO/PEDOT-PSS/g-NQD/LiF/Al. These simple devices that use -NQDs with 16 CdS shells as active layer yield an external quantum efficiency (EQE) of up to 0.12% and a maximum luminance approaching 1000 Cd/m^2 (in air). [Figure 1] Since this device contains neither any luminescent electron/hole injecting layers nor any additional encapsulation, they produce electroluminescence (EL), which is solely due to NQDs excited via direct charge injection. The observed performance is already comparable to that of the more sophisticated all-inorganic NQD LEDs that operate on similar direct carrier injection. Further studies on shell thickness dependence of EQE reveal that g-NQD (>12 CdS monolayer shells) devices show EQEs about one order of magnitude higher than those of thin-shell NQD (4 ML) devices, as well as much greater stability for operation under ambient conditions. Although current performance of the g-NQD devices is still below the record numbers achieved for more sophisticated NQD-LEDs, this work demonstrates that the thick shells of g-NQD provide dramatic improvement of stability and performance for LED applications.

Established synthetic protocol for blue emitting g-NQDs: Jennifer Hollingsworth's team has established the synthetic protocol for CdZnS (core)/ ZnS (shell) and CdS (core) / ZnMgS(shell) g-NQDs that emit in the blue region of the spectral range (415-465nm)[Figure 2]. To date, we have achieved the best color tunability with the CdZnS-based system, largely because the alloyed nature of the core allows for compositional control over the core emission wavelength. Red-shifting upon shell addition has been minimal for both systems compared to the CdSe-based g-NQD counterparts. Size disparity and quantum yields need to be optimized, with the highest quantum yields (>40%) observed only for the middle-shell thicknesses (3-5 monolayers) and lower emission efficiencies (10-20%) obtained for the thicker shell systems (8-10 monolayers).

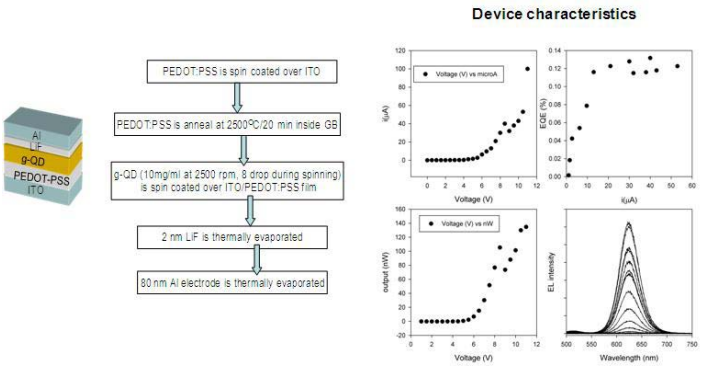

Figure 1. Schematic of prototyped LED device and performance data. Despite the simplicity of the structure, this device exhibit the performance comparable to more state of the art all in-organic NQD LEDs.

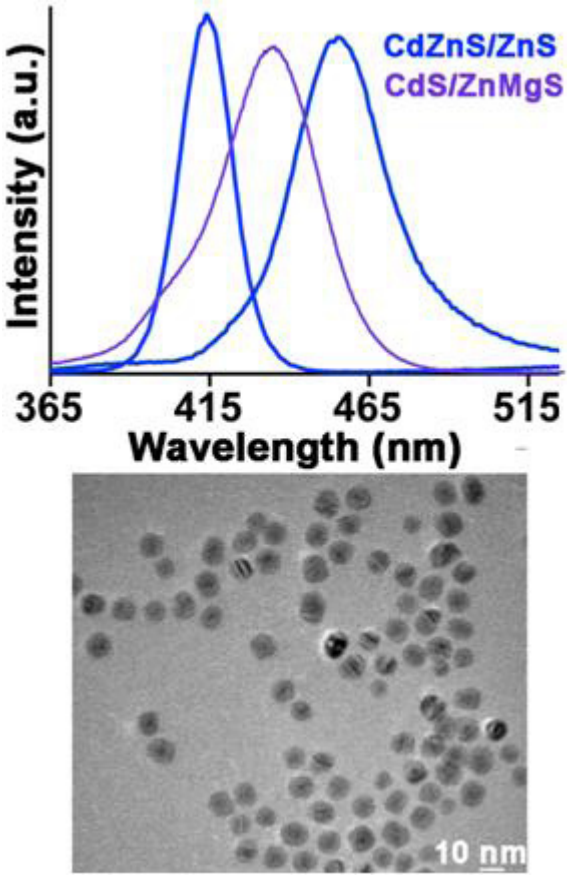

Figure 2. Emission spectra and TEM image of g-NQDs emitting in blue spectral range.

Evaluating the potential of g-NQD as red phosphor for down conversion LEDs

Down conversion, white-light LEDs, in which blue light of an InGaN LED chip is down converted to longer wavelengths, have tremendous potential at mass market of illumination devices. Current commercially available white

LEDs exhibit poor color-rendering properties due to the lack of green and red component in emission spectra of converter material YAG:Ce. NQDs have been considered for this application due to their size tunable emission color. However, the strong dependency of NQDs PL emission properties upon its ligand coating has lead to poor efficiency and thermal stability of standard -NQD based phosphor. Our g-NQDs that emit at 620 nm, have already been demonstrated to emit efficient PL at temperature >350 °C without the presence of ligand coating. In addition our g-NQD also exhibit good excitability with blue light and low unwanted green/yellow absorbance that are highly desirable for phosphor applications. For these reasons, here we expand the scope of our project to systematically evaluate the potential of g-NQD as red phosphor s and develop prototype down conversion LEDs. As the first step, Janardan Kundu and Jennifer Hollingsworth are now developing a simple electroluminescence device, in which a commercially available blue emitting electroluminescent phosphor acts as an excitation source to the g-NQD/PLMA polymer composite layer deposited on the ITO substrate [Figure 3(a)]. The Red emission component of g-NQD is clearly observable in the electroluminescence spectra of g-NQD phosphor composite device under 350V, 30KHz AC bias [Figure 3(b)].

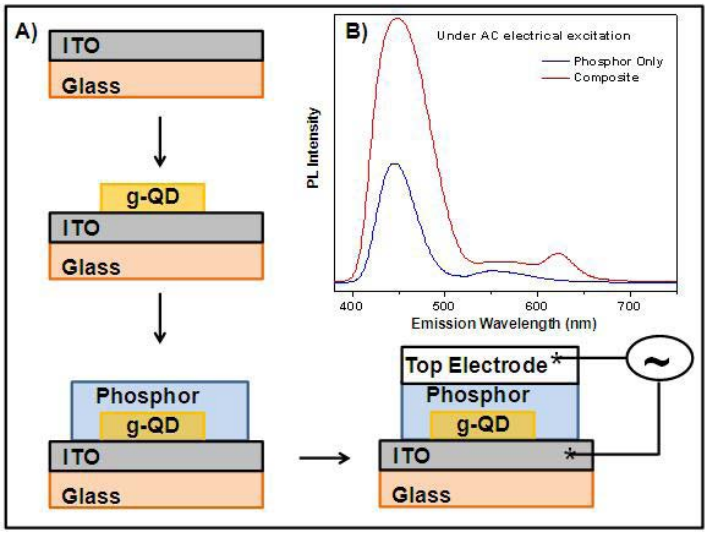

Figure 3. Prototype electroluminescence device: (a) Schematic showing the fabrication process and (b) Electroluminescence spectra of phosphor only (blue) and composite (red) devices.

Future Work

g-NQD/PAD integration and fabrication of all-solid-state LEDs: we will complete the development of vacuum thermal process for the growth of functional g-NQD/PAD composite films in the second year and optimize the process to ultimately achieve novel all-solid-state LED active layer. We will, in parallel, optimize the simple prototype g-NQD device structures and later integrate with g-NQD/PAD composite active layer to demonstrate an all-solid-state LED.

We will also integrate the g-NQD/PAD composite active layer to GaN p-i-n diode and Ag/PAD GaN/g-NQD/P-NiO diode structures.

Evaluating the potential of g-NQD as red phosphor for down conversion LEDs: We are currently focusing on optimizing ratio of the blue phosphor and g-NQDs to achieve stronger red emission. We will also directly compare the stability of g-NQDs with thinner shell NQDs under continuous operation. In addition, we will attempt to demonstrate an advantage afforded by the large effective g-NQD Stokes shift with respect to reduced self re-absorption in high-density films compared to thinner shell systems.

Development of synthesis routes for green and blue-emitting g-NQDs: We will continue to optimize the synthesis of blue emitting g-NQDs to reach higher QY. We will also explore ZnSe cores coupled with a ZnS shell system for green emitting g-NQDs.

Finally on the third year, we will integrate all these efforts to demonstrate high-efficiency, low-cost single-color and white-light LEDs.

Conclusion

Up to this moment, we have (1) established all the capabilities necessary for fabrication and characterization of LEDs; (2) solved/identify major technical problems in our attempt to ward g-NQD-PAD integration and; (3) achieved a very simple LED structure that could rival the performance of the best all-inorganic LEDs. In addition to these accomplishments, we are expanding the scope of our project to evaluate the potential of our g-NQDs as a red phosphor for white light LEDs.

Publications

Pal, B. N., S. Brovelli, Y. Ghosh, V. I. Klimov, J. A. Hollingsworth, and H. Htoon. New type of core-shell nanocrystal quantum dots for applications in light emitting diodes . Presented at *MRS 2011 Spring Meeting.* (San Francisco, April 25-29).

New Catalytic Methods for Selective C-C Bond Cleavage in Lignin: Towards Sustainable and Renewable Chemicals and Fuels

Louis A. Silks III
20100160ER

Introduction

We are developing new catalysts for the selective unraveling and monomer unit extraction of the natural polymer lignin. Lignin is a non-food biomass that makes up the woody component of lignocellulose. The DOE estimates that the US could produce as much as 1.3 billion tons/y of lignocellulosic biomass, enough to replace 30% of the current US petroleum consumption. Efficient transformation of lignocellulose into usable chemicals and fuels remains a major challenge, particularly due to the difficulties associated with lignin breakdown. Lignin is resistant to natural decomposition processes, and has been considered a nuisance or roadblock in the conversion of biomass to fuels. Methods to depolymerize lignin would therefore potentially be a key breakthrough towards the production of bioderived fuels and chemicals. Our catalytic oxidation of lignin is targeted to convert lignin into smaller, soluble, more useful components using less energy and generating less waste than current methods. Such a process will have dual usage: it would provide a way to improve biofuels processing by removing lignin, as well as provide a new route to valuable aromatic compounds necessary for jet fuels (DOD applications) and industrial applications (Industry has expressed a strong interest in our lignin depolymerization program for their aromatic chemical feedstock needs).

Benefit to National Security Missions

The proposed work will significantly contribute to the development of alternative and renewable sources of energy, facilitate reduction of CO2 emissions, and contribute new technologies to enable us to live in a more sustainable fashion. Catalysts currently used with great success in the petroleum industry are not compatible with the highly functionalized compounds derived from biomass, and thus, new catalytic approaches are fundamentally required for the unraveling of complex organic molecules of biological origin. Moreover, this project directly impacts the sustainable and renewable energy needs the US.

Progress

Efficient transformation of lignocellulose into more valuable products remains a major challenge, particularly due to the difficulties associated with breakdown of lignin. New methods to depolymerize lignin would represent a major breakthrough towards the production of bio-derived chemicals and fuels. An aerobic oxidation could be an inexpensive, environmentally friendly approach to convert lignin into smaller, soluble components. As described below, we have developed several vanadium catalysts capable of aerobic oxidation under mild conditions and have carried out studies to understand the mechanisms of these reactions and explore the substrate scope and selectivity.

A greater understanding the mechanism of vanadium-mediated oxidations could enable the development of more effective vanadium catalysts, and could elucidate factors underlying the overall reaction selectivity. Detailed investigations of the mechanism of alcohol oxidation by dipicolinate vanadium(V) have been carried out. The role of the pyridine in the reaction has been studied. Kinetic studies of the alcohol oxidation suggest a pathway where the rate-limiting step is a bimolecular reaction involving attack of pyridine on the C-H bond of the isopropoxide ligand. The oxidations of mechanistic probes cyclobutanol and tertbutylbenzylalcohol support a two-electron pathway proceeding through a vanadium(III) intermediate. The alcohol oxidation reaction is promoted by more basic pyridines and facilitated by electron-withdrawing substituents on the dipicolinate ligand. The involvement of the base in the elementary alcohol oxidation step determined for dipicolinate vanadium(V) is a substantial departure from what has been previously proposed and may provide a new handle for controlling selectivity in vanadium-mediated lignin oxidations. This work was accepted for publication in the *Journal of the American Chemical Society*.

Based on the results of the mechanistic study described above, a new catalytic system was discovered capable of aerobic oxidation under very mild conditions. A number of different additives, solvents, and vanadium catalysts

were tested, and it was found that the combination of the complex (HQ)2VV(O)OiPr (HQ = 8-hydroxyquinolinate) and NEt3 is a highly active catalyst for aerobic alcohol oxidation. Conversion is significantly diminished in the absence of triethylamine. The substrate scope was also investigated; benzylic, allylic, and propargylic alcohols were readily oxidized to the corresponding aldehydes while aliphatic and sterically hindered alcohols showed little or no conversion. This catalytic system is advantageous in that it features an inexpensive base metal catalyst, produces water as the by-product of oxidation, and provides a significant improvement in atom economy over traditional stoichiometric oxidants. The oxidations of several lignin model complexes are currently being tested using the optimized catalytic system. The model systems have been constructed and are stable isotope labeled in strategic positions to all mechanistic interpretations. A manuscript has been written and will be submitted to *Angewandte Chemie* for consideration as a communication.

Future Work

Preparation of V and Mn complexes and the investigation of their stoichiometric and catalytic reactivity with lignin models, air, and H2O2. For molybdenum-based oxidations, the coordination mode of the substrate plays a critical role in determining product selectivity. Therefore, V and Mn complexes with bidentate and tridentate ligands (allows for a variety of coordination sites at the metal) will be prepared, as it is anticipated that these ancillary ligands may play a role in determining the ultimate product selectivity. Tuning the steric and electronic environment by ligand control will have significant effects on the regio- and chemoselectivity of the reaction.

1. Ligands stable to hydrolysis will be investigated. These ligand systems are also chosen as they may be readily synthetically modified to address trends in reactivity and selectivity discovered in initial mechanistic studies. The Schiff base ligand will allow for facile immobilization of the catalyst on a solid support and will be useful in aqueous systems. The V and Mn complexes will be characterized by a variety of spectroscopic techniques, including IR, NMR and UV-vis spectroscopies, as well as X-ray crystallography.

2. Explore the mechanism of reaction to develop more effective catalysts. The enzyme lignin peroxidase, found in white rot fungi, has been proposed to degrade lignin by generating oxidizing carrier species (such as ·OH or the veratryl alcohol radical cation) which subsequently react directly with the lignin. It is anticipated that the reaction mechanism of the V and Mn catalysts may differ from this enzymatic pathway. Both V and Mn can react by one-electron oxidation or hydrogen atom abstraction pathways, and preliminary studies described above have implicated a two-electron pathway for vanadium under certain conditions.

3. Explore the reactivity with commercial lignins: organosolv, kraft.

Conclusion

We are designing and contructing new catalysts based on vanadium and manganese (both bio-inspired) for the oxidation of lignins mediated by air or hydrogen peroxide. This work has the goals; (a) The synthesis and characterization these complexes, investigation of catalytic reactivity with lignin model compounds; (b) Elucidation of the mechanism of the reaction allow us to develop more effective and selective catalysts; (c) Upon selection of the best performing catalyst(s) begin study with commercially available lignins such as organosolv and kraft lignin. This project then, would provide sustainable and renewable sources of these important industrial compounds.

Probing the Structure of Superconducting States with Rotating Magnetic Field

Roman Movshovich
20100172ER

Introduction

Superconducting materials may have a significant impact on the energy use and requirements of the future. Superconductors provide means for loss-less energy transmission and energy storage among other important applications. The symmetry of the superconducting gap is one of the most important properties of a superconductor that might reveal its underlying microscopic mechanism. It is commonly the first question posed after the discovery of a new superconductor. Thermal transport and specific heat often provide important clues into the structure of the superconducting gap. For a fully gapped Fermi surface, both low temperature electronic specific heat and thermal conductivity in the superconducting state decay exponentially as a function of temperature, while the presence of nodes, where the super-conducting gap goes to zero, manifests itself in a power-law temperature dependence of these quantities. For example, thermal conductivity of CeCoIn5 in a magnetic field rotating within the a-b plane displayed four-fold oscillations, which was attributed to the presence of nodes in the superconducting gap that are located along the [110] direction, suggesting symmetry of the superconducting order parameter. Specific heat measurements, which too revealed four-fold oscillations in a field rotated within the a-b plane. With recent theoretical advances, a combination of ARCK tools (Angle-Resolved specific heat C and magneto-thermal conductivity κ) has the potential of becoming a powerful probe of the symmetry of the superconducting order parameter. We will validate the general correctness of our present theoretical understanding by performing ARCK on CeCoIn5 down to 20 mK and fields up to Hc2 ≈ 12 T. By combining both thermal conductivity and specific heat measurement capabilities at a single facility, together with the underpinning theoretical support required for this project, we will take the lead in this emerging field of ultralow-energy quasiparticle spectroscopy.

Benefit to National Security Missions

Superconductivity was the first examples of a macroscopic phase that arose from fundamentally quantum interactions. Since discovery, superconductivity was a foremost field of research, both basic as applied. Basic research in superconductivity these days is focusing on unconventional superconductivity, where novel phenomena and novel states of matter are discovered at great pace. This field of superconductivity is also directly related to applications, since most of the recently discovered high temperature superconductors belong to this class of materials. DOE/SC and NSF are therefore primary agencies, Basic Understanding of Materials is the primary mission that this project is relevant to.

Progress

We investigated superconducting state in ambient pressure non-centrosymmetric (NCS) superconductor LaRhSi3. It is an analogue of CeRhSi3, which superconducts under pressure. A number of NCS superconductors that contain Ce with its f-electron have been shown to be likely unconventional superconductors, where the superconducting energy gap disappears at some points or lines on the electronic Fermi surface (i.e. for some wave vectors k in the momentum space). The outstanding question is whether the unconventional nature in NCS materials is due to the presence of the f-electrons with associated magnetic fluctuations, as is the case for a number of heavy fermion U (with 5f-electrons) and Ce (with 4f-electron) compounds, or is directly related to the NCS crystal structure of these systems. We suspect not that LaRhSi3 is a Type I superconductor, and therefore the canonical route for using thermal conductivity to identify whether superconductor is unconventional, via field variation of the residual linear in temperature term, cannot be used. However, there are clearly several sharp features in thermal conductivity of LaRhSi3 that indicate phase transitions, creating a very rich phase diagram. Numerous anomalies in thermal conductivity of LaRhSi3 may be associated intermediate state, a mixture of superconducting and normal regions in a Type I superconductor. In that case, one might not expect a canonical square root dependence of thermal conductivity on the magnetic field at low fields. However, the nodal quasiparticles in unconventional superconductors should still be contributing to the heat current. This situation was not considered theoretically before, and

if LaRhSi3 is indeed an unconventional superconductor, it would represent a unique case of an unconventional Type I superconductor. We measured specific heat in single crystal sample on LaRhSi3 but so far did not identify a bulk phase transitions within superconducting state on LaRhSi3. We will continue to explore this scenario both theoretically and experimentally.

We have built specific heat cell for a rotator, with a calibrated RuO thermometer, and are ready to perform first measurements of specific heat in a rotated field. We are also building the next generation cell where it will be possible to rotate the sample stage with respect to the frame with fine control after the sample is mounted on the specific heat platform. This will ensure more accurate alignment of the sample with respect to the rotation axis.

On the Theory front, we developed, in collaboration with Vorontsov (MSU) and Vekhter (LSU), a multiband theory for calculating the specific heat and thermal conductivity in rotating magnetic fields in the superconducting state, an extension of the single band theory, [1-3] that was used to analyze several superconductors using simplistic Fermi surface model. Among characteristic features captured by this theory is the inversion of anisotropy patterns, [1] crucial for correct identification of the order parameter symmetry. Such inversions have been observed experimentally [4]. We tested our theory for a generic two-band model with d-wave pairing symmetry of the superconducting order parameter and successfully reproduced the experimentally observed four-fold symmetry. The multi-band code with simple circular Fermi surfaces was also used to describe observed thermodynamic and transport features [5] of iron-based superconductors, both in zero and finite magnetic fields, and successfully connect the experimental findings to the theoretical model [6]. In order to compare these calculations directly with experiments, we need to account for the real Fermi surface anisotropies of the conduction bands and electronic properties near the Fermi energy. The realistic Fermi surface is important because the anisotropy patterns shift in the T-H phase diagram depending on the relative position of gap nodes and specific parts of the Fermi surface [7]. We have begun with incorporating down-folded, but realistic electronic dispersions and Fermi surfaces for the Ce-115 family that will lead to realistic modeling of anisotropic properties in the superconducting state. In the next step, we will be able to use the rotational magnetic field dependence on specific heat and thermal conductivity in the superconducting state to reliably identify the pairing symmetry based on realistic Fermi surface parametrization.

With regard to personnel, we have hired a senior postdoc to work full time on the experimental part of this project, Franzisca Weickert from High Field Laboratory / Max Plank Institute for Chemical Physics of Solids, who started on November 1 2010. Mathias Graf has hired a theory postdoc, Tanmoy Das, who will work half-time on this ER project. Dr. Das has started in September. He comes from Arun Bansil's group at Northeastern University, and has done some nice work on cuprates using effective models derived from ab-initio.

Future Work

Thermal conductivity measurements under rotating magnetic field are proving to be a powerful probe of the structure of the superconducting energy gap and location of its nodes. CeCoIn5, originally discovered at LANL with Tc=2.3 K, was shown to be unconventional, with lines of nodes, via specific heat and thermal conductivity in zero magnetic field, based on the zero-temperature universal thermal conductivity and a power-law temperature dependence of thermal conductivity. CeCoIn5 was the first HFS where thermal conductivity in magnetic field rotated in the (a,b) plane displayed four-fold oscillations, which was attributed to the presence of nodes in the superconducting gap that are located along the [110] direction, suggesting symmetry of the superconducting order parameter. Similar thermal conductivity studies were subsequently used by the same group for the identification of the superconducting gap structure in a number of different superconductors, including organic, and a Pr-based (possibly electric quadrupolar origin) HFS. However, the need for a deeper understanding of the thermodynamic and transport phenomena under rotating magnetic fields was exposed by the subsequent specific heat measurements, which too revealed four-fold oscillations in a field rotated within the a-b plane, where the experimentally observed minima in the specific heat, under a rotating magnetic field, would place the nodes along the [100] and [010] directions, suggesting symmetry, in clear contradiction with the interpretation of the thermal conductivity measurements. This controversy pushed the development of more complicated theories of specific heat and thermal conductivity for nodal superconductors in rotating fields, which predicted that the positions of maxima and minima with rotating field, for both specific heat and thermal conductivity, should switch in the H-T plane, compared to the T=0 K expectations. We will look for this switching, thereby validating our understanding of Abrikosov vortex physics.

There are several superconducting samples that have been grown at MPA-CMMS that are relatives of 115 compounds. They include Pauli limited Ce_2PdIn_8, a "two $CeIn_3$ layer" compound, and $CePt_2In_7$, a "two spacer $PtIn_2$ layer" compound. We will investigate both of these compounds with ARCK technique. In addition, we will perform ARCK measurements on the very high purity UPt_3 samples from Pr. Halperin's group at Northwestern University.

Conclusion

Our ARCK measurements, over a broad range of field (from zero to Hc2 = 12 T) and temperature (from Tc down to 20 mK), will validate the available theoretical model, which reconciled the initially contradictory results in the higher

temperature regime. A detailed comparison between experimental results and theory will necessitate further refinement of theoretical models and shed light on the appropriateness of the approximations made in the model calculations. Using ARCK as the new ultralow-energy quasiparticle spectroscopy tool, we will establish the symmetry and structure of superconducting order parameters in a number of systems of current high interest.

References

1. Vorontsov, A., and I. Vekhter. Nodal structure of quasi-two-dimensional superconductors probed by a magnetic field. 2006. *Physical Review Letters.* **96** (23): 237001.

2. Vorontsov, A. B., and I. Vekhter. Unconventional superconductors under a rotating magnetic field. I. Density of states and specific heat. 2007. *PHYSICAL REVIEW B.* **75** (22): 224501.

3. Vorontsov, A. B., and I. Vekhter. Unconventional superconductors under a rotating magnetic field. II. Thermal transport. 2007. *PHYSICAL REVIEW B.* **75** (22): 224502.

4. An, K., T. Sakakibara, R. Settai, Y. Onuki, M. Hiragi, M. Ichioka, and K. MacHida. Sign reversal of field-angle resolved heat capacity oscillations in a heavy fermion superconductor CeCoIn5 and dx2-y2 pairing symmetry. 2010. *Physical Review Letters.* **104** (3): 037002.

5. Kim, H., R. T. Gordon, M. A. Tanatar, J. Hua, U. Welp, W. K. Kwok, N. Ni, S. L. Bud'ko, P. C. Canfield, A. B. Vorontsov, and R. Prozorov. London penetration depth in Ba(Fe_{1-x}T_x)₂As₂(T = Co, Ni) superconductors irradiated with heavy ions. 2010. *Physical Review B (Condensed Matter and Materials Physics).* **82** (6): 060518 (4 pp.).

6. Vorontsov, A. B., and I. Vekhter. Nodes versus minima in the energy gap of Iron Pnictide superconductors from field-induced anisotropy. 2010. *Physical Review Letters.* **105**: 187004.

7. Vekhter, I., and A. Vorontsov. Searching for zeroes: Unconventional superconductors in a magnetic field. 2008. *Physica B: Condensed Matter.* **403** (5-9): 958.

Biocatalysts: A Green Chemistry Approach to Industrially Relevant Compounds

Andrew T. Koppisch
20100182ER

Introduction

Catechol and catechol-derived products are globally consumed commodities of importance to a wide range of industrial applications, including textile and pharmaceutical synthesis, pesticide production and the specialty chemical industry. Catechol, like the majority of all phenol derivatives, is currently produced on an industrial scale (global consumption >20,000 metric tons per year) via distilling of thermally cracked crude oil, or by oxidation of benzene. Not only are these processes environmentally harmful, production costs are dictated by the price of crude oil. The main goal of this project is to develop a photosynthetic, environmentally friendly route to production of these important industrial products. This will be undertaken by metabolically engineering photosynthetic organisms with a unique enzyme discovered by our team which will afford it a means to produce the catechol precursor, 3, 4-dihydroxybenzoic acid. Further metabolic engineering processes will be pursued to provide a means to yield adipic acid, which is the primary component of nylon (Figure 1).

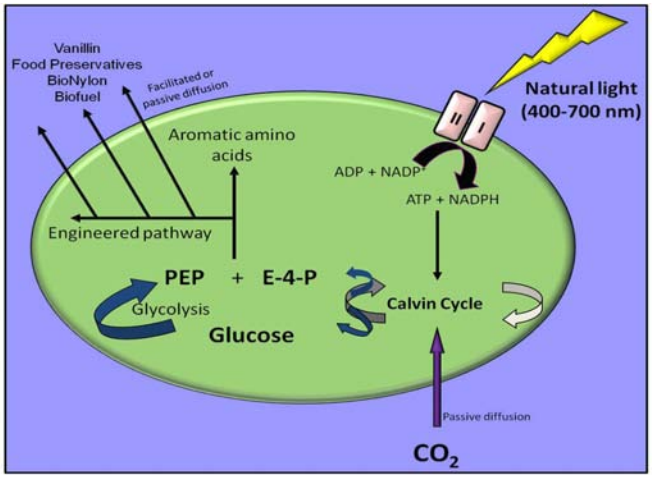

Figure 1. Engineering of phototrophic organisms to produce compounds used in a number of applications to society.

Benefit to National Security Missions

This work aims to produce commodity chemicals independent of the petroleum industry, and to do so via an approach that itself mediates environmental greenhouse gasses. This is directly in line with stated DOE-EERE missions in renewable energy and materials, and environmental stewardship. It also provides fundamental biological and engineering studies in phototrophs, which is of interest to other governmental agencies such as NIH or NSF.

Progress

We have pursued several goals in the first year of our ER project. We have three general specific aims: a) assembly, construction, and transformation of appropriate gene vectors into bacterial hosts to afford our catalysts the ability to make various commodity chemicals; b) optimization of the growth and maintenance conditions of our phototrophic host for commodity chemical production and c) pursue structural studies of the key members in our enzymatic process.

In the first months of our project, our laboratories were outfitted with equipment to facilitate culture of photosynthetic organisms. Two such organisms were obtained and growth protocols established. Further, we have compiled a small gene library from numerous soil-borne organisms encoding enzymes that are typically involved in multiple degradative catabolic pathways. Enzyme properties were previously determined, in most cases, and the enzyme activity verified for several in a eubacterial host. Initial experiments indicate that catechol production in heterotrophic strains (strains that utilize glucose or other solid carbon sources as the main means of cellular growth), which harbors two of our isolated genes, accumulates to an appreciable level in the growth media. Furthermore, additional plasmids are in construction that contains all of our genes of interest, and permutations thereof, to afford efficient enzyme production on a single transformable piece of DNA. This is expected to facilitate the production of the commodity chemicals of interest.

In addition, our team is in the process of incorporating a flow cytometry-based approach as a means to analyze the health, viability and robustness of our genetically modified phototrophs (G-MORPHs). Analysis of our G-MORPHs (strains that survive through photosynthesis using carbon dioxide as its main source of carbon for cell growth) using flow cytometry enables us to assess the culture health (as a fraction of the total that are surviving vs. those that are dead), and also to measure the properties that are associated with rapidly growing cells vs. those that are associated with slower growing cells (culture robustness). We estimate that this tool will be a very important mechanism for us to quantify the affects our genetic manipulations have on newly constructed G-MORPHs, and also a way to identify and isolate those that are not significantly affected by the process.

Our team is also pursuing large scale production of a key enzyme in our process for structural studies. Recent communications indicate that the N-terminal histidine tag amended to our original construct to facilitate protein purification is unsuitable for the subsequent protein crystallization. We have constructed two plasmids to alleviate this, both of which have segments encoding protease cleavage sites (either thrombin or TEV protease sites) amended to the gene sequence, which will allow us to remove the purification tag. Multi-milligram preparations of his-tag free enzyme are currently being developed, and upon establishment of this protocol extension to larger scale should follow readily.

After approximately 12 months of ER support, our team has submitted two invention disclosures to LANL tech transfer division and is currently working with the LANL intellectual property lawyers to develop these into full patents.

Future Work

In the future, we plan to engineer a phototrophic organism to produce the catechol precursor, 3, 4 dihydroxybenzoate (DHB).

Second, further engineering of the recombinant DHB producing organism will be undertaken to afford a strain which can produce cis, cis muconate (nylon precursor). Third, we will further optimize growth and maintenance conditions for enhancement of DHB and cis, cis muconate production, and to conduct advanced structural studies on our key enzyme for this process.

In order to address the first goal, we will transform cells with asbF, which is a novel enzyme discovered by our team. We have observed that integration of asbF into other bacteria outfits them with a means to make 3,4-DHB. Various reports document protocols for introduction of exogenous plasmids into cyanobacteria/algae and a number of promoters will be tested to effect optimum DHB production. Accomplishment of goal one is observable upon isolation of DHB from culture extracts of the recombinant strain.

Further engineering of the strain in aim 1, by introducing a second construct to the strain with genes encoding DHB decarboxylase and catechol 1,2-dioxygenase. This will provide the organism a means to cis, cis-muconate, which is transformed to adipic acid in one chemical step. Quantification of adipic acid production will also be undertaken.

Third, we will conduct studies to optimize the production of both aforementioned products in the recombinant host. The effect of various environmental variables on chemical production, such as light intensity, media nutrients and CO2 concentration will be explored to optimize production. We will also attempt to obtain a high-resolution neutron structure of the key enzyme of this process using unique LANL resources, which is expected to aid future engineering developments.

Conclusion

We aim to equip G-MORPHs with a means to produce a number of industrially important commodity chemicals, including catechol and nylon precursors, via metabolic engineering approaches being implemented in our laboratories. Tens of thousands of tons of these commodities are consumed annually across the globe, and currently they are almost exclusively produced from petroleates. Our work provides a renewable, petroleum-independent route to these commodities. Furthermore, since phototrophic organisms only require light and carbon dioxide for growth, our approach also provides a means to mitigate environmental greenhouse gases in this process.

Ultrafast Cathodoluminescence for Improved Gamma-Ray Scintillators

Jeffrey M. Pietryga
20100183ER

Introduction

Energy resolving gamma-ray detectors are crucial to national security, nonproliferation, and basic research. Principally, there is a need to identify radioactive materials (such as fissile material) and detect their movement. Energy resolving gamma-ray detectors are superior to "yes/no" gamma-ray detectors because they provide isotope identification information. Thus, the former can reduce high false positive rates on portal monitors used to prevent movement of fissile material. Energy resolving gamma-ray detectors need high efficiency conversion of the gamma-ray energy into charge. For large-scale applications, scintillators are usually employed wherein the gamma-ray energy is converted into photons, typically in a large, single crystal detector such as LaBr. When gamma-rays interact with matter, much of the energy is converted into energetic electrons that cascade into showers of lower and lower energy electrons. In single-crystal scintillators, the electrons produce visible photons in a relatively well-understood manner.

Semiconductor nanocrystals are of significant interest as scintillators because of their high-Z, high emission quantum yields, solution processibility and low cost in comparison to large single crystals. However, conversion of electron energy into photons is more complex in nanomaterials because of the influences of interfaces, quantum confinement and the material heterogeneity. While nanomaterials will interact with gamma-rays the same as other materials (it's an atomic process), it is largely unknown how they will respond to the energetic electrons that result. This disconnect makes it impossible to predict the performance of these promising materials, and thus current efforts are reduced to wasteful trial-and-error. Instead, exciting with an electron gun (as a surrogate for gamma-rays) and collecting the resulting emission, known as cathodoluminescence (CL), allows one to probe the same excitation and relaxation processes with a specificity impossible to achieve with actual gamma-rays. In this project, we will use a short pulse (10s of femtoseconds) ultra fast laser to excite a metal photocathode to create similarly short pulses of electrons. These short, synchronizable pulses will allow us to measure the transient CL on picoseconds timescales, which will yield important evidence regarding the nature of excitation and relaxation mechanisms in the nanomaterials. Finally, analysis of these mechanisms will provide feedback to the rational design and synthesis of the active materials for high performance energy-resolving gamma-ray scintillators that are operable at room temperature.

Benefit to National Security Missions

Energy resolving gamma-ray detectors are vital to nuclear nonproliferation and security as these devices impair material diversion and movement/smuggling of fissile materials. Semiconductor nanocrystals are recognized candidates for application as highly fieldable, high-energy resolution, scalable scintillators. This project aims to determine the extent of their utility for this purpose and thereby aid in threat reduction.

Progress

The ultimate goal of this project is a transient CL capability to probe the excitation branching ratios that energetic electrons produce upon interaction with fluorescent semiconductor nanocrystal and composite nanomaterials. Thus the project could be considered to comprise three major component efforts: 1) building a short-pulse laser-driven electron gun and CL chamber, and establishing controllable, reproducible production of low-fluence, synchronizable electron pulses; 2) baseline studies of known nanocrystal materials, such as cadmium selenide/zinc sulfide core/shell nanocrystals, to optimize system and sample parameters (laser power, electron-gun voltage, sample thickness and loading density, substrate, etc.) and to produce a database of spectral signatures that can be readily compared to known excitation states of semiconductor nanocrystals; 3) development of new nanocrystals and/or composites that show maximum luminescence signal and minimal non-radiative losses based on the initial baseline studies and continuous feedback from ongoing CL studies.

Clearly, each subsequent step builds on the successful completion of the previous, so our main objective for

the first year was to optimize the CL apparatus itself. As pictured and discussed in the proposal, a prototype version was constructed previous to the current project. The first major task was to build this rough proof-of-concept short-pulse electron gun into a fully functional CL instrument capable of stable, routine operation (Figure 1a). First, a more compact electron gun assembly (consisting of a gold film electrode and a series of accelerating and steering electron optics) was constructed. This allows us to place it in a newly built antechamber separated from the main sample chamber by a gate valve (Figure 1b). A second turbopump attached directly to the antechamber allows the electron gun to remain under vacuum while the main chamber is refilled to, e.g., switch samples, and a new in situ collection electrode mounted on a push-pull manipulator can be extended into the beam for quick current measurements without moving the sample. Not cycling the electron gun between vacuum and atmosphere repeatedly will increase its longevity and the reproducibility of its electron pulses. We also mounted a custom-made sample holder onto two coupled translational stages within the sample chamber to allow us to scan a sample within the plane normal to the electron beam (Figure 1c). Although modifications will continue to be made throughout the lifetime of this proposal, these additions were the most fundamental in nature, and in comparison, subsequent work on the apparatus will be relatively minor tweaks that will not require significant downtime.

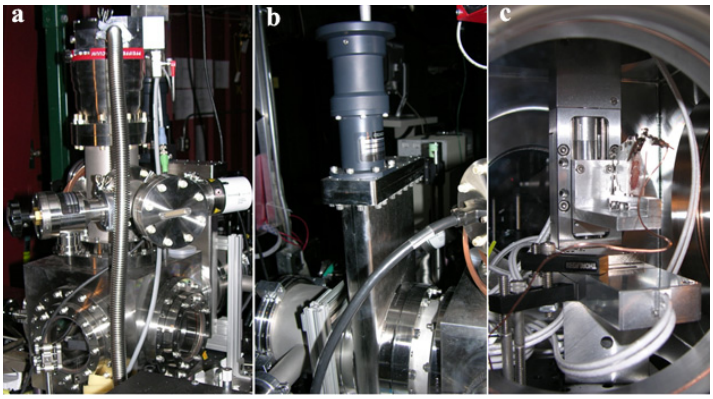

Figure 1. a) The CL instrument features many new features to enhance stability and reproducibility. b) The electron gun now sits in a designated antechamber behind a gate valve that allows it to remain under vacuum through a whole series of experiments. c) The custom sample holder and translational stages allow fine scanning of a 1" X 1" sample.

After hiring Lazaro Padilha as the dedicated postdoc for this project in June, successful operation of the rebuilt CL instrument was demonstrated in July, when the beam was directed onto a commercial phosphor screen (Figure 2a). Over the ensuing months, the durability and reproducibility of the instrument was established by achieving the same profile after stopping and restarting the experiment, both with the same cathode and with a replacement cathode. Finally, in September, a simple drop-cast film of red-emitting QDs was mounted next to the phosphor screen, and the first image of CL was collected by a simple digital camera (Figure 2b).

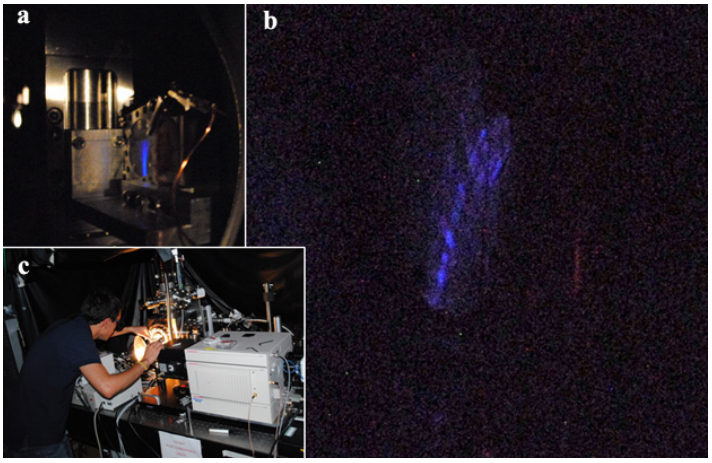

Figure 2. a) The beam can be visualized using a commercially available phosphor screen (blue light). b) The first CL collected from a real QD sample (faint red streak at right), along with light from scattered electrons that hit the nearby phosphor screen (blue at left). c) Postdoc Lazaro Padilha optimizing the collection of CL and its direction into the streak camera (to his right).

Future Work

With the first main task accomplished, efforts will turn to performing the first baseline studies of simple QD systems whose excitation signatures are well established. Towards that, Padilha, as an expert in ultra-fast spectroscopy, will first create an optimal collection pathway to capture and direct the CL signal into a streak camera (Figure 2c), which is a very sensitive way to capture simultaneously time- and energy-resolved spectra. Once the detection side is ready for operation, a series of thin film samples will be created and analyzed on both ordinary glass and electrically grounded, conductive substrates. A range of QD samples, including CdSe, CdSe/ZnS, $CuInS_2$, $CuInS_2$/CdS, and PbS/CdS are already on hand to allow population of a substantial database of CL traces of QDs varying in size, emission energy, ionization potential, and numerous other properties. When analyzed, this database will allow us to identify common factors in determining the branching ratios between "good" (i.e., emissive) relaxation pathways and "bad" (dark) channels of energy loss. These factors will be used to design the first generation of "ideal" scintillating QDs and predict the type of matrix (polymer, conductive or dielectric oxides, etc.) that would most enhance luminescence. Iterative testing and redesign will then lead to successive generations of rationally designed QDs will increasingly advantageous branching ratios, and hence, close to optimal scintillating performance. It is anticipated that after the conclusion of this project, the final, most success-

ful materials will then be used in radioluminescence experiments using x-rays and, eventually, elemental gamma sources prior to eventual follow-on efforts to fashion a fully functional scintillator element for benchmarking of the effective energy resolution.

Conclusion

A transient cathodoluminescence capability will be developed in order to probe the excitation branching ratios that energetic electrons produce upon interaction with nano-sized matter. Once we are able to determine branching ratios directly (via monitoring of transient emission), synthetic efforts will be applied to optimize these branching ratios for maximum populations of a single electron-hole pair per nanocrystal because these excitations result in efficient light emission (scintillation). In this manner, nanomaterials will be optimized for energy resolving gamma-ray detector performance.

Understanding and Controlling Complex States of Matter in New Iron-arsenide Superconductors through Strain and Disorder

Eric D. Bauer
20100210ER

Introduction

Superconductivity is an important technology for a variety of applications including energy transmission, energy storage, and sensor design. The discovery superconductivity in the iron-arsenide materials roughly one year ago has set off a flurry of international activity. These superconductors are more metallic and isotropic than their cuprate counterparts and show great promise for future energy applications. In addition, the similarity of the phase diagrams of the iron-arsenides and the high temperature cuprates, in which an antiferromagnetic state in the parent compound is suppressed with charged doping giving rise to a dome of superconductivity, suggests that these new superconductors may help finally unlock the secret pairing mechanism for generating such high transition temperatures (e.g Tc=55 K in SmFeAs(O,F)).

However, some striking differences between the phase diagrams are now emerging. Isoelectronic substitutions and pressure studies on the iron-arsenides demonstrate that strain and disorder are also equally effective at suppressing the antiferromagnetic state and inducing superconductivity. In the cuprates, pure disorder (without changing carrier concentration) is always detrimental for superconductivity. This then begs the question as to what is the interplay between local structure, magnetism, and superconductivity that allows disorder and strain to promote superconductivity in the iron-arsenides. Our novel approach, which combines the materials synthesis capabilities in

MPA-CMMS in bulk single crystals and thin films in MPA-STC, will determine how strain and disorder affects the local atomic structure in the iron-arsenide planes to suppress the antiferromagnetic order and induce superconductivity in this new family of superconductors.

Benefit to National Security Missions

The understanding of the role of disorder and strain in generating superconductivity in the new iron-arsenide superconductors ties directly into the central theme of LANL's Materials Grand Challenge of emergent phenomena. The novel approach described herein for inducing disorder and strain into these superconductors in a precisely controlled manner may lead to new ways to enhance their superconducting properties. Furthermore, since these three-dimensional superconductors show promise for superior energy-transmission performance over their anisotropic cuprate counterparts, the knowledge (and subsequent possible control) gained through the success of this project ties in well with the Lab's long-term energy security strategy.

Progress

We have made progress on two main tasks in our project aimed at understanding how strain and disorder affect the properties of the new iron-pnictide superconductors that lead to superconductivity, and to probe the nature of the superconducting state. In collaboration with Daniel Dessau (University of Colorado, Boulder), we used angle resolved photoemission spectroscopy to make direct measurements of the electronic structure and Fermi surface of the untwinned uniaxial state of $CaFe_2As_2$, which undergoes a simultaneous structural phase transition from a tetragonal to a orthorhombic structure, and a magnetic transition to a antiferromagnetic state. In this parent compound of the iron arsenic high temperature superconductors, we observe differences in the Fermi surface geometries along the orthogonal Fe-Fe bond directions, consistent with the development of an exotic type of charge order, called nematic charge density wave order. Furthermore, the doping dependence of this order extrapolates to a possible quantum critical point of the disappearance of this order at doping levels corresponding to the heavily overdoped regime of these materials, where superconductivity exists in the absence of magnetic/charge ordering. Thus, our results provide information about subtle structural and electronic effects that may cause the superconductivity.

The nature of superconductivity in these iron-pnictide materials including the pairing mechanism and the symmetry of the superconducting order parameter—both fundamentally important quantities for understanding any new superconductor--remains unclear despite intense experimental and theoretical efforts. We address

the nature of superconductivity through investigation of the low-temperature heat capacity. By analyzing the temperature dependence of this physical quantity, we gain information about the symmetry of the superconducting order parameter, which allows us to speculate on the origin of superconductivity in these exciting materials. We have measured the specific heat of $Ba(Fe_{1-x}Co_x)_2As_2$ samples in the under-doped regime (i.e., both magnetic and superconducting), optimal regime (maximal superconducting transition temperature of 20 K), and overdoped regime (just superconducting). Our results [1-4] indicate that the temperature variation of the electronic specific heat as well as its field dependence cannot be described by single clean s-wave (conventional superconductivity mediated by phonons) or d-wave (superconductivity mediated by excitations other than phonons, such as magnetic excitations) models and, rather, the data require an anisotropic superconducting gap. The temperature and field dependencies of the superconducting part of heat capacity have similar behavior for all doping concentrations indicating that the gap structure does not change significantly as a function of doping. A substantial residual linear term in the specific heat in $Ba(Fe_{1-x}Co_x)_2As_2$ is also observed, which suggests that nanoscale inhomogeneity may be an important factor in Co-doped $BaFe_2As_2$ and we are currently investigating this possibility in annealed samples.

We have made several attempts at growing $CaFe_2As_2$ thin films in MPA-STC, however, due to technical difficulties, the synthesis of these films was not successful. In parallel, we have set up a contract with Professor Xiaoxing Xi at Temple University to hire a postdoc to work both at Temple and here at LANL to grow thin films of various iron-pnictide materials on different strain-inducing substrates to directly investigate the effects of strain in the iron-arsenic layer on superconductivity. With Professor Xi's world-renowned expertise in growing thin films of these materials, combined with the expertise of Lab Fellow Quanxi Jia, who will mentor the postdoc effectively, we expect to make a number of iron-pnictide thin films by the end of the fiscal year and begin their characterization. We have made several attempts at growing $CaFe_2As_2$ thin films in MPA-STC, however, due to technical difficulties, the synthesis of these films was not successful. In parallel, we have set up a contract with Professor Xiaoxing Xi at Temple University to hire a postdoc to work both at Temple and here at LANL to grow thin films of various iron-pnictide materials on different strain-inducing substrates to directly investigate the effects of strain in the iron-arsenic layer on superconductivity. Preliminary attempts at Temple University have yielded superconducting thin films of optimally doped $Ba(Fe_{1-x}Co_x)_2As_2$. In particular, we have made 1 µm-thick $Ba(Fe_{1-x}Co_x)_2As_2$ film on Lanthanum Aluminate substrate with a T_c onset of 22 K and T_{c0} = 16 K for this film, comparable to the best quality thin films made by other groups. During our research, we have found that there is no arsenic deficiency is these films, which attests to their high quality. We have also found a variation of the superconducting transition temperature with film thickness, which may indicate sensitivity to strain and we are currently optimizing the parameters of the thin film growth to obtain the best quality sample. With Professor Xi's world-renowned expertise in growing thin films of these materials, combined with the expertise of Lab Fellow Quanxi Jia, who will mentor the postdoc effectively, we expect to make a number of iron-pnictide thin films on piezoelectric substrates to precisely control the strain applied to this new class of superconductors in the coming year.

Future Work

Our novel approach, which combines the materials synthesis capabilities in MPA-10 in bulk single crystals and thin films in MPA-STC, will determine how strain and disorder affects the local atomic structure in the iron-arsenide planes to suppress the antiferromagnetic order and induce superconductivity in this new family of superconductors. This approach demands that we accurately control both the applied strain, which we will accomplish through the synthesis of epitaxial thin films of the iron-arsenide materials on both lattice mis-matched substrates and on appropriate piezo-electric "substrates", and the induced disorder, which we will achieve through isoelectronic substitution in single-crystalline AFe_2As_2 (A=Ca, Sr, Ba) and through ion-bombardment on these stoichiometric materials. Carefully selected measurements on these bulk and thin film samples will provide essential information about the symmetry of the superconducting order parameter—currently one of the most outstanding issues in these materials. The combination of charge-sensitive, x-ray absorption spectroscopy and spin-sensitive nuclear magnetic resonance local structure probes will delineate how the induced changes in the local Fe or As environment alters the spin density wave order and accompanying superconductivity that will be a critical test of existing and future theories. In addition, the synthesis of these materials will enable several studies of the superconducting order parameter in real and momentum space, which are critical guides for determining the mechanism of superconductivity for any material.

Conclusion

Our discoveries will uncover synthetic design principles that offer new routes to enhancing the already high transition temperatures in the new iron-arsenide superconductors and make them even more attractive for energy applications. At this crucial time when the scientific community is intensely exploring these materials, this novel approach provides an exceptional opportunity to make a large impact that would propel LANL to the top of this ever-growing field.

References

1. Wang, Q., Z. Sun, E. Rotenberg, F. Ronning, E. D. Bauer, and D. S. Dessau. Uniaxial nematic-like electronic structure and Fermi surface of untwinned CaFe2As2. *Science.*

2. Gofryk, K., A. S. Sefat, E. D. Bauer, M. A. McGuire, B. C. Sales, D. Mandrus, J. D. Thompson, and F. Ronning. Gap structure in the electron-doped iron-arsenide superconductor Ba(Fe0.92Co0.08)(2)As-2: low-temperature specific heat study. 2010. *NEW JOURNAL OF PHYSICS.* **12**: 023006.

3. Gofryk, K., A. S. Sefat, M. A. McGuire, B. C. Sales, D. Mandrus, J. D. Thompson, E. D. Bauer, and F. Ronning. Doping-dependent specific heat study of the superconducting gap in Ba(Fe(1-x)Cox)(2)As-2. 2010. *PHYSICAL REVIEW B.* **81** (18): 184518.

4. Gofryk, K., A. B. Voronstov, I. Vekhter, A. S. Sefat, E. D. Bauer, J. D. Thompson, and F. Ronning. Effect of annealing on the specific heat of Ba(Fe1-xCox)2As2. *Physical Review B.*

Publications

Gofryk, K., A. S. Sefat, E. D. Bauer, M. A. McGuire, B. C. Sales, D. Mandrus, J. D. Thompson, and F. Ronning. Gap structure in the electron-doped iron-arsenide superconductor Ba(Fe0.92Co0.08)(2)As-2: low-temperature specific heat study. 2010. *NEW JOURNAL OF PHYSICS.* **12**: 023006.

Gofryk, K., A. S. Sefat, M. A. McGuire, B. C. Sales, D. Mandrus, J. D. Thompson, E. D. Bauer, and F. Ronning. Doping-dependent specific heat study of the superconducting gap in Ba(Fe(1-x)Cox)(2)As-2. 2010. *PHYSICAL REVIEW B.* **81** (18): 184518.

Developing Actinide Catalysis for Cleaning Dirty Fossil Feedstocks

Jaqueline L. Kiplinger
20100228ER

Introduction

This project outlines innovative directions in actinide chemistry that supports the Lab's mission in Energy Security. The primary focus is to determine whether actinides can be used to efficiently catalyze the breakdown of petroleum into more useful component materials. In addition, this work will provide basic understanding of the chemistry of these reactions that may lead to ever improved approaches to efficient transformation of raw carbon-rich materials into starting materials for fuel and polymer synthesis. Results from our group demonstrate that thorium and uranium alkyl and aryl complexes show extraordinary behavior towards aromatic N-heterocycles, which are some of the most recalcitrant contaminants in fossil fuel feedstocks. The current effort takes advantage of the ability of actinides to engage in C-N cleavage and dearomatization chemistry with multiple N-heterocycle substrates per metal. These transformations represent new reactivity behavior for pyridine ring systems which have not been observed for transition metal or lanthanide complexes. This project will not only improve our fundamental understanding of key steps in hydrodenitrogenation (HDN) processes (such as C-N bond cleavage and dearomatization) but will also assess whether milder conditions than those currently used are viable.

Benefit to National Security Missions

These proposed studies relate directly to the Lab's mission in Energy Security by providing much-needed insight into directions for the development of new hydrodenitrogenation (HDN) catalysts. What is learned from HDN studies will be, by extension, applicable to HDO (oxygen removal) and HDS (sulfur removal) processes. Furthermore, understanding the chemistry between actinides and N-heterocycles finds application in the country's nuclear energy future as well as nonproliferation issues since poly(vinylpyridine)-based Reillex-HPQ resin is used in separation columns for actinide processing at TA-55 and elsewhere in the world.

Progress

Noteworthy Accomplishments & Highlights:

1. Developed a new class of precursor materials for thorium science
2. Developed a new class of precursor materials for uranium science
3. Discovered a reliable synthesis route to a key uranium-benzyne complex
4. Mapped out the thermodynamic profiles for reaction chemistry between uranium-benzyne complex and pyridine, thiophene, and furan

Out of the project's need for reproducible synthetic routes to thorium and uranium starting materials, the initial stages of this project were focused on developing new safe, mild reproducibly high-yielding methods for accessing thorium and uranium halide complexes. These compounds are critical to our ability to prepare the pre-catalyst compounds for the project.

For non-aqueous thorium chemistry, $ThBr_4(THF)_4$ and $ThCl_4$ have been the most commonly used precursors, but their syntheses suffer from several inconvenient drawbacks, which have, in turn, greatly hampered progress in thorium research. For example, the synthesis of $ThBr_4(THF)_4$ requires thorium metal, an expensive material available at only a small number of institutions. Furthermore, its synthesis is highly dependent on the type of thorium metal used (turnings, powder or chips) and the $ThBr_4(THF)_4$ complex is thermally sensitive. The syntheses for $ThCl_4$ require special equipment and more dangerous protocols that involve elevated temperatures (300-500°C).

Seeking a better and safer approach for our project, we refluxed commercially available thorium nitrate $Th(NO_3)_4(H_2O)_5$ (**1**) with concentrated hydrochloric acid to produce $ThCl_4(H_2O)_4$ (**2**) in quantitative yield under mild conditions. We then used a novel combination of

anhydrous HCl and trimethylsilyl chloride (Me_3Si-Cl) to remove the coordinated water molecules and replace them with dimethoxyethane (DME) (**3**), 1,4-dioxane (**4**), or tetrahydrofuran (THF) (**5**) solvent molecules to make three new thorium chloride reagents (Figure 1). Preliminary reaction chemistry has shown that these new thorium reagents display versatile reaction chemistry and can be used to prepare Th-halide, Th-O, Th-N and Th-C compounds and materials on multigram scales.

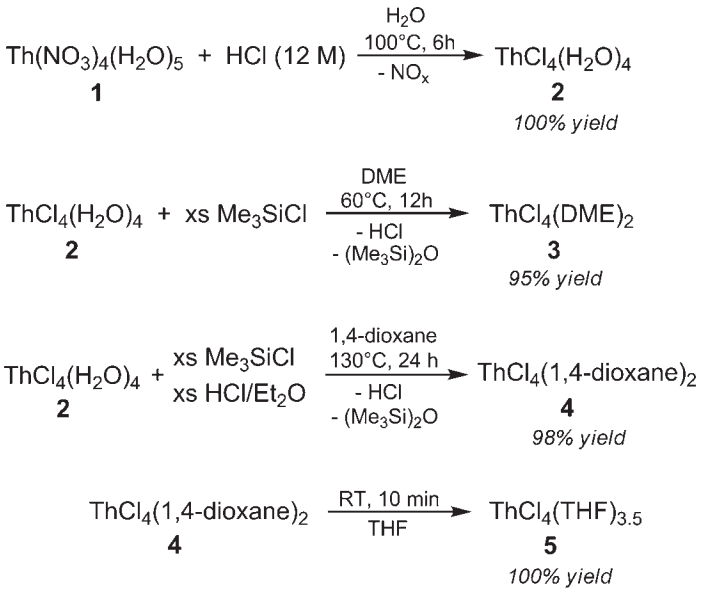

Figure 1. Synthetic scheme for the preparation of the new thorium chloride starting material complexes, $ThCl_4$(DME) (1), $ThCl_4$(1,4-dioxane)2 (2), and $ThCl_4(THF)_{3.5}$ (3).

Similarly, UCl_4 and $UI_3(THF)_4$ have served as the most popular starting materials for uranium chemistry. However, problems exist with the syntheses of both compounds. For example, the method of choice for the synthesis of UCl_4 has been the reaction of $UO_3 \cdot 2H_2O$ with hot (190 °C) hexachloropropene, a highly toxic chemical, and special precautions must be taken to avoid uncontrolled radical reactions. In contrast, the synthesis of $UI_3(THF)_4$ needs to be performed in the presence of HgI_2 at temperatures slightly below 10°C and is usually low-yielding because of the formation of unwanted by-products caused by the ring-opening of THF. In addition, $UI_3(THF)_4$ is thermally sensitive and must be stored at low temperature.

As shown in Figure 2, we discovered that 1,4-dioxane can also be used to prepared two new uranium(III) and uranium(IV) iodide starting materials, UI_3(1,4-dioxane)$_{1.5}$ (**6**) and UI_4(dioxane)$_2$ (**7**). Of particular note is that these complexes are stable above ambient temperature and are useful precursors to a variety of U-O, U-N, U-C and U-halide compounds, including a safe, room temperature synthesis of $[UCl_4(dioxane)]_2$ (**8**), which is a practical synthetic alternative to UCl_4.

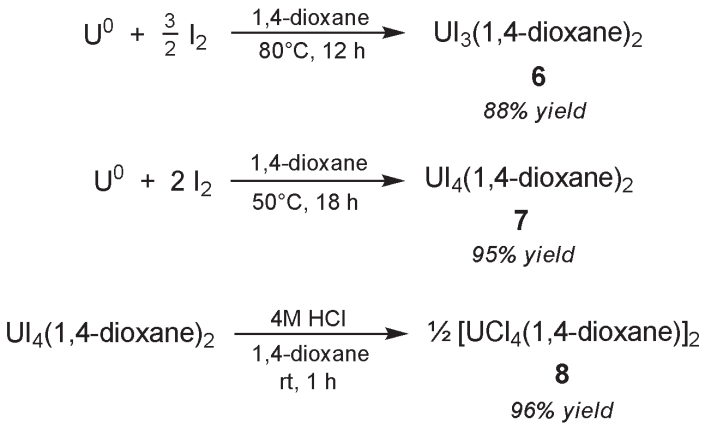

Figure 2. Synthetic scheme for the preparation of the new uranium(III)/(IV) iodide and uranium(IV) chloride starting material complexes, UI_3(1,4-dioxane)$_{1.5}$ (6), UI_4(1,4-dioxane)2 (7), and $[UCl_4$(1,4-dioxane)$]_2$ (8), respectively.

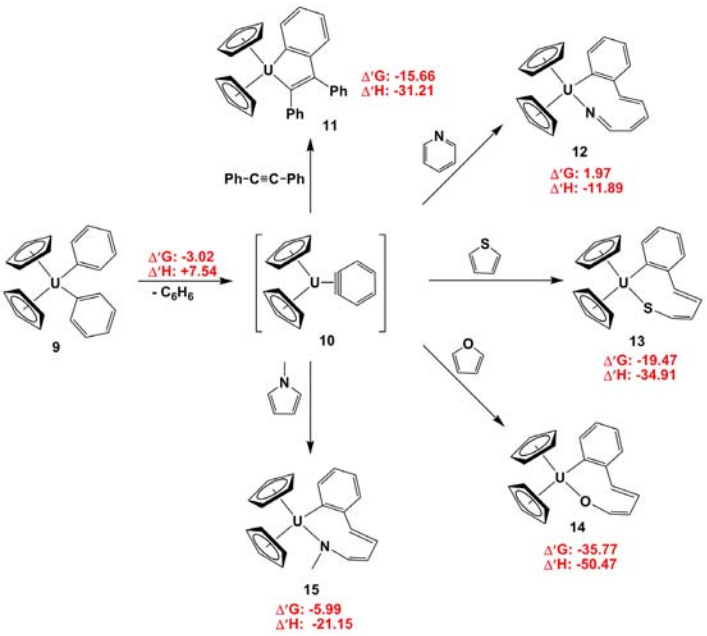

Figure 3. Thermodynamic calculations for the formation of the uranium benzyne complex (10) and its reaction chemistry with diphenylacetylene (to give 11), pyridine (to give 12), thiophene (to give 13), furan (to give 14), and methylpyrrole (to give 15).

During late Summer 2010, we completed the development of the new thorium and uranium starting materials and the project was finally staffed with a theoretical postdoc and an experimental postdoc. The easy access to starting materials enabled rapid experimental progress of our project. As illustrated in Figure 3, the initial chemistry that has been explored both theoretically and experimentally has been the ability of the uranium benzyne complex, $(C_5Me_5)_2U(C_6H_4)$ (**10**), to cleave strong C-N, C-S and C-O bonds in substrates that are commonly found in crude

petroleum and are the most difficult to process (i.e. break apart and remove during the refining process). We proposed that the uranium benzyne complex, $(C_5Me_5)_2U(C_6H_4)$, should react with (coordinated) pyridine, thiophene and furan at the C_α position resulting in C-N, C-S and C-O cleavage to give ketimide, thiolate, and alkoxide phenyl complexes, respectively. In addition to the strong U-N, U-S, and U-O bonds that are formed upon ring opening of the heterocycles, the extended conjugation in the products will also serve as a thermodynamic driving force for these reactions.

The uranium benzyne complex, $(C_5Me_5)_2U(C_6H_4)$ (**10**), is formed by the elimination of benzene from the diphenyl precursor, $(C_5Me_5)_2U(C_6H_5)_2$ (**9**). The thermodynamics of the formation of the uranium benzyne complex and its reaction chemistry with diphenylacetylene (Ph-C≡C-Ph, to give **11**), pyridine (NC_5H_5, to give **12**), thiophene (SC_4H_4, to give **13**), furan (OC_4H_4, to give **14**), and methylpyrrole ($MeNC_4H_4$, to give **15**) were examined. The calculations were carried out with B3LYP/6-31+G(d) using Stuttgart pseudopotentials. The results from these initial theoretical studies are quite promising and the calculations show that – as we proposed – every transformation is thermodynamically favorable, with the benzyne complex formation being the least thermodynamically favorable process (ΔG = -3.02 kcal/mol, ΔH = 7.54 kcal/mol). The C-N, C-S, and C-O cleavage processes are energetically ranked as follows: $C\text{-}N_{pyridine}$ (ΔG = 1.97 kcal/mol, ΔH = -11.89 kcal/mol) > $C\text{-}S_{thiophene}$ (ΔG = -19.47 kcal/mol, ΔH = 34.91 kcal/mol) > $C\text{-}O_{furan}$ (ΔG = -35.77 kcal/mol, ΔH = -50.47 kcal/mol), with C-O and C-N cleavage being most and least favored (though still exothermic). Importantly, these results suggest that the C-N, C-S, and C-O cleavage chemistry should take place at, or around, room temperature!

Experimentally, the synthesis of uranium diphenyl $(C_5Me_5)_2U(C_6H_5)_2$ complex (**9**) was mapped out. This complex is in rapid equilibrium with benzyne complex, $(C_5Me_5)_2U(C_6H_4)$ (**10**), at room temperature. To date, chemistry of the uranium benzyne system with pyridine, thiophene, and phthalazine (polyaromatic *N*-heterocycle) has been examined. The reactions are clean and are not consistent with simple C-H activation chemistry, rather the ^{1}H NMR spectra suggest that a different type of reaction pathway has taken place. Of course, we anticipate that C-N and C-S cleavage have taken place, but we cannot be certain until crystal structures of the products from these reactions are obtained. This is actively being pursued. Regardless, the fact that thiophene even displays reaction chemistry with the uranium benzyne is rather significant since the molecule chemically behaves like benzene (C_6H_6) and usually is chemically inert.

Future Work

While we are clearly at an early stage, this new uranium benzyne chemistry is opening up new frontiers in the understanding of actinide chemical reactivity with nitrogen, sulfur, and oxygen heterocycle substrates that are commonly found in crude petroleum and are the most difficult to process (i.e. break apart and remove during the refining process). Currently, theoretical calculations are ahead of the experimental studies and are quite promising. The experimental studies need to catch up with theory. We need to unambiguously determine the identity of the benzyne chemistry product through X-ray crystallography. We plan to extend the uranium benzyne chemistry to thorium to compare the reactivity of the two actinide systems with C-N, C-S, and C-O bonds. Theoretical calculations will help us understand the experimental results in real-time. The potential of this new system is just being realized, and further studies are certain to have high impact across the chemistry community. Additionally, this work will provide further insight into directions for the development of new HDN catalysts, which continues to be a technological and cost-prohibitive gap that is currently limiting the U.S. from exploring the use of lower-quality petroleum feedstocks while transitioning from energy derived from fossil fuels.

Conclusion

As evidenced by this project, the DOE complex and LANL clearly benefits from simple exploratory research. We have developed simple, safe, inexpensive and high-yielding solution routes to several new anhydrous thorium (IV), uranium (III) and uranium(IV) halide complexes that that will permanently change (for the better) the starting material landscape of actinide chemistry. Our work contrasts the older, low-yielding and more dangerous methods. These new complexes possess exceptional thermal stability and are easy to prepare on a large scale. Furthermore, they are excellent starting materials to a wide range of thorium(IV), uranium(III), and uranium(IV) alkoxide, amide, organometallic and halide compounds. We anticipate that these new thorium and uranium compounds will become important reagents in synthetic actinide chemistry and enable future progress in thorium and uranium materials science and nuclear fuel cycle research.

Publications

Cantat, T., B. L. Scott, and J. L. Kiplinger. Convenient access to the anhydrous thorium tetrachloride complexes ThCl4(DME)2, ThCl4(dioxane)4 and ThCl4(THF)3.5 using commercially available and inexpensive starting materials. 2010. *Chemical Comunications.* **46**: 919.

Planetary Analog Geochemical Explorations with Laser-Induced Breakdown and Raman Spectroscopies

Roger C. Wiens
20100230ER

Introduction

The ability to quantitatively characterize and interpret both mineralogical and chemical compositions from complex geological samples is an enormous challenge for planetary exploration. The most informative distinctions between terrestrial, lunar, Martian, Venusian, and asteroidal geochemistry are extracted from subtle differences and require sophisticated analysis. Remote Raman and Laser Induced Breakdown Spectroscopy (LIBS) developed at Los Alamos National Laboratory (LANL) for NASA are exciting new geochemistry tools which were R&D100 prize winners in 2003. Raman spectroscopy is fundamentally sensitive to molecular structure while LIBS primarily determines elemental compositions. We have demonstrated that one can use an integrated remote Raman-LIBS instrument for planetary geological exploration.

Recently, seminal work demonstrated new data calibration techniques that extract greatly improved chemical and mineral accuracies from these two analytical techniques. In this project, combined LIBS-Raman analysis of planetary analog samples is providing new understanding of surface chemistry of lunar samples and small-scale analyses of carbon-rich asteroidal materials. We are also synthesizing planetary analog samples of ice-bearing lunar polar deposits and analog Venusian rocks. The current critical need is to explore geological analogs for Venus, lunar, and asteroidal samples and identify the relevant geochemical parameters detected from a Raman-LIBS instrument. This entails investigating volatile elements such as hydrogen, carbon, nitrogen, and oxygen, which are highly important to planetary science, but which more traditional planetary instruments are not capable of analyzing.

Benefit to National Security Missions

The laser-induced breakdown spectroscopy and Raman spectroscopy techniques that will be extensively used and tested in this project have very wide applicability to many of the lab's and DOE's missions. They are used for nuclear detection (i.e., uranium isotopes), explosives detection, chem-bio detection, detection of environmental hazards such as Pb or Be in soils, carbon sequestration studies, production of silicon wafers for solar arrays, as well as for NASA space exploration.

Progress

We report progress on the tasks listed in the Technical Description: We have acquired most of the Venus analog minerals that are needed for our experiments. We have carried out analyses of analog Venus minerals at elevated temperature and pressure, although we plan to carry out more analyses. Several interesting features of these analyses have been observed, as noted in the publications listed below. We have also carried out LIBS and remote Raman spectroscopy calibrations in a simulated Venus environment of 92 bars of CO2. These calibrations show that LIBS can indeed achieve 5% accuracy and precision for some of the critical elements in this environment. These results have also been noted in the publications listed below. For the lunar work, we started out by preparing for lunar samples. NASA requires the samples to be stored in a safe when not being analyzed. We obtained a surplus safe last fall and installed it in our LIBS lab. We then submitted the request for lunar pyroclastic glass samples to be analyzed. The request was turned down this time, based mostly on the need to first demonstrate the technique on non-lunar relevant samples and publish those results. We will therefore proceed with the other analyses—of lunar simulants—and then resubmit our lunar sample request. We currently have a sample of JSC-1 lunar soil stimulant. This was analyzed under vacuum conditions simulating the Moon, from a distance of 3.5 m. We used approximately ten standards for calibration. The results showed that accuracy and precision for most major elements is below +/-10%, which is our goal. We are particularly interested in the capability to analyze hydrogen abundances under lunar conditions. Several of the standards had measurable water, up to 3% by weight. The hydrogen in these samples was not detected by LIBS. However, it is possible that this water was present in the form of alteration products. If this were the case, the water would have been pumped away in our vacuum chamber. We are currently checking for the presence of these minerals to ascertain

if this was indeed the case.

We did an analysis of water ice as well as ice mixed with lunar soil simulant under vacuum conditions and were able to observe nice hydrogen and oxygen peaks.

The lunar glass sample analysis mentioned in our plan will be done later. Lunar-related abstracts to date from this work are listed below. We have not yet started analysis of carbon-rich asteroidal material.

Future Work

The ability to quantitatively characterize and interpret both mineralogical and chemical compositions from complex geological samples is an enormous challenge for planetary exploration. The most informative distinctions between terrestrial, lunar, Martian, Venusian, and asteroidal geochemistry are extracted from subtle differences and require sophisticated analysis. Remote Raman and Laser Induced Breakdown Spectroscopy (LIBS) developed at LANL for NASA are exciting new geochemistry tools (R&D100 winners). Recently the leaders of this LDRD project demonstrated new multivariate analysis (MVA) techniques that extract greatly improved chemical and mineral analysis from LIBS and Raman spectra. LANL is building a LIBS instrument that will fly to Mars, for which many Mars analog samples have been studied. In this LDRD project analog and real samples of other planetary bodies (the Moon, Venus, asteroids) will be studied with LIBS and Raman spectroscopy to understand the benefits of these techniques for these samples as well as to carry out important science on the analog and actual planetary samples.

Tasks:

1. Acquire or synthesize analog Venus minerals (tremolite, eastonitic mica, fluorite, anhydrite, galena, and hematite) for LIBS-Raman analysis.
2. Carry out analyses of analog Venus minerals, including simulated carbonate-bearing basalt, in CO2 at Venus pressure and elevated temperature.
3. Perform calibrations in Venus environment. Determine accuracies and detection limits for elements.
4. Publish and present results of Venus analog work.
5. Obtain lunar pyroclastic glass sample.
6. Obtain lunar soil or soil simulant. Construct vacuum cold finger for LIBS/Raman analyses.
7. Analyze lunar glass sample for volatiles.
8. Analyze lunar soil/ice mixtures.
9. Perform calibrations for lunar environment. Determine accuracies and detection limits for elements.
10. Give presentations on lunar samples and publish results.
11. Perform analyses of carbon-rich asteroidal material, observing distributions of C and H. Perform calibrations.
12. Give presentations on asteroidal materials and publish results.

Conclusion

In terms of space instrumentation, the power and importance of remote analytical capability for both mineralogy and chemistry provided by a combined LIBS-Raman instrument cannot be overstated; competing methods that require drill or scoop sampling with ingestion into a rover analytical module are fraught with high complexity, cost, and risk. The scientific results from these studies are very important in their own right, but they will also position LANL to provide our LIBS-Raman technology for missions to the Moon and to Venus.

Presentations

Clegg S.M., Barefield J.E., Humphries S.D., Wiens R.C., Vaniman D.T., Sharma S.K., Misra A.K., Dyar M.D. (2009) Remote laser induced breakdown spectroscopy (LIBS) geochemical investigation under Venus atmospheric conditions. Fall AGU.

Sharma S.K., Misra A.K., Clegg S.M., Barefield J.E., and Wiens R.C. (2009) Time-resolved remote-Raman spectroscopic study of minerals at high temperature and under supercritical CO2 relevant to Venus exploration. Fall AGU.

Clegg S.M., Barefield J.E., Wiens R.C., Sharma S.K., Misra A.K., Dyar M.D., Lambert J., Smrekar S., and Treiman A. (2010) Venus geochemical analysis by remote laser induced breakdown spectroscopy (LIBS). Lunar Planet. Sci. XLI, 1631.

Vaniman D., Wiens R.C., Clegg S., and Maurice S. (2010) Sample analysis in the lunar environment using Laser Induced Breakdown Spectroscopy. Lunar Science Forum 2010, 7/20-22, Mountain View, CA.

Wiens R.C., Clegg S., Sharma S., Maurice S., Dyar M.D. (2010) Proposed remote Raman-LIBS geochemical exploration on the surface of Venus. LIBS 2010, Sept. 13-17, Memphis. LA-UR 10-03652.

Mezzacappa A., Nortier L.-M., Clegg S., Wiens R.C., Melikechi N. (2010) Investigation of LIBS under low pressure for application to planetary exploration. LIBS 2010, Sept. 13-17, Memphis. LA-UR 10-03649.

Wiens R., Barraclough, B., Vaniman D., Bender S., Nelson T., Dallmann N., Storms S., Stiglich R., Dingler R., Little C., Sharma S., Maurice S., Esposito L. (2010) Laser-induced breakdown spectroscopy (LIBS) on Mars and Venus. 2010

Earth and Space Science Capability Review, LANL, 23-June, 2010.

Sharma S.K., Misra A.K., Clegg S.M., Barefield J.E., Wiens R.C., Quick C.R., Dyar M.D., McCanta M.C., and Elkins-Tanton L. (2010) Venus geochemical analysis by remote Raman-LIBS spectroscopy (Raman-LIBS) 2010 Chemistry Capability Review, LANL, 23-June, 2010.

Clegg S.M., Barefield J.E., Humphries S.D., Wiens R.C., Vaniman D.T., Sharma S.K., Misra A.K., and Dyar M.D. (2010) Remote Raman – Laser Induced Breakdown Spectroscopy (LIBS) Geochemical Investigation under Venus Atmospheric Conditions. Fall AGU.

Publications

Sharma, S. K., A. K. Misra, S. M. Clegg, J. E. Barefield, R. C. Wiens, T. E. Acosta, and D. E. Bates. Remote-Raman spectroscopy study of minerals under supercritical CO2 relevant to Venus exploration. *Spectrochimica Acta A.*

Sharma, S., A. Misra, S. Clegg, J. Barefield, R. Wiens, and T. Acosta. Time-resolved remote Raman study of minerals under supercritical CO2 and high temperatures relevant to Venus exploration. 2010. *PHILOSOPHICAL TRANSACTIONS OF THE ROYAL SOCIETY A-MATHEMATICAL PHYSICAL AND ENGINEERING SCIENCES.* **368** (1922): 3167.

One-Dimensional Nanomaterials for Enhanced Solar Conversion

Samuel T. Picraux
20100237ER

Introduction

To meet the earth's future energy needs, the efficiency of solar energy harvesting must be increased and the cost decreased. This requires new approaches which go beyond simply re-engineering currently established methods. One of the greatest, but least-explored, opportunities for enhancing the light-to-electric conversion process is to exploit energy transfer concepts made possible by nanoscale materials design. The objective of this project is to discover and determine the underlying scientific issues required to implement an enhanced light harvesting approach for electrical energy generation based on composite one dimensional nanowire structures. Nanoscale materials offer opportunities to achieve materials properties not possible in bulk materials. The project will use a new approach to solar cell design using one-dimensional materials, where the light absorption and charge collection constraints are decoupled. Vertical nanowire arrays provide strong diffuse scattering, resulting in nearly 100% light absorption over a broad wavelength region within a shallow depth. This enables highly efficient charge carrier generation in the semiconducting wires. Radial p-i-n junctions in the nanowires provide strong local electric fields for highly efficient carrier separation in the lateral direction. Contacts to the nanowire core and shell then provide carrier collection from the wires. The key concept derives from the one-dimensional design of these structures—in essence light absorption is controlled by the vertical direction and charge separation by the lateral direction. In addition, and of critical importance, these nanoscale materials are produced by low cost chemical vapor deposition techniques that are suitable for large scale manufacturing and do not require single crystal silicon substrates.

Benefit to National Security Missions

This project addresses fundamental challenges in implementing low-cost solar cell concepts and is directly relevant to the DOE renewal energy mission. The objective is to achieve crystalline solar cell efficiencies at the low cost of thin film approaches. The proposed transformational science will develop composite nanoscale materials concepts that will enable decoupling of photon and electron collection. This coupling currently limits silicon solar cell design. These concepts are also important to the remote sensing and threat reduction areas, for example in developing new approaches to highly sensitive, near infrared sensing.

Progress

During the first year of this project we have made significant progress on the needed tools and scientific understanding of issues related to the control of photovoltaic performance in nanostructured materials. The purpose of this research is to develop the understanding required for a new approach to solar cells based on nanostructuring materials. The key scientific issues involved are: 1) to understand one dimensional nanostructured materials design for strong, broad-band absorption of light; 2) to understand rapid charge separation and recombination processes in nanoscale structures with large electric field gradients, and 3) to fabricate nanowire structures with these characteristics of strong light absorption and good carrier collection.

In the area of nanomaterials design and fabrication we have specifically focused on the synthesis of silicon nanowire structures with uniform radial shells of controlled electrical doping and with a growth morphology leading to smooth, defect-free surfaces and interfaces. A critical factor has been to block Au diffusion along the sidewalls of the nanowires upon switching from axial to radial nanowire growth. This has been accomplished by control of the growth temperatures and, in the case of Ge nanowire cores for the Si nanowire radial shells, by growth of a short Si blocking layer before switching to radial nanowire growth (see Figure 1). This technique has resulted in high quality smooth silicon nanowire surfaces and interfaces as shown in Figure 2 for both Ge/Ge and Ge/Si core/shell structures by eliminating Au sidewall contamination which can result in rough catalytic sidewall growth as well as lead to shorter carrier lifetimes and poor efficiencies. This new approach to block Au diffusion has been modeled and has provided new understanding of how to block this source of contamination. These synthesis developments are critical to high

performance photovoltaic structures with minimal carrier recombination.

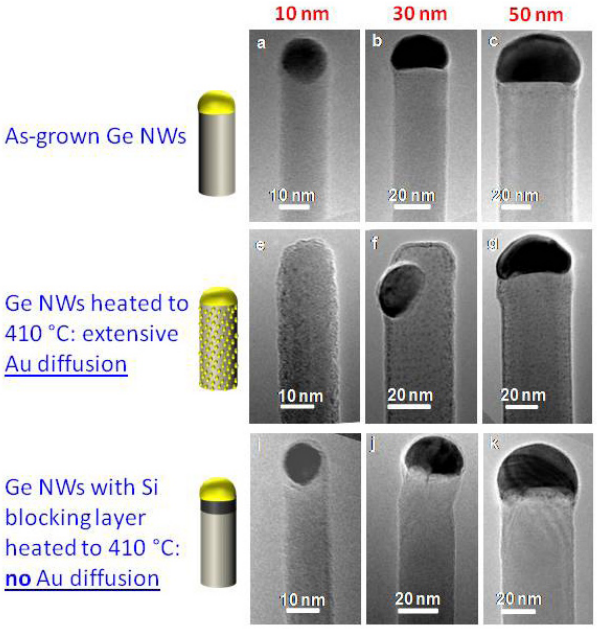

Figure 1. Germanium nanowires for 10, 30, and 50 nm diameter after growth (top row), heating which results in Au diffusion as indicated by small black dots and loss of dark top Au catalytic growth seed (middle row), and after growth of a silicon blocking layer followed by the same heating cycle.

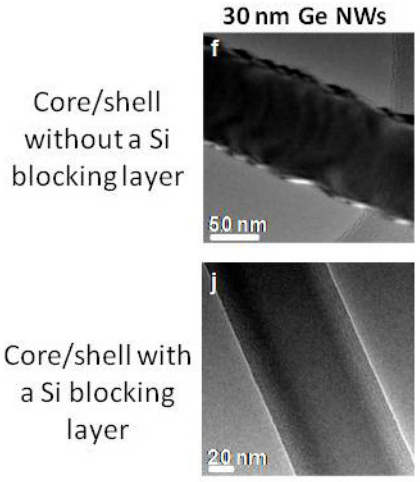

Figure 2. Growth of germanium core/shell radial structure with Au diffusion on sidewalls leading to rough, poor quality shell (top row) and with silicon blocking layer to prevent Au diffusion resulting in smooth, high quality epitaxial shell growth (bottom row).

In a second area we are developing methods to measure the electron-hole carrier diffusion lengths and recombination times in nanowires. There have been only a couple studies of recombination times in nanowires and systematic understanding of the influence of surfaces and interfaces on this recombination is needed for this project. Also there are no reported results for radial nanowires with doping from heavily doped p+ to intrinsic to heavy n+ radial electrical doping profiles, structures which are required for solar energy collection and which we are now able to grow with good morphology and doping control. The objective of these optical characterization studies is to understand and minimize carrier recombination under the high build-in electric fields in these nanostructures. Platforms for the study of the photocurrent and lifetimes in nanowires and our first minority carrier lifetime measurements in p-n junction nanowires demonstrating this new capability have now been demonstrated. We have also developed a new capacitively-coupled photoresponse measurement method for nanowires. This latter characterization tool is anticipated to be valuable in the study of defects in the radial nanowires which could induce carrier recombination and ultimately limit photovoltaic efficiencies.

In a third area we are using finite-difference time-domain simulations to describe the optical properties of the NW arrays. By combining the modeling with optical measurements we will be able to establish the optimum nanowire array geometry required for strong, broad-band carrier absorption. The diameter and length of the individual nanowires and the inter-nanowire spacing within the array are being designed to maximize optical absorption and minimize reflection, and thus optimize solar photon collection. This approach is appropriate for the Si nanowire structures with large dielectric discontinuities and multiple scattering. We are using an integrating sphere to measure the optical properties of the arrays for comparison with simulation. In model structures good optical performance can be achieved with NWs only 10 um long. This is a promising result that implies nanowire solar cells could use less than 5% of the Si required for conventional crystalline Si solar cells.

Future Work

The scientific issue we will address is to understand and control photovoltaic performance in nanostructured materials with nanoscale variations in material composition and electronic doping. To achieve our goals we must understand one dimensional (1D) nanostructured materials design for strong, broad-band collection of light; understand charge generation in 1D structures with unprecedented electric field gradients; understand rapid charge separation and recombination control under such nanoscale separation conditions; and determine the feasibility of achieving efficient radial single crystal nanowire solar cells. The fundamental science to be developed will not only be relevant to energy harvesting, but also to a wide range of 1D nanomaterials electrical and optical applications. Such materials have attracted great attention, but have received little scientific study to understand how to extend and exploit these benefits beyond this specific empirical example. Our approach to the 1D nanostructured materials synthesis

will be to use the chemical vapor deposition technique for nanostructure growth by the vapor-liquid-solid method. Our future work will focus on fabricating high quality p-i-n axial and radial, single Si nanowires and measurements of their electrical and optical properties. We will design, fabricate, and measure single Si nanowire structures for optimum PV response and then extend this work to fabrication and study of prototype solar cells.

Conclusion

This project will develop new understanding and control of the photovoltaic performance in nanostructured materials through variations in material composition and electronic doping. Using silicon nanowires as our model system, we will: 1) understand one dimensional nanostructured materials design for strong, broad-band absorption of light; 2) understand rapid charge separation and recombination processes in nanoscale structures with large electric field gradients; and 3) fabricate prototype solar cells to determine the feasibility of this approach for low cost, efficient solar cells.

Publications

Dayeh, S., J. Huang, A. Gin, and S. T. Picraux. Synthesis, Fabrication, and Characterization of Ge/Si Axial Nanowire Heterostructure Tunnel FETs. 2010. In *IEEE Nano 2010 .* (Seoul, Korea, 17-20 Aug. 2010). , p. 85. Seoul: IEEE.

Dayeh, S., J. Huang, A. Gin, and S. T. Picraux. Elimination of Gold Diffusion in the Heterostructure Core/Shell growth of High Performance Ge/Si Nanowire HFETs. 2010. In *IEEE Nano 2010 International Conference.* (Seoul, Korea, 17-20 Aug. 2010). , p. 95. Seoul: IEEE.

Dayeh, S., J. Huang, A. Gin, and S. T. Picraux. Elimination of Au diffusion for high performance core/multi-shell germanium/silicon nanowire heterostructure transistors. To appear in *Nano Letters.*

Dayeh, S., and S. T. Picraux. Axial Ge/Si Nanowire Heterostructure Tunnel FETs. 2010. In *SiGe, Ge, and Related Compounds 4: Materials, Processing, and Devices.* (Las Vegas, NV, 12-14 Oct. 2010). Vol. 33, p. 22. New Jersey: Electrochemical Society.

Kar, A., P. Upadhya, S. Dayeh, S. T. Picraux, A. J. Taylor, and R. P. Prasankumar. Probing ultrafast carrier dynamics in silicon nanowires (Invited). To appear in *Journal Selected Topics in Quantum Electronics.*

Le, S. T., P. Jannaty, A. Zaslavsky, S. Dayeh, and S. T. Picraux. Growth, electrical rectification, and gate control in axial in situ doped p-n junction germanium nanowires. 2010. *Applied Physics Letters.* **96**: 262102.

Le, S. T., S. Dayeh, S. T. Picraux, and A. Zaslavsky. Growth and electrical rectification in axial in-situ doped p-n junction germanium nanowires. 0920. In *The Second International Workshop on Nanotechnology and Application – IWNA 2009.* (Vietnam National University, Ho Chi Minh City, 16 Sept. 2009). , p. 40. Ho Chi Minh City: --.

Picraux, S. T., S. A. Dayeh, P. Manandhar, D. E. Perea, and S. G. Choi. Silicon and Germanium Nanowires: Growth, Properties and Integration (Invited Overview). 2010. *Journal of Materials.* **62** (4): 35.

Sierra-Sastre, Y., S. Dayeh, S. T. Picraux, and C. Batt. Epitaxy of Ge Nanowires from Biotemplated Au Nanoparticle Catalysts. 1209. *ACS Nano.* **4**: 2010.

Swadener, J. G., and S. T. Picraux. Coherent interface limits at high misfit strain in Si/Ge axial nanowire heterostructures. To appear in *Nano Letters.*

Electron Spin Injection, Transport and Detection in Semiconductor Nanowires

Samuel T. Picraux
20100261ER

Introduction

Today's electronics industry is based on electron charge transport in bulk (3D) or planar (2D) semiconductors. However, there is a belief that by further exploiting the fact that electrons have spin, semiconductor devices can be made energy efficient (low power), smaller and thus faster with versatile functionality, and this is the focus of the rapidly growing field of "semiconductor spintronics." Concurrently, there is great interest in electronic devices based on 1D nanowires, which hold promise for unconventional device architectures allowed by their unique dimensionality. Both fields—semiconductor spintronics and 1D nanowires—are now sufficiently mature to marry these ideas. Therefore this project will investigate electron spin injection, transport, and detection in semiconductor nanowires. This area holds great promise for new advances in materials physics science and for a new generation of low power and high speed electronics, quantum information processing systems, and single electron spintronic devices. This team is uniquely suited to pursue this new direction and, to the best of our knowledge, no spin injection, transport, and detection measurements or analyses with semiconductor nanowires have been performed prior to the initiation of this project.

Benefit to National Security Missions

This project is central to LANL's materials mission and leadership in the subcategory of emergent phenomena, which specifies the need for exploitation of nanostructures, quantum confinement and crystalline interfaces to produce new properties and new functionalities in designed materials. By manipulating electron spin in a semiconductor, low power devices may be realized with compact size for multi-functionality, and with high speed and performance. Silicon-based nanowires and nanowire heterostructures will enable significant advances through long mean free paths and coherence times. Demonstration of spin electronics in Si nanowires will generate worldwide attention and form a robust platform for a nanoscale spintronics program at LANL.

Progress

The focus of this project is to combine the areas of semiconductor spintronics and one-dimensional nanowire synthesis. The integration of these two areas will enable the investigation of electron spin injection, transport, and detection in semiconductor nanowires with potential for a new generation of spintronic devices. The focus in the first year of this project has been on the design and fabrication of the nanowire structures and devices required to achieve spin injection, transport, and detection. In the area of nanowire design we have been synthesizing both silicon and germanium nanowires with intermediate electrical doping for diameters ranging from 20 to 100 nm. A key step has been developing nanowire growth procedures for uniform doping across the nanowire length, as well as ferromagnetic contacts with thin dielectric barriers on the nanowires for filtered spin-polarized charge injection through a tunnel barrier. Engineering the contact resistance for filtering single spin charge carriers at the ferromagnetic contact/nanowire interface is the major challenge for successful control of the spin injection, as well as for spin detection by the reverse process, and has been the primary initial effort of this project. For the ferromagnetic contacts we are using cobalt. For the planned technique to electrically inject and detect the spin-polarized carriers on the same nanowire we must be able to independently switch the spin polarization for different contacts as we vary the strength of the magnetic field. For this purpose we have used electron beam lithography followed by cobalt deposition and lift off to form nano- to microscale Co regions of varying thicknesses with different coercive field strengths. We are currently using longitudinal Kerr rotation optical measurements to establish the field-induced switching strengths. Issues with field strength and magnetic boundaries are currently being addressed for structures compatible with our nanowire geometries. For the tunnel barriers which require control at thicknesses in the sub-one- nanometer regime we are developing aluminum oxide barriers which are formed by sequential aluminum deposition and oxidation. This process will be greatly improved by the arrival in November, 2010, of an atomic layer deposition system which

will allow highly uniform Al2O3 conformal depositions on the nanowires with monolayer control providing superior ability for adequate control of the ferromagnetic contact/nanowire contact resistance. An additional important area of basic materials science progress has been in developing techniques to growth Ge/Si core/shell nanowire structures. We have developed an all in situ process to grow these radial structures with high quality smooth shells for the first time. This process has involved the development and understanding of forming a silicon blocking layer under the Au growth catalyst upon completion of growth of the Ge core which prevents Au diffusion down the nanowire sidewalls. Without this blocking layer the smooth, high quality Si shells on Ge cores cannot be grown (see Figure 1 for high resolution transmission electron microscopy images of our single crystal radial Ge/Si core/shell structures). This development is important because it provides a new approach to tunnel barriers for spin injection which has not been used previously and is anticipated to provide much better materials control of the spin injection process. Additional progress in the processing has involved developing the fabrication steps to combine both the tunnel barriers and ohmic contact barriers on the same nanowires. These combined contact structures are required to independently establish the electrical properties of the same nanowire for which the spin-polarized injection is being studied. Initial studies are aimed at electron injection and detection on n-doped nanowires using the multi-terminal Hanle effect approach Preliminary theoretical analysis has suggested the tunnel spin injection approach will be superior to Schottky barrier approaches and is also helping to guide the doping levels and tunnel thicknesses to be used for optimal contact resistances, spin injection, and resulting magnetoresistance values. We anticipate our first spin injection demonstration in the near future.

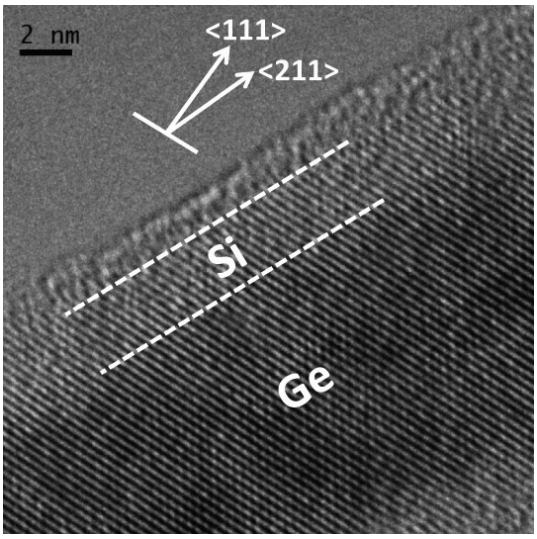

Figure 1. Single crystal Ge/Si core/shell nanowire demonstrating high quality epitaxial radial growth by the vapor-liquid-solid technique with smooth sidewalls and no gold contamination.

Future Work

The scientific challenge we will address is to understand the injection, transport, and detection of electron spins in semiconducting nanowires. A silicon nanowire contacted with ferromagnetic metal contacts with a thin insulator in between will allow tunneling to occur primarily for those electrons in the ferromagnetic contact with the majority spin. This approach will permit a spin polarized current to flow into the nanowire. The spin current will be detected by another ferromagnetic contact. By application of magnetic fields parallel and perpendicular to the plane of the ferromagnetic contacts, the device resistance can be varied, allowing representation of "on" and "off" states by electron spins, rather than by the large currents typically employed in semiconductors logic devices. This method will allow us to unambiguously detect spins and analyze spin transport in semiconducting nanowires for the first time. Our proposed work aims to: 1) investigate electron spin injection, transport and detection in silicon or germanium nanowires as a function of temperature, electrical and magnetic fields; 2) establish the influence of nanowire diameter, doping, and surface passivation on electron spin dynamics; and 3) study spin transport in radial and axial nanowire Si/Ge heterostructures and the new physics resulting from strain, and band-structure modifications. Both theoretical and experimental techniques will be employed in this project.

Conclusion

This project will use theory and experiment to study the manipulation of spins in silicon-based nanowires grown by our chemical vapor deposition method. Electron spin injection and transport will be detected and quantified by magneto-impedance, spin valve and Hanle effect techniques. The influence of temperature, and electric and magnetic fields will be measured. Effects of surface passivation and diameter on spin transport in nanowires will be determined. In addition, we will exploit our ability to synthesize Si/Ge nanowire heterostructures to explore spin transport across hetero-interfaces and to examine the effects of strain on spin transport in radial heterostructures.

Publications

Dayeh, S., J. Huang, A. Gin, and S. T. Picraux. Elimination of Gold Diffusion in the Heterostructure Core/Shell growth of High Performance Ge/Si Nanowire HFETs. 2010. In *IEEE Nano 2010 International Conference.* (Seoul, Korea, 17-20 Aug. 2010). , p. 95. Seoul: IEEE.

Dayeh, S., J. Huang, A. Gin, and S. T. Picraux. Elimination of Au diffusion for high performance core/multi-shell germanium/silicon nanowire heterostructure transistors. To appear in *Nano Letters.*

Dayeh, S., and S. T. Picraux. Ge/Si Core/Multi-shell Heterostructure FETs. 2010. In *Electrochemical Society: SiGe, Ge, and Related Compounds 4: Materials, Processing,*

and Devices. (Las Vegas, NV, 11-14 Oct. 2010). , p. 56. Las Vegas: Electrochemical Society.

Dayeh, S., and S. T. Picraux. Direct Observation of Nano-scale Size Effects in Ge Semiconductor Nanowire Growth. 2010. *Nano Letters.* **10**: 4032.

Le, S. T., P. Jannaty, A. Zaslavsky, S. Dayeh, and S. T. Picraux. Growth, electrical rectification, and gate control in axial in situ doped p-n junction germanium nanowires. 2010. *Applied Physics Letters.* **96**: 262102.

Picraux, S. T., S. Dayeh, P. Manandhar, D. E. Perea, and S. G. Choi. Silicon and Germanium Nanowires: Growth, Properties and Integration (Invited Overview). 2010. *Journal of Materials.* **62** (4): 35.

Transformational Approach for the Fabrication of Semiconductor Nanowires: "Flow" Solution-Liquid-Solid Growth

Jennifer A. Hollingsworth
20100285ER

Introduction

Semiconductor nanowires (SC-NWs) constitute "next-generation" nanoscale building blocks for a range of applications from nanoelectronics and photonics to energy-harvesting. SC-NWs can be fabricated using either vapor- or solution-phase methods, where solution-phase approaches offer advantages in simplified processing and scale-up, as well as almost unlimited choice of materials systems from Group III-V to Groups IV, II-VI, IV-VI, and I-III-VI2 semiconductors (e.g., InP, InAs, GaP, GaAs, ZnTe, CdSe, PbSe, and CuInSe2). Despite these advantages compared to vapor-phase approaches, the solution-phase methods suffer from two fundamental flaws: (1) the solution-phase approach has not been applied to patterned, vertical SC-NW growth at surfaces and (2) there is currently no clear way to use these methods to grow complex axial heterostructures. Overcoming these limitations would move the field of solution-phase SC-NW fabrication forward to the point that this approach could be realistically considered for real-world applications. Therefore, our overall research goal is to develop a novel solution-phase SC-NW growth method that aims to address these limitations. We call this new approach Flow-Solution-Liquid-Solid (FSLS) growth.

Like conventional SLS, FSLS entails thermally decomposing chemical precursors in the presence of molten metal nanoparticles, which promote the nucleation and growth of the SC-NWs. Unlike SLS, FSLS will allow us to introduce precursors into a reaction vessel by way of a continuously supplied flow of carrier solution, rather than all at once in a single injection. In this way, unreacted precursor and by-products will be constantly removed, approximately steady-state precursor concentrations will be maintained, and different precursors will be able to be supplied in an alternating fashion. Further, rather than utilizing "free-standing" metal nanoparticle catalysts, FSLS will make use of nanoparticles adhered to solid substrates. The coupled ability to flow precursors past bound catalyst particles will enable us to synthesize complex axial heterostructures and to fabricate patterned, vertical SC-NW arrays.

Benefit to National Security Missions

The proposed work addresses two key LANL Materials: Discovery Science to Strategic Applications Grand Challenge FY10 Priorities: Develop (1) the underlying materials science, physics and chemistry to support materials needs in energy efficiency and (2) intrinsic techniques to control functionality with novel architectures resulting from new synthesis, fabrication and processing concepts. Further, it supports the Energy and Earth Systems Grand Challenge FY10 Priority to develop transformational science and technology that enables clean, efficient power generation, addressing energy efficiency and security mission areas.

Progress

Task 1: Transforming Solution-Liquid-Solid (SLS) growth into Flow-SLS (FSLS) growth. In support of this task, a commercial microfluidic reactor (Syrris FRX flow reactor) was modified to perform SLS nanowire (NW) growth from solid substrates. This was accomplished by inclusion of a custom glass microfluidic chip, chip holder, and Mitos edge connector (designed in collaboration with The Dolomite Centre Ltd.) into the flow reactor. The chip allows for a substrate bearing metal catalyst nanoparticles (or a thin metal film – see below) to be incorporated into the flow stream of solution-phase precursors, to be held at a desired reaction temperature for the duration of a nanowire reaction, and then to be removed from the chip for analysis and any further processing.

Achieving an important goal of Task 1, we have successfully demonstrated the first synthesis of compound semiconductor NWs by FSLS. Specifically, we used our new setup to grow vertically aligned ZnSe on GaAs substrates, and CdSe and CdTe on Si substrates. More recently, we also attempted growth of the first axially heterostructured NW by this method. We synthesized CdSe/CdTe NWs, potentially up to three segments of each composition. To realize FSLS and to minimize competing quantum dot growth in flow, we had to modify the reactant/ligand concentrations and metal/chalcogen ratios compared to those employed in the literature for standard SLS. The substrate-bound bismuth catalyst nanoparticles were

achieved by depositing thin Bi layers onto the substrates (with or without substrate pre-cleaning with HF) using e-beam evaporation. These films break apart into Bi droplets at the growth temperatures employed. Differences in the Bi films thicknesses (assessed using RBS) and quality have been the largest contributor to a lack of reproducibility in the FSLS NW growth process. Therefore, for this project, we purchased a combined DC sputtering/thermal evaporation system, where the sputtering component will allow reproducible deposition of the low-melting Bi metal with large-area and batch-to-batch uniformity of better than 2.5% (to be installed FY11). As an alternative approach, we used pre-synthesized Bi nanoparticles. We initially had difficulty getting the pre-synthesized NPs to stay in place during NW growth, and use of thin polymer layers to adhere the particles sometimes prevented NW growth. We solved this issue by employing a simple bifunctional ligand (3-mercaptopropyl methoxysilane) to stick the Bi nanoparticles to the substrate.

Obtaining adequate electron microscopy images and related elemental analysis data for our surface-bound nanowires remains a significant challenge. A new high-res SEM on order for LANL-CINT should provide improved image quality and elemental analysis sensitivity. Conventional TEM requires the substrate-bound nanowire samples to be thinned to TEM transparency, a laborious and often unsuccessful endeavor, especially when the objects of interest are sparsely spaced. For these reasons, we are pursuing collaboration with J. Huang, Sandia National Laboratories CINT Core TEM facility, as his sample holder permits analysis of un-thinned specimens, i.e., ~as-prepared.

Significantly, in addition to demonstrating "firsts" with respect to flow-SLS nanowire growth, we have explored a large range of reaction condition phase space. For these fundamental studies, we have targeted CdTe and CdSe, as these are the best-understood nanowire systems grown by conventional SLS. First, we studied the effect of precursor concentration on growth rates and mechanism (Figure 1). These observations suggested that at high precursor concentrations, a different growth mechanism, possibly a seeded-growth process, took place rather than the SLS growth mechanism. We also explored the effect of flow rate (from 0.2 mL/min to 0.02 mL/min) on nanowire growth. We observed that nanowires grown at the slowest flow rate (0.02 mL/min) showed a dramatic shift in growth mechanism from the "seeded-growth" characteristic of faster flow rates to a completely SLS growth regime. Thus, by combining high precursor concentrations with low flow rates, we were able to get high density (albeit short nanowires) all-SLS growth, where the density was enhanced by increasing the fraction of Bi nanoparticles that progressed from a swelling/nucleation stage to a growth stage (Figure 1). Related trends were also observed for CdSe, though, in this case, the CdSe occasionally grew as faceted pillars. Such growth mechanism-related changes in structure have also been observed for vapor-liquid-solid (VLS) nanowire growth. Thus, our flow-SLS approach does appear to allow us access to reaction parameter phase space that is more traditionally associated with flow-based vapor-phase processes. We are currently preparing a manuscript based on these findings.

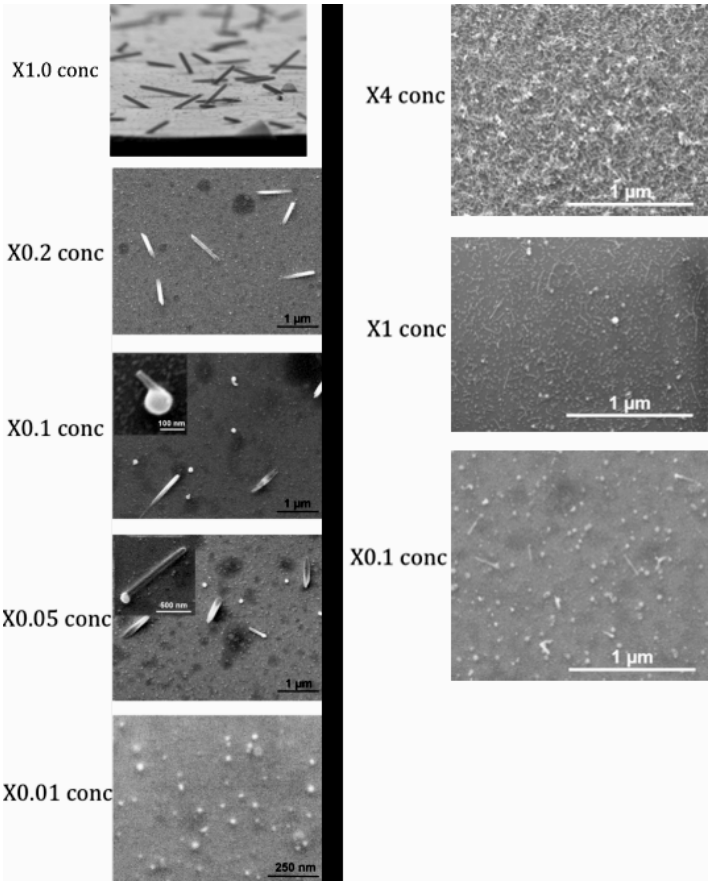

Figure 1. Left Panel (moderate flow rate of 0.2 mL/min): "High" concentrations (x1 concentration compared to those used in conventional flask reactions) of Cd and Te precursors yield wire-like morphology but lacking evidence of Bi nanoparticle catalyst tips, thus lacking conclusive evidence that the growth mechanism was indeed catalyzed (SLS) growth. At lower concentrations (x0.2-0.05 conc.), SLS-grown nanowires with visible Bi tips become evident in addition to the structures without tips. At very low concentrations (x0.01 conc.), nanowire structures did not grow; however, Bi nanoparticles swollen with precursor elements were found on the substrate. Right Panel (low flow rate of 0.02 mL/min): All concentrations resulted in SLS-type growth, with enhanced nanostructure density obtained at the highest concentrations.

Task 2: For this task, we have obtained the required conductive polymers for fabrication of hybrid photovoltaic devices comprising our nanowires as the electron transport material and the polymer as the hole-transport material. We have also obtained conductive ITO-coated substrates and will soon attempt FSLS NW growth on these device-

relevant substrates. Lastly, we have developed the first SLS synthesis method for Cu_2ZnSnS_4, an "earth-abundant" semiconductor with a solar-relevant bandgap and high absorption coefficient. Once this procedure is optimized, we will transfer the approach to the FSLS system. We also successfully prepared the first SLS Cu_3P_2 nanowires, which we intend to use as a model system for developing another "energy-relevant"/earth-abundant system, namely, a preparation for Zn_3P_2 nanowires (Figure 2). Lastly, given the lack of fundamental or applied studies in the literature to date, we are also synthesizing known near-IR/IR nanowire systems (CdTe, InP, and PbS) for comparison to our newly developed materials.

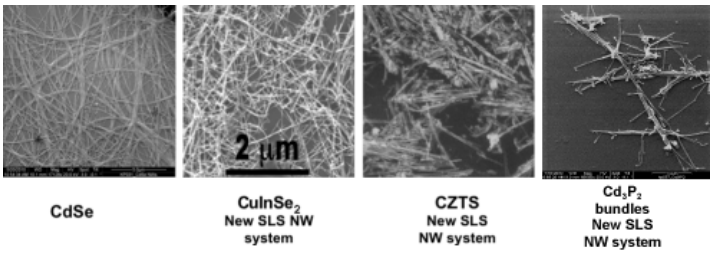

Figure 2. Scanning electron microscopy (SEM) images of nanowires grown by SLS in-flask, emphasizing syntheses developed in our laboratory for energy-harvesting applications.

Spectroscopy. We have established and begun to apply a variety of spectroscopic tools including transient absorption spectroscopy, photoluminescence (PL), and time-resolved PL techniques to investigate electronic structure, energy relaxation and inter/intra wire charge and energy-transfer processes. We will shortly start transient-absorption and time-resolved PL studies on diameter-controlled NWs and NW/polymer complexes. We have also begun combined electrical/optical characterization on individual nanowire field-effect transistors, successfully fabricating necessary individual NW devices using an e-beam lithography process (Figure 3). Lastly, we have started a correlated structural/optical-spectroscopy study on individual nanowires.

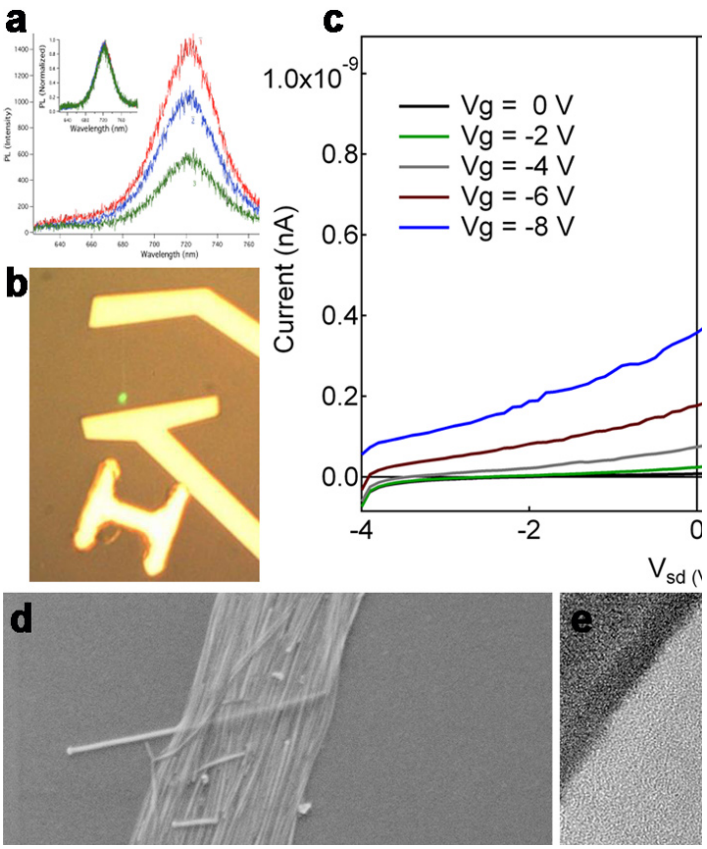

Figure 3. (a) Single-CdSe-NW emission spectra taken at different positions along the NW length. (b) Single-CdSe-NW device: faint white line is the NW, and green dot is the laser spot. (c) Current versus voltage plot showing strong gate dependence of single CdSe-NW-device. (d) SEM image and (e) TEM image of recently synthesized, high-quality, quantum-confined CdTe NWs. Single-NW analytical and device capabilities have been developed in Year 1 for CdSe NWs and will be extended in Year 2 to "energy-relevant" systems, e.g., CdTe.

Future Work

Task 1: Transform SLS into FSLS for Advanced Solution Growth of SC-NWs --

We have achieved FSLS and have developed an initial understanding of growth conditions affecting the mode of growth and NW density; however, in Year 2 of the project we need to optimize growth conditions to achieve more consistently vertical growth and longer NW growth. To this end, we will continue to explore key parameter space building on lessons learned from Year 1. We will also emphasize patterning of the catalyst particles and optimized substrates to facilitate regular and vertical nanowire growth, e.g., microfabricated "cups."

Task 2: Assess Utility of FSLS Method for Energy Harvesting Applications --

Photovoltaic example: We will significantly advance the

state-of-the-art in hybrid inorganic/polymer solar cells by fabricating NW-based devices wherein SCNWs will provide substantially improved charge transport. Here, we will emphasize synthesis of solar-relevant NWs: Cu_2ZnSnS_4, Zn_3P_2 and CdTe, and fabrication of simple PV devices.

Thermoelectric example: We will use FSLS to conclusively demonstrate for the first time nanoscale axial heterostructuring in solution-grown SC-NWs toward high-efficiency thermoelectrics.

Conclusion

We will enable for the first time the solution-phase synthesis of complex axially heterostructured semiconductor nanowires (SC-NWs), as well as the ability to fabricate patterned, vertical SC-NW arrays from solution. These new capabilities will address the factors that are currently limiting the utility of solution-phase-grown SC-NWs for key applications in energy harvesting -- SC-NW-based photovoltaics and thermoelectrics. In addition to developing new functional nanomaterials synthesis and fabrication capabilities, we will provide a practical demonstration of enabled photovoltaic and thermoelectric devices.

Publications

Hollingsworth, J. A.. Novel functional semiconductor nanocrystal quantum dots and nanowires for applications involving energy conversion. Invited presentation at *2010 Materials Research Society Spring Meeting.* (San Francisco, April 5-9).

Laocharoensuk, R., N. Smith, J. Baldwin, A. Gin, and J. A. Hollingsworth. Versatile Solution-Phase Approach for Fabrication of Metal-Semiconductor Heterostructured Nanowires. Presented at *2010 Materials Research Society Spring Meeting.* (San Francisco, 5-9 April 2010).

Laocharoensuk, R., N. Smith, K. Palaniappan, J. K. Baldwin, and J. A. Hollingsworth. Integration and Development of Solution-Phase Techniques for Fabrication of Novel Heterostructured Nanowires. Presented at *2010 Materials Research Society Fall Meeting.* (Boston, Nov. 29-Dec. 3 2010).

Unraveling Electron-Boson Interactions in High-Tc Superconductors With Ultrafast Infrared Spectroscopy

Rohit P. Prasankumar
20100298ER

Introduction

The first high-T_c superconductor (HTSC) was discovered over 20 years ago, spurring a worldwide effort to study and utilize these materials. However, the mechanism underlying this unique phenomenon is arguably the greatest unsolved mystery in condensed matter physics. In particular, it is not understood whether electrons in these materials form Cooper pairs through interactions with other particles, known as bosons (e.g., phonons (quantized lattice vibrations)), or through strong electronic correlations alone. Conventional experimental and theoretical techniques have thus far been unsuccessful in unambiguously determining this pairing "glue" in HTSCs. Further progress on this critical problem will thus require the application of novel experimental and theoretical methods.

The goal of this project is therefore to couple the new experimental technique of ultrafast infrared spectroscopy (UIS) with novel theoretical models to investigate electron-boson interaction dynamics in HTSCs. UIS has, to the best of our knowledge, never been demonstrated, and stands to significantly impact our understanding of HTSCs. This technique will allow us to probe electron-boson coupling by photoexciting relevant bosonic modes and temporally resolving the resulting changes in the complex conductivity, σ(ω, t). If a particular bosonic mode is the pairing glue in HTSCs, then directly photoexciting it should affect the conductivity of the superconducting state; conversely, if no conductivity change is detected after photoexcitation, this likely indicates that the photoexcited mode is not directly linked to Cooper pairing. This experiment alone should provide much insight on the important question of whether certain bosons are the pairing glue in HTSCs. Analysis of the data using our theoretical models for the photoinduced changes in σ(ω, t) could then be used to uncover the specific bosonic mode that serves as the pairing glue between electrons.

In short, the use of ultrafast infrared spectroscopy to examine the dynamics of low energy excitations in HTSCs, coupled with advanced theoretical models, is an innovative approach for exploring electron-boson interactions in HTSCs. Most significantly, it has the potential to finally uncover the pairing glue in these extensively studied systems and answer a question that has puzzled scientists for over 20 years.

Benefit to National Security Missions

The DOE Office of Science, in particular Basic Energy Sciences, has made understanding superconductivity a priority research direction, signified by the workshop on "Basic Research Needs for Superconductivity" that was held in 2006. The research described in this proposal directly addresses many of the issues identified in the report from this workshop, along with the Basic Understanding of Materials grand challenge at LANL, and will thus be very relevant to these areas.

Progress

We have made significant progress during the first year of this project. On the experimental side, we have finished building our ultrafast infrared spectroscopy system and applied it to study ultrafast dynamics in several different materials. In particular, we have performed mid-infrared (IR) pump, terahertz (THz)-probe experiments on type-II InAs/GaSb semiconductor superlattices (SLS) (Figure 1). These devices are currently used for efficient, high temperature mid-IR photodetection, with applications in night vision imaging and chemical identification. These first ultrafast optical experiments on these nanostructures are particularly relevant to detector operation, since a mid-IR pump photon is absorbed and the resulting conductivity is detected with sub-picosecond time resolution using THz probe pulses. We are currently preparing a publication on these results, which should provide insight on the fundamental limitations to fast modulation of type-II-based SLS photodetectors.

We have also used our UIS system to perform optical/mid-IR pump, THz-probe experiments on graphene. This is arguably the "hottest" material in current condensed matter physics, as evidenced by the awarding of the 2010 Nobel Prize in Physics to its discoverers. These experiments are still in progress but promise to reveal unique physics relevant to electron-phonon coupling in

these materials. Finally, we have performed some initial optical/mid-IR pump, THz-probe studies on the high-T_c superconductor YBCO to address the primary goals of this proposal. Preliminary optical pump, THz-probe measurements demonstrated that we could get a signal from YBCO that qualitatively compared to previously published results. We expect to perform more mid-IR pump, THz-probe experiments in FY11 to provide insight on the pairing mechanism in high-T_c superconductors. This will enable us to connect to our theoretical calculations of time-resolved optical conductivity in high-T_c superconductors, as follows.

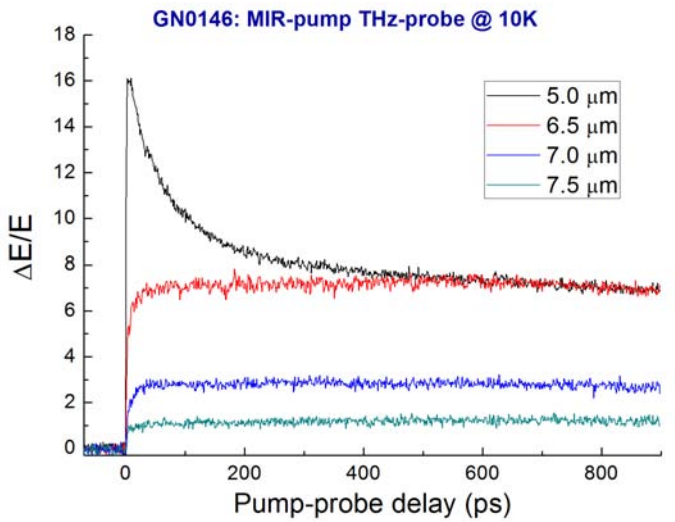

Figure 1. Mid-IR pump, THz-probe experiments on a type-II SLS as a function of pump wavelength.

Theoretically, we have focused on establishing a complete framework for calculating the time-resolved optical conductivity in HTSCs. As a first step, we have succeeded in deriving a set of coupled rate equations for the electronic and lattice baths in superconductors. The derivation is a combination of microscopic quantum modeling of electron-lattice coupling and classical modeling of electron-photon coupling. We have solved these rate equations for temperatures for both electron and phonon pumping. Our results show the existence of a kink structure as the electronic temperature rises above the superconducting transition temperature. This finding is new and should be tested carefully by experiments.

As a second step, we have derived the electronic single-particle Green's function, which provides information about the quasiparticle excitation properties, and calculated the time-resolved electronic spectral function. We have shown that when phonons are directly photoexcited, new features can be revealed in the electronic spectral function [1]. This finding is very important by providing a "smoking gun" for identifying the nature of bosonic modes, to which electrons are strongly coupled, and should enable straightforward comparison to our forthcoming experimental results. This study, if confirmed experimentally, will provide direct evidence for electron-phonon coupling, and is not only relevant to mid-IR pump, THz-probe experiments but also to time-and-angle-resolved photoemission spectroscopy (TR-ARPES) experiments with a mid-IR pump pulse.

Overall, we expect this project to yield groundbreaking results in the next year, as we now have laid the theoretical and experimental groundwork for accomplishing our primary objective of studying electron-boson interactions in high-temperature superconductors, with the potential to yield substantial insight on the pairing mechanism in these fascinating systems.

Future Work

Experimentally, we have optimized our UIS system and applied it to measurements on several materials as described above. However, we experienced problems during our initial UIS measurements on YBCO, due to the difficulty in finding cryostat window materials that simultaneously transmit mid-IR and THz radiation. We have since overcome this problem by fabricating a novel window design comprised of two different materials, and expect to successfully perform the first mid-IR pump, THz-probe experiments on YBCO in FY11. As described above, we expect these experiments to shed new light on the pairing glue in HTSCs. In parallel, we plan to extend our initial UIS measurements on graphene, as our unique capability to do these experiments on this hotly studied material could provide insight on graphene-based phenomena unavailable from any other technique. Finally, we will extend these measurements to other HTSCs to determine the universality of electron-boson coupling in these systems, as well as other materials of current interest, such as topological insulators.

Our theoretical studies will be pursued in parallel with the experimental efforts. We will use the models developed thus far to calculate the time evolution of σ(ω, t) and compare it with experiments to understand its origin. Finally, we will develop a real-time non-equilibrium optical conductivity model within a density-matrix theory and compare the calculated and experimentally measured σ(ω, t).

Conclusion

The potent combination of advanced ultrafast techniques and sophisticated theoretical modeling described here provides a unique opportunity to disentangle electron-boson interactions in HTSCs while pioneering an original approach to studying the microscopic origin of high-T_c superconductivity. Our approach has the potential to finally uncover the pairing mechanism in high-T_c superconductors, which could lead to room temperature superconductivity and will certainly enable many new applications of HTSCs in areas such as power transmission and magnetic resonance imaging.

References

1. Tao, J., and J. X. Zhu. Theory of the time-resolved spectral function of high-temperature superconductors with bosonic modes. 2010. Physical Review B. **81**: 224506.

Publications

Tao, J., and J. X. Zhu. Theory of the time-resolved spectral function of high-temperature superconductors with bosonic modes. 2010. *Physical Review B.* **81**: 224506.

GO FISH, A Smart Capture and Detection Strategy for Intact and Viable Pathogens

Harshini Mukundan
20100308ER

Introduction

The project aims to generate novel technology to track viable pathogens of national security interest and global health concern, thereby addressing a very significant gap in this area. This directly enhances the capabilities of LANL's Complex Biological systems grand challenge. In 2009, Dr. Terry Wallace said that the "emphasis areas for strategic growth in CLES are in *Energy, Climate & Environment; Complex Biological Systems; Fundamental Understanding of Materials; and Forensics and Sensing"*. This work greatly advances the technological capabilities of the LANL Biosecurity center as well.

Benefit to National Security Missions

The project aims to generate novel technology to track viable pathogens of national security interest and global health concern, thereby addressing a very significant gap in this area. This directly enhances the capabilities of LANL's Complex Biological systems grand challenge. In 2009, Dr. Terry Wallace said that the "emphasis areas for strategic growth in CLES are in *Energy, Climate & Environment; Complex Biological Systems; Fundamental Understanding of Materials; and Forensics and Sensing"*. This work greatly advances the technological capabilities of the LANL Biosecurity center as well.

Progress

Siderophore Synthesis: *We have synthesized and characterized enterobactin, the E. coli siderophore.* We evaluated two routes to make enterobactin analogs, 1) a solid phase building block technique and 2) synthesizing the tri-serine core using Sn based template, followed by protecting group manipulations to give the desired targets. Attempts to prepare the enterobactin core *via* solid phase route led to products that gave inconclusive mass spectra. We will probably not purse this route in light of recent results that show we can efficiently, and on large scale, prepare synthetic enterobactin, as well as the modified enterobactin through solution-phase routes (method 2, below). The second method has yielded a substantial amount of pure enterobactin, and allowed us to synthesize an enterobactin analog based on the tri-serine core, with two catechol groups along with a linkable protected amine tether. We are currently applying a combinatorial approach to generate a library of enterobactin related compounds with various side chains for further study. *We have successfully synthesized enterobactin and its target analogs and are currently undertaking steps to generate a library of compounds to investigate the intriguing biology of these compounds*.

The tethered analogue strategy uses solid phase bead synthesis to sequentially add each amino acid residue. The serine cyclization using SnCl4 is not feasible using diaminopropionic acid, hence this route was deemed to be appropriate to make an amide core analogue.

The hurdles encountered using the SnCl4/serine cyclization strategy were:

- The stability of the final product was compromised if all the amines were not functionalized with aromatic residues.
- In order to get a 2:1 ratio of residues (two catechols and one tether group) it was necessary to use acid chlorides with similar steric hindrance that would create equal reactivity. If otherwise, the transformation resulted in both the tri-substituted catechol and tri-substituted tether as the two major products.

Characterization of receptor-enterobactin binding: Enterobactin is recognized and internalized by a multi-protein porin system. The ferric enterobactin transporter protein cluster consists of proteins FepA to FepG. While FepA is inserted into the outer membrane and represents the **f**erric **e**nterobactin rece**p**tor with a K_d= 0.1 nM for ferric enterobactin, FepB is a periplasmic binding protein that binds ferric enterobactin for transport across the inner membrane by the FepCDG ABC transporter. We cloned and over-expressed both, the binding receptor FepA and the intermediate transporter FepB, independent from each other. FepA was over-expressed in quantities of approximately 120 mg of purified protein/ litre culture. The purified protein was inserted into micelles to preserve its native fold and enable liquid-state NMR based ligand-binding studies of the

monomeric protein. Since FepA is already a 78 kDa protein, consistent out of a 22 stranded beta-barrel with a 25 kDa inserted recognition and binding domain, the additional size of the obtained micelles has a significant influence of the quality of the NMR spectra. We were able to trim the size of the micelles to a minimum of ~ 25-30 kDa using a combination of *E.coli* lipids and two different detergents. The quality of the NMR spectra of this ~105 kDa protein-micelle complex could be further improved by using per-deuterated *E.coli* lipids. For this purpose, we extracted and purified lipids out of 100% perdeuterated *E.coli* culture.

The binding of the modified enterobactin synthesized to receptors has been characterized using NMR studies, ahead of schedule. The obtained initial results of those ligand-titration experiments formed the basis for NMR-based ligand interaction and binding studies using synthetic enterobactin and first structural studies were effectively completed.

We have also established cell-based systems and cultures for Mycobacteria and Escherichia for siderophore characterization. Approvals and permits for the same are now added to the IBC and cultures have started.

As shown above, we have developed synthetic strategies for modified enterobactin and successfully synthesized significant quantities of the same. We have also cloned and characterized the enterobactin receptor and are well poised to evaluate the binding and internalization of the modified enterobactin to the receptor in the next month.

Future Work

Alternative tethering strategies for enterobactin are being explored. Binding studies for tethered enterobactin are being initiated. Biological assays and binding affinity constant measurements are scheduled for FY11. We will also initiate synthesis of other siderophores

Conclusion

Progress is ahead of schedule. We anticipate delivering on proposed milestones in 2011 on target.

Ultra-Fast DFT-Quality Forces for Molecular Dynamics Simulations of Materials

Arthur F. Voter
20100366ER

Introduction

The molecular dynamics (MD) simulation method, in which atoms are evolved in time according to the classical equations of motion, has become a standard and powerful tool in materials science. If the underlying model for the forces between the atoms is accurate, high-quality predictions of molecular and material behavior can be made. This helps researchers interpret experiments, develop new models, and generally understand how materials behave in full microscopic detail. Electronic structure methods, such as density functional theory (DFT), can be used to provide very accurate forces on the atoms. However, the computational cost of DFT is extremely high, typically limiting MD simulations to at most picoseconds for relatively small systems of a few hundred atoms. In contrast, MD simulations using empirical interatomic potentials, although not as accurate, can reach much longer times, up to roughly a microsecond. Moreover, using accelerated molecular dynamics methods, this time scale can then be pushed even further, to milliseconds and sometimes beyond. In this project, we are developing a new approach for calculating interatomic forces, aimed at achieving roughly the accuracy of DFT with a speed close to that of empirical potentials. We are developing a self-adaptive data-mining approach, in which force and local geometry information from every DFT evaluation is saved in a large database for future use. During a simulation, the force on each atom is obtained by selecting clusters of atoms from the database that are similar to the neighbors around the atom of interest. We then apply a novel physics-based interpolation to approximate the force on the central atom. If we succeed, this will enable predictive-quality materials simulations on large systems for long times (e.g., microseconds and beyond), which has not been possible before.

Benefit to National Security Missions

This project is aimed at developing a capability for very fast, very accurate force calculations for molecular dynamics simulations of materials, so that longer time scales can be achieved than ever before with good accuracy. This capability will be valuable in designing advanced materials for nuclear reactors and nuclear waste storage. It will also be useful for designing alloys for aerospace and energy applications. In the area of alternative energy, it will be useful for designing catalysts for fuel cells, and for improving processing steps for growth of solar cells or superconducting films.

Progress

A key part of this project is designing a method to quickly extract, from the database, clusters that have a close geometrical match to the target cluster. The target cluster is made up of the atom for which we want to calculate the force, along with all the atoms that surround it out to some cutoff distance. One focus so far has been on improving the accuracy and robustness of the covariance-based (CB) cluster-matching approach that we originally proposed. The CB approach is fast, but it defines the distance between two atomic configurations in a non-traditional way. Hence we need to carefully analyze the relationship between the two distances, i.e., the fast but approximate CB, and the exact rotation-based (RB) one. Our goal is to make sure that the error we are making by substituting RB by CB will not lead to distorted results. We made several improvements on the existing version of the CB distance computation. One modification is that we now use weight functions to increase the length of the CB vector representing a configuration. Since each atom is given as a point in 3d, the covariance matrix has dimensions 3x3, and hence the number of its eigenvalues is only 3. This is too short for accurately representing a configuration of as many as 50 atoms. By weighting the neighbors differently, we can append more sets of eigenvalues to the vector representing the configuration, thereby increasing the accuracy. Optimizing the set of these weights is one of our goals.

Another modification we made was using an inversion of each configuration in a preprocessing step; i.e., we invert the distance from the central atom to each neighbor. Because in the covariance-based approach, greater distances to the neighbors contribute more, this inversion has the effect of making the closer neighbors more important (rather than less important), as they should be

chemically. More importantly, this approach resolves the formerly troubling issue of how to compare clusters with different numbers of neighbors. In this new approach, any extra neighbors beyond the cutoff (e.g., those added to make two clusters have the same number of neighbors) simply become zero-length vectors after the inversion.

We implemented the above changes and a number of smaller ones. In our tests, the Pearson and the rank-based correlation coefficients between CB and RB distances were in most cases above 0.8. This represents an improvement over our previous results by about 25%. Computational retrieval speed is also important; the current computer code can retrieve the ten nearest clusters from a database of 1500 Si clusters in 0.5 ms. This is compatible with our goal of a few ms per atom for the final force speed.

We are also considering a variant of the original method to be implemented once the clusters are extracted from the database. We can store the Hessian, which represents the derivatives of the force components, in the database along with each cluster geometry. We can then use the Hessian to approximate the forces for the target cluster through straightforward Taylor expansion. Moreover, this requires only one cluster to be retrieved. This approach is computationally simple and tractable, yet it has rigorous mathematical convergence properties if the set of configurations in the database is made dense enough. Additionally we have given some speculation to creating an alternate formulation which invokes chemical arguments about bonding and valence in the context of the Hessian based idea. This may lead to a theory for creating an on-the-fly chemically based potential. In either case, insights gleaned through chemistry could dramatically improve the computational performance and accuracy of the method.

A preliminary study on the Hessian based method was carried out on Si and a model potential for Al. For Si, we find that the Hessian elements decay rapidly, so that the number of atoms in the target cluster and the database configurations can be kept small. In metals we found the decay to be slower.

Our current thinking is that the kinetics of growth and nucleation for the {311} defect in crystalline silicon will be a good test case for our method because it is an interesting and technologically valuable problem, one that cannot be studied using currrently available techniques. We have an accurate tight-binding reference potential for Si developed by Lenosky et. al. Although this tight-binding potential is less accurate than DFT, it is much less costly. We believe it is accurate enough to serve as the reference method while developing our algorithms, and its lower computational cost will allow us to perform tests more quickly. We are now testing the accuracy of forces computed using this tight-binding model on finite-sized clusters of silicon. Figures 1-3 shows the improving accuracy for the force on the central atom, compared to the result from tight binding on the full system, as the radial cutoff distance is increased from 5 to 7 Angstroms.

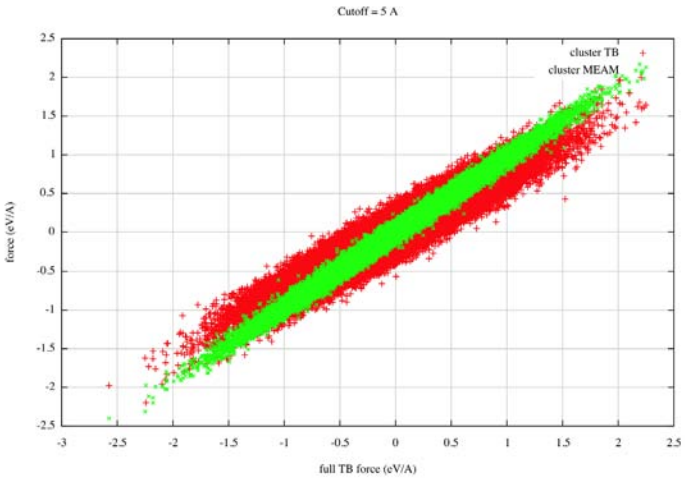

Figure 1. Accuracy of the force on the central atom of a cluster of silicon atoms using tight binding and a cluster radius of 5 Angstroms. The large number of clusters were generated from thermal sampling. The correct result is the full tight binding calculation (x axis). If the cluster-based force is perfectly accurate, the symbol (red cross) will fall exactly on the diagonal line. Also shown (in green) are the forces from an existing approximate interatomic potential of the modified embedded atom form.

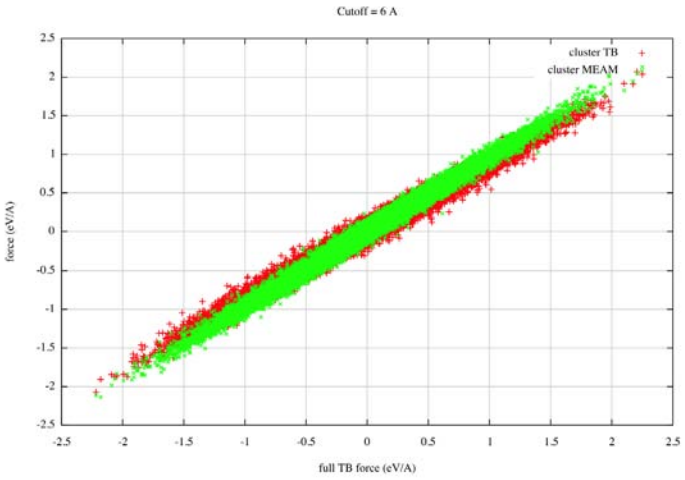

Figure 2. Accuracy of the force on the central atom of a cluster of silicon atoms using tight binding. As in Figure 1, but here the cutoff radius is 6 Angstroms. Note the improved accuracy.

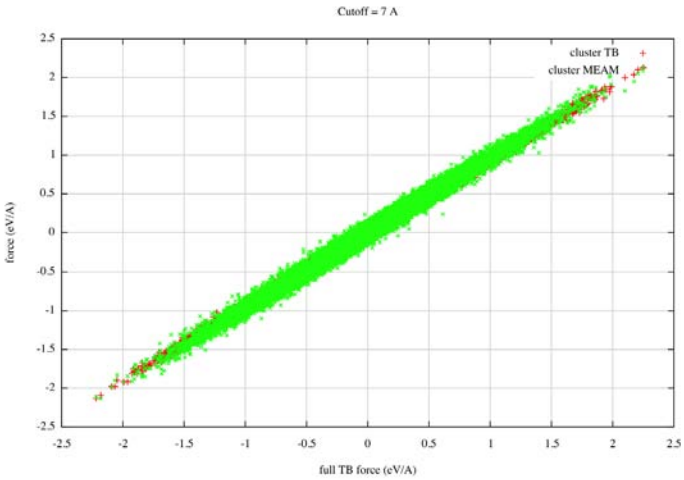

Figure 3. Accuracy of the force on the central atom of a cluster of silicon atoms using tight binding. As in Figure 1, but here the cutoff radius is 7 Angstroms. Note the improved accuracy.

Future Work

We will continue developing the data-mining approach built on an adaptive, self-filling database, to return DFT-quality forces at a speed close to that of an empirical potential. The database will be populated on the fly with clusters of atoms whose DFT force on the central atom is known. We will continue optimizing and tuning the fast search algorithm for retrieving clusters from the database whose geometries are similar to the neighbors of an atom whose force is currently needed. We will continue developing the "physics-based interpolation" procedure that will be applied to achieve the high-dimensional interpolation over the known cluster forces to approximate the desired force. If an insufficient number of clusters is retrieved, a new DFT calculation will be performed, and the new cluster(s) will be added to the database. We will pursue ways to parallelize this procedure that are not possible with conventional DFT. Error control will be built in. We hope to develop this overall procedure to achieve a speed in the milliseconds per atom per time step in the limit of a fully populated database. The methodology and codes will be developed and tested on silicon defect diffusion. Time permitting, we will apply the method to carbon clustering in bcc iron and the interaction of carbon with defects in iron.

Conclusion

Our goal is to design a procedure for calculating fast, accurate interatomic forces for molecular dynamics simulations of materials. This opens the way for predictive-quality simulations on much longer time scales than is currently possible, allowing processes such as fracture, plastic deformation, impurity precipitation and film growth to be simulated and the results compared directly to experiment. This capability will be valuable in designing advanced materials for nuclear reactors and nuclear waste storage, for designing alloys for aerospace and energy applications, designing catalysts for fuel cells, and for improving processing steps for growth of solar cells or superconducting films. We are making good progress towards this goal.

Controlling Charge Recombination Processes in "Giant" Nanocrystal Quantum Dots Toward High-Efficiency Solid-State Lighting

Jennifer A. Hollingsworth
20100469ER

Introduction

The most widely used sources of artificial illumination remain incandescent and fluorescent lamps, but these are not optimized for efficiency or longevity. Significant economic and environmental savings—~20% of electricity is consumed in lighting—could be achieved if efficient and robust low-cost alternatives were available for general lighting purposes. The primary alternative as perceived by industry and government is so-called 'solid-state lighting' (SSL). As described in the DOE SSL Roadmap, SSL differs fundamentally from existing technologies, and its development is central to DOE's—and LANL's—mission in energy efficiency. Existing technologies, most notably nitride-based and organic or polymer-based light emitting diode (LED) technologies, have thus far fallen short of providing the desired combination of properties: high-efficiency, long-term robustness, low-cost, and facile color-tunability. An ideal "building block" for LED technologies would possess the high-efficiency and innate robustness of nitride-based technologies coupled with low-cost processibility and color tunability. Here, we aim to establish a new class of colloidal semiconductor nanocrystal quantum dot (NQD)—the "giant" NQD (g-NQD)—as the ideal building block for high-efficiency, general-use SSL through three research goals:

- Fundamental photophysics: understand charge-recombination processes toward controlling/optimizing electronic→photonic conversion pathways.
- Materials-by-design: establish general synthesis capability for engineering key physical and electronic structure parameters controlling electronic→photonic conversion processes.
- Proof-of-principle devices: test hypothesis that g-NQDs provide significant performance improvements.

Benefit to National Security Missions

The proposed work addresses key LANL-identified Materials and Energy Grand Challenge FY10 Priorities: e.g., Develop (1) the underlying materials science, physics and chemistry to support materials needs in energy efficiency and (2) intrinsic techniques to control functionality with novel architectures resulting from new synthesis, fabrication and processing concepts. Thereby, the science developed here will provide the necessary fundamental understanding that will enable significant progress in SSL technology, where, according to the DOE, "No other lighting technology offers as much potential to save energy and enhance the quality of our building environments, contributing to our nation's energy and climate change solutions."

Progress

Task 1: Synthesize/structurally characterize g-NQD "test subjects" representing a range of physical/electronic-structure parameter space

To date, we have modified the synthesis parameters for the prototype (CdSe)CdS g-NQD system to drastically improve size/shape dispersity. This has resulted in a clear correlation between optimized structural and optical properties. Specifically, we have systematically studied the effects of shell-growth time, starting CdSe core and subsequent shell crystalline phases, ligand identity and concentration, and global reaction solution concentration on size and shape dispersity, as well as on ensemble and single-NQD optical properties. This work is assisted by basic optical measurements (photoluminescence, absorption spectroscopy, powder X-ray diffraction, transmission electron microscopy, and advanced spectroscopy – see below).

We have made significant progress in our aim to understand electronic structure and physical structure (interfacial alloying and core-size) effects on g-NQD properties. In this discussion, electronic structures are defined as follows: classic Type I refers to the case where the electron and hole are confined to the QD core; classic Type II refers to the case where the electron or hole is confined to the core, while the other carrier resides in the shell; and so-called quasi-Type II behavior refers to the case where both carriers reside in the core, but one of the carriers has a substantially higher probability of extend-

ing into the shell region. To date, we have synthesized intentionally alloyed CdSe/CdS systems. At the 4-shell (4 monolayers of shell material) level, these QDs show unexpected differences in spectral shifting as a function of shell composition within the first 2 shell layers (Figure 1). Also using the CdSe/CdS system, we have synthesized thick-shell materials starting from different core sizes, where theory predicted that electronic structure would transition from Type I to quasi-Type II to unconventional Type I (both carriers localized in shell) by simply adjusting the core size from large (>5 nm) to ultrasmall (<1.5 nm). We have succeeded in achieving some degree of color tunability (610-660 nm); however, it is not yet clear whether our results support theoretical predictions pertaining to core-size effects on electronic structure. Lastly, we explored the effect of shell composition on blinking and observed a clear trend toward non-blinking behavior only for the predominantly CdS shell systems [1].

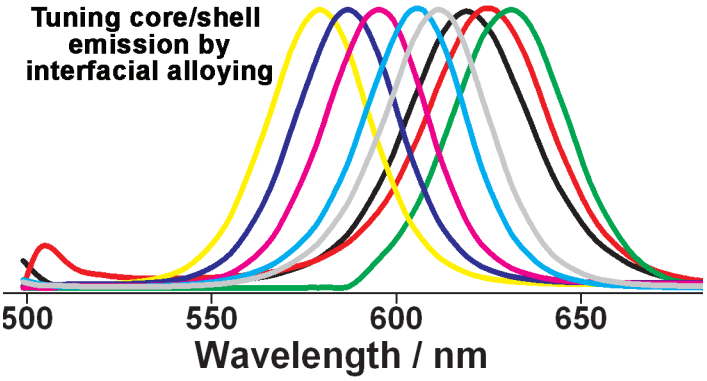

Figure 1. Photoluminescence spectra for a series of (CdSe) CdSexSy/CdS alloyed (core)shell NQD systems revealing the strong influence of interfacial alloying over emission energy.

We have also explored electronic-structure effects in the case of InP QDs. Here, we modified optical properties by applying a range of different shell materials – ZnS, ZnSe, CdS, CdSe, where each core/shell combination is hypothesized to afford a different electronic structure ranging from Type I to Quasi Type II to Type II. The likely extreme differences in electronic structures for these core/shell systems are thought to result in the vastly varying, and highly tunable, photoluminescence energies that we observe experimentally (extending from 2.1 to 1.1 eV; InP bulk band gap is 1.34 eV) (Figure 2). Recently, we collaborated with A. Piryatinski (T-4) to develop a model for understanding the shell-dependent energy shifts as a function of electronic structure. Significantly, his theoretical understanding correlates well with our experimental results.

To further assist synthesis efforts, we have begun to screen batches of g-NQDs for size-correlated optical properties. This approach allows us to move beyond simple measurements of ensemble-level emission quantum yields to assess the fraction of emitting g-NQDs in a population as a function of shell thickness. To this end, we have established a routine capability for *correlated* atomic force microscopy (AFM)/fluorescence microscopy. This work was done by a talented SULI student, Jason Grider (Rice Un.) (half funded by this project). We were assisted by Peter Goodwin, MPA-CINT, who graciously offered his time (to train Jason) and his equipment. The approach allowed us to apply a "physical" meaning to our solution-phase QY measurements and to, thereby, better understand how the changes we make in synthesis protocols translate to correlated NQD-level size/optical properties.

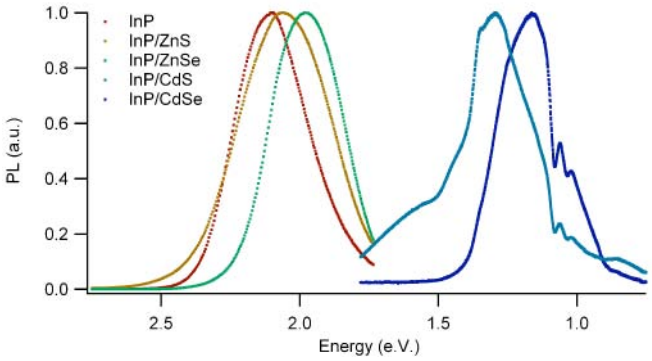

Figure 2. Photoluminescence spectra for a novel series of InP-based (core)shell g-NQD systems. Emission energies are controlled by tuning NQD electronic structures.

Task 2: Advanced ultrafast spectroscopy studies to provide mechanistic insight into non-radiative and radiative charge-recombination processes

We conducted single-nanocrystal spectroscopic studies of 16-monolayer-thick CdS shell CdSe/CdS g-NQDs. Using both continuous-wave and pulsed excitation, we observed strong emission features due to both neutral and charged biexcitons as well as multiexcitons of higher order. The development of pronounced multiexcitonic peaks in steady-state photoluminescence of individual nanocrystals, as well as continuous growth of the emission intensity in the range of high pump levels, point toward a significant suppression of nonradiative Auger decay, which would normally render multiexcitons nonemissive species [2]. These observations open interesting opportunities for studies of multiexciton phenomena using well-established methods of single-NQD spectroscopy, as well as new exciting prospects for applications that have been previously hampered by nonradiative Auger decay (Figure 3). More recently, biexciton quantum yields were determined as a function of shell thickness. Quantum yields as high as 90% were observed (*manuscript in preparation*).

Toward understanding the relationships between g-NQD electronic structure and excitonic behavior, we have conducted temperature- and magnetic-field-dependent measurements of time-resolved photoluminescence (PL) and fluorescence line narrowing (FLN). These important studies

have exposed the extrinsic control that we have achieved with the development of the novel g-NQD core/shell architecture over the electron-hole exchange interaction. The electron-hole exchange interaction (EI) in spherically shaped, quantum-confined semiconductor nanocrystals (NCs) of CdSe gives rise to an optically forbidden ("dark") exciton ground state that is several meV below an optically allowed ("bright") exciton. This dark-bright splitting has a profound effect on exciton dynamics and, specifically, leads to a nearly two-order-of-magnitude increase in the exciton radiative lifetime as a sample is cooled from room-temperature to liquid-helium temperature. EI has also been shown to dramatically affect other important physical properties of nanostructures, such as exciton spin dynamics, coherent interdot coupling and electron transfer kinetics to external quenchers. Here, we showed that the dark-bright energy splitting can be tuned over an order of magnitude by tuning the electron-hole spatial overlap in core-shell CdSe/CdS NCs with a variable shell width (submitted, *Nature Mater.*) (Figure 3).

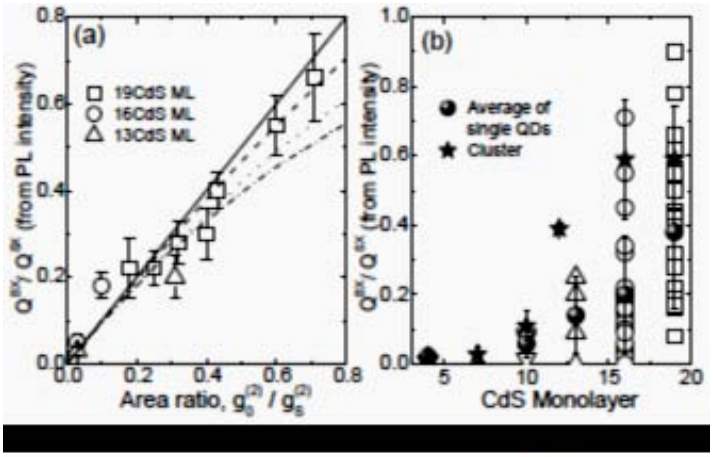

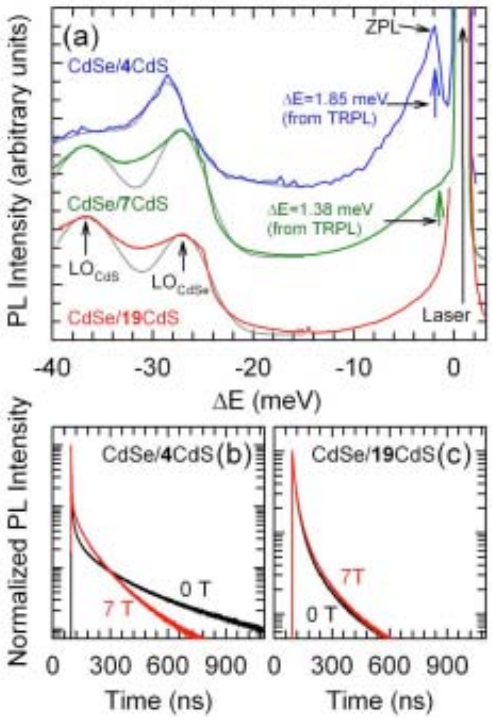

Figure 3. Top Panel: (a) Direct comparison between exciton and biexciton quantum yields (QBX/QSX) from PL intensity and area ratio for single g-NQDs. Theoretical estimation of QBX/QSX values are added assuming real QSX = 1 (solid), 0.8 (dashed), 0.5 (dotted) and 0.3 (dot-dashed), respectively. (b) QBX/QSX obtained from variations of the PL intensity for a large number of single QDs (open symbols). Botton Panel: Fluorescence line narrowing (FLN) spectra and magnetic field dependence of the emission dynamics. (a) FLN spectra at 1.55 K for CdSe/4CdS (blue curve, excitation energy EEX=2.101eV), CdSe/7CdS (green curve, EEX=2.138eV) and CdSe/19CdS NCs (red curve, EEX=2.138eV). A portion of the excitation laser is included for reference and set to zero for direct comparison between the different NCs. The actual value of the excitation energy for each set of data is reported in the same color as the respective FLN spectrum. The values for the Stokes shift, ΔE, between the excitation pump and the zero-phonon line (ZPL) extracted from the Boltzmann fit of the τR(T) data in Figure 1.e are indicated by arrows. Gaussian fits of the CdSe and CdS LO phonon bands are reported as grey curves. Surface phonons were not included in the fitting procedure. PL decay curves at the emission maxima (excitation energy= 3.06 eV) at 0 T (black curve) and 7 T (red curve) for (b) CdSe/4CdS, and (c) CdSe/19CdS NCs.

Additionally, we are developing the capability to achieve the first single-NQD spectro-electrochemistry study, which will provide the fundamental understanding essential for the optimization and control of charged-exciton emission for light emission applications. NQD charging has to date limited the practical implementation of NQD light-emitting devices.

Task 3: Demonstrate superior properties of g-NQDs for light-emission applications in proof-of-principle LED

We have developed the necessary techniques (thin-film growth and g-NQD film preparation) to fabricate prototype device structures based on device designs from the literature. Specifically, we fabricated ITO/NiO/NQD layer/Zn-Sn oxide/Ag constructs, the first light-emitting devices comprising g-NQDs as the active layer. g-NQDs were compared with more conventional, thinner-shell NQDs, and shown to provide low turn-on voltages and stable and uniform electroluminescence as a first proof-of-concept for the utility of this new materials system for light-emission applications.

Future Work

We will continue to conduct highly correlated synthesis and advanced spectroscopy studies (Tasks 1 and 2) toward development of a Materials-by-Design approach to identifying and realizing candidate g-NQD systems. We will determine which g-NQD electronic and structural properties dictate the unique and important properties of suppressed

blinking, Auger recombination, and photobleaching. Device fabrication and testing will be de-emphasized in Year 2, as Year 1 results provided an adequate proof-of-principle light-emitting diode demonstration, and device development is the topic of another LDRD ER project.

Conclusion

Conventional nanocrystal quantum dots (NQDs) are characterized by several basic properties that have limited their utility in light-emission applications: (1) deleterious sensitivity to surface chemistry and chemical environment, (2) the requirement for a surface layer of "protective" but electronically insulating organic molecules, and (3) efficient non-radiative Auger recombination. We recently discovered that these properties no longer apply in the case of our novel "giant" NQDs. In this effort, we expect to generalize these exciting initial results to the full range of NQD materials systems to achieve ideally efficient, robust, and color-tunable building blocks for next-generation solid-state lighting.

References

1. Vela, J., H. Htoon, Y. Chen, Y. S. Park, Y. Ghosh, P. Goodwin, J. H. Werner, N. P. Wells, J. L. Casson, and J. A. Hollingsworth. Effect of shell thickness and composition on blinking suppression and the blinking mechanism in 'giant' CdSe/CdS nanocrystal quantum dots. 2010. *Journal of Biophotonics (Special Issue on Nanobiophotonics).* **3** (10-11): 706.

2. Htoon, H., A. V. Malko, D. Bussian, J. Vela, Y. Chen, J. A. Hollingsworth, and V. I. Klimov. Highly emissive multiexcitons in steady-state photoluminescence of individual "giant" CdSe/CdS core/shell nanocrystals . 2010. *Nano Letters.* **10** (7): 2401.

Publications

Ghosh, Y., A. Steinbruck, A. M. Dennis, H. Htoon, and J. A. Hollingsworth. Giant (core)shell compound semiconductor nanocrystal quantum dots: From light emission applications to bioimpact. Presented at *2011 Materials Research Society Spring Meeting.* (San Francisco, April 25-29, 2011).

Hollingsworth, J. A.. Novel functional semiconductor nanocrystal quantum dots and nanowires for applications involving energy conversion. Invited presentation at *2010 Materials Research Society Spring Meeting.* (San Francisco, April 5-9, 2010).

Hollingsworth, J. A., A. Steinbruck, Y. Ghosh, and A. Dennis. Direct and indirect redox processes of semiconductor nanocrystal quantum dots: Implications for biological applications. Invited presentation at *241st American Chemical Society National Meeting & Exposition.* (Anaheim, March 27-31, 2011).

Hollingsworth, J. A., H. Htoon, B. N. Pal, J. Kundu, and Y. Ghosh. "Giant" nanocrystal quantum dots: Uniquely stable and efficient building blocks for light emitting diodes. Presented at *241st American Chemical Society National Meeting & Exposition .* (Anaheim , March 7-31, 2011).

Htoon, H., A. V. Malko, D. Bussian, J. Vela, Y. Chen, J. A. Hollingsworth, and V. I. Klimov. Highly emissive multiexcitons in steady-state photoluminescence of individual "giant" CdSe/CdS core/shell nanocrystals . 2010. *Nano Letters.* **10** (7): 2401.

Vela, J., H. Htoon, Y. Chen, Y. S. Park, Y. Ghosh, P. Goodwin, J. H. Werner, N. P. Wells, J. L. Casson, and J. A. Hollingsworth. Effect of shell thickness and composition on blinking suppression and the blinking mechanism in 'giant' CdSe/CdS nanocrystal quantum dots. 2010. *Journal of Biophotonics (Special Issue on Nanobiophotonics).* **3** (10-11): 706.

DARTS Thermal Storage Technology

Stephen J. Obrey
20100622ER

Abstract

DARTS Thermal Storage (**D**iels **A**lder **R**eaction **T**hermal **S**torage) is a new method for the capture, storage and release of thermal energy using the reversible heat of chemical reactions. In contrast to traditional thermal storage methods that use sensible and latent heat of phase transitions for thermal storage, DARTS utilizes a chemical reaction to store the thermal energy in the form of chemical bonds. The primary objective of this project is the technical demonstration of DARTS technology to modify and enhance the performance of a heat storage/transfer fluid. This project details the fabrication and characterization of a designer DARTS-modified heat transfer fluid. A preliminary technological assessment of this concept is carried out using Second Law analysis that results in a direct comparison of state-of-the-art heat transfer fluids with a DARTS-modified fluid. This preliminary technological assessment showed that DARTS fluid performance is favorable, showing marked improvement over traditional heat transfer fluids as a direct result of its enhanced heat capacity.

Background and Research Objectives

DARTS Thermal Storage is a new method for the capture, storage and release of thermal energy using reversible chemical reactions. In contrast to traditional thermal storage methods that use sensible and latent heat of phase transitions for thermal storage, DARTS stores thermal energy in the form of chemical bonds. Chemical engineers have known for many years that industrial scale chemical reaction has an enormous potential to adsorb and desorb thermal energy. Heats of reaction can be much higher than those found in phase transitions. For instance, the water-gas shift reaction, Eq.1, is an industrially important reaction where the carbon monoxide and water yield

$$CO + H_2O \rightleftharpoons CO_2 + H_2$$

carbon dioxide and hydrogen-requiring the addition of 42 kJ/mol of heat to drive the reaction. At small scale, 42 KJ/mol is inconsequential but at industrial scale the 42 kJ/mol is an enormous heat load. Just to maintain the reaction temperature during the shift reaction in an IGCC power plant producing CO_2 and H_2 demands almost a 10% parasitic energy load. Thermochemically similar to the water gas shift reaction, DARTS reactions are reversible in nature. At lower temperatures DARTS react with an exothermic release of heat but when DARTS is heated to elevated temperatures an endothermic reaction occurs to regenerate the starting materials.

This effort was designed to be a preliminary demonstration of DARTS technology to enhance a heat storage/transfer fluid. This collaborative effort between C-division and AET-divisions focused on 1) the development and integration of a DARTS chemical reaction a heat transfer fluid, and 2) the technical evaluation of the potential impact of the DARTS modified heat transfer fluid in comparison to state of the art heat transfer fluid technology. These chemical fluids were characterized, their thermochemical and physiochemical properties evaluated and tabulated to provide input for a preliminary technology evaluation.

Contrary to traditional heat transfer fluids, properties of DARTS fluids are expected to change significantly as the temperature changes that could be potentially problematic in application. At low temperatures, the DARTS fluid will have fairly predictable fluid properties, but as temperatures increase, the viscosity, density, diffusivity, and thermal properties (heat capacity and conductivity) will become effectively anisotropic as the chemical nature of the fluid changes. This will potentially impact pressure drop per unit length of heat exchanger, rate of reaction, and net thermal flux. As the impact of these fluid properties is presently unknown it is our intention to develop a baseline understanding of these factors in sufficient detail to estimate performance and identify unforeseen technical challenges. With estimates of physical properties in-hand, performance estimations can then be base-lined against the current state of the art.

Scientific Approach and Accomplishments

Fluid development and characterization

The integration of DARTS chemical reactions into a heat transfer carrier fluid was undertaken by first identifying

suitable DARTS chemical reactants. Once identified, these reactants were integrated into chemical components representative of the known industrially important heat transfer fluids, Therminol® and polydimethylsilicone, see Figure 1. Two DART fluids were synthesized. The first was based on the modification of the chemical backbone found in Therminol®, DARTS-BP1, and the second was a chemical modification of dimethyl silicone, DARTS-SI. The baseline engineering analysis required the acquisition of specific fluid properties as a function of temperature. The key fluid thermochemical properties associated with the DARTS reaction were determined using Differential Scanning Calorimetry as well as more rigorous equilibrium measurements. The thermochemistry and the effective heat capacity of the DARTS fluid was measured at temperatures up to 275°C, as shown in Figure 2. It is interesting to note the divergence of the specific heat of these two fluids at ~200°C as a result of extra thermal capacity due to the presence of the DARTS chemical reaction. Experimental difficulties precluded direct measurement of thermal properties above 275°C therefore, these properties were extrapolated using statistical thermodynamic techniques. Although our estimations were conservative, as much as 20% variability in the DARTS contribution to the specific heat is foreseeable. Key values for Therminol® and dimethylsilicone were extracted from the product literature. Similarly, values for the DARTS fluids were either directly measured, extracted from the literature or were estimated using literature using chemically similar materials.

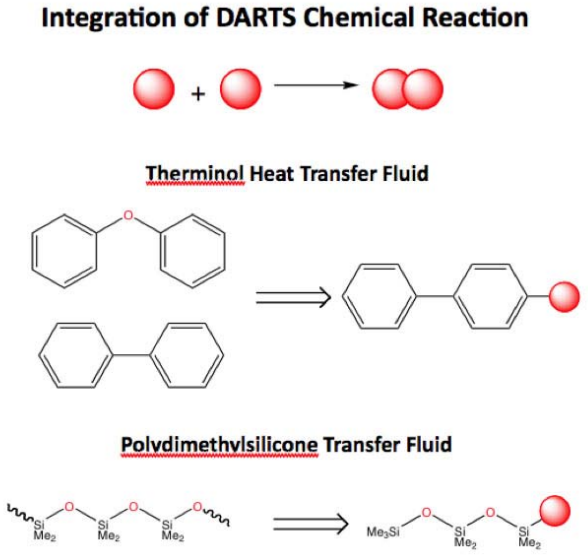

Schematic describing the integration of DARTS with fluid backbones.

Preliminary DARTS Technological Assessment

A method for comparing the heat transfer and fluid flow performance of DARTS was developed under the context of eventual utilization in a power production scenario via steam generation. Two performance goals for the development of new heat transfer fluids were identified. These goals are to 1) maximizing heat flux in heat exchangers, while at the same time 2) minimizing the pressure drop and the required pumping power.

In this analysis, a Second Law (of Thermodynamics) or entropy generation analysis [1] was employed as a method to evaluate DARTS fluid performance. Entropy generation occurs in all processes including fluid flow under a pressure gradient and heat transfer through thermal gradients. The Second Law analysis allows these losses, or thermodynamic irreversibilities, to be put on a common scale. By putting both fluid friction and heat transfer losses on a scale of entropy generation; Second Law analysis can clearly determine the optimal flow configuration that minimizes the combination of these losses. By comparing the entropy generation in two heat transfer fluids, we are able to discern the combinations of fluid properties, or performance measures that will determine which heat transfer fluid will perform most favorably.

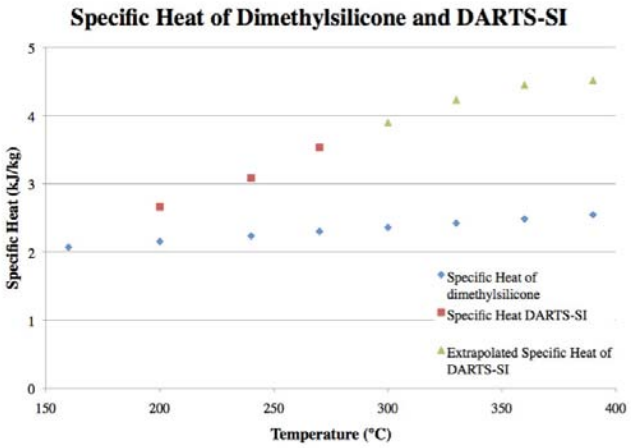

Specific Heat of Therminol® and DARTS-BP1. Divergence of Specific Heat at 200° C is due to DARTS.

Comparison of the DARTS heat transfer fluid with Therminol® and dimethylsilicone was carried out under the context of heat transferred via the heat exchanger for conversion into work output (shaft work of the steam turbine minus work required by the pumps for the heat transfer fluid and steam) through a steam cycle. This analysis resulted in the development of a descriptive expression of the augmentation entropy generation number, $N_{S,a}$, which is the basis for comparing the performance of heat transfer fluids transport properties for conversion into useful work.

The augmentation entropy generation number is essentially a ratio of the total entropy generation in a modified fluid divided by the total entropy generation in a reference fluid when the two fluids are used as heat transfer fluids under the same conditions. The total entropy generation is directly proportional to the loss of available work (work that

could have been converted to shaft work) caused by fluid flow and heat transfer irreversibilities during operation. As a measure of lost available work, the entropy generation in a system using a modified fluid should be lower than the entropy generation in a system with the baseline fluid. A requirement for the modified fluid to produce a net benefit during operation of the power plant is that $N_{S,a} < 1$. Small values of $N_{S,a}$ are desirable. The preliminary examination of the augmentation entropy generation number using experimentally derived and extrapolated DARTS fluid properties the exergy analysis shows that the value of the augmentation entropy generation ratio is favorable for DARTS fluids. Once more system properties can be verified, reanalysis *via* the exergy analysis is recommended.

To illustrate the applicability and impact of these DARTS heat transfer fluids a system level model was developed using the DARTS fluid in a power generation scenario. In this system, heat is collected from a high temperature source with the DARTS heat transfer fluid. This fluid is then run through a thermal storage heat exchanger used to produce high pressure steam. This thermal storage heat exchanger generates steam, which is subsequently used to produce mechanical work using the thermal storage heat exchanger heat transfer fluid as a high temperature source reservoir and standard background temperature as a low temperature reservoir. By comparing the DARTS fluid performance to a standard reference fluid, Therminol®, the influence of the DARTS fluids can be realized, Figure 3. Under the circumstances examined, there is a noticeable dependence on the thermal source temperature. At source temperatures below 400 K there is no contribution from the DARTS chemical reaction and thus the $W_{DARTS\ Enhanced}/W_{Reference}$ is approximately 1.00 but as the Source Temperature rises the impact of DARTS chemical reactions becomes more influential as represented by the gradual increase in $W_{DARTS\ Enhanced}/W_{Reference}$ from 1.00 to greater than 1.10 at Source Temperatures approaching 650K. It is interesting to note that maximum $W_{DARTS\ Enhanced}/W_{Reference}$ ratio closely matches the temperature at which the DARTS thermal contribution also maximizes. At this point, the $W_{DARTS\ Enhanced}/W_{Reference}$ is greater than 1.10. In other words, a DARTS modified Heat Transfer Fluid can increase the overall system efficiency and thus the total work available for power production by over 10% over state of the art systems.

Project Summary

Two new DARTS modified heat transfer fluids were synthesized and characterized. A Second Law Engineering analysis was used to develop system performance measures that are based only on the thermochemical and fluid properties of DARTS fluid designs. This engineering analysis evaluates system losses in heat exchangers, system pressure drop and the required pumping power. Based on preliminary fluid properties generated, the results of the Second Law analysis came back favorable showing and increase in available exergy for the DARTS system. Furthermore, the system model was developed as a method to compare the DARTS and state of the art fluids that showed that implementation of DARTS technology can result in greater that 10% enhancement in power generating scenario.

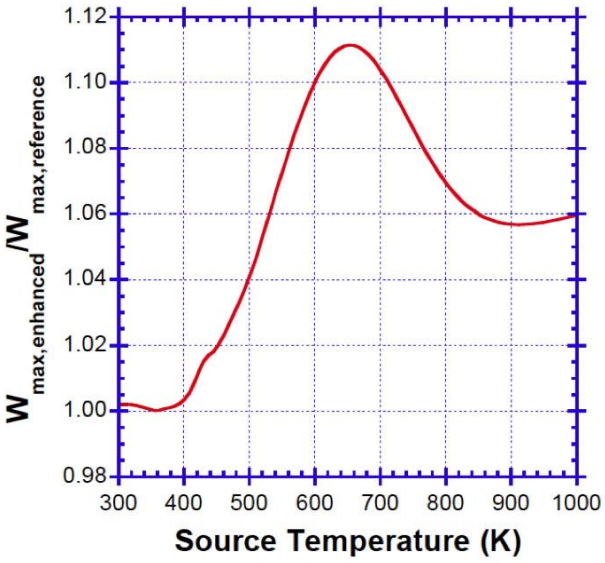

Plot relating the increase in available work as a result of integration of DARTS chemical reactions into Heat Transfer Fluids.

Impact on National Missions

This technology demonstration is a first generation example of DARTS technology to store energy in a thermal reservoir for later reuse. These fluids are directly applicable to concentrated solar power generating stations as both a fluid and as a thermal storage media which could allow production plants to meet energy demand both at day time and night time. As such, DARTS thermal storage technology could find widespread application in next-generation power production. These efforts directly tie into the Laboratory's Energy and Earth Systems Grand Challenge and missions in energy security. Results from the research have laid the groundwork to supply potential technology to meet DOE mission goals. Advances in this area are also of significant basic scientific interest and serve to raise the Laboratory's profile in sustainable energy research and attract talented investigators in the field to LANL.

Detection of Respiratory Infection by Scent

Jurgen G. Schmidt
20080317ER

Abstract
Rapid detection of the emergence of pandemic respiratory infection requires the development of novel, instrumentation free first line detection capabilities. We suggest that the innate pathogen specific enzyme activity of viral surface proteins can be deployed to allow the release of an odorant in the presence of virus and the detection at the primary location of infection - the human nose. During this project we generated functional substrates and explored their use as "moderators" enabling instrumentation free detection. This detection scheme is illustrated in Figure 1.

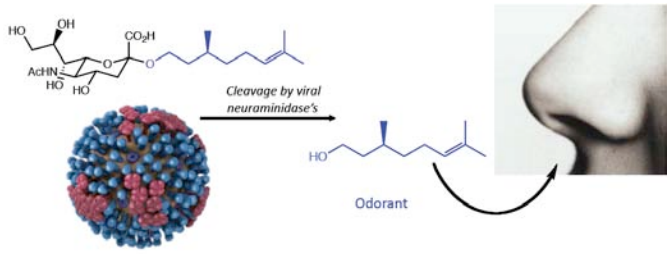

Figure 1. Influenza enzymes cleave a man made substrate to release an odorant. The "event" is detected instrumentation free, pre-symptomatic and directly by the olfactory receptors of the nose.

Background and Research Objectives
Human respiratory viruses such as influenza A, B and C, respiratory syncytical virus (RSV) and human rhinovirus (HRV) account for over 150 million infections and 200,000 hospitalizations every year in United States. Although novel antiviral drugs for the treatment of influenza are available, their efficiency depends on an early diagnosis. Current technologies for the detection of these infections are time consuming. The deployment of a biosensor in a point of care (POC) or over the counter (OTC) patient setting is clearly limited by the requirement of skilled personnel for the application of the detection device. Real time markers of exposure become even more important for the emergence of pandemic strains, where self-diagnosis and early detection at borders become important means to identify and potentially isolate infected populations early in the progression of the disease. This project will provide novel means for ubiquitous sensing to mitigate the national security threat of pandemic influenza.

Upper respiratory viral and bacterial agents primarily infect the mucus membrane and surface cells in the nose. The primary contact of the virus with the host are cell surface carbohydrates (neuraminic acid) which bind to viral hemagglutinin receptors. After infection and replication a second viral surface protein cleaves neuraminic acid residues to free the viral progeny from host cell debris to facilitate a new round of infection. This neuraminidase is a prolific enzyme that provides fast turnover of the carbohydrate substrates.

The location of respiratory infection, the mucus membranes of the nose, present one the most ubiquitous biosensor surfaces with exquisite selectivity and subsequent amplification of the stimulant exposure into neurotransmission.

While current detection of influenza is either laboratory or POC based and cannot be easily scaled in a pandemic. Biosensors, dipsticks and antibody based tests all require trained personal and an infrastructure (e.g. refrigeration). Detection of influenza by enzyme triggered odorant release will allow fieldable, self-diagnostics based on smell in the most ubiquitous sensor available – the nose.

During this project we have designed and executed syntheses of substrates for a viral enzyme that release an odorant. This allows for detection of the virus by olfactory receptors in the nose. The detection utilizes amplification by multiple enzyme turnovers and olfactory receptor coupled signal amplification. These key facets allow for instrumentation free, selective, highly sensitive and potentially pre-symptomatic detection that can be performed by a "lay-man" outside of a POC setting.

Scientific Approach and Accomplishments
The design of the substrates for neuraminidase cleavage requires the attachment of an odorant at the anomeric positions (natural attachment point) of the neuraminic

acid sugar. We have designed and executed syntheses that accommodate a wide range of potential odorants. During this project it became clear that most reported standard coupling reactions are not successful in generating a " standard" protocol that we envisioned as one universally applicable reaction for a combinatorial library approach. The coupling under oxidative conditions, while successful for simple odorants, destroys the double bond structural feature widely found in odorant molecules. Initial attempts found coupling yields for these reactions to be low and products were obtained in only 10-20% after purification. Figure 2 exemplifies our modified synthetic route to attach odorant alcohols. This alternate approach to current "standard protocols" in carbohydrate synthesis is compatible to generate potentially thousands of compounds. The reactions yield between 30 and 50% of the product after purification and have now been optimized for combinatorial exploration of structural and "scent" diverse libraries of targets. All compounds were purified and their structure confirmed by 1H, 13C – NMR (Nuclear Magnetic Resonance) and mass spectrometry.

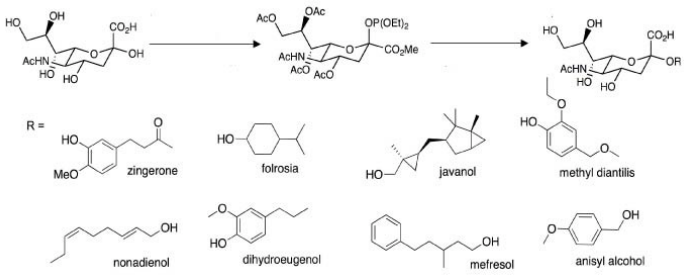

Figure 2. Schematic representation of the synthetic route to odorant – neuraminic acid chimera. The depicted odorant alcohols represent a small sample of possible structures.

We have therefore achieved one of our major goals to design our synthesis to be amendable to automation and combinatorial screen for a diverse set of chemicals.

During the course of the project it became evident that odorants more volatile that those carrying alcohol groups are to be included to allow for "ex vivo" applications. We have explored the synthetic options and after intense screening and optimization found a method to attach esters and ketones through an oxygen bond to the neuraminic acid. This task while initially thought of as "trivial" led to a first synthesis, to our knowledge, using enol ethers to form a C-O bond at the anomeric center of a sugar. We are currently preparing a manuscript to publish this valuable synthetic method that can give access to a wide range of currently unknown sugar derivatives.

A reproducible High Performance Liquid Chromatography was developed to gain access to highly purified samples. Development of reliable purification methods was essential to afford odorant free odorant-sugar chimera, as residual un-reacted odorant would have given rise to false positive results in the biological assays.

While initial biological experiments on the neuraminidase cleavage of the substrates were conducted with commercial purified enzyme, we have also shown the release of the odorant with "real" influenza samples. In the biology section of this project influenza virions have been expressed and UV (ultra violet light) inactivated. The PCR (polymerase chain replication) amplification of potential remaining viral genes and attempts to culture the virus showed no residual viral infectivity. Commercial neuraminidase activity assays proved that the enzymatic reactivity is retained. The samples were BSL-1 level certified and used in our mass spectrometry facility.

Substrate samples showed the prerequisite absence of residual scent, however, most of them developed the expected characteristic scent of the underlying odorant on exposure to neuraminidase. This pathogen dependent scent evolution was evident over minutes to hours on exposure both to purified neuraminidase and inactivated influenza virus. The scent as predicted was ranging from noticeable to irritating when opening incubation plates, which subjectively shows the utility for instrumentation free scent based detection. We have used mass spectrometry as the analytical method to follow the enzyme cleavage of the substrates (Figure 3). The disappearance of the substrate with higher mass is accompanied by the appearance of the odorant and neuraminic acid fragments at lower mass. Finally we have shown that in the absence of neuraminidase enzymes the substrates remain intact in solution and over extended periods of time. Substrates in neat dry form are shelf stable compounds that were unaffected by ambient degradation over the course of the project period.

We would like to point out additional and intangible benefits afforded to us during the LDRD funding of the project. We had the opportunity to work with several summer intern students on the scent detection and chemical syntheses at Los Alamos. Researching the nature of pathogen detection by release of scent as an immediate application of a synthetic molecule was a "favorite" for two summer students, while training them in the fundamental chemical methods of carbohydrate chemistry. In addition we have trained two postdoctoral associates funded and mentored under this project, one of them has in the meantime joined the staff at a major pharmaceutical company. This project will lead to a patent application and two manuscripts for publication are currently in preparation.

Acknowledgement: We gratefully acknowledge Vigon International Inc. for providing us with free fragrance and odorant samples.

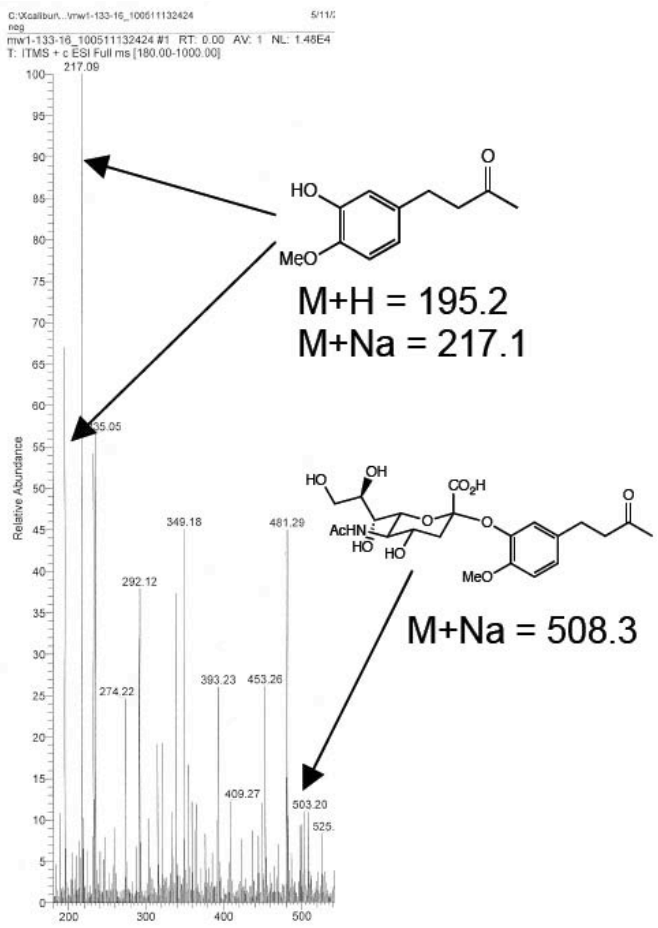

Figure 3. The mass spectrum of a substrate in the presence of influenza virons shows the disappearance of the starting material (M=508) and the appearance of the odorant (M= 195/ 217).

Impact on National Missions

The recent emergence of a novel influenza strain H1N1 (Swine Flu) made the news headlines. Novel detection methods to indicate the presence of influenza to monitor global outbreaks of influenza will become essential tools to mitigate and counter the spread of influenza infections. This research will enable direly needed novel detection techniques for this emerging health threat. The basic research supports the DOE mission of National Security. The detection of influenza by instrumentation free means can be extended to other pathogens of interest among others water and food security. In addition this project will further lead to enhanced capabilities for the DOD, DHS and the HHS in the detection of emerging biothreats.

Publications

Kale, R. R., H. Mukundan, D. N. Price, J. F. Harris, D. M. Lewallen, B. I. Swanson, J. G. Schmidt, and S. S. Iyer. Development of a “carboassay”. Detection of Influenza virus using capture and reporter biotinylated biantennary S-sialosides. 2008. *Journal of the American Chemical Society.* **130**: 8169.

Spins in Organic Semiconductors

Brian K. Crone
20080323ER

Abstract

Today's electronics are based on the electron charge. The last few years have seen extensive research in exploring the spin degree of freedom for the design of new electronic devices. This interest is motivated by the prospect of using spin, in addition to charge, as an information carrying physical quantity in electronic devices, and thus improving the device functionality and performance in an entirely new way; a set of ideas that has been called spintronics. Key requirements for success in this effort include the following: efficient injection of spin polarized charge carriers through one device terminal; efficient transport and sufficiently long spin relaxation times within the semiconductor; effective control/manipulation of the spin polarized carriers in the structure (e.g., by using a gate bias) to provide the desired functionality; and effective detection of the spin polarized carriers at a second device terminal. Ferromagnetic (FM) metals can be used as a source of spin polarized (SP) charge carriers, and they can also serve to detect a SP current. Spin relaxation lifetimes in conventional, inorganic semiconductors are primarily limited by the spin-orbit and hyperfine interactions. However, organic materials are composed of light elements - basically carbon and hydrogen – that have weak spin orbit and hyperfine interactions for the relevant electronic states near the gap and consequently long spin relaxation times. Thus organic semiconductors offer potential as the active material for spintronics applications. However, the spin-orbit interaction is also responsible for selection rules that allow optical generation/detection of polarized electron spin distributions. Optical injection and detection was important in the development of electrical spin injection in inorganic semiconductors. The purpose of this work was to develop both optical and electrical methods to inject and detect spins in organic semiconductors and demonstrate the advantages of these materials for spintronic applications.

Background and Research Objectives

The ability to control an electron's *spin* degree of freedom in solids is central to the operation of a new generation of "spintronic" devices that have the potential to overcome the power consumption and speed limitations of conventional electronic circuits, and that are promising candidates for the physical implementation of quantum information processing and computing ideas. Very recently there has been dramatic progress in the electrical injection, transport, and detection of spin polarized charge carriers in inorganic semiconductors such as GaAs. The use of magneto-optical spectroscopies using circularly polarized light has been absolutely essential in achieving this success. Due to the *spin-orbit interaction* inherent in these materials, right- and left-circularly polarized light couples differently to spin-up or spin-down electrons. As a result, spin-polarized electrons can be generated and detected using circularly polarized optical probes.

In parallel to these developments, *organic* semiconductors are revolutionizing important technological areas including information display, large area electronics, solid state lighting, and solar energy generation due to their ability to be economically processed in large areas, their compatibility with low temperature processing, the tunability of their electronic properties and the simplicity of thin film device fabrication. Organic semiconductors are typically made from conjugated hydrocarbons and thus contain the only the very light elements carbon and hydrogen. Because the spin-orbit (S-O) interaction results from motion of electrons in the Coulomb electric field of the host-lattice nuclei, S-O coupling is very weak for light elements, which makes them promising materials for the active layer in spintronic devices.

As a result, the corresponding optical selection rules that have been so successfully exploited in inorganic semiconductors do not apply in organic semiconductors, and progress in understanding electron spin based processes has been comparatively slow. Heavy elements can be incorporated into organic semiconductors which locally "turn on" a strong spin-orbit interaction. In this way it is possible to introduce spin-selective optical selection rules, analogous to those that have successfully utilized in inorganic semiconductors. We specifically considered the use of metal-organic compounds containing heavy

transition-metal ions such as platinum. For conventional organic semiconductors, the spin-orbit interaction is extremely small -- but by including heavy metal-organic components in the organic semiconductor, a significant spin-orbit interaction is introduced.

It is difficult to electrically inject a spin polarized current from a magnetic contact into a non-magnetic organics semiconductor. This is due to the establishment of equilibrium at the injecting interface, which maintains the non-spin polarized (non-magnetic) nature of the charges in the organic semiconductor. Electrical injection of spin polarized current requires some method to pull the interface out of equilibrium, such as an insulating tunnel barrier. This technique is well established for inorganic semiconductors. An important aspect of the research was to explore the similarities and differences between the organic and inorganic semiconductor cases. There are important physical differences between organic and inorganic semiconductors, including much larger carrier mobilities and much shorter spin coherence lifetimes in the inorganic materials.

Scientific Approach and Accomplishments

Our research into spins in organics has taken a multi-pronged approach. We have investigated: 1) experimental magneto-optical properties of metal organic molecular dopants for optical spin injection into organic semiconductors [1], 2) ab initio quantum chemical modeling of these metal organic molecules [1], 3) theory of spin injection and transport in organic semiconductors [2], 4) device modeling of spin based organic semiconductor structures [3,4], and 5) new methods to measure spin polarizations in semiconductors [5,6]. We will address these topics in order.

We studied photoluminescence from the metal organic molecules octaethyl-porphine platinum (PtOEP) and porphine platinum (PtP) as a function of temperature and magnetic field in organic hosts. PtOEP is typical of the phosphorescent dopants used in organic light emitting diodes (OLEDs) in which the octaethyl substitutions are utilized to increase solubility and enable solution processing. We first considered PtOEP in the conjugated polymer host poly-dioctylfluorene (PFO). This material system is typical of ones used in organic light emitting diodes (OLEDs). We observed a strong temperature and magnetic field dependence of the zero phonon emission lines and a strong circular polarization of the emission in an applied magnetic field. We then investigated the emission properties of PtOEP in an octane host in which the interactions between the PtOEP and this host are much weaker and the emission lines are much narrower than for the PFO host. Finally we investigated unsubstituted PtP in an octane host for which the emission spectra are simpler than for PtOEP. Figure 1(a) shows the measured PL spectrum of dilute PtP in octane over a wide spectral region at T=6K and in zero magnetic field. A family of zero-phonon lines is observed in the vicinity of 2.02eV, along with a series of phonon-assisted transitions at lower energies. Figure 1(b) shows higher-resolution spectra in the zero-phonon region at zero magnetic field and at various temperatures, while Figure 1(c) shows similar spectra at a fixed low temperature of 1.7K with increasing magnetic field. There are three main lines in the PtP emission spectrum. It is known from previous studies of the optical properties of PtP in octane that there are two distinct substitutional positions occupied by PtP in the octane crystal. Two optical emission lines result from molecules in each of these substitutional sites. The higher energy emission line from one of the sites is very close in energy to the lower energy emission line in the second site. The result is a three line spectrum in which the center line consists of two separate components. At the lowest temperature and zero applied magnetic field only the two lowest energy lines are observed and they are both rather weak. As the temperature is increased, at zero magnetic field, the lowest energy line intensity decreases slightly with increasing temperature, but the intensity of the two higher energy lines increases rapidly with increasing temperature. The energies of the three emission lines do not change with temperature. At low temperature, the intensity of the two low energy emission lines increase rapidly with applied magnetic field. Both lines shift to lower energy and broaden with increasing magnetic field.

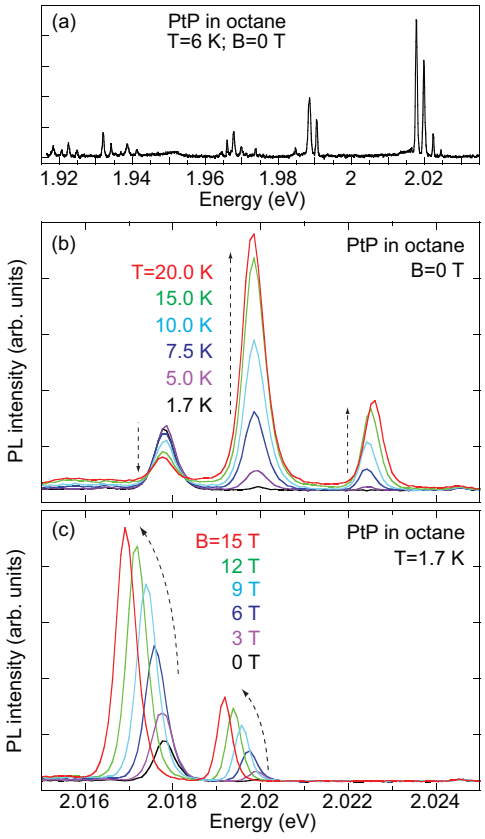

Figure 1. Measured photoluminescence spectrum of dilute PtP in octane: a) in a wide spectral region at T=6K and zero magnetic field, b) at zero magnetic field and with increasing temperature from 1.7K to 20K, and c) at T=1.7K and with increasing magnetic field from 0T to 15T.

We performed a series of electronic structure calculations on the PtP molecule to determine the properties of its low energy electronic excited states. We use the results of the electronic structure calculations to define a model for the temperature and magnetic field dependence of the emission lines. The model results are in good quantitative agreement with the experimental observations in PtP and with the observed circular polarization of the PtOEP emission in an applied magnetic field. They qualitatively explain the observed temperature and magnetic field dependence of PtOEP emission. Figure 2(a) shows the calculated photoluminescence spectra of PtP for zero magnetic field at the temperatures used in the measurements presented in Figure 1(b). Figure 2(b) shows the calculated photoluminescence spectra of PtP as a function of magnetic field at the T=1.7K used in the measurements presented in Figure 1(c).

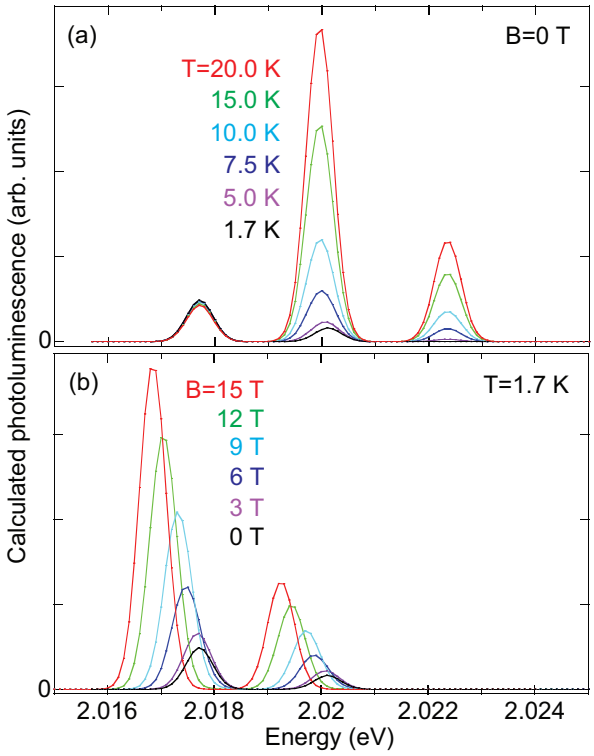

Figure 2. Calculated photoluminescence spectrum of PtP: a) at zero magnetic field and at the temperatures used in the experimental results of Figure 1b), and b) at a temperature of T=1.7K and at the magnetic fields used in the experimental results of Figure 1c).

There is a good correspondence between the measured and calculated results. At very low temperature only the lowest energy states are thermally occupied and contribute to photoluminescence. As the temperature is increased, the higher energy states become thermally occupied and because these states have a stronger optical matrix element, the total luminescence intensity increases with increasing temperature. As a magnetic field is applied, the original eigenstates are mixed to give new eigenstates. In the new eigenstates, optical transition strength is transferred from the higher energy state to the lower energy states. As the magnetic field is applied the two lower lying states split apart in energy, shift to lower energy and receive optical transition strength from the higher lying state. Thus the emission lines increase in strength, broaden and shift to lower energy with increasing magnetic field.
We have theoretically investigated spin injection from ferromagnetic metals into organic semiconductors. This work has shown that one can't inject a spin polarized current from a magnetic metal directly into a semiconductor. This is easily explained by the concept of thermal equilibrium. If a magnetic metal is in equilibrium with a non-magnetic semiconductor, then currents will flow to maintain this equilibrium. This means the spin polarization in the semiconductor will remain zero. To enable spin polarization in the semiconductor one needs to pull the interface out of equilibrium, for instance by inserting a barrier between the metal and semiconductor as has been demonstrated in inorganic semiconductors. Tunneling through an insulating layer provides a spin selective mechanism to inject charge carriers into organic semiconductors. Localized molecular states close to the injecting ferromagnetic contact is the primary contributor for the tunnel current. Spin transmission and hence spin injection strongly depend on the height of the barrier. As the barrier become more transparent (either by decreasing the barrier height or by decreasing the thickness of the barrier or through an increasing electric field), spin injection decreases.

We have developed a model to describe transport and recombination of spin polarized electrons and holes injected from ferromagnetic contacts into a conjugated organic semiconductor. Transport in the semiconductor is treated by the spin dependent continuity equations coupled with Poisson's equation. Recombination of injected electrons and holes is modeled as a Langevin process. The boundary conditions used to solve the continuity equations are given by specifying the spin polarized particle currents at the boundaries. Injected spin currents are related to the charge currents via the transport parameters of the ferromagnetic contacts. Spin injection strongly depends on the contact polarization and the conductivity of the contact material. In the case of conventional ferromagnetic metal contacts, the relatively weak polarization and high conductivity hinder spin polarized injection. Spin injection can be greatly enhanced if (spin dependent) tunneling is the limiting process, which may be described by contact resistances. The dependence of the current polarization on these contact resistances is explored. On the other hand, we have demonstrated that if the injecting contacts are made from half-metallic materials with low conductivity, spin injection is strong even for thermionic injection and the spin current approaches the charge current.
Typical spin injection and detection schemes rely on tunneling to avoid the conductivity mismatch problem. However, tunneling introduces a strong applied voltage bias dependence to the polarization. Using a combination of magneto-optical and electronic transport techniques, we

investigated the process of spin detection in lateral spin transport devices. Our results show that spin detection sensitivities do not simply follow trivially from the spin-polarized conductivities of the contacts, but rather can be enhanced or suppressed due to the electric fields that exist in real semiconductor channels. We have used experiments and theory to show that the bias dependence of the spin polarized tunneling current in combination with field dependence of the spin transport can be used to control, in a predictable way, the sensitivity of spin detection in lateral ferromagnet/semiconductor structures. Thus, not only can spin polarized electrons be made to induce both positive or negative voltages at spin detection electrodes, but also some detector sensitivities can be enhanced over ten-fold with applied bias. Part of our effort has focused on alternative, noise-based schemes to measure the dynamical properties of electron spins in semiconductors. Whereas most traditional studies of dynamics employ pump-probe methods to perturb and then measure the recovery of a spin system (such as ultrafast spectroscopy, or pulsed ESR), the Fluctuation Dissipation Theorem guarantees that the same dynamical information is available if one can "listen" to the intrinsic fluctuations of the spins while in thermal equilibrium. We have demonstrated that such noise-based approaches can actually work, using n-type GaAs as a canonical solid-state spin system. We used sensitive optical magnetometry based on off-resonant Faraday rotation to measure the frequency spectra of stochastic electron spin noise as a function of electron density, temperature, and interaction volume. We have applied these techniques to study the spin fluctuations of electrons and holes that are quantum-mechanically confined in zero-dimensional semiconductor quantum dots.

Impact on National Missions

This project supported DOE missions in basic science and threat reduction by providing the fundamental understanding of spin-based processes in organic materials needed to enable new technologies including quantum information processing and computing. These technologies will support our national security by providing powerful tools for data encryption and decryption.

References

1. Diaconu, C. V., E. R. Batista, R. L. Martin, D. L. Smith, B. K. Crone, and S. A. Crooker. Temperature and magnetic field dependent photoluminescence properties of platinum porphyrins in organic hosts. *Journal of Applied Physics.*
2. Yunus, M., P. P. Ruden, and D. L. Smith. Spin-polarized charge carrier injection by tunneling from ferromagnetic contacts into organic semiconductors. *Applied Physics Letters.*
3. Yunus, M., P. P. Ruden, and D. L. Smith. Ambipolar electrical spin injection and spin transport in organic semiconductors. 2008. *Journal of Applied Physics.* **103**: 103714.
4. Ruden, P. P., and D. L. Smith. Modeling spin injection and transport in organic semiconductor structures. 2010. In *Organic spintronics.* Edited by Vardeny, Z. V.. , p. 31. Boca Raton: CRC Press.
5. Crooker, S. A., J. Brandt, C. Sandfort, A. Greilich, D. R. Yakovlev, D. Reuter, and A. D. Wieck. Spin noise of electrons and holes in self-assembled quantum dots. 2010. *Physical Review Letters.* **104**: 036601.
6. Crooker, S. A., L. Cheng, and D. L. Smith. Spin noise of conduction electrons in n-type bulk GaAs. 2009. *Physical Review B.* **79**: 035208.

Publications

Chantis, A. N., D. L. Smith, J. Fransson, and A. V. Balatsky. Scanning tunneling microscopy detection of spin polarized resonant surface bands: The example of Fe(001). 2009. *Physical Review B.* **79** (16): 165423.

Chantis, A. N., and D. L. Smith. Theory of electrical spin-detection at a ferromagnet/semiconductor interface. 2008. *Physical Review B.* **78** (23): 235317.

Crooker, S. A., E. S. Garlid, A. N. Chantis, D. L. Smith, K. S. M. Reddy, Q. O. Hu, T. Kondo, C. J. Palmstrom, and P. A. Crowell. Bias-controlled sensitivity of ferromagnet-semiconductor electrical spin detectors. 2009. *Physical Review B.* **80** (4): 041305(R).

Crooker, S. A., J. Brandt, C. Sandfort, A. Greilich, D. R. Yakovlev, D. Reuter, A. D. Wieck, and M. Bayer. Spin noise of electrons and holes in self-assembled quantum dots. 2010. *Physical Review Letters.* **104** (3): 036601.

Crooker, S. A., L. Cheng, and D. L. Smith. Spin noise of conduction electrons in n-type bulk GaAs. 2009. *Physical Review B.* **79** (3): 035208.

Pershin, Yu. V., N. A. Sinitsyn, A. Kogan, A. Saxena, and D. L. Smith. Spin polarization control by electric steering: proposal for a new spintronic device. 2009. *Applied Physics Letters.* **95** (2): 022114.

Ruden, P. P., and D. L. Smith. Modeling spin injection and transport in organic semiconductor structures. 2010. In *Organic Spintronics.* By Vardeny, Z. V.. , p. 31. Boca Raton: CRC Press.

Yunus, M., P. P. Ruden, and D. L. Smith. Spin injection effects on exciton formation in conjugated organic semiconductors. 2008. *Applied Physics Letters.* **93** (12): 123312.

Yunus, M., P. P. Ruden, and D. L. Smith. Macroscopic modeling of spin injection and spin transport in organic semiconductors. 2010. *Synthetic Metals.* **160** (3-4): 204.

Strain-induced Novel Physical Phenomena in Epitaxial Ferroic Nanocomposites

Quanxi Jia
20080394ER

Abstract

The vast range of structures and properties of complex metal-oxides such as ferroelectric and ferromagnetic materials provides an excellent case platform to investigate novel device functionalities. By combining efforts from both theoretical prediction and experimental verification, we have used a phase-field model for investigating and predicting the magnetoelectric coupling effects on ferroelectric/ferromagnetic epitaxial nanocomposite films. We have grown epitaxial ferroelectric nanocomposite films with desired functionalities, and demonstrated a proof-of-principle improved and/or enhanced functionalities potentially for novel devices. Our experimental results open up a wide array of possible applications of ferroelectric and ferromagnetic materials. Importantly, our works holds great promise for enhancing various fundamental and applied studies of functional metal-oxides. LANL's thrusts in functional materials, nanotechnology, and sensors all benefit from this project.

Background and Research Objectives

Perovskite metal-oxides have become the subject of many theoretical and experimental studies in recent years due to their versatile physical properties that conventional metallic elements and covalent semiconductors do not possess. Their important technological applications make these materials very attractive in electronic industry. In such complex metal-oxides, the anisotropic lattice-strain caused by the lattice-mismatch between the substrate and the film plays a critical role in their physical properties.

With the remarkable progress in epitaxial growth of high quality metal-oxide films, ferroelectric (FE) and/or ferromagnetic (FM) materials, in particular, have emerged as a fertile ground for exploring new physical phenomena such as complementary functionalities and new devices. Nevertheless, due to the lattice strain imposed on epitaxial nanostructured films, the physical properties of FE and/or FM nanocomposites are quite different from those of their bulk single-crystal counterparts. In addition, because of complicated interplay between the lattice strain, solid solubility, structural and chemical compatibility, and thermal stability, the experimental design in combining these materials for maximum coupling is still in its "trial and error" stage. Furthermore, a theoretical description of such epitaxial nanocomposite films that is critical to material scientists for experimental guidance is still lacking.

Our research objectives were i) addressing these gaps by using a phase-field model to investigate and to predict the magnetoelectric coupling effect in ferroelectric/ferromagnetic epitaxial nanocomposite films; ii) growing such epitaxial nanocomposite films with desired functionalities; and iii) using these materials as model systems to demonstrated proof-of-principle nanostructured materials that shows improved and/or enhanced functionalities for novel devices. Our goal was to seek a fundamental understanding of the relationship between the strain and the physical properties as well as the method to manipulate the strain state in ferroelectric and ferromagnetic nanocomposites, which are all crucial for the application of these materials in the next generation electronic devices.

Scientific Approach and Accomplishments

Scientific approaches

Instead of fitting experimental data using a given physical model to explain the experimental results, we used our theoretical modeling tool to guide our experiments. The phase-field method has recently emerged as a powerful computational approach to modeling and predicting mesoscale (in the range of nanometers to microns) and microstructural evolutions in materials. We used this approach to simulate the magnetoelectric coupling in strained nanocomposite films. As an example, we studied the vertically aligned epitaxial nanocomposite $BaTiO_3$-$CoFe_2O_4$, where $BaTiO_3$ is ferroelectric with large piezoelectricity and $CoFe_2O_4$ is ferromagnetic with large magnetostriction. We further applied this approach to the study of other forms of nanocomposites such as particulate and layered laminar-like ones, taking into con-

sideration of the thickness of ferroelectric and magnetic layers.

We investigated three particular epitaxial nanocomposite architectures: the vertically aligned nanocomposite, the layered laminar-like nanocomposite, and the particulate nanocomposite. Based on our more than ten years experience in growing complex metal-oxide films, we used pulsed laser deposition (PLD) to grow the first two architectures whereas PAD, a chemical solution technique, was used to construct the particulate nanocomposite. We also fabricated proof-of-principle nanocomposite systems to demonstrate improved and/or enhanced functionalities for novel electronic devices.

Accomplishments

We made tremendous progress for this project. This can be testified by a total 20 refereed journal articles supported by this LDRD project, one patent application, and three prestigious awards garnered by the principle investigator and co-investigator. The papers published in high profile journals include Nature Mater., Phys. Rev. Lett., Advanced Mater., Appl. Phys. Lett., Phys. Rev. B, and J. Appl. Phys. The principle investigator, Quanxi Jia, was elected as a Fellow of American Physical Society and a Fellow of American Ceramic Society. The co-investigator, Turab Lookman, was the recipient of LANL's Fellows award.

In the following, we summarize the key technical accomplishments. For example, we successfully used theoretical model to predict the effect of strain on the ferroelectric properties of $BaTiO_3/SrTiO_3$ superlattice; we used theoretical model to predict ferroelectric domain structures of single-crystal like $BiFeO_3$ thin films; we systematically studied the strain control in multifunctional thin films such as $BiFeO_3$; we studied the strain relaxation behavior in ferroelectric films on selected substrates; we experimentally demonstrated nanocomposite $BiFeO_3$ (BFO):Sm_2O_3 (SmO) films, and observed that there is a reduction in the dielectric loss for the BFO/SmO nanocomposite, compared to the pure films of the two phases; and we discovered a novel approach to control strain in the vertically aligned epitaxial nanocomposite metal-oxide films. Detailed description of the experiments and theoretical modeling can be found from our publications. In the report, we highlight the strain relaxation behavior in ferroelectric films on controlled substrate, and the effect of chemical composition and processing parameters on the structural and physical properties of two-phase vertically aligned nanocomposite (VAN) $(BiFeO_3)_x$:$(Sm_2O_3)_{1-x}$ thin films.

Strain relaxation behavior in ferroelectric films on controlled substrate

Strain effect on ferroelectric thin films has been widely investigated in recent years since it plays an important role in determining the physical properties of the materials when the thickness of the films scaled down to nanometers [1,2]. Recent researches indicate that the ferroelectric properties can be noticeably enhanced by inducing proper strains in the highly epitaxial films [2]. On the other hands, theoretical studies demonstrated that the dislocations generated during strain relaxation would also affect the ferroelectric properties significantly [3]. Therefore, understanding of the interface nature and strain relaxation is crucial for controlling the properties of ferroelectric thin films.

We investigated the strain relaxation behavior of (Pb,Sr) TiO_3 thin films on $NdGaO_3$ substrates during the cooling process. To understand the strain relaxation in slowly cooled and fast cooled samples, High resolution x-ray diffraction was employed to evaluate the dislocation densities in both samples for comparison. Our analysis indicated a notable difference in the interfacial behavior between the fast cooled and slowly cooled samples. The fast cooled sample exhibits an obvious elongated out-of-plane lattice and it sharply relaxes in just a few unit cells above the interface. Then it increases back to the bulk value slowly. On the other hand, the slowly cooled sample shows a totally different behavior [4].

We believe that the reduction in dislocation density and interfacial strain relaxation during the slowly cooling process may be associated with the evolution of threading dislocations. Beyond the critical thickness, dislocation half loops begin to nucleate near the film surface. The dislocation half loops grow and extend downwards as the film grows, and thus release the misfit stress at the interfaces. However, for the fast cooled sample, many of the dislocations may not get to the interface after the faster cooling down process, in other words, lots of dislocation half loops or the threading dislocations may still remain in the fast cooled sample, as observed in our studies and also reported on some other as-deposited perovskite oxide thin films by other groups. Since these dislocations have not reached the film-substrate interface, the lattices of the area beneath the dislocations are still strained, causing a larger out-plane lattice parameter at the interface, as shown in Figure 1 (a). During the slowly cooling process, the isolated small dislocation half-loops get enough time to keep growing and combining with each other. This results in the elimination of most of the threading dislocations and the extension of the dislocations to the film-substrate interface. Hence, the dislocation density reduces, the strain near the interface releases, and a shorten lattice is observed at the interface for the slowly cooled sample as schematically illustrated in Figure 1 (b). The evolution of the dislocations is very similar to the case of $BaTiO_3$ or $SrTiO_3$ films during high-temperature annealing as reported by others [5,6].

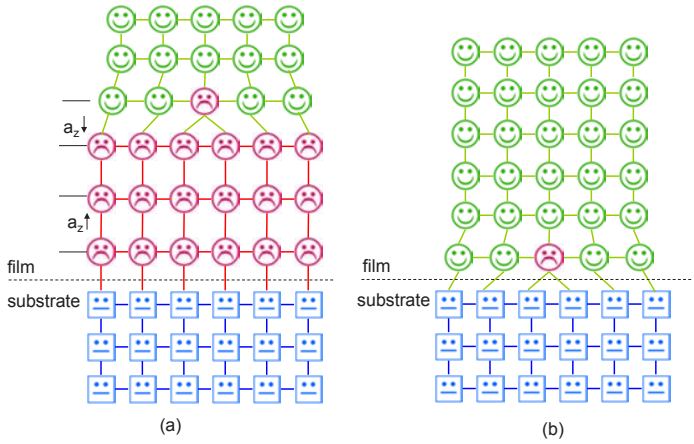

Figure 1. Schematic view of dislocation evolution during the slowly cooling process.

Effect of chemical composition and processing parameters on the structural and physical properties of vertically aligned nanocomposite (VAN) $(BiFeO_3)_x:(Sm_2O_3)_{1-x}$ thin films

We processed single-crystal like $(BFO)_x:(SmO)_{1-x}$ VAN thin films with various compositions and deposition frequencies on $SrTiO_3$ substrates, and observed that the out-of-plane lattice parameter/strain is sensitive to the composition x and deposition frequency (as shown in Figure 2) [7].

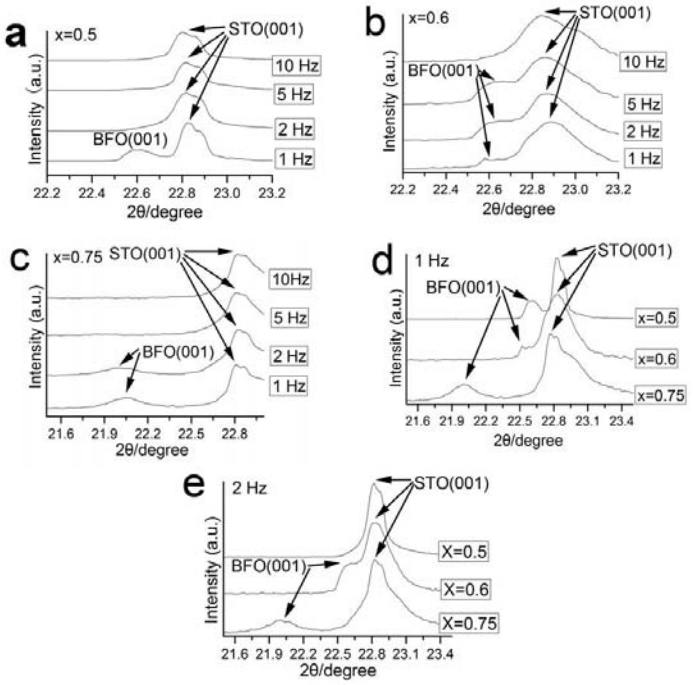

Figure 2. Local x-ray diffraction theta~2theta scans of BFO(001) peak as a function of deposition frequency for films with a) x = 0.5; b) x =0.6; c) x = 0.75; and as a function of film composition for films deposited at frequency of d) 1Hz; e) 2Hz.

The overall trend is that, as the deposition frequency decreases and the BFO content increases, the out-of-plane lattice parameter of BFO increases and the strain switches from compressive strain (x=0.5 and 0.6) to slightly tensile strain (x=0.75). On the other hand, the out-of-plane lattice parameter of SmO decreases and the strain switches from tensile (x=0.5 and 0.6) to slightly compressive (x=0.75). This suggests that both film composition and deposition frequency play a very important role in the overall strain control. When the film composition in the neighborhood of x=0.5, the VAN films show obvious vertical strain control rather than the substrate strain control. However when the composition reaches a certain limit (e.g., x=0.75), the VAN structure lost its vertical strain control and the substrate strain control dominates the overall film strain. We believe that the systematic variations in the BFO out-of-plane strain is most likely related to the size variation. This can be understood through the thin film growth kinetics. Lower deposition frequency results in longer resting time in between laser pulses and thus longer atomic diffusion path and larger column width. This observation can also explain the systematic variation in BFO's out-of-plane compressive strain. As the frequency reduces, the BFO column width increases and the total amount of the vertical column boundaries reduces. These will cause the reduction in the vertical strain control in between BFO and SmO columns and therefore the out-of-plane compressive strain of BFO reduces.

In summary, we showed that the VAN thin films exhibited a highly ordered vertical columnar structure with high structural quality. We demonstrated the strains of the two phases in both out-of-plane and in-plane directions could be tuned by the deposition parameters during growth, e.g. deposition frequency and film composition of the nanocomposite. The strain tunability was found to be directly related to film composition and the systematic variation of the column widths in the nanocomposite. Our experimental results for the first time suggest a promising avenue in achieving tunable strain in functional oxide thin films by using VAN structures [8].

Impact on National Missions

This research ties to the mission of DOE Office of Science for fundamental understanding of materials. The ability to design and fabricate materials to yield specific functionalities is central to the Grand Challenge in Materials: discovery science to strategic applications. LANL's thrusts in functional materials, nanotechnology, and sensors directly benefit from this project. This project not only provides a better understanding of the fundamental physics and physical chemistry as well as materials issues of ferroelectric and ferromagnetic films, but also solves technologically important issues related to nanotechnology.

References

1. Nagarajan, V., S. P. Alpay, C. S. Ganpule, B. Nagaraj, B. Aggarwal, E. D. Williams, A. L. Roytburd, and R. Ramesh. Role of substrate on the dielectric and piezoelectric behavior of epitaxial lead magnesium niobate-lead titanate relaxor thin films . 2000. *Appl. Phys. Lett..* **77**: 438.

2. Haeni, J. H., P. Irvin, W. Chang, R. Uecker, P. Reiche, Y. L. Li, S. Choudhury, W. Tian, M. E. Hawley, B. Craigo, A. K. Tagantsev, X. Q. Pan, S. K. Streiffer, L. Q. Chen, S. W. Kirchoefer, J. Levy, and D. G. Schlom. Room-temperature ferroelectricity in strained SrTiO3. 2004. *Nature.* **430**: 758.

3. Li, Y. L., S. Y. Hu, S. Choudhury, M. I. Baskes, A. Saxena, T. Lookman, Q. X. Jia, D. G. Schlom, and L. Q. Chen. Influence of interfacial dislocations on hysteresis loops of ferroelectric films. 2008. *J. Appl. Phys..* **104**: 104110.

4. Lin, Y., C. Dai, Y. R. Li, X. Chen, C. L. Chen, A. Bhalla, and Q. X. Jia. Strain relaxation in epitaxial (Pb,Sr)TiO3 thin films on NadGaO3 substrates. 2010. *Appl. Phys. Lett..* **96**: 102901.

5. Sun, H. P., X. Q. Pan, J. H. Haeni, and D. G. Schlom. Structural evolution of dislocation half-loops in epitaxial BaTiO3 thin films during high-temperature annealing. 2004. *Appl. Phys. Lett..* **85**: 1967.

6. Su, D., T. Yamada, V. O. Sherman, A. K. Tagantsev, and N. Setter. Annealing effect on dislocations in SrTiO3/LaAlO3 heterostructures. 2007. *J. Apl. Phys..* **101**: 064102.

7. Bi, Z., J. W. Lee, H. Wang, H. Yang, Q. X. Jia, and J. L. MacManus-Driscoll. Tunable lattice strain in vertically aligned nanocomposite (BiFeO3)x(Sm2O3)1-x thin films. 2009. *J. Appl. phys..* **106**: 094309.

8. MacManus-Driscoll, J. L., P. Zerrer, H. Wang, H. Yang, J. Yoon, S. R. Foltyn, M. G. Blamire, and Q. X. Jia. Spontaneous ordering, strain control and manipulation in vertical nanocomposite heteroepitaxial films. 2008. *Nature Materials.* **7**: 314.

Publications

Beaud, P., S. L. Johnson, E. Vorobeva, U. Staub, C. J. Milne, Q. X. Jia, and G. Ingold. An Ultrafast Structural Phase Transition Driven by Photo-Induced Melting of Charge and Orbital Order. 2009. *Phys. Rev. Lett..* **103**: 155702.

Bi, Z., J. W. Lee, H. Wang, H. Yang, Q. X. Jia, and J. L. MacManus-Driscoll. Tunable Lattice Strain in Vertically Aligned Nanocomposite (BiFeO3)x(Sm2O3)1-x Thin Films. 2009. *J. Appl. Phys..* **106**: 391409.

Choudhury, S., J. X. Zhang, Y. L. Li, L. Q. Chen, Q. X. Jia, and S. V. Kalinin. Effect of Ferroelastic Twin Walls on Local Polarization Switching: Phase-Field Modeling. 2008. *Appl. Phys. Lett..* **93**: 162901.

Choudhury, S., Y. L. Li, L. Q. Chen, and Q. X. Jia. Strain Effect on Coercive Field of Epitaxial Barium Titanate Thin Films. 2008. *Appl. Phys. Lett.* **92**: 142907.

Fouchet, A., H. Wang, H. Yang, J. Yoon, Q. X. Jia, and J. L. MacManus-Driscoll. Spontaneous Ordering, Strain Control and Multifunctionality in Vertical Nanocomposite Heteroepitaxial Films. 2009. *IEEE Trans. Ultrasonics, Ferroelectrics, and Frequency Control .* **56**: 1534.

Li, Y. L., S. Y. Hu, S. Choudhury, M. I. Baskes, A. Saxena, T. Lookman, Q. X. Jia, D. G. Schlom, and L. Q. Chen. Influence of Interfacial Dislocations on Hysteresis Loops of Ferroelectric Films. 2008. *J. Appl. Phys..* **104**: 104110.

Lin, Y., C. Dai, Y. R. Li, X. Chen, C. L. Chen, A. Bhalla, and Q. X. Jia. Strain relaxation in epitaxial (Pb,Sr)TiO3 thin films on NadGaO3 substrates. 2010. *Appl. Phys. Lett..* **96**: 102901.

Lookman, T., and P. Littlewood. Nanoscale heterogeneity in functional materials. 2009. *MRS Bulletin.* **34**: 822.

MacManus-Driscoll, J. L., P. Zerrer, H. Wang, H. Yang, J. Yoon, S. R. Foltyn, M. G. Blamire, and Q. X. Jia. Spontaneous Ordering, Strain Control and Manipulation in Vertical Nanocomposite Heteroepitaxial Films. 2008. *Nat. Mater .* **7**: 314.

Porta, M., T. Castan, P. Lloveras, and T. Lookman. Interfaces in ferroelastics: Fringing fields, microstructure, and size and shape effects . 2009. *Phys. Rev. B.* **79**: 214117.

Porta, M., T. Lookman, and A. Saxena. Effects of criticality and disorder on piezoelectric properties of ferroelectrics. 2010. *J. Phys. Condensed Matter.* **22**: 345902.

Sheng, G., J. X. Zhang, Y. L. Li, S. Choudhury, Q. X. Jia, Z. K. Liu, and L. Q. Chen. Domain Stability of PbTiO3 Thin Films Under Anisotropic Misfit Strains: Phase-Field Simulations. 2008. *J. Appl. Phys.* **104**: 054105.

Sheng, G., J. X. Zhang, Y. L. Li, S. Choudhury, Q. X. Jia, Z. K. Liu, and L. Q. Chen. Misfit Strain – Misfit Strain Diagram of Epitaxial BaTiO3 Thin Films: Thermodynamic Calculations and Phase-Field Simulations. 2008. *Appl. Phys. Lett..* **93**: 232904.

Soukiassian, A., W. Tian, V. Vaithyanathan, J. H. Haeni, L. Q. Chen, X. X. Xi, D. G. Schlom, D. A. Tenne, H. P. Sun, X. Q. Pan, K. J. Choi, C. B. Eom, Y. L. Li, Q. X. Jia, C. Constantin, R. M. Feenstra, M. Bernhagen, P. Reiche, and R. Uecker. Growth of Nanoscale BaTiO3/SrTiO3 Superlattices by Molecular-Beam Epitaxy. 2008. *J. Mater. Res.* **23**: 1417.

Staruch, M., L. Stan, F. Ronning, J. D. Thompson, Q. X. Jia, J.

Yoon, H. Wang, and M. Jain. Magnetotransport properties of epitaxial Pr0.5Ca0.5MnO3 films grown by a solution technique. 2010. *J. Magnetism and Magnetic Mater..* **322**: 2708.

Yang, H., H. M. Luo, H. Wang, I. O. Usov, N. A. Suvorova, M. Jain, D. M. Feldmann, P. C. Dowden, R. F. DePaula, and Q. X. Jia. Rectifying Current-Voltage Characteristics of BiFeO3/Nb-doped SrTiO3 Heterojunction. 2008. *Appl. Phys. Lett.* **92**: 102113.

Yang, H., H. Wang, G. F. Zou, M. Jain, N. A. Suvorova, D. M. Feldmann, P. C. Dowden, R. F. DePaula, J. L. MacManus-Driscoll, A. J. Taylor, and Q. X. Jia. Leakage Mechanisms of Self-assembled (BiFeO3)0.5:(Sm2O3)0.5 nanocomposite Films. 2008. *Appl. Phys. Lett.* **93**: 142904.

Yang, H., H. Wang, J. Yoon, Y. Q. Wang, M. Jain, D. M. Feldmann, P. C. Dowden, J. L. MacManus-Driscoll, and Q. X. Jia. Vertical Interface Effect on the Physical Properties of Self-assembled Nanocomposite Epitaxial Films. 2009. *Adv. Mater..* **21**: 3794.

Yang, H., Y. Q. Wang, H. Wang, and Q. X. Jia. Oxygen concentration and its effect on the leakage current in BiFeO3 thin films. 2010. *Appl. Phys. Lett..* **96**: 909012.

Zhang, J. X., Y. L. Li, S. Choudhury, L. Q. Chen, Y. H. Chu, F. Zavaliche, M. P. Cruz, R. Ramesh, and Q. X. Jia. Computer Simulation of Ferroelectric Domain Structures in epitaxial BiFeO3 thin films. 2008. *J. Appl . Phys.* **103**: 094111.

Genetically Engineered Polymer Libraries

Jennifer Martinez
20080395ER

Abstract

Biomaterials are used as medical implants (hip replacements, vascular grafts, dental fillings, sensors), therapeutic drug delivery agents, wound-healing devices, or biosensor platforms. If the material is to be implantable within or on the surface of the body, it must appear "native" and thus must interact with human cells in particular ways. Upon implantation, the surface of materials become coated with proteins found in blood and interstitial fluids. Cells sense the adsorbed proteins and subsequently respond to the surface as either foreign or native. Those surfaces that advantageously absorb extracellular adhesion proteins avoid encapsulation and proceed with cell adhesion and proliferation. Instead of redesigning man-made materials to function in the body, we are letting Nature select in vivo polymers that are most biocompatible.

This work is currently being protected by patenting. A complete report can be obtained by contacting the LDRD Program Manager at Los Alamos National Laboratory.

Probing Unconventional Superconductivity in Heavy Fermion Thin Films

Vladimir Matias
20080519ER

Abstract

In this project we attempted to grow epitaxial thin films of the superconducting compound $CeCoIn_5$. $CeCoIn_5$ is a so-called heavy-fermion superconductor with unconventional and interesting physical properties not fully understood and explained yet. Investigating and understanding these superconductors will help to find new superconductors with higher transition temperatures and improve existing ones. Two important investigations, which can be done with thin films of this material are: probing the symmetry of the superconducting state, and probing a novel inhomogeneous superconducting phase in this material that does not exist possibly elsewhere. We deposited thin films by pulsed laser deposition (PLD) and e-beam evaporation. The best films were made with PLD with high In content and high deposition temperature, and at lower In content and lower temperature on MgF2 substrates. We were able to show that epitaxy is possible in thin films despite of the low melting point and the rather high vapor pressure of In. These films are now being further investigated for their electrical transport properties and magnetic states.

Background and Research Objectives

Superconductivity is a physical phenomenon whereby a material loses all resistance to electric current below a certain transition temperature. There are many classes of superconductors, among which are the high temperature superconductors that contain copper oxide with a superconducting transition temperature around 100 K (or about -300 °F). Superconducting materials may dramatically increase efficiency of electrical energy distribution and use.

We are exploring the physical nature of superconductivity in a class of compounds known as 'heavy fermion' materials, sometimes referred to as heavy electron systems. Fermion is another word for electrons in this case, and the adjective 'heavy' refers to the conduction electrons in these materials that are strongly bound to the atoms. These materials contain rare-earth or actinide elements, such as cerium or uranium, and can exhibit unusual superconductivity that is still poorly understood and whose mechanism is still under scientific debate. LANL discovered a plutonium-containing compound in this '115' class of superconductors with a critical temperature of 18 K and the search is still on for even higher transition temperatures. Our project aims to make thin layers of these superconductors for scientific study of their unusual superconducting properties. The project combined LANL's advanced thin film technology currently used for high temperature superconductors with the LANL-established expertise in 'heavy fermion' materials to access new physical measurements and shed new light on unconventional superconductivity. We studied specifically the growth of thin films of $CeCoIn_5$ [1]. We intend to use the thin films for model studies of electrical transport across grains within the material. A particular result of this work will be to test the symmetry of superconductivity in these materials, which is presumed to be not spherically symmetric [2]. Furthermore, thin films offer the unique possibility to control the dimensionality of the samples, which will lead to further insight into the spatially inhomogeneous superconducting phases that have been discovered for larger samples of this material [3]. Insights from this work should lead researchers to better understand the limits of superconductivity and how to increase the superconducting transition temperature.

There are several groups worldwide investigating the thin film deposition of $CeCoIn_5$. Up to now, most groups only succeeded in fiber-textured films [4-6], i.e. one preferred crystal orientation perpendicular to the substrate, but random orientation in the plane of the substrate. For most advanced experiments, truly epitaxial films are necessary, i.e. preferred orientation also within the plane. The group in Kyoto is close to achieving this [7] but no results are published to date. However, the group has made the first 2D 'heavy fermion' materials providing the best evidence yet that heavy fermions undergo a special quantum phase transition [8]. The difficulty in depositing epitaxial $CeCoIn_5$ thin films is, besides the high reactivity of Ce and the low melting point and the relatively high vapor pressure of In. The low melting point leads to the formation of large molten spheres of In on the substrate, which cannot participate in the phase for-

mation. The vapor pressure leads to an additional loss of In during deposition at elevated temperatures. Therefore, the In content has to be carefully adjusted.

Scientific Approach and Accomplishments

For the deposition of heavy-fermion thin films we attempted two approaches. One is pulsed laser deposition (PLD) from a variety of targets, the other one is electron-beam and thermal co-evaporation in an approach similar to molecular beam epitaxy (MBE), as shown in Figure 1.

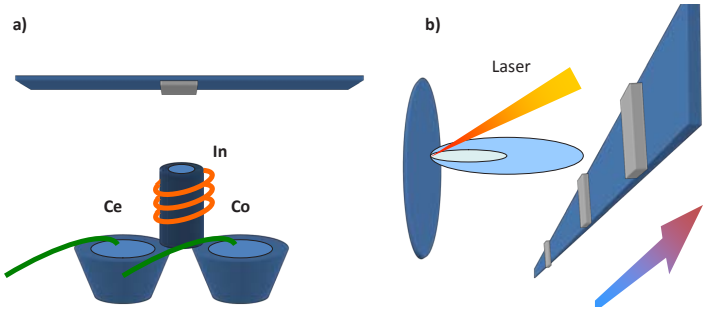

Figure 1. Schematic illustration of the two deposition methods used in this project, pulsed laser deposition (a) and electron-beam evaporation (b).

The heavy-fermion compounds contain very reactive elements, such as cerium, which require ultra high vacuum, below 10^{-7} torr, during film deposition to prevent oxidation. Therefore, we had to modify our vacuum chambers to the needs for growing these intermetallic heavy-fermion films. We added evaporation sources to augment our co-evaporation capability and internal bake-out systems to bring the base pressure to 10^{-8} torr. We also utilized combinatorial approaches for sample synthesis to increase our sample throughput. We used a reel-to-reel system with up to 20 samples to minimize the need to open the chamber. In addition to single crystal substrates, we also used long flexible tapes of ion-beam assisted deposition (IBAD) grown MgO layers on Hastelloy tapes as template, which further speeded up the process (the carrier is the template!) and reduced costs. The phase formation in the films was analyzed by x-ray diffraction, the stoichiometry by inductively coupled plasma spectroscopy (ICP) and energy dispersive x-ray spectroscopy (EDX), for spatially resolved analysis. EDX as well as the investigation of the surface morphology by scanning electron microscopy (SEM) was carried out at the Center for Integrated Nanotechnologies (CINT) at LANL. The electrical transport properties of selected samples were measured in a 4-point measurement geometry in a Quantum Design PPMS He3 system.

With the PLD approach we have succeeded in depositing $CeIn_3$ and $CeCoIn_5$ thin films, but not as single phase because there is always excess In. Some of our best samples to date by PLD were made with In-rich targets and at temperatures of around 500°C. However, the crystallites of $CeCoIn_5$ in these films can be epitaxial with the substrate, as shown in the SEM micrograph in Figure 2.

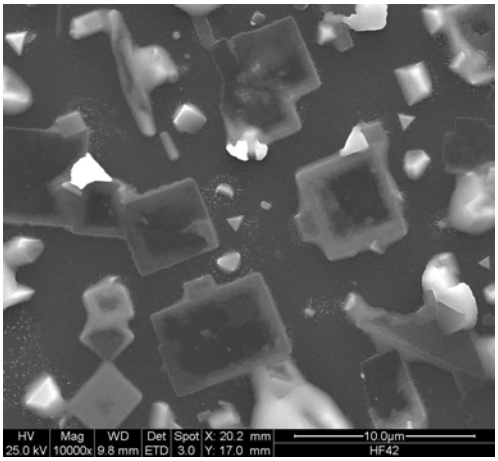

Figure 2. Electron microscopy surface image of a $CeCoIn_5$ thin film on MgO substrate, showing square shaped crystallites with well-defined orientation with respect to the substrate.

The main problem for obtaining single phase film growth is that In does not wet the substrate and tends to form islands which are In-rich. SEM images together with EDX analysis show the formation of these large In-rich particles. With these films we could for the first time show that epitaxy is possible despite of the low melting point of In [9]. Recently, we found complete epitaxy of CeCoIn5 films on MgF2 substrates at low growth temperature of about 400°C. Figure 3 shows an x-ray phi scan for this sample with the fourfold symmetry of an epitaxial layer. Electrical transport has been measured to low temperatures and we observe a superconducting transition temperature of 2.1 K, as shown in Figure 4. This is slightly depressed compared to that of bulk crystals whose Tc is 2.3 K. The main substrates that we use are MgO and MgF_2; the latter one itself has an excellent lattice match to $CeCoIn_5$. To improve the wetting we deposit buffer layers before deposition of Ce-In compounds. We were able to get excellent epitaxial films of Cr on MgO and on MgF2. We were utilized *in situ* reflection high-energy electron diffraction (RHEED) to observe epitaxy and atomic layer smoothness in real time. We were also utilizing time-of-flight ion scattering spectroscopy for analysis of our thin film samples. We believe that the *in situ* monitoring approach is necessary to successfully make these films. We found that the growth conditions for epitaxy by co-evaporation and PLD in the low-In content regime requires low deposition temperatures. This is in agreement with recent results by a Japanese group that reported first films of $CeIn_3$ and $CeCoIn_5$ [9,10].

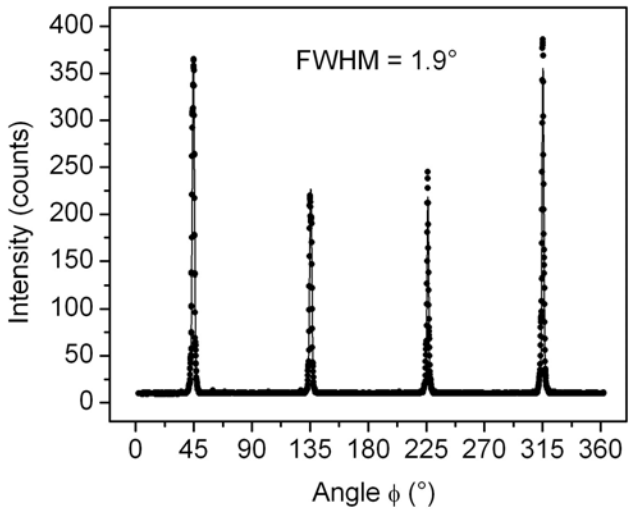

Figure 3. X-ray analysis of a $CeCoIn_5$ thin film on MgF2 substrate, showing full epitaxy and a fourfold symmetry.

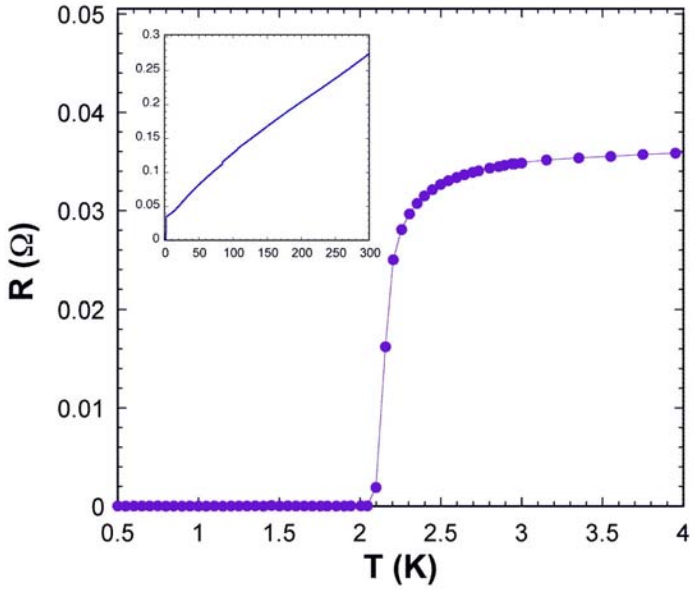

Figure 4. Temperature dependence of the resistance in a CeCoIn5 thin film, showing a zero-resistance superconducting transition at 2.1 K.

From this work we learned that our present deposition systems can be used for synthesis of these intermetallics and that the vacuum level, at 10^{-8} torr, in our current vacuum chambers is high enough for this work. We explored a large number of growth parameters and found several regimes where we could grow this material. However, the current systems were used for a number of different projects in parallel, which made a continuous high-throughput investigation difficult. For future experiments a dedicated ultra-high vacuum, perhaps MBE chamber, designated solely for this work should be built and used to deposit high-quality epitaxial $CeCoIn_5$ films. Our films are recently being used to image magnetic vortices in the superconducting state by magnetic force microscopy. Other groups investigating terahertz spectroscopy also have an interest in exploring subgap optical conductivity in these films and we plan to supply them with our thin film samples.

Impact on National Missions

This project will support the DOE mission in Office of Science by enhancing our understanding of unconventional superconductivity and through the search for new superconducting materials. Understanding the mechanisms which lead to superconductivity in these strange metals will help to find new materials with higher transition temperatures (maybe even room temperature) and improve existing superconducting materials. It will be used to strengthen and secure the power grid, it is used to built smaller and lighter motors and generators for airplanes and ships, for degaussing ships (i.e. the ships are not visible under radar), as detectors and many more. Superconductivity is potentially a key technology for national energy security.

References

1. Petrovic, C., P. G, Pagliuso, M. F. Hundley, R. Movshovich, J. L. Sarrao, J. D. Thompson, Z. Fisk, and P. Monthoux. Heavy-fermion superconductivity in CeCoIn5 at 2.3 K. 2001. *Journal of Physics - Condensed Matter.* **13** (17): L337.

2. Movshovich, R., M. Jaime, J. D. Thompson, C. Petrovic, Z. Fisk, P. G. Pagliuso, and J. L. Sarrao. Unconventional superconductivity in CeIrIn5 and CeCoIn5 : Specific heat and thermal conductivity studies. 2001. *Physical Review Letters.* **86** (22): 5152.

3. Bianchi, A., R. Movshovich, C. Capan, P. G. Pagliuso, and J. L. Sarrao. Possible Fulde-Ferrell-Larkin-Ovchinnikov Superconducting State in CeCoIn5. 2003. *Physical Review Letters.* **91** (18): 187004.

4. Soroka, O. K., G. Blendin, and M. Huth. Growth of CeCoIn5 thin films on a - and r -Al2O3 substrates. 2007. *Journal of Physics - Condensed Matter.* **19**: 05606.

5. Izaki, M., H. Shishido, T. Shibauchi , Y. Matsuda, and T. Terashima. Superconducting thin films of heavy-fermion compound CeCoIn5 prepared by molecular beam epitaxy. 2007. *Applied Physics Letters.* **91** (12): 122507.

6. Zaitsev, A. G., A. Beck, R. Schneider, R. Fromknecht, D. Fuchs, J. Geerk, and H. v. Löhneysen. Deposition of superconducting CeCoIn5 thin films by co-sputtering and evaporation. 2009. *Physica C.* **469** (1): 52.

7. Shibauchi, T., H. Shishido, K. Yasu, Y. Mizukami, T. Terashima, and Y. Matsuda. Epitaxial thin films of heavy-fermion superconductor CeCoIn5 . Presented at *American Physical Society March Meeting 2010.* (Portland, OR, March 15-19, 2010).

8. Shishido, H., T. Shibauchi, K. Yasu, T. Kato, H. Kontani, T. Terashima, and Y. Matsuda. Tuning the dimensionality of the heavy fermion compound CeIn3. 2010. *Science.* **327**: 980.

9. Haenisch, J., F. Ronning, R. Movshovich, and V. Matias. Pulsed laser deposition of CeCoIn5 thin films. To appear in *Physica C.*

Publications

Dubi, Y., R. R. Biswas, and A. V. Balatsky. Phase fluctuations in finite thickness disordered superconducting thin films. *Europhysics Letters.*

Haenisch, J., F. Ronning, R. Movshovich, and V. Matias. Pulsed laser deposition of CeCoIn5 thin films. 2009. *Physica C.* **470**: XXX.

Photocatalytic Materials Based on Quantum Confined Semiconductor Nanocrystals

Milan Sykora
20080523ER

Abstract

The goal of the summarized research was to exploit the possibility of developing a new class of nanoscale photocatalytic materials, which upon solar irradiation can produce molecular hydrogen via photochemical decomposition of organic substrates or water. The approach is based on exploitation of unique properties of semiconductor nanocrystaline quantum dots (NQDs) in assemblies where they are coupled to established molecular redox catalysts. In the photocatalytic assemblies the NQD functions as light absorber and a charge generator, which activates a molecular catalyst via charge transfer. In the constructed assemblies the goal was to take advantage of unique properties of NQDs, such as high light harvesting efficiency, size-tunable absorption spectra and redox properties. The research performed lead to development of new nanoscale fabrication methods, an understanding of the electronic interactions at the semiconductor-molecule and semiconductor-semiconductor interfaces, which are necessary first steps towards the construction of a practical device. The summarized research made important progress in supporting the drive toward national energy security, a key DOE mission.

Background and Research Objectives

The objective of the research was to exploit the possibility of developing a new class of nanoscale photocatalytic materials, which upon solar irradiation can produce molecular hydrogen via photochemical decomposition of organic substrates or water (Figure 1). The approach is based on exploiting unique properties of semiconductor nanocrystaline quantum dots (NQDs) in assemblies where they are coupled to established molecular redox catalysts. In the photocatalytic assembly NQD functions as a light absorber and a charge generator, which activates a molecular catalyst via charge transfer (CT). In construction of the assemblies the goal was to take advantage of unique properties of NQDs, such as high light harvesting efficiency, size-tunable absorption spectra and redox properties. The goal of the research was to address fundamental problems that are necessary first steps towards development of a practical solar energy conversion device. Specifically:

- Development of new nanoscale fabrication methods for chemical coupling of NQDs to molecular catalysts and nanocrystalline metal oxides and new approaches to characterization of these structures.
- Development of understanding of factors that dictate the efficiency and dynamics of heretofore virtually unstudied electronic interactions at NQD-semiconductor and NQD-molecule interfaces.
- Fabrication of an NQD-based assembly with the ability to efficiently harvest the solar radiation and has the potential to use the harvested energy to oxidize organic substrates or water. Such assembly is a key component of the photoanode of the potential device. In addition to the obvious potential practical benefit, the pursuit of the above objectives provided important insights in some of the most intensely studied areas of chemistry.

Scientific Approach and Accomplishments

In pursuing our goal of constructing photocatalytic assembly shown in Figure 1, we have chosen a three step, modular approach:

- Develop methods for chemical and electronic coupling of NQDs with molecular catalyst and study their interactions upon irradiation with light
- Develop methods for chemical and electronic coupling of NQDs with TiO_2 electron transporting material and study their interactions upon irradiation with light
- Construct assembly comprising TiO_2/NQD/catalyst and study interaction of the components upon light irradiation

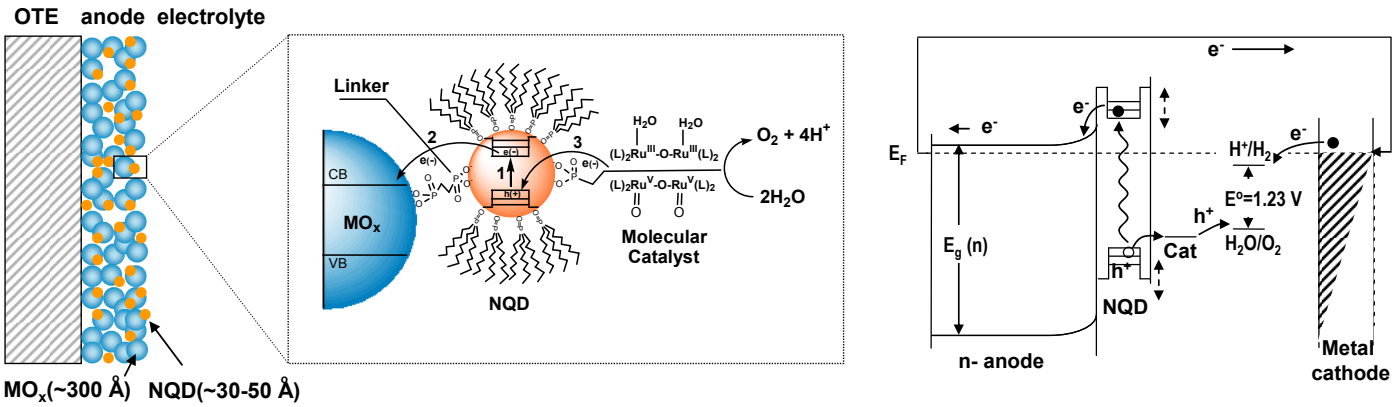

Figure 1. Left: Schematic diagram of the nanoscale photocatalytic assembly based on coupling of semiconductor NQDs and molecular catalysts. Irradiation of the NQD with visible light leads to generation of one or more electron-hole pairs (1), followed by rapid photoinjection of an electron into the conduction band (CB) of the metal oxide (MOx = TiO2 (2). Right: Energy diagram of the photoelectrolytic cell in which the composite material could be used as a photoanode (Cat is the molecular catalyst). Hydrogen production occurs at a metal (e.g., Pt) cathode. Development of the actual device is not the objective of the current project.

Construction and studies of NQD-catalyst assemblies

Studies of NQD-catalyst coupling by Infrared Spectroscopy

A necessary first in construction of the photocatalytic assemblies is identifying means for chemical coupling of the NQD and a catalyst. As prepared, NQDs comprise an inorganic core overcoated with a layer of organic ligand molecules –passivating layer. In our application the goal is to partially or completely substitute the passivating layer with molecular catalysts. While ability to modify the passivating layer in a controlled way is important for many applications, progress in this area has been generally hindered by limited understanding of the NQD surface chemistry and lack of experimental techniques for studies of surface chemistry of the NQDs. In our research we found that Attenuated Total Reflectance Fourier Transform Infrared Spectroscopy (ATR-FTIR), when properly adapted, can be used as a very powerful tool for studies of NQD surface chemistry. Our approach is schematically shown in Figure 2 a. Briefly, a thin film of NQDs deposited on the ATR crystal is exposed to solution of catalysts functionalized with anchoring group (e.g. carboxylic acid) allowing attachment to NQD surface. Following the exposure of the NQD film to the solution of the catalysts the ATR-FTIR spectrum of the film is monitored continuously for several hours. During that time dramatic changes in the spectral properties of the NQD film are observed (see Figure 2d), which are indicative of changes taking place at the NQD surfaces. While changes in the intensities of various spectral bands indicate the dynamics of the surface substitution, the positions of the bands indicate how the catalysts bind to the NQD surface. Based on the observed spectral changes, such as those shown in Figure 2d we made the following observations:

- The substitution of the passivating ligand with the catalyst is rapid taking less than 15 minutes after the exposure of the film to the catalyst
- The interaction between the catalyst and the CdSe NQD film leads to the deprotonation of the carboxylic acid functional group on the catalyst. This occurs as a result of the chemical attachment of the complex to the surface of the NQDs.
- The catalysts couple to the NQD surface via bridging binding mode (see Figure 2).

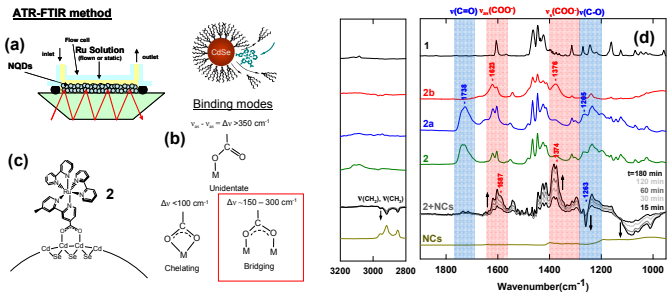

Figure 2. (a) Schematic representation of the ATR-FTIR experiment. (b) Possible modes of attachment of the carboxylic acid anchoring group to NQD surfaces and corresponding difference in frequencies of symmetric and asymmetric stretches of the carboxylic acid group. (c) The proposed mode of coupling of the Ru-polypyridine complexes to the surface of CdSe. (d) ATR-FTIR spectra observed following exposure of CdSe NQD film to acetonitrile solution of complex 2 (2+NCs). Also shown are spectrum of complex with no linking group (1), fully protonated (2a) and deprotonated (2b) forms of the complex and the film of NQDs(NCs).

To be able to better interpret our experimental results we have initiated collaboration with the theory group of Dr. Sergei Tretiak at the Center for Integrated Nanotechnology (CINT) at LANL. The results of modeling of the process of catalyst-NQD assembly formation using Density Functional Theory (DFT) were consistent with the experiment and provided important insights on how the redistribution of electron densities associated with the coupling may affect the efficiency of the photoinduced charge transfer in the resulting assemblies. The results of the experimental and theoretical studies for series of Ru-polypyridine catalysts are summarized in a recently completed publication to be submitted to Journal Langmuir.

Studies of NQD-catalyst coupling by Photoluminescence

A second approach that we used to investigate the interaction between the NQDs and catalysts is based on studies of photoluminescence (PL) of the NQD/catalyst mixtures in solution. Very recently, it was demonstrated that PL studies of NQDs in solution can be used, with the aid of isotherm models, to quantitatively monitor substitution of one surface ligand for another. We have adapted this approach to investigate the formation of NQD-catalyst assemblies. The sample results are summarized in Figure 3. As shown in the Figure, in the presence of a catalyst the PL intensity of the NQDs is dramatically reduced, while the PL intensity of the catalyst is enhanced. This effect, however, is observed only in case when the catalysts are functionalized with an anchoring group. These results, which are consistent with our ATR-FTIR studies discussed above, indicate that when the NQDs are exposed to catalysts functionalized with carboxylic acid anchoring groups, the catalysts chemically couple to the NQD surface. When we monitored the evolution of the PL spectra of the NQDs shortly after injection of the solution of the catalyst we found that formation of the NQD-catalyst assemblies is very rapid occurring with formation half-time of 1.08 seconds, where the formation lifetime is time needed for half of the NQDs to have single catalyst adsorbed on their surface, on average.

To more quantitatively analyze the structure of the formed assemblies we have performed studies where the concentration of the catalyst in solution was systematically varied, while the NQD concentration was constant. The concentration dependent variation in the PL intensity of the NQDs of several sizes was modeled using Langmuir isotherm model. This analysis provided following insights:

- The Langmuir constant, which reflects the relative affinity of the adsorbing group towards the surface is approximately order of magnitude larger for catalyst than for the ligands, which explains large rate of the substitution process.
- Although the fractional surface coverage of the NQD with the catalyst is NQD size independent, the absolute surface coverage, expressed in terms of number of catalysts per NQD is strongly dependent on the NQD size. For example, (see Figure 3) for smaller NQDs with radius r=1.2 nm ($CdSe_{501}$) excess of six catalysts present in solution per single NQD leads to one catalyst

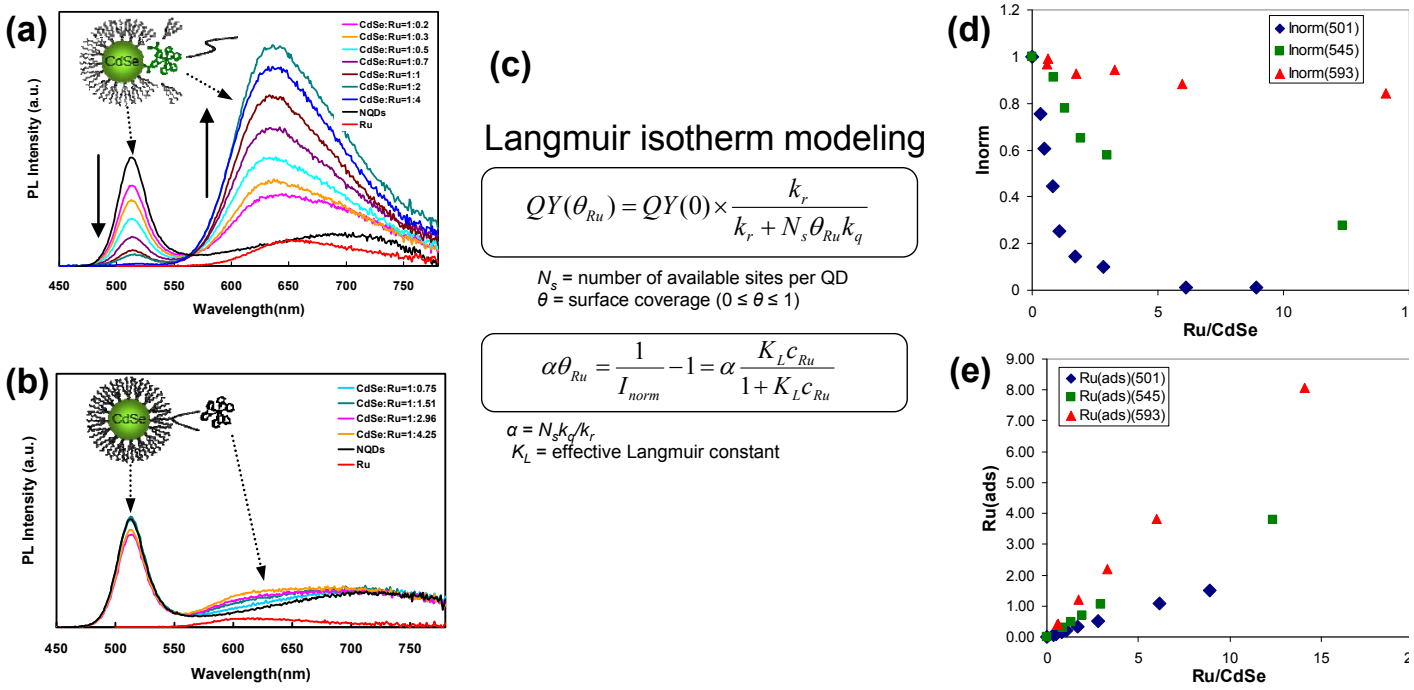

Figure 3. PL spectra of the NQD/catalyst mixtures with various catalyst concentrations (a) catalyst with linking group (b) catalyst without linking group. (c) Isotherm model used to analyze the PL data. (d) Normalized NQD PL intensity as a function of catalyst concentration for three sizes of NQDs (e)Surface coverage of the NQD by catalyst as a function of NQD/catalyst ratio in solution.

adsorbed per NQD on average. The same excess of catalyst for larger NQD, with r=2.3 nm ($CdSe_{593}$) leads to approximately four catalysts adsorbed on NQD, on average. This result is a reflection of larger number of sites available on the surface of larger NQDs.

The results summarized above provide important guidelines on how to construct the NQD-catalyst assemblies with specific composition. They are summarized in a recently completed publication to be submitted to Journal Advanced Materials.

In further studies of the PL spectra o the NQD-catalyst assemblies we have found that upon coupling the PL spectra of the catalyst shift to higher energies, which indicates that the electronic structure of the complexes changes upon adsorption onto the NQD surface. We found that the spectral shift is a result of the deprotonation of the carboxylic acid group of the catalyst in the process of adsorption onto the NQD surface. This result is consistent with the results of our ATR-FTIR studies.

To further understand the effect on deprotonation on the electronic properties of the catalyst we performed a DFT theoretical study of the electronic structure of the protonated and deprotonated catalysts in collaboration with the theory group of Dr. Sergei Tretiak. Our calculations show that the shift is a result of more delocalized character of the electron transition orbitals in the deprotonated species and a strong destabilization of the three lowest unoccupied orbitals localized on the substituted and unsubstituted ligands, all of which contribute to the lowest-energy optical transitions. The above results have been recently published in Journal Physical Chemistry Chemical Physics.

Studies of NQD-catalyst electronic interactions.

Construction of the working photoanode requires proper understanding not only how to couple the catalysts to the NQDs but also how the NQDs and catalyst interact. For the assembly to function as a photocatalyst the photoexcitation of the NQD must lead to an NQD->catalyst CT. To understand the interaction we have performed steady state and time resolved PL and absorption studies. In our studies we have found that the NQD->catalyst CT occurs only in some of the assemblies. More specifically, we found that mode of interaction is dependent on NQDs size (Figure 4); for small (r<2nm) NQDs the dominant interaction is NQD->catalyst energy transfer (ET). The ET is efficient (>90%) and fast (<1ns) due to the large spectral overlap between the absorption spectrum of the complex and the PL spectrum of the NQD. Only for very large NQDs (r>2nm) we observed that the excitation of the NQDs is accompanied by significant quenching of the catalyst PL, which is an evidence of (CT) between NQDs and the catalyst (Figure 4). In the assemblies where the dominant process is CT our studies of relaxation dynamics suggests that the CT is much faster than ET, with corresponding time constant <10 ps. The publication summarizing our results is currently in preparation.

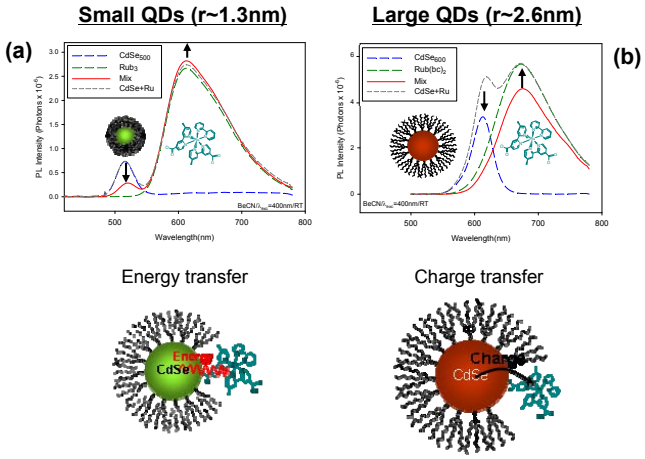

Figure 4. Dependence of electronic interaction between NQD and catalyst on NQD size. (a) The PL of NQD is quenched and PL of catalyst is enhanced. This indicates NQD to catalyst energy transfer. (b) PL of NQD and the catalyst is quenched. This is indicative of NQD to catalyst charge transfer.

In our investigation of the NQD-catalyst electronic interactions we observed that photoexcitation of CdSe NQDs with excitation energies >3.1 eV leads to rapid photodegradation of the NQDs. Although, this effect was reported previously we have made an important observation that the photodegradation only occurs if the NQD solutions are exposed to air. Through further studies we have found that the degradation mechanism is in fact photoinduced oxidation. The photooxidation in solution has a distinct energy threshold that is solvent dependent. These observations are relevant to this project as the formation of oxygen on the photoanode is one of the long-term goals. However, we believe that these results have broader implication for any NQD-based application where high energy or high intensity irradiation is required. The results of our studies in this area are being summarized in two manuscripts currently in preparation.

Construction and studies of NQD/TiO_2 interface

In the second component of our modular approach we have developed fabrication methods for and studied the charge transfer properties of the TiO_2/NQD assemblies. Although, reports are available in literature on preparation of such assemblies, we have found that number of improvements in the fabrication process were needed before we could study the light induced processes at the NQD/TiO_2 interface. First, we made transition from commonly used, "doctor blading" to screen printing approach for preparation of TiO_2 films, which allowed us to prepare materials

with highly reproducible properties (e.g., thickness, porosity, optical transparency). Next, we optimized the method for infiltration of the TiO_2 films with NQDs to achieve infiltration with approximately 100% coverage of the TiO_2 surface with NQDs. We have also discovered that upon air exposure the NQDs infiltrated in the TiO_2 films undergo rapid photo-induced oxidation when irradiated with simulated solar light. To overcome this problem we developed procedures for fabrication of the composites under fully anaerobic conditions. With these improvements we were able to prepare very reproducible and stable materials for studies of photoinduced interfacial CT. Contrary to our preliminary results and reports available in literature, we found that efficient NQD->TiO_2 CT is not contingent upon the use of organic linkers to provide electronic coupling between NQD and TiO_2. We found that in the assemblies where the NQDs are adsorbed onto TiO_2 surface directly, the photoinduced NQD->TiO_2 electron transfer is nearly 100% efficient. We also found that the efficiency of the CT increases significantly with the reduction in the length of the NQDs passivation ligands. Our results are summarized in a publication to be submitted to ACS Nano.

Construction and properties of TiO_2/NQD/catalyst assembly

As a final step in our modular approach we have attempted to construct the TiO_2/NQD/catalyst assembly and study its properties under irradiation. To construct the assembly we have first prepared the TiO_2/NQD assemblies using the methods developed in section B. Next we exposed these assemblies to solutions of catalysts functionalized with anchoring carboxylic acid groups under controlled conditions as discussed in section A (Figure 5). Our results strongly indicate that:

- The TiO_2/NQD/catalyst assembly forms effectively as indicated by clear signatures of all the components in the absorption spectrum of the assembly
- Upon irradiation the changes in the absorption spectra provide strong indication that the charge separation across the assembly is effective with the catalyst being present in its active form.

These encouraging preliminary results provide a basis for future investigation of the photacatlytic activity of the TiO_2/NQD/catalyst assemblies developed in this project.

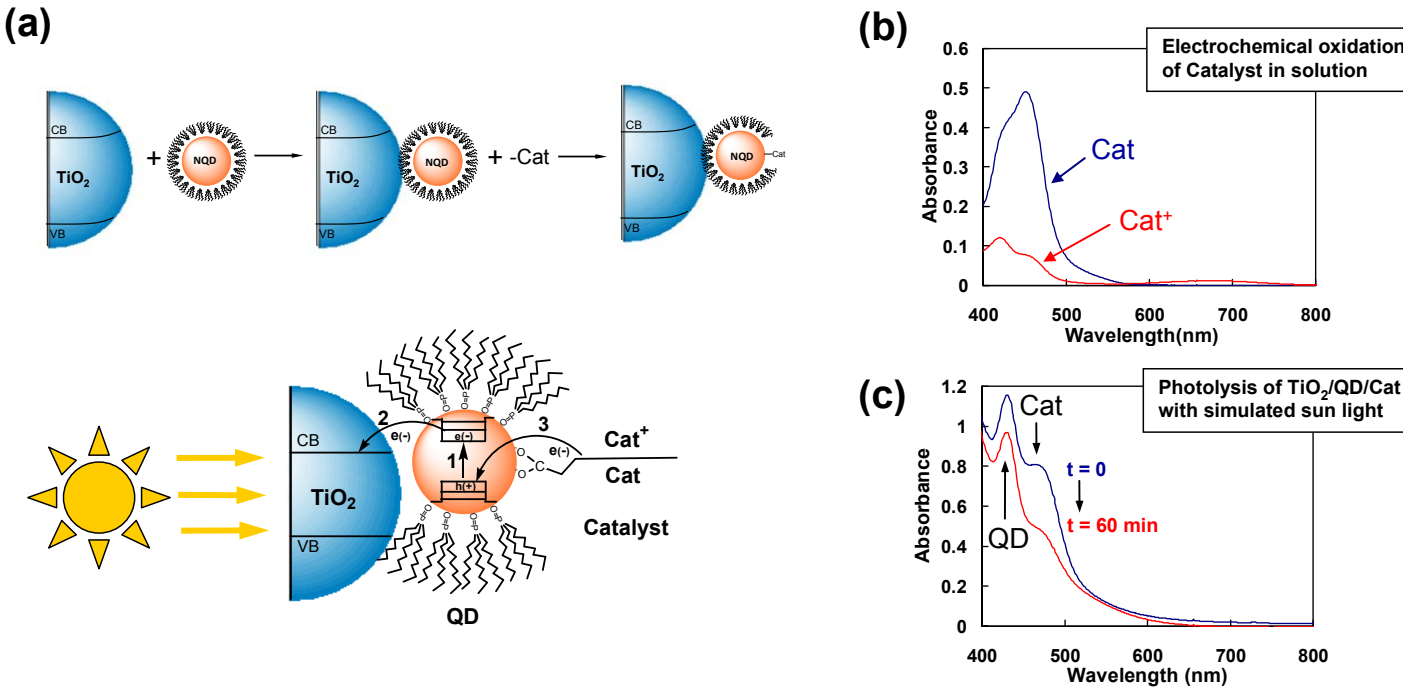

Figure 5. (a) Schematic diagram showing the process of formation of TiO_2/NQD/Catalyst assembly and the detailed structure of the assembly. (b) Changes in the absorption spectrum of the catalyst induced by electrochemical oxidation in solution. (c) Changes in the absorption spectrum of the TiO2/NQD/Catalyst assembly upon simulated white light irradiation. The decrease in the absorption in the spectral range at ~470 nm indicates that the catalyst is oxidized (activated) upon irradiation.

Impact on National Missions

The work performed under this project is one example of an effort towards better understanding of how nanoscale materials can be utilized to improve the efficiencies of the solar energy conversion technologies. In this context, the results generated in the project represent an important step towards building long-term national energy security, which is a key DOE mission.

Publications

Badaeva, E., V. Albert, S. Kilina, A. Koposov, M. Sykora, and S. Tretiak. Effect of deprotonation on absorption and emission spectra of Ru(II)-bpy complexes functionalized with carboxyl groups. 2010. *PHYSICAL CHEMISTRY CHEMICAL PHYSICS.* **12** (31): 8902.

Sykora, M., A. Koposov, J. McGuire, R. Schulze, O. Tretiak, J. Pietryga, and V. Klimov. Effect of air exposure on surface properties, electronic structure, and carrier relaxation in PbSe nanocrystals. 2010. *ACS Nano.* **4** (4): 2021.

Design of Robust Waste Nuclear Waste Forms via Radioparagenesis

Christopher R. Stanek
20100528ER

Abstract

Although public support for the expansion of nuclear power is increasing, significant growth is liable to be hindered by the seemingly intractable nuclear waste problem. A particularly difficult aspect of the waste problem is that any solution must be predictable with great confidence at time scales not conducive to experimental verification. However, we have recently discovered a phenomenon that allows for improved predictability of long-term waste form performance. Specifically, using electronic structure methods, we have found that unconventional compounds and crystal structures can form via the chemical transmutation occurring during radioactive decay (e.g. rocksalt ^{137}BaCl formation from the β- decay of ^{137}CsCl). We refer to this phenomenon as "radioparagenesis." We propose to employ insights gained via radioparagenesis to design robust waste forms and discover novel materials with interesting properties. In this feasibility project, we have designed and subsequently commenced an accelerated isotope experiment at the Isotope Production Facility. The novelty of this experiment is that we are using highly radioactive, short-lived isotopes, typically used as tracers, to create materials that are amenable to bulk characterization techniques, e.g. X-ray diffraction. The specific goal of the verification component is to experimentally observe radioparagenetic ^{107}AgS from the decay of ^{107}CdS. We also present corresponding density functional theory predictions of radioparagenetic phase formation.

Background and Research Objectives

Several obstacles exist that are preventing significant expansion of nuclear energy, including: construction cost of new plants, proliferation risk of nuclear material, safety concerns and nuclear waste disposal. Of these outstanding issues, nuclear waste possesses the highest potential to benefit from technological advances. Furthermore, the waste problem may be the largest obstacle – a sustainable solution will likely result in the realization of a so-called "nuclear renaissance."

A glaring weakness of the current approach to nuclear waste disposal is the lack of predictability at long time scales. Indeed, waste solutions are engineered so that performance at the beginning of life (*i.e.* $t = 0$) is sufficient to hopefully withstand the aggressive radiation fields and chemical changes that occur. A better solution for nuclear waste begins with fuel reprocessing. The first advantage of this approach is a significant reduction on the volumetric load of a geologic repository. For example, the removal of the burnable actinides (Pu, Am, Np and Cm) and the short-lived fission products (Cs and Sr) from spent fuel results in a load decrease of 225 times. Second, in addition to importantly minimizing the volume in (and therefore number of) geologic repositories, reprocessing spent nuclear fuel presents ***an opportunity to design customized waste forms for specific fission products.*** By using spent nuclear fuel as a waste form (the solution proposed in the license application for Yucca Mountain), fission products with disparate chemistries are encapsulated in the same waste form. As a simple example, ^{99}Tc has a half-life of 2.13×10^5 years, while ^{137}Cs has a half-life of 30.07 years. Clearly, an optimized solution for nuclear waste does not entail a singular disposal strategy for fission products so chemically and physically different. Rather, customized waste forms can be designed to encapsulate particular fission products and account for peculiarities in fission product physics and chemistry.

The encapsulation of fission products in crystalline waste forms has been considered for over thirty years. But research in this area has focused on either the radiation or leach resistance of host phases. This focus has supported the design philosophy mentioned above, *i.e.*: maximize performance at $t = 0$ and hope that is sufficient. Again, this approach lacks the predictability required for a reasonable solution. However, without sophisticated modeling and simulation tools, this is the best that could be done, since even the shortest experiments on actual fission products require more than 100 years.

We propose to turn this problem on its head by "backward" designing waste forms from the end of their life to the beginning, which is made possible by the new concept of *radioparagenesis* recently introduced by our team. This concept allows us to understand how chemical transmutation (the conversion of one element or isotope to another, in this case during radioactive decay) impacts the stability of a waste form. We assert that it is fundamentally incorrect to view nuclear waste as a static entity. Rather, by understanding the chemical and structural evolution that occurs during the decay of certain fission products to chemically distinct daughters (*e.g.* ^{137}Cs ® ^{137}Ba), we are not only in a position to understand how the performance is impacted by the chemical evolution, but ultimately we may understand how to design waste forms whose stability actually increases over time.

We define radioparagenesis as: the formation of unconventional crystal structures (*e.g.* rocksalt BaCl) for compounds formed during the chemical transmutation that occurs during radioactive decay. Our initial example of **^{137}**CsCl ® **^{137}**BaCl (see Figure 1) clearly demonstrates that radioparagenetic phases defy intuition and conventional bonding arguments (see Jiang *et al. Phys. Rev. B* **79** (2009) 132110). That is, based on ionic bonding theory, one would expect the formation of $BaCl_2$ rather than BaCl, since Ba is a rigidly 2+ cation. However, our results suggest that radioactive decay may be an unconventional synthesis method resulting in the formation of compounds and structures that cannot be synthesized via conventional means. Indeed, as will be discussed in the following proposed work section, we are investigating the possibility of using this approach to synthesize materials for non-nuclear applications that exhibit fascinating properties. Initial discussion of this result was featured in *Innovation* magazine.

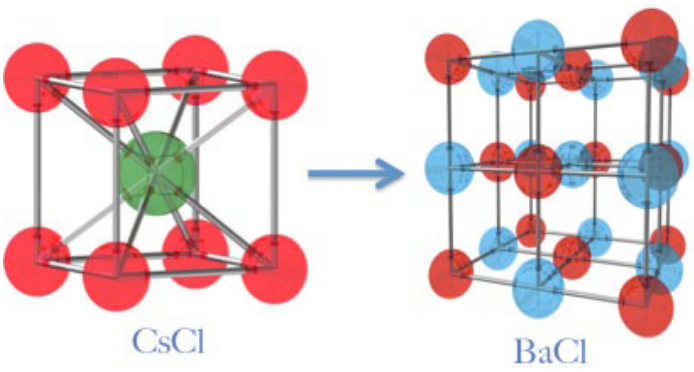

Figure 1. Depiction of chemical transmutation of 137Cs to 137Ba via β- decay in CsCl (spacegroup: Pm m, No. 221), resulting in the radioparagenetic formation of rocksalt BaCl (spacegroup: Fm m, No. 225). Red atoms denote Cl, green Cs and blue Ba.

For nuclear waste forms, there are two important and distinct implications of radioparagenesis that are worth explaining, as they seem to have been a source of confusion in a recent LDRD-DR proposal, namely: (1) effects of radioparagenetic phase formation on waste form stability and performance, and (2) design of robust waste forms using radioparagenetic insights. For (1), it is critical to understand that the **^{137}**CsCl ® **^{137}**BaCl example is not at all representative of a robust waste form. Rather it was chosen as a computationally feasible example to demonstrate the phenomenon. To be clear, we are quite certain that CsCl is not a robust encapsulation host for ^{137}Cs. However, the relative simplicity of the CsCl and BaCl rocksalt structures clearly illustrate how radioparagenesis may affect waste form performance, i.e. via the formation of unexpected phases. For example, we found that BaCl exhibits more metallic than ionic bonding character. Diffusivity in metals is much different than ionic crystals. Therefore, if the waste form was expected to exhibit ionic bonding throughout its life, then it is clear that the unexpected formation of a radioparagenetic phase would result in different behavior than anticipated.

However, applied in this way, radioparagenesis only allows one to determine how much worse a waste form will perform than anticipated. Much more powerful is the ability to use these insights to design a waste form with predictive performance ((2) from above). For example, we have recently performed simulations pertaining to the encapsulation of ^{90}Sr, which ultimately decays to ^{90}Zr. If the desired end state of a ^{90}Sr waste form is $^{90}ZrO_2$ (the pronounced stability of which is well known), we have found that this phase will form if the starting compound is SrO_2. And although SrO_2 is not the preferred structure for Sr oxide (which prefers to be a 2+ cation, therefore SrO is preferred), it can be readily synthesized and perhaps has acceptable properties. However, and again, this is a demonstrative example of a new paradigm for waste form design rather than a suggestion for a ^{90}Sr waste form. Indeed, a simple definition of desired end state, though novel, is an over simplification. However, from these preliminary simulations, there are hints that compounds of interest should be complex oxides such as $A_5B_3O_{12}$ garnets or $A_4B_3O_{12}$ δ–phase. These compounds are already known to be radiation tolerant, and may exhibit the chemical flexibility required to withstand chemical transmutation during the entire life of the waste form. In any case, this approach allows for predictability not available via the current approach or via vitrification in to glass waste forms, which are, of course, inherently metastable.

Scientific Approach and Accomplishments

For this feasibility project, we have focused on validating

the effect of radioparagenesis. Three significant accomplishments were made during the course of this project. This first step was to identify and design a feasible experiment. Recall, the relevant experiments for actual fission products of interest would require at least 100 years. During our FY10 feasibility project, we have designed and commenced an accelerated experiment using ^{109}Cd to validate the phenomenon of radioparagenesis. We explicitly note that $^{\boldsymbol{109}}$Cd is neither a fission product of any relevance, nor a surrogate for any particular fission product. It is, however, an ideal isotope for the verification of radioparagenesis, for the following reasons :

- it has a half life conducive to an LDRD project (461 days),
- the resulting daughter product, ^{109}Ag, is chemically distinct from Cd (e.g. Ag cations are rigidly 1+, while Cd cations are 2+),
- ^{109}Cd decays via electron capture, resulting in no recoil damage to the crystal structure,
- only moderately high energy gamma radiation (88keV) is produced during decay allowing for samples of measureable quantity and manageable radioactivity, ***i.e.*** 500 µg ~ 1Ci, and
- $^{\boldsymbol{109}}$Cd is readily synthesized via proton irradiation of indium at the Isotope Production Facility (IPF).

To date, a measureable quantity of ^{109}Cd has been produced via a 7-day proton irradiation of natural indium and converted to ^{109}CdS. Furthermore, a plan for structural characterization relying on X-ray diffraction has been devised and is described in the next paragraph.

The second accomplishment of this project was the actual synthesis of $^{\boldsymbol{109}}$CdS and a corresponding characterization plan. For the production of hundreds of µg quantities of Cd-109, an indium target must be irradiated at IPF with an intense 100 MeV proton beam. An inconel encapsulated indium target was fabricated for this purpose and irradiated in the high energy slot at IPF during August of 2009, utilizing the proton energy range between 92 MeV and 72 MeV. The full beam power available at IPF was used and an integrated beam charge of 42,000 µAh was accumulated on the target in the one-week irradiation. A total of 1.34 Curies of Cd-109 was produced in the target at the end of bombardment (EOB), translating into a production approximately 500 µg of Cd-109 atoms. Figure 2 shows a picture taken in the hot cell of the ring-shaped burn mark on the target caused by the high intensity proton beam.

The target was transported in a Type B container to the TA-48 hot cells for chemical processing during which the target was punctured, heated, and the molten indium was dissolved in concentrated hydrochloric acid. The solution was purified using a series of ion-exchange columns. CdS was precipitated from the solution of cadmium chloride using ammonium sulfide. After allowing the powder to sit for a week, it turned from a light yellow color (the cubic hawleyite form) to an orange yellow (the hexagonal greenockite form). The solid was vacuum filtered onto a black 0.2 um polycarbonate membrane which was placed into an XRD holder that had a stainless steel bottom section and a beryllium dome and allowed to dry overnight. The sample holder was sealed, removed from the hot cell, and brought to the XRD for analysis.

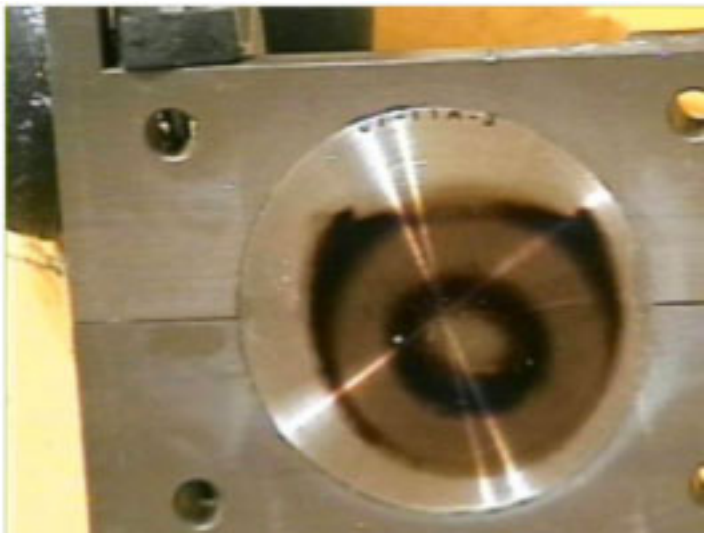

Figure 2. In-hot-cell picture of the 2" diameter encapsulated indium target after irradiation.

The optimal diffraction configuration including detector, monochromators, slits, shielding, sample holder, and sample loading logistics were determined. Several cold mock up samples of CdS were run to determine these parameters. In addition, the initial attempt at obtaining a diffraction pattern from the radioactive CdS sample yielded valuable information regarding the background of the gamma radiation measured at the NaI(Tl) scintillation detector[1]. The result of these experiments led to a configuration where diffraction intensity and resolution were optimized, while minimizing the background effects from the gamma radiation. This initial work also included the development of the safety envelope including procedures and radiological work permit. All diffraction experiments were run on a Bruker D8 discover with CuKa radiation (Gobel mirror) and NaI(Tl) scintillation detector.

Three attempts were made to observe diffraction from the radioactive CdS sample. The sample on a filter paper was mounted on a round aluminum stub inside a stainless steel cup and capped with an x-ray transparent beryllium dome. The first attempt assumed the sample was at the center of the holder, and at the proper height. Diffraction was not observed, and a step in the background pattern showed the sample to be too low. A second attempt at the correct height didn't show diffraction either. The final attempt scanned the x-ray beam over the entire sample holder

surface in order to find the sample, but no diffraction was observed. The aluminum peaks from the sample holder were also not observed in any of the three attempts. The lack of the aluminum peaks, which were observed on a blank sample holder and filter paper, suggest the sample is in place and blocking the x-rays from the aluminum. This would suggest the sample is not polycrystalline. It must also be considered that the x-ray diffraction signal was less than the background from the gamma radiation, and is lost in the noise. Finally, a significant portion of the sample may have flaked off the filter paper leaving too small a portion to observe diffraction, but enough to prevent diffraction from the aluminum holder.

Our final accomplishment was to use density functional theory (DFT) to predict the evolution of the $Cd_{1-x}Ag_xS$ experiment. Indeed, DFT is the only viable approach to consider the effects of chemical evolution on crystalline stability (*i.e.* empirical potentials cannot be derived for compounds that exhibit such great change in chemical environment). In this project, we have performed calculations, illustrated in Figure 3, that show the formation of a heretofore unobserved rocksalt phase at ~1 half-life.

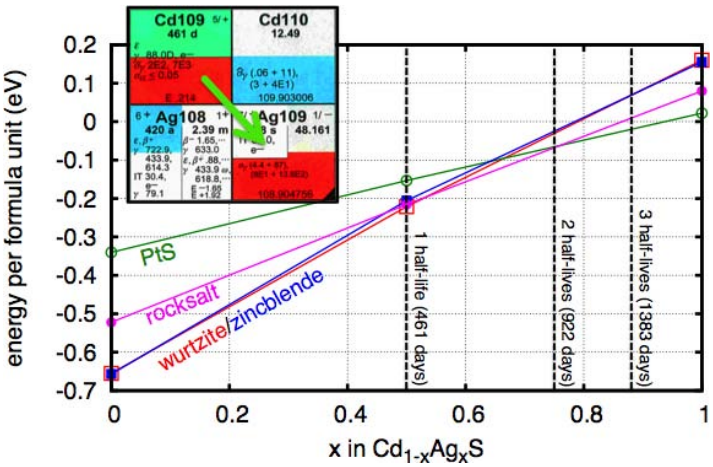

Figure 3. DFT results for Cd1-xAgxS showing the preference of the rocksalt structure at ~1 half-life. The Cd-109 decay is shown in the inset.

Although we have not yet validated radioparagenesis, we have taken large steps toward designing and performing the challenging experiments required for validation. We were fortunate to transition this feasibility project in to a successful LDRD-DR proposal. Therefore, through this feasibility project, we have a "running start."

Impact on National Missions

Since this was only a feasibility project, and although our motivation is solutions to the nuclear waste problem, we focused our effort on demonstrating the viability of our idea and converting it in to an LDRD-DR program. The DR project will open a new route for the design of robust waste forms, thus positioning LANL at the forefront of the competition for DOE-NE programs and for a leadership role in the international nuclear waste community. To specifically facilitate the development of DOE-NE programs, Sara Scott (Director of Civilian Nuclear Programs) has agreed to mentor this project. We will proactively apprise the Fuel Cycle Research and Development (FCRD, previously GNEP and AFCI) program of our progress, as one of their eight stated FY11 goals is to *"Continue to develop alternative waste forms that are tailored to specific radionuclides and potential geologic media."* Longer-term, we foresee this project potentially contributing to the Fission Fusion Materials Facility (FFMF) of MaRIE via a Center for Nuclear Waste Solutions - since all components of a facility of this type uniquely reside at LANL, and near to FFMF.

Publications

Jiang, C., B. P. Uberuaga, K. E. Sickafus, F. M. Nortier, J. J. Kitten, N. A. Marks, and C. R. Stanek. Using "radioparagenesis" to design robust nuclear waste forms. 2010. *ENERGY & ENVIRONMENTAL SCIENCE.* **3** (1): 130.

Jiang, C., C. R. Stanek, N. A. Marks, K. E. Sickafus, and B. P. Uberuaga. Predicting from first principles the chemical evolution of crystalline compounds due to radioactive decay: The case of the transformation of CsCl to BaCl. 2009. *PHYSICAL REVIEW B.* **79** (13): 132110.

Jiang, C., C. Stanek, N. Marks, K. Sickafus, and B. Uberuaga. Radioparagenesis: The formation of novel compounds and crystalline structures via radioactive decay. 2010. *PHILOSOPHICAL MAGAZINE LETTERS.* **90** (6): 435.

A Predictive Molecular Site-Specific Natural Abundance Isotopic Signature Capability for Attribution of Chemical, Nuclear, and Biochemical Threats

Toti E. Larson
20100543ER

Abstract

Our research has the ultimate goal of identifying atomical site-specific stable isotope signatures in organic and inorganic molecules. We hypothesized that unique stable isotope signatures from particular molecular sites can address many forensics needs by uniquely tracking and reporting the molecule's environmental history. Full or even partial development of this research will find direct application in nuclear, chemical, and biological threat forensics applications. This research offers significant advances over current isotope ratio mass spectrometry (IRMS) techniques that focus primarily on large primary kinetic isotope effects (PKIE) that occur during the formation or breakage of covalent bonds in a molecule. In contrast, our proposed technique will probe all sites in a molecule, allowing us to also monitor non-covalent isotope effects (NCIE) that result from chemical processes that do not involve covalent bond formation or breakage. Examples of processes that result in NCIE include distillation, liquid-liquid extraction, liquid-solid adsorption, and gas-solid adsorption. Here we conducted a series of experiments specifically designed to probe NCIE associated with three of these processes. Samples were analyzed using quantitative ^{13}C Site-specific Natural abundance Isotope Fractionation Nuclear Magnetic Resonance spectroscopy (SNIF-NMR) and d^{13}C compound-specific isotope ratio mass spectrometry (CS-IRMS). Results from this research demonstrate that we have the needed precision for the quantitative measurement of natural abundance carbon isotope variations at the molecular site-specific level that result from NCIE. We have demonstrated that the complex inter-molecular interactions in non-ideal solutions do indeed affect the site-specific isotope distributions in molecules, an observation that is only possible using our SNIF-NMR techniques. These results form the basis needed to demonstrate how one could use SNIF-NMR to develop a more robust forensics attribution tool.

Background and Research Objectives

Natural abundance Isotope Ratio Mass Spectrometry (IRMS) has been utilized as a forensics attribution tool to determine the geographical origin of illicit drugs [1], micro-organisms [2], humans and animals [3], and to associate links between starting materials/products of the synthesis of illicit drugs [4] or high-explosives [5]. These last two approaches rely on large Primary Kinetic Isotope Effects (PKIE) that occur during chemical bond cleavage and formation. Although a carbon isotope link was established between the high explosive RDX and a precursor material, hexamine, it was recognized that the global carbon isotope value is affected by at least three variables: the PKIE related to C-N bond cleavage/formation, incomplete reaction, and the starting global IRMS carbon isotope value of the hexamine. This demonstrates the inherent limitation of using a single IRMS ratio measurement when attempting to attribute multi-step, multivariate, and complex processes typically used to process (synthesize, isolate, and purify) chemical, biochemical, and nuclear materials.

The key requirement for accurate forensics attribution lies in the ability to differentiate subtle differences in processing techniques while simultaneously identifying the overall batch production pathways. Inter- and intramolecular interactions that occur during processing are directly responsible for Non-Covalent Isotope Effects (NCIE). To observe and interpret NCIE it is necessary to measure stable isotope fractionations at the site-specific (atomical) level. Knowledge of site-specific fractionations will provide a new and robust forensics tool for attribution.

Quantitative ^{13}C Site-specific Natural abundance Isotope Fractionation Nuclear Magnetic Resonance spectroscopy (SNIF-NMR) and Compound Specific IRMS (CS-IRMS) have the needed precision to measure NCIE and PKIE in the same molecule. We therefore have the capability to develop a forensic tool that attributes threats by identifying unique molecular fingerprints imposed by the processes of chemical synthesis, isolation, compounding, and/or purifying. Consequently, we conducted a feasibility study and demonstrated that site-specific stable isotope signatures caused by NCIE are interpretable, robust, and diagnostic of a specific process. We initially proposed to investigate potential NCIE associated with chemical reactions that are used in nuclear processing

of plutonium as well as reactions associated with the well-known Arbuzov chemical reaction that is used in the synthesis of Dichlor, a common precursor in the synthesis of high priority chemical warfare agents. Upon the comments of several reviewers and considering the complexity associated with these experiments, we simplified our experimental design to explore NCIE associated with three specific types of non-covalent interactions: gas-solid, gas-liquid, and liquid-liquid. Importantly, the physical processes that we studied bracket the physical processes associated with plutonium processing, making our research applicable to nuclear forensics applications. This simpler design allowed us to explore, in much greater detail, site-specific isotope effects that result from non-ideal interactions between different compounds. The objective is to use resulting site-specific isotope effects to probe inter- and intra-molecular interactions between different chemical functional groups.

This objective is aligned with the overall scientific goal of developing a fundamental understanding of the physical chemical principles that influence and/or control the "communication effects in isotopic fractionation" resulting in NCIE. We believe that solving these objectives will allow us to measure and interpret accurately unique signatures that address many forensics capability needs. Our overarching hypothesis is that an understanding of the theoretical basis that causes atomical isotopic fractionation will provide a predictive forensic tool to attribute threats by identifying unique molecular fingerprints imposed by the processes of synthesizing, isolating, compounding, and/or purifying. Thus answering questions such as, but not limited to: What types of purification techniques were applied? What temperature specific steps of the reaction pathway were conducted? What reaction yield was obtained? What type of chemical or biochemical reactor was employed during production? What is the country or location of origin of solvents and reagents used in the processing technique (geolocation)? How long were the materials stored prior to deployment (degree of degradation)?

Scientific Approach and Accomplishments

We conducted a series of experiments that were specifically designed to probe three different physical systems that can exhibit site-specific isotopic fractionation: 1) adsorption (gas-solid), 2) distillation (gas-liquid), and 3) extraction (liquid-liquid). These three systems compliment the liquid-solid adsorption system reported by Botosoa, et. al. [6] that showed "unexpected fractionation in site-specific ^{13}C isotopic distribution". These experiments were conducted at Los Alamos National Laboratory and samples were collected for stable isotope measurement. Due to restrictions of analysis time for the quantitative ^{13}C Site-specific Natural abundance Isotope Fractionation Nuclear Magnetic Resonance spectroscopy (SNIF-NMR), subsets of samples from each experimental suite were measured using SNIF-NMR. All samples collected were measured using d^{13}C compound-specific isotope ratio mass spectrometry (CS-IRMS), since this technique has a much higher throughput. The key difference with these measurement techniques is that SNIF-NMR measures the $\delta^{13}C$ value of carbon at each molecular site whereas CS-IRMS averages the $\delta^{13}C$ of all carbons in a molecule.

Adsorption (gas-solid phase): The interaction between a gas and a solid phase was probed for NCIE using simple capillary column gas chromatography. The difference in elution time of $^{13}CO_2$ relative to $^{12}CO_2$ as a result of CO_2 flow through a packed (sample gas) or unpacked (reference gas) capillary column was measured using IRMS techniques. Masses 44, 45, and 46 were analyzed in continuous time series by IRMS (Figure 1). Mass 45 CO_2, composed primarily of $C^{13}O^{16}O^{16}$, elutes before mass 44 CO_2 composed of $C^{12}O^{16}O^{16}$. This suggests that non-covalent surface interactions between CO_2 and the solid substrate result in NCIE. Mass 46 CO_2, composed primarily of $C^{12}O^{16}O^{18}$, also shows multiple positive excursions. As of this writing, a complete analysis of the actual adsorption interactions between CO_2 and the solid substrate has not been conducted, which will be required to explain the meaning of these differences. Regardless, this reproducible effect could be computationally modeled rigorously due to the tractability of the small CO_2 molecule on a solid surface.

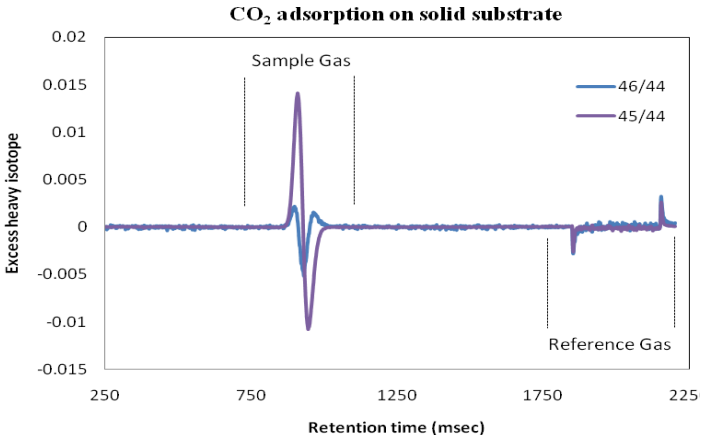

Figure 1. Gas-solid adsorption of 12CO_2 resulting in faster elution of 13CO_2 while reference shows no retention difference in unpacked column.

Distillation (gas-liquid phase): Azeotropic solutions were selected because they are non-ideal mixtures that deviate from Raoult's Law. The two ternary azeotropes shown in Figure 2 are constant boiling solutions that exhibit identical vapor and liquid phase compositions (verified by monitoring the temperature during the distillations). In other words, an azeotrope cannot be separated by distillation, unlike more common mixtures (for example, the alcohol/water mashes separated by moonshiners). Consequently, isotopic fractionation during distillation is not due to temperature effects. Thus, by measuring the changes in carbon isotope ratios during distillation of azeotrope mixtures we can probe any isotope fractionation that results from the inter-molecular interactions that vary from site to site

(Figure 2). Non-ideal solutions, such as these azeotropes, have not been effectively computationally modeled – the problem is intractable due to the large number of potential inter-molecular interactions. We contend that site-specific carbon fractionation will provide the tool that will allow computational models to be constructed for these complex interactions.

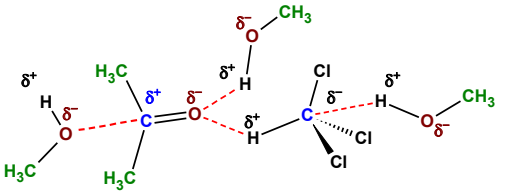

Acetone / Chloroform / Methanol - Saddle Point Azeotrope
46.7 / 23.4 / 29.9 (% Liquid and Vapor Composition at BP = 48.9 ^{0}C)

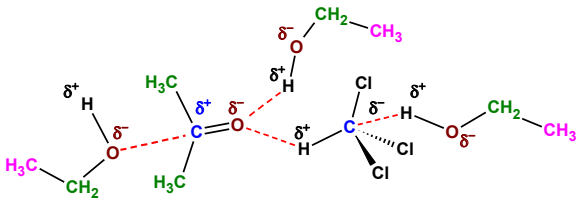

Acetone / Chloroform / Ethanol - Positive Azeotrope
65.3 / 10.4 / 24.3 (% Liquid and Vapor Composition at BP = 52.6 ^{0}C)

Figure 2. Non-ideal solutions to probe site-specific fractionations caused by molecular interactions. d13C fractionation expected to show blue carbons > green carbons > pink carbons.

Figure 3 shows the results we measured from distillation of the azeotropes and the pure components. While we expected to see isotopic fractionation caused by the distillation of the azeotropes, we did not anticipate such large fractionation from either ethanol, where both carbons show a Δ $\delta^{13}C/^{12}C$ >12 ‰, or methanol, where the single carbon shows a Δ $\delta^{13}C/^{12}C$ >5 ‰. In contrast, when we distilled pure ethanol and methanol, the enrichment of ^{13}C was much reduced. Almost 60 years ago, Baertsch, Kuhn, and Kuhn showed in a 1953 Nature paper [7] that distillations of methanol and chloroform "surprisingly" enrich the heavier ^{13}C isotope, while other heavy isotopes (^{18}O and ^{37}Cl) enrich in the still pot. They offer as explanation for this fractionation effect "the possible existence of a general rule stating that, in isotopic molecules having a central atom, the molecular variety containing the heavier isotope of the central atom will exhibit a somewhat higher vapor pressure than the variety containing the lighter isotope as central atom." Fifty years later, in 2003, Wang and Huang [8] repeated the distillation of methanol and ethanol and discussed the "inverse" ^{13}C and ^{2}H isotope fractionation where compounds containing enriched ^{13}C and ^{2}H preferentially evaporate and concluded that hydrogen bonding must play a role [8]. While a higher vapor pressure for the heavier isotope has been postulated to be due to a smaller intermolecular binding energy in the liquid phase [7,9] there is no clear explanation for the large increase in ^{13}C enrichment for the ethanol or methanol azeotrope. It is our contention that site-specific fractionation data will provide the information necessary to derive a full understanding of these phenomena. For example, in the distillation of ethanol there is difference in enrichment from site to site: the global enrichment between still pot and the vapor is Δ $\delta^{13}C/^{12}C$ = 4.2 ‰, but CH_3 group shows a Δ $\delta^{13}C/^{12}C$ = 2.1‰ and the CH_2 shows three times as much enrichment at Δ $\delta^{13}C/^{12}C$ = 6.3‰.

Extraction (liquid-liquid phase)

Liquid-liquid extraction is a critical conponent of the Plutonium-Uranium Extraction (PUREX) process used in nuclear reprocessing. We conducted a liquid-liquid extraction of two immicible fluids, acetonitrile and pentane. To determine if the hydrophobic interactions between the C_5H_{12} (pentane) and CH_3CN (acetonitrile) will show an isotopic fractionation, acetonitrile was extracted with fresh pentane five separate times, and each extraction was measured for $\delta^{13}C/^{12}C$ using IRMS. The change between initial acetonitrile ($\delta^{13}C/^{12}C$ = -12.23±0.12‰) and acetonitrile after five extractions was Δ= -0.37; whereas the change between the intial pentane ($\delta^{13}C/^{12}C$ = -19.55±0.15‰) and processed pentane was Δ= 0.91. This indicates that the acetonitrile became enriched in ^{12}C while the pentane became enriched in ^{13}C. Thus, hydrophobic inter-molecular interactions between the pentane and acetonitrile cause an apparent isotopic fractionation; albeit, under the conditions of this preliminary experiment, a considerably smaller effect than that observed in the azeotropic distillations.

Impact on National Missions

This research supports a broad range of national security programs, and strengthens LANL's core mission of reducing global threats and solving emerging national security challenges through innovative science-based prediction and development of signatures that can be used in the attribution of current and future threats. Full, or even partial, development of the proposed research will find direct application in nuclear, chemical, and biological threat forensics application as well as to significant commercial prospects and IP potential when used in product identification and/or protection (*i.e.*, generic vs. patented pharmaceuticals or commodities). The process of NCIE is so fundamental in nature that any interaction among materials can be probed and tools developed to describe cause and effect. We have intentionally chosen "process and material" broadly as the proposed research can impact basic science for other applications in LANL's portfolio to study interactions in material, chemical, biological and physical sciences.

References

1. Galimov, E., V. Sevastyanov, E. Kulbachevskaya, and A. Golyavin. Isotope ratio mass spectrometry: d13C and d15N analysis for tracing the origin of illicit drugs. 2005. *Rapid communications in mass spectrometry.* **19**: 1213.

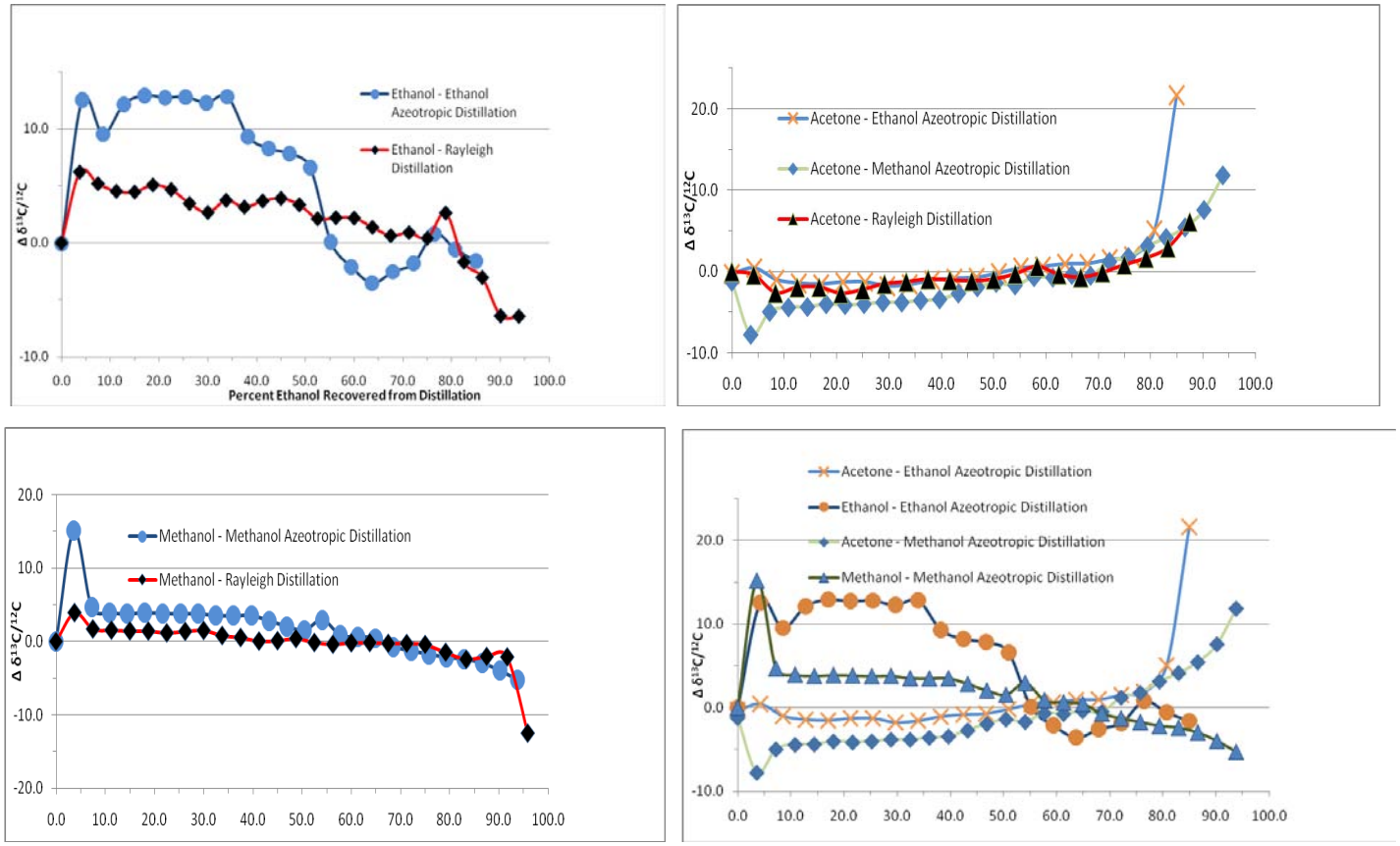

Figure 3. Azeotropic and Rayleigh distillations showing the change in δ13C for ethanol, acetone, and methanol versus per cent recovered. Bottom right compares the acetone:chloroform:ethanol (65.3:10.4:24.3 wt%, BP 52.6 oC) azeotrope to the acetone:chloroform:methanol (46.7:23.4:29.9 wt%, BP 48.9 oC) azetrope.

2. Kreuzer-Martin, H., M. Lott, J. Dorigan, and J. Ehleringer. Microbe forensics: Oxygen and hydrogen stable isotope ratios in Bacillus subtilis cells and spores. 2003. *Proceeding of the National Academy of Sciences of the United States of America.* **3**: 815.

3. Ehleringer, J. R., G. J. Bowen, L. A. Chesson, A. G. West, D. W. Podlesak, and T. E. Cerling. From the Cover: Hydrogen and oxygen isotope ratios in human hair are related to geography. 2008. *Proceedings of the National Academy of Sciences.* **105** (8): 2788.

4. Carter, J., E. Titterton, M. Murray, and R. Sleeman. Isotopic characterisation of 3,4-methylenedioxyamphetamine and 3,4-methylenedioxymethylamphetamine (ecstasy). 2002. *Analyst.* **127**: 830.

5. Lock, Claire M., and . . Investigation of isotopic linkage between precursor and product in the synthesis of a high explosive. 2008. *Forensic Science International.* **179**: 157.

6. Botosoa, E. P., E. Caytan, V. Silvestre, R. J. Robins, S. Akoka, and G. S. Remaud. Unexpected Fractionation in Site-Specific 13C Isotopic Distribution Detected by Quantitative 13C NMR at Natural Abundance. 2007. *Journal of the American Chemical Society.* **130** (2): 414.

7. Baertschi, P., W. Kuhn, and H. Kuhn. Fractionation of isotopes by distillation of some organic substances. 1953. *Nature.* **171**: 1018.

8. Wang, Y., and Y. Huang. Hydrogen isotopic fractionation of petroleum hydrocarbons during vaporization: Implications for assessing artificial and natural remediation of petroleum contamination . 2003. *Applied Geochemistry.* **18**: 1641.

9. Grootes, P. M., W. G. Mook, and J. C. Vogel. Isotopic fractionation between gaseous and condensed carbon dioxide. 1969. *Zeitschrift für Physik A Hadrons and Nuclei.* **221** (3): 257.

Publications

Larson, T., J. Fessenden, and J. Heikoop. Differentiating nuclear processing from multiple sources of anthropogenic nitrate in a complex groundwater system using dual isotope systematics. Invited presentation at *Forensic Isotope Ratio Mass Spectrometry.* (washington, D.C., 11-14 April 2010).

Polaron Dynamics of Hypervalent Urania and Other Complex Materials

Steven D. Conradson
20100545ER

Abstract

The interesting properties of some complex functional materials originate in "polarons," charge defects around which the atoms are displaced from their positions in the crystal lattice. We had previously obtained indirect evidence from structural studies that hypervalent urania, UO_{2+x}, an extensively studied industrial chemical used as nuclear fuel, possessed what appeared to be the most radical dynamical polaron in any material. Ultrafast pump-probe optical reflectivity measurements on UO_2 have now confirmed that the initial, optically induced, charge-separated state relaxes via a thermally activated path within 1–3 psec into an intra-gap state, consistent with the substantial rearrangement of the neighboring atoms characteristic of a polaron. This polaron then exhibits a 20–170 psec relaxation mode coupled to the spin ordering and a 0.5–3 μsec relaxation mode that displays unusual temperature dependence, implying a complicated mechanism consistent with an unusual polaron. These results corroborate the behavior observed with chemical doping. DFT calculations compared with O K edge X-ray Absorption Spectroscopy (XAS) measurements confirm that these remarkable behaviors also affect the electronic structure, which is predicted for dynamical polarons. In addition, the same optical measurements applied to $SrTiO_3$, which possesses a super-paraelectric type polaron, give analogous results. We have therefore met the objectives of this project, to be well positioned to perform effective, time resolved x-ray scattering experiments at a synchrotron that will help elucidate the structures of these optically-induced polarons for comparison with the static ones in $UO_{2=x}$ compounds made by adding excess O to UO_2.

Background and Research Objectives

Many of the properties of scientifically intriguing and technologically valuable complex materials are likely to originate in atomic scale inhomogeneities or defects that are dynamical, i.e., in motion rather than immobilized at a specific site in the crystal lattice, or that interact strongly with each other so as to promote collective and cooperative behavior. When these two properties occur simultaneously, their combination can result in the aggregation of the inhomogeneities into transitory, self-organized, nanoscale structures, a phenomenon that we have termed "nanoscale heterogeneity" because it involves the formation of a second ordered structure within the host lattice. These properties are poorly understood because they involve the transport or percolation between atoms of charge, spin, displacements, energy, and other properties that, although localized on atoms in these compounds, nevertheless modify the interatomic interactions within sets of thousands or even millions of atoms, far exceeding our current modeling capabilities. It is therefore important to identify the range and scope of these behaviors in the mid-range between good/conventional metals that possess freely itinerant electrons that tend to distribute or delocalize these properties throughout the material, and insulators that trap the excess charge, spin, etc. very deeply on the defects. The light actinides are good candidates for this purpose because of their position at the crossover between localized electronic behavior that promotes, e.g., paramagnetism, and itinerant behavior that produces, e.g., ferromagnetism and superconductivity.

The motivation for this project was also described by the words of a participant at a Materials Guiding Coalition workshop on emergent phenomena; "The future of condensed matter is measuring ultrashort length scales on ultrafast time scales." This statement summarizes two of the Office of Basic Energy Science Grand Challenges, understanding the properties of matter that emerge from complex correlations and characterizing fluctuations and matter far from equilibrium. This project was intended to address these issues by converging three areas of current interest to science and the laboratory – correlated materials, actinides, and dynamical processes in condensed matter – with the ultimate goal of elucidating the structures involved in dynamical processes on the atomic and nanometer length scales, especially those associated with collective phenomena in complex materials.

The scientific basis for this is the failure of conventional approaches to explain many of the compelling characteristics of complex matter. One of the most important

of these both scientifically and technologically is the quasiparticle called a polaron, the combination of a charge defect and its associated lattice distortion, that often occurs in mixed valence oxides and when mobile results in unusual properties such as high temperature superconductivity. It is likely that these phenomena still defy description because their complex behaviors originate not in their static aspects but instead in the dynamical aspects of the interactions of their intrinsic inhomogeneities with the host lattice and each other. These interactions are the critical ones because they drive the aggregation and self-organization of the inhomogeneities into larger, transitory structures, thus giving a novel conceptual image of complex matter in which its constantly shifting patterns almost animate it, analogous to biomolecules.

Scientific Approach and Accomplishments

We have recently discovered that the most extreme example of a dynamical, collective, multi-site distribution occurs in hypervalent urania – UO_{2+x}, $0 \le x \le 0.33$, a chemical that has been extensively studied for 60 years and which has an average annual production of around 40 ktonnes because it is fuel for nuclear reactors. Our understanding of the structural chemistry of UO_{2+x} has been tumultuous since our XAFS results [1] showing U(VI) sites with 1.7 Å U-O bonds like the highly oblate trans dioxo complexes in high valence molecular complexes contradicted 40 years of neutron scattering [2, 3] that had indicated much more symmetric U(V) sites ($U\text{-}O_{min}$>2.15Å) as occur in some ternary uranates. We have now solved this problem by showing (Figure 1) that x-ray pdf corroborates the broad, multisite U-O XAFS results whereas our neutron data on exactly the same samples gave the literature values. This ostensible contradiction is, however, known to actually indicate that the U-O distribution for x>0 is dynamical, involving tunneling of the atoms involved between the sites for multiple, nearly degenerate configurations [4,5]. We find that the U(IV) O=U(VI)=O polaron in UO_{2+x} is much more radical than the O^{2-}-Cu(II)-O^{-} one in cuprates [4,5]. It involves two electrons on 5–6 atoms instead of just one electron on three atoms, the enormous 30% range requires a total change in the bonding, and the overall site geometry changes from spherical with 8–12 near neighbors to highly oblate with 6–8 neighbors. Another conundrum is the absence of inhomogeneous broadening in O K XAS spectra (Figure 2); electronic homogeneity concomitant with crystallographic disorder is a rare or possibly unique phenomenon.

The research plan was intended to meet three overlapping objectives: to perform the additional measurements and calculations on the defects and their dynamical properties in UO_{2+x} required to credibly extend this work to time resolved x-ray measurements – primarily characterization of the time scales of interest; to expand the scope of the techniques being applied by adding Inelastic Neutron Scattering (INS) and time resolved pump-probe optical measurements; and to add to our knowledge of and expertise with dynamical correlated systems by performing experiments on additional materials. Reportable results were obtained for the first and third of these. The original structural measurements were performed on chemically-doped UO_2, adding adventitious O to give UO_{2+x} whose charge inhomogeneities resulting from the mixed valence form polarons. Polarons can also be created in pure, homogeneous materials by optical pumping. This creates charge-separated excited polaronic states that, if the displacement of atoms around the charge lowers the energy into the band gap of the original structure, will be stabilized. If the polarons in the chemically doped compounds are unusual then the optically induced ones should exhibit analogous properties, motivating experiments on these systems to complement those on the chemically doped ones.

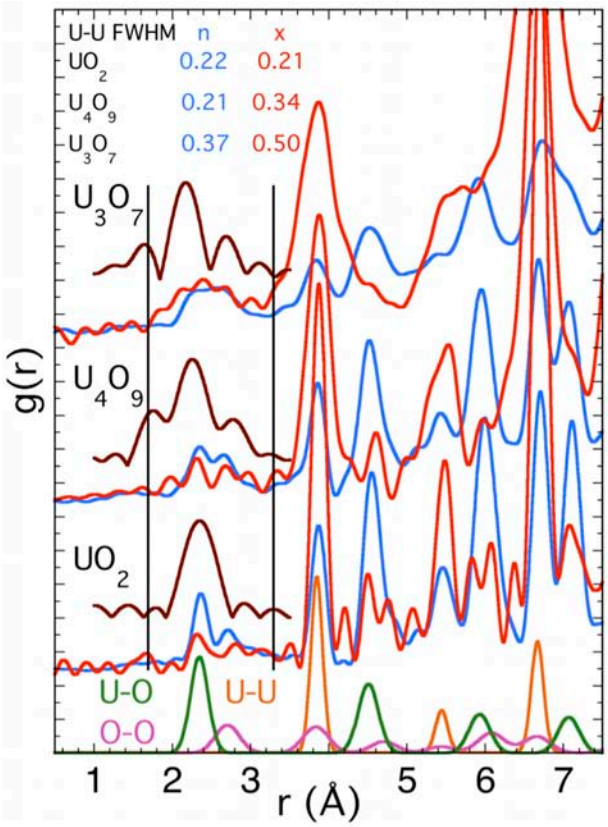

Figure 1. Neutron (blue) and x-ray (red) pair distribution functions and phase-corrected χ(R) EXAFS moduli at 30 K (brown) of indicated compounds, plus the partial neutron pdfs from UO_2 (bottom) for identifying the shells. The vertical lines at 1.7 and 3.3 Å bracket the U-O distances found by the x-ray measurements. The amplitude relative to the largest peak and the spacing of the "ripple" produced by the use of square windows in calculating χ(R) from the phase-corrected spectra are demonstrated by the UO_2 spectrum; features in the other EXAFS spectra that have larger amplitudes relative to the primary U-O peak and different intervals between peaks must originate in U-O pairs. The widths of the U-U pair at 3.8 Å from neutrons and x-rays are listed at the top.

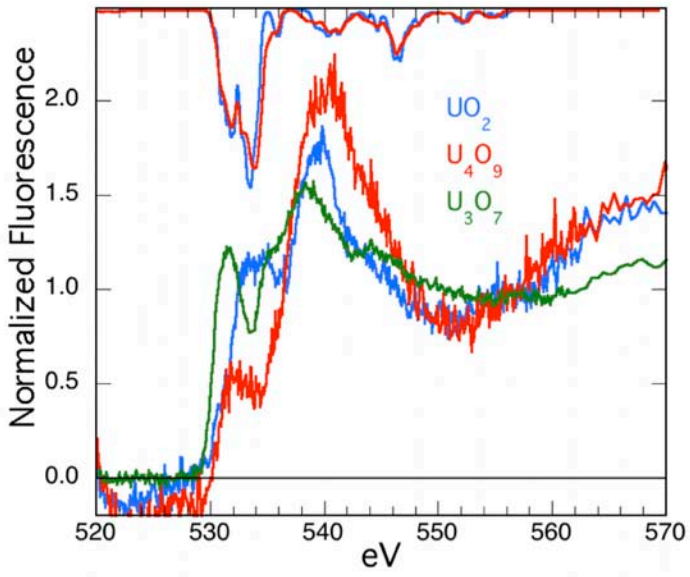

Figure 2. Fluorescence O K edge XAS of indicated compounds. These spectra were corrected for self-absorbance by comparison with NRIXS data. Inverted at the top are the densities of states from DFT calculations for UO_2 and UO_2+x that include extra O atoms that are arranged as the quad interstitial defects but that are locally very similar to the O positions for the cuboctahedral cluster.

Direct measurement of optically-induced polaron in UO_2 single crystal

Femtosecond (fsec) pump-probe reflectivity measurements revealed ultrafast hopping dynamics of photoexcited 5f electrons in UO_2. Fsec pump-probe techniques access the full scope of processes, the formation of the original charge separated state, its relaxation to a polaron, and the ultimate loss of the polaron by recombination of the photoelectron and its hole. By varying the time delay between the pump and probe pulses that are split from a 250-kHz, 80-fs pulsed laser, transient reflectivity, $\Delta R/R$, was measured at 5-300 K. The 1.5-eV and 3-eV $\Delta R/R$ show the electron and lattice dynamics (Figure 3). These show that 5f electrons instantly hop to neighbor U sites where the psec rise times of the intra-band relaxation indicate that they presumably effect the lattice deformation that is the signature of a polaron. The sign flip of $\Delta R/R$ at the magnetic transition temperature at 31 K demonstrates that the binding of U^{3+}-U^{5+} is magnetic-ordering mediated, indicating that the pairs are Hubbard excitons. Half-frequency oscillations as shown in the inset confirm the presence of coherent acoustic phonons following photoexcitation. The spin-independent relaxation channel of this mid-gap state that we presume is a polaron is found to be on µsec time scales at low temperatures compared with psec to nsec typical for such polarons in transition metals. Longer lifetimes are associated with polarons that become bound to defects. Since these measurements were performed on a highly ordered single crystal is it likely that the long lifetimes result from interactions of two or more polarons, analogous to the clustering of the adventitious O atoms in chemically doped material.

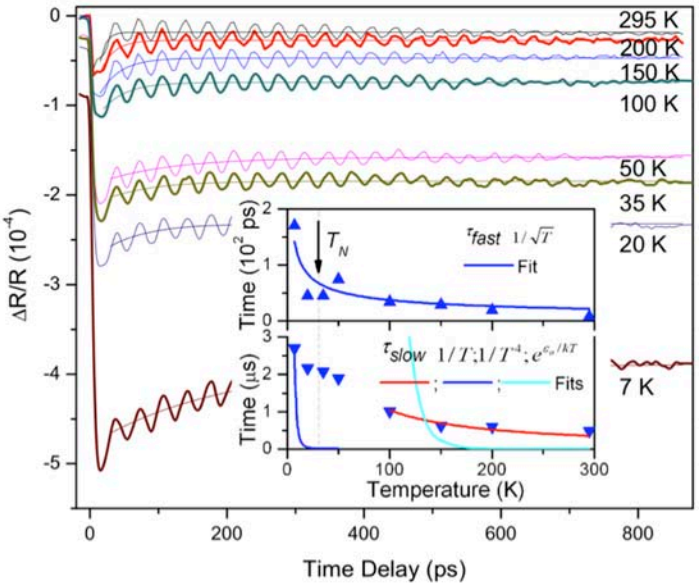

Figure 3. Optical reflectivity of UO_2 crystal at 1.55 eV within the gap at indicated temperatures and times following a 3.1 eV pump pulse into the conduction band. Insets show the (upper) fast and (lower) slow relaxation times as a function of temperature, fit with the indicated functional forms.

Modeling of defects in UO_{2+x}.

In previous theoretical studies [7] we investigated the structure of UO_{2+x} using density functional theory (DFT) calculations. Our simulations were unable to identify any U-O bonds shorter than ≈2.2 Å, partially contradicting the EXAFS results. In order to better understand this discrepancy we expanded our initial static calculations by running *ab initio* molecular dynamics simulations at select temperatures, subsequently probing the dynamical UO_{2+x} structure. These simulations showed the expected broadening of the static atomic pair distribution functions, but U-O bonds < 2.0 Å [8]. We then studied surface oxidation of UO_2. Oxygen atoms were added to UO_2 (111) surfaces. In bulk UO_{2+x} the extra oxygen ions tend to form clusters due to favorable interactions at the electronic levels. The surface UO_{2+x} ions exhibit different bonding properties; with U-O bond lengths centered around 1.8 Å rather than the 2.2 Å found in bulk, corroborating the EXAFS. Similar properties emerge from clusters containing three or more uranium vacancies. Altogether this implies that under specific assumptions the DFT simulations reproduce the experimental EXAFS measurements. We have also shown that internal nanometer sized voids (essentially vacancy clusters) would also exhibit oxidation properties that mimic the characteristic features of (111) surfaces. Another important result from the calculations is that the electronic

structure calculated for the adventitious O arranged to give minimum bonds of 2.2 Å does not match the measurement for U_4O_9, corroborating the hypothesis of a dynamical polaron that substantially perturbs this arrangement of atoms and their electrons (Figure 2).

Investigations of dynamical polarons in other materials: $SrTiO_3$

Another important material where poorly understood polaronic effects play a crucial role is $SrTiO_3$ (STO). STO belongs to the class of perovskite oxides with Ti^{4+} ion placed in the center of O^{2-} octahedron. The Ti-O bond has a finite dipole moment and the off-center displacement of the Ti ion should lead to formation of a ferroelectric (FE) state at low temperature. It is, however, not observed because of the extreme "softness" (vibrational energy < 1meV) of this mode that causes quantum fluctuations of the position of Ti ion that exceed the separation of the two metastable ferroelectric states [9, 10]. The very small restoring force nevertheless allows a large displacement with consequent high polarizability. This quantum paraelectricity can be found in a many complex oxides. External perturbations such as strain, doping, or a strong electric field may either "harden" the associated vibrations or reduce the fluctuation amplitude of Ti ion and induce the ferroelectric transition [11, 12, 13]. For example, several groups have reported a giant, photo-induced, dielectric effect in STO in which above band-gap photo-excitation gives rise to a dramatic (~100x) increase in the dielectric constant [14, 15]. Theoretical studies attribute this dielectric enhancement to large polarons resulting from strong coupling of photo-excited electrons to the displacement. These polarons extend over ~1000 lattice sites and can be considered as transient ferroelectric domains that are responsible for the "super-paraelectric" response to externally applied electric fields.

To verify the feasibility of future x-ray measurements we applied ultrafast optical spectroscopy to indirectly probe the dynamics of the polaron formation and relaxation in STO. Figure 2 shows the temperature dependent relaxation dynamics of the polaron at 2.4 eV following above-band-gap excitation. Two different components are evident in the time-resolved signals – fast initial decay and subsequent slow relaxation. The relaxation is in the µsec regime, corresponds well with the previously observed fluorescence decay [16, 17], and can be attributed to the recombination of the self-trapped polaron state. The fast component has never been observed before and corresponds to the process happening at the few-picoseconds timescale. The decay constant of 1.5 ps is very close to the theoretically predicted 1-2 ps time interval necessary for self-trapping of an optically induced super-paraelectric polaron. The amplitude of this fast process shows the same temperature dependence (Figure 3a) as both the fluorescence coming from the polaron state (Figure 3b) and the dielectric enhancement attributed to the large polaron polarization (Figure 3c). Interestingly, all of these processes are strongly suppressed above ~ 40 K, which corresponds to the putative ferroelectric transition temperature. This behavior supports theoretical predictions that the 1.5 ps component in the time-resolved signal represents the dynamics of photo-induced large polarons.

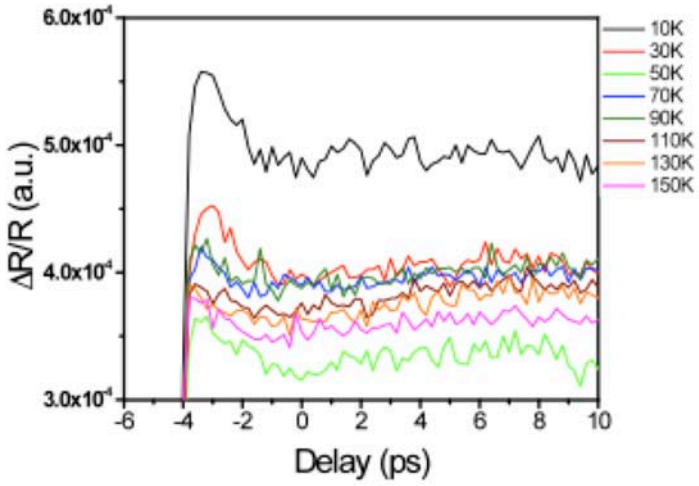

Figure 4. Temperature dependent relaxation dynamics of polaronic state in STO at 2.4 eV following above-band-gap excitation of crystal with ultrafast laser pulse.

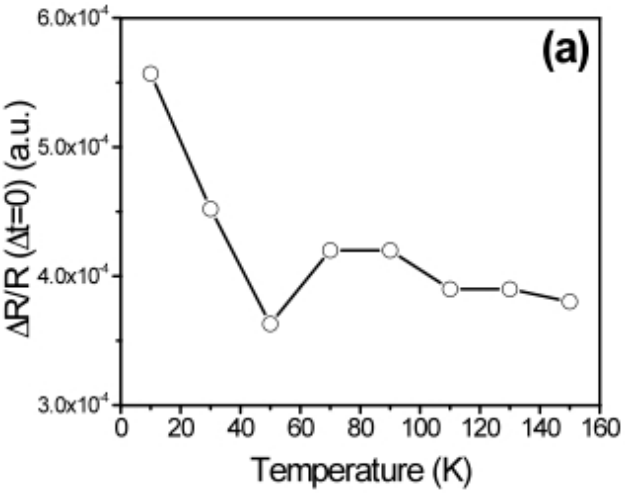

Figure 5. Temperature dependence of self trapping of super-paraelectric polaron in STO measured directly by optical reflectivity at 2.4 eV following above-the-gap excitation pulse.

Impact on National Missions

Since UO_2 and Mixed Oxide (MOX, $U_xPu_{1-x}O_2$) will be the fuel for nuclear reactors for some time into the future, improvements in performance and the associated issues of fuel fabrication, processing, and disposal as well as environmental issues and radiation effects will be dominated by the chemistry of UO_2. More accurate descriptions of this chemistry are therefore essential in future optimization. A critical issue is the extent to which this chemistry is deter-

mined by the dynamical rather than the time-averaged or static properties of the structure and speciation; the oxo species produces much more internal stress, and leaching of UO_2^{2+} from UO_{2+x} implies that the reactions can involve the transient species and are not necessarily restricted to the time average ones. This new conceptual basis for the charge distribution and resultant chemical properties in UO_{2+x}, if accepted and disseminated by the community, could have an enormous impact on atomic scale modeling of oxide fuels because the correct approach to understanding these materials is radically different than the existing, overly simplistic one. These experiments and subsequent ones that they stimulate will therefore provide critical input to improve the accuracy of the predictive models being developed by DOE's Nuclear Energy Office and its Energy Innovation Hubs. In addition, the elucidation of this extreme polaron would be expected to have a substantial impact on the physics of polarons in complex oxides and related materials.

References

1. Conradson, S. D., D. Manara, F. Wastin, D. L. Clark, G. H. Lander, L. A. Morales, J. Rebizant, and V. V. Rondinella. Local structure and charge distribution in the UO2-U4O9 system. 2004. *INORGANIC CHEMISTRY.* **43** (22): 6922.

2. Garrido, F., A. C. Hannon, R. M. Ibberson, L. Nowicki, and B. T. Willis. Neutron diffraction studies of U4O9: Comparison with EXAFS results. 2006. *INORGANIC CHEMISTRY.* **45** (20): 8408.

3. Garrido, F., L. Nowicki, and L. Thome. Channeling investigation of the crystalline structure of U<sub>4. 2006. *Physical Review B (Condensed Matter and Materials Physics).* **74** (18): 184114.

4. CONRADSON, S. D., I. D. RAISTRICK, and A. R. BISHOP. AXIAL OXYGEN CENTERED LATTICE INSTABILITIES AND HIGH-TEMPERATURE SUPERCONDUCTIVITY. 1990. *SCIENCE.* **248** (4961): 1394.

5. EGAMI, T., B. H. TOBY, S. J. BILLINGE, H. D. ROSENFELD, J. D. JORGENSEN, D. G. HINKS, B. DABROWSKI, M. A. SUBRAMANIAN, M. K. CRAWFORD, W. E. FARNETH, and E. M. MCCARRON. LOCAL STRUCTURAL ANOMALY NEAR TC OBSERVED BY PULSED NEUTRON-SCATTERING. 1991. *PHYSICA C.* **185** (2): 867.

6. SALKOLA, M. I., A. R. BISHOP, S. A. TRUGMAN, and J. M. DELEON. CORRELATION-FUNCTION ANALYSIS OF NONLINEAR AND NONADIABATIC SYSTEMS - POLARON TUNNELING. 1995. *PHYSICAL REVIEW B.* **51** (14): 8878.

7. Andersson, D. A., J. Lezama, B. P. Uberuaga, C. Deo, and S. D. Conradson. Cooperativity among defect sites in AO(2+x) and A(4)O(9) (A=U,Np,Pu): Density functional calculations. 2009. *PHYSICAL REVIEW B.* **79** (2): 024110.

8. Andersson, D. A., F. J. Espinosa-Faller, B. P. Uberuaga, and S. D. Conradson. Configurational stability and migration of large oxygen clusters in UO(2+x): Density functional theory calculations. *PHYSICAL REVIEW B.* **79** (2): 024110.

9. MULLER, K. A., and H. BURKARD. SRTIO3 - INTRINSIC QUANTUM PARA-ELECTRIC BELOW 4-K. 1979. *PHYSICAL REVIEW B.* **19** (7): 3593.

10. BEDNORZ, J. G., and K. A. MULLER. SR1-XCAXTIO3 - AN XY QUANTUM FERROELECTRIC WITH TRANSITION TO RANDOMNESS. 1984. *PHYSICAL REVIEW LETTERS.* **52** (25): 2289.

11. Haeni, J. H., P. Irvin, W. Chang, R. Uecker, P. Reiche, Y. L. Li, S. Choudhury, W. Tian, M. E. Hawley, B. Craigo, A. K. Tagantsev, X. Q. Pan, S. K. Streiffer, L. Q. Chen, S. W. Kirchoefer, J. Levy, and D. G. Schlom. Room-temperature ferroelectricity in strained SrTiO3. 2004. *NATURE.* **430** (7001): 758.

12. Ang, C., A. S. Bhalla, and L. E. Cross. Dielectric behavior of paraelectric KTaO3, CaTiO3, and (Ln(1/2)Na(1/2)) TiO3 under a dc electric field. 2001. *PHYSICAL REVIEW B.* **64** (18): 184104.

13. Itoh, M., R. Wang, Y. Inaguma, T. Yamaguchi, Y. -J. Shan, and T. Nakamura. Ferroelectricity induced by oxygen isotope exchange in strontium. 1999. *Physical Review Letters.* **82** (17): 3540.

14. Takesada, M., T. Yagi, M. Itoh, and S. Koshihara. A gigantic photoinduced dielectric constant of quantum paraelectric. 2003. *Journal of the Physical Society of Japan.* **72** (1): 37.

15. Hasegawa, T., S. Mouri, Y. Yamada, and K. Tanaka. Giant photo-induced dielectricity in SrTiO₃. 2003. *Journal of the Physical Society of Japan.* **72** (1): 41.

16. Hasegawa, T., M. Shirai, and K. Tanaka. Localizing nature of photo-excited states in SrTiO₃. 2000. In *International Conference on Luminescence and Optical Spectroscopy.* Vol. 87-89, p. 1217.

17. Hasegawa, T., and K. Tanaka. Photo-induced polaron states in strontium titanate. 2001. In *Thirteenth International Conference on Dynamical Processes in.* Vol. 94-95, p. 15.

From Sensor to Scientist: Optimizing the Delivery of Hyperspectral Information for Efficient Signature Detection

Christopher M. Brislawn
20100572ER

Abstract

This project has demonstrated that the communications bandwidth of thermal hyperspectral imagery can be reduced by at least one order of magnitude (relative to 32-bit floating point representations) using the Joint Photographic Experts Group's JPEG 2000 international image coding standard without causing an unacceptable loss of accuracy in highly demanding chemical signature exploitation tasks. This reduction is based solely on coding the data at reduced sample precision and does not include significant additional bandwidth reductions that would be possible using JPEG 2000's region-of-interest and resolution scalability features. The study was conducted using state-of-the-art operational hyperspectral airborne imaging sensors collecting data against both gas plume and solid material targets, analyzed using comparably advanced chemical signature exploitation algorithms.

This report begins with an overview of the background behind the use of hyperspectral imaging in the Proliferation Detection Program of the United States Department of Energy and the image coding technology contained in the JPEG 2000 standard. JPEG 2000's role in national and international standards for military imagery is discussed, as are our objectives in applying JPEG 2000 to hyperspectral imagery. The scientific approach to the study using the Kakadu software implementation of JPEG 2000 is then presented along with the results of five very demanding chemical signature exploitation experiments. Attention is focused on one particular experiment involving gas plume detection and identification that highlights the performance differences between JPEG 2000 Part 1 (``Baseline'') algorithms and more advanced JPEG 2000 Part 2 approaches. The report concludes with a brief discussion of the implications of these results for national missions. The full report can be obtained by contacting the LDRD Program Manager at Los Alamos National Laboratory.

Statistical Modeling for Nuclear Fuel Rod Damage

Cynthia J. Reichhardt
20100612ER

Abstract
Continuum modeling of a nuclear reactor requires incorporation of damage that occurs on scales well below the engineering scale level, and this damage must be modeled outside of a continuum approach. In this project we studied the application of a statistical bubble concentration model to bridge length scales between ab-initio/atomistic simulations of gas atom formation in fuel rods and gas release mechanisms at the engineering scale for the fuel rod. Our extreme value technique requires information about both the microscopic mechanism responsible for the growth and formation of gas bubbles and about macroscale structural properties of the fuel such as grain boundary density and grain boundary angle distribution. During this short term project our focus was on establishing in detail how to apply the potentially very powerful extreme value statistics method to the fuel rod system.

Background and Research Objectives
We consider gas bubble growth in ceramic fuel rods. Due to the insolubility of the gas in the fuel matrix, gas atoms accumulate at grain boundaries within the material and form bubbles that can migrate toward the hottest region of the fuel rod, forming a central void. For engineering scale computations of fuel rod properties, it is important to know the concentration of porosity within the fuel as a function of time. However, direct simulations of the bubbles on the scale of the entire fuel rod are computationally infeasible with current resources. Thus, we proposed using a statistical technique to carry microscopic porosity levels up to the continuum scale. The statistical model provides a bridge between two disparate length scales.

Scientific Approach and Accomplishments
Our statistical approach to determining the porosity distribution is based on the behavior of gas atoms at grain boundaries. From the microscopic side, we identify which grain boundaries are associated with the fastest rate of gas bubble growth. From the macroscopic side, we make the assumption that the behavior of the system is dominated by the fastest growing gas bubbles. In this case, knowledge of the average gas bubble growth rate is not sufficient to predict the behavior of the material. Instead, we must focus on the extreme statistics of the system.

For the microscopic gas bubble growth modeling, we investigated the manner in which gas bubbles accumulate at grain boundaries in ceramic fuels. Gas atoms are continuously produced as the fuel burns. A gas such as Xe is immiscible in the fuel matrix and will precipitate into a bubble at the earliest opportunity. Gas bubbles that have formed in the ceramic matrix are not mobile, but the gas bubbles accumulate on the grain boundaries through the following mechanism. The gas bubbles are repeatedly subjected to energy deposition from passing fission fragments released as the fuel burns. This energy is sufficient to re-solve the gas atoms from the bubble back into the fuel matrix, destroying the bubble. The gas atoms can then form a new bubble, which will be destroyed again. The largest, persistent gas bubbles will form at locations in the fuel where the rate of bubble reformation is highest. These locations are the highest energy grain boundaries, where the local lattice strain acts as a potential that confines the gas atoms and draws them back into the bubble. We use a generalized model to study the fraction of high-energy grain boundaries present in a sample under different conditions, as shown in Figure 1.

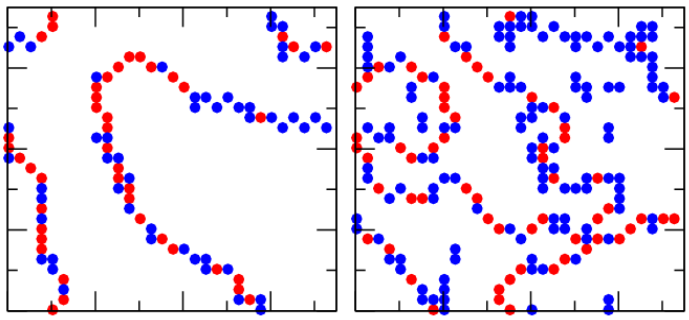

Figure 1. Grain boundary configurations from a simulation model under two different thermal conditions.

The distribution of grain boundaries is also an input for the statistical model. Of particular importance are the disordered grain boundaries, since these are able to stabilize the largest bubbles. In this modeling effort, we consider only a representative model for grain boundary formation. In a full application of the statistical model, which was beyond the scope of this project, we would use the grain boundary distribution inside the fuel element, which is determined not only by the manner in which the fuel was fabricated, but also by the burn history of that particular portion of the fuel, since coarsening or polygonization can occur in different parts of the fuel. The information fed into the statistical model from the mesoscopic side is the average population of grain boundaries as a function of thermal history, or in a simplified model, as a function of temperature alone.

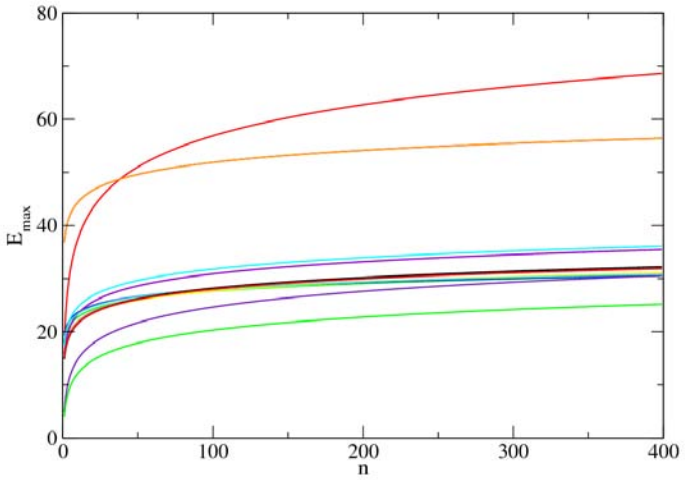

Figure 2. The maximum grain boundary energy as a function of the size of the sampling area as predicted by the statistical model for a variety of grain boundary formation conditions.

The statistical model bridges the two scales as follows. Consider a mesoscopic portion of a fuel element which is presently at temperature T. The size of this element L is taken to be equal to the size of a mesh element in a finite element simulation of the fuel rod. The length scale L is compared to the average grain boundary size l for temperature T. We assume that we have sampled the grain boundary distribution n=L/l times, and we use extreme value statistics to identify the highest energy grain boundary that would occur for this distribution. We then use the microscopic information to assign a fuel bubble size to this volume element based on the grain boundary energy. In the simplest version of the model, we consider only a single fuel bubble size per volume element; it would be possible to extend this to a bubble size distribution since the extreme value statistics produces a full distribution and not merely a single value for the grain boundary energy. The result is a physically-based, non-deterministic model for heterogeneous gas bubble size distribution based on the local temperature and physical size of the finite elements used to model the fuel rod. An advantage of this statistical technique is that it is not sensitive to the size of the finite element mesh; rescaling the mesh automatically rescales the model. The gas bubble size distribution can then be used in the finite element calculation to determine properties such as strength or thermal conductivity. Examples of the results from the statistical model for various simulated grain size distributions appear in Figure 2.

Impact on National Missions

This project supports the Grand Challenge issue of linkage of processes occurring at different scales of length and time as part of the “Fundamental Understanding of Materials and their Dynamic Response” challenge. It also supports the Nuclear Energy component of the “Carbon-Neutral Energy” Grand Challenge. It supports the FY10 LDRD Strategic Investment Plan areas of the science of nuclear fuel materials as well as the materials grand challenge areas of defects and interfaces and of extreme environments. The multi-scale linking method we consider is a fundamentally new S&T approach to the multi-length scale modeling problem and offers an important new capability for LANL missions.

Anthropogenic CO2 in the Atmosphere Measured Directly and through Indicator Species

Michael D. Di Rosa
20100613ER

Abstract

Carbon dioxide (CO_2) in the atmosphere is measured in total amount the world over but is not easily divided into a natural portion and that contributed by the burning of fossil fuels. The best means to date of measuring airborne anthropogenic carbon involves collecting air in flasks for later analysis. Akin to surveying a landscape by microscope, the sampling of air at handfuls of points for anthropogenic content is unlikely to give us the broad perspective researchers will need to track the distribution of fossil-fueled carbon on a global scale. Ideally, in the near future, scientists will be able to determine the amount of fossil-fueled CO_2 (FF-CO2) by methods that are as easy and reliable to implement as those used to measure total CO_2. We relate what we believe will be our important contributions in this area.

Background and Research Objectives

Measurements of airborne FF-CO2 are important to our understanding of global carbon constitution and transport. Such measurements might become arbiters in anticipated international agreements on greenhouse-gas emissions limits, where we imagine that maps of FF-CO2 on a global scale would show where such emissions originate. Today, however, our best means of partitioning atmospheric CO_2 into anthropogenic and biogenic origins begins by collecting air in flasks, a method too limited in atmospheric coverage to serve a comprehensive scientific program in carbon constitution, let alone treaties on greenhouse-gas limits.

It is helpful at this point to note that the carbon atom within CO_2 can be one of three isotopes, designated ^{12}C, ^{13}C, and ^{14}C, with the number indicating the sum of neutrons and protons composing the carbon atom (which, by definition, always has six protons). Almost all—99%—of the carbon is ^{12}C and uninteresting for our purposes. Ingeborg Levin [1, 2], knowing that fossil-fuel carbon is absent ^{14}C [3], developed in 1980 the now standard method for detecting the intrusion of fossil-based carbon into the air. Sampling stations collect air and concentrate CO_2 for a week or more. The level of ^{14}C is then determined later following sample preparations and measurement techniques that take several days to complete. While accurate, the method must collect a very rare isotope in enough quantity to measure—the isotope ^{14}C represents only one one-trillionth of all the carbon in the atmosphere. The benchmark method in atmospheric science for determining FF-CO2 is thus relegated to infrequent, point sampled, and protracted measurements by the very scarcity of what it seeks.

By comparison, ^{13}C is abundant, constituting about 1% of atmospheric carbon. Research is now afoot to see whether measurements of $^{13}CO_2$ can determine FF-CO2 instead, minus the tedium of measuring $^{14}CO_2$. So far, measurements of $^{13}CO_2$ show promise as a direct indicator of FF-CO_2 [4]. Figure 1 charts the ratio of ^{13}C to ^{12}C for different sources of carbon by a convenient factor termed $\delta^{13}C$, which is set to zero at a datum near that of uncontaminated air. Natural gas and petroleum, both of which are fossil fuels, are alone at greatly negative values of $\delta^{13}C$ and separate from the range of factors indicative of carbon within living plants and microbes. By extension, measured ratios of atmospheric $^{13}CO_2$ to $^{12}CO_2$ can show carbon's provenance, whether from natural or fossil-fueled sources. Presently, measurements of $^{13}CO_2$ are made with large but common laboratory instruments that receive air collected in flasks, and in this regard bear similarity to measurements of $^{14}CO_2$. But measurements of $^{13}CO_2$ can be made nearly instantaneously by comparison, needing a few hours rather than days for results. Yet like the $^{14}CO_2$ measurements, the process provides only point measurements, offering coverage only by carriage.

Dissatisfaction with these slow point-by-point measurements has motivated research into other albeit indirect techniques for measuring FF-CO2 over large swaths of sky. As mentioned, measurements of total CO_2 are easily made over long atmospheric paths. Whether by a ground instrument that looks up, or by a satellite-borne instrument that looks back at earth, the total amount of CO_2 within that instrument's view over many kilometers is derived from the radiation, and sometimes the absorption, that is characteristic of CO_2 at infrared wavelengths. Are there atmospheric proxies for FF-CO2 that could be measured as readily and easily as total CO_2?

Gamnitzer and coworkers [5] note that a number of such proxies for FF- CO2 have been tried, including chlorofluorocarbons, sulfur-containing pollutants, and species related to incomplete combustion. Their own measurements at a single point of $^{14}CO_2$, total carbon monoxide (CO), and total CO_2 left Gamnitzer and colleagues highly dubious of CO as a fossil-fuel tracer. To them, "($^{14}CO_2$) measurements seem to be indispensable for reliable estimates of fossil fuel CO_2". In contrast, Rivier and colleagues [6] found merit in correlating anthropogenic CO_2 with trends of several tracers, though their study lacked comparisons against direct measurements of FF-CO2. Such diametric conclusions are emblematic of a research topic that is just beginning, complex, and maybe mired in vigorous debate until techniques arise that can more directly resolve the main question, which is whether FF-CO2 has easily measured surrogates.

Direct, continuous measurements of FF-CO2 over skyward distances and alongside those of likely tracers would best help the atmospheric community evaluate FF-CO2 proxies. However, such comparisons are unlikely to appear under the present methods by which we measure ^{14}C and its suitable replacement ^{13}C. Our research under this LDRD program has developed the technical and material resources to introduce such measurements—of FF-CO2 and potential tracers over long atmospheric paths—that we believe will advance the science of monitoring and mapping anthropogenic carbon.

Scientific Approach and Accomplishments

Project members Clegg and Fessenden recently published with colleagues their work [7] on single-point measurements of $^{13}CO_2$ and $^{12}CO_2$ made outdoors during a test where small amounts of $^{13}CO_2$ were injected into the ground and allowed to seep into the air. They derived $\delta^{13}C$ (recall Figure 1) values from their *in-situ* and rapidly-made measurements for comparison with $\delta^{13}C$ values obtained through the standard method, where collected air samples are sent to a laboratory for analysis. Their work produced two significant outcomes. First, their rival method for measuring $^{13}CO_2$ and $^{12}CO_2$ directly outdoors yields values of $\delta^{13}C$ in very good agreement with those from the standard. Second, their technique has the sensitivity needed to detect and quantify anthropogenic airborne carbon.

To these two important outcomes we add an insight. At the technical core of the instrument developed by Clegg and deployed in Bozeman [7] beats the heart of a field known as laser spectroscopy. It suffices to say that inside is a precision laser that can be tuned in its invisible, infrared wavelength to areas where $^{13}CO_2$ and $^{12}CO_2$ each but distinctively absorb infrared light. The more each is present in the gas, the more laser-light each absorbs. Ordinarily, one measures the laser power absorbed by the gas and then relates the absorption to the amount of the absorbing species. Such a direct measurement of laser-beam absorption is what, in essence, that instrument uses.

But there are other if indirect ways of measuring laser-light absorption. One is known as LIDAR, which stands for light detection and ranging and has not the accidental ring of the more familiar and earlier acronyms of RADAR and SONAR. In all three technologies, one sends out waves and analyzes what returns by reflection. An elementary LIDAR instrument is a $200 laser rangefinder, which sends a pulse of laser light toward an object and then counts the elapsed time for a reflection to return as a measure of the object's distance. The more sophisticated LIDAR instruments of the atmospheric sciences use only the faint reflections of laser light from molecules, aerosols, and dust in the air. In our case, amounts of $^{13}CO_2$ and $^{12}CO_2$ would be indicated by diminished levels of light returned to the LIDAR receiver when laser light is tuned to their respective absorption wavelengths. In all, the extension of the technology within Clegg's instrument to LIDAR could make measurements of FF-CO2 quickly, outdoors, and mapped over atmospheric paths of many kilometers for the very first time.

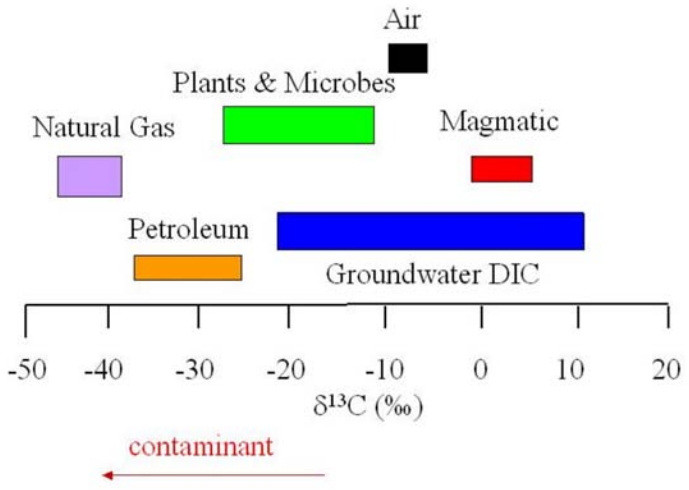

Figure 1. Isotopic variation of delta-13C (measured in ‰) from CO_2 sources typically found in geologic sequestration systems.

However, between that notional LIDAR idea and our objective of providing "direct measurements of FF-CO2 and its proxies over skyward lengths" stood several technical problems. The first was adapting the laser-based technique to LIDAR. Second, we recall that LIDAR provides an indirect measure of the beam absorption, and so by itself cannot provide maps of the absolute amounts of $^{13}CO_2$ and $^{12}CO_2$. We thus needed a way to calibrate LIDAR measurements, ideally through an independent measurement made along the same view of the sky seen by the LIDAR instrument. Lastly, we needed a means of measuring FF-CO2 proxies along the same view of the sky as the LIDAR instrument. Happily, our resolution to these issues produced a unique instrument and a new concept in LIDAR.

Schematically speaking, the overall plan was simple. The LIDAR instrument would report signals proportional to $^{12}CO_2$ and $^{13}CO_2$ at spatial increments along a skyward column.

At the same time, we would examine through standard methods of infrared spectroscopy an adjacent, collinear skyward column. A spectrometer of suitable performance would see both $^{12}CO_2$ and $^{13}CO_2$, and measurements of each would be converted (through known algorithms) to a total amount of each molecule in the atmospheric column. The conversion of LIDAR signals to absolute concentrations would then be adjusted for consistency with these measurements of total columnar amounts. The infrared spectrometer used to calibrate the LIDAR retrievals would also measure carbon monoxide, methane, and other proposed tracers of FF-CO2 at the same time. At once, we would chart along relevant atmospheric paths the absolute amounts of $^{13}CO_2$ and $^{12}CO_2$, the FF-CO2, and the amounts of proposed FF-CO2 proxies for comparison.

The Magdalena Ridge Observatory (MRO) at New Mexico Tech is an ideal facility for the planned measurements. Their 2.4-meter-diameter telescope has a port for the spectrometer we designed. While it might seem otherwise, the sheer diameter of the 2.4-m telescope offers no particular advantage in gathering light from an extended source like the sky. However, the tight field of view (19 arc minutes) intrinsic to the large telescope is important because it limits the spectrometer's view of the sky to a narrow cone that approximates the divergence of the laser beam used in the LIDAR system. The LIDAR and spectrometer measurements would thus be obtained for closely matched sections of the atmosphere. The LIDAR system operates independently and uses its own collection of three hobbyist telescopes, shown in Figure 2, to collect reflected laser light. The LIDAR system will be placed in the dome of the telescope and aimed at the same section of sky.

Our spectrometer is a Fourier-transform (FT) spectrometer specialized to our needs and incorporating a detector of infrared light from among the latest generation of low-noise infrared sensors. When complemented as we did with internal components unusual for a commercial FT spectrometer, this detector makes possible the measurements of both $^{12}CO_2$ and the less abundant $^{13}CO_2$ in the manner we need. Atmospheric $^{13}CO_2$ and $^{12}CO_2$ are readily seen in high-resolution solar spectra [8]. However, our spectrometer will view the open daytime sky and collect data on CO_2 and other species in whatever direction necessary without need for a bright solar backlight.

We mentioned earlier that our laser-based method for measuring CO_2 works best when the laser is continuously on. One could adapt the technique to LIDAR by pulsing the laser on-and-off, like a laser rangefinder, but the result would be unsatisfactory. A full day might not provide enough time to map the concentrations of $^{13}CO_2$ and $^{12}CO_2$ over a path of a few kilometers. Instead, we drew on basic concepts and hardware from optical and RF communications to design a LIDAR system where the laser operates continuously and signals are retrieved continuously. We estimate that measurements of $^{13}CO_2$ and $^{12}CO_2$ made in this way over a path of several kilometers can be accomplished in 30 minutes.

Figure 3 diagrams our LIDAR concept. With the laser steadily on, a common device in fiber-optic communications alternates the phase of the laser light between 0 and 180 degrees (0 and π radians) in a mathematically unique way known as a pseudo-random sequence [9]. The telescope (Figure 2) collects the sky-scattered laser light, and an optical detector along with RF-communications hardware converts the phase of the retrieved light to pluses and minuses that multiply the total (and positive) signal from the detector. As depicted in the graph of Figure 3, the final signal alternates between positive and negative values, as set by the phase, and by excursions that indicate the total amount of light received.

Figure 2. The three 10-inch reflector telescopes (photographed with caps) that collect reflected light in the LIDAR system.

We provide in Figure 4 a numerical simulation of the LIDAR signal versus time when the laser beam propagates through four weakly absorbing regions, as in Figure 3, over a path of 12 kilometers. In its raw form, the LIDAR signal (the black trace) appears chaotic. What information it might contain is obscured further by the simulation's addition of random noise (the red trace) that accounts for detector noise and other imperfections. The LIDAR signal juts above the noise by a miserable ratio of 5 to 1, at least until we take advantage of our pseudo-random sequence.

The black trace of Figure 5 shows the positions, shapes, and concentrations of the absorbing regions we entered in the simulation. We note that the ideal LIDAR signal indicates how much the laser beam has been absorbed between where it starts (at zero kilometers) and a distant point. The red curve of Figure 5, referenced to the right vertical scale, shows this ideal LIDAR retrieval in units of column-integrated concentration, where its four steps divulge the underlying four regions. Our raw LIDAR signal (Figure 4) is then compared against our random-looking but unique key of a sequence in a calculation called called cross-correlation that unlocks the LIDAR retrieval. The blue circles were obtained from this procedure and, as shown, recover the ideal expectation with remarkable fidelity despite the signal's humble appearance in structure and magnitude as not much more than noise. Our publication on the method's theory with proof-of-concept results is being prepared.

We attempted an initial experimental test at the Magdalena Ridge Observatory, but instrumental complications precluded a useful measurement during the short term of this reserve project.

We now have the unique technical and analytical resources to make valuable contributions to the atmospheric science community's search for a tracer of anthropogenic emissions. The general designs and methods behind our spectrometer and LIDAR instruments might also be of use to the broader scientific community.

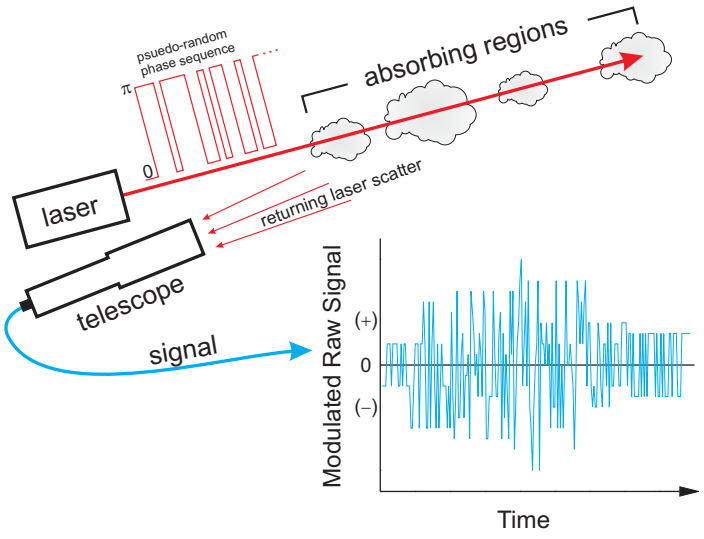

Figure 3. Cartoon of LIDAR concept. A laser beam shines continuously while the phase of its output (technically, the phase relationship between RF sidebands that are impressed on the light frequency) is modulated by a binary psuedo-random sequence. The binary phase sequence is converted to positive and negative content for the raw LIDAR signal, and encodes the range. The modulation amplitudes of the LIDAR signal encode the amount of light received for a given range.

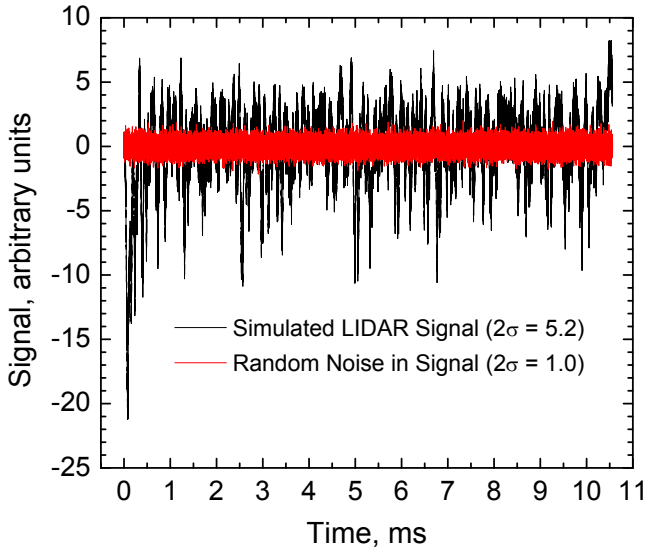

Figure 4. A simulated continuous LIDAR signal obtained for a maximum-length-binary phase-shift key (PSK) of numerical period 32,767 and having an overt signal-to-noise of 5.2. The approximately 10 ms signal contains the temporal period of the PSK and the simultaneous LIDAR retrieval. Four weakly-absorbing regions spread over 12 km were assumed for the simulation (see the black trace of Figure 5).

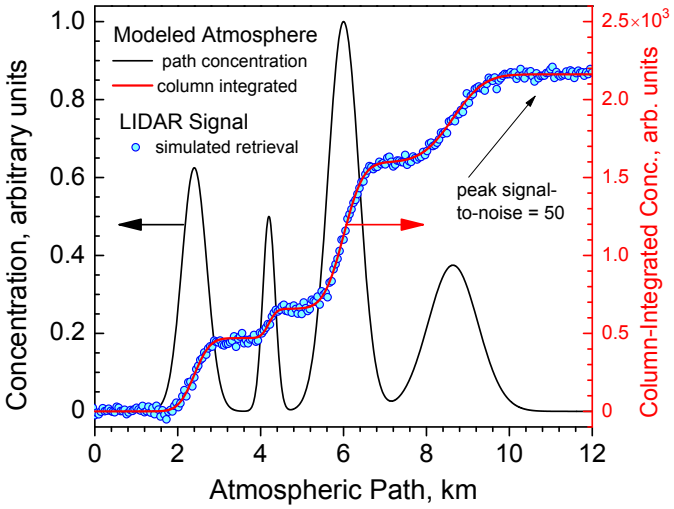

Figure 5. Simulations show that our technique bears promise for measuring the CO_2 content of the atmosphere. As input to the simulation, the black trace shows four absorbing regions of varying positions, shapes, and CO_2 concentrations over a 12 km path of the atmosphere. The red curve (referenced to the right scale) is the ideal LIDAR retrieval, given by the pathwise accumulation of concentration. Analysis of the simulated LIDAR signal (Figure 4) produced the blue circles, which nicely match the ideal retrieval.

Impact on National Missions

The DOE, NOAA, and NASA recognize in their environment and climate programs that measurements of anthropo-

genic CO_2 are critical to our understanding of global carbon transport. We suspect the DOE would oversee programs in greenhouse-gas (GHG) emissions verification should international agreements on GHG limits be ratified. NNSA and the intelligence community are generally interested in detecting human activities, as anthropogenic carbon might betray. The capacity to detect anthropogenic activity also seems suited to NNSA's nonproliferation programs. NASA's annual solicitation for Research Opportunities in Space and Earth Sciences routinely includes topics of atmospheric composition. The DOE Office of Science portfolio will, we expect, include research in carbon sequestration, to which our work can apply.

References

1. Levin, I., K. O. Munnich, and W. Weiss. The effect of anthropogenic CO2 and 14C sources on the distribution of 14CO2 in the atmosphere. 1980. *Radiocarbon.* **22** (2): 379.

2. Levin, I., B. Kromer, M. Schmidt, and H. Sartorius. A novel approach for independent budgeting of fossil fuel CO2 over Europe by 14CO2 observations. 2003. *Geophysical Research Letters.* **30** (23): art. no. 2194.

3. Fergusson, G. J.. Reduction of atmospheric radiocarbon concentration by fossil fuel carbon dioxide and the mean life of carbon dioxide in the atmosphere. 1958. *Proceedings of the Royal Society of London, Series A (Mathematical and Physical Sciences).* **243** (1235): 561.

4. Pataki, D. E., D. R. Bowling, and J. R. Ehleringer. Seasonal cycle of carbon dioxide and its isotopic composition in an urban atmosphere: Anthropogenic and biogenic effects. 2003. *Journal of Geophysical Research.* **108** (D23): art. no. 4735.

5. Gamnitzer, U., U. Karstens, B. Kromer, R. E. M. Neubert, H. A. J. Meijer, H. Schroeder, and I. Levin. Carbon monoxide: A quantitative tracer for fossil fuel CO2?. 2006. *Journal of Geophysical Research.* **111**: art no. D22302.

6. Rivier, L., P. Ciais, D. A. Hauglustaine, P. Bakwin, P. Bousquet, P. Peylin, and A. Klonecki. Evaluation of SF6, C2Cl4, and CO to approximate fossil fuel CO2 in the Northern Hemisphere using a chemistry transport model. 2006. *Journal of Geophysical Research.* **111**: art. no. D16311.

7. Fessenden, J. E., S. M. Clegg, T. A. Rahn, S. D. Humphries, and W. S. Baldridge. Novel MVA tools to track CO2 seepage, tested at the ZERT controlled release site in Bozeman, MT. 2010. *Environmental Earth Sciences.* **60** (2): 325.

8. Wallace, L., W. Livingston, K. Hinkle, and P. Bernath. Infrared spectral atlases of the sun from NOAO. 1996. *Astrophysical Journal Supplement Series.* **106**: 165.

9. Tan, A. H., and K. R. Godfrey. The generation of binary and bear-binary pseudorandom signals: An overview. 2002. *IEEE Transactions on Instrumentation and Measurement.* **51** (4): 583.

A Novel Technique for Introduction of Fission Gas Xe in Solids

Ross E. Muenchausen
20100623ER

Abstract
A novel method for the fabrication of test samples for fission gas behavior studies in nuclear fuel materials is described. We demonstrated an experimental set up for fabrication of such test samples and applied it to the fabrication of a set of ceramic oxides (including depleted uranium dioxide). It was demonstrated that properties of such test samples resemble those associated with fission gas accumulation in reactor-irradiated nuclear fuels. Thus a new powerful technique for experimental simulation of conditions typical to a nuclear fuel environment has been implemented. This achievement makes a tangible contribution to the Los Alamos National Laboratory mission and grand challenges.

Background and Research Objectives
Degradation of nuclear fuel and cladding materials properties in a nuclear reactor environment may be attributed to a combined effect of elevated operating temperature, radiation damage accumulation and physico-chemical changes. When a ^{235}U nucleus fissions, two fission fragments are produced with bimodal mass and energy distributions. Generation of fission gas (FG) elements (Xe and Kr) in nuclear fuels and their release to the fuel-clad gap is considered to be one of the major factors that limit the fuel performance (both from the economical and safety viewpoints). Despite of the vital importance of FG behavior, basic data on diffusion, solubility, bubble nucleation, lattice location and etc., even in traditional nuclear fuel materials such as UO_2, is lacking. The reason is that there is no conventional technique for fabrication of reference samples containing controllable and uniform concentration of FGs. Therefore these basic parameters cannot be experimentally measured.

The main research objective of this proposal was to apply the ion beam assisted deposition (IBAD) method to the fabrication of test samples doped with Xe atoms (which is the most abundant FG product), and characterize the microstructure and Xe depth distribution. This novel approach for FG doping was conceived in the second half of FY10 and had been funded for the last three months of this year. In this short timeframe we fabricated a set of ceramic oxides doped with Xe (including depleted UO_2 (DUO_2)) and characterized them. Thus all objectives of the program were met and a unique capability, rich in applications to multiple nuclear energy related projects currently running at Los Alamos National Laboratory (LANL), is developed.

Scientific Approach and Accomplishments
Our scientific approach was divided into four tasks. Technical and scientific achievements summarized below are given for evaluation of our accomplishments for each task. To achieve the set goals we focused efforts of our research team at two directions, which were performed in parallel. The first direction, incorporated into task 1 was to initiate deposition of depleted UO_2 (DUO_2) films. The second direction, incorporated into tasks 2-4, was to develop a better understanding of the IBAD process by using surrogate ceramic materials. The use of non radioactive surrogates, instead of DUO_2, provides a rapid way to optimize deposition conditions and to characterize the test samples.

A vacuum deposition system equipped with an electron beam evaporation source and an assisting ion gun was dedicated for the IBAD synthesis of DUO_2 films doped with FG species (Xe and Kr). The deposition system is located in the Target Fabrication Facility (TFF) and now is a part of MST-7 group experimental capabilities. A DUO_2 pellet, serving as a target material for the electron beam evaporator, was fabricated at MST-8 group and shipped to the TFF. An image of the pellet is shown in Figure 1. An Integrated Work Document (IWD) was prepared for the DUO_2 deposition and additional safety requirements for working with radioactive materials were implemented [1]. A first deposition process of DUO_2 film doped with Xe by IBAD method was conducted.

We have also fabricated three types of ceramic oxide materials doped with Xe atoms: MgO, Al_2O_3 and HfO_2. The HfO_2 was chosen because it is a well accepted surrogate for UO_2 due to the similarity in physico-chemical properties. Thus IBAD deposition conditions and attendant microstructural features determined for the HfO_2 can be directly applied to DUO_2. In deciding on MgO

and Al_2O_3, we considered these materials in connection with the inert matrix concept or dispersion composite ceramic fuel forms. It was established by grazing incidence X-ray diffraction (GIXRD) measurements that Al_2O_3 doped with Xe by using IBAD performed at room temperature was amorphous. Partial recrystallization of Al_2O_3 -Xe was achieved only after annealing. Whereas diffraction patterns obtained from as deposited MgO-Xe and HfO_2 -Xe were indicative of crystalline materials: cubic MgO and a mixture of tetragonal and monoclinic HfO_2.

We have experimentally evaluated a major parameter affecting the concentration of incorporated Xe atoms: the effect of the assist Xe ion current density to the film deposition rate ratio. IBAD conditions providing controllable introduction of Xe in the range of 1.5 – 5 at% were determined for Al_2O_3<Xe>.

We have also performed a detailed study of microstructure and Xe depth profile changes in Al_2O_3<Xe> induced by post deposition annealing at 800 ^oC for 1 hour. A paper describing the IBAD method for FG introduction using the example of Al_2O_3-Xe was submitted to the Journal of Nuclear Materials [2]. We found that the size and spatial distributions of Xe bubbles, in our post-annealed Al_2O_3-Xe IBAD films, are similar to the fission gas bubbles observed in UO_2 irradiated with thermal neutrons (see Figure 2). We also demonstrated that the microstructure of our as-deposited Al_2O_3-Xe IBAD films have features in common with other irradiated nuclear fuel materials (namely dispersion metal fuels).

Chemical composition analysis of Al_2O_3-Xe films, performed by Rutherford backscattering spectroscopy (RBS), found no evidence for Xe release from the alumina film after annealing. This is an additional encouraging result coincident with Xe behavior in actual nuclear fuels.

In summary, we have successfully executed the program and implemented a new experimental technique that offers an opportunity to develop a systematic approach to elucidating the underlying physics of FG behavior.

In closing, it is worth mentioning that during this project we invented another application of the IBAD technique, addressing another issue in the nuclear energy area. Materials utilized in nuclear reactors are exposed to various energetic particles, which result in radiation damage accumulation and swelling. Due to the swelling initial volume (and shape) of various components may change and result in failure. One of the reasons for swelling is preferential absorption of interstitials at dislocations and as a result enhanced concentration of vacancies, which form cavities (the so-called dislocation bias effect). Once the dislocations formed, the cavities grow in size and material swells. To avoid this deleterious effect equally efficient sinks for vacancies and interstitials must be introduced into a material. We believe that coatings fabricated by our IBAD method and containing well arranged voids (similar to those shown in Figure 2) may demonstrate exceptional tolerance to radiation damage. The reason is that, based on theoretical predictions, voids of a certain size (specific to each material) act as annihilation centers for both vacancies and interstitials with the same efficiency (so called neutral sinks). Such voids filled with noble gases can be introduced in any material fabricated by IBAD. Swelling attributed to the dislocation bias effect should be suppressed in such coatings. An invention disclosure on fabrication of such swelling resistant coating was submitted [3] and experimental testing of this hypothesis is underway.

Figure 1. Optical image of depleted UO_2 pellet.

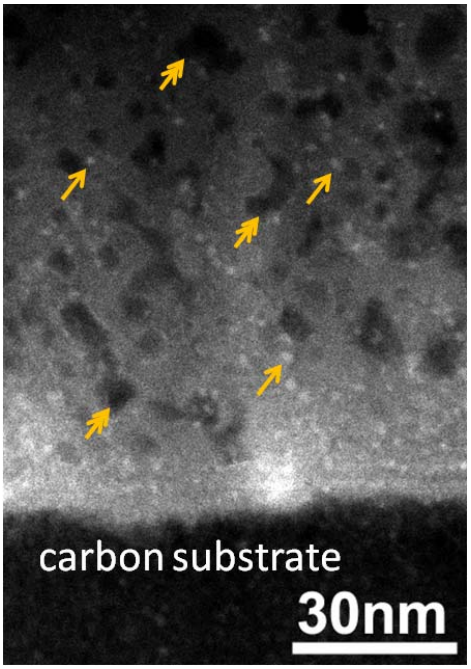

Figure 2. Cross-sectional high-angle angular dark field scanning transmission electron microscopy (HAADF/STEM) image obtained from a post-annealed alumina Al_2O_3-Xe IBAD film deposited on carbon substrate and annealed in vacuum at 800 oC for 1 hour. Single arrows indicate Xe bubbles. Double arrows indicate cavities or voids.

Impact on National Missions

This program contributes not only to the existing LANL mission (such as Energy Security) and grand challenges () but also to new concepts such as the MaRIE (Matter-Radiation Interactions in Extremes) project, since the goal of our work involves one the MaRIE core tasks, namely swelling of nuclear fuel due to accumulation of FGs. We believe that this new capability will expand LANL's expertise and capabilities in the area of nuclear materials properties evaluation and modeling.

Successful application of the IBAD method to the DUO_2 film fabrication came to the Fuel Cycle Research and Development Program attention. This program is sponsored by the Department of Energy. The IBAD method that we developed was included into this program as a major tool for studies of FG behavior in ceramic nuclear fuels.

References

1. Bennett, B., and D. J. Devlin. Ion beam coating of UO2. 2010. *IWD: MST-7-35-213-B106-4.*

2. Usov, I. O., J. Wov, D. J. Devlin, Y. B. Jiang, J. A. Valdez, and K. E. Sickafus. A novel method for incorp[orating fission gas elements into solids. *Journal of Nuclear Materials.*

3. Usov, I. O.. Coatings resistant to irradiation induced swelling. 2010. *Invention Disclosure 10-181.*

Publications

Bennett, B., and D. J. Devlin. Ion beam coating of UO2. 2010. *IWD: MST-7-35-213-B106-4.*

Usov, I. O.. Coatings resistant to irradiation induced swelling. 2010. *Invention disclosure 10-181.*

Usov, I. O., J. Won, D. J. Devlin, Y. B. Jiang, J. A. Valdez, and K. E. Sickafus. A novel method for incorporating fission gas elements into solids. *Journal of Nuclear Materials.*

Bio-Directed Assembly of Multicolored One-Dimensional Quantum Dot Light-Emitting Devices

Gabriel A. Montano
20080784PRD3

Introduction

The goal of the funded research project is to use organizational properties of biological systems to create efficient and inexpensive platforms usable for various nanotechnology applications. For example, we have exhibited the use of active biological molecules to drive assembly of multicolored quantum dots into ordered structures for Light Emitting Devices (LED). Technology developed in this research project is also being utilized to develop nanoplasmonic platforms as well as for light-harvesting and energy transfer systems. Further, bio-templating architectures are also being utilized as platforms for investigating fundamental physical and biophysical properties of nanomaterials and for mimicking active transport mechanisms in cells for use in microfluidics transport of nano-scaled materials. Our approach is interdisciplinary, incorporating aspects of molecular biology, chemistry and engineering, and spanning the fields of nanoelectronics, nanophotonics and nanoscale assembly. By combining the merits of biology-enabled self-assembly, the research and technology described eliminates complicated and costly microfabrication processes. Further project development will enable manufacturing of integrated nanoscale devices for a vast array of electronic, photonic and fluidic applications.

Benefit to National Security Missions

The proposed research directly ties into the area of Energy Security. The ability to generate inexpensive efficient photonic and electronic devices is of the utmost importance to both the US and the world. Further, this research relates directly to projects outlined in BES for nanoscience initiatives, specifically emergent properties at the nanoscale.

Progress

This project is focused on bio-assembly strategies for development of nano-optical and nano-electronic architectures and devices. As described in previous reports, we have exhibited the ability to control one-dimensional assembly of nanomaterials such as quantum dots and gold nanoparticles. (See 2009 report for project details) Examples of resultant assemblies can be observed in previous submitted reports. In regard to both ordered one-dimensional QD assemblies and plasmonic gold nanoring architectures, results are to be written up shortly. Much of the time since the last report was spent verifying previous results for publication. It was our intention to have manuscripts already submitted, however due to Dr. Liu's 2010 hiring by Sandia National Laboratory as a Principle Member of the Technical Staff, a result in large part due to her work as a LANL Director's Funded Postdoctoral Fellow, manuscript preparations are still being made. However, during the last year using the microtubule-kinesin based system and in collaboration with Sandia colleagues, Dr. Liu has shown the ability to control lipid tubule based systems which mimic vesicle processing in cellular systems as well as provide a platform for dynamic microfluidics transport. Figure 1 is a schematic of the described lipid tubule formation. This system shows the ability of using the active bio-assembly strategy described throughout this project to create novel lipid tubule systems. In brief, lipid vesicles are tethered to the microtubules and as the micrtubules are shuttled along the surface by kinesin motors, lipid tubules are formed from the giant lipid vesicle reservoirs. An example of such tubule formation from giant vesicle reservoirs is also shown in Figure 2. The described work represents a novel mechanism for controlled lipidic tubule formation, a novel bio-templated strategy for microfluidics design.

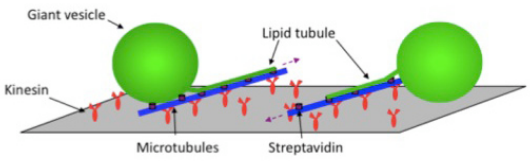

Figure 1. Illustration of microtubule processing on inverted kinesins on solid substrate and pulling on giant vesicles to form lipid nanotubes.

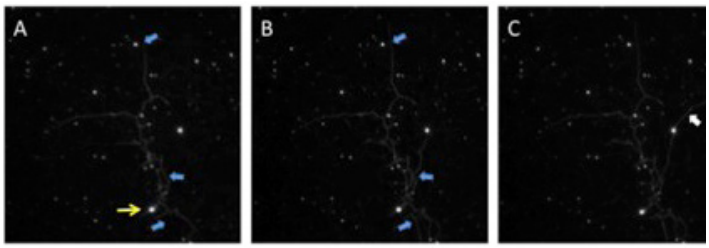

Figure 2. Lipid tubule extensions from 5% DOPE-biotin/ DOPC giant vesicles. Structures formed after A) 5 minutes, and C) 9 minutes. Line arrow identifies the giant vesicle that appears to be the main reservoir of membrane for the tubulated network; dark block arrows identify where tubule growth occurs A) before and B) after a period of minutes, and the white block arrow reveals a linear tubule extending off a giant vesicle.

Conclusions and Future Work

We have made significant progress toward development of nanophotonic and nanoelectronic assemblies. As described previously, Dr. Liu has exhibited the ability to synthesize one dimensional- multi-colored arrays of QD's and well as exhibited controlled ring assembly of various nanoparticles. Further, bio-assembly strategies employed have also been shown to be useful in creating dynamic lipidic tubule formations, structures that mimic biological vesicle budding mechanisms as well as useful in long-range microfluidics transport. We will continue work on the described projects in collaboration with Dr. Liu, a newly hired Primary Member of the Technical Staff at Sandia National Laboratory and CINT user.

This research project was developed far beyond our initial proposed development of QD-LED devices. While one of the goals of this proposal was to develop QD-LED architectures, the focus shifted to our ability to control the bio-templating strategies and use of such architectures to develop other photonic and electronic nano-scaled assemblies, as well as use the architectures as a framework to investigate fundamental physics of nanomaterials and microfluidic transport vehicles. We will continue to focus our efforts on development of the bio-templating strategies in collaborative efforts while utilizing combined expertise in development of nano-device architectures.

Dr. Liu's work on this project was recognized as a highlight presentation at the 2010 MRS spring meeting as reported in the MPA newsletter. Further, as mentioned above, Dr. Liu has successfully obtained a permanent staff position at Sandia National Laboratory, in part due to her work on this funded LDRD project.

Publications

Polsky, R., C. Washburn, G. Montano, H. Liu, T. Edwards, D. Lopez, J. Harper, S. Brozik, and D. Wheeler. Reactive ion etching of gold-nanoparticle-modified pyrolyzed photoresist films. 2009. *Small.* **5** (22): 2510.

Local Atomic Arrangements in Phase Change Materials

Thomas E. Proffen
20080791PRD4

Introduction

In optical and electronic memory device technology a deposited crystalline phase is liquefied with a laser and solidified with quenching to form an amorphous one. Low intensity light or an electrical pulse ´reads' the distinct reflectivity or resistivity in the amorphized region while a longer and more intense source can render it crystalline once again, enabling re-writable media. Optical storage devices are nearing terabyte data storage densities, and emphasis is quickly shifting to electronic nonvolatile memory. To date improvements in the underlying phase-change materials(PCM) have largely been made through a trial and error process. We have pursued the use of state-of-the-art local structure studies, using neutron and synchrotron X-ray total scattering techniques, to address these deficiencies and provide a better understanding of the crystal chemistry, local structure, bonding, and properties in well-established and novel phase-change materials. Along with these milestones, we have advanced scattering capabilities necessary for their understanding.

Benefit to National Security Missions

An energy efficient nonvolatile memory with fast switching speeds has the potential to revolutionize our data storage infrastructure and realize substantial leaps in computing power. This project will support the missions of the Office of Science by enhancing our understanding of complex disordered materials on the atomic level. This project also supports the other DOE missions by enhancing experimental techniques to study complex materials. These advances will broadly impact government agencies and programs.

Progress

This project is aimed at understanding the interplay between structure and property in phase-change chalcogenide alloys. Our most significant areas of progress have been in preparing and characterizing thin films of the canonical phase change materials GeSb2Te4 and Sb2Te. We prepared GeSb2 Te4 and Sb2Te thin films of thicknesses between 50 nm and several microns by sputtering from a stoichiometric target, at LANL's Center for Integrated Nanotechnologies. Initially we experimented with several substrates, with the goal of providing optimal samples for synchrotron and neutron studies. Samples were deposited on polyimide and on silica for synchrotron studies. For the silica deposition, half the substrate was masked during deposition, aiding in data reduction procedures. Multi-layer films were deposited on vanadium foil in order to explore neutron measurements of thin films.

At the Advanced Photon Source earlier this year we explored in situ thermal annealing of the thin films for the first time, using a commercially available heat stage with minor modifications of the beamline. The measurements were very successful. We found data reduction was possible for films as thin as 50 nm and also for films deposited on either polyimide or silica. We collected temperature dependent data for 1 um thick samples for several heat ramping rates. There were some significant findings from these studies. (1) The amorphous (as-deposited) phase has a strongly correlated structure up to 8 Å, a length scale not accessible with complimentary techniques, including EXAFS/XANES. (2) We found, as others have, that the nearest neighbor (Ge-Te, Sb-Te) coordination is shorter and sharper than in the crystalline phase, an unusual property for inorganic solids. This is in contrast to the next nearest neighbor (Te-Te) coordination, which is broader than in the crystalline phase. (3) For the technologically relevant metastable crystalline phase we found a disordered rocksalt crystal structure describes the average structure well, however, large atomic displacement parameters suggest a superposition of local (disordered) structural states. We are in the process of exploring this atomic structure with larger models. These measurements have allowed us to extract correlation length scale, bond lengths, and chemical short range order (ordering of Ge, Sb, and vacancies) in the different states of this material, and we are currently preparing a manuscript summarizing these findings. We are collaborating with world-leading scientists in this field to correlate our observations to charge transport and optical reflectivity properties, and compare our

results to several ab initio calculations completed for prototype phases of Ge2Sb2Te5 and Ge1Sb2Te4.

These experimental strides have been made hand in hand with several key methods advancements for determining local atomic structure of disordered crystalline and amorphous materials. (1) The ability to distinguish separate peak contributions to pair correlation functions was previously limited. We developed a program MIXSCAT that extracts differential pair distribution functions using respective x-ray and neutron data sets. This program has been published for the wider scientific community. (2) Incoherent scattering contributions present a significant challenge in neutron total scattering experiments, especially for many nanomaterials. We have developed a method for correcting such contributions, and have made this routine available for use and published our procedure for the scientific community. (3) We have demonstrated that amorphous and polycrystalline thin film samples can be studied in transmission geometry at a synchrotron source by conventional x-ray total scattering methods. We found data reduction is possible for films deposited on polymer and glass substrates and films as thin as 50 nm. These methods can be adapted for a wide variety of thin film materials and sample environments where local atomic structure and behavior of thin film samples are of interest.

Future Work

Current phase-change materials are group 15 and 16 alloys with octahedral-like atomic arrangements in the crystalline state. Successful candidates have large optical or electrical contrast between phases, thermal and chemical stability, fast switching speed for the phase change, and scalability. We will continue efforts to investigate how lattice distortions, vacancy concentrations, chemical short-range order, crystalline length scale, and local bonding environments affect these properties in PCM. We have several key milestones aligned: (1) With synchrotron scattering measurements scheduled for later this year we will complete *in situ* crystallization studies for thin film materials based on the Sb70Te30 eutectic (Sb2Te), where crystallization is believed to be growth controlled. This will allow important comparisons to be made with GST compositions. (2) We have planned complementary neutron scattering experiments and anomalous x-ray scattering experiments both GeSb2Te4 and Sb2Te. If successful, this will allow us to completely separate the contribution of separate pair correlations to the total pair distribution function experimentally (without structure models). (3) We have plans to study PCM nanoparticles with a collaborator at the Molecular Foundry, Lawrence Berkeley National Laboratory, in order to investigate the crystal chemistry and local atomic structure in finite particles with amorphous and ordered GeTe structures. The characteristics and behavior of these materials will be compared with traditional PCM and their promise for technological applications will be explored.

The merit of this proposed work lies in the promise of better understanding of the crystal chemistry, local structure, bonding, and properties in well-established and novel phase-change materials, and the advancement of scattering capabilities necessary for their understanding.

Conclusion

This project is aimed at understanding the interplay between structure and property in the remarkable class of existing phase-change materials and expanding the number and types of compounds available for future data storage technology. This work will complement LANL strengths in theory and engineering, bringing the much anticipated electronic nonvolatile universal memory closer to reality. In the broadest sense, this work will advance the methods of characterization available for amorphous-crystalline phase transitions in solids, bridging an important gap in solid state characterization as it is pursued today.

Publications

Aksel, E., J. Forrester, J. L. Jones, P. A. Thomas, K. Page, and M. Suchomel. Monoclinic crystal structure of polycrystalline Na0.5Bi0.5TiO3. *Applied Physics Letters.*

Im, W. B., K. Page, S. P. DenBaars, and R. Seshadri. Probing local structure in the yellow phosphor LaSr2AlO5:Ce3+, by the maximum entropy method and pair distribution function analysis. 2009. *Journal of Materials Chemistry.* **19** (46): 8761.

Melot, B. C., K. Page, R. Seshadri, E. M. Stoudenmire, L. Balents, D. L. Bergman, and T. Proffen. Magnetic frustration on the diamond lattice of the A-site magnetic spinels CoAl2-xGaxO4: The role of lattice expansion and site disorder. 2009. *Physical Review B.* **80**: 104420.

Page, K., C. E. White, E. G. Estell, A. Llobet, and T. Proffen. Treatment of hydrogen background in bulk and nanocrystalline neutron total scattering experiments. To appear in *Journal of Applied Crystallography.*

Page, K., T. C. Hood, T. Proffen, and R. B. Neder. Building and refining complete nanoparticle structures with total scattering data. *Journal of Applied Crystallography.*

Page, K., T. Proffen, M. Niederberger, and R. Seshadri. Probing local dipoles and ligand structure in BaTiO3 nanoparticles. 2010. *Chemistry of Materials.* **22**: 4386.

Page, K., T. Proffen, and R. B. Neder. Structure of Nanoparticles from Total Scattering. To appear in *Modern Diffraction Methods.* By Mittemeijer, E., and U. Welzel.

Page, K., and T. Proffen. tructure from Neutron Total

Scattering: the Pair Distribution Function Approach. To appear in *Neutrons and Nanoscience.* By Hurd, A. J., and S. Sinha.

Wurden, C., K. Page, A. Llobet, C. E. White, and T. Proffen. Extracting differential pair distribution functions using MIXSCAT. 2010. *Journal of Applied Crystallography.* **43** (3): 635.

Energy Transfer Processes in Type-Specific Single-Walled Carbon Nanotubes

Stephen K. Doorn
20080797PRD4

Introduction

Single-Walled Carbon Nanotubes (SWNT) have remarkable optical and electrical properties. These photophysical properties are heavily dependent on the sidewall purity, diameter and chirality (a property of the geometry) of the tube. While this heterogeneity offers many opportunities in sensing and electronic applications, full utilization of these properties requires the development of well defined materials. This includes controlling the energy transfer (ET) that occurs between distinct tube types and between the tube and environment. Control of ET is important because it can enhance and/or quench the detectable photophysical properties of the tubes, and allows tunability of their absorption range. Current research on bulk samples is lacking because the heterogeneity inherently limits the sensitivity and reproducibility of the measurements. However, new separation techniques allow access to chirality-enriched samples and offer the possibility of engineering samples with specific bandgap and reactivity properties. We are proposing to utilize enriched chirality samples to engineer and enhance ET reactions between specific tube types and between SWNTs and molecules in ensemble systems and at the single molecular level.

Benefit to National Security Missions

This project supports the development of advanced functional nanomaterials that support threat reduction, energy security, human health, and basic science missions in DOE and other government agencies.

Progress

In the past year Juan Duque's efforts have been aimed at several aspects of understanding fundamental photophysical processes between single-walled carbon nanotubes (SWNTs) and their surroundings for energy transfer processes aimed at energy harvesting and sensing applications. We highlight three major accomplishments:

1. Solubility of SWNTs in solutions.
2. Raman spectroscopy of different SWNT chiralities.
3. Formation of SWNT gels.

Solubility of SWNTs in solutions: We studied the solubility and dispersability of SWNTs in oleum and surfactant suspensions. We found that small diameter SWNTs disperse at higher concentrations in aqueous surfactants and dissolve at higher concentrations in oleum than do large-diameter SWNTs. These results highlight the importance of SWNT diameter distribution in order to optimize processes dependent on solubility, since solubility and dispersibility are key parameters for macroscopic SWNT processing techniques including fiber spinning, and thin-film production, as well as for fundamental research in type selective chemistry, optoelectronics, and nanophotonics. This work was accomplished in collaboration with Rice University and Bordeaux University in France. This collaborative effort resulted in a publication earlier this month in ACS Nano ("Diameter Dependent Solubility of Single Walled Carbon Nanotubes" DOI: 10.1021/nn100170f). Understanding the interfacial interaction between SWNTs and the local environment and control over the dispersability of the tubes in solutions allows tunability over the energy transfer processes between different SWNT species and their local environment and has helped us further understand the mechanism of SWNT separation.

Raman spectroscopy of different SWNT chiralities: Resonant Raman scattering experiments using excitation wavelengths in the visible, near infrared and ultra violet (UV) regions were performed on enriched fractions of semiconducting and metallic SWNTs. This type of work is the first of its kind in the SWNT community and aims to answer fundamental question of the exciton-phonon coupling of SWNTs and their transition energies. Raman excitation profiles for the G-band in semiconducting samples reveal a strong asymmetry in the intensities of the resonance coupling to incident and scattered photons and can be understood as a consequence of the presence of non-Condon effects. These behaviors hold significant consequence for our ability to understand and manipulate excitation and emission processes, and understanding of observed transition energies, all with important implications for envisioned energy transfer

applications. This work is being conducted in collaboration with a group from NIST lead by Ming Zheng, a group in Boston University lead by Prof. Anna Swan and a group in Rice University lead by Prof. Jun Kono. As result, we are preparing several manuscripts that will be submitted to Physical Review Letters and Science.

Formation of SWNT gels: We have identified a new approach to obtain SWNT-silica nanocomposite silica gels which retain SWNT emission properties upon encapsulation with silica (SiO2). By modifying the surfactant composition adsorbed on the SWNT surface, we were able to control the interactions between the tubes and their local environment and in some cases the tubes were virtually insensitive to changes in the surrounding environment. Subsequent supercritical drying of the Si-SWNT gels resulted in monolithic low-density solution-free composites with significant near-infrared emission intensity. These unique solid platforms of fluorescent SWNTs will enable ultrasensitive optical sensors for bio-weapons, gases, and basic research in areas like low temperature excitonic dynamics, exciton-phonon coupling, and energy transfer for photovoltaic applications. We aim to design and engineer the functionality of nano-structured materials, specifically SWNT-aerogel nanocomposites, by controlling inter-tube and matrix interactions. Such control will allow mitigation and/or enhancement of key energy transfer processes needed for targeted energy and sensing applications. This work is in collaboration between MST-7, C-PCS and MPA-CINT.

These accomplishments are helping us to understand the optical and electronic structures of SWNTs and consequently will help us engineer and design new experiments involving single molecular spectroscopy for energy transfer, biological tagging, and chemistry at the single tube level.

Future Work

SWNT suspensions with tailored bandgap and narrow electronic properties will be developed. This will allow engineering of suspensions in which the intertube interactions between select types will be studied. Optical and electronic enhancement will be investigated between specific diameter semiconductors, allowing the identification of the most efficient ET pathway for photophysical processes and energy harvesting. Metallic-semiconductor interactions will give insight to the electronic and optical quenching pathways SWNTs undergo. These parameters will be studied as a function of the difference in bandgap energies and relative chirality overlaps. The energy transfer between SWNTs and photoactive organic and inorganic molecules, or dopants, will also be studied. This will provide further knowledge of energy processes that specific SWNTs undergo by offering a point of reference to evaluate the efficiency and ET yield of each tube type. Examples include squarylium dye which does not overlap with SWNT absorbance and quantum dots which have easily manipulated absorbance and emission profiles. Engineering of the surfactant structure around the SWNTs will also be important to control the bandgap and Fermi level which then allows tunability of the degree, type and rate of interactions between tube types and tube-dopant. Photoluminescence excitation (PLE) maps and Raman spectroscopy will be the primary analysis tools for these studies because they provide information on the specific interactions that affect the electronic and optical structure of SWNTs. Therefore, we will analyze the energy flow in the system and the electronic properties of the tubes as a function of the photoluminescence, surfactant and relative SWNT side-wall structure. We can also extract information on the tube energy levels and the most energy-favorable path for ET processes between tube-tube and tube-dopants by selecting and adjusting the desired bandgap and Fermi level via surfactant selection, thus allowing control over the ET rates.

Conclusion

This project will be the first of its kind to correlate the ET of various tube-tube and tube-molecule interactions both in ensembles and at the single molecular level. It aims to define the electronic transitions that occur in a variety of SWNT systems to improve the control and predictability of the electronic and optical properties of SWNTs. The results of this project will answer fundamental questions on intertube and tube-molecule ET so that SWNT suspensions can be engineered with predictable photophysical properties, and thus have an impact on optoelectronic, sensing, and energy harvesting applications.

Publications

Duque, J. G., C. G. Densmore, and S. K. Doorn. Saturation of surfactant structure at the single-walled carbon nanotube surface. 2010. *Journal of the American Chemical Society.* **132**: 16165.

Duque, J. G., G. Gupta, L. Cognet, B. Lounis, S. K. Doorn, and A. M. Dattelbaum. A new route to flourescent swnt/silica nanocomposites: balancing fluorescence intensity and environmental sensitivity. *Nano Letters.*

Duque, J. G., H. Chen, A. B. Swan, E. H. Haroz, J. Kono, X. Tu, M. Zheng, and S. K. Doorn. Revealing new electronic behaviors in the Raman spectra of chirality-enriched carbon nanotube ensembles. 2010. *Physica Status Solidi B.* **247**: 2768.

Duque, J. G., H. Chen, A. K. Swan, A. P. Shreve, S. Kilina, S. Tretiak, X. Tu, M. Zheng, and S. K. Doorn. Violation of the Condon approximation in semiconducting carbon nanotubes. *Nature.*

Duque, J., A. Nicholas G. Parra-Vasquez, N. Behabtu, M. Green, A. Higginbotham, B. Katherine. Price, A. Leonard, H. Schmidt, B. Lounis, J. Tour, S. Doorn,

L. Cognet, and M. Pasquali. Diameter-Dependent Solubility of Single-Walled Carbon Nanotubes. 2010. *ACS NANO.* **4** (6): 3063.

Kalugin, N., I. Kalichava, J. Fallt, C. D. Barga, C. Cooper, J. Duque, E. Gonzales, S. Doorn, E. Shaner, and A. Gin. The characterization of non-planar graphene nanowires with an Œ© shape cross-section. 2010. *Carbon.* **48** (12): 3405.

In situ X-ray Microdiffraction Study of Nanomechanical Behavior

Amit Misra
20090513PRD1

Introduction

Investigations into the role of plasticity in the mechanical behavior of materials have great importance to the field of materials science, especially for nano-materials where submicron and nanoscale devices are built near the size of their microstructural features. The creation of such small components requires a thorough understanding of the mechanical properties of materials at these small length scales. Integration of nanoscale materials into bulk composite materials systems such as nanolayered copper-niobium developed at LANL opens the opportunity to develop bulk materials with ultra-high strengths. Recent DOE, BES workshop report on Materials under Extreme Environments has called for structural materials that are tolerant to damage under extreme mechanical stresses. The evolution of damage in nanocomposite materials remains an open question. In this work, x-ray diffraction techniques, including synchrotron white-beam x-rays, are being utilized to evaluate the defect densities in plastically deformed nanolayered composites. Especially, synchrotron x-ray microdiffraction observation of a deformed nanopillar sample will provide insights into the dislocation hardening mechanisms that have been not possible from post mortem studies that show minimal retained defects. This study will provide the fundamental understanding crucial to the design of nanomaterials that are ultra-high strength and possess damage tolerance.

Benefit to National Security Missions

This project supports the missions of DOE and other agencies in areas of defense, nuclear energy, and other mission spaces by providing fundamental understanding of damage tolerance of ultra-high strength nanolayered composite materials. In particular, it provides the scientific underpinning of damage tolerant nanolayered composites for materials under extreme environments for a broad range of defense, nuclear energy and transportation applications.

Progress

Using electron beam evaporation with optimized deposition parameters, we have grown a good quality and thermally stable epitaxial Cu/Nb nanoscale multilayered composite materials with individual layer thickness of 20nm. The film exhibits mostly continuous layers of Cu and Nb with minimum pinch-off between layers of Cu and Nb that is found prevalent in the nanoscale multilayers deposited at much higher temperatures. Our observations suggest the importance of maintaining quasi-single crystal growth and continuity from one layer to the next in order to grow high quality quasi-single crystal Cu/Nb nanoscale multilayers of desired thicknesses. This quasi-single crystal Cu/Nb nanoscale multilayer samples will enable us to follow closely the Laue diffraction spots from the multilayers of Cu and Nb and observe how they evolve during the deformation of the sample and thereby learn about the nanoplasticity mechanisms that are at play in the deformation of our nanoscale multilayered materials.

Initial deformation experiments were performed as follows: nanopillar compression samples from the 20nm Cu/20nm Nb multilayer films on sapphire substrates were made via focused-ion-beam machining technique. These pillars had a nominal diameter of 1000 nm and height of 600 nm. The samples were then taken to Advanced Light Source (ALS) at Berkeley to obtain Laue microdiffraction patterns from individual pillars. Then the samples were taken to Stanford University to perform pillar compression to a plastic strain of approximately 10% and brought back to ALS beamline the same day for measurement of the Laue microdiffraction from the same pillar after deformation. The exact same Laue spot from the Cu layers were measured before and after deformation. The same process was repeated for Nb.

Analysis of the measured Laue spots in Cu indicates uniform broadening. The measure of this spot size increase indicated a uniform increase in statistically stored dislocation density from approximately 7 x 10^14 /m^2 to 1.2 x 10^15 /m^2. The deformation in Nb is accommodated both elastically as well as plastically. There appears to be recovery in both crystals and/or interface of Cu and Nb during the deformation. For

an annealed single crystal of Cu, the initial dislocation density is on the order of 10^10 /m^2. The dislocation density increase after equivalent plastic strain in annealed Cu would be almost two orders of magnitude. In the nanolayers, the initial dislocation density is very high because of the high interface area per unit volume. The interface contains a cross-grid of misfit dislocations of an average of 2 nm spacing and given the 20 nm spacing of the interfaces this amounts to a very high estimated dislocation density per unit volume in the as-synthesized materials, on the order of 10^17 /m^2. Our results show that the measured initial dislocation density in nanolayered Cu is very high as compared to annealed Cu, although less than the theoretical upper bound estimate. Furthermore, the increase in the dislocation density after deformation is marginal, when compared to the bulk annealed single crystalline metals. This indicates that the interfaces in the nanolayered Cu/Nb are very effective in trapping and annihilating dislocation content during mechanical deformation.

Most recently, we further studied the **evolution** of plasticity in the nanoscale Cu/Nb single crystal multilayers ***during*** successive uniaxial compression experiments using *ex situ* synchrotron-based Laue X-ray microdiffraction at Beamline 12.3.2 in the Advanced Light Source (ALS), Berkeley Lab. Studying how the dislocation configurations and densities evolve *during* deformation is crucial in understanding the yield, work hardening and recovery mechanisms in the nanolayered materials. Using this approach, we first characterized the initial plasticity state in the Cu and Nb nanolayers (as fabricated pillars, before any compression/deformation) at ALS, and then brought it to Stanford Nanomechanical Lab (we collaborated with Prof. Nix's group at Stanford – one of his senior Ph.D. students, Lucas Berla, was helping us with the pillar compressions) to perform first pillar compression, and then brought it back to ALS again to characterize the plasticity state after the first compression (by observing amongst others X-ray ring width broadening, shifts as well as intensities). We subsequently did these experiments back and forth between ALS Berkeley and Stanford Lab in Bay Area for four successive pillar compressions (total strains = 1%, 2%, 10% and 20%). In so doing, we studied the plasticity evolution that occurred in the course of successive compressions on the nanoscale Cu/Nb multilayer pillars and found significant X-ray ring width broadening in both Cu and Nb layers (which indicates storage of statistically stored dislocations) **initially** (up to strains of about 4%) which was then followed by the saturation of the X-ray ring width broadening (up to large strains of 20%). This indicates that the interfaces in the nanolayered Cu/Nb are very stable and effective in trapping and annihilating dislocation content during mechanical deformation, and explains why the Cu/Nb nanolayers can be deformed to large plastic strains without any onset of plastic instabilities.

Future Work

This work will utilize the unique capability of synchrotron white-beam x-ray diffraction (SXRD) technique as a local probe of strain gradients and geometrically necessary dislocations to study the nanomechanical response of nanolayered materials. A synchrotron white-beam x-ray diffraction technique utilizing focused x-ray beam into the submicron and nanometer resolution has proved to be a unique, powerful tool for the study of plasticity due to its sensitivity to local lattice rotation. This capability becomes crucial when the plasticity mechanisms of crystalline materials at submicron and nanoscales are increasingly known to deviate from their bulk (classical) mechanisms leading to their unexpected mechanical behaviors. Understanding and controlling plasticity and the mechanical properties of materials on this scale could thus lead to new and more robust nanomechanical structures and devices.

Especially, following the size and shape of Laue x-ray microdiffraction spots from a given nanopillar compression sample of a nanolayered sample as a function of compressive strain will provide insights into the dislocation hardening mechanisms that have been not possible yet. By observing the evolution of plasticity in the course of successive compressions of pillars, we could further study the stability and deformability to large plastic strains of other nanolayer systems with different interface structures than Cu/Nb. When other nanolayered systems exhibit stability/deformability to different extents, then it would be insightful to demonstrate if it is correlated with the evolution of dislocation densities in the nanolayered system in the course of large strain deformation.

In addition to leveraging the state-of-the-art synthesis, and nanomechanical and structural characterization capabilities at LANL, this research project will utilize world-class synchrotron x-ray microdiffraction capabilities, such as Paul Scherrer Institute in Switzerland and Advanced Light Source at Berkeley. The ability to understand and control the mechanical properties of these nanolayered composites is important for potentially many scientific as well as technological applications requiring extremely high strength and damage tolerant materials. This research will characterize magnetron sputter deposited nanolayered metallic composites such as copper-niobium. The key goals are to characterize the defect densities accumulated in the nanolayered materials as a function of the (i) nanolayering dimension and (ii) interface structure.

Conclusion

This research will provide fundamental insights into the damage tolerance of nanolayered metallic composites subjected to large strain plastic deformation. Specifically, it will elucidate the nature of interfaces in composite materials and nanostructuring length scales that are ideal for designing damage tolerant nanocomposites that may have applications as super-strong, light-weight engineering

materials and structural components in nuclear energy reactors.

Publications

Budiman, A. S., S. M. Han, P. Dickerson, N. Tamura, M. Kunz, Q. M. Wei, and A. Misra. Plasticity in the Nanoscale Cu/Nb Single Crystal Multilayers as Revealed by Synchrotron Laue X-ray Microdiffraction. *Journal of Applied Physics.*

Budiman, A. S., and A. Misra. Growth and Structural Characterization of Epitaxial Cu/Nb Multilayers. To appear in *Thin Solid Films.*

Novel Fabrication of Metal-Semiconductor Heterostructured Nanowires

Jennifer A. Hollingsworth
20090514PRD1

Introduction

Semiconductor nanowires (SCNWs) have tremendous potential as building blocks in the assembly of nanoscale devices and nanocircuits for optoelectronics and electronics applications. For these applications, however, electrical contacts must be made to the SCNWs. To date, electron-beam lithography is the common approach employed to define contacts for constructing, for example, single-SCNW devices. The contacts created via this approach are considerably larger than the SCNWs themselves, limiting many advantages of nanoscale systems. To address this problem, fabrication of integrated nanoscale contacts have been proposed, but only a few demonstrated: (1) the localized electroless deposition of gold on the tips of CdSe nanorods, (2) the lithographic patterning of metallic Ni on Si NWs to form NiSi/Si/NiSi metal/SC/metal NWs, and (3) the electrodepositions of Au/CdS/Au NWs. These techniques are limited by choice of metal, inadequate size control, and/or the low quality of the electrodeposited SCs. Therefore, a new and more versatile approach for fabrication of functional nanoscale metal-SCNW interfaces is required to facilitate SCNW device applications. Here, we will employ a novel technique that couples two solution-phase growth methods to allow controlled synthesis of nanoscale semiconductor-metal contacts for vastly improved integration into optoelectronic and electronic devices.

Benefit to National Security Missions

This project will support the DOE missions in Energy Security and Threat Reduction by providing critical supporting technologies that will enable the further miniaturization of functional devices with enhanced efficiencies. For example, the materials fabrication strategies developed will be applicable to photovoltaics and sensor technologies.

Progress

The electrochemical work-station setup in the first-year for electrochemical synthesis (Setup 1), which consists of a potentiostat and an electrochemical deposition cell that was custom-made to support membrane electrode assemblies, was used to synthesize Au nanowires of various lengths. The focus this year was on fine-tuning this synthesis to control deposition such that the Au filled the porous alumina membranes either to the top or nearly to the top of the membrane. Although we were previously able to deposit Bi solution-liquid-solid (SLS) catalyst into the porous membranes and onto the templated Au nanowires, and subsequently to grow CdSe nanowires by the SLS mechanism, the resulting constructs were not ideal. Specifically, we observed two general problems: (1) if the CdSe nanowire grew from a Au nanowire surface, the CdSe component was short and narrower (often significantly) in diameter compared to the Au, rendering the CdSe component more rod-like than wire-like, and (2) longer CdSe nanowires grew only from Bi that had separated from the Au and resided on the top of the alumina membrane surface, with these nanowires being very long and thin and without any structural relationship to the thicker Au component. This year, the postdoc has emphasized modifications to the fabrication of the membrane-Au-Bi system to (1) improve the SLS CdSe growth and (2) to improve the interaction between the Bi and the Au and, thereby, the interaction between the CdSe and the Au. Specifically, thin alumina membranes (quality optimized as much as possible, as discussed below) were constructed that allowed the postdoc to fill, or nearly fill, the membranes with Au. Even in this case, electrodeposition of Bi exclusively into the pores proved difficult and insufficiently irreproducible. Therefore, Bi was deposited by e-beam evaporation. The Bi partially enters the pores and partially resides on the membrane surface. A pre-synthesis anneal melts the Bi and encourages it to enter the pores. Alternatively, polishing has been used as a means to removed Bi from the top surface of the membrane and ensure its presence exclusively in the pores. Currently, the influence of the distance between the top of the Au nanowires and the top of the membrane (from 0 nm to 10's of nm's) on our ability to limit CdSe nanowire growth to the Au interface is being explored as a key parameter.

Using this approach, the postdoc has successfully synthesized Au-CdSe hybrid nanowires comprising

approximately equal 500 nm segments and uniform diameter across the interface (Figure 1). This is a significant advance from the short and thin (or the detached long and ultrathin) CdSe nanowire segments produced in the first year of the project. While chemical yield of these hybrid structures remains low, the approach is clearly on the right track toward realizing the primary goal of the project.

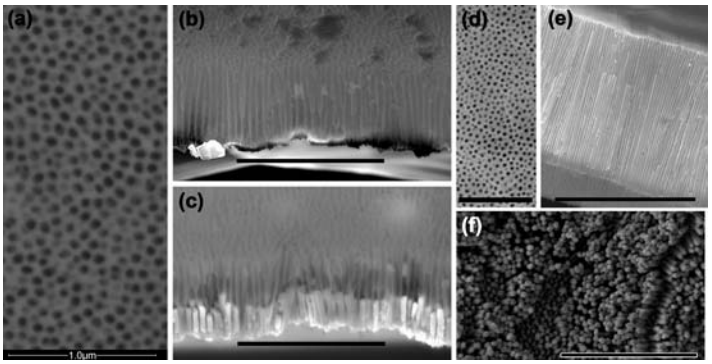

Figure 1. Optimized porous anodic alumina templates: (a)-(b) Ultrathin membranes on solid substrate support. (c) Au rods electrochemically grown within an ultrathin membrane. (d)-(e) Thick, free-standing small-diameter membranes. (f) Au nanowire vertical array formed in a freestanding membrane.

Utilizing our Electrochemical Setup 2, we have continued to fabricate a range of ultra-thin porous anodic alumina membranes. Compared to last year, we have optimized the method and have established clear materials parameter requirements for successful synthesis of uniform (laterally and vertically) porous membranes (Figure 2).

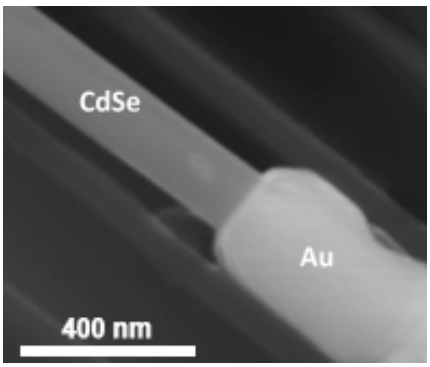

Figure 2. Scanning electron microscopy (SEM) image of Au rod / CdSe semiconductor nanowire hybrid nanostructure.

Namely, we have found that high quality metal films are critical for the successful preparation of the ideal porous membrane. We have determined that to prepare the alumina membranes, we need to be able to controllably grow thick aluminum films (500-2000 nm). Our experience with Al films prepared to date using existing LANL (and SNL) equipment, however, has shown that these films are characterized by variations in thickness and grain size. These variations render the alumina membranes prepared from the aluminum films irregular in pore size and uncontrolled in terms of the percent of pores that access the underlying Au layer. Both of these factors inhibit our ability to grow well-defined arrays of metal nanowires and to optimize our approach. For this reason, this project will benefit from a new CINT capability that is currently being acquired, a combined DC sputtering/thermal-evaporation deposition system that offers a unique confocal sputtering capability for rapid deposition of highly uniform aluminum films (+/- 2.5%).

In the past two, we have achieved an important breakthrough in our ability to grow NW/nanometal contacts. Namely, given the challenges to our initial approach described above, we sought an alternative approach to adhere Bi catalyst particles to Au NW/rods. We found that we were able to modify a literature report for synthesizing semiconductor heterobranched-NWs (Ref. 1: Dong et al. J. Am. Chem. Soc. 2007) to allow us to fabricate semiconductor/metal NW heterostructures. For this, we used a polymer (PEI: polyethyleneimine) to adhere Bi nanoparticles to Au nanorods, which were synthesized electrochemically but subsequently liberated from their templates. We have found that Au rod/Bi nanoparticle assemblies are sufficiently easy to separate from free-Bi nanoparicles when the Au rods are relatively large in diameter (>200 nm), while thinner Au rods are less easy to separate by centrifugation / sedimentation techniques. However, smaller diameter Au rods are desired for applications requiring more comparable semiconductor/metal-contact sizes. To address this deficiency in our approach, we incorporated a magnetic segment (Ni) into the Au rods to allow for magnetic separation of the bound-Bi from the free-Bi nanoparticles. The Au/Bi constructs were suspended in a reaction solution for SLS-based CdSe NW growth. Adhesion of Bi nanoparticles to the Au rods and successful growth of the semiconductor NWs were assessed by SEM and TEM characterization (Figure 3). Currently, all of these novel composite semiconductor/metal nanoscale structures are being tested for electronic and optical properties.

The postdoc has also been instrumental this year in establishing our new flow-SLS synthesis capability and is preparing to use the flow reactor to grow semiconductor nanowires from her alumina templates.

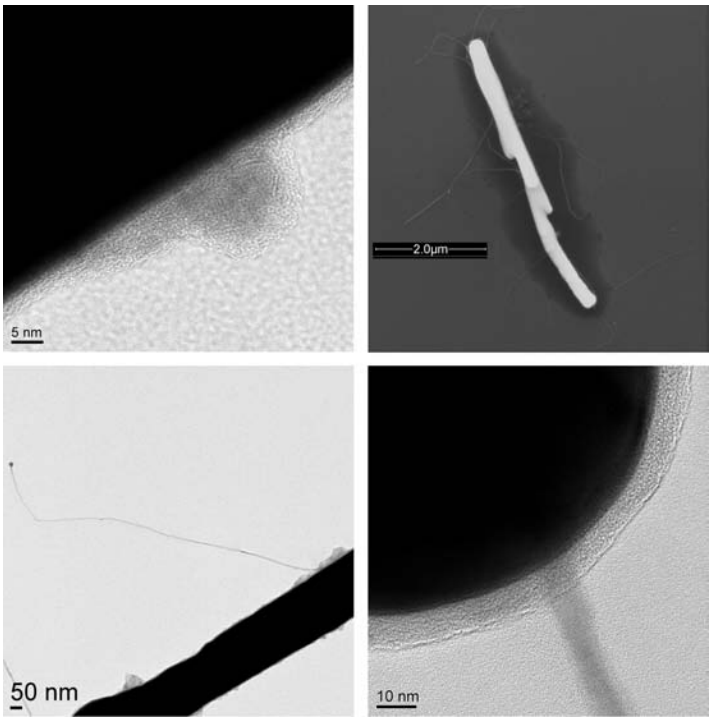

Figure 3. (top-left) Transmission electron microscopy (TEM) image of a Bi nanoparticle adhered to a Au rod and surrounded by PEI polymer. (top-right) SEM image of a Au rod with numerous CdSe nanowires growing from it. (bottom-left) TEM image of a Au rod with a CdSe nanowire growing from it. A Bi nanoparticle is evident at the end of the nanowire. (bottom-right) Higher resolution TEM image of a CdSe nanowire extending from a Au rod. The nanowire growth starts at the Au interface and projects through the PEI polymer layer.

Future Work

Previously, we identified a key technological need for a more versatile approach for the fabrication of functional nanoscale metal-semiconductor nanowire interfaces in order to facilitate semiconductor-nanowire device applications. We proposed a novel technique that couples two solution-phase growth methods: Solution-Liquid-Solid (SLS) semiconductor-nanowire growth with template-based metal electrodeposition. In the SLS method, low-melting metal catalysts (e.g., In, Bi, and Sn) support the growth of high-quality semiconductor-nanowires—upon supersaturation of chemical precursors in the molten catalyst, the semiconductor-nanowire nucleates and then grows with high crystallinity. The template-directed synthesis is ideal for metal growth, and it is a facile method for fabricating multi-segmented metal nanowires (e.g., Au with Bi tips, where the Bi would serve as the SLS catalyst) via sequential reductions of metal ions into a nanopore template. The unique combination of these techniques, we predicted, would enable fabrication of heterostructured metal-semiconductor nanowires integrated at the nanoscale. This approach proved to be a valid one; however, it was not able to provide for high yields of the targeted hybrid structures due to the various reasons described in the Progress section of this report. We will continue to pursue this approach as it allows the possibility for creating ordered vertical arrays of metal-contacted semiconductor nanowires. In parallel, though, we will expand on our newer approach to forming metal-semiconductor nanoscale contacts -- see heterobranched Au-rod/semiconductor nanowire constructs in Progress. Here, we will demonstrate synthetic control by manipulating contact density. We will show versatility and generalizability by employing a variety of metal rod compositions (e.g., Ag, Pt) and semiconductor nanowire compositions (e.g., CdTe). The resulting nanowires are being and will continue to be structurally characterized, and their optical / electrical properties will be investigated by single-nanowire photoluminescence spectroscopy and gate-dependent I-V measurements, respectively. Finally, with rods comprising both gold and magnetic-metal segments in hand, we will proceed with magnetic separation, bismuth incorporation, and nanowire growth using these systems. We will explore whether this added functionality can also facilitate post-growth magnetic manipulation and assembly of the nanowires.

Conclusion

The primary aim is to develop a novel method for creating nanoscale electrical contacts. Successful coupling of the now distinct metal and semiconductor nanowire growth techniques will allow us to establish a general route to new, hybrid nanoscale structures, including technologically important (but currently impractical) high-density, vertically addressable nanowire assemblies, enhancing LANL's reputation in the growing field of nanomaterials design and integration. Simply put, the new class of metal-semiconductor nanowires will expedite the revolution of nanoscale electronic devices and circuitry.

References

1. Dong, A., R. Tang, and W. E. Buhro. Solution-based growth and structural characterization of homo- and heterobranched semiconductor nanowires. 2007. *Journal of the American Chemical Society.* **129** (40): 12254.

Publications

Laocharoensuk, R., N. Smith, J. K. Baldwin, A. Gin, and J. A. Hollingsworth. Versatile Solution-Phase Approach for Fabrication of Metal-Semiconductor Heterostructured Nanowires. Presented at *Materials Research Society Spring Meeting 2010.* (San Francisco, 5-9 April 2010).

Laocharoensuk, R., N. Smith, K. Palaniappan, J. K. Baldwin, and J. A. Hollingsworth. Integration and development of solution-phase techniques for fabrication of novel heterostructured nanowires. Presented at *Materials Research Society Fall Meeting 2010.* (Boston, Nov. 29-Dec. 3 2010).

Nanogenerators Driven by Both Magnetic and Mechanical Waves

Quanxi Jia
20090519PRD2

Introduction

Wireless devices are promising in real-time biomedical monitoring and operation, but their practical applications are limited by the short lifetime of present power sources. In order to work in a long-term of period and avoid the cost of battery replacement, these devices should be self-powered or powered by the energy from non-contact sources such as mechanical or magnetic waves. Nowadays, the development of nanotechnology dramatically reduces the size of the devices into nano-scales. It is indispensable that nanogenerators are developed so that they can be used to power these devices. Recently, piezoelectric nanogenerators, which could transform vibrational or mechanical energy directly to electricity to power nano devices, were reported. However, when the wireless devices are embedded into a substance, the body may absorb and decrease the applied vibration energy. We have explored different electronic films and ceramic like materials to develop the nanogenerator that can be driven by both magnetic and mechanical waves. Compared to mechanical source, a magnetic source is easier to control by adjusting the frequency and intensity of the magnetic field. Therefore, the nanogenerators may not only be an efficient power source, but also enable the wide application of nano wireless devices.

Multiferroic magnetoelectric (ME) materials, which simultaneously exhibit ferroelectricity and ferromagnetism, have recently been extensively investigated due to their both scientific interest and technological promise for novel multifunctionalities. For example, high performance devices such as magnetic sensors, microwave phase shifters, and electrical and/or magnetic tunable devices can be readily fabricated based on this class of materials. As the objective of this project is to develop innovative electronic devices using such materials in thin film form, the first task is to grow high quality ME thin film materials using the techniques available at Los Alamos National Laboratory.

The ME effect was first observed in single phase materials nearly 50 years ago. The largest value of ME voltage coefficient for a single phase material has been detected in Cr_2O_3 crystals, where the ME voltage coefficient is around 20mV/cm-Oe. The ME effect in single phase material, although scientifically interesting, has always shown small values of ME voltage coefficient. From a technological point of view, the appearance of such an effect only at low temperatures also limits its applications. In other words, the weak ME effects at very low temperature cannot meet the requirements of practical applications. Recently, $BiFeO_3$ thin film has attracted a lot of attention due to its large multiferroic ME coupling at room temperature. Most of these films have been fabricated by either pulsed laser deposition or sol-gel methods. Although pulsed laser deposition can deposit epitaxial $BiFeO_3$ thin films, the deposition conditions are critical for high performance films and the technique itself is expensive. Sol-gel method is a chemical solution technique which does not need complicated setup. However, polycrystalline $BiFeO_3$ thin films, which show degraded properties, are often produced by this technique. In the following, we highlight two main efforts to achieve high performance ferroelectric and ferromagnetic thin films based both pulsed laser deposition (PLD) and polymer assistant deposition (PAD), a cost effective and patented process at Los Alamos National Laboratory.

Benefit to National Security Missions

This research ties to the mission of DOE Office of Science for fundamental understanding of materials. LANL's thrusts in functional materials, nanotechnology, and sensors directly benefit from this project. Microsensors for a range of national security problems, including monitoring weapons inventories, could ultimately benefit from this work.

Progress

Recently piezoelectric/magnetostrictive composites have been reported and showed giant magnetoelectric (ME) coupling at room temperature. For example, the voltage coefficient of Terfenol-D/PZT bulk laminates is 2-4 V/cm-Oe. The fabrication method for bulk metal/oxide laminates is by using hard epoxy to bind each layer together. However, this method does not work

out for thin film heterostructures which are the future for miniature devices. One of the challenges for the integration of ferroelectric materials with magnetic materials such as Terfenol-D is the oxidation of the magnetic material at the processing temperature and environment. To deposit a $BaTiO_3$ thin film on Terfenol-D substrate, we need to significantly decrease $BaTiO_3$ deposition temperature. We discovered that an increase of the laser power can significantly reduce the deposition temperature during $BaTiO_3$ growth. In this experiment, we used $LaAlO_3$ substrate since it has similar lattice parameter as $BaTiO_3$. When the laser power increased to 3.5 J/cm^2, epitaxial $BaTiO_3$ thin films were fabricated at a deposition temperature as low as 400C, much lower than a substrate temperature of 750 C or above commonly used for pulsed laser deposition where the laser energy of 2 J/cm^2 is used. At this low temperature, the interface diffusion between the $BaTiO_3$ and the Terfenol-D could be decreased and the oxidation of Terfenol-D could be avoided.

Polymer assistant deposition offers the opportunity to grow crack free epitaxial metal oxide films. We used PAD to deposit ultra-thin epitaxial $BiFeO_3$ (10 nm per layer) films on $BaTiO_3$, $SrTiO_3$ and $LaAlO_3$ (001) substrates. High resolution x-ray diffraction (XRD) measurements shows that $BiFeO_3$ thin films deposited on these three different substrates are high quality epitaxial films, while the detailed crystal structure of $BiFeO_3$ thin films changes with the substrate due to the mismatch between the substrate and the $BiFeO_3$ materials. The lattice parameters of $BiFeO_3$ thin film deposited on $LaAlO_3$ are a = b = c = 0.3944 nm with $\alpha = \beta = \gamma = 89.42^o$. In other words, the crystal structure of $BiFeO_3$ is rhombohedra, the same as the bulk $BiFeO_3$ single crystal. Since there is a large lattice mismatch between the $BiFeO_3$ and $LaAlO_3$ (~6%), the $BiFeO_3$ thin film is fully relaxed and does not constrained by the substrate. The thin film deposited on $LaAlO_3$ shows antiferromagnetic properties in the out-of-plane direction and a weak ferromagnetic in the in-plane direction with a saturated magnetization of 5 emu/cc. For the $BiFeO_3$ thin film deposited on $SrTiO_3$ substrate (the lattice parameter of $BiFeO_3$ is 1% smaller than $SrTiO_3$), the lattice parameters of $BiFeO_3$ are a = b = 0.3904 nm, c = 0.4046 nm with $\alpha = \beta = \gamma = 90^o$. It is obvious that the $BiFeO_3$ on $SrTiO_3$ has a tetragonal structure. The in-plane lattice parameter of the $BiFeO_3$ is the same as the $SrTiO_3$. This indicates that the in-plane lattice of $BiFeO_3$ has been constrained by the substrate. As a result, the lattice parameter in the out-of-plane is elongated. High resolution TEM confirmed that the $SrTiO_3$ and $BiFeO_3$ are coherent at the interface. The saturated magnetization in the in-plane direction change to 30 emu/cc, six times larger than that of $BiFeO_3$ thin film deposited on $LaAlO_3$ substrate. To do the comparison, $BaTiO_3$ substrate was also used since the lattice parameter of $BaTiO_3$ is 1% larger than that of $BiFeO_3$. The lattice parameters of as deposited $BiFeO_3$ thin film are a = b = 0.4001nm, c = 0.3872 nm with $\alpha = \beta = \gamma = 90^o$. The lattice parameter in the in-plane direction is elongated while the lattice parameter in the out-of-plane direction is constrained.

Future Work

We will develop a nanogenerator that can be driven by both magnetic and mechanical waves. Compared to mechanical source, a magnetic source is easier to be controlled by adjusting the frequency and intensity of the magnetic field. Therefore, the nanogenerators may not only be an efficient power source, but also enable the wide application of nano wireless devices.

To develop nanogenerators, our tasks and approaches are composed of patterned carbon nanotube arrays and BaTiO3/Ni-ferrite thin films, by using both piezoelectric effect (converting mechanical energy to electrical energy) and magnetoelectric effect (converting magnetic energy to electrical energy). First, carbon nanotube arrays with well-controlled patterns will be fabricated on silicon or other ceramic substrates. The nanotube array changes the 2D substrate to a 3D template, which facilitates the fabrication of complex composite structures. Following that, piezoelectric $BaTiO_3$ (BTO) and magnetic $NiFe_2O_4$ (NFO) films will be subsequently coated on the carbon nanotube arrays. A large magnetoelectric coupling from BTO/NFO composite is expected due to the strain transition at the interface. We will investigate the magnetoelectric coupling in the nano-scaled BTO/NFO composites (in comparison with the composites in the bulk format). To fabricate these materials, we will use both pulsed laser deposition (PLD) and polymer assistant deposition methods, both are available at LANL, to deposit BTO and NFO on nanotube array templates. The microstructure of the nanocomposites will be characterized by XRD and TEM. The structure-property relationship of this composite is expected to be established through such systematic investigation. The output voltage as a function of both mechanical and magnetic signals will be investigated thereafter.

Our goals are to (i) develop a new pattern design method in nanostructured materials by using carbon nanotube arrays; (ii) investigate the magnetoelectric coupling of nanoscaled BTO/NFO composites; and (iii) develop nanogenerators driven by both mechanical and magnetic waves.

Conclusion

We successfully deposited ferroelectric $BaTiO_3$ films on Terfenol-D by pulsed laser deposition. By increasing the laser power during the film deposition, we could reduce the substrate temperature which is important to integrate these two materials. We further studied the structural and the transport properties of $BiFeO_3$ films deposited by polymer assisted deposition on different substrates. The lattice strain has a significant effect on both the structural and transport properties.

Publications

Xiong, J., V. Matias, H. Wang, J. Zhai, B. Maiorov, D. Trugman, B. W. Tao, Y. R. Li, and Q. X. Jia. Much Simplified IBAD-TiN Template for High Performance Coated Conductors. 2010. *J. Appl. Phys..* **108**: 083903.

Zhai, J., Y. Y. Zhang, G. F. Zou, L. Yan, J. Xiong, P. Shi, and Q. X. Jia. Epitaxial multiferroic BiFeO3 thin film grown by polymer assistant deposition. Invited presentation at *MS&T'10.* (Houston, 17-21 Oct. 2010).

Zhai, J., Y. Y. Zhang, G. F. Zou, L. Yan, M. J. Zuo, J. Xiong, P. Shi, and Q. X. Jia. Structure control of epitaxial BiFeO3 thin film by polymer assistant deposition. *J. Mater. Res..*

Zhai, J., Y. Y. Zhang, G. F. Zou, L. Yan, M. J. Zuo, J. Xiong, and Q. X. Jia. Multiferroic epitaxial BiFeO3 thin film grown by polymer assistant deposition. Presented at *MRS Spring Meeting.* (San Francisco, CA, 5-9 April 2010).

Zhang, Y. Y., C. J. Sheehan, J. Zhai, G. F. Zou, H. M. Luo, J. Xiong, Y. T. Zhu, and Q. X. Jia. Polymer-embedded Carbon Nanotube Ribbons for Stretchable Conductors. 2010. *Adv. Mater..* **22**: 3027.

Zou, G., H. M. Luo, Y. Y. Zhang, J. Xiong, Q. Wei, M. Zhuo, J. Zhai, H. Wang, D. Williams, N. Li, E. Bauer, X. H. Zhang, T. McCleskey, Y. R. Li, and A. K. Burrell. A Chemical Solution Approach for Superconducting and Hard Epitaxial NbC Film. 2010. *ChemComm.* **46**: 7837.

Hybrid Semiconductor-metal Nanostructures for Amplification of Surface Plasmons

Jeffrey M. Pietryga
20090523PRD2

Introduction

Near the beginning of the 20th century, Einstein discovered the "photoelectric effect," in which light hitting a metal surface can cause electrons to move, and even to be ejected from the metal if the energy is high enough. Light interacts with nano-sized metal particles in a somewhat different way, by causing all the free flowing conductive electrons within the particle to slosh back and forth collectively. These motions are called "surface plasmons," and they are responsible for the intense colors of solutions of metal nanoparticles (such as in some types of stained glass). Because of their intensity, these light-absorbing transitions have tremendous potential for use in photonic circuitry (the next generation of ultra-fast computers based on moving photons instead of electrons), as well as in enhancing the spectroscopy of nearby molecules (such as for detection of single molecules of chemical threat agents by Surface-enhanced Raman Spectroscopy). However, these plasmon excitations are hard to extract from the nanoparticles, because they are quickly dampened within a very short distance from the surface. Thus, practical application of these effects has been limited. A possible solution to this problem is the development of methods for plasmon amplification. A recent theoretical paper [1] discusses the possibility of plasmon amplification using direct stimulated emission of plasmons from a proximal system of resonant dipole emitters, such as semiconductor quantum dots (QDs). We propose to use this new physical process, which is similar to that applied to make the intense, coherent light of lasers, to amplify plasmons by many orders of magnitude. In a nutshell, we will surround a metal nanoparticle with fluorescent nano-sized semiconductors of specifically chosen size and material. We will then use a light source to excite the semiconductors, and they will pump their energy directly into the plasmon vibrations of the metal nanoparticle. The additive effect of the contribution of 10s to 100s of semiconductors will create a non-linear increase in the spatial extent and gain lifetime of surface plasmons, which will finally allow their practical application in plasmon lasers, circuitry and single-molecule chemical agent detectors.

Benefit to National Security Missions

This project will support the DOE mission in Threat Reduction, by enhancing our understanding of plasmon amplification, which could ultimately lead to a new class of chemical threat agent sensor with orders of magnitude higher sensitivity. It also supports Office of Science missions, especially in energy and within the purview of CINT. The exquisite sensitivity of this technique may also contribute to tracking trace materials in the weapons program.

Progress

Tremendous progress has been made on the materials synthesis effort of the project, which is the primary purpose of this work. The ultimate goal was to create a series of plasmonic-dielectric-semiconductor (core-shell-shell) hybrid nanostructures which would be probed for effects such as plasmon amplification using some of the advanced spectroscopic tools available on the Quantum Dot Team within C-PCS. The work would use published results from a previous postdoc [2] as a starting point, but required significant advances in synthesis of colloidal plasmonic structures, with and without dielectric shells, first. It was anticipated that for the first year, Bisnhu Khanal would focus on expanding known methods for colloidal gold (Au) particle synthesis, including those which he developed during his previous work at Rice University, to develop reliable routes to a range of novel shape- and composition-controlled plasmonic structures. However, Dr. Khanal has already produced a wide range of gold (Au) plasmonic structures, including spherical Au nanoparticles and Au nanorods ranging in aspect ratio from 2 through 100. Further, he has also already established a reliable protocol for production of Au@Ag core@shell nanoparticles and nanorods with controllable shell thickness. These materials have become popular among many other members of the team for a number of potentially productive side projects, particularly in the use of plasmonic particles for enhancing sunlight capture and energy transfer in nanocrystal thin-film photovoltaics.

Such quick progress has allowed Dr. Khanal to move on

to the second phase of the materials work, which is to coat the plasmonic structures with a dielectric layer and couple them to other nanoparticles. Despite the previous report, the growth of a shell of silica (SiO_2) of controlled thickness proved to be far from trivial. After careful experimentation with the reaction conditions, Dr. Khanal was able to accomplish it not only for Au nanoparticles, but also for Au nanorods, Au nanoplatelets (Figure 1) and the Au@Ag core@shell nanorods. Finally, coupling of semiconductor nanoparticles of a number of formulations has also recently been demonstrated, with straightforward control over and size, QD composition and loading, and the separation distance. We are in the final stage of submitting this novel nano-engineering method to the high profile international journal *Nature Nanotechnology*.

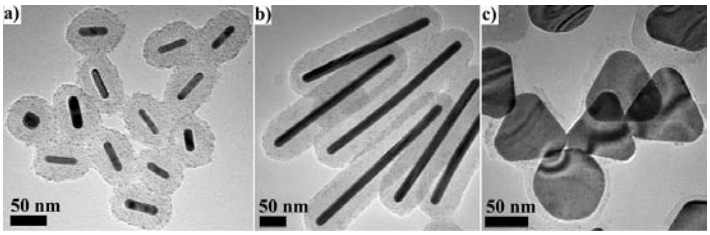

Figure 1. Transmission Electron Microscopy (TEM) image of metal/dielectric/semiconductor hybrid nanostructures composed of a) single-crystalline AuNRs; b) pentahedrally twinned AuNRs; and c) gold platelets.

As a result of this success, other members of the Quantum Dot team have already been able to start the advanced spectroscopic studies of the hybrid particles. Specifically, Young-Shin Park has been attempting to observe single-particle absorption and fluorescence of the hybrid structures. Preliminary results are interesting, but indicate that a series of "control" particles, including simple silica particles, and silica particles with only semiconductor nanoparticles (no Au cores), will be necessary to fully deconvolve and interpret the signatures that were observed. Such control particles will be available very soon. Finally, Anshu Pandey's initial studies of particle ensembles have implied that all plasmonic systems, in which plasmonic Au cores are coupled to plasmonic Ag nanoparticles in the shell, could also be very interesting. Dr. Khanal was able to make simple modifications to the methods he already developed to produce simple versions of these new structures as well.

In addition, Dr. Khanal developed a method for the direct growth of a continuous semiconductor shell directly on top of Au nanorods (Figure 2) which opens a new direction for the investigation of the effect of surface plasmons on processes within the semiconductor or vice versa. His materials are already being studied by a number of spectroscopists within our team.

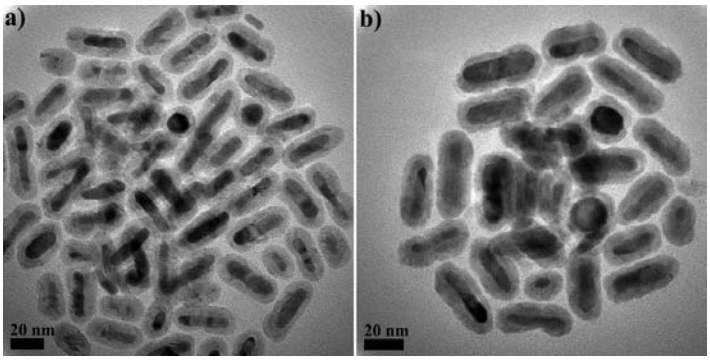

Figure 2. TEM image of direct growth of a) CdS or b) PbS on AuNRs.

Future Work

Interest in the manipulation of the plasmon resonances of metal nanostructures has grown tremendously in the context of using surface plasmons are utilized to carry, store, and process information. Practically, however, the utility of "plamonic circuits" is restricted by strong damping that limits the propagation length of surface plasmon polaritons to a few microns. This research will have a strong and significant impact on the existing problems of surface plasmon damping. We expect that our work will result in the experimental demonstration of plasmon amplification, which can potentially lead to the development of sources of coherent plasmons ("plasmon lasers"). Plasmon amplification can also be utilized for producing giant field-enhancement factors, useful in sensing applications utilizing surface-enhanced spectroscopic techniques (such as SERS). Finally, we will investigate the corollary effects of the plasmons on the properties of the nearby QDs. It is expected that the large electric fields produced by the plasmonic metal nanoparticles can greatly affect the absorption cross-sections, relaxation rates and energy transfer processes of the QDs. Each effect is also expected to demonstrate unique dependence on parameters such as separation distance and the overlap of metal and QD spectral features which will need to be probed using a carefully varied set of these new nanostructures. Finally, we will probe the effect of the plasmons on the non-linear optical properties of the QDs, including their two-photon absorption cross-sections. All of these effects are of great potential importance in the use of these unique hybrid structures in photovoltaics.

Conclusion

We hope to experimentally demonstrate that surface plasmons can be amplified by indirect excitation using nearby semiconductor nanocrystals. Previously, this effect has only been seen theoretically. If this is successful, it opens to door to a host of applications that could take advantage of extremely strong plasmon fields. This includes photonic computing (based on photons instead of much slower electrons), plasmonic lasers (or "spasers") enhanced Raman-based chemical fingerprint detectors

for pollutants, chemical agents, explosives, etc., with potentially single-molecule sensitivity, and photovoltaics.

References

1. Bergman, D. J., and M. I. Stockman. Surface plasmon amplification by stimulated emission of radiation:. 2003. *Physical Review Letters.* **90** (2): 027402/1.

2. Liu, N., B. Prall, and V. Klimov. Hybrid gold/silica/ nanocrystal-quantum-dot superstructures: Synthesis and analysis of semiconductor-metal interactions. 2006. *JOURNAL OF THE AMERICAN CHEMICAL SOCIETY.* **128** (48): 15362.

New Generation of Fluorescent Probes for In-Vivo Imaging

Jennifer Martinez
20090534PRD3

Introduction

Selection of suitable probes for in-vivo imaging has been a challenge for decades. Noble metal nanoclusters (NCs) (made of 4-30 atoms, ≤ 1nm) have strong fluorescence. NCs were originally made in gas phase. Recently, Martinez and colleagues developed strategies to synthesize water-soluble nanoparticle-free nanoclusters. We are creating nanoclusters of defined size/fluorescence, using biological molecules as templates to guide their formation. DNA, proteins, and peptides are being used to create clusters as part of a molecular recognition unit. We are creating a multifunctional molecule (i.e. in DNA) that both templates nanoclusters and contains a recognition unit to bind proteins.

Benefit to National Security Missions

This project is largely focused on biological threat reduction and health science as applicable for NIH and DoD/DHS agencies. Control at the nanoscale, as exercised in this project, builds underlying capability for renewable energy missions.

Progress

DNA an attractive tool for biothreat detection because of: 1. Complimentary base pairing. 2. Rapid enzymatic means of replication. 3. Low cost. Many of the same features make DNA an attractive tool for the synthesis of: 1. Two- and three-dimensional nanostructures. 2. Templating inorganic materials. In the medical diagnostics arena, the molecular specificity of DNA is often used to accurately confirm the presence of one or many DNA molecules. This simultaneous measurement of multiple DNA sequences requires many difference fluorophores. We are using DNA to not only template nanomaterials (fluorescent nanoclusters), but to use them for multiplex analysis of DNA or proteins. Among the DNA bases, cytosine is well known for its ability to bind Ag+ ions. Taking advantage of Ag+-base binding, other groups have each developed nice strategies to synthesize Ag-nanoclusters templated, most typically, in cytosine-rich single-stranded DNA. While Dickson and coworkers produced individual silver nanoclusters with distinct emissions, most of the clusters were produced under different buffer and salt conditions, which likely limits their practical use. Conversely, while Fygenson and colleagues produced clusters under one reaction condition, the resultant clusters had broad excitation and emission profiles. Because most multiplex assays are performed under one buffer condition (typically physiological pH), there is still a need for a palette of nanoclusters that each emit at different wavelengths in the same conditions (i.e. pH, buffer, temperature). We synthesized and photophysically characterize Ag-nanoclusters, which were templated on DNA under one reaction condition (near physiological pH), with distinct, and narrow, excitation and emission profiles tuned to common laser lines (Figures 1 and 2).

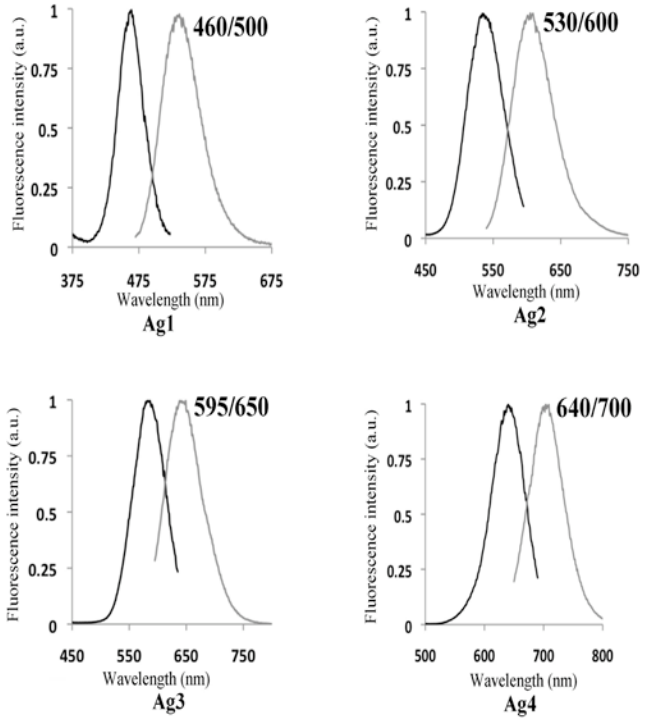

Figure 1. Fluorescence of four different Ag-DNA nanoclusters.

Nanocluster	Emission peak (nm)	Lifetime (ns)	Fractional intensity	Quantum yield
AG1	550	2.5 0.59	38 62	0.002 ± 0.0002
AG2	600	2.86 0.8	59 41	0.107 ± 0.014
AG3	650	3.47 1.32	64 36	0.640 ± 0.014
AG4	700	3.6		0.524 ± 0.034

Figure 2. Fluorescence properties for four different Ag-DNA nanocluster.

While advancements in nanocluster synthesis have been made, the use of metallic nanoclusters for biological- or chemical-sensing is still in its infancy. We have developed and used an intrinsically fluorescent recognition ligand based on a DNA aptamer-templated AgNC for specific and sensitive protein detection. Aptamers are nucleic acids (DNA or RNA) that are evolved to specifically bind proteins or low-molecular-weight inorganic or organic substrates. Because of their specificity and good binding constants, aptamers have been used for detection of heavy metals, proteins, cancer cells, and for the nanoscale assembly of biomolecules. Our intrinsically fluorescent recognition ligand combines the strong fluorescence of oligonucleotide templated AgNCs with the specificity and strong binding affinity of DNA aptamers for their target proteins, to develop a new strategy for detection of specific proteins. Thus, the AgNC-aptamer assembly serves as both a fluorescent label and a specific binding ligand. Our in situ method is a single step that requires no covalent attachment of aptamer nor protein to fluorophore, and is thus a simple and inexpensive labeling and detection method.

Using simple surfactants with gold or silver, we have made silver wires, gold triangular disks, and gold triangular rings. These materials are currently being assembled using DNA ligands.

Future Work

The goal of our work is to produce stable, biocompatible nanoclusters with complete control over their sizes in order to tune their fluorescent properties. To achieve this goal, we will: 1. Explore bio-inspired and traditional methods of NC synthesis. 2. Characterize NC morphology and photophysical properties. 3. Demonstrate the utility of NCs in biological imaging and sensing. We will use synthetic (1. dendrimers, 2. polymers) and biological (1. peptides, 2. proteins, 3. DNA) templates to generate size-controlled nanoclusters. State-of-the-art facilities available at LANL will be used to characterize the newly developed nanoclusters. Nanocluster size and morphology will be determined by: 1. Electron microscopy. 2. Mass spectrometry. 3. Scattering techniques. Raman, single-molecule, and time-resolved laser spectroscopies will be employed to characterize their photophysical properties in collaboration with Drs. Jim Werner and Andy Shreve.

Conclusion

To synthesize nanoclusters with specific photophysical properties is a challenge with profound implications. In general, biological sensors require stable and small-sized probes with wide-ranging fluorescence, which are developing here. By synthesizing nanoclusters that span a wide range of fluorescence frequencies and are much smaller than the biological molecules (proteins etc), we can understand the dynamic changes in different proteins, simultaneously, without disrupting their structures and movements. Our nanoclusters can be used for a variety of other purposes including catalysis, light harvesting, biological sensing and fluorescence imaging. Our clusters are being actively applied toward biothreat detection.

References

1. Bao, Y., H. Yeh, C. Zhong, S. Ivanov, J. Sharma, M. Neidig, D. Vu, A. Shreve, R. Brian. Dyer, J. Werner, and J. Martinez. Formation and stabilization of fluorescent gold nanoclusters using small molecules. 2010. *Journal of Physical Chemistry C.* **114** (38): 15879.

2. Yeh, H., J. Sharma, H. Yoo, J. Martinez, and J. Werner. Photophysical characterization of fluorescent metal nanoclusters synthesized using oligonucleotides, proteins and small molecule ligands. 2010. In *Reporters, Markers, Dyes, Nanoparticles, and Molecular Probes for Biomedical Applications II ; 20100125 - 20100127 ; San Francisco, CA, United States.* Vol. 7576, p. var.pagings.

3. Sharma, J., H. Yeh, H. Yoo, J. Werner, and J. Martinez. A complementary palette of fluorescent silver nanoclusters. 2010. *CHEMICAL COMMUNICATIONS.* **46** (19): 3280.

4. Yeh, H., J. Sharma, J. Han, J. Martinez, and J. Werner. A DNA-silver nanocluster probe that fluoresces upon hybridization. 2010. *Nano Letters.* **10** (8): 3106.

5. Yeh, null., null. Sharma, null. Yoo, and null. Martinez. Fluorescence enhancement of DNA-silver nanoclusters from guanine proximity. 2010. *DOE.*

6. Yoo, H., J. Sharma, H. Yeh, and J. Martinez. Solution-phase synthesis of Au fibers using rod-shaped micelles as shape directing agents. 2010. *CHEMICAL COMMUNICATIONS.* **46** (36): 6813.

Publications

Bao, Y., H. Yeh, C. Zhong, S. Ivanov, J. Sharma, M. Neidig, D. Vu, A. Shreve, R. Brian. Dyer, J. Werner, and J. Martinez. Formation and stabilization of fluorescent

gold nanoclusters using small molecules. 2010. *Journal of Physical Chemistry C.* **114** (38): 15879.

Sharma, J. K., H. C. Yeh, H. Yoo, J. H. Werner, and J. S. Martinez. In-situ generation of aptamer templated silver nanoclusters for label-free protein detection. To appear in *Chemical Communication.*

Sharma, J., H. Yeh, H. Yoo, J. Werner, and J. Martinez. A complementary palette of fluorescent silver nanoclusters. 2010. *CHEMICAL COMMUNICATIONS.* **46** (19): 3280.

Yeh, H., J. Sharma, H. Yoo, J. Martinez, and J. Werner. Photophysical characterization of fluorescent metal nanoclusters synthesized using oligonucleotides, proteins and small molecule ligands. 2010. In *Reporters, Markers, Dyes, Nanoparticles, and Molecular Probes for Biomedical Applications II ; 20100125 - 20100127 ; San Francisco, CA, United States.* Vol. 7576, p. var.pagings.

Yeh, null., null. Sharma, null. Yoo, and null. Martinez. Fluorescence enhancement of DNA-silver nanoclusters from guanine proximity. 2010. *DOE.*

Yoo, H., J. K. Sharma, and J. S. Martinez. Solution-phase synthesis of trigonal and hexagonal Au rings. *Angew. Chemie Int. Ed..*

Yoo, H., J. Sharma, H. Yeh, and J. Martinez. Solution-phase synthesis of Au fibers using rod-shaped micelles as shape directing agents. 2010. *CHEMICAL COMMUNICATIONS.* **46** (36): 6813.

Study of Chemical and Electronic Structure in Metal-Containing Nanoparticles and Nanoclusters

Andrew P. Shreve
20090539PRD4

Introduction

The geometry and electronic structure of metal-containing nanoclusters and nanoparticles will be studied. These nanomaterials are used in applications because of their behavior. For example, small gold clusters have unexpected light emission properties. However, their chemical structure and behavior are not well understood. How these properties control the overall performance of the particles is also still unknown. Spectroscopic, structural, and imaging methods will be used. Results of these studies will determine the structure of the nanoparticles and guide their use in applications.

Benefit to National Security Missions

The structure and properties of metal nanoparticles is at the forefront of fundamental reseach in chemistry and materials science. These particles are used for biological sensing and imaging. They are also being considered for use in solar energy systems. Sometimes they are also found in the environment. Thus, a better understanding of their properties is strongly tied to DOE Office of Science needs. Such understanding is also relevant to environmental missions, applied energy missions, and biological studies.

Progress

Study of metal nanoclusters and metal sites in nanomaterials has proceeded. Several different approaches are being used. A new type of gold nanocluster made by templated growth on small molecules has been studied using optical methods. This experiment allows the sample heterogeneity to be assessed. Such measurements tell us whether multiple structures or conformations are present. The same techniques have also been implemented at low-temperature. This advance required modification of a commercial instrument. This characterization work led to a publication.

An important experimental tool to study metal-containing clusters is Extended X-Ray Absorption Fine Structure (EXAFS) spectroscopy. This experiment is carried out at synchrotron facilities. To use this technique, we have developed a successful user proposal at the Stanford Synchrotron Light Source. Data have been collected from several experimental runs. Much work has been performed to identify sample-handling methods that give a large enough concentration of metal clusters for the x-ray studies. Work has also shown how to make samples that are stable enough under x-ray exposure to give useful data. Data on both gold and silver-containing clusters have been obtained. Analysis of these data is ongoing and complicated. However, already, data on silver clusters grown using different DNA sequences have been analyzed. The results show that the cluster size and structure depends on the DNA sequence used.

In addition, light is being used to study the chemical structure and properties of metal clusters. These studies are very challenging because of unwanted background signals. However, a new technique is being investigated that may give better data. Initial data have been obtained. However, whether experimental conditions can be found that produce informative signals is still a question.

Future Work

We will continue to study the structures of nanoclusters and nanoparticles. Initially, we will study small gold or silver clusters. These systems are important because of their unexpected light emission. Our methods will include: 1. Light scattering, 2. Light absorption, 3. X-ray scattering, and 4. X-ray absorption. Later, we will extend these methods to study other particles. For example, actinide-containing particles are equally important. However, they are more complicated because of their electronic structure. They are also often a mix of several different species. The same methods will be used for their study. The goal of the work is to improve understanding of the chemical structure of clusters and how structure is linked to their properties.

Conclusion

The work will show how systematic experimental

studies can characterize complex nanoparticles. Overall, the types of materials studied are used in catalysis, optical communication, biological imaging, energy applications, and sensors. The work here will lead to results that could improve their performance in all these application areas.

Publications

Bao, Y., H. Yeh, C. Zhong, S. Ivanov, J. Sharma, M. Neidig, D. Vu, A. Shreve, R. Brian. Dyer, J. Werner, and J. Martinez. Formation and Stabilization of Fluorescent Gold Nanoclusters Using Small Molecules. 2010. *JOURNAL OF PHYSICAL CHEMISTRY C.* **114** (38): 15879.

Dopant Distribution and Interface Studies of Si and Ge Nanowire Heterostructures

Samuel T. Picraux
20090540PRD4

Introduction

The structure/composition and the electronic transport properties of individual nanowire heterostructures are basic enabling elements for the application of nanowires for energy, electronic, and photonic applications. Heterostructured nanowires hold the greatest promise for their eventual application but relatively little control or understanding of the electrical doping and composition control during synthesis of the heterostructured interfaces and the resulting electrical properties has been achieved up to now. Because of the importance of nanowires as a new approach to photovoltaic applications, this work is especially timely. Both radial and axial p-n junction semiconductor nanowire heterostructures hold promise for high performance solar cells as well for low power remote sensing and high performance electronics and photonics, and these are the subject of the studies to be carried out in this project.

Benefit to National Security Missions

This project will support the DOE missions in energy research, threat reduction, and nuclear weapons by advancing our fundamental understanding of nanoscale electronic materials for new materials synthesis, new photovoltaic approaches to solar cells, chemical and biological sensing, thermoelectric energy conversion, and electronics systems for future low power, miniaturized applications.

Progress

During the first year of this project we have demonstrated significant progress in understanding the compositional abruptness of heterostructured nanowire interfaces grown via the vapor-liquid-solid (VLS) growth process. This basic understanding is equally relevant to the formation of abrupt electrical dopant profiles during nanowire growth. Specifically we have demonstrated significantly increased abruptness in the compositional transition between Si and Ge in Si/Ge nanowire axial heterostructures by in-situ trimethylgallium alloying of the liquid Au catalyst with Ga. At the same time, Si/Ge heterostructure growth from a Ga-Au alloy allows for a significant decrease in structural kinks which form in a high percentage of nanowires grown from pure Au. For nanowire heterostructure applications such as in tunnel field effect transistors or thermoelectric devices, the formation of straight, compositionally abrupt heterointerfaces is important for optimizing device performance. However, for group IV semiconductors such as Si and Ge, abrupt heterojunction formation has been a challenge due to the relatively high solute solubilities in the commonly used liquid Au catalyst during vapor-liquid-solid growth. Consider growth of a nanowire axial heterostructure synthesized by first growing a segment from species A. After growth of sufficient length, species A is removed from the reactor while simultaneously introducing species B. As the growth is mediated through a liquid metal alloy nanoparticle, the transition region width is dictated by the depletion rate of species A from the liquid, which in turn is dictated by its relative solubility in the liquid. Recently, it was shown by others that compositionally-abrupt axial heterojunctions could be made in Si-Ge nanowires using solid Al-Au catalyst particles. For their case of growth from a solid catalyst, the solid solubility of both Si and Ge in the Al-Au alloy is very low, thus allowing for a compositionally abrupt interface. However, this approach of nanowire growth from a solid catalyst does not provide a useful approach to nanowire device structures due to the inherently slow growth rates in the solid phase. We have taken a new approach of using a liquid Ga-Au alloy catalyst to create a sharper axial heterojunction in Ge-Si, relative to that obtained using pure Au. This novel alloy lowers the solubility of Si and Ge in the liquid which sharpens the interface, while at the same time reduces the growth rate, thus promoting a significant reduction in kinking. For example, considering a ~65nm diameter nanowire, for the transition from Ge to Si, the solubility of Ge is significantly decreased and the interface sharpness increases from a width of 45 nm to 22 nm for growth at 380 °C using a $Au_{0.67}Ga_{0.33}$ alloy, as compared to growth from pure Au. At the same time, the growth rate decreases from 2.8 nm/s for kinked Si segments grown from a pure Au catalyst, to 0.2 nm/s with a 10X improvement in unkinked Ge/Si

heterostructure growth from approximately 95% kinking to <10% (See Figure 1). Since the growth rates are only a little less than Au-catalyzed growth rates, we determine that nanowire growth from the Ga-Au alloy proceeds via the vapor-liquid-solid growth process, making it practical for heterostructure device growth. Detailed analyses demonstrate 100% Ge to Si compositional change with good morphology control. While the underlying mechanisms for kinking that drive a nanowire to change growth direction is not well understood, it is known that this effect is sensitive to the kinetics of growth and becomes a significant issue when changing the growth precursors or temperature. Our work provides motivation to further explore alternative catalyst metals and metal alloys with Au in order to tailor interfacial abruptness by manipulating the semiconductor and dopant solubility in the catalyst. Furthermore, the same growth approach from a low-solubility liquid can also be applied to controlling the heterojunction width between doped axial segments to create more abrupt junctions, as for example in a p-n junction nanowire for PV applications. In a Si axial p-n nanowire, the p-n junction width can be greater than 100 nm. Preliminary Si p-n junctions by Au catalysts have been grown and this alloying technique will now be applied to these structures. By making a more abrupt p-n junction, the built-in potential at the interface will be sharper thus increasing the carrier separation and ultimately increasing the electrical output.

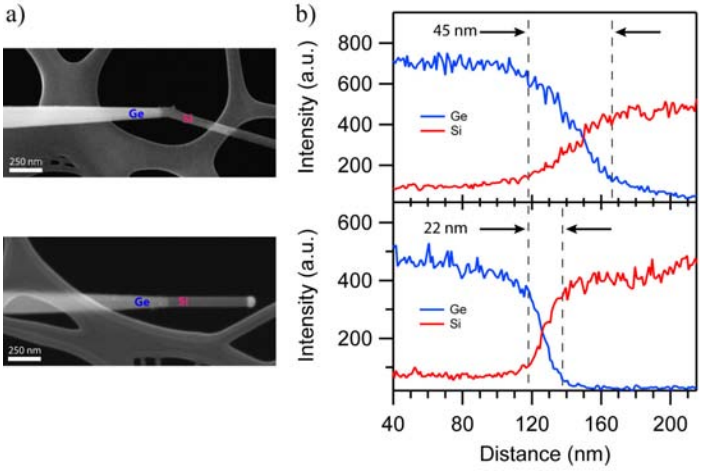

Figure 1. A high percentage of Si-Ge axial heterostructure nanowires grown from a pure 60 nm Au catalyst nanoparticle exhibit a kinked morphology (a, top panel) after the junction and have an average interfacial width of 45 nm (b, top panel) as measured by EDAX analysis. A high percentage of nanowires grown from a Au0.67Ga0.33 catalyst alloy are straight, i.e. do not kink (a, bottom panel) and have a more abrupt interface of 22 nm (b, bottom panel).

Future Work

Established facilities at CINT to synthesize radial and axial p-n junction Si and Ge nanowires will be used. The wires will be grown via the metal-catalyzed vapor-liquid-solid mechanism using a cold-walled CVD reactor. The study will focus on nanowire heterostructures grown from the described AuGa alloy. We also plan to exploit other alloys such as AuSb and AuBi as a means to explore the limits of controlling axial interfacial width. The nanowire morphology will be characterized using scanning electron microscopy, while the crystalline quality of the interfaces will be probed using transmission electron microscopy. Having established our ability to control axial interfacial width of heterostructured nanowires, I (Daniel Perea) will use my expertise in atom probe tomography to map the 3-dimensional composition of individual free-standing axial and radial p-n junction semiconductor nanowires. This work has never been accomplished before for nanowire heterostructures. Atom probe analysis requires that the nanowires be grown atop specially-designed Si micropost array substrates which will be microfabricated using the existing tools available within the Integration Laboratory at the CINT Core facility. Atom probe analysis will be performed using the Local Electrode Atom Probe (LEAP) at Northwestern University which is available to outside users. I will focus on directly mapping the dopant concentration and distribution as well as heterointerface abruptness as a function of synthesis conditions and alloy compositions. I will also fabricate nanowire devices to measure electronic transport properties. As LEAP analysis is unable to determine the electrical activity of the dopants, I will collaborate with experts at Arizona State University (Prof. M. McCartney at ASU has previously collaborated with my mentor T. Picraux) to perform electron holography to determine the charge distributions in a p-n junction nanowire for the first time. A quantitative comparison between electron holography and LEAP results can provide a direct estimate of dopant activation in nanowires.

Conclusion

We will learn how to create silicon and germanium nanowire heterostructures with precise control of electrical doping and composition in the radial and vertical directions. This new capability is anticipated to enable a revolutionary new approach to the fabrication of nanowire arrays for use as low cost, high efficiency solar cells. The knowledge learned is also anticipated to lead to new approaches to high efficiency chemical, biological and radiation sensing.

Publications

Perea, D. E., N. Li, A. Misra, and S. T. Picraux. Synthesis of abrupt interfaces without kinking in VLS-growth of Si-Ge axial nanowire heterostructures by novel in situ catalyst alloying . *Nano Letters.*

Perea, D. E., and S. T. Picraux. Controlling the transition region width of VLS-grown axial nanowire heterostructures by catalyst alloying. Presented at

Materials Research Society. (Boston, 29-30 Nov. 2010).

Perea, D. E., and S. T. Picraux. Control of Interface Sharpness in Nanowire Axial Heterostructures by Catalyst Alloying. Presented at *Los Alamos Postdoc Career Fair.* (Los Alamos, 1 Sept. 2010).

Perea, D. E., and S. T. Picraux. Controlling Heterointerface Abruptness in Vapor-Liquid-Solid Grown Semiconductor Nanowires via a Gold/Gallium Alloy Catalyst; . Presented at *Postdoc Research Day.* (Los Alamos, 16 June 2010).

Perea, D. E., and S. T. Picraux. Control of interface sharpness in nanowire axial heterostructures by catalyst alloying. Presented at *Center for Integrated Nanotechnologies User Conference.* (Albuquerque, 10-11 Aug. 2010).

Picraux, S. T., S. A. Dayeh, P. Manandhar, D. E. Perea, and S. G. Choi. Silicon and Germanium Nanowires: Growth, Properties, and Integration. 2010. *Journal of Materials.* **62** (4): 43.

Control of Shape, Dispersion and Size of Disorder in High-Temperature Superconducting Films and its Effect on in-Field Superconducting Properties

Leonardo Civale
20090542PRD4

Introduction

The large scale introduction of high temperature superconductors (HTS) into the electric grid would result in significant energy savings through higher efficiency, as well as enhanced power quality and reliability. US industries are currently producing long lengths of "second generation" HTS wires based on films of $REBa_2Cu_3O_7$ (REBCO, where RE=Y, Gd etc.), also known as *coated conductors.* Although their properties are already good enough for some applications, other uses require further improvements. In particular, it is necessary to increase their critical current density, J_c, which is controlled by the presence of nanoscale disorder or "defects" in the crystalline structure of the superconductor. Such defects act as "pinning centers", i.e., traps that preclude the motion of the vortices inside the superconductors, which would otherwise move and produce dissipation. Not all defects are equally useful, and their effectiveness in precluding dissipation depends in a complex way on their size, shape, composition, and distribution. The purpose of this project is to artificially create nanoscale defects into films of $REBa_2Cu_3O_7$ to improve their pinning properties, particularly in the presence of large magnetic fields. We have much experience in this topic, and we have previously obtained HTS with record high J_c. Those previous studies demonstrate that the best results are obtained through a combination of different types of defects, so in this project we are focusing on developing methods to artificially engineer "mixtures" of defects in a controllable fashion. The "pinning" properties of those mixtures of defects are almost unknown, so we are exploring them using several different experimental techniques, including studies at very high magnetic fields at the pulsed-field facilities of the National High Magnetic Field Laboratory at LANL.

Benefit to National Security Missions

This project will advance the physics and materials science of vortex pinning in high temperature superconductors (HTS) contributing to DOE/SC goals. The results of this work will advance the state of the art performance of HTS wires that contribute to goals of DOE/OE to improve electricity transmission and energy reliability. These materials will also contribute to electric power generation, transmission and utilization for DOD, DHS, and other agency programs

Progress

Initially, Dr Miura's received on-the-job training on the systems and tools needed for his studies, namely (1) electrical resistivity measurements in DC and pulsed facilities at the NHMFL to determine the upper critical field H_{c2} (where superconductivity disappears and the material becomes normal) and the irreversibility field H_{irr} (where vortex matter goes through a solid-liquid transition and J_c vanishes), (2) J_c measurements by transport using two different systems, and (3) magnetization studies in a commercial MPMS from Quantum Design to explore J_c as well as its decay with time, a phenomenon due to thermal fluctuations known as flux creep.

Using all these tools and techniques, Dr. Miura has studied the effect of various combinations of hybrid artificial disorder of different dimensionality on the angular dependence of H_{irr} up to 60 T and on the dependence of J_c on temperature and magnetic field strength and orientation [1]. He used a metal organic deposition technique to grow ~0.6 um-thick films of pure YBCO and $(Y,Gd)Ba_2Cu_3O_7$ with 1 wt % additions of dispersed $BaZrO_3$ nanoparticles (YGdBCO+ 1wt%BZO) at ISTEC, Japan. The planar-view transmission electron microscopy (TEM) images of the films without and with BZO are shown in Figures 1(a) and 1(b), respectively. Both films have a low density of large $RE_2Cu_2O_5$ precipitates. The YGdBCO+1wt%BZO film has a high density of *c*-axis correlated twin boundaries (planar 2D defects, yellow arrows) and uniformly dispersed 25 nm-size BZO particles (macroscopic 3D defects, circles). To produce strong vortex pinning a defect should have a size similar to the vortex core, which is the non-superconducting central filament of the vortex that becomes trapped. The core size for these films (at temperatures well below T_c) is indicated by the size of the yellow dots sketched in Figures 1(a) and 1(b). For

B = 1 T the inter-vortex distance is ~50 nm (the distance between the yellow dots sketched in the figures), which is the same order of magnitude as the distance between BZO nanoparticles (~60 nm) or between twin boundaries (TBs) (~34 nm). This indicates that the $RE_2Cu_2O_5$ precipitates are too big and too sparse to produce significant pinning, but the combination of 2D (TBs) and 3D (BZO nanoparticles) defects can work as an effective pinning landscape even in a high magnetic field.

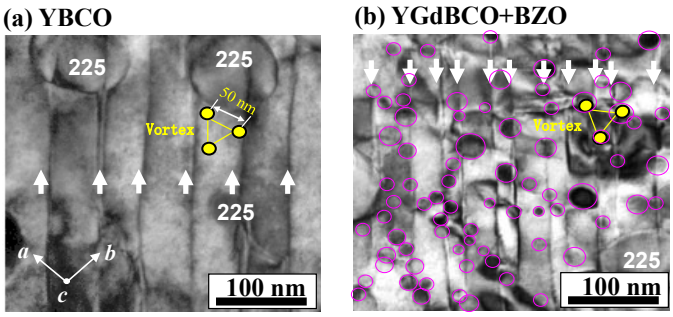

Figure 1. TEM images of REBCO films (a) without and (b) with BZO additions.

To investigate the effect of these mixtures of 2D and 3D defects on the angular dependence of J_c, we measured $J_c(B,theta)$, where theta is the angle between the magnetic field and the crystallographic *c*-axis. Figures 2(a) and (b) show J_c(theta) at 77 K, 1 T and 65 K, 1 T for the YBCO and YGdBCO+1wt%BZO films. The YBCO film shows an anisotropic J_c(theta) and a small *c*-axis peak due to *c*-axis 2D defects (TBs) at both 77 K and 65 K. On the other hand, the YGdBCO+1wt%BZO film shows nearly isotropic angular dependence, and the minimum J_c of the film is 3 times higher than that of YBCO due to the combination of 2D and 3D defects (see Figure 1(b)).

In order to investigate the effect of hybrid defects on the angular dependence of H_{irr} up to 60 T, we measured the resistivity for pure YBCO and 1wt%BZO and 3wt%BZO doped films using pulsed fields at NHMFL-LANL. The main results are shown in Figure 3. For H||*ab*, our three films have very similar H_{irr}, indicative of similar *ab*-plane correlated pinning (e.g., stacking faults or intrinsic pinning). The similarity also indicates that the nanoparticles present in the YGdBCO+BZO do not influence H_{irr}||*ab*. On the other hand, for all fields up to 60 T, H_{irr} is slightly higher for 3wt%BZO than for 1wt% BZO and YBCO. The YGdBO+3wt%BZO film shows significantly higher H_{irr} for H||45°. The behavior of H_{irr} for YGdBCO+BZO is probably related to a combination of 2D and 3D defects.

To analyze the results described above Dr. Miura has been studying theoretical concepts in vortex matter, such as single vortex pinning in different regimes, and analyzed the results obtained according to different models applicable to strong pinning produced by nanoparticles. In particular, the results of the individual vortex regime (where J_c is constant) were analyzed by a recent theory by Alex Koshelev (Argonne National Laboratory) with whom we have a close collaboration.

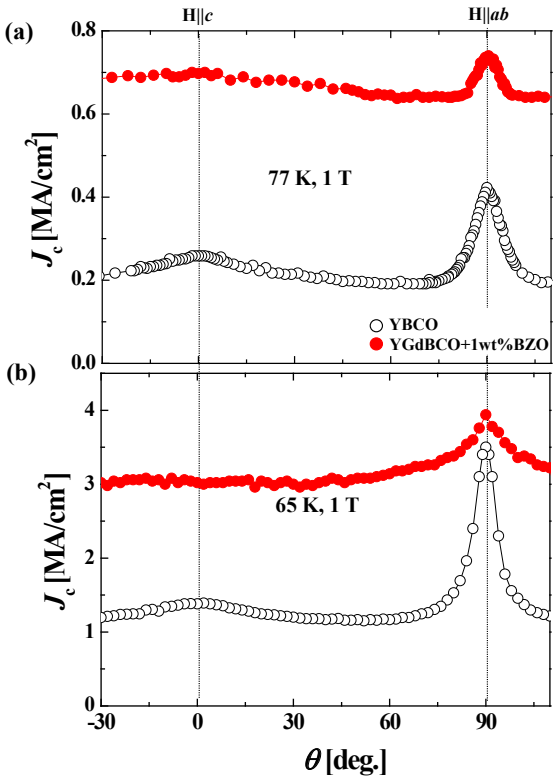

Figure 2. Jc as a function of angle at (a) 77 K & 1 T and (b) 65 K & 1 T for both pure YBCO and for YGdBCO+1wt%BZO films.

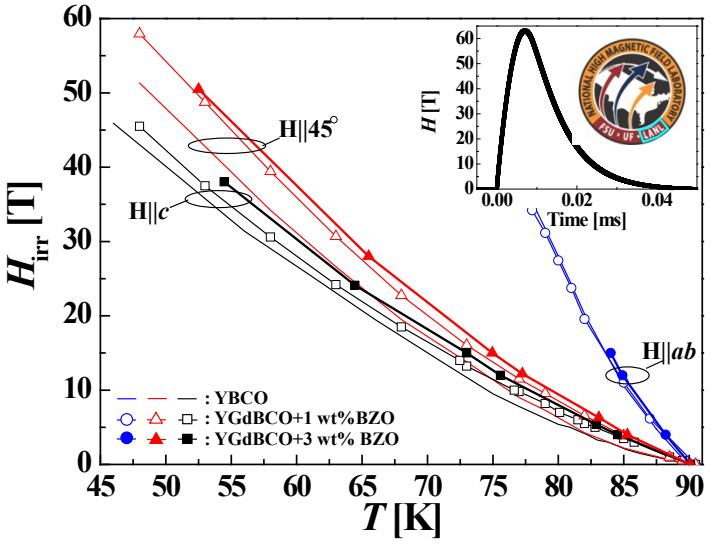

Figure 3. Irreversibility fields as a function of temperature for H||ab, H||c, and H||45 degrees for pure YBCO and for YGdBCO1wt%- and YGdBCO3wt%BZO films. The inset shows the time profile of a magnet pulse.

The understanding and manipulation of the mixed pinning landscapes due to a combination of various dimensional defects is critical to improving J_c and H_{irr}. Our results indicate that nanoengineered films are an enabling technology for high magnetic field applications. These results have recently been submitted for publication.

Finally, Dr. Miura is currently involved in analyzing the recent results obtained in pnictide films where a change in the apparent anisotropy was observed. He worked closely with a former post-doc in MPA-CMMS and STC (Scott Baily) in learning algorithms for performing the non-trivial task of analyzing the upper critical field angular dependence according to the two-band theory [2]. This also led him to start the study of the different effects that can be responsible for the very high upper critical field, higher than the predicted Pauli limit.

Future Work

We will continue to study $REBa_2Cu_3O_7$ films with mixtures of nanorods and nanoparticles grown by pulsed laser deposition, metal organic deposition and other processes. By tuning composition, oxygen pressure, temperature and growth rate, we will obtain unprecedented control of the film growth mode and the shape, dispersion and size of the second-phase inclusions.

We will investigate J_c, H_{irr}, vortex phases and transitions of these films over wide temperature and magnetic field ranges, including angular dependence up to 65 T using pulsed fields only accessible at the NHMFL-LANL. Presently known vortex phases are associated with a single type of disorder and are largely unexplored above 20 T; we will elucidate the nature of the phases in the presence of pinning center mixtures. This research will lead to novel sample preparation methods, enhancement of J_c and H_{irr}, and deeper understanding of vortex pinning.

Conclusion

We are developing methods to nano-engineer inhomogeneities in HTS films of $REBa_2Cu_3O_7$ with unprecedented levels of control. By introducing combinations of defects and tuning their size, shape and distribution, we expect to obtain wires with significantly higher performance than currently available. By exploring the “pinning” properties of these defect mixtures over a wide range of temperatures and magnetic fields using several techniques, we expect to gain fundamental physical understanding of the underlying mechanisms to guide further optimization. This will strongly increase the viability of using HTS for the electric grid and other power applications.

References

1. Miura, M., S. A. Baily, B. Maiorov, L. Civale, J. O. Willis, K. Marken, T. Izumi, K. Tanabe, and Y. Shiohara. Vortex liquid-glass transition up to 60 T in nanoengineered coated conductors grown by metal organic deposition. 2010. *APPLIED PHYSICS LETTERS.* **96** (7): 072506.

2. Baily, S. A., Y. Kohama, H. Hiramatsu, B. Maiorov, F. F. Balakirev, M. Hirano, and H. Hosono. Pseudoisotropic Upper Critical Field in Cobalt-Doped SrFe2As2 Epitaxial Films. 2009. *PHYSICAL REVIEW LETTERS.* **102** (11): 117004.

Publications

Miura, M., B. Maiorov, S. A. Baily, N. Haberkorn, J. O. Willis, T. Izumi, Y. Shiohara, and L. Civale. Mixed pinning landscape at high temperature in nanoparticle-introduced YGdBa2Cu3Oy films grown by metal organic deposition. *Physical Review B.*

Atomic Interface Design of Nanocomposites for Extreme Mechanical Loadings

Irene J. Beyerlein
20100596PRD1

Introduction

In recent years, there has been an increasing demand for next generation structural nanomaterials that can withstand extreme mechanical loadings, such as those generated in severe plastic deformation (SPD) and shock loadings. One material that has exhibited extraordinarily high strength, ductility, and resistance to radiation and mechanical loading is the nanostructured copper-niobium (Cu-Nb) multilayer composite made by physical vapor deposition at LANL While LANL scientists have shown that bimetal composite nanolayers have superior damage resistance to extreme environments, only one material combination has been studied Cu-Nb. A leading candidate composite material combination for advanced structural applications has yet to be identified and hence the potential of nanolayered composites remains untapped. The problem is the inability to model at the atomistic scale just any bi-material interface. To overcome this, Dr. Zhang proposed to develop new atomic scale theoretical methodologies and techniques that will enable for the first time study of a variety of nanocomposites. The breakthrough in his work will be the atomic scale mechanisms that distinguish one nanomaterial from another in its robustness to extreme environments, such as high temperature, radiation, and shock

Benefit to National Security Missions

Dr. Zhang's research will lead to controlled synthesis of structural-sized nano-composite metals that--by virtue of their high density of bi-metal interfaces--will be an order of magnitude more resistant to extreme mechanical conditions (shock) and environments (radiation, high temperatures) than currently available materials. These shock- and radiation-resistant bulk nanocomposites will greatly benefit nuclear power applications (longer lifetimes of structural components), weapons applications (armor development and penetrator technology) and transportation, where high strength, high-temperature resistance, lightweight, and damage tolerance are critical for boosting energy efficiency. In this way, our DR supports LANL missions to 1) solve emerging national security (energy) challenges, and 2) be a leader in materials and process modeling. In addition, novel nanomaterials in bulk form will open new opportunities for material testing in MARIE, such as real-time, in-situ diagnostic of bi-metal interfaces in deformation under a wide range of strain rates and temperatures.

Progress

Recently, much theoretical and experimental effort has been carried out on nanostructured composite materials with the aim of developing materials that can withstand extreme mechanical loadings, such as severe plastic deformation (SPD), shock loadings and irradiation. One composite material candidate that has exhibited extraordinarily high strength, ductility, and resistance to radiation and mechanical loading is the nanostructured copper-niobium (Cu-Nb) multilayer composite made by physical vapor deposition at LANL. When the layer thicknesses are on the order of a few tens of nanometers or less, composite deformation behavior becomes controlled by the Cu-Nb interface instead of the Cu phase or Nb phase. The interface blocks, stores, nucleates, and removes dislocations, the essential defects that enable plastic deformation. Most studies to date have concentrated on Cu-Nb interfaces in an ideal, low energy state. Under the extreme mechanical loading conditions of interest, however, the interface can deviate significantly from ideal. It can become amorphous, accumulate defects, roughen, and change its crystallography. These structural changes can alter the way the interface responds to extreme loadings, how it interacts with dislocations, and hence, the overall mechanical properties of the composite.

The goal of the scheduled work is three-fold. The first objective is to develop different interface models for large-scale molecular dynamics (MD) simulations (via SPaSM code or others) to study the atomic-scale interface mechanisms in multilayer (Cu-Nb) systems. The second objective is to develop an analytical description of these MD results that will enable relating the atomic mechanisms operating at the interface to the mechanical behavior of the composite under extreme

loads. The third objective is to construct interatomic potentials for other prime composite material candidates, via the ab initio method (via VASP code), that reliably describe behavior far from equilibrium. In the past seven months, since his date of hire, April 5, 2010, Ruifeng Zhang has begun work on the first task, which involves atomistic scale modeling, and the third tasks, which involves density functional theory.

Recently in LANL, much effort has been dedicated to the study of a certain type of Cu–Nb interface, the classical Kurdjumov–Sachs (KS) crystallographic orientation. Prior modeling of this interface has shown that it acts as a very strong barrier to dislocation propagation. Transmission of a dislocation from one phase to another across this interface is possible and details of this important interaction have been reported in the literature. These previous studies started with a pre-existing dislocation that was inserted in either the Cu or Nb phase at the beginning of the simulation. However, because slip transmission is difficult and the layer thicknesses are very fine (~10 nm or less), it is likely that the dislocations gliding in the phases under deformation in the real material originated from the Cu-Nb interface rather than in the Cu or Nb phase. To date, dislocation nucleation from the interface and the effects of interface geometry and pattern on the dislocation nucleation have not been studied using atomic-scale simulations.

To study the mechanism of dislocation nucleation and correlate it with atomic interface structure, two types of experimentally observed Cu/Nb incoherent interfaces were constructed using MD: the KS orientation mentioned earlier and the Nishiyama-Wasserman (NW) orientation. It was found that these two interfaces have different interfacial patterns (See Figure 1). Preliminary atomistic simulations under tensile loading have shown that dislocations can nucleate from both interfaces in the ideal form. Specifically nucleation sites corresponded to points where the Cu and Nb atoms were perfectly aligned. Significantly the density of such nucleation sites and hence the number of dislocations nucleated under a given loading state will differ between the KS and NW interfaces. Dr. Zhang studied the deformation of these interfaces under various conditions (shock, uniaxial strain, uniaxial stress). In each case, the number and type of dislocations nucleated from each interface varied depending on the interface structure. This suggests that the slip activity and hence plastic deformation is controlled by interface. For the purposes of integrating these atomic scale results into meso-scale modeling, he has been developing the atomistic model to determine the activation energy for nucleation of a single, three-dimensional dislocation loop from the interface (See Figure 2). Development of the MD model was non-trivial since it involved devising a new method to isolate one loop without interactions from the others. (All previous work in the literature considered only a one-dimensional dislocation.) With this new method, we are able to quantify the activation energy for nucleation as a function of loop size. Dr. Zhang's results on the relationship between physical and functional properties of the interface will open the way to further improve the mechanical properties of Cu/Nb nanocomposites via atomic design of its interface.

Dr. Zhang is also developing a new potential for Nb, which will be valid under high rates of strain and shock. To date, Dr. Zhang has shown that the other inter-atomic potentials for Nb are not suitable for our high-rate applications.

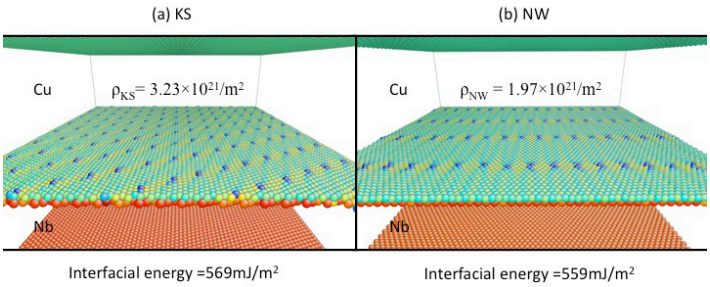

Figure 1. Comparison of the atomic structure of two Cu-Nb interfaces (a) Kurdjamov-Sachs and (b) Nishiyama-Wasserman.

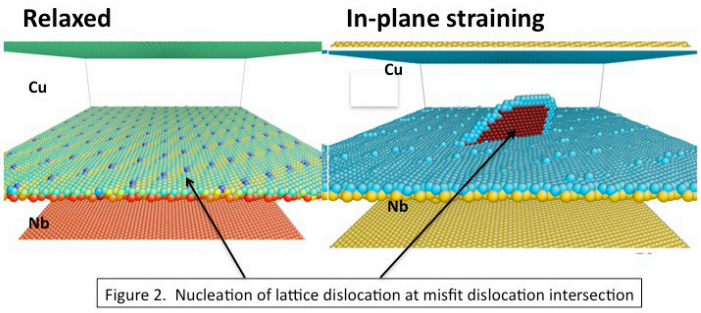

Figure 2. Nucleation of a single, three dimensional loop from a Cu-Nb interface.

Future Work

Nanostructured copper-niobium (Cu-Nb) multilayer composite made by physical vapor deposition at LANL has exhibited extraordinarily high strength, ductility, and resistance to radiation and mechanical loading. Unlike their conventional counterparts, in these Cu-Nb nanocomposites the interface dominates dislocation nucleation, motion, and removal. Thus far, their interfaces have been largely studied in an ideal, low energy state. Under extreme mechanical loadings, the interface can become amorphous, accumulate defects, roughen, and change its crystallography. These structural changes can alter the way the interface responds to extreme strains and strain rates and hence can either enhance or degrade the overall strength of the nanocomposite. The behavior of the interface and hence its relationship to the overall material performance is unknown. Moreover, previous successes

with the Cu-Nb composites suggest that there may be other similar potential material candidates with dissimilar crystal structures, such as Cu-V (Ta, Mo etc.). The number of nanocomposite combination is prohibitively large to explore via experimentation and trial and error alone.

To address these issues, Dr Zhang proposes novel numerical approaches via first principle ab initio calculations and molecular dynamics simulation 1) to determine how mechanical-induced atomic-scale structural changes influence the way the interface nucleates, interacts with, and removes dislocations and 2) to investigate other two-phase immiscible material systems for outstanding resistance to extreme mechanical loadings.

Conclusion

Dr. Zhang's DF research results will determine which material composite systems will be robust in extreme conditions such as shock and irradiation. Stronger and more robust materials in next generation nuclear (e.g., fuel cladding), weapons applications (armor and penetrator technology), and transportation systems (where high strength to weight ratio is critical) will be safer, more economical, and sustainable. In this way, his research supports LANL's mission to solve emerging national security (energy) challenges.

Multi-scale Computational Approach for Studying Radiation Resistant Nanoclustered Alloy

Blas P. Uberuaga
20100598PRD1

Introduction

Nanostructured ferritic alloys (NFAs) (with usual composition 12– 14 wt% Cr, 0.25 wt% Y and 0.5 wt% Ti) are considered excellent candidate materials for structural applications for next generation nuclear reactors as they exhibit exceptionally high-temperature creep strength due to the presence of highly stable nanometer sized Y-Ti-O precipitates (NPs) – often complex oxides such as $Y_2Ti_2O_7$ (a pyrochlore) and Y_2TiO_5 – formed during consolidation. Understanding the stability of these complex oxides requires an investigation of the precise structure, compositions, and role of defects like grain boundaries on the stages of nucleation and growth of these NPs. In this report, we present an analysis of the research problem based on an extensive literature survey and inputs from experimentalists at LANL. Experimentally it has been observed that Y_2O_3 precipitates exhibit similar structural features as these complex oxides, such as formation of core-shell structures. We present a plan to develop a phase-field based multi-scale approach to understand the nucleation and growth of Y_2O_3 precipitates under applied stress in Fe-Cr alloys. Further, the role of defects like grain boundaries on defect energetics will be discussed using $SrTiO_3$ as a model system. It will be shown that ab-initio calculated defect energetics matches well with molecular statics calculations performed at LANL.

Benefit to National Security Missions

Precipitation hardening is a common method of strengthening in metals and alloys like Ni-based superalloys used for turbine or nanostructured Ni-alloy for fusion and fission applications. Within ferritic alloys, alloys like PM2000 and MA956 are precipitation hardened where the nanoclusters are Y-Al complex oxides. Unlike these alloys (where NPs are formed intentionally during processing), nano sized precipitates are formed due to radiation in alloys like HCM12A, T91 and HT9. The proposed phase-field based multi-scale framework constitutes an important step in studying microstructural evolution in these alloys. Overall, this study will greatly benefit the future development and understanding of advanced metallic alloys at LANL

Progress

Phase-field approach to model microstructural evolution of Y_2O_3 in Fe-Cr Alloys

Precipitates of Y_2O_3 in Fe-Cr alloys exhibit interesting microstructural features. For example, it has been observed experimentally[2] that as the precipitate grows beyond 12nm in size they exhibit a change in morphology from round to more faceted structures (Figure 1). This change morphology is expected to affect the mechanical properties of the alloy. To model the evolution of the precipitates using phase field, accurate estimation of the material parameters is essential. Central to the development of a phase-field model for microstructural evolution is to describe the total free energy of the system and an accurate estimation of the mobility of the precipitate-matrix interface. The total free energy comprises of bulk or chemical energy, the interfacial energy and the elastic energy. In the following section we present a plan to describe individual energies as well as the mobility of the precipitate-matrix interface.

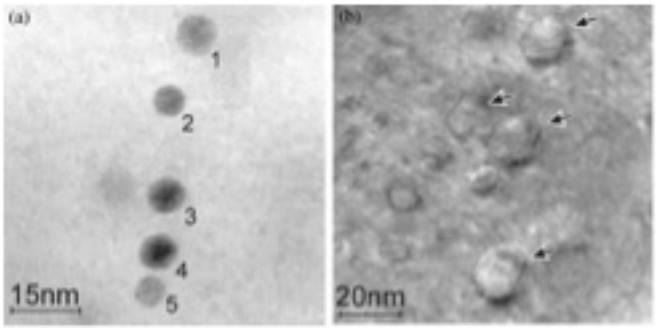

Figure 1. TEM micrograph of Y_2O_3 precipitates from Ref [2].

Bulk energy: The bulk free energy density will be estimated from the free energy of a solid solution of Y and O in Fe as well as free energy of Y_2O_3 precipitates.

Free energies will be obtained using ab-initio calculations in combination with cluster expansion and monte carlo simulations. Part of the estimation of these free energies will be done in collaboration with Prof. Dane Morgan's research group at University of Wisconsin, Madison.

Interfacial energy: To estimate the interfacial energy contribution to the total energy, it is essential to evaluate the interfacial orientation relationship between the precipitates and the matrix. Extensive literature search has been performed to find experimentally observed orientation relationship between the precipitates and the matrix. Klimiankou et al. [3] reported that precipitates of Y_2O_3 follows Kurdjumov–Sachs relation with $[110]_{YO}$ || $[111]_{FeCr}$ and $(1\text{-}11)_{YO}$ || $(\text{-}101)_{FeCr}$. We plan to estimate the interfacial energy using ab-initio calculations [4]. However as the lattice parameter of the ferritic matrix and the Y_2O_3 precipitates differ considerably, the orientation relationship reported by Klimiankou et al. needs to be verified. Dr. Amit Misra's group at LANL as a part of an EFRC program is conducting TEM studies of Y_2O_3 precipitates in Fe matrix. We are collaborating with Dr. Misra's group to better understand the interfacial structure and verify orientation relationship reported by Klimiankou et al.

Elastic energy: To calculate the elastic energy, elastic constants are assumed to be homogenous and isotopic. Elastic constants will be obtained from ab-initio calculations. Elastic solution will be obtained under stress-free boundary conditions using Kachaturyan's theory of microelasticity[5,6].

Interface mobility: The mobility of the interface is related to the diffusion coefficients of Fe, Y and O in Fe matrix. The diffusion coefficients of these species can be obtained from ab-initio calculations in combination with cluster expansion and kinetic monte carlo simulations. However, such a numerical approach to estimate diffusion coefficients is highly computationally intensive and falls short of experimental accuracy. Hence, we plan to use experimentally measured diffusion coefficients by Allinger using SANS.[7]

The computational will provide atomic and electronic structure at Fe-Y_2O_3 interface. Further, the evolution of morphology of Y_2O_3 precipitates, size distribution as a function of temperature and applied stress as well as relevant physical factors controlling the morphology such as diameter, thickness and aspect ratio of the precipitates can be obtained from this computational approach.

Ab-initio based Defect Energetics in $SrTiO_3$

A major challenge in materials science is to understand the highly complex equilibrium structure and properties of interfaces in multi-component systems. The atomic arrangement at the interface is quite different from that of bulk solid and thus exhibits unique properties. For example, the atomic and electronic structure at a grain boundary can lead to enhanced diffusion behavior of atoms along the grain boundary. Such diffusion behavior can have a pronounced effect on microstructure evolution. To understand diffusion at the grain boundary, as a first step defect energetics were calculated at the grain boundary as well as in the bulk in multicomponent ionic oxide, $SrTiO_3$, a technologically important electroceramic. The objective is to understand the difference in structural properties of defects like vacancies and interstitials at different types of grain boundaries using an ab initio approach. $SrTiO_3$ is used here as a model system to gain some insight into the possible behaviors that will need to be considered for the NFAs – as there is extensive literature on grain boundaries in $SrTiO_3$, it serves as a good model[8]. Table 1 shows a comparison of defect formation energy in two different types of grain boundaries using ab-initio and molecular statics. Currently work is in progress to understand the electronic properties of these defects.

	Oxygen Vacancy (eV)	Oxygen Interstitial (eV)	Strontium Vacancy (eV)
Ab-initio	2.8	8.4	0.13
Molecular Statics	2.6	13.5	-1.1

Figure 2. Comparison of ab-initio and MS calculated difference in defect formation energy between grain boundaries with two different types of atomic arrangements.

Future Work

This theoretical project will use atomistic and mesoscale (micrometer) simulation techniques to examine nanostructured ferritic alloys (NFAs). These are metallic materials with nanometer-sized oxide particle embedded within and have shown great exceptional strength and radiation tolerance and are thus considered prime candidates for future generation nuclear energy applications. However, there is currently no fundamental understanding of how these materials obtain these exceptional properties. This work will provide the fundamental understanding of both the structure of these materials and how that structure leads to the observed properties. We will perform electronic structure calculations to determine the properties of the interface between the oxide particles and the metal matrix, including the behavior of defects near the interface. The goal of this task, primarily relying upon density functional theory, will be to determine the thermodynamic and kinetic quantities of defects near the metal/ceramic interface. This information will be used to develop a model at the mesoscale -- a phase field model -- that can then simulate the performance and behavior of the

material under irradiation. In particular, the model will examine the ability of the nanoparticles to retain their shape under irradiation and how that ability depends on the composition and properties of the particles. By understanding how the oxide particles improve the performance of the material, we will be able to guide the future design of new NFAs that meet the demands of extreme applications.

Conclusion

Future nuclear reactors will demand even more from the materials that comprise them, in terms of mechanical strength and radiation tolerance, to extract the most energy from the fuel. This requires new materials that can withstand these extreme environments. One candidate for such applications is a nanostructured ferritic alloy. However, while these materials hold great promise, the origins of their exceptional behavior are unknown. By studying these materials at the atomic level, we will develop the necessary fundamental understanding that will allow for the design of improved materials that will form the foundation of future generation reactors.

References

1. Ukai, S., T. Nishida, H. Okada, T. Okuda, M. Fujiwara, and K. Asabe. Development of oxide dispersion strengthened ferritic steels for. 1997. *Journal of Nuclear Science and Technology.* **34** (3): 256.

2. Klimiankou, M., R. Lindau, and A. Moslang. HRTEM Study of yttrium oxide particles in ODS steels for fusion reactor application. 2003. *JOURNAL OF CRYSTAL GROWTH.* **249** (1-2): 381.

3. Klimiankou, M., R. Lindau, and A. Moslang. TEM characterization of structure and composition of nanosized ODS particles in reduced activation ferritic-martensitic steels. 2004. In *11th International Conference on Fusion Reactor Materials (ICFRM) ; 20031207 - 20031212 ; Kyoto, JAPAN.* Vol. 329, A Edition, p. 347.

4. Wang, Y., Z. K. Liu, L. Q. Chen, and C. Wolverton. First-principles calculations of beta”-Mg5Si6/alpha-Al interfaces . 2007. *Acta Materialia.* **55**: 17.

5. Choudhury, S., Y. L. Li, C. Krill III, and L. Q. Chen. Effect of grain orientation and grain size on ferroelectric domain switching and evolution: Phase field simulations. 2007. *Acta Materialia.* **55** (4): 1415.

6. SHATALOV, G. A., and KHACHATU.AG. CALCULATING ENERGY OF INTERSTITIAL IMPURITY ATOM INTRUSION INTO OCTAHEDRAL AND TETRAHEDRAL SITES OF A BCC LATTICE. 1968. *PHYSICS OF METALS AND METALLOGRAPHY-USSR.* **25** (4): 56.

7. Hin, C., B. D. Wirth, and J. B. Neaton. Formation of Y₂O₃ nanoclusters in nanostructured ferritic alloys during isothermal and anisothermal heat treatment: A kinetic Monte Carlo study. 2009. *Physical Review B (Condensed Matter and Materials Physics).* **80** (13): 134118 (11 pp.).

8. Alfthan, S. von, N. Benedek, L. Chen, A. Chua, D. Cockayne, K. Dudeck, C. Elsasser, M. Finnis, C. Koch, B. Rahmati, M. Ruhle, S. Shih, and A. Sutton. The Structure of Grain Boundaries in Strontium Titanate: Theory, Simulation, and Electron Microscopy. 2010. In *The Structure of Grain Boundaries in Strontium Titanate: Theory, Simulation, and Electron Microscopy.* Vol. 40, p. 557.

Unique Semiconductor Nanowire Heterostructures in Physics and Applications

Samuel T. Picraux
20100601PRD2

Introduction

Our work in the past two years concentrated on size effects in semiconductor nanowires and designing material systems that utilize the ability to synthesize heterostructure materials in unconventional ways in these nanoscale systems. Our earlier progress report discussed some of the aspects of nanoscale size effects and confined radial (core/shell) heterostructure Germanium/Silicon nanowires and nanowire transistors. Here we have fabricated a "***green tunnel transistor***" on axial nanowire heterostructures with levels of performance better than any achieved tunnel transistor performance to date. We demonstrated a 100 % germanium-silicon axial nanowire heterostructures and asymmetric Schottky-barrier tunnel field-effect transistors with high on-currents, on/off ratios, and totally eliminated ambipolar conduction behavior. This work has advanced the state of the art of nanowire electronics.

Benefit to National Security Missions

While there have been a gazillion reports on semiconductor nanowires (NWs) and NW heterostructures promising different electronic and opto-electronic device applications, most of the experimentally realized devices to date are one-dimensional analogs of conventional planar devices. In other words, the true potential of semiconductor NWs to grow and fabricate devices beyond conventional practice has yet to be realized. One of the compelling aspects of the vapor-liquid-solid (VLS) growth of semiconductor NWs is the ability to modulate doping and composition during their layer-by-layer growth, thereby enabling energy band-edge engineering along their axis for enhancing and providing additional control over charge transport in semiconductor devices. Earlier composition modulation in VLS grown Si-SiGe heterostructure NWs has been limited to less than 30 % [1,2]. To surmount this problem and obtain abrupt Ge-Si heterostructure NWs, researchers at IBM TJ Watson and Purdue University used a solidified growth mediating alloy to achieve 100 % composition modulation [3], however over length scales comparable to those typically achieved with planar growth [4], and compromised by radial over-coating of pre-grown segments, both of which preclude useful device applications.

At Los Alamos, we have been growing 100% composition modulation Ge-Si axial NW heterostructures since 2008 (Figure 1), and have advanced our level of understanding of their growth and material properties to design and demonstrate unique tunnel transistors with excellent performance characteristics.

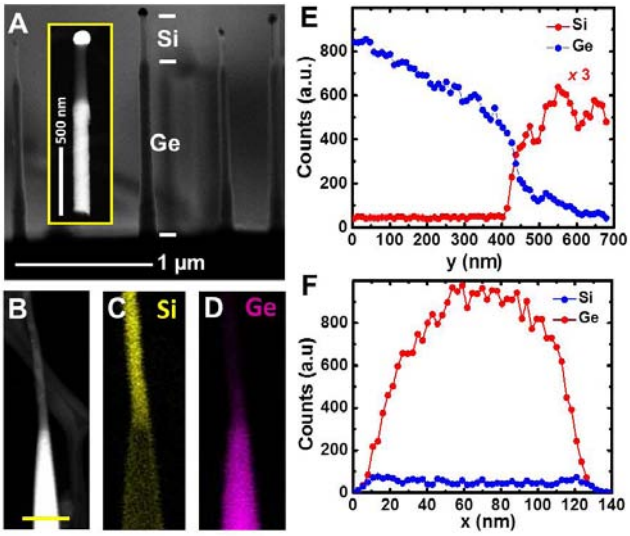

Figure 1. (A) Cross-sectional SEM image of epitaxial Ge-Si heterostructure NWs on a Ge(111) substrate. The inset shows a z-contrast SEM image of a 100 nm diameter Ge-Si axial heterostructure with a Au tip. (B to D) HAADF-STEM image and elemental maps of a Ge-Si axial NW heterostructure with 30 nm diameter Si segment and 80 nm diameter Ge segment. Maintaining Ge NW growth during temperature ramp results in larger Ge diameter but prevents Au diffusion from evolving on its surface.

The merits of this unconventional design stem from the ability to implement bandgap engineering along the

charge transport direction (NW axis), in contrast to being perpendicular to the transport direction in conventional planar devices. Such bandgap asymmetry have allowed us to fabricate state-of-the-art Schottky barrier heterostructure tunnel field-effect transistors (H-TFETs) that benefit from controlled yet different energy band-offsets at the source (drain) device terminals, allowing high on-currents (low off currents) and therefore low static power dissipation. Such performance can be enabled uniquely from this kind of devices where additional built-in fields and bandgap asymmetry along the channel length add to abrupt yet different barrier heights at the metal/Si and metal/Ge interfaces, all of which help in assisting carrier tunneling and transport in one direction but not the other. We discuss below the motivation to fabricate such devices, discuss our new design, and present experimentally realized performance.

Progress

The growth of the axial NW heterostructures is non-trivial and starts with growing a Ge NW followed by a temperature ramp and growth of a Si segment while preventing loss or diffusion on the sidewalls of the mediating growth seed. Details on the VLS growth of Ge can be found in ref. [5]. The wires are afterwards suspended by sonication into an Isopropanol solution and transferred to SiO_2/Si substrates with pre-patterned grid to fabricate devices.

Conventional complementary metal oxide (CMOS) transistors utilize back-to-back p-n junction diodes. In their on state, the surface of the junction under the gate is "inverted" therefore reducing any barrier for charge transport and the device can be turned on. In the off state, few carriers can be thermally emitted above the diode energy barriers and contribute to an off-state current. While this has not been a problem for CMOS till early 2000s, reducing transistor sizes to boost current and operating frequencies lead to undesired and intolerable levels of off-state currents (one can literally feel the levels of heating in laptops, for example, increase over the past few years). This is a direct result of what is referred to as "short-channel effects" where the supply voltage terminals (source and drain electrodes) control the voltage in the channel and overpower the gate electrode (which is supposed to switch the device on and off) and an excessive amount of gate leakage current flows through the channel (instead of the ideal zero current). Therefore, as the device dimensions become smaller (an essential requirement for high speed), CMOS devices exhibit high off currents at zero gate voltages leading to a lot of wasted power when the device should be really off (Figure 2). Being a diffusive current in the off-state, the maximum rate at which the transistor switches off is, in best cases, a change of one decade of current per 60 mV of gate voltage, referred to inverse subthreshold slope of 60mV/decade as indicated in Figure 2.

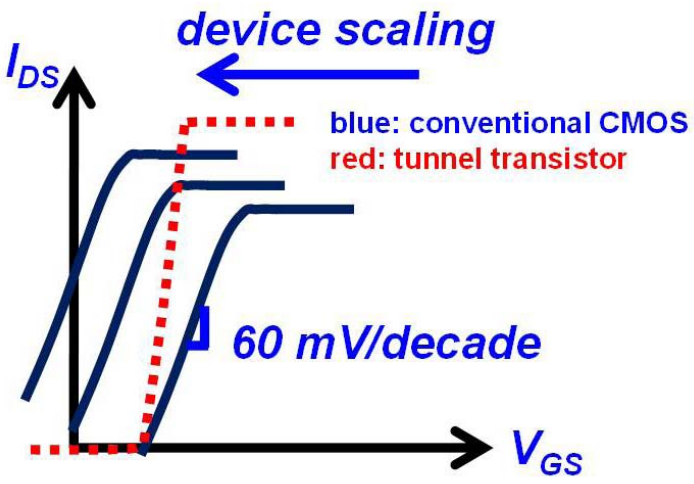

Figure 2. Illustration of the transfer characteristics (transistor on-off current as function of gate voltage) for an n-type MOS device which shows higher current as the device is scaled down but larger intercept with the y-axis (off-state current). A tunnel transistor on the other hand enables faster modulation of the current (better than 60 mV/decade) and therefore low off-state current.

It is therefore desired to have devices that can switch from on-state to off-state over a very narrow gate voltage window (Figure 2, red dashed line). Field-assisted tunneling is one charge transport mechanism that is independent of temperature (thermal emission), and is dependent on the charge carrier effective mass (material bandgap), the tunneling barrier width and height, as well as applied electric fields. It follows then that axial NW heterostructures should be ideal material system for this kind of transistors because (i) excellent electrostatic and electric field control can be achieved in the three-dimensional NW geometry and (ii) the tunneling barrier heights and widths can be asymmetric with a heterostructure NW material (refer to band diagrams in Figure 3).

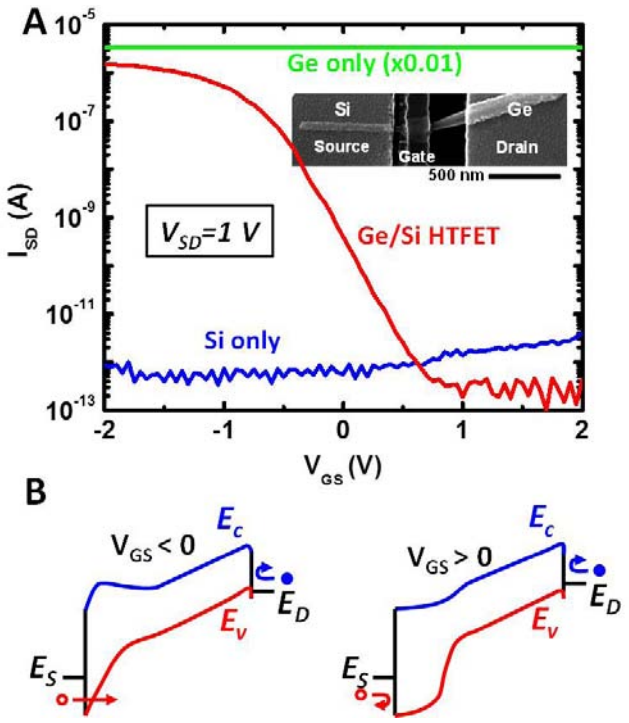

Figure 3. (A) Transfer curves of a p+Ge–i-Si NW heterostructure Schottky barrier FET showing an on-off current ratio, Ion/Ioff, of 10^7. Devices fabricated in the same process on reference p+Ge segments showed no gate modulation and those on reference Si segments showed ambipolar behavior over a larger V_{GS} range. (B) Energy band-edge diagrams illustrating device operation where VD is applied to the Si side. Left panel: Positive V_{GS} assists hole tunneling at the Si side of the device. Right Panel: Negative V_{GS} blocks hole tunneling at the Si side. High p+Ge shell doping prevents field penetration into the channel and electron barrier modulation at the Ge side leading to sustained off state for positive gate voltages.

Nickel contact electrodes have been utilized as source and drain contacts for the heterostructure transistor channels, whose bands then align as shown in Figure 3. Pure silicon or pure germanium NW transistors from the same growth run have been fabricated for comparison. Figure 3a shows the transfer curves of these devices. It can be readily seen that Si on its own exhibits very low current levels with no gate modulation in the gate-voltage window shown here. Also, Ge exhibits large currents (due to heavy p-type doping) with no gate modulation. Remarkably, the Ge/Si heterostructure NW transistor exhibits an impressive 10^7 on/off current ratio, no leakage current branch at positive gate voltages (no ambipolar behavior), and a drive current of 50 microamp/micrometer. This is more than 100 times better than that achieved before in Si NWs [6] and in carbon nanotubes [7]. Such overall performance is well above any other achieved tunnel FET performance available to date and the low attainable off currents are indicative of the low power dissipation in the off-state using this kind of transistor opening the door for enabling a truly green transistor using this kind of one-dimensional heterostructure NW transistors.

Future Work

This project supports the DOE missions in threat reduction, energy independence, and nuclear weapons by advancing our fundamental understanding of nanoscale electronic materials for new materials synthesis, chemical and biological sensing, thermoelectric energy conversion, and electronics systems for future low power, miniaturized applications. We already see a number of new device and system concepts emerging that are anticipated to be important to these areas. The demonstrated devices have a great potential for low-power, low noise, linear and high performance analog and digital electronics.

Conclusion

In this report, we have discussed our most recent work on fabricating a tunnel transistor on axial nanowire heterostructures with levels of performance better than any achieved tunnel transistor performance to date. Specifically, we demonstrate 100 % germanium-silicon axial nanowire heterostructures and asymmetric Schottky-barrier tunnel field-effect transistors with high on-currents, on/off ratios, and totally eliminated ambipolar conduction behavior, typically observed in homogenous device counterparts. This experimentally realized performance, paves the road for a new generation of band-edge engineered novel electronic devices that can operate at high frequencies but at very low off-state dissipation power. Since a significant fraction of U.S. electricity goes to current electronics, improvement in those electronics can have large economic and environmental benefits.

References

1. Wu, y., R. Fan, and P. Yang. Block-by-Block Growth of Single-Crystalline Si/SiGe Superlattice Nanowires. 2002. Nano Letters. **2**: 83.

2. Clark, T., P. Nimmatoori, K. Lew, L. Pan, J. Redwing, and E. Dickey. Diameter dependent growth rate and interfacial abruptness in vapor-liquid-solid Si/Si1-xGex heterostructure nanowires. 2008. NANO LETTERS. **8** (4): 1246.

3. Wen, C. -Y., M. C. Reuter, J. Bruley, J. Tersoff, S. Kodambaka, E. A. Stach, and F. M. Ross. Formation of Compositionally Abrupt Axial Heterojunctions in Silicon-Germanium Nanowires. 2009. SCIENCE. **326** (5957): 1247.

4. People, R., and J. C. Bean. Calculation of critical layer thickness versus lattice mismatch for. 1985. Applied Physics Letters. **47** (3): 322.

5. Dayeh, S., and S. T. Picraux. Direct observation of nanoscale size effects in Ge semiconductor nanowire growth. 2010. Nano Letters. **10** (10): 4032.

6. Moselund, K. E., H. Ghoneim, M. T. Bjork, H. Schmid, S. Karg, E. Lortscher, W. Reiss, and H. Riel. VLS-grown Silicon Nanowire Tunnel FET. 2009. In IEEE Device Research Conference Technical Digest. (Santa Barbara, 22-24 Jun. 2009). , p. 23. New You: IEEE.

7. Appenzeller, J., Y. -M. Lin, J. Knoch, and P. Avouris. Band-to-band tunneling in carbon nanotube field-effect transistors. 2004. Physical Review Letters. **93** (19): 196805/1.

Publications

Dayeh, S. A.. Electron transport in indium arsenide nanowires. 2010. *Semiconductor Science and Technology.* **25** (2): 024004 (20 pp.).

Dayeh, S., and S. T. Picraux. Direct observation of nanoscale size effects in Ge semiconductor nanowire growth. 2010. *Nano Letters.* **10** (10): 4032.

Le, S., P. Jannaty, A. Zaslavsky, S. A. Dayeh, and S. T. Picraux. Growth, electrical rectification, and gate control in axial in situ doped p-n junction germanium nanowires. 2010. *Applied Physics Letters.* **96** (26): 262102.

Picraux, S. Tom., S. Dayeh, P. Manandhar, D. Perea, and S. Choi. Silicon and germanium nanowires: Growth, properties, and integration. 2010. *JOM.* **62** (4): 35.

Sierra-Sastre, Y., S. Dayeh, S. T. Picraux, and C. Batt. Epitaxy of Ge nanowires grown from biotemplated Au nanoparticle catalysts. 2010. *ACS Nano.* **4** (2): 1209.

Polymer-Coated Surfactant Micro-reactors for Applications in Chemical Sensing, Contaminant Remediation and Synthetic Biology

James M. Boncella
20100624PRD3

Introduction

This research project is directed toward the generation of a new detection system for materials of interest such as organophosphates. These compounds are the chemical constituents of nerve agents and pesticides. It will utilize a biotechnology approach to make a system that will specifically recognize the desired analyte (organophosphate). Upon recognition, the system will glow when exposed to ultraviolet light (blacklight). This type of detection scheme is enabled by our ability to encapsulate anionic compounds in vesicles (cell-like structures that form from soap-like molecules under specific conditions). Because this scheme will use DNA which is randomly generated using DNA finger printing techniques, a successful system can be "evolved" to improve the detection process. This would be a completely new way to do chemical detection with an almost unlimited potential for improvement because of the tremendous variability that is possible with DNA polymers. For example, a DNA polymer that is 30 base pairs long has more than a billion billion possibilities of unique structures that would be able to recognize organophosphates. The potential for finding a specific structure that will recognize one and only one type of organophosphate is extremely high. This would allow us to make a sensor that only responds to one compound (say, a specific nerve agent). Furthermore, the method that we will use to find this DNA polymer will be completely unique and will itself represent a major breakthrough in this area of research.

Benefit to National Security Missions

This work is intended to generate a new method for the detection of phosphate chemicals or metabolites in solution. If successful, it will be a new way of detecting pesticide or chemical weapons residues in samples of interest. This type of detection scheme will be of interest to agencies including the Department of Homeland Security, the intelligence services as well as those parts of DOE who have interest in detecting small molecules.

Progress

Methylphosphonic acid has been modified so that it can be detected with our DNA aptamer (an aptamer is a single strand DNA oligomer that can recognize small molecules by binding to them) scheme. The initial screening is currently underway to find a DNA sequence that binds the modified methylphosphonic acid. The preliminary results are extremely encouraging. We are using a new screening method that does not require growing bacterial cell cultures to generate large amounts of aptamer. We are currently at the point where we have identified several candidate DNA aptamers and now need to have the sequences of these molecules determined.

Future Work

The overall goal of the project is to generate a chemical detection scheme for organophosphates (pesticides/ nerve agent residues) that will only respond to a specific, desired compound.

The tasks that will be performed are as follows:

1. Demonstrate that short strands of RNA or DNA (known as aptamers) can be encapsulated in chemical bubbles know as vesicles that form from soap-like molecules. (Already accomplished.)

2. Show that libraries of the DNA/RNA (that are commercially available) can recognize the organophosphate by inducing a fluorescent response (glowing when exposed to ultraviolet light). (Already accomplished.)

3. Develop a selection process to separate the DNA/ RNA fractions that recognize the compound(s) of choice (in the process of being validated as occurring).

4. Once selected, synthesize large quantities of the recognition agent DNA/RNA using DNA fingerprint techniques.

5. Incorporate the useful aptamer into a system that can detect the analyte of choice in a real water sample.

Conclusion

The goal of this project is to produce a new way to detect/ sense organophosphate

chemicals which are the constituents of pesticides and nerve agents. This technology would offer a more selective and possibly more sensitive way to monitor these agents. It could also be used to determine whether someone was manufacturing these materials in a clandestine way by examining the wastes from such a process.

Growth of Actinide-Nanocomposites using Hyperbaric Laser Chemical Vapor Deposition.

William L. Perry
20100626PRD3

Introduction

Since the discovery of the first man-made actinides over 60 years ago, researchers have been fascinated by their complex chemistry, crystal structure(s), and physical properties – as they possess 5f electrons in their outer shells. Currently, methods for producing dense actinide materials and alloys suitable for use as nuclear fuel are limited to dry mixing/pressing or melting at high temperatures. Novel processing methods and development of unique alloys are needed to better understand the inherent electronic and material properties. The aim of this project is to fabricate refractory materials (such as zirconium, tantalum, and tantalum hafnium carbides and nitrides) that will be embedded with surrogate nanoparticles (initially cerium or cesium instead of uranium or thorium) *in situ* using laser-initiated and CVD approaches.

Benefit to National Security Missions

This project will support the DOE missions in Energy Security and Threat Reduction by providing advancement in support technologies that include nuclear power generation and propulsion systems.

Progress

Work on this project officially began on August 9, 2010 and was therefore active less than two months. During this short time, much of the effort was spent on project planning and designing/acquiring parts for the laser chemical-vapor deposition (CVD) apparatus that will be used for the first-generation experiments. The set-up (schematic shown in Figure 1) was successfully built and used in several preliminary growth experiments. The gas-phase reactions take place in a stainless steel vacuum chamber that is enclosed by a furnace to maintain an elevated temperature in the chamber during the reaction. A 532 nm Nd:YAG laser (0.1 – 10 W) enters the chamber through one sapphire window, and a camera is setup through another sapphire viewport 90° to the laser entry and monitors the reaction progress in real-time. The entire chamber is resting on a translation stage that allows movement in x, y, and z directions to aid in laser alignment. Swagelok VCR fittings and braided stainless steel hoses are used throughout the remainder of the setup which feeds to the top of the chamber through the enclosing furnace. Directly attached to the reaction chamber is a mechanical pressure gauge (pressure monitoring in this device is not adversely affected by high temperatures), a cold trap, and the solid precursor introduction container. All of these devices, including the hosing between, are wrapped with heat tape and insulation that is heated throughout the duration of the experiment. A valve separates the remaining system components, which include a port to introduce gases, a secondary digital pressure gauge, and a vacuum pump.

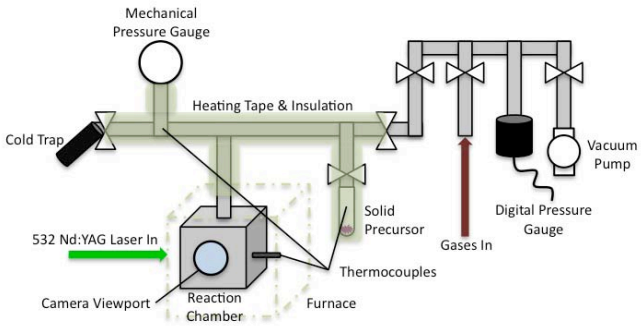

Figure 1. Illustration of the LCVD System.

A considerable amount of effort was also spent using the thermodynamic program EkviCalc (BeN Systems) to generate a list of candidate systems that are predicted to successfully form the transition metal carbides of interest. Specifically, the aim is to grow refractory materials in the form of fibers using laser CVD. Hafnium, tantalum, rhenium, and zirconium carbides are all target materials for fabrication, and these systems were investigated thermodynamically under a variety of reaction conditions. The carbon source, metal-halide precursor, temperature, and pressure were all varied within the program in an attempt to find the optimal conditions for metal carbide formation which are also practical to carry out with the experimental set-up that was built. Figure 2 shows the most promising preliminary results, with ZrC the target product (all

possible products listed in the legend to the right), from the thermodynamic calculations using ZrI_4 (a) and $ZrCl_4$ (b) as solid zirconium precursors and methane (CH_4) as the carbon source for both. When used in a 1:1 mole ratio, it is apparent that ZrC(s) formation begins to dominate over the other solid by-products at ~1800 °C, a reasonable temperature that can be obtained with a well-focused laser beam. The vapor pressure of the solid precursors is an important factor that must also be considered, and that of ZrI_4 and $ZrCl_4$ is at least 55 Torr at 350 °C – theoretically enough for a reaction to occur if the system is kept at this temperature.

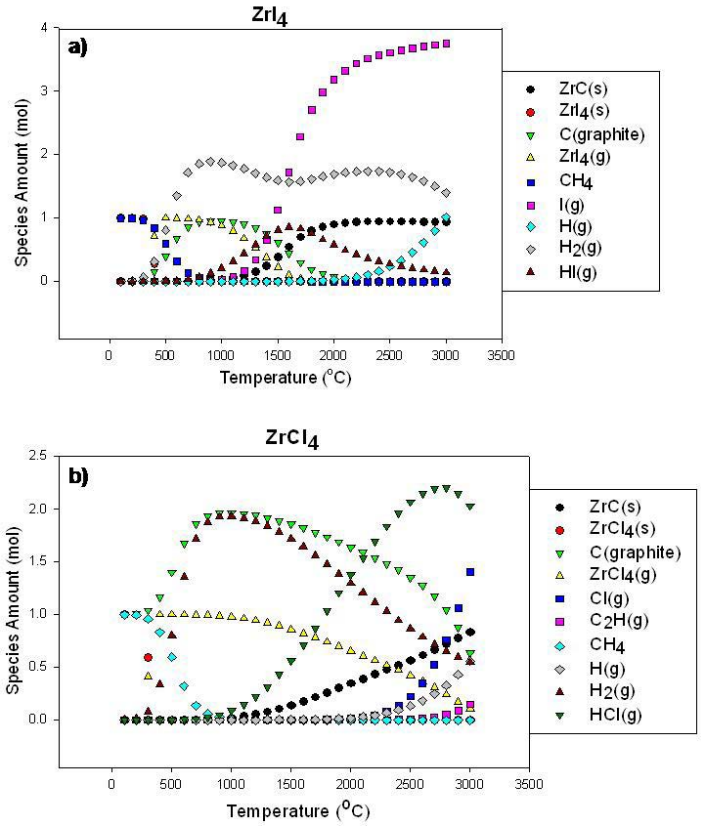

Figure 2. Ekvicalc Thermodynamic Results of the Gas-Phase Reaction of the (A) ZrI_4, and (B) $ZrCl_4$ Systems with Methane.

Several experiments were carried out using ZrI_4 and CH_4, with mixed results. The extreme air-sensitivity of ZrI_4 is one hurdle; it was determined that the experiment will not work (i.e. no deposition observed) if the precursor has the slightest sign of oxidation. In all attempted experiments, the precursor was heated to 350 °C and the reaction chamber to 375 °C to facilitate maximum attainable vapor pressure (~50 Torr) of ZrI_4. Methane was introduced at 50 Torr, and parameters such as substrate, laser power, and reaction time were varied. Depending on those variables, two morphologies were observed: a short fiber was grown on an alumina substrate (SEM image in Figure 3a) and a nanorod-containing coating was deposited on a tungsten wire (Figure 3b). Energy-dispersive X-ray spectroscopy (EDX) analysis performed on the samples while in the SEM does not support ZrC formation, although further analysis is still needed to determine the composition of the deposited materials.

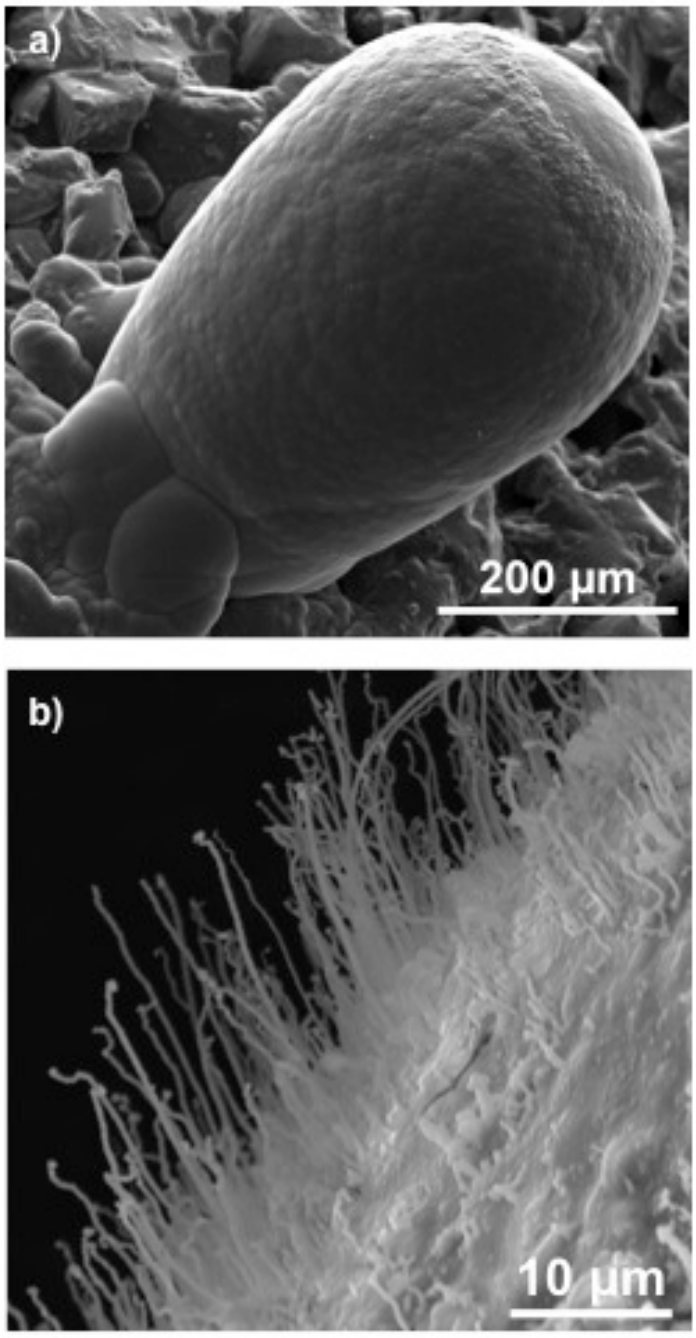

Figure 3. SEM Images of Experimental 3-D Structures on (A) Alumina Substrate, and (B) Tungsten Wire Substrate.

Future Work

Much future work still remains to obtain the target refractory materials. Other metal precursor/carbon-source gas combinations will be tested in an attempt to fabricate refractory metal carbides, and the CVD products will be further analyzed not only using SEM (to image porosity and overall morphology, as well as do gross atomic analysis

using EDX), but also x-ray photoelectron spectroscopy (to quantitatively determine elemental composition) and x-ray diffraction (to determine atomic packing arrangement). An optical two-color pyrometry temperature measurement system is currently being built and tested so that real-time temperature measurements can be made of the material as it deposits. This data is critical in order to publish novel growth of these materials. Following successful growth of several candidate refractory fibers, non-radioactive nanoparticles will be incorporated into the fibers as they are being fabricated. Doping of non-refractory fibers will be attempted first, such as carbon, as the growth conditions are more straightforward and will allow focus to be made on the optimum incorporation of the nanoparticles.

Conclusion

The novel synthesis of refractory nanocomposites for potential applications as nuclear fuel materials will create: (1) an enhanced understanding of the fundamental properties of the actinides in pure and alloyed form, (2) more reliable/safe nuclear reactors, and (3) a potentially irreversible means of disposing of nuclear waste/materials. LANL is the ideal location for these types of experiments as it is one of just a few places in the world performing HP-LCVD research and is the world's premiere facility for handling radioactive materials.

Molecular Level Investigation of Tunable Energetic Mixtures

David S. Moore
20070766PRD4

Abstract
This study on shock-induced initiation of intermetallic reactions provides the first insight into the critical molecular-level processes responsible for ultra-fast shock induced reactions in multi-component energetic mixtures, and their dependence on system heterogeneity. The results have a broad impact on conventional reactive material systems and supply the fundamentals to directly manipulate and optimize chemical behavior. This understanding will enable the design of a new class of application-based energetic materials, demonstrating tunable sensitivity, reaction kinetics, and energy yield.

Background and Research Objectives
Explosive materials (e.g., HMX, PBX) generate rapidly expanding gases, which can cause unnecessary collateral damage. A safer alternative is in intermetallic- forming reactive mixtures, which can undergo ultra-fast shock-induced reactions, releasing significant heat during the formation of solid products, and thereby provide for the controlled defeat of targets. The challenge associated with reactive mixtures has been to determine the molecular-level mechanisms that govern the initiation and kinetics of shock-induced reactions. We are studying the shock-induced initiation of intermetallic reactions through combined laser-driven shock-compression experiments and computer modeling, performed on a range of binary reactive systems, in order to determine the influence of heterogeneity on the molecular-level processes responsible for reaction. Multi-component reactive films (e.g., V/Si, Mo/Si, Al/PTFE) up to 2 µm in thickness are deposited onto transparent substrates using e-beam deposition and/or spin casting. A novel dynamic masking technique, in which a mask is translated between the source and substrate during deposition, is employed to construct films with a predefined thickness gradient. This method, performed in forward and reverse mask mode with reactive complements, is used to fabricate bi-layer films with an internal interface, inclined to the substrate normal by a specified angle. Measures of the total film thickness, roughness, and interface angle, necessary for proper interpretation of results, are characterized through SEM, AFM, and profilometry.

A Ti:sapphire laser system, focused at the substrate/film interface to a spot size of 75 µm, is then used to drive an ultra-fast, supported shock wave (10-20 ps rise-time, >200 ps shocked duration) through the bi-layer. Spatially flat shocks can be produced using a field-flattener. Ultra-fast dynamic ellipsometry is employed at the film/air interface to obtain time- and spatially-resolved surface displacements in a single given experiment, and detect short timescale phase shifts corresponding to the onset of molecular-level reactions. Varying the film species (metals, metalloids, polymers), interface angle during deposition (gradient and non-gradient), and laser-drive energy, provides great flexibility in further studying the role of heterogeneity in the kinetics of shock-induced reactions at the molecular-level. This experimental work is complemented by multi-scale numerical simulations, used to develop and validate new predictive models for the controlled, ultra-fast initiation of intermetallic reactions.

Scientific Approach and Accomplishments
We completed addition of the dynamic masking system to our bell jar vapor deposition system necessary to produce multi-component films with a predefined thickness gradient. We successfully deposited a series of amorphous Si films with a thickness gradient, and characterized their uniformity using SEM.

We found a complex ultrafast dynamic ellipsometry (UDE) time response after shocking these films using our ultrafast laser shock system. We realized this complex time response could be due to changes in particle velocity due to reaction or phase transformation, or to changes in the shocked material index of refraction. The initial films cleverly used silicon both as a window and as one of the reaction components, but we discovered that the shock response of amorphous silicon was not very well understood. However, we also discovered a large body of work on the shock response of single crystal silicon. We then devised a method to produce thin film samples of single crystal silicon, and located a photolithography/MEMS vendor willing and able to manufacture the required array of supported thin film samples from a single

crystal silicon blank. We have since used these samples to acquire an extraordinary set of UDE results on the ultrafast time response of shocked single crystal silicon. We implemented two approaches to analyze the time dependent UDE data. One involves a time dependent change in the index of refraction of the shocked material with either sigmoidal or logarithmic approach to a new constant value. The other involves a first order reaction with progress variable, and calculates the time dependent index of refraction. To implement, the UDE ellipsometric data are fit using four variables instead of three, with the fourth describing the time dependent index of refraction.

However, the similar UDE contributions from changes in shocked material index of refraction and the shock velocity necessitated an additional diagnostic. We constructed a 400 nm UDE diagnostic to independently measure the shock velocity (using both 800 nm – transparent to silicon – and 400 nm – reflects from silicon – probes), which will allow us to pin down one of the fitting variables in our UDE methodology and thereby extract the remaining variables (particle velocity and index of refraction) with greater confidence and accuracy. These experiments are in progress and will be completed by other DE-9 staff as Dan Eakins departed from Los Alamos January 2010 to Imperial College London as a Lecturer.

We have also produced Mo/Si and V/Si binary films with a sharp (near vertical) step between the two layers. The spatially resolved UDE data are being obtained and will be analyzed using similar tools to those developed for the non-gradient films. Continuum-level simulations of this configuration have been performed using the multi-material Eulerian shock code, CTH, to estimate the magnitude of particle-velocity mismatch at such an interface.

Impact on National Missions

The results from this study are directly applicable to threat reduction mission needs, enabling the design of a new class of application-based energetic materials for controlled defeat of targets.

Publications

Eakins, D. E., and N. N. Thadhani. Mesoscale simulation of the configuration-dependent shock-compression response of Ni+Al powder mixtures. 2008. *Acta Materialia.* **56** (7): 1496.

Eakins, D. E., and N. N. Thadhani. Shock compression of reactive powder mixtures. 2009. *International Materials Reviews.* **54** (4): 181.

First-Principles-Based Equations of State Including Multi-Phase Chemical Equilibrium

Milton S. Shaw
20080695PRD1

Abstract
The goal of this project was to refine and extend computational methods for building an equation of state for chemical explosive detonation products. The principal vehicle for achieving this was the development of a Monte Carlo simulation method specially designed to capture the complexities of chemistry under extreme conditions of temperature and pressure. A very efficient procedure was implemented for evaluating equilibrium averages with electronic structure-based (quantum chemistry) energies in place of approximate functional forms. Many steps in a reference system (characterized by a computationally inexpensive "model" potential) are used to generate a single electronic structure configuration. This effectively reduces by up to three orders of magnitude the number of electronic structure calculations required to build ensemble averages.

Replacement of approximate potentials with highly accurate ab initio energy evaluation, especially in the context of Monte Carlo in a reactive ensemble, promises considerable improvement in accuracy over that of previous work. Namely, it permits evaluation of statistical properties accounting for rare events (in this case, chemical reactions among fluid components) on a highly accurate and reactive potential energy surface, but without actually having to sample those regions of the potential most sensitive to error (i.e., the chemical reaction barrier tops). In addition to enhancing the predictive capability of the Laboratory's continuum detonation models, these developments should be of broad interest to computational scientists in government, industrial, and academic contexts.

Background and Research Objectives
Detonation fronts moving through energetic materials leave hot, dense fluids in their wake. The macroscopic, continuum-mechanical description of this fluid incorporates two components:dynamical equations embodying conservation of mass, momentum, and energy, and constitutive expressions relating equilibrium thermodynamic properties of the material (also known as equation of state, or EOS). While the former are capably provided by classical mechanics (e.g. Navier-Stokes), truly predictive hydrodynamics also require that the latter be of very high precision (~1%). Empirical EOS reconstruction is frustrated by the material conditions following detonation; high explosives (HE) produce immense pressure at temperatures exceeding those obtainable in diamond anvil experiments by up to a factor of three.. Additional features of the product mixture, such as chemical equilibrium among fluid components or between fluid and solid phases, are difficult to assess even qualitatively in the laboratory. Computer simulation provides an essential means of circumventing the practical obstacles to obtaining accurate and meaningful data for matter under such extreme conditions.

Scientific Approach and Accomplishments
Over the course of the two year duration of the project, we have made considerable progress in our efforts to improve the accuracy and efficiency of atomistic Monte Carlo simulation. Our focus in particular has been description of molecular fluids subjected to extreme temperatures and pressures, approximating thermodynamic conditions that follow detonation of high explosive compounds.

We formulated a new Monte Carlo method for efficiently sampling accurate ab initio and density functional theory (DFT) energies in lieu of approximate model potentials. Our method uses Boltzmann sampling of a pair potential to statistically decorrelate successive evaluations of a much more accurate and computationally expensive DFT potential. A sequence of single-particle steps made in the reference system (described by the pair potential) is combined to yield a composite step made in the full system (described by DFT). Through a slight modification of the acceptance probability, one recovers Boltzmann sampling of the full system. By statistically decorrelating samples of the DFT potential, fewer evaluations of it are required to obtain ensemble averages having low variance. The efficiency of this decorrelation process is significantly enhanced by maximizing the overlap of the distribution of reference system states with that of full system states. This, in turn, is achieved by variation of

the full system temperature and pressure such that an a priori estimate of the acceptance probability for composite steps is maximal. Monte Carlo simulation at the new, optimal conditions can then be performed; we have dubbed this procedure the optimized-Nested Markov Chain Monte Carlo (o-N(MC)^2) method. We published a largely methodological discussion [1] in the Journal of Chemical Physics as well as presenting a talk at the 2009 APS Shock Compression of Condensed Matter Conference and the associated conference proceedings [2].

After laying the theoretical groundwork, we applied our technique to the description of compressed nitrogen fluid as described by the Perdew-Burke-Ernzerhof exchange-correlation functional and a 6-31G* basis set. The required simulations took ~6 months and represented the most accurate potential applied to the largest simulation performed to date on this system. The Monte Carlo simulation results were then reworked to yield the nitrogen Hugoniot, the locus of states accessible upon shock loading of an initial state. Our Hugoniot results reflected precision levels of ~2% were in quantitative agreement with experiments. This implementation was published in the Journal of Chemical Physics [3]. This work was also presented at a talk at the 2009 APS Shock Compression of Condensed Matter Conference and in the conference proceedings [4].

In the process of improving the thermodynamic description of molecular fluids at high pressure and temperature, we discovered that elements of our methodology could be applied to modeling spectroscopic signals recorded for such systems. Using a rapidly-evaluatable reference potential as in our thermodynamic work, we collected statistics on dense fluid nitrogen using Monte Carlo sampling of an accurate density functional theory potential and its forces. Introduction of a novel methodology then enabled us to convert the DFT forces into Raman line shifts as a function of pressure (density). The results were in quantitative agreement with experiments previously performed at LANL, and reported in Chemical Physics Letters [5].

In the last few months of the project, we developed the principal features of a method combining the best features of the optimized Nested Markov Chain Monte Carlo with Hybrid Monte Carlo. In essence, this allows the use of molecular dynamics, with all of its advantages, as the trial move within the optimized method. The implementation is currently being tested.

Impact on National Missions

This project supports the DOE/NNSA mission in Nuclear Weapons (and e.g. Homeland Security and Office of Science) by enhancing our understanding of the extreme pressure and temperature environment occurring in the detonation of chemical high explosives including near-first-principles prediction capability.

References

1. Coe, J. D., T. D. Sewell, and M. S. Shaw. Optimal sampling efficiency in Monte Carlo simulation with an approximate potential. 2009. *Journal of Chemical Physics.* **130** (16): 164104.

2. Coe, J. D., T. D. Sewell, and M. S. Shaw. Optimized nested Markov chain Monte Carlo sampling: theory. 2009. (Nashville, TN, 28 June - 3 July 2009). Vol. CP1195p. 525. New York: AIP.

3. Coe, J. D., T. D. Sewell, and M. S. Shaw. Nested Markov chain Monte Carlo sampling of a density functional theory potential: equilibrium thermodynamics of dense fluid nitrogen. 2009. *Journal of Chemical Physics.* **131** (7): 074105.

4. Shaw, M. S., J. D. Coe, and T. D. Sewell. Optimized nested Markov chain Monte Carlo sampling: application to the liquid nitrogen Hugoniot using density functional theory. 2009. (Nashville, TN, 28 June - 3 July 2009). Vol. CP1195p. 529. New York: AIP.

5. Coe, J. D., T. D. Sewell, M. S. Shaw, and E. M. Kober. A quantum chemical method for calculating vibrational line shifts in diatomic fluids. 2008. *Chemical Physics Letters.* **464** (4-6): 265.

Publications

Coe, J. D., T. D. Sewell, M. S. Shaw, and E. M. Kober. A quantum chemical method for calculating vibrational line shifts in diatomic fluids. 2008. *Chemical Physics Letters.* **464** (4-6): 265.

Coe, J. D., T. D. Sewell, and M. S. Shaw. Optimal sampling efficiency in Monte Carlo simulation with an approximate potential. 2009. *Journal of Chemical Physics.* **130** (16): 164104.

Coe, J. D., T. D. Sewell, and M. S. Shaw. Nested Markov chain Monte Carlo sampling of a density functional theory potential: equilibrium thermodynamics of dense fluid nitrogen. 2009. *Journal of Chemical Physics.* **131** (7): 074105.

Coe, J. D., T. D. Sewell, and M. S. Shaw. Optimized nested Markov chain Monte Carlo sampling: theory. 2009. In *Shock Compression of Condensed Matter - 2009.* (Nashville, TN, 28 June - 3 July 2009). Vol. CP1195, p. 525. New York: AIP.

Shaw, M. S., J. D. Coe, and T. D. Sewell. Optimized nested Markov chain Monte Carlo sampling: application to the liquid nitrogen Hugoniot using density functional theory. 2009. In *Shock Compression of Condensed Matter - 2009.* (Nashville, TN, 28 June - 3 July 2009). Vol. CP1195, p. 529. New York: AIP.

Study of Hybrid Semiconductor/Molecular Systems for Photo-production of Hydrogen

Andrew P. Shreve
20080700PRD1

Abstract
This is the final report of a two-year Laboratory Directed Research and Development (LDRD) postdoctoral research project. Charge transfer is a basic step needed for solar energy conversion. However, optimizing charge transfer in materials is hard. New experimental tools and studies are needed to provide fundamental knowledge of rates and mechanisms for charge-transfer steps. This research project mostly addressed the development of instrumentation for study of light-induced charge transfer. Specifically, great improvement in instruments for time-resolved step-scan Fourier Transform infrared spectroscopy was demonstrated. These new methods were then used to study structure of molecules in their excited states. Compounds studied were transition-metal-containing molecules used for photo-induced charge injection into semiconductors.

Background and Research Objectives
Solar-based methods are attractive for energy generation. These methods rely upon light absorption to make excited states of molecules or semiconductors. From the excited states, charge transfer leads to charge collection. Finally, for fuel production, light-absorbers and charge-transfer reagents are linked with catalysts. These catalysts can transform chemical compounds to make fuels. For light absorption and catalysis, transition-metal-based molecules are often used. However, there remain fundamental questions regarding the structure of photo-excited states in transition-metal compounds.

Infrared spectroscopy is a very useful tool for the study of excited states of molecules [1-4]. However, since excited states don't survive for very long, the infrared spectra must be measured using time-resolved methods. Time-resolved infrared spectra provide information about the speed of excited-state relaxation or charge-transfer steps. They also probe structural changes in molecules that follow excitation with light. Unfortunately, time-resolved infrared spectroscopy has often been limited by low signal-to-noise ratios. For nanosecond and longer time scales, this limitation has arisen because only low-repetition rate laser sources have been available for the excitation step. However, there are now inexpensive kHz-repetition-rate lasers with enough power to excite molecules. Using this new generation of lasers for time-resolved infrared spectroscopy should lead to a big improvement in signal-to-noise ratios. Such an advance will allow more sensitive studies of charge-transfer steps useful for solar technologies. Developing and using such instrumentation has been one of the major activities of this project.

Scientific Approach and Accomplishments
This section describes the development of new instrumentation and the use of this instrumentation for the characterization of molecular excited states.

Instrumentation Development

The most common method for time-resolved infrared spectroscopy on nanosecond and longer time scales is step-scan Fourier Transform Infrared (ssFTIR). In a step-scan Fourier Transform experiment, the relative geometric delay between the arms of a two-arm optical interferometer is held at a particular value. Then, a kinetic process being studied is measured at that fixed value. For example, one might use a laser pulse to excite a molecule, and then measure infrared light passing through the sample at various times after the initiation point. Next, the interferometer is moved to another fixed delay setting. This movement is the "step" of the step-scan method. The kinetic measurements are then repeated at this new setting. From this sequence, a data set is generated that consists of infrared intensity versus time following photo-excitation for every point of an interferogram. These data can then be reorganized to provide the interferogram versus time following photo-excitation. In Fourier Transform spectroscopy, the interferogram is related to the spectrum by a Fourier Transform operation. Thus, Fourier Transform of the interferograms led to the infrared spectrum at each time point.

To efficiently excite molecules with light in the ssFTIR experiment, lasers with relatively large per-pulse energies (> 100 μJ) are needed. Up until a few years ago, such lasers were only available as low-repetition rate systems, typically generating only a few light pulses each

second. For example, most such lasers operated at a pulse repetition frequency of 10 Hz (10 pulses per second). Thus, the usual method of using step-scan instruments has been to measure data from only a single excitation pulse per interferometer step, with interferometer steps occurring at the low repetition rate of the laser. A typical interferogram requires of order 4000 steps. Further, obtaining good signal-to-noise for the measured infrared signals typically requires averaging about 100 laser pulses. Thus, the total acquisition time if operating at 10 Hz is several hours. In this specific example, at best, it would take 11.1 hours to measure a spectrum. Such very long measurement times cause numerous problems with long-term instabilities arising from temperature changes, sample damage, electronic and detector drift, and other similar issues.

Fortunately, within the last few years, several inexpensive lasers have been developed that provide t high per-pulse energies with kHz (or higher) pulse repetition rates. Thus, if one could use, for example, a 4 kHz repetition rate laser as an excitation source, then the same experiment just described could be done in as little as 1.67 minutes.

Motivated by these considerations, we have developed an instrument for time-resolved ssFTIR using a kHz pulsed laser source. While straightforward in principle, combining step-scan instrumentation with a kHz repetition excitation laser requires addressing several major issues. In our case, we use a Biorad FTS-60 FTIR instrument. The Biorad instrument is built so that step-scan mode is achieved by synchronizing two continuously scanning interferometer arms. These arms are synchronized so that a fixed delay is maintained between them. To maintain this fixed delay, one of the arms is slightly "dithered" in position with a 16 kHz modulation. A reference laser signal is monitored at this frequency to provide feedback to the interferometer mechanism. Thus, the laser source must be synchronized with this instrumental modulation in order to avoid introduction of additional noise. The electronic and optical details of the implementation we have developed are shown in Figures 1 and 2.

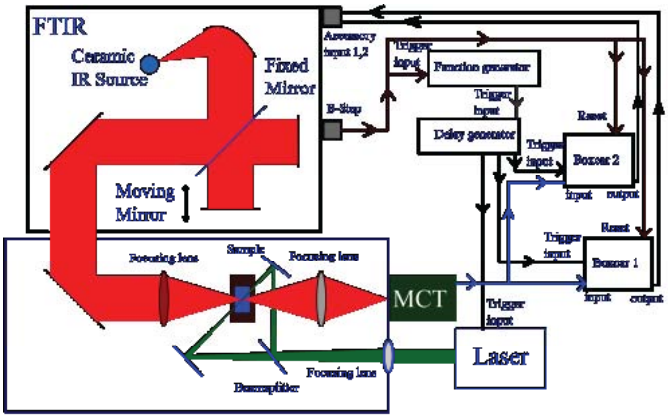

Figure 1. Schematic of the nanosecond ssFTIR and the connectivity of the FTIR. Data collection starts with an initiation signal from the FTIR going to the signal generator and providing a reset signal to the boxcar integration modules. The output from the signal generator is passed through a delay generator, which sends pulses to the boxcars and laser. The homemade purged box contains the sample chamber where the sample is excited from two sides. In the last step the boxcars send the data back to the FTIR for acquisition and processing.

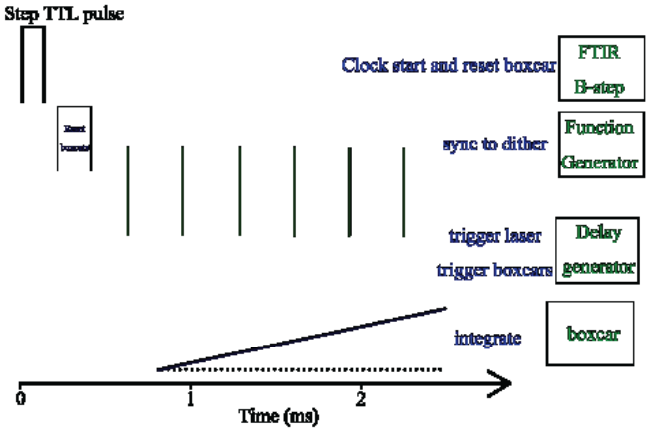

Figure 2. A detailed illustration of the synchronization of the data collection at each step. The FTIR produces an electronic pulse at each step of the interferogram, which is used to start the data collection. The pulse from the FTIR is used to reset the boxcars and is input into a signal generator. The signal generator produces a burst of pulses triggered at 4 kHz rate (typically) and sent to the delay generator. The delay generator synchronizes the pulses to the 16 kHz dither frequency of the FTIR and triggers the laser and boxcars. The boxcars then sample, integrate the and average the infrared signal synchronized with the individual laser pulses. As described in the text, both a pre-pulse and a post-pulse sample is taken for each laser pulse. The averaged signal from each of the boxcars is provided to the FTIR for processing.

In our case, we have normally designed the experiment to obtain an infrared spectrum at a specific time delay following the excitation pulse. This design uses so-called boxcar integration modules for the electronic sampling. In most cases, such single-time infrared spectra are all that are needed to study structural changes that occur upon photo-excitation. For each laser pulse, we measure two infrared signals by setting two sampling gates of the boxcar modules. One gate (the reference signal) precedes the excitation pulse. The other gate (the probe signal) is set to a specific time delay following the excitation pulse. A typical time delay is a few hundred nanoseconds. The reference signal leads to an interferogram that generates a ground-state spectrum. The probe signal leads to a spectrum that includes contributions from the fraction of molecules excited by the laser pulse. These signals are averaged over hundreds of excitation laser pulses. Taking the difference of the two spectra leads to a spectrum produced by the photo-excitation process. Here, depletion of the ground

state corresponds to negative features and production of the excited state leads to positive features. The true excited state spectrum can also be produced by adding a small amount of the ground state spectrum back into the difference spectrum to compensate for the depletion of ground state. In a typical experiment, less than 10% of the molecules are excited in each laser excitation pulse.

Application

To illustrate these methods, we measured the infrared spectra associated with excitation of the transition-metal based molecule $Ru[bpy_3]^{2+}$ (bpy stands for bipyridine). This compound and its structural relatives are used in photovoltaic and photochemical applications. Also, one previous study measured the mid-infrared spectral region of this compound after photo-excitation [5]. However, since this study used 10 Hz lasers for excitation, the signal-to-noise was very poor even after days of signal averaging. Thus, in addition to producing useful scientific results, we were able to assess the improvement in signal-to-noise that our new instrument can provide.

Results from our study are shown in Figure 3. The ground state spectrum is shown in Panel A. The difference spectrum associated with photo-excitation is shown in Panel B. The reconstructed excited-state spectrum obtained by adding 0.073 times the ground state spectrum into the difference spectrum is shown in Panel C. These data were obtained with a total acquisition time of about 50 minutes. Previous experiments on the same system with a 10 Hz excitation source required upwards of 14 hours for data acquisition. Further, the resulting spectrum was of much lower spectral resolution, so analysis of the transient spectrum was difficult. In our case, there are clear peaks in the excited-state spectrum. The positions of these peaks are consistent with the view that photo-excitation causes transfer of an electron from the Ru atom to a bipyridine. Further, from these peak positions, we can confirm that the electron is located on only one of three bipyridines. As an aside, we have also shown that this same instrumentation yields significant improvement in obtaining transient infrared spectra from metal-ion containing proteins. Such proteins are important components in biological and biomimetic energy transduction processes. The much improved signal-to-noise and the shorter data acquisition times are a substantial advance over existing technologies. A more detailed description of experiments and applications are presented in a submitted manuscript.

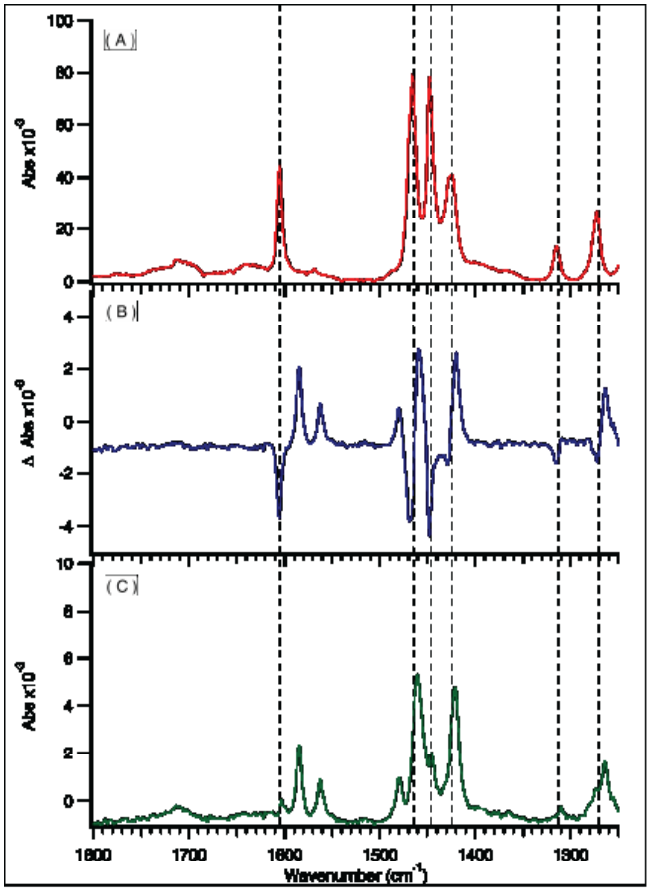

Figure 3. A) Ground state absorption spectrum of [Ru(bpy)3]2+. B) The difference spectrum associated with photoexcitation of [Ru(bpy)3]2+. C) Excited state spectrum obtained by adding 7.3% of the ground state spectrum to the photoexcitation difference spectrum.

Follow on work will investigate a series of transition-metal-containing molecules useful as light-absorbing compounds with photo-induced charge transfer activity. Preliminary work has shown that other ligands such as terpyridine and phenanthroline can also be studied with the methods developed here. In addition, in some cases, energy- and charge-transfer processes occur on time scales faster than a few nanoseconds. Thus, studies may also require use of ultrafast time-resolved infrared spectroscopy. Additional work in the project has developed an instrument for femtosecond time-resolved infrared spectroscopy. This instrument is based on optical parametric amplifiers, and a schematic is shown in Figure 4. Some initial infrared data obtained after ultrafast excitation of malachite green, an organic molecule, are shown in Figure 5. The ability to measure transient infrared signals following photo-excitation on time scales from femtosecond to millisecond (or longer) will enable the investigation of numerous photo-induced energy transduction steps in molecular-based photovoltaic and photocatalytic systems.

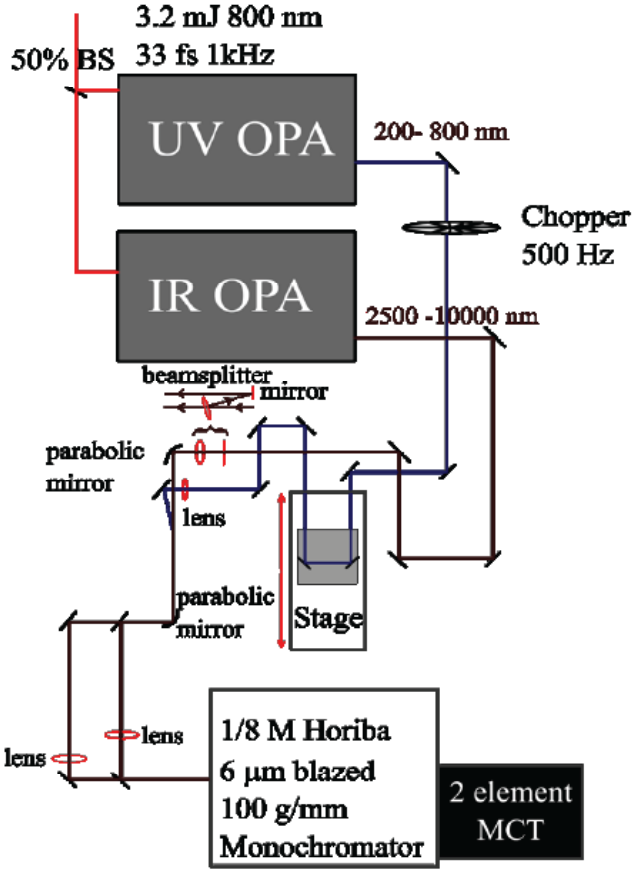

Figure 4. The schematic of the femtosecond time-resolved infrared instrument developed here. Two optical parametric amplifiers were used, one to produce an excitation pulse and the second to produce infrared light to probe the excited state. A stage is used on the pump side for scanning the time delay of the excitation pulse with respect to the probe.

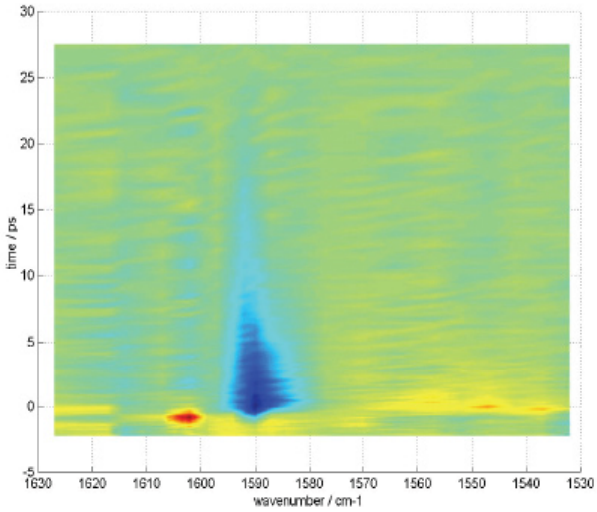

Figure 5. Time-resolved infrared signals obtained from malachite green are shown with infrared wavelength (wavenumber) on the horizontal axis and delay time on the vertical axis. Blue colors correspond to depletion of the ground state, and red colors correspond to new signals associated with the photo-excitation process.

Impact on National Missions

The development of new sources of energy to provide alternatives to fossil fuels is an immediate and urgent national security need. One promising avenue is the use of transition-metal compounds as components of photovoltaic or photocatalytic systems. Such systems can convert sunlight into electricity or chemical fuels. However, study of the structure of photo-generated excited states remains challenging, which limits optimization of molecules useful for such applications. The development of new characterization tools in this project will allow study of both dynamics and structural changes in molecules of interest. Ultimately, this work will open up new opportunities for long-term optimization of solar energy technologies.

References

1. Chen, P. Y., and R. A. Palmer. Ten-nanosecond step-scan FT-IR absorption difference time-resolved spectroscopy: Applications to excited states of transition metal complexes. 1997. *Applied Spectroscopy.* **51** (4): 580.

2. Schoonover, J. R., G. F. Strouse, K. M. Omberg, and R. B. Dyer. Time-resolved, step-scan FTIR spectroscopy of excited states of transition metal complexes. 1996. *Comments on Inorganic Chemistry.* **18** (3): 165.

3. Schoonover, J. R., and G. F. Strouse. Time-resolved vibrational spectroscopy of electronically excited inorganic complexes in solution. 1998. *Chemical Reviews.* **98** (4): 1335.

4. Turner, J. J., M. W. George, F. P. A. Johnson, and J. R. Westwell. Time-resolved infrared spectroscopy of excited states of transition-metal species. 1993. *Coordination Chemistry Reviews.* **125** (1-2): 101.

5. Omberg, K. M., J. R. Schoonover, J. A. Treadway, R. M. Leasure, R. B. Dyer, and T. J. Meyer. Mid-infrared spectrum of [Ru(bpy)3](2+). 1997. *Journal of the American Chemical Society.* **119** (30): 7013.

Publications

Magana, D., D. Parul, R. B. Dyer, and A. P. Shreve. Implementation of time-resolved step-scan FTIR using a kHz repetition rate pump laser. *Applied Spectroscopy.*

Synthesis and Characterization of Novel Metal-Organic Frameworks for Hydrogen Storage

Toti E. Larson
20080780PRD2

Abstract

Metal Organic frameworks (MOFs) may play a critical role for hydrogen storage and separation applications and may solve other environmental, energy and national security problems. This project specifically addresses the use of MOFs to increase storage capacity and separation efficiency of select gases. Considerable effort is placed on the design, synthesis, and characterization of new MOFs for these specific applications. Specifically, MOFs were designed with unsaturated metal coordination site on the walls of the channels to enhance the framework-guest interaction and increase guest molecule adsorption capacity. Results from experiment indicate that this style of MOF design effectively increase the enthalpy of hydrogen adsorption and improve adsorption capacities. It is expected that the work completed here will contribute significantly to the use of hydrogen storage and potential chemical threat adsorption applications.

Background and Research Objectives

Hydrogen is the key to a CO_2 limited society. Unfortunately the extreme low density of even liquid hydrogen has a major consequence in its use, storage and transport. To have appreciable amounts of hydrogen stored as a fuel we must both have very high pressure and cryo-cooled tanks, which represent a significant hazard in general applications. However, many materials have hydrogen densities much greater than that of liquid hydrogen and do not require the use of high pressures. Also the hydrogen must be released at relatively low temperatures and come out without impurities. Another major issue is regeneration (or rehydrogenation) of the storage material. The DOE has set very aggressive targets for the performance of such materials and these are based on a system not a material. For example, the DOE sets targets at 5.5 wt% of hydrogen capacity for the system which includes pumps tanks and anything else required releasing the hydrogen for use. This work aims at designing, synthesizing and testing novel Metal-organic frameworks (MOFs) for hydrogen storage/separation as well as exploring their use in other application fields related to environmental, energy and national security problems. Since the discovery of the first MOF compound, hundreds of different MOFs have been developed and reported. MOFs are generally synthesized by self-assembly of metal ions/clusters as coordination centers and organic ligands as linkers. They possess intriguing chemical and physical properties and are structurally tunable, thermally stable and mechanically sound. MOFs are increasingly proving to be a superior class of materials for state-of-the-art applications in crystal engineering, chemistry, and materials science.

Scientific Approach and Accomplishments

I have worked for this project since July 7, 2008. During the past two year, I have completed the required training and work authorization requirements involving safety and security. For research task, I have synthesized and structurally characterized a series of novel MOFs for tailored applications, such as hydrogen storage, CO_2 capture, sampling of chemicals, etc.. I investigated reticular design of their functionalized pore wall structures, and showed some of their remarkable applications, especially in the areas of storage and separation. I also designed and assembled several instruments for gas separation and variable-pressure gas-loading cells in conjunction with neutron scattering instruments, allowing *in-situ* and real-time examination of guest uptake/release processes in MOF compounds at the molecular site-specific level. Recently, I also investigated MOFs application for high-efficiency sampling, preservation, and sensing of chemical threat agents. The following research tasks were accomplished during the past two years:

Design and syntheses of tailored MOFs for hydrogen storage

I have synthesized a series of MOF compounds from reactions of different functionalized ligands with metal salts under various reaction conditions. These MOFs have different pore sizes and polar pore walls and exhibit excellent gas adsorption and separation capacities. Specifically, they can be categorized into three types.

MOFs with unsaturated metal coordinated sites on the walls of channels, which enhance the framework-guest interaction and thus increase the chemical threat agent adsorption capacity.

As shown in Figure 1A-D, four MOFs with different open metal sites were synthesized and characterized. Reactions of benzene-1,3,5-carboxylic acid (H_3BTC) with metal nitrate (Cu^{II} or Zn^{II}) create two novel MOFs with the similar molecular structures: $Cu_3(BTC)_2(H_2O)_3$ and $Zn_3(BTC)_2(H_2O)_3$ (Figure 1A,1B). Both MOFs contain paddle wheel $M_2(CO_2)_4$ molecular building block units (MBBs). The open metal sites are originally occupied by water molecules, which can be easily removed via heat the materials at 150 ºC for 4 h without decomposition of host frameworks of MOFs. Replacing the metal cations with the same ligand, another two kinds of MOFs, $Ln(BTC)(H_2O)$ (Ln = La - Yb) and $Zn_2Ca(BTC)_2(H_2O)_2$ were also solvothermally synthesized (Figure 1C,D). Their coordinated water molecules can also be easily removed to offer open metal sited. These MOFs with open metal sites exhibit excellent hydrogen adsorption capacities (Figure 2A). The result shows that MOFs with open metal sites strength the enthalpies of hydrogen adsorption and improve the hydrogen uptake capacities.

(MOFs containing functionalized organic ligands with active -NH_2, -Br, and -NO_2 groups (Figure 1E-H), which offer strong polar sites on the pore walls.

These results will serve as a baseline for our development of new MOFs tailored for sampling or sensing chemical threat agents. For example, we synthesized and characterized four MOFs with the similar structures of Zn_2(TPT-X)$_2$(Dzbo), (TPT-X = terephthalate, 2-aminoterephthalate, 2-nitroterephthalate, or 2-bromoterephthalate; dzbo = 1,4-diazabicyclo[2.2.2]octane) (Figure 1E-H). These functionalized organic linkers will strengthen the framework-guest interaction, respectively. We will identify how these MOF materials selectively respond to the compound of interest and preserve an irreversible effect when exposed.

These MOFs with functionalized organic linkers exhibit various hydrogen adsorption capacities (Figure 2B). The result shows that MOFs with functionalized organic linkers enhance the hydrogen uptake capacities via intermolecular hydrogen bonding interactions.

MOFs exhibiting a wide range of pore sizes, which can be used for adsorption and separation of hydrogen (for example, the sizes of pores of several MOFs are between the van der Waals kinetic diameters of H_2 and N_2, and thus are suitable for H_2/N_2 separation).

As shown in Figure 1 I-L, we designed and synthesized four novel MOFs with various pore or window sizes with different metal and ligand. Their pore sizes can range form 0.3 to 3.2 nm. I investigated how the pore sizes of these MOF materials can influence their hydrogen adsorption/separation capacities. The result indicates MOFs with 0.4 ~ 0.8 nm pore sizes are most suitable for hydrogen storage (Figure 2C).

Design and assembly of special devices for gas storage and separation-catalysis

Two special devices for gas storage and separation-catalysis have been designed and assembled. In details, *in-situ* neutron diffraction gas-sorption evaluation cell can monitor complex compositional and exact gas sorption sites inside pores of MOFs at various pressure and temperature condition. As the lightest element, the hydrogen atom contains only one electron and thus has the weakest X-ray scattering cross-section of all of the elements. In contrast, the scattering power of neutrons does not vary with the number of electrons in an element, and neutron diffraction is much more sensitive to the positions of hydrogen (or its isotopes such as deuterium) and other light elements, making neutron scattering well suited for studying hydrogen-containing or other gas-containing materials. In addition, as neutrons are more penetrating than X-rays, one can probe samples inside high-pressure vessels, within

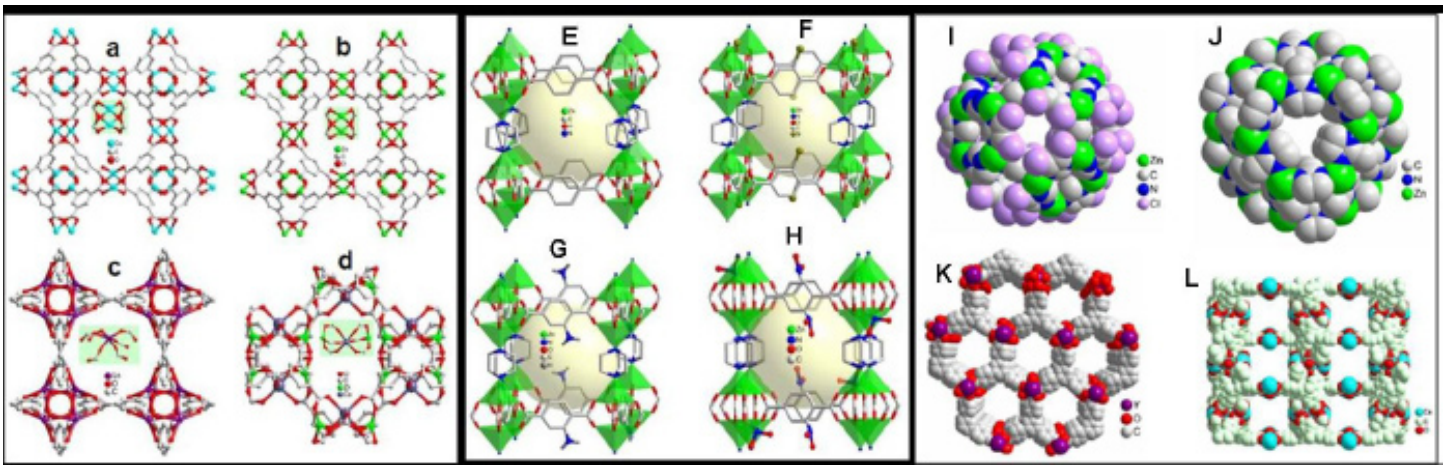

Figure 1. A schematic demonstration a series of MOFs with different functionalized groups or various pore sizes.

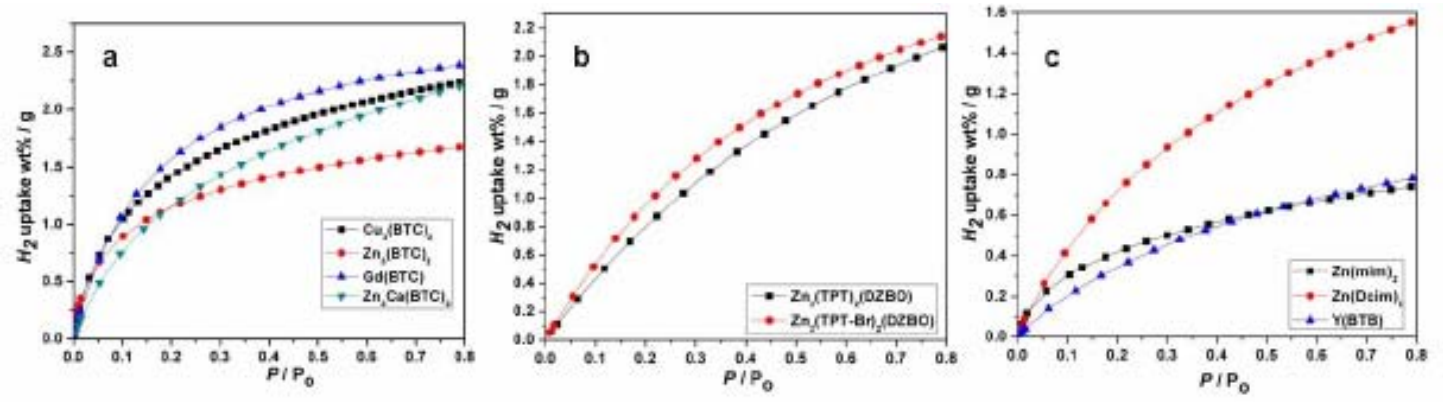

Figure 2. Hydrogen uptakes in three types of MOFs at 77K

refrigerators and furnaces, or measure deeply buried local structures within a bulk host material. Hence, the home-made gas cell are designed and assembled for *in-situ* neutron scattering analysis. On the other hand, gas separation-catalysis evaluation apparatus is assembled for various applications of MOFs including hydrogen purification, gas separation, as well as catalysis.

Chemical threat agent adsorption investigation

I also developed MOFs application for high-efficiency sampling, preservation, and sensing of chemical threat agents. We specially designed and synthesized a new MOF $Zn_2Ca(BTC)_2$ (BTC = benzene-1,3,5-tricarboxylate) for adsorption of chemical threat agents. This MOF have been structurally characterized by single-crystal X-ray diffraction. Structural analysis exhibits that the title compound self-assembles a three-dimensional porous framework with open metal sites on the channel walls. So the open metal sites can service as valid active sites for chemical threat agent adsorptions. I started to investigate their adsorption capacity for one of hydrolytic products (methylphosphonic acid) of nerve agents since we cannot work the real chemical threat agent, which will be a flexible simulation to real agents. The result shows open metal nodes in MOFs is valid bonding sites for the adsorption of methylphosphonic acid.

In conclusion, a series of novel MOFs have been synthesized and structurally characterized. Their hydrogen storage capacities have been investigated. Through exploring new chemistry and synthetic approaches, the present research produced novel materials that can store large amounts of hydrogen. It is expected to contribute significantly to the utilization of hydrogen in future transport/mobile applications. The results of this research also provided basis for utilizing similar techniques in environmental and threat-reduction applications. Example of other applications includes fast and reversible detection of trace amounts of high explosives and chemical threat agents via MOF's various physical and chemical properties of organic pore walls or metal clusters in MOFs.

Impact on National Missions

This project supports the DOE mission in Energy Security and Environmental stewardship by developing novel metal-organic frameworks (MOFs) for hydrogen storage and purity as well as their applications in other fields, such as storage/separation of carbon dioxide and sensing of chemical threat agents. It is also important to other Laboratory missions (e.g., Homeland Security).

References

1. Zou, R., A. Addel-Fattah, H. Xu, Y. Zhao, and D. Hickmott. Storage and separation Applications of nanoporous metal-organic frameworks. 2010. *CrystEngComm.* **12**: 1337.

2. Zou, R., A. Addel-Fattah, A. Burrell, T. Larson, T. McCleskey, Q. Wei, M. Janicke, D. Hickmott, T. Fimoreeva, and Y. Zhao. Porous metal-organic frameworks containing alkali-bridged two-fold interpenetration: Synthesis, gas Adsorption, and fluorescence Properties. 2010. *Crystal Growth & Design.* **10**: 13011306.

3. Zou, R., H. Xu, A. Burrell, J. Cape, N. Henson, T. Timofeeva, T. Larson, and Y. Zhao. A porous metal-organic replica of α-PbO2 for capture of nerve agent surrogate. To appear in *Journal of the American Chemical Society.*

Publications

Zou, R., A. Abdel-Fattah, A. Burrell, T. Larson, T. McCleskey, Q. Wei, M. Janicke, D. Hickmott, T. Timofeeva, and Y. Zhao. Porous metal-organic frameworks containing alkali-bridged two-fold interpenetration: Synthesis, gas adsorption, and fluorescence Properties. 2010. *Crystal Growth & Design.* **10**: 13.

Zou, R., A. Abdel-Fattah, H. Xu, Y. Zhao, and D. Hickmott. Storage and separation applications of nanoporous metal-organic frameworks. 2010. *CrystEngComm* . **12**: 1337.

Zou, R., H. Xu, A. Burrell, J. Cape, N. Henson, T. Timofeeva, T. Larson, and Y. Zhao. A porous metal-organic replica of α-PbO2 for capture of nerve agent surrogate. To appear in *Journal of the American Chemical Society.*

Semiconductor Nanowire Heterostructures

Samuel T. Picraux
20080785PRD3

Abstract

Heterostructured nanowires offer the possibility of engineering surface effects, strain, energy band-edge and modulation-doped one-dimensional structures across both, the nanowire radius and its axis, for novel electronic and optoelectronic devices. Synthesis of such heterostructures requires an advanced level of understanding of simultaneous processes occurring during their growth and demands supreme control over their structure, composition and doping. Due to their free surfaces, size-dependent phenomena emerges strongly at small sizes, generally at a diameter of ~ 30 nm or less for germanium, which is a size of interest in novel (opto-)electronic and thermoelectric nanoscale devices and systems. In this project, we have directly measured these nanoscale size effects and provided a comprehensive model that accurately described and correlated observed reduction of nanowire growth rates at small diameters to concurrent increases in germanium solute concentration in a gold-germanium liquid growth-mediating seeds. Building on this understanding, we modified the interfacial energy difference between the nanowire sidewalls and the gold mediating growth seed to inhibit gold diffusion during the growth of core/multi-shell germanium/silicon radial nanowire heterostructures. This resulted in excellent surface morphology and controlled epitaxy of radially designed Ge/Si core/multi-shell structures. We fabricated from these heterostructure nanowires p-type nanowire field-effect transistors that have resulted in significantly improved transconductances and hole mobilities as well as record maximum on-currents for p-type devices.

Background and Research Objectives

Semiconductor nanowires (NWs) allow the realization of one dimensional (1D) structures that exhibit unusual electronic and optical properties, as well as unique device architectures. They are grown by the vapor-liquid-solid (VLS) mechanism in which gas precursors containing reactant material catalytically decompose and incorporate at a metal nanoparticle surface, supersaturate in the particle, and lead to crystallization at the liquid-solid interface resulting in 1D NW growth. Since the diameter, and consequently the electronic and optical properties of NWs, is dependent on the size of the metal nanoparticle, understanding and controlling the diameter-dependent growth behavior in semiconductor NWs is important. Controversies in the literature regarding size dependence [1] arises from mixed-complex reactions when compound semiconductor NWs are considered [2], or due to low precursor partial pressures and/or Au loss by diffusion from the Au seed at the nanowire tips occurs for elemental semiconductor NWs [3,4]. We use extreme level of control over NW diameter and placement, as well as over NW growth conditions for superb NW morphology, as demonstrated in Figure 1, to probe nanoscale size effects on their growth. Our results establish the validity and universality of these size effects to semiconductor NWs and provide routes for achieving smallest NW diameters and in turn controlling their heterostructure growth.

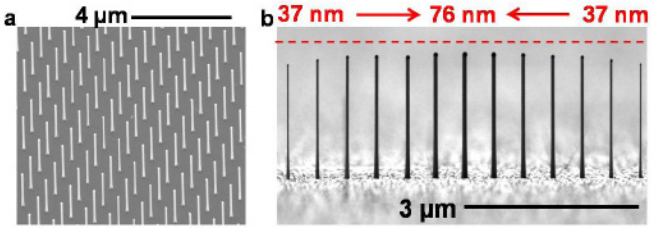

Figure 1. Ge NW growth from e-beam lithography patterned arrays. a) An array of Ge NWs with 1 µm spacing and 60 nm diameter. b) Linear array of Ge NWs with 0.5 µm spacing. The dashed red line highlights the systematic changes in nanowire length at different diameters.

The formation of high quality epitaxial core/shell materials composed of a semiconducting nanowire (NW) surrounded by one or more single crystal shells offer the opportunity for new control of charge transport in nanostructures. By forming shells of different materials

or electrical conduction type on NWs, strain [5], quantum size [6] and electronic band offset effects [7] can be tailored to manipulate spatial distribution of charge carriers and achieve novel opto-electronic device properties. For example, a shell doped NW with a second passivating and charge carrier confining shell can allow the formation of high-mobility and high on-current devices for optimal transistor performance. Core/shell NWs based on the Ge/Si system with its 4.1% lattice mismatch are among the most interesting from both technological and basic "band-gap engineering" perspectives. While Si and Ge NWs are readily grown by the vapor-liquid-solid (VLS) method using liquid Au alloy droplets as the catalytic growth medium, the required temperatures for wire or shell growth are quite different (~300 and 500 C for Ge and Si, respectively). This disparity in synthesis temperatures results in highly detrimental Au diffusion when growing higher temperature shells, such as for the Ge core/Si shell heterostructures [8]. To eliminate Au diffusion, previous work approaches have either used O_2 during growth [9] or etching of the Au seed ex-situ prior to growing Si shells [10], both of which introduce contaminants that adversely affect the nanowire properties. We devised and implemented a novel growth procedure allowing in-situ synthesis of Ge/Ge and Ge/Si core/multi-shell nanowires by engineering the growth interface between the growth-mediating Au seed and the nanowire sidewalls. The result is excellent surface morphology and, no Au diffusion, and enabling the controlled epitaxy of core/multi-shell nanowires. In a direct assessment of this procedure approach for the growth of fabricating radially designed Ge/Si core/multi-shell structures, we demonstrate high performance heterostructured p-type nanowire field-effect transistors devices with previously unachieved levels of performance and significantly improved transconductances and hole mobilities and with the highest reported maximum on-currents for p-type devices.

Scientific Approach and Accomplishments

Germanium NWs grow epitaxially on Ge (111) surfaces in the vertical orientation as shown in Figure 1 leading to mostly <111> oriented vertical wires for all Ge NW diameters down to sub-10 nm diameters. The Ge NW length decreases with decreasing diameter for a given growth time for all growth conditions. For the sake of space and simplicity, we describe here the general growth behavior with time, in-situ measurements of solubility, and doping effects, and leave out temperature and pressure effects. Figure 2a shows a plot of the NW lengths as function of diameter for different growth times where a rapid decrease in the NW length occurs for diameters ≤ 30 nm. Supersaturation, Δμ, decreases with NW diameter according to Equation 1 where $\Delta\mu_0$ denotes the supersaturation in the planar limit (i.e., d approaches infinity), omega is the atomic volume of the growth species, d is the diameter of the NW below the liquid droplet, and α_{vs} is the average surface energy density of the nanowire surface facets.

$$\Delta\mu = \Delta\mu_0 - \frac{4\Omega\alpha_{vs}}{d}$$

This results in a reduced growth rates as the NW diameter decreases according to Equation 2 where v=dL/dt is the growth velocity, and b is a kinetic coefficient independent of supersaturation. A plot of $v_{1/2}$ as function of 1/d (Figure 2b) allows us to extract a cut-off diameter of ~ 3.5 nm for undoped Ge NWs. At this diameter, Δμ=0 and NW growth ceases.

$$\sqrt{v} = \sqrt{b}\frac{\Delta\mu_0}{kT} - \sqrt{b}\frac{4\Omega\alpha_{vs}}{kT}\frac{1}{d}$$

To validate this attribute, we carried in-situ transmission electron microscope measurements to measure the equilibrium Ge concentration in Au-Ge alloys at the NW tip, the results of which are plotted in Figure 2c. As the NW diameter decreases, the equilibrium Ge concentration in the Au-Ge alloy increases as demonstrated in Figure 2c. If one considers an input Ge concentration at the surface of the Au-Ge droplet to be C_{in}, as shown in Figure 2c, the larger diameter will encounter a larger concentration overdrive, i.e. a larger supersaturation, leading to faster growth rates for the larger diameter. This experiment and observation constitute the first direct measurement of the Gibbs-Thomson effect in semiconductor NWs.

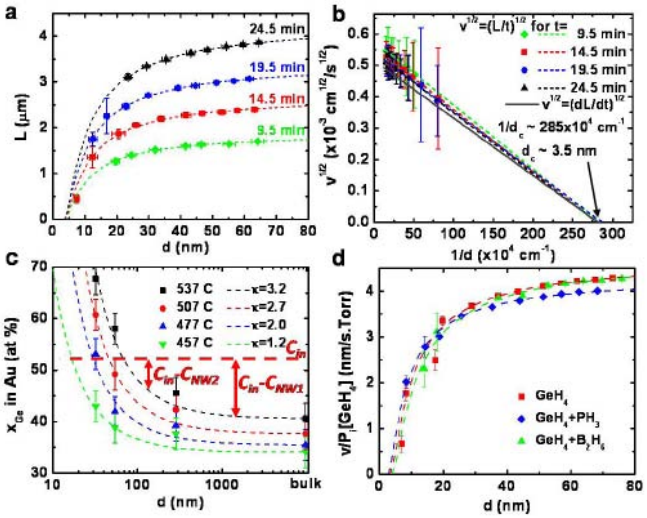

Figure 2. Plot of the NW length as function of diameter for different growth times at the resulting in a linear increase of NW length with time for all. b) Plot of the square root

of the growth velocity for the data shown in (a) calculated using v=L/t and using v=dL/dt resulting in the same cut-off diameter. c) Ge atomic % as a function of diameter at different temperatures. Symbols are experimental data points; dashed lines are fits according to xNW=xGe bulk. exp(4κΩαvs/dkT). d) Plot of the growth rate normalized by the GeH4 partial pressure showing a reduction in the growth rate when PH3 is present during growth.

One important aspect of the growth of NWs is the ability of in-situ doping for implementing unconventional devices. While size effect trends remain essentially the same with flowing dopant gases (Figure 2d), we found that the introduction of PH_3 in particular leads to a reduction of the NW surface energy, and therefore, a reduction of the second (negative) term in equation (1), leading to prevalent supersaturation to even smaller diameters. As shown in Figure 2d, the normalized growth rate to GeH_4 reactor pressure shifts to the left enabling sustained growth down to ~ 2.9 nm cut-off diameter. This shows that by manipulating the surface chemistry, one not only can achieve smaller diameter NWs but also utilize this aspect to modify surfaces and enable growths that are not possible otherwise as we show in the core/shell heterostructure NW growth below.

For the case for core/shell NW growth, the growth temperature has to be elevated in order to induce vapor-solid growth of the shell material on the NW sidewalls. During the temperature ramp, Au becomes unstable and diffuses on the NW sidewalls, thereby leading to its decoration with Au dots. These Au dots cause surface roughening in the shell materials as shown in Figure 3a. Utilizing the catalytic effect of the liquid Au growth seed, we deposited at 280 °C a thin Si interfacial barrier layer underneath the Au to increase the surface energy on the NW sidewalls and prevented Au diffusion to the Ge surface. Subsequent temperature elevation to those suitable for Ge and Si shell growths have resulted in epitaxial Ge/Si core/multi-shell NWs without any observed Au on the NW sidewalls as verified by high resolution electron microscopy and X-ray analysis. Figure 1b shows an example of a single crystal Ge/Si core/shell NW. Such control over core/shell growth allows realization of core/multi-shell NWs for high on-currents and transconductances in heterostructure FET (HFET) devices, not accessible before in planar or NW growth techniques. We therefore grew i-Ge/p+-Ge/i-Si core/multi-shell Ge/Si NWs to increase the gate coupling with holes confined in the Ge core. NWs with and without Au diffusion were fabricated (Inset of Figure 3b) and tested. The output curves of two Ge/Si NW HFET devices with gate length, LG=1 µm, is shown in Figure 3c. Solid lines are measured on devices with no Au diffusion and dashed lines are measured on devices with Au diffusion that resulted in a rough surface morphology and shown for the same sequence of gate voltage steps. Transfer curves for the same devices are shown in Figure 3d. The on-currents and transconductances measured on NW HFETs with no Au diffusion are significantly higher than those measured on NW HFETs with Au present on the NW sidewalls. This is attributed to the higher surface roughness scattering and reduced hole mobilities in NWs with Au diffusion and rough surface morphology. The normalized maximum on-current is I_{max}=520 µA/V compared to an earlier best result of 211 µA/V [11].

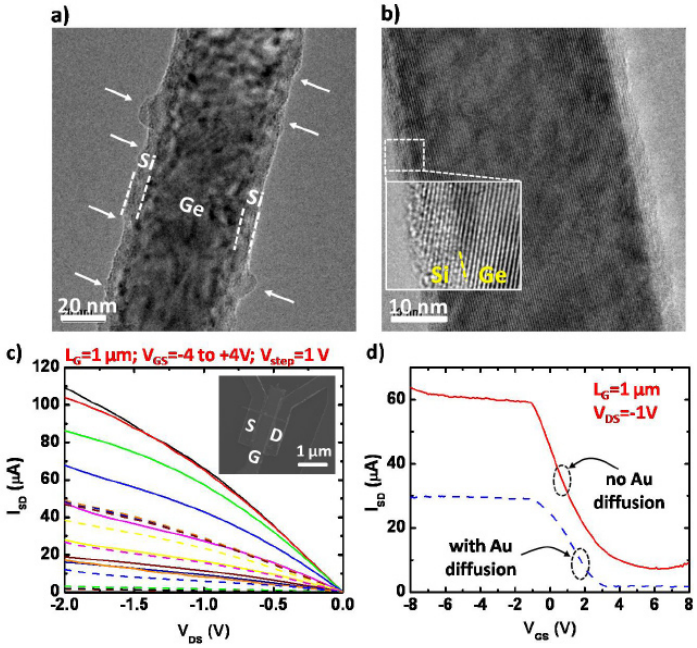

Figure 3. TEM images of Ge/Si core/shell NWs with (a) and without (b) Au diffusion. Au diffusion catalyzed the growth of thicker Si shells and rough surface morphology marked by white arrows in (a). Single crystal Ge/Si core/shell NW with smooth morphology is shown in (b). Inset is a zoom-in high resolution TEM image at the edge of the NW in (b) showing lattice fringes extending from the Ge core to the Si shell with a well-defined interface. c) Output curves of Ge/Si core/multi-shell NW HFETs with (dashed) and without (solid) Au diffusion for the same channel length of 1 µm. Inset is a top-view SEM image of a representative device. d) Transfer curves corresponding to the same devices in (a) showing higher on-current and transconductance for the device with no Au diffusion.

Impact on National Missions

This project supports the DOE missions in threat reduction, energy independence, and nuclear weapons by advancing our fundamental understanding of nanoscale electronic materials for new materials synthesis, chemical and biological sensing, thermoelectric energy conversion, and electronics systems for future low power, miniaturized applications. We already see a number of new device and system concepts emerging that are anticipated to be important to these areas. The demonstrated devices have a great poten-

tial for low-power, low noise, linear and high performance analog and digital electronics.

References

1. Givargizov, E. I.. Fundamental aspects of VLS growth. 51. *Journal of Crystal Growth .* **31**: 2.

2. Borstrom, M. T., G. Immink, B. Ketelaars, R. Algara, and E. P. A. M. Bakkers. Synergetic nanowire growth. 2. *Nature Nanotechnology.* **2**: 54.

3. Kodambaka, S., J. Tersoff, M. C. Reuter, and F. M. Ross. Diameter-independent kinetics in the vapor-liquid-solid growth of Si nanowires. 62. *Physical Review Letters.* **96**: 096105.

4. Schmid, H., M. T. Bjork, J. Knoch, H. Riel, and W. Riess. Patterned epitaxial vapor-liquid-solid growth of silicon nanowires on Si(111) using silane. 2008. *Journal of Applied Physics.* **103**: 024304.

5. Peng, X., and P. Logan. Electronic properties of strained Si/Ge core/shell nanowires. 2010. *Applied Physics Letters.* **96**: 143119.

6. Yang, L., R. N. Musin, X. Q. Wang, and M. Y. Chou. Quantum confinement effect in Si/Ge core-shell nanowires: first-principles calculations. 2008. *Physical Review.* **B77**: 195325.

7. Pekoz, R., and J. Y. Raty. From bare Ge nanowire to Ge/Si core/shell nanowires: a first-principles study. 2009. *Physical Review.* **B80**: 155432.

8. Goldthorpe, I. A., A. F. Marshall, and P. C. McIntyre. Synthesis and strain relaxation of Ge-core/Si-shell nanowire arrays. 2008. *Nano Letters.* **8**: 4081.

9. Kodambaka, S., J. B. Hannon, R. M. Tromp, and F. M. Ross. Control of Si nanowire growth by oxygen. 2006. *Nano Letters.* **6**: 1292.

10. Goldthorpe, I. A., A. F. Marshall, and P. C. McIntyre. Inhibiting strain-induced surface roughening: dislocation-free Ge/Si and Ge/SiGe core – shell nanowires. 2009. *Nano Letters.* **9**: 3715.

11. Hu, Y., J. Xiang, G. Liang, H. Yan, and C. M. Lieber. Sub-100 nm channel length Ge/Si nanowire transistors with potential for 2 THz switching speeds. 2008. *Nano Letters.* **8**: 925.

Publications

Dayeh, S. A.. Electron transport in indium arsenide nanowires. 2010. *Semiconductor Science and Technology.* **25**: 024004.

Dayeh, S. A., C. Soci, X. Bao, and D. Wang. Advances in the synthesis of InAs and GaAs nanowires for electronic applications. 2009. *Nano Today.* **4**: 347.

Dayeh, S. A., D. Susac, K. L. Kavanagh, E. T. Yu, and D. Wang. Structural and electrical properties of zincblende and wurtzite InAs nanowires. 2009. *Advanced Functional Materials.* **19**: 2102.

Dayeh, S. A., E. T. Yu, and D. Wang. Surface diffusion and substrate: nanowire adatom exchange in InAs nanowire growth. 2009. *Nano Letters.* **9**: 1967.

Dayeh, S. A., E. T. Yu, and D. Wang. Diameter dependent transport properties in InAs nanowire field effect transistors. 2009. *Small.* **5**: 77.

Law, J., S. A. Dayeh, D. Wang, and E. T. Yu. Scanning capacitance characterization of potential screening in InAs nanowires. 2009. *Journal of Applied Physics.* **105**: 014306.

Lee, S. T., P. Jannaty, A. Zaslavsky, S. A. Dayeh, and S. T. Picraux. Growth, electrical rectification, and gate control in axial In situ doped p-n junction germanium nanowires. 2010. *Applied Physics Letters.* **96**: 262102.

Picraux, S. T., S. A. Dayeh, P. Manandhar, D. E. Perea, and S. G. Choi. Silicon and germanium nanowires: growth, properties, and integration. 2010. *Journal of Materials.* **62**: 35.

Raychaudhuri, S., S. A. Dayeh, D. Wang, and E. T. Yu. Precise semiconductor nanowire placement through dielectropheresis. 2009. *Nano Letters.* **9**: 2260.

Sierra-Sastre, Y., S. A. Dayeh, S. T. Picraux, and C. A. Batt. Epitaxy of Ge nanowires from biotemplated Au nanoparticle catalysts. 2010. *ACS Nano.* **4**: 1209 .

The Kondo Lattice Problem

Joe Thompson
20080894PRD4

Abstract
Strong interactions among electrons force a correlated, collective response to their physical and chemical environments. Experimental and theoretical work over the past three decades to understand these correlated responses have failed to provide a microscopic or even firmly based phenomenological understanding of the complex underlying physics of such systems. A recent conceptual breakthrough from our examination of one large class of electronically correlated materials, so-called Kondo-lattice materials, has provided an entirely new phenomenological description of the complex physics. This project has had the goal of exploring the predictive consequences of this phenomenology, especially regarding the possible emergence of unconventional superconductivity from this model. Additionally, we have explored whether a more basic microscopic understanding of this phenomenology can be developed.

Background and Research Objectives
The Kondo-lattice materials can be described by a dense, periodic array of localized f-electrons coupled to a sea of 10^{23} itinerant electrons. Understanding its various exotic properties, such as unconventional superconductivity, defines the so-called Kondo-lattice problem. The building block of the problem, namely the single-impurity problem that describes a single localized electron coupled to 10^{23} itinerant electrons, has been intensively studied in 20th century and is well understood. However, a solution to the Kondo-lattice problem remains obscure despite three decades' of theoretical and experimental effort. So far, it has been generally believed that the essential physics of the problem comes from the competition between two fundamental magnetic interactions characterized by their energy scales: a Kondo energy scale T_K, that results from the local (Kondo) interaction of an individual f-spin and resembles the single-impurity Kondo problem, and an exchange energy scale T^*, that originates from the long-range (Ruderman-Kittel-Kasuya-Yosida (RKKY)) interaction of neighboring f-spins and tends to correlate f-spins into collective excitations. However, theories along this line have not been able to give a comprehensive solution to the large amount of experimental data, even though such a picture has been quite successful in interpreting the qualitative features of the low temperature phase diagram of Kondo-lattice materials. In light of this, we have been pursuing the problem from a different aspect. We base our research on experimental analysis and develop a new conceptual framework based on a phenomenological two-fluid model [1-4] in which the Kondo and RKKY interactions give rise to two interpenetrating 'fluids'—one of itinerant electrons with very heavy effective mass and the other of weakly interacting local magnetic moments . Our ultimate goal is to explore the new framework and develop it into a standard theory for the Kondo-lattice problem. We also investigate other problems raised by latest experiment.

Scientific Approach and Accomplishments
Our work is a fruitful result of close collaborations between experiment and theory. The following progress has been made from either our theoretical analysis of existing experimental data or experimental realization of our theoretical proposal.

A new conceptual framework for the Kondo-lattice problem

We have proposed a new conceptual framework based on our previous studies of the two-fluid model. Figure 1 summarizes our results and shows that the physics of the Kondo lattice can be separated into three distinct regimes depending on temperature. The two fluids, a fluid of emergent heavy electron Kondo liquid and a fluid of residual unhybridized magnetic moments, describe the gradual nature of the heavy electron emergence below T^* from the high temperature localized f-spins. In contrast to a conventional picture, the RKKY interaction is always the dominant one for most Kondo-lattice materials. This work has been accepted for publication in Journal of Physics: Conference Series and appears on-line as **Y.-F. Yang *et al.*, arXiv:1005.5184 (2010).**

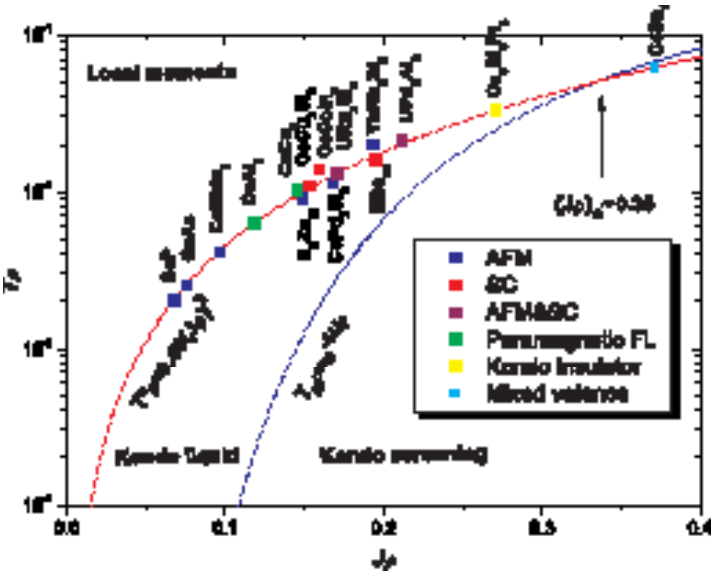

A general phase diagram proposed for heavy electron materials based on our new framework. The expected values of two characteristic temperature scales, the RKKY scale T and the Kondo scale TK, are compared in the figure and all materials are placed according to their T*. J is the local Kondo coupling and rho is the conduction electron density of states. For most materials, T* is much larger than TK. The f-electrons are localized above T* and become partially itinerant forming a heavy electron Kondo liquid below T*. At very low temperatures around TK, the itinerant heavy electrons condense into some exotic states, such as unconventional superconductivity.*

Theory for electron tunneling and point contact spectroscopy

Experimental point-contact spectroscopy and scanning tunneling spectroscopy studies [5] of Kondo-lattice compounds probe the energy-dependent electronic states and observe a spectral asymmetry between plus and minus voltages (energies) below T^*. Building on our new conceptual framework for the Kondo lattice, we have developed the first semi-microscopic scenario based on quantum interference between 'light' and 'heavy' electrons that accounts for these experimental observations. A comparison between experimental results and our model calculations are shown in Figure 2. The same hybridization between f-electrons and conduction electrons that leads to the emergence of the heavy electron Kondo liquid gives rise to the quantum interference of electrons and explains the asymmetry in the conductance spectra. Results of this research appeared in **Y.-F. Yang, Phys. Rev. B: Rapid Communications 79, 241107 (2009).**

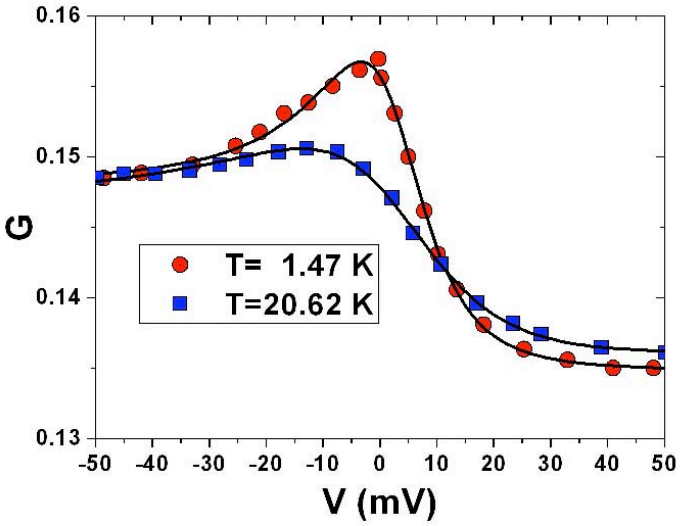

Comparison of experimental (symbols from [5]) and our theoretical (solid lines) point contact conductance spectra G as a function of the bias voltage at two different temperatures. The asymmetry in the spectra around zero-bias voltage results from quantum interference of two hybridized channels, the conduction-electron channel and the f-electron channel, for the electron current.

A new route to new superconductors

We have applied our phenomenology to provide a natural explanation for the evolution of the experimentally determined spin susceptibility (Knight shift) in the superconducting state of the Kondo-lattice material $CeCoIn_5$. We find that the unconventional superconductivity originates from the condensation of electronic excitations intrinsic to the Kondo liquid. Because the characteristic temperature scale T^* of the Kondo liquid is given by the magnetic interaction between the Ce ions in these materials, our analysis further concludes that the superconducting transition temperature is actually controlled by this single magnetic interaction. This conclusion, which would not have followed from conventional views of the Kondo lattice, points to a qualitatively new direction for discovering new superconductors with higher transition temperatures. See **Y.-F. Yang *et al.*, Phys. Rev. Lett. 103, 197004 (2009).**

Connecting Mott and Kondo-lattice physics

Using analytical many-body and numerical techniques, we have shown that a generalization of the Kondo-lattice problem, the Anderson lattice problem, can be mapped under certain circumstances onto the so-called Mott-Hubbard model that considers the consequences of strong Coulomb repulsion on the motion of electronic charges. This is a rather important result because the Mott-Hubbard model is used commonly to describe the physics of

strongly correlated d-electron materials, in particular the high temperature superconductors based on copper-oxide. The mapping that we have discovered now provides a link between the physics of strongly correlated f-electron systems, such as Kondo-lattice systems based on Pu and related heavy-electron superconductors, and technologically important d-electron systems. Because of the extensive theoretical underpinning of the Mott-Hubbard model, the bridge that we have made now to the Anderson lattice problem opens the path to a microscopic theory of our phenomenological model of the Kondo lattice. See **K. A. Al-Hassanieh *et al.*, Phys. Rev. Lett. 105, 086402 (2010).**

Superconducting Swiss cheese

Intrinsic electronic inhomogeneity is a hallmark of strongly correlated d-electron materials, such copper-oxide superconductors and certain materials that exhibit a colossal change in electrical resistivity when subjected to small magnetic fields. Electronic inhomogeneity, however, has rarely, if ever, been considered to appear in an f-electron Kondo lattice. Motivated by observations made in the course of developing our conceptual framework for the Kondo lattice, we have analyzed the superconducting properties of Kondo-lattice/heavy-electron superconductors and discovered strong evidence for electronic inhomogeneity that is revealed when small amounts of non-magnetic impurities are introduced into these systems. This inhomogeneity is hidden in the absence of foreign atoms. The picture that emerges from these studies is that foreign atoms produce an electronic 'Swiss cheese', analogous to what is found in copper-oxide superconductors that contain small amounts of certain non-magnetic impurities. Unlike the copper-oxide superconductors, however, this unexpected manifestation of electronic inhomogeneity in Kondo-lattice superconductors appears to be a generic response that is independent of the specific type of added impurity. An account of this discovery is under consideration by **Nature Communications**.

Impact on National Missions

Complex correlations among electrons control the physical properties of unconventional superconductors and actinide materials that are important for DOE missions for energy security and understanding materials. This work has attacked the unsolved problem of complex correlations from a completely new perspective, with the goal of understanding how they control physical properties.

References

1. Nakatsuji, S., D. Pines, and Z. Fisk. Two fluid description of the Kondo lattice. 2004. Physical Review Letters. 92: 016401.
2. Curro, N. J., B. L. Young, J. Schmalian, and D. Pines. Scaling in the emergent behavior of heavy-electron materials. 2004. Physical Review B. 70: 235117.
3. Yang, Y. F., and D. Pines. Universal behavior in heavy-electron materials. 2008. Physical Review Letters. 100: 640409.
4. Yang, Y. F., Z. Fisk, H. O. Lee, J. D. Thompson, and D. Pines. Scaling the Kondo lattice. 2008. Nature. 454: 611.
5. Park, W. K., J. L. Sarrao, J. D. Thompson, and L. H. Greene. Andreev reflection in heavy-fermion superconductors and order parameter symmetry in CeCoIn5. 2008. Physical Review Letters. 100: 177001.

Publications

Yang, Y. F., N. J. Curro, Z. Fisk, D. Pines, and J. D. Thompson. A predictive standard model for heavy electron systems. To appear in Journal of Physics: Conference Series.

Al-Hassanieh , K. A., Y. F. Yang, I. Martin, and C. D. Batista. Effective low-energy model for f-electron delocalization. 2010. Physical Review Letters. 105: 086402.

Durakiewicz, T., P. S. Riseborough, C. D. Batista, Y. F. Yang, P. M. Oppeneer, J. Joyce, and E. D. Bauer. Quest for band renormalization and self-energy in correlated f-electron systems. 2010. Acta Physica Polonica A. 117: 264.

Yang, Y. F., R. Urbano, N. J. Curro, D. Pines, and E. D. Bauer. Magnetic excitations in the Kondo liquid: Superconductivity and hidden magnetic quantum critical fluctuations. 2010. Physical Review Letters. 103: 197004.

Yang, Y. F. The Fano effect in the point-contact spectroscopy of heavy electron materials. 2009. Physical Review B. 79: 241107(R).

Classical/Quantum Mechanical Simulations of Electronic Nanomaterials

Sergei Tretiak
20080795PRD4

Abstract
In this project we used a combination of ab initio techniques, such as density functional theory (giving an accurate electronic structure of a system), with classical force field calculations (providing reasonably fast geometries, packing and dynamics for large molecules) to predict and to explain experimental results on dynamics, transport, and optical properties of several hybrid composites and nano-scaled materials. We applied our new methodologies to a variety of materials, which are promising for optoelectronics and sensing, and several bio-applications such as drug delivery, cancer diagnostics and therapy.

Background and Research Objectives
The idea of harnessing molecular building blocks to assemble nanometer-scale devices promises many fascinating applications in fields ranging from electronic to medical technologies. Unfortunately, our fundamental understanding of the underlying physics and chemistry of such complex structures lag the experimental observations; the major reason being the computationally unmanageable number of atoms in such systems. In this project we developed a new theoretical approach able to predict and to explain experimental results on dynamics, transport, and optical properties of several hybrid composites and nano-scaled materials. Our goal was to be able to compute the optical and transport properties of complex molecular composites. Our developed methodology was applied to: i) Adsorbed Deoxyribonucleic Acid (DNA) strands or other bio-molecules on metallic surfaces. Here the unique Scanning Tunneling Microscope (STM) spectra of bases promised resolution of the structure and fast sequencing of DNA. To interpret experimental results, the Postdoc simulated tunneling spectra and identifyiedthe underlying electronic features; ii) Semiconductor quantum dots to clarify the role of soft ligand layer and surface roughness on electron-electron and electron-phonon coupling important in experimentally observed efficient carrier multiplication processes. These systems are promising for harvesting of solar energy; iii) Molecular-functionalized carbon nanotubes to investigate computationally photoinduced structural relaxation and uncaging. This has a potential to make carbon nanotubes into highly luminescent materials. Many other applications are envisioned and broad dissemination of these methods is expected. Besides providing fundamental theoretical understanding of transport, and photoexcited properties of complex molecular composites, this research is envisioned for developing a fast and accurate “virtual computational nano-scale laboratory” to be used in a variety of projects with significant LANL, DOE, and NIH investments, and supports a number of experimental efforts currently carried out at LANL/CINT.

Scientific Approach and Accomplishments
This project combines two approaches: ab initio methods (giving an accurate electronic structure of a system) and force field (FF) methods (providing reasonably fast geometries, packing, and dynamics for large molecules). We proposed to: i) construct new FF potentials using quantum mechanical calculations (e.g., Density Functional Theory, DFT) to be performed on a set of representative units; ii) conduct FF simulations of the dynamics of the entire system at specific temperature, pressure, etc; iii) DFT and time-dependent DFT calculations of electronic structure of ground and excited states using selected resulting geometries (snapshots); iv) develop a computational package to allow non-adiabatic photo-induced dynamics based on correlated excited states in time-dependent DFT method. Using this approach, the ultimate goal is to predict and to explain experimental results on several nanoscale molecular composites/hybrids.

Over the project duration we investigated optical response and phonon induced dynamics in pure CdSe quantum dots (QD) and QDs functionalized by different organic molecules [1,2]. Currently, our main focus is on organic ligands that cover the QD surface. The role of ligands is expected to be crucial in the carrier multiplication processes experimentally observed in these systems and promising for the harvesting of solar energy. Surface ligands also impact phonon-assisted carrier dynamics that competes with carrier multiplication. In contrast to

the common point of view, we found that ligands strongly impact charge relaxation in QDs for high-energy excitations. No molecular orbitals of ligands appear as trap states inside or near the band gap of the QD. We found that the surface ligands introduce new electronic states which are strongly delocalized over the ligands and the dot surface and open new relaxation paths for the nonradiative charge relaxation, increasing relaxation rates [3]. These results are obtained for small $Cd_{33}Se_{33}$ clusters passivated by different organic molecules and extended to larger systems ($Cd_{111}Se_{111}$) which are comparable to the common QDs used in experiments. The main focus of these studies is the trap states inside the band gap of the QD originated from the detachment of one of the ligands from the surface. These investigations have resulted in several published articles [1-3] and other papers to be submitted soon. Our results were also presented in several conferences. We also investigate optical and transport properties in dye-functionalized metallic clusters self-assembled on the DNA template. Some of our results have been already published [4]. All these composites hold great promise in the areas of bio-inspired self-assembly of electronic circuits.

We also studied charge and energy transfer mechanisms in CdSe QDs functionalized with ruthenium Ru(II) complexes. New photovoltaic and photocatalysis applications have been recently proposed based on these hybrid systems, while the exact mechanism and direction of the charge transfer controlling their photochemistry is still under debate. As a first step, we investigated how the addition of protonated and deprotonated carboxyl groups to the Ru(II)-bipyridine changes the electronic and optical properties of the complex [5]. We also have shown that the structure of these molecules allows one to express their excitations in terms of wavefunctions localized on individual ligand via the Frenkel exciton model. This simple effective model is able to accurately explain the optical activity, localization properties, and splitting patterns of the low-energy excited states [5]. Next, we focus on how the Ru(II) complex binds to the QD and how the adsorbed complex affects the electronic structure of the QD. Our calculations predict that deprotonation of the carboxyl group favors the QD-complex interaction. This occurs via “bridging” attachment of two Cd atoms with two oxygens. The calculated vibrational modes associated with such bridging bonding are in good agreement with vibrational spectroscopy data for these systems confirming the stability of hybrids interacting via bridging attachment.

Our results on excitonic and electron-phonon couplings in semiconductor carbon nanotubes (CNTs) and quantum dots were also summarized in the book [6,7] that was published by World Scientific/Pan Stanford (a science publishing company of high reputation) this summer (Figure 1). This project was extended by studies of photocurrent and its dependence on the photoexcitation energies in CNTs.

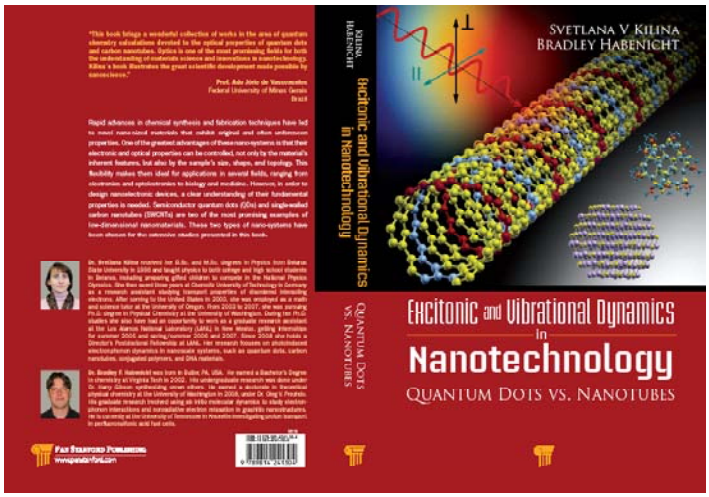

Cover of the published book on excitonic and electron-phonon couplings in semiconductor carbon nanotubes and quantum dots illustrated light interaction with these systems.

Finally, we also investigated the conformational inter- and intra-molecular disorder and its impact on the electronic structure of amorphous conjugated polymers, which are the commonly used materials for organic optoelectronic devices. Classical molecular dynamics is used to determine probable molecular arrangements, and first-principle calculations based on DFT are used to compute the electronic structure. We also calculated the participation ratios to characterize electronic localization properties of amorphous organic polymers. We found that these quantities for polyfluorenes differ drastically from those of poly-phenylenevinylenes, because of the long side chains that prevent the close packing and interactions among molecules, which should affect transport properties of these materials [8]. These results are useful for calculations of charge mobilities in these materials.

Impact on National Missions

This project directly addresses LANL institutional goals in basic understanding of materials, energy security, and threat reduction. Furthermore, the project strongly connects to thrusts of the DOE-funded Center for Integrated Nano-Technology (CINT) by impacting priorities in nanotechnology, multi-scale material modeling, and sensing.

References

1. Kilina, S., S. Ivanov, and S. Tretiak. Effect of Surface Ligands on Optical and Electronic Spectra of Semiconductor Nanoclusters. 2009. Journal of the American Chemical Society . 131: 7717,Äì7726.

2. Kilina, S., D. Kilin, and O. Prezhdo. Breaking the Phonon Bottleneck in PbSe and CdSe Quantum Dots: Time-Domain Density Functional Theory of Charge Carrier Relaxation. 2009. ACS NANO. 3 (1): 93.

3. Isborn, C., S. Kilina, X. Li, and O. Prezhdo. Generation of Multiple Excitons in PbSe and CdSe Quantum Dots by Direct Photoexcitation: First-Principles Calculations. 2008. Journal of Physical Chemistry C. 112: 18291,Äì18294.

4. Kilin, D., K. Tsemekhman, S. Kilina, A. Balatsky, and O. Prezhdo. Photoinduced Conductivity of a Porphyrin-Gold Composite Nanowire. 2009. Journal of Physical Chemistry C. 113: 4549.

5. Badaeva, E., V. Albert, S. Kilina, A. Koposov, M. Sykora, and S. Tretiak. Effect of deprotonation on absorption and emission spectra of Ru(II)-bpy complexes functionalized with carboxyl groups. 2010. PHYSICAL CHEMISTRY CHEMICAL PHYSICS. 12 (31): 8902.

6. Svetlana Kilina coauthors book on nanotechnology. 2009. PADSTE HIGHLIGHTS . http://in.lanl.govorgsadse.

7. Habenight, B., and S. Kilina. Excitonic and Vibrational Dynamics in Nanotechnology: Quantum Dots vs Carbon Nanotubes. 2009. Vol. I, 1 Edition, p. 1. Pan Stanford Publishing : World Scientific Book.

8. Kilina, S., E. Batista, P. Yang, S. Tretiak, A. Saxena, R. Martin, and D. Smith. Electronic structure of self-assembled amorphous polyfluorenes. 2008. ACS NANO. 2 (7): 1381.

Publications

Kilina, S., D. Kilin, and O. Prezhdo. Breaking the Phonon Bottleneck in PbSe and CdSe Quantum Dots: Time-Domain Density Functional Theory of Charge Carrier Relaxation. 2009. ACS NANO. 3 (1): 93.

Badaeva, E., V. Albert, S. Kilina, A. Koposov, M. Sykora, and S. Tretiak. Effect of deprotonation on absorption and emission spectra of Ru(II)-bpy complexes functionalized with carboxyl groups. 2010. PHYSICAL CHEMISTRY CHEMICAL PHYSICS. 12 (31): 8902.

Svetlana Kilina coauthors book on nanotechnology. 2009. PADSTE HIGHLIGHTS . http://in.lanl.govorgsadse.

Habenight, B., and S. Kilina. Excitonic and Vibrational Dynamics in Nanotechnology: Quantum Dots vs Carbon Nanotubes. 2009. Vol. I, 1 Edition, p. 1. Pan Stanford Publishing : World Scientific Book.

Kilin, D., K. Tsemekhman, S. Kilina, A. Balatsky, and O. Prezhdo. Photoinduced Conductivity of a Porphyrin-Gold Composite Nanowire. 2009. Journal of Physical Chemistry C. 113: 4549.

Kilina, S., S. Ivanov, and S. Tretiak. Effect of Surface Ligands on Optical and Electronic Spectra of Semiconductor Nanoclusters. 2009. Journal of the American Chemical Society . 131: 7717,Äì7726.

Kilina, S., and O. Prezhdo. Breaking the Phonon Bottleneck in PbSe and CdSe Quantum Dots: Time-Domain Density Functional Theory of Charge Carrier Relaxa. 2009. ACS Nano. 3: 93.

Isborn, C., S. Kilina, X. Li, and O. Prezhdo. Generation of Multiple Excitons in PbSe and CdSe Quantum Dots by Direct Photoexcitation: First-Principles Calculations. 2008. Journal of Physical Chemistry C. 112: 18291,Äì18294.

Vanadium Catalyzed Aerobic Oxidations

John C. Gordon
20090492PRD1

Abstract

Current petroleum reserves may be insufficient to meet the growing worldwide demand for energy. Non-food derived biomass (lignocellulose) is currently the only renewable carbon resource available, but new technologies are needed to transform lignin and cellulose into useful chemicals and fuels. Dipicolinate vanadium complexes have been studied as potential catalysts for oxidative cleavage of carbon-carbon and carbon-hydrogen bonds in lignin and cellulose. The aerobic oxidation of several lignin and cellulose model complexes was studied. Mechanistic studies of alcohol oxidation have been carried out, suggesting that more than one pathway is accessible, and that pyridine plays a role the elementary C-H bond breaking step. These results demonstrate the potential utility of vanadium complexes in the selective disassembly of lignin.

Background and Research Objectives

In light of growing worldwide demand for energy, concerns over global warming, and diminishing fossil fuel reserves, the search for renewable alternatives to petroleum-based fuels and chemicals is becoming increasingly urgent. Non food-derived biomass (lignocellulose) is attracting attention as a potential renewable feedstock for production of chemicals and fuels. Efficient transformation of lignocellulose into more valuable products remains a major challenge, particularly due to the difficulties associated with breakdown of lignin. Although some promising selective conversions of cellulose to useful materials have recently been reported, less progress has been made with lignin, which is typically incinerated in the paper and forest industry. New methods to depolymerize lignin and cellulose would represent a major breakthrough towards the production of bio-derived chemicals and fuels.

Cellulose is composed of strands of glucose monomers connected by β-1,4-glycosidic linkages, which are cross-linked together through an extensive hydrogen bonding network. The glycosidic linkages in cellulose allow it to be broken down by acid or enzyme catalyzed hydrolysis. In contrast, lignin is an irregular polymer containing methoxylated phenoxy propanol units, which are connected through carbon-carbon and carbon-oxygen (ether) linkages. Several different types of linkages occur in lignin; these are classified according to their chemical structure, with β-O,4- and β-1-linkages being among the most prevalent. Because it is so difficult to break apart the carbon-carbon and carbon-oxygen linkages, lignin is resistant to chemical degradation, playing an important role in nature in protecting plants from attack by microorganisms.

The goal of this project was to explore a new strategy of using an earth-abundant transition metal (vanadium) catalyst to break apart lignin and cellulose. This could lead to selective methods to transform lignin and cellulose into more useful chemicals and fuels. We selected vanadium for investigation because in oxidation reactions, vanadium complexes are known to break carbon-carbon and carbon-hydrogen bonds. Vanadium is also an ideal candidate for oxidation of lignin and cellulose because it has a high oxidation potential in oxidation state +5, but can still be regenerated by air. Using air as the terminal oxidant is ideal from both economic and environmental perspectives, as it is inexpensive and water is the only byproduct of oxidation.

Scientific Approach and Accomplishments

Reactions of dipic vanadium complexes with lignin and cellulose model compounds

Our initial studies focused on developing an understanding of how homogeneous vanadium complexes react with lignin and cellulose model compounds. Due to the inherent chemical complexity of both cellulose and lignin, it is difficult to analyze chemical reactions of these polymers, both in terms of determining the extent of conversion and the products formed. For this reason, we began by studying the reactivity of smaller organic compounds that mimic the structural frameworks of lignin and cellulose. Diols were used to model the vicinal –OH framework of cellulose and the β-O,4-linkage of lignin was modeled using compounds with 1,2-alcohol

ether substituents.

It was found that the vanadium(V) complex (dipic)V(O)O^{i}Pr (**1**) reacts with both the cellulose and lignin models to form complexes where the substrate is bound to the vanadium center in a chelating fashion. This type of interaction was detected for both diol and 1,2-hydroxyether substrates by ^{1}H NMR, and complexes of pinacol, pinacol monomethyl ether, 2-phenoxyethanol, and 1,2-diphenyl-2-methoxyethanol were characterized crystallographically (Figure 1).

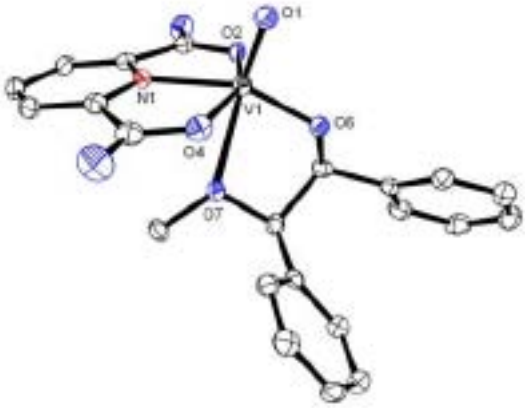

Figure 1. Vanadium(V) complex of 1,2-diphenyl-2-methoxyethanol.

The vanadium(V) complexes reacted cleanly upon thermolysis in pyridine solvent. Carbon-carbon bond cleavage was observed for pinacolate complex (dipic)V(O)(Hpin) (**2**), yielding acetone and the vanadium(IV) complex (dipic)V^{IV}(O)(pyr)$_2$ (**3**). A very similar C-C bond cleavage was observed for pinacol monomethyl ether complex **4**, which reacted at 100 °C over 6 h to afford **3**, acetone, and 2-methoxypropene (Figure 2). In other substrates having a C-H bond adjacent to the alcohol, this bond was broken selectively in pyridine solvent to yield the aldehyde or ketone product. For example, 1-phenyl-2-phenoxyethoxide complex **5** reacted in pyr-d_5 solvent to afford **3** and 2-phenoxyacetophenone (Figure 2).

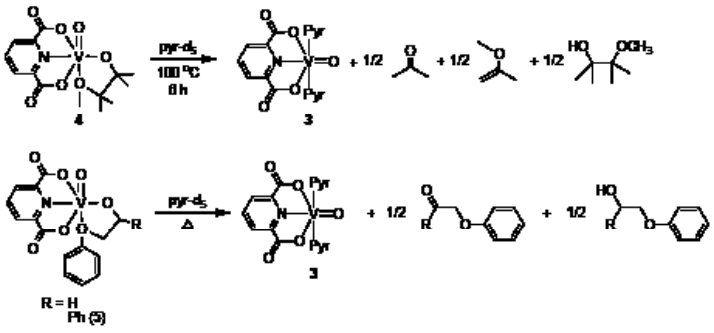

Figure 2. Reactions of lignin model complexes.

The catalytic oxidation of the cellulose models pinacol and 1,2-diphenylethanediol was carried out. In both cases, catalysis was achieved using air and mild heating (100 °C), affording products of carbon-carbon bond cleavage. Complex **1** was found to be an effective catalyst for the aerobic oxidation of pinacol in NMP (NMP = *N*-methyl-2-pyrrolidone) solvent. Nearly complete conversion of pinacol to acetone was observed. Oxidation of 1,2-diphenylethanediol occurred even more rapidly. In pyridine-d_5 solvent, complete conversion (40 turnovers) was observed. A control reaction with no vanadium catalyst showed only 2-4% oxidation of 1,2-diphenyl-ethanediol and no reaction of pinacol under the catalytic conditions (air, heat). This shows that the vanadium plays a key role in the oxidation reaction. Prior to these discoveries, only a few examples of the aerobic oxidation of diols using homogeneous vanadium catalysts had previously been reported.

Finally, the oxidation of glucose, the monomeric unit in cellulose, was testing using the *cis*-dioxo complex [(dipic)V(O)$_2$]HPy (**6**). Reaction of glucose-$^{13}C_6$ with complex **6** in pyr-d_5 solution (100 °C) afforded CO_2 and formic acid, as well as some unreacted glucose, which were detected by ^{13}C NMR spectroscopy. The formation of carbon dioxide indicates that the oxidation is not selective, and the initial products are oxidized more rapidly than glucose itself. The complete oxidation of glucose to carbon dioxide suggests that the dipicolinate vanadium complexes might be better suited for breaking down lignin, which is more resistant than cellulose to chemical degradation.

Mechanistic study of the vanadium-mediated alcohol oxidation reaction.

The development of more effective catalysts is often facilitated by an understanding of the reaction mechanism, or how the reaction proceeds. Several experiments were carried out to explore how the dipicolinate vanadium system oxidizes simple alcohol substrates; these reactions are closely related to the catalytic oxidations of lignin and cellulose model compounds.

Several experiments were performed using mechanistic probes, substrates where the products of oxidation give information about the mechanism of the oxidation. Dipic complexes of cyclobutanol (dipic)V^{V}(O)OCy (**7**) (OCy = cyclobutanoxide) and α-*tert*-butylbenzylalcohol (dipic)V^{V}(O)(TBA) (**8**) (TBA = α-*tert*-butylbenzylalkoxide) were prepared. Thermolysis of a pyridine-d_5 solution of **7** at 100 °C for 30 min resulted in formation of cyclobutanone in 93% yield. The absence of ring-scission products in this reaction argues against radical intermediates, and is more consistent with a two-electron pathway involving V^{III} intermediates. Thermolysis of **8** in pyr-d_5 solution at 100 °C for 20 minutes formed the ketone product 2,2-dimethylpropiophenone in 98% yield, consistent with a hydride transfer or hydrogen atom transfer pathway. Remarkably, carrying out the reaction of **7** in CD_3CN gave a different result, with the predominant organic product being benzaldehyde (92%), consistent with radical intermediates.

The reaction of isopropoxide complex **1** with pyridine to generate acetone and the vanadium(IV) complex **3** was studied (Figure 3). The reaction is first order in vanadium through at least three half-lives, and no reaction was observed in the absence of pyridine. Conducting the reaction in mixtures of acetonitrile and pyridine solvent revealed a surprising dependence on the concentration of pyridine (Figure 4). Preparation of the deuterated isopropoxide complex **1-d_7** allowed for determination of a primary kinetic isotope effect (k_H/k_D) of about 5.7 (pyr-d_5 solvent). Activation parameters of $\Delta H^{\ddagger}$ = 25.5(1) kcal/mol and $\Delta S^{\ddagger}$ = -18(2) eu were determined from an Eyring plot (319-360 K, pyr-d_5 solvent), consistent with a bimolecular reaction. The involvement of pyridine in the elementary alcohol oxidation step determined for dipicolinate vanadium(V) is a substantial departure from what has been proposed for other vanadium catalysts and is a completely new type of mechanism for vanadium-mediated alcohol oxidation. Using a base to promote alcohol oxidation could provide a new handle with which to tune reactivity of vanadium catalysts.

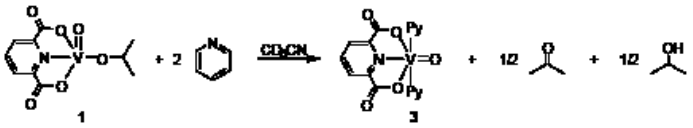

Figure 3. Reaction of complex 1 with pyridine.

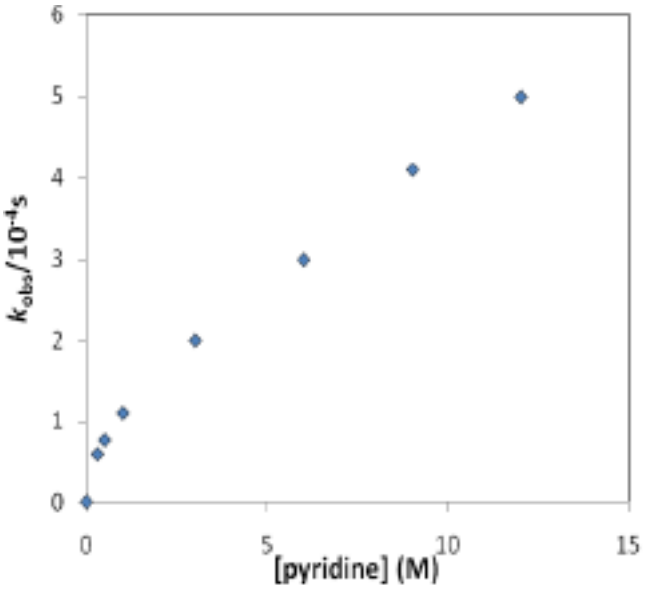

Figure 4. Observed pyridine dependence of the reaction of 1 to afford 3 and acetone.

Catalytic oxidations of lignin model complexes

Catalytic oxidations of several lignin model complexes have been tested. Using the (dipic)V(O)O^{i}Pr catalyst (5 mol %), 1,2-diphenyl-2-methoxyethanol was oxidized in DMSO-d_6 solvent (94% conversion after 20 hours), affording benzaldehyde (78%) and methanol (73%) as the major products. Minor products of this reaction included benzoin methyl ether, methyl benzoate, and benzoic acid. Lignin model 1-phenyl-2-phenoxyethanol could also be oxidized by air using **1** (10 mol%) in DMSO-d_6 solvent. After 1 week at 100 °C, 95% conversion had occurred to yield a mixture of formic acid, benzoic acid, phenol, and 2-phenoxyacetophenone (Figure 5). The substrate 2-phenoxyethanol, having no backbone phenyl substituents, was only partially oxidized (20% or less) under these conditions.

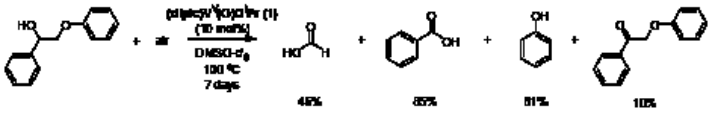

Figure 5. Oxidation of lignin model 1-phenyl-2-phenoxyethanol.

Impact on National Missions

Overall, using the vanadium catalyst and air as the oxidant is a completely new method for breaking carbon-carbon bonds in the lignin model complexes (this is the first example of catalytic aerobic oxidative C-C bond cleavage of 1,2-hydroxyether complexes). This approach affords aromatic monomers from the lignin model complexes under mild conditions. The results described above suggest the potential utility of dipicolinate vanadium complexes to produce valuable chemicals from biorenewable sources such as lignin. Furthermore, the homogeneous nature of the catalyst provides new opportunities for ligand design to optimize activity and selectivity in these reactions.

References

1. Hanson, S. K., R. T. Baker, J. C. Gordon, B. L. Scott, and D. L. Thorn. Aerobic Oxidation of Lignin Models Using a Base Metal Vanadium Catalyst. To appear in *Inorganic Chemistry.*

Publications

Hanson, S. K., R. T. Baker, J. C. Gordon, B. L. Scott, and D. L. Thorn. Aerobic Oxidation of Lignin Models Using a Base Metal Vanadium Catalyst. To appear in *Inorganic Chemistry.*

Hanson, S., R. Tom. Baker, J. Gordon, B. Scott, L. A. Silks, and D. Thorn. Mechanism of alcohol oxidation by dipicolinate vanadium(V): Unexpected role of pyridine. 2010. *Journal of the American Chemical Society.* **132** (50): 17804.

Hanson, S., R. Tom. Baker, J. Gordon, B. Scott, and D. Thorn. Aerobic Oxidation of Lignin Models Using a Base Metal Vanadium Catalyst. 2010. *INORGANIC CHEMISTRY.* **49** (12): 5611.

Environmental & Biological Sciences

LABORATORY DIRECTED RESEARCH AND DEVELOPMENT

Understanding Drug Resistance and Co-infectivity in HIV and TB Infections

Bette T. Korber
20090098DR

Introduction

Mycobacterium tuberculosis, which causes tuberculosis (TB), has ravaged mankind for several thousand years and claims over 4000 lives worldwide every day. TB infections are increasing, particularly in Africa and Eastern Europe, and the WHO estimates that ~2 billion people are infected. HIV/AIDS is estimated to infect 33 million people, with over 2.1 million dying of AIDS each year. AIDS and TB each cause tremendous human suffering, and combined these two diseases have a terrible synergy. People die rapidly when co-infected, and untreatable extensively drug resistant TB (XDR-TB) is emerging in regions of the world where the two epidemics are coincident. XDR-TB is gaining ground; 57 countries/territories have now reported XDR-TB strains, and TB is a contagious air born pathogen. Rapid diagnostics to track, treat, and understand these diseases are urgently needed.

Diagnosis of TB and identifying drug resistant forms of TB for treatment remains a very challenging global health problem; current diagnostic methods require culture and can take weeks to get results, while life saving treatment can depend on rapid diagnosis. We are developing novel methods to detect TB biomarkers in different tissue samples for use in rapid diagnosis. Furthermore, while the characteristic patterns of mutations that confer resistance to specific classes of HIV drugs are defined, those associated with TB are still being mapped. New state of the art sequencing methods are enabling us characterize the genetic diversity in both HIV and TB infections, and to track the evolution of both pathogens as a function of treatment. These approaches will permit early diagnosis and help track virulence factors to guide drug treatment. Ultimately, we hope to utilize the diagnostic and genetic analysis tools developed in the initial phases of the project to better understand HIV-TB co-infections. LANL has a strong foundation in the evolutionary analysis of pathogen genetic diversity, and the development of detection assays for TB and other agents. This DR has enabled us to bring together our experimental and theoretical expertise in these areas, develop new experimental and analysis methods, and to work biologically interesting samples that provide new insights into the biology of these two pathogens.

Benefit to National Security Missions

We are developing new methodologies for diagnostics and metagenomics for application to the extreme scenarios of a very rapidly evolving small virus with a 10,000 base genome (HIV), and a slowly evolving large bacterial genome of roughly 4 million bases (TB). The methods are being developed in the context of asking critical scientific questions regarding HIV and TB, two of the most serious public health problems of our times. These methods could readily be transitioned to a broad spectrum of other pathogens, addressing threat reduction, human health, and basic science missions relevant to DOE, DHS, and other government agencies. As we develop new detection methods for drug resistance and disease progression, we are improving our understanding of the associated biological and evolutionary processes. These methods can potentially be used to both improve patient care and to track the movement of drug resistant forms of HIV and TB pathogens globally. Furthermore, the technologies and tools we are developing to combat current real world problems of TB and HIV could be adapted and applied if infectious bio-organisms are ever used as a weapon.

Progress

In the first two years of this project we have developed the analysis tools to use ultradeep sequencing to track immune escape and drug resistance in HIV-infected people. Old sequencing methods allowed us two examine up to 50 viruses per sample, but ultradeep sequencing has enabled us to sequence 10,000-50,000 viruses; to use this data we have had to develop analytical methods to reveal rare variants and evolutionary pathways. Our first technical challenge was primer design; we had to find conserved regions of appropriate length in the HIV genome, design optimal biobarcodes to distinguish sequence sources, and attend to the biochemistry of annealing. These methods have been used in each of our studies to date [1, 2], and a web-based informatics application and paper are

currently being written. Our next challenge was to devise computational ways to clean up and analyze such massive genetic data sets. Our first pass at this was a study of the emergence of drug resistance over time in HIV infected individuals [3]. In a second study, we used 454 ultradeep sequencing of HIV to study viral escape from the initial immune responses. We found that:

- A single virus initiates infection.
- The virus explores a vast array of ways to evade the immune response.
- The earliest immune responses were initiated earlier than previously thought, as illustrated in Figure 1 [1].

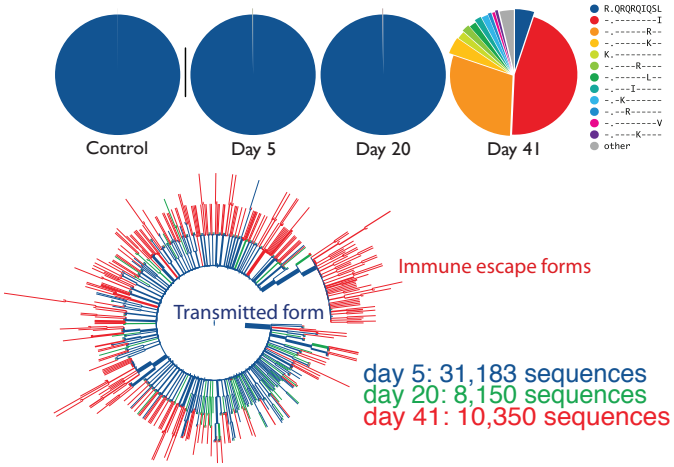

Figure 1. HIV rapidly evolves many ways out of the initial immune response after infection. The pie graphs show the frequency of different escape mutant forms in the region targeted by a human killer T cell response. The phylogenetic tree underneath shows the evolution of the virus during early infection. The virus explodes in diversity in the 2nd three weeks of infection.

We have also explored viral evolution under immune pressure in acute infection in SIV infected macaques, the best animal model available for HIV vaccine studies [2]. SIV is a monkey disease related to HIV. We have explored the reconstruction of phylogenetic trees from large datasets of sequences obtained by deep sequencing technologies. We are adapting Bayesian inference programs to be able to handle such large data sets, and optimized for the high sequence identity in these sets. We are using these methods to calculate in vivo mutation rates from sequences, a critical parameter for modeling HIV dynamics.

Finally, we are collaborating in an HIV drug resistance study. Our S. African colleagues have shown that the anti-retroviral drug Tenofovir used in a vaginal gel used during sex results in 39% protection from infection [4]. We are using use deep sequencing to evaluate whether the prophylactic use of the Tenofovir resulted in increased frequencies of known resistant mutations in the study population. In preparation for this study, we performed a pilot study to assess the sensitivity of 454 sequencing for detection of Tenofovir resistance mutants in a dilution series and from known patients; the results indicated our methods are extremely sensitive and quantitative, shown in Figure 2. Our collaborators are currently preparing DNA from the study samples for shipment to LANL for sequencing and analysis.

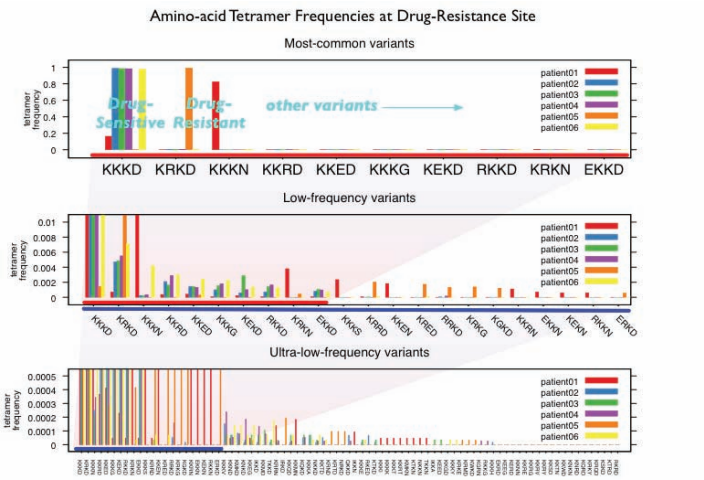

Figure 2. Deep sequencing reveals low- and ultra-low-frequency detection of drug resistant forms of the virus that are invisible to tradition methods. Results for 6 different chronically infected South African patients are shown. The three panels show increasing numbers of variants detected with decreasing vertical scales. Sequence variants can be detected at levels of less than 0.02% of the total virus in the sample.

We are also attempting to develop sensitive methods for detecting TB biomarkers, with particular progress with detection of the TB molecule LAM in easily drawn samples such as serum and urine. We have developed exquisitely sensitive methods for detection of LAM, using methods that mimic recognition of bacteria by our innate immune system in which LAM is bound to a membrane, and Figure 3 illustrates the application of this method to human samples [5,6]. With sufficient sensitivity, we can detect infections before symptoms appear. Furthermore, understanding mechanisms by which LAM interacts with the host is important for gaining understanding of the pathology of tuberculosis. No three-dimensional structure of LAM has yet been reported. Therefore we built an all-atom molecular model of LAM based on structural details assembled from the literature consisting of 2139 atoms, with a MW of 16,100 [5]. The all atom model revealed a relatively large non-peptide glycolipid with a width of 14 nm. Currently we are exploring how LAM interacts with the membrane through structural modeling.

We have also obtained our first five TB genomic sequences from extensively drug resistant samples from KwaZulu

Natal for a pilot study for defining key drug resistance mutations. We have combined this data with 13 previously published TB genomes, and successfully aligned all genes in these 18 genomes, enabling us to create the first full genome phylogeny of TB, based on all variable positions. The preliminary results are very interesting and offer a new perspective on the spread of XDR TB and drug resistance. Our results show there are many genetically diverse forms of TB co-circulating in South Africa, and suggest that either there are many mutational pathways to XDR TB and few common drug resistance mutations, or alternatively, that sample cultures are more complex than was previously realized and phenotypic designations based on these cultures need to be reconsidered. We are working with colleagues in S. Africa to design experiments to resolve these questions in the last year of our DR.

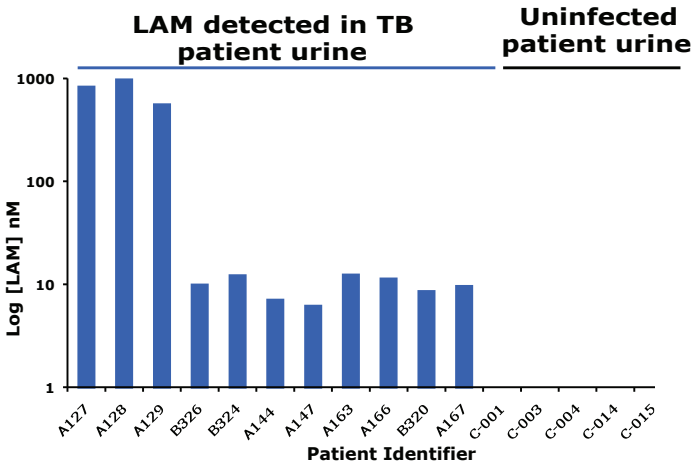

Figure 3. Measurements of tuberculosis molecular markers in patient serum and urine samples. Detection of LAM correlate with active disease, and longitudinal studies are underway to determine if this may be used to help guide therapy. Using methods developed through this DR we can detect the TB LAM biomarker at levels < 1 fm, 100,000 times more sensitive than the bottom of this chart.

Future Work

Through our ongoing the studies of HIV and TB, we are helping shape the cutting edge of new sequencing and biomarker detection technology as it can be applied to human pathogens, while working on better understanding of the basic biology of infectious diseases of the utmost importance for public health. We are building a network of collaborators for both HIV and TB studies, and as a consequence LANL will be hosting a TB meeting to explore opportunities for developing tracking and diagnostic assays for drug resistant TB. Sensitive and specific immunoassays and oligonucleotide probes for the simultaneous detection of multiple markers will be developed using both the waveguide-based optical biosensor and a nanotechnology biobarcode-based amplification diagnostic method.

Conclusion

The WHO designates TB and HIV/AIDS as two of the three most deadly diseases confronting mankind. These pathogens, each deadly in its own right, operate synergistically, and HIV-induced suppression of the immune system allows activation of latent TB, leading to progressive, contagious, and drug resistant TB. The biology underlying the interaction between these two pathogens is not understood. We are developing an applying new technologies that will enable us to identify markers of disease progression for TB, design diagnostics for HIV and TB drug resistance and progression, and study the evolution of these two pathogens in infected and co-infected individuals.

References

1. Fischer, W., V. V. Ganusov, E. E. Giorgi, P. T. Hraber, B. F. Keele, T. Leitner, C. S. Han, C. D. Gleasner, L. Green, C. C. Lo, A. Nag, T. C. Wallstrom, S. Wang, A. J. McMichael, B. F. Haynes, B. H Hahn, A. S. Perelson, P. Barrow, G. M. Shaw, T. Bhattachraya, and B. T. Korber. Transmission of single HIV-1 genomes and dynamics of early immune escape revealed by ultra-deep sequencing. 2010. *PLoS One.* **5** (8): e12303.

2. Cale, E. M., P. Hraber, E. E. Giorgi, W. Fischer, T. Bhattacharya, T. Leitner, W. W. Yeh, C. Gleasner, L. D. Green, C. S. Hahn, B. Korber, and N. Letvin. CD8+ T lymphocytes recognize but fail to contain the accumulation of SIV epitope escape mutations. *Immunity.*

3. Tsibris, A., B. Korber, R. Arnaout, C. Russ, C. C. Lo, T. Leitner, B. Gaschen, J. Theiler, R. Paredes, Z. Su, M. D. Hughes, R. M. Gulick, W. Greaves, E. Coakley, C. Flexner, C. Nusbaum, and D. R. Kuritzkes. Quantitative deep sequencing reveals dynamic HIV-1 escape and large population shifts during CCR5 antagonist therapy in vivo. 2009. *PLoS One.* **4** (5): e5683.

4. Karim, Q. Abdul. Effectiveness and safety of tenofovir gel, an antiretroviral microbicide, for the prevention of HIV infection in women. 2010. *Science.* **329** (5996): 1168.

5. Mukundan, H., D. N. Price, M. Goertz, G. B. Montano, A. S. Anderson, R. Parathasarathy, G. S. Gnanakaran, S. Kumar, S. Iyer, and B. Swanstrom. Interaction of Lipoarabinomannan with membrane mimetic architectures: A novel detection strategy for amphiphilic biomarkers. *Tuberculosis.*

6. Makundan, H., D. N. Price, Y. Valdez, L. Via, C. Barry, and B. Swanstrom. LAM partitions into HDL particles in patient serum samples: Implications in TB diagnostics and PAMP clearance. *Journal of Infectious Disease.*

Publications

Fischer, W., V. V. Gaunsov, E. E. Giorgi, P. T. Hraber, B. F. Keele, T. Leitner, C. S. Han, C. D. Gleasner, L. Green, C. C. Lo, A. Nag, T. C. Wallstrom, S. Wang, A. J. McMicael, B. F. Haynes, B. H. Hahn, A. S. Perelson, P. Borrow, G. M. Shaw, T. Bhattacharya, and B. T. Korber. Transmission of single HIV-1 genomes and dynamics of early immune escape revealed by ultra-deep sequencing. 2010. *PLoS One.* **5** (8): e12303.

Lynch, R. M., R. Rong, B. Li, T. Shen, W. Honnen, J. Mulenga, S. Allen, S. Zolla-Pazner, A. Pinter, S. Gnanakaran, and C. A. Derdeyn. Subtype-specific conservation of Isoleucine 309 in the Env V3 domain is linked to immune evasion in subtype C HIV-1 infection. 2009. *Virology.* **404** (1): 5970.

Mukundan, H., H. Xie, D. Price, J. Kubicek-Sutherland, W. Grace, A. Anderson, J. Martinez, N. Hartman, and B. I. Swanson. Quantitative multiplex detection of pathogen biomarkers on multichannel waveguides. 2010. *Analytical Chemistry.* **82** (1): 136.

Neher, R., and T. Leitner. Recombination rate and selection strength in HIV intra-patient evolution. 2010. *PLoS Computational Biology.* **6** (1): e1000660.

Rebecca, M., T. Shen, S. Gnanakaran, and C. Derdeyn. Appreciating HIV-1 diversity: subtypic differences in Env. 2009. *AIDS Research and Human Retroviruses.* **25**: 237.

Tsibris, A. M., B. Korber, R. Arnaout, C. Russ, C. C. Lo, T. Leitner, B. Gaschen, J. Theiler, R. Paredes, Z. Su, M. D. Huges, R. M. Gulick, W. Greaves, E. Coakley, C. Flexner, C. Nusbaum, and D. R. Kuritzkes. Quantitative deep sequencing reveals dynamic HIV-1 escape and large population shifts during CCR5 antagonist therapy in vivo. 2009. *PLoS One.* **4** (5): 5683.

Distributed Metabolic Regulation: the Key to Synthetic Biology for Carbon Neutral Fuels

Pat J. Unkefer
20090117DR

Abstract

Transcription factors (TFs) control phenotype – the function and structure of organisms – by regulating gene expression. Gene regulation occurs in response to stimuli; this response manifests itself in the binding of a transcription factor effector molecule (TFEs) by TFs. This binding modulates the affinity of the TFE/TFs binary complex for its specific DNA binding site in the gene's operator region, and thus facilitates or inhibits transcription. This project seeks to discover effectors of, and the DNA operator sequence recognized and bound by transcription factors (TF) in *Burkholderia xenovorans.* We are successfully applying our combined approach of frontal affinity chromatography with mass spectrometery detection (FAC-MS) to discover the effectors with TF-binding DNA microarray to find the DNA operator sequences to which the TF binds. This project also seeks to test our hypothesis that at least some and probably many operator sequences interact with more than a single TF and that these interactions with the TF provide modulation of the TF function.

Background and Research Objectives

We are successfully demonstrating our approach to solving the long-standing challenge of discovering the effectors of transcription factors controlling target genes. We are also showing that our hypothesis that transcription factors could function as signal processors is also correct for some transcription factors. The work is supporting the development of additional project concepts and preliminary data for proposals aimed at developing new anti-microbial drugs.

Effector prediction from genetic context - Using the contextual analysis method we developed and reported last year, which compares across bacterial species the functional context of gene clusters in close sequence proximity to TF genes, we have been able to predict metabolic pathways whose expression is potentially regulated by the target TF. These predictions allow us to quickly assemble focused metabolite libraries from which to screen the actual effector molecule(s) for a given TF. Before our work, "blind" or uninformed searches for TF effectors had been the state of the art for discovering the function of a TF not already associated with a metabolic pathway. Without prediction of effector structure classes, these methods have great difficulty in discovering the effector.

After constructing informed libraries, we clone, express, purify, and immobilize the target TF on Biotin and GST HPLC binding columns. Then using the informed libraries of potential effectors, we performed FAC-MS experiments. Originally, the protein binding arrays are then used with the purified GST-TF fusion to identify the DNA operator. We have developed a green fluorescent protein (GFP)/TF fusion, which is intrinsically fluorescent. The GFP/TF fusion can be observed on the protein-binding array with greater sensitivity. Finally we are developing a functional assays to demonstrate effector modulated TF binding to its double stranded DNA operator sequence. The validity of this approach has been established with MetJ, a TF with a known effector S-adenosyl methionine (SAM). We used a mixture of effector and structurally related compounds to test and establish the relationship between the breakthrough volume and their relative binding affinity to the TF. The difference in the elution times of compounds in the library allows us to rank their relative binding affinities.

Scientific Approach and Accomplishments

Our progress, outlined below, demonstrates a high fraction of success in finding both the metabolite effectors and DNA operator sequences for these TFs of unknown function. As is to be expected with proteins, not all TFs lend themselves to both technologies in the original approach; as noted in the progress outlined below, we are finding other ways to find the effectors of such TFs by taking advantage of our predicted function and other data. We have also shown that our hypothesis many TFs will bind multiple metabolite effectors is true for MetJ as described in the last paragraph of the report.

Progress on Discovering TF Effectors and DNA operator sequences

TF BxeB3018

Using our contextual analysis approach outlined in Figure 1, we predicted that TF *BexB3018* would regulate the expression of genes involved in glycine, serine and threonine metabolism. From this prediction we constructed an informed library containing fifteen commercially available and structurally dissimilar metabolites. Of these candidates, 1-amino acetone bound tightest to *BexB3018* (Figure 2). Another potential tight binding effector is dihydroxyfumarate. The TF binding microarray was used to develop a consensus DNA sequence recognized and bound by this TF (5'-AGAANNNNNNTTCT-3'). A genome-wide DNA operator scan revealed this operator sequence repeated upstream of twenty one genes, many of which are involved in the predicted metabolic function and others encoding three TFs and several genes of unknown function that may be associated with the function of the TF. We are working to confirm that amino acetone modulates the binding of TF *BexB3018* to the operator DNA sequence. A manuscript describing this work is in draft.

TF BxeA0736

Using our approach we predicted that TF *BxeA0736* was involved in tryptophan degradation. Using this as a guide we tested the set of available (8) metabolites (tryptophan, kynurenine, tyrosine, phenyalanine, tyrosine, anthranilic acid, 4-4-hydroxybenzoic acid, 4-hydroxy anthranilic acid and 3,4-dihydroxybenzoic acid) produced in this metabolism. Of these L-kynurenine was found to bind tightly to TF *BxeA0736* providing strong evidence in support of our original prediction of the metabolic function regulated by this TF. We also showed that ADT, ADP and L-kynurenine form stabilizing interactions with this TF, probably by interacting with DNA recognition/binding site. The TF-binding microarray allowed the identification of a consensus sequence of CATATAAT for this TF. Because of the physical limitation of the DNA microarray it is likely that this is a truncated sequence. The consensus sequence is located near and upstream of the TF gene, consistent with it being the TF-bound sequence. Using this larger region as the DNA substrate we have gained evidence that the DNA actually wraps around the octomeric structure of this TF with the widely spaced representatives of the consensus sequences being bound by each of several TFs within this octomeric structure. This is the first evidence of this rare mechanism being used for any member of this family of TFs. We are examining this further. A manuscript of this work is in draft.

TF BXeA0425

We predicted that TF *BXeA0425* was involved in regulation of a major facilitator transporter mechanism. Because this information does not provide as specific insight as we in the other cases we simply screened all of our libraries of metabolites in central metabolism because our TF targets had been chosen for their high degree of conservation in *Burkholderia*. From this structurally diverse set of central metabolites, we identified choline as binding tightly to the TF. The TF-binding microarray allowed used to identify a consensus sequence of –CC-C-CCCTAACAA-; this sequence as used to scan the DNA operator regions genome wide. It was found upstream of three genes. We are examining these upstream regions to experimentally (gel shift and DNA finger-printing) test this sequence as a component of the DNA sequence recognized by this TF. If confirmed or

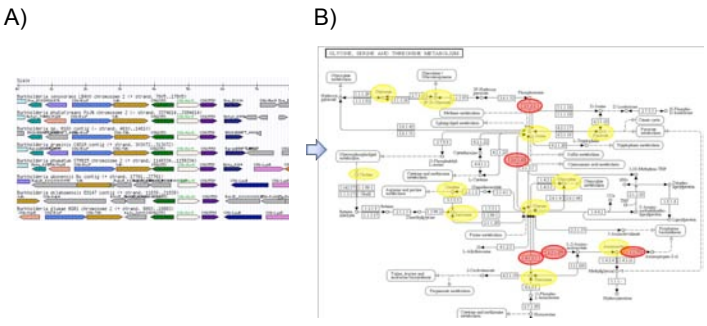

Figure 1. Contextual analysis of Transcription Factor Effectors. A) Alignment of genes clustered around TF BexB3018 (White Arrow) across eight Burkholderia genomes. Conserved genes are color-coded. B) Based on the functional annotation, proteins encoded by conserved genes clustered around TF BexB3018, are highlighted on red ovals on the KEGG metabolic map. The compounds highlighted in yellow ovals are commercially available and were selected to test in our initial targeted effector libraries.

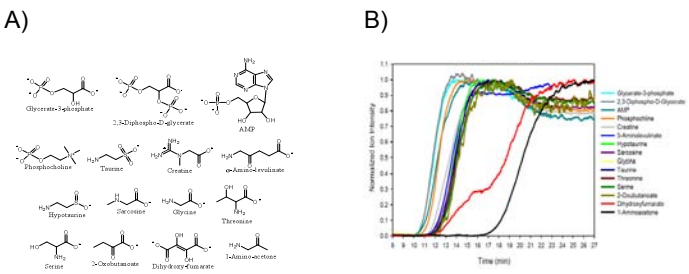

Figure 2. FAC-MS analysis of potential effectors of TF BexB3018. A) Fifteen compound library of metabolites involved in Glycine, serine, and threonine metabolism. B) FAS-MS trace of the normalized ion intensity of M+1 positive ions derived from the compounds listed diagrammed in A). The long breakthrough times for 1-amino acetone and dihydroxyfumarate indicate specific high-affinity binding to BexB3018 characteristic of TF effectors.

refined it can be used to gain additional information on the genes regulated by this TF and test further the function of choline as an effector of this TF.

TF Bxe2842

Bex2842 has been postulated in the literature to bind aminophenol. We are working to validate this postulation; because it has proved extremely difficult to over-express in the quantities needed for FAC-MS, we have crystallized the TF to confirm the binding and to examine the effects of binding on structure of the TF. The TF binding microarray was not helpful in finding the binding site therefore we simply inspected the intergenomic regions of the gene for this TF and found the motif 5'-TTTGCNNNNNNNNNNTTT GTNNNNNNNNNNTTTGC-3' in the upstream region and the motif 5'-TTTGCNNNNNNNNNNTTTGTNNNNNNNNT TTGT-3' in the downstream region. These motifs provide the requisite repeated sequences characteristic of DNA sequences bound by TFs. We are testing this prediction with DNA footprinting, a standard method to gain such information.

TF BxeB0878

Our prediction method suggested that *BxeB0878* is involved in arginine/proline metabolism or lysine biosynthesis. FAC-MS analysis showed that proline and hydroxy-proline derivatives are bound by the TF. This is strong support for our prediction of its overall regulatory function. Because some of the candidate effector metabolites are not readily available we are exploring synthesis for them (four metabolites). The TF-binding microarray will be employed next to test for the DNA sequence recognized by this TF. A manuscript is being crafted on this work.

Progress on our TFs as Signal Processors Hypothesis
Our studies of the TF, MetJ, have opened the door to study regulation at a completely new level. Specifically we are addressing and proving our hypothesis we put forward in the proposal for this work that at least some TFs would act as "signal processors" as a result of interacting with more than one metabolite. Our findings show that metabolites that were previously rejected as effectors for MetJ can be reinterrogated with our high-throughput FAC-MS method, and new questions can be asked about their interaction with the target TF. We showed that in addition to the known effector of MetJ, S-adenosyl-methionine (SAM), MetJ also interacts strongly with adenine and methylthioadenosine. The binding of a TF to a DNA operator is commonly induced by a confirmation change caused by the binding of a TEF. Binding of novel ligands to the effectors' binding sites could have several effects. First, the binding of a novel ligand could cause a new conformational change in the TF that leads to binding to an existing known operator, or even to a completely new and unknown operator, thus regulating a different system. Also, it could cause secondary regulation by binding the TF and inhibiting its ability to bind the activating ligand or effector (SAM for MetJ). More experiments will be required to obtain answers to what may be the biological function of these novel MetJ complexes to Ade, MTA and what DNA operators and metabolic systems could be affected. A manuscript has been submitted describing this work.

As the project continues, we will be completing the characterization of the currently targeted transcription factors, preparing manuscripts on this work and preparing several proposals for external funding to extend this work. For example a proposal is expected to be submitted to Defense Threat Reduction Agency on developing specific inhibitors of a transcription factor that controls multi-drug resistance in many pathogens and in particular Burkholderia species of particular importance to military deployments.

Impact on National Missions

Establishing the capability to discover the effectors of transcription factors creates the opportunity to control many different genes and genetic networks in microorganisms important to National Security Missions. Such important organisms and goals include microbes for producing or processing biofuels or creating and / or producing antimicrobials (antibiotic) needed to combat such threats as select agents or infectious diseases that our deployed military or diplomatic personnel may encounter.

Publications

Bauer, A., W. Hlavacek, P. Unkefer, and F. Mu. Using Sequence-Specific Chemical and Structural Properties of DNA to Predict Transcription Factor Binding Sites. To appear in *PLos.*

Bauer, A., W. Hlavacek, and F. Mu. Using sequence-specific chemical and structural properties of DNA to predict transcription factor binding sites. Presented at *q-Bioconference.* (Santa Fe, June 26-28. 2009).

Marti-Arbona, R., M. Teshima, P. Anderson, K. Nowak-Lovato, E. Hong-Geller, P. Unkefer, and C. Unkefer. Discovery of Transcription Factor Function: Multiple Metabolites Interact with MetJ. *Journal of Biological Chemistry.*

Marti-Arbona, R., M. Teshima, P. Anderson, P. Unkefer, and C. Unkefer. FAC-MS uncovers new effectors for old transcriptional regulators: Discovery of novel transcription factor effectors for MetJ. Presented at *Gorden Research Conferences "Enzymes, coenzymes and metabolic pathways.* (New Hampshire, 5-10 July 2009).

Marti-Arbona, R., M. Teshima, T. Maity, J. Dunbar, C. Unkefer, and P. Unkefer. Discovery of novel transcription factor effectors for metJ. . Presented at *238 ACS national meeting.* (Washington, DC, 1-20 Aug.

2009).

Marti-Arbona, R., T. Maity, J. Dunbar, C. Unkefer, and P. Unkefer. Discovery and function annotation of novel transcription factors. Presented at *Gorden Research Conference "Enzymes, Coenzymes and Metabolic Pathways".* (New Hampshire, 18-23 July 2010).

Mu, F., A. Bauer, J. Faeder, and W. Hlavecek. Using systems biology techniques to determine metabolic fluxes and metabolic pool sizes. 210. In *Handbook of Chemoinformatics Algorithms.* Edited by Faulon, J., and A. Bender. Vol. I, First Edition, p. 399. Boca Raton, FL: CRC Pres.

Mu, F., C. Unkefer, and P. Unkefer. Using sequence-specific chemical and structural properties of DNA to predict transcription factor binding sites. To appear in *PLos Computational Biology.*

Tuhin, S., D. Close, Y. Valdez, R. Marti-Arbona, T. Nygen, P. Unkefer, A. Bradbury, and J. Dunbar. Improved discovery of DNA regulatory motifs by using fluorescent protein-labeled transcription factors in a universal protein binding microarray. *PLos.*

Integrated Experimentation and Hybrid Modeling for Prediction and Control of Multiphase Flow and Reaction in CO_2 Injection and Storage

James W. Carey
20100025DR

Introduction

The prediction and control of multiphase flow and reaction in geologic media is one of the great challenges in the Earth and Energy Sciences. This challenge has come into even greater focus with the recognition that the environment cannot sustain the CO_2 released from oil, gas, and coal combustion. These carbon-based fuels form the backbone of the world economy and have enabled nearly all of the technological innovations of the past 100 years. As developing countries with large populations strive to attain higher standards of living, their emphasis will be on the utilization of even more inexpensive and abundant fossil fuel. A promising approach for avoiding this impending environmental crisis is the geologic sequestration of CO_2 in depleted oil reservoirs and deep saline aquifers.

As a response to global warming, geologic disposal of CO_2 represents an enormous challenge: a single 1-GW coal-fired power plant produces a volume of about 10 m x 1 km^2 of supercritical CO_2 each year. Predicting the fate of CO_2 in the subsurface requires a fundamental understanding of multiphase, reactive flow and transport where competing physical and chemical processes generate complex, heterogeneous flow and reaction patterns. The injection of CO_2 into a saline aquifer upsets a system that has been close to chemical equilibrium and hydrodynamic steady-state for millennia. Determining the long-term mobility of the buoyant, immiscible CO_2 is essential to making this technology viable. Our project integrates the innovative, cutting-edge experimental and numerical approaches to directly observe CO_2 flow and reaction and will use these results to develop and validate predictive models of CO_2 mobility.

Benefit to National Security Missions

This proposal supports LANL's Grand Challenge goals in Energy and Earth Systems. It accomplishes this by enabling geologic sequestration of CO_2 which will allow the continued use of fossil fuels without continuing to emit harmful quantities of CO_2 to the environment. Our proposal support's DOE's top priority of carbon sequestration as a means of mitigating the impacts of fossil fuel consumption. On a more fundamental level, the proposed research maps directly to the Basic Energy Sciences Advisory Committee's Grand Challenge to "Characterize and Control Matter Away From Equilibrium" as "crucial for energy supply and security."

Progress

Fiscal Year 2010 is the first year of our LDRD project on multiphase flow and reaction of CO_2. The project is off to a great start with progress on key personnel actions, new instrument design, initiation of experimental and modeling tasks, development of first results, and presentation and submission of these results to the research community. We briefly summarize this below.

Personnel: We created and began a three-year subcontract with Oregon State University (Professor Dorthe Wildenschild, PI) that is central to our experimental tomographic and core flooding work. We created and began a three-year subcontract with the University of Illinois (Professors Al Valocchi and Charlie Werth, co-PIs) that is essential to our work on hybrid modeling and experimental microfluidics studies. In addition, we have hired five postdoctoral research fellows.

Instrumentation: A key focus area is the development of unique instrumentation for *in situ* study of supercritical CO_2 behavior in porous media. We have designed and fabricated a high-pressure microfluidics cell that will allow optical and fluorescent microscope observations of flow and reaction at conditions ranging to 60 ^oC and 150 atmospheres. This will be the first instrument of its kind and utilizes a sapphire window to simultaneously control pressure and allow optical observations.

Our project has also designed a unique core-flood system for conducting *in situ* high-pressure, high-temperature multiphase fluid flow experiments through porous media. The core-holder is x-ray and neutron transparent and will be used for tomographic imaging. In addition, the system supports tri-axial stress loading with a flexible array of sensors such as acoustic, thermal,

strain gauges, etc. In the coming year, we will construct the device.

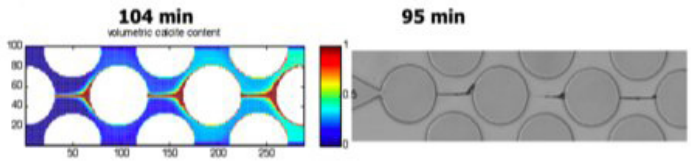

Figure 1. Simulated microfluidics experiment showing deposition of calcite (a) and an image of calcite precipitation in a micromodel experiment (b) shown at comparable times.

Research Progress: At the end of our first year, we already have interesting experimental and computational results that have been presented at national meetings and submitted to or appeared in leading journals. The experimental work includes studies of the displacement of immiscible fluids in synthetic, homogeneous porous medium using 2-dimensional microfluidics methods. These direct, optical observations provide essential information on efficiency of fluid displacement, the reactive surface areas between multiple phases and the trapping of fluids by capillary forces. The experiments demonstrated systematic behavior that depends on relative fluid viscosity and capillary number. We are preparing these results for publication. In another set of microfluidics experiments, we studied calcite precipitation processes similar to what may occur during geologic sequestration. Two fluids bearing calcium and bicarbonate were injected along parallel paths and where they mix a precipitate of calcite formed (Figure 1). We have used lattice Boltzmann modeling methods to simulate this process. Further results are available in [1].

We conducted 3-dimensional fluid displacement with core-flood devices and high-resolution, x-ray computed tomography to observe multiphase behavior in a heterogeneous sintered glass bead porous medium. The *in situ* tomographic images permitted analysis of fluid drainage and imbibition processes for three sets of fluids: air-water, octane-water and light oil-water. These span a range of interfacial tensions, densities, and viscosities that allow our team to probe analogs to the CO_2-brine system for the effects of interfacial tension, viscosity, and flow rate on trapping of fluids by capillary forces. See [2] for more details.

Density-induced mixing of CO_2-laden waters is one of the most hotly debated subjects in sequestration. Much theoretical work has been conducted but no experiments. We have constructed a Hele-Shaw cell (transparent 2-D plate; Figure 2) for examining density-induced advection of fluids that are analogs to density-induced mixing of CO_2-saturated brine in geologic reservoirs. We used the water-propylene glycol system, which is miscible and produces solutions denser than either phase. Photographs allowed the team to measure enhanced mixing of the fluids due to gravitationally driven mixing; numerical simulations demonstrated our ability to model the onset of advection and will allow application to the CO_2 sequestration problem. See [3] for more details.

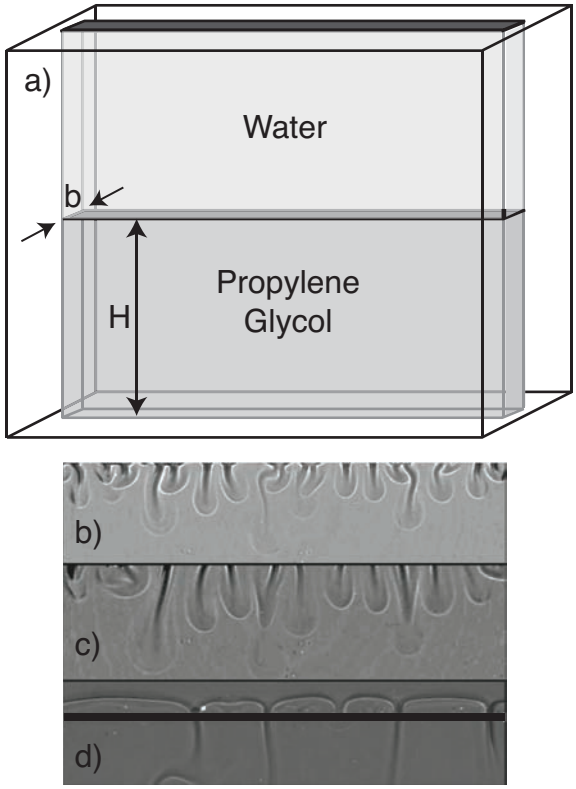

Figure 2. Schematic diagram of Hele-Shaw cell showing initial state with water above polypropylene glycol (a). Three photographs at differing times showing development of density-induced mixing as water dissolves into polypropylene glycol (b, c, and d).

We use computer simulations to develop and demonstrate understanding of our experimental systems. We also use these to extend the experiments to long time periods that are inaccessible within the laboratory. At fine scales (< 1 cm), we have continued the development of our lattice Boltzmann method as we move toward our goal of a 3-D, parallel multicomponent, multiphase reactive code. This work includes simulations of multicomponent pore-scale precipitation processes (e.g. Figure 1 and [1]) and multiphase displacement patterns observed in microfluidics experiments

We are integrating fine-scale phenomena with large-scale simulations using a hybrid modeling approach. At the lattice Boltzmann scale, we are using quad tree methods to locally refine grids and have benchmarked this against classical vorticity simulations (Figure 3; [4]). At larger scales, we are using a mimetic finite difference approach to local grid refinement. This method uses error analysis to velocity fields to automatically identify regions of the grid that require higher resolution. This will lead the way to an automated grid refinement process. At the

continuum scale, we have developed a flash method for variable switching that will work more efficiently with our adaptive mesh refinement methods. We have also recently submitted a manuscript in which we have developed a kinetic-continuum hybrid theory for modeling of complex fluid transport. This generalizes previous hybrid approaches based on a particularly specified lattice Boltzmann model and finite-difference/finite-volume numerical solver, ensuring that our hybrid modeling strategy will be valid for a wider range of fluid transport processes. This hybrid theory will be an important building block for coupling the pore-scale and continuum-scale codes. See [5] for more details.

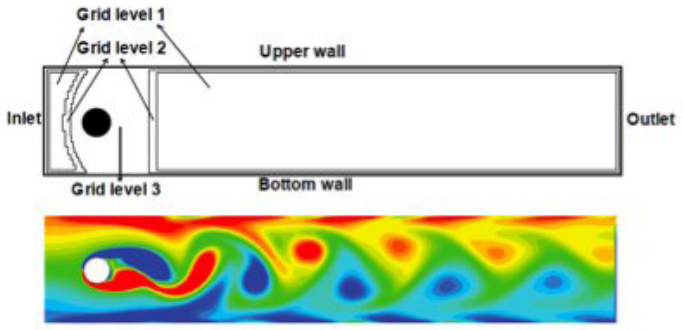

Figure 3. Lattice Boltzmann simulation of flow over an asymmetrically placed cylinder in a channel using the quadtree method of grid refinement. Top: grid distribution; Bottom: Vorticity contours

Future Work

The first year's work has been dominated by experiments on analog fluid systems and development of computational capabilities. In our second year, we will begin conducting experiments on supercritical CO_2 systems at high-pressure and temperature using our microfluidics and core-flood facilities. Optical and tomographic imaging will provide some of the first direct observations of the dynamics of CO_2-brine interaction within porous media. These novel experiments will provide benchmarking data for our hybrid modeling approach, in which we incorporate pore-scale phenomena in large-scale simulations.

Conclusion

We have made substantial progress in experimental investigations of analog systems to the CO_2-brine-water system using microfluidics, x-ray tomography, and Hele-Shaw methods to elucidate multiphase fluid flow and reaction. These experiments were used in the development of sophisticated numerical simulations conducted on a range of scales designed to allow quantitative prediction of multiphase processes in the subsurface. As we develop these tools further and apply them to supercritical CO_2 storage, we will form the basis of engineering CO_2 injection projects to minimize the mobility of CO_2. The direct observations allow validation of predictive computer codes, which will ultimately be used to evaluate the long-term effectiveness of CO_2 sequestration as a means of mitigating greenhouse gas-induced warming.

References

1. Zhang, C., K. Dehoff, N. Hess, M. Oostrom, T. Wietsma, A. Valocchi, B. Fouke, and C. Werth. Pore-scale study of transverse mixing induced $CaCO_3$ precipitation and permeability reduction in a model subsurface sedimentary system. 2010. *Environmental Science and Technology.* **44** (20): 7833.

2. Wildenschild, D., R. T. Armstrong, A. L. Herring, I. M. Young, and J. W. Carey. . Exploring capillary trapping efficiency as a function of interfacial tension, viscosity, and flow rate. (Amsterdam, 19-23 September 2010).

3. Backhaus, S.. Laboratory measurements of large-scale carbon sequestration flows in saline reservoirs. *Physical Review Letters.*

4. Chen, Y., Q. Kang, Q. Kai, and D. Zhang. Lattice Boltzmann method on quadtree grids. *Physical Review E.*

5. Shi, Y., Q. Kang, and P. C. Lichtner. Theory of kinetic-continuum hybrid modeling for complex multiscale fluid transport: Use of lattice Boltzmann method coupled with conventional continuum numerical methods. *Physical Review E.*

Publications

Backhaus, S.. Laboratory measurements of large-scale carbon sequestration flows in saline reservoirs. *Physical Review Letters.*

Chen, Y., Q. Kang, Q. Kai, and D. Zhang. Lattice Boltzmann method on quadtree grids. *Physical Review E.*

Kang, Q., P. C. Lichtner, and D. R. Janecky. Lattice Boltzmann method for reacting flows in porous media. 2010. *Advances in Applied Mathematics and Mechanics.* **2** (5): 545.

Lipnikov, K., D. Moulton, and D. Svyatskiy. {Multilevel multiscale mimetic (M3) method for two-phase flows in porous media. *SIAM Multiscale Modeling and Simulation .*

Shi, Y., Q. Kang, and P. C. Lichtner. Theory of kinetic-continuum hybrid modeling for complex multiscale fluid transport: Use of lattice Boltzmann method coupled with conventional continuum numerical methods. *Physical Review E.*

Wildenschild, D., R. T. Armstrong, A. L. Herring, I. M. Young, and J. W. Carey. . Exploring capillary trapping efficiency as a function of interfacial tension, viscosity, and flow rate. To appear in *10th Greenhouse Gas and*

Technology Conference. (Amsterdam, 19-23 September 2010).

Zhang, C., K. Dehoff, N. Hess, M. Oostrom, T. Wietsma, A. Valocchi, B. Fouke, and C. Werth. Pore-scale study of transverse mixing induced $CaCO_3$ precipitation and permeability reduction in a model subsurface sedimentary system. 2010. *Environmental Science and Technology.* **44** (20): 7833.

Transformative Bioassessment of Engineered Nanomaterials: Materials by Design

Rashi S. Iyer
20100027DR

Introduction

Engineered nanomaterials (ENMs) provide the potential to address such national and global issues as energy security and weapons of mass destruction through realized and potential applications in energy harvesting, efficient lighting, biomedical science, catalysis, and sensor technologies. The rapid pace of ENM development, however, is outpacing our ability to understand their biological effects. This lack of knowledge is increasingly impacting their potential for 'real-world' applications. It is becoming apparent that the field of toxicology needs to be reinvented to address the field of engineered nanomaterials. Conventional bio-assessment protocol (cell to animal to human) and particle-by-particle analyses are neither sufficiently accurate nor rapid. Thus, a concerted and systematic effort/capability is needed to address this issue. To fully realize the potential of ENMs, future development will ideally be informed by both function/application and health considerations, where the latter will ultimately determine the feasibility of use as production scales increase and new regulations are introduced. Based on our unique combination of capabilities (biology, materials science and computational), LANL has the ability to lead the emerging field of nanotoxicology and to enable the intelligent design of new ENMs possessing controlled bioimpact. We propose an unprecedented approach that couples innovative and highly relevant artificially reconstructed human tissue equivalents with powerful computational methods. The expected outcome is a sophisticated and world-class biological interrogation system that will represent a unique capacity to facilitate the design of 'high-function biosafe' nanomaterials.

Benefit to National Security Missions

Engineered nanomaterials address national and global issues such as energy security and WMD through applications in energy harvesting, efficient lighting, biomedicine, catalysis, and sensor technologies. Our unprecedented approach couples innovative reconstructed human tissue equivalents with powerful computational methods. The expected outcome is a sophisticated and world-class biological interrogation system that will represent a unique capacity to facilitate the design of 'high-function biosafe' nanomaterials. This capability will strategically establish LANL as a premier materials center and realize, to the fullest extent, the potential of DOE's five nanoscience centers while addressing challenges recognized by the NIH and DOD.

Progress

ENMs represent a fascinating new category of 'chemical agent' due to their unprecedented complexity in properties and potential for size-dependent biological interactions. Critically, the potential for bio-impact cannot be assessed by simply knowing the ENM 'chemical formula,' as is essentially the case for traditional chemical threats. Individual particle-by-particle testing using conventional approaches (cell→animal→human) for assessing the bio-impact of chemical agents are grossly inadequate to address the extent of the ENM problem, thus jeopardizing the promise of these materials. The majority of currently funded studies focus primarily on biomedical applications and very little is known on the health impact these new materials may have. The overarching goal of our larger proposed effort was to enable predictive and high-throughput screening of the bio-impact of ENMs. The overall goal of our proposed work is the "Creation of a framework for a streamlined, rapid approach enabling the prediction of 'properties-dependent' ENM biological impact using novel human experimental platforms." This is an unprecedented approach that couples innovative and highly relevant artificially reconstructed human tissue equivalents with powerful computational methods. Importantly, demonstrating the use of a 3-D tissue bio-platform for the rapid assessment of ENMs would immediately establish a new state-of-the-art capability for the toxicological analyses of nanomaterials.

As our model ENM system, we synthesized semiconductor nanomaterials – nanocrystal quantum dots (NQDs) and nanowires; functionalized carboxylated fullerenes, silver nanowires and gold spherical

particles. All synthesized ENMs were characterized using multiple characterization tools. These comprise a technologically important class of ENM for which the physicochemical properties can be precisely controlled using the synthesis and characterization capabilities available in our laboratories (LANL Center for Integrated Nanotechnologies, CINT). The ability to control and knowledgeably characterize the ENM of interest is critical to any systematic study of properties-bioimpact correlations. We evaluated the biochemical and molecular level responses of an in vitro reconstructed 3-D skin and lung tissue on exposure to several classes of nanomaterials (CdSe dots and wires, fullerenes, Au, Ag wires, control polymers). Initial experiments facilitated the validation of our proposed experimental approach, providing a key 'proof-of-principle.' We established basic parameters of exposure (dose and time) to the different ENM types. We performed proteomic and genome level analyses of our exposed tissues. In addition, we established and developed biochemical assays that will be used to interrogate our tissue models. All data obtained from the proteomic experiments were analyzed using the IPA software for pathway and network analysis. Output from the bioinformatic analysis was used to develop multiscale tissue models that comprised of the different levels of data (molecular, cellular and tissue). Our results indicate that there are significant differences in the biological responses as a function of size, shape and composition. Initial correlative studies of cellular responses and physical chemical properties of the selected ENMs suggested a property-dependence bioimpact. We have also made significant progress initiating collaborations with government and industrial partners.

The overarching goal of our effort is the creation of a framework for a streamlined, rapid approach enabling the prediction of "properties-dependent" engineered nanomaterials (ENM) biological impact using novel human experimental platforms. We have made progress on several tasks:

1. Develop Human Tissue Platform for Bioassessment of Reference ENM's.

- We have successfully developed and established the use of artificially reconstructed organ-tissues, specifically lung and skin tissue (Figure 1) experimental systems (representing inhalation and dermal exposure) to precisely assess biological responses to ENM's. We have also developed in house skin tissues with and without a stratum corneum. This enables us to understand the barrier function of skin and its role in the penetration of ENMs in the skin organ and also to extrapolate our results to actual human skin tissue.

- We have synthesized reference ENMs with controlled shapes, sizes and surface chemistries (Figure 2). Each ENM is fully characterized to catalog physicochemical parameters and the impact of the microenvironment on these properties.

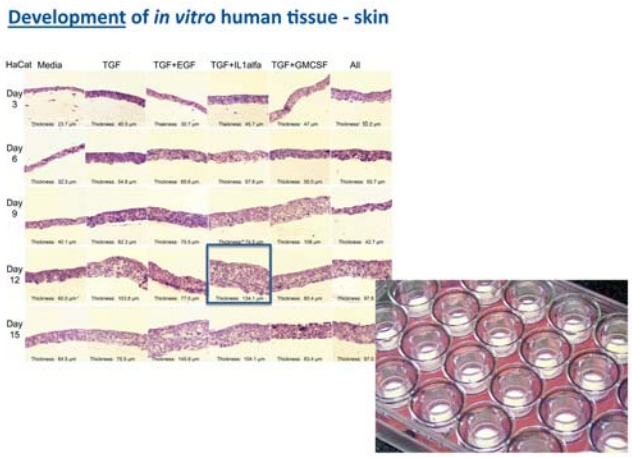

Figure 1. Reconstructing an in-house skin tissue using either HEK or HaCat cell lines. We also use commercially available engineered tissues.

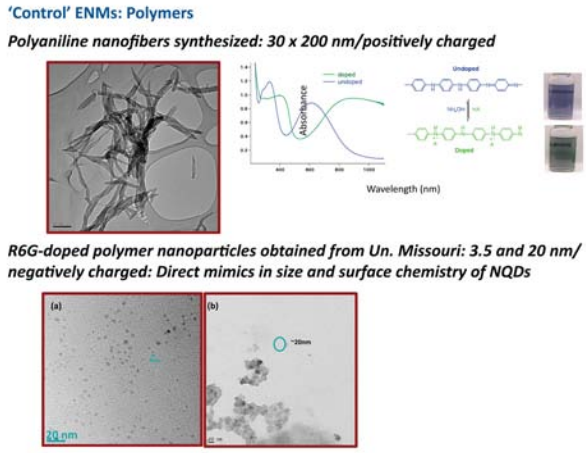

Figure 2. Synthesis and characterization of control polyaniline fibres and RGG-doped polymer nanoparticles for standardization of toxicological analysis.

2. Assess physical interaction and transport in lung and skin tissue using ENMs with controlled size, shape, surface chemistry, and reactivity.

   The goal of this task is to understand the ability of ENMs to penetrate, transport and localize both at the macro- and microscale of the tissue. We employed both experimental and modeling tools to elucidate the physical interaction and transport of ENMs in dermal and lung tissue. Initial experiments indicate that the interaction and penetration of CdSe quantum dots might be a function of their charge.

3. Toxicological assessment of ENMs: Pathological responses and identification of signature molecular responses for mechanistic-level understanding. This task includes the investigation of properties-dependent ENM biological responses at the tissue, cellular and molecular level followed by a systematic bioinformatic analysis and profiling of the experimental data. ENMs were screened to determine their potential to induce overt toxic responses and monitor molecular level responses in exposed tissue. In preliminary experiments, the size and shape of the ENM appeared to have a significant impact on the degree of toxicity. Our results suggest that positively charged QDs are significantly more toxic that the negatively charged QDs. In addition, 3- and 4-nm sized QDs are relatively more toxic than the 5-nm sized QDs.

4. Multiscale modeling of tissue responses: Towards a predictive capability. In this task we will develop an integrated tissue modeling framework called 'Hierarchial Interrogative Computational Tissue Model' (HIT). HIT will incorporate ENM distribution, membrane interactions, effects at the molecular, cellular and tissue level, and correlate them with physiological changes of cells and tissues (Figure 3). Based on our initial observations we have developed a mutliscale model that incorporates the experimental observation obtained from task 1 and 2.

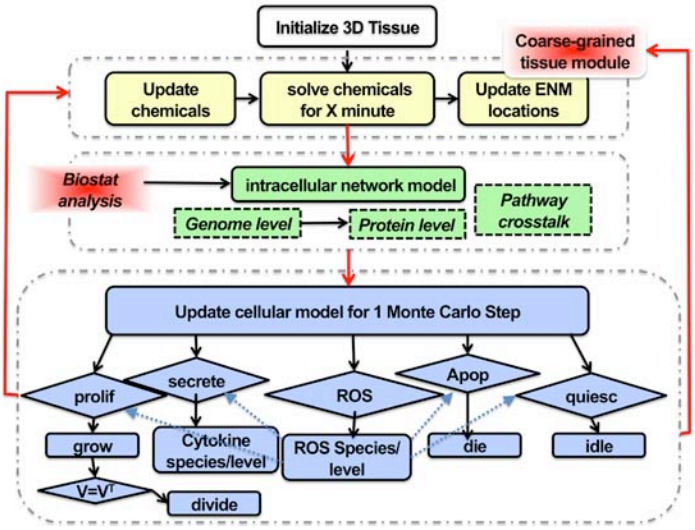

Figure 3. Multiscale tissue model of nanobio-interactions.

Conclusion

The nation has a vested interest in enabling the uninterrupted advancement of nanotechnology in order to accomplish our goals of national security and public health through aggressive and immediate actions in addressing the challenge of nanomaterial risk assessment. We will couple our innovative organ-tissue bio-model with multi-scale computational approaches toward enabling predictive nanotoxicology. Finally, while significantly simplifying the scope of bio-analysis, our approach will enable the consideration of 'bio-impact' as part of materials design strategies.

One-Step Biomass Conversion: Looking to Nature for Solutions to Energy Security

Paul A. Langan
20080001DR

Abstract

Cellulosic biomass is the fibrous material derived from plant cell walls. Comprised of lignin, hemicellulose and cellulose in varying ratios dependant on crop, the components of biomass can serve as a source of carbon-based feedstock for fuel and chemical production in much the same way as crude oil serves as the carbon feedstock in petrochemical refineries, partially replacing these conventional refineries. However, the conversion of biomass into simple fermentable sugars constitutes a core barrier for producing products from this biomass platform. The main aim of this project was to develop innovative science and technology to pretreat biomass so that it can be cost-effectively converted into sugars and other products. Our research plan was organized into three goal-oriented objectives and was executed through five technical thrusts each with a leader. An important part of our approach was the establishment of collaborations in order to bring on board key expertise and capabilities that complemented those at Los Alamos. Significant technical achievements have been reported in over 30 publications, have resulted in a patent being filed, the award of several tens of millions of dollars worth of experimental beam time at central X-ray and neutron facilities throughout the world, several awards, news releases and highlights, and have produced five front cover articles. Importantly, these accomplishments have led to several new promising leads for more efficient pretreatment strategies.

Background and Research Objectives

Biofuels are an alternative to conventional energy sources that increase our Nation's energy security by reducing dependence on imported oil. Our growing biofuels industry is largely based on the use of starch in grains such as corn to produce ethanol. However, there are advantages in using cellulosic biomass as an alternative feed stock, and in producing more advanced biofuels and bioproducts than ethanol. Biomass is the fibrous material derived from plant cell walls [35]. Comprised of lignin, hemicellulose, and cellulose in varying ratios dependant on crop, the components of biomass can serve as a source of carbon-based feedstock for fuel and chemical production in much the same way as crude oil serves as the carbon feedstock in petrochemical refineries, partially replacing these conventional refineries. The development of biofuels and other bioproducts from biomass has attracted considerable commercial and government investment. Early results from these efforts indicate that many factors are important at different points in the life cycle of a biomass process, and contribute towards its overall cost-competitiveness. *However, it remains clear that converting biomass into fermentable sugars is the main cost-burden.*

The cellulosic part of biomass is difficult to break down into sugars because of its crystalline fibrous nature [36]. Furthermore, cellulose fibers are encrusted in the branched polymers of hemicellulose and lignin. Lignin adds structural rigidity to plant cell walls, but it also protects the cellulosic component from hydrolyzing enzymes that can release sugars [37]. Several different approaches are being developed to pretreat biomass so that its complex architecture can be disrupted, thereby making it accessible to water and enzymes for an accelerated conversion to sugar. These include dilute acid, steam explosion, hydrothermal processes, organic solvents in aqueous media, biological and enzymatic processes, ammonia fiber explosion (AFEX), strong alkali processes, ionic liquids (ILs) ,and highly-concentrated acid treatment [38]. *The main aim of this project was to develop innovative science and technology to pretreat biomass so that it can be cost-effectively converted into sugars and other products.* However, we wanted to do this not through incremental improvements, but by a revolution in cost-efficiency through a scientific breakthrough in our approach to pretreatment.

We started looking for this breakthrough in nature. Although many fungi degrade parts of the cell wall, white rot fungi are unique in their ability to degrade it completely. Our initial focus was on identifying the key lignin degradation mechanisms of the fungus *P. chrysosporium* and then combining them with depolymerizing enzymes in a consolidated biomass conversion process. Our research plan was organized into three goal-oriented sections that address the following major objectives.

1. Define the key cofactors, mediators, and enzymes in the fungal degradation of lignin.

2. Characterize the structure of biomass and how it is degraded by interaction with these cofactors, mediators, and enzymes.

3. Combine key cofactors, mediators, and enzymes with cellulases and hemicellulases in a consolidated biomass conversion process.

This plan was executed through several technical thrusts each with a leader. The use of multidisciplinary thrusts positioned us in a complementary but competitive way to larger biofuels programs and allowed us to be responsive to diverse opportunities. We have been able to submit proposals for several spin-off projects and collaborations.

Another important part of our approach was the establishment of collaborations, Memo's of Undertsanding (MOUs), subcontracts, and Non-Disclosure Agreements (NDAs) in order to bring on board key expertise and capabilities that complemented those at Los Alamos; an MOU with Ken Hammel's group at USDA Forest Products Laboratory (FPL) allowed us to make significant progress towards meeting objective 1 [6, 8-13,34], collaborations with Al French's group at USDA Agricultural Research Service (ARS), Yoshi Nishiyama at the Center for Biomass Studies (CERMAV) in Grenoble University, Pat Mariano's group at the University of New Mexico (UNM), and Masahisa Wada's group at the department of Wood Science Group in Tokyo University allowed is to make significant progress towards objective 2 [1-5,7, 15-20, 22, 23, 25, 29, 30].

In the last year of the project our objectives were modified. This was because although we had found a number of novel mediators for one family of lignin degrading enzymes called lignin peroxidases (LiPs) it looked unlikely that they would perform better than the well-known putative mediator of LiP, veratryl alcohol (VA). Furthermore it also looked unlikely that LiP could be produced in industrially relevant quantities. We therefore decided to switch focus to another family of lignin degrading enzymes called manganese peroxidase (MnP), which are known to use Mn as a mediator. Our current efforts to understand the action of MnP are progressing well [10] and our project has contributed strongly to other projects that involve the development of oxidizing metal-based chemical pretreatments and which are looking promising [LDRD DR20100089].

Although we switched priorities from LiP to MnP in the last year we have recently made significant progress in developing a system for producing LiP in the lab, and in identifying the key mechanisms of how it degrades lignin [20]. These advances are of potential significance for genetically altering the lignin composition of plants to enhance degradation and for making bioproducts from lignin.

Our objectives were also broadened in the last year to include the development and optimization of other types of pretreatments. Collaboration with Connie Schall's group at Toledo University allowed us to make important fundamental discoveries about the treatment of biomass with ILs [18, 19]. Collaboration with the DOE funded Great Lakes Bioenergy Research Center (GLBRC) allowed us to develop a proposed modification to the AFEX pretreatment process that has the potential to significantly increase its efficiency [21, 33]. In this same collaboration we made important progress towards objective 3 and the co-optimization of pretreatments and cocktails of enzymes.

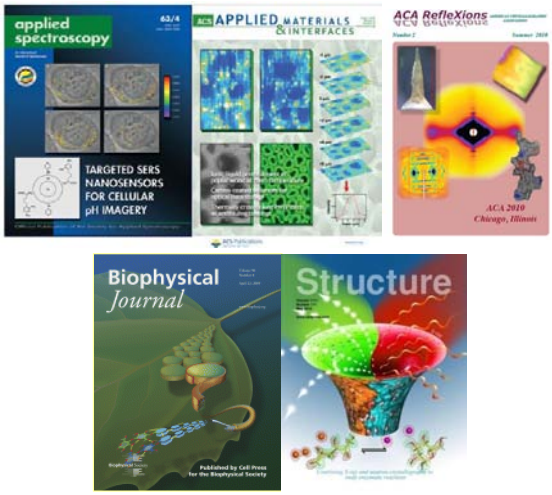

Figure 1. Cover artwork from Applied Spectroscopy 2009, American Chemical Society Applied Materials and Interfaces 2010, the American Crystallographic Association Reflexions 2010, the Biophysical Journal 2009 and Structure 2010.

Scientific Approach and Accomplishments

The technical approach taken by the project was organized into five thrusts:

1. Fungal cultures and mass spectrometry (MS) degradomics

2. Theory

3. Multiplatform microspectroscopy

4. Enzyme science

5. Crystallography

The most significant technical accomplishments are described below. These accomplishments have been reported in over 30 publications, have resulted in a patent being filed, the award of several tens of millions of dollars worth of experimental beam time at central X-ray and neutron facilities throughout the world, several awards and news releases and highlights from LANL, USDA and other institutions, and have produced five front cover articles, Figure 1. A Website has been constructed with information about

our capabilities. We were directly involved in the organization of a conference "Energy for the 21st Century" Santa Fe May 2009 and a special session "Renewable Energy and the Environment" at the "International Conference on Neutrons in Biology" Santa Fe, October 2009 which highlighted work from this project. *Importantly, these accomplishments have led to several new promising leads for more efficient pretreatment strategies.*

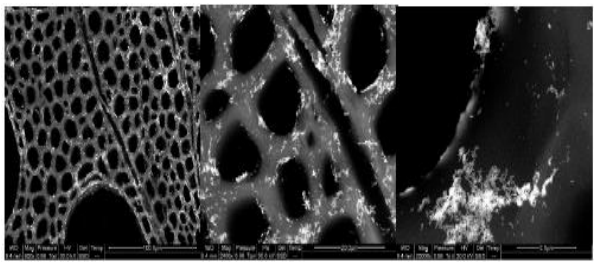

Figure 2. Ionic liquid-swollen -Au nanoparticle impregnated poplar at magnitudes (L-R) 600x, 2400x and 20000x. Bright spots are 40 nm Au nanoparticles.

Microscopy

The microscopy thrust was to employ a series of microscopic platforms to study the structural properties of biomass (poplar), and its response to fungal, chemical and/or biochemical treatments. A highlight was our time lapse microscopic movies of the swelling and buckling of poplar biomass as it was treated with IL 1-ethyl-3-methylimidazolium acetate [19]. Swelling reaches a maximum at two hours after treatment and can then be reversed with the expulsion of the IL simply with water. Interestingly, we have discovered that this effect can serve as a general approach to introduce chemicals and materials into the cell wall structures, see Figure 2 [18]. We used XRF spectroscopy to quantify uptake and confocal NIR SERS microscopy to verify penetration of particles up to 4μm into the poplar cell wall. This work was submitted in a patent disclosure, S121057 "Ionic liquid pretreatment of poplar wood at room temperature: Swelling and incorporation of nanoparticles" United States as a Provisional Patent Application (2010). We have also performed measurements indicating that the IL/Au- and IL/Ag- impregnated poplar samples may show enhanced destruction under conventional microwave oven action over controls. If confirmed, this new pretreatment strategy using industrial microwave ovens may be cost effective at scale-up. We have also shown that impregnated samples when subjected to surface-enhanced Raman microscopy show a strong surface-enhanced effect. This technique can be used to significantly increase the speed in Raman microscopy image acquisition, as well as the ability to place nanosensors at the cell wall to measure chemical environment at the wall during fungal or biochemical treatments. This technique proved to be generally applicable to biochemical analysis [16, 17].

Another highlight has been work done in collaboration with another LDRD-DR project (DR20100089) in which we have been investigating various metallic oxidizing agents to delignify poplar biomass at room temperature, including V-based complexes. We have performed microscopic characterization of more than 10 specific compounds, as well as investigated the roles or addition of peroxide or control of pH. Our results show that some of these compounds in the proper conditions invoke rapid release of gas from the poplar surface and over time oxidize the macroscopic material to much smaller clusters which appear to be relatively purified cellulose. Work is continuing to optimize conditions. This method has the potential to simplify or eliminate the need for enzyme cocktails in biomass pretreatment.

Theory

Novel computational studies were performed at both atomistic and coarse-grain scales to investigate the stability of cellulose under different conditions and also to investigate to what extent this stability is controlled by hydrogen bonding. The combination of theoretic studies with experimental results from our crystallographic thrust is a major scientific success story and has been highlighted in LANL and USDA news releases, and reported by news agencies worldwide. These studies involved developing and applying for the first time statistical mechanical methods and Replica Exchange Molecular Dynamics simulations to oligosaccharides [3, 5, 7, 15, 22, 25, 26]. Other significant successes included the combination of quantum mechanics with kinetic analysis and enzyme catalyzed studies (with our collaborators at UNM) to understand bond cleavage in lignin [20] as shown in Figure 3, and the combination of theory with enzymatic studies of cocktails to understand and optimize AFEX pretreatment [21, 33].

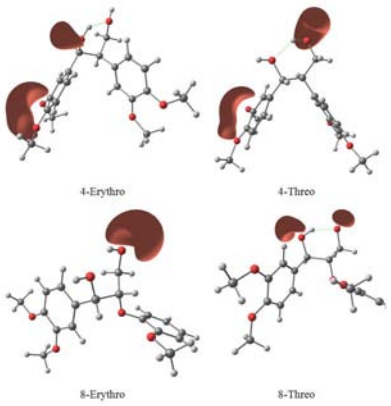

Figure 3. The oxidative cleavage of different bonds in lignin was investigated by synthesizing different fragments of lignin and then using different chemical and LiP enzymatic experimental methods to cleave them. These experimental results were combined with theoretical quantum mechanics calculations to produce a predictive understanding of lignin. In this figure some of these lignin fragments with an electrostatic potential map (in red) are shown [20].

Crystallography

A unique capability at Los Alamos is our neutron Protein Crystallography Station (PCS) which is being used to elucidate the mechanisms of enzymes involved in the production of biofuels including xylanases and xylose isomerase [14, 24, 28]. However, other central X-ray and neutron facilities are being used [4, 19, 23, 27]. A success of this thrust has been its contribution to creating an X-ray scanning microprobe community at BioCAT at the Advanced Photon Source (APS) of Argonne National Laboratory, the first of its kind in the USA. Our work in using this technique to understand biomass has provided new insights into biomass structure and its conversion during pretreatment with IL, amines, and fungal enzymes [1-4, 19, 23, 26, 27]. Results from this thrust are closely integrated with those from the theory and microscopy thrusts. In particular, fundamental insights provided by this thrust on the structure of cellulose (Figure 4) and how it changes during pretreatment have contributed greatly toward the proposed development of a more efficient AFEX pretreatment.

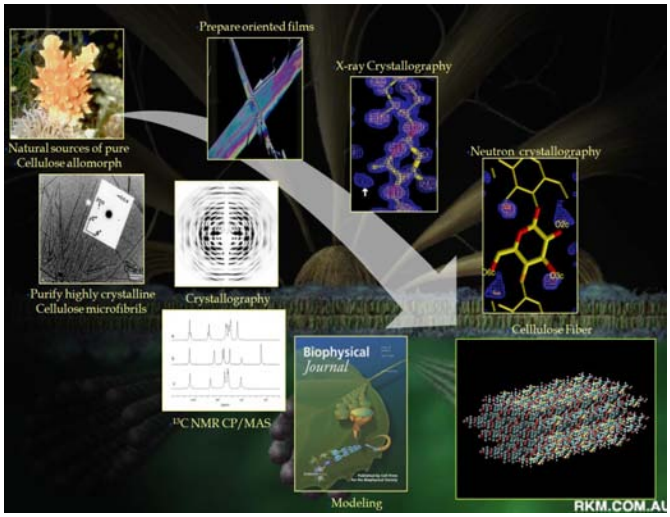

Figure 4. This figure represents how in the crystallography thrust several experimental methods including X-ray crystallography, neutron crystallography, electron microscopy and NMR are combined with theory to obtain a complete structural and dynamic understanding of cellulose fibers and how they change during pretreatment.

Enzyme Science

A long sought after success for this thrust was the establishment of a liquid fungal culturing system in order to produce ligninolytic and non-ligninolytic conditions. This system is now operational and producing LiP enzymes. Expression of active LiP in bacteria proved more problematic. It became clear in this thrust that large quantities of LiP necessary to be industrially relevant would not be possible with current technologies. More success was obtained in our studies of optimizing cocktails of cellulose and hemicelluloses degrading enzymes. With our collaborators at GLBRC we found that by optimizing AFEX pretreatment condition with enzyme cocktails we could obtain a significant increase in the efficiency of the conversion of biomass to sugars, a promising result with important implications [21, 33], Figure 5. Building on the ground work and progress achieved in this area the thrust leader, David Fox, was awarded an LDRD Early Career Investigator Award that has close ties to this project.

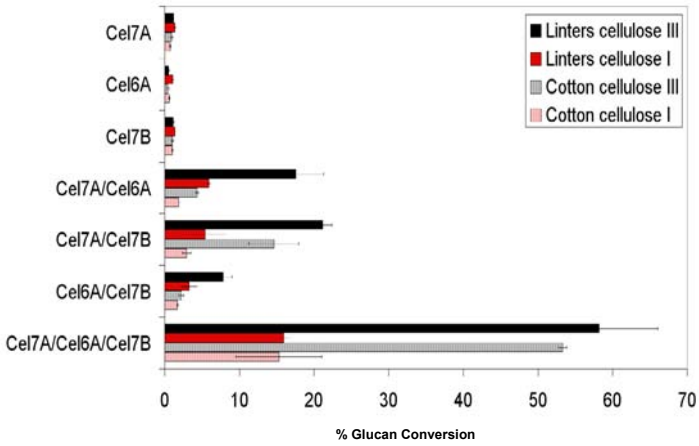

Figure 5. Optimizing AFEX pretreatment to produce cellulose III rather than cellulose I, and different cocktails of the enzymes Cel7A, Cel6A, and Cel7A significantly increases the efficiency of biomass conversion. This figure is from [33].

Fungal cultures and MS degradomics

Our MOU with USDA FPL focused on the production of metabolites that fungi secrete into their surroundings to deconstruct lignocellulosic biomass. Several compounds were identified, with one fungus secreting a previously unknown metabolite. This metabolite is aromatic, as shown by the finding that it becomes radiolabeled when ^{14}C-labeled phenylalanine is supplied to the wood cultures. In associated work, we have identified a transporter protein, located in the cell membrane of *P. chrysosporium*, which is up-regulated during ligninolytic metabolism and thus may have a role in the secretion of biodegradative metabolites. Also identified during this study was a ligninolytically up-regulated, membrane-associated alcohol oxidase which likely has a role in production of the hydrogen peroxide needed to support the action of lignin-degrading peroxidases during wood deconstruction by *P. chrysosporium*.

In summary several promising results have been obtained in each of our technical thrusts with important implications for optimized pretreatments. Several very productive collaborations have been established to bring expertise and capabilities into this program to complement what already exists at Los Alamos. These promising results and productive collaborations have resulted in several follow on projects, some already funded, others anticipated.

Impact on National Missions

The technology leads developed in this project contribute towards Laboratory missions and grand challenges in en-

ergy security and carbon neutron fuel cycles. Importantly, this project has contributed greatly to follow-up projects based on the multidisciplinary technologies developed. Several are already funded and some anticipate funding. In particular, this project played an important role in laying the foundation for LANL leadership in the National Alliance for Advanced Biofuels and Bioproducts, a multi-institute consortium that was recently awarded $44M of funding from the American Reinvestment Recovery Act.

References

1. Wada, M., Y. Nishiyama, H. Chanzy, T. Forsyth, and P. Langan. The structures of cellulose. 2008. *Powder diffraction.* **23** (2): 92.

2. Wada, M., Y. Nishiyama, H. Chanzy, T. Forsyth, and P. Langan. The structures of celluloses. 2008. *Advances in X-ray Analysis.* **51**: 138.

3. Nishiyama, Y., G. Johnson, A. French, T. Forsyth, and P. Langan. Neutron crystallography, molecular dynamics, and quantum mechanics studies of the nature of hydrogen bonding in cellulose Ib. 2008. *Biomacromolecules.* **9**: 3133.

4. Wada, M., L. Heux, Y. Nishiyama, and P. Langan. X-ray crystallographic, scanning microprobe X-ray diffraction, and cross-polarized/magic angle spinning 13C nuclear magnetic resonance studies of the structure of cellulose III(II). 2009. *Biomacromolecules.* **10**: 302.

5. Shen, T., and G. Gnanakaran. The stability of cellulose: A perspective from the statistical mechanics of hydrogen bond networks. 2009. *Biophysical Journal.* **96**: 3032.

6. Shary, S., A. Kapich, E. Panisko, J. Magnuson, D. Cullen, and K. Hammel. Differential expression in Phanerochaete chrysosporium of membrane-associated proteins relevant to lignin degradation. 2008. *Applied and Environmental Microbiology.* **23**: 7252.

7. Shen, T., P. Langan, A. French, G. Johnson, and S. Gnanakaran. Conformational flexibility of soluble cellulose oligomers: chain length and temperature dependance. 2009. *Journal of the American Chemical Society.* **131**: 14786.

8. Martinez, D., J. Challacombe, I. Morgenstern, and E. Tal. Genome transcriptome and secretome analysis of wood decay fungus Postia placenta supports unique mechanisms of lignocellulosic conversion. 2009. *Proc. Nat. Acad. Sci. USA .* **106**: 1954.

9. Yelle, D., K. Hammel, J. Ralph, and F. Lu. Evidence for cleavage of lignin by a brown rot basidiomycete. 2008. *Environ. Biol. .* **10**: 1844.

10. Hammel, K., and D. Cullen. Role of fungal peroxidases in biological lignolysis. 2008. *Curr. Opin. Plant. Biol..* **11**: 349.

11. Kinne, M., M. Poraj-Kobielska, S. Ralph, M. Hofrichter, and K. Hammel. Oxidative ether cleavage by an extracellular fungal peroxugenase. 2009. *J. Biol. Chem..* **284**: 29343.

12. Kinne, M., R. Ullrich, K. Hammel, K. Scheibner, and M. Hofrichter. Regioselective preparation of (R)-2-(4-hydroxyphenoxy)propionic acid with a fungal peroxygenase. 2008. *Tetrahedron Letters .* **49**: 5950.

13. Kinne, M., M. Poraj-Kobielska, E. Aranda, R. Ullrich, and K. Hammel. Regioselective preparation of 5-hydroxypropranolol and 4 ‘-hydroxydiclofenac with a fungal peroxygenase . 2009. *Bioorganic & Medicinal Chemistry Letters .* **19**: 3085.

14. Kovalevsky, A., A. Katz, H. Carrell, L. Hanson, M. Mustyakimov, S. Fisher, L. Coates, B. Schoenborn, G. Bunick, J. Glusker, and P. Langan. Hydrogen location in stages of an enzyme catalyzed reaction: time of flight neutron structure of D-xylose isomerase with bound D-xylulose. 2008. *Biochemistry.* **47**: 7595.

15. Shen, T., P. Langan, S. Gnanakaran, A. French, and G. Johnson. Shift in conformational flexibility of soluble cellulose oligomers with increasing chain length. 2008. (Salt Lake City, 22-26 March 2009). p. 2008. Salt Lake City: Journal of the American Chem Soc..

16. Nowak-Lovato, K., B. Wilson, and K. Rector. SERS nanosensors that report pH of endocytic compartments during FceRI transit. To appear in *Analytical and Bioanalytical Chemistry.*

17. Nowak-Lovato, K., and K. Rector. Targeted Surface-Enhanced Raman Scattering Nanosensors for Whole-Cell pH Imagery. 2009. *Applied Spectroscopy .* **63** (4): 387.

18. Lucas, M., B. Macdonald, G. Wagner, S. Joyce, and K. Rector. Ionic liquid pretreatment of poplar wood at room temperature: Swelling and incorporation of nanoparticles. 2010. *Applied Materials and Interfaces.* **2** (8): 2198.

19. Lucas, M., G. Wagner, Y. Nishiyama, L. Hanson, I. Samayam, C. Schall, P. Langan, and K. Rector. Reversible swelling of the cell wall of poplar biomass by ionic liquid at room temperature. *Bioresource Technology .*

20. Cho, D., R. Parthasarathi, A. Pimentel, G. Maestas, H. Park, U. Yoon, D. Dunnaway-Mariano, S. Gnanakaran, P. Langan, and P. Mariano. The Nature and Kinetic Analysis of Carbon-Carbon Bond Fragmentation Reactions of Cation Radicals Derived from SET-Oxidation of Lignin Model Compounds. To appear in *Journal of Organic Chemistry.*

21. Chundawat, S., and E. Tal. Physicochemical characterization of alkali-pretreated lignocellulosic biomass. 2010. *Genomic Science: Systems biology for energy and the environment DOE/SC-0122 .*

22. Shen, T., S. Gnanakaran, P. Langan, A. French, and G. Johnson. Conformational variability of soluble cellulose oligomers. 2010. *Science Highlights of the TSC Directorate of Theory, Simulation, and Computation LA-UR-10-01992.*

23. Langan, P.. Getting to know Cellulose. 2010. *Annual science report of the Advanced Photon Source, Argonne National Laboratory, ISSN 1931-5007.*

24. Kovalevsky, A., Z. Fisher, H. Johnson, M. Mustyakimov, M. Waltman, and P. Langan. Preliminary Joint X-ray and Neutron Protein Crystallographic Studies of Endoxylanase II from fungus Trichoderma longibrachiatum. *Acta Crystallographica F.*

25. Bellesia, G., A. Asztalos, T. Shen, P. Langan, A. Redondo, and S. Gnanakaran. In Silico studies of crystalline cellulose and its degradation by enzymes. To appear in *Acta Crystallographica D.*

26. Wada, M., Y. Nishiyama, G. Bellesia, T. Forsyth, S. Gnanakaran, and P. Langan. Rearrangement of Hydrogen Bonding during the Treatment of Cellulose with Ammonia: Neutron Crystallographic Structure of Ammonia-Cellulose I. *Journal of the American Chemical Society.*

27. Nishiyama, Y., M. Wada, L. Hanson, and P. Langan. Time-resolved X-ray diffraction microprobe studies of the conversion of cellulose I to ethylenediamine-cellulose I. 2010. *Cellulose.* **17**: 735.

28. Kovalevsky, A., L. Hanson, S. Fisher, S. Mason, T. Forsyth, M. Mustyakimov, M. Blakeley, D. Kean, J. Glusker, and P. Langan. Metal ion roles and the movement of hydrogen during reaction catalyzed by D-Xylose Isomerase: a joint X-ray and neutron diffraction study. 2010. *Structure.* **18**: 688.

29. Wada, M., L. Heux, Y. Nishiyama, and P. Langan. X-ray crystallographic and cross-polarized/magic angle spinning 13C nuclear magnetic resonance studies of the structure of the complex of cellulose I with EDA. 2009. *Cellulsoe.* **16**: 943.

30. Nishiyama, Y., P. Langan, and T. Forsyth. Looking at hydrogen bonds in cellulose. To appear in *Acta Crystallographica D.*

31. Rickman, J.. LANL NEWS RELEASE: Breaking the ties that bind cellulose. 2009. *LANL NEWS RELEASE.*

32. Bliss, R.. NEWS RELEASE: Inside look at cellulose provides insights into cotton crystals. 2009. *NEWS & EVENTS USDA ARS.*

33. Chundawat, S., G. Bellesia, N. Uppugundle, L. de Costa Sousa, D. Gao, A. Cheh, C. Bianchetti, S. Gnanakaran, P. Langan, G. Phillips, V. Balan, and B. Dale. Restructuring hydrogen bond network within crystalline cellulose enhances its depolymerization kinetics. *Proceedings of the national academy of sciences USA..*

34. Wei, D., C. Houtman, A. Kapich, C. Hunt, D. Cullen, and K. Hammel. Laccase and its role in production of extracellular reactive oxygen species during wood decay by the brown rot basidiomycete Postia placenta. . 2010. *Applied Environmental Microbiology .* **76** (7): 2091.

35. Caroll, A., and C. Somerville. Cellulosic biofuels. 2009. *Annual Reviews in Plant Biology.* **60**: 651.

36. Chen, Y., A. Stipanovic, W. Winter, D. Wilson, and Y. Kim. Effect of digestion by pure cellulose on crystallinity and average chain length for bacterial and microcrystalline celluloses. 2007. *Cellulose .* **14**: 283.

37. Chandra, R., R. Bura, W. Mabee, A. Berlin, B. Pan, and J. Sadler. Substrate pretreatment: The key to effective enzymatic hydrolysis of lignocellulosics?. 007. *Biofuels.* **108**: 67.

38. Yang, B., and C. Wyman. Pretreatment: the key to unlocking low-cost cellulosic ethanol. 2008. *Biofuels bioproducts & Biorefining.* **2** (1): 26.a

Publications

Bellesia, G., A. Asztalos, T. Shen, P. Langan, A. Redondo, and S. Gnanakaran. In Silico studies of crystalline cellulose and its degradation by enzymes. To appear in *Acta Crystallographica D.*

Bliss, R.. NEWS RELEASE: Inside look at cellulose provides insights into cotton crystals. 2009. *NEWS & EVENTS USDA ARS.*

Cho, D., R. Parthasarathi, A. Pimentel, G. Maestas, H. Park, U. Yoon, D. Dunnaway-Mariano, S. Gnanakaran, P. Langan, and P. Mariano. The Nature and Kinetic Analysis of Carbon-Carbon Bond Fragmentation Reactions of Cation Radicals Derived from SET-Oxidation of Lignin Model Compounds. To appear in *Journal of Organic Chemistry.*

Chundawat, S., G. Bellesia, N. Uppugundle, L. de Costa Sousa, D. Gao, A. Cheh, C. Bianchetti, S. Gnanakaran, P. Langan, G. Phillips, V. Balan, and B. Dale. Restructuring hydrogen bond network within crystalline cellulose enhances its depolymerization kinetics. *Proceedings of the national academy of sciences USA..*

Chundawat, S., and E. Tal. Physicochemical characterization of alkali-pretreated lignocellulosic biomass. 2010.

Genomic Science: Systems biology for energy and the environment DOE/SC-0122 .

Hammel, K., and D. Cullen. Role of fungal peroxidases in biological lignolysis. 2008. *Curr. Opin. Plant. Biol..* **11**: 349.

Kinne, M., M. Poraj-Kobielska, E. Aranda, R. Ullrich, and K. Hammel. Regioselective preparation of 5-hydroxypropranolol and 4 '-hydroxydiclofenac with a fungal peroxygenase . 2009. *Bioorganic & Medicinal Chemistry Letters .* **19**: 3085.

Kinne, M., M. Poraj-Kobielska, S. Ralph, M. Hofrichter, and K. Hammel. Oxidative ether cleavage by an extracellular fungal peroxugenase. 2009. *J. Biol. Chem..* **284**: 29343.

Kinne, M., R. Ullrich, K. Hammel, K. Scheibner, and M. Hofrichter. Regioselective preparation of (R)-2-(4-hydroxyphenoxy)propionic acid with a fungal peroxygenase. 2008. *Tetrahedron Letters .* **49**: 5950.

Kovalevsky, A., A. Katz, H. Carrell, L. Hanson, M. Mustyakimov, S. Fisher, L. Coates, B. Schoenborn, G. Bunick, J. Glusker, and P. Langan. Hydrogen location in stages of an enzyme catalyzed reaction: time of flight neutron structure of D-xylose isomerase with bound D-xylulose. 2008. *Biochemistry.* **47**: 7595.

Kovalevsky, A., L. Hanson, S. Fisher, S. Mason, T. Forsyth, M. Mustyakimov, M. Blakeley, D. Kean, J. Glusker, and P. Langan. Metal ion roles and the movement of hydrogen during reaction catalyzed by D-Xylose Isomerase: a joint X-ray and neutron diffraction study. 2010. *Structure.* **18**: 688.

Kovalevsky, A., Z. Fisher, H. Johnson, M. Mustyakimov, M. Waltman, and P. Langan. Preliminary Joint X-ray and Neutron Protein Crystallographic Studies of Endoxylanase II from fungus Trichoderma longibrachiatum. *Acta Crystallographica F.*

Langan, P.. Getting to know Cellulose. 2010. *Annual science report of the Advanced Photon Source, Argonne National Laboratory, ISSN 1931-5007.*

Lucas, M., B. Macdonald, G. Wagner, S. Joyce, and K. Rector. Ionic liquid pretreatment of poplar wood at room temperature: Swelling and incorporation of nanoparticles. 2010. *Applied Materials and Interfaces.* **2** (8): 2198.

Lucas, M., G. Wagner, Y. Nishiyama, L. Hanson, I. Samayam, C. Schall, P. Langan, and K. Rector. Reversible swelling of the cell wall of poplar biomass by ionic liquid at room temperature. *Bioresource Technology .*

Martinez, D., J. Challacombe, I. Morgenstern, and E. Tal. Genome transcriptome and secretome analysis of wood decay fungus Postia placenta supports unique mechanisms of lignocellulosic conversion. 2009. *Proc. Nat. Acad. Sci. USA .* **106**: 1954.

Nishiyama, Y., G. Johnson, A. French, T. Forsyth, and P. Langan. Neutron crystallography, molecular dynamics, and quantum mechanics studies of the nature of hydrogen bonding in cellulose Ib. 2008. *Biomacromolecules.* **9**: 3133.

Nishiyama, Y., M. Wada, L. Hanson, and P. Langan. Time-resolved X-ray diffraction microprobe studies of the conversion of cellulose I to ethylenediamine-cellulose I. 2010. *Cellulose.* **17**: 735.

Nishiyama, Y., P. Langan, and T. Forsyth. Looking at hydrogen bonds in cellulose. To appear in *Acta Crystallographica D.*

Nowak-Lovato, K., B. Wilson, and K. Rector. SERS nanosensors that report pH of endocytic compartments during FceRI transit. To appear in *Analytical and Bioanalytical Chemistry.*

Nowak-Lovato, K., and K. Rector. Targeted Surface-Enhanced Raman Scattering Nanosensors for Whole-Cell pH Imagery. 2009. *Applied Spectroscopy .* **63** (4): 387.

Rickman, J.. LANL NEWS RELEASE: Breaking the ties that bind cellulose. 2009. *LANL NEWS RELEASE.*

Shary, S., A. Kapich, E. Panisko, J. Magnuson, D. Cullen, and K. Hammel. Differential expression in Phanerochaete chrysosporium of membrane-associated proteins relevant to lignin degradation. 2008. *Applied and Environmental Microbiology.* **23**: 7252.

Shen, T., P. Langan, A. French, G. Johnson, and S. Gnanakaran. Conformational flexibility of soluble cellulose oligomers: chain length and temperature dependance. 2009. *Journal of the American Chemical Society.* **131**: 14786.

Shen, T., P. Langan, S. Gnanakaran, A. French, and G. Johnson. Shift in conformational flexibility of soluble cellulose oligomers with increasing chain length. 2008. In *Journal of the American Chemical Society.* (Salt Lake City, 22-26 March 2009). , p. 2008. Salt Lake City: Journal of the American Chem Soc..

Shen, T., S. Gnanakaran, P. Langan, A. French, and G. Johnson. Conformational variability of soluble cellulose oligomers. 2010. *Science Highlights of the TSC Directorate of Theory, Simulation, and Computation LA-UR-10-01992.*

Shen, T., and G. Gnanakaran. The stability of cellulose: A perspective from the statistical mechanics of hydrogen bond networks. 2009. *Biophysical Journal.* **96**: 3032.

Wada, M., L. Heux, Y. Nishiyama, and P. Langan. X-ray crystallographic, scanning microprobe X-ray diffraction, and cross-polarized/magic angle spinning 13C nuclear magnetic resonance studies of the structure of cellulose III(II). 2009. *Biomacromolecules.* **10**: 302.

Wada, M., L. Heux, Y. Nishiyama, and P. Langan. X-ray crystallographic and cross-polarized/magic angle spinning 13C nuclear magnetic resonance studies of the structure of the complex of cellulose I with EDA. 2009. *Cellulsoe.* **16**: 943.

Wada, M., Y. Nishiyama, G. Bellesia, T. Forsyth, S. Gnanakaran, and P. Langan. Rearrangement of Hydrogen Bonding during the Treatment of Cellulose with Ammonia: Neutron Crystallographic Structure of Ammonia-Cellulose I. *Journal of the American Chemical Society.*

Wada, M., Y. Nishiyama, H. Chanzy, T. Forsyth, and P. Langan. The structures of cellulose. 2008. *Powder diffraction.* **23** (2): 92.

Wada, M., Y. Nishiyama, H. Chanzy, T. Forsyth, and P. Langan. The structures of celluloses. 2008. *Advances in X-ray Analysis.* **51**: 138.

Wei, D., C. Houtman, A. Kapich, C. Hunt, D. Cullen, and K. Hammel. Laccase and its role in production of extracellular reactive oxygen species during wood decay by the brown rot basidiomycete Postia placenta. . 2010. *Applied Environmental Microbiology .* **76** (7): 2091.

Yelle, D., K. Hammel, J. Ralph, and F. Lu. Evidence for cleavage of lignin by a brown rot basidiomycete. 2008. *Environ. Biol. .* **10**: 1844.

Flash before the Storm: Predicting Hurricane Intensification using LANL Lightning Data

Christopher A. Jeffery
20080126DR

Abstract
During the 2005 hurricane season, a LANL electromagnetic pulse detection and geo-location system called LASA, developed for nuclear non-proliferation, observed abundant lightning activity within hurricanes Katrina, Rita and Wilma. Lightning activity from Rita peaked as the hurricane transitioned from Category 3 to 5 [1]. These remarkable observations of the hurricane eye-wall region, a region that has been thus far opaque to conventional remote sensing and often too violent for in situ measurements, motivated the predictive challenge of this project: discover, investigate, and monitor the convective activity in the critical eye-wall region and, thereby, enable the numerical prediction of hurricane intensification – a spectacular large-scale dynamical organization, driven by small-scale eye-region processes, where wind speeds can increase by 100 mph in 24 hours.

Background and Research Objectives
In the wake of the devastating 2005 hurricane season, government agencies, scientific boards and advisory panels unanimously called for urgent increases in hurricane research and improvements in hurricane forecast accuracy. In coordination with this national agenda, our LDRD project had the following high-profile science & technology objectives:

1. Develop a new dual VLF/VHF total lightning mapping system in the New Orleans area, capable of remotely probing the violent and opaque hurricane eye-wall.

2. Discover and quantify the dynamics and convective structure of the hurricane eye-wall region as revealed for the first time in the 3D spatial structure, intensity and evolution of the lightning data.

3. Develop a new hurricane model with prognostic cloud electrification, and a data assimilation machinery capable of assimilating proxies (e.g. column saturation, latent heating) for the LANL lightning flash rate observations.

The great relevance and timeliness of these objectives has been central to the high impact of this project; our project aligns not only with LANL's energy security priorities, but also with a recent National Science Board report calling for a new national hurricane research initiative; and a recent NOAA science advisory board report advocating "novel methods for data assimilation founded on improved observations of the hurricane". Additionally, the new dual VLF-VHF lightning mapping array that we have built in the Gulf of Mexico is of great long-term technological value to the US space-based nuclear denotation monitoring system (USNDS).

Scientific Approach and Accomplishments
Our project had three key components [2]:

1. Development of a new dual VLF-VHF "total lightning mapping" array technology, and establishment of a new RF lightning array in the Gulf of Mexico.

2. Development of the first-ever hurricane forecast model that includes cloud electrification and lightning prediction;

3. Development of a new data assimilation scheme to ingest lightning data into our unique hurricane forecast model.

We discuss our accomplishments for each task separately below.

Gulf Lightning Mapping Array
We have developed a new dual-band VLF/VHF lightning mapping array in the New Orleans area [3]. We rely on the generosity of our host organizations to provide space and power for the individual sensors: the Louisiana Marine Consortium (LUMCON), Louisiana Department of Wildlife and Fisheries, Town of Jean Lafitte, Rotorcraft Leasing Co. LLC, U.S. Fish & Wildlife Service, and the U.S. Coast Guard. The new array is capable of determining the location of a lightning event (both cloud-to-ground lightning and inter-cloud lightning) that occurs several 1000 kilometers away. This information is transmitted in real-time back to LANL using satellite internet. The primary purpose of the array is to monitor the eyewall region of hurricanes in the Gulf of Mexico for a sudden

burst of lightning activity that is a potential indicator of rapid intensification. The array collected its first hurricane data on September 10th, 2008, from Hurricane Ike. Two distinct technologies are employed in the array: VLF mapping and VHF mapping, and we discuss each separately below.

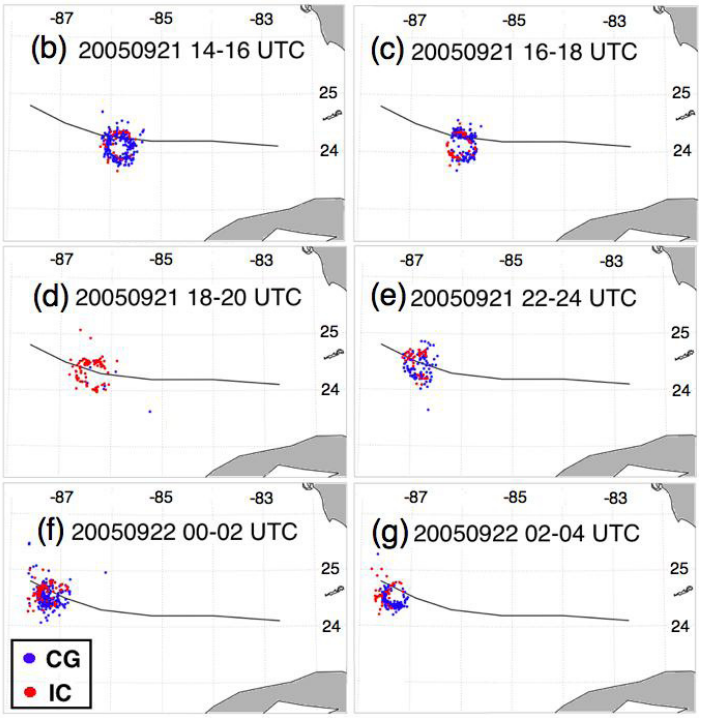

Figure 1. Panels (b-g) shows a map of 2-hour accumulated intra-cloud (IC, red) and cloud-to-ground (CG, blue) lightning flashes for Rita overlain by the NHC Best Track in the thick black line. The UTC times shown define the period of analysis of the lightning.

Over the course of this project, the original LASA VLF lightning observations of hurricane's Rita and Katrina were reprocessed and re-analyzed in great depth, to provide a first insight into the three-dimensional electrical activity of rapidly intensifying hurricanes [4]. This information is crucial for modelers aiming at better forecasting hurricane intensity, which is inherently related to key *structural* aspects of the storm often misrepresented in numerical models. Analysis of the intra-cloud narrow bipolar events (NBEs) for Rita revealed a general increase in discharge heights during the period of rapid intensification. Figure 1 shows the spatial evolution of the CG and NBE (labeled IC) events within the eyewall. During the intensification stage (1400–2000UTC, Figs. 1b-d), lightning occurred in a nearly symmetric pattern around the eyewall (e.g., [1]) similar to Hurricane Andrew in 1992. As the storm reached maximum intensity (2200-0000UTC, Figure 1e), and before the onset of the eyewall replacement cycle (0002UTC on 22 September 2005), the symmetric pattern of lightning was not as well-defined (Fig. 1f). Within a short period of time (0200-0400UTC) a more well-defined eyewall was mapped out by both NBE and CG lightning flashes (Figure 1g).

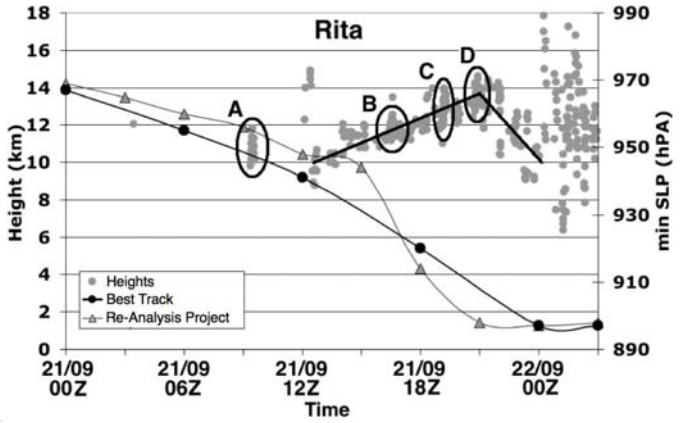

Figure 2. Time-height plot of narrow bipolar events (NBE) for Hurricane Rita with minimum central pressure overlaid. The black ovals labeled A through D highlight lightning bursts. The solid black line represents the approximate best fit slope of the NBE discharge heights as a function of time.

Figure 2 shows the three-dimensional view of the eyewall lightning activity [4]. Starting three hours before rapid intensification, the source heights of the NBE discharges increased continuously from ~10 km to ~14 km. This observation suggests that intense convective bursts in the eyewall lofted the charge regions to progressively higher altitudes, similar to observations of intensifying severe continental storms and tornadic storms. After the continuous increase in NBE discharge heights, an abrupt decrease in heights and a sharp increase in CG flash rate occurred during the onset of a period of maximum intensity. This behavior is, again, similar to that of continental storms in which a descent of precipitation cores, and therefore charge regions, is often followed by a sharp increase in CG flash rate.

These results suggest that NBEs are useful in tracking and mapping the evolution of individual strong convective elements embedded in the eyewall during rapid intensification. The evolution of NBE heights is particularly revealing, and suggests that the general increase in height of the intra-cloud lightning is an aggregate consequence of numerous short-lived convective events rotating rapidly around the eyewall of Rita.

Our shorter-range VHF lightning mapping technology has the ability to image the three dimensional structure of cloud charge layers, providing detailed dynamical and structural information remotely and under severe weather conditions. An example of the type of high resolution information produces by this system is shown in Figure 3 for a thunderstorm system observed on August 21, 2009 between 16:50 and 16:55 UTC. The three dimensional charge structure of the storm, associated with regions of intense convection in the storm's core, is clearly visible in the figure.

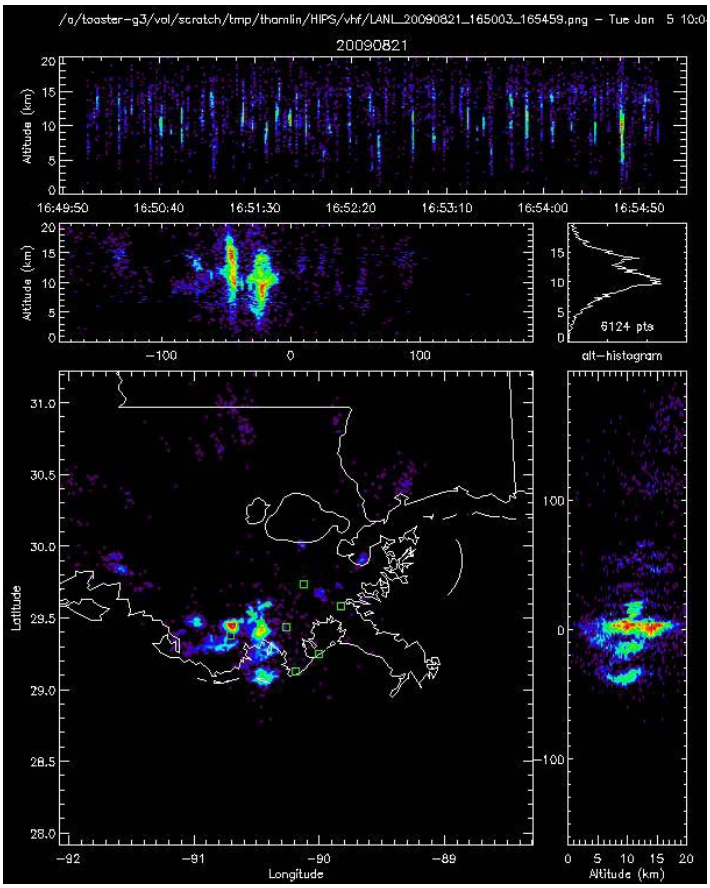

Figure 3. VHF mapping of the 3D charge structure of a convective system on August 21, 2009. Top panel: altitude vs time plot of recorded events; middle left panel: integrated altitude vs longitude plot of events; middle right panel: altitude histogram of events; bottom left panel: latitude-longitude plot of events; bottom right panel: integrated altitude vs latitude plot of events.

LANL Hurricane Model with Cloud Electrification

We have developed a novel hurricane model with prognostic lightning that is described in detail in [5] and [6]. The model includes conservation equations for the three momentum fields, potential temperature, gas density, water vapor density, number and density of cloud water, rain water density, number and density of cloud ice, snow density, graupel density, turbulence kinetic energy density, and the space charge densities associated with each hydrometer. Space charge density equations within the hurricane model are included within a lightning module option that simulates the local time rate of change of a one-dimensional form of the electric field due to charging and discharging (lightning). Lightning initiation/discharge in the model occurs whenever the ambient electric field exceeds the breakeven (or fair weather) electric field threshold, which was assumed to decrease exponentially with height, with the electric field and space charge densities being decreased by a constant value of 10% through the column upon discharge.

The model was tested and evaluated using a high-resolution simulation establishing relationships between lightning and eyewall convection during a rapid intensification phase of hurricane Rita. Simulations were performed with a grid spacing of 2km (1000x800x86) and a 0.25 second time step. All simulations utilized DOE's XT-5 Cray machine (Jaguar) hosted at the Oak Ridge National Laboratory using between 2000 to 32,000 processors.

The simulation produces significant lightning activity within strong convective events found within the eyewall, based on a test case from which high fidelity lightning observations are available [4,6]. Specifically, our analysis focused on two electrically-active eyewall convective events that had properties similar to events observed by the LANL lightning mapping array. The counterclockwise rotating convective events were characterized by updraft speeds exceeding 10 m/s, a relatively larger flash rate, confined in a layer between 10 and 14 km, and a propagation speed that was 10 m/s less than the primary circulation. Within an hour of the first event, the simulated minimum surface pressure dropped by approximately 8 mb. This pressure drop appears to be the result of a large pulse in vertical motions associated with the convective event merging with rainband convective cells being drawn inward towards the eyewall.

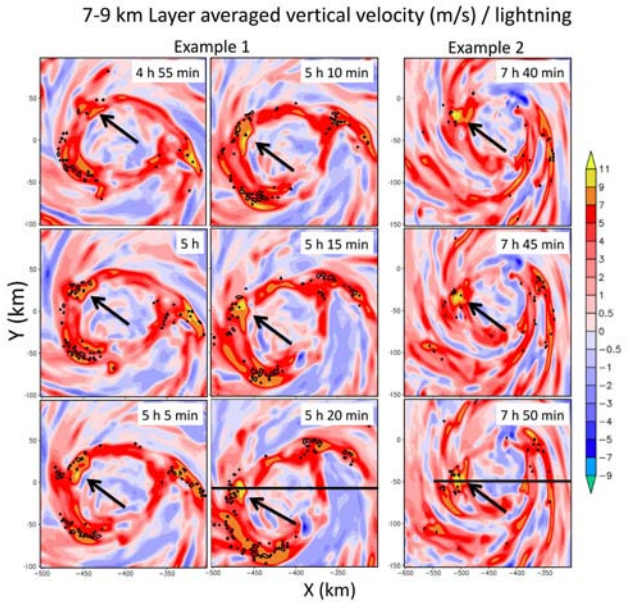

Figure 4. Horizontal cross sections of 7-9 km layer-averaged vertical velocity (in m s-1) at selected times of the 2 km simulation (time shown on the upper right corner of each panel) overlaid with horizontal projection of accumulated 5-min lightning discharge zoomed over the eyewall. In this figure two examples of convective events rotating around the eyewall are shown. The black arrow indicates the location of the convective event of interest.

Vertical cross-sections of the simulated net space charge across two simulated convective events and across the

eyewall are shown in Figure 4. The simulated gross charge structure in the events resembles an inverted tripole, which consists of a main positive charge region sandwiched in between two layers of negative charge. Our recent observational study [4] found, however, that the gross charge structure in Rita's eyewall was of opposite polarity, namely a normal tripole. Previous high-resolution modeling studies on thunderstorm electrification showed that the simulated gross charge structure of a thunderstorm was very sensitive to the non-inductive charging scheme selected in the model. Such discrepancies in simulated charge structure are mainly attributed to the different in-cloud conditions and apparatus used to reproduce the critical charging curves of graupel. Figure 4 shows that space charge in the simulated eyewall is found within regions having liquid water content values near 0.5 g m^{-3} and graupel mixing ratios ranging between 2.5 and 5 g kg^{-1}, which are generally located atop updrafts. Another interesting aspect of Figure 4 is that lightning varies marked across the simulated hurricane. Though the convective events have much more lightning than the bulk of the eyewall, space charge magnitude, electric fields and vertical motions are almost unchanged.

Thus, in summary, the LANL hurricane model is able to predict a large increase in lightning activity concurrent with pulses of intense convective activity. This modeled relationship between enhanced vertical motions, a significant pressure drop, and heightened lightning activity suggests that can be used to remotely diagnose future changes in hurricane activity. Further, since the model can relate lightning activity to latent heat release, this functional relationship, once validated against a derived field produced by dual-Doppler radar data, can be used to initialize eyewall convection in a hurricane model.

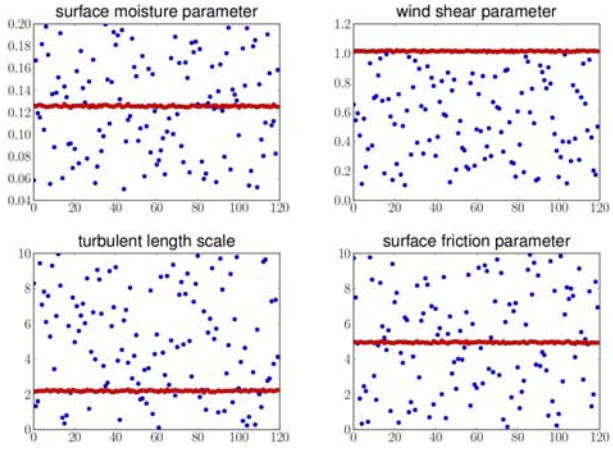

Figure 5. Initial parameter spread (blue) and assimilated parameter spread (red) for observations at 14100 seconds.

Lightning Data Assimilation

In this project the Ensemble Kalman Filter (EnKF) was used to calibrate the LANL hurricane model for the case of rapidly intensifying Hurricane Guillermo (1997) from which a unique three dimensional wind and radar dataset collected in situ during flight reconnaissance mission is available. The EnKF is up-to-date of the most popular methods for data assimilation, which requires an ensemble of model simulations, which coupled with the observations, produces an improved model forecast. To implement the EnKF into the LANL model a parallel ensemble simulation package was developed which allows its users to run multiple simulations at the same time, thanks to the high performance of the Cray XT5 clusters hosted at Oak Ridge National Laboratory.

Once the ensemble of simulations was completed, the three dimensional observational data was used in the EnKF. One of the main limitations of this algorithm is the limited amount of data that can be processed at one time. To overcome this limitation we developed a novel implementation of the EnKF that efficiently assimilates large amounts of data into the LANL model. This is done via a matrix-free approach that allows the computation of the EnKF without the need to store or even create the matrices in the algorithm.

The model calibration of the LANL hurricane model for Hurricane Guillermo was carried out using a highly reliable three-dimensional dual-Doppler data set. The three dimensional data set was collected every 30 min to observe the inner core structural changes of Hurricane Guillermo from 1830 UTC 2 August to 0030 UTC 3 August as it rapidly intensified from a Category 1 into a Category 3 on the Saffir-Simpson scale. The raw data set, which tracks dBZ (radar return), was processed with well-established published techniques to derive the horizontal wind field as well as latent heat field. These three fields are key for a direct comparison between the data and the model.

The objective of our data assimilation was to pin down three parameters that are critical to hurricane intensification: surface process parameters, surface friction, and surface moisture. Other model uncertainties included balance between resolved and unresolved transport of moisture contains high uncertainty. Furthermore , while vertical wind shear is known to be detrimental to hurricane intensification, Guillermo underwent rapid intensification within a sheared environment, and hence this parameter was also tested within the EnKF implementation.

An ensemble of HIGRAD simulations consisting of 120 members was created by perturbing the aforementioned four parameters using a Latin Hypercube sampling scheme that provides a reasonable spread without underlying assumption about the distribution of the parameters. The assimilation is performed at each instance when observations for latent heat data are available. The time instances are from 14100 seconds to 30300 seconds at 1800 seconds increments. Figure 5 shows the estimated parameters (red) for each ensemble member for 14100 seconds with latent

heat data, and the initial parameter spread (blue). After carrying the EnKF, each parameter is shown to converge to a single value for all ensemble members giving an estimation of what the "true" parameter value should be for the observations at 14100 seconds.

Because latent heat can be used as a surrogate/proxy for lightning, assimilation of lightning data obtained by either VLH/VHF sensors can provide accurate estimates of key parameter values and model calibration for hurricanes. Lightning observations can be readily detected over large distances with high temporal resolution, unlike radar mapping. This advantage is especially important over oceans where radar does not reach, since hurricanes form and intensify a long way from land.

Impact on National Missions

This project has supported DOE's Threat Reduction by enhancing our understanding of the strength and organization of eyewall convective processes that trigger rapid hurricane intensification, and by developing a new hurricane model to improve forecast accuracy. We contributed to energy security by developing a new Gulf lightning observing system to anticipate threats to the oil infrastructure. Our project leveraged investment in nuclear security to help solve problems of national importance. During the summer of 2009, we were interviewed by the Associated Press and by the Weather Channel; this publicity highlighted our new application of nuclear non-proliferation technology to the problem of hurricane intensity forecasting.

References

1. Shao, X., J. Harlin, M. Stock, M. Stanley, A. Regan, K. Wiens, T. Hamlin, and M. Pongratz. Katrina and Rita were lit up with lightning. 2005. *EOS Transactions.* **86** (42): 4.

2. Jeffery, C., J. Reisner, and X. Shao. An overview of LANL's new hurricane lightning project. (San Francisco, 14-18 Dec. 2009).

3. Shao, X., N. O'Connor, T. Hamlin, C. Jeffery, and C. Ho. First observations with Los Alamos dual-band Lightning Mapping Array. (San Francisco, 14-18 Dec. 2009).

4. Fierro, A., X. Shao, T. Hamlin, J. Reisner, and J. Harlin. Evolution of eyewall convective events as indicated by intra-cloud and cloud-to-ground lightning activity during the rapid intensification of Hurricanes Rita and Katrina. *Monthly Weather Review.*

5. Reisner, J., and C. Jeffery. A smooth cloud model. 2009. *Monthly Weather Review.* **137**: 1825.

6. Fierro, A., and J. Reisner. High resolution simulation of the electrification and lightning of Hurricane Rita during the period of rapid intensification. *Journal of the Atmospheric Sciences.*

Publications

Chylek, P., and G. Lesins. Multi-decadal variability of Atlantic hurricane activity: 1851-2007. 2008. *Journal of Geophysical Research.* **113**: 22106.

Fierro, A., X. Shao, T. Hamlin, J. Reisner, and J. Harlin. Evolution of eyewall convective events as indicated by intracloud and cloud-to-ground lightning activity during the rapid intensification of Hurricanes Rita and Katrina. *Monthly Weather Review.*

Fierro, A., and J. Reisner. High resolution simulation of the electrification and lightning of Hurricane Rita during the period of rapid intensification. *Journal of the Atmospheric Sciences.*

Harlin, J., X. Shao, T. Hamlin, N. O'Connor, T. Lavezzi, and C. Jeffery. LASA Observations of lightning in hurricanes. Presented at *American Geophysical Union Fall Meeting.* (San Francisco, 15-19 Dec., 2008).

Henderson, B., D. Suszcnysky, K. Wiens, T. Hamlin, C. Jeffery, and R. Orville. Lightning and radar observations of Hurricane Rita landfall. *Monthly Weather Review.*

Jeffery, C., J. Reisner, and X. Shao. An overview of LANL's new hurricane lightning project. Presented at *American Geophysical Union Fall Meeting.* (San Francisco, 14-18 Dec. 2009).

Jeffery, C., and N. Jeffery. Theory and computation of wavenumber-2 Vortex Rossby Wave instabilities in hurricane-like vortices. Presented at *Geophysical Turbulence Phenomena.* (Boulder, 27-29 Feb., 2008).

O'Connor, N.. The Los Alamos National Laboratory Hurricane Intensification Prediction System. 2010. *M. S. Thesis, New Mexico Institute of Mining and Technology.*

Reisner, J., and C. Jeffery. A smooth cloud model. 2009. *Monthly Weather Review.* **137**: 1825.

Shao, X., J. Harlin, D. Suszcynsky, and C. Jeffery. Hurricane lightning: a new campaign to investigate hurricane intensification by using lightning observations. Presented at *American Meteorological Society 88th Annual Meeting.* (New Orleans, 20-24, Jan., 2008).

Shao, X., N. O'Connor, T. Hamlin, C. Jeffery, and C. Ho. First observations with Los Alamos dual-band Lightning Mapping Array. Presented at *American Geophysical Union Fall Meeting.* (San Francisco, 14-18 Dec. 2009).

Shao, X., and A. Jacobson. Model simulation of VLF/LF lightning signal propagation over intermediate ranges. 2009. *Transactions on Electromagnetic Compatibility.* **51**: 519.

Genomes to Behavior: Predicting Bacterial Response by Constrained Network Interpolation

John M. Dunbar
20080138DR

Abstract

The DOE Office of Science envisions direct prediction of microbe behavior (response to stimuli) from a genome sequence. To achieve this, we aimed to extrapolate behavior from experimentally well-characterized model organisms to close relatives. We focused on the bacterium *Burkholderia thailandensis* as a model organism and sought to extend gene expression patterns to other species in the *Burkholderia* genus that impact climate, biosecurity, and public health missions of interest to DOE, DoD, and NIH.

Our objectives were to experimentally characterize the response of the model organism to a variety of external stimuli, then use comparative genomics techniques to assess conservation of the response patterns in 8 other species. We encountered unanticipated technical challenges that slowed our progress towards achieving the project goal. Nonetheless, we solved several fundamental problems, acquired experimental data that exceeded our original targets and that increased the publically available gene expression data for *Burkholderia* by ten-fold, and established a solid foundation to pursue the project goal with funding support from DoD and NIH.

A major impact on program development and national missions has yet to be realized. The project contributed to 18 research proposals to external sponsors, and at least 3 additional NIH proposals are currently being prepared for submission to enable demonstration of the original project goal. External funding of $5.4 for related projects was acquired, and $6.5M is pending in additional research proposals. Eleven manuscripts have been published or are in review, four drafted manuscripts are being revised for submission, and seven additional manuscripts are in preparation. The project established a new experimental capability in the Bioscience Division that is seeding program development. The project contributed support for ten TSMs, four postdocs, and five graduate students, three external collaborations, and helped project members to organize and host an annual Quantitative Biology (qBio) conference.

Background and Research Objectives

The DOE Office of Science envisions direct prediction of microbe behavior (response to stimuli) from a genome sequence; however, the lack of methods currently makes this impossible. Consequently, the DOE, DoD, DHS, and NIH rely on slow, expensive empirical methods to determine the response of new strains and species to particular stimuli and to identify the genetics underpinning response. For example, knowledge of strain virulence is needed in biothreat risk assessment, but can only be estimated at present through burdensome animal studies. Similar hurdles occur in bioenergy and waste remediation. This creates an increasingly severe bottleneck as the accumulation of genome sequences (already >1000 partial or complete) greatly outstrips the capacity for experimental analysis.

To alleviate this bottleneck, we aimed to extrapolate behavior from experimentally well-characterized model organisms to close relatives. This conceptual approach avoids the intractable task of predicting behavior *de novo*. In fact, the concept is based on an established precedent: extension of known protein functions from one organism to another based on protein sequence or structural similarity. We focused on the bacterial genus *Burkholderia.* This genus contains species that impact climate, biosecurity, and public health missions of interest to DOE, DoD, and NIH. We used *Burkholderia thailandensis* as the model organism and aimed to extend behavior to closely related biothreat agents and other species in the genus. To extrapolate cellular behavior, genomes must be compared to assess the conservation of gene inventory and gene regulation. Gene inventory defines a cell's potential capabilities. Gene regulation determines which capabilities are actually used in various conditions. Comparing gene inventory is a well-established capability (Figure 1). On the other hand, assessing conservation of gene regulation is undeveloped; this is the primary challenge in extending behavior among genomes.

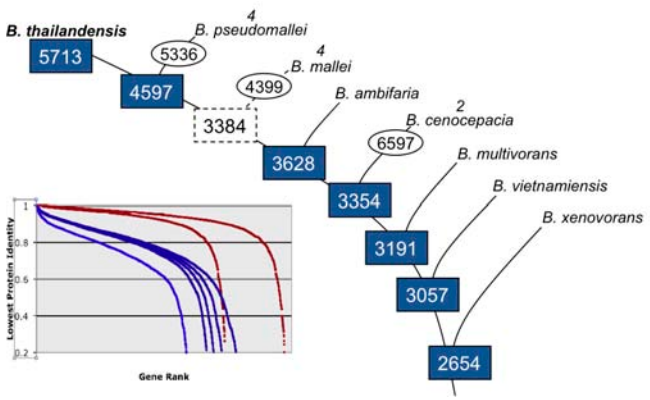

Figure 1. Conservation of gene inventory among Burkholderia species. The cartoon tree illustrates the evolutionary relationships among the species. The most distant neighbor of B. thailandensis is B. xenovorans. If more than 1 genome was available per species, the number is indicated above the species names. The numbers at each node of the tree are the genes common to all genomes above the node. For example, pseudomallei strains have 5336 common genes and they have 4597 in common with thailandensis. The inset panel shows the similarity of common proteins from each organism relative to thailandensis. The right-most curve compares proteins from thailandensis and pseudomallei. The left-most curve compares proteins from thailandensis and xenovorans. Performing such comparisons is a well-established, although time-consuming, capability in comparative genomics.

Scientific Approach and Accomplishments

The central obstacle in assessing conservation of gene regulation is lack of knowledge of the organization and components of regulatory networks in a cell. For a few model organisms (e.g. *E. coli*, *Bacillus subtilis*) there are specialty databases that catalogue regulatory components (e.g., promoters, transcription factor binding sites, regulatory protein-protein interactions). But for most organisms, including *Burkholderia* species, detailed information about gene regulation is nonexistent or severely limited. We pursued two parallel approaches to address this problem.

In the first approach, we attempted to quantify the general conservation of DNA regions containing regulatory elements. The DNA regions between genes (i.e, "intergenic regions") often contain regulatory elements such as binding sites for regulatory proteins. This approach exploits the same logic used for transitive annotation of protein functions—the overall degree of sequence conservation reflects the likelihood of functional conservation. Surprisingly, even for this coarse level of assessment, supporting computational infrastructure is lacking. Despite the past 15 years of tool development in comparative genomics, genome-wide comparison of regulatory regions is non-trivial.

In the second approach, we attempted to characterize specific regulatory circuits and the general architecture of the regulatory network in *Burkholderia thailandensis* in order to refine the assessment of conservation. This general task involved documenting the gene expression response of *B. thailandensis* to numerous growth conditions, determining interactions among a suite of regulatory proteins, and establishing a new experimental capability at LANL to discover the DNA recognition sequences of specific gene regulator proteins. We focused in particular on two-component regulatory systems because bacteria exploit these systems to sense environmental stimuli, and transduce the stimuli into an adaptive gene expression response.

For both approaches, our progress was severely undermined by a faulty assumption at the project outset. We assumed that the 18 *Burkholderia* genome sequences available from Genbank's Reference Sequence database had high quality, reliable gene maps. Instead, we discovered that the gene maps for each genome were full of erroneous gene start sites. The errors in gene start sites arise from the imperfection of gene-prediction algorithms. The errors create large inconsistencies among genomes (Figure 2) that impede the extraction and comparison of regulatory regions and the analysis of gene expression data. We found that the NIAID-funded Bioinformatics Resource Center that was established in 2004 to improve the annotation quality of *Burkholderia* genomes had completely ignored this fundamental problem. This finding reflected the groundbreaking nature of our project. If our objective of performing genome-wide comparisons of regulatory regions among multiple bacterial genomes were commonplace, the problem of inconsistent gene maps would have been widely recognized and solved previously.

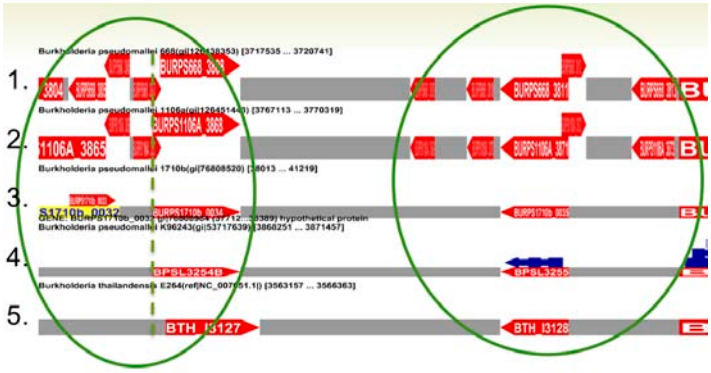

Figure 2. Examples of inconsistencies in gene maps for 5 Burkholderia genomes. The genomes, numbered 1 to 5 represent 4 pseudomallei strains and 1 thailandensis strain. For this portion of the genomes, the gene maps should be identical, yet numerous inconsistencies are apparent. The red arrows represent genes and their orientations. The grey boxes are the DNA regions between genes; these regions often contain elements that regulate gene expression. Inconsistencies in the diagram include variable presence/ absence of genes and variation in gene start sites.

Addressing this problem set back our project timeline by a year. As described in recently submitted publications[1, 2], we thoroughly characterized the problem, devised a solu-

tion that increased the percentage of *Burkholderia* genes with consistent start sites from the initial 45% to 85% (Figure 3), validated the accuracy of our approach, and showed that our approach provides numerous improvements to genome annotation and facilitates identification of true evolutionary divergence that can influence cellular behavior. We also developed stand-alone software enabling the external research community to apply our approach in an automated fashion to 39 other clusters of existing genomes. By illuminating and solving a very fundamental and widespread problem, we made a significant contribution to the field of comparative genomes. This is a significant, albeit unanticipated, highlight of the project. Having solved this problem, we can now achieve our original objective: assess across the *Burkholderia* genus the conservation of inter-genic DNA regions containing regulatory elements.

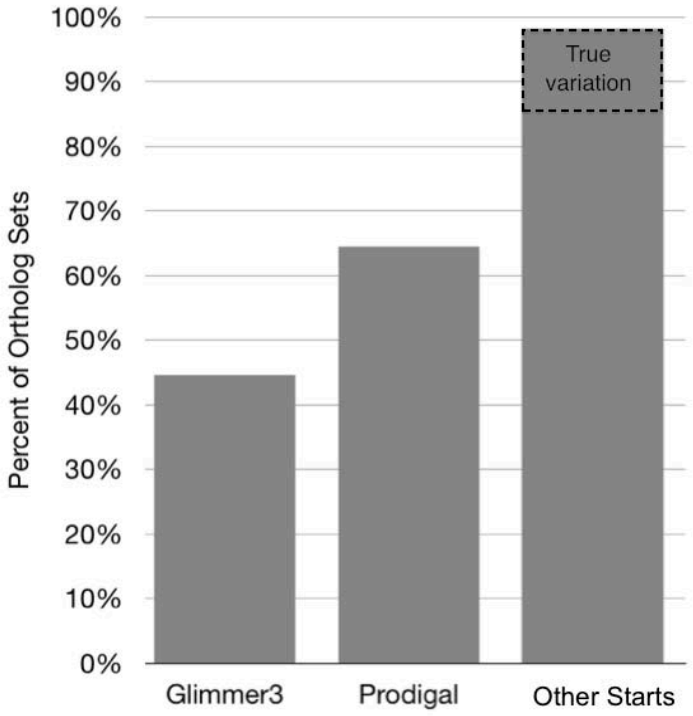

Figure 3. Consistency of the start sites for orthologous genes. Over 2500 sets of orthologous genes across the Burkholderia genus were examined. Using the original gene maps produced by Glimmer3 (the most widely used gene prediction software), only 45% of the sets of orthologs had consistent start sites. Better results were obtained with Prodigal, the gene prediction tool recently created by the DOE Joint Genome Institute at Oakridge National Lab. We improved upon the Prodigal results by showing that 98% of the ortholog sets (rightmost bar) could in principle possess consistent start sites, but that about 15% of the ortholog sets harbor true inconsistencies owing to real evolutionary divergence.

Another significant achievement of the project is the compendium of data acquired for reconstruction of regulatory networks in *Burkholderia*. The quantity and spectrum of experimental data we acquired exceeded the original project goals. We measured the gene expression response of the model organism, *Burkholderia thailandensis*, in 40 different conditions. The conditions included exposure to different carbon and energy sources, stress conditions, physical regimes, and nutrient limitations. In total, we collected 170 gene expression profiles using custom designed Affymetrix microarrays—one of the highest-quality measurement platforms. This collection of expression profiles is one of the largest available for bacteria, comparable to the landmark collections for *Escherichia coli* and *Shewanella,* and increases the publically available data for *Burkholderia* by tenfold. The set of *Burkholderia thailandensis* profiles represents numerous single-factor experiments but also includes multi-factorial time-series experiments revealing the progression of cellular response to different stimuli. The set is augmented by other types of data including two transcriptome sequencing datasets (demonstrating a new capability at LANL), regulatory protein-protein interactions obtained with a unique technology invented recently at LANL by Dr. Geoff Waldo, regulatory protein-DNA interactions (demonstrating a new capability at LANL), and compilation of published regulatory interactions from over 100 articles focusing on *Burkholderia* species. The size and diversity of the data compendium is exceptional.

As most of the data were acquired in FY10, analysis and integration of the data is still in progress. We reconstructed a putative regulatory network for *Burkholderia thailandensis* that can now be assessed for conservation across the genus. Our preliminary analyses also indicate that the organism's responses to diverse stimuli can be distilled into a few basic response patterns. These data are being prepared for publication in at least ten manuscripts, three of which have already been submitted or drafted, and have been exploited for 23 proposals to external sponsors, including four pending proposals designed to support continuation of the project to achieve the original project goal. In short, the exceptional data collection represents a significant step toward achieving the ambitious goal of the project, and is a valuable resource for program development in the LANL Bioscience Division.

Aside from these major highlights, we had many notable tangential achievements. For example, we successfully modeled the quantitative behavior of two well-defined regulatory circuits in order to expand our understanding of how DNA sequence variation between genomes can alter the behavior of a regulatory circuit. From these studies, we obtained novel insights into mechanisms regulating gene expression and we defined minimal parameters for construction of effective predictive models[3-5]. Separately, our gene expression studies of *Burkholderia thailandensis* have revealed a possible mechanism underpinning an unusual bacterial physiological state that contributes to chronic infections, heightened antibiotic resistance, and higher mortality (Dunbar, J., S. Buddenborg, J. Gans, B. Gao, T. Maity, Y. Valdez. "Transcriptome profiling reveals

physiological tradeoffs underlying heightened multidrug resistance". In preparation). We are pursuing investigation of this unifying mechanism and extension of the behavior observed in *thailandensis* to *Burkholderia* pathogens through NIH. We also developed and demonstrated a novel capability to model protein complexes, optimizing the interactions of multiple proteins as a means to constrain the conformational landscape. This innovative work is in review for publication[6].

Impact on National Missions

The project targeted a fundamental bottleneck identified by DOE Office of Science within the Life Sciences. However, a major impact on program development and national missions has yet to be realized. Demonstrating the capacity to extend behavior from a model organism to close relatives is crucial to achieving a major impact. Successful demonstration would substantially increase the value of model systems, and reduce the need for experimental work on more difficult or higher risk organisms by 10-100 fold. While the project made a substantial step towards achieving this goal, unanticipated technical challenges slowed progress. The project is about 8-12 months away from a proof-of-principle demonstration. The project contributed to 18 research proposals to external sponsors, and at least three additional NIH proposals are currently being prepared for submission to enable demonstration of the original project goal. Eleven manuscripts have been published or are in review, four drafted manuscripts are being revised for submission, and seven additional manuscripts are in preparation. The project contributed to acquisition of $5.4M of external funding from Office of Science and DTRA, and $6.5M is pending in additional research proposals. The project established a new experimental capability in the Bioscience Division that is already seeding program development, and contributed support for ten TSMs, four postdocs, five graduate students, and collaborations with three external teams. The project also supported the Annual q-bio Conference and Summer School on Cellular Information Processing by enabling project members to organize and host the conference [7-9]. The q-bio conference is now the premier international meeting covering highly focused experimental and theoretical studies of biological systems. The summer school attracts students from major research universities. Both the conference and school have been key recruiting tools and have substantially increased the reputation of Los Alamos in the area of systems biology.

References

1. Dunbar, J., J. D. Cohn, and M. E. Wall. Consistency of gene starts among Burkholderia genomes. *BMC Genomics.*

2. Raghavan, S., J. D. Cohn, J. Dunbar, and M. E. Wall. Genome majority vote improves gene preditions. *Nucleic Acids Research.*

3. Dreisigmeyer, D. W., J. Stajic, I. Nemenman, W. S. Hlavacek, and M. E. Wall. Determinants of bistability in induction of the Escherichia coli lac operon. 2008. *IET Systems Biology.* **5**: 293.

4. Martin, R. G., E. S. Bartlett, J. L Rosner, and M. E. Wall. Activation of the Escherichia coli marA/soxS/rob regulon in response to transcriptional activator concentration. 2008. *Journal of Molecular Biology.* **380**: 278.

5. Wall, M. E., D. A. Markowitz, J. L. Rosner, and R. G. Martin. Model of transcriptional activation by MarA in Escherichia coli. 2009. *PLoS Computational Biology.* **5**: e1000614.

6. Tung, C. S.. A novel method utilizing motif interacting geometry to model PhoB dimer in the E.coli transcription initiation complex. *Nature.*

7. Edwards, J. S., J. R. Faeder, W. S. Hlavacek, Y. Jiang, I. Nemenman, and M. E. Wall. q-bio 2007: a watershed moment in modern biology. 2007. *Molecular Systems Biology.* **3**: 148.

8. Nemenman, I., W. S. Hlavacek, J. S. Edwards, J. R. Faeder, Y. Jiang, and M. E. Wall. Selected papers from the First q-bio Conference on Cellular Information Processing. 2008. *IET Systems Biology.* **2**: 203.

9. Nemenman, I., W. S. Hlavacek, Y. Jiang, and M. E. Wall. Editorial: Selected papers from the Second q-bio Conference on Cellular Information Processing. 2009. *IET Systems Biology.* **3** (5): 297.

Publications

Chen, G., B. H. McMahon, and C. S. Tung. Molecular dynamics simulations of phosphorylation-induced conformational transitions in the Mycobacterium tuberculosis response regulator PrrA. 2009. *Los Alamos National Laboratory, LAUR 08-05233.*

Dreisigmeyer, D. W., J. Stajic, I. Nemenman, W. S. Hlavacek, and M. E. Wall. Determinants of bistability in induction of the Escherichia coli lac operon. 2008. *IET Systems Biology.* **5**: 293.

Dunbar, J., J. D. Cohn, and M. E. Wall. Consistency of gene starts among Burkholderia genomes. *BMC Genomics.*

Edwards, J. S., J. R. Faeder, W. S. Hlavacek, Y. Jiang, I. Nemenman, and M. E. Wall. q-bio 2007: a watershed moment in modern biology. 2007. *Molecular Systems Biology.* **3**: 148.

Frauenfelder, H., G. Chen, J. Berendzen, P. W. Fenimore, H. Jansson, B. H. McMahon, I. R. Stroe, J. Swenson, and R. D. Young. A unified model of protein dynamics. 2009. *Proceedings of the National Academy of Science.* **106**: 5125.

Martin, R. G., E. S. Bartlett, J. L Rosner, and M. E. Wall. Activation of the Escherichia coli marA/soxS/rob regulon in response to transcriptional activator concentration. 2008. *Journal of Molecular Biology.* **380**: 278.

Nemenman, I., W. S. Hlavacek, J. S. Edwards, J. R. Faeder, Y. Jiang, and M. E. Wall. Selected papers from the First q-bio Conference on Cellular Information Processing. 2008. *IET Systems Biology.* **2**: 203.

Nemenman, I., W. S. Hlavacek, Y. Jiang, and M. E. Wall. Editorial: Selected papers from the Second q-bio Conference on Cellular Information Processing. 2009. *IET Systems Biology.* **3** (5): 297.

Raghavan, S., J. D. Cohn, J. Dunbar, and M. E. Wall. Genome majority vote improves gene preditions. *Nucleic Acids Research.*

Tung, C. S.. A novel method utilizing motif interacting geometry to model PhoB dimer in the E.coli transcription initiation complex. *Nature.*

Wall, M. E.. Structure-function relations are subtle in genetic regulatory networks. *Mathematical Biosciences.*

Wall, M. E., D. A. Markowitz, J. L. Rosner, and R. G. Martin. Model of transcriptional activation by MarA in Escherichia coli. 2009. *PLoS Computational Biology.* **5**: e1000614.

Complex Biological and Bio-Inspired Systems

Robert E. Ecke
20080673DR

Abstract

The understanding and characterization of the fundamental processes of the function of biological systems underpins many of the important challenges facing American society, from the pathology of infectious disease and the efficacy of vaccines, to the development of materials that mimic biological functionality and deliver exceptional and novel structural and dynamic properties. These problems are fundamentally complex, involving many interacting components and poorly understood bio-chemical interactions. We use the basic science of statistical physics, kinetic theory, cellular biochemistry, soft-matter physics, and information science to develop cell level models and characterize materials that mimic biological function. Specific objectives are to determine how cells respond to mechanical forces, to chemical composition and related gradients, and to other cell-signaling mechanisms. These efforts may lead to the development of bio-sensors to detect hazards from pathogenic viruses to chemical contaminants. Other potential applications include the development of efficient bio-fuel alternative-energy processes and the exploration of novel materials for energy usages. Finally, we use averaging over less important degrees of freedom to develop computational models that predict cell function and systems-level response to disease, chemical stress, or biological pathogens.

Background and Research Objectives

Biological systems are canonical examples of complex nonlinear systems. Models of these systems are as diverse as the systems themselves, incorporating varying levels of detail, with the relevant resolution ranging from atomic and molecular to whole organisms and populations of interacting species. Although we are broadly interested in these systems, we focus much of our work on cellular processes, and much of the subject area of this project lies within the emerging field of systems biology, with emphasis on modeling, computation, and theory. Another significant focus is bio-inspired systems, such as carbon nano-tubes, thin-film self-assembling materials, and membrane-based colloidal particles.

Modern systems biology aims to extend understanding of the cell at the molecular level to understanding at the systems level, which is important because cellular behavior depends largely on complex nonlinear cellular processes, which are often regulatory systems with information-processing functions. Bio-systems are comprised of numerous interconnected molecular parts, each of which may be considered a complicated molecular machine (e.g., a cellular response can involve interactions of hundreds of proteins, each of which may have multiple functions and be regulated in different ways). For a given system, we may have a list of the component parts, and we may know a great deal about each part from traditional approaches of molecular and cellular biology, in which parts of a system are typically studied in isolation. We usually lack, however, a predictive understanding of how the parts of a system work together, and how system behavior emerges from the dynamical nonlinear interactions of the system components.

Systems-level understanding of dynamical cellular processes depends on the ability to assay the key quantities of a system as they change in time and space in response to an environmental perturbation. This need is being addressed experimentally with various high-throughput technologies, such as micro-arrays, and with technologies based on mass spectroscopy for monitoring collections of post-translational protein modifications and profiling the abundances of small-molecule metabolites in the metabolic network of a cell.

Computational systems biology develops cell level models by analyzing high-throughput datasets and using the vast knowledge base of molecular and cellular biology. Two major approaches to data analysis are commonly taken. The currently dominant one involves statistical analysis of data. The other approach, which we follow here, is based on mathematical models of systems that incorporate physics and chemistry. A capability to develop and validate such models of cellular systems will be important for accurate predictions of cellular behavior and DOE/LANL missions in bio and energy security, in which there is a need, for example, to rationally engineer the metabolism of plants and microbes for bio-fuel

production.

Physical or chemical systems that mimic or are inspired by natural ones play important roles in building good models of cell function by providing better understanding of the physics and chemistry of constituent cell parts. Also, studies of bio-inspired systems can form the basis for synthesizing interesting new materials. In that context, we will explore the mechanical deformations of viruses using nonlinear elastic theory, the properties of interfaces, and the coordination of our mainly theory-computation-modeling approach with experimental methods that span activities in soft materials research and biological physics. When simulating optical experiments probing bio-systems or to describe many processes involving quantum-mechanical phenomena, atomistic modeling based on classical molecular dynamic simulation is frequently not sufficient. To describe these processes first-principles based quantum-chemical approaches are required.

Scientific Approach and Accomplishments

Our approach is mostly theoretical and computational but always with an eye towards experimental collaborations. We describe our results somewhat according to scale from the molecular level of DNA, RNA and proteins through the cellular level to the intercellular domain.

Using molecular-level simulations of complex-molecule/DNA complexes in the presence of a model cell membrane, we determined the required conditions for the complex to arrive intact at the membrane and the lifetime of the complex as it resides attached to the membrane. Our simulations directly pertain to critical issues arising in emerging gene delivery for therapeutic applications, where a molecular carrier is required to deliver DNA segments to the interior of living cells.

No simple model exists that accurately describes the melting behavior and breathing dynamics of double-stranded DNA as a function of nucleotide sequence. This is especially true for homogenous and periodic DNA sequences, which exhibit large deviations in melting temperature from predictions made by additive thermodynamic contributions. We extended the nonlinear Peyrard-Bishop-Dauxois (PBD) model of DNA to include a sequence-dependent stacking term, resulting in a model that can accurately describe the melting behavior of homogenous and periodic sequences [1]. Using comparison between experiments and our numerical simulations, we showed that our extended PBD model facilitates thermodynamic and dynamic simulations of important genomic regions. We also used our model to study the affects of tera-Hertz radiation on DNA dynamics.

We derived a theoretical expression for photon emissions from a single molecule driven by laser excitation [2]. The frequencies of the fluoresced photons are explicitly considered. Calculations are performed for the case of a two-level dye molecule, showing that measured photon statistics will display a strong and unintuitive dependence on detector properties. Moreover, we demonstrated that the certain observed phenomena result from correlations between photons with well-separated frequencies.

MicroRNAs have the potential to regulate diverse sets of messenger RNA targets. In addition, mammalian genomes contain numerous natural antisense transcripts, most of which appear to be non-protein-coding RNAs (ncRNAs). We have identified and characterized a highly conserved non-coding antisense transcript for a critical enzyme in Alzheimer's disease [3]. Our data demonstrate an interface between two distinct groups of regulatory RNAs in the computation of gene expression. Moreover, bioinformatics analyses revealed a theoretical basis for many other potential interactions among natural antisense transcripts and microRNAs at the binding sites of the latter.

A critical roadblock to the production of bio-fuels from cellulosic biomass is the efficient degradation of crystalline cellulose to glucose. A microscopic understanding of how different physical conditions affect the overall stability of the crystalline structure of cellulose could facilitate the design of more effective protocols for their degradation. One of the essential physical interactions that stabilizes crystalline cellulose is a network of hydrogen bonds: both intra-chain hydrogen bonds between neighboring monomers of a single cellulose polymer chain and inter-chain hydrogen bonds between adjacent chains. We construct a statistical mechanical model of cellulose assembly at the resolution of explicit hydrogen-bond networks. With the help of a lattice-based model, we capture the plasticity of the hydrogen bond network in cellulose owing to frustration and redundancy in the placement of hydrogen bonds [4]. This plasticity is responsible for the stability of cellulose over a wide range of temperatures. Stable intra-chain and inter-chain hydrogen bonds are identified as a function of temperature that could possibly be manipulated toward rational destruction of crystalline cellulose.

Structures, dynamics, and stabilities of different sized cellulosic macromolecules need to be considered when designing enzymatic cocktails for the conversion of biomass to biofuels since they can be both productive substrates and inhibitors of the overall process. We studied [5] the conformational variability, hydrogen bonding, and mechanical properties of short, soluble cellulose chains, an example of which is shown in Figure 1, as a function of chain length. As the chain length is increased, the conformations of the macromolecules become more rigid and likely to form intra-chain hydrogen bonds, like those found in crystals.

Nuclear pore complexes (NPCs) act as effective and robust gateways between the nucleus and the cytoplasm, selecting for the passage of particular macromolecules across the nuclear envelope. NPCs comprise an elaborate scaffold that defines an approximately 30 nm diameter passageway

connecting the nucleus and the cytoplasm. To test whether a simple passageway and a lining of transport-factor-binding macromolecules are sufficient for selective transport, we designed a functionalized membrane that incorporates just these two elements as illustrated in Figure 2. We demonstrated [6] that this membrane functions as a nano-selective filter, efficiently passing transport factors and transport-factor-cargo complexes that specifically bind the lining macromolecules, while significantly inhibiting the passage of proteins that do not. This inhibition is greatly enhanced when transport factor is present. We showed that this artificial system faithfully reproduces key features of trafficking through the NPC. To further elucidate the transport mechanisms, it is important to understand the transport on the single molecule level in the experimentally relevant regime when multiple particles are crowded in the channel. We explored the effects of inter-particle crowding on the non-equilibrium transport times through a finite-length channel by means of analytical theory and computer simulations [7].

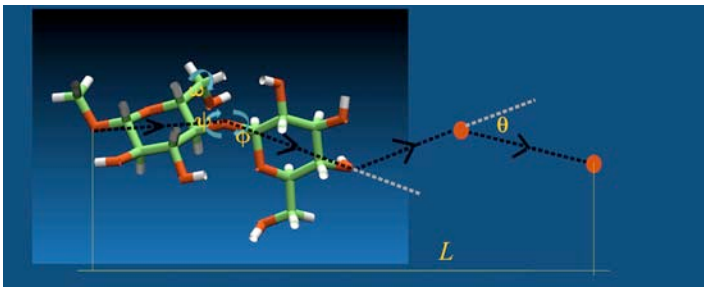

Figure 1. Structure of a cellulosic oligomer that needs to be considered when designing enzymatic cocktails for the conversion of biomass to biofuels. Molecules like this can both enhance and inhibit the conversion process.

Biochemical processes typically involve huge numbers of individual steps, each with its own dynamical rate constants. For example, kinetic proofreading processes rely upon numerous sequential reactions in order to guarantee the precise construction of specific macromolecules. We studied the transient properties of such systems and fully characterized their time to completion distributions [8]. In particular, we provide explicit expressions for the mean and the variance of the kinetic proofreading completion time. We find that, for a wide range of parameters, as the system size grows, the completion time behavior simplifies: it becomes either deterministic or exponentially distributed, with a very narrow transition between the two regimes. In both regimes, the full system dynamical complexity is trivial compared to its apparent structural complexity. Similar simplicity will arise in the dynamics of other complex biochemical processes. In particular, these findings suggest not only that one may not be able to understand individual elementary reactions from macroscopic observations, but also that such an understanding may be unnecessary.

We extended this work to the study of dynamical properties of discrete stochastic two branch kinetic proofreading schemes. Using the Laplace transform of the corresponding chemical master equation, we obtain an analytical solution for the completion time distribution. In particular, we provide expressions for the specificity and the mean and the variance of the process completion times. We also show that, for a wide range of parameters a process distinguishing between two different products can be reduced to a much simpler three-point process. Our results [9] allow for the systematic study of the interplay between specificity and completion times as well as testing the validity of the kinetic proofreading model in biological systems.

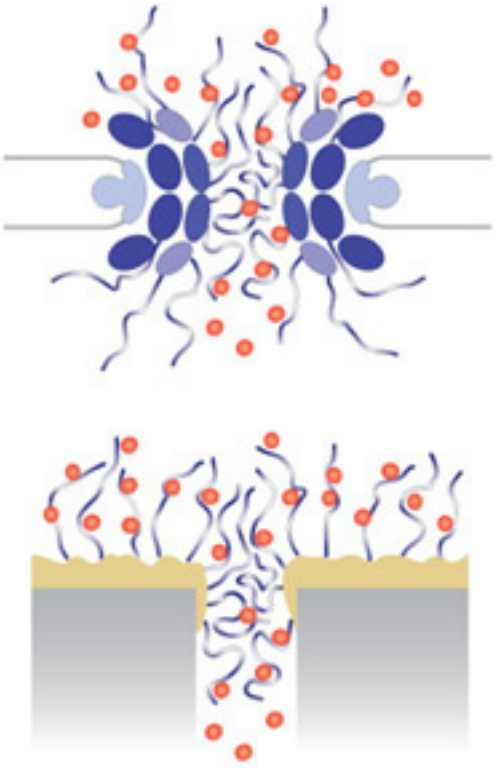

Figure 2. A schematic illustration of the real nuclear pore complex (above) and an artificial one (below) created in the laboratory. Transport factors (red) help proteins move through the complex, assisted by other proteins (twisting lines).

Interactions of molecules, such as signaling proteins, with multiple binding sites can be modeled using reaction rules. Rules comprehensively, but implicitly, define the individual chemical species and reactions that molecular interactions can potentially generate. Although rules can be automatically processed to define a biochemical reaction network, the network implied by a set of rules is often too large to generate completely or to simulate using conventional procedures. To address this problem, we developed DYNSTOC, a general-purpose tool for simulating rule-based models, which implements a null-event algorithm for simulating chemical reactions in a homogenous reaction compartment. We demonstrate [10] the ability of DYN-

STOC to simulate models accounting for multisite chemical reactions and binding processes that are characterized by large numbers of reactions. Pursuing these ideas further, we developed RuleMonkey [11], which implements a network-free method for simulation of rule-based models. RuleMonkey enables the simulation of rule-based models for which the underlying reaction networks are large and is typically faster than DYNSTOC for benchmark problems that we have examined.

Agent-based models were employed to describe numerous processes in immunology. Simulations based on these types of models have been used to enhance our understanding of immunology and disease pathology. We reviewed various agent-based models relevant to host-pathogen systems and discussed their contributions to our understanding of biological processes [12]. We also described some limitations and challenges of agent-based models and encouraged efforts towards reproducibility and model validation.

We showed [13] that the random fluctuations of cellular constituents carry within them valuable information about the underlying genetic network. This ever-present cellular noise acts as a rich source of excitation that, when processed through a gene network, carries a distinctive fingerprint that encodes a wealth of information about that network. We demonstrated that in some cases the analysis of these fluctuations enables the full identification of network parameters, including those that may otherwise be difficult to measure. This establishes a powerful approach for the identification of gene networks and offers a new window into the workings of these networks.

Phylogenetics is the study of the relationships among groups of organisms that are obtained by analyzing molecular sequencing data. By using statistical methods, shown schematically in Figure 3, one can estimate the degree to which different organisms are related to each other in an evolutionary sense. This has particular importance in ongoing epidemics where the ability of, for example, viruses to evolve can determine the efficacy of treatments or vaccines. We recently reconstructed specific events associated with an epidemic using the phylogenetic analysis of viral sequences [14]. This type of analysis is used in helping construct practical vaccines for HIV, an effort we contributed to recently [15, 16].

Demographic models built from genetic data play important roles in illuminating prehistoric events. We introduced [17] an inference method based on the spectrum of genetic variations within and between populations. For candidate models we numerically compute the expected spectrum using a diffusion approximation. As applications, we model human expansion out of Africa and the settlement of the New World, using non-coding DNA sequenced in 68 individuals from 4 populations.

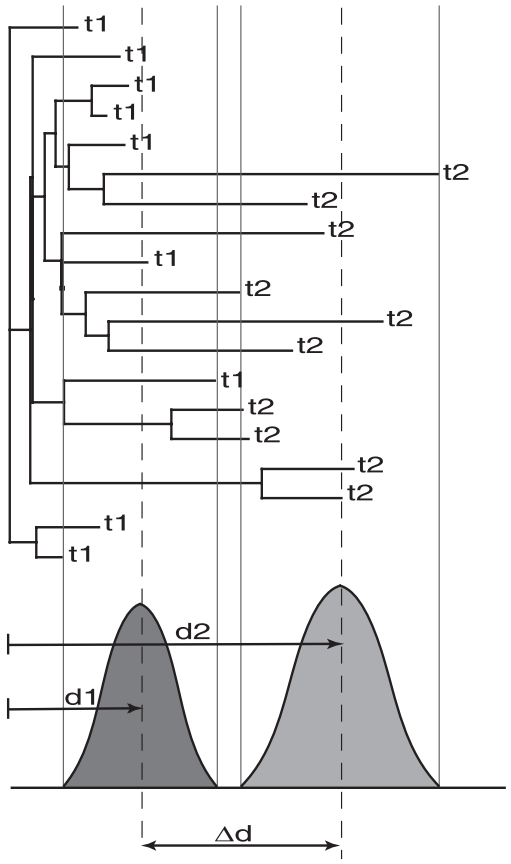

Figure 3. Schematic illustration of the statistical construction of a phylogenetic tree from genetic sequence data.

Impact on National Missions

This project supports Energy Security, Threat Reduction, and the missions of the DOE Office of Science through its far reaching efforts to accurately model biological systems at the molecular and cellular level with applications to bio-fuels, to novel sensors and to materials with broad use for energy or threat reduction. It has contributed directly to capability development in the bio-fuels area and in the area of rule-based modeling of cell signaling.

References

1. Bel, G., and F. L. Brown. Theory for Wavelength-Resolved Photon Emission Statistics in Single-Molecule Fluorescence Spectroscopy. 2009. *Physical Review Letters.* **102** (1).

2. Bel, G., and F. L. Brown. Theory for Wavelength-Resolved Photon Emission Statistics in Single-Molecule Fluorescence Spectroscopy. 2009. *Physical Review Letters.* **102** (1): 018303.

3. Munsky, B., I. Nemenman, and G. Bel. Specificity and completion time distributions of biochemical processes. 2009. *Journal of Chemical Physics.* **131** (23): 235103.

4. Faghihi, M. A., M. Zhang, J. Huang, F. Modarresi, M. P. Van der Brug, M. A. Nalls, M. R. Cookson, G. St-Laurent, and C. Wahlestedt. Evidence for natural antisense transcript-mediated inhibition of microRNA function. 2010. *Genome Biology.* **11** (5): R56.

5. Jovanovic-Talisman, T., J. Tetenbaum-Novatt, A. S. McKenney, A. Zilman, R. Peters, M. P. Rout, and B. T. Chait. Artificial nanopores that mimic the transport selectivity of the nuclear pore complex. 2009. *Nature.* **457** (7232): 1023.

6. Bel, G., B. Munsky, and I. Nemenman. The simplicity of completion time distributions for common complex biochemical processes. 2010. *Physical Biology.* **7** (1).

7. Colvin, J., M. I. Monine, J. R. Faeder, W. S. Hlavacek, D. D. Von Hoff, and R. G. Posner. Simulation of large-scale rule-based models. 2009. *Bioinformatics.* **25** (7): 910.

8. Colvin, J., M. I. Monine, R. N. Gutenkunst, W. S. Hlavacek, D. D. Von Hoff, and R. G. Posner. RuleMonkey: software for stochastic simulation of rule-based models. 2010. *Bmc Bioinformatics.* **11**.

9. Bauer, A. L., C. A. Beauchemin, and A. S. Perelson. Agent-based modeling of host-pathogen systems: The successes and challenges. 2009. *Information Sciences.* **179** (10): 1379.

10. Santra, S., H. X. Liao, R. J. Zhang, M. Muldoon, S. Watson, W. Fischer, J. Theiler, J. Szinger, H. Balachandran, A. Buzby, D. Quinn, R. J. Parks, C. Y. Tsao, A. Carville, K. G. Mansfield, G. N. Pavlakis, B. K. Felber, B. F. Haynes, B. T. Korber, and N. L. Letvin. Mosaic vaccines elicit CD8(+) T lymphocyte responses that confer enhanced immune coverage of diverse HIV strains in monkeys. 2010. *Nature Medicine.* **16** (3): 324.

11. Santra, S., H. X. Liao, R. J. Zhang, M. Muldoon, S. Watson, W. Fischer, J. Theiler, H. Balachandran, A. Buzby, D. Quinn, R. J. Parks, C. Y. Tsao, A. Carville, K. G. Mansfield, B. F. Haynes, B. T. Korber, and N. L. Letvin. Mosaic Vaccines Elicit Cd8+T Cell Responses in Monkeys That Confer Immune Coverage of Diverse Hiv Strains. 2010. *Journal of Medical Primatology.* **39** (4): 282.

12. Alexandrov, B. S., V. Gelev, Y. Monisova, L. B. Alexandrov, A. R. Bishop, K. O. Rasmussen, and A. Usheva. A nonlinear dynamic model of DNA with a sequence-dependent stacking term. 2009. *Nucleic Acids Research.* **37** (7): 2405.

Publications

Alexandrov, B. S., V. Gelev, A. R. Bishop, A. Usheva, and K. O. Rasmussen. DNA breathing dynamics in the presence of a terahertz field. 2010. *Physics Letters A.* **374** (10): 1214.

Alexandrov, B. S., V. Gelev, S. W. Yoo, A. R. Bishop, K. O. Rasmussen, and A. Usheva. Toward a Detailed Description of the Thermally Induced Dynamics of the Core Promoter. 2009. *Plos Computational Biology.* **5** (3): e1000313.

Alexandrov, B. S., V. Gelev, S. W. Yoo, L. B. Alexandrov, Y. Fukuyo, A. R. Bishop, K. O. Rasmussen, and A. Usheva. DNA dynamics play a role as a basal transcription factor in the positioning and regulation of gene transcription initiation. 2010. *Nucleic Acids Research.* **38** (6): 1790.

Alexandrov, B. S., V. Gelev, Y. Monisova, L. B. Alexandrov, A. R. Bishop, K. O. Rasmussen, and A. Usheva. A nonlinear dynamic model of DNA with a sequence-dependent stacking term. 2009. *Nucleic Acids Research.* **37** (7): 2405.

An, G., J. Faeder, and Y. Vodovotz. Translational systems biology: Introduction of an engineering approach to the pathophysiology of the burn patient. 2008. *Journal of Burn Care & Research.* **29** (2): 277.

Bauer, A. L., C. A. Beauchemin, and A. S. Perelson. Agent-based modeling of host-pathogen systems: The successes and challenges. 2009. *Information Sciences.* **179** (10): 1379.

Beauchemin, C. A., J. J. McSharry, G. L. Drusano, J. T. Nguyen, G. T. Went, R. M. Ribeiro, and A. S. Perelson. Modeling amantadine treatment of influenza A virus in vitro. 2008. *Journal of Theoretical Biology.* **254** (2): 439.

Bel, G., B. Munsky, and I. Nemenman. The simplicity of completion time distributions for complex biochemical processes. 2010. *Physical Biology.* **7** (1): 16003.

Bel, G., and F. L. Brown. Theory for Wavelength-Resolved Photon Emission Statistics in Single-Molecule Fluorescence Spectroscopy. 2009. *Physical Review Letters.* **102** (1): 018303.

Bel, G., and I. Nemenman. Ergodic and non-ergodic anomalous diffusion in coupled stochastic processes. 2009. *New Journal of Physics.* **11**: 083009.

Berry, I. Maljkovic, K. Aperia, M. Kothari, M. Daniels, B. Korber, C. Kuiken, and T. Leitner. The evolutionary rate dynamically tracks changes in HIV-1 epidemics: Application of a simple method for optimizing the evolutionary rate in phylogenetic trees with longitudinal data. 2009. *Epidemics.* **1**: 230.

Chernyak, V. Y., and N. A. Sinitsyn. Pumping Restriction Theorem for Stochastic Networks. 2008. *Physical Review Letters.* **101** (16): 160601.

Choi, C. H., Z. Rapti, V. Gelev, M. R. Hacker, B. Alexandrov, E. J. Park, J. S. Park, N. Horikoshi, A. Smerzi, K. O. Ras-

mussen, A. R. Bishop, and A. Usheva. Profiling the thermodynamic softness of adenoviral promoters. 2008. *Biophysical Journal.* **95** (2): 597.

Colvin, J., M. I. Monine, J. R. Faeder, W. S. Hlavacek, D. D. Von Hoff, and R. G. Posner. Simulation of large-scale rule-based models. 2009. *Bioinformatics.* **25** (7): 910.

Colvin, J., M. I. Monine, R. N. Gutenkunst, W. S. Hlavacek, D. D. Von Hoff, and R. G. Posner. RuleMonkey: software for stochastic simulation of rule-based models. 2010. *Bmc Bioinformatics.* **11**: 404.

Dreisigmeyer, D. W., J. Stajic, I. Nemenman, W. S. Hlavacek, and M. E. Wall. Determinants of bistability in induction of the Escherichia coli lac operon. 2008. *Iet Systems Biology.* **2** (5): 293.

Faghihi, M. A., M. Zhang, J. Huang, F. Modarresi, M. P. Van der Brug, M. A. Nalls, M. R. Cookson, G. St-Laurent, and C. Wahlestedt. Evidence for natural antisense transcript-mediated inhibition of microRNA function. 2010. *Genome Biology.* **11** (5): R56.

Gutenkunst, R. N., R. D. Hernandez, S. H. Williamson, and C. D. Bustamante. Inferring the joint demographic history of multiple populations from multidimensional SNP data. 2010. *PLoS Genetics.* **5** (10): e1000695.

Gutenkunst, R. N., R. D. Hernandez, S. H. Williamson, and C. D. Bustamante. Inferring the Joint Demographic History of Multiple Populations from Multidimensional SNP Frequency Data. 2009. *Plos Genetics.* **5** (10): e1000695.

Ham, M. I., V. Gintautas, M. A. Rodriguez, R. A. Bennett, C. L. Maria, and L. M. Bettencourt. Density-dependence of functional development in spiking cortical networks grown in vitro. 2010. *Biological Cybernetics.* **102** (1): 71.

Hu, B., G. M. Fricke, J. R. Faeder, R. G. Posner, and W. S. Hlavacek. GetBonNie for building, analyzing and sharing rule-based models. 2009. *Bioinformatics.* **25** (11): 1457.

Jovanovic-Talisman, T., J. Tetenbaum-Novatt, A. S. McKenney, A. Zilman, R. Peters, M. P. Rout, and B. T. Chait. Artificial nanopores that mimic the transport selectivity of the nuclear pore complex. 2009. *Nature.* **457** (7232): 1023.

Kilina, S., E. Badaeva, A. Piryatinski, S. Tretiak, A. Saxena, and A. R. Bishop. Bright and dark excitons in semiconductor carbon nanotubes: insights from electronic structure calculations. 2009. *Physical Chemistry Chemical Physics.* **11** (21): 4113.

Lipniacki, T., B. Hat, J. R. Faeder, and W. S. Hlavacek. Stochastic effects and bistability in T cell receptor signaling. 2008. *Journal of Theoretical Biology.* **254** (1): 110.

Monine, M. I., R. G. Posner, P. B. Savage, J. R. Faeder, and W. S. Hlavacek. Modeling Multivalent Ligand-Receptor Interactions with Steric Constraints on Configurations of Cell-Surface Receptor Aggregates. 2010. *Biophysical Journal.* **98** (1): 48.

Motter, A. E., N. Gulbahce, E. Almaas, and A. Barabasi. Predicting synthetic rescues in metabolic networks. 2008. *Molecular Systems Biology.* **4**: 168.

Munsky, B., B. Trinh, and M. Khammash. Listening to the noise: Random fluctuations reveal gene network parameters. 2009. *Molecular Systems Biology.* **5**: 318.

Munsky, B., I. Nemenman, and G. Bel. Specificity and completion time distributions of biochemical processes. 2009. *Journal of Chemical Physics.* **131** (23): 235103.

Nag, A., M. I. Monine, J. R. Faeder, and B. Goldstein. Aggregation of Membrane Proteins by Cytosolic Cross-Linkers: Theory and Simulation of the LAT-Grb2-SOS1 System. 2009. *Biophysical Journal.* **96** (7): 2604.

Nemenman, I., W. S. Hlavacek, Y. Jiang, and M. E. Wall. Selected papers from the Second q-bio Conference on Cellular Information Processing. 2009. *IET Systems Biology.* **3** (5): 297.

Nemenman, I., W. S. Hlavacek, Y. Jiang, and M. E. Wall. Selected papers from the Second q-bio Conference on Cellular Information Processing. 2009. *Iet Systems Biology.* **3** (5): 297.

Ramachandran, S., H. Tang, R. N. Gutenkunst, and C. D. Bustamante. Human population genetics and genomic. 2010. *Human Genetics: Problems and Approaches, 4th Addition, Springer Verlag by Vogel and Motulsky.* : 589.

Santra, S., H. X. Liao, R. J. Zhang, M. Muldoon, S. Watson, W. Fischer, J. Theiler, H. Balachandran, A. Buzby, D. Quinn, R. J. Parks, C. Y. Tsao, A. Carville, K. G. Mansfield, B. F. Haynes, B. T. Korber, and N. L. Letvin. Mosaic Vaccines Elicit Cd8+T Cell Responses in Monkeys That Confer Immune Coverage of Diverse Hiv Strains. 2010. *Journal of Medical Primatology.* **39** (4): 282.

Santra, S., H. X. Liao, R. J. Zhang, M. Muldoon, S. Watson, W. Fischer, J. Theiler, J. Szinger, H. Balachandran, A. Buzby, D. Quinn, R. J. Parks, C. Y. Tsao, A. Carville, K. G. Mansfield, G. N. Pavlakis, B. K. Felber, B. F. Haynes, B. T. Korber, and N. L. Letvin. Mosaic vaccines elicit CD8(+) T lymphocyte responses that confer enhanced immune coverage of diverse HIV strains in monkeys. 2010. *Nature Medicine.* **16** (3): 324.

Schultz, A. K., M. Zhang, I. Bulla, T. Leitner, B. Korber, B. Morgenstern, and M. Stanke. jpHMM: Improving the reliability of recombination prediction in HIV-1. 2009.

Nucleic Acids Research. **37**: W647.

Shen, T. Y., P. Langan, A. D. French, G. P. Johnson, and S. Gnanakaran. Conformational Flexibility of Soluble Cellulose Oligomers: Chain Length and Temperature Dependence. 2009. *Journal of the American Chemical Society.* **131** (41): 14786.

Shen, T. Y., and D. Hamelberg. A statistical analysis of the precision of reweighting-based simulations. 2008. *Journal of Chemical Physics.* **129** (3): 034103.

Shen, T. Y., and S. Gnanakaran. The Stability of Cellulose: A Statistical Perspective from a Coarse-Grained Model of Hydrogen-Bond Networks. 2009. *Biophysical Journal.* **96** (8): 3032.

Weronski, P., and M. Elimelech. Novel numerical method for calculating initial flux of colloid particle adsorption through an energy barrier. 2008. *JOURNAL OF COLLOID AND INTERFACE SCIENCE.* **319** (2): 406.

Yang, J., M. I. Monine, J. R. Faeder, and W. S. Hlavacek. Kinetic Monte Carlo method for rule-based modeling of biochemical networks. 2008. *Physical Review E.* **78** (3): 031910.

Yang, J., M. I. Monine, J. R. Faeder, and W. S. Hlavacek. Kinetic Monte Carlo method for rule-based modeling of biochemical networks. 2008. *Physical Review E.* **78** (3): 031910.

Zilman, A.. Effects of Multiple Occupancy and Interparticle Interactions on Selective Transport through Narrow Channels: Theory versus Experiment. 2009. *Biophysical Journal.* **96** (4): 1235.

Zilman, A., J. Pearson, and G. Bel. Effects of Jamming on Nonequilibrium Transport Times in Nanochannels. 2009. *Physical Review Letters.* **103** (12): 128103.

Zilman, A., S. Di Talia, T. Jovanovic-Talisman, B. T. Chait, M. P. Rout, and M. O. Magnasco. Enhancement of Transport Selectivity through Nano-Channels by Non-Specific Competition. 2010. *Plos Computational Biology.* **6** (6): e1000804.

Using Small Molecules to Control RNA Conformations

Karissa Y. Sanbonmatsu
20090163ER

Introduction

A riboswitch is a molecule inside a bacterium that turns genes on or turns genes off. The riboswitch is controlled by small molecules present inside the cell, such as vitamins, amino acids, and metabolites. They are exciting because they represent a new form of gene control that was only recently discovered. They have applications in the development of new antibiotics. How they work is not understood in atomic detail. If we can understand how they work, then we can design better ones.

More specifically, these switches have a normal configuration that occurs when the small molecule is not present. The normal configuration, for example, does not allow gene expression. When the small molecule is present, the switch folds into an alternative configuration that turns the gene on, allowing gene expression. Riboswitches can easily discriminate between very similar small molecules. Considering that a prototype riboswitch-based biosensor chip has been constructed, riboswitches are excellent candidates for next generation biosensors. The sensitivity to minute differences between ligands also makes the riboswitch a promising target for antibacterial drug design. So far, these switches have only been found in bacteria. Therefore, antibiotics that target riboswitches are thought to have very few side effects, since the switches have not been found in humans.

Our goal is to understand how these switches switch. We will address the questions:

1. How does the small molecule bind?
2. How does binding result in switching?
3. How tunable is the switch? In particular, we will investigate the hypotheses:
   - Stabilization of a compact binding domain upon ligand recognition occurs through a series of intermediate states.
   - Switching occurs by morphing between the two-riboswitch states through a series energetically favorable intermediates, as opposed to unfolding and refolding.

Benefit to National Security Missions

Because the study focuses on genetic switches that are biosensors, the project is directly related to the "Biological Sensor Systems" of the "Ubiquitous Sensing" grand challenge, as well as the sensing component of the "Biology of Infectious Agents" key capability. The project is also related to the "Biology of Infectious Agents" by its applications to antibiotic design. We are currently preparing and will be preparing proposals for NIH, DARPA and DOE.

Progress

We made tremendous progress during FY2010, including several important discoveries that will help us to design molecular switches. We were able to optimize our new technique to measure the operating characteristics of molecular switches. We achieved amazing agreement between simulation and experiment. We discovered that salt is critical for the operation of the switch, and, that both salt and the sensed small molecule must be present for the switch to work properly.

Optimized experiments to determine the operational principles of genetic switches.
We have used our novel 2-piece switching system to uncover part of the mechanism of switching in riboswitches. In our new method, we split the switch into two pieces (Figure 1). When we add the second piece to the mix, we are able to observe automatic switching from state 1 to state 2. We discovered that certain parts of the genetic switch have a large affect on the capability to switch properly. Certain alterations make the switch completely unusable. We identified the most critical parts of the switch required for switch function. The study is was accepted and is in press [1] at "Nucleic Acids Journal," which has an impact factor higher than "Physical Review Letters".

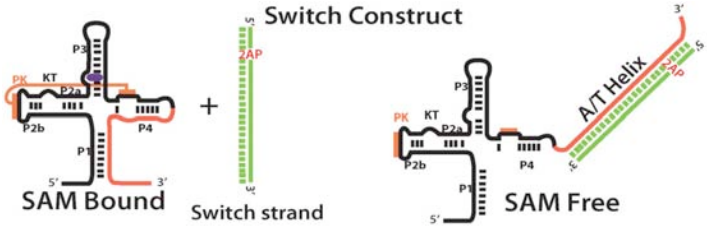

Figure 1. Schematic of novel 2-piece switching system that measures the rate of switching. The switch is made out of ribonucleic acid (RNA), which is the molecular cousin of deoxyribonucleic acid (DNA). The diagram shows the two-dimensional structure of the switch, with small molecule bound(purple). Each double helix is labeled P1, P2, P3, P4, etc. An interaction that occurs in three dimensions is shown with the label "PK". The switch is first cut into 2 pieces. The small piece (green) is labeled with a glowing molecule ("2AP"). When the small piece is added, it rips apart the large structure and forms a new helix, which no longer glows (right panel). The small molecule (purple) that is detected by the biosensor actually prevents the green strand from invading and ripping apart the structure. By mutating key contacts, we were able to discover which parts are crucial for switching.

Achieved close agreement between theory and experiment

We performed biochemical experiments measuring the mobility of each piece of the riboswitch using fluorescence. These were performed for many different biochemical environments. We then performed all-atom molecular dynamics simulations of the same systems. The simulations used a simplified force field potential that has just a few free parameters. This technique is closely tied to experimental data and is also quite easily adjustable to experimental data. The first simulations showed overall similarity to experiments but differed significantly in some important parts of the riboswitch. We developed new analytical measures to enable direct comparison to experiment. We isolated those parts that differed and modified the corresponding force field potential for the parts showing differences from experiment. This is the first such agreement ever for a riboswitch system.

Studied the effect of salt on the genetic switch

We did a wide range of experiments focused on determining the effect of ionic concentration and electrostatic environment on the switch. This included experiments of the binding part of the switch. We also performed switching studies that probed the effect of Magnesium ions. We found something startling – both the small molecule that triggers switching and salt are important for the operation of the riboswitch. The riboswitch is controlled by a tiny small molecule. It is an unsolved problem (for many years) regarding how such a tiny small molecule can cause a huge change in the conformation of the switch. We have evidence that the salt works together with the small molecule to cause the gigantic configurational movement of this riboswitch. Our studies are consistent with a dynamic equilibrium between two switching states that favors one state. When the small molecule and the salt are present, the equilibrium changes to the other state.

Our new method and discovery have led to unprecedented insight regarding the mechanism of the molecular switch called a 'riboswitch'. They have led to our goal of trying to figure out how tunable the riboswitch may be.

Future Work

We will perform a more careful study of the effect of salt on the genetic switch. We will then perform computer simulations of the effect of salt on the genetic switch. We will tune our simulation parameters to improve the agreement between computer models and actual experiments that occur in the real world. Next, we will expand our computer models of the system without salt. We will perform new experiments that heat up the genetic system by turning up the temperature. We will watch exactly how the genetic switch melts as a function of temperature. We will then make computer models to try to match the real world experiments. We will tune the computer parameters to improve agreement. Finally, we will watch single gene switches using single molecule experiments. This will give us a more detailed picture of how gene switches work.

Conclusion

We have used computers and biochemistry experiments to understand a new kind of genetic switch. Biochemistry experiments were performed to understand the overall process of switching. Then, computers were used to simulate the inner workings of the switch. In the future, we hope to improve the performance of the switch.

References

1. Hennelly, S. P., and K. Y. Sanbonmatsu. Tertiary contacts control switching of the SAM-I riboswitch. To appear in *Nucleic Acids Research.*

Publications

Hennelly, S. P., and K. Y. Sanbonmatsu. Tertiary contacts control switching of the SAM-I riboswitch. To appear in *Nucleic Acids Research.*

Whitford, P. C., A. Schug, J. Saunders, S. P. Hennelly, J. N. Onuchic, and K. Y. Sanbonmatsu. Nonlocal helix formation is key to understanding S-adenosylmethionine-1 riboswitch function. 2009. *Biophysical Journal.* **92** (2): L7.

Whitford, P. C., J. K. Noel, S. Gosavi, A. Schug, K. Y. Sanbonmatsu, and J. N. Onuchic. An all-atom structure-based potential for proteins: bridging

minimal models with all-atom empirical forcefields. 2009. *Proteins: Structure, Function, and Genetics.* **75** (2): 430.

Functional Gene Discovery Using RNAi-based Gene Silencing

Elizabeth Hong-Geller
20090202ER

Introduction

Human pathogens have evolved sophisticated mechanisms by which to attack the host immune system. Yersinia pestis, the causative agent of plague, is a CDC Category A pathogen with bioweapon potential, and thus represents a high-value target for the development of novel therapeutic strategies. Y. pestis employs multiple virulence strategies during host infection, including the type III secretion system (TTSS), a "syringe-like" needle complex that injects virulence proteins, or Yop effectors, into the host cell. In the proposed study, we will identify host proteins that are targeted by Y. pestis during infection using RNA interference (RNAi), a powerful tool for analyzing gene function by silencing, or inactivating, target genes through the specific destruction of their mRNAs. We will perform high-throughput genome-wide screens and more directed automated confocal microscopy studies to select for genes, that when silenced, lead to inhibition of Y. pestis infection. From these functional genomics studies, we will identify host proteins targeted by Y. pestis and thus, be able to exploit their associated mechanisms of pathogenicity to develop therapeutic countermeasures against Y. pestis infection. We expect that development of genomic screens using our human siRNA library will establish a robust methodology by which to ascribe function to previously uncharacterized genes, a major challenge in biomedical research given that approximately half of all predicted human genes have no known function.

Benefit to National Security Missions

This project will support the DOE/NNSA mission in Threat Reduction by enhancing our understanding of host-pathogen interactions and biodefense capabilities. It is important to support other missions of the Laboratory as well (e.g., Homeland Security), but not to the exclusion of the DOE/NNSA missions. We have already secured funding from DTRA to use our methodology to investigate host-genes targeted by *Burkholderia pseudomallei*.

Progress

To identify host proteins essential for microbial pathogenicity, we have established a platform for genome-wide loss-of-function high-throughput screens (HTS) employing RNA interference (RNAi), a powerful tool for loss-of-function studies used to analyze gene function by silencing target genes through the specific destruction of their mRNAs, which encode for expression of specific proteins. We have focused our studies on the Yersinia species, including Y. pestis, the etiological agent of bubonic and pneumonic plague, because of its high virulence and potential threat for social devastation, and Y. enterocolitica, a causative agent of gastrointestinal disease. We have obtained two RNAi libraries that cover the Kinase and Druggable target genes families. We have developed an assay based on cytokine activation of a regulatory protein, the transcription factor NF-kB, linked to a fluorescence or luminescence reporter gene. Infection with Yersinia blocks the cytokine activation step, leading to decreased levels of reporter gene expression. Inhibition of Yersinia infection with the RNAi library constructs will restore reporter gene expression. (Figure 1) We have currently screened the entire kinase library and a small selection of the druggable target library using this assay. We have identified ~25 human genes, that when silenced, leads to decreased Yersinia infectivity. (Figure 2) These genes fall into multiple functional categories, including signal transduction, cell stress and apoptosis, protein folding, cell adhesion, and membrane potential. Among the initial hits from the genomic screen was HSP90 (heat shock protein 90), which upon downregulation, leads to increased viability of human cells in response to Yersinia enterocolitica infection. Using a small molecule inhibitor against HSP90 (17-AAG), we obtained a higher percentage of primary human dendritic cells surviving the impact of Yersinia infection. We are currently validating a number of the other candidate genes to confirm their role in *Yersinia* infection. Identification of these targeted host proteins during *Yersinia* infection would greatly elucidate *Yersinia* virulence mechanisms and serve as the basis for design of novel inhibitor therapeutics that block *Yersinia* infection. Furthermore, we expect to develop a RNAi-

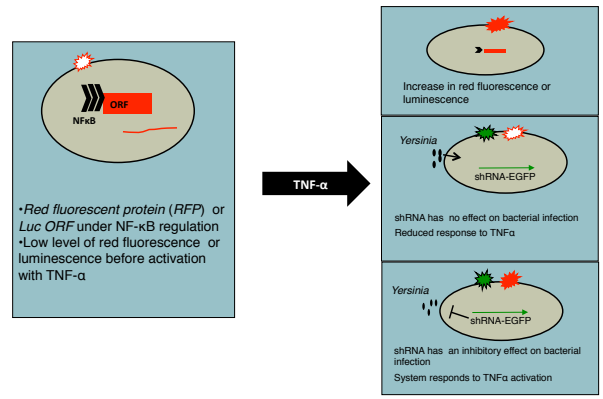

Figure 1. Assay development to screen for shRNAs that block Yersinia infection

TARGET PATHWAY				
Signal Transduction	Cell stress and Apoptosis	Protein Folding	Cell Adhesion	Membrane potential
Gene Function				
•**MAP3K14**, binds TRAF and stimulates NFkB •**MAP2K1**, regulates ERK activation •**MAP3K3**, directly regulates ERK pathways by activating MEK1/2 •**LKB1/PJS**, involved in SR-BI activation of AKT •**ERK4/MAPK7**, translocates in the nucleus and activates many TFs •**CK2**, cell cycle and cell growth regulation •**PIK3R2**, regulatory subunit 2β of PI3K •**PI3-K-C2A**, class 2 α-polypeptide of PI3K family, involved in cell proliferation, survival, migration and intracellular protein trafficking; may be involved in integrin-dependent signaling •**ACTR-IIB**, activin A type II B receptor, transmembrane cell growth and differentiation factors belonging to TGFβ superfamily	•**HSP90AB1**, regulates apoptosis through AKT, BIRC5, and Apaf1 signaling, also FKBP38 direct inactivation •**HSPH1**, role in ER stress response through GSK3 •**SGK1**, has an important role in cell stress response, negative regulation of apoptosis •**MAP3K3**, directly regulates stress-activated protein kinase (SAPK) by activating SEK •**ULK2**, regulates authophagy in response to mTOR signaling •**WNK3**, binds to Casp3 and prolongs cell survival upon stress stimulus; Ca+-transport regulation •**ABL/JTK**, non-receptor Tyr kinase involved in cell differentiation, stress response, and apoptosis (activates AKT)	•**HSP90AB1**, has a key role in folding newly synthesized proteins or stabilizing the structure and promoting proper function of many signal transduction proteins •**HSPH1**, senses unfolded proteins	•**ABL/JTK**, non-receptor Tyr kinase involved in actin cytoskeleton organization •**SGK1**, has a negative regulation of microtubule polymerization •**DMRV/GNE**, a rate-limiting enzyme in the sialic acid biosynthesis pathway, thus having a crucial role in cell adhesion and signal transduction	•**WNK1**, regulates Na and Cl-ion transport, activates MAP3K3 and SGK1 •**SGK1**, activates certain K, Na, and Cl-ion channels •**SGK2**, regulates K -ion channels, has a role in epithelial ion transport •**MONaKA/PXK**, regulates both Na,K-ATPase enzymatic and ion pump activities

Figure 2. Table of host genes identified in shRNA screen

based high-throughput research capability that can be used to ascribe function to human genes in many complex host response processes.

Future Work

We have developed a robust RNAi-based platform for HTS functional genomics and discovery of host proteins that play a role in *Yersinia* pathogenicity. We expect this methodology and the shRNA reagents can be broadly applied to study host response to other pathogens or chemical agents. In this third and final year, we will continue to validate the genes identified in Table 1 by creating stable cell lines that express the shRNAs and using alternative methods of gene knock-down such as small molecule inhibitors to assess Yersinia infection phenotypes. We will try to confirm a similar role for these host targets in Y. pestis and correlate function with Y. enterocolitica infection from the original screen. We will also perform hypothesis-drive cell and molecular biology assays to discover the molecular mechanisms by which Yersinia manipulates these target host genes. We will also continue to screen the remaining shRNAs from the druggable target library to increase the number of potential host targets fro drug discovery against infectious disease. We plan to publish our experimental work in the next year and pursue follow-on opportunities for funding from different agencies.

Conclusion

This project will contribute significantly to the study of host-pathogen interactions, a key strategic research capability that supports the LANL mission of biothreat reduction and protection of national security. Yersinia pestis, a potential agent of bioterrorism, is a CDC Category A pathogen, signifying great potential risk for adverse impact on public health. The proposed research will seek to identify host proteins targeted by Y. pestis during infection. New strategies to counteract Y. pestis infection, based on increased fundamental understanding of Y pestis virulence, can greatly impact our ability to contain potential outbreaks of plague in the population.

Publications

Hong-Geller, E., K. Nowak-Lovato, S. Micheva-Viteva, and S. Lauer. Regulation of host chemokine response by the pathogenic Type III secretion system. To appear in *Chemokines: Types, Functions, and Structural Characteristics.* Edited by Walker, K..

Hong-Geller, E., and S. Micheva-Viteva. Functional gene discovery using RNA interference-based genomic screen to combat pathogen infectin. 2010. *Current Drug Discovery Technologies.* **7**: 94.

Micheva-Viteva, S., K. Rector, and E. Hong-Geller. Functional gene discovery in Y. pestis infection using RNAi-based gene silencing. 2009. In *2009 Chemical and Biological Defense Science and Technology Conference.* (Dallas, TX, 16-20 Nov. 2009). , p. 262. Dallas: DTRA.

Micheva-Viteva, S., K. Rector, and E. Hong-Geller. Functional gene discovery using RNAi-based gene silencing. To appear in *2010 Chemical and Biological Defense Science and Technology Conference.* (Orlando, FL, 15-19 Nov. 2010).

Micheva-Viteva, S., K. Rector, and E. Hong-Geller. Functional gene discovery using RNAi-based gene silencing. To appear in *High Content Analysis.* (San Francisco, 12-14 Jan. 2011).

A Visionary New Approach to Assess Regional Climate Impacts on Vegetation Survival and Mortality

Nathan G. Mcdowell
20090305ER

Introduction

Models of climate change and its impacts on ecological systems must be accurate at regional scales for predictions to be of use to policy-makers. By regional scale, we mean at the level of individual states and smaller. We propose to dramatically improve climate change and climate impacts modeling at the regional scale through a two component, integrated project. Our first component will test cutting edge theory of plant survival and mortality with both empirical and modeling efforts to develop the first mechanistic model of vegetation dynamics in response to climate. Our second component will improve downscaled predictions of climate over the 50 year timespan. By downscaled we mean taking climate predictions made at the global level and scaling them to the scale of individual states and smaller. We are integrating these two facets into an improved model of regional climate change and ecological impacts.

Benefit to National Security Missions

This project supports the Office of Science and other agency missions to understand and predict climate change and its ecological impacts.

Progress

Vegetation mortality

We investigated the potential for the observed vegetation mortality event at the Los Alamos National Environmental Research Park to inform us of the potential cause of death of the pinon trees at the site. Our analysis of the long term leaf water potential records, and our increasing understanding of pinon mortality resulting from allied LANL projects, indicated that the three month period of static leaf water potentials was actually consistent with both hydraulic failure and carbon starvation as modes of death. This means that, given appropriate fitting of the free parameters associated with both physiological mechanisms, the model can be made to fit the observations using either set of assumptions. This result, while being a negative science result and thus not amenable to publication, has been instrumental in navigating our scientific efforts towards measurements that will likely soon yield data capable if distinguishing between the two hypotheses.

In addition we have published a study investigating the ecological consequences of the carbon starvation model for long term vegetation trends (Fisher et al. 2010). This represents the first time that this explicit mechanism has been incorporated into a dynamic vegetation model and has generated motivation to measure the relevant parameters in fieldwork studies (there are currently three funded proposals that tackle this topic directly).

This work on vegetation dynamics clearly demonstrates that vegetation mortality and regrowth, as community level processes, cannot be considered in isolation from ecosystem structure. Indeed, the same mortality model can generate vastly different results depending on how functional diversity in plant resilience, and the sharing of water resources are proscribed. This lead to discussions with NCAR on potential improvements to the Community Land Model ecology representation, and the integration of a combined mortality- vegetation dynamics model into CLM. This model is now in the testing phase, but it due to form the core of the next release of the CLM model (CLM5.0).

Furthermore, this development, which was facilitated by the LDRD-ER project, lead to Rosie Fisher's appointment as an NCAR scientist leading this development, and thus lays the foundation for close LANL- NCAR collaborations both ongoing and in the future.

Further investigations of the mechanisms of vegetation mortality have focused in the methodologies for inverse parameterisation of non-structural carbohydrate stores using experimental data from a tropical forest ecosystem. This site was chosen to demonstrate this technique on account of the mature status of the observations and analyses. We have designed a technique to infer the constraints in the distribution of NSCs in a population from ecosystem level mortality and carbon economics data. A manuscript on our findings, which suggest that trees are a factor of 2-3 times more

resilient that existing parameterizations assume, is in the latter stages of preparation (Fisher, Vrught, McDowell et al)

McDowell has published numerous papers regarding vegetation mortality, listed in the publications section, that were supported either directly, i.e. through work with Rosie Fisher, or indirectly, through stimulating discussions and T&E support with this ER team. He has also given numerous invited presentations, including to DOE and multiple Universities.

Regional climate

In order to test hypotheses about the effects of vegetation change on Southwest climate, Rausher and Ringler worked on customizing the regional climate model WRF for use over the western United States. Over the summer they continued to test different configurations of WRF, including the use of different boundary conditions (NCEP/NCAR Reanalysis, North American Regional Reanalysis (NARR)), different physics options (e.g., cumulus and radiation schemes), and the effects of including the Community Land Model on the simulation. So far the biases compared to observations are still larger than we prefer (precipitation should be within +/- 20% of observations and temperature biases within 1-2 degrees). In addition, with the addition of the new land surface model (CLM) I was getting different solutions with different numbers of processors. Dr. Rausher has presently switched compilers from PGI to INTEL and reduced optimization. In addition to testing, she added new output variables to WRF for diagnosis, and has modified the code so that CO_2 can be transient (necessary for climate change simulations).

Coupled vegetation-climate regional modeling

We have compiled the driver dataset and high resolution datasets to drive the version of CLM native to WRF (3.5) and have commenced these simulations. Initial results indicate that a physiological signal of the drought is indeed manifested in the model, and further tests are necessary to determine the impact on vegetation dynamics. We are scheduled to present this work at AGU, and as a publication in the spring. This work is novel in several respects- its high spatial resolution, the focus of the model on semi-arid systems, and the diagnosis of a mortality event.

In addition to the coupled model system (WRF-CLM), Rosie Fisher and Sara Rauscher are currently running CLM at high resolution (~30 km) off-line with atmospheric data forcing (NARR). In this way, CLM can be validated quickly, and we can efficiently perform mortality experiments. We know have the scripts to obtain the data from the NCAR mass store system and to convert the data into the necessary format to force CLM. The data conversion process is ongoing, as it requires obtaining 60,000 files (three hourly data for nearly 30 years) from the NCAR mass store system, and processing them.

Future Work

The remaining tasks are to finish the coupling of WRF and ED-CLM and write one or more manuscripts describing the coupling and the associated hypothesis testing.

Conclusion

This project has, and will continue, to develop fundamental understanding of climate change and of ecological impacts. Our coupled WRF-ED-CLM model is allowing regional scale predictions of climate change and its impacts, and is leading to continued knowledge gain and model improvements. Improved understanding will allow this tool to be more accurate, greatly enhancing our ability to inform policy makers of coming changes within their regions.

Publications

Fisher, R., N. G. McDowell, D. Purves, P. Moorcroft, S. Sitch, P. Cox, C. Huntingford, P. Meir, and I. Woodward. Assessing uncertainties in a second-generation dynamic vegetation model due to ecological scale limitations. 2010. *New Phytologist.* **187** (3): 666.

McDowell, N. G., C. Allen, and L. Marshall. Growth, carbon isotope discrimination, and mortality across a ponderosa pine elevation transect. 2010. *Global Change Biology.* **16** (1): 399.

Rauscher, S. A., F. Kucharski, and D. B. Enfield. The role of regional SST warming variations in the drying of Meso-America in future climate projections. To appear in *Journal of Climate.*

Seth, A., S. A. Rauscher, M. Rojas, A. Giannini, and S. J. Camargo. Enhanced Spring Convective Barrier for Monsoons in a Warmer World? . To appear in *Climatic Change Letters.*

Membrane Micro-chromatography: A Novel Approach to Preparative Nucleic Acid Sample Processing

Goutam Gupta
20090363ER

Introduction

The lateral flow microarray (LFM) device allows detection of specific signatures from a pathogen as well as host biomarkers that report different stages of infection caused by the pathogen. The LFM is ideally suited for the detection of nucleic acid signatures from the pathogen and host. Prior to detection, the nucleic acid from the pathogen or host will be isolated and amplified. Also, appropriate probes will be spotted on the LFM that capture the pathogen signatures or host biomarkers by hybridization or sequence identity. The final step will involve the colorometric detection of the hybridized target sequences (i.e., pathogen signatures and/or host biomarkers) on the LFM platform. This project focuses on two specific applications:

- Discovery of host markers for early infection due to specific influenza A subtypes;
- Monitoring the efficacy of a therapeutic protein expressed in a transgenic grape to protect against fatal Xylella fastidiosa (Xf) infection by examining the expression of key Xf and grape genes.

Benefit to National Security Missions

This project will support DOE missions in threat reduction and non-proliferation by providing a previously unavailable capacity to detect DNA signatures and biological threats under field conditions. Additionally, the technology supports missions in homeland security by providing the capability to detect, identify and respond to a biological threat.

Progress

Traditionally infectious diseases are diagnosed by monitoring symptoms that include distinct changes that occur at the tissue and organ level in patients and that can be detected by simple imaging methods. Recently, detection of specific biomarkers is also included as a part of diagnosis. In this LDRD-ER project, our goal has been to develop and apply a novel method that is capable of detecting infection at a stage much earlier than the occurrence of tissue damage and organ failure. This pre-symptomatic diagnosis is achieved by a nucleic acid based lateral flow platform that detects several disease-specific gene biomarkers in a multiplex format (Figure 1). The pattern of expression of these biomarkers is indicative of the onset and progression of a given disease. Here, we report our progress in the discovery and validation of such biomarkers for a) Pierce's Disease in grapes and b) seasonal flu in humans.

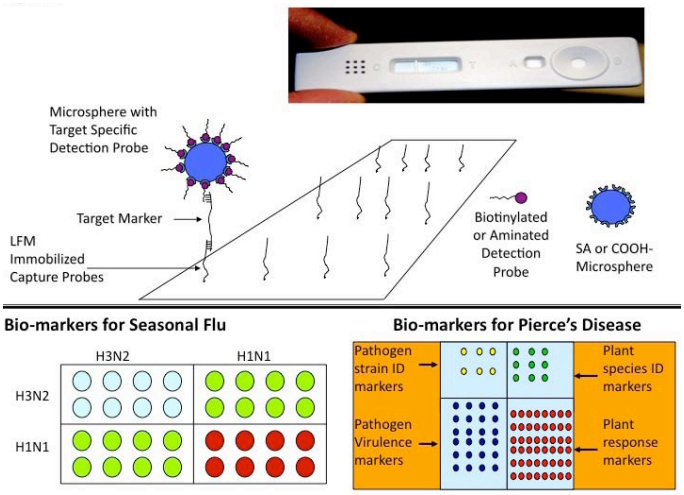

Figure 1. Schematic view of the Lateral Flow Microarray (LFM) platform: (top) the device; (middle) the assay system of recognition of the target sequence by the capture probe immobilized on the platform and the detection probe attached to the bead; (bottom) the host biomarkers for H1N1 and H3N2 and biomarkers for PD.

a) A Platform For Efficacy Studies On Transgenic Grapes

Pierce's Disease (PD) is caused by a gram-negative bacteria *Xylella fasitidiosa* (Xf), which is transmitted by sharpshooters to the grape xylem. Xf colonization results in the clogging of the xylem and total shutdown of water transport through the grape plant. Leaf scorching appears to be the obvious symptom of Xf-induced PD. However, visually prominent "leaf scorching" occurs three to six months after the initial exposure of Xf, which may be too late to protect the infected plant. We, therefore, set out to discover PD-specific biomarkers that can be monitored to predict the

onset and progression of PD. For this, we chose two sets of grape plants: one Thompson Seedless variety (TS) that is susceptible to Xf and develops PD whereas the other (also TS) that is resistant to PD. The transgenic TS lines differ from the regular TS plants only in that they express a Xf-killing protein. Previously we reported the design of this Xf-killing protein by combining both recognition and clearance functions of plant defense [1]; (United States Patent 7432419 Publication Date: 10/07/2008). Several PD-susceptible and PD-resistant plants were inoculated with million copies of Xf. Leaf scorching and xylem clogging were then monitored. The symptoms began to appear only after three months. RNA samples were collected from 30 PD-susceptible plants and multiple PD-resistant lines each containing 15 plants. Real-time PCR (polymerase chain reaction) probes were design to test the expression of 40 genes belonging to both Xf and grape genomes. By extensive literature survey of studies on Xf pathogenesis and PD in grapes, we chose two classes of genes: one belonging to Xf virulence and the other corresponding to the grape pathways induced by stress and dehydration during Xf colonization. The use of both PD-susceptible and PD-resistant plants offers a route to discovery and also validation of the grape biomarkers for subsequent adaptation to nucleic acid lateral flow. Genes that are related to the development PD should be up- or down-regulated in PD-susceptible plants. If the pattern of expression of the same genes is reversed in the PD-resistant plants, then we are sure that we have been able to discover and validate grape biomarkers for PD. Similarly, the expression of the virulence factors in PD-susceptible plants would be higher than that in the PD-resistant plants because a significant fraction of transmitted Xf is killed in the PD-resistant plants. Figure 2 (top) shows the expression of a small subset of 6 grape biomarkers for PD. Note that the PD-susceptible and PD-resistant plants show an opposite pattern of expression. Figure 2 (bottom) shows the expression of Xf virulence genes PD-susceptible and PD-resistant plants; note that these genes are down-regulated in the PD-resistant plants. Based on our analysis of gene expression data in PD-susceptible and PD-resistant plants, we have selected 15 grape and 5 Xf biomarkers that are predictive of PD. Adaptation of these biomarkers to lateral flow could help manage PD outbreaks in the field by predicting time and onset of infection in potentially exposed grape plants.

b) Discovery of host markers Due To Two Influenza A Subtypes

Two influenza strains H1N1 and H3N2 are commonly encountered in seasonal flu. H1N1 refers to the presence of the two envelope proteins, hemeagglutinin Type 1 and neuraminidase Type 1, whereas H3N2 corresponds to the presence of the two envelope proteins, hemeagglutinin Type 3 and neuraminidase Type 2. H1N1 is more pathogenic than H3N2. We set out to design a LFM platform that can report the early stages of infection by

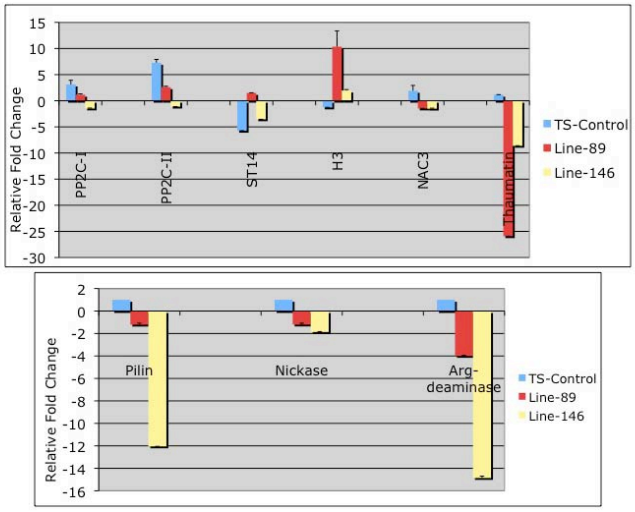

Figure 2. (Top) Validation of grape biomarkers for PD and (bottom) Xf biomarkers for PD. Note that the expression patterns of grape biomarkers are reversed in the resistant lines relative to the susceptible line. Also, since Xf is largely cleared, the level of expression of the Xf genes are significantly lower in the resistant lines.

H1N1 and H3N2. A comprehensive set of host markers for early infection is better derived from the innate immune repertoire, which consists of the pro- and anti-viral genes (or proteins) and the factors in the signaling processes that induce or regulate them. The pro-viral factors, by their presence or specific expression pattern, supports the early steps in the viral lifecycle whereas the anti-viral factors inhibit the early steps. In this project, we have primarily focused on signaling due to the pattern recognition receptors (PRRs). Such PRRs include TLR3 on the endosome and cytosolic RIG-I, MDA-5, and PKR, which sense small viral RNA. We considered two classes of genes:

- The ones that are associated with the signaling due to the PRR pathways.
- The pro- and anti-viral genes that are induced by the PRR pathways.

For this, we have examined the expression of these two classes of genes by two influenza A virus sub-types, i.e., high pathogenicity (A/Beijing/262/95 H1N1- H1N1 in short) strain and low pathogenicity (A/Sydney/5/97 H3N2-H3N2) strain, both of which are relevant to human and swine flu. Normal human bronchial epithelial cells (NHBE) were used as a model of infection for identifying host markers that are common to both of them as well as those that are unique to each of them. The putative influenza A specific host markers were discovered by whole genome (50,000 genes) microarray analysis. These genes were mapped to various pathways. Finally, approximately 200 genes belonging to biologically relevant pathways were validated by re-measuring expression or mRNA levels using real-time quantitative PCR and protein levels by

ELISA. This has lead to the successful identification of reliable subsets of host genes that are either unique to one of the two strains or common to both of them. Figure 3 shows the informative genes belong to the innate immune response pathways. Interestingly, our research has found anti-viral host genes are expressed at a higher level in the low pathogenic H3N2 strain but are expressed at a lower level in the high pathogenicity H1N1 strain. In summary, we have discovered a robust set of host markers that are common to H1N1 and H3N2 as well as those that are unique to either one of them. This discovery presents us with the unique opportunity to assess a nucleic acid based lateral flow assay for possible applications to pre-clinical or clinical diagnostics.

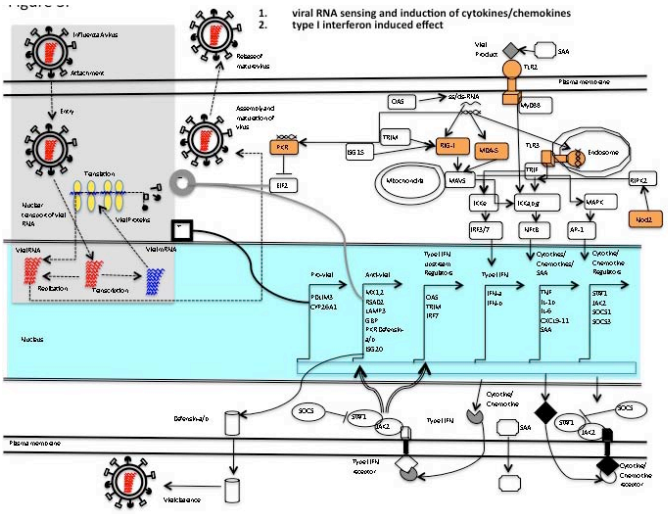

Figure 3. The host response due to H1N1 and H3N2 during the early phase of viral lifecycle (shown on left as a shaded area. The pathways involved in the viral RNA recognition by the host pattern recognition receptors (shaded brick yellow) induce production of cytokines/chemokines and other pro- and anti-viral genes.

Future Work

LFM fabrication

Nucleic acid segments from relevant host and pathogen genes will be selected and adapted for detection on the lateral flow platform.

Sample preparation

Nucleic acids will be isolated and purified from the pathogen and/or host cells.

Target Amplification

The target sequences will first be amplified by conventional PCR with thermocycling and selected PCR products will further be tested by real-time PCR for quality control. After establishing quality control, isothermal Nucleic Acid Specific Based Amplification (NASBA) will be performed on the target sequences.

Detection on LFM

The amplified targets (from pathogen and host) will be detected on the LFM by a sandwich type assay. The nucleic acids on the substrate surface and the nucleic acids linked to the colored beads will bind or couple to each other only if the genetic information is matching. This simultaneous binding of the probes on the colored bead and LFM surface is made visible by colorometric changes.

Conclusion

A significant advance in the surveillance and management of infectious diseases requires *accurate identification of these markers for a particular infection* and *rapid, sensitive,* and *efficient detection of these markers on a platform amenable to laboratory and field use*.

This project builds a LANL capability in:

- Identification and validation of nucleic acid signatures for pathogen-specific infection (markers for both the pathogen and the host).
- Design of a nucleic acid based lateral flow assay that detects the host and pathogen markers of infection using RNA from infected cells.

References

1. Kunkel, M., M. Vuyisich, G. Gnanakaran, G. E. Bruening, A. M. Dandekar, E. Civerolo , J. J. Marchalonis , and G. Gupta. Rapid clearance of bacteria and their toxins: development of therapeutic proteins. 2007. *Critical Reviews in Immunology* . **27** (3): 233.

Publications

Dandekar, A. M., A. M. Ibanez, H. Gouran, F. Martinelli, R. L. Reagan, C. Leslie, G. McGranahan, G. Bruening, P. Pardington, A. Chaudhary, and G. Gupta. Boosting of host innate immunity for protection against infectious diseases. Invited presentation at *International Conference on Antimicrobial Research.* (Valladolid, Spain, 3-5 Nov. 2010).

Dandekar, A. M., F. Martinelli , C. E. Davis, A. Bhushan, W. Zhao, O. Fiehn, K. Skogerson, G. Wohlgemuth, R. D'Souza, R. Soumen, R. L. Reagan, L. Dawei, R. B. Cary, P. Pardington, and G. Gupta. Analysis of early host responses for asymptomatic disease detection and management of specialty crops. 2010. *Critical Reviews in Immunology.* **30**: 277.

Pardington, P., A. Zeytun, A. Chaudhary, R. B. Cary, and G. Gupta. Early host responses due to influenza A infection. Invited presentation at *Eighth International Conference on Pathways, Networks, and Systems Medicine.* (Ixia, Rhodes, Greece, 9-14 Jul. 2010).

Pardington, P., M. Norvell, A. Chaudhary, and G. Gupta. Protection against infectious disease by boosting host innate immunity . Invited presentation at *Fifth Biological Therapeutics Research and Development* .

(San Francisco, 20-22 Oct. 2010).

Zeytun, A., A. Chaudhary, P. Pardington, R. B. Cary, and G. Gupta. Induction of cytokines and chemokines by toll-like receptor signaling: strategies for control of inflammation. 2010. *Critical Reviews in Immunology.* **30**: 53.

Isotopic Tracer for Climate Relevant Secondary Organic Aerosol

Thomas A. Rahn
20090425ER

Introduction

Aerosols by definition are simply fine solid particulates or liquid droplets suspended in a gas. In Earth's atmosphere these can take many forms - from fine dust particles to clusters of inorganic molecular species to amalgams of complex organics and as a whole, they have a profound influence on Earth's radiation budget, cloud and precipitation distribution and climate. The least understood of the atmospheric aerosols are the Secondary Organic Aerosols (SOA), those aerosols that result from the oxidation and coalescence of volatile organic gaseous compounds. In this proposed work, we will begin to unravel some of the intricacies of the formation and evolution of these SOA by applying state of the art isotopic and ultrahigh resolution mass spectrometry techniques, as well as chemometric techniques. In particular, we will develop novel analyses of the carbon and oxygen isotopic content of SOA that will elucidate pathways of oxidation and details of structure that have heretofore been elusive. These techniques will be applied to SOA generated in a series of controlled experiments in our laboratory at LANL. In addition we will utilize the National High Magnetic Field Laboratory to analyze the SOA by ultrahigh resolution mass spectrometry thus providing precise empirical formulas for SOA produced in these experiments. We will then begin the process of comparing these laboratory results to actual atmospheric samples collected in a few select environments to determine how the origin of volatiles and subsequent processing and environmental exposure control the evolution of these complex compounds.

Benefit to National Security Missions

By identifying the production pathways of secondary organic aerosol formation, this project will support DOE's Office of Science Atmospheric Science Program's stated mission "to develop a comprehensive understanding of the atmospheric processes that control the transport, transformation, and fate of energy related chemicals and particulate matter" and in particular the focus of "characterization of aerosol properties, and transformations". Such work can also impact sensing and forensic missions.

Progress

The second year milestones for the project are to continue experiments of SOA generation and IRMS analysis, perform analyses at the National High Magnetic Field Laboratory (NHMFL) and to develop field sampling protocol for aerosols collection and initiate sampling. A sampling protocol has been developed for SOA collection from the chamber. A similar protocol with higher flow rate will be used for field sampling.

SOA generation

We have generated SOA from ozonolysis reaction of four different monoterpens (α-pinene, β-pinene, limonene, D-carene) and one sesquiterpene (caryophellene). This was achieved by injecting 2 ppm of the individual terpenes in to the Teflon chamber (1.5m^3) and allowed the gaseous phase terpene to react with ozone without the presence of light and OH radical scavenger under dry condition. SOA was formed right after the injection of ozone into the chamber. Particle number concentrations were recorded for this experiment. Highest particle number formation was recorded from the reaction of caryophyllene with ozone where as ozonolysis of beta pinene yielded the list number of particles under the same condition. The produced SOA was collected on pretreated quartz fiber filters at a flow rate of 9.5 l/min for at least 3 h. These filter samples were used for stable carbon isotope analysis of SOA and for detail chemical analysis of SOA at the NHMFL using an ultra high resolution mass spectrometer by our collaborator Lynn Mazzoleni at Michigan Technological University.

Stable isotope analysis

The stable carbon isotopic composition ($\delta^{13}C$) of total SOA was measured using and elemental analyzer coupled to an isotope ratio mass spectrometer. Prior to that the $\delta^{13}C$ values of the individual terpenes were measured using a bulk analysis of the liquid terpenes by elemental analyzer (EA) coupled to our isotope ratio mass spectrometer, and by a gas chromatograph coupled to isotope ratio mass spectrometer via a

combustion furnace (GC-IRMS). For some terpenes, up to 1‰ difference was observed between the EA and GC-IRMS measurements. We hypothesize that the reason for this difference is due to impurities in the liquid compounds used for bulk (EA) analysis. The total carbon isotope ratio ($\delta^{13}C$) of SOA produced from ozonolysis of different terpene ranged between -32.6‰ to 28.1‰. In general the $\delta^{13}C$ value of the SOA is depleted in ^{13}C compared to their precursor by about 1‰ with the exception of caryophyllene which is enriched by 0.9‰ (Figure 1).

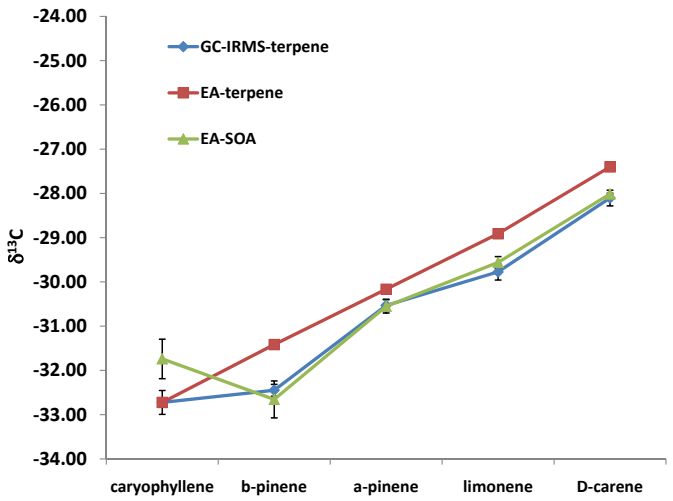

Figure 1. Stable isotope composition of secondary organic aerosol and liquid terpenes (precursors) measured with EA and GC-IRMS

Previous studies of the isotopic composition of SOA produced from beta pinene showed that the bulk $\delta^{13}C$ of SOA has a very similar isotopic composition as the precursor whereas, when the bulk SOA is separated into its individual molecular components, they could be strongly depleted or enriched with the heavy isotope compared to the precursor terpene depending on their formation process (Fisseha et al., 2009). Further analyses of these individual components will be performed in order to assess the variability of individual compounds within SOA.

Ultra-high resolution mass spectrometry

We have performed a number of analyses at the ultra-high resolution mass spectrometry facility at Woods Hole Oceanographic Institute. Results of these analyses yield insight into the types of reactions that occur during the formation of SOA from the precursor materials: the terpenes and ozone. Shown in Figure 2 is one dataset that relates the double bond equivalency (DBE) of a single SOA experiment (three hours of SOA collected on a teflon filter) to the number of carbon atoms in the fragments. DBE is a measure of hydrogen deficiency in a molecule, and is related to the number of double and triple bound carbon atoms in that molecule. The precursor material in Figure 2, alpha-pinene, has an initial DBE of 3. The hot spots at DBE=3 and DBE=6 shown in Figure 2 are indicative of the initial alpha-pinene reacting with ozone without significant change to the binding structure of the precursor material but the hot spots at DBE=5 and to a lesser degree at 4, 7 and 8, are indicative of processes that are currently under investigation. Other work at Woods Hole is leading to new insight into other aspects of SOA such as its composition and stability under various atmospheric conditions.

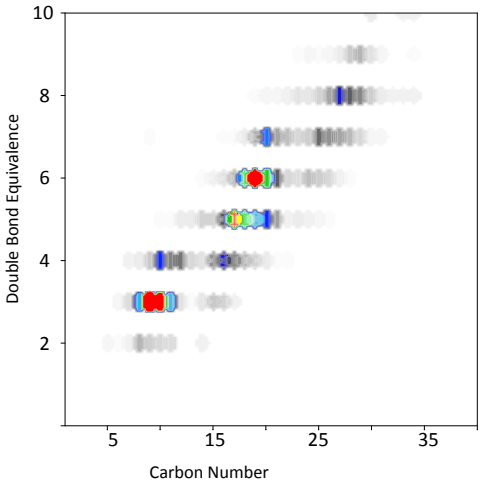

Figure 2. The relationship between carbon number and Double Bond Equivalence (DBE)

Future Work

Secondary Organic Aerosols (SOA) comprise as much 70 percent of the global carbonaceous aerosol burden by mass. Because aerosols have multiple feedback mechanisms to Earth's radiation budget, a complete understanding of the formation and fate of aerosols is imperative for understanding their influence on global climate. SOA in particular are poorly understood due to the multitude of precursors responsible for their formation and because they are a complex, heterogeneous mixture of organic species. Because the atmosphere is, in general, an oxidizing environment, the evolution from precursor organic gas species to aerosol results from reaction of biogenic and anthropogenic organic gases with various oxidizing species. The oxygen atoms that are found in SOA are derived, for the most part, from reactive oxygen species that have been shown to carry a mass independent signature in the stable isotopes of oxygen. The ^{17}O anomaly from reactive oxygen species that is transferred to the secondary organic compound reaction products can thus serve as a quantitative signature of the pathways of SOA generation. We are currently working on our next step in SOA analysis, optimized methodology for sensitive ^{17}O measurement.

Conclusion

We have presented the stable carbon isotopic composition of secondary organic aerosol produced from the ozonolysis of terpenes. We also have presented characterization unique signatures of reaction pathways related to ozone

reaction with various terpenes. Preliminary results have been presented this past year at the 2010 American Chemical Society Meeting and up to date results are in preparation for several manuscripts and presentation at the American Geophysical Union meeting in Dec. 2010.

References

1. Fisseha, R., H. Spahn, R. Wegener, T. Hohaus, G. Brasse, H. Wissel, R. Tillmann, A. Wahner, R. Koppmann, and A. Kiendler-Scharr. Stable carbon isotope composition of secondary organic aerosol from beta-pinene oxidation. 2009. *JOURNAL OF GEOPHYSICAL RESEARCH-ATMOSPHERES.* **114**: D02304.

Publications

Putman, A., T. Rahn, L. R. Mazzoleni, R. F. Derseh, and J. Offenberg. Characterization of secondary organic aerosols from the ozonolysis of a-pinene. . To appear in *Central Regional Meeting of the American Chemical Society.* (Dayton, Ohio, 16-19 June 2010).

Evolving a Thermostable Cellulase by Internal Destabilization and Evolution

Andrew M. Bradbury
20090443ER

Introduction

Cellulose is the "backbone" of all plant material, and the predominant material in all plant matter. While biofuel generation has largely focused on the sugar/starch containing plant matter, these are the foundation of the global food market while cellulose materials are largely the "waste" from food production. The main research goal of this proposal is to create a highly thermostable version of a widely used cellulase, for which thermostability has been a long desired goal. This could be used in the generation of bioethanol, or other biofuels, and would facilitate the use of cellulose, rather than maize, as feedstock, so permitting the use of otherwise marginal land. By carrying out this goal, we will also have carried out an important secondary goal: the demonstration of the universality of a new protein thermostabilization method we recently developed by its application to an important industrial enzyme. We expect success in this project to position LANL well to exploit future funding in bioenergy for which enzyme and protein thermostabilization are required.

Benefit to National Security Missions

By developing a new method to stabilize cellulases, this project will support the DOE mission in energy security. Cellulases are enzymes that breakdown cellulose to sugars suitable for fermentation. However, commercial cellulases tend not to be sufficiently thermostable for industrial processes, a problem we hope to solve.

Progress

The main research goal of this project is to create a highly thermostable version of a cellulase normally produced by a fungus, Trichoderma reesei, for which thermostability has been a long desired goal, for its applications in biofuel production. For any directed evolution project, there is need of an optimized expression system and a high-throughput screening assay. The full length and truncated versions of the gene encoding this cellulase were cloned and expressed in E. coli, a bacterium used in research. This expression system gave measurable activity using Carboxymethyl Cellulose (CMC) as the substrate when the reaction was carried out at 50°C for 24h. There are two types of activity assays available for cellulases. One is Carboxy methyl Cellulose agar based, wherein the active clones are spread on agar plate containing CMC and the plate is stained using Congo Red dye. Haloes corresponding to CMC consumption by endoglucanase are then observed around active clones. The other assay is liquid based wherein enzyme is incubated with CMC solution and then 2,4-dinitro salicylic acid (DNS) is added. Cellulase activity is seen by conversion of the color of the substrate from yellow to red. We optimized the DNS based assay for use in a high-throughput manner in 96-well microtitre plates.

We attempted to improve the expression of EG1 in deep well plates using different bacterial host strains (such as BL21, Origami2 and Rossettablue) and co-expression of five different chaperones (proteins that improve folding - dnaK-dnaJ-grpE groES-groEL, groES-groEL, dnaK-dnaJ-grpE, groES-groEL-tig and tig). However, no alternative host strain or chaperone co-expression improved cellulase activity or expression. The relatively low activity of this cellulase when expressed in E. coli, required us to embark upon a program to improve the enzyme activity for CMC. For this, we used a technique termed Iterative Saturation Mutagenesis at eight flexible sites within the protein. This involves identifying those amino acids that are the most mobile in the protein, and then creating small libraries in which the original amino acid is replaced with all the twenty natural amino acids. We created eight such libraries, and identified one clone Gln284Leu (I) from one of the libraries that gave improved activity. This clone was used as a template for a second round of saturation mutagenesis at the remaining sites followed by screening using the previously developed HT screening method. This procedure was carried out three times, until we obtained a clone containing three mutations: Thr371Phe, Gln284Leu, Gly230Ala (III) that was able to show activity after only 30 minutes of CMC reaction (compared to 24 hours for the wild type) (Figure 1). The increased activity of this mutant allowed us to use it for the insertion of destabilizing loops.

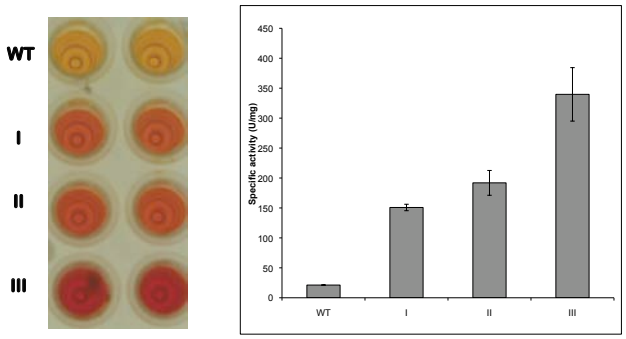

Figure 1. Improved activity of the mutant enzymes we created. WT is the original "wild type" enzyme. I, II and III are the improved variants. The darker the color, the greater the activity. On the right, the activity is graphed, with higher bars indicating greater activity.

Six sites (three comprising amino acids that were relatively rigid, and three comprising amino acids that were flexible) were chosen for loop insertion. The insertion of the destabilizing loops led to the expected loss of much of the activity. Mutagenesis was carried out on these six clones to recover the activity loss using a mutational technique termed error-prone PCR. Screening was carried out using the CMC-DNS based test, but after screening about 4000 clones, no mutants with improved activity as compared to the template (mutant III + loop) were observed.

This disappointing result led us to realize that an additional test prior to direct enzymatic screening was required since the mutagenesis library can have a large population of mis-folded proteins. The use of a pre-screening step that can eliminate those clones with mis-folded cellulase will reduce the downstream screening efforts required to obtain improved clones. There are many folding reporters described in the literature that can be used for such folding pre-selection. These include ß-lactamase based filtering on ampicillin gradients, GFP-based folding reporters and yeast display. The basic idea is that the gene-of-interest (GOI) is fused to a reporter gene, and if the protein of interest folds well, the reporter protein also folds correctly and gives a desired signal. This can be antibiotic resistance (ß-lactamase), fluorescence (GFP) or display levels (yeast display). We have shown the effectiveness of ß-lactamase folding reporters in our laboratory for selecting correctly folded cellulases (of a different kind from the organisms called T. emersonii) from a library of random clones. Consequently, we recloned our cellulase gene (from T. reesei) upstream of the ß-lactamase gene and screened about 4000 clones but were unable to find a good clone. It seems the ampicillin based filtering did not work for this enzyme.

Consequently we decided to use yeast display as a folding reporter, since for a protein to be correctly displayed on the surface of yeast, it has to be very well folded. This allows us to select for correctly folded proteins by selecting those yeast that are displaying cellulase on their surface. Furthermore, this approach has the potential advantage that the activity of the cellulase on the surface can be directly tested, without needing to purify the protein. The cellulase gene EG1 and the three mutants described above were subcloned into our yeast display vector. Expression of the cellulase on the yeast cell surface was assessed with an antibody that recognized a small tag at the end of the cellulase. We were able to show activity of the displayed cellulase using the DNS assay described above (Figure 2). This makes selection and screening of improved mutants easier since only the correctly folded proteins will be displayed on the yeast surface and their activity can be directly assessed using the DNS test. We were able to show good activity of the starting enzyme and the three improved mutants, but loop insertion reduced the enzyme activity significantly, but did not abolish it (Figure 3). This is the perfect starting point from which to start an evolutionary experiment. We are now in the process of preparing error-prone PCR libraries in the yeast display system to select for improved variants that contain loops. We expect these to have greater stability.

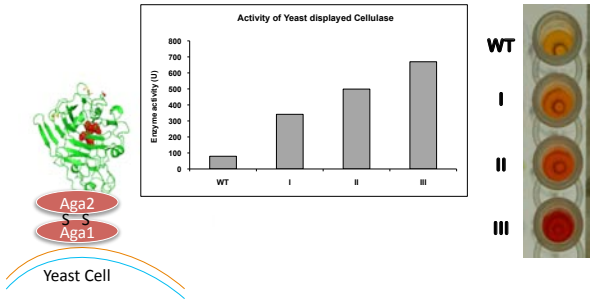

Figure 2. When cellulase is "displayed" on the surface of yeast (left) it maintains its activity, as shown by the DNS assay (center and right). This allows rapid screening and selection of improved clones.

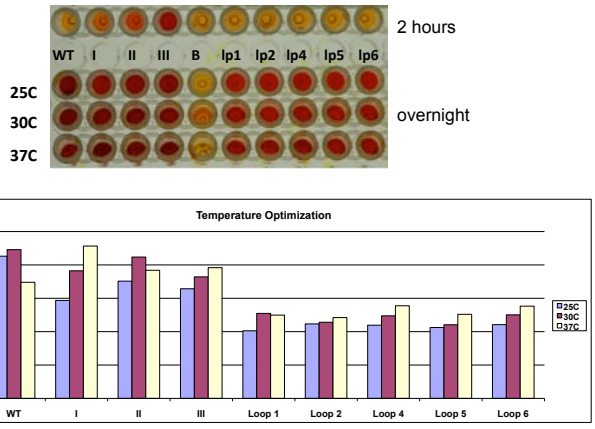

Figure 3. Insertion of loops within the cellulase expressed on the surface of yeast reduces the activity. WT is the original wild type enzyme, I, II and III are the improved variants, and loop 1, 2, 4, 5 and 6 are cellulase molecules that have destabilizing loops inserted. B, in the top is a blank well to assess the background assay levels.

Future Work

Since we now have an optimized yeast display system for the expression of T.reesei cellulase, we will construct the mutagenesis libraries in this system and screen the clones for recovery of the activity lost due to insertion of destabilizing loops. Once such mutants are obtained, further rounds of loop insertion and mutagenesis for recovery of activity will be carried out. After 2-3 rounds, we will synthesize the cellulase gene without loops and test it for thermostability. Once a thermostable cellulase mutant is obtained, it will be purified and biochemically characterized for its application in the biofuel process.

Conclusion

We have optimized the cellulase expression system in bacteria as well as yeast. The selection and screening system of cellulase activity has been optimized in high-throughput format. Cellulase activity has been enhanced by almost 16-fold by carrying out three rounds of Iterative Saturation Mutagenesis. Six sites have been selected for insertion of destabilizing loops in the cellulase. The loop insertion reduced the activity levels significantly. Mutagenesis libraries have been created using error prone PCR. Direct screening of error prone PCR libraries gave no improved clones. Lactamase based filtering was tried as pre-screening strategy but that was not very useful. Yeast display system for expression of cellulase has been optimized. Using Flow Cytometry, we can monitor both the expression levels on the yeast cell surface as well as the enzyme activity. Wild type, B-FIT clones and the loop mutants have been cloned and expressed in yeast display system. We are in the process of making libraries of these new clones.

A Molecular View of Cellulase Activity: A Single-Molecule Imaging and Multi-Scale Dynamics Approach

Peter M. Goodwin
20100129ER

Introduction

Cellulases are enzymes that accelerate the conversion of cellulose to sugars. A detailed understanding of cellulase action is crucial for the efficient conversion of cellulosic biomass to biofuels and other useful hydrocarbon products. The enzyme-catalyzed hydrolysis of cellulose is complex. Several enzymes (cellulases) are known to act together during the conversion of cellulose to sugar. The specific aims of this project are to:

1. Use single-molecule fluorescence imaging to get a molecular level picture of cellulase action and synergy.

2. Create all-atom and coarse-grained computer simulations of cellulase activity on cellulose.

3. Use our experimental and computational results to attain a molecular-level understanding of cellulase function.

Benefit to National Security Missions

One of the most important scientific and engineering problems on the national energy agenda is bioenergy. Developing bioenergy is germane to both national security and the environment. A major roadblock to using biomass for energy is the cost of converting recalcitrant lignocellulosic biomass to sugars that can then be used to produce fuels and other products. Further cost reductions and improvements in enzyme activity are necessary to make cellulosic fuel economically viable. The goal of this project, a molecular level understanding of the cellulase-catalyzed hydrolysis of cellulose, is the logical means to this end.

Progress

Experimental

Since our goal is to monitor the same cellulase molecule moving on its cellulose substrate over intervals longer than the average time to photobleach a fluorescent reporter, we desire a labeling approach that allows regeneration of the fluorescent label on the cellulase bound to its substrate. We are pursuing two approaches.

The first approach uses the coiled coil protein interaction between a pair of E- and K-peptide coils to label the cellulase. We express the protein to be labeled as an amino- or carboxyl-terminus fusion with the E-coil. We then fluorescently label the expressed protein by adding fluorophore-labeled K-coils. Coiled-coil interaction between the E- and K-coil results in the binding of the fluorescent K-coil to the E-coil protein fusion. Regeneration of the fluorescent label bound to the E-coil protein fusion is accomplished by exchange of the bound fluorescent K-coil with other fluorescent K-coils in solution. Background emission due to unbound fluorescent K-coils is reduced by the addition of quencher-labeled E-coils. Previous work has demonstrated that E/K-coil exchange takes place on the timescale of a minute. To date we have designed and synthesized two sets of E/K-coils. We are in the process of labeling the K-coils with fluorophores and the E-coils with quenchers. We have also expressed and purified three E-coil containing fusion proteins that will be used to test this labeling approach in single-molecule imaging experiments. Our approach to labeling cellulases using E- and K-coil peptides is shown in Figure 1.

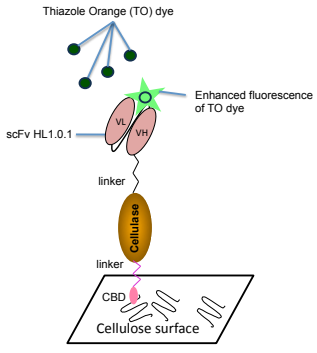

Figure 1. Fluorogen activating protein approach to regenerative fluorescent labeling of an immobilized cellulase. Legend: scFv - single-chain variable fragment; VL - light chain immunoglobulin; VH - heavy chain immunoglobulin; CBD - cellulose binding domain.

The second approach will label the cellulase with a fluorogen activating protein (FAP). Szent-Gyorgyi et

al. have demonstrated fluorescence enhancements ranging from ~2000 to ~20000-fold for malachite green (MG) and thiazole orange (TO) based fluorogens bound to several FAPs selected from a library of human single-chain antibody fragments.[1] We will express cellulases as fusions with the appropriate FAP. The cellulase-FAP fusion will become fluorescent upon binding of the cognate fluorogen to the FAP. Regeneration of the fluorescent label will be take place by exchange of the FAP-bound fluorogen with fluorogens in solution. We have expressed two FAPs (HL1.0.1 and H6) in E. coli and tested these against their respective cognate fluorogens (TO and MG) and fluorogen derivatives (TO1-2p and MG-2p). We have expressed and purified biotinylated versions of these FAPs suitable for surface immobilization and are testing the FAP/fluorogen approach in single-molecule imaging experiments. Our approach to labeling cellulases using fluorogen activating proteins is shown in Figure 2.

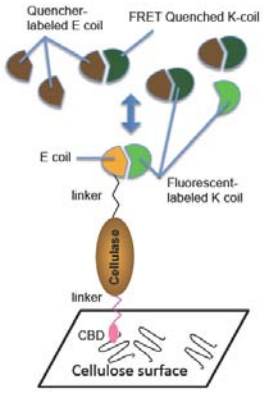

Figure 2. E/K-coil approach to regenerative fluorescent labeling of immobilized cellulases. Legend: FRET - fluorescence resonance energy transfer; CBD - cellulose binding domain.

Both of the above labeling approaches require that we produce recombinant protein fusions of the cellulases we want to study with either a fluorogen activating protein or the E-coil peptide. As a first step we attempted to produce a recombinant T. reesei cellulase (Cel7A). We first expressed Cel7A in a bacterial host (E. coli) but the purified protein showed no catalytic activity. We then expressed Cel7A in yeast (P. pastoris). As expected from earlier work Cel7 expressed in P. pastoris is hyperglycosylated compared to the native T. reesei protein. We deglycosylated the expressed protein to levels similar to that of native Cel7A from T. reesei. However this protein also showed no catalytic activity.

Theory and Simulation

We have developed a coarse-grained dynamical model that captures the key events associated with the enzymatic degradation of cellulose. Our model accounts for the mobility and action of a single enzyme as well as multiple enzymes on a homogeneous cellulose surface. This model also incorporates recent findings from time-resolved atomic force microscopy experiments that capture the motion of cellulases on cellulose. Preliminary results from this model show the dependencies on enzyme affinity, enzyme loading and coverage for the biomass degradation process. This represents the first microkinetic model for enzymatic conversion of biomass that takes into account the spatial properties of the substrate with the intrinsic stochastic properties due to cellulase adsorption/desorption and processivity on a cellulose surface and can be used to explain single molecule imaging and atomic force microscopy experiments on cellulases on cellulose. Copyright/patent of this software is being explored with Technology Transfer Division.

Future Work

Experimental

We will consult with other groups working in this field to find a workable expression system for the production of recombinant cellulases. It is likely that this will be the T. reesei fungus itself. Given that we do not have the resources to express proteins in the fungus we will likely abandon this approach unless we can team up with an external collaborator who is willing to supply us with recombinant cellulases.

As an alternative to using recombinant cellulases, we will instead purify the cellulase components we wish to study from a commercially available mixture of T. reesei cellulases. The advantage of this approach is that we can readily purchase the necessary quantities of active enzymes. The disadvantage is that we will not be able to use the regenerative labeling approaches we are developing. Instead, we will use conventional chemical approaches to label the purified enzymes with fluorescent reporters. Photobleaching of the chemically linked fluorescent label(s) will limit the time we can observe the motion of a single enzyme molecule.

We will use total internal reflection fluorescence microscopy (TIRFM), to monitor the activity of individual fluorescently-labeled T. reesei endoglucanases and exoglucanases interacting with cellulose substrates during cellulase-catalyzed hydrolysis of cellulose.

Theory and Simulation

Ours is the first microkinetic model for enzymatic conversion of biomass that takes into account the spatial properties of the substrate with the intrinsic stochastic properties due to cellulase adsorption/desorption and processivity. This work was recently presented at the 32nd Annual Symposium On Biotechnology For Fuels and Chemicals held in Florida. It generated a lot of interest. NREL scientists expressed keen interest and were eager to collaborate with us. A team of NREL scientists is expected to visit LANL later this fall. The high performance computing community considers the expansion of this model as a perfect application

in exascale computing. We are currently in discussion with Computer, Computational, and Statistical Sciences Division on porting this code to the next generation architecture.

Conclusion

The ultimate goal of this project is a molecular-level understanding of the cellulase-catalyzed hydrolysis of cellulose. Single-molecule fluorescence imaging of and computer simulation of individual cellulases interacting with the cellulose substrate will be used to obtain direct insight into the molecular mechanisms of cellulase synergy as well as detailed information on cellulase kinetics. This molecular-level model of cellulase activity will be crucial for the rational design of improved cellulases and cellulase mixtures.

References

1. Szent-Gyorgyi, C., B. Schmidt, Y. Creeger, G. Fisher, K. Zakel, S. Adler, J. J. Fitzpatrick, C. Woolford, Q. Yan, K. Vasilev, P. Berget, M. Bruchez, J. Jarvik, and A. Waggoner. Fluorogen-activating single-chain antibodies for imaging cell surface proteins (vol 26, pg 235, 2008). 2008. *Nature Biotechnology.* **26** (4): 470.

2. Boer, H., and T. Teeri. Characterization of Trichoderma reesei cellobiohydrolase Cel7a secreted from Pichia pastoris using two different promoters. 2000. *Biotechnology and Bioengineering.* **69** (5): 486.

3. Igarashi, K., A. Koivula, M. Wada, S. Kimura, M. Penttila, and M. Samejima. High Speed Atomic Force Microscopy Visualizes Processive Movement of Trichoderma reesei Cellobiohydrolase I on Crystalline Cellulose. 2009. *JOURNAL OF BIOLOGICAL CHEMISTRY.* **284** (52): 36186.

Publications

Chundawat, S. P. S., G. Bellesia, N. P. Uppugundla, L. da Costa Sousa, D. Gao, A. Cheh, U. Agarwal, C. M. Bianchetti, G. N. Phillips Jr., P. Langan, V. Balan, S. Gnanakaran, and B. Dale. Restructuring crystalline cellulose hydrogen bond network enhances its depolymerization rate. *Science* .

Gaiotto, T., H. B. Nguyen, J. Jung, A. M. Bradbury, S. Gnanakaran, J. G. Schmidt, G. S. Waldo, and P. M. Goodwin. A photophysical study of two fluorogen-activating proteins bound to their cognate fluorogens. Presented at *Single Molecule Spectroscopy and Imaging IV.* (San Francisco, CA, 22-27 January, 2011).

Bacterial Invasion Reconstructed Molecule by Molecule

James H. Werner
20100215ER

Introduction

Understanding the mechanisms of host-pathogen interactions are a crucial first step to developing countermeasures to infection, whether natural or man-caused. We are developing advanced laser-based microscopic methods to explore bacterial infection of human host cells with unmatched spatial and temporal resolution. This work exploits state of the art 3D single molecule tracking technology developed in our lab to study the kinetics of bacterial virulence factors in live human host cells. We are also building a new instrumental capability for this laboratory, super-resolution optical imaging, that will be used to directly visualize the bacteria-host interface with unmatched spatial resolution.

The host-pathogen system we are working on is Salmonella Typhimurium infection of human cells. This system is ideally suited for super-resolution visualization methods as the identities of key human host receptors are already known, but the spatial organization occurs at length-scales below the wavelength of visible light. This study will be the first to reveal the spatial organization of this bacteria-host interface at near nanometer resolution, greatly increasing our knowledge of bacteria-host interactions, not only for this one bacteria-host system, but for a whole class of virulent bacteria that all employ a highly conserved type three secretion system for infection.

Benefit to National Security Missions

This work helps LANL missions in Biosecurity science and Complex Biological systems, by creating instrumentation to study bacteria-host interactions with unprecedented detail. This work should create a much better understanding of bacterial infection mechanisms on a molecular level. This work will position our team to respond aggressively and competitively to proposal calls from the NIH, DARPA, and DTRA.

Progress

We have made substantial progress in the first year of this project. We identified and hired an outstanding postdoctoral research associate, Dr. Jason Han (Figure 1), to work full time on this effort. In his first year here, we constructed a single molecule localization microscope based largely upon the design of Betzig and coworkers (Science 2006). Microscope construction consisted of writing instrument control software to

Figure 1. Photograph of the super-resolution microscope built by Dr. Jason Han (pictured).

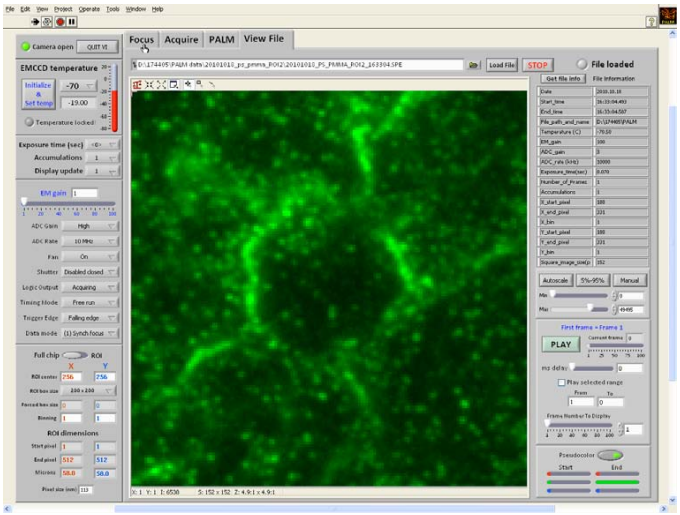

Figure 2. A screen-shot capture of the software interface

control laser timing and CCD image aquisition in a Labview environment. A screen-shot of the instrument control software is shown in Figure 2. In addition to instrument control software development, there was a substantial hardware component to microscope construction, with the procurement and alignment of excitation and readout lasers at a variety of wavelengths (405, 488, 561, and 632 nm). These lasers need to be carefully over-lapped in a total-internal reflection based microscopy. In addition to instrument control hardware and software, we wrote a complete software package for image analysis to construct 10 nanometer resolution images from the obtained single molecule micrographs. We have tested the instrument capabilities and resolution by studying nano-structure features created at air/water interfaces and diblock copolyjmer morphologies (Figure 3). Quite recently, we employed active feed-back methods of a 632 nm laser retro-reflection to eliminate z-focus drift during image aquisition. Dr. Han has also become familiar and proficient in learning the intricacies of our 3D tracking apparatus. We have used this system to explore protein traffic in live cells and are working towards examining 3D tracking of individual GFP-labeled bacterial effectors.

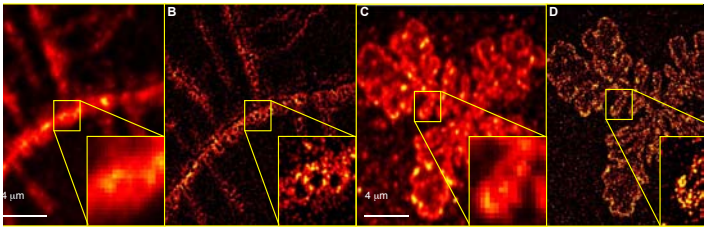

Figure 3. A) and C) are fluorescence images diblock copolymer structures as would be seen via conventional fluorescence microscopy. B) and D) are the images formed by super-resolution optical microscopy based upon single fluorophore localization. The scale bar is 4 microns long.

From a cellular biology standpoint, Dr. Elizabeth Hong-Geller has made substantial progress in labeling human host cells and bacteria for this project. Stable (i.e. drug resistant) cell lines and transfectants have been made for the human protein Rac1 and the important cellular receptor alpha5 beta1 integrin to photoswitchable proteins. We have been actively working on protocols for cell fixation that “freeze” protein dynamics while keeping the background levels suppressed to levels suitable for single molecule detection and imaging. These cells have been studied using ensemble and single molecule fluorescence methods available in our laboratory.

Future Work

Our future goals are to examine the bacteria-host interface of a human-bacteria interaction, examining the distrubution of key host and bacteria proteins with the super resolution microscope we built in the first year of the project. We are also working on imaging the actin cytoskeleton (the structural framework) of human cells before and after bacterial infection using super-resolution imaging. We have begun tracking individual green fluorescent protein (GFP) molecules in solution, using proprietary and award-wining 3D molecular tracking technology developed in our laboratory. In the future, we will track GFP labeled bacterial protein effectors in human cells to better understand the initial stages of bacterial infection of a human host cell.

Conclusion

We expect a number of key outcomes of this research. First, we will create a new super resolution microscope that will be a valuable research tool for exploring the finer details of cellular structure. Second, we will directly test scientific hypotheses concerning bacteria-host interaction dynamics in ways only now technically feasible, due to state of the art 3D molecular tracking technology developed by our group. Finally, this work will provide mechanistic insights into conserved infection strategies used by many high-risk pathogens, and as such, will substantially increase our knowledge of the molecular basis of host-pathogen interactions.

References

1. Betzig, E., G. H. Patterson, R. Sougrat, O. W. Lindwasser, S. Olenych, J. S. Bonifacino, M. W. Davidson, J. Lippincott-Schwartz, and H. F. Hess. Imaging intracellular fluorescent proteins at nanometer resolution. 2006. *Science.* **313** (5793): 1642.

2. Werner, J. H., P. M. Goodwin, and A. P. Shreve. Three Dimensional Imaging at Nanometer Resolutions. 2010. *US Patent 7,675,045 .*

Metabolic Regulation of Light-harvesting and Energy Transfer

Gabriel A. Montano
20100257ER

Introduction

The energy from sunlight that strikes the earth in one hour (4.3x1020J) is more than the global yearly demand (4.1x1020 J). While having tremendous potential, solar energy production currently provides less than 1% of total energy consumption. This is due in part to a lack of efficient capture and conversion into a useful energy supply in either the form of biomass or by man made solar collection devices. Bacteria and plants have evolved photosynthetic machinery that efficiently capture and store energy from sunlight, however attempts to manufacture efficient bio-hybrid and bio-inspired solar energy devices with similar efficiency have proved problematic. The physical energy capture and conversion processes of photosynthesis, such as light-harvesting, are remarkably efficient and serve as a model for development of efficient solar energy systems. However, these photosynthetic processes are complex, highly evolved, and carefully regulated metabolically. The complexity of this regulation makes it difficult to ascertain how such precise and dynamic control occurs.

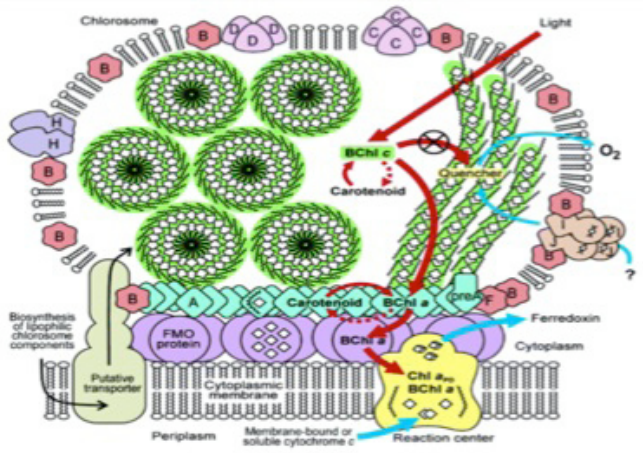

Figure 1. C. tepidum photosynthetic unit including chlorosome light harvesting complex. The chlorosome shows two proposed models of Bchl c oligomerization resulting in characteristic absorption spectrum.1

The chlorosome antenna complexes of green bacteria combine efficiency with novel self-assembly mechanisms to create robust light-harvesters (Figure 1). Our project goal is to understand the role of metabolic regulation in developing an optimized photosynthetic light-harvesting complex. By doing so, we hope to increase our fundamental understanding of the metabolic regulation of light-harvesting complexes as well as advance research in artificial photosynthetic design and other bio-energy applications. Knowledge gained will have an impact on our understanding of complex biological systems, in particular, bio-energy related systems. Further, as an ideal model system, understanding dynamic response of chlorosomes is ideal in pursuit in development of dynamic and responsive materials, particularly in bio-inspired light-harvesting design.

Benefit to National Security Missions

Developing new forms of energy is fundamental to the laboratory mission. The current research project is directly related to the LDRD grand challenges of *Complex Biological Systems* and *Energy and Earth Systems*. For example, under the Complex Biological Systems Grand challenge, one of the goals is ***Biology by Design: The goal of this priority is to model and engineer biological systems to resolve national challenges in energy…***. This project directly addresses this goal. Further under the Energy and Earth Systems challenge is the goal of ***Concepts and materials for Clean Energy-- Integrating solar energy capture with energy storage and/or CO2 capture and chemical reduction, using "hard materials," "soft materials," "bio-inspired systems, biological systems, or combinations of these.*** Further, developing mechanisms of energy transfer from molecular scale assembly is a fundamental focus with CINT. The research proposed will lead to new program development in bioenergy and bio-inspired design within CINT and with programs within Basic Energy Sciences and has already fostered new collaborations with international leaders in photosynthetic research.

Progress

The first few months of this project were spent on initial setup and modification of our laboratory design in order to 1) grow and maintain anaerobic bacteria

and 2) optimize a main source of characterization, a laser scanning confocal microscope (LSCFM) with picosecond fluorescence lifetime imaging microscopy (FLIM) capabilities. Further, an initial model that allows for simulation of energy transfer propogation in chlorosomes was developed allowing for incorporation of energy traps that could mimic conditions under various environments such as aerobic/anaerobic or high/low light conditions.

As described, our goal is to investigate metabolic regulation of light-harvesting and energy transfer in chlorosome light-harvesting complexes. The mechanisms of control can occur on different time scales (picoseconds to days) and it is our goal to understand levels of regulation on picoseconds, minutes, hours and days time scales as well as to determine levels of heterogeneity within a given population. In order to perform such a task, we are using a suite of capabilities either pre-existing or recently added. Bacteria are grown anaerobically in a Coy anaerobic chamber that contains a mini-prep area capable of growing small amounts of bacteria in stringently controlled anaerobic conditions that can be adjusted accordingly. For example, it is possible to alter anaerobic and light conditions to grow bacteria under varying levels and types of stress. This will become important as discussed in future work. Currently, bacteria have been cultured and grown under previously reported conditions[2] in order to determine optimal growth conditions and develop baseline growth curves.

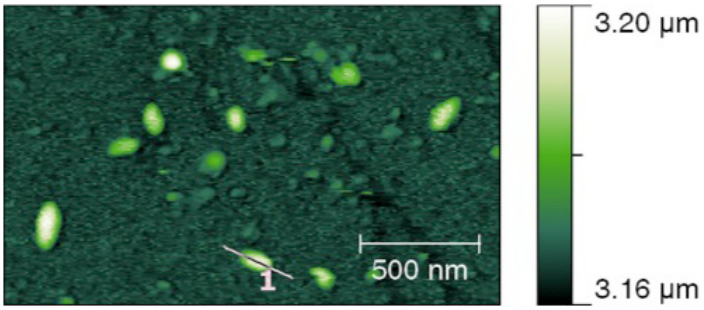

Figure 2. AFM of isolated C. tepidum membrane fragments.

We have spent considerable time investigating initially grown bacterial cultures via both Atomic Force Microscopy (AFM) and optical microscopy. AFM has been used to determine heterogeneity of chlorosome structure in a given population. Figure 2 shows an image of isolated *Chlorobium tepidum* membranes using in situ AFM. The chlorosomes are the large ellipsoidal structures sitting on top of the membrane substrate. Analysis was performed on chlorosome dimensions and heterogeneity and results are shown in Table 1. These results represent a baseline as to chlorosomal dimensions and also give us an idea of heterogeneity that exists within a given culture of bacteria. Further, a curious result was that in respect to width, chlorosomes exhibited less heterogeneity. This result may indeed provide a clue as to the nature of chlorosomal biosynthesis. Space prevents discussion of this process at this time but is being further investigated.

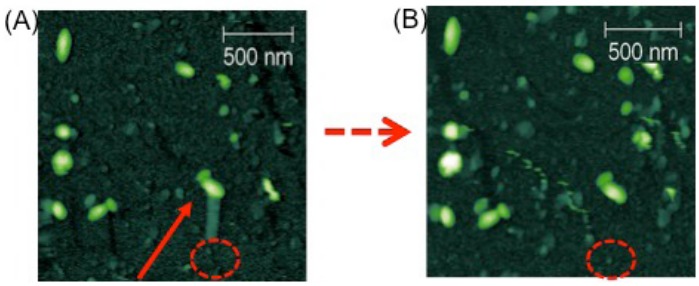

Figure 3. (A) C. tepidum chlorosome shifted upwards by probe during scan, leaving visible path as evidence. (B) C. tepidum Membrane substructure left underneath indicating a protrusion with width of 15 nm.

A second function of AFM as an investigative tool is shown in Figure 3 in a method termed "nanomanipulation". Figure 3a shows an isolated *C. tepidum* membrane. The arrow points to a chlorosome that has been pushed away by the AFM tip with gently applied pressure, with the drawn ellipsoid indicating the starting position of the chlorosome. Figure 3b is a following scan of the same area. A protruding membrane structure can be observed where the chlorosome previously existed. This result exhibits our potential to use *in situ* AFM to determine three-dimensional organization of the green bacterial photosynthetic unit, a heavily debated topic. While this was not the initial intent of our AFM studies, it is an exciting outcome that we are exploring further. This method also will allow us to determine changes in stoichiometric relationships between the various components of the photosynthetic unit directly addressing regulation of chlorosome antenna biosynthesis by investigating isolated membranes of *C. tepidum* grown under various conditions.

	length [nm]	width [nm]	height [nm]
Averages (N = 180)	141	79.3	21.7
Standard Deviation	26	11.5	4.3
Fractional Standard Deviation	0.19	0.14	0.20

Table 1. Chlorosome structural dimensions from AFM Topography Images

Lastly, we have performed initial fluorescence lifetime imaging experiments of *C. tepidum* cells. Currently, we are exploring optimal conditions for obtaining fluorescence lifetime measurements of single cells. This is a non-trivial task, however our initial results have indicated we are able to resolve chlorosome lifetime differences between oxidized (~14ps) and reduced (~40 ps) *C. tepidum* cells.

We are currently optimizing the optics setup in order to allow for the highest time resolution possible for a single cell in the shortest acquisition time. This is necessary to investigate dynamic responses in single cell chlorosome light-harvesting and energy transfer processes.

Future Work

It is our hope to have the optics of our optical microscopy system optimized within the next couple of months. Upon completion, we will begin to investigate living cells via FLIM. We will begin with cultures grown under traditional conditions, however quickly progress to cultures grown under various conditions of aerobic and light stress. Further, design of our microscope incubation chamber, as previously described, allows for alteration of conditions while continually obtaining data. Thus, we will be able to investigate rapid mechanisms of metabolic regulation such as quinone regulation. AFM will also be performed on isolated membranes from *C. tepidum* grown under various conditions to determine effects of metabolic regulation on chlorosome structure and stoichiometric relationship to the other photosynthetic components. Similar experiments will be performed on *Chloroflexus aurantiacus* cells as well as genetically modified *C. tepidum*.

Project research will aim to understand the role of metabolic control in developing an optimized photosynthetic light-harvesting complex, increasing our fundamental understanding of the metabolic regulation of light-harvesting complexes and advancing research in artificial photosynthetic design and other bio-energy applications.

Conclusion

The project research will result in a greater understanding of the relationship of metabolism to light-harvesting and energy transfer in photosynthesis. It is our hope to get a detailed understanding of the metabolic control necessary for development of functional and optimized antenna complexes allowing development of a model for metabolic regulation of light-harvesting structure/function. The metabolic regulation of the self-assembled pigments within the chlorosome present an excellent candidate for studying processes of metabolically regulated bio-design. Further, better understanding has implications that transfer to all areas of bio-inspired design, particularly in complex biological systems and energy-related systems.

References

1. Li, H., N. Frigaard, and D. Bryant. Molecular contacts for chlorosome envelope proteins revealed by cross-linking studies with chlorosomes from Chlorobium tepidum. 2006. *Biochemistry.* **45** (30): 9095.

2. Montano, G., B. Bowen, J. LaBelle, N. Woodbury, V. Pizziconi, and R. Blankenship. Characterization of Chlorobium tepidum chlorosomes: A calculation of bacteriochlorophyll c per chlorosome and oligomer modeling. 2003. *Biophysical Journal.* **85** (4): 2560.

Understanding Arctic Hydrologic Response to Climate Change

Bryan J. Travis
20100312ER

Introduction

The impact of global climate change is predicted to disproportionately affect arctic systems. Many of the changes in the Arctic documented over the past several decades (shrinking lakes, changes in flows and chemical loading of rivers, vegetation distributions, and thermokarst expansion) are intimately linked with the hydrology of permafrost dominated landscapes. The rate and timing of these hydrological changes will have a direct impact on the fate of the approximately 1600 Gt of carbon presently sequestered in frozen arctic soils. At present, our ability to monitor ongoing activity and predict the spatial and temporal scales over which future changes in the arctic hydrological cycle will occur is greatly limited by current modeling and remote sensing technologies. Current models of permafrost thawing focus exclusively on the thermal diffusion of temperature changes and neglect the role of hydrologic flow in transporting heat into the subsurface. Presently, there are no remote sensing technologies that can directly detect changes in permafrost. This project addresses these two fundamental challenges by combining numerical modeling of groundwater and heat flow through frozen soils with the development of novel algorithms to apply to remote sensing data that will provide new tools to infer permafrost distributions and changes.

Benefit to National Security Missions

Predicting the timing and spatial patterns of permafrost changes in response to global climate change, and associated carbon release, is of direct relevance to DOE Office of Science climate change programs. The hydrologic and geomorphic impacts of permafrost thawing are highly relevant to the energy industry and the Departments of Defense, Commerce and State in that defense bases, transportation routes, ports and energy infra-structure will be impacted these changes. The natural resource impacts have direct relevance to the USGS, USFWS, BLM and state agencies. The remote sensing technologies develop have a direct application to NNSA and DOD programs.

Progress

In FY2010 our project made significant advancements on all of our three research fronts: permafrost model development, development of novel remote sensing algorithms for feature detection and extraction, and collection of data for model testing and simulation in support of the project's fundamental research objectives. Under the lead of PI Travis the following model development tasks have been implemented into the Arctic Hydrology (ARCHY) code: microbial transformation of soil carbon, snow dynamics, talik formation due to groundwater flow, and coupling of surface vegetation with subsurface dynamics.

Soil carbon is a primary focus of arctic climate research. How much of the soil carbon locked up in permafrost will be released if the climate warms? Our ARCHY model addresses this question by coupling heat transport, permafrost thawing or freezing, water and vapor transport (vertical and/or lateral), and microbial community activity (with associated transport of substrates, gases, nutrients, and the nitrogen cycle). A student, Irena Ossola, is comparing our model simulations to field data from Toolik Lake, Alaska, data that includes both temperature vs depth as well as CO_2 and CH_4 surface emissions, as a function of time. A second, major expansion of the ARCHY model is nearly complete; this couples a surface vegetation ecology model to the subsurface dynamics.

Dynamic snow model has been added as a complex time-dependent boundary condition to our subsurface mass and heat and bioreactive transport model (ARCHY). Snow cover can affect heat transport and extent of permafrost thawing by acting as an insulating layer. Significant changes in average snow cover will affect not only the depth of the active layer, but may also lead to talik formation (a layer of soil that is unfrozen year round), which will also impact microbial activity and production of CO_2 and CH_4. UGS student Peter Revelle researched snow dynamics during the summer of 09. A snow component is now operational in ARCHY.

Previous models of subsurface heat transport

and permafrost thawing have ignored the impact of groundwater flow through transmissive layers. With our ARCHY model we are starting to address the change in timescale of permafrost thawing due to groundwater flow through transmissive layers. Initial simulations have shown that water flow in such thin but transmissive layers can significantly shorten the time for thawing of permafrost beneath lakes.

Co-PI Rowland has lead efforts collecting field data on permafrost dynamics in response to sudden warming associated with landsurface dynamics along the Selawik River in northwest Alaska. This work has lead to institutional collaborations with Idaho State University and the US Fish and Wildlife Service Region 7. During field efforts in-kind logistical support from the USFWS has greatly facilitated research efforts. Rowland and CO-I Cathy Wilson have also led an effort to analyze remotely sensed imagery of arctic lakes to use variability in lake dynamics as proxy for changes in permafrost extent and distribution.

Under the supervision of Co-I Brumby development has progressed on creating algorithms for extracting hydrologic and vegetation features from radarsat 2 quad-polarization synthetic aperture radar imagery. During the past FY, a new post-doc Dr. Chandana Gangodagamage was hired to work on satellite imagery analysis tasks. Also working on remote sensing was graduate student Daniela Moody (ISR-2) who assisted with development of new feature extraction algorithms based on sparse, learned, over-complete dictionaries.

Wilson is developing strong collaboration with University of Alaska and ORNL researchers working on impacts of permafrost degradation on hydrology, thermokarst and carbon cycles. She is leading an effort to transition current LDRD ER work to programmatic work through the development of a science plan for Arctic carbon cycle experiments with ORNL on behalf of DOE BER, and the development of a white paper for NSF and DOE BER with the University of Alaska for the land component of a Regional Arctic System Model.

The following presentations at the upcoming annual AGU meeting arose entirely or in part from research funded or related to ER work:

Simulation of Active Layer CO2 and CH4 Emissions in Response to Rainfall Events. *I. Ossola; B. J. Travis*

Coupling hydrologic and hydraulic models in the Mackenzie Basin to quantify the spatial and temporal distribution of surface and subsurface water storages. *R. E. Beighley; K. G. Eggert; R. L. Ray; C. J. Wilson; M. K. Greene; G. L. Altman; J. C. Rowland; B. J. Travis; D. M. Lawrence*

The potential influence of thaw slumps and sea-level rise on the Arctic carbon cycle (*Invited*). *J. C. Rowland; B. T. Crosby; B. J. Travis*

Quantification of interannual and inter-seasonal variability of lake areas within discontinuous permafrost of the Yukon Flats, Alaska. *G. Altmann; J. C. Rowland; C. J. Wilson; D. Verbyla; L. Charsley-Groffman*

Assessing differences in topographic form between arctic and temperate drainage basins: Possible implications for dominant erosion processes. *J. P. Prancevic; J. C. Rowland; C. J. Wilson; P. Marsh; H. Wilson*

A dynamic ecosystem process model for understanding interactions between permafrost thawing and vegetation responses in the arctic. C. Xu*, B. J. Travis, R. A. Fisher, C. J. Wilson, N. McDowell.*

The following manuscripts are currently in preparation for submission to peer reviewed journals:

Rowland, J.C., Wilson, C.J., Brumby, S., and Pope, P.A., Arctic river mobility and sensitivity to climate change, for submission to Geology.

Rowland, J.C., Travis, B.J., and Wilson, C.J., The influence of regional groundwater flow on permafrost thawing and talik development, for submission to Geophysical Research Letters.

Rowland, J.C., Wilson, C.J., Brumby, S., and Pope, P.A., Erosion and channel dynamics of the Yukon River, Yukon Flats Alaska, 1974-Present. for submission to Geomorphology.

Travis, B.J., Wilson, C.J., Rowland, J.C., Ossola, I., Description and validation of a coupled mass and heat transport model with microbial transformation of soil carbon in the arctic. for submission to Geochemistry, Geophysics, Geosystems.

Ossola, I., Travis, B.J., Impact of rainfall events on active layer CO_2 and CH_4 emissions, for submission to Nature or Geophysical Research Letters.

Hayes, D.J., Hinzman, L.D., McGuire, A.D., Norby, R.J., Oechel, W.C., Rogers, A., Schuur, E.A.G., Thornton, P.E., Walsh, J.E., Wilson, C.J., Wullschelger, S.D., Experiments to Quantify the Ecosytem-Climate Interactions of a Warming Arctic. For submission to EOS.

Xu, C., Travis, B.J., Fisher, R.F., McDowell, N., Ossola, I., Wilson, C.J., Wullschleger, S.D. Hydrological Cycle Simulation in ARCHY-ED.

Future Work

In the coming FY our main project focuses will the implementation and testing of the modeling and remote sensing technologies developed in the first project year. On the remote sensing front, the primary focus will be on upscaling of the detection and quantification of landscape features and attributes related to permafrost presence/

absence and change. Specifically, we will explore how best to integrate observations of spatially discrete attributes to watershed and regional scales and how to automate such integrations.

Modeling efforts will be directed at investigating the process controls on Arctic hydrology and carbon cycle dynamics at a range of temporal and spatial scales. These simulations are critical in defining what processes control landscape responses to climatic change. Ongoing model development and improvements in computational efficiency will closely linked and motivated by the results of these simulations.

Conclusion

We will produce two new technologies:

1. The first fully coupled heat and fluid transport model with the capability to predict the interactions between permafrost thawing, changes in hydrology and land surface responses.

2. A software platform with integrated statistical relational learning algorithms.

With these two advancements, we will:

- Determine rates, timing, magnitude, and scales of hydrologic changes arising from permafrost thawing.

- Assess the evolution of hydrologic conditions amenable to activation of biotic and geomorphic processes that will drive carbon release.

Major changes in the arctic regions will impact climate, food supplies and land usage.

Publications

Rowland, J. C., C. E. Jones, G. Altmann, R. Bryan, B. T. Crosby, G. L. Geernaert, L. D. Hinzman, D. L. Kane, D. M. Lawrence, A. Mancino, P. Marsh, J. P. McNamara, V. E. Romanovsky, H. Toniolo, B. J. Travis, and C. J. Wilson. Arctic Landscapes in Transition: Responses to Thawing Permafrost. 2010. *EOS, Transactions, American Geophysical Union.* **91** (26): 229.

Deciphering the Controlled Chaos of Intrinsically Disordered Proteins

Dung M. Vu
20100328ER

Introduction

Many cellular proteins are intrinsically disordered. Oftentimes, these proteins undergo folding upon binding to their cellular targets. The advantages of having an unstructured shape and exhibiting a high degree of flexibility allow intrinsically disordered proteins (IDPs) to bind to multiple partners and to modulate their functional pathways. However, it is this transient nature that also makes IDPs susceptible to many human diseases such as cancers, neurodegenerative diseases and cardiovascular diseases. Therefore to understand the underlying causes of these diseases and to derive effective treatments, it is crucial to understand the correlation between the underlying structures of these IDPs to their biological functions.

Alpha-Synuclein is an ideal model protein to study the structural and functional characteristics of IDPs. It is relatively small (140 residues) and it displays many of the unique characteristics of IDPs. Although the function of alpha-synuclein is relatively unknown, it has been widely implicated as the major causative protein in numerous neurodegenerative diseases such as Parkinson's disease. Therefore, the central goal of this project is to elucidate the underlying mechanisms and molecular interactions of alpha-synuclein that defines its function and pathological formation into filamentous aggregates. Because of the intrinsic structural heterogeneity of alpha-synuclein, structural and functional characterizations of this protein have proven to be very challenging. To help overcome this obstacle, we propose to integrate vibrational spectroscopic techniques along with advanced computational methods to characterize the structure, function, and dynamics of alpha-synuclein.

Benefit to National Security Missions

We expect the computational and experimental methods developed in this study can be applied to the understanding of other IDPs that are important in many human diseases. Understanding the structures, folding, and functions of IDPs will help advance the Laboratory's mission by developing a predictive understanding of complex biological systems and developing applications to solve health and the environmental issues that are relevant to DOE, DHHS, and other government agencies.

Progress

Year 1 of our project was spent recruiting two new external postdocs, one experimental and one computational, acquiring and constructing samples for our vibrational spectroscopic experimental studies, setting up model systems and carrying out our computational molecular dynamics (MD) simulations. Our experimental postdoc, Divina Anunciado, comes to us from University of Illinois at Urbana-Champaign. She joined our team in September. She has a strong scientific background in biology, chemistry and biophysics. Our computational postdoc, Jianhui Tian, comes to us from Rensselaer Polytechnic Institute. He joined our team in July. He has a strong scientific background in physics, mathematics, chemistry and theory. With these talented additions to our team, we anticipate that we will make significant progress in our project during Year 2 and Year 3 of our project.

For our theoretical and computational work, we carried out long timescale simulations of alpha-synuclein in an aqueous environment to characterize its conformational ensemble of structures. As a starting structure, we used the nuclear magnetic resonance (NMR) structure of alpha-synuclein in a lipophilic environment. This NMR structure is composed of two helices that span residues 3-37 and 45-92 and a disordered C-terminal region. The MD simulation was run to simulate the molecular structure over a period of 355 nanoseconds resulting in the analysis of 710,000 conformations of the protein. In addition, we also performed the simulations at different temperatures to ensure that our results were not biased towards our starting conformation.

We characterized the conformational heterogeneity of alpha-synuclein in water by assessing how the secondary structure of this protein evolved with time. Results from this analysis are shown in Figure 1. As the protein evolves to form a random coil, the N-terminal helices

begins to break up, however, other helices are transiently formed within residues 1-90 of alpha-synuclein. Parts of the C-terminal tail start to form beta-strands independent of the rest of the protein. These strands form and break regularly throughout the simulation. In addition, the MD simulation also shows that the amyloid fibril forming region of the protein has a slight tendency to form beta-sheets and hydrogen bonded beta-bridges.

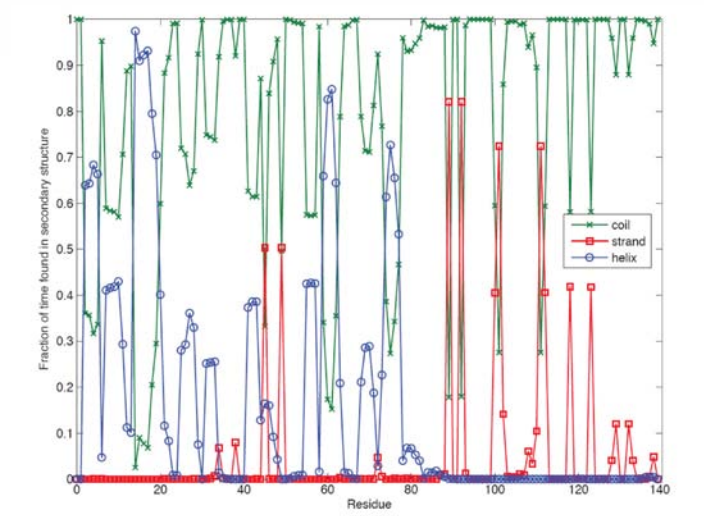

Figure 1. The probability of the residues 1-140 from alpha-synuclein displaying a particular secondary structure.

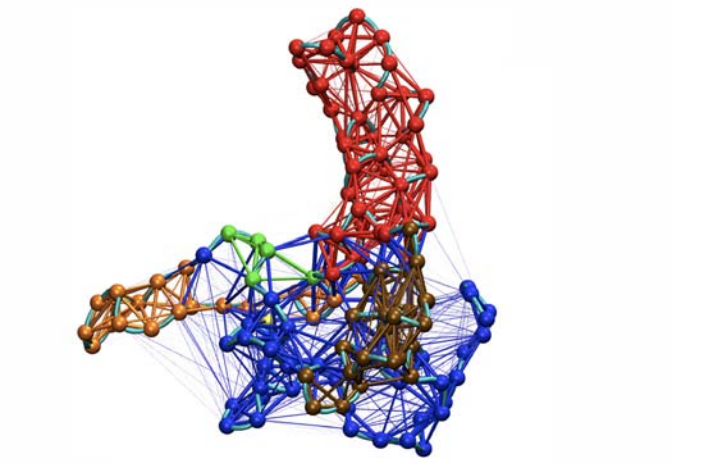

Figure 2. A representative collapsed structure of alpha-synuclein from the MD simulation. The colors (blue, red, green and brown) denote the four distinct structural communities derived from network analysis.

Alpha-synuclein exists as compact structures in an aqueous environment. These collapsed structures were determined by calculating the radius of gyration of alpha-synuclein (Figure 2). This compaction in size is largely due to long-range contacts between sequentially distant regions of alpha-synuclein. At higher temperatures, this compactness remains and even shows a smaller radius of gyration. The observed compact size of alpha-synucelin at high temperatures contradicts the current polymer models of IDPs, which predict that the radius of gyration of an unstructured peptide would increase with temperature.

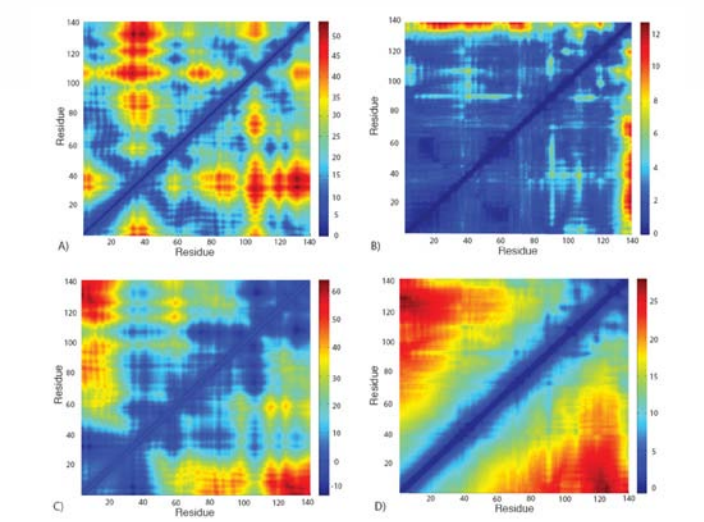

Figure 3. Long-range contacts are formed in alpha-synuclein. A) The average distance and B) standard deviation of distance (in angstroms) between residues in alpha-synuclein during the MD simulation. The difference in C) average distance and D) standard deviation between residues observed in the MD simulation and those estimate using the worm-like polymer model for a peptide.

The compact structures of alpha-synuclein are composed of a large distribution of structures with varying long-range contacts. In order to characterize these structures, we calculated the average distance and standard deviation of distance between the backbone carbon atoms of all residues in alpha-synuclein during the MD simulation. As seen in Figure 3, long-range contacts are transiently formed between residues in the C-terminus region (residues 120-140) and the N-terminus region (residues 1-20) as well as some residues in the amyloid fibril forming regions of alpha-synuclein (residues 55-65 and 80-100). In addition, the N-terminus region also forms contacts with the amyloid fibril forming region (60-90). These contacts probably shield the hydrophobic region of the amyloid fibril forming region from being exposed to the aqueous environment and hence reduce the tendency to form fibrils under normal physiological conditions. However, the exact contacts and nature of the collapsed states observed in the MD simulations depend on the initial conditions used. Several transient salt bridges have also been identified: between the positively charge N-terminus and Glu130 and Glu131, Lys6-Glu130, Lys21-Glu62, Glu28-Lys43, Lys96-Glu123, Glu35 with both Lys43 and Lys45, Lys58-Glu114, Lys60-Asp115.

In addition, we tried to assess whether fragments of the protein could be identified that would allow us to easily compare our computational results with our infrared experiments. In order to identify these fragments, we built a network based on the MD simulation of the protein.

This frequency-weighted contact network was constructed in which a node represents a residue in the protein and an edge was used to represent a contact in the protein. Surprisingly, we found that alpha-synuclein could not be fragmented into smaller continuous segments. What we observed was that alpha-synuclein could be divided into four distinct communities (Figure 1). Because the communities are discontinuous in sequence, we predict that the conformational behavior of the protein will be different from that of its fragments.

The results from this work havbe been presented at two conferences: the inaugural Gordon Research Conference on Intrinsically Disordered Proteins (July 2010) and 24th Annual Symposium of the Protein Society (August 2010). Since the research field of IDPs is a newly emerging field, our research presentations at these national conferences generated a lot of interest from the external scientific community. We have also submitted a manuscript on this work to the Proceedings of the National Academy of Sciences.

Progress on the experimental front has been limited. First we had to acquire and produce the alpha-synuclein constructs (full-length protein and deletion mutants) to allow us to begin our IR measurements. We have worked to improve our production of alpha-synuclein by increasing our growth induction to at least 10 hours. Although this resulted in more of our protein being found in the inclusion body fragments, we were able to purify this insoluble protein via a denaturing chemical route to eventually obtain purified soluble protein. We are in the process of characterizing this protein in the unbound and bound ligand form.

Future Work

1. We will focus on characterizing the folding pathway of this protein. This will include understanding the disordered state distributions and identifying intermediate structures along this pathway. We will determine how our infrared measurements of alpha-synuclein at different solution conditions (i.e. temperature, pH, ionic strength) compares with our MD simulation. This will allow us to test our computational models as well as provide more detailed insight into our experimental results.

2. We will focus on the early protein events that dictate the formation of intermediate species along the self-assembly pathway into filamentous aggregates.

3. We will integrate theory, simulations and experiment to build a general model to describe the dynamics of alpha-synuclein and other IDPs. These results will allow us to put forward guidelines for a predictive tool that can be used to identify signatures of IDPs and regions of significant disorder in proteins.

Conclusion

We have shown with our MD simulations and theoretical analysis that the current polymer models cannot adequately characterize IDPs. All self-avoiding polymer models would estimate that alpha-synuclein would be more expanded in size with limited long-range residue contacts. Clearly current computational and theoretical methods are not adequate to tackle the problem of trying to understand the nature and dynamics of IDPs. These results need to be tested and validated with vibrational spectroscopic experiments. We are poised to carryout these tasks in Year 2 and Year 3 of our project.

Publications

Sethi, A., D. M. Vu, and S. Gnanakaran. Secondary structure propensities of alpha-synuclein. *Proceedings of the National Academy of Sciences.*

Algal Lipid Regulatory Networks

Scott N. Twary
20100456ER

Introduction

Algae are the leading candidates for biodiesel production due to their potential to produce 10 to 100 times more oil/ lipids than plants. Algae produce and accumulate lipids as energy dense food to survive environmental stress. Current algal lipid production systems are not cost competitive, however. To make the systems more efficient, we need to be able to grow large number of algae cells with high levels of lipids that can be used for fuel. It is poorly understood how the algae cell determines what to do with its food and energy. Developing an understanding of the factors controlling and limiting lipid biosynthesis can lead to effective production systems. This project will reveal the how the cell controls lipid biosynthesis optimizing algal biofuel production. The overall result will be to decrease our dependence on petroleum-based energy production and produce environmentally friendly fuels. We will identify the genetic changes that occur in algal cells during nitrogen limitation. This environmental stress induces lipid production. Measuring coordinated changes in the cell will allow us to identify key components controlling lipid production. This project will also modify the activity of key genetic steps to direct food and energy towards lipid production. By combining LANL's innovative capabilities we can identify key regulatory mechanisms and optimize biofuel production.

Benefit to National Security Missions

This work directly addresses the challenges outlined by EERE and DARPA for the development of productive algal biodiesel systems. The results of this project will define the fundamental mechanisms controlling lipid biosynthesis. Algal strains suitable for industrial production systems will be developed. These systems will provide greater energy security through decreasing dependence on petroleum based fuels. CO2 recapture into high value products will enhance environmental stewardship.

Progress

The objectives of this project are to identify the changes that occur in algae when the cells progress from rapid growth to lipid accumulation. Nitrogen stress has previously been identified as inducing lipid accumulation. We have developed a bioreactor system that can monitor and regulate many growth conditions including O_2, CO_2, pH, light, and cell density. Automated sampling systems allow for extensive sample collection and preservation. We can monitor how much nitrogen is used by the algae during its growth to precisely define the period of nitrogen depletion and the beginning of this stress. Four key time points were defined. First cells grow rapidly in the presence of excess nitrogen. Second cells use all of the media nitrogen, sense this environmental change and turn on lipid production. Third cells continue to grow yet they increase their content of valuable fuel lipids. Fourth maximum lipid production and accumulation occurs. To figure out what changes are occurring inside these algae cells, we need to rapidly extract and preserve the desired cellular components. Nannochloropsis salina contains a recalcitrant cell wall resulting in difficulty lysing cells without also destroying the internal contents. We have developed and optimized protocols for cell lysis while preserving DNA, RNA, lipids, and other cell metabolites. Techniques include bead beating with garnet beads, heat treatments to accelerate cell membrane disruption, organic solvent refluxing, and acoustic disruption.

During an initial algal growth experiment we noted oxygen consumption increasing during the day. Algae are photosynthetic organisms and thus produce oxygen when the lights are on. The increase in oxygen consumption, therefore, suggests that bacteria are also present in this culture consuming the oxygen through respiration. Isolation and culturing identified five potential unique bacterial strains. These strains were identified through 16S rDNA sequencing and belong to the marine genus of Algoriphagus, Marinobacter, Limnobacter, Oceanicola, and Henriciella. Antibiotic screening was performed to identify both algal and bacterial susceptibility to a variety of differing classes of antibiotics. Streptomycin and cefotaxime treatments were toxic to bacteria but also inhibited algal growth. A process was developed for culture purification. Antibiotics were followed by enzyme and detergent

washes to remove any surviving bacterial cells. Pure algal cultures were obtained and maintained for further experiments. This process allows us to create and maintain bacteria free algae stocks obtained from any source. The effects and interactions of the bacterial contaminants on lipid production are unknown at this time. Typical industrial production systems, though, are a complex mix of algae and other organisms. These interactions may be beneficial or detrimental to both algal growth and lipid production.

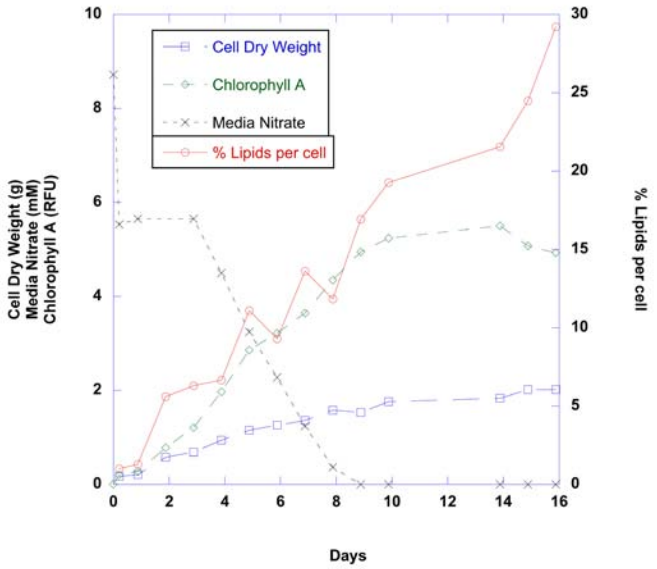

Figure 1. Growth parameters and lipid production of Nannochloropsis salina during nitrogen depletion.

We have completed two fermentor growth cycles with a pure Nannochloropsis salina cell culture. Algae cells progressed from rapidly growing to lipid production and accumulation. Lipids increased 336 % after depletion of nitrogen from the media (Figure 1). The main neutral lipid, triacylglycerol, was composed of C14 to C20 fatty acid chains. Cell samples were collected every four hours including both light and dark periods during the 20 day growth cycle. Expressed genes were purified from critical time points and submitted for sequencing and comparative analysis through JGI LANL. Cellular metabolites from the exact same sample will be extracted and analyzed by LC/LTQ/FT mass spectrometry. Cellular metabolism and carbon distribution should differ significantly between periods of rapid cell growth and periods of lipid accumulation. By comparing the genes expressed and relating these to metabolite pools, we can determine the key genes involved with lipid production in Nannochloropsis salina. This will be the first elucidation of lipid genetics in this organism.

We have improved our fermentor growth conditions by the addition of LED lighting increasing light intensity close to sunlight. This will allow for more rapid growth through greater photosynthetic capacity. We have also enhanced monitoring of headspace O_2 and CO_2 to better understand respiratory fluxes in the system.

We now have extensive collections of algae cell samples. We will complete tests to identify coordinated changes in genes expressed with cellular metabolites. This information will allow us to develop theories of how lipid production is controlled. Optimizing production of this valuable fuel commodity will increase its profitability and marketability.

Future Work

The objective of this project is to reveal how the green algae Nannochloropsis salina alters its processing of food and energy to produce neutral lipids, a valuable green fuel. Algae are leading candidates for biodiesel production because they have the potential to produce 10-100 times more oil than higher plants have. Overcoming the critical limitation to commercialization requires increasing lipid biosynthesis further. Algae respond to environmental stresses, such as nitrogen starvation, by producing energy rich oils as food reserves. The interactions of the critical nutrient, nitrogen, with carbon (algae food and energy) are closely coordinated in the cell to maintain the cells ability to grow and reproduce. Optimizing algal biodiesel production requires an understanding of the fundamental partitioning of carbon and energy between growth and lipid biosynthesis.

The goals of this project are to:

1. Identify key biochemical and genetic changes that initiate lipid biosynthesis during nitrogen limitation.

We have completed the isolation of expressed genes at different critical time points. We can identify unique changes that can be directly related to changes in cellular production of key compounds. We will develop specific tests for these genes. Their measured response will help determine the role they play in lipid production.

2. Identify characteristic metabolites that may play a regulatory role in environmental signaling and in inducing subsequent lipid production.

The cell is able to sense and respond to environmental cues. These messages are transmitted internally into the cell and signal changes and adaptations so the cell can optimize growth and survivability. We will identify key molecules in the cell that can be critical components of this system.

3. Identify the genetic regulatory elements involved in carbon partitioning to lipids.

The algae cell can make significant changes in how it utilizes food and energy. We will identify global elements in the cell that trigger these changes. Small RNA molecules and gene regulatory elements will be isolated and tested for their impact. We will also genetically modify the algae

to change their ability to control these key genes and determine the effects on lipid production.

Conclusion

The goal of this research is to create an algae strain with enhanced biodiesel lipid production. This will be a primary component in developing a cost effective industry. This project will identify the key regulatory processes allocating carbon and energy in algae cells between biomass and lipid production. Genetic modification of each critical step will allow for optimal lipid production. Advances in understanding the complex regulation of biosynthesis will allow for the creation of an algae biofuel crop. Algae biodiesel production will decrease our dependence on petroleum based energy and contribute to environmental sustainability through carbon neutral fuels.

Modeling the Global Circulation and Evolution of Influenza A Virus

Alan S. Perelson
20100479ER

Introduction

Each year, 5-15% of the world becomes infected with influenza, and an average of 36,000 people in the United States, and 500,000 people in the world, are estimated to die as a result. Moreover, the highly pathogenic avian influenza A-H5N1 and swine origin influenza A-H1N1 strains currently pose pandemic threats. The global patterns of influenza virus circulation and evolution remain unknown, and understanding these patterns in detail will increase our ability to respond to and prevent seasonal and pandemic influenza infections. Influenza outbreaks are strongly seasonal in temperate regions of the globe, affecting populations primarily in winter months, and follow more complicated patterns in regions closer to the equator. The central hypothesis of this proposal is that global influenza circulation patterns can be predicted by weather features. Based on this hypothesis, we plan to develop a mathematical model of the annual global movement and evolution of influenza A virus as a function of weather phenomena, at the scale of several geographical regions per country (Figure 1). We will use multiple regression analysis to determine which weather-related features, such as latitude, time of year, humidity, temperature and cloud cover, are correlated with influenza outbreaks. Given these factors, a worldwide model of influenza spread and evolution will be constructed, integrating susceptible-infected-recovered (SIR) models for each region. Viral genetic and antigenic evolution will be included in these models, together with the evolution of host susceptibility. Each region will experience its own outbreaks, which will then spread to other regions, both near and far. Precise annual geographic patterns of circulation within East and Southeast Asia, and of transmission to temperate regions of the northern and southern hemispheres, will be predicted.

Benefit to National Security Missions

This work hopes to uncover basic features determining the world-wide circulation and evolution of influenza A. It has direct application to the basic mission of NIH, CDC and other agencies, such as DARPA and DHHS, now concerned with the effects of an influenza pandemic caused either by the new swine origin H1N1 or the H5N1 bird flu. The model will both address basic science questions as well as be used for examining intervention strategies, such as vaccination and the use of antivirals, to slow the spread of influenza.

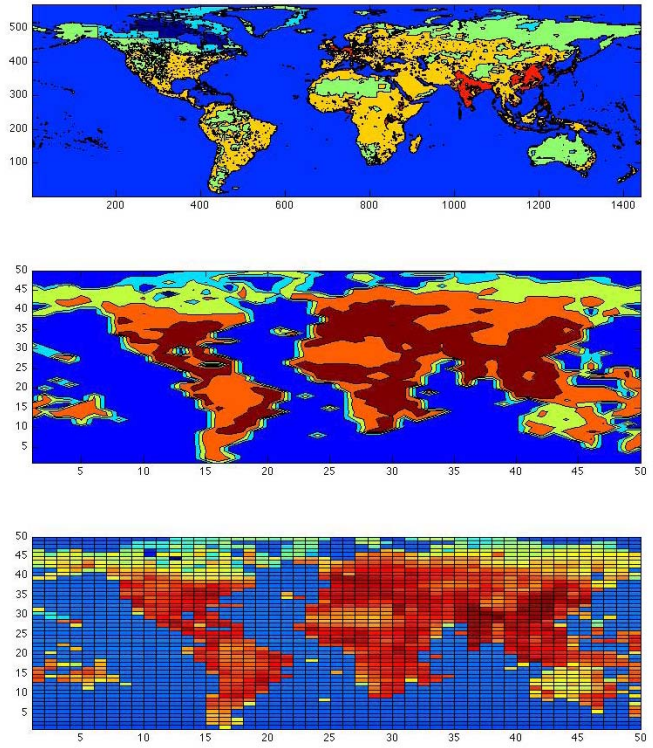

Figure 1. This figure shows the global world population density. The top panel shows a fine grained view of the population density, plotted as the log of the density to account for the very disparate levels of populations. The bottom panel shows a coarse grained version of the original data on a 50x50 grid. We will use these grids to couple epidemic models within each cell, using human movement patterns, to the global circulation of disease. Importantly, we will examine the type and coarseness of the grid to ensure convergence of the mathematical model. (The center panel simply shows a smoothed version of the 50x50 grid to allow for a visual comparison of what the coarse-grain procedure has done.)

Progress

Our studies have initially focused on exploring various modeling approaches that will be used to model the global circulation of influenza. We have identified several important criteria for any reasonable model. Most important is including human movement, which acts as a population mixer on different spatial scales. On a continent scale, influenza spreads predominantly as a result of commuters with long (perhaps across states) commutes; this is mainly due to the large number of commuters and their commuting frequency. Thus, any model must include commuter travel patterns, and we have identified US Census data with such information. At the intercontinental scale, the overwhelming form of travel is via airline flights, and we have begun assimilating international flight data, which describes thousands of airport connections and flow rates between them. Given this data, two questions arise. First, how important is local human movement between large, international cities, relative to movement between and within those cities? This is important because high quality census data, as is collected in the US, is not available for most other countries. Second, how important are the details of travel? For example, do we need to know the distribution of trip lengths? Do we need to know which cities people often or rarely travel to? How important are cities that are small in population, but provide a major airline hub in a certain geographical region?

Answering these questions form the current focus of our work. We have developed two modeling strategies. The first is known as a "coupling" model because each geographical region is "aware" of disease elsewhere because of a coupling coefficient in the mathematical model. No actual movement of people is described in such a model. The second model is known as a metapopulation model, and such models have explicit terms that describe where people are and where they live, thereby including details of human movement. We have explored the mathematical conditions under which the more accurate metapopulation model reduces to the coupling model, and we are generalizing that to the global scale. Although it would be preferable to always use the more accurate metapopulation model, it scales as O(N squared) rather than O(N), where N is the number of geographical regions included; clearly, for an accurate global model, including many regions that span all continents in both hemispheres is important (Figure 1). However, we have found that the coupling model is not particularly accurate for influenza, with the main error being in the timing of the epidemic. We are currently exploring to what extent the timing information would be inconsistent with actual data. In parallel, all of these models are being tested using various evolution equations, including deterministic and stochastic. All of these variants have been coded, tested, and compared.

How will we know that our theoretical model is accurate? To answer this question we will begin analyzing past influenza epidemics. We have identified two methods that we believe will aid us in understanding correlations in the spread of the disease, which can be used to validate our mathematical model. The first method is the well-known space-time correlation function method in which various variables are analyzed to explore potential sources of correlations that span both space and time. (Most often, only time correlations are explored.) The second set of methods we will implement are wavelet methods that allow us to examine "power" locally in space and in time, in contrast to Fourier methods that treat an entire data set at once. Together, these methods will allow us to see space-time correlations at the local level in space and time. This will allow us to see where time correlations might arise, for example, in Southeast Asia, but not propagate across continents.

Once these models and analysis tools are in place, we will turn to adding biophysical information to our model. For example, we will begin to develop a model for influenza transmission in air to account for humidity effects.

Future Work

To develop a global circulation model for influenza A virus, we shall first assemble data on global weather, airline networks and traffic, and influenza outbreaks. Weather and airline traffic data are readily available, and significant data is available on influenza outbreaks worldwide. Second, we will develop a coarse-grained patch model for the Earth based on weather information; i.e., we will subdivide the world into population regions whose boundaries are defined by relatively homogeneous weather conditions within. Third, we will develop SIR models corresponding to each region or patch. We will validate aspects of the model/code based on retrospective modeling of pandemics such as the 1968-1969 Hong Kong pandemic. We will compare with previous models of these pandemics. Fourth, multiple regression analysis will be used to determine which weather-related factors are correlated with influenza outbreaks for a given geographical region. For each region for which influenza outbreak data is available, weather-related factors will be analyzed for their contributions to outbreaks. Factors that will go into the analysis include latitude, time of year, solar UV index, cloud cover, temperature, relative humidity, and absolute humidity. Monthly averages, maxima and minima of UV index, cloud cover, temperature, and relative and absolute humidity will be examined. Fifth, given the factors that are shown to be important predictors of outbreaks for each region, a worldwide model of influenza spread and evolution will be constructed. An SIR model will be constructed for each region, incorporating important weather-related factors found earlier; outbreaks will only be allowed to occur in proportion to the degree of permissiveness of environmental and host conditions. Lastly, we will use our model to test multiple intervention strategies involving antiviral drug and vaccine

administration, airline flight pattern alterations, and passenger screening. We will simulate interventions in seasonal and pandemic influenza outbreaks.

Conclusion

The goal of this project is to develop a mathematical model of the annual global movement and evolution of influenza virus as a function of weather phenomena, such as latitude, humidity, temperature and cloud cover at the scale of several geographical regions per country. Such a model will help us understand worldwide influenza virus circulation, and substantially improve our predictive capability for vaccine strain selection and targeted antiviral drug use, in order to protect populations from both seasonal and pandemic influenza more efficiently. This proposal thus attempts to answer basic questions about influenza evolution and global circulation.

Identifying High Risk Species Critical for the Emergence of Pandemic Influenza

Jeanne M. Fair
20080230ER

Abstract
Management and detection of highly pathogenic influenzas in wild and domestic animal populations require a better understanding of the determinants of host range. The major host range determinant for influenza is the binding site for the virus, sialic acid that varies between mammals and bird cell membranes. We tested the hypothesis that the characterization of sialic acid of species in each order in the Class Aves can be used as a phylogenetic guide map to host range for influenza and that data can then be used to guide biosurveillance efforts for strains of concern for influenza [1]. This hypothesis was based on the fact that to gain entrance into cells, human influenza viruses bind preferentially to sialic acid containing N-acetylneuraminic acid α2,6-galactose (SAα2,6Gal) linkages, while avian and equine viruses bind preferentially those containing N-acetylneuraminic acid α2,3-galactose (SAα2,3Gal) linkages. By characterizing and comparing sialic acid in the respiratory, digestive tracts, and on red blood cells between important bird species and investigating correlations between the three physiological landscapes for a wide range of bird species we developed a mapping system for the host range of influenzas in birds.

Background and Research Objectives
Management and detection of highly pathogenic influenzas in animal populations requires a better understanding of the determinants of host range. The major host range determinant for influenza is the binding site for the virus, sialic acids (Sia) that varies between mammalian and avian cell membranes [2]. The specific hypothesis behind the proposed research is that the characterization of Sia in each Family in the Class Aves can be used as a phylogenetic guide map to the host range for influenza and that data can then be used along with species distribution information to guide surveillance efforts for strains of public health concern [1]. To begin to understand this interaction we first set out to characterize sialic acid species in the respiratory, digestive tracts, and on erythrocytes between five peridomestic and phylogenetically different bird species. We then investigated for correlations between these three physiological landscapes in order to conduct a sialic acid survey in a wide range of bird species using the simplest tissue(s) to acquire yet still describe an animal's sialome. Sialic acid characterization in birds is being measured using a new method that makes use of stable isotope labeled substrates (neuraminyllactose) for binding to both neuraminidase and hemagglutinin present on the surface of the virus, resulting in a risk assessment for priority species.

The data collected from this research effort identified species differences in the sialome that can help point to species or groups of birds that we need to be concerned about for potential increase in the probability for reassortment of the influenza virus due to similarities in sialic acid with humans. In short, this would enhance our Nation's ability to find "mixing vessels." Mixing vessels are those species that can be infected by both human and avian adapted viruses and thus might transmit novel resorted (mixed) viruses to humans. The end results of this project will be a much needed phylogenetic guide map created by overlaying Sia quantification and linkage data with species distribution information that will result in a prioritization of avian species that may asymptomatically carry influenza viruses of public health concern. This project helped build a science foundation for the challenge of avian influenza surveillance around the world and how we can be more effective in detecting influenzas in the environment.

Scientific Approach and Accomplishments
In order to successfully complete the scope of work for our project of completing a phylogenetic analysis of the key receptor protein, sialic acid (Sia) in birds, we needed to: 1) obtain blood samples from numerous avian species, 2) develop a novel database, and finally, 3) isolate and quantify Sia using cutting-edge stable isotope technology at Los Alamos National Laboratory (LANL). We gratefully collaborated with a multitude of researchers in the field and with zoological parks across North America. During the three years of this project we have obtained over 1300 blood samples from a majority of the 23 Orders needed for the comparative analysis. Blood samples

from the over 800 birds were collected in 2009 from numerous collaborators that include the Saint Louis Zoo, Brookfield Zoo, Monterey Bay Aquarium, the Albuquerque Zoo, and researchers within the United States Geological Survey and National Wildlife Research Center. To investigate variation in Sia's that may be due to infection or age and sex, we collected tissue and blood samples from mallards that were part of an influenza infection study at the National Wildlife Research Center in Fort Collins, CO, as well as a cohort of breeding American kestrels of different ages and sexes in Colorado.

The sample and analysis database, development by Dr. Jankowski, is a relational database programmed in Microsoft structured query languange (MsSQL). It is housed on a LANL MsSQL server and accessible to multiple users on and off campus depending on access privileges. The database is capable of tracking molecular to landscape scale data and interacts with a geographic information system (GIS) in order to accommodate spatial analyses. Certain data standards are being developed in collaboration with the Wildlife Disease Information Node of the National Biological Information Infrastructure. The database contains information on the bird collection specimen type, sialic Sia content analysis as well as spatial and geographical identification of Sia types in tissue sample. The materials and methods leading to the database inputs are also contained within the database.

Laboratory protocols for total Sia quantitation in chickens, pigeons, and bluebirds were successfully developed in the second year using both classical methods and the newly developed stable isotope technologies (Figure 1). These protocols were then used on a myriad of species' samples. Analyses of HPLC-mass spectrometer (MS) results for total Sia quantification were performed using Center for Disease Control standards and preliminary results in pigeons were validated by the Glycotechnology Core Resource at UC San Diego demonstrating a working assay. Our team synthesized several neuraminic acid moieties with different stable isotope labeling patterns ($^{13}C_{3,5,7,}$ etc.) as well as optimized the protocol for rapid LCMS detection and analysis. These compounds can be used to quantitate the sialic acid present in biological samples using LCMS using the labeled compounds as an internal standard that is chemically identical to the compound detected. After the sialic acid is harvested, a known amount of labeled sialic acid was added before purification. Any loss of compound that occurs will also occur to the chemically identical labeled compound. Detection of the labeled and unlabeled sialic acid with MS gives the relative amounts of each compound, easily seen as two peaks mass shifted by 3-7 mass units. Thus, this new method allowed for verification of other literature methods for sialic acid detection and quantification and provides a rapid means (within hours, even using complex samples) of analyzing multiple samples.

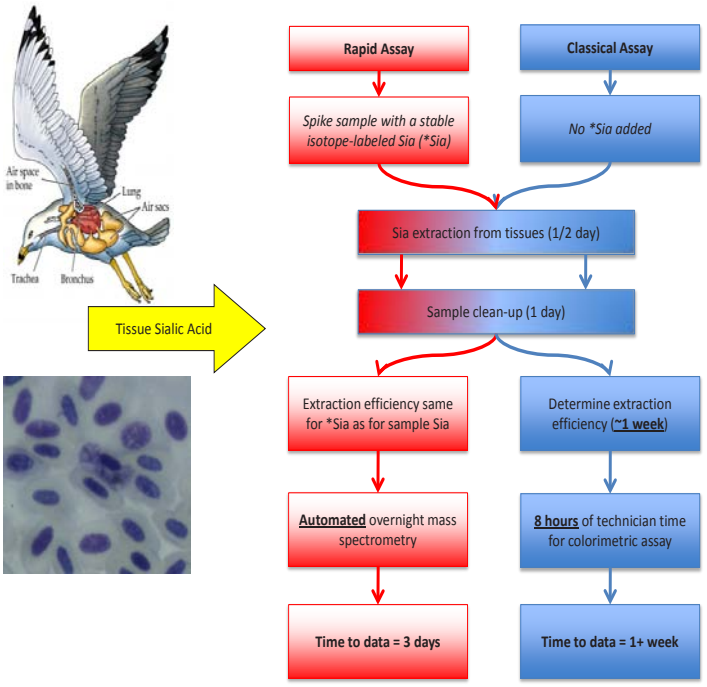

Figure 1. Combing both classical and newly developed mass spectrometry methodologies we developed a thorough suite of laboratory assays for both quantifying and identifying sialic acid in a variety of tissues and species.

Bovine fetuin that is used as a control protein for Sia was analyzed and also showed a strongly consistent standard curves. Between-assay runs showed reproducible results in the MS. Amounts of a common type of Sia (Neu5Ac) varied from 10 to 14 pm/µg total protein in red blood cells (RBC) (n = 155). There were many differences according to the taxonomic group (Figure 2 and Table 1). We have detected Sia concentrations as low as 0.5 pm/µg total protein in avian RBCs using our current MS protocols and have discovered the presence of a form of Sia (N-glycolylneuraminic acid, Neu5Gc) on pigeon RBC membranes considered rare in birds [3]. The time of this assay is 30 minutes per sample and the lowest volume being currently used is 50 µl RBCs. This volume size allowed for analysis of blood samples from small birds (e.g. Order Passeriformes) and the time will allow for multiple samples to be run overnight by the mass spectrometer. This was important as Passeriformes (songbirds) were recently found to harbor more influenzas as previously thought [4]. We developed lower detection thresholds of Sia via fluorescent marker labeling. We attempted to use flow cytomety to investigate the linkage difference in Sia in blood samples but the clumping of the red blood cells could not be eliminated so we utilized that fact and used hemmagglutination methods with fresh blood samples from over 30 species and 200 individuals. Hemmagglutination relies on clumping and is a reliable method that allows for the assessment of sialic acid linkage in a sample in a rapid and simple manner [5].

Taxonomic Group	Common Names of Species Sampled	More α2-6?	Number of Samples	2-6:2-3 Ratio	Lower 95%	Upper 95%
Class						
Mammals	Dogs, Cats	No	9	0.66	0.02	1.30
Aves (birds)	See below	YES	98	1.72	1.52	1.91
Bird Order						
Columbiformes	Pigeons, Doves	YES	7	2.43	1.73	3.13
Passeriformes	Song birds	YES	64	1.90	1.66	2.13
Anseriformes	Ducks and geese	No	16	1.14	0.68	1.61
Galliformes	Chickens and grouse	No	11	1.04	0.48	1.60
Bird Family (first letter of *order*)						
Emberizidae (P)	Towhees	YES	6	3.04	2.37	3.71
Cardinalidae (P)	Grosbeaks	YES	8	2.61	2.03	3.19
Tyrannidae (P)	Wood-pewee	YES	3	2.46	1.52	3.40
Columbidae (C)	Rock pigeons, the common pigeon	YES	7	2.43	1.81	3.05
Mimidae (P)	Crissal thrasher	No	1	2.41	0.78	4.05
Parulidae (P)	Warblers	YES	4	2.24	1.42	3.06
Sittidae (P)	Nuthatch	YES	3	1.97	1.02	2.91
Fringillidae (P)	Finches	YES	13	1.86	1.40	2.31
Picidae (P)	Sapsuckers	No	4	1.67	0.86	2.49
Turdidae (P)	American robins, bluebirds	YES	11	1.50	1.01	1.99
Anatidae (A)	Many Ducks	No	16	1.14	0.73	1.55
Phasianidae (G)	Chickens	No	11	1.04	0.55	1.53
Corvidae (P)	Jays, Magpie	No	8	0.88	0.30	1.45

Table 1. Sialic acid linkage ratio (α2-6:α2-3) for a sampling of tested species. A ratio greater than 1.0 indicates a taxonomic group that has more of the human flu receptor (α2-6) than the bird flu receptor (α2-3). Humans have a ratio of about 1.0, pigs have a ratio that is higher than 1.0 whereas horses and cows have a ratio that is lower than 1.0. Thus humans have about the same amount of α2-6, pigs have more α2-6 than α2-3 and horses and cows have more α2-3 than α2-6 (6). Red colored rows are groups that would be of concern for reassortment of human and avian influenzas.

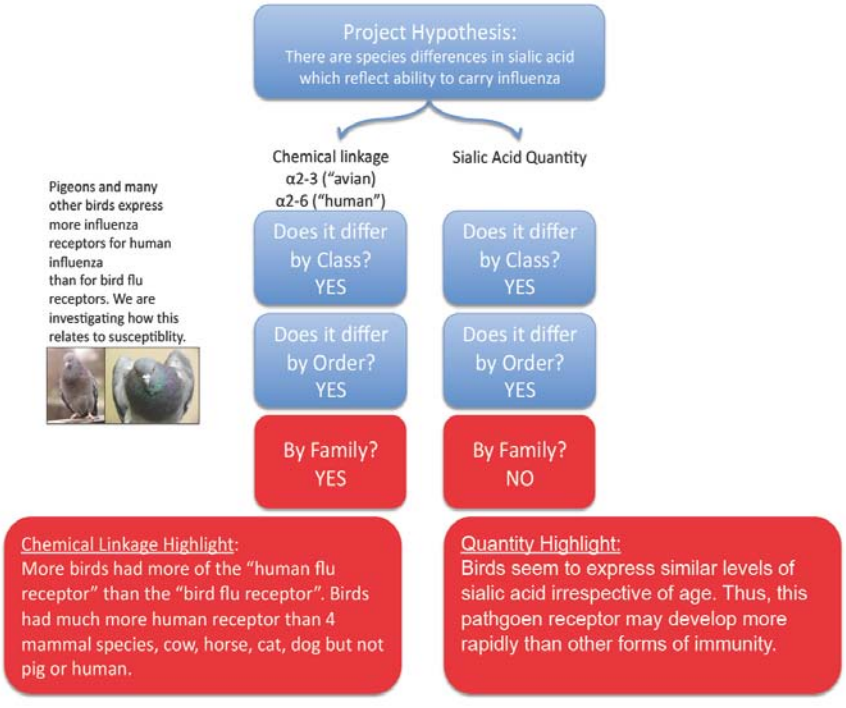

Figure 2. Answering the project hypothesis of using sialic acid as a phylogenetic map for identifying species that could be critical for the assortment and propagation of influenzas in the environment we identfied Orders and Familes that should be included in biosurveillance efforts for influenza.

Impact on National Missions

This project supported the biothreat reduction missions within DOE, DHS, and other government agencies by enhancing the understanding of emerging diseases in non-human populations, focusing on avian and pandemic influenza. This project also supported our ability to improve world-wide human health due the strong link between influenza in birds and human health because influenza epidemics in human populations occur when viruses that typically inhabit the avian gastrointestinal tract mutate or reassort, enabling them to cross the species barrier to infect people. Biosurveillance of avian influenzas in wild birds has been a priority for the last decade globally. However, biosurveillance is expensive and can easily miss infections of highly pathogenic avian influenza in bird populations. Therefore, monitoring for influenzas must be focused on the priority species that will be critical for possible reassortments with human influenza leading to a pandemic. The results from this work will be used to map the risk of influenza in wild and domestic bird populations and in cost effective and more efficient surveillance of influenza in the environment.

This work lead to multiple other collaborations and funding that included investigating the histology of Sia that is under way via collaboration with UC San Diego Glyobiology Research and Training Center. Other collaborations that were a direct result from this project that will continue into the future include working with Dr. Jen Owens a disease ecologist at Michigan State University, and the National Wildlife Research and Wildlife Centers. In addition, this project lead to a funded collaboration with New Mexico State University and with two Master's students using the data and ideas for their thesis'. Sialic acid is also the receptor site for other diseases such as Newcastle disease virus and malaria. Birds are considered as a global model for the behavior of the parasite that causes malaria, Plasmodium. This project allowed for the phylogentic mapping and comparisons of the sialome in birds that now can be used to answer numerous other questions related to disease ecology and evolution.

This study addressed a potentially catastrophic public health problem — the increased possibility of a pandemic influenza strain due to current circulation of H5N1 in both wild and domestic birds, in other mammals hosts, and in humans. Attempts to eradicate or control H5N1 have been unsuccessful, and will continue to be a problem into 2011 along with the newly emerged subtype, H1N1 that may now have more opportunities to merge with H5N1. The scientific gains of this research include a better understanding of the potential host range of birds in order to have effective, focused, and meaningful surveillance of influenza in host populations. This work filled knowledge gaps in the types and quantities of sialic acid birds that will lead to an increased knowledge of influenza viral evolution by default. In this current work, sample acquisition and total Sia quantity and linkage methodology have been successfully developed and measured for avian species. Methodology for stable isotope Sia measurement in birds have been developed which allows for faster analysis with increased sensitivity thresholds.

References

1. Suzuki, Y., T. Ito, and T. Suzuki. Sialic acid species as a determinant of the host range of influenza A viruses. 2000. *Journal of Virology.* **74** (24): 11825.

2. Stallnecht, D., and S. Shane. Host range of avian influenza virus in free-living birds. 1988. *Veterinary Research Communication.* **12**: 125.

3. Schauer, R., G. Srinivasan, B. Coddeville, B. Zanetta, and Y. Guerardel . . Low incidence of N-glycolylneuraminic acid in birds and reptiles and its absence in the platypus. 2009. *Carbohydrate Research* . **344** (12): 1494.

4. Fuller, T., G. Saatchi, and E. Curd. Mapping the risk of avian influenza in wild birds in the US. 2010. *BMC Infectious Diseases.* **10** (1): 187.

5. Koehle, H., and H. Kauss. Improved analysis of hemagglutination assays for quantitation of lectin activity. 1980. *Analytical Biochemistry* . **108** (2): 227.

6. Ito, T., Y. Suzuki, L. Mitnaul, A. Vines, H. Kida, and Y. Kawaoka. Receptor specificity of influenza A viruses correlates with the agglutination of erythrocytes from different animal species. 1997. *Virology.* **227** (2): 493.

Publications

Cohen, M., N. Varki, M. Jankowski, N. Nemeth, J. Fair, and P. Gagneux. Secreted mucins are better preserved in frozen tissues . *Journal of Histology.*

Fair, J., K. McCabe, Y. Shou, and B. Marrone. Immunophenotyping of Chicken Peripheral Blood Lymphocyte Subpopulations: Individual Variability and Repeatability. . 2008. *Veterinary Immunology and Immunopathology.* **In Press**: In Press.

Fair, J., K. Taylor-McCabe, Y. Shou, and B. Marrone. Immunophenotyping of avian lymphocytes: implications and future for understanding disease in birds. To appear in *Studies in Avian Biology.*

Fair, J., K. Taylor-McCabe, Y. Shou, and B. Marrone. Immunologic and clinical responses following West Nile virus infection in domestic chickens (Gallus gallus domesticus). To appear in *Poultry Science.*

The Effect of Acoustical Waves on Stick-Slip Behavior in Sheared Granular Media: Implications for Earthquake Recurrence and Triggering

Paul A. Johnson
20080268ER

Abstract

Among the most fascinating, recent discoveries in seismology have been the phenomena of dynamically-triggered slip, including triggered earthquakes and triggered-tremor, as well as triggered slow, silent-slip during which no seismic energy is radiated. Dynamic earthquake triggering remains a compelling mystery: how do transient seismic waves with micrometer displacements trigger earthquakes, often with failure occurring long after the waves have passed? How can triggering take place at distances of hundreds of kilometers, from the earthquake generating the seismic waves? Because fault nucleation depths cannot be probed directly, the physical regimes in which these phenomena occur are poorly understood. Thus determining physical properties that control diverse types of triggered fault sliding and what frictional constitutive laws govern triggered faulting variability is challenging. We are characterizing the physical controls of triggered faulting with the goal of developing constitutive relations by conducting laboratory and numerical modeling experiments in sheared granular media. In order to simulate granular fault zone gouge in the laboratory, glass beads are sheared under constant normal stress, while subject to transient perturbation by acoustic waves. We find that triggered slip events—triggered laboratory earthquakes—take place under predictable conditions, but always at low effective stresses (effective stress is equal to the applied stress minus the pore pressure). In our laboratory studies we see many kinds of triggered slip events observed in the Earth such as instantaneous triggering, delayed triggering and triggered slow slip. Further, we observe a shear-modulus decrease corresponding to dynamic-wave triggering. Modulus decrease in response to dynamical wave amplitudes of roughly a micro strain and above is a hallmark of elastic nonlinear behavior. Our Discrete Element modeling results show that the dynamical waves increase the material non-affine elastic deformation during shearing, simultaneously leading to instability and slow-slip. Non-affine deformation is a measure of the translation and reorganization of the beads as they are perturbed by acoustical waves while being sheared.

Background and Research Objectives

At 4:57 a.m. on June 28, 1992, a very strong earthquake occurred in the High Desert of Southern California. The magnitude (M) 7.3 event was centered near the town of Landers (Figure 1a). Something remarkable took place as a result of this earthquake: as seismic waves broadcast from the event traveled northward, other earthquakes were *dynamically triggered,* not only nearby but as far north as Yellowstone and Montana more than 1000 km distant; elevated micro seismicity, termed *delayed triggering*, lasted for several months afterwards. Following Landers, other recent earthquakes were found to induce dynamic wave triggering, including the 1999 M7.1 Hector Mine (California), the 1999 M7.4 Izmit (Turkey) and the 2002 M7.9 Denali (Alaska) earthquakes. More recently, in 2002, a Japanese researcher discovered a long term Earth rumbling he called "tremor". Soon thereafter it was discovered that tremor too could be dynamically triggered. In fact, the entire suite of slip along faults, from tremor, to slow "silent" slip to earthquakes can all be triggered by seismic waves from other earthquakes. One can imagine that static stress changes due to a large earthquake could trigger nearby earthquakes (known as *aftershocks*) and this is common. Further, it is not hard to accept that dynamic triggering very near a large earthquake may take place as well (but was not widely recognized until the Landers event); however, dynamic wave triggering at large distances is surprising, and delayed triggering at these distances is even more surprising. The seismic-wave strain-amplitudes are extremely small once the waves have propagated more than several fault radii, of order 0.1-1 micro strain [*strain=(particle velocity)/(wave velocity)*]; however it has been shown that only several micro strain are necessary to induce dynamic triggering. To put this in perspective, for a wavelength of 1m, a micro strain corresponds to a displacement of 10^{-6} meter! *How does dynamic triggering (immediate and delayed) take place under such small perturbations?* That has been the basis of our work: *to quantify the effects of seismic waves on fault rupture and determine how small strains trigger earthquakes (immediate and delayed) and what the underlying physical mechanism(s) may be.*

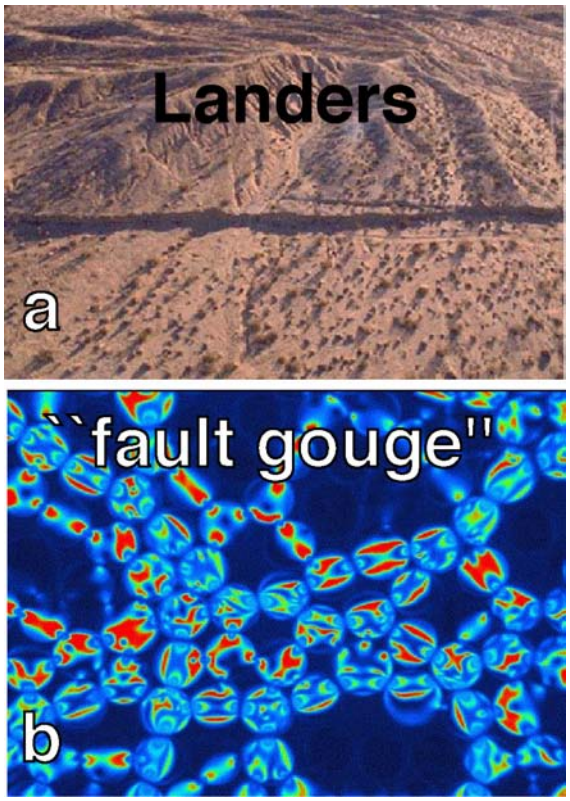

Figure 1. (a) Arial view of the Landers Fault in California. The Landers Earthquake of 1992 produced the first verifiable observations of dynamic earthquake triggering. (b) Force chains in surrogate fault gouge (polymer beads). The light colors show "force chains" that were formed when stress was applied to the bead pack. Force chains can be seen due to what is known as the photoelastic effect, that provides the means for regions of stress concentration to be imaged (courtesy of Bob Behringer).

Many mechanisms for triggering have been proposed and one or more must exist that can explain triggering in both wet fault cores (triggering is frequently associated with geothermal areas) and dry fault cores. *No* proposed mechanism can explain delayed triggering—hours, days, even months after the passage of the wave. We hypothesize there may be a *universal cause of triggering* that may be nonlinear in nature but with potentially multiple physical origins.

In two recent papers published in the journal *Nature* [1,2], we proposed that dynamic elastic nonlinearity of fault gouge may be the cause of triggering, via a modulus softening-to-weakening mechanism (softening means the modulus decreases). Gouge, the material in a fault core, is rock that has been highly fractured and "worked" by the adjacent crustal blocks into a granular state. Glass/polymer beads, broadly termed "granular media", have been found to be a good surrogate for fault gouge in experiment and modeling due to their easily quantifiable physics and similar behaviors to real Earth fault processes. Figure 1b shows granular media illustrating "force chains" where the material strength resides. Thinking simply, one must shear and break some or all of the force chains to induce failure. The force chain concept can be applied broadly, e.g., in cracked solids where asperities in the crack act as the force chains.

In refs. [1,2] we demonstrated from laboratory studies in granular media, that modulus decrease takes place under acoustic wave perturbation. Modulus (proportional to velocity) dependence with wave amplitude is a nonlinear response. It is very small in most materials, e.g., metals, single crystals, etc., but is large in granular media, much larger than in rock (unless highly damaged) where it is also observed. As pressure is applied, the nonlinear effect is diminished. *Thus if nonlinearity has anything to do with triggering, experiments show, (i) seismic strain amplitudes must be >10^{-6}; and (ii), effective pressures (confining-pore pressure) at fault nucleation depths (~5-15 km) must be small*. This could happen in locations where fluid pressures are high (e.g., Yellowstone), and/or where horizontal stresses are very low making the fault more easily mobilized (e.g., San Andreas Fault). Significantly, strain amplitudes larger than ~10^{-6} are only observed near a large earthquake source, and at large distances when rare, source-related focusing produces such strains. *Logically, the fault must also be in a critical state, near failure, otherwise it is impossible to imagine the triggering scenario*.

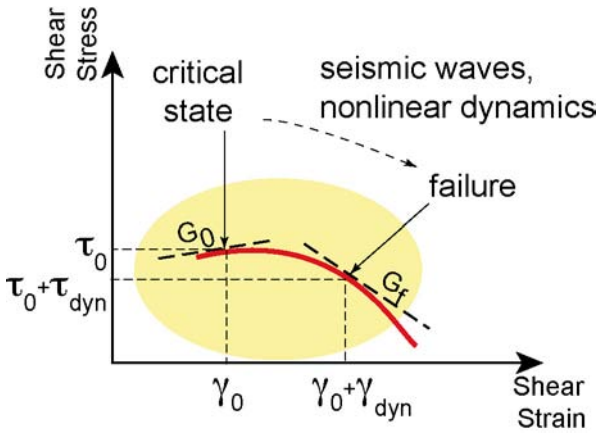

Figure 2. Shear modulus, softening-to-weakening in fault gouge. The figure shows shear stress (tau) vs. shear strain (gamma) [bold/red]. The material is in an equilibrium state (tau zero and gamma zero) maintained by adjacent fault blocks. The shear modulus G is defined by the slope of the stress-strain curve. A typical seismic wave does nothing but pass by, and the shear modulus G0 remains unchanged. A wave at nonlinear strains causes shear modulus decrease, meaning the modulus, measured as the tangent to the curve (dashed line), must move to the right along the stress-strain curve, to failure. If the equilibrium modulus is in a critical state near failure, the modulus softening causes weakening and failure. If the gouge is not in a critical state, modulus softening occurs but no failure is induced.

Modulus softening is not necessarily related to material weakening; weakening of the gouge must take place

to initiate slip. Our proposed, phenomenological model states that shear modulus softening induces shear material weakening, leading to failure in the presence of large strain acoustic wave in the lab, or a seismic wave in the Earth. We leave out the details—they can be found in reference *2*—but in Figure 2 we show how this might happen.

Scientific Approach and Accomplishments

Our approach has been to quantify the effects of acoustic/seismic waves on fault rupture. Specifically we addressed, (i) how small strains trigger earthquakes (immediate and delayed) and the underlying physical mechanism(s) of triggering; and (ii) how and why waves change recurrence and induce fault gouge memory. We conducted earthquake laboratory studies supported by numerical modeling studies of sheared granular media. In order to see if such triggering may be induced, we began stick-slip experiments while simultaneously applying acoustic waves, in collaboration with Penn State University (C. Marone). Lab studies of granular friction applying stick-slip have emerged as a powerful tool for investigating fault zone processes including post-seismic slip, interseismic frictional restrengthening, and earthquake nucleation. The Penn State group has been working on granular friction for many years, but have never included acoustics.

In typical experiments in the absence of acoustic waves, one observes consistent, repeatable "normal" earthquakes, the stick-slips (Figure 3). We think of these "normal" events as recurrence of a large earthquake that take place with a rough periodicity. Bursts of vibration were applied when the shear stress was in a critical state, in keeping with the proposed model. When acoustic waves are applied very interesting things happen.

We observed instantaneous triggering almost immediately, and saw that it occurred easily under a range of conditions (Figure 3a). *Delayed triggering* was observed but complex. For instance, it can appear during or immediately following a vibration (not shown), or in one or more follow-on earthquake cycles (e.g., pink/cross-hatched regions in Figure 3b), indicating a material memory of the wave perturbation. A significant surprise was that vibration causes increased recurrence (note the overall cycle lengthening—statistically significant), another indicator of fault-gouge memory. This is remarkable, because logically, the "normal" earthquakes should cause a violent material reset, erasing the effect of the acoustical waves. *It would appear that what we were looking for, dynamic triggering and delayed triggering, occur in the experiment but it is very complex. Other, significant physics—memory and recurrence disruption—occur as well*. The complex behaviors have their origin in the force chains that maintain the material strength, but in manners to be understood by modeling (see below). In a paper published in Nature in 2008 [3], we showed that the triggering of laboratory earthquakes took place, and that the nonlinear mechanism was plausible.

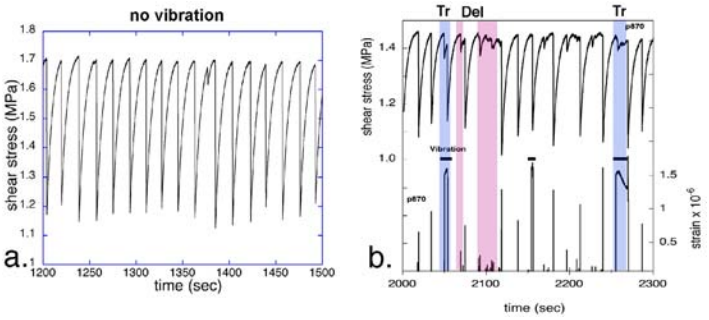

Figure 3. Earthquakes in the laboratory. (a) Shear stress vs. experimental run time (no vibration). The recurrence (time between "earthquakes") is quite constant. Occasionally small, inter-event slips appear (e.g. 1375 sec) but they are rare. (b) (top) Same experiment but with acoustic vibration. The thick horizontal lines show where vibrations were applied. (bottom) The acoustic emission is plotted as time-averaged acceleration (scale on right-hand vertical axis). The largest amplitudes correspond to applied vibrations. We observe acoustic emission from "normal" earthquakes (e.g., 2015 sec.), triggered events (solid blue), delayed triggered events (pink, cross-hatched). Disruption in the recurrence rate is clear—it becomes inconsistent due to the acoustic waves, an indication that memory of vibration is maintained through numerous major stick cycles. We believe this is how delayed triggering takes place. The fault gouge material has a long term memory of applied vibration.

Over the duration of the funded work we have discovered many phenomena in the laboratory that look like those in the Earth. For instance, there is a fascinating group of observations regarding triggered slow, silent slip. Slow slip can have displacements as large as the biggest of earthquakes—but it can only be identified geodetically because it emits no (or very little) seismic energy. We find that triggered, slow, silent-slip occurs at very small confining pressures (~10-30 atmospheres) that are smaller than those where dynamic earthquake triggering takes place (40-70 atmospheres). Experimental evidence suggests that the nonlinear dynamical response of the gouge material induced by dynamic waves may be responsible for the triggered slip behavior: the slip-duration, the stress-drop and along-strike slip displacement are proportional to the triggering wave amplitude. Further, we observe a shear-modulus decrease with dynamic-wave triggering. Modulus decrease in response to dynamical wave amplitudes is a hallmark of elastic nonlinear behavior, as previously noted. We believe that the dynamical waves increase the material "non-affine elastic deformation" during shearing, simultaneously leading to instability and slow-slip (non-affine refers to translation and distortion of groups of beads). In the Earth, triggered slow-slip on the San Andreas Fault at Parkfield, CA., due to the December, 2003 M*agnitude* 6.5 San Simeon Earthquake [4] shows very similar characteristics to what we observe in the laboratory, suggesting an extremely low *in situ* effective stress or a weak fault and a nonlinear-dynamical triggering mechanism.

Simultaneous to the laboratory earthquake studies, we have been conducting Molecular Dynamical Modeling of sheared beads in contact, leveraging with collaborators at ETH in Zurich, Switzerland (M. Griffa and J. Carmeliet) [Figure 4]. In short, we find in simulations that, as waves shake the model sheared beads, non-affine deformation becomes widespread. When it is sufficiently diffuse, slip is triggered [5]. This is a highly nonlinear process. Our overarching hypothesis of a nonlinear triggering mechanism is borne out by laboratory experiments and numerical modeling, and supported by field observations.

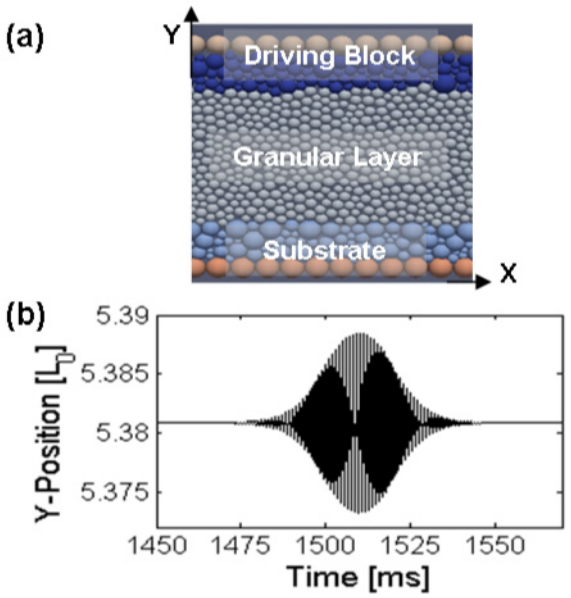

Figure 4. (a) Molecular Dynamics model composed of the "driving layer" (top), the granular layer (center) and the "substrate" (bottom). Normal load is applied along the Y-axis and shear load is imposed along the X-axis. (b) Imposed time variation applied to the substrate's bottom along the Y axis direction to test for dynamic wave triggering. The wave amplitude is expressed in relation to particle radius.

We have made great strides in characterizing the physics leading to and during triggering, and we believe we understand how it happens. Understanding the triggering nucleation process takes us a step closer to predictability. We do not pretend that the elusive goal of prediction will come easily or soon; however we know far more about fault processes now than we did at the beginning of this work. Our work is a portion of the mosaic that will ultimately lead to earthquake forcasting of one type or another.

Impact on National Missions

Triggering is an intriguing scientific question that confounds, as well as a topic important for time-dependent earthquake forecasting. Predictive models will have to include triggering (dynamic & quasistatic) and wave effects on recurrence and memory. *There is a large class of diverse applications of this work that include predicting unexpected breakdown or avalanche behavior.* Predicting that an incipient crack can run-away due to moderate amplitude sound has many defense applications. For instance, in systems where cracks exist in materials where small-amplitude vibration is present, unexpected failure may take place, such as in a reentry vehicle. A very different example is predicting slope stability subject to strong ground motion or avalanches occurring from a sound impulse. Subject to large vibration these are obvious effects. *Under moderate amplitudes, they are routinely ignored*.

References

1. Gomberg, J., and P. Johnson. Dynamic triggering of earthquakes. 2005. *Nature.* **473**: 30.

2. Johnson, P. A., and Xiaoping Jia. Nonlinear dynamics, granular media and dynamic earthquake. 2005. *Nature.* **437** (7060): 871.

3. Johnson, P., H. Savage, M. Knuth, J. Gomberg, and C. Marone. The effect of acoustic waves on stick-slip behavior in sheared granular media: implications for earthquake recurrence and triggering. 2008. *Nature.* **451**: 57.

4. Brenguier, F., M. Campillo, C. Hadziioannou, N. M. Shapiro, R. M. Nadeau, and E. Larose. Postseismic relaxation along the San Andreas fault at Parkfield from continuous seismological observations. 2008. *Science (Washington D C).* **321** (5895): 1478.

5. Griffa, M., E. Daub, R. Guyer, P. Johnson, C. Marone, and J. Carmeliet. Vibration-induced unjamming of sheared granular layers and the micromechanics of dynamic earthquake triggering. *Physical Review Letters.*

Publications

Brunet, T., X. Jia, and P. A. Johnson. Transitional, elastic-nonlinear behaviour in dense granular media. 2008. *Geophysical Research Letters.* **35**: L19308.

Daub, E., D. Shelly, R. Guyer, and P. Johnson. Brittle and ductile friction and the physics of tectonic tremor. *Nature.*

Griffa, m., E. Daub, R. Guyer, P. Johnson, C. Marone, and J. Carmeliet. Vibration-induced unjamming of sheared granular layers and the micromechanics of dynamic earthquake triggering. *Physical Review Letters.*

Guyer, R. A., and P. Johnson. . 2009. In *Nonlinear Mesoscopic Elasticity: the complex behaviour of granular media including rocks and soil.* By Guyer, R., and P. A. Johnson. , First Edition, p. 410. Berlin: Wiley-VCH.

Johnson, P. A., H. Savage, M. Knuth, J. Gomberg, and C. Marone. The effect of acoustic waves on stick-slip behavior in sheared granular media: implications for

earthquake recurrence and triggering. 2008. *Nature.* **451**: 57.

Johnson, P., P. Bodin, J. Gomberg, F. Pearce, Z. Lawrence, and F. Menq. Inducing in situ, nonlinear soil response applying an active source. 2009. *Journal of Geophysical Research.* **114**: B05304.

Johnson, P., P. LeBas, M. Knuth, B. Carpenter, E. Daub, R. Guyer, and C. Marone. Nonlinear dynamical triggering of slow slip. *Nature.*

Developing a Remote Sensing of the Solar Surface

Joseph E. Borovsky
20080321ER

Abstract
This LDRD/ER project is a statistical reanalysis of decades of solar-wind measurements to discern the structure of the solar-wind plasma, the origin of the structure, the evolution of the structure, and the impact of the structure on physical processes throughout the solar system and to determine whether the structure measured near the Earth carries information about physical processes ongoing at the solar surface where the wind is born.

Background and Research Objectives
The solar wind emanates from the Sun and affects the space environment around the Earth. Our recent work indicates that there is a systematic structure to this wind. This LDRD/ER project is motivated by a desire to understand the nature of this structure and to understand the generation of this structure by the Sun. This LDRD/ER Project has three research objectives. (1) To survey the properties of the solar wind that emanates from different features on the Sun. (2) To map in situ measurements of the solar wind by the ACE spacecraft to their specific regions of origin on the solar surface. (3) To develop a technique to use existing solar-wind instruments to make remote measurements of the structured solar wind as it escape from the Sun. The project involves theory and the analysis of existing satellite data.

Scientific Approach and Accomplishments
The scientific approach is statistical and event data analysis of measurements taken by spacecraft in the solar wind. The primary data set is plasma data from the Los Alamos SWEPAM instrument onboard the NASA ACE satellite near Earth, and measurements from the Helios-1 and Helios-2 spacecraft closer to the Sun and the Voyager-1, Voyager-2, and ULYSSES spacecraft further from the Sun were used.

The major accomplishments of the LDRD project are 1) a firming up of a model of the solar wind in which the solar-wind plasma is confined in a spaghetti of fossil magnetic flux tubes that are created at the solar surface, 2) a matching of solar-wind measurements made at Earth with models and observations for the magnetic structure at the solar surface, and 3) an assessment of the impact of the spaghetti structure on the physics of the solar wind and on solar-wind/magnetosphere coupling. The spaghetti structure is depicted in Figure 1.

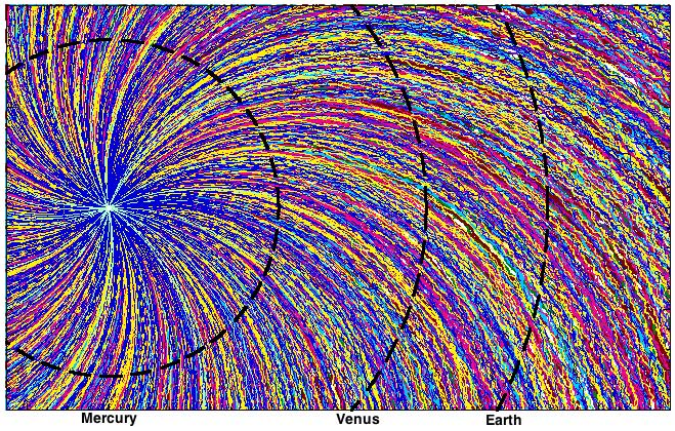

Figure 1. A depiction of the flux-tube structure of the solar wind. The viewer is looking down on the ecliptic plane. The diameters of the orbits, the radius of the Sun, and the diameters and braiding angles of the flux tubes at 1 AU are approximately to scale. The pattern of flux tubes convects radially outward with the solar-wind speed and the tubes undergo transverse Alfvenic motions. Ejecta disturbances are not shown. The braiding angles of the flux tubes is envisioned to give rise to the angular spread in magnetic-field directions about the Parker spiral.

The firming up of the model came about by a statistical analysis of current sheets in the solar-wind plasma, looking at the spacings and orientations of the sheets, their relation to changes in the properties of the plasma, and their statistical evolution with distance from the Sun. The data analysis demonstrated that the structure of the solar wind is formed into a braiding of magnetic flux tubes and that these tubes are long-lived fossil structures.

The matching of solar-wind measurements (the spaghetti of flux tubes) with the properties of the solar surface (the chromospheric magnetic carpet) was very success-

ful and points to the Sun as the origin of the structure in the solar wind. Studying the details of small-scale features in the solar-wind structure is enabling physical processes at the solar surface to be remotely analyzed.

The fossil structure of the solar wind was found to dominate the Fourier spectrum of solar-wind measurements. The spectrum of the fossil structure (which dominates the spectral power) was found to have the properties of the Kolmogorov turbulence spectrum, leading to warnings about the interpretation of solar-wind fluctuations as an active turbulence. The fossil-structure interpretation versus the turbulence interpretation leads to very different assessments of (1) the flow properties of the solar wind, (2) the transport of energetic particles into and out of the solar system, and (3) the heating and radial evolution of the solar-wind plasma.

Impact on National Missions

Understand the nature of the solar wind leads to more-accurate modeling of the way the solar wind drives space weather in the Earth's magnetosphere, which leads to more-accurate predictions of dangerous spacecraft charging and of the intensities of penetrating radiation. Understanding the nature of the solar wind leads to a better understanding of how energetic particle bursts near the Sun travel to the Earth.

Publications

Borovsky, J. E.. Flux tube texture of the solar wind: Strands of the magnetic carpet at 1 AU?. 2008. *Journal of Geophysical Research.* **113**: A08110.

Borovsky, J. E.. On the variations of the solar-wind magnetic field about the Parker-spiral direction. 2010. *Journal of Geophysical Research.* **115**: A09101.

Borovsky, J. E.. Contribution of strong discontinuities to the power spectrum of the solar wind. 2010. *Physical Review Letters.* **105**: 111102.

Borovsky, J. E.. The velocity and magnetic-field fluctuations of the solar wind at 1 AU: Statistical analysis of Fourier spectra. *Journal of Geophysical Research.*

Borovsky, J. E., and M. H. Denton. Solar-wind turbulence and shear: A superposed-epoch analysis of corotating interaction regions at 1 AU. To appear in *Journal of Geophysical Research.*

Borovsky, J. E., and S. P. Gary. On viscosity and the Reynolds number of MHD turbulence in collisionless plasmas: Coulomb collisions, Landau damping, and Bohm diffusion. 2009. *Physics of Plasmas.* **16**: 082307.

Gary, S. P., and J. E. Borovsky. Damping of long-wavelength kinetic Alfven fluctuations: Linear theory. 2008. *Journal of Geophysical Research.* **113**: A12104.

Podesta, J. J., J. E. Borovsky, and S. P. Gary. A kinetic Alfven wave cascade subject to collisionless damping cannot reach electron scales in the solar wind at 1 AU. 2010. *Astrophysical Journal.* **712**: 685.

Podesta, J. J., and J. E. Borovsky. Scale invariance of normalized cross-helicity in the inertial range of solar wind turbulence. To appear in *Physics of Plasmas.*

Tessein, J. A., C. W. Smith, B. T. MacBride, W. H. Matthaeus, M. A. Forman, and J. E. Borovsky. Spectral indices for multi-dimensional interplanetary turbulence at 1 AU. 2009. *Astrophysical Journal.* **692**: A12104.

A New Approach to Unravel Complex Microbial Community Processes

Cheryl R. Kuske
20080464ER

Abstract

Soil organic matter is the largest pool of terrestrial carbon on Earth. Soil microbiota (bacteria, fungi, microfauna) are responsible for stabilization and release of this pool via complex processes such as decomposition. Although key to carbon flux in terrestrial ecosystems, microbial decomposition is one of the major unknowns for prediction of carbon sequestration, ecosystem responses to climate change, and contaminant mitigation. Our project identified the active bacteria and fungi in soils that differed in associated plant material and regional climate, using a novel combination of stable isotope experiments and metagenomic analysis. This project used a unique Tunable Diode Laser Spectroscopy (TDL) system in soil experiments to monitor decomposition rates and partitioning of different carbon sources in soil. Collectively, we have identified key microbial species capable of cellulose degradation for which we can now use as markers for soil cellulose decomposition, and have demonstrated their collective rates of activity under different conditions.

Background and Research Objectives

Soil organic matter is the largest pool of terrestrial carbon on Earth. Soil microbiota (bacteria, fungi, microfauna) are responsible for stabilization and release of this pool via complex processes such as decomposition. Although key to carbon flux in terrestrial ecosystems, microbial decomposition is one of the major unknowns for prediction of carbon sequestration, ecosystem responses to climate change, and contaminant mitigation. We undertook a series of studies to couple new technologies in soil investigations of the active microbial communities across several soils.

Our research objectives were to:

- Determine the role of carbon type (easily consumed sugars vs. recalcitrant substrates such as cellulose), moisture, and soil geochemical features in regulating the abundance, composition and activity of the soil microbial community, and consequently the decomposition process. Through these studies our goal was to identify actively respiring bacteria and fungi in the presence of simple (acetate) and complex (cellulose) substrates among the very complex and diverse background of soil microbiota.
- Couple three emerging technologies into an experimental soil system. The first of these is stable isotope probing (SIP), where a ^{13}C-labeled substrate is added to a soil system and is monitored by its incorporation into microbial DNA of the decomposition-active microbes. The second is high-throughput metagenomics, where the collective DNA of the soil under investigation is sequenced across the community of genomes (a cell's DNA) as a single unit. The third is a unique tunable diode laser (TDL) used for spectroscopic measurement of the rate of CO_2 flux, which provides a relative measure of decomposition rates and allows us to identify which soil substrates are being preferentially used.

This combination of new techniques was applied to microcosms of field soil samples from LANL's woodland observatory and other ecosystems, to provide an understanding of soil biota that control degradation of plant carbon and their rates of activity under different conditions. Scientific contributions that have resulted from this project include 1) development of a sensitive stable isotope probing (SIP) approach to track use of 13C-labeled substrates that is applicable to many soils, 2) identification of the active soil bacteria and fungi that are capable of degrading cellulose across multiple soils using SIP, coupled with new high-throughput metagenomic sequencing techniques, 3) application of a novel tunable diode laser system to use with soils, to monitor the isotopic composition ($d^{13}C$ and $d^{18}O$) of CO_2 decomposed by soil microbes, and 4) assessment of the effects of cellulose addition, periodic aeration, and pulses of moisture on soil decomposition rates and associated abundance of soil bacteria and fungi.

Scientific Approach and Accomplishments

In the first year of the project, we developed the SIP approaches for simple carbon (acetate) and complex car-

bon (cellulose), the metagenomic procedures, and microcosm systems for analysis of CO_2 flux by gas chromatograpy and using the TDL. In the second year, we applied these approaches to soils of the LANL woodland observatory and other soils from different geographic regions in the U.S. These experiments continued in the third year.

Accomplishments in year three are highlighted in two elements below:

SIP/metagenomic experiments

Summary

We completed ^{13}C-cellulose SIP experiments on five different soils that differ in soil characteristics that influence carbon decomposition rates. Analysis of ^{13}C-enriched soil DNA by three complementary metagenomic approaches revealed common features of cellulose degradation across the soils, as well as bacterial and fungal species specific to each soil. Two manuscripts on this work are in draft form for submission to the International Society for Microbiology Journal.

Background

The identification of bacterial communities, the manner, and efficiency to which different carbon types are degraded are not well understood. As global carbon dioxide levels continue to rise, a potential net result is an increase in plant biomass. This plant biomass is the dominant source of fixed carbon both above and below ground. Plants provide carbon to the microbial community either as readily oxidizable carbon such as simple sugars, amino acids typically originate from root exudates, or recalcitrant carbon (i.e. lignin, cellulose) from plant litter. In year one of the project we examined soil microbial use of a simple carbon, acetate. To identify key microbial taxa and patterns of use for a complex carbon (cellulose), we compared active bacterial and fungal communities in soils obtained from five geographic regions with different soil properties.

Approach

Soil microcosms were established by addition of ^{13}C-UL-maize cellulose. Total carbon dioxide concentrations in ^{13}C-maize cellulose amended and non-amended treatments were measured over a period of thirty days via gas chromatography. The active cellulolyic microbial communities were resolved using the technique of DNA-SIP combined with rDNA Sanger and pyro-tag sequencing of the time zero, enriched and non-enriched fractions, targeting the SSU rRNA gene (bacteria), LSU rRNA gene (fungi), and fungal cellobiohydrolase genes. Libraries were analyzed using readily available software to assess any changes in diversity, richness, biomass, and taxonomic affiliations of the enriched genes with cellulose.

SIP/metagenomic Results

- Established stable isotope probing (SIP) procedures for use with soil microcosms to isolate soil microbial community DNA representing the active communities (Figure 1).
- Identified the active cellulolytic bacterial and fungal communities across five geographically and edaphically different soils using Sanger and pyrotag sequencing, and related this information to soil geochemical data from each soil.
- Logarithmic relationships were observed with total carbon dioxide produced the aforementioned treatments with the starting organic matter and nitrogen concentration, suggesting that these edaphic properties strongly influence the activity of the microbial communities in microcosms (Figure 2).
- The patterns of cellulose use and microbial community response (as measured by changes in biomass, richness, diversity, and composition) were different across the different soils. Hierarchical dendrograms illustrate a clear enrichment for distinct, cellulose-degrading bacterial communities in replicate microcosms (Figure 3).
- Even though these soils differed in many physical and chemical properties, some of the most active cellulolytic bacterial communities were similar (at the order level) across these soils. Members of the orders *Burkholderiales*, *Caulobacteriales*, *Rhizobiales*, subdivision 1 *Acidobacteria*, *Spingobacteriales,* and *Xanthomonadles* were consistently found in the enriched fractions across all soils. The genera within these orders differed, which probably reflects differential preferences for pH, mineral or temperature conditions.
- In contrast, a different fungal group responded to cellulose in each of the different soils. Enriched cellulolytic fungi included members of the *Arthrobotrys*, *Dactylaria*, *Trichocladmium*, *Cladophialophora*, and *Chaetomium*.
- To better understand the distribution, structure, and function of cellulose-degrading fungi in these soils, we amplified and sequenced the cellobiohydrolase gene (GH7 family – a key cellulose degrading fungal gene) from time zero, enriched, and non-enriched microcosm DNAs. The members of this functional gene clustered into five major clades (related groups) that are instrumental in decomposing soil cellulose (Figure 4).

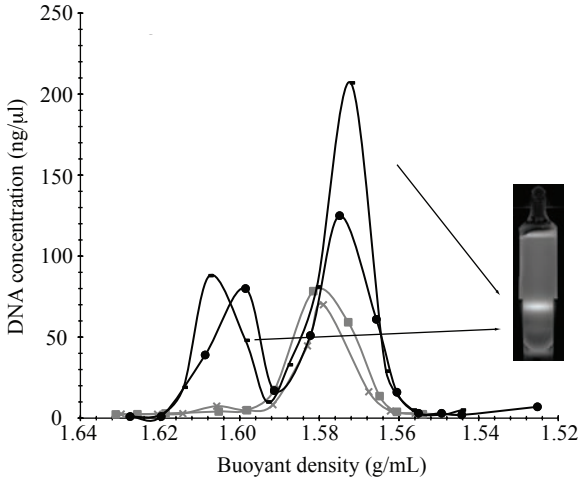

Figure 1. Elution profile of 13C-labelled and 12C-unlabelled DNA from duplicate 13C-cellulose amended (black lines) and non-amended control (grey lines) soil microcosms. Soil DNA is fractionated by high-speed ultracentrifugation in ethidium-bromide cesium chloride solution.

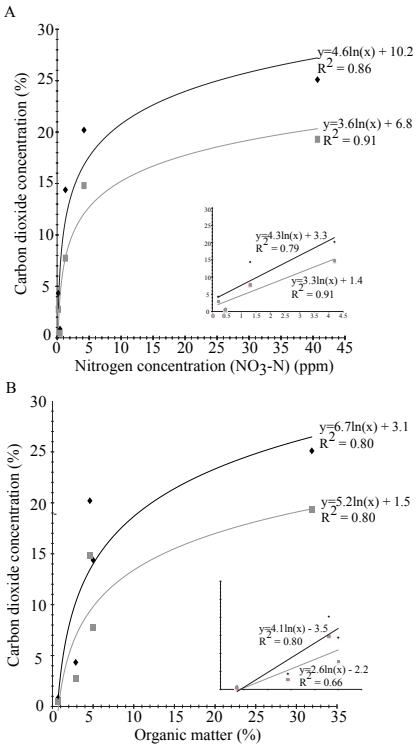

Figure 2. Relationship of edaphic properties to total carbon dioxide production. Panels A & B, respectively, depict the logarithmic relationship with final carbon dioxide concentrations (day 30) to the initial nitrogen concentration (ppm), and % organic matter. Figures illustrate the relationship for the cellulose-amended microcosms (black points and line) along with the non-amended controls (gray points and line). Inlet figures for each panel represent the relationship for nitrogen (0 to 4.5) and % organic matter (1 to 6). Trendline equation and R-squared value are depicted to the right of the lines.

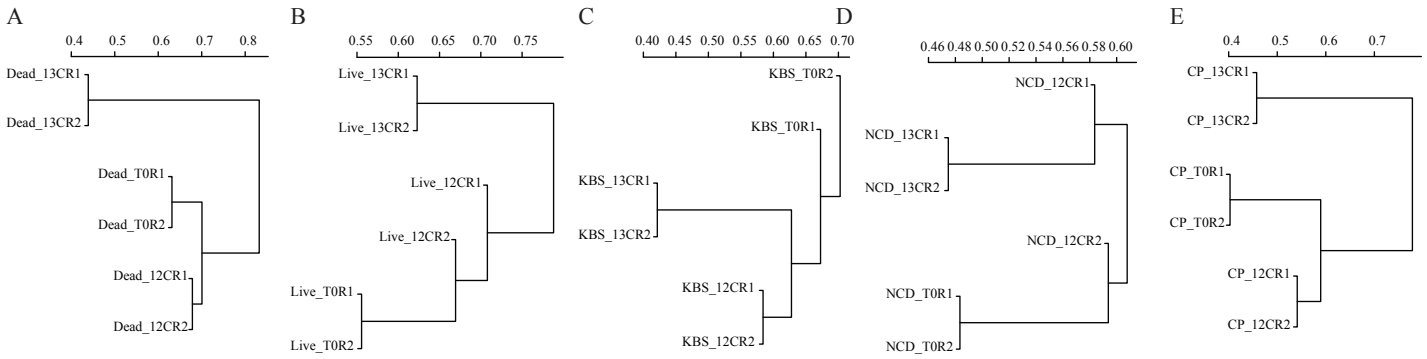

Figure 3. Hierarchical agglomerative cluster dendrogram of community relatedness of time zero, day 30 nonenriched, and day 30 cellulose-enriched bacterial communities, showing enrichment of a different bacterial community, and tracking of replicate microcosms, in each of five soil types: dead pinon pine (A), live pinon pine (B), native MI grassland (C), loblolly pine (D), and longleaf pine (E). Scale bar indicates the relative distance of the communities based on a Bray-Curtis matrix.

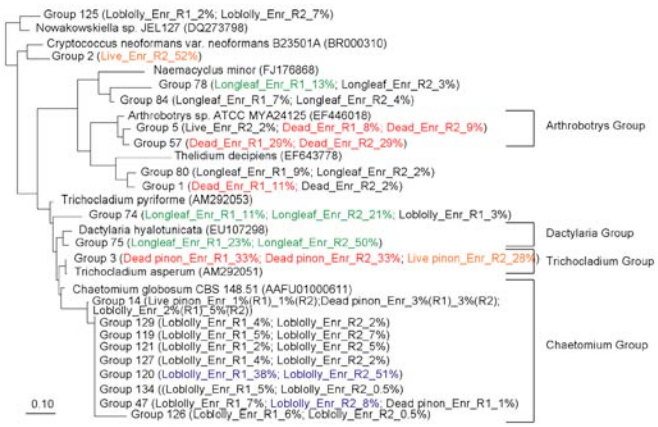

Figure 4. Phylogenetic position of active cellulolytic fungi from five different soils, identified by in situ addition of 13C-cellulose.

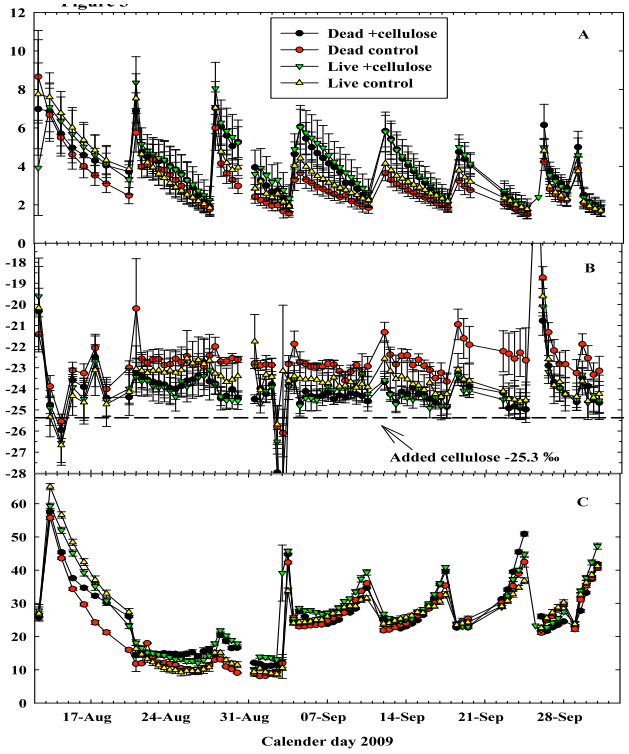

Figure 5. Rates of CO_2 flux measured in soil microcosms derived from the root zones of dead or live pinyon pines, to which cellulose was either added or withheld. Weekly spikes are associated with watering, which was done equally to each jar in each treatment. (3A): Soil respiration rates for the four treatments (see legend caption in figure for treatment symbols). Average soil CO_2 efflux was higher in most of the cellulose-added jars. (3B): The carbon isotope composition of soil respiration for the four treatments. The cellulose-added jars shifted their isotopic signature towards that of the added cellulose, indicating increased use of the added cellulose. (3C): The oxygen isotope composition of soil respiration for the four treatments. The lack of difference between treatments provides confidence that our experimental infrastructure is operating properly.

Soil TDL and microbial community dynamics:

Summary

A soil microcosm experiment was conducted to evaluate the effects of added cellulose, periodic pulsed water addition, and aeration (by stirring) on soil community respiration rates and relative abundance of soil bacteria and fungi. Two soils with identical geochemical background that differed in organic carbon content were compared. Time-course measures of the rate of CO_2 flux from the microcosms, and the relative abundance of natural ^{13}C and ^{12}C isotopes in the released CO_2, was conducted using a tunable diode laser, and weekly samples were collected for microbial community analysis.

Background

The combined activities of soil microorganisms, resulting in CO_2 respiration from soil, has been difficult to track. The efflux of CO2 from soils has been measurable, but determining the substrates being consumed, their rates of consumption, or preference of members of the microbial community for certain substrates has not been quantifiable. In year three of this project, we conducted a time course microcosm experiment using soils collected from widely-spaced trees to track the effects of additional cellulose, periodic pulsed water addition, and aeration on the rates of soil respiration, the substrate being preferentially used (added cellulose or natural soil organic matter), and whether these measures could be scaled to the landscape.

Approach

We developed a soil jar system for use with the tunable diode laser to test the respiration rates of soil microcosms experiments amended and non-amended with cellulose across root-zone soils of live and dead piñon pines. Total microbial biomass and bacterial & fungal biomass were measured to track the biomass of the microbial community responsible for carbon flux. The TDL was used to monitor changes in the rate of CO_2 efflux from the soils, and to determine the proportion of carbon that was derived from the added cellulose or the natural soil organic matter.

Results

1. The most dramatic observation with these data is that the variability among the twelve tree root zone soil samples chosen for this study was surprisingly large. The initial microbial biomass measures were widely divergent, and initial tunable diode laser CO_2 flux rates also documented this variability. Each of the twelve microcosms exhibited a different trajectory in overall

microbial biomass, in relative abundance of bacteria or fungi, and in carbon used during the course of the experiment. The initial samples for this study were collected from a very patchy landscape where initial soil conditions could be highly divergent. Despite the replicate variability in natural pinyon root zone soils (which was higher than in any prior study we've conducted), and in the resulting dynamics in soil microcosms, several trends were apparent:

2. Soils to which additional cellulose was added usually showed increased rate of CO_2 release, regardless of wetting or aeration treatment, and the isotopic signature shifted toward that of the added cellulose, indicating increased use of the cellulose substrate in those microcosms (Figure 5). This was not true of all of the field sampled soils, however, and for some microcosms additional cellulose was not, or negatively, correlated with rate of CO_2 release.

3. The relative abundance of soil bacteria and soil fungi changed dramatically in the microcosms over time, but did not exhibit the same trajectories in soils from different trees. In some microcosms bacterial and fungal abundance increased over the course of the experiment while in others it decreased. Soil bacteria and fungi did, however, track in parallel in each microcosm, suggesting that both broad groups were responding similarly to the conditions in that microcosm.

4. Wetting and aeration by stirring displayed additive effects on soil microbial activity as measured by rate of CO_2 release, and these effects are transient, occurring within hours of the event.

Accomplishments

Our project identified the active bacteria and fungi in soils that differed in associated plant material and regional climate, using a novel combination of stable isotope experiments and metagenomic analysis. This project used a unique Tunable Diode Laser Spectroscopy (TDL) system in soil experiments to monitor decomposition rates and partitioning of different carbon sources in soil. Collectively, we have identified key microbial species capable of cellulose degradation for which we can now use as markers for soil cellulose decomposition, and have demonstrated their collective rates of activity under different conditions.

We presented this work through posters at international professional meetings (American Society for Microbiology 2009, International Society for Microbial Ecology 2010), at the 2009 LDRD Day, and at two DOE program reviews. We have one manuscript published and three others in preparation.

Impact on National Missions

This project synthesized novel stable isotope approaches, high throughput metagenomics platforms and new measurement technologies in order to better understand and characterize carbon cycling in soils. Soil carbon is one of the largest sources of CO_2 in global atmospheric CO_2, and soil decomposition processes are key to tracking and predicting the effects of increased atmospheric CO_2 and global warming. They also influence the movement of organic pollutants and toxic metals, supporting missions in DOE/SC, and other government agencies. Our research has demonstrated new combinations of technologies and research approaches that enable us to address soil processes as a system science. Our experimental results on soil systems provide information needed to develop reliable markers for the active participants in soil carbon cycling. This LDRD project has provided results contributing to two successful research projects now funded by the DOE (Young Investigator Award, McDowell; and Science Focus Area in Soil Metagenomics & Terrestrial Carbon Cycling, Kuske).

Publications

Powers, H., J. Hunt, P. Hanson, and N. McDowell. A dynamic soil chamber system coupled with a tunable diode laser for online measurements of delta13C and delta18O of soil respired CO2. 2009. *Rapid Communications in Mass Spectrometry.* **23** (9): 121.

Nonequilibrium Mechanics of Geomaterials

James A. Ten Cate
20080603ER

Abstract

In 1996 peculiar rate effects were noted in Los Alamos acoustic resonance experiments on several oil and gas bearing rocks. The effects were seen in both sedimentary and crystalline rocks and in geomaterials like concrete. They resemble creep and creep recovery. However, they can be induced by a sinusoidal acoustic drive at strains three orders of magnitude smaller than usual creep experiments. These strains are only a few tenths of a microstrain, on the order of seismic disturbances 100s of km from an earthquake. The effects have also been shown to be macroscopically reversible and repeatable. They are important because they can mask measurements of basic rock properties (e.g., sound speed) by as much as 10%. The unique character of these rate effects caused them to be called *slow dynamics.* A quantitative experimental and numerical study of slow dynamics is the work reported here. Resonance experiments were performed on several samples in a temperature-controlled isolation chamber. Very-slow stress-strain measurements were performed on the same samples and the results compared. Further experiments on the long-term recovery were performed. Results have been submitted for publication. In order to understand of the nature of slow dynamics, we also generalized an Ising-like model to describe the experiments. The model successfully describes the hysteretic response seen in our quasi-static experiments. In the Ising model a rock is represented as a chain of rigid units with a specific mass and displacement that are coupled to one another through hysteretic elastic elements. Emphasis was placed on examining the range of relaxation times that characterize slow dynamics recovery. Analytically and numerically, this work confirms that the elements are broadly distributed. The recovery, which extends for 1000s of seconds, can be described by a slow function of time like logarithmic as seen in our experiments.

Background and Research Objectives

Work by Los Alamos researchers during the past decade has pioneered a new direction in the study of nonlinear-elastic, dynamic behavior in materials. Certain materials display surprisingly large nonlinearities, especially granular materials. Geomaterials are prototypes for these (apparently) unrelated solids. These also include granular materials, sintered and damaged metals, some ceramics, and high explosives. Rate effects dominate as well, sometimes masking values of properties like sound speed by more than 10%. Moreover, rate effects appear at wave strains smaller than parts per million. These are disturbances equivalent to those of seismic waves 100's of km from an earthquake epicenter. Consolidated granular materials are conditioned and recover in a very peculiar way for very long durations after the wave disturbance. Conditioning and recovery are manifestations of a nonequilibrium phenomenon termed "slow dynamics." Slow dynamics is behavior somewhat similar to creep, yet induced at strains 3 orders of magnitude smaller than most creep behavior. Unlike creep, slow dynamics is also induced by a sinusoidal, acoustic drive. The uniformity of measurements of slow dynamics over a wide variety of complex materials suggests a new way to characterize and understand their behavior. Though there are some clues as to the processes leading to the bulk behavior, the microphysics of the nonequilibrium behavior remains unclear. Careful experiments to explore slow dynamics have been few. Most have been only qualitative. Further, many geomaterials are highly sensitive to environmental changes. To truly understand and untangle nonlinearity and slow dynamics requires very stable, long-term measurements. The work performed here consisted of several measurements of slow dynamics in an environmentally stable and isolated lab space. Further, we explored the link between creep in quasi-static stress-strain measurements and slow dynamics measurements on the same samples. These experiments have gone beyond what was achieved before and has resulted in several publications, both describing results of new experiments and new ways to model slow dynamics behavior. Our hope is that our work will have a major impact on diagnostics of materials (e.g., concrete monitoring in nuclear reactors) and on earthquake mechanics, and seismic wave propagation.

Scientific Approach and Accomplishments

Our work proceeded along two parallel and simultaneous streams of work. New experiments were being performed while modeling of those experiments developed. Two competing theories are currently used to describe the dynamical behavior of poorly cemented materials. One is a purely phenomenological model frequently used to describe any generalized hysteretic system (called a Preisach model). The limitations of the Preisach model to describe experiments on poorly cemented granular systems like rocks have never been explored (or challenged) until now. This model has now been generalized. We used an Ising-like model to describe the behavior. The results of that modeling study have been submitted for publication. Quantitative slow dynamics experiments are rare as well. Two sets of experiments have been completed. Both sets are now either published or accepted/in press. The first is a suite of measurements to explore the limitations of Preisach model with varying rate stress-strain measurements. We discovered that quasi-static hysteresis loops, loops seen in rocks since the beginning of the last century are not repeatable. Rate dependency is present in these experiments. The area of the hysteresis loop was plotted as a function of measurement rate for a wide range of rates and as the experiment was performed slower and slower, the area of the loop disappeared. This is not a surprising result for the hysteresis seen in magnetism but has never been observed or reported in rocks until now. Moreover, this behavior has been found to occur at a very accessible time scale for experiments. These results have been published in *Geophysical Research Letters*. In our experiments, a very long measurement (several days) is sufficient for a sandstone sample to completely "lose" its hysteretic behavior. The resulting stress-strain curve for a very long measurement is purely nonlinear. What we have done in this experiment is to remove the time dependent, nonequilibrium behavior of the rock's dynamics and isolated just its nonlinearity. This result and a full detailed description can be found in the paper. At the higher end of the frequency scale, at kHz frequencies where "slow dynamics" appears, separating the nonequilibrium behavior from the nonlinear behavior was more challenging. A very long duration experiment in a very thermally stable environment has been performed where the sample was disturbed as little as possible during measurements. In contrast to the very long stress-strain measurements, the sample's stiffness was also measured at a very slow rate. A new quasi-equilibrium was thus reached during every measurement point. Additionally, work related to conditioning and recovery in slow dynamics has shown that *both* processes of slow dynamics go as the logarithm of time, similar to creep experiments at much higher strains. This work has been submitted and accepted for publication in *Pure and Applied Geophysics*. Work on the modeling front has also produced a paper recently submitted for publication. Experiments were modeled in which slow dynamics is seen as "transient" events. Here the slow dynamics is seen in recovery of the system to a variety of perturbations. In order to get a better understanding of the nature of slow dynamics and the role of these perturbations, we generalized an Ising-like model incorporating slow dynamics. The model successfully describes the hysteretic response to quasi-static stress protocols involving a displacement field coupled to the elastic state field. In this model a rock is represented as a chain (length L) of rigid units with a specific mass and displacement that are coupled to one another through hysteretic elastic elements (springs). This generalization was studied analytically, using Fokker-Planck methods, and numerically for the case of response to a step in stress. Emphasis has been placed on examining the spectrum of relaxation times that characterize the approach to equilibrium following the disturbance. Both analytic work (the Fokker-Planck treatment) and numerical work (direct integration of the stochastic differential equations) confirm that this spectrum is broadly distributed. Consequently the approach to equilibrium in slow dynamics recovery, which extends for 1000s of seconds, can sensibly be described by a slow function of time like logarithmic as shown in our experiments.

Impact on National Missions

This project primarily supported the DOE/NNSA mission in Science with an enhanced understanding and ability to measure and model consolidated, imperfectly cemented materials. These range from geomaterials like concrete to high explosives. The project also supported the missions of science for Nuclear Weapons (e.g., high explosives) and Energy Security. The work has resulted in a new potential research direction as well. The nuclear energy emerging technologies program (NEET) has been identified as a possible user of this research. Degradation and monitoring of aging concrete in light water reactors is an emerging problem and this work bears directly on that. A call for new proposals for the NEET program is due out this fall and the work done on this project will be the basis for the proposed research. For example, the nonequilibrium behavior of concrete seems to be directly related to the amount of fatigue. If indeed slow dynamics is an emergent form of creep as we have proposed, measurements of slow dynamic time constants may be able to predict early onset of damage and degradation. No new staff has been brought on during the project but collaborations with two researchers at the University of Bath (doing finite element modeling combined with optimization) may yield more work In the future.

Publications

Claytor, K. E., J. R. Koby, and J. A. TenCate. Limitations of Preisach theory: Elastic aftereffect, congruence and end point memory. 2009. *Geophysical Research Letters.* **36** (L06304): L06304, 1.

Kim, H. A., J. A. TenCate, and R. A. Guyer. Hysteretic Elastic Materials. To appear in *Proceedings of Meetings on Acoustics, XV International Conference on Nonlinearity in Elastic Materials.* (otranto, Italy, 4-11 July 2010).

Pasqualini, D., and R. A. Guyer. Hysteretic elastic systems: transient response. *Geochemisry, Geophysics, and Geosystems.*

TenCate, J. A.. Slow dynamics of earth materials: an experimental overview. To appear in *Pure and Applied Geophysics.*

Evolution and Function of Microbial Signatures

Murray A. Wolinsky
20080618ER

Abstract

The primary goal of this proposal is to advance the science underlying microbial signatures. For us, signatures are relatively short nucleic acid sequences that can be used to identify bacteria or viruses of interest. Signatures are of great practical importance in medical diagnostics, biodefense, microbial forensics and related disciplines, but they also pose fundamental scientific questions pertaining to evolution, functional organization, microbial diversity and speciation, which have been inadequately addressed.

Currently the most successful techniques for identifying useful nucleic acid detection or diagnostic signatures rely on the computational comparison of the sequences for target groups of interest with the sequences for all background organisms. Any differences that appear between the target sequences and the background sequences represent potentially useful signatures.

This work aims at trying to understand the biological significance of these signature elements "after the fact": knowing that these signatures distinguish target groups of interest from background groups, what can we learn about their roles and distribution?

This work has the potential to shed light on the definition of microbial species and to develop new methods for predicting sequence function. The k-mers we are studying are also becoming increasingly important for applications. In particular, "metagenomics," which attempts to assess the properties of biological communities using high-throughput (but incomplete) sequencing relies on k-mers to determine which organisms are present and what biological functions are being performed. Also, k-mer based approaches are being used by Dr. Bette Korber and her team to design "mosaic" vaccines which show great promise in protecting against HIV (and potentially other viral and bacterial threats).

Background and Research Objectives

When we started our effort, there was relatively little interest in k-mers as biological signatures. This has changed, primarily due to the emergence of new sequencing technologies. These new technologies produce large amounts of sequence data in a short time and at relatively little cost, but the resulting data is generally in the form of large numbers of relatively short "reads" or fragments. While it is possible in principle to *assemble* these short reads into longer consecutive stretches (and thereby better recover the actual sequence and provide results similar to more traditional sequencing) it is relatively costly and time-consuming to do so. In consequence, a number of approaches have been studies that attempt to use the short reads directly. The use of k-mers in this context has become relatively common and underlies a number of approaches to the analysis of *metagenomic* data.

A large number of metagenomic analyses and tools have arisen to exploit these new sequencing technologies. The focus of these studies is generally a community or population of some sort (e.g., all organisms in a soil or water sample, or all bacteria that live in a person's mouth) and the goals of these studies are typically to identify which micro-organisms are present, including, in particular, whether there are any novel organisms present and to determine which biological functions are being performed, again, identifying any novel genes or functions.

Our interest in k-mers arose independently of the new sequencing technologies. We have a long-standing effort to develop assays for the detection of biothreat agents for the Department of Homeland Security (DHS). These assays are chemical diagnostic tests which indicate whether a particular biothreat agent is present or absent in a specified sample. The assays we work with are nucleic acid assays and are specified by providing a set of (typically three) short sequences that can be used to perform the test. Our methods relied on finding *conserved* and *unique* stretches of nucleic acids (DNA or RNA) that distinguish the targets of interest from all background organisms. That is, the signatures we were concerned with must be both conserved (present in all strains of the target organisms) and unique (absent in all other organisms). It is by no means guaranteed that such

signatures will exist: in fact, there are many cases of interest where there are no signatures in this sense. At the other extreme, some groups of organisms (e.g., *Yersinia pestis*) have tens of thousands of signatures. Most organisms fall somewhere in between: typically there are of the order of a few to a few hundred signatures per target. These facts immediately raise the question: what, if anything, determines the number of signatures that a particular organism, or group, will possess? In other words, can one relate the distribution of signatures of organisms to their biological or phylogenetic properties?

We began by asking some simple questions:

- Can the distributions of microbial signatures (short nucleic acid sequences) be predicted?
- Do signatures support a coherent definition of microbial species? What are the implications of signature distribution for microbial diversity?
- How are signatures related to regulation and function?
- Can robustness of signatures be predicted?

At present, we have *not* been able to answer any of these question definitively – but our progress on these issues is reported below.

Scientific Approach and Accomplishments

The most tangible accomplishments of this effort are three-fold.

First, we have developed a large set of computational tools for the identification and analysis of k-mers in genomic sequence data. We have designed fast and simple SQL queries to count k-mers of any size. We have also developed methods to count k-mers using the R programming environment. R is mainly used for statistical computing such as clustering and graphics, but many bioinformatic tools are also available from add-on packages in BioConductor (Gentleman et al 2004). In particular, the BioStrings package includes memory efficient string containers and other utilities for fast manipulation of large sequences. Finally, we have also written a number of Perl scripts to count k-mers from many genomes in parallel using multi-core processors.

Further, we have developed tools for comparing k-mer distributions. There are nearly 3,000 microbial genome sequences (complete and assembly) available at NCBI and the accurate and comprehensive description of these sequenced strains is crucial to allow grouping and searching of the k-mer distributions. For example, identifying those genomes that were sequenced from a vaccine strain or other avirulent strains is a necessary step before comparative analyses. The recently described minimum information about a genome sequence (MIGS) standard proposed by Field et al. (2008) is another step in capturing and organizing the genome project metadata.

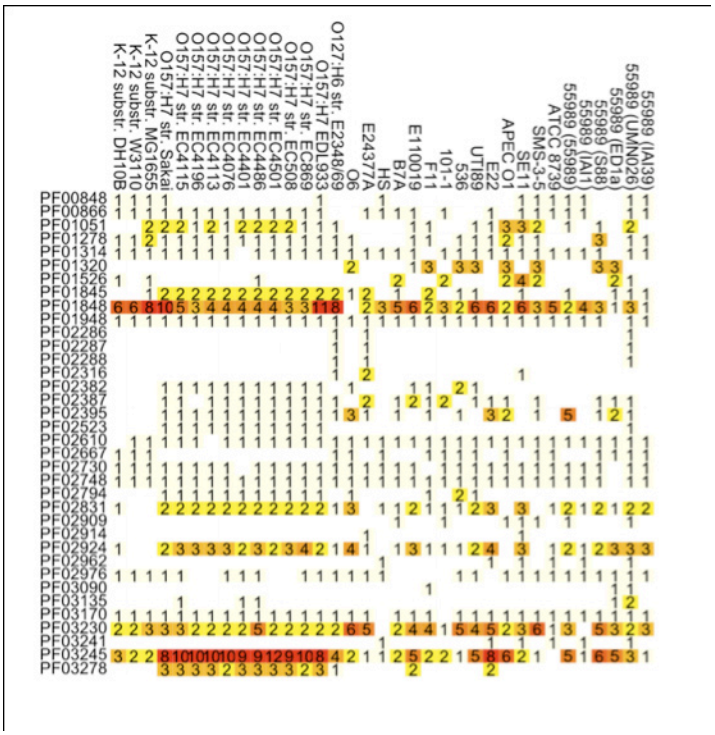

Figure 1. The number of k-mers in each genome are summarized into a string known as a phylogenetic profile. These profile patterns are arranged in tables and analyzed using the profiles package in R. This profile tables show a very small subset of the number of Pfam domains (rows) across 35 E. coli strains (columns).

To answer these questions, we have developed a pathogen-host related ontology to describe the pathogen life cycle (some terms were already defined for biothreat pathogens, see Schriml et al. 2010) and then annotated all complete genomes and some assembly genomes to terms in this new ontology. These annotations include codes describing the evidence for pathogenicity and references to the primary literature. Most importantly, these annotations will be available on our public website at and in an R package called `genomes` that we developed to organize genome sequencing project metadata. The first part of this package includes metadata from publically available sources like NCBI and was available in the April 2010 BioConductor release (and a publication describing this package is in review, Stubben 2010). The TvFac database will be described in the upcoming Database Issue of Nucleic Acids Research (Stubben et al 2011).

The detailed descriptions of genome projects will allow researchers to quickly group and compare k-mer distributions among pathogens or other groups. However, a new

set of tools is needed to cluster and analyze these large datasets. In many cases, we first summarize the distribution of k-mers (or motifs, domains and other conserved sequences) across all genomes into a string known as a phylogenetic profile (Figure 1). We have developed a complementary package called `profiles` to view, analyze and cluster these patterns and relate the results back to phenotypic groups in the `genomes` package. The profiles package will be available in the upcoming BioConductor release and an application paper will be submitted to the journal Bioinformatics (Stubben and Wolinsky 2010).

Identifying over-represented 12-mers in microbial genomes.

We have obtained the empirical distribution of DNA k-mers of varying lengths for all sequenced genomes and identified a number of critical features. For example, the frequency distributions from pathogens containing abundant mobile genetic elements are often characterized by peaks in the k-mer distribution at intermediate lengths (k=12), corresponding to the number of insertion sequence elements (Figure 2). We have collected all these abundant or over-represented 12-mers into a single table (with at least 10 copies in one or more genomes) and are currently analyzing and preparing the results for publication (Stubben and Wolinsky 2010). In particular, we want to distinguish mobile elements from non-mobile, conserved sequences and identify the function of each (e.g., mobile elements are often related to virulence and conserved sequences to regulatory functions).

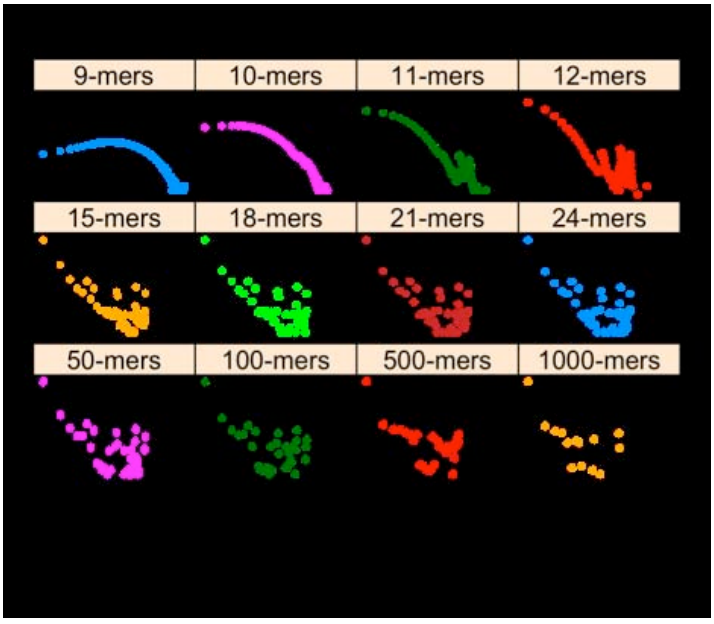

Figure 2. Frequency distribution of DNA k-mers from the plague pathogen, Yersinia pestis. Peaks in the 12-mer distribution (top right) correspond to the number of annotated insertion sequences and this pattern is typical of pathogens with abundant mobile genetic elements.

Prioritizing amino acid k-mers for drug target identification

We have also obtained the empirical distribution of amino acid 9-mers for all sequenced genomes and identified common peptides in *Burkholderia* that may provide suitable drug targets. There are 512 billion possible combinations of amino-acid 9-mers (20 different amino acids), so the raw tables are quite large and provided an number of computational challenges (to cluster this data we looked at speed improvements for large tables using the `bigmemory` package and parallel computing in R). We also counted the number of unique profile pattern strings (Figure 3).

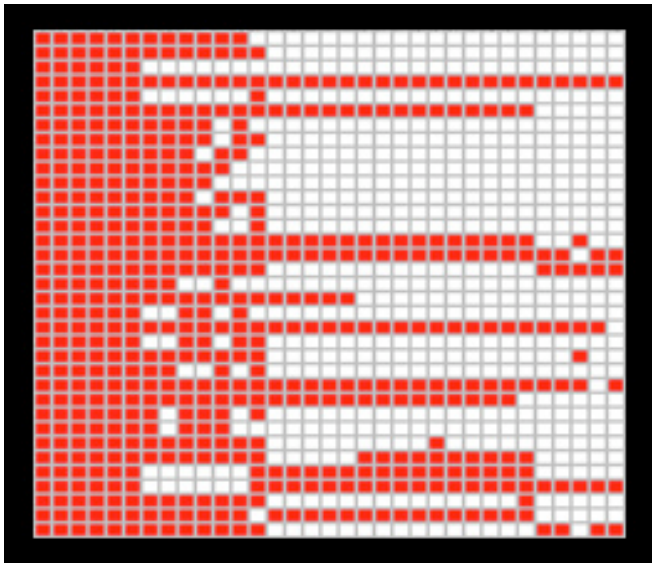

Figure 3. Top profile patterns for amino acid 9-mers found in all 6 B. pseudomallei genomes and their distributions among the remaining Burkholderia neighbors. The top rows shows there are 266,873 different 9-mers found only in B. pseudomallei and B. mallei.

Second, we have obtained the primary dataset we were after: to the best of our knowledge, we now have the first species-level phylogenetically organized set of nucleic acid k-mer signatures for varying sequence lengths. The analysis of this data is now in progress.

One of our major goals was to develop mathematical models that predict number of signatures and compare with computational "measurements" on microbial populations. Specifically, by choosing a broad class of microbes (e.g., *Proteobacteria*) and counting signatures, then progressing to smaller sub-groupings and counting signatures, we can get empirical signature distributions that can be compared to theoretical models. If we get good fits, we will obtain values for microbial evolutionary speciation rates and for total microbial population sizes. Thus our methods may furnish independent ways of estimating microbial biodiversity.

CI	YPTB Locus	Definition	50-90 Cluster	Total non-pathogens	Total pathogens	Pathogen strains
0.01	2410	Magnesium transport ATPase mgtB	1035	3	8	Bme, Bma, Bp
0.03	2913	Deoxyribopyrimidine photolyase phrB	2801	0	6	Vc
0.06	2705	Putative manganese transport protein	1611	3	8	Ba, Bma, Bp
0.12	3827	Outer membrane biogenesis protein	2798	0	5	-
0.13	0181	Putative protohaeme IX biogenesis	3642	0	5	-
0.16	0756	Superoxide dismutase C sodC	1306	0	9	Bme, Cb, Ft,
0.39	1340	Lysine specific permease cadR	563	2	9	Ba, Bma, Bp,
0.42	0242	Glycerophosphoryl diester	2411	0	7	Bma, Bp
0.45	2699	Hypothetical protein	3924	0	7	Bma, Bp
0.76	1424	Hypothetical protein	1031	3	9	Bma, Bp, Ft,
0.87	3166	Thiol:disulphide interchange protein dscB	3283	0	5	-
2.38	0188	Frataxin-like protein cyaY	2139	2	6	Vc
3.15	3505	Stringent starvation protein sspB	1207	3	7	Cb, Vc
ND	1167	Phosphate starvation protein	3911	0	6	-
ND	1251	Ecotin	3380	0	6	-
ND	2026	MviN-like protein	1296	3	9	Bma, Bp, Cb
ND	2995	Putative surface antigen	2296	2	7	Vc

Figure 4. Selected targets. Virulence-associated genes identified by computational methods and selected for experimental screening. These targets have been ranked by their competitive index (CI) value in Y. pseudotuberculosis. The CI value shown is the mean of the CI calculated from 3 spleens individually plated in triplicate. The top six candidates are deemed virulence-related by our experimental criteria. Hits to pathogens include all five members of the Enterobacteriaceae (Ec, Se, Sf, St, Yp) plus some additional strains.

We are also studying how signature lengths affect these distributions. Do the features of the distributions of signature counts remain fixed or are there signature lengths for which these distributions show marked changes? Answering this question will shed light on whether microbial species constitute a meaningful and discrete level of biodiversity. We have finally been able to produce the empirical datasets that we need to address these issues and the modeling work is in progress.

Third, our most interesting results to date were published in BMC Genomics (BMC Genomics 2009, 10:501). This paper reported on a comparative analysis of multiple genomes and attempted to find signatures of pathogenicity that were present in diverse pathogens. Experimental testing of our computational predictions was performed by an external collaborator (Dr. Melanie Duffield at Defene science and technology laboratory, Porton Down, UK) and verified many of our predictions.

Specifically, we computationally identified 13 targets as potential broad-spectrum virulence factors worthy of experimental testing. These targets were selected by identifying proteins common to pathogenic bacteria that are rarely found in non-pathogens. Six of these 13 targets were identified as critical to virulence of *Y. pseudotuberculosis*, (a model organism used for testing), including 3 genes previously unassociated with virulence.

This work has been the basis of a number of proposals, including an effort funded by the U.S. Defense Threat Reduction Agency (DTRA), and performed primarily by Genetic Chemistry to perform lead generation (i.e., develop therapeutic countermeasures) for use against *Burkholderia pseudomallei*.

Figure 4 is taken from that paper and shows the identity of some of the targets we identified. Figure 5 shows the location of these targets in a "pathogenicity space." The identified targets appear in yellow and green.

Impact on National Missions

Better understanding of microbial signatures supports biothreat reduction and basic bioscience missions in DOE, DHS, and other government agencies. The work will develop a scientific basis for understanding how the evolution of pathogens may impact our techniques for their detection.

This work has directly contributed to obtaining DHS funding for a spin-off forensics effort ($500K for a one-year effort and an additional $500K for a second year) as well as a larger bioassay effort headed by Karen Hill (approximately

$2.5 million total, of which about $550K represents work that is related, though distinct, to the work being performed on the LDRD).

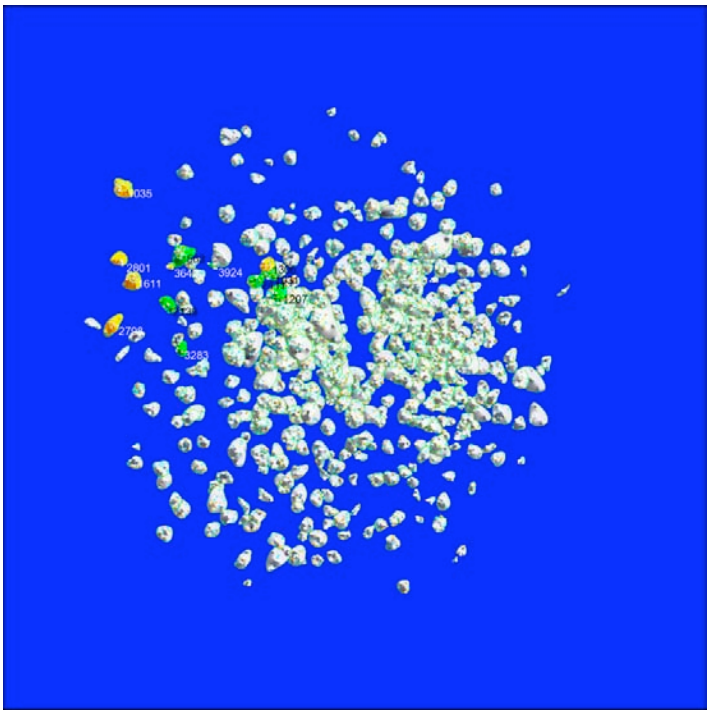

Figure 5. Visualization of potential broad-spectrum targets (signatures) in a "pathogenicity space." Targets shown in yellow and green were predicted to be good candidates for countermeasure development. Targets shown in yellow have been experimentally verified to be involved in pathogenicity.

Unexpectedly, we anticipate this work leading to a partial reshaping of our current DHS forensics effort. The goals of the original DHS forensics effort were centered on assay development and phylogenetic analyses; however, the sponsor is now primarily interested in different approaches to obtaining signature data. The software we have developed, as part of this effort will help us respond to our sponsor's shifting interests.

We entered into a small work-for-others agreement with a company called Genetic Chemistry, Inc. based on the signature work undertaken here. This work is exciting because the goal of that effort is to use some of our early results as targets for treatments (drugs) for a disease (melioidosis, caused by the pathogen *Burkholderia pseudomallei*). If this work is successful, our effort will directly contribute to the development of a new therapeutic treatment.

This work has also supported a post-doc, Dr. Chris Stubben, who will shortly become a staff member at LANL, in large part due to the work that is reported here. This work also supported a number of summer students, including Forest Altherr.

Further, the work has led to a number of collaborations, both internal and external, that we plan to build upon in the future. Internally, this work has led to collaborations with Drs. Ben McMahon, Paul Fenimore, and Peter Hraber (all of T-6), Dr. Nick Hengartner (CCS-3), and Dr. Joel Berendzen (P-21). These individuals all contributed to this effort and we expect to continue the working relations that were established. In addition, also internally, we have started to work with Dr. Geoff Waldo (B-9), whose experimental capabilities nicely complement our computational methods. Together with Dr. Waldo, we recently submitted a large ($8.6 million) DTRA Phase II proposal based on work reported here. This work has also led to important external collaborations. In addition to allowing us to maintain existing external collaborations (Dr. Melanie Duffield, UK; Dr. Elliot Lefkowitz, U. Alabama at Birmingham; Dr. Charles Daitch, Akonni Biosystems, Frederick, MD), this project has led to new working relations with Dr. Yuriy Fofanov (U. Houston); Dr. Jonathan Wong (Canadian defense research laboratory); and Dr. Melody Mills (NIH, Bethesda, MD), and Dr. Stan Goldman (Genetic Chemistry, Inc., California).

Finally, this work contributed indirectly to a 2010 LANL Small Team Distinguished Performance Award that three of the individuals who were (partially) supported by this effort (Wolinsky, Stubben, Fenimore) received.

References

1. Field, D.. The minimum information about a genome sequence. 2008. *Nature biotechnology.* **26**: 541547.

2. Gentleman, R. C.. Bioconductor: open software development for computational biology and bioinformatics. 2004. *Genome Biology.* **5**: R80.

3. Kurtz, S., A. Narechania, J. C. Stein, and D. Ware. A new method to compute k-mer frequencies and its application to annotate large repetitive plant genomes. 2008. *BMC Genomics.* **9**: 517.

4. Schriml, L. M.. GeMInA, Genomic metadata for infectious agents. 2010. *Nucleic acids research.* **38**: D54.

Publications

McMahon, B.. Indexing the tree of life. 2010. *LA-UR: 10-03700.*

Stubben, C.. genomes: an R package for analyzing genome sequencing project metadata. *Standards in Genomic Sciences.*

Stubben, C., F. Altherr, A. Appert, P. Li, and M. Wolinsky. TVFac: a database for identifying toxins and virulence factors. To appear in *Nucleic acids research.*

Stubben, C., M. Duffield, J. Song, J. Gans, and M. Wolinsky. Steps toward broad-spectrum therapeutics: discovering virulence-associated genes present in diverse human pathogens. 2009. *BMC Genomics.* **10**: 501.

Stubben, C., and M. Wolinsky. Comparing phylogenetic profile patterns using the profiles package in R. To appear in *Bioinformatics.*

Stubben, C., and M. Wolinsky. Function and evolution of over-represented 12-mers in microbial genomes. To appear in *BC Genomics.*

Stubben, C., and M. Wolinsky. Prioritizing virulence-associated peptide sequences for drug target identification in Burkholderia pseudomallei. To appear in *BMC Genomics.*

Coupling of Genetics and Metabolism and the Orgin of Life

Hans J. Ziock
20080716ER

Abstract

The goal of this project has been to demonstrate in an artificial process the most important capability of any living system, namely the use of external energy and resources to replicate its information system (a nucleic acid polymer). For that task, the project undertook a modification of an experimentally proven light-driven information-metabolic process that we previously developed. The modification consists of adapting the existing chemistry that generates container materials to one capable of ligating DNA [the joining two short DNA (DeoxyriboNucleic Acid) strands into a longer continuous strand], thereby enabling the reproduction of the information-metabolic complex itself. An initial version of the desired ligation has been accomplished. When coupled with the earlier work on container material production and the demonstration that the container will spontaneously assemble once enough container material has been produced, in addition to the more recent demonstration that the container will both capture resources from the environment and hold onto the information-metabolism complex in a number of different configurations, we have an operational demonstration of most of the key features of a system that has minimal life-like behavior. Future work to further develop the DNA ligation process for the application side, namely the demonstration of a non-enzymatic direct (switchable) light-driven DNA ligation would potentially have an extraordinary impact in biochemistry and therapeutics.

In addition to the above experimental work we have developed a new definition of information, the central ingredient of life. The definition takes into account the Laws of Thermodynamics and is based on the principle of selection. It not only provides insight as to how information first originated, but it also predicts the growth of information (both the amount and the content) with time.

Background and Research Objectives

In spite of the lack of a universal definition of life, there is general agreement that life involves a closely coupled system consisting of 3 components: information, metabolism, and a container, and one that is capable of reproduction and evolution. Information can be thought of as the key component and in organic life is encoded by DNA and/or RNA (RiboNucleic Acid), the genetic material of living organisms. However, as the generation and copying of information requires energy, active living organisms also require a metabolism. Finally, as the metabolism generates waste heat, that must be rejected, along with random, non-information bearing coding a boundary/container is also needed. Hence a living system MUST contain all 3 components.

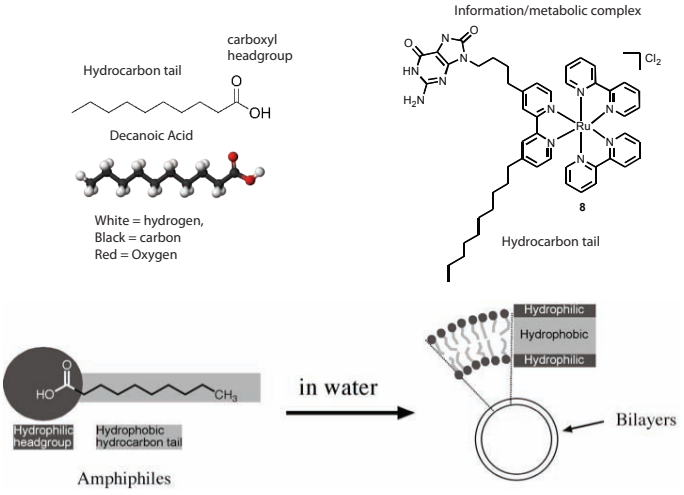

Figure 1. An edge-on view of our container structure that has the form of a bilayer made up of decanoic acid. Decanonic acid is a 10 carbon fatty acid that has an ionizable carboxyl group (COOH) at one end that likes to interact with water (i.e., is hydrophilic) and which is attached to 9 carbon hydrocarbon chain that prefers to avoid any contact with water (i.e., is hydrophobic). These affinities result in a bilayer structure. The addition of a hydrocarbon tail to other molecules causes the hydrocarbon tail to insert itself into the bilayer so as to avoid water.

When attempting to artificially produce a system that has the properties that mimic those of natural life, one must take into account that modern life is extraordinarily complex and far more so than the earliest living systems. In fact, if one is stating from the bottom-up, one

should aim to build a system that is as simple as possible, yet meets the previously listed requirements. This is the approach that we have pursued following the suggestion of our former coworker and on-going collaborator Steen Rasmussen [1]. To avoid the tremendous complications and complexity of resource transport through a "cell" boundary/container, transcription machinery and protein production machinery, our protocell has all its active chemistry take place directly in association with the container, and uses the information/genetic material directly as part of the metabolism, thereby avoiding any need for protein production. In earlier work [2] we had shown that we are able to directly use a single and specific nucleobase to enable a light driven reaction that is able to cleave resource molecules to yield container molecules. These molecules were also observed to spontaneously coalesce to form spherical containers (vesicles), the structure of the vesicles being a thin bilayer (See Figure 1) of container molecules. In follow-on work conducted together with our collaborators, we showed that the resource molecules would be absorbed by the container bilayer and subsequently converted into additional container molecules causing the containers to grow [3,4]. Furthermore, by the addition of container-loving moieties to our information and metabolic components these components were shown to be taken up and remain anchored to the container. Having successfully shown a coupled information/metabolic system that would associate with the container and that would produce more container molecules from resource molecules (food), the next key element in our attempt to produce a minimal protocellular system that possessed life-like properties was the generation of a metabolic process capable of producing copies of the information component of the protocell. To achieve that and maintaining out underlying principle of simplicity, we focused our efforts on adopting our already proven metabolic system to allow it to be used to join (ligate) two short pieces (oligomers) of DNA into a continuous strand and to do this in a process that took advantage of the property of the DNA bases to pair with their complementary bases and thereby form an exact opposite of the original strand. (See Figure 2 and note that a complementary copy of a complementary strand yields an exact duplicate of the original strand.) As will be explained in the subsequent section, several additional simplification steps were undertaken to make success more likely, but still demonstrate the underlying principles.

In a parallel theoretical study we also reexamined the concept of information and how it could have first originated. This was undertaken due to the close links between information and life and also to address the issue of how information together with life could have first originated, an issue that had not been satisfactorily resolved in the past. To investigate this we started out with the non-standard approach of asking the question what is not information and why it is not information. By inverting the answers and repeating the process numerous times we developed new insights into the question of what is information, how it first originated, and its inherently close ties to life.

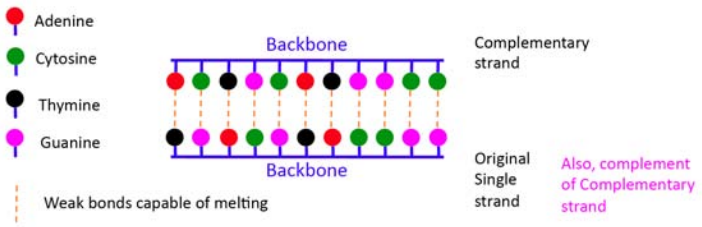

Figure 2. A DNA strand consists of a chemically linked backbone that maintains the bases in a strand in a fixed order. The nucleobases themselves however form specific weak chemical bonds with each other, an Adenine (A) always pairing with a Thymine (T) and a Cytosine (C) always pairing with a Guanine (G). Thus they can form double strands. At elevated temperatures, the weak bonds "melt" and the double-stranded DNA disassociates into two single strands. Note that the complement of a complement is an exact copy of the original single-stranded DNA.

Scientific Approach and Accomplishments

To ligate two short oligomers into a continuous longer strand that was an exact copy of a starting longer strand we modified the two short oligomers as follows. To one, we added a protecting group. The protecting group was identical to the group that we had previously successfully removed with our metabolism to transform a precursor of a container molecule into a functional container molecule. To the other oligomer we added an activating group, the principle being that the removal of the protecting group from the first oligomer would yield a site that could then chemically interact with the activating group of the second oligomer and form a chemical bond that joins the two short oligomers into a longer continuous strand. Although seemingly straightforward in theory as described above, achievement of success experimentally proved to be difficult. As organic molecules and moieties such as our protecting group are relatively complex molecules, with many potential reactive sights, preparation of the desired products was neither simple nor straightforward. The preparation involved the need to "protect" the non-desired reactive site so that the protecting group could be attached only to the one desired specific site on the short oligomer, and also so that the attachment took place to the correct site of the protecting molecule itself. Following the formation of the desired linkage between the protecting group and the first oligomer, the previously "protected" non-desired reactive sites themselves had to be "deprotected" to yield a functional system that would interact properly with the second oligomer. Likewise the system had to be designed so that once the final protective group was cleaved by our metabolism, the two oligomers would form the desired linkage yielding the longer continuous final product. The above process involved numerous steps yielding numerous intermediate products, some desired and some unwanted. The different products had to be characterized, with alternative/modified reaction steps being implement-

ed as needed to yield the desired products. At other times purification methods needed to be developed to separate the desired products from undesired products formed as side reactions. The series of steps used and intermediate products formed for forming a protected thymine are shown in Figure 3, and the deprotection reaction is shown in Figure 4.

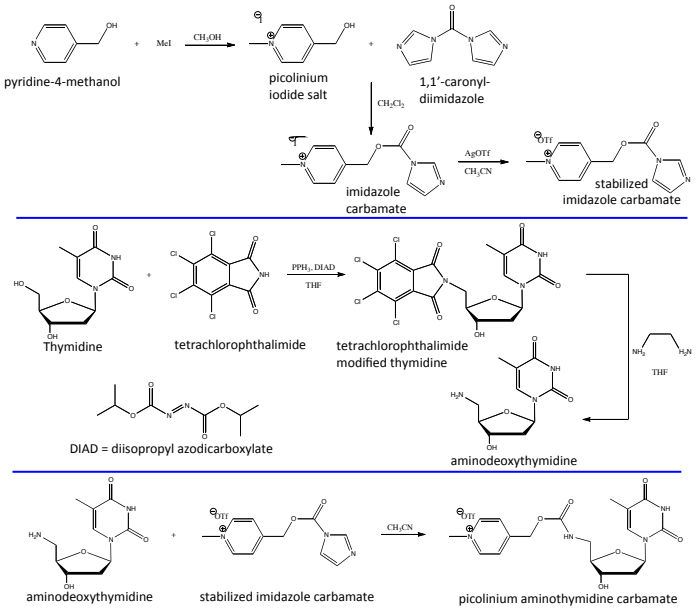

Figure 3. The starting reactants, reaction steps, intermediate products, and final product which is a protected thymidine.

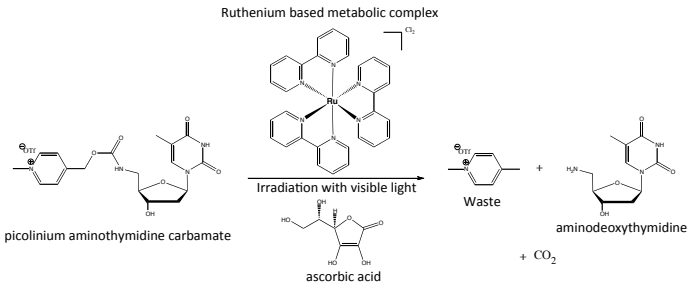

Figure 4. The reaction to cleave the protecting group from the protected thymidine.

Achieving the desired products proved to be sufficiently difficult so that rather than directly attaching the protecting group to a short oligomer (a strand of linked DNA nucleobases), we added the protecting group to a single nucleobase. We were able to show that the desired protected single nucleobase was indeed formed and had the desired structure. We subsequently showed that we were able to cleave off the protecting group in the presence of our metabolic system when the system was exposed to light, while deprotection did not occur if light was not present, nor when our metabolic system was not present. Finally, we were able to show the ability to ligate the single nucleobase to our second activated oligomer following the light/metabolically driven deprotection of the single nucleobase. The reaction is schematically shown in Figure 5. Investigation of a temperature dependence of the ligation reaction showed increased ligation yields (up to 30% preliminarily) at lower temperatures, with decreasing yields as temperature was increased. The observed temperature dependence is expected if base-pairing of the oligomer and single nucleobase occur. At low temperature the dNA strand folds over on itself as shown with the complementary bases forming the links indicated by the horizontal solid lines in Figure 5. When folded as such, there is one overhanging base [the adenine (A)], which is able to then base pair with its complementary base [the protected/deprotected thymine (T). At elevated temperatures, the weak base pairing bonds indicated by the horizontal lines dissociate and the folded DNA unfolds making the probability that the thymine is in the right position to form a bond far less likely.

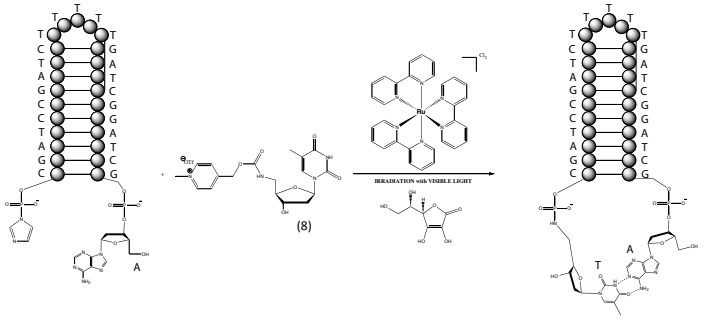

Figure 5. The scheme used to ligate a thymidine to a short oligomer. The oligomer chosen takes on a hairpin structure at low temperature which folds back on itself, the weak bonds between complementary bases forming a semi-stable double stranded like structure with a loop at one end. The folded-back structure has an unpaired adenosine at its end, which will tend to associate with any free protected thymidine in solution. Once associated and deprotected that thymine now has a significantly enhanced probability for being joined to the oligomer yielding a longer fully backbone linked oligomer. The use of a hairpin structure simplifies the complexity of the overall process, but preserves the base-pairing concept.

We were also able to gain some preliminary evidence that indicates we may have been successful in producing a protected oligomer that we were able to ligate to a longer secondary oligomer. Unfortunately this was achieved in the closing days of the project and hence has not been confirmed.

The new definition of information that we developed is based on the concept of selection. Using the fact that information is a non-equilibrium state (i.e. not a random state; a given random state being equally likely as any other similar random state) and that by the Second Law of Thermodynamics any non-equilibrium state decays with time to an equilibrium condition, we realized that the only

way that information could survive long term is through the process of replication and selection. [Without replication any non-equilibrium state would with time decay to an equilibrium (random) state and hence a non-information state. Thus the only way that information could be maintained long term is if it is replicated at a rate faster or equal to the rate at which it naturally decays due to the Second Law of Thermodynamics.] Thus our definition of information is simply "something that has been selected, the selection criterion being that the information directly or indirectly contributes to its replication;" the replication being the requirement needed to have the information to exist long term (longer than its inherent decay time). The definition includes the ability for information to self-generate itself; namely any chemical compound or system that is produced at random at a fixed rate by some energy gradient, and that is able to make copies of itself or part of itself will have a larger population than if it did not have that self-replication ability. As such, it will have a larger probability of eventually transforming into a version that is able to reproduce itself at a rate faster than its inherent decay time. A mathematical analysis shows that any replication ability does indeed have a larger population than a similar system without a replication ability. The same analysis shows that the population however maintains at a steady level provided that the decay rate is faster than the replication rate. However, the moment the replication rate exceeds the decay rate the population explodes exponentially and one effectively has the origin of life.

Furthermore, the Second Law of Thermodynamics also indicates that any copying process will inevitably involve some level of mistakes (random changes). Those mistakes that prove to be advantageous and yielding more copies of themselves than the original self-replicating system will tend to be selected. Thus our definition has built into it the concept of "natural selection" and further predicts the growth in both the amount of information and the quality of information with time. An information system with self-replication abilities thus has the properties of life.

The selection-based definition of information also deals with human-based information. Although such information is not capable of self-reproduction, the information, if correct and useful, is reproduced by humans. It is the correctness/usefulness of this human-based information that is what contributes to its selection for reproduction. Our work also examines the issue of what the information ultimately provides and why information/knowledge is so advantageous. [6]

In closing the project has also resulted in a Ph.D. for Sarah Maurer (University of California, Santa Cruz).

Impact on National Missions

This project supports the DOE/NNSA mission of supporting US leadership in science and technology and the origin of life issue pursues a question that has been pursued for generations. We have developed a technique for using light to drive and control DNA replication (a critical step in developing light controlled therapeutics and self-healing organic nanomaterials), learned about systemic issues related to the origin of life, and developed a more universal definition of information while understanding its relationship to life. Developing and gaining insights into what information is has universal applications. The work associated with this projected has also resulted in a NASA grant and another two grants dealing with radiation detection. The work on information has resulted in new contacts and several funding possibilities that are being pursued.

References

1. Rasmussen, S.; Chen, L.; Nilsson, M.; Abe, S.; Bridging nonliving and living matter, **Artificial Life** (Summer 2003) vol.9, no.3, p.269-316

2. DeClue, MS; Monnard, PA; Bailey, JA; Maurer, SE; Ziock, HJ; Rasmussen, S; Boncella, JM; Nucleobase Mediated, Photocatalytic Vesicle Formation from an Ester Precursor, **Journal of the American Chemical Society** (Jan 28 2009) Vol.131, iss.3, p.931-+

3. Maurer, SE, Deamer, DW, Boncella, JM, Monnard, P, Chemical Evolution of Amphiphiles: Glycerol Monoacyl Derivatives Stabilize Plausible Prebiotic Membranes, **Astrobiology** (Dec, 2009) Vol.9, iss.10, p.979-987.

4. S.E. Maurer, M.S. DeClue, A.N. Albertsen, M. Dörr, D.S. Kuiper, H. Ziock, S. Rasmussen, J.M. Boncella, and P.-A. Monnard, Interactions between catalyst and amphiphilic structures and their implications for a protocell model, Accepted for publication **ChemPhysChem**, manuscript cphc.201000843

5. S.E. Maurer, A. Albertsen1 J. Cape, J.M. Boncella, L. Spencer, H.-J. Ziock, S. Rasmussen, and P.-A. Monnard, Designing a Protocell: Attempt at a Systemic Design Linking Information, Metabolism and Container, Artificial Life XII, Proceedings of the Twelfth International Conference on the Synthesis and Simulation of Living Systems, Odense, Denmark, Harold Fellermann, Mark Dörr, Martin M. Hanczyc, Lone Ladegaard Laursen, Sarah Maurer, Daniel Merkle, Pierre-Alain Monnard, Kasper Stoy and Steen Rasmussen (Eds.), **MIT Press, Proceedings of ALIFE XII**, http://mitpress.mit.edu/catalog/author/default.asp?aid=38533

6. Stirling A. Colgate and Hans Ziock, A Definition of Information, the Arrow of Information, and its Relationship to Life, currently in press, **Complexity**, DOI 10.100/cplx20364

Publications

Protocells, bridging nonliving and living matter. 2008.

DeClue, M. S., P. - A. Monnard, J. A. Bailey, S. E. Maurer, G. E. Collis, H. - J. Ziock, S. Rasmussen, and J. M. Boncella. Nucleobase mediated, photocatalytic vesicle formation from ester precursor . 2009. *Journal of the American Chemical Society.* **131**: 931.

Fuchslin, R. M., H. Fellermann, A. Eriksson, and H. - J. Ziock. Coarse-graining and scaling in dissipative particle dynamics. 2009. *The Journal of Chemical Physics.* **130**: 214102.

Monnard, P. A., M. S. DeClue, and H. Ziock. Amphiphile nanostructures as model for artificial cell-like entities. 2008. *Current Nanoscience.* **4**: 71.

Rasmussen, S., J. A. Bailey, J. M. Boncella, L. Chen, G. Collis, S. Colgate, M. S. DeClue, H. Fellermann, G. Goranovic, Y. Jiang, C. Knutson, P. - A. Monnard, F. Mouffouk, P. Nielsen, A. Sen, A. Shreve, A. Tamulis, B. Travis, P. Weronski, J. Zhang, X. Zhou, H. Ziock, and W. H. Woodruff. Assembly of a minimal protocell. 2008. In *Protocells: Bridging Nonliving and Living Matter.* Edited by Rasmussen, S., M. A. Bedau, L. Chen, D. Deamer, D. C. Krakauer, N. H. Packard, and P. F. Stadler. , p. 125. Cambridge, Massechusetts: MIT Press.

Tamulis, A., V. Tamulis, H. Ziock, and S. Rasmussen. Influence of water and fatty acid molecules on quantum photo-induced electron tunneling in self-assembled photosynthetic centers of minimal protocells. 2008. In *Multiscale Simulation Methods for Nanomaterials.* Edited by Ross, R. B., and S. Mohanty. , First Edition, p. 9. Hoboken, N.J: Wiley.

Zhou, X., Y. Jiang, S. Rasmussen, and H. Ziock. A method to bridge different-level coarse-grained models by estimating free energies of high-dimensional conformations: jump-in-sample simulations. 2008. *The Journal of Chemical Physics.* **128** (17): 174107.

Protein-protein Interactions in Host Response to H1N1

Geoffrey S. Waldo
20100520ER

Abstract

Complete knowledge of protein-protein interactions between flu virus and host innate and adaptive immunity proteins are key to developing treatment and detection modalities. There are no techniques for monitoring the spatiotemporal aspects of these processes in real time during the course of infection. We will develop and validate promising technologies for monitoring protein localization and interactions in real-time in living cells, and benchmark these using well-established NS1-target interactions. In Figure 1, NS1 interacts with several aspects of the host immunity. One of the first 'known' interactions is with p85 (see lower right part of cell in Figure 1). Conventional antibody blots, targeted genetic mutations have implicated the multifunctional viral NS1 protein and suggested how it contributes to efficient virus replication and virulence by participating in a multitude of protein–protein and protein–RNA interactions (Figure 1). One of the first interactions during infection is between NS1 and p85-beta, which is part of the p110 innate immunity inflammatory response regulatory pathway.

Background and Research Objectives

To evaluate the feasibility of using the 3-body split-GFP to study protein interactions between NS1 and components of the host immune pathway. Interactions between host protein (H, p85) and pathogen effector (Y, NS1) are monitored as depicted in Figure 2. Objectives: (1) demonstrate distinguishing interactors from non-interactors (2) establish the assay in living cells (3) get an idea about the limitations and considerations needed to use the assay in general. Our objective is to demonstrate that the split 3-body GFP can distinguish known NS1 interactors and non-interactors in (1) test tube using cell lysates (2) living cells. Specifically: (1) wild-type p85-alpha doesn't interact with NS1 protein; but wild-type p85-beta does interact with NS1, (2) the M582V mutant of p85-alpha does interact with NS1 (Li et al. 2008), (3) NS1 interacts with wild-type p85-beta (its natural target) but the NS1 Y89F mutant does not interact with p85-beta (Hale et al, 2006). We expect that the NS1 Y89F wouldn't interact with either the p85-alpha or the p85-alpha M582V mutant.

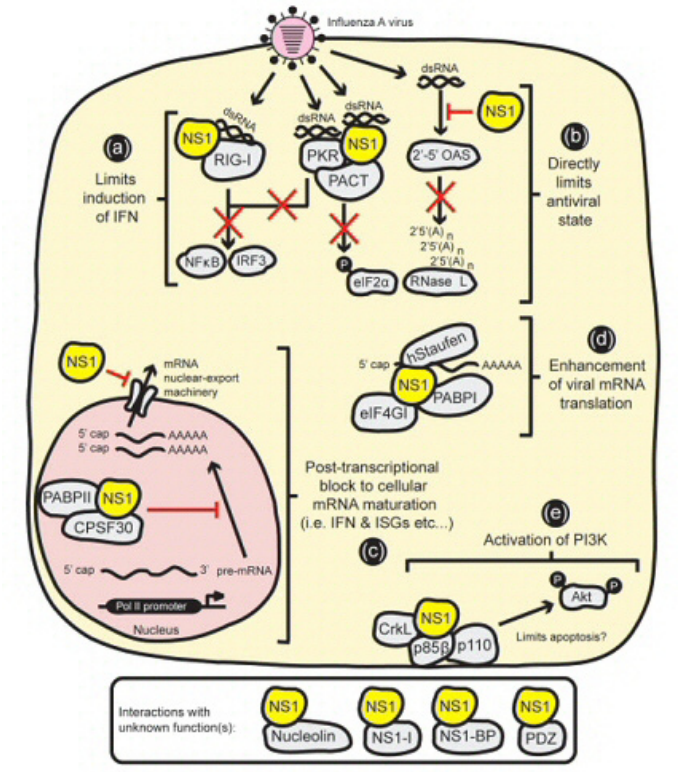

Figure 1. Multifunctional role of the Flu A NS1 protein

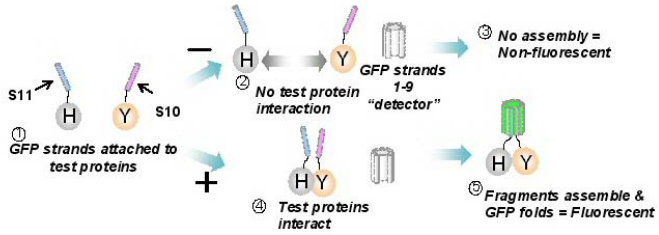

Figure 2. Principle of split GFP protein interaction detector. Fragments S11 and S10 of GFP are brought together by host (H) and pathogen (Y) proteins. Then GFP strands 1-9 can fold with S11 and S10, giving a fluorescent signal.

Scientific Approach and Accomplishments

Our approach is to use the split GFP 3-body system as

depicted in Figure 2. Our controls include (1) wild-type p85-alpha doesn't interact with NS1 protein; but wild-type p85-beta does interact with NS1, (2) the M582V mutant of p85-alpha does interact with NS1 (Li et al. 2008), (3) NS1 interacts with wild-type p85-beta (its natural target) but the NS1 Y89F mutant does not interact with p85-beta (Hale et al, 2006). We expect that the NS1 Y89F wouldn't interact with either the p85-alpha or the p85-alpha M582V mutant. In our approach, we expect that the interacting proteins should give a positive signal (GFP fluorescence) while the negative, non-interacting protein mutant should give a low GFP signal. We expect these to make good test cases, because 1) the interactors and non-interactors differ by a single amino acid (conservative change) and 2) these interactors and non-interactors have been established and validated using conventional immunoprecipitation and co-purification/binding assays in the literature.

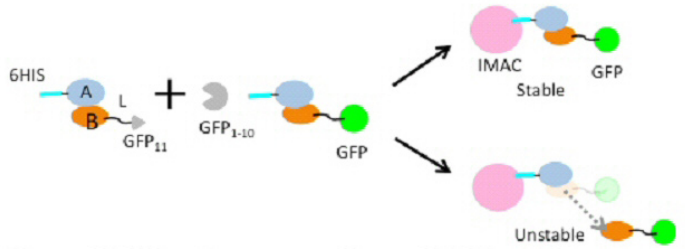

Figure 3. Simple screen for validation of predicted protein complexes. If Proteins A and B in fact form a stable complex in the cell, the immobilization of Protein A would be expected also to immobilize protein B, which carries a fluorescent signal.

Validating control NS1 and p85 constructs using IMAC pull-down assay.

We used a well-established method to confirm that the expected interactions occurred. The assay is depicted in Figure 3. Protein complexes that are stable can be bound to the IMAC beads by attaching a 6HIS tag to one of the proteins. The other protein is tagged with GFP, so fluorescent beads tell us that the complex formed. When applied to the NS1 and p85 trial complexes, as expected, the NS1 wild-type interacts with the p85-alpha M582V mutant. All the other pairs do not interact, as expected. This is an important confirmatory experiment. All proteins had been expressed and quantified by SDS-PAGE, and the concentrations of the proteins were micromolar, comparable to what the concentrations would be in the cell-based experiments. The p85 was captured on IMAC beads via the 6HIS tag, and the associated GFP-labeled NS1 came along for the ride (forming a complex with the p85, see upper right, Figure 4).

Testing control NS1 and p85 constructs using 3-body complementation in vitro.

Bicistrons were used to express the same NS1 and p85 controls as in Figure 4, but this time the NS1s had the S10 GFP tag, and the p85s had the S11 tag. The GFP 1-9 detector was added to the cell lysates in white assay plates. After overnight incubation, the p85 M582V + NS1 pair gave a signal of 19,000 fluorescence units. The other three non-interacting pairs averaged about 3000 fluorescence units, a ratio of ca. 6. In a separate experiment we added GFP 1-10 instead, to detect just the S11-tagged p85s. The signals from all four pairs was about 25,000, showing that the lower signal in the GFP 1-9 system didn't come about from lack of p85. All the experiments had comparable concentrations of target proteins, and we concluded that the GFP 1-9 was faithfully reporting the interactions between the species.

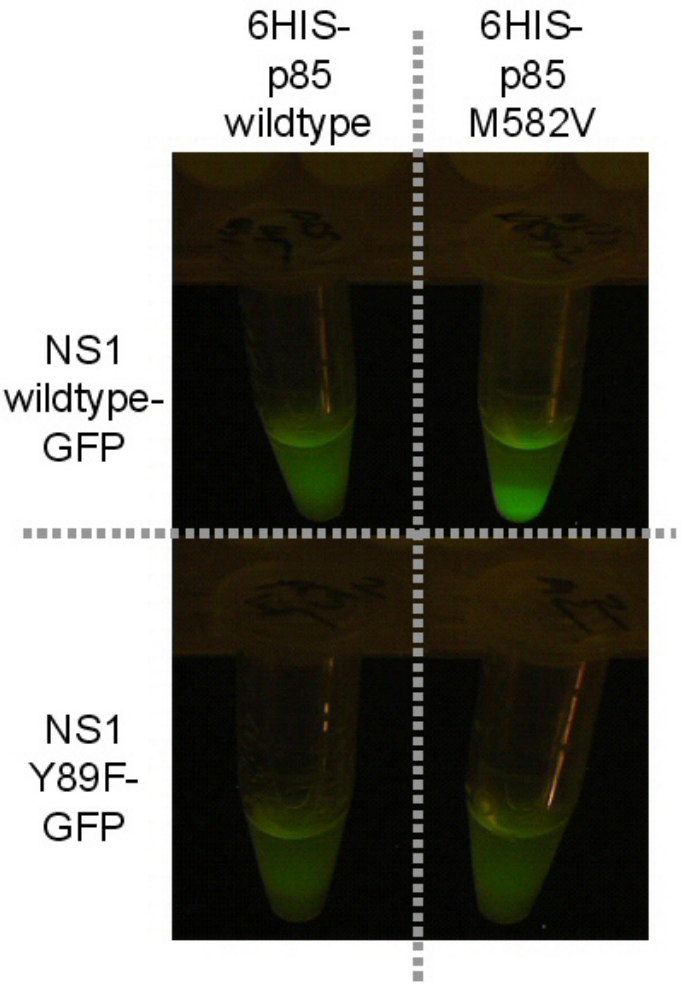

Figure 4. 4 possible pairs depicted were expressed and mixed as indicated. The p85 had a 6HIS tag and the NS1 had a GFP tag. Fluorescent beads confirm the p85 M582V interacts with NS1 wild type (upper right). Concentrations of proteins 1 uM.

Testing control NS1 and p85 constructs using 3-body complementation in vivo.

We repeated the bicistron experiments in living E. coli cells. We tried two orientations: (1) S10-p85 + NS1-S11, and (2) S10-NS1 + p85-S11. The GFP 1-9 was co-expressed in the cells. We tried several concentrations of Antet (to vary the amount of target protein), several concentrations of IPTG

(to vary the amount of GFP 1-9), and imaged at various times to see how the fluorescence developed. The ratio of fluorescence between interactors and non-interactors seemed to not vary much with Antet or IPTG, (only the absolute signal decreased as we lowered Antet or IPTG). Figure 5. shows the results for the 100 nM Antet, and 1 mM IPTG (both promoters are fully-on at these concentrations, meaning the maximum amount of protein is being made). The first orientation (S10-p85/NS1-S11) shows a slower appearance of fluorescence vs. S10-NS1/p85-S11. At 4 hr the positive interactor stands out clearly for both orientations. At 8 h post-induction, the difference between interactors and non-interactors is clear for S10-p85/NS1-S11 (orientation 1). For the second orientation, the positive interactor is only slightly brighter than the non-interactors.

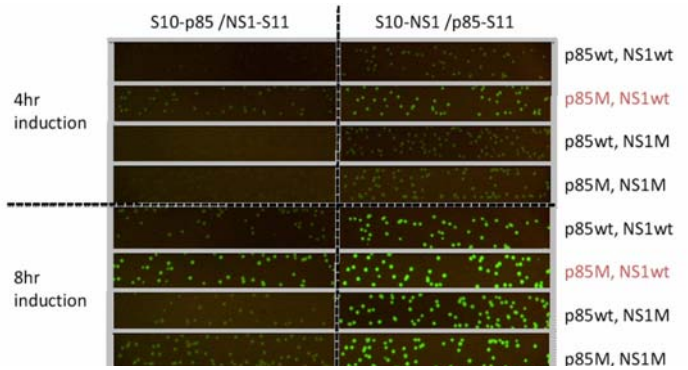

Figure 5. The two columns show the two orientations of the constructs; the rows are labeled by the identities of the NS1 and p85 (interactors (red text) or non-interactors (black text)). There are two time points shown (4 h post-induction, 8 h post-induction).

Expressing large, complex mammalian protein p85 in bacteria presents a number of challenges. Despite this, we are clearly able to distinguish interactors resulting from a single point mutation, from non-interactors. The dynamic range between interactors and non-interactors appears dependent on orientation and kinetics (time of induction). This research has clearly established the feasibility of using the LANL split-GFP in-vivo protein interaction reporter for detecting protein interactions. Several new questions have been raised by these results

1. What is the source of the background from the non-interactors?
2. How important is orientation?
3. What effect does linker-length have between the tag and the target?
4. What is the 'best' way to establish the 'negative' signal level (that coming from non-interactors)? How does the system perform in mammalian cells using this set of controls?
5. What is the intrinsic background from the affinity of the split GFP components independent of the target , and can it be 'evolved' or 'engineered' to maximize the dynamic range? These questions will be addressed in future research.

Impact on National Missions

While the underlying technology we have developed is sophisticated enough to perform many assays in high-throughput format at low cost when fully matured. In order to gain wide-spread acceptance the methodology must be carefully validated using experiments that are tedious, precise, and involve living systems and considerable human and experimental resources. We achieved the goal of our small feasibility project. The preliminary data will be used to write competitive research proposals to exploit the technology for understanding host/pathogen biology. This directly supports the lab mission in human health and biosurveillance.

References

1. Hale, B., D. Jackson, Y. Chen, R. Lamb, and R. Randall. Influenza A virus NS1 protein binds p85 beta and activates phosphatidylinositol-3-kinase signaling. 2006. *Proceedings of the National Academy of Sciences of the United States of America.* **103** (38): 14194.

2. Li, Y., D. Anderson, Q. Liu, and Y. Zhou. Mechanism of influenza A virus NS1 protein interaction with the p85 beta, but not the p85 alpha, subunit of phosphatidylinositol 3-kinase (PI3K) and up-regulation of PI3K activity. 2008. *Journal of Biological Chemistry.* **283** (34): 23397.

Pre-Symptomatic and Strain Specific Diagnosis of Influenza

Basil I. Swanson
20100522ER

Overview

The focus of this project was to evaluate the application of the Hartman Interferometer for the reagent-free, sensitive detection of influenza viruses using carbohydrate ligands that were synthesized at Los Alamos National Laboratory. The LANL developed carbohydrate ligands (Kael, et. al., JACS, 2008) were demonstrated to be strain specific using an optical waveguide-based sensor that was also developed at Los Alamos [1]. In using the Los Alamos optical biosensor, it was necessary to employ a reporter antibody that had been conjugated with an organic dye to "report" the presence of the influenza virus particles. The potential advantage of the Hartman Interferometer is that this reporter antibody would not be necessary thereby simplifying the assay and eliminating the step requiring an added reagent. Moreover, this approach would only require carbohydrate ligands and, therefore, be potentially more robust. To achieve this, a Hartman interferometer was obtained via collaborations with Nile Hartman and nGimat Ltd, Atlanta, for evaluation over the course of this project. The project goals were to optimize the instrument, evaluate it for standard measurements and then evaluate the feasibility of detection of influenza viruses in complex biological samples.

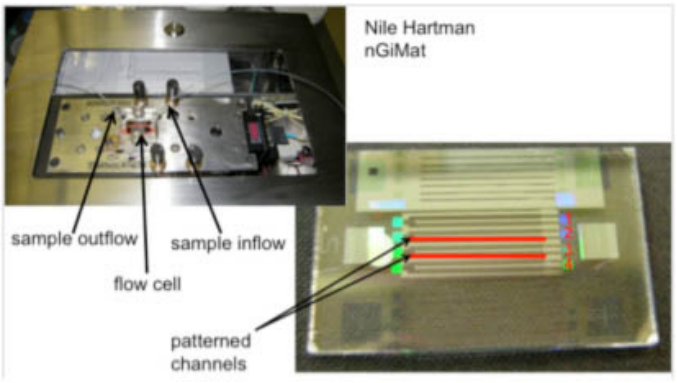

Figure 1. The Hartman Interferometer and a waveguide interferometer chip with patterned channels.

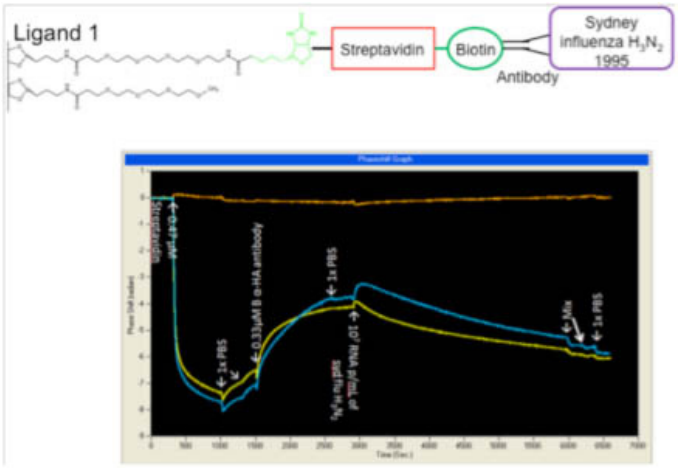

Figure 2. Evaluation of binding of influenza viruses to functionalized interferometer chips with anti-H1N1 antibody.

Experimental Approach

The Hartman interferometer and associated patterned waveguides are shown in Figure 1. The waveguides are fabricated and patterned to incorporate a reference channel for calibration. The waveguides were selectively functionalized with biotinylated silane-based self-assembled monolayers (LANL technology, Anderson, et. al., Langmuir, 2008, [2]), using patterning techniques to functionalize each of the three sensing channels with different recognition ligands (either antibodies or carbohydrates) and to functionalize the reference channel with the same underlying SAM but with no recognition ligand. Functionalized waveguides were then loaded on the instrument and calibrated for stability. Preliminary experiments simply measured the binding of biotin (conjugated to the self-assembled monolayer surface) to streptavidin labeled with quantum dots (655 nm emission). The quantum dot conjugation allowed for significant mass increase to facilitate detection by interferometry and also to cross-validate results on our waveguide-based optical biosensor platform. The Hartman Interferometer senses changes in the effective index of refraction at the surface of the sensing chip and the binding of streptavidin that had been conjugated to a quantum dot would

induce a large change in the refractive index. We were able to measure a concentration dependent change in the index of refraction with the binding of biotin to streptavidin QD. Despite the strong binding affinity between the two, the signal took a long time to stabilize (60-75 minutes) between additions.

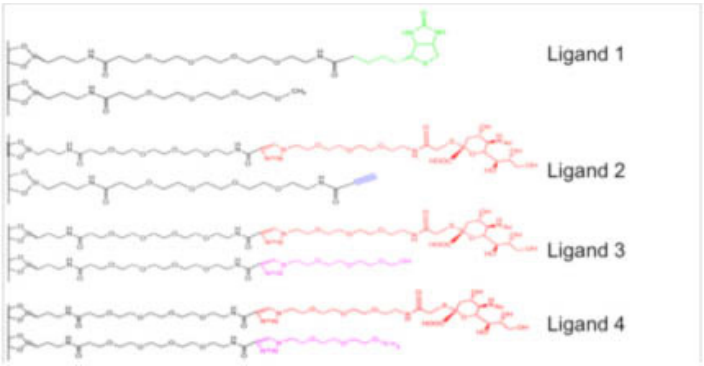

Figure 3. The different conjugation chemistry approaches evaluated during this project.

Given the successful validation of biotin-avidin conjugation, waveguides were cleaned and functionalized with self-assembled monolayers, followed by conjugation of a biotinylated anti-influenza H1N1 antibody to the surface using biotin-avidin chemistry. After significant signal stabilization, UV inactivated A/Beijing/95 influenza virus was added to the surface and a specific change in index of refraction was measured as indicated in Figure 2. The stabilization of the signal took a very long time (2-3 hrs), most likely indicating slow diffusion of the influenza virus. Given the size and mass of the influenza virus particles, the rate of diffusion is expected to be much slower than that of a protein (e.g., streptavidin). In order to speed up the assay time, we evaluated several ways of rapid mixing of contents in the flow cell including the use of a peristaltic pump and a syringe pump. However, the instrument was extremely sensitive to the flow and pressure perturbations caused by the pumps and therefore, we were not able to effectively use them in the experiment.

Although disappointed by the time required to stabilize the measurement, we proceeded to evaluate the binding of influenza virus to carbohydrate ligands developed by our group. To better evaluate the chemistry, we performed the experiments in tandem on the waveguide-based optical biosensor platform (where the detection is achieved by a fluorescently labeled reporter antibody rather than changes in refractive index) and on the interferometer. Four different ligand conjugation chemistry approaches (Figure 3) were evaluated on both platforms. Ligand 2 resulted in a high non-specific interaction in both transduction approaches (fluorescence and interferometric) and was abandoned. Ligands 3 and 4 showed promising results on the waveguide-based optical sensor platform (low non-specific signals, specific detection of 10^7 particles/mL influenza A). However, the results on the interferometer chip were not quantitative, reliable or reproducible. Indeed, a mock preparation (all cell lysate components without virus), also gave very similar results on the interferometer platform (but not on the optical biosensor, see Figure 4). As a result, we re-evaluated the antibody-virus interactions indicated in Figure 2. Indeed, the mock also gave similar results using this functionalization.

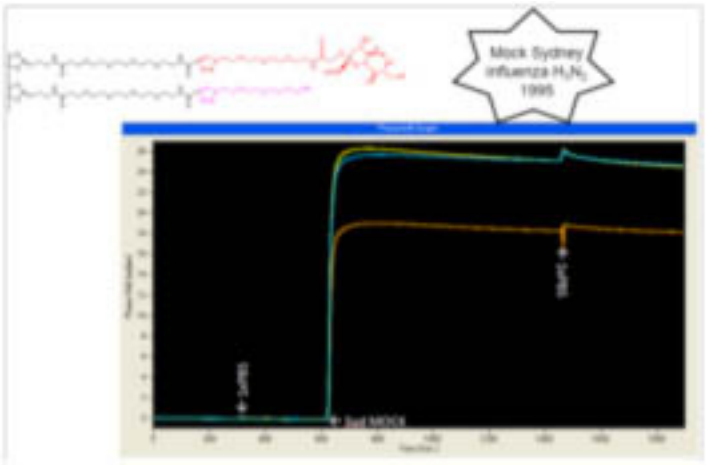

Figure 4. Hartman interferometer signal and changes in refractive index associated with mock preparation

Conclusions

We were able to successfully evaluate the Hartman interferometer for laboratory measurement of biotin-avidin conjugation and purified influenza virus detection, using carbohydrate ligands developed at LANL. Unfortunately, assays of complex samples using the Hartman interferometer resulted in significant roadblocks. Our results clearly indicate that large protein components and other materials in complex biological samples result in large changes in the index of refraction thereby giving a high background signal. This high background signal makes it difficult to measure a specific binding of the target influenza and thereby reduces both sensitivity and specificity. At this point, it is not clear if biological molecules in complex fluids bind directly to the surface sensing film to give a high non-specific background signal or if the large changes in index of refraction result from the complex fluid in close proximity to the sensing film. We note that the Hartman interferometer is sensitive to changes in the effective index of refraction for the fluid up to ~ 200 nm above the sensor surface. So, whereas the Hartman interferometer can be effectively used for detection of purified targets under controlled laboratory conditions, extension to real-world detection in complex samples remains questionable using the current approach. Also, the platform is highly sensitive to changes in environment, including changes in room temperature, humidity and other factors. Further, diffusion of large particles takes a long time and stabilization of the chip for repeat measurements is time consuming and intensive. A different approach (both engineering and chemistry) is required to make this platform amenable for use with real-world samples.

References

1. Kale, R., H. Mukundan, D. Price, J. Foster. Harris, D. Lewallen, B. Swanson, J. Schmidt, and S. Lyer. Detection of intact influenza viruses using biotinylated biantennary S-sialosides. 2008. *JOURNAL OF THE AMERICAN CHEMICAL SOCIETY.* **130** (26): 8169.

2. Anderson, A., A. Dattelbaum, G. Montano, D. Price, J. Schmidt, J. Martinez, W. Kevin. Grace, K. Grace, and B. Swanson. Functional PEG-modified thin films for biological detection. 2008. *LANGMUIR.* **24** (5): 2240.

Flow Cytometry Technology Applied to the Characterization and Optimization of Algal Cells for Biofuel Production

Babetta L. Marrone
20100523ER

Abstract

The importance of alternative energy resources has become increasingly apparent over the years with renewable sources, including algal biofuel, receiving much interest. Some algae produce lipids when starved of nitrogen and these lipids can, in turn, be harvested and refined for biofuel. Algal biofuel technology could be a promising advancement in the development of alternative, renewable energy, but much research is needed to prove sustainability. In order to help improve and maximize algal biorefinery processes an assay characterizing algal growth and metabolism related to biofuel production was developed. Using flow cytometry (FCM), which measures individual cells in a flowing sample stream, we measured morphology and functional features of algal cells related to lipid production and cell cycle in *Nannochloropsis salina*. The flow cytometry assays that we developed can be used in live cells and therefore will allow for selection of high lipid producing cells by flow sorting followed by culturing of those samples for further molecular and chemical analyses.

Background and Research Objectives

The overall objective of this project was to develop advanced state-of-the art flow cytometry-based technologies to provide a detailed characterization and comprehensive understanding of algal growth and metabolism relevant to biofuel production, and apply these technologies to maximize biorefinery processes. Studies were aimed at developing methodologies and collecting data related to a variety of cellular activities in algal species and strains of interest.

Flow cytometry (individual cell measurement in a flowing sample stream) is an established technology for rapid, sensitive, and quantitative high throughput analysis of cellular morphology and function (Figure 1). We proposed to adapt flow cytometry methods that are routinely used for analysis of mammalian cells to analysis of algal cells. Application of flow cytometry to algal cell analysis will build a knowledge base for understanding algal cell biology, which will enable the development of improved biorefinery technologies.

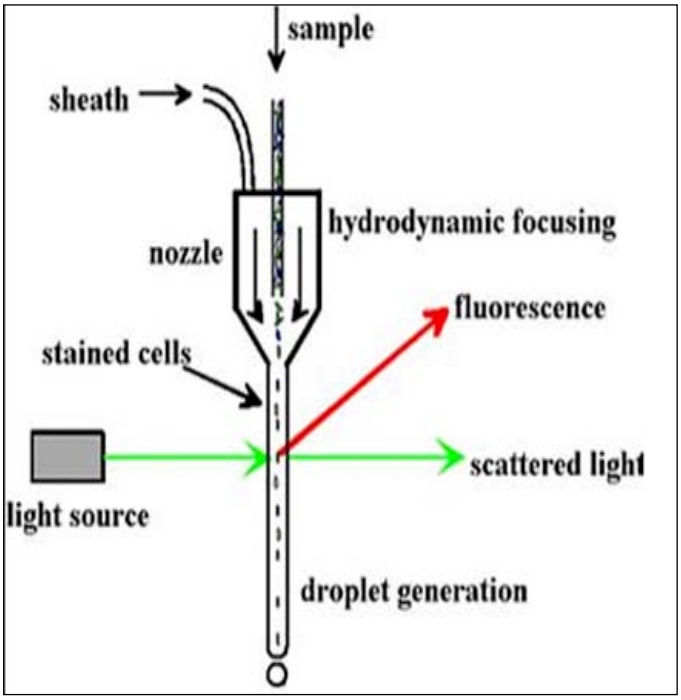

Figure 1. Flow cytometry is the multiparameter analysis of single cells (or particles) as they are passed through a flowing sample stream. The cells are hydro-dynamically focused, such that each cell is individually interrogated by a light source (often a laser). How much the light is scattered by the cell, as well as any emission of light that has been excited within or on the surface of the cell, is detected and utilized for characterization. Thus, different populations within heterogeneous samples can be identified and if desired, sorted. A BD FACSCalibur flow cytometer was used for most experiments. This instrument has 4 different bandpasses to measure fluorescence (530, 585, 670, 661) in addition to both side and forward scatter. It has two lasers (488 nm and 635 nm). Image adapted from http://missinglink.ucsf.edu/lm/molecularmethods/images/flow%20cytometry_clip_image002.jpg.

Flow cytometry is an ideal technology for algal analysis. Single cell analysis of thousands of cells by flow cytometry provides detailed information about the cell population distribution that cannot be achieved using bulk

analysis methods. The ability to analyze cells in suspension with little or minimal sample preparation, and to access biochemical activity in individual live cells, provides unique insight into cell function. The ability to sort individual cells for further analysis, growth in culture, or cloning and selection is another advantage of flow cytometry technology. A wide variety of fluorescent tags for cellular analysis is available commercially and will be fully utilized for this project.

There are several published reports of flow cytometry applied to the study of algal biology, indicating that the proposed approaches are feasible. These studies include analysis of lipid production and composition in algal cells, used in the pharmaceutical and nutraceutical industries, as well as a number of different measurements used to assay for ecotoxicity, including enzyme inhibition, light scatter; and population-based parameters such as growth, yield, and chlorophyll production.

Nannochloropsis salina (N.s.) is a marine single cell microalgae that completes photosynthesis for its nutrients. This particular organism has been identified as high-lipid producing and thus a feasible candidate for large-scale cultivation for biofuel. Some have found this particular strain capable of producing up to 70% oil under nitrogen depletion [1].

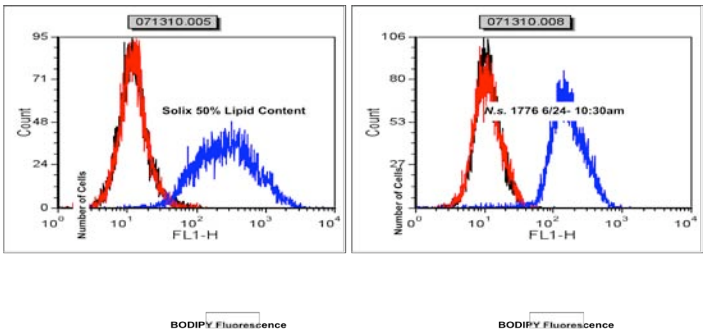

Figure 2. These results show successful staining of algae cells with BODIPY 505/515 dye. Additionally the fluorescence shows differences between Solix N.s. and LANL N.s. samples. We also see that the DMSO alone does not affect the cellular auto-fluorescence. Black: Unstained Red: Unstained with 6 µl of 50% DMSO Blue: BODIPY 505/515. 10 µm in 50% DMSO

Scientific Approach and Accomplishments

To develop a method for monitoring lipid content in algal culture, we conducted three main tasks:

Determine the optimal conditions to stain live algal cells for the detection of lipids using the dye BODIPY 505/515 [2]

We examined the best concentration of dye and the best solvent for the dye using both flow cytometry and fluorescent microscopy. Results were compared between lab-grown algae and samples provided by Solix in Fort Collins, CO. By first testing for the optimal dye concentration using both flow cytometry and microscopy, greater than 10 µM caused too much fluorescent background in microscopy. DMSO, dimethylsulfoxide, is known to assist dyes in permeating cells, but high concentrations can be toxic to the cell. We found that a working stock concentration of 10 µM dissolved in 1:2 DMSO and Phosphate Buffered Saline (PBS) was the optimal condition to stain *N. salina* with BODIPY (Figure 2). A final concentration of 3% DMSO in solution was not harmful to the cell. This DMSO/PBS solution does not affect the algae's auto-fluorescence or light scatter. By examining under the microscope, the cell shape, size and fluorescence could be determined and also indicated successful detection of lipids.

Validate our lipid staining method using algae samples with known lipid content

Solix, our commercial partner, has provided algal samples with a known lipid content. The *N.s* strain received has 30% and 50% lipid content and the *Nannochloropsis oculata* (*N.o.*) strain received has 40% lipid content. These percentages were determined by dry weight measurements conducted by Solix. Samples were stained with BODIPY 505/515 as above and evaluated by flow cytometry. We found that the fluorescence intensity of BODIPY-stained cells was greater in the 50% lipid *N.s*. samples than in the 30% lipid *N.s*. samples. However, the BODIPY fluorescence of the 40% lipid *N.o.* sample did not follow the expected trend. This could be attributed to the effectiveness of the staining procedure between *N.o.* vs. *N.s* or to strain differences in BODIPY staining.

Evaluate lipid content during a time course of N.s. cultivation using BODIPY dye

Using the BODIPY 505/515 staining protocol, we evaluated samples from a multi-day time-course of *N.s.* growth for changes in auto-fluorescence and lipid content using flow cytometry. (Samples were provided by Scott Twary, B-8). Cells were stained and measured by flow cytometry. The first sample was rapidly growing with nitrogen available while the second sample was undergoing nitrogen depletion, which causes the algae to produce an increasing amount of lipids. These samples were all taken during the light cycle (16 hours light: 8 hours dark). We found that in the nitrogen-depleted environment there was an increase in BODIPY fluorescence, indicating increased lipid content.

Development of a DNA staining protocol to use in conjunction with BODIPY to measure cell cycle stage

Several DNA staining dyes were evaluated for their ability to stain DNA in live *N.s.* cells. The dye HOESCHT 33342 was selected base on the ability to combine this dye with BODIPY for simultaneous, multi-color measurement of lipid content and DNA content.

Additional work supported by this project included: mea-

surement of cell size as an indicator of lipid production; an extensive literature search on algal flow cytometry.

The flow cytometry technology and capabilities of the National Flow Cytometry Resource (NIH grant P41 RR01315) were utilized for this project.

Conclusion

We have developed an easy, robust assay for analysis of algal cell lipid content by flow cytometry using the dye BODIPY 505/515. The method is ready to be standardized for application to monitoring of lipid content in algal cultivation systems. It will be used to monitor algal lipid production in the NAABB project, in algal biology studies and in algal harvesting and extraction R&D. In conjunction with DNA measurement, it will be used to sort living *N.s.* cells for proteomic research on lipid metabolism pathways.

Impact on National Missions

The results that we obtain from this feasibility study have been used as preliminary data in proposals to external sponsors in the area of algal biofuels R&D. We are using the flow cytometry assays on a routine basis to monitor algae harvesting processes, as part of a new project funded by DOE, National Alliance for Advanced Biofuels and Bioproducts (NAABB). We expect that the flow cytometry assays will become a routine, easily standardized method for monitoring algal cultivation ponds and biorefinary processes; and will facilitate systems biology research and protein engineering studies on algal biofuels species.

References

1. Boussiba, S., A. Vonshak, Z. Cohen, Y. Avissar, and A. Richmond. Lipid and biomass production by the halotolerant microalga Nannochloropsis salina. 1987. *Biomass.* **12**: 37.

2. Cooper, M. S., W. R. Hardin, T. W. Peterson, and R. A. Cattolico. Visualizing “green oil” in live algal cells. 2010. *Journal of Bioscience and Bioengineering.* **109** (2): 198.

Detecting and Defending Against Viral Threats in Cyberspace

Michael E. Fisk
20100533ER

Abstract
Cyber systems are ubiquitous in modern society, from everyday communication to systems that control and manage our nation's financial, energy, and defense systems. The integrity of cyber systems is critical for maintaining a functioning society, but our ability to provide robust and secure systems is increasingly uncertain. The focus of our work was detecting the actions of intruders once they are already inside cyber networks. Our challenge is to prevent a singular vulnerability from turning into a complete loss of integrity of the entire cyber system. To achieve this objective requires understanding the temporal dynamics of network activity and developing methods to detect abnormal patterns and changes. In turn, accurate detection requires modeling complex normal behavior that varies from computer to computer, and user to user, and that has diurnal and weekly patterns. In the short duration of this ER, we were able to make significant progress toward several key technical objectives as well measures of the team coalescing into a whole greater than the sum of its parts.

Background and Research Objectives
Cyber systems are ubiquitous in modern society, from everyday communication to systems that control and manage our nation's financial, energy, and defense systems. The integrity of cyber systems is critical for maintaining a functioning society, but our ability to provide robust and secure systems is increasingly uncertain. The focus of our work was on detecting the actions of intruders once they are already inside cyber networks. This distinguishes our approach from the majority of the literature that deals with detecting intrusions into the perimeter of a network as they occur. Large networks will always have some vulnerability somewhere at some point in time. Our challenge is prevent that singular vulnerability from being leveraged in ways that result in lack of integrity of the entire cyber system or of large parts of the system.

Today's best intruders use a phishing e-mail or other explicitly allowed communication to get a computer inside a protected network to execute malicious software. From this beachhead, trust relationships, authorized connections, and stolen credentials are used to traverse internal networks. These techniques lie close to the theoretical limit of detection and require much more sophisticated detection techniques. We characterize this new detection regime as *whole-network* detection rather than *individual-host* detection (Figure 1). To avoid colliding terminology, we use the math and computer science terminology of *graphs* to refer to abstract networks (including computer communication networks).

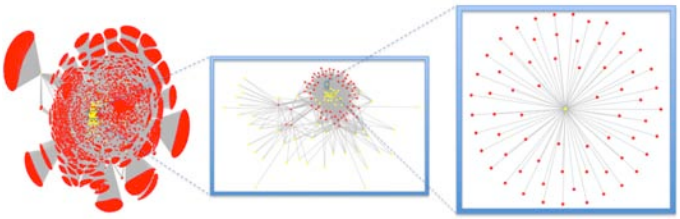

Figure 1. We will move cyber detection from local features (right) to regional (center) and global (left) properties that capture more subtle attacks.

Viral attacks are the most nefarious since they either be extremely fast spreading or they can spread slowly with low observability at any given network cross-section (most classic detection algorithms focus on specific cross-sections such as firewall perimeters.). The viral nature of this threat implies that there will be patterns of activity across multiple nodes in the graph. The scope of this 1-year project was to develop methods for identifying viral anomalies in graphs.

Our approach was based on a data-driven cycle of increasing understanding, modeling, discovery of data that does not fit the models, and updating models or, in the case of anomaly detection, presenting those anomalies themselves as results. We also sought to establish a new inter-disciplinary team to execute this approach.

Scientific Approach and Accomplishments
Despite the short project duration and a small team, we had a number of notable achievements:

- Two invited talks at the annual Joint Statistical Meeting (JSM) [4,5]
- Poster submission (under review) to ACSAC 2010 [3]
- Three program development talks with potential PADGS customers (STRATCOM, 24th Air Force, NSA) as well as results featured in discussions with a DARPA Program Manager.
- Established a new team that spans 5 groups and disciplines, including recruiting one faculty member from UNM to become a Scientist in CCS-6 and one new PhD student from UNM Computer Science.
- Hosted open seminars from Terran Lane (UNM), Genevieve Bartlett (USC), Curt Storlie (UNM), and David Marchette (Navy).
- Superset of the team successfully competed for a full DR project starting in FY11.

Our technical results were in three major areas: data pre-processing, malware methods, and graph detection. Data pre-processing refers to the manipulation of observed data to facilitate analysis. Malware methods are methods to understand and detect malicious software and its movement in the network. Graph detection involves the use of statistical methods to detect anomalies arising from processes based in a graph.

Data Pre-Processing
Data collected from a computer network can be very complex, and interdependency abounds. One difficult task is to partition the data into subsets that look similar to each other, so that a clearer picture of normal behavior can be discerned. For example, web traffic can be partitioned out of the data and a separate analysis can be performed on this data. To this end, we have developed several tools to process the network data at high speed. These tools include:

1. Raw tools which translate the data into a portable binary format, which can be parsed rapidly on a parallel machine.
2. Parallel tools, which process and filter the output of the binary log data to a greatly reduced dataset that is amenable to further analysis or visualization.
3. Analysis tools, that analyze the web server logs to determine various characteristics of web clients.

Malware methods
Malware detection is an important part of an overall anomaly detection effort. Malware running on a machine indicates not only that machine is infected, but that its neighbors could possibly be compromised. Understanding the dynamics of malware in realistic networks is an important facet of our work. To this end, we have produced an LA-UR report studying the propagation of malware in a real-world social network [2,9].

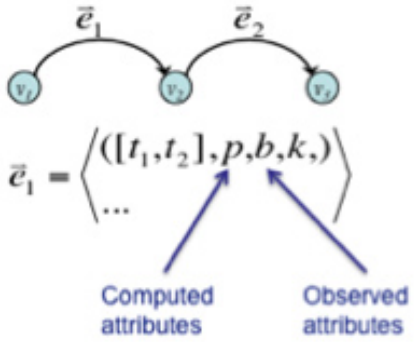

Figure 2. Our temporal graph construction

Graph detection
We have made progress in several aspects of graph anomaly detection:

Temporal Graphs

We have developed a construction for temporal graphs. Cyber datasets frequently result in multi-graphs where there is more than one edge between a pair of nodes. Unfortunately, many graph algorithms are designed and studied for simpler graphs that do not have redundant edges. We therefore use a construction shown in Figure 2 where redundant edges are expressed as a vector of attributes on a single edge. Because we are often interested in temporal aspects of graphs, every vector element of every edge has start-time and end-time attributes. Other attributes measured by sensors (such as size, network protocol information, etc) or computed (such as edge probability) are also included [3]. With this construction, basic, static graph structure can be directly analyzed while also preserving enough information to allow us to drill-down into the dynamics to create partitions or sub-graphs.

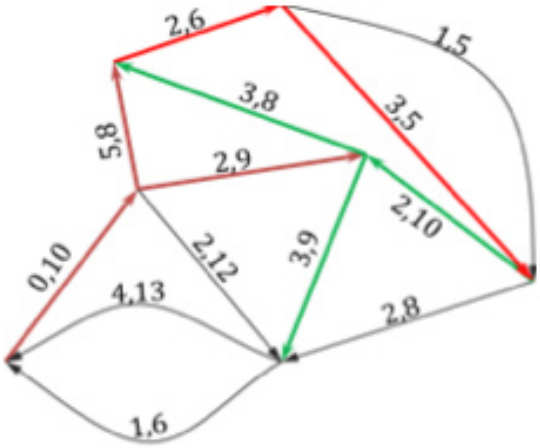

Figure 3. Decomposition of a multigraph into graphlets. Edges of the same color belong to the same graphlet. Black thin lines denote single-edge graphlets.

Time-Constrained Subgraphs

We have defined several types of *paths* in a temporal graph that correspond to types of malicious activity. A *telescoping path* is a multi-hop interactive session (for example, SSHing from one host to another and to another). We define such a path as a sequence of edges where the time interval of each edge (its start and end times) is encompassed by the time interval of its predecessor edge. A second type of path is the *precursor path* where the start time of each edge must occur after the start time of its predecessor. Note that paths are directed graphs and need not be linear. Enumerating paths partitions edges of a graph into zero or more sub-graphs (and a remainder of non-path edges). Figure 3 shows a graph that has been partitioned into three telescoping subgraphs with the remaining edges not part of any multi-edge path [1].

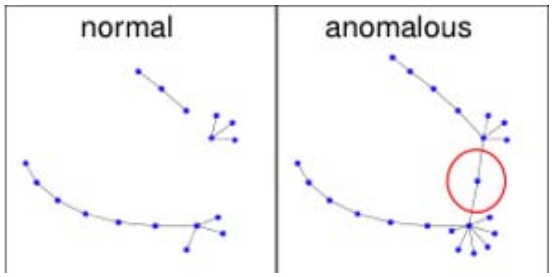

Figure 4. The addition of a few edges changes global properties (number of connected components changes from 3 to 1) and paths (maximum path length doubles).

Anomalous Rate Subgraphs

We have produced a method for scanning a graph over time and identifying anomalous *paths* in the graph. Models are built to reflect normal behavior over time, and then paths are enumerated and compared with the model to determine anomalous paths in the graph (Figure 5)[4].

Graph and Subgraph Structural Features

The shape and diameter of path subgraphs capture the invariants of certain kinds of attacks where an intruder compromises a single host and then jumps from host to host through authenticated, trusted connections to explore the network and discover high-value information. In contrast, legitimate users typically visit (login to) a single host or reach a target host after one or two hops. An intruder's search through a network is also prone to *fumbling* (a term coined by Michael Collins) – the fact that the intruder lacks perfect targeting knowledge and is prone to small numbers of failed or anomalous attempts (in contrast to automated *scanning* which causes very large numbers of failed attempts).

We examined graphs for global features that are normally stationary or cylcostationary, but that are sensitive to this kind of behavior. For example, we have shown that the addition of a single edge can and does change global properties such as the number of connected components as well as path-length properties (Figure 4) [6]. We also identified attributes of graphs that can be used to classify activity by individual user purely through statistical features [8].

Time-Series Anomalies. Given candidate graphs or subgraphs and features over those graphs in time, we then apply novel detection algorithms. These methods are similar to those used to identify anomalous-rate subgraphs. They are multi-faceted models that capture on/off bursts and diurnal and weekly patterns of univariate and multivariate time-series and provide a probabilistic measure of how likely observed values are [5,4,7].

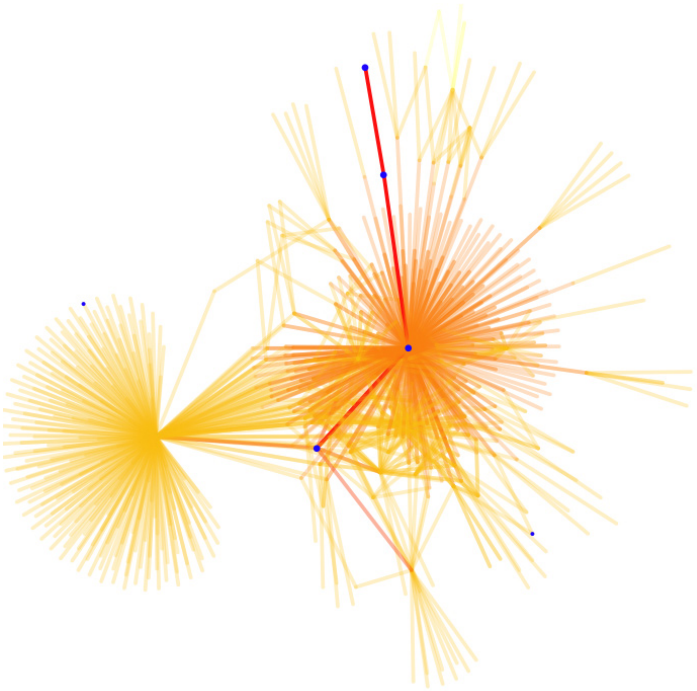

Figure 5. A heat map showing the detection of an anomalous path in red. The heat increases as we approach this path.

Impact on National Missions

The immediate impacts of this 1-year project have been modest thus far, but have influenced other activities and are likely to have longer-term impacts. This project will positively impact cyber security missions executed by both LANL's internal security program and Global Security programs with secondary benefits on our commercial CRADAs. Our advances have gotten us closer to contemporary, undetectable adversaries, and have built a base for the future. More broadly, we have engaged a new IS&T community around graph analysis and data-intensive computing. There will be secondary impact on other sensing, situational awareness, and detection problems that can be represented as networks such as space events, biological networks, and semantic networks. Finally the data-intensive demands of this problem will lead to experience, insight, and tools for scalable data management and analysis for all domains from physics simulations to astronomical

data analysis and bioinformatics.

References

1. Sandine, G., A. Brugh, M. Fisk, A. Hagberg, J. Neil, and M. Warren. Making protocol graphs from NetFlow records. 2010. *LA-UR 10-06098.*

2. Yan, G., G. Chen, S. Eidenbenz, and N. Li. Towards a deep understanding of malware propagation in online social networks. 2010. *LA-UR 09-08100.*

3. Djidjev, H., and G. Sandine. Graph-based network traffic analysis for intrusion detection. 2010. *LA-UR 10-06320.*

4. Neil, J., C. Storlie, C. Hash, and A. Brugh. GraphScan: scan statistics for the detection of anomalous paths in a graph. 2010. *2010 Joint Statistical Meetings, Vancouver, B.C. Canada. Invited presentation. LA-UR 10-05147 .*

5. Wiel, S. Vander, C. Storlie, M. Fisk, H. Djidjev, and G. Sandine. Graph anomalies in cyber communication. 2010. *2010 Joint Statistical Meetings, Vancouver, B.C. Canada. Invited presentation. LA-UR-10-05146..*

6. Sandine, G., A. Hagberg, J. Neil, and S. Vander Wiel. Protocol graph anomaly detection: global graph invariants and graph metrics. 2010. *LA-UR 10-00756.*

7. Sandine, G., A. Hagberg, J. Neil, C. Storlie, and S. Vander Wiel. Relative entropy for anomaly detection in computer networks. 2010. *LA-UR 10-06099.*

8. Tan, K., G. Yan, J. Yeo, and D. Kotz. Privacy analysis of user association logs in a large-scale wireless LAN. 2010. *LA-UR 10-05378.*

9. Yan, G., S. Chen, and S. Eidenbenz. RatBot: anti-enumeration peer-to-peer botnets. 2010. *LA-UR 10-03929.*

Publications

Djidjev, H., and G. Sandine. Graph-based network traffic analysis for intrusion detection. 2010. *LA-UR 10-06320.*

Neil, J., C. Storlie, C. Hash, and A. Brugh. GraphScan: scan statistics for the detection of anomalous paths in a graph. 2010. *2010 Joint Statistical Meetings, Vancouver, B.C. Canada. Invited presentation. LA-UR 10-05147 .*

Sandine, G., A. Brugh, M. Fisk, A. Hagberg, J. Neil, and M. Warren. Making protocol graphs from NetFlow records. 2010. *LA-UR 10-06098.*

Sandine, G., A. Hagberg, J. Neil, C. Storlie, and S. Vander Wiel. Relative entropy for anomaly detection in computer networks. 2010. *LA-UR 10-06099.*

Sandine, G., A. Hagberg, J. Neil, and S. Vander Wiel. Protocol graph anomaly detection: global graph invariants and graph metrics. 2010. *LA-UR 10-00756.*

Tan, K., G. Yan, J. Yeo, and D. Kotz. Privacy analysis of user association logs in a large-scale wireless LAN. 2010. *LA-UR 10-05378.*

Wiel, S. Vander, C. Storlie, M. Fisk, H. Djidjev, and G. Sandine. Graph anomalies in cyber communication. 2010. *2010 Joint Statistical Meetings, Vancouver, B.C. Canada. Invited presentation. LA-UR-10-05146..*

Yan, G., G. Chen, S. Eidenbenz, and N. Li. Towards a deep understanding of malware propagation in online social networks. 2010. *LA-UR 09-08100.*

Yan, G., S. Chen, and S. Eidenbenz. RatBot: anti-enumeration peer-to-peer botnets. 2010. *LA-UR 10-03929.*

A Systematic Single Cell Genomics Approach to Studying the Dominant Unculturable Microbiota of Important Environmental Communities

Shunsheng Han
20100541ER

Abstract
Microbes survive in everywhere and all conditions on the earth. They impact on our lives from inside of our body to outside environments. Most of the microbes cannot be grown in standard lab conditions. We developed single cell genomics capability at LANL to get genomic information from single cell. The one-year LDRD support was used to improve our single cell technology in two aspects. One is to prove the feasibility of artificial polyploidy on bacterial cells and the other is to improve the whole genome amplification process. We made significant progress in both fronts: artificial polyploidy has been verified improving sequencing results, and whole genome amplification efficiency is related with GC content of a genome.

Background and Research Objectives
The major challenge in studying environmental bacteria is that most bacterial species cannot be grown under standard laboratory conditions, making their study extremely difficult to impossible. Metagenomics is a new scientific discipline that has appeared in the last several years and involves the sequencing of many organisms at the same time, typically within defined communities such as the human microbiome[1]. As a scientific field, metagenomics attempts to resolve four questions:

- who is there?
- in what proportions?
- what they are doing?
- how will they react or contribute to environmental change, such as global warming?

Many technological tools must still be developed to answer these questions. Currently, random shotgun sequencing and 16S sequencing surveys have been used to elucidate answers for a number of simple systems. However these technologies can only provide a limited glance into which kinds of bacteria are present for more complex environments due to the sheer number of organisms present in a community (e.g. an estimated million species within a single gram of soil)[2]. A greater challenge remains to obtain information at the genomic level that provides a more complete sequencing profile and enables a more detailed analysis of microbial interactions within their environment. The major reason is that the assembly of complete genomes from the direct sequencing of complex microbial communities is not yet possible.

Whole genome amplification from single cells (also known as Single Cell Genomics) is a novel approach that is beginning to become used to resolve genomic sequence information without the need to culture cells[3]. However, SCG is hard because we are getting DNA from a single cell - we need to remove amplification bias and generate overlapping fragments to close sequence gaps. We made progress in the following area to improve this state-of-the-art technology:

- Increasing the cellular content of DNA by preventing cell division within single cells.
- Improving the whole genome amplification process to reduce the bias observed with typical amplification strategies.

Combined, these improvements will increase the genome coverage of single cell genomics. A manuscript for the second portion of the project is in preparation and the first method has been demonstrated feasible and need further development for higher efficiency and consistency. The two aspects of the work will be summarized below:

Scientific Approach and Accomplishments
Increasing the cellular content of DNA by preventing cell division
Single Cell Genomics was proposed by Roger S Lasken[4]. DNA from individual cells can be amplified for use as templates in genomic sequencing. The multiple displacement amplification (MDA) can generate micrograms of DNA starting with templates of the several femtograms present in a typical bacterium. MDA is based on isothermal (30 °C) strand displacement DNA synthesis

in which the highly processive ϕ29 DNA polymerase repeatedly extends random primers on the template as it concurrently displaces previously synthesized copies and to expose single strand DNA as new templates. The ability to sequence from single cells using the amplified DNA was demonstrated by Raghunathan et al[3]. with flow sorted Eschericia coli, Myxococcus xanthus, and B. subtilis. Whole genome sequencing with amplified DNA from single cell has been attempted on sequenced genomes Escherichia coli and Prochlorococcus and de novo sequence of unculturable bacteria such as TM7, flavobacteria, and Prochlorococcus[5-7]. The fundamental problem of SCG as presently carried out lies in the fact that only a single copy of genomic DNA serves as the template. Consequently, when that piece of DNA is fragmented (as happens when obtaining the genome from a single cell), all linking information is lost. When coupled with amplification and sequencing bias, this results in incomplete genome coverage that cannot be overcome without addressing the core problem: a single genomic template.

We have demonstrated that artificial polyploidy, when used for SCG, produces better genome coverage with fewer gaps (Figure 1). Artificial polyploidy was achieved by blocking cell division while chromosomes continued to replicate. In our study, we used a chemical reagent to block cell division of *E. coli* and *B. subtilis*. Sequencing of treated *E. coli* single cells results in 95% genome coverage comparing to 75% coverage from an untreated control. These results confirm the proposed approach will significantly improve the performance of single cell genomics. In several following up study, results from this approach varied, likely due to the packaging of DNA after the chemical treatment or the chemical reagent itself. We are working to pinpoint the issue and stabilize the performance of the method.

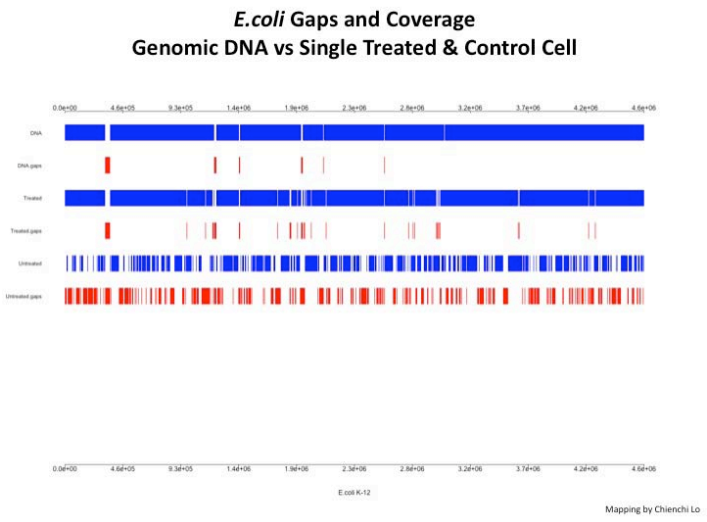

Figure 1. Better sequence coverage from treated single cell. E. coli genome were sequenced with purified DNA directly (top), DNA amplified from single cell treated with chemical to block cell division (middle) and DNA from untreated cell. Blue bar indicated covered region and red bar indicated gaps.

Improving the whole genome amplification process to reduce the bias

Whole genome amplification via Multiple Displacement Amplification (MDA) allows for non-specific amplification of even very small amounts of DNA template. As many molecular techniques require a relatively large amount of DNA, MDA provides a powerful means to allow for a variety of molecular analyses that would not be possible otherwise. While many studies have looked for biases in amplification of DNA, none have closely examined these biases when starting with a community of microorganisms. We explored the impact of GC bias on the representation of an artificial microbial community following MDA and a potential solution of varying the GC content of priming DNA.

MDA has made possible the analysis of very small amounts of DNA including clinical samples and single cells. This results from the ability of the enzyme phi29 to displace double stranded DNA and its extreme processivity. MDA has proved vastly superior to its predecessor whole genome amplification techniques in terms of reduced bias and yield of product. While MDA exhibits reduced bias it still does not result in even coverage of the genome and this becomes increasingly problematic with smaller amounts of starting material. The known biases involve reduced coverage at centromeres and telomeres, preference for plasmid DNA, GC bias, and random high and low levels of coverage due to stochastic early priming and amplification. Interestingly the issue of GC bias continues to be debated as some authors have not found a relationship between GC content and coverage. However, amplification bias due to GC content has not been examined at all when in comes to mixed communities. In fact, GC bias in MDA may be compounded in this scenario due to extensive regions of elevated or reduced GC content compared with relatively low GC variation across DNA from a single organism. Bias in this context is particularly problematic as conclusions in microbial ecology, whether in soil or the human gut, are often based on changes in quantity of taxon-specific DNA. While MDA has not been used on a large scale for transcriptomics studies, significant bias in amplification of cDNA may also present a challenge for analysis.

To test whether MDA evenly amplifies DNA from a mixed bacterial community we created an artificial community composed of DNA from *Anaeromycobacter dehalogenans, Clostridium botulinum* and *Pectobacterium carotovorum*. Averaged across their whole genomes they have 75% GC content, 28% GC content, and 50% GC content respectively. We amplified this mixed community and then tested whether different genomes were amplified to different degrees using qPCR. We also explored a range of GC content for the priming DNA ranging from 20%-80% GC in an effort to lessen the expected bias against the low and high GC genomes.

Total DNA yield following MDA for the different hexamer

conditions is shown in Figure 2. Here we see that amplification efficiency was very low using low GC hexamers (20-40%) and increased dramatically by an order of magnitude at 50%, which is the assumed proportion in commercial kits. Yield was maximized using 70% GC hexamers while decreasing slightly with 80% GC hexamers although not significantly.

The three genomes were amplified at very different rates. Figure 3 shows the dramatic difference in amplification of the three genomes. *P. carotovorum*, had an average amplification of 525x with maximum amplification of 4572x. *C. botulinum*, the low GC genome showed an average amplification of only 12x with a maximum of 122x. *A. dehalogenans*, the high GC genome, amplified an average of 25x with a maximum of 273x**.** *P. carotovorum* peaks in average yield at 70%, *A. dehalogenans* peaks at 80%, and *C. botulinum* peaks at 50%. This trend mirrors the GC content of their genomes.

Our results indicate that the GC content of template DNA and hexamers can have a significant impact on total yield and the relative yield of the component genomes in a community. Total yield was shown to be significantly increased using high GC content hexamers and significantly decreased using low GC hexamers. We believe that low GC content hexamers cannot efficiently prime the MDA reaction due to their decreased ability to bond to complementary DNA. As this bonding becomes tighter it will more efficiently prime the reaction and thus yield is increased. It is maximized at 70% GC. Yield begins to decrease at 80% GC hexamers presumably because they begin to bond too tightly to one another and thus become less efficient at priming the MDA reaction. Yield may also decrease using very high GC hexamers because the mid-GC genome, which was always the largest proportion of post MDA DNA, has fewer complementary sites available for bonding.

We found that moderate GC genomes exhibit extreme overamplification relative to high and low GC genomes. They show thousands fold amplification in many samples whereas the other genomes generally show one to two orders of magnitude less amplification. Presumably, the high GC genome is not denatured as well as the mid GC genome and therefore is not well amplified. Its yield does increase with GC content of hexamers reaching its optimum at 80% GC. The low GC genome is amplified poorly with low GC hexamers as well as high because no genome is well amplified using low GC hexamers and as GC content is increased there become fewer binding sites available for the hexamers on the genome. Our results may make ecological inference following MDA of a mixed community extremely difficult and should be used with great care.

As stated in the introduction GC bias has been somewhat controversial in the MDA literature: sometimes it is found, other times not. We believe this likely reflects the different tests researchers have used and the probable mechanism of GC bias. If GC bias is mostly a result of priming bias, then looking over very small windows will not show significant bias. In this case one would have to look over very large regions to see the bias because MDA amplicons

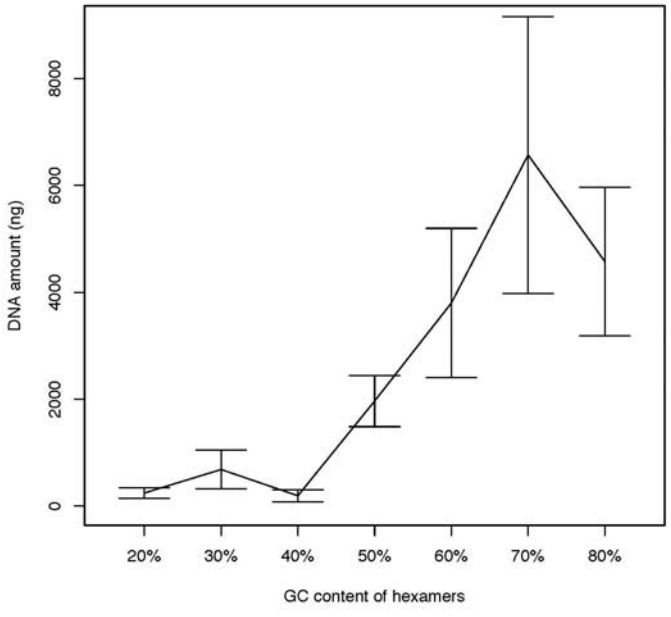

Figure 2. Effect of varying the GC content of hexamers on total DNA yield GC content of reaction priming hexamers were varied and total DNA yield was quantified using a fluorescence based assay. Error bars represent 95% CI.

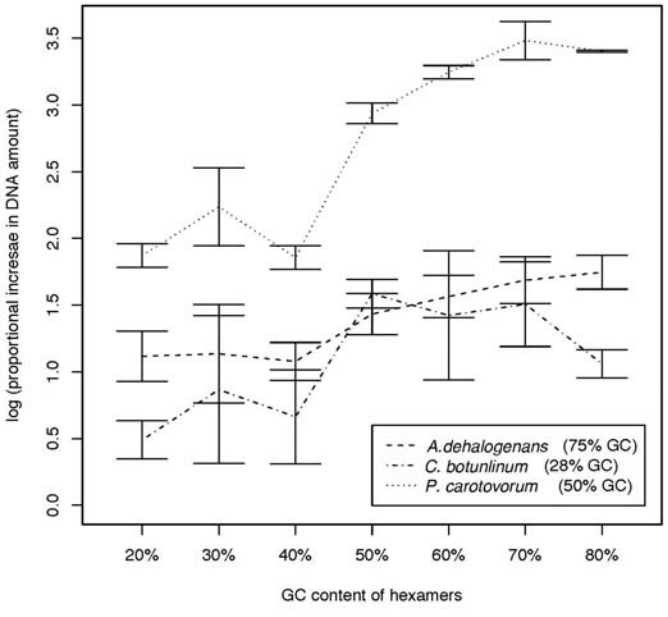

Figure 3. Effect of varying the GC content of hexamers on the yield of the three target genomes GC content of reaction priming hexamers were varied and DNA yield for individual genomes were calculated via qPCR and species specific primers. Error bars represent 95% CI.

are generally greater than 70 kbp in length and may extend into regions with very different GC content than the region that actually initiated the bias. If GC bias is the result of difficulty in strand displacement or polymerization through variant GC regions then looking over relatively small regions should show bias. Since the researchers that have found bias have looked across either the whole genome or very large section of DNA for a relationship between GC content and amplification and the study that found no relationship looked at very tight windows of 100bp, the evidence seems to point to differential priming or early amplification as the main cause of amplification bias. Our study supports this hypothesis as we looked at the overall effect of amplification bias starting with large discontinuous swaths of divergent GC content. Our bias is much higher than that reported previously, but no one has looked at GC bias before following MDA of a mixed community and is probably related to the fact that our regions of divergent GC content are not continuous. The only other paper that did investigate MDA of a mixed community showed strong preferential amplification of certain species. In our own analysis of these data we found that the genome closest to 50% GC is amplified much more than either the high or low GC genomes and therefore support our own findings.

In conclusion, we have shown a strong bias of MDA towards mid GC content genomes. Low and high GC genomes are difficult to amplify, but probably for different reasons. The low GC genome is difficult to amplify likely because the most complementary hexamers, those with low GC content, do not prime the reaction efficiently. The high GC genome is difficult to amplify likely because it does not denature easily and is thus difficult to prime. Across the board there is a beneficial effect of using high GC hexamers, especially 70%. Our results will improve yield in MDA and add a cautionary note to using MDA on environmental samples when one is interested in preserving information on abundance.

Impact on National Missions

The technology developed here will improve the efficiency of single cell genomics, which has been applied in many front of biology research, such as public health, biosurveillance, and climate change. This technology will provide tool to generate comprehensive genomic information from many different environments so that further biological function and impact can be studied.

References

1. Handelsman, J. (2004) Metagenomics: application of genomics to uncultured microorganisms. *Microbiol Mol Biol Rev*, **68**, 669-685.

2. Tringe, S.G., von Mering, C., Kobayashi, A., Salamov, A.A., Chen, K., Chang, H.W., Podar, M., Short, J.M., Mathur, E.J., Detter, J.C. *et al.* (2005) Comparative metagenomics of microbial communities. *Science (New York, N.Y*, **308**, 554-557.

3. Raghunathan, A., Ferguson, H.R., Jr., Bornarth, C.J., Song, W., Driscoll, M. and Lasken, R.S. (2005) Genomic DNA amplification from a single bacterium. *Applied and environmental microbiology*, **71**, 3342-3347.

4. Dean, F.B., Nelson, J.R., Giesler, T.L. and Lasken, R.S. (2001) Rapid amplification of plasmid and phage DNA using Phi 29 DNA polymerase and multiply-primed rolling circle amplification. *Genome research*, **11**, 1095-1099.

5. Marcy, Y., Ouverney, C., Bik, E.M., Losekann, T., Ivanova, N., Martin, H.G., Szeto, E., Platt, D., Hugenholtz, P., Relman, D.A. *et al.* (2007) Dissecting biological "dark matter" with single-cell genetic analysis of rare and uncultivated TM7 microbes from the human mouth. *Proceedings of the National Academy of Sciences of the United States of America*, **104**, 11889-11894.

6. Woyke, T., Xie, G., Copeland, A., Gonzalez, J.M., Han, C., Kiss, H., Saw, J.H., Senin, P., Yang, C., Chatterji, S. *et al.* (2009) Assembling the marine metagenome, one cell at a time. *PLoS ONE*, **4**, e5299.

7. Zhang, K., Martiny, A.C., Reppas, N.B., Barry, K.W., Malek, J., Chisholm, S.W. and Church, G.M. (2006) Sequencing genomes from single cells by polymerase cloning. *Nature biotechnology*, **24**, 680-686.

Publications

Fitzsimons MS, Daughton AR, Snook JP, Daligault HE, Zhang X, Dichosa AEK, and Han CS. Strong bias in Multiple Displacement Amplification of microbial communities. Biotechnique. (Submitted)

Multi-scale Analysis of Multi-physical Transport Processes of Electroosmosis in Porous Media

Qinjun Kang
20080727PRD2

Introduction

Electrokinetic phenomena, such as electrophoresis and electroosmosis, were discovered nearly 200 years ago, and have had a wide range of applications in many fields since then. However, simulation and analysis of these phenomena is a great challenge because of the multi-physics nature of the problem. This problem will be further complicated if chemical reactions occur in the bulk fluid or at the fluid-solid interface. The primary objective of this project is to develop a comprehensive numerical framework to investigate electrokinetic flow coupled with reactive transport in porous media. We are approaching this problem in three stages by:

1. Developing an innovative model for coupled electrokinetic flow and reactive transport in porous media, accounting for multi-physical transport processes, including fluid flow, electric potential distribution, ion convection and diffusion, as well as chemical reaction.

2. Performing nano to micro upscaling analysis of these multi-physical transport processes.

3. Validating the numerical model through theoretical analysis and available experimental data.

The successful accomplishment of the proposed research will provide:

- An improved understanding of the multi-physical electrokinetic transport phenomena coupled with chemical reaction in micro/nanofluidic devices.

- Innovative techniques to bridge atomistic modeling based on first principals with mesoscale modeling based on statistical-analysis.

- A better understanding of the effect of nanoscale structures on the microscale devices.

This research will have direct implications in a broad spectrum of research highly relevant to LANL missions, including new energy exploitation (fuel cells and biofuels), fossil energy prospecting (oil and gas), environmental protection (decontamination of radionuclides in solids), biological applications (enzymatic analysis, DNA analysis, and proteomics), and biomedical applications (clinical pathology and bio-smoke alarm).

Benefit to National Security Missions

This project will support the DOE/NNSA missions in Energy Security, Environmental Quality, and the missions of the Office of Science by enhancing our understanding of multi-physical (hydro-, thermo-, and electro-dynamic) transport processes of electroosmosis in natural porous media.

Progress

In the past year, significant progress has been made in the following areas:

Nonlinear effective properties of unsaturated porous media

As well known, the effective properties of multiphase materials, such as the thermal conductivity and electric permittivity, depend on not only the properties and the volume fraction of each inclusion, but also the geometrical microstructures and the phase interaction effects between the components. No analytical models have been found that deal successfully with effective properties of multiphase materials with random geometrical microstructures and phase interactions up to now.

In this work, we investigated the nonlinear responses of effective properties of unsaturated porous materials using a numerical framework. The multiphase microstructure is reconstructed through a random generation-growth method, and the transport governing equations are solved efficiently by a lattice Boltzmann model. After validated by the experimental data, the present framework is used to study the nonlinear behavior of thermal conductivity and electrical permittivity caused by the saturation degree and the phase interaction for multiphase materials. The results show that the effective thermal conductivity of

unsaturated porous materials increase and then decrease with the phase interaction ratio (Figure 1), while the effective permittivity decrease monotonously with the phase interaction. Mechanism analyses indicate that these nonlinear behavior lies in the role of the liquid phase in the transport. For the thermal conductivity, the liquid phase plays a "bridge" role because its conductivity is between those of the solid and the gas. A better bridge network would enhance the overall effective thermal conductivity. However for the electrical permittivity, the liquid phase plays the leading actor of transport. A better liquid phase connection will lead to a higher effective electrical permittivity of the multiphase system.

This work has been published in the International Journal of Nonlinear Science and Numerical Simulations (Impact Factor is 8.479).

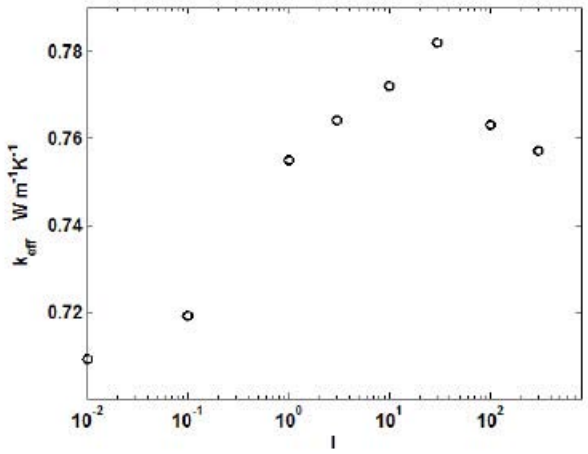

Figure 1. Effective thermal conductivity as a function of phase interaction ratio

Electroosmosis of dilute electrolyte solutions in silica microporous media

Electro-osmosis in porous media has been studied for nearly two hundred years because of its importance in geophysical systems, and this phenomenon is also critical to electrokinetic decontamination of soils and long-term geological storage of nuclear wastes. Although there have been several theoretical studies on electro-osmotic phenomena in porous media, it is still a big challenge to predict the physicochemical transport behavior accurately and efficiently, especially in complex microporous media.

In this work, the physicochemical transport due to electro-osmosis of dilute electrolyte solutions (<1×10-3 mol/L) through microporous media with granular random microstructures has been modeled by our three-step numerical framework. First, the three-dimensional microstructures of porous media are reproduced by a random generation-growth method. Second, the effects of chemical adsorption and electrical dissociation at the solid-liquid interfaces are modeled to determine the electrical boundary conditions, which vary with the ionic concentration, pH, and temperature. Finally the nonlinear governing equations for electrokinetic transport are solved using a highly efficient lattice Poisson-Boltzmann algorithm. The simulation results indicate that the electro-osmotic permeability through the granular microporous media increases monotonically with the porosity (Figure 2), ionic concentration, pH, and temperature. When the surface electric potential is higher than about -50 mV, the electro-osmotic permeability exponentially increases with the electric potential. The electro-osmotic permeability increases with the bulk ionic concentration even though the surface zeta potential decreases correspondingly, which deviates from the conclusions based on the thin layer model. The electro-osmotic permeability increases exponentially with pH, and linearly with temperature. The present modeling results improve our understanding of hydrodynamic and electrokinetic transport in geophysical systems, and help guide the design of porous electrodes in micro-energy systems.

This work has been published in Journal of Geophysical Research--Solid Earth.

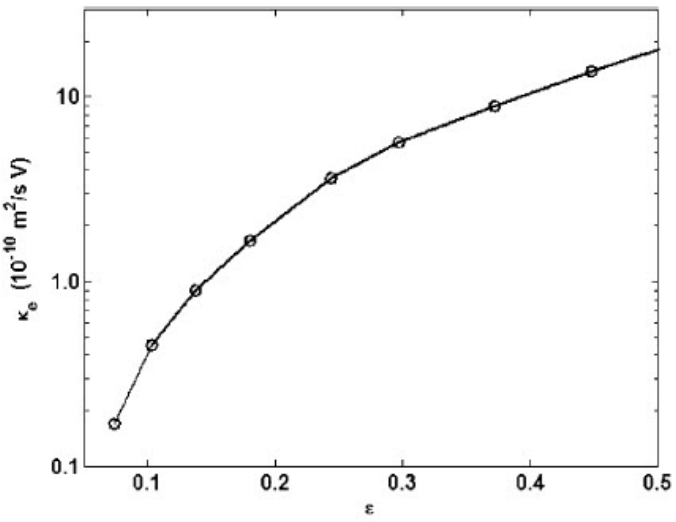

Figure 2. Electroosmotic permeability as a function of porosity at bulk concentration 1 × 10−5 mol/L and electric potential −50 mV.

Electrochemomechanical energy conversion efficiency in nanofluidic channels

When an electrolyte solution flows in a channel, the channel wall surfaces will be charged because of the physical and chemical interactions between ions and surfaces. A pressure-driven flow through a narrow channel therefore carries a net electrical charge with it, inducing both a current and a potential. These so-called streaming currents and streaming potentials can drive an external load and therefore represent a means of converting hydrostatic energy into electrical power (Figure 3). Such an electrokinetic effect in energy conversion devices has received much attention in the context of microfluidic and nanofluidic devices because of its potential attractive

conversion efficiency and clean process of power generation1. High energy-conversion efficiency and high output power are the requirements for such a device to be practical. Physical modeling of electrokinetic energy conversion is needed to guide the design and optimization of these properties.

Our work on this point is focusing on:

- Analyze the multiphysicochemical transport mechanisms in the microfludic and nanofluidic energy conversion using theoretical and numerical tools.
- Predict the energy conversion efficiency and identify the key factors that limit the efficiency.
- Propose new design and optimization schemes to improve the energy conversion efficiency.

This work has been published in Microfluidics and Nanofluidics.

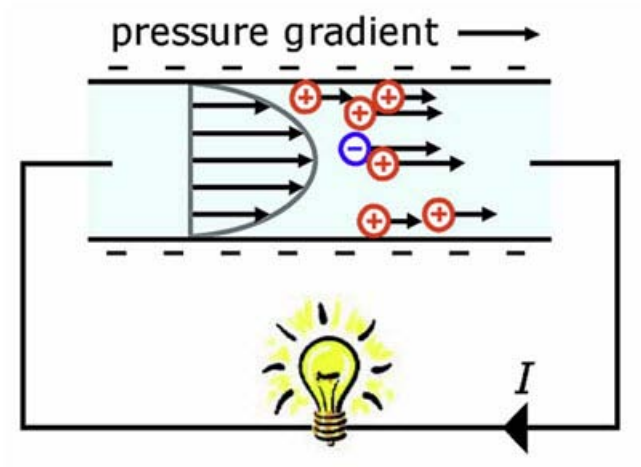

Figure 3. Schematic of electrochemomechanical energy conversion in a nanofluidic channel

Future Work

Electroosmosis is the motion of polar liquid through a porous material or a biological membrane under the influence of an applied electric field. Since its discovery, this phenomenon has had a wide range of applications in many fields. Therefore, a better understanding of multi-physical (hydro-, thermo-, and electro-dynamic) transport processes of electroosmosis in porous media is critical to a wide range of fields. However, this problem is notoriously difficult and none of the existing (macroscopic, mesoscopic, or microscopic) methods can individually solve this multi-scale multi-physical transport phenomena accurately with present-day computers. Therefore it is critical to develop multi-scale modeling and analysis tools to capture the effects of microscale geometry on the macroscale multi-physical transport processes of electroosmosis in porous media.

This project will involve:

1. Developing innovative models for reproducing the multi-scale random microstructures of porous media through new numerical models to reflect the macroscale statistical information obtained from measurements.
2. Performing micro->meso->macro upscaling analysis of multi-physical transport processes of electroosmosis in the porous structures, including fluid flow, electric potential distribution, ion convection and diffusion.
3. Developing a novel hybrid model to integrate the models for different scales so that the important information at the small scale can be captured without resolving the small scale in the entire computational domain.

The successful accomplishment of the proposed research will provide:

- An improved understanding of multi-physical transport phenomena of electroosmosis through multi-scale structures of porous media.
- Innovative techniques to bridge atomistic modeling with mesoscale modeling based on statistical-analysis and continuum modeling.

This approach will have direct implications in a broad spectrum of energy and environmental research, including new energy exploitation (fuel cells and biofuels), fossil energy prospecting (oil and gas), environmental protection (decontamination of radionuclides in solids), biomedical engineering applications, and novel materials design.

Conclusion

This project will enable a science-based understanding of electroosmosis, a phenomenon discovered 200 years ago, and having had a wide range of applications in many fields since then. However, a better understanding of it is still lacking. In this project, an advanced numerical method will be developed and research results will be published in leading journals. This approach will have direct applications in a broad spectrum of energy and environmental research, including new energy exploitation (fuel cells and biofuels), fossil energy prospecting (oil and gas), environmental protection (decontamination of radionuclides in solids), biomedical engineering applications, and novel materials design.

Publications

Chen, Q., M. Wang, and Z. Guo. Field Synergy Principle for Energy Conservation and Applications. 2010. *Advances in Mechanical Engineering.* **2010**: 129313.

Kang, Q., M. Wang, P. Mukherjee, and P. Lichtner. Mesoscopic Modeling of Multi-Physicochemical

Transport Phenomena in Porous Media. 2010. *Advances in Mechanical Engineering.* **2010**: 142879.

Mukherjee, Partha P., M. Wang, Q. Kang, and P. C. Lichtner. Pore-Scale modeling of transport in charged porous media. Presented at *Computational Methods in Water Resources XVII International Conference.* (San Francisco, CA, 6-10, July 2008).

Wang, M.. The Physical Chemistry of Materials: Energy and Environmental Applications. 2010. *Materials Today.* **13** (3): 67.

Wang, M. R., C. C. Chang, and R. J. Yang. Electroviscous effects in nanofluidic channels. 2010. *Journal of Chemical Physics.* **132** (2).

Wang, M. R., Q. Chen, Q. J. Kang, N. Pan, and E. Ben-Naim. Nonlinear effective properties of unsaturated porous materials. 2010. *International Journal of Nonlinear Sciences and Numerical Simulation.* **11** (1): 49.

Wang, M. R., and Q. J. Kang. Electrokinetic Transport in Microchannels with Random Roughness. 2009. *Analytical Chemistry.* **81** (8): 2953.

Wang, M. R., and Q. J. Kang. Modeling electrokinetic flows in microchannels using coupled lattice Boltzmann methods. 2010. *Journal of Computational Physics.* **229** (3): 728.

Wang, M. R., and Q. J. Kang. Electrochemomechanical energy conversion efficiency in silica nanochannels. *Microfluidics and Nanofluidics.* **9** (2-3): 181.

Wang, M., Q. J. Kang, and N. Pan. Thermal conductivity enhancement of carbon fiber composites. 2009. *Applied Thermal Engineering.* **29** (2-3): 418.

Wang, M., Q. Kang, H. Viswanathan, and B. Robinson. Modeling of electro-osmosis of dilute electrolyte solutions in silica microporous media. To appear in *Journal of Geophysical Research.* **In Press**.

Wang, M., Q. Kang, and E. Ben-Naim. Modeling of electrokinetic transport in silica nanofluidic channels. 2010. *Analytica Chimica Acta.* **664** (2): 158.

Wang, M., Q. Kang, and H. Viswanathan. Electroosmosis of dilute electrolyte solutions in microporous media. Presented at *The 2nd ASME International Conference of Micro/Nanoscale Heat and Mass Transfer.* (Shanghai, China).

Carbon and Oxygen Isotopic Variability in Succulent Plants and Their Spines: A New Tool for Climate and Ecosystem Studies in Desert Regions

Claudia Mora
20090526PRD2

Introduction

This project will examine the environmental parameters (e.g., light, temperature, relative humidity) which control carbon and oxygen isotope variations in succulent plant water and newly grown stem and spine tissue. Growth experiments under controlled conditions will provide a quantitative understanding of how to interpret isotope variations preserved in spines grown in series along the stems of long-lived cactuses. These spines are retained for decades to centuries and potentially provide the highest resolution proxy record of past environmental variability in arid regions, which typically have few other climate proxies (e.g., tree rings, lake sediments) available for study. A new climate proxy for cacti would represent a breakthough in our ability to understand the sensitivity of arid regions to past climate change, and to better predict ecosystem changes in response to future climate change. Arid and semi-arid lands are still the "nether lands" of climate research understanding, despite representing almost 45% of global land area and some of the most sensitive and critical regions. We need new ways to quantify past, and therefore potential future, impacts of climate change on arid ecosystems. This project seeks to provide such a tool by allowing us to utilize stable isotope ratios in cactus spines as chemical records of past environments and climate change.

In other parts of the arid ecosystem, widespread tree mortality is observed. The relationship of tree mortality to climate, in particular to periods of extended drought, has been previously examined in carbon isotope and tree physiology studies. Those results cannot uniquely differentiate specific mechanisms which lead to life or death in a given individual. Oxygen isotope time series, in concert with carbon isotope studies, will provide additional constraints on the physiological response of trees which contribute to their survival or demise.

Benefit to National Security Missions

This project will support the DOE Office of Science mission in Biological and Environmental Research (BER) to understand relationships between climate change and Earth' ecosystems. The project will improved the scientific basis for assessing the potential impacts of climate change on arid ecosystems. More broadly, stable isotope signatures and methodologies are applicable to a number of problems in threat detection and attribution.

Progress

English's key accomplishments in the past year include the creation and operation of a new stable isotope preparation Laboratory at TA-51, the completion of an online discrimination and gas exchange experiment, determining the processing procedures and developing the capability to extract cellulose from tree rings for an isotopic mortality study of western US forest species, the analysis of over 1,200 carbon and oxygen isotope samples, a guest appearance as a biogeochemical expert on the National Geographic Channels television special "America Before Columbus", and co-mentoring eight undergraduate and post-baccalaureate students.

The Stable Isotope Preparation Laboratory (SIPL) at TA-51 was built in previously unused space and has now processed over 3,500 unique samples for isotopic and other analyses. The development of this lab and the accompanying IWD's and WPF's have improved the safety and efficiency of all chemistry operations at TA-51. The lab has the capability to process a wide range of sample types for isotopic analysis, including but not limited to whole wood, cactus spines, waters, sucrose, starch, cellulose. The lab has also become a classroom for high school, post-baccalaureate, and post-masters students working on a variety of projects at TA-51 who are interested in cutting edge ecological research. Using this lab, and the MAT253 mass spectrometer at TA-48, English has determined that cellulose extracted from whole wood in live and dead conifer trees from western US forests processed using the Jayme-Wise and modified Brendel methods yield consistently offset results that are indistinguishable from each other. These data are unique, and show that we can proceed to analyze stable carbon isotopes in whole wood and oxygen isotopes using the modified Brendel method, a safer and more efficient method. These experimental results bolstered

a collaborative research project with Alison Macalady and Tom Swetnam at the Tree Ring Laboratory, University of Arizona, examining the causes of drought induced mortality in Piñon/Juniper forests across the Southwestern US.

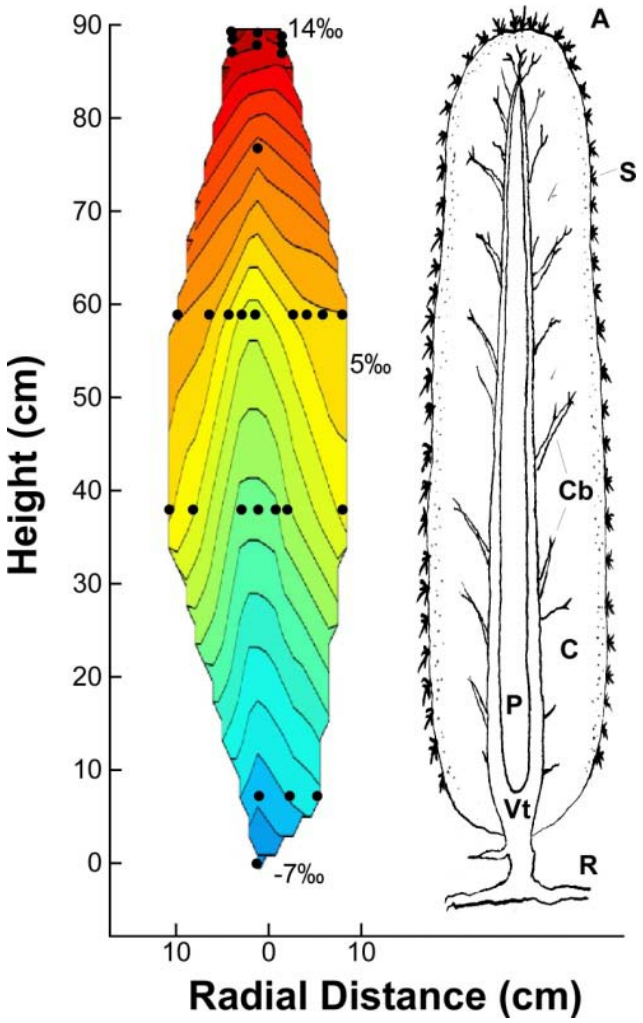

Figure 1. Contours of oxygen isotope ratios reflect the anatomy and physiology of a living saguaro cactus.

English examined the real-time isotopic characteristics of CO_2 gas exchange of cactus over diurnal cycles, in collaboration Drs. David G. Williams and Dustin Bronson, University of Wyoming. These experiments grew potted cactus collected in Tucson, AZ in the TA-51 greenhouse under controlled temperature conditions. Real time analyses were made using an infrared gas analyzer (for CO_2 abundance) and tunable diode laser trace gas analyzer. We found that three species of cactus exhibited similar patterns of diurnal CO_2 uptake and discrimination, however, we were unable to find a morning or evening pulse associated with increased levels of C3 photosynthesis. The publication of these results will shed light on the photosynthetic mechanisms of plants with a Crassalacean Acid Metabolism and the isotopic impact of these processes on the isotopic record produced in the spines of cactus. Sanna Sevanto is now a collaborator on this project and will help to develop numerical, process based models of oxygen isotopic variation in cactus spines using data from natural and potted cactus. Figure 1 shows actual isotopic contours of $d^{18}O$ and the anatomy of a living saguaro cactus. A model of water potentials inside cacti is being developed from these data to reflect the $d^{18}O$ composition of water in the plant based on external (climate) and internal (physiology) processes.

In addition to his research on succulents, English has pursued a new avenue in his academic career – examining the carbon and oxygen isotopic signals that dying conifer trees leave in their tree rings. This research takes advantage previous research performed by Drs. Nate McDowell and Claudia Mora on tree ring carbon and oxygen isotopes, as well as the mass spectrometer capabilities operated by Dr. Mora at TA-48. English is presently examining the proximal causes of western US forest mortality and how this is expressed in a dying trees last rings. We now have $\delta^{13}C$ chronologies from over 20 trees in western US forests. Figure 2 shows the composited $\delta^{13}C$ chronologies from three dead (closed circles) and three living (open circles) Juniper trees at Los Alamos. These data suggest that these trees at this site may have been more water stressed than the live trees, and thus more susceptible to beetle infestation. These data will be presented at the 2010 American Geophysical Union meeting in December.

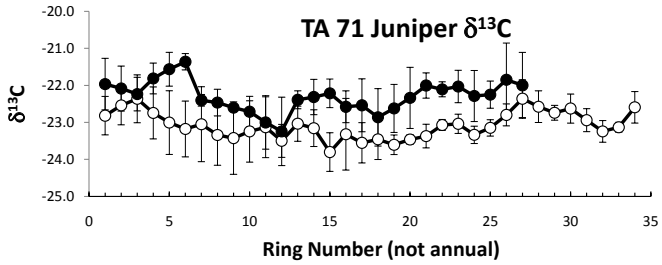

Figure 2. Stable carbon isotope chronologies from dead (closed circles) and living (open circles) juniper trees suggest that trees at this site which died may have been more water stressed than the live trees, and thus more susceptible to beetle infestation.

Finally, English continues to mentor numerous high school through post-bac students in ecological isotope research, an important part of his academic training. Students from the University of Wyoming, New Mexico Institute of Mining and Technology, and Los Alamos High School have honed their skills in framing and executing oxygen and carbon isotope studies of South American cacti, nitrogen isotope signatures in cactus spines, and developing techniques for sugar and starch extraction from woody materials for isotope analysis.

Future Work

Spiny succulent cactuses and euphorbs are vital to the functioning of arid and semi-arid ecosystems by providing

reliable sources of water, nutrients and energy in times of drought. These iconic plants and the ecosystems they inhabit are especially vulnerable to climate change, human and natural disturbance, and exist in regions with few other high resolution, centuries-long proxy records of climate. Stable carbon and oxygen isotopic variations in spines grown by long-lived cactus species record time-series evidence of changing climate and environment over a range of timescales (days to decades), however, little is known about the relative importance of different environmental parameters on these variations. A deeper understanding of which parameters control isotopic variability in cactus spines may provide a novel proxy for environmental variability in treeless, arid regions, and allow us to better predict how future climate change or human disturbance may affect these foundation species and their ecosystems. Using the results of our controlled growth and monitoring experiments, we will develop a model of water potential inside cacti as a precursor to developing a robust numeric model to:

- Reconstruct past environmental variables based on stable isotopes in cactus spines.
- Quantify the uncertainty associated with these reconstructions.

Conclusion

Arid and semi-arid lands are still the “nether lands” of climate research understanding, despite representing almost 45% of global land area and some of the most sensitive and critical regions. We need new ways to quantify past, and therefore potential future, impacts of climate change on arid ecosystems. This project seeks to provide such a tool by allowing us to utilize stable isotope ratios in cactus spines as chemical records of past environments and climate change.

Publications

Bronson, D. R., N. B. English, D. L. Dettman, and D. G. Williams. Paradoxical patterns of seasonal photosynthetic gas exchange and water-use efficiency in a constitutive CAM plant, the giant saguaro cactus (Carnegiea gigantea). . *Oecologia.*

English, N. B., D. L. Dettman, D. R. Sandquist, and D. G. Williams. An easy path from precipitation amount to d18O values in the spines of columnar cactuses, Carnegiea gigantea. Presented at *Geological Society of America Annual Meeting.* (Portland, OR, 18-21 Oct. 2009).

English, N. B., D. L. Dettman, S. Sevanto, D. R. Bronson, and D. G. Williams. An easy path from precipitation amount to d18O values in the spines of columnar cactuses, Carnegiea gigantea. . *Methods in Ecology and Evolution..*

English, N. B., N. McDowell, C. I. Mora, N. L. Stephenson, A. J. Das, and C. D. Allen. Investigating the underlying causes of tree mortality with carbon and oxygen isotopes in tree-rings. . Presented at *American Geophysical Union Annual Meeting.* . (San Francisco, 11-17 Dec. 2010).

English, N., D. Dettman, D. Sandquist, and D. Williams. Daily to decadal patterns of precipitation, humidity, and photosynthetic physiology recorded in the spines of the columnar cactus, Carnegiea gigantea. 2010. *JOURNAL OF GEOPHYSICAL RESEARCH-BIOGEOSCIENCES.* **115**: G02013.

English, N., D. Dettman, and D. Williams. A 26-year stable isotope record of humidity and El Nino-enhanced precipitation in the spines of saguaro cactus, Carnegiea gigantea. 2010. *PALAEOGEOGRAPHY PALAEOCLIMATOLOGY PALAEOECOLOGY.* **293** (1-2): 108.

Placzek, C., J. Quade, J. Betancourt, P. Jonathan. Patchett, J. Rech, C. Latorre, A. Matmon, C. Holmgren, and N. English. CLIMATE IN THE DRY CENTRAL ANDES OVER GEOLOGIC, MILLENNIAL, AND INTERANNUAL TIMESCALES. 2009. *Annals of the Missouri Botanical Garden.* **96** (3): 386.

Probing Molecular Physics of Biological Nano-channels: from Viruses to Biosensors

Benjamin H. Mcmahon
20090527PRD2

Introduction

Proper functioning of living cells requires selective molecular transport into and out of the cell, and between different cell compartments. Many such channels carry selective transport without an input of metabolic energy and without large scale structural transitions from a 'closed' to an 'open' state; the transport is based on diffusion only. Understanding the selective transport through such 'always open' channels is a fundamental biological problem, poses challenging physical questions and has potentially far-reaching technological applications. This project is specifically about transport through one particular channel of this kind, the Nuclear Pore Complex, which gates nucleo-cytoplasmic transport in all eukaryotic cells.

The project also studies another subject of high practical and fundamental interest: the mechanism of entry of viruses into to the cell nucleus. Survival of the virus depends on its ability to deliver its genetic material to the cell nucleus and replicate before the infected cell is destroyed by the immune system. This process is inherently stochastic, as it depends on the transport of a single protein-DNA complex into the nucleus and the computational modeling is crucial for further progress.

This project focuses on the development of conceptual models that capture only the essentials of what is known about the transport mechanism and its selectivity for the nuclear pore, and how these transport mechanisms can be used by viruses to infect the cells.

Benefit to National Security Missions

This project will support the DOE mission in Promoting Science by enhancing our understanding of basics biophysics involved in the nuclear-cytoplasmic particle exchange. The work also provides the foundational understanding of cell processes that enable development of strategies to combat both natural disease and bio-WMDs, as well as to understand how to probe eukaryotic biology in the general context of climate and environment. In this way, this work supports missions of Threat Reduction by understanding the mechanisms of host -- viral pathogens interactions. It also develops the connection between protein biophysics and materials science / physical chemistry, shedding insight on both.

Progress

We have continued the research on the biophysics of transport through the Nuclear Pore Complex (NPC), using several approaches. NPC is a biological nano-gate that regulates all the transport between cell nucleus and cytoplasm. The long-term goal of the research is to provide an integrated description of how conformational changes of the NPC constituents determine the dynamics of transport through it and, in particular, its selectivity. The conceptual understanding arising from the study of the NPC will be leveraged for design of artificial nano-sorting devices based on the same principles. Currently, we are one of the very few groups in the world working on the subject.

We have continued to develop computational tools towards understanding the structure and dynamics of the unfolded proteins that fill the lumen of the NPC. This requires novel methods to describe the behavior of assemblies of unfolded proteins, because the standard state of the art molecular dynamics simulations can only probe the events on time and length scales much shorter than the relevant ones. Therefore, we are using coarse-grained approach based on polymer physics and statistical mechanics. In this approach, the unfolded proteins are represented as flexible polymeric chains and the models can be treated either by analytical methods or by computer simulations. We have done this part in collaboration with Prof. Rob Coalson and Prof. David Jasnow and the graduate student Mr. Michael Opferman from the Pittsburgh University. Mr. Opferman has spent the summer at Los Alamos, developing a simulation code to describe these polymers in the presence of the transport factors. In parallel, we have developed simple approximate analytical models that capture the essential properties of the polymer-transport factor mixtures.

Preliminary results of the models seem to explain the

in vitro experiments on the nano-mechanic behavior of the filaments with and without transport factors. The model has also uncovered hitherto unknown collective structural transitions in the assemblies of these polymers, induced by the presence of the transport factors. We believe that these transitions are important in the gating and transport mechanisms of the NPC. These findings are currently being summarized in a paper. Currently, we are working on introducing more realistic features into the model in geometries mimicking the actual NPC. We have established collaboration with Dr. Gnanakaran (T-6) and Dr. Welch (T-4) in order to supplement the coarse-grained models with direct atomistic simulations at short time and length in a more general context of studying the behavior of unfolded proteins.

We have also continued our previous work on stochastic models of transport through the NPC and related nanochannels. In one work, together with experimental collaborators at the Rockefeller University, we investigated how the competition between different species influences the transport selectivity. The works explains recent experimental results [1]. In another project, together with Dr. Golan Bel (LANL), we investigated how the crowding inside a nano-channel affects the transport times through it. Proper understanding of these phenomena is imperative for interpretation of single-molecule tracking experiments, which can follow dynamics of transport of a single fluorescently labeled transport factor with a resolution of several nanometers. The results are reported in [2]. We are currently establishing collaborations with experimental groups at Texas A&M University and UC Berkeley, to apply our theoretical tools to the analysis of the fluorescent measurements of single-molecule transport through the NPC and other biological channels.

Future Work

One may view the nuclear pore as a tube of ~35 nm in diameter whose walls are composed of essentially fixed structural proteins. The tube is lined by unstructured unfolded polypeptide filaments that are grafted to the walls and protrude to the tube lumen. Small molecules (<6-7 nm) in size can diffuse freely through the pore. Larger molecules have to be shuttled through by special transport proteins. The major challenge is to understand how the basic kinetic mechanisms of stochastic transport interplay with other effects, related to the filament conformation and dynamics. These include:

- Stochastic transport models with crowding: The nuclear pore complex operates in the extremely crowded environment of the cell. Although our work provides some answers, it is still largely unknown how it achieves selective transport in both directions ('in' and 'out') in the presence of vast amount of background molecular noise.

- Conformation of the filaments: Accumulating experimental evidence shows that the conformation of the filament layer and its dynamic transitions during the particle passage play an important role in the transport mechanism. Its role will be investigated using the methods of polymer physics and Brownian dynamic simulations.

- Single molecule level: Transport has to be understood. New experimental techniques allow tracking of single particles inside the channel; motion is highly stochastic. The project will develop stochastic models of the dynamics of particle passage in presence of molecular crowding.

- Viral entry into the nucleus: Viruses employ various strategies for delivery of their genome to the nucleus. In particular, DNA-protein complexes of many viruses are extremely big in terms of cell dimensions. For instance, HIV 'preintegration-complex' is ~56 nm in size – larger than the pore diameter. This poses a major question: how the delivery of these large objects into the nucleus is achieved?

Conclusion

We expect to understand the biophysics of a selectivity of nuclear-cytoplasmic exchange through the nuclear pore and, as a result, some important aspects of the dynamics of a viral entry into a nucleus of a eukaryotic cell. It is expected that, in the future, this understanding may lead the way for a design of potent anti-viral vaccines and therapies.

References

1. Zilman, A., and T. Jovanovic-Talisman. Enhancement of transport selectivity through nano-channels by non-specific competition. 2010. *PLoS Computational Biology.* **6**: e1000804.

2. Zilman, A., and G. Bel. Effects of crowding on non-equilibrium transport through nano-channels. 2010. *Journal of Physics: Condensed Matter.* **22**: 4540.

Publications

Jovanovic-Talisman, T., J. Tetenbaum-Novatt, A. S. McKenney, A. Zilman, R. Peters, M. P. Rout, and B. T. Chait. Artificial nanopores that mimic the transport selectivity of the nuclear pore complex. 2009. *Nature.* : 457.

Zilman, A.. Effects of multiple occupancy and inter-particle interactions on selective transport through narrow channels: theory versus experiment . 2009. *Biophysical Journal.* **96**: 1235.

Zilman, A., J. Pearson, and G. Bel. Effects of jamming on non-equilibrium transport times through nano-channels . 2009. *Physical Review Letters.* **103**: 128103.

Zilman, A., S. Di Talia, T. Jovanovic-Talisman, B. T. Chait, and M. P. Rout. Enhancement of transport selectivity through narrow channels by non-specific competition: a novel kinetic mechanism . 2010. *PLoS Computational Biology.* **6**: e1000804.

Zilman, A., V. Ganusov, and A. Perelson. Stochastic models of lymphocyte proliferation and death. 2010. *PLoS ONE.* **5**: 125.

Zilman, A., and G. Bel. Effects of crowding on non-equilibrium transport through nano-channels. 2010. *Journal of Physics. Condensed Matter.* **22**: 454.

Theoretical Investigations of Ribosome Dynamics

Karissa Y. Sanbonmatsu
20090530PRD2

Introduction

This project will be an important step in laying the groundwork for more accurate design of more effective antibiotics. A very important and critical health risk to our nation is the presence bacteria that cause life-threatening illnesses. Approximately 5% of all hospital patients in the US carry or are infected with superbugs that cannot be treated with existing drugs. Specifically, these bacteria are resistant to many antibiotics. Anthrax and Plague can be easily engineered to become resistant to existing antibiotics.

We will study the number one target for antibiotic drugs: an extremely complicated but naturally occurring "molecular machine" inside bacteria that cause disease.

Our project has pushed the envelop of computer models in biology by performing the largest computer simulation in the world. We are the first to study spontaneous motion of the parts of the molecular machine in atomic detail. The machine occurs in all living things. It implements the instructions in DNA. However, the machines in bacteria are barely different from the machines in humans. Antibiotics leverage these differences to kill the bacteria but not the human. However, these particular antibiotics have severe side effects.

In the project, we will have a close connection with experiments. We are mapping out the exact atomic interactions that make the machine work. These interactions are sites for potential new drugs that might be more effective than drugs in use today.

Benefit to National Security Missions

The project is relevant to antibiotic design, which is important for threat reduction and developing effective countermeasures. Specifically, biological agents need to be treated with antibiotics capable of killing them. Our project focuses on a relevant antibiotic target (the ribosome).

Progress

We have performed the largest simulation in the world of a macromolecular complex for the field of computational biology [1]. We have also established the methodology necessary to understand the drug target at a level useful for designing new drugs [1]. We produced a general modeling method to quantify the energies of the inner motions of the machine. That is, we now have the ability to compute how the energies change when the parts of the machine move.

This work was performed in the context of a big molecule that moves inside the machine. We use a combination of models that have different levels of detail. Some models even include every single atom in the machine and all of the tiny little water molecules that are packed around the machine and inside the machine. We show that the shape of the machine determines how it moves and how it works.

There are many predictions that have resulted from this study. Single-molecule experiments and experiments that use powerful x-ray beams are consistent with the features we see in our computer models.

Specifically, we have shown that our modeling technique is valid by comparing to other modeling techniques and comparing to experiments.

We also found exceptional agreement with the scale, and distribution of fluctuations determined through x-ray beam studies. Together, these comparisons demonstrate that our modeling techniques can accurately describe the motions accessible with current experimental techniques, which allow us to confidently make predictions about the finer details.

Since there is a wealth of information known about experimental rates of movement of the machine, this connection allows for more direct comparison between experiments and theoretical calculations. We have also produced a new method to map one set of experimental techniques to another set of experimental techniques. In particular, we use our simulations to convert kinetic

rates in energy landscape barriers [2]. Cryogenic imaging groups are now attempting to make energy landscapes. Therefore, our technique can connect kinetic data with cryogenic imaging.

This direct comparison will be an instrumental measure for the accuracy of such models. This process of refining our models will provide additional insights into the details of the machine energies.

Future Work

In the future, we will perform very long simulations of the machine. We will study how energies change as the parts of the machine move. We will study very large motions of the molecular machine. We will introduce more details from experimental studies into our computer models.

Conclusion

We have improved our understanding of a critical drug target (the ribosome). Currently, this target is not understood well enough to design more effective antibiotics for harmful drug resistant bacteria. By making computer models of the target, we have increased our chances of designing a drug that can kill these bacteria. By performing the largest biomolecular computer simulation in the world, we have pushed the state-of-the-art.

References

1. Whitford, P. C., P. Geggier, R. B. Altman, S. C. Blanchard, J. N. Onuchic, and K. Y. Sanbonmatsu. Accommodation of aminoacyl-tRNA into the ribosome involves reversible excursions along multiple pathways. 2010. *RNA Journal.* **16** (6): 1196.

2. Whitford, P., J. Onuchic, and K. Sanbonmatsu. Connecting Energy Landscapes with Experimental Rates for Aminoacyl-tRNA Accommodation in the Ribosome. 2010. *JOURNAL OF THE AMERICAN CHEMICAL SOCIETY.* **132** (38): 13170.

Publications

Whitford, P., J. Onuchic, and K. Sanbonmatsu. Connecting energy landscapes with experimental rates for aminoacyl-tRNA accommodation in the ribosome. 2010. *Journal of the American Chemical Society.* **132** (38): 13170.

Whitford, P., P. Geggier, R. Altman, S. Blanchard, J. Onuchic, and K. Sanbonmatsu. Accommodation of aminoacyl-tRNA into the ribosome involves reversible excursions along multiple pathways. 2010. *RNA-A PUBLICATION OF THE RNA SOCIETY.* **16** (6): 1196.

Biocompatibility and Nanotoxicity: Characterization and Manipulation of Interactions at the Biomolecule-Nanomaterial Interface

Sandrasegaram Gnanakaran
20090538PRD3

Introduction

In recent times, the organic/inorganic/bio molecular functionalization of nanomaterials has attracted much attention for potential applications in various areas of microelectronic devices, chemical sensors, biochips, proteomics, medicine, and so on. Despite of growing interest on nanomaterials with their different forms, such as fullerenes, single- and multiple-walled nanotubes, nanoparticles, nanofibers, and so forth, relatively little is known about their biomolecular recognition, the ability of biological complexes to recognize and bind with high affinity and specificity. Nanomaterials show unusual toxicity properties, membrane damage, protein denaturation, DNA damage, immune reactivity, genotoxicity in human lymphocytes, and cytotoxicity. Nanoparticles can enter cells and cross the blood–brain barrier as well as blood-testis barriers, results in unexpected health effects. Recent studies on these topics highlight its potential risks to humans and ecosystems. In view of that, nanoparticles do pose a hazard alert and calls for systematic investigation intended for balance between benefit and risk. Hence, research on toxicological effects of nanomaterials gets increasing attention. However, certain standard experiments (cytotoxicity assays) that are well suited to assess chemical toxicity provide conflicting results for nanomaterials assessment that thrust for development/ validation of accurate/alternate models for toxicity evaluation due to an urgent need to monitor the untoward effects of nanoparticles It is expected that the performance of our research task would endow with new insights on the mechanisms of the toxicity of nanomaterials, as well as relevant scientific information to make current conclusion concerning the potential benefits and risks and cost-effective management of nanomaterials.

Benefit to National Security Missions

Due to rapid advancement and development, a wide variety of nano-structured materials are now employed in pharmaceutics, cosmetics, biomedical products, and industries. Hence, the interaction of these materials with biological molecules has generated intense scientific curiosity in DOE national laboratories and attracted other government agencies concerning the safety and risks. By bridging experimental knowledge with effective computational information, management and prediction of various aspects of bio-nano molecular reactivities, the proposed work may also helpful in addressing potential puzzling factors in dealing with the experimental design of nanomaterial toxicity studies and their interpretation.

Progress

During the past year, we have undertaken studies to understand the nature of interactions between biomolecules and nano-particles of silver metal atoms. Overall purpose of these studies is to characterize the interactions of Nanomaterials with biomolecules such as proteins, lipid bilayer membranes and their building blocks, physiochemical and electronic structure properties and relate them into measurements on biological responses.

Initial investigations considered a systematic investigation on a series of silver nanoparticles to extract the physical properties with the motivation to identify the reactive species among them. Electronic structure calculations considered silver nano-particles of size 1 thru 6 (Agn(n=1-6)) that are optimized in DFT (b3lyp)/lanl2dz methods in neutral, anionic and cationic forms in solvent environment. Nucleic acids bases and zwitterionic amino acid conformations were optimized using DFT (b3lyp)/6-311++g(d,p) basis set in solvent environment. A density function theory based chemical reactivity descriptors were calculated according to strategies published by us previously. Chemical hardness, the descriptor for the stability shows that the Ag_2, Ag_4 and Ag_6 particles are highly stable species than Ag_3 and Ag_5 nps. The values for electrophilicity (reactivity descriptor) predict that, the reactivity of Ag_3 is the highest among all Ag-nps studied. Charge transfer analysis provides insights on the mode of Ag_3 interaction with biomolecules. We find that Ag_3 np acts as electron donors with bases such as adenine, cytosine, guanine and with amino acids such as Arg, Gln, His, Ile, Lys, Met, Phe, Pro, Trp and Tyr.

Recently, we have initiated investigations on silver nanoparticles interacting with phospholipids containing head groups with different charges. These interactions are relevant for understanding the biocompatibility and cell affinity of metal nanoparticles for biosensing and drug delivering applications. We examined the interaction between phospholipid head groups and Ag_3 nps since our previous work identified Ag_3 as the most chemically reactive species among the selected Ag-nps. Geometries of neutral, anionic, and cationic phopholipid head groups with Ag_3 were optimized using the DFT-B3LYP approach with combined basis sets, 6-311++G(d,p) and LANL2DZ. We show that the interaction of Ag3 nps with phospholipid head group is governed by two major bonding factors: (a) the anchoring phosphotidyl O−Ag, and (b) the nonconventional N−H···Ag and C−H···Ag hydrogen bonds. The binding to Ag-nps is stronger for complexes anchoring phosphotidyl O−Ag with zwitterionic and anionic complexes. Results indicate that interaction of the Ag_3 with the phosphoethanolamine head group is the strongest, while interaction of the trimethylammonium propane of the cationic head group is the weakest. Bader's "atoms in molecules" theory is used to determine the nature of interactions that exhibit both electrostatic and covalent characters.

Future Work

1. Relevant experimental data on biological activities/ toxicities of metal nanoparticles will be compared to gain relationship with theoretical descriptors.

2. Nanomaterials including carbon nanotube (CNT), Boron-Nitrogen nanotube (BNT) with constituents of biomolecules such as amino acids to small peptide fragments (with it significance to nano-bio interactions) and phospholipids will be selected and their interactions will be investigated using abinitio/ density functional theory and considerably larger nano-bio system will be studied using hybrid QM/MM approaches.

3. Nano materials and their interactions with biomolecules such as enzymes, proteins, nano composites and the dynamics aspects will be covered using molecular mechanics/molecular dynamics approaches.

4. Probe how the nano-bio interactions can be manipulated to create nanostructured materials with extraordinary functional properties.

Conclusion

We have demonstrated for the first time that chemical hardness, electrophilicity and charge transfer descriptors are very useful for establishing and detecting the chemical structure-reactivity relationships of metal nanoparticle and for identifying the nature of interactions with biomolecular system. Our results shed light on how peptides and lipids interact with silver nanoparticles. We identify Ag3 as the most reactive out of size 1 thru 6 (Agn(n=1-6)) indicating the influence of size and charge on the properties of silver nanoclusters. Quantification of charge transfer of silver nano-particles with biomolecular constituents shows modes of interaction.

We have also characterized the interaction between Ag_3 and membrane head groups with the purpose of generating an efficient model for toxicity behavior and to establish a quantitative structure-activity relationship model for silver nanoparticles. We find that Ag_3 differentially interacts with the lipid head group depending on the head group charges. The interactions with phosphoethanolamine and trimethylammonium propane head groups are the strongest and weakest, respectively. Interestingly, significant contributions to the interactions are also observed from non-conventional hydrogen bonds. We believe that our work is beginning to provide microscopic insights on the interaction of nano-materials with biological molecules that will help with understanding the toxicity of these materials and, eventually, to fill the knowledge gaps concerning risk in the applications of these materials on the human health care systems.

Publications

Cho, D. W., R. Parthasarathi, A. Pimentel, G. Maestas, H. J. Park, U. C. Yoon, D. Dunaway-Mariano, S. Gnanakaran, P. Langan, and P. Mariano. Nature and kinetic analysis of carbon-carbon bond fragmentation reactions of cation radicals derived from SET-oxidation of lignin model compounds. 2010. *Journal of Organic Chemistry.* **75** (19): 6549.

Giri, S., D. R. Roy, S. Duley, A. Chakraborty, R. Parthasarathi, M. Elango, R. Vijayaraj, V. Subramanian, R. Islas, G. Merino, and P. K. Chattaraj. Bonding, Aromaticity, and Structure of Trigonal Dianion Metal Clusters. 2010. *JOURNAL OF COMPUTATIONAL CHEMISTRY.* **31** (9): 1815.

Mandal, A., M. Prakash, R. M. Kumar, R. Parthasarathi, and V. Subramanian. Ab Initio and DFT Studies on Methanol-Water Clusters. 2010. *JOURNAL OF PHYSICAL CHEMISTRY A.* **114** (6): 2250.

Parthasarathi, R., Y. He, J. Reilly, and K. Raghavachari. New Insights into the Vacuum UV Photodissociation of Peptides. 2010. *JOURNAL OF THE AMERICAN CHEMICAL SOCIETY.* **132** (5): 1606.

Analysis of Protein Structure-Function Relations in Antibiotic Biosynthesis and Signal Transducing Receptors

Louis A. Silks III
20100603PRD2

Introduction

The challenge for studying protein structures, their complexes and the structural dynamic of these proteins by Nuclear Magnetic Resonance (NMR) spectroscopy is the protein size-dependent relaxation behavior of the NMR signal. With an increasing size of the proteins, not only the signal overlap increases, also the signal intensity and the line-width of a signal decreases. To solve or at least reduce this problem, other relaxation effects, like the exchange with NMR active nuclei of the solvent, can be prevented by perdeuteration. The number of NMR signals can be reduced by amino acid type specific perdeuteration and ^{13}C-depletion or vice versa the specific ^{13}C and ^{1}H enrichment of a limited number of spins systems in an otherwise fully perdeuterated and ^{13}C

Benefit to National Security Missions

Using these isotopic enriched compounds we will accomplish:

1. The high-resolution liquid-state NMR structures of the C-domain, the structural complexes with it's native interaction partners to gain insight into the biosynthetic processes to consequently support research for the syntheses of new and effective antibiotics and to specific inhibit the biosynthesis of bacterial and fungal toxins.

2. The NMR structure of one micelle embedded antibiotics export protein to study the role of this family of proteins in the development of antibiotic resistance.

3. The structure and the analysis of the substrate specificity of one niacin-binding GPCR to analyze its role in blood sugar level regulation and as an alternative target to treat type II diabetes.

4. Make synthesis protocols available for the growing scientific community interested in studying structures and structural dynamics of membrane proteins and in exchange establish a bacterial cell-free protein production system. These projects shall be accomplished and published within the time frame of two years.

Progress

The development of methods for the elucidation of protein structures, to study their interactions with ligands and other proteins, to analyze complex inter-domain communications, is accelerating. As a result, research that employs biophysical methods to investigate biological molecules and dynamic interaction events has dramatically evolved and allows studies of highly complex systems. These are biological systems like:

- Non-ribosomal peptide bond-forming condensation domains (C-domains), proteins that are essential for the biosynthesis of antibiotics (erythromycin, vancomycin, daptomycin and penicillin), fungal and bacterial toxins and virulence factors (aflatoxin, vibriobactin, enterobactin, mycolic acid in *M. tuberculosis*), chemotherapeutics, antiviral and antifungal compounds.

- Membrane proteins responsible for the export of these secondary metabolites, that show a high homology to proteins responsible for the import of carbohydrates.

- G-protein coupled receptors (GPCRs), membrane proteins responsible for signal transduction in mammalian cells.

The challenge for studying protein structures, their complexes and the structural dynamic of these proteins by Nuclear Magnetic Resonance (NMR) spectroscopy is the protein size-dependent relaxation behavior of the NMR signal.

In collaboration with L. A "Pete" Silks (B8) and Ryszard Michalczyk (B8) specifically isotopic enriched amino acids and amino acid precursor for the cell-free and bacterial expression of selectively labeled proteins and perdeuterated detergents for NMR spectroscopic analysis of membrane proteins will be synthesized.

Together we will perform these syntheses at the LANL Stable Isotope Resource using the in-house expertise and the support of Silks and Michalczyk. The mentioned projects should be accomplished in an order of priorities: (1) synthesis of [3,3'-$^{2}H_{2}$, 1,2-$^{13}C_{2}$, ^{15}N] of Ile and Val, (2) [^{15}N ; ^{13}C depleted; U- ^{2}H; $^{13}C^{1}H_{3\ -methyl}$] of Ile, Leu, Val, Met and [^{15}N; ^{12}C; ^{2}H; $^{13}C^{1}H_{\ -aromatic}$] of Phe, (3) [$^{15}N$; ^{12}C; ^{2}H; $^{13}C^{1}H_{-e}$] of Phe, Tyr, Trp and His, (4) [1-$^{2}H^{R}$, 1-^{13}C, 2-^{2}H, 3-$^{2}H^{R}$, 3-^{13}C] and U-^{13}C glycerol, (5) U-^{2}H fatty acids for the synthesis of U-^{2}H t-octylphenoxyl-polyethoxyethanol (Triton X-100) and u-^{2}H 1-palmitoyl-2-hydroxy-*sn*-glycero-3-[phosphor-RAC-(1-glycerol)] (LPPG).

Alex has made significant synthetic progress in making stable isotope amino acids. Using these isotopic enriched compounds he has been working in the following:

1. The high-resolution liquid-state NMR structures of the C-domain, the structural complexes with its native interaction partners to gain insight into the biosynthetic processes to consequently support research for the syntheses of new and effective antibiotics and to specific inhibit the biosynthesis of bacterial and fungal toxins.

2. The NMR structure of one micelle-embedded antibiotics export protein to study the role of this family of proteins in the development of antibiotic resistance.

3. The structure and the analysis of the substrate specificity of one niacin-binding GPCR to analyze its role in blood sugar level regulation and as an alternative target to treat type II diabetes.

4. Making synthesis protocols available for the growing scientific community interested in studying structures and structural dynamics of membrane proteins and in exchange establish a bacterial cell-free protein production system.

During this period Alex Koglin co-authored a review in the Natural Products Reports journal detailing his research on nonribosomal peptides that have a variety of medicinal activities including activity as antibiotics, antitumor drugs, immunosuppressives, and toxins. Their biosynthesis on multimodular assembly lines as a series of covalently tethered thioesters, in turn covalently attached on pantetheinyl arms on carrier protein way stations, reflects similar chemical logic and protein machinery to fatty acid and polyketide biosynthesis. While structural information on excised or isolated catalytic adenylation (A), condensation (C), peptidyl carrier protein (PCP) and thioesterase (TE) domains had been gathered over the past decade, little was known about how the NRPS catalytic and carrier domains interact with each other both within and across elongation or termination modules. This manuscript catalogs the recent breakthrough achievements in both X-ray and NMR spectroscopic studies that illuminate the architecture of NRPS PCP domains, PCP-containing didomain-fragments and of a full termination module (C-A-PCP-TE).

Future Work

Continue making stable isotope labeled amino acids with Dr. Cliff Unkefer (Director of the National Stable Isotope Resource). Further the field of NMR spectroscopy with continued collaboration with Harvard Medical School and Professors Walsh and Wagner.

Conclusion

This would could revolutionize the field of structural biology in that new powerful NMR spectroscopy techniques are being developed by Dr. Koglin.

Quantitative Modeling of Cellular Noise

Michael E. Wall
20100604PRD2

Introduction

Dr. Munsky's research is truly pioneering in its ambition and achievements. As a student he realized that people who study noise in cellular systems ignore the full richness of the data. Although behaviors are routinely measured for thousands of cells in a population, only the mean and variance were used in modeling. Munsky reasoned that the full dynamical distribution would provide a wealth of information for modeling. He began a systematic research program to test this hypothesis, developing unique tools for identifying parameters of stochastic systems models. He recently published an article in Nature/EMBO Molecular Systems Biology (the top systems biology journal) demonstrating that these tools work when applied to lac operon gene expression data. As described in his research proposal, Brian is now poised for large-scale validation of his pioneering methods using LANL's National Flow Cytometry Resource: the automated sampling capabilities of this resource are not available at competing labs, creating an opportunity for Munsky to make LANL a world leader in modeling single-cell behavior. His work is already attracting attention from the best single-cell / synthetic biology labs nation-wide, and for very good reasons: until now, treatment of single-cell behavior was roughly equivalent to modeling a protein structure using just the mass and radius of gyration; Munsky's achievement literally enables researchers to add an entirely new dimension to understanding of cellular behavior.

Benefit to National Security Missions

The work addresses the problem of modeling stochastic systems in general and seeks to validate methods using bacterial and yeast gene regulation as a test bed. The results will advance all technical problems that involve modeling of stochastic behavior, cross-cutting the needs of many agencies and missions including DOE (biothreat reduction and using microbes for biofuel production), NIH (design of therapeutics for bacterial or viral infection), and broad problems in chem-bio, materials, chemistry, bioscience, health research, and bioenergy research.

Progress

Dr. Munsky has made significant progress to advance the project objectives. He has developed new efficient software for the identification of gene regulation based upon cell-to-cell variability. This software is currently under process for LANL copyright (LA-CC-10-103) and is soon to be released to the public in open source format. He taught these methods to 40 students during a quantitative biology summer school, which he helped to organize at LANL.

Dr. Munsky has applied his software and algorithms to the identification of the regulatory mechanisms of an important gene in yeast. He has recently completed a book chapter on the analysis and identification of stochastic gene regulation. He has published a paper in IET System Biology on a similar topic. Dr. Munsky has given a number of invited talks on the topic of this project, including at the Santa Fe Complex (April, 2010); the 2010 Congress of the International Society for the Advancement of Cytometry (Seattle, May, 2010); the University of Washington (May, 2010); and The University of New Mexico (Nov. 2010). Dr. Munsky also recently won the 2010 Leon Heller Postdoctoral Publication prize and presented a prestigious Physics/ Theory Colloquium talk at LANL (Oct, 2010).

Dr. Munsky's algorithms and approaches are currently being used by collaborators at the University of California at Santa Barbara (Drs. Mustafa Khammash and David Low), Massachusetts Institute of Technololgy (Drs. Alexander van Oudenaarden and Gregor Neuert), the University of California at San Francisco (Dr. Christopher Voigt) and Duke (Dr. Linchong You). Many of these projects are nearing fruition, and many more significant accomplishments are anticipated and will be reported on a future datasheet.

Dr. Munsky's approaches are also contributing a newly funded DR (20110051DR, Illuminating the Dark Matter of the Genome: Small RNAs as Novel Targets for Bioterrorism Counter-measures). In this project, of which Dr. Munsky is a Co-Investigator, LANL will hire a postdoc to extend Dr. Munsky's approaches to the study

of small RNA dynamics during host pathogen interactions.

Dr. Munsky has refereed for a number of journals, including Physical Review Letters, Physical Review E, Automatica, and IET Systems Biology.

Future Work

The project focuses on development of integrated computational/experimental protocols to identify predictive models of important biomedical processes, including:

- The E. coli gene (pap), which causes urinary tract infections.
- The Hog1 pathway, which relates to cancer growth.
- Various genes (plac, ptet, etc...), which are used to build synthetic organisms for biofuel applications.
- sRNA dynamics important during host-pathogen interactions.

The research will use the National Flow Cytometry Resource's advanced equipment to measure millions of individual cells and construct detailed histograms of transient cell responses under myriad controllable inputs (temperature, nutrient levels, chemical inducers, etc...). Most researchers examine only the means and sometimes variances of such data, ignoring other aspects. However, these approaches enable capturing of the full qualitative and quantitative shapes of these non-gaussian histograms and thus extract more information from each experiment. In preliminary studies, integrated experimental/computational approaches have been used to identify and validate predictive stochastic models for gene regulation in bacteria and yeast. This project will use experiments to identify stochastic models, but then use these models to design better experiments (i.e., find more revealing experimental conditions to explore). Iterating these steps will produce more thorough quantitative characterizations of biological processes and make it easier to develop predictive models and design medical treatments.

Conclusion

This project will have many levels of impact. First, the models will improve understanding of numerous biomedical problems, including:

- Systems linked to bacterial infections, antibiotic resistance, and bioterrorism countermeasures.
- Processes related to cancer.
- Influenza virulence.

Second, the methods will improve quantitative modeling of synthetic genes being considered for biomedical research, biofuels, and biochemical sensors. The publicly-released software and experimental protocols will help other researchers to identify stochastic models for numerous applications in academia and industry. By enabling fast and precise analyses, the work will enable researchers to solve currently unapproachable problems.

Publications

Bel, G., B. Munsky, and I. Nemenman. The simplicity of completion time distributions for common complex biochemical processes. 2010. *Physical Biology.* **7** (1): 016003 (9 pp.).

Munsky, B., and M. Khammash. Identification from stochastic cell-to-cell variation: A genetic switch case study. 2010. *IET Systems Biology.* **4**: 356.

Roles of Fungi in Terrestrial Ecosystem Carbon Cycling

Cheryl R. Kuske
20100625PRD3

Introduction

Processes mediated by soil fungi control carbon cycling at local to global scales, but the impacts of climate change factors, such as elevated CO_2, on this diverse group of microorganisms are lacking from monitoring efforts and in predictive models of terrestrial ecosystem responses. A vast array of soil fungi, including key players in carbon cycling, are not culturable and are best detected and monitored in the environment using molecular techniques. This project aims to develop new metagenomic (DNA of the entire soil microbial community) and metatranscriptomic (collectively expressed genes of the microbial community that identify active processes) approaches to identify and track changes in soil fungal composition and function in response to elevated CO_2 and other climate change factors in a landscape-level field experiment and laboratory manipulation experiments. In soils under varied climate change conditions, we combine metagenomics and metatranscriptomics with targeted approaches to detect and monitor specific fungal genes that we know are involved in key carbon cycling processes. This study uses soil samples collected over a two year time course, from the DOE's pine FACE site in NC, and other FACE sites, and explores the interactive effects of soil depth, nitrogen-fertilization and elevated atmospheric CO_2 on the composition and carbon cycling activities of soil fungi.

Benefit to National Security Missions

The most direct agency relevance for this project is to DOE missions in carbon cycling, climate change response, genomics technology development, and understanding complex systems.

Progress

In August, a year-long effort to develop a method for generating metatranscriptomes from soil came to fruition with the successful sequencing of a soil metatranscriptome using 454 titanium technology. This generated over 140,000 sequence reads representing actively expressed genes in the soil. Preliminary data analysis indicates that 52% of the eukaryotic sequences are fungal (Figure 1). Composition of the fungal sequences mirrors results of previous gene-specific sequencing efforts at this same site, which indicates that the fungal phyla Ascomycota and Basidiomycota comprise most of the sequences (Figure 1; ca. 60%); these two phyla likely dominate active taxa at this site and should be among the primary organisms targeted for understanding carbon cycling. We are currently in the process of mining this dataset for functional genes that are important in various aspects of carbon cycling and so far have identified potentially novel genes involved in the degradation of chitin, a complex polymer common in soil from which microbes extract nitrogen and carbon.

Figure 1.

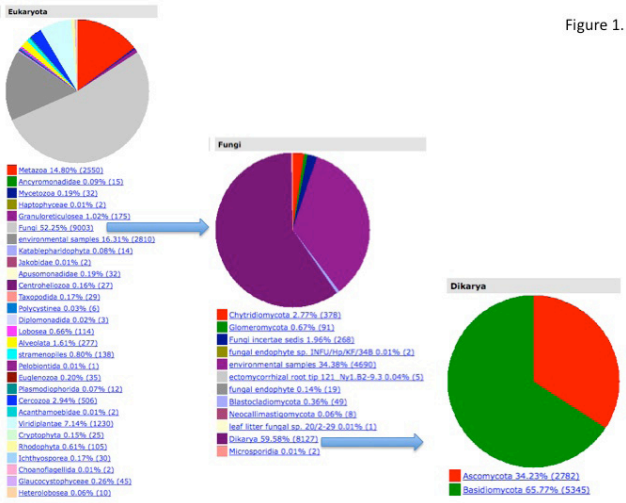

Figure 1. Hierarchical breakdown of the composition (%) of eukaryotic sequences in the preliminary metatranscriptome sequencing run as annotated using MG-RAST.

In July and September 2010, soil cores were collected from nitrogen-fertilized and non-fertilized treatments plots exposed to ambient and elevated CO_2 (four treatments total) at the pine FACE site and fractionated at different depth intervals for a detailed analysis of fungal composition and gene expression profiling. These are the terminal samples in a two year study, which are

currently being sequenced by the DOE's Joint Genome Institute.

In addition, we have drafted a manuscript summarizing a survey of >10,000 fungal cellobiohydrolase genes (a gene involved in cellulose degradation) at three open-top-chamber (OTC) sites and two DOE FACE sites as well as the database of sequenced fungal cellobiohydrolase genes that we have generated thus far. Our results clearly demonstrate that fungal cellulose degrading communities are distinct among ecosystem types, responses to elevated CO_2 are subtle and taxon-specific and cellulose degrading fungal communities are dominated by novel taxa or taxa not yet recognized as cellulose-degrading.

Future Work

1. Continue development of a fungal community transcription approach based on high-coverage transcriptome sequencing of fungal messenger RNAs to identify all fungal genes that are being expressed in CO_2-enriched and non-enriched sites. This dataset will be the first of its kind and will be used as a test subject for generating some of the first bioinformatic analysis tools for eukaryotic community transcriptomes.

2. Develop and use a sensitive molecular probing technique (reverse transcriptase PCR) to examine the expression levels of key functional genes such as cellobiohydrolase (cbh) and chitinase.

3. Use these tools in replicated field experiments to track the response of complex groups of soil fungi to over a decade or elevated atmospheric CO_2 conditions, and the influence of N fertilization and soil depth on those responses.

Conclusion

Globally, soil stores more carbon on Earth than plant biomass, and fungal activities in soil that control storage of this carbon, or its release back into the atmosphere, are critical to stability of global atmospheric conditions. The metagenomics and metatranscriptomics techniques we develop will provide a powerful approach to understanding the roles of fungi, a major soil component in all terrestrial soils and sediments, to complex carbon cycling in terrestrial ecosystems. Filling this knowledge gap is essential for accurate assessment of climate change impacts on natural and agricultural systems and prediction of air quality and altered weather patterns.

Stochastic Spatially Explicit HIV Dynamic Models

Alan S. Perelson
20100627PRD3

Introduction

Today's drug therapies against HIV can suppress the amount of virus measured in the blood of patients, but cannot completely cure the infection. New models may help provide insights into mechanisms of HIV persistence and help us attain the ultimate goal of HIV eradication. Current HIV models, while successful in predicting the need for therapy, have failed in helping guide the end game of HIV infection - i.e. full eradication of the virus and hence cure. We feel that a new generation of models is needed that takes into account many features that existing models have neglected - namely that the viral infection need not be homogeneous in space (by that we mean that there may be more virus in one part of the body than others) and that certain aspects of the infection process may be random (by that we mean that if one considers what happens say to an infected cell whether it lives or dies by a certain time may be random rather than fully determined as it is in existing models). Our goal in this project is develop models that take into consideration spatial heterogeneity as well stochastic (i.e random) effects. We will use these models to help interpret published data on HIV infection and the effects of therapy.

Benefit to National Security Missions

Quantitative models that can help us understand the interactions between a host and pathogens, and mitigate such interactions while they are still in an early stage of development. The work proposed here will help advance our knowledge in viral infections and the effects of drug therapy. The work could impact how new infections are treated and provide new fundamental knowledge about viral infections. This would support our mission of scientific discovery and innovation in basic health research as well as defense against biological weapons. The work is also highly relevant to various DHHS programs at NIH and CDC as well as DOD programs in DTRA (Defense Threat Reduction Agency) such as their Transformational Medical Technology (TMT) program.

Progress

This project is being done by a postdoctoral fellow, Jingshan Zhang. He has completed his required computer, safety and security training and has familiarized himself with the lab computer systems and available software. He has been doing extensive reading of the literature relevant to this project and is in discussions with PI Perelson and others in T-6 about his research project and the best way to proceed. He has done preliminary calculations about the rate of spread of HIV via diffusion and about the rate at which HIV infected cells migrate through tissue and hence could spread HIV. He has done some preliminary calculations about the stochastic nature of early HIV infection and examined early infection in the context of a branching process model.

Future Work

Today's drug therapies against HIV can lower the viral load in patients, but cannot completely cure the infection. Interestingly, even for patients with HIV suppressed below the limit of detection of current assays, the viral load often becomes transiently detectable. The reason for these intermittent "viral blips" is not well understood. The study of this phenomenon will help improve therapies for HIV infection in which one's goal is to completely eradicate the virus. To understand the origin of blips, I will theoretically probe the possible mechanisms by which the viral load could go up and down dynamically.

The theoretical method we will use includes dynamical and stochastic effects in viral replication and release. Most theoretical models of HIV population dynamics yield a steady state, where the virus population level remains stable, and which under therapy can be driven to zero. These models assume the infected cells release virus at a constant rate regardless of how long the cell has been infected. In fact there is a time lag between infection and generation of new virus, and it is well-known that time delays can lead to oscillations. After the time lag the viral production rate may change, leading to other dynamical effects. Moreover, existing theories

are deterministic, implicitly assuming infinite population sizes.We will explore whether stochastic effects in finite systems enhance fluctuations in the virus population level and give rise to “blips”. Furthermore, most existing models on HIV dynamics are spatially uniform. However, spatial heterogeneity in viral load, drug concentration, and cell type may also be important. If drug level is low in some regions, local viral replication might occur and such virus leaking into blood might be viewed as a blip. Models of this type, while developed for HIV, will also be applied to other viral infections.

Conclusion

We expect that the outcome of this project will be a new set of more realistic models of HIV infection that take into consideration the fact that the amount of HIV may be different in different parts of the body. Further, the new models will allow some events to be random rather than deterministic. Thus, for example whether a virus particle will be destroyed or continue to survive longer will be modeled as a random event with the virus lifetime given by a probability distribution. We anticipate that these models will help us in attaining our goal of curing HIV.

Creating a Mathematical Foundation for High-Dimensional Search and Optimization Algorithms to Solve Complex Nonlinear Models

Bruce A. Robinson
20070560PRD1

Abstract

A sound mathematical foundation, combined with testing on canonical search problems and real-world applications, is essential for advancing the field of optimization beyond its current state, and for solving emerging mission-relevant problems. The goal of this project was to advance the numerical optimization algorithms and demonstrate the utility of these advances on real world problems. Thus, this work is answering general, methodological questions on the science of optimization and mathematical model development. In addition, the methods developed in this project were applied to natural systems models to provide insights about scientific questions of environmental interest. In particular, genetic algorithms were developed for single and multi-objective optimization problems, as well as a genetically inspired Markov Chain Monte Carlo algorithm. Several significant application areas were investigated using these new methods, including surface hydrology and hydrogeophysical model inversion problems in unsaturated zone hydrology. By acting as a catalyst to push the frontiers of science in these ongoing projects, we are contributing to the Laboratory's efforts in energy security and complex natural systems while advancing the state of the art in optimization methods.

Background and Research Objectives

Numerical simulation models, along with theory and experiments, have become fundamental tools for understanding complex nonlinear systems. However, successful application of complex models is not straightforward: many of the parameters and internal states in these models require calibration/updating before meaningful predictions and uncertainty estimates can be made. Global optimization algorithms based on evolutionary search are increasingly being used for estimating parameters and states in these models. Many recent studies have demonstrated that hybrid and adaptive methods that extract information from the sampling history to continuously update the proposal distribution during the search are dramatically more efficient than more traditional static methods. However, the field of optimization relies on heuristic approaches to test for efficiency, rather than more formal theoretical approaches. This calls into question the validity of hybrid and adaptive search and optimization methods for solving high-dimensional state and parameter estimation problems. A sound mathematical foundation, combined with testing on canonical search problems and real-world applications, is essential for advancing the field of optimization beyond its current state, and for solving emerging mission-relevant problems.

In this project, we: 1) developed formal convergence proofs of hybrid and adaptive search methods for the solution of nonlinear single and multi-objective optimization problems, 2) continued the development of hybrid and genetically adaptive search methods, and 3) applied these methods to environmental and other modeling problems of strategic importance to the Laboratory. This research was enabled by the opportunity to collaborate with world-class theoretical and numerical analysts and physical scientists at LANL, a large selection of mission-relevant models and emerging problems to choose from, and the excellent parallel computing facilities at LANL.

Scientific Approach and Accomplishments

In this project we have developed a novel concept of genetically adaptive multimethod search that significantly enhances the efficiency of single and multiobjective evolutionary optimization, and have developed the mathematical foundation and numerical implementation of a novel Markov Chain Monte Carlo algorithm (Differential evolution adaptive Metropolis, or DREAM) for computationally efficient posterior inference in a Bayesian framework. The algorithmic advances have been accepted / published in applied mathematical journals, and the usefulness and applicability of these methods has been demonstrated by application to various sampling and inverse problems in different fields of studies. We have extended the mathematical and numerical advances developed within this project to particle filtering approaches for combined parameter and state estimation.

In the area of applications, the project's advances in parameter estimation and uncertainty estimation have led to significant contributions in hydrologic modeling

and hydrologic laboratory and field methods. For instance, in one study, we demonstrated that only a very limited number of discharge observations is needed to appropriately calibrate streamflow forecasting models, that data of throughfall contain insufficient information to parameterize canopy interception models appropriately, that water uptake by plant roots is difficult to estimate in the presence of significant uncertainty associated with the hydraulic properties of the soil, and that most of the uncertainty in streamflow forecasting is due to uncertainty with the observed rainfall data. The project has also placed LANL at the center of the current debate on the most appropriate methods for uncertainty estimation in hydrology. Particularly, there is strong disagreement whether an uncertainty framework should have its roots within a proper statistical (Bayesian) context, or whether such a framework should be based on a different philosophy and implement informal measures and weaker inference to summarize parameter and predictive distributions.

On one study, we compared a formal Bayesian approach with a more common, but less formal approach for assessing uncertainty in conceptual watershed modeling. Our results demonstrated that formal and informal Bayesian approaches have more common ground than the hydrologic literature and ongoing debate might suggest. The main advantage of formal approaches is, however, that they attempt to disentangle the effect of forcing, parameter and model structural error on total predictive uncertainty. This is key to improving hydrologic theory and to better understand and predict the flow of water through catchments. Another study considered application of MCMC simulation to parameter inference in the extensively used Sacramento Soil Moisture Accounting (SAC-SMA) model, a lumped conceptual watershed model that describes the transformation from rainfall into basin runoff using six state variable reservoirs. Inputs to the model include mean areal precipitation (MAP) and potential evapotranspiration (PET) while the outputs are estimated evapotranspiration and channel inflow. This real-world study poses an interesting challenge for MCMC samplers due to the complexity of the model's response surface. We found that that DREAM exhibits superior performance in terms of the number of iterations required to reach the global optimum. In addition, our algorithm achieves a significantly lower root mean squared error than its counterpart derived with the state-of-the-art SCE-UA algorithm. Thus, the algorithms available to date converge prematurely to a sub-optimal region in the parameter space, contradicting many published studies in the literature that have shown that SCE-UA is a reliable and efficient optimizer of nonlinear watershed models. These results suggest that DREAM enhances the efficiency of MCMC simulation, and simultaneously estimates values of the SAC-SMA model parameters that improve the reliability of flood forecasts.

In another study, we test the feasibility of coupled hydrogeophysical inversion for determining the hydraulic properties of a model dike using measurements of electrical resistance tomography (ERT) and soil moisture content using Time Domain Reflectometry (TDR). Our analysis uses a two-dimensional (2D) finite element hydrological model (HYDRUS-2D) coupled to a 2.5D finite element electrical resistivity code (CRMOD), and includes explicit recognition of parameter uncertainty by using a Bayesian and multiple criteria framework with the DREAM and AMALGAM population based search algorithms. To benchmark our inversion results, soil hydraulic properties determined from ERT data are compared with those separately obtained from detailed in situ soil water content measurements using TDR. Our most important results are as follows.

- TDR and ERT data theoretically contain sufficient information to resolve most of the soil hydraulic properties.
- The DREAM-derived posterior distributions of the hydraulic parameters are quite similar when estimated separately using TDR and ERT measurements for model calibration.
- Among all parameters, the saturated hydraulic conductivity of the dike material is best constrained.
- The saturation exponent of the petrophysical model is well defined, and matches independently measured values.
- Measured ERT data sufficiently constrain model predictions of water table dynamics within the model dike. This finding demonstrates an innate ability of ERT data to provide accurate hydrogeophysical parameterizations for flooding events, which is of particular relevance to dike management.
- The AMALGAM-derived Pareto front demonstrates trade-off in the fitting of ERT and TDR measurements.

Altogether, we conclude that coupled hydrogeophysical inversion using a Bayesian approach is especially powerful for hydrological model calibration. The posterior probability density functions of the model parameters and model output predictions contain important information to determine if geophysical measurements provide constraints on hydrological predictions.

Our recent studies have shown the importance of an accurate numerical solution that maintains mass balance. Conceptual rainfall-runoff models have traditionally been applied without paying much attention to numerical errors induced by temporal integration of water balance dynamics. Reliance on first-order, explicit, fixed-step integration methods leads to computationally cheap simulation models that are easy to implement. Computational speed is especially desirable for estimating parameter and predictive uncertainty using Monte Carlo Markov Chain (MCMC) methods. Confirming earlier published work, we show here that computational speed of first-order, explicit, fixed-

step integration methods comes at a cost: for a case study with a spatially lumped conceptual rainfall-runoff model, it introduces artificial bimodality in the marginal posterior parameter distributions, which is not present in numerically accurate implementations of the same model. The resulting effects on MCMC simulation include:

- Inconsistent estimates of posterior parameter and predictive distributions.
- Poor performance and slow convergence of the MCMC algorithm.
- Unreliable convergence diagnosis using the Gelman-Rubin statistic.

We studied several alternative numerical implementations to remedy these problems, including various adaptive-step finite difference schemes and an operator splitting method. Our results show that adaptive-step second-order methods, based on either explicit finite differencing or operator splitting with analytical integration, provide the best alternative for accurate and efficient MCMC simulation. Fixed or adaptive step implicit methods may also be used for increased accuracy, but they cannot match the efficiency of adaptive-step explicit finite differencing or operator splitting. Of the latter two, explicit finite differencing is more generally applicable and is preferred if the individual hydrologic flux laws cannot be integrated analytically, as the splitting method then loses its advantage.

Although in part of our project we formulated a general Bayesian framework that properly treats all individual error sources it will take several years before such a method becomes completely operational. This is because of computational requirements. Explicit treatment of individual error sources requires an ensemble approach in which forcing, model, parameter and calibration data error are formulated as probability distributions that are combined in a hierarchical manner, calculated using Bayes law, and inferred using Markov Chain Monte Carlo simulation using DREAM. For the foreseeable future it therefore seems likely that more simplistic methods will remain the preferred choice. We therefore recently developed a generalized likelihood function that relaxes the assumptions of normally distributed errors and extends the applicability of previously used likelihood functions to situations where residual errors are correlated, heteroscedastic, and non-Gaussian with varying degrees of kurtosis and skewness. The approach focuses on a correct statistical description of the data and the total model residuals, without separating out various error sources. Application to Bayesian uncertainty analysis of a conceptual rainfall-runoff model simultaneously identifies the hydrologic model parameters and the appropriate statistical distribution of the residual errors. When applied to daily rainfall-runoff data from a humid basin we find that:

- Residual errors are much better described by a heteroscedastic, first-order auto-correlated error model with a Laplacian distribution function characterized by heavier tails than a Gaussian distribution.
- Compared to a standard least-squares approach, proper representation of the statistical distribution of residual errors yields tighter predictive uncertainty bands and different parameter uncertainty estimates that are less sensitive to the particular time period used for inference.

Application to daily rainfall-runoff data from a semi-arid basin with more significant residual errors and systematic under-prediction of peak flows shows that:

- Multiplicative bias factors can be used to compensate for some of the largest errors.
- A skewed error distribution yields improved estimates of predictive uncertainty in this semi-arid basin with near-zero flows.

We conclude that the presented methodology provides improved estimates of parameter and total prediction uncertainty. Due to its generality, it may be useful for handling complex residual errors in other hydrologic regression models as well.

In more recent work, we have further enhanced the efficiency of DREAM by sampling from a past archive of points. Standard DREAM requires at least $N = d$ chains to be run in parallel, where d is the dimensionality of the posterior. Unfortunately, running many parallel chains is a potential source of inefficiency, as each individual chain must travel to high density region of the posterior. The lower the number of parallel chains required, the greater the practical applicability of DREAM for computationally demanding problems. We have extended DREAM with a snooker updater and show by simulation and real examples that DREAM can work for d up to 50-100 with far fewer parallel chains (e.g. $N = 3$) by generating jumps using differences of pairs of past states. Our recent developments further include multi-try Metropolis (MTM) sampling in which multiple different candidate points are generated in each individual chain, these points are then evaluated in parallel and the best point with highest likelihood is picked using some modified Metropolis ratio. This MTM – DREAM approach works much more efficiently for high-dimensional problems; a variety of tests will be conducted in future work to demonstrate this conclusion.

Finally, several recent contributions to the environmental modeling literature have demonstrated an inability of standard model evaluation criteria to adequately distinguish between different parameter sets and competing model structures, particularly when dealing with highly parameterized models. The Simple Least Squares (SLS) approach, advocated by Gauss and being applied in virtually all model-data synthesis studies, that summarizes a n-dimensional vector of error residuals, onto a single dimension F, results

in a colossal information loss of the data. This frustrates the search for good parameter values and introduces equifinality. We recently developed the Differential Evolution Particle Filter (DEPF) to better reconcile hydrologic models with observations. As main building block DEPF uses the DREAM sampling scheme developed in this project. Two illustrative case studies using conceptual hydrologic modeling show that DEPF requires far fewer particles than conventional Sequential Monte Carlo approaches to work well in practice, and provides important insights into the information content of discharge data and non-stationarity of hydrologic model parameters. DEPF is especially designed for implementation on distributed computer networks. The development herein follows formal Bayes, yet DEPF readily accommodates informal likelihood functions or signature indices if those better represent the salient features of the data and simulation model used.

Impact on National Missions

The methods developed are integral to the advancement of the science and development of next-generation environmental models in many programs tied to the DOE energy security mission, including groundwater resource, contaminant transport, oil and gas, nuclear waste disposal, and carbon sequestration applications. These methods are being considered for incorporation in the toolsets being developed to conduct groundwater remediation risk assessments for contaminated sites in the DOE complex and elsewhere.

Publications

Behrangi, A., B. Khakbaz, J. A. Vrugt, Q. Duan, and S. Sorooshian. Comment on: Dynamically dimensioned search algorithm for computationally efficient watershed model calibration' by Bryan A. Tolson and Christine A. Shoemaker. 2008. *Water Resources Research.* **43**: W01413.

Blasch, K. W., T. P. A. Ferre, and J. A. Vrugt. Environmental controls on drainage behavior of an ephemeral stream: An example of the limitations of simple correlative data analyses. To appear in *Stochastic Environmental Research and Risk Assessment.*

Blasone, R. S., J. A. Vrugt, H. Madsen, D. Rosbjerg, G. A. Zyvoloski, and B. A. Robinson. Generalized likelihood uncertainty estimation (GLUE) using adaptive Markov Chain Monte Carlo sampling. 2008. *Advances in Water Resources.* **31**: 630.

Braak, C. J. F. ter, and J. A. Vrugt. Differential evolution Markov chain with snooker updater and fewer chains. 2008. *Statistics and Computing.* **18** (4): 435.

Clark, M. P., A. G. Slater, D. E. Rupp, R. A. Woods, J. A. Vrugt, H. Gupta, T. Wagener, and L. Hay. Framework for understanding structural errors (FUSE): a modular framework to diagnose differences between hydrological models. 2008. *Water Resources Research.* **44**: W00B02.

Diks, C. G. H., and J. A. Vrugt. Comparison of point forecast accuracy of model averaging methods in hydrologic applications. To appear in *Stochastic Environmental Research and Risk Assessment.*

Feyen, L., J. A. Vrugt, B. Nuallin, J. van der Kniff, and A. de Roo. Parameter optimization and uncertainty assessment for large-scale stream flow forecasting. 2007. *Journal of Hydrology.* **332**: 276.

Feyen, L., M. Khalas, and J. A. Vrugt. Semi-distributed parameter optimization and uncertainty assessment for large-scale streamflow simulation using global optimization. 2008. *Hydrological Sciences Journal.* **53** (2): 293.

Gourley, J. J., S. Giangrande, Y. Hong, Z. L. Flamig, T. Schuur, and J. A. Vrugt. Impacts of polarimetric radar observations on hydrologic simulation. To appear in *Journal of Hydrometeorology.*

Harp, D. R., Z. Dai, A. V. Wolfsberg, J. A. Vrugt, B. A. Robinson, and V. V. Vesselinov. Aquifer structure identification using stochastic inversion. 2008. *Geophysical Research Letters.* **35**: L08404.

Hinnell, A. W., T. P. A. Ferre, J. A. Vrugt, S. Moysey, J. A. Huisman, and M. B. Kowalsky. Improved extraction of hydrologic information from geophysical data through coupled hydrogeophysical inversion. 2010. *Water Resources Research.* **46**: doi:10.1029/2008WR007060.

Keating, E., J. Doherty, J. A. Vrugt, and Q. Kang. Optimization and uncertainty assessment of strongly non-linear groundwater models with high parameter dimensionality. To appear in *Water Resources Research.*

Kluitenberg, G. L., T. Kamai, J. A. Vrugt, and j. W. Hopmans. Effect of probe deflection on dual probe heat-pulse thermal conductivity measurements. 2010. *Soil Science Society of America Journal.* **7452010** (5): doi:10.2136/sssaj2010.0016N.

Koller, J., Y. Chen, G. D. Reeves, R. H. W. Friedel, T. E. Cayton, and J. A. Vrugt. Identifying the Radiation Belt Source Region by Data Assimilation. 2007. *Journal of Geophysical Research - Space Physics.* **112**: A06244.

Scharnagl, B., J. A. Vrugt, H. Vereecken, and M. Herbst. Information content of incubation experiments for inverse modeling of carbon pools in the Rothamsted model: a Bayesian approach. 2010. *Biogeosciences.* **7**: 763.

Schoups, G., J. A. Vrugt, F. Fenicia, and N. C. van de Giesen. Inaccurate numerical implementation of conceptual hydrologic models corrupts accuracy and efficiency of MCMC simulation. To appear in *Water Resources Re-*

search.

Schoups, G., and J. A. Vrugt. A formal likelihood function for parameter and predictive inference of hydrologic models with correlated, heteroscedastic and non-Gaussian errors. To appear in *Water Resources Research.*

Stauffer, P. H., J. A. Vrugt, H. J. Turin, C. W. Gable, and W. E. Soll. Untangling diffusion from advection in unsaturated porous media: experimental data, modeling and parameter uncertainty assessment. 2009. *Vadose Zone Journal.* **8** (2): 510.

Tittonell, P., M. T. van Wijk, M. C. Runo, J. A. Vrugt, and K. E. Giller. Analyzing trade-offs in resource and labor allocation by smallholder African farmers using inverse modeling techniques. 2007. *Agricultural Systems.* **95**: 76.

Vereecken, H., J. A. Huisman, H. Bogena, J. Vanderborght, J. A. Vrugt, and J. W. Hopmans. On the value of soil moisture measurements in vadose zone hydrology: a review. 2008. *Water Resources Research.* **44**: W00D06.

Vrugt, J. A.. Comment on: How effective and effcient are multiobjective evolutionary algorithms at hydrologic model calibration?. 2007. *Hydrology and Earth System Sciences.* **11**: 1435.

Vrugt, J. A.. Comment on: "Multi-strategy ensemble evolutionary algorithm for dynamic multiobjective optimization. To appear in *Memetic Computing.*

Vrugt, J. A., B. A. Robinson, and J. M. Hyman. Self-adaptive multimethod search for global optimization in real parameter spaces. 2009. *IEEE Transactions on Evolutionary Computation.* **13** (2): 243.

Vrugt, J. A., C. G. H. Diks, and M. P. Clark. Ensemble Bayesian model averaging using Markov chain Monte Carlo sampling. 2008. *Environmental Fluid Mechanics.* **8** (5-6): 579.

Vrugt, J. A., C. J. F. ter Braak, C. G. H. Diks, D. Higdon, B. A. Robinson, and J. M. Hyman. Accelerating Markov chain Monte Carlo simulation from self adaptive differential evolution with randomized subspace sampling. 2009. *International Journal of Nonlinear Sciences and Numerical Simulation.* **10** (3): 273.

Vrugt, J. A., C. J. F. ter Braak, H. V. Gupta, and B. A. Robinson. Equifinality of formal (DREAM) and informal (GLUE) Bayesian approaches in hydrologic modeling?. 2009. *Stochastic Environmental Research and Risk Assessment.* **23** (7): 1011.

Vrugt, J. A., C. J. F. ter Braak, H. V. Gupta, and B. A. Robinson. Reply to comment by Keith Beven on equifinality of formal (DREAM) and informal (GLUE) Bayesian approaches in hydrologic modeling?. 2009. *Stochastic Environmental Research and Risk Assessment.* **23** (7): 1061.

Vrugt, J. A., C. J. F. ter Braak, M. P. Clark, J. M. Hyman, and B. A. Robinson. Treatment of uncertainty in hydrologic modeling: doing hydrology backwards with Markov chain Monte Carlo simulation. 2008. *Water Resources Research.* **44**: 2007WR006720.

Vrugt, J. A., J. van Belle, and W. Bouten. Pareto front analysis of flight time and energy use in long distance bird migration. 2007. *Journal of Avian Biology.* **38**: 432.

Vrugt, J. A., P. H. Stauffer, T. Wohling, B. A. Robinson, and V. V. Vesselinov. Inverse modeling of subsurface flow and transport properties using recent advances in global optimization, parallel computing, and sequential data assimilation. 2008. *Vadose Zone Journal.* **7** (2): W00B02.

Vrugt, J. A., and B. A. Robinson. Treatment of uncertainty using ensemble methods: Comparison of sequential data assimilation and Bayesian model averaging. 2007. *Water Resources Research.* **43**: W01411.

Vrugt, J. A., and B. A. Robinson. Improved evolutionary optimization from genetically adaptive multimethod search. 2007. *Proceedings of the National Academy of Sciences of the United States of America.* **104**: 708.

Wohling, T., J. A. Vrugt, and G. F. Barkle. Comparison of three multiobjective optimization algorithms for inverse modeling of vadose zone hydraulic properties. 2008. *Soil Science Society of America Journal.* **72**: 305.

Wohling, T., and J. A. Vrugt. Combining multi-objective optimization and Bayesian modeling averaging to calibrate forecast ensembles of soil hydraulic models. 2008. *Water Resources Research.* **44**: 2008WR007154.

The Role of NS1 in Disrupting Immune Responses During Influenza Infection: A Modeling and Experimental Approach

Alan S. Perelson
20070645PRD2

Abstract

Influenza kills an average of 36,000 people in the United States each year, and influenza pandemics can pose greater threats. Currently, only four drugs in two drug classes are approved for the treatment of influenza, and resistance to these drugs has developed rapidly in some strains. Using more than one drug at a time, or combination therapy, to treat influenza may delay the development of drug resistance and provide improved treatment outcomes for severe cases. In order to understand the impact of combination therapy on the spread of both wild type and drug resistant influenza A, we have developed an epidemiological model of an influenza outbreak in a closed population. We find, surprisingly, that in some realistic parameter regimes combination therapy may not reduce the size of an influenza outbreak. However, we predict that combination therapy will reduce the probability of the emergence of drug resistant strains. Also, when outbreaks due to drug resistant strains do emerge, our model predicts that combination therapy will hasten the prevalence of these strains, compared to monotherapy. In other work in this project, we have laid the groundwork for further experiments to elucidate whether influenza can possess an enzymatic activity called hyaluronidase activity that would be hypothesized to cause severe disease due to highly pathogenic virus strains. In addition, we have generated samples to be analyzed in future work to determine whether vitamin D has an impact on influenza infection.

Background and Research Objectives

Seasonal influenza kills 36,000 people each year in the U.S. alone. While the 2009-2010 H1N1 pandemic has been relatively mild, the world faces the threat of a severe pandemic from an avian strain known as highly pathogenic H5N1. This strain has infected more than 500 humans to date, with a case fatality rate of approximately 60%. One question of importance in an influenza epidemic is how best to use antiviral medications, in order to minimize the size of an epidemic and the development of drug resistance. Combination therapy, which is not used for influenza, is a strategy that should be considered. This topic has been only partially examined, using epidemiological modeling.

Much also needs to be understood about the biology of influenza virus infection. Cells of the body respond immediately upon encountering the virus with an innate immune response. The production of a protein, called cathelicidin, that forms part of the innate immune response is greatly stimulated by vitamin D; cathelicidin has been shown to be extremely important in preventing tuberculosis infection. Yet no study has examined whether there is any effect of vitamin D on influenza virus infection.

Another part of the innate immune response involves signaling through cell surface receptors called TLRs. H5N1 influenza causes severe disease in part by signaling through one of these receptors, called TLR4. It is possible that H5N1 virus particles could fragment large molecules called hyaluronic acid molecules, which can signal through TLR4, triggering severe disease. This enzymatic activity of cutting hyaluronic acid into fragments is called hyaluronidase activity. No influenza virus has been shown to have hyaluronidase activity.

Little is known about these interactions between influenza and the immune system. We are attempting to redress these gaps in knowledge in a quantitative way, and then based on experimental findings to develop mathematical models to describe each system.

The ultimate goal of this work is to understand how influenza subverts the immune response in order to generate a successful infection. If these mechanisms can be quantitatively elucidated, then new treatments might be designed. Further, we may be able to better understand why strains such as 1918 flu and highly pathogenic H5N1 are so deadly.

Scientific Approach and Accomplishments

This project involves both experimental and theoretical components. In order to carry out experiments, a variety of training and safety requirements were met. All LANL-wide and work-specific training was completed, and Institutional Biosafety Committee approval has been

obtained for all work. We also achieved approval of a new BSL-2 room for influenza work. All work has been conducted following Laboratory safety practices as specified in the Integrated Work Documents signed and approved for this work.

An assay system for an enzymatic activity called hyaluronidase activity has been set up and validated. Our goal was to test whether influenza viruses themselves possess hyaluronidase activity, i.e., whether the virus particles can cut hyaluronic acid molecules. In collaboration with Scott Hennelly, PhD, of LANL, and Robert Stern, MD, Prof. Emeritus, UCSF, we completed the assay validation process, but were unable to determine whether any strain of influenza possessed this activity. This is in part because it is difficult to obtain pure preparations of influenza surface proteins. We hope to pursue this topic further in future studies.

Additional experiments for this study have been conducted using human lung cells in culture infected with a contemporary strain of human seasonal influenza. Samples have been generated from this project that will be analyzed in future work. The kinetics of the production of these host and influenza molecules will be measured from these samples, using techniques such as quantitative real-time PCR and assays to semi-quantitatively measure the production of infectious virus particles. Based on the data, mathematical models can be developed to describe the kinetics of vitamin D levels, cathelicidin production, and infection, and other host cell responses correlated with disease severity, at the multicellular level. Fitting the models to data will allow estimation of model parameters.

On the theoretical side, we have developed an epidemiological model of influenza infection, with which we can examine the effects of antiviral therapy for both prevention and treatment, using any combination of three drugs, such as oseltamivir and zanamivir, neuraminidase inhibitors, and amantadine, an M2 channel blocker. For both amantadine and, increasingly, oseltamivir, antiviral resistance has appeared; resistance to zanamivir, which is much less commonly used, has yet to develop on a significant scale. Thus, there is considerable interest in whether combination therapy consisting of both amantadine and oseltamivir could still be effective, and whether more widespread use of zanamivir could slow down the development of resistance to any or all of these drugs. The model allows the emergence of flu strains resistant to any of the drugs alone or in combination. The model also follows the spread of resistant virus through the population. The surprising result, thus far, is that combination therapy, depending on the circumstances, may or may not be expected to reduce the size or delay the progression of an influenza epidemic. However, combination therapy is predicted to reduce the probability of the emergence of drug resistant strains and outbreaks. Nonetheless, perhaps counter-intuitively, combination therapy may also lead to the rapid emergence of strains resistant to any two drugs used for treatment, when drug resistant outbreaks do appear. The model has been explored for predictions of which combinations of drugs used for prevention and treatment will minimize both the numbers of cases and the development of drug resistance, over the short and long terms. This work will be submitted for publication soon.

The ultimate goal of this work is to understand how influenza subverts the immune response in order to generate a successful infection. If these mechanisms can be quantitatively elucidated, then new treatments might be designed. Further, we may be able to better understand why strains such as 1918 flu and H5N1 are so deadly.

Influenza infection has caused tens of millions of deaths in human history. There is a chance that bird flu (H5N1) may start a new and severe global pandemic, and other strains of influenza, such as the present pandemic strain, are also capable of causing severe disease. This work will elucidate some of the basic mechanisms used by influenza to defeat the host immune defenses. If we can better understand how influenza proteins interact with host proteins to manipulate host cell defenses we may be able to develop new drugs that will be able to better protect us against influenza infection.

Impact on National Missions

This project supports the DOE mission in reducing biological threats; influenza is on the list of identified threat agents. It also supports the missions of DHS and NIH in responding to biological threats.

This project supports the Laboratory's mission of scientific discovery and innovation, with respect to biosecurity. The Laboratory has a strong focus on understanding host-pathogen interactions, and on discovering novel ways to protect the nation from disease threats. This project is helping us to understand the ways in which influenza infections occur and spread in society, and may lead to future projects to discover new drug targets for treating influenza. The data generated from this project will be submitted for publication, and will serve to demonstrate Laboratory capabilities in high-throughput qPCR, influenza research, and epidemiological modeling, all of which will form a basis for submitting applications for funding for new work on influenza and other respiratory pathogens, and on broader areas of research relevant to our nation's biosecurity.

Pore-Scale Modeling of Multiphase Flow and Reaction in Charged Porous Media

Qinjun Kang
20070760PRD4

Abstract

In the present scenario of a global concern over energy security and environmental issues, the physics of transport and reaction encompassing multiple length scales prevalent in natural and synthetic porous media in the presence of charged surfaces is poised to play a key role. In this project, it is intended to develop for the first time a comprehensive modeling framework involving reactive transport and interfacial processes in porous media at the sub-micron and micron length scales. The overriding objective is to develop a science-based approach toward fundamental understanding of the underlying transport and reaction in charged porous media and answer some of long-standing questions in the broad spectrum of energy and environmental research, including subsurface contaminant migration, geological CO_2 sequestration, and fuel cell technology. Our pore-scale modeling framework is based on the Lattice Boltzmann (LB) method, a powerful numerical tool developed at Los Alamos. In this project, the pore-scale modeling formalism has been applied in the fields of fuel cell research, as well as novel electrode architectures with lithium-Ion chemistry in electrochemical energy storage systems. This project has led to strong research collaborations with MPA-11 and the Engineering Research Institute within LANL and also with the Department of Mechanical Engineering, UC Irvine. This project has also resulted in a number of publications and a project funded by the UC Lab Fees Research Program, which enabled PI (Qinjun Kang) to bring in a postdoctoral research associate. The postdoctoral fellow of this project, Partha Mukherjee, has joined Oak Ridge National Laboratory as a scientist. The collaboration between him and Qinjun Kang in the area of clean energy research is expected to continue.

Background and Research Objectives

Reactive transport in natural and man-made porous media is ubiquitous, particularly in various energy, earth, and environment systems. Examples include electrochemical energy conversion devices (fuel cells and batteries), stimulation of petroleum reservoirs, geologic storage of carbon dioxide and nuclear wastes, subsurface contaminant migration, bioremediation etc. However, the inherently complex morphology of such porous media coupled with multi-physical (physico-electrochemical), reactive (chemical/electrochemical) transport and interfacial processes over multiple length scales (nano/micro/meso/macro) makes this problem notoriously difficult and consequently poses several open questions of fundamental and scientific interest. In the aforementioned examples, most of the key processes, including fluid mobility, chemical transport, adsorption, and reaction, are ultimately governed by the pore-scale interfacial phenomena, which occur at scales of microns. However, because of the wide disparity in length scales, it is virtually impossible to solve the pore-scale governing equations at the scale of interest. As a result, a continuum formulation (macroscopic approach) of reactive transport in porous media based on spatial averages and empirical parameters is often employed. As the spatial averaging is taken over length scales much larger than typical pore and grain sizes, spatial heterogeneities at smaller scales are unresolved. These unresolved heterogeneities, together with the empirical parameters often unrelated to physical properties, lead to significant uncertainties in reactive transport modeling at the larger scale. In addition, current continuum models of surface complexation reactions ignore a fundamental property of physical systems, namely conservation of charge. Therefore, to quantitatively investigate the effects of pore scale heterogeneity on the emergent behavior at the larger scale, and to reduce uncertainties in the numerical modeling of reactive transport processes at the scale of interest, it is imperative to better understand these processes at the pore scale and to incorporate pore-scale effects in the continuum scale.

In this project, it is intended to develop for the first time a comprehensive pore-scale modeling framework involving multiphase (air/water), reactive (chemical/electrochemical) transport and interfacial processes in the presence of electrical charge in the sub-micron and micron length scales in porous media.

Scientific Approach and Accomplishments

We base our comprehensive pore-scale modeling

framework for investigating transport in the presence of charged mineral surface in porous media on the Lattice Boltzmann (LB) method, a powerful numerical tool developed at Los Alamos. Due to its kinetic nature, the LB method is particularly suitable for applications involving non-equilibrium dynamics and complex geometries. We have developed a suite of LBMs and computer codes to simulate multiphase flow and reaction in porous media at the pore scale. Our multi-component reactive LBM represents the state-of-the-art of existing pore-scale models for reactive transport and takes into account coupled multiple processes, including fluid flow, diffusion and advection of species, adsorption-desorption and mineral precipitation/dissolution reactions, as well as the evolution of pore geometry due to dissolution/precipitation. Homogeneous reactions are described either kinetically or through local equilibrium mass action relations. Heterogeneous reactions are incorporated into the LBM through boundary conditions imposed at the mineral surface. The LBM can provide detailed information on local fields, such as fluid velocities, solute concentrations, mineral compositions and amounts, as well as the evolution of pore geometry due to chemical reactions. Our multiphase LBM can readily handle fluid/fluid and fluid/solid interactions and therefore is capable of accounting for capillary pressure and fluid wettability.

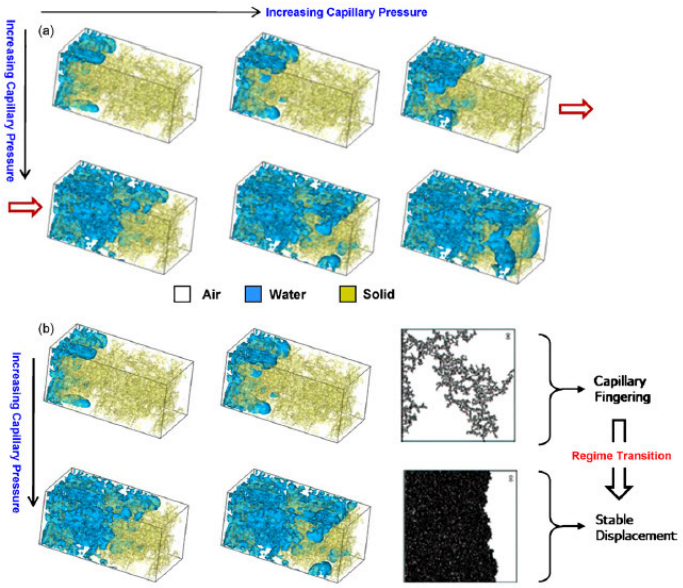

Figure 1. Lattice Boltzmann simulation of advancing liquid water front with increasing capillary pressure through the initially air-saturated reconstructed catalyst layer microstructure from the primary drainage simulation.

The Director's Postdoctoral Fellow of this project, Partha Mukherjee, has been instrumental in applying the pore-scale modeling formalism in the fields of fuel cell research, which involves transport and reaction in disparate porous structures. Figure 1 displays the steady state invading liquid water fronts corresponding to increasing capillary pressures from the primary drainage simulation in the reconstructed catalyst layer (CL) microstructure characterized by slightly hydrophobic wetting characteristics with a static contact angle of 100°. At lower capillary pressures, the liquid water saturation front exhibits finger like pattern, similar to the displacement pattern observed typically in the capillary fingering regime. The displacing liquid water phase penetrates into the body of the resident wetting phase (i.e. air) in the shape of fingers owing to the surface tension driven capillary force. However, at high saturation levels, the invading non-wetting phase tends to exhibit a somewhat flat advancing front. This observation, as highlighted in Figure 1(b), indicates that with increasing capillary pressure, even at very low capillary number (Ca), several penetrating saturation fronts tend to merge and form a stable front. The invasion pattern transitions from the capillary fingering regime to the stable displacement regime and potentially lies in the transition zone in between. In an operating fuel cell, the resulting liquid water displacement pattern pertaining to the underlying pore-morphology and wetting characteristics would play a vital role in the transport of the liquid water and hence the overall flooding behavior.

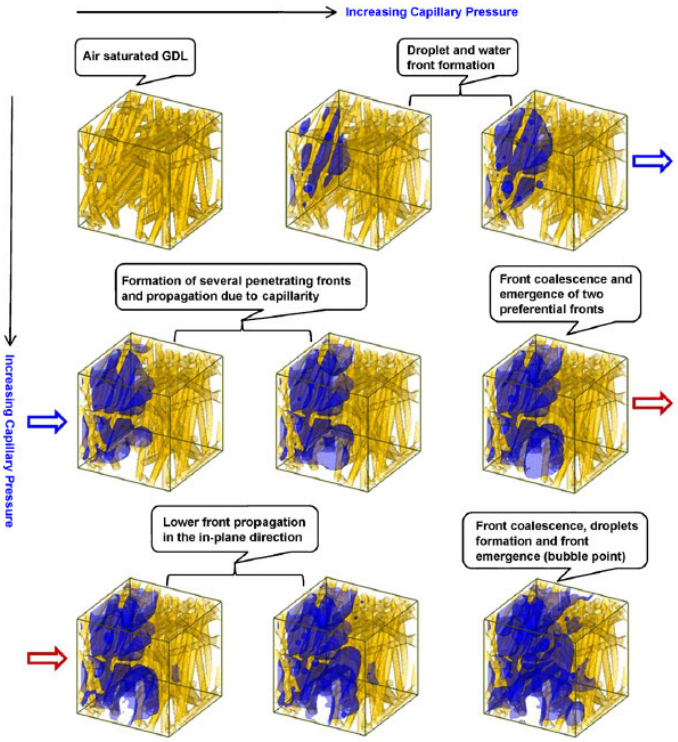

Figure 2. Lattice Boltzmann simulation of advancing liquid water front with increasing capillary pressure through the initially air-saturated reconstructed gas diffusion layer microstructure from the primary drainage simulation.

Figure 2 shows the liquid water distribution as well as the invasion pattern from the primary drainage simulation with increasing capillary pressure in the initially air-saturated reconstructed carbon paper gas diffusion layer (GDL) characterized by hydrophobic wetting characteristics with a static contact angle of 140°. The reconstructed GDL structure used in the two-phase simulation consists of 100×100×100

lattice points in order to manage the computational overhead to a reasonable level. Physically, this scenario corresponds to the transport of liquid water generated from the electrochemical reaction in a hydrophobic CL into the otherwise air-occupied GDL in an operating fuel cell. At the initially very low capillary pressure, the invading front overcomes the barrier pressure only at some preferential locations depending upon the pore size along with the emergence of droplets owing to strong hydrophobicity. As the capillary pressure increases, several liquid water fronts start to penetrate into the air occupied domain. Further increase in capillary pressure exhibits growth of droplets at two invasion fronts, followed by the coalescence of the drops and collapsing into a single front. This newly formed front then invades into the less tortuous in-plane direction. Additionally, emergence of tiny droplets and subsequent growth can be observed in the constricted pores in the vicinity of the inlet region primarily due to strong wall adhesion forces from interactions with highly hydrophobic fibers with the increasing capillary pressure. One of the several invading fronts finally reaches the air reservoir, physically the GDL/channel interface, at a preferential location corresponding to the capillary pressure and is also referred to as the bubble point. It is important to note that the mesoscopic LB simulations provide fundamental insight into the pore-scale liquid water transport through different GDL structures and would likely enable novel GDL design with better water removal and flooding mitigation.

Additionally, Partha has initiated the modeling capabilities of reaction in charged porous media to the investigation of novel electrode architectures with lithium-Ion chemistry in electrochemical energy storage systems, which represent a key clean energy research area for powering hybrid electric vehicles and portable appliances.

Partha has also been very active in developing project proposals involving multi-scale reactive transport phenomena with particular emphasis in energy research. He has also initiated research collaborations with MPA-11 and the Engineering Research Institute within LANL and also with the Department of Mechanical Engineering, UC Irvine. His research accomplishments include a number of peer-reviewed journal articles, invited book chapters, conference presentations, and proposals.

Impact on National Missions

This project supports the DOE/NNSA missions in Energy Security, Environmental Quality, and the missions of the Office of Science by enhancing our understanding of underlying multiphase flow and reaction in porous media at the pore scale in the presence of charged surfaces. Our modeling approach has been applied to the study of transport phenomena in electrochemical energy conversion devices, including fuel cells and batteries, and has provided unique insights that other approaches cannot. This project also led to a project (Fractal Electrodes for Lithium-Ion Batteries) funded by the UC Lab Fees Research Program, which enabled PI (Qinjun Kang) to bring in a postdoctoral research associate. The collaboration between the Postdoc Fellow (Partha Mukherjee) and PI (Qinjun Kang) continues after this PRD project was over.

Publications

Kang, Q., M. Wang, P. P. Mukherjee, and P. C. Lichtner. Mesoscopic Modeling of Multi-Physicochemical Transport Phenomena in Porous Media. 2010. *Advances in Mechanical Engineering.* **2010** (142879): 11.

Mukherjee, P. P., C. Wang, and Q. Kang. Mesoscopic modeling of two-phase behavior and flooding phenomena in polymer electrolyte fuel cells. 2009. *Electrochimica Acta.* **54** (27): 6861.

Mukherjee, P. P., M. Wang, Q. Kang, and P. C. Lichtner. Pore-scale modeling of transport in charged porous media. Presented at *Computational Methods in Water Resources XVII International Conference.* (San Francisco, CA, 6-10, July 2008).

Mukherjee, P. P., M. Wang, Q. Kang, and P. C. Lichtner. Modeling of transport in charged porous media. Presented at *5th Annual Meeting of Center of Environmental Kinetics Analysis (CEKA).* (Pennsylvania State University, 22-24 Oct. 2008).

Mukherjee, P. P., Q. Kang, R. Mukundan, and R. L. Borup. Pore-Scale Modeling of Flooding Behavior in the PEFC Gas Diffusion Layer: Durability Effect. 2010. **to be submitted**.

Mukherjee, P. P., Q. Kang, R. Mukundan, and R. L. Borup. Numerical Modeling of Two-Phase Behavior in the PEFC Gas Diffusion Layer. Presented at *ECS Transactions.*

Mukherjee, P. P., Q. Kang, and C. Wang. Pore-Scale Modeling of Two-Phase Transport in Polymer Electrolyte Fuel Cells - Recent Progress and Perspective. To appear in *Energy & Environmental Science Journal.*

Mukherjee, P. P., V. P. Schulz, Q. Kang, J. Becker, and A. Wiegmann. Two-Phase Behavior and Effect of Compression in the Polymer Electrolyte Fuel Cell Gas Diffusion Medium. Presented at *Electrochemical Society Meeting.* (Vienna, Austria, Oct.2009).

Mukherjee, P. P., and Q. Kang. Electrodics in Electrochemical Energy Conversion Systems: Microstructure and Pore-Scale Transport. To appear in *Microfluidics and Nanofluidics Handbook.*

Mukherjee, P. P., and Q. Kang. Pore-Scale Modeling of Flooding Behavior in the PEFC Gas Diffusion Layer: Microstructure Effect. 2010. **to be submitted**.

Teixidor, G. T., B. Y. Park, P. P. Mukherjee, Q. Kang, and M.

J. Madou. Modeling fractal electrodes for Li-ion batteries. 2009. *Electrochimica Acta.* **54** (24): 5928.

Modeling Fast Basal Sliding of Ice Sheets for Climate and Sea Level Prediction

William H. Lipscomb
20070765PRD4

Abstract

Recent observations show that outlet glaciers and ice streams in Greenland and West Antarctica have accelerated and thinned dramatically, with atmospheric and oceanic warming the likely cause. Given the potential catastrophic impacts of rapid sea level rise, it is critical to predict how ice sheets will respond to future climate warming. This is not yet possible because fundamental physical processes are not represented in ice-sheet models and are only beginning to be understood. The goal of this project was to improve predictive ice sheet models by including realistic treatments of:

- Basal sliding in regions underlain by deformable subglacial sediments (e.g., ice streams).
- The link between this type of sliding and subglacial hydrology that can evolve in response to changes in the overlying ice sheet.

These processes are crucial for predicting the evolution of ice streams and outlet glaciers, which can flow 10 to 100 times faster than ice that is frozen to the bed. The new process models have been implemented and are being tested in a state-of-the-art ice-sheet model (Glimmer-CISM), the ice-sheet component of the Community Climate System Model (CCSM). This model will be used by glaciologists and climate modelers worldwide for regional studies and for global climate projections. In particular, model results from Glimmer-CISM and CCSM will be incorporated in the reports of the Intergovernmental Panel for Climate Change (IPCC). The most recent IPCC assessment report specifically noted the need for better ice sheet models.

Background and Research Objectives

Recent observations show that outlet glaciers and ice streams in Greenland and West Antarctica have accelerated and thinned dramatically. Complete disintegration of the Greenland and West Antarctic ice sheets would raise sea level by more than 10 m. Given the catastrophic impacts of rapid sea level rise, it is critical to predict how ice sheets will respond to future climate warming. This is not yet possible, however, because ice sheet models are missing fundamental physics and because key processes (e.g., meltwater penetration/drainage and subglacial sediment deformation) are only beginning to be understood and accounted for. Lipscomb, the proposal sponsor, has coupled the GLIMMER ice sheet model to the Community Climate System Model (CCSM). Like most current models, GLIMMER is based on the shallow-ice approximation, which is valid for slow flow (~10 m/y) in ice sheet interiors but not for rapid sliding (~100 to 1000 m/y) in ice streams and outlet glaciers, which control the large-scale response to climate change. Accurate modeling of fast-flowing regions, which is critical for predictive capability, requires two general model improvements:

1. "Higher-order" physics (i.e., horizontal stress gradients).
2. Improved treatment of basal sliding and subglacial hydrology.

The first is now available in Glimmer-CISM (CISM = Community Ice Sheet Model), a next-generation version of the original GLIMMER model. This proposal focused on the second set of improvements, including realistic treatment of sliding in areas underlain by subglacial sediments and the link between the subglacial sediments that control sliding, the subglacial hydrology, and changes in the overlying ice sheet. The first involved the implementation of "Coulomb-friction" basal boundary conditions, and the second involved linking the yield stress of subglacial sediments to subglacial hydrological characteristics. Realistic treatment of sliding over subglacial sediments allows for improved representation of ice streams in 3D ice sheet models. By then linking ice stream sliding to time-dependent basal hydrology, regions of ice streaming develop and evolve naturally in ice sheet models.

Scientific Approach and Accomplishments

During his postdoctoral fellowship, Stephen Price focused on general development of an improved ice sheet dynamics model (i.e., one that includes horizontal stress

gradients) and model development specific to his LANL-funded postdoc.

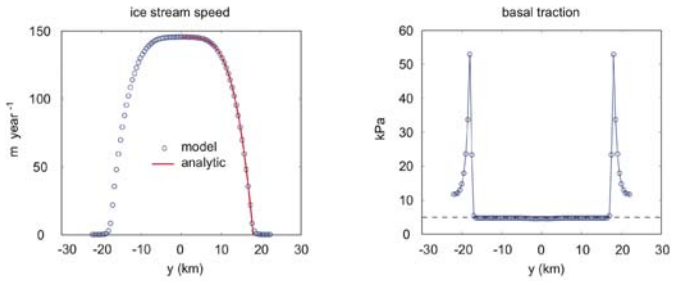

Figure 1. Across-flow profiles for ice speed (left panel) and basal traction (right panel) for Coulomb-friction ("plastic") basal boundary conditions with a prescribed yield stress of 5 kPa within the ice stream and >> 5 kPa outside of it. The red line in the left panel is an analytic solution for ice stream "plug" flow, from Raymond (1996). Note that the model demonstrates the transfer of basal traction from the ice stream interior to just outside of the lateral shear margins (right panel), as observed in real life (e.g. Price et al., 2002).

General model development included the following:

1. The addition of multiple stable ice-thickness evolution solvers (for predicting the change in ice sheet geometry over time). These include a scheme based on LANL-developed "incremental remapping" (IR) and a scheme based on piecewise-parabolic-matching.

2. The addition of the ability to simulate regions of floating ice (e.g., ice shelves or ice tongues), which is fully coupled to land-bound, grounded ice. This scheme was benchmarked against, and compared well with, a) other ice shelf models and b) observations from the Ross Ice Shelf in West Antarctica.

3. The addition of a freely moving grounding line (the point of transition/coupling between grounded and floating ice). Work is still underway to verify that grounding line migration in the model (known to be highly susceptible to grid resolution and numerical artifacts) is consistent with a series of benchmarking experiments, specifically designed to validate grounding line behavior in numerical models.

4. Work to port a "higher-order" momentum balance solver to the Glimmer-CISM ice sheet model. The output from this solver compares well with that from another higher-order solver in Glimmer-CISM. For several test cases spanning the end-member flow regimes for an ice sheet (internal deformation with no sliding versus all sliding and no internal deformation), the two solvers compare well with one another and against a number of benchmark test cases.

5. Construction of an ice-shelf / ocean coupler, based on a widely applied boundary-layer theory, in which heat and salt fluxes between the ocean and an overlying ice shelf are used to couple the boundary conditions for ice shelf and ocean circulation models in a consistent manner.

6. Work with colleagues at LANL, Oak Ridge National Laboratory, and Sandia National Laboratory to implement the Trilinos solver package for use in Glimmer-CISM. The outcome of this work is that the computationally expensive, elliptic solution to the momentum balance equations is now done in parallel, rather than in serial. In addition, model users now have access to a much wider range of linear and non-linear solvers and preconditioners, for use in improving model performance.

7. Work with U.S. and U.K. colleagues towards a public release of Glimmer-CISM, which will be the first open source, freely available, higher-order ice sheet model. The code release is scheduled for April 2010.

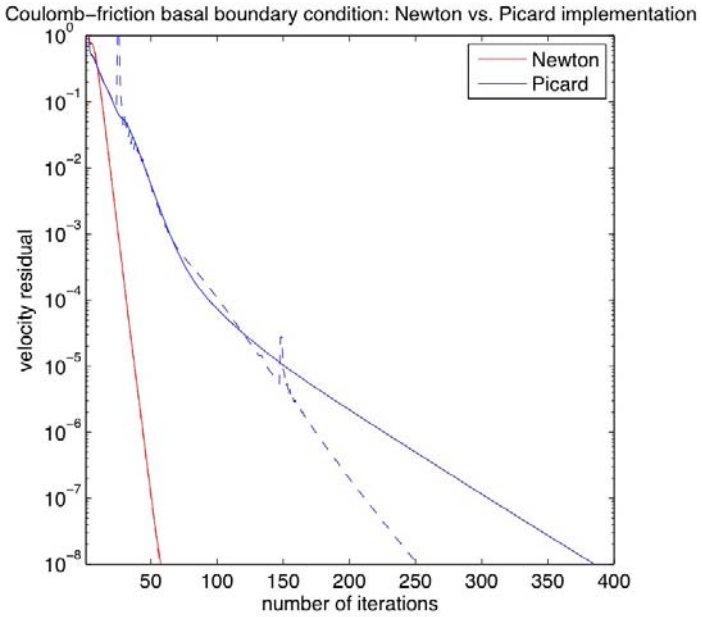

Figure 2. Momentum balance residual versus iteration count for test case implementations of the Coulomb-friction ("plastic") basal boundary conditions (e.g. the analytic solutions shown in Figures 1 and 4). The solid lines are for a 20x40 domain and the dashed lines are for a 40x80 domain (i.e. 2x resolution). With Newton implementation (red), the solid and dashed lines lie atop one another, indicating that the number of Newton iterations is resolution independent. For this test case, the relative computational savings when using the Newton method is a factor of ~5-8.

Model development specific to the goals of simulating regions of fast sliding in ice sheets has included the following:

1. The addition of a simple Picard-type iteration to approximate Coulomb-friction glacier sliding. This implementation has been used successfully in previous ice stream/ shelf models [1,4], which simplify the momen-

tum balance by assuming depth-integrated horizontal stress gradients. Initial experiments indicated that this method also worked for our fully three-dimensional model (Figure 1), although it was sometimes slow to converge.

2. Alteration of the boundary condition implementation from [1] using Newton-methods, akin to those applied to elastic friction/contact problems. (This work was done in cooperation with colleague Georg Stadler at The Univ. of Texas, Austin.) This implementation is ~5-8 times faster than the originally implemented Picard-based method (Figure 2). Additionally, this work has led to a more accurate representation of modeled boundary tractions (Figure 3), important for obeying conservation of energy and for accurate coupling of basal boundary conditions to ice sheet thermomechanical evolution. Portions of this work were presented at the 2010 DOE Climate Change Modeling workshop. A poster on this work will be presented at the annual European Geophysical Union (EGU) meeting in May 2010.

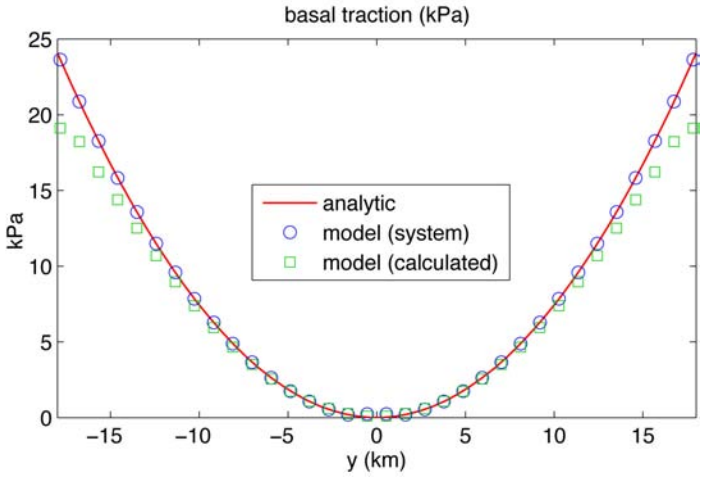

Figure 3. Across-flow profile of basal traction. The solid red line is an analytical solution taken from Schoof (2006). The symbols are from the modeling conducted here, which attempts to match the analytical solution. The blue circles show the basal traction calculated internally ("system", using the new method) and the green squares show the basal traction calculated a posteriori, (the standard method) by applying finite-differencing to the converged velocity and viscosity fields. While the model solution is indeed consistent with the analytical solution, as shown by the blue circles, the standard method of calculation would suggest that the model solution is in error by as much as ~20%.

3. Work with colleagues at the University of Cambridge on incorporating a basal-processes model in Glimmer-CISM. The basal-processes model takes information on basal hydrology (e.g., basal melting / freezing rate) and known subglacial-interface properties (e.g., whether the interface is bedrock or moldable sediment and, if the latter, what are the sediment's rheological and hydrological properties) and provides the larger model with an estimate for the required yield stress (implemented as the basal boundary condition using (1) and (2) above). Results now being prepared for publication were presented at the 2009 West Antarctic Ice Sheet (WAIS) meeting, the 2009 fall American Geophysical Union (AGU) annual meeting, the 2010 DOE Climate Change Modeling Workshop, and will be presented at the annual EGU meeting in May 2010 (Figure 4). Ongoing work involves updating the basal processes model to allow for interaction with an explicit, non-local, subglacial hydrology model, and applying the coupled model to explore the influence of hydrology and basal processes on evolution of the West Antarctic ice sheet.

4. Development and application of a straightforward and quantifiably robust method for the tuning of basal sliding parameters. This is a necessary step in obtaining a reasonable initial condition for simulations of future ice sheet mass balance. As a proof of concept, this tuning procedure has been applied to the Greenland ice sheet. The tuned model state will be used to initialize perturbation experiments exploring the response (e.g., sea level rise) of the Greenland ice sheet to environmental forcing over the next century. Results from these experiments were presented at the annual CCSM meeting in June 2009, at the 2009 fall AGU meeting, and at the 2010 CCSM Land Ice Working Group meeting. This work is currently being prepared for publication and is the subject of an invited talk, to be presented at the annual EGU meeting in May 2010.

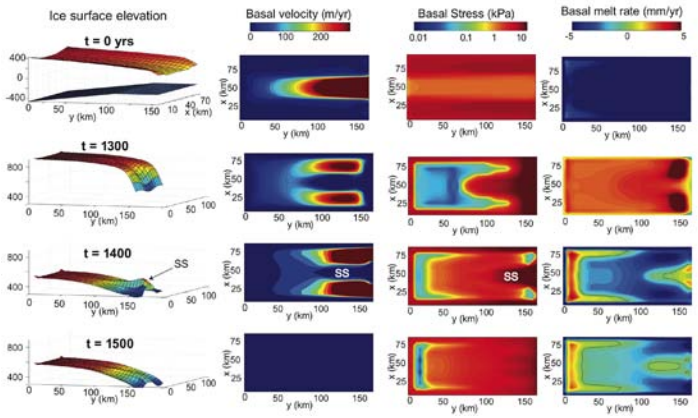

Figure 4. Snapshots of ice surface elevation, basal velocity, basal stress, and basal melt rate, showing part of a cycle from thick-warm-slippery-fast ice to thin-cold-sticky-slow ice, resulting from the coupling of Coulomb-friction basal boundary conditions to the thermomechanical evolution of the ice stream. Such coupling provides an explanation for observations of slow down (Whillans Ice Stream) and stagnation (Kamb Ice Stream) of ice streams in West Antarctica. In the example above, the coupled model also produces a persistent "sticky spot"-like feature (SS), analogous to that observed on modern-day Kamb Ice Stream.

Price has presented his work to the Climate, Ocean and Sea Ice Modeling (COSIM) group and Group T-3 at LANL. In April 2009 he presented results from his work at the DOE Climate Change Modeling workshop in Bethesda, MD. At the June 2009 CCSM workshop, he presented an update on model experiments of the Greenland ice sheet, estimating the potential dynamic contribution to sea-level rise from several key outlet glaciers. In August 2009, he was an invited instructor at an international summer school on ice sheet modeling (http://websrv.cs.umt.edu/isis/index.php/Summer_Modeling_School) at Portland State University. In September 2009, he was co-author on an oral presentation given at the WAIS meeting and was an invited participant and speaker at the Univ. of Chicago *Collaborations in Mathematics and Geosciences Workshop on Automatic Differentiation and Ice Sheet Modeling*. During fall 2009 he contributed to two NASA Venture-Class proposals that, if successful, will provide funding for two LANL postdocs working on ice sheet modeling and partial funding for a LANL scientist (1/6 FTE for five years). In December 2009, he presented results from various aspects of his research at the fall AGU meeting, where he was the lead author on one oral presentation, a co-author on one oral and two poster presentations, and a co-chair of the Cryosphere session *Constraining and Improving Models of Glacier Dynamics Using Observations*. At the February 2010 CCSM Land Ice Working Group meeting he presented an oral presentation on estimating the minimum future contribution to sea-level rise as a result of Greenland ice sheet dynamics. This same work is the subject of an invited talk he will present at the annual EGU general assembly meeting in Vienna, Austria, in May 2010. At this same meeting, he is lead author on a poster presentation discussing his work on implementing dynamic basal processes in ice sheet models, and is a co-author on two other presentations (one poster, one oral). At the DOE Climate Change Modeling workshop in April 2010, he presented an update on his work on implementation of basal processes in ice sheet models.

Price became a LANL staff member (Scientist 2) in April 2010, at the conclusion of his postdoctoral fellowship.

He was co-author of a paper published in the Journal of Glaciology:

Catania, G.A., T.A. Neumann, and S.F. Price. 2008. Characterizing englacial drainage in the ablation zone of the Greenland ice sheet. J. Glaciol., 54(187), 567-578.

Along with LANL colleagues, he is co-author on a new manuscript (in press) and on a new manuscript in review:

Dukowicz, J.K., S.F. Price, and W.H. Lipscomb. Consistent approximations and boundary conditions for ice sheet dynamics from a principle of least action. J. Glaciol. (in press).

Dukowicz, J.K., S.F. Price, and W.H. Lipscomb. Incorporating arbitrary basal topgraphy in the variational formulation of ice sheet models. J. Glaciol. (submitted).

In February 2009 he authored a *News & Views* article in *Nature Geoscience*:

Price, S.F. 2009. From the front. *Nature Geosc.*, **2**(1), doi:10.1038/ngeo424.

Impact on National Missions

This project has supported the DOE mission of the Office of Science by enhancing our understanding of physical processes that control the response of ice sheets to climate change. The project also has supported NASA's mission to understand the changing climate; NASA satellite data is being used to develop and validate improved models of basal sliding of ice sheets. The most significant result of the project is an ice sheet model with more accurate and realistic treatments of ice dynamics and basal boundary conditions, including sliding over a plastic bed and sliding parameterizations linked to the evolution of subglacial hydrology. These improvements have been incorporated in Glimmer, the Community Ice Sheet Model (Glimmer-CISM), which in April 2010 will become the first open-source, publicly available ice sheet model with higher-order ice dynamics. This model will be used by glaciologists and climate modelers worldwide for regional studies and global climate projections. In particular, Glimmer-CISM will be used for coupled climate change experiments as part of the Community Climate System Model (CCSM). Results from CCSM simulations with dynamic ice sheets will be included in the next assessment report (AR5) of the Intergovernmental Panel for Climate Change and will lead to improved projections of 21st century sea-level rise.

References

1. Bueler, E., and J. Brown. Shallow shelf approximation as a "sliding law" in a thermomechanically coupled ice sheet model. 2009. *Journal of Geophysical Research.* **114**: doi:10.1029/2008JF001179.
2. Price, S. F., R. A. Bindschadler, C. L. Hulbe, and D. D. Blankenship. Force balance along an inland tributary and onset to Ice Stream D, West Antarctica. 2002. *Journal of Glaciology.* **48** (160): 20.
3. Raymond, C. F.. Shear margins in glaciers and ice sheets. 1996. *Journal of Glaciology.* **42** (140): 90.
4. Schoof, C.. A variational approach to ice stream flow. 2006. *Journal of Fluid Mechanics.* **556**: 227.

Publications

Catania, G. A., T. A. Neumann, and S. F. Price. Characterizing englacial drainage in the ablation zone of the Greenland ice sheet. 2008. *Journal of Glaciology.* **54** (187): 567.

Dukowicz, J. K., S. F. Price, and W. H. Lipscomb. Incorporating arbitrary basal topgraphy in the variational formulation of ice sheet models. *Journal of Glaciology.*

Dukowicz, J. K., S. F. Price, and W. H. Lipscomb. Consistent approximations and boundary conditions for ice sheet dynamics from a principle of least action. To appear in *Journal of Glaciology.*

Price, S. F.. From the front. 2009. *Nature Geoscience.* **2** (1): 93.

Spectroscopic Studies and Photonic Applications of "Giant" Nanocrystal Quantum Dots

Victor I. Klimov
20080703PRD1

Abstract

Semiconductor nanocrystals (NCs), know also as nanocrystal quantum dots, are nanosized crystalline particles that show high photoluminescence quantum yields and size-dependent emission colors tunable through the quantum-confinement effect. Because of these properties, NCs are attractive materials for various photonic applications including optical amplification and lasing. Practical utilization of nanocrystals in lasing technologies is, however, hindered by their low photo-stability at high excitation intensities required to obtain the optical-gain regime and fast nonradiative carrier losses resulting from Auger recombination. Recently, we have developed a new type of composite core-shell NCs that comprise a small core of CdSe overcoated with a very thick shell (up to 20 monolayers) of a wider gap material such as CdS (Y. Chen et al. J. *Am. Chem. Soc.* **130**, 5026, 2008). The overall size of these composite particles is quite large (10 – 20 nm), therefore, they have been dubbed "giant" NCs or g-NCs. Compare to traditional dots, g-NCs show greatly increased absorption cross-sections, enhanced emission efficiencies, and improved environment and photo-stability. Our initial studies also indicate that they exhibit reduced rates of Auger recombination. All of these properties are beneficial for photonic applications, especially, in lasing technologies. The goal of this project has been to evaluate the potential of g-NCs in optical amplification and lasing through comprehensive studies of their electronic and optical properties conducted in conjunction with microstructural characterization and theoretical modeling of electronic states and carrier relaxation dynamics.

Background and Research Objectives

Colloidal NCs have been the subject of intense research due to potential applications in low-threshold lasers, biological tags, third-generation photovoltaics, and light emitting diodes (LEDs). All of these technologies can benefit from the unique properties of NCs such as a size-tunable energy gap, high photoluminescence (PL) quantum yields, good stability, and chemical processibility. Many of these potential applications are, however, hindered by Auger recombination, wherein the energy of one electron-hole pair (exciton) is non-radiatively transferred to another charge carrier. In NCs, this process occurs on sub-nanosecond timescales, and reduces optical gain lifetimes, restricts the available time to extract multiple excitons generated via carrier multiplication, limits LED brightness due to the build-up of charged NCs, and leads to PL intermittency ("blinking") that is typically observed in single-NC studies.

While the physics underlying Auger recombination in NCs is still not fully understood, general considerations suggest that the rate of this process is directly dependent upon the strength of carrier-carrier Coulomb coupling and the degree of spatial overlap between the electron and hole wave functions involved in the Auger transition. Previous approaches to reducing Auger recombination rates have utilized the manipulation of both of these parameters. For example, using elongated NCs (quantum rods), one can separate interacting excitons along the rod axis, which leads to decreased exciton-exciton Coulomb coupling. One can also reduce the rate of Auger transitions by separating electrons and holes between the core and the shell regions of core-shell heterostructured NCs that exhibit a so–called type-II localization regime. The latter approach has been especially successful in the case of CdTe(core)/CdSe(shell) nanostructures, as indicated by a recent observation of intense multiexciton lines in emission spectra of individual NCs. Finally, a recent report attributed the suppression of Auger recombination in CdZnSe/ZnSe NCs to the formation of a "smooth" confining potential resulting from a graded composition of the NC interfacial layer. This explanation is based on recent theoretical work by Efros and co-workers, which directly links the Auger decay rate to the steepness of the interfacial potential.

The objective of our research has been to analyze dynamical and spectral properties of multiexcitons in a novel class of NCs that comprise a CdSe core and a thick CdS shell of up to 20 CdS monolayers (Figures 1a and b). We developed these so-called g-NCs in an attempt to improve chemical- and photo-stability against ionization by isolating a small emitting core from its chemical environment with a thick shell (single-composition or graded

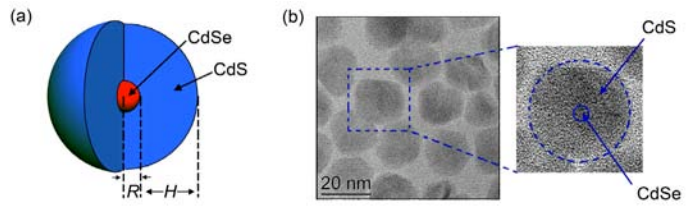

Figure 1. (a) A schematic of the g-NC structure where R is the CdSe core radius and H is the CdS shell thickness. (b) A transmission electron microscopy image of g-NCs with R = 1.5 nm and H = 6.7 nm. Blue lines in the expanded view on the right illustrate the relative size of a core compared to the total size of a g-NC.

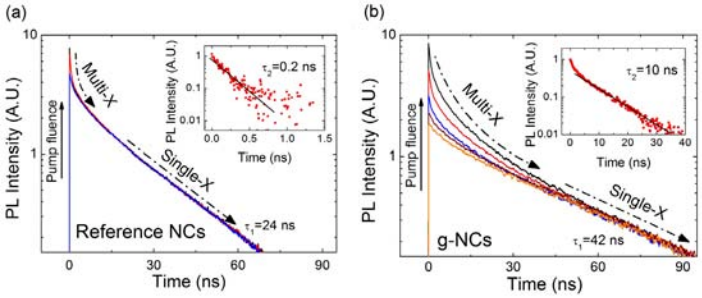

Figure 2. (a) Time-resolved PL intensity of reference CdSe/ZnS core-shell NCs (dilute hexane solution) emitting at 1.92 eV for different excitation fluences (2 to 200 μJ/cm2); pump photon energy is 3.1 eV. Traces normalized at t = 60 ns completely overlap at t > 2 ns, indicating that relatively early in time all of the multiexcitons have already decayed. τ1 is the single exciton lifetime. Inset: the extracted biexciton dynamics show the 200 ps decay due to Auger recombination. (b) The same for g-NCs (12 monolayer CdS shell, R=1.5-nm and H=3.9-nm); PL is monitored at 2.00 eV. Traces normalized at t = 90 ns become indistinguishable only for t > 40 ns, indicating that in this case multiexcitons are long lived. Inset: The extracted biexciton dynamics shows slow 10-ns decay.

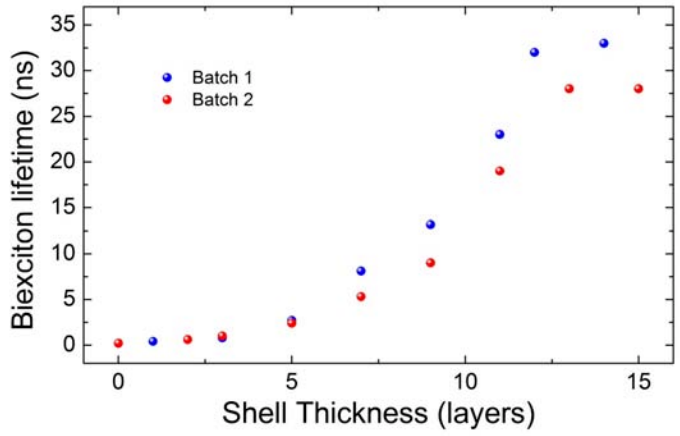

Figure 3. Biexciton lifetimes as a function of shell thickness measured for CdSe/CdS NCs from two different batches.

composition) of a wider-gap material and to effectively create a solution-phase structural mimic of an epitaxial quantum dot. It was also hypothesized that this approach would lead to suppressed PL blinking, as the thick shell would prevent carriers from leaving the NC, inhibiting the formation of non-emitting charged NCs. The synthesized g-NCs indeed exhibited greatly improved chemical- and photo-stability and suppressed blinking, a result that has been confirmed by an independent study of similar structures. Recently it has been shown that individual CdSe/CdS g-NCs can still emit even when they are charged (so-called "grey" states), and therefore, it is likely that previously observed reduced blinking is likely not only due to suppressed ionization but is also a consequence of extended Auger recombination lifetimes.

Scientific Approach and Accomplishments

The most important accomplishment of this project is the demonstration of a significant suppression of nonradiative Auger recombination. For at least two decades, the achievement of this goal has been an important milestone in the NC research. Here, by conducting direct time-resolved spectroscopic studies of g-NCs, we show that the Auger lifetime of a two-exciton state (biexciton) in these nanostructures is by a factor of at least 50 (!) longer than in standard CdSe NCs emitting at the same wavelength. As a result of these exceptionally slow recombination dynamics, even multiexcitons of a very high order (13th and possibly higher) exhibit high emission efficiencies and contribute to optical gain. This allows us to obtain optical amplification over unprecedented bandwidth of more than 500 meV and with record low excitation thresholds.

In order to obtain the lifetime of multiexcitons (typically very short-lived due to Auger recombination), we measure a time-resolved photoluminescence intensity of a sample at low excitation intensities, when only single excitons contribute to the signal. Then we compare the results of these measurements with those conducted at high excitation intensities when multiple excitons are generated per single NC. In the case of standard CdSe NCs used as a reference (Figure 2a), the high- and low-pump-intensity dynamics only differ at very early times (<1ns) indicating that in this case multiexcitons are extremely short-lived. The same experiment conducted on a sample of g-NCs (Figure 2b) indicates that the multiexeciton dynamics become significantly slower. Specifically, while standard NCs show a biexciton lifetime of about 0.2 ns, the biexciton lifetime in g-NCs is ~10 ns, i.e. 50 times longer. This result indicates a very significant *suppression* of Auger recombination in this new type of core-shell nanoparticles (Garcia-Santamaria, F., et al. *Nano Lett.* **9**, 3482, 2009).

After demonstrating that Auger recombination can be effectively suppressed in g-NCs, we have focused our efforts on trying to understand the fundamental physics behind this effect. Especially important insights have been provided by measurements of biexciton lifetimes as a function

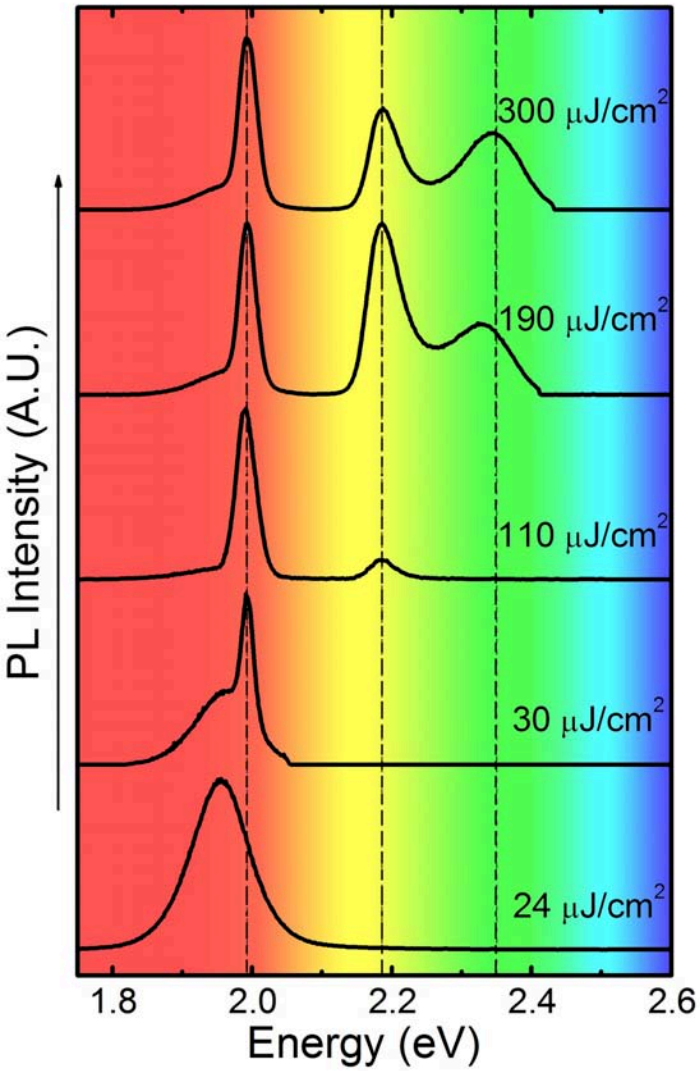

Figure 4. Emission spectra of a close-packed film of g-NCs (11 monolayer CdS shell) measured using 3.1 eV, 100 fs pump pulses with different per-pulse fluences (indicated in the figure); the pump-spot diameter is 60 μm. These spectra illustrate the development of three ASE peaks at 1.99 eV, 2.19 eV and 2.34 eV that span the range of colors from red to green.

of CdS shell thickness. The data obtained for two series of samples (Figure 3) have been mutually consistent and offered very interesting new information:

- The biexciton lifetime does not scale linearly with volume (this linear scaling is typically seen in standard NCs) but rather exhibits a sharp growth at a critical shell thickness of about 7 monolayers.
- The biexciton lifetime saturates for shell thicknesses over 12 layers.

The main conclusion drawn from these results is that a simple increase in the g-NC volume compared to standard NCs cannot explain a very significant lengthening of Auger lifetimes. On the other hand, our data are consistent with the most recent theories in which Auger recombination is considered in terms on an interfacial process mediated by charge carrier collisions with the NC surface. As a result, the efficiency of Auger recombination becomes directly dependent on the steepness of the interfacial potential. A progressive increase in the number of monolayers in the shell leads to smoothening of the interfacial potential, which eventually results in suppression of Auger decay in g-NCs.

The suppression of Auger recombination can greatly benefit lasing applications of NCs since optical gain in these structures involves stimulated emission from multiexciton states. We have fabricated films of g-NCs and tested their optical-gain performance. We observe that the threshold for the development of amplified spontaneous emission (ASE) drops down to just a few tens of microjoules per centimeter squared, which is one-to-two orders of magnitude lower than in samples made of standard NCs. We also observe other unusual optical-gain behaviors for these novel structures such as multi-band ASE spectra, in which the band-edge emission co-exist with stimulated emission features due to transitions involving excited electronic states. Figure 4 shows the emission spectra of a film of g-NCs excited using progressively higher pump intensities (increase bottom to top). The overall spectral range of optical amplification extends over more than 500 meV, which is greater than the optical gain bandwidth observed for any known lasing material. This result indicates a great promise of g-NCs for applications in practical lasing technologies.

Impact on National Missions

In this project, we have demonstrated that a novel class of core-shell NCs consisting of a small CdSe core over-coated with a thick CdS shell show very long multiexciton lifetimes that indicate a significant, possibly complete, suppression of Auger recombination in these nanostructures. We analyze possible reasons for this suppression including the large effective volume of these NCs and a peculiar spatial distribution of electronic wave functions, which results in reduced electron-hole overlap and weak exciton-exciton repulsion. We conclude that while the above factors could indeed provide some reduction of Auger recombination rates, there may also be an important contribution from smoothing of the interfacial potential that results from the likely formation of a gradient alloy layer at the core-shell interface. This would be analogous to the situation in epitaxial quantum dots, where Auger recombination is an inefficient process. As a final proof of suppression of Auger recombination, we conduct ASE experiments. The ASE measurements indicate an extraordinarily large bandwidth of optical gain (>500 meV) that results from contributions of multiexcitons of high order to stimulated emission.

This work can potentially enable novel type of compact, tunable lasers, providing thus a contribution to several technologically important areas such as optical amplification, fiber optics, telecommunication, and remote sensing. All of these

areas are of significant interest to the DOE Office of Basic Energy Sciences. These studies have also applications in areas such as transmission and reception of electromagnetic radiation. These applications are of interest to Threat Reduction.

Publications

Garcia-Santamaria, F., R. Viswanatha, R. D. Schaller, and V. I. Klimov. Do nanocrystal quantum dots have to be "giant" to exhibit suppression of Auger recombination?. Presented at *2009 March Meeting of American Physical Society.* (Portland, OR, 15-19 March 2010).

Garcia-Santamaria, F., Y. Chen, R. Wiswanatha, J. Vela, R. D. Schaller, J. A. Hollingsworth, and V. I. Klimov. Suppression of Auger recombination in giant nanocrystal quantum dots. Presented at *Gordon Research Conference on Clusters, Nanocrystals and Nanostructures.* (South Hadley, MA, 19 - 24 July 2009).

Santamaria, F. Garcia, Y. Chen, R. D. Schaller, J. A. Hollingsworth, and V. I. Klimov. Multi-frequency, low-threshold amplified spontaneous emission from giant quantum dots. Presented at *2008 Fall Meeting of Material Research Society.* (Boston, MA, 1 - 5 December 2008).

Santamaria, F. Garicia, Y. Chen, J. Vela, R. D. Schaller, J. A. Hollingsworth, and V. I. Klimov. Suppressed Auger recombination in giant nanocrystals boosts optical gain performance. 2009. *Nano Letters.* **9** (10): 3482.

Modeling control of viruses by immune responses

Alan S. Perelson
20080726PRD2

Abstract

Humans during their lifetime encounter many pathogens that can cause disease. The immune system is responsible for clearance of these pathogens. Clearance of intracellular pathogens, such as viruses, is mainly achieved by a special population of immune system cells, CD8 T-cells, that can kill pathogen-infected cells. Although for several viruses the importance of CD8 T cells in pathogen clearance has been established, many quantitative properties of the infection, such as the growth dynamics of the pathogen, and the dynamics of pathogen clearance by the CD8 T-cell response, are unknown in detail. This project has provided basic information about these dynamic processes, particularly during HIV-infection.

Background and Research Objectives

Humans during their lifetime encounter many pathogenic microorganisms, and the adaptive immune system is responsible for clearance of many of the encountered pathogens from the host. Clearance of intracellular pathogens (such as viruses) is mainly achieved by a special type of immune cells, CD8 T cells, which are able to kill pathogen-infected cells. For several viral infections, the importance of CD8 T cells in clearance of the pathogen from the host has been clearly established. However, many quantitative properties of pathogen dynamics in the host, including the possible pathogen clearance by the CD8 T cell response, are lacking for most infections of higher mammals such as monkeys and humans. For example, there is still a hot debate about whether the limited availability of host cells susceptible to infection (target cells) or the host's CD8 T cell response control HIV early in infection. The efficacy at which CD8 T cells clear virus-infected cells is generally unknown for most infections. Without a solid framework for estimating the efficacy of T cell responses in vivo, we are not be able to predict which qualities of T cells correlate best with protection against virus infection. Thus, the main goals of our research have been:

- To develop quantitative methods for estimation of the in vivo killing efficacy CD8 T cells during acute and chronic viral infections.
- To estimate the killing efficacy of HIV-specific CD8 T cells during the acute phase of the infection.

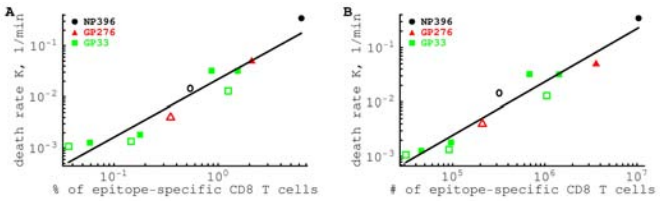

Figure 1. The estimated death rate of peptide-pulsed targets due to killing by epitope-specific CD8 T cells is proportional to the average percent (panel A) or average number (panel B) of epitope-specific CD8 T cells in the spleen [2]. Estimates are given for targets pulsed with NP396, GP276, or GP33 peptides from lymphocytic choriomeningitis virus (LCMV). Filled symbols are for killing by effector CD8 T cells, and open symbols are for killing by memory CD8 T cells. Lines show the linear regression for the log-log transformed estimates of the death rate and density of CD8 T cells. Slopes for the regressions are not statistically different from one (panel A: slope=1.13, p=0.30; panel B: slope=0.98, p=0.80).

Scientific Approach and Accomplishments

We have used data from a set of experiments to quantify the killing efficacy of CD8 T cells, specific to several epitopes of lymphocytic choriomeningitis virus (LCMV) infection [1]. For that virus we have formulated a mathematical model that describes recruitment of targets from the blood to the spleen and killing of targets in the spleen by the virus-specific CD8 T cells [2]. The model was fitted to the experimental data and estimates of the model parameters were obtained. Analysis revealed that killing of target cells in the mouse spleen followed the law of mass-action [4]. According to this law the death rate of target cells due to T cell mediated killing is simply proportional to the total number of virus-specific CD8 T cells in the spleen (Figure 1). This has important implications for the development of T cell based vaccines since it suggests that increasing the number of memory CD8 T cells by vaccination should proportionally increase the rate of killing of virus-infected cells by the T cells response, and as a result lead to a faster clear-

ance of the infection. We have also found that memory T cells are less efficient killers in vivo than are effector T cells. This suggests that the level of memory T cells needed for protection should exceed that generated following live infection. Overall, these results suggest practical guidelines for calculating the level of memory CD8 T cells that will be needed to be induced by vaccination to provide sterilizing immunity. Failure of antibody-based vaccines to prevent infection of humans with HIV has shifted the focus of vaccine development towards CD8 T cells. Many of the current HIV vaccine candidates are aimed at developing large numbers of memory CD8 T cells that are thought to be able to control virus replication. In particular, CD8 T cells have been shown to be important in the control of replication of simian immunodeficiency virus (SIV) during the chronic stages of the infection [3]. However, it is still unknown whether CD8 T cells have any influence on HIV during the acute phase of the infection. Many researchers have thought that depletion of viral target cells was the major reason for the decline of the virus after peak viremia was reached. To address this issue, we have analyzed data on the dynamics of HIV and the escape of the virus from the CD8 T cell response during the acute phase of the infection. Viruses can escape T cell responses by mutating (i.e., changing) the parts of the virus recognized by T cells. We extended our previous mathematical model [5,6], which allowed us to estimate the rate at which CD8 T cells specific to a single viral epitope kill cells infected with HIV (Figure 2), to allow for T cells to recognize multiple epitopes. We found that at the peak of viral load, HIV-specific CD8 T cells, specific to a single viral epitope, contribute to 10-40% of the death of infected cells. Since virus-infected cells generally express 2-10 epitopes, our results suggest that CD8 T cells make a major contribution to the control of HIV growth during acute infection, forming the basis for the development of T cell based vaccines against HIV.

Vaccination is one of the most successful medical achievements of the last century. Due to our limited understanding of the correlates of protection, most vaccines have been developed by a trial and error approach and we have failed to deliver vaccines for important diseases like AIDS or malaria. It is generally believed that most of the currently used vaccines provide protection by inducing high titers of pathogen-neutralizing antibodies [7]. The new vaccines that are currently being developed for devastating chronic infections, such as human immunodeficiency virus (HIV), are designed to stimulate T cell responses. Which properties of T cell responses correlate best with protection are not yet well understood. Our research has been aimed at developing quantitative tools to access the quality of T cell responses generated by vaccines or live infections. We have developed novel mathematical models to quantify the efficacy at which T cells induced after infection with viruses kill virus-infected cells. Using these models, we have shown that killing of targets by T cells follows the law of mass-action, which states that the death rate of targets is simply proportional to the magnitude of the T cell response. This result forms the basis for a prediction of the level of memory T cells needed to provide protection following infection with a virus. We have also shown that CD8 T cells play an important role in regulating replication of HIV during the acute phase of the infection by selecting variants that are not recognized by the T cell response. This work provides a compelling argument for the development of T-cell based vaccines again HIV infection.

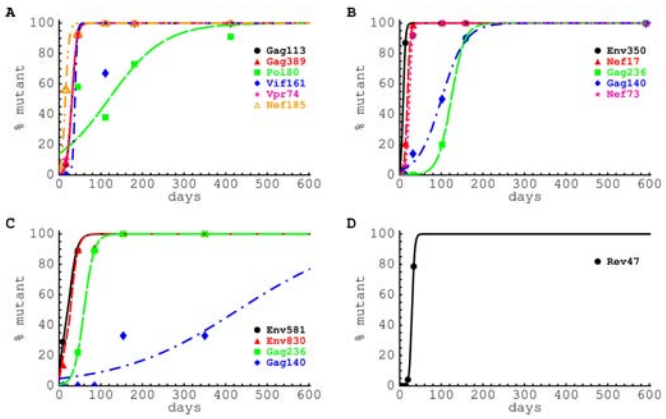

Figure 2. Experimentally measured changes in the frequency of escape mutations in the virus population and the prediction of the mathematical model fitted to data from patients CH40 (panel A), CH77 (panel B), CH58 (panel C), and SUMA0874 (panel D). There is heterogeneity in rates at which virus escapes recognition by the CD8 T cell response in different CTL epitopes. For example, in patient CH77 (panel B), there is rapid fixation of mutations in Nef and Env. Escape mutations in Gag (epitope TW10) occur later in the infection and occur at a much slower rate. Given that a large TW10-specific CD8 T cell response is detected in this patient, a slow rate of escape implies a high fitness cost of the escape mutation [3,4].

Impact on National Missions

This research will directly and specifically impact LANL/DOE missions and goals. One of the strategic grand challenge of LANL is to understand and harness "Complex Biological Systems", including exploring implications for national security and health. This LANL objective falls within the framework of DOE's strategic plan's priority of "Harness the Power of Our Living World". One of the unresolved challenges in immunology is how to predict the efficacy of T cell based vaccines. Work done in this project addresses this challenge.

References

1. Barber, D., E. Wherry, and R. Ahmed. Cutting edge: rapid in vivo killing by memory CD8 T cells. 2008. *Journal of Immunology.* **171** (1): 27.

2. Ganusov, V., and R. J. De Boer. Estimating in vivo death rates of targets due to CD8 T-cell mediated killing. 2008. *Journal of Virology.* **82** (23): 11749.

3. Jin, X., S. E. Tuttleton, S. Lewin , A. Gettie, J. Blanchard, C. E. Irwin, J. T. Safrit, J. Mittler, L. Weinberger, L. G. Kostrikis, L. Zhang, A. S. Perelson, and D. D. Ho. Dramatic rise in plasma viremia after CD8 (+) T cell depletion in simian immunodeficiency virus-infected macaques. 1999. *Journal of Experimental Medicine .* **189** (6): 991.

4. Ganusov, V., D. L. Barber, and R. J. De Boer. Killing of targets by effector CD8 T cells in the mouse spleen follows the law of mass-action. *Journal of Virology.*

5. Ganusov, V., and R. J. De Boer. Estimating costs and benefits of CTL escape mutations in SIV/HIV infection. 2006. *Journal of Public Library of Science Computational Biology .* **2** (3): 24.

6. Goonetilleke, N., M. K. Liu, J. F. Salazar-Gonzalez, G. Ferrari, E. Giorgi, V. Ganusov, B. F. Kelle, G. H. Learn, E. L. Turnbull, M. G. Salazar, K. J. Weinhold, S. Moore, N. Letvin, B. F. Haynes, M. S. Cohen, P. Hraber, T. Bhattacharya, P. Borrow, A. S. Perelson, B. H. Hahn, G. M. Shaw, B. T. Korber, and A. J. Michael . The first T cell response to transmitted/founder virus contributes to the control of acute viremia in HIV-1 infection. 2009. *Journal of Experimental Medicine.* **206** (6): 1253.

7. Plotkin, S. A.. Vaccines: correlates of vaccine-induced immunity. 2008. *Clinical Infectious Diseases.* **47** (3): 401.

Publications

Asquith, B., J. M. A. Borghans, V. Ganusov, and D. Macallan. Lymphocyte kinetics in health and disease Trends. 2009. *Journal of Immunology .* **30** (4): 182.

Ganusov, V.. Estimating in vivo death rates of targets due to CD8 T cell-mediated killing . 2008. *Journal of Virology .* **82** (23): 11749.

Ganusov, V. V., A. E. Lukacher, and A. M. Byers. Similar in vivo killing efficiency of polyoma virus-specific CD8 T cells during acute and chronic phases of the infection. To appear in *Virology.*

Ganusov, V. V., J. M. A. Borghans, and R. J. De Boer. Explicit kinetic heterogeneity: a new method for interpreting data from stable isotope labeling experiments. 2010. *Public Library of Science Computational Biology.* **6** (2): 3000666.

Ganusov, V., J. M. A. Borghans, and R. J. De Boer. Explicit kinetic heterogeneity: a new method for interpreting data from stable isotope labeling experiments. 2010. *Public Library of Science .* **6** (2): e1000666.

Ganusov, V., and R. J Boer. Tissue distribution of lymphocytes and plasma cells and the role of the gut: response to Pabst et al. 2008. *Journal of Trends Immunology .* **29** (5): 209.

Giorgi, E. E., P. Hraber , T. Leitner, B. F. Kelle, C. S. Han, C. Gleasner, L. Green, C. Lo, A. Nag, T. Wallstrom, S. Wang, A. McMichael , B. F. Haynes, B. H. Hahn, A. S. Perelson , P. Borrow, G. M. Shaw, T. Bhattacharya , and B. Korber. Transmission of single HIV-1 genomes and dynamics of early immune escape revealed by ultra-deep sequencing. . To appear in *Public Library of Science .*

Goonetilleke, N., M. K. P Liu, J. F. Salazar-Gonzalez, G. Ferrari, V. Ganusov, E. L. Turnbull, M. G. Salazar, B. F. Keele, K. J. Weinhold, S. Moore, N. Letvin, B. F. Haynes, M. S. Cohen, P. Borrow, A. S. Perelson, B. T. Korber, B. H. Hahn, G. M. Shaw, and A. J. McMichael. The first T cells of acute HIV infection: Transient responses contribute to control of viremia. 2009. *Journal of Experimental Medicine .* **206** (6): 1253.

Lyadova, I. V., M. A. Kapina, G. S. Sepelkova, V. V. Sosunov, K. B. Majorov, T. V. Radaeva, H. J. van den Ham, V. Ganusov, R. J. de Boer, R. Racine, and G. M. Winslos. Tuberculosis progression is promoted by genetically-determined inflammatory responses rather than by the inability of the host to restrict mycobacterial growth. 2010. *Public Library of Science One.* **5** (5): e0469.

Zilman, A., V. V. Ganusov, and A. S. Perelson. Stochastic models of lymphocyte proliferation and death. *Public Library of Science One.*

Fluvial Geomorphic Response to Permafrost Thawing: Implications for the Global Carbon Budget and Arctic Hydrology

Cathy J. Wilson
20080788PRD3

Abstract

Warming and thermal degradation of permafrost and ground ice is anticipated to significantly alter the quantity, distribution and flow pathways of water across the Arctic. These changes will occur both on the surface and in the subsurface. Associated with changes in hydrology and permafrost will likely be the acceleration of landsurface processes that control the storage, release and routing of carbon, sediments, nutrients and trace elements across the landscape. The impact of these changes will likely alter water, energy and carbon budgets across the Arctic and impact model predictions of terrestrial feedbacks on global climate. These terrestrial processes will likely have significant impacts on both the atmosphere and oceans. The processes controlling these changes, however, largely occur at scales far below the resolution of current coupled global models. This research was focused on detecting and predicting changes in the terrestrial arctic to develop a process-based understanding of these hydrologic and geomorphic systems in order to find effective methods of incorporating these changes into global scale models. The research relied heavily on combining numerical modeling of arctic hydrologic systems with remote sensing. The remote sensing is being used to both understand arctic processes and detect change in these systems. The project showed that Arctic river mobility (the rate at which rivers recycle the sediment in their floodplains) is slower than rivers in other parts of the world, but that climate change is causing Arctic river mobility to accelerate, which may lead to larger fluxes of carbon out of permafrost to oceans and the atmosphere.

Background and Research Objectives

Permafrost constitutes 24 percent of the exposed land mass in the Northern Hemisphere. It is estimated that approximately 1,200 Gt of carbon are presently trapped in permafrost (compared to 1,500 Gt in non frozen soils globally), much of which may be released into the atmosphere as a result of global warming and subsequent thawing of permafrost. The thawing of permafrost is also expected to significantly alter arctic hydrology. One potentially critical, but completely unexplored, impact of permafrost thawing is the geomorphic response of arctic river systems.

In many river systems flowing through permafrost much of the bank stability is derived in part from frozen banks. As permafrost warms and the upper few meters of arctic floodplains begin to thaw, bank erosion rates are likely to increase significantly, resulting in more rapid channel migration rates and altering river morphologies. Increased river mobility will erode and mobilize carbon presently trapped in floodplains and potentially accelerate the thawing of deeper permafrost below the active river channels. Erosion of carbon from floodplains may promote sequestration in oceans or conversely accelerate its release to the atmosphere by facilitating oxidation and biological degradation. The potential thawing of deeper permafrost by actively migrating rivers may be a critical, but overlooked, feedback in the current debate regarding how quickly permafrost will respond to global warming.

The focus of this research has been the quantification of Arctic river mobility and dynamics to provide a both a baseline assessment of the rates of Arctic river processes and to detect changes in river mobility during the past four decades of climate warming. The findings of this work will be used to develop models to quantify and predict the impact of climate change on the fluxes of carbon from Arctic river systems to oceans and the atmosphere.

Scientific Approach and Accomplishments

This work has relied on the analysis of remote sensing data using LANL-developed GeniePro automated feature extraction software. Analysis, based on Landsat data for six river systems indicates the rates of channel mobility of Arctic rivers is at least an order of magnitude lower than has been observed in temperate and tropical systems. Additionally these results suggest that river bank erosion rates are relatively constant across Arctic rivers regardless of river size. An implication of this result is that the presence of permafrost is a rate limiting control on bank erosion in the Arctic and that warming and

thawing of permafrost may accelerate river bank erosion across the Arctic. More detailed study of high-resolution imagery from the Yukon River in Alaska suggests that the rates of river bank erosion may have increased from the 1970s to mid-1980s to the present day. This data set also allows for a more detailed assessment of the timing and controls on river bank erosion. This work has been the subject of a number of conference presentations and is being prepared for peer reviewed publication in two separate manuscripts.

Related to this work has been the application of the LANL-developed Arctic Hydrology (ARCHY) model to quantify the influence of surface water and groundwater interactions on permafrost thawing. This work is the subject of an additional manuscript currently in preparation. This research has involved field work on both the Yukon River near Fairbanks Alaska, and the Selawik River in northwest Alaska. The field site on the Selawik will provide data to test models on river bank erosion and has the potential to become a long term study site to determine the affect of landsurface changes on carbon cycles in the Arctic. A major outcome of this Postdoctoral project has been its role as a catalyst for Arctic terrestrial research at LANL. Through internal collaborations related to this Postdoctoral project several areas for broader laboratory research on both remote sensing and hydrology in the Arctic have led to successful proposal efforts for both LDRD and DOE funding sources. Finally, this research has led to a number of external collaborations encompassing field work, remote sensing analysis, and climate modeling. These collaborations include: the USFWS Region 7 (Alaska); Idaho State University; University of Alaska Fairbanks; National Hydrology Research Centre, Environment Canada, Saskatoon, Saskatchewan, Canada; National Center for Atmospheric Research; San Diego State University; and University of California, Santa Barbara.

Impact on National Mission

This work addresses the DOE OBER goal to achieve a predictive understanding of how greenhouse gas emissions impact the Earth's climate and biosphere, including improving the world's most powerful climate models and working to understand carbon cycling in terrestrial systems. The project will significantly improve our estimates of the impact of climate change on Arctic river fresh water, carbon, nutrient, sediment and trace element inputs to the Arctic Ocean. These are key inputs for Arctic ocean biogeochemistry, circulation and sea ice behavior. The Arctic ocean and its behavior is a critical driver of the Northern hemisphere weather, as well as global ocean circulation and global climate.

Publications

Rowland, J. C., C. E. Jones, G. Altmann, R. Bryan, B. T. Crosby, G. L. Geernaert, L. D. Hinzman, D. L. Kane, D. M. Lawrence, A. Mancino, P. Marsh, J. P. McNamara, V. E. Romanovsky, H. Tonolio, B. J. Travis, E. Trochim, and C. J. Wilson. Arctic landscapes in transition: responses to thawing permafrost. 2010. *EOS Transactions, American Geophysical Union.* **91** (26): 229.

Rowland, J. C., G. E. Hilley, and A. Fildani. A test of submarine leveed channel initiation by deposition alone. To appear in *Journal of Sedimentary Research.*

Rowland, J. C., M. T. Stacey, and W. E. Dietrich. Turbulent characteristics of a shallow wall-bounded plane jet: experimental implications for river mouth hydrodynamics. 2009. *Journal of Fluid Mechanics.* **627**: 423.

Rowland, J. C., W. E. Dietrich, G. Day, and G. Parker. Formation and maintenance of single-thread tie channels entering floodplain lakes: Observations from three diverse river systems. 2009. *JOURNAL OF GEOPHYSICAL RESEARCH-EARTH SURFACE.* **114**: F02013.

Rowland, J. C., W. E. Dietrich, and M. E. Stacey. Morphodynamic controls on subaqueous levee formation: experimental implications for river mouth morphology. *Journal of Geophysical Research Earth Surface.*

Determinaing the Mechanisms of Enzymes Xylose Isomerase and HIV Protease using Neutron Crystallography

Paul A. Langan
20080789PRD3

Abstract

Most of our understanding of how proteins, and in particular enzymes, function comes from determining their structure. Previously, it has been done mainly with X-ray crystallographic techniques. We are advancing neutron protein crystallography, a complementary method to X-ray diffraction, in order to reveal finer details of enzymatic reactions than X-ray crystallography alone can provide. The catalytic mechanism of the enzyme D-xylose isomerase, important for bioethanol production from lignocellulosic biomass, has been probed with neutron diffraction and structures were refined utilizing both X-ray and neutron data to give better, more complete and accurate structures than can be achieved by each technique. A modified mechanism has been proposed on the basis of a number of X-ray and neutron structures, while these results paved the way for new research toward constructing a more efficient D-xylose isomerase for industry. Crystallization and neutron diffraction techniques were applied to successfully grow large crystals of per-deuterated HIV-1 protease in complex with clinical drug amprenavir. The postdoc fellow's research and contribution to running the neutron Protein Crystallography Station was recognized by a Postdoc Distinguished Performance Award (LANL 2009).

Background and Research Objectives

Knowledge of three-dimensional structure of proteins is central to protein engineering for commercial applications and also in structure-assisted drug design. Protein structure is also vital for our understanding of how enzymes, nature's macromolecular catalysts, run chemical reactions and for drawing structure-function relationships. Since most industrial and drug-target proteins are enzymes, the knowledge of their exact mechanisms is of paramount importance to help guide protein engineering efforts to produce more efficient enzymes, and to design better medicines that can save many lives. X-ray crystallography has been the major technique to provide information on structure. However, its inability to detect hydrogen (H) atoms in the majority of known macromolecular structures due to weak scattering power of H has hampered its usefulness for determining mechanisms of enzymatic reactions. Most chemical reactions rely on the transfer of H atoms between enzymes, substrates and solvent molecules. As a consequence, many enzyme mechanisms are not well understood, leading to less efficient industrial processes and less effective drugs.

Neutrons, on the other hand, are scattered by atomic nuclei, while their scattering power does not depend on the number of electrons present in an atom, as is the case for atomic scattering of X-ray photons. Thus, neutrons can reveal the positions of H atoms (and its isotope deuterium, D), that comprise almost half of all atoms present in proteins, as easily as those for carbon, oxygen and nitrogen. Importantly, enzyme structures obtained using neutron protein crystallography contain information on the locations of H and D atoms even at quite low resolutions of 2.2-2.5Å [1], whereas X-ray structures need to have resolutions of better than 1Å in order to observe some H atoms. In order to improve the contrast in neutron diffraction some or all H atoms can be exchanged with D, which has much stronger neutron scattering power than H, by deuterated solvent D_2O or by expressing the protein in deuterated media respectively.

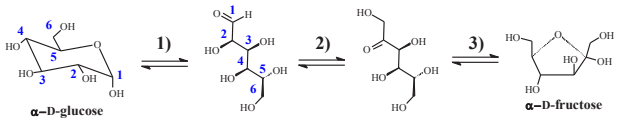

Figure 1. D-glucose-to-D-fructose interconversion reaction. The reaction catalyzed by XI has been represented as consisting of three major steps 1) ring opening 2) isomerization 3) ring closure.

XI is an enzyme capable of interconverting aldo-sugars D-glucose and D-xylose into their keto-isomers D-fructose and D-xylulose, respectively; it can be found in many bacteria and fungi [2] (Figure 1). It has found major commercial application in the production of high fructose corn syrup from starch [2]. Recently, XI has been utilized in the production of bioethanol from lignocellulosic biomass [3]. The industrial ethanol-

fermenting yeast *Saccharomyces cerevisiae* can efficiently utilize hexose sugars, like D-glucose, from biomass, but cannot grow on or ferment pentoses, like D-xylose and L-arabinose, which together can amount to 50% of sugars in biomass feedstocks. It can, however, digest D-xylulose. This deficiency of *S. cerevisiae* is the key challenge for DOE bioenergy mission to achieve cost-effectiveness and profitability of lignocellulosic ethanol. Introducing a metabolic pathway by genetic engineering approach to express XI into yeast is very attractive for alleviating this deficiency in the bioethanol production [4]. However, XI is a very slow enzyme, has low affinity for the substrates, does not function well at acidic conditions and is prone to inhibition by xylitol, the reduced analog of xylose. Understanding the XI mechanism via neutron protein crystallographic technique will not only pave the way to the application of this methodology for HIV-1 PR and other proteins, but will also help current protein engineering efforts to generate a better-performing XI enzyme for bioethanol industry.

The objectives of this research proposal were:

1. Develop neutron crystallography techniques to derive the enzyme mechanism of D-xylose isomerase (XI);

2. Apply those techniques to HIV-1 (human immunodeficiency virus type 1) protease (PR);

3. Determine the mechanism of PR and aid drug design for HIV-1.

We met objectives 1 and 2 fully, and made good progress to meeting objective 3.

Scientific Approach and Accomplishments

Neutron protein crystallography is an emerging structural biology technique [5, 6]. It has never been applied to formulating an enzyme mechanism before. The major drawback of this method has always been the difficulty in producing protein crystals of sufficient size, *i.e.* > 1 mm^3. While in case of X-ray protein crystallography it is sufficient to grow any crystals, for neutron protein crystallography the need is transferred into a different realm: generally crystals have to be orders of magnitude bigger than those required for X-ray diffraction. Therefore, to achieve the goals of this proposal, first, methodology and techniques for crystal growth of XI and HIV-1 PR were designed. A crystallization robot (Oryx 8, Douglas Instruments) and the deuteration laboratory in B division were used to optimize crystal size. Utilizing Oryx 8 we were able to determine the crystallization phase diagram for XI and perform fine scanning of crystallization conditions. This approach gave very precise protein and precipitant concentrations that allowed us to grow large XI crystals of required quality for running neutron diffraction experiments (Figure 2). We have exploited the Protein Crystallography Station (PCS) at LANSCE [7, 8] to study the XI mechanism with the time-of-flight (TOF) neutron diffraction method. PCS is being run as a user facility serving the national and international scientific community. Beamtime is allocated based on peer-review of submitted proposals by a scientific committee consisting of university professors and scientists from other DOE labs. This project received high grades and was granted ~100 days total of beamtime in 2008, 2009 and 2010, which allowed us to collect complete neutron datasets for a number of XI complexes. Since PCS is greatly oversubscribed we also pursued beamtime at Institute Laue Langevin (ILL, Grenoble, France) and were awarded ~50 days total on beamline D19 in 2009 and 2010. The beamtime awards at ILL equal to over $2 million dollar grants if the beamtime were bought on commercial basis. Based on the crystallization methods derived for XI, we were able to grow large crystals of HIV-1 PR in complex with clinical inhibitor amprenavir. We were awarded 12 days of beamtime at ILL on instrument LADI-III to collect the neutron diffraction data and currently await the allocation of the beamtime. During the course of the project we developed crucial collaborations with experts in XI enzyme, with the group led by Dr. J. P. Glusker of Fox Chase Cancer Center (Philadelphia, PA). We also established collaboration with Dr. B. L. Hanson of the University of Toledo, the head of the X-ray Crystallography Instrumentation Center, who was and continues to be active in collecting key room temperature X-ray diffraction data on XI complexes and other proteins.

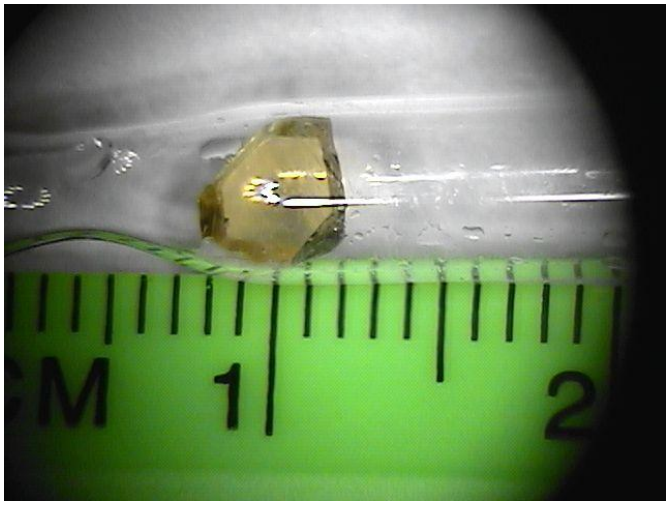

Figure 2. Crystal of XI sealed in a quartz capillary, ready for neutron diffraction experiment.

To determine the catalytic mechanism of XI we employed a combination of X-ray and neutron diffraction experiments and refined structures jointly utilizing both X-ray and neutron crystallographic data. X-ray data give accurate positions of heavy atoms, like carbon, oxygen and nitrogen, while neutron data provide locations of H and D atoms. As a result, a protein structure refined jointly with two sets of diffraction data is more accurate and complete. All crystallographic data were collected at room temperature. This way we avoided any structural artifacts that may arise due to freezing a protein crystal. In addition, enzymes are nor-

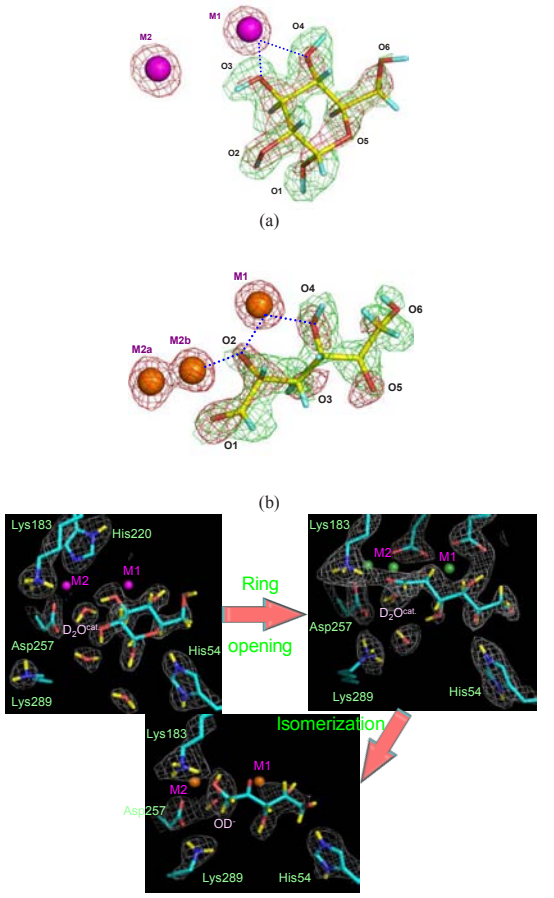

Figure 3. Superposition of neutron (green) and electron density maps for cyclic (a) and linear (b) glucose. M1 and M2 are both Cd2+ in (a) and Ni2+ in (b). (c) neutron density for the enzyme-substrate (left), enzyme-intermediate (right), and enzyme-product complexes.

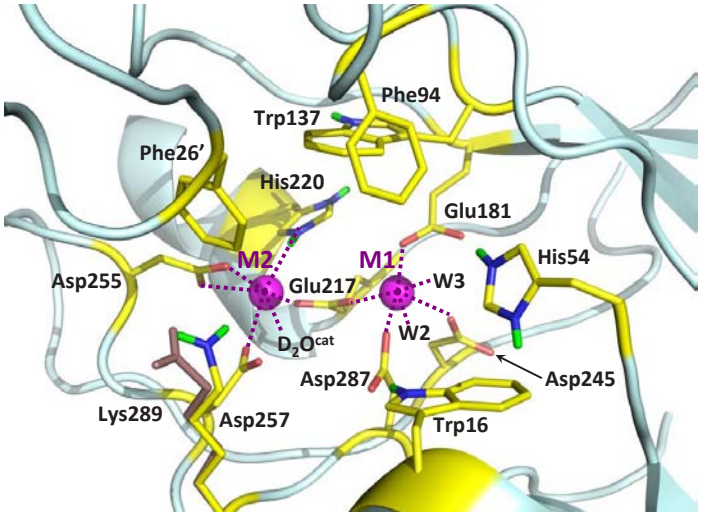

Figure 4. XI active site

mally active at temperatures close to ~30°C, thus, room temperature is closer physiological conditions and the enzyme structures are more relevant for elucidating the reaction mechanisms. A series of X-ray structures of XI in complex with substrates, products and inhibitors were determined in order to select complexes worthy of neutron crystallographic experiments. This led to determining joint X-ray/neutron structures of XI that represent snapshots along the enzyme's catalyzed reaction:

1. *apo*-XI containing no metal cations or a substrate at physiological pH of 7.7;
2. XI complexed with two Co^{2+} co-factors;
3. XI complexed with two Cd^{2+} co-factors and cyclic deuterated glucose;
4. XI complexed with two Ni^{2+} co-factors and linear deuterated glucose;
5. XI complexed with two Mg^{2+} co-factors and linear deuterated xylulose product.

For the first time, the enzyme reaction inhibiting effects of transition metals have been exploited in this study in order to trap intermediates along the reaction pathway [9-18]. XI is a metallaenzyme, with absolute need for divalent metal cations to be present in its active site for full activity. Metals such as Mg^{2+}, Co^{2+} and Mn^{2+} activate XI, whereas most other transition, alkali-earth and rare-earth metals inhibit the enzyme. The sugar conversion reaction proceeds through 3 major stages depicted in Figure 1: 1) sugar substrate ring opening (2) isomerization of the linear substrate and (3) product ring closure. Yet, until this study it was not known at which stage the metal inhibitors stopped the XI-catalyzed reaction. We determined that Cd^{2+} inhibits the reaction at the point of the cyclic sugar substrate binding, but Ni^{2+} allows the ring opening step to occur and stops the reaction before the next stage, isomerization (Figure 3).

The catalytic site of XI is depicted in Figure 4. The joint X-ray/neutron structures have allowed us to trace the possible movements of hydrogen atoms and to propose a modified mechanism for the sugar conversion reaction. The latter is based on our major findings (Figure 3): a) M2-bound solvent molecule is water until after the isomerization step. when it is observed as a hydroxide anion (OH^-); b) key catalytic residues His54 and Lys183 are protonated, and thus positively charged, throughout the reaction; c) Ni^{2+} occupies two distinct sites in M2 position, M2a and M2b, strengthening the proposal that metal movement is crucial for activating the catalytic water to start the isomerization step; d) Lys289 residue (which has never before been implicated in playing a role in the reaction) is neutral before, but is protonated after the ring opening; e) O5 oxygen of the sugar that is hydrogen-bonded to His54 stays deprotonated after the ring opening and acquires a negative charge. Based on these finding we proposed that

1) the ring opening step is not initiated by a permanent donation of H atom from His54 to O5, rather O1 may lose its proton that ends up on Lys289 through a water network; 2) Lys183 does not protonate O1 of the linear sugar substrate to commence the isomerization reaction, but it must be the catalytic water activated by the moving M2 metal that protonates O1 and becomes OH^-.

The proposed mechanism is hard to verify without theoretical calculations. Consequently, we initiated quantum-chemical studies of XI by means of Quantum Enzymology (QuE) approach that is based on $O(N)$ quantum mechanical methods developed at LANL by Dr. Challacombe of T Division. We have developed collaboration with Dr. Challacombe and Dr. Bock of T-1 aimed to develop QuE for studying enzyme mechanism and ultimately perform quantum-chemical mutagenesis. QuE has the advantages over the conventional $O(N^3)$ quantum-mechanical/molecular-mechanical (QM/MM) methods because it can calculate large models solely with QM much faster without the introduction of heavy parameterization. The use of pure QM for the many-atom models is critical to correctly describe the long-range electrostatic effects of the reaction in the enzyme active-site cavity, hydrogen bonding, charge transfer over long distances, and other weak inter-atomic interactions with long-range effects, which play essential roles in the reactions occurring in the enzyme active site.

During the course of the Director's-funded postdoctoral fellowship the work was recognized by Los Alamos Awards Program (LANL 2008) and nominated for J.R. Oppenheimer Distinguished Postdoc Fellowship (LANL 2009). The research and contribution to running PCS was recognized by a Postdoc Distinguished Performance Award (LANL 2009), jointly with Dr. S.Z. Fisher.

Our additional objectives (for future research) that grew out of this project are to perform XI mutagenesis studies by generating mutant libraries and develop enzyme activity assays for constructing XI variants that would be more efficient on D-xylose and L-arabinose substrates, would perform well at acidic conditions (pH of ~5) and temperatures normally used for yeast growth and ethanol fermentation. To achieve our new goals will require additional joint X-ray/neutron structures of XI at low and high pH values, its complexes with inhibitors at low pH, and complexes with L-arabinose. We will also have to develop a high-throughput enzyme assay for testing the activity of mutants in libraries.

Impact on National Missions

Protein engineering has applications for national missions that range from bioenergy, to biological remediation of waste streams, to biosecurity, each of which multiple Federal stakeholders.

References

1. Niinura, N., and R. Bau. Neutron Protein crystallography. 2008. *Acta Crystallographica A.* **64**: 12.

2. Bhosale, S., and E. Tal. Molecular and Industrial Aspects of Glucose Isomerase. 1996. *Microbiology Reviews.* **60**: 280.

3. Maris, A. van, and E. Tal. Alcoholic Fermentation of Carbon Sources in Biomass Hydrolysates by Saccharomyces cerevisiae: Current Status. 2006. *Antonie van Leeuwenhoek .* **90**: 391.

4. Kuyper, M.. High-Level Functional Expression of a Fungal Xylose Isomerase: the Key to Efficient Ethanolic Fermentation of Xylose by Saccharomyces cerevisiae?. 2003. *FEMS Yeast Res.* **4**: 69.

5. Lakey, J.. Neutrons for biologists: a beginner's guide, or why you should consider using neutrons. 2009. *J. R. Soc. Interface .* **6**: 567S.

6. Langan, P., Z. Fisher, A. Kovalevsky, M. Mustyakimov, A. S. Valone, C. Unkefer, M. J. Waltman, L. Coates, P. D. Adams, P. V. Afonine, B. Bennett, C. Dealwis, and B. P. Schoenborn. Protein structures by spallation neutron crystallography. 2008. *Journal of Synchrotron Radiation.* **15** (3): 215.

7. Kovalevsky, A., and E. Tal. Macromolecular Neutron Protein Crystallography at the Protein Crystallography Station. To appear in *Acta Crystallorgaphica.*

8. Kovalevsky, A.. Macromolecular Neutron Crystallography at PCS. To appear in *Acta Crystallographica .*

9. Katz, A. K., X. M. Li, H. L. Carrell, B. L. Hanson, P. Langan, L. Coates, B. P. Schoenborn, J. P. Glusker, and G. J. Bunick. Locating active-site hydrogen atoms in D-xylose isomerase: Time-of-flight neutron diffraction. 2006. *PROCEEDINGS OF THE NATIONAL ACADEMY OF SCIENCES OF THE UNITED STATES OF AMERICA.* **103** (22): 8342.

10. Kovalevsky, A., L. Hanson, S. Zoe. Fisher, M. Mustyakimov, S. Mason, V. Trevor. Forsyth, M. Blakeley, D. A. Keen, T. Wagner, H. L. Carrell, A. Katz, J. Glusker, and P. Langan. Metal Ion Roles and the Movement of Hydrogen during Reaction Catalyzed by D-Xylose Isomerase: A Joint X-Ray and Neutron Diffraction Study. 2010. *STRUCTURE.* **18** (6): 688.

11. Glusker, J., and E. Tal. Using Neutron Protein Crystallography to Understand Enzyme Mechanism. To appear in *Acta Crystallographica.*

12. Kovalevsky, A., A. Katz, H. L. Carrell, L. Hanson, M. Mustyakimov, S. Zoe. Fisher, L. Coates, B. Schoenborn, G. Bunick, J. Glusker, and P. Langan. Hydrogen location

in stages of an enzyme-catalyzed reaction: Time-of-flight neutron structure of D-xylose isomerase with bound D-xylulose. 2008. *BIOCHEMISTRY.* **47** (29): 7595.

13. Kovalevsky, A.. Hydrogen Location in Stages of an Enzyme-Catalyzed Reaction: Time-of-Flight Neutron Structure of D-Xylose Isomerase with Bound D-Xylulose. Invited presentation at *American Conference on Neutron Scattering.* (ottawa, 26 June).

14. Kovalevsky, A.. Structural Enzymology with Neutrons: The Mechanism of D-Xylose Isomerase. Invited presentation at *Bioscience division colloquium.* (Los Alamos, 23 July 2009).

15. Kovalevsky, A.. Revised Mechanism of Sugar Interconversion by Enzyme Xylose Isomerase Employing Time-of-Flight Neutron Crystallography. Invited presentation at *American crystallographic association.* (Toronto, 25 July 2009).

16. Kovalevsky, A.. Locating hydrogen atoms in enzymes: A neutron structure of D-xylose isomerase with bound D-xylulose. Invited presentation at *Keystone symposium.* (Breckenridge, 8 Jan 2010).

17. Glusker, J.. Locating hydrogen atoms in enzymes: A neutron structure of D-xylose isomerase with bound D-xylulose. Invited presentation at *IUCr.* (Osaka, August 23).

Publications

Fisher, S. Z., A. Y. Kovalevsky, J. F. Domsic, M. Mustyakimov, D. N. Silverman, R. McKenna, and P. Langan. Preliminary joint neutron and X-ray crystallographic study of human carbonic anhydrase II. 2009. *ACTA CRYSTALLOGRAPHICA SECTION F-STRUCTURAL BIOLOGY AND CRYSTALLIZATION COMMUNICATIONS.* **65** (5): 495.

Fisher, S. Zoe., A. Kovalevsky, J. Domsic, M. Mustyakimov, R. McKenna, D. Silverman, and P. Langan. Neutron Structure of Human Carbonic Anhydrase II: Implications for Proton Transfer. 2010. *BIOCHEMISTRY.* **49** (3): 415.

Ghosh, A., S. Kulkarni, D. Anderson, L. Hong, A. Baldridge, Y. Wang, A. Chumanevich, A. Kovalevsky, Y. Tojo, M. Amano, Y. Koh, J. Tang, I. Weber, and H. Mitsuya. Design, Synthesis, Protein-Ligand X-ray Structure, and Biological Evaluation of a Series of Novel Macrocyclic Human Immunodeficiency Virus-1 Protease Inhibitors to Combat Drug Resistance. 2009. *JOURNAL OF MEDICINAL CHEMISTRY.* **52** (23): 7689.

Kovalevsky, A. Y., S. Zoe. Fisher, S. Seaver, M. Mustyakimov, N. Sukumar, P. Langan, T. Mueser, and B. Leif. Hanson. Preliminary neutron and X-ray crystallographic studies of equine cyanomethemoglobin. 2010. *ACTA CRYSTALLOGRAPHICA SECTION F-STRUCTURAL BIOLOGY AND CRYSTALLIZATION COMMUNICATIONS.* **66** (4): 474.

Kovalevsky, A. Y., T. Chatake, N. Shibayama, S. -Y. Park, T. Ishikawa, M. Mustyakimov, S. Z. Fisher, P. Langan, and Y. Morimoto. Preliminary time-of-flight neutron diffraction study of human deoxyhemoglobin. 2008. *ACTA CRYSTALLOGRAPHICA SECTION F-STRUCTURAL BIOLOGY AND CRYSTALLIZATION COMMUNICATIONS.* **64** (4): 270.

Kovalevsky, A., A. Katz, H. Carrell, L. Hanson, M. Mustyakimov, S. Fisher, L. Coates, B. Schoenborn, G. Bunick, J. Glusker, and P. Langan. Hydrogen location in stages of an enzyme-catalyzed reaction: time-of-flight neutron structure of D-xylose isomerase with bound D-xylulose.. 2008. *Biochemistry.* **47**: 7595.

Kovalevsky, A., L. Hanson, S. Zoe. Fisher, M. Mustyakimov, S. Mason, V. Trevor. Forsyth, M. Blakeley, D. A. Keen, T. Wagner, H. L. Carrell, A. Katz, J. Glusker, and P. Langan. Metal Ion Roles and the Movement of Hydrogen during Reaction Catalyzed by D-Xylose Isomerase: A Joint X-Ray and Neutron Diffraction Study. 2010. *STRUCTURE.* **18** (6): 688.

Kovalevsky, A., T. Chatake, N. Shibayama, S. Park, T. Ishikawa, M. Mustyakimov, Z. Fisher, P. Langan, and Y. Morimoto. Direct Determination of Protonation States of Histidine Residues in a 2 angstrom Neutron Structure of Deoxy-Human Normal Adult Hemoglobin and Implications for the Bohr Effect. 2010. *JOURNAL OF MOLECULAR BIOLOGY.* **398** (2): 276.

Langan, P., Z. Fisher, A. Kovalevsky, M. Mustyakimov, A. S. Valone, C. Unkefer, M. J. Waltman, L. Coates, P. D. Adams, P. V. Afonine, B. Bennett, C. Dealwis, and B. P. Schoenborn. Protein structures by spallation neutron crystallography. 2008. *Journal of Synchrotron Radiation.* **15** (3): 215.

Langan, P., Z. Fisher, A. Kovalevsky, M. Mustyakimov, A. Sutcliffe Valone, C. Unkefer, M. J. Waltman, L. Coates, P. Adams, P. Afonine, B. Bennett, C. Dealwis, and B. Schoenborn. Protein structures by spallation neutron crystallography. 2008. *Journal of Synchrotron Radiation.* **15** (3): 215.

Vorontsov, I., T. Graber, A. Kovalevsky, I. Novozhilova, M. Gembicky, Y. Chen, and P. Coppens. Capturing and Analyzing the Excited-State Structure of a Cu(I) Phenanthroline Complex by Time-Resolved Diffraction and Theoretical Calculations. 2009. *JOURNAL OF THE AMERICAN CHEMICAL SOCIETY.* **131** (18): 6566.

Analysis of Protein Structure-Function Relations in Antibiotic Biosynthesis and Signal Transducing Receptors

Louis A. Silks III
20090524PRD2

Abstract

The challenge for studying protein structures, their complexes and the structural dynamic of these proteins by Nuclear Magnetic Resonance (NMR) spectroscopy is the protein size-dependent relaxation behavior of the NMR signal. With an increasing size of the proteins, not only the signal overlap increases, also the signal intensity and the line-width of a signal decrease. To solve or at least reduce this problem, other relaxation effects, like the exchange with NMR active nuclei of the solvent, can be prevented by perdeuteration, in which all of the hydrogen atoms are replaced by deuterium. The number of NMR signals can be reduced by amino acid type specific perdeuteration and ^{13}C-depletion, or conversely, the specific ^{13}C and ^{1}H enrichment of a limited number of spins systems in an otherwise fully perdeuterated and ^{13}C-depleted sample.

Background and Research Objectives

The development of methods for the elucidation of protein structures, to study their interactions with ligands and other proteins, and to analyze complex inter-domain communications, is accelerating. As a result, research that employs biophysical methods to investigate biological molecules and dynamic interaction events has dramatically evolved and allows studies of highly complex systems. These are biological systems like:

1. Non-ribosomal peptide bond-forming condensation domains (C-domains), proteins that are essential for the biosynthesis of antibiotics (erythromycin, vancomycin, daptomycin and penicillin), fungal and bacterial toxins and virulence factors (aflatoxin, vibriobactin, enterobactin, mycolic acid in *M. tuberculosis*), chemotherapeutics, antiviral and antifungal compounds

2. Membrane proteins responsible for the export of these secondary metabolites, that show a high homology to proteins responsible for the import of carbohydrates

3. G-protein coupled receptors (GPCRs), membrane proteins responsible for signal transduction in mammalian cells. The challenge for studying protein structures, their complexes and the structural dynamic of these proteins by Nuclear Magnetic Resonance (NMR) spectroscopy is the protein size-dependent relaxation behavior of the NMR signal.

Scientific Approach and Accomplishments

In collaboration with L. A "Pete" Silks (B-8) and Ryszard Michalczyk (B-8), specifically isotopic enriched amino acids and amino acid precursors for the cell-free and bacterial expression of selectively labeled proteins and perdeuterated detergents for NMR spectroscopic analysis of membrane proteins were be synthesized. Together we performd these syntheses at the LANL Stable Isotope Resource using the in-house expertise and the support of Silks and Michalczyk. Originally planned projects included:

- synthesis of [3,3'-$^{2}H_{2}$, 1,2-$^{13}C_{2}$, ^{15}N] of Ile and Val
- [^{15}N ; ^{13}C depleted; U- ^{2}H; $^{13}C^{1}H_{3\ -methyl}$] of Ile, Leu, Val, Met and [^{15}N; ^{12}C; ^{2}H; $^{13}C^{1}H_{\ -aromatic}$] of Phe
- [^{15}N; ^{12}C; ^{2}H; $^{13}C^{1}H_{-e}$] of Phe, Tyr, Trp and His
- [1-$^{2}H^{R}$, 1-^{13}C, 2-^{2}H, 3-$^{2}H^{R}$, 3-^{13}C] and U-^{13}C glycerol
- U-^{2}H fatty acids for the synthesis of U-^{2}H t-octylphenoxyl-polyethoxyethanol (Triton X-100) and u-^{2}H 1-palmitoyl-2-hydroxy-sn-glycero-3-[phosphor-RAC-(1-glycerol)] (LPPG).

Alex made significant progress in synthesizing stable isotope amino acids. Using these isotopic enriched compounds he worked in the following:

- The high-resolution liquid-state NMR structures of the C-domain, the structural complexes with its native interaction partners, to gain insight into the biosynthetic processes to consequently support research for the syntheses of new and effective antibiotics and to specific inhibit the biosynthesis of bacterial and fungal toxins.

- The NMR structure of one micelle-embedded antibiotics export protein to study the role of this family of proteins in the development of antibiotic resistance.
- The structure and the analysis of the substrate specificity of one niacin-binding GPCR to analyze its role in blood sugar level regulation and as an alternative target to treat type II diabetes.
- Making synthesis protocols available for the growing scientific community interested in studying structures and structural dynamics of membrane proteins and in exchange establish a bacterial cell-free protein production system.

During this period Alex Koglin co-authored a review in the Natural Products Reports journal detailing his research on nonribosomal peptides that have a variety of medicinal activities including activity as antibiotics, antitumor drugs, immunosuppressives, and toxins. Their biosynthesis on multimodular assembly lines as a series of covalently tethered thioesters, in turn covalently attached on pantetheinyl arms on carrier protein way stations, reflects similar chemical logic and protein machinery to fatty acid and polyketide biosynthesis. While structural information on excised or isolated catalytic adenylation (A), condensation (C), peptidyl carrier protein (PCP) and thioesterase (TE) domains had been gathered over the past decade, little was known about how the NRPS catalytic and carrier domains interact with each other both within and across elongation or termination modules. This manuscript catalogs the recent breakthrough achievements in both X-ray and NMR spectroscopic studies that illuminate the architecture of NRPS PCP domains, PCP-containing didomain-fragments and of a full termination module (C-A-PCP-TE).

Impact on National Missions

Our isotopic enriched compounds can contribute to:

- The high-resolution liquid-state NMR structures of the C-domain, the structural complexes with its native interaction partners to gain insight into the biosynthetic processes and consequently support research for the syntheses of new and effective antibiotics and to specific inhibit the biosynthesis of bacterial and fungal toxins
- The NMR structure of one micelle embedded antibiotics export protein to study the role of this family of proteins in the development of antibiotic resistance
- The structure and the analysis of the substrate specificity of one niacin-binding GPCR to analyze its role in blood sugar level regulation and as an alternative target to treat type II diabetes
- Make synthesis protocols available for the growing scientific community interested in studying structures and structural dynamics of membrane proteins and in exchange establish a bacterial cell-free protein production system.

Publications

Frueh, D. P., A. Leed, H. Arthanari, A. Koglin, C. T. Walsh, and G. Wagner. Time-shared HSQC-NOESY for accurate distance constraints measured at high-field in N-15-C-13-ILV methyl labeled proteins . 2009. *JOURNAL OF BIOMOLECULAR NMR* . **45** (3): 311.

Koglin, A.. Structural insights into nonrobosomal peptide enzymatic assembly lines. 2009. *Natural Products Reports.* **26** (8): 987.

Koglin, A., C. T. Walsh, D. P. Frueh, H. Arthanari, and G. Wagner. A Double TROSY hNCAnH Experiment for Efficient Assignment of Large and Challenging Proteins . 2009. *JOURNAL OF THE AMERICAN CHEMICAL SOCIETY.* **131** (36): 12880.

Koglin, A., E. R. Strieter, Z. D. Aron, and C. T. Walsh. Cascade Reactions during Coronafacic Acid Biosynthesis: Elongation, Cyclization, and Functionalization during Cfa7-Catalyzed Condensation . 2009. *Journal of the American Chemical Society.* **131** (6): 2113.

Information Science & Technology

LABORATORY DIRECTED RESEARCH AND DEVELOPMENT

Synthetic Cognition through Peta-Scale Models of the Primate Visual Cortex

Luis Bettencourt
20090006DR

Introduction

This project seeks to understand and implement the computational principles that enable high-level sensory processing and other forms of cognition in the human brain. To achieve these goals, we are creating synthetic cognition systems that emulate the functional architecture of the primate visual cortex. By using petascale computational resources, combined with our growing knowledge of the structure and function of biological neural systems, we will match, for the first time, the size and functional complexity necessary to reproduce the information processing capabilities of cortical circuits. Several major scientific and technological breakthroughs are anticipated. First, the hypothesis pervading much of Artificial Intelligence for the last 50 years, that synthetic cognition approaching human levels of performance can be achieved simply by matching the scale of the human brain, can finally be tested. Second, more complex neural processing mechanisms, such as spiking dynamics, synaptic plasticity, and lateral and feedback connections between cortical neurons, will be assessed quantitatively with respect to the resulting performance gains in real time cognitive tasks. Here, we proposed a comprehensive theoretical, computational and experimental program to implement models of the primate visual cortex, faithful in scale and complexity to the biological system, using petascale computational platforms such as Roadrunner. Our ultimate objective is to create a real time synthetic cognitive system that approaches or surpasses human visual performance.

Benefit to National Security Missions

The project supports the Department of Energy Office of Science by creating a new generation of powerful petascale computational systems that approach human visual cognition. It supports applied science missions including battlefield awareness, nuclear threat detection, counterterrorism, and stockpile monitoring, while addressing one of the deepest questions of fundamental science. We currently have a new offshoot of the project funded by DARPA and are in dialogue to several agencies interested in remote sensing [1].

Progress

The project has reached key milestones along its four main objectives. First, regarding scaling up current models of visual cortex, the project has reached system sizes and speeds that are much larger than any by peer groups at MIT, and any other institutions worldwide. This was due to model developments and the implementation of our codes both in terms of CELL (the architecture of roadrunner) and GPUs. We are now able to process large format video (HD) in real time, using GPU clusters, and smaller formats faster than real time. These computational advantages are making us competitive for funding with several agencies seeking surveillance and remote sensing applications [1].

Scientifically, we investigated how system self-organization and performance scales up with size and amount of learning and developed the capability for the system to learn and analyze video content [2]. These analyses are leading to new model developments, such as the reorganization of our computational code in a way that includes feedback and lateral connections, which are essential elements of a model operating without feed-forward input, see below.

We have now made substantial progress along the second objective, which is concerned with analyzing mechanisms and architectures that are not currently part of the main model. This includes lateral connectivity in functional cortical layers, spiking neural dynamics, and feedback from higher visual areas onto lower ones. Regarding lateral connections we have shown that these can help capture long-range correlations that belong to objects across the small receptive of neurons in primary visual cortex [4,5**]**. Using lateral connectivity creates fields of cell activation that correspond to long range object contours and allows the system to de-clutter images. Spiking neural models allow for a finer control of temporal aspects of neural processing that may be explored in the brain to code for information. We have made substantial progress in studies of dynamical mechanisms to bind local features together and of learning rules that are explicitly temporal such as time dependent synaptic plasticity. Finally, we

have started several studies that analyze and implement feedback dynamics in neural image processing. We have shown that different learning rules for feedback connections implement different probabilistic mechanisms of estimation, and of visual attention connected to object localization and segmentation in images. These insights and derived models are now being implemented on our main production codes.

Our theoretical and computational work is guided and informed, whenever possible, by experiments in human visual cognition and via brain imaging during visual tasks [3]. We have now performed a large number of visual perception experiments with over 60 human subjects. These experiments are designed to reveal the time course of human visual perception and shed light on non-linear mechanisms by which consecutive images may be interfere and impair the perception of target objects. To do this we developed several protocols of a general class of tasks called "speed-of-sight" where an individual is asked to identify an object given a very brief presentation of an image (~ 20 ms). We tested extensively the difficulty of these tasks at different image viewing intervals, in different experimental designs (using a yes/no protocols, 2 alternative forced choice and rating of response preference) and under different masking conditions. We have found that there are differential masking effects pointing to – in contrast to previous hypotheses – nonlinear feed back in visual processing even at very fast exposure times. These results are important as they point to a more complex interpretation of early speed of sigh experiments and expose the need for feedback in cortical models of vision.

In addition we have started to produce brain imaging of these tasks in order to have a pre-conscious assessment of mechanisms of human visual cognition and its fine temporal development, though Electro-Encephalography experiments (EEG). We have also started experiments at the MIND institute, using MEG and fMRI techniques that may allow us better source localization of signals in the brain. Preliminary results from these experiments show specific signals correlated with object identification, which we are relating to temporal dynamics and location of neuronal populations.

Finally a paramount component of our approach – for which we have an institutional advantage at LANL – is the implementation of our models in terms of the largest and fastest high performance computers. There are two aspects of the implementation of our models in state of the art high performance machines. The first is the traditional one of dividing up the computational task in terms of multiple processors (CPUs). The newest hybrid computers pose another challenge: their computational power is largely predicated on accelerator elements known as CELL in the roadrunner architecture and more commonly now as Graphics Processing Units (GPUs) in newer ones. We have developed computer code that takes advantage of both these architectures and that allows us unprecedented speed of video processing, which for smaller formats is now faster than real time. We hope to capitalize these investments in terms of using clusters of GPUs and CELL (including Cerrillos and roadrunner if possible) in the near future. We have presently two proposals for time on Roadrunner and have acquired a 16Tflop dedicated GPU cluster, which will be located at CNLS. Access and intense use of these computational resources is paramount to keep us at the forefront of computational developments in the field and for

In summary the project has made substantial progress along all its scientific and technical objectives and is in line or ahead of it with our original planning. We expect to make more substantial scientific progress in the final year with the principal objective of improving object recognition accuracy and creating generative models capable of also recreating and restoring images under feedback and lateral interactions.

Future Work

During this 3rd and last year our research will be primarily concerned with 4 main points. The first deals with the computational theory and model implementations of cortical models that include in consistent ways feed-forward, feed-back and lateral connections, as well as issues of timing (which are characteristic of spiking models). We have developed theory and are creating implementations of fully generative models that can at once classify objects, and recreate them. These models are more complex, but have distinctive advantages: they are robust to changes in viewpoint of objects and to corruptions of images under noise or distortions. They can at once perform object classification and image restoration. We expect that this approach will lead to significant gains in object recognition performance. Second, we will integrate dynamical and feed forward codes with these theoretical developments in new models that use LANL's computational advantages to generate real time, real world image and video processing. Third, we will develop new theory and computational implementations that exploits temporal continuity of moving images to help learning and classification. And fourth, we will integrate our experimental effort with feedback and feed-forward models of cortical processing to validate model choices and establish a new theoretical understanding of image masking and other visual illusions that affect human psychology.

Conclusion

Our objective is to deliver new synthetic cognition systems that match or surpass human visual performance in real-time object identification tasks.The project comprises four tasks: 1) to scale up hierarchical feed-forward networks to match the number of elements, connectivity and diversity

of feature detectors in the visual cortex; 2) to include physiological elements such as spiking dynamics, lateral and feedback interactions, and time-dependent synaptic plasticity; 3) to measure brain activity, at both the single cell and systems levels, along with behavioral performance, on visual detection tasks; and 4) to develop full-scale real time models of the visual cortex. We are on track to match and in some cases to surpass our original objectives and create the new state of the art in synthetic visual cognitive systems and their applications.

Please see our website **http://synthetic-cognition.lanl.gov** for more information and publications.

References

1. Brumby, S. P., G. Kenyon, W. Landecker, C. Rasmussen, S. Swaminarayan, and L. M. A. Bettencourt. Large-Scale Functional Models of Visual Cortex for Remote Sensing. (Washington, DC, 13-15 Oct 2009).

2. Bettencourt, L. M. A., S. Brumby, V. Gintautas, M. I. Ham, S. Barr, P. Loxley, K. Sanbonmatsu, S. Swaminayaran, J. George, G. Kenyon, and I. Nemenman. Image categorization through hierarchical models of the primate visual system . (Chicago, 17-21 Oct 2009).

3. George, J. S., S. Barr, M. Ham, C. Renaudo, J. Hammond, V. Gintautas, S. Brumby, K. Sanbonmatsu, I. Nemenman, L. Bettencourt, and G. Kenyon. Not so Fast: Optimized masks increase processing time for object detection on speed-of-sight tasks . (Chicago, 17-21 Oct 2009).

4. Loxley, P., L. M. A. Bettencourt, and G. Kenyon. Ultra-fast detection of salient contours through horizontal connections in the primary visual cortex . To appear in *Physical Review Letters.*

5. Gintautas, V., L. M. A. Bettencourt, and G. Kenyon. Model cortical association fields account for the time course and dependence on target complexity of human contour perception. To appear in *PLoS Computational Biology.*

Publications

Barr, S., V. Gintautas, J. L. Hammon, M. Ham, S. Brumby, G. T. Kenyon, and L. M. A. Bettencourt. Preliminary Results from the Comparison of Human Visual Performance to Biologically Inspired Computer Object Categorization. Presented at *Decade of the Mind.* (Albuquerque, 13-15 Jan 2009).

Bettencourt, L. M.. The Rules of Information Aggregation and Emergence of Collective Intelligent Behavior . 2009. *topics in Cognitive Scienc* . **1** (4): 598 .

Bettencourt, L. M., S. Brumby, V. Gintautas, M. I. Ham, S. Barr, P. Loxley, K. Sanbonmatsu, S. Swaminayaran, J. George, G. Kenyon, and I. Nemenman. Image Categorization through Hierarchical Models of the Primate Visual System. Presented at *Neuroscience 09* . (Chicago, 17-21 Oct 2009).

Brumby, S. P., G. Kenyon, W. Landecker, C. Rasmussen, S. Swaminarayan, and L. M. A. Bettencourt. Large-Scale Functional Models of Visual Cortex for Remote Sensing. 2009. In *Applied Imagery Pattern Recognition (AIPR 2009): Visions: Human, Animal, and Machines.* (Washington DC, 13-15 Oct 2009). , p. 1. Washington: IEEE.

George, J. S.. Casting Light on Neural Function: A Subjective History. 2010. In *Imaging the Brain with Optical Methods* . Edited by Roe, A.. , p. 1. Heidelberg: Springer.

George, J. S., G. T. Kenyon, M. I. Ham, I. Nemenman, and L. M. Bettencourt. Modeling Consequences of Microscopic Eye Movements on Visual Spatial Perceptio. Presented at *Organization for Human Brain Mapping.* (San Francisco, 18-23 June 2009).

George, J. S., S. Barr, M. Ham, C. Renaudo, J. Hammond, V. Gintautas, S. Brumby, K. Sanbonmatsu, I. Nemenman, L. Bettencourt, and G. Kenyon. Not so Fast: Optimized Masks Increase Processing Time for Object Detection on Speed-of-Sight Tasks . Presented at *Neuroscience 09.* (Chicaho, 17-21 Oct 2009).

Kenyon, G. T.. Extreme Synergy:: Spatiotemporal Correlations Enable Rapid Image Reconstruction from Computer Generated Spike Trains . 2010. *Journal of Vision.* **10** (3): 1.

RADIUS: Rapid Automated Decomposition of Images for Ubiquitous Sensing

Lakshman Prasad
20090104DR

Introduction

Today's explosive growth in the quality and quantity of geospatial imagery calls for the automation of tedious and time-consuming image analysis tasks for timely Intelligence gathering and decision support. Analysts in the Intelligence Community are overwhelmed with this flood of data, resulting in lapses and delays in intelligence assessment. Automated tools to detect features of interest reliably at a rate faster than human experts can are nonexistent. The state-of-the-art in computer-based image analysis largely relies on classifying image pixels based on spectral values (e.g. color) into features. This is a time-consuming operation as geospatial images are comprised of hundreds of millions of pixels. Further, uniformity of spectral values alone is not sufficient for extracting complex features. Our project addresses this bottleneck by taking a radically new approach to image analysis that achieves significant data reduction as well as human-centric feature extraction. Rather than look at all pixels in an image, we focus on a small but salient subset of image pixels that lie on boundaries between image features. These edge pixels provide incomplete but valuable structural information about objects and features. The main scientific goal of our project is to model human visual perception by computer algorithms and obtain completions of edges by 'joining the dots (edge pixels)' and thus delineating features of interest. Computing with a sparse subset of image pixels will result in rapid analysis, while the use of image edge pixels assures meaningful feature extraction leading to object recognition and image understanding. To ensure very high throughput, the project will realize these algorithms on state-of-the-art desktop multiprocessor parallel architectures. This high-risk scientific undertaking of computationally mimicking human visual perception has the high payoff of developing much-needed fast and powerful tools that expedite image analysis to assist Intelligence gathering for national security and defense applications.

Benefit to National Security Missions

This project addresses the DOE mission of Threat Reduction by developing a critical capability of timely and reliable information extraction from imagery for national security applications. Additionally it supports the DOE Office of Science mission by addressing the computational modeling and simulation of human visual perception for advancing information science and technology. The generality of the problem addressed, namely image feature extraction, also supports other mission applications including environmental monitoring for remediation and restoration and space and materials image data analysis.

Progress

Summary

The RADIUS project has successfully developed a new and highly efficient method of hierarchically decomposing an image into polygonal features at multiple scales. This is crucial to the analysis of a wide range of imagery in applications such as proliferation detection, homeland security, and defense, to name a few. The method has been implemented via parallel algorithms to take advantage of today's multiprocessor, multicore desktop computing architectures.
The processor-scalable algorithms and software implementing the method developed perform at rates of an average of 10 million pixels per second on a single desktop computer. The software is three orders of magnitude faster than the state-of-the-art image segmentation methods in use.

Science

The image decomposition method developed is founded on algorithmically emulating broad principles of perceptual organization as evidenced in human vision to exploit structural and statistical regularities in the ensembles of polygons at each stage of decomposition. The image decomposition is realized as a progressive bottom-up synthesis of polygonal primitives obtained by triangulating a sparse but perceptually significant subset of an image, namely edge pixels. Geometric and

statistical criteria are used to detect structural and spectral coherences at each level of the hierarchy that determine the groupings of polygons into larger polygons, delineating image features at progressively increasing scales (Figure 1). The exploitation of edges as perceptual cues, the use of perceptual organization to complete edges into polygonal features, and the use of ensemble regularities (ecological statistics) to detect affinities among polygons and adaptively compute parameters internally without the need for external supervised guidance, are all novel aspects and strengths of the method developed.

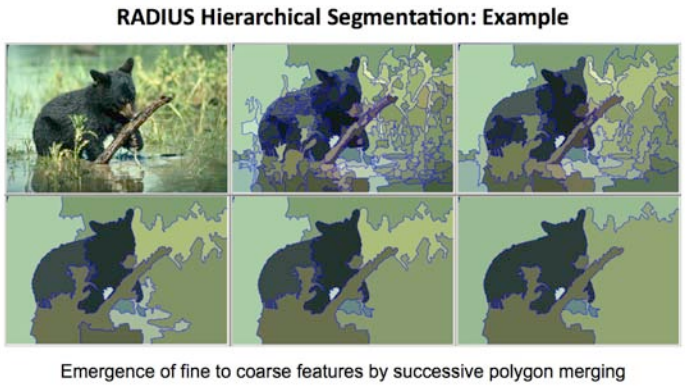

Figure 1. Perceptual agglomeration of polygonal features to obtain a hierarchy.

Technology Functionality

The image decomposition method developed provides semantically meaningful polygonal features at various scales in images. Its hierarchical nature provides context for small-scale features in terms of the large-scale features they are embedded in at coarser levels of the hierarchy, as well as reveals the composition of complex features in terms of their constituent subfeatures. Thus, for example, a vehicle can be a subfeature on a road or in a parking lot, a building can be part of an urban city block or part of an industrial complex. This capability sets the stage for automating feature analysis and understanding in the remainder of the project.

Benchmarks

The image decomposition method has been benchmarked for performance against the well-known Berkeley Segmentation Benchmark Dataset consisting of a set of 300 images, each of which has multiple ground truth segmentations provided by humans. The probabilistic Rand index(PRI)—a measure of the similarity of two clusterings of a dataset was used to evaluate the project's method with respect to the human benchmark. The method scored 0.82 on the PRI; well above that of published state-of-the-art methods, the best of which scored 0.77. The mutual agreement among the different humans' segmentation across the dataset was only 0.875. Thus the project's method has a high performance as well as efficiency.

Application to anomaly and change detection

We have recently developed a general framework to detect salient and anomalous features in images, as well as interesting changes between images based on our hierarchical image decomposition. Detecting unusual features has to take into account what is 'usual'. This means learning an often complex statistical distribution that captures the normative variation in an image, and then detecting features that do not conform to this norm. This is a hard machine-learning problem that has been extensively researched. Our hierarchical segmentation method provides a means of obtaining regions of an image, each of whose spectral variability is statistically simpler to learn than that of the whole image (Figure 2). This helps meaningfully contextualize the quest for outliers to within these regions, circumventing the hard problem of learning a complex distribution. This has significant implications to broad-area search (Figure 3) with important applications in implementing national security related image analysis.

Milestones and Publication Summary

A US patent, "iShapes: Image Segmentation by Hierarchical Agglomeration of Polygons using Ecological Statistics" describing the developed method has been filed.

Software implementing the hierarchical segmentation method has been licensed to a key commercial company specializing in geospatial image analysis.

NDAs with other commercial entities for potential licenses are being negotiated.

A proposal to DOE NA-42 based on the method developed addressing application to render-safe operations by analyzing radiographs has been funded and is progressing as a concurrent derivative project.

Two proposals; one to DOE NA-42 for radiograph analysis, the other to DHS for analysis of mm wave and X-ray backscatter imagery for domestic security have been submitted and are pending award decisions.

The project has produced nine accepted papers in peer-reviewed conferences and two more awaiting decision.

Future Work

Based on our progress at the end of the second year of our three-year project, we will focus on applications of our hierarchical image decomposition method to label features in images based on their appearance (i.e., shape, size, colors) and context (i.e., their relationship to other features in their neighborhood, their internal composition in terms of finer subfeatures, and their membership in a larger composite feature in the hierarchy. We will develop

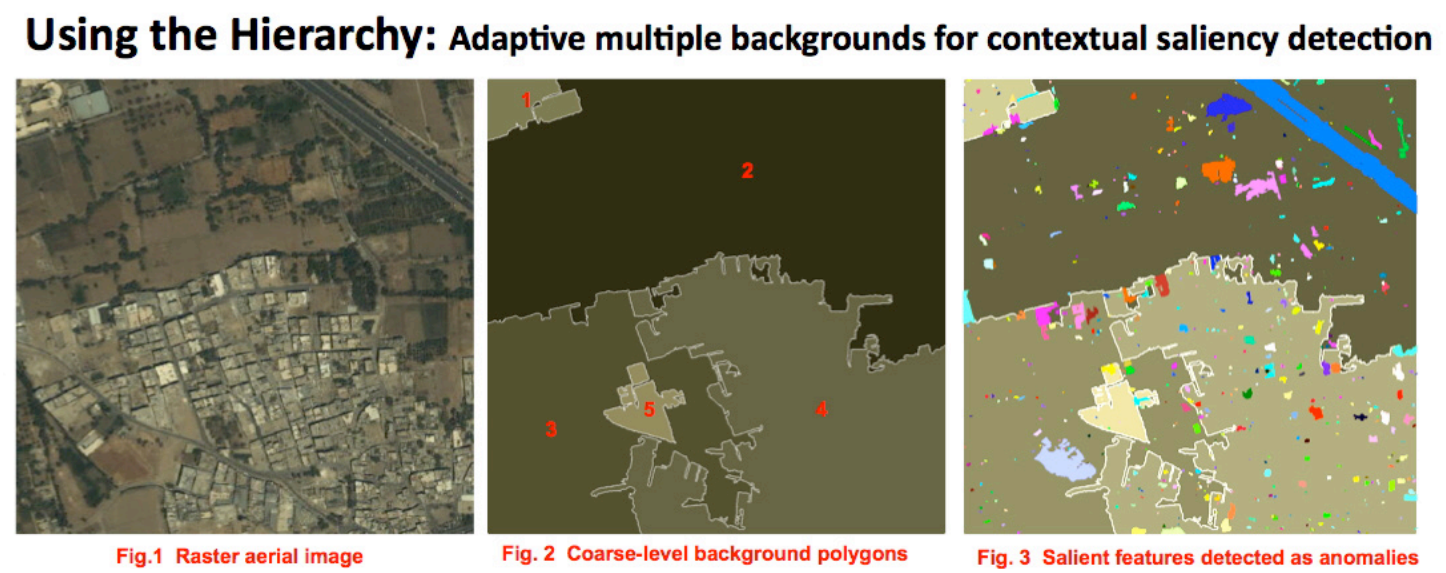

Figure 2. Adaptive background salient feature detection using hierarchical background regions.

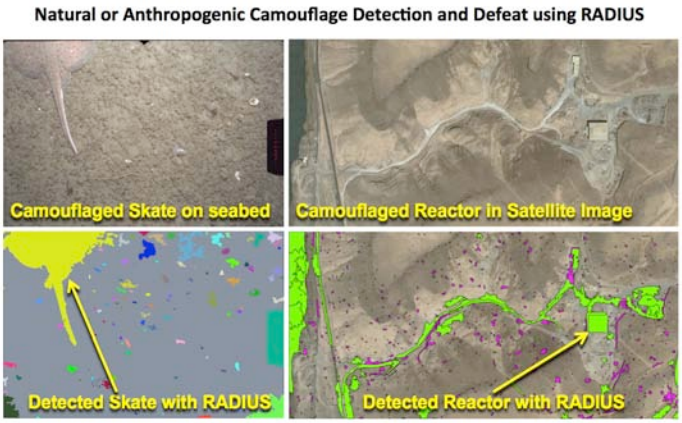

Figure 3. Overcoming camouflage using adaptive background saliency detection.

methods to detect and characterize semantic relationships using ontological decision trees of complex targets such as an industrial facility or an urban area, which are comprised of multiple subfeatures of specific categories. Additionally, we will exploit the hierarchical structure of our image decomposition to query images for features that distinguish themselves from their surroundings or have changed in a distinctive way over time. This is particularly valuable for narrowing down the search time and effort to focus on the novel. This capability to focus attention to interesting areas of an otherwise large and complex image is critical to many national security applications ranging from broad area search to aerial video surveillance and automated target detection.

Conclusion

Scientifically, the project will provide computational insights into emulating human-centric image understanding. Technologically, the project will develop a capability to rapidly extract and assess information from satellite and aerial imagery. Specifically, the project will deliver efficient computer algorithms and software that will scale in performance on single processor and multiprocessor platforms. This will enable the extraction of manmade and natural features and contextually relate them to identify complex and composite scenarios such as urban infrastructure, nuclear facilities and lines of communication. These identifications will be responses to analyst queries for features of interest, thus facilitating and expediting Intelligence assessment.

Publications

Dillard, S., J. Grazzini, and L. Prasad. 6th International Symposium on Visual Computing. To appear in *Region and edge-adaptive sampling and boundary completion for segmentation.* (Las Vegas, 29 Nov.-1 Dec. 2010).

Grazzini, J., S. Dillard, and L. Prasad. Simultaneous hierarchical segmentation & vectorization of satellite images through combined non-uniform anisotropic data sampling and triangulation. 2010. In *Image and Signal Processing for Remote Sensing XVI* . (Toulouse, France, 20-24 Sep. 2010). Vol. 7830, p. 78300F. On-line: SPIE Digital Library.

Grazzini, J., and P. Soille. Iterative ramp sharpening for structure/signature-preserving simplification of images. 2010. In *20th International Conference on Pattern Recognition.* (Istanbul, Turkey, 23-26 Aug. 2010). , p. 4585. On-line: IEEE Computer Society.

Grszzini, J., S. Dillard, and P. Soille. Multichannel image regularization using anisotropic geodesic filtering. 2010. In *20th International Conference on Pattern Recognition.* (Istanbul, Turkey, 23-26 Aug. 2010). , p. 2664. On-line: IEEE Computer Society.

Matsekh, A., E. Rosten, A. Skurikhin, and L. Prasad.

Numerical aspects of spectral segmentation on polygonal grids. To appear in *PARA 2010: State of the Art in Scientific and Parallel Computing.* (Reykjavik, Iceland, 6-9 Jun. 2010).

Prasad, L., and J. Theiler. A structural framework for anomalous change detection and characterization. 2009. In *SPIE Defense and Security Symposium.* (Orlando, FL, April, 2009). , p. 7341. Bellingham, WA: SPIE.

Prasad, L., and S. Swaminarayan. A Framework for Perceptual Image Analysis. 2009. In *43rd Asilomar Conference on Signals, Systems, and Computers.* (Pacific Grove, CA, 1-4 Nov. 2009). Vol. CD-ROM, CD-ROM Edition, p. 867. Bryan, Texas, U.S.A.: IEEE.

Sankaranarayanan, K., and J. Davis. Learning directed, intention-driven activities using co-clustering. To appear in *7th IEEE International Conference on Advanced Video and Signal-Based Surveillance.* (Boston, USA, 29 Aug.-1 Sep.2010).

Sankaranarayanan, K., and J. Davis. Attention-based target localization using multiple instance learning. To appear in *6th International Symposium on Visual Computing.* (Las Vegas, Nevada, 29 Nov.-1Dec. 2010).

Optimization and Control Theory for Smart Grids

Michael Chertkov
20100030DR

Introduction

The national interest in a broad class of problems loosely characterized as the smart grid is rapidly growing. At its core, the smart grid is the modernization of our existing electric power systems through improvements in efficiency, increased robustness and resiliency, integration of time-variable renewable generation, and reduction of environmental impacts. To date, the focus of most commercial entities has been on development of hardware such as smart meters and green technologies. However, with the exception of a handful of academic researchers, there has been limited research on optimization, control and more broadly, the information science required to effectively utilize this hardware. Our proposal targets development of the basic information science that will effectively bridge this gap. Using our expertise in information theory, network analysis, infrastructure analysis and power engineering, we will develop new algorithms for optimal design of the nation's next generation power transmission and distribution system that address the realities and challenges of the future grid.

We focus on three core information science challenges in Grid Design, Grid Control and Grid Stability by considering a set of challenging problems. First, we study efficient and robust integration of geographically widespread renewable generation by solving large, cutting-edge optimization problems that incorporate difficult constraints imposed by the transmission of electrical power. Second, we consider two load balancing problems in the low-voltage distribution grid: development of robust and efficient distributed control techniques and algorithms based on queuing theory. We will also develop efficient control algorithms for maintaining an operational distribution grid via switching of redundant lines. Third, we will develop a preventive toolbox capable of detecting instabilities and failures prior to their occurrence. We are focusing on estimating the probability of power outages, identifying their signatures and precursors, and developing detection algorithms for alerting the transmission grid operator.

Benefit to National Security Missions

This smart grid effort enables the laboratory to expand its infrastructure planning and analysis programs, currently focused mainly on infrastructure security and sponsored by the Department of Homeland Security, to a broader set of programs in energy infrastructure planning and efficiency analysis with the Department of Energy as primary sponsor. The project thereby positions the lab closer to the center of mass in energy research. In a broader sense, infrastructure analysis tools like ours build the ability to understand the complicated infrastructure of the nuclear weapons complex.

Progress

We used a power grid model with M generators and N consumption units to optimize the grid and its control. Each consumer demand is drawn from a predefined finite-size-support distribution, thus simulating the instantaneous load fluctuations. Each generator has a maximum power capability. A generator is not overloaded if the sum of the loads of consumers connected to a generator does not exceed its maximum production. We focus on the asymptotic limit and we show that interconnects allow significant expansion of the parameter domains for which the probability of a generator overload is asymptotically zero. We also have extended this work to account for renewables.

The current electric power grid is a result of incremental growth over the past 100 years under assumptions that a grid provides reliable and controllable generation of energy cheaply and with limited environmental impact. Moving into the twenty-first century, many of these assumptions will no longer hold; the existing grid is ill-equipped to handle the new requirements that it is being subjected to. We developed a novel hybridization algorithm to upgrade the existing electric power network to feasibly achieve future renewable energy generation goals. The algorithm was integrated with state-of-the-art electric power analysis approaches to produce feasible transmission networks to accommodate 20% wind power by 2030 goals.

We showed how distributed control of reactive power can serve to regulate voltage and minimize resistive losses in a distribution circuit that includes a significant level of photovoltaic (PV) generation. To demonstrate the technique, we considered a radial distribution circuit with a single branch, consisting of sequentially-arranged residential-scale loads that consume both real and reactive power. In parallel, some loads also have PV generation capability. We postulated that the inverters associated with each PV system are also capable of limited reactive power generation or consumption, and we posed and analyzed the problem of optimal dispatch of each inverter's reactive power to both maintain the voltage within an acceptable range and minimize the resistive losses over the entire circuit.

We proposed an optimization approach to design cost-effective electrical power transmission networks. That is, we aim to select both the network structure and the line conductances (line sizes) so as to optimize the trade-off between network efficiency (low power dissipation within the transmission network) and the cost to build the network. We developed a heuristic approach to solve this non-convex optimization problem using a continuation method to interpolate from the smooth, convex problem to the (non-smooth, non-convex) combinatorial problem, and the majorization-minimization algorithm to perform the necessary intermediate smooth but non-convex optimization steps.

We developed an approach to predict power grid weak points, and specifically to efficiently identify the most probable failure modes in load distribution for a given power network. This approach was tested on two examples. We found that if the normal operational mode of the grid is sufficiently healthy, the failure modes, also called instantons, are sufficiently sparse, i.e. the failures are caused by load fluctuations at only a few buses.

The anticipated increase in the number of plug-in electric vehicles (EV) will put additional strain on electrical distribution circuits. Many control schemes have been proposed to control EV charging. Here, we develop control algorithms based on randomized EV charging start times and simple one-way broadcast communication allowing for a time delay between communication events. Using arguments from queuing theory and statistical analysis, we seek to maximize the utilization of excess distribution circuit capacity while keeping the probability of a circuit overload negligible.

Renewable energy sources such as wind and solar have received considerable attention as clean power options for future generation expansion. However, these sources are intermittent and increase the uncertainty in the ability to generate power. We studied how to best site the charging EV stations in terms of how they can support both the transportation system and the power grid. We developed two test cases to study the benefits and the performance of these systems.

Future Work

The basic structure of the electrical power grid has remained unchanged for a hundred years. It has become increasingly clear, however, that the hierarchical, centrally-controlled grid of the twentieth century is ill-suited to the needs of the twenty-first. A future grid, in which modern sensors, communication links, and computational power are used to improve efficiency, stability, and flexibility, has become known as the "smart grid." Much of the hardware that will enable smart grids is in development or already exists: "smart" meters and appliances that respond to pricing signals, distributed wireless sensor networks, improved batteries for plug-in hybrid electric vehicles (PHEVs) that enable distributed storage, and so on. While much of the needed hardware necessary to enable the smart grid may be in place, the Information Science and Technology (IS&T) foundation for the smart grid design, operation, and risk assessment requires major development.

Our proposal targets development of the basic information science that will effectively bridge this gap. Using our expertise in information theory, network analysis, infrastructure analysis and power engineering, we will develop new algorithms for optimal design of the nation's next generation power transmission and distribution system that address the realities and challenges of the future grid.

In the area of Grid Design, we study efficient and robust integration of geographically distributed renewable generation by solving cutting-edge optimization problems that incorporate difficult constraints imposed by the transmission of electrical power. In Grid Control, we consider two load balancing problems in the low-voltage distribution grid: development of robust and efficient distributed control techniques and algorithms based on queuing theory to enable high penetration of small-scale distributed generation and plug-in hybrid vehicles. In Grid Stability, we will develop a toolbox capable of detecting instabilities and failures for preventing costly outages. All three problems require the development of efficient new algorithms.

Conclusion

This project is driven by emerging technologies such as renewables, storage, and meters and accordingly specifies the technical challenges in Power Grid Design, Power Grid Control and Power Grid Stability. Rather than tackle the full complexity and requirements of the grid, from security to operations to pricing, we focus on a set of problems where we have well-developed Information Science & Technology (IS&T) capabilities, and thus make a significant impact. The new IS&T challenges for smart grids require coherent advances in analysis and control, stability and

reliability metrics, state estimation, data aggregation and assimilation, and communication for the grid.

Publications

Bent, null., null. Berscheid, and G. Loren [Los Alamos National Laboratory]. Toole. Transmission network expansion planning with simulation optimization. 2010. *DOE.*

Chertkov, M., F. Pan, and M. Stepanov. Predicting Failures in Power Grids. To appear in *IEEE Transactions on Smart Grids.*

Chertkov, null., null. Turitsyn, null. Backhaus, and null. Sule. Distributed control of reactive power flow in a radial distribution circuit with high photovoltaic penetration. 2009. *DOE.*

Johnson, J., and M. Chertkov. A Majorization-Minimization Approach to Design of Power Transmission Networks. To appear in *49th IEEE Conference on Decision and Control .* (Atlanta, Dec).

Kadloor, S., and N. Santhi. Understanding Cascading Failures in Power Grids. *IEEE Transactions on Smart Grids.*

Pan, F., R. Bent, A. Bercheid, and D. Israelevitz. Locating PHEV Exchange Stations in V2G. To appear in *IEEE SmartGridComm 2010 .* (NIST, Oct 2010).

Santhi, N., and F. Pan. Detecting and mitigating abnormal events in large scale networks: budget constrained placement on smart grids. To appear in *HICSS44.* (Kau, Jan).

Sulc, P., K. Turitsyn, and S. Backhaus. Options for Control of Reactive Power by Distributed Photovoltaic Generators. To appear in *Proceedings of the IEEE.*

Toole, G. Loren., M. Fair, A. Berscheid, and R. Bent. Electric power transmission network design for wind generation in the Western United States: Algorithms, methodology, and analysis. 2010. In *2010 IEEE PES Transmission and Distribution Conference and Exposition: Smart Solutions for a Changing World ; 20100419 - 20100422 ; New Orleans, LA, United States.* , p. var.pagings.

Turitsyn, K., N. Sinitsyn, and S. Backhaus. Robust Broadcast-Communication Control of Electric Vehicle Charging. To appear in *IEEE SmartGridComm 2010 .* (NIST Maryland, Oct 2010).

Turitsyn, K., P. Sulc, and S. Backhaus. Distributed control of reactive power flow in a radial distribution circuit with high photovoltaic penetration. To appear in *IEEE PES General Meeting 2010.* (Minneas, July 2010).

Turtisyn, K., P. Sulc, S. Backhaus, and M. Chertkov. Local Control of Reactive Power by Distributed Photovoltaic Generators. To appear in *IEEE SmartGridComm 2010 .* (NISTMaryland, Oct 2010).

Zdeborova&acute, , A. Decelle, and M. Chertkov. Message passing for optimization and control of a power grid: model of a distribution system with redundancy. 2009. *Physical Review E (Statistical, Nonlinear, and Soft Matter Physics).* **80** (4): 046112 (9 pp.).

Zdeborova, L., S. Backhaus, and M. Chertkov. Message Passing for Integrating and Assessing Renewable Generation in a Redundant Power Grid. 2010. In *2010 43rd Hawaii International Conference on System Sciences (HICSS-43) ; 5-8 Jan.* (2010 ; Honolulu, HI, USA). , p. 1.

Automated Change Detection in Remote Sensing Imagery

James P. Theiler
20080040DR

Abstract

The aim of this project was to identify meaningful changes in multiple images, with each image taken of the same scene. As well as recording actual changes on the ground, the imagery will include uninteresting differences caused, for instance, by variations in illumination, calibration, or atmospheric distortion. The central effort in this project is to develop tools for distinguishing these pervasive but incidental differences from the more interesting changes that actually occurred in the scene.

Background and Research Objectives

Change detection, especially in remote sensing imagery, is a tool with many uses: environmental monitoring, facility surveillance, agricultural surveying, illicit crop identification, camouflage defeat, moving target indication, small target detection in broad area search, and emergency response. *Automated* change detection offers a way to deal with the overwhelming quantity of image data, and the growing variety of image modalities, available for both remote sensing and intelligence applications. These data potentially contain important nuggets of useful information, but the nuggets are buried in the background. Our objective on this project was to combine recent advances in machine learning, particularly in anomaly detection, with ongoing efforts in remote sensing image analysis.

Given two images of the same scene, taken at different times, possibly with different instruments, and inevitably under different conditions, the goal is to find the interesting changes that have taken place in the scene. What constitutes an "interesting change" depends on the specific application, but often it is not known in advance what particular kinds of changes are being sought.

The aim of *anomalous* change detection is to identify those changes that are unusual, compared to the ordinary changes that occur throughout the image. This notion of distinguishing anomalous changes from pervasive differences is illustrated in Figure 1. In any realistic scenario, a human analyst will decide whether a given change is interesting or meaningful. What anomalous change detection offers is a way to cull through a large aggregation of imagery to identify the changes that are unusual and that should be passed along to the human analyst. Although it is difficult to devise a mathematical characterization of what constitutes an "interesting" change, the definition of "unusual" can be made more rigorous, and provides a metric that we can use for optimizing algorithms.

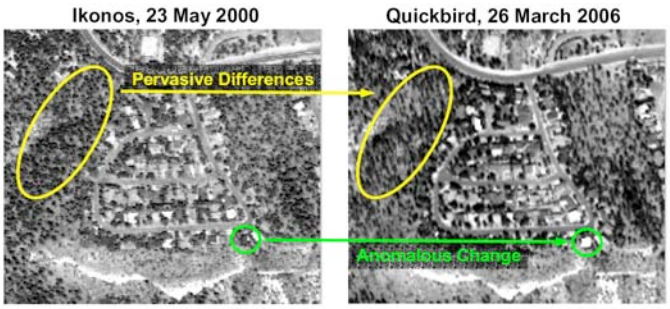

Figure 1. Two satellite images are taken of the same neighborhood in Los Alamos, The images are taken six years apart, with cameras on two different satellites. "Pervasive differences" refer to differences, for instance in illumination or calibration or contrast, that occur throughout the image. The "anomalous changes," on the other hand, are localized and the nature of those changes is unlike the pervasive differences. The aim of anomalous change detection (ACD) is to distinguish, in a formal machine learning sense, the anomalous changes from the pervasive differences.

Since the ordinary or pervasive differences occur throughout the image, there is an abundance of data with which to "learn" the nature of these pervasive differences. Once the patterns of pervasive difference are characterized, then deviations from those patterns can identify the anomalous changes.

Scientific Approach and Accomplishments

Validation of algorithms

The ultimate test of any detection algorithm is how well it detects what is really interesting in real imagery. Anomaly detection, however, is problematic on two counts: one, what is "really interesting" is in the eye of the beholder; and two, anomalies are by definition rare. This makes it difficult to find enough of them to do statistical comparisons of algorithms, and that makes it is easy to be misdirected by anecdotal results. With a keen appreciation for the caveats and limitations of simulated data, we developed a simulation framework to address some of these problems with anomalous change. This framework draws a distinction between pervasive differences, which occur throughout the images, and anomalous changes which occur in only a few pixels. It is the anomalous changes that we want, in our operational scenarios, to draw to the attention of the analyst. Figure 2 illustrates how the simulation framework can take a single image and produce a pair of images that exhibits pervasive differences at most pixels but an anomalous change at one pixel.

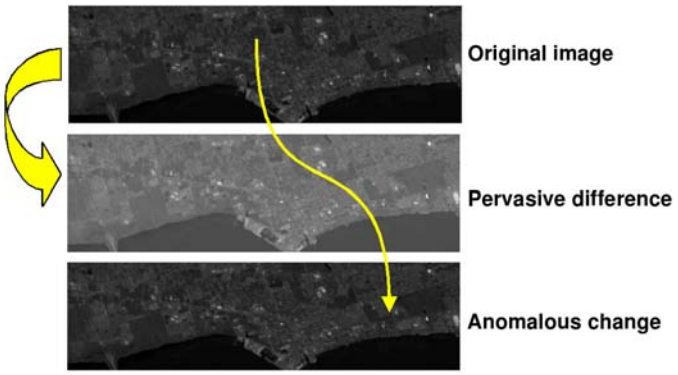

Figure 2. Simulation framework: Starting with a single image, one can generate pervasive differences, which are applied to every pixel in the image; and anomalous changes, which alters only a single pixel, for instance by replacing that pixel with another pixel taken from somewhere else in the image. The bottom two images in the figure can then be used as input to a change detection algorithm. A successful algorithm will find the anomalous change and distinguish it from the pervasive differences. Since the simulation can be run multiple times, statistical measures of performance can be computed. This enables comparison of algorithms under controlled conditions.

We initially developed the simulation framework for evaluating purely spectral ACD algorithms – these are algorithms with treat each pixel of the image independently. The simulation framework was initially designed for single-pixel anomalous changes, but we subsequently developed a variant for simulating sub-pixel anomalous changes (these are changes in the scene that are smaller than the pixel size). A further extension incorporated spatial structure in the imagery and enabled the simulation of spatially extended anomalous changes. It is important to emphasize that none of these are "pure" *ab initio* simulations, but always start with real imagery so that the basic statistical properties of real imagery are incorporated into the simulations.

Both as a starting point for our simulations, and as a valuable sanity check, this project maintained a database of real imagery that (in some cases) included markup identifying the "real" anomalies. This included hyperspectral longwave infrared (LWIR) data from the Los Alamos developed Optimized Remote Chemical Analysis Spectrometer (ORCAS) sensor, some ground-based LWIR data from a previous project, a collection of datasets from the Airborne Visual/InfraRed Imaging Spectrometer (AVIRIS), a pair of hyperspectral images that were part of the Rochester Institute of Technology (RIT) "blind test" experiment (), and some examples from a larger archive of Landsat data, with triples of images, taken many years apart. We also obtained some hyperspectral imagery from colleagues at the Air Force Research Laboratory, that includes images taken hours, days, and months apart, and which further includes real anomalous changes in the form of folded-up tarps that were placed in the scene from time to time. These data are shown in Figure 3. (The performance curves shown in Figure 4 and Figure 5 are based on these data.)

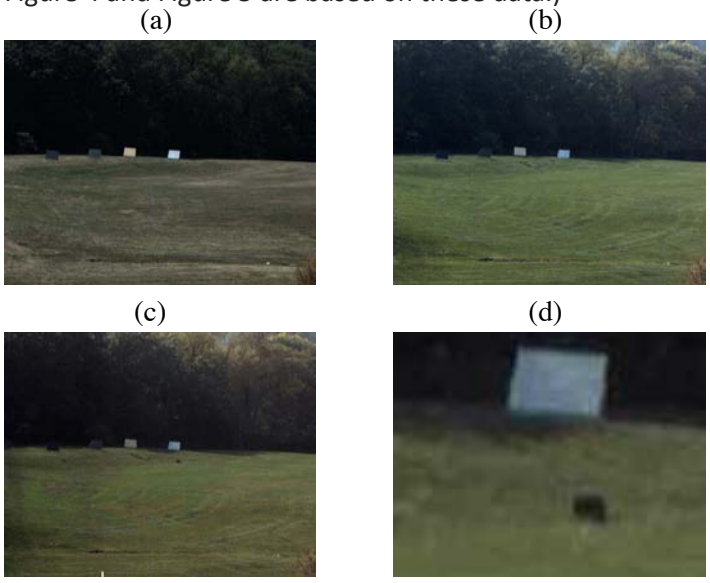

Figure 3. A change detection experiment was carried out at the Air Force Research Laboratory using a hyperspectral sensor, taking images that were several months apart. The image contained grass and trees, with varied seasonally, and some panels which were unusual compared to the rest of the scene, but since they are in both images, they do not represent an anomalous change. (a) Image taken Aug 25; (b) Image taken Oct 14; (c) second image taken Oct 14 with some folded-up tarps added placed in the grass; (d) inset from panel c shows one of the folded-up tarps.

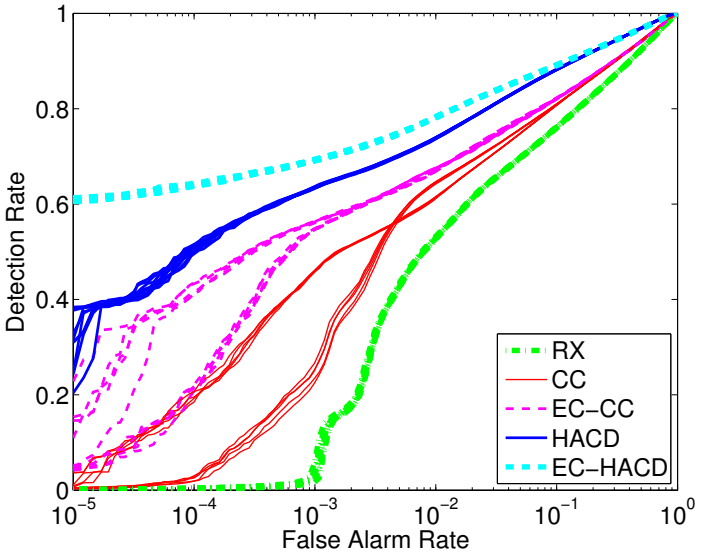

Figure 4. ROC (Receiver Operator Characteristic) curves show how detection rate varies with false alarm rate. A better detector will achieve a high detection rate at a given false alarm rate. Note that very low false alarm rates are of interest, so the false alarms are plotted on a log axis. Shown here is the performance of various detectors (RX and CC are existing Gaussian-based anomalous change detectors; HACD is a detector we developed, which is also based on a Gaussian distribution. The EC-CC and EC-HACD are the variants of these detectors that model the data with elliptically-contoured distributions. These plots are based on a simulation framework: the pervasive differences are from the Aug 25 and Oct 14 data, and the anomalous changes are simulated.

Distribution-based change detection

One of the main intellectual contributions of this project was to introduce and develop "distribution-based" anomalous change detection algorithms. This approach differs from what had been the state of the art: "subtraction-based" change detection. In the subtraction-based methods, a linear or nonlinear transform is applied to one or both images, with the goal of making the images as similar as possible: the idea is to minimize the pervasive differences, using tools such as ordinary least squares, total least squares, covariance equalization, canonical correlation analysis, or neural networks. The transformed images are then subtracted from each other to produce a residual image, and anomalous changes are identified at those pixels where the residuals are largest.

By contrast, the distribution-based approach avoids the need for this subtraction step in the middle. We model the pervasive differences and the anomalous changes in terms of two separate probability distributions, and use statistical principles to optimally distinguish them. For the pervasive differences, the model is data-driven, and can be as complex as the data permit. This data-driven modeling is one of the main technical challenges on the project. The difficulties are exacerbated for hyperspectral data -- although though there are typically (but not necessarily, depending on the operational situation) a large number of samples (pixels), when those pixels are modeled in a high-dimensional space, then one is fighting the curse of dimensionality. Modeling the anomalous changes is conceptually more problematic: anomalies are generally defined in terms, not of what they are, but of what they are not. And a data-driven model does not make sense because there is little or no data. Nonetheless, we found that by modeling the anomalous changes in terms of specific, but broad distributions, the open-endedness of the anomaly's definition is preserved, yet optimization is still well-defined, and effective ACD algorithms can be derived. In this regard, the model for anomalous changes plays a role that is similar to that of a prior in Bayesian modeling. One simple model is a broad uniform distribution for anomalous changes. We proposed a (slightly) more sophisticated model that took the anomalous change distribution to be the product of the marginal densities of the pervasive difference distribution. This provided a way to model anomalous changes without being confounded by individual anomalies; that is, it seeks pixels where the change from one image to the other is unusual, without being distracted by pixels that are themselves unusual.

One of the discoveries on this project was that many of the subtraction-based ACD algorithms could be recast in terms of the distribution-based approach. In so doing, we elucidated implicit assumptions in existing algorithms. For instance, linear subtraction-based algorithms could be derived by assuming that the pervasive difference distribution was Gaussian. Further, by loosening that assumption and considering a broader class of distributions, we could generalize these existing algorithms.

Purely spectral ACD algorithms

For multispectral and hyperspectral imagery, each pixel consists of a vector of radiances or reflectances across a spectrum of different electromagnetic wavelengths. For instance, a commercial digital camera collects values for red, green, and blue – a multispectral or hyperspectral sensor will collect values for many more "colors," often into wavelength regimes where the human eye cannot even see. With so much information at each pixel, it is possible to perform useful analysis by considering only this spectral information, and neglecting the spatial aspects of the imagery. For the distribution-based approach, we are modeling the distribution of individual pixels. With Gaussian distributions as a starting point, we are able to generate a family of quadratic change detection algorithms, some of which had been previously developed in the context of subtraction-based change detectors, and one of which was developed by us: the hyperbolic anomalous change detection (HACD) algorithm.

One of the most effective generalizations we found was to replace the Gaussian distribution with an elliptically-contoured multivariate t-distribution; like the Gaussian, this distribution is characterized by a mean vector and a covariance matrix, but unlike the Gaussian, it has a fatter tail that is characterized by a simple scalar parameter. These fatter tails are typically observed in real data, and we found that the ACD algorithms that were generated from this distribution outperformed their Gaussian counterparts, and that the extra scalar parameter could easily be fit to the data. These results are shown in Figure 4 for simulated anomalous changes and in Figure 5 for real anomalous changes.

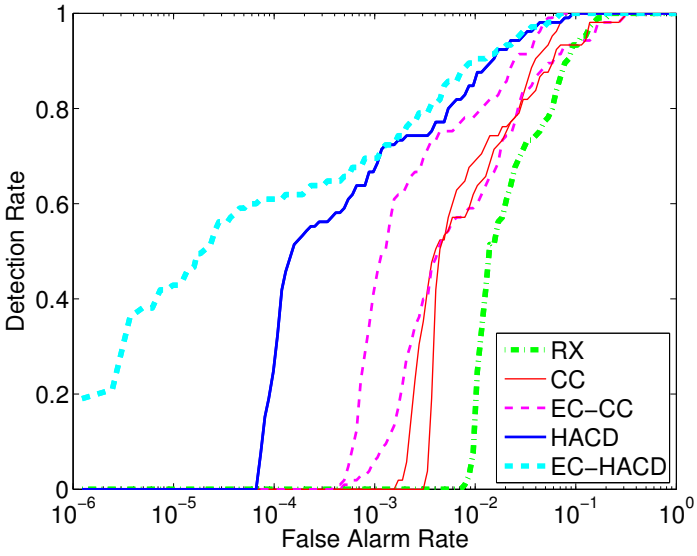

Figure 5. ROC curves for various anomalous change detectors. This is for the same data as used in Figure 4, but instead of the simulation framework, we used the actual anomalies given by the folded-up tarps.

A step beyond parametric modeling of the probability distribution that represented the data is non-parametric modeling of the boundary between pervasive differences and anomalous changes. Since this boundary is an inherently less complex entity than the explicit probability distributions, more effective statistical modeling is possible. That is the concept behind the support vector machine (SVM). We employed a state-of-the-art implementation that exploited the fast processing of General Purpose Graphical Processing Units (GPGPUs). Our SVM used a radial basis kernel, and we found that this outperformed Gaussian ACD algorithms. Our work with the SVM involved considerable customization because anomalous change detection requires a very low false alarm rate, and both the training and the testing of the algorithms were computationally expensive.

Preliminary results with a quadratic kernel SVM have been very encouraging. Here, the low false alarm rate requirement can be more naturally incorporated into the algorithm, and the final algorithm can be expressed in a simple quadratic form.

The quadratic SVM provides one way to obtain an effective covariance matrix for the data; we also investigated a new approach, called the sparse matrix transform, for estimating the covariance matrix. Unlike the SVM and other regularization schemes, the sparse matrix transform is *not* rotation-invariant, but instead exploits the tendency for real data to exhibit eigevectors that are approximately aligned with the natural axes.

Although the notion of change detection is most easily understood when there are two images, extensions to multi-image change detection were also explored.

Spatio-spectral ACD algorithms

Although we continue to develop algorithms that look for *pixels* that have changed in interesting ways, we ultimately want to find what *objects* have appeared or disappeared or changed in a scene. Recognizing that segmentation of imagery into actual discrete objects can be a difficult and open-ended task, we have taken two approaches. One is to stick with the pixel-based representation of the imagery, but to use spatial operators (smooth, dilate, erode, etc.) as part of the change detection scheme. The other is to explicitly partition the image into discrete patches and either to treat these patches as if they were pixels in the change detection algorithms, or to else use them as a starting point for hierarchical image segmentation, which is potentially valuable when the scale of the anomaly is not known beforehand. The efficiency of this segmentation depends on the quality of detected edges. To improve edge detection, we have investigated schemes for grouping oriented segments in highly cluttered images, and developed an iterative, multi-scale tensor voting approach.

While purely spectral approaches are well suited for hyperspectral imagery, spatio-spectral methodology is an important part of our research into the utility of change detection in persistent surveillance with panchromatic video imagery.

Co-registration

Image misregistration is probably the greatest confound to accurate change detection. Corresponding pixels in a pair of images must correspond to the same point on the ground. To enforce this in an automated way requires a fast detector of corresponding interest points, and calibrating camera distortion is an important part of that. More accurate co-registration will produce better change detection, but there will always be some residual misregistration. Thus, it is important to characterize (and optimize) the robustness of change detection to this inevitable misregistration. In an effort to "close the loop" between the co-registration and the change detection steps, we developed a more active way to achieve robustness to residual errors in registration. This approach involves local

co-registration adjustments that are driven by minimizing the anomalous change detection statistic; we developed an asymmetric and a symmetric variant, depending on whether the analyst knows ahead of time which image harbors the anomalous change. A more comprehensive investigation of both approaches, which also included subpixel adjustments, was recently completed.

Accomplishments

Over the past three years, this project has developed algorithms from a distribution-based approach and shown that they can exhibit and exceed state-of-the-art performance on remote sensing imagery. In addition to developing new algorithms, we have provided a mathematical description of the problem that explains how a number of existing change detectors are related to each other. (In fact, we showed that two of these detectors – "optimized covariance equalization" and "multivariate alteration detection" – are equivalent. This had not been known.) This description allowed us to develop further generalizations and to better understand which detectors work best in which situations. We have addressed a range of practical issues as well, developing extensions to spatio-spectral and multi-image change detection, as well as a local co-registration adjustment scheme for mitigating the considerable difficulties introduced into the change detection problem by misregistration of the imagery. Finally, we remark that the development of a simulation framework gave us the leverage to not only evaluate and compare different algorithm variants, but to elucidate the circumstances under which one algorithm would be preferred over another.

Impact on National Missions

This project supported the DOE missions in nonproliferation and national security by developing the technology to enhance an analyst's ability to identify new and/or altered sites from broad area imagery. Furthermore, the techniques rely on innovative statistical estimation tools, and this supported DOE's broader scientific mission.

Publications

Bachega, L., C. A. Bouman, and J. Theiler. Hypothesis Testing in High-Dimensional Space with the Sparse Matrix Transform. To appear in *Sixth IEEE Sensor Array and Multichannel Signal Processing Workshop.* (Israel, 4-10 Oct 2010).

Cao, Guangzhi, C. A. Bouman, and J. Theiler. Weak signal detection in hyperspectral imagery using sparse matrix transform (SMT) covariance estimation. 2009. In *2009 First Workshop on Hyperspectral Image and Signal Processing: Evolution in Remote Sensing (WHISPERS) ; 26-28 Aug.* (2009 ; Grenoble, France). , p. 1.

Eads, D., and E. Rosten. Experiences using SciPy for computer vision research. 2009. *Proc. 7th Python in Science Conference.* : 22.

Foy, B. R., J. Theiler, and A. M. Fraser. Hyperspectral target detection using machine learning in a reduced dimensional space. 2008. *Proc. MSS (Military Sensing Symposia) Passive Sensors Conference.* : 1.

Foy, B. R., J. Theiler, and A. M. Fraser. Decision Boundaries in Two Dimensions for Target Detection in Hyperspectral Imagery. 2009. *Optics Express.* **17** (20): 17391.

Foy, B. R., J. Theiler, and C. R. Quick. Band selection for multispectral target detection using hyperspectral data. Presented at *Proc. MSS (Military Sensing Symposia) Conference on Battlefield Survivability and Discrimination.* (Orlando, FL, Feb 2009).

Foy, B. R., and J. Theiler. Change detection for hyperspectral sensing in a transformed low-dimensional space. To appear in *Proc. MSS (Military Sensing Symposium).* (Orlando, FL, 22-25 Feb 2010).

Harvey, N. R., R. Porter, and J. Theiler. Ship Detection in Satellite Imagery Using Rank-Order Grayscale Hit-or-Miss Transforms. 2010. In *Visual Information Processing XIX ; 6-7 April 2010 ; Orlando, FL, USA.* Vol. 7701, p. 770102 (12 pp.).

Loss, L. A., G. Bebis, M. Nicolescu, and A. Skurikhin. Investigating how and when perceptual organization cues improve boundary detection in natural images. 2008. In *2008 IEEE Computer Society Conference on Computer Vision and Pattern Recognition Workshops (CVPR Workshops) ; 23-28 June 2008 ; Anchorage, AK, USA.*

Loss, L., G. Bebis, M. Nicolescu, and A. N. Skurikhin. An iterative multi-scale tensor voting scheme for perceptual grouping of natural shapes in cluttered backgrounds. 2009. *Computer Vision and Image Understanding.* **113**: 126.

Love, S. P., T. C. Hale, L. J. Jolin, J. E. Barefield, W. H. Atkins, and J. J. Tiee. The ORCAS long-wave infrared hyperspectral sensor. 2008. In *Military Sensing Symposium (MSS).* (Orlando, FL, Feb 2008). , p. 0. Atlanta, GA: SENSIAC.

Matsekh, A., A. Skurikhin, L. Prasad, and E. Rosten. Numerical Aspects of Spectral Segmentation on Polygonal Grids. *Lecture Notes in Computer Science.*

Matsekh, A., and J. Theiler. Block-diagonal representations for covariance-based anomalous change detectors. To appear in *Proc. IGARSS.*

Porter, R., A. Fraser, R. Loveland, and E. Rosten. A recurrent velocity filter for detecting large numbers of moving objects. 2008. *Proc. SPIE.* **6969**: 69690C.

Porter, R., D. Hush, N. Harvey, and J. Theiler. Toward Interactive Search in Remote Sensing Imagery. 2010. In *Cyber Security, Situation Management, and Impact As-*

sessment II; and Visual Analytics for Homeland Defense and Security II ; 5-9 April 2010 ; Orlando, FL, USA. Vol. 7709, p. 77090V (10 pp.).

Porter, R., N. Harvey, and J. Theiler. A change detection approach to moving object detection in low fame-rate video. 2009. In *Visual Information Processing XVIII ; 14-15 April 2009 ; Orlando, FL, USA.* Vol. 7341, p. 73410S (8 pp.).

Prasad, L., and J. Theiler. A structural framework for anomalous change detection and characterization. 2009. In *Visual Information Processing XVIII ; 14-15 April 2009 ; Orlando, FL, USA.* Vol. 7341, p. 73410N (10 pp.).

Prasad, L., and S. Swaminarayan. Hierarchical image segmentation by polygon grouping. 2008. In *2008 IEEE Computer Society Conference on Computer Vision and Pattern Recognition Workshops (CVPR Workshops) ; 23-28 June 2008 ; Anchorage, AK, USA.*

Rosten, E., R. Porter, and T. Drummond. Faster and Better: a machine learning approach to corner detection. 2009. *IEEE Transactions on Pattern Analysis and Machine Intelligence (PAMI).* : (online).

Rosten, E., and R. Loveland. Camera distortion self-calibration using the plumb-line constraint and minimal Hough entropy. 2009. *Machine Vision and Applications.* : (online).

Scovel, C., D. Hush, I. Steinwart, and J. Theiler. Radial kernels and their reproducing kernel Hilbert spaces. 2010. *To appear in: Journal of Complexity.*

Skurikhin, A. N.. Proximity graphs based multi-scale image segmentation. Presented at *International Symposium on Visual Computing.* (Las Vegas, NV, 1-3 December 2008).

Skurikhin, A. N., and P. L. Volegov. Object-oriented hierarchical image vectorization. 2008. In *International Conference on Geographic Object Based Image Analysis (GEOBIA).* (Calgary, Canada, 6-7 August 2008). Vol. XXXVIII-4/C1, p. 0. .: ISPRS.

Steinwart, I.. Two oracle inequalities for regularized boosting classifiers. 2009. *Statistics and its Interface.* **2**: 217.

Steinwart, I., D. Hush, and C. Scovel. Optimal rates for regularized least squares regression. 2009. *Proc. 22nd Annual Conference on Learning Theory.* : 79.

Steinwart, I., D. Hush, and C. Scovel. Training SVMs without offset. To appear in *J. Machine Learning Research.*

Steinwart, I., J. Theiler, and D. Llamocca. Using support vector machines for anomalous change detection. To appear in *Proc. IGARSS.*

Steinwart, I., and A. Christmann. Sparsity of SVMs that use the epsilon-insensitive loss. 2009. *Neural Information Processing Systems.* **21**: 1569.

Steinwart, I., and A. Christmann. Estimating conditional quantiles with the help of the pinball loss. To appear in *Bernoulli.*

Theiler, J.. Quantitative comparison of quadratic covariance-based anomalous change detectors. 2008. *Applied Optics.* **47**: F12.

Theiler, J.. Sensitivity of anomalous change-detection to small misregistration errors . 2008. *Proc. SPIE.* **6966**: 69660X.

Theiler, J.. Subpixel anomalous change detection in remote sensing imagery. 2008. In *IEEE Southwest Sympsoium on Image Analysis and Interpretation.* (Santa Fe, 24-26 March 2008). , p. 165. New York: IEEE.

Theiler, J., B. R. Foy, B. Wohlberg, and C. Scovel. Parametric probability distributions for anomalous change detection. To appear in *Proc. MSS (Military Sensing Symposia).* (Orlando, FL, 22-25 Feb 2010).

Theiler, J., C. Scovel, B. Wohlberg, and B. Foy. Elliptically contoured distributions for anomalous change detection in hyperspectral imagery. 2010. *IEEE Geoscience and Remote Sensing Letters.* **7** (2): 271.

Theiler, J., G. Cao, L. R. Bachega, and C. A. Bouman. Sparse matrix transform for hyperspectral image processing. To appear in *Journal of Selected Topics in Signal Processing.*

Theiler, J., G. Cao, and C. A. Bouman. Sparse matrix transform for fast projection to reduced dimension. To appear in *Proc. IGARSS.*

Theiler, J., N. R. Harvey, R. Porter, and B. Wohlberg. Simulation framework for spatio-spectral anomalous change detection. 2009. In *Algorithms and Technologies for Multispectral, Hyperspectral, and Ultraspectral Imagery XV ; 13-16 April 2009 ; Orlando, FL, USA.* Vol. 7334, p. 73340P (12 pp.).

Theiler, J., and A. M. Matsekh. Total least squares for anomalous change detection. 2010. In *Algorithms and Technologies for Multispectral, Hyperspectral, and Ultraspectral Imagery XVI ; 5-8 April 2010 ; Orlando, FL, USA.* Vol. 7695, p. 76951H (12 pp.).

Theiler, J., and B. R. Foy. EC-GLRT: Detecting weak plumes in non-Gaussian hyperspectral clutter using an elliptically-contoured generalized likelihood ratio test. 2009. In *International Geoscience and Remote Sensing Symposium (IGARSS).* (Boston, MA, 6-11 July 2008). , p. I. Boston: IEEE.

Theiler, J., and C. Scovel. Uncorrelated versus independent elliptically-contoured distributions for anomalous change detection in hyperspectral imagery. 2009. In *Computational Imaging VII ; 19-20 Jan.* (2009 ; San Jose, CA, USA). Vol. 7246, p. 72460T (12 pp.).

Theiler, J., and D. Hush. Statistics for characterizing data on the periphery. To appear in *Proc IGARSS.*

Theiler, J., and S. Adler-Golden. Detection of ephemeral changes in sequences of images. 2009. *37th Applied Imagery Pattern Recognition Workshop (AIPR '08): Multiple Image Information Extraction.* : 1.

Wohlberg, B., and J. Theiler. Improved change detection with local co-registration adjustments. 2009. In *IEEE Workshop on Hyperspectral Image and Signal Processing: Evolution in Remote Sensing.* (Grenoble, France, 26-28 Aug 2009). , p. 1. .: IEEE.

Wohlberg, B., and J. Theiler. Symmetrized local co-registration optimization for anomalous change detection. 2010. In *Computational Imaging VIII ; 18-19 Jan.* (2010 ; San Jose, CA, USA). Vol. 7533, p. 753307 (10 pp.).

Wohlberg, B., and J. Theiler. Local Co-Registration Adjustment for Anomalous Change Detection. *IEEE Trans. Geoscience and Remote Sensing.*

Information Science and Technology: Metagenomics

Nicolas W. Hengartner
20080662DR

Abstract

Shotgun sequencing of uncultured microbial communities is the current frontier of the bioinformatics revolution resulting from advances in sequencing technology that is providing data in quantities unimaginable a few years ago. But without concerted efforts in developing suitable analysis tools, the amount of data will quickly outpace the ability of scientists to analyze it. This effort seeks to develop *de novo* quantitative genomic analysis tools that leverage existing knowledge databases, are readily extensible to new information, and scale linearly with the size of datasets. It promises near real-time analysis of metagenomic datasets that will make the dark matter of biology visible.

Interwoven in this project is the creation of a novel and powerful approach based on identifying informative signatures, incremental development of bioinformatics tools that can feed into existing analysis pipelines, and the construction of a statistical methodology for analyzing large, complex datasets.

Background and Research Objectives

Microbial communities are complex 'supra-organisms' of bacteria, archaea, single-cell eukaryotes and viruses that function together as a whole in order to survive and thrive in their natural environments. Microbes make up the majority of the living biomass on Earth and, as such, are major contributors to carbon cycling and to the biogenic production and destruction of other greenhouse gases, including N_2O and methane. Characterizing the collective genomes of microbial communities, a nascent field known as metagenomics, can help provide insights into the "dark matter" of biology.

The current strategy for metagenomics is to sequence, from uncultured environmental samples, tens of millions of short read sequences of Deoxyribonucleic Acid (better known by its acronym DNA). The challenge of metagenomics is one of extracting information from these reads. Existing analysis pipelines were originally developed to sequence the human genome and are ill suited to analyzing metagenomic data because (1) *there is an information gap* due to little or no redundancy in the reads and the fact that a priori we do not know the phylogenetic profile of the community, making it difficult to reconstruct the genomes in a sample; (2) *there is a computational gap* since modern sequencing technology produces ever more but shorter reads that challenge existing algorithms for assigning phylogeny and function to individual reads; and (3) *there is a signal gap* arising from shorter DNA reads significantly reducing the signal to noise ratio.

This project is developing, *de novo*, information science tools to enable the analysis of imetagenomic DNA reads in near real time. Improving the analysis time is important, as current methods take several years of CPU time. In addition to speed, our goal is to make the analysis quantitative rather than qualitative, readily extensible to accommodate new data as more fully sequenced genomes become available, and sensitive enough to identify small changes in microbial populations arising from changes in the environment. The last item is paramount to enabling comparative metagenomic analysis.

Scientific Approach and Accomplishments

We propose a paradigm shift from seeking to reconstruct, completely or partially, the genomes of organisms in the microbial community to seeking to identify the phylogeny and function of as many DNA reads as possible. Such read-by-read analysis using existing technologies is possible via fragment recruitment to existing fully sequenced genomes (either DNA or amino acids) using a matching algorithm known as BLAST. This strategy is computationally expensive, fails with short reads (less than 100 bp) and confounds sequence similarities arising from inheritance with similarities arising from functional pressure (natural selection). To resolve these issues, we proposed to leverage the existing corpus of over 1000 fully sequenced bacterial genomes to identify highly significant local signatures that we organize with respect to their specificity within the tree of life, and according to existing functional classification of proteins.

We define a significant signature to be any contiguous sequence of 10 amino acids found in at least two ge-

nomes belonging to different genera. Genera are one level up from species in a biological taxonomy. The resulting signatures are either indicative of functional pressure that forces conservation of beneficial motifs, or of inheritance from a close relative (phylogeny). We can distinguish between these two cases by placing the signature on the tree of life at the node of the most specific common ancestor. This provides a phylogenetic label for each signature. Similarly, functional labels for signatures are possible by exploiting an existing functional database of genes.

The surprise is the prevalence of significant signatures in bacterial genomes: about 0.5% of all possible 10-mers in a genome are found in a relatively distant organism. For Escherichia coli , this represents about a thousand signatures. This is impressive, considering that the expected number of random matches between two organisms is about 1/10. The number of signatures increases when comparing more closely related organisms. Figure 1 shows the distribution of signatures shared between Escherichia coli and 22 distantly related bacteria as a function location on the genome (x-axis). Vertical lines indicate a signature that matches most of the 22 bacteria. Notice the spatial distribution of signatures.

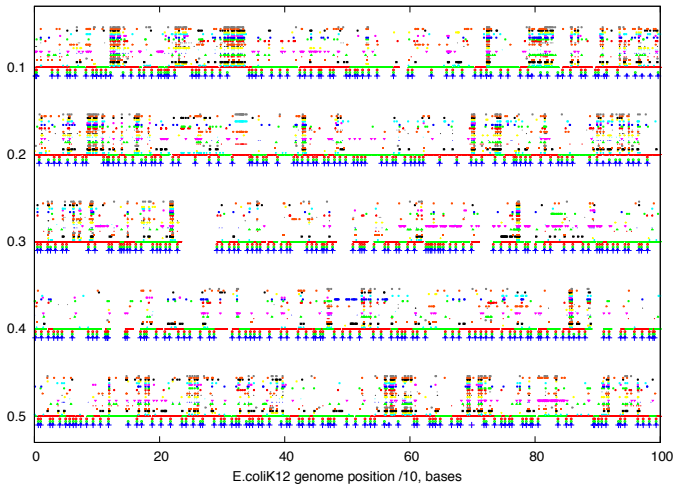

Figure 1. Location of matching signatures in Escherichia coli to one of 22 distantly related bacteria as a function of position in E. Coli (x-axis). Vertical lines indicate signatures that are shared between E. Coli and most of the 22 microbes.

Because the signatures are in terms of conserved peptides through evolution, we expect that some of our signatures will identify proteins in organisms never sequenced before. That is, we rely on natural selection to provide some guarantee that the signatures we find are general. This fact is supported by the observation that nearly 1/3 of all the genes in Escherichia coli contain at least one signature to an evolutionarily distant organism. This implies that the lists of signatures we are constructing are useful for analyzing the genome of an organism that has never been sequenced before.

One can compare this first step of finding signatures as a dictionary-building step that will help us classify DNA reads. Each signature is assigned phylogeny and, where possible, function. We then match each read to the list of signatures, which in turn allows us to assign phylogeny and function to the read, building up a phylogenetic and functional profile of the community (i.e. who does what).

We observed that a significant fraction (~85%) of 400 base-pair long reads that contain at least one signature, contain multiple signatures. Comparing the annotation of the multiple signatures within a read is revealing: ~15% of the reads had multiple signatures with the same phylogenetic label and ~50% of the reads had multiple signatures with labels consistent with a hierarchy implied by the evolutionary tree. But ~20% of the reads had multiple signatures with labels that are at odds with the phylogeny. Since the phylogenetic labels of our signatures were derived using a sparse sample of genomes, we think that many of these contradictory labeled reads may be indicative of novel organisms. That is, our signature method is capable of discovering genes from organisms not represented in our existing database. We expect that some of these “novel genes” may belong to Eukaryotes, Archaea or viruses/phages, which are not yet included in the signature calculation.

The computational challenges we need to solve are not unique to metagenomics. Google faces the same challenges in characterizing the content of webpages. So not surprisingly, tools Google has found to work well for their problem space (e.g. indexing and MapReduce) also work well for us. So in essence, we are developing a “google metagenome.” The net result is an analysis pipeline that produces results in a manner of hours rather than weeks. Comparison of computation times on test metagenomic datasets of oral pathogens and soil microbial communities shows that our method is a hundred thousand times faster than a comparable analysis using the standard BLAST algorithm. Figure 2 shows the profile of functional assignment of reads in various FACE sites. Some functions, like those associated to carbohydrates, and amino acids and derivatives, are ubiquitous and show little differences between the samples beyond statistical noise. Other functions, like respiration (think photosynthesis) are present at various levels of prevalence in the samples.

These ideas and related technology have been encapsulated into a patent application. Our decision to produce a patent delayed publication of the above aspects of our methodology.

We expect genes containing a signature to be related. This can be ascertained by multiple sequence alignment of genes containing a signature of interest. Similarly, multiple sequence alignment of reads identified by a given signatures can help filter out false positives. The computational complexity of strict multiple sequence alignment grows as

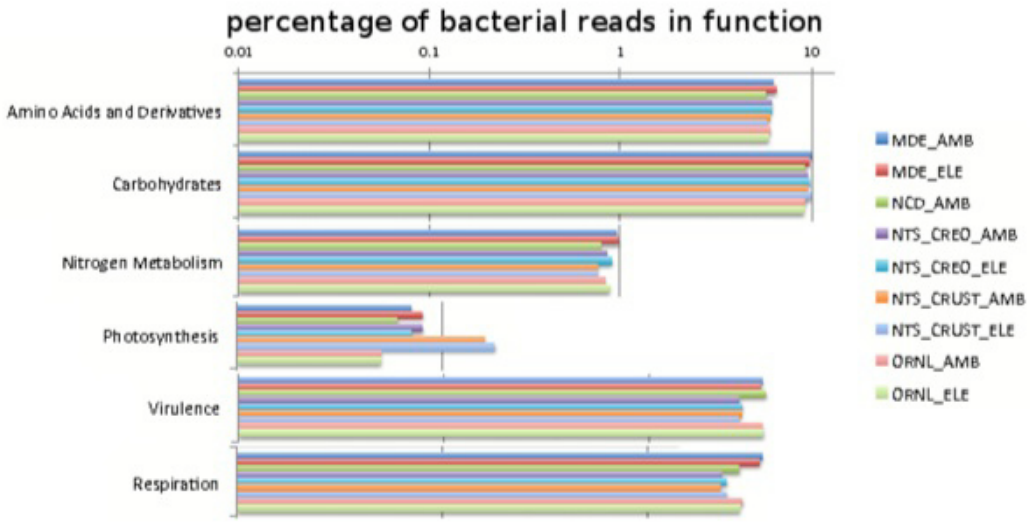

Figure 2. Functional profile of several FACE metagenomic samples, organized by functional category. Ubiquitous categories show the same profile across the different samples, and our method is able to show statistically significant differences in environmental specific functions, such as respiration/photosynthesis.

the square of the number of sequences. That is, the algorithm will not scale. We have developed a fuzzy matching algorithm, called the Velvetrope, to enable useful comparisons of multiple sequences that have the potential of identifying false positives. It does this by rapidly finding all areas of pairwise similarity between an anchor sequence and some set of other sequences. Our algorithm uses only bitwise operations at every step that can be trivially run in parallel with minimal memory requirements. Hence it is well suited to be implemented on a Graphical Processing Unit (GPU) and clusters. The algorithm, while not returning a full multiple alignment, finds regions of high similarity between sequences and aggregates the result as an overlay onto the anchor sequence. The result is somewhere between a local and multiple alignment and answers questions that neither can address independently. The advantage of this approach over BLAST-type alignments is that it can find areas of similarity ignored by the latter, such as areas of conserved structures under transposition. A manuscript detailing the algorithm has been submitted to Bioinformatics, and we are actively pursuing release of the software under the Lesser General Public License.

The true test of usefulness of a novel method is its ability to enable new scientific discoveries. In the last year of this project, we have worked with Dr. Kuske on analyzing arid soil metagenomic data from the Department of Energy (DOE) funded Free Air Carbon Dioxide (CO_2) Experiment (FACE) sites. Our preliminary analysis was able to detect and quantify small but statistically significant changes in microbial populations that could be attributed to higher levels of CO_2. But more data, in the form of replicates, are needed to measure the intrinsic heterogeneity in phylogenetic profiles before we can make a stronger statement on the impact of CO_2 on microbial communities. Figure 3 shows a plot of differences between the phylogenetic profiles overlaid on a phylogenetic (evolutionary) tree for microbial communities at elevated and ambient CO_2 levels, color-coded by statistical significance. An upward pointing triangle indicates an increase of signatures at a given node; a downward pointing triangle indicates a decrease. Observe the consistency of the significant differences along established phylogenies – each branch of the tree goes up or down in unison (more or less).

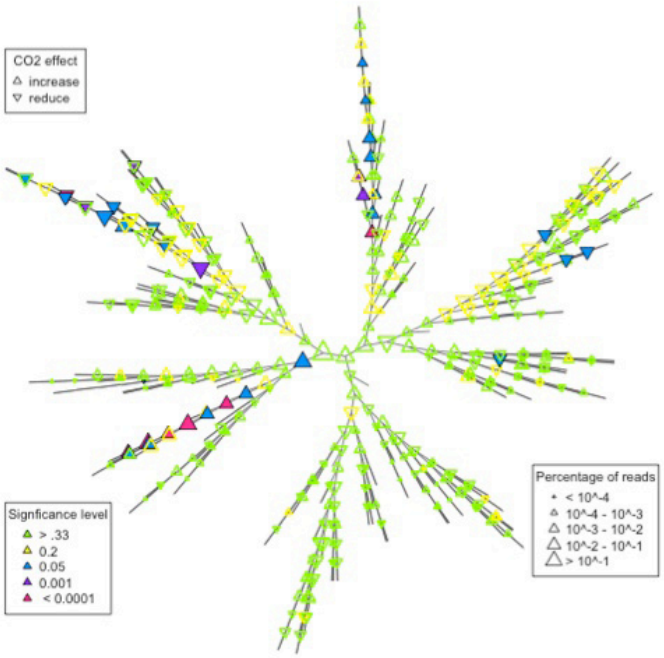

Figure 3. Plot of differences between phylogenetic signatures in reads from two microbial communities, one subjected to increased levels of CO_2 while the other being at ambient levels of CO_2. The differences are colored according to their statistical significance, and the triangles

point indicate an increase (upwards pointing) or a decrease (downward pointing). The differences are organized and displayed on a phylogenetic tree. Notice how the changes are consistent along the various branches on the tree.

We have worked closely with our colleagues at the Joint Genome Institute (JGI) to help transition our novel ideas into existing analysis pipelines. To this end, we have worked on parallel analysis techniques, and developed bioinformatics tools useful to the existing metagenomics analysis pipeline.

We have also developed algorithms and software to classify 16s ribosomal RiboNucleic Acid (rRNA) extracted from uncultured environmental samples using targeted primers into taxonomic groups. This algorithm was instrumental in estimating the phylogenetic profile of oral metagenomic samples.

Genome reconstruction remains one of the central tasks of the JGI. To enable assembly from metagenomic data, we proposed that sequence data should be preprocessed by using fragment recruitment to bin the reads into phylogenetically homogeneous groups. The reads in each bin is then subjected to statistical assembly. The resulting production pipeline was applied to genome reconstruction of the oral microbial fauna.

Other bioinformatics algorithms and software developed in the context of this project include an automatic protein classifier and an algorithm for estimating genome size from single cell amplification sequencing methods. In addition, this project has supported the development of a Markov naïve Bayesian classifier and a metagenomic pathway signature detector.

This close collaboration with JGI has produced three peer-reviewed papers, with an additional five papers in various stages of completion.

Finally, this project has supported basic research on two aspects of statistical analysis of complex datasets. The first set of results rests on the observation that many aspects of post-processing of the data can be recast as (non-parametric) regression problems in high dimensions. We have developed a novel and powerful smoothing technique for high dimensional data. This method has surprisingly good performance, both in simulation and on classical test datasets. The theoretical reason is that our method is adaptive to the smoothness of the unknown regression function. To our knowledge, our smoother is the first practical adaptive multivariate smoother. Second, we have developed an efficient algorithm for estimating extreme quantiles of a distribution. The latter work has lead to some unexpected new algorithms for Monte-Carlo integration that uses the Lebesgue formulation of the integral instead of the common Riemann formulation. This work has produced five papers and an R add-on package available at CRAN.

Impact on National Missions

The goal of our project was to make possible the analysis of shotgun metagenomics data in near real time. Our analysis tool allows one to see the dark matter of biology (microbial communities). This opens the possibility of characterizing existing microbial communities, quantifying the impact of environmental insults on these communities and monitoring the evolution/recovery of these communities over time. For example, one of the biggest uncertainties in long-term climate predictions centers on the response of microbial communities to increased CO_2, changes in temperature, and changes of pH in the ocean. Our methods are also well adapted to following the fate of released biological agents.

Phylogenetic profiles of environmental samples provide a novel type of signature for the origin/provenance of objects and individuals that exploits the genetic profiles of accompanying microbes.

Finally, the signature tags themselves are of interest. They provide specific DNA hybridization tags based on observed functions tags that can be made specifically to monitor particular microbial communities. Such markers may prove useful for microbial communities associated to biofuels, indicators of health status of individuals based on cohabitation of microbial fauna, and the detection/characterization of pathogens.

Publications

Burr, T., N. Hengartner, E. Matzner-Lober, S. Myers, and L. Rouviere. Smoothing Low Resolution Gamma Spectra. To appear in *IEEE Transaction on Nuclear Sciences.*

Clark, S., N. Hengartner, and J. Berendzen. Velvetrope: a Parallel, Bitwise Algorithm for Finding Homologous Regions Within Multipole Sequences. *Bioinformatics.*

Cornillon, P. A., N. Hengartner, and E. Matzner-Lober. Interative Bias Reduction Multivariate Smoothing in R: The IBR package. *Journal of Statistical Software.*

Guyader, A., N. Hengartner, and E. Matzner-Lober. Simulation and Estimation of Extreme Quantiles and Extreme Probability Distributions. *Journal of the Royal Statistical Society, Series B.*

Guyader, A., N. Hengartner, and E. Matzner-Lober. Multilevel Monte Carlo Simulation and Estimation of Extreme Quantiles and Probabilities. To appear in *2011 SIAM Conference on Computational Sciences and Engineering* . (no, , 28 Feb 2011 - 4 Mar. 2011).

Hengartner, N., E. Matzner-Lober, L. Rouviere, and T. Burr. Multiplicative Bias Corrected Nonparametric Smoothers. To appear in *Canadian Journal of Statistics.*

Liu, K., N. Hengartner, and G. Xie. Markov naïve Bayesian classifier (Markov NBC) for metagenomic Reads Assign-

ment . 2010. *LANL B Division Reports.*

Liu, K., T. Wong, G. Xie, and N. Hengartner. Improving naïve Bayesian classifier for metagenomic reads assignment. 2009. In *The 2009 International Conference on Bioinformatics & Computational Biology.* (Las Vegas, July 13-16, 2009). , p. 1020. Las Vegas: BIOCOMP.

Woyke, T., G. Xie, A. Copeland, J. M. Gonzalez, C. Han, H. Kiss, J. Saw, P. Senin, C. Yang, S. Chatterji, J. Cheng, J. Eisen, M. Sieracki, and R. Stepanauskas. Assembling the marine metagenome, one cell at a time. 2009. *Public Library of Science.* **4** (4): e5299.

Xie, G., P. Chain, C. Lo, K. Liu, J. Gans, J. Meritt, and F. Qi. Community and Gene Composition of a Human Dental Plaque Microbiota Obtained by Metagenomic Sequencing. To appear in *Oral Microbiology.*

Xu, J., and G. Xie. Metagenomic Analyses of Saliva Microbiotas from Caries-sensitive Patients and Healthy Controls . 2010. *Los Alamos B Division Report.*

Statistical Physics of Networks, Information and Complex Systems

Robert E. Ecke
20080671DR

Abstract

With the LDRD project "Statistical Physics of Networks, Information and Complex Systems" the Center for Nonlinear Studies (CNLS) underpinned the science of Information Science and Technology (IS&T) in the P,T,D and CCS-divisions of Los Alamos National Laboratory. Built around the central themes of complexity, nonlinearity and statistical mechanics as applied to Information Science, the project provided a multidisciplinary focal point for studying complex behavior, exchange and transportation of information in computer networks, biological cell systems, quantum systems and classical optimization problems. While providing specific themes, this center project also created a scientific backbone structure that allowed IS&T researchers to explore insights and techniques from other fields. The resulting diversity is reflected in the list of accomplishments.

Participants have constructed new algorithms for computing conditional probabilities in communication networks. They have developed new search techniques for finding and retrieving data. They have proposed and tested new, hybrid optimization methods for locating global optima in complex networks. They have worked out statistical mechanics limits of complex information networks. They have revealed fundamental properties of the capacity of quantum communication systems. They have developed new protocols for web searches and web-based computation. They have developed new mathematical models amenable to rigorous, analytical mathematical analysis while including real-world conditions. They have revealed cooperative, non-linear behavior in neural networks and shed light on visual information processing of the human brain.

Background and Research Objectives

Information theory studies communication systems. In its simplest realization, a communication system consists of one sender, one receiver and a transport channel to guide the signal that may be subject to noise. More generally, though, a communication system may consist of a network of many sender/receiver nodes each of which harbors quantities, known as variables. The variables take on numerical values with (generally unknown) probability so that the actual values are uncertain before they have been measured. The exchange of signals, the mutual influence of nodes or the measurement of the variables can reduce the uncertainty of the variable values in a subset of nodes, which corresponds to information exchange. Claude Shannon showed that if the uncertainty measure is expected to satisfy a set of reasonable conditions, it has to be proportional to the entropy function: the higher the entropy, the more uncertainty there is regarding the values of the variables.

The questions that are addressed in determining 'information' can range from physical properties to data content to the outcome of computational processes. Examples of questions can be: 'given that a particle of type A (or a spin-up) occupies a lattice site, what particle (or spin) occupies the neighboring lattice site?', or 'given a series of images is the particle shown in pixel y the same particle as that one shown in pixel z on one of the other images?; 'given a history of computer activities, is a detected anomaly caused by a targeted, malicious computer attack?', or 'given a list of electrical energy sources in an energy grid, is a specific appliance drawing energy from a particular source?'. Clearly, many different systems, natural and man-made, can be characterized as communication systems. The information-theoretic approach is especially useful when the system's complexity or size requires a systematic, quantitative description.

In addition to exhibiting complex behavior, communication systems are subject to heating (increasing noisiness), failures of transmission, and general noise processes. Communication systems are prone to errors and random fluctuations and their robustness may make the difference between a well-functioning safety system and the occurrence of a disaster that could have been avoided. The parameters of the communication system can change in time and the topology of the network that transmits the information can be altered radically, possibly undergoing changes that resemble phase transitions.

By introducing cost functions that quantify the importance of desirable properties, the challenge of designing

communication systems and of understanding and managing information can be posed as an optimization problem. The quantities that determine the capacity of information transport are determined by calculating higher order conditional probabilities. The calculation of entropy from these probabilities is often challenging but entropy obeys its own algebra, the application of which can lead to general insights. Well-defined classes of mathematical models are amenable to rigorous mathematical analysis but many of the current models lack the richness of real-world applications. Effects of randomness have been studied in idealized statistical mechanics systems such as spin glasses. These studies have also revealed that systems with random interactions can undergo phase transitions.

Complexity, the statistical mechanics approach to large system limits and a host of phenomena caused by nonlinear and/or chaotic dynamics, are CNLS-themes that wove threads of commonality into the research of this project.

The first research objective of the project was the study of the structure of communication systems. This part included the development and understanding of fast and robust optimization algorithms, as well as the use of network analysis to make crucial deductions. Some of the methods developed determine conditional probabilities that reveal the efficiency of information flow, the robustness of transmission or the capacity of information transmission, and the calculation of other properties that characterize the communication network. A second objective consisted of unraveling how communication systems work in nature. This objective examined questions such as 'how does human vision work?', 'can similar techniques be implemented to create improved pattern recognition methods (synthetic cognition)?', 'how do swarms and correlated agents improve search efficiency?', and 'can quantum information be transmitted with a higher capacitance than classical information?' A third objective focused on the mathematical modeling of communication systems. This objective involved questions such as 'how can simplified models that are amenable to rigorous mathematical analysis be generalized to include crucial real-world features?', 'how can new computation models that distribute the computation and utilize data storage architecture be implemented?', 'which models describe the dynamics of epidemics successfully and what can we learn from them?'.

Scientific Approach and Accomplishments

The research conducted was mostly theoretical, although some of the vision work and the neural network studies involved experimental work carried out by participants. Many of the efforts employed information theory explicitly. The project produced more than sixty papers in the open literature, some of which appeared in the highest profile journals: eight in Physical Review Letters, one in Science, one in Nature Physics and one in the Proceedings of the National Academy of Science. The common denominators of complexity, nonlinear science and statistical mechanics analysis tied together disparate sciences, provided a common language and allowed cross-fertilization by implementing methods from other fields. The project nucleated new projects such as the Smart Grid and Cyber Security efforts and generated outside funding from companies (NEDO) and from the National Institute of Health.

Institutionally, the project provided focus to the LANL IS&T research. From the scientific perspective, the coordinated broad-phalanx approach produced a larger number of results than we can discuss in this report. We confine our description of the accomplishments to a limited number of discussions, grouped by the above listed objectives.

The study of the structure of communication systems

As mentioned above, communication systems are networks with nodes that have one or multiple variables associated with them. These variables take on values that are inherently uncertain. Their statistical nature poses challenges: as repeated measurements of the same quantity yield different results even under optimal control conditions, one can, at best, determine what the 'most likely' answer is to the question that the measurement investigates and what the uncertainty is. The particular question may be 'what is the value of the variables on the nodes?' if the parameters of the system are known (inference), or 'what are the most likely parameters of the system that are consistent with the measurement of the node variables?' (learning). In a particularly relevant illustration, Misha Chertkov, Florent Krzakala, Lenka Zdeborova and collaborators showed that the challenge of tracking particles in a series of images can be solved in an unusually fast and efficient manner by a message passing technique that identifies likely answers. The particular method is a specific realization of a more general method known as Belief Propagation [1]. Misha Chertkov had shown that the belief propagation method can be exact under conditions in which the algorithm was previously believed to be only approximate [2]. Lenka Zdeborova and Florent Krzakala showed that a different realization of the same Belief Propagation method can well approximate the time evolution of an ensemble (a set of similar states) of spins with random interactions under challenging conditions, such as a phase transitions or with temperature chaos [3]. The problem of calculating the quantum mechanical ground state energy of a spin system with random interactions and random field -- one of the problems recognized as 'intractable' -- has been tackled with belief propagation. Matt Hastings proposed a related but improved algorithm that solved this long-standing problem with a heuristic optimization method [4].

Different optimization methods work well under different conditions. Jasper Vrugt and James Hyman have developed multi-purpose meta-optimization techniques: multi-method approaches that are self-adaptive, which means that they operate with algorithms that select the method

during the calculation [5]. The application of these methods for hydrological purposes were shown to greatly extend the problems that can be addressed numerically, including the challenge of determining the sensitivity to input parameters [6].

Unraveling how communication systems work in nature

How does the human mind process images? The brain's ability to recognize patterns and detect changes is puzzling. The solution to this puzzle may improve pattern recognition techniques and machine learning methods (the challenge of synthetic cognition). Recent research has shown that the brain processes by creating hierarchical maps. The mind builds up an image from visual input by assembling features into larger and larger groups or levels. The mind then updates the different groups at different speeds: the small features such as 'up' and 'down' of a particular observed edge of an object may get updated faster than the information than the information about the overall shape of the object, for instance. This process may occur at the level of hard-wired connections, corresponding to different subgroups of neurons. Luis Bettencourt, Vadas Gintautas and Michael Ham have developed general methods for identifying relevant subgraps in complex systems [7] and they have implemented these techniques to find groups of coordinating neurons in neural networks [8].

In quantum communication, the transported information is encoded in quantum bits: instead of a '0' or a '1', quantum bits (qu-bits) can also take on a superposition of '0' and '1' states. These single qu-bit states can also be described as the 'spin-up' and 'spin-down' states of a spin1/2-particle. The coherent superposition of a qu-bit is a state in which the associated spin does not point up or down but there exists a single, reversible operation (a spin rotation) that turns the corresponding state into a spin-up state deterministically (each repetition of the operation yields a spin-up state in similarly prepared spins). We now consider two senders a and b emitting a qu-bit via two different channels to their respective receivers. Quantum mechanically, the two quantum bits can be in a coherent superposition of two-qu-bit states. We consider a superposition of one state in which the spins of receiver a and b both point up and a state in which spins a and b point down. Now, we say that '0' corresponds to the two-qu-bit system in which both of those states are added; '1' corresponds to the subtraction of those states. In either case, a spin measurement of a single qu-bit has fifty percent chance of yielding spin-up and fifty percent of yielding spin-down. It seems therefore, that channels a and b, taken separately do not carry any information. However, if receivers a and b collaborate they can find out if the two qu-bits were in the '0' or '1' state. All they have to do is to measure spin a in the x-direction after applying a two-qu-bit called a controlled-not gate: if spin a is 'up', change the 'up' of spin b to a 'down' and the 'down' of spin b to an up, otherwise leave the spins untouched. If, after that operation, spin a points in the 'x' direction, the two-qu-bit was in the '0'-state. If spin a was found to point in the negative 'x'-direction, the two-qu-bit system was in the '1'-state. Therefore, two cooperating receivers, each using a communication channel that does not transport information by itself, can extract information encoded in the qu-bit quantum entanglement. Jon Yard and collaborators pointed out that two zero-capacity quantum channels can transport information [9] and they discussed the origins of this effect [10]. Matt Hastings discussed the algebra of 'superadditivity' of quantum communication [11].

Nature, presumably by means of evolutionary selection, has developed improved search techniques. By having the searchers communicate, ants for instance are surprisingly adept at locating food resources. Luis Bettencourt and Vadas Gintautas have discovered a method for quantifying the advantage gained by searches that employ communicating search agents [12].

Mathematical modeling of communication systems

Effects of randomness (also called disorder) are generally challenging to predict. In addition to simulation, from which it is sometimes difficult to generalize, randomness can be described rigorously by classes of simplified models called random graphical models. Random geographical graphs have reveal main trends and crucial features in complex networks such as computer and social networks, as well as epidemics and emergency response in natural disasters. Milan Bradonjic and Aric Hagberg have developed new classes of geographical graphs for extending the current models to include important real-world effects [13]. Marko Rodriguez and Joshua Shinavier have developed a general algebra to map multi-relational network connections to single-relational graphs [14].

Impact on National Missions

Information, its processing, transport and vulnerability are priority matters of national security. Moreover, information systems in computer networks, biological systems (bio-informatics, neural computation), and social dynamics play crucial roles in several national security challenges. By providing a strong, multidisciplinary center of academic excellence with pastors, students and visitors, by steering researchers to application relevant challenges of general interest but with specific focus, by facilitating the transfer of much needed methods and concepts across the boundary of traditional science areas, and by actively nucleating new efforts in "Smart Grid" problems and Cyber security the CNLS has strengthened the laboratory's IS&T, which is recognized not only as a grand challenge, but also as a Pillar of the Laboratory.

References

1. Chertkov, M., L. Kroc, F. Krzakala, M. Vergassola, and L. Zdeborova. Tracking particles by passing messages between images. 2010. *Proceedings of the Academy of*

Sciences. **107** (17): 7663.

2. Chertkov, M.. Exactness of belief propagation for some graphical models with loops. 2008. *Journal of Statistical Mechanics: Theory and Experiment.* : P10016.

3. Zdeborova, L., and F. Krzakala. Generalization of the cavity method for adiabatic evolution of Gibbs states. 2010. *Physical Review B.* **81**: 224205.

4. Hastings, M. B.. Inference from matrix products: a heuristic spin-glass algorithm. 2008. *Physical Review Letters.* **101** (16): 167206.

5. Vrugt, J. A., B. A. Robinson, and J. M. Hyman. Self-adaptive multimethod search for global optimization in real-parameter spaces. 2009. *IEE Theory of evolutionary computation.* **13** (2): 243.

6. Vrugt, J. A., and B. A. Robinson. Treatment of uncertainty using ensemble methods: comparison of sequential data assimilation and Bayesian model averaging. 2007. *Water Resources Research.* **43**: W01411.

7. Bettencourt, L. M. A., V. Gintautas, and M. I. Ham. Identification of functional information subgraphs in complex networks. 2008. *Physical Review Letters.* **100**: 238701.

8. Gintautas, V., L. M. A. Bettencourt, and M. I. Ham. Identification of functional information subgraphs in cultured neural networks. 2009. *Biomedical Neuroscience.* **10** (1471): 22.

9. Smith, G., and J. Yard. Quantum communication with zero-capacity channels. 2008. *Science.* **321**: 1812.

10. Hayden, P., M. Horodecki, A. Winter, and J. Yard. A decoupling approach to the quantum capacity. 2008. *Information Dynamics and Open Systems.* **15** (1): 7.

11. Hastings, M. B.. Superadditivity of communication capacity using entangled inputs. 2009. *Nature Physics.* **5** (4): 255

12. Bradonjic, M., A. Hagberg, and A. G. Percus. The structure of geographical threshold graphs. 2009. *Special Issue of Internet Mathematics.* **5**: 113.

13. Rodriguez, M. A., and J. Shinavier. Exposing multi-relational networks to single-relational network analysis algorithms. 2009. *Journal of Informetrics.* **41**: 29.

Publications

Ben-Naim, E., M. B. Hastings, and D. Izraelevitz. Statistics of partial minima. 200. *Journal of Physics A: Mathematical and Theoretical.* **40** (47): F1021.

Ben-Naim, E., and P. L. Krapivsky. Stratification in the preferential attachment network. 2009. *Journal of Physics A: Mathematical and Theoretical.* **42** (47): 475001.

Bettencourt, L. M. A., V. Gintautas, and M. I. Ham. Identification of functional information subgraphs in complex networks. 2008. *Physical Review Letters.* **100**: 238701.

Beveridge, A., and M. Bradonjic. On the mixing of geographical threshold graphs. *Discrete Applied Mathematics: The Journal of Combinatorial Algorithms, Informatics and Computational Sciences.*

Bianconi, G., N. Gulbahce, and A. E. Motter. Local structure of directed networks. 2008. *PHYSICAL REVIEW LETTERS.* **100** (11): 118701.

Bianconi, G., and N. Gulbahce. Algorithm for counting large directed loops. 2008. *JOURNAL OF PHYSICS A-MATHEMATICAL AND THEORETICAL.* **41** (22): 224003.

Boettcher, S., B. Goncalves, and H. Guclu. Hierarchical regular small-world networks. 2008. *Journal of Physics A.* **41** (25): 252001.

Bradonjic, M., A. Hagberg, and A. G. Percus. The structure of geographical threshold graphs. 2009. *Special Issue of Internet Mathematics.* **5**: 113.

Bradonjic, M., E. Kohler, and R. Ostrovsky. Near-optimal radio use for wireless network synchronization. *Theoretical Computer Science.*

Bradonjic, M., T. Muller, and A. Percus. Coloring geographical threshold graphs. *Discrete Mathematics and Theoretical Computer Science*.

Bradonjic, M., and L. Lazos. Clustering methods for cognitive radio networks based on biclique graphs. *The International Journal of of Computer and Telecommunications Networking.*

Burr, T. L., and G. Chowell. Signatures of non-homogeneous mixing in disease outbreaks. 2008. *MATHEMATICAL AND COMPUTER MODELLING.* **48** (1-2): 122.

Carmi, S., P. L. Krapivsky, and D. ben-Avraham. Partition of networks into basins of attraction. 2008. *Physical Review E.* **78** (6): 066111.

Chernyak, V. Y., M. Chertkov, S. V. Malinin, and R. Teodorescu. Non-equilibrium thermodynamics and topology of currents. 2009. *Journal of Statistical Physics.* **137** (1): 113.

Chernyak, V. Y., and M. Chertkov. Fermions and loops on graphs: II A monomer-dimer model as a series of determinants. 2008. *Journal of Statistical Mechanics: Theory and Experiment.* **1742**: 5468.

Chernyak, V. Y., and M. Chertkov. Fermions and loops on graphs: I. Loop calculus for determinants. 200. *Journal of Statistical Mechanics: Theory and Experiment.* **1742**: 5468.

Chertkov, M.. Exactness of belief propagation for some graphical models with loops. 2008. *Journal of Statistical Mechanics: Theory and Experiment.* **1742**: 5468.

Chertkov, M.. Reducing the error floor. 200. *IEE Information Theory Workshop.* **1/2**: 230.

Chertkov, M., L. Kroc, F. Krzakala, M. Vergassola, and L. Zdeborova. Tracking particles by passing messages between images. 2010. *Proceedings of the National Academy of Science.* **107** (17): 7663.

Chertkov, M., V. Chernyak, and R. Teodorescu. Belief Propagation and Loop Series on Planar Graphs . 2008. *Journal of Statistical Mechanics.* : P05003.

Chertkov, M., and M. G. Stepanov. An efficient pseudo-codeword search algorithm for linear programming decoding of LDPC codes. 2008. *IEEE TRANSACTIONS ON INFORMATION THEORY.* **54** (4): 1514.

Chilappagari, S. K., M. Chertkov, M. G. Stepanov, and B. Vasic. Instanton-based techniques for analysis of error floors of LDPC codes. 2009. *IEE Journal on Selected Areas in Communications.* **27** (6): 855.

Chowell, G., L. M. Bettencourt, N. Johnson, W. J. Alonso, and C. Viboud. The 1918-1919 influenza pandemic in England and Wales: spatial patterns in transmissibility and mortality impact. 2008. *PROCEEDINGS OF THE ROYAL SOCIETY B-BIOLOGICAL SCIENCES.* **275** (1634): 501.

Chowell, G., P. Diaz-Duenas, J. C. Miller, A. Alcazar-Velasco, J. M. Hyman, P. W. Fenimore, and C. Castillo-Chavez. Estimation of the reproduction number of dengue fever from spatial epidemic data. 2007. *Mathematical Bioscience.* **208** (2): 571.

Devetak, I., and J. Yard. Exact cost of redistributing multipartite quantum states. 2008. *PHYSICAL REVIEW LETTERS.* **100** (23): 230501.

Feyen, L., J. A. Vrugt, B. O. Nuallain, J. van der Knijff, and A. De Roo. Parameter optimisation and uncertainty assessment for large-scale streamflow with the LISFLOOD model. 2007. *Journal of Hydrology.* **332** (3/4): 276.

Feyen, L., M. Kalas, and J. A. Vrugt. Semi-distributed parameter optimization and uncertainty assessment for large-scale streamflow simulation using global optimization. 2008. *Hydrological Science Journal.* **53** (2008): 293.

Gintautas, V., A. E. Champagne, F. G. Kondev, and R. Longland. Thermal equilibration of Lu-176 via K mixing. 2009. *Physical Review C.* **80** (1): 015806.

Gintautas, V., A. Hagberg, and L. M. A. Bettencourt. When is social computing better than the sum of its parts?. To appear in *Social Computing, Behavior Modelng and Prediction.* (Phoenix, 2009).

Gintautas, V., L. M. A. Bettencourt, and M. I. Ham. Identification of functional information subgraphs in cultured neural networks. 2009. *Biomedical Neuroscience.* **10** (1471): 22.

Gintautas, V., and A. Hubler. A simple, low cost, data-logging pendulum built from a computer mouse. 2009. *Physics Education.* **44**: 488.

Guclu, H., D. Kumari, and M. Yuksel. Ad-hoc limited scale-free models for unstructured peer-to-peer networks. 2008. In *P2p'08: Eight International Conference on peer-to-peer computing.* (Aachen, Germany, 2008). , p. 0. New York: IEE.

Gumel, A. B., M. Nuno, and G. Chowell. Mathematical assessment of Canada's pandemic influenza preparedness plan. 2008. *Canadian Journal of Infectious Diseases Medicine and Microbiology.* **19** (2): 185.

Ham, M. I., V. Gintautas, M. A. Rodriguez, R. A. Bennett, C. L. Santa Maria, and L. M. A. Bettencourt. Density-dependence of functional development in spiking cortical networks grown in vitro. 2010. *Biological Cybernetics.* **102**: 71.

Ham, M. I., V. Gintautas, and G. Gross. Spontaneous coordinated activity in cultured networks: analysis of multiple ignition sites, primary circuits, burst phase delay distributions and functional structures. 2008. *Journal of Computational Neuroscience.* **24**: 346.

Hamza, E., S. Michalakis, B. Nachtergaele, and R. Sims. Approximating the ground state of gapped quantum spin states. 2009. *Journal of Mathematical Physics.* **50** (9): 95213.

Hastings, M. B.. Superadditivity of communication capacity using entangled inputs. 2009. *Nature Physics.* **5** (4): 255.

Hastings, M. B.. Observations outside the light cone: algorithms for nonequilibrium and thermal states. 14. *Physical Review B.* **77**: 144302.

Hastings, M. B.. Inference from matrix products: a heuristic spin-glass algorithm. 2008. *Physical Review Letters.* **101**

(16): 167206.

Hastings, M. B.. Quantum belief propagation: an algorithm for thermal quantum systems. 2007. *Physical Review B.* **76** (20): 201102(R).

Hastings, M. B., and A. W. Harrow. Classical and quantum tensor product expanders. 2009. *Quantum Information Computation.* **9** (3-4): 336.

Hayden, P., M. Horodecki, A. Winter, and J. Yard. A decoupling approach to the quantum capacity. 2008. *Information Dynamics and Open Systems.* **15** (1): 7.

Hubler, A. W., and V. Gintautas. Experimental evidence for mixed reality states. 2008. *Complexity.* **13**: 7.

Hyman, J. M., and J. Li. Epidemic models with differential susceptibility and staged progression and their dynamics. 2009. *Mathemetical Bioscience Engineering.* **6** (2): 321.

Krzakala, F., and L. Zdeborova. Hiding quiet solutions in random constraint problems. 2009. *Physical Review Letters.* **102** (23): 238701.

Lee, S. Y., R. Teodorescu, and P. Wiegmann. Shocks and finite-time singularities in Hele-Shaw flow. 2009. *Physica D.* **238** (14): 1113.

Lopez, E., R. Parshani, R. Cohen, S. Carmi, and S. Havlin. Limited path percolation in complex networks. 2007. *PHYSICAL REVIEW LETTERS.* **99** (18): 188701.

Miller, J. C., and J. M. Hyman. Effective vaccination strategies for realistic social networks. 2007. *Physica A.* **386** (2): 780.

Munsky, B., I. Nemenman, and G. Bel. Specificity and completion time distributions of biochemical processes. 2009. *Journal of Chemical Physics.* **131** (23): 235103.

Rodriguez, M. A., V. Gintautas, and A. Pepe. The relationship between concert and listening behavior. 1. *First Monday.* **14** (1): 2009.

Rodriguez, M. A., and J. H. Watkins. Faith in the algorithm, Part 2: computational eudaemonics. 2009. *Lecture Notes Artificial Intelligence.* **5712**: 813.

Rodriguez, M. A., and J. Shinavier. Exposing multi-relational networks to single-relational network analysis algorithms. 2009. *Journal of Informetrics.* **41**: 29.

Rohlf, T., N. Gulbahce, and C. Teuscher. Damage spreading and criticality in in finite random dynamical networks. 2007. *Physical Review Letters.* **99** (24): 248701.

Smith, G., and J. Yard. Quantum communication with zero-capacity channels. 2008. *Science.* **321**: 1812.

Sorathia, S., F. M. Izraelev, G. L. Celardo, V. G. Zelevinsky, and G. P. Berman. Internal chaos in an open quantum system: from Ericson to conductance fluctuations. 2009. *Europhysics Letters.* **88**: 27003.

Srinivasan, R., R. Pepe, and M. A. rodrigues. A clustering-based semi-automated techniques for cultural ontologies. 2009. *Journal of American Society for Information Science and Technology .* **60** (3): 608.

Vrugt, J. A., B. A. Robinson, and J. M. Hyman. Self-adaptive multimethod search for global optimization in real-parameter spaces. 2009. *IEE Theory of evolutionary computation.* **13** (2): 243.

Vrugt, J. A., C. J. F. ter Braak, C. G. H. Dicks, B. A. Robinson, J. M. Hyman, and D. Higdon. Accelerating Markov chain Mone-Carlo Simulation by differential evolution with self-adaptive randomization subspace sampling. 2009. *International Journal of Nonlinear Sciences and Numerical Simulation.* **10** (3): 273.

Vrugt, J. A., C. J. F. ter Braak, M. P. Clark, J. M. Hyman, and B. A. Robinson. Treatment of input uncertainty in hydrological modeling: doing hydrology backward with Markov chain Monte-Carlo simulation. 2008. *Water Resources Research.* **44**: W00B09.

Vrugt, J. A., and B. A. Robinson. Treatment of uncertainty using ensemble methods: comparison of sequential data assimilation and Bayesian model averaging. 2007. *Water Resources Research.* **43**: W01411.

Wolf, M. M., F. Verstraete, M. B. Hastings, and J. I. Cirac. Area laws in quantum mechanics: mutual information and correlations. 2008. *Physical Review Letters.* **100** (7): 070502.

Yard, J., and I. Devetak. Optimal quantum source coding with quantum side information at the encoder and decoder. 2009. *IEE Transactions on Information Theory.* **55** (11): 5339.

Zdeborova, L.. Statistical physics of hard optimization problems. 2009. *Acta Physica Slovaca.* **59** (3): 169.

Zdeborova, L., A. Decelle, and M. Chertkov. Message passing for optimization and control of a power grid: model of a distribution system with redundancy. 2009. *Physical Review E.* **80**: 046112.

Zdeborova, L., and F. Krzakala. Generalization of the cavity method for adiabatic evolution of Gibbs states. 2010. *Physical Review B.* **81** (22): 224205.

Zdeborova, L., and M. Mezard. Constraint satisfaction problems with isolated solutions are hard. 2009. *Journal of Statistical Mechanics: THeory and Experiment.* **1742**: 5468.

Zdeborova, L., and S. Boettcher. A conjecture on the maximum cut and bisection width in random regular graphs. 2010. *Journal of Statistical Mechanics: Theory and Experiment.* **1742** (5468): P02020.

Information Science and Technology: Streaming Data

Sarah E. Michalak
20080729DR

Abstract

A key challenge in Information Science and Technology (IS&T) is extracting information from massive streams of data that are arriving in real-time. This project's contribution was to perform the research necessary to enable visualization, analysis, and storage solutions for massive streaming data.

To that end, we have developed: (1) methods for using emerging microparallelism, e.g. Cell procesors and GPUs, for real-time and near-real-time pipelining and processing; (2) statistical and signal processing methods for real-time or near-real-time baselining, anomaly detection and signal detection of high-dimensional data; and (3) novel file system architectures for real-time data ingest and writing out of data identified to be of interest. The overarching research challenge presented by this work is the combination of the amount and intricacy of the data that must be processed with the complexity of the algorithms required for processing it. In many cases, a further challenge is that of data fusion: multiple streams of data must be acted on simultaneously in real-time in order to accomplish the necessary processing.

While this work is motivated by the astronomical problem of real-time detection of radio transients, the methods are general and more broadly applicable. Further, with this research, we have developed a LANL research team that is addressing cutting-edge issues that arise in the real-time extraction of information from streaming data so that scientific research is enabled.

Background and Research Objectives

This work is motivated by the astronomical problem of real-time detection of radio transients. Being able to search the sky and identify anomalous events in real-time using a telescope with a huge collecting area has been called the "holy grail" of radio-astronomy [1]. This is one of several applications, including gene sequencing and cyber security, that were explored as inspiration for our work. We chose radio-astronomy because of its strategic relevance to work at Los Alamos National Laboratory (LANL) and for the broad research challenges it presents. Thus while the research outlined in the next paragraph is being performed in the context of radio-astronomy, it is more generally applicable to settings in which real-time anomaly detection is required.

We have performed the research necessary to enable key pieces of a real-time radio-transient detection system that includes: 1) processing of the data; 2) temporary storage of the data that permits transferring the data identified to be of interest to long-term storage; 3) novel algorithms for excision of radio-frequency interference (RFI; signals of terrestrial origin that are not of interest) and identification of signals of interest; and 4) creation of images of the sky. A multi-disciplinary team that includes individuals with expertise in the novel use of emerging hardware for real-time problems, file systems, statistical and signal processing methods for streaming data, and visualization was assembled for this work.

Real-time and near-real-time data pipelining, data processing, and image processing are facilitated by the use of emerging micro-parallelism, specifically GPUs and Cell processors. A key research challenge in gaining maximum performance from standard x86-64 processors, GPUs and Cell processors is that of efficiently exploiting the spatial and temporal locality of the data. Cell processors have been applied to the challenge of processing the incoming data, referred to as "correlation" and to certain RFI mitigation techniques, while GPUs have been used to increase the rate of image processing using the CLEAN algorithm via acceleration of the identification of the N brightest points in an image.

Two complementary ring buffer file systems have been developed to permit real-time data ingest and some processing of the data, which could include transferring the data identified to be of interest to long-term storage.

Statistical and signal processing methods for RFI mitigation and transient detection have been developed and investigated. These methods reduce RFI so that false positive detection rates are decreased and true positive detection rates are increased. Some of these RFI mitiga-

tion techniques have been ported to a prototype real-time streaming data pipeline.

The problem of extracting information from massive streaming data has many aspects. This project has identified key research problems in this space and extended the state-of-the-art in the identified areas. In performing this work, we have built collaborations with individuals in LANL's ISR Division, UNM and the Long Wavelength Array (LWA) project, UC-Berkeley and the Allen Telescope Array (ATA) project, and UC-Santa Cruz.

Scientific Approach and Accomplishments

Major research accomplishments include the following:

Processing (Correlation) of Incoming Data

Correlation is the processing that must be performed in order to extract meaningful signals from the data collected by radio antennas. Correlators have traditionally been built using custom hardware, e.g., FPGAs [2, 3]. More recently, software-based correlators, e.g. DiFX and LOFAR's BlueGene/L correlator, have been developed [4, 5]. Researchers have also investigated GPUs [6] and Cell processors [7] in this context. Numerous large antenna array radio telescopes (ATA, SKA, and LOFAR) are currently being developed (see ; ; http://www.lofar.org/). Correlation for these antenna arrays requires enormous computation and communication rates that can only be achieved by unique architectures that scale effectively both in area and power. The LWA would like to include a capability that uses the measurements from 256 antennas to search the visible sky in real-time to detect transient events of interest. Accomplishing this requires real-time calculations on the measurements from all of the 32,640 different antenna pairs that derive from the 256 antennas. The process of aperture synthesis uses the correlation of antenna pairs (called baselines) to measure the Fourier components of the sky brightness distribution to synthesize a much larger aperture antenna from a collection of smaller antennas. At full scale and with antenna signal bandwidths of ~67 MHz, the problem requires ~70 Tflops of continuous processing and 256 GB/s of sustained bandwidth. Methods for achieving this real-time processing rate via standard processors (Opterons) and Cell processors were researched. A major research challenge was efficiently exploiting the spatial and temporal locality of the antenna data to generate an effective algorithm given the architecture of the Cell processor**.** In a 2008 performance study, we found that a Cell-based solution outperforms a dual-core Opteron by ~21X and outperforms a quad-socket, dual-core Opteron node by ~6X. Moreover, the Cell-based solution requires ~1/19 of the power and ~1/5 of the space of the Opteron solution. Power and space are important considerations in radio astronomy since the available power and space are frequently limited for compute equipment that must be kept in the field. These results have been detailed in a technical report [26], with related results in [7].

Funds to support extending and transferring this capability to the LWA site were secured. With these funds, the LANL-developed correlator software has been licensed to LWA for use at its site as part of its Prototype All-Sky Imager (PASI) capability, which will permit real-time identification of radio-transients on a limited bandwidth. In addition, these funds enabled purchase and configuration of a cluster for PASI, which has been transferred to LWA. Thus, the LANL correlator work will enable ground-breaking science at LWA, with results to be published once data are collected.

In addition, LDRD reserve funding for related work has been committed for FY11. Specifically, working jointly with other LANL researchers, emerging hardware applied to spatial-temporal databases of the sky will be leveraged to enable new capabilities in astroinformatics.

Ring Buffer with Write-Out Capability for Temporary Storage of Incoming Data

The capture of high-bandwidth streaming real-time data is a problem that has traditionally been resolved by placing severe limitations on duration. Data can only be gathered for a small amount of time (seconds to hours) before the available storage medium is filled to capacity, at which point the capture must be stopped until the system is reset, such as in the ETA radio telescope [9]. Alternatively, one can invest in large supercomputing centers, such as the Large Hadron Collider Computing Grid, which distributes its data over 140 primary installations in over 33 countries to process and store data; see . We are currently developing a third alternative which uses a ring buffer model in order to capture data continuously, but normally only retain it for brief periods (minutes to hours) on the assumption that the large majority of data is not needed for analysis. (A ring buffer provides temporary storage for data in which by default the oldest data are overwritten once the ring buffer's capacity is filled.) This system is capable of operating 24/7 for an indefinite period of time and will preserve any segment of data which might be useful, discarding it if analysis shows it useless after all or transferring it to permanent storage otherwise.

Current high-capacity storage systems are not designed to cope with the simultaneous problems of (1) real-time data capture, (2) quality of service guarantees, (3) concurrent read access without compromising real-time writes, and (4) continuous uninterrupted operation over long periods. File/storage systems such as Panasas, PVFS, and Ceph are designed to support very high aggregate bandwidths [10],

but not to guarantee a particular data rate for a single data stream. Thus, they cannot guarantee a specified data rate for long-term operation, and since streaming real-time data can never be regenerated, these systems are not well suited to this problem. An astronomical event of major interest may be observable for a very short time period, yet a storage system recalibration may take far longer than that and the data may never make it into the buffer.

We have designed and implemented a ring buffer system prototype that is capable of maintaining data capture speeds near the limit of the underlying hardware, and yet still transfer "important" data out to other storage without compromising the accumulation of incoming data. These quality of service guarantees ensure that the system can maintain steady operation up to the endurance of the hardware while reliability mechanisms protect against data loss in the event of hardware failure. Scalability is emphasized, with the intention of supporting any number of concurrent data streams, only limited by how much data can be tracked at the global view. Results were accepted for, via a peer-review process, and have been presented at the 26th IEEE Symposium on Massive Storage Systems and Technologies (MSST 2010) [31].

Since then research has focused on hard drive profiling (accurately measuring and using knowledge of the physical layout of a hard drive to support real-time guarantees); small element indexing (efficiently storing an unknown amount of indexing information on a real-time data collection system with an eye towards future retrieval and search); and scalability and reliability (methods for scaling the system upward and maintaining reliability in the face of hardware failure over a broad set of devices and for managing and searching on a "large" system). This work will continue as thesis research at UC-SC through the LANL ISSDM program, with a goal of producing a fully developed system, including high-speed indexing methods, search over large sets of semi-discrete systems, and adaptive reliability methodologies, with results to be submitted for publication. Once an operational system is completed, it will be presented to laboratory researchers and programs such as cybersecurity.

We have also developed a Filesystem in Userspace (FUSE; http:// fuse.sourceforge.net/) based ring buffer file system (FuseRBFS) that complements the ring buffer design described above. In particular, it provides an easy-to implement ring buffer that can be architected to specifications such as the maximum rate of data inflow and the frequency and size of transfers to permanent storage, but does not include quality of service guarantees. To our knowledge, there is no other research on using FUSE in this manner; see [8, 11] for other work on ring buffers for real-time streaming data.

FUSE is a loadable kernel module for Unix-like computer operating systems that allows non-privileged users to create their own file systems without editing the kernel code. This is achieved by running the file system code in user space, while the FUSE module provides a bridge to the actual kernel interfaces. We can enhance the FUSE scaling capability when it is applied to key parallel storage systems such as IBM's GPFS, Panasas's PANFS, SunMicro 's Lustre, pNFS, and PVFS2. A prototype system has been developed, with an overhead study, testing with large buffers, and a basic API implementation completed. Preliminary results of this work were accepted for presentation, via a peer-reviewed process, at the 2009 International Conference on Parallel and Distributed Processing Techniques and Applications [44]. On-going and future research involves applying the FuseRBFS to large datasets, conducting scaling, performance, and capability studies using a large system, and investigating whether the FuseRBFS architecture might be applicable to the LWA. The results of this work will be submitted to 2011 HPDC, the 20th International ACM Symposium on High-Performance Parallel and Distributed Computing.

RFI Mitigation and Transient Detection

Discovering transient astrophysical phenomena are an exciting and growing area in modern astronomy [12, 13, 33]. Further, it has significant overlap with LANL's space situational awareness (SSA) needs. It is impossible for individuals to continuously monitor all of space over many different wavelengths and respond to anomalies quickly enough to permit real-time follow-up. Automatic monitoring and anomaly detection is needed to cull interesting events from vast streams of data collected from space, and we have developed capabilities for near real-time fusion and analysis of high-dimensional radio astronomy data.

A major problem in detecting interesting transient events from radio-astronomy data is that various terrestrial noise sources also produce transients, i.e. radio frequency interference (RFI). Working jointly with researchers at UC-Berkeley and the ATA, we analyzed 44 streams of spectra recorded from directional antennas at the ATA that monitor different regions of the sky for rare astronomical events in the radio domain [15]. These astronomical events appear as chirps in the spectra and should be observed in only a few antennas. (Signals that occur in too many antennas are likely terrestrial.) Noise signals in this data include 60 Hz power variation, occasional sensor saturation, periodic radar blips in a narrow frequency band, wideband terrestrial pulses of energy and wandering power levels within channels due to instrumentation instabilities. If not mitigated, interference signals are the dominant anomalous events discovered and easily swamp any potential very rare astronomical pulse of interest [14, 16].

We applied a statistical approach to mitigate the effects of outliers, 60 Hz signals and wandering power levels on chirp detection that incorporated estimation of antenna sensitivities and subsequent antenna weighting. This analysis

produced an event stream that was much better at differentiating signal from noise than the methods previously used. Giant pulses from the Crab pulsar were detected with stronger signal-to-noise ratios even as the false alarm rate was reduced. We have also experimented with an adaptive approach to interference cancellation (AIC) in which interference affecting a target antenna is assumed to simultaneously affect some antennas in a reference set. The interfering signal is estimated and removed by regressing the target on the reference set. To our knowledge these methods have not previously been used for radio-astronomy data; see [16, 17] for related methods and characterization of RFI signatures for radio-astronomy data. A simulation study to further explore these methods when known signals are embedded into a noisy background has been completed. Results showing that Huber filtering with energy truncation is complementary to AIC are being prepared for submission to *The Astrophysical Journal* [23].

Visualization of Images of the Sky

CLEAN is a standard algorithm used in the radio-astronomy community to rid images of noise that occurs when widely spaced antennas are used [18, 21, 32]. It is computationally intensive and also time-consuming on the part of the individual producing the image. A quick method of doing CLEAN using commonly available COTS hardware would save time and allow for experimentation on the part of the researcher producing the image. Specifically, the end images might be displayed almost immediately, allowing the astronomer to edit the parameters and adjust the end point of the algorithm in real-time and providing fast results as he or she works to extract signal from noise.

We chose to accelerate the algorithm via GPUs since they are widely available and the image data CLEAN operates on is a data type the GPU handles well. GPUs have been investigated for other stages of the radio-astronomy pipeline, most notably in the correlation of data received by antennas [19], but to our knowledge not yet for the CLEAN algorithm, although it is suggested in [20]. We used NVidia GPUs and the NVidia CUDA library [22] for our work.

The CLEAN algorithm has two parts: identification of the N brightest points in the image and a series of convolutions via FFTs. The FFTs were easily implemented and fast on the GPU, as there is CUDA support for this. Typically, the N brightest points are identified by a sort. However, a full sort is not truly required, but instead only an unsorted top-N point algorithm that identifies the N brightest pixels in an image.

At present, there is no algorithm for Top N identification native to the GPU, and this problem has been identified in one of the GPU libraries (Thrust) as being difficult. Challenges include the lack of fast memory on the GPU. We implemented the identification of the Top N brightest pixels on the GPU by developing a novel method that relies on stochastic optimization and uses memory efficiently. To our knowledge this is the first direction selection implemented on the GPU; related work is in [28, 30, 34]. The method compares favorably to an implementation using standard GPU programming techniques using a CUDA sort in terms of both performance and the image size that can be processed. Performance studies have shown speed-ups of up to 18X relative to a CUDA sort. We have been able to select the Top N from images up to four times the size of those that the CUDA sort can process for many values of N. Maintaining the N points and the image in memory approach the available global memory on the GPU for these large values, so is a limiting factor. Finishing touches are being put on a manuscript describing these results [27] so that it can be submitted to the 25th IEEE International Parallel & Distributed Processing Symposium by the 10/1/10 deadline. We are also considering submitting our code to the open-source Thrust library. We will seek future funding for related novel stochastic computational methods and for developing a full GPU-enhanced CLEAN algorithm. LWA has also expressed an interest in our research on the CLEAN algorithm.

Prototype Data Processing and Analysis Pipeline

Some of the RFI mitigation and transient detection methods developed for the ATA data have been optimized for standard CPUs for the real-time setting and ported to the cell processor. The CPU optimization permits a 17X performance gain over standard CPU serial code, enabling the analysis of over 6700 antenna datastreams in real time. This research has been extended to the development of a prototype pipeline, in which the data are piped from an input node to a data processing node to an output node that captures the processed data. With this prototype pipeline, a performance gain of 8X is achieved, which illustrates the importance of reflecting the entire pipeline or system when determining achievable, sustained performance. The challenges inherent in, methods used, and results of this work have been detailed in a manuscript submitted to *Journal of Computational and Graphical Statistics* [25]. To our knowledge, this is the first work to present these challenges to a statistical audience. This work and related future research could enable LANL to taking a leading role in the field of statistical methods for streaming data, and funding for follow-on work will be sought in FY11.

Impact on National Missions

The general problem of real-time detection of anomalous events has broad applicability including to cyber security, threat reduction, data from sensor networks, and systems data (biological or otherwise) in which a vector of data is recorded at every time step. In addition, much of LANL's work involves streaming data. Existing laboratory weapons work, which will likely be more focused on non-proliferation than design in the coming years, and situational awareness programs, including space, weather, and infrastructure situation awareness, have streaming data aspects. Many, if not most, emerging programs at

the laboratory include some aspect of streaming data. Energy Security and Bio-Security, two areas of focus for the laboratory with newly-formed centers; treaty monitoring and verification; and cyber security are just a few of the emerging programmatic areas at LANL and they all involve streaming data. In short, the proliferation of inexpensive sensors of all kinds makes streaming data capability one of LANL's most important capabilities in the next decade.

This project has developed a research team with cutting-edge streaming data capabilities, including real-time processing and pipelining and methods for the analysis, visualization, and storage of massive streaming data. This capability will enable LANL to respond to key challenges of national interest. The external researchers who collaborated with us on this work and the funding received for related follow-on work further underscore the crucial nature of this research.

Thus, the outlook for the capability developed by this LDRD project to be used for future program building and delivery is bright, and the team is well-positioned to continue their research on methods for visualization, processing and analysis, and storage of massive streaming data and contribute to the CS, visualization, statistics, astronomy, and other substantive-field literatures.

References

1. Ulvestad, J.. Personal Communication . 2008. *October 22, 2008.*

2. Parsons, A., D. Backer, A. Siemion, H. Chen, D. Werthimer, P. Droz, T. Filiba, J. Manley, P. McMahon, A. Parsa, D. MacMahon, and M. Wright. A Scalable Correlator Architecture Based on Modular FPGA Hardware, Reuseable Gateware, and Data Packetization. 2008. *PUBLICATIONS OF THE ASTRONOMICAL SOCIETY OF THE PACIFIC.* **120** (873): 1207.

3. Parsons, A., D. Backer, Chen Chang, D. Chapman, H. Chen, P. Crescini, C. de Jesus, C. Dick, P. Droz, D. MacMahon, K. Meder, J. Mock, V. Nagpal, B. Nikolic, A. Parsa, B. Richards, A. Siemion, J. Wawrzynek, D. Werthimer, and M. Wright. PetaOp/second FPGA signal processing for SETI and radio astronomy. 2006. In *2006 Fortieth Asilomar Conference on Signals, Systems and Computers ; 29 Oct.* (-1 Nov. 2006 ; Pacific Grove, CA, USA). , p. 2031.

4. Deller, A. T., S. J. Tingay, M. Bailes, and C. West. DiFX: A software correlator for very long baseline interferometry using multiprocessor computing environments. 2007. *PUBLICATIONS OF THE ASTRONOMICAL SOCIETY OF THE PACIFIC.* **119** (853): 318.

5. Romein, J., P. Chris. Broekema, E. Van Meijeren, K. Van Der Schaaf, and W. Zwart. Astronomical real-time streaming signal processing on a blue Gene/L supercomputer. 2006. In *SPAA 2006: 18th Annual ACM Symposium on Parallelism in Algorithms and Architectures ; 20060730 - 20060802 ; Cambridge, MA, United States.* Vol. 2006, p. 59.

6. Harris, C., K. Haines, and L. Staveley-Smith. GPU accelerated radio astronomy signal convolution. 2008. *EXPERIMENTAL ASTRONOMY.* **22** (1-2): 129.

7. Nieuwpoort, R. V. van, and J. W. Romein. Using Many-Core Hardware to Correlate Radio Astronomy Signals. 2009. In *2009 ACM SIGARCH International Conference on Supercomputing ; 8-12 June 2009 ; Yorktown Heights, New York, NY, USA.* , p. 440.

8. Rajasekar, A., F. Vernon, T. Hansen, K. Lindquist, and J. Orcutt. Virtual Object Ring Buffer: A Framework for Real-time Data Grid. . *San Diego Supercomputing Center SDSC/UCSD Technical Report.*

9. Patterson, C., B. Martin, S. Ellingson, J. Simonetti, and S. Cutchin. FPGA cluster computing in the ETA radio telescope. 2007. In *Annual International Conference on Field Programmable Technology ; 20071212 - 20071214 ; Kitakyushu, JAPAN.* , p. 25.

10. Devulapalli, A., D. Dalessandro, P. Wyckoff, N. Ali, and P. Sadayappan. Integrating parallel file systems with object-based storage devices. 2007. In *2007 ACM/IEEE Conference on Supercomputing, SC'07 ; 20071110 - 20071116 ; Reno, NV, United States.* , p. var. pagings.

11. Tilak, S., P. Hubbard, M. Miller, and T. Fountain. The ring buffer network bus (RBNB) DataTurbine streaming data middleware for environmental observing systems. 2007. In *3rd IEEE International Conference on e-Science and Grid Computing ; 20071210 - 20071213 ; Bangalore, INDIA.* , p. 125.

12. Bower, G.. ASTRONOMY: Mining for the Ephemeral. 2007. *Science.* : 759.

13. White, R. R., S. M. Evans, W. T. Vestrand, M. S. Warren, J. A. Wren, and P. R. Wozniak. Thinking telescopes and the future astronomical meta-network. 2006. In *1st Workshop on Heterogeneous Telescope Networks ; 20050718 - 20050721 ; Exeter, ENGLAND.* Vol. 327, 8 Edition, p. 758.

14. Cordes, J. M., and M. A. McLaughlin. Searches for fast radio transients. 2003. *ASTROPHYSICAL JOURNAL.* **596** (2, 1): 1142.

15. Siemion, A., J. Von Korff, P. McMahon, E. Korpela, D. Werthimer, D. Anderson, G. Bower, J. Cobb, G. Foster, M. Lebofsky, J. Van Leeuwen, and M. Wagner. New SETI sky surveys for radio pulses. 2010. *Acta Astronautica.* : 1342.

16. Winkel, B., J. Kerp, and S. Stanko. RFI detection by automated feature extraction and statistical analysis.

2007. *ASTRONOMISCHE NACHRICHTEN.* **328** (1): 68.

17. Bhat, N. D., J. M. Cordes, S. Chatterjee, and T. J. Lazio. Radio frequency interference identification and mitigation using simultaneous dual-station observations. 2005. *RADIO SCIENCE.* **40** (5): RS5S14.

18. Hogbom, J. A.. Aperture synthesis with a non-regular distribution of. 1974. *Astronomy and Astrophysics Supplement Series.* **15** (3): 417.

19. Dale, K., D. Mitchell, R. Wayth, S. Ord, L. Greenhill, D. Luebke, and H. Pfister. AstroGPU - A Graphics Hardware-Accelerated Real-Time Processing Pipeline for Radio Astronomy. 2007. *AstroGPU.*

20. Fluke, C., D. Barnes, B. Barsdell, and A. Hassan. Astrophysical Supercomputing with GPUs: Critical Decisions for Early Adopters. 2010. *arxiv.org.*

21. AIPS: astronomical image processing system. 2010. *National Radio Astronomy Observatory.*

22. NVIDIA CUDA: NVIDIA CUDA C programming guide. 2010. *NVIDIA.*

23. Hogden, J., S. Vander Wiel, G. Bower, D. Werthimer, A. Siemion, and S. Michalak. Comparison of RFI mitigation strategies for pulse detection. 2010. *Los Alamos National Laboratory Technical Report in preparation.*

24. Monroe, L., J. Wendelberger, and S. Michalak. A fast and memory-sparing probabilistic selection algorithm for the GPU. 2010. *Los Alamos National Laboratory Technical Report in preparation.*

25. Michalak, S., A. DuBois, D. DuBois, and S. Vander Wiel. Developing systems with real-time streaming statistical analysis capabilities. *Journal of Computational and Graphical Statistics.*

26. DuBois, A., C. Connor, S. Michalak, G. Taylor, and D. DuBois. Application of the IBM Cell processor to real-time cross-correlation of a large antenna array radio telescope. 2009. *Los Alamos National Laboratory Technical Report LA-UR-09-03483.*

27. DuBois, A., C. Connor, S. Michalak, G. Taylor, and D. DuBois. Application of the IBM Cell processor to real-time cross-correlation of a large antenna array radio telescope. 2009. *Los Alamos National Laboratory Technical Report #LA-UR-09-03483.*

28. Bader, D.. An improved, randomized algorithm for parallel selection with an experimental study. 2004. *Journal of Parallel and Distributed Computing.* **64** (9): 1051.

29. Chen, Hsing-bung, null. Michalak, J. Bent, and G. Grider. FuseRBFS* - A Fuse based Ring Buffer File System for Data Intensive Scientific Computing ; vol.2. 2009. In *2009 International Conference on Parallel and Distributed Processing Techniques and Applications.* (PDPTA 2009 ; 13-16 July 2009 ; Las Vegas, NV, USA). , p. 517.

30. Leischner, N., V. Osipov, and P. Sanders. GPU sample sort. Presented at *International Parallel and Distributed Processing Symposium.* (Atlanta, GA, 19-23 Apr. 2010).

31. Bigelow, D., S. Brandt, J. Bent, and H. B. Chen. Mahanaxar: quality of service guarantees in high-bandwidth, real-time streaming data storage. Presented at *26th IEEE Symposium on Massive Storage Systems and Technologies (MSST2010) .* (Incline Village, NV, 3-7 May 2010).

32. CLARK, B. G.. AN EFFICIENT IMPLEMENTATION OF THE ALGORITHM CLEAN. 1980. *ASTRONOMY AND ASTROPHYSICS.* **89** (3): 377.

33. Cordes, J. M., T. J. Lazio, and M. A. McLaughlin. The dynamic radio sky. 2004. *NEW ASTRONOMY REVIEWS.* **48** (11-12): 1459.

34. Rajesekaran, S., and J. H. Reif. Derivation of randomized sorting and selection algorithms. 1993. In *Parallel Algorithm Derivation and Program Transformation ; 30 Aug.* (-1 Sept. 1991 ; New York, NY, USA). , p. 187.

Publications

Bigelow, D., S. Brandt, J. Bent, and H. B. Chen. Managing high-bandwidth real-time data storage. 2009. *Los Alamos National Laboratory Technical Report LA-UR-09-06133.*

Bigelow, D., S. Brandt, J. Bent, and H. B. Chen. Mahanaxar: quality of service guarantees in high-bandwidth, real-time streaming data storage. Presented at *26th IEEE Symposium on Massive Storage Systems and Technologies.* (Incline Village, NV, 3-7 May 2010).

Chen, H. B., S. Michalak, J. Bent, and G. Grider. FuseRBFS - a Fuse based ring buffer file system for data intensive scientific computing. 2009. In *International Conference on Parallel and Distributed Processing Techniques and Applications.* (Las Vegas, NV, 13-17 Jul. 2009). , p. 517. Athens: CSREA Press.

DuBois, A., C. Connor, S. Michalak, G. Taylor, and D. DuBois. Application of the IBM Cell processor to real-time cross-correlation of a large antenna array radio telescope. 2009. *Los Alamos National Laboratory Technical Report LA-UR-09-03483.*

Hogden, J., S. Vander Wiel, G. Bower, D. Werthimer, A. Siemion, and S. Michalak. Comparison of RFI mitigation strategies for pulse detection. 2010. *Los Alamos National Laboratory Technical Report in preparation.*

Michalak, S., A. DuBois, D. DuBois, and S. Vander Wiel. Developing systems with real-time streaming statistical analysis capability. *Journal of Computational and Graphical Statistics.*

Monroe, L., J. Wendelberger, and S. Michalak. A fast and memory-sparing probabilistic selection algorithm for the GPU. 2010. *Los Alamos National Laboratory Technical Report in preparation.*

Developing Adaptive High-Order Divergence-Free Methods for Magneto-Hydrodynamics Turbulence Simulations

Shengtai Li
20090210ER

Introduction

Turbulence is a common phenomenon in plasmas. Plasma is the 4th state of matter in addition to the solid, liquid, and gaseous states. It is remarked that 99% of universe consists of plasmas, which are ubiquitous from Galaxy and star formation, solar wind and space weather forecast, to the electron-magnetic field in our daily life. It is convenient to treat such turbulent plasmas in magneto-hydrodynamic (MHD) framework. However, due to the lack of highly accurate simulation software, the research and development of compressible MHD turbulence is still in its infancy. The MHD turbulence simulation demands methods with both high-order accuracy and divergence-free preserving property for the magnetic field to study the energy cascade from large eddy to small wave structure. No existing computational solver achieves all these goals.

The goal of this project is to develop efficient, accurate, and robust high-order methods and software for unsteady MHD simulations, and use the software and simulations to study compressible MHD turbulence. We propose a new methodology to develop our numerical methods. Rather than using only one mesh to discretize the physical domain as a conventional method, we generate a dual mesh from the primal mesh to facilitate solving the MHD equations for the magnetic field with high-order accuracy while preserving its divergence-free property. To improve the efficiency and robustness of our high-order method, we will develop an adaptive method using both the adaptive mesh refinement and adaptive order for different regions, and solve an auxiliary equation to track the pressure correctly.

The software will be parallelized and tested using our parallel computing resources, and then will be applied in MHD turbulence simulations. These simulations will be used to study the properties of MHD turbulence in inter-stellar medium and solar wind, where massive observation data are available. We will also use the software for other MHD simulations, such as magnetic jet in astrophysics and magnetic reconnection in solar atmosphere.

Benefit to National Security Missions

This project will enhance broadly important computational methods that will impact a wide variety of mission areas including computing, fusion energy, high energy physics, and the NNSA weapons mission by addressing several needs in the new NNSA Astrophysics Initiative. These are important mission areas for DOE and other government agencies.

Progress

In the past fiscal year, We have three key accomplishments. First we have developed a robust, user-friendly, and efficient 2D software package for MHD simulations using our high-order divergence-free methods. Secondly, we have successfully extended our 2D numerical method and software to 3D problem. Thirdly, we have performed large-scale MHD simulations to study the accretion disk problem in astrophysics, magnetic field amplification by supernova blast shocks propagating in a turbulent density medium, and MHD turbulence simulations to study the properties of the compressible MHD turbulence. We have found many new results using our new high-order methods.

For the first key accomplishment, we have enhanced the code capabilities for problems with different physics. With overlapping grid, we have added efficient solver for isothermal equations of state and new high-order discretization for high-derivative terms (viscosity, resistivity, thermal conduction, and Hall MHD). We have extended our third-order method to the fourth-order. We find that the four face reconstructions is not enough for the four-order divergence-free reconstruction over the whole cell. We also find that the divergence-free method is crucial in achieving the expected order of accuracy and preserving the numerical stability for limited reconstruction. We also proposed a new limiter to reduce the undershoot/overshoot near the discontinuities. The paper, which describes the first fourth-order divergence-free method for MHD simulations, has been published by Journal of Computational Physics.

To make our software package more efficient, robust and user-friendly, we reduce the number of ghost cells, which are used in communication between different processors in parallel computation, from 4 to 2. We optimize the data layout and store the data in cache as long as possible, which reduces the total CPU time to half. We also developed a parallel data input/output (I/O) algorithm for processors to read/write data independently without communication. This reduces the I/O time by a factor of 10.

In the second key accomplishment, we find it is not trivial to extend our method from 2D to 3D. We have proposed a new method that reduces the computational cost of the reconstruction by a factor of 4. For the divergence-free reconstruction, we reduced the number of freedoms proposed by other authors and use the overlapping grid to construct more accurate polynomials over the whole cell. We have also extended the high-order non-oscillatory reconstruction of the 2D method to 3D. We have built a suite of 3D test cases and have verified that our code indeed achieves the expected order of accuracy.

We have investigated the feasibility to apply our method to adaptive mesh refinement (AMR). We have found that our method cannot be used for AMR with refinement ratio of an even number, which are popular in almost every AMR package. We are developing an AMR package with refinement ratio of 3 for our method.

In the third key accomplishment, we have performed simulations for astrophysical accretion disk problem, supernova blast shocks propagating in a turbulent density medium, and MHD turbulence problems. We find that the higher-order method is better in preserving the angular momentum than the low-order method for the accretion disk problem. The simulations for the supernova blast shock show that the background weak magnetic field can be greatly amplified (by a factor of 50), which can be used to explain the strong magnetic field enhancement inferred from observations of supernova remnants (Figure 1). We have performed large-scale 2D, 2.5D, and 3D MHD decaying turbulence simulations. Our results show that we have achieved lower numerical dissipation and longer inertial range with our higher-order method than the low-order method (Figure 2). Therefore we have reproduced the published results with a lower resolution grid. To study the mode conversion during the turbulent nonlinear stage, we initialize the problem with a set of fast MHD wave. We find that due to the shock steepening and nonlinear wave interaction, the waves quickly become turbulent and the fast waves have been converted into the slow waves. We have developed numerical analysis techniques using Matlab.

We have also performed force-driven MHD turbulence simulations for both 2D and 3D problems. We found that the magnitude of the magnetic field can be amplified by a larger factor than published results. We have also performed simulations on an elongated box in solar wind applications to study the turbulent dynamics of the flux tube of solar wind. We have studied the scale decomposition and scale locality in compressible turbulence. We prove theoretically that inter-scale transfer of kinetic energy is dominated by local interactions.

We have three papers published on peer-reviewed Journal, one accepted, three more to be submitted. We have presented three talks related to this project among which two are invited.

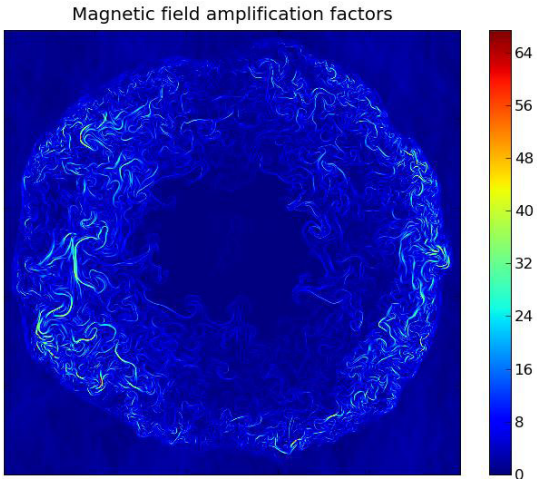

Figure 1. The magnetic fields are amplified by a factor of 60 during a supernova shock propagating in a turbulent medium, which can be used to explain the strong magnetic field enhancement inferred from observations of supernova remnants. The simulations are done using our high-order divergence-free method on a 8000x8000 grid.

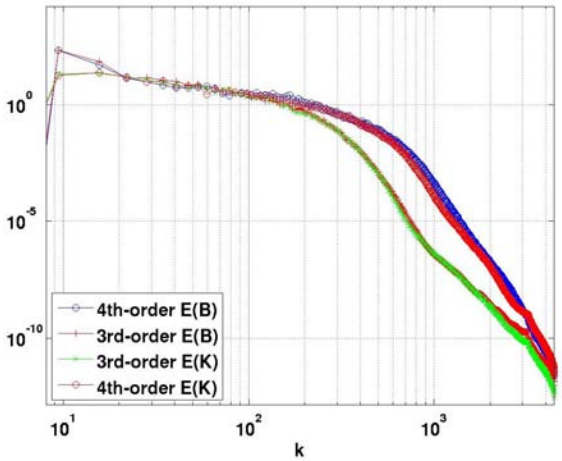

Figure 2. The cascade spectrum for kinetic energy (E_k) and magnetic energy (E_b) for a decaying compressible 2.5D MHD turbulence. The long tail means the dissipation range due to the numerical viscosity. It shows that the fourth-order method has a longer inertial range (before the dissipation range) than the third-order method.

Future Work

We will develop a high-order structured adaptive mesh refinement (AMR) code that uses our current 2D and 3D solver as a basic solver for a single grid. Our current AMR framework works for the second-order method. To achieve high-order accuracy in an AMR grid, we will develop new algorithms for communications and interpolations between different refinement levels.

We will continue to use our current uniform grid solver to study the MHD turbulence problems. Using the large-scale simulations, we will verify the theory we have proposed recently on the spectral property of the energy cascade of the compressible MHD turbulence. In the meantime, we will use the new high-order AMR solver to study the MHD astrophysical jet problem.

We will also propose to develop a new time integration method for both our uniform and AMR grid solvers. The current time integration uses multi-stage Runge-Kutta method. The number of stages is usually larger than the order of accuracy of the methods. Because we need a spatial reconstruction for grid cell and communication between different blocks in a parallel computation, it is not efficient. The new time integration will extend the second-order Lax-Wendroff type integration to higher order. It is requires only one reconstruction and one communication for one time step.

If we have time and resource, we will investigate how to implement our code and solver for future exa-scale computing machine, especially for GPU-accelerated parallel machine.

Conclusion

A new software package, which will be the first one with high-order accuracy, for MHD simulations will be produced. This package is an ideal tool for simulations not only for MHD turbulence but also for other applications involving magnetic field: magnetic jet, magnetic confinement fusion, high energy density physics, etc. By simulation and data analysis, we will gain new understanding on MHD turbulence. Our project will address a critical need in current MHD simulations and will have immediate impact in astrophysics and plasma physics. A number of publications on high-quality journal will be produced.

Publications

Aluie, H.. Scale decomposition in compressible turbulence. *Journal of Fluid Mechanics.*

Aluie, H.. Scale-locality in compressible turbulence. *Journal of Fluid Mechanics.*

Collins, D. C., H. Xu, M. Norman, H. Li, and S. Li. Cosmological AMR MHD with ENZO. 2010. *Astrophysical Journal Supplement Series.* **151**: 308.

Li, S.. High-order central scheme on overlapping cells for magneto-hydrodynamic flows with and without constrained transport method. 2008. *Journal of Computational Physics.* **227**: 7368.

Li, S.. A fourth-order divergence-free method for MHD flows. 2010. *Journal of Computational Physics.* **229**: 7893.

Li, S.. Comparison of refinement criteria for structured adaptive mesh refinement. 2010. *Journal of Applied and Computational Mathematics.* **233**: 3139.

Li, S.. Higher order divergence-free methods for 3D MHD flows on overlapping grid. To appear in *The ASP Conference Series on the 5th International Conference on Numerical Modeling of Space Plasma Flows.* (San Diego, 13-18 Jun. 2010).

Li, S., and M. J. Buoni. High-order divergence-free method for MHD in three dimensions. 2009. *to be submitted.*

Xu, H., H. Li, D. C. Collins, M. Norman, and S. Li. Evolution and distribution of magnetic fields from AGNs in galaxy clusters. I The effect of injection energy and redshift. To appear in *Astrophysical Journal.*

Xu, H., H. Li, D. Collins, S. Li, and M. Norman. Turbulence and dynamo in galaxy cluster media: implication on the origin of cluster magnetic fields. 2008. *Astrophysical Journal Letters.* : L14.

Efficient Interdiction

Feng Pan
20090250ER

Introduction

The goal of this research project is to develop efficient algorithms and models for the problem of network interdiction. In the interdiction mission an interdictor seeks to minimize the ability of an adversary to achieve high consequence activities. Conversely, the evader seeks to maximize the likelihood of success and impact of successful execution. Such a min-max problem can be posed mathematically in terms of graph analysis: the interdictor seeks to identify a set of vital arcs on an activity network whose removal minimize the maximum reliable path from a source to a destination node, while the evader seeks to find and traverse the best unimpeded path. The activity graph may represent a transportation network, but more generally may correspond to resource allocation in an activity network.

The interdiction problem has applications in many areas within threat reduction such as identifying key border control nodes, disrupting nuclear smuggling efforts or suicide bomber logistical support, and analysis of vulnerabilities in critical infrastructures. LANL has several programs that address the interdiction problem, but they concentrate on analysis instead of research on new capabilities. In fact, one may argue that threat reduction in toto, a major thrust within LANL, is essentially the problem of interdiction. In addition to our focus on efficient interdiction our project results may impact other research areas where combinatorial optimization problems appear such as resource allocation in operations research or coding theory in statistical physics.

Benefit to National Security Missions

This project will support multiple national security missions by providing basic science for threat reduction through modeling and decision support capabilities of interdiction problems. The network interdiction problem has mission relevance to DOE, DHS, and other government agencies.

Progress

Network Interdiction on a bipartite graph has a simple min-max formulation and is yet a hard computational problem. Bipartite interdiction model is important for its applications in allocating resources to enhance border security. The solution methods to bipartite interdiction model can be used as subroutines in solving interdiction problem on general networks. To fully understand bipartite network interdiction, we gave a formal proof that the problem is NP-Hard and also proved that it was also hard to approximate this problem with polynomial algorithms within certain bounds. We then showed that to an efficient greedy algorithm could achieve this bound. However, this inapproximability is based the worst computational cases. Currently, we are developing efficient algorithms which will work well on general networks.

One of network interdiction's applications is to detect nuclear smuggling. The model is often built on a network with estimated data, e.g., travel time and reliability. In the reality, these quantities are unlikely known deterministically. As a result shortest paths need to be calculated in a stochastic network prior to any interdiction decisions. We are interested in investigating the criticality measures of stochastic shortest paths including what the probability that a path, edge, or node is on a shortest path is. This problem is known as #P-Complete (a counterpart of NP-Complete for counting problems). The existing methods for this problem are based on state space partition and Monte Carlo simulation. In our research on this problem, we discovered that there were correlations between the probability of a path, edge and node being optimal and certain graph centrality measures. After performing simulation on different types of networks and analyzing the simulation results, we were able to use some deterministic path analysis to reduce the scale of stochastic shortest path problem. In addition, we were able to show the correlation between polynomial-time graph centralities and criticality measures. This discovery may lead to scalable algorithms and enhanced Monte Carlo simulations for the stochastic shortest path problem.

Decomposition algorithms are powerful in solving some network interdiction problems. In a decomposition

algorithm, the original problem is divided into smaller subproblems which can be solved independently. The solutions from the subproblems are then assembled in a master program, which is usually smaller than the original problem and is more structured. However, the master program is still NP-Complete and needs to be solved repeatedly through iterations. Because the network structure in the interdiction problem, we discovered that the master program is equivalent to the hitting set problem, which has known polynomial approximation algorithms. Also, the master program can be directly approximated by a minimum cut problem, which is known an easy problem. Currently, we are investigating these two approaches. The success in these decomposition methods will allow the interdiction models to be used in applications with large networks.

Interdiction models are difficult in the number of solution operations scaled exponentially with the size of the networks and in the bi-level min-max structure. For some problems, the min-max models can be aggregated into a single minimization problem which opens the possibility of much faster algorithms (as the two steps can now be processed simultaneously). We have been studying the problem where such aggregation is possible, thus focusing on developing optimization techniques based on Belief Propagation and Lagrangian relaxation to solve the aggregated optimization problem efficiently. We are also developing Belief Propagation techniques which can be directly applied to min-max structure.

Network interdiction is one of the models for resource allocation on networks. We investigated two network resource allocation models closely related to the interdiction models. A coverage model was developed to direct antennas to minimize the sum of costs of uncovered points. Dynamic programming and heuristics were developed as the solution methods for the coverage model. Allocating firewall rules to improve internet security while balance the increased loads is another application in the area of cybersecurity. Currently, only heuristics are known for this problem. We developed a mixed integer program which would give the optimization solution and incorporate uncertainties. The development of solution algorithms for this problem is currently work-in-progress.

During this period, the team presented their work in INFORMS annual meeting 2009, SIAM Discrete Mathematics 2010, CPAIOR 2010, and ICDCN 2010, and several papers have been submitted, including accepted papers in Lecture Notes in Computer Science and IEEE-HICSS.

Future Work

Combinatorial optimization problems appear in various research areas and the computational complexity of these problems is a critical barrier to theoretical research and application development. This difficulty is amplified because of the uncertainties in real-world applications. The goal of this research is to develop such efficient algorithms for computationally hard combinatorial problems and provide fundamental understanding these problems when uncertainties presents, in particular the problem of network interdiction.

We discussed some of the future works in the last section. We will continue developing heuristic algorithms along several novel approaches. Recent research showed the success of belief propagation (BP) algorithms in solving inference problems (e.g., statistical physics, error-correcting coding theory.). Research on social networks has introduced the concept of centrality measures that identifies those arcs that are critical to connectivity within a network. These two areas are in close vicinity of combinatorial optimization. However, it is original to directly apply them in developing algorithms and robust models of incomplete information for general optimization problems. Our research will take the challenge to explore optimization algorithms and uncertainty modeling along these new dimensions.

We started with deterministic networks with special structures: planar road/rail networks, and the bipartite interdiction model. The development focuses on dynamic centrality measures of these networks and graphical models/loop calculus in BP. In year three, we will complete the ongoing work in stochastic shortest paths, decomposition algorithms and firewall allocation. We will also develop efficient heuristics based on iteratively solving polynomial network problems (e.g., min cut) and distributed algorithms (e.g., BP) for interdiction models related to smart grids.

Conclusion

The object of this research is to remove the critical barriers of computational difficulty and uncertainty modeling in combinatorial optimization problems. The success of this research will impact the areas in counterproliferation and complex infrastructure modeling.

Publications

Cuellar, L., F. Pan, J. Roach, and K. J. Saeger. Distributional properties of stochastic shortest paths for nuclear smuggled material. To appear in *International Multi-Conference on Complexity, Informatics and Cybernetics.* (Florida, 27-30 March. 2011).

Dimitrov, N. B., D. P. Michalopoulos, D. P. Morton, M. V. Nehme, F. Pan, E. Popova, E. A. Schneider, and G. G. Thoreson. Network deployment of radiation detectors with physics-based detection probability calculations. 2009. *Annals of Operations Research.* : 1.

Gomez, V., H. J. Kappen, and M. Chertkov. Approximate inference on planar graphs using loop calculus and

belief propagation. 2010. *Journal of Machine Learning Research.* **11**: 1273.

Gutfraind, A., A. Hagberg, D. Izraelevitz, and F. Pan. Interdicting markovian evader. *INFORMS Computing Society 2011.*

Gutfraind, A., A. Hagberg, and F. Pan. Optimal interdiction of unreactive Markovian evaders. 2009. In *Lecture notes in computer science (CPAIOR 2009).* Edited by Hooker, J., and W. J. van Hoeve. , p. 102. Berlin / Heidelberg: Springer.

Hagberg, A.. Structure and dynamics of cybersecurity networks. Presented at *2009 Siam Annual Meeting.* (Denver, Co, 6 - 10 July 2009).

Kasiviswanathan, S. P.. Matrix interdiction problem. 2010. In *Integration of AI and OR Techniques in Constraint Programming for Combinatorial Optimization Problems.* By Lodi, A., M. Milano, and P. Toth. , p. 219. Berlin / Heidelberg: Springer.

Kasiviswanathan, S. P., B. Zhao, B. Urgaonkar, and S. Vasudevan. Bandwidth provisioning in infrastructure-based wireless networks employing directional antennas. 2010. In *International Conference on Distributed Computing and Networking.* (India, 3-6 January, 2010). , p. 295. Berlin / Heidelberg: Springer.

Pan, F., M. Bradonjic, and A. Hagberg. Interdicting shortest paths on random geometric graphs. Presented at *INFORMS Annual Meeting.* (San Diego, 11-14 October, 2009).

Pan, F., N. Santhi, and M. Chertkov. Message-passing algorithms for solving bipartite network interdiction. Presented at *2009 INFORMS Computing Society Conference.* (Chareston, SC, 11-13 Jan. 2009).

Pan, F., N. Santhi, and M. Chertkov. Network interdiction by securing edges. Presented at *The 20th International Symposium of Mathematical Programming .* (Chicago, Illinois, 23 - 28 Aug. 2009).

Pan, F., and S. P. Kasiviswanathan. Placing directional antennas in infrastructure- based wireless networks. To appear in *IEEE International Conference on Communications.* (Japan, 5-9 June. 2011).

Santhi, N., and F. Pan. A heuristic for restricted rank semi-definite programming with combinatorial applications. Presented at *The 20th International Symposium of Mathematical Programming.* (Chicago, Illinois, 23 - 28 Aug. 2009).

Santhi, N., and F. Pan. Detecting and mitigating abnormal events in large scale networks: Budget constrained placement. To appear in *Hawaiian International Conference on System Science.* (Hawaii, 4-7 January, 2011).

A Hybrid Transport-Diffusion Method for Radiation Hydrodynamics

Jeffery D. Densmore
20090420ER

Introduction

Radiation-hydrodynamics calculations involve the coupled modeling of x-ray regime radiation transport and hydrodynamic material motion. Typically, simulating radiation transport comprises the bulk of the computational effort in these types of problems. One technique for modeling radiation transport is Monte Carlo simulation. This method is very accurate, but can also be prohibitively expensive in optically thick regions, i.e., where the mean distance between photon collisions is much smaller than the size of the region. An alternative to Monte Carlo is the diffusion approximation, which is computationally inexpensive but only valid in optically thick regions. Thus, in realistic problems that contain both optically thick and optically thin regions, replacing a Monte Carlo calculation with the diffusion approximation is impractical if one desires accurate solutions.

In this project, we will develop a hybrid transport-diffusion method for simulating radiation transport as part of a radiation-hydrodynamics calculation. This hybrid technique will combine the diffusion approximation and Monte Carlo to yield efficient simulations without sacrificing accuracy. Specifically, our hybrid method will employ the diffusion approximation in optically thick regions, where Monte Carlo is expensive and this approximate theory is accurate, and resort to Monte Carlo in optically thin regions, where an accurate radiation-transport solution is required.

Benefit to National Security Missions

This project supports the DOE/NNSA mission in Nuclear Weapons by enhancing the basic science that underlies our ability to perform massive simulations. In addition, basic science studies related to astrophysics, inertial confinement fusion, and high energy density physics will also benefit.

Progress

In the past year, we have completed implementing a hybrid transport-diffusion method for the Sphyramid mesh in Milagro [1], our radiation-only production-level software package. This mesh models one-dimensional spherical geometries with a three-dimensional Cartesian-geometry pyramid such that cell faces are planar. The Cartesian coordinate system and planar surfaces of the Sphyramid mesh results in a much simpler Monte Carlo simulation than one performed in the original spherical coordinates, which is why this mesh is employed in Milagro. Our implementation consisted of discretizing an appropriate diffusion equation on this mesh, extracting the probabilities for various events from the resulting discretized equation, and incorporating these probabilities into the Monte Carlo transport process in Milagro. Furthermore, we accounted for two parallelization techniques when calculating the probabilities and in the transport process itself: domain replication, where each processor contains a complete copy of the mesh, and domain decomposition, where, because of memory limitations, the mesh is subdivided amongst the processors and thus particles must travel between processors during the coarse of the simulation.

We have also developed a hybrid transport-diffusion method for the RZWedge mesh employed by Milagro [2]. This mesh models two-dimensional cylindrical geometries with a three-dimesional Cartesian-geometry wedge, in the same manner and for the same reasons that the Sphyramid mesh is used for spherical geometries. We have implemented this hybrid method into Milagro, as well. The implementation details in this case are similar to those discussed above, except that the RZWedge mesh also features local refinement such that a spatial cell may have more than one neighboring cell across each face. This technique is commonly employed in Eulerian hydrodynamics calculations, which, as part of larger radiation-hydrodynamics simulations, our hybrid transport-diffusion method is intended for.

In addition, we have extended our hybrid methodology to account for photon frequency dependence [3]. In this technique, we employ a frequency-integrated diffusion equation for frequencies below a certain threshold, while above this threshold we use Monte

Carlo. This division is justified by the fact that the opacity is typically a decreasing function of frequency, and therefore a spatial region can be optically thick for low frequencies but optically thin for high frequencies. As in the frequency-independent case, the frequency-integrated diffusion equation is discretized to generate probabilities for various events, including now how particles transition across the frequency threshold. We are in the process of implementing this frequency-dependent extension into Milagro.

Next year, we plan on continuing our implementation through to Wedgehog, our production-level callable library that provides radiation-transport capability to multiphysics application codes. Because Wedgehog uses many, if not most, of the same components that Milagro does, this work should be fairly straightforward. This integration will allow our hybrid transport-diffusion method to be employed as part of a realistic radiation-hydrodynamics calculation.

Future Work

Radiation-hydrodynamics simulations are an important aspect of many of DOE's missions, with applications in astrophysics, inertial confinement fusion, and high energy density physics. These types of calculations model the nonlinear coupling between x-ray regime radiation transport and hydrodynamic motion. In addition to this multiphysics feature, radiation-hydrodynamics calculations are inherently multiscale; in optically thick regimes the photon mean-free path (mfp) and mean-free time (mft) are several orders of magnitude smaller than the length and time scales upon which the solution varies. Furthermore, many problems also contain optically thin regions, where the mfp and mft are of the same order as the solution's characteristic length and time scales. We note that simulating radiation transport typically comprises the bulk of the computational effort in radiation-hydrodynamics calculations.

Our objective is to develop a hybrid method for modeling radiation transport in radiation-hydrodynamics calculations. This hybrid technique will employ the diffusion approximation in optically thick regimes, where Monte Carlo simulation in prohibitively expensive and diffusion theory is valid, and resort to Monte Carlo in optically thin regimes where an accurate radiation-transport solution is required. Thus, our hybrid method will be able to yield efficient simulations without sacrificing accuracy.

Our preliminary work on this hybrid methodology has shown promising results, with efficiency gains of several orders of magnitude over pure Monte Carlo. We will extend our existing scheme in several ways that increases its physics capability and utility. First, we will address the issue of photon frequency. We will also develop a technique that automatically determines what parts of phase space to simulate with diffusion versus Monte Carlo. Finally, our resulting hybrid scheme will be implemented into production-level software, directly benefiting DOE's efforts in astrophysics, inertial confinement fusion, and high energy density physics.

Conclusion

The result is a hybrid transport-diffusion method that is implemented into production-level software and capable of modeling complex problems relevant to DOE missions. The benefits of this research are twofold. First, radiation-hydrodynamics simulations are often performed using the diffusion approximation throughout the problem domain, a practice that is computationally inexpensive but can lead to inaccurate solutions. In addition, many problems of interest are currently intractable because a pure Monte Carlo simulation would be prohibitively expensive, while the diffusion approximation is completely insufficient. Our hybrid transport-diffusion method will be able to remedy both of these situations.

References

1. Densmore, J. D.. Discrete Diffusion Monte Carlo for the Sphyramid Mesh. 2009. *CCS-2:09-04(U).*

2. Densmore, J. D.. Discrete Diffusion Monte Carlo for the RZWedge_Mesh. 2010. *CCS-2:10-01(U).*

3. Densmore, J. D., and T. J. Urbatsch. Frequency-Dependent Discrete Diffusion Monte Carlo. 2010. *CCS-2:10-20(U).*

Publications

Densmore, J. D.. Discrete Diffusion Monte Carlo for the Sphyramid Mesh. 2009. *CCS-2:09-04(U).*

Densmore, J. D.. Discrete Diffusion Monte Carlo for the RZWedge_Mesh. 2010. *CCS-2:10-01(U).*

Densmore, J. D., and T. J. Urbatsch. Frequency-Dependent Discrete Diffusion Monte Carlo. 2010. *CCS-2:10-20(U).*

Robust 3D Moving Mesh Adaptation Based on Monge-Kantorovich Optimization

John M. Finn
20090424ER

Introduction

Mesh or grid generation is at the heart of many numerical simulations of physics problems. The grids provide points or boundaries at which the numerical simulation is performed. This project involves optimal grid generation for the numerical solution of nonlinear partial differential equations, e. g. the equations of hydrodynamics or the equations of magnetohydrodynamics (MHD). The grid adaptation is optimal in two senses. First, it assures that the estimated grid error is distributed equally on grid cells, with a finer grid in areas in which the error estimate is larger. This leads to the minimization of the total grid error. Second, for time stepping, this assures that the grid moves a minimal amount relative to the grid at the previous time step. Results so far indicate that this latter property prevents grid tangling, or folding. Grid tangling, in which grid cells collapse with crossed boundaries, is a serious problem, for example in Lagrangian codes. A Lagrangian code for hydrodynamics is a code in which the grid follows the flow. For many applications this is advantageous, but in many situations this leads to grid tangling.

We have begun to extend our preliminary work[1] in a simple two dimensional (2D) physical region (the unit square) to more complex regions in 2D[5]. Examples include regions with missing areas and regions with curved boundaries. We have also begun to extend the work to three dimensions (3D) in a cube[5], and will continue to generalize to a more complex set of physical domains. We plan to use this grid adaptation strategy in moving mesh hydrodynamics and MHD codes in 2D and 3D. We will use well developed error estimators for which our method will concentrate the grid where the error estimate is largest. We will then apply these adaptive grid codes to several challenging problems. These include: 1) propagation of shocks, 2) hydrodynamics problems in which a Lagrangian grid tangles, and 3) MHD simulations. We will compare with commonly used methods to assess the efficiency and accuracy of our methods.

Benefit to National Security Missions

This project endeavors to enhance simulation codes involving, for example, hydrodynamics, radiation hydrodynamics, magnetohydrodynamics, and particle-in-cell (plasma kinetic theory) codes that are immediately relevant to the DOE/NNSA nuclear weapons mission. Such computational tools should also impact astrophysics, high energy-density physics, fusion energy, space plasma physics, and other basic science mission areas.

Progress

We have developed Monge-Kantorovich optimization theory for grid generation and adaptation[1]. In this work, Monge-Kantorovich theory adapts a grid at each time step to an evolving error estimate, while minimizing a measure of the grid velocity, specifically the average of the grid velocity squared. We have more recently shown how to formulate a generalized Monge-Kantorovich adaptation scheme using the average of the magnitude of the grid velocity to an arbitrary power p [2]. (In the context, our earlier work[1] used $p=2$.) We showed that the grid in our previous work[1] generated good grids, with little tendency to tangle. We also showed that the lack of tangling in these grids is related to the fact that they minimize the average grid distortion. In the more recently formulated equations with p other than 2, we concluded that $p=2$ produces the best grids from two points of view. One was a cross comparison of grids for two different values of p. The other measure was the mean grid distortion. By all these measures, $p=2$ provided the best grid, specifically being optimal with respect to minimizing grid tangling. Furthermore, the equations for the grid with $p=2$ are much more efficiently solved than those for different values of p. We have published a paper on this subject, "Generalized Monge-Kantorovich optimization for grid generation and adaptation in *SIAM Journal of Scientific Computing*, Vol. **32**, pp. 3524-3547 (2010).

We have also constructed a fluid dynamic formulation of the above Monge-Kantorovich grid generation for general values of p[3]. The point of this work is to

compare generalized Monge-Kantorovich grid generation for arbitrary *p* with the commonly used deformation method, which produces a grid by integrating an ordinary differential equation in time. Unlike Monge-Kantorovich grid generation and adaptation, however, the commonly used deformation method does not minimize any important grid measure. We first compared our Monge-Kantorovich results for arbitrary *p* with the commonly used deformation method. We found the former to generate much better grids, especially near *p=2*. We published a paper on this work, "The fluid dynamic approach to equidistribution methods for grid generation and adaptation", *Computer Physics Communications*, Vol. **132**, pp. 330-346 (2011).

We have also studied the use of Monge-Kantorovich grid generation with p=2, in the context of an initial value code for a partial differential equation[4]. These flows are of the type which is particularly challenging for Largangian codes, in the sense that they typically cause the grid to fold. We investigated the issue of whether the Monge-Kantorovich method for the grid works better if it is defined relative to the grid used in the previous time step (the sequential method) or to the grid used in the initial conditions (the direct method.) We performed numerical tests for a wide variety of challenging flows. We concluded that in all cases the direct method worked much better. The sequential method showed a tendency to follow the flow to a degree, and it eventually led to a tangled grid, although long after the time at which a Lagrangian grid would tangle. The direct method showed no such tangling tendencies, even for the most challenging examples. We extended this work to three dimensions with challenging 3D flows. We found that the direct Monge-Kantorovich method with *p=2* worked well in all cases. We published a paper on this topic, "Robust, multidimensional mesh motion based on Monge-Kantorovich equidistribution", *Journal of Computational Physics*, Vol. **230**, pp. 87-103 (2010).

Future Work

This project involves optimal grid generation for the numerical solution of nonlinear partial differential equations, e. g. the equations of hydrodynamics, radiation hydrodynamics, or magnetohydrodynamics (MHD). The grid adaptation scheme we will investigate is optimal in two senses. First, it assures that the grid is concentrated in the area in which the estimated error is large, in a systematic manner. Second, for time stepping, this assures that the *p=2* norm of the grid displacement (relative to the grid at the previous time step) be minimized. Grid tangling is a serious problem in, for example, Lagrangian codes, and the displacement minimization property has the potential to deliver untangled grids.

We plan to extend our preliminary work in a simple two dimensional (2D) physical region (the unit square) to more complex regions in 2D. Examples of such physical regions include non-simply connected regions (regions with holes) and regions with curved boundaries. We will then extend the work to complex physical regions in three dimensions (3D). We plan to use this grid adaptation strategy in moving mesh hydrodynamics and MHD codes in 2D and 3D. We will use well developed error estimators for which our method will adapt the grid. We will then apply these adaptive grid codes to several challenging problems of importance to DOE/NNSA programs. These include: 1) propagation of shocks, 2) Hydrodynamic problems in which fine structures appear, and 4) magnetohydrodynamic problems of importance to fusion research and astrophysics. We will compare our results with those obtained with commonly used methods to assess the efficiency and accuracy of our methods.

Conclusion

Grid adaptation in numerical codes uses a fine grid in areas with large numerical errors and a coarse grid elsewhere. Adaptive gridding allows more efficient computer time and memory than uniform grids. There are two issues: grid adaptation methods are often ad-hoc, suboptimal and hard to quantify; these methods are prone to tangling, and the code must be restarted with ad-hoc modifications to mitigate the tangling. Our work is based on optimization theory, minimizing grid error by packing the grid in areas of large error estimate, while minimizing the distortion of the grid. Results so far show that the latter does a very good job of preventing grid tangling.

References

1. Delzanno, G. L.. An optimal robust equidistribution method for two-dimensional grid generation based on Monge-Kantorovich optimization. 2008. *Journal of Computational Physics.* **227**: 9841.
2. Delzanno, G. L.. Generalized Monge-Kantorovich optimization for grid generation and adaptation in L_p. To appear in *SIAM Journal of Scientific Computing.*
3. Delzanno, G. L.. The fluid-dynamic approach to equidistribution methods for grid generation and adaptation. To appear in *Computer Physics Communications.*
4. Chacon, L.. Robust, multidimensional mesh motion based on Monge-Kantorovich equidistribution. To appear in *Journal of Computational Physics.*
5. Finn, J. M.. Grid generation and adaptation by Monge-Kantorovich optimization in two and three dimensions. 2008. In *17th International Meshing Roundtable.* (Pittsburgh, PA, 12-15 Oct,., 2008). , p. 551. Berlin: Springer Verlag.

Publications

Chacon, L.. Robust, multidimensional mesh motion based on Monge-Kantorovich equidistribution. To appear in *Journal of Computational Physics.*

Delzanno, G. L.. The fluid dynamic approach to equidistribution methods for grid generation and adaptation. To appear in *SIAM Journal of Scientific Computing (SISC).*

Delzanno, G. L.. Generalized Monge-Kantorovich optimization for grid generation and adaptation in Lp. To appear in *Computer physics communications.*

Delzanno, G. L., L. Chacon, J. M. Finn, Y. Chung, and G. Lapenta. An optimal robust equidistribution method for two-dimensional grid generation based on Monge-Kantorovich optimization. 2009. *Journal of Computational Physics.* **227** (23): 9841.

Finn, J. M., G. L. Delzanno, and L. Chacon. Grid generation and adaptation by Monge-Kantorovich optimization in two and three dimensions. 2009. In *Proceedings of the 17th international meshing roundtable.* Edited by Garimella, R. V.. , p. 551. Berlin: Springer Verlag.

A Novel Brownian-Poisson Algorithm for Modeling Ion Transport through Artificial Ion Channels

Cynthia J. Reichhardt
20100273ER

Introduction

Artificial nanochannels can be used to create highly sensitive single molecule detectors which are capable of detecting small quantities of biomolecules or infectious agents. These sensors would have longer life and operating characteristics better suited to field work than currently used biological nanochannels. Our project would permit the rapid optimization of nanochannels for devices intended to detect particular molecules, shortening the time required to create a working device.

Recent experimental advances have led to the fabrication of highly controlled artificial ion channels suitable for use in sensors and in a wide array of applications. The artificial channels are much more robust than channels produced by biological means, and their functionalization is more easily controlled since it does not require manipulation of a bacteria genome. A fundamental understanding of the interaction of hydrated ions with the artificial ion channels is still lacking and device development has proceeded purely through trial and error. In our project, we will develop a hybrid simulation tool capable of treating the discrete interactions of ions in the artificial channels. Our simulation can be used to rapidly test a series of nanochannel configurations, including different surface charge treatments, different channel opening angles, different ion charge species, and different functionalization of the channel mouth, for possible use in applications. The simulations can be performed more rapidly and with fewer resources than the equivalent experiments, and will permit the efficient identification of the most efficient operating regime of the artificial channel for a given device application. We will also explore new device applications beyond the most common area of biomolecule sensing, including ion channels for fuel cell applications and ion channel logic elements which could be used to control lab-on-a-chip devices.

Benefit to National Security Missions

Artificial nanochannels can be used to create highly sensitive single molecule detectors which are capable of detecting small quantities of biomolecules or infectious agents. These sensors would have longer life and operating characteristics better suited to field work than currently used biological nanochannels. Our project would permit the rapid optimization of nanochannels for devices intended to detect particular molecules, shortening the time required to create a working device.

Progress

During the past year, we have integrated and tested key components of our combined Brownian dynamics, Poisson solver, and analytic approach to modeling ion transport through artificial ion channels, and have carried out a study of ion-ion interaction effects in a strongly constrained ion channel geometry. When ions pass through the channel they induce a charge at the dielectric boundary between the membrane and the aqueous solution, resulting in a self-energy that can be of order the thermal energy in narrow channels. We have implemented and tested an efficient iterative Poisson solver which generates lookup tables filled with precalculated values of the electric field and potential produced by a charged ion sitting at specific positions within the ion channel. For the best numerical accuracy, we calculate the electric field near the interfaces at some distance away from the interface in order to guarantee that the discretized surface charges can be treated as point-like charges. We have developed a three-dimensional Brownian simulation model which accepts the input of the Poisson solver and uses it to compute the forces acting on the ions as they pass through the channel and interact with each other. Our simulation includes both the self-interaction caused by the charge induced by the ions on the channel walls as well as the direct charge-charge interactions. To check the simulation, we performed a comparison with a semi-analytic Poisson-Nernst-Planck analysis of individual charges moving through a narrow but finite channel. We are also now carrying out analytical field-theoretic calculations of the crucial self-energy effects which produce energetic barriers to the permeation of the channel by the ions. In our first simulation study of a strongly constrained ion channel geometry,

we consider the passage of interacting ions through a series of connected funnels. When the ions occupy the funnels but are not forced to move through them by an external electric field, the ions adopt highly symmetric configurations within the funnels in order to minimize their electrostatic interaction energy. Application of an electric field leads to a complex transport behavior which is highly dependent on the number of ions within each funnel. In the case of few ions per funnel, a relatively straightforward transport along the funnel axis is established. As the number of ions per funnel increases, we find jamming and clogging effects in which the ions interfere with each other as they attempt to pass through the bottleneck region of the funnel. The jamming effects result in an overall decrease of the ion velocity at fixed electric driving field as the density of ions is increased. The clogging effects are much more complicated and can produce regimes of negative differential conductivity of the ions in which the velocity of the ions decreases as the electric driving field is increased. This type of behavior can be exploited for device applications, but it will first require further quantification and study. The results of our study in the jamming regime have just been published. We are preparing a separate manuscript describing the clogging behavior. The PI has also been invited to present this work at domestic and international conferences. We are in contact with the experimental group at UC-Irvine that is presently working on noise signatures in rectifying artificial ion channels. Our jamming study offers insight into the nature of the collective interactions that may be responsible for the unusual noise signatures which have been measured. Prior to our study, there was no theoretical tool capable of accounting for the effects of the complex many-body interactions between ions outside of the highly diluted regime. Our combined analytical and simulation approach offers new insight into the interacting ion regime and can provide the understanding required for future device development work.

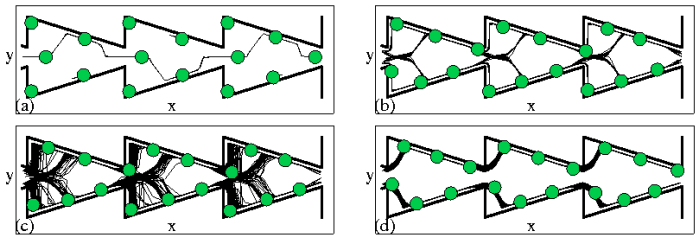

Figure 1. Image of instantaneous ion positions (circles) and ion trajectories over a fixed time (light lines) in a funnel geometry showing four different types of flow. (a) Flow of only a portion of the ions in a winding channel. (b) Flow of all ions through braided channels that switch in a regular pattern. (c) Chaotic flow of all ions. (d) Ordered flow of all ions in a static pattern.

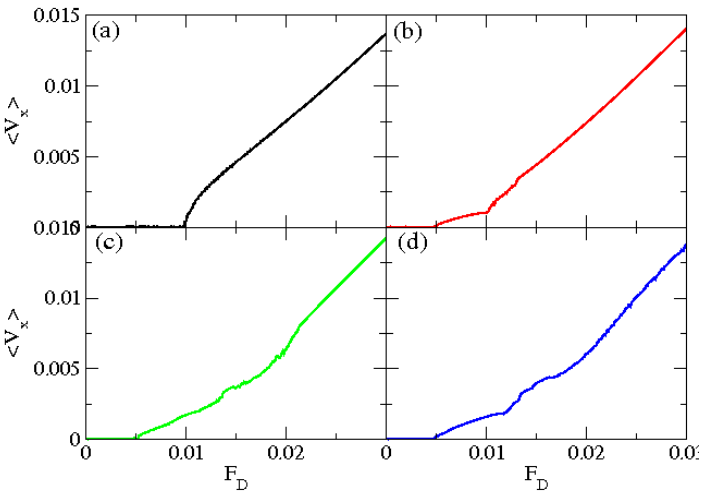

Figure 2. Current-voltage transport curves for ions in the funnel trajectory in different transport regimes. (a) Ordered flow. (b-d) Several examples of transitions between ordered and disordered flow, displaying regimes of negative differential conductivity.

Future Work

We will develop a powerful new multi-scale simulation tool for the study of ion transport in artificial ion channels by combining a Brownian dynamics particle-based simulation of the ions, a Poisson solver for the electrostatic interactions with the nanopore walls, and a Poisson-Nernst-Planck analysis of the nonlinear response. Our simulation method will overcome the limitations of existing ion channel models which consider only short time scales and a small number of ions. This is crucial for future device applications based on ion channels made with artificial nanopores, where interactions between multiple ion species can produce ion transistors or diodes. Our approach is optimized for the rapidly developing area of artificial nanopore applications, ranging from new sensor technologies to novel microfluidic logic devices for use in lab-on-a-chip designs. We will test our simulation and analysis method by comparing the results to recent experimental work on nanopore diode devices. Our simulation toolkit will permit the detailed analysis of experimental data and provide a predictive tool for determining parameter regimes where novel ion transport behavior should appear experimentally, including transport mechanisms for interacting ions and screening charge interactions with the channel walls or with elongated molecules such as DNA. After our toolkit has been thoroughly tested against the behavior of an isolated ion in a channel, we will apply it to studies of the dynamics of ion motion through channels, particularly in the poorly understood cases where multiple ions are present in the channel simultaneously and in channels close to the crossover size between discrete and continuum charge dynamics. This study is important not only for understanding ion transport through channels in the collective regime, but also for developing tailored

nanochannels for devices such as biomolecule sorters or sensors.

Conclusion

We will develop a predictive simulation for artificial nanochannels that can be used for future device development. Artificial nanochannels show great promise for use as highly sensitive and robust sensors of biomolecules or infectious agents. Ion transistors and logic circuits made from nanochannels could be used to control advanced lab-on-a-chip circuitry or to perform highly efficient DNA sequencing. With the help of our predictive tool, completely new areas such as fuel cell applications of the nanochannels can be explored.

Publications

Reichhardt, C. J. O., and C. Reichhardt. Commensurability, jamming, and dynamics for vortices in funnel geometries. 2010. *Physical Review B (Condensed Matter and Materials Physics).* **81** (22): 224516 (14 pp.).

Parallel Algorithms for Robust Phylogenetic Inference

Tanmoy Bhattacharya
20100395ER

Introduction

Individuals share traits due to their common ancestry. The correlations created by this common ancestry have long fascinated statisticians attempting to analyze biological data. The task of constructing such histories, which are also known as `phylogenetic' trees, is an important branch of theoretical biology, because these reconstructed histories are needed to account for the correlations in the data. The ability to reconstruct such histories forms an important core capability at the Laboratory.

With the advent of petascale computing, however, traditional phylogenetic inference is undergoing a revolution. Instead of simply estimating the most likely history, scientists are using powerful computers to calculate the entire range of likely histories, together with their probabilities. The importance of quantifying uncertainty and propagating it to subsequent stages of analyses is only now being appreciated. Soon, it will be a cornerstone capability, necessary for maintaining the leadership of the Laboratory in these sciences.

The problem, however, is that software has not kept pace with the hardware. Dramatic computational speed-ups have occurred using modern parallel architectures, but software tools for phylogenetic inference have lagged behind. For the most part, phylogenetic algorithms are still primarily serial. Such algorithms are not well suited to large data sets needed for the next generation of problems. The space of trees in these problems cannot be searched efficiently by these methods. For this reason, uncertainty is often underestimated. The present work addresses this gap and aims to provide new algorithms and implementations for large scale `Bayesian' phylogenetics on today's powerful parallel machines.

Benefit to National Security Missions

Phylogenetic reconstruction has been a core competency at the Laboratory for over a decade. It is useful in many different fields: for understanding interactions between the host and pathogen in population data, for designing vaccines and therapeutics against rapidly evolving pathogens, and for determining the origins of pathogenic strains. The next generation of problems in these fields will require much larger amounts of sequence data to be analyzed. These analyses will need to come with uncertainty estimates. Experimental advances have already started to make such data available. This project directly addresses the limitations of the existing algorithms. It will develop the required algorithms, and will also provide implementations of these algorithms for practicing bioscientists.

Progress

Since we proposed this work, there have been a number of advances in the tools used to program hierarchical parallel machines. The programming language Haskell, being a purely functional language, has significant advantages for parallel programming. Phylogenetic problems map naturally onto the primitives of functional programming. The tree is the primary data structure in these types of programs. A tree can be 'evaluated' by the 'fold' operation, which is an elementary concept in functional languages. As noted, the compilers for these languages are maturing. Because of the natural fit between our problem and functional languages, we decided that it would be very valuable to rewrite our existing phylogenetic code in Haskell. We are in contact with one of the primary developers for Haskell, the Glasgow Haskell Compiler team, who have recently become interested in developing tools for parallel programming.

We have almost finished rewriting the existing Markov Chain Monte Carlo (MCMC) methods in Haskell on a serial machine, and we are working on tying the low-level likelihood calculations to the existing Roadrunner code. We expect the first workable version to be ready early next year. When available, this will provide a uniform programming interface on both serial and parallel machines and much more natural expression structures for the algorithms that we plan to develop. This development will also make our work independent of any particular hardware platform, so that our code

can be deployed more widely. Finally, this approach separates the tuning of the proposal structure from parallel code development, leading to faster turn around.

We now discuss progress on the algorithmic side of our project. One of our goals in the first year was to find simplified scenarios for studying the properties of the 'likelihood surface,' which is used to assess the probability of different trees. In order to generalize phylogenetic algorithms to the setting of networks, we need to have test cases that are well understood, but which avoid some of the complications of the general setting. Our original plan was to look for such a test case in the setting of small networks, where exhaustive search is feasible. We still consider that a promising direction, but we realized that significant simplifications arise in other settings as well. In particular, the likelihood surface simplifies under the assumption of exponential growth, which occurs in acute infection. In this situation, the likelihood can be determined without MCMC methods, provided large samples are available. This test case involves datasets with large numbers of sequences, which gives us insight on a key complication that arises in the general case.

This year, we had the good fortune of gaining access to several datasets from HCV, SIV, and acute HIV infections obtained from various other LDRD DR and NIH funded projects at the laboratory. The use of this real data guarantees that we are working in a biologically relevant regime. Much of our work this year, therefore, has involved the characterization of the likelihood surface for large numbers of sequences in the case of exponential growth. Many of the results obtained in this study have already been valuable to the other projects, and have been presented at conferences for that reason.

In Figure 1, we illustrate why exponentially growing populations are especially important. When the population size is constant, random sequencing leads to highly correlated data, and the amount of information increases only slowly with the number of samples. When the population grows exponentially, on the other hand, the data is less correlated, and the amount of information grows more rapidly with the number of samples. For this reason, we extended 'importance sampling' methods, which were developed for a small number of sequences [1–3], to this case of large number of sequences from an exponentially growing population. We then applied them to study the relevant likelihood surface.

As a result of this work we now understand, for an exponentially growing population, why the shape of the likelihood surface is heavy tailed and approximately 'log normal' near its peak. We have verified our method on simulated data (see Figure 2), and we have applied these methods to real HIV data (Figure 3). (HIV is the virus responsible for AIDS.) Our work has already provided useful biological information about the *in vivo* viral evolution rate in HIV. This work will help us in the later stages of tuning the parameters of the model. But it is also biologically important in its own right, so it has been presented as a talk and is currently being written up as a paper.

With this understanding of the near-peak structure, and with the development tools already at hand, we should soon be able to extend the likelihood functions away from trees onto more general structures. As we develop these algorithms, we can now test them in two simplified test cases: (1) with a small number of sequences, where exhaustive searches are possible; and (2) with a large number of sequences drawn from a rapidly growing population. We expect these test cases to help us understand how to extend the likelihood functions from trees to more general structures.

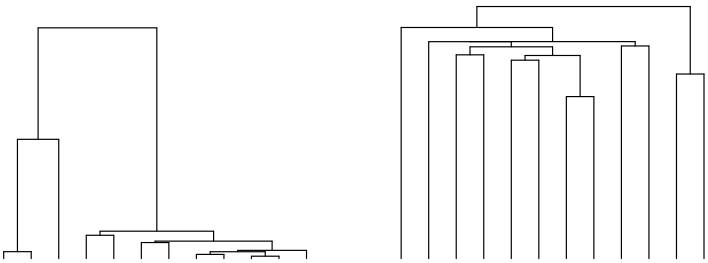

Figure 1. The shape of the phylogenetic tree is very different for constant sized populations (left) and rapidly expanding populations (right). Increasing the number of samples in a constant sized population increases the amount of phylogenetic information, estimated by the total length of all the branches in the tree, proportionally to the log of the sample size, whereas in an exponentially growing population, the information increases almost linearly.

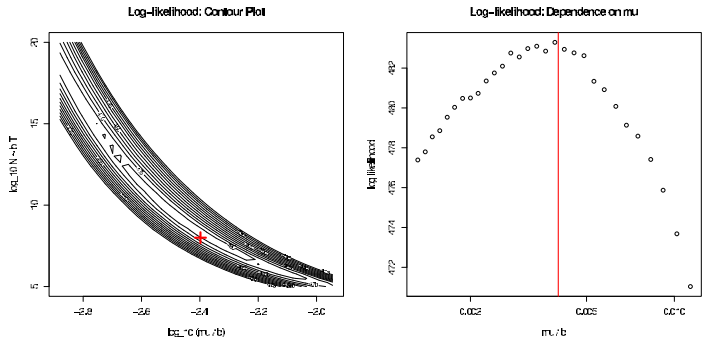

Figure 2. The shape of the likelihood surface near the peak as determined by our method for simulated data sets. The red cross on the contour plot (left) and the red line on the cross-section (right) show the true values are well reproduced within errors.

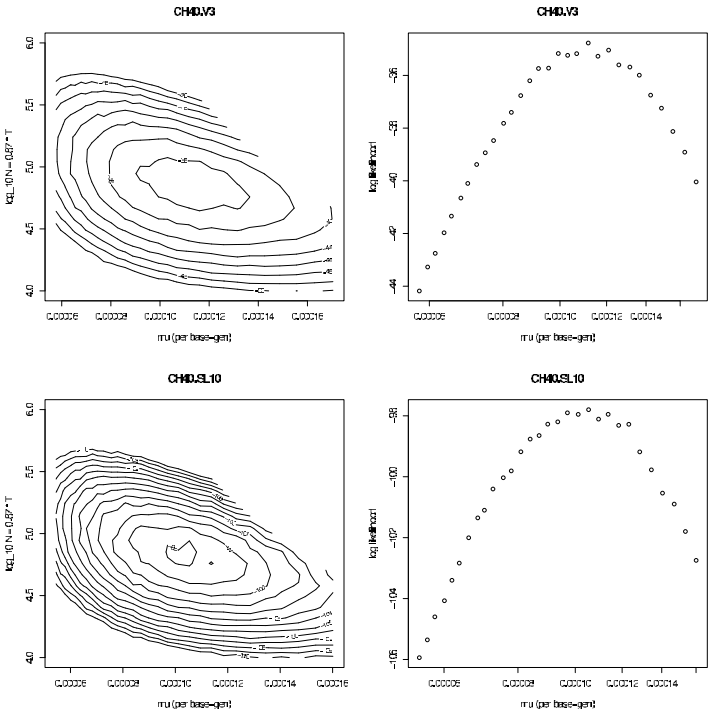

Figure 3. The likelihood surface, shown as a contour plot (left) and as a cross section (right) determined by our method for two regions of the genome (V3 and SL10) from an HIV infected patient (CH40) sequenced deeply using the recently available 454 technology. The peaks occur are seen to occur at very similar parameter values as expected.

Future Work

As noted earlier, the increasing availability of computational power, coupled with dramatic increases in the quantity of experimental data, is leading to a crisis in the field of phylogenetics. Instead of determining a single evolutionary history (`phylogeny') that best fits the observations, it is becoming possible to determine a large number of histories that are consistent with observations, together with their relative probabilities. By providing a more complete solution, such methods can profoundly enrich our ability to provide reliable answers to scientifically interesting questions. But two primary obstacles are currently impeding this progress: effective parallelization and heuristic search for the best tree. We plan to overcome these problems by (i) developing algorithms for adapting MCMC methods to massively parallel multi-level hybrid architectures, and by (ii) developing algorithms that can more effectively sample the discrete space of tree topologies. Towards the first of these goals, we will identify opportunities for microparallelism. We will also implement Metropolis Coupled MCMC algorithms to harness large-scale parallelism. The second task will involve finding more effective ways of moving through tree space, by passing from one tree to the next through network space.

Taken together, these two advances will enable us to build a package for Bayesian phylogenetics that will be portable to the novel architectures, and able to handle the required large data sets.

Conclusion

This project will modernize the core capability of the laboratory for phylogenetic analysis. It will do so by providing a Bayesian sampler that can be used on a wide variety of platforms, and which will harness the power of the new and emerging massively parallel computer architectures acquired by the Laboratory. The codes developed will be optimized for the current generation of hierarchical distributed compilers. But these codes will be written in a functional language, which will make it easy to port them to other architectures, including those that are just now emerging. We have described two key parts to our project. First, we are implementing known algorithms for the problem in a modular way, so that they can be used on parallel architectures. Second, we are developing new algorithms to solve the severe `mixing' problems that currently prohibit use of large data sets.

References

1. Felsenstein, J., M. K. Kuhner, J. Yamato, and P. Beerli. Likelihoods on coalescents: a Monte Carlo sampling approach to inferring parameters from population samples of molecular data. 1999. Statistics in Molecular Biology, Institute of Mathematical Statistics Lecture Notes - Monograph Series Volume 33.

2. Stephens, M., and P. Donnelly. Inference in molecular population genetics. 2000. JOURNAL OF THE ROYAL STATISTICAL SOCIETY SERIES B-STATISTICAL METHODOLOGY. **62** (4): 605.

3. Tavare, S.. Sampling theory for neutral alleles in a varying environment. 1994. Philosophical Transactions of the Royal Society of London B Biological Sciences. **344** (1310): 403.

Robust Unsupervised Operation Under Uncertainty Through Information Theoretic Optimization of Complex Systems.

Aric A. Hagberg
20100460ER

Introduction

The pace of technological advance in information science and technology is opening up new opportunities to accelerate scientific discovery. However, our increased ability to measure and observe complex natural and social systems also threatens to drown us in data. The fundamental question of finding the relevant information in a large and rich stream of information is the main objective of our research.

Successful new mathematical and computational methods must be able to extract information from streaming data originating from distributed sensors in natural and social environments such as high throughput experiments in genetics, astronomy and high-energy physics. They will also guide sensors to actively pursue new pieces of information in noisy environments that can help fulfill a task or answer a question.

We will develop and apply the principles of information theory, with techniques from inference, and Bayesian statistics, to provide a systematic approach to multi-level (hierarchical) modeling of classes of complex systems. We expect that our methods will apply to the discovery of structure in complex systems with unknown interaction structure. It will also generate predictions for the behavior of complex systems with quantified uncertainty, and new data assimilation schemes and unsupervised learning algorithms that are guided by uncertainty reduction.

These methods will create new robust approaches to knowledge extraction from large (streaming) data and the development of adaptive learning and control algorithms for application of strategic interest to LANL's Grand Challenges in information science and technology, ubiquitous sensing, complex systems and to DOE's missions of energy security, nuclear non-proliferation, and environmental stewardship.

Benefit to National Security Missions

Explosive progress in information technology is making possible vast increases in the amount of information that can be measured and retrieved from natural and engineered complex systems. The scientific underpinnings to make the most out of this information are still missing and severely handicap LANL and DOE---specifically in missions of energy security, systems biology, nuclear nonproliferation, and environmental stewardship. Our project will create a mathematical framework for analysis and control of such complex natural and engineered systems.

Progress

The project has focused on the theory and design of optimal algorithms for collective search of stochastic sources. We have also developed a new theory that makes direct connections to real-world problems in analysis and anomaly detection in computer networks.

We have shown how collective searches can result in faster information gain and created models in which these results are made explicit. We have done the following:

- developed a theory for one or more agents searching cooperatively for a stationary, stochastic source;
- generalized single-searcher algorithms to multiple searchers; created parallel simulations of searchers;
- formulated a theory for classifying when multiple searchers should work together to improve efficiency; and
- demonstrated improved efficiency through searcher coordination.

Some of these results are published [1] and more are now being prepared for publication [2].

In addition we developed new concepts that connect our optimization approach to the theory of optimal experimental design and to mechanisms of feedback in neural networks. This makes explicit connections to literature in information theory, statistical estimation

and unsupervised (machine) learning [3].

Finally, we developed approaches to discovering patterns in computer network communications. This work forms a basis for determining which global structural changes are relevant for finding unusual activity [4] and for evaluating which measurements are useful for detection [5].

Future Work

We will develop a mathematical framework based on information theory for solving general optimization and prediction problems in the presence of uncertainty.

Our main goals and tasks are:

Construct mathematical framework:

Information theory provides a principled, general approach for designing objective functions that include fundamental properties of complex natural and engineered systems, such as stochastic heterogeneous variables, design constraints and quantitative performance goals.

Design algorithms for optimization and real time data assimilation:

Information theoretic objective functions support seamless data assimilation in real time. e.g. via Bayesian schemes. We will develop methods and algorithms for systematic approximation of information quantities of many variables that locally minimize uncertainty at each time.

Target problems of strategic importance to LANL and DOE:

- Discovering functional network structure in natural and engineered systems.
- Spatial coordinated search for stochastic sources (e.g. nuclear, pollutant) that can resist damage to parts of the system and interference in communications while automatically coordinating multiple (parallel) sensor/agents.
- Adaptive control of engineered systems through creation of a formalism and computational optimization methods so that a designer or engineer can specify rewards for the adaptive, unsupervised operation of complex engineered systems (e.g., distributed robots or infrastructure networks).

Conclusion

We will create a general class of methods, based on fundamental mathematics and computer science, to identify where information is and to solve general problems in complex systems. We will apply our formalism to network reconstruction (biology, infrastructure) for identifying the most relevant bio-chemical processes in high level functions (metabolism, infection), and to assure quality of service of the electrical power grid or other infrastructure.

The project will focus on fundamental concepts and specific applications where challenging data sets and experiments become available, including distributed sensor networks, robotics, and biological, social and technical network applications.

References

1. Gintautas, V., A. Hagberg, and L. M. A. Bettencourt. Cooperative searching for stochastic targets. 2010. *Journal of Intelligence Community Research and Development.* : 000.

2. Gintautas, V., A. Hagberg, and L. M. A. Bettencourt. Synergy-based infotaxis motion of swarms. 2010. *Unpublished.*

3. Bettencourt, L. M. A.. The Rules of Information Aggregation and Emergence of Collective Intelligent Behavior. 2010. *Topics in Cognitive Science.* (1): 598.

4. Sandine, G., A. Hagberg, J. Neil, C. Storlie, and S. Vander Wiel. Relative entropy for anomaly detection in computer networks. 2010. *LA-UR 10-06099.*

5. Hagberg, A., J. Neil, G. Sandine, and S. Vander Wiel. Protocol Graph Anomaly Detection: Global graph invariants and graph metrics. 2010. *LA-UR 10-00756.*

Publications

Bettencourt, L. M. A.. The Rules of Information Aggregation and Emergence of Collective Intelligent Behavior. 2010. *Topics in Cognitive Science.* (1): 598.

Gintautas, V., A. Hagberg, and L. M. A. Bettencourt. Synergy-based infotaxis motion of swarms. 2010. *Unpublished.*

Gintautas, V., A. Hagberg, and L. M. A. Bettencourt. Cooperative searching for stochastic targets. 2010. *Journal of Intelligence Community Research and Development.* : 000.

Hagberg, A., J. Neil, G. Sandine, and S. Vander Wiel. Protocol Graph Anomaly Detection: Global graph invariants and graph metrics. 2010. *LA-UR 10-00756.*

Sandine, G., A. Hagberg, J. Neil, C. Storlie, and S. Vander Wiel. Relative entropy for anomaly detection in computer networks. 2010. *LA-UR 10-06099.*

Nonconvex Compressed Sensing

Rick Chartrand
20080128ER

Abstract

This project is concerned with the ability to reconstruct images and other signals from very few linear measurements. Our methods exploit the *sparsity* (or *compressibility*) inherent in real-world signals, meaning that they can be described accurately using much less information than their usual representations (such as stating every pixel value). Theoretical results show that the number of measurements needed to reconstruct a signal is commensurate with its *complexity*, rather than its size. Our approach pushes this further, making use of the special geometric properties of *nonconvex* functions, in order to reconstruct signals from many fewer measurements than other competing methods based on convex functions.

Over the course of the project we developed very efficient algorithms, making use of sophisticated mathematics from the research field of optimization. A benchmark test problem had its computation time reduced from over an hour to under 5 seconds.

The project developed methods that are useful in many different application areas, from medical imaging to remote sensing to basic science to homeland security. Our methods are playing a crucial role in a multimillion-dollar DARPA project in space situational awareness.

Before the project, the PI was a little-known researcher in applied mathematics, having only recently changed fields from pure mathematics. He is now an established authority in the fields of sparse signal reconstruction and algorithms for nonconvex optimization, with many citations and invitations.

Background and Research Objectives

The young field from which this project comes is known as *compressive sensing*. This is because one perspective on the results is that they tell us that we can directly measure a compressed version of an image or other signal, without knowledge of the signal itself. But the perspective that best represents most of the work in compressive sensing is that we now know how to reconstruct signals from fewer data than ever before.

College freshmen in linear algebra classes learn that to solve a system of linear equations, one must have as many equations as there are variables. If not, the system is *underdetermined*, and the system has infinitely many solutions. So it is if one has data that come from linear measurements of a signal, that are fewer in number than the size of the signal's digital representation (such as the number of pixels in an image). Standard approaches would tell us that we don't have enough information to be able to determine the signal. But this is true only if every solution of the system that is mathematically possible makes equal sense. In fact, most signals that arise in nature or from human activity can be described *sparsely*, or using much less information than would be needed to convey the entirety of a digital representation.

Compressive sensing exploits this sparsity by seeking sparse solutions to a system of equations, by means of solving an optimization problem. In fact, a strategy that works very well in principle is to simply find the sparsest solution to the system of equations, the one that can be described using the fewest nonzero components. However, to find the sparsest solution directly is completely intractable. There are so many possibilities to check that, for problems of a useful size, all the world's computers working for trillions of years wouldn't even scratch the surface.

At this point, some background concerning *convex functions* is in order. A convex function can be thought of as one whose graph is essentially like a bowl (or bowl-like surface of the appropriate dimension, in the millions or billions for typical applications). The chief property of a bowl in this instance concerns minimization. A miniature robot at any point of the bowl's surface, equipped with only the simple program "always go downhill," will necessarily reach the lowest point on the bowl. Similarly, convex functions can be minimized easily, using efficient algorithms.

The success of compressive sensing can be regarded as arising from the ability to find the sparsest solution of a system by instead finding the minimum of a particular

convex function. Thus, a completely intractable problem has been replaced by one that is computationally very simple. Figure 1 contains a simple example (from [1]; cf. [2]) showing how one can reconstruct an image from a lot less data than needed by traditional methods.

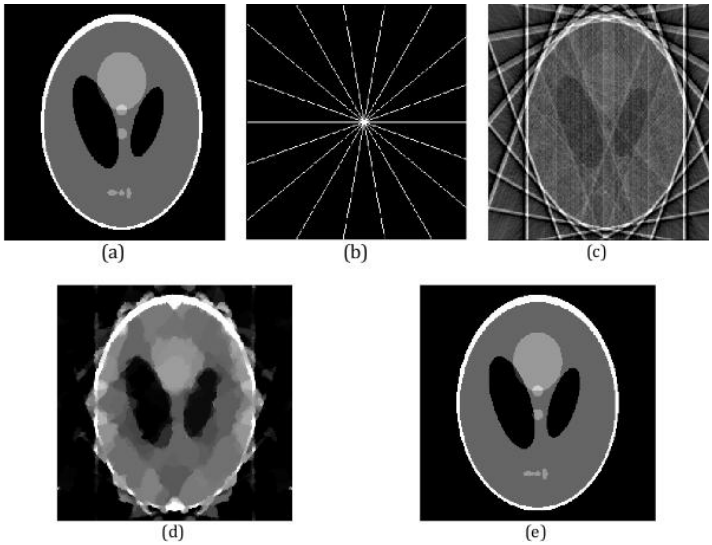

Figure 1. (a) The Shepp-Logan phantom, a common test image in medical imaging. The image is 256 X 256 pixels in size. (b) A sampling mask, showing which pixels of the Fourier transform of (a) will be sampled and used as data. We sample along radial lines in the Fourier domain; this makes the data tantamount to having one radiograph for each line. (c) A reconstruction using filtered backprojection, the state-of-the-art in X-ray CT reconstruction software in clinical use. The result is poor, because there are too few data. (d) A reconstruction using a compressive approach, using convex functions. Again, there are too few data for a good reconstruction. (e) Reconstruction using the nonconvex approach of [1]. The reconstruction is perfect!

The nonconvex functions we considered in this project are entirely different. A downward-heading robot would encounter unfathomably many pitfalls in which he could get stuck (in the example of Figure 1, the number of pitfalls would take a page and a half to write). Attaining the lowest point on the graph would seem to require magical knowledge of where on the pitted bowl to start the descent in order not to get stuck, or else extreme luck. However, in this project we developed simple and efficient algorithms that solve the minimization problem very reliably. The result is that we are able to reconstruct signals from much less data than are needed by the convex methods of compressive sensing.

The research objectives can be divided into three categories:

Theory
The objectives were to provide rigorous, mathematical justification for the very successful numerical results we have obtained. There are two kinds of theorems that were sought. The first was to establish that using nonconvex functions would result in needing fewer measurements to be able to reconstruct a signal, as well as be more robust to noisy measurements. This objective was completely met, as witnessed by results in [3] and [4]. The second was to justify the empirical fact of being able to minimize our nonconvex functions, without getting stuck. We were only able to obtain partial results in this direction, before needing to move on to other project priorities.

Algorithms
The primary algorithmic objective was to develop efficient algorithms for minimizing our nonconvex functions, to decrease computation time and make very large applications feasible. This turned out better than expected, due to the development of an algorithm [1] that makes clever use of the *fast Fourier transform* (or FFT). The FFT is a highly optimized computational routine, whose computation time scales very well as the problem size increases.

Applications
One of the project's goals was to develop applications of our superior reconstruction abilities, for the sake of both scientific impact and obtaining funding. Applications that were worked on over the course of the project include:

1. Neuroscience, where a 3-D reconstruction of electrical activity in the brain would be obtained from 256 electrical measurements on the scalp;
2. Magnetic resonance imaging (MRI), where scan times could be greatly reduced and still produce images of diagnostic quality;
3. X-ray computed tomography (CT), which could be replaced by single X-ray projections along a handful of angles, reducing radiation dose;
4. Oceanography, where oceanographic fluctuations could be recovered at finer scales than currently possible from existing tidal records;
5. Sonar, where images of a scene could be reconstructed from less information, alleviating the burden of slow through-water data transmission rates;
6. Radiography, where our optimization methods were leveraged to improve results for the Inertial Confinement Fusion project;
7. Hyperspectral imaging, where materials could be identified from their spectra from among a very large number of materials in a spectral library;
8. Space situational awareness, as described in the Addendum; and
9. An intelligence application, about which no more can be said.

These applications formed part of publications [1, 5, 6, 7], grant proposals, and programs.

Scientific Approach and Accomplishments

Most of the details of the theoretical approach are beyond the scope of this report. The fundamental underlying concept is *concentration of measure*, which relates to certain geometric and probabilistic properties, often counterintuitive, of very high-dimensional spaces. An example relevant to this project is the following: imagine a wire frame, consisting of struts extending from -1 to +1 along each of the *N* axes of *N*-dimensional Euclidean space. Now wrap this frame in canvas, pulling the fabric tight in every direction. In 3 dimensions, for example, the resulting shape is an octahedron, an 8-sided regular solid. Now consider the volume contained inside our tent. The 3-dimensional version has volume 4/3, but the 10-dimensional version has a volume of only 0.0002. In real applications, *N* can reach into the billions, at which point the volume is unfathomably small. Our 3-dimensional picture of an octahedron becomes very misleading; the high-dimensional tent is extremely spiky. This turns out to be intimately connected to the recovery of sparse signals. The set of signals consistent with a small amount of data forms a high-dimensional analog of a plane. A spiky body is more likely to intersect such a plane at a low-dimensional vertex (where most coordinates are zero), than along a high-dimensional face (where more coordinates are not zero).

Using a probabilistic analysis exploiting similar geometric ideas, we were able to prove that if one uses nonconvex functions, perfect recovery of a sparse signal will occur under weaker hypotheses than were previously known [3]. Moreover, under the more realistic conditions of having noise in the measurement data, we obtained bounds on the possible error in the reconstruction that were tighter than had previously been obtained [4].

In order to develop more efficient algorithms, we used techniques developed by researchers in mathematical optimization. These techniques were developed in the context of convex functions, but we were able to extend them very successfully to the nonconvex case. Our most efficient algorithm made use of a sophisticated technique known as *operator splitting*, taking a complicated optimization problem and decomposing it into two, much easier problems. The derivation of the method is founded in the mathematical field of convex analysis, but we were able to show that the procedures could be applied to nonconvex functions. The results were remarkable. The example of Figure 1 first appeared in [2], the computation requiring over an hour. The algorithm of [1] performs the same computation in 5 seconds (using simple code in a slow, prototyping language).

The most natural applications of the project are in medical imaging, such as CT and MRI. The project led to a collaboration with a medical imaging researcher in the Radiology Department of the University of Chicago. A version of the nonconvex algorithms used in this project was used to improve the quality of images in breast tomosynthesis, an imaging modality that replaces CT with about a dozen radiographs from different angles [6].

This LDRD project has established the PI as an authority in sparse image and signal reconstruction, and algorithms for nonconvex optimization. His publications on the topic have 256 citations (source: Google Scholar), including papers having 89 and 60 citations, despite being less than 3 and 2 years old, respectively. He gave 11 invited talks over the course of the project, and was invited to be the Lead Guest Editor of a Special Issue on Compressive Sensing [9]. He now receives dozens of paper refereeing requests per year (up from just a few, before the project).

Impact on National Missions

This project has had an impact on a number of aspects of LANL's mission. Unique capabilities have been developed for radiographic imaging, which could be deployed in applications pertaining to stockpile stewardship and homeland security. The PI was invited (by an sponsor that we will not name) to take part in a multimillion-dollar proposal for an intelligence application, which is ongoing. The project's methods play a crucial role in the ongoing DARPA project described in an addendum that can be obtained by contacting the LDRD Program Manager at Los Alamos National Laboratory.

References

1. Chartrand, R.. Fast algorithms for nonconvex compressive sensing: MRI reconstruction from very few data. 2009. (Boston, June 28 -- July 1, 2009). p. 262. Piscataway: IEEE.

2. Chartrand, R.. Exact reconstructions of sparse signals via nonconvex minimization. 2007. *IEEE Signal Processing Letters.* **14**: 707.

3. Chartrand, R., and V. Staneva. Restricted isometry properties and nonconvex compressive sensing. 2008. *INVERSE PROBLEMS.* **24** (3).

4. Saab, R., R. Chartrand, and O. Yilmaz. Stable sparse approximations via nonconvex optimization. 2008. (Las Vegas, 31 Mar. - 4 Apr. 2008). p. 3885. Piscataway: IEEE.

5. Sidky, E. Y., R. Chartrand, and Xiaochuan Pan. Image reconstruction from few views by non-convex optimization. 2007. In *2007 IEEE Nuclear Science Symposium Conference Record ; 26 Oct.* (-3 Nov. 2007 ; Honolulu, HI, USA). , p. 3526.

6. Sidky, E. Y., I. Reiser, R. M. Nishikawa, Xiaochuan Pan, R. Chartrand, D. B. Kopans, and R. H. Moore. Practical iterative image reconstruction in digital breast tomos-

ynthesis by non-convex TpV optimization. 2008. (2008 ; San Diego, CA, USA). Vol. 6913p. 691328.

7. Chartrand, R., and B. Wohlberg. Total-variation regularization with bound constraints. 2010. In *IEEE International Conference on Acoustics, Speech, and Signal Processing.* (Dallas, 14-19 Mar. 2010). , p. 766. Piscataway: IEEE.

8. Chartrand, R., and W. Yin. Iteratively reweighted algorithms for compressive sensing. 2008. p. 3869.

9. Chartrand, R., R. Baraniuk, Y. Eldar, M. T. Figueiredo, and J. Tanner. Introduction to the Issue on Compressive Sensing. 2010. *IEEE JOURNAL OF SELECTED TOPICS IN SIGNAL PROCESSING.* **4** (2): 241.

10. Publications

11. Bollt, E., R. Chartrand, S. Esedoglu, P. Schultz, and K. Vixie. Graduated adaptive image denoising: local compromise between total variation and isotropic diffusion. 2009. *ADVANCES IN COMPUTATIONAL MATHEMATICS.* **31** (1-3): 61.

12. Chartrand, R.. Exact reconstructions of sparse signals via nonconvex minimization. 2007. *IEEE Signal Processing Letters.* **14**: 707.

13. Chartrand, R.. Nonconvex compressive sensing and reconstruction of gradient-sparse images: random vs. tomographic Fourier sampling. 2008. In *2008 15th IEEE International Conference on Image Processing - ICIP 2008 ; 12-15 Oct.* (2008 ; San Diego, CA, USA). , p. 2624.

14. Chartrand, R.. Nonconvex regularization for shape preservation. 2007. In *2007 IEEE International Conference on Image Processing, ICIP 2007 ; 16-19 Sept.* (2007 ; San Antonio, TX, USA). , p. 293.

15. Chartrand, R.. Nonconvex compressed sensing and error correction. 2007. In *2007 IEEE International Conference on Acoustics, Speech and Signal Processing, ICASSP '07 ; 20070415 - 20070420 ; Honolulu, HI, United States.* Vol. 3, p. III889.

16. Chartrand, R.. Fast algorithms for nonconvex compressive sensing: MRI reconstruction from very few data. 2009. In *2009 IEEE International Symposium on Biomedical Imaging: From Nano to Macro, ISBI 2009 ; 20090628 - 20090701 ; Boston, MA, United States.* , p. 262.

17. Chartrand, R.. Numerical differentiation of noisy, nonsmooth data. To appear in *International Journal of Applied Mathematics.*

18. Chartrand, R., K. R. Vixie, B. Wohlberg, and E. M. Bollt. A gradient descent solution to the Monge-Kantorovich problem. 2009. *Applied Mathematical Sciences.* **3** (22): 1071.

19. Chartrand, R., R. Baraniuk, Y. Eldar, M. T. Figueiredo, and J. Tanner. Introduction to the Issue on Compressive Sensing. 2010. *IEEE JOURNAL OF SELECTED TOPICS IN SIGNAL PROCESSING.* **4** (2): 241.

20. Chartrand, R., and B. Wohlberg. Total-variation regularization with bound constraints. 2010. In *IEEE International Conference on Acoustics, Speech, and Signal Processing.* (Dallas, 14-19 Mar. 2010). , p. 766. Piscataway: IEEE.

21. Chartrand, R., and V. Staneva. Restricted isometry properties and nonconvex compressive sensing. 2008. *INVERSE PROBLEMS.* **24** (3).

22. Chartrand, R., and V. Staneva. Nonconvex regularization for image segmentation. 2007. In *2007 International Conference on Image Processing, Computer Vision & Pattern Recognition.* (IPCV 2007 ; 25-28 June 2007 ; Las Vegas, NV, USA). , p. 193.

23. Chartrand, R., and W. Yin. Iteratively reweighted algorithms for compressive sensing. 2008. In *33rd IEEE International Conference on Acoustics, Speech and Signal Processing ; 20080330 - 20080404 ; Las Vegas, NV.* , p. 3869.

24. Saab, R., R. Chartrand, and O. Yilmaz. Stable sparse approximations via nonconvex optimization. 2008. In *33rd IEEE International Conference on Acoustics, Speech and Signal Processing ; 20080330 - 20080404 ; Las Vegas, NV.* , p. 3885.

25. Sidky, E. Y., I. Reiser, R. M. Nishikawa, Xiaochuan Pan, R. Chartrand, D. B. Kopans, and R. H. Moore. Practical iterative image reconstruction in digital breast tomosynthesis by non-convex TpV optimization. 2008. In *Medical Imaging 2008: Physics of Medical Imaging ; 18-21 Feb.* (2008 ; San Diego, CA, USA). Vol. 6913, p. 691328.

26. Sidky, E. Y., R. Chartrand, and Xiaochuan Pan. Image reconstruction from few views by non-convex optimization. 2007. In *2007 IEEE Nuclear Science Symposium Conference Record ; 26 Oct.* (-3 Nov. 2007 ; Honolulu, HI, USA). , p. 3526.

Foundations for Practical Pattern Recognition Systems

Reid B. Porter
20080182ER

Abstract

In recent years a theoretical base has been developed for a large class of pattern recognition systems that allows performance to be understood and quantified in far greater detail than ever before. However, the main results have been for standalone black-box type systems, and the main objective has been to remove the user from the design and validation process as much as possible. In practical environments the pattern recognition system is rarely used in isolation and human users are almost always involved in the design, interpretation and validation of system predictions. The objective of this project is to provide deeper understanding and better control of pattern recognition systems as they are used in practical environments. The first major accomplishment was a theoretical base for a different class of pattern recognition system that allows users to inspect and understand how the system makes predictions. The second major accomplishment includes a number of pattern recognition solutions to specific problems encountered in real-world data analysis environments.

Background and Research Objectives

Theory and Practice

The fundamental pattern recognition problem is to build a model of some desired behavior by generalizing from a finite collection of examples of the behavior. Successful solutions to this problem find applications in nearly all aspects of computational science, including bioinformatics, signal processing, computational chemistry and data mining. Although the optimal behavior is well defined it typically cannot be achieved in practice due to a lack of information and resources.

In terms of theory, there are three sources of error (deviation from optimal): 1) representation, 2) estimation and 3) computation. 1) The representation error is due to the mismatch between our choice of model class and the true underlying behavior. 2) The estimation error is due to the fact that we have only a finite number of examples of the desired behavior. 3) The computation error reflects the lack of optimality due to limited computational resources (i.e. the resources needed to both produce and implement the model). A large number of pattern recognition techniques have been suggested, driven largely by the discovery of new methods to minimize these three errors.

In terms of practice, there are two main differences between how theory dictates we should build pattern recognition systems and how pattern recognition systems are used in practical data exploitation environments. 1) Theory dictates we build black-box models where the model class is chosen for particular mathematical properties, which are often different to properties that users desire in practice, such as ease of implementation and ease of interpretation. 2) Theory also dictates the main objective of the pattern recognition system is to remove the user from design and validation as much as possible. In practical environments the pattern recognition system is rarely used in isolation, and human users are intimately involved in the data preparation, system design as well as interpretation and validation of results. How to empower users to efficiently develop, inspect and understand pattern recognition systems is an open question.

State of the Art – Support Vector Machines

Support Vector Machines (SVMs) are a pattern recognition system that have found wide success and use a combination of methods to address representation, estimation and computation errors simultaneously. Kernel functions provide SVMs a rich function set to model a large variety of behavior (minimizing representation error), statistical learning theory provides tight bounds on future performance (minimizing estimation error), and optimization theory provide polynomial time learning algorithms (minimizing computation error).

SVMs enjoy a solid theoretical base and are a good choice for many applications. However there are other applications where they are outperformed by other methods. In addition, SVMs make predictions using a large (possibly infinite) linear combination of terms, which means it can be difficult for users to understand

and interpret predicted results. SVMs have several tuning parameters, which are difficult for non expert users to choose. And finally, SVMs are defined over the space of real numbers, and typically use transcendental functions (e.g. tanh, log, exponential), which means they can only be approximated by digital computers.

State of the Art – Decision Trees

A second model class that is used equally, if not more broadly, in practical pattern recognition systems, is exemplified by the decision tree. This model class is often represented as a set of *if-then-else* logical conditions. Advocates claim that this type of model provides greater transparency and is more understandable to users, and also provides a more natural framework to include multiple types of inputs (discrete, nominal, continuous). These practical advantages have led to the wide spread adoption of Decision Tree classifiers in the bioinformatics and financial application domains.

Decision tree classifiers have been successfully applied to many practical problems, and have produced extremely high performance solutions for commercial and industrial applications. However, the estimation error for this model class is poorly understood and computation error suffers from heuristic learning algorithms and poorly defined stopping conditions. The wide spread use of SVMs in many applications clearly demonstrates the benefit of pattern recognition solutions with known estimation error and good control on computation error. This goal of the project was to combine the benefits of both fields of research and our specific objectives were:

- **Decision Tree Learning Algorithms:** To better understand the underlying assumptions of decision tree classifiers and to produce new learning algorithms for decision tree classifiers that could simultaneously address estimation, representation and computation errors.
- **Real World User Environments:** To develop new design criteria for pattern recognition systems that can help improve their usability, transparency and verifiability in real world environments.

Scientific Approach and Accomplishments

Decision Tree Learning Algorithms

We investigated two different approaches to Decision Tree theory. In the first approach we investigated and built upon recent theoretical work on Dyadic Decision Trees (DDT) [1]. In the second approach, which we call Ordered Hypothesis Machines (OHM), we developed Decision Tree theory using tools from non-linear signal processing [2]. Pursuing the two approaches in parallel helped increase our understanding of how the three errors interact in Decision Tree classifiers and produced two new learning algorithms that control the balance of estimation, representation and computation errors in different ways. Specifically, the DDT learning algorithm is the best choice in applications with discrete and nominal data types and a relatively small number of dimensions. The OHM learning algorithm is the best choice for real-valued data types and outperforms existing Decision Tree Algorithms in high dimensions. Our

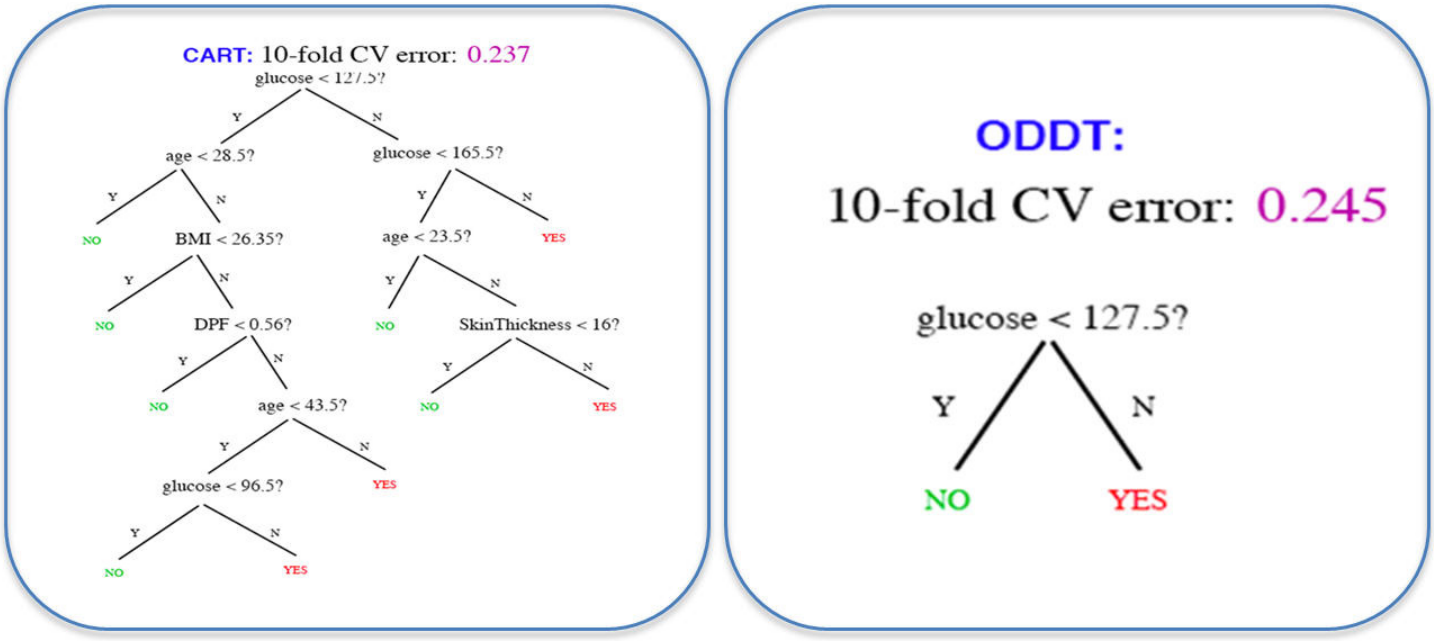

Figure 1. Example result showing Left) the classifier produced by the traditional decision tree learning algorithm (CART) and Right) the classifier produced by our algorithm (ODT).

accomplishments in this area are described in more detail in the next few paragraphs.

Dyadic Decision Trees (DDT)

DDT provides a solution method that exactly minimizes an error estimate based on the training data, which can be directly linked to *estimation* error. This means the approach is consistent (with infinite samples the method approaches optimal) which improves upon the traditional decision tree learning algorithms such as C4.5. [3] and Classification and Regression Trees (CART) [4]. We developed solutions that yield faster run times, use less memory, and simplify the user interface compared to existing methods. Specifically we have transformed the traditional bottom-up (dynamic programming) algorithm into a top-down (memorized) algorithm, which allowed us to add a "look-ahead pruning" heuristic that significantly improved the run time and memory usage. We also replaced the typical "dynamic dictionary" data structure with a "universal hash table" which further improved the run time. Finally, we developed an efficient and automated algorithm for selecting the tuning parameters, which lead to a simpler user interface and low error rates. This work has appeared has the Journal of Machine Learning Research [5]. In Figure 1 we show a typical result where our method obtains a solution that has comparable performance to CART, but produces a much simpler, and easier to understand result.

Ordered Hypothesis Machines (OHM)

Just as linear models generalize the sample mean and weighted average, weighted order statistic models generalize the sample median and weighted median. This analogy can be continued informally, to generalized additive models in the case of the mean, and Stack Filters in the case of the median. Both of these model classes have been extensively studied for signal and image processing, but in pattern recognition their treatment has been significantly one sided. Generalized additive models are now a major tool in pattern classification, largely due to the development of Support Vector Machine learning algorithms. In this project we developed a classification framework for Stack Filters and developed several new learning algorithms.

Specifically, we developed the concept of rank-order margin to control complexity in the Stack Filter model class and developed learning algorithms based on a pre-specified partitioning of the input space. This highlighted the connection between Stack Filter Classifiers and Decision Tree classifiers: both classifiers produce similar decision boundaries but the two approaches place different constraints on how partitions, induced by decision boundaries, can be assigned. We compared performance of the Stack Filter Classifier on several real-world benchmark problems and obtained improved performance over the widely used C4.5 and CART decision tree learning algorithms, and comparable performance to our new DDT learning algorithm. This work was presented at the International Symposium on Mathematical Morphology in 2009 [6].

We then developed a continuous domain learning algorithm for Stack Filter Classifiers which we call Ordered Hypothesis Machines (OHM). OHM classifiers can be considered generalizations of Stack Filter Classifiers where the dimension of the input space expands to infinity. This is analogous to Support Vector Machines, which also operate over a possibly infinite expansion of the input space. Also similar to Support Vector Machines, we were able to develop efficient learning algorithms for OHM classifiers using convex optimization. Despite these similarities SVM and OHM are fundamentally different classifiers. SVMs produces a classifier where a test point is classified based on the sum of relationships to a subset of the training samples, whereas OHM predicts a test point based on its relationship to a single exemplar within a subset of training samples. This leads to a classifier that is easier to understand and implement than SVMs. An article describing OHM and its comparison to SVMs was submitted to the Journal or Mathematical Imaging and Vision [7]. In Figure 2 we compare the performance on a synthetic test set where we observe OHM has superior performance over CART, especially in high dimensions.

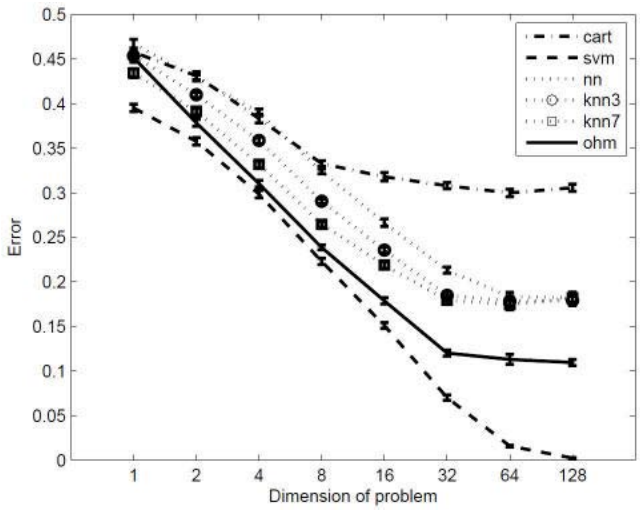

Figure 2. A comparison of OHM to CART, SVM and Nearest Neighbor methods as dimension increases highlights the strengths of the approach in high dimensions compared to traditional decision tree learning algorithms.

In summary, applying the Stack Filter model class to classification problems provides a new way to understand how representation, estimation and computation errors can be controlled for decision tree classifiers. This framework increases the size of the model class (reducing representation error), provides a way to control the complexity of the model class (reducing estimation error) and provides efficient convex optimization based learning algorithms (reducing computation error). Our most recent publication on this topic (to be published) describes how this framework can also be applied to other Pattern Recognition design problems including Neyman Pearson and Multiclass learn-

ing objectives [8].

Real World User Environments

In the standard pattern recognition problem we attempt to build a model that relates observed data X to a categorical variable Y ϵ {a, b, c, d, ... } that encodes high-level information. This approach typically requires a user during the design phase to provide training data, which consists of known examples of {X, Y} pairs. While this leads to a clear problem statement for the pattern recognition system, it is often not a good match to the practical user environments where pattern recognition systems are used. Our second objective was to investigate and develop new problem statements for pattern recognition systems that better match user environments. We investigated and developed problem statements for Query-By-Example as well as a new variation of anomaly detection called Rare Category Detection. Together, these problem statements show how pattern recognition systems can be used to build interactive data exploitation systems for real-world problems. These accomplishments are described in more detail in the next few paragraphs.

Query-By-Example

In many applications a user is less interested in carefully labeling training samples (by providing {X, Y} pairs), as they are in providing examples of the content of interest (Examples = {X, X,... }) and having the system return similar examples (Results = {X, X, ... }). This is known as Query-By-Example and it is a widely used in information retrieval systems. In this project we developed a new similarity measure, which quantifies the relative concentration of the query image distribution to the input image distribution, and allows us to employ our previously developed computationally efficient pattern recognition methods to this problem. This work was presented at the Asilomar Conference on Signals, Systems & Computers in 2009 [9] where we applied the technique to a content-based search problem in image data. An example result is shown in Figure 3.

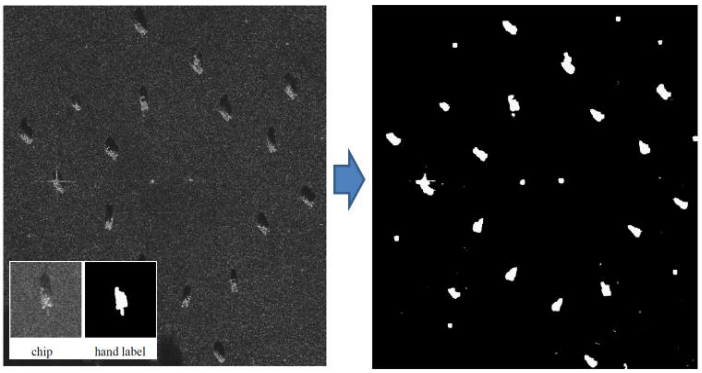

Figure 3. An example of content based search using our pattern recognition approach. The chip on the left is an example of the images used as a query example. The image on the right shows the output from the system which highlights where the match was strongest.

Rare Category Detection

In other real-world applications, we are less interested in learning a model of the data as we are in learning a sampling strategy that minimizes the number of samples required to observe at least one example from each category: {a, b, c, d, ...}. Unlike the traditional pattern recognition objective, which attempts to identify all categories as accurately as possible, this objective produces models that bring new categories of information to the user's attention as quickly as possible. The objective assumes once users are shown a new category, they will do the rest: either discount the information as uninteresting, or initiate follow up analysis. We call this new problem statement Rare Category Detection (RCD).

We presented this new learning objective and quantified its performance in [10] using an astronomical dataset containing seven categories of objects shown in Figure 4. The plots show the number of examples a user must inspect to discover these rare categories, and directly optimizing for a user-in-the-loop produces an order of magnitude less work for the user.

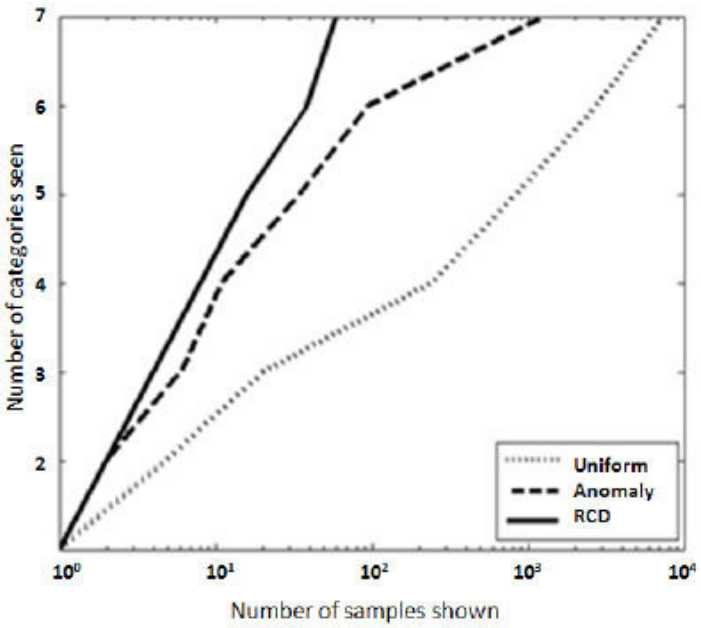

Figure 4. An comparison of the Rare Category Detection design criteria compared to uniform sampling and standard anomaly detection shows how user productivity can be improved by over an order of magnitude.

Impact on National Missions

Advancing the state-of-the-art in pattern recognition will provide an ability to digest and analyze orders of magnitude more data than we currently can, and vastly reduce data storage and exploitation costs. This project uniquely obtains these performance improvements by increasing the productivity of users in practical data analysis environments. By equipping users with pattern recognition tools they can understand and apply with confidence to tedious

and labor intensive tasks, this project provides users with more time to concentrate on the more subtle and difficult data interpretation tasks.

This project supports the NNSA mission in Nonproliferation by increasing our understanding and improving performance of mission critical pattern recognition systems used, for example, in the identification and classification of proliferation signatures in satellite imagery and video. This application was the topic of a recently published IEEE Signal Processing Magazine article, which was developed under this project to better highlight the practical applications of our work [11].

Finally, this project also supports the Department of Homeland Security (DHS) needs in nuclear forensics, for example, by providing computational tools to assist knowledge capture and knowledge management of the nuclear fuel cycle. This is the topic of a three-year DHS project "Knowledge Capture Tool Kit for Forensic Signatures Using Nuclear Material Images" which was based on technical progress made during this project.

References

1. Blanchard, G., C. Schafer, and Y. Rozenholc. Optimal dyadic decision trees. 72. *Machine Learning.* **66** (2-3): 209.

2. Astola, J., and P. Kuosmanen. Fundementals of nonlinear digital filtering. 1997. In *Fundementals of nonlinear digital filtering.* By Astola, J., and P. Kuosmanen. , p. 1. New York: CRC.

3. Quinlan, J. R.. C4.5: Programs for machine learning. 1993.

4. Breiman, L., J. Friedman, R. Olshen, and C. Stone. Classification and Regression Trees. 1984.

5. Hush, D., and R. Porter. Algorithms for optimial dyadic decision trees. 2010. *Machine Learning.* **80** (1): 85.

6. Porter, R., B. Zimmer, and D. Hush. Stack Filter Classifiers. 2009. In *9th International Symposium on Mathematical Morphology and Its Application to Signal and Image Processing .* (Groningen, The Netherlands, 2-4 July). , p. 282. Berlin: Springer-Verlag.

7. Zimmer, B., D. Hush, and R. Porter. Ordered Hypothesis Machines. *Journal of Mathematical Imaging and Vision.*

8. Porter, R., D. Hush, and B. Zimmer. New loss functions for ordered hypothesis machines. Presented at *SPIE Electronic Imaging .* (San Francisco, 23-27 Jan. 2011).

9. Porter, R., C. Ruggiero, and D. Hush. Density-based similarity measures for content based search. 2009. In *Proceedings of the 43rd Asilomar conference on Signals, systems and computers .* (Pacific Grove, California, 2-5 Nov. 2009). , p. 390. New Jersey: IEEE.

10. Porter, R., D. Hush, N. Harvey, and J. Theiler. Toward interactive search in remote sensing imagery. 2010. In *Visual Analytics for Homeland Defense and Security II, Proceedings of the SPIE.* (Orlando, March 2010). , p. Proceedings of the SPIE. Orlando: SPIE.

11. Porter, R., A. Fraser, and D. Hush. Narrowing the semantic gap in wide-area motion imagery. 020. *IEEE Signal Processing Magazine.* **27** (5): 56.

Publications

Hush, D., and R. Porter. Algorithms for Optimal Dyadic Decision Trees. 2010. *Machine Learning Research.* **80** (1): 85.

Porter, R., A. Fraser, and D. Hush. Narrowing the semantic gap in wide area motion imagery. 2010. *IEEE Signal Processing Magazine.* **27** (5): 56.

Porter, R., B. G. Zimmer, and D. Hush. Stack Filter Classifiers. 2009. In *International Symposium on Mathematical Morphology.* (Groningen, The Netherlands, 24-27 August). , p. 282. Berlin: Springer.

Porter, R., C. Ruggiero, and D. Hush. Density-based similarity measures for content based search. 2010. In *Asilomar Conference on Signals, Systems, and Computers .* (Pacific Grive, CA, 1-4 Nov). , p. 390. Ca: IEEE.

Porter, R., C. Ruggiero, and J. D. Morrison. A Framework for Activity Detection in Wide-Area Motion Imagery. 2009. In *Visual Information Processing XVIII, Proceedings of the SPIE.* (Orlando, Florida, 10 March). , p. 73410O. Orlando: SPIE.

Porter, R., D. Hush, N. Harvey, and J. Theiler. Toward interactive search in remote sensing imagery. 2010. In *Proceedings of SPIE.* (Orlando, , March, 2010). , p. 1. Orlando: SPIE.

Porter, R., D. Hush, and B. Zimmer. New loss functions for ordered hypothesis machines. Presented at *SPIE Electronic Imaging.* (San Francisco, 23-27 Jan. 2011).

Zimmer, B., D. Hush, and R. Porter. Ordered Hypothesis Machines. *Journal of Mathematical Imaging and Vision.*

Multilevel Adaptive Sampling for Multiscale Inverse Problems

John D. Moulton
20080300ER

Abstract

Characterizing uncertainty in physical systems, based only on limited and indirect data, is critical to applications such as groundwater management, contaminant remediation, and tomographic screening. Statistical inference, through the Bayesian framework, provides a solid theoretical foundation for this analysis. However, this approach characterizes uncertainty indirectly by sampling the posterior distribution. This sampling is computationally intensive for the high-dimensional problems typical of multiscale applications. In particular, each sample from the posterior requires many runs of the forward model. As a result this analysis is often restricted to linearized and over simplified models, reducing its relevance and applicability.

In contrast, efficient multilevel solvers have been developed for a broad range of realistic problems. We leverage key concepts used in these solvers to develop multilevel sampling techniques. Specifically, we considered Electrical Impedance Tomography (EIT) as a canonical inverse problem. Here the model, or forward map, is diffusion. In the heterogeneous media of interest to tomographic applications, diffusion is a challenging multiscale process. Using concepts from multilevel solvers we developed samplers that use approximations of the forward model to accelerate exploration of the posterior distribution. In addition, we developed adaptive sampling algorithms that built on differential evolution. We established a theoretical foundation for this adaptive extension. This research has advanced the efficiency of these methods, making them a more practical and viable tool.

We used our experience and results from this research to successfully compete for funding in two proposals. In addition, we attracted a new postdoc to continue this work in multilevel methods for uncertainty quantification.

Background and Research Objectives

Statistical inference, through the Bayesian framework, provides a powerful approach to characterizing the solution of inverse problems. The canonical inverse problem that we focus on is electrical impedance tomography (EIT). The goal of EIT is to recover the spatially varying electrical conductivity of an object from measurements of the voltage and current on its boundary. The mathematical model that maps the state (e.g., conductivity) to the measured data (e.g., voltage and current) is called the forward model. The multiscale nature of the diffusion process described by this forward model makes advances here relevant to a wide variety of applications. In the Bayesian framework, solving the inverse problem corresponds to quantifying statistics about the posterior distribution of the state (e.g., conductivities) conditioned on the measurements. Although this method is very flexible, the calculation of statistics over the posterior distribution is typically done through Monte Carlo sampling. This sampling is a computational burden for complex multiscale forward models. To avoid this burden applications often restrict their analysis to simplified forward models, in turn limiting the utility of their analysis.

The multiscale nature of the forward model in EIT has been addressed in robust multilevel solvers. However, the potential synergy of multilevel solvers with Monte Carlo sampling has been overlooked. These solvers achieve optimal algorithmic scaling by combining coarse-scale corrections with a simple smoothing iteration. The accuracy of the coarse-scale models is critical to this optimal scaling. The best coarse-scale models are derived with general multiscale concepts, such as variational coarsening. The objective of this work was to build on these multiscale concepts to drive the development of new efficient multilevel sampling algorithms. To this end we first targeted approximations in the forward map, with sampling of the isotropic fine-scale conductivity. In this work it became clear that sampling the more general anisotropic problem that arises on coarser scales was necessary to develop a multilevel sampler for EIT. In addition, the efficiency of sampling at each level is important to overall performance. This is challenging because the posterior distribution is high dimensional and may be multi-modal. To address this need we developed adaptive sampling strategies. Based on concepts of differential evolution, these new methods evolve multiple

chains simultaneously, and hence, are inherently parallel. We established a theoretical foundation for these algorithms.

Scientific Approach and Accomplishments

In this work we consider steady-state EIT as a canonical inverse problem in which the forward map is multiscale diffusion. Here, the problem is to recover the spatially-dependent conductivity inside an object given data on its boundary. The data is the voltage that is measured on the boundary for a prescribed pattern of boundary currents. In the Bayesian framework the solution is described by the statistics of the posterior distribution. We draw samples from the posterior using a Markov chain Monte Carlo (MCMC) procedure. Then we calculate statistics over the posterior with these samples. This indirect approach only requires the simulation of the forward map. However, due to the high cost of the forward model many practitioners do not consider the full Bayes formulation. Instead their analysis is limited to computing the maximum a posterior (MAP) estimate, or they consider a linearized forward model. The goal of this research is to design adaptive multilevel sampling techniques that facilitate the efficient analysis of the full forward model. These techniques will impact the broad class of problems with complex multiscale forward models.

We consider a stylized EIT problem on a two-dimensional square domain. We use an orthogonal grid to discretize the forward map with bilinear finite elements. An isotropic (scalar) conductivity representing the true state is discretized on the same grid. To establish a baseline for comparison with more complex MCMC methods, we use a single-site Metropolis MCMC sampler. Both binary and gray-scale proposal distributions were used. With this well known method we computed a set of samples drawn from the high-dimensional multimodal posterior distribution. Also, we computed various measures of efficiency. Next we explored techniques that use components of a multilevel solver (e.g., multigrid) in the sampler. Specifically, we focused on two modified sampling strategies that support the use of approximations in the forward model. These were the delayed acceptance Metropolis-Hastings [1,2] and an augmented posterior sampler [3]. In both cases, the forward map was approximated by limiting the number of V-cycles in the black box multigrid (BoxMG) solver [4], and significantly reduced the computational cost of the solution.

However, in these advanced methods sampling and approximation are still driven at the finest scale. This design leads to a fixed speedup, and not the algorithmic scalability needed for large three-dimensional inverse problems. To obtain scalability we need to integrate key concepts from multilevel solvers (e.g., multigrid) directly into an adaptive multilevel sampler. A key challenge in this integration is that at coarser scales the conductivity may be anisotropic. Specifically, in most EIT applications we seek to recover the spatially dependent isotropic (scalar) conductivity. Of particular interest is the recovery of fine-scale spatial structures, such as inclusions or layers. However, accurately capturing the influence of these fine-scale structures on the coarse-scale solution requires an anisotropic (full tensor) conductivity. The forward model for EIT with an anisotropic conductivity is well developed. The corresponding multilevel solution algorithms are well developed also. But the solution of this more general inverse problem may be unique only up to a coordinate transformation.

Fortunately, the discrete representation of the forward map is unique. To explore the potential of sampling this discrete form, we used BoxMG to coarsen the set of forward maps that we created earlier. At the fine-scale this set is described by the multi-modal posterior distribution. With BoxMG we generated probability distributions for both the stencil weights and the anisotropic conductivities at coarser scales. These distributions showed a rapid decrease in multi-modality, becoming uni-modal at coarser scales. Thus, the posterior distribution is much easier to sample at coarser scales. In addition, the computational cost of each forward model simulation is considerably less at coarser scales. These facts motivate building the posterior up from coarser scales in pursuit of a scalable algorithm for three-dimensional problems.

We have made progress on a multilevel sampling method that builds posterior distributions from the coarse scale to the finest scale. The critical step is efficiently sampling the general coarse-scale anisotropic problem [5]. There are two fundamental challenges in this coarse-scale problem. First, the data is unresolved, raising questions of how best to coarsen it in the absence of fine-scale conductivity information. In our current work we use the standard bilinear basis functions. This weighting is consistent with homogenization approaches. The second challenge is addressing the issue of non-uniqueness. Here we take advantage of the fine-scale problem being isotropic, and the coordinate system being fixed. In addition, we sample the eigenvalues and rotation angle of the tensor. As an alternative we plan to consider the direct sampling of the weights in the discrete forward map. Note that both samplers admit the most general model to ensure that the information we obtain may be interpreted at finer scales. To refine this solution we will use a hierarchical view of the forward map that is motivated by the coarsening in the BoxMG multigrid method. Repeating the refinement and sampling process will lead to a scalable algorithm.

During this work we found increasing interest in leveraging multilevel concepts in uncertainty quantification. In some cases, the problems involved parameters whose representation across scales was amenable to simple averaging and interpolation techniques. In these cases, the use of simulations with varying fidelity is more readily used to accelerate the solution of inverse problems. For example, dark matter simulations at multiple resolutions were used to

help estimate cosmological parameters in [6]. This encouraged us to explore other aspects of multilevel sampling while we were developing the coarse-scale EIT sampler. In particular, we extended the concepts used in the t-walk sampler, to a two-level setting. Here recursion naturally leads to a multilevel sampler. The t-walk [7] is in some ways related to DREAM, but is motivated by a principle of invariance not adaptivity. The t-walk uses two chains, with each sampling from the same distribution. It uses the current value from one chain to propose a new value for the other chain. This allows each chain to make larger moves from sample to sample, reducing the correlation between successive samples and decreasing Monte Carlo variance. Our extension uses the current sample from the coarse model to propose a new sample from the fine model, and vice versa. Thus we reduce the number of evaluations of the costly fine model we need. This framework is applicable to the EIT problem, once the more complex maps between resolutions for conductivity proposals are developed.

Significant progress on adaptive techniques for MCMC sampling has been made as well. This aspect of sampling is key to the efficiency at each level of the multilevel sampler, as well as its overall efficiency. In recent work we showed that the efficiency of MCMC sampling could be improved using a self-adaptive Differential Evolution learning strategy within a population based evolutionary framework. This scheme is dubbed DiffeRential Evolution Adaptive Metropolis or DREAM. For global exploration it runs multiple different chains at the same time. Also, DREAM automatically tunes the scale and orientation of the proposal distribution during the search. We have proved the ergodicity of DREAM [8]. Using tests with nonlinearity and multi-modality we showed that DREAM is generally better than other adaptive MCMC sampling approaches. However, DREAM requires the number of chains to be greater than half the number of parameters. This trait is undesirable for high-dimensional problems, as each chain must evolve to the target distribution (burn in). Recent research led to a modification of Differential Evolution strategies that reduces the number of chains to three [9], has now been extended to DREAM [10]. Thus, increasing its flexibility and practical applicability. In addition, we adapted the DREAM algorithm to handle dynamical models in which sequential Monte Carlo methods, such as the particle filter, are appropriate. Here the DREAM sampler effectively reduced the number of particles required. This approach is particularly useful in accounting for model uncertainty under the Bayesian paradigm.

Impact on National Missions

For decision making a description of the uncertainty of the system state (e.g., contaminant plume boundary) is required, as opposed to a single "best estimate", because decisions must account for a realistic range of plausible states. Although methods in statistical inference provide a solid foundation for this analysis, they are too slow for large systems. This research advanced the efficiency of these methods, making them a more viable tool. The areas of impact include the calculation of weather patterns, describing the subsurface environment, and medical imaging. This work is relevant to missions in DOE and other government agencies, such as nuclear weapons diagnostics and climate modeling.

This research was critical in establishing new directions for one of our core projects under the Advanced Scientific Computing Research (ASCR) program in the DOE Office of Science. This project is titled "Predictability with Stochastic Partial Differential Equations" and it is focused on sensitivity analysis and uncertainty quantification. We built on our successful work on adaptive MCMC samplers, such as DREAM, and multi-resolution forward models to propose new research in sample-based Uncertainty Quantification (UQ) techniques. This core project was renewed for the next three-year funding cycle. In addition, a new program from DOE's Office of Environmental Management was developed last year. This project is titled the Advanced Simulation Capability for Environmental Management (ASCEM). It is a multi-lab project to develop a state-of-the-art tool and approach for understanding and predicting contaminant fate and transport in natural and engineered systems. This tool will then be used for standardized assessments of performance and risk in Environmental Management's cleanup and closure activities across the DOE complex. This research provided critical knowledge and experience that we used to develop our role and funding profile in this large project. ASCEM is a significant programmatic effort and is likely to run for five to ten years.

These projects enabled us to attract a new postdoc to continue our research in this growing area of multilevel methods for uncertainty quantification.

References

1. Christen, J. A., and C. Fox. Markov chain Monte Carlo using an approximation. 2005. *Journal of Computational and Graphical Statistics.* **14** (4): 795.

2. Moulton, J. D., C. Fox, and D. Svyatskiy. Multilevel approximations in sample-based inversion of the Dirichlet-to-Neumann map. 2008. *Journal of Physics: Conference Series.* **124**: 012035.

3. Higdon, D., C. S. Reese, J. D. Moulton, J. A. Vrugt, and C. Fox. Posterior exploration for computationally intensive forward models. To appear in *Handbook of Markov chain Monte Carlo: methods and applications.* Edited by Gelman, A., G. Jones, and X. L. Meng.

4. Dendy, J. E.. Black Box Multigrid. 1982. *Journal of Computational Physics.* **48**: 366.

5. Moulton, J. D., D. Higdon, and T. L. Graves. Characterizing coarse-scale anisotropy in the Dirichlet-to-Neumann map. 2010. *In preparation.*

6. Lawrence, E., K. Heitmann, M. White, D. Higdon, C. Wagner, S. Habib, and B. Williams. The Coyote Universe III: simulation suite and precision emulator for the nonlinear matter power spectrum. 2010. *Astrophysical Journal.* **713** (2): 1322.

7. Christen, J. A., and C. Fox. A general purpose sampling algorithm for continuous distributions (the t-walk) . 2010. *Bayesian Analysis.* **5** (2): 263.

8. Vrugt, J. A., C. J. F. terBraak, C. G. H. Diks, D. Higdon, B. A. Robinson, and J. M. Hyman. Accelerating Markov chain Monte Carlo simulation from self adaptive differential evolution with randomized subspace sampling. 2009. *International Journal of Nonlinear Sciences and Numerical Simulation.* **10** (3): 273.

9. terBraak, C. J.F., and J. A. Vrugt. Differential evolution Markov chain with snooker updater and fewer chains. 2008. *Statistics and Computing.* **18** (4): 435.

10. Vrugt, J. A., C. J. F. terBraak, and J. M. Hyman. Differential evolution adaptive metropolis with sampling from past states. 2010. *In preparation..*

Publications

Braak, C. J. ter, and J. A. Vrugt. Differential evolution Markov chain with snooker updater and fewer chains. 2008. *Statistics and Computing.* **18** (4): 435.

Higdon, D., C. S. Reese, J. D. Moulton, J. A. Vrugt, and C. Fox. Posterior exploration for computationally intensive forward models. To appear in *Handbook of Markov chain Monte Carlo: methods and applications.* Edited by Gelman, A., G. Jones, and X. L. Meng.

Moulton, J. D., C. Fox, and D. Svyatskiy. Multilevel approximations in sample-based inversion of the Dirichlet-to-Neumann map. 2008. *Journal of Physics: Conference Series.* **124**: 012035.

Moulton, J. D., D. Higdon, and T. L. Graves. Characterizing coarse-scale anisotropy in the Dirichlet-to-Neumann map. 2010. *In Preparation.*

Rings, J., J. A. Vrugt, G. H. W. Schoups, J. A. Huisman, and H. Vereecken. Bayesian model averaging using ensemble particle filtering and Gaussian mixture modeling. 2010. *In preparation.*

Vrugt, J. A., C. J. F. terBraak, and J. M. Hyman. Differential evolution adaptive metropolis with sampling from past states. 2010. *In preparation.*

Vrugt, J. A., C. J. F. terBraak, C. G. H. Diks, D. Higdon, B. A. Robinson, and J. M. Hyman. Accelerating Markov chain Monte Carlo simulation from self adaptive differential evolution with randomized subspace sampling. 2009. *International Journal of Nonlinear Sciences and Numerical Simulation.* **10** (3): 273.

Adaptive Algorithms for Inverse Problems in Imaging

Brendt E. Wohlberg
20080341ER

Abstract

This project proposed a geometric framework within which it is possible to understand a very important recent class of approaches to modeling image (and other) data for performing inverse problems such as removal of noise and blur, and resolution enhancement. Instead of constructing models by mathematical analysis, which can not be expected to deliver accurate models for very complex data, the model is learned from example data itself. Research on this project has addressed a variety of issues, including the central problem of constructing a geometric framework within which the diverse existing methods can be understood, and improvements in specific application areas. The project has produced a number of conference and journal publications, with further publications under review or in preparation, an open source software distribution in support of some of the published work, and collaborations with leading external researchers, which is expected to lead to further funding to pursue this extremely promising approach to modeling image data for inverse problems.

Background and Research Objectives

Image data are ubiquitous, occurring in such diverse fields as experimental physics, biology, geosciences, nonproliferation surveillance, and medical diagnosis. The family of problems including denoising, blur removal, resolution enhancement, and inpainting represent an important part of the analysis of such data. Solving such problems effectively requires some form of model of the data so that it can be distinguished from the degradation to be removed. These models are usually simplified representations designed by mathematical analysis, and cannot accurately represent all of the properties of complex data, such as images of natural scenes, radiological images, etc. In this project, in contrast, we learn appropriate data models from large sets of examples of the problem domain data, promising more accurate reconstructions and also the ability to adapt to new types of data (e.g. from a specialized scientific instrument), with unusual properties that are not compatible with the assumptions made by standard approaches for these kinds of problem. The general approach is motivated by a geometric view of the problem, distinguishing between the full space of all data that can possibly be represented, and the much smaller space (or "manifold") of uncorrupted example data. Within this view, the desired reconstruction is achieved by finding a representation, which is close both to the measured data and the space of uncorrupted data. The objective of this project has been to construct principled methods of applying this geometric view in practical image reconstruction problems.

Scientific Approach and Accomplishments

The research goals and accomplishments may be divided into a number of distinct categories:

The Manifold Model and Theoretical Issues

While there has been a very rapid growth in the literature on exemplar-based methods over the previous few years, the vast majority of authors have concentrated on specific applications, rather than constructing a coherent geometric view of the approach, one of the goals of this project. The notable exception [1] has independently proposed the manifold model associated with this project, but with a focus on analytically known manifolds, and without serious consideration of the different methods required when the manifold is known only from a discrete set of data points, which is one of the primary questions addressed by this project. Aspects of this problem, such as estimating local manifold properties from sampled data, have proved to be significantly more difficult than originally envisaged. Nevertheless, while overall progress on this central problem has been disappointing, very recent theoretical advances [2] offer the potential for significant future progress. Accomplishments have been as follows:

- A number of diverse methods widely used for exemplar-based approaches can be posed and understood within the proposed geometric view. Furthermore, some aspects of the relative performance of these methods can be explained by this view, and some interesting issues have been discovered by computational experiment. Results have been presented at

two SIAM Imaging Science conferences, and a journal paper is currently in preparation.

- One of the most significant problems in a principled approach to exploiting the geometric view of exemplar-based methods is in estimating the local manifold curvature, which is critical in determining how many neighboring points to utilize in solving the inverse problem. (The intuition is as follows: if the manifold is almost flat, one can obtain a better estimate by considering other samples at some distance from the working point, but when there is significant curvature, distant points reduce the accuracy of a local tangent estimate.) Recent work by Maggioni *et. al.* [2], aimed at estimating the local dimensionality of a set of points sampled from a manifold, may be exploited to give the required curvature estimate. This research,in collaboration with a summer student (now returned to University of Colorado at Boulder) and his PhD adviser (Francois Meyer), is ongoing, and is expected to lead to a number of publications. Discussion is also in progress on obtaining funding for further work on this aspect of the problem, and a proposal is expected to be submitted next year.

Applications

The problem of inpainting (filling in missing areas in an image with visually feasible content) was selected as an application area to demonstrate the value of the proposed approach. A new algorithm offering performance competitive with the state of the art has been developed, the details of which have been presented at a major conference, and have recently been submitted as a journal paper. (An example of the performance of this algorithm is presented in Figures 1 and 2.) There are ongoing collaborations in this area with Francois Meyer (University of Colorado) and Denis Simakov (previously at the Weizmann Institute).

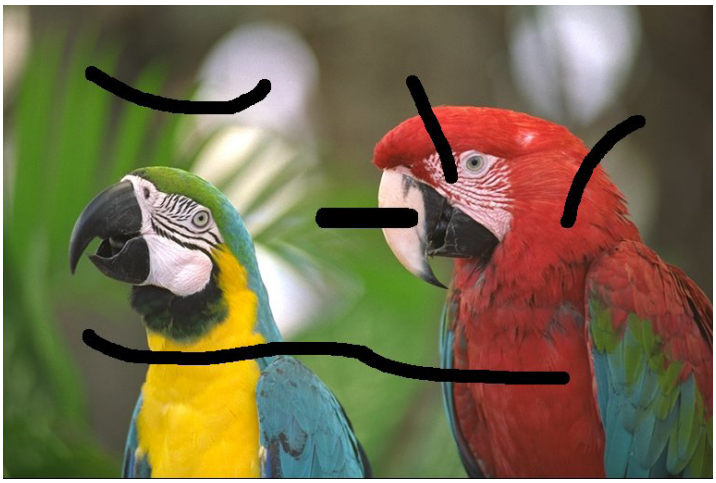

Figure 1. Inpainting test image.

Figure 2. Image inpainted by the LANL method.

Auxiliary Problems and Related Methods

Some research effort has also been directed towards important problems which play a supporting role with respect to the main goals, including efficient nearest neighbor search algorithms for identifying nearby samples in large sets of vector data (a manuscript is in preparation), optimal parameter selection in regularization methods (a conference paper and a journal paper have been published), and regularization methods for inverse problems such as denoising and deblurring (three conference papers and one journal paper have been published).

Software

An open source software distribution containing Matlab code implementing many of the algorithms developed during this project is available, and an updated version reflecting recent developments will be released shortly.

Impact on National Missions

Image and related data play an important role of a number of DOE missions, including Nuclear Weapons (e.g., proton radiography of dynamics experiments) and Threat Reduction (e.g. satellite and airborne imagery). Such data also plays an important role in surveillance and reconnaissance, space science (e.g. astronomical imagery), medical and bioscience (e.g. diagnostic imagery), and has potential applications in numerous other fields. Advances in the analysis, including restoration and other inverse problems, of such data clearly advance the ability to extract useful information. This project has not yet had any immediately measurable impact on these missions, but is expected to do so via its contribution to algorithms for imaging inverse problems, in areas such as those listed above.

References

1. Peyre, G.. Manifold models for signals and images. 2009. *COMPUTER VISION AND IMAGE UNDERSTANDING.* **113** (2): 249.

2. Little, A. V., J. Lee, Yoon-Mo Jung, and M. Maggioni. Estimation of intrinsic dimensionality of samples from noisy low-dimensional manifolds in high dimensions with multiscale SVD. 2009. In *2009 IEEE/SP 15th Workshop on Statistical Signal Processing (SSP) ; 31 Aug.* (-3 Sept. 2009 ; Cardiff, UK). , p. 85.

Publications

Lin, Y., B. Wohlberg, and H. Guo. UPRE method for total variation parameter selection. 2010. *Signal Processing.* **90** (8): 2546.

Lin, Y., and B. Wohlberg. Application of the UPRE method to optimal parameter selection for large scale regularization problems. 2008. In *IEEE Southwest Symposium on Image Analysis and Interpretation.* (Santa Fe, NM, 24 - 26 Mar. 2008). , p. 89. New York: IEEE.

Rodriguez, P., and B. Wohlberg. Efficient Minimization Method for a Generalized Total Variation Functional. 2009. *IEEE Transactions on Image Processing.* **18** (2): 322.

Rodriguez, P., and B. Wohlberg. A Generalized Vector-Valued Total Variation Algorithm. Presented at *IEEE International Conference on Image Processing.* (Cairo, Egypt, 7 - 10 Nov. 2009).

Rodriguez, P., and B. Wohlberg. An Efficient Algorithm for Sparse Representations with lp Data Fidelity Term. Presented at *Proceedings of 4th IEEE Andean Technical Conference (ANDESCON).* (Cusco, Peru, 15-17 Oct. 2008).

Wohlberg, B.. Inpainting with sparse linear combinations of exemplars. 2009. In *International Conference on Acoustics, Speech, and Signal Processing.* (Taipei, Taiwan, 19 - 24 Apr. 2009). , p. 689. Piscataway, NJ: IEEE.

Wohlberg, B.. Inpainting by Joint Optimization of Linear Combinations of Exemplars. 2010. *Submitted to IEEE Signal Processing Letters.*

Wohlberg, B., and P. Rodriguez. An l1-TV algorithm for deconvolution with salt and pepper noise. 2009. In *International Conference on Acoustics, Speech, and Signal Processing.* (Taipei, Taiwan, 19 - 24 Apr. 2009). , p. 1257. Piscataway, NJ: IEEE.

Designing Communication Methods for Bottom-Up Self-Assembled Nanowire Networks of Emerging Computer Architectures

Hsing-Lin Wang
20080380ER

Abstract

Our goal is to engineer novel computer architectures based on self-assembled nanocomponents through an integrated experimental, simulation-based, and theoretical approach. The bottom-up (self-assembled) approach is fabrication-friendly, cheaper, and would eventually scale up to more complex systems compared to today's top-down (fabrication) designs. We adopt a network and system-on-chip-based approach and focus on the interconnect challenge because interconnects have become more important than the transistors as a limiting factor of performance on modern chips. The challenges we address are: 1) master the particular technology of self-assembling conductive silver nanowires that densely interconnect traditional silicon components, 2) develop appropriate schemes that will allow reliable communication in such an irregular, heterogeneous, and unreliable network, and 3) implement new computing paradigms in random nano-wire networks. The research is guided by the following main questions: 1) What connectivity graphs can we obtain, and what are the control parameters for the self-assembly process? 2) How can we reliably and efficiently communicate in such irregular networks, given a set of limited resources and a lack of global information and connectivity? and 3) How can we develop and implement an adaptive learning algorithm for pattern classification in a self-assembled nanowire circuit?

Background and Research Objectives

After more than 30 years of exponential computing power growth under Moore's law, sequential computing as we know it is now finally hitting a wall. The raw number of transistors cannot simply be turned into effectively usable computing power anymore, which has led chip manufacturers into offering multiple cores on one chip since that is essentially the main path to still reach more performance without fundamental architectural changes and new paradigms. While the growth in the number of cores per chip is expected to continue in the next few years, we are interested in the next generation technologies that would enable the research community to go beyond Moore's law. However, there is a lack of consensus on what type of technology and computing architecture holds most promises to keep up the current pace of progress. To avoid the increasing difficulties (e.g., due to economical limits, reliability, complexity of the design process, etc.) of today's top-down manufacturing process and the ongoing technology scaling towards atomic dimensions, molecular self-assembly is often mentioned as the holy grail of nanotechnology, which would allow to easily and cheaply build systems of enormous complexity, involving Avogadro numbers (6.10^23) of simple components. The grand challenge consists in using this functional and structural complexity for performing efficient communication and computations. If successful, we could expect a quantum leap in performance compared to today's traditional computing machines. However, bottom-up self-assembly processes commonly produce highly unreliable, irregular, and heterogeneous assemblies, thus the need for alternative, robust, and decentralized communication and computer architectures. In recent years, the importance of interconnects on electronic chips has outrun the importance of transistors as a dominant factor of performance [1,2]. The reasons are twofold: 1) the transistor switching speed for traditional silicon is much faster than the average wire delays and 2) the required chip area for interconnects has dramatically increased. The ITRS semiconductor roadmaps [3] list a number of critical challenges for interconnects and states that "it is now widely conceded that technology alone cannot solve the on-chip global interconnect problem with current design methodologies." In this proposal, we solely focus on the interconnect networks by combining experiments, theory, and simulations. We adopt a system- and network-on-chip approach [4], which has been shown to be a promising solution to go around current interconnect limitations.

Background and Related Work

The common approach for nano-scale electronics consists in trying to fabricate as regular and as perfect structures as possible, such as crossbars [5] or other array-like structures [6], which is inherently difficult. Little work exists that takes into account the typical irregular ar-

rangement of bottom-up self-assembled structures. On the other hand, Tour et al. [7] showed that it is relatively easy to compute logical functions with a random arrangement of molecular switches and interconnections. Teuscher et al. have shown [8-10] that irregularly assembled networks-on-chip with specific wire-length distributions have major advantages in terms of communication characteristics and robustness over regular and locally interconnected topologies. Here, we will use self-assembling nanowires to build complex networks in a bottom-up way. Nanowires can be grown in various ways using diverse materials, such as metals and semiconductors. We have previously demonstrated that Ag nanowires can be fabricated on top of conducting polymer membranes via a spontaneous electrodeless deposition (self-assembly) method [11,12]. Polyaniline (PANI) is one of the most promising conducting polymers for commercial applications due to its easy synthesis, a low price tag, and environmental stability. Finally, we have also addressed the challenge of using this functional and structural complexity for performing efficient computations. More specifically, we show that the self-assembled nanowire network can be used to implement a non-classical computing paradigm inspired by neuromorphic computation ideas. The network adapts to perform a specific computation task, instead of being programmed, and the system design becomes the provision of self-organizing principles.

Scientific Approach and Accomplishments

Demonstrate the growth of Ag nanowires (AgNWs) with a wide range of morphologies and characterize the electrical properties of the wires.

We have demonstrated the fabrication of AgNWs with a wide range of structure, size, and morphologies, see Figure 1. Our results show that the structure of these nanowires is dominated by the growth kinetics, which is also associated with experimental parameters such as concentration and temperature. We have also characterized their electrical properties and found that they are morphology dependent. The electrical properties of AgNWs were measured by displacing nanowire onto an interdigitated gold electrodes supported on high-resistivity silicon substrate. A perfect linear relationship between the current and voltage was found for all AgNWs as we measure the I-V responses between a low voltage range (-0.05 to 0.05 V). The electrical conductivity of a smooth AgNW with a diameter of 120 nm was 2.81 x 10^6 S/m, and that of a coarse AgNW with cubic cross-section was 1. 34 x 10^6 S/m, slightly lower than that of bulk silver (6.25 x 10^7 S/m). The electrical properties of these nanowires are crucial in defining underlying parameters of the random nanowire network.

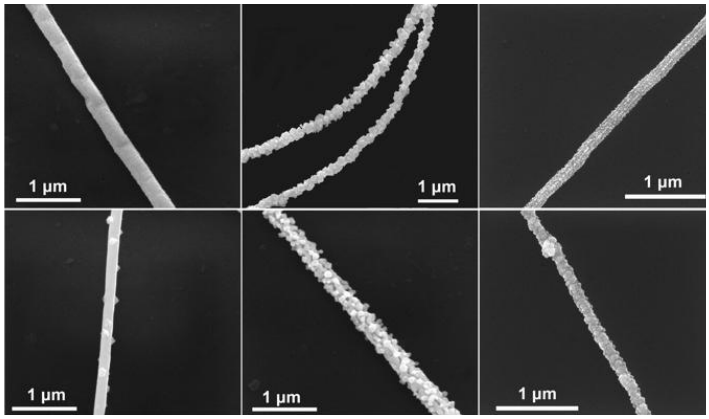

Figure 1. SEM micrographs of silver nanowires with various morphologies.

Fabrication of Au electrode on various substrates and polyaniline patterns.

A whole variety of interdigitated electrodes on glass and silicon surfaces have been prepared with different spacings between two electrodes. Of particular importance is to develop a unique procedure to fabricate interdigitated polyaniline pattern using deep reactive ion etching (RIE) method. To the best of our knowledge, this is the first time it was demonstrated that micrometer sized polyaniline patterns were prepared via RIE method. These polyaniline patterns allows us to control growth of AgNWs and induce anisotroby between two specific polyaniline structures.

The second approach we have employed was coating a thin buffer layer between the substrates and the PANI films. This buffer layer is expected to enhance the adhesion of PANI films to the substrates. A ~100 nm thick photoresist or polyimide dielectric film was spin-coated and thermal-cured on the high resistivity silicon substrate, which has been experimentally shown the capability of enhancing the adhesion of PANI films to the substrates, e.g. the PANI films survived for at least hours without the formation of any cracks or peeling off. With this enhancement of adhesion, we carried out the photolithographic patterning and RIE etching, and excellent micro-scale PANI grids were achieved, making the silver nanowire network or guided growth possible.

Chemical Synthesis of Silver nanowires using polyol synthetic route

We use a modified $CuCl_2$-mediated method to synthesize the silver nanowire. Briefly, a 5 mL of ethylene glycol, EG was preheated to 155 °C under magnetic stirring. To this, 80 µL of a 4mM copper (II) chloride dihydrate, $CuCl_2.2H_2O$ solution in EG was added. Then equal parts of a 0.094 M silver nitrate, $AgNO_3$ (99+%, Aldrich) solution in EG and a 0.376 M polyvinylpyrrolidone, PVP (MW = 55,000, Aldrich) solution in EG were mixed thoroughly and 3 mL of the mixture was quickly added to the vial. The vial was capped and the reaction was monitored by its color change. The

average reaction time was around 40 minutes. The end product is silver nanowires which were stored in water. By varying the experimental parameters, we can fine-tune the diameter and aspect ratio of the silver nanowire.

We have demonstrated the guided growth of Silver nanowire on a prefabricated polyaniline surface.

The PANI surface has physical protrusions, which allow the Ag growth along specific directions. Growth of silver nanowires across polyaniline patterns is achieved by immersing a patterned polyaniline structure into a solution of 25 mM AgNO3 solution for a period of 30 minutes. As can be seen from Figure 2, the schematic representation of the fabrication procedure of making patterned polyaniline is shown on the left and on the right of Figure 2 exhibits silver nanowires grew between the patterned polyaniline structure. Our results suggest the control growth of silver nanowires using a self-assembly method. Our results further suggest the fabrication of silver nanowire network with on a predefined patterned surface to form networks that are capable of validating our hypothesis and develop high function machine learning capability.

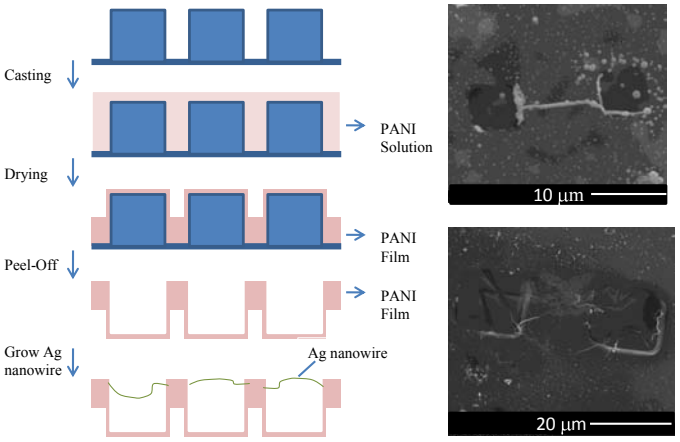

Figure 2. (left) Schematic representation of fabrication procedures making patterned polyaniline and (right) silver nanowires grows between two polyaniline patterned structures.

We have designed an online algorithm for adaptive learning in random linear networks, Figure 3.

The network represents a virtual class of input-output functions in which (supervised) learning takes place. By choosing a specific location and voltage for the control nodes one particular input-output function gets instantiated. To design and analyze pattern classification algorithms in these random networks we have performed: 1) model reduction and computation with an effective input-output function that describes exactly the behavior of the network, 2) analysis of an off-line learning algorithm for two class pattern recognition, 3) design and analysis of an on-line learning algorithm, and 4) an analysis of the class of input-output functions that these self-assembled, random networks implement that has revealed its simple mathematical structure.

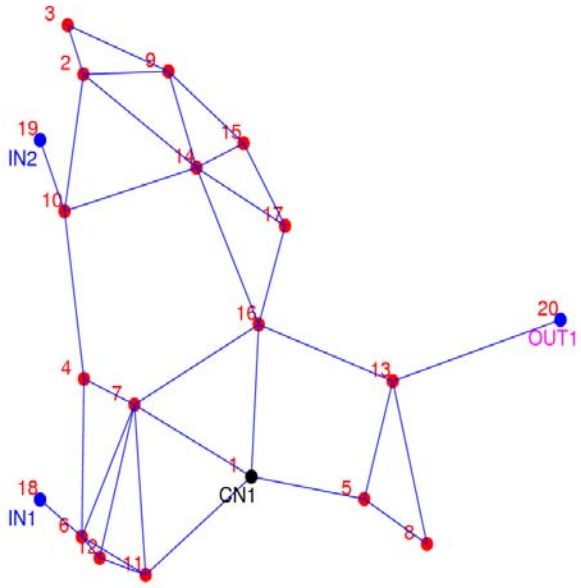

Figure 3. A random geometric network with input nodes I =[18,19], one output node O=[20], and one control node C=[1].

For example, in the absence of any control nodes, the input-output function is described by a stochastic matrix, i.e., a matrix whose rows consists of positive real numbers, with each row summing to one. This finding suggests that the random network can be used to describe the transitions of a Markov chain over a finite state space. The dimension of this space is equal to the number of input nodes while the input voltages can be chosen to represent state probabilities, see Figure 4. Furthermore, in the presence of control nodes, the input-output function is described by a stochastic matrix in which the control nodes play the role of probabilistic sources. This also suggests a generalization of the original input-output model in which a second random network can implement a stochastic model that injects prior information into the control nodes.

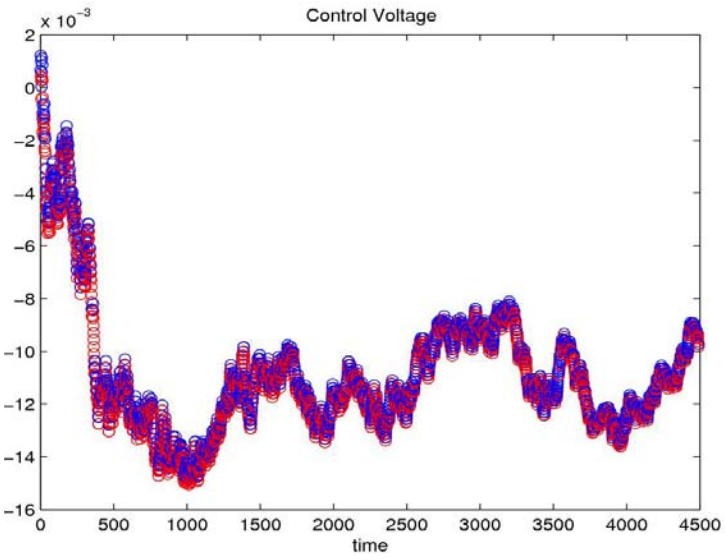

Figure 4. The on-line evolution of the control voltage (left) and separating hyperplane (right) as input examples are presented to the network (left). The optimal control voltage is 0.01.

We explored the design trade-offs of irregular, heterogeneous, and unreliable nanoscale networks.

The important measures we care about for our complex on-chip network models are the information transfer, congestion avoidance, throughput, and latency. We use two control parameters and a network model inspired by Watts and Strogatz's small-world network model to generate a large class of different networks. We then evaluated their cost and performance and introduced a function that allows us to systematically explore the trade-offs between cost and performance depending on the designer's requirement. Figure 5 shows the design space of the aggregate objective function, which combines the hops, the wire length, and the power consumption of different network topologies. We observe that the optimal network (represented by the lowest point of the surface plot) for this experiment is not a mesh but a small-world graph (with p=0.1). We further evaluated these networks under different traffic conditions and introduced an adaptive and topology-agnostic ant routing algorithm that does not require any global control and avoids network congestion.

We proposed a simple model for self-assembled networks where conducting nanowires with specific wire-length distributions are dropped randomly onto a substrate to establish contacts between computing nodes.

We evaluated various design trade-offs of such randomly assembled networks. Previous work was based on uniform wire-length distribution, and did not consider the effect of short circuits nor did it include a thorough performance and cost evaluation. The new model also considers the effect of short circuits between wires. We show that compared to previous work, our self-assembled random network model with a power-law wire-length distribution performs much better at a lower wiring cost. Furthermore, we determined the optimal number of wires to be placed on the grid to satisfy certain performance and cost constraints.

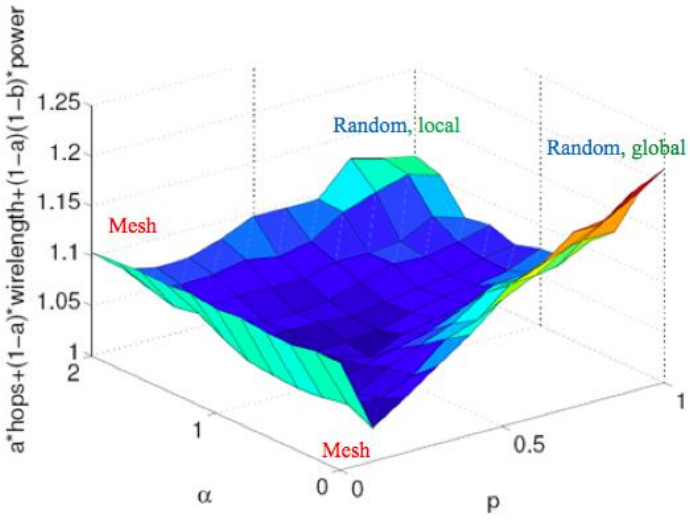

Figure 5. Aggregate objective function of different network topologies. p is the rewiring probability (according to Watts-Strogatz), alpha determines how local or global the connections are. The smaller alpha, the more local the network. We start with a regular mesh and the rewires the connections with probability p and according to the power low distribution l^(-alpha), where l is the Euclidian distance between the nodes. a and b determine what performance metrics one wants to favor.

Impact on National Missions

Bottom-up design and fabrication processes have been identified as one of the most promising methodologies to go beyond Moore's law and to continue the current pace of progress in computing power [13]. The computing power typically limited by the size of the electronic components and available real estate. We seek novel approach in fabricating nanoscaled conducting wire and we propose ways to used self-assembly (fabrication-free) method to construct extremely thin wires which form networks that will allow faster processing speed and develop machine-learning capability relates to artificial intelligence. Network science also impacts a broad mission space, including threat reduction, communication, and data mining relevant for DOE and other government agencies. This project developed science to support new computational paradigms and network communication. The science has the potential to support missions in high-performance computing, which has important implications in sensor design, to understand and eventually contain epidemic of infectious diseases, diagnosis and remote sensing. It also promotes the ability to identified threats, such as explosives and weapon of mass destruction reduction. All of the above capability developments benefit the entire mission space of DOE. Last

but not least, the project promotes the design of the next generation processors, which will benefit society at large due to the omnipresence of computers, in particular in the embedded systems domain.

References

1. Ho, R.. The Future of Wires. 2001. *Proceedings of the IEEE.* **89** (4): 490.

2. Meindl, J. D.. Interconnect Opportunities for Gigascale Integration. 2003. *IEEE Micro.* **238**: 28.

3. International Technology Roadmap for Semiconductors. 2009. *http://www.itrs.net/reports.html.*

4. Benini, L., and G. de Micheli. Networks on Chips: A new SoC Paradigm. 2002. *IEEE Computer.* **35** (1): 70.

5. Chen, Y., G. Jung, D. A. Ohlberg, X. Li, D. Stewart, J. Jeppesen, K. Nielsen, J. Fraser. Stoddart, and R. Stanley. Williams. Nanoscale molecular-switch crossbar circuits. 2003. *Nanotechnology.* **14** (4): 462.

6. DeHon, A.. Array-Based Architecture for FET-Based, Nanoscale Electronics. 2003. *IEEE Transactions on Nanotechnology.* **21**: 23.

7. Tour, J. M., W. L. Van Zandt, C. P. Husband, S. M. Husband, L. S. Wilson, P. D. Franzon, and D. P. Nackashi. Nanocell Logic Gates for Molecular Computing. 2002. *IEEE Transactions on Nanotechnology.* **1** (2): 100.

8. Teuscher, C.. Irregular Interconnect Fabrics for Self-Assembled Nanoscale Electronics, . 2006. *2nd IEEE International Workshop on Default and Fault Tolerant Nanoscale Architectures.* : 60.

9. Teuscher, C.. Small-world power-law interconnects for nanoscale computing architectures. 2006. In *2006 6th IEEE Conference on Nanotechnology, IEEE-NANO 2006 ; 20060617 - 20060620 ; Cincinnati, OH, United States.* Vol. 1, p. 379.

10. Christof, T.. Nature-inspired Interconnects for Emerging Large-Scale Network-on-Chip Designs. To appear in *Chaos.*

11. Li, W. G., Q. X. Jia, and H. L. Wang. Facile synthesis of metal nanoparticles using conducting polymer colloids. 2006. *POLYMER.* **47** (1): 23.

12. Wang, H., W. Li, Q. X. Jia, and E. Akhadov. Tailoring conducting polymer chemistry for the chemical deposition of metal particles and clusters. 2007. *CHEMISTRY OF MATERIALS.* **19** (3): 520.

13. DeHon, A., and H. Naeimi. Seven Strategies for Tolerating Highly Defective Fabrication. 2005. *IEEE Design & Test of Computers.* : 306315.

Publications

Christof, C., and A. A. Hansson. Non-traditional irregular interconnects for massive scale SoC . 2008. *Proceedings - IEEE International Symposium on Circuits and Systems.* : 2785.

Ganguly, A., K. Chang, S. Deb, P. P. Pande, B. Belzer, and C. Teuscher. Scalable Hybrid Wireless Network-on-Chip Architectures for Multi-Core Systems. To appear in *IEEE Transactions on Computers.*

Gao, Y., C. Chen, H. Gau, J. Bailey, E. Akhadov, D. Williams, and H. Wang. Facile synthesis of polyaniline-supported Pd nanoparticles and their catalytic properties toward selective hydrogenation of alkynes and cinnamaldehyde. 2008. *CHEMISTRY OF MATERIALS.* **20** (8): 2839.

Jeon, S., P. Xu, N. MacK, L. Chiang, L. Brown, and H. Wang. Understanding and controlled growth of silver nanoparticles using oxidized N-methyl-pyrrolidone as a reducing agent. 2010. *Journal of Physical Chemistry C.* **114** (1): 36.

Pande, P. P., A. Ganguly, K. Chang, and C. Teuscher. Hybrid wireless network on chip: a new paradigm in multicore design. 2009. In *2009 2nd International Workshop on Network on Chip Architectures (NoCArc 2009) ; 12 Dec.* (2009 ; New York, NY, USA). , p. 71.

Shih, H., D. Williams, N. Mack, and H. Wang. Conducting polymer-based electrodeless deposition of Pt nanoparticles and its catalytic properties for regioselective hydrosilylation reactions. 2009. *Macromolecules.* **42** (1): 14.

Shih, H., D. Williams, N. Mack, and H. Wang. Conducting Polymer-Based Electrodeless Deposition of Pt Nanoparticles and Its Catalytic Properties for Regioselective Hydrosilylation Reactions. 2009. *MACROMOLECULES.* **42** (1): 14.

Teuscher, C., F. J. Alexander, and I. Nemenman. Novel computing paradigms: Quo vadis? . 2008. *PHYSICA D-NONLINEAR PHENOMENA.* **237** (9): 5.

Teuscher, C., H. L. Wang, A. A. Hansson, and E. Akhadov. Future and Emerging Computing Paradigms and Machines.. 2008. *ADTSC Science Highlights.*

Teuscher, C., I. Nemenman, and F. J. Alexander. Novel computing paradigms: Quo vadis?. 2008. *PHYSICA D-NONLINEAR PHENOMENA.* **237** (9): V.

Teuscher, C., N. Gulbahce, and T. Rohlf. Assessing random dynamical network architectures for nanoelectronics. 2008. *2008 IEEE/ACM International Symposium on Nanoscale Architectures, NANOARCH.* : 16.

Teuscher, C., N. Gulbahce, and T. Rohlf. An assessment of

random dynamical network automata for nanoelectronics. 2009. *International Journal of Nanotechnology and Molecular Computation.* **14**: 397.

Teuscher, C., N. Parashar, M. Mote, N. Hergert, and J. Aherne. Wire cost and communication analysis of self-assembled interconnect models for Networks-on-chip. 2009. In *2nd International Workshop on Network on Chip Architectures, NoCArc 2009, In conjunction with the 42nd Annual IEEE/ACM International Symposium on Microarchitecture, MICRO42 ; 20091212 - 20091212 ; New York, NY, United States.* , p. 83.

Xu, P., B. Zhang, N. MacK, S. Doorn, X. Han, and H. Wang. Synthesis of homogeneous silver nanosheet assemblies for surface enhanced Raman scattering applications. 2010. *Journal of Materials Chemistry.* **20** (34): 7222.

Xu, P., N. Mack, S. Jeon, S. Doom, X. Han, and H. Wang. Facile fabrication of homogeneous 3D silver nanostructures on gold-supported polyaniline membranes as promising SERS substrates. 2010. *Langmuir.* **26** (11): 8882.

Xu, P., S. H. Jeon, N. H. Mack, S. K. Doorn, D. Williams, X. Han, and H. L. Wang. Field-assisted synthesis of functional metal nanoparticles using conducting polymers. 2010. *Nanoscaled.* **2**: 146.

Xu, P., S. Jeon, H. T. Chen, H. Luo, G. Zou, Q. X. Jia, J. Won, M. Anghel, C. Teuscher, D. William, X. Han, and H. L. Wang. Facile Synthesis and Characterization of Silver Nanowires through an Electrodeless Deposition Routes Using Polyaniline. To appear in *Journal of Physical Chemistry C. .*

Xu, P., X. Han, B. Zhang, N. Mack, S. Jeon, and H. Wang. Synthesis and characterization of nanostructured polypyrroles: Morphology-dependent electrochemical responses and chemical deposition of Au nanoparticles. 2009. *Polymer.* **50** (12): 2624.

Xu, P., X. Han, C. Wang, B. Zhang, X. Wang, and H. Wang. Facile synthesis of polyaniline-polypyrrole nanofibers for application in chemical deposition of metal nanoparticles. 2008. *Macromolecular Rapid Communications.* **29** (16): 1392.

Xu, P., X. Han, C. Wang, B. Zhang, X. Wang, and H. Wang. Facile synthesis of polyaniline-polypyrrole nanofibers for application in chemical deposition of metal nanoparticles. 2008. *MACROMOLECULAR RAPID COMMUNICATIONS.* **29** (16): 1392.

Stochastic Transport on Networks: Efficient Modeling And Applications to Epidemiology

Nicolas W. Hengartner
20080391ER

Abstract

A variety of problems arising in biosecurity, public health, and basic science research can be viewed as special cases of the general problem of studying a stochastic transport on networks. For example, the evolution and spread of contagious diseases in a human population can be modeled as the transport of a pathogen on social network. And basic biochemical processes involving single molecules, which arise in modeling cancer and other molecular diseases, can be modeled as interacting particles governed by complex stochastic dynamics on cellular regulatory and metabolic networks. The same is true for models of pathogen invasion, such as AIDS, into a host. And many processes in nano technology, in particular in nano-motors, are modeled using stochastic processes on reaction networks.

Detailed computational studies of such stochastic processes on networks are notoriously difficult because bulk modeling (or averaging/mean field approximations) do not capture the intrinsic randomness. The best algorithms simulate the underlying dynamics one event by event. The computational complexity of such algorithms grows exponentially with both the number of interacting particles, the number possible of outcome from each event, and the length of the simulation horizon. For example, the LANL epidemic simulation tool EpiSims is capable of modeling one to four million individual within a city over one day; longer time horizons are be achieved by replicating that day. But that model is not capable of modeling an outbreak of a contagious disease on entire continental US in near real-time.

This project has developed novel algorithms, based on disparate tools from physics, computer science, and information theory, to simulate these stochastic interaction events fast and statistically accurate. The general idea being pursued revolves around coarse-graining stochastic events, so that entire spread of an epidemic or multiple chemical reactions can be modeled as a series of complex, macroscopic steps. Towards achieving this goal, this project also supported fundamental research in simulating extreme events, modeling epidemics, and molecular chemical reactions, random graphs models, and statistical analysis of complex and multivariate data.

Background and Research Objectives

Modeling stochastic transport effects on networks is an essential part of biochemistry, epidemiology, and other diverse sciences. Unfortunately, no algorithm yet exists that can model the transport effectively (that is, near real time simulations for realistic sized networks), taking into the account stochastic properties of the transport and heterogeneity of kinetic parameters to produce statistically accurate results. Expanding on our recent work on stochastic properties of biochemical networks, we exploit tools from statistical field theory and adiabatic methods from quantum mechanics to the analysis of stochastic network transport, specifically in the context of epidemiology and single molecule reactions. The strategy is to take advantage of natural hierarchies in the transportation dynamics on networks to perform what we call physics-inspired “coarse-graining.” Practically, this means that we can separate the nodes in the network according to the time-scale of their influence, enabling us to “statistically aggregate” the effects nodes with smaller-scale dynamics, to produce larger-scale dynamics on a reduced network. The challenge is to operate this reduction in a manner that preserves the correct statistical distribution of the observables. This is achieved by relying on three properties of complex transport networks: time scale separation (adiabaticity), existence of standard building blocks (motifs), and modular and hierarchical architecture. Using these properties, we derive stochastic corrections to deterministic dynamics for common network transport models using a variety of statistical field-theoretic techniques, implement them in terms of efficient computer simulation algorithms, and to apply them to Influenza epidemics, using the developed tools for efficient modeling of the disease.

Identifying and quantifying extreme events in the data produce by these simulations are of great interest. Again, naïve Monte Carlo simulations of extreme and rare events (achieved by running independent copies

of the simulator of the dynamics on the network) are computationally impractical. New algorithms focused on estimating and simulating extreme behavior is needed, and addresses in this project. Finally, the data produced by the simulations are typically high dimensional. In an effort to provide a comprehensive solution, we have studied nonparametric smoothing in high dimensions. The latter suffers from the curse of dimensionally caused by the sparseness of data in high dimensions. Our solution to alleviate the impact of the curse of dimensionality is to exploit the smoothness of the underlying (unknown) regression function by designing adaptive smoothers. While theoretical results on adaptive smoothing abound, there exist to our knowledge, no practical multivariate adaptive smoothers beyond the one we have developed in the context of this project.

Scientific Approach and Accomplishments

We have developed a universal approach for analysis and fast simulations of stiff stochastic biochemical kinetics networks, which rests on elimination of fast chemical species without a loss of information about mesoscopic, non-Poissonian fluctuations of the slow ones. Our approach, which is similar to the Born-Oppenheimer approximation in quantum mechanics, follows from the stochastic path integral representation of the cumulant generating function of reaction events. In applications with a small number of chemical reactions, it produces analytical expressions for cumulants of chemical fluxes between the slow variables. This allows for a low-dimensional, interpretable representation and can be used for coarse-grained numerical simulation schemes with a small computational complexity and yet high accuracy. As an example, we derive the coarse-grained description for a chain of biochemical reactions, and show that the coarse-grained and the microscopic simulations are in an agreement, but the coarse-grained simulations are three orders of magnitude faster.

Fundamentally, we have studied a non-equilibrium statistical system on a graph or network. Identical particles are injected, interact with each other, traverse, and leave the graph in a stochastic manner described in terms of Poisson rates, possibly dependent on time and instantaneous occupation numbers at the nodes of the graph. We show that under the assumption of constancy of the relative rates, the system demonstrates a profound statistical symmetry, resulting in geometric universality of the statistics of the particle currents. This phenomenon applies broadly to many man-made and natural open stochastic systems, such as queuing of packages over the Internet, transport of electrons and quasi-particles in mesoscopic systems, and chains of reactions in bio-chemical networks. We illustrate the utility of our general approach using two enabling examples from the two latter disciplines.

We exploit the above ideas in modeling chemical reactions at the single molecule level. In particular, we investigated non-equilibrium statistical system on networks, in which indentical particles are injected and allowed to interact with one another while moving on the network. Particules exit the system conditionally independently given the history, time, and possibly the instanteneous number of occupied nodes in the network. Under the assumption of constancy of the relative rates, the system demonstrates a profound statistical symmetry, resulting in geometric universality of the statistics of the particle currents. This phenomenon applies broadly to many man-made and natural open stochastic systems, such as queuing of packages over the Internet, transport of electrons and quasi-particles in mesoscopic systems, and chains of reactions in bio-chemical networks. We illustrate the utility of this general approach using two enabling examples from the two latter disciplines. Figure 1 shows a biochemical system of reactions to which the principle of Geometric Universality of Currents was applied to determine statistics of reaction events.

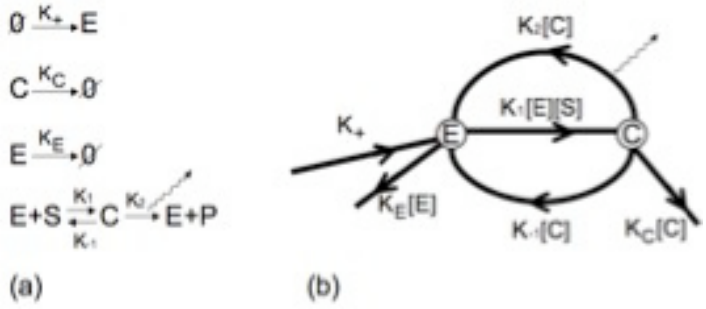

Figure 1. A biochemical system of reactions to which the principle of Geometric Universality of Currents was applied to determine statistics of reaction events. (a) Set of reactions that include a complex Michaelis-Menten process, as well as enzyme creation and degradation. (b) Equivalent Jackson network with kinetic rates, which are proportional to the number of molecules, represented by the nodes. First and second nodes represent free enzymes and enzyme-substrate complexes, respectively.

We successfully applied these ideas to simulate and understand stochastic pump effect and geometric phases in dissipative and stochastic systems and robust quantization of molecular motion in stochastic environments. For the latter, we formulate the Pumping-Quantization Theorem (PQT) that identifies the conditions for robust integer quantized behavior of a periodically driven molecular machine. Implication of PQT on experiments with catenane molecules are discussed. Figure 2 shows the six metastable of a 3-catenane molecule. Control of coupling parameters for smaller rings to 3 stations on the larger ring can induce motion of smaller rings around the center of the larger ring. We show that even though this motion is stochastic, it can be controlled on average with arbitrary precision.

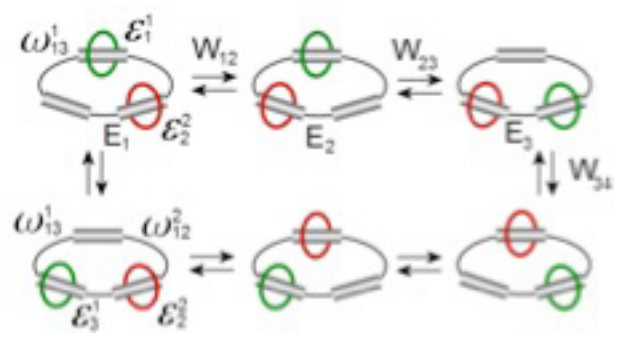

Figure 2. Network of 6 metastable states of a 3-catenane molecule. Control of coupling parameters for smaller rings to 3 stations on the larger ring can induce motion of smaller rings around the center of the larger ring. We show that even though this motion is stochastic, on average in can be controlled with arbitrary precision.

Enzyme-mediated reactions that proceed through multiple intermediate conformational states before creating a final product molecule, is yet another example. One often wishes to identify such intermediate structures from observations of the product creation. We address this problem by solving the chemical master equations for various enzymatic reactions. Our approach is to devise a perturbation theory analogous to that used in quantum mechanics that allows us to determine the first and the second cumulants of the distribution of created product molecules as a function of the substrate concentration and the kinetic rates of the intermediate processes. The mean product flux (or "dose-response" curve) and the Fano factor are both realistically measurable quantities, and while the mean flux can often appear the same for different reaction types, the Fano factor can be quite different. This suggests both qualitative and quantitative ways to discriminate between different reaction schemes, and we explore this possibility in the context of four sample multistep enzymatic reactions. We argue that measuring both the mean flux and the Fano factor can not only discriminate between reaction types, but can also provide some detailed information about the internal, unobserved kinetic rates, and this can be done without measuring single-molecule transition events.

Early evolution of host-pathogen infection is another example of the importance and usefulness of understanding single molecule stochastic dynamics on networks. An important aspect of stochastic viral infection models is the possibility of "extinction" in which the numbers of all participating species go to zero, even though averages over many realizations grow exponentially. The stochastic systems that we consider have linear mean field dynamics. The generating function for such systems satisfies a first order linear partial differential equation. We show that by integrating the characteristic equations backwards in time from the origin we can compute a vector x(t), whose components give the time-dependent probability of extinction starting from a single particle of species s. The extinction probability for all other initial conditions can be obtained from this fundamental solution. The fixed points of the characteristic equations give the various single particle extinction probabilities. Figure 3 shows the distribution of times until an infection begun with a single virion goes extinct for different values of the reproductive ratio. The colored histograms are from stochastic simulations of a viral infection model ad the dotted black lines are obtained from integrating the characteristic equations backwards in time.

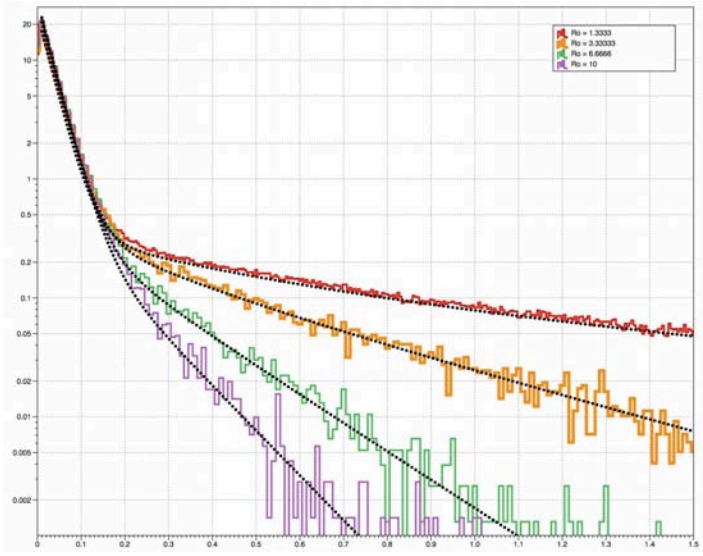

Figure 3. Distribution of times until an infection begun with a single virion goes extinct for different values of the reproductive ratio. The colored histograms are from stochastic simulations of a viral infection model and the dotted black lines are obtained from integrating the characteristic equations backwards in time.

The importance in epidemiology of modeling the stochastic transportation on the underlying network is shown in our work on developing an alternative to Rvachev and Longini's transportation operator. That problem considers only interconnected well-mixed subpopulations, yet depending on how one treats immigration and travel, very different qualitative behavior of the epidemic emerges.

But porting these ideas over to epidemic modeling on social networks is made challenging by the fact that contact networks change over over time. A path forward toward porting the network coarsening ideas to epidemiology is to model the network as a stochastic process. Random Intersection Graphs (RIG) provide a natural framework for modeling social networks. These networks randomly link individuals to mixing groups, and connect individuals that share the same mixing group. As for the Erdos-Renyi random graph model, the RIG exhibit a phase transition between being disconnected and containing a connected giant component. The qualitative behavior of an epidemics on a RIG is strongly impacted by that phase transition. We have analyzed the emergence of that giant component

for general RIG and now have necessary and sufficient conditions for when that component emerges. The analysis techniques generalize existing methods for analysis of component evolution: we analyze survival and extinction properties of a dependent, inhomogeneous Galton-Watson branching process on general RIGs. Our analysis relies on bounding the branching processes and inherits the fundamental concepts of the study of component evolution in Erdos-Renyi graphs. The main challenge comes from the underlying structure of RIGs, where the number of offspring follows a binomial distribution with a different number of nodes and different rate at each step during the evolution.

Simulating extreme values from a black-box is an important problem. For example, the black-box might be a simulators of stochastic transport on a network we considered previously. Naïve Monte-Carlo method for rare event that occur less than 10^{-6} need at leat one million draws. Obtaining that many draws from our simulators may be out of reach given our current computational power. To enable us to get such sample, we have adapted an idea from interacting particle systems that exploits multi-level rebranching. For univariate statistics of the blackbox, we can calculate finite sample distributional properties of the algorithm (as opposed to asymptotic results as the number of particle tends to infinity), which we use to show that our method achieves the logarithmic efficiency. An interesting addendum to this work, is a new method for doing Monte Carlo integration that exploits the Lebesgue formulation of the integral instead of Riemann's.

One purpose of our simulators is to produce synthetic data that can be readily analyzed. For example, one may want to relate the number of infected individuals to the number of infected individuals in the past. Because of the network, that relationship is likely to be nonlinear. But nonparametric method for analyzing nonlinear time series (with large lags) suffers from the curse of dimensionality. The latter is a reflection of the sparesness of data in high dimensions, which forces smoothers to average over large neighborhoods, thereby introducing bias. We show that iterative method for estimating biases to corect the smoother can lead to smoother that adapt to the underlying smoothness of the conditional expectation. And while much is known about the theory of adaptation, our algorithm give a first practical implementation of a multivariate nonparametric smoother. The benefits of our method are an 10%-50% improvement in the out of sample prediction errors over competing state-of-the-art smoothers.

Impact on National Missions

This project supports DOE and DHS missions in bio-security by developing advanced tools for understanding of progression of epidemics, as well as early (stochastic) events in the interactions of a host and a pathogen. Furthermore, the project supports the DOE Energy security mission by enhancing the understanding of biochemical networks, an essential component for biofuels development. Finally, the development of general-purpose simulation strategies of stochastic transport on networks, practical simulation tools for extreme quantiles, and multivariate adaptive smoothers enhances our overall information sciences and technology capability.

Publications

Burr, T., N. Hengartner, E. Matzner-Lober, S. Myers, and L. Rouviere. Smoothing Low Resolution Gamma Spectra. To appear in *IEEE Transactions on Nuclear Sciences.*

Chernyak, V. Y., and N. A. Sinitsyn. Robust quantization of a molecular motor motion in a stochastic environment. 2010. *Journal of Chemical Physics.* **131**: 181101.

Chernyak, V., and N. A. Sinitsyn. Discrete changes of current statistics in periodically driven stochastic systems. To appear in *Journal of Statistical Mechanics.*

Cornillon, P. A., N. Hengartner, and E. Matzner-Lober. Interative Bias Reduction Multivariate Smoothing in R: The IBR package. *Journal of Statistical Software.*

Cornillon, P., N. Hengartner, and E. Matzner-Lober. Iterative Bias Correction Smoothing of High Dimensional Data. To appear in *Scandinavian Journal of Statistics.*

Dahal, H. P., Z. - X. Hu, N. A. Sinitsyn, and A. V. Balatsky. Edge states in a honeycomb lattice: effects of anisotropic hopping and mixed edges. 2010. *Physical Review, B.* **81**: 155406.

Daniels, W., N. Hengartner, M. Rivera, and D. Powell. Epidemiological Modeling: An alternative to Rvachev and Longini's transportation operator. 2010. *LANL Technical report (Manuscript in progress).*

Dreisigmeyer, D., J. Stajic, I. Nemenman, W. Hlavacek, and M. Wall. Determinants of bistability in induction of Escherichia coli lac operon. 2008. *IET Systems Biology.* **2**.

Edwards, J., J. Faeder, W. Hlavacek, Y. Jiang, I. Nemenman, and M. Wall. q-bio 2007: a watershed moment in modern biology. 2007. *Mol. Syst. Biol..* **3**: 148.

Guyader, A., N. Hengartner, and E. Matzner-Lober. Simulation and Estimation of Extreme Quantiles and Extreme Probability Distributions. *Journal of the Royal Statistical Society.*

Guyader, A., N. Hengartner, and E. Matzner-Lober. Multilevel Monte Carlo Simulation and Estimation of Extreme Quantiles and Probabilities. To appear in *2011 SIAM conference on computational sciences and engineering.* (Reno, NV, 28 Feb. - 4 Mar. 2011).

Hengartner, N., E. Matzner-Lober, L. Rouviere, and T. Burr. Multiplicative Bias Corrected Nonparametric Smooth-

ers. To appear in *Canadian Journal of Statistics.*

Mugler, A., E. Ziv, I. Nemenman, and C. Wiggins. Serially-regulated biological networks fully realize a constrained set of functions. 2008. *IET Systems Biology.* **2**.

Nemenman, I., W. Hlavacek, J. Edwards, J. Faeder, Y. Jiang, and M. Wall. Editorial: Selected papers fromthe First q-bio Conference on Cellular Information Processing. 2008. *IET Systems Biology.* **2**.

Nunner, T., N. A. Sinitsyn, M. Borunda, A. Abanov, C. Timm, T. Jungwirth, J. Inoue, and V. Dugaev. Anomalous Hall effect in two-dimensional electron gas. 2007. *Physical Review, B.* **76**: 235312.

Pershin, Y., N. A. Sinitsyn, A. Kogan, A. Saxena, and D. Smith. Spin polarization control by electric stirring: proposal for a spintronic device. 2009. *Applied Physics Letters.* **95**: 022114.

Ronde, W. H., B. Daniels, A. Mugler, N. A. Sinitsyn, and I. Nemenman. Statistical properties of multistep enzyme-mediated reactions. 2009. *IET Systems Biology.* **3**: 429.

Sinitsin, N., and I. Nemenman. Anomalous diffusion in coupled stochastic processes. 2009. *New Journal of Physics.* **11**: 083099.

Sinitsyn, N. A.. Stochastic pump effect and geometric phases in dissipative and stochastic systems. 2009. *Journal of Physics.* **42**: 193001.

Sinitsyn, N. A., and A. Saxena. Geometric phase for non-Hermitian Hamiltonian evolution as anholonomy of a parallel transport along a curve. 2008. *Journal of Physics, A.* **41**: 392002.

Sinitsyn, N. A., and I. Nemenman. Noncyclic geometric phase in stochastic kinetics: corrections to Michaelis-Menten kinetics and application to a cell growth model. To appear in *IET System Biology.*

Sinitsyn, N. A., and J. Ohkubo. Hannay angle and geometric phase shifts under dissipative evolution. 2008. *Journal of Physics, A.* **41**: 262002.

Sinitsyn, N. A., and V. Chernyak. Pumping-Restriction Theorem for stochastic networks. 2008. *Physical Review Letters.* **101**: 39002.

Sinitsyn, N. A., and V. Dobrovitski. Geometric control over the motion of magnetic domain walls. 2008. *Physical Review, B.* **77**: 212405.

Sinitsyn, N., N. Hengartner, and I. Nemenman. Coarse-graining stochastic biochemical networks: quasi-stationary approximation and fast simulations using a stochastic path integral technique. 2009. *Proc. Natl. Acad. Sci. (USA).* **106**: 10546.

Sinitsyn, N., and I. Nemenman. Universal geometric theory of mesoscopic stochastic pumps and reversible ratchets. 2007. *Phys. Rev. Lett.* **99**: 220408.

Teuscher, C., I. Nemenman, and F. Alexander. Novel computing paradigms: Quo vadis?. 2008. *Physica D.* **237**: v.

Critical and Crossover Behaviors at Jamming Transitions

Charles Reichhardt
20080448ER

Abstract

In this project, we used a combination of theory, simulation, and experiment to study jamming transitions. The simplest picture of a jamming transition is when a loose collection of particles that can flow like a liquid becomes densified and acts like a solid. A common example includes the jamming of grain flowing through a hopper. There has been growing evidence that the jamming phenomenon has universal properties that span an enormous range of systems including granular media, soft matter, biological matter, deforming materials, and even the glass transitions. Universal properties arise when the underlying mechanism of the transition is a critical phenomenon associated with a continuous phase transition. What makes the jamming transition particularly challenging is the fact that it is a nonequilibrium system, and little is known about critical phenomena in nonequilibrium systems.

Background and Research Objectives

The goal of this project was to develop a fundamental understanding of the jamming process in granular and other materials. These seemingly simple materials, which include dry sand and powders, exhibit flow behavior far different from ordinary solids, liquids, and gases. Understanding the peculiar behavior of granular materials is vital for predicting and controlling them under a variety of industrial, civil engineering and scientific conditions. Jamming plays an important role in determining the behavior of a granular medium. When the grains are widely separated or slowly moving, they can flow in a manner similar to a fluid, but when the grain separation decreases or the grain speed increases, the grains suddenly jam and resist further motion in an abrupt transi-

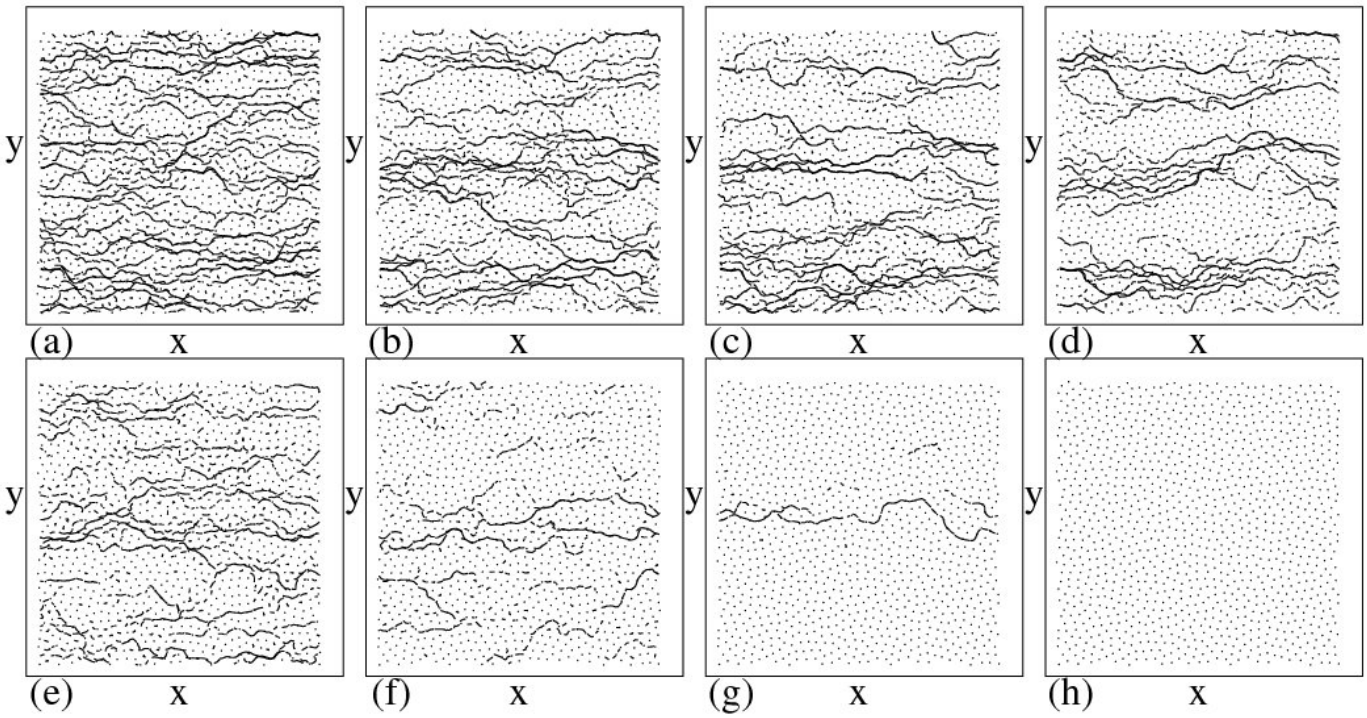

Figure 1. Top panels: A system organizing into a fluctuating state over time. Lower panels: A system organizing into a homogeneous jammed state over time. These two states are separated by a directed percolation transition.

tion to a solid state. The fluid to solid transition associated with jamming is extremely poorly understood but is essential for any application of granular materials. For example, granular media forming a levy is normally in a solid state, but it can unjam in a catastrophic transition to a fluid state which causes the levy to fail. In constrast, when granular media is flowing, such as when a mold for a highly-filled polymer-based explosive is filled, a sudden transition into the solid state can interfere with the filling process. We studied the jamming process and the transition between fluid and solid states and applied powerful concepts from statistical physics which have been successful in describing ordinary solids and liquids.

Scientific Approach and Accomplishments

In our work we have identified several key discoveries related to jamming. Using theoretical modeling and simulations we have shown that the transition from jammed (pinned) states to unjammed (moving) states for the class of systems of colloids and superconducting vortices does indeed fall into the class of nonequilibrium phase transitions with critical phenomena associated with a directed percolation transition, in which the system organizes into either a jammed or unjammed state (see Figure 1) [1]. Experimentally this effect has been realized for colloid systems [2] and vortex systems [3] where the same critical exponents are found in spite of the completely different physical nature, temperature and size scales of the systems. This result provides further evidence that there are indeed universal behaviors associated with jamming, and our next step is to understand whether this phenomenon occurs in materials science such as in dislocation motion. Based on our results, we have initiated collaborations within the laboratory under ASI to examine if dislocation systems exhibit the same behavior. This could have a profound impact on understanding the behavior of materials that are essential to the programs at Los Alamos and to the NNSA.

Our second accomplishment was determining that the addition of quenched disorder could be considered as another parameter for inducing jamming, and finding the nature of the jamming transition in the presence of quenched disorder. A simple picture of this system is particles flowing through randomly placed obstacles. As the obstacle density increases, the particle flow ceases at some point. Such systems are relevant to flow in porous media, models of friction, and to other types of disordered media. We established that for dense particle systems and low obstacle densities, the same jamming phenomenon associated with a critical transition occurs with the same critical exponents found in previous studies without quenched disorder; however, for increasing obstacle densities, the system no longer exhibits the critical phenomena but instead enters a new phase that we term clogging. The clogging transition is characterized by the coarsening of the system into separated regions of high and low particle density, such as shown in Figure 2 for a clogged state. In contrast, a jammed system has very little heterogeneity in the particle density. Additionally, the clogged state is characterized by a slow buildup of the heterogeneity which is accompanied by coarsening dynamics, while the jammed system becomes jammed in a time that decreases exponentially as the jamming threshold is approached, and the jamming transition is characterized by a power law behavior in time. This shows that not all systems that exhibit a cessation of flow display jamming phenomena, and also indicates that clogging and jamming are in fact different types of transition, with clogging having a specific set of behaviors. In particular, clogged systems are much more fragile than jammed systems. They are clogged for only one direction of the particle flow and not for other directions, while jammed systems are jammed in all directions equally [4].

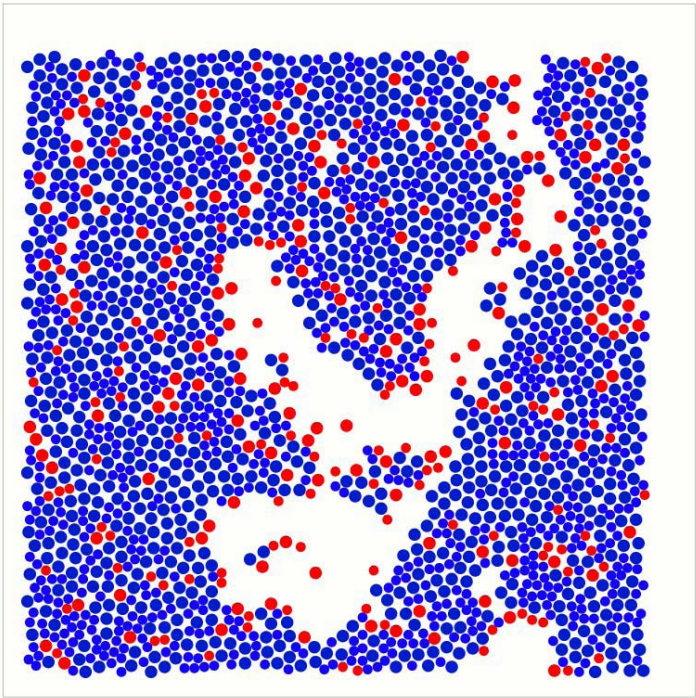

Figure 2. Heterogeneous clogged state in a system containing quenched disorder. Red dots are fixed obstacles.

Another one of the goals of the project was to understand if jamming as understood for simpler symmetrical particles without friction changes if elongated particles or frictional effects are included. We examined a system of granular polymers (Figure 3) where connected grains form a string structure with a limited bending radius [5,6]. In this system we found that the jamming density decreases as the chain length is increased, in agreement with experiment. There are several differences from the symmetrical particle case. In particular, the power law behavior associated with criticality for the symmetrical particles was lost. This suggests that the granular polymer system undergoes a different type of jamming transition. For the addition of friction to the particles, we also observed some deviations in both simulation and experiment from the typical jamming scenario. There are now two jamming transitions. The first is the formation of a fragile contact network, and the second

is the ordinary jamming transition seen for frictionless grains [7]. The first transition has been termed a fragile jamming transition and may be associated with a phenomenon called rigidity percolation.

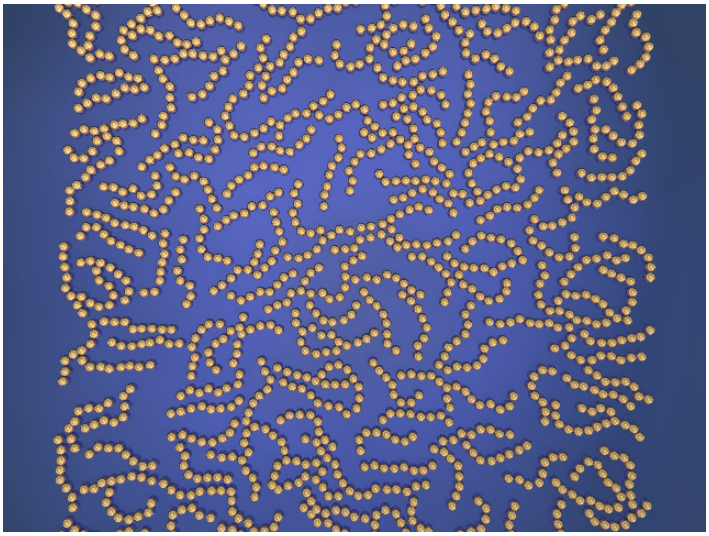

Figure 3. A granular polymer system undergoes a distinct type of jamming transition, different from the jamming that occurs for unconnected disks.

Part of this project has been to study the changes in the fluctuations as the jamming transition is approached from both above and below. We find that the fluctuations become increasingly intermittent and go from an exponential form to a power law form at the jamming transition. The power spectrum of the fluctuations also changes to a 1/f signature [8].

Finally, we have shown that the universal aspects of jamming also occur in systems such as bidisperse colloidal assemblies [9] and vortex flow in type-II superconductors [10,11,12,13,14]. Some of these results have recently been confirmed in experiments [3]. In the superconducting system we showed that the vortex-vortex interactions can lead to a jamming transition in the presence of geometrical restrictions of the vortex flow. The resulting improved pinning of the vortices has important implications for creating superconductors that can carry higher supercurrents, and could be useful for device design. Argonne National Laboratory has recently initiated several experiments to study jamming in superconducting systems based on our results and in conjunction with several basic energy science initiatives.

Impact on National Missions

Jamming underlies numerous physical problems including oil exploration, aging, material failure, pollutant propagation in porous media, solid waste transportation and storage, weapons manufacturing, plastic-based explosives, and characterization of materials out of equilibrium. DOE missions relevant to this research include energy and environmental research, weapons physics, materials science, modeling and simulation.

References

1. Reichhardt, C., and C. J. O. Reichhardt. Random organization and plastic depinning. 2009. *Physical Review Letters.* **103**: 167301.

2. Corte, L., P. M. Chaikin, J. P. Gollub, and D. J. Pine. Random organization in periodically driven systems. 2008. *Nature Physics.* **4**: 420.

3. Okuma, S., Y. Tsugawa, and A. Motohashi. Transition from reversible to irreversible flow: Absorbing and depinning transitions in a sheared-vortex system. *Physical Review Letters.*

4. Groopman, E., C. Reichhardt, Z. Nussinov, and C. J. O. Reichhardt. The jamming transition and crossover to clogging for disks with quenched disorder. *Nature Physics.*

5. Reichhardt, C. J. O., and L. M. Lopatina. A ball and chain polymer model. 2009. *Science.* **326**: 374.

6. Lopatina, L. M., C. J. O. Reichhardt, and C. Reichhardt. Jamming in granular polymers. *Physical Review Letters.*

7. Bandi, M. M., M. K. Rivera, F. Krzakala, and R. E. Ecke. Fragile granular jamming. *Physical Review Letters.*

8. Reichhardt, C. J. O., and C. Reichhardt. Fluctuations, jamming, and yielding for a driven particle in disordered disk assemblies. To appear in *Physical Review E.*

9. Reichhardt, C., and C. J. O. Reichhardt. Disordering transitions and peak effect in polydisperse particle systems. 2008. *Physical Review E.* **77**: 041401.

10. Reichhardt, C.. Vortices wiggled and dragged. 2009. *Nature Physics.* **5**: 15.

11. Reichhardt, C., and C. J. O. Reichhardt. Moving vortex phases, dynamical symmetry breaking, and jamming for vortices in honeycomb pinning arrays. 2008. *Physical Review B.* **78**: 224511.

12. Reichhardt, C., and C. J. O. Reichhardt. Switching and jamming transistor effect for vortex matter in honeycomb pinning arrays with ac drives. 2010. *Physical Review B.* **81**: 024510.

13. Reichhardt, C. J. O., and C. Reichhardt. Commensurability, jamming, and dynamics for vortices in funnel geometries. 2010. *Physical Review B.* **81**: 224516.

14. Reichhardt, C. Reichhardt C.J. Olson. "Jamming and diode effects for vortices in nanostructured superconductors. 2010. *Physica C.* **470**: 779.

Publications

Bandi, M. M., M. K. Rivera, F. Krzakala, and R. E. Ecke. Fragile granular matter. *Physical Review Letters.*

Libal, A., C. Reichhardt, and C. J. Olson Reichhardt. Enhancing mixing and diffusion with plastic flow. 2008. *Physical Review E.* **78** (3): 031401.

Mangan, N., C. Olson Reichhardt, and C. Reichhardt. Reversible to irreversible flow transitions in periodically driven vortices. 2008. *Physical Review Letters.* **100** (18): 187002.

Reichhardt, C.. High-temperature superconductors: Vortices wiggled and dragged. 2009. *Nature Physics.* **5**: 15.

Reichhardt, C. J. O., and C. Reichhardt. Fluctuations, jamming, and yielding for a driven probe particle in disordered disk assemblies. To appear in *Physical Review E.*

Reichhardt, C. J. Olson, and L. M. Lopatina. A ball-and-chain polymer model. 2009. *Science.* **326**: 374.

Reichhardt, C. J., and C. Reichhardt. Commensurability, jamming, and dynamics for vortices in funnel geometries. 2010. *PHYSICAL REVIEW B.* **81** (22): 224516.

Reichhardt, C. Reichhardt C.J. Olson. "Jamming and diode effects for vortices in nanostructured superconductors. 2010. *Physica C.* **470**: 779.

Reichhardt, C., and C. J. Olson Reichhardt. Disordering transitions and peak effect in polydisperse particle systems. 2008. *Physical Review E.* **77** (4): 041401.

Reichhardt, C., and C. J. Olson Reichhardt. Moving vortex phases, dynamical symmetry breaking, and jamming for vortices in honeycomb pinning arrays. 2008. *Physical Review B.* **78**: 224511.

Reichhardt, C., and C. J. Olson Reichhardt. Random organization and plastic depinning. 2009. *Physical Review Letters.* **103**: 168301.

Reichhardt, C., and C. J. Olson Reichhardt. Switching and jamming transistor effect for vortex matter in honeycomb pinning arrays with ac drives. 2010. *Physical Review B.* **81**: 024510 1.

Wan, M. B., C. J. Olson Reichhardt, Z. Nussinov, and C. Reichhardt. Rectification of swimming bacteria and self-driven particle systems by arrays of asymmetric barriers. 2008. *Physical Review Letters.* **101** (1): 018102.

Time-reversible Born-Oppenheimer Molecular Dynamics

Anders M. Niklasson
20080562ER

Abstract

First principles Born-Oppenheimer molecular dynamics, which is based on a rigorous quantum mechanical formulation such as density functional theory, is currently the gold standard for almost all atomistic simulations in materials science, chemistry and molecular biology. Unfortunately, Born-Oppenheimer molecular dynamics is limited by some fundamental shortcomings, such as a very high computational cost or unbalanced and irreversible molecular trajectories with a systematic drift in the total energy and temperature. By restoring underlying physical properties of the dynamics, in particular the reversibility, we have managed to overcome some of the most serious problems that so far have been hampering a direct application of Born-Oppenheimer molecular dynamics in large-scale atomistic simulations. The outcome of our exploratory research is a novel theoretical framework for a new generation first principles molecular dynamics enabling highly efficient and accurate simulations. Our new approach has successfully been implemented in several codes that are used or are being developed at LANL with a direct impact on current and future research in, for example, high-energy explosives and materials science.

Background and Research Objectives

Quantum mechanics was developed during a few years in the mid 1920's. It can briefly be summarized by the Schrodinger equation with its special forms for Fermions and Bosons combined with a few recipes for obtaining measurable physical observables. Essentially all problems in chemistry, materials science, and biology should be possible to predict and understand directly from quantum mechanics if the constituent particles of the systems are known. However, the computational complexity for solving even very small problems is enormous. Only by applying a hierarchy of approximations is it possible to make calculations of any realistic materials systems. Possibly one of the most important and well-tested approximations includes the separation of the nuclear and electronic degrees of freedom in the Born-Oppenheimer approximation, where the fast electrons are assumed to be in a relaxed equilibrium around approximately stationary nuclei. Solving the Schrodinger equation and calculating the forces acting on the nuclei, within the Born-Oppenheimer approximation, the dynamics of a system can be analyzed. In this way we can study, for example, chemical reactions, phase transitions, evolving protein structures, and elastic properties of condensed matter, even at temperatures and pressures that cannot be reached within normal laboratory conditions. Born-Oppenheimer molecular dynamics has emerged as one of the most important theoretical tools in computational materials science and can be viewed as the gold standard of molecular dynamics simulations. However, challenges in nanoscience, biofuels and molecular biology, for example, require significant algorithmic improvements to allow simulations of much larger size and complexity than previously possible. In this project we have explored and developed general ab initio molecular dynamics technologies based on the new opportunities provided by the time-reversible loss-less integration approach to Born-Oppenheimer molecular dynamics that recently was invented at Los Alamos National Laboratory (LANL) by the proposal authors [1].

The time-reversible Born-Oppenheimer technique was originally only an ad-hoc invention to overcome fundamental problems with long-term energy stability and accuracy of molecular dynamics simulations. Figure 1 illustrates the ability of time-reversible Born-Oppenheimer molecular dynamics (TR-BOMD) in comparison to regular Born-Oppenheimer molecular dynamics (BOMD). Because of a non-linear optimization or equilibrium relaxation of the electronic degrees of freedom required within the Born-Oppenheimer approximation for each new molecular configuration, the reversibility present in a true dynamical system was broken in Born-Oppenheimer simulations. The irreversibility leads to a systematic drift of the energy, i.e. the system is unintentionally heated up or cooled down, which leads to uncontrollable errors and uncertainties. This serious shortcoming was considered an unsolvable problem that only partly could be avoided by a substantial increase of the computational effort. The time-reversible Born-Oppenheimer technique solved this problem and opened the door to a

new generation of first principles molecular dynamics simulation methods with unprecedented accuracy and speed. The purpose of this project was to pursue this goal and explore and developed efficient Born-Oppenheimer molecular dynamics techniques enabled by the new time-reversible approach. Our findings have been highly successful leading to a rigorous theoretical framework that may form the backbone of a new generation high-performance quantum based molecular dynamics that is significantly better suited to handle present and future challenges in computational materials science, chemistry and biology.

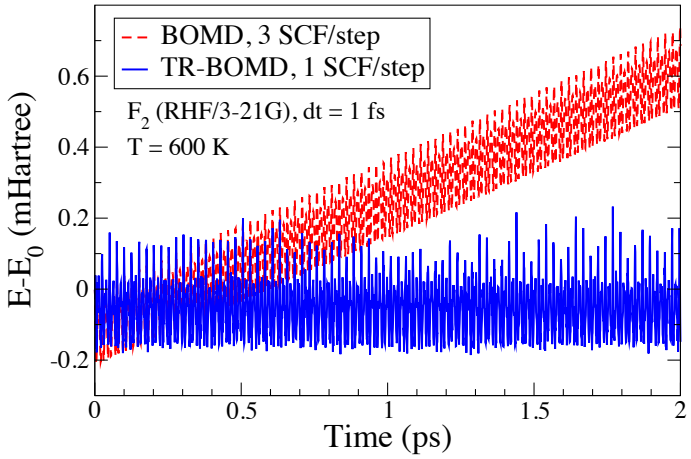

Figure 1. Conventional Born-Oppenheimer molecular dynamics (BOMD) with an electronic propagation based on a linear interpolation between time steps vs. a time-reversible propagation (TR-BOMD). The time-reversible scheme avoids the unphysical systematic drift in the energy and the computational cost as measured by the number of SCF cycles per time step is lower [1].

Scientific Approach and Accomplishments

In the initial step of our exploratory research we searched for a more rigorous theoretical foundation of the ad-hoc time reversible integration scheme that originally was proposed [1]. This would allow a deeper understanding of the underlying dynamics and allow generalizations and improvements beyond what would otherwise be possible. By trying to map various forms of the original time-reversible integration schemes to an extended Lagrangian description that corresponds to a true physical dynamical system this goal was achieved. There was certainly no guarantee that this could be accomplished and there is no unique way in which this could be performed through a straightforward derivation. Only by trial and error and some good luck was this key result achieved. The new ``*extended Lagrangian Born-Oppenheimer molecular dynamics*'' was published in Physical Review Letters [2] and formed the basis of all the continuing research.

Thanks to the extended Lagrangian framework we could analyze and understand important features of the new dynamics. It also enabled generalizations beyond our original expectations. In particular, thanks to the extended Lagrangian scheme it was possible to apply (almost directly) higher-order geometric integration schemes that previously were limited to celestial or classical molecular dynamics. These schemes allow a much higher degree of accuracy to a fraction of the computational cost of conventional (Verlet or leap-frog) integration schemes used in Born-Oppenheimer molecular dynamics [3]. Figure 2 shows an example of the high-degree of accuracy that is allowed with a new form of higher-order symplectic integration schemes, to no additional computational cost.

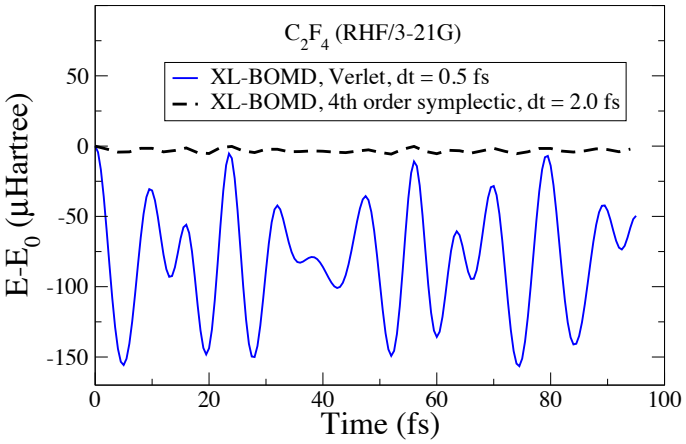

Figure 2. The accuracy, as measured by the amplitude of the total energy oscillations for a small molecule. The extended Lagrangian Born-Oppenheimer molecular dynamics scheme (XL-BOMD) allows for higher order symplectic integration of the equations of motion that can improve the accuracy by orders of magnitude to no extra cost. This is of great importance when small energy differences have to be resolved [3].

Thanks to the extended Lagrangian scheme we also realized a serious limitation in our dynamics. Because of perfect reversibility combined with the relation between the electronic and nuclear degrees of freedom, there was no way for numerical errors to dissipate. In a perfect lossless scheme numerical errors would accumulate and eventually lead to large error fluctuations and divergence. By weakly coupling our extended Lagrangian dynamical system to an external bath through the electronic degrees of freedom, numerical noise could be removed through dissipative force terms. We achieved this damping without including any significant perturbations on the molecular trajectories [4]. The problem of noise accumulation is of particular importance when approximate sparse matrix algebra is used, which is necessary in complex large-scale atomistic simulations. Figure 3 illustrates the problem with numerical noise and the effect of our new dissipative force terms.

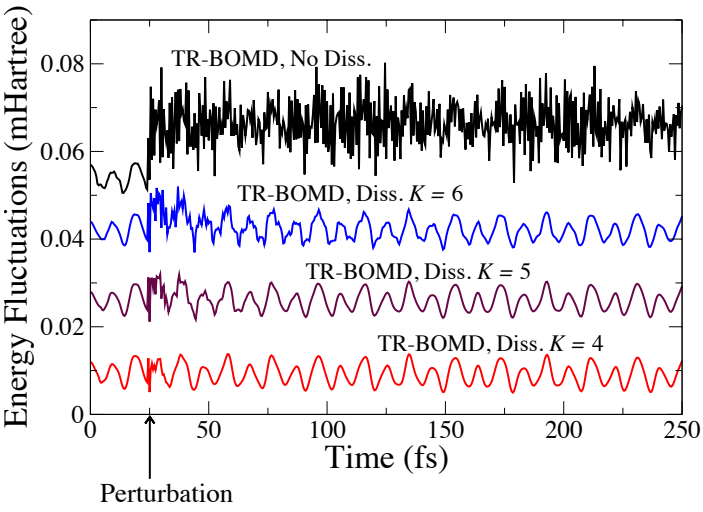

Figure 3. The behavior of numerical noise in the total energy introduced by a single perturbation with and without dissipation of various order [4].

Another key achievement was to understand the importance of stability under incomplete approximate self-consistent field (SCF) optimization. The SCF optimization is used to calculate the relaxed ground state electronic structure at which the nuclear forces are calculated. The SCF optimization can only be performed approximately and sometimes only with very poor convergence, especially for large systems. It is therefore very important to guarantee a stable dynamics even under incomplete SCF convergence. By optimizing an integration constant we found that the new extended Lagrangian framework was stable also under weak (infinitesimal) SCF convergence in contrast to almost all previous schemes, including some of the original time-reversible schemes proposed by the PI and co-workers [2-4]. This may sound like a technical detail, but providing stability under incomplete SCF convergence is in fact often crucial in practical simulations.

Originally the extended Lagrangian formulation of Born-Oppenheimer molecular dynamics was given in terms of the electronic density (or density matrix). However, a large class of first principles molecular dynamics codes is based on the electronic wave functions. Because the total energy and the forces are invariant under rotations of the wave functions, the phase of the wave functions is not uniquely determined. This creates a serious phase alignment problem in the integration of the electronic degrees of freedom. In previous Born-Oppenheimer molecular dynamics schemes, aligning each new wave function to ground state wave functions in previous time steps solved this problem. However, that approach would break time-reversibility and lead to a systematic drift in the total energy. After a significant amount of trial and error we managed to find a surprisingly simple solution to this problem that both keeps reversibility and is stable under approximate weak SCF convergence [5]. Our new form of wave function extended Lagrangian Born-Oppenheimer molecular dynamics allows practical implementation in a number of widely used electronic structure plane-wave pseudo potential codes, such as VASP, Quantum Espresso and ABINIT, which significantly improves the scientific impact of our findings.

In molecular dynamics simulations of metals or at high temperatures, a non-integer occupation of the electronic states has to be included in a free energy molecular dynamics. Within the extended Lagrangian formulation this is easily achievable through a Fermi distribution of the electronic eigenstates with the corresponding entropy term included. This important free energy molecular dynamics was also developed within the extended Lagrangian formulation [6,7]. Figure 4 shows the free energy conservation of our new dynamics.

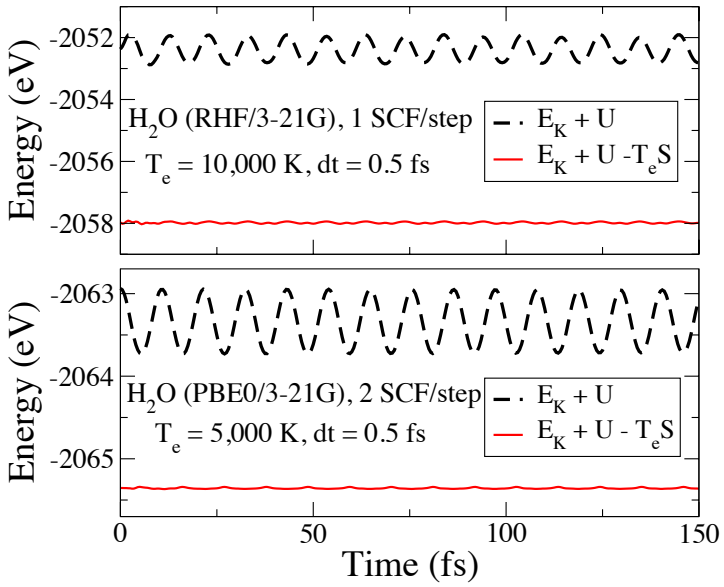

Figure 4. Demonstration of the conservation of the free energy v.s. the total energy in extended Lagrangian free energy molecular dynamics [7].

Two graduate students (Anders Odell and Peter Steneteg) were involved in various parts of the research project and their highly valuable contributions will also become an important part of their thesis work.

The new extended Lagrangian Born-Oppenheimer molecular dynamics has been implemented in several electronic structure codes that are used or are being developed at LANL. These codes include FreeON, LATTE, VASP, and CP2K. The PI has also been in contact with authors of other widely used codes, such as BigDFT, Quantum Espresso, and CASTEP. This will further extend the impact of our LDRD-ER research.

Despite the success, it feels like the research is ended prematurely. An extended but reduced funding would significantly increase the final impact of our accomplishments, especially in following up and supporting some of the cur-

rent implementations that are far from trivial.

Impact on National Missions

The direct or indirect applications of Born-Oppenheimer molecular dynamics range from the problem of high-temperature stabilization of δ-Pu to the folding structures of protein molecules in human cells, all issues with close ties to the DOE missions in Nuclear Weapons, Threat Reduction, and Office of Science, which will benefit from enhancing our fundamental understanding of materials. Our work has provided novel molecular dynamics simulation tools that overcome some significant and fundamental shortcomings of current first principles molecular dynamics. These problems include a high computational cost, numerical instabilities, and a systematic drift in the total energy. This is of particular importance for large-scale simulations of non-equilibrium systems that are necessary, for example, studying reactions of high-energy explosives. The new extended Lagrangian Born-Oppenheimer molecular dynamics was implemented in a self-consistent tight-binding code (LATTE) designed for this purpose. The LATTE code forms the theoretical backbone of both an LDRD-ER and a DR proposal with the purpose of understanding and simulating high-energy explosives. Our new extended Lagrangian scheme has therefore currently a direct impact on DOE and LANL missions in this field of research. Furthermore, the PI was invited to write a full BES proposal based on this ending ER proposal for the development of a new generation high-performance molecular dynamics schemes designed for overcoming computational problems of significance to the Nations future energy needs, including excited state molecular dynamics studies of light harvesting materials. The BES proposal has not yet been awarded.

References

1. Niklasson, A. N., C. J. Tymczak, and M. Challacombe. Time-reversible born-oppenheimer molecular dynamics. 2006. *Physical Review Letters.* **97** (12): 123001.

2. Niklasson, A. N.. Extended Born-Oppenheimer molecular dynamics. 2008. *PHYSICAL REVIEW LETTERS.* **100** (12): 123004.

3. Odell, A., A. Delin, B. Johansson, N. Bock, M. Challacombe, and A. N. Niklasson. Higher-order symplectic integration in Born-Oppenheimer molecular dynamics. 2009. *JOURNAL OF CHEMICAL PHYSICS.* **131** (24): 244106.

4. Niklasson, A. N., P. Steneteg, A. Odell, N. Bock, M. Challacombe, C. J. Tymczak, E. Holmstrom, G. Zheng, and V. Weber. Extended Lagrangian Born-Oppenheimer molecular dynamics with dissipation. 2009. *JOURNAL OF CHEMICAL PHYSICS.* **130** (21): 214109.

5. Steneteg, P., I. Abrikosov, V. Weber, and A. N. Niklasson. Wave function extended Lagrangian Born-Oppenheimer molecular dynamics. 2010. *PHYSICAL REVIEW B.* **82** (7): 075110.

6. Niklasson, A. N.. A note on the Pulay force at finite electronic temperatures. 2008. *JOURNAL OF CHEMICAL PHYSICS.* **129** (24): 244107.

7. Niklasson, A. M. N., P. Steneteg, and N. Bock. Extended Lagrangian free energy molecular dynamics. 2010. *In manuscript.*

Publications

Niklasson, A. M. N.. Extended Born-Oppenheimer molecular dynamics. 2008. *Physical Review Letters.* **100** (12): 123004.

Niklasson, A. M. N.. A note on the Pulay force at finite electronic temperatures. 2008. *J. Chem. Phys..* **129**: 244107.

Niklasson, A. M. N.. Density matrix methods in linear scaling electronic structure theory. *Springer Verlag, Linear-Scaling Techniques in Computational Chemistry and Physics: Methods and Applications.* Edited by Leszcynski, J., R. Zalesny, and M. G. Papadopoulos.

Niklasson, A. M. N., P. Steneteg, A. Odell, N. Bock, M. Challacombe, C. J. Tymczak, E. Holmstrom, G. Zheng, and V. Weber. Extended Lagrangian Born-Oppenheimer molecular dynamics with dissipation. 2009. *J. Chem. Phys..* **130**: 214109.

Niklasson, A. M. N., and N. Bock. Extended Lagrangian free energy molecular dynamics. 2010. *In Manuscript.*

Niklasson, A. N., M. Challacombe, C. J. Tymczak, and K. Nemeth. Trace correcting density matrix extrapolation in self-consistent geometry optimization. 2010. *JOURNAL OF CHEMICAL PHYSICS.* **132** (12): 124104.

Niklasson, A. N., M. Challacombe, C. J. Tymczak, and K. Nemeth. Trace correcting density matrix extrapolation in self-consistent geometry optimization. 2010. *JOURNAL OF CHEMICAL PHYSICS.* **132** (12): 124104.

Odell, A., A. Delin, B. Johansson, N. Bock, M. Challacombe, and A. M. N. Niklasson. Higher-order symplectic integration in Born-Oppenheimer molecular dynamics. 2009. *J. Chem. Phys..* **131** (24): 244106.

Steneteg, P., I. Abrikosov, V. Weber, and A. N. Niklasson. Wave function extended Lagrangian Born-Oppenheimer molecular dynamics. 2010. *PHYSICAL REVIEW B.* **82** (7): 075110.

Quantum Cryptographic QCard Proof-Of-Concept

Jane E. Nordholt
20100516ER

Abstract

Quantum communications (QC) such as quantum key distribution (QKD) can provide unconditional security against the looming threats to current public-key cryptography from new mathematical algorithms, more powerful conventional computers, and ultimately, quantum computers, however quantum communications have found little commercial interest. Current implementations are large, expensive, and only operate in a restricted point-to-point mode over unused or "dark" fibers. The Los Alamos National Laboratory (LANL) QC team has solved many of these problems such as coexistence between a QC signal and a conventional signal so that a second "dark" fiber is not needed to secure each conventional communications link with QC. However a more advanced QC architecture and miniaturization of key components are needed. In this project key elements of a new QC paradigm have been developed: a miniaturized hybridized electro-optics module which demonstrates that the key element of a portable QC system is feasible, and the information assurance protocols needed to implement a portable device. Our new portable device, referred to as a Qcard, would be periodically connected to a trusted authority (TA) with whom it would make large quantities of secure random numbers or "keys." These keys could then be used in remote settings to securely communicate with other users who have a Qcard or other connection to the TA; to access securely facilities; to distribute keys to distant locations not served by the TA; or to provide digital signatures. This means the user with a Qcard, for example embedded in a smart phone, could make an absolutely secure phone call or Internet connection. Qcard is possible because of several significant advances by the LANL QC team, most importantly the prototype device developed in this project and the new information security protocols also developed herein.

Background and Research Objectives

In today's highly networked world, point-to-point communications that cannot take advantage of the network have limited to no commercial interest and very little use even in high-security, government systems. Quantum communications provide unconditional security using the laws of physics and information theory but have not been able to take advantage of networked communications or portable systems. The objective of this project is to make quantum communications commercially viable by demonstrating the key components of a quantum smartcard or Qcard. A Qcard would be a portable QC system that would communicate with a TA. The TA would authenticate users; produce unconditionally secure key with each user; and provide the information to users that would allow them to communicate with other users using quantum security. Such a Qcard could be part of a smart phone or used as a fillgun to key user computers, smart phones, or encryptors at remote locations. Not only would the Qcard store quantum keys in secure memory, but it would also store a nonsecret database, which when used with the quantum keys would provide secure keys in common with any desired user. Should a user wish to communicate with a user not in the database, the Qcard would contact the TA using whatever communication methods it has available such as cellular telephone or internet and without reducing the security of the quantum keys, receive information that would allow secure communication with the other user. This flexibility provides the portability and security needed to make QC commercially viable.

Although the LANL QC team has already shown its ability to perform QC over active fiber optics and miniaturize such things as the conventional protocol processing needed for QKD into an FPGA, a miniaturized electro-optics module capable of QC is needed as well as theoretical development of the security protocols a Qcard would implement.

Scientific Approach and Accomplishments

A Qcard would be periodically coupled to a charging station with a connection to a fiber optic network linking it

to the TA. During this connection the Qcard would perform user authentication and QKD with the TA. Although the initial idea was that the Qcard would authenticate itself and its user using conventional communications secured with quantum keys already on the device, a simpler and more secure method has been developed using quantum secure ID and password authentication. The user would have a memorizable password, the Qcard would have a secure identification number, and would collect biometric information such as key elements of the user's fingerprint. All of this information would be used to determine the way in which random bits are sent to the TA. The password information would never be sent. It would only be used to determine the quantum states in which it random bits are transferred. If the information transfer is performed by two parties who know this password information, both will produce the same random number. These random numbers can be securely compared by the user and TA. Only if the Qcard the TA agree on this extended password information would the user and device be recognized and they begin performing QKD. By performing QKD with the TA, the user's Qcard and the TA create shared, secret random numbers.

Two users who have secure random numbers in common with the TA and can communicate conventionally with a TA can securely produce common random numbers using only unsecured conventional communications. For example if user A wanted to communicate with user B, user A can contact the TA and be told which bits to flip in one of his keys in order to have the same random number as one of user B's keys. Information on which bits to flip can be communicated in the open without compromising security because only user A and the TA, know the secret key that will be modified. In this project an advanced version of this technique has been developed to allow users to check the validity of the keys; allow communication with a network or users; change keys when the network of users changes; and allow the use of separate send and receive keys. These protocols are the subject of a patent application, "SECURE MULTI-PARTY COMMUNICATION WITH QUANTUM KEY DISTRIBUTION MANAGED BY TRUSTED AUTHORITY." The separate Qcard device patent application is entitled "QUANTUM KEY DISTRIBUTION USING CARD, BASE STATION AND TRUSTED AUTHORITY." Both patent applications have been filed.

A hybridized electro-optics module has also been developed and tested. The module is the first of its kind and has demonstrated the electro-optics of a small transmitter. It is shown in Figure 1. The Qcard electro-optic prototype has a laser chip that is followed by a collimating lens and laser isolator. The isolator protects the laser from optical feedback which could be problematic both in laser operation and overall security. The isolator is followed by a waveplate that is necessary to inject light into the modulator at the correct polarization angle. A lens then focuses the light into the modulator. The output of the modulator is connected to a fiber optic pigtail so that it can be easily tested in LANL systems.

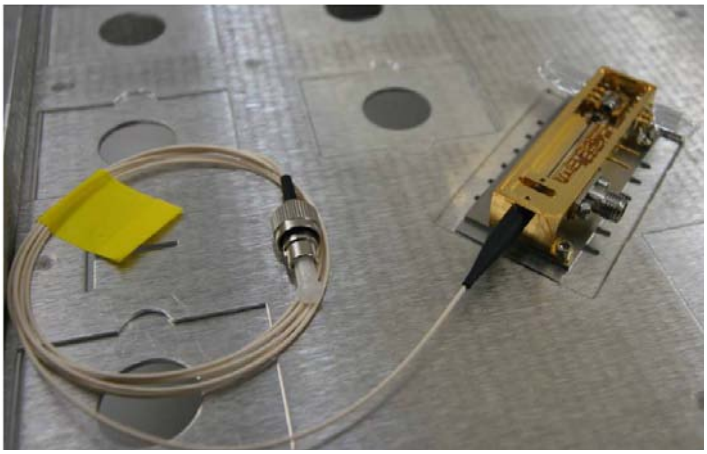

Figure 1. The prototype Qcard electro-optics module with its fiber optic pigtail. The device is ~5 cm in length and ~2 cm in width including the electrical connectors.

Impact on National Missions

Many parts of the US government have a need for increased cybersecurity and, with the coming advent of the quantum computer, better cryptography. The Qcard opens up new ways to use quantum cryptography and offers flexibility and portability that will allow QKD to enable solutions in these areas. This work will make the Qcard feasible for secure communications and personnel authentication. The Qcard will also make it possible to miniaturize QKD transmitters for space and treaty verification. Qcard can also be used as part of a smart cable system for securing infrastructure such as the smartgrid or supervisory, control, and data acquisition (SCADA) systems.

Combination Drug Therapy for Influenza H1N1 Infection

Alan S. Perelson
20100518ER

Abstract

Influenza kills an average of 36,000 people in the United States each year, and influenza pandemics can pose greater threats. Currently, only four drugs are approved for the treatment of influenza, and resistance to these drugs has developed rapidly in some strains. Using more than one drug at a time, or combination therapy, to treat influenza may delay the development of drug resistance and provide improved treatment outcomes for severe cases. As part of our project we have calculated the probability of a drug resistance mutation arising in a typical influenza infection. We find that all possible single drug resistance mutations will be generated and that most likely all possible pairs of drug resistance mutations will also be generated during a typical weeklong infection. Thus, to treat an infected individual and to be sure that drug resistance will not diminish the activity of therapy, a combination of drugs should be used. Ribavirin, a drug that is used in the treatment of other viral diseases, is currently in clinical trials for use in combination therapy for influenza. Ribavirin acts in part by inducing mutations in viral genomes as they replicate, but is also effective against viruses through stimulating an innate antiviral response in human cells. This response frequently involves increasing the expression of many genes, particularly those involved in the interferon response. In one major part of this project, we are studying this interferon stimulated gene response to ribavirin in cultured human lung cells during influenza infection. Our goal is to try to dissect at which point ribavirin acts in this interferon signaling pathway, in order to understand better how ribavirin works, but also to come one step closer to discovering new drug targets for modulating the human innate antiviral response in order to combat a broad spectrum of viral infections.

Background and Research Objectives

Each year, an average of 36,000 deaths can be attributed to influenza in the United States, among the elderly, the very young, and those with pre-existing medical conditions. Influenza A virus pandemics can cause greater numbers of deaths, as happened during the 1918-19 pandemic, and also typically cause a shift towards causing deaths in younger segments of the population, as was the case during the 2009-2010 pandemic as well as previous pandemics. We currently face the threat of a pandemic from highly pathogenic avian influenza A H5N1, which is known to have infected more than 500 people to date, with a cumulative case fatality rate of approximately 60%.

Because influenza causes severe disease and death each year in the United States, and because of the threat of severe pandemics, it is important for us to develop effective drug treatment strategies for preventing death due to influenza. An ideal drug therapy would be both highly efficacious and slow to succumb to the development of drug resistant strains. Treating people with more than one drug at a time, or "combination therapy", can both improve treatment outcomes and slow the development of drug resistance. Combination therapy is used in the treatment of many diseases, such as HIV/AIDS, tuberculosis, and cancer, for these reasons. Currently, only two classes of drugs are approved by the FDA for treatment of influenza in the United States, the adamantanes (amantidine and rimantidine), which are ion channel blockers, and neuraminidase inhibitors (Tamiflu and Relenza). These drugs have almost exclusively been used singly when treating flu infections. Thus, resistance has developed rapidly in some flu strains to either one or the other of these drug classes. Because resistance to our existing influenza medications can develop rapidly, and because highly pathogenic influenza A H5N1 often causes death even when treated with currently available drugs, combination therapy is now being studied and considered for the treatment of influenza infection.

One drug that is in the late stages of being studied in clinical trials of combination therapy for influenza infection is called ribavirin. This drug mimics one of the building blocks of RNA, which is the genetic material of many viruses, including influenza viruses. When an infected cell attempts to replicate a virus's genetic material – its RNA – then the active, metabolized form of ribavirin is incorporated instead of the appropriate RNA building block. When this new RNA is again copied, the copying enzyme encounters ribavirin and finds it ambiguous,

and frequently introduces an error into the genome. In this way, ribavirin introduces mutations into viral genomes. Because nearly all such mutations reduce or eliminate infectivity, ribavirin in effect cuts down on the amount of infectious virus an infected cell can produce.

Ribavirin has been proposed to act in additional ways, as well. For another RNA virus, hepatitis C virus (HCV), ribavirin is an FDA approved therapy. Evidence is mounting that one additional and important way in which ribavirin acts in HCV infection is through stimulating innate defenses in our body's cells. Most human cells, and in particular liver cells targeted by HCV and lung epithelial cells that are targeted by influenza virus, are capable of synthesizing and releasing molecules called interferons (IFNs) that signal that there is nearby danger from a pathogen. Broadly speaking, IFN signaling within and between cells reduces the amount of new proteins made in cells and hence is an attempt to prevent pathogens from hijacking the body's cells to replicate themselves. Ribavirin increases activity in IFN stimulated pathways. One way in which it acts is through interacting with a protein called mTOR that acts on this pathway, but there are other, independent effects of ribavirin on this pathway that are not well understood. How and whether ribavirin acts on IFN signaling pathways has never been studied in the context of influenza infection.

One goal of this project is to determine whether, and if so, then how ribavirin acts on IFN stimulated pathways in the context of influenza infection. There are many different IFN signaling molecules that act at different times during the early, innate response to an infection, and these molecules, in turn, act on a large number of sometimes overlapping and sometimes distinct target molecules within cells. We want to disentangle the activities within infected cells treated with ribavirin, in order to develop a more fine grained understanding of at which points in these signaling pathways ribavirin is acting. To achieve these goals, we are conducting experiments, and the results from these experiments will be used in follow on projects to mathematically model the IFN signaling within infected cells and the actions of ribavirin. Because ribavirin may act as a mutagen and also because it has serious side-effects, including causing anemia, it would be advantageous to find alternative molecules that generate the beneficial effects of ribavirin without its side effects.

This project will help us to understand better how this drug works, and thus how we may better use it or find substitutes for it. The project may also guide us one step closer to discovering new drug targets for modulating the human body's innate immune response to viral infection. If the precise pathways that ribavirin can act on can be identified, then new drugs may be developed with improved, broad-spectrum antiviral activity, and without the side effects of ribavirin as well.

Scientific Approach and Accomplishments

In order to assess the need for combination therapy for influenza, we and others have constructed mathematical models of influenza infection in humans, in mice and in cell culture [1-7]. Fitting these models to data has allowed us to estimate parameters governing the rate of replication of influenza in these various systems. Then using estimates of the mutation rate of influenza that govern the chance that one base in the genetic code of influenza will be miscopied when the virus replicates, has allowed us to compute how many variant viruses carrying mutations one might expect to arise during the course of infection. We found that during a typical seasonal flu infection all possible single mutant variants of influenza and approximately 22% of all possible double mutant variants will be produced (see Figure 1). Thus, if a drug, such as oseltamivir (Tamiflu) that requires only a single change in the virus' neuraminidase to become partially resistant to the drug, we expect such drug resistant variants to be generated [8]. Whether these variants will grow to high levels in an infected person and be spread to others still needs to be determined. Nonetheless, these initial calculations suggest that within individuals with severe influenza infection combinations of drugs should be more effective than single drug therapy.

In preliminary studies, both in vitro and in experimental animals, in which combinations of drugs have been used, synergistic interactions have been observed that have allowed the combination therapy to perform well even if virus is resistant to one of the drugs in the combination. These combination therapies involve combining ribavirin with oseltamivir and amantidine. If ribavirin acts to stimulate the innate immune system, then the combination may be effective even if the virus is resistant to one of the drugs in the combination therapy. Thus, we have been exploring

Number of nucleotide changes	Probability of generation of mutants	Number of mutants produced per infection (mean ± SD)	Number of all possible mutants	Fraction of all possible mutants produced (seasonal H3N2, H1N1, etc)	Fraction of all possible mutants produced (highly pathogenic avian influenza A H5N1 and others*)
1	0.027	$1.4\times10^{10}\pm1.2\times10^{5}$	4.2×10^{4}	100%	100%
2	0.00038	$1.9\times10^{8}\pm1.4\times10^{4}$	8.8×10^{8}	$22\%\pm1.6\times10^{-3}\%$	$100\%\pm3.5\times10^{-3}\%$
3	0.0000036	$1.8\times10^{6}\pm1.3\times10^{3}$	1.2×10^{13}	$1.5\times10^{-5}\%\pm1.1\times10^{-8}\%$	$7.5\times10^{-5}\%\pm2.5\times10^{-8}\%$

Figure 1. Probability of generating influenza mutants and fraction of all possible mutants produced during infection.

how ribavirin acts during influenza infection.

To accomplish this, we are studying the expression of several dozen interferon (IFN) stimulated genes in cultures of human lung epithelial cells infected with influenza A virus and in uninfected controls, and treated with ribavirin, IFN-α, or both, or none as controls. Because ribavirin acts synergistically with IFN-α in HCV infection, we are also testing this combination of drugs in this study. We are using a human lung epithelial cell line designated "A549", which supports influenza infection and demonstrates a response to IFN. We are using a well-characterized strain of influenza A virus, influenza A/Beijing/262/95, a seasonal H1N1 strain that was isolated in Beijing in 1995. We are using high but physiological doses of ribavirin and IFN-α, comparable to what could be achieved in humans.

The gold standard for measuring gene expression quantitatively is a technique called quantitative real-time polymerase chain reaction (qPCR). Several months ago, our collaborator Dr. Norman Doggett at LANL acquired state-of-the-art instruments, manufactured by Fluidigm, for high-throughput qPCR measurements. Using this instrument we shall acquire over 60,000 data points in a small fraction of the time required for similar experiments using more traditional methods, and at a fraction of the cost as well, due to decreased reagent costs.

We have tested and validated inputs into our experiments, and are this week preparing samples for analysis next week in the Fluidigm instrument. This will generate data showing the impact of ribavirin on IFN signaling in the context of influenza infection in human lung cells. If we find an effect, this data will be used to support seeking further funding to pursue ribavirin's use in combination therapy for viral infections.

Impact on National Missions

This project supports the Laboratory's mission of scientific discovery and innovation, with respect to biosecurity. The Laboratory has a strong focus on understanding host-pathogen interactions, and on discovering novel ways to protect the nation from disease threats. This project is helping us to understand the ways in which an important drug in our global antiviral medication arsenal works, and may lead to future projects to discover new drug targets for even more effective, broad-spectrum antiviral medications. The data generated from this project will be submitted for publication, and will serve to demonstrate Laboratory capabilities in high-throughput qPCR, influenza research, and research on antiviral drugs, all of which will form a basis for submitting applications for funding for new work on ribavirin and influenza, and on broader areas of research relevant to our nation's biosecurity.

References

1. Baccam, P., C. Beauchemin, C. Macken, F. Hayden, and A. Perelson. Kinetics of influenza A virus infection in humans. 2006. *Journal of Virology.* **80** (15): 7590.
2. Beauchemin, C. A., J. McSharry, G. Drusano, J. Nguyen, G. Went, R. Ribeiro, and A. Perelson. Modeling amantadine treatment of influenza A virus in vitro. 2008. *JOURNAL OF THEORETICAL BIOLOGY.* **254** (2): 439.
3. Lee, H. Y., D. Topham, S. Y. Park, J. Hollenbaugh, J. Treanor, T. Mosmann, X. Jin, B. Ward, H. Miao, J. Holden-Wiltse, A. Perelson, M. Zand, and H. Wu. Simulation and Prediction of the Adaptive Immune Response to Influenza A Virus Infection. 2009. *JOURNAL OF VIROLOGY.* **83** (14): 7151.
4. Miao, H., J. Hollenbaugh, M. Zand, J. Holden-Wiltse, T. Mosmann, A. Perelson, H. Wu, and D. Topham. Quantifying the Early Immune Response and Adaptive Immune Response Kinetics in Mice Infected with Influenza A Virus. 2010. *JOURNAL OF VIROLOGY.* **84** (13): 6687.
5. Mitchell, H., D. Levin, S. Forrest, C. Beauchemin, J. Tipper, J. Knight, N. Donart, C. Layton, J. Pyles, P. Gao, K. Harrod, A. S. Perelson, and F. Koster. High replication efficiency of 2009 (H1N1) pandemic influenza: kinetics from epithelial cell culture and computational modeling . *Journal of Virology.*
6. Smith, A. M., F. R. Adler, J. L. McAuley, R. N. Gutenkunst, R. M. Ribeiro, J. A. McCullers, and A. S. Perelson. Effect of PB1-F2 expression on influenza A virus infection kinetics . *PLoS Computational Biology.*
7. Smith, A., and A. S. Perelson. Influenza A virus infection kinetics: Quantitative data and models . *Wiley Interdisciplinary Reviews: Systems Biology and Medicine* .
8. Perelson, A. S., L. Rong, and F. G. Hayden. Combination therapy for influenza. *Science.*

Fast and Accurate Detection of Linear Tracks from Ordered Points

Allen L. McPherson
20100536ER

Abstract

This nine-month LDRD project was designed to assess the feasibility of developing fast and accurate algorithms for detecting linear tracks of moving points within a 2-D field. The project consisted of four tasks. First, we performed an assessment of two potential algorithms, analyzing and defining their predicted computational efficiency. Second, we implemented a prototype version of one of these algorithms on a conventional workstation. This implementation accurately detected synthetic tracks in a random background field. Third, we analyzed the effect of errors on the existing algorithm and modified it to include these error parameters in its operation. This analysis also helps to determine the minimum amount of data required to accurately detect a track in the presence of errors. Finally, we performed experiments to assess the potential speed-up of this algorithm using parallelism and hardware acceleration. The result of this feasibility study is a prototype implementation, along with more accurate error and performance analysis that can be used as a foundation for further development of this application.

Background and Research Objectives

A naïve algorithm might look for a track by first choosing a point, then pairing it with all other points, and finally checking to see if any third point is collinear with the pair. This algorithm is extremely inefficient and, even with parallelism, would not run near the desired interactive rates. Using the point's timestamp, much more efficient algorithms can be developed. In essence, the problem comes down to striking a vector through the 3-D set of points (x, y, t) to see if those that intersect it represent a track.

Our task was to analyze two potential algorithms for their computational efficiency and to implement one of them as a proof of concept. Our analysis concluded, at least for the specific case of linear tracks, that a streaming algorithm would be the best potential candidate. Our implementation, on a conventional workstation, successfully detects synthetic tracks within a random background field from an error-free set of points.

We also analyzed the problem in the presence of spatial errors in the point locations. We analyzed this error and its effect on our algorithm. The spatial error adds uncertainty and the potential for false detections. We have, to a basic extent, quantified this uncertainty and determined the number of points that could cause false detections for various sizes of positional errors. We have also modified our algorithm and implementation to adjust its data traversal algorithm to account for these errors. A more detailed analysis of all errors and a modification of the detection mechanism will be required to accurately detect tracks in the presence of these errors.

Finally, we have performed analysis and experiments to assess the potential for speeding up the implementation of this algorithm to near interactive rates. The algorithm is trivially parallelizable, and given the potential compute capability that can be devoted to the problem, it is likely that this performance requirement can eventually be met.

Scientific Approach and Accomplishments

The algorithm we chose to implement uses the sorted nature of the point data to accelerate the search for points along a potential track. It is computationally expensive to sort data but much faster to search it once it has been sorted. We make use of the fact that the incoming points are already sorted in time to speed the search for potential tracks. The algorithm places a grid over the 2-D field and deposits incoming points into their appropriate grid cell. As each point arrives, the algorithm creates pairs from neighboring points to generate a potential track vector. This vector is then used to efficiently traverse the grid looking for other points that may lie along the track (see Figure 1). All of the selected points along this traversal are then checked to see if they are collinear with the original pair and if their time stamps are consistent with those of the pair. If so, a track is detected.

The prototype successfully detects tracks within a random background. These tracks and the background points are synthetically generated to represent points with no errors. In this case the likelihood of a false de-

tection is essentially zero. There may be some spatial error in the point's location and this error adds the potential for false detections. We have analyzed this potential and incorporated updated traversal mechanisms into our prototype code. The upshot of this analysis is that somewhere between 5 and 50 random background points may falsely be attributed to a potential track. Our algorithm must be modified to account for these errors and the minimum number of required points to detect a track must be raised (potentially to over 100) if we are to accurately detect tracks in the presence of errors.

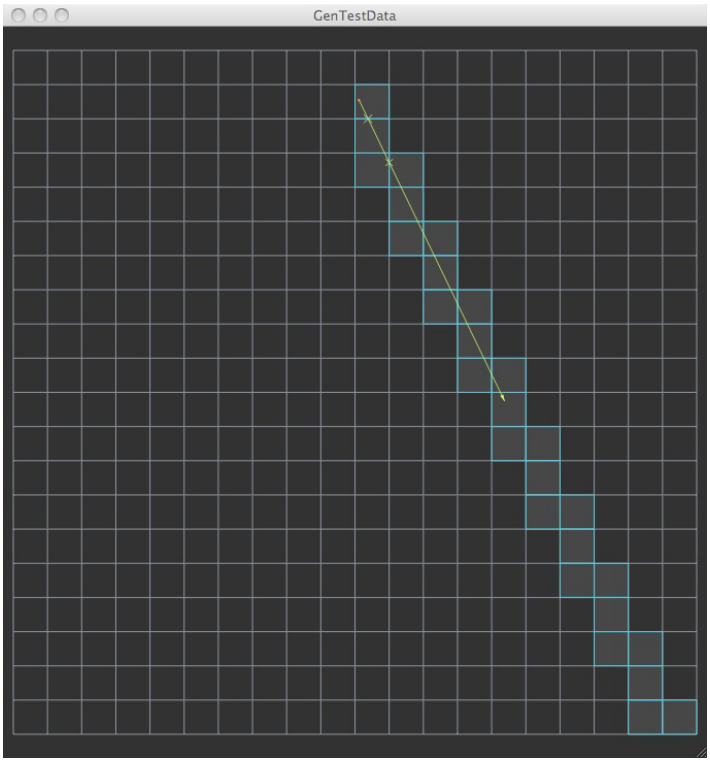

Figure 1. Example of ray traversing grid overlay.

Our prototype software was implemented on a standard Apple Mac workstation using their provided development environment. This environment enables rapid prototyping and elegant user interfaces, but sacrifices speed of execution. We performed some experiments to assess potential performance increases by moving to a more efficient development environment. In one case, typical of much of the code in the prototype, we re-implemented the synthetic track generation software (see Figure 2) using efficient data structures and libraries to achieve a speedup of 100 times over the original. The algorithm is also trivially parallel—points can be processed independent of other points. Given the computing power available in parallel clusters of computers it is our assessment that this algorithm can eventually approach interactive rates (specifically for linear tracks).

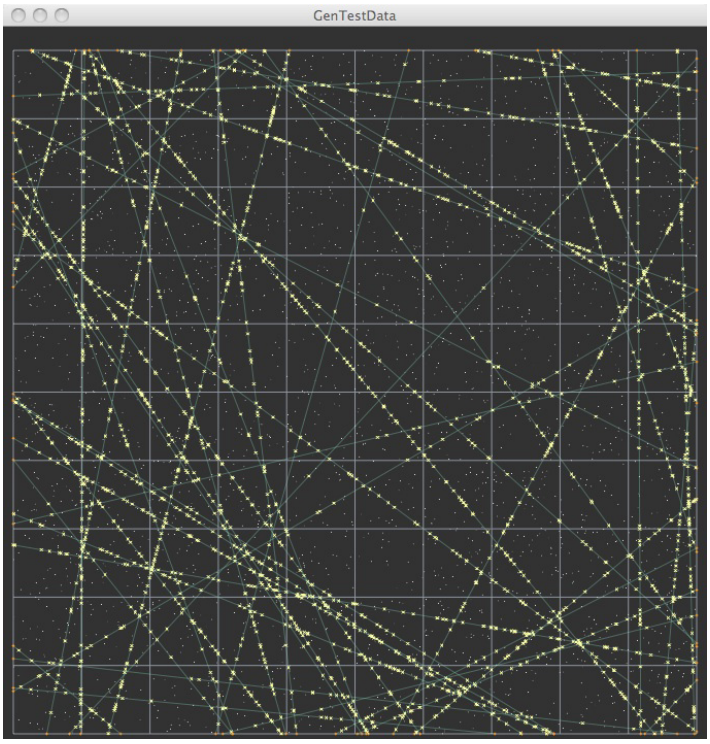

Figure 2. Example of synthetic point and track generation.

Impact on National Missions

This project's impact on national missions is described in an addendum that can be obtained by contacting the LDRD Program Manager at Los Alamos National Laboratory.

OpenCL Abstractions for Scientific Computing

Benjamin K. Bergen
20100557ER

Abstract
This project developed several mid-level code abstractions that form the basis for a new programming model for hybrid and heterogeneous computing systems. This programming model is a first step towards enabling Exascale simulation runs.

Background and Research Objectives
The OpenCL (Open Computing Language) framework is a new cross-platform approach to programming multicore, manycore and accelerated architectures. OpenCL attempts to provide single-source portability while still allowing the programmer to develop hand-tuned, architecture-specific code when needed. However, this necessarily low-level approach is difficult even for experienced developers. The primary intent of this project was to develop mid-level abstractions that would ease OpenCL development and make the framework more accessible.

Scientific Approach and Accomplishments
To develop and test our abstractions, we leveraged a demo code that was developed by the authors for the 2009 Supercomputing conference. Using the experience gained from the original development, we gradually re-factored the code to use our new abstractions. This approach allowed us to test our new code and data structures for feasibility and to verify the behavior of the modified code. Using this approach, we were successful in creating a new set of abstractions that replaced the low-level direct OpenCL calls in the original demo code.

Impact on National Missions
Though not explicitly stated as a goal in the proposal, the body of this work has resulted in a new programming model that is a viable possibility for moving to Exascale HPC systems. This model is made possible by combining the mid-level abstractions developed through this project. In particular, this work forms the building blocks necessary to exploit a greater degree of task-level parallelism on the new class of hybrid/heterogeneous compute nodes that will likely be used in Exascale systems. In addition to allowing increased concurrency, our model is well suited for use in developing fault-tolerant application models. Hard and soft error faults are potentially the greatest challenge that developers will face in developing Exascale simulation codes.

References
1. Bergen, B., M. Daniels, and P. Weber. A Hybrid Programming Model for Compressible Gas Dynamics using OpenCL. To appear in *International Journal of High Performance Computing Applications.*

The PetaFlops Router: Malleable Supercomputers for Application Co-design

Zachary K. Baker
20100559ER

Abstract
The PetaFlops Router is based on Field Programmable Gate Arrays (FPGA) and a programmable network switch. The PetaFlops Router takes a new approach to the computing problem, allowing both the computer architecture and the software running on it to develop in a mutually compatible fashion. This year we moved the project significantly forward, developing several key technologies. These include embedded processor for system control, PCI-E hardware for interfacing with standard PC hosts, the reconfigurable network hardware for building custom networks, and new programming methodologies. These technologies allowed us to demonstrate that a computer system could be effectively "co-designed" to fit a problem, where algorithm needs drive hardware design, and hardware design steers some aspects of application structure.

Background and Research Objectives
Achieving high performance on petascale computers is difficult because little information is exchanged between computer architects and application designers. This is a particular challenge because the design phase of a computer system is long and tends to have the maneuverability of a freight train. Application designers, on the other hand, often support an application built on decades of library development and legacy code. The PetaFlops Router takes a new approach to this problem, allowing both the computer architecture and the software running on it to develop in a mutually compatible fashion. This is achieved by providing the ability to build customized instruction sets and network architectures for a particular application. These customizations can evolve with the development of the application, allowing the co-design philosophy to function throughout the lifetime of an application/system pairing. Compare this to a traditional computer design cycle, where the meaningful design input from the users effectively ends years before delivery.

The PetaFlops Router is based on Field Programmable Gate Arrays (FPGA) and a programmable network switch. FPGAs, a reconfigurable integrated circuit technology that is widely used in the telecommunications industry, can provide the performance expected of Application-Specific Integrated Circuits (ASICs) and yet be customized for many different classes of applications. Not only can the PetaFlops Router system be optimized through reconfiguration of the intra-chip logic, but also by re-routing the flow of information through the inter-chip network using the programmable network switch. This represents a key innovation of the system: to adapt the entire computer architecture to the particular application, including the low-level network fabric. The PetaFlops Router takes the structure of application data movement into account, allowing an application designer to adapt both the algorithm and architecture to match each other. The flexibility provided by the adjustable network structure makes the system ideal for a wide range of scales, from a small embedded system to large HPC installations. Each node has scalable, flexible connections to other nodes, sensors, or through a backplane to additional crossbars and other racks.

Beyond the FPGAs and attached co-processors, the PetaFlops Router includes a highly capable network switch that operates on high-speed serial interconnect (Figure 1). The basis of the network is a crossbar switch, a commodity networking device. While crossbars have been used historically to connect together groups of nodes, our placement of a crossbar on every node allows a significant extension of capability.

By putting a crossbar on every processing node, essentially any network topology desired can be built from a collection of nodes. The crossbars can be modified at runtime to act as network switches, or can be configured by an application to build a particular network topology. This allows the network system to evolve with the development of the application.

Scientific Approach and Accomplishments
During this year's reserve funding, we continued exploring the matched filter as a demonstration kernel. The matched filter is a vital kernel for extracting useful data from hyperspectral imagery. The term "Hyperspectral" implies that the spectra collected covers a very large swath of the frequency spectrum.

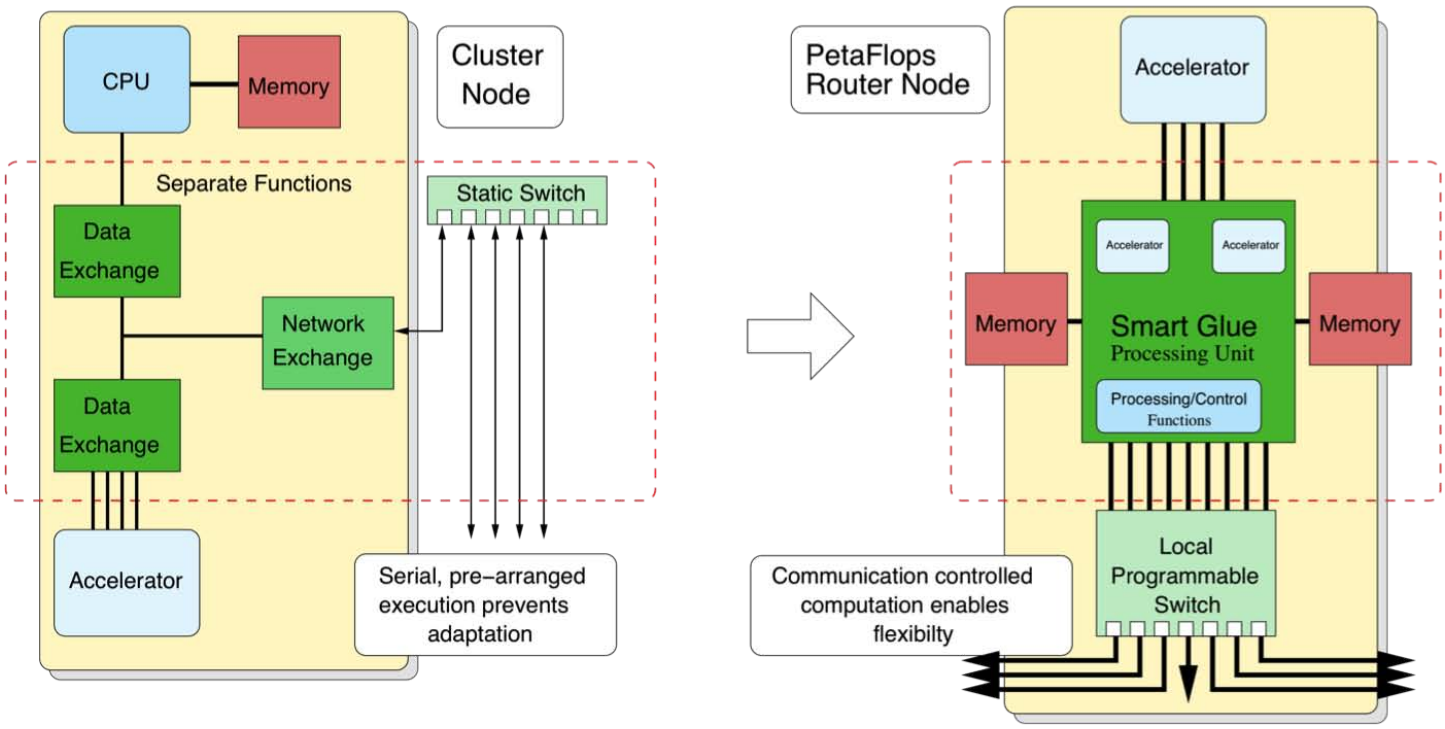

Figure 1. Illustration of PetaFlops Router approach. The PetaFlops Router brings data closer to computation through the use of reconfigurable hardware.

We implement a reduced set of operations for the match filter. Using pre-processed signature templates, the operations required are simplified. The kernel remains a realistic application as the signature templates can be generated offline with no loss of practicality. The simplification focuses attention on the real-time costs of data transfer and bulk computation.

One of key deliverables this year was to demonstrate that a PFRouter system could adapt to an application. We implemented several custom instructions to support the hyperspectral operation. These were integrated with the PFRouter system to demonstrate that custom instructions could appreciable accelerate computation. At the same time we implemented a set of instructions to more closely match the "functional" programming paradigm. This is exciting because it brings a new perspective to co-design, where hardware can adapt to the programming methodology.

PCI Express Connectivity via SRAM FPGAs

The ability to use an SRAM FPGA to communicate with PCI Express (PCIe) systems provides several benefits to the PetaFLOPs Router concept. First, FPGAs can be used to manage the dataflow and data processing of a computation in the context of systems built using off-the-shelf PCIe hardware. Instead of having all data flow through host CPU memory requiring CPU intervention, the FPGAs can transfer data directly to and from accelerators, like GPUs, without requiring the extra latency of having the CPU manage the data transfer. Second, PCIe provides a standard way to extend off-the-shelf computing systems to use FPGA hardware to provide more optimized network capabilities as well as an entry point for ingesting data streams from sensors. In the latter case, the FPGA provides the interface between the sensor and the rest of the system, providing some initial processing of the incoming data and providing this data to the rest of the system via PCIe. A good example of the latter use case can be found with PC chassis populated with FPGA boards, which is shown in Figure 2.

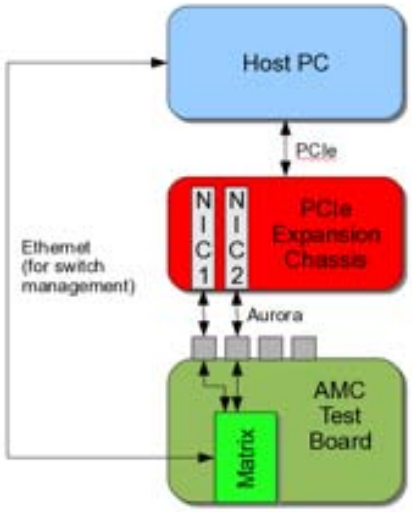

Figure 2. Managed crosspoint switch network demonstration. This allows the PetaFlops Router allows the network to be optimized to the application.

We have developed a few PCIe interfaces for the Xilinx FPGAs, the earliest supporting programmed I/O transfers and the latter versions supporting bus-mastered DMA. The designs have proven to be very stable and portable, having been tested on at least 6 different FPGA boards and both the Virtex-5 and Virtex- 6 FPGA families. Virtex-6 is important since it provides native support for both PCIe root complexes as well as Gen 2 PCIe.

The current software leverages the Jungo WinDriver PCI Express Software Developers Kit to developing the driver and application software to talk to the Xilinx FPGAs over PCIe. As noted above, the low-level software supports programmed I/O as well as DMA transfers. DMA transfers from Xilinx card to other FPGA or GPU cards are also supported with our low-level software. From the API perspective, the main issue is knowing the physical address of the DMA destination, whether it is in the host PC or another peripheral card. Following standard practice, completion of DMAs to and from a host is handled through interrupts.

Customized, Circuit-switched Network

With the two ML605-based network interface cards (NICs) working in Figure 3, the final demonstration we developed was a small, customized circuit-switched network using the Mindspeed crosspoint switch on the Matrix AMC card. This can provide the PetaFLOPs router with the ability to customize a network topology based on the specific needs of an algorithm.

Figure 3. Photograph of compute and network cards in PCI-E slots. This interface allows reconfigurable hardware to efficiently communicate with standard HPC compute nodes.

In this demonstration, the two NICs in the PCIe expansion chassis now communicate through the Matrix card mounted on an AMC test board. The card-edge (copper) network connections from the Matrix card are routed to four CX4 connectors on the edge of the AMC test board, enabling the Matrix's crosspoint switch to connect the two NICs with a custom, circuit-switched connection.

At this point, we are testing the connectivity between the two NICs through the Matrix card's Mindspeed switch for a fixed configuration. Additional NICs can be added and the Ethernet connection to the NXP microcontroller on the Matrix can be used to manage crosspoint switch operation, allowing the application to dynamically change the interconnection topology, as needed.

Development of the mMIPS soft processor for use in PFRouter supporting Smart Glue, communication and data transfer

The mMIPS soft processor is a 32-bit CPU that uses a small subset of MIPS instructions. Use of the soft CPU has allowed us to quickly prove out ideas in hardware at hardware speeds rather than develop full hardware implementations. Adding a standardized bus system to the CPU has allowed other intellectual property (IP) to be quickly developed and combined to make larger and more complex systems. The C compiler for the CPU was modified to allow the use of larger instruction stores, so that we can have more complex programs. These features combined have made the mMIPS a useful vehicle for testing ideas and exploring the space of the PFRouter hardware system.

Smart Glue was further developed to automate the generation of the VHDL hardware and formalized several of the pieces of the Smart Glue system. This built on some work completed previously and relied heavily on the mMIPS CPU. The assembler was modified to be more flexible and much of the code was extended to allow new instructions and possible uses. This continues to be developed and should support efficient memory transfers.

High-level simulation of PetaFlops router system

A very important part of designing large-scale system is understanding how they will perform as they scale. Because we are using only a handful of nodes in our functional demonstrations, it is important to simulate how a larger model will perform. The modeling effort included a software simulation of the mMIPS processor, instruction and data stores, and network communication. The simulator was a modification of existing software and replaced more complex CPU simulations with the mMIPS processor. This allows the same software that is used in hardware to be used in a simulated environment. The simulator is fully threaded, where the CPU, separate hardware devices and monitors all run in separate threads. This allows the simulation to include multiple CPUs with their simulated hardware. There is a hypervisor that controls the launch of the simulated CPUs and allows the hardware to be built and controlled dynami-

cally. The simulation includes a network card that can be connected with an actual network and allows the system to interact with other hosts or possible other PFRouter hardware. This will be useful for testing out ideas and running more complex software with high visibility.

Future work will be to combine more of these efforts to provide a system to more easily port algorithms of interest to the PFRouter system. Understanding how these parts and pieces interoperate and the bottlenecks, will point out the where the system will need to be further developed and optimized.

Functional Programming on the PetaFlops Router

Goals

The goal of this part of the work was to apply functional programming to the PetaFlop Router. Functional programming emphasizes evaluation of functions in lieu of sequential execution of instructions. Functional programming languages offer an approach to writing algorithms in terms of functions without specifying implementation details such as memory locations or order of execution. Decoupling computation and data is a distinct advantage for parallel architectures.

With the limited time availability, Haskell Arrows were selected as they were viewed as a close match to FPGA capabilities. The hope was to write some simple algorithms using Haskell Arrows and then hand translate the code into the PF Router assembler infrastructure.

Arrows/Stream Processing in Haskell

While there is a single API for arrows (Figure 4), there are many possibilities for an implementation. We were interested in a streaming version. There are three stream implementations publically available.

StreamList implemented the arrows as operating on lists. This is the simplest and most direct view of Arrows operating on streams. Unfortunately this is extremely limiting when using multiple streams since streams are required to be of the same length.

StreamAuto was used to overcome this problem. Rather than working on streams directly a run function was used to pass elements of a stream (list) to the Arrows. StreamAuto is based on finite automata and used continuation passing style in its implementation. This implementation seemed to be limited in that for every input there needed to be one output.

StreamProc was the final implementation based on stream processors. Its implementation was similar to StreamAuto but where as StreamAuto would produce an output for every input StreamProc has separate Put operation and Get operation. This allowed for operations that would consume more data than was produced (reductions and filters) and operations that would produce more data than was consumed (generators). This feature was used in the dot product for example.

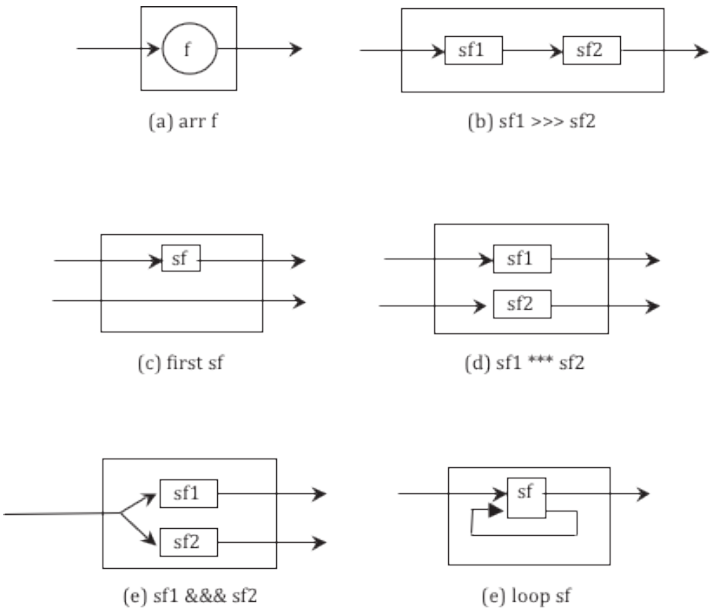

Figure 4. Examples of common operators we have implemented for the "Arrows" programming methodology.

Impact on National Missions

Physics simulations are highly dependent on data management performance. We have tackled the problem by applying Field Programmable Gate Array (FPGA) technology. In the past we have spent appreciable effort attempting to move FPGA technology in the high performance computing arena by directly implementing compute architectures on the FPGAs. This is a difficult and tedious process, and often left to PhD candidates that spent several years on a single kernel. The speedups could be significant, but performance improvements were often based on specific customizations that reduced the flexibility. These problems reduced the acceptance of FPGA as commodity accelerators in favor of GPUs, Cells, etc.

Our new approach is the idea that FPGA should be network and data processors connecting computational elements. We have demonstrated that the network can be malleable to adapt to the application, and that the application can be built to take advantage of the hardware. We believe this experience and these advancements will inform the design of supercomputers in the future, as well as find use in embedded applications. As well, the various technologies we have developed will find a home in many applications for other programs at LANL.

DOVE: Discovery Of Vegetation over the Earth Using High Resolution Remote Sensing Data

Dongming M. Cai
20100582ER

Abstract

Detection and classification of stress and tree mortality down to individual trees on the Earth would bring a major breakthrough in regional and global vegetation modeling. Stress and mortality are among the largest uncertainties in understanding and predicting the global vegetation response to climate change. In this study, we have developed a new two-stage machine learning framework to identify vegetation and assess its state of health, healthy vs. dead status. Leveraging on both supervised and unsupervised learning algorithms, the performance of this new classification system has given impressive accuracy to identify the vegetation from its background, and to distinguish healthy and dead trees. This project supports the DOE missions in global climate monitoring and energy security by developing key capabilities in remote sensing, machine learning, vegetation modeling, and CO_2 dynamics.

Background and Research Objectives

Today, about a trillion canopy trees on Earth consist of around 100,000 species. These trees play a critical role to absorb terrestrial CO_2 and keep CO_2 to an appropriate level that is suitable for human being to live on earth. Recently, many studies [1-2] have indicated the trend of tree mortality is increasing in many regions, which raises two critical questions: 1) is tree mortality increasing on a global scale? and if so, 2) how does the increase of tree mortality impact absorption or emission of CO_2? Unfortunately, there is no current capability available to monitor vegetation changes, and correlate and predict tree mortality with CO_2 change, and climate change on a global scale.

Different survey platforms (methods) have been used for forest management. Typical ground-based forest surveys measure tree stem diameter, species, and alive or dead. The measurements are low-tech and time consuming, but the sample sizes are large, running into millions of trees, covering large areas, and spanning many years. These field surveys provide powerful ground validation for other survey methods such as photo survey, helicopter GPS survey, and aerial overview survey. Satellite imagery has much larger coverage. It is easier to tile the different images together, and more important, the spatial resolution has been improved to match or exceed aerial survey platforms. Today, the remote sensing satellite data have reached sub-meter spatial resolution for panchromatic channels (IKONOS 2: 1 m; Quickbird-2: 0.61 m) and meter spatial resolution for multi-spectral channels (IKONOS 2: 4 meter; Quickbird-2: 2.44 m). Therefore, this high resolution satellite imagery can allow foresters to discern individual trees. This vital information should allow us to quantify physiological states of trees, e.g. healthy or dead, shape and size of tree crowns, as well as species and functional compositions of trees. This is a powerful data resource, however, due to the vast amount of the data collected daily (Quickbird-2: 7~11 terabit/day), it is impossible for human analysts to review the imagery in detail to identify the vital biodiversity information.

Dynamic global vegetation models (DGVMs), the most exciting recent advance in forest modeling, can simulate the distribution, physiology and biogeochemistry of these trees and other vegetation at global scales. These DGVMs are essential to predict future regional and global climate because of the critical role of vegetation in regulating the lower boundary layer of the atmosphere [3]. Current DGVMs suggest that global forest carbon storage is a key parameter in the response of Earth's climate system to anthropogenic CO_2 emissions over the next century. However, the predictions of the DGVMs on land uptake (absorption) of CO_2 are surprisingly divergent [4], which makes vegetation dynamics one of the largest sources of uncertainty in Earth system models [5-6]. In a recent paper published in Science, Purves and Pacala posed the key limitation to the issue with DGVMs: "Because of a lack of data or theory, current DGVMs reduce biodiversity (over 100,000 tree species) to a small number of plant functional types (PFTs) within which all parameters are constant."

In order to build a high-fidelity global vegetation model, as suggested by plant ecologists Nate McDowell and Rosie Fisher at LANL, the realistic biodiversity of trees must be incorporated in a natural "bottom-up" ap-

proach, i.e. a PFT is determined by the tree compositions in a particular area, not in the traditional "top-down" method to simulate the biodiversity by a small number of PFT patches. Such a new global vegetation model will predict vegetation dynamics at an unprecedented level of spatial, temporal, and mechanistic detail.

Our research goal is to develop a new machine learning tool that, in an automated fashion, identifies the composition and stress levels of individual trees from high resolution satellite imagery. The information will be then aggregated into a mechanistic PFT (plant functional type) patches at spatial scales appropriate for modeling, and to scale up the method to account for the distribution of trees on a global scale. A capability to enable analysis and classification of individual trees would bring a major breakthrough in regional and global vegetation monitoring and modeling.

Scientific Approach and Accomplishments

For this study, we have focused on developing a two-stage machine learning framework to identify (classify) tree stress levels and healthy vs. dead status by applying image processing techniques and machine learning algorithms. In the first stage, our goal is to separate the vegetation from the rest of terrestrial structures, man-made and natural, such as buildings, roads, rocks, and etc. The second stage focuses on assessing the state-of-health of individual trees, live vs. dead, to be more specific. The architecture of this machine learning framework is shown in Figure 1, which aims to transform the raw data into the vital vegetation information.

Feature extraction is a process to identify the most informative characteristics for the representation of an object, i.e. a profile for a tree type in this study. The primary features could be the differences among tree species in terms of edge, color, texture, geometry and other secondary features.

After a set of features are extracted from the imagery, the classification algorithms are used to discern different types of objects, which in this study will be tree species and their associated characteristics. Classification algorithms can be generally divided into two categories: supervised learning and unsupervised learning. A supervised classification algorithm uses both the positive and negative examples. Ideally, the algorithm maximizes the difference between the two classes to achieve an optimal separation. An unsupervised classification needs only one class --- either the positive examples or negative ones. In general, supervised algorithms achieve a better performance than the unsupervised algorithms. Both supervised and unsupervised algorithms were successfully used in the applications of classification and anomaly detection [7-10]. In this study, we proposed to combine the advantages of both supervised and unsupervised learning and innovate the classification as a two-stage model.

We selected Southwestern USA as our test-bed since two investigators from this team (Nate McDowell and Rosie Fisher) have been working on vegetation model development in this area. Quickbird-2 data have been acquired from the DigitalGlobe Corporation. The classification results will be compared with the ground-surveyed data.

Progress

Since February 2010 excellent progress has been made in developing a new machine learning framework to identify live and dead trees in this project. We have successfully developed and tested a two-stage model using supervised and unsupervised learning techniques for tree classification. In stage 1, because the number of these distinct land cover objects classes will be limited, vegetation vs. road, the supervised algorithms will provide more accurate separation. The result for vegetation identification is illustrated in next figure.

In Figure 2, the left panel (A) shows an exemplar color image from Quickbird. The image was taken in March 2006 for an open area at Los Alamos, NM, where individual trees, roads, and rocks can be clearly seen and distinguished from each other. The right panel (B) was used to validate how well the classification algorithm performs in

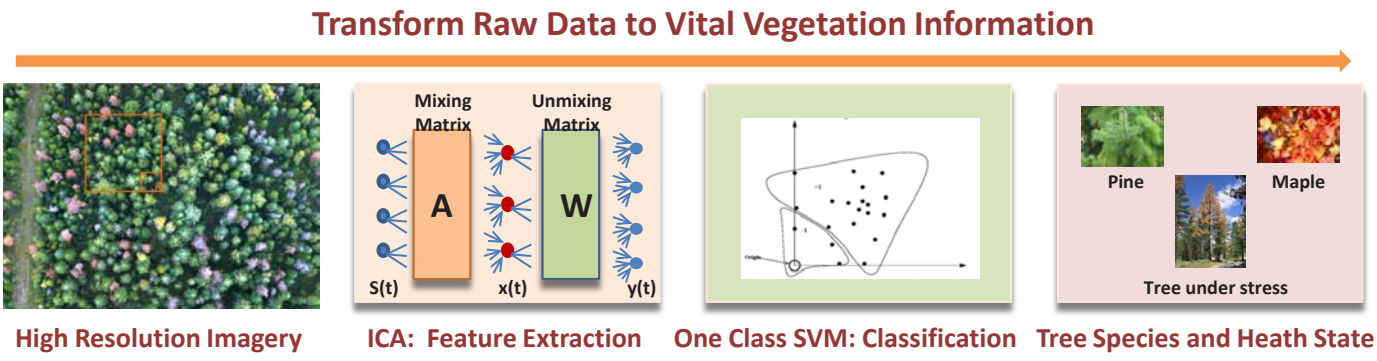

Figure 1. Architecture of the new machine learning framework. The remote sensing data x(t), assumed to be a linear mixtures of independent trees species, are separated by the Independent Component Analysis (ICA) as the feature sets y(t). The one-class SVM uses the features to profile the individual tree species and their state of health.

separating the vegetation from its background. The vegetation in panel A was identified by the supervised learning algorithm in red color, laid on top of the original image, and the resulting image is presented in panel B. It demonstrates that the algorithm accurately separates the vegetation from the roads and rocks.

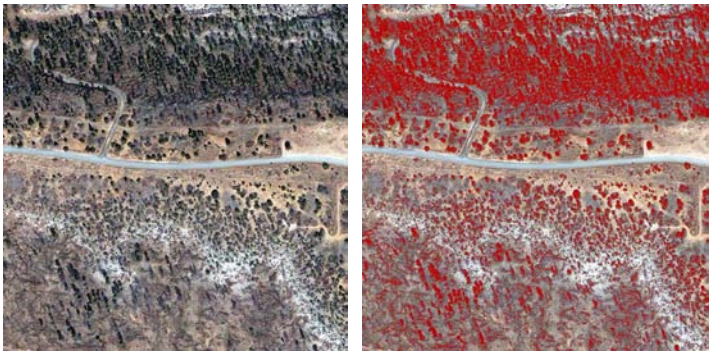

A B

Figure 2. Excellent performance in separating the vegetation from the background. A: the original image; B: The identified vegetation (in red color) is overlaid on top of the original image to assess the classification accuracy.

In stage two, an unsupervised classification algorithm was applied to identify live and dead trees. After the classification algorithm was developed in the area shown in Figure 1A, on a blind test, we applied the classifier to an image from LANL's National Environmental Research Park.

Figure 3 shows the result in categorizing (distinguishing) the state-of-health of individual trees, live vs. dead status. The original image is shown in panel A in which not many trees are live. However, it would certainly take time and experience to identify and label which one is live or dead in the image. The middle panel (B) presents the result to label the live and dead trees by applying the unsupervised classification algorithm we developed in stage two. Comparing to the ground-surveyed data shown in panel C, the live and dead trees identified by the computer algorithms are aligned with the ground-truth data in good accuracy.

Conclusion

In this feasibility study, we have developed a new two-stage machine learning framework to identify vegetation and then assess its state of health, live vs. dead status. Leveraging both supervised and unsupervised learning algorithms, the performance of this new classification system has given impressive accuracy to identify the vegetation from its background, and to distinguish healthy and dead trees.

Future Work

We plan to extend algorithm development to identify the level of stress for individual trees, which will identify the early warning signs and signatures of tree mortality. In addition, we will expand the study areas to include a variety of terrestrial conditions, e.g. different tree types and densities. The results will significantly improve the prediction capability of vegetation models and provide the needed ground truth data to validate dynamic interaction among terrestrial vegetation, CO_2 emission, and climate change.

Impact on National Missions

This project supports the DOE missions in global climate monitoring, and energy security. Quantifying terrestrial impacts and feedbacks associated with climate change is critical to greenhouse gas treaty verification because of the large carbon storage, and emission potential, of terrestrial forests. Success of this project will represent an enormous advance by addressing one of the largest uncertainties in

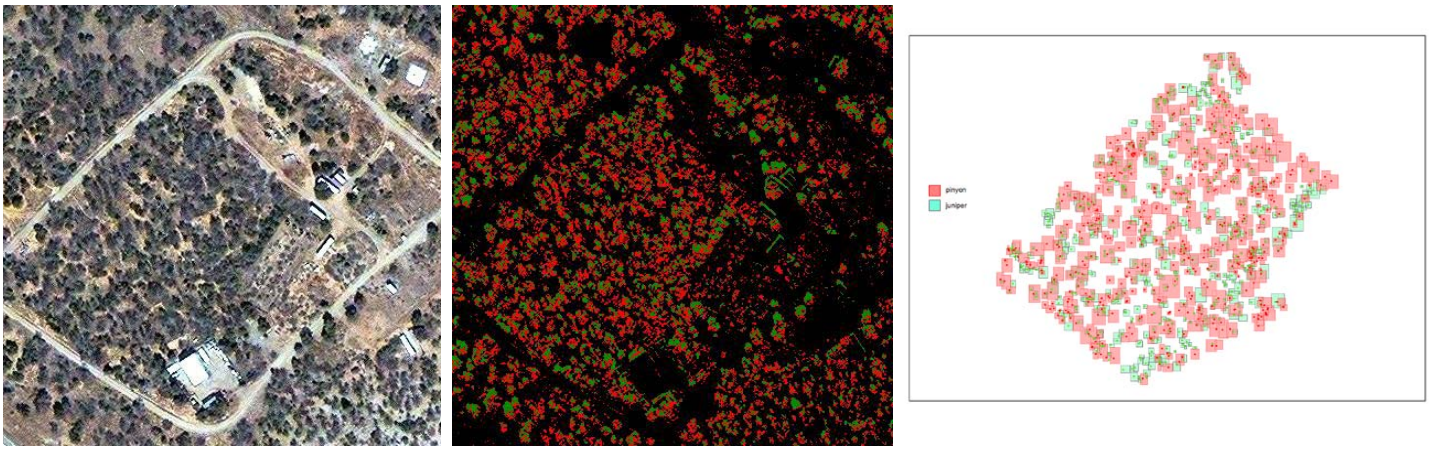

A B C

Figure 3. Performance in identifying live trees and dead trees using unsupervised leaning algorithms. A: original satellite image for the environmental research park; B: live trees (in green) and dead trees (in red) identified by the computer classification algorithm; and C: the ground-surveyed data. The dead pinon trees are labeled in red and live juniper trees are in green.

predicting the global response of Earth to Global Climate Change, with development of key capabilities in remote sensing, machine learning, vegetation modeling, and CO_2 dynamics.

References

1. Allen, C., A. Macalady, H. Chenchouni, D. Bachelet, N. McDowell, M. Vennetier, T. Kitzberger, A. Rigling, D. Breshears, E. H. Hogg, P. Gonzalez, R. Fensham, Z. Zhang, J. Castro, N. Demidova, J. Lim, G. Allard, S. Running, A. Semerci, and N. Cobb. A global overview of drought and heat-induced tree mortality reveals emerging climate change risks for forests. 2010. *Forest Ecology and Management.* **259** (4): 660.

2. McDowell, N., W. Pockman, C. Allen, D. Breshears, N. Cobb, T. Kolb, J. Plaut, J. Sperry, A. West, D. Williams, and E. Yepez. Mechanisms of plant survival and mortality during drought: why do some plants survive while others succumb to drought?. 2008. *NEW PHYTOLOGIST.* **178** (4): 719.

3. Bonan, G. B.. Forests and climate change: forcings, feedbacks, and the climate benefits of forests. 2008. *Science.* **320** (5882): 1444.

4. Friedlingstein, P., P. Cox, R. Betts, L. Bopp, W. von Bloh, V. Brovkin, P. Cadule, S. Doney, M. Eby, I. Fung, G. Bala, J. John, C. Jones, F. Joos, T. Kato, M. Kawamiya, W. Knorr, K. Lindsay, H. D. Matthews, T. Raddatz, P. Rayner, C. Reick, E. Roeckner, K. -G. Schnitzler, R. Schnur, K. Strassmann, A. J. Weaver, C. Yoshikawa, and N. Zeng. Climate-carbon cycle feedback analysis: results from the C<sup>4. 2006. *Journal of Climate.* **19** (14): 3337.

5. Purves, D., and S. Pacala. Predictive models of forest dynamics. 2008. *Science.* **320** (5882): 1452.

6. Fisher, R., N. McDowell, D. Purves, P. Moorcroft, S. Sitch, P. Cox, C. Huntingford, P. Meir, and F. Ian. Woodward. Assessing uncertainties in a second-generation dynamic vegetation model caused by ecological scale limitations. 2010. *NEW PHYTOLOGIST.* **187** (3): 666.

7. Cai, D. M., M. Gokhale, and J. Theiler. Comparison of feature selection and classification algorithms in identifying malicious executables. 2007. *Computational Statistics & Data Analysis.* **51** (6): 3156.

8. Cai, D. M., J. Theiler, and M. Gokhale. Detecting a malicious executable without prior knowledge of its patterns. 2005. In *Data Mining, Intrusion Detection, Information Assurance, and Data Networks Security 2005 ; 28 March 2005 ; Orlando, FL, USA.* Vol. 5812, 1 Edition, p. 1.

9. Theiler, J., and D. M. Cai. Resampling approach for anomaly detection in multispectral images. 2003. In *Algorithms and Technologies for Multispectral, Hyperspectral, and.* Vol. 5093, 1 Edition, p. 230.

10. Brumby, S., J. Theiler, J. Bloch, N. Harvey, S. Perkins, J. Szymanski, and A. Cody. Young. Evolving land cover classification algorithms for multi-spectral and multi-temporal imagery. 2002. In *Imaging Spectrometry VII ; 20010801 - 20010803 ; San Diego, CA, United States.* Vol. 4480, p. 120.

Publications

Cai, D. M., N. G. McDowell, S. Brumby, R. Fisher, S. Brennan, and K. Edlund. DOVE: Discovery Of Vegetation over the Earth Using High Resolution Remote Sensing Data. Presented at *2010 Earth and Space Capability Review.* (Los Alamos, 21-24 June 2010).

Cai, D. M., N. G. McDowell, S. J. Elliot, S. P. Brumby, and F. V. Pabian. Automated identification of tree mortality using high resolution Quickbird Imagery. 2010. *In preparation.*

Cai, D. M., S. J. Elliot, J. Theiler, P. A. Pope, and N. G. McDowell. Assessing vegetation changes with image change detection and classification. 2010. *In preparation.*

Fundamental Research in Quantum Communications

Richard J. Hughes
20100597ER

Abstract

Single-photon (quantum) communications provide the ultimate security assurance provided by the laws of quantum physics. Owing to the Heisenberg Uncertainty Principle, an adversary cannot attempt to eavesdrop on quantum communications without being discovered because of the inevitable disturbance that this would introduce. And quantum communications cannot be passively tapped because each photon is an indivisible elementary particle that cannot be split. During this research project we have invented the first multi-party quantum communications and practical quantum authentication protocols. Ultimately, these protocols could be implemented on a hand-held quantum communications device, which has considerable commercial potential. We have performed the first demonstration of an entirely new quantum-enabled cyber security concept that leverages the network environment to provide communications security even between nodes that lack direct quantum communications. This methodology could be implemented as an overlay on existing campus, enterprise, access or metro-area transparent networks, with node-to-node path lengths as large as 60km using current technology.

Background and Research Objectives

Securing cyberspace is an extraordinarily difficult challenge. Hardly a day goes by without a news report highlighting the need for improved cyber security technologies to protect our economic and National security. In this nine-month project we began the foundational research for a revolutionary new cyber security capability, which will harness the unique security features of new quantum (single-photon) communications protocols. Quantum communications offers the attractive feature of security rooted in laws of quantum physics, providing "forward security": in contrast to conventional approaches, today's quantum-secured communications cannot be compromised by unanticipated future technological advances. However, to be of utility for cyber security, quantum communications must be developed beyond its present point-to-point instantiations to provide communications security even between users who share no direct quantum communications link. Recent theoretical developments have extended the advantages of quantum communications from two-party quantum key distribution (QKD) to new quantum cryptographic protocols such as quantum secure identification. We have invented new multi-party QKD protocols providing quantum security between parties who share no direct quantum communications channel, and Quantum Enabled Security (QES) for securing multiple data streams on a single optical channel. These developments open up multiple uses of quantum communications, including: a handheld quantum communications device providing access control, authentication and a secure telephone call capability; and a photonic layer security overlay on optical fiber networks providing anti-tap, authentication, anti-jam, and anonymous routing capabilities. During this foundational research project we developed these theoretical concepts into practical protocols that can be implemented on real optical channels with loss and noise. These inventions resulted in the filing of a patent application for QES, and a provisional filing for multi-party QKD protocols.

Scientific Approach and Accomplishments

Our research concerns secure communications scenarios in which multiple users are capable of performing quantum communications with a central trusted authority (TA), but not directly with other users. Each user will use quantum communications with the TA to establish shared, secret encryption and authentication keys, not only with the TA, but with the non-secret, off-line assistance of the TA, with other users. First, the TA must be convinced that it is performing quantum communications with a given user, and not some unauthorized third party. We have devised a practical password-based quantum secure identification (QSID) protocol. Our QSID protocol enables an honest user to convince an honest TA that he knows a secret, human-memorable password, while a dishonest user can do no better than to guess the password. Likewise, the probability that a fake TA can deceive an honest user to learn the password is no greater than guessing the password. Each honest user can leverage authentication for the user's messages with the TA from the results of the identification protocol.

Based on this authentication, a user may establish secure communications with another user via quantum key distribution (QKD) with the TA as follows. User 1 uses QKD to generate a secret key with the TA, and user 2 uses QKD to generate a distinct secret key (unknown to user 1) with the TA. The TA may now communicate (in the clear) a list of which bits user 2 must flip so that his key becomes equal to user 1's. This does not compromise security because actual bit values are never revealed. Now user 2 can establish secure communications with user 1, even though they have had no direct quantum communications. We have invented a secure protocol elaborating on this simple concept that provides authenticated multi-party quantum key establishment for both pair-wise and group keys. In a first laboratory experiment we have demonstrated that the shared secrets produced by these quantum protocols can be used to secure data from tapping by adversaries. Optical data is spread over a large amount of temporal bandwidth, using spreading codes that are changed frequently according to the secret bit sequences established by quantum communications. In this way any adversary would be unable to "keep up," even in principle.

Impact on National Missions

The capability resulting from this research will be an attractive way to address cyber security needs within many existing network environments, such as: certain DoD and NNSA complexes; between government agencies in the Washington, DC area; the SmartGrid, power, water, and financial networks; IAEA treaty monitoring; within constrained environments such as a US Embassy or a military aircraft; and LANL's own network. The QES methodology also has commercialization potential as a low-cost, all optical method to secure fiber-to-the-home (FTTH) and fiber-to-the-premises (FTTP) passive optical access networks.

Name Disambiguation and Semantic Networks

Mary Linn M. Collins
20100621ER

Abstract

Name disambiguation is a problem of singular importance. As the attempted terrorist attack on December 25, 2009 illustrated, collecting information about an individual is of little use if critical, related information about the same individual is stored under a different name. Understanding terrorist networks, proliferation networks, and co-authorship graphs in science all depend on matching names to individuals. A proliferation network and co-authorship graph for the Pakistani nuclear scientist A. Q. Khan, for example, will be accurate only if the system that generates the network understands that A. Q. Khan, Abdul Qadeer Khan, Abdul Quadeer Khan, and Abdul Guadeer Khan are one and the same.

An individual's name may be presented in multiple ways in databases, cables, or publications for various reasons: the presence or absence of initials, variations in transliteration, inconsistent use of titles or honorifics, even simple misspellings. Alternatively, multiple individuals may have the same name, requiring disambiguation based on context. Advances in name disambiguation require algorithms that enable machines to 1) identify strings in text or metadata that represent names; 2) match names by detecting variations in strings; 3) extract information from the text or metadata that provides context for the name; and 4) represent the results in a semantic network. Applying advances in name disambiguation to national security requires, in addition, that the algorithms be scalable and reliable, and that human analysts be included in the workflow to validate machine results.

Los Alamos National Laboratory (LANL) has a unique combination of capabilities that can be applied to this problem: digital library expertise in author disambiguation; analysts with expertise in proliferation and the nuclear fuel cycle; and distributed high-performance computing. This report describes a four-month LDRD-ER Reserve Project that studied the problem of context-driven name disambiguation using these capabilities.

Background and Research Objectives

An unclassified analysis of the attempted terrorist attack on Christmas Day 2009 explained what a system should be able to do:

"Abdulmutallab applies for a multi-entry visa. The terrorist database (TIDE) is checked and found to contain no such record. The State Department issues a visa. Later, a TIDE record for Abdulmutallab is added to TIDE. The split-second this record is added to TIDE, the State Department is notified the visa may need [to be] reconsidered…

"…For all this to work, the system needs to realize that despite name variations and inconsistent data, the identity in the terrorist database is the identity in the visa system " [1].

Why is it so hard to create such a system?

The first problem is extracting information from the source. If the source is structured metadata, the issue is fairly straightforward. Metadata parsers can extract information from each field of metadata and convert it to the appropriate representational format. If the source is unstructured text, the issue is anything but straightforward. Entity extraction is a topic of current research [2, 3, 4, 5, 6, 7] and several commercial and open-source tools are available, but the accuracy of these tools is, at best, 90%.

The second problem is representing extracted information in a form that makes it interoperable across disparate systems, such as TIDE and the State Department visa database referred to above. Standards are being developed for the Linked Data Web and semantic web technologies, but these standards are still emerging and are not widely used [8].

The third problem is resolving differences between similar names to determine if they represent the same person. This is the key problem, as solving the first two problems without solving this problem will not result in accurate name and identity disambiguation.

Our primary research objective was to address these three problems by customizing or developing algorithms

to 1) identify strings in unstructured text that represent names; 2) match names by detecting variations in strings; 3) extract information from the text or metadata that provides context for the name; and 4) represent the results in a semantic network.

Scientific Approach and Accomplishments

Identifying strings in unstructured text that represent names

There are several ways to recognize variations of a name in unstructured text such as news articles or message traffic. The approach we took involves a series of text processing steps.

The first step is to find the candidate names within the text. This can be done by a combination of sentence structure analysis and recognition of name honorifics and titles such as "Mr." or "Al-". For example, the open-source text analysis tool ANNIE (A Nearly-New Information Extraction System) [9], which runs within the GATE (General Architecture for Text Engineering) framework [10], utilizes a gazetteer of titles, common first names, and common descriptive words combined with a part of speech tagger and uppercase tokenizer. Like other existing tools, it does not recognize all proper names but it can be modified as its modules are extensible.

One way to increase its accuracy is to expand the gazetteer to include honorifics and name parts from more languages. Another is to tag all capitalized nouns and check against common existing words such as place names.

Matching names by detecting variations in strings

Once the candidate names have been found, the second step is to compare the names to the name being searched. This step involves using name tokenizing and name matching. Tokenizing involves the identification of the different parts of the name, including title and honorifics as well as first and last names where possible. This is highly dependent on the origin of the name searched. For instance, a Muslim name might include a series of honorifics, politeness markers, or name variations such as "Bin" (the son of), "Abu" (the father of), and "Abdul" (the servant of) [11, 12].

These name parts might be included, or not, and might appear in different parts of the name, in different orders, and might be the primary name used. Hyphenated surnames may be identified individually, as one or the other half of the name. The parts must be identified and included in the match algorithm, but there must also be a match when these tokens are not included.

Once the name or name parts are identified, the name matching problem becomes a variation on string matching. There are two major types of name variations that create difficulties in matching: transliteration of the name from its language of origin to English sounds and characters (Qathafi, Kaddafi, Qadafi, Gadafi, Gaddafi), and misspellings such as letter transposition or substitution (Smith, Smyth, Smit).

Three classes of name matching algorithms are commonly used:

- **Soundex** generally keeps the first letter of the name and bins the remaining letters into numbers that refer to similar sounds. So, in English, B, F, P, and V are often mapped to a single letter, as are D and T. The vowels are all dropped, as are H, W, and Y. When the same number appears multiple times together, the duplicates are dropped [13].
- **Damerau–Levenshtein** distance is a string edit distance algorithm that measures the number of insertions, deletions, and substitutions needed to transpose one string to another [14, 15].
- **Editex** is a combination of the two that looks at the string edit distance of letters that are associated with each other in Soundex-type bins. If the letters are in the same bin, the cost to edit is only half as much as if they are not, and letters can be in more than one bin [16].

We tested the different algorithms using several small sets of transliteration variations on the same Arabic name, as well as a larger set of 90,000 non-matching common names to look for false positives. We found the best results using the Editex algorithm with modifications for Arabic, as well as some preprocessing associated with the tokenization described above and accounting for common language-specific transliteration choices.

Three metrics were used to measure the accuracy of the algorithms:

- Matching the same names with different transliterations. The metric is the number of missed matches as well as the average size of the gap from matching to non-matching.
- Matching the set of names from the first metric against 110 non-matching Arabic names to find the number of false matches.
- Matching a subset of the test names against the 90,000 other random names to find the average number of false matches per name.

Figure 1 summarizes the results for all of the algorithms. Clearly, the best name-matching algorithm tested for this set of Arabic names is the Editex algorithm tailored for use with Arabic names. This tailoring involved preprocessing to

Algorithm	Names Missed	Cutoff Size	Mismatched Arabic	Mismatched Common (average out of 90,000)
Soundex	76	-	4	111
Levenstein	0	4.5	831	6700
Editex	3	7.3	782	6681
Tailored Editex	0	8.6	11	40

Figure 1. Summary of match algorithms. The first column indicates how many names were missed that should have matched. The second column refers to the distance between the match and non-match average values. The third and fourth columns list the number of matches that were identified mistakenly.

remove "al" followed by a space or dash, as in the tokenizing described above, and also steps to remove "h" immediately in front or after consonants. The letter binning was also modified to account for different pronunciations.

This appears to be a promising direction, but there are several modifications we can make. We can enhance the matching algorithm by using a much larger set of sample data on high-performance computers. Letter binning can be improved to assign sets of letters to bins instead of individual letters and we can run a learning algorithm on a large set of name data to discover the best match set of bins.

We can also enhance the preprocessing step to account for more language-specific name modifications, and include tokenizing to match or eliminate honorifics and titles. We need to design automated and analyst-mediated processes to determine the area of origin of the name in order to better utilize algorithms tailored to specific languages. Finally, the edit distance needs to be normalized to the maximum possible edit distance (the combined lengths of the two names) to account for the variation in name length, and provide a normalized match number.

Extracting information from text or metadata that provides context

Even if the names themselves are matched perfectly, there still remains the problem of distinguishing separate entities (persons) with the same or very similar name. This requires the use of contextual information to determine differences between the entities. Some level of context definition can be found from analysis of the text content alone, but we added an external taxonomy to aid in defining the contexts in which the names are both searched and found, such as cables or articles.

Our focus taxonomy is on nuclear technology and expertise, primarily defined along the nuclear fuel cycle. We began with a draft set of subject words and phrases, which define an area of interest. A set of sample nuclear texts was analyzed using the Natural Language Toolkit (NLTK) [17] to determine the phrases of interest and how often they appear in the text. This resulted in a set of weighted terms that were adjusted based on our subject matter expertise in nuclear technology.

The weighted keyword list was developed using a combination of word and phrase count analysis of related texts, in combination with subject matter knowledge to highlight the best fit phrases. For example, five scientific articles about uranium enrichment [18, 19, 20, 21, 22] and laser enrichment [23, 24, 25, 26, 27] were analyzed to find the most common words and phrases used in the articles. Only significant words were used, as determined through subject matter knowledge, and weights were assigned based on word counts normalized to the total count within each concept. So, for example, nuclear is assigned a weight of 0.40, uranium 0.22, and plutonium 0.20.

The weighted set of keywords can be used to determine if different texts concern the same subject. This, in turn, makes it possible to more accurately identify the expertise of a given name (person) associated with a given text, and to use this information to disambiguate names and persons.

The taxonomy needs to be enhanced to a much finer level of detail, and to include more terms and concepts, particularly in follow-on work that moves the project to a classified environment. We would improve the match algorithm by considering word distance, taking into account the word distance between keywords and also between keywords and names. More work will be done to ensure that all variations in the keywords are captured, such as "U235", "U-235", and "235U." The set of keywords will change depending on the context of interest, i.e., manufacturing expertise, scientific expertise, or equipment. Finally, the keywords will be tested against much larger datasets.

Representing the results in a semantic network

A taxonomy in the form of a hierarchical list is highly simplified as it does not represent relationships between concepts or different facets of a given concept. In a nuclear taxonomy, for example, "Uranium" may be listed under the category of "Nuclear Material" but it is also associated with other categories, such as "Light Water Moderated Reactors," where uranium is the fuel.

Complexities such as these can be represented better in a

concept map than in a hierarchical list. Figure 2 is a high-level nuclear concept map that shows relationships as well as the semantic distance between concepts. For instance "Mining" is closer to "Milling" than it is to "Fuel Fabrication" as the numbered steps in the category of "Fuel Cycle" are considered to be an ordered process.

Even this representation does not capture all nuances, as the same concepts may be used in different contexts. For instance, different words may be used when thinking about a specific technology in terms of export control vs. expertise, as in a visa application.

We explored the use of semantic networks and graphs to represent several kinds of information besides concepts.

Figure 3 shows a semantic graph for names that have the same Soundex encoding. Figure 4 shows a semantic graph that associates a given Soundex encoding and author name with concepts in the paper written by the author. Finally, Figure 5 shows all of the information about a particular author extracted from several bibliographic records containing structured metadata.

The semantic graphs in Figures 3, 4, and 5 were created on a high-performance computer as proofs-of-concept. The importance of semantic networks and graphs becomes most obvious when high-performance computers and very large amounts of data are involved, as well as a structured taxonomy or ontology to enable inferencing across sub-graphs. The speed of inferencing dwarfs what humans are capable of, but the data has to be accurate or the inferences will not be.

Impact on National Missions

Real-time inferencing across very large datasets and sub-graphs to resolve identities of terrorists and proliferators is a critical national need. LANL has unique capabilities in terms of subject matter expertise and high-performance computing that can be applied to this problem.

In the four-month project described here we succeeded in laying the foundation for this work. Specifically, we:

- Customized algorithms for extracting names, matching them, and resolving ambiguities re: entities (persons) by using contextual information
- Identified improvements that need to be made to the algorithms for specific languages
- Developed portions of a nuclear taxonomy
- Created proof-of-concept semantic networks and graphs

We hope, now, to combine the unique capabilities of machines and humans and to apply them to the problem of name disambiguation on the scale required to ensure global security.

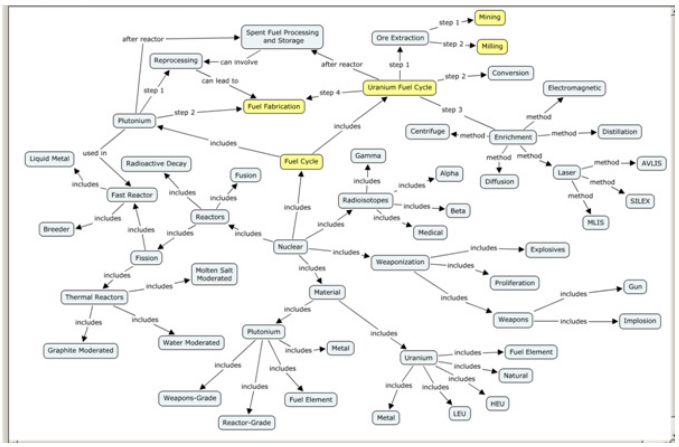

Figure 2. High-level nuclear concept map. Not all concepts and relationships are shown in order to ensure readability. Concepts in yellow are referred to in the text.

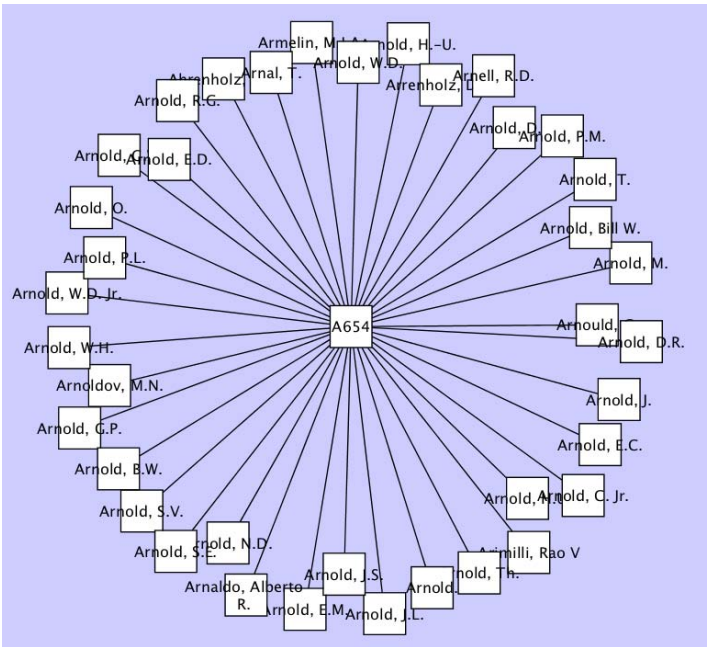

Figure 3. Semantic graph showing all of the author names associated with the Soundex encoding A654 from a small subset of the Research Library's collection.

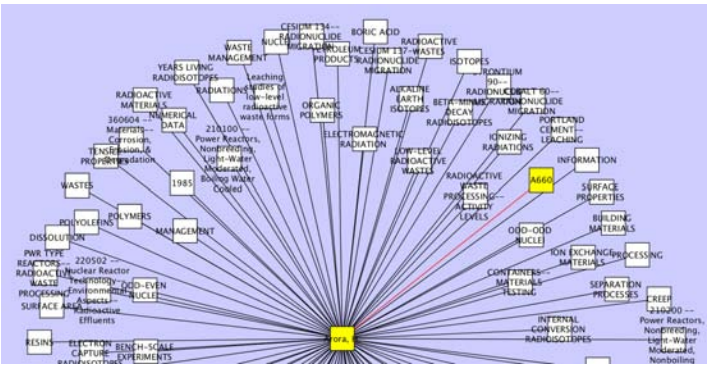

Figure 4. Semantic graph showing an author name, the Soundex encoding A660 associated with that author name, and the topics the author has written about.

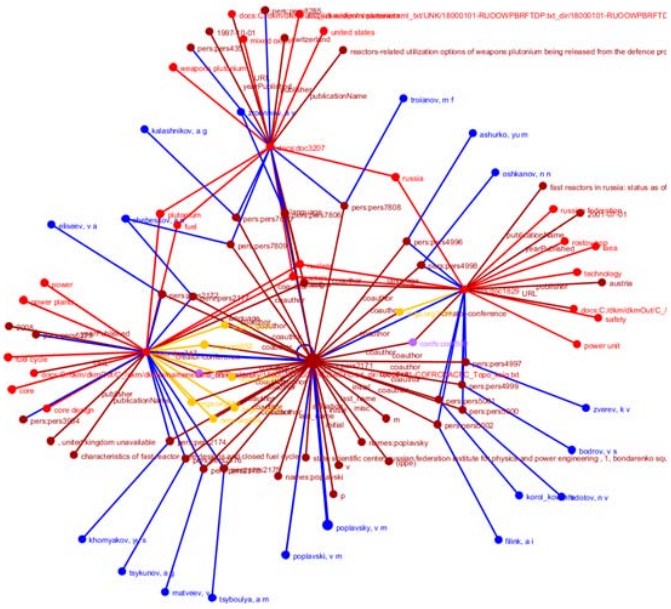

Figure 5. Semantic graph showing information about an author, including the names of co-authors, extracted from multiple structured bibliographic records and integrated in a semantic database.

References

1. A. R. Qureshi. Design and development of an early warning system to prevent terrorist attacks. 2009. In *Proceedings - 2009 2nd IEEE International Conference on Computer Science and Information Technology.* , p. 222. 445 Hoes Lane - P.O.Box 1331 Piscataway, NJ 08855-: IEEE Computer Society.

2. N. Tongtep. A feature-based approach for relation extraction from thai news documents. 2009. In *Intelligence and Security Informatics - Pacific Asia Workshop, PAISI 2009.* Vol. 5477, p. 149. Tiergartenstrasse 17 Heidelberg, D-69121, Germany: Springer Verlag.

3. H. Traboulsi. Arabic named entity extraction: a local grammar-based approach. 2009. In *Proceedings of the 2009 International Multiconference on Computer Science and Information Technology (IMCSIT).* , p. 139. Piscataway, NJ, USA: IEEE.

4. R. B. Bradford. Entity refinement using latent semantic indexing. 2010. In *2010 IEEE International Conference on Intelligence and Security Informatics (ISI 2010).* , p. 126. Piscataway, NJ, USA: IEEE.

5. E. Chan. Text analysis and entity extraction in asymmetric threat response and prediction. 2010. In *2010 IEEE International Conference on Intelligence and Security Informatics (ISI 2010).* , p. 202. Piscataway, NJ, USA: IEEE.

6. W. R. Osman. Ambiguity in text mining. 2008. In *2008 International Conference on Computer and Communication Engineering.* , p. 1172. Piscataway, NJ, USA: IEEE.

7. J. Jonas. The Christmas Day Intelligence Failure – Part I: Enterprise Amnesia vs. Enterprise Intelligence [Weblog]. 2010.

8. Advanced Knowledge Technologies. ANNIE (A Nearly-New Information Extraction System).

9. University of Sheffield. GATE (General Architecture for Text Engineering). 2010.

10. A. F. Beeston. Arabic Nomenclature: A summary guide for beginner. 1971.

11. D. B. Appleton. Periodic Arabic Names and Naming Practices. 2003.

12. National Archives. The Soundex Indexing System. 2007. **2010** (7/23).

13. V. S. LETOKHOV. LASER SEPARATION OF ISOTOPES. 1977. *Annual Review of Physical Chemistry.* **28**: 133.

14. J. A. PAISNER. ATOMIC VAPOR LASER ISOTOPE-SEPARATION. 1988. *APPLIED PHYSICS B-PHOTOPHYSICS AND LASER CHEMISTRY.* **46** (3): 253.

15. M. YAMAMOTO. OPTIMUM OPERATING-CONDITIONS FOR A LASER URANIUM ENRICHMENT PLANT. 1977. *Applied Energy.* **3** (4): 287.

16. C. WEITKAMP. HYPERFINE-STRUCTURE AND ISOTOPE SHIFT MEASUREMENTS ON U-235 AND LASER SEPARATION OF URANIUM ISOTOPES BY 2-STEP PHOTO-IONIZATION. 1978. *Optics Communications.* **26** (2): 177.

17. W. D. METZ. URANIUM ENRICHMENT - LASER METHODS NEARING FULL-SCALE TEST. 1974. *Science.* **185** (4151): 602.

18. R. Schuette. Uranium enrichment by the separation-nozzle process. 1976. *Naturwissenschaften.* **63** (9): 407.

19. S. VILLANI. PROGRESS IN URANIUM ENRICHMENT. 1984. *NATURWISSENSCHAFTEN.* **71** (3): 115.

20. S. M. Badawy. Uranium isotope enrichment by complexation with chelating polymer adsorbent. 2003. *Radiation Physics and Chemistry.* **66** (1): 67.

21. P. Dart. Phonetic string matching: lessons from information retrieval. 1996. In *19th Annual International ACM SIGIR Conference on Research and Development in Information Retrieval .* , p. 166. USA: ACM.

22. F. J. DAMERAU. A TECHNIQUE FOR COMPUTER DETECTION AND CORRECTION OF SPELLING ERRORS. 1964.

Communications of the ACM. **7** (3): 171.

23. T. Heath. Linked Data - The Story So Far. 2009. *INTERNATIONAL JOURNAL ON SEMANTIC WEB AND INFORMATION SYSTEMS.* **5** (3): 1.

24. E. Klein. Natural Language Processing with Python. 2009.

25. I. Hore-Lacy. Uranium Mining, Processing, and Enrichment. 2004.

26. V. I. Levenstein. Binary codes capable of correcting deletions, insertions, and reversals. 1966. *Soviet Physics Doklady.* **10** (8): 707.

27. Alternatives for uranium enrichment. 1991. *Membrane Technology.* **1991** (9): 1.

Multiscale Variational Approaches to Markov Random Fields

Michael Chertkov
20090516PRD1

Introduction

Graphical models, also known as Bayesian networks or Markov random fields, are statistical models for complex systems of random variables represented as a graph. The nodes of this graph correspond to random variables while its edges denote statistical interactions among those variables. Graphical models have now come to play a central role in many computational fields such as image restoration, computer vision, information theory, statistical signal processing in oceanography and seismology and biological applications. However, optimal inference and estimation in these models is generally intractable for very large problems. This has driven research and development of principled yet tractable approaches to approximate inference for this rich class of models. These approaches typically involve a distributed message-passing algorithm that serves to propagate information throughout the graph. The performance of these method, however, often suffers in graphical models which exhibit strong long-range correlations. Handling such situations is precisely the goal of multi-scale methods such as the renormalization group method of statistical physics or the multi-grid method for solving large-scale linear systems. It is the aim of this project to develop a new class of algorithms that combine modern advances in approximate inference and appropriate multi-scale algorithms inspired mainly by the renormalization group method of statistical physics. Our basic strategy is to first consider equivalent reformulation of the inference problem as a multi-scale model by defining an equivalent graphical model depended on an extended set of variables including new auxiliary variables that can be used to represent large-scale interactions of the model. Then, recently developed variational methods can be applied in this extended model where the new auxiliary variables provide additional degrees of freedom to obtain a more accurate solution.

Benefit to National Security Missions

This project will support the DOE mission in Office of Science by enhancing our understanding of Inference and Optimization Techniques. Our multiscale approach is relevant to long-range correlations and non-local measurements such as seismic or gravity inversion in geophysics, tomography, and radiography of all types, with several national security applications.

Progress

In the past year we have continued work on combinatorial approaches to approximate inference in graphical models inspired by approaches in statistical physics. In June 2009, we presented the paper “Orbit-Product Representation and Correction of Gaussian Belief Propagation” at the International Conference of Machine Learning. This works build upon Jason’s prior work in graduate school on walk-sums in Gaussian graphical models and on Micheal Chertkov’s prior work on loop series correction to belief propagation (BP) in discrete-variable graphical models. We developed an interpretation of inference in the Gaussian model (essentially computing a matrix determinant) as computing a weighted product over all orbits (closed walks) of the graph and demonstrate that BP captures a certain subset of these orbits. Using this interpretation, we bound the error of BP and propose methods to compute corrections to BP.

In September 2009, we presented our work on Gaussian BP at the Physics of Algorithms Workshop (Jason was a co-organizer of this workshop). This presentation included extensions of our orbit-product framework to analyze Generalized Belief Propagation (GBP) [of Yedidia et al] in the context of Gaussian graphical models. The basic idea behind GBP is to use exact inference within small subgraphs together with message-passing between subgraphs to obtain a better approximation that captures small cycles of the graph. Our analysis confirms this intuition for Gaussian models, providing error-bounds dependent on the length of the shortest orbit omitted by GBP. However, we also show that the subgraphs used in GBP must be chosen properly to avoid over-counting orbits, which can destabilize the iterative algorithm or results in inaccurate estimates. We are currently preparing a conference paper on GBP, and plan a longer journal article combining both conference

papers to be submitted in the fall.

In related work, we have developed an extension of these methods aimed at analysis of belief propagation in binary-variable graphical models. A key ingredient of this approach is a method of Kac and Ward that allows the partition function of the planar Ising model in statistical physics (a seemingly intractable sum over all states of the model) to be expressed simply as a determinant of a matrix which generates non-backtracking orbits of the graph. Using this construction, we have shown that it is possible to express the BP estimate of the partition function of the (non-planar) Ising model as a nonbacktracking orbit-product of the graph. Ultimately, we hope to use the representation to derive new results for the convergence and accuracy of BP in binary-variable graphical models, analogous to those we have already derived in the Gaussian model. A by-product of this work has been the invention of a new approach to approximate inference in graphical models. Whereas belief propagation may be seen as inference on the computation tree of the graph (the infinite tree cover of the graph), a more general approach is to construct iterative algorithms that can be interpreted as inference on other infinite planar covers of the graph. Similar as in GBP, this allows retaining many cycles of the graph so as to given a better approximation to the original graphical model. Inference in this planar cover may be implemented using a combination of message-passing ideas and Gaussian elimination to compute determinants of planar subgraphs of the non-planar graph.

Jason has also made contributions to an allied project, Optimization and Control of Smart Grids, adapting methods for learning sparse graphical models (part of his graduate work) to the problem of near-optimal design of power transmission networks. We pose the network design problem of selecting the network (both its graph structure and line conductances) to minimize a combination of the power dissipation within the network and cost of resources needed to build the network. Building on work of Ghosh, Boyd and Saberi and of Candes and Boyd, we developed a principled optimization approach to solve this problem and have recently submitted the "A Majorization-Minimization Approach to Design of Power Transmission Networks" to the IEEE Conference of Decision and Control.

Future Work

We will develop a new class of approximate inference methods which blend recently developed variational-combinatorial approaches from the graphical modeling literature with a multiscale approach inspired by renormalization group theory in statistical physics. Inference in the graphical models can be reduced to computation of the log-partition function, also known as the cumulant generating function in statistics. Hence, we will focus our efforts on developing a multiscale variational method to approximate the log-partition function. This will combine three key elements: (1) combinatorial methods to decompose the log-partition function as a sum of interactions defined on subregions of varying size, (2) a multiscale method to approximate complex multi-variable interactions from a coarse-scale representation of the field, and (3) variational methods to improve the quality of approximation by optimizing over all reparameterizations of the model. This approach is similar to multigrid methods in linear algebra, but differs in that we address non-linear models and also pose a single, global optimization criterion based on "re-summing'' effects across multiple scales.

The proposed methods are relevant to a wide range of problems of interest to LANL that can be posed as one of inference or estimation in a graphical model. Consider reconstruction from a two-dimensional media, like network of sensors or compact computer disc. As the density of information increases, it becomes difficult to resolve individual bits, leading to inter-symbol interference. Then, the optimal inference strategy reduces to estimation of an intractable two-dimensional graphical models. The multiscale approach is especially important in problems involving long-range correlations and non-local measurements such as seismic or gravity inversion in geophysics, tomography, and radiography of all types. These methods may also prove relevant in monitoring non-equilibrium dynamical systems that exhibit interactions at multiple scales.

Conclusion

It is expected that by combining the multi-scale method with modern computational heuristics for graphical models, such as belief propagation and the variational approach, we can achieve improved performance (both better accuracy and faster convergence of distributed iterative algorithms) in those most challenging applications where current methods either fail or are inaccurate. This will then be an important advance for solving a wide range of challenging computational problems in science and engineering.

Publications

Johnson, J., D. Bickson, and D. Dalev. Fixing Convergence of Gaussian Belief Propagation. 2009. In *International Symposium on Information Theory (ISIT).* (Seoul, June 2009). , p. 1674. Piscataway, NJ, USA: atawa.

Johnson, J., V. Chernyak, and M. Chertkov. Orbit-Product Representation and Correction of Gaussian Belief Propagation. 2009. In *International Conference on Machine Learning (ICML).* (Montreal, June 2009). Vol. 38, p. 473. New York: ACM.

Johnson, J., and M. Chertkov. A Majorization-Minimization Approach to Design of Power Transmission Networks. To appear in *49th IEEE Conference on Decision and Control.* (Atlanta, Georgia, , Dec. 2010).

Netrapalli, P., J. Johnson, and M. Chertkov. Greedy Learning of Planar Ising Graphical Models. Presented at *Artificial Intelligence and Statistics (AISTATS 2011).* (Ft. Laudedale, Florida, Apr, 2011).

Quantum Information Processing: Capabilities and Limitations

Robert E. Ecke
20090520PRD2

Introduction

The possibility of manipulating quantum states raises exciting possibilities for engineering and computer science. Because quantum systems are hard to simulate on conventional computers, computers utilizing quantum coherence should be intrinsically more powerful than their conventional counterparts. For example, exponentially faster quantum algorithms exist for factoring integers, for algebraic and optimization problems, and for simulating physical systems. Quantum mechanical noise is a challenging obstacle for experimental realizations of quantum computation. One promising idea to fight noise is error correction. The quantum capacity of a noisy process is the amount of quantum data that can be protected, in the limit of many transmissions affected by that noise; classical capacity is defined similarly. Determining these capacities from a description of the noise is an open problem. Another proposal to combat noise seeks to engineer exotic materials with topological order, as they are believed to have noise-resistant collective excitations that could be used to build a quantum computer. As a Richard P. Feynman Postdoctoral Fellow in Theory and Computing, Jon Yard works to determine the quantum and classical capacities for practical noise models and will seek better theoretical understanding of quantum capacity. He is using quantum information concepts he has developed, to better understand physical systems exhibiting topological order, and how they can be used to protect quantum information. His objective is new algorithms for solving classically hard problems on a quantum computer.

Benefit to National Security Missions

Understanding how quantum information processing can promote or jeopardize cybersecurity supports Threat Reduction. Quantum information helps understand properties of matter, such as superconductivity, bearing on materials and device design for the Energy and Office of Science missions. Long-term leadership in cutting-edge computation supports all Laboratory missions.

Progress

With collaborators Matthias Christandl, and with Fernando Brandão, Yard discovered a fundamentally new property of quantum conditional mutual information, which is an entropic quantity central to the connection between entanglement and topological order, while having equal importance in the study of quantum communication in general. Many quantities of interest in quantum information theory, such as channel capacities and measures of entanglement, are given as optimization problems involving quantum conditional information. However, in several important cases, the best-known expressions are not effectively computable, requiring optimizations over infinitely many variables. The recent breakthrough obtained by Yard and his collaborators unexpectedly relates this quantity to the distance from the set of quantum states having only classical correlations. This in turn gives several important insights for the structure of quantum states and settles several open questions in quantum information theory and computer science. Among these was the resolution of two longstanding open questions – one concerning the structure of approximate quantum Markov chains, and the other concerning technical properties of a much-studied measure of entanglement called Squashed Entanglement. This work also gave a new classical algorithm for detecting entanglement in quantum states, and gave a new characterization of the quantum generalization of the class of computational problems called NP. Indeed, the famous P vs. NP problem of computer science asks whether it is easier to verify a proof than it is to find the proof oneself. This new result proves that if the proofs are given by several unentangled quantum states, to be verified by quantum computers that can only communicate classically, there is no advantage over having just a single quantum proof, settling an open question in computer science. A key observation that lead to this breakthrough was a careful use of the information-theoretic “state redistribution” protocol that Yard had previously discovered with collaborator Igor Devetak.

With collaborator Graeme Smith (IBM), Yard has been working toward identifying optical communication channels that have zero quantum capacity by themselves, but which nonetheless can have a nonzero capacity when used together. While such channels were shown to exist by Yard and Smith in their 2008 Science paper, a practical example that can be realized in a laboratory is still missing. They found that such a channel would necessarily consist of at least two optical modes, and they have isolated conditions on such channels that would suffice to find such an example. However, two-mode Gaussian quantum channels - of which such a channel will be an example - have not been given a complete characterization to date. This work is thus expected to lead to other new results on the capacities of two-mode channels for transmitting secure and quantum information. They have since found such an example numerically, and are working now on understanding the numerics so they may give a mathematical proof and characterization of how this effect can be explored in a laboratory.

Yard has also continued his research on entropic signatures of entanglement and topological order. Building on previous work, he has identified a class of model Hamiltonians - known as quantum double Hamiltonians - whose topologically ordered ground states lead to a direct connection between his previously discovered "state redistribution protocol" for quantum communication and a well-established entropic measure of topological order. He has also identified that this connection can be made rigorous for states that are holographic, meaning the number of degrees of freedom grows with the area of the state. Previously, the connection was only heuristic. He still is pursuing ways of making this connection applicable to a wider and more robust class of topologically ordered states.

Future Work

Jon Yard's recent Science paper showed that quantum capacity could be much larger than expected for some types of noise, and perhaps should be replaced with a more general concept. In particular, it showed that there are pairs of channels, each with zero quantum capacity when used on their own, such that when used together, quantum information can be transmitted through the pair at a nonzero rate. That is, the capacity of quantum channels is not additive: the capacity of the tensor product of two channels is not the sum of their individual capacities. This very surprising result suggests that a generalization of the notion of channel capacity, able to describe how channels combine, is needed. Yard will work toward developing such a generalization. He will also determine quantum and classical capacities for practically relevant noise models (such as electromagnetic field modes affected by Gaussian noise). He will also demonstrate relationships between an information-theoretic characterization of multipartite quantum correlations that he discovered, involving the quantum conditional mutual information, and entropic measures of topological order. Topological order appears in the quantum Hall effect and may play a role in other strongly interacting materials such as high-temperature superconductors, so there may be applications of his measure of multipartite correlations in these contexts. Yard will develop new algorithms for solving classically hard problems on a quantum computer. These include computing topological invariants, such as whether a knot can be untied without cutting, implementing Fourier transforms over new types of groups, and simulating physical systems. He will also find ways to efficiently perform certain entangled quantum measurements with a quantum computer, leading to practical coding schemes and providing key subroutines for classes of quantum algorithms.

Conclusion

Determining the quantum capacity of quantum channels will help in developing designs for reliable quantum computers and in improving quantum methods for secret key distribution. Yard's work on classical capacity could provide methods for achieving higher data rates in existing free-space and fiber optical networks. The algorithms he will design will help us understand whether and how one might design public-key cryptographic systems (e.g. for ecommerce, banking, and authenticated digital communication) resistant to quantum codebreaking. New algorithms, and theoretical concepts form quantum information, could help understand the properties of physical systems, for example, materials properties important in energy efficiency engineering.

Publications

Brandao, F., M. Christandl, and J. Yard. Faithful Squashed Entanglement. *Communications in Mathematical Physics.*

Yard, J., and I. Devetak. Optimal quantum source coding with quantum side information at the encoder and decoder. 2009. *IEEE Transactions on Information Theory.* **55** (11): 5339.

Quantum Knowledge: A Revolutionary Approach to Measurement

Michael Zwolak
20100619PRD2

Introduction

This is a theoretical physics project, with potential experimental collaborations in the later phases. It begins with a recently-developed theory of agents, observation, and decision-making, which constructs an object that can interact with quantum systems in its environment to solve simple problems faster than can be done classically. This is a new way of observing and making decisions, centered around "quantum knowledge."

In the course of this project, this theory will be thoroughly explored and validated, including making testable predictions where possible. Furthermore, the theory of quantum knowledge will be applied to clarify and reconcile tensions and paradoxes within quantum theory, which have plagued it for nearly a century. The most ambitious goal of this theory is to resolve the tension between classical and quantum physics by showing that classical experience fits self-consistently within quantum theory.

In parallel, concrete applications of the theory will be developed. Potential applications arise in quantum metrology, quantum information theory, and quantum algorithms. The plan is to devise powerful techniques by modeling quantum devices as agents that gather and utilize information.

Finally, collaborations with experimental groups will be pursued in order to test predictions made by the theory of quantum knowledge and to implement and demonstrate new algorithms and measurement techniques.

Benefit to National Security Missions

This project supports the missions of the Office of Science by enhancing our understanding of quantum theory, and our ability to probe and measure complex natural systems. It also supports the Homeland Security mission of the Laboratory by assisting the development of quantum computers, secure quantum communications, and improved precision sensing.

Progress

The current research goal is to design improved techniques for gathering information about quantum systems, and to better understand the physical limits of such information gathering. In particular, we are exploring a paradigm called quantum knowledge. Based on the observation that data about quantum systems can, itself, be quantum information, quantum knowledge has the potential to revolutionize how we think about information gathering.

During FY 2010, we applied quantum knowledge to enhance quantum state discrimination. In collaboration with Sarah Croke (Perimeter Institute), we found an elegant streaming protocol for discriminating between two quantum pure states, if N copies of the unknown state are available in an array. This protocol condenses all the information available in the array of copies into a single quantum bit, using coherent information processing (quantum computation) on each copy sequentially, and then obtains a result by measuring this single memory bit.

In late 2010 (FY 2010-11), we refined this process and extended it to discrimination between K distinct pure states. We also identified a candidate (and potentially very powerful) way of extending this technique to finitely correlated lattice states, also known as matrix product states (MPS). MPS are a hot topic in condensed matter physics, believed to accurately describe 1-D lattice systems' ground states. In an MPS, entanglement between lattice sites is limited but nontrivial, so key properties of laboratory-produced MPS can be hidden from local observations. We expect our algorithm to provide the most efficient possible way of probing and measuring these properties, using only a small quantum memory. We are currently drafting a paper on this topic.

Finally, we are intensively investigating the limits of *classical* techniques for statistical estimation of quantum systems' properties. This supports and complements our work on coherent ("quantum knowledge") inference, since the extra effort required to implement a quantum protocol is only advantageous if that protocol (provably)

improves on the best that can be achieved classically. In the course of establishing these bounds, we found that existing protocols for quantum state and property estimation can be substantially improved, leading to independent benefits for quantum technologies.

Future Work

We will proceed on several fronts. First, we will further develop the theory of quantum agents and quantum knowledge, seeking in particular to understand:

- whether it is self-consistent,
- how much of the ``measurement problem'' can be resolved with it,
- what amount of decoherence is sufficient to make quantum agency unadaptive,
- how this theory relates to the many-worlds hypothesis, and
- what testable predictions can be made about the feasibility of quantum agents.

The second main thrust of this research is continued development of improved techniques for quantum metrology and estimation. The goal here is to surpass classical limits on sensitivity, while using very modest quantum resources. Candidate problems include quantum state estimation (a.k.a. tomography), state discrimination, and the detection of extraordinarily weak forces. Challenges include discriminating complex states of many-body systems, and finding and measuring robustly quantum degrees of freedom outside of sheltered laboratory conditions.

We will also use ideas from quantum knowledge to inspire novel quantum algorithms and communication protocols. Protocols for coherent state discrimination and adaptive data compression (which achieve high efficiency on tiny quantum computers) are already being designed. Adaptive communication protocols show great promise. A variety of other computational problems may be addressed using the same intuitions.

Conclusion

The first goal of this project is improved understanding of quantum measurement. This will fill a longstanding gap in our most fundamental physical theory. The second goal is improved quantum measurement technology. This will assist design of quantum computers; more broadly, it should have repercussions for a broad range of sensing applications, important to science, industry, and national security. The third goal is development of new quantum information-processing protocols. This will enhance the utility of quantum computers (when they are built) and quantum communication devices (which already exist), as well as illuminating the fundamental limits of quantum information theory.

Towards Human Level Artificial Intelligence: A Cortically Inspired Semantic Network Approach to Information Processing and Storage

Luis Bettencourt
20080724PRD2

Abstract

Multi-relational graph modeling and analysis is becoming more prevalent in the area of information storage and processing. A testament to this statement is the enormous amount of funding being directed to the Web of Data community (aka. Semantic Web community) of the domain of computer science. Beyond the application to problems of information storage and processing on the Web, the LDRD research was focused on the applicability of multi-relational graphs to information and storage that is cortically inspired. As such, this research focused on the development of theories and applications of multi-relational graphs to cognitive logics.

Background and Research Objectives

A multi-relational graph is a graph/network that makes use of multiple relations over the vertices of the graph. Other names for such graphs are semantic graphs and edge labeled graphs. Network science and graph theory are primarily concerned with single-relational graphs, where all edges have the same meaning. For instance, in single-relational graphs, all edges mean "friendship," "kinship," etc., but not all of them together within the same structure. As such, there are limits to what can be modeled with single-relational graphs. In order to rectify the inherent limitations of such structures, there has been a push to develop multi-relational graph analysis techniques and apply them to various domains of modeling and analysis.

The objectives of the LDRD funded research were to 1) develop a general theory of multi-relational graph analysis, and 2) apply it to cortically-inspired information processing. The remainder of this summary will discuss these two points at length.

Scientific Approach and Accomplishments

A general theory for multi-relational graph analysis was developed using two approaches. The relation types concern both of these approaches with how to traverse a multi-relational graph in such a way as to bias the traverser. If an expressive traversal language can be developed, then the full body of single-relational graph analysis algorithms can be mapped over to the multi-relational domain in a semantically feasible way. The two mathematical approaches to the development of an expressive multi-relational traverser are presented below.

Tensor-based approach: an algebraic ring with the binary operations of * and + was developed. The operation * (ordinary matrix-multiplication) was used to perform a step in the graph and the operation + (entry-wise addition) was used to merge the paths of different steps. Moreover, the Hadamard operation o (entry-wise multiplication) was introduced to allow for the filtering of particular branches of a path. With this algebra defined, it was demonstrated that all known single-relational graph analysis algorithms could be ported over to the multi-relational domain while preserving the semantics of the multi-relational graph. This work was presented in [1].

Binary relational algebra approach: a relational algebra for combining binary relations was developed. This approach borrowed from the n-ary relational algebra developed by E.F. Codd in 1970 [2]. In the binary algebraic model, an f-join operation was developed that allows for the joining of graph edges according to a predicate defined by some f. For those unfamiliar with relational algebra, the join operation can be rewritten as a Cartesian product followed by a selection and projection. The f-join (along with other operations) demonstrated the same expressivity as the tensor-based approach mentioned previous. However, unlike the tensor-approach, the binary relational model has the convenient feature of being computationally feasible -- as ordinary matrix multiplication is expensive to compute. This work was presented in [3].

Given these two theories of multi-relational graph traversals, a programming language was the demonstrated,

in concrete implementation, the usefulness and expressiveness of these two algebraic theories. However, to ensure Turing completeness, branching and looping were introduced. Such operations were not presented in the algebras. This language is called Gremlin [] and has become a standard in the graph database community as it currently is being used by as a query/manipulation language for 4 different graph databases.

What has been described so far was only the first half of the objectives of the funded research. In order to apply this theory and language to the problem of cortically inspired information storage and processing, there needed to be a way to store large multi-relational graphs and a way to process them in a cortically-inspired way. Storage was made possible through collaborations with the graph database community. Cortically-inspired processing was made possible through two methods: non-monotonic logics and biased random walks.

Ordinary predicate logic is monotonic in that once a statement is proved true, it remains true. Ordinary predicate logics are also completely deductive in that they only derive more sophisticated theorems from a set of provided axioms. Unfortunately, cognitive logic doesn't obey the premises of mathematical logic [4]. In the space of non-monotonic logics statements can be derived through ampliative methods such as induction, abduction, and exemplification. A particularly interesting non-monotonic logic is the evidential logic developed by Pei Wang [5]. Evidential logics allow for the updating of "truth" based on future information as well as inference methods not based solely on deduction. The evidential logic was represented according to the multi-relational graph tensor algebra in [6]. For the sake efficiency, a random walk model was developed in [7]. In conclusion, a cortically inspired information storage and processing system was developed using multi-relational graphs.

Impact on National Missions

This research, being theoretical in nature, contributes primarily to a deeper understanding of multi-relational graph structures in modeling and analysis. However, of applied, practical significance, a programming language was developed that is being used by the graph analysis community. The language's mailing lists boasts almost 100 members with over 400 downloads of the compiler and virtual machine. While the primary researcher (Dr. Marko A. Rodriguez) has since left the Laboratory, the capabilities have moved into the public sector and as such, are being used both in academia and the commercial sector.

References

1. Rodriguez, M. A., and J. Shinavier. Exposing Multi-Relational Networks to Single-Relational Network Analysis Algorithms. 2009. *Journal of Informetrics.* **4** (1): 41.
2. Codd, E. F.. A Relational Model of Data for Large Shared Data Banks. 1970. *Communications of the ACM.* **13** (6): 377.
3. Rodriguez, M. A., and P. Neubauer. A path algebra for multi-relational graphs. Presented at *The 2nd International Workshop on Graph Data Management Techniques and Applications (GDM 2011).* (Hannover, Germany, 16 April 2011).

Publications

Ham, M. I., V. Gintautas, M. A. Rodriguez, R. Bennet, C. L. Santa Maria, and L. M. A. Bettencourt. Density-Dependence of Functional Spiking Networks in Vitro. 2010. *Biological Cybernetics.* **102** (1): 71.

Rodrigez, M. A., A. Pepe, and J. Shinavier. The Dilated Triple. 2009. In *Emergent Web Intelligence.* Edited by Chbeir, R., A. Hassanien, A. Abraham, and Y. Badr. , p. 1. Heidelberg: Springer Verlag.

Rodriguez, M. A.. Grammar-Based Random Walkers in Semantic Networks. 2008. *Knowledge-Based Systems.* **21** (7): 727.

Rodriguez, M. A., J. Bollen, and H. Van de Sompel. Automatic Metadata Generation using Associative Networks. 2009. *ACM Transactions on Information Systems .* **27** (2): 1.

Rodriguez, M. A., and A. Pepe. On the Relationship Between the Structural and Socioacademic Communities of a Coauthorship Network. 2008. *Journal of Informetrics.* **2** (3): 195.

Rodriguez, M. A., and J. Geldart. An Evidential Path Logic for Multi-Relational Networks. 2009. *Association for the Advancement of Artificial Intelligence.* **SS-09** (09): 114.

Rodriguez, M. A., and J. Shinavier. Exposing Multi-Relational Networks to Single-Relational Network Analysis Algorithms. 2009. *Journal of Informetrics.* **4** (1): 29.

Srinivasan, R., A. Pepe, and M. A. Rodrigez. A Comparison Between Ethnographic and Clustering-Based Semi-Automated Techniques for Cultural Ontologies. 2009. *Journal of the American Society for Information Science and Technology.* **60** (2): 1.

Finite State Projection for Accurate Solution of the Master Equation

Michael E. Wall
20080730PRD2

Abstract
When experiments are too expensive or otherwise impossible to perform, computational models help fill the gaps in our understanding. However, many natural systems are inherently discrete and stochastic, and the models needed to gain reliable insight are overwhelmingly complex. For example, in biology some important regulatory proteins are present in quantities of a few per cell. Standard tools for stochastic analyses do not suffice here. Drawing upon automatic control theory, dynamical systems, and model reduction, this project further developed the Finite State Projection (FSP) algorithm to enable the difficult task of stochastic analysis for low probability transient events.

Background and Research Objectives
Random events are a cornerstone of a variety of subjects, from statistical physics to control theory. They are also central to problems in biology that address cell chemistry, evolution, and studies of infectious disease. Most researchers use the master equation to study such events. Unfortunately, it is difficult to solve for all but the simplest systems.

Dr. Munsky invented a fast way of solving the master equation. He developed the Finite State Projection (FSP) algorithm, which enables one to ignore unimportant contributions to the master equation. The method is having a large impact already.

This project addressed a big hurdle in applying the FSP: many biological systems have millions of interacting components, preventing sufficient simplification of the master equation. The goal of this project was to make the FSP approach work even in these extremely complicated cases. Dr. Munsky developed methods for further reducing the complexity of the equations by focusing only on the variables that are relevant to answering specific questions. These methods used control theory and information theory techniques. He also demonstrated the utility of the FSP approach by applying it to specific biological problems.

Scientific Approach and Accomplishments
Many natural systems are inherently discrete and stochastic, and the models needed to gain reliable insight are overwhelmingly complex. For example, in biology some important regulatory proteins are present in quantities ranging from one or two copies to thousands per cell. Standard tools for stochastic analyses, such as stochastic simulation algorithms, do not suffice to deal with this diversity of scale. Drawing upon extensive theory from automatic controls, dynamical systems, and model reduction, the Finite State Projection (FSP) algorithm was developed to enable the difficult task of stochastic analysis for low probability transient events. Where previous methods simulate individual process trajectories, the FSP directly describes the dynamics of the system's probability distribution.

For many systems, the FSP method outperforms all other computational techniques to provide precise error bounds on low probability transient events, but there remains much room for improvement. In this project, Dr. Munsky extended the FSP approach to efficiently and accurately handles a vast range of complex stochastic systems that cannot be analyzed with any current approach. Real systems often include far more variables than can be experimentally altered or measured. With control theory-based model reduction techniques and coarse graining modeling approaches, Dr. Munsky developed systematic means of identifying the key characteristics of complex models. Reduced models were specifically tailored to analyze the correlations between (i) the alterable quantities (inputs), and (ii) the measurable quantities (outputs), while aggregating or eliminating the vast number of extraneous variables and mechanisms that can be neither affected by inputs nor detected from outputs. Working with a number of theoretical collaboraters, Dr. Munsky extensively tested and compared reduced models to large scale Monte Carlo algorithms for their efficiency and accuracy in analyzing complex systems from cellular biology and epidemiology. Working with experimental collaborators, he developed models of stochastic gene regulation for specific biological systems.

The following are accomplishments of this project:

Stochastic model validation for the Pap (pili) epigenetic switch (with Brooke Trinh, David Low, Bruce Braaten and Mustafa Khammash--UCSB).

This ongoing task introduces a model to predict regulation of pili expression in uropathogenic E. coli. Dr. Munsky inferred model parameters using in vitro Mobility Shift Assays and in vivo Florescence Activated Cell Sorting techniques. The result is highly predictive model, which can now be extended to discover new behaviors in this and similar biological systems.

Simplicity of Completion Time Distributions for Common Complex Biochemical Processes (With Golan Bel and Ilya Nemenman--CNLS/CCS3)

Many cellular processes involve a large number of distinct, reversible steps. For example, in kinetic proofreading, cells use serial reactions to precisely construct large protein complexes. In this work, we study the dynamics of such systems and statistically characterize the time required to complete a process. We determined equations for the mean and the variance of the completion time for a kinetic proofreading process, and numerically analyzed more complicated systems. As the system size grows, the completion time can cease to be random or can become exponentially distributed. In other words, the full complex system starts looking like it has a simple transition from one simple behavior to another. We expect the behaviors of many complex cellular processes to simplify in a similar manner, and suggest that cellular behavior might be robust to the details of elementary reactions.

Specificity and Completion Time Distributions of Biochemical Processes (With Golan Bel and Ilya Nemenman--CNLS/CCS3)

In the previous task we examined a system of serial reactions. In this task we considered a branched system that leads to two possible outcomes. We determined equations not only for the completion time distribution but also for the tendency of the system to follow the desired branch. We also showed that the full system behaves like a simple three-point process. Our model paves the way for understanding the interplay between specificity and completion times as well as testing the validity of different models for biological systems.

Identification of Gene Regulatory Networks Based Upon Stochastic Gene Expression and Flow Cytometry Measurements (with Brooke Trinh, David Low, Mustafa Khammash--UCSB and Babetta Marrone, B9-LANL).

We showed that randomness could be exploited to reverse engineer genetic regulatory networks. Cellular noise changes as it propagates through a molecular network, carrying with it a distinctive fingerprint with information about the structure of the network. We demonstrate that analysis of noise can enable identification of all network parameters, including those that may otherwise be difficult to measure. Our approach is general and can be used to identify other cellular networks.

Identification of Gene Regulatory Networks Based Upon Stochastic Gene Expression and Fluorescence in Situ Hybridization (FISH) Measurements (with Gregor Neuert (MIT) Alex van Oudenaarden (MIT) and Mustafa Khammash (UCSB)).

Investigators at MIT have used a newly developed method to count the number of mRNA molecules in individual yeast cells exposed to different environmental conditions. We applied FSP to the data to identify multiple competing models of gene regulation for this system, and evaluated competing models using maximum likelihood methods. We plan to bring the experimental capability to LANL for future experiments.

Impact on National Missions

This project will support the DOE mission in Threat Reduction. The tools developed will impact many fields in science, medicine, and industry. They can be applied to problems throughout LANL and DOE in genomics, fluid dynamics, global climate, social networks, disease spread, and material science. Understanding cellular networks is a major stated goal of DOE/OS/BER and multiple NIH institutes.

Publications

Bel, G., B. Munsky, and I. Nemenman. Simplicity of completion time distributions for common complex biochemical processes. 2009. *Physical Biology.* **7**: 016003.

Munsky, B., B. Trinh, and M. Khammash. Listening to the noise: random fluctuations reveal gene network parameters. 2009. *Molecular Systems Biology.* **5**: 318.

Munsky, B., I. Nemenman, and G. Bel. Specificity and completion time distributions of biochemical processes. 2009. *Journal of Chemical Physics.* **131**: 235103.

Munsky, B., and M. Khammash. Transient analysis of stochastic switches and trajectories with applications to gene regulatory networks. 2008. *IET Systems Biology.* **2**: 323.

Munsky, B., and M. Khammash. Using noise transmission properties to identify stochastic gene regulatory networks. 2008. In *46th IEEE Conference on Decision and Control.* (Cancun, Mexico, Dec, 2008). , p. 768. Cancun: IEEE.

Munsky, B., and M. Khammash. Identification of a stochastic model for the genetic toggle switch. To appear in *IET Systems Biology.*

Munsky, B., and M. Khammash. Stochastic gene expression: modeling, analysis, and identification. To appear in *The control handbook.* Edited by Levine, B..

Statistical Physics of Optimization

Michael Chertkov
20080787PRD3

Abstract

In this project Statistical Physics of Optimization we used the experience collected over decades by physicists in the studies of matter in order to understand, and predict, new relations between the microscopic (local) and macroscopic (global) properties of complex systems. Particularly handy in this task are techniques developed in studies of disordered systems such as spin glasses, or structural glasses this is because complex systems, such as hard optimization problems, power grid or logical Boolean formulas used for electronic design verification, are very rarely ordered, homogeneous or strongly symmetric, often they are not even embedded in an Euclidean space. On the other hand studies of optimization problems provides insight that permits new understanding of disordered physical materials such as glasses or spin glasses.

The main results of this project are both in development of theoretical methods and applying new methods to practical problems. The main theoretical results concern our work on random ensembles of constraint satisfactions problems and the study of their complex energy landscapes, we found several fundamental properties of the planted ensemble, and generalized the current static approach to a description of a long time dynamics in these systems. These works served as inspiration for the discovery of deep connections between the physics of the glass transition and bulk melting – this is a significant step forward in understanding the fundamental properties of glassy materials. We also proved non-existence of a spin glass phase in the random filed Ising model thus solving a twenty years open question. The applications driven side is illustrated in our work on inference of parameters in particle tracking and the optimization and integration of renewable resources in a model of the smart grid.

The following groups in LANL will benefit from the knowledge and capabilities acquired during this project Complex System Group (T-13, now part of T-4), Center for Nonlinear Studies (CNLS), Information Science Group (CCS-3) and the center for Information Science and Technology.

Background and Research Objectives

Optimization and inference are fundamental in many areas of science, from computer science and information theory to engineering and statistical physics, as well as to biology or social sciences. Optimization and inference typically involve a large number of variables, e.g. particles, agents, cells or nodes, and a cost function depending on these variables, such as energy, measure of risk or expenses. In this project we addressed the following fundamental questions that concern general combinatorial optimization setting: How to recognize if given instance of an optimization problem is hard and what are main reasons for this? How to find efficiently an approximate solution of a hard problem? What are the relations between hard optimization problems and frustrated disordered systems such as spin glasses and structural glasses? Do insights from hard optimization problems provide some new understanding of physics of disordered systems? Answering these questions is among others crucial for developing new algorithms for optimization problems.

We applied concepts from the statistical physics of disordered systems to problems of computer science, information theory and artificial intelligence. Insights coming from models and methods of statistical physics are fruitful in these domains and bring novel predictions, understanding and practical results. Our work concentrated both on development of theoretical methods and applying new methods to practical problems. The theoretical side is illustrated in our work on random ensembles of constraint satisfactions problems and the study of their complex energy landscapes, we found several fundamental properties of the planted ensemble, and generalized the current static approach to a description of a long time dynamics in these systems. These works served as inspiration for the discovery of deep connections between the physics of the glass transition and bulk melting – this is a significant step forward in understanding the fundamental properties of glassy materials. We also proved non-existence of a spin glass phase in the random filed Ising model thus solving a twenty years open question. The applications driven side is illustrated

in our work on inference of parameters in particle tracking and the optimization and integration of renewable resources in a model of the smart grid.

Scientific Approach and Accomplishments

Our research combines physics-based ideas with standard optimization methods and with learning and inference methods from artificial intelligence. Common denominator in our work is often the use of message passing approach, such as belief propagation, to tackle both the theoretical and algorithmic questions. In statistical physics the message passing approach translates into the cavity method that is used to study disordered systems with complex energy landscape. Bellow we list in more detail the most significant results on this project that have been published in high impact scientific journals (e.g. one in Proc. Nat. Acad. Sci., two in Phys. Rev. Let., one paper selected for editor's suggestions in Phys. Rev. B).

Particle tracking

In many experiments high-speed cameras are used to take images of many moving objects to infer trajectories or parameters of the equations of motion. According to the context, these objects are for example particles in a turbulent flow, bacteria, cars, or soldiers. In most current approaches one first reconstructs the trajectories of individual objects and then one infers parameters of interest. We suggested and validated an approach to infer parameters of the equations of motion without reconstructing individual trajectories. We show that the problem can be rephrased as a maximization of a partition function of a matching (linear assignment) problem. We use the belief propagation algorithm to approximate this partition function and its maximum. We illustrate precision of the method in the regime of high densities (or low image frequency) where reconstruction of the individual trajectories is no more possible. The method can be easily generalized to other problem, where the laws of motion of the objects are known or are to be tested, but their parameters are unknown. See Figure 1 for illustration.

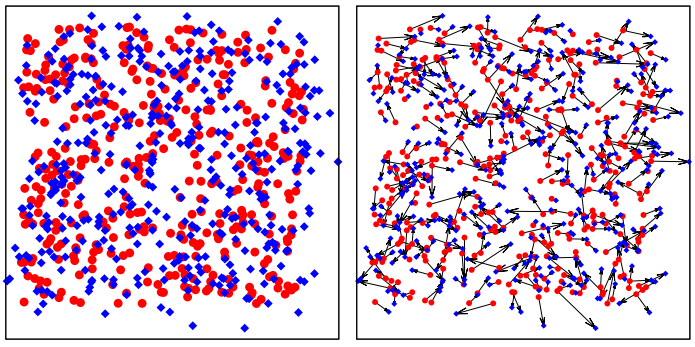

Figure 1. An example of particle tracking, with N=400 particles moving from their original positions (red circles) to new one (blue diamonds). The particles are transported by a turbulent fluid flow. The parameters describing the local stretching, shear, vorticity and diffusivity of the flow are a=0.28, b*=0.54, c*=0.24 and T*=1.05. The figure on the right shows the actual motion of each particle. Evidently, the simple criterion of particle proximity fails to pick the actual trajectories, and the mapping of the particles between the two images is intrinsically uncertain. Nevertheless, the inference algorithms we developed rapidly obtain excellent predictions a=0.32, b=0.55, c=0.19 and T=1.00 for the parameters of the flow.*

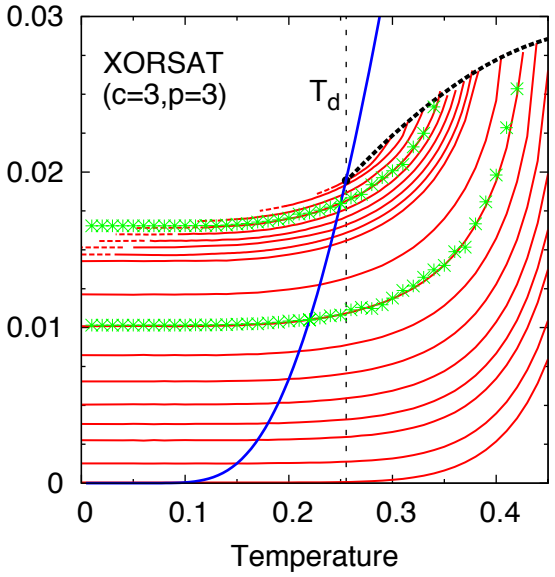

Figure 2. Red lines depict the evolution of different basins of attraction in the landscape (states) in a mean field glassy model with Ising spins interacting via random 3-body interactions, the lattice being a random graph of coordination fixed to 3. Energy of different states is plotted as a function of the temperature. The blue line corresponds to the thermodynamic energy of the system at a given temperature and the vertical line depicts the glass phase transition in the system.

We developed smart grid model with redundancy and renewable resources.

We consider the power grid with M generators and N consumption units. Each consumer demand is drawn from a predefined distribution, thus mimicking instant uncertainty in the load. Each generator has a maximum power cap. A generator is not overloaded if sum of loads of consumers connected to the generator does not exceed the power cap. In the standard grid each consumer is connected only to its designated generator, while we consider a more general organization of the grid when a consumer selects one generator depending on the load from a pre-defined consumer-dependent and sufficiently small set of generators which can all serve the load. We show that the redundancy allows significant expansion of the domain of

parameters where the probability for a generator overload is asymptotically zero. Our results also translate into an algorithmically efficient and distributed message-passing control scheme achieving the asymptotically optimal selection of loaded links. In the same setting we also discussed the integration of fluctuating renewable generation in [6]. We explored the capacity of the renewable generation by determining the level of "firm" generation capacity that can be displaced for different levels of redundancy.

The random field Ising model (RFIM)

RFIM is a benchmark model for disordered systems with a wide range of applications, from vortices pining in superconductors to binary liquids in porous media.

In this model Ising spins are placed at the vertices of a graph (e.g. a periodic lattice) and interact ferromagnetically, on top of that each spin is subject to a random magnetic field. The model has attracted interest in theoretical physics since more than thirty years. Several authors argued that a spin glass phase precedes the ferromagnetic transition in the RFIM. We showed rigorously that an equilibrium spin glass phase does not exist in the random field Ising model, in any dimension, for any type of geometries. The proof is remarkably simple and relies of a special case of the Fortuin-Kasteleyn-Ginibre inequality, from which it follows that the spin glass susceptibility cannot diverge out of the critical ferromagnetic point, hence the RFIM does not exhibit a spin glass phase and this disproves conclusions of previous authors. This result closes a twenty years old debate and is one of the rare rigorous proofs of a non-trivial statement in the filed of disordered systems.

The problem of partitioning a graph into two groups of a given size appears often in applications

Linear time heuristic algorithms are widely studied and used. The problem is tricky to treat with message passing algorithms because of the existence of a global constraint that fixes the size of the two groups. We worked out a way to fix the groups sizes in a local way within the belief propagation equations. We showed that such a BP is very efficient and we anticipate it can be used as a part of modern partitioning solvers. The treatment of combinatorial problems with methods of statistical physics leads unexpectedly to some rather strong mathematical statements. One conjecture of the kind discovered within this sub-project concerns two famous NP-complete problems: the maximum cut and minimal bisection of graphs. It follows from the cavity solution of the two problems that in random regular graphs the maximum cut size asymptotically equals the number of edges in the graph minus the minimum bisection size. Such a result is surprising from the graph theory point of view and mathematically challenging.

We studied the planted ensemble of constraint satisfaction problems (CSPs)

CSPs are benchmarks of hard optimization problems. Statistical analysis of random formulas of CSPs sheds light on the origin of the algorithmic hardness and helped understanding performance of heuristic algorithms. We studied constraint satisfaction problems on the so-called "planted" random ensemble, where the formula is chosen in such a way that a certain predefined configuration of variables is satisfying that formula. We showed that for a certain large class of problems many of the properties of the usual random ensemble are quantitatively identical in the planted random ensemble. We described the structural phase transitions, and the easy/hard/easy pattern in the average computational complexity. In consequence we are able to create benchmark random formulas that are impossible to solve in available time (if the hidden solution is not uncovered). More importantly, planting provides us with a random formula and an equilibrium solution in a region of parameters where Monte-Carlo equilibration time diverges: this provides a very simple trick to simulate efficiently a priori "impossible-to-simulate" models.

One big remaining question about hard random optimization problems was: Can we say something analytically about the behavior of the dynamics?

In mean field glassy models, with the exception of very simple unrealistic models, the dynamics was indeed analytically inaccessible. Understanding of the dynamics, however, is absolutely crucial, both for physics and computer science applications. Using ideas that appeared in the study of the planted formulas, we managed to generalize the cavity method to describe the adiabatic evolution of every state in the glassy energy landscape of mean field models as the temperature is changed. In mean field glassy systems the equilibration time of local dynamics is exponentially large, hence a Monte-Carlo procedure such as simulated annealing is not able to sample the ground states. A practically relevant question is instead: What is the limiting energy of a very slow (but not exponentially) simulated annealing? Our method of adiabatic following of glassy states allows to compute this limiting energy. From the computer science perspective this means that for a first time we were able to analyze how well simulated annealing can possibly perform in problems such as random K-satisfiability or random graph coloring. See Fig.[2] for illustration.

The following properties are in the present literature associated with the behavior of super-cooled glass-forming liquids: faster than exponential growth of the relaxation time, dynamical heterogeneities, growing point-to-set correlation length, crossover from mean field behavior to activated dynamics.

We show that these properties are also present in a much simpler situation, namely the melting of the bulk of an ordered phase beyond a first order phase transition point. This is a promising path towards a better theoretical, nu-

merical and experimental understanding of the above phenomena and of the physics of super-cooled liquids. We discussed in detail the analogies and the differences between the glass and the bulk melting transitions. Moreover, we show that for a class of Ising-spin models undergoing a first order transition -- namely the p-spin model on the so-called Nishimori line -- the melting dynamics can be exactly mapped to the equilibrium dynamics. In this mapping the dynamical ---or mode-coupling--- glass transition corresponds to the spinodal point, while the Kauzmann transition corresponds to the first order phase transition itself. Both in mean field and finite dimensional models this mapping provides an exact realization of the random first order theory scenario for the glass transition. The corresponding glassy phenomenology can then be understood in the framework of a standard first order phase transition.

Impact on National Missions

Our goal was to use statistical physics models to predict, understand and improve behavior of complex systems such as hard optimization problems or glasses. Deep understanding of such problems allows exploring new frontiers in information science. LANL researchers have been developing related approaches within the Complex System Group (T-13, now part of T-4), Center for Nonlinear Studies (CNLS), Information Science Group (CCS-3) and the center for Information Science and Technology. All these programs will benefit from our work as it steps forward in combining insights from computer science, information theory, artificial intelligence, machine learning, and physics. In particular novel were the works on the connection between hard optimization problems and the various application of the message passing algorithms that will further be explored in the above groups. This project brought to the laboratory a long-term visitor Florent Krzakala and two summer students Aurelien Decelle and Michele Castellana.

Publications

Chertkov, M., L. Kroc, F. Krzakala, M. Vergassola, and L. Zdeborova. Tracking particles by passing messages between images. 2010. *Proceedings of National Academy of Sciences.* **107**: 766.

Krzakala, F., F. Ricci-Tersenghi, and L. Zdeborova. Elusive Glassy Phase in the Random Field Ising Model. 2010. *Physical Review Letters.* : 207208.

Krzakala, F., and L. Zdeborova. Hiding Quiet Solutions in Random Constraint Satisfaction Problems. 2009. *Physical Review Letters.* **102**: 238701.

Krzakala, F., and L. Zdeborova. Following Gibbs States -- The Energy Landscape of Mean Field Glassy Systems. 2010. *Euro Physics Letters.* **90**: 66.

Krzakala, F., and L. Zdeborova. Glassy dynamics as a melting process. *Journal of Chemical Physics.*

Sulc, P., and L. Zdeborova. Belief propagation for graph partitioning. 2010. *J. Physics A.* **43**: 28.

Zdeborova, L., A. Decelle, and M. Chertkov. Message Passing for Optimization and Control of Power Grid: Toy Model of Distribution with Ancillary Lines. 2009. *Physical Review E.* **80**: 046112.

Zdeborova, L., S. Backhaus, and M. Chertkov. Message Passing for Integrating and Assessing Renewable Generation in a Redundant Power Grid. Presented at *HICSS 43.* (Kaui, 5-8 Jan. 2010).

Zdeborova, L., and F. Krazakala. Generalization of the cavity method for adiabatic evolution of Gibbs states. 2010. *Physical Review B.* **81**: 224.

Zdeborova, L., and S. Boettcher. Conjecture on the maximum cut and bisection width in random regular graphs. 2010. *Journal of Statistical Mechanics.* : P02020.

Physics

LABORATORY DIRECTED RESEARCH AND DEVELOPMENT

Double Beta Decay

Steven R. Elliott
20090053DR

Introduction

The answer to the question: "Is the neutrino its own anti-particle?", is critical for theories of particle mass. It is also needed to help uncover the reasons matter dominates over anti-matter in our Universe. The neutrino mass will not only tell us about the energy scale at which the Standard Model breaks down, but also has implications for the large-scale structure of the Universe. Finally, lepton-number violation is significant in its own right.

Neutrinoless double-beta decay is the only practical method for investigating the particle/anti-particle question. If the neutrino is its own anti-particle, neutrinoless double-beta decay will have the best sensitivity to neutrino mass of any laboratory technique. Calculations of the nuclear matrix elements for this process have driven the advancement of nuclear shell-model codes. Our double-beta decay program will greatly influence the wider-particle physics, nuclear physics, astrophysics and cosmology endeavors.

If this nuclear decay process exists, one would observe mono-energetic beta emission originating from certain isotopes. This is in contrast to classical single beta decay, in which the beta particles (electrons) are spread over a wide range of energies. One isotope that may undergo double-beta decay is Ge-76. Germanium-diode detectors fabricated from material enriched in Ge-76 have established the best half-life limits and the most restrictive constraints on the effective Majorana mass. This material holds great promise for future advances in double-beta decay experimental techniques. Eventually, these future experiments could detect a double-beta decay lifetime as long 10^27 y, which produces only about 1 event per ton per year. At this sensitivity, we can look for neutrino mass values near that indicated by the atmospheric neutrino oscillation results.

The primary goal of this proposal is to establish the experimental and theoretical technology for a "near background-free" search for neutrinoless double-beta decay in Ge-76.

Benefit to National Security Missions

The Nuclear Physics Long Range Plan strongly endorses research in this area of double beta decay. The DOE Office of Nuclear Physics has defined this research as a mission need. The similarity of requirements means that this R&D will be applicable to certain environmental monitoring applications. Furthermore, this work will develop sensor technology for Threat Reduction, e.g. Nonproliferation, and for materials management in the weapons program.

Progress

During the past two years we have made significant progress on the so-called first cryostat: the device that we want to build to show that the experimental design is ready for Ge detectors fabricated from enriched Ge. We plan to build this cryostat and install detectors made from natural-isotopic-abundance Ge. If this "prototype" works successfully, then we will continue on with a separate project to build a similar cryostat with enriched Ge. We have purchased and tested the 35 detectors that we require for the first cryostat. In addition we have made progress on a better understanding of the various types of background that could make our search for double beta decay difficult, beginning construction of the first cryostat of detectors and theory efforts.

We have continued to do a number of projects, which investigate the background contributions for a double beta decay experiment. Much of our recent work in this area has exploited the nearby proximity of the neutron facility at LANSCE. We have just published a paper on neutron interactions in lead, to determine a rate for a particularly troublesome background reaction. We have made progress analyzing similar data we have for Ge and Cu. We took similar data on the material CZT and Ar. The Cu data is nearly ready for publication. An analysis of the Ge sample for cosmogenic production of backgrounds was recently accepted for publication in Physical Review C. We have also completed taking data to understand surface alpha backgrounds and the analysis of that data is nearing completion, with a student's dissertation

being complete. We are presently taking data to measure long-lived cosmogenic isotopes in Pb.

We have been working closely with the designers of the Sanford Underground Laboratory (SUL) at Homestake to prepare for occupation of an underground laboratory there. We will be one of the initial experiments to reside in that facility. Through our direction, SUL has prepared a design of a laboratory that will meet our requirements for the R&D associated with this proposal. There has been a bit of delay in the anticipated beneficial occupancy date of the finished lab. However, some of this schedule risk has been mitigated by a plan to install a temporary lab to begin the time critical electroforming of the low-activity shield parts. This step is very time consuming and hence it is important to get it started soon. This temporary lab has been completed and we anticipate beneficial occupancy in December after installation of a fire suppression system. We now anticipate having access to the full lab in late 2011.

We have operated our mechanical, electrical, and thermal test cryostat to better understand the cryostat design. See Figure 1. After year 1 we identified 2 thermal issues that required redesign prior to construction of the first cryostat. A modification and further testing found additional issues that have been resolved and further tests are planned.

We have finished the design of the calibration system. We have finalized the conceptual design of a flexible line source and have engineered the system. We will assemble a prototype and test in the coming months.

We have made significant progress on the shield and calibration engineering. The shield will be composed of a large mass of Cu and Pb. In year 1, we purchased the required lead and Cu. In Year 2, we purchased the required plastic that is used as a neutron shield. Our design engineer has completed a concept design and engineering is very far along. See Figure 2.

We have ordered and received 35 Ge detectors, which will comprise that needed for the first cryostat. See Figure 3. These detectors arrived over years 1 and 2. We nearing completion of acceptance testing of these detectors and 19 of them are being delivered to SUL.

Theory work on matrix element operators has begun. Jonathan Engel from the University of North Carolina has begun a series of visits to work with our theory group on this part of the effort.

This work has led to positive reviews for the proposed MAJORANA DEMONSTRATOR. In particular our mid-term review was positive.

Figure 1. A photograph of the mechanical, electrical, and thermal test cryostat.

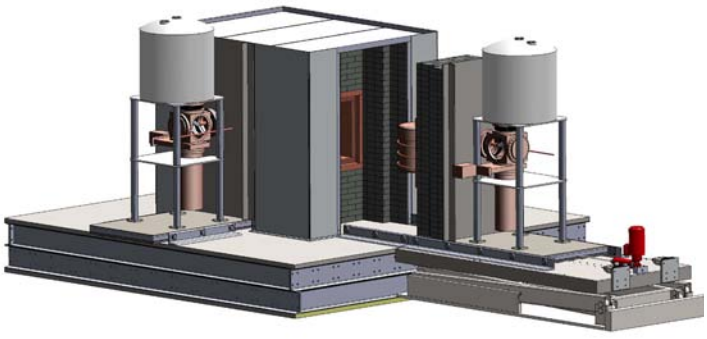

Figure 2. An engineering drawing of the shield.

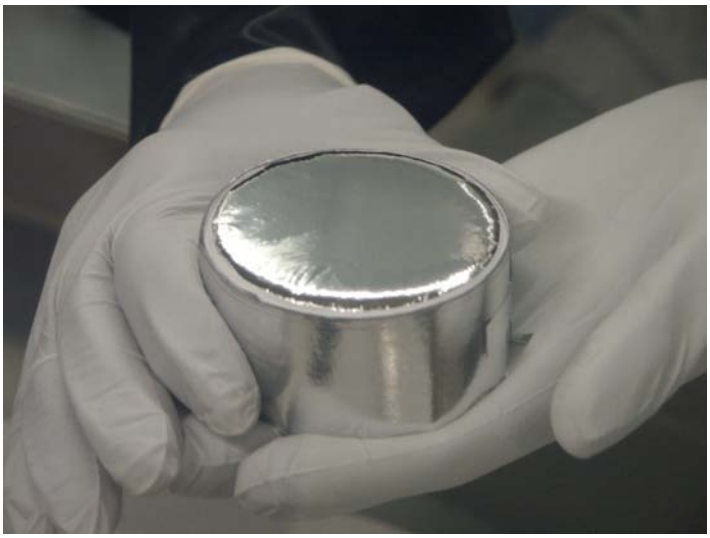

Figure 3. A photograph of a Ge detector.

Future Work

We will finish the analysis of the (n,n') data we took at LANSCE on Cu, Ge, CZT and Ar. We hope to publish all these data sets during the coming two years.

We will analyze the Pb cosmogenic data and publish the results. The qualitative results show that such isotopes do form in Pb and therefore they must be taken into account in any background model of an experiment that uses Pb shielding.

We will continue to analyze data from our activated detectors. Whether we will be able to understand this data well enough to publish is still an open question. Nevertheless, the data have taught us much about cosmogenic activities in Ge detectors and we will learn much more. In particular, we have learned that our external-source calibrations do not necessarily mimic the behavior of internal-source response. This is a critical piece of information for double beta decay and we will better understand it as a result of this work. Already this is no longer an unknown-unknown.

We will test the new string design in our thermal and mechanical test cryostat and verify the thermal performance of our design. We expect these parts to be delivered early next year and will perform the test soon thereafter. The results will be used to confirm the final design for the cryostats.

We will assembly and test a prototype of the calibration system. The parts are on order now and we will verify the operation of the system. We will also perform accelerated testing to confirm long-term repeated operation of the apparatus.

We will complete testing of the 35 detectors and store them all underground to be ready for installation into the prototype cryostat.

All of these efforts will help to finalize the design of the initial cryostat and we will have the parts in place to assemble that cryostat by year's end. This work has helped greatly in getting us ready to build the cryostats for the enriched detectors.

The theory work will continue with work on the matrix elements being published this year.

Conclusion

The results from this project will demonstrate that the proposed technique is capable of reaching the sensitivity required for future double beta experiments. These experiments have the potential to elucidate the origin of the matter-antimatter asymmetry of the Universe and hence address the question of why galaxies, stars, and planets were possible.

Publications

Elliott, S. R.. Double Beta Decay: Solid-State and Semiconductor Detectors. Presented at *Conference on the Intersections of Particle and Nuclear Physics.* (San Diego, CA, May 2009).

Elliott, S. R.. Toward a tonne-scale Ge experiment: the Majorana Demonstrator. Invited presentation at *Workshop on Germanium-Based Detectors and Technologies.* (Berkeley, CA, May 2010).

Elliott, S. R.. Experimental Overview of Neutrinoless Double Beta Decay. Invited presentation at *International Workshop on Double Beta Decay and Related Neutrino Measurements.* (Hawaii, October 2009).

Elliott, S. R.. Neutrinoless Double Beta Decay. Invited presentation at *238th American Chemical Society National Meeting.* (Washington DC, August 2009).

Elliott, S. R., V. E. Guiseppe, R. A. Johnson, B. H. LaRoque, and S. G. Mashnik. Fast-Neutron Activation of Long-Lived Isotopes in Enriched Ge. To appear in *Physical Review C.*

Gehman, V. M., S. R. Elliott, and D. M. Mei. Systematic Effects in Pulse Shape Analysis of HPGe Detector Signals for Neutrinoless Double-Beta Decay. 2010. *Nuclear Instruments and Methods.* **615**: 83.

Guiseppe, V. E., M. Devlin, S. R. Elliott, N. Fotiades, A. Hime, R. O. Nelson, D. M. Mei, and D. V. Perepelitsa. Neutron inelastic scattering and reactions in natural Pb as a background in neutrinoless double-beta decay experiments. 2009. *Physics Review C.* **79**: 054604.

Mei, D. M., Z. B. Yin, and S. R. Elliott. Cosmogenic Production as a Background in Searching for Rare Physics Processes. 2009. *Astroparticle Physics.* **31**: 417420.

others, T. H. Burritt and. Surface-alpha backgrounds for the Majorana neutrinoless double-beta decay experiment. 2008. *Journal Physics Conference Series.* **136**: 042051.

others, V. E. Guiseppe and. The production of 68Ge in Ge detectors due to fast neutrons. Presented at *April Meeting of the American Physical Society.* (Denver, CO, May 2009).

others, V. E. Guiseppe and. The MAJORANA Project. Presented at *Implications of Neutrino Flavor Oscillations.* (Santa Fe, NM, July 6-10, 2009).

Turbulence By Design

Malcolm J. Andrews
20090058DR

Introduction

The prediction, design and control of turbulence have challenged our ingenuity for thousands of years. Roman water systems, air flight, climate, and Inertial Confinement Fusion (ICF) highlight the range of scientific problems that involve fluid turbulence. Los Alamos National Laboratory (LANL) has led developments of high fidelity fluid flow diagnostics, and the discovery that starting conditions can influence the development of hydrodynamic turbulence and material mixing in buoyancy driven flows. These leading edge advances have come about through studies of buoyancy driven turbulence in ICF targets. This Directed Research (DR) project couples a well-balanced set of unique LANL facilities and advanced diagnostics with experts in theory and computation. This synergistic expert team are determining the role of designed starting conditions and characterizing their effect on the development of material interpenetration, mixing, and turbulence. Thus, a timely opportunity has arisen to develop a new paradigm for buoyancy driven turbulence, namely "Turbulence by Design" (TbD), with LANL fluid dynamics research at the leading edge. The central goal of this DR is to determine the extent to which certain starting conditions can be used to predict and design turbulent transport/material mixing, Figure 1. The broad impact of this research includes the ability to design ICF targets for net energy gain, determination of early-time astrophysical processes, a better understanding of climate and ocean flow dynamics and, more generally, a scientific basis for understanding the development of buoyancy driven turbulence and its prediction/design/control.

Benefit to National Security Missions

This project will support the DOE and NNSA mission in Nuclear Weapons and Energy by determining the effect and use of initial conditions on Inertial Confinement Fusion, and code validation for Stockpile Stewardship. Additional high impact on climate, energy generation and usage, astrophysics, and any technological area that involves turbulence.

Progress

Major scientific achievements for the second twelve (12) months of the project include:

WE formulated a connection between our Ordinary Differential Equation (ODE) solver for initial perturbation power spectrum development and the BHR turbulence model, thus allowing BHR to incorporate an initial condition representation. Moreover, the ODE spectrum solver permits the evaluation of the need to account for initial conditions, and a dynamic set of BHR coefficients, and the exploration of "metrics" (Rollin & Andrews, 2010).

The three dimensional initial conditions (ICs) of the single mode curtain have been set up in the simulation, and reshock times have been varied experimentally and in simulations to understand the impact of initial condition modes upon the turbulent transition. Multi-mode gas curtain ICs were simulated to address the potential impact of three dimensional (3D) fluctuations on the shocked gas-curtain transition to turbulence. Various ways of superimposing synthetic noise to the baseline (non-perturbed, single-mode) gas curtain were tested. Simulated configurations with carefully controlled ICs were considered, differing from each other on the specifics of modeled low-amplitude multimode fluctuations. This was achieved through two strategies: a) by slightly offsetting the nozzles in the shock direction, and, b) by adding a 3D perturbation to the initial (simulated) concentration field; by combining them, four different realistic IC cases were considered (Figure 1).

Metrics that incorporate knowledge of the ICs are being used to understand and predict turbulent transition, and they are being computed for both the simulations and experiments (Figure 2). This information will be used to design a new nozzle configuration that will become turbulent upon first shock (Prestridge et al., 2011; Gowardhan et al., 2010; Grinstein et al., 2011).

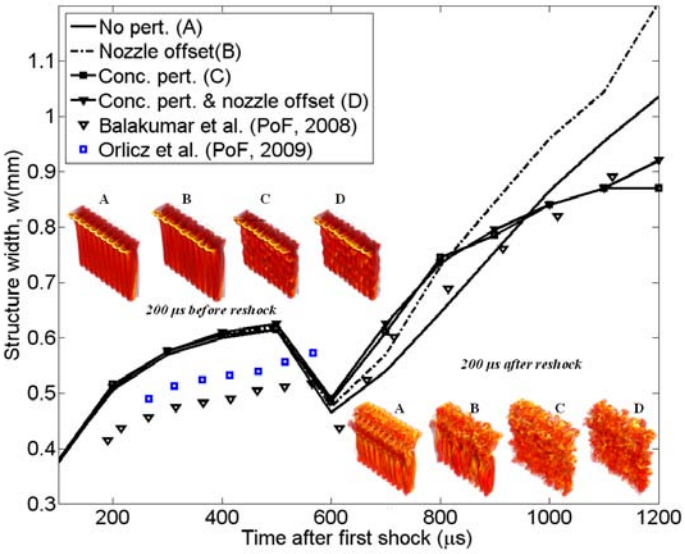

Figure 1. Gas Curtain mixedness from computational and laboratory experiments. Growth rates are fairly consistent before reshock (time~600_s); late-times measures and simulated flow organization are quite sensitive to initial conditions – particularly to their long wavelengths.

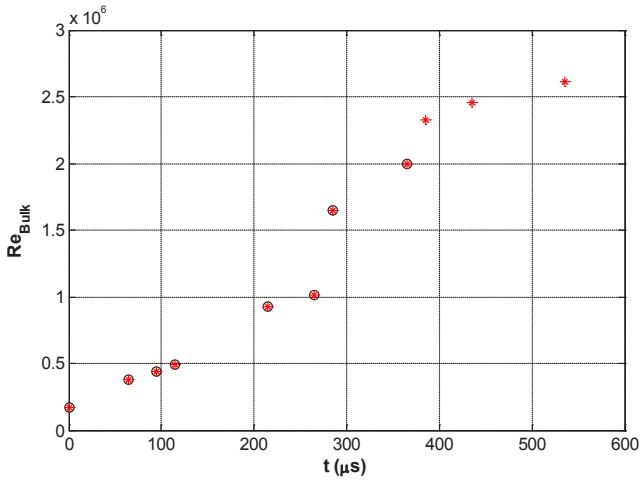

Figure 2. Bulk Reynolds number of singly-shocked curtain versus time. Reynolds number incorporates modes in initial conditions , Re=At_U(__)_/_, and indicates that flow may transition upon reshock at 280μs or later in time.

Formulation of turbulence model parameters, based on linear and nonlinear analyses and substantiated by computer simulations, has produced a parameter that incorporates dynamical and morphological properties of the initial interface and predicts the delays or speeds up the development of the transition in Rayleigh-Taylor turbulence (Ristorcelli and Hjelm, 2010). Similar work on Richtmeyer-Meshkov driven turbulence is underway, with ongoing numerical simulations. One parameter, based on the zero crossing frequency of the RM interface, appears to be the leading order parameter in determining turbulence and transition in shock and reshock situations. An analytic stability theory that combines RM with KH is being developed to understand the nature of the secondary instabilities that are likely responsible for the transition, and perhaps even parameterization of the fully turbulent flow.

Last year we performed 3-D Direct Numerical Simulations with various initial conditions (single, two-mode and multi-mode perturbations). In the multimode case, we also examined the de-mixing problem (see Figure 3). These are the first fully resolved numerical simulations of instability driven turbulent mixing, and will form one of our canonical datasets against which we will be testing our methodologies for "Turbulence By Design" (Livescu et al., 2010).

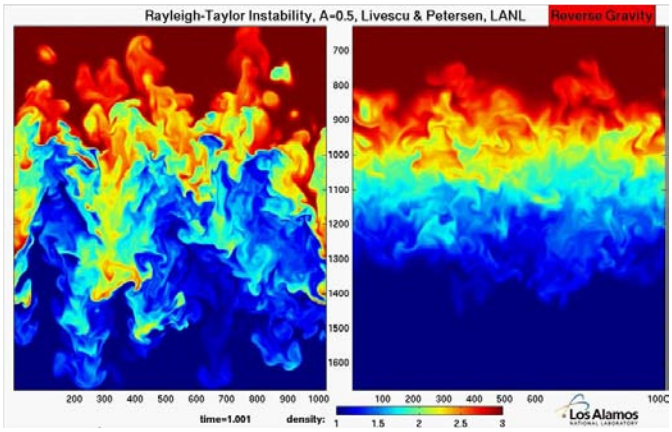

Figure 3. RT De-mixing: The mix layer on the left has de-mixed on the right due to a reversal in gravity.

Future Work

Recent work at Los Alamos National Laboratory (LANL) has shown that buoyancy-driven turbulence can be affected at late time by initial conditions, and memory of the initial conditions is not lost. This is a remarkable discovery that suggests an important opportunity to predict and "design" late-time buoyancy driven turbulence, i.e. Turbulence by Design (TbD), with transformative impact on our understanding and prediction of Inertial Confined Fusion (ICF), free-convection, environmental and technological flows, and general fluid mixing processes. Often, and especially in turbulence research, the assumption is made that initial conditions (ICs) wash out (loss of memory) and that the turbulence develops to a universal self-similar end state. However, there is a growing body of fundamental research that indicates only special turbulent flows are truly self-similar. Indeed, empirically-based turbulence modification is commonly used for example with golf-ball dimples. At the heart of our TbD blue-print for turbulence prediction and thus design lies the hypothesis that initially seeded small amplitude, long wavelength, perturbations can develop at late-time and be used to control turbulence

transport and material mixing.

Our work over the last year of this project will center around the determination of practically useful "metrics" that look at the initial perturbation spectra and the late-time spectra to determine the outcome of RT and RM drivers. We are also working toward a transition of our results into specification of IC's for turbulence models, as indicated in "A" above, and thus a broader impact for the results. Indeed, the incorporation of our work into the BHR turbulence model, demonstrates the broad impact of this hypothesis extends well beyond our interest in buoyancy and shock driven flows and incorporates the possibility of scientifically designing boundary conditions/ shapes for passive turbulence control. Thus, we envision a transformative opportunity for LANL to define a new paradigm for turbulence research that leaves behind the universal "fully-developed" equilibrium concept, and embraces late-time turbulence in ICF through prescribed ICs that enhance, suppress, or maintain turbulence intensity/structure for practical gain as related to LANL Grand Challenges. The late-time "signatures" or "metrics" of ICs also imply a better understanding of mix dominated buoyancy problems such as supernovas, solar ponds, ocean over-flows, and heat-transfer enhancement by rotating flows, and thus address a broad class of technological problems with the potential of revolutionary advances and discoveries.

Conclusion

This fundamental research will control the development of turbulence by design of starting conditions. Our focus is Inertial Confinement Fusion, with the goal of enhanced energy gain, lower energy costs, and reduce US dependence on foreign energy sources. However, more immediate impacts will be felt since oil trapping salt domes in Texas and the Gulf are also buoyancy formed structures whose location, size, and orientation depend on how they start and thus lend their prediction to our research. Other applications include more efficient engine fuel sprays, reduction of drag, cooling technologies, and weather prediction.

References

1. Balasubramanian, S., K. Prestridge, B. J. Balakumar, G. C. Orlicz, and C. D. Tomkins. Experimental study of initial condition dependence for turbulence design in shock-driven flows. (Moscow, 12-17, July, 2010).

2. Gowardhan, A. A., F. F. Grinstein, and A. J. Wachtor. Three Dimensional Simulations of Richtmyer-Meshkov Instabilities in Shock-Tube Experiments. 2010. (Orlando, 4-7 Jan. 2010). Vol. Paper # 2010-1075p. 1. AIAA: AIAA.

3. Grinstein, F. F., A. A. Gowardhan, and A. J. Wachtor. Simulation of Shock-Driven High-Re Turbulent Mixing. (Moscow, 12-17 July, 2010).

4. Livescu, D., J. R. Ristorcelli, M. R. Petersen, and R. A. Gore. New phenomena in variable-density Rayleigh-Taylor Turbulence. To appear in *Phys. Scripta.*

5. Rollin, B., and M. J. Andrews. On the 'early-time' evolution of variables relevant to turbulence models for the Rayleigh-Taylor instability. (Montreal, Canada, 1-5, Aug., 2010).

6. Ristorcelli, J. R., and N. Helm. Initial conditions for the turbulence moments at an unstable quiescent stochastic material interface. To appear in *Journal of Turbulence.*

Publications

Andrews, M. J.. LDRD-DR: Turbulence by design: 1st year review. 2009. *Poster given at the HED&P&F Capability Review, LANL, May 13, 2009. LA-UR 09-02673..*

Andrews, M. J.. Turbulence by design. 2009. *Poster, LDRD Day, Los Alamos National Laboratory, September 15, 2009. LA-UR # 09-05195. .*

Andrews, M. J.. LDRD-DR: Turbulence by design: 1st year review. Presented at *LDRD-DR 1st year review.* (Los Alamos National Laboratory, 13 May 2009).

Andrews, M. J., A. Duggleby, and Y. Doron. A PDF of molecular mix measurements in high Schmidt number Rayleigh-Taylor turbulence. Presented at *Turbulent Mixing and Beyond.* (Trieste, Italy, 27 July - 7 August, 2009).

Andrews, M. J., F. F. Grinstein, D. Livescu, and K. Prestridge. LDRD-DR: Turbulence by Design. 2009. *Poster presentation, at Boost Fest, Sandia National Laboratory, April 4, 2009. LA-UR 09-02673..*

Andrews, M. J., F. F. Grinstein, E. Kwickles, and R. Linn. Security and Environmental Fluid Dynamics (EFD). To appear in *Handbook of Environmental Fluid Dynamics.* Edited by Fernando, J..

Andrews, M. J., and B. Rollin. Incorporation of initial conditions in turbulence models for Rayleigh-Taylor instability driven mixing. Presented at *FEDSM2011/ AJK2011.* (Hamamatsu, Japan, 24-28 July, 2011).

Bakosi, J., and J. R. Ristorcelli. Exploring the beta distribution in variable density turbulent mixing. To appear in *Journal of Turbulence.*

Balasubramanian, S., B. J. Balakumar, G. Orlicz, C. Tomkins, and K. Prestridge. Initial conditions effects in shock-driven instabilities. 2009. In *APS Division of Fluid Dynamics Annual Meeting.* (Minneapolis, 22-24 Nov. 2009). Vol. 54, 19 Edition, p. 203. Minneapolis:

American Physical Society .

Balasubramanian, S., G. C. Orlicz, K. Prestridge, B. J. Balakumar, G. R. Friedman, and C. D. Tomkins. Turbulence by Design: Richtmyer-Meshkov Experiments. Presented at *1st Annual Los Alamos Postdoc Research Day (LAPRD).* (Los Alamos, 16 June, 2010).

Balasubramanian, S., K. Prestridge, B. J. Balakumar, G. C. Orlicz, and C. D. Tomkins. Experimental study of initial condition dependence for turbulence design in shock-driven flows. Invited presentation at *12th International Workshops on the Physics of Compressible Turbulent Mixing (IWPCTM 12).* (Moscow, 12-17, July, 2010).

Balasubramanian, S., K. Prestridge, B. J. Balakumar, G. C. Orlicz, and G. R. Friedman. Influence of initial conditions on turbulence and mixing in Richtmyer-Meshkov flows in the presence of re-shock. Presented at *41st AIAA Fluid Dynamics Conference & Exhibit.* (Honolulu, Hawaii, 27-30 June, 2011).

Balasubramanian, S., K. Prestridge, B. J. Balakumar, and G. R. Friedman. Effect of multi-mode initial conditions in shock-driven flows. Presented at *63rd Annual Meeting of APS-DFD.* (Longbeach, CA, 22-24 Nov., 2010).

Banerjee, A., and M. J. Andrews. 3D Simulations to investigate initial condition effects on the growth of Rayleigh–Taylor mixing. 2009. *International Journal of Heat and Mass Transfer.* **52** (17): 3906.

Banesh, A., M. J. Andrews, and D. Ranjan. Effect of Shear on mixing in R-T mixing layers at low Atwood numbers. Presented at *63rd Annual Meeting of APS-DFD.* (Long Beach, CA, 22-24 Nov., 2010).

Gowardhan, A. A., F. F. Grinstein, and A. J. Wachtor. Three Dimensional Simulations of Richtmyer-Meshkov Instabilities in Shock-Tube Experiments. 2010. In *AIAA ASM.* (Orlando, 4-7 Jan. 2010). Vol. Paper # 2010-1075, p. 1. AIAA: AIAA.

Gowardhan, A. A., and F. F. Grinstein. Simulation of Material Mixing in Shocked Gas-Curtain Experiments. Presented at *63rd Annual Meeting of APS-DFD.* (Long Beach, CA, 22-24,Nov., 2010).

Gowardhan, A., and F. F. Grinstein. Simulation of Material Mixing in Shocked Gas-Curtain Experiments. 2009. In *APS Division of Fluid Dynamics Annual Meeting.* (Minneapolis, 22-24 Nov. 2009). Vol. 54, 19 Edition, p. 203. Minneapolis: APS.

Gowardhan, A., and F. F. Grinstein. Simulation of Material Mixing in Shocked Gas-Curtain Experiments. Presented at *WINNER, 1st Annual Los Alamos Postdoc Research Day (LAPRD).* (Los Alamos, 16 June, 2010).

Grinstein, F. F.. On integrating large eddy simulation and laboratory turbulent flow experiments. 2009. *Transactions of the Royal Society.* **A** (367): 2931.

Grinstein, F. F.. On Integrating LES and Laboratory Turbulent Flow Experiments. Presented at *Discussion Meeting on "Applied Large Eddy Simulation" of the Royal Society.* (London, 27-28 October 2008).

Grinstein, F. F.. Simulating vortex dynamics, transition, and turbulent mixing in high Reynolds-number flows. Presented at *Tutorial at "Turbulent Mixing and Beyond" Conference.* (Trieste, Italy, 5 August 2009).

Grinstein, F. F.. On credibility and convergence of hydro aspects of recent high resolution boost simulations (U). 2009. In *NEDPC.* (LLNL, 29-31 Oct. 2009). Vol. LA-CP-10-000163, p. 1. LLNL: LLNL.

Grinstein, F. F.. On the Simulation of Vortex Dynamics and Transition in High Reynolds-Number Inhomogeneous Flows. Invited presentation at *Invited Lecture, 1st Annual Workshop on "LES for Jet Flows".* (NASA GRC, Cleveland, OH, 2-3 June, 2010).

Grinstein, F. F.. Simulating Vortex Dynamics and Transition in High Reynolds-Number Flows. Invited presentation at *3rd International Conference on Jets, Wakes and Separated Flows.* (Cincinnati, 27-30 Sept., 2010).

Grinstein, F. F.. Simulating Vortex Dynamics and Transition in High Reynolds-Number Flows. To appear in *Phys. Scripta .*

Grinstein, F. F.. Verification and Validation of CFD based Turbulent Flow Experiments. To appear in *Encyclopedia of Aerospace Engineering, Volume 1 Fluid Dynamics and Aerothermal Dynamics, Computational Fluid Dynamics.* By Shyy, W., and R. Blockley.

Grinstein, F. F., A. A. Gowardhan, and A. J. Wachtor. Simulation of Shock-Driven High-Re Turbulent Mixing. Invited presentation at *IWPCTM12 Workshop.* (Moscow, 12-17 July, 2010).

Grinstein, F. F., A. Gowardhan, and A. J. Wachtor. On the Simulation of Shock-Driven Material Mixing in High Reynolds-Number Flows. To appear in *Phys. Scripta .*

Grinstein, F. F., A. Gowardhan, and A. J. Wachtor. Simulations of Richtmyer-Meshkov Instabilities in Planar Shock-Tube Experiments. To appear in *Physics of Fluids,.*

Grinstein, F. F., A. Gowardhan, and A. Wachtor. On the Simulation of Shock-Driven Material Mixing in High Reynolds-Number Flows. 2009. In *APS Division of Fluid Dynamics Annual Meeting.* (Minneapolis, 22-24 Nov. 2009). Vol. 54, 19 Edition, p. 203. Minneapolis: APS.

Grinstein, F. F., M. J. Andrews, and B. Rollin. Progress on the LDRD-DR 'Turbulence by Design' (U) . Invited presentation at *NECDC-2010.* (Los Alamos, 18-22, 2010).

Grinstein, F. F., and A. A. Gowardhan. Effects of Initial Conditions on the Planar Richtmyer-Meshkov Instability. Presented at *63rd Annual Meeting of APS-DFD.* (Long Beach, CA, 22-24, Nov., 2010).

Grinstein, F. F., and A. Gowardhan. On the simulation of shock-driven material mixing in high Reynolds-number flows. Presented at *Turbulent Mixing and Beyond .* (Trieste, Italy, 6 August 2009).

Grinstein, F. F., and W. J. Rider. Turbulence: Monotone-Integrated and Implicit Large-Eddy Simulation. 2010. In *Scholarpedia Encyclopedia of Physics (Fluid dynamics), http://www.scholarpedia.org/article/Turbulence:_Monotone-Integrated_and_Implicit_Large-Eddy_Simulation ..* Edited by Schilling, O.. , p. 1. www: www.

Livescu, D.. Direct Numerical Simulations of turbulence. Presented at *High energy Density Plasmas and Fluids Capability Review.* (Los Alamos National Laboratory, 13 May 2009).

Livescu, D., H. Yu, and R. McLarren. Temperature effects on the Rayleigh-Taylor instability. *Phys. Fluids .*

Livescu, D., J. R. Ristorcelli, M. R. Petersen, and R. A. Gore. New phenomena in variable-density Rayleigh-Taylor Turbulence. To appear in *Phys. Scripta.*

Livescu, D., J. R. Ristorcelli, and R. A. Gore. Mixing asymmetry in variable density turbulence. Presented at *62nd APS Dvision of Fluid Dynamics Annual Meeting.* (Minneapolis, MN, 24 November 2009).

Livescu, D., M. J. Petersen, S. Martin, and P. McCormick. Spikes and bubbles in turbulent mixing: High Atwood number Rayleigh-Taylor instability. 2009. *Poster to be presented at the 62nd APS/DFD annual meeting, Minneapolis, 2009..*

Livescu, D., M. R. Petersen, and R. A. Gore. Turbulence and mixing characteristics in the variable-density Rayleigh-Taylor mixing layer. Invited presentation at *NECDEC-2010.* (Los Alamos, 18-22 Oct., 2010).

Livescu, D., M. R. Petersen, and R. A. Gore. Turbulence characteristics in the variable-density Rayleigh-Taylor mixing layer. Presented at *63rd Annual Meeting of APS-DFD.* (Long Beach, 22-24 Nov., 2010).

Livescu, D., and J. R. Ristorcelli. Mixing asymmetry in variable density turbulence. 2009. In *Advances in Turbulence XII.* Edited by Eckhardt, B.. Vol. 132, p. Not known. Berlin: Springer.

Petersen, M. R., D. Livescu, R. A. Gore, and K. Stalzberg-Zarling. High Atwood number Rayleigh-Taylor instability with gravity reversal. Presented at *JOWOG 32MIX.* (Los Alamos, 19-22 April, 2010).

Petersen, M. R., D. Livescu, and R. A. Gore. Direct numerical simulations of Rayleigh-Taylor instability with gravity reversal. Presented at *63rd Annual Meeting of APS-DFD.* (Long Beach, CA, 22-24 Nov., 2010).

Prestridge, K.. Richtmyer-Meshkov mixing and turbulence experiments. Invited presentation at *Invited seminar, Center for Turbulence Research, Stanford University.* (Stanford University, 4 May, 2010).

Prestridge, K.. Turbulent mixing in shocked variable-density flows. Invited presentation at *Invited seminar, Dept. of Mechanical Engineering, Arizona State University.* (Arizona, 4 May, 2010).

Prestridge, K. P., B. J. Balakumar, C. Tomkins, and S. Balasubramanian. Experiments for understanding shock-driven mixing and turbulence. Presented at *High Energy Density Plasmas and Fluids (HEDPF) Capability Review.* (Los Alamos National Laboratory, 13 May 2009).

Prestridge, K. P., B. J. Balakumar, G. Orlicz, C. Tomkins, C. Zoldi-Sood, and R. A. Gore. Understanding Turbulence in Richtmyer-Meshkov unstable flows. Presented at *NEDPC.* (Lawrence Livermore National Laboratory, 27 October, 2009).

Prestridge, K. P., B. J. Balakumar, G. Orlicz, and C. Tomkins. High resolution experimental measurements of Richtmyer-Meshkov turbulence in fluid layers after reshock. Presented at *APS Shock-Compression of Condensed Matter.* (Nashville, TN, 2 July 2009).

Prestridge, K. P., B. J. Balakumar, G. Orlicz, and C. Tomkins. Understanding experimental diagnostics and results for code and model validation. Presented at *Turbulent Mixing and Beyond.* (Trieste, Italy, 27 July 2009).

Reckinger, S. J., D. Livescu, and O. V. Vasilyev. Wavelet-Based Simulations of Rayleigh-Taylor Instability. Presented at *63rd Annual Meeting of APS-DFD.* (Long Beach, CA, 22-24 Nov., 2010).

Reckinger, S. J., D. Livescu, and O. V. Vasilyev. Adaptive Wavelet Collocation Simulation of Rayleigh-Taylor Instability. To appear in *Phys. Scr. .*

Reckinger, S., D. Livescu, and O. Vasilyev. Compressibility effects on single mode Rayleigh-Taylor instability. 2009. *Poster given at Turbulent Mixing and Beyond Conference, Trieste, Italy, July 27, 2009..*

Ristorcelli, J. R., N. Hjelm, and T. Clark. LBM turbulence:

multi-component turbulence without interface tracking. Invited presentation at *Symposium on Combustion and Turbulence.* (Cornell, Ithaca, NY, 3-4 Aug., 2010).

Ristorcelli, J. R., and D. Livescu. Correcting anisotropic gradient transport of k. To appear in *Flow Turb. Comb.*

Ristorcelli, J. R., and N. Helm. Initial conditions for the turbulence moments at an unstable quiescent stochastic material interface. To appear in *Journal of Turbulence.*

Ristorcelli, R. J.. Stochastic linear stability theory: obtaining statistics for moment closure models. Presented at *Turbulent Mixing Colloquium.* (Los Alamos National Laboratory, 1 July 2009).

Rollin, B., and M. J. Andrews. Progress Toward Specifying Initial Conditions for Variable Density Turbulence Models. 2009. In *APS Division of Fluid Dynamics Annual Meeting.* (Minneapolis, 22-24 Nov. 2009). Vol. 54, 19 Edition, p. 102. Minneapolis: APS.

Rollin, B., and M. J. Andrews. On the 'early-time' evolution of variables relevant to turbulence models for the Rayleigh-Taylor instability. Presented at *FEDSM2010.* (Montreal, Canada, 1-5, Aug., 2010).

Rollin, B., and M. J. Andrews. On Initial Conditions for Turbulent Rayleigh-Taylor Mixing. Presented at *63rd Annual Meeting of APS-DFD.* (Long Beach, CA, 22-24 Nov., 2010).

Rollin, B., and M. J. Andrews. A Mathematical Model of Rayleigh-Taylor and Richtmyer-Meshkov Instabilities for Viscoelastic fluids. To appear in *Phys. Rev. E.*.

Wei, T., D. Livescu, and M. J. Andrews. The effects of initial conditions on single and two-mode Rayleigh-Taylor instability. Presented at *63rd Annual Meeting of APS-DFD.* (Long Beach, Ca, 22-24 Nov., 2010).

New and Enhanced Capabilities in Quantum Information Processing

Eddy M. Timmermans
20090476DR

Introduction

This project is intended to search out and exploit new connections between several areas of quantum physics and information science to build new tools and technologies that support the Laboratory mission.

- We will develop the new field of quantum sensing, using the power of quantum mechanics to create sensors of forces and fields performing beyond the current state of the art. This requires both theory to develop optimum measurement strategies, and experiment to provide the tightly-controlled quantum systems which can implement these strategies.
- We will explore the many interlocking aspects of many-body physics, atomic and optical physics, and quantum control essential to understanding, controlling, and predicting the properties of materials. The focus will be on understanding those materials relevant to energy, such as high Tc superconductors.
- We will use the tools of quantum information science to gain new insights into the power and potential of quantum computers to solve otherwise intractable problems and to increase information security. In particular we hope to find new classes of algorithms for quantum computers and new techniques for increasing the range of quantum key distribution for provably secure protection of information.

Benefit to National Security Missions

This project will support the DOE missions of the Office of Science by enhancing our understanding of basic quantum physics and of the properties of matter. It will also support the nonproliferation mission by investigating methods for quantum sensing. The understanding of superconductors will benefit energy transmission technology.

Progress

This project is finding and exploiting new connections between several areas of quantum physics and information science and building new tools and technologies tjat support the Laboratory mission. In the second year of the project we have made progress in three of these areas:

QUANTUM INFORMATION THEORY

Our focus here is on finding ways to use quantum technologies to increase the security and capacity of communication channels.

- The LANL Quantum Communication team designed, built, and demonstrated a test-bed system for performing polarization-based quantum key distribution (QKD) in optical fiber. This system extended our previous work on fiber-based transmitters and incorporated an all-new fiber-based receiver to create a fiber-optic communication link suitable for Quantum Communication. Previously it had not been possible to use optical fiber to connect polarization-based quantum encryption equipment, because the polarization state of light is severely distorted as it travels through fiber. Our work overcomes this limitation by transmitting fiducial polarization states, measuring the distorted states at the receiver, and using in-fiber polarization control to counter the distortion. We have developed a control algorithm that can compensate for any amount of fiber-induced distortion in less than three seconds. Once tracking has been established, the algorithm will compensate for any further polarization changes with an update rate of 3 Hz. With the all-fiber transmitter and receiver we have demonstrated a quantum bit-error-rate due to polarization errors under 1%.
- Wojciech Zurek and visitor William Wootters collaborated on a “Quick Study” article in Physics Today explaining their celebrated no-cloning theorem, the theoretical result which makes quantum key distribution provably unbreakable.

Technology for Quantum Control and Quantum Information Processing
Felipe Da Rosa and his colleagues have been considering the possibility of engineering the composition or geometry of a system to make the Casimir force (due to the fundamental and unavoidable fluctuations in the electromagnetic vacuum) turn from attraction to repulsion. A repulsive atom-surface force would be an important new quantum technology, enabling, for example, completely passive guiding and trapping of atoms for quantum information processing. They have now shown that, even with the additional flexibility afforded by engineered metamaterials, it is very unlikely that the Casimir force can be made repulsive in a useful way. This result is of wide interest because there are now many groups around the world working on Casimir physics. Many of these groups presented their work at a 2009 international conference on this topic organized in Santa Fe by Diego Dalvit and his colleagues in the LANL Casimir team.

Together with Gennady Berman, Alexander Nesterov, a quantum institute supported visitor has been investigating the dynamics of non-hermitian systems. In these systems, the coupling with an environment does not only lead to decoherence but the amplitude of the system's states leak into other channels. They discovered that the dynamics of such systems exhibits behavior that can be exploited for the purposes of quantum processing, a somewhat surprising conclusion that may affect the development of mesoscopic quantum processing architectures.

Quantum Many-body Physics
Haitao Quan and his collaborators have worked on several aspects of quantum many-body systems relevant to quantum information processing. They are studying decoherence, a phenomenon due to the interaction of a system with its environment, which is the greatest fundamental barrier to practical quantum information processing. They have considered decoherence induced by a many-body dynamic environment undergoing a non-equilibrium (quantum) phase transition. As the environment "monitors" the quantum system, its sensitivity -- and, consequently, efficiency of decoherence -- is amplified by a phase transition, as is often the case in the real world detectors (bubble chambers, photographic emulsions, or rhodopsin in our eyes). They have shown that decoherence happens almost exclusively as the critical point of the environment is traversed, and they have found a simple expression that relates decoherence to the universal critical exponents in a way that parallels theory of topological defect creation in non-equilibrium phase transitions.

Together with Cristian Batista, Yasuyuki Kato, a quantum institute supported postdoc, discovered a new thermodynamic phase in the triangular Kondo-lattice model. The phase is a consequence of an intrinsic quantum effect (the Bhom-Aharanov phase) and produces spontaneous Quantum Hall effects (in the absence of a magnetic field). The ordered state that produces this quantum macroscopic phenomenon is a chiral liquid.

Future Work
The main scientific issue to be addressed is exploiting more fully the potential of quantum mechanical coherence and entanglement, particularly in areas that cross boundaries between traditional scientific disciplines.

Working at the intersection of information science and quantum physics, we will address the important question of identifying the origin of the power of quantum computing. Most physicists believe that entanglement is key, but much remains to be understood. The goal here is to gain additional insight and understanding of this key issue. We expect to investigate network quantum information theory, quantum conditional information, and their roles in understanding and computational modeling of complex quantum systems. Another challenge for quantum information processing is to develop quantum algorithms for problems whose computational complexity renders them insoluble on classical hardware. In this project, we will seek new quantum algorithms for an important class of problems in the mathematical theory of knots.

We will also investigate the emerging field of quantum sensing. Here the goal is to find ways to build instruments with sensitivities to forces, accelerations, and electromagnetic fields which exceeds the standard limits due to shot noise, etc. Tasks include the theoretical issue of devising optimum measurement strategies, and the practical challenge of implementing those strategies on suitable quantum hardware, such as trapped ions or ultracold atoms.

Finally, we will build a coalition to work at the fertile overlap of atomic and optical physics, quantum information science, and condensed matter physics. Here one goal is to devise new techniques for computing quantum systems in the face of exponential complexity. Another is to link the very clean quantum phase transitions observed in ultracold gases to the quantum critical behavior that is important in many materials, such as unconventional superconductors.

Conclusion
The quantum institute is in the process of broadening its base, including work on quantum many-body physics and, possibly, involving optical and atomic-molecular applications. Success in this project would mean:

1. The theoretical exploration of new quantum sensing technologies with sensitivity beyond the current state of the art. Applications range from surface microscopy to precise measurements of gravity and electromagnetic fields. Part of this work will support

the experimental development of a technology that can demonstrate beyond-the-standard limit resolution.

2. New techniques and computational tools for understanding, controlling, and predicting the properties of materials and other many-boson systems, including those relevant to energy such as high-Tc superconductors. This work includes new insights into quantum phase transitions and topological states of matter.

3. New insights into the advantages of quantum information, uncovering classes of mathematical problems that can be solved with quantum codes and that are currently intractable. The project will also have explored techniques for improving the range of applicability of quantum key distribution, which enables completely secure distribution of cryptographic key material.

Publications

Berman, G. P., A. R. Bishop, B. M. Chernobrod, A. A. Chumak, and V. N. Gorshkov. Suppression of scintillations and beam wandering in free space gigabit rate optical communication based on spectral encoding of a partially coherent beam. 2009. In *Photonics West.* (San Jose, 24-29 January). Vol. 7200, p. 72000H. Digital Library: The international Society for Optical Engineering.

Berman, G. P., B. M. Chernobrod, A. R. Bishop, and V. N. Gorshkov. Uncooled infrared and terahertz detectors based on micromechanical mirror as a radiation pressure sensor. 2009. In *Photonics West.* (San Jose, 24-29 January, 2009). Vol. 7204, p. 720403. Digital Library: The International Society for Optical Engineering.

Rice, P., and I. J. Owens. Comparison between continuous wave and pulsed laser EQKD Systems. 2009. *To Be Submitted.*

Yard, J., and I. Devetak. Optimal quantum source coding with quantum side information at the encoder and decoder. 2009. *IEEE Transactions on Information Theory.* **55** (11): 5339.

Revolutionary Science at the Intersection of Extreme and Transient Events, Natural Hazards, and National Security

Harald O. Dogliani
20090477DR

Introduction

This LDRD project falls under the technical leadership of the Institute for Geophysics and Planetary Physics (IGPP). The project goal is to advance the science of extreme phenomenology associated with astrophysics, space physics, geoscience and climate change issues. These include: seismic and volcanic events, arctic climate change, regional climate change impacts, application of advanced modeling and simulation techniques applied to space plasma and astrophysical transient events, and development of novel concepts in support of a broader set of issues. While simultaneously satisfying LDRD requirements, this project is integrated with the broader natural sciences mission of IGPP. IGPP uses General and Administrative (G&A) and LDRD resources to assess science needs and opportunities, develop strategies, and support cutting edge basic scientific research. LDRD is strictly limited to the support of R&D. A key element of this LDRD project is the promotion and strengthening of the Los Alamos workforce to advance its scientific excellence.

Benefit to National Security Missions

This research advances Los Alamos capabilities associated with its DOE energy security, climate change, geophysical hazards, and astrophysics missions. It also keeps the Los Alamos workforce on the cutting edge of science directly tied to weapon simulations and space and/or surface based detection of nuclear activities.

Progress

Climate Science

In an effort to understand the time evolution of carbon dioxide and other carbon-containing greenhouse gases, a variety of techniques are used to better understand key chemical processes. Secondary organic aerosols are formed by the interaction of volatile organic carbon molecules and ozone. Measuring the resultant secondary organic aerosols (SOA) that are produced as well as the carbon isotopic content can shed information on the extent of the processing that the volatile organic compounds have undergone in the troposphere. A group of researchers at Los Alamos with a collaborator from Michigan Tech are measuring the carbon content of SOA produced in the laboratory and comparing those results to SOA collected in the atmosphere in an effort to quantify the relative contribution of various reactants and pathways that produce these aerosols that are key species influencing global climate.

The study of perturbations in electron density in the D-layer ionosphere can help one understand the energy coupling between thunderstorms and the ionosphere. A method was developed to retrieve certain ionospheric parameters (height, absorption) in space and time from recorded negative cloud-to-ground lightening time waveforms. Observed oscillatory signatures suggest strong coupling with atmospheric gravity waves while other coupling mechanisms have not been observed to date. This is leading to follow-on LDRD research.

Sebastian Mernild developed *IceHydro*, a runoff routing model for the Greenland ice sheet. In this model, the simulation domain is divided into grid cells that are linked via an eight-direction (N, NE, E, SE, etc.) flow network. There are two runoff components in each grid cell: slow-response and fast-response. The slow time scale is the time required for snow or ice melt in an individual grid cell to reach the routing network that moves this moisture downstream at the fast time scale. Associated with these two time scales are different water transport mechanisms: the slow time scale accounts for transport within the snow and ice matrices, and the fast time scale generally represents channel flow, either superglacial, englacial, or subglacial. IceHydro has been linked to the program SnowModel, a spatially distributed snow-evolution and ice melt modeling system designed to be applicable over a wide range of snow and glacier landscapes, including Greenland, and climates found around the world, where snow and ice variations play an important role in hydrological cycling.

Using a digital elevation map, the Greenland ice sheet has been divided into several hundred sub-catchments and tested for a sub-catchment (Kangerlussuaq, West

Greenland). IceHydro has further been run and tested at the scale of a single glacier (Mittivakkat Glacier; East Greenland), using tracer measurements to tune the model; the output compares well with hydrograph data (Fig. 4). By the end of 2010, the model will be implemented for the entire ice sheet, giving the spatial distribution of runoff to the ocean.

Meanwhile, Lipscomb has implemented a dynamic ice sheet model in the Community Earth System Model (CESM), which was publicly released in June 2010. (This work was supported by the DOE SciDAC project.) The implementation includes a new physically based surface-mass-balance scheme for ice sheets. CESM will be used at global and regional scales for Greenland mass-balance studies planned during the second year of the project.

A study of the Santa Fe Municipal Watershed to understand the local impact of climate change and disturbances indicates that while precipitation is the dominant climatic control on streamflow, the Santa Fe River flow regime is also highly sensitive to temperature shifts, particularly through changes in snow accumulation and melt. In addition water availability in the Watershed is highly dependent on vegetation water use, and the spatial pattern of vegetation throughout the landscape exerts a strong control on streamflow timing and magnitude. This suggests that proper land management may ameliorate the impact.

Geophysics

Los Alamos scientists in collaboration with colleagues from Stanford and the US Geological Survey, both chaired a special session and presented recent results at the Geological Society of America Annual Meeting in October 2009. The topical session, entitled "Slow slip and non-volcanic seismic tremor in Cascadia and beyond: Observations, models, and hazard implications", included critical observational or modeling constraints that bear on all aspects of the recently discovered episodic non-volcanic tremor and slow slip events both within and outside of the Cascadia Subduction Zone (CSZ). The recent discovery of non-volcanic tremor and slow aseismic slip has resulted in a flurry of research activity across many geologic and geophysical disciplines. The two phenomena are often coupled and recurrent, in which case they are called Episodic Tremor and Slip (ETS). Research suggests that non-volcanic tremor and slow slip are both members of a family of unusually slow earthquakes. These slow earthquakes occur in diverse tectonic environments and appear to have the same mechanism as ordinary earthquakes, but differ from normal earthquakes in their source location and moment-duration scaling. Unlike ordinary earthquakes, which grow explosively in size with increasing duration, slow earthquakes, whether large or small, grow at a constant rate. The hazard implications of tremor and slow-slip are also quite important. Tremor and slow-slip are typically found on the deep extension of faults, just below the region of the fault that produces the more familiar, and dangerous, "ordinary" earthquakes. Thus, the slip from these slow events could load, or even trigger, large earthquakes in the shallower portion of the fault zone. ETS events are observed along the CSZ from northern California to Vancouver Island, Canada. Major cities affected by a disturbance in this subduction zone could include Vancouver, Seattle, Portland, and Victoria.

Los Alamos scientists with collaborators from UC San Diego, the Institute of Environmental Assessment and Water Research (Barcelona, Spain) and the Weizmann Institute of Science (Rehovot, Israel) have published an article in the Journal of computational Physics describing an approach that reduces the uncertainty of computational simulation of "non-Fickian" transport. The approach allows for better simulation of a substance dissolved in fluid (solute) as it is transported in porous media, as can be encountered in the flow of water in porous strata. Fickian transport describes the diffusion of mass through media.

A class of non-Fickian diffusion can involve reactive material whose "identity" changes as it diffuses and a more general approach must be used to properly account for the reactive nature of the mass. The team derived a deterministic equation for a probability density function of the concentration of a solute that undergoes heterogeneous reactions such as precipitation or dissolution. Ultimately the approach enables one to convert any particle-tracking legacy code into a simulator for describing such non-Fickian transport.

Many major cities of the U. S. (e.g., San Francisco, Los Angeles, Seattle, Boston, Charleston) and the world (e.g., Jerusalem, Ankara, Tokyo, Manila) are situated in regions of high earthquake potential. Despite decades of research and anecdotal claims, study of earthquakes has never become a predictive science. Instead, research is focusing on mitigating earthquake hazards by a better understanding of effects of sedimentary basins on amplifying earthquake damage, of strain accumulation, and of earthquake triggering. One fruitful approach is the study of "gouge," the granular material that develops along earthquake faults by comminution (process in which solid materials are reduced in size) of adjacent rock. The importance of gouge is becoming apparent through experimental studies of its rheological properties, using a rheometer (A rheometer is a laboratory device used to measure the way in which a liquid, suspension or slurry flows in response to applied forces. It is used for those fluids which cannot be defined by a single value of viscosity and therefore require more parameters to be set and measured than is the case for a viscometer. It measures the rheology of the fluid.), detailed microscopic investigation, and numerical modeling. The tiny particles that comprise gouge can roll during earthquakes, allowing the gouge to flow. This flow is controlled in part by angularity and aspect ratio of individual grains, and on overall slip

rate. The team is characterizing the dependency of flow rheology (quasi-static, inertial) on shear rate. For angular particles (compared to smooth, spherical particles), an initial volume of gouge (characterized as "excess volume") is maintained at low slip rates in quasi-static flow. This excess volume *decreases* at higher slip rates, as force chains in the gouge collapse, before increasing again in the inertial regime. It is speculated that an angular, granular medium such as gouge moving at low strain rates is in a metastable, delicate balance, dilated state, and hence may be especially sensitive to vibrations and/or dynamic stress. Thickness variations in a granular flow layer (gouge) can control fault slip-surface topography, hence the locus of stress accumulation. Strength of the granular (gouge) layer ultimately determines whether and/or where slip occurs on a fault. The overall goal of the work is a better prediction, not of earthquakes themselves, but of risk if/when earthquakes occur.

Space Science and Astrophysics
Enhanced ion cyclotron fluctuations have been observed by NASA spacecraft in the inner magnetosphere of Jupiter and Saturn as well as from their inner moons. However it has unexpectedly not been observed from the Cassini spacecraft around Titan. Simulations at Los Alamos showed that while indeed there is growth of the cyclotron instabilities, even under ideal wave growth conditions, ion cyclotron waves are not likely to grow above the substantial background "noise," so that enhanced waves near the pickup ion frequency are not likely to be observed as distinct from the widespread broadband noise of the outer magnetosphere.

A Rice-LANL jointly developed Monte Carlo radiation transport code is being enhanced to more effectively model a number of astrophysical sources. Last year results were published that investigated the radiative accretion flow of Sagittarius A*. Application of General Relativistic Magnetohydrodynamic and Monte Carlo codes resulted in good fits to the broadband flaring and quiescent spectra from the accretion disk around the supermassive black hole at the center of Milky Way with several sets of input data. This year, the Monte Carlo code is being modified to account not only for the magnitude of the considered magnetic fields but also the full-angle dependence of the synchrotron emission to allow for 3-dimensional field structures. Similarly, recent progress has been made incorporating 3-dimensional bulk plasma flow effects.

Understanding electron-positron plasmas is important in understanding aspects of gamma-ray bursts, magnetically striped pulsar winds accretion disks and active galactic nucleus jet phenomenology. Application of a Los Alamos developed state-of-the-art particle-in-a-cell (PIC), code VPIC, has been used to study the relativistic pair reconnection. More than twenty five 2- and 3- dimensional simulations have been run. Among the 3-dimensional simulations are the largest to-date within the community in terms of the simulation sizes, number of particles used and the duration of the simulation. The large size is essential to properly account for some key phenomenology , e.g. relativistic tearing and kink modes. Sufficient lengths in all directions are needed to capture the modes correctly to follow the full non-linear development. The key finding is that the overall conversion from magnetic to particle energy can be explained by dynamics of multiple magnetic islands through a betatron-like mechanism.

Future Work

Research will follow certain themes. Within the Space and Astrophysics disciplines we continue to address cosmological modeling and simulation associated with gamma-ray events, neutron star physics, super nova evolution, cosmological structure formation and the earth's plasma environment. Much of the simulation will stretch the state-of-art modeling codes using adaptive mesh refinement and other techniques. This capability will allow refined resolutions from megaparsecs to kiloparsecs to analyze galaxy clusters and the distribution of mass. With an increasing stress to understand the earth's environment and an increasing demand for better predictive fidelity of space situational assessments, space science will look at sponsoring fundamental work that ultimately supports this national mission. Exploration of plasma sheet, magneto sheet, magnetospheric and reconnection dynamics of the Earth's upper atmosphere will be needed to explain episodic and severe phenomenology, key space situational assessment issues.

Studies in climate change will strive to improve the models describing hydrology-ice sheet-permafrost interactions. We will begin to steer to a more precise understanding the material properties of ice; its rheology and morphology to increase the fidelity of ice field dynamics as it pertains to climate change predictive capabilities.

We will continue to advance the understanding of earthquake initiation, subduction zones, and flow through porous media. As opportunity arises, we will investigate how land mass elasticity can change icefield behavior, and seek to better couple the icefield, atmosphere, ocean and geological boundaries as required.

Our operational business model is to continue with state-of-the-art workshops and conferences, to help guide future investments and to germinate new science and guidance on ongoing science. IGPP sponsored twelve (12) workshops and sponsored twenty-four (24) projects each that included post-docs and numerous other collaborators from various universities, such as UCI, MSU, NMT, UNM, NMSU, UCLA, UCSC, UCSD, UTD, UCD, UI, OU, and UA. The workshops are not funded by LDRD, but LDRD researchers play a major role in their technical content.

Conclusion

Progress has been made towards the goals of better understanding climate change, earthquake, space and cosmological phenomenology.

The overarching goals are:

- Increasing accuracy of predicting evolving climate change, especially of extreme events or significant changes in regional landscapes such as caused by sea level rises or other long term weather changes that will induce energy and political infrastructure stress.
- Understand earthquake precursors and watershed dynamics
- Increase in-depth understanding of upper atmospheric/low space phenomena that ultimately affect the safety and security of space assets; and
- Seek to improve our understanding of the evolution of the universe, to include dark matter and dark energy.

References

1. Hilburn, G., E. Liang, S. Liu, and H. Li. Monte Carlo simulations of the broad-band spectra of Sagittarius A* through the use of general relativistic magnetohydrodynamics. 2010. *MONTHLY NOTICES OF THE ROYAL ASTRONOMICAL SOCIETY.* **401** (3): 1620.
2. Hilburn, G., E. Liang, Siming Liu, and Hui Li. Monte Carlo simulations of the broad-band spectra of Sagittarius A* through the use of general relativistic magnetohydrodynamics. 2010. *Monthly Notices of the Royal Astronomical Society.* **401** (3): 1620.
3. Bhattacharya, S., H. Yang, and P. Ricker. Impact of cluster Structure and Dynamical State on Scatter in Sunyaev-Zeldovich Flux-mass Relations. *Astrophysical Journal.*
4. Shaw, L. D., D. Nagai, S. Bhattacharya, and E. T. Lau. Impact of cluster Physics on the Sunyaev-Zel'dovich Power Spectrum. *Astrophysical Journal.*
5. High, W. F.. Optical Redshift and Richness Estimates for Galaxy Cluster Selected with the Sunyaev-Zel'dovich Effect. *Astrophysical Journal.*
6. Placzek, C. J., B. S. Linhoff, L. R. Riciputi, and J. M. Heikoop. Mechanisms and Geologic distribution of Mass independent 238U/235U Fractionation. To appear in *American Geophysical Union Annual Fall Meeting.* . (San Francisco, CA, 13-17-2010).
7. Placzek, C. J., B. S. Linhoff, and J. M. Heikoop. Mass Independent 238U/235U Fractionation and Weathering Processes. To appear in *Geological Society of American Annual Fall Meeting .* (Denver, CO, Oct 31-Nov. 3, 2010).
8. Wilson, D. C., R. Aster, S. Grand, J. Ni, and W. S. Baldridge. high-resolution receiver function imaging reveals Colorado Plateau lithospheric architecture and mantle-supported topography. 2010. *Americal Geophysical Union.*
9. Mernild, S., and G. Liston. The Influence of air temperature inversions on snowmelt and glacier mass balance simulations, Ammassalik Island, Southeast Greenland. 2010. *Journal of Applied Meteorology and Climatology.* **49** (1): 47.
10. Mernild, S., G. Liston, C. Hiemstra, and J. Christensen. Greenland Ice Sheet Surface Mass-Balance Modeling in a 131-Yr Perspective, 1950-2080. 2010. *JOURNAL OF HYDROMETEOROLOGY.* **11** (1): 3.
11. Mernild, S., G. Liston, K. Steffen, and P. Chylek. Meltwater flux and runoff modeling in the ablation area of Jakobshavn Isbrae, West Greenland. 2010. *JOURNAL OF GLACIOLOGY.* **56** (195): 20.
12. Mernild, S. H., I. M. Liston, Y. Howat, K. Ahn, B. H. Steffen, B. Jakobsen, and B. Hasholt. Freshwater flux to Sermilik Fjord, SE Greenland. 2010. *The Cryosphere Discussion.* **4**: 10.
13. McGrath, D., K. Steffen, I. Overeem, S. H. Mernild, B. Hasholt, and M. van den Broeke. Sediment Plumes in Kangerlussuaq, West Greenland. To appear in *Journal of glaciology.*
14. Mernild, S. H., G. E. Liston, K. Steffen, M. van den Broeke, and B. Hasholt. Runoff and mass-balance simulations from the Greenland Ice Sheet at Kangerlussuaq. 2008. *The Cryosphere.*
15. Mernild, S. H., G. e. Liston, K. Steffen, and P. Chylek. Meltwater flux and runoff modeling in the ablation area of the Jakobshavn Isbrae, West Greenland. 2010. *Journal of Glaciology.* **56** (195): 2032.
16. Mernild, S. H., G. E. Liston, P. Chylek, M. S. Seidenkraztz, and B. Hasholt. Climate-driven fluctuations in freshwater to Sermilik Fjord, East germany. To appear in *The Holocene.*
17. Mernild, S. H., B. Hasholt, G. E. Liston, and M. van den Broeke. Runoff simulations from the Greenland Ice Sheet at Kangerlussuaq. To appear in *Hydrology Research.*
18. Yde, J. C., N. T. Knudsen, B. Hasholt, and S. H. Mernild. Chemical weathering and solute export in Southeast Greenland. To appear in *Chemical Geology.*
19. Li, H.. Particle Energization in 3D Magnetic Reconnection in Relativistic Pair Plasmas. To appear in

Physical Review Letters.

20. Cowee, M. M., S. P. Gary, H. Y. Wei, R. L. Tokar, and C. T. Russell. An explanation for the lack of ion cyclotron wave generation by pickup ions at Titan. To appear in *Journal of Geophysical Research.*

21. Srinivasan, G., D. M. Tartakovsky, M. Dentz, H. Viswanathan, B. Berkowitz, and B. A. Robinson. Randon walk particle tracking simulations of non-Fickian transport in heterogeneous media. 2010. *Journal of Computational Physics.* **229** (11): 4304.

22. Tartakovsky, D. M., and S. Broyda. PDF equations for advective-reactive transport in heterogeneous porous media with uncertain properties. 2010. *Journal of Contaminant of Hydrology.* **10**: 009.

23. WoldeGabriel, G., S. H. Ambrose, D. Barboni, R. Bonnefille, and L. Bremond. The Geological, Isotopic, Botanical, Invertebrate, and Lower Vertebrate Surroundings of Ardipithecus ramidus. 2009. *Proceedings of the National Academy of Sciences.* **10**: 1126.

24. White, T. D., B. Asfaw, Y. Beyene, Y. Haile-Selassie, C. O. Lovejoy, G. Suwa, and G. WoldeGabriel. Ardipithecus ramidus and the Paleobiology of Early Hominids. 2009. *Proceedings of the National Academy of Sciences.* **326**: 75.

25. White, T. D., S. H. Ambrose, G. Suwa, and G. WoldeGabriel. Response to comment on the paleonvironment of ardipithecus ramidus. 2010. *National Academy of Sciences.* **328** (1105): 1126.

26. Lay, E. H., and S. M. Shao. High temporal and spatial-resolution detection of D-layer fluctuations by using time domain lightning waveforms. To appear in *Journal of Geophysical Research - Space Physics.*

27. Tague, C., and A. Dugger. Ecohydrology and climate change in the mountains of the western U.S. - A review of research and opportunities. *Geography Compass.*

Publications

Burt, D. M., L. P. Knauth, K. H. Wohletz, and M. F. Sheridan. Surge deposit misidentification at Spor Mountain, Utah and elsewhere: A cautionary message for Mars. . 2008. *Volcanology and Geothermal Research.* : 755.

Carlson, J., M. White, and N. Padmanabhan. A critical look at cosmological perturbation theory techniques. 2008. *Astrophysical Journal.* : 479.

Chaudhuri, A., H. Rajaram, and H. Viswanathan. Alteration of fractures b precipitation/dissolution in gradient reaction environments: computational results and stochastic analysis. 2008. *Water Resources Research.* : 23.

Chaudhuri, A., H. Rajaram, and H. Viswanathan. Bouyant convection resulting from dissolution and pereability growth in vertical limestone fractures. 2009. *Geophysical Research Letters.* : 36.

Duan, H., G. Fuller, J. Carlson, and Y. Z. Qian. Flavor Evolution of the neutroni8zaiton neutrino burst from an O-Ne-Mg Core-Collapse Supernova. 2008. *Journal of Applied Physics.* : 100.

Duan, H., G. M. Fuller, and J. Carlson. Simulating nonlinear neutrino flavor evolution. 2008. *Computational Science and Discovery.* : Vol 1.

Heitmann, K., M. White, C. Wagner, S. Habib, and D. Higdon. The Coyote Universe I: Precision determination of the nonlinear matter power spectrum. 2009. *Astrophysical Journal.* : 50.

Hill, T. W., M. F. Thomsen, M. G. Henderson, R. L. Tokar, A. J. Coates, H. J. McAndrews, G. R. Lewis, D. G. Mitchell, C. M. Jackson, C. T. Russell, M. K. Dougherty, F. J. Crary, and D. T. Young. Plasmoids in Saturn's magnetotail. 2008. *Journal of Geophysical Research.* : 113.

Hinz, E. A., J. F. Ferguson, L. Pellerin, and A. F. Ramenofsky. A geophysical investigation of subsurface structures and quaternary geology of San Marcos Pueblo, NM . 2008. *Archaeological Prospection.* : 247.

Huebner, W. F., L. N. Johnson, D. C. Boice, P. Bradley, S. Chocron, A. Ghosh, P. T. Giguere, R. Goldstein, J. A. Guzik, J. J. Keady, J. Mukherjee, W. Patrick, C. Plesko, J. D. Walker, and K. Wohletz. A comprehensive program for countermeasures against potentially hazardous objects. . 2010. *Solar System Research.* **43**: 334.

Jiang, W., S. Liu, C. Fragile, C. Yu, and C. Fryer. Cascade and damping of Alfv' en-Cyclotron fluctuations: application to solar wind turbulence. 2009. *Astrophysical Journal.* **698**: 163.

Ogden, D. E., K. H. Wohletz, G. A. Glatzmaier, and E. E. Brodsky. Numerical simulations of volcanic jets: Importance of vent overpressure. 2008. *Geophysical Research.* : 113.

Ogden, D. E., S. W. Kieffer, X. Lu, G. McFarquhar, and K. H. Wohletz. Fluid Dynamics of High Pressure Volcanic Eruptions. 2009. *Geophysical Research.* : 238.

Wohletz, K. H., D. Steedman, P. Giguere, and D. Zhang. PHO mitigation simulations using computational fluid and solid mechanics. 2008. *Los Alamos National Laboratory Report.* : 10.

Zoglauer, A.. Application of neural networks to the identification of the compton interaction sequence in compton igagers. 2008. *IEEE.* : 701137.

New Generation Hydrodynamic Methods: from Art to Science (U)

Donald E. Burton
20100015DR

Introduction

When solids are deformed extremely rapidly, they behave very much like fluids. For that reason, the field of study focused on extremely fast solid deformation is known as "*hydro*dynamics." Hypervelocity impact such as an explosively launched penetrator striking an army tank or an asteroid striking the earth are examples of solids exhibiting hydrodynamic behavior.

The process of simulating hydrodynamic events is similar to the more commonly recognized branches of science known as computational fluid dynamics ("CFD") and computational solid mechanics. Just as these two branches have their own particular difficulties, hydrodynamics presents its own difficulties and in some ways shares a special combination of the difficulties from both of these other branches.

Specifically, CFD has relatively simple models for how fluids behave under stress but has to deal with the difficulties associated with shock waves in high speed flows. These shock waves represent mathematical discontinuities, and so they are challenging to capture algorithmically in general geometries and for general situations. Meanwhile, stress analysts do not have to deal with shocks, but do have the burden of dealing with highly complicated material models, including materials that creep or develop cracks. In hydrodynamics, the worst of both scenarios collide. While the solids under extreme loading behave mostly like fluids, it is not acceptable to completely disregard their solid strength characteristics. So, the complexities of material modeling still impacts hydrodynamics. At the same time, the rapid loading of the material causes shocks to form, and dealing with these shocks is absolutely critical. For example, high explosive detonation occurs when the shock wave induces chemical reactions that reinforce the shock.

Hydrodynamics is faced with these difficulties, along with others that it shares with CFD and stress analysis such as multi-body contact and mixing of materials. Despite these many challenges associated with phenomena of hypervelocity flow, there actually remain challenges even at a more rudimentary level, that of simulating the basic laws of physics on computational meshes. In other words, hydrodynamics is still plagued with problems developing algorithms that enforce the conservation of momentum and energy when the associated governing equations are approximated on a mesh.

To date, no perfect method for solving the hydrodynamics equations has been found. This research project proposed a new scheme called "cell-centered hydrodynamics" (CCH), which appears to be highly promising. Preliminary theoretical analysis and a prototype implementation suggests the method to be superior to traditional methods for all test problems investigated.

Benefit to National Security Missions

Hydrodynamic simulations are central to many missions of the NNSA and other agencies. The DOE's Advanced Scientific Computing (ASC) program has developed codes that have become successful simulation tools, but most of the hydrodynamics algorithms have a common origin dating back to the 1950s and constitute a common mode of failure for these new-generation applications across the DOE complex.

Numerical errors associated with current methods are relatively small providing they are applied to problems similar to those for which the methods were developed. However, as these codes are applied to increasingly challenging problems with higher expectations for accuracy, the numerical errors that used to be acceptable will not be in the future, and it is necessary to consider more advanced hydrodynamic methods.

The project proposes to develop the theory and numerical algorithms for this new hydrodynamics simulation method, implement it in an established code framework, complete with the other challenges mentioned above, evaluate its performance relative to historical methods, and extend it as needed to address practical applications.

The risk associated with developing a new hydrodynamics method is high. To be successful, the new method must not only offer substantial improvements over existing methods, it must be functionally equivalent. That is, it must have the same realm of physical applicability and support similar interfaces to related physics modules. Whether it can be adapted for the full range of applications addressed by ASC codes remains to be determined.

Progress

The project was reviewed by an external panel in March 2010. Their summary concluded that the LDRD project "is highly relevant to the strategic directions of the laboratory. It has made substantial progress despite having been funded for only a few months, and is ahead of its planned schedule. The project team is first-rate and the technical work is of the highest quality."

The particular type of hydrodynamic simulation method pursued in this project is called "Lagrangian hydrodynamics." It has that name because, unlike CFD simulations where the mesh is stationary and the fluid moves through it, here the mesh moves with the material. The chief reason for pursuing a Lagrangian approach is that the specialized history of a material plays a large role in how it responds under these loading conditions. It is advantageous to keep the identity and history of that material associated with a cell in the mesh so that it can be modeled properly.

The LDRD stays focused on this cell-centered Lagrangian approach, and divides its work into five areas: Theory, implementation, verification, exploratory studies, and publication. In the first area, theory, the project has made substantial progress toward developing a self-consistent theoretical formulation for Lagrangian hydrodynamics. This formulation addresses not only the fundamental issues of momentum conservation, energy conservation, and thermodynamics, but retains functional equivalence relevant to real-world applications and also areas of particular concern to both old and new methods. To address functional equivalence, the project has extended the theory to include curvilinear geometry necessary for one- and two-dimensional problems, continuum mechanics necessary for modeling solids, and material mixtures. The project team has paid particular attention to entropy errors associated with walls as well as a limiting case of isentropic compression. Work has also been done on extending the method to an alternative Eulerian hydrodynamics method, i.e. the method used in CFD where the mesh does not move.

However, the team still faces challenges in the development of algorithms that eliminate all of the known errors commonly plaguing hydro methods. The team is continuing to explore new ideas in order to produce breakthrough technology. Two new exploratory efforts are now underway. One is pursuing novel ideas that introduce additional auxiliary conservation laws as constraints for making cells cooperate in their motion. Another is the enlistment of Professor Philip Roe at the University of Michigan in a cooperative effort with AWE's Andy Barlow to work together on new ideas.

In the area of implementation, the project team has made considerable progress on developing an implementation suitable for large-scale simulations. The project team has written several prototype implementations in a relevant code framework (the code FLAG). To date, calculations have been done in one, two, and three dimensions, including several curvilinear geometries. Essential capabilities for modeling solids have been written, and are being tested.

Verification of the code implementation involves applying it to problems with known solutions. Preliminary experience with the FLAG implementation suggests the new method is consistently superior to historical schemes. In particular the project team found improved robustness, accuracy, and symmetry preservation, along with a reduction in mesh imprinting and entropy errors.

Preliminary results have been presented at several international forums: MultiMat09 (Pavia), JOWOG-42 (Aldermaston 2009, Livermore 2010), NEDPC-09 (Livermore), NECDC-10 (Los Alamos).

Future Work

The future work falls within the five areas mentioned in the previous section.

- Theory: The team will continue to develop and extend current theory to encompass hydrodynamic and numerical capabilities required for a general purpose hydrodynamics code. It is also continuing to develop and test novel concepts in both production quality and prototype coding.
- Implementation: Phased implementation in an established hydrocode framework beginning with a limited 2D prototype and progressing to 1D & 2D curvilinear geometry, 3D geometry, ALE, complex materials, contact discontinuities, and curvature corrections will continue in the coming year.
- Testing & verification: As implemented capabilities become available, they will be tested against other codes and analytical solutions. Testing will be weighted toward assessing the method with regard to its ultimate applications.
- Exploratory studies: This area is undergoing a mild redirection. Whereas it was initially going to focus on potential application in Eulerian codes and advanced computer architecture, these funds are being directed somewhat to continue the fundamental theoretical work for breakthrough hydrodynamics algorithms.

- Publication and Outreach: This year, at least one refereed journal article is planned along with one or more conference proceedings.

Conclusion

The project team anticipates the effort will improve the ability of the national laboratories and other institutions to execute their core missions. This will result from significant improvements in the fidelity of hydrodynamic simulations. The effort will give rise to products on several levels. The theory, algorithms, and assessment of the method will be published in open forums. There will be a verified hydrocode implementation suitable for large-scale simulations and compatible with ASC code requirements, along with code modules that can be adapted to other codes. There will be a prototype application for advanced computer architectures.

References

1. Burton, D. E., and M. J. Shashkov. Mimetic formulation of cell-centered Lagrangian hydrodynamics. (Pavia, Italy, 21-25 Sep. 2009).

2. Burton, D. E., and M. J. Shashkov. Mimetic formulation of cell-centered hydrodynamics (CCH), LA-UR-09-06533. (Livermore, CA, 2-30 Oct. 2009).

3. Burton, D. E., and M. J. Shashkov. Mimetic formulation of cell-centered Lagrangian hydrodynamics (CCH), LA-UR-09-03454. (Aldermaston, UK, 8-12 June 2009).

4. Runnels, S., and D. Burton. LANL cell-centered hydro research, LA-UR-10-04062. (Livermore, CA, 21-24 Jun. 2010).

5. Burton, D., T. Carney, S. Runnels, and M. Shashkov. Exploration of a cell-centered Lagrangian hydrodynamics method, LA-UR-10-06548. (Los Alamos, NM, 18-22 Oct. 2010).

Publications

Burton, D. E., and M. J. Shashkov. Mimetic formulation of cell-centered Lagrangian hydrodynamics. Invited presentation at *Numerical Methods for Multi-Material Fluids & Structures, LA-UR-09-05875.* (Pavia, Italy, 21-25 Sep. 2009).

Burton, D. E., and M. J. Shashkov. Mimetic formulation of cell-centered hydrodynamics (CCH), LA-UR-09-06533. Presented at *NEDPC 2009.* (Livermore, CA, 2-30 Oct. 2009).

Burton, D. E., and M. J. Shashkov. Mimetic formulation of cell-centered Lagrangian hydrodynamics (CCH), LA-UR-09-03454. Presented at *JOWOG 42 2009.* (Aldermaston, UK, 8-12 June 2009).

Burton, D., T. Carney, S. Runnels, and M. Shashkov. Exploration of a cell-centered Lagrangian hydrodynamics method, LA-UR-10-06548. Presented at *NECDC 2010.* (Los Alamos, NM, 18-22 Oct. 2010).

Runnels, S., and D. Burton. LANL cell-centered hydro research, LA-UR-10-04062. Presented at *JOWOG 42 2010.* (Livermore, CA, 21-24 Jun. 2010).

Cosmological Signatures of Physics Beyond the Standard Model: Petascale Cosmology Meets the Great Surveys

Katrin Heitmann
20100023DR

Introduction

The unveiling of the secrets of the large-scale Universe by sky surveys has transformed cosmology, fundamental physics, and astrophysics. Dark energy and dark matter are at the focus of an intense global effort to fathom the deep mysteries posed by their existence. Next-generation observations promise new discoveries and an unprecedented jump in our knowledge of the Universe. The extraction of deep science requires a theoretical and computational understanding and a modeling capability fully as revolutionary as the surveys themselves.

The focus of our project is the prediction and extraction of physics beyond the Standard Model of cosmology from large scale structure probes. We targeting the following, fundamental questions: (i) What are the detectable signatures of a dynamical dark energy? (ii) How does a modification of general relativity alter the nonlinear regime of structure formation? (iii) What are the effects of plausible dark matter candidates on the mass distribution? (iv) What are the imprints of non-standard initial conditions on the large scale distribution of galaxies?

To answer these questions, two newly developed capabilities, unique to our effort at Los Alamos, are very significant: (i) A new cosmology code which takes full advantage of Roadrunner, the fastest supercomputer in the world. This capability, unmatched world-wide, will allow us to simulate the entire observable Universe down to galactic scales for the first time. These simulations will establish new benchmarks for the state of the art in predicting cosmological statistics for large-scale structure surveys. (ii) A new statistical framework, that melds precision predictions with observations, and removes the computational barrier to Monte Carlo analyses of cosmological data. This framework can combine datasets from different observations, detailed simulation predictions, and systematic and statistical error models. It will be essential for interpreting data, and for optimizing observational strategies.

Benefit to National Security Missions

Our project targets questions about the nature of dark energy, and is therefore highly relevant to DOE/SC sponsored missions such as the Large Synoptic Survey Telescope (of which Los Alamos is a member institution) and NASA sponsored missions such as WFIRST (Wide-Field Infrared Survey Telescope). A major component of our project involves innovative concepts for high-performance computing targeted at future hybrid architectures on our way to exa-scale computing. Another major component targets the analysis of heterogeneous data sets, both very relevant to DOE/SC and DOE/ASCR.

Progress

During the first year of the project we have made substantial progress on several fronts. In order to detect features in the dark energy equation of state which would hint at an explanation of the accelerated expansion of the Universe beyond the cosmological constant, we have developed a new non-parametric reconstruction scheme. This new method allows us to extract one of the most important quantities to characterize dark energy in a model-independent way. The new method was tested and verified on simulated data and has been applied to real observations. One paper has been published [1] and one is currently under review [2]. We carried out an extensive analysis of the imprints of dynamical dark energy models which have a considerable dark energy component in the early evolution of the Universe. We derived signatures of such models for the mass function of clusters of galaxies and contrasted the results with the sensitivity of future surveys. We concluded that the high precision of future surveys will allow us to get constraints on such models. A paper is currently under review [3]. This part of our work constitutes a major advance in answering the first questions stated in the introduction about imprints of dynamical dark energy. In addition, we derived the most accurate predictions for the mass function (the number count of clusters as a function of their mass) ever for a class of cosmologies with constant equations of state, again going beyond the current paradigm of the

cosmological constant. Figure 1 shows the mass function measurement for three different epochs. A paper is under review [4].

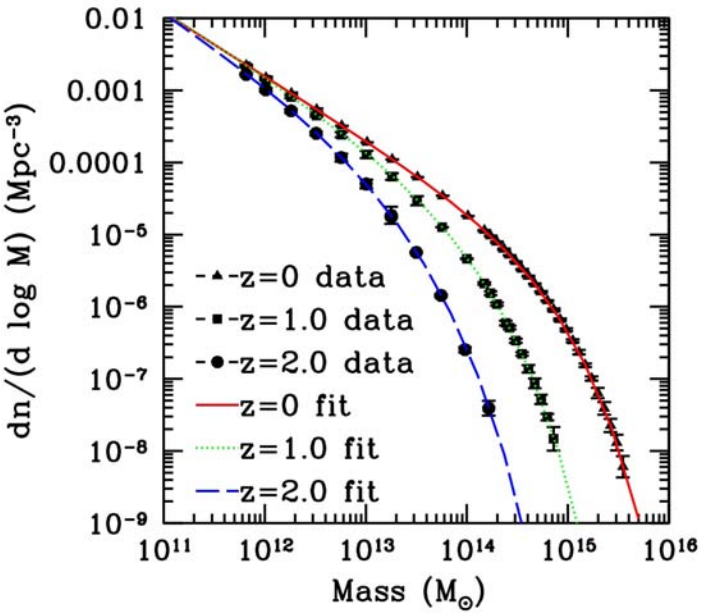

Figure 1. Dark matter mass function measured from simulations at three different epochs (triangles: today, squares and circles: past) and the best fit to the simulation data.

We have carried out an analysis of 9 of the largest large scale structure simulations every performed and extracted the baryon acoustic oscillation signal in the Lyman-alpha forest from these simulations. A paper on this work has appeared in the Astrophysical Journal [5]. Figure 2 shows a snapshot of one of the simulations. Displayed are the dark matter halos that host galaxies. We have developed a high-precision prediction scheme for one of the most important cosmological statistics, the matter power spectrum. This new prediction tool has been made publicly available and is already in use by the community. A paper has been published in the Astrophysical Journal [6]. We have started to investigate the signatures of primordial non-Gaussianities on the large-scale structure distribution of the Universe. The progress in this area positions us well to answer the fourth questions stated in the introduction. In order to generate simulations that have enough dynamic range to mimic upcoming large surveys such as the Large Synoptic Survey Telescope, we have extended our simulation capabilities extensively. We have added a high-resolution module to our simulation code. We have ported the code to some of the fastest supercomputers in the world. A paper describing this new code has been published [7] and a second invited paper is in preparation. In addition, we have developed a new hydrodynamics capability for the code to incorporate more physics into our simulations. In order to analyze the simulations in an efficient way, we have developed a new suite of analysis tools. These tools can run with the code "on-the-fly" and have been also integrated into ParaView, a visualization tool that now allows the simultaneous analysis and visualization of large data sets. This part of the project has led to two publications [8,9], and two more are in preparation. In addition, work was carried out on exploring different parameters to describe and reconstruct dark energy properties [10], using galaxy peculiar velocities from large-scale supernova surveys as a dark energy probe [11], connecting photometric and spectroscopic redshifts with a sophisticated statistical framework [12], investigating the properties of large scale structure in the Universe [13], and using a Bayesian framework to combine simulations and physical observations for statistical inference [14]. So far the project has led to 14 publications (several more are almost finished) and has been presented at ~30 workshops, conferences, and Universities worldwide. The code development carried out in this project enabled the successful competition for the Early Science Program at ANL, leading to 6 million core hours per year for two years on Intrepid (a Blue Gene P system) and 150 million core hours on Mira (a future 10 Petaflop machine at Argonne).

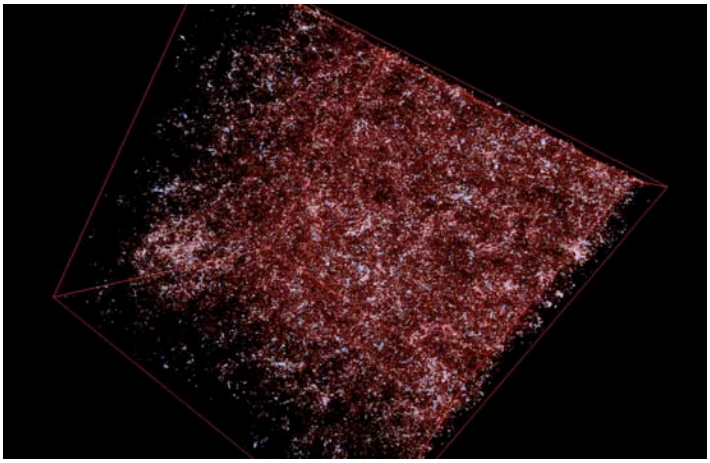

Figure 2. Visualization of halos from a dark matter simulation. The underlying simulation advanced 64 billion particles in a volume of 750 Mpc/h on a side. The halos shown are clumps of dark matter particles and are the hosts of the galaxies observed in the Universe.

Future Work

Cosmology is entering one of its most scientifically exciting phases. The last two decades have culminated in the celebrated Standard Model of cosmology. Yet, two pillars of the Standard Model, dark matter and dark energy -- together accounting for 95% of the mass-energy of the Universe -- remain its greatest mysteries. To venture beyond the current boundaries, cosmological survey capabilities are being spectacularly improved. Interpretation of future observations is impossible without a theory, modeling, and simulation effort fully as revolutionary as the new surveys.

To discover signatures of new physics using structure formation probes, our approach is to (i) develop new theoretical ideas and introduce them into the modeling and simulation capabilities, (ii) generate observational predictions (``simulated skies'') and extract unique features of the new physics in different statistics of the large scale structure distribution, (iii) determine the sensitivity of observations to these features and the other physics (or systematic errors) that could mimic them, and (iv) contrast the predictions to observations. Our aim is to incorporate the new physics in a general way, i.e., to implement classes of models and analyze generic behaviors of quantities of interest rather than working with one possible model after another -- a possibly hopeless task, with limited science return.

In the second and third year of the project we will focus on answering the following questions: (i) How does modification of general relativity alter the nonlinear regime of structure formation? (ii) Dark matter: What are the effects of plausible dark matter candidates on the mass distribution? (iii) Physics of the early Universe: What are the imprints of non-Gaussian initial conditions and nontrivial inflation models on the large-scale distribution of galaxies? We have set up all the required tools to answers these questions during the first year.

Conclusion

Observations indicate that the Universe consists of 70% of a mysterious dark energy and 25% of a yet unidentified dark matter. Understanding the physics of this dark sector is one the foremost challenges in all of physics today. This project will make important contributions to further this understanding. We will provide the essential theoretical and modeling framework to interpret results from major upcoming dark energy missions. Only by performing complex simulations and modeling tasks will we be able to analyze the wealth of upcoming data and shed light on the physics of the dark Universe.

References

1. Holsclaw, T., U. Alam, B. Sanso, H. Lee, K. Heitmann, S. Habib, and D. Higdon. Nonparametric reconstruction of the dark energy equation of dtate. To appear in *Physical Review D.*

2. Holsclaw, T., U. Alam, B. Sanso, H. Lee, K. Heitmann, S. Habib, and D. Higdon. Nonparametric dark energy reconstructing from supernova data. *Physical Review Letter.*

3. Alam, U., Z. Lukic, and S. Bhattacharya. Galaxy clusters as a probe of early dark energy. To appear in *The Astrophysical Journal.*

4. Bhattacharya, S., K. Heitmann, M. White, Z. Lukic, C. Wagner, and S. Habib. Mass function predictions beyond LCDM . To appear in *The Astrophysical Journal.*

5. White, M., A. Pope, J. Carlson, K. Heitmann, S. Habib, P. Fasel, D. Daniel, and Z. Lukic. PARTICLE MESH SIMULATIONS OF THE Ly alpha FOREST AND THE SIGNATURE OF BARYON ACOUSTIC OSCILLATIONS IN THE INTERGALACTIC MEDIUM. 2010. *ASTROPHYSICAL JOURNAL.* **713** (1): 383.

6. Lawrence, E., K. Heitmann, M. White, D. Higdon, C. Wagner, S. Habib, and B. Williams. THE COYOTE UNIVERSE. III. SIMULATION SUITE AND PRECISION EMULATOR FOR THE NONLINEAR MATTER POWER SPECTRUM. 2010. *ASTROPHYSICAL JOURNAL.* **713** (2): 1322.

7. Pope, A., S. Habib, Z. Lukic, D. Daniel, P. Fasel, K. Heitmann, and N. Desai. The Accelerated Universe. 2010. *Computing in Science & Engineering.* **12** (4): 17.

8. Hsu, Chung-Hsing, J. P. Ahrens, and K. Heitmann. Verification of the Time Evolution of Cosmological Simulations via Hypothesis-Driven Comparative and Quantitative Visualization. 2010. In *2010 IEEE Pacific Visualization Symposium (PacificVis 2010) ; 2-5 March 2010 ; Taipei, Taiwan.* , p. 81.

9. Ahrens, J., K. Heitmann, M. Petersen, J. Woodring, S. Williams, P. Fasel, C. Ahrens, C. H. Hsu, and B. Geveci. Verification of scientific simulations via hypothesis-driven comparative and quantitative visualization. To appear in *IEEE Computer Graphics and Applications.*

10. Pan, A. V., and U. Alam. Reconstructing dark energy: a comparison of different cosmological parameters. *Physical Review D.*

11. Bhattacharya, S., A. Kosowsky, J. Newman, and A. Zentner. Galaxy peculiar velocities from large-scale supernova surveys as a dark energy probe . *Physical Review D.*

12. Kaufman, C., D. Bingham, S. Habib, and K. Heitmann. Efficient emulators for computer experiments using compactly supported correlation functions. *Journal of the American Statistical Association.*

13. Shandarin, S., S. Habib, and K. Heitmann. Origin of the cosmic network in Lambda CDM: Nature vs nurture. 2010. *PHYSICAL REVIEW D.* **81** (10): 103006.

14. Higdon, D., K. Heitmann, E. Lawrence, and S. Habib. Using the bayesian framework to combine simulations and physical observations for statistical inference. 2011. In *Large-scale inverse problems and quantification of uncertainty.* Edited by Biegler, L., G. Biros, O. Ghattas, M. Heinkenschloss, D. Keyes, B. Mallick, L. Tenorio, B. van Bloemen Waanders, K. Wilcox, and Y. Marzouk. p. 87. West Sussex: Wiley.

Publications

Ahrens, J., K. Heitmann, M. Petersen, J. Woodring, S. Williams, P. Fasel, C. Ahrens, C. H. Hsu, and B. Geveci. Verification of scientific simulations via hypothesis-driven comparative and quantitative visualization. 2010. *IEEE Computer Graphics and Applications.* **30** (6): 16.

Alam, U., Z. Lukic, and S. Bhattacharya. Galaxy clusters as a probe of early dark energy. To appear in *The Astrophysical Journal.*

Bhattacharya, S., A. Kosowsky, J. Newman, and A. Zentner. Galaxy peculiar velocities from large-scale supernova surveys as a dark energy probe . To appear in *Physical Review D.*

Bhattacharya, S., K. Heitmann, M. White, Z. Lukic, C. Wagner, and S. Habib. Mass function predictions beyond LCDM . To appear in *The Astrophysical Journal.*

Higdon, D., K. Heitmann, E. Lawrence, and S. Habib. Using the bayesian framework to combine simulations and physical observations for statistical inference. 2011. In *Large-scale inverse problems and quantification of uncertainty.* Edited by Biegler, L., G. Biros, O. Ghattas, M. Heinkenschloss, D. Keyes, B. Mallick, L. Tenorio, B. van Bloemen Waanders, K. Wilcox, and Y. Marzouk. , p. 87. West Sussex: Wiley.

Holsclaw, T., U. Alam, B. Sanso, H. Lee, K. Heitmann, S. Habib, and D. Higdon. Nonparametric dark energy reconstructing from supernova data. *Physical Review Letter.*

Holsclaw, T., U. Alam, B. Sanso, H. Lee, K. Heitmann, S. Habib, and D. Higdon. Nonparametric reconstruction of the dark energy equation of dtate. To appear in *Physical Review D.*

Hsu, Chung-Hsing, J. P. Ahrens, and K. Heitmann. Verification of the Time Evolution of Cosmological Simulations via Hypothesis-Driven Comparative and Quantitative Visualization. 2010. In *2010 IEEE Pacific Visualization Symposium (PacificVis 2010) ; 2-5 March 2010 ; Taipei, Taiwan.* , p. 81.

Kaufman, C., D. Bingham, S. Habib, K. Heitmann, and J. Frieman. Efficient emulators for computer experiments using compactly supported correlation functions. *Journal of the American Statistical Association.*

Lawrence, E., K. Heitmann, M. White, D. Higdon, C. Wagner, S. Habib, and B. Williams. The coyote universe. iii. simulation suite and precision emulator for the nonlinear matter power spectrum. 2010. *Astrophysical Journal.* **713** (2): 1322.

Pan, A. V., and U. Alam. Reconstructing dark energy: A comparison of different cosmological parameters. *Physical Review D.*

Pope, A., S. Habib, Z. Lukic, D. Daniel, P. Fasel, K. Heitmann, and N. Desai. The Accelerated Universe. 2010. *Computing in Science & Engineering.* **12** (4): 17.

Shandarin, S., S. Habib, and K. Heitmann. Origin of the cosmic network in Lambda CDM: Nature vs nurture. 2010. *PHYSICAL REVIEW D.* **81** (10): 103006.

White, M., A. Pope, J. Carlson, K. Heitmann, S. Habib, P. Fasel, D. Daniel, and Z. Lukic. Particle mesh simulations of the Lyα forest and the signature of baryon acoustic oscillations in the intergalactic medium. 2010. *Astrophysical Journal.* **713** (1): 383.

Information Science for Understanding Complex Quantum Matter

Malcolm G. Boshier
20100045DR

Introduction

The challenge motivating this project was famously articulated 25 years ago by Richard Feynman. He pointed out that simulating quantum many-body systems on a computer is exponentially difficult: just storing the state of a system with N parts requires an exponentially large memory. Exact simulation of large quantum systems on classical computers is thus impossible (e.g. Roadrunner might manage to do 42 spin-½ particles, but a future exaflop machine, 1000x faster than Roadrunner, could only increase this number to 52). Exponential complexity is the reason why a recent BES report discussing high-Tc superconductivity laments that "We do not even know whether the 2D Hubbard model has a stable superconducting ground state". Fundamental difficulties like these motivate our search for completely new ways to compute many-body quantum systems. Together, our capabilities in quantum information (QI) science and in quantum many-body physics can address this challenge. Feynman's visionary solution to the quantum complexity problem was effectively a restricted form of quantum computing: use a controllable quantum system with the same Hamiltonian as the system of interest to emulate its behavior. While easier than universal quantum computation, this quantum emulation is still technically extremely demanding because of the unavoidable coupling between a quantum system and its environment, which acts to destroy superposition through decoherence and to remove energy through dissipation. However, laboratory control over quantum systems, especially with QI techniques from ultracold atomic physics, is reaching a point where quantum emulation looks feasible. This unprecedented level of control opens up novel opportunities for probing complexity in quantum many-body systems. QI also inspires a second solution to the complexity issue: new algorithms to simulate (approximately, but efficiently) a large class of quantum systems on present day classical computers. Together, these QI-derived techniques could transform the simulation of quantum many-body systems.

Benefit to National Security Missions

The tools of quantum emulation and quantum-information-inspired algorithms developed in this project will provide powerful new ways compute the properties of complex quantum systems. This work is directly relevant to the missions of DOE/SC, in particular the Basic Understanding of Materials and, to a somewhat lesser extent, Fundamental Chemistry. The controllable quantum systems we will build for emulation may also have sensing applications ultimately useful to missions in DOE/NNSA, DOE/NN and the Intelligence Community.

Progress

Boshier's experimental team has focused on realizing smooth, laser-"painted" potentials to confine ultracold Bose-Einstein condensates (BECs). This is an essential prerequisite for creating the uniform density BECs which will eventually enable us to make a quantum emulator of a homogeneous system (in contrast to all previous experiments with cold atoms, which are rendered inhomogeneous and less ideal by the presence of a confining magnetic potential). They have proved the smoothness of the painted potential by exciting persistent currents in a painted toroid. The condensate rotates indefinitely without dissipation, proving that the potentials are flat. The technique has turned out to be more powerful than originally anticipated, allowing us to demonstrate for the first time that the flow of a BEC in a toroidal geometry is quantized. This was done in a very simple and direct way: the BEC is created in a trap with a rotating barrier that is then lowered to produce a superfluid state. The confining potential is turned off and the BEC imaged after a period of expansion. The resulting density distribution has a hole at the center if the original BEC was rotating, and our measurements show that the hole size is quantized in values corresponding to winding numbers (a measure of the rotation velocity) from zero to five. Our work also confirms that the painted toroid is smooth enough to function as a one-dimensional homogeneous system, complementing the two dimensional painted box systems we also plan to use in later stages of the project.

Several aspects of the painted toroid experiment have been explored theoretically by the project members. First, it turns out that winding number is a robust quantum number that is not changed easily, even if the system has dissipation. Mozyrsky has considered how this important aspect of the experimental result could be used to realize a "BEC flux qubit", in which the two states of the qubit correspond to different winding numbers [1,2]. This work may provide a new strategy for quantum information processing with trapped BECs as well as a new paradigm to explore fundamental properties and manifestations of quantum mechanics at macroscopic level. Second, Timmermans and his team have been considering the quantum mechanical theory of the dynamic rotating ring potential, which is a key part of the experiment. Third, Zurek, Damski, and colleagues have been applying their expertise in phase transition dynamics to address the issue of why the winding number observed in the experiment, while quantized, is not reproducible. This is both an interesting question in fundamental many-body physics and an important technological issue for some applications of the technique.

The team has also made progress in several other areas of the project. The effect of disorder and dissipation in quantum emulators is going to be a topic of investigation later in the project timeline. Dalvit and visiting student Moreno have already begun considering the effects of disorder: in analogy to Anderson localization of waves induced by a random potential, they have shown that atom-surface interactions between a Bose-Einstein condensate and a rough surface also produce localization phenomena. Quantum fluctuations of the electromagnetic field serve as a means to imprint the surface disorder onto matter waves, which show either algebraic or exponential density localization depending the noise spectrum of the surface. This work has just been accepted for publication in Physical Review Letters [3]. Timmermans and collaborators have developed the theory of pseudo-spin interactions in cold atoms, which is at the heart of our plan to use phase separation of a two-component BEC in a homogeneous potential to emulate quantum phase transition dynamics [4]. Zurek, Damski, and their collaborators have investigated a simple, but powerful, model of decoherence by considering a single spin coupled to a ring of spins, which emulates an environment. They have also studied soliton formation in a 1D system driven through the BEC phase transition and shown that the number of solitons formed may be used to extract critical exponents from experiments such as those which could be performed with our toroidal BEC [5]. Damski and Chien have studied dynamics of an ultra-cold atomic BCS superfluid driven by a gradual decrease of the pairing interaction, and considered how a cold fermion cloud implementation of this system could be a quantum emulator of a conventional superconductor [6]. Experimental realization of such driving in conventional superconductors would require a real-time change of either dopant concentration or lattice structure, which is essentially impossible. They found interesting dynamics of the Cooper pairs, which should stimulate future experiments on out-of-equilibrium fermionic gases. Finally, Lybarger has been refining designs for a new type of "programmable" surface electrode ion trap, which should enable powerful emulation of condensed matter systems using trapped ions.

Future Work

Our primary goal is to make several significant advances in quantum emulation experiment and theory. A secondary goal is to enhance the state of the art in several important QI technologies.

LANL today possesses the two key ingredients for success in this plan: exquisite laboratory control over quantum systems with interesting Hamiltonians, and state of the art theory to devise clever strategies and targets for emulation. We intend to build emulators based on two different QI technologies: Bose-Einstein condensates (BECs) and trapped ions. These complementary architectures harness original Los Alamos work both in theory and experiment which give LANL unique advantages in the race to build useful quantum emulators. LANL's theoretical expertise in decoherence, quantum computing, quantum phase transitions, and quantum many-body physics will both provide the crucial emulator and algorithmic theory and steer the project in exciting directions.

The classes of problems within reach of our techniques are large. We will consider systems governed by many-body Hamiltonians containing Ising/Heisenberg (spin-spin interactions) or Bose-Hubbard (tunneling and on-site interactions) terms. Interesting complexity and realism will arise from controllably introducing frustration, disorder, decoherence, and dissipation to the systems. We will compute both static properties and dynamics, including those of quantum phase transitions (QPTs), with emphasis on scaling behavior and on what QPT effects persist away from temperature T = 0.

To avoid being stymied by an unforeseen technical obstacle, we are developing in parallel two complementary QI architectures, trapped ions (emulating small number of fermions with spin-spin interactions) and BEC (emulating large numbers of interacting bosons in both simple and disordered potentials). These two threads will help focus, but not constrain, the more theoretical components on QI-inspired algorithms and quantum many-body theory.

Conclusion

This project is attempting to develop a range of new techniques to simulate large quantum systems. This is a task that is intractable on conventional computers because of the intrinsic complexity of quantum mechanics. This barrier to exact calculation is extremely important because

it prevents us from modeling energy-relevant systems such as high-temperature superconductors from first principles, and so improving their performance. In this project we are using both experimental and theoretical tools derived from the field of quantum information processing to create new tools for simulating large quantum systems.

References

1. Solenov, D., and D. Mozyrsky. Metastable states and macroscopic quantum tunneling in a cold-atom Josephson ring. 2010. *Physical Review Letters.* **104** (15): 150405.

2. Solenov, D., and D. Mozyrsky. Cold atom qubits . To appear in *Journal of Theoretical and Computational Nanotechnology.*

3. Moreno, G. A., R. Messina, D. A. R. Dalvit, A. Lambrecht, P. A. Maia Neto, and S. Reynaud. Disorder in quantum vacuum: Casimir-induced localization of matter waves. To appear in *Physical Review Letters.*

4. Santamore, D. H., and E. Timmermans. Pseudospin and spin-spin interactsions in ultracold alkali atoms. *New Journal of Physics.*

5. Damski, B., and W. Zurek. Soliton creation during a Bose-Einstein condensation. 2010. *Physical Review Letters.* **104** (16): 160404.

6. Chien, C., and B. Damski. Dynamics of a quantum quench in an ultra-cold atomic BCS superfluid. *Physical Review A.*

Publications

Chien, C., and B. Damski. Dynamics of a quantum quench in an ultra-cold atomic BCS superfluid. *Physical Review A.*

Damski, B., and W. Zurek. Soliton creation during a Bose-Einstein condensation. 2010. *Physical Review Letters.* **104** (16): 160404.

Moreno, G. A., R. Messina, D. A. R. Dalvit, A. Lambrecht, P. A. Maia Neto, and S. Reynaud. Disorder in quantum vacuum: Casimir-induced localization of matter waves. To appear in *Physical Review Letters.*

Santamore, D. H., and E. Timmermans. Pseudospin and spin-spin interactsions in ultracold alkali atoms. *New Journal of Physics.*

Solenov, D., and D. Mozyrsky. Metastable states and macroscopic quantum tunneling in a cold-atom Josephson ring. 2010. *Physical Review Letters.* **104** (15): 150405.

Solenov, D., and D. Mozyrsky. Cold atom qubits . To appear in *Journal of Theoretical and Computational Nanotechnology.*

CLEAN Detection & Identification of Dark Matter

Andrew Hime
20100063DR

Introduction

Testimony to the scientific imperative to directly detect and identify the dark matter in the universe is provided in a suite of national studies and task force reports. LANL scientists have co-invented a conceptually simple and economic means to achieve the multi-ton targets necessary to directly detect and study dark matter in our galactic halo. This program, dubbed CLEAN for Cryogenic Low Energy Astrophysics with Noble liquids, is unique in the world for its ability to exploit, interchangeably, targets of liquid argon and liquid neon in the same "single-phase" scintillation detector operating deep beneath the Earth's surface. This project permits demonstration of our novel concept through the design and construction of the Mini-CLEAN detector (Figure 1). We combine this important and timely experimental opportunity with a theoretical program to establish the physical nature of dark matter through a comprehensive study of the experimental data within the broader framework of physics Beyond the Standard Model (Figure 2).

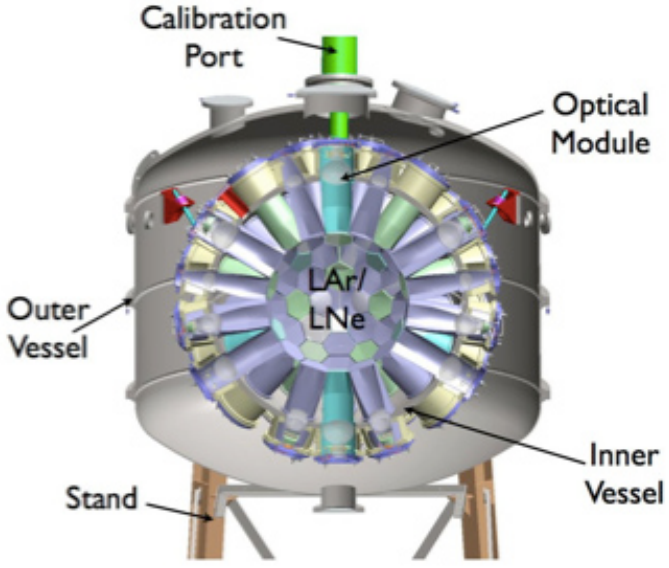

Figure 1. A conceptual drawing of the MiniCLEAN detector. The central target of liquid cryogen will be contained in and Inner Vessel (IV) that contains 92 ports to house the optical cassettes providing a "cold seal" to the IV and viewing the inner target via acrylic light guides. The front faces of these light guides provide a 4-pi wavelength-shifting sphere that shifts the extreme ultraviolet light into the "blue" where it can be detected by the photomultiplier tube array. The IV is contained inside an Outer Vessel (OV) which provides thermal shielding for the IV and that acts as basic containment of the central cryogen.

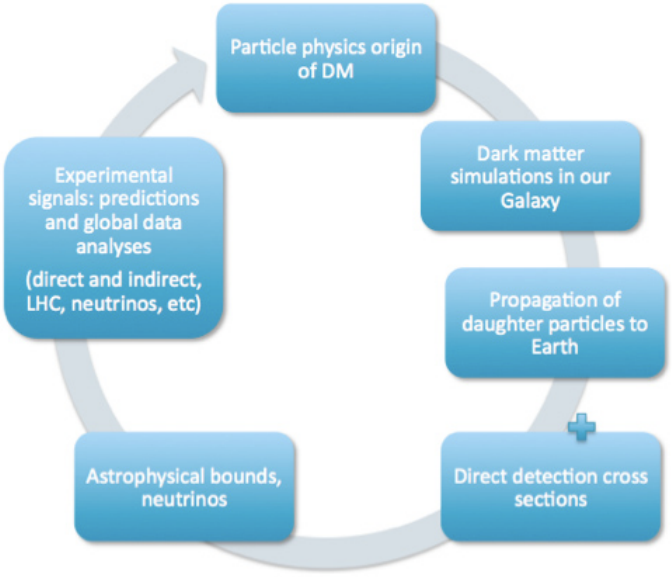

Figure 2. Within each of the well-motivated dark matter scenarios, we will determine the key properties of the dark matter particles: mass, interaction cross-sections, and annihilation rates. Several steps are required in order to make quantitative experimental predictions. We will need to understand the properties of the dark matter distribution in our galaxy, how the annihilation products propagate to earth, how the dark matter particles interact with detectors and whether there are astrophysical constraints from dark matter capture in the sun.

Benefit to National Security Missions

This project directly addresses mission(s) of the DOE Office of Science for discovery and innovation in basic research to understand the universe by developing novel experimental and theoretical techniques to directly detect and identify the dark matter in the universe. It is a centerpiece of LANL's Grand Challenge to understand the universe Beyond the Standard Model. The development of these basic and fundamental techniques can be applied to other missions such as non-proliferation and homeland security.

Progress

Experimental Program: The first year of this project afforded significant progress in the realization of the MiniCLEAN dark matter detector. A thorough engineering design for the major components of the central detector, including the outer vacuum vessel (OV), inner cryogenic vessel (IV), and a conceptual design for the optical cassette array is complete. The OV has been fabricated, the complete set of photomultiplier tubes has been purchased, and fabrication of the IV is underway. Infrastructure underground at SNOLAB is well in place and discussions are underway to develop a MoU and Project Execution Plan with SNOLAB management.

The IV proved to be a significant challenge and several iterations on its design had to be performed before a model was achieved that can meet technical specifications. An engineering design for the IV was nonetheless completed, successfully put through procurement and is now in fabrication. Nonetheless the complexity and cost of the IV has meant a significant change in schedule. Assembly and commissioning of the MiniCLEAN detector at SNOLAB is now anticipated for FY12.

Efforts are now being directed in taking the conceptual design for the optical cassette array to a full engineering design and in developing the assembly plan for inserting these modules into the IV in a radon-free environment underground. A prototype of the optical cassette will be constructed and used to test all optical and thermal components of the design before fabricating the entire array consisting of 92 modules.

In addition to the progress seen for the central detector, significant progress has been made in the design of all external subsystems, including cryogenic and purification systems, calibration systems, electronics and data acquisition, external water shield and muon veto. A dedicated Monte Carlo simulation and analysis software package is mature. The simulation has been used to optimize the design of the detector and calibration systems to ensure that the experiment can meet its scientific goals with respect to scintillation light yield, position reconstruction capability, and attack against radioactive backgrounds.

In April, 2010 the experimental and theoretical program for dark matter at LANL was met with enthusiasm and high endorsement from the Nuclear, Particle, Astrophysics and Cosmology (NPAC) capability review panel. An expert committee was struck to review MiniCLEAN in July, 2010 to examine the MiniCLEAN project with respect to its scientific and technical progress, management, costs, and schedule. The report from this internal committee was very positive and was followed by an equally positive review in August, 2010 from SNOLAB's Experiment Advisory Committee (EAC).

Theoretical Program: The primary focus of our theoretical effort has been on understanding the Dark Matter distribution in the Galactic Halo. We have performed several high-resolution dark matter simulations to model the velocity distribution of dark matter under conditions similar to our own Milky Way galaxy. We have simulated a spherical region of the Universe 12.5 Mpc in diameter, with cosmological parameters set to match the current best-fit results of the Wilkinson Microwave Anisotropy Probe (WMAP). The dark matter particle mass was 5.3 $x10^5$ solar masses. Evolving 70 million dark matter particles from a red-shift of 64 to the present, we extracted 35 dark matter halos with total masses between 3 x 10^{11} and 2 x 10^{12} solar masses. The velocity dispersion of the dark matter was found to follow an approximately Gaussian profile, with a width similar to the velocity of a test particle on a circular orbit (220 km/sec for the Milky Way). However, there were significant deviations from the Gaussian on the tail of the distribution. This has important implications for a class of models involving the so-called inelastic dark matter, in which only the particles in the tail of the velocity distribution interact with the detector.

Furthermore, the density distribution of dark matter is inhomogeneous, which will have consequences for the signal expected from direct dark matter detection experiments. The experiments are affected by the small-scale inhomogeneities that are beyond the resolution of today's codes (and will remain so for the foreseeable future). Therefore, calculating the probability of encountering a clump of dark matter in our local environment requires an additional theoretical work, combined with targeted simulations, which we are pursuing.

As the first clumps of dark matter come together, they strip some of the material off each other resulting in a "smooth" dark matter component. To understand how much material ends up in the smooth component and how much remains bound in the clumps, one needs to know the density profiles of the first clumps. To understand this, we are presently conducting a series of simulations of models with a broken power-law power spectrum.

We are also working to understand the cross-sections of dark matter interactions with the nuclei in our experimental apparatus. In particular, we are focused

on possible multi-nucleon interactions which requires a combination of effective field theory analysis and nuclear physics.

Future Work

This project encompasses two major and synergistic thrust areas that leverage LANL expertise and positions us to take a world lead in experimental and theoretical physics in the quest to detect and identify the dark matter in the universe:

Experimental Program: Our focus in FY11 will be upon fabrication of all major components of the central MiniCLEAN detector. With the OV now fabricated and the IV under fabrication, engineering and procurement will be dedicated to quality control and oversight of the IV and the engineering design and testing of a prototype optical module. We will be working closely with SNOLAB management to establish a technical review process, MoU and Project Execution Plan with the aim to begin assembly and commissioning of the MiniCLEAN detector underground in FY12. Parallel efforts will continue to refine our simulation code, calibration scheme and background model.

Theoretical Program: We will continue an integrated and comprehensive theory program that will collectively consider the interpretation of a suite of laboratory experiments and astrophysical observations in the framework of physics beyond the Standard Model. We will work to understand the profiles of the earliest formed halos using a combination of analytical arguments and numerical modeling. We will then trace the merger history of these halos to predict the present day substructure of our halo. We will also investigate the halo-to-halo variations in the dark matter distribution, given our simulation with hundreds of halos, and the impact of this variation on uncertainty in the dark matter direct detection rates. We plan to validate the large-scale substructure seen in our simulations against the observations of the disruptions in galactic disks. Finally, we will continue working on pinpointing the rule of multi-nucleon interactions in dark matter cross sections.

Conclusion

Experimental Program: Significant progress has been made towards a realization of the MiniCLEAN experiment for the direct detection of dark matter, including fabrication of the OV, procurement of the IV, and a conceptual design for the optical cassettes. A major milestone was met in the final design and procurement for fabrication of the IV. Complexity and cost associated with the IV means that assembly and commissioning of the MiniCLEAN detector is now anticipated for FY12. Following successful internal review, the MiniCLEAN collaboration will be working closely with SNOLAB to establish a technical review, a MoU and project execution plan.

Theoretical Program: A theoretical platform and set of universal tools is under development that will allow an analysis of all the available data from direct-detection experiments, indirect-detection experiments, and the LHC with the goal of inferring the parameters of the underlying dark matter model.

Probing Brain Dynamics by Ultra-Low Field Magnetic Resonance

Michelle A. Espy
20100097DR

Introduction

We seek to experimentally measure and understand, for the first time, the temporal and spatial dynamics of cognition in the human brain. Specifically, we will measure the neural activity associated with visual cognition in ways that have not yet been demonstrated. We will combine high temporal and spatial resolution into a single measurement modality. We propose to achieve this by combining new neuroscience methods in ultra-low field (ULF) magnetic resonance imaging with existing neuroscience resources at LANL. Our research objective is to observe neural activity in the human brain with temporal (ms) and spatial (mm) resolution. Such a tool will be capable of resolving the location and dynamics of visual cognition, and capable of answering key hypotheses in neuroscience. Our technical approach is to initially employ multi-modality techniques to integrate data from conventional, separate measurements of MRI at high field and MEG. We will also develop new techniques for functional MRI measurements at ULF, and explore the feasibility of direct imaging of neural currents using ULF-MRI. We will employ simultaneous MEG and functional MRI at ULF to allow us to characterize the location and dynamics of the transient neural responses associated with visual cognition such as identification of a familiar object or face.

Benefit to National Security Missions

Understanding the Brain is an identified LANL Grand Challenge relevant to a number of NNSA/DOE, DOD/DARPA and Intel agency mission areas in surveillance and information processing for nonproliferation and national security. The basic technologies being developed are broadly applicable in energy, environment, biomedical and materials science in addition to the targeted breakthrough applications in basic and clinical neuroscience.

Progress

In support of Objective 1, we have developed and are implementing 1) the visual protocols for retinotopic mapping in separate magnetoencephalography (MEG) and functional magnetic resonance imaging (fMRI) studies, 2) the MEG protocol for frequency tagging, and 3) "amoeba" and number recognition tasks for both MEG and fMRI. These protocols are similar to those used in the psychophysics experiments for the synthetic cognition DR. These experiments, conducted separately at the MIND institute in Albuquerque, will enable us to develop methods for single pass analysis and a foundation for comparison/integration with new multi-modal methods developed at LANL. We have identified and implemented experimental protocols for this mapping (task 1), programmed stimulus generation software compatible with the hardware (task 1), and are developing analysis tools (task 2). Experiments were completed in September and October of 2010 (task 3). An example of a protocol for fMRI, and results are shown in Figure 1.

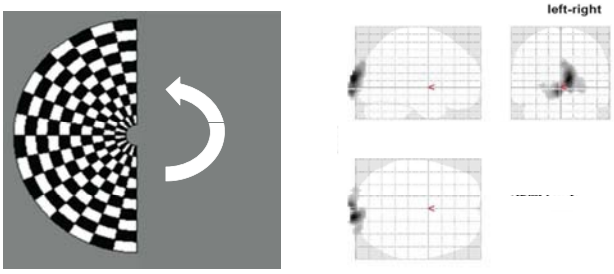

Figure 1. Left: Example of rotating checkerboard stimulus and Right: areas of visual field stimulated as determined by functional magnetic resonance.

We have made significant progress toward Objective 2, in developing the protocol for fMRI at ultra-low fields (ULF). We have identified and modeled the methods for a pulse sequence similar to traditional flow-based methods in fMRI (in particular the Flow-sensitive alternating inversion recovery or FAIR technique), task 1. We have made modifications to account for the much shorter tissue relaxation times associated with ultra-low field MRI (about 5 times shorter than conventional approaches). We are in the process of designing hardware for execution of the pulse sequence

and flow phantom experiments are underway. These phantom experiments provide a basis for tasks 2-5. In fact, although the final ULF fMRI experiments are not scheduled until year 3 of the proposal, we believe we can conduct preliminary experiments at lower fields by the end of 2010. The design of the pre-polarization sub-system is complete, after completion of significant R&D efforts in magnet materials (task 2). Design of the dense sensor array is largely complete and construction has begun (task 3). Tasks 4 and 5 are scheduled to be completed by the second year of the project, but as previously mentioned, we believe our preliminary fMRI work with existing hardware will make significant progress in these areas by the end of the first year. We are on schedule for all five tasks associated with this objective. The dense sensor array is shown in Figure 2. An example of the fMRI flow phantom is shown in Figure 3.

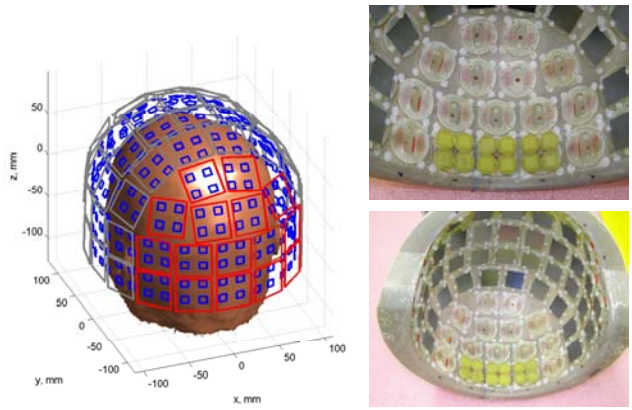

Figure 2. Left: Model of dense array for combined magnetoencephalography (MEG) and ultra-low field MRI. The blue squares indicate MEG sensor locations, and the larger squares indicated positions of MRI channels. The red squares are locations that will be populated first. Right: photographs of the array under assembly.

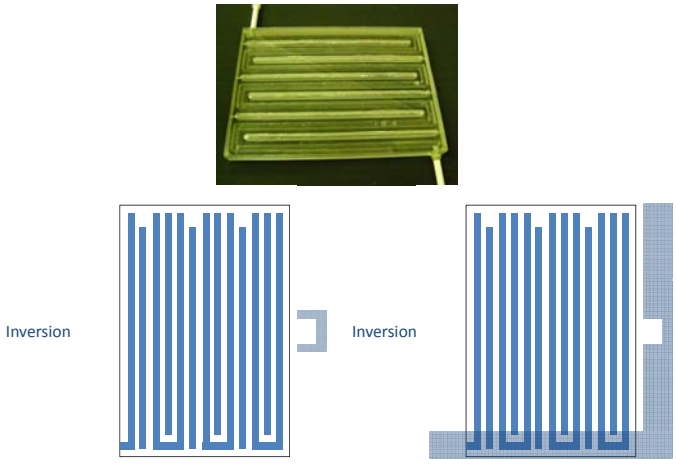

Figure 3. Upper: Flow phantom for functional magnetic resonance based on arterial spin labelling. Lower: Left and right show labeled and unlabeled regions. On the labeled (left) image, only a small region is labeled and then after some evolution time, imaged. On the control (right) image, the entire region is labeled and then imaging occurs after evolution. The difference between the two images will provide information about flow.

To support our demonstration of direct neural current imaging (DNI), Objective 3, we are developing the experimental capability to execute an unprecedented experiment exploiting the highly synchronous and wide-spread brain activity associated with sleep. We believe that the large cortical area and strong brain signals associated with sleep cycles provide a good chance for establishing the interaction of neural signals with the spin population. We have completed theoretical estimation of the expected DNI signal (task 1) and are undertaking the design of the experimental pulse sequences and hardware (task 2). The experiments require use of a specialized EEG system that can tolerate the pulsed magnetic fields associated with MRI. We are in the process of obtaining a system from collaborators. These experiments will be conducted in spring 2011. Final implementation for experiments and analysis (task 3), according to the project timeline was scheduled for years 2-3 of the project, and we believe we are on schedule.

Objective 4 is to resolve the sequence and location of visual cognition exploiting progress from objectives 1-3 (in years 2-3 of the proposal). We believe our significant progress to-date positions us on track to make significant inroads to understanding the “when” and “where” of visual cognition in single transient responses.

Future Work

Recently it has become practical to perform MR at much lower field strengths compared to conventional MRI techniques. The so-called ultra-low field (ULF) regime, is compatible with simultaneous MEG. ULF MRI has unique advantages for measuring the direct interaction between magnetic fields arising from neural activity and the MRI signal, called direct neural-current imaging or DNI. DNI is considered the “holy grail” of functional neuroimaging because it would provide direct tomographic imaging of neural activity. ULF MRI also has intriguing prospects for functional MRI through the mapping of hemodynamic responses or metabolic activity. Combining MEG with functional data via fMRI or DNI may also allow for single pass analysis of functional dynamics combined with spatial localization. In order to achieve the scientific objectives of the project we proposed the following four technical objectives:

- Perform neuroscience experiments using existing resources in MEG and high field fMRI. Conduct visual recognition tasks and make separate MEG and fMRI measurements in the brain, to allow multimodality integration.

- Develop the ability to perform fMRI at ULF. Extend our experimental capability beyond any presently available and show the feasibility of functional MRI based on blood flow, blood oxygenation, metabolic or tracer measurements at ULF.

- Demonstrate direct neural current imaging at ULF. In principle, MRI allow direct detection of neuronal currents, which would allow tomographic reconstruction of neural activity. This is a high-risk objective, however success would revolutionize the field of human functional neuroimaging.

- Resolve the sequence and location of visual cognition. Leverage and optimize our world-class capability in ULF-MRI to employ simultaneous MEG and fMRI or DNI to monitor neural activity during visual processing associated with behavioral tasks. This will allow us to determine the "when" and "where" of visual cognition in single transient responses.

Conclusion

In addition to providing important and unique new tools for human functional neuroimaging, the proposed work will provide new insight into how the brain processes information. Eventually this will enable us to harness the power of artificial intelligence, improve human-machine interfaces, or construct bio-mimetic sensors and networks approaching human performance. This LDRD project will position LANL to lead the world and serve the nation with a world-class capability in functional neuroscience, that can provide input to specific applications important for the Laboratory mission, and provide powerful new biomedical techniques for basic and clinical neuroscience and medical imaging.

References

1. Magnelind, P., J. Gomez, A. Matlashov, T. Owens, J. H. Sandin, P. Volegov, and M. Espy. Interleaved Co-Registration of MEG and ULF MRI Using a 7 Channel Low-Tc SQUID System. To appear in *IEEE Transacations on Applied Superconductivity* .

Publications

Magnelind, P., J. Gomez, A. Matlashov, T. Owens, J. H. Sandin, P. Volegov, and M. Espy. Interleaved Co-Registration of MEG and ULF MRI Using a 7 Channel Low-Tc SQUID System. To appear in *IEEE Transactions on Applied Superconductivity* .

Bridging Equilibrium and Non-equilibrium Statistical Physics

Robert E. Ecke
20100531DR

Introduction

The twentieth century saw unprecedented advances in our understanding of the properties of matter, culminating in the application of these ideas to produce the technology of the modern age from electronic devices to space age structural materials. Much of this science has been based on thinking about materials near thermal and mechanical equilibrium, with uniform or periodic atomic structure. In contrast, many of the scientific challenges of the twenty-first century involve behavior of greater complexity: competing interactions, geometric frustration, spatial and temporal intrinsic inhomogeneities, nano-scale structures and physics that spans many scales. In this project, we focus on a broad class of emerging problems that will require new tools in non-equilibrium statistical physics, building on foundations in equilibrium statistical mechanics that will find applications in new material functionality, in predicting complex spatial dynamics, and in understanding novel states of matter. This work will encompass materials under extreme conditions involving elastic/plastic deformation, competing interactions, intrinsic inhomogeneity, frustration in condensed matter systems, scaling phenomena in disordered materials from glasses to granular matter, quantum chemistry applied to nano-scale materials, soft-matter materials and spatio-temporal properties of both ordinary and complex fluids. To further exploit the connection with the studies of matter under extreme conditions, the 2009/2010 CNLS Ulam scholar was Ekhard Salje, a senior expert on materials science phase transitions from Oxford University, whose expertise bridges statistical physics, materials and environmental sciences.

Benefit to National Security Missions

Non-equilibrium processes are related to emergent new materials functionality, to turbulence and mixing, and to structural properties of materials. The application of our theory, modeling and simulation approaches to non-equilibrium processes helps build fundamental science capability in areas related to Office of Science Programs in materials science, to developing efforts in climate modeling in DOE, to LANL efforts in MaRIE, and to interactions with NSF/DOE programs at NHMFL, at CINT, and at the Lujan Center.

Progress

In the area of electronic transport, we have developed an exciton scattering model, which allows one to treat various photoexcitation-induced processes, including intra- and inter-band Coulomb scattering, in semiconductor nanostructures and bulk. We have applied the developed model to analyze the efficiency of multiple exciton generation in bulk and nanocrystalline chalcogenide materials. The theoretical/computational analysis of this efficiency has given us insight into the relative contributions of various pathways of multiple exciton generation, which is of critical importance for practical realization of a new generation of inexpensive and highly efficient solar cells. In work on transport in strongly correlated electron systems (SCES), we investigated SCES models with cluster dynamical mean-field theory. From a self-consistent two-impurity model, we have elucidated the characteristic energy scales (in particular, the puzzling coherence scale) of heavy fermion materials and the relation between superconductivity and magnetic fluctuations. In other electron transport materials, we interpreted the large thermoelectric effects in graphene, from an interplay of band structure, disorder and thermal activation. Finally, we examined the thermodynamical properties near generic quantum phase transitions, and proposed that the divergence in Gruneisen ratio and the accumulation of entropy can be employed to probe a quantum critical point.

We are actively exploring the mechanical properties of materials in a different context. In the first context, we are investigating how stress is distributed in idealized 2D granular materials. In particular, we designed an experimental setup that uses a hopper-like device to create an ensemble of two-dimensional granular materials. This set-up will be used to study the internal force distribution in a granular material that is packed under gravitational settling. The forces are measured using a sophisticated photo-elastic response analysis

of stressed bi-refrigent plastic disks. The results will be used to test fundamental ideas of how the force varies with depth for granular materials - behavior that is at the core of determining failure thresholds for granular storage facilities such as grain silos. In related work on materials in a geophysical context, we look at mechanical properties of materials under shear. Deep in the earth's crust, high temperatures and pressures change the frictional properties of rocks from brittle to ductile, which alters the manner of mechanical deformation. Our research focuses on two poorly understood ways that faults slip in the lower crust: transient strain localization, and non-volcanic tremor. We find that in ductile rocks, deformation can occur transiently in a narrow shear band when driven away from steady state by earthquake rupture in the upper crust, in agreement with field observations of rocks exhibiting both broad and localized shear deformation. We have also shown that a semi-brittle model for friction produces non-volcanic tremor, and we used our model in conjunction with seismic observations to constrain the physical conditions in the lower crust.

We have adapted the technology of time dependent density functional theory to provide a more general treatment of many-body physics under non-equilibrium conditions. We derived a closed equation of motion for the current density of an inhomogeneous quantum many-body system under the assumption that the time-dependent wave function can be described as a geometric deformation of the ground state wave function. By describing the many-body system in terms of a single collective field we provide an alternative to traditional approaches, which emphasize one-particle orbitals. The quantum fluctuations of such collective field can become pronounced near a critical point. In Figure 1, we show the density fluctuation pattern of a two-dimensional Bose-Einstein Condensate with localized potential near the critical potential depth for which the corresponding excitation becomes unstable. The pattern, which bears a striking resemblance to the Chladni patterns that reveal modes of vibration on a classical, mechanical surface, was calculated in this project and illustrates the role of intrinsic inhomogeneities.

An important aspect of our work on non-equilibrium statistical physics is the flow of fluids in different contexts. The first is MHD turbulence. Unlike its hydrodynamic counterpart, the theory of magnetohydrodynamic (MHD) turbulence is much less developed despite its importance in nuclear fusion, space weather, and astrophysics. The coupling between the flow and the magnetic fields in MHD systems is not well understood, as illustrated by the efforts to describe magnetic reconnection events. We have developed a new multi-scale analysis approach to attacking the problem. Our efforts have succeeded in showing that interactions in MHD turbulence take place between scales of similar size and that the velocity and magnetic fields decouple in a statistical sense at sufficiently small scales. We have also shown that the magnetic field at the largest scales has no role in the cascade dynamics in MHD turbulence, contrary to what was widely believed. Our results are based on mathematical analysis and are supported by high-resolution numerical simulations. These should have significant implications on devising reduced models of MHD turbulence as well as providing physical insight into this rich problem. In other work on fluids, we added Radial-Basis-Function interpolation algorithms for irregular grids to the new ocean model being developed at LANL. We anticipate using these algorithms to implement an immersed boundary method within the new model that can be used to represent the ocean bottom topography, the geometry of moving ice shelves, continental boundaries and other complex and/or moving boundaries that occur in the ocean.

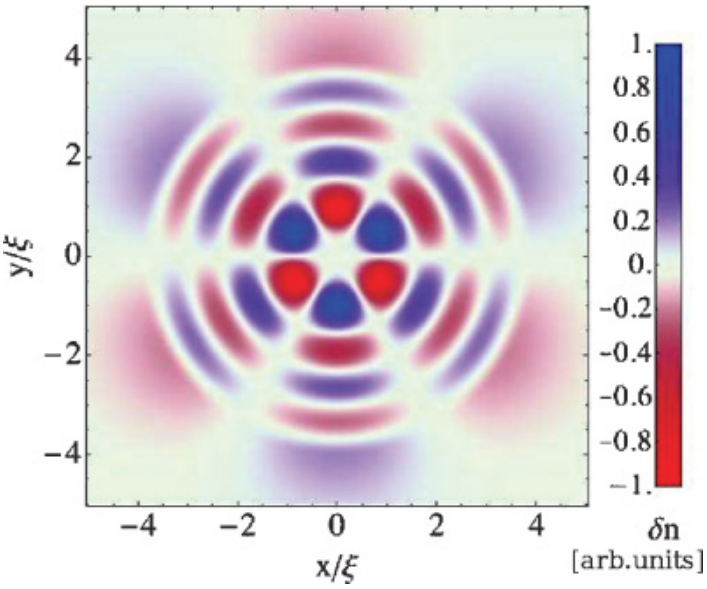

Figure 1. Density fluctuations (blue is positive and red is negative) of a mode-five atomic Bose Einstein Condensate state.

Future Work

The goals and objectives of this project rely upon the inter-disciplinary connections that are present in the CNLS environment. We identify specific goals that will be pursued in this project, but many of the connections will be unforeseen and unanticipated.

In the area of self-organized structure, we will exploit the developing recognition that the non-equilibrium properties of glassy materials may have a physical analog in the behavior of granular materials. In related work on granular materials we will study driven thin layers of granular materials and explore applications of ideas of rigidity percolation and jamming to real physical configurations of granular particles. We will use new concepts in shear transformation theory applied to these granular systems, to real geophysical earthquakes, and to the properties of

land ice evolution.

In the area of continuum mechanics, we propose to establish a clear link between the microscopic and mesoscopic dislocation density in order to understand heterogeneous nucleation in materials of interest to the matter under extreme conditions efforts.

We will develop a cluster Dynamical Mean-Field Theory (DMFT) for attacking the Kondo-lattice problem. We will explore the prospect for nonlinear condensate wavefunction engineering and, possibly, self-organized criticality in quantum many-body systems.

In the area of climate research, we will extend current work on climate models and model hierarchies that satisfy the conservation laws at the numerical level and reconsider the assumption of "Balanced Dynamics" common to large-scale dynamics, in the light of efforts to reduce the resolution of global climate models below the kilometer-level.

Conclusion

This project exploits the expertise and unique capabilities of the Center for Nonlinear Studies to affect and guide inter-disciplinary research in statistical physics. The project exploits common threads of non-linear physics, non-equilibrium physics, hydrodynamics and applied mathematics to impact strategic interests to the Laboratory including matter under extreme conditions and nano-technology. Our work will contribute fundamental insights and transfer concepts and techniques of quantum chemistry, non-equilibrium statistical mechanics, continuum mechanics, applied mathematics (including graph and network theory) and many-body theory to meet new challenges in materials science, granular materials, nano-science, climate research and strongly correlated electron systems.

Publications

Aluie, H., and G. L. Eyink. Localness of energy cascade in hydrodynamic turbulence. II. Sharp spectral filter. 2009. *Physics of Fluids.* **21** (11).

Aluie, H., and G. L. Eyink. Scale Locality of Magnetohydrodynamic Turbulence. 2010. *Physical Review Letters.* **104** (8).

Atanasov, V., and A. Saxena. Tuning the electronic properties of corrugated graphene: Confinement, curvature, and band-gap opening. 2010. *Physical Review B.* **81** (20).

Badaeva, E., V. V. Albert, S. Kilina, A. Koposov, M. Sykora, and S. Tretiak. Effect of deprotonation on absorption and emission spectra of Ru(II)-bpy complexes functionalized with carboxyl groups. 2010. *Physical Chemistry Chemical Physics.* **12** (31): 8902.

Camassa, R., P. O. Rusas, A. Saxena, and R. Tiron. Fully nonlinear periodic internal waves in a two-fluid system of finite depth. 2010. *Journal of Fluid Mechanics.* **652**: 259.

Chernyak, V. Y., M. Chertkov, D. A. Goldberg, and K. Turitsyn. Non-Equilibrium Statistical Physics of Currents in Queuing Networks. 2010. *Journal of Statistical Physics.* **140** (5): 819.

Chernyak, V. Y., and N. A. Sinitsyn. Robust quantization of a molecular motor motion in a stochastic environment. 2009. *Journal of Chemical Physics.* **131** (18).

Dandoloff, R., A. Saxena, and B. Jensen. Geometry-induced potential on a two-dimensional section of a wormhole: Catenoid. 2010. *Physical Review A.* **81** (1).

Daub, E. G., M. L. Manning, and J. M. Carlson. Pulse-like, crack-like, and supershear earthquake ruptures with shear strain localization. 2010. *Journal of Geophysical Research-Solid Earth.* **115**.

Daub, E. G., and J. M. Carlson. Stick-slip instabilities and shear strain localization in amorphous materials. 2009. *Physical Review E.* **80** (6).

Dawson, J. F., B. Mihaila, and F. Cooper. Dynamics of particle production by strong electric fields in non-Abelian plasmas. 2010. *Physical Review D.* **81** (5).

Eyink, G. L., and H. Aluie. Localness of energy cascade in hydrodynamic turbulence. I. Smooth coarse graining. 2009. *Physics of Fluids.* **21** (11).

Gao, X. L., J. M. Tao, G. Vignale, and I. V. Tokatly. Continuum mechanics for quantum many-body systems: Linear response regime. 2010. *Physical Review B.* **81** (19).

Goel, S., K. A. Velizhanin, A. Piryatinski, S. Tretiak, and S. A. Ivanov. DFT Study of Ligand Binding to Small Gold Clusters. 2010. *Journal of Physical Chemistry Letters.* **1** (6): 927.

Gottesman, D., and M. B. Hastings. Entanglement versus gap for one-dimensional spin systems. 2010. *New Journal of Physics.* **12**.

Grigorenko, I., and H. Rabitz. Optimal design strategies for electrostatic energy storage in quantum multiwell heterostructures. 2010. *Journal of Chemical Physics.* **133** (5).

Hermundstad, A. M., E. G. Daub, and J. M. Carlson. Energetics of strain localization in a model of seismic slip. 2010. *Journal of Geophysical Research-Solid Earth.* **115**.

Kalas, R. M., D. Solenov, and E. Timmermans. Reentrant stability of Bose-Einstein-condensate standing-wave

patterns. 2010. *Physical Review A.* **81** (5).

Katan, C., M. Charlot, O. Mongin, C. Le Droumaguet, V. Jouikov, F. Terenziani, E. Badaeva, S. Tretiak, and M. Blanchard-Desce. Simultaneous Control of Emission Localization and Two-Photon Absorption Efficiency in Dissymmetrical Chromophores. 2010. *Journal of Physical Chemistry B.* **114** (9): 3152.

Khare, A., K. O. Rasmussen, M. R. Samuelsen, and A. Saxena. Exact solutions of the two-dimensional discrete nonlinear Schrodinger equation with saturable nonlinearity. 2010. *Journal of Physics a-Mathematical and Theoretical.* **43** (37).

Kobayashi, T., J. Du, W. Feng, K. Yoshino, S. Tretiak, A. Saxena, and A. R. Bishop. Observation of breather excitons and soliton in a substituted polythiophene with a degenerate ground state. 2010. *Physical Review B.* **81** (7).

Larkin, J., M. M. Bandi, A. Pumir, and W. I. Goldburg. Power-law distributions of particle concentration in free-surface flows. 2009. *Physical Review E.* **80** (6).

Larkin, J., W. Goldburg, and M. M. Bandi. Time evolution of a fractal distribution: Particle concentrations in free-surface turbulence. 2010. *Physica D-Nonlinear Phenomena.* **239** (14): 1264.

Lee, A. T., E. Chiang, X. Asay-Davis, and J. Barranco. Forming Planetesimals by Gravitational Instability. I. The Role of the Richardson Number in Triggering the Kelvin-Helmholtz Instability. 2010. *Astrophysical Journal.* **718** (2): 1367.

Li, H., S. V. Malinin, S. Tretiak, and V. Y. Chernyak. Exciton scattering approach for branched conjugated molecules and complexes. IV. Transition dipoles and optical spectra. 2010. *Journal of Chemical Physics.* **132** (12).

Mertens, F. G., N. R. Quintero, and A. R. Bishop. Nonlinear Schrodinger equation with spatiotemporal perturbations. 2010. *Physical Review E.* **81** (1).

Mihaila, B., A. Cardenas, F. Cooper, and A. Saxena. Stability and dynamical properties of Rosenau-Hyman compactons using Pade approximants. 2010. *Physical Review E.* **81** (5).

Nisoli, C., D. Abraham, T. Lookman, and A. Saxena. Thermally Induced Local Failures in Quasi-One-Dimensional Systems: Collapse in Carbon Nanotubes, Necking in Nanowires, and Opening of Bubbles in DNA. 2010. *Physical Review Letters.* **104** (2).

Nisoli, C., J. Li, X. L. Ke, D. Garand, P. Schiffer, and V. H. Crespi. Effective Temperature in an Interacting Vertex System: Theory and Experiment on Artificial Spin Ice. 2010. *Physical Review Letters.* **105** (4).

Nisoli, C., N. M. Gabor, P. E. Lammert, J. D. Maynard, and V. H. Crespi. Annealing a magnetic cactus into phyllotaxis. 2010. *Physical Review E.* **81** (4).

Perdew, J. P., and J. M. Tao. When does static correlation scale to the high-density limit as exchange does?. 2010. *Journal of Molecular Structure-Theochem.* **943** (1-3): 19.

Quintero, N. R., F. G. Mertens, and A. R. Bishop. Generalized traveling-wave method, variational approach, and modified conserved quantities for the perturbed nonlinear Schrodinger equation. 2010. *Physical Review E.* **82** (1).

Shen, Y., F. Williams, N. Whitaker, P. G. Kevrekidis, A. Saxena, and D. J. Frantzeskakis. On some single-hump solutions of the short-pulse equation and their periodic generalizations. 2010. *Physics Letters A.* **374** (29): 2964.

Tao, J. M., S. Tretiak, and J. X. Zhu. Prediction of excitation energies for conjugated polymers using time-dependent density functional theory. 2009. *Physical Review B.* **80** (23).

Vasseur, R., and T. Lookman. Effects of disorder in ferroelastics: A spin model for strain glass. 2010. *Physical Review B.* **81** (9).

Zhu, L. J., R. Ma, L. Sheng, M. Liu, and D. N. Sheng. Universal Thermoelectric Effect of Dirac Fermions in Graphene. 2010. *Physical Review Letters.* **104** (7).

Development of a Magnetically Driven Target for Thermo-Nuclear Burn Studies (U)

Robert G. Watt
20070518DR

Abstract

This LDRD project developed a magnetically driven cylindrical confinement system for the creation of a small volume of material under extreme conditions. Using a low cost multi-MA electrical current source, an aluminum cylinder was driven radially inward until it impacted on a series of nested, progressively less massive gold shells whose purpose was to provide a very high velocity inner-most gold shell. The velocity of this last shell is intended to ultimately be at a level where further impact on an object in the center will produce a region in which material conditions are sufficient for many types of physics studies not currently possible in the laboratory. The concept utilizes the fact that the final velocity of a small mass impacted by a larger mass can exceed the impact velocity by as much as a factor of two in a single collision. It is possible to use several sequential collisions to produce an object moving much faster than the original source object. In a cylindrical geometry, this process can potentially produce a cylindrically converging Au shell with a radial velocity above 100 km/sec driven by impact with an Al shell converging with a radial velocity of only a few km/sec. An Inertial Confinement Fusion (ICF) target could be placed inside the last multiplier shell comprised of a gold pusher shell surrounding frozen DT in the central void. In this application the conditions achieved would be similar to those anticipated inside the gold inner capsule of the double shell implosion target design [1] at the National Ignition Facility (NIF) [2]. Future versions of this type system therefore might provide an inexpensive complement to the study of fusion at large laser facilities.

Background and Research Objectives

The physics community has a need for volumes of material at very high density, temperature, and pressure for a wide variety of studies. While the technique developed here has many applications, we will use ICF as a benchmark application. The nation has invested 4B$ in the development of a large laser system at the National Ignition Facility in the pursuit of the grand challenge of fusion ignition. The final conditions inside the igniting DT core at NIF consist of DT densities in the 100-200 g/cc range and ion temperatures between 2 and 10 keV depending on the type of capsule design. The pressure in the final pusher shell outside the fuel exceeds 10^9 atmospheres. The key to achieving these extreme conditions is the ability to drive the outer surface of the DT at velocities in the 15 - 40 cm/us range, again dependent on the target design. (The highest velocities are needed to drive plastic or Be single shell capsules at NIF. The lower range is sufficient to drive a double shell capsule with an inner Au pusher shell.) Alternative ways of achieving such velocities are worth investigating so that dependence on a single driver technology (laser radiation) and potential failure of that technology to achieve the required velocity will not cause failure of the pursuit of the grand challenge. Magnetically driven cylindrical implosion systems have been demonstrated in the last several decades that achieve conditions an order of magnitude or more below the velocity range needed but the extension to higher velocity has not been studied. The goal of the present project is to show through simulation and confirming experiment that the concept of velocity multiplication through multiple sequential collisions can be used to bridge the gap between the fairly routine 0.5-1 cm/us range of velocities of a magnetically driven Al liner and a desired 15-25 cm/us range required for use in ICF to crush frozen DT inside a Au pusher. Bridging this gap would provide an alternative, hydro-dynamically coupled means of achieving the conditions required for ignition in DT. Removing laser or x-ray drive from the problem will allow a very cost effective alternative for the study of fusion in the laboratory.

The project is developing the electrical and mechanical techniques required to take energy from a high current source (30MA with 100 us duration) and utilize it to create an Al shell moving inward at a velocity approaching 1 cm/us. Subsequent collisions with cushioned, less massive Au shells will sequentially increase that velocity into the 15-25 cm/us range in later physics experiments. In effect, the cylindrical system of nested shells acts as the mechanical analog of an electrical pulse compression system capable of increasing power at the expense of energy. The final goal is the demonstration of current extraction from the generator into the load assembly,

velocity multiplication within the load assembly, and the ability to accurately simulate the experiments with existing MHD and radiation-hydrodynamics codes available at LANL. Follow on work will then utilize those codes for design of experiments in relevant areas using the platform developed under this project, as well as perform such experiments. Those experiments will reside within the center of the last shell driven by this platform. Robust agreement between predictions using many simulation codes and experimental data produce by this project will lend credence to the simulations. If we then simulate the final 10-12 shell system and achieve the desired end state, a strong case can be made for actual construction and fielding of a full scale system able to attempt DT burn in an ICF target driven magnetically.

Scientific Approach and Accomplishments

In this project a High Explosive Pulsed Power (HEPP) 1.4 m long *Ranchero* [3] Flux Compression Generator (FCG) was used to drive a 2.2 mm thick, 7.6 cm inside radius Al liner radially inward. The 18.3 MA current pulse drove the Al inward until it ran into a plastic cushion surrounding the first of five Au shells (the multiplier assembly) and gave up much of its kinetic energy to the Au. Like a ping pong ball bouncing off a billiard ball which impacts it at some velocity, the second Au shell could bounce off of the first Au shell with up to a factor of 2 higher velocity, if it was very much less massive than the first shell. The collisions of subsequent shells in the multiplier then increase the velocity further. In this subsystem demonstration, the first Au shell bounced off the Al and reached an inside velocity of 0.256 cm/us. The Au on Au multiple collision process then proceeded through 5 Au shells and 4 collisions, each of which could have ideally contributed around a factor of 1.4 velocity increment. The final Au shell reached 0.91 cm/us, for a velocity multiplication ratio of 3.55. Simulations of the shell bounce predicted final velocities of 1.07-1.2 cm/us, making it apparent that some additional loses are not currently modeled adequately in the codes. The final Au shell, which has a density near 19.3 g/cc, can crush an object or experiment inside it much more successfully than an Al shell with similar velocity whose density remains near 2.7 g/cc if the Al were to drive the central object directly. Both velocity multiplication and density increase are needed for successful future applications. In this subsystem demonstration, the magnetically driven Al liner collapse, the transfer of kinetic energy to the Au multiplier assembly, and the subsequent stable velocity multiplication were demonstrated through about one half of the ultimate set of shells required for fusion applications in ICF. The addition of the final 5 shells and an increase in the Al velocity at impact with the multiplier assembly, achieved by changes to the implosion system geometry, will be needed to create final velocities in the 15-25 cm/us range desired.

The *Ranchero* FCG produced a 27 us risetime, 18.3 MA current pulse that was applied to a dual cavity implosion assembly. Use of two adjacent implosion cavities driven

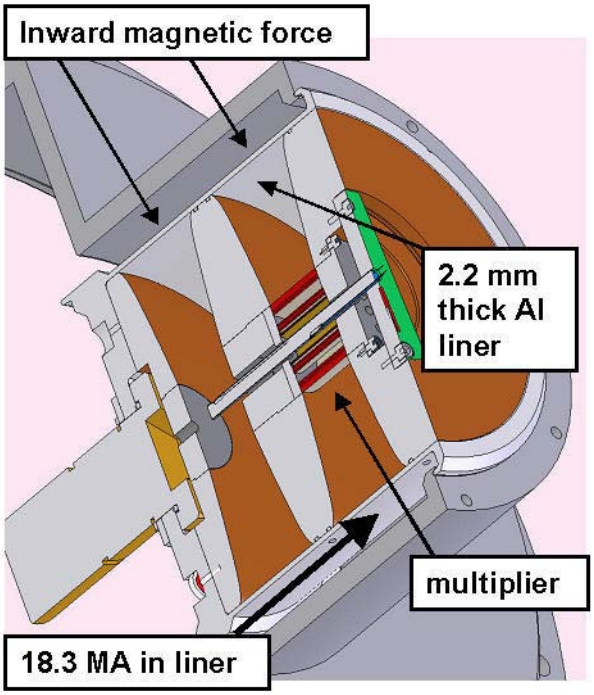

Figure 1. 3D CAD model of a dual cavity implosion load. This load, which includes a 3 shell multiplier in the right hand cavity, was used in the first implosion shot. The annotations show the location of various parts of the load and indicate the current flow through the liner as well.

Figure 2. Photograph of the 5 shell multiplier assembly used in the second implosion shot.

by the same current pulse allowed simultaneous measurement of both the driven Al liner in the absence of a multiplier assembly and the velocity of the final Au shell in the multiplier assembly driven by an identical Al liner on a single shot using Photon Doppler Velocimetry (PDV). Figure 1 shows the implosion system used in the first implosion shot. Various items are indicated in the dual cavity system along with the location of current flow. Figure 2 shows the multiplier subassembly comprised of 5 Au shells and their plastic cushions used on the second implosion shot. The cushions are used to increase the kinetic energy transfer efficiency. The Au shells had a mass ratio of 40% from shell to shell, which controls the ideal velocity increment. Each shell was about 10% of its outer radius thick which helps suppress instability growth during implosion. Simulations, which agreed well with the measured Al velocity history, also suggest that the ideal Au on Au velocity ratio is not approached until after the first several collisions have occurred. The general behavior of the system is as predicted by several hydrodynamics codes. The accuracy of the current measurement is approximately 3% . Using the measured current profile, adjusted up or down in peak current by less than that 3%, as an input to the simulation codes, all of the codes used predicted Al velocity histories in excellent agreement with the measured Al velocity. Figure 3 shows a comparison between the measured (magenta circles) and simulated (black line) velocity history for the Al liner in the second implosion shot, using the Raven 1D MHD code [4] driven by 98.5% of the peak measured load current. The final value of the Au shell velocity is typically over-estimated by the codes. (In the Raven simulation the final velocity predicted was 1.07 cm/us whereas 0.91 cm/us was observed.) Experience over the last several decades suggests that the strength of cross linked plastic polymers such as those used here for the cushions is much larger than our current strength models can account for at high strain and high strain rate. This may explain the lower than predicted measured Au velocity. The detailed acceleration history observed on the inside of the Au shell, which accelerates in three discrete steps, verifies that the codes are accurately simulating the dynamics of the pressure waves inside the Au and plastic components, despite getting the final velocity wrong by .

In the course of the project a number of accomplishments occurred.

1. Al liners were stably thrown over large distances using HEPP generators.

2. Long time duration velocity measurements of the outer and inner surfaces of the Al liner and the inner surface of the last Au shell of a 5 shell multiplier were measured using PDV probes.

3. Stable, azimuthally symmetric Al and Au implosions were observed with velocity multiplication within ~ 20% of that predicted. The Al liner was imaged in x-rays prior to multiplier impact.

4. DT burns at velocities above ~ 15 cm/us, as well as velocity multiplication, were demonstrated using numerous simulation codes.

5. 2D instability growth was shown to be survivable using several rad-hydro codes, which had extensive experimental validation in other venues. Predicted yield remained high so long as surface perturbations were less than 1-2 um peak-valley, which is straightforward to attain with current fabrication capabilities.

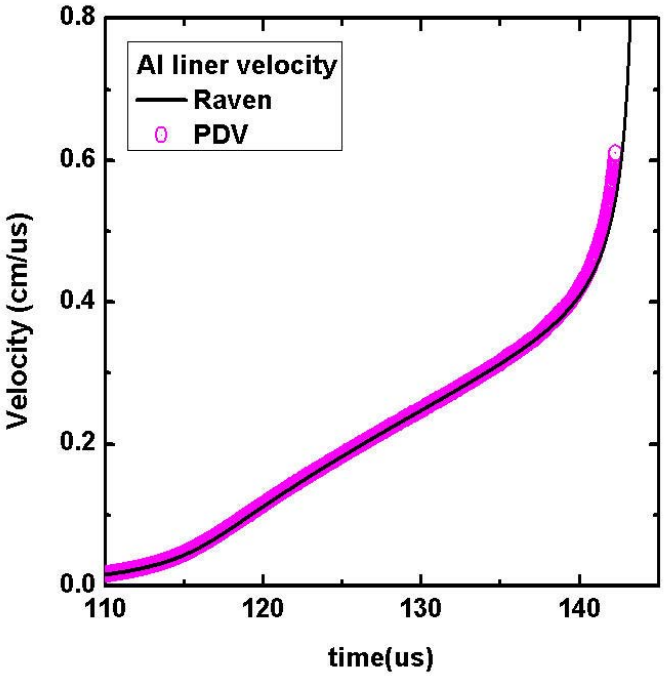

Figure 3. 1D Raven MHD code comparison to the Al liner trajectory velocity history data for the second implosion shot.

Impact on National Missions

The tie to the nation's energy needs lies in the application of the system to studies of ICF fusion, providing an alternative tool in the national grand challenge of ignition. With DT ion temperatures in the several keV range and DT gas densities above 100 g/cc, the conditions ultimately achievable in an ICF target with this type of system are similar to those expected in double shell capsule implosions at the National Ignition Facility. The cylindrical implosion geometry, is different than the spherical implosion geometry at NIF. The implosion does not require the same laser and x-ray drive for ablation of the outer capsule surface as is the case at NIF. The cylindrical geometry also has different constraints of the successful achievement of ignition and burn. Consequently, such a system provides an alternate platform for the study of DT fusion. We cannot here go into details regarding the tie to weapons physics.

References

1. Amendt, P.. Indirect-drive non-cryogenic double-shell ignition targets for the National Ignition Facility: Design and analysis. 2002. *Phys. Plasmas.* **9** (5): 2212.

2. Paisner, J. A., J. A. Boyes, S. A. Kumpan, W. H. Lowdermilk, and M. S. Sorem. NIF . 1994. *Laser Focus World.* **30**: 75.

3. Goforth, J. G.. Ranchero: A high current flux compression generator system for heavy liner experiments. 1997. In *Seventh International Conference on Megagauss Magnetic Field Generation and Related Topics.* (RFNC-VNIIEF, 1997). Vol. , Edition, p. 254. RFNC-VNIIEF: .

4. Oliphant, T. A., and K. H. Witte. Raven. 1995. *LA-10826.*

Publications

ATCHISON, W., P. TURCHI, and D. LEMONS. THE QUEST FOR THE WHOLLY STABLE LINER. 2007. *X-4.*

Atchison, W., A. Kaul, C. L. Rousculp, and R. G. Watt. Optimization of a Ranchero driven high energy liner driver system (U) . Presented at *MegaGauss XII.* (Moscow, Russia, 13-18 July 2008).

Colgate, S. A., R. G. Watt, W. Atchison, J. Goforth, J. Guzik, D. Holtkamp, A. Kaul, R. Kirkpatrick, R. Menikoff, H. Oona, P. Reardon, C. Rousculp, A. G. Sgro, and T. E. Tierney. Equilibrium ignition by a cold adiabat: ICF via multi-collision velocity multiplication. 2008. *T-2.*

Colgate, S., R. G. Watt, W. Atchison, and C. Rousculp. Equilibrium ignition by a cold adiabat: ICF via multi-collision velocity multiplication (U) LA-UR-08-06915. 2008. *Presentation to be given at Sandia National Laboratory, Nov. 6, 2008.*

Goforth, J.. A new 40 MA Ranchero explosive pulsed power system . To appear in *IEEE Pulsed Power Conference.* (Washington, DC, USA, June 29, 2009).

Guzik, J. A., S. A. Colgate, J. Goforth, D. Holtkamp, A. Kaul, R. Kirkpatrick, Hui Li, R. Menikoff, H. Oona, P. Reardon, and C. Rousculp, S. Sgro, T. Tierney. A LDRD project to develop a fusion target driven by velocity multiplication using colliding shells (U) LA-CP-08-01191 . Presented at *NECDC 2008.* (Livermore National Laboratory, Ca., Oct. 20-24, 2008).

Guzik, J., R. Watt, and C. Rousculp. Feature Sensitivity Study For Fusion Target Driven By Velocity Multiplication Of Colliding Shells. 2008. *P-24.*

Oona, H.. Generator modification and characterization of the Ranchero explosive generator. To appear in *XII international conference on megagauss magnetic field generation and related topics.* (Novosibirsk, Russia , July 13, 2008).

Sgro, A. G.. Studies of a magnetically driven liner for TN burn (U) LA-CP-08-. Presented at *NECDC 2008 LA-CP-08-01230.* (Livermore, Ca., 20-24 Oct. 2008).

Sgro, A. G.. Studies of a magnetically driven liner for TN burn (U). 2008. *X-1-PTA.*

Sgro, A. G.. Studies Of A Magnetically Driven Liner For TN Burn (u). 2008. *X-1.*

Sgro, A. G.. Magnetically Driven Liner For Tn Burn Studies (u). 2008. *X-1.*

Sgro, T.. Magnetically driven liner - glide plane interactions. Presented at *NEDPC 2009, LA-CP-09-00666.* (Livermore, Ca., Oct. 26-30, 2009).

WATT, R., S. T. COLGATE, W. ATCHISON, L. I. HUI, G. E. IDZOREK, A. N. KAUL, R. O. KIRKPATRICK, R. A. MENIKOFF, P. REARDON, C. ROUSCULP, M. SALAZAR, A. SGRO, T. TIERNEY, and P. TURCHI. DEVELOPMENT OF A MAGNETICALLY DRIVEN TARGET FOR THERMO-NUCLEAR BURN STUDIES (U). 2007. *P-22.*

Watt, R. G.. Development of a LASNEX MHD model of an A liner driven by a high explosive pulsed power generator (U). 2009. *P-24.*

Watt, R. G.. LA-UR-101305 MS-2 preshot report. 2010. *Internal Documentation.*

Watt, R. G.. LA-UR-10-1621 Multishell completion handout. 2010. *For Distribution Intenally.*

Watt, R. G.. LA-UR-10-1981 MS-2 postshot report. 2010. *Internal Documentation.*

Watt, R. G., S. A. Colgate, W, L. Atchison, J. H. Goforth, J. Griego, J. Guzik, D. Holtkamp, G. Idzorek, R. Kirkpatrick, R. Menikoff, R. Meyer, H. Oona, P. Reardon, C. L. Rousculp, A. G. Sgro, and L. Tabaka. Status of LDRD-DR 20070518 Development of a magnetically driven arget for thermo-nuclear burn studies. (U) . 2009. *NEDPC 2009, Oct. 26-30, 2009, LLNL LA-UR-09-06620 .*

Watt, R. G., S. Colgate, W. L. Atchison, L. Hui, G. Idzorek, A. Kaul, R. Kirkpatrick, R. Menikoff, P. T. Reardon, C. L. Rousculp, M. A. Salazar, A. G. Sgro, T. E. Tierney, and P. J. Turchi. LDRD 20070518-DR development of a magnetically driven target for thermo-nuclear burn studies (U). 2007. *P-22.*

Watt, R. G., S. Colgate, W. L. Atchison, L. Hui, G. Idzorek, A. Kaul, R. Kirkpatrick, R. Menikoff, P. T. Reardon, C. L. Rousculp, M. A. Salazar, A. G. Sgro, T. E. Tierney, and P. J. Turchi. Development of a magnetically driven target for thermo-nuclear burn studies (U). 2007. *P-22.*

Watt, R. G., W. Atchison, S. Colgate, J. Goforth, J. Guzik, D. Holtkamp, A. Kaul, R. Kirkpatrick, H. Li, R. Menikoff, H. Oona, P. Reardon, C. Rousculp, A. Sgro, and T. Tierney. An LDRD Project to Develop a Fusion Target Driven by Velocity Multiplication Using Colliding Shells (U). 2008. *P-24.*

Watt, R. G., W. Atchison, S. Colgate, J. Goforth, J. Guzik, D. Holtkamp, A. Kaul, R. Kirkpatrick, L. Hui, R. Menikoff, H. Oona, P. Reardon, C. Rousculp, A. G. Sgro, and T. E. Tierney. LDRD 20070518-DR Midterm Review: A Project To Develop A Magnetically Driven Target For Thermo-nuclear Burn Studies (u). 2008. *P-21.*

Watt, R. G., W. Atchison, and S. Colgate. LDRD 20070518-dr midterm review: a project to develop a magnetically driven target for thermo-nuclear burn studies (U) LA-CP-08-00675. 2008. *Presentation to LANL LDRD Office, May 22, 2008.*

Watt, R. G., W. Atchison, and S. Colgate. LDRD 20070518-DR Development of a Magnetically Driven Target for Thermo-nuclear Burn Studies (U) LA-CP-07-1593. Presented at *NEDPC 2007.* (Los Alamos, NM, 22-26 Oct. 2007).

Watt, R. G., W. Atchison, and S. Colgate. Development of a Magnetically Driven Target for Thermo-nuclear Burn Studies (U) . Presented at *JOWOG37 2008.* (Los Alamos, NM, 11-14 Feb. 2008).

Watt, R. G., W. L. Atchison, S. A. Colgate, J. Gofoeth, J. Griego, J. Guzik, D. Holtkamp, G. Idzorek, R. Kirkpatrick, R. Menikoff, R. Meyer, H. Oona, P. Reardon, C. L. Rousculp, A. G. Sgro, and L. Tabaka. Status of LDRD-DR 20070518 development of a magnetically driven target for thermo-nuclear burn studies (u). 2010. *P-24.*

Watt, R. G., W. L. Atchison, S. A. Colgate, J. Goforth, D. Herrera, D. Holtkamp, G. Idzorek, R. Kirkpatrick, E. Lopez, J. Lynch, R. Menikoff, R. Meyer, H. Oona, P. Reardon, C. L. Rousculp, A. G. Sgro, L. Tabaka, and D. Torres. Postshot Report, MS-1: Development of Magnetically Driven Target for Thermo-Nuclear Burn Studies (u). 2010. *P-24.*

Watt, R. G., W. L. Atchison, S. A. Colgate, J. Goforth, J. Griego, D. Herrera, D. Holtkamp, G. Idzorek, R. Kirkpatrick, E. Lopez, R. Menikoff, R. Meyer, H. Oona, P. Reardon, C. L. Rousculp, A. G. Sgro, L. Tabaka, and D. Torres. Potshot report for MS-0 fired August 6, 2009 (u). 2009. *P-24.*

Watt, R. G., W. L. Atchison, S. A. Colgate, J. H. Goforth, J. Griego, D. Herrera, D. Holtkamp, G. Idzorek, R. Kirkpatrick, E. Lopez, R. Menikoff, R. Meyer, H. Oona, P. Reardon, C. L. Rousculp, A. G. Sgro, L. Tabaka, and D. Torres. Postshot report for MS-0 fired August 6, 2009 (U). 2009. *LA-UR 09-06959 .*

Watt, R. G., W. L. Atchison, S. Colgate, J. Goforth, J. Griego, D. Holtkamp, G. Idzorek, R. Kirkpatrick, R. Menikoff, R. Meyer, H. Oona, P. Reardon, C. L. Rousculp, A. G. Sgro, and L. Tabaka. Recent results in the development of a magnetically driven target for thermo-nuclear burn studies (U). 2009. *P-24.*

Watt, R. G., W. L. Atchison, S. Colgate, J. Goforth, J. Griego, D. Holtkamp, G. Idzorek, R. Kirkpatrick, R. Menikoff, R. Meyer, H. Oona, P. Reardon, C. L. Rousculp, A. G. Sgro, and L. Tabaka. Status report on the development of a magnetically driven target for thermo-nuclear burn studies (U). 2009. *P-24.*

Watt, R. G., W. L. Atchison, S. Colgate, L. Hui, J. A. Guzik, A. Kaul, R. Kirkpatrick, R. Menikoff, C. L. Rousculp, A. G. Sgro, and T. E. Tierney. LDRD 20070518-DR a project to develop a magnetically driven target for thermo-nuclear burn studies (U). 2008. *P-22.*

Watt, R., W. L. Atchison, S. A. Colgate, J. H. Goforth, D. Holtkamp, A. Kaul, R. Kirkpatrick, R. Menikoff, H. Oona, C. L. Rousculp, A. G. Sgro, and L. Tabaka. LDRD-2007-0518-DR experiment MS-0 Pre-shot report. 2009. *P-24.*

Prompt and Radiochemical NTS Diagnostics and New Measurements (U)

David J. Vieira
20080009DR

Abstract
This project addressed the Laboratory's nuclear performance Grand Challenge, in support of Stockpile Stewardship. In particular, we are refined our understanding of nuclear performance by advancing two diagnostics that have not been well studied in the past. Our goal was to combine the latest nuclear data and reanalysis of neutron pinhole imaging and arsenic radiochemistry diagnostics to provide new constrains on weapons simulations. An extensive set of new weapons simulations were undertaken for a limited set of underground tests to explore how these advanced diagnostics (along with other prompt and radiochemical data) helped differentiate between different simulation models and the different mechanisms which they are based on. With a carefully constrained test, we sought to obtain an improved first-principle understanding of key processes that determine nuclear performance and improve our confidence in certifying the nuclear stockpile without testing.

Background and Research Objectives
In this project we refined the analysis and interpretation of existing underground test data, tested and improved explosion code calculations, and produced new cross section calculations and measurements for the arsenic production and destruction network. New scientific developments were needed to go beyond the currently baseline weapons physics program, in order to fully utilize the information contained within the irreplaceable archival data. In particular, we have made advances in three major areas:

1. Producing refined neutron pinhole images and developing their interpretation.

2. Calculations and measurements of $^{73\text{-}75}$As nuclear cross sections to interpret this existing arsenic radiochemistry diagnostic.

3. Performed an extenstive set of weapons simulation calculations for a selected set of underground test with which to contrast the refined pinhole images and arsenic radiochemical data along with a host of other prompt and radiochemical diagnostic data.

Much of this work is classified, so we present only a high level, unclassified overview here. Please refer to the many classified reports and papers given in the publication list for this project for more specifics.

Scientific Approach and Accomplishments
In our LDRD project we developed two diagnostics that have not been extensively studied before. These are reaction-in-flight neutron pinhole images and the arsenic isotope ratio ^{73}As/^{74}As radiochemical diagnostic. Both are sensitive to the spectrum of high-energy neutrons produced during thermonuclear burn. An extensive new set of explosion code calculations have been performed to examine what new information and constraints these "new" diagnostics provide.

We have perfomed a re-analysis of neutron pinhole (PINEX) images for three events tested at the Nevada Test Site (NTS). This analysis included a set of time-resolved PINEX images for one event which enabled us to make a real-time movie of the thermonuclear burn. This provided valuable information about the dynamics of the burn that was compared to device simulations. The importance of this work was acknowledged by LANL through the awarding of a small-team distinquished performance award.

For two other events, the reaction-in-flight (RIF) and time-integrated (TI) PINEX images were carefully re-analyzed. RIF PINEX images are of interest because the camera is time gated to image only neutrons of a certain energy, typically 16.5-18.5 MeV, that are produced by a deuterium or tritium reacting with a 14-MeV neutron in a "knock-on" process. These are the so-called reaction-in-flight neutrons. The time-integrated PINEX image looks at all the fast neutrons, so it is dominated by the 14-MeV neutrons. The ratio of RIF/TI images was analyzed in this LDRD project to provide valuable new information about the thermonuclear burn and those processes affect it. This provides an important new metric with which to test and improve our weapons simulation codes. As such this is one of the major accomplishments

of this LDRD project. Follow-on work to apply this new metric to other NTS events is now planned to be supported by the Stewardship Science program.

A second major area of work for this project was in the calculation and measurement of the arsenic reaction production and destruction network as needed to calculation and interpretation of $^{73}As/^{74}As$ radiochemical results. 14-MeV neutrons convert ^{75}As to ^{74}As by the (n,2n) reaction. ^{74}As, in turn, is converted to ^{73}As by another (n,2n) reaction. Knowing these (n,2n) reactions and their associated neutron capture and (n,p) or (n,np) reactions which destroy ^{73}As and ^{74}As are central to calculation the $^{73}As/^{74}As$ ratio.

In a series of measurements using the DANCE (Detector for Advanced Neutron Capture Experiments) at the Lujan Center at LANSCE and the Triangle University Nuclear Laboratory (TUNL) at Duke University with our Stewardship Science Academic Alliance collaborators from Duke University, North Carolina State, the University of North Carolina, and the University of California, Berkeley, we remeasured the ^{75}As neutron capture, (n,2n), and (n,p) reaction cross sections. This work is being prepared for publication (see publication list). Using this information a new set of Hauser-Feshbach calculations for the arsenic network has been performed. This has been evaluated and will be published in the next version of ENDF/B-VII data evaluation. From this we have produced 618-group NDI libraries for the arsenic isotopes and produced the assoicated continuous energy Monte Carlo libraries that are needed for the weapons simulation codes. Similiarly we have developed the full multi-group transport libraries for the ytterium production and destruction network so that the ytterium radiochemical diagnostic can also be calculated. By so doing we have developed a new capability to simulate (in 2D codes) non-actinide radiochemistry diagnostics that are loaded into different parts of the device. This is a significant accomplishment not only for this project, but for the Stockpile Stewardship program as a whole.

To verify and further improve this arsenic cross section set, we undertook a series of measurements on radioactive targets of ^{73}As ($t_{1/2}$=80 d) and ^{74}As (18 d). For this we used the Isotope Production Facility (IPF) to produce Curie-quantities of these arsenic isotopes via Ge(p,xn) reactions using the high-intensity (250 mA) proton beam at LANSCE. The germanium targets were then processed in our hotcell facility at TA-48 to extract the arsenic and make radioactive targets. With the first target, we attempted to measure the important $^{74}As(n,p)$ destruction reaction using the lead slowing-down spectrometer at the weapons neutron research facility at LANSCE. This experiment was a partial success and a second experiment is planned in the near future to complete this measurement. This second experiment will be supported by the Stewardship Science program. An additional target has been made to measure the $^{73}As(n,2n)^{72}As$ reaction using the TUNL facility at Duke. This measurement is important in improving the crucial $^{74}As(n,2n)$ reaction; this reaction must be calculated since a measurement in not currently possible. At TUNL we will perform an activation experiment to determine that amount of ^{72}As produced, but given that both ^{73}As and ^{74}As are simultaneously produced at IPF, we had to wait ~8 months for the shorter-lived ^{74}As (which emits interfering high-energy γ-rays) to decay away before attempting this measurement. We are now prepared to attempt this measurement with Stockpile Stewardship support. These experiments with radioactive targets are extremely challenging and require a confluence of many of our unique capabilities at Los Alamos (IPF, hotcell radiochemistry, special instruments at LANSCE). This LDRD project has enabled us to become proficient in making and handling these radioactive targets and performing forefront experiments with them. Although these measurements are still in progress, this work has established an important new capability for the Laboratory.

The third focus area was the undertaking of high-fidelity explosion code calculations to compare to the re-evaluated PINEX images and arsenic radiochemical results. As mentioned above, the first step of this work involved the construction of new reaction libraries for arsenic and ytterium. With this implemented, over 150 calculations for the three NTS tests were performed with a variety of different models. This was a tour-de-force effort which provided significant new information about these models and how they affect nuclear performance. This work highlighted the sensitivity and importance of the RIF/TI PINEX images and the arsenic radiochemistry in addressing a long-standing issue in the simulation of nuclear weapons. Although we can not adequately highlight these results here because they are classified, this was a major outcome of this LDRD project with important ramifications for the Stockpile Stewardship program. Please see the LA-CP reports listed in the publication list for details.

Impact on National Missions

As mentioned above this work directly benefits the Stockpile Stewardship program. Many of the advances and new capabilities established by this work will endure and be further refined to improve our understanding of nuclear weapons processes at a fundamental level and advance our weapons simulation capabilities upon our nuclear aresnal is annual certified. This work has also promoted a healthy collaborative team effort within Los Alamos and fostered external collaborations with several universities and with other national laboratories. As such this work has attracted several young scientists which have since been converted to staff.

Publications

Cheng, B. L., and T. J. Gorman. Radiochemical Modeling of Coalora (U). 2010. *Los Alamos National Laboratory Report LA-CP-10-01305.*

DeYoung, A.. RIFs as a New Constraint on Mix Models (U).

2009. *Nuclear Explosives Design Physics Conference - NEDPC, Lawrence Livermore National Laboratory, Livermore, CA, Oct. 26-30, LA-CP-09-01284..*

Gorman, T. J.. Development of a Nuclear Testbed for Boost (U). 2008. *Weapons Science Capability Review, Los Alamos National Laboratory, Los Alamos, NM, May 5-8, 2008..*

Gorman, T. J.. Beyond Initial Conditions Non-DPE (U). 2008. *Weapons Science Capability Review, Los Alamos National Laboratory, Los Alamos, NM, May 5-8, 2008.*

Gorman, T. J., T. McKee, and D. J. Vieira. New Radiochemical Calculations of Three NTS Experiments (U). 2009. *JOWOG 32P, Los Alamos National Laboratory, Los Alamos, NM May 18-20, 2009, LA-CP-09-00552..*

Keksis, A. L.. Neutron Capture Measurements on Arsenic (U). 2008. *Radiochemistry Inter-Laboratory Working Group - ILWOG 41, AWE Aldermaston, UK, Sept. 6-15, 2008, LA-UR-08-05692..*

Obst, A. W.. Coalora TIP/TRP Orientation (U). 2008. *Los Alamos National Laboratory memo to X-Division, dated Sept. 23, 2008, LA-CP-08-01162..*

Raut, R., A. S. Crowell, B. Fallin, C. R. Howell, C. Huibregtse, J. H. Kelley, T. Kawano, E. Kwan, G. Rusev, A. P. Tonchev, W. Tornow, D. J. Vieira, and J. B. Wilhelmy. Cross-Section Measurements of Neutron Induced Reaction on GaAs using Monoenergetic Beams from 7.5 to 15 MeV. *Physical Review C.*

Vieira, D. J.. Prompt and Radiochemical NTS Diagnostics and New Measurements: A LDRD Project on Boost (U). 2008. *Weapons Science Capability Review, Los Alamos National Laboratory, Los Alamos, NM, May 5-8, 2008..*

Vieira, D. J.. Radiochemistry and PINEX Diagnostics Focused on Boost - A LDRD/DR Project. 2009. *Fission Workshop, Los Alamos National Laboratory, Los Alamos, NM, Feb. 5-6, 2009..*

Vieira, D. J.. Radiochemistry and PINEX Diagnositcs Focused on Boost - A LDRD/DR Project (U). 2009. *N-Division Seminar, Lawrence Livermore National Laboratory, Livermore, CA, March 30, 2009, LA-CP-09-0317..*

Vieira, D. J.. Arsenic Radiochemical Diagnostics (U). 2009. *Nuclear Explosives Design Physics Conference (NEDPC), Lawrence Livermore National Laboratory, Livermore, CA, Oct. 26-30, 2009, LA-CP-09-01478..*

Williams, M.. A Formation of Time Integrated Mix (U). 2009. *Nuclear Explosives Design Physics Conference (NEDPC), Lawrence Livermore National Laboratory, Livermore, CA, Oct. 26-30, 2009, LA-CP-09-01431..*

al, A. DeYoung et. PINEX and Arsenic Radiochemical Diagnostics Focused on Boost (U). 2010. *Defense Research Review (in preparation).*

Global Monitoring of the Sky with Thinking Telescopes: Finding and Interrogating Cosmic Explosions

W T. Vestrand
20080039DR

Abstract
This project created technology for a ground-breaking integrated grid of persistent monitoring telescopes and rapid response follow-up telescopes in order to find and to interrogate the optical light from space objects and cosmic explosions. Our project integrated Information Science, Robotic Instrumentation, and Distributed Sensor Network technology into a full, end-to-end, spatially distributed search engine for persistently monitoring the night sky. This fully autonomous robotic network is designed to feed its observations back to real-time decision engines, pose new questions for interrogation, conduct triage, and optimize the network hardware configuration for real-time knowledge extraction. We used the optical observations collected by this system, along with context observations at other wavelengths, to gain new insights into the physics of Nature's most powerful explosions---Gamma Ray Bursts (GRBs).

Background and Research Objectives
Our goal was to build and operate a grid of autonomous robotic telescopes – Thinking Telescopes – that observe the full night sky searching for optical transients, simultaneously monitor more than 10 million persistent sources, recognize anomalous behavior, select targets for detailed interrogation, and make real-time, follow-up observations – all without human intervention. This challenging goal required significant achievements in robotic instrumentation, distributed networks, artificial intelligence, advanced database technology, and time-domain astrophysics. The principal focus of our scientific effort was developing an understanding of Gamma Ray Bursts (GRBs). But, the tools and methodologies developed on this project have general applicability to areas of Defense, Intelligence, and Homeland Security, and have direct applicability to specific problems in Space Situational Awareness. A key objective of the applied scientific effort was to demonstrate, with real operating hardware, how this integration of cutting edge technologies can be applied to Space Situational Awareness.

Scientific Approach and Accomplishments
On March 19, 2008 eight of the telescopes in our autonomous Thinking Telescopes network detected a spectacular optical transient that for a few seconds became bright enough to be even visible to the naked eye (Wozniak et al 2009). The transient was associated with GRB 080319B (Racusin et al. 2008), a gamma-ray burst (GRB) at a luminosity distance of about 6 Gpc (7.5 Billion light-years), making it the most luminous optical object ever recorded by humankind. Our comprehensive sky monitoring and multicolor optical follow-up observations of GRB 080319B covered the development of the explosion and the afterglow before, during, and after the burst.

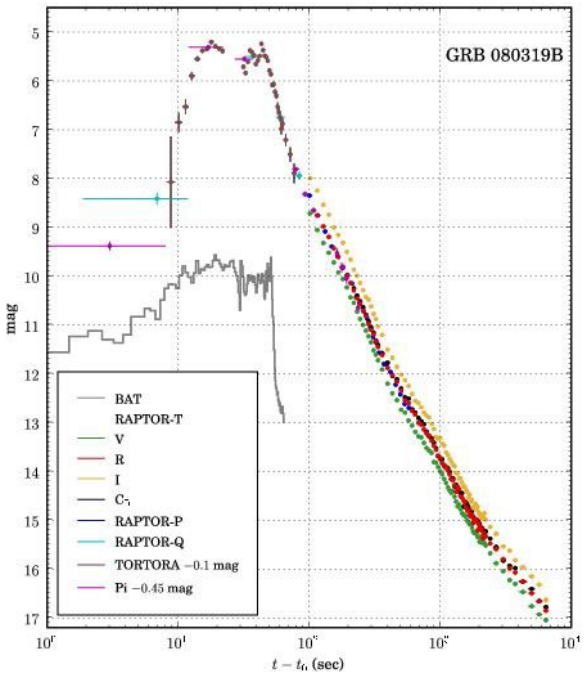

Figure 1. Optical light curve of GRB 080319B, "the naked eye burst". The transient was independently detected and followed over a high dynamic range by three fully autonomous instruments on the RAPTOR telescope network: a simultaneous multi-color imager RAPTOR-T, a wide-field survey array RAPTOR-P, and an all-sky monitor

RAPTOR-Q. A non-detection in RAPTOR-Q data rules out the presence of a significant optical precursor for ~ 30 minutes prior to BAT trigger at t0. The RAPTOR measurements of the prompt optical emission during the gamma-ray burst (t−t0 = 0–60 s.) agree with the data collected by other instruments reporting detections: TORTORA and Pi-of-the-sky. Unfiltered observations were adjusted to R-band equivalent scale.

The unmatched dynamic range of our robotic system allowed us to measure the evolution of the extremely bright transient over more than 12 magnitudes and measure properties that are normally not detectable (Figure 1). We found that the optical and gamma-ray variability during the explosion are correlated consistent with the behavior we discovered for prompt optical emission in GRBs (Vestrand et al. 2005, 2006). But the record brightness of GRB 080319B is much greater than expected from our analysis of previous gamma-ray bursts. A theory effort by one of the members of our team, Alin Panaitescu, in collaboration with P. Kumar at UT Austin, found that this extreme optical behavior is best understood as synchrotron self-Compton (SSC) emission (Kumar and Panaitescu 2009). After a gradual onset of the gamma-ray emission, there is an abrupt rise of the prompt optical flux, suggesting that light cannot escape at the beginning of the burst. As the burst continues, our simultaneous multicolor light curves show a rapidly decaying red component due to large-angle emission, and an emerging blue forward-shock component, as the burst slams into the surrounding environment. While providing little evidence that a reverse shock dominates the early afterglow, these observations strengthen the case for the universal role of the SSC mechanism in GRBs.

Our persistent monitoring of the site of GRB 080319B also provided important limits on the relative strength of optical precursor emission from gamma-ray bursts. These measurements help us address the question: Is there any hint that a gamma-ray burst is just around the corner? Our RAPTOR-Q monitored the burst location for several hours before the onset of gamma-ray emission and showed no evidence for emission brighter than R~10^{th} magnitude. These are the best constraints ever on precursor emission and provide an upper limit on the brightness of precursor outbursts to less than ~3% of the counterpart peak brightness.

Another key accomplishment came from our study of the early afterglows from all GRBs with measured distances. In the most comprehensive study of afterglow behavior to that date, we discovered that optical afterglows show just four kinds of behavior: fast-rising with an early peak, slow-rising with a late peak, flat plateaus, and rapid decays (Panaitescu and Vestrand 2008). We found that the fast-rising optical afterglows display correlations among peak flux, peak epoch, and post-peak power-law decay index. We also found that the afterglows with plateaus and slow-rises show a similar correlation between peak flux and peak time.

Having found these relationships in the observed properties of gamma-ray afterglows, we explored the question: What are the physical processes that generate the linked properties? In Panaitescu and Vestrand (2008), we suggested that the correlations could arise if the observer's location is originally outside the GRB jet's aperture for peaked afterglows. For afterglows with plateaus from outflows, we hypothesize a non-uniform angular distribution of the ejecta kinetic energy.

Later in the project, we updated this work by examining the expanded sample of optical afterglows that were collected during the project and explored another possible explanation for the diversity of optical afterglows---the onset of blastwave deceleration (Panaitescu and Vestrand 2010). Again, we found that the optical light-curves of GRB afterglows display either peaks or plateaus. We identified 15 afterglows of the former type and 20 of the latter. We found the optical energy release is similar for both types and is correlated to the GRB output, the correlation being stronger for peaky afterglows. That suggests that the prompt (burst) and delayed emissions of peaky afterglows are from the same relativistic ejecta and that the optical emission of plateau afterglows arises more often from ejecta that did not produce the burst emission. We therefore proposed that peaky optical afterglows are from impulsive ejecta releases and that plateau optical afterglows originate from long-lived engines, the break in the optical light-curve (peak or plateau end) marking the onset of the entire outflow deceleration. Exploring the peak luminosity--peak time correlation, we found the distribution of peaky afterglows displays a "zone of avoidance" (no luminous late time peaks) with an edge which is likely to arise from variations (among afterglows) in the density of the surrounding material. The fluxes and epochs of optical plateau breaks follow an anti-correlation which probably arises from an upper limit to the afterglow output.

We also conducted a study that compared optical afterglows with x-ray afterglows for the same events. Sixty percent of the afterglows well-monitored in both the optical and X-ray showed comparable decays and simultaneous light-curve breaks. The other 40 percent display three types of decoupled light-curves:

1. Chromatic optical light-curve breaks (that could be due to the peak of the radiation spectrum moving though the optical band).

2. X-ray flux decays faster than in the optical (suggesting that the X-ray emission is from local inverse-Compton scattering).

3. Energy dependent X-ray light-curve breaks (which suggest that the X-ray emission is from external up-scattering).

Figure 2. The RAPTOR-K sky monitoring array. This array has the ability to image the full sky every seven minutes down to 16th magnitude using 30 second exposures.

Figure 3. This small observatory called RQD2 (RAPTOR-Q Design 2) is the prototype for nodes in a global network, capable of continuous persistent monitoring of the night sky. The observatory employs five wide field of view imagers that altogether view about 90% of the sky above 14 degrees elevation with the sensitivity of 10th magnitude in 10 seconds.

In collaboration with our colleagues at U. C. Berkeley, our RAPTOR measurements of the early optical emission from GRBs were combined with their infrared measurements to place interesting constraints on the nature of dust in extremely distant star forming regions. The combined broadband (optical/infrared) observations of the afterglow from GRB071025 show that source must be at a distance of about 12.5 Billion light-years ($4.4 < z < 5.2$). Further, the red spectral energy distribution (even in regions not affected by the Lyman α break) provides secure evidence of a large dust column. The inferred extinction curve is inconsistent with any observed template for dust in our galaxy, but well fitted by models of dust formed by supernovae. Together with recent studies of high-z quasars, our combined observations (Perley et al. 2010) suggest a transition in dust properties in the early Universe, possibly associated with a transition between supernova-dominated and asymptotic giant branch-dominated modes of dust production.

We also had several achievements in the construction of new instrumentation that enabled the persistent sky monitoring for our gamma-ray burst and Space Situational Awareness studies. We completed the construction of the RAPTOR-K, a wide-field, persistent optical monitoring array with unprecedented capability (Figure 2). It is composed of 16 wide-field telescopes carried on a single rapidly slewing mount. Each telescope has a 2Kx2K E2V back-illuminated CCDs at the focal plane and has a 3-sigma limiting magnitude of $R\sim16^{th}$ magnitude in 30 seconds. Altogether the 16 telescopes have an instantaneous field-of-view of ~1,000 sq-degrees. In normal operation, the array is capable of patrolling the full visible sky above 20 degree elevation on 6-minute circuit. It is roughly 30 times more sensitive than any other full sky optical monitor capable of finding transients with durations measured in minutes. This system is a fully autonomous robot and runs without human intervention.

We designed, tested, and deployed a new portable observatory called RQD2 (Raptor-Q/demonstrator-2), which is fully autonomous and easily deployable to remote locations around the World (Figure 3). It is a small portable robotic observatory developed for the purpose of real-time sky condition monitoring that also has the capability to detect bright astronomical transients. In fact, the prototype for this system made key observations of the naked eye GRB. RQD2 consists of five wide field telescopes that, altogether, simultaneously view 14,500 square degrees---approximately 90% of the sky above 12 degrees elevation. The limiting sensitivity of the RQD2 system for a 10 second exposure is $R\approx10^{th}$ on a clear, moonless, night. The system normally detects about 55,000 objects in each set of exposures. Using those measurements our real-time photometry pipeline and machine learning algorithms are able assess the conditions over the full sky every 20 seconds That information can then be feed back into the network to help trigger observations by narrow field telescopes at that site and plan the tasking of time critical observations throughout the global network.

Fully autonomous operation is a key feature of our system. An ability to delegate increasingly complex data analysis and decision making tasks to machines (software agents) is the key to success in this area. We developed an ap-

proach that employs state of the art Machine Learning (ML) algorithms to dramatically simplify the problem of finding optimal decision boundaries in high dimensional feature spaces. We focused on supervised learning techniques that require training by a human analyst prior to application on new data, but generally are more mature and offer better performance. To that end, we developed a software framework that enables us to quickly extract new features from a standard set of our data products and evaluate (cross-validate) the performance of candidate ML classifiers over a range of models and parameters. Support for feature selection allows us to explore alternative feature spaces by weighting the relative importance of each dimension in the input data. Our ML tool set has been integrated into the software package that can be rapidly deployed to a new node on the network.

To develop and deploy the Machine Learning algorithms in a real-time operational system one needs to construct the infrastructure capable of handling data intensive computing. To meet that need we built a parallel database server composed of three storage/processing nodes. Those processing (slave) nodes are managed by a master node running hardware virtualization layer and multiple operating systems without performance overhead. Each slave node runs a postgres database server with table partitioning scheme that enables fast parallel loading of the RAPTOR sky monitoring data. The master node runs pgpool-II software for managing parallel queries and data consistency. Altogether the system has 40TB of usable storage,120 GB of RAM memory, 48 Intel Xeon cores, and 16 network channels.

We also developed a mechanism for efficient search and retrieval of RAPTOR data that is distributed throughout the global network. This was challenging because the physical location of required imagery, or even knowledge of which image supports an event in question, is often unknown. We developed an approach, called RAPSTER, that leverages design patterns and lessons learned from the public internet peer to peer file sharing community. As each site node processes imagery it reports to a RAPSTER database which constructs temporal and spatial indexes of available imagery. This database is then capable of constructing a list of imagery which intersects an arbitrary region of interest across the celestial sphere, optionally filtered by time. A request is then submitted to a distributed storage mesh for each required image. The mesh decides which location holds the desired image and streams it back.

Finally, we developed demonstrations that showed how this technology can be applied to Space Situational Awareness. For resident space objects, we conducted campaigns that established both the metric accuracy and sensitivity of the system. We also created a self-generated photometric catalog that helped highlight the strength of our new approach.

Impact on National Missions

The technology developed on this project represents a pathfinder for a revolutionary new approach to Space Situational Awareness (SSA)—an area of growing importance to the Nation. Our construction of and live demonstrations of operating robotic hardware that conduct wide-field persistent monitoring, anomaly detection, and autonomous real time robotic follow-up garnered significant attention in the government. These demonstrations led one government sponsor to fund us to build autonomous robotic hardware for them and fund new programmatic research on our Thinking Telescopes technology. Our innovative robotic instrumentation work was also one of the flagship efforts that were key in demonstrating that the DOE National Laboratories could make important contributions to SSA. But the new approach that we developed employing autonomous robotic, distributed, instrumentation for situational monitoring also has general applicability to areas of Defense, Intelligence, and Homeland Security.

References

1. Wozniak, P. R., W. T. Vestrand, A. D. Panaitescu, J. A. Wren, H. R. Davis, and R. R. White. GAMMA-RAY BURST AT THE EXTREME: “THE NAKED-EYE BURST” GRB 080319B. 2009. *ASTROPHYSICAL JOURNAL.* **691** (1): 495.

2. Racusin, J. L., S. V. Karpov, M. Sokolowski, J. Granot, X. F. Wu, V. Pal,ÄôShin, S. Covino, A. J. van der Horst, S. R. Oates, P. Schady, R. J. Smith, J. Cummings, R. L. Starling, L. W. Piotrowski, B. Zhang, P. A. Evans, S. T. Holland, K. Malek, M. T. Page, L. Vetere, R. Margutti, C. Guidorzi, A. P. Kamble, P. A. Curran, A. Beardmore, C. Kouveliotou, L. Mankiewicz, A. Melandri, P. T. O,ÄôBrien, K. L. Page, T. Piran, N. R. Tanvir, G. Wrochna, R. L. Aptekar, S. Barthelmy, C. Bartolini, G. M. Beskin, S. Bondar, M. Bremer, S. Campana, A. Castro-Tirado, A. Cucchiara, M. Cwiok, P. D,ÄôAvanzo, V. D,ÄôElia, M. Della Valle, A. Postigo, W. Dominik, A. Falcone, F. Fiore, D. B. Fox, D. D. Frederiks, A. S. Fruchter, D. Fugazza, M. A. Garrett, N. Gehrels, S. Golenetskii, A. Gomboc, J. Gorosabel, G. Greco, A. Guarnieri, S. Immler, M. Jelinek, G. Kasprowicz, V. La Parola, A. J. Levan, V. Mangano, E. P. Mazets, E. Molinari, A. Moretti, K. Nawrocki, P. P. Oleynik, J. P. Osborne, C. Pagani, S. B. Pandey, Z. Paragi, M. Perri, A. Piccioni, E. Ramirez-Ruiz, P. W. Roming, I. A. Steele, R. G. Strom, V. Testa, G. Tosti, M. V. Ulanov, K. Wiersema, R. A. Wijers, J. M. Winters, A. F. Zarnecki, F. Zerbi, P. Meszaros, G. Chincarini, and D. N. Burrows. Broadband observations of the naked-eye gamma-ray burst GRB 080319B. 2008. *NATURE.* **455** (7210): 183.

3. Vestrand, W. T., P. R. Wozniak, J. A. Wren, E. E. Fenimore, T. Sakamoto, R. R. White, D. Casperson, H. Davis, S. Evans, M. Galassi, K. E. McGowan, J. A. Schier, J. W. Asa, S. D. Barthelmy, J. R. Cummings, N. Gehrels, D. Hullinger, H. A. Krimm, C. B. Markwardt, K. McLean, D. Palmer, L. Parsons, and J. Tueller. A link between

prompt optical and prompt γ-ray emission in. 2005. *Nature.* **435** (7039): 178.

4. Vestrand, W. T., J. A. Wren, P. R. Wozniak, R. Aptekar, S. Golentskii, V. Pal'shin, T. Sakamoto, R. R. White, S. Evans, D. Casperson, and E. Fenimore. Energy input and response from prompt and early optical afterglow emission in Œ≥-ray bursts. 2006. *Nature.* **442** (7099): 172.

5. Kumar, P., and A. Panaitescu. What did we learn from gamma-ray burst 080319B?. 2008. *Monthly Notices of the Royal Astronomical Society.* **391** (1): L19.

6. Panaitescu, A., and W. T. Vestrand. Taxonomy of gamma-ray burst optical light curves: identification of a salient class of early afterglows. 2008. *MONTHLY NOTICES OF THE ROYAL ASTRONOMICAL SOCIETY.* **387** (2): 497.

7. Panaitescu, A., and W. T. Vestrand. Optical and x-ray afterglows of gamma-ray bursts: peaks, plateaus, and possibilities. *Monthly Notices of the Royal Astronomical Society.*

Publications

Hoffman, D., T. Harrison, and J. Coughlin et al. New Beta Lyrae and Algol candidates from the Northern Sky Variability Survey. 2008. *Astronomical Journal.* **136** (3): 1067.

Kozlowski, S., and C. S. Kochanek et al. SDWFS-MT-1: A self-obscured luminous supernova at z~0.2. To appear in *Astrophysical Journal.*

Kumar, P., and A. Panaitescu. What did we learn from gamma-ray burst 080319b?. 2008. *Monthly Notices of Royal Astronomical Society.* **391** (1): L19.

Panaitescu, A.. X-ray flares, plateaus and chromatic breaks of GRB afterglows from up-scattered forward-shock emission. 2008. *Monthly Notices of Royal Astronomical Society.* **383** (3): 1143.

Panaitescu, A.. An external-shock origin of the relation for gamma-ray bursts. 2009. *Monthly Notices of the Royal Astronomical Society.* **393** (3): 1010.

Panaitescu, A., and W. T. Vestrand. Taxonomy of gamma-ray burst optical light curves: identification of a salient class of early afterglows. 2008. *Monthly Notices of Royal Astronomical Society.* **387** (2): 497.

Panaitescu, A., and W. T. Vestrand. Optical afterglows of gamma-ray bursts: peaks, plateaus, and possibilities. *Monthly Notices Royal Astronomical Society.*

Perley, D. A., and J. S. Bloom et al. Evidence for supernova-synthesized dust from the rising afterglow of GRB071025 at z~5. 2010. *Monthly notices of the Royal Astronomical Society.* **406** (4): 2473.

Perley, D., J. Bloom, and N. Butler et al. The troublesome broadband evolution of GRB 061126. 2008. *Astrophysical Journal.* **672** (1): 449.

Rossi, A., and S. Schulze et al. The Swift/Fermi GRB 080928 from 1 eV to 150 keV. *Astronomy and Astrophysics.*

Vestrand, W. T., H. Davis, and J. Wren et al. Autonomous global sky surveillance with real-time robotic follow-up: night sky awareness through Thinking Telescopes technology. 2009. In *Advanced Maui Optical and Space Surveillance Technologies Conference.* (Maui, 14-16 Sept. 2008). , p. p.E71. Maui: Maui Economic Development Board.

White, R., H. Davis, W. T. Vestrand, and P. Wozniak. Distributed intelligence in an astronomical distributed sensor network. 2008. *Astronomische Nachrichten.* **329** (3): 278.

White, R., and A. Allan. An overview of the heterogeneous telescope network system: concept, scalability and operation. 2008. *Astronomische Nachrichten.* **329** (3): 232.

Wozniak, P., W. T. Vestrand, and A. Panaitescu et al. Gamma-Ray Burst at the extreme: 'the naked eye burst' GRB 080319B. 2009. *Astrophysical Journal.* **691**: 495.

Wren, J., W. T. Vestrand, P. Wozniak, and H. Davis. A portable observatory for persistent monitoring of the night sky. 2010. In *Observatory Observations: Strategies, Processes, and Systems.* (San Diego, 29-30 June 2010). Vol. 7737, p. 773723. : SPIE.

Yuan, F., and P. Schady et al. GRB 081008: from burst to afterglow and the transition phase in between. 2010. *Astrophysical Journal.* **711** (2): 870.

al, E. Rykoff et. Looking into the fireball: ROTSE-III and Swift observations of early GRB afterglows. 2009. *Astrophysical Journal.* **702**: 489.

al, F. Yuan et. Prompt optical observations of GRB 080330 and GRB 080413A . 2008. In *2008 Nanjing Gamma-Ray Burst conference.* (Nanjing, China, October 2008). Vol. 1065, p. 433. Melville, New York: American Institute of Physics.

Carrier Multiplication in Nanoscale Semiconductors for High-Efficiency, Generation-III Photovoltaics

Victor I. Klimov
20080057DR

Abstract

The solution to the global energy challenge requires revolutionary breakthroughs in areas such as the conversion of solar energy into electricity. One such breakthrough is high-efficiency generation of multiple electron-hole pairs (excitons) from absorption of single photons known as carrier multiplication (CM). For more than 20 years it has been recognized theoretically that such a process has the potential to significantly increase the power conversion efficiency of photovoltaic devices via an enhanced photocurrent for a fixed photovoltage. In 2004, using a novel experimental approach, we discovered that semiconductor nanocrystals (NCs), in distinction from bulk materials, undergo this process very efficiently within the range of solar photon energies. In this project, we conduct theoretical and experimental studies of the fundamental physics of CM and relevant phenomena (e.g., photoionization and charge extraction from the NCs) that will ultimately lead to the development of novel principles, materials, and architectures for making use of this process in practical photovoltaic technologies. Specifically, to identify the factors that control the energy onset and the efficiency of multiexciton generation, we perform detailed studies of the CM mechanism in nanoscale semiconductors as well as the nature of competing processes such as NC photoionization. We also conduct quantitative studies of CM yields as a function of the nanostructure shape (e.g., spherical nanoparticles versus nanorods), underlying structure (e.g., different compositions within the same group of compounds) and heterostructuring (e.g., core-only particles versus core-shell structures). Finally, we investigated charge-transfer processes in engineered nanostructures such as type-II heterojunctions. The utilization of such structures can simplify extraction of charges from the NCs, and thus, make practical use of the CM phenomenon. The results of this project should help researchers in the development of novel nanoscale materials with CM efficiencies that approach the "ideal" efficiency as defined by energy conservation.

Background and Research Objectives

The objective of this project was to study the basic science of the formation of multiple electron-hole pairs (excitons) upon absorption of a single photon of sufficient energy in semiconductor NCs and to determine the feasibility of exploitation of this effect in photovoltaic (PV) devices. CM has the potential to increase the power conversion efficiency of PV above the Shockley-Quiesser limit of 31% for single junction devices (the lowest-cost platform). The increase in efficiency is possible because CM results in the formation of two or more excitons per absorbed blue solar photon, which can increase photocurrent if the excitons can be extracted prior to exciton-exciton annihilation (Auger recombination). We were the first to discover that:

- The energetic onset of this process decreases significantly in NCs relative to bulk materials.
- The electron-hole creation energy (the energy required to generate a new exciton) is also reduced.

These finding indicate the significant promise of NCs for the realization of high-efficiency low-cost solar cells (*generation-III PV*).

Our work in this project had the following objectives:

- Investigation of the fundamentals of the CM process and competing process including the development of novel theoretical approaches.
- Development of experimental techniques for reliable measurements of CM efficiencies and isolation from "extraneous" effects.
- Studies of interfacial process in the context of charge extraction from the NCs.
- Development of novel infrared (IR) materials for PV applications.
- Studies of single- and multiexciton effects in NCs of group-IV indirect-gap semiconductors.
- Fabrication and characterization of prototype NC-based devices.

This project has allowed a coherent program of sufficient scope that it can have a significant technical impact and maintain the Laboratory's established recognition as leader in a rapidly developing field of chemically synthesized semiconductor nanostructures.

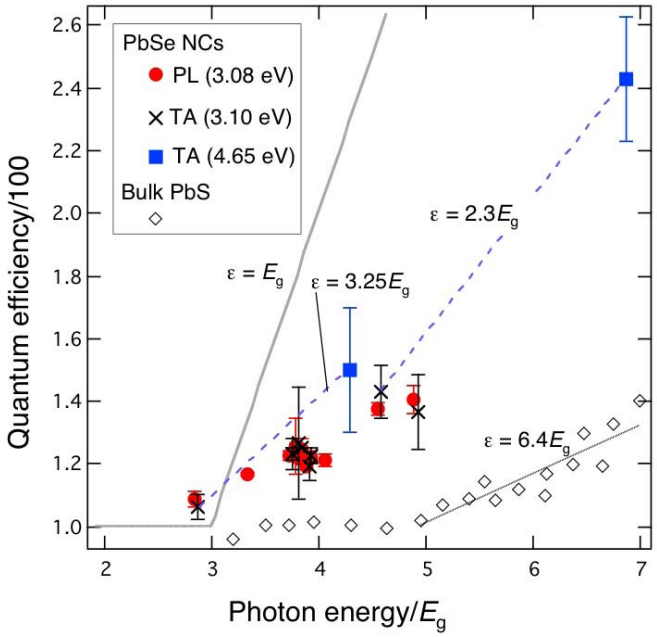

Figure 1. Quantum efficiencies for photon conversion into excitons using TA and time-resolved PL for PbSe NCs (circles, crosses, and squares) relative to bulk PbS (open diamonds). The horizontal axis is the photon energy normalized by the band-gap energy.

Scientific Approach and Accomplishments

Carrier multiplication and extraneous processes

We reported the first experimental observation of CM in NC materials in 2004 (Schaller & Klimov, *Phys. Rev. Lett.* **92**, 2004). In this work, we detected the CM effect in PbSe NCs on the basis of a distinct decay component due to Auger recombination of multiexcitons. Later, similar dynamical signatures of CM were observed in NCs of other compositions including PbS, PbTe, CdSe, InAs, and Si. However, in addition to a large body of experimental data demonstrating high-efficiency CM in NCs, several recent reports have questioned the claim of enhanced CM in NCs and even its existence, in at least some NC systems. In this project, we have addressed this apparent controversy regarding CM in NCs and analyzed potential reasons for observed discrepancies (J. McGuire et al., *Acc. Chem. Res.* **41**, 2008; J. McGuire et al., *Nano Lett.* **10**, 2010). Specifically, we have considered factors such as sample-to-sample variations, differences in detection techniques, and the influence of extraneous effects (such as photoionization) that could lead to CM–like signatures in spectroscopic measurements.

As part of these studies, we applied side-by-side two different spectroscopic techniques, time-resolved photoluminescence (PL) and transient absorption (TA), for evaluating CM efficiencies in PbSe NCs. Both techniques show clear signatures of CM with efficiencies that are in good mutual agreement. NCs of the same energy gap show moderate batch-to-batch variations (within ~30%) in apparent multiexciton yields and larger variations (more than a factor of 3) due to differences in sample conditions (stirred vs. static solutions). These results indicate that NC surface properties may affect the CM process. They also point toward potential interference from extraneous effects such as NC photoionization that can distort the results of CM studies.

CM yields measured under conditions when extraneous effects are suppressed via intense sample stirring and the use of extremely low pump levels (0.02 - 0.03 photons absorbed per NC per pulse) indicate that both the electron-hole creation energy and the CM threshold in NCs are reduced compared to those in bulk solids (Figure 1). These results are consistent with a confinement-induced enhancement of the CM process in NC materials.

Carrier multiplication theory

We have focused on model development and numerical simulations to reveal microscopic mechanisms that contribute to CM in quantum-confined NCs. Specifically, we have developed a theoretical concept for treating CM as a Coulomb-mediated scattering process between the single-exciton and biexciton bands. This generic model naturally interpolates between earlier proposed models where the interband (single-biexciton-band) Coulomb interaction is assumed to be either weak [Schaller, Agranovich & Klimov, *Nature Phys.* **1**, 189 (2005); Rupsaov & Klimov, *Phys. Rev. B* **76** 125321 (2007)] or strong [Shabaev, Efros & Nozik, *Nano Lett.* **6**, 2856 (2006)]. In our new model, we also account for the effects of arbitrary duration optical pulses, which is in contrast to earlier work where CM was only considered for steady-state excitation.

To perform numerical simulations, the time-dependent density matrix model accounting for the interband Coulomb interaction using second-order perturbation theory has been developed (Velizhanin & Piryatinski, *J. Chem. Phys.* **133**, 2010). This model has been parameterized to experimentally describe studied PbSe and PbS NCs by implementing the four-band effective-mass treatment proposed by Kang and Wise [*J. Opt. Soc. Am. B*, **14**, 1632 (1997)]. Within this framework, different CM pathways naturally arise as the interband Coulomb induced correlations (scattering events) perturb the Hartree-Fock electron-hole states described by the Kang-Wise model. Furthermore, our model predicts a CM pathway that was not considered earlier, which is a direct excitation of the single-exciton resonances followed by scattering to the biexciton manifold. The calculations demonstrate that direct and virtual single-exciton channels have equal contributions whereas the virtual biexciton channel is two orders of magnitude weaker. Calculated and measured total CM efficiencies are in reasonable agreement. Currently, the focus of our theoretical study is on the effect of the phonon-assisted intraband relaxation accompanied by the

interband Coulomb scattering on the CM efficiency.

Development of novel IR materials
Colloidal Ge nanocrystals.

One goal of our project is to understand the effect of material electronic structure on exciton-exciton interactions, and especially, the CM process. To address this issue, we sought to produce and examine materials with unique band structures, including germanium (Ge), which has an indirect band gap in the bulk, and IR type-II heterostructured materials in which the electron and hole of the lowest-energy exciton are separated into two different spatial regions of the NC. Both of these systems, however, first required substantial synthetic development.

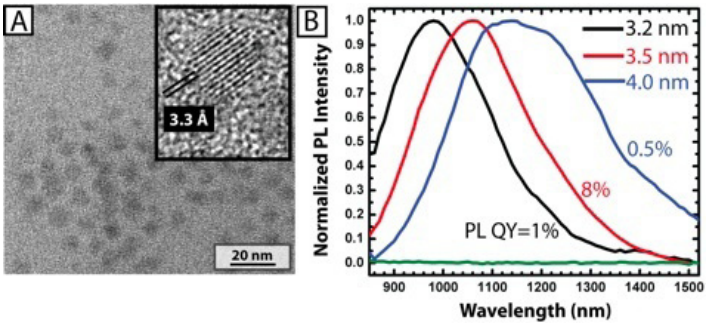

Figure 2. (A) Transmission electron microscopy (TEM) images of Ge NCs (4.0±1.7 nm) whose photoluminescence (PL) peak centers at 1160 nm (blue curve in Figure 1B). Inset shows high-resolution TEM image of a single Ge NC. The lattice spacing, measured by taking fast Fourier transform of the image, matches the (111) d-spacing of cubic Ge. (B) Normalized PL spectra (excited at 808 nm) of Ge NCs capped with octadecene (ODE) at room temperature. Green curve shows PL (not normalized) of Ge NCs (3.8±0.8 nm) capped with trioctylphosphine (TOP).

In bulk Ge, the maximum of the valence band lies at a different point in momentum space than the minimum of the conduction band in indirect-gap semiconductors, which makes interband transitions highly inefficient. As a result, indirect materials have very weak absorption at the band edge, and very long radiative lifetimes. The most well-known example of an indirect material is silicon (Si), and there is a report of CM in Si NCs [Beard et al. *Nano Lett.* **7**, 2506, 2007]. An indirect-gap material with a large but still unrealized potential in PV is Ge. Germanium's bulk band gap (~0.7eV) is narrower than that of silicon (1.1 eV), which provides more complete coverage of a solar spectrum, especially in the regime of CM. In addition, Ge NCs of appropriate size could have effective band gaps at the same energies as the more thoroughly studied PbSe and InAs NCs, allowing direct, isoenergetic comparison between Ge and these direct-gap systems.

However, as of last year, IR-emitting Ge NCs were unknown. Instead, numerous accounts of solution-based syntheses of Ge NCs reported emission at visible wavelengths, which showed questionable size dependence and could easily arise due to known emission from GeO_x species. Using an existing preparation of non-emissive Ge NCs as a starting point, we were able to synthesize 3-6 nm diameter Ge NCs (Figure 2) with size-tunable IR PL with quantum yields up to 8% (Lee et al, *J. Am. Chem. Soc.* **131**, 2009). TA and PL studies of these materials indicate that Ge NCs (Robel et al., *Phys. Rev. Lett.* 2009) may display partial confinement-induced pseudo-direct behavior in the same manner as Si NCs (Sykora et al., *Phys. Rev. Lett.* **100**, 2008).

Type-II IR-active PbSe/CdSe/CdS hetero-NCs.

Type-II heterostructured NCs have been the subject of an increasing number of reports, including from our project team, with a special focus on how the spatial separation of electrons and holes influences radiative and Auger recombination rates. In this work, we were particularly interested in studying a system based on the well-characterized PbSe NCs. This would allow us to specifically study how CM changes in a series of samples taken during heterostructure growth, as one of the carriers was increasingly drawn away from the original PbSe core. Truly heterostructured PbSe NCs were a relatively recent advance of our team (Pietryga et al, *JACS* **130**, 2008), and as such, there were no examples of PbSe type-II NCs.

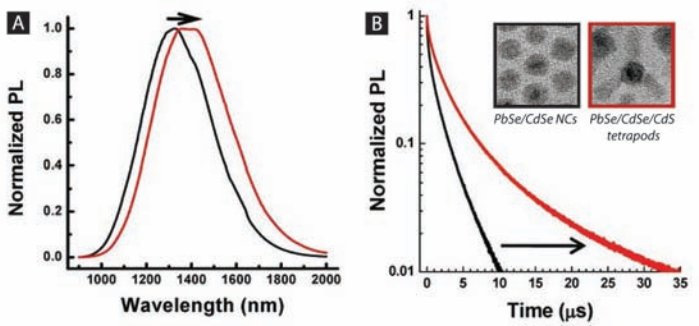

Figure 3. (A) The red shift of PL following overgrowth of PbSe/CdSe particles with CdS. (B) The PL lifetime gets longer following overcoating with CdS; this indicates a type-II behavior that is spatial separation of an electron and a hole. Inset: Growth of CdS at high temperature produces a core-shell geometry (left), while at high temperature the reaction with CdS precursors results in a tetrapod geometry (right).

In our work we focused on PbSe/CdSe/CdS heterostructures, in which excited holes would remain in the PbSe core while excited electrons would be increasingly drawn into the CdS shell as it grows thicker and thicker during synthesis (D. Lee et al., *J. Am. Chem. Soc.* **132**, 2010); Figure 3. The synthesis was carried out in a three-step process. First, PbSe NCs were synthesized and then PbSe/CdSe core/shell NCs, with a thick (>1.5 nm) shell of CdSe, were formed via the partial cation replacement method we recently published. Finally, we grew a shell of CdS using slow addition of precursors at a range of temperatures (150 - 250 °C). Higher temperatures resulted in the expected core/shell/shell NCs (inset of Figure

3B, left), with PL shifting to the red with growth as expected (Figure 3A), but with reduced quantum yields. Surprisingly, TEM revealed that these lower temperature NCs were not typical core/shell/shell, but rather tetrapods in which the CdS had grown as arms extending radially away from the central PbSe/CdSe core/shell (inset of Figure 3B, right). The exact cause of this difference in growth is still under investigation. Preliminary time-resolved studies, however, suggest that both the core/shell/shell and tetrapod systems may exhibit type-II behavior. Forming a CdSe shell on PbSe NCs generally increases the radiative lifetime (Figure 4B). This increase is similar to that observed in other type-II systems, as a result of a decline in electron and hole wavefunction overlap.

Investigation of dimensionality effects on CM

We have conducted studies of shape-controlled IR NCs. Such elongated materials exhibit different degrees of quantum-confinement in their radial and axial directions. Uncertainty regarding the mechanism of CM makes the impact of such anisotropic confinement unknown, which is the primary reason for our interest in such studies. Anisotropy could either increase CM efficiency due to reduction in the symmetry of the electronic states, or such effects could decrease CM efficiency due to re-emergence of translational momentum-related barriers to efficient CM. However, there is also a practical aspect to measurement of CM efficiencies in elongated NCs, which is related to devices. Elongated NCs offer an efficient means of carrier transport to electrodes in photovoltaics, whereas in spherical NCs a less efficient carrier hopping transport is necessary.

Specifically, we have made significant efforts to synthesize elongated PbSe NCs, which is non-trivial given the isotropic, rock-salt crystal structure. A report does exist regarding the successful gold-seeded synthesis of such materials, but despite several attempt we have been unable to reproduce it as stated. Elongated PbSe NCs were successfully synthesized using variations on the reported synthetic route that exhibit a band edge near 1650 nm based upon PL measurements. TEM measurements indicate an aspect ratio of ~1.8:1. Pump-power dependent TA experiments exciting with 1.55 eV photons indicate that some trapping does take place in these materials, however, we are able to observe Auger recombination in these materials with a biexciton lifetime of about 130 ps, which is notably slower than in spherical PbSe NCs that emit in the same energy range (~80 – 90 ps). Excitation with 3.1eV photons indicates that CM is observable in these materials and with an efficiency that is ~150%, which would represent *an increase* in efficiency relative to spherical NCs.

Fabrication and characterization of prototype devices

Semiconductor NCs are promising materials for applications in PV structures that could benefit from size-controlled tunability of absorption spectra, the ease of realization of various tandem architectures, and perhaps, increased conversion efficiency in the ultraviolet through CM. The first practical step toward utilization of the unique properties of NCs in PV technologies could be through their integration into traditional silicon-based solar cells. In this project, we have explored a concept of hybrid photovoltaics by fabricating and studying structures that combine colloidal NCs with amorphous silicon (a-Si) deposited via RF-magnetron sputtering (Sun et al., *Nano Lett*. **9**, 2009).

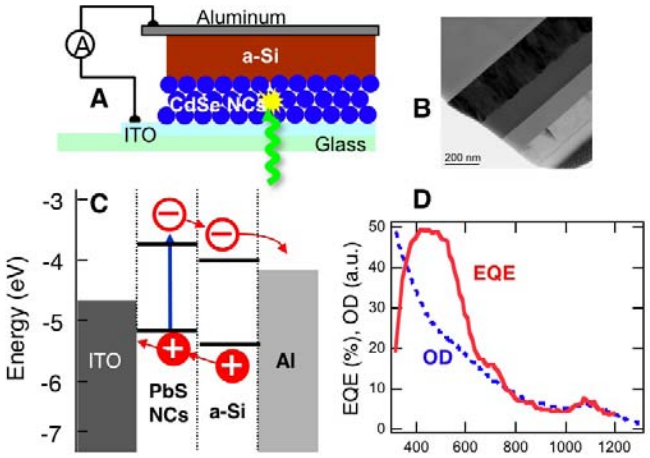

Figure 4. A hybrid a-Si/PbS NC structure. (A) Schematics of the device. (B) Cross-sectional TEM image of the device. (c) Alignment of electronic states at the a-Si/PS NC interface. (d) External quantum efficiency (EQE) and absorption (OD) spectra.

Schematics of a hybrid PV device comprising PbSe NCs along with a diagram of electronic states are displayed in Figure 4A-C. According to the alignment of conduction-band levels, the electrons that are photo-generated in PbS NCs can be transferred into a-Si and then collected at the Al electrode. Further, the positions of the valence-band states at the PbS NC/a-Si interface favor hole transfer from silicon into NCs followed by collection at the indium tin oxide (ITO) electrode. Thus, this structure is expected to show photocurrent due to both a-Si and NCs.

Indeed, the fabricated devices show the expected performance. In Figure 4D, we compare the spectrum of external quantum efficiency (EQE) of the hybrid PV structure with the NC absorption spectrum. The EQE at low energies (wavelength, λ, > 800 nm) mimics the spectral shape of NC absorption, indicating that in this spectral range, the photocurrent is primarily due to the NCs. For wavelengths shorter than ~800 nm, the EQE shows faster growth with decreasing λ than the NC absorption, which is a signature of a contribution from charges generated in the a-Si layer. Thus, as is expected based on the diagram in Figure 4C, this hybrid structure allows one to collect photo-generated carriers from both the NC and the a-Si material components.

The use of narrow-gap PbS NCs allows us to extend the device operational range into the IR region, and thus, efficiently harvest low-energy photons. For example, for the structure in Figure 4, the 1100 nm photons are converted

into electrical charges with EQE of ~7%. Further, these devices also show high quantum efficiencies in the visible (EQE up to ~50%), which is a result of both a steep increase in absorbtivity of the PbS NCs at shorter wavelengths and the increasing contribution from carriers generated in the a-Si layer.

The above results show the significant promise of hybrid a-Si/NC PVs. An encouraging practical aspect of this work is that magnetron sputtering, which is a common industrial fabrication technique, is apparently compatible with colloidal NCs, which could facilitate practical applications of these hybrid PV devices.

Impact on National Missions

This project directly supports DOE mission in Energy Security, specifically, in areas of alternative energy sources and energy efficiency. The proposed studies also address several critical research areas relevant to LANL challenges in "Carbon-Neutral Energy" and "Design, Synthesis and Properties of Photoactive Nanostructures." Several DOE reports have recognized that the solution to the global energy challenge "*will require scientific breakthroughs and truly revolutionary developments*" (*Basic Research Needs for Solar Energy Utilization*, Washington April 18-21, 2005). One such breakthrough, which can potentially result in revolutionary advances in the area of solar-energy conversion has been the discovery of CM in semiconductor nanocrystals. This process has the potential to considerably increase the performance of solar cells through increased photocurrent. Specifically, the detailed balance considerations indicate that CM can increase the power conversion efficiency of a single-junction solar cell up to 42%. To take full advantage of this phenomenon, the CM performance should approach the efficiency limit as defined by energy conservation. Fundamental insights gained from the studies conducted in this project should help researchers in the design of "ideal" CM structures operating at the energy-conservation-defined limit.

Publications

Durach, M., A. Rusina, V. I. Klimov, and M. I. Stockman. Nanoplasmonic renormalization and enhancement of Coulomb interactions. 2008. *New Journal of Physics.* **10**: 105011.

Glennon, J. J., R. Tang, W. E. Buhro, R. A. Loomis, D. A. Bussian, H. Htoon, and V. I. Klimov. Exciton localization and migration in single CdSe quantum wires at low temperatures. 2009. *Physical Review B.* **80** (8): 081303.

Joo, J., J. M. Pietryga, J. A. McGuire, S. H. Jeon, D. J. Williams, H. L. Wang, and V. I. Klimov. A reduction pathway in the synthesis of PbSe nanocrystal quantum dots. 2009. *Journal of American Chemical Socienty.* **131** (30): 10620.

Klimov, V. I., J. A. McGuire, R. D. Schaller, and V. I. Rupasov. Scaling of multiexciton lifetimes in semiconductor nanocrystals. 2008. *Physical Review B.* **77** (19): 195324.

Lee, D. C., I. Robel, J. M. Pietryga, and V. I. Klimov. Infrared-active heterostructured nanocrystals with ultralong carrier lifetimes. 2010. *Journal of American Chemical Society.* **132**: 9960.

Lee, D. C., J. M. Pietryga, I. Robel, D. J. Werder, and R. D. Schaller. Colloidal synthesis of infrared-emitting germanium nanocrystals. 2009. *Journal of American Chemical Society.* **131**: 3436.

McGuire, J. A., J. Joo, J. M. Pietryga, R. D. Schaller, and V. I. Klimov. New aspects of carrier multiplication in semiconductor nanocrystals. 2008. *Accounts of Chemical Research.* **41**: 1810.

McGuire, J. A., M. Sykora, I. Robel, L. . Padilha, J. Joo, J. M. Pietryga, and V. I. Klimov. Spectroscopic signatures of photocharging due to hot carrier transfer in solutions of semiconductor nanocrystals under low-Intensity ultraviolet excitation . To appear in *ACS Nano.*

McGuire, J., M. Sykora, J. Joo, J. M. Pietryga, and V. I. Klimov. Apparent versus true carrier multiplication yields in semiconductor nanocrystals. 2010. *Nano Letters.* **10**: 2049.

Pietryga, J. M., D. J. Werder, D. J. Williams, J. L. Casson, R. D. Schaller, V. I. Klimov, and J. A. Hollingsworth. Utilizing the lability of lead selenide to produce heterostructured nanocrystals with bright, stable infrared emission. 2008. *Journal of American Chemical Society.* **130** (14): 4879.

Pietryga, J. M., K. K. Zhuravlev, M. Whitehead, V. I. Klimov, and R. D. Schaller. Evidence for barrierless Auger recombination in PbSe nanocrystals: A pressure- dependent study of transient optical absorption. 2008. *Physical Review Letters.* **101**: 217401.

Piryatinski, A., and K. A. Velizhanin. An exciton scattering model for carrier multiplication in semiconductor nanocrystals: Theory. 2010. *Journal of Chemical Physics.* **133**: 084508.

Robel, I., R. Gresback, U. Kortshagen, R. D. Schaller, and V. I. Klimov. Universal size-dependent trends in Auger recombination in direct- and indirect-gap semiconductor nanocrystals. 2009. *Physical Review Letters.* **102**: 177404.

Schaller, R. D., S. A. Crooker, D. A. Bussian, J. M. Pietryga, J. Joo, and V. I. Klimov. Revealing the exciton fine structure in PbSe nanocrystal quantum dots. 2010. *Physical Review Letters.* **105**: 067403.

Sun, B. Q., A. T. Findikoglu, M. Sykora, D. J. Werder, and V. I. Klimov. Hybrid photovoltaics based on semiconductor

nanocrystals and amorphous silicon. 2009. *Nano Letters.* **9**: 1235.

Sykora, M., L. Mangolini, R. D. Schaller, U. Kortshagen, D. Jurbergs, and V. I. Klimov. Size-dependent intrinsic radiative decay rates of silicon nanocrystals at large confinement energies. 2008. *Physical Review Letters.* **100** (6): 067401.

Probing Physics Beyond the Standard Model through Neutron Beta Decay

Alexander Saunders
20080116DR

Abstract

This project explored Physics Beyond the Standard Model by using neutron beta decay in three ways, each at the cutting edge of the field. First, it used ultra-cold neutrons, neutrons that have such low temperature that they can be stored for hundreds of seconds in material bottles, to measure the lifetime of the neutron. This lifetime, with a value of about 15 minutes, is only known to about one second. Unfortunately, existing experiments disagree at the six second level. The present work was unique in using a gravito-magnetic trap to store the ultra-cold neutrons while they decay, thus eliminating the leading uncertainties in previous work. Second, this project established the technology that will be used for the next generation of neutron beta decay correlation experiments, which will measure the correlations between the outgoing particles from neutron decay and the original polarization of the neutron. Finally, we advanced the theory of neutron beta decay in two ways: first, by linking low energy neutron experiments to high energy kaon decay experiments that follow similar decay processes, and second, by exploring the impacts that different values of the decay correlations and neutron lifetime can have on the new physics emerging beyond the standard model.

Background and Research Objectives

The Standard Model (SM) of nuclear and particle physics describes the fundamental constituents of Nature and their interaction down to distances d >10^{-16} cm, corresponding to an energy scale of ~250 GeV. A number of observations (such as dark matter, the excess of matter over antimatter, neutrino masses) strongly suggest the existence of new degrees of freedom and interactions at distances d < 10^{-16} cm, corresponding to energies greater than 250 GeV. Unveiling this next layer of reality is one of the main goals of the international nuclear and particle physics community for the next few decades and is well captured by the LANL Grand Challenge in science entitled "Beyond the Standard Model to Understand the Universe – Stellar Formation, Cosmology, Dark Energy, Dark Matter" [1]. In this endeavor, two complementary approaches are possible: short-distance degrees of freedom can be directly excited at high energy collider experiments, or they can be detected through their quantum mechanical virtual contributions to low energy observables. This second option makes high-sensitivity low-energy probes, such as neutron decay, an attractive ground for searches of physics beyond the SM.

The CKM quark mixing matrix: within the SM, the three-generation quark flavor mixing due to the misalignment of weak and mass eigenstates is described by the unitary Cabibbo-Kobayashi-Maskawa (CKM) matrix:

$$V_{CKM} = \begin{pmatrix} V_{ud} & V_{us} & V_{ub} \\ V_{cd} & V_{cs} & V_{cb} \\ V_{td} & V_{ts} & V_{tb} \end{pmatrix}$$

Each element of the matrix describes the mixing between a given pair of quark flavors: V_{ud}, for example, describes the mixing between the up and down quarks. If the CKM matrix elements determined from various experiments assuming the standard model did not satisfy a mathematical condition called unitarity, it would be conclusive evidence of physics beyond the standard model; one possible explanation of non-unitarity would be the existence of a fourth generation of heavy quarks. To the degree that the matrix can be confirmed to be unitary, it would set limits on the possible models of new physics.

The most stringent unitarity test is given by studying the elements of the first row of the CKM matrix, namely the deviation of $\Delta = (|V_{ud}|^2 + |V_{us}|^2 + |V_{ub}|^2 - 1)$ from zero. V_{ub} is small relative to V_{ud} and thus its contribution to the unitarity sum when added in quadrature is below the uncertainty due to V_{us} and V_{ud}. V_{us} is determined using high energy kaon decay experiments; its error is currently dominated by the uncertainty in the theoretical calculations required for extracting the value of V_{us} from

the measurements; one of the goals of this project was to reduce this uncertainty through a calculation of the K → π matrix element based on new techniques never applied before. The world's understanding of V_{ud} and V_{us} at the outset of the project is displayed in Figure 1.

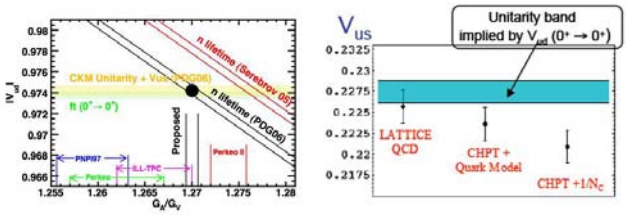

Figure 1. Left side: Measurement of the neutron lifetime (diagonal band) along with neutron decay correlation coefficients (horizontal axis) is necessary to extract the value of Vud (vertical axis), and hence test the unitarity of the CKM matrix. Depending on which experiments and calculations are compared, the value of Vud may deviate from unitarity by up to three standard deviations. Right side: Vus versus different theoretical input on the K to Pi decay matrix element (labeled in red), with the unitarity band obtained by using Vud from nuclear beta decay. The results of the three calculations differ by up to 2%, despite having individual 1% uncertainties.

The largest element, V_{ud}, can be measured using the decay of the free neutron. Although no single measurement of neutron beta decay allows the direct extraction of V_{ud} , the simultaneous measurement of two parameters in neutron decay, such as the *A* parameter (the correlation between the decaying neutron's spin and the momentum of the emerging beta particle) and the neutron lifetime allow the extraction of the value of V_{ud}. The *A* parameter is already being measured at high precision by an ongoing LANL experiment, called UCNA, which has recently begun releasing its results[2][3]. The value of the neutron lifetime is in doubt, because a newly released experiment [4] disagrees with the accepted value [5] at the six-sigma uncertainty level. Thus, although the claimed uncertainty from the individual experiments is about one second, the effective uncertainty is approximately six seconds. What remains is to measure the neutron lifetime at the highest possible precision and proceed to development of experiments to measure the rest of the neutron decay parameters.

Motivated by the above considerations, we conducted a three-part project to probe CKM unitarity and new physics scenarios via neutron decay:

- We completed the design and construction of a new experiment to measure the neutron lifetime, described below. It uses a new approach to measure the neutron lifetime with independent and smaller systematic uncertainties from previous experiments. Its initial uncertainties will be small enough to resolve the six sigma discrepancy between the recent neutron lifetime measurement and the accepted value.
- We developed the underlying technology for the next generation of neutron decay correlation experiments, in order to improve the accuracy of our determination of CKM unitarity to a level beyond the reach of any existing set of experiments. The existing UCNA experiment measures the correlation between the neutron beta particle momentum and the spin of the neutron; the next generation will also detect the decay protons and precisely measure the energy of the beta particles, using new detectors. This will allow elimination of the leading systematic uncertainties in the present generation of experiments.
- Our nuclear theory effort reduced the theoretical uncertainty on $\Delta = (|V_{ud}|^2 + |V_{us}|^2 + |V_{ub}|^2 - 1)$ below the 0.001 level and investigated the significance of CKM unitarity constraints or violation ($\Delta \neq 0$) on new physics scenarios at the TeV scale.

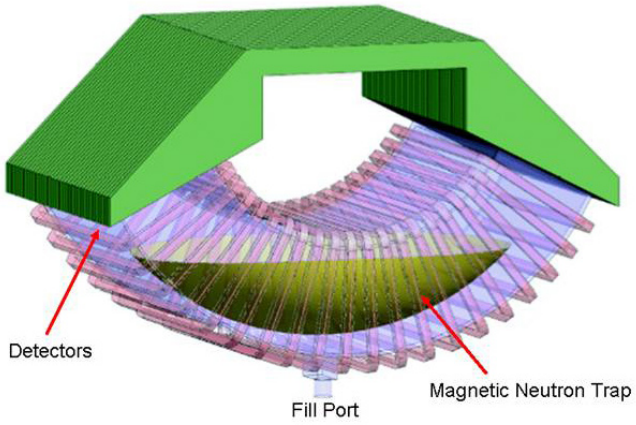

Figure 2. The apparatus for the UCN neutron lifetime experiment. Neutrons are filled into the magnetic trap from the bottom trap door. Their decay products are detected using wire chambers at each end of the experiment, while the neutrons themselves can be directly detected by flooding the trap with wire chamber gas.

Scientific Approach and Accomplishments

The first goal of the project was developing and building a prototype experiment that can measure the neutron lifetime. The ultimate goal of the full experiment is to measure the neutron lifetime to a precision better than any previous experiment (<1 s), and with entirely unique systematic uncertainties. The goal of this part of the LDRD project was to design and build a prototype that can make a measurement of the neutron lifetime to about the 10 second level or better. The experiment is based on storing ultra-cold neutrons (UCN) in a gravito-magnetic trap[6]; that is, a trap which is closed on the bottom and sides by an array of permanent magnets and on the top by gravity. Since UCNs can rise only about one meter before falling back in the Earth's gravity, the trap is about one meter high

by one meter wide by two meters long. The layout of the experiment is shown in Figure 2.

Construction of the experiment continued throughout the project, and was completed just as the project ended. Assembly and testing of the magnetic trap took place at an offsite contractor, while the construction and assembly of all the support structures and vacuum hardware was completed at Los Alamos. While construction continued on the trap hardware, we pursued our studies of the dominant systematic uncertainties of this experiment, which are the presence of long-lived quasi-bound neutron states in the trap and the variability of the efficiency of detecting the neutrons as a function of time. Either of these effects can lead to substantial systematic uncertainty in the measured lifetime of the neutron. We developed novel solutions to these problems, by controlling the orbits of neutrons in the trap and by developing monitor detectors that have no time dependence in their efficiency.

Both of the neutron counting methods initially proposed for the experiment, counting neutrons emptied from the trap to an external detector and counting decay beta particles from neutron decay transported in a toroidal guide field, suffer from having a strong dependence on the phase space distribution of the neutrons in the trap, which in principle can vary strongly as function of time. The former of these methods would suffer from long unloading times and would be susceptible to phase-space-dependent unloading times. Detecting decay beta particles would introduce phase space dependent efficiencies (decays near the trap wall would be detected less efficiently than decays from the center of the volume because a higher fraction of the electron orbits near the wall could intercept the magnet).

A solution to these problems for the lifetime experiment was to turn the trap into the neutron detector by mounting electrodes on the magnet surface and introducing counter gas into the system to count surviving neutrons. A gas mixture with small elastic cross sections to allow ~10 s counting time and large cross sections for producing charge particles was required for this solution to work. The short counting time and unbiased counting throughout the trap volume eliminate the problems introduced by a mix of chaotic and quasi-periodic orbits. A mixture of $^{10}BF_3$ and argon gases was investigated as a possible medium for detecting the neutron directly. An initial test was conducted detecting neutrons in a sample cell using a mixture of ^3He and argon gases.

In pursuit of the second goal of the project, to develop the next generation of neutron beta decay experiments, we have continued exploring improved measurements of neutron decay correlations using UCNs and the silicon detectors being developed in this project. The most promising appear to be the parameters b and B. b is the Fierz interference term in the neutron decay that distorts the shape of the electron spectrum, if scalar or tensor interactions due to physics beyond the Standard Model interfere with the vector or axial vector interactions in the Standard Model. B is the correlation between the neutron spin and the momentum of the anti-neutrino. There is recent interest in precision measurement of B as it has been shown to be sensitive to certain classes of supersymmetric extensions to the Standard Model [7].

B could be measured by adapting the existing UCNA decay magnet to electrostatically accelerate the decay protons to about 20 keV and replacing the existing detectors with silicon detectors. The silicon detectors allow detection of the (accelerated) protons in coincidence with the electrons. This allows determination of the proton asymmetry as a function of electron energy, as required to extract B. We estimate that a statistical uncertainty of approximately 10^-4 can be obtained. This is sufficient to put new limits on the supersymmetric models described above. We have published a paper outlining the concept of a UCN measurement of B [8]. The silicon detectors and the associated hardware were tested offline and are now ready for an integrated test in the existing UCNA magnet using UCNs from the LANL facility.

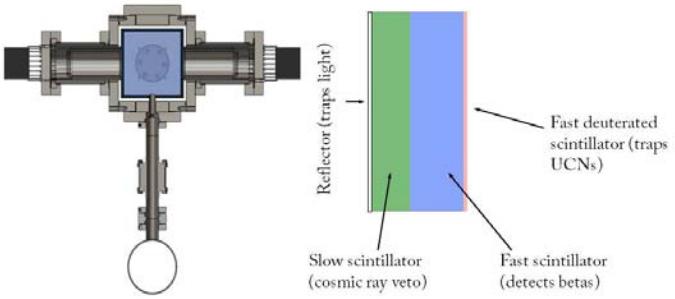

Figure 3. The "b" calorimeter traps the UCNs and detects all the light generated in the scintillator walls by any decay beta particles, while simultaneously vetoing cosmic ray backgrounds. The calorimeter is built from a multilayer scintillator that allows the differentiation between decay electrons and background.

UCNb is a precision measurement of the energy spectrum of the decay electron to detect a shift with respect to the Standard Model prediction at the 10^{-3} level. To make a measurement of this type the detector must have a very low background rate and energy resolution sufficient to resolve the spectral features. The UCNb detector is a box, constructed from scintillating plastic, that is filled with UCN through a small hole as shown in Figure 3. The outside of the box is covered by a high efficiency diffuse reflector. The box acts much like an integrating sphere for light intensity measurements. Light produced by electrons stopping in the scintillator is contained in the box until it reaches a photocathode surface. The inner layer of the box is constructed from a material with a sufficiently high Fermi potential to trap the UCN. An outer layer of scintillator, with

a different scintillation decay time constant, is used as a cosmic ray veto. An initial prototype of the detector box has been assembled and tested offline.

Finally, we have completed our theoretical investigations of the consequences of the next generation of neutron beta decay experiments. The theory effort in this LDRD-DR project had two main goals, aimed to assess the impact and significance of the proposed experimental effort. During the last years of the project, the theory effort has focused on studying the implication of precise determinations of V_{ud} and V_{us} on extensions of the Standard Model (SM) at the TeV scale.

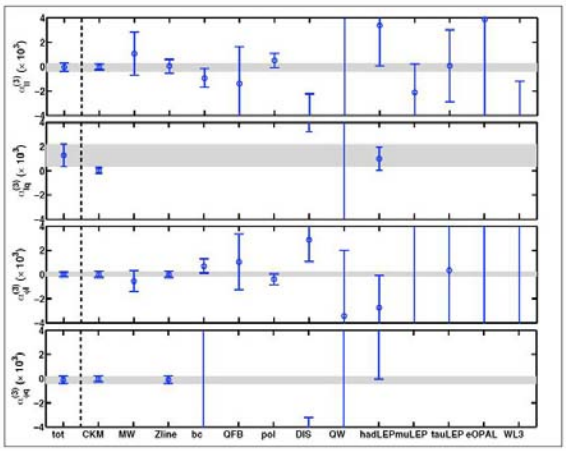

Figure 4. The 90% C.L. allowed regions for the coefficients αn = v2/Λ2 (v=176 GeV) of the four effective operators that induce violations of Cabibbo universality. The first column displays the constraint from all precision observables except Δ .The second column displays the constraint coming exclusively from Δ. The remaining columns display the constraint derived from various subsets of precision measurements (both at high and low-energy). The Δ constraint implies an effective scale of new physics Λ> 11 TeV (90% CL).

We have investigated in a model-independent framework the impact of quark-lepton universality (CKM unitarity) tests on physics beyond the Standard Model. In terms of new physics corrections at the TeV scale, we have derived the low-energy effective Lagrangians describing muon decay and beta decays. We have performed the phenomenological analysis assuming nearly flavor-blind new physics interactions, under the well motivated assumption that flavor breaking at the TeV scale is suppressed by a symmetry principle or by the hierarchy Λ_{flavor} >> TeV. We have shown that, in this limit, the extraction of V_{ud} and V_{us} from any decay mode should give the same result and the only significant probe of physics beyond the SM involves the quantity $\Delta = (|V_{ud}|^2 + |V_{us}|^2 + |V_{ub}|^2 - 1)$. We have shown that Δ receives contributions from four short distance operators, two of which correspond to corrections to the W-fermion-antifermion vertex, the other two parameterizing four-fermion contact interactions. This result applies to any weakly coupled extension of the Standard Model, thus allowing us to study the interplay of Δ with other precision measurements in a model-independent way. The main conclusions of our analysis [9] are:

1. The current phenomenological constraint $\Delta = (-1\pm6)\times10^{-4}$ bounds the scale of all four effective operators contributing to quark-lepton universality violation to be Λ >11 TeV (90 \% C.L.) (Figure 4). For the four-fermion operator $O_{lq}^{(3)}$ involving two left-handed quark doublet and two left-handed lepton doublets, the Δ constraint improves existing bounds from LEP2 cross-section measurements by one order of magnitude.

2. Another way to state this result is as follows: should the central values of V_{ud} and V_{us} move from the current values, precision electroweak data would leave room for sizable deviations from quark-lepton universality (roughly one order of magnitude above the current direct constraint). Essentially only the four-fermion operator $O_{lq}^{(3)}$ could be responsible for $\Delta \neq 0$, as the others are tightly bound from Z-pole observables.

Our conclusions imply that the study of semileptonic processes and Cabibbo universality tests provide constraints on new physics beyond the SM that currently cannot be obtained from other electroweak precision tests and collider measurements.

Impact on National Missions

This project supported the DOE mission in Nuclear Physics by enhancing our understanding of physics beyond the standard model. This project provided measurements of neutron decay properties, a main goal of the DOE Nuclear Physics Long Range Plan. Fundamental nuclear science underlies the weapons program and nuclear threat reduction, both major centers of effort for Los Alamos Lab, the DOE, and the nation.

References

1. Los Alamos Science in the 21st Century. 2006. *Los Alamos National Lab Grand Challenge Report.*

2. Pattie, R. W., J. Anaya, H. O. Back, J. G. Boissevain, T. J. Bowles, L. J. Broussard, R. Carr, D. J. Clark, S. Currie, S. Du, B. W. Filippone, P. Geltenbort, A. Garcia, A. Hawari, K. P. Hickerson, R. Hill, M. Hino, S. A. Hoedl, G. E. Hogan, A. T. Holley, T. M. Ito, T. Kawai, K. Kirch, S. Kitagaki, S. K. Lamoreaux, C. -Y. Liu, J. Liu, M. Makela, R. R. Mammei, J. W. Martin, D. Melconian, N. Meier, M. P. Mendenhall, C. L. Morris, R. Mortensen, A. Pichlmaier, M. L. Pitt, B. Plaster, J. C. Ramsey, R. Rios, K. Sabourov, A. L. Sallaska, A. Saunders, R. Schmid, S. Seestrom, C. Servicky, S. K. Sjue, D. Smith, W. E. Sondheim, E. Tatar, W. Teasdale, C. Terai, B. Tipton, M. Utsuro, R. B. Vogelaar, B. W. Wehring, Y. P. Xu, A. R. Young, and J. Yuan. First measurement of the neutron β asymmetry with ultracold neutrons. 2009. *Physical Review Letters.*

102 (1): 012301 (4 pp.).

3. Liu, J., M. P. Mendenhall, A. T. Holley, H. O. Back, T. J. Bowles, L. J. Broussard, R. Carr, S. Clayton, S. Currie, B. W. Filippone, A. Garcia, P. Geltenbort, K. P. Hickerson, J. Hoagland, G. E. Hogan, B. Hona, T. M. Ito, C. Y. Liu, M. Makela, R. R. Mammei, J. W. Martin, D. Melconian, C. L. Morris, R. W. Pattie Jr., A. Perez Galvan, M. L. Pitt, B. Plaster, J. C. Ramsey, R. Rios, R. Russell, A. Saunders, S. J. Seestrom, W. E. Sondheim, E. Tatar, R. B. Vogelaar, B. VornDick, C. Wrede, H. Yan, and A. R. Young. Determination of the axial-vector weak coupling constant with ultracold neutrons. *Physical Review Letters.*

4. Serebrov, A. P.. Neutron lifetime measurements using gravitationally trapped ultracold neutrons. 2005. *Physics-Uspekhi.* **48** (8): 867.

5. Review of particle physics. 2006. *Journal of Physics G: Nuclear and Particle Physics.* **33**: 1.

6. Walstrom, P. L., J. D. Bowman, S. I. Penttila, C. Morris, and A. Saunders. A magneto-gravitational trap for absolute measurement of the ultra-cold neutron lifetime. 2009. *NUCLEAR INSTRUMENTS & METHODS IN PHYSICS RESEARCH SECTION A-ACCELERATORS SPECTROMETERS DETECTORS AND ASSOCIATED EQUIPMENT.* **599** (1): 82.

7. Profumo, S., M. J. Ramsey-Musolf, and S. Tulin. Supersymmetric contributions to weak decay correlation coefficients. 2007. *Physical Review D.* **75** (7): 75017.

8. Wilburn, W. S., V. Cirigliano, A. Klein, M. F. Makela, P. L. McGaughey, C. L. Morris, J. Ramsey, A. Salas-Bacci, A. Saunders, L. J. Broussard, and A. R. Young. Measurement of the neutrino-spin correlation parameter B in neutron decay using ultracold neutrons. 2009. *Revista Mexicana de Física.* **55** (2): 119.

9. Cirigliano, V., J. Jenkins, and M. Gonzalez-Alonso. Semileptonic decays of light quarks beyond the Standard Model. 2010. *NUCLEAR PHYSICS B.* **830** (1-2): 95.

Publications

Cirigliano, V.. Precision tests of the Standard Model with leptonic and semileptonic kaon decays. 2008. *The FlaviaNet Working Group on Kaon Decays.*

Cirigliano, V., C. Lee, M. J. Ramsey-Musolf, and S. Tulin. Flavored quantum Boltzmann equations. 2010. *Physical Review D.* **81** (10): 103503 (25 pp.).

Cirigliano, V., J. Jenkins, and M. Gonzalez-Alonso. Semileptonic decays of light quarks beyond the Standard Model. 2010. *NUCLEAR PHYSICS B.* **830** (1-2): 95.

Cirigliano, V., M. Giannotti, and H. Neufeld. Electromagnetic effects in Kl3 decays. 2008. *Journal of High Energy Physics.* **11**: 6.

Cirigliano, V., Y. Li, S. Profumo, and M. J. Ramsey-Musolf. MSSM baryogenesis and electric dipole moments: an update on the phenomenology. 2010. *JOURNAL OF HIGH ENERGY PHYSICS.* (1): 002.

Walstrom, P. L., J. D Bowman, S. I. Penttila, C. Morris, and A. Saunders. A magneto-gravitational trap for absolute measurement of the ultra-cold neutron lifetime . 2009. *Nuclear Instruments and Methods in Physics Research, Section A.* **599** (1): 82.

Wilburn, W. S., V. Cirigliano, A. Klein, M. F. Makela, P. L. McGaughey, C. L. Morris, J. Ramsey, A. Salas-Bacci, A. Saunders, L. J. Broussard, and A. R. Young. Measurement of the neutrino-spin correlation parameter B in neutron decay using ultracold neutrons. 2009. *Revista Mexicana de Física.* **55** (2): 119.

Cosmic Explosions Probing the Extreme: X-Ray Bursts, Superbursts, and Giant Flares on Neutron Stars

Sanjay Reddy
20080130DR

Abstract

Cosmic explosions range from x-ray bursts and superbursts, to giant flares that occur on neutron stars, to supernova explosions that mark the end of the life of regular stars. Differing in detail, they are all complex phenomena in which radiation hydrodynamics, nuclear, plasma, and neutrino physics all play role. Our project combined theoretical and computational efforts to develop the tools needed to simulate these explosive phenomena and predict their observable aspects. Our calculations focused on the microphysical aspects relating to the equation of state, thermal and electrical conductivities, nuclear reactions and photon opacities, and the macroscopic modeling of transport and hydrodynamics.

Background and Research Objectives

Neutron stars are quite literally at the center of a variety of explosive phenomena in the cosmos, including x-ray bursts, superbursts, giant flares, and supernova explosions. X-ray bursts are the most common thermonuclear explosions in space, occurring on the surface of an accreting neutron star. As hydrogen and helium from the companion star accumulates on the surface, nuclear explosions become possible thanks to the large surface gravity (a few times 10^{12} m/s^2) and high surface temperature (10^6 K). The possibility and nature of the explosions depends on the rate of accretion of material and the local ambient conditions. These explosions are observed as type I x-ray bursts [1]. Since their discovery in 1976 by Grindlay et al. and Belian, Conner and Evans, about 100 type I x-ray burst sources have been identified. The burst itself lasts between 10-100 seconds; their recurrence frequency ranges from one every few hours to one every few days. This recurrent behavior on the same source makes a useful tool to study neutron star properties and nuclear burning under extreme conditions [2]. More recently in (Cornelisse et al., 2000) discovered long-duration bursts called superbursts, which last 1000 times longer and recur only every several years. These bursts are also believed to arise from unstable thermonuclear burning, *i.e.* the ignition of carbon deeper inside the neutron star [3]. In addition to these thermonuclear phenomena, highly magnetized neutron stars called magnetars host very powerful magnetic explosions called giant flares. These very rare phenomena (only a few observed to date) are expected to originate in the deeper regions of the neutron star crust where large magnetic fields reorganize catastrophically, triggering flares which not only release about 10^{46} ergs on a time scale of a few seconds, but also excite oscillations deep inside the neutron star [4].

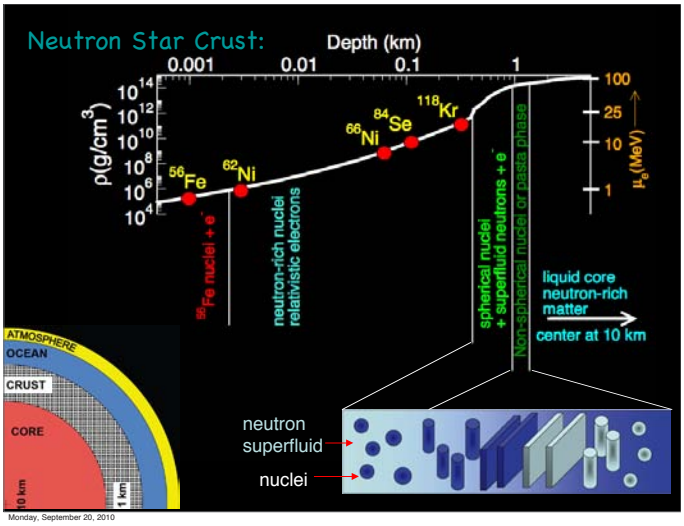

Figure 1. The figure illustrates the internal structure of the neutron star crust. The density profile, the composition, and the increasing pressure and electron Fermi energy are shown.

Theoretical attempts to understand these varied phenomena in neutron stars have identified the physical processes that are most important in the outer 1-2 kms of the neutron stars. Nuclear reactions, thermal and electrical conductivity, and neutrino cooling processes all play a role in determining the energetics, duration and recurrence times of explosions occurring on neutron stars. The outer 1-2 kms of the neutron star contains a strongly coupled plasma of fully ionized nuclei in a liquid state at shallow depths, called the ocean, and a solid state at greater depths, called the crust. The structure of neutron stars is illustrated in Figure 1, where the key physical attributes and the variation of density and com-

position with depth are shown. One of the research objectives of this project was to combine theoretical efforts in nuclear physics, plasma physics and condensed matter physics to provide a microscopic framework for the outer 2 kms of the neutron stars. A second related objective was to improve macroscopic models of these explosive phenomena, especially x-ray bursts, and study how the ambient conditions determined by physics of layers deeper inside affected the observable bursts.

To build a realistic model for accreting neutron stars, it is necessary to follow the sequence of nuclear reactions that transform the hydrogen and helium nuclei. At the surface, nuclear burning quickly builds up a variety of proton-rich nuclei through a process called the rapid proton (rp) capture process. As additional material from companion arrives onto the surface, the heavy proton-rich nuclei get buried ever more deeply. With increasing pressure and electron energy, electron-capture transforms the proton-rich mix into a neutron-rich mix. Eventually the nuclei get dense enough to fuse even at low temperature, releasing energy deep in the crust. The change in composition with depth is a key factor determining the crustal properties

Another major effort in this project was focused on studying the photon emission from cosmic explosions. A number of astrophysical surveys, both ground-based: e.g ESSENCE, Pan-STARRS, Palomar Transient Factory, and satellite: Swift, are dramatically increasing the number of observed cosmic explosions. These observations have discovered a wide range of "abnormal" supernovae that place strong tests on our understanding of normal supernovae. Indeed, these observations have seriously shaken our understanding of type Ia supernovae.

Our goal in modeling emission from cosmic explosions was to develop the tools necessary to model both these exotic explosions as well as more normal supernovae. Most cosmic explosions are extremely energetic and hot. One might naively think that the light we see from these explosions arises from the initial energy of the explosion. When the exploding shock first breaks out of the star, this is true. Swift has now observed explosions of this "shock breakout". But as the explosion expands into the universe, it cools. Without a sustaining source of energy, cosmic explosions would be quite dim. Two sources of sustaining energy are typical: the decay of radioactive elements such as ^{56}Ni, and shock heating. Our codes are ideally suited for modeling shock heating, so we concentrated on the systems where this heating dominates. Our study required understanding the environments surrounding the supernova explosion, which is set up by their progenitor stars.

Scientific Approach and Accomplishments

Several efforts were combined to build a realistic model of the neutron star crust, especially for the case of accreting neutron stars. These efforts and their main findings are discussed briefly below. They have important implications for the ambient conditions necessary for explosive burning both at the surface (x-ray bursts) and in the ocean (superbursts), and the magnetic field evolution in highly magnetized neutron stars.

1. **New nuclear reactions** that play a role as nuclei are subject to increasing density were discovered and reported in Ref. [5]. These showed that the heat released by these reactions was fairly independent of initial composition, suggesting that all accreting neutron stars have similar deep crustal heating profiles.

2. **A new mechanism for heat conduction** was discovered as a result of our attempts to provide a microscopic description of the neutron superfluid in the crust. We developed a theory that described the coupled fluctuations of the lattice of nuclei, the phase of the superfluid, and the electron density. Our theory predicted that fluctuations of the superfluid, called superfluid phonons, could effectively store and transport heat. This new mode was more effective than electrons at conducting heat at the highest temperatures and magnetic fields [6].

3. **Electron conduction in an impure crust** was shown to be significantly lower than predicted by simple formulae that assumed that impurities were randomly distributed in a background crystal. Using large-scale molecular dynamic studies, where the motion of each ion is explicitly simulated with high performance computing tools, we obtained a new understanding of the transport properties of complex mixtures [7].

4. **A robust superfluid** is formed when neutrons in the crust combine in pairs to form a quasi-bound state called a Cooper pair. Using sophisticated algorithms to simulate quantum system, with an approach called Quantum Monte Carlo, we showed that the binding energy of the pair (also called the superfluid gap) was significantly larger than earlier expectations [8]. This implies superfluid behavior would persist to higher temperature, thus affecting bursting and magnetized neutron stars.

5. **Strong crusts** are harder to break and will release more energy if broken. Giant flares, the very high energy explosions observed in magnetized neutron stars, may indeed require very strong crusts. The strength of the crust, characterized by the strain required to break it, was not known until a collaboration between Kadau (LANL) and Horowitz(IU, Bloomington) led to large-scale computer simulations using LANL computers and programs. We demonstrated that neutron star crusts are indeed very strong [9].

6. The **first numerical simulation of superbursts** and multiple x-ray bursts were performed by Alexander Heger, and showed that they were sensitive to the heat flux from the deeper layers. Our model integrates our new

insight (reported above) into nuclear reactions, thermal properties ,and conduction to predict the diverse behavior of neutron stars at different accretion rates. This work will be submitted to the Astrophysical Journal shortly.

7. **Thermal relaxation of the crust** after prolonged bouts of accretion has been observed in some systems. Such behavior depends on the same properties of the neutron star crust that also play a role in explosive phenomena. With external collaborator Page (UNAM, Mexico) we have incorporated our physics models for the crust reactions and thermal properties to simulate this relaxation and its dependence on the accretion history. This work shows that a wide range of behavior can be expected depending on the rate and time over which material was accreted. The results of this work should be published soon.

   Our efforts to study the photon emission from supernova concentrated on systems where shock heating was important. For this reason we had to study both the progenitors of these explosion and the explosion mechanism itself. In what follows we describe the main results of this study and its relevance to supernova light-curves.

8. **Our study of diverse type Ia progenitors** argues strongly that there must be more than one type Ia progenitor [10] . Although the thermonuclear supernova community has focused on "Chandrasekhar-mass" progenitors (so-termed because the white dwarf progenitor slowly accretes until it reaches the Chandrasekhar mass), other astrophysicists have long argued that such progenitors simply don't occur in nature. Thanks in part through our efforts, the supernova community is moving toward different progenitors. We have done detailed studies of the emission from one possible progenitor, the merger of two white dwarfs. We have found that such progenitors do not easily match the standard supernova light-curve (Fryer et al., submitted to ApJ). This has made lightweight (sub-Chandrasekhar) models more appealing, and we will focus follow-up studies on these new progenitors (Ruiter et al., submitted to ApJ).

9. **Link between progenitors and explosion mechanisms** was explored in our work on explosions from stellar collapse. We studied both gamma-ray burst and supernova progenitors [11-12]. Our engine studies included a wide range of effects, including the effect of material falling back onto the neutron star after the launch of an explosion [13]. Here again, we focused on exotic objects, with view to using the exotic to better understand normal supernovae [14]. Our studies included photons over a range of wavelengths, including the most high-energy photons produced in supernova remnants [15-16].

10. **Pair-instability supernovae** may occur in very massive early stars. Our work has developed the tools to simulate these explosions and their light curves. This effort is important for a number of satellite missions, including the James Webb Space Telescope and smaller missions such as the Joint Astrophysics Nascent Universe Satellite. We have developed collaborations with both of these missions.

Our efforts equipped LANL with the capability to model a wide range of diagnostics from supernovae. These projects include shock breakout calculations for the Swift satellite, transient calculations for many ground-based surveys, including the upcoming Large Synoptic Survey telescope (recently ranked at the top of future ground-based missions under the Astrophysics decadal survey), and the WFIRST satellite (ranked at the top of future space-based missions in this same survey). We have developed strong collaborations with both of these missions. Our work on explosions, nucleosynthesis, and gamma-ray emission (needed for our emission calculations) led to us being added to the scientific team for the NuSTAR satellite (a funded NASA mission to be launched in Feb. 2012). We are helping finalize observing plans for this mission, which demonstrates the importance of theoretical studies for NASA missions. A major goal of project was to tie LANL theory to a number of NASA missions, making possible a large ($1 million) NASA center here at LANL.

Our work on supernova light-curves allowed us to test new transport algorithms using the Roadrunner machine. New algorithms are important for the health of the ASC program. Coupled to the success of the topical collaboration, this work allowed us to demonstrate the value of the astrophysical postdoctoral initiative at LANL. This program to hire computational physicists is scheduled to hire 3-4 post-docs every year, supported by the stockpile stewardship program. The first 5 post-docs have already accepted offers. Most are funded through weapons program projects within XTD and XCP divisions. This program will bring in scientists that can both pursue cutting-edge astrophysics and contribute to laboratory programs.

Impact on National Missions

The development of a coordinated effort that combines state of the art methods in nuclear, particle, plasma and condensed matter physics to address key problems in astrophysics will have an important impact on scientific goals of relevance to the Department of Energy in basic physical sciences. The multi-physics and high-performance computing aspects of this project provide both new theoretical tools for applications elsewhere and tests existing tools widely used in some terrestrial applications in extreme astrophysical environments.

This effort enabled us to develop a focused effort on the nuclear and neutrino physics aspects of cosmic explosions. Our research in this area, and our role in leading such ef-

forts nationally were recognized by the Department of Energy, which awarded LANL a nationwide grant to lead a topical collaboration center for studies relating to "Neutrinos and Nucleosynthesis in Hot and Dense Matter". The collaboration includes scientists, students and postdoctoral fellows from 11 participating institutions working on several aspects of cosmic explosions.

References

1. Brown, E. F., and L. Bildsten. The ocean and crust of a rapidly accreting neutron star:. 1998. *Astrophysical Journal.* **496** (2): 915.

2. Page, D., and S. Reddy. Dense matter in compact stars: Theoretical developments and observational constraints. 2006. *ANNUAL REVIEW OF NUCLEAR AND PARTICLE SCIENCE.* **56**: 327.

3. Strohmayer, T. E., and A. L. Watts. Discovery of fast X-ray oscillations during the 1998 giant flare. 2005. *Astrophysical Journal, Letters.* **632** (2): L111.

4. Strohmayer, T., and L. Bildsetn. New views of thermonuclear bursts. 2006. In *Compact stellar X-ray sources.* Edited by Lewin, W. H. G., and M. van der Klis. , p. 113. Cambridge, UK: Cambridge University Press.

5. Gupta, S., T. Kawano, and P. Moller. Neutron reactions in accreting neutron stars: A new pathway to efficient crust heating. 2008. *PHYSICAL REVIEW LETTERS.* **101** (23): 231101.

6. Aguilera, D., V. Cirigliano, J. Pons, S. Reddy, and R. Sharma. Superfluid heat conduction and the cooling of magnetized neutron stars. 2009. *PHYSICAL REVIEW LETTERS.* **102** (9): 1101.

7. Daligault, J., and S. Gupta. Electron-ion scattering in dense multi-component plasmas: Application to the outer crust of an accreting neutron star. 2009. *ASTROPHYSICAL JOURNAL.* **703** (1): 994.

8. Gezerlis, A.. Low-density neutron matter. 2010. *PHYSICAL REVIEW C.* **81** (2): 025803.

9. Horowitz, C., and K. Kadau. Breaking strain of neutron star crust and gravitational waves. 2010. *PHYSICAL REVIEW LETTERS.* **102** (19): 191102.

10. Ruiter, A., K. Belczynski, and C. Fryer. RATES AND DELAY TIMES OF TYPE Ia SUPERNOVAE. 2009. *ASTROPHYSICAL JOURNAL.* **699** (2): 2026.

11. Fryer, C. L., P. A. Mazzali, J. Prochaska, E. Cappellaro, A. Panaitescu, E. Berger, M. van Putten, E. P. van den Heuvel, P. Young, A. Hungerford, G. Rockefeller, Sung-Chul Yoon, P. Podsiadlowski, K. Nomoto, R. Chevalier, B. Schmidt, and S. Kulkarni. Constraints on type Ib/c supernovae and gamma-ray burst progenitors. 2007. *Publications of the Astronomical Society of the Pacific.* **119** (861): 1211.

12. Belczynski, K., D. E. Holz, C. L. Fryer, E. Berger, D. H. Hartmann, and B. O'Shea. On the origin of the highest redshift gamma-ray bursts. 2010. *Astrophysical Journal.* **708** (1): 117.

13. Fryer, C. L.. Neutrinos from fallback onto newly formed neutron stars. 2009. *Astrophysical Journal.* **699** (1): 409.

14. Fryer, C. L., P. J. Brown, F. Bufano, J. A. Dahl, C. J. Fontes, L. H. Frey, S. T. Holland, A. L. Hungerford, S. Immler, P. Mazzali, P. A. Milne, E. Scannapieco, N. Weinberg, and P. A. Young. Spectra and light curves of failed supernovae. 2009. *Astrophysical Journal.* **707** (1): 193.

15. Liu, Siming, Zhong-Hui Fan, and C. L. Fryer. Stochastic electron acceleration in shell-type supernova remnants. II. 2008. In *High Energy Gamma-Ray Astronomy: 4th International Meeting on High Energy Gamma-Ray Astronomy ; 7-11 July 2008 ; Heidelberg, Germany.* Vol. 1085, p. 344.

16. Liu, Siming, Zhong-Hui Fan, C. L. Fryer, Jian-Min Wang, and Hui Li. Stochastic electron acceleration in shell-type supernova remnants. 2008. *Astrophysical Journal.* **683** (2): L163.

Publications

Aguilera, D., V. Cirigliano, J. Pons, S. Reddy, and R. Sharma. Superfluid heat conduction and the cooling of magnetized neutron stars. 2009. *Physical Review Letters.* **102**: 091101.

Belczynski, K., D. E. Holz, C. L. Fryer, E. Berger, D. H. Hartmann, and B. O'Shea. On the origin of the highest redshift gamma-ray bursts. 2010. *Astrophysical Journal.* **708** (1): 117.

Belczynski, K., M. Dominik, T. Bulik, R. O'Shaughnessy, C. Fryer, and D. E. Holz. The effect of metallicity on the detection prospects for gravitational waves. 2010. *Astrophysical Journal Letters.* **715** (2): L138.

Belczynski, K., M. Dominik, T. Bulik, R. O,ÄôShaughnessy, C. Fryer, and D. Holz. THE EFFECT OF METALLICITY ON THE DETECTION PROSPECTS FOR GRAVITATIONAL WAVES. 2010. *ASTROPHYSICAL JOURNAL LETTERS.* **715** (2): L138.

Belczynski, K., T. Bulik, C. L. Fryer, A. Ruiter, F. Valsecchi, J. S. Vink, and J. R. Hurley. On the maximum mass of stellar black holes. 2010. *Astrophysical Journal.* **714** (2): 1217.

Bennett, M. E., R. Hirschi, M. Pignatari, S. Diehl, C. Fryer, F. Herwig, A. Hungerford, G. Magkotsios, G. Rockefeller,

F. Timmes, M. Wiescher, and P. Young. The effect of ¹²C + ¹²C rate uncertainties on s-process yields. 2010. *Journal of Physics: Conference Series.* **202**: 012023.

Budge, K. G., C. L. Fryer, and A. L. Hungerford. Supernova theory: simulation and neutrino fluxes. 2008. In *The XXIII International Conference on Neutrino Physics and Astrophysics ; 25-31 May 2008 ; Christchurch, New Zealand.* Vol. 136, 2 Edition, p. 022040 (6 pp.).

Budge, K. G., C. L. Fryer, and A. L. Hungerford. Supernova theory: simulation and neutrino fluxes. 2008. In *The XXIII International Conference on Neutrino Physics and Astrophysics ; 25-31 May 2008 ; Christchurch, New Zealand.* Vol. 136, 2 Edition, p. 022040 (6 pp.).

Budge, null., C. L. Fryer, and A. S. Hungerford. Supernova theory: Simulation and neutrino fluxes. 2008. *Journal Name: Journal of Physics. Conference Series (Online).* **136** (2): Medium: X; Size: 6 pages.

Budge, null., C. L. Fryer, and A. S. Hungerford. Supernova theory: Simulation and neutrino fluxes. 2008. *Journal Name: Journal of Physics. Conference Series (Online).* **136** (2): Medium: X; Size: 6 pages.

Daligault, J., and S. S. Gupta. Electron-Ion Scattering in Dense Multi-Component Plasmas: Application to the Outer Crust of an Accreting Neutron Star. 2009. *Astrophysical Journal.* **703**: 994.

Falcone, A. D., D. A. Williams, M. G. Baring, R. Blandford, V. Connaughton, P. Coppi, C. Dermer, B. Dingus, C. Fryer, N. Gehrels, J. Granot, D. Horan, J. I. Katz, K. Kuehn, P. Meszaros, J. Norris, P. S. Parkinson, A. Peer, E. Ramirez-Ruiz, S. Razzaque, X. Wang, and B. Zhang. The gamma ray burst section of the white paper on the status and future of very high energy gamma ray astronomy: a brief preliminary report. 2008. *AIP Conference Proceedings.* **1000**: 611.

Falcone, A. D., D. A. Williams, M. G. Baring, R. Blandford, V. Connaughton, P. Coppi, C. Dermer, B. Dingus, C. Fryer, N. Gehrels, J. Granot, D. Horan, J. I. Katz, K. Kuehn, P. Meszaros, J. Norris, P. S. Parkinson, A. Peer, E. Ramirez-Ruiz, S. Razzaque, X. Wang, and B. Zhang. The gamma ray burst section of the white paper on the status and future of very high energy gamma ray astronomy: a brief preliminary report. 2008. *AIP Conference Proceedings.* **1000**: 611.

Falcone, A. D., D. A. Williams, M. G. Baring, R. Blandford, V. Connaughton, P. Coppi, C. Dermer, B. Dingus, C. Fryer, N. Gehrels, J. Granot, D. Horan, J. I. Katz, K. Kuehn, P. Meszaros, J. Norris, P. Saz. Parkinson, A. Pe,Äôer, E. Ramirez-Ruiz, S. Razzaque, X. Wang, and B. Zhang. The gamma ray burst section of the white paper on the status and future of very high energy gamma ray astronomy: A brief preliminary report. 2008. In *Santa Fe Conference on Gamma-Ray Bursts ; 20071105 - 20071109 ; Santa Fe, NM.* Vol. 1000, p. 611.

Fragos, T., B. Willems, V. Kalogera, N. Ivanova, G. Rockefeller, C. L. Fryer, and P. A. Young. Understanding compact object formation and natal kicks. II. The case of XTE J1118 + 480. 2009. *Astrophysical Journal.* **697** (2): 1057.

Fragos, T., B. Willems, V. Kalogera, N. Ivanova, G. Rockefeller, C. L. Fryer, and P. A. Young. UNDERSTANDING COMPACT OBJECT FORMATION AND NATAL KICKS. II. THE CASE OF XTE J1118+480. 2009. *ASTROPHYSICAL JOURNAL.* **697** (2): 1057.

Fryer, C. L.. Applying lessons from SN studies to GRBs. 2009. In *Gamma Ray Bursts: Sixth Huntsville Symposium ; 20-23 Oct.* (2008 ; Huntsville, AL, USA). Vol. 1133, p. 97.

Fryer, C. L.. Neutrinos from fallback onto newly formed neutron stars. 2009. *Astrophysical Journal.* **699** (1): 409.

Fryer, C. L., P. J. Brown, F. Bufano, J. A. Dahl, C. J. Fontes, L. H. Frey, S. T. Holland, A. L. Hungerford, S. Immler, P. Mazzali, P. A. Milne, E. Scannapieco, N. Weinberg, and P. A. Young. Spectra and light curves of failed supernovae. 2009. *Astrophysical Journal.* **707** (1): 193.

Fryer, C. L., and S. Diehl. On the road to understanding Type Ia progenitors: Precision simulations of double degenerate mergers. 2008. In *Hydrogen-Deficient Stars ASP Conference Series.* (Eberhard Karls University, Tübingen, Germany, 17-21 September, 2007). Vol. 391, p. 335. San Francisco: Werner and Thomas Rauch. .

Geballe, T. B., G. C. Clayton, M. Asplund, F. Herwig, and C. L. Fryer. O-18 and the origins of HdC and R CrB stars. 2008. In *3rd International Workshop on Hydrogen-Deficient Stars ; 20070917 - 20070921 ; Tubingen, GERMANY.* Vol. 391, p. 51.

Geballe, T. B., G. C. Clayton, M. Asplund, F. Herwig, and C. L. Fryer. O-18 and the origins of HdC and R CrB stars. 2008. In *3rd International Workshop on Hydrogen-Deficient Stars ; 20070917 - 20070921 ; Tubingen, GERMANY.* Vol. 391, p. 51.

Gezerlis, A., S. Gandolfi, K. E. Schmidt, and J. Carlson. Heavy-light fermion mixtures at unitarity. 2009. *Physical Review Letters.* **103** (6): 060403.

Gezerlis, A., and J. Carlson. Strongly paired fermions: Cold atoms and neutron matter. 2008. *Physical Review C.* **77**: 032801(R).

Gupta, S., T. Kawano, and P. Moller. Neutron reactions in accreting neutron stars: a new pathway to efficient

crust heating. 2008. *Physical Review Letters.* **101**: 231101.

Horowitz, C. J., and K. Kadau. Breaking Strain of Neutron Star Crust and Gravitational Waves. 2009. *Physical Review Letters.* **102**: 19102.

Liu, S., Z. H. Fan, C. L. Fryer, J. M. Wang, and H. Li. Stochastic electron acceleration in shell-type supernova remnants. 2008. *Astrophysical Journal.* **683**: L163.

Liu, Siming, Zhong-Hui Fan, C. L. Fryer, Jian-Min Wang, and Hui Li. Stochastic electron acceleration in shell-type supernova remnants. 2008. *Astrophysical Journal.* **683** (2): L163.

Liu, Siming, Zhong-Hui Fan, C. L. Fryer, Jian-Min Wang, and Hui Li. Stochastic electron acceleration in shell-type supernova remnants. 2008. *Astrophysical Journal.* **683** (2): L163.

Liu, Siming, Zhong-Hui Fan, and C. L. Fryer. Stochastic electron acceleration in shell-type supernova remnants. II. 2008. In *High Energy Gamma-Ray Astronomy: 4th International Meeting on High Energy Gamma-Ray Astronomy ; 7-11 July 2008 ; Heidelberg, Germany.* Vol. 1085, p. 344.

Liu, Siming, Zhong-Hui Fan, and C. L. Fryer. Stochastic electron acceleration in shell-type supernova remnants. II. 2008. In *High Energy Gamma-Ray Astronomy: 4th International Meeting on High Energy Gamma-Ray Astronomy ; 7-11 July 2008 ; Heidelberg, Germany.* Vol. 1085, p. 344.

Pethick, C. J., N. Chamel, and S. Reddy. Superfluid dynamics in neutron star crusts. To appear in *NEW FRONTIERS in QCD 2010, KYOTO, JAPAN.* (Kyoto, January-March, 2010).

Ruiter, A. J., K. Belczynski, and C. Fryer. Rates and delay times of type Ia Supernovae. 2009. *Astrophysical Journal.* **699** (2): 2026.

Ruiter, A., K. Belczynski, and C. Fryer. RATES AND DELAY TIMES OF TYPE Ia SUPERNOVAE. 2009. *ASTROPHYSICAL JOURNAL.* **699** (2): 2026.

Sharma, R., and S. Reddy. Anisotropic electronic screening and damping in magnetars. *PHYSICAL REVIEW C.*

Steiner, A., and S. Reddy. Superfluid response and the neutrino emissivity of neutron matter. 2009. *Physical Review C.* **79**: 015802.

Tierney, T. E., H. E. Tierney, G. C. Idzorek, R. G. Watt, R. R. Peterson, D. L. Peterson, C. L. Fryer, M. R. Lopez, M. C. Jones, D. Sinars, G. A. Rochau, and J. E. Bailey. Blast wave energy diagnostic. 2008. *Review of Scientific Instruments.* **79** (10): 10E919 (4 pp.).

Tierney, T. E., H. E. Tierney, G. C. Idzorek, R. G. Watt, R. R. Peterson, D. L. Peterson, C. L. Fryer, M. R. Lopez, M. C. Jones, D. Sinars, G. A. Rochau, and J. E. Bailey. Blast wave energy diagnostic. 2008. *Review of Scientific Instruments.* **79** (10): 10E919 (4 pp.).

Tierney, T., H. Tierney, G. Idzorek, R. Watt, R. Peterson, D. Peterson, C. Fryer, M. Lopez, M. Jones, D. Sinars, G. Rochau, and J. Bailey. Blast wave energy diagnostic. 2008. *Review of Scientific Instruments.* **79** (10): 10E919.

Tierney, T., H. Tierney, G. Idzorek, R. Watt, R. Peterson, D. Peterson, C. Fryer, M. Lopez, M. Jones, D. Sinars, G. Rochau, and J. Bailey. Blast wave energy diagnostic. 2008. *Review of Scientific Instruments.* **79** (10): 10E919.

Young, P. A., C. I. Ellinger, D. Arnett, C. L. Fryer, and G. Rockefeller. Finding tracers for supernova produced ²⁶Al. 2009. *Astrophysical Journal.* **699** (2): 938.

Young, P. A., and C. L. Fryer. The local environments of long-duration gamma-ray bursts. 2007. *Astrophysical Journal.* **670**: 584.

al., C. L. Fryer et. Constraints on Type Ib/c supernovae and gamma-ray burst progenitors. 2007. *The Publications of the Astronomical Society of the Pacific.* **119** (861): 1211.

Novel Signatures of Beyond the Standard Model at the Large Hadron Collider

Rajan Gupta
20080661DR

Abstract

A new era in high-energy physics began when the Large Hadron Collider (LHC) began colliding protons at a center-of-mass energy of 7 TeV. It will explore particle masses or distance scales in Nature not previously explored. Its discovery potential will be the focus of the high-energy physics community for years to come. A discovery of dark matter at the LHC will revolutionize cosmology, particle and astrophysics.

The Standard Model (SM) of elementary particles is very successful at describing all interactions of the known fundamental particles at energy scales up to 100 times the mass of the proton. Despite this success, a number of fundamental questions remain unanswered, such as the nature of the Higgs sector---whether the particle is elementary or composite, the mechanism that stabilizes the electroweak scale against quantum corrections, the number of spatial dimensions at the weak scale, and whether an as yet unobserved symmetry called supersymmetry is realized by nature at the electroweak scale to both stabilize it and lead to grand unification. This is an unsatisfactory situation and we need the answers to these and a number of related questions, both to take the next logical step in theory design and in suggesting further measurements and analyses.

This project addresses these issues by focusing on the experimental signatures of new physics at the LHC. This work investigates decays of proposed supersymmetric particles in which various normal, SM particles can be used as triggers or aids in interpreting the new data. It will explore the hierarchy of these particles to understand which theoretical constructs fit observations and if they are candidates for dark matter. In addition, the effort will also identify experimental techniques that can guide in searches for novel events and in elucidating the nature of new physics.

Background and Research Objectives

The Standard Model is a descriptive theory of the interactions between the fundamental particles known to exist – quarks, leptons and gauge bosons. It agrees extremely well with experimental observations, having no significant deviations. Yet there is a sector of the Standard Model of which we know very little, except to know that it exists. This is the part of the theory that gives mass to the fermions, quarks and the W and Z bosons. The Standard Model predicts the existence of a new particle - dubbed the Higgs boson – whose postulated condensation and interactions with the other Standard Model particles generates all the known fundamental masses.

While the Standard Model has a parsimonious explanation for the origin of electroweak symmetry breaking, it does not explain *why* the symmetry breaking occurs: it is simply a placeholder. Another more fundamental problem with the Standard Model Higgs boson is the following. The interactions of the top quark to the Higgs boson, and the interaction of the Higgs boson to itself, at the quantum level generate corrections to the energy or mass of the Higgs boson. The problem is that if the Standard Model is a correct description of Nature down to distance scales much smaller than the characteristic electroweak scale (10^-16 cm), then these corrections are so large that electroweak symmetry breaking at the experimentally known scale is generically impossible. It can only occur if fundamental parameters of the theory are fine tuned against one another. More generally, if there are new degrees of freedom (beyond the Standard Model) that couple to the Higgs boson, then they too will generically generate large corrections to the mass of the Higgs boson. In short, many particle physicists reject the Standard Model because they believe that its description of electroweak symmetry breaking is unsatisfactory.

A quest for particle physicists has therefore been to find theories of Nature that

- Dynamically break the electroweak symmetry
- Makes the size of the electroweak scale natural
- And remain consistent with all known data

There are a number of theories that achieve these objectives to varying degrees of success, however none are completely compelling, and no theories solve all of these problems.

Since the LHC will probe Nature at a greater and previously unexplored energy, it is anticipated that it will produce new particles having mass between 100 GeV – few TeV. The masses, gauge quantum numbers, and interactions of these new particles will provide essential clues about the fundamental theory of Nature at these energies. It is expected that the new theory revealed by the discoveries of the LHC will resolve the long-outstanding mysteries described above. Reconstructing the underlying theory from experimental data will be a challenge and among the most important physics efforts at the LHC.

The purpose of this DR was to investigate and address the following questions:

1. How do we test different theories? How do we measure the interactions?

2. Are there characteristic signatures for some theories?

3. Are there ``better" theories? Can we improve or clarify existing ideas for physics at the TeV scale?

Scientific Approach and Accomplishments

Supersymmetry is an attractive framework for new physics at the electroweak scale because it automatically stabilizes the mass of the Higgs boson against quantum corrections. It however makes the incorrect prediction that each Standard Model should have a partner having the same mass but differing by ½ unit of spin. Supersymmetry must therefore be broken, but without destabilizing the electroweak scale. There is a related issue: the size of electroweak symmetry breaking is tied to the size of the supersymmetry breaking scale. Supersymmetry alone does not explain why the electroweak scale has the value it does, it only stabilizes it.

Communicating supersymmetry breaking through gauge interactions is an old idea that dates to the early 1980s [1,2,3]. Since gauge interactions are flavor-blind, this is an elegant way to break supersymmetry in the Standard Model without introducing flavor changing neutral current processes. A disadvantage of gauge mediation however is that it does not generate a mass term for superpartners of the Higgs bosons (the Higgsinos).

A new ingredient in our work [Ibe and Kitano; 4] is to assume that the Higgs multiplets are composites that arise from the strong dynamics that break supersymmetry. That is, the Higgs boson is not fundamental, but extended, much like how the proton and neutron are composed out of confined quarks. They then generate masses for the Higgsinos, a significant improvement on previous model-building efforts. Their theory has only two parameters, and remarkably there is a range for them that can simultaneously solve a number of phenomenological problems [4].

They further their focus on constructing elegant models of communicating supersymmetry breaking to the supersymmetric Standard Model (SSM), in way that is consistent with all known data. They build on the observation of [5] that it may be enough to find a local, rather than global, minimum that breaks supersymmetry. In [6] they construct a class of simple models of the ISS scenario, with a range of parameters satisfying the phenomenologically preferred region identified in [4]. They constructed additional models of gauge mediation in [7] with a general algorithm for finding local supersymmetry breaking minima in [8].

In typical supersymmetry model-building attempts, the SM and their superpartners are assumed to occur in complete SUSY multiplets. In Ref. [9], Graesser, Kitano and Kurachi reconsider this assumption for the superpartners of the Higgs boson. The phenomenology at the LHC is quite different if this assumption is changed. Ref. [9] constructs an effective field theory describing this scenario. The new ingredient is the key assumption that the breaking of supersymmetry and its communication to the SSM is realized non-linearly, rather than linearly. They further assume the existence of additional light particles that are composites out of the sector that breaks supersymmetry. The most interesting candidate would be the Higgs boson itself, or a massive spin-2 particle.

Interactions coupling the Standard Model particles (+ superpartners) to the light composites, in a manifestly supersymmetric, and therefore internally consistent, manner, are then described. This technical result is non-trivial, since the composites do not appear in complete supersymmetric representations.

They further showed:

- That only one Higgs boson is needed to give mass to both up and down-type quarks, explicitly disproving the standard lore that two Higgs doublets are needed if supersymmetry is realized non-linearly.

- That a spin-2 particle can partially unitarize the goldstino-goldstino scattering channel.

- This spin-2 particle can be produced at the LHC with a large enough rate to make discovery possible, as shown in Figure 1.

In short, the experimental signatures of this scenario are novel: the LHC will discover superpartners to all of the SM particles, except the Higgs boson; the Higgs boson is composite; and the discovery of a spin-2 resonance is interpreted as due to strong supersymmetric dynamics at the TeV scale, rather than the first Kaluza-Klein excitation of an extra dimension.

If supersymmetry is correct then the LHC will produce a number of new particles. Identifying the masses, quantum numbers and interactions of these new particles will provide critical information needed to infer the underlying theory at the TeV scale. It is therefore important to identify measurements that can be made to distinguish theories, with a minimum number of theoretical assumptions.

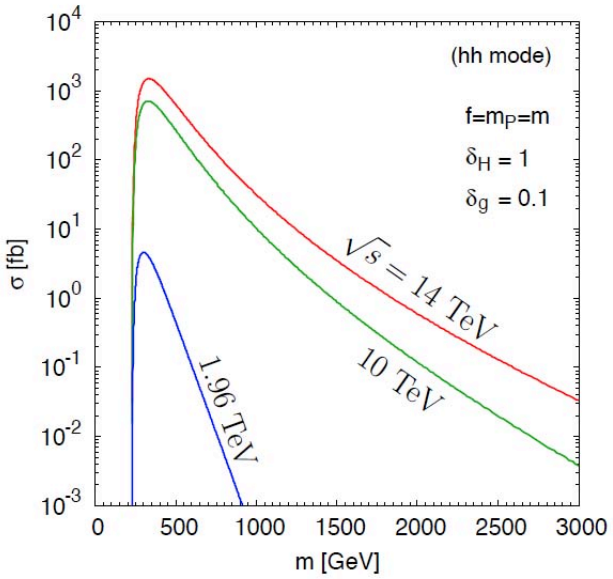

Figure 1. The production cross-section to two Higgs bosons through the spin-2 resonance, as a function of the graviton mass, for three choices of the center of mass energy. Note that production cross-sections at the Large Hadron Collider (green,red) are sizable for sub-TeV mass, while those at the Tevatron (blue) are small enough to not be excluded. Figure from [9].

In Ref. [10] Graesser and Shelton focus on final states involving jets, missing energy and third generation particles such as the b quark or the tau lepton. These final states may provide for a potentially richer phenomenology and insight into the underlying theory, as compared to decay chains producing electrons and muons instead of taus. The taus or b quarks can be produced at the LHC through processes as shown in Figure 2. The lightest neutralino (the dark matter particle) escapes the detector and appears as ``missing energy".

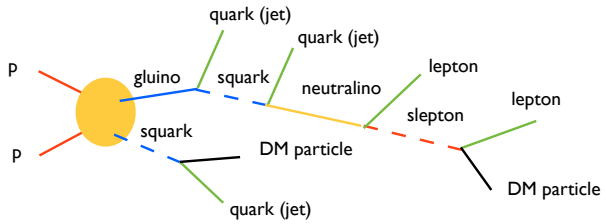

Figure 2. Production of jet, lepton and missing energy final states at the Large Hadron Collider through a sample supersymmetric process.

Ref. [10] investigates how specific distributions, formed out of the kinematics of these events, depend on the underlying theory assumptions. Such a model-independent approach had not been done before for these final states, as previous articles focus on specific model parameter points. They find a number of important results.

Stops and sbottoms contribute differently to the shape of the b-l distributions, suggesting these distributions can be used to separate stop and sbottoms in an event sample containing both. This observation will help disentangle supersymmetric processes from one another. Next, signing the charge of the b-quark is found to increase the experimental sensitivity to the quantum numbers of the superpartners.

Similar results are found for distributions involving tau leptons. Here the polarization of the tau is partially inherited by its visible decay products, unlike for the decays of the b quark. Because of this effect, lepton-tau distributions in particular can identify the relative quantum numbers of the slepton and stau superpartners. Finally the authors suggest that theoretical distributions should be compared to data by fitting to the peak of the observed distributions, which are better characterized than the end-points (which are softened due to the lost neutrino).

These results have motivated further work on b-l distributions. There it is shown how a charge asymmetry involving the b-quarks and leptons can be used to discriminate theories, as illustrated in Figure 3.

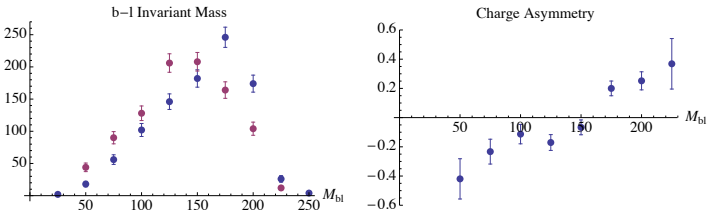

Figure 3. Left: Bottom quark jet+ lepton mass distributions for two possible charge assignments (blue,red). Right: Charge asymmetry. A measurement of these experimentally observable distributions provides important information on the underlying structure of the theory. Assumed approximately 10 years of running at the Large Hadron Collider. From M.Graesser, J. Ruderman and J. Shelton, unpublished.

Theories for new physics at the TeV scale typically predict the existence of a number of new particles. That is, they predict a *discrete* spectrum. In the lead-up to the start of the LHC, it is important to investigate whether there are more general possibilities. This point has been recently emphasized by Georgi [11,12], who has proposed a new class of theories he dubbed ``unparticles". In these theories the Standard Model fields couple to a hidden sector conformal field theory (CFT) through irrelevant operators. The two main distinctions of this class of theories com-

pared to other classes are: the spectrum is *continuous*; and if there is a mass gap, it is well below the electroweak scale. Collisions of Standard Model particles at the LHC would then excite states in the hidden sector CFT, leading to novel phenomena.

The physics of CFT's (and by extension unparticles) is encoded in correlation functions of gauge-invariant operators. The work of Friedland, Giannotti and Graesser [13,14] is inspired by a number of issues surrounding the simplest of these, namely the correlator involving two operators (the ``two-point correlator).

These puzzles are:

1. What is the physical meaning of the complex phase in the two-point correlator?

2. What does it mean that the spectral representation of vector operators is not finite?

3. In the momentum-space representation, the two-point function diverges at integer dimension.

All of these puzzles should have a simple resolution.

In this context Grinstein, Intriligator, and Rothstein (GIR) partly address some of these issues, and raise additional ones [15]. First, they point out that the dimensions of operators in a CFT are bounded by unitarity. They next show in a weakly coupled CFT (e.g., [16]) that contact interactions involving Standard Model fields are necessarily present, and that they cancel the divergences that appear at integer dimension (puzzle #3). The existence of contact interactions is important for phenomenology, since GIR find, at least for vector operators, they always dominate over the novel CFT contributions found by Georgi.

To confront these issues, Refs. [13,14] find a simple framework that possesses all the properties of unparticles, while also satisfying the constraints of unitarity. Moreover, they ask: do GIR's findings about the contact interactions – which in [15] only apply to weak coupling – also extend to strong coupling?

Motivated by the AdS/CFT correspondence [17-19], [13,14] focus on theories in warped space-time backgrounds. Specifically, they consider the well-known Randall-Sundrum models having a single brane [20,21]. By the celebrated AdS/CFT correspondence, these backgrounds in five(!) space-time dimensions are conjectured to describe certain strongly coupled conformal field theories in four(!)-dimensions.

Refs. [13,14] show:

- That these brane models provide realizations of unparticles.

- The unitarity bound on CFT vector operators is obtained in a simple manner by considering brane-to-brane scattering and applying the optical theorem.

- The mysterious phase appearing in the two-point correlator – (puzzle #1) - has a simple interpretation here: it is due to the production and escape of particles through the horizon.

- They confirm that the contact interactions and cancellations of divergences found by GIR at weak coupling also extend to strong coupling.

- These contact interactions cancel divergences appearing at integer dimension (puzzle #3), and dominate scattering amplitudes, but that interactions at a finite distance are dominated by the CFT.

- That the contact interactions are not really fundamental: at short enough distances the contact interactions are resolved (puzzle #2). The last point is illustrated in Figure 4.

The importance of [13,14] has been to show that the Randall-Sundrum models [20,21] provide a realization of unparticles. The RS models are intuitively simpler to understand than the abstractions of conformal field theories.

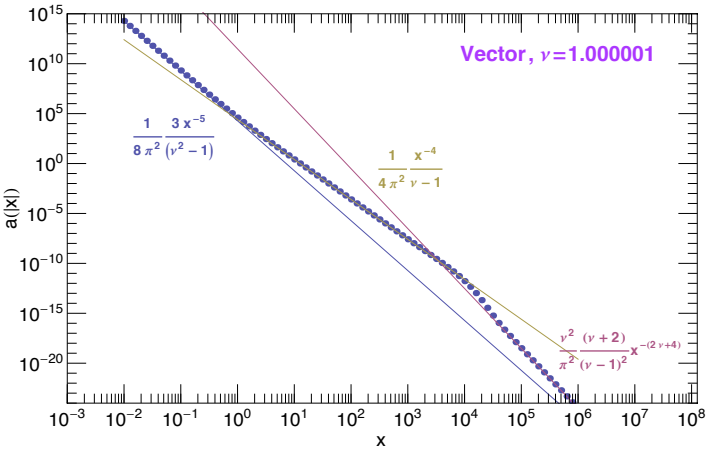

Figure 4. The Euclidean transverse two-point correlator. The horizontal axis gives the distance between the sources. The plot shows the transition from purely 5-dimensional flat space behavior (left), through a four-dimensional massive spin-1 exchange behavior (middle), to purely 4-dimensional CFT behavior at large distances (right). Figure from [14].

Impact on National Missions

We support the high energy physics component of the DOE Office of Science mission by addressing four of its six long-term goals: discover the Higgs' particle, measure matter-antimatter asymmetry, probe the high energy frontier, and directly discover dark matter particles. Our instrumentation expertise will build capability for nuclear nonproliferation.

References

1. Alvarez-Gaume, L., M. Claudson, and M. Wise. Low Energy Supersymmetry. 1982. *Nuclear Physics B.* (207): 96.

2. Dine, M., W. Fischler, and M. Srednicki. Supersymmetric Technicolor. 1981. *Nuclear Physics B.* **189**: 575.

3. Dine, M., and W. Fischler. A Phenomenological Model of Particle Physics Based on Supersymmetry. 1982. *Physics Letters B.* (110): 227.

4. Ibe, M., and R. Kitano. Sweet spot supersymmetry . 2007. *Journal of High Energy Physics.* **0708** (016): 1.

5. Intriligator, K. A., N. Seiberg, and D. Shih. Dynamical SUSY breaking in meta-stable vacua. 2006. *Journal of High Energy Physics .* **0604**: 021.

6. Ibe, M., and R. Kitano. Sweet spot supersymmetry and composite messengers . 2008. *Physics Letters B.* **663**: 242.

7. Ibe, M., and R. Kitano. Minimal direct gauge mediation . 2008. *Physical Review D.* **77**: 075003.

8. Kitano, R., and Y. Ookouchi. Supersymmetry breaking and gauge mediation in models with a generic superpotential. 2009. *Physics Letters B.* (675): 4.

9. Graesser, M., R. Kitano, and M. Kurachi. Higgsinoless Supersymmetry and HIdden Gravity . 2009. *Journal of High Energy Physics.* **0910** (077): 26.

10. Graesser, M., and J. Shelton. Probing Supersymmetry with Third Generation Cascade Decays . 2009. *Journal of High Energy Physics.* **0906**: 039.

11. Georgi, H.. Unparticle Physics. 2007. *Physical Review Letters.* **98**: 221601.

12. Georgi, H.. Another Odd Thing About Unparticle Physics. 2007. *Physics Letters B.* **650**: 275.

13. Friedland, A., M. Giannotti, and M. Graesser. On the RS2 realization of unparticles . 2009. *Physics Letters B.* **678**: 149.

14. Friedland, A., M. Giannotti, and M. Graesser. Vector Bosons in the Randall-Sundrum 2 and Lykken-Randall models and unparticles. 2009. *Journal of High Energy Physics .* **0909**: 033.

15. Grinstein, B., K. Intriligator, and I. Rothstein. Comments on Unparticles . 2008. *Physics Letters B .* **662**: 367.

16. Banks, T., and A. Zaks. On the Phase Structure of Vector-Like Gauge Theories with Massless Fermions. 1982. *Nuclear Physics B .* (196): 189.

17. Maldacena, J.. The Large N limit of superconformal field theories and supergravity. 1999. *International Journal of Theoretical Physics .* **38** (4): 1113.

18. Gubser, S., I. Klebanov, and A. M. Polyakov. Gauge theory correlators from noncritical string theory. 1998. *Physics Letters B.* (428): 105.

19. Witten, E.. Anti-de Sitter space and holography. 1998. *Advanced Journal of Theoretical Mathematics and Physics.* (2): 253.

20. Randall, L., and R. Sundrum . An Alternative to compactification. 1999. *Physical Review Letters .* (83): 4690.

21. Randalll, L., and J. Lykken. The Shape of Gravity . 2000. *Journal of High Energy Physics.* **0006** (014): 1.

Publications

Friedland, A., M. Giannotti, and M. Graesser. On the RS2 realization of unparticles . 2009. *Physics Letters B.* **678**: 149.

Friedland, A., M. Giannotti, and M. Graesser. Vector Bosons in the Randall-Sundrum 2 and Lykken-Randall models and unparticles . 2009. *Journal of High Energy Physics .* **0909**: 033.

Graesser, M., R. Kitano, and M. Kurachi. Higgsinoless supersymmetry and hidden gravity . 2009. *Journal of High Energy Physics .* **0910** (077): 26.

Graesser, M., and J. Shelton. Probing Supersymmetry with Third Generation Cascade Decays. 2009. *Journal of High Energy Physics .* **0906**: 039.

Ibe, M., and R. Kitano. Minimal direct gauge mediation . 2008. *Physical Review D.* **77**: 075003.

Ibe, M., and R. Kitano. Sweet spot supersymmetry and composite messengers . 2008. *Physics Letters B.* **663**: 242.

Kitano, R.. Study of chargino-neutralino production at hadron colliders in a long-lived slepton scenario. 2008. *Journal of High Energy Physics .* **11**: 045.

Kitano, R.. A clean slepton mixing signal at the LHC. 2008. *Journal of High Energy Physics .* **03**: 023.

Kitano, R., H. Murayama, and M. Ratz. Unified origin of baryons and dark matter . 2008. *Physics Letters B.* **669**: 145.

Kitano, R., and Y. Ookouchi. Supersymmetry breaking and gauge mediation in models with a generic superpotential. 2009. *Physics Letters B.* (675): 4.

High-Precision Spectroscopic Search for Variation of the Fine-Structure Constant

Justin R. Torgerson
20080663DR

Abstract
We pursued three promising areas to investigate physics beyond the standard model by searching for time variation of fundamental constants and in particular, time variation of the Fine Structure Constant (α) which determines the strength of electromagnetic interactions. To date, only astrophysical data suggest that α may have been different in the distant past, but modern evidence for this effect would have a dramatic impact on our theoretical understanding of our Universe. We achieved the bulk of our goals for this work and developed a state-of-the-art capability for precision spectroscopy at LANL. At the time of this writing, we are still working diligently to achieve our final goal of an absolute frequency measurement in a single trapped ytterbium ion, and anticipate success with this final goal. We also worked in collaboration with UC Berkeley to develop an apparatus to measure time variation of α in an atomic dysprosium system. The apparatus is now complete and data is currently being collected. We anticipate a world-class competitive result in the coming months. Finally, we established a strong, multi-institutional collaboration to attack a problem of both keen scientific and technological interest: a solid-state optical clock based on a low energy (7.8 eV) transition in the nucleus of the rare isotope ^{229}Th.

Background and Research Objectives
Recent discoveries in astrophysics and cosmology continue to provide ample motivation to look for variation of fundamental constants (FCs). These discoveries include the determination that the cosmic microwave background has an unexpected large-scale structure, that the expansion of the universe is still accelerating, and that it mostly contains dark energy and dark matter. Theories to explain these observations suggest that varying fundamental constants are possible, perhaps even required. Of particular interest among FCs are the dimensionless coupling constants that determine the strength of the fundamental forces. Foremost among these is the coupling constant of the electromagnetic force, the fine-structure constant (α). Richard Feynman was pithy about α: "It's one of the greatest damn mysteries of physics: a magic number that comes to us with no understanding by man."

Some astrophysical measurements of quasars, whose light gives us a window billions of years into the past, have been interpreted to show that α was different in the past, shifting the spectra of some atoms and ions far from what can be reconciled in any other way [1]. Most recently, more data have been added and, when combined with the original data, they allow for a more complicated interpretation: that α may vary as a function of position in space [2].

Our original objective was to construct experimental arrangements that were particularly sensitive to time variations of α. One system of choice was based on well-chosen transitions in ions of ytterbium that we found to be more sensitive to α (and therefore changes in α) than any transitions that had been considered before [3,4]. Another system of choice was a pair of nearly degenerate levels in atomic dysprosium. We began to pursue measurements in both of these systems. However, halfway into our experimental setup, our colleagues at the National Institute of Standards and Technology (NIST) in Boulder produced a result than exceeded our near-term goals [5]. With their outstanding result in mind, we diverted some of our resources from the ytterbium ion trapping effort and added a new goal for our project that was in line with our original goal for understanding physics beyond the standard model, can support nation missions in safety and security, and has the potential for generating significant external funding: to design a system for observing the decay of an extremely low energy nuclear excited state in ^{229}Th (^{229m}Th) and to use it as the basis for a solid state portable nuclear clock. A key connection with our ytterbium ion trapping effort is that the transition between the ground state of ^{229}Th and the ^{229m}Th excited state could be 100,000-1,000,000 times more sensitive to changes in α than any atom-based method, such as those based on ytterbium ions and dysprosium atoms [6].

Scientific Approach and Accomplishments
With our ytterbium ion trapping work, the goal set

at our midterm review was to make an absolute optical frequency measurement of a 3.1 Hz wide transition in a trapped Yb^+ ion. This would prove our capability as truly world-class, and is a feat that has been accomplished in only two laboratories worldwide. The target transition's frequency is 688,358,979,309,306 Hz (near a wavelength of 436 nm). Driving this transition with a resolution of a few 10's of Hz is the best that has ever been achieved and our goal was to approach this level of sensitivity. A partial energy level diagram of the Yb^+ ion in shown in Figure 1.

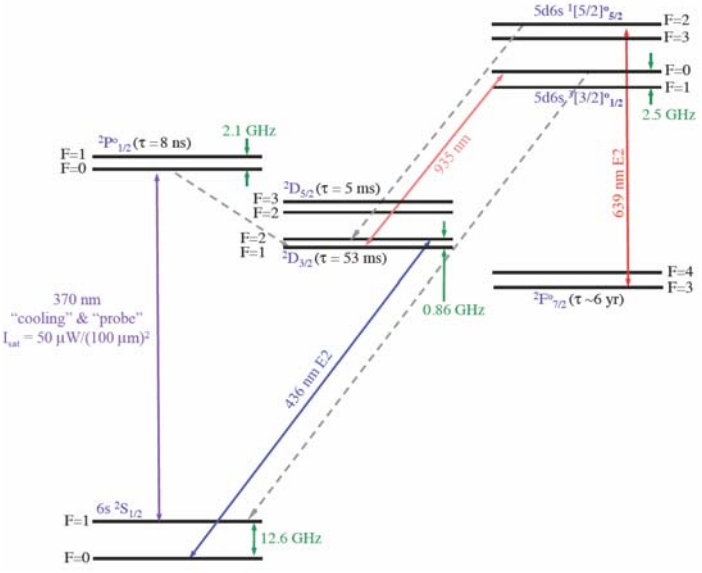

Figure 1. Partial energy-level diagram of Yb+. Laser lines are shown in solid colors. The dashed grey lines represent collisional decay paths while the dashed red lines represent electronic decay paths.

At the writing of this report, we are searching for the transition and our apparatus is 100% operational. However, our knowledge of the stability of the frequency comb we are using to drive the transition of interest is limited. The long term stability is known to a few parts in 10^{12} by comparison to a rubidium clock, but we have no way of determining the short term stability of the comb (over a period of 1 s or less). Another way to say this is that we do not know the number of photons within the 3 Hz bandwidth of the transition we are trying to drive on the timescale of a few 10s of seconds.

It should be pointed out that the approach we have chosen to follow here, the first-ever direct- drive of the narrow transition with a femtosecond-laser frequency comb (FLFC), offers the potential of significant simplification over the more standard approach of locking a high stability laser to the FLFC and then driving the transition with the stable laser. The latter approach requires yet another laser system and a high stability cavity and approximately one additional man-year of effort for each transition and each wavelength. The former dispenses with these complications at the price of a more difficult search at the beginning.

A new experiment to measure parity violation in the same Yb^+ system will use most of the apparatus we have already constructed, and the current measurement we are pursuing will offer only a minor distraction to this follow-on experiment since the apparatus is already operational and collecting data.

During the process of making our apparatus 100% operational, we achieved several additional interim goals of note. These are:

1. We performed a detailed study of radiative and collisional decay mechanisms in excited states of Yb^+. It was imperative that we quantify these effects in our system so that we could understand their effects on stability of our trapped ions. The results of our work are published in Physical Review [7].

2. We identified several new transitions that were highly sensitive to changes in α and worked with atomic theorists at the University of New South Wales to determine which transitions are both accessible and highly sensitive. Through this work, we identified a collection of transitions that are the most sensitive to α ever investigated. The work is published in Physical Review [4].

3. We successfully performed the first-ever trapping and sympathetic cooling of doubly-charged Yb ions. Our work with Yb^{2+} represents the first trapped-ion investigation with a doubly-charged species and opens a new paradigm for trapped-ion laser spectroscopy studies as well as optical frequency standards. We also succeeding in trapping and cooling isotopically pure Yb^{2+} ions: This represents a double milestone of progress in work with multiply-charged ions. To date, only one other multiply-charged ion has been trapped and laser cooled in an ion trap ($^{232}Th^{3+}$ which Natures gives to us already isotopically pure). A manuscript describing this work is finished pending addition of several references and will be submitted to Physical Review imminently.

4. We performed the first-ever measurement of the lifetime of the all-important $^2D_{3/2}$ metastable state in a single ^{171}Yb ion which is the excited state of the $^2S_{1/2}$->$^2D_{3/2}$ transition near 688 THz that we are currently investigating. The experimental work has been completed, analyzed and the manuscript describing this work is under preparation. It will be submitted to Physical Review within a few weeks as work on driving the $^2S_{1/2}$->$^2D_{3/2}$ transition is completed.

5. We measured the amplitude, transition width and frequency of hyperfine transitions in the ground state of $^{171}Yb^+$ ions. Through these careful measurements we were able to align laser polarizations with the applied ambient magnetic field and to quantify the size of the

magnetic fields and calibrate the currents used to apply magnetic fields. These are critical measurements for precision spectroscopy of the $^2S_{1/2}$->$^2D_{3/2}$ transition, and any other precision spectroscopy that can be performed with this system or similar systems in the future. Our method is novel, as compared with the current state-of-the-art, and our former postdoc, Saidur Rahaman is preparing a technical note for publication on the method.

6. We developed a new technique to load isotopically-pure samples of 5 stable isotopes of Yb. This method combines an in-house-built diode laser system locked to a miniature atom beam source of our design.

7. We accurately measured the frequencies of all of the $^2S_{1/2}$->$^2P_{1/2}$ "laser cooling" transitions $^2D_{3/2}$->$^1[3/2]_{1/2}$ "repump" transitions in all of these isotopes and accurately measured the hyperfine splittings in $^{171}Yb^+$.

8. We developed LANL's only FLFC that is currently locked to a rack of cesium and rubidium atomic clocks that are continuously monitored. The FLFC provides about 100,000 individual spectral features that can be used as optical frequency references, or, in our case, to drive optical transitions in trapped ions. We recently acquired a GPS-stabilized rubidium clock pair that will extend our long-term stability to about 4:10^{14}. (For reasons already mentioned, we cannot accurately quantify the short-term FLFC frequency stability.) A schematic of LANL's FLFC is show in Figure 2.

9. We constructed a novel and efficient diode laser system based on a diode laser cooled to -20 C and published the result in Reviews of Scientific Instruments [8].

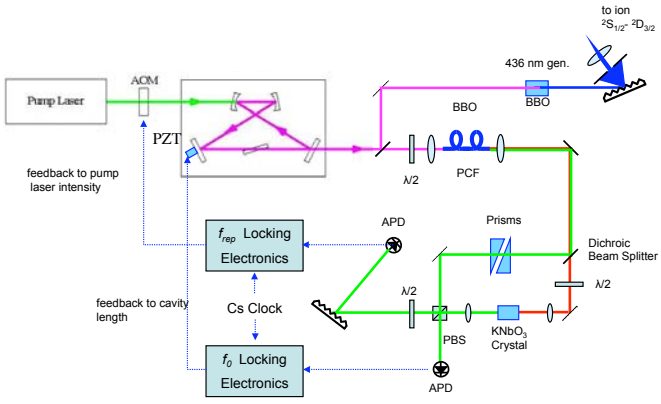

Figure 2. Schematic of LANL's femtosecond laser frequency comb (FLFC). In the upper right corner, the frequency synthesis is shown diagrammatically which illustrates that the FLFC light is being used to directly drive narrow transitions in Yb+ - a novel and important advance in atomic spectroscopy.

Measurements with the atomic dysprosium system are being conducted in collaboration with Prof. Dmitry Budker at UC Berkeley. This collaboration is particularly advantageous to us since there exists in his lab a dysprosium atomic-beam source. In collaboration with us, this experiment previously reached a sensitivity of $(-2.7 \pm 2.6) \times 10^{-15}$ yr^{-1}, which approached the best laboratory limits at the time [9]. This result was limited by several technical systematic problems from an imperfect apparatus. We have now completed construction of a new measurement apparatus with more ideal properties such as better vacuum, magnetic shielding, and more homogeneous electric fields in the test region of the apparatus. Figure 3 shows a schematic of the new, dedicated spectrometer that we have designed and constructed to reduce the influence of the systematic effects due to the background pressure, residual magnetic fields, inhomogeneities in the rf electric field, as well as other systematic effects expected to be important below the 1-Hz level. We are currently taking data on the time stability of α and expect to be able to publish new results in the coming months.

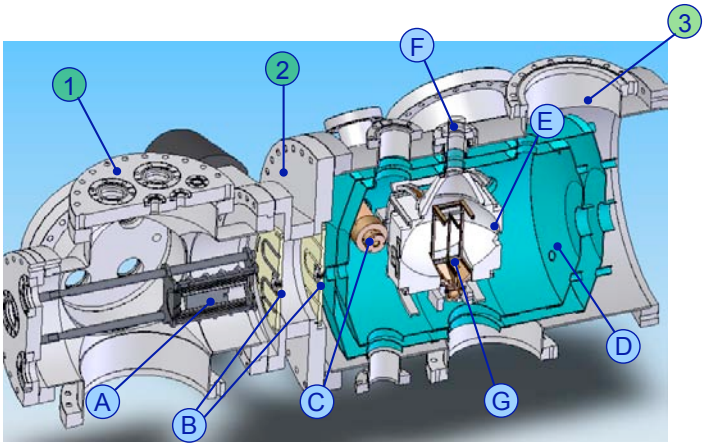

Figure 3. Cutaway drawing of the new Dy spectrometer as built. 1) oven chamber, 2) gate valve, 3) interaction chamber, A. Dy effusive oven, B. collimator, C. laser access port, D. two-layer magnetic shield, E. optical collection system, F. PMT viewport, G. rf electrodes.

We have also designed new rf electrodes using finite-element numerical analysis. Similar to the parallel-plate electrodes of the original apparatus, the new rf electrodes utilize a standing-wave mode of a terminated rectangular coaxial transmission line. Since most of the inhomogeneities of the first-generation electrodes are due to the exponentially decaying higher-order TE and TM modes near the rf feed, the dimensions of the transmission line near the rf feed are smaller than the rest of the electrode in order to keep the phase gradients away from the interaction region. An impedance-matched conical "transition region" links the feed location to the rf-atom interaction region.

In addition to these effects, the largest systematic effect is the ac Stark shifts due to the rf field amplitude. While the size of the effect for the small transition frequencies

would require amplitude stability of better than 10^{-3}, for a transition frequency on the order of 1 GHz, only a modest control at a level of 10 percent is required.

Most recently, we successfully laser cooled the transverse motion of Dy. There exist ten possible trap states with energy below the upper level of the cooling transition at 421 nm. However, consistent with our estimates, it does not appear that these states will prevent cooling of the transverse motion and we are now considering a future generation of this experiment in a magneto-optical trap (MOT). For this generation of the experiment, transverse cooling has the potential to increase the signal/noise of the optical fluorescence and reduce our statistical uncertainty as well as to reduce or eliminate several systematic effects. This result was published in Physical Review [10] and several updates on the progress of this experiment have also been published recently [11,12].

Finally, we researched new ideas and developed a coherent approach toward using the lowest-energy nuclear transition (from the nuclear ground state) known into an optical frequency standard with unprecedented utility. As stated earlier, this transition exists in ^{229}Th and the transition wavelength is 160±10 nm. Not only can this system be developed into a solid-state nuclear clock, but the properties of the transition and the ^{229}Th nucleus provide an ideal system for searches for physics beyond the standard model at unprecedented levels. The details of this work are largely presented in our recent publication in Physical Review Letters [13]. One crucial piece of this advancement is the ability to read out the "state" of the nucleus with high speed to determine whether or not it has been excited. One idea to perform this measurement is shown in Figure 4, where it is shown how the state of the atomic electrons changes in response to a change in the state of the nucleus.

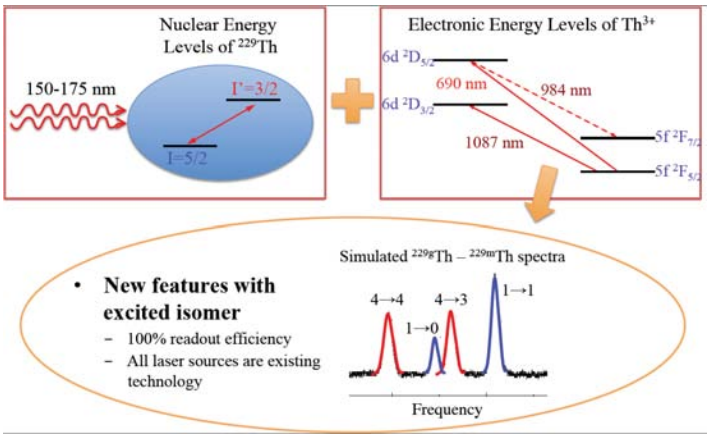

Figure 4. The state of the atom containing the 229Th nucleus is affected by the state of the nucleus. Previously unknown features in the hyperfine spectrum of the Th3+ ion are illustrated here. A similar effect will occur for an atomic or ionic transition in 229Th.

Impact on National Missions

Measurement of a nonzero variation of α on physics and metrology would play a crucial role in the development of a unified theory of Nature. LANL's work on Yb^{2+} is also of interest to the National Institute for Science and Technology (NIST), since it can be the basis for a new optical frequency standard of exceptional stability. We are developing powerful frequency synthesis techniques based upon optical frequency comb technology that can be immediately applied to sensitive detection of atoms and molecules such as mercury (as mentioned above) and others. We are working closely with external funding agencies such as NA-22 to develop our new FLFC frequency synthesis techniques for standoff detection of material of interest. Our work on the ^{229}Th nuclear clock is also of serious interest to DARPA and we have been specifically encouraged by DARPA to pursue this idea with them. In this vein, we are in the process of answering the QuASAR (Quantum Assisted Sensing and Readout) BAA (Broad Agency Announcement) with a proposal to develop a ^{229}Th-based solid-state nuclear clock for national security.

As a final note, this LDRD project attracted one bright, young physicist who has moved into programmatic work and is expected to be offered a staff position within the coming fiscal year.

References

1. Webb, J. K., M. T. Murphy, V. V. Flambaum, V. A. Dzuba, J. D. Barrow, C. W. Churchill, J. X. Prochaska, and A. M. Wolfe. Further evidence for cosmological evolution of the fine structure constant. 2001. *Physical Review Letters.* **87** (9): 913011.

2. Ye cannae change the laws of physics. 2010. *The Economist, September 4th, 2010 - a review of a paper expected to print in Physical Review Letters later this year..*

3. Dzuba, V. A., V. V. Flambaum, and M. V. Marchenko. Relativistic effects in Sr, Dy, Yb II, and Yb III and search for variation of the fine-structure constant. 2003. *Physical Review. A.* **68** (2): 022506.

4. Porsev, S. G., V. V. Flambaum, and J. R. Torgerson. Transition frequency shifts with fine-structure constant variation for Yb II. 2009. *Physical Review A (Atomic, Molecular, and Optical Physics).* **80** (4): 042503 (6 pp.).

5. Rosenband, T., D. B. Hume, P. O. Schmidt, C. W. Chou, A. Brusch, L. Lorini, W. H. Oskay, R. E. Drullinger, T. M. Fortier, J. E. Stalnaker, S. A. Diddams, W. C. Swarm, N. R. Newbury, W. M. Itano, D. J. Wineland, and J. C. Bergquist. Frequency ratio of Al⁺ and Hg⁺ single-ion optical clocks; metrology at the 17th decimal place. 2008. *Science.* **319** (5871): 1808.

6. Berengut, J. C., V. A. Dzuba, V. V. Flambaum, and S. G. Porsev. Proposed experimental method to determine α sensitivity of splitting between ground and 7.6 eV isomeric states in ²²⁹Th. 2009. *Physical Review Letters.* **102** (21): 210801 (4 pp.).

7. Schauer, M. M., J. R. Danielson, A. -T. Nguyen, L. -B. Wang, X. Zhao, and J. R. Torgerson. Collisional population transfer in trapped Yb+ ions. 2009. *PHYSICAL REVIEW A.* **79** (6): 062705.

8. Nguyen, A. -T., L. -B. Wang, M. M. Schauer, and J. R. Torgerson. Extended temperature tuning of an ultraviolet diode laser for trapping and cooling single Yb+ ions. 2010. *Review of Scientific Instruments.* **81** (5): 053110.

9. Cingoz, A., A. Lapierre, A. -T. Nguyen, N. Leefer, D. Budker, S. K. Lamoreaux, and J. R. Torgerson. Limit on the temporal variation of the fine-structure constant. 2007. *Physical Review Letters.* **98** (4): 040801/1.

10. Leefer, N., A. Cingoz, B. Gerber-Siff, A. Sharma, J. R. Torgerson, and D. Budker. Transverse laser cooling of a thermal atomic beam of dysprosium. 2010. *PHYSICAL REVIEW A.* **81** (4): 043427.

11. Leefer, N. A., A. Cingoz, D. Budker, S. J. Ferrell, V. V. Yashchuk, A. Lapierre, A. -T. Nguyen, S. K. Lamoreaux, and J. R. Torgerson. VARIATION OF THE FINE-STRUCTURE CONSTANT AND LASER COOLING OF ATOMIC DYSPROSIUM. 2009. In *7th Symposium on Frequency Standards and Metrology ; 20081005 - 20081011 ; Pacific Grove, CA.* , p. 34.

12. Cingoz, A., N. A. Leefer, S. J. Ferrell, A. Lapierre, A. -T. Nguyen, V. V. Yashchuk, D. Budker, S. K. Lamoreaux, and J. R. Torgerson. A laboratory search for variation of the fine-structure constant using atomic dysprosium. 2008. *EUROPEAN PHYSICAL JOURNAL-SPECIAL TOPICS.* **163**: 71.

13. Rellergert, W., D. Demille, R. R. Greco, M. P. Hehlen, J. R. Torgerson, and E. Hudson. Constraining the evolution of the fundamental constants with a solid-state optical frequency reference based on the Th229 nucleus. 2010. *Physical Review Letters.* **104** (20): 200802.

Publications

Cingoz, A., A. Lapierre, A. -T. Nguyen, N. Leefer, D. Budker, S. K. Lamoreaux, and J. R. Torgerson. Limit on the temporal variation of the fine-structure constant. 2007. *Physical Review Letters.* **98** (4): 040801/1.

Cingoz, A., N. A. Leefer, S. J. Ferrell, A. Lapierre, A. -T. Nguyen, V. V. Yashchuk, D. Budker, S. K. Lamoreaux, and J. R. Torgerson. A laboratory search for variation of the fine-structure constant using atomic dysprosium. 2008. *EUROPEAN PHYSICAL JOURNAL-SPECIAL TOPICS.* **163**: 71.

Danielson, J. R., M. Schauer, S. Rahaman, Bouzhou Sun, Jiepeng Zhang, J. Torgerson, Xinxin Zhao, and Li-Bang Wang. Isotope Selective Trapping of Singly and Doubly Charged Yb Ions in an RF Trap. 2010. In *2010 Conference on Lasers and Electro-Optics (CLEO) ; 16-21 May 2010 ; San Jose, CA, USA.* , p. 1.

Ferrell, S. J., A. Cingoz, A. Lapierre, A. -T. Nguyen, N. Leefer, D. Budker, V. V. Flambaum, S. K. Lamoreaux, and J. R. Torgerson. Investigation of the gravitational-potential dependence of the fine-structure constant using atomic dysprosium. 2007. *Physical Review A (Atomic, Molecular, and Optical Physics).* **76** (6): 062104.

Leefer, N. A., A. Cingoz, D. Budker, S. J. Ferrell, V. V. Yashchuk, A. Lapierre, A. -T. Nguyen, S. K. Lamoreaux, and J. R. Torgerson. VARIATION OF THE FINE-STRUCTURE CONSTANT AND LASER COOLING OF ATOMIC DYSPROSIUM. 2009. In *7th Symposium on Frequency Standards and Metrology ; 20081005 - 20081011 ; Pacific Grove, CA.* , p. 34.

Leefer, N. A., A. Cingoz, D. Budker, S. J. Ferrell, V. V. Yashchuk, A. Lapierre, A. T. Nguyen, S. K. Lamoreaux, and J. R. Torgerson. A laboratory search for variation of the fine-structure constant using atomic dysprosium. 2008. *European Physical Journal.* **163**: 71.

Leefer, N., A. CingoÃàz, B. Gerber-Siff, A. Sharma, J. R. Torgerson, and D. Budker. Transverse laser cooling of a thermal atomic beam of dysprosium. 2010. *Physical Review A - Atomic, Molecular, and Optical Physics.* **81** (4): 043427.

Nguyen, A. -T., L. -B. Wang, M. M. Schauer, and J. R. Torgerson. Extended temperature tuning of an ultraviolet diode laser for trapping and cooling single Yb+ ions. 2010. *Review of Scientific Instruments.* **81** (5): 053110.

Porsev, S. G., V. V. Flambaum, and J. R. Torgerson. Transition frequency shifts with fine-structure constant variation for Yb II. 2009. *Physical Review A.* **80**: 042503.

Rellergert, W., D. DeMille, R. R. Greco, M. P. Hehlen, J. R. Torgerson, and E. Hudson. Constraining the Evolution of the Fundamental Constants with a Solid-State Optical Frequency Reference Based on the Th-229 Nucleus. 2010. *PHYSICAL REVIEW LETTERS.* **104** (20): 200802.

Rellergert, W., S. Sullivan, R. Shojaei, D. DeMille, R. Greco, M. Hehlen, J. Torgerson, and E. Hudson. Optical transition of the 229Th Nucleus in a Solid-State Environment. Presented at *Bulletin of the American Physical Society, 41st Annual Meeting of the Division of Atomic, Molecular, and Optical Physics.* (Houston, TX, 25-29 May, 2010).

Schauer, M. M., D. Feldbaum, A. T. Nguyen, L. B. Wang, X. Zhao, and J. R. Torgerson. Trapping and spectroscopy

of singly- and doubly-charged ytterbium ions. Presented at *39th Annual Meeting of the Division of Atomic, Molecular, and Optical Physics.* (State College, PA, 27-31 May, 2008).

Schauer, M. M., J. Danielson, D. Feldbaum, M. S. Rahaman, B. Sun, X. Zhao, and J. R. Torgerson. Trapping and Optical Detection of Doubly-charged Ytterbium Ions. Presented at *40th Annual Meeting of the Division of Atomic, Molecular, and Optical Physics.* (Charlottesville, VA, 19-23 May, 2009).

Schauer, M. M., J. Danielson, S. Rahaman, B. Sun, J. Zhang, X. Zhao, and J. R. Torgerson. Microwave and Optical Spectroscopy of Ytterbium Ions. Presented at *Bulletin of the American Physical Society, 41st Annual Meeting of the Division of Atomic, Molecular, and Optical Physics.* (Houston, Texas, 25-29 May, 2010).

Schauer, M. M., J. R. Danielson, A. -T. Nguyen, L. -B. Wang, X. Zhao, and J. R. Torgerson. Collisional population transfer in trapped Yb+ ions. 2009. *PHYSICAL REVIEW A.* **79** (6): 062705.

Schauer, M. M., J. R. Danielson, A. T. Nguyen, L. B. Wang, X. Zhao, and J. R. Torgerson. Collisional population transfer in trapped Yb+ ions. 2008. *Physical Review A.* **79**: 6062705.

Understanding the Feedback of Active Galaxies in Galaxy Clusters

Hui Li
20090174ER

Introduction

Clusters of galaxies are the largest gravitationally bound objects in the Universe. They are made up by dark matter (the dominant component) and the ordinary matter (called baryons). Interestingly, because the ordinary matter can dissipate by shocks and other physical processes, there is currently a lack of detailed understanding of the baryonic component in galaxy clusters. This has seriously hindered the application of galaxy clusters as reliable probes for cosmology. We propose to investigate the feedback of Active Galaxies in galaxy clusters to address this lack of understanding, building upon the distinctive capabilities at Los Alamos. Our new cosmological magnetohydrodynamics will allow us to model accurately the evolution of magnetic energy in the clusters for the first time.

Benefit to National Security Missions

This project will support the DOE mission in Office of Science by enhancing our understanding of how galaxy clusters evolve when important physical processes are included. These results will provide important constraints on the energy contained in clusters, which can be utilized to help constrain the key cosmological parameters for Dark Matter and Dark Energy. Our effort will strengthen Laboratory's competencies in Basic Sciences, especially in large-scale computer modeling.

Progress

We have completed a suite of cosmological MHD simulations (> 20 simulation runs) using the Institutional Computing machines (Lobo and Coyote) to investigate the evolution of magnetic fields in clusters with different initial energy inputs from various active galaxies (AGNs). These runs are motivated by the variety of observed AGNs in galaxy clusters. Our most significant results include: 1) A detailed characterization of multiple energy components in clusters. We found that, in a well relaxed cluster, the thermal energy is dominant, followed by the turbulent kinetic energy which is a factor of ~ 5 lower. The magnetic energy is about a factor of ~ 10 smaller than the thermal energy. This result provides critical information for modeling the energy contents of galaxy clusters as they are used for constraining the cosmological parameters. 2) Based on simulations, we have derived the radial profiles for the thermal, turbulent, and magnetic energies. These profiles are needed in order to make detailed comparison with X-ray, Sunyaev-Zel'dovich effect and radio observations of clusters.

By varying the injected energy from AGNs, from 10^{57} ergs to 10^{60} ergs, we have shown that the MHD turbulence in the intra-cluster medium (ICM) is a robust environment for amplifying magnetic fields via a small-scale dynamo process that eventually produces cluster-wide magnetic energy that saturates at a fraction of the total turbulent energy. This robustness implies that nearly all clusters that had an AGN in the early formation history will be guaranteed to have magnetic fields. We further predict that the total magnetic energy in a cluster is proportional to its turbulent energy.

We have performed further detailed analysis to understand the microphysical processes that govern the saturation of the magnetic field amplification. The saturation is affected first by the energy density balance between the turbulence energy and magnetic energy at small scales. Because the turbulence driving is episodic, the magnetic saturation is at a sub-equipartition level. The magnetic field strength is a critical input parameter for modeling the nonthermal radiation (both gamma-rays and radio emissions) from clusters.

We have also formed new collaboration with scientists from University of New Mexico to use the Extended Very-Large-Array to observe several galaxy clusters so that we can make comparisons between our simulation results and the observations. The observing proposal has been approved by EVLA and observations are planned for early 2011.

Future Work

We will continue the development of robust model for

the origin of cluster-wide magnetic fields in galaxy clusters. Another suite of large-scale simulations of AGN feedback in galaxy clusters is underway. These simulations will help us understand in more detail the saturation mechanism so that we can deduce a firm correlation between the magnetic field distribution and other cluster properties (density and turbulence level). These simulation results will be compared with the planned observations as well as available observations. Further comparison between our model and the observations of radio halos and relics will be conducted.

Conclusion

The proposed research addresses an important problem in modern astrophysics and cosmology. Clusters are being used as one of the important probes of fundamental cosmological parameters. Since clusters are made by both the dark matter and ordinary matter (baryons) components, our research will provide the physics underpinning for understanding the cluster baryon dynamics. The simulations being conducted are providing a quantitative understanding and description on the origin and magnitude of magnetic fields in clusters. This has important implications for modeling the X-ray, radio, gamma-ray and SZ effect observations (distortions in the spectrum of the cosmic microwave background caused by clusters). Detailed comparisons between the simulations and observations allow us to place constraints not only on our models but also on the cosmological parameters.

Publications

Collins, D., H. Xu, M. Norman, H. Li, and S. Li. Cosmological AMR MHD with Enzo. 2010. *Astrophysical Journal Supplements.* **186**: 308.

Xu, H., H. Li, D. Collins, S. Li, and M. Norman. Turbulence and Dynamo in Galaxy Cluster Medium: Implications on the Origin of Cluster magnetic fields. 2009. *Astrophysical Journal Letters.* **698**: L14.

Xu, H., H. Li, D. Collins, S. Li, and M. Norman. Evolution and Distribution of Magnetic Fields from AGNs in Galaxy Clusters. I. The Effect of Injection Energy and Redshift. To appear in *Astrophysical Journal.*

The First Characterization of Large Interstellar Dust

Rohan C. Loveland
20090176ER

Introduction

Our solar system is traveling at 26 km/s through the Local Interstellar Cloud (LIC), which is a partially ionized cloud within 3 parsecs (pc, about 3 light years or 31 trillion kilometers) of the sun that is warmer and less dense than regions around it. Our limited understanding of the LIC has been gained through measurements of the spectral attenuation of star light, neutral atoms that flow to the inner Solar System, and interstellar dust (ISD), but is still largely unknown. ISDs are particularly difficult to measure due to their size and paucity; hence only a few sparse data sets exist. These data include in situ impact detections with space experiments, which have poorly determined velocity and mass measurements, and ground-based measurements of the plasma that is created when an ISD enters Earth's atmosphere (i.e. a "meteor'). An important subset of ISD is the large grains. Large grains are relatively unaffected by Lorentz forces in the interstellar medium, thus we can use large ISD to accurately determine their original provenance and allow direct measurement of debris generated during the disk formation stage of nearby stellar systems. Unfortunately, large ISD grains are typically invisible to most observational techniques because their contribution to the total cross section for extinction is low.

We propose to provide the first characterization of large interstellar dust grains (ISD) that are typically invisible to most observational techniques due to their paucity. Our research will include data collection and analysis of ground-based radar data, in addition to applying models that are unique to LANL. Our goal is the characterization of ISD grains in order to discover the fundamental properties of the LIC. This information will be used to constrain models of stellar accretion and evolution.

Benefit to National Security Missions

This project will support the missions of the Office of Science by enhancing our understanding of interstellar dust and its impact on Earth's atmosphere. In addition, we will be able to characterize the flux of particles and their potential impact on Earth orbiting satellites, including nuclear detection sensors.

Progress

Substantial progress has been made towards the LDRD goals, both in terms of practical requirements (e.g. getting the data declassified), and scientific aspects (e.g. refinement of density calculation techniques).

Approximately 4 Tb of ALTAIR radar data, containing ~100,000 meteoroid streaks, have been acquired and rendered usable through declassification. Pioneering techniques for declassifying large datasets through the LANL system were developed to deal with this; all of the raw data has now been declassified.

Data reduction tools for identifying meteoroid streaks have been developed, based on Delaunay triangulation and iterative closure. Tools for linking and filtering streaks based on SNR, duration etc. have also been developed, as have automated scripts for applying these to multiple Terabytes of data.

Due to quantization issues preventing a simple conversion of range to range rate using differencing, a novel method of calculating range rates using Doppler shifted phase has been developed, with aliasing removal made possible using differencing derived constraints.

Algorithms for converting the radar monopulse information to 3-D trajectories have also been developed, as have density estimation methods based on the ballistic equation and a scattering model allowing conversion of the SNR to radar cross section.

These methods have been applied to generate densities for ~15,000 streaks. Based on these densities and corresponding range rates, a sub-population of interstellar meteoroids comprising ~5% of the total have been conclusively identified, thus fulfilling one of the original primary goals of this effort. Work has begun on orbital calculations in order to allow the identification of meteoroid sources.

Work on modeling head echo polarization features in order to identify fragmentation has also been conducted, as has a computer model of the coupled processes of

collisional heating, radiative cooling, evaporative cooling and ablation, and deceleration – for meteors composed of defined mixtures of mineral constituents.

The LDRD has resulted in collaborations with Stanford University, Boston University, the University of Washington, and NASA Marshall Space Flight Center. Presentations by LANL personnel and university collaborators have been made at the URSI, CEDAR, and Meteoroids 2010 conferences. A second project investigating electromagnetic phenomena resulting from meteoroid impacts has been recently funded, partially as a result of the work carried out so far in this LDRD.

Future Work

In the light of what we've learned so far we will pursue two main avenues of investigation. The first will be to construct a meteoroid flux map, while the second will be the development of models for individual meteoroid properties, such as composition and density.

The construction of a flux map will enable us to understand what the various sources of the meteoroids are that we see in our data. A key to the problem of investigating interstellars is being able to separate them from the sporadics, which make up the vast majority of what is present in our data. Determining whether we have actually seen any interstellars at all is critical; doing so will require the large scale data exploration which will of necessity be partially automated.

The investigation of individual meteoroid properties, such as composition and density, reveals information about the nature of the underlying sources. The sensitivity of the ALTAIR radar should allow us to contribute to, and refine, the current state of knowledge. This will be accomplished by combining empirical measurements of characteristics such as 3-D trajectory and deceleration with models of radar cross-sectional area using radar return signal amplitudes.

Conclusion

Our research will refine and contribute to the understanding of meteoroids on both a macroscopic and individual basis, through the construction of a flux map and the characterization of individual meteoroid properties. If interstellars are found to be present in our data, we will be in a strong position to contribute to, and refine, the current level of understanding about meteoroids and their sources. This will in turn advance our general understanding of space weather and how it affects both our satellites and spacecraft.

Publications

Close, S., T. Hamlin, M. Oppenheim, L. Cox, and P. Colestock. Dependence of radar signal strength on frequency and aspect angle of nonspecular meteor trails. 2008. *Hournal of Geophysical Research.* **113** (A06203): 1.

Loveland, R., A. Macdonell, S. Close, M. Oppenheim, and P. Colestock. Comparison of methods of determining meteoroid range rates from LFM chirped pulses. *Journal of Geophysical Research - Radio Science.*

Vertatschitch, L., J. Sahr, P. Colestock, and S. Close. Meteoroid head echo polarization features studied by numerical electromagnetics modeling. *Journal of Geophysical Research - Radio Science.*

Zinn, J., S. Close, P. Colestock, A. Macdonell, and R. Loveland. Analysis of ALTAIR 1998 meteor radar data. *Journal of Geophysical Research - Space Physics.*

Soild Helium-4: A Supersolid or Quantum Glass?

Matthias J. Graf
20090217ER

Introduction

The discovery of the putative supersolid state in solid Helium-4 in 2004 restarted a race for new measurements and theories to prove or disprove the existence of this exotic state of matter. This enigmatic state of matter is the crystalline analog of superfluidity and superconductivity. Essentially, the supersolid phase is the last remaining quantum phase that can exhibit persistent particle current of vacancies or interstitials with no dissipation, the analog to zero viscosity in a superfluid or zero resistance in a superconductor. Hence, the discovery and investigation of this phase is of fundamental importance to quantum physics and has created a stir far beyond the quantum solid and quantum fluid community.

We propose to explore the nature of the low-temperature phase in Helium-4, where the possible supersolid is reported by torsional oscillator measurements. The extremely low-temperature and high-pressure part of the Helium-4 phase diagram is the subject of our investigations. We investigate the consequences of disorder and contrast a supersolid scenario with a possible quantum glass state, torsional oscillator, elastic shear modulus, specific heat, thermal conductivity, and dielectric susceptibility experiments.

Benefit to National Security Missions

This proposal answers to the missions of the Office of Science and LANL's Grand Challenge "Fundamental Understanding of Materials" by advancing the state-of-the-art quantum state modeling and experimentation in condensed matter physics at ultralow temperatures and high pressures, with ramifications to the Grand Challenge "High Temperature Superconductivity and Actinides".

A better understanding of supersolid or quantum glass behavior may lead to better control and toward predictive capabilities for thermodynamic and mechanical materials properties for a large class of materials exhibiting disorder.

Progress

Our theoretical work focuses largely on the possible glassy state due to dislocations that might be responsible for the unusual behavior of solid Helium-4 at ultralow temperatures. We expanded our phenomenological glass model to account for general glass relaxation processes known from dielectric or structural glasses. An extension of our glassy scenario to more general distributions of relaxation times has led to better agreement with torsion oscillator experiments, see Figure 1. Consequently, we were invited to present these results at the international conference QFS 2009 at Northwestern University, Evanston, in August 2009.

Our hypothesis of a glassy component responsible for the anomalous behavior is also supported by new torsion oscillator measurements of our external collaborators headed by Davis at Cornell University and published in the journal of Science [1]. They found, using a new generation of ultrahigh precision torsion oscillators that solid Helium-4 exhibits very long relaxation times (sometimes lasting up to days) in the period shift and damping of the Helium-4 samples. These results clearly point toward the presence of uncrystallized glassy components down to 10 mK. So far the lowest temperatures measured in this quantum solid. Their data analysis was strongly motivated by our theoretical predictions and subsequent interactions with his group.

Since then we have continued to further develop a theory of glassy and viscoelastic dynamics of defects in solid Helium-4. We list details of these developments.

Thermodynamics - Pursuing our theory development, we found that glassy dynamics and glassy freeze-out allow us to address the anomalies observed in torsion oscillator, shear modulus, and pressure vs. temperature measurements. Developing a unified approach, we investigated the thermodynamic signatures of either supersolidity or glassy response in specific heat measurements to address the question of the existence of a true phase transition in solid Helium-4 at low temperatures. Remarkably, this is still a hotly debated question after six years of discovery. Our calculations indicate that

the observed excess specific heat at low temperatures is more consistent with a cross-over transition due to glassy relaxation processes of two-level tunneling systems than a Bose-Einstein condensation of vacancies. This calculation and data analysis further corroborates our proposed glassy interpretation of the observed anomaly [2].

Torsion oscillator - Our theory for the glassy response in torsion oscillators covers now a wide range of different distribution functions for glassy relaxors [3]. We demonstrated that the glass scenario accounts for many torsion oscillator experiments reported in the literature, see for example Figure 1. We presented these findings during an invited talk at the international conference QFS (Quantum Fluids and Solids) in 2009 and consequently published these results [4]. Based on this success, we developed a model with a glassy backaction for the coupled torsion oscillator experiment by Kojima's group at Rutgers. For the first time, a comprehensive interpretation of single and double torsion oscillators based on a linear response function analysis is possible. We presented these results at the workshop Supersolid 2010 in Paris and submitted a paper to J. Low Temp. Phys. [5].

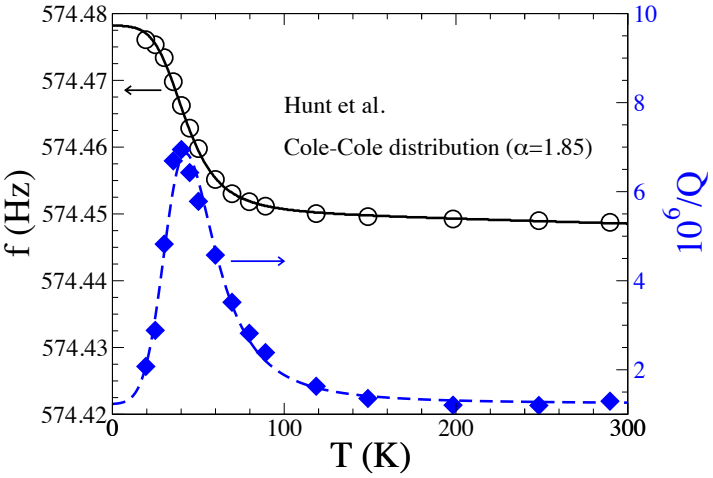

Figure 1. The resonant frequency (left axis) and dissipation (right axis) versus temperature of a high-precision torsion oscillator. Our model with a glassy backaction (solid lines) results in excellent agreement with the experimental data by B. Hunt and coworkers, when using a Cole-Cole distribution for relaxation times. The Cole-Cole exponent alpha=1.85 deviates from unity, indicating glassiness.

Shear modulus - Our most recent study of the anelastic response seen in shear modulus measurements is based on a glassy backaction onto the elastic deformation of a solid. The approach is similar to the linear response formulation of the torsion oscillator [6]. In this latest work, we account for the expected frequency dependence of the changes in the elastic modulus and the phase lag or dissipation as a function of temperature. Since a glass exhibits viscoelastic properties, we also developed a generalized Maxwell model comprised of elastic springs and dash-pots to describe the anelastic shear modulus in terms of a viscoelastic theory [7]. In a related study we investigated elastic deformations and their influence on a putative supersolid transition, which was submitted for publication by our long-term external collaborator Nussinov [8].

Heat transport - We continued our external collaboration with Vekhter at LSU to use thermal conductivity measurements as a probe for a potential phase transition in solid Helium-4. The modeling of lattice and vacancy contributions to the heat transport of existing measurements is so far consistent with conventional heat transport and scattering processes. There are big uncertainties in the modeling of various scattering processes due to a lack of proper crystal characterization of defects. Fortunately, new experiments have been performed by the Manchester group of Golov, extending to lower temperatures than previously and to ultrahigh purity samples with concentrations of as few as 10^{-15} Helium-3 atoms. We hope that our calculations will also apply to these new thermal conductivity measurements to ultimately address the question of an enigmatic glass vs. quantum coherent state.

Note a change in the scope of work: Unfortunately, our planned neutron scattering experiments (PDF and diffraction as well as small-angle scattering) with our external collaborator Goodkind from UCSD experienced another technical set-back due to the lack of low-temperature capabilities and a shortage of technical personnel at the Lujan center at LANSCE. After the second cancellation of our planned experiments at LANSCE, we decided not to pursuit these experiments any longer, until LANSCE has a proven track record of low-temperature capabilities and dedicated support in the milli-Kelvin regime.

In addition, we hired a postdoc, Jung-Jung Su, who has been working 50% FTE on this project since the end of July 2009. We also acquired much needed computational hardware and software to support our numerical approaches.

Future Work

We will further address the fundamental quantum physics question of a possible supersolid or quantum glass state in solid He-4. Currently, it is hotly debated whether the anomalies are due to supersolidity, quantum (dislocation) glass, quantum plasticity, or a conventional dislocation network.

Our research has the central theoretical goal: Develop a theory of a (quantum) glass state of He-4. Combined with bulk properties determined by thermal conductivity, shear modulus, torsion oscillators, we will provide important insights and interpretation for this anomalous ground state.

Within the framework of our glassy backaction model, we started developing a theory for the dielectric function, which also shows anomalous behavior similar to shear modulus and torsion oscillator. Finally, we have begun

developing models to include effects of velocity perturbations in torsion oscillator experiments or strain in shear modulus experiments. The effect of rim velocity dependence remains puzzling as it suppresses the frequency change similar to the temperature. Clearly a unification of rotation and strain effects will present a breakthrough and will be an important test for any theory. We expect that a "mechanical" temperature similar to jamming in granular materials may explain this phenomenon, rather than the loss of long-range coherence of a supersolid state.

Conclusion

In a nutshell, the supersolid phase is the last remaining quantum phase that can exhibit persistent particle current of vacancies or interstitials with no dissipation, similar to superfluidity or superconductivity.

The outcome of this research will either confirm the putative supersolid state or provide an alternative explanation, namely, that of a quantum glass or dislocation network and its effects on mechanical, elastic and thermal properties. Either way the results will impact the way we think about supersolidity and its hallmark signatures.

References

1. Hunt, B., E. Pratt, V. Gadagkar, M. Yamashita, A. V. Balatsky, and J. C. Davis. Evidence for a superglass state in solid Helium-4. 2009. *Science.* **324** (5927): 632.

2. Su, J., M. Graf, and A. Balatsky. A Glassy Contribution to the Heat Capacity of hcp He-4 Solids. 2010. *JOURNAL OF LOW TEMPERATURE PHYSICS.* **159** (3-4): 431.

3. Graf, M. J., A. V. Balatsky, Z. Nussinov, I. Grigorenko, and S. A. Trugman. Torsional oscillators and the entropy dilemma of putative supersolid ⁴He. 2009. In *Journal of Physics: Conference Series.* (Amsterdam, Netherlands, Aug. 2008). Vol. 150, p. 032025 (6 pp.). London: IOP.

4. Graf, M. J., Z. Nussinov, and A. V. Balatsky. The glassy response of solid Helium-4 to torsional oscillations. 2010. *Journal of Low Temperature Physics.* **158** (3-4): 550.

5. Graf, M. J., J. J. Su, H. P. Dahal, I. Grigorenko, and Z. Nussinov. The glassy response of double torsion oscillators in solid Helium-4 . *J. Low Temp. Phys..*

6. Su, Jung-Jung, M. J. Graf, and A. V. Balatsky. Glass Anomaly in the Shear Modulus of Solid ⁴He. 2010. *Physical Review Letters.* **105** (4): 045302 (4 pp.).

7. Su, J. J., M. J. Graf, and A. V. Balatsky. Shear modulus in viscoelastic solid 4He . *J. Low Temp. Phys..*

8. Arpornthip, T., A. V. Balatsky, M. J. Graf, and Z. Nussinov. The Influence Of Elastic Deformations On The Supersolid Transition . *Phys. Rev. B.*

Publications

Graf, M. J., A. V. Balatsky, Z. Nussinov, I. Grigorenko, and S. A. Trugman. Torsional oscillators and the entropy dilemma of putative supersolid ⁴He. 2009. In *25th International Conference on Low Temperature Physics (LT25) ; 6-13 Aug.* (2008 ; Amsterdam, Netherlands). Vol. 150, p. 032025 (6 pp.).

Graf, M. J., A. V. Balatsky, Z. Nussinov, I. Grigorenko, and S. A. Trugman. Torsional oscillators and the entropy dilemma of putative supersolid ⁴He. 2009. *Journal of Physics: Conference Series.* **150** (3): 032025.

Graf, M. J., J. J. Su, H. Dahal, I. Grigorenko, and Z. Nussinov. The glassy responses of double torsion oscillators in solid Helium-4. *submitted to J. Low Temp. Phys..*

Graf, M. J., Z. Nussinov, and A. V. Balatsky. The glassy response of solid ⁴He to torsional oscillations. 2010. *Journal of Low Temperature Physics.* **158** (3-4): 550.

Hunt, B., E. Pratt, V. Gadagkar, M. Yamashita, A. V. Balatsky, and J. C. Davis. Evidence for a Superglass State in Solid He-4. 2009. *SCIENCE.* **324** (5927): 632.

Su, J. J., M. J. Graf, and A. V. Balatsky. Shear modulus in viscoelastic solid Helium-4. *submitted to J. Low Temp. Phys..*

Su, J., M. Graf, and A. Balatsky. A Glassy Contribution to the Heat Capacity of hcp He-4 Solids. 2010. *JOURNAL OF LOW TEMPERATURE PHYSICS.* **159** (3-4): 431.

Su, J., M. Graf, and A. Balatsky. Glass anomaly in the shear modulus of solid He₄. 2010. *Physical Review Letters.* **105** (4): 045302.

A Novel Millimeter-Wave Traveling-Wave Tube Based on an Omniguide Structure

Evgenya I. Simakov
20090265ER

Introduction

Millimeter (mm)-wave devices are proving to have many important applications from imaging to communication. Among the greatest impediments to exploiting this regime of the electromagnetic spectrum are the difficulties in building sources with sufficient power suitable for practical applications. This project's goal is to construct a novel traveling-wave tube (TWT) amplifier at mm-waves (100 GHz) that employs a dielectric photonic band gap (PBG) structure. A TWT is a vacuum electronics tube amplifier that operates with a purpose of delivering high microwave power across a wide frequency bandwidth. Present state-of-the-art millimeter wave TWT development has reached fundamental limitations in both frequency and bandwidth that can be overcome with a use of a periodic electromagnetic structure (so called "PBG structure"), that is at the cutting edge of the electrical engineering technology applied to a real world problem. An extremely broadband TWT based on the PBG concept would enable new applications in mm-wave communications, radar receivers, radio astronomy, and remote mm-wave spectroscopy. A cylindrically symmetric version of a PBG structure, called an "omniguide," is attractive for a proof-of-principle demonstration. Omniguide TWT structures have great potential for generating high average power (up to 1 kW) with simultaneously large bandwidth (greater than 20 per cent) and linear dispersion [1]. In addition, being cheap to fabricate, omniguides enhance the commercial transferability of the W-band TWT technology. Because of new national security spectroscopy missions that would be enabled by this technology, this research directly addresses specific needs of the laboratory grand challenge "Detection of nuclear materials (Ubiquitous sensing)".

Benefit to National Security Missions

This project, through the development of new mm-wave sources, will impact a broad range of technical problems including imaging, sensing, and communication. These technical areas are crucial for supporting threat reduction, nuclear material detection, and other missions important to DOE (NN), DHS (DNDO), DOD (DARPA) and other government agencies.

Progress

The most significant outcome of the second year of the project was the first experimental demonstration of gain (power amplification in the presence of an electron beam) at 94 GHz in the omniguide tube (Figure 1) [2]. This proved the physical concept of using silica dielectric omniguide structure as a high frequency traveling wave tube amplifier.

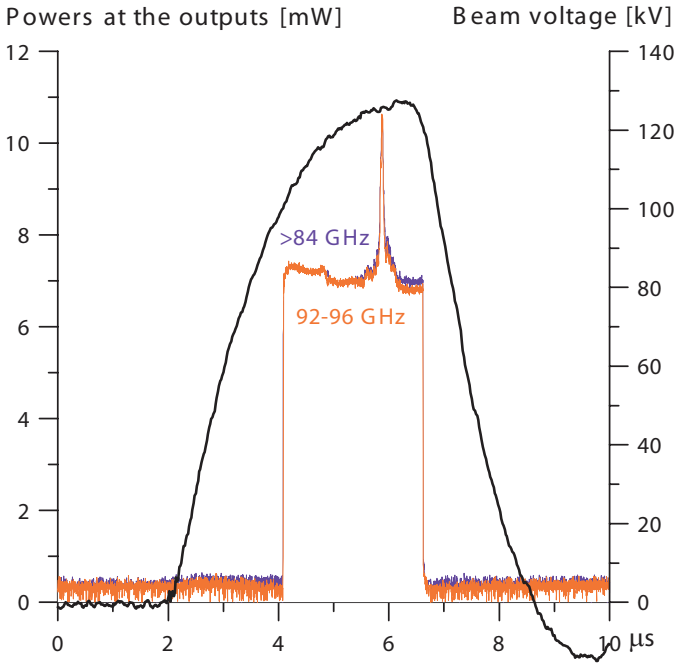

Figure 1. Measurement of the output power from the omniguide TWT. About 3 dB of gain is observed at 6 us, corresponding to the beam voltage of about 125 kV.

We started the year with replacing the electron gun cathode which was exposed to air during the ISR-division-wide shutdown in May of 2009 and poisoned by the oxygen. The design of the new electron gun was improved compared to the old design to reduce arching at high voltage. The beamline was then realigned for two reasons. First, the electron beam helical trajectory induced by the new cathode had to be eliminated; and second, the beam diameter had to be reduced to the

size small enough to pass through the omniguide tube. Significant efforts were also undertaken to improve the RF waveguide test stand for the gain measurement experiment. It included a repair of EIK input RF source for a high power gain test, and replacement of some of the waveguide components with new components with lower ohmic and reflection loss. A new omniguide tube was also manufactured and was 0.6 inches longer than the old tube (overall length of the new tube was 4.6 cm) and was supposed to provide higher gain (Figure 2). The new tube was tested for RF transmission with a network analyzer and performed according to the design.

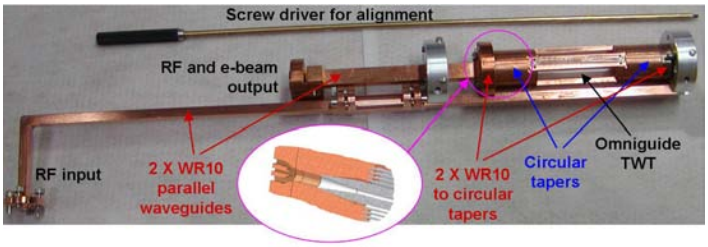

Figure 2. An assembled 46 mm long omniguide structure with the attached custom waveguide ports and adjustable aluminum mounts for the beamline. A part of the omniguide with a mode taper to a pair of WR10 waveguides is shown in the CAD section on top of the photograph.

The gain experiment started in January 2010. The gain experiment produced three very important and promising results. First, the omniguide dielectric tube performed well with the electron beam and did not show any charge accumulation. The tube was inspected after many shots and we did not discover any damage of the silica tubes which could potentially affect the performance. Second, reproducible amplification of RF radiation at 94 GHz by the electron beam in the omniguide was demonstrated. Third, the value of the gain was consistent with theoretical calculations for the beam current and voltage which were achieved in the experiment.

It was discovered however that the present beamline did not produce the electron beam of the sufficient quality. As a result, we were unable to pass the desired 2A of the electron beam through the omniguide at an optimum voltage (Figure 3). Thus, the observed gain varied between 1 and 3 dB, instead of the desired 10 dB. The problem was attributed to scraping of a high current 20 A electron beam to less than 2 A electron beam for focusing to a small aperture of the omniguide tube. Scraping of high energy beam produced plasma which deflected the rest of the beam in a random manner.

To overcome the problem we were forced to switch to a new beamline, with a 2 A electron gun. The new beamline required some extensive modifications before it could be used for the omniguide experiment. At this moment, the following modifications were accomplished. First, we have purchased most of the readily available necessary components. Second, we finished an extensive modification of a 2A gun for ensuring high vacuum pumping speed. Third, we successfully integrated a magnet used for the electron beam confinement with a DC power supply, and tested their operation. Fourth, we made drawings and ordered some custom components with expected delivery by the beginning of November, 2010. Finally, the new beamline with the installed electron gun passed the high vacuum tests. To complete the transfer of the omniguide experiment to the new beamline, the following steps still have to be accomplished. First, we will test the new electron gun at high voltage in November, 2010. Second, we will align the beamline with the electron beam. At that point we will finally be ready to test the omniguide with an electron beam of the proper voltage and current. It should result in demonstration of a 4 dB gain per centimeter of omniguide length with the omniguide being 4.6 cm long.

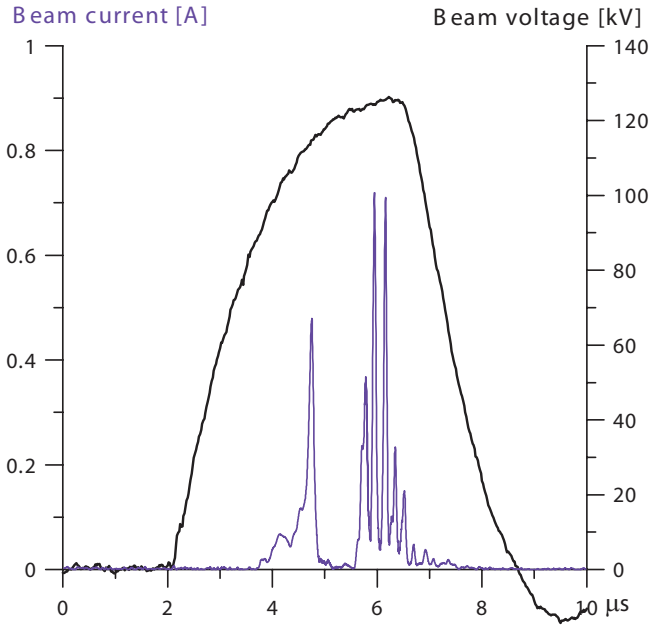

Figure 3. The voltage and current of the electron beam at the omniguide input (after passing the scraper). Only some narrow spikes of current get through the scraper/ collimator with the peak amplitude strongly reduced from initial 20 amperes produced by the electron gun.

Future Work

The successful completion of this project will yield a new mm-wave power-generating device, which is very compact, high power, high bandwidth and cheap to fabricate. The work can be divided into three interrelated areas as follows: testing of the omniguide traveling wave tube with an electron beam, working on improving the omniguide tube design, working on improving the test stand (electron beamline) itself. Specifically during the third year we will:

- Complete the assembly of a new beamline with a 2

A electron gun, which will produce higher quality 2 A electron beam than we could get before. This new beamline will improve our control of the beam transmission through the omniguide structure, accuracy and stability. We will overcome problems which we faced with the old beamline, namely generating plasma due to scraping of a 20 A beam into a 2 A beam, which prevented the complete beam transmission and generation of high power. We will test the new gun, align the beam focusing magnet, and tune the beam to have 2 microseconds beam pulse at a voltage of 110 kV with a current of 2 A focused inside of 0.6 mm wide aperture.

- Demonstrate 10 to 20 dB gain in an omniguide tube at 94 GHz. We will also measure amplification as a function of beam voltage and do a high power test with 100 W EIK as an input source. We will demonstrate the bandwidth of 10 per cent.

- Redesign the tube's output coupler to increase its bandwidth to 20 per cent. We will also work on coupler design to improve its power limit. Although silica cylinders which form the tube are capable of withstanding high gradients, the current design for the output coupler has metallic parts, which may be vulnerable to breakdown.

Conclusion

At the end of this project there will exist a new mm-wave power-generating device, that is very compact, high power, high bandwidth and cheap to fabricate. The new device will allow improved nuclear material detection and also can be used by our military forces in radars and secure communications.

References

1. Smirnova, E. I., L. M. Earley, and B. E. Carlsten. Fabrication and low-power tests of a W-band omniguide traveling-wave tube structure. 2008. *IEEE Transactions on Plasma Science.* **36** (3): 763.

2. Shchegolkov, D., L. Earley, W. Brian. Haynes, R. Renneke, E. Smirnova, and N. Yampolsky. 20.2: Testing of the omniguide traveling-wave tube. 2010. In *2010 IEEE International Vacuum Electronics Conference, IVEC 2010 ; 20100518 - 20100520 ; Monterey, CA, United States.* , p. 497.

Publications

Shchegolkov, D., L. Earley, W. Brian. Haynes, R. Renneke, E. Smirnova, and N. Yampolsky. 20.2: Testing of the omniguide traveling-wave tube. 2010. In *2010 IEEE International Vacuum Electronics Conference, IVEC 2010 ; 20100518 - 20100520 ; Monterey, CA, United States.* , p. 497.

Smirnova, E. I., L. M. Earley, W. B. Haynes, R. M. Renneke, and D. Yu. Shchegolkov. Omniguide traveling-wave tube structure testing with a 120 keV electron beam. Presented at *36th International Conference on Plasma Science.* (San Diego, CA, 31 May - 5 June, 2009).

Development of a Muon to Electron Conversion Experiment at LANSCE/MaRIE: Search for Physics beyond the Standard Model

Takeyasu Ito
20090269ER

Introduction

The ultimate goal of this research is to perform an experiment to search for a process in which a muon is converted to an electron in the field of an atomic nucleus without the emission of neutrinos. The muon is a particle that has very similar properties to those of the electron, except that the muon is much heavier than the electron. This process is highly suppressed in the Standard Model, a widely accepted theory that describes the ultimate constituents of matter and radiation, as we understand them. However, this theory is at best incomplete and the above-mentioned process is predicted by many extension of the Standard Model. Therefore, if found, this process unambiguously signifies the existence of physics beyond the Standard Model, providing a new breakthrough in our understanding of the Universe.

The LANSCE accelerator at LANL turns out to be the best facility at which to perform such an experiment. The original goal of this ER project was to further develop the physics basis for the experiment to a point where it is possible for us to seek an external funding to construct the experiment. Issues to be studied on the ER project included:

Beam delivery and experimental siting

- Can the necessary amount of beam with the necessary beam structure be delivered to the mu-e experiment in a way that is consistent with other activities at LANSCE?
- Where can the mu-e experiment be sited?

Beam extinction

Achieving a high extinction (the ratio of the accelerator current between beam-off vs beam-on, needs to be ~10^{-9}) is very important in order to suppress beam related background. We need to study the "base" extinction achievable just with the front-end chopper.

Expected sensitivity

Although we made progress in 1 and 2 above in FY09, we decided to join the Mu2e collaboration in Fermi National Laboratory, our competitor, because it became clearer that the Mu2e project was likely to go ahead and had a higher chance of success in getting funded. Our responsibility in the Mu2e project includes:

- Design the muon-stopping target. The muon-stopping target is at the heart of the Mu2e experiment, where muons stop to form muonic atoms where the expected muon-electron conversion process would occur. In the current design, the muon-stopping target consists of a series of thin aluminum disks. A careful optimization of the design of the muon-stopping target is crucial in maximizing the overall sensitivity of the experiment. This involves maximizing the muon stopping while minimizing the energy loss of the outgoing signal electrons in the target material.
- Design the muon stopping target monitor. The muon stopping in the target will be monitored by observing the muonic aluminum x rays using a germanium detector.
- Design the proton absorber. The proton absorber slows down or absorbs the protons from the muon-stopping target due to muon capture in order to reduce the count rate at the tracking detector. The design needs to be properly optimized so that it effectively reduces the proton rate at the detector without affecting the energy of the signal electrons.

These tasks are in line with the expertise of the PI, who has an extensive experience in optimizing stopping target and detection of exotic atom x-ray measurements.

In this FY, we continued our study of the LANSCE accelerator properties while we ramped up our effort on the Mu2e muon-stopping target design optimization and the design of the muon stopping target monitor.

Benefit to National Security Missions

This project will contribute to our basic understanding of forces and processes in the universe governed by the "Standard Model." It directly addresses issues in

the LANL "Beyond the Standard Model" Grand Challenge and impacts basic understanding of physics that underlies nuclear weapons, a key DOE mission.

Progress

In this FY, we made progress on two fronts: 1) study of the LANSCE accelerator properties and 2) design optimization of the Mu2e muon-stopping target.

Last FY, we identified a couple of modes in which the LANCE accelerators can be operated to meet the requirements. One of such modes is to use the H+ beam at 20 Hz when the H- beam is delivered to the Lujan center. One possible contribution to the background in this mode of running is from H+ particles created by H- particles getting stripped upstream and downstream of the accelerator. In order to evaluate such contributions, we performed a series of measurements using image plates. The accelerator was run in the H- mode (which is the only mode it can run currently), and an image plate was inserted into the H+ beamline. The image plate detected any H+ particles that were generated by H- particles getting stripped and were transported down to the H+ beamline. From a preliminary analysis of the data, we determined that the contribution from the vacuum stripping downstream of the accelerator is small and is at an acceptable level for the mu-e experiment. However, the contribution from the front-end part of the accelerator is rather large, although it could potentially be reduced and kept at an acceptable level by improving the vacuum. A more detailed analysis including an estimate of such effects based on a model calculation is currently underway. Preliminary results were presented at the LINAC10, the 25th Linear Accelerator Conference. Together with the data we had taken previously on the effectiveness of the front-end chopper, we plan to publish the results in an accelerator journal.

As part of the target design task, we performed the following studies:

1. Evaluation of allowed contaminants in the target and the required elemental purity of the target. If the energy spectrum of the decay-in-orbit electrons from the impurity atoms has a higher end-point energy than that for the target material (=aluminum), then the decay-in-orbit electrons can contribute to a background. Oxygen atoms are in particular problematic, because it has the highest decay-in-orbit end-point energy among all elements. We evaluated the allowed amount of oxygen contamination in the target material.

2. Evaluation of the target heating. The target disks are heated due to the beam muons and electrons that stop or go through them. The heating of the target was evaluated, and it was confirmed that enough heat could be dissipated solely by radiation.

3. Evaluation of the possible force due to eddy currents that the target disks can experience when the detector solenoid quenches. The muon-stopping target is located in the warm bore of a superconducting solenoid. The target disks need to be held with a minimum amount of materials. The largest force that the target support structure should be able to handle is the force due to eddy currents during magnet quench. The size of the force was evaluated, which is to be used in the engineering design of the target support.

We also completed a very preliminary engineering design of the target support structure.

On the muon stopping target monitor, we started to work on the engineering design of the germanium detector mount. We plan to have a test run at Paul Scherrer Institute in Switerland or TRIUMF (Canada's nuclear physics laboratory) next summer, in which we plan to stop slow muons in aluminum target and to observe muonic aluminum x rays. We have acquired a germanium detector to prepare for the test run.

Future Work

Our goal for FY11 is to complete the muon-stopping target design. To this end, we will perform a detailed simulation study to optimize the stopping target design. In particular we will study the following issues:

1. Optimize the target geometry for flat target disks. We will vary various parameters, such as the thickness and radius of each disk, and the inter-disk spacing. The goal is to come up with a geometry that minimizes the outgoing electrons' energy loss while maintaining the required muon stopping.

2. Study the effects of the target supporting structure. The goal is to come up with a realistic engineering design of the stopping target support that is consistent with the physics requirements.

3. Explore non-flat disk geometries of the stopping target.

4. Optimize the design of the proton absorber including both the material choice and the geometry

Once a realistic engineering target design is arrived at, we will produce a prototype target. We will also produce a prototype proton absorber.

We will also continue to work on the design of the muon stopping-target monitor. Here possible radiation damage to the detector and the size of the signal need to be taken into consideration. It is beneficial to the project if we gain experience in detecting muonic x rays. We plan to take our germanium detector either to Paul Scherrer Institute in Switzerland or to TRIUMF in Canada, where a muon beam is available.

We also plan to document everything we learned from our

study on the possibility of building a mu-e conversion experiment at LANSCE. If, for some reason, the Mu2e project at Fermilab does not get a go-ahead, such a document will form a basis of a possible future project to build such an experiment at LANSCE.

Conclusion

We are making progress both on studying the LANSCE accelerator properties in the context of building a mu-e conversion experiment and on the design of the FNAL Mu2e experiment's muon-stopping target. We plan to document the results of our study on the possibility of building a mu-e conversion experiment at LANSCE at the end of FY11. We also plan to conclude our design effort on the muon stopping target, the muon stopping target monitor, and the proton absorber for the Mu2e experiment, which we believe to be a great contribution to the Mu2e project.

Publications

Ito, T.. Possibility of a muon electron conversion experiment at LANSCE: search for physics beyond the standard model. Presented at *LANSCE users' group meeting.* (Santa Fe, NM, 30 Sep - 1 Oct, 2009).

McCrady, R. C., T. Ito, M. Cooper, and A. Saunders. Stripping of H-beams by residual gas in the linac at the Los Alamos Neutron Science Center. To appear in *25th International Linear Accelerator Conference (LINAC10).* (Tsukuba, Japan, 12-17 September, 2010).

Unconventional Methods for Quantum-enhanced Metrology

Malcolm G. Boshier
20090284ER

Introduction

Precision measurement is crucial to many areas of national security and industrial technology, and basic science, for characterization and control of complex systems. The act of performing any physical experiment is, in fact, a measurement, and therefore metrological techniques are central to all we know about the world. There are obviously many practical applications as well; sensing of all types is rapidly becoming paramount for more complete knowledge of what is built, stored, or moved across borders, behind barriers, or underground. Reduction of the time or total energy in sensing can make the process harder for an adversary to detect. Hence reducing the resources required to make measurements to a given precision, or increasing the precision attainable with given resources, is a critical task for scientific, technological, and national security applications.

Toward these ends, we will develop quantum-informational techniques that we expect will lead to new devices capable of measuring many physical quantities to what may be extraordinary precision while requiring significantly fewer resources than devices based on traditional measurement protocols. In particular, we will use single atoms trapped on-chip and employ them for quantum enhanced measurements of externally applied fields and forces of interest, surpassing the shot-noise "limit" to measurement. We will also investigate using nonlinear interactions in ultracold atomic gases to perform interferometry with precision below the standard quantum limit. Theoretically, we will explore nonlinear quantum metrology and its application to such devices. Through multi-atom couplings produced during a measurement, enhanced sensitivity may be achieved.

Benefit to National Security Missions

This project will support the DOE mission in Threat Reduction and the "ubiquitous sensing" Laboratory Grand Challenge by enhancing our understanding of how sensing can be improved beyond standard limits using quantum technology. We will work to transition it to programs supporting this mission, such as those sponsored by the IC. The project also supports the mission of the Office of Science for better understanding of fundamental quantum behavior, including that of complex materials.

Progress

The project has two experimental threads, one with trapped ions and the other with ultracold Bose-Einstein condensates (BECs), and a complementary theory thread.

In the trapped ion thread we have now brought the laboratory to the point where everything is in place to implement the phase estimation algorithm which is one of the below-standard quantum limit (SQL) measurement strategies we are pursuing. Through upgrades and enhancements in the laser systems, the imaging system, and the data acquisition and experiment control system, we are now able to reliably prepare ions in the ground state of the trap potential with greater than 90% fidelity, and then coherently control their subsequent evolution over almost 1ms. A novel transfer cavity system for stabilizing the frequencies of three of the four lasers required in the experiment has been an essential component of this part of the project. We expect that workers in other areas of atomic and optical physics will find it to be a useful technology.

We are simultaneously pursuing a second experimental approach to sub-SQL metrology, namely a nonlinear interferometry scheme invented by Carl Caves at UNM [1]. This technique promises measurement precision which not only exceeds the SQL, but can also surpass the so-called Heisenberg limit where measurement uncertainty scales as 1/N, with N being the number of resources involved in the measurement (in this case, the number of atoms in the BEC). The key requirement for implementing Caves' scheme is that the BEC wavefunction not change size appreciably with the number of atoms N. We realized that the toroidal condensates created with our painted potential technology satisify this requirement very well because the BEC is effectively frozen into the ground state of the potential in the two radial coordinates, but completely free to move in the azimuthal direction (i.e. around the circumference of the torus). We

have now performed extensive numerical simulations of Caves' interferometer scheme as it would be applied in our apparatus, and the results are extremely promising. One initial cause for concern was that when the condensate is put into a superposition of two internal states (i.e. following the "beamsplitter" in the interferometer description of the process), the slightly different interaction strengths of each state with itself and with the other state would drive a complex evolution that would in turn decrease the spatial overlap and hence the fringe contrast. We now know from our simulations that this is not the case, and so we will now move forward with the experimental implementation.

The theory thread, in addition to supporting the two experiments, has also been considering the main goal in quantum metrology: the estimation of parameters at resolutions that are classically impossible. Methods for quantum metrology can be interpreted as quantum algorithms in the so-called quantum query model, where one is given a black-box that implements an unknown operation, and such operation encodes the parameter to be estimated. For example, the typical case in single parameter estimation is that where the black-box implements an unknown spin rotation around a given axis, and the magnitude of the rotation is the parameter to be estimated. For this reason, it is important to study the costs of different quantum methods for black-box estimation. An important such method is adiabatic quantum computing, where the goal is to estimate the black-box by performing continuous-time evolutions by interleaving the black-box with other, known, evolutions. Adiabatic quantum computing is important because it is equivalent to the standard model of quantum computation. Lower bounds on the cost of adiabatic-like quantum algorithms (in the query model) where unknown until we recently showed that general quantum processes that prepare a target state (eigenstate of a Hamiltonian) require a minimum time proportional to the ratio of the length of the eigenstate path to the gap [2]. This result sets a lower bound on the cost of algorithms for black-box estimation and, in particular, it shows that adiabatic quantum methods could in principle estimate parameters with quadratically improved precisions over classical methods. In addition, we recently proposed and studied the so-called spectral gap amplification problem (GAP) that considers questions such as "what are the optimal quantum strategies to compute low-temperature parameters of quantum systems?". We showed that there exists a large family of systems for which a quadratic gap amplification is possible. For this family, zero-temperature properties can be obtained with a quadratic enhancement in precision when compared to "classical" methods for the same goal. We plan to submit this work for publication in the near future.

A second part of the theory thread considers the problem of using BECs to detect rotational motion of surfaces in close proximity. It turns out that provided the rotating surface is non-flat, it can induce an anisotropic Casimir-Polder potential that modifies the dynamics of the condensate and can drive quantized vortices via quantum vacuum fluctuations. In particular, we have studied the case of a lamellar Si grating rotating above a BEC and shown that contactless transfer of angular momentum from the surface to the atomic cloud is possible. The resulting quantum torque is strong enough that quantized vortices should be observable under realistic experimental conditions at separation distances around 3 microns [3]. Both this work and a second paper giving the general exact theory of atom-grating interactions [4] have been submitted for publication. The detection of rotation via the BEC in this analysis is done at the SQL, basically because the initial state of the BEC is assumed to be simply a coherent state. The next step will be to study the possibility of going beyond SQL detection of rotation by means of exotic initial BEC states, such as superposition states.

Future Work

The long-term goals of our program for quantum-enhanced measurement include the development of methods for measurement far beyond the capabilities of present probes of electromagnetic fields and forces. The near-term goals involve proof-of-principle demonstrations of such methods (with modest initial enhancements beyond standard classically-enabled technologies) and theoretical investigation of novel protocols that may be derived from quantum information processing algorithms and information-theoretic principles.

We expect that precision measurement beyond the standard quantum limit (also known as the "shot noise" limit), approaching the Heisenberg limit, can be implemented in our trapped-ion quantum information processing system. In particular, we plan (i) to make determinations of parameters such as frequency, magnetic field, and force (via displacement or rotation) to a given precision using fewer resources than standard methods (such as Ramsey spectroscopy or standard displacement measurement); or (ii) to make these determinations to a higher precision using similar resources to standard methods. A quadratic, or greater, reduction in resources or increase in precision, respectively, should be possible with these methods. We plan to demonstrate such gains in the lab when measuring real parameters through a direct comparison of the proposed and standard methods.

Concurrent explorations of unconventional nonlinear quantum methods for metrology will provide guidance for the experiments and establish the capability of possible future experimental methods. These will focus on many-body coherent interactions during the measurement process. Such interactions can lead to drastic minimization of the resources required for measurements made using experimental probes amenable to large-scale entanglement, such as atomic ensembles or collections of interacting quantum bits. A nonlinear scaling of the parameter estimation precision, inversely proportional to the number of

particles raised to the power of the degree of interactions, may be attainable, leading to significant gains in measurement speed and precision.

Conclusion

We hope to be able to develop, and in some cases demonstrate, proof-of-principle techniques that will allow for enhanced measurement of physical quantities whose determination is required for threat reduction and basic environmental measurement. Techniques derived from quantum algorithms will allow far more precise measurement of many parameters of interest using reduced resources, possibly enabling sensing of adversaries without detection or reductions in energy requirements for portable sensing technologies.

References

1. Boixo, S., A. Datta, M. J. Davis, A. Shaji, A. B. Tacla, and C. M. Caves. Quantum-limited metrology and Bose-Einstein condensates. 2009. *Physical Review A (Atomic, Molecular, and Optical Physics).* **80** (3): 032103 (16 pp.).

2. Boixo, S., and R. D. Somma. Necessary condition for the quantum adiabatic approximation. 2010. *Physical Review A - Atomic, Molecular, and Optical Physics.* **81** (3): 032308.

3. Impens, F., A. M. Contreras-Reyes, P. A. Maia Neto, D. A. R. Dalvit, R. Guérout, A. Lambrecht, and S. Reynaud. Driving quantized vortices with quantum vacuum fluctuations. To appear in *Europhysics Letters.*

4. Contreras-Reyes, A. M., R. Guérout, P. A. Maia Neto, D. A. R. Dalvit, A. Lambrecht, and S. Reynaud. Casimir-Polder interaction between an atom and a dielectric grating. To appear in *Physics Review A.*

Publications

Boixo, S., and R. D. Somma. Necessary condition for the quantum adiabatic approximation. 2010. *Physical Review A - Atomic, Molecular, and Optical Physics.* **81** (3): 032308.

Contreras-Reyes, A. M., R. Guérout, P. A. Maia Neto, D. A. R. Dalvit, A. Lambrecht, and S. Reynaud. Casimir-Polder interaction between an atom and a dielectric grating. To appear in *Physics Review A.*

Impens, F., A. M. Contreras-Reyes, P. A. Maia Neto, D. A. R. Dalvit, R. Guérout, A. Lambrecht, and S. Reynaud. Driving quantized vortices with quantum vacuum fluctuations. To appear in *Europhysics Letters.*

First Unambiguous Measurement of Jet Fragmentation and Energy Loss in the Quark Gluon Plasma

Gerd J. Kunde
20090303ER

Introduction

We propose to work on the Compact Muon Solenoid (CMS) experiment [1] at the Large Hadron collider with the goal to measure properties of the quark-gluon plasma via a new probe, the modification of particle production from the decay of the fundamental but unstable constituents of matter. We call this effect 'modification of the fragmentation functions'.

Collisions of lead nuclei at the highest energies ever created in a laboratory will lead to the production of a plasma of elementary particles, such as quarks and gluons. While detected previously the properties of this new state of matter are not known.

We propose an integrated approach of physics analysis, software infrastructure and highly integrated state-of-the-art ultra-high speed data and signal processing electronics. We propose to study the strongly interacting quark-gluon plasma by tagging strongly interacting particles traversing the plasma with a non-interacting electromagnetic probe [2,3]. Comparison of the plasma measurement with a vacuum measurement will lead to a quantitative measurement of the density and temperature of the plasma.

The probe manifests in the detector as pair of muons (a heavy version of the electron). The detector is designed to measure these muons. We will enhance the capabilities of the CMS detector by adding high-speed electronics to cleanly detect these muons in the background of all the other particles produced, therefore enabling the measurement.

Benefit to National Security Missions

One of the eleven science questions for the 21st century (National-Research-Council) addresses the properties of new states of matter such as the quark-gluon plasma, a stated goal of the DOE Office of Science long range plan. Threat reduction is a secondary goal enabled by the ultra-high speed data processing.

Progress

The Compact Muon Solenoid (CMS) experiment has begun recording proton-proton collisions at the world's highest energies using the Large Hadron Collider at CERN in March 2010, to date this effort yielded already 9 reviewed publications. These includes two papers which were pushed by the CMS heavy ion group, one on particle multiplicities and one about particle correlations. These papers were received by the community with great interest and lots of discussion. They will serve as a baseline for the QGP measurements which will follow in the last year of this ER.

The first heavy ion run started November 3rd 2010. Much of the past 12 month of our ER effort were spend preparing for first run of Pb-Pb collisions at unprecedented energies; in terms of theory predictions, analysis software development and hardware testing and development. A problem has been discovered with the readout of the silicon pixel tracker that is at the heart of the experiment. Insufficient buffering capacity exists in the frontend readout electronics to store all of the particle hits that occur during central Pb-Pb collisions with high multiplicity at high collision frequencies.

Our technical solution to this problem is twofold: Firstly we were involved in finding a solution for the first two years of data taking, at low collision rates, by helping to devise a trigger hold-off scheme that allows for emptying the aforementioned buffers before accepting new events. This required rigorous testing of the system performance, adding the hold-off scheme to the readout system as well as testing the solution at CERN. We are now reasonably confident that the first year of Pb-Pb data talking should be possible with a minimal dead time introduced by the pixel hold-off. We will be at CERN during the first heavy ion collisions to help assess the performance of the system and devise possible solutions should there be any surprises.

Secondly, custom FPGA based hardware was designed and constructed by us that can electronically inject hits from simulation or from real, previously recorded, events into the front end drivers of the CMS silicon pixel read-

out system. These injected events are distributed according to the LHC beam bucket fill structure and interaction probability and will allow us to perform tests of the readout hardware, not possible via software simulation alone. By varying the number of added hits and the trigger frequency, we are studying the failure modes of the readout system. Information gleaned from this exercise will guide us in the preparation for run two, with more bunches in the machine. In addition these data will help the design of replacement hardware for CMS, which will operate correctly for high luminosity heavy ion collisions in 2013.

We have completed the design, construction and testing of the required custom FPGA hardware. Much of the VHDL code necessary to program the FPGAs has been written and tested, our custom hardware is presently being operated in the test bench setup of the CMS experiment.

In September, we did our first test of the new hardware at CERN. Using the Virtex6 development board and the new Spartan 3 cards developed at LANL, we were able to start exercising the Front End Drivers (FED) for the Pixel system. This new testing hardware generates data according to the LHC beam fill structure, folded with physics simulation of Heavy Ion (HI) interactions, to simulate as closely as possible the real hit distribution in the pixel detector. This enables us to study more closely the response of the FEDs to the real HI data taking, which is currently underway. We will continue our tests in the middle of November at CERN, at the same time as Heavy Ion data are being taken. Comparing real data behavior with our simulation is crucial to get a full understanding of the underlying problem and ultimately to develop the solution.

On the physics side, we are currently leading the dilepton analysis effort in CMS Heavy Ions in the person of our postdoc Catherine Silvestre, she was elected by CMS to be the convener of the dilepton group which is holding weekly meetings. The LANL's physics push led the CMS heavy ion group to accept the analysis of obtaining Z^0 cross sections from the first year Pb-Pb data as a very high priority and therefore this publication will be one of the first heavy ion papers. This new and important measurement was never before attempted for heavy ion collisions. In preparation for this goal, a very successful mid-summer mock data challenge was held and within a week of obtaining simulation data, the Z^0 cross section was extracted. This involved the determination of trigger and reconstruction efficiencies as well as acceptance corrections. After the revelation of the monte carlo truth, it was clear that the dilepton team had performed very well.

The recent push, before the data taking, was geared towards improving reconstruction efficiencies, by evaluating various tracking schemes, and to improving measurements of reconstruction efficiencies, by embedding into monte carlo and future real events.

In the theory of heavy ion collisions, one of the least understood experimental results is the large suppression in the production rate of energetic particles relative to the same rate in proton-proton collisions. Specifically, it is not clear whether quark and gluon energy loss effects or a possible universal modification of their fragmentation in observable hadrons, dominates this suppression pattern. To shed light on this problem, we calculated the decay functions of heavy charm and beauty quarks in the vacuum and in the background of a thermal medium – the quark gluon plasma [4]. We demonstrated that these fragmentation functions are not significantly altered at high temperature. Consequently, the mechanism of the observed meson suppression is related to inelastic energy loss processes in the plasma.

We also completed accurate calculations of Z boson + jet production at the LHC [5]. This final state is one of the principal experimental channels that LHC experiments will use to determine quark and gluon energy loss in the plasma. Electroweak bosons, in conjunction with jets in high energy collider experiments, are also one of the principle final-state channels that can be used to test the accuracy of the perturbation theory of strong interactions calculations. This assess the potential of the experiments to uncover new physics through comparison between data and theory. We demonstrated conclusively that beyond the most naïve theoretical estimates, known as tree level calculations, Z boson measurements do not constrain the energy of the leading recoil jet with better than 25% accuracy. Precise baseline experimental measurements of these distributions in p+p collisions and theoretical calculations, such as the one that we have performed, are necessary to enable physics extraction in the upcoming heavy ion runs. Last, but not least, we have made theoretical prediction for the expected modification of the Z-tagged recoil jet spectrum in Pb-Pb collisions at the LHC.

Future Work

The qualitatively new experimental approach proposed here is the measurement of jets tagged by Z0s at the Large Hadron Collider (LHC). We will also concurrently develop the supporting perturbative many-body Quantum Chromodynamics (QCD) theory.

This breakthrough approach will allow in the future for the first time the reconstruction of the full jet fragmentation function and its in-medium modification. (Fragmentation functions describe the probability of a quark or gluon to produce a given momentum final state hadron.) These new data will severely constrain the current theoretical models of jet energy loss and thus allow for a precise determination of the plasma properties

Experimental goals:

- Develop a solution for the high luminosity readout system.
- Measure as a first step the Z0 cross section and esti-

mate the nuclear modification factor in Pb-Pb collisions at the LHC.

- Present and publish the results.
- Write proposal to DOE for future founding of the LHC studies.

Theoretical goals:

- A non-universal, and consequently non-factorizable, redistribution of the jet fragments due to collisional and radiative processes in the QGP initiated by many-body jet-medium interactions;
- The possibility of a universal modification of fragmentation distributions in the presence of a thermalized medium.

The first approach naturally extends the current studies of leading particle suppression, but requires detailed new insight into bremsstrahlung processes for much higher jet energies than presently available at RHIC.

Conclusion

The project will lead to measurements of the properties of the quark-gluon plasma (QGP) such as its temperature and density, which are currently not very well constraint. The quark-gluon plasma was discovered at the Relativistic Heavy Ion Collider (RHIC) in near the speed of light collisions of gold nuclei. The QGP properties can now be measured quantitatively at the Large Hadron Collider (LHC). In addition to the measurement there is a large discover potential for new physics which will revolutionize our understanding of universe.

References

1. Enterria, D., M. Ballintijn, M. Bedjidian, D. Hofman, O. Kodolova, C. Loizides, C. Lourenço, C. Mironov, S. Petrushanko, C. Roland, G. Roland, F. Sikler, and G. Veres. CMS Physics Technical Design Report: Addendum on High Density QCD with Heavy Ions. 2007. *Journal Physics G: Nuclear Particle Physics 34 2307.* **J. Phys. G** (34): 2307.

2. Srivastava, D., C. Gale, and T. Awes. Dilepton tagged jets in relativistic nucleus nucleus collisions: A Case study. 2003. *Physical Review C.* : 054904.

3. Kunde, G. J., H. van Hecke , K. Hessler, and C. Mironov. Z0-tagged quark jets at the large hadron collider . 2009. *The European Physical Journal C - Particles and Fields Volume 61, Number 4, 785-788 .* **European Phys. Journal C** (61, 4): 785.

4. Vitev, I., and B. Zhang. Jet tomography of high-energy nucleus-nucleus collisions at next-to-leading order. 2010. *Physical Review Letters.* **104** (13): 132001.

5. Neufeld, R. B.. Jets associated with Z⁰ boson production in heavy-ion collisions at the LHC. 2010. In *26th Winter Workshop on Nuclear Dynamics ; 2-9 Jan.* (2010 ; Ocho Rios, Jamaica). Vol. 230, 1 Edition, p. 012035 (6 pp.).

Publications

Neufeld, R. B.. Jets associated with Z⁰ boson production in heavy-ion collisions at the LHC. 2010. In *26th Winter Workshop on Nuclear Dynamics ; 2-9 Jan.* (2010 ; Ocho Rios, Jamaica). Vol. 230, 1 Edition, p. 012035 (6 pp.).

Vitev, I., and B. Zhang. Jet tomography of high-energy nucleus-nucleus collisions at next-to-leading order. 2010. *Physical Review Letters.* **104** (13): 132001.

Breakthroughs in Magnetic Reconnection Enabled by Petaflop Scale Computing

Lin Yin
20090306ER

Introduction

Magnetic reconnection is a fundamental process that occurs within hot ionized gases known as plasmas. This process often releases energy explosively as the magnetic field undergoes a rapid reconfiguration. Scientists believe this process plays an important role in space, laboratory and astrophysical phenomena, with a variety of real and potential applications. This research is leading to new advances in this field by utilizing the world's fastest supercomputers to perform unprecedented three-dimensional (3D) simulations. The primary focus is to better understand what causes magnetic reconnection to suddenly develop and how it proceeds in real applications. The research involves a combination of theory and large-scale computer simulations that describe the plasma at the most basic level. The project is utilizing the computer code VPIC, which has been carefully designed to run on new supercomputers, including the Roadrunner machine at Los Alamos. This project also uses theoretical approaches in order to better understand the results of these computer calculations. These tools are leading to groundbreaking new discoveries regarding the complicated 3D evolution of this process for both space and laboratory plasmas.

Benefit to National Security Missions

This project will support the DOE mission in Nuclear Weapons by enhancing our understanding of high temperature plasmas and by pushing the limits of large-scale simulations using the new hybrid computing technology on the Roadrunner supercomputer. The project supports the energy mission by advancing our understanding of magnetic reconnection, which is an important dynamical process in magnetic fusion machines. This research may indirectly benefit the nonproliferation mission since magnetic reconnection is also important in modeling the near-Earth space environment to better understand and mitigate the risks to satellites from extreme space weather events.

Progress

In the past year, we have made significant progress in understanding how magnetic reconnection evolves in 3D configurations relevant to the Earth's magnetosphere, a protective bubble of plasma surrounding our planet. In addition, we have performed computer simulations designed to mimic a laboratory experiment (MRX device at Princeton), where detailed measurements are available. Our initial simulations were performed on *Roadrunner* during the 2009 open science campaign, but during the past year we have utilized the *Kraken* supercomputer at Oakridge, performing a series of runs using up to 100,000 processors. For the upcoming 2011 calendar year, we were recently awarded 30 million processor hours on the *Jaguar* machine at Oakridge to continue these studies. Here we briefly summarize two important results emerging from this research.

For configurations relevant to the Earth's magnetosphere, we have demonstrated that magnetic reconnection occurs through a process that is intrinsically three-dimensional, and involves the formation rope-like structures called *flux ropes*. We have developed a new theory that explains many of these features and have submitted a paper to *Nature Physics* describing these calculations using up to 1.3 trillion particles. These calculations demonstrate that reconnection naturally gives rise to intense layers of current due to the movement of electrical charges in the plasma. These current layers then break-up and form rope-like structures that can interact in complex ways. This project has uncovered large differences in how this occurs in real 3D applications in comparison to previous 2D models. As illustrated in Figure 1, the current layers break-up into oblique flux ropes in 3D, but this process is artificially suppressed in the previous 2D models. These new results imply that magnetic reconnection in large 3D systems proceeds through a turbulent scenario involving the continual formation and interaction of flux ropes as illustrated in Figure 2. This complexity increases for larger systems as more flux ropes are permitted to grow. Our recent scaling study indicates that the average energy conversion rate may slow down due to this complexity. In addition, the magnetic field is becoming chaotic when multiple flux ropes interact, which may have important implications for acceleration and transport of energetic particles in the Earth's magnetosphere. Many of these new predictions

should be observable in existing and upcoming satellite missions. To test these ideas, we have begun to collaborate with researchers at UC Berkeley in order to compare our results with satellite measurements.

Using our 3D simulation capability, we are also addressing another longstanding question involving the influence current driven plasma instabilities on magnetic reconnection. Our primary focus is a particular type of plasma instability that occurs in both space and laboratory experiments. As illustrated in Figure 3, we are performing 3D simulations relevant to both space and laboratory plasmas with the goal of validating our results on the basic properties and influence of this instability. During the past year, these calculations have demonstrated the plasma instability can induce a strong kinking of the electron layer, which under certain conditions may develop into a fully turbulent evolution. Under these conditions, these waves may play an important role in modifying the basic mechanisms responsible for energy conversion. We are presently comparing the properties of these waves in the computer simulations with experimental measurements from the Magnetic Reconnection eXperiment (MRX) at Princeton.

During the past year, we have authored or co-authored 10 new publications relating to this research topic, and have given six invited talks. We are working on two more publications describing the above 3D results.

Future Work

During the last year of this project, our first goal is to further analyze the large data sets and complete some additional publications describing these results. Our new simulations in 2011 will exploit the *Jaguar* computer to perform somewhat larger 3D calculations. The focus will be including greater realism in order to make direct contact with satellite observations in the Earth's magnetosphere, where rope-like structures are routinely observed. The precise formation mechanism has been the subject of considerable controversy and this project has the potential to resolve these long standing questions.

Conclusion

Scientists believe that magnetic reconnection plays a central role in a wide variety of applications such as magnetic storms around our planet, solar flares and laboratory fusion machines. To understand and accurately model magnetic reconnection in real systems is very challenging. However, the required computing power is now available for researchers who are able to utilize the new peta-scale supercomputers with over 100,000 processors. This project has greatly enhanced the ability of Los Alamos researchers to exploit these computers for modeling high temperature plasmas. These advancements in our basic understanding of magnetic reconnection may lead to several practical applications. For example, the results of this project may have direct application to modeling the plasma environment surrounding the Earth where communication and GPS satellites play a crucial role in modern society.

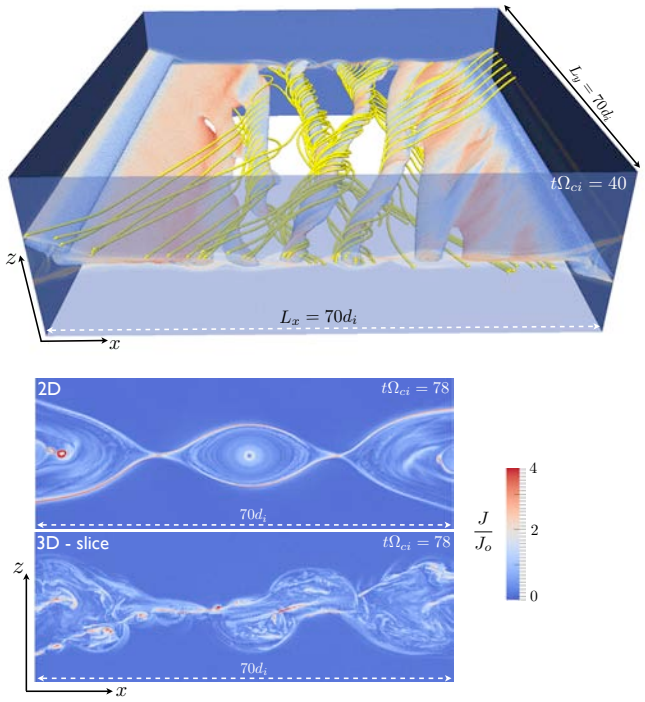

Figure 1. Evolution of current density in equivalent 2D (top) and 3D (bottom) simulations. The thin electron current sheets generated during the onset of reconnection break-up into secondary flux-ropes in the 3D simulation, but these layers remain stable in the equivalent 2D simulation The 3D run was performed on Kraken using 4.4 billion cells and ~1 trillion particles. For further details see Daughton et, al. 2010.

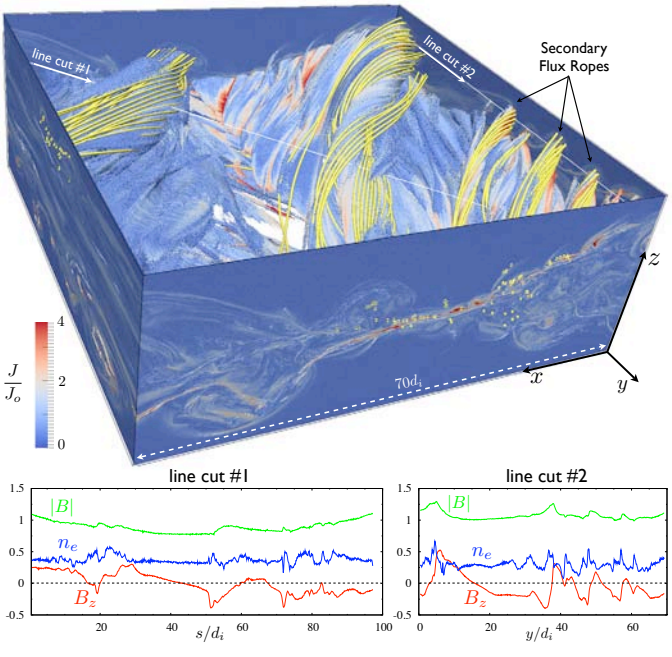

Figure 2. The extended electron current sheets break-up into rope-like structures giving rise to a turbulent evolution. The three-dimensional structure is illustrated by an

isosurface of particle density colored by current density, along with a some selected magnetic field lines (yellow). This is the same case as the bottom panel of Figure 1 and further details are discussed in Daughton et al., 2010.

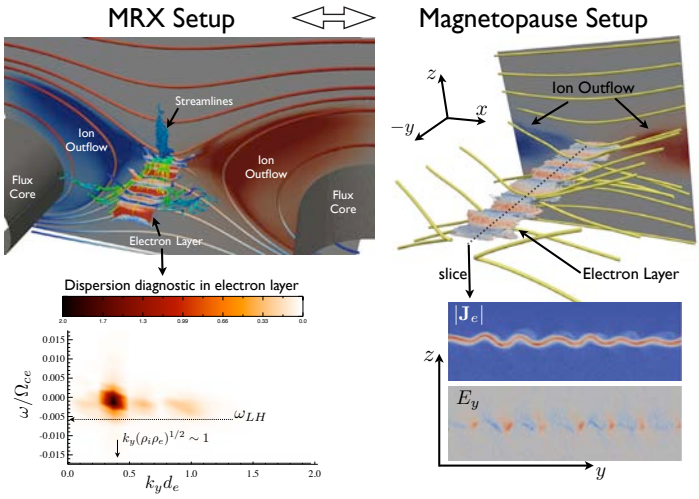

Figure 3. In 3D simulations, the electron current sheets are also unstable to a type of plasma instability which gives rise to a flapping of the electron layer. We are studying the dynamics of this instability for 3D setups to mimic the laboratory reconnection experiment MRX (left panels) and also using open boundary conditions (right panel) to mimic large systems in space. Details are described in Roytershteyn et al, 2010 (in prep).

Publications

Bowers, K. J., B. J. Albright, L. Yin, W. Daughton, V. Roytershteyn, B. Bergen, and T. J. T. Kwan. Advances in petascale kinetic plasma simulation with VPIC and Roadrunner. 2009. *Journal of Physics: Conference Series.* **180**: 012055.

Daughton, W., V. Roytershteyn, H. Karimabadi, L. Yin, B. Albright, B. Bergen, and K. Bowers. Role of Electron Physics in the Development of Turbulent Magnetic Reconnection in Collisionless Plasmas. *Nature Physics.*

Daughton, W., V. Roytershteyn, H. Karimabadi, L. Yin, B. Albright, and S. Gary. Secondary Island Formation in Collisional and Collisionless Kinetic Simulations of Magnetic Reconnection. To appear in *in AIP Conference on Modern Challenges in Nonlinear Plasma Physics.*

Daughton, W., and V. Roytershteyn. Emerging parameter space map of magnetic reconnection in collisional and kinetic regimes. *Space Science Reviews.*

Egedal, J., A. Le, Y. Zhu, W. Daughton, M. Oieroset, T. Phan, R. Lin, and J. Eastwood. Cause of super-thermal electron heating during magnetotail reconnection. 2010. *Geophysical Research Letters.* **37**: L10102.

Egedal, J., N. Katz, L. Chen, B. Lefebvre, W. Daughton, and A. Fazakerley. Cluster observations of bi-directional beams caused by electron trapping during anti-parallel reconnection. 2009. *Journal Geophysical Research.* **115**: A03214.

Egedal, J., W. Daughton, J. F. Drake, N. Katz, and A. Le. Formation of a localized acceleration potential during magnetic reconnection with a guide field. 2009. *Physics of Plasmas.* **16**: 050701.

Karimabadi, H., V. Roytershteyn, C. Mouikis, L. Kistler, and W. Daughton. Flushing effect in reconnection: Effects of minority species of oxygen ions. 2010. *Planetary and Space Science.* : doi:10.1016/j.pss.2010.07.014 .

Le, A., J. Egedal, W. Daughton, J. Drake, W. Fox, and N. Katz. Magnitude of the Hall fields during magnetic reconnection. 2010. *Geophysical Research Letters.* **37**: L03106.

Le, A., J. Egedal, W. Daughton, W. Fox, and N. Katz. Equations of State for Collisionless Guide-Field Reconnection. 2009. *Physical Review Letters.* **102**: 085001.

Quest, K., H. Karimabadi, and W. Daughton. Linear theory of anisotropy driven modes in a Harris neutral shee. 2010. *Physics of Plasmas.* **17**: 022107.

Royterhsteyn, V., W. Daughton, L. Yin, B. Albright, K. Bowers, S. Dorfman, Y. Ren, H. Ji, M. Yamada, and H. Karimabadi. Driven magnetic reconnection near the Dreicer limit. 2010. *Physics of Plasmas.* **17**: 055706.

Disentangling Quantum Entaglement

Wojciech H. Zurek
20090312ER

Introduction

We will explore basic concepts of how information about a system can be extracted from its environment. This technique is known as either "environment as a witness" or "Quantum Darwinism." It is a natural extension of decoherence, which is one of the key themes of the project. It is motivated by very fundamental questions in quantum mechanics, and promises application to quantum detection as well as many body physics.

We shall use the newly established understanding of entanglement in quantum systems to study properties of many-body systems. In particular, we will develop codes that can simulate them efficiently. The efficiency of the simulation technique is based on the realization that entanglement - while still pervasive - has a limited reach for the states of interest in applications (i.e., ground states and low-lying excitations of many body systems relevant to, e.g., high-temperature superconductivity and other applications). This makes it possible to find (in the, e.g., 2^N dimensional state space of N spins) the basis of states that reduces the required memory from exponential to polynomial in the system size.

In addition to the above entanglement-based strategy, our plan is to also study and to take advantage of decoherence. Decoherence is present when the system is interacting with its environment: Even modestly sized quantum systems are next to impossible to isolate. This proposal will investigate decoherence, and whether it can help simulate open quantum systems. We expect a simplification because decoherence suppresses quantum entanglement responsible for the computational expense of representing a quantum state on a classical computer (e.g., which requires 2^N complex numbers for the state of N spins). This leads one to expect that states of the system plus environment have precisely the sort of structure that makes them amenable to efficient simulation.

Benefit to National Security Missions

Our studies should allow us to investigate large class of many-body quantum systems of interest to advancing nanoscience, condensed matter physics, and materials science. This will impact variety of fields in which the fundamental role of quantum phenomena is now being recognized by numerous sponsors including DOE.

Progress

We have carried out studies of the propagation of quantum information throughout the environment in two distinct models:

In a model that consists of multiple spins we have studied (with Zwolak and Quan) the effect of partially mixed environment on "Quantum Darwinism"[1,2]. We have concluded that while information gathering is more difficult, the same total information about the system can be ascertained as long as the environment is not completely mixed. This observation (based on a combination of computer experiments and theoretical studies) was published in two papers (a Physical Review Letter in late 2009 and a recent Physical Review A). Salient points include a Shannon "channel capacity" understanding of the effect of the mixed environment and an observation that decoherence makes it possible to simplify the computation of the information theoretic quantities that are needed to characterize "Quantum Darwinism". We have started the next steps that use channel capacity estimates and other information theoretic tools (Fano inequality, Chernoff's bound, etc.) to see how to simplify calculations in realistic cases and make computer simulations easier.

We have also studied (with Riedel, GRA based in UC Santa Barbara) very realistic and specific model of information dispersal by photon scattering [5]. The result is a huge redundancy (many orders of magnitude larger than redundancies obtained in the studies of more artificial models). This is an exciting development that appeared Physical Review Letters. The next step would be to find out what happens when the photon environment is partially mixed.

These results support "quantum Darwinism" approach to the transition from quantum to classical [8], and help chart future course of our research [6,7].

In a separate development, we have (with Quan) proposed a method to experimentally evaluate adiabaticity of quantum transitions in systems with "anticrossing", and we have tested its effectiveness on the quantum Ising model [3,4]. The basic point is that as one drives the system through the anticrossing at some arbitrary rate, and the drives it back at the same rate, it will remain in its instantaneous ground state (as desired) only when such driving is sufficiently slow. This, if the system returns to the starting state after the "round trip", then it is very likely that the transition was, as a whole, adiabatic. Otherwise, for a part of the trip the rate of the transition was too high to allow for adiabaticity. This test of adiabaticity will be especially important in implementing adiabatic quantum computing, as it allows one to test for adiabaticity without prior knowledge of the size of the energy gap at anticrossing. (Such gaps are generally unknown in the proposed applications of adiabatic quantum computers.) The paper describing this appeared recently in "New Journal of Physics".

Future Work

The role of entanglement in determining complexity of quantum simulations was elucidated few years ago. The research focus was, so far, primarily on algorithms, rather than on "doing physics", which is our ultimate aim. The range of approaches that have been proposed to date is broad, although based on the same unifying recognition of the role of entanglement. The simplest ones are based on so-called Jordan-Wigner transformations. They allow one to reduce a specific (but interesting) class of spin models from exponential to O(N) computational complexity by a time-independent transformation. Broader class of models can be studied using Vidal's time-dependent approach of adjusting computational basis to suite the entangled state the specific Hamiltonian. These models have been by now generalized to more than 1-D "in principle" (but, to date, only rarely "in practice"). Finally, there are proposed approaches (Vidal's "MERA") that attempt to capitalize on the renormalization group-like approach to entanglement, and treat infinite systems.

The original motivation for studying many-body systems was condensed matter, but with recent advances of atomic physics it appears that the closest experimental connection will be in the trapped atom / optical lattice experiments. Our proposal is motivated by the need to "keep up" with them. In many of these systems (Bose-Einstein condensates) Hubbard model is a reasonable representation, and there is a long-standing suspicion that it may also play a role in (high-TC) superconductivity. Last not least, there are specific high-impact projects involving e.g. DNA, nanotech, etc. The idea of taking advantage of decoherence is central to our proposal. Dealing with decoherence involves, by now, a set of well understood procedures, some of which we have originated. We therefore expect to be successful in devising efficient codes and applying them to problems of interest.

Conclusion

We will model open quantum systems, taking into account the role of the environment. Further, we will investigate the extent to which the suppression of entanglement in the system (due to decoherence by the environment) can be utilized to understand behavior of many body systems. These two achievements will allow us to both streamline the task of simulating open quantum systems and extend the boundaries of systems efficiently simulated on a classical computer. Overall, this proposal will enable the development of novel and robust computational tools and also an in-depth understanding of open quantum systems.

References

1. Zwolak, M., H. T. Quan, and W. Zurek. Redundant imprinting of information in nonideal environments: Objective reality via a noisy channel. 2010. *Physical Review A - Atomic, Molecular, and Optical Physics.* **81** (6): 062110.

2. Zwolak, M., H. T. Quan, and W. H. Zurek. Quantum Darwinism in a mixed environment. 2009. *Physical Review Letters.* **103** (11): 110402 (4 pp.).

3. Quan, H. T., and W. H. Zurek. Testing quantum adiabaticity with quench echo. 2010. *NEW JOURNAL OF PHYSICS.* **12**: 093025.

4. Damski, B., and W. Zurek. Quantum phase transition in space in a ferromagnetic spin-1 Bose-Einstein condensate. 2009. *NEW JOURNAL OF PHYSICS.* **11**: 063014.

5. Riedel, C. Jess., and W. Zurek. Quantum darwinism in an everyday environment: Huge redundancy in scattered photons. 2010. *Physical Review Letters.* **105** (2): 020404.

6. Wootters, W., and W. Zurek. The no-cloning theorem. 2009. *PHYSICS TODAY.* **62** (2): 76.

7. Zurek, W. H.. Causality in condensates: gray solitons as relics of BEC formation. 2009. *Physical Review Letters.* **102** (10): 105702 (4 pp.).

8. Zurek, W. H.. Quantum Darwinism. 2009. *NATURE PHYSICS.* **5** (3): 181.

Publications

Damski, B., H. T. Quan, and W. H. Zurek. Critical dynamics and decoherence. 2009. *LA-UR 09-06655, to be submitted to arXiv eprint server and Nature Physics.*

Damski, B., and W. H. Zurek. Soliton creation during a Bose-Einstein condensation. 2009. *arXiv:0909.0761 and LA-UR 09-05090, submitted to Physical Review Letters.*

Damski, B., and W. H. Zurek. Quantum phase transition in space in a ferromagnetic spin-1 Bose-Einstein conden-

sate. 2009. *New Journal of Physics.* **11**: 063014.

Wootters, W. K., and W. H. Zurek. The no-cloning theorem. 2009. *Physics Today.* : 76.

Zurek, W. H.. Causality in Condensates: Gray Solitons as Relics of BEC Formation. 2009. *Physical Review Letters.* **102**: 105702.

Zurek, W. H.. Quantum Darwinism. 2009. *Nature Physics.* **5**: 181.

Zwolak, M., H. T. Quan, and W. H. Zurek. Quantum Darwinism in a Mixed Environment. 2009. *Physical Review Letters.* **103**: 110402.

Backward Stimulated Raman and Brillouin Scattering of Laser in the Collisional Regime

Lin Yin
20090394ER

Introduction

The objective is to develop a validated predictive capability for laser-plasma interaction (LPI) that will enable more successful experimental designs in inertial confinement fusion (ICF) experiments that may, one day, impact our ability to derive energy from fusion. Furthermore, this work will impact our understanding for laser-driven ion acceleration which has potential applications from fusion to medical accelerators. This project aims to develop the world's first truly first-principles model of LPI in laser-driven hohlraums. The proposed work uses the Roadrunner petaflop supercomputer and applies the state-of-the-art VPIC kinetic plasma simulation code, recently adapted to run efficiently on Roadrunner.

Success of this project will have several prospective payoffs: First, it directly supports the achievement of fusion ignition on the National Ignition Facility, which has manifold tie-ins into high-profile, exciting science, including carbon-neutral energy production, high energy density physics, laboratory astrophysics, and weapons science.

Moreover, by learning to control LPI, we can guide the search for new, high gain, high efficiency operating regimes for NIF ignition (including fast ignition) that simply cannot be attempted now because our understanding of the basic nonlinear physics of LPI is incomplete and phase space is simply too large to sample experimentally in an economical way.

Finally, a high-risk/high-reward application of LPI is in novel plasma gain media (so-called Raman amplifiers) to generate extremely high power, short pulse lasers. If demonstrated experimentally, these new amplifiers could enable short pulse laser intensities and energy densities inaccessible today without going to very large, expensive facilities. Potential applications include fast ignition inertial confinement fusion, novel high fluence ion beams for nuclear physics studies, and hadrontherapy of tumors.

Benefit to National Security Missions

This project supports the nuclear weapons mission in two ways:

1. Laser Plasma Interaction science underpins high energy density and boost physics experiments at the National Ignition Facility.

2. Improved verification and validation of the VPIC plasma code on Roadrunner supercomputer will improve modeling of processes in nuclear weapons.

Progress

Extensive VPIC simulations and analysis for this project have been conducted on heterogeneous multi-core supercomputer Roadrunner of LANL and Jaguar of ORNL. Computer simulations of "stimulated scattering" of laser light in the trapping regime are performed in single- and multi-laserspeckle, mm-scale plasma media. A suite of VPIC simulations have been run to validate the physics using both LANL Trident short-pulse, signal speckle experiments in the strong laser intensity regime (peak intensity > 10^{16} W/cm^2) and Raman amplification experiments on the LLNL Jupiter laser facility where average laser intensity is lower (~10^{14} W/cm^2). The predicted nonlinear physics associated with electrons "trapped" in plasma waves is observed in simulations of both experiments and quantitative agreement is obtained [1] (Figure 1). Surprisingly, "at scale" simulations of these large plasma volumes show for the first time that substantial electron trapping occurs and may ultimately limit the amount of laser scattering occurring, even at low average laser intensity.

Regarding the effects of binary particle collisions on determining the onset threshold for stimulated Raman backscatter low temperature plasmas [2] (Figure 2), it has been demonstrated that nonlinear trapping effects, which lead to the enhancement of backscatter, are reduced by collisional detrapping resulting from both parallel and perpendicular diffusion in velocity space. Furthermore, it has been shown that competition between particle trapping and collisional detrapping leads to a temporal delay in the onset of trapping enhanced SRBS, and that this in turn leads to an increase in the onset laser intensity threshold for SRBS enhancement.

2D VPIC simulations [3] (Figure 3) of Trident short pulse

experiments show the time-dependent nature of SRS backscatter. We found that individual, sub-picosecond, bursts of enhanced SRS backscatter occur at discrete wavelengths (frequencies), shifted from linear resonance due to electron trapping. Such shifting results in broad, time-integrated spectra observed in TRIDENT experiments.

Our understanding of the effects of collisional detrapping and heating on the development of enhanced backscatter in the kinetic regime has been used to properly interpret results from LPI experiments at both LANL Trident and LLNL Jupiter laser facilities.

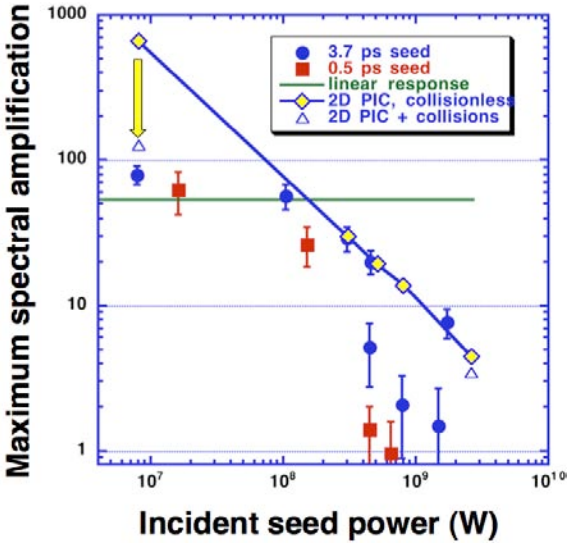

Figure 1. Experimental validation of VPIC Raman amplification simulations. The experiments were done by R. Kirkwood et al. at the LLNL Jupiter laser facility [1]. The solid points are the measured amplification of a small seed pulse propagating in plasma where a long pump pulse is propagating. Nonlinear LPI coupling among seed, pump, and plasma waves gives rise to the amplification scaling seen. The open points are collisionless (diamonds) and collisional (triangles) 2D VPIC runs. The arrow indicates the importance of including binary collisions in the modeling, particularly at small incident seed power.

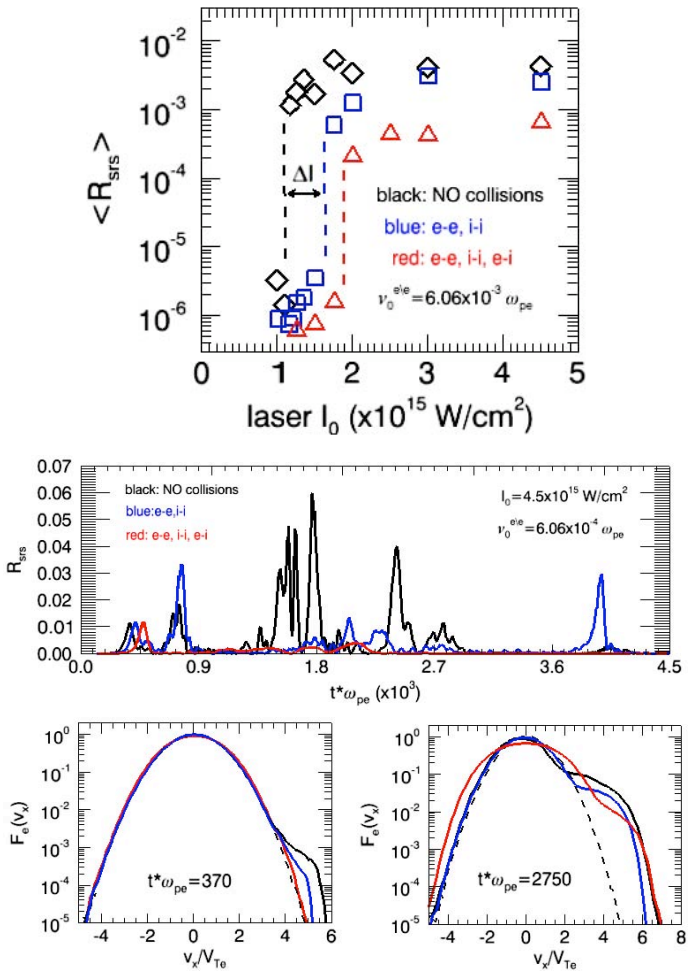

Figure 2. De-trapping of electrons resulting from binary coulomb collisions delays the onset of kinetic SRS enhancement and increases the onset laser intensity threshold. Onset of SRS enhancement is determined predominantly by PARALLEL diffusion, however perpendicular diffusion cannot be neglected and must be included [2]. Collisional heating changes the local electron plasma wave dispersion and plasma linear resonance as a function of time, reducing SRS backscatter.

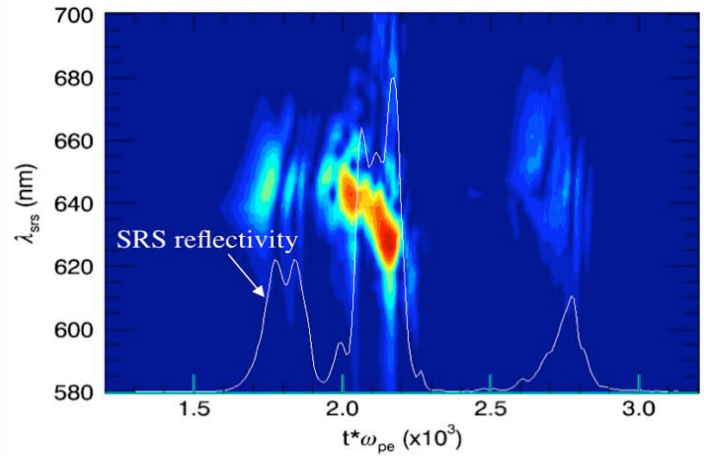

Figure 3. 2D VPIC simulations [3] of Trident short pulse experiments show the time-dependent nature of SRS backscatter. Individual, sub-picosecond, bursts of enhanced SRS backscatter occur at discrete wavelengths (frequencies), shifted from linear resonance due to electron trapping. Such shifting results in broad, time-integrated spectra observed in TRIDENT experiments.

Future Work

In FY11, we will continue to model LPI in collisional and collisionless regimes to study nonlinear kinetics of stimulated Raman and stimulated Brillouin scattering. These calculations are important from a basic physics standpoint and are relevant to upcoming fusion ignition experiments on the National Ignition Facility. Our ongoing efforts further develop this kinetic modeling capability to explore nonlinear physics in crossed-beams in macroscopic (mm-sized) plasma media. These large-scale simulations, which have not been done before, will be validated against experiments of the National Ignition Campaign. Work will be documented in scientific journals and presentations at scientific meetings and workshops.

Conclusion

We expect two key things to result from this study. The first is to illuminate the underlying nonlinear physics of laser-plasma instabilities (LPI), a problem of critical importance to the success of fusion ignition on the National Ignition Facility, paying special attention to the role of binary collisions in the physics. The second is to use this understanding to identify plasma parameter regimes which are relatively safe from LPI and to pose possible mitigation strategies to avoid their effects. This is an important basic science study directly related to mitigation of risk on a multi-billion dollar experiment. In the interest of developing a validated predictive model of LPI in inertial confinement fusion experiments, future work can employ this capability to explore LPI in mm-sized inertial fusion plasma media. These simulations will be much needed for the understanding of future experiments at the National Ignition Facility at LLNL. Simulation efforts such as these could also have other, far-reaching consequences, including future high energy density physics (HEDP) experiments on the NIF and Omega facilities as well as pushing the state-of-the-art in supercomputing.

References

1. Kirkwood, R. K., Y. Ping, S. C. Wilks, N. Meezan, P. Michel, E. Williams, D. Clark, L. Suter, O. Landen, N. Fisch, E. O. Valeo, V. Malkin, D. Turnbull, S. Suckewer, J. Wurtele, T. L. Wang, S. F. Martins, C. Joshi, L. Yin, B. J. Albright, H. A. Rose, and K. J. Bowers . Observation of amplification of light by Langmuir waves and its saturation on the electron kinetic timescale. *Phys. Rev. Lett.*.

2. Finnegan, S. M., L. Yin, J. L. Kline, B. J. Albright, and K. J. Bowers. Influence of binary Coulomb collisions on nonlinear stimulated Raman backscatter in the kinetic regime. *Physics of Plasmas.*

3. Finnegan, S. M., J. L. Kline, L. Yin, D. S. Montgomery, R. A. Hardin, K. A. Flippo, B. J. Albright, K. J. Bowers, T. Shimada, and R. P. Johnson. Modeling short-pulse single hot spot laser plasma interaction experiments using the VPIC particle in cell code. *Physics of Plasmas.*

Publications

Bowers, K. J., B. J. Albright, B. Bergen, L. Yin, K. J. Barker, and D. J. Kerbyson. 0.374 Pflop/s Trillion-Particle Kinetic Modeling of Laser Plasma Interaction on Roadrunner. 2008. *Proceedings of the 2008 ACM/IEEE conference on Supercomputing, SC'08, Austin, Texas, IEEE Press, Piscataway, NJ, USA* . : 1.

Bowers, K. J., B. J. Albright, L. Yin, W. Daughton, V. Roytershteyn, B. Bergen, and T. Kwan. Advances in petascale kinetic plasma simulation with VPIC and Roadrunner. 2009. *Journal of Physics: Conference Series.* **180**: 012055.

Finnegan, S. M., J. L. Kline, L. Yin, D. S. Montgomery, R. A. Hardin, K. A. Flippo, B. J. Albright, K. J. Bowers, T. Shimada, and R. P. Johnson. Modeling short-pulse single hot spot laser plasma interaction experiments using the VPIC particle in cell code. *Physics of Plasmas.*

Finnegan, S. M., L. Yin, J. L. Kline, B. J. Albright, and K. J. Bowers. Influence of binary Coulomb collisions on nonlinear stimulated Raman backscatter in the kinetic regime. *Physics of Plasmas.*

Kirkwood, R. K., Y. Ping, S. C. Wilks, N. Meezan, P. Michel, E. Williams, D. Clark, L. Suter, O. Landen, N. Fisch, E. O. Valeo, V. Malkin, D. Turnbull, S. Suckewer, J. Wurtele, T. L. Wang, S. F. Martins, C. Joshi, L. Yin, B. J. Albright, H. A. Rose, and K. J. Bowers . Observation of amplification of light by Langmuir waves and its saturation on the electron kinetic timescale. *Phys. Rev. Lett.*.

Kline, J. L., D. S. Montgomery, C. Rousseaux, S. D. Baton, V.

Tassin, R. A. Hardin, K. A. Flippo, R. P. Johnson, T. Shimada, L. Yin, B. J. Albright, H. A. Rose, and F. Amiranoff. Investigation of stimulated Raman scattering using short-pulse diffraction limited Laser beam near the instability threshold. 2009. *Lasers and Particle Beams.* **27**: 185.

Rose, H. A., W. Daughton, L. Yin, and A. B. Langdon. Intensity dependent waiting time for strong electron trapping events in the onset regime of speckle stimulated Raman scatter. *Physics of Plasmas.*

Transport in Magnetized Dense Plasmas for Magneto-Inertial Fusion

Xianzhu Tang
20090410ER

Introduction

Controlled fusion is an attractive carbon-neutral energy source. Fusion has been achieved in the laboratory by imploding a fuel pellet (the so-called inertial confinement fusion or ICF) or magnetically confining a 100 million degree temperature plasma (the so-called magnetic confinement fusion or MCF). Both ICF and MCF require huge capitol investment for their development, the first to build powerful laser systems, and the second to build magnetics and sustain a large body of plasma. A hybrid approach, the so-called magneto-inertial fusion (MIF), combines the strength of ICF and MCF by imploding a magnetized plasma target with slow pushers, and offers a path towards fusion energy with orders of magnitude lower developmental cost.

This project develops the physics basis underlying the transport of particle, heat, and radiation in the MIF magnetized dense plasma target. A computational model of these transport phenomena is critical for the selection and optimization of MIF plasma target and predicting the behavior. Computational exploration of physics phenomena is an exceptionally cost effective approach to initial investigations of new systems and will provide guidance for the eventual fabrication of the experimental system and early experiments.

Benefit to National Security Missions

This project will support the DOE mission in energy security by enhancing our understanding of the transport physics in magnetized dense plasma for magneto-inertial fusion energy development. This is a program within the portfolio of the Office of Fusion Energy Sciences. In addition, transport phenomena are extremely important for nuclear weapons design, hence this project will also support the NNSA weapons mission.

Progress

We have made substantial progress in two areas of the proposed research. The first is on plasma transport near the wall and the associated plasma-materials interaction issue. LANL postdoc Natalia Krashenennikova and the PI are the primary contributors in this area. The second is on a special request from LANL's magneto-inertial fusion (MIF) experimentalists (Scott Hsu at P-24 and his MIF collaborators) on assessing the enhanced dwell time by using a thick plasma liner for MIF compression. LANL postdoc Grigory Kagan and the PI are the primary contributors in this area.

In the first area, Motivated by the Magnetized Target Fusion (MTF), a systematic investigation of the equilibrium properties of a 1D and 2D plasma sheath with a magnetic field parallel to the wall was carried out by using analytical theory and kinetic simulations. The so-called plasma sheath refers to a narrow region of plasma next to a material surface, in which the ion and electron have significantly different number densities and hence a large electric field exists. In our investigation, initially uniform plasma in thermal equilibrium consisting of equal temperature collisionless electrons and ions is allowed to interact with a perfectly absorbing conducting wall, which charges positively due to large ions gyro-radii. The analysis of the steady-state plasma and field profiles reveals the importance of the relation between electron and ion thermal gyro-radii and plasma Debye length, which is the characteristic length of charge separation when a plasma wave propagates through an unmagnetized plasma. In particular, the sheath width scaling, the details of the particle and field profiles, the break-down of force balance components, and the onset of the instabilities exhibit different behaviors in three distinct regimes. More recent focus has been on the 2D Kelvin-Helmholtz instability in the 2D sheath, which we found to be unstable in MTF regime. The Kelvin-Helmholtz instability is a classical fluid instability driven by flow shear. In our specific case, the flow shear is induced by the strong electric field and the magnetic field in the MIF plasma sheath. The importance is that the saturation of the instability can dominate the plasma loss to the wall in comparison with the conventional collisional effect. Our work has resulted in an invited talk at APS/DPP annual meeting in 2009, two papers in Physics of Plasma, and a submitted manuscript to Journal of Nuclear Materials. This series of work motivated additional studies of the effect of a magnetic field intercepting the wall at a small angle, and the effect of strong collision. For the oblique magnetic

field, we clarify the competition between electron parallel streaming and the gyro-orbit loss of the ions, which determines whether the wall is charged negatively or positively. A strong collisionality, which is possible for a high density plasma, would introduce such a strong drag that it can reverse the direction of the electric field in the presheath plasma. Our calculation also indicates the presence of a collision-induced electron instability. We are currently completing three manuscripts on the subject.

In the second area, postdoc Grisha Kagan has carried out a detailed analysis on how a thick plasma liner can be used instead of a conventional thin liner to improve the dwell time of a MIF target, which would have a higher fraction of thermonuclear burn. The subtle physics of the dwell time of a liner compressed MIF target is clarified with two analyses. One is in the strong shock regime, where the incoming liner Mach number is much greater than one. The second is in the slower liner regime, where compressional heating of the liner is taking into account. Using both models, we identified the physics governing the liner-target interface movement and the back propagating shock in the post-shocked liner. The regime for "infinite" dwell time is specified for both the large M liner and the slow liner using a quasi-simple spherical wave model. One manuscript is currently being finalized for publication.

Future Work

This project addresses critical scientific issues underlying the performance and potential of magneto-inertial fusion (MIF), an innovative approach to fusion energy that combines attractive features of both magnetic and inertial confinement fusion. There have been many proposed ideas to achieve MIF, but a leading approach is to use an imploding metal or plasma "liner" to compress a magnetized "target" plasma to thermonuclear temperatures. If this is successful, MIF will permit fusion energy development without billion-dollar facilities, thus circumventing one of the most serious obstacles for conventional fusion development. MIF is a key area of investment for the new joint NNSA/SC program in High Energy Density Laboratory Plasmas (HEDLP). Two critical open scientific issues underlying our ability to assess, design, and optimize MIF systems are (1) the physics of transport in HED plasmas with ultra-high magnetic fields and (2) the role of plasma-materials interaction in setting the energy loss rate. For issue (1), we will continue to use state-of-the art computational tools to understand the roles of magnetic geometry, topology, and plasma micro-turbulence on thermal and radiation transport in the previously unexplored regime of magnetized HEDLP. For issue (2), the magnetic sheath transport will be further resolved to understand the impact of impurity generation and transport, and to assess the enhanced radiation losses. A third, emerging, issue of great importance on how to optimize dwell time using thick plasma liner, will be tackled in response to request of LANL's MIF experimental program.

Conclusion

We expect both a qualitative and quantitative assessment of particle, heat, and radiation transport in magnetized dense plasma targets when compressed by a material liner. The transport rate would determine whether the magneto-inertial fusion concept can reach fusion ignition temperature and would guide target selection and optimization. If successful, it contributes to the ultimate goal of achieving controlled fusion energy and help safeguard our nation's energy security.

References

1. Krasheninnikova, N., X. Tang, and V. Roytershteyn. Scaling of the plasma sheath in a magnetic field parallel to the wall. 2010. *Physics of Plasmas.* **17** (5): 057103.

2. Krasheninnikova, N., and X. Tang. Equilibrium properties of the plasma sheath with a magnetic field parallel to the wall. 2010. *Physics of Plasmas.* **17** (6): 063508.

Publications

Krasheninnikova, N., X. Tang, and V. Roytershteyn. Scaling of the plasma sheath in a magnetic field parallel to the wall. 2010. *Physics of Plasmas.* **17** (5): 057103.

Krasheninnikova, N., and X. Tang. Equilibrium properties of the plasma sheath with a magnetic field parallel to the wall. 2010. *Physics of Plasmas.* **17** (6): 063508.

Novel Cone Targets for Efficient Energetic Ion Acceleration for Light Ion-Driven Fast Ignition Fusion

Kirk A. Flippo
20090466ER

Introduction

Intense particle beams are important components of a host of applications, including fast ignition inertial confinement fusion, high energy density physics, warm dense matter, novel nuclear physics studies, and medical therapy. However, understanding production mechanisms of these intense particle beams is in its infancy, yet it is crucial for designing and optimizing systems.

The goal of this project is to understand the fundamental physics of ion beams produced from some unique flat-top cone targets and to improve their performance. These cone-targets enhance the conversion efficiency and ion energies, which could lead to the realization of Ion Fast Ignition (IFI) fusion energy using light ions, a concept recently championed by LANL. The project aims at understanding, specifically, the hot electron behavior in the targets, which affect how these ion beams behave. Understanding and controlling these beams would not only make IFI fusion and energy independence closer to reality, but would also affect any potential application that would benefit from such beams, such as ion (hadron) cancer therapy, medical isotope production, radioactive waste transmutation, proton radiography, active interrogation, probing warm dense matter and laboratory astrophysics.

Benefit to National Security Missions

This project will enhance our understanding of laser-based ion acceleration relevant for ion Fast Ignition Fusion by enabling compact directed energetic particle and x-ray sources. Laser-based accelerator technology can also impact nuclear wastes transmutation, active interrogation of SNM, proton radiography and stockpile stewardship via warm dense matter studies - missions of interest to DOE, DHS, and other government agencies. This work also underpins the goal of producing compact ions sources for medical isotope production and hadron cancer therapy of interest to the DHHS/NIH.

Progress

We have now completed our second experimental run for this project, the 2010 Trident run. We have shot new structured flat-top cone targets (micro-grooves on the flat-top) to determine the TNSA sheath (vitrual cathode) and source size of the laser-accelerated ion beam as a function of energy, along with other structured targets to see the direct laser light acceleration of electrons, a process that we have discovered via x-ray emission 2-D imaging and simulations last year. We have deployed the most extensive suit of diagnostics to ever run at one time at the Trident facility to help us understand the laser-matter interaction. We have built and fielded a new high resolution ion energy analyzer (Thomson Parabola), three electron-positron spectrometers, a flat crystal x-ray spectrometer, a new ion beam activation autoradiograh pack, a 2 or 3 omega probe beam line for looking at the target and sheath expansion, a Raman backscatter diagnostics, a backscatter focal diagnostic, neutron diagnositcs, and we now have two x-ray K-alpha imagers to look at orthogonal views of the target's x-ray emission to determine interaction of the laser with the cone walls to achieve even higher energies than the recored breaking energies observed in the '09 Trident laser time, which was the subject of a press release from the lab, and one of the selected press releases of the APS-Division of Plasma Physics (DPP) Conference in 2009. This beam time plus the previous one have let us accomplished goals 1,2,4,5, with goals 3 and 6 to be done for the final remaining beam time. We have discovered a completely new laser absorption mechanism called the direct laser light acceleration (DLLA) mechanism. The understanding of this mechanism is the subject of manuscript submitted to Physical Review Letters [1]. This new mechanism will have a huge impact on the field as it should be able to be harnessed to boost ion energies even further, it will also be of special importance to the inertial confinement fusion community due to its implications for fast ignition fusion physics (electron and ion), as it may lead to electron too energetic to be useful for electron fast ignition in a cone geometry. Our next experimental campaign will concentrate of using this new mechanism to achieve higher gains in energy and efficiency.

We are currently analyzing data from the 2010 run (ended July 8th) with our collaborators from the University of Illinois, Urban-Champaign; the University of Missouri,

Columbia; the University of Nevada, Reno; ForschungsZentrum Dresden-Rossendorf (FZD); Nanolabz; and Sandia National Laboratories. Scientist from FZD are currently running simulations for the current round of experiments to help with the understanding of our results. This project involves over 20 scientists, of whom 8 are graduate students, 8 are Postdocs, and 6 are staff. This set of experiments was particularly resource intensive with the amount of diagnostics built and fielded, but positions us very well to diagnose the next round of experiments, where we will attempt to focus the ion beam in specially shaped cone/hemi hybrid targets and produce focused beams of carbon.

Interest in these experiments continues to run high, the PI has given 3 invited talks: The Antimatter Creations Using Intense Lasers Workshop (Berkeley, CA), The Advanced Accelerators Conference (Annapolis, MD), and the Anomalous Absorption Conference (Snowmass, CO), and 2 of our postdocs have invited talks at the APS-DPP this year in November. We have a paper under review, one at Physical Review Letters. We are currently working on 3 additional high impact papers to be submitted to PRL or equivalent, plus two articles for Physics of Plasmas for each of the invited talks in November. This work was also featured in an interview for educational videos produced within a CRADA from the DOE.

Future Work

The goal will focus on understanding the fundamental physics of ion acceleration from some unique 100 micron scale flat-top cone (FTC) targets that have the ability to enhance the ion energies and laser energy to ion energy conversion efficiency of these Target Normal Sheath Accelerated (TNSA) ion beams as seen in preliminary experiments at the LANL Trident laser facility. This observed enhancement could lead to the realization of Fast Ignition (FI) fusion using light or medium Z ions. The project aims at understanding, specifically, the hot electron transport using K-alpha x-ray imaging, which effects the efficiency, topology, and focusability of these ion beams.

We intend to:

- Using Radiochromic Film Imaging Spectroscopy, measure the energy of the ions as well as the conversion efficiency obtained by shooting these cone targets with the new Enhanced Trident Laser (80-100 J at 500 fs).
- Using K-alpha x-ray crystal imaging and spectroscopy, determine the hot electron production and transport which then will be correlated with the ion beam acceleration characteristics and other studies with similar cone geometries (without flat tops) and just the flat-tops (without cones), known as reduced mass targets (RMTs) which are about 100-300 microns in diameter.
- Developing with our partners (Nanolabz) Pd or Pt FTCs which, when heated, should lead to a catalytic reaction producing nanolayers of carbon, which will allow us to accelerate mono-energetic carbon beams.
- Measure the energy and efficiency of any mono-energetic carbon beams produced.
- Model the cones using 2D and 3D PIC simulations, PICLs from UNR and VPIC on the LANL Roadrunner supercomputer to understand the physics of the cone laser light guiding and hot electron generation along with possible methods for better control.
- Study the possibility of shaping the flat-tops of the cones for ion focusing and spectral control.

Conclusion

The project has yielded the world's record in proton energies for lasers in '09, and is expected to yield ion energies with efficiencies on the order of 10-20%. We have also observed mono-energentic ion structures from the cone targets, and are working toward improving these characteristics to open many new application in compact forms, including hadron cancer therapy, isotope production, radioactive waste transmutation, proton radiography, active interrogation, fast ignition, probing warm dense matter, and laboratory astrophysics. These applications will benefit the US public in a multitude of ways becoming a new base of technological development and economic growth.

Publications

Flippo, K. A., E. d'Humieres, S. A. Gaillard, J. Rassuchine, D. C. Gautier, M. Schollmeier, F. Nurnberg, J. L. Kline, J. Adams, B. Albright, M. Bakeman, K. Harres, R. P. Johnson, G. Korgan, S. Letzring, S. Malekos, N. Renard-LeGalloudec, Y. Sentoku, T. Shimada, M. Roth, T. E. Cowan, J. C. Fernandez, and B. M. Hegelich. Increased efficiency of short-pulse laser-generated proton beams from novel flat-top cone targets. 2008. *Physics of Plasmas.* **15**: 056709.

Flippo, K., S. A. Gaillard, T. Kluge, and M. Bussmann. Advanced Laser Particle Accelerator Development at LANL: From Fast Ignition to Radiation Oncology. To appear in *11th Advanced Accelerator Concepts Workshop, AIP Conf. Proc. .* (Annapolis, MD, 14-18 June, 2010).

Gaillard, S. A., K. A. Flippo, D. C. Gautier, J. L. Kline, J. Workman, F. Archuleta, R. Gonzales, T. Hurry, R. Johnson, S. Letzring, D. Montgomery, S. -M. Reid, T. Shimada, Y. Sentoku, T. E. Cowan, J. Rassuchine, M. Lowenstern, and E. Mucino. Proton, electron and K-alpha emission from micro-scale copper cone targets. 2009. In *2009 IEEE 36th International Conference on Plasma Science (ICOPS) ; 1-5 June 2009 ; San Diego, CA, USA.* , p. 1.

Gaillard, S. A., K. A. Flippo, M. E. Lowenstern, and J. E. Mucino. Proton acceleration from ultrahigh-intensity

short-pulse laser-matter interactions with Cu micro-cone targets at an intrinsic ~10-8 contrast. 2010. *J. Phys.:Conf. Series.* **244**: 022034.

Gaillard, S. A., T. Kluge, K. A. Flippo, M. Bussmann, B. Gall, T. Lockard, M. Geissel, D. T. Offermann, M. Schollmeier, Y. Sentoku, and T. E. Cowan. Nearly 70 MeV laser-accelerated-proton beams from micro-cone targets via laser grazing. *Physical Review Letters.*

Kluge, T., M. Bussmann, S. A. Gaillard, K. Flippo, D. C. Gautier, B. Gall, B. Lockard, Y. Sentoku, K. Zeil, S. Kraft, U. Schramm, T. E. Cowan, and R. Sauerbrey. Wakefield Accelerated Electron Beams from Ultra-Thin Solid Foils. 2010. *2nd International Conference on Ultra-Intense Laser Interaction, AIP Conference Proceedings.* **1209**: 51.

Kluge, T., M. Bussmann, S. Gaillard, K. Zeil, S. Kraft, U. Schramm, T. Cowan, R. V. Sauerbrey, K. Flippo, null. Gautier, T. Lockard, null. Sentoku, M. Lowenstern, J. E. Mucino, and null. Gall. Low-divergent, energetic electron beams from ultra-thin foils. 2010. *Journal Name: Verhandlungen der Deutschen Physikalischen Gesellschaft.* (HANVER 2): Medium: X; Size: 1 pages.

Kluge, T., S. A. Gaillard, M. Bussmann, and K. Flippo. Theoretical Understanding of Enhanced Proton Energies from Laser-Cone Interactions. To appear in *11th Advanced Accelerator Concepts Workshop, AIP Conf. Proc.* (Annapolis, 14-17 June, 2010).

Miley, G. H., X. Yang, H. Heinrich , K. Flippo, S. Gaillard, D. Offermann, and D. C. Gautier. Advances in proposed D-Cluster Inertial Confinement Fusion Targets. 2010. *J. Phys.:Conf. Series.* **244**: 32036.

Nuernberg, F., M. Schollmeier, K. Harres, M. [Institut fuer Kernphysik. Roth, E. [Laboratoire pour l'Utilisation des Lasers Inte, A. [GSI Helmholtzzentrum fuer Schwerionenforschung, D. C. Carroll, P. [Department of Physics. McKenna, K. Flippo, D. C. Gautier, B. M. Hegelich, M. [Sandia National Laboratories. Geissel, O. [Department of Physics. Lundh, K. [School of Mathematics and Physics. Markey, D. [Rutherford Appleton Laboratory. Neely, and J. [Fakultaet fuer Physik. Schreiber. Radiochromic film imaging spectroscopy of laser-accelerated proton beams. 2009. *Journal Name: Review of Scientific Instruments.* **80** (3): Medium: X; Size: page(s) 03330.

Perez, F., L. Gremillet, M. Koenig, S. D. Baton, P. Audebert, M. Chahid, C. Rousseaux, M. Drouin, E. Lefebvre, T. Vinci, J. Rassuchine, T. Cowan, S. A. Gaillard, K. A. Flippo, and R. Shepherd. Enhanced Isochoric Heating from Fast Electrons Produced by High-Contrast, Relativistic-Intensity Laser Pulses. 2010. *PHYSICAL REVIEW LETTERS.* **104** (8): 085001.

Rassuchine, J., d&psila, S. D. Baton, P. Guillou, M. Koenig, M. Chahid, F. Perez, J. Fuchs, P. Audebert, R. Kodama, M. Nakatsutsumi, N. Ozaki, D. Batani, A. Morace, R. Redaelli, L. Gremillet, C. Rousseaux, F. Dorchies, C. Fourment, J. J. Santos, J. Adams, G. Korgan, S. Malekos, S. B. Hansen, R. Shepherd, K. Flippo, S. Gaillard, Y. Sentoku, and T. E. Cowan. Enhanced hot-electron localization and heating in high-contrast ultraintense laser irradiation of microcone targets. 2009. *Physical Review E (Statistical, Nonlinear, and Soft Matter Physics).* **79** (3): 036408 (5 pp.).

General Relativity as a Probe of Cosmology

Daniel Holz
20090518ER

Introduction

We are in the midst of a revolution in astrophysics and cosmology. There has been an explosion of observational data, leading to a radical transformation in our understanding of our universe on the largest scales. The field of general relativity, with the advent of gravitational wave observatories, is also poised for major advances in the coming years. While the first direct detection of gravitational waves will be much celebrated, it is the ensuing astrophysical and cosmological observations that will have the greater scientific impact. Research in general relativity, and astrophysics and cosmology, is phenomenally vibrant and dynamic. The interplay of these fields offers particular promise, and it is here that we are focusing our work.

This proposal centers on gravitational waves and gravitational lensing: two uniquely powerful cosmological probes furnished by general relativity. The next generation of observational surveys can be expected to revolutionize the study of statistical lensing, and gravitational lensing is expected to become one of the most powerful probes of dark energy. In addition, as "first sound" for LIGO (and, hopefully, LISA) arrives, the birth of the age of gravitational-waves is imminent. We propose two complementary research directions, both of which can be expected to lead to elucidation of the nature of dark energy and dark matter.

Benefit to National Security Missions

This project supports the DOE mission by directly addressing dark matter and dark energy, which form the heart of the unknowns in cosmology, and play a major role in research at the DOE Office of Science.

Progress

Gravitational-waves are expected to be seen for the very first time in the next few years by the Laser Interferometric Gravitational-wave Observatory. This project explores the cosmological constraints which can be generated from the observations of these gravitational-waves. The main scientific result of this project thus far is establishing that future gravitational-wave observatories could provide exquisite (sub-percent level) constraints on both the dark energy equation-of-state (responsible for the accelerated expansion of the Universe) and the growth factor (responsible for the development of stars and galaxies in the Universe). We have shown how the effects of gravitational lensing, a potential source of noise in gravitational-wave experiments, can be mitigated. And, finally, we have shown that black hole binaries, the most promising source of gravitational-wave observatories, are expected to occur in significantly larger numbers than previously anticipated.

This has been an immensely productive project thus far. Although it has only been funded for ~18 months, it has already generated four published papers [1–4] that have generated a fair amount of attention. For example, while I was visiting MIT last April to give a Colloquium, the LIGO collaboration (based at MIT and Caltech) expressed tremendous interest in these results. They may alter the direction of this ~$500M experiment based on our findings.

Future Work

This proposal centers on gravitational waves and gravitational lensing: two uniquely powerful cosmological probes furnished by general relativity. The next generation of observational surveys can be expected to revolutionize the study of statistical lensing, and gravitational lensing is expected to become one of the most powerful probes of dark energy. In addition, as "first sound" for LIGO (and, hopefully, LISA) arrives, the birth of the age of gravitational-waves is imminent. We propose two complementary research directions, both of which can be expected to lead to elucidation of the nature of dark energy and dark matter.

We have been actively developing a completely independent standard candle: the gravitational-wave driven inspiral of binary compact objects. These standard sirens are the gravitational-wave analogs of standard candles. The radiation emitted during the inspiral phase is well described using the post-Newtonian expansion of general relativity for the compact-object binary. Because

these binary systems are relatively simple and well modeled, the gravitational waves they generate determine the source's luminosity distance with high accuracy. The goal of this proposal is to explore how well LIGO will be able to constrain cosmology, utilizing short/hard gamma-ray burst events as standard candles. We are analyzing the precision with which the Hubble Constant can be determined, and then will utilize this to constrain the dark energy equation-of-state. We will also further explore gravitational lensing at high-redshift, in an attempt to characterize and understand the effects of lensing on supermassive binary black holes sources of gravitational waves. This can have ramifications for cosmological constraints from LISA, a proposed space-borne gravitational-wave observatory.

Conclusion

The main results of this project will be tools which will further our understanding of dark matter and dark energy. We will thus make progress in understanding some of the most profound questions: how old is the Universe? what is the Universe made out of? what is the ultimate fate of the Universe?

References

1. Belczynski, K., M. Dominik, T. Bulik, R. O'Shaughnessy, C. Fryer, and D. E. Holz. The effect of metallicity on the detection prospects for gravitational waves. 2010. *Astrophysical Journal Letters.* **715** (2): L138.

2. Hirata, C. M., D. E. Holz, and C. Cutler. Reducing the weak lensing noise for the gravitational wave Hubble diagram using the non-Gaussianity of the magnification distribution. 2010. *Physical Review D.* **81** (12): 124046 (11 pp.).

3. Cutler, C., and D. E. Holz. Ultrahigh precision cosmology from gravitational waves. 2009. *Physical Review D.* **80** (10): 104009 (15 pp.).

4. Nissanke, S., D. E. Holz, S. A. Hughes, N. Dalal, and J. Sievers. Exploring short gamma-ray bursts as gravitational-wave standard sirens. To appear in *Astrophysical Journal.*

Publications

Belczynski, K., M. Dominik, T. Bulik, R. O'Shaughnessy, C. Fryer, and D. E. Holz. The effect of metallicity on the detection prospects for gravitational waves. 2010. *Astrophysical Journal Letters.* **715** (2): L138.

Bloom, J., D. Holz, S. Hughes, and K. Menou. Coordinated Science in the Gravitational and Electromagnetic Skies. 2009. *Astro2010: The Astronomy and Astrophysics Decadal Survey, Science White Papers, no. 20.*

Cutler, C., and D. E. Holz. Ultrahigh precision cosmology from gravitational waves. 2009. *Physical Review D.* **80** (10): 104009 (15 pp.).

Hirata, C. M., D. E. Holz, and C. Cutler. Reducing the weak lensing noise for the gravitational wave Hubble diagram using the non-Gaussianity of the magnification distribution. 2010. *Physical Review D.* **81** (12): 124046 (11 pp.).

Nissanke, S., D. E. Holz, S. A. Hughes, N. Dalal, and J. Sievers. Exploring short gamma-ray bursts as gravitational-wave standard sirens. To appear in *Astrophysical Journal.*

Characterizing the Th-229 Isomer: A Nuclear Clock Candidate

Xinxin Zhao
20100184ER

Introduction

Atomic clocks are widely used today in precision measurement, navigation (GPS), and for defense and intelligence applications such as sensing, localizing targets and explosions from space. A 10-fold improvement in the accuracy of GPS satellite's clock would have important impact in threat reduction and intelligence applications, especially for single shot event. In this project, we propose to study the underlying science for a new class of clocks, called a nuclear clock. This nuclear clock would be based on the energy difference between the ground and the lowest-lying isomeric nuclear level in ^{229}Th. Compared to atomic clocks, a nuclear clock would be inherently more accurate and robust with respect to variations in its environment (such as EM fields and atomic collisions). As such the development of such an ultra-high precision clock would truly have a transforming impact enabling new fundamental physics tests at unprecedented accuracy and important applications as mentioned above. Because no direct measurement of the ^{229m}Th isomer has been made, we propose to directly measure the gamma decay of the ^{229m}Th isomer for the first time and characterizing the property of the isomer.

Benefit to National Security Missions

This project is the first step towards precision measurements with the isomer transition and lays the scientific foundation for a ^{229}Th nuclear clock. Success of the project will have transforming impact in navigation (GPS), military, as well as important applications in threat reduction and intelligence programs.

Progress

We have made great progresses on the project. We have set up the detector system in vacuum (~1 micro torr) for detecting vacuum ultra-violet (VUV) photons. We have found a lab for the new experiment setup (TA48/rm 410). The system is compact enough to fit in the fume hood. The PMT detector was cooled with a thermo-electric cooler (TEC)/chiller to achieve a dark count rate of less than 0.2 Hz, five times better than our estimates in the proposal. We have custom made and tested the source plates assembly which consists of a stack of polished MgF_2 plates for collecting the Th-229 recoils from the U-233 decay. We have started the search and found a decay signal since early August and have completed many measurements.

Due to the historical uncertainty in the transition wavelength, we first measured the light emission using the R8486 PMT, which has a wide detection range from 115 nm to 320 nm. The emission decay observed after 4 hours of recoil implantation using the U-233 source (red dots in Figure 1) fits well to the sum of four exponentials with three of the four time constants fixed: MgF_2 phosphorescence, MgF_2 fluorescence due to Pb-212 beta decay and Ra-224 alpha decay. We also fixed the ratio of the amplitudes (7.33 for 4 hours of implantation) between the Pb-212 and Ra-224 components. With this model, we isolated a 1 Hz component (16.5 hr) as a possible signal of interest. The residue ripples are attributed to the modulation of MgF_2 phosphorescence/fluorescence by room temperature fluctuations. We are currently working on the final set of measurements to characterize this component.

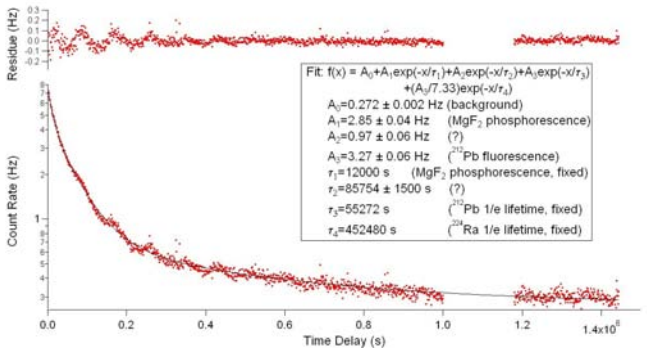

Figure 1. Emission decay after a 4 hour recoil implantation period with U-233source measured with R8486 (red square dots) and a four-exponential fit (solid black line). Three known time constants and the ratio of Ra-224 to Pb-212 activities were fixed in the fit. The residue ripples (top panel) are attributed to the modulation of MgF2 phosphorescence/fluorescence by room temperature fluctuations.

On the manpower front, we recruited a new postdoc, Dr. Yenny Natali Martinez from Rice University. Natali is a very promising young scientist, just graduated with fourteen publications, five of which are in Physical Review Letters. We attended the APS/DAMOP meeting in May and learned a growing interesting in the hunt for this unique nuclear transition.

Future Work

With a signal that is possibly from the isomer in hand, we are focusing on new measurements to rule out all of the non-isomeric possibilities and to determine the lifetime and wavelength of the isomeric transition.

Conclusion

Preliminary results are very encouraging. This discovery once proven to be true lays the ground work for a new emerging field of nuclear manipulation with coherent light sources.

A Plasma-Based Ultrafast THz Source

George Rodriguez
20100189ER

Introduction

Terahertz (THz) science and technology is one of the most intriguing and challenging research fields to emerge in the 21st Century. Terahertz radiation is loosely defined by the electromagnetic spectrum whose frequency range is between 0.1 to 30 THz (10^12 cycles per second). Situated between infrared light and microwave radiation, THz radiation is not well suited to generation and detection techniques commonly employed in these well-established neighboring bands. In fact, the terahertz region of the electromagnetic spectrum has proven to be one of the most elusive. High atmospheric absorption constrained early interest and funding for THz science. However, the past 10-15 years have seen a revolution in THz systems, as advanced materials and laser research provided newer and higher-power sources. Consequently, the terahertz research continues to emerge as a development area for future applications in optical imaging and sensing technologies. Some of the anticipated applications using THz radiation include tomography, bio-chemical forensics, THz electronic devices, and security scanners for portal screening. Yet, despite these advances, there still is a desperate need for a high peak power THz source capable of producing pulses above the microjoule per pulse energy level. For many applications, today's THz sources are still too weak [1, 2]. To overcome this limitation, the main goal in this project is to develop a wideband pulsed THz source with energies in microjoule range [3]. The work represents a significant advance in the field of THz science. Our research approach uses two-color laser beams that focused to high intensity in a gas that causes gas atoms to ionize and form a plasma filament. The strong ionization in the gas occurs on the time scale of the input laser beams, femtoseconds. Subsequent motion of the liberated electrons in the ionization process produces transient electric current pulse that emits THz radiation much like a radiating antenna. The THz radiation emitted is a beam that is coherent in space and time. This project uses advanced laser-plasma physics models and experiments to develop an optimized source for increased output and tuning across the entire terahertz spectral range of this plasma based THz source.

Benefit to National Security Missions

This work supported under this project benefits technologies for THz-based sensor systems relevant to programs within the intelligence and security agencies. This includes THz spectroscopy instrument technologies for trace chemical or bulk material detection using spectral analyses, chemical forensics, or non-destructive imaging methodologies. This work in this project underpins Laboratory's missions in plasmas and beams as well as in fundamental understanding of materials.

Progress

In FY10 we achieved progress in our experimental characterization and physics understanding of terahertz (THz = 10^{15} Hertz) generation from ultrafast laser-plasma interactions in gases. First, we report that the experimental apparatus for THz generation and characterization was completed. We commissioned a high repetition rate (1 kilohertz - kHz) ultrafast titanium-sapphire laser system and built a new THz generator gas cell along with vacuum-based THz spectrometer. The experimental setup and THz spectrometer illustrated in Figure 1.

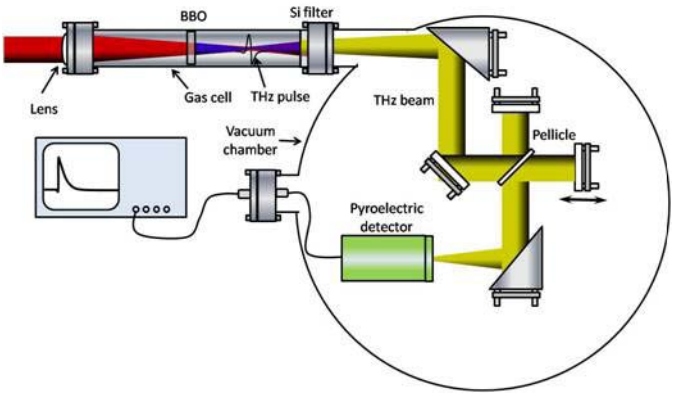

Figure 1. Experimental layout showing that THz beam is generated by mixing the fundamental laser beam at 800 nm and its second harmonic laser field at 400 nm, generated from a frequency-doubling Beta-Barium Borate crystal in a gas cell. Ionization of the gas by the two laser beams is necessary for THz generation. A

silicon filter is used filter out the THz pulse from the optical pulses. The THz interferogram is measured using Michelson interferometer located inside a vacuum chamber.

The spectrometer measures the THz pulse temporal interferogram. An interferogram is an amplitude autocorrelation of the pulse time structure. From the interferogram, we can mathematically compute the spectrum of the pulse using the Fourier Transform. Next, we proceeded with experiments aimed studying the THz output scaling properties versus input optical energy, gas species (air, neon, argon, krypton, xenon), and gas concentration [4]. Results from these experiments indicate that broad band (> 30 THz), microjoule-level, 30 femtosecond (fs) THz pulses are readily generated when driven with our laser system. Input laser pulse energy of 6 millijoule per pulse is used. The laser wavelength is 800 nanometers (nm), and the second color at 400 nm is produced in a special nonlinear crystal beta barium borate (BBO) contained in the gas cell. This two-colored laser beam is focused into the gas for ionization and produces the plasma filament. From the filament emerges the newly created THz beam. Figure 2 shows a representative THz spectrum generated in argon gas.

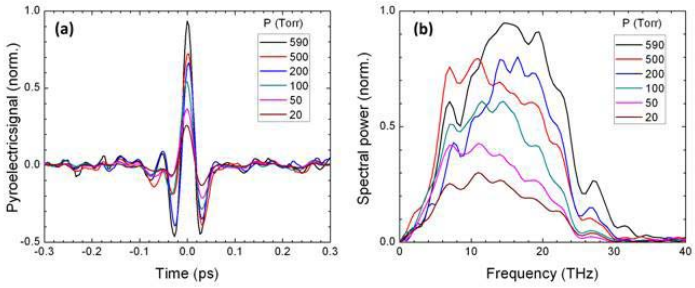

Figure 2. A representative example THz interferogram temporal waveforms and corresponding power spectra for the following Argon gas at pressures between 20 Torr and 590 Torr. Note the the temporal is extremely short ~30 fs with very large spectral content to beyond 30 THz.

A 30 THz pulse represents extremely broad spectral content in the far-infrared wavelength region range between 10 -300 microns. We studied THz generation under varying drive laser conditions and gas parameters. Figure 3 shows the data from these studies where we plot THz output pulse energy versus (a) input laser energy and (b) gas pressure for a series of gases: air, neon, argon, krypton, and xenon. The results show that laser field ionization and induced gas-plasma filamentation are the conditions that generate THz. Although overall optical-to-THz pulse energy conversion efficiency appears low at 1 part in 6000, the THz pulse energy (approximately 1 uJ) and peak power (30 MW) remain as some of the highest ever generated from a laser-based drive source at 1 kHz repetition rates. In addition to these experiments, a simple 1-D theoretical model was used to describe results, albeit the adequacy of a 1D model is still lacking. Results of first year experiments were published in the journal *Optics Express* [4]. As the first year of this project ended, experimental efforts concentrated on more sensitive spectral pulse detection techniques (to 100 THz) and on plasma filament effects on transverse spatial beam profile. The theory component of this project is addressing these issues and a more sophisticated model is under development. We describe progress on this front next.

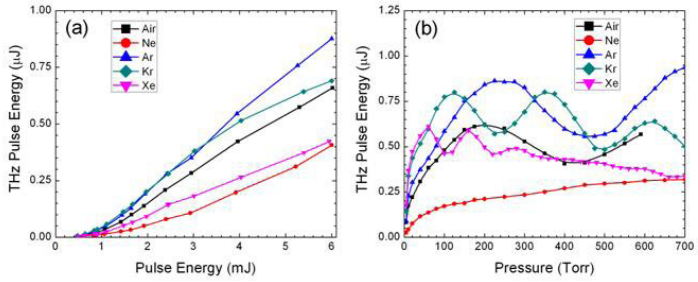

Figure 3. THz output pulse energy versus (a) input 800-nm pulse energy (P=590 Torr) and (b) pressure (E=5.4 mJ/pulse) for the following gases: air, neon, argon, krypton, and xenon.

The generation of THz radiation inside laser-produced filaments is an inherently a 3D process requiring an accurate model of both laser-induced ionization and pulse propagation through the inhomogeneous plasma. We use a full 3D electromagnetic pulse propagation computer code, PULSE, to calculate the laser-gas interaction, plasma formation, and far field THz spatio-temporal pulse generation. Over the past year, we have developed a laser ionization model appropriate for the operating regime of on-going experiments. In particular, for the intensities and frequencies of interest, the dominant regime of ionization (i.e. plasma production) is multi-photon and tunnel ionization. We were able to obtain both analytical and semi-analytical solutions for the ionization rate and incorporated them into our simulation model. It is quite clear that the loss of laser energy from ionization will have a significant impact on the propagating laser field. To make the simulations self-consistent, we update the electric field appropriately. Finally, the simple model for the plasma current in earlier models from which the THz signal was calculated lacked the contribution from plasma generation. We have developed a more sophisticated model for the current evolution and incorporated it into the code. We are currently testing the updated code in the regimes that are relevant to the experiment and early 3D computational results for comparison with experiments are expected in early FY2011.

Future Work

In FY2011, we will use input from the computational model to optimize THz generation through manipulation of the input laser properties (pulse shape, phasing, or beam focusing conditions). Second, the spectral tuning properties of the THz beam will studied by introduction of tuning elements in the THz beam, or by active control via spatio-

temporal manipulation of the driving laser beam. Narrow band tuning within the spectrum of the entire pulse is sometimes desired because chemical and material resonances in this frequency range are often on the order a few THz (a fraction of the overall 30 THz bandwidth). Selective channeling of THz energy into these resonances requires one to tune to these resonances for efficient excitation and subsequent detection.

Conclusion

The goal of this proposal is to experimentally and theoretically develop a plasma-based ultrashort pulse coherent terahertz (THz) source with peak pulse energies in the microjoule range. The THz source is based on ultrafast two-color laser generated plasma filaments in gases. We continue our work on establishing a high-peak-power tunable THz pulse over the wide range of frequencies (to 30 THz). Needed is a THz source for a myriad of applications in materials science, active THz sensing and imaging, non-linear THz optics, THz electronics, forensics, and others.

References

1. Sherwin, M. S., C. A. Schmuttenmaer, and P. H. Bucksbaum. Opportunities in terahertz science. 2004. *Report of a DOE-NSF-NIH Workshop held February 12 – 14, 2004, Arlington, VA, USA.*

2. Reimann, K.. Terahertz radiation: a table-top source of strong pulses. 2008. *Nature Photonics.* **2** (10): 596.

3. Kim, K. Y., A. J. Taylor, J. H. Glownia, and G. Rodriguez. Coherent control of terahertz supercontinuum generation in ultrafast laser-gas interactions. 2008. *Nature Photonics.* **2** (10): 605.

4. Rodriguez, G., and G. L. Dakovski. Scaling behavior of ultrafast two-color terahertz generation in plasma gas targets: energy and pressure dependence. 2010. *Optics Express.* **18** (14): 15130.

Publications

Rodriguez, G.. Parametric studies of ultrafast two-color terahertz generation in gas plasma filaments. Invited presentation at *3rd International Symposium on Filamentation.* (Crete, Greece, 31 May - 5 Jun. 2010).

Rodriguez, G., N. Krasheninnikova, and M. J. Schmitt. Analytical and simulation study of laser-ionized plasma. Presented at *52nd Annual Meeting of the APS Division of Plasma Physics.* (Chicago, IL, USA, 8 2 Nov. 2010).

Rodriguez, G., and G. Dakovski. Scaling behavior of ultrafast two-color terahertz generation in plasma gas targets: energy and pressure dependence. 2010. *OPTICS EXPRESS.* **18** (14): 15130.

Rodriguez, G., and G. L. Dakovski. Parametric studies of two-color ultrafast terahertz generation in gas plasma filaments. Presented at *37th IEEE International Conference on Plasma Science.* (Norfolk, VA, USA, 20-24 Jun. 2010).

Hawking-Unruh Effect in Atomic Bose-Einstein Condensates

Emil Mottola
20100191ER

Introduction

The primary goal of this project is to test the hypothesis of the Hawking-Unruh effect, namely that an accelerated mirror will radiate with a thermal spectrum, predicted in relativistic field theories and black hole physics, in the concrete analog system of cold atomic Bose-Einstein condensates (BEC's) in the laboratory. By carrying out detailed calculations for an accelerated "mirror" of sound waves in a BEC generated by a laser induced potential, we are studying the practical feasibility for detecting an analog of the Hawking-Unruh effect in a realistic laboratory experiment for the first time. The general scientific interest in black hole phenomena and Einstein's legacy guarantees that the results of our research will be a highly visible scientific accomplishment. It will enhance the public image and scientific capabilities of the Laboratory by helping to attract future staff and help retain our excellent scientists and engineers.

In this project, we focus on the most promising strategy for detection of the Hawking-Unruh radiation in a BEC. Our approach relies on the prediction of radiation produced by an accelerating laser "mirror" potential, i.e. the Davies-Fulling-Unruh effect. The key idea that distinguishes a BEC mirror environment from other analog Hawking proposals is that the acceleration of the laser mirror can be accurately controlled over a large dynamic range while this is not possible for the velocity gradient in a BEC. Since very large accelerations can be achieved with accurately controlled lasers focused on a BEC, it is possible to achieve temperatures as large as mK. Thus, this extremely important prediction of fundamental physics may be measurable for the first time in the laboratory, and quite possibly in a cold atom BEC experiment at Los Alamos National Laboratory.

Benefit to National Security Missions

This is a basic research project, relevant to DOE OS programs in Particle Physics, Quantum Field Theory, Gravitation, Bose-Einstein Condensates, Many-Body and Statistical Physics. Verification of the Hawking-Unruh effect in a BEC experiment would be a major achievement. If realized at Los Alamos, it would be a significant boost to the program in cold atoms at the Quantum Institute. The basic knowledge gained about BECs and detailed numerical codes could form the basis of a larger program in applications of cold atoms to fundamental gravitational physics.

Progress

The first step in calculating quantities relevant to real BEC experiments is choosing the simplest nontrivial, non-equilibrium, quantum dynamical model. For this purpose we have investigated both the two dimensional Hartree-Fock-Bogoliubov (HFB) approximation for the coupled condensate-one particle (equal time) matrix Green's function, and the more systematic large N approximation. Both HFB and Large N are well known to be consistent with indispensable physicals properties including the conservation of particle number, momentum and energy. Both reduce to the classic Gross-Pitaevskii equation when quantum fluctuations are negligible. Large N preserves the Goldstone theorem for the spontaneous breaking of phase symmetry in the condensate and the second order nature of the BEC phase transition, while HFB recovers the Bogoliubov approximation at low temperature. We have developed a Fortran code to solve both HFB and Large N in two spatial dimensions, with initialization as the ground state in an external potential (the "mirror") for the first time. The code has been benchmarked against several analytically controlled approximations and determined to be accurate and reliable. Preliminary numerical results have been obtained which confirm the order of magnitude estimates of mirror parameters, including shape, height and acceleration that are suitable for observing BEC analog Hawking-Davies-Fulling-Unruh effect.

In the numerical implementation of HFB a modal representation of the Green's function/condensate dynamics has been found which preserves the fundamental invariants under arbitrary truncation of the modal expansion. This is not necessary when the modes can be represented by Fourier modes, but will prove useful for detailed comparison with experimental results.

As a test problem for the codes and to compare with

analytical results, relaxation to the steady state under the influence of an external, one dimensional, potential translating at constant velocity << speed of sound has been simulated. We find in the approach to a steady state as modeled by the HFB Green's function (G)/condensate dynamics, a finite drag, consistent with recent analytical results of David Roberts (T-04 Oppenheimer fellow) and Andrew Sykes (CNLS postdoc). As their results are the subject of discussion in the literature, this use of the code to study quantitatively the drag and damping dynamics of a BEC should attract wide interest.

In parallel to this code development we have also developed a general formalism for finite frequency dependent mirror reflectivity which will make possible the calculation of the spectrum and total energy emitted by its arbitrary motion, relevant for realistic BEC laboratory experiments. The formalism has been applied to the relativistic problem of arbitrary mirror motion and reflectivity in one dimension, and a paper is in preparation on this new result. Extension to two dimensional BEC geometries are straightforward, and we are currently comparing the parameters of the model to realistic parameters attainable by laser-painting the potential on a two dimensional BEC as anticipated in the laboratory experiment. The analytic formula is currently being used to test the code as well.

A third line of research involves the incorporation in the theoretical framework of the full non-equilibrium dynamics induced by the mirror motion. To that end we have developed techniques in the quantum many-body problem which go beyond the usual perturbative framework of expansion in a weak coupling parameter (in the BEC the mean interparticle spacing compared to the much larger healing length). We have investigated the systematics of the loop expansion in high temperature gauge theories beyond the leading order hard thermal loop (HTL) approximation, and calculated the two-loop electron proper self-energy in a high temperature plasma. The many-body resummation methods developed apply equally well to the high density but low temperature regime appropriate for atomic BEC's. This work has been completed with an external collaborator (Zsolt Szep) and is published in:
Systematics of High Temperature Perturbation Theory: The Two-Loop Electron Self-Energy in QED
Emil Mottola and Zsolt Szep, **Phys. Rev. D81**:025014 (2010)
Several other papers are in preparation extending the effective action capturing the collective effects in both relativistic and non-relativistic many-body systems to non-equilibrium plasmas and atomic BEC's.

With the important preliminary steps in code development and testing, and exploration of more sophisticated analytic techniques to accurately model the BEC dynamics, accomplishing several benchmarks in the first year of this project, we anticipate rapid progress and a series of publications detailing our first completed results in the second year FY2011.

One of us (E. M.) was invited to the Spanish Relativity Meeting, Sept. 6-10, 2010 for a plenary talk on *New Horizons in Gravity: Dark Energy and Condensate Stars.* This international meeting (see its website for more details) had more than 100 participants, and most of the world's experts in analog gravitational systems, with whom this project was discussed. Interest in the results of this project are very high, and future invited talks at major meetings are anticipated when the first results are reported.

Future Work

Detailed calculations for an accelerated "mirror" of sound waves in a BEC generated by a laser induced potential in progress are:

- Determine the robustness of the spectrum and total energy emitted by the moving laser "mirror" potential, and sensitivity of the result to the precise boundary conditions and high frequency cut-off in the reflectivity.
- Replace the mirror of infinite extent with one with finite transverse dimension, in two dimensions, and recalculating the spectrum, total energy and statistical correlations of the radiation emitted.
- Compute the density profile of condensate and resulting time and position dependence of the sound speed as modeled by the Gross-Pitaevskii equation, in both the HFB and Large N approximations first in an infinite condensate, and then in a sample of finite spatial extent.
- Determine the critical acceleration of the laser that will "melt" the condensate in the physically realizable experimental configuration and its dependence on density, atomic scattering length, laser intensity and other control parameters.
- Study the drag and production of vortices at the mirror edges and the contributions of the normal fluid component in the BEC, by including the nonlinear backreaction effects of the phonon modes on the condensate. Investigate the effects of vorticity on the signal.
- Determine the effects of laser mirror shape, geometry and trajectory for optimization of the signal in the BEC.
- Study the properties of the new theoretical approaches to many-body nonequilibrium dynamics in the BEC which we have recently developed, and compare to BEC experiments.

Conclusion

We are investigating the Hawking-Unruh prediction under a wide variety of external conditions. This will lay the groundwork for the first possible experimental confirmation of the effect. Verification of the Davies-Fulling-Hawking-Unruh effect in a BEC experiment would be a major achievement. If realized at Los Alamos, it would be a significant boost to the program in cold atoms at the LANL Quantum Institute. In addition to enhancing the prestige of existing LANL program in this area, the basic knowledge gained about BECs could form the basis of a larger program in applications of cold atoms to fundamental gravitational physics.

Publications

Mottola, E., and Z. Szep. Systematics of High Temperature Perturbation Theory: The Two-Loop Electron Self-Energy in QED. 2010. *Physical Review.* **D81**: 025014.

Cold Atoms in Quantum Periodic Potentials

Bogdan F. Damski
20100296ER

Introduction

This work is focused on studies of new solid state systems from the most basic, i.e., quantum level. This will advance our understanding of many-body quantum physics that provides a key insight into superconductors, superfluids, nano-scale devices, etc. Practical applications of the new systems/materials that we will study include quantum processing/computing, advanced emulation of challenging condensed matter systems like superconductors, and sensing.

We will capitalize here on a revolutionary progress taking place in atomic and molecular physics. This progress is driven by efforts to study the most challenging quantum systems in easily controllable (cold atom/ion) setups. It allows us to consider new forms of matter whose experimental realization was impossible a few years ago.

We will theoretically focus on many-body quantum systems exposed to quantum external fields. These fields can be in a superposition of various strengths/structures. They can be physically realized in either cold ion or cold atom systems. In the former system the quantized fields are emulated by laser-driven interactions between ions, while in latter system they come from quantized photon fields trapped in optical cavities made of high-quality mirrors.

As a result of interactions with quantum external fields, the systems that we consider have unique properties because atoms/ions can be there in a simultaneous superposition of various quantum phases. We'll develop a new theory of quantum phase transitions to account for this. We'll investigate stability of these new phases and experimental prospects for their realization. We'll focus on both the static and dynamic properties of these systems. We will advance current analytical techniques used for studies of quantum many-body systems (typically magnetic materials) and develop numerical approaches that can handle these problems efficiently.

Benefit to National Security Missions

This work will uncover properties of new physical systems whose potential applications may include quantum processing/computing, advanced emulation of challenging condensed matter systems like superconductors, and sensing. All of them are of interest to various federal agencies. On the technical level, this work contributes to the fundamental understanding of new materials through first principles quantum studies (bottom-up approach). This topic is also attracting attention of numerous sponsors including DOE.

Progress

We have developed a spin model that allows for detailed investigations of many-body physics in a quantum (magnetic) field. The model is made of the Ising spin chain coupled to a central spin-1/2. The central spin, a quantum subsystem, is prepared in a superposition of its two up/down states. Its interaction with the Ising chain is engineered in such a way that it creates an effective quantum magnetic field acting on Ising spins. We have developed an approach allowing for creation of the quantum superposition of ferromagnetic and paramagnetic phases (ground states) of the Ising chain, which is the key goal of our project.

The great advantage of our model is that its quantum state can be exactly analytically solved. Therefore, we have been working on extraction of useful information out of these analytical, but complicated, expressions. We have developed approximate analytical techniques for handling these expressions and exact numerical codes to evaluate them. The two approaches have been found to be in good agreement.

We have focused first on correlation functions: the most important objects in the field of quantum phase transitions. We have found that quantum nature of the potential does modify non-trivially correlations by introducing a new correlation length scale and a new decay rate. Both results shall be experimentally accessible in the future in cold ion systems exposed to laser-engineered interactions.

We have also studied several other observables (e.g., local magnetization) and found that they all depend on quantum fidelity. In our system quantum fidelity is the overlap

between two ground states of the Ising chain calculated at different magnetic fields acting on its spins. This allowed us to understand how the size of the quantum system exposed to a quantized potential affects the observable properties. In particular, we found that for too large systems the effects associated with quantum nature of the potential disappear and, interestingly, their decay rate encodes the critical exponent characterizing divergence of the correlation length near a phase transition point. Quantum fidelity has been recently extensively studied by many condensed matter/quantum information researchers. We have discovered that its functional dependence on system size and the coupling strength has never been properly characterized in the thermodynamic limit. To describe it analytically, we have employed a renormalization group theory and linked universality class of the system to the decay rate of the quantum fidelity. This general result, in particular, quantifies for the first time the celebrated Anderson catastrophy (disappearance of quantum fidelity of large systems) near a quantum phase transition point. To confirm our scaling predictions remarkably compact and accurate analytical solution for the quantum fidelity of the Ising chain was found. Several other spin models (XY, extended Ising, etc.) have been solved as well to verify our general predictions that depend on the symmetry (universality class) of the system rather than its microphysics.

One manuscript on quantum fidelity has been already submitted to Physical Review Letters [1], while a follow-up paper is currently in final stages of preparation. In addition to that, two more papers on quantum phase transitions have been written and published [2,3].

Future Work

We will study cold atoms/ions exposed to quantum potentials. More work is needed to understand the interplay between the system size and the fluctuations of the quantized potential in these systems. To bring our calculations close to experiments, we will also consider the effects of finite temperature (previous calculations have been done at zero temperature typically considered in the context of quantum phase transitions). To extend our studies to systems that are not exactly solvable (like the Ising chain considered so far), we will develop tensor network algorithms that will efficiently reduce the system computational complexity from exponential to polynomial in the system size.

We will also work on a specific scheme that should allow for a straightforward realization of the models that we study in current experiments with cold ions/atoms.

Our final goal is to develop a theory of quantum phase transitions in quantum potentials describing novel aspects of these systems (simultaneous superpositions of distinct quantum phases). We will investigate stability of these systems in various phases and evaluate experimental prospects for their observation. We will study their static (equilibrium) properties, but also research their dynamic response to driving (e.g., time dependent magnetic fields).

Conclusion

We will study properties of the new materials made of strongly interacting particles coupled to quantum fields. Our work will characterize the unique properties of these novel systems guiding future experimental work in this field. It will advance understanding of many-body quantum physics (a key theory describing nano-scale systems) and contribute to development of high-impact practical devices of potential interest to quantum processing/computing, advanced emulation of challenging condensed matter systems like superconductors, and sensing.

References

1. Rams, M. M., and B. Damski. Quantum fidelity in the thermodynamic limit . *Physical Review Letters.*

2. Dziarmaga, J., and M. M. Rams. Adiabatic dynamics of an inhomogeneous quantum phase transition: the case of z > 1 dynamical exponent. 2010. *New Journal of Physics.* **12**: 103002.

3. Niederberger, A., M. M. Rams, J. Dziarmaga, F. M. Cucchietti, J. Wehr, and M. Lewenstein. Disorder-Induced Order in Quantum XY Chains. 2010. *Physical Review A.* **82**: 013630.

Publications

Dziarmaga, J., and M. M. Rams. Adiabatic dynamics of an inhomogeneous quantum phase transition: the case of z > 1 dynamical exponent. 2010. *New Journal of Physics.* **12**: 103002.

Niederberger, A., M. M. Rams, J. Dziarmaga, F. M. Cucchietti, J. Wehr, and M. Lewenstein. Disorder-Induced Order in Quantum XY Chains. 2010. *Physical Review A.* **82**: 013630.

Rams, M. M., and B. Damski. Quantum fidelity in the thermodynamic limit. *Physical Review Letters.*

BEC Waveguide Optics

Eddy M. Timmermans
20100302ER

Introduction

The cold atom Bose-Einstein condensates (BEC's), gas systems of atoms that have been laser-cooled to the lowest temperatures ever reached in a laboratory, exhibit the characteristics of atom lasers and of superfluidity simultaneously. As atom lasers, all atoms can be made to move in perfect lockstep coherence and the BEC acts as a single, giant quantum wave which can exhibit large contrast fringes (wiggles) when two waves intersect. This ability promises unprecedented atom optics applications for sensing rotations (gyroscopes), for sensing weak forces (metrology) and for imaging. As a superfluid system, an object can be dragged through the gas without causing drag or dissipation (heating). Another counter-intuitive property of superfluidity is exhibited by the Josephson junction that connects weakly connected superfluids: the sudden alteration of the relative energy of the fluids causes a back-and-forth current to set in instead of the classically expected flow from the most energetic region into theregion of lower energy. Quantum mechanically, the weak connection and quantum nature can also greatly increase the uncertainty of the number of particles that find themselves on either side, which greatly increases the contrast of the interference fringes and, hence, the accuracy of optical sensing devices. In this project, we explore by means of theory and simulation the intriguing potential of BEC-physics for realizing novel atom optical applications by guiding the BEC-waves along well-defined directions. We will also explore the prospect of using many-body quantum physics and the unusual ability of cold atom technology to manipulate superfluid properties of the BEC to realize optical devices that reach the quantum limit of resolution.

Benefit to National Security Missions

The development of a practical, coherent atom optics are part of the quantum efforts which fit in the charter of the information science grand challenge. The scientific goals satisfy calls in the broad agency announcements of DOE-BES, ASFR and ONR. The promise of metrology applications of unparalleled sensitivity may also find long-term applications in the threat-reduction part of the laboratory.

Progress

The waveguide potential that confines the Bose-Einstein condensate (BEC) is a focused laser beam that can paint a potential minimum with equipotential surfaces that are cylindrical tubes with their ends connected. If the trapped Bose-Einstein condensate is the matter laser wave that is guided, the ring potential realizes the simplest geometry of a multiply connected superfluid.

We have explored the physics of effective gauge fields that can be implemented in such BEC wave guide systems. In the context of the toroidal trap, we found that a Berry-phase gauge can be implemented with a two component spin Bose-Einstein condensate. The doughnut-shaped two component BEC can take on vortex states with integer and half-integer charge winding numbers and with an integer number of spin rotation numbers. By varying the polarization of the sample, one can fulfill the conditions under which the system's charge winding number and/or spin rotation number could increase by one quantum. Not only does this system provide an example of an effective gauge field that can be simulated in cold atom physics, but it also gives a gauge field that has its own dynamics. The combination of gauge physics and quantization would also be new to the field of cold atom physics.

We have shown that an additional focused, red-detuned laser beam can create a potential barrier that acts as a constriction on the BEC in the waveguide. Rotating the barrier along the ring then creates a Josephson junction. As in Superfluid Quantum Interference Devices (SQUIDs), the system can take on a state that is a linear superposition of two flux states.

Another unusual knob in the BEC waveguide system is the Feshbach resonance control of the inter-particle interactions, which will play an important role in demonstrating that non-linearity can induced sensitivity that scales faster than the standard shot limit. For that system, the equation of state of strongly interacting bosons needs to be understood. Nearly a century after the first observation of the lambda transition in liquid helium, a quantitative, first principles description of strongly cor-

related bosons remains a challenge. Most of the proposed descriptions fall within the Hohenberg and Martin classification of conserving and gapless approximation, which implies that they either violate Goldstone's theorem or general conservation laws. These approximations predict Bose-Einstein condensation of interacting (even weakly interacting) boson particles to a be a first order transition whereas we expect it to be second order. We have devised a new theoretical framework that treats the normal and anomalous (depletion) densities on the same footing. The resulting description brings many highly useful and powerful advantages that were previously unavailable in the same package. The description satisfies Goldstone's theorem (yielding excitation frequencies that vanish in the long wavelength limit). The description yields a second-order Bose-Einstein transition. The calculations yield reasonable values for the depletion in a wide range of $\ rho^{1/3} a$ values where ρ denotes the density and a the scattering length that characterizes the boson-boson interactions. A mean-field level determination of the critical temperature gives a variation with scattering length that is identical with the most sophisticated resummation schemes that have been published so far.

We have completed a study of the narrow Feshbach resonances and found a universal momentum dependency of the binary atom scattering amplitude. This finding implies that the effective interaction potential which gives the binary scattering characteristics represented by the scattering amplitude will be universal as well, in the sense that all narrow resonance scattering amplitudes exhibit the same dependency on relative momentum. As the scattering amplitude is universal, we can expect that the effective potential will be universal in the same sense. In this same system, we found that a narrow resonance of sufficient amplitude gives rise to a BEC excitation spectrum with a roton feature. At higher amplitudes, the homogeneous system becomes unstable and the system takes on a ground state that simultaneously exhibits long-range phase coherence as well as breaking translational order by exhibiting crystalline order in the single-particle density.

We have developed a spin-spin description of the binary atom interactions of two-component cold atoms. By selecting two specific hyperfine states in an external magnetic field, the cold atom experimentalists have created effective spin 1/2 systems that behave as magnetic systems do. As these systems can be cooled to temperatures that are lower than the energy of characteristic excitations, these systems promise to simulate quantum magnetism. We have developed a description of their mutual interactions that involve short-range ising-like interactions. We have shown that this description gives new insight by developing a framework for describing the spin dynamics of N bosons trapped in a tight potential, all occupying the same orbital state. The spin degrees of freedom behave as controlled macrocopic quantum magnet that can exhibit spin squeezing, macroscopic quantum tunneling and can be used to demonstrate Heisenberg limited interferometry.

Future Work

The development of novel techniques to create and alter the external potential that traps and guides cold atom gas systems is opening up the prospect of realizing some of the long-promised advantages of atom optics over traditional light-based optics. Guiding Bose-Einstein condensates (BEC's) along well-defined directions can overcome the long-standing problem of dispersion and effectively realize the atom optical elements needed to create a practical optics. In addition, the creation of merging wave-guide profiles (y-junctions) can realize beam-splitting and can result in interference measurements that would overcome the low accuracy of atom counting techniques. We will develop the theoretical description and conduct the necessary numerical simulations of the potential-induced dimensional reduction of the BEC in optical cold atom wave guide potentials and of the dynamics of the BEC at beam-splitters. We will study the interesting prospect of realizing an effective gauge potential by squeezing the guide-potential in the transverse direction (transverse to the direction of BEC-propagation) in a time and spatially dependent manner. We will study the novel prospect of nonlinear wavefunction engineering such as the creation and testing of stable standing wave patterns and of the creation of two-dimensional vortex states. We will show that the time-dependent manipulation of cold atoms can combine the cold-atom demonstrated control of superfluid BEC-properties with optical applications and result in Heisenberg-limited multi-step measurement protocols. We will show that the combination of magnetic fields and two-photon (Raman) transitions can demonstrate and test macroscopic quantum tunneling in an environment of unprecedented control.

Conclusion

Since its realization the BEC technology been widely successful at demonstrating superfluid properties, but the development of a practical BEC-based atom optics has slowed to a trickle. We will show that guiding the BEC-wave along atom wave guides can overcome major hurdles and that manipulating the superfluid properties of the BEC can increase the accuracy of BEC-based sensors to reach the quantum limit. This project will guide the development of a waveguide BEC-optics, creating a mathematical description of the wave-dynamics and exploring the prospect for increasing the sensing accuracy even further by manipulating the superfluid properties.

Publications

Solenov, D., and D. Mozyrsky. Metastable states and macroscopic quantum tunneling in a cold atom Josephson ring. 2010. *Physical Review Letters.* **104**: 150405.

Digital Trigger for the High Altitude Water Cherenkov (HAWC) Observatory

Brenda L. Dingus
20100310ER

Introduction

This project will enable the highest energy observations of photons from astrophysical sources to help us better understand the universe in which our planet resides. These observations probe the fundamental physics of extreme gravitational and electromagnetic fields near black holes. The technique uses the novel detection of showers of particles in the atmosphere interacting with a large water detector located at 13,500' altitude in Mexico. A first generation version of this detector, called Milagro, was built at LANL. This project will fund a digital trigger for this High Altitude Water Cherenkov (HAWC) TeV gamma-ray observatory. We will use the latest technology for this trigger. The objective of this new trigger is threefold.

1. The trigger will allow more information to be recorded about each gamma ray and therefore reduce the systematic uncertainties in flux measurements.

2. The trigger will result in a lower energy threshold for the detector, by excluding non gamma-ray events through pattern recognition algorithms.

3. New triggers for exotic physics, such as magnetic monopoles or SUSY Q balls, will be possible with this more complex trigger. Therefore, this effort will enhance the success of the HAWC observatory and will maintain LANL's leadership in this forefront scientific field of high energy astrophysics.

Benefit to National Security Missions

High energy emission from astrophysical sources has been ranked by National Academy studies as forefront fundamental research. DoE Office of Science, NSF, and NASA support this research. In addition, this research will increase LANL's capabilities in forefront technologies of particle detection, computation, remote sensing, and digital electronics.

Progress

An important objective of this LDRD project is to increase the low energy response of the High Altitude Water Cherenkov (HAWC) Observatory. With better low energy sensitivity, we will be able to observe high-energy transient signals, such as gamma-ray bursts and flaring active galactic nuclei. The lowest energy observations have a very high rate background, so with this LDRD proposal we are investigating a digital trigger to reduce this background.

Our tasks this year have focused on four different activities: 1) investigating the capabilities of commercially available field programmable gate arrays (FPGAs) 2) programming an FPGA to make a simple multiplicity trigger, 3) characterizing the nature of the signals that will be input to the trigger, and 4) increasing our understanding of GRBs in this energy regime by studying data from the Fermi observatory.

There are many commercially available FPGAs. The challenge of this project is that the number of input channels (900) is large. Also, we would like to be able to record and read out the input information to verify that the trigger algorithms are being correctly implemented. We have purchased 3 different commercial modules of which one can be used in a tiered approach to incorporate all 900 inputs. This FPGA is on a board in a VME (Virtual Machine Environment) crate that can be read out and programmed using VME protocols. Using our current algorithms, ~15 of these units would be required to implement a digital trigger for HAWC.

The other two FPGA units were simpler and cheaper and allowed us to investigate different algorithms. A multiplicity trigger has been developed with only 5 inputs, but work is under way to investigate using these simpler units for the first few HAWC tanks that are deployed.

We have also spent considerable effort characterizing the 900 inputs. Specifically, the rate of these input signals is an important parameter that is difficult to determine from simulations. Instead we must look at typical inputs from a prototype of the HAWC tanks. We have assembled such a tank in Texas at the manufacturers plant, but the rate depends on the altitude of the tank. The HAWC site was chosen because of its very high altitude

of 13500'. The first HAWC tank is now being constructed at the HAWC site and we will soon learn key parameters that will influence the design of the trigger.

The final task is to better understand the signal for which we are searching. The highest energy gamma-rays observable by NASA's Fermi Observatory almost overlap with the lowest energy gamma-rays that will be observable by HAWC. We have participated in the analysis of the Fermi data and determined unique characteristics of the high energy emission that HAWC will be able to investigate. Figure 1 shows a the flux vs time that was detected by Fermi from a gamma-ray burst at lower energies and the detection that is expected in HAWC if this emission extends only four-times higher in energy. This further motivates the importance of developing a trigger with lower energy response to be sensitive to these phenomena.

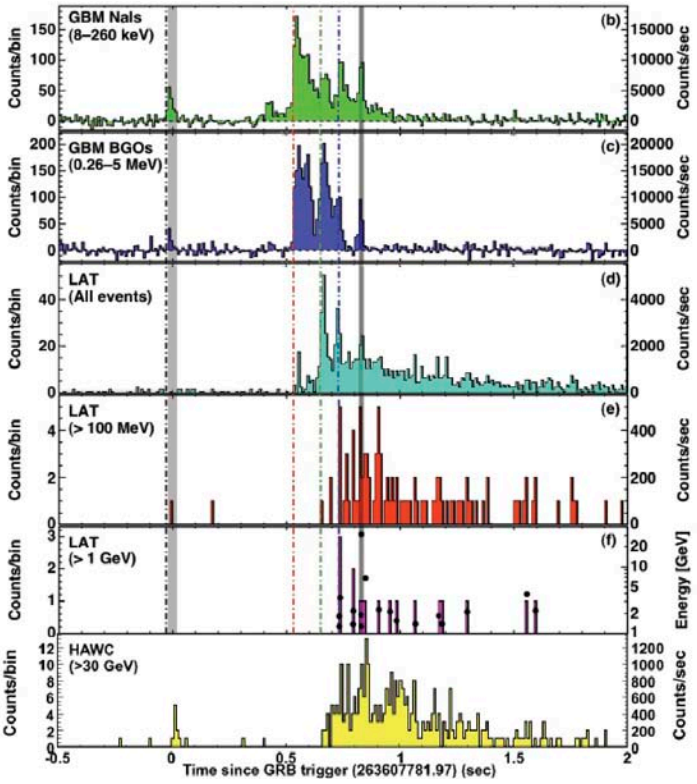

Figure 1. The gamma-ray burst from 10 May 2009 as observed by the Fermi satellite in 4 different energy bands and the expected observation in the higher energy band of HAWC if the spectrum continues to 4 times higher energy.

Also, this year NSF and DOE High Energy Physics have decided to fund the construction of HAWC in FY11-14. Thus, this LDRD work is being implemented at a very opportune time. The capabilities of the LDRD-funded trigger were appealing to the review committee, and they were especially interested in triggers for exotic phenomena, such as Q balls. We plan this work over the next two years.

Future Work

We propose to develop and install a digital trigger system for the HAWC observatory. Milagro used a simple multiplicity trigger requiring a given number of photomultiplier tubes(PMTs)receive a signal within a 170 nanosecond time window. The trigger was implemented with off-the-shelf electronics. With HAWC, we are investigating FPGAs (field programmable gate arrays) to create a modern, robust, easily monitored, flexible trigger system to replace the simple multiplicity trigger that is the baseline design for HAWC. There are three primary objectives of this FPGA-based trigger.

1. Maintain a stable trigger system. One of the largest contributors to the systematic uncertainties for the Milagro data analysis was determining the variable trigger and live PMT fraction. With an FPGA trigger, we will monitor the participation of all PMTs in the formation of the trigger. Such a trigger is required to measure astrophysical fluxes with lower systematic errors in order to search for episodic flaring sources, such as active galactic nuclei, and to combine the HAWC data with other instruments at TeV and lower energies.

2. Reduce the low energy threshold. Many gamma-ray sources cut off at higher energies either due to the maximum energy particles that can be accelerated in the sources or due to the attenuation of gamma rays either in the source or in transit. However, lower energy gamma rays produce fewer hit PMTs on average, and the rate of low multiplicity events is more susceptible to noise, such as single muons. A pattern recognition algorithm can be programmed with FPGAs to reject much of the noise, which is randomly dispersed in the array, and still keep the low energy gamma rays, which have a more centralized core.

3. Enable multiple, specialized triggers for exotic phenomena, such as Q-balls. Other algorithms will be developed for different science goals.

Conclusion

Nature accelerates particles to energies over a million times higher than man made accelerators. This project will result in discovery of astrophysical accelerators and measure the highest energy gamma-ray emission from these objects. The gamma rays are one of the most direct probes of the fundamental physics of extreme gravitational and electromagnetic fields and will increase our understanding of black holes and other astrophysical accelerators.

Publications

Abdo, A. A., M. Ackermann, M. Ajello, K. Asano, W. B. Atwood, M. Axelsson, L. Baldini, J. Ballet, G. Barbiellini, M. G. Baring, D. Bastieri, K. Bechtol, R. Bellazzini, B. Berenji, P. N. Bhat, E. Bissaldi, E. D. Bloom, E. Bonamente, J. Bonnell, A. W. Borgland, A. Bouvier, J. Bregeon, A. Brez, M. S. Briggs, M. Brigida, P. Bruel, J. M. Burgess, T. H. Burnett, G. A. Caliandro, R. A. Cameron, P. A. Cara-

veo, J. M. Casandjian, C. Cecchi, O. Celik, V. Chaplin, E. Charles, C. C. Cheung, J. Chiang, S. Ciprini, R. Claus, J. Cohen-Tanugi, L. R. Cominsky, V. Connaughton, J. Conrad, S. Cutini, C. D. Dermer, A. de Angelis, F. de Palma, S. W. Digel, B. L. Dingus, E. Silva, P. S. Drell, R. Dubois, D. Dumora, C. Farnier, C. Favuzzi, S. J. Fegan, J. Finke, G. Fishman, W. B. Focke, L. Foschini, Y. Fukazawa, S. Funk, P. Fusco, F. Gargano, D. Gasparrini, N. Gehrels, S. Germani, L. Gibby, B. Giebels, N. Giglietto, F. Giordano, T. Glanzman, G. Godfrey, J. Granot, J. Greiner, I. A. Grenier, M. -H. Grondin, J. E. Grove, D. Grupe, L. Guillemot, S. Guiriec, Y. Hanabata, A. K. Harding, M. Hayashida, E. Hays, E. A. Hoversten, R. E. Hughes, G. Johannesson, A. S. Johnson, R. P. Johnson, W. N. Johnson, T. Kamae, H. Katagiri, J. Kataoka, N. Kawai, M. Kerr, R. M. Kippen, J. Knodlseder, D. Kocevski, C. Kouveliotou, F. Kuehn, M. Kuss, J. Lande, L. Latronico, M. Lemoine-Goumard, F. Longo, F. Loparco, B. Lott, M. N. Lovellette, P. Lubrano, G. M. Madejski, A. Makeev, M. N. Mazziotta, S. McBreen, J. E. McEnery, S. McGlynn, P. Meszaros, C. Meurer, P. F. Michelson, W. Mitthumsiri, T. Mizuno, A. A. Moiseev, C. Monte, M. E. Monzani, E. Moretti, A. Morselli, I. V. Moskalenko, S. Murgia, T. Nakamori, P. L. Nolan, J. P. Norris, E. Nuss, M. Ohno, T. Ohsugi, N. Omodei, E. Orlando, J. F. Ormes, M. Ozaki, W. S. Paciesas, D. Paneque, J. H. Panetta, D. Parent, V. Pelassa, M. Pepe, M. Pesce-Rollins, V. Petrosian, F. Piron, T. A. Porter, R. Preece, S. Raino, E. Ramirez-Ruiz, R. Rando, M. Razzano, S. Razzaque, A. Reimer, O. Reimer, T. Reposeur, S. Ritz, L. S. Rochester, A. Y. Rodriguez, M. Roth, F. Ryde, H. F. Sadrozinski, D. Sanchez, A. Sander, P. M. Parkinson, J. D. Scargle, T. L. Schalk, C. Sgro, E. J. Siskind, D. A. Smith, P. D. Smith, G. Spandre, P. Spinelli, M. Stamatikos, F. W. Stecker, M. S. Strickman, D. J. Suson, H. Tajima, H. Takahashi, T. Takahashi, T. Tanaka, J. B. Thayer, J. G. Thayer, D. J. Thompson, L. Tibaldo, K. Toma, D. F. Torres, G. Tosti, E. Troja, Y. Uchiyama, T. Uehara, T. L. Usher, A. J. van der Horst, V. Vasileiou, N. Vilchez, V. Vitale, A. von Kienlin, A. P. Waite, P. Wang, C. Wilson-Hodge, B. L. Winer, K. S. Wood, X. F. Wu, R. Yamazaki, T. Ylinen, and M. Ziegler. A limit on the variation of the speed of light arising from quantum gravity effects. 2009. *NATURE.* **462** (7271): 331.

Abdo, A. A., M. Ackermann, M. Ajello, K. Asano, W. B. Atwood, M. Axelsson, L. Baldini, J. Ballet, G. Barbiellini, M. G. Baring, D. Bastieri, K. Bechtol, R. Bellazzini, B. Berenji, P. N. Bhat, E. Bissaldi, R. D. Blandford, E. D. Bloom, E. Bonamente, A. W. Borgland, A. Bouvier, J. Bregeon, A. Brez, M. S. Briggs, M. Brigida, P. Bruel, J. M. Burgess, D. N. Burrows, S. Buson, G. A. Caliandro, R. A. Cameron, P. A. Caraveo, J. M. Casandjian, C. Cecchi, O. Celik, A. Chekhtman, C. C. Cheung, J. Chiang, S. Ciprini, R. Claus, J. Cohen-Tanugi, L. R. Cominsky, V. Connaughton, J. Conrad, S. Cutini, V. d,ÄôElia, C. D. Dermer, A. de Angelis, F. de Palma, S. W. Digel, B. L. Dingus, E. Silva, P. S. Drell, R. Dubois, D. Dumora, C. Farnier, C. Favuzzi, S. J. Fegan, J. Finke, G. Fishman, W. B. Focke, P. Fortin, M. Frailis, Y. Fukazawa, S. Funk, P. Fusco, F. Gargano, N. Gehrels, S. Germani, G. Giavitto, B. Giebels, N. Giglietto, F. Giordano, T. Glanzman, G. Godfrey, A. Goldstein, J. Granot, J. Greiner, I. A. Grenier, J. E. Grove, L. Guillemot, S. Guiriec, Y. Hanabata, A. K. Harding, M. Hayashida, E. Hays, D. Horan, R. E. Hughes, M. S. Jackson, G. Johannesson, A. S. Johnson, R. P. Johnson, W. N. Johnson, T. Kamae, H. Katagiri, J. Kataoka, N. Kawai, M. Kerr, R. M. Kippen, J. Knodlseder, D. Kocevski, N. Komin, C. Kouveliotou, M. Kuss, J. Lande, L. Latronico, M. Lemoine-Goumard, F. Longo, F. Loparco, B. Lott, M. N. Lovellette, P. Lubrano, G. M. Madejski, A. Makeev, M. N. Mazziotta, S. McBreen, J. E. McEnery, S. McGlynn, C. Meegan, P. Meszaros, C. Meurer, P. F. Michelson, W. Mitthumsiri, T. Mizuno, A. A. Moiseev, C. Monte, M. E. Monzani, E. Moretti, A. Morselli, I. V. Moskalenko, S. Murgia, T. Nakamori, P. L. Nolan, J. P. Norris, E. Nuss, M. Ohno, T. Ohsugi, N. Omodei, E. Orlando, J. F. Ormes, W. S. Paciesas, D. Paneque, J. H. Panetta, V. Pelassa, M. Pepe, M. Pesce-Rollins, V. Petrosian, F. Piron, T. A. Porter, R. Preece, S. Raino, R. Rando, A. Rau, M. Razzano, S. Razzaque, A. Reimer, O. Reimer, T. Reposeur, S. Ritz, L. S. Rochester, A. Y. Rodriguez, P. W. Roming, M. Roth, F. Ryde, H. F. Sadrozinski, D. Sanchez, A. Sander, P. M. Parkinson, J. D. Scargle, T. L. Schalk, C. Sgro, E. J. Siskind, P. D. Smith, P. Spinelli, M. Stamatikos, F. W. Stecker, G. Stratta, M. S. Strickman, D. J. Suson, C. A. Swenson, H. Tajima, H. Takahashi, T. Tanaka, J. B. Thayer, J. G. Thayer, D. J. Thompson, L. Tibaldo, D. F. Torres, G. Tosti, A. Tramacere, Y. Uchiyama, T. Uehara, T. L. Usher, A. J. van der Horst, V. Vasileiou, N. Vilchez, V. Vitale, A. von Kienlin, A. P. Waite, P. Wang, C. Wilson-Hodge, B. L. Winer, K. S. Wood, R. Yamazaki, T. Ylinen, and M. Ziegler. FERMI OBSERVATIONS OF GRB 090902B: A DISTINCT SPECTRAL COMPONENT IN THE PROMPT AND DELAYED EMISSION. 2009. *ASTROPHYSICAL JOURNAL LETTERS.* **706** (1): L138.

Abdo, A. A., M. Ackermann, M. Arimoto, K. Asano, W. B. Atwood, M. Axelsson, L. Baldini, J. Ballet, D. L. Band, G. Barbiellini, M. G. Baring, D. Bastieri, M. Battelino, B. M. Baughman, K. Bechtol, F. Bellardi, R. Bellazzini, B. Berenji, P. N. Bhat, E. Bissaldi, R. D. Blandford, E. D. Bloom, G. Bogaert, J. R. Bogart, E. Bonamente, J. Bonnell, A. W. Borgland, A. Bouvier, J. Bregeon, A. Brez, M. S. Briggs, M. Brigida, P. Bruel, T. H. Burnett, D. Burrows, G. Busetto, G. A. Caliandro, R. A. Cameron, P. A. Caraveo, J. M. Casandjian, M. Ceccanti, C. Cecchi, A. Celotti, E. Charles, A. Chekhtman, C. C. Cheung, J. Chiang, S. Ciprini, R. Claus, J. Cohen-Tanugi, L. R. Cominsky, V. Connaughton, J. Conrad, L. Costamante, S. Cutini, M. DeKlotz, C. D. Dermer, A. de Angelis, F. de Palma, S. W. Digel, B. L. Dingus, E. Silva, P. S. Drell, R. Dubois, D. Dumora, Y. Edmonds, P. A. Evans, D. Fabiani, C. Farnier, C. Favuzzi, J. Finke, G. Fishman, W. B. Focke, M. Frailis, Y. Fukazawa, S. Funk, P. Fusco, F. Gargano, D. Gasparrini, N. Gehrels, S. Germani, B. Giebels, N. Giglietto,

P. Giommi, F. Giordano, T. Glanzman, G. Godfrey, A. Goldstein, J. Granot, J. Greiner, I. A. Grenier, M. -H. Grondin, J. E. Grove, L. Guillemot, S. Guiriec, G. Haller, Y. Hanabata, A. K. Harding, M. Hayashida, E. Hays, J. A. Morata, A. Hoover, R. E. Hughes, G. Johannesson, A. S. Johnson, R. P. Johnson, T. J. Johnson, W. N. Johnson, T. Kamae, H. Katagiri, J. Kataoka, A. Kavelaars, N. Kawai, H. Kelly, J. Kennea, M. Kerr, R. M. Kippen, J. Knodlseder, D. Kocevski, M. L. Kocian, N. Komin, C. Kouveliotou, F. Kuehn, M. Kuss, J. Lande, D. Landriu, S. Larsson, L. Latronico, C. Lavalley, B. Lee, S. -H. Lee, M. Lemoine-Goumard, G. G. Lichti, F. Longo, F. Loparco, B. Lott, M. N. Lovellette, P. Lubrano, G. M. Madejski, A. Makeev, B. Marangelli, M. N. Mazziotta, S. McBreen, J. E. McEnery, S. McGlynn, C. Meegan, P. Meszaros, C. Meurer, P. F. Michelson, M. Minuti, N. Mirizzi, W. Mitthumsiri, T. Mizuno, A. A. Moiseev, C. Monte, M. E. Monzani, E. Moretti, A. Morselli, I. V. Moskalenko, S. Murgia, T. Nakamori, D. Nelson, P. L. Nolan, J. P. Norris, E. Nuss, M. Ohno, T. Ohsugi, A. Okumura, N. Omodei, E. Orlando, J. F. Ormes, M. Ozaki, W. S. Paciesas, D. Paneque, J. H. Panetta, D. Parent, V. Pelassa, M. Pepe, M. Perri, M. Pesce-Rollins, V. Petrosian, M. Pinchera, F. Piron, T. A. Porter, R. Preece, S. Raino, E. Ramirez-Ruiz, R. Rando, E. Rapposelli, M. Razzano, S. Razzaque, N. Rea, A. Reimer, O. Reimer, T. Reposeur, L. C. Reyes, S. Ritz, L. S. Rochester, A. Y. Rodriguez, M. Roth, F. Ryde, H. F. Sadrozinski, D. Sanchez, A. Sander, P. M. Parkinson, J. D. Scargle, T. L. Schalk, K. N. Segal, C. Sgro, T. Shimokawabe, E. J. Siskind, D. A. Smith, P. D. Smith, G. Spandre, P. Spinelli, M. Stamatikos, J. -L. Starck, F. W. Stecker, H. Steinle, T. E. Stephens, M. S. Strickman, D. J. Suson, G. Tagliaferri, H. Tajima, H. Takahashi, T. Takahashi, T. Tanaka, A. Tenze, J. B. Thayer, J. G. Thayer, D. J. Thompson, L. Tibaldo, D. F. Torres, G. Tosti, A. Tramacere, M. Turri, S. Tuvi, T. L. Usher, A. J. van der Horst, L. Vigiani, N. Vilchez, V. Vitale, A. von Kienlin, A. P. Waite, D. A. Williams, C. Wilson-Hodge, B. L. Winer, K. S. Wood, X. F. Wu, R. Yamazaki, T. Ylinen, M. Ziegler, Fermi LAT Collaboration, and Fermi GBM Collaboration. Fermi Observations of High-Energy Gamma-Ray Emission from GRB 080916C. 2009. *SCIENCE.* **323** (5922): 1688.

Ackermann, M., K. Asano, W. B. Atwood, M. Axelsson, L. Baldini, J. Ballet, G. Barbiellini, M. G. Baring, D. Bastieri, K. Bechtol, R. Bellazzini, B. Berenji, P. N. Bhat, E. Bissaldi, R. D. Blandford, E. D. Bloom, E. Bonamente, A. W. Borgland, A. Bouvier, J. Bregeon, A. Brez, M. S. Briggs, M. Brigida, P. Bruel, S. Buson, G. A. Caliandro, R. A. Cameron, P. A. Caraveo, S. Carrigan, J. M. Casandjian, C. Cecchi, O. Celik, E. Charles, J. Chiang, S. Ciprini, R. Claus, J. Cohen-Tanugi, V. Connaughton, J. Conrad, C. D. Dermer, F. de Palma, B. L. Dingus, E. Silva, P. S. Drell, R. Dubois, D. Dumora, C. Farnier, C. Favuzzi, S. J. Fegan, J. Finke, W. B. Focke, M. Frailis, Y. Fukazawa, P. Fusco, F. Gargano, D. Gasparrini, N. Gehrels, S. Germani, N. Giglietto, F. Giordano, T. Glanzman, G. Godfrey, J. Granot, I. A. Grenier, M. -H. Grondin, J. E. Grove, S. Guiriec, D. Hadasch, A. K. Harding, E. Hays, D. Horan, R. E. Hughes, G. Johannesson, W. N. Johnson, T. Kamae, H. Katagiri, J. Kataoka, N. Kawai, R. M. Kippen, J. Knodlseder, D. Kocevski, C. Kouveliotou, M. Kuss, J. Lande, L. Latronico, M. Lemoine-Goumard, M. Llena. Garde, F. Longo, F. Loparco, B. Lott, M. N. Lovellette, P. Lubrano, A. Makeev, M. N. Mazziotta, J. E. McEnery, S. McGlynn, C. Meegan, P. Meszaros, P. F. Michelson, W. Mitthumsiri, T. Mizuno, A. A. Moiseev, C. Monte, M. E. Monzani, E. Moretti, A. Morselli, I. V. Moskalenko, S. Murgia, H. Nakajima, T. Nakamori, P. L. Nolan, J. P. Norris, E. Nuss, M. Ohno, T. Ohsugi, N. Omodei, E. Orlando, J. F. Ormes, M. Ozaki, W. S. Paciesas, D. Paneque, J. H. Panetta, D. Parent, V. Pelassa, M. Pepe, M. Pesce-Rollins, F. Piron, R. Preece, S. Raino, R. Rando, M. Razzano, S. Razzaque, A. Reimer, S. Ritz, A. Y. Rodriguez, M. Roth, F. Ryde, H. F. Sadrozinski, A. Sander, J. D. Scargle, T. L. Schalk, C. Sgro, E. J. Siskind, P. D. Smith, G. Spandre, P. Spinelli, M. Stamatikos, F. W. Stecker, M. S. Strickman, D. J. Suson, H. Tajima, H. Takahashi, T. Takahashi, T. Tanaka, J. B. Thayer, J. G. Thayer, D. J. Thompson, L. Tibaldo, K. Toma, D. F. Torres, G. Tosti, A. Tramacere, Y. Uchiyama, T. Uehara, T. L. Usher, A. J. van der Horst, V. Vasileiou, N. Vilchez, V. Vitale, A. von Kienlin, A. P. Waite, P. Wang, C. Wilson-Hodge, B. L. Winer, X. F. Wu, R. Yamazaki, Z. Yang, T. Ylinen, and M. Ziegler. FERMI OBSERVATIONS OF GRB 090510: A SHORT-HARD GAMMA-RAY BURST WITH AN ADDITIONAL, HARD POWER-LAW COMPONENT FROM 10 keV TO GeV ENERGIES. 2010. *ASTROPHYSICAL JOURNAL.* **716** (2): 1178.

Gonzalez, M. M., M. Carrillo-Barragan, B. L. Dingus, Y. Kaneko, R. D. Preece, and M. S. Briggs. BROADBAND, TIME-DEPENDENT, SPECTROSCOPY OF THE BRIGHTEST BURSTS OBSERVED BY BATSE LAD AND EGRET TASC. 2009. *ASTROPHYSICAL JOURNAL.* **696** (2): 2155.

Pasquale, M. De, P. Schady, N. P. Kuin, M. J. Page, P. A. Curran, S. Zane, S. R. Oates, S. T. Holland, A. A. Breeveld, E. A. Hoversten, G. Chincarini, D. Grupe, A. A. Abdo, M. Ackermann, M. Ajello, M. Axelsson, L. Baldini, J. Ballet, G. Barbiellini, M. G. Baring, D. Bastieri, K. Bechtol, R. Bellazzini, B. Berenji, E. Bissaldi, R. D. Blandford, E. D. Bloom, E. Bonamente, A. W. Borgland, A. Bouvier, J. Bregeon, A. Brez, M. S. Briggs, M. Brigida, P. Bruel, T. H. Burnett, S. Buson, G. A. Caliandro, R. A. Cameron, P. A. Caraveo, S. Carrigan, J. M. Casandjian, C. Cecchi, O. Celik, A. Chekhtman, J. Chiang, S. Ciprini, R. Claus, J. Cohen-Tanugi, V. Connaughton, J. Conrad, C. D. Dermer, A. de Angelis, F. de Palma, B. L. Dingus, E. Silva, P. S. Drell, R. Dubois, D. Dumora, C. Farnier, C. Favuzzi, S. J. Fegan, G. Fishman, W. B. Focke, M. Frailis, Y. Fukazawa, S. Funk, P. Fusco, F. Gargano, D. Gasparrini, N. Gehrels, S. Germani, N. Giglietto, F. Giordano, T. Glanzman, G. Godfrey, J. Granot, J. Greiner, I. A. Grenier, J. E. Grove, L. Guillemot, S. Guiriec, A. K. Harding, M. Hayashida,

E. Hays, D. Horan, R. E. Hughes, M. S. Jackson, G. Johannesson, A. S. Johnson, W. N. Johnson, T. Kamae, H. Katagiri, J. Kataoka, N. Kawai, M. Kerr, R. M. Kippen, J. Knodlseder, D. Kocevski, M. Kuss, J. Lande, L. Latronico, M. Lemoine-Goumard, F. Longo, F. Loparco, B. Lott, M. N. Lovellette, P. Lubrano, A. Makeev, M. N. Mazziotta, J. E. McEnery, S. McGlynn, C. Meegan, P. Meszaros, C. Meurer, P. F. Michelson, W. Mitthumsiri, T. Mizuno, C. Monte, M. E. Monzani, E. Moretti, A. Morselli, I. V. Moskalenko, S. Murgia, P. L. Nolan, J. P. Norris, E. Nuss, M. Ohno, T. Ohsugi, N. Omodei, E. Orlando, J. F. Ormes, W. S. Paciesas, D. Paneque, J. H. Panetta, D. Parent, V. Pelassa, M. Pepe, M. Pesce-Rollins, F. Piron, T. A. Porter, R. Preece, S. Raino, R. Rando, M. Razzano, A. Reimer, O. Reimer, T. Reposeur, S. Ritz, L. S. Rochester, A. Y. Rodriguez, M. Roth, F. Ryde, H. F. Sadrozinski, A. Sander, P. M. Parkinson, J. D. Scargle, T. L. Schalk, C. Sgro, E. J. Siskind, P. D. Smith, G. Spandre, P. Spinelli, M. Stamatikos, J. -L. Starck, F. W. Stecker, M. S. Strickman, D. J. Suson, H. Tajima, H. Takahashi, T. Tanaka, J. B. Thayer, J. G. Thayer, D. J. Thompson, L. Tibaldo, K. Toma, D. F. Torres, G. Tosti, A. Tramacere, Y. Uchiyama, T. Uehara, T. L. Usher, A. J. van der Horst, V. Vasileiou, N. Vilchez, V. Vitale, A. von Kienlin, A. P. Waite, P. Wang, B. L. Winer, K. S. Wood, X. F. Wu, R. Yamazaki, T. Ylinen, and M. Ziegler. SWIFT AND FERMI OBSERVATIONS OF THE EARLY AFTERGLOW OF THE SHORT GAMMA-RAY BURST 090510. 2010. *ASTROPHYSICAL JOURNAL LETTERS.* **709** (2): L146.

Probing the Origin of Matter in the Universe

Vincenzo Cirigliano
20100394ER

Introduction

To a very good approximation, the laws of physics do not distinguish between matter and antimatter. Yet, the observed Universe is made up of matter and not antimatter. In order to produce the current asymmetry, in the primordial hot plasma one microsecond after the big bang there must have been a tiny imbalance of one part in a billion between matter and antimatter. As the Universe evolved and cooled down, most of the antimatter annihilated with matter, leaving the very small initial excess of matter to make up the observed stars and galaxies. Understanding how the observed imbalance has developed during cosmic evolution is one of the great open questions at the interface of cosmology, particle physics and nuclear physics.

A number of explicit mechanisms have been proposed to explain the origin of the matter-antimatter asymmetry. This project aims to address in a quantitative way theoretical predictions within the so-called weak scale baryogenesis scenario, in which the asymmetry develops at relatively late times in the cosmic evolution. Relatively late time means that the primordial plasma had temperatures comparable to the energy scale that can be reached in current laboratory experiments. Hence, the appeal of this scenario is that it can be tested through terrestrial experiments that can either produce the particles responsible for the baryogenesis mechanism or feel their virtual quantum mechanical excitations.

Benefit to National Security Missions

Elucidating the origin of the matter-antimatter asymmetry is one of the priorities of the DOE Office of Science (for both Nuclear Physics and High Energy Physics). This is one of the questions at the heart of our basic understanding of matter and the laws that govern the universe. Our work addresses this priority and develops theoretical tools that can be potentially applied in other areas of interest to the Nuclear Physics Office of Science, such as nuclear and particle astrophysics.

Progress

As a first step in this project, we have analyzed a simplified model of particle mixing (two spinless particles) in presence of a time-varying CP violating mass matrix (C=charge conjugation, P=parity). Within this simple model, we have shown how to derive from first principles, using non-equilibrium field theory, the quantum Boltzmann equations that describe the dynamics of flavor CP violating flavor oscillations and collisions in the early universe. Although applied to a simplified model, our derivation is based on a new power counting based on the hierarchy of relevant time scales (Compton time scale, collision time scale, flavor oscillation time scale).

Besides developing the basic tools, our analysis provides a novel, simple physical picture for the generation of flavor-diagonal CP asymmetries (i.e. differences in the propagation of particles and antiparticles that carry definite "flavor" quantum numbers) in the early universe during the electroweak phase transition. In this epoch the early universe undergoes a phase transition, with bubbles of "broken electroweak phase" nucleating and expanding (see Figure 1 for a cartoon representation of the physics involved). The interesting dynamics happens near the bubble boundaries, where on a characteristic length scale Lw the order parameter (vacuum expectation value of the Higgs field) goes from zero to a finite value. As the order parameter changes, so do the mass matrices of all particle species that couple to the Higgs. So starting from a CP-conserving equilibrium initial states, a CP asymmetry arises through coherent flavor oscillations, as the particles cross the boundary between broken and unbroken electroweak phase.

We have solved the Boltzmann equations numerically for the density matrices, investigating the impact of collisions in various regimes that correspond to different mixing particles in realistic extensions of the Standard Model. We have found that the CP asymmetry is essentially determined by the ratio of wall thickness to the flavor oscillation length, reaching a maximum when these two time (length) scales are comparable (see Figure 2).

The results of this first step of the investigation have

been published in V. Cirigliano, C. Lee, M. Ramsey-Musolf, S. Tulin, "Flavored Quantum Boltzmann Equations", Phys. Rev. D 81, 103503, 2010.

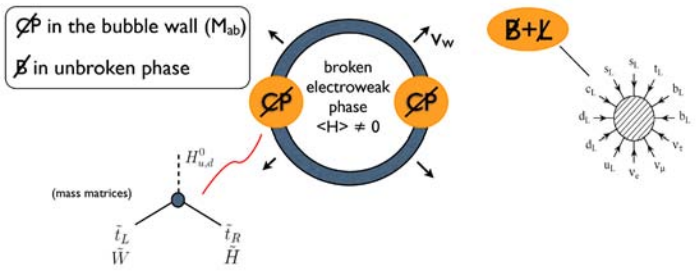

Figure 1. Schematic representation of the main ingredients involved in electroweak baryogenesis. At the electroweak phase transition, bubble of broken electroweak phase nucleate and start expanding. CP violation is localized at the boundary between broken and unbroken phase: it occurs through off-diagonal elements in the mass matrices of particles coupling to the Higgs (order parameter). Baryon (B) and lepton (L) number violating processes are active only in the unbroken phase, outside of the bubbles.

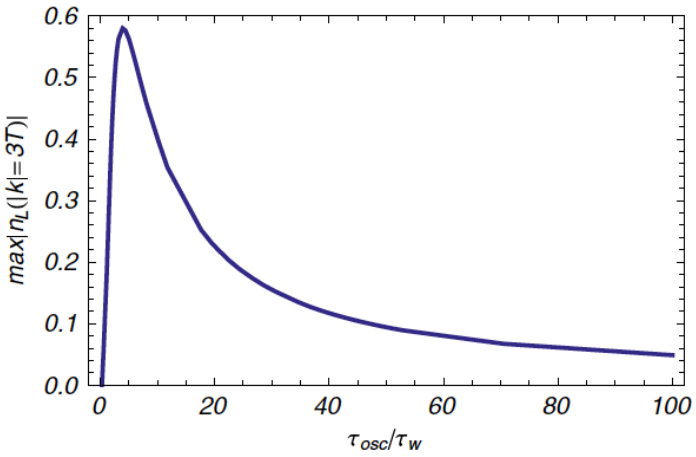

Figure 2. CP asymmetry generated in the toy model as a function of the ratio of oscillation length and wall thickness. The maximum value corresponds to a "resonant" condition, when the wall thickness and the oscillation length are comparable.

Future Work

The aim of this proposal is to link in a quantitative way the origin of the matter-antimatter asymmetry of the Universe to physics at the electroweak scale, which we are about to probe experimentally through the Large Hadron Collider (LHC) and low-energy signals of CP violation. Our research will focus on obtaining a sound quantitative understanding of the amount of baryon asymmetry produced during the electroweak phase transition at a temperature of about 100 GeV, within the Minimal Supersymmetric extension of the Standard Model (MSSM).

The next immediate step on which we are working on is the extension of the simplified model of mixing scalars to the case of a space-time dependent mass matrix (as opposed to only time-dependent). In this case, the system is spatially non-homogeneous and diffusion currents are expected to arise. We need to takle two main tasks: (i) writing down first principle quantum kinetic equations for the density matrices describing mixing particles at the phase transition boundary; (ii) solving these equations numerically, without simplifying approximations. This step will enable first-principles study of realistic weak-scale baryogenesis models.

Conclusion

The goal of the project is to validate or rule out one of the most appealing mechanisms for generating the matter-antimatter asymmetry of the Universe. We will remove the current theoretical uncertainties and we will perform quantitative tests of the scenario, based on experimental constraints from a wide array of experiments. The project is making steady progress towards the state goal.

The taxpayer should be proud to support our research project, as it addresses one of the deepest mysteries of science: what happened to the antimatter? Moreover, this research supports experimental programs in which the federal funding agencies are currently heavily investing.

Publications

Cirigliano, V., C. Lee, M. Ramsey-Musolf, and S. Tulin. Flavored quantum Boltzmann equations. 2010. *Physical Review* . **D 81**: 103503.

Revolutionizing Short-Pulse Laser Generation using Stimulated Raman Scattering

Evan S. Dodd
20100413ER

Introduction

Stimulated Raman scattering (SRS) in laser-plasma interactions has typically been studied in order to avoid its detrimental effects on inertial confinement fusion (ICF). However, this physical process can be used to amplify short laser pulses without the expensive optical components used in the current state-of-the-art chirped-pulse amplification (CPA) technique. Elimination of these components allows two revolutionary changes to be made to short-pulse amplification. First, intensity limits due to the CPA technique can be greatly exceeded in the laboratory setting. And also, this technique can be applied to both existing lasers as an up-grade as well as to new laser systems built in the future. Second, the sensitivity of the gratings in CPA lasers prevents their use in environments where temperature and vibrations are present. This work will allow short-pulse lasers to move from laboratories and user facilities into more real world settings. Short-pulse lasers have been used in a number of applications, including: laser-plasma acceleration of ion and/or electrons; high-brightness short-pulse x-ray sources; and the fast-ignition concept for ICF. Any significant improvement in amplification technology will have direct relevance to a wide range of basic and applied research.

Backscattered light from SRS can significantly affect capsule implosion and burn for ICF targets. Because of this fact, much effort has been applied to model the physics of SRS and its subsequent nonlinearities. This existing expertise will be applied toward the development of the proposed novel amplification technique. The LLNL code pF3d, which is currently used to assess backscatter for targets at the National Ignition Facility (NIF), contains the physics needed to model SRS-based laser amplifiers. LANL has recently developed a kinetic-based particle-trapping model and implemented it into pF3d for the nonlinear propagation of Langmuir waves that can dominate the saturation of SRS. It has typically been difficult for theory and simulation to predict experimentally measured reflectivities, and the newly implemented model now allows pF3d to better reproduce experiment.

Initial experimental results from other research groups have been promising, but limited due to saturation of the amplification process. This project will apply the numerical models that were developed at LANL for ICF to the problem of SRS amplification. Initial results from calculations using these models will be validated with data from experiments done by an external collaborator as a part of this project. The project will then use the validated models to plan a new set of optimized experiments, which will be performed later in the project.

Benefit to National Security Missions

The novel short-pulse laser amplifier resulting from this research can be an enabling technology. It will have direct relevance to facilities for high-energy density physics experiments, fusion energy and charged particle beam acceleration. Any application that utilizes such a facility or technology will benefit.

Progress

Our successful project proposal set a time-line and set of intermediate deliverables for each fiscal year, which would ensure successful completion of the overall project goals, and we have successfully completed our FY10 deliverables.

First, we have hired a highly qualified post-doctoral researcher, Jun Ren, who had been performing similar research as a post-doc at Princeton University. In a very short period of time Jun has begun making important contributions to the success of this project. She has been performing analysis of spectroscopic data to characterize the plasma conditions of the target to be used in our laser amplification experiments. These conditions are needed to perform predictive calculations of the subsequent experiments.

Second, our external collaborators at Applied Energetics have performed the initial experimental work that was promised. Experiments were properly set-up and executed that have resulted in obtaining spectral data from the capillary-discharge generated plasma needed for characterization of the conditions. Initial measurements of the SRS amplification were also attempted near the end of FY10, but were not conclusive. Calculations aimed at un-

derstanding the amplification saturation mechanisms have been performed, but are inconclusive based on the data.

The actual SRS amplification experiments pass two laser pulses through the plasma, a short-pulse to be amplified and a second longer pulse to provide the energy for amplification. The actual amplification not only depends on these pulses, but on the plasma conditions. These conditions are estimated from spectral lines measured when the plasma is generated, but no pulses propagate through it. Figure 1 shows an example of the lines measured by our collaborators from a discharge that creates plasma from Xenon gas. The horizontal axis shows the wavelength of the lines and the vertical axis shows the line evolution with time. The plasma conditions are changing with times, so the lines are also.

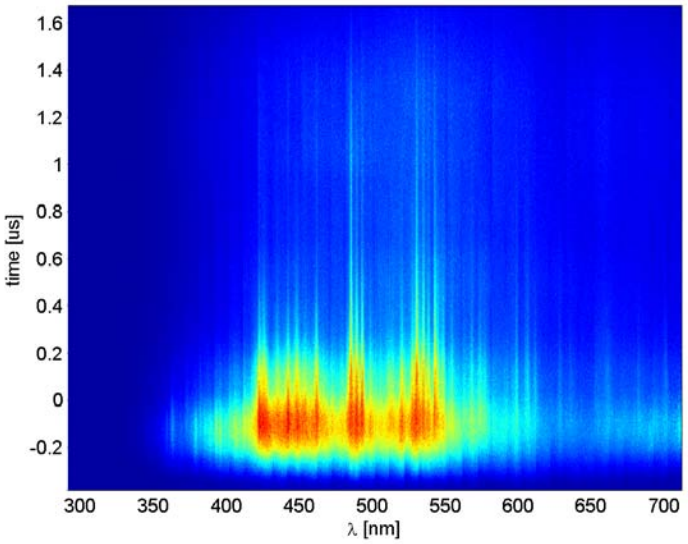

Figure 1. An example of the time-dependent spectra measured from the capillary discharge, which are being used to characterize the plasma conditions during the amplification experiments. This was data was taken without a laser pulse propagating in the plasma

A commercial software package called PrismSPECT is then used to find the plasma conditions. This product will take as input a set of plasma conditions and generate a set of synthetic spectra, which will be compared with the data from our experiments. One example of such software generated spectra can be seen in Figures 2, which is intended to be compared with the data from Figure 1 a t = -181.4 ns. By iterating over many sets of temperatures and densities, we will estimate the actual conditions of the plasma that is being generated by the capillary discharge.

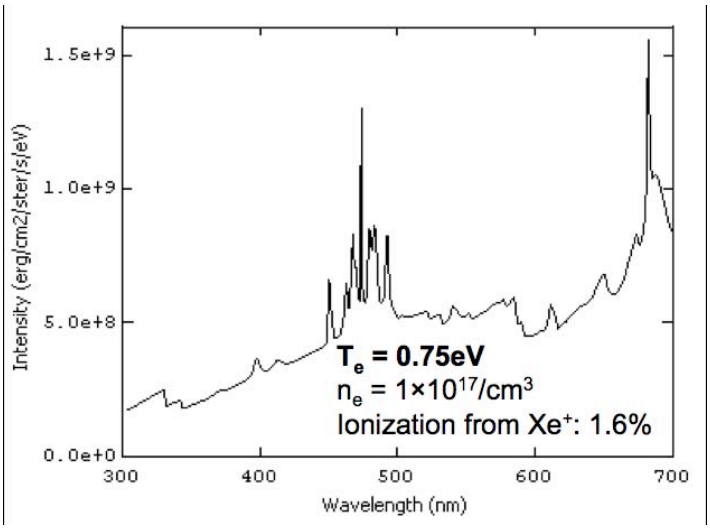

Figure 2. One example of the synthetic spectra calculated using PrismSPECT, which we are comparing with the data to determine the plasma conditions present in our capillary discharge. This has resulted in a range of possible conditions, which is being narrowed down with laser propagation experiments.

Future Work

The kinetic saturation of SRS is thought to dominate the short-pulse amplification process. LANL is thus uniquely positioned to use its modified version of pF3d to optimize the laser and plasma conditions for SRS-based amplification. However, the model was developed from kinetic particle-in-cell simulations (PIC) of the microscopic-scale plasma physics and implemented into the macroscopic-scale fluid and light-propagation code, pF3d.

Our modeling effort will now begin to include the LSP PIC code. It can contribute to our work in two important ways, and thus provides an efficient path forward. The first way is the initially intended role for PIC simulations in our project, which is as a verification method for the trapping model implemented in pF3d. This is necessary because the model is untested at the plasma conditions in our experiments. Since PIC is a computationally intensive technique, LSP simulation results from small sub-domains will be compared with experimental data pF3d results as a test of our technique. This testing will ensure that our model in pF3d continues to produce the same answer as PIC and to verify that electron trapping in Langmuir waves is the dominant saturation mechanism. The second way that LSP will contribute is to model the capillary discharge that creates our plasma for the experiments. By modeling the discharge itself, a greater confidence in our understanding of the plasma conditions will be gained. And ultimately, we would like to initialize the PIC and pF3d simulations of the SRS amplification with this calculated discharge plasma.

After this process of verification, optimized experiments will be designed and then fielded by our collaborators that

demonstrate an increase in the amplification of laser pulses. We plan to begin these experiments at the end of the projects second year. It is this predictive capability that is our ultimate goal. If this work is successful, then LANL will be able to design new laser-based HED facilities to further its mission-oriented research with this capability, and engage in fundamental research at novel physical conditions.

Conclusion

The ultimate goal of this research is to demonstrate significant amplification (>25 times) over a long scale length plasma (> 1 mm). We will show that a newly developed model for nonlinear SRS at ICF conditions is relevant to the development of this technology. In particular, we will show that our models: first, agree with measurements made by our external collaborators; and two allow us to optimize the amplification process through calculation (i.e. increased amplification).

Surface Fitting for Thermodynamically Consistent Evaluation of Tabular Equations of State

John W. Grove
20100438ER

Introduction

The goal of this project is to produce algorithms and supporting software for piecewise smooth representations of thermodynamic free energies based on surface fitting methods for tabular equations of state. Our intent is to address known problems with current evaluation and table development schemes and to provide tools that can be used in hydrodynamic application codes.

The free energy surface fits reproduce the tabulated data in an optimal sense subject to the constraints of physics. Mathematically this problem is one of constructing a convexity constrained shape-preserving optimal fit of the equation of state (EOS) data. Specifically we compute smoothing tensor product B-splines [1-2], to produce optimal fits that are appropriately convexity/shape constrained. The resultant surface fit parameters are suitable for storage as part of the SESAME [3] database to allow for exact reproducibility for verification and validation (V&V) purposes.

Our approach consists of two parts, compute free energies from SESAME data and use discrete Legendre transforms [4] to impose the convexity. The result is a tensor product spline function for the free energy that can be differentiated to evaluate thermodynamic data.

Benefit to National Security Missions

The use of general equation of states in hydrodynamic simulations is central to almost all applications for which hydrodynamics is relevant. Our project is directed towards addressing the specific needs of hydrodynamic solvers for valid EOS evaluations. By providing methods and tools that ensure consistent and stable EOS evaluations we will significantly enhance the ability of hydro codes to be used for predictive science. In particular we will ensure that numerical errors produced by thermodynamically inconsistent EOS evaluations are not present in a computation and that the evaluations produce appropriate physically constrained results.

Progress

A surface fitting method using tensor product spline fits for specific internal energy and pressure as a function of the temperature and density has been implemented in the analysis tool AMHCTOOLS [5] which is in wide usage as part of the Eulerian Applications ASC project. Several significant issues were addressed to produce good over the entire range of the Sesame data. Logarithmic transforms were used since the Sesame files have extensive dynamic range (ten or more orders of magnitude in pressure and temperature). An iterative method was used to automatically compute an optimal smoothness factor for the fit, as well as selecting an appropriate tensor product knot set. Finally the automatic selection of the fitting weights was also implemented since the Sesame data showed significant unphysical oscillations for many EOS models. Numerical experimentation showed that a good choice for the knot weights was the reciprocal of the second derivative of the data. With this choice of weights the spline fitting tools in the Dierckx library [6] were able to produce smooth tensor product splines that fit the data well across the entire domain (Figure 1).

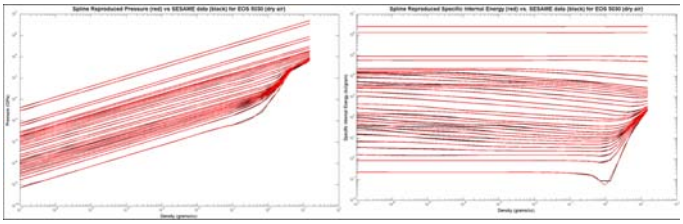

Figure 1. Comparison of spline reproduced isotherms with raw SESAME data.

The surface fits for the pressure and specific internal energy were then integrated to compute a Helmholtz free energy (Figure 2). Our work showed that the amount of data compression for the tensor product fit is about 75% of that required for the Sesame table, assuming one uses quintic order splines. This reduction is largely the result of the reduced number of knots needed to fit the data in the high density/temperature range of the table where in log space the pressure and energy surfaces are relatively flat.

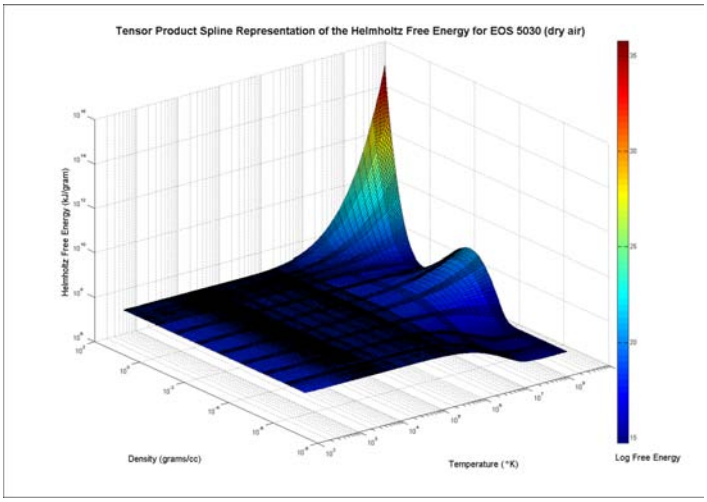

Figure 2. Helmholtz Free Energy Computed from EOS 5030 (dry air).

Two presentations related to this work were presented.

- "*Equations of State in the Eulerian Applications Project*", presented January 19, 2010 in the X division code users Verification and Validation seminar. The talk described how equation of state models are incorporated into production code and discussed numerical issues associated with their use and how the EOS surfacing fitting work can address important issues in this regard.
- "*So you Want to Use a Real Equation of State*", presented at the 2010 SIAM Annual meeting, July 12-16. This talk discussed how equation of state issues affect solver algorithm design and implementation as also describe some of the current work on EOS modeling using surface fitting.

A draft paper describing our work on surface fitting applied to EOS usage is under preparation. An article related to this work recently appeared in Acta Mathematical Scientia as part of a special issue dedicated to Professor James Glimm.

For the purposes of cross verification, the EOSPAC library [7] and a new utility code were incorporated into the AMCHTOOLS equation of state tools. This allows us to compare the effect of the interpolation method on the evaluation of the various thermodynamic quantities as functions of density and temperature

A mathematical analysis of consistent tensor product spline representations of pressure, specific internal energy, and Helmholtz free energy was conducted. This method suggests that an appropriate spline representation can be based on fits to temperature divided differences between the free energy and its cold curve value at constant density. From such an expression one can easily derive formulas for the pressure, specific internal energy, and higher order thermodynamic derivatives using derivatives of this quantity with respect to density and temperature (Figure 3). Since these derivatives are readily computed from a tensor product spline expression, this offers a viable method for describing the entire EOS in terms to one univariate spline (the cold curve free energy) and one bivariate tensor product spline (for the divided difference expression). Utility routines for performing the operations cited above were added as new operations to the Dierckx tensor product spline library.

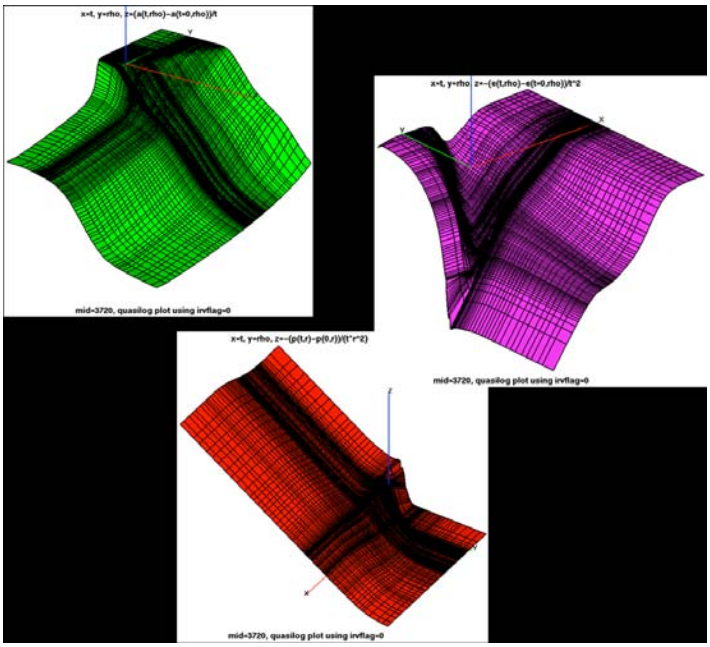

Figure 3. Free Energy Surfaces for EOS 3720 (aluminum) Generated using the Energy Divided Difference Method.

A summer student (Jonathan Robey) supervised by the PI implemented linear –Legendre-transform into the EOS library. This tool will be used to transform the Helmholtz free energy into other thermodynamic forms, specifically the Gibb's free energy (pressure-temperature based), specific internal energy (specific volume-specific entropy based), and specific enthalpy (pressure-specific entropy based). We also have implemented the beneath-and-beyond algorithm [8] for computing the convex hull of a single variate function. This algorithm will be uses for the convexification of our generated free energies.

Future Work

The focus of our second year effort of this project will include the application of convex analysis theory and tools to construct the convex hulls of our generated free energies. This step ensures that application codes see a thermodynamically realistic equation of state. We will also be pursuing the completion of a complete EOS software interface that can be used as a standalone library by ASC and other hydro-codes. One critical issue here will be to optimize the evaluation of the equation of state properties when called for the hydro solver. Documentation work on our EOS library will be pursued and we will be preparing articles

describing this work to be published in the open literature. Validation studies for the quality of the fitting EOS surfaces are ongoing as part of our program development.

Conclusion

This project will produce algorithms for the construction of piecewise smooth representations of thermodynamic free energies for use in equation of state evaluation. The surfaces are intended to provide optimal fits to tabular equation of state data such as provided by the SESAME equation of state library constrained to conform to thermodynamic stability, which is equivalent to convexity of the specific interface energy as a function of specific entropy and specific volume. These methods will be incorporated within a computational equation of state tool (*e.g.* EOSPAC) for use in production and research codes, as well as equation of state development.

References

1. Dierckx, P.. Curve and Surface Fitting with Splines. 1993.

2. Boor, C. de. A Practical Guide to Splines. 1978.

3. Sesame: the Los Alamos national laboratory equation of state database. 1992. *Los Alamos National Laboratory.*

4. Lucet, Y.. Faster than the fast Legendre transform, the linear-time Legendre transform. 1997. *Numerical Algorithms.* **16** (2): 171.

5. Grove, J.. Amhctools: user guide and programming manual. 200. *Los Alamos National Laboratory Release Number LA-UR-05-7424.*

6. Dierckx, P.. The Dierckx fitpack libary. 1993. *netlib.org.*

7. Pimentel, D.. Eospac version 6 user's manual. 26. *Los Alamos National Laboratory report, LA-UR-06-0213.*

8. Preparata, F. P., and M. L. Shamos. Computational geometry. 1988.

Publications

Grove, J.. Pressure-velocity equilibrium hydrodynamic models. 2010. *Acta Mathematica Scientia.* **30B** (1): 563.

LES Modeling for Predictive Simulations of Material Mixing

Fernando Grinstein
20100441ER

Introduction

The mixing of initially separate materials in a turbulent flow by the small scales of turbulent motion is a critical element of many LANL programs including: 1) urban contaminant dispersal important for threat reduction, 2) the heat, mass, CO2, and salinity fluxes in ocean models needed for climate prediction, 3) plasma mixing during inertial confinement fusion, 4) combustion, 5) material processing, 6) nuclear weapons performance, and many other applications in engineering, geophysics, and astrophysics. Our broad research goal is to develop and validate a rational, first-principles theory and associated algorithm for simulation of material mixing by a turbulent velocity field. The precise physical problem we address is: the creation of a capability to calculate the (small) unresolved scales of material mixing generated by (small) unresolved scales of fluid motion. We will pursue this goal by accomplishing several separate goals in theory, computation, and analysis. The work aims at developing a new paradigm for mixing simulations and as a consequence has scope that includes, but far exceeds practical weapons applications. The expected impact is on, 1) extending recent new methodologies from turbulence to address material mixing issues, 2) providing a physical underpinning for this extension.

Benefit to National Security Missions

The mixing of initially separate materials in a turbulent flow by the small scales of turbulent motion is a critical and often poorly understood element of many LANL programs: 1) nuclear weapons performance and inertial confinement fusion, 2) urban contaminant dispersal in threat reduction, 3) combustion, 4) climate, and a host of other applications in engineering, geophysics, and astrophysics.

Progress

Year 1: finite scale analysis of the flow and material fields are used to obtain finite scale equations (FSE). An equation of the small sub-grid scales of the mixing field will be derived, based on extended self-similarity and renormalization ideas applied to a statistical moment equation. Years 1 & 2 : Algorithm development and Flux-Corrected Transport code development will also be required to implement the algorithm and test it. We are on track to addressing the planned goals for the first two years.

We have derived the finite scale version of the passive scalar concentration equation with new terms that represent the effects of finite time averaging. The consequences of the new terms that arise from the averaging over finite scales of length and time have been mathematically analyzed through an extensive derivation of the moment equations for the 1) mean concentration, 2) the scalar variance, 3) the scalar mixing rate variance and 4) the scalar turbulent flux. From a theoretical standpoint, the results of the moment analysis represent a precise and self-consistent process that produces new and physically relevant terms with a meaningful physical interpretation. The energy and enstrophy exchanges for the scalar between the different scales of the motion have been clarified. A similar analysis for the velocity field is being undertaken. This is a substantial breakthrough in the field of Large Eddy Simulation (LES). In addition, the moment procedure applied to a coarse-grained set of equations is generic and can be applied to all LES methods to understand the physical nature of the LES closure and serve as a consistency and realizability check. A manuscript delineating this process and its consequences is being written and several talks have been planned for dissemination and discussion.

We have identified the code developments needed to implement and test our finite scale equations (FSE) material mixing algorithm and set up a detailed work plan. The plan is to simulate material mixing in a convergence study of increasing resolution, where the length scales of the mixing varies from being much smaller than a cell (coarse resolution) to where the mixing length scale is

well-resolved by the mesh, and compare with previous and new direct numerical simulation reference data, as well as relevant large eddy simulations previously reported. Actual progress with the code developments (at NRL) have been much slower than expected because of our inability to effectively transfer the allocated LDRD-ER funds to cover NRL's work in a timely fashion through an Interagency Agreement (IA) between LANL and NRL. The rules prevented NRL from starting actual work until the IA was fully approved by both parts and NRL received the funds – which only happened at the end of May 2010. However, a significant part of the planned code development work was completed by the end of FY10, and the rest is being carried out by NRL in the early part of FY11 (at no additional cost from LDRD funds).

Future Work

Mixing is usefully characterized by the length scales of the fluid physics involved: 1) large-scale advection which brings relatively large regions of the fluids together, 2) an intermediate length scale associated with the convective stirring due to velocity gradient fluctuations, and, 3) a small scale interpenetration resulting from molecular diffusion. We are primarily concerned with numerical simulation of the first two processes as is appropriate to nonequilibrium transients in a mixing process with low volume fraction and low diffusivity of the heavier fluid. Our goal is the derivation of a convective stirring length scale concerned with characterizing the material mixing at length scales much smaller than the size of a computational cell. The proposed research can be conveniently organized in five steps. Steps 1 and 2 are primarily theoretical. Steps 3 and 5 are primarily computational. Step 4 is both.

1. Length scale of the sub-grid material field: a finite-scale equation (FSE) for the sub-grid length scales characterizing the mixing field is to be derived. Extended self-similarity and renormalization of statistical equation will be invoked.

2. Algorithm development: modified equation analysis is used to design an algorithm that matches the FSE derived from governing equations.

3. Direct numerical simulation (DNS) database creation: Very high resolution DNS and data analysis and averaging are conducted for the initial value problem of material mixing by a stationary forced turbulence].

4. Code development: implement and test the algorithm. We simulate material mixing in a convergence study of increasing resolution, where the length scales of the mixing varies from being much smaller than a cell (coarse resolution) to where the mixing length scale is well-resolved by the mesh. Initial conditions for the FSE consistent with those of the DNS will be designed.

5. Validation: ILES algorithms are used to compute averages of the DNS databases.

Conclusion

Our end product is to provide a prototype (tested) algorithm that can be used in the context of an ASC code and other LANL applications in which mix prediction is central. From the applied point of view our goal is to achieve high-resolution quality results on very low-resolution grids with a parameter free approach. In the bigger picture, our approach helps illustrate that better physics and rigorously derived finite scale algorithms provide a viable alternative to the "more cells and bigger computers" strategy for LANL applications.

Publications

Grinstein, F. F.. Simulating vortex dynamics and transition in high Reynolds-number flows. To appear in *Physica Scripta (2010).*

Grinstein, F. F.. Verification and validation of CFD based turbulent flow experiments. To appear in *Encyclopedia of Aerospace Engineering, Volume 1, Fluid Dynamics and Aerothermal Dynamics, Computational Fluid Dynamics, John Wiley & Sons (2010)..* Edited by Shyy, W., and R. Blockley.

Understanding Dynamical Diversity of Extrasolar Planets

Hui Li
20070171ER

Abstract
The discovery of 170 extrasolar planets (the total number now is more than 400) in the past decade has stimulated an explosive growth in studying the basic processes that regulate planet-system evolution. At least two fundamental mysteries have emerged. One is that proto-planet embryos that are formed farther out in protoplanetary disks could migrate towards their central stars through tidal interactions with their nascent gaseous disks. This seriously limits the time available for these embryos to grow into giant planets, contrary to the discoveries of many giant planets both in our Solar system and many extra-solar planet systems. Another mystery is how the orbital evolution of protoplanets/embryos produces the observed large diversity in semi-major axis and eccentricity distributions, which are completely different from solar system planets. This project is aimed at addressing these challenges by performing extensive hydrodynamic simulations of protoplanetary disks with protoplanets and studying the orbital evolution of planets. Our models, run on supercomputers, have yielded some important insights on how to prevent the protoplanet migration and how to excite their orbital eccentricity. These results have provided further understanding on the planet formation processes that are consistent with the current observations. This research has helped to establish LANL as an important institution in this booming field in astronomy and astrophysics.

Background and Research Objectives
After centuries of speculation about planets orbiting stars other than our Sun, the discovery came in 1995 when an extrasolar planet with Jupiter-like-mass was inferred to be orbiting a nearby Sun-like star. The past decade has seen the amazing discovery of > 400 extrasolar planets. But they have also brought new challenges. Notably, extrasolar planets discovered thus far have shown a tremendous diversity in their orbital properties. Observations found that Jupiter-mass extrasolar planets have semi-major axes ranging from 0.02 astronomical unit (AU) (!) to 6 AU (Jupiter is at 5.2 AU), and large eccentricities (solar system planets are on nearly circular orbits). Because the key orbital properties of planets (e.g., location, eccentricity, mass, etc.) are believed to originate from the early phases of planet formation when the protoplanet is still embedded in the surrounding protoplanetary disks, one naturally asks: ``What determined the orbital evolution of these extrasolar planets?''

During the past several years, we have made important progress in addressing the migration problem. We discovered a new instability in protoplanetary disks, produced by the potential vorticity evolution in the disk because the spiral waves/shocks act like continuous ``pumps'' in generating positive and negative vorticity. We found that, under a broad physical conditions, the instability growth is faster than the protoplanet migration timescale. When the instability saturates nonlinearly, multiple vortices are produced. These vortices exert strong but incoherent torques on the planet. Consequently, the planet's migration is greatly altered and could eventually be halted. This finding offers a potential resolution to the planet migration problem.

To address the observed dynamical diversity of extrasolar planets and their migration, we will focus on three new, yet critical aspects:

1) The role of the newly discovered secondary instability.

2) The role of the disk self-gravity.

3) The role of multiple protoplanet embryos.

This will be achieved by performing large-scale, high-resolution planet-disk simulations and by conducting analytic studies of the flow stabilities.

Scientific Approach and Accomplishments
We have completed a major study on understanding the influence of disk viscosity on the migration of protoplanets. We discovered that, when the disk viscosity becomes small, the gas density in the disk around the planet shows systematic changes so that the net torque on the planet motion is greatly reduced. This is because the density evolution is determined by the damping of

density waves driven by the planet. So, when the viscosity is low, this feedback process is quite efficient so the torque on the planet is greatly reduced. This causes the migration of planets to slow down drastically and, in some cases, the migration is completely halted. We have carefully examined the dependence of important feedback process on the disk viscosity, planet mass, and disk sound speeds. This result has important implications on the migration rate of planets and on the crucial question whether small mass planet can survive in the protoplanetary disks or not. We find that planets will be able to survive if the disk viscosity is small. This work is published in the Astrophysical Journal Letters. In addition, we have completed a systematic study on the migration of low mass planets over long-term (> 100,000 years). We find that there exists a wide range of disk viscosity in which migration is halted and the disk condition is favorable for giant planet formation. This result has been published in the Astrophysical Journal Letters.

We have also completed a linear theory analysis of the Rossby vortex instability (RVI) in the presence of magnetic field. The RVI was discovered by us a few years ago and we have shown that it plays an important role in determining the flow dynamics in the co-orbital region of a planet. Our new work elucidated the influence of magnetic fields on this instability. We find that, when the magnetic field becomes stronger, the RVI is gradually stabilized by the magnetic fields. We attribute this stabilizing effect to the tension of the fields. This work will have implications for understanding both the linear and nonlinear outcome of the RVI when disk magnetic fields are present. This work has been published in the Astrophysical Journal.

Further important improvements were made to our numerical simulation package. In addition to already high resolution and highly efficient implementation of the disk-planet interaction schemes, our newly developed fully two-dimensional disk self-gravity solver has been proven to be extremely efficient and accurate. Furthermore, we have developed the adaptive mesh refinement schemes to enable very high resolution near the planet so that the gas flow around the planet can be accurately followed and studied. Thus far, we have been able to make simulation runs that are of the highest resolution and the longest evolution time when compared to other groups in the community. Adequate computing resources from LANL's Institutional Computing machines have made this possible. A full description of our advanced simulation package has been published in Astrophysical Journal Supplements.

Impact on National Missions

Through this project, we have developed new theories on how protoplanet migrate in gaseous disks, which provide important physical understanding of the vast amount of astronomical observations. It has also helped us to develop new computational capabilities in hydrodynamics and large-scale computing. In fact, the new numerical schemes we have developed were much superior to the previous schemes that were available in the community. This research has pushed the limits of supercomputing and help to establish the Laboratory as a leading institution in computational protoplanetary research. Protoplanetary science is becoming a major research area in astronomy. We are making an important impact in this field and this work has enhanced the DOE mission in basic science.

Publications

Li, H., S. Lubow, S. Li, and D. Lin. Type I Planet Migration in Nearly Laminar Disks. 2009. *Astrophysical Journal Letters.* **690**: 52.

Li, S., M. J. Buoni, and H. Li. A Fast Potential and Self-Gravity Solver for Nonaxisymmetric Disks. 2009. *Astrophysical Journal Supplements.* **181**: 244.

Li, S., and H. Li. A Fast Parallel Simulation Code for Interaction between Proto-Planetary Disk and Embedded Proto-Planets. 2009. *LA-UR-09-2968.*

Li, S., and H. Li. Verification of Runaway Migration in a Massive Disk. 2009. *LA-UR-09-6019* .

Yu, C., H. Li, S. Li, S. Lubow, and D. Lin. Type I Planet Migration in Nearly Laminar Disks - Long Term Behavior. 2010. *Astrophysical Journal.* **712**: 198 .

Yu, C., and H. Li. Nonaxisymmetric Rossby Vortex Instability with Toroidal Magnetic Fields in Radially Structured Disks. 2009. *Astrophysical Journal.* **702**: 75.

Precision Cosmology and the Neutrino Sector

Salman Habib
20080031ER

Abstract
The Standard Model of particle and nuclear physics is now known to provide only a very partial description of the fundamental constituents of the Universe. Solid -- now overwhelming -- evidence for Beyond Standard Model (BSM) physics first came from cosmological observations and terrestrial neutrino experiments. Significantly, precision cosmology and the neutrino sector are intimately related and each provides complementary information about the other. Cosmology provides the best-known limits on the sum of all neutrino species, currently very difficult to constrain with terrestrial experiments. In addition, cosmological observations can probe new directions in neutrino physics such as the existence of sterile neutrinos, which have no Standard Model interactions. With these motivations, we conducted an integrated research program in our project that connected state state-of-the-art experiments, observations, and theory, to shed light on the neutrino mass, the effective number of neutrinos, and the sterile neutrino sector. We also worked on the design of future neutrino oscillation experiments.

As next-generation cosmological and accelerator neutrino experiments become more sophisticated, theory must keep up with observational advances. The main thrust in our project was to develop a computational capability that would allow precision predictions for the neutrino sector. This work was accomplished by collaborating with researchers at the Paul Scherrer Institute. Our project also included work on the design of future neutrino experiments, particularly the Long-Baseline Neutrino Experiment (LBNE) to be carried out at Fermilab.

This project supported the DOE Office of Science (HEP/NP) mission by enhancing our understanding of the neutrino sector using ground-based and satellite experiments and observations. The high-performance computing and verification and validation pieces of the proposal tied in to aspects of NNSA threat reduction and stockpile stewardship programs. New capabilities developed during this project include a petascale neutrino cosmology code. A post-doc who worked on this project is continuing her career at LANL and is likely to be converted to a staff member. Follow-on funding that resulted partially as a result of the work performed in this project includes a new theory grant from DOE High Energy Physics and support for the experimental program from the same Office.

Background and Research Objectives
The Standard Model (SM) of particle physics provides a remarkably successful description of the electroweak and strong interactions that govern particle and nuclear physics. Despite this success, we now know that the SM is incomplete. Observational evidence for this comes from two, very different, directions. Cosmological evidence for the dominant components of the Universe – dark energy and dark matter – finds no explanation in the SM. Nonzero neutrino masses and mixings from flavor conversion experiments provide compelling evidence for physics beyond the Standard Model (BSM). Significantly, the two fields that first pointed to the existence of BSM physics – cosmology and the neutrino sector – are inextricably connected, and inform on each other in important ways. This rich area of contact [1] was the focus of this proposal.

Although precision particle and nuclear physics experiments have a long history, precision cosmology is a relatively new field. Precision cosmology refers to arenas where

- Observations can be conducted with excellent control over systematic and statistical uncertainty, especially with regard to astrophysical uncertainties.
- Where theoretical interpretation and analysis rests on either a complete foundational basis or on the existence of a reliable phenomenology.

To provide some sense of where precision cosmology is headed, the current targets of measurement and theoretical uncertainties for several fundamental parameters are at levels as low as 0.1-1%!

Precision cosmology provides key, complementary observational probes of the neutrino sector. Cosmological observations can be very sensitive to the neutrino mass and less so to mass splittings and mixing angles, while terrestrial experiments strongly constrain the mass differences, but provide less stringent constraints on the absolute mass. Cosmology also provides constraints on the total neutrino energy density, including the existence of possible additional sterile neutrino degrees of freedom (a sterile neutrino does not possess any SM interactions). In turn, the neutrino sector has significant implications for cosmology. Sterile neutrinos, generated in the early Universe by active-sterile conversion, are viable candidates for dark matter, either warm (WDM), or cold (CDM). A fourth sterile neutrino with a mass around an electron volt or a little less, would have profound consequences for cosmology. The interplay between terrestrial neutrino oscillation experiments and these cosmological settings is important, not only in the constraints that terrestrial experiments impose on neutrino properties, but also in how cosmology might point the way towards future terrestrial neutrino oscillation experiments. It must be borne in mind that all cosmological information is *model-dependent*, thus uncertainties in particle physics translate into uncertainties in cosmological parameters and *vice versa*. It is therefore imperative that cosmological studies of the neutrino sector must necessarily involve close collaborations between observers, experimentalists, and theorists. This feature was an important facet of our project.

From the point of view of precision cosmology, neutrino physics can be probed by two complementary sets of cosmological data: fluctuations of the cosmic microwave background (CMB), and the large-scale structure (LSS) of the Universe. The CMB constrains neutrino properties by features in its temperature and polarization spectra generated by the primary anisotropies (acoustic peaks and Silk damping) and secondary ones (CMB lensing by cosmic structure). These anisotropies are being mapped by Planck (in space) and by the South Pole telescope (SPT) and the Atacama Cosmology Telescope (ACT). Neutrino-sensitive LSS observations include galaxy surveys such as the Sloan Digital Sky Survey (SDSS), weak lensing surveys, and observations of quasar spectra. These observational data sets provided the central setting for our project. We took an integrated approach to addressing three problems we believe to be the most promising scientifically as well as timely in terms of observations and experimental results. These are the total neutrino mass, the number of neutrino species, and constraints on the sterile sector. The analysis requires significant advances in theoretical predictions for the effects of neutrinos on the CMB and LSS, and in combining observational and experimental data with results from large-scale simulations to yield the required constraints with robust error bounds.

Scientific Approach and Accomplishments

Our research program consisted of the analysis of CMB and LSS data, modeling and simulation, and, based on new constraints for the neutrino sector, design studies for new oscillation experiments. The dynamical effects of neutrinos on the CMB and LSS influence both, the small amplitude, or *linear* regime of fluctuations as well as the *nonlinear* regime of structure formation. These regimes can only be computed through detailed simulations. To get reliable constraints on the neutrino sector from the simulations and cosmological data, one must:

- Control parametric degeneracies.
- Find good statistical estimators which lead to robust constraints.
- Accurately model CMB lensing.
- Explore LSS probes of small-scale physics.
- Perform reliable LSS simulations which capture all the relevant physics.

Success in these tasks will lead to new robust constraints on the neutrino sector and in turn allow the design new oscillation experiments.

The primary focus of this project was to build a computational capability to carry out the scientific program enabled by ongoing and next-generation observational surveys. The primary difficulty with carrying out simulations of structure formation with neutrinos is that neutrinos contribute only a small fraction of the mass in the Universe. Consequently, in simulations, the particles that represent the neutrinos are very light compared to the particles that represent the dark matter and normal matter. When particles with large mass imbalances are included in a cosmological simulation, there are serious artifacts due to numerical scattering and diffusion. These artifacts present a serious barrier to precision simulation of the neutrino sector.

To get around this barrier, there are two approaches. The first blends analytic approximations with numerical calculations and the second aims to correct the basic problem in the simulations. The first approach is easier to implement but errors are harder to estimate, whereas the second is numerically much more difficult, but has much better defined error controls. We chose the second approach. This approach requires carrying out simulations with very large numbers of particles (tens to hundreds of billions) in order to make sure that the particle masses of the neutrino tracers are roughly equal to the masses of the other tracer particles. Simulations at this scale require the use of petascale supercomputers.

We built a new code using the IPPL simulation framework for particle simulations developed at the Paul Scherrer Institute, led by Dr. Andreas Adelmann. Code tests are now

underway. Yves Ineichen, Dr. Adelmann's student, visited in Nov/Dec 2009 to help add a new initializer to the IPPL code for neutrino simulations. The same initializer can be used to work with our own hybrid cosmology simulation code, based in what we are calling the Hardware-Accelerated Cosmology Code (HACC) framework, recently validated on Roadrunner, the world's first petascale platform.

In terms of connections to observations, work proceeded on multiple fronts. The effects of neutrino mass on the high-resolution (large multipole) CMB temperature anisotropy can be detected by Sunyaev-Zeldovich surveys such as SPT and ACT (Figure 1). However, in order for this signal to be extracted from various sources of confusion, careful modeling of gas physics is required. One of our post-docs, Suman Bhattacharya, participated in this work [2].

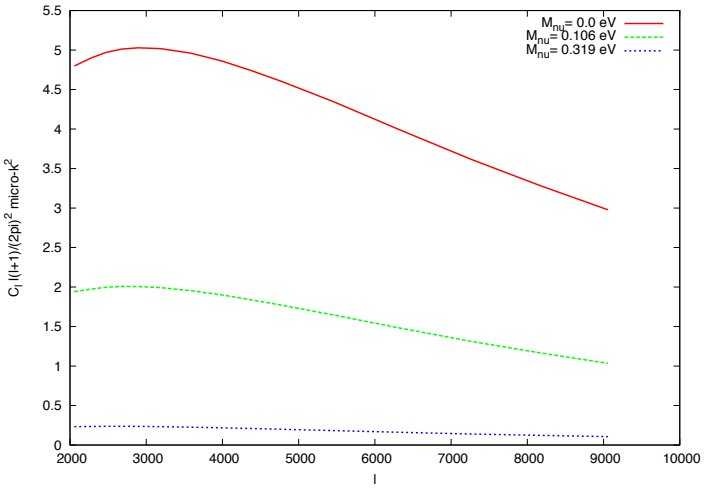

Figure 1. The effect of neutrino mass on the Sunyaev-Zeldovich power spectrum as measurable by the South Pole Telescope and the Atacama Cosmology telescope. The neutrino signal must be disentangled from secondary effects caused by radio sources and galaxy clusters.

The analysis of precision cosmological simulations can only be performed by Markov Chain Monte Carlo methods. These require very large numbers of simulations, typically in the tens of thousands to hundreds of thousands. We have recently applied sophisticated statistical methods to reduce the number of required simulations to only of order hundreds, using high-dimensional interpolation to construct 'look-up' emulators as a replacement for brute force simulation – a procedure we have termed 'cosmic calibration'. Our emulators for the cosmic microwave background temperature anisotropies now include neutrino properties as an input. These emulators have 10 degrees of freedom and cover a dynamic range more or less consistent with that of Planck, the latest cosmic microwave background satellite mission, which will announce results within a year. The aim was to produce emulators with errors at the sub-percent level, a very challenging requirement for a system with so many degrees of freedom. We are preparing the emulator for public release.

Impact on National Missions

This project supported the DOE Office of Science (HEP/NP) mission by enhancing our understanding of the neutrino sector using ground-based and satellite experiments and observations. This scientific area is also a major thrust within the National Science Foundation. High performance computing, particularly heterogeneous supercomputing, and verification and validation pieces of the proposal tied in to aspects of NNSA threat reduction and stockpile stewardship programs. The major new capability developed during this project was a petascale neutrino cosmology code. In terms of recruiting at LANL, a post-doctoral research associate who worked on this project is continuing her career at LANL in beam physics and is likely to be converted to a staff member. Follow-on funding that resulted partially as a result of the work performed in this project includes a new theory grant from DOE High Energy Physics (cosmological probes of particle physics) and support for the experimental program from the same Office (for work on neutrino oscillation experiments).

Our petascale cosmology effort was recently awarded 150 million CPU-hours at Argonne National Laboratory's new IBM BG/Q Mira system (20 Petaflop in 2012). One of the key aims of these runs will be to produce precision predictions for neutrino properties as probed by next-generation cosmological observations, such as the Large Synoptic Survey Telescope (LSST). LSST is the highest-ranked project in the Astro2010 Decadal Review and is expected to come on line in 2016. LANL is an institutional member of LSST.

References

1. Hannestad, S.. Neutrinos in cosmology. 2004. *New Journal of Physics.* **6**: 108.

2. Shaw, L. D., D. Nagai, S. Bhattacharya, and E. T. Lau. Impact of cluster physics on the Sunyaev-Zel'dovich power spectrum. 2010. *arXiv:1006.1945.*

Publications

Shaw, L. D., D. Nagai, S. Bhattacharya, and E. T. Lau. Impact of cluster physics on the Sunyaev-Zel'dovich power spectrum. 2010. *arXiv:1006.1945.*

Finding the First Cosmic Explosions

Daniel Holz
20080080ER

Abstract

Although we understand the birth of the Universe, and the growth of large-scale structure (such as galaxies and superclusters), we have a very limited understanding of how the first stars form, how they live, and most importantly, how they die. The first generation of stars are distinguished by being of primordial composition, meaning that they are composed of the elements forged in the Big Bang (mostly Hydrogen and Helium). These stars are expected to be unusually massive (possibly hundreds of times more massive than our Sun), and they end their lives in spectacular explosions. In this project we have explored the properties of these objects. We have, for the first time, calculated the expected rate of these explosions in the Universe. We have also explored what they look like; how bright the explosions are expected to be, and their colors and spectra. We have analyzed these explosions within the context of our standard Big Bang cosmological model, showing that this population of stars can impact the distribution of gamma-ray bursts (the most distant cosmic explosions we have seen). Finally, we have shown that the distribution of metallicity (which is what sets the types of stars, and is a direct result of the first generation of stars) plays a crucial role in the expected distribution of binary compact objects (black holes and neutron stars). This is a finding of immense topical relevance, as it directly impacts plans for the Laser Interferometer Gravitational-wave Observatory (LIGO), a ~$500 million dollar observatory expect to begin observations in 2014.

Background and Research Objectives

The very first stars in the Universe end their lives in the most powerful thermonuclear explosions in all of nature. Although these events are intrinsically extraordinarily bright, we have yet to directly observe them. These stars, a critical underpinning of our cosmological model, only exist on paper and in large computer simulations. In this project we have analyzed the formation and evolution of these very first objects in the Universe. We have addressed critical questions, including the event rates of these objects as a function of cosmological epoch, as well as the lightcurves of the explosions associated with their stellar deaths. We have found that these objects form early in the Universe, and that they are extraordinarily bright (comparable to the brightest conventional supernovae in the Universe, but lasting an order of magnitude longer). In addition, we have shown that gravitational lensing significantly impacts what is observed at such an early epoch. In particular, the incidence of strong lensing dramatically increases, and this must be incorporated into future estimates of the luminosity function of the first stellar deaths. In Figure 1 we show SN2006gy, the brightest supernova ever discovered. Although discovered at low redshift, SN2006gy is representative of what we hope to find at much higher redshifts.

Figure 1. An image of SN2006gy, the brightest supernova ever discovered. It was discovered right at the beginning of this project, and is thought to be a pair instability supernova of the sort studied in the project.

Simulations of the formation of the first stars in the Universe suggest that these stars were extremely massive, hundreds of times more massive than typical stars today. These stars formed from primordial matter, consisting of only hydrogen and helium, at a time when the Universe was less than 1% of its current age (just a few 100 million years after the Big Bang). They likely lost little mass in their evolution, and ended their lives in immensely

powerful thermonuclear explosions (that were up to a factor of 100 times more powerful than Type Ia supernovae, the tremendously bright cosmological standard-candles). Although they are a critical underpinning of modern cosmology, clear confirmation of the existence of this first generation of stars continues to elude us. While we have a mature theoretical edifice describing the collapse of the very first structures in the Universe, and the subsequent birth of the first stars, we have neither direct nor circumstantial evidence that these processes actually occurred, nor that this first generation of stars ever existed.

In this project we modeled the lightcurves (the spectrum and amount of emitted light) of the explosions, determining how bright they are, and how often they happen. We also modeled cosmic magnification, which causes very distant objects to be significantly brightened due to the gravitational effects of intervening matter. This proposal exploits gravitational lensing, a uniquely powerful tool to probe the high-redshift Universe. The gravitational effects of matter near the line-of-sight to a distant object impacts the observed brightness and shape of the source. In extreme cases, this lensing can cause tremendous increases (>100X) in the apparent brightness of a distant source. In addition, as the sources move to higher redshifts, the likelihood for these strong lensing effects increases. Gravitational lensing offers the possibility of transforming the death of a first star at the very edge of the Universe into an event easily observable by modern surveys. Most lensing studies to date have focused on sources at low redshifts (z<5), since it has not been thought that there would be significant numbers of bright, compact sources at much higher redshift. In this project we are extending lensing calculations to very high redshifts.

The goal of this proposal was to explore the properties of the very first objects in the Universe. Though a combination of numerical and analytic techniques, this project dramatically increased our understanding of the very earliest objects in the Universe.

Scientific Approach and Accomplishments

The project has been tremendously productive, producing 8 papers published in major journals.

A number of sub-projects directly address properties of the first objects in the Universe. In particular, the papers "Pulsational pair instability as an explanation for the most luminous supernovae"[1], "Mixing in Zero and Solar Metallicity Supernovae" [2], "The destruction of cosmological minihalos by primordial supernovae" [3], and "Cosmological Radiative Transfer Comparison Project II: The Radiation-Hydrodynamic Tests" [4], produced simulations of the first stars, and in particular, provided the very first lightcurves for the spectacular explosions associated with the end-stages of their evolution. These papers represent a major advance in the field.

A number of papers further developed the gravitational-lensing techniques relevant to the project, including [5] and [6]. In [5] we show that the effects of gravitational lensing are important, especially at high redshift, while in [6] we develop techniques to account for and correct the lensing. In a particularly topical aspect of the project, a paper on the detectability and origin of the recent, very exciting observations of high-redshift gamma-ray bursts was written. Titled "On The Origin Of The Highest Redshift Gamma-Ray Burst GRB 080913", [7], the paper explores population synthesis models of GRBs, focusing on the very earliest populations. GRB 080913, discovered by SWIFT, was the most distant gamma-ray burst (GRB) known to-date, with a spectroscopically determined redshift of z=6.7 (although it has since been surpassed; more on this below). The detection of a burst at such an early epoch of the Universe significantly constrains the nature of GRBs and their progenitors. To evaluate these constraints, we performed population synthesis studies of the formation and evolution of early stars and calculate the resulting formation rates of short- and long-duration GRBs at high redshift. The peak of the GRB rate from Population II stars occurs at z=7 for a model with efficient/fast mixing of metals, while it is found at z=3 for an inefficient/slow metallicity evolution model. We show that for at z=6.7 essentially all GRBs originate from Population II stars, independent of the adopted metallicity evolution model. At this epoch Population III (metal free) stars, representing the very first generation of stars, most likely have already completed their evolution, and Population I stars (representing the present population) have just begun forming. We argue that Population II stars (having small, but non-zero metallicity) are the most likely progenitors of both long GRBs (collapsars) and short GRBs (NS-NS or BH-NS mergers) in the redshift range 6<z<10. Since the predicted rates, after correction for modeling and observational biases, are very similar at these epochs we cannot definitively conclude which of these two progenitor scenarios is more likely in the case of GRB 080913. Further information about these high-redshift events, such as their spectral energy distribution and host galaxy properties, will be needed for a much larger sample to consolidate the progenitor models considered here.

These results are crucially related to the earliest generation of stars. It is a major observational advance that GRBs are being directly observed at redshifts greater than eight, corresponding to the earliest known cosmic explosions ever detected. These are therefore our earliest observational clue to the nature of the first generation of stars, and this was a fundamental development in this proposal.

The most important result of this proposal, and the culmination of many of the different avenues being pursued, was our final project looking at the effects of metallicity on these early populations of stars [8]. In particular, Pop III are distinguished as originating in extremely low metallicity environments (so that they are composed out of the material produced in the Big Bang [mostly Hydrogen and

Helium]). We showed that recent observations indicated that low metallicity environments persist until late in the Universe (and even until the current epoch). This has important ramifications for our understanding of the evolution of stars and the formation of galaxies. In particular, our results show that the incidence of binary neutron stars and, especially, binary black holes, can be significantly enhanced. These systems are the most important sources for the Laser Interferometer Gravitational Observatory (LIGO), a ~$500 million dollar observatory currently operating in Hanford, Washington and Livingston, Louisiana. Our results may inform the particular configuration of these detectors, arguing for a focus on the low-frequency regime (below 1 kHz), and indicating that the sensitivity in the high-frequency regime is of less importance.

In summary, our project has been immensely successful. We have made major contributions to our understanding of how stars form and evolve in the Universe. We have calculated how often these stars are born, and what they look like as they live and die. We have shown how the rates of different types of stars are related to the metallicity distribution of their surrounding environments. And, finally, we have established that this metallicity directly impacts the life and death of stars, and thereby sets the distribution of neutron star and black hole binaries. This final result impacts the design of one of the foremost observational facilities in the US in the next decade.

Impact on National Missions

This project ties into the missions in a number of important ways. First, we are simulating the thermonuclear explosions of the first generation of stars. This has direct programmatic relevance, and the codes we have been using for radiation transport are related to codes being used for stockpile stewardship. This project is part of a larger V&V effort at LANL, where we are using astrophysical scenarios as testbeds for important physical processes relevant to the missions.

In addition, this project has generated a number of important collaborations, including those with Edo Berger (Harvard) and Brian O'Shea (Michigan State). A graduate student has also been supported (Candace Church, at UC Santa Cruz), as well as a postdoc (Dan Whalen; now a McWilliams Fellow at Carnegie Mellon University). In addition to increasing LANL's visibility outside of the laboratory, this project helps with recruiting talented individuals to LANL. In particular, Candace Church (who was entirely supported as a graduate student through this LDRD grant) is starting a postdoc at LANL in X division.

In summary, this project has produced first-rate science, which enhances LANL's reputation in the outside world. The results from this project directly improve LANL's ability to perform its mission, through important V&V. And the project has established important collaborations, enhancing LANL's recruitment of first-rate scientists.

References

1. Woosley, S. E., S. Blinnikov, and A. Heger. Pulsational pair instability as an explanation for the most luminous supernovae. 2007. *Nature.* **450**: 390.

2. Heger, A., S. Woosley, and C. Joggerst. Mixing in Zero- and Solar-Metallicity Supernovae. 2009. *Astrophysical Journal.* **693** (2): 1780.

3. Whalen, D., B. van Veelen, B. O'Shea, and M. Norman. The destruction of cosmological minihalos by primordial supernovae. 2008. *Astrophysical Journal.* **682**: 49.

4. Iliev, I., and D. Whalen. Cosmological radiative transfer comparison project - II. The radiation-hydrodynamic tests. 2009. *Monthly Notices of the Royal Astronomical Society.* **400**: 1283.

5. Sarkar, D., A. Amblard, D. Holz, and A. Cooray. Lensing and supernovae: Quantifying the bias on the dark energy equation of state. 2008. *ASTROPHYSICAL JOURNAL.* **678** (1): 1.

6. Sarkar, D., A. Amblard, D. Holz, and A. Cooray. Lensing and supernovae: quantifying the bias on the dark energy equation of state. 2008. *Astrophysical Journal.* **678**: 1.

Publications

Belczynski, C., D. Holz, C. Fryer, M. Dominik, and T. Bulik. The Effect of Metallicity on the Detection Prospects for Gravitational Waves. 2010. *Astrophysical Journal Letters.* **715** (2): L138.

Belczynski, K., D. E. Holz, C. L. Fryer, E. Berger, D. H. Hartmann, and B. O'Shea. On the origin of the highest redshift gamma-ray bursts. 2010. *Astrophysical Journal.* **708** (1): 117.

Heger, A., S. Woosley, and C. Joggerst. Mixing in Zero- and Solar-Metallicity Supernovae. 2009. *Astrophysical Journal.* **693** (2): 1780.

Hirata, C. M., D. E. Holz, and C. Cutler. Reducing the weak lensing noise for the gravitational wave Hubble diagram using the non-Gaussianity of the magnification distribution. 2010. *Physical Review D.* **81** (12): 124046 (11 pp.).

Hu, W., D. Holz, and C. Vale. CMB cluster lensing: cosmography with the longest lever arm. 2007. *Physical Review D (Rapid Communications).* **76** (12): 127301.

Iliev, I., D. Whalen, G. Mellema, K. Ahn, S. Baek, N. Gnedin, A. Kravtsov, M. Norman, M. Raicevic, D. Reynolds, D. Sato, P. Shapiro, B. Semelin, J. Smidt, H. Susa, T. Theuns, and M. Umemura. Cosmological radiative transfer comparison project - II. The radiation-hydrodynamic tests. 2009. *MONTHLY NOTICES OF THE ROYAL ASTRO-*

NOMICAL SOCIETY. **400** (3): 1283.

Joudaki, S., D. Holz, and A. Cooray. Weak lensing and dark energy: The impact of dark energy on nonlinear dark matter clustering. 2009. *Physical Review D.* **80** (2): 023003.

Sarkar, D., A. Amblard, D. Holz, and A. Cooray. Lensing and supernovae: quantifying the bias on the dark energy equation of state. 2008. *Astrophysical Journal.* **678**: 1.

Tinker, J., A. Kravtsov, A. Klypin, K. Abazajian, M. Warren, G. Yepes, S. Gottlober, and D. Holz. Toward a halo mass function for precision cosmology. 2008. *Astrophysical Journal.* **688** (2): 709.

Woosley, S. E., S. Blinnikov, and A. Heger. Pulsational pair instability as an explanation for the most luminous supernovae. 2007. *Nature.* **450**: 390.

Materials and Device Optimization towards Room Temperature Spin-Transport through Single-Walled Carbon Nanotubes

Stephen K. Doorn
20080164ER

Abstract

The primary objective of this project was to develop single walled carbon nanotubes (SWNTs) as channels for efficient transport of electron spin information. This goal has significant implications for development of advanced computing concepts based on spintronics. Accomplishing this goal required advances in several areas of materials and nanoscience. These included synthesis and manipulation of high quality carbon nanotube arrays. Synthesis of high quality magnetic thin films. Magnetic electrode patterning and fabrication of functioning spin electronics devices. Advanced materials magnetic and spectroscopic characterization. Ultimately, materials compatibility issues prevented the attainment of our primary objective. However, each of the component parts was accomplished. Of particular note was our ability to make significant advances in Raman spectroscopic characterization of the nanotube components. This LDRD effort also led directly to development of important new capabilities for materials synthesis and characterization that did not previously exist at LANL. These capabilities will further support the goals of the Department of Energy Office of Basic Energy Sciences (DOE-BES) funded Center for Integrated Nanotechnologies (CINT). The capability and fundamental understanding developed in this project will also drive new program development efforts in nanotube photophysics and graphene chemistry.

Background and Research Objectives

Our purpose was to develop integrated structures based on carbon nanotubes that will allow the manipulation of electron spin for electronics and computing applications (spintronics). The ultimate goal is to produce a carbon-nanotube structure capable of transmitting, manipulating, and preserving information carried in electron spin orientation at room temperature. Adding the extra dimension of spin control to computation will enable tremendous leaps in computing speed and in device and memory density. Our aim was to combine new advances in synthesis of defect-free carbon nanotubes with novel ferromagnetic thin films to approach this goal. Ideally our device design would lead to maximized injection of spin-information while minimizing its loss within the nanotube-based devices. Our research objectives included:

- Maximize spin-polarization of our electrode materials through improvements in their domain structure via advances in epitaxial materials synthesis.
- Maximize spin injection into the nanotubes through engineering of the electrode/nanotube interfacial composition and interaction.
- Minimize spin loss through minimizing spin scattering in the nanotube by use of suspended chemical vapor deposition (CVD)-grown single-walled structures that eliminate defect scattering sites.

This first-time demonstration of spin transport through single-walled nanotubes (SWNTs) was aimed at approaching the room-temperature application barrier. This would be obtained through simultaneous optimization of the magnetic and carbon-based materials involved. We anticipated gaining a fundamental understanding of spin-loss mechanisms in these integrated materials. Additionally, significant advances in new magnetic interface materials and the development and exploration of the integrated functionality of these novel nanoscale devices were also envisioned.

Ultimately, we were able to achieve all of the individual pieces required to meet our primary objective. However, integration into a final room-temperature spin device was not achieved. This resulted from significant materials compatibility challenges that we were unable to overcome. None-the-less, we successfully achieved the following: We developed a capability for routine generation of ultralong, dense arrays of highly aligned carbon nanotubes. We developed an approach for transferring the nanotubes to patterned substrates in predefined locations. We developed synthesis protocols for high-quality thin films of $La_{0.7}Sr_{0.3}MnO_3$ (LSMO). We developed approaches to patterning the required magnetic electrodes from both LSMO films and Ni and Co. Furthermore, we expanded the scope of this project to include a greater component of developing Raman

spectroscopic characterization tools. We also explored the properties of graphene as a potential transport channel.

Scientific Approach and Accomplishments

Our approach was to grow high quality carbon nanotubes in well-aligned arrays that could then be transferred to magnetic device substrates. The tubes would be assembled over trenches to avoid substrate interactions. Raman and transport characterization would follow. Such characterization required development of new advanced capabilities for these tools at LANL. Initial efforts at device generation revealed significant materials compatibility and device engineering issues in our approach. These required us to redefine our original strategies for generating our electronic devices. The initial lithographic techniques used to pattern the required ferromagnetic electrodes were inadequate. They did not provide the proper alignment of the several overlapping features we envisioned and damaged the nanotube components. Additionally, we envisioned depositing our high-temperature ferromagnetic films ($La_{0.7}Sr_{0.3}MnO_3$, or LSMO) over our nanotubes. Alternatively, the nanotubes might be grown over initially deposited films. However, we found the reducing environment of the nanotube growth would destroy the films. Conversely, the oxidizing environment of the film deposition would destroy the nanotubes. Our final strategy was to directly pattern our entire device structure from a large-scale LSMO film. Pre-grown nanotubes would then be incorporated into the devices by using a direct transfer technique. Thus, all three problems would be solved.

To accomplish this new strategy, the thrust of our efforts were directed toward making significant progress in these critical areas:

- Develop a LANL capability to fabricate dense arrays of parallel SWNTs.
- Develop an approach to directly transfer the SWNT arrays from their growth substrate to the electronic device structures.
- Develop and evaluate multiple approaches to synthesis of LSMO films.
- Design and pattern new LSMO device structures to integrate with the SWNT arrays.
- Develop advanced magnetic and spectroscopic characterization tools.

These accomplishments are detailed below:

Synthesis of Nanotubes

We developed a new capability at LANL for growth of arrays of long (mm to cm) SWNTs. The approach enabled growth of SWNTs in a tube furnace using chemical vapor deposition (CVD) with ethanol as the carbon source. We have successfully developed techniques to grow well-aligned (highly parallel) arrays. These are produced on both single crystal quartz and SiO2 coated silicon substrates. The resulting arrays grow in the plane of the substrate. This is necessary for incorporating them into spintronics devices. Example arrays are shown in Figure 1.

Ultralong nanotubes grown on Silicon

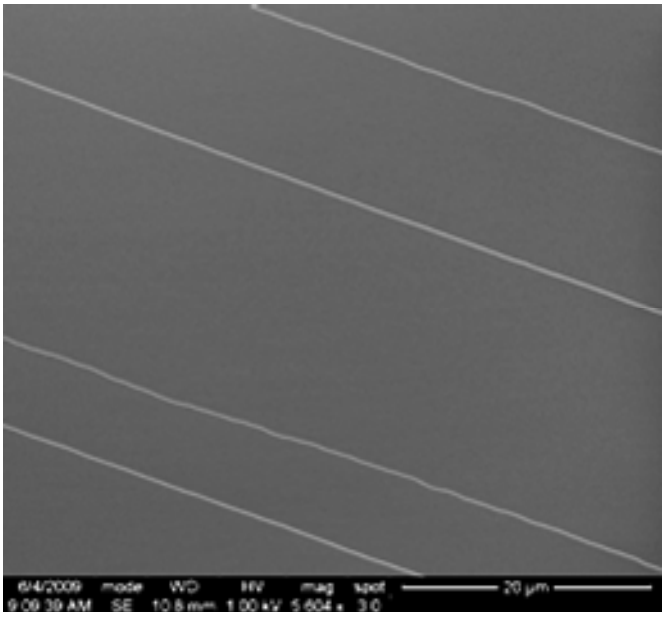

Ultralong nanotubes grown on Quartz

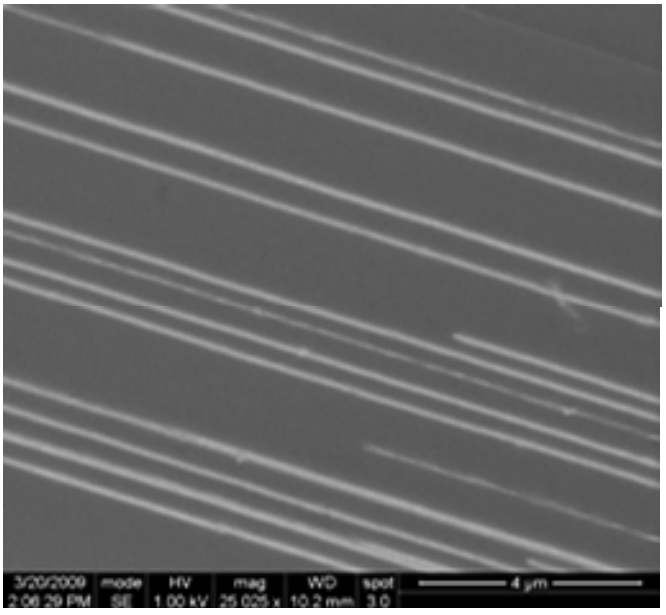

Figure 1. Upper: Scanning electron micrograph (SEM) of array of parallel ultralong carbon nanotubes grown on Si/SiO2 substrate. Lower: SEM image of array of parallel ultralong carbon nanotubes grown on quartz substrate.

Development of Nanotube Transfer Technique

We worked with collaborators at Duke University to develop the technology for transferring SWNT arrays from the

growth substrate onto pre-patterned microchips. A polymer coated substrate is used to effectively lift off an existing SWNT array from its growth substrate. A polymer layer is first deposited on the SWNT array to be transferred. The layer is then peeled from the substrate. The assembly is then pressed onto the destination substrate (device structure). The polymer is subsequently removed with an acetone wash, leaving behind pristine SWNTs in well-defined locations. The technique can now be applied reproducibly with the required accuracy in final SWNT location.

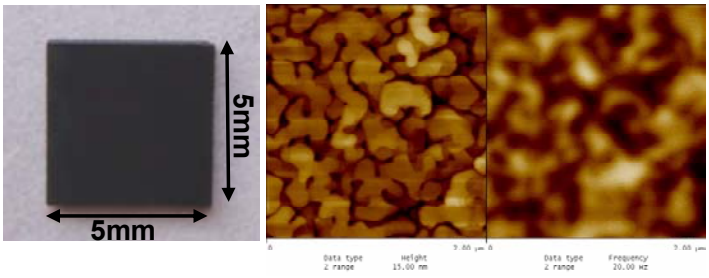

Figure 2. Left: Optical image of a 120 nm thick film of LSMO grown on LaAlO3 substrate. (4 μm)2 topography (center) and magnetic domain structure (right) for the LSMO film. Note film RMS roughness is 1.4 nm.

Synthesis of Ferromagnetic LSMO Films

We have developed two approaches to deposition of LSMO thin films. LSMO is of interest for our electrode materials because it exhibits ferromagnetism at relatively high temperatures. We are using our newly developed radio-frequency (RF) off-axis sputtering deposition capability for growing high-quality LSMO thin film electrode materials. Properties were optimized by growing the films at 800°C and an Argon (60%) to O2 (40%) mix at a chamber pressure of 50 mTorr. We have also evaluated methods to improve the magnetic properties of these thin film materials through post-deposition annealing procedures. Annealing of the films in oxygen at 975°C for three hours is found to improve the domain structure of the films. Films were also grown on silicon, $LaAlO_3$, and MgO substrates. The highest quality results were obtained on $LaAlO_3$. Currently optimized films are illustrated in Figure 2. We have also explored using a pulsed laser deposition (PLD) technique for LSMO growth. The quality of the resulting films is not as high as with the RF approach. However, the films can be generated more quickly and provided a suitable source of material to establish our electrode etching approach for final device fabrication (see below).

Device Patterning and Development

Our final strategy for device fabrication was to directly pattern electrode structures from LSMO films via an etching or ion milling process. For LSMO electrode patterning we have designed a prototype electrode structure and the protocol for fabricating this structure. Masks for patterning of photoresist were also completed. We have successfully deposited the necessary masks on LSMO test films. Etching of the patterns has been tested. Argon ion etching is capable of etching the LSMO films, but required prolonged etching times. Film deformation and loss of the desired magnetic properties resulted. To overcome this difficulty, Al and Ti masks were incorporated into the etching process to prevent LSMO film heating. Ti masks were found most suitable. Ti masking led to successful patterning (see Figure 3), but also led to degradation of the film magnetic properties. How to overcome this final challenge remains an open question.

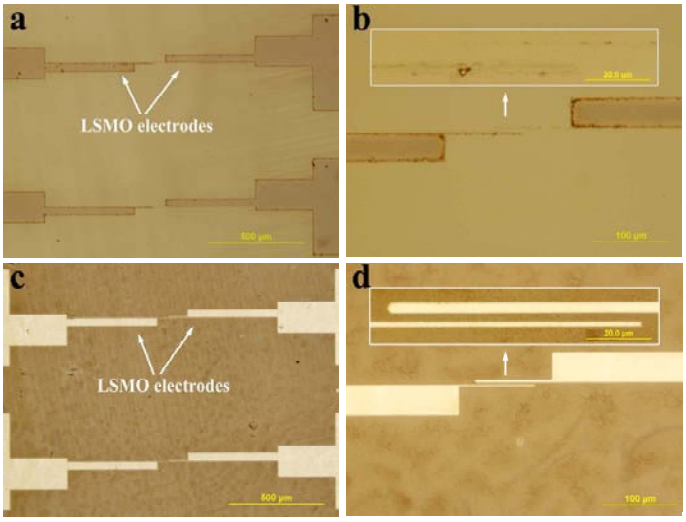

Figure 3. Optical images of LSMO microelectrodes etched with (a, b) Al and (c, d) Ti as etching masks. The insets in (b) and (d) show their respective enlarged images. The results clearly indicate the effectiveness of Ti masks for LSMO etching, although the issue related to their magnetic properties needs to be further addressed.

In parallel to the LSMO electrode route we have tried constructing devices by electron-beam patterning of nickel and cobalt electrodes. These were successfully incorporated into silicon microchips with trench structures, over which SWNT arrays have been directly transferred (Figure 4). Unfortunately, the metal electrode structures do not yet adhere well to the device assemblies. Thus, functioning devices have not yet been demonstrated by this route.

Magnetic Materials Characterization

We have used a combination of advanced atomic force microscopy (AFM) and magnetic force (MFM) techniques and scanning electron microscopy (SEM) to characterize the properties of the LSMO films and the SWNTs. Measurements of magnetization (M) and resistivity (ρ) versus temperature for the LSMO films were used to further characterize sample homogeneity. The data provided important feedback into improvement of film characteristics. The magnetization and resistivity display sharp features at the Curie temperature. By tracking the relative sharpness of the magnetic feature it is possible to make a relative determination of sample quality. The key growth variables of interest include growth (growth time, temperature, and deposition rate) and post-anneal conditions (time and temperature). We found that a high-temperature O_2

post-anneal has a profound positive impact on the overall quality of our films. This condition reduced the spread of Curie temperatures within the film while also lowering the overall resistivity of the film. This conclusion is borne out both in M(T) and ρ(T) measurements (Figure 5). These results also correlated well with improvements in domain structure observed via MFM. Raman, SEM, and AFM, measurements of the SWNT arrays have shown the SWNTs to be of high quality and suitable for incorporation into our device structures.

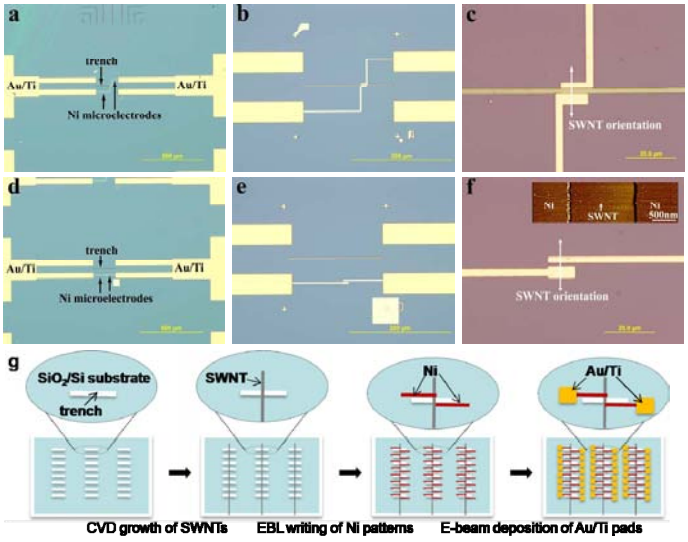

Figure 4. Optical images of Ni electrodes-integrated spin-valve devices based on suspended (a-c) and supported (d-f) sections of an individual SWNT. The inset in (f) shows the AFM image of the as-fabricated supported device. (g) Scheme showing the fabrication of suspended SWNT-based spin-valve devices with Ni electrodes.

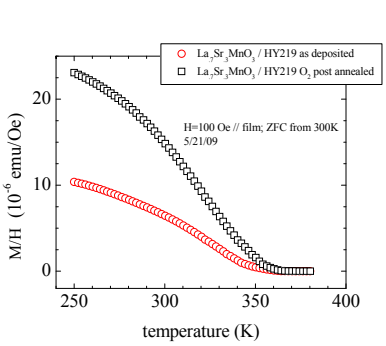

Notes:

- T_C in manganites dependents on Mn valence
- Mn valence determined by Sr doping and oxygen stoichiometry
- Inhomogeneities leads to distribution of T_cs in sample
- Sharp rise at T_C indicates that sample is homogeneous
- M(T) of as-deposited sample shows clear signs of inhomogeneities
- Annealing improves magnetic quality of film but sample still contains distribution of Curie temperatures

Figure 5. LSMO magnetization (M) as a function of temperature for as generated (red circles) and post-annealed in O2 at 975 degrees C (black squares) films. Sharper transition in the post-annealed sample shows annealing yields higher quality LSMO films.

Raman Characterization

Raman spectroscopy was expected to be a primary tool for evaluating how spin transport efficiencies depended on substrate and defect interactions. We therefore expanded our project scope to better understand nanotube Raman response for specific conditions. The presence of typically large diameter nanotubes in our synthesis made it important to understand Raman response arising from excitation of relatively high level electronic transitions. Most importantly, these would include the third and fourth transitions (labeled as E_{33} and E_{44}) in semiconductors. Significant results from these studies include the demonstration of a breakdown in scaling laws used to describe E_{33} and E_{44} energy behavior. We also for the first time demonstrated a predicted cross-over of E_{33} and E_{44} energies. We also carried out a detailed investigation of how Raman frequencies depended on nanotube diameters. This was required to better characterize our tube structures. Equally important was the need to understand the nature of Raman response in metallic nanotubes. We mapped this response for the largest range of metallic structures to date. We also demonstrated the surprising excitonic nature of metallic optical excitations. Finally, we made the first ever observations of long-predicted energy splitting in the metallic transitions. These discoveries are highlighted in three publications listed in our supporting material.

Graphene

Graphene (single layer carbon) is rapidly gaining in interest for electronics applications. We therefore further expanded the scope of our studies to include developing a capability for advanced Raman spectroscopy of graphene. This would feed into any use of the material as a spin channel. We successfully obtained the first ever near-infrared Raman spectra of mono and bilayer graphene. This work was done in collaboration with Prof. Marcos Pimenta of Brazil. Raman in this spectral range allowed us to probe graphene band-structure near the Dirac point, which determines all electronic transport behavior. We were able to demonstrate for the first time nonlinearities in electron-phonon couplings. This work is now published in two publications noted in the supporting material. Working with Stephane Berciaud of Columbia University, we also explored Raman behavior of graphene supported over trenches. This work serves as a parallel to our interest in enhanced spin transport in carbon structures suspended away from the substrate. We anticipate an additional publication from this work and continued collaboration with both the Pimenta and Berciaud groups.

Impact on National Missions

Mission Impact: This research supports the development of advanced functional nanomaterials in support of threat reduction, energy security and basic science missions in DOE and other government agencies. Developing SWNT spintronics materials provides understanding and control of fundamental properties at the nanoscale to enable energy-efficient next-generation computing in support of advanced materials modeling. This work and the resultant new capabilities have also supported the goals of CINT. As a DOE user facility, the new capabilities are also serving as a draw to new users.

Capability Development: Pursuit of the project goals led to the creation of the following capabilities that previously did not exist at LANL: Capability for reproducible growth of highly aligned arrays of ultra-long carbon nanotubes. Creation of protocols for directed transfer of nanotubes to patterned substrates. Capability for synthesis of LSMO films. Establishment of a new capability for advanced micro-Raman spectroscopy of nanomaterials. The impact of this capability reaches beyond applications in nanotube and graphene synthesis. The Raman instrumentation is also now a critical tool in several CINT nanowire research efforts. Finally, the ER effort is spinning off new capability for synthesis of large area graphene films of interest for electronics and photonics applications.

Publications

Araujo, P. T., I. O. Maciel, P. B. C. Pesce, M. A. Pimenta, S. K. Doorn, H. Qian, A. Hartschuh, M. Steiner, L. Gregorian, K. Hata, and A. Jorio. Nature of the constant factor in the relation between radial breathing mode frequency and tube diameter for single-wall carbon nanotubes. 2008. *Physical Review B.* **77**: 241403(R).

Doorn, S. K., P. T. Araujo, K. Hata, and A. Jorio. Excitons and excciton-phonon coupling in metallic single-walled carbon nanotubes: resonance Raman spectroscopy. 2008. *Physical Review B.* **78**: 165408.

Haroz, E. H., S. Bachilo, R. B. Weisman, and S. K. Doorn. Curvature effects on the E33 and E44 exciton transitions in semiconducting single-walled carbon nanotubes. 2008. *Physical Review B.* **77**: 125405.

Mafra, D. L., L. M. Malard, S. K. Doorn, H. Htoon, J. Nilsson, A. H. Castro Neto, and M. A. Pimenta. Observation of the Kohn anomaly near the Dirac point of bilayer graphene. 2009. *Physical Review B.* **80**: 241414(R).

Malard, L. A., D. L. Mafra, S. K. Doorn, and M. A. Pimenta. Resonance Raman scattering in graphene: probing phonons and elesctrons. 2009. *Solid State Communications.* **149**: 1136.

The First Precise Determination of Quark Energy Loss in Nuclei

Ivan M. Vitev
20080201ER

Abstract

The rate of energy loss of the basic building blocks of the proton - quarks and gluons - in nuclear matter is unknown and constitutes the largest gap in our current understanding of the fundamental nuclear interactions at relativistic energies. As a consequence, it also hampers the quantitative determination of the properties of a new state-of-matter created in relativistic heavy ion collisions - the quark-gluon plasma. To bridge this gap, we carried out a joint theoretical and experimental project to provide the foundation for the first precise determination of quark energy loss in nuclei. We developed theoretical techniques and computational tools to reliably calculate the stopping power of cold nuclear matter. A unique opportunity to perform the benchmark measurements was presented by the Fermilab E906 experiment and our project reinvigorated its proton-nucleus program. We built a new muon identification system for E906 to achieve the world's best sensitivity to quark energy loss effects. Theoretically justified numerical simulations have guided the optimization of this detector design. We anticipate that the upcoming landmark measurements at E906 will establish the shortest radiation lengths ever observed in nature. Results from our project were shown to be critical for the accurate modeling and reliable interpretation of the data from current and future heavy ion experiments. This research has helped keep LANL at the forefront of contemporary nuclear science at high energies.

Background and Research Objectives

The energy loss of a charged particle, as it traverses dense matter, is a fundamental probe of the matter properties. Following the pioneering work of Hans Bethe [1] on the collisional stopping power (energy loss per unit length) for electrons, precise theoretical calculations and experimental measurements of this quantity became one of the great early successes of the classical and quantum theories of electromagnetic interactions. The stopping power, $-dE/dx$, in the limit of large energies is dominated by radiative energy loss. It is related to the radiation length, X_0, of charged particles in matter as follows: $dE/dx = -E/X_0$. Precise knowledge of the stopping power and radiation length of materials is widely used today in X-ray tomography, muon and proton radiography (including national security applications), and high energy nuclear and particle physics detector development and instrumentation.

The fundamental constituents of nuclei (quarks and gluons) predominantly interact via their "color" charge. The forces between them are described from first principles by the theory of strong interactions, Quantum Chromodynamics (QCD), and are much larger in magnitude than the electromagnetic force. In the last decade, advances in high energy many-body QCD have allowed us to quantify, albeit with significant uncertainty, the stopping power of a novel ultra-hot and dense state of nuclear matter – the quark-gluon plasma (QGP) [2]. Alongside the excitement of this new discovery comes the realization that the biggest gap in our current knowledge of nuclear reactions in extremis is the stopping power of cold nuclei for color-charged particles. In proton-nucleus collisions (p+A) at the Relativistic Heavy Ion Collider (RHIC), where a QGP is not formed, a similarly large suppression of particle production at small angles relative to the incident proton beam is observed, indicative of large nuclear stopping power. Mutually exclusive explanations of this intriguing phenomenon have been proposed, ranging from reduced probability for certain types of quark and gluon interactions at high center-of-mass (C.M.) energy (called nuclear shadowing) to energy loss, $-dE/dx$, of these strongly interacting particles in large nuclei. Current data and future dimuon measurements at RHIC cannot distinguish among conflicting theoretical models.

Given the pressing need for a benchmark determination of the energy loss of quarks and gluons in large nuclei, its far-reaching implications for QCD phenomenology and the interpretation of data from current and future heavy ion experiments, and the opportunity for LANL to play a leadership role in this high-impact area of research, our goal was to carry out a joint theoretical and experimental project to provide the first precise determination of the stopping power of cold nuclear matter for strongly interacting particles. To reliably establish the QCD mechanisms of quark energy loss and precisely measure $-dE/$

dx for large nuclei, the following criteria must be satisfied:

- Robust theoretical calculations of many-body scattering effects at high energies.
- Sufficiently low C.M. energy, outside of the region where shadowing effects are significant.
- An unambiguous experimental signature.
- Minimal final-state interactions of the detected particles.

We have determined that the Drell-Yan process - the production of a pair of weakly interacting particles called leptons – is the ideal experimental channel to look for signatures of quark energy loss. In the Drell-Yan process, a quark (anti-quark) from the beam hadron undergoes energy loss in the large nucleus and then annihilates with an anti-quark (quark) in the nuclear target. Therefore, this process directly measures the interactions of the initial-state quark in the nuclear medium.

The platform for our project is a recently approved new experiment, E906, at the Fermi National Accelerator Laboratory (Fermilab) [3]. This experiment collides a 120 GeV proton beams on hydrogen and deuterium targets and detects muon pairs. Its 120 GeV beam energy is sufficiently low to eliminate contributions from nuclear shadowing and makes E906 the ideal experiment for quark energy loss measurements. Our project aimed to significantly improve the physics reach of E906 by optimizing the critical p+A program that will likely establish the shortest radiation length ever measured in nature.

To summarize, there were two equally important research objectives in this proposal: theoretical and experimental. Our primary theoretical goal was to carry out the first rigorous calculation of the stopping power, $-dE/dx$, and radiation length, X_0, for cold nuclear matter in QCD. We planned to implement these new theoretical results in numerical simulations of proton-nucleus collisions to calculate unambiguous experimental observables that can be used to precisely constrain the above quantities. The primary experimental goal of this proposal was to develop a new critical program of dimuon measurements at the E906 experiment at Fermilab to study the quark energy loss effects and pinpoint the stopping power of cold nuclear matter.

Scientific Approach and Accomplishments

Theoretical accomplishments

The prototypical radiative energy loss for fast electrons grows linearly with the incident particle energy, *E*, and the medium size, *L*. In contrast, for color-charged particles, quantum interference effects that are specific to QCD can dramatically alter this simple dependence. With this motivation, we developed a theory of radiative energy loss of quarks in nuclear matter, where the destructive quantum interference effects for initial-state and final-state interactions are properly treated [4]. To accomplish this task, we employed an elegant algebraic approach to quark propagation in matter, which has proven extremely useful for summing large numbers of scattering diagrams for a wide range of physics problems. We found that quantum interference effects can reduce the stopping power of cold nuclear matter for quarks by as much as a factor of ten. Nevertheless, in the limit of very large quark energies, initial-state energy loss in large nuclei significantly exceeds final-state energy loss even in the QGP. Our theoretical results show that the radiation length X_0 that characterizes the former process is of the order of 10^{-13} cm – the shortest radiation length known to date. For comparison, the well-known radiation length of tungsten is $X_0 = 3.2 \times 10^{-1}$ cm.

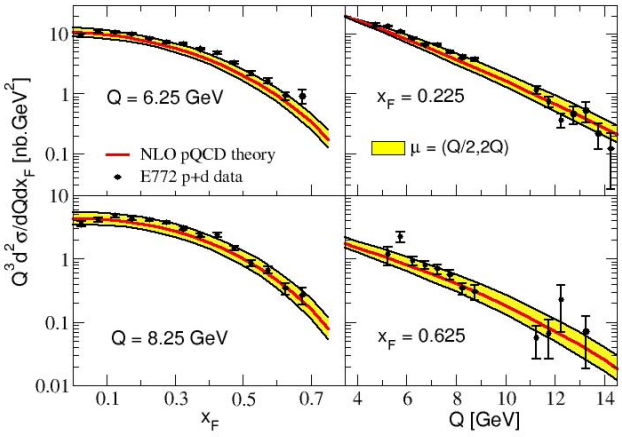

Figure 1. Comparison of our theoretical results for the Drell-Yan production cross section at a C.M. energy of 38.8 GeV to existing data from Fermilab experiment E772. Bands indicate the uncertainty in the theoretical predictions.

An equally important accomplishment is the identification and simulation of signature observables that can be used to experimentally determine the stopping power of large nuclei. One such observable is the suppression of the Drell-Yan cross section in nuclear matter, in the direction of the incident proton beam, relative to the Drell-Yan cross section in "elementary" proton-proton collisions. We developed a code to calculate this cross section with high precision (known as next-to-leading order) and validated the new simulation tool against existing experimental data. Excellent agreement between data and theory is shown in Figure 1 [5]. Yellow bands represent the uncertainty that is inherent in the theory of strong interactions. As a next step, we incorporated the calculated energy loss effects when light targets, such as deuterium, are replaced with heavy nuclear targets ranging from beryllium (Be) to tungsten (W). Figure 2 shows the attenuation in the number of the produced lepton pairs in the direction of the proton beam, designated by $x_F \sim 1$ [5]. Our predictions reflect the state-of-the-art knowledge of subatomic particle interactions in large nuclei. We also recognize the possibility that experimental results may differ from even the most detailed theoretical predictions. The computational tools

that we have developed will be employed to promptly and accurately determine the stopping power of cold nuclear matter as soon as data becomes available.

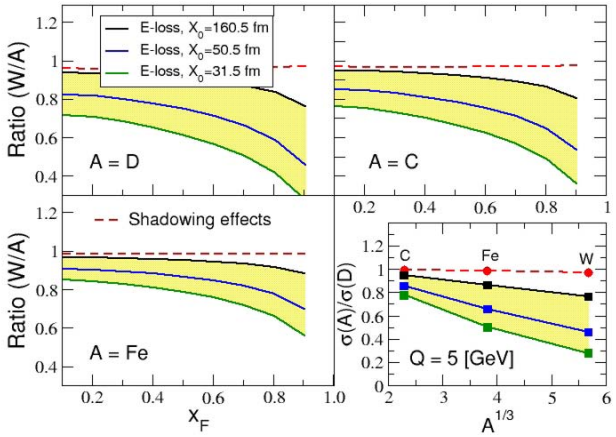

Figure 2. Theoretical predictions for the attenuation of the Drell-Yan production cross section as a function of the radiation length X0. Energy loss in large nuclei is clearly distinguishable from minimal shadowing effects.

Last but not least, we have demonstrated the connection of the newly constructed theory of quark energy loss in cold nuclear matter to the experiments at RHIC and the Large Hadron Collider. In these experiments, emphasis has been placed on the final-state interactions of quarks and gluons in the strongly-interacting QGP at temperatures in excess of 10^{12}K. Our work was the first to demonstrate that initial-state cold nuclear matter energy loss effects cannot be neglected in the interpretation of the experimental results. In fact, if this important piece of physics is not properly accounted for, the extracted density of the QGP may be overestimated by more than a factor of two. We have established quantitatively the magnitude of cold nuclear matter effects for several experimentally accessible channels:

- Direct photon production in deuterium-copper (d+Cu), deuterium-gold (d+Au), copper-copper (Cu+Cu), and gold-gold (Au+Au) reactions at RHIC [6];
- Production of heavy particles, known as D and B mesons, in Au+Au and Cu+Cu reactions at RHIC and lead-lead reactions at the LHC [7];
- Production of jets, collimated showers of energetic subatomic particles, in Au+Au and Cu+Cu heavy ion collisions at RHIC [8].

Experimental approach and accomplishments

A study of the Drell-Yan process via high-energy dimuon measurements at E906, will give the ultimate sensitivity to the stopping power of large nuclei [9]. We have performed detailed simulations to optimize the beam luminosity, target selection, and magnet and detector configurations for the E906 experiment. Realistic event generators were used to simulate full hard scattering events in p+A collisions, including both the Drell-Yan dimuon signal and correlated backgrounds. We then filtered the events through a realistic detector response to identify and reconstruct the Drell-Yan events and derive the quark energy loss values. The Drell-Yan events will be measured in the dimuon mass range of 4.0 – 9.0 GeV where other known physics processes have minimal contributions. With an expected dimuon mass resolution of better than 0.25 GeV, our simulations show that the backgrounds will be well separated from the Drell-Yan signal [10].

To operate at the highest possible beam luminosity, E906 must effectively reject very large backgrounds. We have constructed a new muon identification system for the E906 experiment to trigger and identify the dimuon events of interest. We have used the technology developed by the Muon Radiography Team at LANL to build the full-scale detector. This proportional tube-based detector was refurbished and tested in FY08 and FY09 at Los Alamos, and was then shipped to Fermilab [11]. During 2010, we successfully retested, fixed and conditioned all 50 16-channel modules at Fermilab. Figure 3 shows the performance of one typical module: cosmic ray signal rates versus operating high voltage for all 16 channels. In the plateau region of the high voltage, all channels have a very uniform response to the cosmic rays [12].

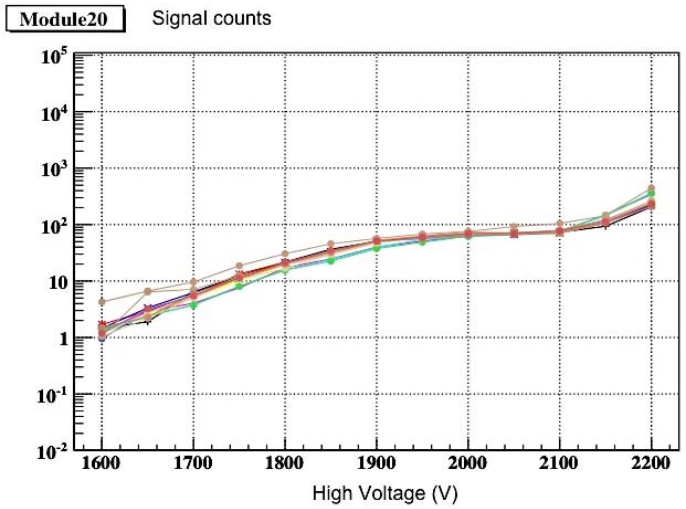

Figure 3. High voltage scan for the detector response with cosmic rays. Shown are signal counts vs applied high voltage from all 16 channels for one muon detector module. The optimal operation high voltage range is measured to be 1800 - 2100V.

One critical experimental issue is to determine the maximal hit rate the detector can handle. We have carried out another simulation to study these background rates. Twenty-six million 120 GeV protons were interacted with a proton target in this very detailed detector simulation that required a lot of CPU time. It took us about one year

to accumulate the needed statistics. The final result shows that the background hit rate per tube could be as high as 1.5 million per second. Therefore, to avoid signal pileup, the response time of the tubes must be unusually fast. We have studied various fast gas mixtures that meet this requirement, while also trying to keep the gas cost down. A satisfactory gas mixture, called MIPP gas, was selected [12]. The resulting count rate versus maximum drift time is shown in Figure 4.

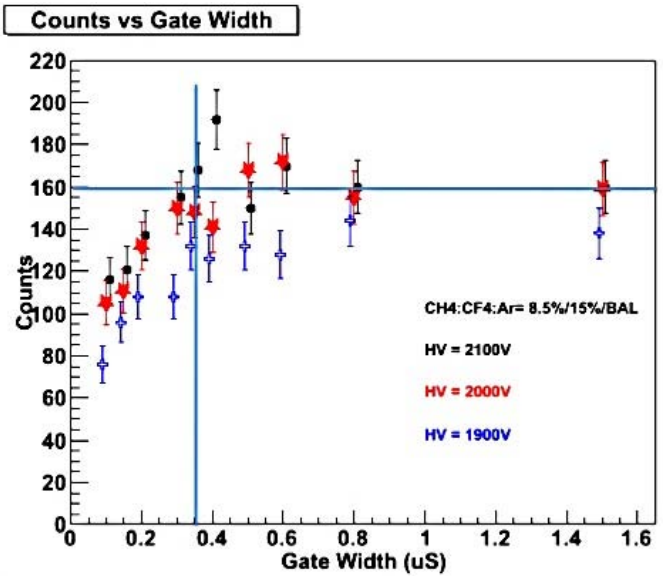

Figure 4. Muon tube maximum drift time study with MIPP gas. Signal counting rates were measured vs allowed maximum drift time (gate width) for 3 different high voltage settings. The maximum drift time was measured to be 0.35 micro-second.

With help from LANL engineers, we have designed and fabricated the module supporting structures using aluminum frames. All parts are presently at Fermilab and ready for final installation, pending the completion of the overall experimental supporting I-beam structure. Figure 5 shows the LANL-contributed muon identification detector modules at the E906 experimental hall, while undergoing testing and conditioning [11,12].

Due to a change in the Fermilab beam operation schedule, the start of E906 was postponed until the end of 2010. We will participate in the first p+p and p+A runs at Fermilab and produce the first direct high-energy quark energy loss measurements in FY11. The experimental project is transitioning to support by DOE funds to accomplish the first measurement of quark energy loss in p+A collisions at Fermilab in the next two years.

Last but not least, this LDRD project has supported the publication of five peer-reviewed papers that include a Physical Review Letter, two Physical Review C publications, a Physics Letters B, and another manuscript to be submitted to Physics Letters B. We have given a total of nine invited and contributed oral and poster presentation that include results from this research. The PI, Ivan Vitev, received a Presidential Early Career Award for Scientists and Engineers (PECASE) in 2009. Benwei Zhang, a key investigator, took a Full Professorship position in his home country at Central China Normal University, Key Laboratory of Quarks and Leptons, in early 2010. Bryon Neufeld, who joined this project more recently, was awarded a Director's Fellowship at LANL.

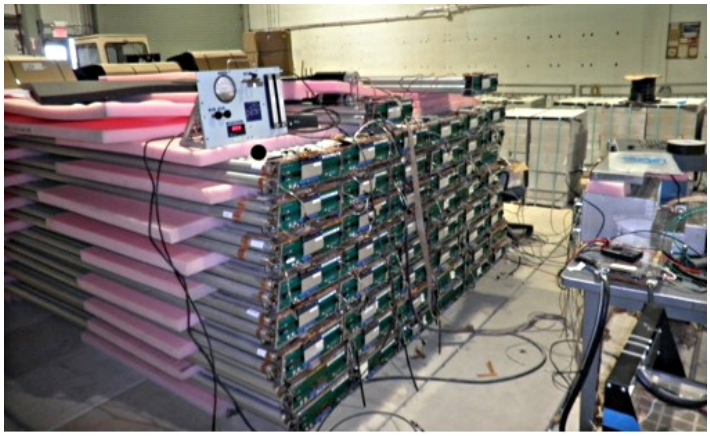

Figure 5. LANL-contributed muon detectors at Fermilab E906 experimental hall for testing and conditioning. Detectors are ready for the final installation.

Impact on National Missions

The theoretical and experimental tools that we developed to investigate and understand subatomic matter were specifically identified as strategic priorities of the LDRD strategic investment plan. Exploration of extreme properties of matter is a cornerstone of the Department of Energy (DOE) nuclear science Long Range Plan and one of the Grand Challenges at Los Alamos - Beyond the Standard Model. The principal strength of this project has been the significant scientific impact on the nuclear physics community at large. Theoretical calculations have established for the first time the stopping power of nuclear matter for quarks and gluons and provided the foundation for a consistent phenomenology of heavy ion reactions. The first unambiguous measurement of quark energy loss in nuclei, resulting from our experimental breakthrough in the use of dimuons, will provide the much-needed "standard candle" for gauging the nuclear response to strongly interacting particles.

References

1. Bethe, H.. Annalen der Physik. 1930. *heory of the passage of fast corpuscular rays through matter.* **5**: 400.

2. Vitev, I., and M. Gyulassy. High p(T) tomography of d + Au and Au+Au at SPS, RHIC, and LHC. 2002. *Physical Review Letters.* **89**: 252301.

3. Reimer, P.. Drell-Yan measurements of nucleon and nuclear structure with the Fermilab main injector: E906. 2006. *E906 Fermilab PAC Proposal.*

4. Vitev, I.. Non-Abelian energy loss in cold nuclear matter. 2007. *Physical Review C (Nuclear physics).* **75**: 064906.

5. Vitev, I., and B. Zhang. Jet tomography of high-energy nucleus-nucleus collisions at next-to-leading order. 2010. *Physical Review Letters.* **104** (13): 132001.

6. McGaughey, P.. Cold nuclear matter effects on QCD processes at fixed target and collider experiments. (Santa Fe, 2-6 Nov. 2010).

7. Neufeld, R., I. Vitev, and B. Zhang. Toward the determination of the shortest radiation length. *Physics Letters B.*

8. Liu, M.. Precision determination of high energy quark energy loss in the Fermilab E906 experiment. Presented at *Fall meeting of the DNP of the APS.* (Waikoloa, 13-17 Oct. 2009).

9. McGaughey, P.. Cold nuclear matter effects on QCD processes at fixed target and collider experiments. Presented at *Division of Nuclear Physics fall meeting.* (Santa Fe, 2-6 Nov. 2010).

Publications

Liu, M.. Future high energy dimuon experiments at Fermilab and JPARC. Invited presentation at *LBL seminar.* (Berkeley, CA, 2007).

Liu, M.. A study of quark energy loss in p+A collisions. Presented at *Quark Matter 2009.* (Knoxville, 29 Mar. - 3 Apr. 2009).

Liu, M.. Precision determination of high energy quark energy loss in the Fermilab E906 experiment. Presented at *Fall meeting of the DNP of the APS.* (Waikoloa, Oct. 13-17).

McGaughey, P.. E906 muon identifier status. Invited presentation at *E906 Collaboration Meeting at Fermilab.* (Batavia, IL, 20-21 June 2008).

McGaughey, P.. Cold nuclear matter effects on QCD processes at fixed target and collider experiments. Presented at *Division of Nuclear Physics fall meeting.* (Santa Fe, 2-6 Nov. 2010).

Neufeld, R., I. Vitev, and B. Zhang. Toward the determination of the shortest radiation length. *Physics Letters B.*

Sharma, R., I. Vitev, and B. Zhang. A light-cone wavefunction approach to open heavy flavor dynamics in QCD matter. 2009. *Physical Review C (Nuclear Physics).* **80**: 054902.

Vitev, I.. Non-Abelian energy loss in cold nuclear matter. 2007. *Physical Review C (Nuclear physics).* **75**: 064906.

Vitev, I.. Theoretical developments in heavy and light flavor energy loss. 2008. In *Quark Matter 2008 .* (Jaipur, India, 4-10 February). Vol. 35, p. 104011. Journal of Physics G: IOP.

Vitev, I.. QCD intersections of nuclear and particle physics at the high-energy frontier. Presented at *Division of Nuclear Physics fall meeting.* (Santa Fe, 2-6 Nov. 2010).

Vitev, I., and B. Zhang. A Systematic study of direct photon production in heavy ion collisions. 2008. *Physics Letters B.* **669**: 337.

Zhang, B.. Theoretical calculations of Drell-Yan production at NLO. Presented at *E-906/Drell-Yan collaboration meeting and DAQ workshop.* (Batavia, 7-8 Jul. 2009).

Zhang, B., and I. Vitev. Direct photon production in d+A and A+A collisions at RHIC. 2009. In *Hot Quarks 2008.* (Estes Park, CO, 17-23 Aug. 2008). Vol. 24, 33 Edition, p. 2649. Modern Physics Letters A: World Scientific.

Entanglement in Quantum Ground States

Michael Chertkov
20080342ER

Abstract
Topological quantum computing is a proposed method for doing Quantum computation that avoids problems with decoherence that currently is preventing other approaches from working. We have proven the existence of topological order in physical systems, such as quantum Hall systems, and have gone a step further to prove robustness of such systems against local perturbations due to imperfections in engineering the underlying quantum interactions. Moreover, we have shown that certain classes of naturally occurring quantum states have efficient representations on classical computers as so called "matrix product states". These advances are of fundamental importance to the future of topological Quantum computing, as well as the evaluation of certain materials in condensed matter physics as reliable resources for quantum computation. This work has also benefited our fundamental understanding of materials and simulation of Quantum systems. We have advanced methods of classical computations related to aforementioned Quantum phenomena but is also guiding further progress in the Quantum Computation Science.

Background and Research Objectives
This project studies the nature of ground states in quantum systems from the point of view of quantum entanglement and topological order. The idea of quantum entanglement is behind the rapidly developing fields of quantum computing and quantum key distribution. Quantum computers that take advantage of entanglement may be able to perform computations that are not tractable on a classical computer. Within the field of quantum computing, the study of quantum entanglement involves looking at very carefully engineered states, which are created by carefully controlling the system. On the other hand, this project looks at the kind of quantum entanglement that is present in naturally occurring systems. We consider the entanglement in ground states of local quantum systems. This offers two possible rewards. First, certain naturally occurring ground states, like those in the quantum Hall effect, have nontrivial entanglement that can be used to do quantum computation, without requiring the careful control required by other approaches. This approach, called topological quantum computation, is possible and potentially a very robust approach to quantum computation due to the insensitivity (topological order) of the relevant quantum states to macroscopic errors. Second, many other naturally occurring ground states have fairly simple entanglement, and can well be described classically. Then, it should be possible to develop novel algorithms to model the ground state and dynamics of these systems using existing classical computers. This can lead to new advances in materials.

Scientific Approach and Accomplishments
Under auspices of this project we had developed new techniques and have derived new results in the following seven subareas:

Stability of Topological Quantum Order.
Using locality properties of a Hamiltonian with an energy gap (spectral gap) between the lowest energy states and the first excited states, we proved robustness of the ground state subspace against external perturbations. In particular, our result proves that any Hamiltonian comprised of the sum of commuting interactions can withstand up to a constant strength (independent of system size) quantum perturbation on each local region of the lattice, without the energy gap closing. In other words, Hamiltonians such as Kitaev's toric code - the most well-known candidate for a quantum memory - have ground state subspaces that are not only topologically robust against internal errors ("flips" between the degenerate ground states encoding the logical qubits in the memory), but also robust against external perturbations that may excite any one of them to the higher energy sectors!

The Quantum Hall Effect Revisited.
For T = L x L, a finite subset of the two dimensional lattice, let H denote a Hamiltonian with periodic boundary conditions, finite range, finite strength interactions and a unique ground state with a non-vanishing spectral gap. Using a tight-binding model of fermionic interactions, we show that the celebrated Quantum Hall Conductance

is quantized in integer multiples of e^2/h. Our main tools involve Lieb-Robinson bounds for quasi-adiabatic evolutions. Our proof of quantization removes the long-standing assumptions of persistent spectral gap throughout the adiabatic evolution of the ground state, as well as any averaging of the conductance over flux space. Instead, we prove quantization up to corrections that decay as a sub-exponential in the linear length L of the system.

Approximating the ground state of gapped quantum spin systems.
We consider quantum spin systems defined on finite sets V equipped with a metric. In typical examples, V is a large, but finite subset of Z^d. For finite range Hamiltonians with uniformly bounded interaction terms and a unique, gapped ground state, we demonstrate a locality property of the corresponding ground state projector. In such systems, this ground state projector can be approximated by the product of observables with quantifiable supports. In fact, given any subset, X, of V the ground state projector can be approximated by the product of two projections, one supported on X and one supported on X^c, and a bounded observable supported on a boundary region in such a way that as the boundary region increases, the approximation becomes better. Such an approximation was useful in proving an area law in one dimension, and this result corresponds to a multi-dimensional analogue.

Matrix Product States for dynamical simulation of infinite chains.
We proposed a new method for computing the ground state properties and the time evolution of infinite chains based on a transverse contraction of the tensor network. The method does not require finite size extrapolation and avoids explicit truncation of the bond dimension along the evolution. By folding the network in the time direction prior to contraction, time dependent expectation values and dynamic correlation functions can be computed after much longer evolution time than with any previous method. Moreover, the algorithm we propose can be used for the study of some non-invariant infinite chains, including impurity models.

Light Cone Matrix Product.
We show how to combine the light-cone and matrix product algorithms to simulate quantum systems far from equilibrium for long times. For the case of the XXZ spin chain at Delta=0.5, we simulate to a time of approx 22.5. While part of the long simulation time is due to the use of the light-cone method, we also describe a modification of the iTEBD algorithm with improved numerical stability, and we describe how to incorporate symmetry into this algorithm. While statistical sampling error means that we are not yet able to make a definite statement, the behavior of the simulation at long times indicates the appearance of either “revivals” in the order parameter as predicted previously or of a distinct shoulder in the decay of the order parameter.

Fermions and Loops on Graphs.
This research is the first in the series devoted to evaluation of the partition function in statistical models on graphs with loops in terms of the Berezin/fermion integrals. We focus on a representation of the determinant of a square matrix in terms of a finite series, where each term corresponds to a loop on the graph. The representation is based on a fermion version of the Loop Calculus, previously introduced by the authors for graphical models with finite alphabets. Our construction contains two levels. First, we represent the determinant in terms of an integral over anti-commuting Grassman variables, with some reparametrization/gauge freedom hidden in the formulation. Second, we show that a special choice of the gauge, called BP (Bethe-Peierls or Belief Propagation) gauge, yields the desired loop representation. The set of gauge-fixing BP conditions is equivalent to the Gaussian BP equations, discussed in the past as efficient (linear scaling) heuristics for estimating the covariance of a sparse positive matrix.

Permanents and Loops.
We consider computation of permanent of a positive non-negative matrix, or equivalently the problem of weighted counting of perfect matchings (evaluation of the Partition Function) over a complete bipartite graph. The problem is known to be sharp-P-hard. Stated as a graphical model, this weighted counting problem allows exact Loop Calculus representation in terms of a minimum of the non-convex bounded Bethe Free Energy functional over marginal beliefs. This Bethe Free Energy optimization problem can be solved by an iterative and distributed message-passing algorithm of the Belief Propagation type. We show that the Loop Calculus multiplicative correction, completing the Belief Propagation estimate for the Partition Function is expressed in terms of a new permanent. We give two alternative derivations of the formula, a direct one based on the Bethe Free Energy and another one utilizing Loop Series transformed in accordance with the Ihara graph-zeta function approach. Assuming that the matrix of the Belief Propagation marginal’s is calculated, we provide two lower bounds and one upper-bound to estimate the multiplicative term. Two complementary lower bounds, one based on the Gurvits-van der Waerden theorem and the other based on the relation between permanent and determinant. We observe that the Gurvits-van der Waerden theorem is invariant with respect to the Belief Propogation transformation, as it gives identical lower bounds when applied to the original permanent and the transformation-induced permanent. We also derive upper bound, based on the Godzil-Gutman representation for permanent of non-negative matrix in terms of an average of a determinant squared.

Impact on National Missions
This project supported the DOE Office of Science Mission in Basic Energy Sciences by improving our understanding of ground state properties of quantum systems such as in materials science and quantum chemistry, and by enhancing

our understanding of which systems are useful for building a quantum computer.

Publications

Chernyak, V., and M. Chertkov. Fermions and loops on graphs: I. Loop calculus for determinants. 2008. *JOURNAL OF STATISTICAL MECHANICS-THEORY AND EXPERIMENT.* : P12011.

Chernyak, V., and M. Chertkov. Fermions and loops on graphs: II. A monomer-dimer model as a series of determinants. 2008. *JOURNAL OF STATISTICAL MECHANICS-THEORY AND EXPERIMENT.* : P12012.

Chertkov, M., R. Teodorescu, and V. Chernyak. Belief propagation and loop series on planar graphs. 2008. *Journal of Statistical Mechanics.* (P05): 003.

GoÃÅmez, V., H. Kappen, and M. Chertkov. Approximate inference on planar graphs using loop calculus and belief propagation. 2010. *Journal of Machine Learning Research.* **11**: 1273.

Hastings, M. B.. Topology and phases in fermionic systems. 2008. *JSTAT.* **01**: L001.

Hastings, M. B.. Observations outside the light-cone: algorithms for non-equilibrium and thermal states. 2008. *Physical Review B.* **77**: 144302.

Hastings, M. B.. A counterexample to additivity of minimum output entropy. 2009. *Nature Physics.* **5** (4): 237.

Watanabe, Y., and M. Chertkov. Belief propagation and loop calculus for the permanent of a non-negative matrix. 2010. *JOURNAL OF PHYSICS A-MATHEMATICAL AND THEORETICAL.* **43** (24): 242002.

Wolf, M. M., F. Verstraete, M. B. Hastings, and J. I. Cirac. Area laws in quantum systems: mutual information and correlations. 2008. *Physical Review Letters.* **100**: 070502.

CP-violating Moments of Atoms and Nuclei

Anna C. Hayes-Sterbenz
20080424ER

Abstract
A permanent electric dipole moment (EDM) of a physical system would indicate direct violation of time-reversal (T) and parity (P), and, thus, CP (charge conjugation and parity) violation through the CPT theorem.

Presently there are several international experimental programs pushing the limits on EDMs in atoms, nuclei, and the neutron to regimes of fundamental theoretical interest. The Standard Model (SM) predicts values for the EDMs of these systems that are too small to be detected in the foreseeable future, and hence a measured nonzero EDM in any of these systems is an unambiguous signal of a new source of CP violation and for physics beyond the SM. In this project we quantified the magnitude of CP-violating moments of those atoms and nuclei of experimental relevance and related these to the EDM of the neutron. Our motivations were directly coupled to the advances in measurement techniques and our results impact LANL EDM project, and the newly proposed EDM measurements at Brookhaven National Laboratory for charged systems such as the proton and deuteron.

Background and Research Objectives
To extract fundamental physics from EDM measurements requires accurate calculations of the EDMs in terms of the underlying CP-violating interaction. This project focused on four key theoretical issues that needed be addressed:

1. The LANL *neutron* EDM experiment is aimed at measuring the dipole moment of the the neutron (d_n) to an unprecedented accuracy of 10^{-28} *e cm*. This requires that the measurement be made with respect to another system that is know to have a negligible EDM. For this the LANL neutron EDM project uses the atomic EDM of ^{3}He. The ^{3}He acts as a polarizer and co-magnetometer in the experiment. A rigorous theoretical verification that the EDM of ^{3}He is not a significant (unknown) systematic background to the measurement is crucial.

2. A new experimental scheme for measuring EDMs of *nuclei* (stripped of their atomic electrons) in a magnetic storage ring is being developed at several heavy ion laboratories, with the largest effort being tat Brookhaven National LAboratory. In this scheme the EDM of the deuteron and of ^{3}He *nuclei* could be measured to an accuracy of better that 10^{-27} *e cm*, which is an order of magnitude better that the present limit on the neutron EDM.

3. If an *atomic* system is not stripped of its electrons, a nuclear EDM is reduced by what is known as Schiff screening. However, atomic EDM measurements are sensitive to a higher-order volume-average CP-violating moment: the Schiff moment. Reevaluation of the full quantum expression for the Schiff moment is needed.

4. The nuclear Schiff moment is predicted to be very enhanced in *octupole deformed nuclei*, and new atomic EDM experiments are planned at Argonne Natl. Lab and TRIUMF for Radium and Radon. Detail calculations for these systems and for the spherical nucleus ^{199}Hg (for which the best atomic EDM measurement exists) within the same theoretical framework are needed to evaluate the relative merits of these measurements.

Scientific Approach and Accomplishments
EDM of 3He
Of the atoms and nuclei examined in this project, 3He was the most important because its relevance to both the neutron EDM experiment and the newly proposed magnetic storage ring experiments at Brookhaven.

To calculate the EDM and the Schiff moment of ^{3}He requires knowledge of the ground state and all the excited states of the nucleus. The full problem cannot be calculated exactly in any models, and it required that we invoke an approximation to the structure of the states of ^{3}He. For this, we employed the no-core shell model, which is an *ab initio* approach to the nuclear many-body problem for light nuclei. In this approach, one starts from realistic two-nucleon or two- plus three-nucleon interactions and performs many-body calculations using a finite harmonic-oscillator basis. The model has the

advantage that it can be used to calculate the structure of states in nuclei using any nuclear interaction, and its accuracy has to be determined by the convergence of the calculations.

An EDM in a nucleus can arise from two main contributions:

- The intrinsic EDMs of the proton and neutron inside the nucleus.
- The two-body *PT*-violating interaction between nucleon.

Thus, our calculation of the EDM of 3He required knowledge of both the individual EDMs of the nucleons and the *PT*-violating nuclear force. These very different quantities can only be related if some understanding exists of both the origin of the symmetry violation and its expression in strong-interaction observables. Constructing an effective field theory (EFT) that incorporates the symmetry violation, as well as the dynamics underlying the usual strong-interaction physics in nucleons and nuclei, provides a suitable framework. The most straightforward model is one in which the PT-violating is described by an interaction involving the exchange of mesons between the nucleon in the nucleus. For this we used a formulation in terms of a one-meson-exchange model, Including π-, ρ-, and ω-meson exchanges.

We solved the three-body problem in an ab initio no-core shell model framework, which requires the diagonalization of the nucleon-nucleon interaction in a truncated harmonic oscillator basis. Several high-precision nucleon-nucleon interactions are available and we compared the results from three of these.

The results for the EDM of 3He were found to be somewhat sensitive to the strong interaction chosen, we found that the pion-exchange dominated the EDM of He-3, in all cases. Our results suggest that a measurement of He-3 EDM would be complementary to the currently planned neutron and deuteron experiments, and would constitute a powerful constraint to the models of the pion-exchange P- and T-violating interactions.

Electric dipole polarizability of hydrogen and helium isotopes

A comparison between the model predictions for electric polarizbility and the available experimental data provides a strong test of our predicted EDM for 3He. This is because the operators involved in the two processes are very similar. The electric polarizability is an electromagnetic sum-rule that is measured in photo-absorption on the nucleus. In adition to providing a test of our EDM calculation, electric polarizatilities are important corrections that need to be taken into account for atom physics calculations of hyperfine transitions.

Theoretical calculations of transition frequencies in hydrogenic atoms and ions have reached a level of precision where small corrections due to nuclear structure and dynamics are necessary to interpret the results of high precision measurements in these systems. This has largely been the result of recent improvements in quantum electrodynamic (QED) calculations. In many cases the experimental errors and estimated sizes of uncalculated QED corrections are much smaller than the nuclear corrections, and one can thus use those measurements (corrected for QED effects) as an experimental determination of various nuclear quantities. Perhaps the most important of these is the electric dipole polarizbility of the nucleus.

We computed the 3H, 3He, and 4He electric dipole polarizabilities starting from a nuclear Hamiltonian derived within the framework of (QCD-based) Chiral Perturbation Theory (including the Coulomb interaction between the protons). Calculations for the electric polarizability of 3H and 3He are in agreement with the experimental determinations. Compared to previous results, we showed that direct calculations of the electric polarizability of 4He using modern nuclear potentials are smaller than published values calculated using experimental photoabsorption data. This work suggests that our estimates for the EDM of 3He are reasonably accurate.

Structure of the particle-hole amplitudes in no-core shell model wave functions

As a final check on the validity of the no-core shell model used to predict the relative magnitude and importance of the EDM of 3He, we compared the prediction of the model with experimental electron scattering data. For the lighest nuclei such as the deuteron and 3He, the model give quite accurate prediction for the electron scattering form factors. But for heavier nuclei, from mass 6 to 12, we uncovered a previously unnoticed flaw with the model

We studied the structure of the no-core shell model wave functions for Li-6 and C-12 by investigating the ground state and first excited state electron scattering charge form factors. In both nuclei, large particle-hole (ph) amplitudes in the wave functions appear with the opposite sign to that needed to reproduce the shape of the electron scattering form factors, the charge radii, and the gamma-ray transition strengths for the lowest two states. The underlying source of the problem seems to lie in the lack of self-consistentcy in the model. In the case of 3He, the calculations can be carried out using sufficiently large models spaces to overcome the problem.

The CP-violating Schiff moment of 3He

If 3He had a large screen nuclear CP-violating Schiff moment, it would manifest itseld in an atomic EDM for 3He, and cause an unaccounted for background in LANL's neutron EDM experiment.

There are two mechanisms for P,T-violation in a nucleus.

One is driven solely by the individual EDMs of nucleons: both neutrons and two protons in 3He. We have shown that, to a good approximation, the EDM and the magnetic moment of the 3He nucleus are carried entirely by the neutron. This contribution is strongly screened by the atomic electrons of 3He and is tiny. The other mechanism leading to P,T-violation in a nucleus is driven by P,T-violating nuclear forces, shown in our earlier calculations to be dominated by one-pion-exchange. We calculated the Schiff moment contribution from a PT-violating one-pion exchange force to be 10^{-9} times smaller that that of the bare neutron.

There is also a contribution to the atomic EDM of 3He from the nuclear magnetic moment. The external electric field forces the electron cloud of the 3He atom to be non-spherical, and this allows the magnetic moment of the nucleus to interact with the magnetic field created by the orbiting electrons, leading to an atomic EDM. This contribution to the atomic EDM of 3He also turned out to be tiny, 10-7 times the EDM of the neutron.

Thus, we concluded that PT-violating moments of the 3He atom can be safely neglected in neutron EDM experiments that used 3He as a polarizer and/or co-magnetometer.

Impact on National Missions

The are several multi-million dollar experiments and proposed experiments aimed at searching for sources of EDMs that are not allowed by the Standard Model of Particle Physics. If a non-zero EDM is measured in any of these experiments it would signal an unambiguous signal of a new source of CP violation and hence fundamentally change our understanding of symmetry violation in the forces of nature. This LDRD project examined the relative merits of these different experiments and quantified important background signals for these. In particular, we find that a measurement of the EDM of stripped 3He atoms would probe a new and unique combination of the CP-violating interaction.

In the course of this work, we uncovered a significant short-coming with the no-core shell model, a model that has been proposed for the calculation of thermonuclear reactions relevant to NNSA's mission. These studies suggest that the no-core shell model is valid for light nuclei up to 4He, but that it introduces serious self-consistency problems for nuclei heavier than mass 4.

Publications

Hayes, A. C., J. L. Friar, and P. Moller. Splitting sensitivity of the ground state and the 7.6 eV isomeric states of 229Th. 2008. *Physical Review C.* **78** (02): 024311.

Hayes, A. C., and A. A. Kwiatkowski. Structure of the Particle-hole Amplitudes in the no-core shell model. 2010. *Physical Review C.* **81** (5): 054301.

Hayes, A. C., and J. L. Friar. Sensitivity of nuclear transition frequencies to temporal variation of the fine structure constant ot the strong interaction. 2007. *Physics Letter B.* **650**: 229.

Stetcu, I., C. P. Liu, J. L. Friar, A. C. Hayes, and P. Navratil. Nuclear Electric Dipole Moment of 3He. 2008. *Physics Letters B.* **665**: 168.

Stetcu, I., C. P. Liu, J. L. Friar, A. C. Hayes, and P. Navratil. Nuclear electric dipole moment of 3He. 2008. In *Capture Gamma-Ray Spectroscopy and Related Topics. 13th International Symposium* . (Cologne, Germany, 25-29 Aug. 2008). Vol. 1090, p. 273. USA: AIP Conferenc Proceedings.

Stetcu, I., S. Quaglioni, J. L. Friar, A. C. Hayes, and P. Navratil. Electric dipole polarizabilities of hydrogen and helium isotopes. 2009. *Physical Review C.* **79** (6): 064001.

Ultrafast Nanoplasmonics for Photonics and Quantum Control at the Nanoscale

Anatoly V. Efimov
20080473ER

Abstract

Fundamental optical diffraction laws prohibit localization of light on spatial scales much smaller than the wavelength (about 1 micrometer). This fact limits the resolution of optical microscopes, precludes optical addressing of individual molecules, nanoparticles or other quantum systems and restricts the miniaturization of photonic circuits. Nevertheless, the diffraction limit can be overcome by using light, which is bound to metallic surfaces and nanostructures – so called surface plasmons (SP) – local fields, which are not subject to the laws of free-space optics. The area of research that studies surface plasmons – plasmonics – is a rapidly growing field that promises practical solutions in optical nanotechnology, sensing, energy, chemistry and materials science.

This project addresses fundamental scientific aspects of generating, manipulating, controlling and using surface plasmons on the sub-wavelenght scale and their interaction with quantum systems. Our specific challenge is to learn how to manipulate these fields, not only spatially, but also, and more importantly, temporally, through studying broadband response of the nanostructures . The temporal aspect in field design is extremely important for ultrafast processes in nature and technology, such as controlling molecular dynamics, steering chemical reactions, selective sensing, signal processing and communication. In order to better understand such processes, we use ultrashort femtosecond optical pulses in our experiments to excite and measure the ultrafast dynamics of the localized fields. It is important to realize that femtosecond time scales are characteristic to many processes in nature, such as fundamental vibrations in molecules and crystals, isomerization reactions responsible for vision and energy transfer between mesosystems. The focus of this project on controlled excitation and manipulation of broadband and ultrafast surface plasmons is a new direction in plasmonics research.

Background and Research Objectives

Optical properties of plasmonic (metallic) nanostructures are substantially more rich as compared to the more conventional all-dielectric systems (dielectric waveguides, optical fibers, linear and nonlinear photonic devices) commonly used to manipulate light. This is because the electromagnetic radiation couples much more strongly to the conduction electrons in metals, whereas in dielectrics the field only slightly polarizes the bound electrons. This enhanced coupling leads to formation of surface-bound field modes - surface plasmons - with unusual dispersion, polarization, confinement properties and valuable local field enhancement and subwavelength localization effects. Often times quantum nature of the electrons in the metal cannot be ignored and thus quantum methods need to be used in the nanostructure design procedure. External excitation of a given nanostructure with an optical field forces the electrons to move, but this motion is restricted by the geometry of the nanostructure. The accumulation of electronic density in certain areas and reduced density in others results in the formation of the local field, which may be much stronger than the external field and be localized to beyond the diffraction limit. Furthermore, the reaction of the nanostructure to a complex laser pulse may involve delayed and nonlinear response. These and other properties of plasmonic nanostructures continue to provide fertile ground for research.

A number of advances that were demonstrated in recent years regarding spatial control of SP fields relied mostly upon the design of metallic nanostructures, which ranged from colloidal metallic nanoparticles to focused ion beam (FIB) milled optical resonant nanoantennas. Waveguiding structures supporting propagating surface plasmon-polaritons (SPP) were demonstrated as well with spatial field localization visualization using, e.g., near-field optical scanning techniques. Interestingly, the vast majority of experiments were performed using continuous wave light sources neglecting any temporal dimension of the problem.

It is evident, however, that new applications of SPs or SPPs require temporal control over localized fields. For instance, plasmonic data processing units will be competitive only if they are faster than electronics, currently limited to gigahertz clock rates. Breaking out of scaling limitations imposed on conventional microelectronics

to gain speed is one primary motivation underpinning the goal to develop optical-plasmonic based devices. Thus, to be viable, plasmonic devices must operate with pico- or femto-second pulses as the carriers of information. Similarly, quantum computers, although at first may not need be this fast, require shaped electromagnetic fields to load initial program, which again highlights the temporal aspect and the need for temporal control of the localized fields. Finally, the characteristic time of operation of future nanomachines is dictated by typical vibrational-rotational molecular frequencies, with characteristic time scales in femto- or picosecond range. Hence, the ability to create, manipulate and characterize surface plasmons in both space *and* time is needed to usher the development of new types of miniaturized photonic devices.

Implementation of these concepts requires the development of coherent sources of broadband, tailored localized plasmonic fields, SPP waveguides for delivery of EM energy to a specific nano-spot, and linear and nonlinear SPP processing elements. Such capabilities require an understanding of the dynamic interactions and properties of SPPs, as well as the development of experimental techniques to controllably tailor, manipulate, and characterize their properties.

It is also important to rely on numerical modeling for the design of proper plasmonic nanostructures possessing a specific functionality. Thus, proper theoretical analysis was one of the objects in this work. Further, manufacture of quality plasmonic nanostructures with subwavelength features for photonic applications requires nanotechnology tools and specific expertise, the development of which was among our objectives. The development of the methods and the tools for plasmon field characterization in space and time with high sensitivity in a broad optical spectral bandwidth was also one of our objectives. Following the development of the machinery for plasmonic research our goal was to investigate the ways to control the local SP field parameters in spatial, spectral and temporal domains using flexibility in structure design and external excitation conditions.

Scientific Approach and Accomplishments

Plasmonic structures for subwavelength light confinement either in waveguiding or localized modality are infinitely more rich as compared to previously studied dielectric structures. Thus, theoretical analysis and numerical modeling are of primary importance to correct and timely design of the most effective geometries. Our theoretical investigations focus on design and characterization of 1) efficient plasmonic antennas; 2) novel plasmonic lattices; 3) temporal control of local SP fields; 4) improved plasmon-polariton waveguides with increased mode confinement and propagation lengths. From the experimental standpoint the manufacture of quality metallic nanostructures is of prime importance. To this end we use advanced nanotechnology tools to 5) prepare metallic slot and strip waveguides waveguides, dipole nanoantennae on evaporated or single-crystal metal films using electron-beam lithography and focused ion beam milling. Linear and nonlinear properties of SPPs 6) are subsequently studied with spectroscopic, interferometric and time-resolved techniques.

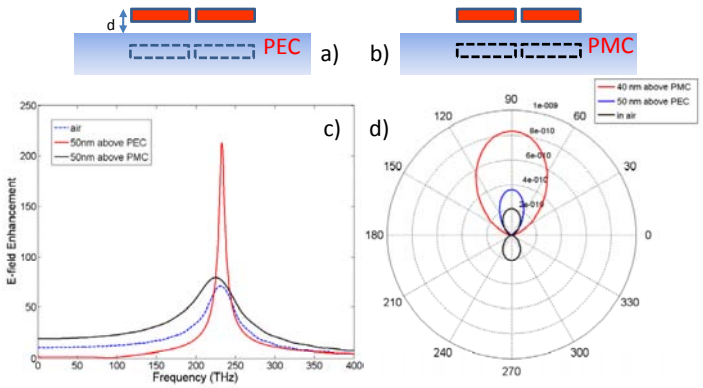

Figure 1. Performance of optical dipole nano-antennae. a) antenna above a perfect electric conductor (PEC); b) antenna above a perfect magnetic conductor (PMC); c) enhancement of the electric field in the antenna gap as a function of optical frequency for a single antenna in air (dashed blue), above PEC (solid red line) and above PMC (solid black curve); d) directional diagrams showing enhanced emission of the PMC-coupled antenna.

1. In the quest to control the response of a plasmonic nanostructure we devised a scheme to shape and actively tune the resonant spectrum of optical antennas and to increase their quality factor, an important characteristic of any resonant structure. By shaping the optical antennas' response spectrum, we can control the absorption, emission and scatter spectra (as well as the corresponding rates) of quantum objects coupled to the antenna. The control mechanism is based on interaction of optical antennas with the substrate above which the antennas are located, Figure 1. The substrate can be a layer of metal or properly designed dielectric multilayer stack, depending on properties sought. The operation of this structure is based on the delayed response of the antenna to the radiation reflected off of the substrate and interference between the radiation from the antenna and its image. This enables shaping the resonant spectrum by controlling the substrate's reflection phase and amplitude as a function of frequency. For example, Figures 1(a) and 1(b) show optical dipole antennas located above a perfect electric conductor and perfect magnetic conductor respectively. In the former case the local field is strongly enhanced because the antenna's radiation is suppressed, while in the latter case the emission is enhanced because the antenna and its image radiate in-phase in this case. More complicated behavior is observed when the antenna is positioned above a multilayer dielectric stack.

2. The behavior of SPs can be controlled through coupling of individual nanostructures, leading to collective response, similar to solid-state crystal materials or photonic crystals. For example, periodic array of metal-dielectric waveguides can be created to exhibit such effects as diffraction anomalies, near-dispersionless band structure, diabolic points, etc [1]. In fact, our findings suggest a deep mathematical analogy between collective SP excitations of such systems and electronic properties of graphene and massless Dirac particles in Quantum Electrodynamics. Using these analogies, certain SP modes can be assigned such characteristics as pseudo-spin and chirality using which a deeper understanding of the SP dynamics is gained [2]. These results could open new directions in light manipulation on the nanoscale.

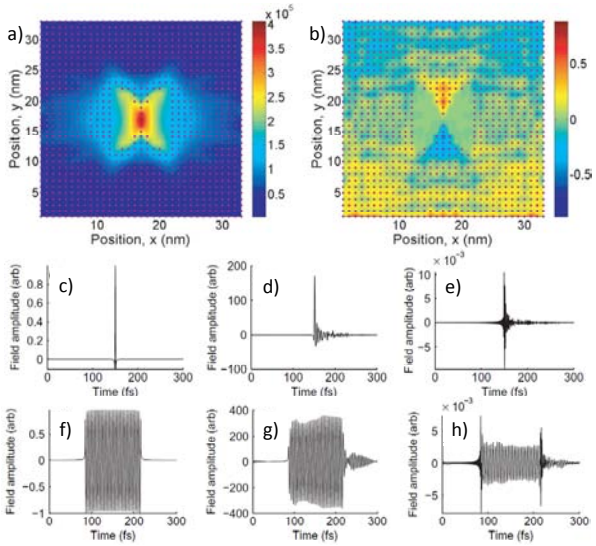

Figure 2. Temporal control of the local field in a bowtie metallic nanostructure. a) normalized local field intensity; b) the real part of the induced electron density distribution; c) Gaussian pulse duration of 1 fs. d) temporal profile of the local field excited in the center of the nanostructure by the pulse (c); e) temporal profile of the external field required to excite the local field of shape (c). Similarly: f) rectangular external field pulse with duration of 100 fs. g) temporal profile of the local field excited by the pulse (f); h) temporal profile of the external field that excites the local field of shape (f).

3. Controlling the temporal response of a plasmonic nanostructure to a given incident optical pulse is another important area of our research. If enhanced local SP fields are to be used in controlling the behavior of atoms, molecules and other quantum systems, then temporal control of the fields themselves is required. Just like the spatial distribution of local field intensity and polarization may not resemble the incident (drive) field, its temporal waveform may significantly differ from the drive as well. With this in mind we studied the ways to control the temporal profile of the local electric field in the vicinity of a small doped semiconductor or metal nanostructure [3]. Unlike in the case of control in a gas or liquid phase, the collective response of electrons in the nanostructure may significantly enhance different frequency components of the field due to the excitation of local (plasmonic) resonances. This enhancement strongly depends on the geometry of the nanostructure and can substantially modify the temporal profile of the local field. We solved the direct problem of finding complex local field given the external field, as well as the inverse problem of finding the external field to generate an arbitrary target temporal profile of the local field. For a given geometry it is found that the nanostructure acts as a phase-amplitude filter and the inverse problem is solved in the first approximation by dividing the target local field by this filter function of the nanostructure. Figure 2 shows some examples of the solutions of the direct and inverse problem for a metallic nanostructure of bow-tie shape. The local field distribution, Figure 2(a) and the charge density, Figure 2(b) are computed with a full quantum description of the electrons coupled to classical field. It is evident that both the direct and the inverse problem can be solved for a known nanostructure.

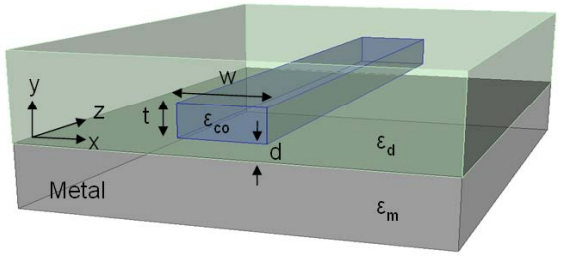

Figure 3. Hybrid metal-dielectric waveguide for efficient subwavelength confinement and propagation of terahertz SPP mode.

4. Efficient subwavelength guiding is of great importance for future development of photonics and terahertz circuits for signal processing, sensing and spectroscopic applications. Usually strong confinement of an SPP mode also results in high propagation loss. With this in mind we studied the hybrid waveguide structure consisting of coupled metallic and dielectric strips in the terahertz region, Figure 3. It was found that compared to metallic microstrip waveguides, the hybrid waveguide offers one order of magnitude longer (!) propagation length while still maintaining subwavelength mode confinement [4]. The investigated waveguide structure could be used as a basic building block for terahertz integrated circuits where generation, detection, and modulation components are all integrated on a single chip. This structure is also promising for efficient terahertz generation via optical rectification of guided modes.

5. For the experimental component of the project we prepare plasmonic nanostructure samples using electron lithography and FIB milling on either evaporated or single-crystal gold films, Figure 4. Although the evaporated gold films are easy to produce, the granular structure of these films leads to increased loss due to field scattering at the grain boundaries. This extra loss adds to the already substantiall intrinsic loss due to the imaginary part of the dielectric function of the metal. Thus, we also developed an in-house method to grow single-crystal gold film flakes with typical dimensions exceeding tens of micrometers. Subsequently, FIB is used to machine nanometer-scale features in individual flakes.

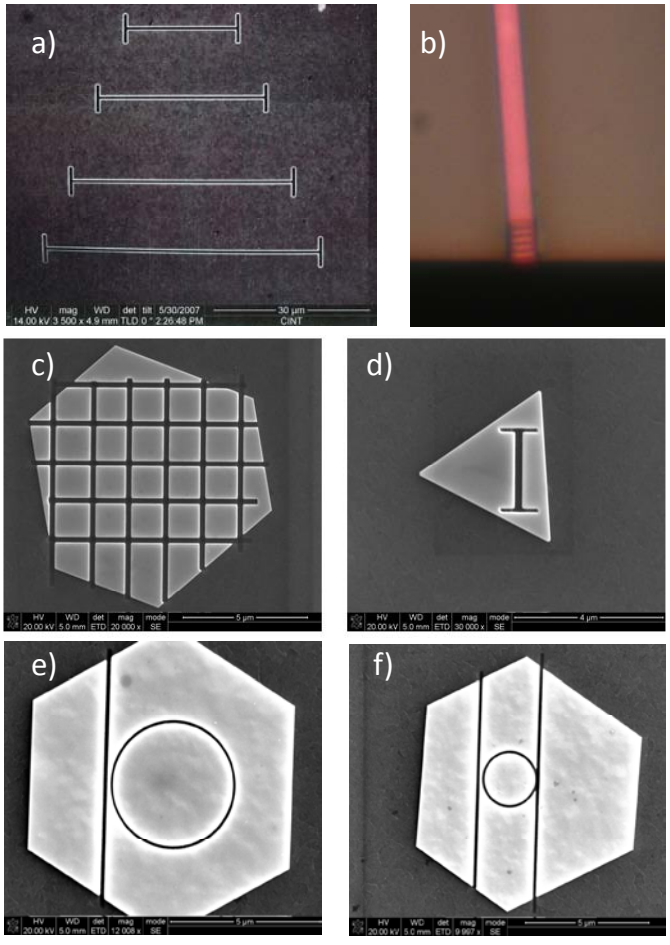

Figure 4. Examples of plasmonic nanostructures: a) slot waveguide in evaporated gold film; b) ridge silicon waveguide with diffraction grating for in- and out-coupling of light; c) and d) FIB-milled slots in single-crystal gold films; e) and f) plasmonic waveguide coupled to a ring resonator FIB-milled in single-crystal gold films.

6. Broadband response of the prepared plasmonic nanostructures was studied in a range of spectroscopic, interferometric and time-resolved systems. For example, Figure 5 shows SEM and optical dark-field images of a pair of plasmonic nanostructures, along with scattered spectra measured in a total-internal reflection microscope system. In Figure 5(a) a periodic array of FIB-milled features at the center of a single gold nanowire forms a Bragg-type resonator. The scattered spectrum displays a strong resonance corresponding to the characteristic period of the array. Similarly, the example spectrum shown in Figure 5(b) has a periodic structure, which in this case indicates the presence of Fabry-Perot type resonances in the short plasmonic waveguides.

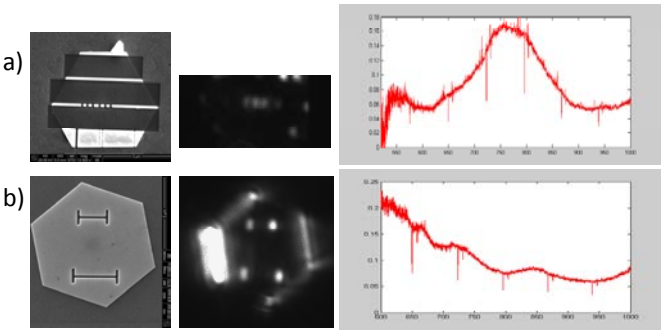

Figure 5. Broadband white-light excitation of a) gold nanowire with Bragg-type resonator FIB-milled at the center; b) slot waveguides of different lengths. Left to right: SEM image, optical image, recorded dark-field spectrum scattered by the nanostructure.

Impact on National Missions

This project supports the DOE missions of the Office of Science and contribute to Threat Reduction and Energy Security missions by enhancing our understanding of the fundamental behavior of electromagnetic fields (light) localized to the nanoscale as well as their interactions with quantum systems for sensing, energy, materials science, signal processing and communications applications.

References

1. Nam, S. H., A. Taylor, and A. Efimov. Diabolical point and conical-like diffraction in periodic plasmonic nanostructures. 2010. *OPTICS EXPRESS.* **18** (10): 10120.

2. Nam, S. H., A. J. Taylor, and A. Efimov. Dirac dynamics in one-dimensional graphene-like plasmonic crystals: pseudo-spin, chirality, and diffraction anomaly. To appear in *Optics Express.*

3. Grigorenko, I., and A. Efimov. Control of the temporal profile of the local electromagnetic field near metallic nanostructures. 2009. *New Journal of Physics.* **11** (10): 105042 (20 pp.).

4. Nam, S. H., A. Taylor, and A. Efimov. Subwavelength hybrid terahertz waveguides. 2009. *OPTICS EXPRESS.* **17** (25): 22890.

Publications

Grigorenko, I., and A. Efimov. Control of the temporal profile of the local electromagnetic field near metallic nanostructures. 2009. *New Journal of Physics.* **11**: 105042.

Nam, S. H., A. Taylor, and A. Efimov. Diabolical point and conical-like diffraction in periodic plasmonic nanostructures. 2010. *OPTICS EXPRESS.* **18** (10): 10120.

Nam, S. H., A. Taylor, and A. Efimov. Subwavelength hybrid terahertz waveguides. 2009. *OPTICS EXPRESS.* **17** (25): 22890.

Probing Physics Beyond the Standard Model with Supernovae

Alexander Friedland
20080636ER

Abstract

One of the greatest challenges of today's science is to find new physics beyond the Standard Model (BSM). Although there are very strong indications that the Standard Model is incomplete, no single preferred scenario has emerged, necessitating a broad search strategy. In addition to collider experiments, an important part in this search is played by astrophysical systems, such as stars and especially supernovae. The extreme conditions in these objects cannot be reproduced on earth, making it possible to test scenarios of new physics that would otherwise remain inaccessible. The goal of this project was to identify BSM scenarios that cause observable effects in a supernova (such as the neutrino signal), or in its progenitor star. This required estimating astrophysical uncertainties, using a combination of analytical arguments and detailed numerical models. We have established that the entire class of BSM models, in which the photon can escape into extra dimensions, can be ruled out by considering the cooling rates in supernovae and red giant stars. We have also constrained the value of the neutrino magnetic moment, based on the changing it would have on stellar evolution. We have modeled the energy and lepton number transport in a collapsed supernova core and estimated the effect of the nonstandard neutrino interactions on it. We have found that convection in the core can have a significant impact on the cooling timescales of the central object. While this may mask the effects of the nonstandard interactions, it is in itself a significant finding. We have discovered that very precise bounds on the nonstandard interactions could be obtained from modeling the collective oscillations of supernova neutrinos. Our code to model collective oscillations, and the set of supercomputer runs, are at this point the most advanced in the world.

Background and Research Objectives

On the smallest scale probed, the Universe is made up of elementary particles, such as electrons, quarks, muons, neutrinos, etc. The interactions between them are described by the Standard Model of particle physics that includes the strong, weak, and electromagnetic forces. Despite its successes, the Standard Model is known to be incomplete. It does not include quantum theory of gravity; it has no place for the Dark Matter or Dark Energy that permeate our Universe; it did not predict the mass of the neutrino, which has recently been demonstrated to be nonzero in many oscillation experiments; finally, on a more technical level, it predicts an extremely unattractive tune-tuning of the Higgs particle mass. All in all, there are extremely compelling reasons to believe that the Standard Model is simply an effective theory and that a more complete fundamental picture of the world is awaiting discovery.

Traditionally, particle physics has been studied in collider experiments. Particles are accelerated to high energies and collided inside a detector, to produce more massive, unstable particles that often live for a tiny fraction of a second. To reach higher energies requires ever-bigger accelerators. The Large Hadron Collider currently operating in Europe provides an impressive illustration of the state-of-the-art accelerator machine. Built at a cost of $10billion by a vast international collaboration of thousands of scientists, this machine is aiming to resolve some of the mysteries of the elementary particle world, by creating inside its detectors the Higgs particle and hypothetical superpartners of the known particles.

Given the immense technical challenge and cost of experiments such as the LHC, it is important to explore all other paths, by which new physics could reveal itself. An important opportunity is provided by astrophysical objects, such as stars and supernovae. What makes supernovae interesting as a laboratory for new physics are the extreme physical conditions that exist in their central regions – conditions that cannot ever be recreated in the lab. For example, the density of the collapsed core, a hundred billion grams per cubic centimeter, exceeds that inside of a nucleon. Even a ghostly particle like a neutrino, which can travel through the entire Sun without scattering even once, gets trapped inside a supernova core. Clearly, in conditions like that certain physical processes that are unobservable in the lab could reveal themselves.

A particularly interesting and fruitful phenomenon for

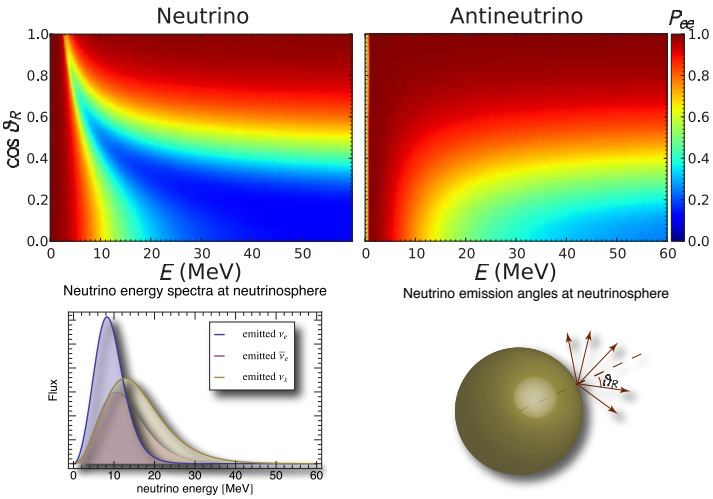

Figure 1. Neutrinos in a supernova undergo collective flavor oscillations. Neutrino evolution depends on its emission angle and its energy. The resulting pattern of the oscillations can be very nontrivial, as this figure shows. Colors indicate the flavor conversion probability, as specified in the legend on the right. The calculation were done on supercomputers at LANL.

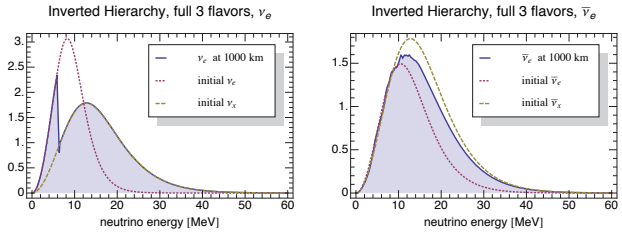

Figure 2. Energy spectra of supernova neutrinos and antineutrinos, showing the imprints of the collective oscillations. The oscillations are treated in the full three-flavor framework.

our purposes turns out to be neutrino flavor oscillations in a supernova. While neutrino oscillations have been observed over the last decade in a variety of experiments – with solar, atmospheric, reactor, and accelerator beam neutrinos – the conditions in the supernova are so unique that neutrino flavor oscillations there happen in ways that are inaccessible on Earth. As we discovered in the course of this project, they can indeed serve as very powerful probes of new physics, with sensitivity exceeding the lab experiments by orders of magnitude.

It should be realized that stars and supernovae are extremely complicated objects with very rich physics. As such, many details about them are at present uncertain. Therefore, the task of our exploration was to estimate not only the effects of new physics, but also the size of the astrophysical uncertainties. *Only those effects of BSM physics that safely exceed the astrophysical uncertainties can be probed.*

The project had several goals:

- Identify processes in core collapse supernovae and their progenitor stars that are sensitive to particle physics beyond the Standard Model.
- Analyze the astrophysical backgrounds and uncertainties.
- Develop the tools modeling processes in supernovae, such as neutrino diffusion and oscillations; make sure these tools can be used going forward, to enhance the Lab's long-term research potential.
- To make predictions and recommendations for experiments under design.

The latter, in particular, emerged in the course of this project as a powerful validation to the effectiveness of the LDRD investment. This year (2010), the focus of the US high-energy community has shifted to the physics potential of the Deep Underground Science and Engineering Laboratory (DUSEL) in South Dakota. A variety of experiments are on the drawing board for DUSEL, including a neutrino beam from Fermilab to a large underground detector at the DUSEL site. A working group of experts has been convened, tasked to understand the full science potential of this experiment. One specific question has been to establish the science potential of the supernova neutrino signal and to specify the detector characteristics that would be optimal for extracting the most physics out of this signal. The PI of this project has been invited to the working group, to advise experimentalists on the features in the neutrino signal. Working on this ER has placed us at the top of the experts on the supernova neutrino signal in the US.

Scientific Approach and Accomplishments

The first class of BSM models we considered was the setup with extra spacetime dimensions, in which the photon can escape from our world "into the bulk". These types of extra-dimensional models have attracted a great deal of theoretical attention over the last ten years. More recently, it has been proposed that they could be tested in the laboratory, in precision positronium (the system of an electron and a positron) decay experiments. In the course of this ER project, we realized that in this framework a photon in plasma should be metastable. We modeled the astrophysical consequences of this observation, in particular, what it implies for the plasmon decay rate in globular cluster stars and for the core-collapse supernova cooling rate. We found that supernovae and red giant stars provide extremely strong constraints on these models. The resulting bounds on the model parameter exceed the possible reach of orthopositronium experiments by many orders of magnitude.

The results of this work have been published in Physical Review Letters [1]. The paper has led to a rethinking of the

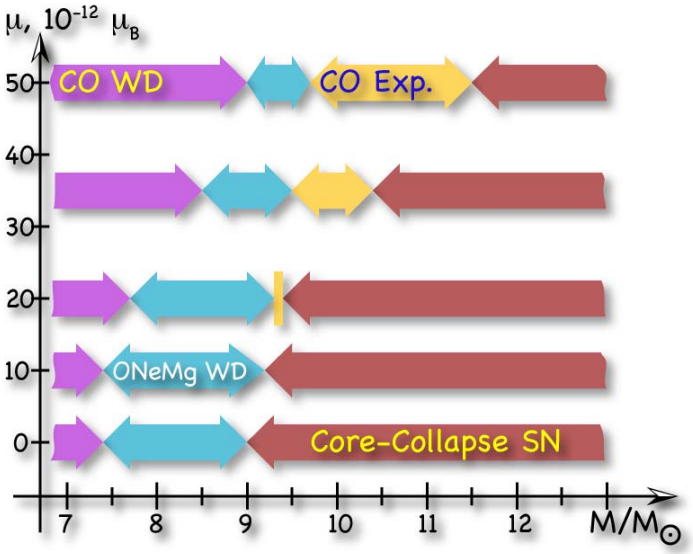

Figure 3. The Figure shows the impact of the additional cooling due the neutrino magnetic moment on the final destiny of a massive star. As the magnetic moment is increased, a new type of supernova appears. This supernova is essentially a Type Ia explosion inside a massive star

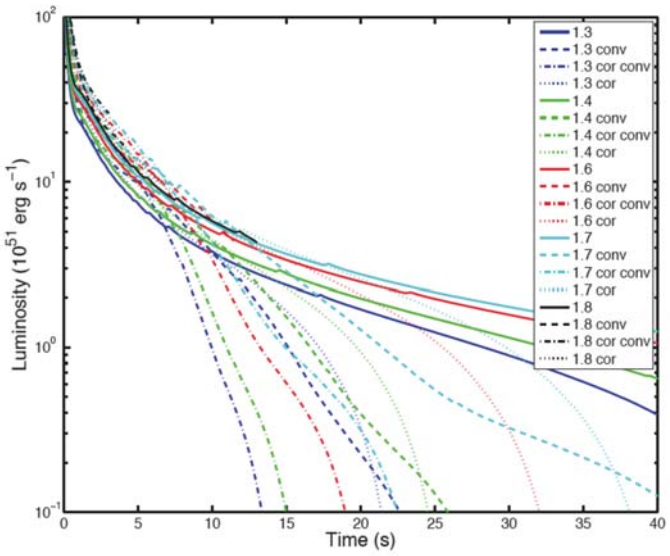

Figure 4. The cooling rates of the supernova core for different models, with and without convection.

physics case for the ortho-positronium decay experiments. We have also developed the implications of these models further in two additional papers [6,7].

We also considered bounds on the neutrino magnetic moment of the neutrino. This scenario has been repeated invoked over the last several decades in connection with neutrino oscillation data. We noted that the additional cooling from the emission of neutrinos from the cores of massive stars could radically alter the evolution of these stars.

To quantify this effect, we added the extra cooling to the detailed models of massive stars and ran the evolution codes. We performed the calculations for a grid of stellar masses and values of the neutrino magnetic moment. We discovered that in a range of stellar masses around 10-11 solar masses, a new type of supernova is predicted to appear: a type Ia explosion, but inside a massive star. The results are graphically shown in Figure 3, with the new region marked "CO exp.". Clearly, objects of this type would stand out in observations, hence providing a constraint of this type of BSM physics. The results are published in the Astrophysical Journal [4].

Our next effort was directed at modeling the cooling process of the cooling of the collapsed core of a supernova, known as the protoneutron star (or PNS). The PNS cools and deleptonizes as neutrinos diffuse outwards driven by strong gradients in electron-neutrino chemical potential and temperature. The timescale for deleptonization is set by the mean free paths of the electron neutrinos, while the one for cooling is set mostly by the nonelectron neutrino mean free paths. Novel neutrino-matter interactions that allow for flavor conversion would modify this transport and therefore would potentially cause observable changes in the neutrino signal. Our preliminary estimates at the preparation stage of this proposal indicated potentially very high levels of sensitivity to such flavor changing interactions.

To simulate this diffusion process we developed a general relativistic, spherically symmetric neutrino diffusion code where structural changes of the star as it looses thermal and lepton degeneracy pressure is treated as a quasi-static relaxation. In addition to the diffusive transport of neutrinos it implements convection using a mixing length theory in regions of the star that are convectively unstable with respect to lepton or entropy gradients. This treatment is approximate, but is able to demonstrate whether or not convection can have a significant impact on the cooling timescales. Our calculations have shown that indeed this is so. As shown in Figure 4, convection can significantly change the cooling process. It noticeably accelerates neutrino emission leading to higher initial luminosities and shorter time-scales. According to our separate estimates, the BSM flavor changing interactions caused a comparable effect. Therefore, we concluded that:

- A more detailed simulation of the convection phenomenon is warranted.
- Only when reliable convection models are constructed, possible bounds on the flavor-changing interactions from the diffusion timescales can be discussed.

This does not, however, mean that the supernova neutrino signal cannot probe nonstandard neutrino interactions. In fact, we uncovered a novel mechanism, by which this signal tightly constrains such effects. The physics, which makes this possible, is the ***collective*** neutrino oscillations.

It is unique to the supernova environment, where the density of the streaming neutrino is so high, that flavor states of different neutrinos become coupled. It was realized by several collaborations over the last three years that the collective oscillations occur close to the protoneutron star and lead to large, unmistakable signatures in the observed spectra (see, for example, Fig. 3, adopted from our calculations in Ref. 2).

Modeling collective oscillations involves solving tens of millions of coupled differential equations – a task for supercomputers. We have been able to take advantage of the supercomputing resources of LANL. An example of the output of our calculations is shown in Figure 1. Our calculations have shown that tiny nonstandard neutrino interactions indeed change the neutrino signal observable on earth [11]. This provides a important scientific goal for the planned large detector at DUSEL.

In the course of this investigation, we also uncovered a fundamental property of the collective oscillations: that the calculations must be done with all three flavors. This result was accepted to Physical Review Letters [2] and chosen for special highlighting by the editors of this journal on the prestigious physics.aps.org website [3].

We have also demonstrated a novel multiangle suppression mechanism for the oscillations that operates close to the neutrinosphere. The paper describing this effect is currently under review at Physical Review Letters [7]. As we have shown with our external collaborators from NCSU and Union C., this effect has a large impact on the predictions for the r-process nucleosynthesis. The paper reporting this finding has been prepared and will be submitted to the journal once an LAUR number for it is received [10].

Our work has been recognized by the scientific community, as evidenced by the large number of invited presentation we have given over the last two years [8,9,12,13,14].

Impact on National Missions

The work funded by this LDRD ER project built a capability that has already directly benefited the DOE Office of Science. The High Energy Physics office of DOE is in the process of transitioning its efforts towards the Long Baseline Neutrino experiment. The experiment will consist of a neutrino beam generated at Fermilab and shot to a large underground detector, or a suite of detectors, at the DUSEL underground facility in South Dakota. Given the substantial cost of this experiment – the estimated price tag is about $1Billion – it is very important that the experiment be optimized to allow the exploration of the full spectrum of physics problems. One such question is how to optimize the far detector configuration for the neutrino burst signal from the next galactic supernova. The work of our team on probing the physics beyond the Standard Model with supernova neutrinos, funded by LANL LDRD, has positioned us as the leader in this field in the US and internationally.

The PI of the project, Alexander Friedland, was invited to participate in the DUSEL working group and in collaboration with Prof. Scholberg (Duke U.) wrote the section of the working group report describing the physics potential of the supernova neutrino detection. The capability developed in the course of this project has placed LANL as the world leader in the supernova neutrino field, with benefits that are expected to accrue in the years to come.

The supernova neutrino LDRD project also involved large-scale supercomputing calculations. Done in collaboration with Huaiyu Duan, who was a postdoc in our group, the work resulted in the development of the world-leading computational capability. In fact, the work produced the biggest set of supercomputer runs in the world in this field. It can be safely stated that LANL is currently has no equals in the world when it comes to supercomputer modeling of collective neutrino oscillations.

Another important benefit of this project has been the recruitment and training of young talent. James Jenkins, who was trained on this project in modeling neutrino transport and other numerical techniques, has since been hired by a defense contractor company in Washington, D.C. Huaiyu Duan has recently become a professor at the University of New Mexico in Albuquerque. The collaboration between Friedland and Duan is continuing, strengthening the ties between the two institutions.

References

1. Friedland, A., and M. Giannotti. Astrophysical bounds on photons escaping into extra dimensions. 2008. *Physical Review Letters.* **100**: 031602.

2. Friedland, A.. Self-refraction of supernova neutrinos: mixed spectra and three-flavor instabilities. 2010. *Physical Review Letters.* **104**: 191102.

3. Friedland, A., and D. Voss. A full-flavored neutrino calculation. 2010. *Physics Synopsis.*

4. Heger, A., A. Friedland, M. Giannotti, and V. Cirigliano. The impact of neutrino magnetic moment on the evolution of massive stars. 2009. *Astrophysical Journal.* **696**: 608.

5. Friedland, A., M. Giannotti, and M. Graesser. On the RS2 realization of unparticles. 2009. *Physics Letters B.* **678**: 149.

6. Friedland, A., M. Giannotti, and M. Graesser. Vector Bosons in the Randall-Sundrum 2 and Lykken-Randall models and unparticles. 2009. *Journal of High Energy Physics.* **0909**: 033.

7. Duan, H., and A. Friedland. Self-induced suppression of collective neutrino oscillations in a supernova. *Physical Review Letters.*

8. Friedland, A.. Observing the development of supernova explosion in neutrinos: an overview. (Detroit, 26-31 July, 2009).

9. Friedland, A.. Supernova neutrinos: imprints of the explosion. (Los Angeles, Sept. 16-17).

10. Duan, H., A. Friedland, G. McLaughlin, and R. Surman. The influence of collective neutrino oscillations on a supernova r-process. 2010. *Awaiting LAUR number; to be submitted to the Journal of Cosmology and Astroparticle Physics.*

11. Friedland, A., and H. Duan. Collective oscillations in a supernova and constraints on nonstandard neutrino interactions. 2010. *in preparation; to be submitted to Physical Review Letters.*

12. Friedland, A.. Oscillations of supernova neutrinos. Presented at *INT DUSEL workshop.* (Seattle, WA, 9-11 Aug. 2010).

13. Friedland, A.. Collective oscillations of supernova neutrinos: three-flavor instabilities and multiangle suppression . Presented at *Neutrino 2010.* (Athens, Greece, 14-19 June 2010).

14. Friedland, A.. Flavor oscillations of supernova neutrinos. Presented at *SnowPAC 2010.* (SNOWBIRD, UT, 23 - 28 March 2010).

Publications

Duan, H., A. Friedland, G. McLaughlin, and R. Surman. The influence of collective neutrino oscillations on a supernova r - process. 2010. *Awaiting LAUR numer; to be submitted to the Journal of Cosmology and Astroparticle Physics.*

Duan, H., and A. Friedland. Self-induced suppression of collective neutrino oscillations in a supernova. *Physical Review Letters.*

Friedland, A.. Self-refraction of supernova neutrinos: mixed spectra and three-flavor instabilities. 2010. *Physical Review Letters.* **104**: 191102.

Friedland, A., M. Giannotti, and M. Graesser. On the RS2 realization of unparticles. 2009. *Physics Letters B.* **678**: 149.

Friedland, A., M. Giannotti, and M. Graesser. Vector Bosons in the Randall-Sundrum 2 and Lykken-Randall models and unparticles. 2009. *Journal of High Energy Physics.* **0909**: 033.

Friedland, A., and M. Giannotti. Astrophysical bounds on photons escaping into extra dimensions. 2008. *Physical Review Letters.* **100**: 031602.

Heger, A., A. Friedland, M. Giannotti, and V. Cirigliano. The Impact of Neutrino Magnetic Moments on the Evolution of Massive Stars. 2009. *Astrophysical Journal.* **696**: 608.

Dissipation and Decoherence in Complex Many-Body Systems

Wojciech H. Zurek
20080728PRD2

Introduction

We will investigate quantum phase transitions and nonequilibrium dynamics in decohering and dissipative many body systems. In general, quantum information processing requires quantum hardware for its implementation. However, it was recently realized (by looking at quantum systems from the point of view inspired by quantum information processing ideas) that a large and interesting category of quantum evolution can be simulated on a classical computer with resources that are only polynomial (rather than exponential) in the size of the system. We will apply this method to simulate time-dependent evolution of quantum systems. One immediate goal is to study the dynamics of quantum phase transitions that are beginning to be investigated experimentally in, e.g. Bose-Einstein condensates (BEC's). However, in the process we expect to improve and generalize this novel method so that it can be applied much more broadly to study the exact quantum time evolutions of systems with approximately 100-10000 independent components (which will include sixth generation quantum computers, but potentially also other systems such as molecules, nuclei, etc.).

Benefit to National Security Missions

This project will support the missions of the Office of Science by enhancing our understanding of materials and comprehension of complex natural systems. This work will also support the Homeland Security mission of the Laboratory by bringing the encryption breaking power of quantum computing one step closer to reality.

Progress

Simulating decoherence and information transfer – We have examined how information about a system is distributed into its environment while undergoing decoherence. We demonstrated that noisy environments can effectively acquire and communicate certain classical information about the system, but at a reduced rate compared to "clean" environments. However, quantum information about coherence in the system is distributed globally into the environment, regardless of its noise level, and is therefore effectively lost. In addition to analytic techniques, we developed a simulation method that can handle symmetric qubit environments with a polynomial computational cost (and thus, we simulated 200 qubits, i.e., a state space of 2^200, which cannot be handled by direct diagonalization). We have a number of new developments that incorporate information-theoretic concepts (Quantum Chernoff Bounds; Data processing inequality; Fannes' and Fano's inequalities), and that promise to bring a universal understanding of information transfer during decoherence. This work supports the LANL mission of gaining a fundamental understanding of materials and of complex natural systems. This work resulted in two articles, one in the prestigious journal Physical Review Letters and the other in Physical Review A (M. Z. et al., Phys. Rev. Lett. 103, 110402 (2009); M. Z. et al., Phys. Rev. A 81, 062110 (2010))

Aspects of nanoscale electronic sensors – We have examined two issues in the behavior of nonequilibrium nanoscale systems: (i) The effect of noise on the ability to detect biomolecules with electronic sensors and (ii) how ionic transport occurs through nanopores. For (i), we investigated decoherence (also known as dephasing in this field) and inelastic scattering effects on rapid DNA sequencing using transverse electronic transport measurements and nanopores. We found that the efficient distinguishability of the bases is not influenced by white noise unless it is unrealistically strong, reaffirming that electronic transport might serve as a mechanism of rapid DNA sequencing. Our work has recently been confirmed experimentally, settling a long-standing debate concerning the feasibility of DNA base detection/sequencing with transport (see, Nature Nanotechnology 5, 286 (2010) and Nano Letters 10, 1070 (2010)). For (ii), we studied how ions move from bulk into a nanopore to create an ionic current. This is process that occurs in natural (biological ion channels) as well as artificial systems (synthetic nanopores, e.g., made for sequencing and molecular detection). We showed that there should be a precipitous drop in ionic current when the radius of the nanopore is shrunk below the radius of the first hydration layer of the ions. This research will help the development of nanopore-based electronic sensors that will create new possibilities for ubiquitous sensors,

and thus this work addresses the LANL mission of Threat Reduction. As well, such sensors open up new avenues for investigation into the complex interface between solids, liquids, and biomolecules, and increase our understanding of how materials behave at the nanoscale. The work resulted in two publications in prestigious journals and one submitted article (M. Z. et al., Phys. Rev. Lett. 103, 128102 (2009); M. K. et al., Biophys. J. 97, 1990 (2009); M. Z. et al., arXiv:1005.2550, to appear in a special issue on nanopores in J. Phys. Cond. Mat. (2010))

Nonequilibrium thermal transport as a probe of biological processes – DNA denaturation has long been a subject of intense study due to its relationship to DNA transcription and its fundamental importance as a nonlinear, structural transition. Many aspects of this phenomenon, however, remain poorly understood. Existing models fit quite well with experimental results on the fraction of unbound base pairs versus temperature. Yet, these same models give incorrect results for other essential quantities, e.g., the predicted base pair fluctuation timescales - relevant to transcription - are orders of magnitude different from experimental ones. We demonstrated that nanoscale thermal transport can serve as a sensitive probe of the underlying microscopic mechanisms responsible for dynamics of DNA denaturation. Specifically, we showed that the heat transport properties of DNA are altered significantly and abruptly as it denaturates, and this alteration encodes detailed information on the dynamics of thermal fluctuations and their interaction along the chain. This finding allows for the unambiguous discrimination between models of DNA denaturation. Measuring the thermal conductance will thus shed new light on the nonlinear physics of this important molecule. An article describing this work (LA-UR 10-05320) is currently being prepared to submit to Science.

Decoherence of topological defects – We are studying the dynamics of quantum phase transitions in the presence of decoherence. In particular, in the absence of decoherence, topological defects are generated – i.e., these are features of the quantum state that can not be changed with local perturbations to the state of the system and are therefore "protected" from local decoherence (a feature that is necessary in quantum computing). However, when driving the system, superpositions of defects are also created. We find that these superpositions are actually extraordinarily sensitive to local noise and will collapse essentially instantaneously from a coherent quantum state to an incoherent mixture of states with a single topological defect that remains protected. We have developed a proposal that will allow for the direct observation of this instability. This finding sheds light on a fundamental issue in the dynamics of quantum phase transitions and also on what types of states might be useful for quantum computing. This work supports the LANL mission of gaining a fundamental understanding of materials and of complex natural systems.

Future Work

Nonequilibrium physics is at the heart of some of the most beautiful and spectacular phenomena in nature, from pattern formation in biological systems to phase transitions in exotic superconductors. Furthermore, the nonequilibrium characteristics of many physical systems form the basis of their projected technological use, yet, in most cases, they remain poorly understood. In particular, a general category of nonequilibrium systems is composed of quantum systems out of equilibrium with their environment, which gives rise to the processes of dissipation and decoherence (D&D). The dynamics of quantum systems, though, are notoriously hard to simulate classically due to the presence of a unique quantum correlation called entanglement. We propose a two-step research program revolving around D&D: 1) Building on our past research on the efficient representation of partially entangled states, we will develop an innovative computational method that can simulate the dynamical behavior of thousands of atoms or particles as it interacts with the outside world. 2) Using this method along with analytical techniques, we will investigate several distinct but interrelated issues involving D&D in complex many-body systems. For all these issues, our current understanding is hampered by the lack of accurate methods to study D&D. In particular, we will (i) calculate physical characteristics of dissipative materials relevant to superconductivity and evaluate the possibility of engineering a dissipative transition to create a room-temperature superconductor; (ii) simulate the precise behavior of decoherence in (solid-state) architectures for quantum computing and delineate approaches for suppressing and correcting for decoherence; and (iii) simulate electronic transport across molecules in the presence of strong D&D in order to assess the effect of the aqueous environment on practical application of nanoscale electronic sensors, and more generally to study open scientific issues and challenges at the interface between solids, liquids, and biomolecules.

Conclusion

The research will result in the development of novel simulation techniques for driven, nonequilibrium, and dissipative quantum and nanoscale systems. In addition, the research will result in a greater understanding of quantum computing. Further, the research will result in setting the underlying theoretical basis of nanoscale, biological/single-molecule sensors. The realization of the end technological goals could revolutionize computing and medical treatments, giving us increased security and health.

Publications

Krems, M., M. Zwolak, Y. V. Pershin, and M. Di Ventra. Effect of Noise on DNA Sequencing via Transverse Electronic Transport. 2009. *Biophysical Journal.* **97**: 1990.

Zwolak, M., H. T. Quan, and W. H. Zurek. Quantum Darwinism in a mixed environment. 2009. *Physical Review Letters.* **103**: 110402.

Zwolak, M., J. Lagerqvist, and M. Di Ventra. Quantized ionic conductance in nanopores. 2009. *Physical Review Letters.* **103**: 128102.

Zwolak, M., J. Wilson, and M. Di Ventra. Dehydration and ionic conductance quantization in nanopores. To appear in *arXiv:1005.2550, to appear in Journal of Physics: Condensed Matter.*

Unconventional Superconductivity in Heavy Fermion Materials

Cristian D. Batista
20090491PRD1

Introduction

Our goal is to modeling unconventional superconductivity of f-electron materials. Some materials can conduct electricity without dissipating energy, i.e., with no energy losses in the form of heat. These materials are known as superconductors, and their unique properties lead to several technological applications. Unfortunately, the known materials that exhibit this property are superconductors only at low temperatures. One of the challenges for future technologies is to find materials that can superconduct at room temperature. To find guiding principles for designing such materials we need to understand the microscopic origin of superconductivity. This is the main purpose of this project. In particular, the project will be focused on f-electron materials that are at the center of the experimental effort of LANL (MPA-10 group). We will study the non-trivial interplay between magnetism and superconductivity in strongly correlated materials. One of the main goals is to derive guiding principles for optimizing the superconducting properties of non-conventional superconductors. In addition, we want to derive effective low-energy models for these materials and unveil the hidden connections between seemingly unrelated families of unconventional superconductors.

Benefit to National Security Missions

This project supports DOE, Office of Science missions by enhancing our understanding of unconventional superconductivity, which is needed for future energy transmission and storage applications, and addresses the Laboratory's mission in superconductivity from 5f electrons. Because the properties of uranium and plutonium are driven by their 5f nature, this work contributes to the understanding of key materials for the weapons program.

Progress

Starting from a Periodic Anderson Model with a momentum dependent hybridization that cancels at the Fermi level, we have derived, for the first time, a low-energy effective Hamiltonian for the mixed valence regime. The low-energy effective theory is obtained under control by performing a Schrieffer-Wolf transformation that is a perturbative expansion in the small ratio between the hybridization amplitude and the conduction bandwidth.

The main impact of our derivation is that it unveils the presence of a new fixed point for the mixed valence regime of 4f-electron compounds (i.e., compounds that are described by a Periodic Anderson Model). As it demonstrated in our derivation, this fixed point is described by an effective single band Hubbard model. The same model is used to describe the properties of the high-temperature superconducting cuprates that have many qualitative aspects in common with several Ce-based superconductors like the 115 family. Our derivation provides a formal way of connecting these similarly unrelated materials. Moreover, it provides an explanation for the f-character pockets that have been recently measured in CeIn3, an antiferromagnetic material that becomes superconducting under pressure.
We have also validated our low-energy effective theory by comparing the numerical results for the original Periodic Anderson Model and the low-energy effective Hamiltonian. The numerical technique that we used it the Density Matrix Renormalization Group that is the state of the art method for solving correlated models in one dimensional lattices.

The impact of our work is reflected by the fact that it was immediately accepted for publication in the prestigious journal Physical Review Letters.

We have also demonstrated that a bare (Coulomb) repulsion between electrons described by a Periodic Anderson model can lead to an effective attraction. The effective attraction is induced by the presence of antiferromagnetic correlations with long enough correlation length. This result is in correspondence with many experimental phase diagrams that show the presence of superconductivity in the neighborhood of an antiferromagnetic phase. An important result is that our pairing

mechanism survives in dimension higher than one and is robust against the inclusion of the longer range part of the Coulomb repulsion. The ultimate reason of this property is that the attractive mechanism is produced by confining of topological defects (solitons). Each hole (moving charge) carries a soliton (or domain wall for the antiferromagnetic ordering) and the antiferromagnetic interaction induces an attractive hole-hole potential that increases linearly in the distance between the holes. The results of this research were published in Physical Review B.

Finally, by starting from an inhomogeneous Hubbard model, we have demonstrated the existence of a d-wave superconducting phase. The model consists of Hubbard "molecules" or plaquettes that are connected by a weak hopping amplitude. The obtained quantum phase diagram includes a charge-density-wave and a d-wave superconducting phase. A remarkable conclusion of our work is that optimal superconductivity is obtained for optimal intra-plaquette kinetic energy frustration. This is an important association because it provides a guiding principle for maximizing the critical temperature of unconventional superconductors and understanding the role of frustration in this process. Our paper has been published in the Physical Review Letters.

There are many other works that have been published under this project (see the list of publications). Most of these works are contributions to the general area of strongly correlated electrons. These ideas were derived along the process of working on the main subject of this project (magnetism and superconductivity). In particular, I would like to highlight the discovery of orbital electric currents in Mott insulators and the possibility of inducing orbital antiferromagnetism by the application of a uniform external magnetic field. These results were published in the Physical Review Letters.

Future Work

This work will be oriented to modeling unconventional superconductivity of f-electron materials. To carry out our study, the postdoc will use both numerical and analytical techniques. The numerical techniques consist of algorithms for solving models of interacting electrons. These techniques are the Density Matrix Renormalization Group (DMRG) and Quantum Monte Carlo (QMC). Our next step is to investigate the effect of the overlap between f atomic orbitals on the low-energy physics of the periodic Anderson model. The goal is to determine if this model has a single-band fixed point that describes the localized to delocalized f-electron transition. This is crucial for connecting the physics of f-electron unconventional superconductors with the high temperature superconductors (cuprates), that exhibit very similar phase diagrams (although their critical temperatures are much higher).

Conclusion

The discovery nearly 20 years ago of high temperature superconductivity in complex copper oxide materials held great promise for revolutionizing electrical power transmission and storage. The promise of this discovery has not been realized fully, in part because we still do not understand how electrons interact strongly to produce unconventional superconductivity in these and related materials formed from f-electron elements. This project focuses on providing basic understanding of the interacting electrons and how these electrons affect the utility of unconventional superconductors for energy applications. By means of the research that is being performed under this research project, we are providing guiding principles for finding superconducting materials with higher critical temperatures. In addition, we are finding novel states of matter that emerge in the neighborhood of the superconducting and magnetic phases out of the same electron-electron interactions that stabilize these phases. The discovery of these novel states of matter may also lead to novel technological applications.

Publications

Al-Hassanieh, K. A., C. A. Busser, and G. B. Martins. Electron transport in strongly correlated nanostructures. 2009. *Modern Physics Letters B.* **23** (18): 2193.

Al-Hassanieh, K. A., C. D. Batista, G. Ortiz, and L. N. Bulaevskii. Field-induced orbital antiferromagnetism in Mott insulators. 2009. *Physical Review Letters.* **103**: 216402 .

Al-Hassanieh, K. A., C. D. Batista, P. Sengupta, and A. E. Feiguin. Robust pairing mechanism from repulsive interactions. 2009. *Physical Review B.* **80**: 115116.

Al-Hassanieh, K. A., F. A. Reboredo, A. E. Feiguin, I. GonzaÃÅlez, and E. Dagotto. Excitons in the one-dimensional hubbard model: A real-time study. 2008. *Physical Review Letters.* **100** (16): 166403.

Hei, F. [Materials Science and Technology Division., null. Department of Physics and Astronomy, G. B. Martins, K. A. Al-Hassanieh, null. Department of Physics and Astronomy, A. E. Feiguin, E. [Materials Science and Technology Division. Dag, and null. Department of Physics and Astronomy. Finite-size scaling analysis of spin correlations and fluctuations of two quantum dots in a T-shape geometry. 2008. *Physica. B, Condensed Matter.* **403** (5-9): 1544.

Heidrich-Meisner, F. [., G. B. Martins, C. A. Busser, null. Al Hassanieh, A. E. Feiguin, G. [Universidad de Alicante]. Chiappe, E. V. Anda, and null. Dagotto. Transport through quantum dots: a combined DMRG and embedded-cluster approximation study. 2008. *European*

Physical Journal - Applied Physics. **67**: 527.

Heidrich-Meisner, F., G. B. Martins, C. A. Busser, K. A. Al-Hassanieh, A. E. Feiguin, G. Chiappe, E. V. Anda, and E. Dagotto. Transport through quantum dots: a combined DMRG and embedded-cluster approximation study. 2009. *European Physical Journal B.* **67** (4): 527.

Isaev, L., G. Ortiz, and C. D. Batista. Superconductivity in Strongly Repulsive Fermions: The Role of Kinetic-Energy Frustration . 2010. *Physical Review Letters.* **105**: 10.

Kohama, Y., A. V. Sologubenko, N. Dilley, V. S. Zapf, M. Jaime, J. Mydosh, A. Paduan-Filho, K. A. Al-Hassanieh, P. Sengupta, S. Gangadharaiah, A. L. Chernyshev, and C. D. Batista . Thermodynamic and transport properties of NiCl2-4SC(NH2)2: Role of strong mass renormalization. To appear in *Physical Review Letters.*

Paduan-Filho, A., K. A. Al-Hassanieh, P. Sengupta, and M. Jaime. Critical Properties at the Field-Induced Bose-Einstein Condensation in NiCl2-4SC(NH2)2. 2009. *Physical Review Letters.* **102**: 077204.

Paduan-Filho, A., K. A. Al-Hassanieh, P. Sengupta, and M. Jaime. Critical properties at the field-induced bose-einstein condensation in NiCl₂-4SC(NH₂)₂. 2009. *Physical Review Letters.* **102** (7): 077204 (4 pp.).

Samulon, E. C., K. A. Al-Hassanieh, Y. -J. Jo, M. C. Shapiro, L. Balicas, C. D. Batista, and I. R. Fisher. Anisotropic phase diagram of the frustrated spin dimer compound Ba3Mn2O8. 2010. *PHYSICAL REVIEW B.* **81** (10): 104421.

Samulon, E. C., Y. Kohama, R. D. McDonald, M. C. Shapiro, K. A. Al-Hassanieh, C. D. Batista, M. Jaime, and I. R. Fisher. Asymmetric Quintuplet Condensation in the Frustrated S=1 Spin Dimer Compound Ba3Mn2O8. 2009. *Physical Review Letters.* **103**: 047202.

Silva, L. G. da, K. Al-Hassanieh, A. Feiguin, F. Reboredo, and E. Dagotto. Real-time dynamics of particle-hole excitations in Mott insulator-metal junctions. 2010. *PHYSICAL REVIEW B.* **81** (12): 125113.

Disorder in Frustrated Systems

Avadh B. Saxena
20090493PRD1

Introduction

As a Director's Funded postdoc Cristiano Nisoli will conduct basic research on a variety of physical problems involving competing interactions and frustration (when the system constraints cannot all be fulfilled simultaneously) using statistical mechanics techniques. Examples include structural glasses, neural networks, economic/social models and countless complex systems. Specifically, his initial focus will be on spin ice materials which are artificial geometrically frustrated system of magnetic nano-islands. Subsequently he will explore the colloidal version of artificial ice. In particular, he will investigate the consequences of altering geometry and the strength of interaction, introducing defects and other properties that impact the nature of frustration. This work will help us understand the origin and properties of disordered states in liquids, soft bio-systems and frustrated magnets, systems extensively studied at LANL, as well as the effect of jamming on disorder. The understanding is likely to lead to designed materials with properties which are relevant for alternative energy applications.

Benefit to National Security Missions

This project will support the DOE Office of Science missions in basic energy and energy security by enhancing our understanding of fundamental properties of disordered materials. In particular, the low-dimensional materials studied may provide some insights into renewable energy. Similarly, study of bacteria, etc. may help understand the biophysical aspects of health research. Our insight into novel materials may also provide new sensors for the weapons and nonproliferation programs.

Progress

During the last year Cristiano worked on different topics and published seven articles in high profile journals. He has continued his work on disorder of Artificial Apin Ice, an artificially frustrated metamaterial at the nanoscale which he had introduced and now many research groups around the world are working to develop it further. On this topic he has published one Physical Review Letters, two Physical Review B, a Nature Physics paper and he was an invited speaker at a conference in UK. His work on Dynamical Phyllotaxis (on which he has published a Physical Review E in 2010), in which he has demonstrated the emergence of botanical patterns in physical systems as well as novel sets of linear and topological excitations, was recognized when a column was devoted to it in Nature Materials and by the American Mathematical Society. He has also worked on the stability of quasi-one-dimensional systems in collaboration with Prof. Douglas Abraham at Oxford University by extending the ideas to carbon nanotubes, DNA and nanowires. He published a Physical Review Letters on this topic in 2010. During the year Cristiano was also awarded honorable mention for the Leon Heller Prize in Theoretical Physics for his work on quasi-one-dimensional systems. In addition, this work was recognized at the Postdoc Research Day by the Outstanding Poster Award, for his work on Artificial Spin Ice.

Future Work

Frustration, a competition between interactions in a material or physical system, not all of which can be satisfied, leads to disorder in neural networks, structural glasses, economic/social models and many other complex systems. The unusual statistical mechanics of such systems is related to the residual entropy at very low temperature in crystalline ice as frustration of hydrogen ion positions. Similar ice rules can emerge in magnetic systems via geometrical frustration of spins. Experiments have designed frustrated nano-islands of a magnetic system--i.e. Artificial Spin Ice. Such materials can transform our understanding of disordered matter and potentially lead to new technologies. The effective temperature of artificial spin ice can be controlled by applying an external magnetic field.

The specific research questions to be answered are: (i) What is the effect of the long range interaction on such a system? (ii) Is there a unique ground state? (iii) What is the dynamics of artificial spin ice? This question can help us understand glass transitions and jamming phe-

nomena. Spin ice provides a way of encoding information and thus could be useful as memory element. We intent to extract information energy in order to relate it to effective thermodynamics. Another important question we intend to answer is: What are the consequences of altering geometry, strength of interaction and introducing defects on the nature of frustration. We will answer these questions by developing models and analyzing them both analytically and by means of simulations.

Conclusion

The fundamental understanding from this project will help us design new disordered materials such as structural glasses, magnetic materials, and colloidal systems which are likely to find applications in alternative energy systems and possibly higher energy efficiency materials.

Publications

Gupta, A. K., C. Nisoli, P. Lammert, V. H. Crespi, and P. C. Eklund. Curvature-Induced D-Band Raman Scattering in Folded Graphene. 2010. *J. Phys.: Cond. Matt.*. **22**: 334205.

Lammert, P. E., X. Ke, J. Li, and C. Nisoli. Direct Entropy Determination and Application to Articial Spin Ice. 2010. *Nature Phys.* . **6**: 786.

Li, J., S. Zhang, J. Bartell, C. Nisoli, X. Ke, and P. E. Lammert. Comparing Frustrated and Unfrustrated Clusters of Single-Domain Ferromagnetic Islands. 2010. *Phys. Rev. B.* **82**: 134407.

Li, J., X. Ke, S. Zhang, D. Garand, C. Nisoli, and P. Lammert. Comparing Artificial Frustrated Magnets by Tuning the Symmetry of Nanoscale Permalloy Arrays. 2010. *Phys. Rev. B.* **81**: 092406.

Nisoli, C.. Polarons Induced Deformations in Carbon Nanotubes. 2009. *Phys. Rev. B.* **80**: 113406.

Nisoli, C.. Spiraling Solitons. A Continuum Model for Dynamical Phyllotaxis and of Physical Systems. 2009. *Phys. Rev. E.* **80**: 0210.

Nisoli, C.. Static and Dynamical Phyllotaxis in a Magnetic Cactus. 2009. *Phys. Rev. Lett.* . **102**: 186103.

Nisoli, C., D. Abraham, T. Lookman, and A. Saxena. Thermally Induced Local Failures in Quasi-One-Dimensional Systems: Collapse in Carbon Nanotubes, Necking in Nanowires, and Opening of Bubbles in DNA. 2010. *Phys. Rev. Lett.* . **104**: 119902.

Nisoli, C., D. Abraham, T. Lookman, and A. Saxena. Thermal Stability of Strained Nanowires. 2009. *Phys. Rev. Lett.* . **102**: 245504.

Nisoli, C., J. Li, X. Ke, D. Garand, and P. Schiffer. Effective Temperature in an Interacting Vertex System: Theory and Experiment on Artificial Spin Ice. 2010. *Phys. Rev. Lett.*. **105**: 047205.

Nisoli, C., N. M. Gabor, P. E. Lammert, J. D. Maynard, and V. H. Crespi. Annealing a Magnetic Cactus into Phyllotaxis. 2010. *Phys. Rev. E.* **81**: 0107.

Measurement of Transverse Single-Spin Asymmetries of Neutral Pion and Eta Meson Production in Polarized p+p Collisions Using the PHENIX Detector at RHIC

Melynda L. Brooks
20090498PRD2

Introduction

Dr. Aidala performs data analysis on data collected by the PHENIX detector at the Relativistic Heavy Ion Collider (RHIC) at Brookhaven National Laboratory (BNL) for polarized proton-proton collisions. The purpose of her data analysis is to try to shed light on how the proton's spin - a fundamental property of the proton - is formed. It was originally thought that the three constituent quarks' spins (up, up and down) would completely determine the spin of the proton. However, data collected to date have shown that the constituent quarks can only account for approximately 30% of the proton's spin. The remaining portion is assumed to come from the spins of the sea of quarks and gluons which bind the quarks together, or from orbital angular momentum carried by the quarks and gluons. By colliding polarized protons on polarized protons and carefully measuring any asymmetry in particles produced, the contributions of the sea quarks and gluons can be extracted. To this end, Dr. Aidala is looking at spin asymmetries for multiple channels—production of several kinds of particles in different kinematic regimes, and for different configurations of the polarized proton beams. These asymmetries can be related back to the quark and gluon contributions to the proton spin, and can also potentially be related back to the orbital angular momentum. With these new data, important constraints are expected to be placed on the proton spin contributions, leading to fundamental new information about how the basic building blocks of nature are formed by their constituents.

Benefit to National Security Missions

This project will support the DOE missions of the Office of Science by enhancing our understanding of the origin of the proton's spin, and adding detector capabilities to the RHIC PHENIX detector, which will also gather data to study the Quark Gluon Plasma.

Progress

The PHENIX Collaboration paper entitled "Double Helicity Dependence of Jet Properties from Dihadrons in Longitudinally Polarized p+p Collisions at $\sqrt{s}$ = 200 GeV," submitted as of this report one year ago, has now been published as Physical Review D81, 012002 (2010). The paper describes a novel measurement attempting to access the orbital angular momenta of quarks and gluons inside the proton. Dr. Aidala took responsibility for the physics discussion in the paper.

A PHENIX Collaboration paper entitled "Measurement of Transverse Single-Spin Asymmetries for J/Psi Production in Polarized p+p Collisions at $\sqrt{s}$ = 200 GeV," in PHENIX internal review at the time of this report last year, has been submitted for publication in Physical Review D. The transverse single-spin asymmetry for J/Psi production was proposed in 2008 as a new observable sensitive to the J/Psi production mechanism, a long-standing question in quantum chromodynamics (QCD), the theory of the strong force, and it is also specifically sensitive to gluon dynamics within transversely polarized protons. She is involved in this work with other LANL collaborators. Dr. Aidala has served as chair of the Paper Preparation Group and wrote the physics description and discussion of results in the paper. The manuscript is available as arXiv:1009.4864.

Another PHENIX Collaboration paper has been submitted to Physical Review D for publication, entitled "Cross Section and Double Helicity Asymmetry for Eta Mesons and Their Comparison to Neutral Pion Production in Proton-Proton Collisions at $\sqrt{s}$ = 200 GeV." Dr. Aidala finalized a number of analysis details regarding the three results in the paper, coordinated the theoretical calculations, and shepherded the paper draft through PHENIX. The spin asymmetry can provide sensitivity to the gluon spin contribution to the spin of the proton now that a parameterization for the fragmentation of quarks and gluons into eta mesons has become available thanks to Dr. Aidala's work described below. The manuscript is available as arXiv:1009.6224.

The above PHENIX paper was submitted simultaneously with a paper by Dr. Aidala and four co-authors entitled, "Global Analysis of Fragmentation Functions for Eta Mesons," accepted for publication by Physical Review D. The fragmentation functions, previously unavailable in the literature, allow perturbative QCD calculations of

eta production to be performed, permitting interpretation of RHIC data from both PHENIX and STAR as well as predictions for measurements at other facilities, for example for hadronization studies in cold nuclear matter at a future Electron-Ion Collider. The manuscript is available as arXiv:1009.6145. This paper and the PHENIX paper above were submitted in coordination and cross-referenced one another.

Dr. Aidala has continued her work with UC Riverside graduate student David Kleinjan on analysis of the transverse single-spin asymmetry in forward, i.e. close to the beam direction, eta meson production using the Muon Piston Calorimeter (MPC) in PHENIX. Preliminary results from the STAR experiment indicate that the single transverse-spin asymmetry of eta production may be larger than that of neutral pion production, providing evidence that the large transverse single-spin asymmetries observed for pions are not a valence quark effect as previously believed. Her careful work with David Kleinjan on data quality assurance eventually uncovered an incorrect cable mapping for the MPC, the correction of which in turn led to greatly improved calibrations for all PHENIX collaborators analyzing the 2008 and 2009 MPC data. Work to obtain results for the transverse single-spin asymmetry is now progressing.

Because of her expertise in eta meson studies, she also played a supporting role in a PHENIX heavy ion paper on the ratio of eta production in gold-gold collisions to that in unpolarized proton-proton collisions entitled "Transverse Momentum Dependence of Eta Meson Suppression in Au+Au Collisions at $\sqrt{s_{NN}}$=200 GeV." She contributed to the analysis of the proton-proton collisions and served on the Paper Preparation Group. The paper has been published as Physical Review C82, 012001 (2010).

Dr. Aidala has continued supervision of a graduate student from UMass Amherst, Amaresh Datta, to analyze PHENIX data on midrapidity, i.e. approximately perpendicular to the beam direction, charged hadron production in proton-proton collisions at a center-of-mass energy of 62.4 GeV. The double-helicity asymmetry analysis, sensitive to the gluon spin contribution to the proton spin, has been complete for more than a year, and at the time of this report last year, her work with Amaresh Datta was focused on measurement of the cross section. An internal discrepancy with a related PHENIX analysis significantly delayed finalizing the cross section results but is now resolved. Work has begun on a paper draft for Physical Review D. The cross section will be published together with the asymmetry measurement, and it will provide important information regarding which theoretical tools of perturbative QCD can best be used to interpret the asymmetry data at this moderate center-of-mass energy.

In additional work with charged hadrons, earlier this year Dr. Aidala released preliminary PHENIX results for her analysis of the double-helicity asymmetry in charged pion production from data taken in 2009 at a center-of-mass energy of 200 GeV. The double-helicity asymmetries of the charged pions are of particular interest because taken in conjunction with the neutral pion asymmetry, already published by PHENIX for the 2005 and 2006 data, the ordering of the asymmetries can provide information on the sign of the gluon's spin contribution, i.e. whether the gluon's spin is parallel or antiparallel to the proton's.

As of October 2010, Dr. Aidala has begun to commit a significant fraction of her time to assembly of the Forward Silicon Vertex Detector (FVTX) at BNL, a PHENIX upgrade detector for which LANL is the lead institution.

Looking toward the long-term future of her field, Dr. Aidala served on the PHENIX Decadal Plan Writing Committee this year to produce a document for BNL management outlining the PHENIX Collaboration's physics priorities and plans for the next ten years.

As a leader in the international community studying QCD in hadrons, Dr. Aidala has organized multiple workshops and conferences over the past year. She served as a co-convener of the Spin Physics Working Group for the 18th International Workshop on Deep-Inelastic Scattering, held in Florence, Italy, co-organized the Workshop on Transverse-Momentum-Dependent Distributions, held in Trento, Italy, and is a member of the Program Committee for the 19th Particles and Nuclei International Conference, to be held at MIT in 2011. In addition, she is a member of the Scientific Advisory Committee for the Niccolo' Cabeo International School on Nucleon Structure, Spin, and Related Subjects, founded in 2010 and to be held annually.

Future Work

Dr. Aidala will continue her work on FVTX assembly, bring her preliminary results for cross sections and double-helicity asymmetries of charged hadrons to publication, and work to achieve a preliminary and then published measurement of the transverse single-spin asymmetry of eta meson production in the PHENIX proton-proton collision data. The latter asymmetry measurement extends previous work on the transverse spin structure of the proton and transverse-momentum-dependent distributions, sensitive to quark and gluon dynamics, and will provide essential data to continue fueling the rapid advance of the study of the origin of the proton's spin.

Conclusion

Dr. Aidala has published or submitted for publication four papers and released two new preliminary results based on PHENIX data, as well as submitted one phenomenology paper independent of PHENIX, since the time of this report last year. These results help to constrain the gluon spin contribution to the proton spin, explore gluon dynamics in the proton, provide data against which to test the applicability of perturbative QCD techniques, and enable perturbative QCD calculations for eta mesons to be performed

for the first time. How quarks and gluons make up the proton is a basic scientific question that has yet to be understood, and answering this will improve our understanding of one of the most fundamental building blocks of nature.

Publications

Adare, A.. Measurement of neutral mesons in p+p collisions at √s = 200 GeV and scaling properties of hadron production. *Physical Review D.*

Adare, A., and E. Tal. Double helicity dependence of jet properties from dihadrons in longitudinally polarized p+p collisions at sqrt(s) = 200 GeV. 2010. *Physical Review D.* **D81** (012002): 1.

Adare, A., and E. Tal. Transverse momentum dependence of η meson suppression in Au+Au collisions at √sNN = 200 GeV. 2010. *Physical Review C.* **82**: 011902.

Adare, A., and E. Tal. Measurement of transverse single-spin asymmetries for J/Ψ production in polarized p+p collisions at √s = 200 GeV. *Physical Review D.*

Adare, A., and E. Tal. Cross section and double helicity asymmetry for eta mesons and their comparison to neutral pion production in proton-proton collisions at √s = 200 GeV. *Physical Review D.*

Aidala, C. A., F. Ellinghaus, R. Sassot, J. P. Seele, and M. Stratmann. Global analysis of fragmentation functions for eta mesons. To appear in *Phys. Rev. D.*

Exploring the Expanding Universe and the Nature of Dark Energy

Katrin Heitmann
20090521PRD2

Introduction

In 1998, two independent teams measuring the light from distant supernovae made an extraordinary discovery: the expansion of the Universe is accelerating. In the last 10 years, this discovery has been confirmed by completely different measurements of the large-scale distribution of galaxies in the Universe, of the cosmic microwave background radiation, and by measuring the abundance of clusters of galaxies in the Universe. The cause of the accelerating expansion is completely unknown, although it has a name – "dark energy". Understanding this cause is the most important question in cosmology. The aim of the current project is to characterize the nature of dark energy with special emphasis on the dark energy equation of state. Currently, dark energy caused by a cosmological constant is consistent with all measurements, but its magnitude is in contradiction with the Standard Model of particle physics by ~100 orders of magnitude. In order to exclude a cosmological constant, the dark energy equation of state would need to be a dynamical quantity. In this project, three major research directions are investigated: (i) How can we extract a time variation in the dark energy equation of state from current and upcoming data in a model-independent way? (ii) What would be the observational signatures of an early dark energy scenario, which would point to different physics than a cosmological constant? (iii) How can we distinguish dark energy from a modification of gravity on the largest scales? The project makes use of sophisticated statistical methods, simulations, and publicly available data.

Benefit to National Security Missions

This project will support the DOE mission of the Office of Science and NASA which have made unraveling the secrets of dark energy one of their top priorities. In addition, as part of this project new statistical methods will be developed which will be important for our national security mission in general.

Progress

The first major aim of this project is to develop a new reconstruction method for the dark energy equation of state. For such a method to be bias-free, it should not rely on very specific model assumptions, in other words it should be parameter free. Together with the statistics group at UC Santa Cruz, a new reconstruction method has been developed as part of this project. The method is based on Gaussian Process Modeling. This method is usually used for regression problems in statistics, it was adapted to the reconstruction problem of the dark energy of state for this project. It was demonstrated that the method yields reliable results for simulated supernova data; our paper will appear in Physical Review D [1]. The simulated data provided a very controlled testbed and allowed the comparison to standard parametric methods. The new GP approach is clearly superior, especially if the data have some feature that need to be captured. Next, the method was applied to real supernova data. The results are in agreement with a cosmological constant, the currently simplest explanation for the accelerated expansion of the Universe. A paper has been submitted to Physical Review Letters [2]. The method is currently extended to include a diverse set of cosmological probes and first results are very promising. In addition, parametric reconstruction methods for different cosmological observables besides the dark energy equation of state have been investigated. A paper on the results in under review [3].

The second major aim of the project is to characterize the imprints of early dark energy on different cosmological probes. A fully self-consistent treatment of dark energy fluctuations has been carried out and the imprint of these fluctuations on measurements of the cosmic microwave background have been determined. It was found that these effects can be measured and different models of early dark energy can be distinguished. An example for the effect of the perturbations on the power spectrum is shown in Figure 1. The results have been published in the Astrophysical Journal [4]. As a follow-on project, the imprints on large scale structure probes have been investigated. Both, the cluster mass function and the Sunyaev-Zeldovich power spectrum are sensitive to early dark energy and with future measurements, it will be possible to rule out or confirm such models.

The results are currently under review in the Astrophysical Journal [5].

The project has made overall very good progress in two of the three major research areas outlined in the introduction.

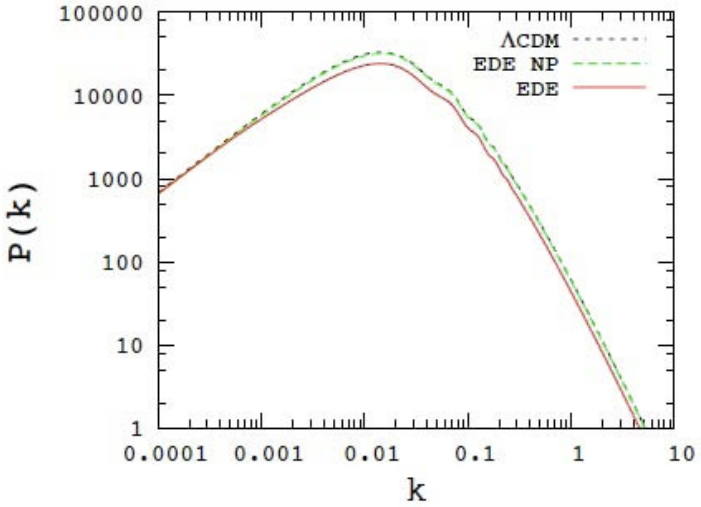

Figure 1. Power spectrum for the standard model of cosmology (black dashed line), an early dark energy model without taking perturbations into account (green dashed line), and the same early dark energy model with the perturbations self-consistently included (red solid line). The effect of the perturbations is clearly visible.

Future Work

This project targets the characterization of dark energy. Currently, the accelerated expansion of the Universe can be explained by introducing a cosmological constant into Einstein's theory of general relativity. A cosmological constant has several theoretical problems: the origin is unclear and the prediction for such a term from the Standard Model of particle physics is ~100 orders of magnitudes different from what we observe. In order to disprove a cosmological constant, the first step is to find a time-dependence in the dark energy equation of state. The first major aim of this project is to develop a new way to constrain such a time dependence in a non-parametric way. This approach has to be applied to supernova measurements as well as large-scale structure probes. Currently, the dark energy equation of state is most commonly parametrized by a two-parameter fit which is too restrictive for gaining a deeper understanding of a possible deviation from a cosmological constant. The second major aim of the project concerns the investigation of early dark energy models and their imprints on current and future cosmological observations. The first step here is to characterize such imprints and to develop a strategy to disentangle them from other effects. Once a unique characteristic has been identified and perhaps seen in observations, more substantive dark energy models could replace the simplistic assumption of a cosmological constant. The third major part of this project concerns the question of how to distinguish a dark energy from modification of general relativity on largest scales. If this turns out to be the reason for the accelerated expansion of the Universe, it would disprove the existence of a cosmological constant. Therefore, a major aim of our project is to find unique signatures in cosmological measurements that can distinguish these scenarios.

Conclusion

During this project a new non-parametric way for characterizing the dark energy equation of state will be developed, substantive dark energy models and their imprints on observations investigated, and modifications of general relativity on very large scales will be confronted with current observational data. This project will advance our understanding of the nature of dark energy, which makes up 70% of the content of the Universe and is one of the biggest puzzles in science today. Multi-billion dollar national and international programs are devoted to understanding the origin of dark energy; our work will help build their theoretical foundations.

References

1. Holsclaw, T., U. Alam, B. Sanso, H. Lee, K. Heitmann, S. Habib, and D. Higdon. Nonparametric reconstruction of the dark energy equation of state. To appear in *Physical Review D.*

2. Holsclaw, T., U. Alam, B. Sanso, H. Lee, K. Heitmann, S. Habib, and D. Higdon. Nonparametric dark energy reconstructing from supernova data. *Physical Review Letter.*

3. Alam, U.. Constraining perturbative early dark energy with current observations. 2010. *Astrophysical Journal.* **714** (2): 1460.

4. Pan, A. V.. Reconstructing dark energy: A comparison of different cosmological parameters. *Physical Review D.*

5. Alam, U., Z. Lukic, and S. Bhattacharya. Galaxy clusters as a probe of early dark energy. To appear in *The Astrophysical Journal.*

Publications

Alam, U.. Constraining perturbative early dark energy with current observations. 2010. *Astrophysical Journal.* **714** (2): 1460.

Alam, U., Z. Lukic, and S. Bhattacharya. Galaxy clusters as a probe of early dark energy. To appear in *The Astrophysical Journal.*

Holsclaw, T., U. Alam, B. Sanso, H. Lee, K. Heitmann, S. Habib, and D. Higdon. Nonparametric dark energy reconstructing from supernova data. *Physical Review Letter.*

Holsclaw, T., U. Alam, B. Sanso, H. Lee, K. Heitmann, S. Habib, and D. Higdon. Nonparametric reconstruction of the dark energy equation of state. To appear in *Physical Review D.*

Pan, A. V.. Reconstructing dark energy: A comparison of different cosmological parameters. *Physical Review D.*

Non-equilibrium Phenomena in Physics, Biology and Computer Science

Michael Chertkov
20090525PRD2

Introduction

We are studying non-equilibrium phenomena in physics, biology, computer and network science.

Our research has four main directions. First, we will work on the dynamics of biological membranes, vesicles and cells. We will develop a new spectral boundary integral code to simulate membrane dynamics and will extend existing analytical models to include effects of membrane interaction with actin and cytoskeleton networks, membrane proteins and the environment. Armed with this code, we will study various intra-cellular biological processes, such as membrane nanotube formation, propulsion of active cells, viscoelastic mobility of blood and other complex biological fluids. Second, we will study statistics of pressure and stress fluctuations in complex fluids. The noisy part of measurements is usually considered to be an inevitable annoyance, but it actually contains valuable information which could be extracted and used in lieu of formal statistical modeling. We will develop a data-driven modeling approach aimed at discovering which microscopic features can be inferred from the measurements. Third, we will utilize methods of non-equilibrium statistical physics for building better computer science algorithms. In particular, we will work on an accelerated Markov Chain algorithm via controlled violation of reversibility. Finally, we will apply concepts and approaches from non-statistical physics to analysis of non-equilibrium (transient) phenomena in power networks.

Benefit to National Security Missions

This project will support the DOE mission in Basic Science by enhancing our understanding of the dynamics of biological membranes, vesicles and cells, statistics of pressure and stress fluctuations in complex fluids and developing modeling approach aimed at discovering which microscopic features can be inferred from the experimental measurements

Progress

New phenomena were discovered while studying the statistics of heat dissipation in single polymer dynamics. The probability distribution function does not have a large-deviation form, and is instead described by a universal exponential tail. (in collaboration with M. Vucelja, M. Chertkov)

The effect of membrane buckling was shown to explain the phase diagram of vesicle motion observed in experiments of Victor Steinberg. (in collaboration with S. Vergeles and V. Lebedev)

The large deviation function of currents and occupation numbers in Jackson queuing networkds were shown to have a universal form. It was proven that the system is not ergodic, and the PDF of final occupation number is different from the PDF of average occupation number. The manuscript has appeared in J. Stat. Phys. (in collaboration with D. Goldberg, M. Chertkov, V. Chernyak)

We studied control of losses and consumption in power grids. Several decentralized control techniques based on the smart inverters were proposed and analyzed. It was shown that these techniques achieve a very solid performance comparable to the control based on global optimization. One manuscript was submitted to IEEE PES conference, and was invited to the super-session on renewable generation. Another manuscript was submitted to IEEE SmartGridComm conference. (In collaboration with S. Backhaus, M. Chertkov, P. Sulc)

A novel computational method based on dynamic programming was proposed for assessing the risks of excessively high voltage drop in feeder lines with significant uncertainty in power generation/consumption. The manuscript was accepted for presentation at IEEE SIBIRCONN conference.

A scheduling technique for Plug-In-Hybrid-Electric-Vehicle charging was proposed and shown to achieve almost optimal performance. This technique allows significant reduction of fluctuations in consumption and reduces the risks of exceeding the maximal power consumption (in collaboration with S. Backhaus, M. Chertkov, N. Sinitsyn).

Future Work

Recent developments in micro-fluidic and optical experimental techniques open new opportunities for observing and manipulating micro- and nano-scale systems. This progress has given rise to a number of new challenges and questions, such as how to analyze experimental data and infer properties of the system provided that it exhibits complexity on multiple scales? Moreover, such systems exhibit a high level of fluctuations, making the task of learning the underlying model even more intricate. The main theoretical complication in dealing with strongly-fluctuating, multi-scale systems is that they are out of equilibrium and there are almost no universal approaches for analyzing them.

We will pursue research in three main directions. First, we will work on the dynamics of biological membranes, vesicles and cells. We will develop a new spectral boundary integral code to simulate membrane dynamics and will extend existing analytical models to include effects of membrane interaction with actin and cytoskeleton networks, membrane proteins and the environment. Armed with this code, we will study various intra-cellular biological processes, such as membrane nanotube formation, propulsion of active cells, viscoelastic mobility of blood and other complex biological fluids. Second, in close collaboration with experimentalists at LANL we will study statistics of pressure and stress fluctuations in complex, e.g., micro-rheological and biological, fluids. The noisy part of measurements is usually considered to be an inevitable annoyance, but it actually contains valuable information which could be extracted and used in lieu of formal statistical modeling. We will develop a data driven modeling approach aimed at discovering which microscopic features can be inferred from the measurements. We will continue work on an accelerated Markov Chain algorithm via controlled violation of reversibility. Finally, we will make further progress on understanding non-equilibrium phenomena in optimization and control of networks, in particular power grids.

Conclusion

The results will improve our understanding of the processes responsible for unusual behavior of biological and synthetic systems on intra- and extra- cellular scales and will suggest new ways of performing quantitative measurements. The numerical codes developed for simulation of membranes can be later integrated into large scale simulations. Understanding the statistical properties of noise in non-equilibrium systems should be useful for developing new micro-rheological experimental techniques. The irreversible modifications of MCMC algorithms could be incorporated into existing codes to accelerate simulations of proteins and macromolecules, biological and artificial networks, and other condensed and soft matter systems. Our efforts in analysis of non-equilibrium phenomena over networks, specifically power grids, will help to design efficient approaches to the network optimization and control.

Publications

Chernyak, V., M. Chertkov, D. Goldberg, and K. Turitsyn. Non-Equilibrium Statistical Physics of Currents in Queuing Networks. 2010. *JOURNAL OF STATISTICAL PHYSICS.* **140** (5): 819.

Turitsyn, K. S., Lipeng Lai, and W. W. Zhang. Asymmetric disconnection of an underwater air bubble: persistent neck vibrations evolve into a smooth contact. 2009. *Physical Review Letters.* **103** (12): 124501 (4 pp.).

Turitsyn, K., M. Chertkov, and M. Vucelja. Irreversible Monte-Carlo algorithms for efficient sampling. To appear in *Physica D.*

Turitsyn, K., N. Sinitsyn, P. Sulc, and M. Chertkov. Robust Broadcast-Communication Control of Electric Vehicle Charging. To appear in *IEEE International Conference on Smart Grid Communications.* (NIST, Maryland, Oct, 2010).

Turitsyn, K., P. Sulc, S. Backhaus, and M. Chertkov. Options for Control of Reactive Power by Distributed Photovoltaic Generators. To appear in *IEEE International Conference on Smart Grid Communications.* (NIST, Maryland, Oct).

Turitsyn, K., P. Sulc, S. Backhaus, and M. Chertkov. Distributed control of reactive power flow in a radial distribution circuit with high photovoltaic penetration. To appear in *Power and Energy Society General Meeting, 2010 IEEE.* (Minneapolis, July 2010).

Theoretical/Computational Research on Particle Acceleration by Intense Laser Pulse

Brian J. Albright
20090528PRD2

Introduction

Generation and acceleration of charged particles are of importance to many fields of activities, such as tumor treatment with proton/ion beams in medical physics, "fast ignition" of fuel capsule with electron/proton beams for inertial fusion energy and radiation sources from electron beams for chemistry, biology and material science.

Conventional technologies to produce and accelerate charged particles are costly, however recently a class of novel particle sources and efficient acceleration methods has emerged following the development of high-power-lasers. When these lasers are tightly focused onto gas jets or solid targets, reaching ultrahigh-intensities of above 10^18 W/cm^2, acceleration fields as high as 10s of TV/m can be produced from the intense laser plasma interactions, surpassing those in conventional accelerators by six orders of magnitude. Electrons or ions in the targets can be accelerated promptly, forming unprecedented beams with low-emittance, short-duration and high-brightness. At LANL, the Trident facility with 250TW, 500fs laser beam is well suited for the study of laser-ion acceleration. A proposed Extreme Light Infrastructure in Europe as well as comparable intensity laser facilities envisioned as part of the LANL MaRIE facility would enable the laser matter interaction in ultra-relativistic regime (I >10^23 W/cm2), opening doors to energetic particles and radiation beams of femtosecond to attosecond duration.

We plan to explore new concepts such as staging of ion acceleration with double foils to improve beam quality and develop theoretical understanding of such processes with the help of large scale Particle-In-Cell (PIC) computer simulations on Lobo, Coyote, and the open Roadrunner supercomputers at LANL, as well as the ORNL Jaguar supercomputer. The proposed work will involve close collaboration with the Trident short pulse experimental team from LANL P-24 in designing and interpreting experiments for laser ion acceleration.

Benefit to National Security Missions

This project will support the DOE mission in Nuclear Weapons by enhancing our understanding of laser-particle sources related to boost in nuclear weapons and ICF physics; it is important for other missions of the Laboratory as well (e.g., Homeland Security), but the emphasis is on DOE/NNSA missions.

Progress

Chengkun has mastered running and analyzing VPIC simulation runs on some of the supercomputers and he has quickly become a leader in the field of laser-ion acceleration. He then reproduced results published by myself and others regarding a new ion acceleration technique, the Break-Out Afterburner (BOA). This is no mean feat, given the complexity of the simulation techniques involved. He developed a new wave-launch capability within VPIC as well as a suite of new diagnostics to analyze the simulations.

Chengkun worked on various projects with high applicability to ongoing experimental efforts at LANL and elsewhere. The bulk of his work was on the proposed technique of employing multiple target foils to condition laser-generated ion beams through the BOA mechanism and prevent long-time energy spread. Chengkun discovered (Figure 1) that use of a second target foil placed behind the nm-scale BOA target, accomplishes three things: 1) it stops the laser, eliminating late-time laser-plasma interaction that degrades beam quality; 2) passage of an ion beam through the second foil exchanges hot co-moving electrons for cold target electrons, thereby slowing beam expansion (which occurs at the ion sound speed, which scales as the square root of the electron temperature); and 3) the production of a second electrostatic sheath at the rear of the second foil produces a "chirp" on the ion beam that counteracts the disadvantageous chirp the beam acquires as a result of the BOA mechanism. These effects are shown in Figure 2 and Figure 3. As a result of this work, he has shown how to maintain high beam quality at only a modest cost in mean beam energy, a substantial advancement toward the feasibility of using laser-ion accelerators for

applications such as ion fast ignition inertial fusion.

Chengkun has also worked on related side projects, including laser acceleration of proton beams, and the use of low-density aerogel targets and gas jets for ion beam collective acceleration and stopping, both of which have much potential applicability in laser-ion and conventional accelerator fields. He has also continued to work on positron and ion wakefield accelerators, which are related to (and complement) laser-ion accelerators and which enables him to remain a scientific leader in these fields. He visited the Max Planck Institute for Quantum Optics in Munich, Germany, for one month during Summer 2010 to collaborate on first-ever ion wakefield accelerator experiments.

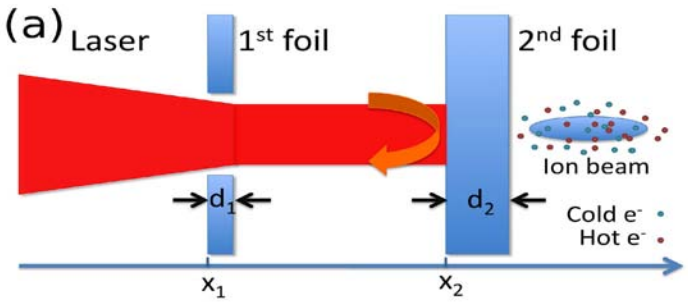

Figure 1. Diagram of the two-foil configuration for tailoring a laser-driven ion beam. In this concept, the laser turns the first foil relativistically transparent and begins a period of enhanced acceleration. To prevent degradation of the quality of the ion beam at late time from laser-interaction with the co-moving electrons, a second foil is used as a fast optical switch to turn off the beam.

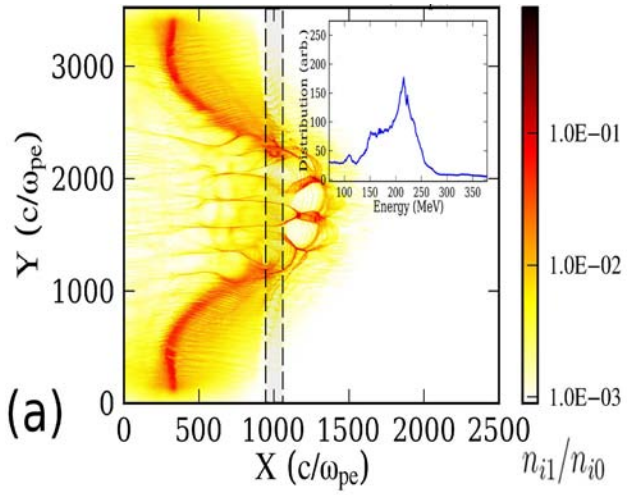

Figure 2. Two dimensional kinetic plasma simulations of multi-foil concept. Shown is ion charge density from laser-interaction with a nanoscale, diamond-like-carbon target. The inset is energy distribution of the ion beam, showing 23% energy spread (without the second foil, no such quasi-monoenergetic beam would be possible).

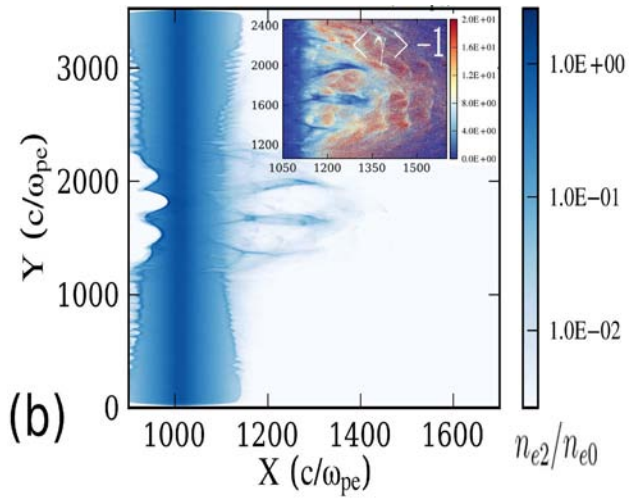

Figure 3. Density and energy (inset) of electrons from the second target foil. One of the benefits of having a second foil is that it enables a tradeoff of co-moving hot electrons (which also lead to late-time expansion of the ion beam) with cold electrons from the second foil. Optimizing this exchange is key to making high quality ion beams using techniques such as the Break-Out Afterburner.

As evidence of his prodigious accomplishments, Chengkun has presented papers and posters in several venues. He showed a poster at the Anomalous Absorption Conference in Snowmass, Colorado (the premier conference in the world for laser-plasma interaction), the European Physical Society Division of Plasma Physics meeting in Dublin, Ireland, the American Physical Society Division of Plasma Physics meeting in Atlanta, Georgia, and he presented a poster on his work at the LANL Accelerators and Electromagnetic Radiation capability review.

Chengkun's work on multiple target foils will be presented by him in a prestigious invited talk at this Fall's American Physical Society Division of Plasma Physics held in Chicago 7-12 Nov., 2010.

Based on his work for this project, Chengkun has authored or co-authored seven scientific papers in the past year, including two Physical Review Letters (one as first author); he has one more paper in preparation based on his last Summer's research. An image he prepared appeared on the cover of *Symmetry* magazine, a popular journal focusing on advances in particle physics.

We anticipate that at least two of the ideas developed in this project may be appropriate for pursuing patents over the next year and the PI has spoken with individuals in the LANL Tech Transfer office about pursuing this work.

Future Work

Several applications for laser-particle accelerators are near-

ing practicality with the work done thus far on this project. Over the next year, we will continue to refine the multi-foil concept for ion beam conditioning as well as explore two new ideas for which preliminary kinetic simulations using the VPIC code show promise:

1. The first is the production of wakefield accelerating structures from electron bunches that naturally form as a consequence of enhanced ion acceleration techniques, like the break-out afterburner (BOA). When these coherent bunches of electrons interact with low-density plasma (e.g., from an aerogel or a gas jet), they can make very intense, extended regions over which particles can be accelerated. We hope to refine these ideas and guide experiments of the same.

2. The second is the use of a curved second foil to focus the ion beams generated by the BOA. An ability to focus these ion beams is critical to missions such as ion based fast ignition and this is a necessary next step toward generation of these sources.

A third task will be for the PI and postdoc to jointly write an LDRD ER proposal to explore computational modeling techniques within kinetic simulations for lasers at extreme scale (intensity higher than 10^23 W/cm^2), where radiation back-reaction and electron-positron pair production become important.

Chengkun will also participate in a collaboration with several outside researchers on an innovative idea for proton wakefield acceleration; this team includes essentially all of the leading researchers in this field. Since the number of collaborators on the form is limited, this list is reproduced here for completeness: From the Max Planck Institute for Physics, Muenchen, Germany: A. Caldwell, O. Reimann, H.V.D. Schmitt, F. Simon, G. Xia; from the Budker Institute for Nuclear Physics, Novosibirk, Russia: K. Lotov; from Duesseldorf University, Duesseldorf, Germany: A. Pukhov, N. Kumar; from CERN, Geneva, Switzerland: R. Assmann, F. Zimmermann, I. Efthymiopoulos, J.P. Koutchouk, S. Hillenbrand; from UCLA, Los Angeles, CA, USA: W. An, C. Joshi, W. Lu, W.B. Mori; from USC, CA, USA: P. Muggli; from Max Planck Institute for Plasma Physics, Greifswald, Germany: O. Gruelke; from University of College London, London, UK: A. Lyapin, M. Wing; from Rutherford Appleton Laboratory, Chilton, UK: R. Bingham; from GoLP/Instituto de Plasmas e Fusao Nuclear, IST, Lisboa, Portugal: J. Vieira; from Heidelberg University, Heidelberg, Germany: A. Schoening.

Metrics for this work include publications in refereed journals, participation in scientific meetings, and presentation of these results at high-level technical conferences and workshops.

Conclusion

Our work is answering the fundamental questions regarding the practical application of high intensity lasers for particle acceleration and the methodology of experimental design and optimization for practical usages. We are exploring new regimes of operation. These unique particles sources with ultra-short duration, excellent collimation and high-intensity will lead to a host of emerging technologies, e.g., ion driven fast ignition, hadron therapy of tumors, radiography, preparation and probing of warm dense matter, compact electron accelerator and ultra-short high-brightness X-ray sources. This work will generate substantial improvement in the state of the art in this field and will both better position LANL for leadership in this important area of science, as well as better position Dr. Huang for employment, either as a staff scientist at LANL or as a university professor.

Publications

Albright, B. J., L. Yin, B. M. Hegelich, K. J. Bowers, C. Huang, A. Henig, J. C. Fernandez, K. A. Flippo, S. A. Gaillard, T. J. T. Kwan, X. Q. Yan, T. Tajima, and D. Habs. Ultraintense laser interaction with nanoscale targets: a simple model for layer expansion and ion acceleration. 2010. *Journal of Physics: Conference Series.* **244** (4): 042022.

Gholizadeh, R., T. Katsouleas, P. Muggli, C. Huang, and W. Mori. Preservation of beam emittance in the presence of ion motion in future high-energy plasma-wakefield-based colliders. 2010. *Physical Review Letters.* **104** (15): 155001.

Hogan, M. J., T. O. Raubenheimer, A. Seryi, P. Muggli, T. Katsouleas, C. Huang, W. Lu, W. An, K. A. Marsh, W. B. Mori, C. E. Clayton, and C. Joshi. Plasma wakefield acceleration experiments at FACET. 2010. *New Journal of Physics.* **12**: 085002.

Huang, C. K., B. J. Albright, L. Yin, H. C. Wu, K. J. Bowers, B. M. Hegelich, and J. C. Fernandez. Improving beam spectral and spatial quality by double-foil target in laser ion acceleration. *Physical Review Letters.*

Huang, C. K., B. J. Albright, L. Yin, H. C. Wu, K. J. Bowers, B. M. Hegelich, and J. C. Fernandez. A double-foil target for improving beam quality in laser ion acceleration. *Physics of Plasmas.*

Lu, W., W. An, M. Zhou, C. Joshi, C. Huang, and W. Mori. The optimum plasma density for plasma wakefield excitation in the blowout regime. 2010. *New Journal of Physics.* **12**: 085002.

Muggli, P., I. Blumenfeld, C. E. Clayton, F. J. Decker, M. J. Hogan, C. Huang, R. Ischebeck, R. H. Iverson, C. Joshi, T. Katsouleas, N. Kirby, W. Lu, K. A. Marsh, W. B. Mori, E. Oz, R. H. Siemann, D. R. Walz, and M. Zhou. Energy gain scaling with plasma length and density in the plasma wakefield accelerator. 2010. *New Journal of Physics.* **12**: 045022.

Tuttle, K.. Crashing the size barrier. 2009. *Symmetry.* **6** (5): 1.

Single-Nanocrystal Photon-Correlation Studies of Carrier Multiplication

Victor I. Klimov
20090532PRD3

Introduction

Carrier multiplication (CM) is the process by which a single absorbed photon produces more than one electron-hole pair in a semiconductor. This process offers the potential of increased power conversion efficiency in low-cost single-junction photovoltaics. With carrier multiplication, the extra energy in a blue solar photon is not wasted. To date, transient absorption, the change in absorption spectral features owing to photoexcitation, has been the tool of choice for detecting CM and quantifying its efficiency. This method is based on a significant difference in the recombination dynamics of multiexcitons, which decay via fast non-radiative Auger recombination, and single excitons, which decay via a slow radiative process. However, this technique is not applicable to nanomaterials in which Auger recombination is not pronounced, such as colloidal quantum rods or epitaxial quantum dots. Furthermore, transient absorption requires that measurements are performed on ensembles of particles, which reveal only an average response that may smear out the response of individual particles based upon nanoparticle size, shape, surface passivation, etc. An alternative technique is studying the time resolved photoluminescence (PL) of nanomaterials after excitation with an ultrafast pulse. Time resolved PL has found successful application in both ensemble and single nanoparticles. When combined with fast electronic photodetectors, time resolved PL is a simple to use and powerful technique; however, this technique has been limited to commercially available silicon photodetectors that are sensitive to wavelengths shorter than about 1 micron.

Here, we will demonstrate a new method for studying CM via the analysis of statistics of infrared (IR) photons from nanomaterials with smaller bandgaps that may find broad application in light harvesting applications such as in third-generation photovoltaics. These studies are enabled by a novel IR sensitive superconducting nanowire single photon detector (SNSPD). The SNSPD detectors have proven to be very powerful tools for time resolved PL studies of ensemble IR nanomaterials and should also find successful application to studying single IR nanostructures. In comparison to traditional "dynamical" ensemble methods, this time resolved PL studies of IR nanostructures offers several advantages including (1) single-nanoparticle sensitivity, (2) elimination of complications associated with ensemble heterogeneities and (3) applicability to structures that do not exhibit resolvable Auger decay. This new technique will be based upon photon anti-bunching, which is a phenomenon of individual chromophores that results from a wait time between successive photon emission events. Nanoparticles containing more than one electron-hole pair exhibit a photon bunching signal that arises from the occurrence of emission of two photons (one for each electron-hole pair contained in the particle).

Benefit to National Security Missions

This work aims to understand the process of carrier multiplication (production of more than one electron-hole pair per absorbed photon of sufficient energy). Carrier multiplication can potentially increase the efficiency of photovoltaics and photocatalytics, which is of relevance to societal energy security, remote power sources, and catalytic chem/bio threat neutralization. This work also contributes to basic understanding of materials and especially electronic and optical properties of nanostructures. Finally, it is relevant from the point of view of fundamental chemistry, especially with regard to the problem of electronic materials by design. Our detector work builds capabilities for remote sensing, e.g. for nuclear nonproliferation.

Progress

Over the past year, the focus of this project has been on the development of a new instrument for single-photon counting in the near-infrared (IR). Photon counting for the visible range of wavelengths typically utilizes silicon avalanche photodiodes or photo-multipier tubes. However, few low noise single photon detectors exist for photon energies below the silicon bandgap (wavelengths longer than ~1 μm), and, until recently, those that did exist did not have sufficient time resolution. In order to develop a capability for fast and reliable detection of single IR photons, we have pursued a new detection technology that is based on a superconducting nanowire

single-photon detector (SNSPD) through a collaboration with the National Institutes of Standards and Technology (NIST).

Originally developed for quantum information purposes, the SSPDs consist of a thin superconducting layer of niobium nitride (NbN) nanowire meander that is ~5-10 nm thick and 200 nm wide. The meandering nanowire typically fills a 10 µm square with a fill factor typically about 50%. The nanowire detector is biased at near 95% of the superconducting critical current and is housed in a cryostat cooled to 2.6 K with a closed-loop He cryocooler. When the nanowire absorbs a photon, a hot spot is created that expels the current and causes the current density in the surrounding area to go above the superconducting critical current. Thus, the superconductivity is lost and a voltage pulse is created that can be read out. Due to the cryogenic temperatures, the SSPD and cryostat need to be in a high vacuum chamber, so the light is coupled into the SSPD through a single mode fiber. This allows the SSPD to have a very low dark noise (<100 Hz) with high sensitivity. Additionally, the SSPD has very little dead time (theoretically 30 ps healing time) that should allow 10's of GHz count rates. Thus, the SSPD appears to be a very powerful detector for ultrafast studies of IR nanomaterials.

In February of this year, we tested a SNSPD system extensively on site at LANL that had been provided by Dr. Sae Woo Nam of the Quantum Information and Terahertz Technology group at NIST in Boulder, Colorado. Over a three week period in February of this year, we used this detector system to study multi-exciton dynamics in a variety of IR emitting quantum-confined nanomaterials, including:

1. Lead-selenide (PdSe) and lead-sulfide quantum dots of several sizes
2. Two sizes of PbSe nanorods
3. Germanium quantum dots
4. PbSe/CdSe/CdS Type II quantum dots

When compared to photoluminescence (PL) upconversion (uPL), the previous standard technique for ultrafast IR PL measurement, the SSPD has reduced time resolution (>40 ps compared to sub-100 fs) but much higher detection efficiency and is much more user friendly. The SSPD was able to measure low pump fluence single exciton dynamics in about an hour that would take uPL 8-10 hours. This then allowed several measurements that were never possible with uPL. Due to the very Gaussian nature of the SSPD instrument response function, the SSPD traces can be deconvolved to extract the true exciton dynamics at very early times (< 60 ps). One major result we achieved was measuring the carrier multiplication (CM) efficiency of novel PbSe nanorods where we saw a slightly enhanced exciton yield as compared to traditional spherical quantum dots (see Figure 1). Here we show the estimated exciton multiplicity per individual nanostructure, <N>, as a function of pump fluence for nanorods and spherical nanocrystals and see a modest increase in yield at higher pump energies for the nanorods.

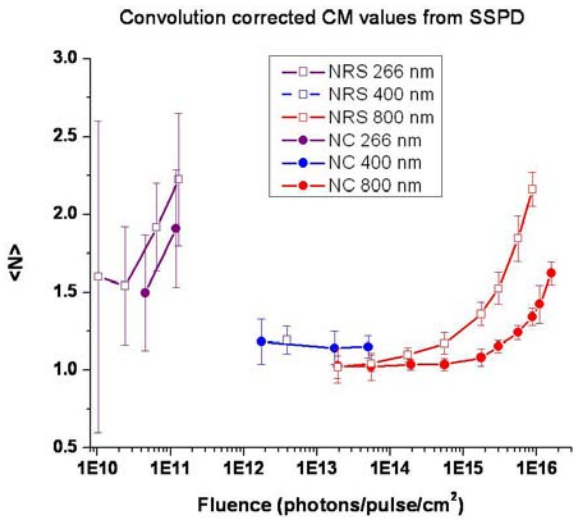

Figure 1. The estimated exciton multiplicity per individual nanostructure, <N>, as a function of pump fluence for nanorods and spherical nanocrystals. These data demonstrate a modest increase in CM yield at higher pump energies for the nanorods.

These preliminary results are very encouraging and are being summarized for publication in two papers, one which describes how we use the SNSPD system for CM efficiency measurements in IR nanomaterials and the second describing our results of studying PbSe nanorods with enhanced CM efficiencies. The application of the SSPD to ultrafast PL lifetime measurements of IR emitting nanomaterials appears to be a breakthrough technique that will greatly accelerate the analysis and screening of synthetic nanomaterial for practical applications such as light-emitting diodes and photovoltaics.

Future Work

In addition to loaning us a SNSPD system in February, our collaborators at NIST earlier this year retrofitted a closed cycle cryo-cooler system we had with a two channel SNSPD system that we currently have up and running in our lab at LANL. This dedicated system is being set up in a new optics lab with a new dedicated laser system for both ensemble and single nanostructure studies. Currently, we are in the last steps of setting up the lab and expect within the next few months to begin single IR nanostructure studies.

With this new dedicated capability here at LANL, we will develop a new method for studying CM via the analysis of statistics of photons emitted by individual nanocrystals. In comparison to traditional "dynamical" ensemble methods, this new technique offers several advantages including single-nanoparticle sensitivity, elimination of complications

associated with ensemble heterogeneities and applicability to structures that do not exhibit resolvable Auger decay. This new technique will be based upon photon anti-bunching, which is a phenomenon of individual chromophores that results from a wait time between successive photon emission events. Nanoparticles containing more than one electron-hole pair exhibit a photon bunching signal that arises from the occurrence of emission of two photons (one for each electron-hole pair contained in the particle).

Photon bunching intensities will be measured and related to CM efficiencies for several photon energies in individual particles. These studies may reveal resonant CM phenomena, which quantum mechanical mechanisms predict, or continuous energy effects, which incoherent scattering models predict. Either finding will inform and constrain theoretical models of CM. It is generally agreed that the mechanism of CM in nanoparticles is the key to producing optimally efficient CM materials.

Conclusion

Superconducting nanowire single photon detector (SNSPD) for studying IR emitting nanomaterials has been acquired here at LANL and has been used to measure the carrier multiplication (CM) efficiencies of a variety of novel materials. This same technology will be applied to single nanostructure photon bunching studies. Photon bunching intensities will be measured and related to CM efficiencies for several photon energies in individual particles and may reveal resonant CM phenomena or continuous energy effects. Either type of finding will inform and constrain theoretical models of CM. It is generally agreed that understanding the mechanism of CM in nanoparticles is the key to producing optimally efficient CM materials, for applications in photovoltaics and elsewhere.

Correlation in Ultracold and Ultrafast Systems

Lee A. Collins
20090533PRD3

Introduction

The project has two parts: one treats very fast processes and the other very cold gases.

The first part follows the reaction of an atom or molecule to a very short pulse of light produced by a laser. As technology has advanced, lasers have been engineered to produce shorter and shorter pulses that now reach lengths on the order of the time scale that an electron moves within an atom. This interval is an attosecond, which is about the time light takes to cross an atom. Long pulses interact weakly with atoms since the electrons have ample time to relax to the slow changes in the light field. However, for the attosecond case, since the pulse and electron interact on the same time scale, the effects on the atom can be dramatic. Even at the level of quantum mechanics, which governs the behavior of microscopic particles, we can still in certain cases, view an electron as orbiting the central nucleus of an atom, much like a planet around the Sun. Since the laser pulse is shorter than the period of the electron, we can take a snapshot at a particular point within its orbit, in much the same way as a strobe light "freezes" motion. By probing at different times, we can construct a series of frames or a movie of the motion of the electron around its path. This particular sequence in which one laser pulse places the electron in a given orbit while a second laser pulse snaps a picture at a later time is refer to as a pump-probe experiment and occupies our main study into the effects of light on matter. We can also use this device to control the process itself by readjusting the state of the system at a particular time. Since electrons form the glue that binds atoms, and molecules, and solids together, an understanding of their behavior at such a basic level can lead to the development of new materials, the real-time control of atomic processes, and the detailed imaging complex systems.

In the second part, we will study a strange state of matter called the Bose-Einstein Condensate (BEC), which for a gas exists just one billionth of a degree above absolute zero, the lowest temperature possible at which all motion ceases. The temperature is so cold that all the atoms move together, and the BEC acts as a unified object with very different properties than a usual gas. For example, disturbances in the medium flow without friction and once set in motion will continue to travel undisturbed for as long as the BEC is stable. This effect is know as superfluidity and exists in many materials under a variety of conditions. In addition, the medium supports certain stable structures such as vortices, much like little whirlpools but with special properties due their quantum nature. Crossed laser beam have been used to form optical lattices, which trap various parts of the BEC. By adjusting the trap depth, various situations can be studied in analogy to solid state materials. One great advantage of the gaseous BECs is their dilute nature allows them to be imaged and easily manipulated so that their properties can be determined in great detail. The first BECs used simple atoms with very short-range interactions. However, new experiments have begun to study BECs consisting of atoms and molecules with more complicated longer-range interactions. We have focused our studies on a particular set with dipoles moments. In a simple analogy, these dipoles can be viewed as bar magnets influencing each other at a distance through their fields. This longer range aspect complicates the description in that all parts of the BEC can now interact with each other. A basic understanding of these systems can have important applications to such areas as high-precision measurements and even quantum computing.

Benefit to National Security Missions

Fast pulse interactions with materials from atoms to solids allow us to probe and control basic quantum processes in order to improve our understanding of basic materials, to better design new materials, and to change reaction rates in chemical processes. In addition, these fast probes provide new imaging techniques for complex systems. Ultracold systems can provide precision measurement devices such as interferometers and gyroscopes, which significantly exceed current optical capabilities. Dipolar condensates also have applications to the construction of quantum devices, which might be the key to high performance computing.

Progress

The project involves the funding for Director's Postdoctoral Fellow Chris Ticknor, who started at Los Alamos on January 19, 2010 and covers two major scientific goals.

The dipolar condensate project has resulted in two publications {1,2], one in Physical Review Letters (PRL) and the other in Physical Review A (PRA) as well as a PRL in preparation {3}. The research has focused on several important aspects of these systems. The first contribution concerns the basic stability of molecular condensates. For the first time, Chris and a collaborator at Harvard determined the rates of three-body processes for dipolar particles, which provides an important guide to the experimental realization and lifetimes of these objects. The second contribution, reported in a sole-author PRA, also concerns scattering effects but this time confined to two dimensions. The calculations determine the consequence of this restriction and its signature in the collision process. Once again, the research was the first of its kind and is vital to current experimental efforts that also are investigating dipolar gases in reduced dimensions. A third contribution focuses more on the condensate as a whole and investigates many-body effects such as superfluidity. The research shows that an obstacle moving in the dipolar gas will generate distinct effect depending on which way it moves in the gas. This anisotropic response offers an important means to understand collective quantum behavior at a fundamental level. This work will be presented in seminars at CNLS and T-1 at LANL, and at an invited seminar at UNM's Center for Quantum Information and Control.

The second goal involves providing theoretical support for a set of basic pump-probe experiments that first excite Helium into correlated states and then ionize these states to determine their basic characteristics. Since the pulses are on the scale of the interaction, these experiments provide new insights into basic quantum mechanical processes not attained by long-pulse lasers. This work is in collaboration with the Technical University of Vienna and the Institute for Theoretical Atomic and Molecular Physics at Harvard. A series of calculations on Helium have recently been completed on which a paper will soon appear. In this case, the pump laser populates several coupled doubly-excited states. The superposition of these states produces a wave packet that moves around the system. A probe laser at various delay times examines the packet throughout its journey between weak and strong mixings of the states and thus provides a real-time map the basic electronic motion that can directly be compared to experiments. This project serves as a first step to treating simple molecules in which additional pathways such as rotation, vibration, and dissociation open.

Future Work

This project has two components: interaction of ultrafast laser pulses with molecules and ultracold long-ranged systems.

We plan to examine the basic interactions of attosecond pulses with small molecules in order to determine the effects of correlation and the ability to manipulate various reaction paths. We plan to extend our large-scale, highly-parallel simulation methods for solving the time-dependent Schrodinger equation for attosecond interactions with atoms to molecules in order to determine the evolution of the electron. This in turn should lead to means of manipulating the mechanisms to tune the outcome. The understanding at such a fundamental level will greatly elucidate these effects in more complicated systems. Our techniques employ the finite-element discrete variable representation (FEDVR), which has shown linear scaling out to thousands of processors. This scaling permits us to extend the technique to the more complicated molecular systems. Our first demonstration will focus on the two-electron hydrogen molecule to understand the attosecond interaction and its effects on photoionization by multiple photons. Knowledge gained here will permit an extension to other molecules such as nitrogen or carbon monoxide that are garnering experimental interest.

For the ultracold component, we shall also extend our FEDVR approach for nonlinear systems to treat dipolar ultracold condensates. We shall focus on understanding the effects of long-range interactions on the basic condensate properties and how these might be manipulated to design simple quantum algorithms as a basis for computing**.** Additionally the ultracold dipolar gases present a highly controlled and clean means to study he collective behavior at a fundamental level.

Conclusion

The ability to examine basic material systems at the time scale of their most fundamental motions opens broad prospects for both deeper understanding and the development of new materials and new probes that can have a broad impact in a variety of areas. These dipolar systems offer a means to study how quantum systems collectively behave when the presence of other particles are felt even from far away, similar to electrons. Long-range ultracold gases permit the study of the basic mechanisms that control state selection and manipulation that have applications to quantum computing and high precision devices such as gyroscopes and interferometers.

References

1. Ticknor, C., and S. T. Rittenhouse. Three-body recombination of ultracold dipoles to weakly bound dimers. 2010. *Physical Review Letters.* **105**: 013201.

2. Ticknor, C.. Quasi-two-dimensional dipiolar scattering . 2010. *Physical Review A.* **81**: 042708.

3. Ticknor, C., R. M. Wilson, and J. L. Bohm. Asymptotic superfluidity in a dipolar BEC. *Physical Review Letters.*

4. Nagale, S., C. Ticknor, L. A. Collins, J. Burgdorfer, B. I. Sch-

neider, and J. Feist. Ultrafast wavepacket dynamics in the doubly excited states of Helium. *Physical Review A.*

Publications

Ticknor, C.. Quasi-two-dimensional dipolar scattering. 2010. *Physical Review A.* **81**: 042708.

Ticknor, C., and R. M. Wilson. Asymptotic superfluidity in dipolar BECs. To appear in *Physical Review Letters.*

Ticknor, C., and S. T. Rittenhouse. Three-body recombination in ultracold dipoles to weakly bound dimers. 2010. *Physical Review Letters.* **105**: 01201.

Experimental Studies On the Origin of Nucleon Spin

Xiaodong Jiang
20090535PRD3

Introduction

Three large-scale experiments on nucleon spin structure led by the LANL P-25 group collected data during FY-09 at Jefferson Lab (JLab) in Newport News, Virginia. The postdoc funded by this project has led the data analysis effort, supervising and guiding eight Ph.D. students through the analysis process to the final publications, anticipated within the next several months. These results will advance our understanding of how the spin and orbital motion of quarks in the nucleon contribute to the nucleon spin. The goal of these experiments, as part of a worldwide effort, is to collect enough data on many relevant observables to eventually build up a 3-dimensional image of quark motion inside a nucleon, similar in a sense to a medical MRI except in this case the patient is in constant motion. These new results will also motivate new measurements using Jefferson Lab's upgraded 12 GeV beam (JLab 12 GeV) in the near future, and build a strong physics motivation for next-generation accelerator facilities such as the electron-ion collider (EIC).

Benefit to National Security Missions

Understanding the nucleon's spin structure is one of the major physics goals of DOE's nuclear physics program. With an operations budget of $120 million/year, JLab is one of the major US nuclear physics facilities operated by DOE. This project, in which LANL plays a lead role, will produce final physics results for three spin experiments, which took up one-third of JLab's FY-2009 accelerator operation. The Jefferson Lab 12 GeV upgrade is the top priority of the Department of Energy's Office of Science's Nuclear Physics Long Range Plan (2007). Advanced nuclear experimentation techniques build capabilities for trace nuclear detection for, e.g., nuclear nonproliferation.

Progress

Dr. Puckett joined LANL in Oct. 2009. His primary effort has been focused on the data analysis of Jefferson Lab experiment E06-010, which collected data during 2008-2009. Dr. Puckett led the physics data analysis and Monte Carlo simulations, closely interacting with and guiding seven Ph.D. students through the analysis process. Dr. Puckett's contributions to the analysis effort included detailed Monte Carlo simulations used to validate the analysis procedures by which the core physics results were extracted from the data. The preliminary results of E06-010, shown in Figure 1, have been officially released in May 2010. These preliminary results have been presented at a number of major conferences, including but not limited to:

1. The 12th International Conference on Meson-Nucleon Physics and the Structure of the Nucleon at the College of William and Mary in Williamsburg, VA. http://conferences.jlab.org/menu10/

2. TMD2010 - Workshop on Transverse Momentum Distributions
   ECT*, Trento, June 21 - 25, 2010 . http://www.pv.infn.it/~bacchett/TMDprogram.htm

3. 2010 Annual Fall Meeting of the APS Division of Nuclear Physics, Santa Fe, NM. http://www.lanl.gov/dnp/

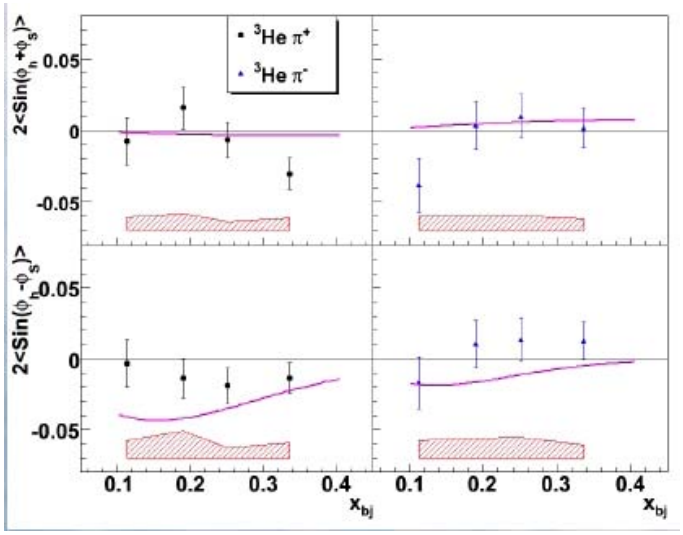

Figure 1. Preliminary results of experiment E06-010 in Jefferson Lab's Hall A. Top left: the Collins single-spin asymmetry(SSA) in the semi-inclusive deep-inelastic

(SIDIS) electroproduction of positive pions, related to the transverse polarization of quarks in a transversely polarized neutron. Top right: the Collins SSA in negative pion electroproduction. Bottom left: The Sivers single-spin asymmetry (SSA) in SIDIS positive pion electroproduction, related to the orbital angular motion of unpolarized quarks in a transversely polarized neutron. Bottom right: The Sivers SSA for negative pions.

Drafts of publications are in preparation in which Dr. Puckett played the dominant role. Publication of the final results is expected in late 2010 to early 2011. The goal of these experiments, as part of a worldwide effort, is to collect enough data on the many relevant and interrelated observables of nucleon spin to eventually build up realistic and accurate 3-dimensional images of the quark motion inside a nucleon. A new experiment proposal (JLab PR10-010, Puckett co-spokesperson) was submitted to the Jefferson Lab Program Advisory Committee (PAC35) in January 2010 to extend the scope of current experiments using the upgraded 12 GeV accelerator at JLab in the near future.

In addition to his primary work on the LANL-led nucleon spin structure experiments, Dr. Puckett has published the final results of a precision measurement of the electric form factor of the proton at high energies, also at Jefferson Lab (experiment E04-108). The measured form factors of the proton are used to construct images of its internal spatial densities of charge and magnetization. Dr. Puckett played a lead role in the experiment and data analysis, and was the lead author of the publication of the final results (see Figure 2) in Physical Review Letters [1]. This experiment was an extension to higher energies of a series of two previous experiments that produced **the most widely cited experimental results from Jefferson Lab to date.** These results have been presented in two conferences at Jefferson Lab, including the 4th Workshop on Exclusive Reactions at High Momentum Transfer and the annual Jefferson Lab Users' Group Meeting, where Dr. Puckett was awarded the 2009 JSA Thesis Prize for his dissertation on the same experiment. Publications of additional physics results from this experiment are in preparation and will be released in the next several months. In light of the improved understanding of the data analysis requirements of this kind of measurement gained from E04-108, Dr. Puckett reanalyzed the data from the predecessor experiment E99-007, in collaboration with its original spokespeople, improving the consistency between the two experiments and within the world database of proton form factors. The new results were presented at the Fall Meeting of the Division of Nuclear Physics of the American Physical Society. A draft publication of the new results has been prepared and will be released in the near future.

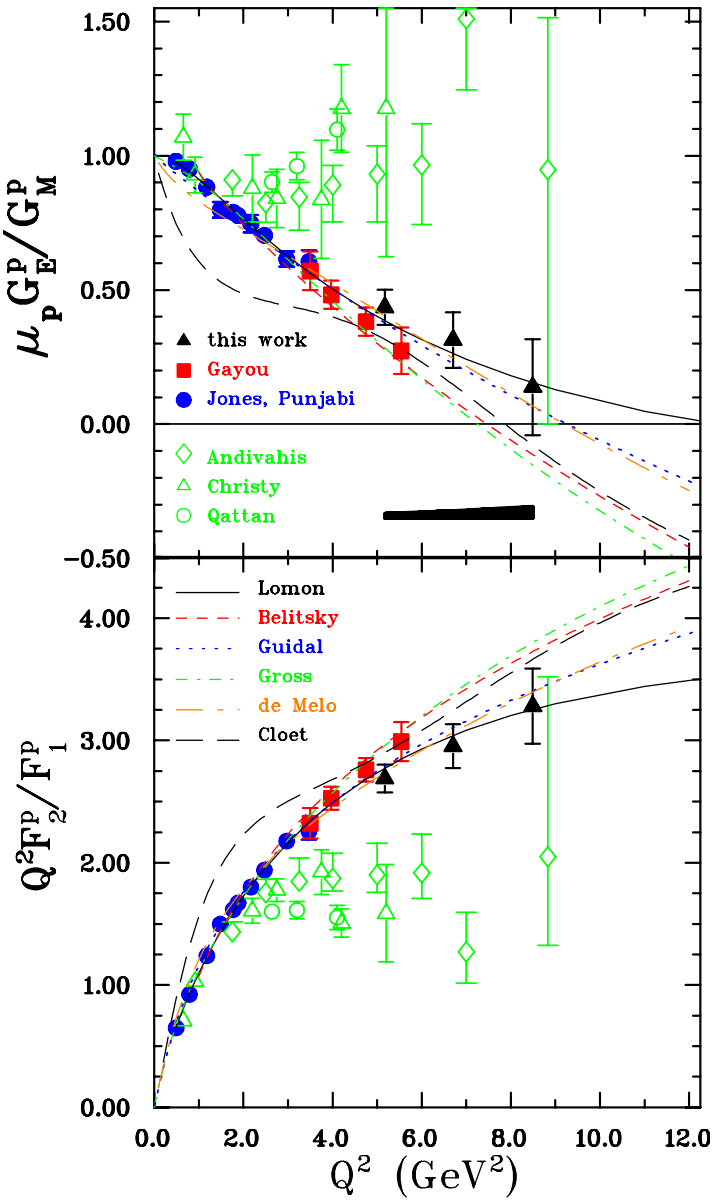

Figure 2. Final results of Jefferson Lab Hall C experiment E04-108, recoil polarization measurements of the proton electromagnetic form factor ratio to Q^2 = 8.5 GeV^2. See reference [1] for details.

Finally, Dr. Puckett is heavily involved in the development of physics proposals for the JLab 12 GeV upgrade era and the physics motivation for a future electron-ion collider (EIC). Efforts include:

- Simulation studies and proposal writing for neutron transverse spin structure measurements in experimental Hall A at JLab using the upgraded accelerator. As a co-PI of this project, Dr. Puckett will submit and present the proposal to the JLab Program Advisory Committee (PAC37) in Jan. 2011.
- Studies of longitudinal proton and neutron spin structure at the JLab 12 GeV upgrade.

- Studies of Charge Symmetry Violation in unpolarized quark distributions (also JLab 12 GeV).
- Measurement of proton form factors at higher energies.
- Feasibility studies and simulations on the extension of these and other physics topics of high current interest to the field to an EIC environment.

Future Work

As detailed in the progress report above, Dr. Puckett's future efforts will focus on two specific areas. The top priority will be to finalize and publish the results of experiment E06-010 on the neutron spin structure. The second effort is the development of follow-up experiments using the upgraded 11 GeV electron beam at JLab, including physics and detector simulations, detector and experiment design, preparation and testing. Two new experiment proposals in which Dr. Puckett is a co-spokesperson were submitted to JLab PAC37 on Dec. 1st, 2010. Pending approval of these proposals, Dr. Puckett will play a lead role in the preparation and execution of the experiments.

Conclusion

Postdoc Puckett is on track to meet or exceed all of the goals laid out in the research proposal. Significant progress and results have already been achieved to date, including publication of the results of part of the proposed research. Ongoing efforts to finalize the results of the completed neutron spin experiments are on track. These first-generation experiments, which provided the world's first data on the neutron transverse spin structure through measurements on Helium-3, have laid the groundwork for future experiments that will vastly improve the precision of our knowledge of the neutron spin structure, with high impact to the worldwide understanding of nucleon spin. These efforts are under way, with Dr. Puckett playing a lead role in the development and execution of the experiments.

References

1. Puckett, A. J. R.. Recoil polarization measurements of the proton electromagnetic form factor ratio to Q^2 = 8.5 GeV^2. 2010. *Physical Review Letters.* **104**: 242301.

Publications

Puckett, A. J. R.. Recoil polarization measurements of the proton electromagnetic form factor ratio to Q^2 = 8.5 GeV^2. 2010. *Physical Review Letters.* **104**: 242301.

Puckett, A. J. R.. Final results of the GEp-III experiment and the status of the proton form factors. To appear in *The 4th Workshop on Exclusive Reactions at High Momentum Transfer.* (Newport News, Virginia, 18-21 May 2010).

al, M. Paolone et. Polarization transfer in the 4He(e,e'p)3H reaction at Q^2 = 0.8 and 1.3 (GeV/c)^2. 2010. *Physical Review Letters.* **105**: 072001.

Cold-Atom-Based Theory and Quantum Simulations for Many-body Physics

Bogdan F. Damski
20090536PRD3

Introduction

We are studying cold atom systems and their use as quantum simulators of superconductors and many-body effects in nanoscale transport. This is a competitive field with broad implications in condensed matter physics, nanoscale science, and quantum information. Quantum simulations use the highly controllable nature of one quantum system (here, a cold atom cloud) to create simplified analogs of complex materials and devices in order to gain direct theoretical and experimental insight into the underlying physical phenomenon. We will develop, theoretically, a scheme for emulations of various superconductors in cold atom setups to address the problems inaccessible in traditional condensed matter settings. In particular, we will develop a theory of the different phases of cold atom systems that incorporates many features of high-Tc superconductors. Further, we will theoretically study properties of these phases and a response of the system to external perturbation (e.g., time dependent magnetic fields). From here, more complex systems will be studied to understand quantum and nonequilibrium effects in nanoscale electronic systems, as well as to provide additional measurement techniques capable of probing the cold atom systems. This will help elucidate the role of electron-electron interactions and dissipation in electronic transport – effects that are difficult to capture in traditional theoretical approaches to transport.

Our work will characterize a promising method for the cold atom emulation of superconductors that will help understand the underlying phenomenon involved. Superconducting materials have the potential to revolutionize power distribution, i.e., create more efficient means of distributing electricity that will be helpful in moving to green sources of energy among other things. Also, we will investigate nonequilibrium and inhomogeneous cold atom systems in order to understand quantum effects in electronic transport, which is crucial in designing functional nanoscale devices.

Benefit to National Security Missions

This work will bring better understanding of high-Tc superconductors: materials with zero electrical resistance. These materials have important applications, e.g., they can eliminate virtually all the loss of energy that goes into resistive heating in the lines transmitting electricity. This research will also advance fundamental understanding of materials on the very quantum level. Both goals are becoming focus areas for numerous sponsors including DOE, for example for both applied and basic aspects of energy research.

Progress

The project has started from studies of the ground state properties of ultra-cold atoms with tunable interactions. It was found that for weakly repulsive interactions cold atoms can simulate a very important paradigm in condensed matter physics: the Landau-Fermi liquid. A detailed study of Fermi liquids can help us understand how atoms can form unconventional Cooper pairs as the interaction varies. This has been widely studied in Helium 3 and A.J.Leggett won a Nobel prize for his work on the subject. So far there have been only limited studies on Fermi liquid properties of ultra-cold atoms. We have proposed to systematically evaluate the parameters required for characterization of a Fermi liquid and address how those parameters can be extracted experimentally. The results are summarized in [1]. Next we will generalize our results to stronger interactions and address possible instability in such systems.

Subsequently studies of how a cloud of ultra-cold atoms respond to density and spin disturbance was performed. Past work on this subject usually ignores the important contribution from the collective excitations of the superfluid and as a consequence the important conservation laws of mass and spin are not respected. We followed well-developed theories in conventional superconductors responding to electromagnetic disturbance and developed a theory that is shown to satisfy the conservation laws. We further applied the theory to Bragg scattering spectroscopy, which is a powerful tool in detecting the superfluid coherence. We have suggested future improvement of experimental techniques. The results are summarized in [2]. Next we generalized our theory to obtain transport coefficients such as shear viscosity and bulk viscosity of

a strongly interacting Fermi gas. There has been a growing interest in the viscosity of quantum fluids such as atomic superfluids and quark-gluon plasma in high-energy physics because they tend to approach certain quantum limits. We found that the shear viscosity decreases as the temperature decreases in the superfluid phase, which contradicts the conclusion from conventional approaches. Recent experimental data from J.E.Thomas' group show decreasing shear viscosity and support our results. The results are summarized in [4]. Moreover, we found that by slight modification, our theory can also explain the behavior observed in optical conductivity of high-temperature superconductors. This implies that the underlying mechanism could be similar and this sheds light on future investigations. We report our results in [5].

We also studied how cold-atom superfluids can simulate non-equilibrium dynamics of conventional superconductors inaccessible in traditional condensed matter setups. We have studied the dynamics of a superfluid approaching a quantum critical point by numerically simulating the equations of motion governing the dynamics of an atomic superfluid. We have analyzed the scaling behavior of non-equilibrium quantities and found that quantum criticality imprints non-equilibrium length and energy scales on the coherence length and the order parameter, respectively. Furthermore, to account for real experimental situations, we studied finite-temperature effects and searched for parameters where signatures of quantum criticality can still be observed. We summarized our results in [3].

Finally, we have studied quantum transport of ultra-cold atoms in optical lattice potentials. We followed a micro-canonical formalism and developed a theory of quantum transport in one dimensional geometry. We are currently developing numerical codes that are capable of simulating the transport of atoms in such a setup. Several experimentally-relevant configurations have been considered. From our preliminary results we found that for two initially disconnected parts, it takes time for correlations to establish after they are connected. By introducing impurities or potential biases, we are investigating the dynamics of correlations building across a quantum point junction. We will compare our analytical and numerical results and publish our findings.

Future Work

In the first part we will generalize a cold-atom based finite-temperature many-body theory to investigate quantum simulations of the pseudogap phase of high-temperature superconductors (HTSCs). This is promising because the pseudogap phase is observed in both systems and ultra-cold atoms have the advantage that interactions and trapping potentials are tunable. It remains a great challenge to explain why electrons form pairs as they do in conventional superconductors but show no superfluidity in the pseudogap phase. Since electrons in HTSCs carry charges while ultra-cold atoms are neutral, not every probing tool can be applied to both systems.

Now that we have better understanding of Bragg spectroscopy of cold atoms, we will investigate its counterpart in superconductors. A promising candidate would be Raman spectroscopy, which may be understood using our unified theory. This can provide more insight into the underlying many-body physics. Previous theoretical work on quantum simulations was limited to either strictly zero temperature or temperatures well above the transition temperature Tc. Our theory has the advantage that it can be applied to a broad range of temperature, including the vicinity of superfluid transition.

Moreover, we will study non-equilibrium superconductor physics in cold atom setups. This will answer how superconductors respond to time-dependent external fields and how critical properties of various superconducting phase transitions can be dynamically observed. This will also clarify the role of non-equilibrium effects in ongoing experiments.

Finally, we will apply our many-body theory to quantum transport in ultra-cold atoms and nano devices such as quantum dots or quantum wires. Ultra-cold atoms can be confined in nano scale and simulate quantum transport in nano devices. It is important to use a unified theory to study quantum transport in both systems. Our goal is to construct a unified theory based on our many-body theory and implement this theory to address how ultra-cold atoms can simulate quantum transport of nano devices.

Conclusion

Our results from quantum simulations will provide more insight into the mechanism of high-temperature superconductivity, which is one of the greatest problems in physics. This can lead to the discovery of novel superconductors with even higher transition temperatures. Superconductivity is one of the most significant discoveries in the 20th century and has important applications in dissipationless power transmission and advanced medical instruments. The unified theory, which we will develop for quantum transport in nanoscale, will lead to new design of nano devices. These new nano devices will play a crucial role in next-generation electronics.

References

1. CHIEN, C. C., and K. Levin. Fermi liquid theory of ultra-cold trapped Fermi gases: Implications for Pseudogap Physics and Other Strongly Correlated Phas. 2010. *Physical Review A.* **82**: 013603.

2. Guo, H., C. C. CHIEN, and K. Levin. Establishing the Presence of Coherence in Atomic Fermi Superfluids: Spin-Flip and Spin-Preserving Bragg Scattering at Finite Temperatures. 2010. *Physical Review Letters.* **105**: 120401.

3. CHIEN, C. C., and B. Damski. Dynamics of a quantum quench in an ultra-cold atomic BCS superfluid . *Physical Review A.*

4. Guo, H., D. Wulin, and C. C. CHIEN. Microscopic Approach to Viscosities in Superfluid Fermi Gases: From BCS to BEC. *Physical Review Letters.*

5. Guo, H., D. Wulin, C. C. CHIEN, and K. Levin. Transport Analogies in Bad Metals and Perfect Fluids: Insights into the Conductivity in high T_c Superconductors. To appear in *New Journal of Physics.*

Publications

CHIEN, C. C., and B. Damski. Dynamics of a quantum quench in an ultra-cold atomic BCS superfluid . *Physical Review A.*

Chien, C., and K. Levin. Fermi-liquid theory of ultracold trapped Fermi gases: Implications for pseudogap physics and other strongly correlated phases. 2010. *Physical Review A - Atomic, Molecular, and Optical Physics.* **82** (1): 013603.

Guo, H., C. Chien, and K. Levin. Establishing the presence of coherence in atomic Fermi superfluids: Spin-flip and spin-preserving Bragg scattering at finite temperatures. 2010. *Physical Review Letters.* **105** (12): 120401.

Guo, H., D. Wulin, C. C. CHIEN, and K. Levin. Microscopic approach to viscosities in superfluid Fermi gases: from BCS to BEC . To appear in *Physical Review Letters.*

Guo, H., D. Wulin, C. C. CHIEN, and K. Levin. Transport analogies in bad metals and perfect fluids: Insights into the conductivity in high T_c superconductors . To appear in *New Journal of Physics.*

Casimir Interactions and Their Applications to Nanomachines and Atom-Chips

Diego A. Dalvit
20090537PRD3

Introduction

The goal of this project is to carry out an intensive theoretical and computational study of the Casimir effect for fundamental and nanotechnological applications. This includes the impact of the effect on both ultracold atoms near macroscopic surfaces (atom-chips) and nanomachines.

In these systems the Casimir interaction is an unavoidable effect. Its knowledge is essential for designing these devices (the effect presents severe challenges, such as the problem of microgears sticking to each other due to attractive Casimir forces, thereby ruining the micromachines), but it could also be used to control them (for example, it provides a contactless force). A reduction or a change of sign of the Casimir force would certainly be important to prevent sticking phenomena in micro-electro-mechanical systems. In this project several configurations involving metals, dielectric, superconductors, and metamaterials are considered in order to use the dependence of the Casimir force on the material to obtain strongly modified forces, and possibly reach the crossover to repulsion.

Benefit to National Security Missions

This project is relevant to DOE mission on nanotechnology and material science, to the DARPA mission by controlling Casimir interations in nanomachines, to the NSF mission on basic science, and to LANL/DOE mission on quantum science and technology.

Progress

Dr. Intravaia has studied Casimir effects in several contexts, both in atom-surface and surface-surface interactions. He was invited to write a review article on Casimir-Polder interactions that will appear as a contributed chapter for the book "Casimir Physics" that will be published by Springer as part of its Lecture Notes in Physics series. He has also looked into the problem of computing Casimir forces between structured surfaces, including gratings and metamaterials. His work involves a formulation of Rayleigh scattering of quantum vacuum fluctuations from complex geometries, and expresses the Casimir force as a multi-scattering process that requires the computation of the frequency-dependent reflection matrices of the Casimir bodies. He is numerically computing such reflection matrices, and in parallel he is developing analytical approaches to predict asymptotic behaviors both at large and small separations.

Together with the chapter for the book on "Casimir Physics", Dr Intravaia has published or submitted for publication a series of papers since he started as Director-Funded postdoc at LANL. One of them involves the Casimir-Foucault interaction and the dependence on temperature of the free energy and entropy. Another one studied the influence of surface plasmons on the temperature dependence of the Casimir force. A third one concerns the application of the modal approach to calculate the Casimir force between multilayer nanostructured surface.

He has also given several invited talks at international conferences, one in Oklahoma at QFEX09 on Influence of External Conditions on Casimir effects, and another in Les Houches, France, on Van der Waals/Casimir and Nanoscale interactions and, very recently, in Dresden on Fluctuation-Induced Forces in Condensed Matter. His talks appeared in the conference proceedings of these conferences. One of them deals with a review of mode contributions to the Casimir effect, another one on the Casimir entropy between perfect crystals, and a third one on the thermal effects of the magnetic Casimir Polder interaction. He presented posters about his research at the International Workshop on Electromagnetic Metamaterials IV, New Mexico.

Renowned experts have also invited Dr. Intravaia to their groups in order to establish or reinforce collaborations. He recently gave talks at the MIT, Yale University, and Harvard University, and he will soon give invited talks at the Ecole Normale Superieure (France) and Université Paris Sud (France).

Future Work

In the near future Dr. Intravaia will continue the study of Casimir forces between complex nanostructures, includ-

ing dielectric/metallic gratings and two-dimensional and three-dimensional metamaterials. He will also start to look into the problem of non-equilibrium Casimir interactions, including heat transfer at the nanoscale in situations out of thermal equilibrium, and in dynamical contexts.

Conclusion

The expected results of this project is a new theory and numerical simulations of tailored Casimir forces between nanomachines and atoms above engineered surfaces. This research will lead to progress in the areas of quantum/atom optics and nanotechnology, and will impact ongoing LANL/DOE programs in nanotechnology and quantum science. This work will have strong impact in fundamental science as well as in technological applications.

The successful experimental implementation of the techniques that will be developed would represent the first demonstration of repulsive Casimir interactions in nanomachines.

Publications

Bimonte, G., H. Haakh, C. Henkel, and F. Intravaia. Optical BCS conductivity at imaginary frequencies and dispersion energies of superconductors. 2010. *JOURNAL OF PHYSICS A-MATHEMATICAL AND THEORETICAL.* **43** (14): 145304.

Haakh, H., F. Intravaia, C. Henkel, S. Spagnolo, R. Passante, B. Power, and F. Sols. Temperature dependence of the magnetic Casimir-Polder interaction. 2009. *Physical Review A (Atomic, Molecular, and Optical Physics).* **80** (6): 062905 (15 pp.).

Haakh, H., F. Intravaia, and C. Henkel. Temperature dependence of the plasmonic Casimir interaction. 2010. *Physical Review A - Atomic, Molecular, and Optical Physics.* **82** (1): 012507.

Henkel, C., and F. Intravaia. ON THE CASIMIR ENTROPY BETWEEN "PERFECT CRYSTALS". 2010. *INTERNATIONAL JOURNAL OF MODERN PHYSICS A.* **25** (11): 2328.

Intravaia, F., S. Ellingsen, and C. Henkel. Casimir-Foucault interaction: Free energy and entropy at low temperature. 2010. *PHYSICAL REVIEW A.* **82** (3): 032504.

Intravaia, F., and C. Henkel. Casimir Interaction from magnetically coupled Eddy currents. 2009. *Physical Review Letters.* **103** (13): 130405 (4 pp.).

Extra-Long-Range Energy Transfer in Hybrid Semiconductor-Metal Nanoassemblies

Victor I. Klimov
20100599PRD1

Introduction

In this project, we will study the effect of surface plasmons (SPs) on dipole-dipole energy transfer (ET) in assemblies of semiconductor nanocrystals. Since SPs are characterized by a large oscillator strength and a significant spatial extent of the electric field, coupling to plasmons increases both the rate and the range of ET. In one example, we will study directional transfer in quantum-dot bi-layers that are combined with metal nanoparticles. We will also investigate the regime of nonlinear transfer where SPs will be used to facilitate a simultaneous transition of excitons from two donor nanocrystals to a single acceptor quantum dot. We expect that this work will be the first unambiguous demonstration of SP-enhanced ET. The observation of robust long-range exciton migration would suggest the possibility of new strategies for light harvesting in photovoltaics, such as using multilayer ET cascades. Plasmon-enhanced ET in nanocrystals is also the first step towards realizing excitonic circuitry, where light may be used, e.g., to perform computations. These results will motivate the study of other more complex phenomena such as SP-assisted nonlinear ET, which could enable active elements of excitonic circuits.

Benefit to National Security Missions

The work conducted in this project is relevant to LANL and DOE interests in both world-class fundamental science and strategic applications. Successful implementation of new strategies for energy transport in hybrid semiconductor/metal assemblies can yield solar-energy-conversion technologies relevant to DOE and LANL missions in Energy Security. At the recent DOE workshop on Basic Research Needs for Solar Energy Utilization, it was recognized that while solar photovoltaics is an important clean energy source, the practical large-scale applications of solar cells would require new concepts and novel materials for solar energy conversion. A novel concept of hybrid semiconductor/metal nanostructures that is explored in this project can potentially help in the realization of such breakthrough technologies that combine low fabrication costs with high power conversion efficiencies.

Progress

Our primary interest has been to demonstrate efficient nonlinear ET, a process by which two excitons of lower energy may recombine to produce a higher energy exciton. This process would have a direct impact on photovoltaic efficiency, since it would enable a first generation solar cell to harvest energy from photons that are below its material bandgap, thereby upgrading it to a significantly more efficient third generation device.

Valuable insights into how such a process could be made to work were obtained from our quantitative model that showed that this process is linearly dependent on the two-photon absorption cross sections of the nonlinear acceptor. Being a three body phenomenon, the process also has a severely limited efficiency due to distance effects between the three interacting states. While we were able to observe evidence of non-linear energy transfer in a disordered ensemble, a higher efficiency is required for practical applications.

In order to resolve these issues we adopted a four part approach. First, we developed the synthesis of CdS/CdSe/CdS/ZnS nanocrystals that have ten-fold higher two-photon absorption cross section than regular CdSe NCs. This development had been addressed in the previous approach.

Second, to achieve even higher cross sections, we used plasmons to enhance the two photon absorption cross sections. We were able to demonstrate values as high as $3x10^5$ GM, that are 30 fold higher than a bare CdS/CdSe/CdS/ZnS NC and 300 times higher than CdSe (Figure 1a). To our knowledge, these represent the highest observed two-photon cross sections for any green emitting fluorophore. By itself, this result has a significant impact in the field of bio-imaging ad two-photon microscopy.

The third thrust focuses on developing new physical principles to reduce the distance scaling for this process. A significant improvement in efficiency could be obtained if two low energy excitons could be “squeezed” into a single emitter giving rise to a Biexciton. While this is expected to significantly increase the efficiency of

nonlinear ET, it also leads to nonradiative biexciton decay via Auger recombination. We therefore also put emphasis on developing new "Auger suppressed" materials. We focused on Copper Indium Sulfide based materials for this study. Specifically, the CIS/CdS system was found to have complete suppression of biexciton recombination on the time scale of a few ns (Figure 1b). Given the high emission efficiencies (>60% typical) that we were able to achieve from this system, it is clearly the material of choice as a nonlinear donor.

A fourth area of research has been to enhance interactions between distant excitons using plasmons. This strategy aims as enhancing the rates of nonlinear ET by introducing radiative coherence between two excitations. We achieved this in silica coated gold spheres that have plasmons that can interact resonantly with NCs attached to the outer silica surface (Figure 1c). Evidence of a radiative coherence is observed in these superstructures, since excitons created on two different NCs within the same superstructure show pronounced cooperative effects. We have been able to observe exciton-exciton cooperative decay even at fluences that are low enough to generate only one exciton per 100 nanocrystals (Figure 1d). By itself, this result represents a significant step forward towards realization of working plasmonic circuitry for applications such as information processing.

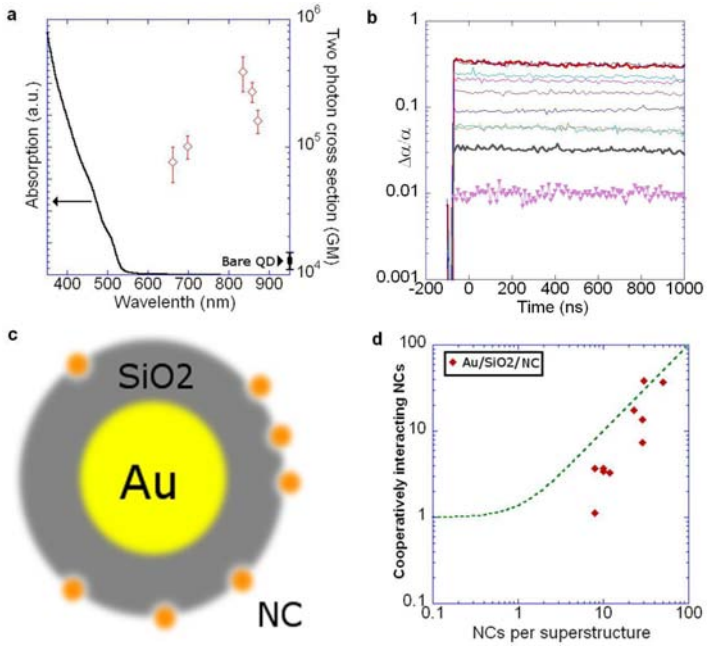

Figure 1. (a) Absorption spectrum of CdS/CdSe/CdS/ZnS NCs (black line), and the two-photon cross sections observed upon attachment to gold nanorods with plasmons at various spectral positions (red diamonds). The two photon cross section of the bare NCs is given by the black square. (b) Suppression of multiexciton decay on the nanosecond timescale in CIS/CdS heterostructures was observed using femtosecond transient absorption experiments. (c) Schematic of a gold/silica/NC superstructure. (d) Cooperative radiative decay is observed in these superstructures. The number of cooperatively interacting NCs (red symbols) closely follows the number of NCs per superstructure. The green line is a Poisson guide to the eye that is expected if all NCs on each superstructure can cooperatively emit radiation.

Future Work

We will now direct our efforts towards two main goals. First all of the four strategies that have already been realized will be integrated into a single plasmonic-excitonic superstructure to achieve efficient nonlinear ET. Second, we intend to explore novel light concentration strategies by utilizing shaped metal structures. Specifically we intend to achieve large scale unidirectional emission from metal-semiconductor hybrids that will enable concentration of diffuse sunlight. This is an important goal for practical applications of nonlinear ET.

Project milestones:

1. The development of hybrid assemblies of semiconductor nanocrystals and metal particles of controlled geometries such as well-defined bi-layers and multilayers.

2. The development of spectroscopic methods for detecting energy transfer dynamics based on time-resolved photoluminescence and transient absorption.

3. Identification of parameters that define the range of energy transfer in hybrid semiconductor/metal nanoassemblies.

4. Experimental demonstration of long-range energy transfer (~100 nm and possibly greater) using the effects of field enhancement in metal nanostructures.

Conclusion

Nonlinear ET represents a novel physical principle that envisages an uphill flow of energy, converting low energy excitations into higher energy ones. Our efforts have been directed towards making this process efficient enough to lead to practical applications. In this regard we have developed novel semiconductor nanocrystal materials that exhibit significantly enhanced nonlinearities. Further these materials were assembled into hybrid metal-semiconductor superstructures that show further enhancements in nonlinear properties of the original NCs. We were also able to demonstrate new materials with suppressed multiexciton recombination that are particularly suited for light concentration. Finally we also demonstrated onset of coherent behavior among distant excitons.

Tracing Fluctuations in the Universe

Katrin Heitmann
20100605PRD2

Introduction

The major focus of the project is to generate sophisticated maps of the Universe by carrying out high-performance simulations of the matter distribution of the Universe and by advancing our understanding of how this matter distribution is connected the distribution of galaxies we observe with large surveys. Once such maps have been created, it is possible to extract new cosmological information from observational data. The project has therefore two challenging components: (i) the simulation of large cosmological volumes for different cosmological scenarios, (ii) the development of reliable models that allows us to populate these simulations reliably with galaxies. Observations in the optical and X-ray will be used for the second step.

Benefit to National Security Missions

The work is most important for scientific discoveries in the field of astrophysics and cosmology and has very strong ties to DOE/SC and NASA. In DOE/SC the work connects to two major offices: HEP and ASCR. The project addresses one of the major questions asked by DOE/HEP and NASA: what is the nature of dark energy and dark matter? The new high-performance codes developed to answer this question addresses very important questions for DOE/ASCR, for example, how to use the next generation hybrid computing machines and how to advance such efforts to the exa-scale era, essential for weapons modeling.

Progress

Dr. Pope has made considerable progress in porting the new large scale structure code MC3 [1] to different supercomputing architectures (Cerrillos/Roadrunner at Los Alamos, Jaguar at ORNL, and the BlueGene system at ANL) and in improving the resolution of the code to resolve length scales an order of magnitude smaller than possible with the current version of the code. These are very important steps to realize the first major aim of the project: developing the best-possible cosmological simulations on the world's fastest supercomputers (note that Jaguar and Roadrunner are the number 1 and 3 in the latest supercomputnig ranking). It also marks important progress in the first sub-task of the project, improving existing cosmological simulation capabilities and develop new analysis tools to analyze the resulting simulations. An invited paper on the new code capability is in preparation. For his work on the code, Dr. Pope won an award from the Los Alamos Award Program for outstanding services. The high-resolution code has been tested carefully and the first very large runs are underway. Figure 1 shows the comparison between the new code and Gadget-2, an established code used by the community. Shown are particles that live in dark matter halos, the hosts of galaxies. The major advantages of the new code are: (i) the code scales to arbitrary big machines and is the first petascale cosmology code, (ii) the code is the first cosmology code that runs on heterogeneous architectures and therefore is an important step to the exascale regime. One simulation is currently being carried out on Roadrunner, encompassing 64 billion particles. This is one of the largest cosmological simulations worldwide. In addition, some smaller simulations have been finished and are currently analyzed. This simulation suite will lead to an important publication. In addition, Dr. Pope mentored a student over the summer and together they ported the code to a GPU (graphics units processing) architecture. This version of the code will be showcased at Supercomputing 2010 (SC10) in November. IBM nominated the GPU version of the code for an award at SC10.

Future Work

The major aim of this project is to connect the dark matter distribution we simulate on high-performance computers to the distribution of galaxies we observe with powerful telescopes. The simulation of cosmological volumes is a daunting task. Currently, the scales involved are too vast to include galaxy formation physics in such simulations and additionally, our models for galaxy formation are not good enough to do so. We therefore simulate the matter distribution for different cosmological scenarios, and by comparing to observations derive prescriptions for populating the simulations with galaxies. After this step, we can extract information about the evolution and content of the Universe. This project

focuses on two aspects: (i) developing the best-possible cosmological simulations on the world's fastest supercomputers, (ii) connecting these simulations to observations to enable the extraction of information about dark energy and dark matter.

Specific tasks in this project therefore include: (i) improving existing cosmological simulation capabilities and develop new analysis tools to analyze the resulting simulations, (ii) based on the evolution of structure extracted from the simulations and comparing to observations, develop new and improved models to populate the simulations with galaxies, (iii) carry out these tasks for different cosmological models, (iv) derive new constraints on cosmological scenarios.

The first task has been successfully carried out. Next, a diverse set of simulations will be carried out for different cosmologies and new models for populating the simulations with galaxies will be developed. Very recent new observations from the Sloan Digital Sky Survey will be used for this task.

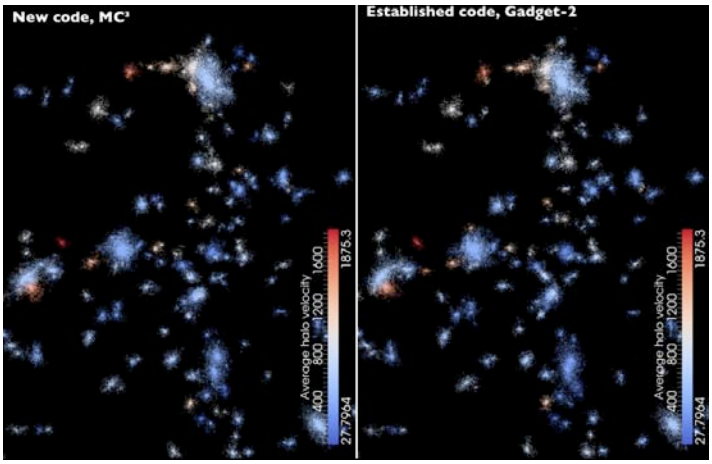

Figure 1. Comparison of the new code and Gadget-2, an established N-body cosmology code. Shown are the particles living in dark matter halos (colored with respect to halo velocities) that host galaxies. The agreement is very good. The major advantage of the new code is scalability and portability: the code can be run on very large heterogenous architectures such as Roadrunner to produce the largest cosmological simulations ever. The code has been designed with future exascale architectures in mind.

Conclusion

The project will lead to (i) improved, world-leading simulation capabilities to follow structure formation in the Universe, (ii) sophisticated models which will allow us to connect the distribution of galaxies to the underlying matter in the Universe at very good accuracy, (iii) new cosmological constraints by comparing different cosmological models to observations, (iv) the development of important new capabilities to analyze future cosmological surveys.

References

1. Pope, A., S. Habib, Z. Lukic, D. Daniel, P. Fasel, K. Heitmann, and N. Desai. The Accelerated Universe. 2010. *Computing in Science & Engineering.* **12** (4): 17.

Publications

Pope, A., S. Habib, Z. Lukic, D. Daniel, P. Fasel, K. Heitmann, and N. Desai. The Accelerated Universe. 2010. *Computing in Science & Engineering.* **12** (4): 17.

Search for CP and CPT Violation in the Neutrino Sector

William C. Louis III
20100607PRD2

Introduction

This project is designed to search for CP and CPT violation in the neutrino sector, where C stands for charge conjugation, P for parity inversion, and T for time reversal. Such a violation would have an enormous impact on nuclear and particle physics because it could possibly explain the matter-antimatter asymmetry in the universe. After the Big Bang, the universe was presumably symmetric in terms of matter and antimatter. However, the universe we observe today consists almost entirely of matter. What has caused this matter-antimatter asymmetry? One possible explanation involves leptogenesis, where a lepton asymmetry in the early universe gets translated into a baryon (or matter) asymmetry. CP or CPT violation in the neutrino sector could then explain how the lepton asymmetry is generated. By analyzing data from the SciBooNE, MiniBooNE, and MicroBooNE experiments at Fermilab, CP violation will be searched for by looking for a difference between electron-neutrino appearance and anti-electron-neutrino appearance. CPT violation will be searched for by looking for a difference between muon-neutrino disappearance and anti-muon-neutrino disappearance.

Benefit to National Security Missions

This work addresses one of the major questions in nuclear, particle, astrophysics, and cosmology, which is the origin of the baryon asymmetry of the universe. A sensitive search for CP and CPT violation can be performed by looking for a difference between neutrino and antineutrino oscillations. Therefore, this work is of great benefit to the Department of Energy Office of Science.

Progress

Warren Huelsnitz has begun learning both the MiniBooNE Analysis Framework and the SciBooNE/MiniBooNE joint analysis that has been partially completed. A crucial aspect of this project is the understanding of the error matrix, which includes both correlated and uncorrelated systematic errors. Warren has started working on the fitting method for the SciBooNE/MiniBooNE joint analysis and on the reduction of systematic errors and methods for improving the fit for neutrino oscillations. In addition, Warren has begun the software design of the data acquisition system for the MicroBooNE experiment. Warren has met with the group that is designing the electronics and has obtained the necessary information for the interface to the data acquisition system.

Future Work

This project will search for evidence of CP and CPT violation in the neutrino sector, where C stands for charge conjugation, P for parity inversion, and T for time reversal, by using results from the SciBooNE, MiniBooNE, and MicroBooNE experiments. SciBooNE is located at a distance of 100 meters from the Booster neutrino source at Fermilab, while MiniBooNE is located at a distance of 500 m. By comparing neutrino and antineutrino event rates in the two detectors, a sensitive search for CPT violation can be made. Therefore, the first goal is a search for CPT violation in the neutrino sector. The second task is to work on the design and development of a new data acquisition system for the MicroBooNE experiment, which will determine whether the low-energy excess observed by MiniBooNE in neutrino mode is due to electron events or gamma events. If the excess is due to electron events, then this will open up the possibility of observing CP violation with the MiniBooNE experiment. Therefore, the second goal is to design a data acquisition system for MicroBooNE. Both goals involve computers and are computational in nature.

Conclusion

This scientific effort will search for a difference between neutrino and antineutrino oscillations. Such a difference would be extremely important because it could possibly explain the reason why the universe we observe today consists almost entirely of matter and not antimatter, even though the universe presumably began with the Big Bang and with an equal amount of matter and antimatter. Therefore, this scientific effort may be able to provide an explanation for why we exist today.

Seeing the Invisible: Observational Signatures of Dark Matter

Alexander Friedland
20100608PRD2

Introduction

We see countless stars by naked eye and myriad of galaxies with powerful telescopes. However, we now have good evidence that the majority of the universe is actually made of an invisible substance called dark matter. Without the gravitational pull of dark matter, many stars would not stay in their orbits around galaxies. Many fewer galaxies would exist to harbor stars since galaxies are made from ordinary matter falling in regions of the Universe with high dark matter density. In addition, dark matter together with dark energy plays a key role in determining the fate of the Universe–whether it will keep expanding forever or eventually collapse back onto itself. Despite its importance, we know very little about the identity and properties of dark matter since it does not emit light. Resolving the mysteries of dark matter is one of the utmost challenges in fundamental physics.

A promising approach to detect dark matter is based on the fact that while dark matter particles do not emit ordinary light, they can still produce visible signatures through decaying or annihilating with other dark matter particles. Dr. Yuksel will investigate the signatures of dark matter annihilation or decay products such as gamma rays, neutrinos, or anti-matter particles and make robust predictions for the experiments and observations. He will then work to incorporate his results into a broader picture of astrophysics, cosmology and physics beyond the Standard Model.

Dr. Yuksel is a recognized world leader in this area. Among his many contributions is a seminal paper on pulsars as being the sources of the excess signal seen at Fermi and PAMELA experiments. His scientific leadership has been recognized by the LANL postdoc committee, which awarded him the Director's Postdoctoral Fellowship for this work.

Benefit to National Security Missions

Detection and identification of dark matter is also a very high priority of the DOE Office of Science (the High Energy Office). Accordingly, LANL has been making a considerable investment in the areas of dark matter detection and modeling. In addition to the dark matter detectors currently under development at LANL, there is also a strong effort in cosmic ray physics, particularly the Milagro experiment and the proposed HAWK experiment. On the theory side, the LANL supercomputing simulations of dark matter by M. Warren et al have been recognized for two decades as world-leading.

The work of Dr. Yuksel outlined in his Director's Fellow proposal will strengthen all these areas and, importantly, will help to integrate them.

Progress

Dr. Yuksel has been pursuing his studies of dark matter and neutrinos as outlined in his research proposal. The primary goals of his research are (1) to determine neutrino properties and their role in astrophysical environments such as supernovae, and, (2) to understand what dark matter is composed of and where it exists in the universe. Both of these challenging tasks should become more feasible as new facilities come on-line and increase the quality and quantity of available data. For this purpose, Dr. Yuksel has participated in a number of workshops at the Ohio State University on "Novel Searches for Dark Matter with Neutrino Telescopes" (July 5-6, 2010), at the Penn State University on "Low Energy Neutrino Physics and Astrophysics" (July 1-2, 2010), and locally organized Santa Fe 2010 Summer Workshop on ``LHC: From Here to Where?'' (July 7-9, 2010). These workshops brought together experts from experimental and theoretical particle astrophysics and formed ideal venues to exchange ideas on how to utilize and expend capabilities of experiments such as IceCube, DeepCore, Fermi, Super-K, and KM3Net for the purpose to better scrutinize the theories of dark matter and neutrinos. Motivated by the challenges and opportunities as identified in these workshops, Dr. Yuksel has begun exploring new ideas towards understanding the identity and properties of dark matter and neutrinos, taking advantage of wide variety of

Motivated by the challenges and opportunities as identified in these workshops, Dr. Yuksel has begun exploring

new ideas towards understanding the identity and properties of dark matter and neutrinos. He has been working on a manuscript in which neutrino induced muon fluxes due to dark matter annihilations in the Sun are presented for well studied CMSSM model as well as other grand unified models such as NUHM2 and flipped SU(5) with universal higgs masses at the GUT scale. In a relevant project, he is also studying the sensitivity of neutrino telescopes to neutrinos arising from dark matter annihilation in the Galactic halo, demonstrating how the dark matter models developed to explain PAMELA positron data and the WMAP/Fermi haze can be deeply constrained. The signatures of these models in the IceCube-DeepCore detector will be assessed (see Figure 1).

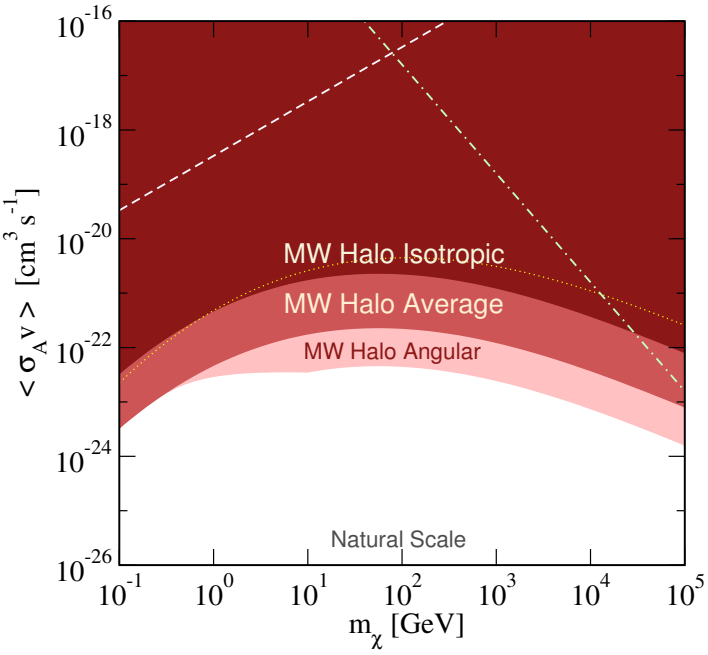

Figure 1. Constraints on the DM total self-annihilation cross-section from various components of the Milky Way halo in a dark matter model in which the principal annihilation products are neutrinos. Since neutrinos are the least detectable Standard Model particles, a limit on their flux conservatively bounds the dark matter total self-annihilation cross section.

Besides these two studies directly relevant to neutrinos and dark matter, Dr. Yuksel has been actively pursuing some other important projects in the field of particle astrophysics. He has recently developed a transport code that can handle propagation of charged particles with very high accuracy in various of magnetic field configurations. This code will be used in modeling variety of open problems in particle astrophysics. For instance, ultra high-energy cosmic rays observed by the Pierre Auger Southern Observatory suggest a marked anisotropy signal with a prominent excess of events from the direction of Cen A, a nearby radio galaxy. Dr. Yuksel is examining the implications of this excess in terms of the magnetic fields at the source, chemical composition of the particles, and, plausible production and injection mechanism of the ultra high-energy cosmic rays (see Figure 2).

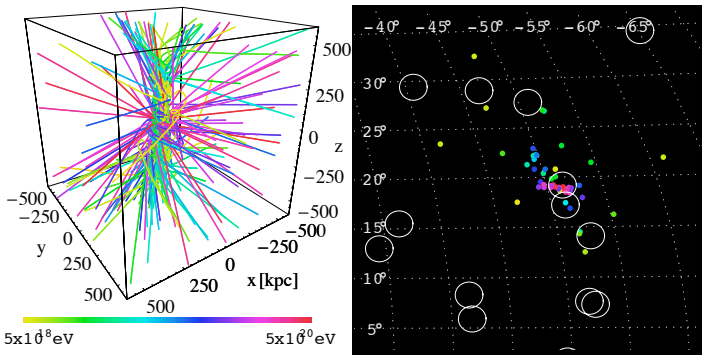

Figure 2. Left: Trajectories of protons (colored according to their energies) as they are leaving the source region. Protons are injected around the origin and their trajectories are determined by the structure of magnetic fields at the source. Right: Auger events around the direction of Cen A are shown with circles and they are to be compared with colored dots of simulated events (assuming source is located at about 4 Mpc distance).

Future Work

Many dark matter candidates have been proposed, from axions to sterile neutrinos to weakly interacting massive particles spanning many orders of magnitude in particle mass. One may hope to reveal the identity of dark matter by direct detection in underground low background experiments, or through missing energy signals at particle accelerators.

A promising alternative approach is based on the fact that while dark matter particles do not emit ordinary light, they can still produce visible signatures through decaying or annihilating with other dark matter particles. The corresponding signals depend on the concentration of dark matter, making precise knowledge of both dark matter distribution and associated astrophysical backgrounds essential. Dr. Yuksel will investigate the signatures of dark matter annihilation or decay products such as gamma rays, neutrinos or anti-matter particles and make robust predictions for the experiments and observations. While this is a challenging task, it is also feasible as the quality and quantity of data is increasing at an unprecedented rate with new facilities now coming on-line, vastly improving past measurements and reaching never-before probed energy scales. In the gamma ray and cosmic ray electron/positron observations, much greater clarity than what had existed in preceding decades has recently been brought by Fermi and PAMELA space missions. Upcoming neutrino telescopes such as Ice-Cube will do the same with neutrinos. Thus, it is timely to combine different parts of the dark matter puzzle, taking into account all new data and observations together with their astrophysical interpretations, in

order to provide better guidance for relevant experimental and theoretical efforts.The results will then be incorporated into a broader picture of astrophysics, cosmology and physics beyond the Standard Model.

Conclusion

Successful accomplishment of this proposed research will enable better discrimination of the candidate theories of dark matter, so that researchers could focus their efforts in more promising avenues. It will provide interpretation for the results of several leading experiments, including the Fermi and PAMELA cosmic ray observatories. It will also help to integrate the results from the direct detection experiments, indirect detection experiments, and supercomputer simulations of dark matter in our galaxy.

Probing Fundamental Physics with Cosmological Surveys

Daniel Holz
20100610PRD2

Introduction

Cosmology is on the brink of a metamorphosis driven by the unprecedented volume of survey data. I will explore ways in which upcoming survey data can shed light on modifications of general relativity, inflationary models, baryonic physics, and galaxy formation. One prediction of cosmological models that is difficult to constrain observationally is the filamentary cosmic web seen in N-body simulations of structure formation. Filaments are interesting because they govern many aspects of structure formation, and are key to understanding how gas is deposited in galaxies and clusters. Filamentary structure is sensitive to the dark energy and other cosmological parameters. It is also sensitive to the initial conditions at the end of inflation, and may contain evidence of modified gravity and non- Gaussianity. Filaments have not been widely studied because they are incredibly diffuse, and do not possess sufficient contrast to detect reliably with current technology. I will develop a stacking technique to detect filamentary structure and characterize its profile observationally using the new survey data, with weak gravitational lensing, galaxy density, and potentially in emission or absorption from gas tracing the dark matter. Both aspects of this work will require use of computing facilities at LANL, and access to the output of cosmological simulations that have been run by member of the cosmology group.

Benefit to National Security Missions

This work directly ties into the standard model for cosmology. It helps us elucidate the essential constituents of our Universe. In addition, the work entails data-intensive computing, with potentially important applications elsewhere.

Progress

In the one month that this project has been running, Alexia has familiarized herself with the LANL computing system, and is beginning analysis of the large cosmological datasets which are being produced at LANL. In particular, she is exploring the importance of different halo finders (friends-of-friend and spherical overdensity) on properties of Sunyaev-Zelodovich maps.

Future Work

We are on the brink of a transformation in cosmological data, including orders of magnitude increase in the number of observed galaxies and galactic clusters, hundreds of thousands of high redshift quasars, and small-scale maps of the cosmic microwave background. This new survey data will further refine the precision to which the cosmological parameters are determined, and they will shed more light on the nature of the dark energy driving the current period of accelerated expansion, which is one of the most important outstanding problems in theoretical physics. But equally interesting, the new data will be sufficiently vast that several new avenues of opportunity will be opened in cosmology. They are (1) to test for modifications of general relativity, such as f(R) models that include other polynomial terms of the Ricci scalar (or 1/R) in the Einstein-Hilbert Lagrangian, models such as DGP which arise due to hidden extra dimensions, or models which arise naturally in string theory; (2) to test for non-Gaussian initial conditions at the end of inflation and evidence of primordial gravitational wave modes, either of which can be used to constrain and/or eliminate vast swaths of inflationary models; (3) to examine more deeply the role of baryonic physics in the formation and shapes of cosmological structures and substructures, and what the ultimate fate of the baryons may be; (4) to connect populations of galaxies to their progenitors at higher redshift so as to probe the evolution of galaxy morphology, metallicity, gas fraction and stellar mass; in short to develop a better understanding of the physics of galaxy formation.

Conclusion

What is the dark energy and dark matter? How are galaxies formed? I will use upcoming surveys (on unprecedented scales) to investigate these fundamental questions. I will develop a pipeline that can be directly used by photometric survey experiments such as DES and LSST for calibration of the redshift distributions. I will also identify astrophysical observables that will identify filamentary structure and use it to illuminate the four scientific areas (1) gravity, (2) inflation, (3) baryons, and (4) galaxies. This work will provide observational tests to

help bridge the theoretical gaps between cosmology, particle physics, string theory, relativity and astrophysics.

Physics of Cosmic Ray Shocks and the High Energy Universe

Hui Li
20100611PRD2

Introduction

Most matter in space and astrophysical systems (stars, galaxies, solar wind, etc.) are made of plasmas. These plasmas, being conductive, generate their own magnetic fields due to large-scale or small-scale dynamo. As microscopic diffusivities are tiny, these magnetized plasmas are turbulent. The behavior of magnetized turbulence is still a major question. It's understanding fundamentally affects our interpretation of space and astrophysical observations and holds the key to many mysteries in space and astrophysical plasmas, such as the production and propagation of cosmic rays. We have developed some very innovative approaches in understanding how turbulence will transfer energy to different length scales and how they will scatter particles and energize them. These studies will provide the physics underpinning for understanding the electron and ion heating in the solar wind and cosmic rays in the interstellar medium.

Benefit to National Security Missions

This research addressed the fundamental question on how magnetohydrodynamic turbulence will behave in various space and astrophysical plasmas, including solar wind and interstellar medium. The tools developed from this study, in addition to the analytic results, will provide the physics underpinning for interpreting many space and astrophysical observations. This will contribute the basic science capabilities at the Laboratory. It also provides the necessary physics basis for many problems associated with the Beyond the Standard Model Grand Challenge at LANL. Nuclear weapons themselves involve turbulent plasmas.

Progress

Starting on July 19, 2010, Dr. Beresnyak continued his studies of the basic properties of MHD turbulence. One paper was published in Astrophysical Journal (ApJ) Letters. One paper is being currently refereed by ApJ. One paper was prepared for submission to a journal. Dr. Beresnyak gave three talks: July SHINE meeting, 274 IAU Symposium (proceedings to be published by CUP), and the October LANL Turbulence workshop.

Dr. Beresnyak also ran new high-resolution simulations of MHD turbulence, analyzed them and the results were prepared for publication.

Future Work

The knowledge of MHD turbulence will be applied to the solar wind environment and inter-stellar medium.

We will study the dynamic behavior of MHD turbulence both upstream and downstream of a shock that is modified by cosmic rays. In order to self-consistently address the problem of MHD flow coupled to the energetic particles, we will use the diffusion approximation for the particles and the corresponding small-scale MHD fluctuations will be calculated analytically on the basis of turbulent cascade. Supercomputing resources will be used to simulate such coupled systems.

Conclusion

We will use our newly developed MHD simulation tools, together with the analytic theory we have completed, to study how shocks in space and astrophysical plasmas can excite turbulence and, at the same time, being modified by the same turbulence. We expect to explore how much energy particles will gain through interactions with the MHD turbulence.

Publications

Beresnyak, A., and A. Lazarian. Scaling laws and diffuse locality of balanced and imbalanced magnetohydrodynamic turbulence. 2010. *Astrophysical Journal Letters.* **722** (1): L110.

Gamma-Ray Bursts and Gravitational Waves from Compact Mergers

Christopher L. Fryer
20070574PRD1

Abstract
Compact binaries play an important role in a wide range of astrophysics problems, from X-ray sources to supernovae to the prime source of gravitational waves for the advanced Laser Interferometer Gravitational-wave Observational (LIGO). In this project, we brought one of the leading scientists in this field, Chris Belczynski, to work with scientists at LANL to both reinvigorate LANL's efforts in Gravitational Wave sources and allow Chris to leverage off of the physics and computational expertise at LANL to drive improvements in population synthesis calculations. This project has led to 63 publications, over 36 in the leading astrophysics journals. LANL scientists are now much more actively involved in the Gravitational Wave community and we have developed strong collaborations that will persist for the next few decades.

Background and Research Objectives
Einstein's theory of General relativity, the effect of matter altering both space and time, remains one of the more exotic concepts in physics. Understanding general relativity is important both to understand the foundations of physics and the universe we live in. Although a number of indirect tests have measured and confirmed general relativity, the pinnacle of our understanding will only be reached when we measure the direct consequence of general relativity: gravitational waves. Scientists believe gravitational waves are emitted when material is accelerated causing a time-varying quadrupole moment in that matter. Indirect detections of this emission, the inspiral of two neutron stars orbiting around each other, led to a Nobel prize in physics. This indirect measurement argued that the inspiral of the orbit was caused by the loss of energy through gravitational wave emission. Advanced LIGO was developed to directly detect the gravitational wave emission predicted by general relativity.

Any accelerating object emits gravitational waves, but these waves are very difficult to detect. For LIGO, scientists quickly determined they would need extreme masses being accelerated at phenomenal rates. They turned to astrophysics, where explosions on a phenomenal scale might produce the signals they could observe. Core-collapse supernovae are an obvious choice. A core-collapse supernova occurs when the iron core of a massive star collapses in on itself, forming a neutron star. This core, roughly the 10,000km in size and as massive as the sun, collapses down to 10km in less than a second. If rotating, this collapse, and the subsequent bounce, produces a rapidly changing quadrupole moment, leading to the emission of gravitational waves. This energetic explosion was not the only cosmic event astronomers found that would produce gravitational waves.

Scientists also realized that the merger of two compact objects (two neutron stars or a neutron star and a black hole) could also produce strong signals. Neutron stars are formed in core-collapse supernovae. Their mass is roughly that of the sun, but they are 10km in radius. They are termed "neutron stars" because in these intense conditions, normal matter in a neutron star is broken apart into bare neutrons. Dropping a gram of material onto a neutron star releases roughly the energy of the Hiroshima atomic bomb. Merging two neutron stars, each with masses well above 10^{33}g is believed to produce the most energetic explosion in the universe: a gamma-ray burst. These mergers are also incredibly strong emitters of gravitational waves. In this project, we want to study the progenitors of these explosions to help the design of detectors observing gravitational waves.

Scientific Approach and Accomplishments
This post-doctoral research fellowship brought Chris Belczynski to LANL to work with LANL scientists to better understand the progenitors of merging compact binaries. The basic approach relied on building off of the population synthesis code developed by Belczynski. As we determined uncertainties in these calculations, we used LANL expertise in computational hydrodynamics, stellar and supernova physics to constrain these uncertainties. We carried out a series of studies using Belczynski's population synthesis code to determine the effect of an uncertainty, then using theory to diminish that uncertainty and recalculating the uncertainty in the

binary progenitors. Where other observations existed (e.g. X-ray binaries), we were able to validate our technique. Our science focused on making direct predictions for the LIGO community and we developed a strong working relationship with this community.

Over the 3 year period of this project, this work produced 63 publications, 36 in leading astrophysics journals. As an indicator of its relevance to the scientific community, we note that this work garnered over 750 citations in this brief period. Some of the highlights include revamping the estimates for black hole masses formed in stellar collapse and modifying the modeling of binary interactions to better study this important uncertainty. These modifications introduced order-of-magnitude changes in the estimates used for gravitational wave detectors and will drastically change the goals for advanced LIGO.

More importantly, it reinvigorated LANL's involvement in the gravitational wave community. After a multi-year hiatus in this community, Fryer is now attending at least one Gravitational Wave meeting every year to ensure that LANL's work ties better to this community. Other LANL scientists such as Dan Holz have also re-involved themselves in this important science.

Chris Belczynski himself catapulted his career, earning a ranking of one of the top 10 physical scientists in Poland during this time period and he has accepted joint positions at universities in Poland and the United States. He will continue to work in both countries and continue to work with LANL. Chris has included LANL in many international proposals to continue this work and has already instigated a program to send students to work with Dan Holz and Chris Fryer at LANL.

Although most of this work focused on double neutron star and neutron star/black hole binaries, we also studied other compact binaries such as the progenitors of type Ia supernovae. Thermonuclear, or type Ia, supernovae are formed when a white dwarf undergoes a thermonuclear explosion, fusing its Carbon/Oxygen core into iron in the largest fusion bomb in the universe. Progenitors include accreting white dwarfs and merging double white dwarf binaries. With Chris Belczynski's student, Ashley Ruiter, we studied the progenitors of these explosions in a series of papers.

Impact on National Missions

In the same way as we approach our program goals, this problem combined numerical calculation with theory, coupled with experimental validation, to make predictions on a problem for which we currently have no data. This approach has a more scientific bent than the "engineering-led" approach historically used at the national laboratories for large-scale simulations relevant to Stockpile Stewardship. It is this scientific approach that the national laboratories must move toward for their problems and Fryer, who works extensively in Verification and Validation at LANL, has used this example to push LANL into this science-based method.

But this research has even stronger implications for LANL for broader scientific goals. Gravitational waves have long been a strong goal of the National Science Foundation. But they are even more important as a diagnostic in understanding nuclear and particle physics in mergers and core-collapse supernovae. Astrophysics is rapidly moving towards using all the available diagnostics from these cosmic explosions to learn basic physics. LANL has used the expertise it has gained in gravitational waves to reintroduce this diagnostic back into its calculations. This so-called "Multi-messenger" era is now a major theme in science and this effort has allowed LANL to play a leading role in this theme.

Publications

Belczynski, K., D. E. Holz, C. L. Fryer, E. Berger, D. H. Hartmann, and B. O'Shea. On the origin of the highest redshift gamma-ray bursts. 2010. *Astrophysical Journal.* **708** (1): 117.

Belczynski, K., M. Dominik, T. Bulik, R. O,ÄôShaughnessy, C. Fryer, and D. Holz. THE EFFECT OF METALLICITY ON THE DETECTION PROSPECTS FOR GRAVITATIONAL WAVES. 2010. *ASTROPHYSICAL JOURNAL LETTERS.* **715** (2): L138.

Belczynski, K., R. E. Taam, E. Rantsiou, and M. van der Sulvs. Black hole spin evolution: implications for short-hard gamma-ray bursts and gravitational wave detection. 2008. *Astrophysical Journal.* **682** (1): 474.

Belczynski, K., R. O'Shaughnessy, V. Kalogera, F. Rasio, R. E. Taam, and T. Bulik. The lowest-mass stellar black holes: catastrophic death of neutron stars in gamma-ray bursts. 2008. *Astrophysical Journal.* **680** (2): L129.

Belczynski, K., T. Bulik, C. L. Fryer, A. Ruiter, F. Valsecchi, J. S. Vink, and J. R. Hurley. On the maximum mass of stellar black holes. 2010. *Astrophysical Journal.* **714** (2): 1217.

Belczynski, K., and R. E. Taam. The most massive progenitors of neutron stars: CXO J164710.2-455216. 2008. *Astrophysical Journal.* **685** (1): 400.

Belczynski, K., and R. Taam. The most massive progenitors of neutron stars: CXO J164710.2-455216. 2008. *ASTROPHYSICAL JOURNAL.* **685** (1): 400.

Fragos, T., M. Tremmel, E. Rantsiou, and K. Belczynski. BLACK HOLE SPIN-ORBIT MISALIGNMENT IN GALACTIC X-RAY BINARIES. 2010. *ASTROPHYSICAL JOURNAL LETTERS.* **719** (1): L79.

Fragos, T., V. Kalogera, B. Willems, K. Belczynski, G. Fabbiano, N. J. Brassington, D. -W. Kim, L. Angelini, R.

L. Davies, J. S. Gallagher, A. R. King, S. Pellegrini, G. Trinchieri, S. E. Zepf, and A. Zezas. TRANSIENT LOW-MASS X-RAY BINARY POPULATIONS IN ELLIPTICAL GALAXIES NGC 3379 AND NGC 4278. 2009. *ASTROPHYSICAL JOURNAL LETTERS.* **702** (2): L143.

Fragos, T., V. Kalogera, K. Belczynski, G. Fabbiano, N. J. Brassington, D. W. Kim, L. Angelini, L. R. Davies, J. S. Gallagher, A. R. King, S. Pellegrini, G. Trinchieri, S. Zepf, and A. Zezas. Transient Low-mass X-ray Binary Populations in Elliptical Galaxies NGC 3379 and NGC 4278. 2009. *Astrophysical Journal.* **702**: L143.

Gondek-Rosinska, D., T. Bulik, S. Oslowski, and K. Belczynski. PROPERTIES OF DOUBLE NEUTRON STARS. 2008. In *30th Spanish Relativity Conference ; 20070910 - 20070914 ; Inst Astrofis Canarias, Tenerife, SPAIN.* Vol. 30, p. 137.

Heinke, C., A. Ruiter, M. Muno, and K. Belczynski. Cataclysmic variables in globular clusters, the galactic center, and local space. 2008. In *Conference on Nature and Evolution of X-Ray Binaries in Diverse Environments ; 20071028 - 20071102 ; St Pete Beach, FL.* Vol. 1010, p. 136.

Ivanova, N., C. O. Heinke, F. A. Rasio, K. Belczynski, and J. M. Fregeau. Formation and evolution of compact binaries in globular clusters. Part II. Binaries with neutron stars. 2008. *Monthly Notices of the Royal Astronomical Society.* **386** (1): 553.

Ivanova, N., C. O. Heinke, F. A. Rasio, K. Belczynski, and J. M. Fregeau. Formation and evolution of compact binaries in globular clusters - II. Binaries with neutron stars. 2008. *MONTHLY NOTICES OF THE ROYAL ASTRONOMICAL SOCIETY.* **386** (1): 553.

Linden, T., J. F. Sepinsky, V. Kalogera, and K. Belczynski. Probing Electron-Capture Supernovae: X-ray Binaries in Starbursts. 2009. *Astrophysical Journal.* **699** (2): 1573.

Linden, T., J. F. Sepinsky, V. Kalogera, and K. Belczynski. Probing electron-capture supernovae: x-ray binaries in starbursts. 2009. *Astrophysical Journal.* **699** (2): 1573.

O'Shaughnessy, R., C. Kim, V. Kalogera, and K. Belczynski. Constraining population synthesis models via empirical binary compact object merger and supernova rates. 2008. *Astrophysical Journal.* **672** (1): 479.

O'Shaughnessy, R., K. Belczynski, and V. Kalogera. Short gamma-ray bursts and binary mergers in spiral and elliptical galaxies: redshift distribution and hosts. 2008. *Astrophysical Journal.* **675** (1): 566.

Oslowski, S., R. Moderski, T. Bulik, and K. Belczynski. Gravitational lensing as a probe of compact object populations in the Galaxy. 2008. *ASTRONOMY & ASTROPHYSICS.* **478** (2): 429.

O,ÄôShaughnessy, R., V. Kalogera, and K. Belczynski. BINARY COMPACT OBJECT COALESCENCE RATES: THE ROLE OF ELLIPTICAL GALAXIES. 2010. *ASTROPHYSICAL JOURNAL.* **716** (1): 615.

Ruiter, A. J., K. Belczynski, M. Benacquista, and K. Holley-Bockelmann. The contribution of halo white dwarf binaries to the laser interferometer space antenna signal. 2009. *Astrophysical Journal.* **693** (1): 383.

Ruiter, A. J., K. Belczynski, and C. Fryer. Rates and delay times of type la Supernovae. 2009. *Astrophysical Journal.* **699** (2): 2026.

Ruiter, A., K. Belczynski, M. Benacquista, S. Larson, and G. Williams. THE LISA GRAVITATIONAL WAVE FOREGROUND: A STUDY OF DOUBLE WHITE DWARFS. 2010. *ASTROPHYSICAL JOURNAL.* **717** (2): 1006.

Sadowski, A., J. Ziolkowski, K. Belczynski, and T. Bulik. The missing population of Be plus black hole X-ray binaries. 2008. In *Conference on Nature and Evolution of X-Ray Binaries in Diverse Environments ; 20071028 - 20071102 ; St Pete Beach, FL.* Vol. 1010, p. 407.

Sadowski, A., J. Ziolkowski, K. Belczynski, and T. Bulik. The Missing Population of Be plus Black Hole X-Ray Binaries. 2008. In *252nd Symposium of the International-Astronomical-Union ; 20080406 - 20080411 ; Sanya, PEOPLES R CHINA.* Vol. 252, p. 399.

Detecting Dark Matter with Cryogenic Liquids

Andrew Hime
20070751PRD4

Abstract
As a postdoctoral fellow, Stanley Seibert has contributed to LANL's objectives for both the Sudbury Neutrino Observatory and MiniCLEAN experiments. Stan played a critical role in SNO's most recent publication, providing one of the primary analyses of the low energy ^{8}B solar neutrino data. This work dramatically improved the precision over previous measurements, and has already contributed to our global understanding of neutrino oscillations. For the MiniCLEAN experiment, Stan has managed the development of our simulation and analysis tools, where his experience with accelerating numerical calculations using graphics processing units has resolved a significant future data processing bottleneck. He has also taken a lead role in laboratory measurements of the properties of the organic fluor, TPB, which is a key component of the MiniCLEAN detector. Stan is also managing the bulk testing of photomultiplier tubes that will be installed in the detector when construction starts next year.

Background and Research Objectives
Stanley Seibert's postdoctoral work at LANL focused on two major experiments: the Sudbury Neutrino Observatory and the MiniCLEAN dark matter experiment. The Sudbury Neutrino Observatory was a heavy water (D2O) Cherenkov detector whose primary goal was to measure solar neutrinos. This both advances our understanding of neutrino physics and also improves our understanding of fusion processes in the Sun. SNO finished data collection in November of 2006, and through Stan's efforts, LANL continues to play a lead role in the final analyses of this unique data set. His primary work on the experiment was directed toward a 5-year effort to dramatically reduce the uncertainties in the measurement by including lower energy events in the analysis. The low energy threshold analysis of the SNO data set is very challenging due to the high level of precision required. At low energies, there is a significant background generated by the natural radioactivity of the detector components. Mitigating this background and modeling it with sufficient accuracy to extract the neutrino signal required a detailed study of the detector response with a wide range of calibration sources. Lowering the energy threshold has necessitated major improvements to our simulation of the detector, a complete reevaluation of all calibration data, and the invention of several new signal extraction techniques to separate the neutrino signal from the backgrounds.

The MiniCLEAN dark matter experiment will search for weakly interacting massive particles, which are hypothesized to make up the dark matter which comprises 25% of the universe. MiniCLEAN is a spherical detector with ~150 kg of liquid argon or liquid neon target imaged by an array of 92 photomultiplier tubes around the surface. The detector will be constructed and installed in the Creighton nickel mine in Sudbury, Ontario, Canada in 2010-2011, with data collection continuing for several years after that. As the institution tasked with primary construction of the detector, LANL has significant responsibilities on the experiment. Stan leads the Simulation and Analysis working group within the MiniCLEAN collaboration, in addition to contributing to the broad R&D effort by the Weak Interactions team to characterize the electrical, mechanical, and optical properties of components that will be installed in the MiniCLEAN detector. He has also developed the position reconstruction algorithm that will be used to locate events in the MiniCLEAN detector and reject those which come from the backgrounds originating from the walls.

Scientific Approach and Accomplishments
As part of the SNO collaboration, Stanley Seibert was one of the key analysts for the low energy threshold measurement of ^{8}B neutrinos from the Sun. This work presents a significant improvement in precision and rigorous treatment of systematic uncertainties using the first two phases of data collection at SNO. The new low energy information adds to our understanding of how different kinds of neutrinos transform into each other as they propagate. Our measurement of the total ^{8}B neutrino flux has halved the uncertainty of previous SNO papers, and will contribute to ongoing astrophysical debates about the chemical composition of the Sun. Figure 1 shows our latest flux result in comparison to previous

SNO results. In addition, this analysis presents the lowest published energy threshold for a water Cherenkov detector, raising the bar for other neutrino experiments, such as the Super-Kamiokande experiment in Japan. The paper was accepted for publication in the May issue of Physical Review C [1].

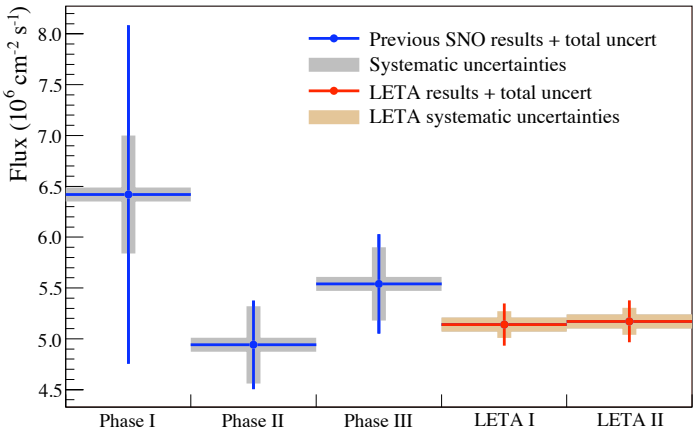

Figure 1. Total boron-8 neutrino flux measured by SNO in previous papers ("Phase I," "Phase II," and "Phase III") compared to the new low energy threshold results ("LETA I," "LETA II"). "LETA I" and "LETA II" refer to two independent analyses of the same data that were performed to verify the results. The "LETA II" analysis was done at LANL.

During his fellowship at LANL, Stan continued work on accelerating physics calculations using commercially available graphics processing units (GPUs). The low threshold SNO analysis made extensive use of GPUs to perform the final statistical analysis of the data set to extract the total flux of ^{8}B neutrinos and their energy spectrum. The speed improvements made possible by the GPU enabled a more sophisticated treatment of systematic uncertainties in detector response, like energy scale and energy resolution. These uncertainties could be propagated in a more accurate way, which was important due to large radioactive backgrounds present in the detector at low energies.

Stan also completed development of a novel method for obtaining the probability of an electron neutrino not transforming into another kind of neutrino, called the "survival probability." Knowledge of how the electron neutrino survival probability varies as a function of neutrino energy is extremely useful, as it shows how neutrinos interact with the matter in the Sun via the Mikheyev-Smirnov-Wolfenstein effect. The SNO collaboration has never been able to report the electron neutrino survival probability function for solar neutrinos because there was no practical way to extract it directly from our data. Thanks to the massive computing power available from off-the-shelf GPUs, Stan demonstrated a technique for obtaining this information, which was also included in the low threshold publication. A survival probability function is much easier for neutrino phenomenologists to interpret when performing model tests on all neutrino experiments simultaneously, and the function published by SNO has already been incorporated into global fits of various models of neutrino oscillation.

After submission of the paper, Stan has become one of the primary internal reviewers of SNO's final ^{8}B analysis. This analysis is applying the techniques that he and his coauthors developed for the previous publication to all three data collection phases at SNO simultaneously. This work is expected to be published later in 2010.

Stan has presented this work on SNO locally at the P-25 Group Seminar, at invited talks for the INFO09 and PHENO10 conferences, and the University of New Mexico. He has also presented portions of this work in contributed talks at APS meetings in 2008 and 2009.

In addition to his work on SNO, Stan has played a key role on the MiniCLEAN dark matter experiment, an LDRD-supported project headed by Andrew Hime. Stan was promoted to a leadership role shortly after starting at LANL, placing him in charge of the software and analysis efforts of the collaboration. This leveraged his prior experience in data analysis on SNO, and his role as designer and primary developer of the simulation and analysis package used by MiniCLEAN, called RAT. While at LANL, Stan managed a team of 10-15 physicists doing software development at 8 institutions, all working to improve the accuracy and power of the detector simulation. He organized a successful simulation and analysis workshop at the University of Pennsylvania in June 2009 which helped define the goals and plan the software work for the next 2 years. RAT has played an important role in the design of the experiment, allowing the collaboration to test out different detector designs and quickly see how they impact the quality of the data we will record. Once the experiment begins data collection in 2011, RAT will also be used to process the data for analysis. Stan has coordinated with other collaborations, like SNO+, on the use of RAT, ensuring that development by both groups is complementary.

A critical stage in the data processing for MiniCLEAN is position reconstruction. The scintillation time distribution in liquid argon, the primary target material used in MiniCLEAN, has superb rejection of natural beta and gamma radiation. A much more challenging task is the rejection of alpha and neutron background-induced nuclear recoils, which would otherwise be indistinguishable from the WIMP-recoil signal MiniCLEAN is searching for. Such background sources are all located outside the inner sphere of liquid argon. Therefore, they can be removed with reasonable efficiency by reconstructing the position of the scintillation event and cutting those events at high radius. Unfortunately, scintillation light from liquid argon is in the extreme ultraviolet band and must be shifted into the visible spectrum before detection with 8" photomultiplier

tubes. MiniCLEAN contains an approximately spherical layer of tetraphenyl butadiene (TPB) that absorbs ultraviolet photons and reemits blue photons with high efficiency. The reemitted photons from TPB are isotropic, however, scrambling some of the position information carried by the original photons. Standard position reconstruction methods cannot easily account for this effect, leading them to produce inwardly-biased estimates for event position.

Stan has developed a new reconstruction algorithm, called "ShellFit," which uses the detailed optical simulation inside of RAT to capture the complex range of photon paths and include those distributions in a maximum likelihood fit for event position and energy. This technique has both minimal bias and much improved resolution over other reconstruction methods that were investigated by the collaboration. He presented this work in a contributed talk at the APS meeting in 2010. The original version of the algorithm was very slow and impractical to use with the high event rates planned for MiniCLEAN, but Stan was able to port the method to the GPU, and improved its performance by a factor of 8. As reconstruction was the slowest stage of event processing, Stan's work has reduced the cost of and electrical power required for data processing for MiniCLEAN by nearly a factor of five.

LANL also has significant R&D responsibilities for the technologies that will go into MiniCLEAN. Stan has contributed to two measurement tasks while at LANL. The first is a study of the optical properties of TPB. An experimental setup designed to illuminate TPB with extreme UV light existed when he arrived, but Stan has taken over the data analysis and mentored several summer students using the apparatus, leading to an undergraduate poster at the APS DNP meeting in 2009. The TPB apparatus is designed primarily to measure the reemission efficiency of TPB, which determines the light yield that will be observed in the full size MiniCLEAN detector. Prior measurements had very large uncertainties, but Stan, in collaboration with other members of the team, has helped to bring this uncertainty down to the 20% level. This work has been very successful, and a paper is now being prepared for publication, as this information will be very useful to other experiments that depend on TPB.

Stan also has extended the TPB apparatus to perform a second important measurement. A literature search revealed a discrepancy in the published spectrum of visible light reemitted by TPB when excited with different wavelengths of extreme UV light. It had been originally thought that the reemission spectrum was independent of incident wavelength, but two papers showed a significant difference in the width and shape of the reemission spectrum. Stan integrated an inexpensive CCD-based spectrometer into the system and developed an analysis technique in order to push the sensitivity of the spectrometer well beyond its typical range. This has allowed Stan to extract a useful reemission spectrum from TPB for two different incident wavelengths when the signal to noise ratio is well below 1. The data confirm that for incident wavelengths of 125 and 160 nm, the reemitted visible light spectra are consistent, but the reemission is not the same for 254 nm light, which was measured by our colleagues at the University of Pennsylvania, as shown in Figure 2. This work will be folded into the RAT simulation code to improve the accuracy of our light yield predictions and the optical model used for position reconstruction.

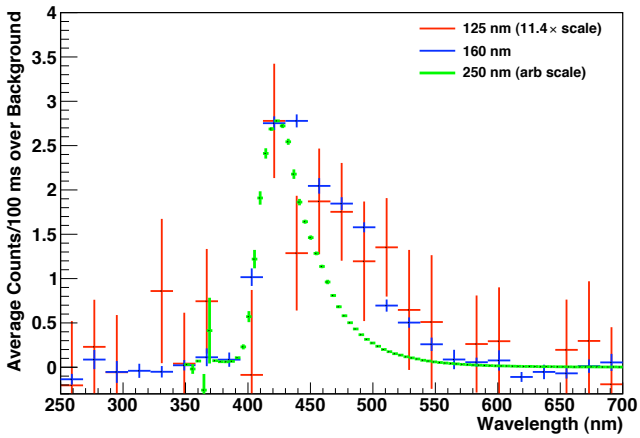

Figure 2. Comparison of the reemission spectrum from TPB for three different incident wavelengths. The 125 and 160 nm incident wavelengths were provided by a deuterium lamp and monochrometer, while the 250 nm measurement was made at University of Pennsylvania using a UV LED source.

The second R&D project that Stan has taken on is the testing of PMTs for use inside MiniCLEAN as well as outside the detector in a large water shield. Instrumenting the water shield allows rejection of cosmic ray muons, which are rare at the underground depth of MiniCLEAN, but nevertheless higher rate than an extremely weak WIMP signal. LANL has 63 PMTs left over from the construction of SNO which have been configured for use underwater, and would therefore be ideal for use in the water shield. However, these PMTs have been unused for nearly 15 years and therefore need thorough testing before being assembled into strings to be lowered into the water tank. In collaboration with MIT, Stan has helped put together a data acquisition system and analysis tools to enable 6 PMTs to be tested simultaneously, and trained a summer student to take over operation of the testbed. The procedure developed by MIT and Stan will shortly be applied to the 100 cryogenic PMTs that will go inside the MiniCLEAN detector.

Impact on National Missions

This project supports DOE Office of Science missions in basic research to elucidate the fundamental properties of neutrinos using the sun as a unique astrophysical source and in the development of novel detector technologies for low-energy solar neutrinos and cosmological dark mat-

ter. The development of such technologies can potentially build upon capabilities for nuclear threat reduction.

References

1. Collaboration), B. Aharmim (et al SNO. Low-Energy Threshold Analysis of the Phase I and Phase II Data Sets of the Sudbury Neutrino Observatory. 2010. *Physical Review.* **C81** (055504): 055504 .

Publications

Collaboration, S. N. O.. Low-Energy Threshold Analysis of the Phase-I and Phase-II Data Sets of the Sudbury Neutrino Observatory. 2010. *Physical Review.* **C81** (055504): 55504 .

Seibert, S.. ShellFit: Reconstruction in the MiniCLEAN Detector. Presented at *April Meeting of the American Physics Society.* (Washington DC, 14 Feb. 2010).

Seibert, S.. Backgrounds in the MiniCLEAN Detector. Presented at *American Physics Society Division of Nuclear Physics.* (Santa Fe NM, 4 Nov. 2010).

Seibert, S.. The Low Energy Threshold Analysis of SNO. Invited presentation at *PHENO10 Symposium.* (Madison WI, 11 May 20101).

Seibert, S.. The MiniCLEAN Experiment. Invited presentation at *Darkness Visible 2010.* (Cambridge England, 3 Aug. 2010).

Seibert, S.. ShellFit: A Reconstruction Algorithm for the DEAP/CLEAN Family of Detectors. To appear in *Nuclear Instruments and Methods.*

Dynamics of Quantum First Order Phase Transitions

Dima V. Mozyrsky
20080689PRD1

Abstract

We investigated the kinetics (i.e. dynamics) of quantum phase transitions in a variety of cold atom systems. Understanding of the dynamics of quantum phase transitions may answer a number of fundamental questions. These questions range from the evolution of the universe at its early stages to the problems of cluster dynamics at nano-scale. Contemporary cold atom systems, such as atoms or molecules confined in a magnetic trap, provide a perfect setup where such phase transitions can be observed and controlled with a desired accuracy. The work sets up a theoretical framework for the description of the dynamics of the first order phase transitions in these systems. We consider cold atom mixture systems at different regimes as well as dynamically controlled cold atom systems of ring geometry that have become available recently.

Background and Research Objectives

Quantum phase transitions, in particular the first-order quantum phase transitions, is a cutting-edge research area in cold atom physics. These phase transitions - the quantum equivalent of water freezing to ice - are relevant to many areas of theoretical physics, ranging from the evolution of the universe at its early stages to cluster dynamics in magnetic systems. At the same time, not many experimental observations have been confirmed. One of the first but not very conclusive results came from experiments on He-isotope liquids. This question has stimulated large experimental and theoretical efforts in the field. The dynamics of a system undergoing a first order phase transition is typically characterized by the process of nucleation. In nucleation, one component forms a droplet (nuclei) separating itself from the other. Unlike numerous commonly-found temperature-driven transitions, low temperature nucleation relies solely on quantum fluctuations and has not yet been consistently observed. Another type of process that closely resembles physics of quantum nucleation is so-called "phase-slip" process. It occurs when the phase of a macroscopic quantum system is altered at some microscopic region (usually inside some potential barrier). As the result of a phase-slip the system, usually of cycle geometry, can support stable currents. The decay of these currents at low temperatures takes place via macroscopic quantum tunneling – the process, when all the involved particles undergo transition in exactly the same fashion (as in quantum nucleation). Cold atom systems provide an excellent opportunity to measure these phenomena. We investigated boson-fermion cold atom mixtures and ultra-cold boson systems to provide theoretical and numerical guidance for experiment.

Our investigation took several directions. We demonstrated that quantum nucleation transition in cold atom mixtures is significantly suppressed by the dissipative processes. As the result, measurements of the nucleation rate need to be carried out in mixtures with certain ratio between masses of the atomic species, where dissipation is minimal. On the other hand, macroscopic quantum tunneling phenomena associated with phase separation is more accessible. Moreover, its rate is controlled by the density rather then the total number of particles, and therefore it can be easily controlled and measured. We proposed to measure the dissipative transition in the nucleation regime by analyzing expansion of an externally initiated droplet. We also investigated possible stable superfluid configurations in the system near the phase separation transition point. Finally, we explored possibilities to observe macroscopic quantum tunneling between current states in a single species boson system. In the following we address all these points in a greater detail.

Scientific Approach and Accomplishments

In the first stage of our project we have investigated the possibility of observing quantum nucleation [1]. We studied kinetics of phase separation transition in boson-fermion cold atom mixtures. Starting from a macroscopic description of a boson-fermion mixture, we derived an effective action that describes the system in terms of the boson density representing an order parameter. We analyzed the characteristic length scale and identified three different regimes of phase separation. The first regime corresponds to nucleation. The droplet of fermion fraction formed during the transition has distinctive bound-

aries. It forms when the densities of the two species are close to the critical density of the mixture. We obtained the asymptotic behavior for the droplet's size dynaimcs and demonstrated that the nucleation is significantly suppressed by dissipation when the fermion particle mass is greater or equal to that of a boson. Therefore, we concluded that experimental observation of quantum nucleation is feasible only in the mixtures with light fermion and heavy boson atoms. In addition, measurable rates (the number of created droplets per unit of time) require highly interacting mixtures. While such mixtures are experimentally possible, they are not easy to prepare and require state-of-the-art trapping and cooling techniques. We, therefore, propose an alternative scheme to probe dissipative dynamics associated with the nucleation [2]. It is based on the analysis of expansion of an externally initiated droplet of fermions. Measurable changes associated with the dissipative transition take place for moderate interactions. As a result, the measurement can be done for relatively dilute easy-to-prepare systems.

Critical dynamics near the absolute instability of the mixture is fundamentally different. Here, the characteristic length scale diverges and the droplet boundary is not well defined. This regime is suitable for observing macroscopic quantum tunneling phenomena. Near the instability the potential barrier separating mixed and phase-separate states is small. The system quantum-mechanically tunnels through this barrier creating an excess of fermion species in relatively large volume of the mixture. We calculated the tunneling exponents as a function of the system parameters, such as density and interaction strengths. We demonstrated that macroscopic quantum tunneling phenomenon can be observed in dilute mixtures which are easily accessible to experiment. In addition, due to the modification of boson-mediated interaction near the absolute instability, this regime presents an opportunity to test novel unconventional superconductivity mechanisms within the boson-fermion framework. In particular we have shown [3] that thermodynamically stable superconducting phase can exist in odd-frequency channel. Further work has to be done to develop microscopic interpretation of this unconventional phase.

We also investigated metastable macroscopic quantum states in a singe species boson system in Bose-Einstein condensation regime [4,5]. In particular, we analyzed transitions between macroscopic current-carrying states in a ring-shaped Bose-Einstein condensate. Estimates for geometric parameters were obtained [4] to support experimental observation of macroscopic quantum transitions in this system. The possibility to create well-controlled Bose-Einstein condensate of ring geometry has been recently confirmed by LANL experimental group within novel "painted potential" trapping technique. Our result indicates that, for experimentally feasible geometries, coherent macroscopic quantum tunneling phenomena should be accessible, see Figure 1, at temperatures of about few nano-Kelvin. While such temperatures are certainly achievable, some modifications to current LANL experimental setup might be necessary.

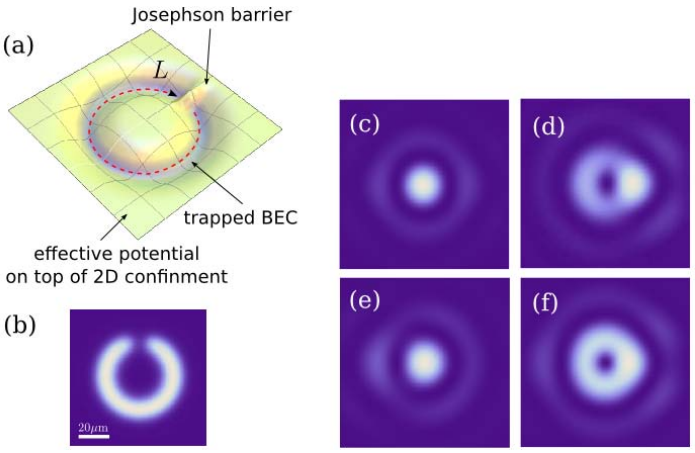

Figure 1. Kinetics of single species cold atom Bose-Einstein Condensate of ring geometry. (a) The effective potential profile created with the "painted potential" technique (schematically). Circular potential well of length L is created on top of the 2D confinement plane. It is cut with the Josephson barrier. (b) The shape of typical condensate cloud. The system has rich structure or current-carrying state visible upon measurement (c, d, e, f). Macroscopic tunneling from the current state should be clearly visible in free expansion measurement (calculated): (c) the free expansion cloud in the case when tunneling took place, (d) expansion cloud indicating that the tunneling did not happen. Similarly for the tunneling from the zero current state (e, f). In both cases absence of density in the center of the expansion cloud hints the presence of non-zero current state.

The current-carrying states in a Bose-Einstein condensate ring are formed due to interplay of several energy contributions. One of them comes from the kinetic energy of the rotation in the bulk of the ring. It raises the energy of a current state and forces the phase of the condensate to change linearly along the ring. The other contribution is due to the phase slip of the condensate. The phase slip corresponds to an abrupt change (jump) in the phase of the condensate. Such change is only possible when the density of the condensate vanishes at that point. This usually causes a substantial increase of energy that is a function of the phase jump. However if an appropriate potential barrier cuts the ring at some point the energy cost of the phase slip inside the barrier becomes comparable to the kinetic energy contribution in the bulk. In this case these two energies create a rich energy profile that has several local minima corresponding to the flow of the condensate along the ring, or current. These are the metastable current-carrying states. However these states are usually higher in energy. Hence, if initially prepared, they will decay back to the zero-current state (for which both

the kinetic energy and the phase slip contributions are minimal). At low enough temperature, few nano-Kelvin [4], the decay process is due to quantum fluctuations – it is the transition of the entire system with the current into the zero-current state via macroscopic quantum tunneling. Observation of this transition requires fine tuning of the geometric parameters of the trapping system. Therefore we advise to begin with the thermal transition which is more easily accessible in currently available higher-temperature systems. This should allow performing fine calibration of the experimental setup necessary to measure macroscopic quantum tunneling effects.

We also demonstrated that as soon as the coherent quantum tunneling is achieved the system can be tuned [6] to quantum two-state regime. In this case the trap should be set rotating (about one revolution a second). Rotation of the trap changes the kinetic energy contribution inside the bulk shifting its minimum towards the states with non-zero current. In this case some of the non-zero current minima become stable (lower in energy). This regime provides a unique opportunity to explore a well controlled quantum system of two macroscopically distinct states (almost visible to a naked eye upon measurement), or quantum bit, within the cold atom framework. The two key factors are important in this regime. First, the transition between the two macroscopic quantum states has to take place within an accessible time interval. Second, the quantum fluctuations present in the system should be sufficiently small to allow unambiguous measurement. These two factors limit the parameter space where macroscopic two-state system is measurable. We analyzed these limitations and concluded that two-state regime can be realized in contemporary cold atom traps [6,7]. We also investigated the prospects of this novel atomic system in quantum information processing. Indeed, the proposed macroscopic two-state system can, in principle, be used to record quantum bit of information. It turns out that even within a relatively simple geometry of current LANL experiments quantum operations involving few such quantum bits can be performed, however further research is necessary to asses full potentials of this novel cold atom system.

To conclude, we investigated kinetics of the collective quantum phenomena associated with first-order quantum phase transitions. Understanding of the dynamics of quantum phase transitions may answer a number of fundamental questions. These questions range from the evolution of the universe at its early stages to the problems of cluster dynamics in magnetic systems. This stimulates large ongoing experimental and theoretical efforts in the field. At the same time, not many experimental observations have been confirmed (one of the first results came from experiments on 3He, 4He systems). Contemporary cold atom systems, such as atoms or molecules confined in a magnetic trap, provide a perfect setup where such phase transitions can be observed and controlled with a desired accuracy. In particular, we demonstrated that quantum-driven first order phase transition is measurable in two species cold atom systems. Moreover, it provides a unique opportunity to test novel collective states such as unconventional superconducting states. We also demonstrated that closely related macroscopic quantum tunneling phenomena can be realized in even simpler one-species cold atom system of ring geometry. This latter system also provides a unique opportunity to create macroscopic quantum Schrödinger-cat-like device in a laser trap. It also opens a pathway for more complex atomic system for sensing applications based on the same coherent phenomena.

Impact on National Missions

The project supports the DOE mission by enhancing our understanding of fundamental properties of complex systems. These areas of research constitute two major grand challenges pursued by the Los Alamos National Laboratory. In the regimes described above, systems exhibiting coherent macroscopic quantum effects have strong potentials for developing new means of sensing and computing for missions such as Threat Reduction.

References

1. Solenov, D., and D. Mozyrsky. Kinetics of phase separation transition in cold-atom boson-fermion mixtures. 2008. *Physical Review Letters.* **100**: 150402.

2. Solenov, D., and D. Mozyrsky. Quantum nucleation and macroscopic quantum tunneling in cold-atom boson-fermion mixtures . 2008. *Physical Review A.* **78**: 053611.

3. Solenov, D., I. Martin, and D. Mozyrsky. Thermodynamical stability of odd-frequency superconducting state. 2009. *Physical Review B.* **79**: 132502.

4. Solenov, D., and D. Mozyrsky. Metastable states and macroscopic quantum tunneling in a cold atom Josephson ring. 2010. *Physical Review Letters.* **104**: 150405.

5. Kalas, R., D. Solenov, and E. Timmermans. Reentrant stability of BEC standing wave patterns. To appear in *Physical Review A .*

6. Solenov, D., and D. Mozyrsky. Macroscopic two-state system with cold atoms: towards BEC flux qubit. *Physical Review Letters.*

7. Solenov, D., and D. Mozyrsky. Cold Atom Qubits. To appear in *Journal of Computational and Theoretical Nanoscience.*

Publications

Kalas, R., D. Solenov, and E. Timmermans. Reentrant stability of BEC standing wave patterns. To appear in *Physical Review A .*

Solenov, D., I. Martin, and D. Mozyrsky. Thermodynami-

cal stability of odd-frequency superconducting state. 2009. *Physical Review B.* **79**: 132502.

Solenov, D., and D. Mozyrsky. Kinetics of the phase separation transition on cold-atom boson-fermion mixtures. 2008. *Physical Review Letters.* **100**: 150402.

Solenov, D., and D. Mozyrsky. Quantum nucleation and macroscopic quantum tunneling in cold-atom boson-fermion mixtures . 2008. *Physical Review A.* **78**: 053611.

Solenov, D., and D. Mozyrsky. Metastable states and macroscopic quantum tunneling in a cold atom Josephson ring. 2010. *Physical Review Letters.* **104**: 150405.

Solenov, D., and D. Mozyrsky. Macroscopic two-state system with cold atoms: towards BEC flux qubit. *Physical Review Letters.*

Solenov, D., and D. Mozyrsky. Cold Atom Qubits. To appear in *Journal of Computational and Theoretical Nanoscience.*

Strongly Coupled Fermion Systems: From Atomic Gases to Dark Matter

Sanjay Reddy
20080731PRD2

Abstract

Here we describe advancements made in our understanding of matter through the use of an innovative approach combining ab-initio computer simulations with density functional theory. A "unitary Fermi gas" is a universal state of matter found in neutron stars and formed in cold atom experiments. Our work has improved by an order of magnitude the calculation of a fundamental parameter of this gas. We also discuss what we have learned about finite size effects in the density functional theory, which is crucial part to applying the theory to nuclei.

We also describe how density functional theory has been used to connect the state of matter in neutron stars and dark matter to observational signatures. These signatures will help us learn more about the nature of matter in extreme conditions in our universe, and could hold the key to understanding one of the most outstanding problems in physics today: the nature of dark matter.

Background and Research Objectives

Our research attempts to better understand the fundamental nature of matter. Although the Standard Model can in principle predict the properties of all matter, in practice, even approximately computing the properties of a few particles—such as a proton comprising only three quarks—is a Herculean computational challenge. Our innovative approach is to develop an accurate model that combines computer simulations (Monte-Carlo), experiments and analytic properties to understand systems of many fermions. Universality in the underlying theory allows this model to be applied to many systems, from cold atoms and superconductors, to nuclear matter, stellar matter, and possibly even the elusive dark matter that holds galaxies together. Some of these systems can be studied in the lab, allowing for the model to be tested and then applied with confidence to those systems outside of experimental control. Our core research object is to develop and apply a set of techniques that allow for a quantitative analysis of fermionic matter in these varied contexts.

Progress has been in developing Density Functional Theory (DFT) techniques for quantitatively modeling these systems, from cold atoms to dark matter. In particular, we have focused our attention on the so-called "Unitary Fermi Gas". This is a strongly interacting quantum gas with resonantly tuned interactions such that interaction parameter -- the s-wave scattering length—is infinite. Since the scattering length is infinite, the only scale in the problem is the density. Thus the equation of state is characterized by a single dimensionless number: ξ - the ratio of the energy of the interacting gas to the energy of a free gas with the same density. An improved calculation would directly impacts the equation of state of cold atom systems and dilute neutron matter in neutron stars.

The main research objectives have been met. These include:

- A systematic study of finite size effects in the DFT for the unitary Fermi gas approach using quantum Monte-Carlo calculations.
- Improvements to the DFT code and incorporation in a scalable parallel code that can access both static and dynamic properties of Fermi systems. This code is presently being used to study the static and dynamic properties of vortex rings.
- Application of DFT to astrophysical problems, including calculating shear properties of nuclear matter in neutron star crusts and properties of the electrosphere in our dark matter, are possibilities for connecting these objects with observational signatures.

Scientific Approach and Accomplishments

One of Forbes' accomplishments with collaborators at LANL has been to use Quantum Monte-Carlo calculations to calculate the value of ξ for finite size systems of 4 to 130 particles in a periodic box, (See Figure 1), performing a careful extrapolation to zero effective range.

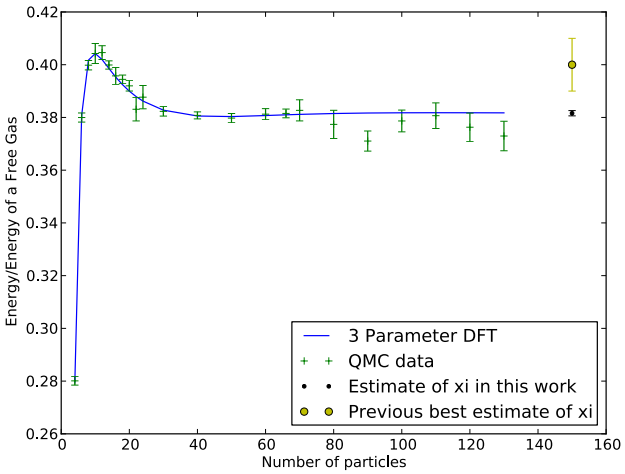

Figure 1. Monte Carlo calculations of the energy of the unitary Fermi gas in a periodic box with varying particle number (point) and the best fit 3-parameter density functional theory (solid). The reduced chi squared is 1.1 indicating that, to within statistical errors, the DFT agrees with the Monte Carlo "data". For comparison, at the right of the plot we show the previous best estimate of $\xi=0.40(1)$ and the value extracted from our fit $\xi=0.382(1)$.

These results alone have increased the precision $\xi=0.382(1)$ by an order of magnitude from the previous best calculation $\xi=0.40(1)$ [1].

Although useful in themselves, these results play a larger role in providing a benchmark for testing the fermion many-body theories being developed to study finite nuclei, nuclear matter in neutron stars, and condensed matter systems. Providing such benchmarks is the main objective behind our successful proposal for a workshop "Fermions from Cold Atoms to Neutron Stars: Benchmarking the Many-Body Problem" accepted to be held at the INT in 2011, for which Forbes is the lead organizer.

Forbes' research focused in particular on Density Functional Theory (DFT): an in-principle exact formalism that allows us to extend *ab initio* calculations of small systems (~100 particles) to larger systems of physical interest that are well beyond the reach of *ab initio* simulation. To this end, we have used these results to rigorously test the DFT for the unitary gas and explore the finite size effects: a crucial component of the program to use DFT to study other finite size systems such as nuclei. We have found that the DFT framework performs remarkably well (see Figure 1) eschewing the need for complicated and somewhat unjustified techniques such as particle number projection in order to capture finite size effects to a high degree of accuracy.

In collaboration with colleagues at the University of Washington, we have prepared two contributions for inclusion in books: one lengthy review for inclusion in a volume of Lecture Notes in Physics [2], and another for inclusion in and edited volume detailing the FINESS workshop. These works detail some of our efforts to use large-scale computing to study static and dynamic properties of Fermi gases.

Work applying the DFT to calculate properties of neutron stars is ongoing. As one descends into the crust of a neutron star and the density increases, neutrons "drip" out of the nuclei and one enters a phase of dilute neutron matter with properties very similar to the unitary Fermi gas along with positively charged clumps of protons. These positively charged regions could organize themselves into complicated structures dubbed "pasta" phases that act as solids with a shear modulus. This solid crust can support vibrations that propagate around the entire neutron star with frequencies that are commensurate in frequency to modulations of observed transient signals.

Using a simplified classical DFT, we have calculated the shear modulus for these phases. Work is ongoing to determine the sensitivity of these calculations to the model parameters. Preliminary indications are that more sophisticated DFT may be required that properly takes into account quantum corrections. This will require the parallel DFT code being developed.

A second major project is investigating a potential dark matter candidate in the form of quark antimatter nuggets. This potentially solves two of the major outstanding problems in cosmology: 1) Baryogenesis or where is all the antimatter? and 2) What is the nature of the hitherto unobserved dark matter that holds our universe together? Our proposal hides the antimatter in macroscopic "nuclei" formed at the QCD phase transition, thus solving both problems.

What is intriguing about this proposal is that, not only is it consistent with present constraints, but it predicts that the dark matter should be directly observable. The idea is that regular matter in our galaxy (hydrogen for example) will annihilate on these antimatter nuggets releasing observable radiation. Our model makes definite predictions about both 511 keV radiation resulting from electron-positron annihilation as well as diffuse radiations in the 10 keV, 10 MeV and micro-wave bands.

All of these emissions have observational constraints, and our preliminary analysis found that—with a few reasonable phenomenological parameters—our model is not only consistent with the observations, but could provide a compelling explanation. In our resubmitted paper [3], we have used semi-classical DFT approximation to determine the density profile of the electrosphere of these quark nuggets. This allowed us to directly compute some of these phenomenological parameters from unambiguous microscopic physics. We found that the phenomenological values required to explain the observations emerged naturally from the microscopic calculation, providing another

piece of strong evidence for our proposal. The comparison of our results with the observations is shown in Figure 2.

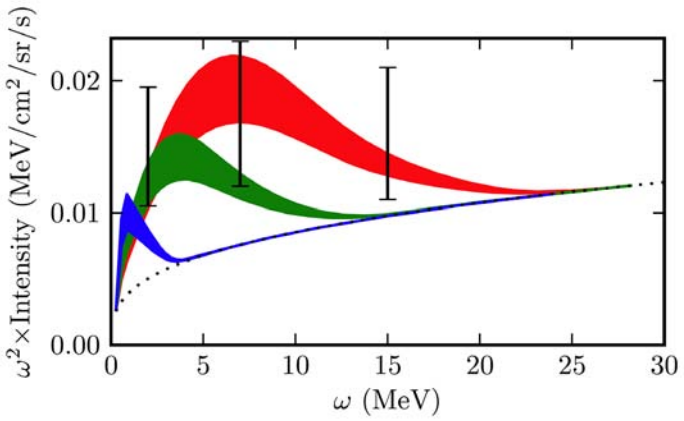

Figure 2. Here we compare the results of our microscopic calculation of the emissions in up to 30 MeV with the COMPTEL data [4]. We have included the known backgrounds (dotted line) showing that -- given a suitable velocity distribution for the incoming electrons (indicated by different colours) -- we can easily explain part or all of the excess. In the absence of strong new background sources, the data certainly cannot rule out our proposal. Note that the overall normalization is set by the observed 511 keV flux along the same line of sight which -- prior to our proposal -- has been considered an independent source. Thus, this provides a stringent test of our theory.

Impact on National Missions

This research on strongly interacting Fermi systems ties in well with Office of Science missions relating to nuclear physics, astrophysics and condensed matter physics. The results of this work have enhanced our basic understanding of materials through our ability to model superfluid and superconducting matter in both the terrestrial and astrophysical context.

References

1. Forbes, M., S. Gandolfi, and A. Gezerlis. Resonantly interacting fermions in a box. 2010. *Physics preprint archive.*

2. Bulgac, A., M. Forbes, and P. Magierski. The unitary fermi gas: From Monte Carlo to density functionals. 2010. *Physics preprint archive.*

3. Forbes, M., K. Lawson, and A. R. Zhitnitsky. Electrosphere of macroscopic “quark model”: A source of diffuse MeV emissions from dark matter. 2010. *Physical Review D.* **82** (8): 083510.

4. Strong, A. W., I. V. Moskalenko, and O. Reimer. Diffuse Galactic continuum gamma rays. A model compatible with EGRET data and cosmic-ray measurements. 2004. *Astrophysical Journal.* **613**: 976.

Publications

Bulgac, A., M. M. Forbes, and P. Magierski. The Unitary Fermi Gas: From Monte Carlo to Density Functionals. 2010. *Preprint Archive.*

Forbes, M. M., and A. R. Zhitnitsky. WMAP Haze: Directly observing dark matter?. 2008. *PHYSICAL REVIEW D .* **78** (8): 83505.

Matter and Light

Katrin Heitmann
20080786PRD3

Abstract

Cosmology relies on melding diverse measurements to understand the composition and evolution of the Universe. Microwave background observations showed that the Universe is flat, but studies of the clustering of matter found only one-third of the matter required. Famously, supernovae observations then showed that dark energy provided the missing energy density, bringing all measurements into concordance. This project is aimed at future surveys that will measure the distribution of galaxies in the Universe with very high accuracy. From these measurements, new cosmological constraints will be derived and these will advance our understanding of the fundamental constituents of our Universe: dark matter and dark energy.

Current and near-future galaxy surveys probe such huge volumes and such a large range of distance scales that it is a computational "grand challenge'' to compare our theoretical understanding of galaxy clustering with the surveys. It is vital to develop efficient statistical and numerical techniques that can enable the making of such comparisons.

Background and Research Objectives

Our current understanding of the Universe relies heavily on measurements of its large-scale structure as probed by the clustering of galaxies. These studies are complicated by the fact that the luminous baryonic matter in galaxies (stars, gas) is only a tracer for the dark matter, whereas theoretical models directly predict the clustering properties of dark matter. This project focuses on understanding the connection between light and matter. Dr. Pope is successfully developing new simulation and prediction capabilities to facilitate this understanding. This will be a crucial step for interpreting new cosmological observations and obtaining constraints on dark energy.

The major focus of the project is to connect theoretical predictions with observational data to derive new cosmological constraints. One of the major tools on the theoretical side is N-body simulations. The size of such simulations has to be enormous in order to cover the observational surveys adequately. It is crucial to develop capabilities that allow us to simulate the whole visible Universe down to galactic scales. This means that simulations have to be carried out covering a dynamical range of a million. Only sophisticated high-performance cosmology codes can enable this task. New supercomputing architectures like the Roadrunner machine at Los Alamos, enable for the first time simulations with sufficient resolution and large volumes, mimicking ongoing and upcoming surveys. These supercomputers are based on hybrid architectures, a mixture of conventional high-performance machines and accelerating units to obtain the desired performance. In order to use these machines, a new paradigm has to be developed for cosmological simulation codes. One major objective of this project was the development of such a code, the first petascale cosmology code. The second major objective was to perform some of the largest cosmological simulations ever to extract the signature of the baryon acoustic oscillation peak from simulations of the Lyman-alpha forest. In these simulations, the matter distribution of the Universe is mapped out via placing bright objects, quasars, into the simulations. The quasars act as "flashlights" to map out the matter distribution between them and an observer. A major aim of the Sloan Digital Sky Survey III is to make a measurement of the baryon acoustic oscillation peak in the Lyman-alpha forest and this project provides some of the theoretical predictions to interpret the measurements. The measurements will be important to advance our understanding of dark energy.

Scientific Approach and Accomplishments

The use of high-performance simulations to model the distribution of matter and galaxies in the Universe is essential as outlined above. Dr. Pope concentrated therefore during the start of the project on developing extremely efficient simulation and analysis tools. Dr. Pope made very impressive progress with this difficult task. A code version that allows for medium resolution simulation has been finished, tested and successfully ran on Roadrunner to produce some of the world's largest simulations. Figure 1 shows a zoom-in to a snapshot from one of these simulations. The excellent mass resolution allowed us to resolve

structures in great detail. A high-resolution extension of the code has been completed. All major analysis tools have been developed and implemented in the code infrastructure. Dr. Pope gave an invited talk at UIUC on his work and published invited proceedings for the SciDAC conference 2009 together with Salman Habib (LANL) [1]. A second invited paper to Computing in Science and Engineering will appear later this year, Dr. Pope is the lead author on this publication [2]. Dr. Pope also delivered an invited presentation on his work at the Snowpac Meeting in Utah on March 27, 2010.

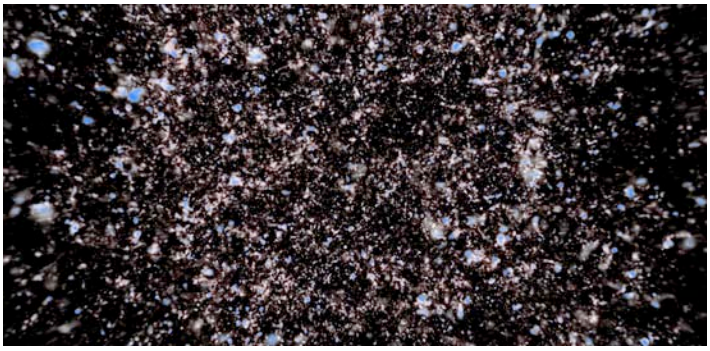

Figure 1. Dark matter halos from a Roadrunner simulation. The simulation encompasses 64 billion particles and we show here a small subsection of the full volume.The halos are colored with respect to mass.

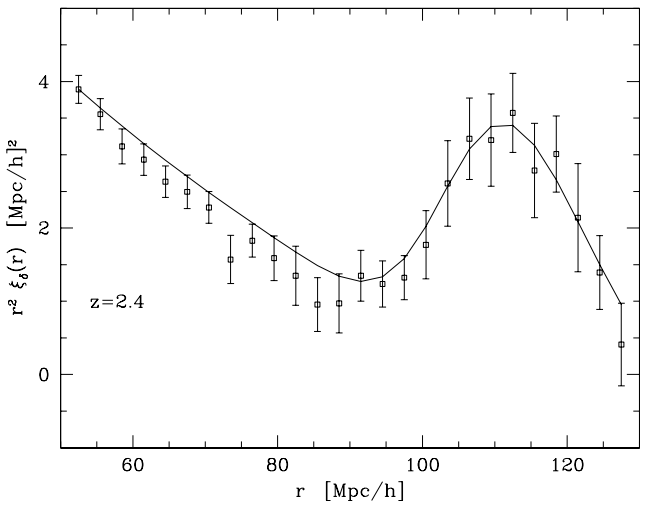

Figure 2. Baryon acoustic oscillation peak in the Lyman-alpha forest. The peak height, position, and width contains information about dark energy.

The Roadrunner simulation suite was used to explore the imprints of baryon acoustic oscillations in the matter distribution of the universe. The baryon acoustic oscillations leave their imprint at a certain scale in the matter distribution. The imprint manifests itself in the correlation function as a distinct peak. The position, height, and shape of the peak hold clues about the origin of dark energy. It was recently proposed that this observation can be obtained from Lyman-alpha forest observations, a major target of the ongoing Sloan Digital Sky Survey III. In order to detect the peak in the Lyman-alpha forest, very large simulations have to be carried out. The baryon acoustic oscillation signal in the Lyman alpha forest was successfully extracted from the Roadrunner simulations (see Figure 2). New clues for observing and analysis strategies have been found. The results have been published in the Astrophysical Journal [3].

Impact on National Missions

The project targets two of the top priorities of the DOE mission: understanding the nature of dark energy and high-performance computing. In addition, the project is relevant for the threat reduction arena in providing new techniques to extract information from diverse and very large data sets.

References

1. Habib, S., A. Pope, Z. Lukic, D. Daniel, P. Fasel, N. Desai, K. Heitmann, C. Hsu, L. Ankeny, G. Mark, S. Bhattacharya, and J. Ahrens. Hybrid petacomputing meets cosmology: the Roadrunner Universe project. 2009. (San Diego, 14 - 18 June, 2009). Vol. 180p. 012019. Journal of Physics: Conference Series: IOP.

2. Pope, A., S. Habib, Z. Lukic, D. Daniel, P. Fasel, N. Desai, and K. Heitmann. The accelerated universe. To appear in *Computing in Science and Engineering* .

3. White, M., A. Pope, J. Carlson, K. Heitmann, S. Habib, P. Fasel, D. Daniel, and Z. Lukic. Particle mesh simulations of the Lyman-alpha forest and the signature of Baryon Acoustic Oscillations in the intergalactic medium. 2010. *Astrophysical Journal.* **713** (1): 383.

Publications

Habib, S., A. Pope, Z. Lukic, D. Daniel, P. Fasel, N. Desai, K. Heitmann, C. Hsu, L. Ankeny, G. Mark, S. Bhattacharya, and J. Ahrens. Hybrid petacomputing meets cosmology: the Roadrunner Universe project. 2009. In *SciDAC 2009.* (San Diego, 14 - 18 June, 2009). Vol. 180, p. 012019. Journal of Physics: Conference Series: IOP.

Pope, A., S. Habib, Z. Lukic, D. Daniel, P. Fasel, N. Desai, and K. Heitmann. The accelerated universe. To appear in *Computing in Science and Engineering* .

White, M., A. Pope, J. Carlson, K. Heitmann, S. Habib, P. Fasel, D. Daniel, and Z. Lukic. Particle mesh simulations of the Lyman-alpha forest and the signature of Baryon Acoustic Oscillations in the intergalactic medium. 2010. *Astrophysical Journal.* **713** (1): 383.

Technology

LABORATORY DIRECTED RESEARCH AND DEVELOPMENT

Nanoscale Superconductivity for Single Photon Detection

Michael W. Rabin
20100006DR

Introduction

Photon detection lies at the heart of numerous applications in national security and fundamental science. Space surveillance, nuclear threat detection, quantum science, and biomolecular imaging all have compelling needs for broadband, high efficiency, low noise, fast single photon detectors. Conventional technologies fall short in at least one of these areas, forcing application-specific compromises. A new class of detector, the superconducting nanowire single photon detector (SNSPD), has the potential to revolutionize the field of single photon detection through a combination of unsurpassed performance in all critical parameters (scalability, broadband efficiency, dark count rate, speed). Current development of these detectors is limited by materials difficulties that affect yield and performance, making it impossible to study the underlying physics and determine the fundamental limits of SNSPD detector operation. We are pursuing two complementary thin-film growth techniques (energetic neutral atom beam lithography & epitaxy, or ENABLE, and polymer assisted deposition, or PAD) and integrating expertise over a wide range of fields to understand and apply nanoscale superconductivity.

Benefit to National Security Missions

In the long term, we anticipate the development of large-format SNSPD-based cameras that will have extraordinary applicability in areas that include:

- Surveillance and reconnaissance in support of nuclear, biological, chemical, and environmental treaty verification.
- All-sky search for small, dark, unknown space objects (space situational awareness or SSA).
- Determining reaction history at picosecond time resolution in thermonuclear burn or ignition experiments

Progress

A series of ENABLE and PAD NbN films ranging from 4-50 nm thickness have been grown. We discovered a strong dependence of film properties on growth conditions and are exploring how to better control film properties through control of growth conditions. Extensive characterization of our PAD and ENABLE grown films was performed to correlate growth conditions with microstructural and physical properties. We have grown superconducting NbN thin films on SrTiO3 substrates by PAD, a chemical solution technique, developed recently to synthesize high-quality epitaxial metal-oxide films with desired structural and physical properties [1]. Stable metal-polymer solutions were used as the film precursor, where the water-soluble polymer not only controls the solution viscosity but also binds the metal ions to prevent the metal ions from hydrolysis and to form a homogeneous solution. We have extended this growth technique to prepare an epitaxial nitride film, e.g., superconducting cubic NbN films have been grown by PAD [2]. Most of the NbN films grown on $SrTiO_3$ by PAD were epitaxial, as revealed by x-ray diffraction. Disappointingly, many of these films exhibited no superconducting transition, even though the films showed the expected phase and texture. Analysis showed oxygen inclusion in the films and a mesh-like or granular surface morphology. The inclusion of oxygen in the film and the island growth of the film can potentially degrade the superconducting properties. Nevertheless, we have deposited epitaxial and superconducting NbN films on $SrTiO_3$ substrates by PAD. The most recent NbN film has a superconducting transition temperature of around 8 K and a metallic-like behavior from 50 K to 300 K. Such a metallic-like resistivity vs. temperature characteristics above the transition temperature is very different from the NbN films grown by other techniques.

A substantial portion of the growth efforts by ENABLE [3-4] focused on changing from a Nb wire electron-beam evaporation source to a high temperature thermal Nb source. The variation in growth parameters with wire consumption were known to be substantial, and thermal epitaxial film growth of related materials (e.g. gallium and aluminum nitride) is well known to be superior to

electron beam methods. Nonetheless, repeated attempts to use a high-temperature thermal Nb evaporation cell resulted in NbN films that failed in every attempt to superconduct. Although the films had good crystalline properties they lacked superconductivity. Analysis of these films showed that BN crucible and components used in the evaporator were decomposing, contaminating the NbN with B, and destroying the superconductivity.

Returning to the electron-beam methods, the cell was placed in a more optimal configuration than before and several structural modifications were made to improve its lifetime and reliability. Since the return to the Nb wire e-beam system, results have been outstanding. We have re-established our ability to produce superconducting NbN and have grown several films with superconducting transition temperature T_c above 10 K with thicknesses of 5 nm or less. These results are important film growth milestones, as films of that thickness and transition temperature will be needed for SNSPD device fabrication. We also moved to capping ENABLE grown films *in-situ* with ~20 nm of AlN to improve the in-air stability of the as-grown films. Figure 1 shows corresponding resistance vs. temperature graphs. In Figure 1b a film of thickness of ~ 5 nm, as determined by TEM, shows a transition T_c=13.9 K with width ΔT_c of 0.6 K. Such films are excellent initial candidates for device patterning.

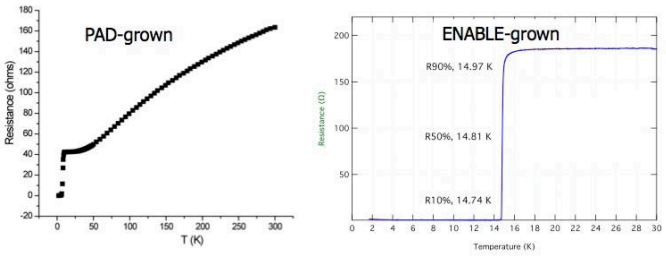

Figure 1. Resistance vs. temperature graphs for superconducting NbN thin films grown by PAD (a, left) and ENABLE (b, right). PAD-grown film has a superconducting transition temperature of Tc=8 K, transition width ~1K, and resistance increasing with temperature above the transition. The ENABLE-grown film has superconducting transition temperature Tc=14.8 K, with transition width ~0.2K, and is 15 nm thick with a 20 nm AlN cap.

Subsequently, we studied the correlations between the films' surface morphology (scanning electron microscopy or SEM) and the internal structure as determined by (scanning) transmission electron microscopy (STEM or TEM). PAD films have porosity due to the evaporation, decomposition and removal steps of solvents and other organics during film deposition. Hence, finding the right deposition conditions for the production of thin, dense films with the required properties is a significant challenge. Figures 2a and 2b show the correlations between surface morphology and internal structure. Figures 2c and 2d show the differences one can obtain with changes in the process parameters. Of interest for the film of Figure 2d is the metallic behavior of this particular film above T_c as opposed to the typical semiconducting behavior observed for most films, see Figure 1a. All e-beam films grown at LANL and examined by electron microscopy were under 15 nm thick. Recent e-beam films, showing high values of T_c (> 10K), had thicknesses of under 10 nm, see Figure 3b. Specific areas of interest include mis-aligned grains or secondary phases, stacking faults, multilayer stacks using AlN spacer layers, and interfacial defects, see Figures 3c, 3d, and 3e. Of interest in the coming year are the correlations of these defects with the superconducting properties of the NbN films and their effects on detector performance.

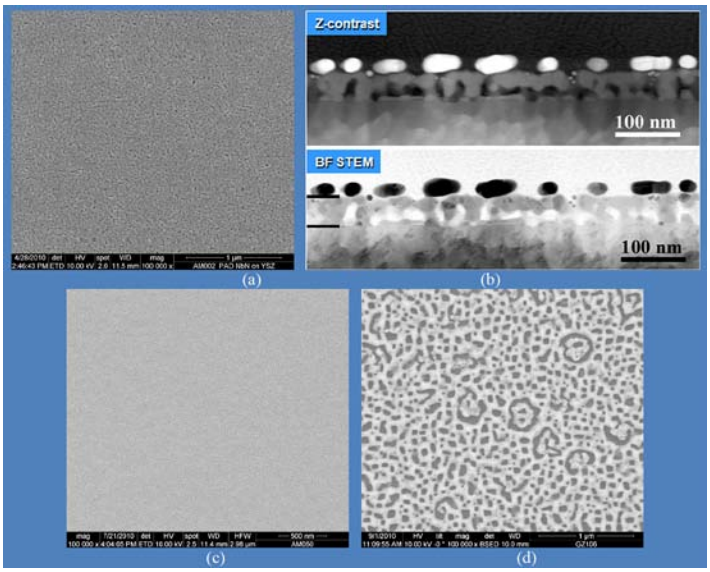

Figure 2. SEM image (a) and STEM z-contrast (phase incoherent) images of an early PAD film showing the connections between surface morphology and internal structure. The NbN film is identified by the two black lines in the bright field (BF) STEM image. The particles on top are Au used to delineate surfaces. SEM images of PAD films showing improved density (c) and a PAD film (d) showing a connected network structure in a film that showed metallic behavior above Tc=8 K.

In parallel, we developed a theory of order parameter fluctuations to account for excess dissipation due to vortex crossings in thin current-biased superconducting films with thickness on the order of the coherence length, and widths much narrower than the magnetic Pearl length in thin films. We found that for technologically relevant thin and narrow films or strips with widths much larger than the coherence length, the barrier for phase slips by the creation of temporary normal regions across the entire film width is too big; thus phase slips become highly improbable. Instead, we propose the process of a vortex crossing the strip from one edge to the other, perpendicular to the bias current, as the dominant mechanism for generalized phase slips resulting in detectable voltage pulses. In Ginzburg-Landau theory, the vortex position inside the

strip is given by the maximum in the kinetic energy due to supercurrents. However, the free energy barrier derived in such a mean-field theory is strongly renormalized by superconducting fluctuations, because fluctuations drastically reduce the barrier and thus increase the rate of vortex crossings and consequent dissipation.

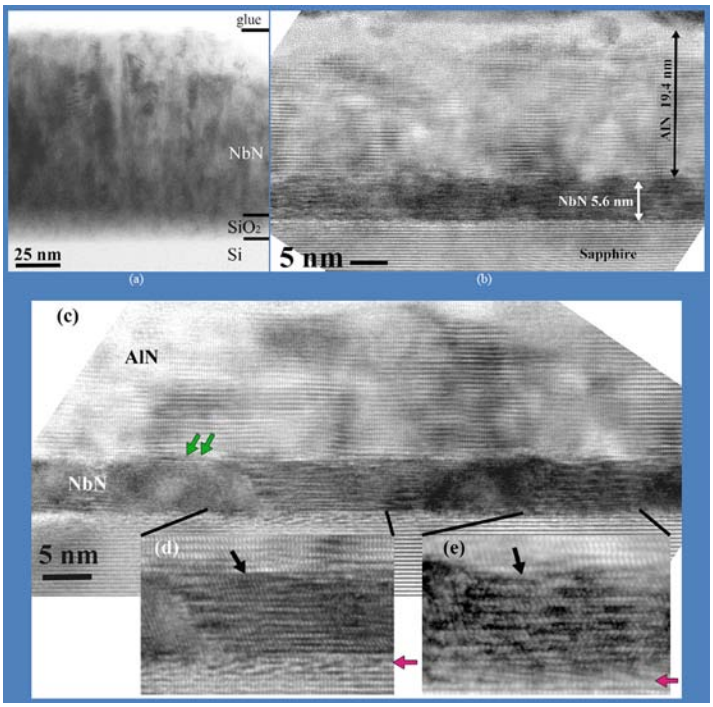

Figure 3. Panel (a) TEM cross-sectional image of a thick magnetron sputtered Nb(Ti)N film. (b) A thin ENABLE-grown (electron beam) NbN film with an AlN capping layer. A number of defects are shown in the TEM image (c) and expanded views (d) and (e). The red arrows indicate some tilted rows of atoms at the interface between the sapphire and NbN film. The black arrows indicate a number of stacking faults in the NbN film. The green arrows indicate either misaligned grains or secondary phases.

Our studies extended the theory of transition rates between metastable states in superconductors [5-6] from quasi-1D to quasi-2D wires. We found for nanowires of length L, thickness d, and width W, with magnetic Pearl length $\Lambda=2\lambda^2/d$ much larger than the superconducting coherence length ξ and magnetic penetration depth λ ($L>\Lambda>>W>>\xi\sim d$) that every crossing by a vortex results in a detectable voltage pulse. By going beyond mean-field approach, we accounted for the first time for the renormalization of the vortex-crossing rate by superconducting phase fluctuations. In addition, we estimated the amplitude of induced voltage pulses (~1 meV) and their respective fluctuation renormalized I-V characteristics. The time evolution of the voltage pulse may be used to differentiate between a photon induced hotspot with voltage pulse and a vortex induced dark count with a different characteristic voltage pulse. Another prediction of our theory is the existence of "cold" dark counts, which correspond to vortex crossings that do not induce a hotspot, and thus may not be measureable with available experimental timing resolutions. However, they generate a background DC voltage in the SNSPD that can be extracted to estimate their occurrence rate. We predict the magnitude and duration of V(t) with time-integrated value $\int V(t)dt=\Phi_0/2\pi c$, with flux quantum Φ_0 and speed of light c.

Future Work

Our two complementary growth techniques, coupled with device characterization, provide us with an exceptional opportunity to develop a theoretical framework that can be validated by controlled experimental studies. Films are being characterized using several diagnostic resources. A theoretical model is being developed for predicting the relationships between material characteristics (crystallinity, grain size, dynamic response) and basic superconducting properties. To allow the controlled design of materials and SNSPD devices, we must understand the relevant physical regimes and parameters for nanowires, the origin of dark counts, and the electrothermal runaway processes and dissipation of thermal energy. Patterned SNSPD devices will be tested electrically and optically between room temperature and 2 K. Electrical characterization will include measurements of $I_c(T)$, kinetic inductance, high frequency properties, and noise power spectral density.

Conclusion

Our goals include nanofabrication of prototype arrays of SNSPDs, an important step toward our ultimate goal of moving SNSPDs from a single or few-pixel technology with limited efficiency, to a high-efficiency single photon imaging array. Substantial work has set the basis for understanding of nanoscale superconductivity (theory, materials & device physics) that is necessary for developing SNSPDs into a technology that will deliver broadband, high-efficiency, high-speed, low-noise single photon detection systems.

References

1. McCleskey, T. M., A. K. Burrell, Q. X. Jia, and Y. Lin. Polymer-assisted deposition of films. 2008. *U.S. Patent 7365118.*

2. Zou, G. F., M. Jain, H. H. Zhou, H. M. Luo, and S. A. Baily et al.. Ultrathin epitaxial superconducting niobium nitride films grown by a chemical solution technique . 2008. *Chemical Communications.* (45): 6022.

3. Hoffbauer, M. A., and A. H. Mueller. Charge-free low temperature method of forming thin film-based nanoscale materials and structures on a substrate. 2008. *U.S. patent 7393762.*

4. Mueller, A. H., E. A. Akhadov, and M. A. Hoffbauer. Low-temperature growth of crystalline GaN films using energetic neutral atomic-beam lithography/epitaxy. 2006. *APPLIED PHYSICS LETTERS.* **88** (4): 014907.

5. Williamson, T. L., M. A. Hoffbauer, K. M. Yu, L. A. Reichertz, M. E. Hawkridge, R. E. Jones, N. Miller, J. W. Ager, Z. Liliental-Weber, and W. Walukiewicz. Highly luminescent In_xGa_{1-x}N thin films grown over the entire composition range by energetic neutral atom beam lithography & epitaxy (ENABLE). 2009. *Physica Status Solidi C.* **6** (S2): S409.

6. MCCUMBER, D. E., and B. I. HALPERIN. TIME SCALE OF INTRINSIC RESISTIVE FLUCTUATIONS IN THIN SUPERCONDUCTING WIRES. 1970. *PHYSICAL REVIEW B.* **1** (3): 1054.

Publications

Boulaevskii, L. N., M. J. Graf, C. D. Batista, and V. G. Kogan. Vortex induced dissipation in narrow current-biased thin-film superconducting strips. 2010. *to be submitted to Physical Review B.*

Luo, H., H. Wang, G. Zou, E. Bauer, T. M. McCleskey, A. K. Burrell, and Q. X. Jia. A Review of Epitaxial Metal-Nitride Films by Polymer-Assisted Deposition. 2010. *Trans. Electrical & Electronic Mater.*. **11**: 54.

Intelligent Wind Turbines

Curtt N. Ammerman
20100040DR

Introduction

The Intelligent Wind Turbine Project is a multi-disciplinary engineering research and development effort. The goal of the project is to make wind power more affordable. We are developing technologies that will increase turbine efficiencies and reduce the number of wind turbine failures. We are constructing better predictive models to understand the effects of realistic wind conditions on turbine health and performance. We are developing new sensing techniques that can detect damage in wind turbine blades. We are also generating control schemes that will both improve turbine efficiency and compensate for structural damage. These project elements will be combined with data gathering and model validation techniques to produce a new class of wind turbine hardware and software tools. These tools will enable wind turbines to intelligently assess their structural health and optimize their power output. Our team is unique in that we can combine these complimentary tasks into a single coordinated effort. This effort will significantly impact the current practice of harvesting wind energy. This effort will also enable Los Alamos National Laboratory (LANL) to bring innovation to this rapidly growing field.

Benefit to National Security Missions

The US Department of Energy (DOE) proposes to meet 20% of the nation's energy needs with wind power by the year 2030. Although wind turbines have a design lifespan of 20 years, they typically fail 2.6 times per year during their first 10 years. The industry is struggling to understand these premature failures and predict and manage the growth of defects. We will transform current engineering practice by advancing and integrating innovative techniques to understand, identify, and manage wind power systems. The same advances in engineering practice will improve the LANL's ability to deliver systems solutions for a wide range of missions.

Progress

We have made significant progress so far this year in several areas. These areas include turbine blade sensing, modeling and simulation, model validation, and wind turbine controls.

In the area of turbine blade sensing, we participated in a cooperative, multi-Laboratory fatigue test of a wind turbine blade. We placed the structural health monitoring (SHM) sensing system that we are developing on the turbine blade (Figure 1).

Figure 1. Wind turbine blade during fatigue test.

In this test, we proved that we can detect a small crack in the blade and follow its growth [1-4]. We will build on these results to inform our own fatigue test that will take place in 2011. The wind turbine blade for this 2011 test (and a companion blade) have been fabricated and are in our facility. To date, we have investigated three different SHM diagnostic techniques on sections of wind turbine blades. These techniques (Lamb wave propagations, frequency response functions, and a time series predictive model) have each yielded sufficient damage detection capability to warrant further investigation. We are also working to reduce weight, cost, and power requirements for the SHM system. In addition, we are developing a wireless sensor node specifically designed for wind turbine blades [5]. This sensor node will be able to detect blade cracks and predict remaining blade life as the turbine is spinning. These sensor nodes will be

self-powered. We have performed initial experiments on a variety of promising energy harvesting techniques [6-8].

In the area of modeling and simulation, we have integrated a turbulence simulator into our WindBlade wind turbine simulation code. We worked jointly on this effort with the National Renewable Energy Laboratory (NREL), which generated this simulator. This turbulence simulator is being used to provide realistic input conditions that enable WindBlade to accurately model turbine wake effects (Figure 2). We have also generated software interfaces so that WindBlade can communicate with the Weather Research and Forecasting (WRF) mode. This WRF interface is particularly important for validation against data from the National Wind Technology Center. We also have created and are expanding a software interface to enable the output from WindBlade to be viewed and manipulated with ParaView [9]. ParaView is an open-source, scientific visualization package. In addition, we are in the process of developing a finite element model of the wind turbine research blade. This model will be used to help place sensors on the blade for the 2011 fatigue test. This model will also be used to provide WindBlade with an accurate structural representation of a wind turbine blade.

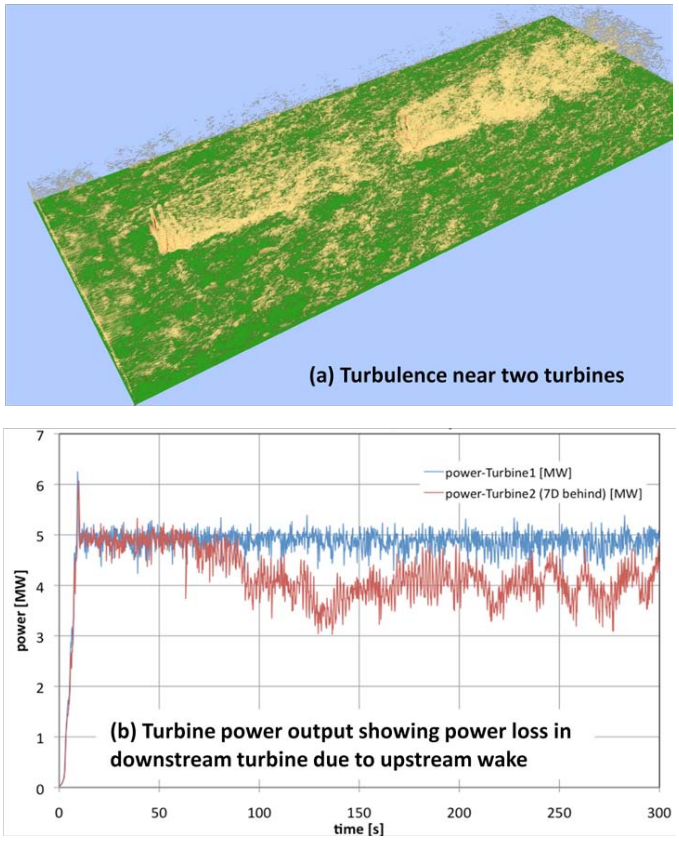

Figure 2. WindBlade simulation showing (a) the turbulence near two, 120-meter-diameter turbines 7 diameters apart, and (b) their respective power output.

In the area of model validation, we have performed several particle image velocimetry (PIV) tests. These tests measure the rotating turbulent vortices behind scaled wind turbines in the New Mexico State University (NMSU) wind tunnel (Figure 3). We have used the results from these PIV test to generate valuable validation datasets [10]. These datasets have already been requested by other research institutions and will be used to validate their wind turbine design codes. In addition, we have purchased a 4.5-meter-diameter turbine that will be installed at LANL in 2011. This turbine will be used to perform the first-ever PIV measurements on a wind turbine in the field. We are currently working to obtain siting, facility, and engineering approval for the installation of this turbine. We are also nearing completion of a small test facility to stage and tune the laser system that will be used for these PIV field measurements. The results obtained from these measurements will provide data for the validation of WindBlade and for software used by the wind turbine industry.

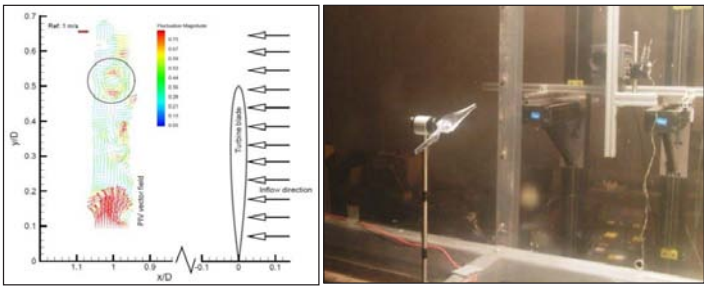

Figure 3. Turbulent vortices measured on scale wind turbine in NMSU wind tunnel.

In the area of active turbine blade control, we are developing an adjoint version of a fluid-structure interaction (FSI) code. This code will enable studies of advanced blade trailing edge actuation concepts. We are working jointly on this effort with the University of California, San Diego (UCSD). This adjoint formulation will be applied first in a 2-D computational fluid dynamics code, and subsequently in a 3-D code. We are also in the early planning stages of a test to demonstrate a damage-mitigating control algorithm. This algorithm will, once blade damage is detected, effect active blade pitch control to minimize damage growth while maximizing power output. We are coordinating with NREL for a 2012 test at their Controls Advanced Research Turbine test facility.

Future Work

In the coming year, we will be performing a fatigue test of our wind turbine blade at NREL. This test will enable us to further refine our SHM sensing techniques. We hope that as a result of this test, we will be able to pinpoint the location and size of incipient cracks in wind turbine blades. This year we will also complete the installation of a small research wind turbine at LANL. With this turbine in place, we will begin taking large-format PIV measurements of airflow both upstream and downstream of this turbine. We will also be implementing the first-ever rotating PIV measure-

ment techniques to visualize the flow around the rotating turbine blade. These measurements will provide researchers with unprecedented insights into the nature of the airflow around an operating wind turbine. We also plan to add capability to the WindBlade code to enable the simulation of aeroelastic turbine blades. This new capability will allow for the two-way interaction between the flexible blade and the moving air. This capability will also enable users of the code to extract operating loads on the rotating turbine blades. In 2012, our project will culminate in a full-scale flight test of three research blades on a 20-meter-diameter turbine. This test will provide proof-of-concept for our SHM sensing nodes. This test will also demonstrate our capability to measure the flow fields with PIV around a relevant-scale turbine. The data from this test will be used to validate a WindBlade simulation of the test turbine.

Conclusion

The expected deliverables for this effort include a validated wind turbine and wind plant simulation tool capable of modeling true wind loading (with realistic terrain, vegetation, and upstream turbines), blade and hub loading, damaged and undamaged rotors, and various control schemes. We will also develop self-powered structural health monitoring hardware nodes capable of being deployed on wind turbines that will enable damage detection and prognosis and will provide damage mitigating control. This project will result in increased wind turbine reliability and efficiency enabling DOE to meet their goal of reducing wind power operation and maintenance costs by 40 percent.

References

1. Park, G., K. M. Farinholt, and C. R. Farrar. SHM of wind turbine blades using piezoelectric active-sensors. To appear in *Proceedings of 5th European Structural Health Monitoring Conference.* (Sorento, Naples-Italy, 29 Jun.-2 Jul. 2010).

2. Claytor, T. N., C. N. Ammerman, G. Park, K. M. Farinholt, C. R. Farrar, and M. K. Aterbury. Structural damage identification in wind turbine blades using piezoelectric active sensing with ultrasonic validation. To appear in *Proceedings of The American Society of Nondestructive Testing 19th Annual Research Symposium and Spring Conference.* (Williamsburg, VA, 22-26 Mar. 2010).

3. Park, G., E. F. Figurido, K. M. Farinholt, and C. R. Farrar. Time series analysis of piezoelectric active-sensing for SHM applications. To appear in *Proceedings of the 17th SPIE Conference on Smart Structures and Nondestructive Evaluation.* (San Diego, CA, 7-11 Mar. 2010).

4. Sobin, A., A. Light-Marquez, K. M. Farinholt, and G. Park. Structural damage identification in wind turbine blades using piezoelectric active-sensing. To appear in *Proceedings of IMAC-XXVIII, A Conference & Exposition on Structural Dynamics.* (Jacksonville, FL, 1-4 Feb. 2010).

5. Taylor, S. G., K. M. Farinholt, G. Park, M. D. Todd, and C. R. Farrar. Application of a wireless sensor node to health monitoring of an operation wind turbine blade. To appear in *Proceedings of IMAC-XXVIII, A Conference & Exposition on Structural Dynamics.* (Jackonville, FL, 1-4 Feb. 2010).

6. Schlichting, A., S. Oullette, C. Carlson, K. M. Farinholt, G. Park, and C. R. Farrar. Multi-source energy harvester to power sensing hardware on rotating structures. To appear in *Proceedings of 17th SPIE Conference on Smart Structures and Nondestructive Evaluation.* (San Diego, CA, 7-11 Mar. 2010).

7. Haynes, C., N. Konchuba, K. M. Farinholt, and G. Park. Estimation and modeling of force transmission in wind turbines. To appear in *Proceedings of IMAC-XXVIII, A Conference & Exposition on Structural Dynamics.* (Jacksonville, FL, 1-4 Feb. 2010).

8. Carlson, C. P., A. D. Schlichting, S. Ouellette, K. M. Farinholt, and G. Park. Energy harvesting to power sensing hardware onboard a wind turbine blade. To appear in *Proceedings of IMAC-XXVIII, A Conference & Exposition on Structural Dynamics.* (Jacksonville, FL, 1-4 Feb. 2010).

9. Ahrens, J., K. Heitmann, M. Petersen, J. Woodring, S. Williams, P. Fasel, C. Ahrens, C. H. Hsu, and B. Geveci. Verifying scientific simulations via comparative and quantitative visualization. 2010. *IEEE Computer Graphics and Applications.* **30** (6): 16.

10. Balakumar, B. J., R. C. Alarcon, J. T. Hoffman, and S. Pol. Detailed flow-field measurements around a small wind turbine, and an array of small turbines, designed using blade element momentum theory. To appear in *ASME/JSME/KSME Joint Fluids Engineering Conference.* (Hamamatsu, Japan, 24-29 Jul. 2011).

Publications

Ahrens, J., K. Keitmann, M. Petersen, J. Woodring, S. Williams, P. Fasel, C. Ahrens, C. H. Hsu, and B. Geveci. Verifying scientific simulations via comparative and quantitative visualization. 2010. *IEEE Computer Graphics and Applications.* **30** (6): 16.

Balakumar, B. J., R. C. Alarcon, J. T. Hoffman, and S. Pol. Detailed flow-field measurements around a small wind turbine, and an array of small turbines, designed using blade element momentum theory. To appear in *ASME/JSME/KSME Joint Fluids Engineering Conference.* (Hamamatsu, Japan, 24-29 Jul. 2011).

Bazilevs, Y., M. C. Hsu, I. Akkerman, S. Wright, K. Takizawa, B. Henicke, T. Spielmanand, and T. E. Tezduyar. 3D simulation of wind turbine rotors at full scale. Part I:

Geometry modeling and aerodynamics. 2010. *International Journal of Numerical Methods in Fluids.* **DOI: 10.1002/fld.2400**: .

Bazilevs, Y., M. C. Hsu, J. Kiendl, R. Wuechner, and K. U. Bletzinger. 3D simulation of wind turbine rotors at full scale. Part II: Fluid-structure interaction. To appear in *International Journal of Numerical Methods in Fluids.*

Carlson, C. P., S. Schlichting, S. Ouellette, K. M. Farinholt, and G. Park. Energy harvesting to power sensing hardware onboard a wind turbine blade. To appear in *Proceedings of IMAC-XXVIII, A Conference & Exposition on Structural Dynamics.* (Jacksonville, FL, 1-4 Feb. 2010).

Claytor, T. N., C. N. Ammerman, G. Park, K. M. Farinholt, C. R. Farrar, and M. K. Aterbury. Structural damage identification in wind turbine blades using piezoelectric active sensing with ultrasonic validation. To appear in *Proceedings of The American Society of Nondestructive Testing 19th Annual Research Symposium and Spring Conference.* (Williamsburg, VA, 22-26 Mar. 2010).

Farrar, C., K. Worden, and G. Park. Complexity: a new axiom for structural health monitoring?. To appear in *Proceedings of the 5th European Workshop on Structural Health Monitoring .* (Sorrento, Italy, 29 Jun.-2 Jul. 2010).

Figueiredo, E., G. Park, K. M. Farinholt, and C. R. Farrar. Use of time-domain predictive models for piezoelectric active-sensing in structural health monitoring applications. *ASME Journal of Vibration and Acoustics.*

Haynes, C., N. Konchuba, K. M. Farinholt, and G. Park. Estimation and modeling of force transmission in wind turbines. To appear in *Proceedings of IMAC-XXVIII, A Conference & Exposition on Structural Dynamics.* (Jacksonville, FL, 1-4 Feb. 2010).

Hsu, M. C., I. Akkerman, and Y. Bazilevs. High-performance computing of wind turbine aerodynamics using isogeometric analysis. To appear in *Computers and Fluids.*

Hsu, M. C., Y. Bazilevs, I. Akkerman, and J. Kiendl. Fluid-structure interaction modeling of wind turbine rotors at full scale. To appear in *4th Southern California Symposium on Flow Physics.* (Irvine, CA, 17 Apr. 2010).

Hsu, M. C., Y. Bazilevs, and I. Akkerman. Isogeometric fluid-structure interaction analysis for wind energy applications. To appear in *UCSD Jacobs School of Engineering 29th Annual Research Exposition.* (Irvine, CA, 15 Apr. 2010).

Hsu, M. C., and Y. Bazilevs. Computational fluid-structure interaction: from wind turbines to cerebral aneurysms. To appear in *22nd International Conference on Parallel Computational Fluid Dynamics.* (Kaohsiung, Taiwan, 17-21 May 2010).

Hush, null., null. Porter, and null. Ruggiero. Density-based similarity measures for content based search. 2009. *DOE.*

Park, G., E. F. Figurido, K. M. Farinholt, and C. R. Farrar. Time series analysis of piezoelectric active-sensing for SHM applications. To appear in *Proceedings of the 17th SPIE Conference on Smart Structures and Nondestructive Evaluation.* (San Diego, CA, 7-11 Mar. 2010).

Park, G., K. M. Farinholt, and C. R. Farrar. SHM of wind turbine blades using piezoelectric active-sensors. To appear in *Proceedings of 5th European Structural Health Monitoring Conference.* (Sorento, Naples-Italy, 29 Jun.-2 Jul. 2010).

Schlichting, A., S. Oullette, C. Carlson, K. M. Farinholt, G. Park, and C. R. Farrar. Multi-source energy harvester to power sensing hardware on rotating structures. To appear in *Proceedings of 17th SPIE Conference on Smart Structures and Nondestructive Evaluation.* (San Diego, CA, 7-11 Mar. 2010).

Sobin, A., A. Light-Marquez, K. M. Farinholt, and G. Park. Structural damage identification in wind turbine blades using piezoelectric active-sensing. To appear in *Proceedings of IMAC-XXVIII, A Conference & Exposition on Structural Dynamics.* (Jacksonville, FL, 1-4 Feb. 2010).

Steinwart, I., D. Hush, and C. Scovel. Training SVMs without offset. *Journal of Machine Learning Research.*

Taylor, S. G., K. M. Farinholt, G. Park, M. D. Todd, and C. R. Farrar. Application of a wireless sensor node to health monitoring of an operation wind turbine blade. To appear in *Proceedings of IMAC-XXVIII, A Conference & Exposition on Structural Dynamics.* (Jacksonville, FL, 1-4 Feb. 2010).

Theiler, J., and D. Hush. Statistics for characterizing data on the periphery. To appear in *IEEE International Geoscience & Remote Sensing Symposium.* (Honolulu, HI, 25-30 Jul. 2010).

Construction and Use of Superluminal Emission Technology Demonstrators with Applications in Radar, Astrophysics, and Secure Communications

John Singleton
20080085DR

Abstract

Our project demonstrates that sources of electromagnetic radiation, such as radio waves, can be made to be superluminal, that is, travel faster than the speed of light. Although this may sound like science fiction, no laws of physics are in fact being broken; the sources involved consist of wave-like disturbances in special antennas made of alumina, and obey the principles of Relativity and Electromagnetism. Most people will be familiar with the idea of a "sonic boom", an intense burst of sound encountered some distance from a high-performance airplane that accelerates through the sound barrier. This occurs because the airplane overtakes the sound waves that it has emitted, pushing them together to make the "boom". In the same way, our superluminal sources overtake their own radio waves (which travel at the speed of light), producing an "electromagnetic boom"; a region of tightly focused and powerful radio waves. This effect has many potential applications, including medicine (focusing beams to excise tumors), radar, long-range communications (e.g. with distant space probes) and security (e.g. disabling stolen cars without harming people in and around them). In addition to building and testing two superluminal technology demonstrators and designing a third, the current project looks at the complex mathematics of the electromagnetic boom (e.g. how to predict and control it) and ties superluminal emission to astronomical phenomena. We have recently shown that pulsars, neutron stars that emit pulses of radiation seen by astronomers on Earth, are natural superluminal sources; using our mathematical models, we are able to predict all of the properties of their radiation. The models are now being adapted to other space phenomena such as gamma-ray bursts and Quasars.

Background and Research Objectives

Between 2004 and 2007, LANL-sponsored experimental [1, 2] and theoretical [3, 4, 5] work directed by the PI of the current program established that polarization currents can be made to travel *superluminally*, that is, made to move faster than the speed of light in a vacuum. This research also showed that these superluminal polarization patterns emit tightly focused packets of electromagnetic radiation that are fundamentally different from the emissions of previously known sources, such as phased arrays.

The idea of superluminal emission was developed from proposals by Ginzburg and colleagues in the early 1970s [6, 7]. The LANL research involved numerical and mathematical studies of radiation sources that exceed the speed of light [3, 4, 5], carried out in collaboration with H. Ardavan of the University of Cambridge. In addition, verification experiments were performed using a proof-of-principle apparatus built at Oxford University (in collaboration with A. Ardavan) using funds acquired by the PI in the UK [1,2].

Although resources were limited, the studies in the period 2004-2007 demonstrated that man-made superluminal sources have great potential for applications relevant to radar [8], medical and directed-energy technologies [2], as well as long-range communications [1]. In addition, the numerical work showed that phenomena seen in astronomical observations of pulsars might be attributable to emission by a rotating superluminal source [3]. In parallel with the US/UK work, a team at Sarov used the ISKRA-5 laser to demonstrate emission by superluminal polarization currents, verifying the fundamental physics involved [9, 10].

These developments [11], and the potential for scientific and technological advances in a promising but little-explored field, formed the basis of our LDRD project, which covered three areas:

- the design, construction and testing of next-generation practical superluminal sources to serve as technology demonstrators for radar, directed energy, and communications applications, as experimental verification for calculations and as ground-based astrophysics experiments (pulsar and gamma-ray burst simulators);

- analytical and numerical calculations of both man-made and natural superluminal sources, continuing the collaboration with Professor Ardavan; and

- the search for natural superluminal sources using astronomical observations.

As will be seen in the following sections, two new technology demonstrators were designed, built and tested (Figure 1), and form the basis of a continuing research program on communications and radar. A small 8-element "Test Bed" device was also built, to enable antenna elements and electronics to be proved (Figure 1(c)).

From comparisons with the above description of the "sonic boom", it will be seen that our superluminal sources need to both (a) travel faster than light and (b) accelerate. In the first technology demonstrator (TD1), the alumina containing the superluminal polarization current forms a circle, so that the acceleration is centripetal (Figure 1(d)). The second technology demonstrator, TD2, is a linear accelerator with 32 elements (Figure 1(e)).

Based on both performance and simulations of the technology demonstrators, a number of patents have been filed or are in the process of being drafted, and there is commercial interest in developing the concept. A fourth superluminal source of THz radiation was designed for security applications; its construction and use is the subject of a funded LDRD-ER proposal. The numerical and astrophysical work resulted in several presentations and publications (see publication list); some of the latter are in the process of being written.

Scientific Approach and Accomplishments

Whilst the competing Russian group demonstrated the feasibility of superluminal emission using polarization shock waves in a plasma generated by the ISKRA-5 laser [9, 10], the method promoted by the LANL group is based on electrostatic control and animation of the polarization current, a technique far more amenable for useful and controllable devices [2]. Figures 1(a), (b) show the basic principle: a series of electrodes is placed on one side of a dielectric such as alumina; a ground plate is mounted on the other side. The application of voltages to the electrodes creates a polarized region underneath; this can then be moved by switching the voltages on the electrodes on and off [1, 2]. Given the sizes of practical devices (~ 0.1 – 1 m), superluminal speeds can be achieved using switching speeds in the MHz-GHz range (timings in the 10s–100s of picoseconds) [2, 11]. More subtle manipulation of the polarization current is of course possible by controlling the magnitudes and timings of the voltages applied to the electrodes [2].

After the Test-Bed machine was demonstrated (Figure 1(c)), Technology Demonstrator 1 (TD1) was the first practical machine designed and constructed by the project. It has 72 electrodes arranged (Figure 1 (d)) around a circular alumina strip. The electric fields are thus applied to the alumina in a radial direction. Previous reports described the unusual nature of the 72 dielectric antenna elements compared to conventional sources such as phased arrays.

Each element contains a transition from a coaxial 50 Ohm mode (the drive signal from the control electronics) to the linear electric field applied between each electrode and the ground plane, plus impedance matching to ensure that signals are not reflected back into the machine. This transition necessitated a considerable design/modeling effort and is now the subject of a patent (see Inventions list); it works well, as several of the antenna elements used in coordination were shown to be more efficient than a similar array of commercially-designed Bluetooth aerials. A simple development of the antenna elements for TD1 was also used in the third machine to be constructed, the linear accelerator, TD2.

Because of the symmetry of TD1, the requirements for driving each electrode are similar, so that the control electronics are constructed on a modular basis. The modular units were also used in the linear accelerator, TD2, and are visible in the photographs of it under construction (Figure 1(e)). All of the circuit board design and final assembly was done in-house at LANL.

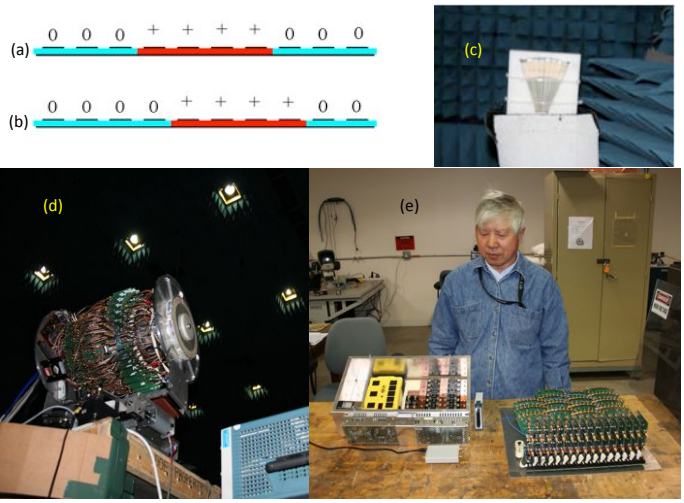

Figure 1. Principles and construction of LANL superluminal sources. (a) Schematic of source; blue shading represents the alumina dielectric, and the black bars are the electrodes. The continuous black line on the opposite side is the ground plane. "0" represents zero voltage applied to an electrode; "+" represents finite voltage. The red shading under the energized electrodes is the resulting polarized region. (b) Source movement; one of the electrodes shown in (a) has been turned off (0), whilst another has been turned on (+); consequently, the polarized region (red) has moved, creating a polarization current. Moving the polarized region arbitrarily fast is just a question of precise timing; the circular machine shown in (d) has been run at 8 times the speed of light. (c) 8-element test-bed superluminal source, used to assess the performance of antenna elements and circuit boards. The alumina dielectric is the white arc, with the electrodes (concealed) above and the ground plane below. The picture was taken in the small LANL anechoic chamber during an experiment. (d) 72 element circular

superluminal source, TD1, shown in the large Kirtland Anechoic Chamber. The alumina ring is visible on the right-hand end of the source. The whole source is mounted on a turntable to allow the angular distribution of the radiation to be mapped. (e) 32 element linear accelerator superluminal source TD2 under assembly, illustrating the modular electronics. This modularity enables components to be exchanged rapidly in the field, and to be interchanged between the three antennas shown in this figure.

Since Summer 2009, testing of TD1 and TD2 has been done in a variety of locations; a very large quantity of data has been collected (the most recent experiments were from September 13 to 17, 2010). Data are under analysis for publication in the scientific literature and for patent purposes. An interim report has been issued concerning the implications for long-range communications; release of this material for journal publication awaits the submission of related patents. In view of the large quantity of data still being processed, we will focus here on two highlights obtained using TD1.

In calibrating emission from new types of antenna such as TD1 or TD2, complications are caused by signals reflected from the ground interfering with direct transmissions between the source and the detector. It is therefore necessary for experiments to be carried out in an area where the reflections from the ground are either well characterized or eliminated. Most experiments were carried out either at Los Alamos Airport (Figure 2(a)), where there is access to both a concrete apron and a flat concrete taxiway approximately 2400 feet long, or at two facilities in Albuquerque, the Kirtland Air Force Base Anechoic Chamber and the Sandia National Laboratory FARM range. The Kirtland Anechoic chamber is a 20 m by 20 m by 20 m shielded room designed to eliminate reflected electromagnetic waves. The FARM (Facility for Antenna and RCS Measurement) range is an outdoor concrete track with an inverted-V-shaped surface that is approximately a quarter of a mile long; the V shape suppresses reflections from the ground.

At each location, the antenna in question was run under several different conditions (e.g. different superluminal speeds) and the resulting angular distribution of the radiation mapped at many different distances (Figures 2(b), (c)). This requires a week to two weeks of experimental time at each range.

The most remarkable effect to emerge is illustrated in Figures 2(b) and (c), which show data gathered at the FARM range. The angular distributions of horizontally-polarized, vertically-polarized, and total power received from TD1 are plotted for distances of 20 and 1100 feet. The most noticeable feature is a peak in intensity at about 41.5 degrees that appreciably narrows as the distance increases; this is completely different than the signal from a conventional antenna such as a phased array, where diffraction effects broaden the beam with increasing distance. On correcting for the effect of ground reflection and analyzing the rate at which the intensity decays with distance, R, it is found that the power on the peak at 41.5 degrees decays as $R^{-1.65}$. Conversely, the signals in the troughs of the distribution at 22.8 and 68.4 degrees both decay as $R^{-2.24}$. Under the same conditions, the radiation from a conventional dipole aerial was found to fall off in power as the conventional inverse-square law, proportional to $R^{-2.0}$.

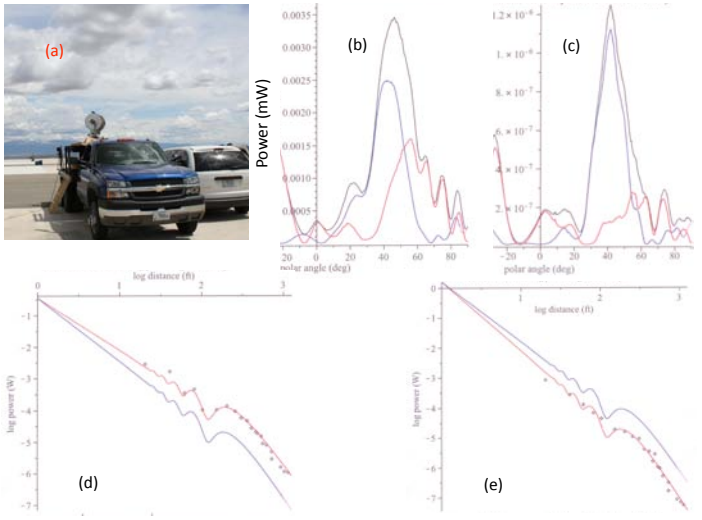

Figure 2. Experiments in the field. (a) The 72-element circular superluminal source TD1 in use at Los Alamos Airport. (b) Power versus angle data taken at a distance of 20 feet from the TD1 source at the FARM range; blue represents emission with horizontal polarization, red vertical polarization and black the total power. The source was running at a speed of around 1.1 times the speed of light. (c) Similar data to (b) for a distance of 1200 feet. Note how the peak at 41.5 degrees has become sharper, and the intensity of the structure around it has fallen away. This is due to temporal focusing (see text). (d) Logarithm of the power versus logarithm of distance for the peak emitted by the superluminal source at 41.5 degrees (shown in (b) and (c) - points and red curve) compared with the signal from a conventional dipole antenna (blue curve). Note how the peak power from the superluminal source falls off more slowly with distance than that from the conventional antenna; at large ranges, this will give superluminal communications considerable advantages. (e) Logarithm of power versus logarithm of distance for the trough in (b) and (c) at 22.8 degrees (points and red curve). Note how temporal focusing leads to this part of the emission falling off more rapidly with distance than that of the conventional dipole antenna (blue curve); temporal focusing is transferring power from these angles to the peak at 41.5 degrees, which consequently becomes sharper ((b), (c)). Such behavior (power falling off more slowly with distance, features becoming sharper at greater distances) is completely different from that of conventional phased arrays and horns, and is a unique consequence of the superluminal nature of our source.

Similar effects were noted at the other ranges; for example, at the Kirtland Anechoic Chamber, peaks in the emission were found to decay as $R^{-1.35}$ and $R^{-1.53}$, whereas the emission from a conventional horn antenna decayed as $R^{-2.00}$.

These slower-than-expected decays with distance are a remarkable, but predicted, aspect of a radiation source that exceeds the wave speed and accelerates. For such a superluminal source, the relation between retarded (source) and reception times need not be one-to-one: multiple retarded times, or even extended periods of retarded time, may contribute to a single instant of reception [4, 11, 12]. The peak in Figure 3 (b), (c) corresponds to radiation emitted over an extended period of source time arriving instantaneously at the detector [2, 4, 12]. This is focusing in the time domain, or *temporal focusing*. Calculations [2, 4, 12] show that, for an ideal superluminal source, at very large distances temporal focusing will lead to an intensity that falls off as R^{-1}. The data obtained from TD1 show the clear emergence of this effect for the first time, pointing to applications in low-power, ultra-long-range communications. We expect the pure R^{-1} decay to dominate at larger distances once other (conventional) emissions from the source have died away; we are applying to NASA for such a test in 2011.

Temporal focusing is not subject to the same diffraction limits as the conventional spatial focusing provided by horns and phased arrays; it makes possible very sharply focused radiation at very large distances from the superluminal antenna. Other data from TD1 now suggest that applications in radar and directed energy are entirely feasible, supporting a LANL patent application (see Patent List).

Turning to the mathematical and numerical work, it should be remembered that the solution of Maxwell's Equations for a source traveling faster than the speed of light is non-trivial. Multiple retarded times must be considered, and there are divergences in the fields. The modeling of the technology demonstrators and astronomical objects such as pulsars demands a considerable amount of mathematical and numerical groundwork; sources that move faster than their own waves have been little considered thus far, and the field is at an early stage of development. Hence, members of the project have been developing the mathematical framework necessary to understand superluminal sources, and publishing papers that are the foundations of this new area of electromagnetism. In addition, one of the students on the project is writing a Master's thesis on her contribution to this mathematical work.

As will be seen from the Publication List, the astronomical part of the project has had notable successes. First, in a recent paper in the journal MNRAS, we show that a simple superluminal source model can explain the emission spectrum of the Crab pulsar over 16 orders of magnitude of frequency using essentially only one adjustable parameter. A subsequent paper shows that similar considerations apply to 8 more pulsars for which good observational data are available (Figure 3). Given that previous models struggled to explain very small fractions of an individual pulsar's emission spectrum, this is a considerable breakthrough. In another paper, we demonstrate that the emission from pulsars that reaches Earth falls off in intensity as 1/distance, rather than the familiar inverse square law; this is a fundamental property of rotating superluminal sources (Figure 3). Finally, two other papers in preparation compare superluminal models with gamma ray bursts.

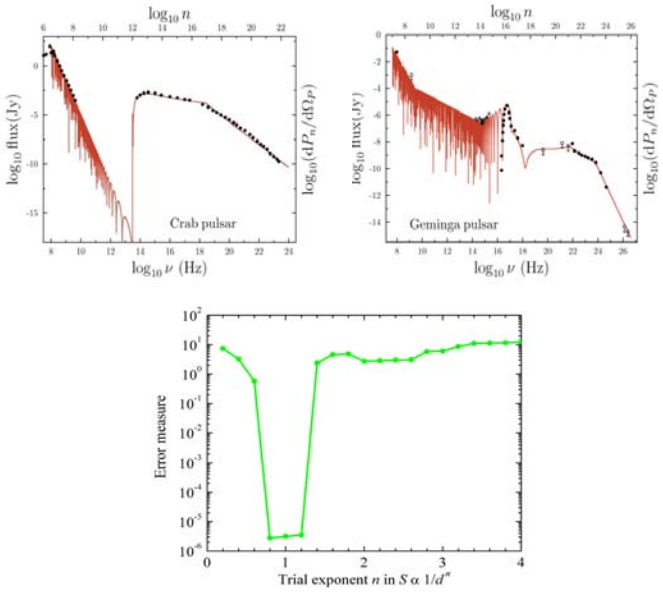

Figure 3. (top) The black points show observational data (where available) of the spectrum of the Crab (left) and the Geminga (right) pulsars, the red lines represent the spectra as predicted by the superluminal model. The overall behavior of pulsar spectra is given by the superluminal nature of the source, the detailed differences are due to resonances in the pulsar atmosphere such as the plasma frequency and the electron cyclotron resonance. (bottom) A maximum-likelihood analysis of observational data on fluxes and distances of radio pulsars strongly suggests that the flux of pulsars observed from Earth contains a component whose intensity falls off as 1/d, where d is distance. The maximum-likelihood analysis determines an initially unknown luminosity function (i. e. fraction of pulsars with a particular luminosity) that fits all of the collected pulsar data. Given a luminosity function 1/d^n, n < 2 supports the superluminal model; n = 2 implies a conventional spherical decay. The best fit was obtained for n = 1.

Impact on National Missions

The new method for generating radio waves, superluminal emission, is an almost completely unexplored technological field. It has potential applications in secure communication, radar, electronic countermeasures, electronic weapons and long-range, low-power transmission. To develop these applications, two prototype transmitters, each

designed to exploit a particular property of superluminal emission, have been constructed using the electronics expertise at LANL. These compact machines are now being used as technology demonstrators for radar, communications and directed-energy, and to verify the computer models of superluminal emission. They will also be used to explore possible spin-off technologies in areas such as medical diagnostics and therapy. A third machine is to be constructed using follow-on funding.

This project supports the DOE mission in nonproliferation by providing secure, low-power surveillance and monitoring technologies. Superluminal sources are also relevant to secure communications, radar and directed-energy applications. They provide insights into the basic principles that govern the Universe, supporting Office of Science missions.

Efforts to develop applications and communicate developments to future sponsors in US industry and government continue, with briefings to DARPA, Boeing, Raytheon and others. A spin-off company, One Over R Inc. is being formed through LANL Tech. Transfer to aid the use and licensing of superluminal technology by US industry. In this context, the intellectual property surrounding superluminal sources is being protected by the filing of patents.

References

1. Singleton, J., A. Ardavan, H. Ardavan, J. Fopma, D. Halliday, and W. Hayes. Experimental demonstration of emission from a superluminal polarization current - a new class of solid-state source for MHz-THz and beyond. 2004. Conference Digest of the 2004 Joint 29th International Conference on Infrared and Millimeter Waves and 12th International Conference on Terahertz Electronics (IEEE Cat. No.04EX857). : 591.

2. Ardavan, A., W. Hayes, J. Singleton, H. Ardavan, J. Fopma, and D. Halliday. Experimental observation of nonspherically-decaying radiation from a rotating superluminal source. 2004. Journal of Applied Physics. **96**: 7760.

3. Schmidt, A., H. Ardavan, J. Fasel, J. Singleton, and A. Ardavan. Occurrence of concurrent 'orthogonal' polarization modes in the Lienard-Wiechert field of a rotating superluminal source. 2007. Proceedings of the 363rd WE Heraeus Seminar on Neutron Stars and Pulsars. : 124.

4. Ardavan, H., A. Ardavan, and J. Singleton. Spectral and polarization characteristics of the nonspherically decaying radiation generated by polarization currents with superluminally rotating distribution patterns. 2004. Journal of the Optical Society of America A (Optics, Image Science and Vision). **21**: 858.

5. Ardavan, H., A. Ardavan, and J. Singleton. Spectral and polarization characteristics of the nonspherically decaying radiation generated by polarization currents with superluminally rotating distribution patterns: reply to comment. 2006. Journal of the Optical Society of America A (Optics, Image Science and Vision). **23**: 1535.

6. Bolotovskii, B. M., and V. L. Ginzburg. The Vavilov-Cerenkov effect and the Doppler effect in the motion of sources with superluminal velocity in vacuum. 1972. Sov. Phys. Usp.. **15**: 184.

7. Ginzburg, V. L.. Vavilov-Cerenkov effect and anomalous Doppler effect in a medium in which wave phase velocity exceeds velocity of light in vacuum. 1972. Sov. Phys. JETP. **35**: 92.

8. Singleton, J., H. Ardavan, and A. Ardavan. Apparatus and method for phase fronts based on superluminal polarization current. 2010. US patent.

9. Bessarab, A. V., A. A. Gorbunov, S. P. Martynenko, and N. A. Prudkoy. Faster-than-light EMP source initiated by short X-ray pulse of laser plasma. 2004. IEEE Trans. Plasma. Sci. **32**: 1400.

10. Bessarab, A. V., S. P. Martynenko, N. A. Prudkoi, A. V. Soldatov, and V. A. Terekhin. Experimental study of electromagnetic radiation from a faster-than-light vacuum macroscopic source. 2006. Radiation Physics and Chemistry. **75**: 825.

11. Bolotovskii, B. M., and A. V. Serov. Radiation of superluminal sources in empty space. 2005. Phys. Usp.. **48**: 903.

12. Ardavan, H., A. Ardavan, and J. Singleton. Frequency spectrum of focused broadband pulses of electromagnetic radiation generated by polarization currents with superluminally rotating distribution patterns. 2003. Journal of the Optical Society of America A (Optics, Image Science and Vision). **20**: 2137.

Publications

Aradavan, H., A. Aradavan, J. Singleton, and M. R. Perez. Mechanism of generation of the emission bands in the dynamic spectrum of the Crab pulsar. 2008. *Monthly Notices of the Royal Astronomical Society.* **388** (2): 873.

Ardavan, A., H. Ardavan, J. Fasel, J. Middleditch, M. R. Perez, A. Schmidt, and J. Singleton. A new mechanism for generating broadband pulsar-like polarization. 2009. In *Proceedings of Polarimetry Days in Rome: Crab Status, Theory and Prospects.* (Rome, 16-17 Oct. 2008). Vol. Proceedings of Science, p. 016. Rome: SISSA.

Ardavan, H., A. Ardavan, J. Singleton, J. Fasel, W. Junor, J. Middleditch, M. R. Perez, A. Schmidt, P. Sengupta, and P. Volegov. Comparison of multiwavelength observtions of 9 broad-band pulsars with the spectrum of the emission from an extended current with a super-

luminally rotating distribution pattern. *Astrophysical Journal.*

Ardavan, H., A. Ardavan, J. Singleton, J. Fasel, and A. Schmidt. Fundamental role of the retarded potential in the electrodynamics of superluminal sources. 2008. *Journal of the Optical Society of America A (Optics, Image Science and Vision) .* **25** (3): 543.

Ardavan, H., A. Ardavan, J. Singleton, J. Fasel, and A. Schmidt. Spectral properties of the nonspherically decaying radiation generated by a rotating superluminal source. 2008. *Journal of the Optical Society of America A (Optics, Image Science and Vision) .* **25** (3): 780.

Ardavan, H., A. Ardavan, J. Singleton, J. Fasel, and A. Schmidt. Morphology of the nonspherically decaying radiation generated by a rotating superluminal source: reply to comment. 2008. *Journal of the Optical Society of America A (Optics, Image Science and Vision) .* **25** (9): 2167.

Ardavan, H., A. Ardavan, J. Singleton, J. Fasel, and A. Schmidt. Response to comment on method of handling the divergences in the radiation theory of sources that move faster than their own waves. 2008. *http://xxx.lanl.gov/.* : 1.

Ardavan, H., A. Ardavan, J. Singleton, J. Fasel, and A. Schmidt. Fundamental role of the retarded potential in the electrodynamics of superluminal sources. 2009. *Journal of the Optical Society of America A- Optics Image Science and Vision.* **26** (10): 2109.

Ardavan, H., A. Ardavan, J. Singleton, J. H. Fasel, and A. Schmidt. Inadequacies in the conventional treatment of the radiation field of moving sources . 2009. *Journal of Mathematical Physics.* **50**: 103510.

Middleditch, J.. Pulsars, cosmology and science with giant telescopes. Invited presentation at *Science with giant telescopes.* (Chicago, 15-18 June 2008).

Middleditch, J.. Supernova 1987A Interpreted through the SLIP Pulsar Model. 2010. *Bulletin of the American Astronomical Society.* **41** (1): 356.

Middleditch, J.. Pulsed Gamma-Ray-Bursts Afterglows. *Astronomy and Astrophysics.*

Middleditch, J., and M. R. Perez. The Kinematics of the SN 1987A Beam/Jet(s). 2008. *Bulletin of the American Astronomical Society .* **40** (2): 206.

Middleditch, J., and M. R. Perez. The SN 1987A Beam/Jet and Its Associated Mystery Spot. 2008. *Bulletin of the American Astronomical Society .* **39** (4): 742.

Perez, M. R., B. McCollum, M. E. van den Ancker, and M. D. Joner. The enigmatic young object: Walker 90/V590 Monocerotis. 2008. *Astrnomy and Astrophysics.* **486** (2): 533.

Schmidt, A. C.. Terrestrial and astronomical radiation sources that move faster than the speed of light in vacuo. 2010. *Master of Science Thesis, University of New Mexico, Department of Mathematics and Statistics.*

Schmidt, A., H. Ardavan, J. Fasel, M. Perez, and J. Singleton. Superluminal emission processes as a key to understanding pulsar radiation. 2008. *Bulletin of the American Astronomical Society .* **39** (4): 917.

Schmidt, A., J. Singleton, H. Ardavan, A. Ardavan, J. Fasel, and J. Middleditch. Quantitative Agreement of Multiwavelength Pulsar Observations with the Spectrum of the Emission from a Rotating Faster-than-light Source Across Sixteen orders of Magnitude of Frequency. 2010. *Bulletin of the American Astronomical Society.* **42** (1): 466.

Schmidt, A., J. Singleton, H. Ardavan, A. Ardavan, J. Fasel, and J. Middleditch. Fitting Fermi LAT Observations of Millisecond Pulsars to the Spectrum of the Emission from a Faster-than-light Source. 2010. *Bulletin of the American Astronomical Society.* **42** (3): 895.

Singleton, J.. Lawbreakers? Superluminal sources in the laboratory and as a model for pulsars. Invited presentation at *23rd Annual New Mexico Symposium.* (Socorro, October 2007).

Singleton, J.. Eighteen-Month Report on LDRD 20080085 DR: Construction and Use of Superluminal Emission Technology Demonstrators with Applications in Radar, Astrophysics, and Secure Communications. 2009. *18 Month Review of the current project..*

Singleton, J.. Preliminary results of experiments performed with the proof-of-concept apparatus TD 1 constructed under LDRD 20080085 DR: Construction and Use of Superluminal Emission Technology Demonstrators with Applications in Radar, Astrophysics, ... 2010. *Preliminary report of experimental data written to support the patent applications associated with this project. The report focuses on demonstrations of the slow decay of radiated power with distance..*

Singleton, J., A. Schmidt, J. Fasel, H. Ardavan, A. Ardavan, and M. R. Perez. Polarization currents that travel faster than the speed of light in vacuo: laboratory demonstrations and a model for pulsar observational data. 2008. *Bulletin of the American Astronomical Society .* **39** (4): 950.

Singleton, J., H. Ardavan, P. Volegov, A. Schmidt, J. Middleditch, and A. Ardavan. Realistic Model for Gamma-ray Bursts Based on Decelerated, Superluminal Polarization Currents. 2010. *Bulletin of the American Astro-*

nomical Society. **42** (3): 846.

Singleton, J., P. Sengupta, J. Middleditch, T. Graves, A. Schmidt, M. Perez, H. Ardavan, A. Ardavan, and J. Fasel. Determination of the Flux-distance Relationship for Pulsars in the Parkes Multibeam Survey: Violation of the Inverse Square Law Gives Support for a New Model of Pulsar Emission. 2010. *Bulletin of the American Astronomical Society.* **42** (1): 603.

Singleton, J., P. Sengupta, J. Middleditch, T. L. Graves, M. R. Perez, H. Ardavan, and A. Ardavan. A Maximum-Likelihood Analysis of Observational Data on Fluxes and Distances of Radio Pulsars: Evidence for Violation of the Inverse-Square Law. *Physical Review Letters.*

Webb, R.. What makes a pulsar tick?. 2010. *New Scientist.* **2752**: 33.

Efficient and Selective Photon Detection

Michael D. Di Rosa
20090189ER

Introduction

The eavesdropper at a party strains to hear the quietest, most hushed conversation in the room for a snippet of privileged information. In applications of light detection, it is similarly the fainter signals within the glare of sun and streetlights that are the more interesting, revealing unusual or unnatural phenomena. But how can one isolate the signal of interest—the quiet speaker to the eavesdropper, and the feeble emitter to the optical detector—from the din? Our snoop might excuse himself to an adjacent room, knowing the wall will preferentially transmit the baritone voice he is keen on hearing from among the crowd of sopranos. Indeed, the wall serves as an acoustic filter, but it also mutes the baritone's voice to unintelligibility. In the technology of light detection, we find a similar compromise between spectral selectivity and signal sensitivity. Techniques that narrow the spectral window through which a detector sees ordinarily reduce the sensitivity of the combined filter-detector system, sometimes so drastically that the system is incapable of seeing the intended weak source of light.

In this LDRD program, we are attempting to break with this customary and often frustrating tradeoff in light detection. We appeal to a class of phenomena known as quantum-coherent effects, where a medium (say a gas or solid) is manipulated in such a way that its atoms act synchronously—coherently—to unusual effect. For example, quantum coherence has recently been used to change a medium from opaque to transparent at the switch of a laser beam and to slow light in a medium to a walker's pace. The same type of quantum coherence can also be used to make a new type of photon detector, where a single photon enters a medium and triggers a beam-like avalanche of similar photons. Quantum-coherent properties dictate that the amplifier is reasonably low in noise, responds only to those photons that have a wavelength specific to 1 part in ten million (equivalent to specifying one's location along a 100-mile stretch to the nearest inch), and is otherwise blind. The promise of such an amplifier is that it will allow researchers in biology, remote sensing, and other fields to measure extremely faint light signals with surgical spectral precision. Other important characteristics of the amplifier include its suitability for imaging applications.

The fundamental process behind our amplifier is known in the scientific literature as amplification without inversion, or AWI. Because AWI can theoretically be generated in many types of systems—including atoms, molecules, and semiconductor materials—our concept ought to be adaptable to different media and thereby tailored to detect photons of various wavelengths. We are using mercury vapor in a first test of AWI for faint-light detection. Mercury has many desirable traits for this first excursion into applications of AWI, but its use also presented technical challenges that, as explained in the progress section, we were able to surmount.

Benefit to National Security Missions

Research on light detection, especially of faint signals and single photons, has numerous applications including detecting chemical/biological agents, low-light imaging, and weapons activities. A new weak-light detection method is consistent with many missions including threat reduction, human health, and basic science of interest to DOE, DHS, and other government agencies.

Progress

As reported previously, we chose mercury (Hg) vapor with its well-known spectroscopy and photophysics to be the medium our archetypal amplifier. The atomic states within Hg that we need to manipulate are not occupied at room temperature. The easiest way to induce Hg into the needed states is to place Hg vapor in a plasma discharge not unlike those used in household fluorescent lamps. However, the plasma discharge is a noisy environment, liable to obscure the very transitions we need to observe.

During the first year of this program, we built our own plasma discharge in which mercury atoms were excited into the right levels for our experiments following our dissatisfaction with commercial mercury discharges. We then followed common experimental prescriptions for obtaining high-resolution spectra that year but were

disappointed with the results. We re-evaluated the underlying physics of the plasma discharge for clues on how to improve our spectral resolution.

We are glad to report our success this past year with a technique that cuts underneath the collisional noise in the plasma and allows us to observe in fine detail the very transitions we will manipulate, a prerequisite for forthcoming experiments in amplification. To date, we have observed the different isotopes and so-called hyper-fine states of mercury at a level of detail and high signal unseen in the literature for this type of simple plasma discharge. Figure 1 shows the progressively better resolution of the constituent mercury isotopes—from the blue data, to the red, to the black—as the technique is optimized. The experimental set-up that produced the spectra of Figure 1 is shown in Figure 2. A form of saturation absorption spectroscopy, the experiment makes use of a laser we built specifically for the AWI study. This elementary research in laser spectroscopy certainly benefits the AWI program yet might also find use in analytical chemistry, where distinguishing one or more isotopes from others is often paramount. We note that our technique can also be adapted to measurements of the velocity of atoms, ions, and their isotopes, as might be important in research topics of flowing or diffusive plasmas.

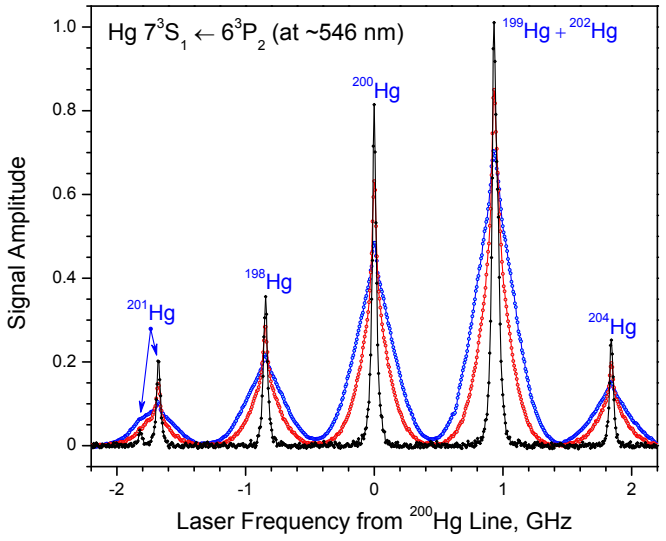

Figure 1. Progression in measurement resolution to the absolute Doppler-free limit, represented by the black diamonds and trace, of the "green line" of atomic mercury. All measurements were obtained from a simple dc plasma discharge of natural Hg in argon. The isotopic composition of the spectra is labeled.

We also obtained high-resolution spectra from our discharge in a way consistent with locking laser frequencies. Through a method called Modulation Transfer Spectroscopy (MTS), we obtained dispersive-looking (asymmetric, like a sine wave) features whose signal crosses zero at the resonance of each isotopic transition shown in Figure 1.

Through a feedback loop we designed, we then steadied the laser frequency at a particular zero crossing of the MTS spectra. We held our laser frequency to the selected atomic transition for hours, as required for our AWI experiments. Additionally, we succeeded in producing a needed second laser wavelength for the AWI experiments from a laser system that had proved troublesome.

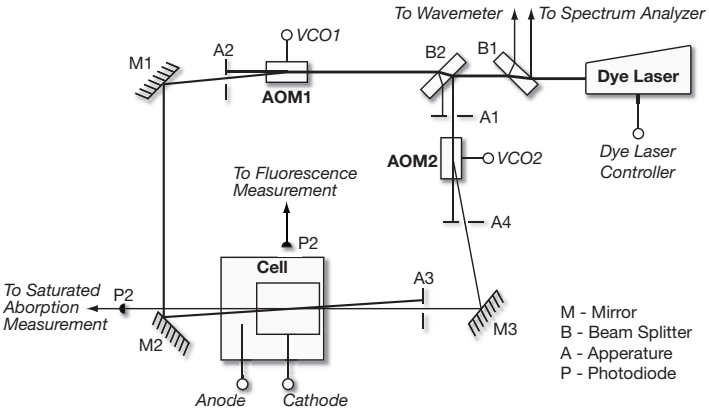

Figure 2. Diagram of the experiment used to measure the Hg spectra of Figure 1. This setup is useful for measuring the spectrum of any low-pressure atomic or molecular gas with sub-Doppler resolution (our "gas" happens to be the plasma discharge of Hg, labeled "Cell"). A minor variation converts the setup to one known as modulation-transfer-spectroscopy, which produces sharp dispersive-looking features useful for locking a laser frequency to an atomic or molecular transition frequency.

The past year's work provided material for two papers by postdoctoral researcher K. M. Mertes and staff member M. D. Di Rosa that are in preparation. They are (1) "High-resolution spectroscopy and laser-lock circuit for excited-state transitions using a direct-current discharge cell," in preparation for Review of Scientific Instruments and (2) an in-depth treatment of our high-resolution spectra and the techniques by which they are obtained, a paper of general theoretical and experimental importance that is lacking in the literature. Two more papers, by D. H. Bradshaw and Di Rosa, on the theory and applications of nonlinear media grew from this project. They are (1) "Vacuum field energy and spontaneous emission in anomalously dispersive cavities," submitted to Physical Review A and (2) "Nonstationary electromagnetics of controllably dispersive media," in preparation for Physical Review A.

Future Work

Now that we have the means, through our plasma discharge and spectroscopy techniques, of locking our laser frequencies precisely to our atomic transitions, we look forward to examining very soon the quantum-coherent phenomenon of AWI in the "clean and quiet" environment of a photolytically-pumped cell containing pure mercury vapor, as planned. A demonstration of AWI as a novel amplifier of faint, spectrally-specific light will then follow.

The primary goal is to demonstrate in the context of light detection and imaging an unusual quantum-coherent phenomenon, called amplification without inversion (AWI). This light amplifier would be the front-end to a common detector, or detector array, and would give the overall system the aforementioned special properties. The research will develop predictive theory for the characteristics of the AWI-amplifier and experimentally test the concept. Gain, bandwidth, and noise will be measured when amplifying faint light (picoWatts or less) and compared with predictions. The detection of single photons looks promising and will be undertaken afterwards. Our theory to date hints that AWI makes for a radically different and low-noise light amplifier, suggesting additional experiments for confirmation of these qualities.

Conclusion

Our sense and knowledge of physical phenomena has expanded innumerable times and ways beyond our human limits by the instruments we develop and then re-examine with discontent for their own limits. In the detection of light, common and modern systems trade efficiency for spectral specificity, a compromise so ingrained that we regard as impossible those instances where we want to detect weak but spectrally exact signals out of a broad spectrum of light. Our initial considerations of quantum-coherent process for light detection that began our program indicated that AWI could be exploited to make a low-noise, highly efficient, and spectrally selective detector, an unusual instrument by present standards. Our experimental success to date and our planned work this year aim to show how an AWI-based detector can sit radically apart from existing technologies and enable applications we previously dismissed.

Publications

Bradshaw, D., Z. Shi, R. Boyd, and P. Milonni. Electromagnetic momenta and forces in dispersive dielectric media. 2010. *Optics Communications.* **283** (5): 650.

Mertes, K. M., and M. D. Di Rosa. Efficient and selective photon detection using amplification without inversion. Presented at *2009 American Physical Society March Meeting.* (Pittsburgh, PA, 16-20 March 2009).

Mertes, K. M., and M. D. Di Rosa. Building an efficient and selective photon detector using amplification without inversion. Presented at *March Meeting of the American Physical Society.* (Portland, Oregon, 15-19 March 2010).

Compact Solid State Tunable THz Source

Nathan A. Moody
20090321ER

Introduction

Terahertz and millimiter-wave devices are proving to have many important applications from imaging to covert communication [1]. Among the greatest impediments to exploiting this regime of the electromagnetic spectrum are the difficulties in building sources with sufficient power and sensors with the needed sensitivity that are suitable for practical applications [2]. We propose to develop a new THz source technology using a novel application of superconductive Josephson junctions that directly addresses many of the critical barriers for practical utilization of the THz spectrum [3-5]. The pioneering approach we pursue could lead to follow-on development of other THz devices, including filters, mixers, oscillators, amplifiers, modulators, and receivers, that would completely revolutionize the field by providing a much-needed suite of compatible components with which to build entire THz systems. Our group has refined a source design which was the product of a preliminary investigation (2007) into the use of Josephson junctions as THz emitters. Our goal is to transition this source design into a working prototype using LANL's unique fabrication capabilities, experience in millimeter-wave systems, and superconductivity expertise.

Benefit to National Security Missions

This project will likely impact a broad range of technical problems including imaging, sensing, and communiation. Enhancing our understanding of THz radiation particularly suited to spectroscopy applications for detection of chemical, nuclear, and biological threats, supporting threat reduction and other missions important to DOE, DHS, and other government agencies.

Progress

Progress in FY2010 was concentrated along three primary goals, each of which factored heavily in the 2nd year of the proposal and advance the state of the art significantly, as evidenced by two publications submitted to high impact journals and an experimental demonstration.

A significant development in FY10 is a simplified demonstration led by our experimental collaborators of THz emission from an intrinsic Josephson junction (IJJ)-based structure similar to that proposed in [6]. The structure is very different from the final design we propose as the final outcome of this project but the confirmation of THz emission from IJJs lends momentum to the overall experiment and definitively confirms the ability to create THz radiation using resonantly coupled oscillations among many closely spaced junctions. The demonstration involved a simplified "mesa" geometry which permitted only small power and single-frequency (as opposed to tunable) operation but indeed showed outcoupled radiation.

The second goal the project emerged at the beginning of the second year. It became apparent that self-synchronization among the many (perhaps tens of thousands) of individual IJJ oscillators was not easily established [7]. This is because synchronization process relies upon the radiation field to couple the oscillators together and such fields are inherently weak when the device is first turned on. Our models show that once powered up, our source is quite robust and stable, but we had not addressed the process of synchronization during initial turn-on. Thus, we identified a significant road-block for utilization of the IJJ-based THz source: establishing and maintaining synchronization among the individual junctions at low (20-30%) emission power. Such phase locking, where power scales as the number of synchronized junctions squared, is required in order to achieve practically useful output power and is a key outcome of this project [3, 8]. We successfully identified a practical modification that not only solves the problem of self-synchronization upon startup, but also enhances stability and provides a method of modulating output power. Modulation of the bias voltage yields frequency tunability (first year outcome). This means the source is frequency tunable but many applications require also that power be dynamically controllable. The method we use to solve the problem of synchronization at startup, a shunt capacitor, also provides a means to modulate output power.

The modification of our design to include a shunt ca-

pacitor is literally a capacitor in parallel with a distributed capacitance throughout a length equal to that of the junction stack, as shown in Figure 1. This change required us to evaluate its effect on the THz emission process and quantify the line width of THz emission. Line width is an important metric in this source project because many spectroscopy applications require a narrow linewidth in order to resolve the spectral peaks of an unknown sample with high specificity. We evaluated the effect of the shunt capacitor addition and found that it had increased the line width and order of magnitude to one part in a million, which means the emitted signal will have bandwidth of 1 MHz when the source is emitting at 1 THz [5]. This is still acceptable for spectroscopy applications so we consider the design modifications to be an important second year successful outcome.

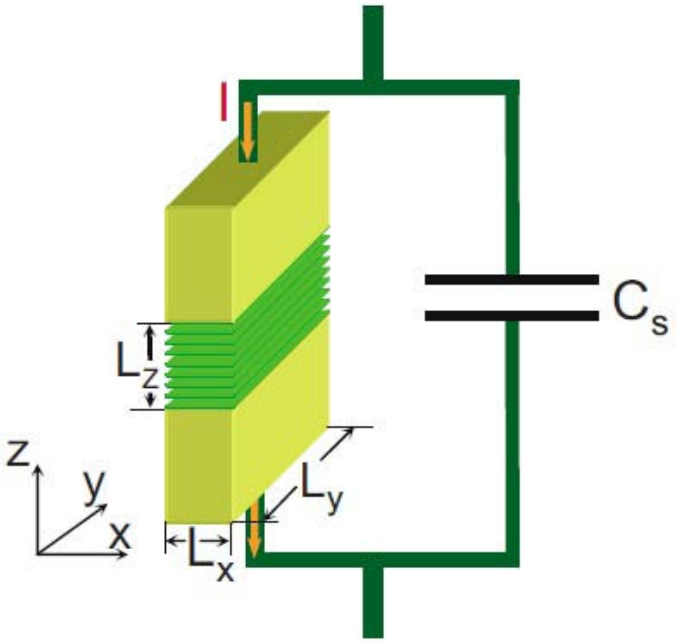

Figure 1. Schematic depiction of intrinsic Josephson junction stack (IJJ), depicted as green planes having dimension Lx, Ly, Lz shunted by an external capacitance Cs to assist synchronization of IJJ emitters.

The final goal involves the fabrication of the proposed structures that maximize out-coupled radiation. These consist of a bismuth-based high temperature superconductor (termed BSCCO) that is grown with its longest axis parallel to the substrate. We have identified the growth process, obtained all precursor materials, and have made initial tests proving our ability to deliver precursors to the substrate at the required rates. A reactor is being prepared under a separate project and is near completion. The growth of the ceramic films will occur early in the third year (FY11) of the project and will then be tested and characterized for use in the THz emission demonstration. Preparation of a cryostat, sample holder, IV measurement probe, and Labview-driven instrumentation have also begun in the last month of FY10, enabling momentum in experimental tasks ahead.

Future Work

The "THz gap" refers to the portion of the electromagnetic spectrum from approximately 0.3 to 5 THz in which there are few practical sources of radiation [9]. This same spectral region, because of its unique propagation characteristics and interaction with matter, corresponds to some of the most exciting applications to date for national security [10]. The well established emission techniques for the neighboring microwave and optical regions of the spectrum have proven ineffective for the THz band, despite over a decade of intense effort. In contrast, the Josephson junction interaction is naturally suited to operate in the THz band, as it naturally converts a dc voltage (1 mV corresponds to 0.483 THz) into millimeter wave radiation via a quantum mechanical tunneling resonance called the Josephson effect. We propose to build solid-state THz sources by harnessing this interaction and have a designed a device using bismuth-strontium-calcium-copper-oxide (BSCCO) intrinsic Josephson junctions (IJJs) which we will transition into a working prototype in the third year. This effort will also be geared to enable follow-on projects.

Our tasks in the final year consists of three major tasks, all closely tied to simulation studies: 1.) develop a BSCCO fabrication process to produce high quality crystals of the desired orientation, 2.) demonstrate that IJJs can be used as a scalable, compact source of THz radiation, and 3.) validate and expand our radiation model using experimental to predict other types of IJJ interactions at THz frequencies.

The goals of each task: 1.) modify our facility to grow BSCCO, demonstrate an ability to grow high purity crystals in the desired crystal orientation, and complete device modeling; 2.) characterize samples, and mount & wire bond samples without degradation; 3.) measure the current and voltage (I-V) characteristics with and without emitted radiation, and demonstrate the ability to sink the associated heat load using a commercially available cryo-cooler.

Conclusion

This work has and will continue to extend our knowledge of and provide raw materials for a new, portable mechanism for creating non-ionizing THz radiation, which is ideal for determining certain properties of materials that are not apparent when using other types of radiation (such as microwave, light, or x-rays). THz radiation can be used to actively interrogate a variety of environments, including human subjects, in search of dangerous materials to protect both soldiers and civilians. Our work could also lead to tissue-safe low cost THz imaging, which could be used to supplement and/or replace harmful x-ray doses typical in medical imaging.

References

1. Federici, J., B. Schulkin, F. Huang, D. Gary, R. Barat, F. Oliveira, and D. Zimdars. THz imaging and sensing for security applications, explosives, weapons and drugs. 2005. *Semiconductor Science and Technology.* (7): S266.

2. Fitch, M. J., and R. Osiander. Terahertz Waves for Communications and Sensing. 2004. *APL Technical Digest.* **25** (4): 348.

3. Bulaevskii, L. N., and A. E. Koshelev. Radiation due to Josephson Oscillations in Layered Superconductors. 2007. *PRL.* **99** (5): 057002.

4. Bulaevskii, L. N., A. E. Koshelev, and M. Tachiki. Shapiro steps and stimulated radiation of electromagnetic waves due to Josephson oscillations in layered superconductors. 2008. *Physical Review B (Condensed Matter and Materials Physics).* **78** (22): 224519.

5. Bulaevskii, L. N., G. B. Halasz, and I. Martin. Line width of radiation from intrinsic Josephson junctions in layered superconductors. To appear in *Journal of Applied Physics.* **Submitted for publication**.

6. Koshelev, A. E., and L. N. Bulaevskii. Resonant electromagnetic emission from intrinsic Josephson-junction stacks with laterally modulated Josephson critical current. 2008. *Physical Review B (Condensed Matter and Materials Physics).* **77** (1): 014530.

7. Martin, I., Gabor B. Halasz, L. N. Bulaevskii, and A. E. Koshelev. Shunt-capacitor-assisted synchronization of oscillations in intrinsic Josephson junctions stack. 2010. *Journal of Applied Physics.* **108** (3): 033908.

8. Bulaevskii, L. N., and A. E. Koshelev. Radiation from a Single Josephson Junction into Free Space due to Josephson Oscillations. 2006. *Physical Review Letters.* **97** (26): 267001.

9. Tonouchi, M.. Cutting-edge terahertz technology. 2007. *Nat Photon.* **1** (2): 97.

10. Moore, D.. Recent Advances in Trace Explosives Detection Instrumentation. 2007. *Sensing and Imaging: An International Journal.* **8** (1): 9.

Publications

Bulaevskii, L. N., A. E. Koshelev, and M. Tachiki. Shapiro steps and stimulated radiation of electromagnetic waves due to Josephson oscillations in layered superconductors. 2008. *Physical Review B (Condensed Matter and Materials Physics).* **78** (22): 224519.

Bulaevskii, L. N., A. E. Koshelev, and M. Tachiki. Shapiro steps and stimulated radiation of electromagnetic waves due to Josephson oscillations in layered superconductors. 2008. *Physical Review B (Condensed Matter and Materials Physics).* **78** (22): 224519.

Bulaevskii, L. N., and A. E. Koshelev. Stabilization of synchronized oscillations and radiation line width of intrinsic Josephson junctions. Invited presentation at *The 7th International Symposium on Intrinsic Josephson Effects and Plasma Oscillations in High T-c Superconductors (PLASMA 2010).* (Hiosaki, Japan, 29 April - 2 May, 2010).

Koshelev, A. E., and L. N. Bulaevskii. Resonant electromagnetic emission from intrinsic Josephson-junction stacks with laterally modulated Josephson critical current. 2008. *Physical Review B (Condensed Matter and Materials Physics).* **77** (1): 014530.

Martin, I., Gabor B. Halasz, L. N. Bulaevskii, and A. E. Koshelev. Shunt-capacitor-assisted synchronization of oscillations in intrinsic Josephson junctions stack. 2010. *Journal of Applied Physics.* **108** (3): 033908.

A Metamaterial-Inspired Approach to RF Energy Harvesting

Md A. Azad
20100241ER

Introduction

Metamaterials are engineered materials that exhibit unique electromagnetic (EM) properties. Visible light, microwaves, infrared, and x-rays are all examples of EM waves. The ability to control such waves is critical to modern technology. One must be able to focus light for microscopy and photography. And one must be able to transmit and receive microwaves for wireless communication. Control of EM waves is achieved through materials. Current research in metamaterials is aimed at improving that control by engineering material properties.

Metamaterials are typically comprised of split-ring resonators (SRRs). These may be regarded as little antennas that capture EM energy, change its form, and then re-emit it. Recently, researchers have shown interest in using SRRs to create high-performance antennas, rather than creating metamaterials in bulk. These "metamaterial-inspired" antennas offer some properties not found in traditional antennas. For example, recent work has shown that SRR antennas can be made to operate efficiently even when their size is much smaller than a traditional antenna.

We intend to design and build these SRR (or metamaterial-inspired) antennas for the purpose of low-power radio frequency (RF) EM energy harvesting. Traditional antennas are often too large or inefficient for such a task. But metamaterial antennas offer an unobtrusive approach to power small electric devices. Indeed, these devices may operate in embedded or inaccessible environments, where maintenance is impossible or undesirable. Examples include bio-sensors embedded in living organisms, covert communication or data exfiltration devices, and monitoring sensors buried in structural members (e.g. bridge pylons). This work leverages the fact that we are often immersed in EM energy. EM energy from radio antennas for example, is predominately wasted. Further, in support of compact wireless devices such as cell phones, technologists have developed a class of very low power electronic devices which can operate on the amount of power harvested by a small metamaterial antenna. These circumstances provide a unique opportunity to diversify our nation's utilization of energy. It is difficult to improve upon several decades of antenna research, but metamaterial concepts provide an optimistic path forward. We expect this work to positively impact wireless communication and tracking in compact devices.

Benefit to National Security Missions

This project will diversify our energy usage and production by creating methods of utilizing now wasted ambient EM energy. This specifically impacts the national security mission of renewable energy. This project will also create a method to remotely provide power to embedded, buried, or inaccessible electronics, thus enabling new modes of covert communications and sensing, data exfiltration, surveillance, and remote sensing and monitoring. As such it is relevant to missions of DOE, DOD, DHS, and intelligence agencies. We believe there could be additional benefits to commercial technologies (e.g. RFID tags), suitable for military application.

Progress

Our progress to date has focused on the general study of metamaterial antennas. Here we have been gaining knowledge in how metamaterial principles can improve the performance of antennas. To accelerate progress, we have also established collaboration with Rick Ziolkowski of the University of Arizona, one of the world leaders in novel antenna designs. Our work has focused on three main parts: 1) simulate and analyze metamaterial-inspired antennas to learn how to optimize them for specific applications, 2) validate simulation results with experiments and measurements, 3) study antenna array effects. We originally thought the last item would not be studied until the third year of this project. We have since discovered that even single antennas feature "array-like" effects that require deeper research to understand.

In terms of progress, we discuss this last point first. Through a series of simulations and measurements, we have determined that power harvesting antennas are particularly sensitive to their electrical connections. Our

antennas send their collected power through an external circuit such as a coaxial cable. This circuit is partially made of metal interconnections that are fabricated near the antennas. We have found these interconnections can radically change the behavior of the antenna. Antenna behavior is also modified by placing antennas near each another. In both cases, the effect is to reduce the efficiency of the antenna, which is detrimental to energy harvesting. We are now beginning to understand these effects quantitatively and we intend to publish some results soon. These difficulties have also forced us to discover new "parasitically-coupled" designs that enable energy extraction without altering the antennas basic behavior. These are antennas that have parts electrically isolated from connection circuits. We are now testing several such designs through simulation and measurement.

On the experimental side, we have completed the construction of an anechoic chamber in which we can measure the performance of our antennas. This chamber was built in ISR-2 labs and is also integrated with a computer-controlled antenna mapping system comprised of an electric field monitor and motorized X-Y-Z stages. We are now using the anechoic chamber to validate our simulation results and test some of our antennas. We are testing microwave frequency antennas in the anechoic chamber and have already demonstrated energy harvesting with some un-optimized designs (see Figures 1 and 2). Actual energy harvesting requires inserting a diode into the antenna structure. The diode changes the alternating currents (AC) in the antenna into direct currents (DC) that can charge a storage capacitor or battery. We found that these diodes can also degrade the antenna behavior. This is an effect we are now beginning to quantify. We are also are testing metamaterials made of scaled down antennas to test array effects. These measurements allow us to test arrays consisting of thousands of antennas. The measurements are performed at CINT labs using terahertz waves.

Our simulation capabilities continue to mature, and we are now regularly using our commercial simulators to perform antenna studies. We have also become increasingly familiar with the weaknesses of these simulators through experimental validation. Our collaborator has helped us perfect these simulations in a very rapid time frame.

Finally, we have purchased and tested a commercial RF energy harvesting system (from Powercast Co.) that utilizes traditional antennas. We intend to use this system to benchmark our new designs. This system is comprised of a transmitter and receiver along with several "harvesting" chips that draw and store energy received from the antennas.

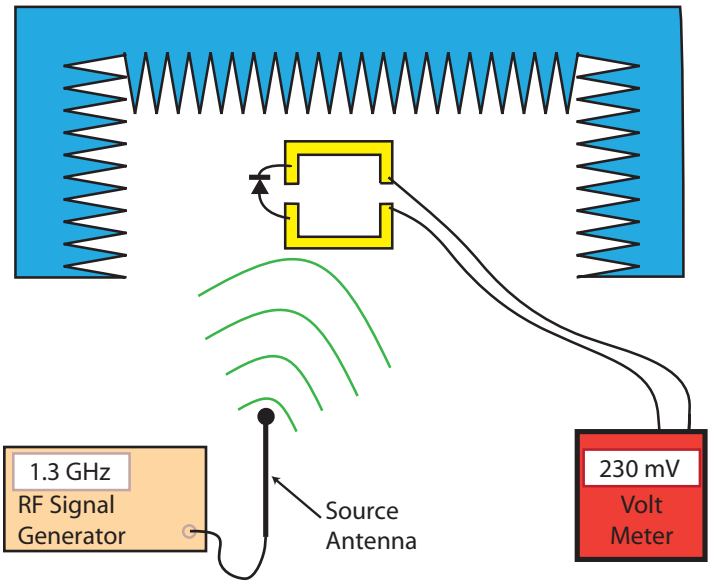

Figure 1. Metamaterial-inspired antennas (yellow) are set up in an anechoic chamber (blue) and connected to a volt meter (red). An RF signal generator (beige) feeds a traditional antenna that radiates RF waves (green) toward the metamaterial antenna. As RF energy is collected, our antenna converts it to DC (direct current, or zero frequency) power, which is indicated as a DC voltage on the meter.

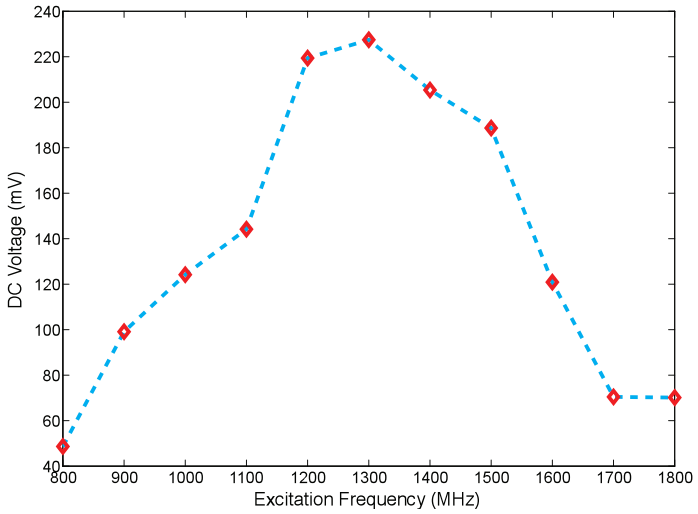

Figure 2. Voltage data measured from one of our metamaterial-inspired antennas. The data shows that our antenna collects power most efficiently at 1.3 GHz (or 1300 MHz), and is able to generate a voltage of 230 millivolts.

Future Work

Our most immediate future work will be to quantify the limits on how well our antennas can perform given our two major design approaches. These approaches were alluded to previously and are: 1) antennas directly connected to power harvesting circuits, 2) antennas parasitically connected to power harvesting circuits. We will obtain this

information by continuing to design, simulate, and measure different antenna designs. Our goal is to reach the theoretical limit of efficiency for one of our metamaterial-inspired designs. We then intend to reduce antenna size by taking advantage of antenna coupling effects. This last point is a consequence of our array studies. Though these effects were first seen as a detriment, we believe they can be used to reduce the antenna size without sacrificing performance. As this work progresses, we intend to record comparisons of our antenna performance with those in our commercial Powercast harvesting system. Finally, we intend to fabricate and test larger antenna arrays. These form the basis of a RF energy harvesting "panel", much like a solar panel is used to collect light energy.

Conclusion

We have already demonstrated metamaterial-inspired antennas that harvest radio frequency energy, and we are now working towards optimization. Our antennas have been designed, simulated, and measured. All of this increases our understanding of the problems and leads to improved designs. Our work will lead to small, highly efficient energy collection. This may be used to power electronic devices that are buried, hidden or otherwise inaccessible. Our work will contribute to energy efficiency by using wasted energy sources such as radio broadcast waves. It should also improve wireless technologies such as more compact cell phones, or covert sensors.

Ultra High Quality Electron Source for Next Generation Vacuum Electronic Devices

Nathan A. Moody
20100262ER

Introduction

As a society, we routinely rely upon a broad class of devices, known as vacuum electronics, to help us communicate, understand weather, maintain air safety, image and diagnose medical conditions, and sustain our national defense. These important devices utilize an electron beam to amplify or create radiation and include the microwave tubes found in satellite and ground communications, x-ray tubes in medical imaging and airport screening systems, civilian and military microwave systems, cellular network nodes, etc. The technology has encountered widely recognized limitations which erode its ability to meet future needs. This vulnerability is directly tied to the method by which the requisite electron beams are created, which is now more than 50 years old.

In response to this need, we are developing a new, ultra-high quality, robust electron source using nanostructured polycrystalline diamond which could not only replace the stagnant state of the art, leading to immediate improvements across a burgeoning industry, but also enable the development of a new generation of high power vacuum electronic devices (i.e., RF sources) that scale to higher power, shorter wavelength, improved efficiency, smaller form factor, and reduced cost. Developments to this effect would leverage the huge existing R&D investments in the vacuum electronics industry while eliminating their inherent limitations.

This project was inspired by a discovery made during earlier experiments on high-current photo-cathodes for the Dual-Axis Hydrodynamic Test Facility (DARHT). In particular, diamond samples were subjected to a high electric field and then illuminated by a laser beam (wavelength 193 nm) to test their emission characteristics. When illuminated, normal photoemission would take place in a predictable manner until the laser fluence reached a particular level, at which time the sample would continue to emit a high current electron beam without the need for laser illumination and until the electric field was turned off. This first-ever observation represents a completely new electronic emission mechanism which is stable, repeatable and does not damage the samples in any way, occurring on different diamond samples with similar boron doping profiles.

Benefit to National Security Missions

The important mission of stand-off detection of nuclear and non-nuclear materials requires smaller, more powerful, and higher frequency sources of GHz and THz radiation for remote interrogation than are currently available. From the physics point of view, vacuum electronics (VE) is the technology of choice for building such high power sources, except for weaknesses associated with creating the requisite electron beam. Our ultra-high quality electron source can directly address this vulnerability and enable VE-based source development to continue.

Progress

Accomplishments for year 1 include the completion of the assembly of essential components of the diamond cathode vacuum test stand. This experimental system consists of a cryogenically pumped vacuum chamber with multiple diagnostic ports and rapid access to the vacuum electron beam diode for test sample insertion and removal. The facility also includes two dedicated laser systems, a Lambda Physik excimer laser operating at a laser wavelength of 193 nanometers and a Spectra Physics flash lamp pumped solid state laser system operating at 1064, 532, 354, and 266 nanometers. The laser systems provide a wide range of diagnostic and operational capability. Some, but not all of the applications of laser radiation would include: a.) Photo-stimulated electron field emission, b.) Desorption of surface contaminates, and c.) Back cathode illumination to promote uniform charge mobility within the diamond structure. System diagnostics include a Stanford Research Systems residual gas analyzer, a Tektronics 684B 4 channel digital oscilloscope, and a Keithley picoammeter.

We have begun to complete repairs and refurbishment of the microwave assisted chemical vapor deposition reactor that had not been used since the time of the DARHT photocathode experiments. This reactor enables the growth of nanostructured diamond and the necessary parts and equipment have been ordered and the

repair work is in progress. In parallel with the experimental systems preparation, both at the ISR-6 test stand and the MST-7 processing laboratory, there is ongoing intensive research into the physics issues involving the charge insertion, mobility, and electron emission of various nanocrystalline diamond heterostructures. This research has a particular focus on issues surrounding the back electrical contact for the cathode structure. Back contact phenomena are of considerable concern for high current solid state devices and this has been well documented in the literature. The substrate/diamond contact interface was also identified as a limiting factor in the DARHT diamond photocathode experiments. To mitigate the contact issue, a novel approach utilizing a platinum/carbon nanotube matrix as a substrate for the nanocrystalline diamond growth is in development. The electrical characteristics of the platinum/nanotube matrix are ideal. The allotropic identity between the nanotubes and diamond then allows the nanotubes to become the precursor for the nucleation and growth of the diamond heterostructure. Preparations are being made for the initial electrical testing of these substrates.

A critical issue in the development of a diamond based, very high current density (greater than 200 amperes per square centimeter) electron beam sources, is the ability to inject large amounts of charge from the metallic electrical contact into the crystalline diamond structure. The methods used to accomplish this may be thought of as the "foundation" of the device and is the primary characteristic upon which the design and performance of this device, as a multi-level condensed matter system is based. The development of a near-perfect conductive back contact will contribute to the improved performance of many types of diamond-based electronic devices beyond our intended applications.

The ultimate goal of this project is to create a high quality, cold (minimal transverse energy) electron source, able to operate over a broad range of applications from continuous (DC) emission to very high frequency emission. The electron mobility within the diamond semi-conductor bulk is finite so the physical conditions within the diamond structure must vary considerably depending on the application and the frequency domain. A common need in all applications is the charge injection through the back electrical contact.

Our approach in meeting this need is to develop a platinum (Pt)/carbon nanotube (CNT) matrix where the CNT's are densely populated in random orientation and imbedded within the Pt metal and conjoined through a thin carbide formed through a Pt-CNT catalysis [1, 2]. One side of the Pt-CNT matrix is a uniform Pt surface and with a high population density of randomly oriented, partially exposed CNT's on the opposite surface. The surface electronic states (work functions) of the Pt and CNT's are nearly perfectly bridged by the carbide formed between the two elements, carbon and platinum. To date, we have fabricated several different types of Pt/CNT composites but have not yet demonstrated a matrix of sufficient quality with reproducibility in the necessary quantities. As of this report, we are testing a new process of bonding a thin Pt foil and a dense CNT "paper" using melt compression.

The exposed Pt/CNT surface will be used as the substrate for the nucleation and growth of diamond nanocrystalline bulk material [3]. As mentioned earlier the goal is unimpeded charge injection into the diamond structure, or bulk. Since both diamond and carbon nanotubes are allotropes of carbon, the transitional growth of diamond through nucleation at the CNT sites is a natural process and low temperature diamond growth methods ensure the survival of the CNT structure. Augmentation of the diamond nucleation process, by seeding the Pt/CNT surface with nanodiamond crystallites may also be done.

The resulting 3D Pt/CNT/diamond heterostructure is highly conductive due to the ballistic transport of electrons through the CNT's. Quantum mechanically, the electron wave function should be conserved within the CNT "bridge" from the Pt into the diamond structure. The extreme population density and random orientation of the CNT's and the inter-atomic carbon-carbon (CNT/diamond) bond provides optimism toward achieving high probability of charge deposition into the nanocrystalline diamond structure.

Parallel to work on the high-conductivity back-contact, we began investigating diamond growth methodologies with an emphasis on electronic properties. More than a decade ago the original high current cathode application of diamond films (DARHT) was identified and the field has matured considerably since then. Namely, polycrystalline, nanocrystalline, and ultrananocrystalline diamond film growth is now generally well understood. Our research effort is to add doping profiles which govern the electronic properties and transitional doping for p to n-type diamond.

On August 6th of this year we filed a US Provisional Patent, application # 61/371,510 (LANL S-112,992). The technology described in the application, shown diagrammatically in Figure 1, is the same as this LDRD-ER however the title is: A PHOTO-STIMULATED LOW ELECTRON TEMPERATURE HIGH CURRENT DIAMOND FILM FIELD EMISSION CATHODE.

Future Work

Year 2: improved faraday cup and laser fluence diagnostics, back illumination of the diamond field emitters, demonstration of high conductivity back contact, and deep ion implantation to achieve de-sired doping concentrations.

Year 3: Optimize growth and post processing to yield diamond samples with a demonstrated ability to sustain photo-initiated high current emission, comparing the performance of both n- and p- doped samples.

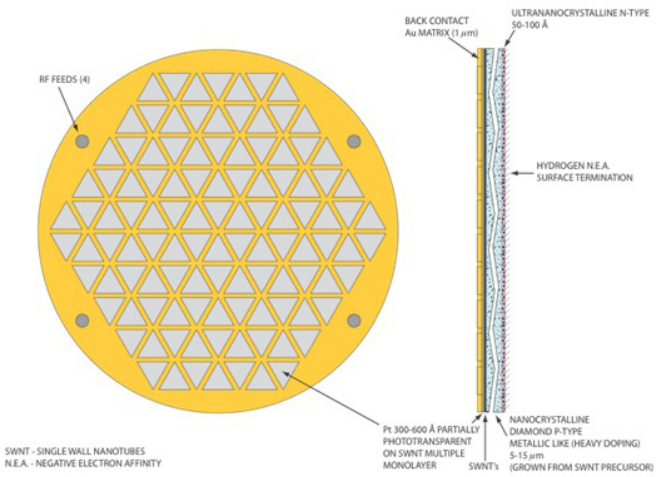

Figure 1. Schematic of a notional diamond cathode configuration designed for RF accelerator applications.

Conclusion

Our research goal is to transition our novel diamond field emitter concept into a versatile, robust electron source whose form factor and emission characteristics can be tailored to any number of specific applications. We are fabricating polycrystalline diamond films and working on the problems which must be solved to demonstrate their revolutionary and robust capacity to serve as an ultra-high quality, high current, high duty factor electron source.

References

1. Kane, A. A., T. Sheps, E. T. Branigan, V. A. Apkarian, M. H. Cheng, J. C. Hemminger, S. R. Hunt, and P. G. Collins. Graphitic Electrical Contacts to Metallic Single-Walled Carbon Nanotubes Using Pt Electrodes. 2009. *Nano Letters.* **9** (10): 3586.

2. Matsuda, Y., W. Deng, and W. A. Goddard. Contact Resistance Properties between Nanotubes and Various Metals from Quantum Mechanics. 2007. *The Journal of Physical Chemistry C.* **111** (29): 11113.

3. Xiao, X., J. Elam, S. Trasobares, O. Auciello, and J. Carlisle. Synthesis of a Self-Assembled Hybrid of Ultrananocrystalline Diamond and Carbon Nanotubes. 2005. *Advanced Materials.* **17** (12): 1496.

4. Shurter, R. P., D. C. Moir, D. J. Devlin, R. W. Springer, and T. A. Archuleta. Development and characterization of diamond film and compound metal surface high current photocathodes. 1997. In *1997 Particle Accelerator Conference.* (Vancouver, 12-16 May 1997). , p. 2829 . Vancouver: IEEE.

Solid State Neutron Detector

Anthony K. Burrell
20100389ER

Introduction

This project details the development of a completely new class of solid state neutron detectors based upon scintillator materials recently discovered at Los Alamos National Laboratory. The traditional neutron absorber used to detect neutrons is 3He, a material that is becoming difficult to obtain throughout the world. Furthermore, the detector system will not employ high-pressure gas or toxic materials and as such will have few limitations on transport. The scintillator comprises a completely new composition. We believe these new scintillators will provide neutron detectors with performance comparable to existing ^{3}He without the cost or difficulties associated with compressed gas. As a result of reduction in cost of over 80% and increased portability of the detector system, more detector systems can readily be deployed. These detectors will also be light, thin, tolerant of extremes temperature and vibration, low in power demand and insensitive to radiation other than neutrons.

Benefit to National Security Missions

Neutron detectors are critical for missions from nuclear physics to nonproliferation and forensics. Conventional neutron detectors typically include devices that operate as ionization chambers or proportional counters. The ^{3}He proportional counters are currently the most widely used thermal neutron detectors for nonproliferation-related activities. Besides the clear problems that the limited supply of ^{3}He is causing, these counters also suffer to some extent from transportation-related disadvantages including the perceived dangers of high pressure gas containment. This device will replace ^{3}He detectors with a cheaper and safer alternative.

Progress

In the past year we have developed the synthesis of inverse opals and currently prepare these materials based upon SiO_2 up to the 2 gram scale. We have refined the synthesis to include holes on the order of 350 nm. The inverse opals have been fully characterized using surface area analysis, X-Ray diffraction and photoluminescence. These materials we also used as the standards in the gamma spectroscopy work.

Modification of the inverse opals was employed to determine the limits of the synthetic technique. Specifically we were interested in the possibility of enhancing or modifying the emission from the native inverse opals. In the initial work we added rare earth metal ions to the sol-gel precursor of the inverse opal. For example, europium acetate was added to the TEOS solution before it was deposited onto the latex beads. After baking the inverse opals were physically identical to the undoped materials. However, the opals now emit red under 350 nm light as shown if Figure 1.

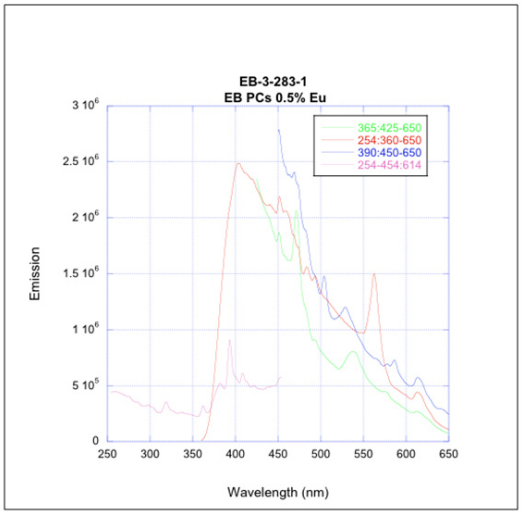

Figure 1. Emission spectra of inverse opals prepared using Eu (0.025%).

Clearly the europium is emissive and stable in the silica lattice. We are in the process of examining the other rare earth metals to discovery what range of wavelengths can be accommodated inside the inverse opal structure. Other rare earth material such as terbium also incorporate into the silica lattice also show emission under uv light (Figure 2) The addition of a red component to the inverse opals opens up a second parallel application. One of the major needs in solid state lighting is a requirement for a warm white phosphor. The

current zirconium coated inverse opals are relatively cool (blue). However, the addition of a red line in the emission spectrum could produce the warm red needed for this application. In the rest of our work we will pay attention to this possible application.

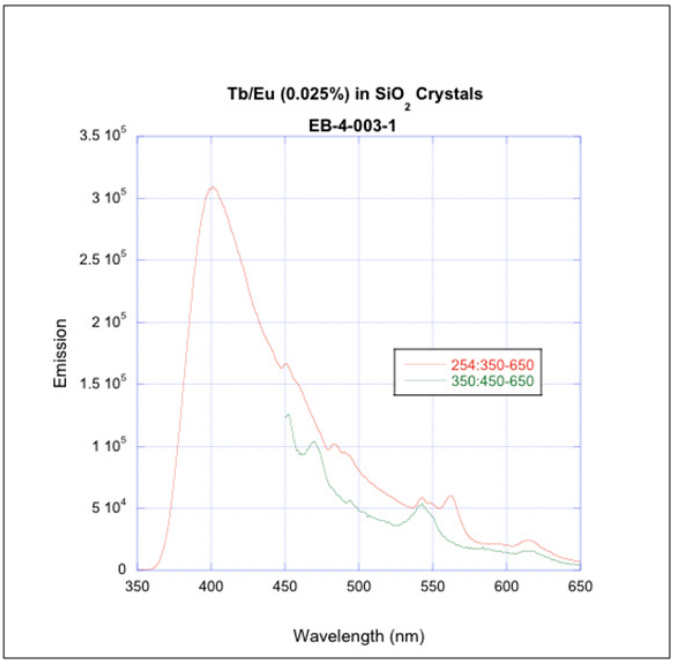

Figure 2. Emission spectrum of inverse opals prepared using Eu/Tb mix (0.25%).

The new prepared pure inverse opals have been coated with a zirconium oxide and the new spectral response of these materials has been examined and is shown in Figure 3. In particular, we needed to confirm that the in house materials were consistent with the preliminary data we obtained from samples obtained from the University of Auckland. This was indeed the case and we have begun preparing a manuscript describing the new emissive materials based upon zirconium coated inverse opals. We anticipate submission to Advanced Materials.

With the LANL prepared zirconium inverse opals in hand we have been investigating the possible systems that will enable filling of the pores with boron or lithium rich materials. Initial work has focused on simple aqueous solutions of borate or lithium ions. The current systems have been sent for gamma spectroscopy and are not satisfactory.

Future work will entail the assessment of different hole sizes and the effect the optical band gap change has on emission. These will be prepared over the remainder of this year. We will assess if the rare earth doped inverse opals have any effect on the emission from the zirconium or hafnium coated inverse opals. We will also determine if a barrier coating on the zirconium or hafnium is advantageous in the ability to index match the fill solution. We have also begun an collaboration with Thomas Proffen at the Lujan Center to look at total scattering in these materials in an attempt to determine the fundamental nature of the emission process and how the interaction of the hafnium or zirconium with the silica causes the emission and more importantly have the nature of the metal affects the emission spectrum.

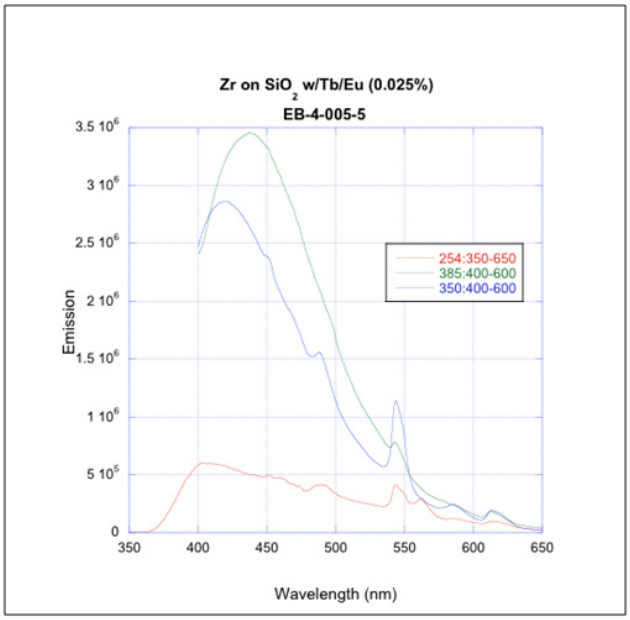

Figure 3. Emission spectrum of inverse opals Eu/Tb mix coated with Zr.

Future Work

We will build a solid state detector system through the use of a new class of scintillators in which simple metal oxide films of Zr or Zn on nano-structured silica or borates result in high quantum yield scintillators. The materials we will employ take advantage of nanotechnology in material that is cheap and can be prepared in very large scale. The detector system will not employ high-pressure gas or toxic materials and as such will have few limitations on transport. The scintillator comprises a completely new composition. We believe these new scintillators will provide neutron detectors with performance comparable to existing 3He without the cost or difficulties associated with compressed gas. As a result of reduction in cost of over 80% and increased portability of the detector system, more detector systems can readily be deployed. These detectors will also be light, thin, tolerant of extremes temperature and vibration, low in power demand and insensitive to radiation other than neutrons.

Project Milestones

- Prepare and characterize photonic crystal scintillators with lifetimes < 20 ns and quantum efficiencies (lifetime vs λ etc).

- Fill photonic crystal scintillators with boron or lithium material that provides an index match and thereby a transparent scintillator.
- Determine neutron capture and gamma exclusion efficiencies of new neutron phosphor.
- Assemble a device consisting of a neutron detector 0.5 mm x 1 cm x 1 cm.

Conclusion

The success of the proposal will be the production of a working prototype solid state neutron detector, which has efficiencies and gamma exclusion properties comparable to the 3He detectors. This will reduce the dependency on 3He which is a scare material and therefore enable wide spread deployment of neutron detectors at ports of entry.

Terahertz Generation Harnessing the Two-Stream Instability

Kip A. Bishofberger
20080210ER

Abstract
The terahertz regime of the electromagnetic spectrum is situated between traditional high- frequency microwave and extremely far-infrared light. Both producing and detecting terahertz waves has been both difficult and the focus of significant efforts world-wide. Because of the very specific absorption and transmission properties of terahertz radiation, there are potentially many high-impact applications including medical imaging, secure or covert communication, and cloaking.

High-power sub-millimeter and terahertz-frequency sources have remained an elusive target of physicists and engineers over the past many years. While lasers and microwave circuitry have conquered higher and lower frequencies, this missing band has a vast range of scientific, commercial, and military applications. A group at LANL has shown that a particular instability in a particle beam, a phenomenon well-known and strongly avoided by most accelerator laboratories, can actually be harnessed, controlled, and utilized to produce high-power terahertz radiation. Simulations predict that this experiment could break open the barrier to this band of frequencies, opening the door to future applications.

Background and Research Objectives
This project focuses on modeling and constructing a sub-millimeter radiative source using a well-known physics phenomenon. This compact device, loosely similar to a laser, is predicted to produce a beam of this radiation, which is applicable to numerous scientific, commercial, and security-based military applications. For example, this frequency range can be used for extremely high-bandwidth communications or image the contents of shipping containers arriving daily at American ports. It is capable of detecting specific environmental hazards. Like lasers today, terahertz sources would be ubiquitous in countless future applications once these sources exist.

Scientific Approach and Accomplishments
We are excited to report the conclusions of our LDRD-funded research. Over the course of the project, our deeper understanding of the physics involved in the process has changed the emphasis of the program. New and unexpected facets of the two-stream process have been published and are the subject of a Ph.D. thesis being defended.

This project has centered around modeling a sub-millimeter radiative device that utilizes a well-known phenomenon called the two-stream instability. This technique allows us to develop a simple, robust source of sub-millimeter radiation, through the terahertz range, while dispensing with complicated metallic structures and difficult tolerances.

- Simulations have yielded a wealth of information about the gain of the device. Before getting funding, we had a simplistic, one-dimensional model of the effect. With two-dimension and three-dimension simulations, we can see that the gain of the device does not degrade significantly [2,4,5]. In fact, within certain specific parameter spaces, the perceived gain is actually higher in the simulations than what the simplistic model predicts [1,6,7]. This result is very exciting, as it shows that a realistic device may actually perform better than our first predictions

- The simulations have established a number of parameters, which affect the growth of the radiative modes. Without these crucial tests, it would have proved improbable that an experimental device would perform as expected. Additionally, other effects, such as how the beam propagates through a beam pipe, determine which mode (which frequency) has the highest gain [2,3]. Again, these results have directly influenced the specifics of the experiment.

- Other results show that the bandwidth of the device is exceedingly large [1-3,9]. This is great news for development of wideband communications and feedback-driven oscillators. By seeding the beam at a “frequency of interest,” it will amplify that

frequency without any finicky adjustments of the beam parameters.

- The one challenge that remains is turning the "beam mode" (Coulombic, space-charge mode) into a "radiative mode," essentially converting the power into a directed beam that can be harnessed for applications. From a gathering of physicists who are experts in this type of coupling, several proposed scenarios were studied on how to efficiently convert the modes. We are publishing results from these calculations; however, the efficiencies are very much less than desirable, typically less than 1% [1,7,9]. The easiest way to couple the radiation out is to add an accelerating stage after the instability grows toward saturation, but this would add a meter or so of length to the originally very compact device.

- An experiment was designed, but with the difficulty of coupling out the power exposed, we were forced to redirect our focus to solving this problem. We have several options available that we wish to test, but resources are not available to complete the experiment, including the out-coupling concepts. In addition, our publications not only describe our new and full understanding of the two-stream terahertz-generation concept, but scrutinize several of these ideas [1,7].

- Included in the final push toward coupling the power into a radiative mode, two workers have developed a new simulation tool, which calculates Coherent Synchrotron Radiation (CSR). This code has been crucial in predicting the amount of radiation that can be coupled out of the beam. As an added benefit, the code has already been used to analyze vastly different beamlines, such as MaRIE and the Navy FEL designs.

The above achievements are all based on the work that has been occurring over the past three years. As testimony to this research, we have:

- a Ph.D. thesis that is currently being defended [7],

- several peer-reviewed articles published, plus several more submitted [2,4,6],

- numerous invited and contributed presentations at conferences [1-5,9],

- a newly developed software code already being used for other projects.

We are grateful for the opportunity that the LDRD program has provided to work on this exciting and significant physics research.

Impact on National Missions

It is important to note that such research can be immediately utilized in a variety of scientific, commercial, and military applications. In particular, Threat Reduction has desired efficient, adaptable devices in this frequency range for remote sensing, communications, and imaging applications. Terahertz radiation is seen as a vital tool: it combines the penetrating power of microwaves with the high resolution of IR and visible imaging [8,10-13].

In addition, it is a significant element of future INTEL and Warfighter Support missions (secure or covert communications, covert imaging, etc), especially involving ultra-wideband amplifier capabilities [10,13]. Finally, DOE/SC and NIH missions are seeking terahertz sources that will enable new medical imaging technologies [11].

It is exciting to know that this LDRD project has successfully paved the way toward a high-power, continuous source of terahertz radiation. We look forward to developing this device for these applications in the future.

References

1. Svimonishvili, T., K. Bishofberger, R. J. Faehl, and B. E. Carlsten. PIC simulation of MM and SUB-MM radiation source based on two-stream instability. 2010. In *2010 IEEE 37th International Conference on Plasma Sciences (ICOPS 2010) ; 20-24 June 2010 ; Norfolk, VA, USA.* , p. 1.

2. Bishofberger, K., T. Svimonishvili, R. J. Faehl, and B. E. Carlsten. Structure-less generation of sub-millimeter radiation. 2009. In *2009 IEEE International Vacuum Electronics Conference (IVEC) ; 28-30 April 2009 ; Rome, Italy.* , p. 275.

3. Svimonishvili, T., K. Bishofberger, R. J. Faehl, and B. E. Carlsten. THZ radiation source based on two-stream instability. 2009. In *2009 IEEE 36th International Conference on Plasma Science (ICOPS) ; 1-5 June 2009 ; San Diego, CA, USA.* , p. 1.

4. Bishofberger, K., B. E. Carlsten, and R. Faehl. Generation of millimeter and sub-millimeter radiation in a compact oscillator utilizing the two-stream instability. 2008. In *IEEE International Vacuum Electronics Conference (IVEC 2008) ; 22 April 2008 ; Monterey, CA, USA.* , p. 164.

5. Bishofberger, K., B. E. Carlsten, and R. Faehl. Millimeter and sub-millimeter radiation from a unique compact oscillator. 2008. In *2008 IEEE 35th International Conference on Plasma Science ; 15-19 June 2008 ; Karlsruhe, Germany.* , p. 1.

6. Carlsten, B. E., K. A. Bishofberger, and R. J. Faehl. Compact two-stream generator of millimeter- and submillimeter-wave radiation. 2008. *Physics of Plasmas.* **15** (7): 073101.

7. Svimonishvili, T.. Modeling of a mm and sub-mm wave radiation source based on two-stream instability. 2010. *University of New Mexico Doctoral Dissertaion.*

8. Bishofberger, K.. PIC Simulations of Terahertz Generation Utilizing the Two-Stream Instability. 2010. In *2010 Advanced Accelerator Workshop.* (Annapolis, Maryland, 13-19 June 2010). , p. 194. New York: American Institute of Physics.

9. Bishofberger, K.. PIC simulations of terahertz generation utilizing the two-stream instability . 2010. In *2010 Advanced Accelerator Workshop.* (Annapolis, MD, 13-19 Jun. 2010). , p. 194. New York: AIP.

10. Wallace, H. B., and M. J. Rosker. A method for analyzing active SMMW imaging system performance. 2008. In *2008 33rd International Conference on Infrared, Millimeter and Terahertz Waves (IRMMW-THz 2008) ; 15-19 Sept.* (2008 ; Pasadena, CA, USA). , p. 1.

11. Bykhovski, A., T. Globus, T. Khromova, B. Gelmont, D. Woolard, and M. Bykhovskaia. An analysis of the THz frequency signatures in the cellular components of biological agents. 2006. In *Conference on Terahertz for Military and Security Applications IV ; 20060417 - 20060418 ; Kissimmee, FL.* Vol. 6212, p. 62120H.

12. Rosker, M. J., H. Bruce. Wallace, and IEEE. Imaging through the atmosphere at terahertz frequencies. 2007. In *IEEE/MTT-S International Microwave Symposium ; 20070603 - 20070608 ; Honolulu, HI.* , p. 772.

13. Jacobs, E., S. Moyer, C. Franck, F. DeLucia, C. Casto, D. Petkie, S. Murrill, and C. Halford. Concealed weapon identification using terahertz imaging sensors. 2006. In *Conference on Terahertz for Military and Security Applications IV ; 20060417 - 20060418 ; Kissimmee, FL.* Vol. 6212, p. 62120J.

Publications

Bishofberger, K., B. E. Carlsten, R. Faehl, and IEEE. Generation of millimeter and sub-millimeter radiation in a compact oscillator utilizing the two-stream instability. 2008. In *9th IEEE International Vacuum Electronics Conference ; 20080422 - 20080424 ; Monterey, CA.* , p. 162.

Bishofberger, K., B. E. Carlsten, and R. Faehl. Generation of millimeter and sub-millimeter radiation in a compact oscillator utilizing the two-stream instability. 2008. In *IEEE International Vacuum Electronics Conference (IVEC 2008) ; 22 April 2008 ; Monterey, CA, USA.* , p. 164.

Bishofberger, K., B. E. Carlsten, and R. Faehl. Millimeter and sub-millimeter radiation from a unique compact oscillator. 2008. In *2008 IEEE 35th International Conference on Plasma Science ; 15-19 June 2008 ; Karlsruhe, Germany.* , p. 1.

Bishofberger, K., B. E. Carlsten, and R. Faehl. Generation of millimeter and sub-millimeter radiation in a compact oscillator utilizing the two-stream instability. 2008. In *2008 IEEE International Vacuum Electronics Conference, IVEC with 9th IEEE International Vacuum Electron Sources Conference, IVESC ; 20080422 - 20080424 ; Monterey, CA, United States.* , p. 164.

Bishofberger, K., T. Svimonishvili, R. Faehl, B. Carlsten, and IEEE. Structure-less Generation of Sub-millimeter Radiation. 2009. In *10th IEEE International Vacuum Electronics Conference ; 20090428 - 20090430 ; Angelicum Univ, Rome, ITALY.* , p. 275.

Bishofberger, K., T. Svimonishvili, R. Faehl, and B. Carlsten. Structure-less generation of sub-millimeter radiation. 2009. In *2009 IEEE International Vacuum Electronics Conference, IVEC 2009 ; 20090428 - 20090430 ; Rome, Italy.* , p. 275.

Bishofberger, K., T. Svimonishvili, R. J. Faehl, and B. E. Carlsten. Structure-less generation of sub-millimeter radiation. 2009. In *2009 IEEE International Vacuum Electronics Conference (IVEC) ; 28-30 April 2009 ; Rome, Italy.* , p. 275.

Carlsten, B. E., K. A. Bishofberger, and R. J. Faehl. Compact two-stream generator of millimeter- and submillimeter-wave radiation. 2008. *Physics of Plasmas.* **15** (7): 073101.

Carlsten, B., K. Bishofberger, and R. Faehl. Compact two-stream generator of millimeter- and submillimeter-wave radiation. 2008. *Physics of Plasmas.* **15** (7): 073101.

Svimonishvili, T.. Modeling of a mm and sub-mm wave radiation source based on two-stream instability.

Svimonishvili, T., K. Bishofberger, R. J. Faehl, and B. E. Carlsten. PIC simulation of MM and SUB-MM radiation source based on two-stream instability. 2010. In *2010 IEEE 37th International Conference on Plasma Sciences (ICOPS 2010) ; 20-24 June 2010 ; Norfolk, VA, USA.* , p. 1.

Svimonishvili, T., K. Bishofberger, R. J. Faehl, and B. E. Carlsten. THZ radiation source based on two-stream instability. 2009. In *2009 IEEE 36th International Conference on Plasma Science (ICOPS) ; 1-5 June 2009 ; San Diego, CA, USA.* , p. 1.

Nano-Fission-Material based Neutron Detectors

Ernst I. Esch
20080221ER

Abstract

Neutron monitors are commonly used for a variety of nuclear physics applications. A scintillating neutron detector consisting of a liquid scintillator loaded with fissionable material has been developed, characterized, and tested in a neutron beam line. The detector shows a significant improvement in neutron sensitivity compared with conventional fission chambers. Recent research indicates that it is possible to load nanoparticles of fissionable material into a scintillating matrix, with up to three orders of magnitude higher loading than typical fission chambers. This will result in a rugged, cost-efficient detector with high efficiency, and short signal rise time.

Background and Research Objectives

Neutron monitors are commonly used for a variety of nuclear physics and non-proliferation applications. Current technology is based on either fission chambers or ^{3}He tubes. The ^{3}He tube has been the work-horse for nonproliferation application for more than 4 decades. However, current ^{3}He shortages are forcing the global security sector to develop new detector technologies. The fission chamber technology is currently used in beam line experiments to determine neutron flux for a variety of neutron interaction measurements. Both technologies offer a variety of challenges that we believe can be remedied by our proposal.

Recent research on nanocomposite based γ-scintillator development, pioneered at Los Alamos, indicate that this approach can be extended to load fissionable nanomaterial into a matrix of plastic scintillator material, with up to three orders of magnitude higher fissionable material loading than typical modern fission chambers. This will result in a rugged, cost efficient fission detector with high efficiency, short signal rise time and the ability to be used in low neutron-flux environments. This technology could ultimately replace fission-chambers in nuclear science as well as 3He tubes, the current workhorse in neutron detector applications for threat reduction and nonproliferation programs.

Within the proposed project, we want to synthesize fissionable nanoparticles and load them into a plastic scintillator matrix. We will investigate the physical properties of the detector material and find the optimal parameters for particle size and loading ratio and matrix type. Our goal is to manufacture nanomaterials in quantities large enough to build and characterize fission detectors. Once the detector material is fabricated, the optical, physical and nuclear properties will be determined, including the optical transmission, radio- and photo-luminescence, nanoparticle crystallinity and size, and detector energy resolution, pulse width, scintillation decay constant and neutron sensitivity. At LANSCE-NS fission chambers are currently in use and it will be possible to cross-calibrate the detector performance as a function of the neutron flux.

Scientific Approach and Accomplishments

We proposed a scintillating neutron detector, consisting of a liquid scintillator loaded with fissionable material. If the fissionable material is small enough (molecular or nano-particles), the fission elements will leave the non scintillation complex and deposit their energy in the scintillating matrix. Recent research indicates that it is also possible to load nanoparticles of fissionable material into a scintillating matrix. This technique allows for a fissionable material loading in the scintillator of more than three orders of magnitude more than a conventional fission chamber. This approach offers several advantages over conventional techniques.

A liquid scintillator loaded with 2% ^{232}Th in the form $Th(NO_3)_4(TBP)_2$ was prepared, as well as a liquid scintillator standard for comparison. The liquid scintillator standard contained the same amount of TBP as was found in the thorium-loaded detector, in order to ensure that the only difference between the two solutions was the presence or absence of the thorium nitrate molecule. Both solutions were transparent to the liquid scintillator emission. The radioluminescence of the thorium-loaded liquid scintillator displays emission peaks in the same locations and with the same relative intensities as the unloaded liquid scintillator. The only difference between the radioluminescence spectra of the two solutions is a

slight increase in the overall intensity of the thorium-loaded liquid scintillator to $3.2x10^6$ counts/s, compared with $2.9x10^6$ counts/s for the liquid scintillator, due to its larger effective atomic number.

Two scintillator modules were prepared for testing in the 90L beam line at the Los Alamos Neutron Science Center (LANSCE). The thorium-loaded scintillator contained 2 g of thorium, in the form $Th(NO_3)_4(TBP)_2$, suspended in a liquid scintillator consisting of 750 mg PPO and 100 mg POPOP in 100 mL toluene. For comparison purposes, the other scintillator module was filled with liquid scintillator to which an amount of TBP equal to the amount in the thorium-loaded scintillator had been added.

Measurements were performed at the 90L flight path at LANSCE. Micropulses arrived every 1786.6 ns. A typical liquid scintillator spectrum is shown in Figure 1. The arrival of the gamma-flash is visible at 0 ns, with neutrons beginning to arrive shortly afterwards. The feature at 225 ns results from electronic noise. As shown in Figure 1, the thorium-loaded scintillator produced more large pulses than the unloaded scintillator. In order to determine whether these extra events result from fission, gamma-ray interactions, or ^{232}Th alpha events, analysis of the data is currently focused on pulse shape discrimination.

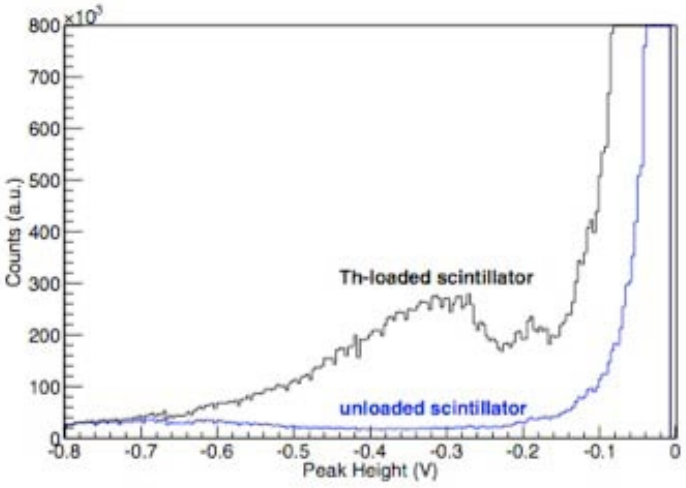

Figure 1. Pulse height distribution for thorium loaded and non-loaded liquid scintillator. The pulse height is displayed in negative numbers.

The ongoing data analysis demonstrated that there is a good chance to perform pulse shape discrimination to distinguish between gammas and neutrons. Figure 2 shows the first attempts of pulse shape discrimination. The analysis revealed that a digitizer with more bits resolution is needed. However a comparison between gamma response and neutron response in Figure 3 clearly displays that a simple threshold analysis might be used as discrimination instead.

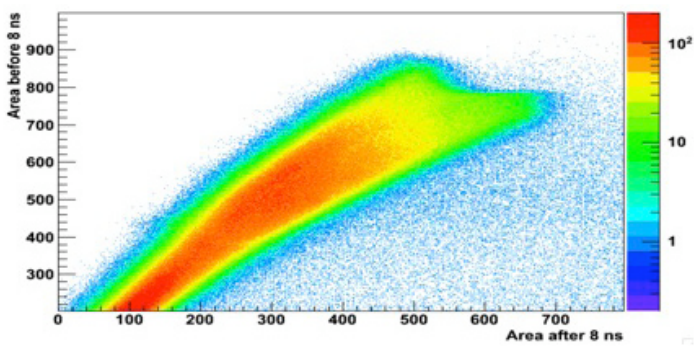

Figure 2. Attempt to do pulse shape discrimination. The result showed that we needed a digitizer with more bit resolution.

In parallel we developed a method for generating fissionable material nano-particles. Our results at LANCSE indicate that Th-232 rather than U-238 could be the actinide isotope of choice for the development of a fissionable scintillator detector, based on results using molecular $Th(NO_3)_4(TBP)_2$ (where TBP = tri-n-butyl phosphate) dissolved in toluene with scintillator cocktail. Switching this molecular thorium complex out for a thorium based nanoparticle could significantly increase material loading and this lays down the synthetic challenge of preparing solvent soluble thorium nanoparticles. Our initial focus was on the attempted synthesis of capped ThF_4 nanoparticles using the synthetic methods developed at LANL for CeF_3 nanoparticle synthesis. Unfortunately the distinctive properties of the tetra-valent f-element (ThIV) vs. the tri-valent f-element (CeIII) rendered this approach largely unsatisfactory. We then turned our attention to literature methods for MIV nanoparticle synthesis (M = Zr, Ce, U & Th) noting previous reports of the incorporation of Th into nanmaterials [1].

There are numerous references to CeO_2 and ZrO_2 nanoparticle syntheses in the literature,[2] and we focused on a room temperature aqueous method for the synthesis of Ce_1-$xZrxO_2$ nanoparticle sols [3]. Adaption of this preparative route led to the synthesis of a sol at pH3, a pH value where $Th(OH)_4/ThO_2$ would under normal conditions have precipitated from solution. This synthesis is readily reproducible and the sol is stable for weeks, if not months. Dynamic light scattering measurements, in collaboration with Nick Smith (MST-7), revealed the presence of ca. 100 nm material in solution which could be attributed to agglomeration of smaller nanoparticles. This was confirmed by TEM (Transmission Electron Microscopy) measurements, in collaboration with Leif Brown (C-CDE), where ca. 5 nm nanoparticles could be clearly observed. These particles were linked into extended ribbon structures which indeed points to agglomeration in the sol. Complimentary diffraction data indicate that the particles are probably composed of cubic ThO_2 with EDS (Energy Dispersive X-ray Spectroscopy) confirming the presence of thorium. Raising the pH of the ThO_2 nanoparticle sol led to solid precipita-

tion. Preliminary attempts to extract these ThO_2 nanoparticles into toluene were promising, particularly when oleic acid was used as the capping agent. TEM data indicates that ThO_2 nanoparticles have been successfully transferred into toluene although both TEM results and dynamic light scattering measurements reveal that the concentration of thorium nanoparticles in toluene is much lower than can be achieved in aqueous solution. Nevertheless, it seems likely that additional research will lead to the extraction of sufficient ThO_2 nanoparticles into a toluene liquid scintillant matrix to enable us to test for the first time if actinide nanoparticles can be employed as fissionable scintillant neutron detectors.

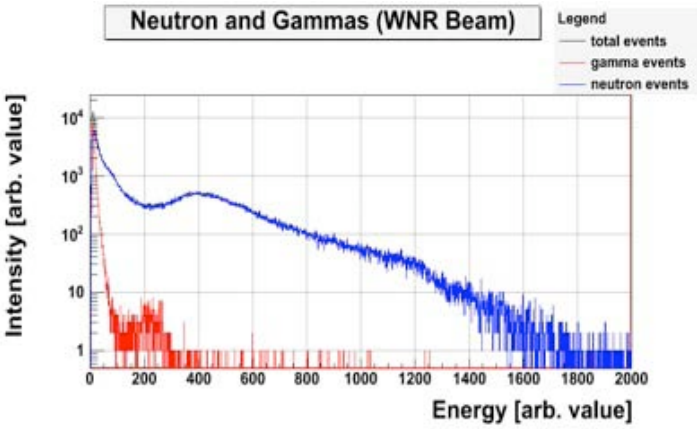

Figure 3. Energy spectrum received for gammas (red) and neutrons (blue).

Impact on National Missions

The proof of principal demonstration of our work could be the technological answer to several issues of the current ^3He shortage for nonproliferation solutions. If the detectors can be made solid and the mass loading can be increased, the detector technology could be an ideal replacement neutron-detector for portal monitors. Also, since the detectors have a neutron energy threshold, no moderation would be needed for multiplicity counting measurements as well as non destructive assay measurements.

References

1. Rousseau, G., M. Fattahi, B. Grambow, L. Desgranges, F. Boucher, G. Ouvrard, N. Millot, and J. C. Niepce. Synthesis and characterization of nanometric powders of UO2+x, (Th,U)O2+x and (La,U)O2+x. 2009. *JOURNAL OF SOLID STATE CHEMISTRY.* **182** (10): 2591.

2. Sivudu, K. Samba, and D. Shailaja. Preparation and characterization of ceria nanoparticles supported on poly(4-vinyl pyridine-co-divinyl benzene). 2006. *Journal of Applied Polymer Science.* **100** (5): 3439.

3. Deshpande, A. S., N. Pinna, P. Beato, M. Antonietti, and M. Niederberger. Synthesis and characterization of stable and crystalline Ce1-xZrxO2 nanoparticle sols. 2004. *CHEMISTRY OF MATERIALS.* **16** (13): 2599.

Publications

Esch, E., S. Stange, A. J. Couture, R. E. Del Sesto, L. Jacobsohn, T. M. McCleskey, E. A. McKigney, R. E. Muenchausen, D. Ortiz-Acosta, R. Reifarth, F. L. Taw, and F. Tovesson. Nano-composite based radiation detectors for beam experiments. Presented at *CAARI 08.* (Ft. Worth, TX, August 08).

Stange, S., E. I. Esch, R. E. Muenchausen, R. E. Del Sesto, F. L. Taw, F. Tovesson, and E. Burget. Nano-fission detector program at LANL. 2009. In *IEEE NSS 09.* (ORlando, FL, Octoberr 09). , p. Dis. Dresden: IEEE.

Efficient Structures for Low-Energy Acceleration of Light Ions

Sergey S. Kurennoy
20080228ER

Abstract

The project goal was to develop high-efficiency normal-conducting RF accelerating structures based on inter-digital H-mode (IH) cavities and the transverse beam focusing with permanent-magnet quadrupoles (PMQ), for ion-beam velocities in the range of a few percent of the speed of light. The H-mode resonator cavities are about ten times more efficient in this velocity range compared to the conventional drift-tube linear accelerator (DTL), and also have transverse dimensions a few times smaller than those of the DTL. However, the beam focusing is inherently difficult in H-cavities. Inserting permanent-magnet quadrupoles (PMQs) inside the H-cavity small drift tubes, as we suggested [1], solves the problem without reducing the accelerating efficiency.

Designing an H-PMQ accelerator for considerable ion-beam currents requires a careful balance of beam-physics and engineering considerations. We succeeded in achieving this balance by combining electromagnetic 3-D modeling with beam dynamics simulations and engineering thermal-stress analysis. Results of combined 3-D analysis of H-PMQ structures, including full IH-PMQ accelerator tanks – electromagnetic computations, beam-dynamics simulations with high currents, and thermal-stress analysis – were presented in [2-7]. They prove that H-mode structures with PMQ focusing can work even at high currents. Due to the structure efficiency, the thermal management is simple and can be realized with cooling channels in vanes [4-6]. The accelerating field profile in the tank is tuned to provide the best beam propagation using coupled iterations of electromagnetic and beam-dynamics modeling [7]. A cold model of the IH-PMQ tank has been manufactured and its measurements showed a good agreement with our calculations.

IH-PMQ accelerating structures following a short radio-frequency-quadrupole accelerator (RFQ) can be used in the front end of ion linacs or in stand-alone applications. For example, a compact deuteron-beam accelerator up to the energy of several MeV can be useful for homeland defense in an intense neutron and gamma source for interrogation of special nuclear materials.

Background and Research Objectives

Compact particle accelerators are important and enabling technologies for a variety of applications from medical therapy to imaging to active interrogation. Our project aims to develop novel compact and efficient accelerator structures for low-energy charged particles. The H-mode resonator cavities are about ten times more efficient at the beam velocities around a few percent of the speed of light compared to the usual DTL. However, keeping the beam transverse size small to avoid losses is more difficult in H-cavities compared to the DTL where the beam focusing is achieved with electromagnetic quadrupole magnets placed inside its large drift tubes. We suggested inserting PMQs inside the H-cavity small drift tubes (DTs) to solve the focusing problem without any reduction of the accelerating efficiency [1]. The high efficiency of the H-PMQ accelerator gives a new option of using small inexpensive radio-frequency (RF) generators as its power source instead of usual large and expensive RF klystrons.

The research objectives of the project were formulated as follows:

- Develop effective H-structures with PMQ focusing for the beam velocities from 3% to 10% of the speed of light using electromagnetic modeling (EM); integrate H-mode DTs and vanes in a resonator-tank design;
- Explore beam dynamics (BD) in such structures with envelope codes and multi-particle simulations to improve the beam quality, within the limitations of having PMQs inside the drift tubes;
- Perform engineering analysis (EA) of the structure cooling with chilled water and explore options for structure fabrication.

Finally, we proposed to fabricate and test a cold model of the IH-PMQ tank (full-scale aluminum model operated at low RF power) to prove the design feasibility. We chose the structure frequency to be 201.25 MHz, within the range of both popular RFQ types (four-rod and four-

vane), so that either one can be used for the initial acceleration. In addition, 201.25 MHz is the frequency of the LANSCE DTL. Therefore, the RF will be available for a future hot model (operated at full RF power with water cooling), if needed, and our design can serve as a step toward replacing the aging DTL.

Scientific Approach and Accomplishments

Designing an H-PMQ accelerator for considerable ion-beam currents requires a careful balance of beam-physics and engineering considerations. Our approach to achieve this balance was by combining electromagnetic 3-D modeling with beam dynamics simulations and engineering thermal-stress analysis. We addressed important challenges in pursuing our research objectives. One was the structure cooling: it must be simple (without water channels inside DT, to keep the DT size small) but efficient to ensure that the DT heating is not excessive, so that the DT temperatures do not exceed the maximal working temperature of the permanent magnets, 200-250°C. Another problem was to keep the beam size well within the relatively small DT aperture. Achieving a balance of the accelerator efficiency, beam quality, and thermal management within the above limitations required multiple iterations of electromagnetic modeling, beam dynamics, and thermal-stress analysis. We have developed the efficient interfaces between the available EM, BD, and EA codes that facilitated the design process. The developed EM-EA interface has been successfully applied to other projects at LANSCE, e.g. in [8].

Significant progress has been made in developing room-temperature H-mode accelerator structures with PMQ beam focusing for low-energy ions. Our initial efforts focused mostly on analyzing just one or a few periods of the H-mode structures [1-5]. In the second year of the project, the focus shifted to the design of a complete interdigital H-mode (IH) tank with PMQ focusing. An IH-PMQ tank includes many periods and two end cells where the magnetic flux turns to make a loop; the end-cell design is complicated but very important since it influences the field profile in the tank. We chose to design a short IH tank, 2-3 feet long, since it was easier to manufacture here at LANL. Its design incorporates all details of the full-length IH tank. The aluminum model of the tank serves as a cold model to be tested at low RF power.

We designed two different short IH tanks. The first IH tank (IH1) [6] can serve as the first stage, after a short radio-frequency-quadrupole (RFQ) accelerator, in a 1-4 MeV IH-PMQ 201.25-MHz deuteron accelerator with 50-mA beam current, for interrogation of SNM in cargo. The tank includes 20 drift tubes (DT) containing PMQs and covers the beam velocity range from 3.3 to 5 percent of the speed of light, corresponding to the deuteron beam energies from 1 to 2.25 MeV, with the accelerating gradient of 2.5 MV/m. Its total length is 63 cm; the cavity inner radius is 11.5 cm. For the nominal duty factor of 10%, the power dissipated in the tank walls is 1.34 kW, which is significantly smaller than the power put into the beam, 6.25 kW. Beam-dynamics simulations for IH1 in an axisymmetric approximation with the Parmila code showed that the 50-mA beam fills a significant part of the aperture that can lead to particle losses. Based on these results, we increased the beam-injection energy from 1 to 1.5 MeV, where the space-charge forces are lower and beam size is smaller. Using the developed iterative procedure, the second short IH tank (IH1L) was designed much faster, in just a few days. It covers the beam velocity range from 4 to 5.5 percent of the speed of light (deuteron beam energies from 1.5 to 2.8 MeV), with 2.5 MV/m gradient. The tank IH1L, shown in Figure 1, is longer, with the total length of 73.5 cm; the cavity inner radius is 12.0 cm. At the nominal duty factor of 10%, the power dissipated in the tank walls is 1.91 kW, while the power put into the beam is 6.5 kW. The RF power input for such power values can be provided with a simple loop on the tank wall.

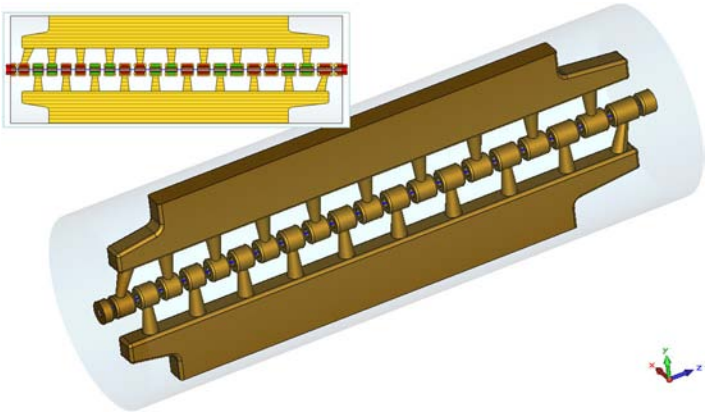

Figure 1. MWS model of a short IH tank (73.5 cm) with gradually increasing cell lengths. The drift tubes are supported by stems attached alternatively to two vanes. The outer cavity wall is removed; the cavity inner volume is shown in light-blue. PMQ magnets inside drift tubes are arranged in pairs as shown in the inset.

EM and BD iterations have been performed to adjust the electric field profile along the tank to be consistent with the PMQ focusing for a 50-mA deuteron beam. We have developed a simple algorithm similar to that in the Parmila linac design code that allows performing quick design iterations based on the on-axis electric field computed by our 3-D electromagnetic (EM) code, MicroWave Studio (MWS). For multi-particle BD simulations we made modifications of the Parmila simulation code and used the input from the MWS. In the IH1 tank the electric field profile was tuned to be flat [6]. For the tank IH1L we made the electric field gradually increasing along the tank at the same rate as the cell length increases, so that the average accelerating gradient per cell is constant [7]. We also adjusted the locations of the accelerating gaps to correspond to the required RF-phase ramp along the structure. All these modifications lead to much better beam dynamics [7].

Following our research plan, we have developed an interface for transferring data between the 3-D EM code, MWS, and engineering codes, COSMOS and ANSYS. We performed iterative EM-engineering analysis of the IH tank and demonstrated the effectiveness of its water cooling with cooling channels located only in the vanes supporting the structure drift tubes [4-6]. The temperatures of PMQ in the tank DTs, as well as the structure stress, remain well within the acceptable range. For the IH1 tank with water cooling in vanes, the highest temperature was below 35° C for 10% duty operation [6], cf. Figure 2. This confirms feasibility of room-temperature H-PMQ accelerator concept since in effective H-mode structures there can be no cooling channels inside DTs while the PMQ temperatures must be kept below 150-200° C.

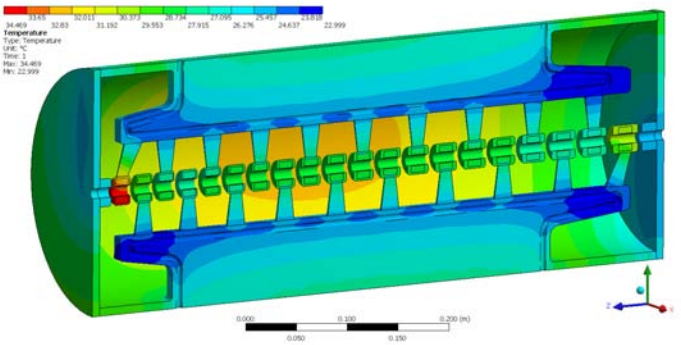

Figure 2. Temperature distribution in the IH tank with two cooling channels in the vanes and two simple cooling loops in the end walls at the nominal 10% duty as calculated by ANSYS.

As was proposed, we have developed an EM-BD interface – a procedure for transferring 3-D EM fields in H-mode structures computed by the MicroWave Studio to the multi-particle tracking codes, like Parmela and TRACK. This procedure now allows us performing detailed multi-particle beam-dynamics simulations with realistic fields from 3-D EM analysis, including both RF fields from the MWS and the magnetic fields of the array of 22 16-segment PMQs computed by the CST Electromagnetic (EM) Studio. We have completed a full 3-D multi-particle analysis of the IH1L tank both with the Parmela code and with the CST Particle Studio (PS). In the process, we developed a routine to input the same initial distribution generated by Parmila, into both tracking codes. Simulations have been performed with up to 100K particles, see Figure 3, and indicated no particle losses down to the fractional level of 10^{-5} [7]. These results prove that the tank can accelerate a 50-mA deuteron beam with the realistic emittance without losses using only two families of the PMQs. Such simulations help exploring the structure sensitivity to manufacturing errors and establish the manufacturing tolerances for the accelerator.

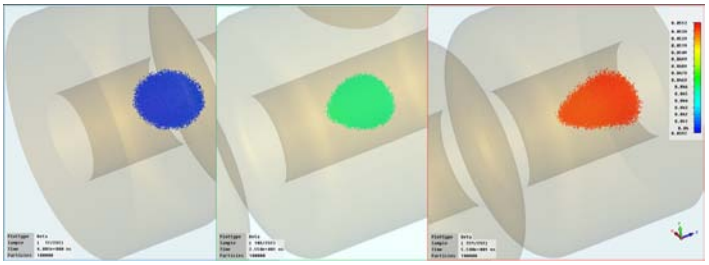

Figure 3. Evolution of a Gaussian bunch with 100K particles in the IH-PMQ tank of Figure 1 computed by the CST Particle Studio: near the entrance, in the middle, and near the exit. Color changes indicate the particle-energy increase (beta-scale shown, beta = v/c).

We explored the frequency and field sensitivity of the working mode in the IH tank to tank dimension variations using 3-D EM MWS modeling. A simple scheme with slug tuners for frequency and field-tilt tuning of the tank was developed and implemented in the cold model [6, 7]. The cold-model design was finalized, and the drawings were completed in Sep. 2009, see Figure 4. The model fabrication took longer than was planned; it was completed in June 2010, cf. Figure 5, and the DT alignment was finished in July. The bead-pull measurements showed a very good agreement with the calculated field profile, on the percent level [9]. The measured frequency was 0.7% higher than the computed one, and was adjusted with the tuners. The reason for this discrepancy was found in an unusual asymptotic dependence of the computed frequency on the mesh size. This dependence was studied and parametrically fitted, and now we can calculate the IH-PMQ tank frequency much more accurately [9].

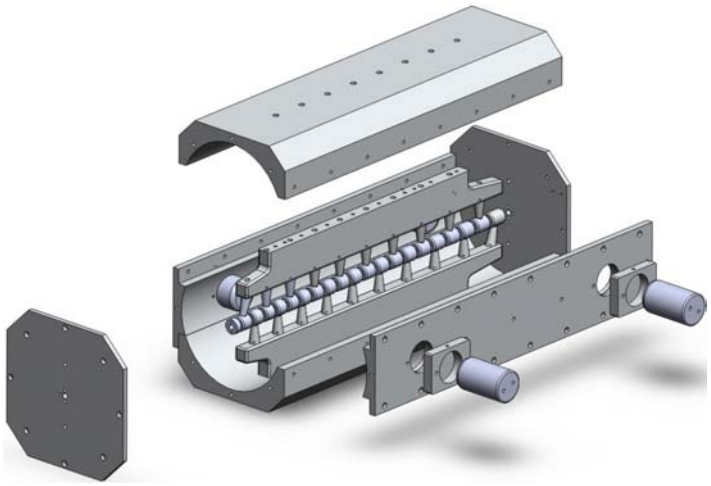

Figure 4. Explosion view of the IH-PMQ tank cold model. Two pairs of slug tuners in the side panels are shown.

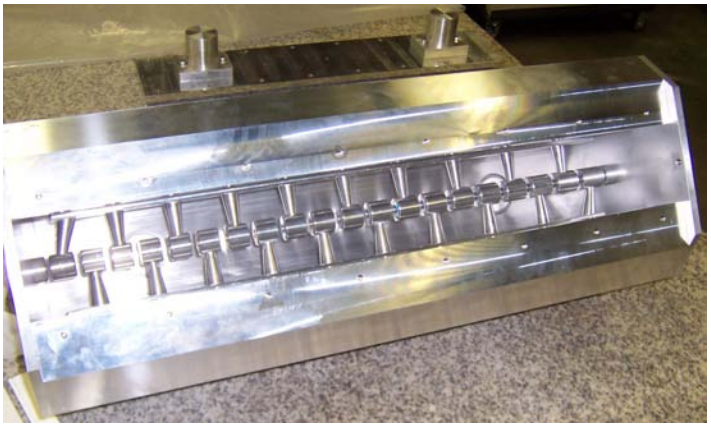

Figure 5. Photograph of the IH-PMQ tank cold model in the lab. One side panel with the slug tuners is removed.

Our project resulted in four invited talks, six conference publications, and four technical notes. We have also recently received a special invitation from the Physical Review Special Topics – Accelerator and Beams to prepare an article on our work toward the H-PMQ structure development. The article [9] is now being prepared for publication.

There is a significant interest to the IH-PMQ accelerator technology from industry and medical-accelerator projects. We had discussions on possible CRADA agreements with three industrial companies. In particular, AccSys Technology Inc (Pleasanton, CA) has been interested in acquiring our H-mode linac technology for medical applications and pursued a CRADA with us. The company even included funds for the CRADA in the budget for CY09; unfortunately, the decision to proceed with the CRADA was postponed due to their uncertain financial situation.

Impact on National Missions

This project supports the DOE missions of Treat Reduction, Non-Proliferation, Homeland Security, and the Office of Science research missions, by providing high-efficiency accelerators of light ions. We envision multiple applications of H-PMQ high-efficiency room-temperature structures, including industrial and medical ones. For example, a compact 4-MeV deuteron accelerator that we developed can drive a mobile intense neutron and gamma source for interrogation of special nuclear materials. Another important application could be a cost-effective replacement of the aging DTL in the LANSCE linear accelerator that would improve its reliability as required for the MaRIE project.

Within this project we have developed new capabilities for accelerator physics and engineering at LANL: the efficient interfaces between the available electromagnetic (EM), beam-dynamics (BD), and engineering-analysis (EA) codes that facilitate the accelerator design process. The EM-EA interface has already been successfully applied to a few other projects at LANSCE, e.g. [8].

References

1. Kurennoy, S. S., L. J. Rybarcyk, and T. P. Wangler. Efficient accelerating structures for low-energy light ions. 2007. (Albuquerque, NM, USA, 25-29 June 2007). p. 3824. New York, NY: IEEE.

2. Kurennoy, S. S., S. Konecni, J. F. O'Hara, and L. J. Rybarcyk. IH accelerating structures with PMQ focusing for low-energy light ions. 2008. In *European Particle Accelerator Conference 2008.* (Genoa, Italy, 23-27 June 2008). , p. 3428. Geneva, Switzerland: European Physical Society.

3. Kurennoy, S. S.. IH accelerating structures with PMQ focusing. 2008. *Los Alamos National Laboratory Report LA-UR-08-03795.*

4. Kurennoy, S. S., J. F. O'Hara, and L. J. Rybarcyk. Compact linac for deuterons. 2008. (Nashville, TN, USA, 25-29 Aug. 2008). p. 428. Nashville, TN, USA: ORNL.

5. Kurennoy, S. S., J. F. O'Hara, E. R. Olivas, and L. J. Rybarcyk. H-Mode accelerating structures with PMQ focusing for low-beta ion beams. 2010. In *1st International Particle Accelerator Conference (IPAC'10).* (Kyoto, Japan, 24-28 May 2010). , p. 828. Kyoto, Japan: IPAC'10.

6. Kurennoy, S. S., J. F. O'Hara, E. R. Olivas, and L. J. Rybarcyk. Efficient low-beta H-mode accelerating structures with PMQ focusing. 2008. (Victoria, BC, Canada, 29 Sep. - 3 Oct. 2008). p. 954. Victoria, BC, Canada: TRIUMF.

7. Kurennoy, S. S., J. F. O'Hara, E. R. Olivas, and L. J. Rybarcyk. Development of IH accelerating structures with PMQ focusing for low-beta ion beams. 2009. (Vancouver, BC, Canada, 4-8 May 2009). p. FR5REP070. Vancouver, BC, Canada: TRIUMF.

8. Kurennoy, S. S., S. Konecni, J. F. O'Hara, and L. J. Rybarcyk. Heating and stress in the LANSCE side-coupled linac RF cavities. 2008. In *European Particle Accelerator Conference 2008.* (Genoa, Italy, 23-27 June 2008). , p. 3431. Geneva, Switzerland: European Physical Society.

9. Kurennoy, S. S., L. J. Rybarcyk, J. F. O'Hara, and E. R. Olivas. H-Mode accelerating structures with PMQ focusing for low-beta beams. To appear in *Physical Review Special Topics - Accelerators and Beams.*

Publications

Kurennoy, S. S.. IH accelerating structures with PMQ focusing. 2008. *Los Alamos National Laboratory Report LA-UR-08-03795.*

Kurennoy, S. S., J. F. O'Hara, E. R. Olivas, and L. J. Rybarcyk. Efficient low-beta H-mode accelerating structures with PMQ focusing. 2008. In *XXIV Linear Accelerator Conference (Linac08).* (Victoria, BC, Canada, 29 Sep. - 3 Oct.

2008). , p. 954. Victoria, BC, Canada: TRIUMF.

Kurennoy, S. S., J. F. O'Hara, E. R. Olivas, and L. J. Rybarcyk. Development of IH accelerating structures with PMQ focusing for low-beta ion beams. 2009. In *Particle Accelerator Conference 2009.* (Vancouver, BC, Canada, 4-8 May 2009). , p. FR5REP070. Vancouver, BC, Canada: TRIUMF.

Kurennoy, S. S., J. F. O'Hara, E. R. Olivas, and L. J. Rybarcyk. H-Mode accelerating structures with PMQ focusing for low-beta ion beams. 2010. In *1st International Particle Accelerator Conference (IPAC'10).* (Kyoto, Japan, 24-28 May 2010). , p. 828. Kyoto: IPAC'10.

Kurennoy, S. S., J. F. O'Hara, and L. J. Rybarcyk. Compact linac for deuterons. 2008. In *42nd ICFA Advanced Beam Dynamics Workshop on High-Intensity High-Brightness Hadron Beams.* (Nashville, TN, USA, 25-29 Aug. 2008). , p. 428. Nashville, TN, USA: ORNL.

Kurennoy, S. S., L. J. Rybarcyk, and T. P. Wangler. Efficient accelerating structures for low-energy light ions. 2007. In *Proceedings of Particle Accelerator Conference 2007.* (Albuquerque, NM, USA, 25-29 June 2007). , p. 3824. New York, NY: IEEE.

Kurennoy, S. S., S. Konecni, J. F. O'Hara, and L. J. Rybarcyk. IH accelerating structures with PMQ focusing for low-energy light ions. 2008. In *Proceedings of European Particle Accelerator Conference 2008.* (Genoa, Italy, 23-27 June 2008). , p. 3428. Geneva, Switzerland: European Physical Society.

Compact Millimeter Wave Spectrometer Based on a Channel Drop Filter

Lawrence M. Earley
20080409ER

Abstract

The main objective of this project is the construction and testing of the novel passive mm-wave spectrometer based on a Photonic Band Gap (PBG) channel-drop filter (CDF). There is a need for a compact wide-band versatile and configurable mm-wave spectrometer for applications in mm-wave communications, radio astronomy, and radar receivers for remote sensing and nonproliferation. PBG CDFs allow channeling selected frequencies from spectra into separate waveguides through a PBG structure. Several PBG CDF devices were designed manufactured and tested. The first device was a single-channel filter operating at around 240 GHz fabricated out of silicon. The second device was a single-channel copper filter operating at around 108 GHz. The third sample was a three-channel device made out of silicon with the channels at around 240 GHz, 260 GHz, and 280 GHz. The size of all the samples was less than 1 inch by 1 inch and just a fifth of an inch in thick. The three-channel spectrometer can be directly employed for detection of methyl chloride. The proposed technology is expandable for frequencies from 60GHz to 1000GHz. Creation of a novel ultra-compact, wide-band, configurable, and easy to operate under all weather conditions mm-wave spectrometer would enable Laboratory missions in both national security and basic research and directly addresses the laboratory grand challenge "Detection of nuclear materials (Ubiquitous sensing)."

Background and Research Objectives

Performing the analysis of millimeter-wave spectra is essential for a broad range of applications. Monitoring of suspected nuclear facilities for compliance with non-proliferation treaties is an important national security issue. Millimeter-waves can be used together with infrared diagnostics to monitor precursors or residue from nuclear purification facilities [1,2]. Decoding infrared emission is crucial to understanding the processes of galaxy formation in astronomy [3,4]. The importance of millimeter-waves in biological sensing is beginning to take a new direction, following the demonstration that THz spectroscopy is sensitive to the dielectric response of small ligands binding to biological molecules, which opens the way for the detection of toxins and pathogens [5]. Expansion of an extremely crowded rf spectrum towards millimeter-waves is of critical importance to military and civil satellite communications [6]. To date, the millimeter-wave band is essentially undeveloped, and there is an evident need for novel components to fully harness the millimeter-wave spectrum.

We have initiated a project at Los Alamos National Laboratory (LANL) to construct and test a novel millimeter-wave passive direct-detection spectrometer based on the photonic band gap (PBG) [7] channel-drop filter [8]. A practical millimeter-wave detection spectrometer must be wide-band, compact, easy to operate, and configurable to adapt to requirements of the mission. The spectrometers currently available at millimeter-wave frequencies are heterodyne spectrometers [3], Fabri-Perot spectrometers [4], and more sophisticated millimeter-wave dispersive gratings or dispersive prisms [9,10]. The main disadvantage of the most popular heterodyne spectrometer is the noise which is introduced into the device by the mixer, and which reduces the sensitivity of the system. Heterodyne systems are also limited in bandwidth. For real-world chemical detection, this may result in lower detection capabilities. A Fabri-Perot system, in turn, has to be tuned to determine the frequency of the incoming signal. This requires the emission to be present for long enough to analyze and may result in some short emissions of dangerous chemicals going undetected. The quasi-optical systems, such as a dispersive grating or a prism, are bulky and employ a large array of detectors (100 detectors or more). Since space and aircraft systems are essentially purchased by the pound, this ultimately implies a higher system cost. A sweeping detector is an alternative, but it again precludes continuous monitoring, resulting in some information being lost. A PBG channel-drop filter-based device has the potential to become a unique, ultra-compact, configurable and easy-to-operate millimeter-wave passive spectrometer.

The photonic band gap channel-drop filter was first proposed by Fan et al. [8]. A CDF is a device which is capable of extracting a certain frequency from a continuous spectrum in the bus channel and passing it to the test chan-

nel. The rest of the spectrum is transmitted unaffected in the bus channel, thus making the CDF attractive for spectroscopic applications at millimeter-waves.

Scientific Approach and Accomplishments

We have initiated a project at Los Alamos National Laboratory (LANL) to construct and test a novel millimeter-wave passive direct-detection spectrometer based on the photonic band gap channel drop filter. Over the course of three years, the project has made significant progress and met most of the deliverables. Several configurations of the PBG CDFs were designed and experimentally evaluated.

Our design of the CDF, which was initially reported in [11], is based on a PBG structure which represents a square lattice of high-resistivity silicon posts (see Figure 1(a)). The filter consists of two parallel photonic crystal waveguides, which are the defects in the lattice in the form of rows of removed posts. Regular metal waveguides can be connected to the PBG waveguides, and the power will transmit from one waveguide into another. The two PBG waveguides are coupled by two micro-cavities. The cavities can be formed by either altering the size of a post [8] or by removing several posts from the structure altogether. In the absence of losses, the whole power at the resonance frequency goes directly into the test output channel (channel #4) (Figure 1(c)). At all other (non-resonant) frequencies, the power from the input waveguide, channel #1, exits directly into the main output waveguide, channel #2 (Figure 1(b)). Channel #3 is the test channel; no power should transmit into channel #3 at any frequency. The complete theory underlying the principles of operation of CDFs with two micro-cavities is described in [8]. Placing a detector at the resonant output, channel #4, provides an opportunity for detection of the single frequency of interest. Multiple CDFs with different frequencies can be stacked in series, and this system will act as a spectrometer. The spectrometer will determine if the unknown spectrum contains the set of given frequencies.

In the first year, we have studied fabrication of a 98 GHz version of the PBG CDF with a MEMS process. The MEMS fabrication process for the channel-drop filter consists of four stages. First stage is fabrication of the high-resistivity (resistivity of 100 Ohm*cm) silicon wafers. Second stage is the creation of the thermal oxide mask on top of the wafer. Third stage is the dry-etching of the wafers to create the PBG structures. And the final stage is the gold-plating of the PBG structure and bonding with the metallic plates. The first two fabrication stages were very successful. The dry-etching process, however, was found to push the limits of the existing technologies. Fabrication of the proof-of-principle filter at the frequency of 98 GHz required etching PBG rods which are 1000 micro-meters high. However we have discovered that etching beyond 650 micro-meters caused degrading of the thermal-oxide mask. Even when it was decided to limit height of the PBG rods to 500 um, the PBG structure suffered from significant undercuts which resulted in poor performance and additional losses. The gold-plating and bonding processes also proved to be successful. We have learned however that at higher frequencies, in particular at the frequencies around 250 GHz, which are important for detection of methyl chloride and other chemicals, the third step of the fabrication process will be successful due to smaller dimensions of the structure. The results of this work were reported at the 33th International Conference on Infrared, Millimeter, and Terahertz Waves Pasadena, CA [11].

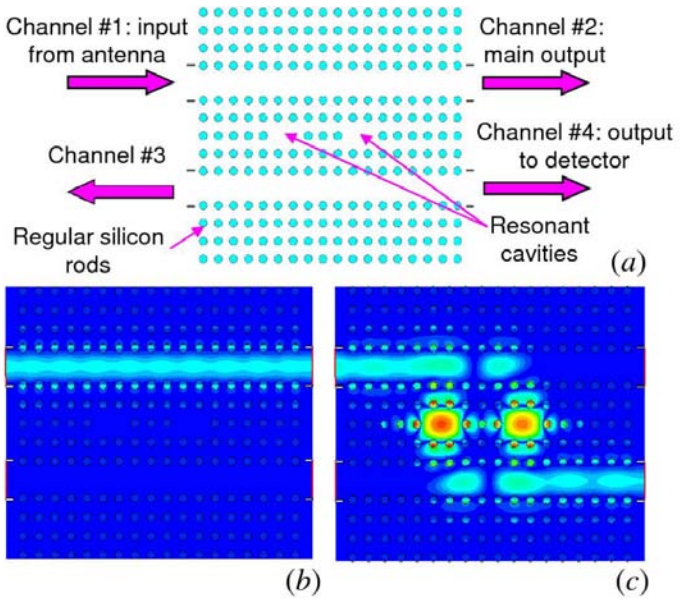

Figure 1. Schematic of a channel-drop filter (a). Electric field energy density for non-resonant frequency (b) and for the resonant frequency (c). Power transmits straight into channel 2 for all frequencies, except for the resonance, when it transmits into channel 4 through the resonant cavities.

Based on the outcome of the first year, the second year progressed as follows. The laboratory equipment was upgraded with the new testing heads that would allow us to conduct mm-wave measurements in the 220-325 GHz frequency range. The CDF was re-designed to operate at the frequency of 235 GHz (Figure 1). The fabrication procedure was re-evaluated and the fabrication of the higher frequency filter was started. New high-resistivity silicon wafers were purchased with the resistivity of 5000 Ohm*cm, which is 50 times higher than in the first year. This should significantly decrease Ohmic losses in the structure. New mask designs were developed to reduce the undercuts during the etching process. These new designs incorporated retaining walls of different shapes that were supposed to confine plasma and make undercuts smaller. The results of the etching were perfect with the undercuts less than 1.5 degrees. The undercuts were the smallest for the designs with retaining walls. The structures were successfully diced from the wafers and bonded to gold plates on top and bottom and cleaned. The detailed fabrication process

was thoroughly documented. Several of the produced devices (Figure 2) were tested in the mm-wave laboratory. All samples produced similar results. Measured transmission characteristics were in excellent agreement with computations. In our best sample, we have observed the frequency of 240 GHz being transmitted into the sampling channel with a linewidth of approximately 1 GHz and transmission of more than 20 dB above the background (Figure 3). The results of this work were reported at the 34th International Conference on Infrared, Millimeter, and Terahertz Waves in Busan, Korea [12], and later at the Progress in Electromagnetics Research Symposium PIERS 2010 in Cambridge, MA, **a**nd a paper was submitted and accepted for publication in the Review of Scientific Instruments [13]. We also submitted a patent application to the LANL IDEAS system.

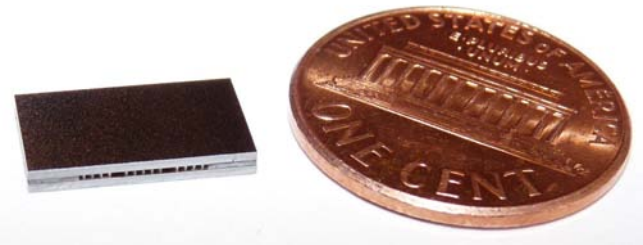

Figure 2. Photograph of the 240 GHz silicon channel-drop filter and scale.

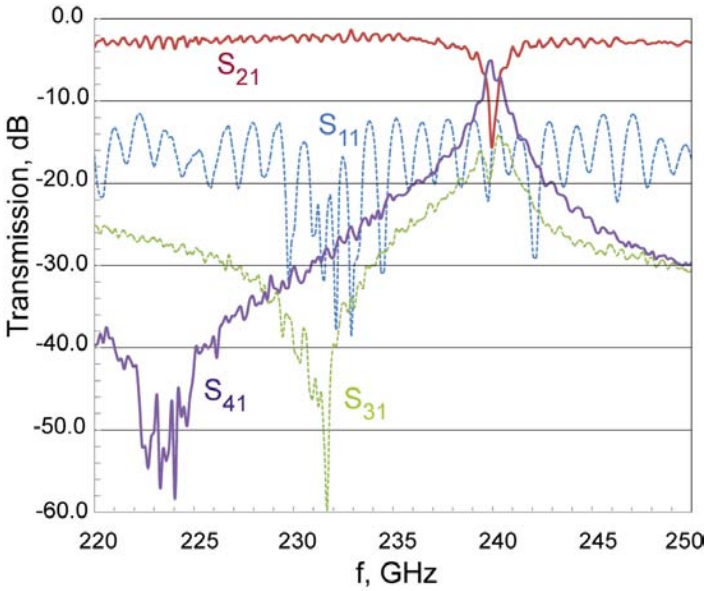

Figure 3. Measured transmission through the single-channel silicon channel-drop filter. Resonant frequency is 240 GHz.

In the second experiment, we have redesigned the W-band CDF to be fabricated with metal rods. We employed the conventional machine shop to fabricate the metal filter. However, it was predicted, that the standard machining tolerance would be insufficient for the proper operation of the filter, and therefore some tuning would be required in the experiment. The metal filter was tested in the laboratory and tuning was performed. At the frequency of 106 GHz a strong peak in transmission was observed, which perfectly agreed with the design. However, the design was not mechanically robust due to metal rods sliding in an out of the filter. To solve the problem, we decided to manufacture the metal filter in a different way. The filter was electroformed as a single copper crystal with no separate parts (Figure 4). Two devises were fabricated and tested in the mm-wave laboratory. The test results from the first sample were in perfect agreement with the design. The frequency of 108.5 GHz was filtered into the test channel with a linewidth of approximately 0.3 GHz and transmission of more than 30 dB above the background. The second sample did not operate properly from start and required tuning. We came up with a tuning idea which included some chemical etching of copper rods. The results of this work were reported at the 34th International Conference on Infrared, Millimeter, and Terahertz Waves in Busan, Korea [12], and later at the Progress in Electromagnetics Research Symposium PIERS 2010 in Cambridge, MA, **a**nd a paper was prepared for submission to the Progress in Electromagnetics Research Journal [14].

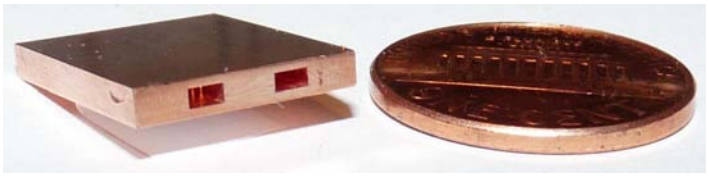

Figure 4. Photograph of the copper 108 GHz channel-drop filter and scale.

Based on the outcome of the second year, the third year progressed as follows. A three-channel CDF was designed with the channels at near 240 GHz, 260 GHz, and 280 GHz. The frequencies of the channels approximately corresponded to the spectral lines of the methyl chloride. The fabrication procedure was re-evaluated once again. High-resistivity silicon wafers with the resistivity of 5000 Ohm*cm were purchased. New mask designs were developed. The three-channel structure was designed with a denser array of posts than the second year structure, which reduced the likelihood of significant undercuts. Therefore the structure of the retaining walls was designed with smaller elements that were supposedly easier to remove. The results of the etching were perfect with the undercuts of about 2 degrees in the samples with no retaining walls, and with undercuts less than 1.5 degrees for the designs with retaining walls. It turned out however, that the retaining walls consisting of small elements were tricky to remove and the remnants of the sacrificial walls tended to get stuck in between the posts of the structure. Therefore, the structures with no retaining walls became our best candidates for the subsequent bonding step and testing. The bonding step was also more complicated than in the second year, since the bigger structure required more precise alignment procedure. So far, two samples were successfully bonded (Figure 5). However, during the labo-

ratory tests none of the two samples performed perfect. One sample demonstrated excessive loss due to an internal crack. And the second sample could not demonstrate 100 per cent transmission into the test channels due to the fragments of the retaining walls being stuck inside of the micro-cavities. The third sample is on the way and will be tested after the end of FY10. In summary, the design and fabrication procedure for the three channel device were generally developed. However, some minor details of fabrication are still to be worked out.

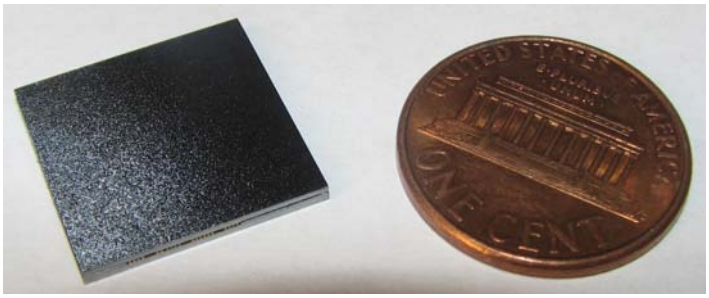

Figure 5. Photograph of the three-channel channel-drop filter and scale.

Impact on National Missions

This project, through the development of a new mm-wave spectrometer, will impact a broad range of technical problems including imaging, sensing, and communication. These technical areas are crucial for supporting threat reduction, nuclear material detection, and other missions important to DOE (NN), DHS (DNDO), DOD(DARPA) and other government agencies.

References

1. Gopalsami, N., S. Bakhtiari, A. C. Raptis, S. L. Dieckman, and F. C. DeLucia. Millimeter-wave measurements of molecular spectra with application. 1996. *IEEE Transactions on Instrumentation and Measurement.* **45** (1): 225.

2. Gopalsami, N., and A. C. Raptis. Millimeter-wave radar sensing of airborne chemicals. 2001. *IEEE Transactions on Microwave Theory and Techniques.* **49** (4): 646.

3. Lazareff, B.. Instrumentation for heterodyne mm-wave astronomy. 2009. In *Instrumentation for heterodyne mm-wave astronomy.* Vol. 37, p. 37.

4. Bradford, C. M., G. J. Stacey, M. R. Swain, T. Nikola, A. D. Bolatto, J. M. Jackson, M. L. Savage, J. A. Davidson, and P. A. Ade. SPIFI: a direct-detection imaging spectrometer for submillimeter. 2002. *Applied Optics.* **41** (13): 2561.

5. Chamberlain, M.. Applied Terahertz Science: The Technology of the Future, and Always Will Be?. 2007. In *Terahertz Frequency Detection and Identification of Materials and Objects.* , p. 1. Netherlands: Springer.

6. Christopher, P.. Mid millimeter waves for broadband satellite communication 72-100 GHz. 2008. In *2008 Wireless Telecomunications Symposium (WTS '08) ; 24-26 April 2008 ; Pomona, CA, USA.* , p. 188.

7. Yablonovitch, E., T. J. Gmitter, and K. M. Leung. Photonic band structure: the face-centered-cubic case employing. 1991. *Physical Review Letters.* **67** (17): 2295.

8. Fan, S. H., P. R. Villeneuve, and J. D. Joannopoulos. Channel drop tunneling through localized states. 1998. *PHYSICAL REVIEW LETTERS.* **80** (5): 960.

9. Lin, Shawn-Yu, V. M. Hietala, Li Wang, and E. D. Jones. Highly dispersive photonic band-gap prism. 1996. *Optics Letters.* **21** (21): 1771.

10. Maystre, D.. Photonic crystal diffraction gratings. 2001. *Optics Express.* **8** (3).

11. Smirnova, E. I., L. M. Earley, C. E. Heath, and D. Yu. Shchegolkov. Design and fabrication of a 100 GHz channel-drop filter. 2008. (Pasadena, CA, 15-19 Sept. 2008). p. 1175. Online: IEEE.

12. Shchegolkov, D. Yu, L. M. Earley, C. E. Heath, and E. I. Smirnova. Design and testing of photonic band gap channel-drop-filters. 2009. (Busan, Korea, 21-25 September, 2009). p. 10.1109/ICIMW.2009.5324590. Online: IEEE.

13. Simakov, E. I., L. M. Earley, C. E. Heath, B. D. Schultz, and D. Yu. Shchegolkov. First experimental demonstration of a photonic band gap channel drop filter at 240 GHz. To appear in *Review of Scientific Instruments.*

14. Shchegolkov, D. Yu., C. E. Heath, and E. I Simakov. Low Loss Metal Photonic Band Gap Channel Drop Filter at 109 GHz. *Progress in Electromagnetics Research.*

Publications

Shchegolkov, D. Yu, L. M. Earley, C. E. Heath, and E. I. Smirnova. Design and testing of photonic band gap channel-drop-filters. 2009. In *The 34th International Conference on Infrared, Millimeter and Terahertz Waves.* (Busan, Korea, 21-25 September, 2009). , p. 10.1109/ICIMW.2009.5324590. Online: IEEE.

Shchegolkov, D. Yu., C. E. Heath, and E. I Simakov. Low Loss Metal Photonic Band Gap Channel Drop Filter at 109 GHz. *Progress in Electromagnetics Research.*

Simakov, E. I., L. M. Earley, C. E. Heath, B. D. Schultz, and D. Yu. Shchegolkov. First experimental demonstration of a photonic band gap channel drop filter at 240 GHz. To appear in *Review of Scientific Instruments.*

Smirnova, E. I., L. M. Earley, C. E. Heath, and D. Yu. Shchegolkov. Design and fabrication of a 100 GHz chan-

nel-drop filter. 2008. In *33rd International Conference on Infrared, Millimeter, and Terahertz Waves.* (Pasadena, CA, 15-19 Sept. 2008). , p. 1175. Online: IEEE.

Novel High Performance Terahertz Metamaterial Photonic Devices

John F. O'Hara
20080414ER

Abstract

The control of electromagnetic (EM) waves influences nearly every aspect of our lives, from cell phone communications to simple photography. Technological advances have made it possible to control EM waves of nearly every type from radio waves to x-rays. There is one notable exception: terahertz (THz) waves. Our project was to use a new type of engineered material to dramatically improve the control of THz waves; these are called metamaterials. We combine natural materials (e.g. metals, insulators, and semiconductors) to create metamaterials that are specifically tuned for THz control. Our main success in this project was to create materials that can be actively tuned, something available in few natural materials. The result was unprecedented levels of functional versatility, leading to new THz devices whose performance far exceeded the state-of-the-art. This has positively impacted the LANL mission by creating new metamaterial capabilities. It has since led to external funding in both fundamental and practical arenas.

Background and Research Objectives

Terahertz science has been pursued heavily since the early 1990's in an effort to make THz waves practical. Still, devices suitable for controlling THz waves simply do not exist and THz technology has thus failed to graduate into real-world usability. Despite this, THz science remains an important pursuit because there are many promising THz applications including: identification of chemical and biological agents, THz imaging inside of closed packages, high-speed communications, and even environmental monitoring. The problem has always been that natural materials are well suited to control almost all electromagnetic waves except THz. This underpinned the motivation of our work. Can we create engineered materials that enable THz technology to advance into real-world practicality? Our work in metamaterials seemed to be the perfect match. Our objective was to use metamaterials concepts to create new devices that controlled THz waves in a much more versatile and practical fashion. In this way we intended to advance THz technology well beyond the state-of-the-art.

The predominant focus of our work was creating THz modulators. These are devices that alter characteristics of the THz waves such as intensity or polarization. Modulators are key elements in almost all EM technologies, but were terribly immature in the THz spectrum. For example, THz modulators often performed prohibitively poorly or required cryogenic cooling to operate, clearly unsuitable for real-world use.

Modulators come in many forms and we investigated both electronic and photonic versions. In almost all cases we studied metamaterials that were a combination of semiconductors and resonator arrays. Figure 1 shows one such device. Without going into technical detail, the resonators are the heart of metamaterial operation. They are engineered to make metamaterials do what natural materials cannot. When we combine these resonators with semiconductors, we change the properties of the resonators in real time, thereby changing the overall metamaterial properties also. This is very useful as a technological tool. As an example, we can cause the metamaterial to go from transparent to opaque. This is analogous to actively changing the shading of sunglasses! In this way we can modulate the intensity of THz waves by passing them through our metamaterial.

Our objective was met with great success and we were able to design a number of different THz modulators with performance far exceeding the state-of-the-art. These will be described in the Accomplishments section.

Scientific Approach and Accomplishments

Our approach to this work was partially described in the previous section. In more detail, we aimed to create hybrid metamaterials that are a combination of semiconductors and resonator arrays. Why would we do this? The answer is to add functionality. Metamaterials are typically created by designing resonators for a particular function. For example, we may desire that the metamaterial reflect waves at 1 THz, but transmit them at 2 THz. This function is usually unchangeable; it is built into the original design. Resonator arrays are simply small metallic patterns on some insulating substrate (usually slightly simpler than those shown in Figure 1). Their shape and

size determines how they will affect the THz waves passing through them. One cannot alter their size and shape after they are fabricated, therefore one can neither alter their response.

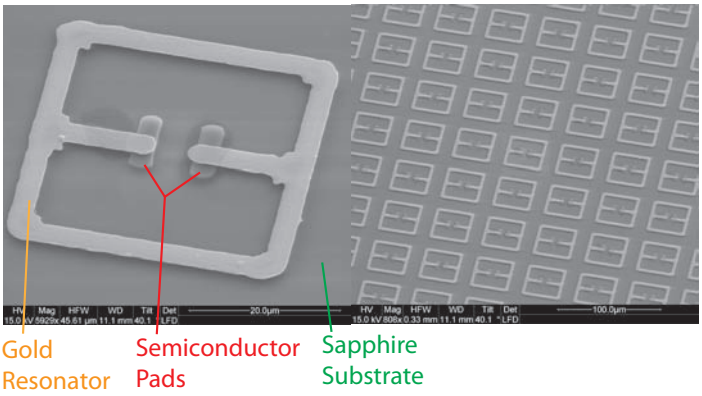

Figure 1. Electron microscope pictures of our dynamic terahertz metamaterial. The right panel shows the array of resonators that, as a whole, make up the metamaterial. The left panel shows a detailed picture of one resonator.

We devised a way around this hurdle. We engineered the resonator array for a particular function, but then changed the substrate underneath it. The function of a resonator array is very sensitive to the properties of substrate. Therefore when we change the substrate, we change the overall metamaterial response. For example, this may cause a metamaterial to pass waves at 1 THz instead of reflecting them. The metamaterial becomes more like clear glass and less like a mirror. What is particularly appealing about this approach is that it is possible to dynamically (or real-time) change the substrate properties by choosing the proper substrate. Semiconductors are one such substrate. By creating hybrid metamaterials comprised of resonators arrays on semiconductors, we can dynamically alter the semiconductor, and thereby dynamically alter the entire metamaterial function. This is the very basis of modulation.

There are a couple of ways to change semiconductor properties. In the photonic approach, laser pulses can illuminate a semiconductor making it then behave like a sheet of metal. This effectively "shorts out" metamaterial resonator arrays. When shorted, their response to THz waves changes drastically. In the electric approach, electronic signals can be used to remove electric charge within a semiconductor, making it behave like an insulator. This dynamically removes the "shorting" effect, having an opposite effect as the laser. In either case, we use external signals to dynamically tune the overall metamaterial response by changing the properties of the semiconductor.

Our accomplishments with this approach have been substantial. In summary, we have demonstrated high-performance, room-temperature THz amplitude and phase modulators, frequency-modulators, polarization control schemes, and thin lenses. Each of these will now be described in greater detail.

We first describe our intensity and phase modulators. Our metamaterial devices modulate the intensity of THz waves by as much as 75% and at speeds of up to 2 MHz [1]. Put in other words, the THz wave intensity can be altered via the modulator at a rate of about once every 0.5 nanoseconds. These devices also operate at room temperature. The previous state-of-the-art at room temperature provided THz modulation on the order of 3%, thus severely limiting its utility. We have further developed smaller metamaterials that may be integrated directly onto THz antennas. Because of their smaller size, these modulators should be able to operate at near gigahertz speeds, sufficiently fast to support high-speed data communication. We are currently writing a paper on the measured results of one such device. This device has also drawn external interest via its ability to be conveniently incorporated into a compact THz spectrometer or THz wireless communication device. This is a substantial improvement over other technologies such as optical choppers, which are limited to kilohertz speeds. In the same vein, we have shown that these modulators can operate over a wide spectral range, despite the fact that metamaterials are typically engineered for a single frequency. This fortunate but unexpected result leverages the fact that metamaterials modulate both phase and amplitude simultaneously, but at complementary frequencies. Using this phenomenon, we have demonstrated broadband THz modulation. This work was published in Nature Photonics [2].

We have also successfully demonstrated a metamaterial that allows THz waves to be frequency modulated. Frequency modulation is the basis of numerous technologies including FM radio, modern radar, and digital communication links. Though it is a core concept in modern technology, it has not been demonstrated at THz frequencies. In our work, we used metamaterials whose response was tunable by illumiation with laser light. By illuminating semiconductor pads within our metamaterial (shown in Figure 1), we caused its response to shift in frequency, thereby changing the "color" of the THz waves passing through it. In this work, one can regard the semiconductor pads in the metamaterial like weights added to a clock's pendulum. When weight is added the pendulum swings more slowly, or equivalently its resonance frequency shifts. Similarly, when we illuminate the pads in our metamaterial, its resonance shifts, thus changing the frequency response. These results were also published in Nature Photonics [3]. We are currently working with the Tech Transfer office of LANL to patent this result. Since no other technology has shown such a simple and effective way to frequency modulate THz waves, we believe this could spawn substantial commercial interest.

During our research we studied a method to control THz polarization. Control of the polarization of electromagnet-

ic waves is highly important in modern technology. Global Positioning System receivers, for example, require circularly polarized signals to function properly. This removes any sensitivity the receiver might have to its orientation. Very little work had ever been done to control the polarization of THz waves when we began this work. And the existing research resulted in technology that was difficult to implement. We devised a new type of metamaterial that allowed us to tune the polarization state of THz waves. Figure 2 shows the resonator design behind this work. Because of the asymmetry of the resonator, the overall metamaterial responds differently to horizontally and vertically polarized THz waves. One of the polarizations travels more slowly through the sample and lags behind the other polarization. This lag is the basis of waveplates, which change linearly polarized waves into circularly polarized waves. We recognized this fact and showed that this resonator design may be used to create THz waveplates. The result was a very simple yet effective waveplate design that also had the added feature of being extremely thin and lightweight. In fact, it was orders of magnitude thinner than conventional waveplate designs. This is a tremendous asset in space-based technology where weight is a crucial performance spec. While our demonstration was at THz frequencies, the concept is scalable to almost any other frequency. This work was published in Optics Express [4].

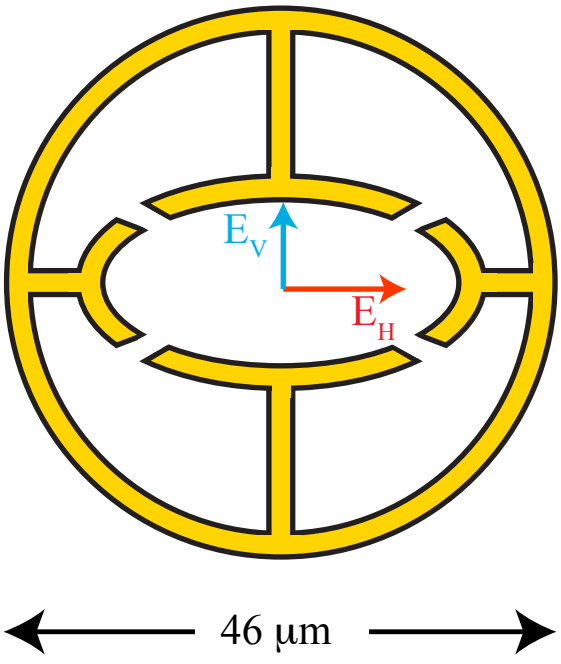

Figure 2. Gold resonator design for polarization controlling terahertz metamaterial. This design causes differently polarized terahertz waves (red arrow versus blue arrow) to travel at different speeds through the metamaterial.

Finally, we studied how our dynamic metamaterials might be used to create THz lenses. Traditional lenses are dielectric slabs that are curved on one or both sides. The thickness variation across the lens enables focusing and imaging. We recognized that our metamaterials can do the same thing, but in a much more compact package. Metamaterial lenses may also be "reflectionless" producing no glare effects that we are accustomed to on glass lenses. This is particularly important for THz technology since most materials used for THz lenses have a high index of refraction, thus producing high glare. We determined that THz lenses can be made ultra-thin, like our waveplate. And, using our hybrid semiconductor designs, these lenses can have dynamic focal lengths. This is akin to creating eyeglasses that are paper thin, completely invisible (no glare), and change their prescription with the flick of a switch! The experimental realization of these lenses is difficult, so only preliminary data has been acquired. However, the concept has drawn interest from external agencies which have invested ~$400k for our team to develop this further.

These research results have boosted our team to worldwide leadership in THz and dynamic metamaterials. We expect that this type of research can continue to produce high-impact results, which support both Laboratory and national missions. Indeed our work thus far has led to numerous new research directions. One specific example was the creation of an ultrafast THz modulator based on surface plasmon polaritons. This concept can be considered a cousin to our metamaterial modulators. Instead of using metamaterial resonators, we modulated THz waves by the control of surface plasmon formation. This work, an offshoot of our project, was published in Applied Physics Letters [5]. Finally, this work has created a solid theoretical foundation by which engineering of metamaterials can be made more efficient. These more theoretical results were published in the journal Metamaterials [6] and the European Physical Journal D [7].

Impact on National Missions

This project has had numerous impacts on the Laboratory and national missions. First, it enhances our fundamental understanding of materials, particularly engineered materials. As such, it has built a capability within LANL for understanding the limitations and applications of metamaterials. Again, this is most relevant in the THz frequency region, where natural materials have proven less than ideal. This capability is both fundamental and practical. On the practical side, this is proven by external funding given to us for the development of a metamaterial gradient index lens. More fundamentally, we were funded ($975k) with LANL theoretical division to study how metamaterials might tune the Casimir force. These funding streams have enabled us to convert one of our former postdocs (Abul Azad) into a staff position. Second, the work has generally drawn the interest of several government agencies including DOD, DOE, and DHS, who are interested in technologies supporting ubiquitous sensing and threat reduction. We continue to pursue such external opportunities based on the results of this project. Third, based in part on this project, our group has become a worldwide metamaterial leader in dynamic and THz metamaterials. This has opened the door

to fruitful collaborations and commercialization opportunities, which we have pursued through patent applications.

References

1. Chen, H., S. Palit, T. Tyler, C. Bingham, J. O. Zide, J. O'Hara, D. Smith, A. Gossard, R. Averitt, W. Padilla, N. Jokerst, and A. Taylor. Hybrid metamaterials enable fast electrical modulation of freely propagating terahertz waves. 2008. *APPLIED PHYSICS LETTERS.* **93** (9): 091117.

2. Chen, H. T., W. J. Padilla, M. J. Cich, A. K. Azad, R. D. Averitt, and A. J. Taylor. A Metamaterial Solid-State Terahertz Phase Modulator. 2009. *Nature Photonics.* **3**: 148.

3. Chen, H., J. O'Hara, A. Azad, A. Taylor, R. Averitt, D. Shrekenhamer, and W. Padilla. Experimental demonstration of frequency-agile terahertz metamaterials. 2008. *NATURE PHOTONICS.* **2** (5): 295.

4. Peralta, X. G., E. I. Smirnova, A. K. Azad, H. T. Chen, A. J. Taylor, I. Brener, and J. F. O'Hara. Metamaterials for THz Polarimetric Devices. 2009. *Optics Express.* **17** (2): 773.

5. Azad, A. K., H. T. Chen, S. R. Kasarla, A. J. Taylor, Z. Tian, X. Lu, W. Zhang, H. Lu, A. C. Gossard, and J. F. O'Hara. Ultrafast Optical Control of Terahertz Surface Plasmons in Subwavelength Hole Arrays at Room Temperature. 2009. *Applied Physics Letters.* **95**: 011105.

6. Holloway, C. L., A. Dienstfrey, E. F. Kuester, J. F. O'Hara, A. K. Azad, and A. J. Taylor. A discussion on the interpretation and characterization of metafilms/metasurfaces: the two-dimensional equivalent of metamaterials. 2009. *Metamaterials.* **3**: 100.

7. O'Hara, J., A. K. Azad, and A. J. Taylor. A method to determine effective metamaterial properties based on stratified metafilms. 2010. *The European Physical Journal D.* **58** (2): 243.

Publications

Azad, A. K., H. T. Chen, S. R. Kasarla, A. J. Taylor, Z. Tian, X. Lu, W. Zhang, H. Lu, A. C. Gossard, and J. F. O'Hara. Ultrafast Optical Control of Terahertz Surface Plasmons in Subwavelength Hole Arrays at Room Temperature. 2009. *Applied Physics Letters.* **95**: 011105.

Azad, A. K., Z. Tian, H. T. Chen, X. Lu, S. R. Kasarla, W. Zhang, A. J. Taylor, and J. F. O'Hara. Ultrafast Optical Control of Terahertz Surface Plasmon Polariton in Subwavelength Hole-Arrays at Room Temperature. 2009. In *Conference on Lasers and Electro-Optics.* (Baltimore, May 31 - June 5, 2009). , p. CWG4. New Jersey: Piscataway.

Azad, A., H. Chen, E. Akhadov, N. Weisse-Bernstein, A. Taylor, and J. O'Hara. Multi-layer planar terahertz electric metamaterials on flexible substrates. 2008. In *Conference on Quantum Electronics and Laser Science Conference on Lasers and Electro-Optics, CLEO/QELS 2008 ; May 4-9 2008 ; San Jose, CA, United States.*

Chan, W. L., H. T. Chen, A. J. Taylor, I. Brener, M. J. Cich, and D. Mittleman. A Spatial Light Modulator For Terahertz Beams. 2009. *Applied Physics Letters.* **94**: 213511.

Chen, H. T., W. J. Padilla, M. J. Cich, A. K. Azad, R. D. Averitt, and A. J. Taylor. A Metamaterial Solid-State Terahertz Phase Modulator. 2009. *Nature Photonics.* **3**: 148.

Chen, H. T., W. J. Padilla, M. J. Cich, A. K. Azad, R. D. Averitt, and A. J. Taylor. A Broadband Terahertz Metamaterial Electrical Modulator. 2009. In *Conference on Lasers and Electro-Optics (CLEO).* (Baltimore, May 31-June 5, 2009). , p. CThX1. New Jersey: Piscataway.

Chen, H., A. Azad, D. Shrekenhamer, W. Padilla, R. Averitt, A. Taylor, and J. O'Hara. Frequency tunable terahertz metamaterials. 2008. In *Conference on and Quantum Electronics and Laser Science Conference Lasers and Electro-Optics, QELS 2008 ; May 4-9 2008 ; San Jose, CA, United States.*

Chen, H., J. O'Hara, A. Azad, A. Taylor, R. Averitt, D. Shrekenhamer, and W. Padilla. Experimental demonstration of frequency-agile terahertz metamaterials. 2008. *NATURE PHOTONICS.* **2** (5): 295.

Chen, H., S. Palit, T. Tyler, C. Bingham, J. O. Zide, J. O'Hara, D. Smith, A. Gossard, R. Averitt, W. Padilla, N. Jokerst, and A. Taylor. Hybrid metamaterials enable fast electrical modulation of freely propagating terahertz waves. 2008. *APPLIED PHYSICS LETTERS.* **93** (9): 091117.

Holloway, C. L., A. Dienstfrey, E. F. Kuester, J. F. O'Hara, A. K. Azad, and A. J. Taylor. A discussion on the interpretation and characterization of metafilms/metasurfaces: the two-dimensional equivalent of metamaterials. 2009. *Metamaterials.* **3**: 100.

O'Hara, J., A. K. Azad, and A. J. Taylor. A method to determine effective metamaterial properties based on stratified metafilms. 2010. *The European Physical Journal D.* **58**: 243.

O'Hara, J., E. Smirnova, A. Azad, H. Chen, and A. Taylor. A circuit model for terahertz metafilms and effective medium implications. 2008. In *Conference on Quantum Electronics and Laser Science Conference on Lasers and Electro-Optics, CLEO/QELS 2008 ; May 4-9 2008 ; San Jose, CA, United States.*

Padilla, W. J., Hou-Tong Chen, J. F. O'Hara, A. J. Taylor, and R. D. Averitt. Opto-electronic control of terahertz metamaterials. 2007. In *Photonics: Design, Technology,*

and Packaging III ; 5 Dec. (2007 ; Canberra, ACT, Australia). Vol. 6801, p. 68010H.

Peralta, X. G., E. I. Smirnova, A. K. Azad, H. T. Chen, A. J. Taylor, I. Brener, and J. F. O'Hara. Metamaterials for THz Polarimetric Devices. 2009. *Optics Express.* **17** (2): 773.

Peralta, X. G., I. Brener, A. K. Azad, H. T. Chen, E. Smirnova, A. J. Taylor, and J. F. O'Hara. THz Polarimetric Components Based on Metamaterials. 2009. In *Conference on Lasers and Electro-Optics (CLEO).* (Baltimore, May 31 - June 5, 2009). , p. CThFF. New Jersey: Piscataway.

Enhanced Battery Performance

Anthony K. Burrell
20100525ER

Abstract
The technical challenges of electrical energy storage cross multiple length scales from nanometers, for the electrode-electrolyte interface, to microns for the electrolyte and claddings. In addition the breath of potential applications for electrical energy storage require multiple engineering solutions. At LANL we have experience in chemical storage (very high energy density) and capacitors (low energy density). However, in the area of batteries LANL has no current track record. Over the next few years the development of battery technologies will be critical to many storage technologies. In the last year we have developed research collaborations with the battery group at Argonne National Lab. This group is the premier battery research group in the United States. At LANL we have several capabilities which can interface well with the ANL group and develop a collaboration that will enable LANL to establish a foundation in battery research.

Background and Research Objectives
The goal of reducing the US dependence on foreign sources of energy requires the development and deployment of many different sources of energy. In recent years the growth of alternative electrical generation from wind and solar has highlighted a significant problem with these sources of electrical energy, they are by their very nature intermittent. In reality while solar and wind are high profile alternative energy resources their intermittent nature effectively eliminates them as major players in electrical energy generation. The most often quoted solution to the implementation of alternative electrical generation is the "Smart Grid" which will enable rapid national shifts in electrical supply and demand. The complex legislative tangle associated with building a new grid across the entire country, dealing with every county and landowner along the way, is nothing compared to the cost. The American Society of Civil Engineers estimates that total needed investment in electric utilities could be as much as $1.5 trillion to $2 trillion by 2030. That would include money for energy generation (wind farms, solar farms, etc.) and all of the power lines to move the energy.

Batteries are chemical energy storage devices with electrochemical processes acting between cathodes, electrolytes, and anodes. Better understanding of their interrelated chemical and physical properties and charge-discharge cycles are critically important in making breakthroughs for future energy storage materials. The key energy storage parameters include capacity, power, charge-discharge rates, and lifetimes; whereas safety, economical, and environmental issues are further concerns. We focus on synthetic control of material architectures to achieve super-ionic transport and capacity, thus to effectively increase power density and energy density. We proposed to develop research collaborations with ANL in the area of battery research to strengthen our fledgling energy storage efforts here at LANL.

Scientific Approach and Accomplishments
The funding was split in two different applications in a effort to develop a working relationship with ANL. These were neutron studies and battery materials development.

Neutron diffraction electrochemical cell

We prepared a designed neutron diffraction electrochemical cell that can "monitor" complex compositional and structural changes *in-situ* during ion insertion and removal in *real-time* experiments using actual battery components. Neutron diffraction is an ideal tool to study lithium-ion battery and fuel cell, in particular, to locate lithium and/or hydrogen positions. It has made great contributions in determination of Li diffusion pathway in $LiFePO_4$, and rationalized the 15-20% capacity loss during the first charge-discharge cycle. Knowledge of the diffusion pathway allows us to fine-tune the fast ionic channels by systematic cation substitution in the crystal structure and/or field-induced texture in bulk material in order to optimize the diffusion rates. The team at ANL is particularly interested in neutron studies to complement their x-ray studies and collaborations based upon electrolyte development and the chelation of lithium in cathode materials are developing.

Battery materials

The electrolyte transfer of ions and electrons between electrodes during charge and discharge cycles should provide high conductivity over a broad temperature range and be electrochemically inert at the electrodes. The active electrode nano-materials should enable us to achieve high discharge rates (>100C) about two orders of magnitude higher than the *state-of-the-art* electrode materials used in today's lithium-ion batteries. We proposed that the super-ionic conductivity during structural phase transition, observed in $NaMgF_3$ perovskite, should work for lithium containing $Li(M)F_3$ perovskites and inversed (M) LiF_3 perovskites. In particular this should be structurally tuned close to T_c. In particular the electrically-inversed $A^-B^{2-}X^+_3$ anti-perovskites, e.g. $BrOLi_3$ and $(Br,I)OLi_3$, can be used to both supply the Li^+ with incorporation of the I^- supply the high probability of thermal vacancies during phase transition and/or melting. This material should act as a super-ionic conductor. During the course of this research project we prepared $BrOLi_3$ using the literature method and examined the Li ion conductivity. Theory indicated that two avenues were available to increase ion conductivity in this system. Firstly, substitution of the bromide for iodide would place strain on the lattice and therefore improve lithium ion mobility. Secondly, substitution of a small amount of the lithium ions by magnesium ions will cause site vacancies in the cationic lattice, due to Mg^{2+} ion and charge neutrality. Both sets of materials were prepared and the ion conductivities were determined. The introduction of lithium ion vacancies appears to have the most promise in the current materials. This work has lead to the successful development of the Fy-11 LDRD ER project Novel Anti-Perovskite Electrolytes for Superionic Lithium Transport.

In addition we have prepared epitaxial examples of the $Li_2MTi_6O_{14}$ (M =Sr, Ba) materials. These materials were fully characterized using x-ray diffraction and lithium loading was determined. These materials need to be prepared using conductive substrates so we can examine the lattice strain under dynamic lithium loading. The bulk materials were prepared using the same solution precursors and these materials have excellent surface area and conductivity work with these materials will continue with ANL.

Impact on National Missions

This research strongly supports the LDRD Energy & Earth Systems Grand Challenge "*to develop transformative new energy technologies*", and we believe will lead to a strong connection to the LDRD Materials Grand Challenge of "*controlled functionality through discovery and application of fundamental materials properties*". It will allow LANL to build the alliances necessary to contribute to the large research programs lead by ANL and other recognized energy storage leaders.

THz Generation, Detection, and Control using Superconducting Josephson Junctions

Nathan A. Moody
20100538ER

Abstract
This project focused on an initial, critical-path step toward developing a tunable source of continuous electromagnetic radiation in the THz range using intrinsic Josephson Junctions (IJJs), sub-micron structures made of high-temperature superconductors (HTS). The initial step targeted in this project consists of growing HTS crystals with a usable orientation. Utilizing these materials for THz emission relies on the AC Josephson effect: a dc voltage applied across two superconductors separated by a thin insulating region causes radio-frequency current oscillations across the junction. A separate project has shown that with proper selection of junction geometry, current oscillations in these devices can be radiated out to free space. The frequency of the oscillation is determined by the applied voltage, with a known relationship of 483.59 GHz/mV, suggesting the possibility of a tunable source of THz radiation. Making a practically useful source of radiation requires pumping current through the HTS ceramic material in a particular direction, relative to the crystalline planes. This required orientation is difficult and has only been tangentially addressed in the literature. This project made initial steps toward the required growth of the HTS crystals from basic precursors.

Background and Research Objectives
Sandwiched between the optical infrared and microwave regions of the electromagnetic spectrum, the THz band (from 0.3-10 THz) has received considerable attention over the past decade as practical applications of these wavelengths have emerged. These include imaging for security and safety, high bandwidth communications systems and chemical detection and analysis [1]. Much of the potential for THz science has gone unrealized to date because of the lack of components, most importantly sources and detectors that function at THz frequencies. By investigating a fundamental material synthesis problem, namely oriented growth of the bismuth-based high temperature superconductor (termed BSCCO), this project supports the larger quest for THz sources and sensitive detectors [2-4] in support of crucial national security missions.

Our research objectives in this LDRD reserve effort consisted of: 1.) identifying the most promising fabrication techniques (MOCVD and PLD), 2.) growing BSCCO crystals from the precursor materials using both methods in parallel, and 3.) performing limited characterization studies (as allowed by budget) to determine crystalline orientation.

Scientific Approach and Accomplishments
Previous work [2, 3, 5-7] has shown that utilization of the intrinsic Josephson junction property of high temperature ceramic superconductors is best accomplished using a material called BiSrCaCuO (2212), or simply 'BSCCO.' Furthermore, the ability to create and out-couple THz oscillations requires a specific crystal orientation with respect to the substrate that enables electrical current to flow in the desired direction [6]. Typical growth techniques of BSCCO yield a crystalline orientation termed *c*-axis orientation, meaning the longest axis of the unit cell is perpendicular to the substrate plane [8]. Our work requires that the longest axis of the unit cell be *parallel* to the substrate plane, a challenge that has not yet been resolved in the literature. This type of growth, termed *a*-axis oriented growth is what this project seeks to demonstrate. There are two general approaches that can be pursued: Pulsed Laser Deposition (PLD) and metal-oxide chemical vapor deposition (MOCVD). Because crystal growth is a critical step in future IJJ-based THz source work, we pursued initial demonstrations using both methods in parallel. Results from each approach are reported below.

Laser Molecular Beam Epitaxy and Pulsed Laser Deposition (PLD)

There are no reports for the growth of *a*-axis BSCCO films by pulsed laser deposition in the literature, so use of this method is truly novel. We selected a substrate that assists in the preferred crystalline growth, called SrTiO_3-110, since its lattice constants closely match that of *a*-axis oriented BSCCO well.

Pulsed laser deposition (PLD) is a growth technique where a laser beam with short and high energy pulses is focused on a target of desired composition. Material is then vaporized from the very top surface of the target and deposited as a film on a substrate. PLD is especially powerful for compounds such as high-temperature superconductors that are difficult to produce in film form by other deposition techniques. The main advantages of PLD are good stoichiometric preservation for multicomponent materials, operation in a wide range of atmosphere, versatile, cost-effective, and fast.

As part of this project, we have designed and setup a laser-molecular beam epitaxy (laser-MBE) system to grow BSCCO films based on the PLD process. **This was a critical deliverable that makes further progress toward IJJ devices at LANL possible.** This state-of-the-art system is particularly well suited for fabricating epitaxial complex oxide films. Laser-MBE combines the merits of PLD and MBE, and has advantages of a high energy density and wide oxygen pressure during film growth. In-situ monitoring by high-pressure reflection high energy electron diffraction enables real-time control of epitaxial growth, permitting atomically controlled lattices (required for this project).

We used this system to deposit BSCCO thin films on $SrTiO_3$-(110) substrates as well as a similar material MgO-(100). The PLD uses an excimer laser with energy of 250mJ per pulse and repetition rate of 5Hz. During film deposition, the oxygen pressure was maintained at 200 mTorr. Samples under different substrate temperatures were deposited (at 450, 600, 700, and 800 °C, respectively) in order to obtain *a*-axis BSCCO films. X-ray diffraction (XRD) analysis is a typical approach to determining orientation; Figure 1 shows the XRD results for the PLD approach. As can be seen from the XRD results, the films on MgO substrate are c-axis oriented as long as the deposition temperature is above 600 °C. The film is feature-less if the substrate temperature is reduced to 450 °C. This leads us to believe that PLD using MgO substrate is not a good path forward. On the other hand, the films on (110) $SrTiO_3$ show very different texture when different substrate temperature is used. Similar to the film on the (100) MgO substrate, c-axis oriented films are obtained when the substrate temperature is above 600 °C. However, 450 °C deposition leads to totally different texture: one peak near 30° is observed. As the position of (200) plane of bulk BSCCO should be around 33.04° (marked by blue dash line in both figures), the strain and other reasons can potentially lead to the peak shift. More detailed analysis will be required to confirm that this peak is really from *a*-axis BSCCO (highly strained film) or second phase material.

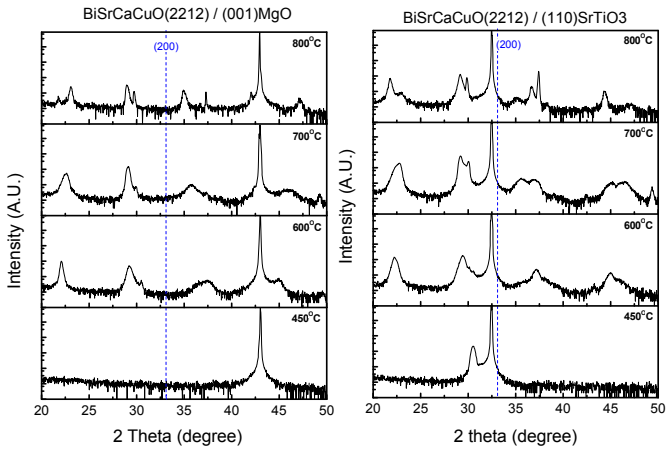

Figure 1. X-ray diffraction (XRD) analysis results for BSCCO samples grown using the pulsed laser deposition (PLD) process. Left: results for growth using MgO-(001) substrate, showing c-axis orientation. Right: results for growth using SrTiO3-(110) substrate. Note that for lower substrate temperature, a peak near 30 degrees appears which may indicate the desired a-axis orientation.

Chemical Vapor Deposition

There have been a few reports of the deposition of BSCCO films using CVD in an orientation other than c-axis [9, 10]. In general the films prefer the c-axis orientation when deposited by physical vapor deposition techniques. However conditions under which a-axis growth occurs may exist. The use of chemical vapor deposition techniques has clear advantages over PLD and other methods beyond just the higher deposition rates. The method also provides a wide range of operating conditions via the independent control of precursor delivery and substrate temperature. This also means it is a more complex process but does offer the potential for developing the desired orientation.

Beginning with the simultaneous arrival of Cu, Bi, Ca, and Sr species to the substrate, the nucleation of the c-axis orientation requires substantial rearrangement. This is affected by the species diffusion and nucleation rates. For the CVD process the diffusion rate is determined by the substrate temperature. The nucleation rate is determined by the degree of super saturation of gaseous species arriving at the surface. Thus, to preferentially nucleate and grow the a-axis orientation a high degree of super saturation (rapid nucleation) combined with low temperature to reduce surface diffusion is desirable. The CVD process is ideal for independently controlling reactant super saturation, reaction and diffusion rates.

We have built a MOCVD reactor specifically for BSCCO deposition demonstration. The reactor consists of a precursor

delivery system, reaction chamber and exhaust system. The precursor delivery contains individual sublimators, associated heaters, and mass flow controllers for carrier gases. The gaseous precursor concentration delivered into the reaction chamber is adjusted through the sublimator temperature along with carrier gas flow rate. In this way the partial pressure of each reactant can be varied. The independently controlled carrier gases are heated to the vaporization temperature and flow through their associated sublimators. On exiting the sublimator they enter a manifold held at or above the highest vaporization temperature (220°C). At a point near the precursor injector is a second ring injector where oxygen is injected into the system. These are positioned at approximately 5 cm above a 1" heated substrate. The system is operated in a reduced pressure of 10 to 15 mmHg and vacuum is pulled from below the heated substrate directing the gas flow across the substrate. The total pressure of the system is maintained between 10 and 15 mmHg through an automatic throttle valve.

Our approach was to first find the conditions needed to transport the precursors into the reaction chamber. This involved a number of runs with varying conditions followed by a qualitative determination of chemistry via XRD, Auger spectroscopy, and/or time of flight secondary ion mass spectroscopy (TOF-SIMS).

The preliminary runs accomplished in this project have shown qualitatively by TOF-SIMS the presence of three of the components, Bi, Ca, and Cu. However, no Sr was detected. XRD analysis for CuO film showed the presence of Cu suggesting the precursor does transport but will require a higher carrier gas flow rate. We have not been able to successfully transport Sr for which there are two likely reasons. The first is the possibility of cold spots at points along the manifold and the reactor injector system. The precursor has a low vapor pressure and we have typically evaporated at or near 200°C. The manifold and injection line are wrapped in heating tape and heated to just above 200°C. However there are numerous valves and bends in the line and it is very easy to imagine spots were the temperature could drop below 200°C and condense out. The second reason could be the decomposition of the precursor in the sublimator. This might happen for a number of reasons such as a decrease in the thermal stability due to the presence of impurities, temperature excursions in the sublimator or a leak in the vacuum system. Since we did have a leak in the Bi sublimator the possibility of oxygen back-streaming into the hot Sr sublimator could easily have resulted in precursor decomposition/oxidation. The difficulties with Sr are not surprising given the narrow temperature range between a reasonable vapor pressure and the decomposition temperature. We now know to separate that part of the system from the manifold and separately inject the Sr material.

Overall, both the PLD and the MOCVD approaches yielded good results. In the case of PLD, a functional system is in place and we have samples which seem to exhibit *a*-axis like qualities. Additional characterization is needed to be certain of these preliminary findings but they are encouraging. A functional reactor is now also in place for the MOCVD approach and we have demonstrated great results in transporting three of the four precursors. These advances make future IJJ-based THz source investigations feasible (at LANL) by providing a path to controlling crystal orientation during thin film growth.

Impact on National Missions

As stated before, the DOE and NSF (2004) has labeled THz research as a frontier in science. This proposal targeted and advanced a critical step, establishing a process for fabrication of *a*-axis oriented films, in the larger goal of answering the most persistent and pressing question in THz research today: lack of a compact THz radiation source. Developments in solid-state source technology could position LANL for leadership in the wide array of DoD, DOE, and NASA missions that center on application of THz radiation: nondestructive testing and evaluation, illicit materials identification, imaging techniques (including computed tomography reconstruction), satellite technologies, and high-speed communications. While these applications could only come from follow-on efforts, this seedling project has bought down considerable risk by establishing and demonstrating two approaches to thin film growth of *a*-axis oriented BSCCO.

References

1. Kemp, Michael C., P. F. Taday, E. C. Bryan, J. A. Cluff, Anthony J. Fitzgerald, and William R. Tribe. Security applications of terahertz technology. 2003. Vol. 5070, p. 44.

2. Bulaevskii, L. N., A. E. Koshelev, and M. Tachiki. Shapiro steps and stimulated radiation of electromagnetic waves due to Josephson oscillations in layered superconductors. 2008. *Physical Review B (Condensed Matter and Materials Physics).* **78** (22): 224519.

3. Koshelev, A. E., and L. N. Bulaevskii. Resonant electromagnetic emission from intrinsic Josephson-junction stacks with laterally modulated Josephson critical current. 2008. *Physical Review B (Condensed Matter and Materials Physics).* **77** (1): 014530.

4. Bulaevskii, L. N.. Detection of electromagnetic waves by use of Josephson oscillations in layered

superconductors. 2009. *PRL.* **Submitted for publication**.

5. Bulaevskii, L. N., and A. E. Koshelev. Radiation from a Single Josephson Junction into Free Space due to Josephson Oscillations. 2006. *Physical Review Letters.* **97** (26): 267001.

6. Bulaevskii, L. N., and A. E. Koshelev. Radiation due to Josephson Oscillations in Layered Superconductors. 2007. *PRL.* **99** (5): 057002.

7. Chen, H., W. J. Padilla, M. J. Cich, A. K. Azad, R. D. Averitt, and A. J. Taylor. A metamaterial solid-state terahertz phase modulator. 2009. *Nat Photon.* **3** (3): 148.

8. Kubota, N., T. Sugimoto, Y. Shiohara, and S. Tanaka. (110)-oriented Bi-Sr-Ca-Cu-O superconducting thin films prepared by metalorganic chemical vapor deposition. 1993. *J. Mater. Res..* **8** (5): 978.

9. Kawahara, T., T. Ishibashi, H. Kaneko, K. Sato, K. Lee, and I. Iguchi. Intrinsic BSCCO Josephson junctions on off-axis substrates. 1999. *Applied Superconductivity, IEEE Transactions on.* **9** (2): 4519.

10. Sugimoto, T., M. Nakagawa, Y. Shiohara, and S. Tanaka. a-Axis oriented Bi---Sr---Ca---Cu---O thin films deposited on (1 0 0) MgO substrates by metalorganic chemical vapor deposition. 1992. *Physica C: Superconductivity.* **192** (1-2): 108.

Publications

Bulaevskii, L. N., I. Martin, and Gabor B. Halasz. Line width of radiation from intrinsic Josephson junctions in layered superconductors. 2010. *Journal of Applied Physics.* **Submitted for publication**.

Martin, I., Gabor B. Halasz, L. N. Bulaevskii, and A. E. Koshelev. Shunt-capacitor-assisted synchronization of oscillations in intrinsic Josephson junctions stack. 2010. *Journal of Applied Physics.* **108** (3): 033908.

Robust, Low Power, and Miniature Mixed Potential Sensors for the Detection and Discrimination of High Explosives

Eric L. Brosha
20100577ER

Abstract

We have successfully demonstrated in this short-term, LDRD Reserve Project (7 month timeline) that it is possible to detect trace amounts (1-10μg) of energetic materials/high explosives (EM/HE) (PETN, TNT, and RDX in this study) using electrochemical, mixed potential gas sensors based on yttria stabilized zirconium oxide (YSZ) solid electrolyte. These sensors are a unique form of the ubiquitous O_2 lambda sensor used today in automobile engine control systems around the world. While the sensing of HE/EM materials using electrochemical transduction methods has been reported in the literature for the detection of certain trace explosive residues in aqueous media, our work shows that it may be possible to build inexpensive HE/EM detection systems based on these inexpensive gas sensors when combined with established vapor sampling/concentrator front-end technology. The use of front-end technology to collect and concentrate the HE vapor emanating from areas and surfaces with trace HE contamination appears to make the intrinsically low vapor pressure of the HE samples less relevant, because the strength of the measured response from the sensors did not scale with the sample's relative vapor pressure, given equal quantities of HE. Moreover, our results show that by using multiple sensors with specifically targeted selectivity to hydrocarbon (HC) and nitrogen oxide (NO_x) chemical components, we were able to discriminate the PETN, TNT, and RDX samples from each other by simply calculating the ratio of NO_x to HC integrated peak areas. Most importantly, the ability the use of multiple sensors each tuned to basic chemical structures comprising HE materials (e.g. nitro, amine, and hydrocarbon groups) will permit the construction of detector systems with lower false positives than present day technologies, with the added benefit of greatly reduced detector costs.

Background and Research Objectives

The goal of this short-term LDRD project was to investigate and prove that it is possible to detect trace quantities of HE substances using novel electrochemical gas sensors originally developed at LANL for automotive/pollution mitigation applications. This LDRD Reserve project builds on a foundation of mixed potential electrochemical sensor science and leverages a substantial investment into new types of inexpensive, robust electrochemical sensors for various gas sensing applications [1-6]. Our technology relies on the use of YSZ as a high temperature oxygen ion conducting solid electrolyte. There are no commercial devices in the market based on the mixed potential phenomenon. This is primarily due to the fact that the mixed potential is dependant on electrochemical oxidation and reduction reaction rates and is therefore a strong function of the electrode composition, electrolyte and electrode/electrolyte/gas three-phase interface morphologies. Addressing this issue, the MPA-11 sensors group at LANL has come up with unique sensor design with improved electrode, electrolyte and 3-phase interface stability by incorporating either metal wire or dense oxide electrodes in combination with a porous electrolyte. The use of stable metal and ceramic electrodes ensures that the morphology of these electrodes and the 3-phase interface is both reproducible from sensor to sensor and is very stable over time [7]. Mixed potential sensor development work at LANL over the last decade has focused on the development of sensors for the detection of CO, HCs, and NO_x for a variety of applications including automotive OBD catalytic converter monitoring, stationary reciprocating engines, and air monitoring [8-10].

The work and results we highlight here, go beyond all previous work and has allowed us to show experimental data that demonstrates a proof-of-principal that it is possible to use this unique class of sensors for the purpose of not only detecting high explosives and energetic materials, but also of discriminating the chemical the type of HE based on the chemistry of the sample.

Furthermore, the use of sensor arrays – increasing the number of selective sensors each targeting specific chemical groups comprising the HE – would permit the design and construction of detector systems that would be positioned to better reduce the high false positive rates endemic to today's widely used explosives detection technologies.

Scientific Approach and Accomplishments

Trace samples of common military high explosives samples (PETN, TNT, and RDX *de minimus* quantities dissolved in organic solvent) were obtained using Accustandards™ high purity analytical calibration standards typically used to calibrate IMS and GC/MS analytical instrumentation. Figure 1 shows the temperature profile of a typical experiment.

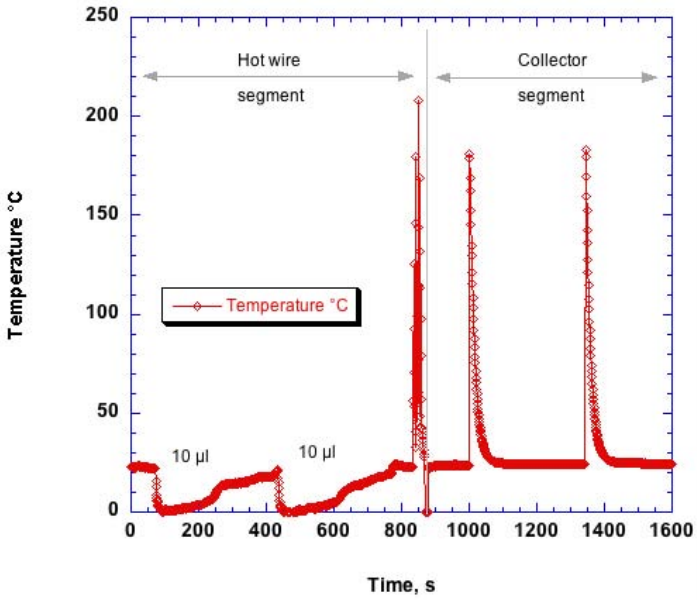

Figure 1. Temperature profile of a typical experiment. The Hot wire segement shows the loading of the hot wire with HE/solvent sample followed by a succession of rapid heating to transfer explosive to the sample collector. The Collector segment shows rapid heating of the felt to desorb the explosives sample and release to the sensors.

The HE/solvent sample was transferred onto a wire with a thermocouple attached to monitor temperature. After evaporation of the organic solvent (sample conc. 100 or 1000 µg/mL in methanol and/or acetonitrile depending on the HE sample), the hot wire was rapidly heated several times to increase the vapor pressure of the sample sufficiently to desorb the HE molecules from the hotwire surface using a succession of 4 pulses separated by a pauses of 8 – 9 seconds. The sampling/concentrating front-end unit was positioned approx. 2.5 cm away from the hot wire; this device served to collect and concentrate the HE sample and was comprised of a high surface area stainless steel felt through which the HE vapor was pulled using a handheld vacuum (flow ca. 400 ft^3/min). Subsequent to trapping the HE molecules on the surface of the felt, the collector felt module was rapidly heated to the desired set point temperature (185°C, 170°C, and 170°C for PETN, TNT, and RDX respectively) in airflow (200 ml/min). Once again, the result of these actions was to release the HE molecules from the surface they were adsorbed to; however, in this second part of the experiment, the HE vapor was directed to the LANL electrochemical gas sensors operating in a miniature tube furnace at 500°C. One sensor was tuned for preferential total NO_2/NO response by the appropriate application of a bias current [11] and the other for hydrocarbon (HC) response [12]. Figure 2 shows the NO_x and HC sensor response to 2µg of PETN.

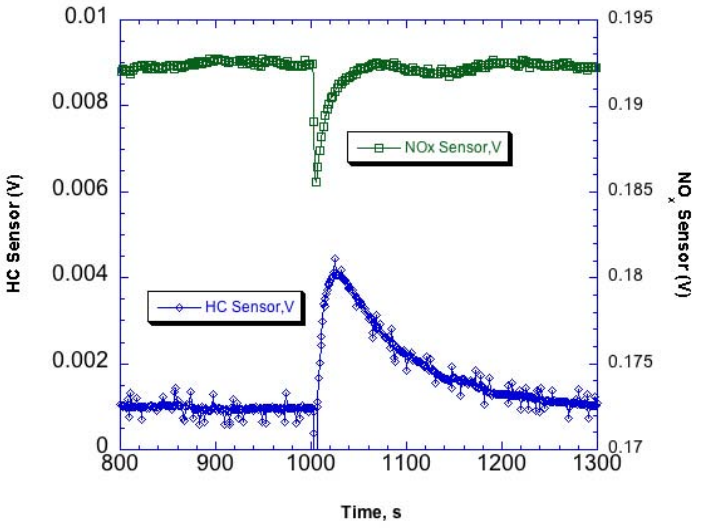

Figure 2. Simutaneous measurement of NOx sensor (bias current = 0.1µA) and HC sensor at 500°C in air being pulled through collector felt and to the sensors. Data show segment for flashing collector felt to 185-190°C for 2 µg of PETN.

The area under each sensor peak was calculated and was found to be proportional to the amount of HE sample placed onto the hot wire and subsequently collected by the felt collector. Figure 3 is a plot of integrated peak area versus sample mass of 4 separate experiments using 0, 1, 2, and 3 µg of PETN. A similar curve was obtained for the HC sensor. These data showed that the sensors responded to increasing trace amounts of HE. Figures 4 and 5 repeat these basic experiments for 10µg of TNT and RDX explosives. These species of HE have a higher and lower vapor pressure compared to PETN respectively (e.g. TNT 10^{-8}>PETN 10^{-11}>RDX 10^{-12} at 25°C). Figure 4 shows the measured total NO_x response from the NO_x sensor and Figure 5 shows the corresponding HC response from the HC sensor; the calculated peak areas are also show in these plots. These three HE species constitute the extent of what samples could be studied in this short term, LDRD reserve project.

Table 1 presents the three high explosives listed left-to-right according to carbon content in the formula unit. The chemical formula has been written so as to quantify the number and nature of the nitro-groups. The ratio of peak area measured by the HC sensor to peak area measured for the total NO_x sensor is tabulated. The fact that a unique ratio of HC/NO_x is obtained for each species of HE identifies a method of discriminating high explosives using this approach.

Peak Area	RDX	PETN	TNT
Ratio	$C_3H_6(NO)_6$	$C_5H_8(NO_2)_4O_2$	$C_7H_5(NO_2)_3$
HC/NO$_x$	4.226	2.437	10.91

Table 1. Calculated ratio of areas (in units of V•s) under the measured response from the total HC/NO$_x$ and HC sensors.

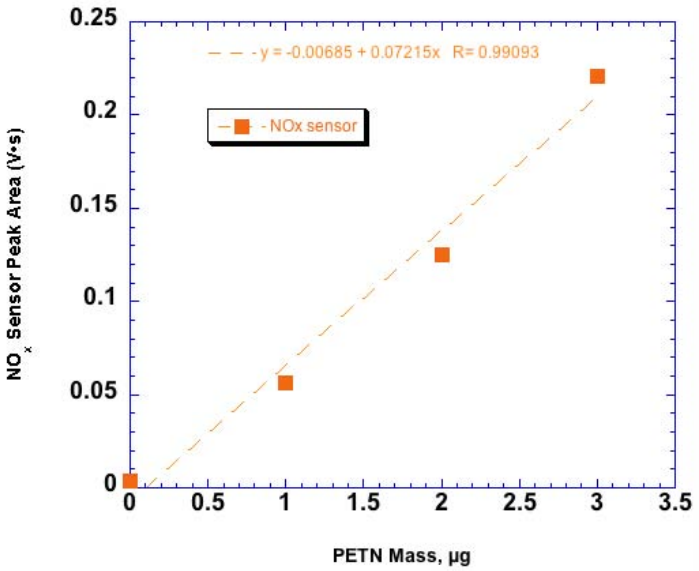

Figure 3. Data for NOx (500°C, current bias = 0.1µA) sensor response for 4 PETN experiments with PETN sample size = 0, 1, 2, and 3 µg collected onto collector felt. Collector felt was flashed at 185-190°C in air at 200 ml/min. The area under the NOx sensor peak was calculated and potted vs. PETN mass.

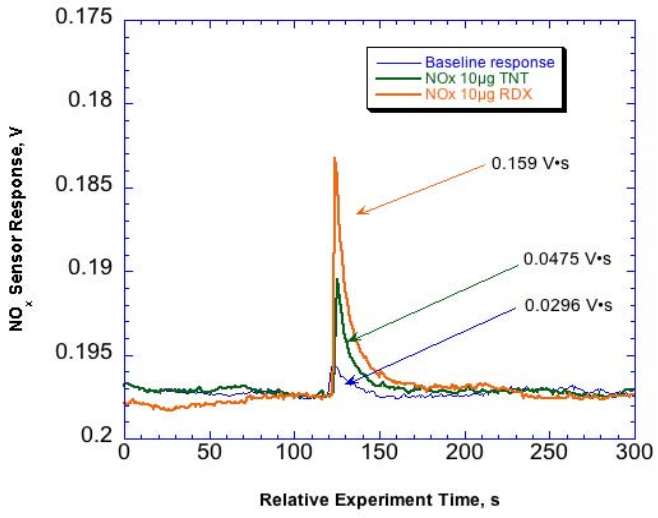

Figure 4. Data for NOx (500°C, current bias = 0.1µA) sensor response for 10 µg of TNT and 10µ of RDX (1µl Accustandards™ at 1000µg/ml conc. MeOH:AcCN = 1:1) Collector felt was flashed at 170°C in air at 200 ml/min. The area under the NOx sensor peak was calculated and indicated here.

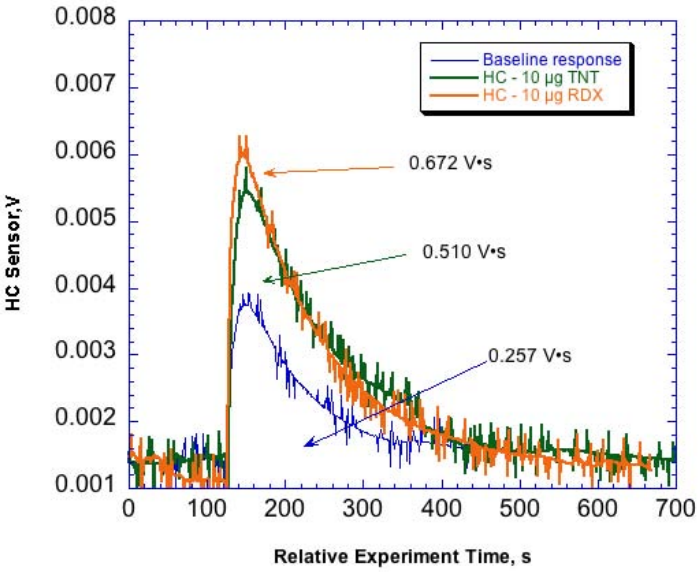

Figure 5. Data for HC (500°C, unbiased) sensor response for 10 µg of TNT and 10µ of RDX (1µl Accustandards™ at 1000µg/ml conc. MeOH:AcCN = 1:1) Collector felt was flashed at 170°C in air at 200 ml/min. The area under the HC sensor peak was calculated and indicated here.

Impact of National Missions

The results from the LDRD reserve proposal directly support Laboratory's mission to develop and apply science and technology to (a) reduce global threats, and (b) solve emerging national security challenges. The Intelligence Reform and Terrorism Prevention Act of 2004 (P.L. 108-458) directed the Department of Homeland Security (DHS) to place high priority on developing and deploying passenger explosives screening equipment. Recent Christmas Day bombing plot (25 Dec 2009) using Pentaerthyritoltetranitrate (PETN, a focus of study in this work) has once again constituted an immediate need to reliably detect bulk and trace amount of explosives not only in a cost-effective way, but in a manner that greatly improves upon existing technology vis-à-vis reducing the rate of false positives while eliminating false negatives.

Addressing such a need, the results from the LDRD research initiative will be leveraged to seek additional funding from different federal agencies interested in explosives interdiction such as the Defense Threat Reduction Agency (DTRA), Department of Homeland Security (DHS), the US Army, and even end-user agencies that sponsor R&D efforts such as the Transportation Security Agency (TSA) and the Federal Aviation Administration (FAA) to develop inexpensive and portable screening systems.

References

1. Garzon, F. H., R. Mukundan, and E. L. Brosha. Solid-state mixed potential gas sensors: Theory, experiments and. 2000. In *12th International Conference on Solid State Ionics ; 6-12 June 1999 ; Halkidiki, Greece.* Vol. 136-137, p. 633.

2. Miura, N., T. Raisen, G. Lu, and N. Yamazoe. Highly selective CO sensor using stabilized zirconia and a couple of oxide electrodes. 1998. *SENSORS AND ACTUATORS B-CHEMICAL.* **47** (1-3): 84.

3. Miura, N., G. Lu, and N. Yamazoe. High-temperature potentiometric/amperometric NO_x sensors. 1998. *Sensors and Actuators B (Chemical).* **B52** (1-2): 169.

4. Martin, L. P., and R. S. Glass. Hydrogen sensor based on YSZ electrolyte and tin-doped indium oxide. 2005. *Journal of the Electrochemical Society.* **152** (4): H43.

5. Mukundan, R., E. L. Brosha, D. R. Brown, and F. H. Garzon. Ceria-electrolyte-based mixed potential sensors for the detection. 1999. *Electrochemical and Solid-State Letters.* **2** (8): 412.

6. Miura, N., T. Shiraishi, K. Shimanoe, and N. Yamazoe. Mixed-potential-type propylene sensor based on stabilized zirconia. 2000. *Electrochemistry Communications.* **2** (2): 77.

7. Sekhar, P. K., E. L. Brosha, R. Mukundan, Wenxia Li, M. A. Nelson, P. Palanisamy, and F. H. Garzon. Application of commercial automotive sensor manufacturing methods for NO_x/NH₃ mixed potential sensors for on-board emissions control. 2010. *Sensors and Actuators: B Chemical.* **144** (1): 112.

8. Brosha, E. L., R. Mukundan, R. Lujan, and F. H. Garzon. Mixed potential NO_x sensors using thin film electrodes. 2006. *Sensors and Actuators B (Chemical).* **119** (2): 398.

9. Mukundan, R., E. L. Brosha, and F. H. Garzon. Solid-state electrochemical sensors for automotive applications. 2002. In *Symposium on Chemical Sensors for Hostile Environments ; 20010422 - 20010425 ; INDIANAPOLIS, IN.* Vol. 130, p. 1.

10. Mukundan, R., E. L. Brosha, D. R. Brown, and F. H. Garzon. A mixed-potential sensor based on a Ce0.8Gd0.2O1.9 electrolyte and platinum and gold electrodes. 2000. In *195th Meeting of the Electrochemical-Society ; 19990502 - 19990506 ; SEATTLE, WASHINGTON.* Vol. 147, 4 Edition, p. 1583.

11. Mukundan, R., K. Teranishi, E. Brosha, and F. Garzon. Nitrogen oxide sensors based on yttria-stabilized zirconia electrolyte and oxide electrodes. 2007. *ELECTROCHEMICAL AND SOLID STATE LETTERS.* **10** (2): J26.

12. Mukundan, R., E. L. Brosha, and F. H. Garzon. Mixed potential hydrocarbon sensors based on a YSZ electrolyte and oxide electrodes. 2003. *JOURNAL OF THE ELECTROCHEMICAL SOCIETY.* **150** (12): H279.

AC Losses in DC Superconducting Cables

Stephen P. Ashworth
20100614ER

Abstract

Nationally, attention is beginning to focus on dc power transmission as the preferred technology to transmit electric power from remote renewable generation to load centers. Superconducting cables have been shown to have a number of advantages in this application as well as, for example, in interconnecting the three synchronous systems in the US at the proposed Tres Amigas Superstation in Clovis, NM. A superconducting cable carrying a dc current should have no energy losses, however in a practical system the currents are not pure dc but will commonly be 'dc + ac ripple'. The amount of ripple depends primarily on the type and quality of the ac – dc conversion system. At the present time the techniques to predict the ripple losses in DC superconducting cables do not exist and there is very limited literature on their measurement.

Within this project we developed the techniques to measure the losses in superconducting wire due to dc +ac ripple currents and show data on the two types of wire presently available (IBAD and RABiTS). One significant finding is that, counter intuitively, the energy losses in the RABiTS wire are higher at lower dc currents. We have also shown that the present state of the art in modeling and simulation for high temperature superconducting wires and cables is not easily extended from pure ac to dc + ac ripple. Absent significant advances in processor speed and memory of 'desktop' computers in the near future (or theoretical breakthroughs) , the dc + ac ripple simulations will need to be run on high performance machines and the software to do this will need to be adapted, or possibly written. This is a significant undertaking.

Background and Research Objectives

Within LANL we have developed world leading expertise in measuring and modeling the ac losses in superconducting tapes, cables and other devices. This expertise is being used in DOE and DHS programs to assist in the design of ac superconducting power cables. However, attention is beginning to switch to dc power transmission as the preferred technology to transmit electric power from remote renewable generation to load centers. DC superconducting cables are also being planned to interconnect the three synchronous systems in the US at the proposed Tres Amigas Superstation in Clovis, NM.

A superconducting cable carrying a dc current should have no energy losses, however in a practical system the currents are not pure dc but will commonly be 'dc + ac ripple'. The ripple will be at frequencies between 60Hz and 20kHz, will have a number of frequency components with various amplitudes depending on the type of ac/dc conversion system. This ripple will generate energy losses and heat in the cable. This has two practical consequences: the heat must be removed by refrigeration, so the refrigeration equipment must be sized appropriately, and temperature gradients will be generated within the cable. If the heat generated is too large the cable may not be operable. At the present time the techniques to predict the ripple losses in DC superconducting cables do not exist and there is very limited literature on their measurement.

Our objective has been to improve the state of the art in both measurement and modeling of dc + ripple currents in high temperature superconductors. Specifically we intended to:

- Develop techniques and perform measurements on HTS single tape conductors to generate data on the losses due to dc currents and fields with ac current and/or field ripple.
- Adapt our ac loss simulation techniques for single tapes to include dc + ripple by exploring the parameter space to develop classes of solution.
- Use the data of (a) to validate the simulations in our modified model for single tapes.

Scientific Approach and Accomplishments

Measurements

The energy loss in a superconductor is the product of the voltage along the superconductor and the current. The current is supplied by the measurement equipment, but the voltage must be measured. In the case of ac currents, the voltages are pure ac and are possible to measure using established techniques. Typically we have to measure voltages in the range 1_V, so we need a noise level below 100nV. This can be achieved for ac signals using highly selective instruments which 'lock' to the ac frequency, however this is not so straightforward for dc signals. A significant part of our experimental effort was directed toward developing the techniques to extract the dc voltage component in the presence of large ac currents with low enough noise to return good data.

There are two US manufacturers of high temperature superconducting wire. These two wires types (identified as IBAD and RABiTS wires) have similar dc characteristics, but very different ac behavior. This difference arise from the magnetic properties of one of the constituents of the of the RABiTS wire. In Figure 1 we show the results of energy loss measurements on the RABiTS wire when carrying dc currents with a superimposed ac ripple. In these measurements ac ripple at 60Hz was held at a constant value and an increasing dc current added, simulating the case of an ac-dc convertor with constant voltage ripple feeding a dc cable with increasing load. The energy losses of this RABiTS wire *decrease* with *increasing* dc current generating a family of curves. In fact the losses decrease by nearly an order of magnitude when the dc current is increased from 50A to 150A. This is due to the losses in the magnetic RABiTS substrate dominating at low dc currents, but being suppressed by the dc magnetic field generated by the dc current at higher dc currents. This measurement provides a vital piece of information for the design of dc cables using the RABiTsS wire: the highest heat load (for fixed ripple amplitude) will occur at low power transmission, *i.e.* low dc current. This is counterintuitive and had not been previously demonstrated.

Figure 2 shows the measured losses for IBAD wire. This exhibits completely different behavior: the measured losses are constant over the range of measurement. This material has no magnetic substrate to contribute losses at low dc currents.

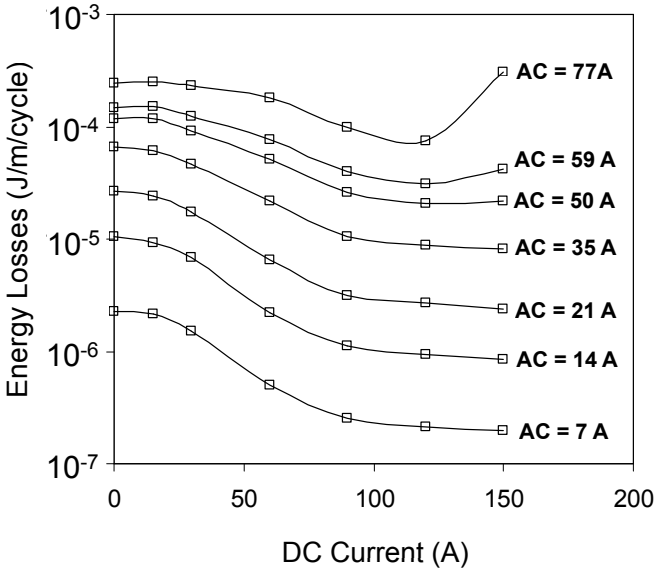

Figure 1. Measured energy losses of a RABiTS wire carrying both a dc and ac ripple current.

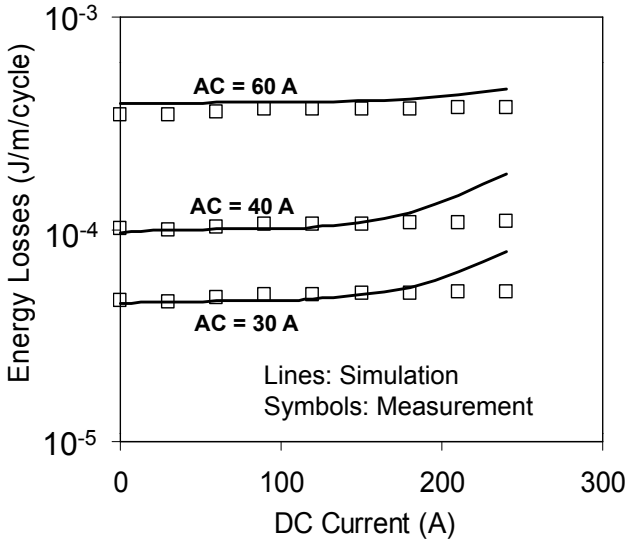

Figure 2. Measured and simulated energy losses of an IBAD wire carrying both a dc and ac ripple current.

Simulation

We carried out numerical simulations using the commercial finite element software package COMSOL. This package solves the electromagnetic and material equations of the system on a grid with appropriate boundary and initial conditions, and is written to run on high specification PC's. This package, modified appropriately in house, has proven very successful in predicting the losses due to pure ac currents with reasonable computation times (a few hours per current value). The simulations require that the initial conditions mimic an actual experiment, and the computation has to be run for a number of ac cycles before it settles

to a steady state. In the pure ac case 4 cycles is sufficient. This is not an artifact of the simulation but represents the actual transient states that would be present in a measurement.

In Figure 2 we also show the simulation results for an IBAD wire with fixed ac ripple but increasing dc current. The measurements show no increase in losses, yet the simulation predicts a significant increase at higher currents. The reason for this discrepancy becomes clear if we examine the simulation losses as a function of time, *i.e.* the number of simulated ac cycles as shown in Figure 3. Unlike the pure ac case, the predicted losses are still decreasing as we run the simulation for greater numbers of ac cycles. Transients set up by 'switching' on the currents have not decayed even after 40 ac cycles. In an experiment this would be less than 1 second and a typical measurement would take about 5 minutes per data point, but a 40-cycle simulation takes nearly 12 hours for each value of current on a high specification PC. Longer simulations are not feasible due to memory limitations.

This presents us with a significant finding for dc cable development. In order to predict dc + ac ripple losses we need to move from 'desktop' PC's to high performance computing. However we would have to put significant effort into developing the software for these machines – it is not available 'off the shelf'. This will take time and funding. If the national programs take the path of developing dc superconducting cables it will be vital to start to establish high performance simulation capabilities sufficiently far in advance of when they will be needed.

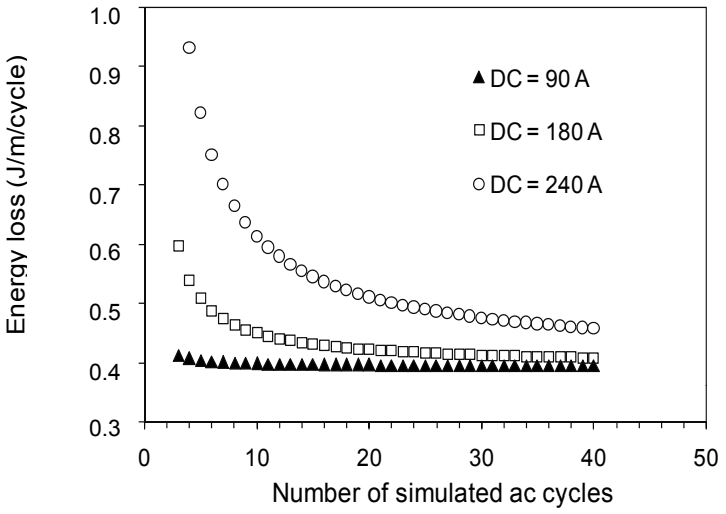

Figure 3. Simulated energy losses of an IBAD wire carrying a dc current and ac ripple current of peak value 60A as a function of the number of ac cycles simulated.

Impact on National Missions

The DOE mission includes developing the technologies to transmit electricity generated by renewable sources. One way of doing this is using dc systems, and in particular superconducting dc systems. This project has started us along the path to understanding, and hence removing, one of the barriers to the deployment of superconducting dc cables.

We can now measure the dc +ac ripple losses in superconducting wire with good accuracy, and we have developed techniques that can be extended to cables. This allows us to supply engineering data to cable manufacturers as needed, allowing the design of efficient cable systems.

Understanding, and minimizing, the effect of ripple on dc cables may allow a more economic design of ac/dc convertor stations. These convertor stations cost upward of $1.5 billion for a 1GW cable: if the cable can operate with a lower specification, and hence lower cost, convertor more wind energy resources can be economically deployed. Similarly, the cost of refrigeration for a dc cable is significant, perhaps $1M per mile of cable. Without an understanding of the ripple losses the tendency will be to over-engineer the cooling system, again increasing costs and perhaps making some wind resources economically unviable. We have also shown that basing the dc cable development "route map" on our experience with pure ac cables would leave us lacking in vital simulation competencies when the time comes to design the first dc cables for the power grid.

Exploring the Physical Basis of Nano/Micro-scale Thermodiffusion Phenomena at Near-Critical Pressures (U)

James L. Maxwell
20100630ER

This report can be obtained by contacting the LDRD Program Director at Los Alamos National Laboratory.

Control/Path Planning Strategies for Nonholonomic, High-Speed, Autonomous Unmanned Ground Vehicles

Charles R. Farrar
20100594PRD1

Introduction

The goal of this work is to develop path planning optimization algorithms for unmanned ground vehicles that incorporate vehicle dynamics concerns such as longitudinal and lateral load transfer, wheel loading, slip, tire slip angle, available lateral and longitudinal traction (traction ellipse), chassis dynamics, wheel to ground interface, camber/toe changes, and changes in center of gravity (CG) location. All these considerations are important for getting the vehicle from point A to point B without mishap in the face of natural and manmade hazards.

Benefit to National Security Missions

The development of a an adaptive architecture for correcting unforeseen circumstances encountered by unmanned ground vehicles (UGVs) will represent a major step forward for artificial intelligence research. This technology can be adapted to a wide variety of DOE-related missions including resilience of high performance computing hardware and the development of robotic devices for assessing and handling of hazardous materials.

Progress

David has been working actively on the high-speed autonomous mobile sensor node (MSN) project since January 2010. To get the project started, David spent considerable time getting groundwork in place. When David first arrived, he spent a significant portion of his time in training. The nature of his work requires energized electrical worker training which took a fair amount of time to complete. David also immediately began getting the required wireless, safety, and camera security approvals in place. One major concern was to find a test site for performing high-speed MSN experiments that would meet the safety and security requirements. After extensive searching a suitable test site was found in White Rock and the approvals for its use were obtained. The nature of high-speed autonomous unmanned systems research requires the development of a custom experimental platform. Extensive searching has not uncovered a suitable commercially available high-speed MSN. David thus began building an MSN using commercially available hardware and sensors. The chassis of the MSN is an E-MAXX remote control truck. Hardware has been procured to convert it to computer control. The required sensors have also been procured. A modular, scalable, software architecture has been adopted for the incorporation of the sensors, servos, and control software. Significant effort has been expended to integrate all the sensing components onboard the MSN. At this point the foundation of the software architecture is in place, and all of the required sensors have been integrated into the framework. The sensors include a camera, Lidar, a compass, and an inertial measurement unit. The servo control for the steering and throttle is functional as well. In addition to the robot, a remote basestation has been setup and is capable of initiating the mobile sensor node control sequences. Field testing of the mobile host system is anticipated to begin in the very near future. A diagram of the MSN can be found in Figure 1.

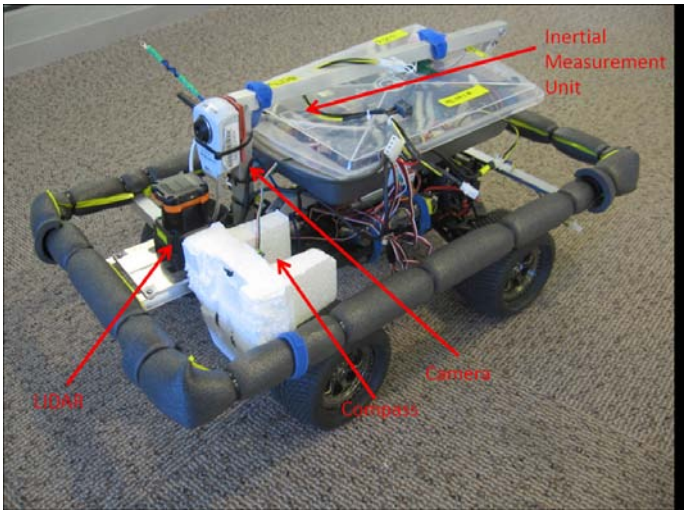

Figure 1. Mobile Sensor Node (MSN) test platform with integrated sensors.

David also spent considerable effort on developing and modeling potential high-speed MSN control systems. One major problem with current field robotics is the potential for their theft or destruction by adversarial agents. For this reason it has been decided to focus on the unmanned vehicle escape and evasion problem. One major

escape and evasion problem hindering the development of autonomous convoys for adversarial environments is the sabotage of MSNs with the Precision Immobilization Technique (PIT). The PIT maneuver is a tactic used by law enforcement to disable fleeing vehicles and could be used by adversarial agents to damage, loot, and capture unattended MSNs. Substantial work has been done in differential game theory on the pursuit evasion problem, but these results generally assume capture has occurred only when the pursuer and evader occupy the same physical location or perhaps are within sensor range of one another. For the PIT maneuver problem the MSNs must not only be in the same physical location and within sensor range of one another. They must also meet specific pose and velocity constraints. In the course of developing PIT maneuver control policies work from the differential game theory, missile guidance, model predictive control, and the planning and scheduling communities have been leveraged. David has developed a modified version of velocity pursuit that respects the nonholonomic nature of the MSN and takes advantage of the variable velocity of the MSN to perform PIT maneuvers on an evading vehicle. This modified version of velocity pursuit has been subjected to preliminary simulation studies, and seems to be a good candidate for executing a PIT maneuver. In addition, preliminary work has also begun on developing a PIT maneuver evasion strategy. Potential evasion strategies are currently being implemented in simulation.

In addition David co-mentored one of the 2010 Dynamic Summer School groups. David's group studied the use of structural health monitoring for pre-flight checks of responsive satellites. As part of this effort David designed a representative satellite test structure for the students to perform their experiments on. The group was able to show that it is possible to estimate the first three natural frequencies of a structure representative of a satellite using embedded piezoelectric patches as sensors and actuators. The group has written a conference paper that will be presented at the International Conference on Modal Analysis XXIX in 2011. An image of the representative cube structure can be found in Figure 2.

During June and July of 2010 David attended the Neuromorphic engineering workshop in Telluride Colorado. During this workshop David interacted with researchers from Georgia Tech to begin developing a prototype analog, time-domain compressed sensor. Some of David's initial ideas on how a time-domain, analog compressed sensor could be built were implemented using Paul Hasler's (Georgia Tech) field programmable analog array board. Lessons learned from this work are currently being used to help guide the development of a digital, time-domain, compressed sensor for applications ranging from structural health monitoring to treaty verification.

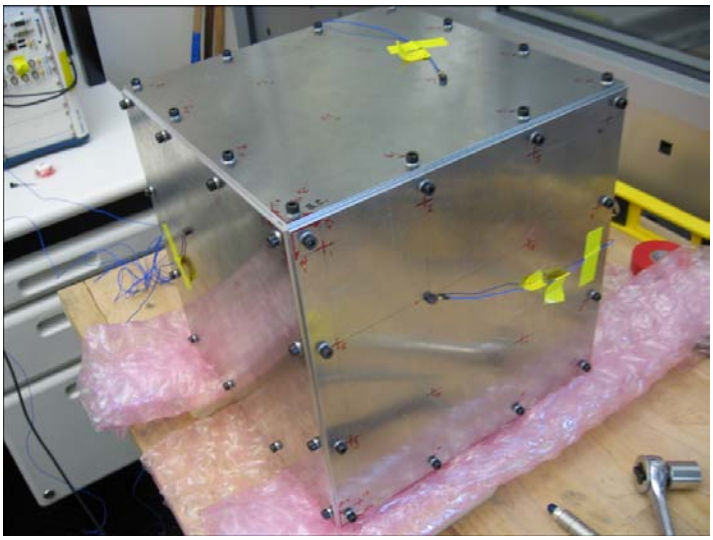

Figure 2. Simulated cube satellite

Future Work

At this point the sensors, and computation hardware have been completely integrated into a functional MSN. Some preliminary software for motion control is also integrated. The most immediate goal is to begin characterizing the vehicle and getting it ready for serious control policy testing. PIT maneuver control policies are mature enough at this point that they are ready to be ported and tested on-board the MSN. Another immediate goal is to develop software to implement cooperative aerodynamics ideas that would allow teams of MSNs to travel at high speeds while enjoying significant energy savings – like a pack of bicyclists drafting the leader. The results of these tests will be used to guide the development of more adaptive MSN software capable of learning from its environment and evading capture by unfriendly agents.

Conclusion

The end state of this work will be field-tested unmanned ground vehicle (UGV) path planning software capable of traversing unimproved terrain at high speed while adapting to unforeseen environmental stimuli. The development of high-speed control and path planning strategies for nonholonomic UGVs will revolutiorize the next generation of safe, high-performance, adaptive, self-sufficient, human competitive UGVs and open up a variety of new UGV applications. The path planning strategies will also be applicable to extraterrestrial UGVs such as Mars rovers.

Publications

Macknelly, D., J. Mullins, H. Wiest, D. Mascarenas, and G. Park. Dynamic characterization of satellite components through non-invasive methods. To appear in *IMAC A Structural Dynamics Conference.* (Jacksonville, FL, 31 Jan – 3 Feb, 2011).

Mascarenas, D., C. Stull, and C. Farrar. Escape and evade control policies for ensuring the physical security of

nonholonomic, ground-based, unattended mobile sensor nodes. To appear in *SPIE Defense, Security and Sensing Conference.* (Orlando, FL, 25-29 April, 2011).

Mascarenas, D., D. Macknelly, J. Mullins, H. Wiest, and G. Park. Characterization of satellite assembly for responsive space applications. To appear in *SPIE Smart Structures and Materials & Nondestructive Evaluation and Health Monitoring Conference.* (San Deigo, CA, 6-10 March, 2011).

Development of an acoustic exotic metamaterial slab using the acoustic radiation force and micro-streaming of high-order Bessel helicoidal beams

Dipen N. Sinha
20100595PRD1

Introduction

The design, development & characterization of acoustic metamaterials (AMs) offer innovative trends in material science, (nano)-technology and other areas of research because of their novel acoustic properties. With such features, it is possible to go beyond the band-gaps, focusing and wave-guiding found in phononic crystals, and create new effective materials. In short, metamaterials provide a new scale-invariant design paradigm to create functional materials that revolutionize our ability to manipulate, control, and detect acoustical radiation. There has been little headway on the experimental development and characterization of AMs, though some work is being currently explored theoretically. At present, the majority of the existing processes has been carried out on macroscopic levels. However, it has been recently recognized that the design, development & characterization of miniaturized samples (usually at the micron-level and below) of AMs is technologically relevant in the context of a wide range of applications in nanotechnology and nano-electronics, for example the production of micro-lenses with high-gain for stronger microscopes, building AEM-based parts for faster computer chips, biological- and chemical-agent detectors, and cloaking military (nano)devices, to name a few. It is therefore of some particular importance to work out novel techniques to achieve efficient design, development & characterization of AMs in micro-volumes. Various conventional (magnetically-based and other) devices have been proposed mainly for the design, development & characterization of optical metamaterials. Nevertheless, the design, development & characterization of AMs in small volumes remains difficult; applying conventional strategies to micro-volumes is generally ineffective. A possible solution to this complex problem is the development of 3D periodic AM microstructure based on the acoustic radiation forces and micro-streaming of counter-propagating ultrasound beams.

Benefit to National Security Missions

The results of this research will be most relevant to agencies, such as DOD and DOC (in the area of non-nuclear forensics), in terms of having a very low cost and easily manufacturable means of creating superlenses with sub-wavelength resolution and highly directional miniature antennas among other applications. Once the proof-of-concept is completed and the intellectual property is protected, we will approach the relevant government program offices through appropriate LANL channels to explore possibilities of addressing their specific needs and see how a more focused project can be developed that allows transitioning this work to support their missions. If we succeed, we will have a new probe of matter to support a range of detection and inspection (e.g. in manufacturing) missions.

Progress

Creation of periodic patterns of nanoparticles in a host curing fluid.

We, F. G. Mitri (postdoctoral fellow) and I, synthesized a composite metamaterial using epoxy diluted with ethyl alcohol. The principal and curing solutions of epoxy (5 Minute® Epoxy, dynamic viscosity = 10 Pa.s, Net Vol. 25 ml, Devcon S-208 20845, FL, USA) were mixed within a plastic container (AMAC plastic products corp., CA, USA) having the following dimensions (12x12x45 mm^3, wall thickness of 1 mm) and diluted with 1 mL of ethyl alcohol. About 3 mg of 5 nm-diameter diamond nanoparticles were poured into the plastic container and the mixture was then slowly hand-steered for one minute using a metallic micro-needle so as to produce a quasi-homogeneous blend solution. Two 15 mm-diameter ultrasound piston transducers (Panametrics V103, Model # 56848, Olympus NDT Inc., MA, USA) were connected to the rectangular plastic chamber on opposite sides and perfectly aligned so as to create a counter-propagating ultrasonic wave-field. The experimental set up is illustrated in Figure 1. The transducers were driven by a RF power amplifier (EIN, Model # 240L, 50 dB, 20 kHz-10 MHz, NY, USA) coupled to two continuous wave (CW) signals obtained from two output channels of function generator (Tektronix AFG 3022B, Dual channel, 25 MHz)

operating at 1 MHz. The ultrasound field was activated for 5 minutes, a duration that corresponds to the epoxy curing cycle. During this time period, clusters of diamond nanoparticles were trapped and patterned due to the acoustic radiation force phenomenon that directs them toward the nodes of the standing wave field so as to form quasi-parallel periodic planes. The spacing of the arranged planes of particle clusters is highly sensitive to the tuning frequency and the physical properties of the host medium (i.e. in this case ethanol-diluted epoxy). After solidification, the transducers were removed and the plastic container was extracted before characterizing the internal morphological structure of the metamaterial with microXCT.

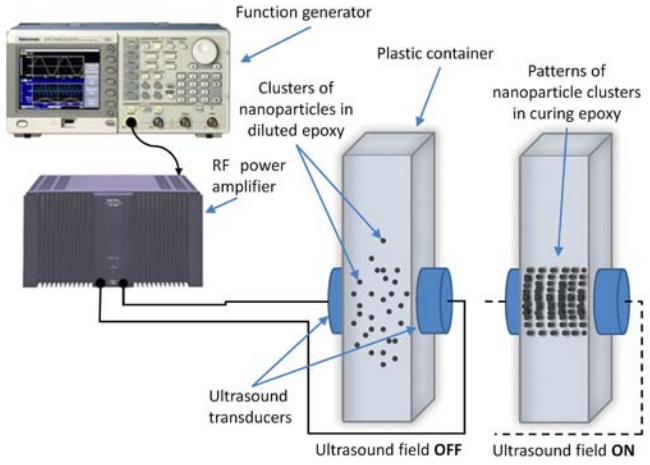

Figure 1. Experimental setup.

Characterization of the nano-particle based metamaterial with micro-computed X-ray tomography (microXCT)

With microXCT, it is possible to verify the quality of the patterns periodicity in addition to other micro-structural features. To accomplish this task, the specimen was scanned (Xradia, Micro-XCT-400, CA, USA) in the Sensors and Electrochemical Devices Group (MPA-11) of the Los Alamos National Laboratory (LANL). Its X-ray tube has an energy ranging from 20-90 keV, and the achievable resolution of the detector using the 2X, 4X, 10X and 20X magnification lenses are ~10 micron, ~5 micron, ~2.5 micron and 1.5 micron, respectively. In X-ray computed tomography, a set of individual radiographs (X-ray projections indicative of integrated X-ray absorption) is collected of a sample from all different viewing directions, and then via the mathematical technique of tomographic reconstruction, the data set of radiographic images from different view angles is used to reconstruct the internal structure of the sample.

Figure 2 (a) shows the 3D rendering of a tomographic section using the 2X detector lens, in which all the patterned planes (i.e. 12 planes) of diamond nanoparticle clusters are clearly visible. Figures 2 (b)-2(d) show the 3D rendered images of volumetric tomographic sections of the assembled metamaterial structure obtained at higher resolutions using the 4X-, 10X- and 20X-lenses, respectively. As the detector resolution increases from ~10 micron (using the 2X lens) to 1.5 micron (using the 20X lens), the field-of-view (FOV) decreases as shown in the figures. The spacing of arranged particles, which corresponds to half the wavelength of 1 MHz ultrasound waves in ethanol-diluted epoxy, is 800 micron. Moreover, an average thickness of each plane of nanoparticle clusters may be estimated, which is found to be about 215 micron.

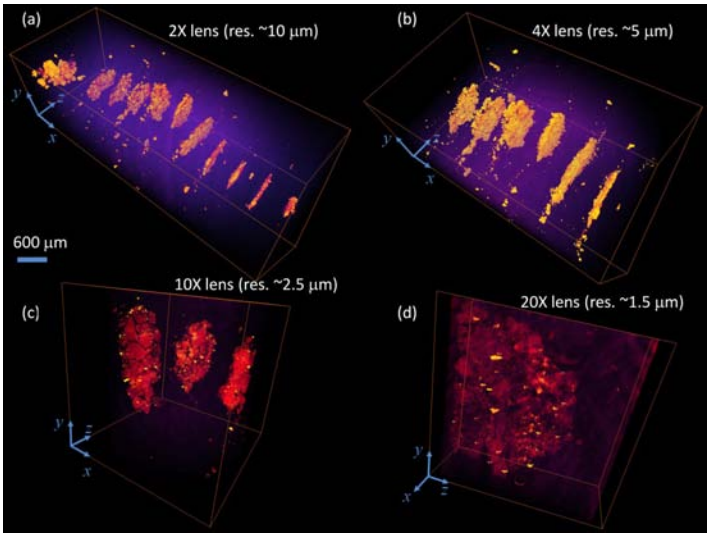

Figure 2. 3D Renderings of the diamond nanoparticle-based metamaterial.

Creation and use of high-order Bessel helicoidal beams (HOBHB) in acoustic scattering and nonlinear wave propagation phenomena

The nonlinear wave propagation of such beams in a nonlinear fluid medium is investigated. Through a sophisticated analysis based on Lighthill's formalism, closed form solutions valid to any order of approximation in the nonlinear wave equation have been established. Analytical solutions up to the forth-order level of approximation were derived and discussed. Lateral magnitude and phase profiles of the beam were also computed and compared and this is shown in Figure 3. The results showed that the beam's width reduces and becomes narrower, the side-lobes decrease in magnitude, and the hollow region diameter (or null in magnitude) increases as the order of nonlinearity increases. Furthermore, the nonlinearity of the medium preserves the non-diffracting feature of the beam's harmonics.

The second aspect is related to the scattering properties of a new type of Bessel beams that mimics the bull's eye singularity in optics. Analytical solutions for the axial scattering by a sphere and numerical simulations showed impor-

tant features not available with conventional beams. The new type of Bessel beams is regarded as a superposition of two equi-amplitude first order Bessel vortex (helicoidal) beams having a unit positive and negative order (known also as topological charge), respectively. This new family is also non-diffracting, possesses an axial null, a geometric phase, and has an azimuthal phase that depends on the transcendental cosine function. It was found that the backward and forward acoustic scattering by a sphere vanish for all frequencies. 3D directivity patterns were computed, and the resulting modifications of the scattering were illustrated for a rigid sphere in water. The results are useful in various areas in particle manipulation and entrapment, nondestructive imaging, digital acoustic communications, and may be extended to other potentially useful applications in optics and other fields of physics.

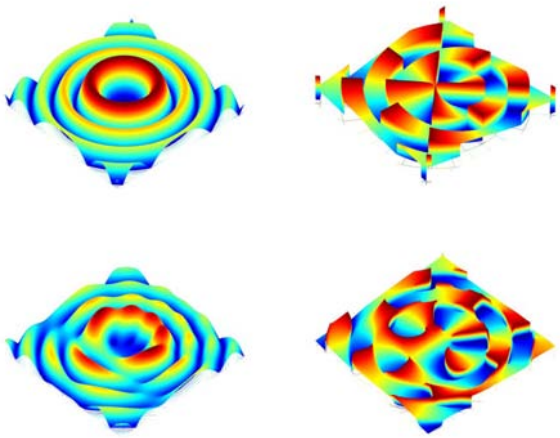

Figure 3. Theoretical magnitude and phase profiles.

The third aspect is related to the off-axial scattering of such beams, which requires tedious derivations coupled with the use of the spherical harmonics. A numerical code to predict the scattering response at any point in space is developed, thus recovering the previous axial scattering results. This investigation extends prior works on the acoustic scattering of a high-order Bessel vortex beam centered on a sphere to the case of an arbitrary position of the incident beam. Theoretical expressions for the incident and scattered field from a rigid immovable sphere were derived.

Future Work

The proposed research consists of the following remaining tasks and research goals.

Creation and use of high-order Bessel helicoidal beams (HOBHB).

The typical Gaussian beams will be replaced by HOBHB to study the improvement that can be gained from these types of beams as these are diffraction free beams.

Exploration of applications of these exotic microstructures.

The final objective of this project is to explore how these exotic materials can be used in applications such as creating novel sensors.

Conclusion

The anticipated results of this project will be a laboratory proof-of-concept to demonstrate the feasibility of producing a stable Acoustic Exotic Material (AEM) microstructure. The successful completion of this research will certainly lead to factual advancements in the field of AEMs research with potential for a wide range of applications. Only our own imagination may limit the wide range of applications of this proposed research spanning basically all areas of applied sciences (Physics, Materials Science, Chemistry, Biology, Geology…). Diverse commercial applications can be developed and patents can be filed based on the proposed technology.

Publications

Mitri, F. G.. Linear axial scattering of a high-order Bessel trigonometric beam by fluid spheres . To appear in *Journal of Applied Physics.*

Mitri, F. G.. Acoustic radiation force on a contrast agent shell in the vicinity of a porous vessel wall . To appear in *Ultrasound in Medicine and Biology.*

Mitri, F. G.. Acoustic beam interaction with a rigid sphere: the case of a first-order non-diffracting Bessel trigonometric beam (FOBTB). To appear in *Ultrasonics.*

Mitri, F. G.. Second-harmonic pressure generation of a non-diffracting acoustical high-order Bessel (vortex) beam of fractional type a. To appear in *Ultrasonics.*

Mitri, F. G.. Axial acoustic radiation force of progressive cylindrical diverging waves on a rigid and a soft cylinder immersed in an ideal compressible fluid . To appear in *Ultrasonics.*

Mitri, F. G.. Acoustic scattering of a high-order Bessel beam of fractional type a incident upon a rigid immovable sphere. 2010. *Journal of the Acoustical Society of America.* **128,** (4): 2314.

Chiral Metamaterials for Terahertz Frequencies

John O'Hara
20080796PRD4

Abstract

Electromagnetic radiation influences nearly every aspect of our lives, from cell phone communication to simple photography. Photography leverages centuries of technology development in focusing, image recording, and of course materials (i.e. glass). Today, scientists are studying "metamaterials" to radically advance such technologies. Metamaterials are engineered materials that exhibit properties not found in nature. Imagine a material that could change color on demand. The military implications would be enormous. Metamaterials enable such behavior. Our project was to use metamaterials for two purposes. First, we showed that metamaterials can fill a technology vacuum in the terahertz frequency range. Terahertz (THz) waves, electromagnetic (EM) waves whose frequency lies between microwaves and the infrared, are notoriously difficult to control. Second, we quantified the effectiveness of a new design strategy for negative index metamaterials. Negative index metamaterials have drawn much interest in their ability to improve imaging technologies.

Our main success in this project was to create chiral THz materials that can be actively controlled. Normal chiral materials rotate the polarization of a wave. Ours does this much more strongly and without altering any other aspect of its polarization qualities! In addition, we showed that this metamaterial behavior can be turned on or off dynamically. This difficult combination of qualities was never before demonstrated. We were also successful in determining limitations of chiral metamaterials. We showed how chirality affected absorption in negative index metamaterials. And with collaborators, we also helped determine the role chirality might play in tuning the Casimir force. All of this has positively impacted the LANL mission by creating new metamaterial capabilities, and helped foster external funding.

Background and Research Objectives

Terahertz science has been pursued since 1990 in an effort to make THz waves practical. Still, devices suitable for controlling THz waves are not yet adequate. One area of development that has remained unusually weak is polarization control. Control over polarization is important in many technologies such as wireless communications and global positioning systems. Before THz technology can become practical, the basic devices for controlling THz waves must be developed, including devices for controlling THz wave polarization. The first objective of this project was to create a new metamaterial that enables us to control the polarization of THz waves.

Metamaterials research has led to many new EM technology ideas. One idea was the notion of negative index materials (NIMs). Negative index materials are not naturally occurring; they must be engineered. With respect to our project, the novelty of NIMs is that they enable "super-resolution" imaging. All imaging schemes are limited in resolution to the wavelength of the EM waves used. For example, millimeter resolution is possible by imaging with EM waves of millimeter wavelength. Nanometer resolution is possible with ultraviolet or x-rays. With NIMs, it is theoretically possible to achieve unlimited resolution at any wavelength. Real NIMs, however, are highly absorbing. In other words, you might make a super-resolution lens out of NIMs, but it is nearly opaque! When we began this work, chiral metamaterials were seen as a new approach that enables negative index (and thus super-resolution), but with much lower absorption. That defined our second research objective: determine whether NIMs with very low absorption could be created using the chiral metamaterial approach.

Our objectives met with great success. We were able to design a THz metamaterial that not only featured tuned chirality, but this chirality was about 10,000 times stronger than in natural materials. Even more important, the chirality could be actively turned on and off. In addition, this metamaterial featured negative refractive index, enabling us to quantify absorption.

Scientific Approach and Accomplishments

Our approach to this work was partially described in the previous section. In more detail, we aimed to create a chiral THz metamaterial. Chirality is a rather vague description and can mean different things. Chirality, like color, is a property of a material. But chirality can mean

that a material is “optically active” or “dichroic”. Optical activity means that the material rotates the polarization plane of an EM wave passing through it. Dichroism means that a wave of one polarization is more highly absorbed than another polarization. Technical details are not necessary to understand the importance. For example, optical activity is critical to the understanding of molecular biology and analytical chemistry. In addition, optical activity is the basis of numerous display technologies, such as LCD computer monitors. Control over optical activity in the THz frequency range may prove particularly useful in biomedical imaging and sensing applications. Our approach was therefore to create a chiral THz metamaterial that could tune optical activity. Dichroism generally represents increased absorption, which we wanted to avoid. Therefore, we aimed for metamaterial designs that featured zero dichroism.

Optical activity originates from the molecular structure of a chiral material. The double-helix DNA molecule is a good example. These molecules are shaped such that the wave must rotate or twist in one direction as it propagates through the material. This is similar to a corkscrew moving through a cork. Like natural materials, chiral metamaterials are designed at the “molecular” level. Our task was to create a metamaterial molecule that twisted the THz wave as it passed through. When these molecules are packed tightly together they form the metamaterial as a whole. The molecule in our metamaterial is a bi-layer structure comprised of two resonators (Figure 1). The top and bottom resonators work together to force the wave to twist as it passes through the array of molecules.

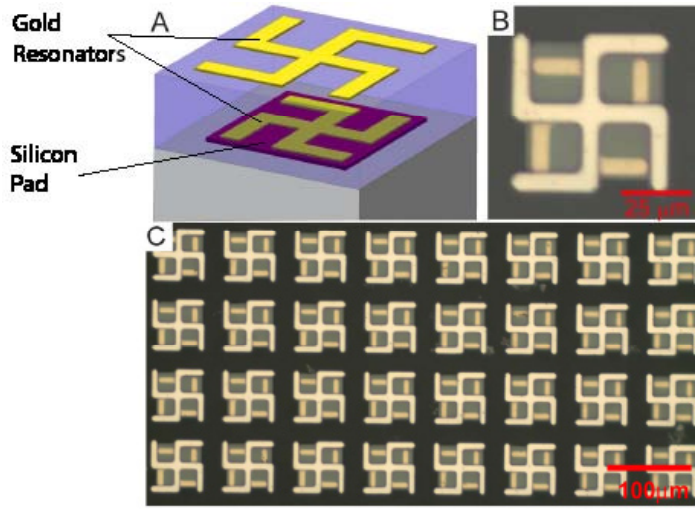

Tunable chiral THz metamaterial. Panel A shows the design of the metamaterial “molecule”. Two gold resonators are separated by a dielectric spacer. Under the bottom resonator is a silicon pad that enables active control of chirality. Panel B shows a picture of one actual molecule taken through a microscope. The silicon pad under the lower resonator is light gray in the picture. Panel C is a picture of part of the array of molecules, which comprises the chiral metamaterial as a whole.

Our design process was constrained by several factors. First, we had to establish a design that twisted the wave. Second, we had to ensure that the wave passed through the metamaterial without any modifications except the twist. Third, we wanted the wave to experience little absorption. This combination was very difficult to achieve. Our design process started with an asymmetric molecule. That is, the top and bottom resonators shown in Figure 1 are oriented oppositely; one is clockwise and the other is counter-clockwise oriented. This combination forces the wave to twist. However, resonators are functional only at particular frequencies. When operated at these “resonant frequencies” resonators exhibit high absorption. Through EM simulations and iterative design we were finally able to create a metamaterial that operated slightly off-resonance. In this way we reduced absorption and maintained the twisting behavior we desired. Numerous design iterations were required to arrive at this point.

Our next task was to modify our design so that it was controllable. Typically, metamaterials have a certain response that is tuned by the size and shape of the resonators. Once fabricated, these metamaterials have a fixed response. It may be a novel response that cannot be obtained in natural materials, but it is fixed nonetheless. Our group at LANL has pioneered metamaterial designs that feature dynamic responses. In our modified designs, an electrical or optical (laser) signal is applied to the metamaterial. This signal changes the behavior of the individual resonators and thereby alters the overall metamaterial response. We were able to add this feature to our chiral THz metamaterial by placing a small silicon pad underneath the lower resonator (Figure 1). In normal operation the metamaterial twists the wave by 12 degrees. When we illuminate the silicon pad with laser light it turns off the lower resonator. This also disables the chirality so the metamaterial can no longer twist the wave. Using the laser, we can actively control how much twist the wave experiences. These design modifications were done using semiconductor analysis and EM simulation tools.

Having reached several suitable designs, we fabricated our metamaterials. Fabrication was performed at the Center for Integrated Nanotechnologies cleanroom in Albuquerque, NM. This was a multi-layer fabrication. Each layer of the metamaterial was consecutively patterned using conventional photolithographic techniques.

We then used our THz characterization labs to measure the metamaterials. We found that our measured results were very consistent with our simulations. Our originally designed THz chiral metamaterial featured optical activity, low absorption, and affected nothing but the polarization rotation (or twist). The twist was found to be 12 degrees, yet the metamaterial was only about 1/18th of a wavelength thick. This corresponded to chirality about 10,000 times stronger than in natural materials such as quartz. We fabricated and measured three other metamaterials

that had even greater chirality. The strongest could twist the EM wave about 45 degrees. However, these stronger metamaterials also produced distortions of the wave, which was an undesirable trade-off.

Next we demonstrated that our metamaterials were dynamic. By illuminating the metamaterial with an infrared laser we could switch the chirality on and off. This was the first demonstration of an engineered material that could actively control the twist of a passing THz wave. It represents an enormous step forward in THz technology (in terms of polarization control). But this technology is generally important to all EM technologies, across the spectrum. Our designs are scalable, meaning this approach should work well at almost any frequency.

Finally, we analyzed our results to see how chirality could affect absorption in NIMs. Mathematical inversion techniques are available to extract "effective parameters" of metamaterials. One example of an effective parameter is refractive index. We performed these extractions and found that we had indeed achieved negative index. Though already demonstrated, this was still a useful result in our work because it allowed us to quantify absorption in a NIM. This was one of our original goals. We found that chirality was not a route to low absorption NIMs, despite earlier conjectures in the community. More importantly, however, we demonstrated something that had never been done. Our metamaterial was dynamic; it had switchable chirality. As such it also had the ability to switch from negative to positive index, on demand! All of these interesting results were prepared into a paper, which has been submitted to Nature Photonics [1] and is currently under review. Many of our results have already been published [2] or presented at various conferences [3-8] as invited works.

One project that has spawned from our original work is the study of how chiral metamaterials might reverse the Casimir force. This is a weak nuisance force that causes nano-machines to stick together. Its reversal would be highly important for future nano-mechanical devices. We are collaborating with Iowa State University to study this phenomenon further. This also supports an external project of more general scope studying the Casimir force and its relation to all types of metamaterial.

Impact on National Missions

This project positively impacted both Laboratory and national missions. First, it enhances our fundamental understanding of engineered materials. As such, it has built LANL's capability to understand the limitations and applications of metamaterials. This is most relevant in the THz frequency region, where natural materials have proven less than ideal. This capability is important for other efforts also. We were funded ($975k) with the LANL Theoretical division to study how metamaterials might tune the Casimir force. Our chiral metamaterials work is going to add value to this project. The work has generally drawn the interest of several government agencies including DOD, DOE, and DHS, who are interested in technologies supporting ubiquitous sensing and threat reduction. We continue to pursue external opportunities based on the results of this project. Lastly, this project helped propel our group to worldwide metamaterial leadership in dynamic and THz metamaterials. This has opened the door to fruitful collaborations and commercialization opportunities, which we have pursued through patent applications.

References

1. Zhou, J., D. Roy Chowdhury, R. Zhao, A. K. Azad, H. Chen, C. M. Soukoulis, A. J. Taylor, and J. F. O'Hara. Active terahertz chiral metamaterial with tunable optical activity. Submitted to Nature Photonics.

2. Zhao, R., J. Zhou, T. Koschny, E. N. Economou, and C. M. Soukoulis. Repulsive casimir force in chiral metamaterials. 2009. Physical Review Letters. 103 (10): 103602.

3. Zhou, J., B. Wang, E. Plum, T. Koschny, V. Fedotov, H. Chen, A. Taylor, J. O'Hara, N. Zheludev, and C. Soukoulis. Chiral metamaterials with negative refractive index. Presented at International Workshop on Electromagnetic Metamaterials, III.(Los Alamos, New Mexico, 18-19 May, 2009).

4. O'Hara, J., J. Zhou, A. Taylor, D. Dalvit, F. da Rosa, P. Milonni, I. Brener, and P. Davids. Metamaterial design considerations for Casimir force control. Presented at New Frontiers in Casimir Force Control.(Santa Fe, New Mexico, 26-28 Sep. 2009).

5. Zhao, R., J. Zhou, T. Koschny, E. Economou, and C. Soukoulis. Repulsive Casimir force in chiral metamaterials. Presented at New Frontiers in Casimir Force Control. (Santa Fe, New Mexico, 26-28 Sep. 2009).

6. Jiangfeng Zhou. , Rongkuo Zhao, C. M. Soukoulis, A. J. Taylor, and J. O'Hara. Chiral THz metamaterial with tunable optical activity. 2010. In 2010 Conference on Lasers and Electro-Optics (CLEO) ; 16-21 May 2010 ; San Jose, CA, USA.p. 1.

7. O'Hara, J. F., J. Zhou, D. Roy Chowdhury, M. T. Reiten, A. K. Azad, H. Chen, L. Earley, A. J. Taylor, C. Soukoulis, R. Zhao, T. Koschny, A. Gossard, and H. Lu. Nonlinear metamaterial investigations from RF to terahertz... and more. Presented at International Workshop on Electromagnetic Metamaterials, IV.(Santa Ana Pueblo, New Mexico, 11-12 Aug. 2010).

8. Zhou, J., R. Zhao, C. Soukoulis, A. J. Taylor, and J. F. O'Hara. Chiral THz metamaterial with optical activity. To appear in Metamaterials 2010: Fourth International Congress on Advanced Electromagnetic Materials in Microwaves and Optics.(Karlsruhe, Germany, 13-16 Sep. 2010).

Publications

Zhou, J., R. Zhao, C. Soukoulis, A. J. Taylor, and J. F. O'Hara. Chiral THz metamaterial with optical activity. To appear in Metamaterials 2010: Fourth International Congress on Advanced Electromagnetic Materials in Microwaves and Optics.(Karlsruhe, Germany, 13-16 Sep. 2010).

O'Hara, J., J. Zhou, D. Roy Chowdhury, M. T. Reiten, A. K. Azad, H. Chen, L. Earley, A. J. Taylor, C. Soukoulis, R. Zhao, T. Koschny, A. Gossard, and H. Lu. Nonlinear metamaterial investigations from RF to terahertz... and more. Presented at International Workshop on Electromagnetic Metamaterials, IV.(Santa Ana Pueblo, New Mexico, 11-12 Aug. 2010).

Jiangfeng Zhou. , Rongkuo Zhao, C. M. Soukoulis, A. J. Taylor, and J. O'Hara. Chiral THz metamaterial with tunable optical activity. 2010. In 2010 Conference on Lasers and Electro-Optics (CLEO) ; 16-21 May 2010 ; San Jose, CA, USA.p. 1.

Zhao, R., J. Zhou, T. Koschny, E. Economou, and C. Soukoulis. Repulsive Casimir force in chiral metamaterials. Presented at New Frontiers in Casimir Force Control. (Santa Fe, New Mexico, 26-28 Sep. 2009).

O'Hara, J., J. Zhou, A. Taylor, D. Dalvit, F. da Rosa, P. Milonni, I. Brener, and P. Davids. Metamaterial design considerations for Casimir force control. Presented at New Frontiers in Casimir Force Control.(Santa Fe, New Mexico, 26-28 Sep. 2009).

Zhou, J., D. Roy Chowdhury, R. Zhao, A. K. Azad, H. Chen, C. M. Soukoulis, A. J. Taylor, and J. F. O'Hara. Active terahertz chiral metamaterial with tunable optical activity. Submitted to Nature Photonics.

Zhou, J., B. Wang, E. Plum, T. Koschny, V. Fedotov, H. T. Chen, A. J. Taylor, J. F. O'Hara, N. Zheludev, and C. Soukoulis. Chiral Metamaterials with Negative Refractive Index. Presented at International Workshop on Electromagnetic Metamaterials III: Toward Real World Applications.(Los Alamos, NM, 18-19 May, 2009).

Zhao, R., J. Zhou, T. Koschny, E. N. Economou, and C. M. Soukoulis. Repulsive Casimir Force in Chiral Metamaterials. 2009. Physical Review Letters. 103: 103602.

Laboratory Directed Research & Development
Los Alamos National Laboratory
PO Box 1663, MS M708
Los Alamos, NM 87545
505-667-1235 (phone)